Applied Ecology and Environmental Research

International Scientific Journal

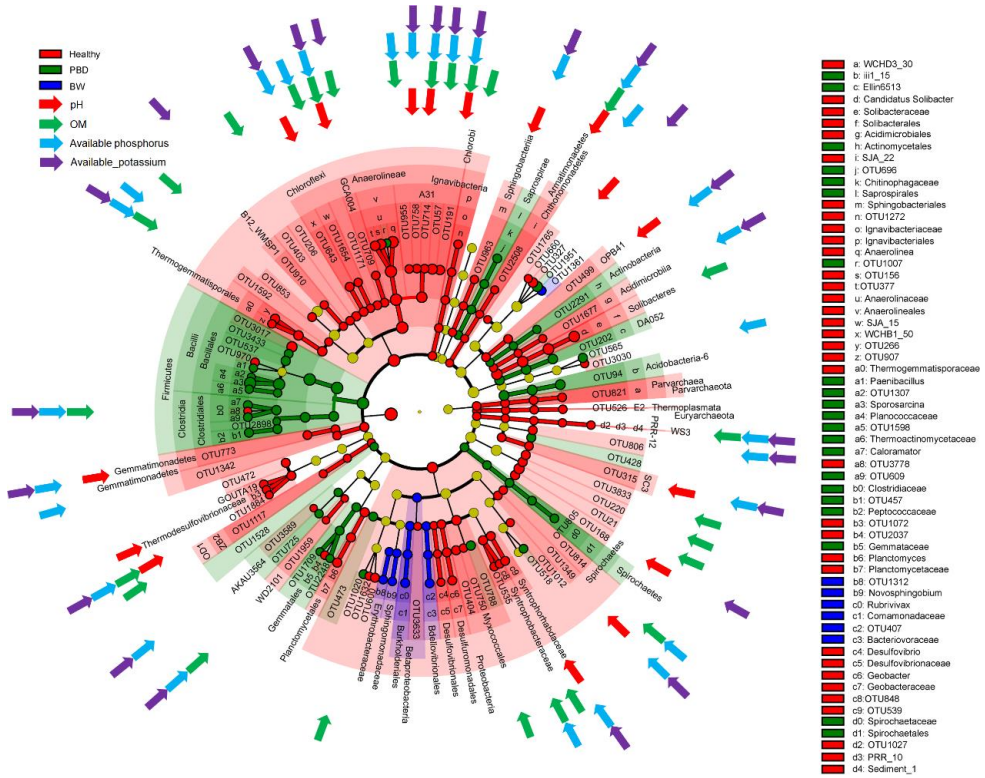

VOLUME 18 * NUMBER 2 * 2020

http://www.aloki.hu
ISSN 1589 1623 / ISSN 1785 0037
DOI: http://dx.doi.org/10.15666/aeer

DROUGHT STRESS TOLERANCE IN TRANSGENIC WHEAT CONFERRED BY EXPRESSION OF A DEHYDRATION-RESPONSIVE ELEMENT-BINDING 1A GENE

MEHMOOD, K.[1,2] – ARSHAD, M.[2*] – ALI, G. M.[3] – SHAH, S. H.[4] – ZIA, M. A.[3] – QURESHI, A. A.[5] – QURESHI, R.[2]

[1]*Department of Biology/Botany, Pir Mehr Ali Shah Arid Agriculture University, Rawalpindi, Attock Sub-Campus, Pakistan*

[2]*Department of Botany, Pir Mehr Ali Shah Arid Agriculture University, Rawalpindi, Pakistan*

[3]*National Institute for Genomics & Advanced Biotechnology (NIGAB), National Agricultural Research Centre (NARC), Islamabad, Pakistan*

[4]*Department of Agricultural Sciences, Allama Iqbal Open University, Islamabad, Pakistan*

[5]*Department of Horticulture, Pir Mehr Ali Shah Arid Agriculture University, Rawalpindi, Pakistan*

**Corresponding author*
e-mail: arshad2uaar@yahoo.com

(Received 1st Apr 2019; accepted 31st Oct 2019)

Abstract. Drought stress hinders root and shoot growth, leaf area, biomass accumulation, plant fresh and dry weight signifying the severe losses of plant growth and development. During drought stress, different genes are activated that increase the drought tolerance efficiency of plants. In this study, *DREB1A* gene was transformed in wheat cv. Lasani-08 to improve drought tolerance efficiency after optimizing in planta *Agrobacterium* mediated transformation protocol. The results reveal that 3.0 mg/l 2, 4-D and 6 h soaking period were found to be the best combination for in planta transformation. The inoculation of seeds with *Agrobacterium* suspension before germination of apical meristem was proved to be the best time for obtaining more transformation efficiency (6.38%) as compared to seeds inoculation after germination of apical meristem. Molecular analyses of transgenic plants through PCR, Southern blotting and RT-PCR confirmed the presence, number of copies and expression profile of transgene in T_1 generation. The drought tolerance efficiency was assessed in T_2 transgenic plants on the basis of agronomical and biochemical analyses. These detailed analyses reveal that *DREB1A* gene has fostering effect on the expression of a large number of genes by means of enhanced germination frequency, germination rate index, shoot, root and coleoptiles lengths, relative water contents, proline contents and total chlorophyll contents of transgenic plants relative to control plants. In summary, our results propose that *DREB1A* is involved in improving drought stress tolerance of transgenic wheat by sustaining growth and yield of plants.
Keywords: *drought stress, DREB1A, in planta transformation, proline contents, relative water contents, transgenic wheat, total chlorophyll contents*

Introduction

Wheat (*Triticum aestivum* L.) is an important cereal crop and it plays a significant role in food security of the world. It is a major crop of Pakistan (Ishaq and Memon, 2016; Mehmood et al., 2016; Abbas et al., 2017). The contribution of wheat to GDP is 3.4% and its share in agriculture value addition is 13.8% (Adeel et al., 2017). Pakistan has to produce extra food grains to meet the dietary needs of the increasing population which is currently over 191.71 million (Pakistan Economic Survey, 2014-15). Overall

http://www.aloki.hu ● ISSN 1589 1623 (Print) ● ISSN 1785 0037 (Online)
DOI: http://dx.doi.org/10.15666/aeer/1802_19992024

dietary needs of the population have reached to twenty million tons wheat (Anjum et al., 2016). However, its productivity is affected by many environmental stresses due to sudden climatic changes and scarcity of water (Alghabari et al., 2015). Due to limitation of water resources, wheat cultivation area has been exposed to water shortage. Due to climatic changes and continuous droughts in summer, the yield losses have been more intensified. Severe yield losses can occur by drought stress because it can happen at any stage of development in wheat especially in arid and semi-arid areas (Farooq et al., 2011). Drought stress obstructs root growth, shoot growth, leaf area, biomass accumulation, plant fresh and dry weight signifying the severe losses of plant development (Xue et al., 2003; Jan et al., 2017). The degree of drought sensitivity is dependent on developmental phase of wheat plants because some developmental stage can cope with the drought, while others are highly sensitive to drought. For example, if wheat is vulnerable to drought stress before anthesis stage, then reduction in plant height, number of ears and leaf area will occur (Hassan et al., 1987). While the number of kernels per ear and weight of kernels of wheat is reduced if the drought stress occurs at lateral stages of development (Sieling et al., 1994). Soil moisture stress at heading stage caused reduction in shoot growth, while no drought effect was evident on root growth (Saidi et al., 2008). Similarly, 37% yield reduction was recorded by shortage of water at booting to maturity stage, while this loss was increased to 44%, when drought stress befell at heading to maturity stage (Prasad et al., 2011).

Plants have adopted many mechanisms to tolerate the effects of drought such as metabolic accumulation of organic solutes including proline, glycine betaine, sugars etc. (Zhu, 2001) wax accumulation (Chen et al., 2003) production of antioxidant enzymes (Mowla et al., 2002), abscisic acid accumulation (Marcotte et al., 1989) and through transcription factors (Jain et al., 2001). During drought stress, different genes are activated and increase the drought tolerance of plants. These include *BADH*, *WXP1* and *DREB1A* (Zhang et al., 2005; Pellegrineschi et al., 2004). Researchers are trying to cope with drought problem using *Agrobacterium* mediated genetic transformation (Cheng et al., 1997; He et al., 2010). In this phenomenon, T-DNA region of the Ti-plasmid is excised, transformed into the host plant tissue and integrated into the genome of the plant (Ali et al., 2016). *Agrobacterium* mediated genetic transformation depends upon different factors affecting the rate of transformation (Amoah et al., 2001; Yenchon and Te-chato, 2012; Wu et al., 2003).

Genetic engineering approach is fast and precise means (Cushman and Bohnert, 2000) of genetic improvement of crops transferring only desirable genes into crop of interest (Jones, 2005). *DREB1A* gene enhanced the drought tolerance ability of transgenic plants triggering the expression of twelve (*CBF3/DREB1A*) target genes in non-stress condition, while 27 extra genes were stimulated in water stress conditions without involving growth retardation (Oh et al., 2005). Target genes of *CBF3/DREB1A* includes RNA binding proteins, transcription factors, KIN (cold inducible) proteins, Phospholipase C, Sugars transport proteins, Osmoprotectant biosynthesis proteins, Carbohydrate metabolism related proteins, Late embryogenesis abundant (LEA) proteins and the Proteinase inhibitors (Seki et al., 2001).

Gene transformation of wheat is still comparatively difficult as compared to other cereals due to relatively longer genome and being tissue culture recalcitrant crop. So, there is strong need to improve and select the proper methodology of genetic transformation. In planta *Agrobacterium* mediated transformation is a cheap and fast method to develop transgenic plants. It was previously used for the development of

http://www.aloki.hu ● ISSN 1589 1623 (Print) ● ISSN 1785 0037 (Online)
DOI: http://dx.doi.org/10.15666/aeer/1802_19992024

transgenic maize (Brunecky et al., 2011), tomato (Shah et al., 2015; Ali et al., 2018), rice (Andrieu et al., 2012), tobacco (Brunecky et al., 2011) and wheat (Borisjuk et al., 2019; Khan et al., 2019).

Keeping in view the above facts, the present study was planned to optimize the in planta transformation protocol for transformation of *DREB1A* gene through *Agrobacterium* strain EHA101 in wheat cultivar Lasani-08. During this study, concentration of 2, 4-D and soaking time of seeds were optimized. Comparison was made between two procedures of seeds inoculation i.e. inoculation before germination of seeds and inoculation after germination of seeds. The T_2 transgenic plants were scrutinized on the basis of agronomical and biochemical characteristics.

Materials and methods

Experimental sites and source of explants

During our previous research study (Khalid et al., 2013), we confirmed that among six wheat cultivars namely Lasani-08, Inqalab 91, Tatara, Chakwal 97, GA-02 and Khyber obtained from Crop Science Institute (CSI), NARC Islamabad, one cultivar Lasani-08 was found to be the best for regeneration. Therefore, in this study we used cv. Lasani-08 and optimized factors affecting in planta transformation and then screening of transgenic plants was done on the basis of agronomical as well as biochemical characteristics. Optimization of in planta transformation protocol as well as transgenic wheat plants carried out in NIGAB, NARC, Islamabad, Pakistan, while screening of drought tolerance of transgenic line was done at Plant Physiology Lab, PMAS, Arid Agriculture University, Rawalpindi, Pakistan.

Agrobacterium-mediated in planta transformation

The experimental procedure of in planta transformation has been shown in *Figure 1*. *Agrobacterium* strain EHA101 carrying binary plasmid PCAMBIA containing *DREB1A* gene under 35 S promoter with *hpt* (plant selectable marker gene) and kanamycin resistance gene (bacterial selectable marker gene) was used in this study (*Fig. 2a*). Seeds of wheat cv. Lasani-08 were washed with tap water to remove dust and surface sterilization was done with 70% ethanol for 30 s, 60% Clorox for 15 min and then washed with autoclaved distilled water 3-5 times to remove the Clorox from the surface of seeds. Sterilized seeds were placed on filter paper and soaked in distilled water supplemented with different concentration of 2, 4-D (2.0, 3.0 and 4.0 mg/l) for 3, 6 and 9 h to get the suitable combination of soaking time and 2, 4-D for maximum transformation efficiency. On the other hands, in case of inoculation after germination, seeds were soaked in distilled water devoid of 2, 4-D until emergence of coleoptiles. Subsequently, seeds were peeled off with the help of forceps at the top of embryo to expose the embryonic apical meristem. O.D of overnight bacterial culture was maintained at $O.D_{600\ nm} = 0.8 - 1.0$ by photonanometer for co-infection. Embryo tip was cut with sharp blade, injured with acupuncture pin No.35 and a drop of *Agrobacterium* suspension was inserted. Then these seeds along with embryonic apical meristem were dipped in inoculation medium (*Agrobacterium* suspension containing 3.0 mg/l 2, 4-D and 300 μM acetosyringone) for 40 min. The culture was placed for 48 h in dark at 28 °C in growth chamber for co-cultivation. The *Agrobacterium* attached with seeds during co-cultivation were eliminated by washing with autoclaved distilled water then

http://www.aloki.hu ● ISSN 1589 1623 (Print) ● ISSN 1785 0037 (Online)
DOI: http://dx.doi.org/10.15666/aeer/1802_19992024

with MS liquid supplemented with 500 mg/l cefotaxime sodium. Sterilized seedlings were transferred in chiller at 5 °C for further development. Pre-selection media (MS liquid supplemented with 3.0 mg/l BAP, 500 mg/l cefotaxime sodium) was used for first 3-5 d. Then culture was transferred to selection media (MS liquid, 250 mg/l cefotaxime and 50 mg/l hygromycin). These seedlings were vernalized for further 2-3 weeks and hygromycin selected seedlings were transferred to glass house under controlled conditions for further growth and development.

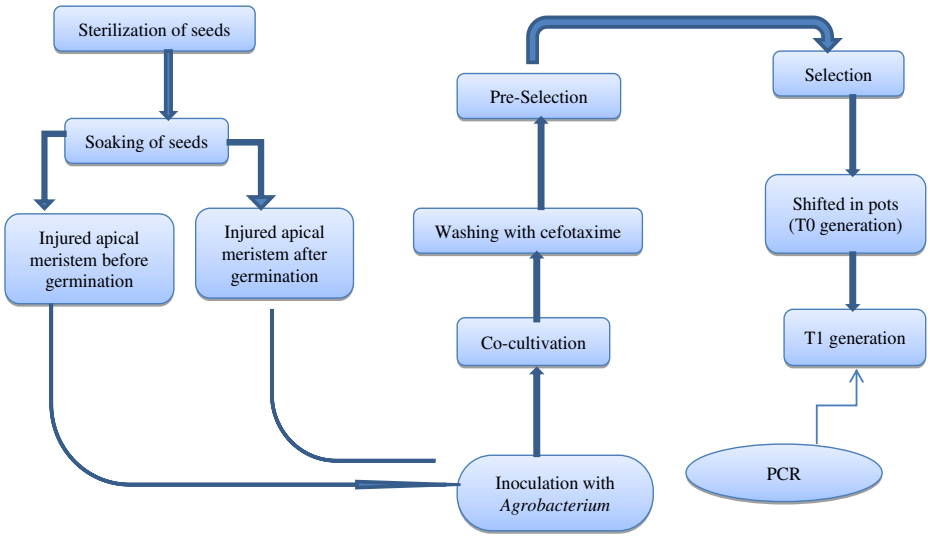

Figure 1. *Flow diagram showing the development of wheat transgenic plants via in planta method of Agrobacterium-mediated transformation*

Confirmation of transgenic plants

The 3-weeks old hygromycin resistant seedlings (T_0 generation) were shifted to glass house till maturity. The transgenic seeds of T_0 generation were further sown to get T_1 generation. When plants of T_1 generation reached up to 2-3 leaf stage, genomics DNA was isolated from fresh leaves by CTAB method (Murray and Thompson, 1980) and then PCR was performed using *DREB1A* gene specific primers; F 5'-TGAACTCATTTTCTGCTTT-3' and R 5'-TAATAACTCCATAACGATA-3'. The product of PCR was run on 1% gel electrophoresis for 30 min at 100 V current and visualized by gel documentation system (Alpha imager HP) under UV light. The 5 µl of each PCR product was loaded in gel with the help of 2.0 µl bromophenol blue for each sample as loading dye. 1 kb ladder was used to compare size of required band (649 bp).

Southern blotting

The copy number of inserted gene in transgenic plants was determined through southern blotting. For probe preparation, plasmid DNA was isolated and amplified by PCR using *DREB1A* primers. About 50 µl of PCR product of plasmid DNA was run on 1.5% gel electrophoresis applying 50 V voltage, 100 A current and 50 W power for 30 min. The required band was visualized under UV light in gel documentation system and cut the gel around the band and transferred the band along with gel in Eppendorf tube. Binding buffer of 600 µl was mixed, incubated for 10 min at 56 °C with continuous shaking at the rate of 500 rpm in incubator. After melting, gel was shifted

http://www.aloki.hu ● ISSN 1589 1623 (Print) ● ISSN 1785 0037 (Online)
DOI: http://dx.doi.org/10.15666/aeer/1802_19992024

into column and centrifugation was done at 14000 rpm for 1 min. Filtrate was discarded and pellet was washed with 700 µl washing buffer having ethanol through centrifugation at 14000 rpm for 1 min and then filtrate was discarded. The 50 µl elusion buffer was added at mid of membrane and incubated for 1 min in centrifuge machine and then started centrifugation at the rate of 14000 rpm for 1 min. The pure DNA was eluted and stored at -80 °C. DNA (10 µg) of three transgenic plants (K1, K2, K3) of T_1 generation obtained from in planta transformation was digested with HindIII endonuclease. Then samples were run on 0.8% agarose gel. Subsequently, it was blotted on a nylon membrane. Non-Radioactively labeled (Fermentas Biotin DecaLabel DNA labeling kit) 649 bp PCR amplified fragment plasmid DNA was used as a probe.

RNA isolation and cDNA synthesis

Leaf sample (80 mg) was homogenized with the help of 1 ml Tri reagent, and then this homogenized mixture was placed at room temperature for 5 min in Eppendorf tubes. 2 µl of chloroform was added in this homogenized mixture and vigorously shaking was done for 15 s. The homogenate was placed at room temperature for 2-15 min and then centrifugation was done at 12000 rpm for 15 min. After centrifugation, a colorless aqueous phase (having RNA) was appeared on the top of Eppendorf tube. This colorless aqueous phase was taken into new Eppendorf tube and 500 µl isopropanol was added into each sample and stored for 5-10 min at room temperature. Again, centrifugation was done for 8 min at 12000 rpm. Supernatant was poured out and 70% ethanol (1 ml for each sample) was used for washing RNA pellet, vertexed following centrifuge at 7500 rpm for 5 min. Ethanol discarded and pellet remained in Eppendorf which was air-dried for 3-5 min. RNAase free water was used to dissolve RNA pellet. This dissolved form of RNA incubated for 10-15 min at 55-60 °C temperature and then stored at -80 °C for further used. For cDNA synthesis, PCR profile was set as 65 °C for 5 min, 42 °C for 80 min and 72 °C for 10 min. 20 µl reaction volumes were used for each sample. Conventional PCR was carried out in two steps. In step one, PCR tubes were placed in PCR machine for 5 min at 65 °C. Each PCR tube contained RNA (4 µl), oligodT (1 µl) and water (9.5 µl). After 5 min, they were chilled in ice for 2-3 min. In step 2, for each sample, a master mixture containing RT buffer (4 µl), dNTPs (1 µl) and RT (0.5 µl) was prepared before starting first step PCR. This master mixture (5.5 µl) was added into chilled PCR tubes getting total volume of 20 µl in each PCR tube. Then, these PCR tubes were immediately placed in PCR machine at 42 °C for 80 min and 72 °C for 10 min (PCR profile was already set). After completion of cDNA synthesis, samples were stored at -20 °C for further use in RT-PCR.

RT-PCR analysis

In order to check the expression of desired gene, RT-PCR analysis was performed. For it, a reaction volume (20 µl) was used in each PCR tube. This reaction volume was made by mixing cDNA (2 µl) with master mixture (18 µl). For master mixture, 10.5 µl water, forward (1 µl) and reverse (1 µl) primers, 2.4 µl $MgCl_2$, 0.4 µl dNTPs, 0.3 µl Taq Polymerase and 2 µl Taq DNA buffer were mixed. PCR profile was set as: initial denaturation temperature 94 °C for 5 min for 1 cycle; for 35 cycles temperature profile was set as denaturation at 94 °C for 1 min, annealing at 50 °C for 1 min and extension at 72 °C for 1 min. At the end of one cycle, final extension temperature was set at 72 °C for 10 min.

http://www.aloki.hu ● ISSN 1589 1623 (Print) ● ISSN 1785 0037 (Online)
DOI: http://dx.doi.org/10.15666/aeer/1802_19992024

Evaluation of drought tolerance of transgenic plants on the basis of agronomical characteristics

The transgenic plants were scrutinized for their drought tolerance at three stages. At first stage, Polyethylene Glycol (PEG) solution was applied on petri plates to induce artificial drought stress (-2, -4, -6 and -8 bars osmotic stress) in laboratory. The stock solution of PEG 8000 (25% w/v) was prepared using autoclaved distilled water. Then dilution of different concentration was prepared starting from 6.0%, 8.0% up to 24.0%. The osmotic potential was measured using osmometer (Osmomate 030) at Central Laboratory PMAS, Arid Agriculture University, Rawalpindi, Pakistan. The reading was taken in osmomol/kg which were converted into MPa using formula = CRT, here C = Osmolality in moles per kg, R = .0083 and T = 25 °C + 273. MPa value was converted into bars by multiplying -10. A graph (standard curve) was plotted between PEG percentage and bar values. Four levels of PEG (-2, -4, -6 and -8 bar) osmotic stress were used to induce drought at germination stage of transgenic and non-transgenic (control) plants by sowing seeds on moist filter papers with different levels of PEG solution at 25 °C. The healthy seeds were sterilized with 60% Clorox for 15 min followed by four to five times washing with autoclaved distilled water. Subsequently, they were placed in petri plates having two filter papers wet with 5 ml of different PEG-solution. Petri plates were kept in growth chamber at 25 °C and data about germination of seeds was recorded daily for 8 days. At second stage, drought stress was induced withholding water to transgenic and control plants in pots under glass house conditions. At third stage, transgenic plants were screened out on the basis of drought tolerance efficiency relevant to crop yield.

Data about germination percentage were recorded after the interval of 24 h up to 8 days. The calculation was made using this formula:

$$\text{Germination (\%)} = \frac{\text{Number of seeds germinated}}{\text{Total number of seeds used}} \times 100 \quad \text{(Eq.1)}$$

Germination rate index was determined using the formula described by Camargo and Vaughan (1973):

$$\text{Germination rate index} = \frac{\text{Number of seeds germinated}}{\text{day}} \quad \text{(Eq.2)}$$

The length of shoot, root and coleoptiles were measured in cm with the help of scale at the 8th day of experiment.

Evaluation of drought tolerance of transgenic plants on the basis of biochemical characteristics

The drought was induced at vegetative stage of T_2 transgenic and control plants withholding water for 8 days. Relative water contents (RWC) of transgenic and control plants were determined following method proposed by Barrs and Weatherley (1962). Fresh leaves were excised from plants, sealed within aluminum file and plastic bag and quickly transferred to lab. Fresh weight was taken immediately after arrival in Laboratory. Then, turgid weight was taken after soaking leaves into distilled water for 6 h at room temperature. Dry weight was taken after drying the samples at 70 °C in an oven. Finally, the calculation of RWC was made with the help of following formula:

http://www.aloki.hu ● ISSN 1589 1623 (Print) ● ISSN 1785 0037 (Online)
DOI: http://dx.doi.org/10.15666/aeer/1802_19992024

$$\text{RWC}\,(\%) = \frac{\text{Fresh weight} - \text{Dry weight}}{\text{Turgid weight} - \text{Dry weight}} \times 100 \quad \text{(Eq.3)}$$

Proline contents (mg/g fresh weight) were determined following the method devised by Bates et al. (1973). Fresh leaf sample (0.25 g) was ground and homogenized with 5 ml of 3% sulfosalicylic acid. Extract was poured into test tubes and allowed to set down the debris. Then, 2 ml of supernatant was taken into another test tube mixed with 2 ml ninhydrin reagent (ninhydrin = 1.25 g, glacial acetic acid = 30 ml and 6 M phosphoric acid; 20 ml) and 2 ml glacial acetic acid. Samples were boiled in water bath at 100 °C for 1 h and then reaction was immediately stopped in ice. After cooling, 4 ml toluene was added into each sample and shaken vigorously for few seconds, and upper layer of toluene appeared after few seconds. Supernatant was collected into another set of test tubes. Absorbance of supernatant was taken by spectrophotometer using the wavelength of 520 nm. Toluene was used as a blank.

$$\text{Proline contents}\left(\frac{\text{mg}}{\text{g}}\text{FW}\right) = \frac{(\text{Absorbance of sample}) \times (\text{k value}) \times (\text{Dilution factor})}{\text{Weight of sample}} \times 100 \quad \text{(Eq.4)}$$

Here FW denotes fresh weight.

Total chlorophyll contents (mg/g fresh weight) were measured in Plant Physiology Lab, PMAS, Arid Agriculture University, Rawalpindi, Pakistan according to the method of Arnon (1949). Fresh leaves (5 g) were immersed in 10 ml of 80% ethanol; tubes were capped and digested the samples at 80 °C for 10 min in water bath. Green extract immediately was cooled down in incubator (as a dark room) to give protection from light because it degrades the chlorophyll. Optical density was measured after 3 h for chlorophyll "b" and chlorophyll "a" at 663 nm and 645 nm, respectively using spectrophotometer. Ethanol (80%) was used as a blank.

$$\text{Total chlorophyll contents}\left(\frac{\text{mg}}{\text{g}}\text{FW}\right) = \frac{(20.2 \times \text{OD at 645 nm}) + (8.02 \times \text{OD at 663 nm})}{\text{Weight of sample}} \times \text{V} \quad \text{(Eq.5)}$$

$$\text{Chlorophyll a contents}\left(\frac{\text{mg}}{\text{g}}\text{FW}\right) = \frac{(12.7 \times \text{OD at 663 nm}) - (2.69 \times \text{OD at 645 nm})}{1000 \times \text{Fresh shoot weight (g)}} \times \text{V} \quad \text{(Eq.6)}$$

$$\text{Chlorophyll b contents}\left(\frac{\text{mg}}{\text{g}}\text{FW}\right) = \frac{(22.7 \times \text{OD at 663 nm}) - (4.69 \times \text{OD at 645 nm})}{1000 \times \text{Fresh shoot weight (g)}} \times \text{V} \quad \text{(Eq.7)}$$

Here: V = Volume of extract (ml); OD = Optical density; FW = Fresh weight.

Drought tolerance efficiency (%)

Comparison between transgenic and control plants was done on the basis of drought tolerance efficiency. The transgenic and control plants of T_2 generation were divided into two groups. Each group contained both transgenic and control plants. Drought stress was applied to one group withholding water, while 2nd group plants were kept as a control with continuous irrigation. Drought tolerance efficiency (DTE) was calculated keeping the yield of both groups by following the equation of Fischer and Wood (1981):

$$\text{Drought tolerance efficiency}\,(\%) = \frac{\text{Yield under stress condition}}{\text{Yield under non-stress condition}} \times 100 \quad \text{(Eq.8)}$$

http://www.aloki.hu ● ISSN 1589 1623 (Print) ● ISSN 1785 0037 (Online)
DOI: http://dx.doi.org/10.15666/aeer/1802_19992024

After calculating drought tolerance efficiency, both values were compared and difference was calculated that how much drought tolerance ability of transgenic plants increased through transformation of *DREB1A* gene.

Improvement in wheat for drought tolerance = (DTE% of transgenic plants) – (DTE% of control plants).

Improvement in transgenic plants regarding average spike length, grains per spike, 100-grain weight was measured in both conditions i.e. normal and stress conditions and compared with control plants.

Statistical analysis

Data were recorded in percentage and statistical analysis was carried out applying ANOVA with two factorial CRD using statistics 8.1. Three replications were used for each treatment. The significance of treatment means was further analyzed using LSD test.

Results

Optimization of soaking time and 2, 4 D for in planta transformation

The effects of two treatments (3 and 9 h soaking time) were non-significantly different from one another, while 6 h soaking time was significantly different from these two treatments showing maximum hygromycin resistant plants (18.31% on average basis) on selection media (*Table 1*). Similarly, no significant differences were found between 2.0 and 4.0 mg/l of 2, 4-D, while 3.0 mg/l 2, 4-D showed significant difference from the other two treatments giving 21.8% hygromycin resistant plants. Subsequently, soaking time 6 h and 3.0 mg/l 2, 4-D yielded 25.12% plants survived on the selection media. Conclusively, seeds were soaked in distilled water containing 3.0 mg/l 2, 4-D for 6 h to get maximum transformation efficiency of our desired gene (*Table 1*).

Table 1. *Effect of various soaking times and 2, 4-D concentrations on transformation efficiency (%)*

Soaking time (h)	Hygromycin resistant plants (%)			
	2 mg/l (2, 4-D)	3 mg/l (2, 4-D)	4 mg/l (2, 4-D)	Mean
3	10.53 e	20.42 b	9.23 e	13.39 b
6	15.97 c	25.12 a	14.85 cd	18.31 a
9	14.85 cd	19.87 b	11.20 de	15.31 b
Mean	13.78 b	21.80 a	11.76 b	

Each value is the mean of three replications. Mean values following by the different letters show significant differences ($p \leq 0.05$). For 2, 4-D, LSD value was 2.22 at $p \leq 0.05$. For soaking time, LSD value was 2.22 at $p \leq 0.05$, while for interaction of 2, 4-D and soaking time, LSD was 3.86 at $p \leq 0.05$

Optimization of apical meristem incubation method for in planta transformation

Table 2 shows that three hundred seeds were surface sterilized for each experiment i.e. inoculation before and after germination of apical meristem. Out of which 250 and 263 seeds were co-cultivated, respectively. After co-cultivation, these seeds were washed with MS liquid media having 500 mg/l cefotaxime then transferred to regeneration media. The regeneration frequency was 48 and 40.68% when seeds were inoculated before and after

http://www.aloki.hu ● ISSN 1589 1623 (Print) ● ISSN 1785 0037 (Online)
DOI: http://dx.doi.org/10.15666/aeer/1802_19992024

germination, respectively (*Table 2*). In case of inoculation after germination, apical meristem was blindly injured through cut end of coleoptiles, so it might be damaged cells of mother germ lines due to which regeneration frequency was low, while in case of before germination embryo was visible and was easily targeted for injury. These results suggested that injury of apical meristem before germination of apical meristem was better than that of after germination. Injury should be made very carefully so that germ line mother cells remained safe from damaging. Hygromycin (50 mg/l) was used in selection media and 25 and 0% hygromycin resistant plants were obtained from seeds which were inoculated before and after germination, respectively (*Table 2*).

Table 2. *Assessment of inoculation method for incubating apical meristem before and after seed germination*

In planta transformation steps	Inoculation of apical meristem before seed germination	Inoculation of apical meristem after seed germination
Number of treated seeds	300	300
Number of co-cultivated seeds	250	263
Number of regenerated seeds	120	107
Regeneration percentage	48%	40.68%
Number of hygromycin resistant plants	30	Nil
Hygromycin resistant percentage	25%	Nil
Number of seeds sown in T_1 generation	50	Nil
Number of germinated seeds	47	Nil
PCR positive plants	3	Nil
Transformation efficiency	6.38%	0%

Transformation efficiency was measured by the number of PCR positive plants divided by the total number of explants cultured on selection medium, expressed in percentage

Molecular analysis of wheat transgenes

Seeds of hygromycin resistant plants (T_0 generation) were pooled, out of which only 50 seeds were sown due to limited space and T_1 generation was obtained. 47 seeds were germinated and when seedlings were at 2 to 3 leaf stage, they were confirmation by PCR using *DREB1A* specific primers. The results indicated that 3 plants were PCR positive showing transformation efficiency of 6.38% (*Table 2; Fig. 2b*). These plants were also found positive by PCR using *hpt* specific primers (*Fig. 2c*). In order to assess the inheritance pattern of transgene, segregation analysis was performed by normal PCR using *DREB1A* specific primers. The segregation ratio of three transgenic plants has been shown in *Figure 3*. The data indicated that segregation ratio was 5:5, 4:5 and 2:7 in K1, K2 and K3 transgenic plants, respectively that exhibited non-Mendalian inheritance pattern (*Table 3*). Trizole reagent was used for isolation of RNA from the leaves of transformed plants. cDNA synthesized from RNA was used for amplification of *DREB1A* gene through PCR using gene specific primers. The results show the differential expression pattern of transgenic plants i.e. some transgenic plants gave good expression, while few produced weak expression (*Fig. 4*). Southern blotting was done to detect the number of copies of desired gene in three transgenic plants (K1, K2 and K3) that indicated 1-2 copies of gene (*Fig. 5*).

http://www.aloki.hu ● ISSN 1589 1623 (Print) ● ISSN 1785 0037 (Online)
DOI: http://dx.doi.org/10.15666/aeer/1802_19992024

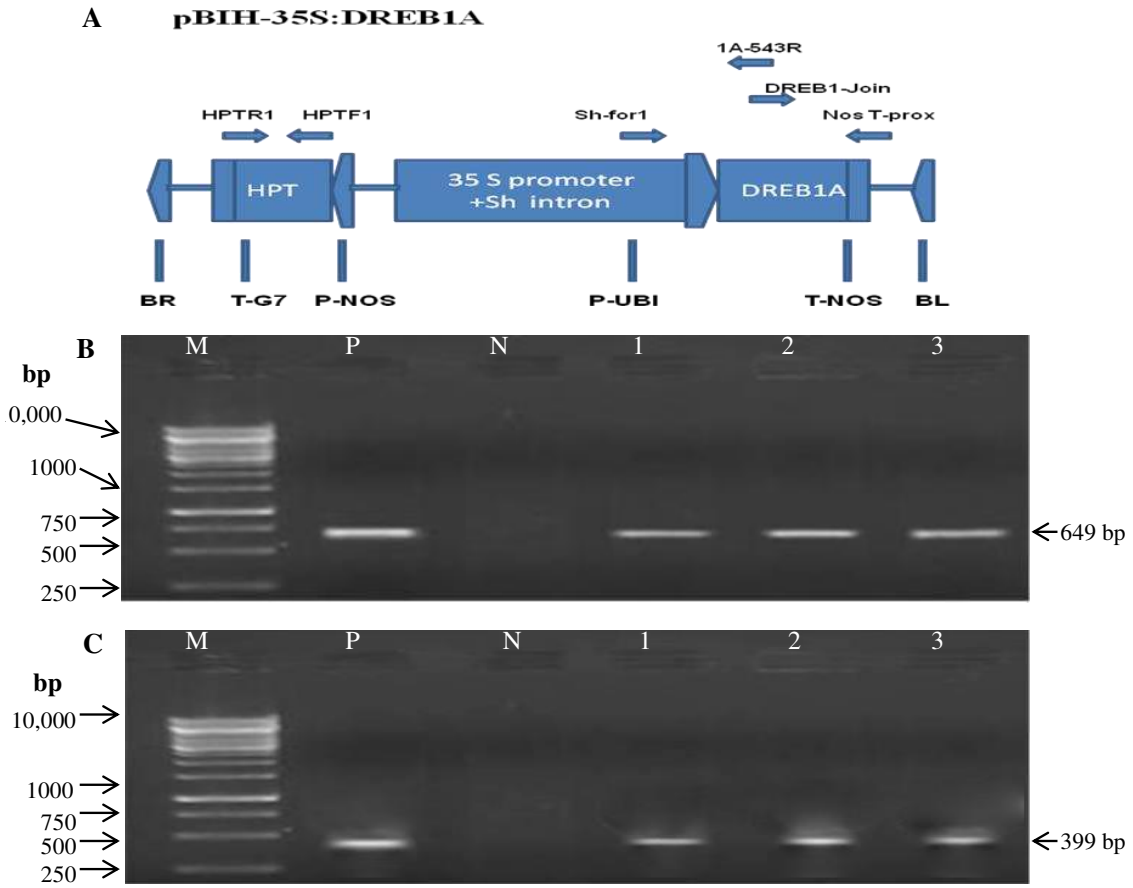

Figure 2. *Confirmation of T_0 and T_1 wheat transgenic plants for the existence of DREB1A (649 bp) and hpt (399 bp) genes within their genomes.* ***A*** *Construct diagram containing DREB1A under 35S promoter. LB: Left border, RB: Right border, T-G7; Terminator, hpt: Hygromycin phosphotransferase gene, T-NOS and P-NOS (terminator and promoter sequences of nopaline synthase gene) (Source: NIGAB, NARC Islamabad, Pakistan).* ***B*** *PCR analysis showing transgenic plants of wheat possessing DREB1A gene (649 bp) using Agrobacterium strain EHA101 (carrying binary plasmid PCAMBIA); Lane M shows 1 kb DNA Ladder (Fermentas), Lane P shows positive control (plasmid pCAMBIA), Lane N shows negative control (non-transgenic wheat). Lanes show 1–3 transgenic plants of wheat.* ***C*** *PCR analysis for presence of hpt gene (399 bp fragment size); Lane M 1 kb DNA Ladder (Fermentas). Lane P positive control (plasmid pCAMBIA), Lane N negative control (non-transgenic wheat), Lanes 1-3 transgenic plants of wheat*

Germination of T_2 transgenic plants improved in response to drought stress

The seeds of the transgenic plants were tested for germination frequency and germination rate index. The transgenic and control seeds were placed on filter paper soaked with different concentrations of PEG solution (-2, -4, -6 and -8 bar osmotic stress) to induce artificial drought stress under controlled condition. *Figure 6* indicated that the transgenic and control plants had significant difference ($P = 0.0000$) at 5% alpha level. Similarly, a significant difference among different treatments of PEG stress as well as among the interaction of transgenic plants, control plants and PEG stress for germination frequency and germination rate index. But there was non-significant difference ($P = 0.2607$) in terms of the interaction of plants and PEG stress at 5% alpha

http://www.aloki.hu ● ISSN 1589 1623 (Print) ● ISSN 1785 0037 (Online)
DOI: http://dx.doi.org/10.15666/aeer/1802_19992024

level. The results showed that the highest germination frequency (94.97%) was recorded in transgenic plants as compared to control plants (80.83%) at -2 bar osmotic stress (*Fig. 6*). Similarly, more germination rate index (5.5) was found in transgenic plants than that of control plants that yielded 2.8 germination rate index (*Fig. 7*).

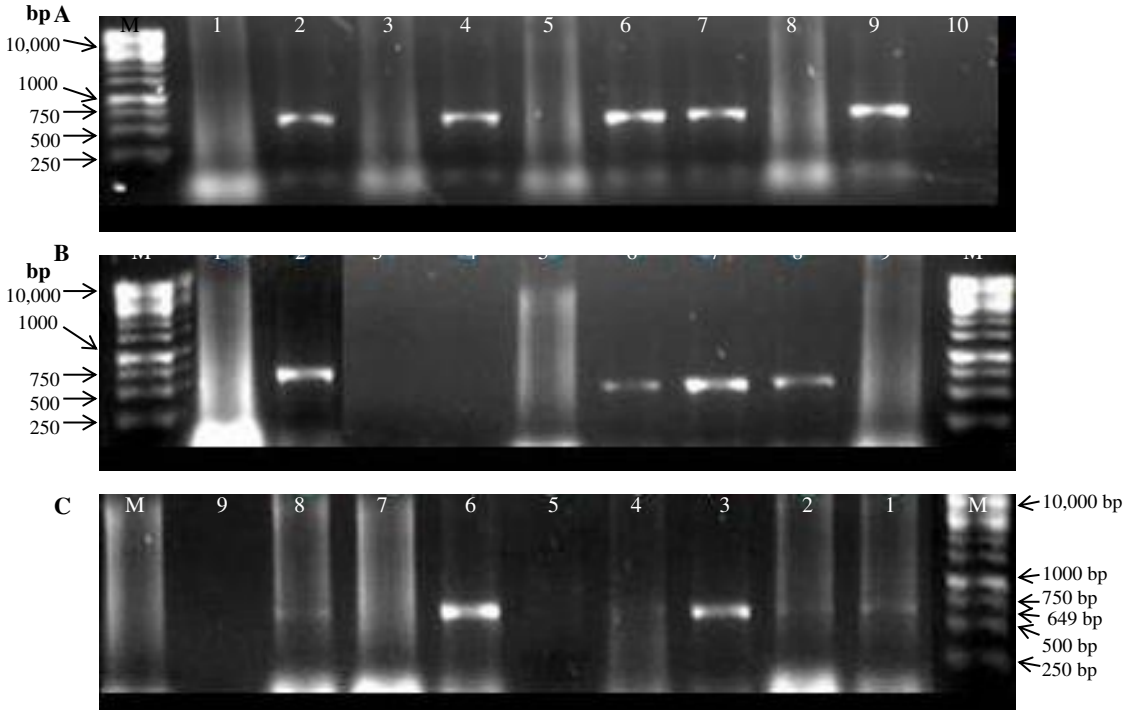

Figure 3. *Segregation analysis of three transgenic plants of wheat (K1, K2 and K3). Seeds obtained from T_1 transgenic plants were sown in pots for T_2 generation. Segregation pattern of DREB1A gene was noticed through PCR using DREB1A specific primers. The segregation ratio was 5: 5, 4: 5 and 2: 7 for three transgenic plants K1, K2 and K3, respectively. The total 28 plants of T_2 generation were tested through PCR for the presence of DREB1A gene using DREB1A specific primers. Results shows that out of these tested plants, 11 plants were PCR positive having DREB1A gene in their genomes. It indicates that transformation was successful in these plants and gene was stably inherited into T_2 generation*

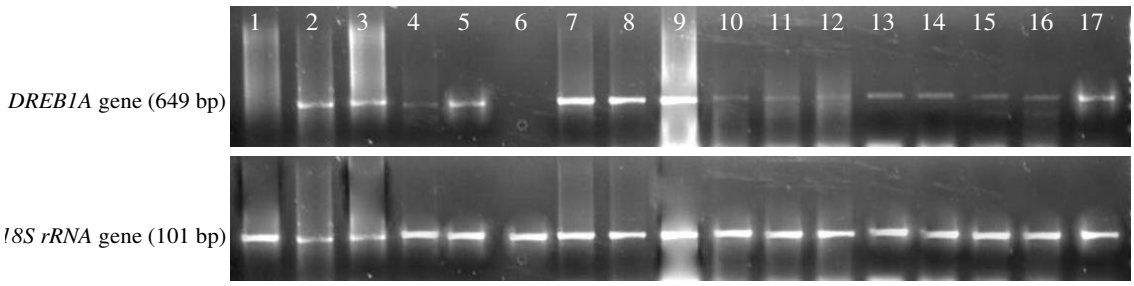

Figure 4. *Expression of DREB1A gene in leaf tissues of T_2 transgenic plants at various levels by semi-quantitative RT-PCR. Here, 18S rRNA gene was used as an internal control. Lane 1 is demonstrating amplicon from control wheat plants. Lanes 2-6 are demonstrating amplicon from K1 transgenic plants. Lanes 7-12 are demonstrating amplicon from K2 transgenic plants. Lanes 13-17 are demonstrating amplicon from K3 transgenic plants*

http://www.aloki.hu ● ISSN 1589 1623 (Print) ● ISSN 1785 0037 (Online)
DOI: http://dx.doi.org/10.15666/aeer/1802_19992024

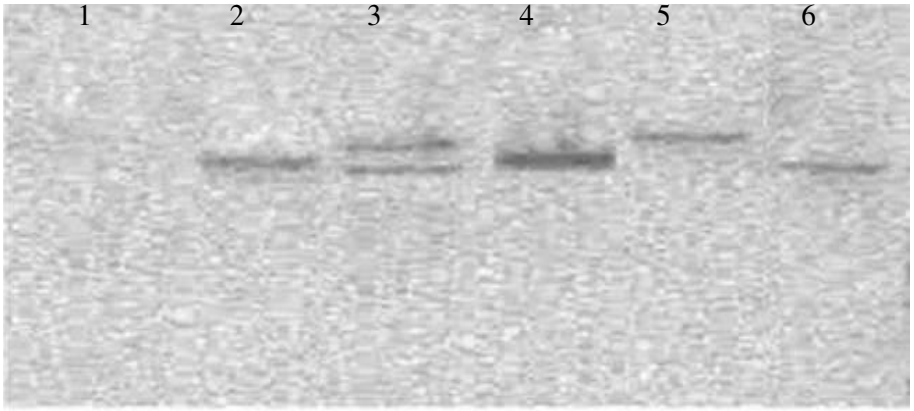

Figure 5. *Southern blotting of T_2 wheat transgenic plants using HindIII endonuclease for DNA digestion of transgenic and control plants and hybridized with DREB1A-Fermentas Biotin DecaLabel probe. Lane 1 is showing negative control (non-transgenic plants), Lane 2 is showing transgenic plants K1, Lanes 3-4 are showing transgenic plants K2, Lanes 5-6 are showing transgenic plants K3*

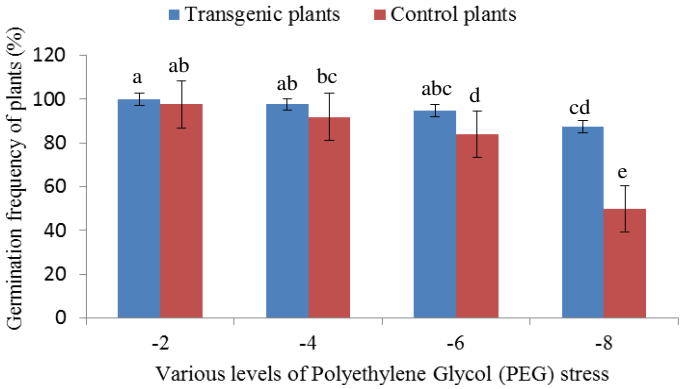

Figure 6. *Effect of various levels of Polyethylene Glycol (PEG) stress on germination frequency (%) of transgenic and control plants of wheat. The error bars indicate standard error. Means not sharing a letter in common differ significantly at 5% probability level*

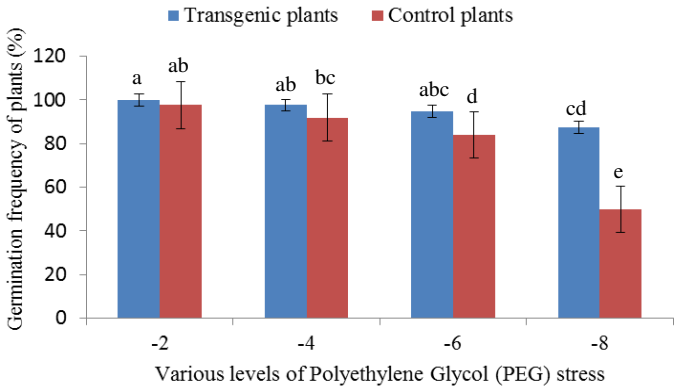

Figure 7. *Effect of various levels of Polyethylene Glycol (PEG) stress on germination rate index of transgenic and control plants of wheat. The error bars indicate standard error. Means not sharing a letter in common differ significantly at 5% probability level*

http://www.aloki.hu ● ISSN 1589 1623 (Print) ● ISSN 1785 0037 (Online)
DOI: http://dx.doi.org/10.15666/aeer/1802_19992024

Table 3. *Segregation analysis of transgenic plants produced by in planta transformation method*

Transgenic plants	Total no. of plants tested	PCR positive plants	PCR negative plants	Segregation ratio
K1	10	5	5	5: 5
K2	9	4	5	4: 5
K3	9	2	7	2: 7
Total	28	11	17	11: 17

Length of shoots, roots and coleoptiles of T_2 transgenic plants improved in response to drought stress

Seedling stage is an appropriate stage for testing drought stress tolerance using PEG-8000 in laboratory condition. During this study, it was confirmed that the increased concentration of PEG prevented the growth, and survival of seedling and PEG concentration was found to be inversely proportional to the shoot length. After 8 days, it was noticed that the lethal effect was more prominent in control plants as compared to transgenic plants. The data in *Figures 8–10* indicate that shoots, roots and coleoptiles length of transgenic plants were significantly different to control plants (non-transgenic plants). The results showed that the shoots, roots and coleoptiles length of transgenic plants were 13.11, 5.77 and 5.6 cm, respectively at -2 bar osmotic stress as compared to their non-transgenic counterparts that showed 12.46, 3.27 and 3.3 cm shoots, roots and coleoptiles length. While at -8 bar osmotic stress, the transgenic plants gave 7.49, 5.4 and 2.93 cm shoot, root and coleoptile lengths which were comparable to their non-transgenic counterparts that produced 3.47, 1.84 and 1.64 cm shoot, root and coleoptiles lengths. Our results showed that shoots, roots and coleoptiles length reduced with the increase in the stress level. But this reduction was more prominent in control plants.

Increased relative water contents of T_2 transgenic plants under drought stress

Water is a limiting factor for plant growth and development. It maintains the turgor pressure in plant cells and involves in all physiological function of plants. So, the plants which maintain the high relative water contents in their cells have good performance under drought stress as compared to the plants having low water contents (Ali et al., 2015). In this regard relative water content was measured in transgenic and control plants at germination stage inducting the drought stress through PEG, while at vegetative stage drought stress was induced withholding water for 8 d. The significant difference ($P = 0.0000$) were recorded between transgenic and control plants and interaction of transgenic and control plants with PEG stress (*Fig. 11*). The highest relative water contents (92.28%) were recorded in transgenic plants as compared to control plants (76.63%) at -2 bar osmotic stress. When PEG stress increased then RWC decreased significantly in control as well as in transgenic plants. But in transgenic plants RWC was not reduced significantly as osmotic stress increased from -2 to -4 bar osmotic stress. *Figure 12* shows the significant difference ($P < 0.05$) between treatments, cultivars (Transgenic and control plants) but non-significant difference ($P = 0.210$) in terms of interaction among treatments and cultivars (Transgenic and control plants). During this experiment, drought stress was induced withholding water for 8 d. The highest relative

http://www.aloki.hu ● ISSN 1589 1623 (Print) ● ISSN 1785 0037 (Online)
DOI: http://dx.doi.org/10.15666/aeer/1802_19992024

water contents (67.46%) was found transgenic plants which were comparable to those of control plants that yielded 40% relative water contents (*Fig. 12*).

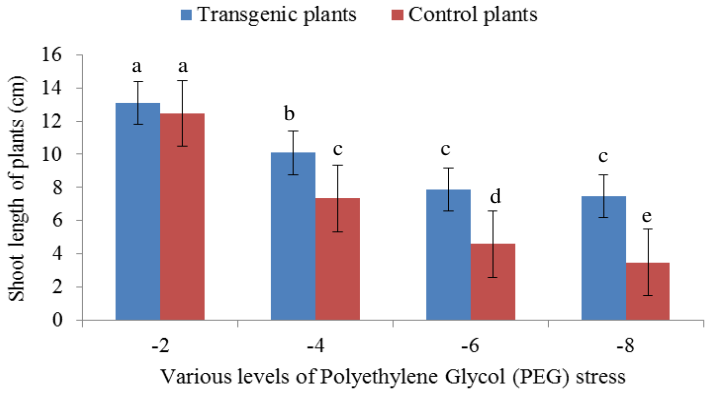

Figure 8. *Effect of various levels of Polyethylene Glycol (PEG) stress on shoot length (cm) of transgenic and control plants of wheat. The error bars indicate standard error. Means not sharing a letter in common differ significantly at 5% probability level*

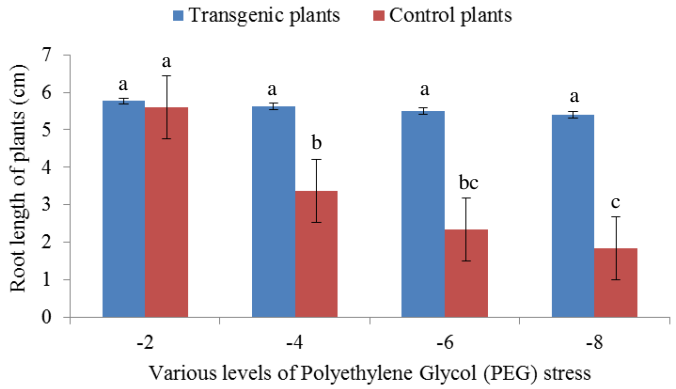

Figure 9. *Effect of various levels of Polyethylene Glycol (PEG) stress on root length (cm) of transgenic and control plants of wheat. The error bars indicate standard error. Means not sharing a letter in common differ significantly at 5% probability level*

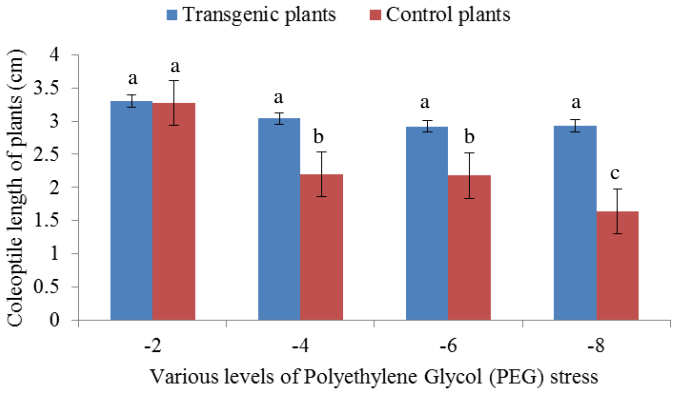

Figure 10. *Effect of various levels of Polyethylene Glycol (PEG) stress on coleoptile length (cm) of transgenic and control plants of wheat. The error bars indicate standard error. Means not sharing a letter in common differ significantly at 5% probability level*

http://www.aloki.hu ● ISSN 1589 1623 (Print) ● ISSN 1785 0037 (Online)
DOI: http://dx.doi.org/10.15666/aeer/1802_19992024

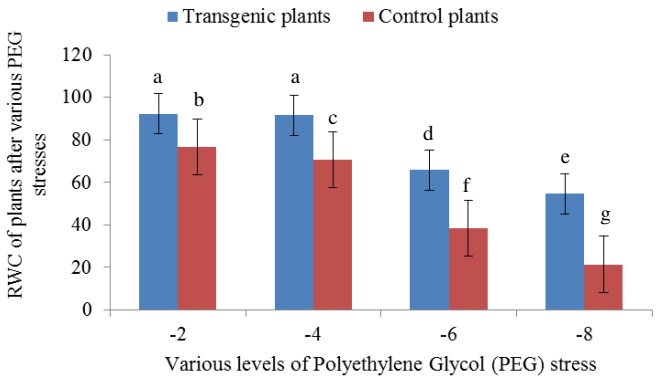

Figure 11. *Effect of various levels of Polyethylene Glycol (PEG) stress on relative water contents (%) of transgenic and control plants of wheat. The error bars indicate standard error. Means not sharing a letter in common differ significantly at 5% probability level*

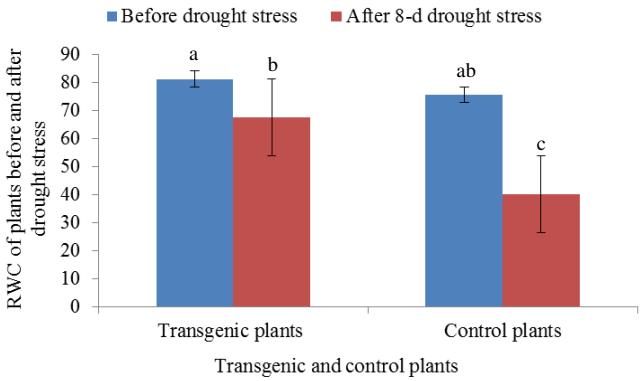

Figure 12. *Effect of 8-d drought stress on relative water contents (%) of transgenic and control plants of wheat. The drought stress was induced by withholding water for continuous 8-d and then drought tolerance was assessed in transgenic plants on the basis of relative water contents (%). The error bars indicate standard error. Means not sharing a letter in common differ significantly at 5% probability level*

Proline contents of T_2 transgenic plants improved in response to drought stress

Osmotic adjustment is the mechanism of drought tolerance in which plant cells accumulate different osmoprotectants such as polyols, proline, proteins and polyols etc. These osmoprotectants protects the cells membranes from stress conditions (Filippou et al., 2014). These compounds accumulated in higher quantities under stressed condition and acted as osmoprotectants (Strange and Yancey, 1994), among these, proline (amino acid) enhances the stability of proteins and membranes under water stress conditions (Anjum et al., 2017). Moreover; its concentration increased with the increase in drought levels (Mujtaba et al., 2007). *Figure 13* shows the significant difference ($P < 0.05$) between transgenic plants and control plants in terms of proline contents and a significant difference between treatments as well as between the interaction of cultivars (transgenic and control plants) and treatments (drought stress by withholding water). The data showed that proline contents increased significantly in transgenic and control plants after drought stress. This increase in proline contents from1.03 µmol/g to 7.06 µmol/g that was more prominent and significant in transgenic plants as compared

http://www.aloki.hu ● ISSN 1589 1623 (Print) ● ISSN 1785 0037 (Online)
DOI: http://dx.doi.org/10.15666/aeer/1802_19992024

to control plants (0.86 µmol/g to 3.50 µmol/g) under normal and drought conditions, respectively. The reason of this higher accumulation of proline contents in transgenic plants might be due to function of *DREB1A* gene that triggers the other genes related to mechanism of production of proline under drought stress. The higher proline contents in transgenic plants indicated that these are more drought tolerance than control plants.

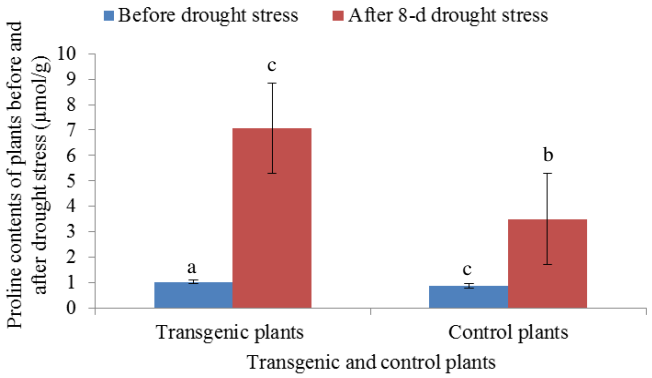

Figure 13. *Effect of 8-d drought stress on proline contents (µmol/g FW) of transgenic and control plants of wheat. The drought stress was induced by withholding water for continuous 8-d and then drought tolerance was assessed in transgenic plants on the basis of proline contents (µmol/g FW). The error bars indicate standard error. Means not sharing a letter in common differ significantly at 5% probability level*

Increased chlorophyll contents of T_2 transgenic lines after drought stress

Chlorophyll is the most effective parameter for the selection of drought tolerant wheat genotype under drought stress conditions (Rad et al., 2012). The data in *Figures 14–16* showed that the chlorophyll contents decreased non- significantly in transgenic plants (before and after drought stress), while they were decreasing significantly in control plants. The significant difference of chlorophyll contents was recorded between transgenic and control plants after drought stress. These results indicated that transgenic plants have capability to sustain their chlorophyll contents in drought stress and behave as drought tolerant wheat plants as compared to control plants. This capability of transgenic plants was developed due to the function of *DREB1A* gene in their genome.

Improved agronomic characteristics of T_2 transgenic plants in term of drought tolerance efficiency

The *Table 4* showed the significant differences ($P < 0.05$) between treatments as well as between transgenic lines and control plants for the parameters (spike length, grains per spike and 100-grains weight). The *Table 4* shows the comparison of transgenic plants with no-transgenic plants (control plants). It was observed that in normal conditions, spike length (10.7 cm), grain per spike (57) of transgenic plants was significantly higher than non-transgenic plants i.e. 10.2 cm (spike length) and 53 (grains per spike), respectively. Similarly, weight of 100 grains (4.72 g) of transgenic lines was a little bit higher than non-transgenic plants (4.63 g). But in case of drought conditions the reduction in spike length, 100 grains weight and grains per spike were much lower in transgenic plants as compared to non-transgenic plants (*Table 4*).

http://www.aloki.hu ● ISSN 1589 1623 (Print) ● ISSN 1785 0037 (Online)
DOI: http://dx.doi.org/10.15666/aeer/1802_19992024

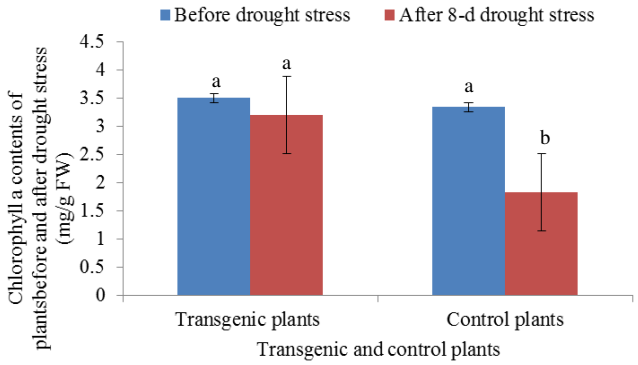

Figure 14. *Effect of 8-d drought stress on chlorophyll a contents (mg/g FW) of transgenic and control plants of wheat. The drought stress was induced by withholding water for continuous 8-d and then drought tolerance was assessed in transgenic plants on the basis of chlorophyll a contents (mg/g FW). The error bars indicate standard error. Means not sharing a letter in common differ significantly at 5% probability level*

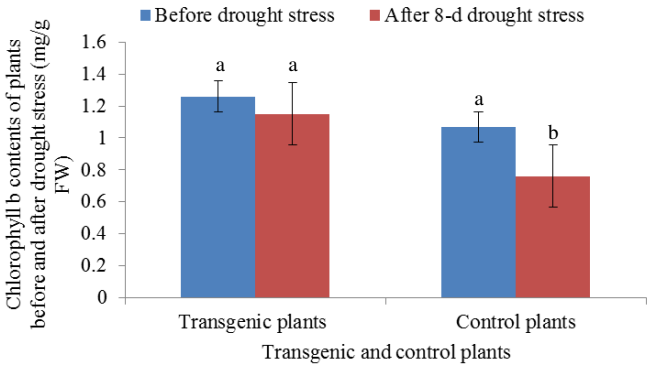

Figure 15. *Effect of 8-d drought stress on chlorophyll b contents (mg/g FW) of transgenic and control plants of wheat. The drought stress was induced by withholding water for continuous 8-d and then drought tolerance was assessed in transgenic plants on the basis of chlorophyll b contents (mg/g FW). The error bars indicate standard error. Means not sharing a letter in common differ significantly at 5% probability level*

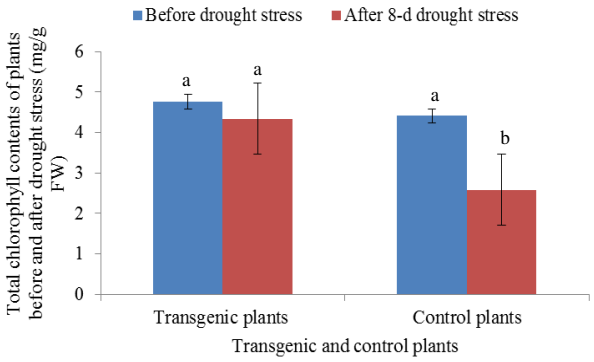

Figure 16. *Effect of 8-d drought stress on total chlorophyll contents (mg/g FW) of transgenic and control plants of wheat. The drought stress was induced withholding water for continuous 8-d and then drought tolerance was assessed in transgenic plants on the basis of total chlorophyll contents (mg/g FW). The error bars indicate standard error. Means not sharing a letter in common differ significantly at 5% probability level*

http://www.aloki.hu ● ISSN 1589 1623 (Print) ● ISSN 1785 0037 (Online)
DOI: http://dx.doi.org/10.15666/aeer/1802_19992024

Table 4. *Improved agronomic characteristics and drought tolerance efficiency of transgenic plants*

Characteristics	Transgenic plants		Control plants	
	Normal condition	Drought stress	Normal condition	Drought stress
Spike length (cm)	10.7 a**	9.6 c	10.2 b	8.5 d
Number of seeds per spike	57 a	46 c	53 b	31 d
100-grain weight (g)	4.72 a	4.25 b	4.63 a	2.15 c
Drought tolerance efficiency (DTE)	90%*		46.43%	
Improvement in DTE	DTE of transgenic plants – DTE of control plants = (90) - (46.43) = 43.57%			

Each value is the mean of three replications. For comparison of spike length, LSD value was 0.36 at $p \leq 0.05$. For comparison of number of seeds per spike, LSD value was 4.32 at $p \leq 0.05$, while for comparison of 1000-grain weight; LSD value was 0.1001 at $p \leq 0.05$. *Calculation based on 100-grain weight in normal and stress condition. **Means not sharing a letter in common differ significantly at 5% probability level

Drought tolerance efficiency (DTE) is a criterion to compare drought tolerance cultivars. It was proposed by Fisher and Wood (1981). It is a good index for determination of drought tolerant wheat cultivars. So, this index was used for transgenic plants and control plants. The data in *Table 4* showed that the drought tolerance efficiency of transgenic plants (90%) was much higher than control plants (46.43%). So, the total improvement in DTE of transgenic plants was 43.57%. This increase in drought tolerance efficiency was due to the presence of *DREB1A* gene in transgenic plants. This transcription factor might trigger other genes to produce such proteins which protect the plants from drought stress and also maintain the water balance in cells of leaves. So, as a result chlorophyll contents stable in leaves and maximum food were synthesized which was stored in the form of grains. It was also used as criteria for drought and heat resistance in spring wheat (Bahar and Yildrim, 2010) they reported the range of 65-98% (DTE %) in drought tolerance wheat cultivars.

Discussion

Wheat ensures the food security of the world, but it is severely affected by scarcity of water due to limited water resources. Drought can occur at any developmental stage of wheat that drastically limits its yield. Plants have to adopt some tolerance mechanisms to endure the severity of water shortage. Genetic improvement of wheat can cope with drought problem using *Agrobacterium*-mediated method. Dehydration-responsive element-binding 1A (*DREB1A*) gene enhances the drought tolerance ability of transgenic plants activating the expression of drought related target genes (Oh et al., 2005). In planta method of genetic transformation is a technique of gene transformation which has low cost, does not require sterilized environment and it avoids laborious hardworking tissue culture steps.

During this study, inoculation before seed germination was found to be optimum for maximum transformation efficiency of in planta transformation because inoculation media fortified with 3.0 mg/l 2, 4-D decreased the cell division and delayed the process of differentiation. As a result, *Agrobacterium* got maximum time to transfer its T-DNA

http://www.aloki.hu ● ISSN 1589 1623 (Print) ● ISSN 1785 0037 (Online)
DOI: http://dx.doi.org/10.15666/aeer/1802_19992024

to apical meristem cells. While in case of inoculation after germination, seeds were soaked in distilled water only without 2, 4-D, so no transformation was obtained. The cell division and differentiation processes in meristematic cells increased rapidly with the increase of soaking time due to which the probability of infection to cells by *Agrobacterium* was decreased. These processes needed to be slow down for infection of target cells by *Agrobacterium* (Razzaq, 2005). The piercing of meristematic cells with needle facilitates *Agrobacterium* to reach and infect the germ line mother cells. In case of inoculation after germination, no hygromycin resistant plants were visualized indicating that there would be two possibilities; first was damaging cells of mother germ lines and second was that *Agrobacterium* could not reach and infect the germ line mother cells due to large number of layers of cells formed on outer surface of germ line mother cells. On the contrary, 25% hygromycin resistant plants were obtained in case of inoculation before germination indicating that at this time, germ line mother cells could easily be targeted and *Agrobacterium* could easily reach and infected the target cells. The similar studies were reported by Razzaq et al. (2005) who conducted in planta transformation of wheat and sixty-three kanamycin resistant plants were reported. Out of these sixty-three plants, only three plants were PCR positive and one plant produced seeds. Bratic (2007) transformed the buckwheat via in planta transformation and compared the efficiency of two different procedures, i.e. vacuum infiltration and infiltration by syringe. It was concluded that vacuum infiltration was more efficient than that of infiltration by syringe. Rao et al. (2008) reported in planta transformation of pigeon pea in which primary transformants were chimeric in nature. Due to this reason, T_0 plants were not tested for the confirmation of gene through PCR. PCR was performed in T_1 generation and 13.71% transformation efficiency was reported. Cheng et al. (2003) analyzed the transgenic wheat by southern blotting and reported that 67% transgenic wheat plants obtained a single copy of transgene. Yao et al. (2006) developed transgenic wheat and reported that in transgenic line, one to four hybridizing bands were displayed, but most of the lines showed single copy of inserted genes. In present study inheritance pattern of transgene was shown as non-Mendelian ratio. Similarly, Yin et al. (2004) reported 10-50% transgenic plants showing non-Mendelian inheritance; either they were produced by gene gun or *Agrobacterium* mediated transformation. They concluded that this non-Mendelian segregation ratio might be due to the nature of the gene and recipient genome.

The results of our study suggested that *DREB1A* gene improved the germination frequency and germination rate index of transgenic seeds as compared to the seeds of control plants. Early and best germination rate of any crop is a pre-requisite to establish new seedlings. The problem of low germination of seeds exists in most of the wheat cultivars especially when moisture level in soil is very low. Water stress limits the germination frequency, germination rate index as well as emergence of seedling due to loss of seed vigor. During this study, it was also noticed that all transgenic seeds obtained from in planta *Agrobacterium tumefaciens* mediated transformation showed non-uniform germination under different PEG stresses. It was due to segregation of *DREB1A*. Our findings are supported by the results of Pellegrineschi et al. (2004); Kasuga et al. (1999) who conducted research studies in wheat and Arabidopsis, respectively and found non-uniform germination. Germination rate index and germination frequency were higher in seeds of transgenic plants as compared to control plants. These were considered good parameters for screening drought tolerant wheat cultivars. Our results also revealed that with increasing PEG stress levels, germination

http://www.aloki.hu ● ISSN 1589 1623 (Print) ● ISSN 1785 0037 (Online)
DOI: http://dx.doi.org/10.15666/aeer/1802_19992024

frequency and germination rate index were decreased. Our findings are harmonious with the earlier research study by Qayyum et al. (2011) who reported that germination time and germination frequency became low with increasing level of osmotic stress from 0 to -8 bars induced by PEG.

High relative water contents are a resistance mechanism to tackle drought stress (Ritchie et al., 1990). So, relative water content is a tool to discriminate drought sensitive and drought resistant wheat cultivars (Fahliani and Assad, 2005). Amirjani and Madhiyeh (2013) and Bayoumi et al. (2008) induced drought stress under field conditions withholding water and noticed that drought tolerance wheat cultivar had higher relative water contents as compared to drought susceptible wheat cultivar. Our findings were similar with the findings of Raziuddin et al. (2010) who reported that drought tolerance wheat cultivars attained maximum relative water contents as compared to other cultivars during stress induced by PEG 6000. Similarly, Rab et al. (2012) assessed the drought tolerance and drought sensitive wheat cultivars hydroponically by inducing drought through 20% PEG and found higher relative water contents (RWC) at cellular levels in drought tolerance wheat cultivar as compared to drought sensitive one. Drought tolerant wheat cultivars maintained higher RWC in their leaves as compared to drought sensitive cultivars (Keyvan, 2010). Ritchie et al. (1990) reported that RWC were stable in early days of water stress in both drought tolerant and drought sensitive genotypes but it decreased significantly after 8 days of water stress in drought sensitive genotypes. From these results it was concluded that transgenic plants exhibited high relative water contents due to overexpression of *DREB1A* gene.

Our findings are consistent with the findings of Qayyum et al. (2011) who reported the progressive increase of proline contents with the increase of osmotic stress from 0 to -08 bar. Similarly, Raziuddin et al. (2010) reported that when PEG-6000 was used to induce drought stress, proline contents increased up to 10 fold in response to 40% PEG. Bayoumi et al. (2008) reported that drought tolerant wheat cultivar had higher proline contents as compared to drought susceptible cultivars. A similar nature of study was conducted by Moaveni (2011) who recorded more accumulation of proline contents in transgenic wheat plants under drought stress as compared to control plants. Valifard et al. (2012) classified two wheat varieties i.e. Zagros (drought tolerant) and Pishtaz (drought susceptible) and reported that proline increased significantly in tolerant one. These results indicate that proline is a part of defense mechanisms which confers water deficit tolerance to wheat cultivars. The increase of proline contents under drought stress has been reported in previous research studies such as Pigeonpea (Kumar et al., 2011), Brassica (Khan et al., 2010) and bean (Stoyanov, 2005) suggesting that it is a common osmolyte which accumulated in drought conditions. Moussa and Abdel-Aziz (2008) reported that the drought tolerant maize genotype "Giza-2" had accumulated more proline contents than that of drought sensitive maize genotype "Trihybrid-321". Proline improves the drought tolerance at cellular level by stabilizing cytosolic pH, protecting protein and enzyme structure, providing organic nitrogen for growth and survival of plants and also acts as a source of energy (Hare et al., 1999; Errabii et al., 2006; Ashraf and Foolad, 2007; Bayoumi et al., 2008).

Present study reports an enhanced accumulation of chlorophyll contents in transgenic wheat plants as compared to their control counterparts under drought stress. Our results of transgenic plants do not agree with the results of Amirjani and Madhiyeh (2013). This research group reported a significant reduction of total chlorophyll contents in transgenic plants under drought stress. In our study, improvement of chlorophyll

http://www.aloki.hu ● ISSN 1589 1623 (Print) ● ISSN 1785 0037 (Online)
DOI: http://dx.doi.org/10.15666/aeer/1802_19992024

contents in transgenic plants might be due to overexpression of *DREB1A* gene triggering drought tolerant genes that produce certain proteins due to which stability of chlorophyll contents was recorded in them as compared to control plants. Consistent with our findings, Moaveni (2011) assessed drought tolerance efficiency of wheat by measuring chlorophyll contents and reported that chlorophyll contents were significantly improved in transgenic plants as compared to control plants. The chlorophyll contents were significantly higher in transgenic plants as compared to control plants. The philosophy of increased chlorophyll contents in transgenic plants might be possible that DREB1A transcription factors switch on others genes producing chemicals that lower the stress level, protect the plant cells and maintain the water balance in cells. While in control plants, chlorophyll contents were limited due to water stress and they could not maintain their structures. The chlorophyll contents are considered as a good parameter to differentiate drought tolerance and drought sensitive germplasms (Rong-Hua et al., 2006). Drought stress decreased the level of water in mesophyll cells of leaves and as a result chlorophyll pigment degraded and damaged the photosynthetic machinery (Bogale et al., 2011).

Drought susceptible index (DSI) and drought resistance index (DRI) have been used to determine the drought tolerance ability of plants (Fisher and Maurer, 1978; Bidinger et al., 1982). These indices were used to differentiate drought tolerance and drought susceptible cultivars (Dong and Liu, 2005). Drought resistance index has a positive or negative value. If this value is more than 1.3 then that the cultivar lies under the category of drought resistant and if this value is less than -1.3 then cultivar lies under the category of drought sensitive (Akcura et al., 2011). Song-ping et al. (2007) calculated the drought resistance index using the formula DRI = Grain Yield under stress / Grain Yield under normal condition. When it was correlated with other parameters then it was found that this index was correlated with coleoptiles length of the recombinant inbreed line (RILs) of rice under moisture stress. Parameshwaarppa (2007) conducted a similar type of study and concluded that the genotypes which had least DSI value gave more yield, the highest drought tolerance efficiency and the highest drought tolerance index as compared to the other cultivars. They were also in argument that these cultivars maintained the highest harvest index under drought stress conditions.

Conclusion

It was concluded that injury and inoculation of apical meristem was found to be better before seed germination as compared to after seed germination. The transformation efficiency (6.38%) was recorded based on PCR positive plants before germination. Under drought stress, germination percentage and germination rate index was higher in transgenic plants as compared to control plants. Proline contents were significantly increased which was a good indicator of drought tolerance. The stability of transgenic plants was higher as compared to control plant owing to more relative water contents, chlorophyll contents as well as length of shoots, roots and coleoptiles. The total improvement of transgenic plants in terms of drought tolerance efficiency (43.57%) was higher in transgenic plants as compared to control plants.

Acknowledgements. This study was financially supported by Indigenous PhD Fellowship Program Higher Education Commission (HEC), Islamabad, Pakistan. The authors gratefully acknowledge the support of HEC for conducting PhD studies and the results presented here are part of PhD research of

http://www.aloki.hu ● ISSN 1589 1623 (Print) ● ISSN 1785 0037 (Online)
DOI: http://dx.doi.org/10.15666/aeer/1802_19992024

principal author. The authors acknowledge the support of National Institute for Genomics and Advanced Biotechnology (NIGAB), NARC, Islamabad, Pakistan for providing the facilities for the production of transgenic wheat. The authors also appreciate Plant Physiology Lab, PMAS, Arid Agriculture University, Rawalpindi, Pakistan for screening of drought tolerance in wheat transgenic line.

REFERENCES

[1] Abbas, R., Mirza, F. I., Afzal, A. (2017): Farm management capacities contribute to sustainability of rural livelihoods and income amongst small farmers in district Layyah, Punjab, Pakistan. – Journal of Rural Development and Agriculture 2: 11-25.

[2] Adeel, M., Siddiqui, B. N., Tareen, W. H., Rayit, A., Shah Fahd, S. (2017): Working efficiency of extension field staff with regard to integrated pest management of cotton in D. G. Khan, Punjab, Pakistan. – Journal of Rural Development and Agriculture 2: 26-40.

[3] Akcura, M., Partigoc, F., Kaya, Y. (2011): Evaluating of drought stress tolerance based on selection indices in Turkish bread wheat landraces. – Journal of Animal and Plant Sciences 21: 700-709.

[4] Alghabari, F., Ihsan, M. Z., Hussain, S., Aishia, G., Daur, I. (2015): Effect of Rht alleles on wheat grain yield and quality under high temperature and drought stress during booting and anthesis. – Environmental Science and Pollution Research 22: 15506-15515.

[5] Ali, N., Zada, A., Ali, M., Hussain, Z. (2016): Isolation and identification of *Agrobacterium tumefaciens* from the galls of peach tree. – Journal of Rural Development and Agriculture 1: 39-48.

[6] Ali, S., Kareem, K., Zia, M. A., Khan, S. U., Shahzad, A., Din, J. U., Ali, G. M. (2018): Expression analysis and introgression of transcriptional factor (DREB1A) in tomato for cold tolerance. – Journal of Pure and Applied Agriculture 3(1): 1-12.

[7] Ali, Z., Ashraf, M., Al-Qurainy, F., Khan, S., Akram, N. A. (2015): Appraising drought tolerance in local accessions of sesbania [*Sesbania sesban* (L.) Merril.] using biomass production, relative membrane permeability and photosynthetic capacity as selection criteria. – Pakistan Journal of Botany 47: 845-850.

[8] Amirjani, M. R., Mahdiyeh, M. (2013): Antioxidative and biochemical responses of wheat to drought stress. – APRN Journal of Agricultural and Biological Science 8: 292-301.

[9] Amoah, B. K., Wu, H., Sparks, C., Jones, H. D. (2001): Factors influencing *Agrobacterium tumefaciens* mediated transient expression of *uidA* in wheat inflorescence tissue. – Journal of Experimental Botany 52: 1135-1142.

[10] Andrieu, A., Breitler, J. C., Sire, C., Meynard, D., Gantet, P., Guiderdoni, E. (2012): An in planta, Agrobacterium-mediated transient gene expression method for inducing gene silencing in rice (*Oryza sativa* L.) leaves. – Rice 5: 1-12.

[11] Anjum, A. S., Zada, R., Tareen, W. H. (2016): Organic farming: hope for the sustainable livelihoods of future generations in Pakistan. – Journal of Rural Development and Agriculture 1: 20-29.

[12] Anjum, S. A., Ashraf, U., Tanveer, M., Khan, I., Hussain, S., Shahzad, B., Zohaib, A., Abbas, F., Saleem, M. F., Ali, I., Wang, L. C. (2017): Drought induced changes in growth, osmolyte accumulation and antioxidant metabolism of three maize hybrids. – Frontiers in Plant Science 8: 1-12. DOI: 10.3389/fpls.2017.00069.

[13] Arnon, D. I. (1949): Copper, enzyme in isolated chloroplasts polyphenoloxidase in *Beta vulgaris*. – Plant Physiology 24: 1-15.

[14] Ashraf, M., Foolad, M. R. (2007): Roles of glycine betaine and proline in improving plant abiotic stress resistance. – Environmental and Experimental Botany 59: 206-216.

[15] Bahar, B., Yildirim, M. (2010): Heat and drought resistances criteria in spring bread wheat: drought resistance parameters. – Scientific Research and Essays 5(13): 1742-1745.

http://www.aloki.hu ● ISSN 1589 1623 (Print) ● ISSN 1785 0037 (Online)
DOI: http://dx.doi.org/10.15666/aeer/1802_19992024

[16] Barrs, H. D., Weatherley, P. E. (1962): A re-examination of the relative turgidity technique for estimating water deficit in leaves. – Australian Journal of Biological Sciences 15: 413-428.
[17] Bates, L. S., Waldran, R. P., Teare, I. D. (1973): Rapid determination of free proline for water stress studies. – Plant and Soil 39: 205-208.
[18] Bayoumi, T. Y., Eid, M. H., Metwali, E. M. (2008): Application of physiological and biochemical indices as a screening technique for drought tolerance in wheat genotypes. – African Journal of Biotechnology 7: 2341-2352.
[19] Bidinger, F. R., Mahalakshmi, Y., Talukdar, B. S., Alagarswamy, G. (1982): Improvement of Drought Resistance in Pearl Millet. – In: IRRI (ed.) Drought Resistance in Crops with Emphasis on Rice. – IRRI, Los Banos, Laguna Philippines, pp. 357-375.
[20] Bogale, A., Tesfaye, K., Geleto, T. (2011): Morphological and physiological attributes associated to drought tolerance of Ethiopian durum wheat genotypes under water deficit condition. – Journal of Biodiversity and Environmental Sciences 1: 22-36.
[21] Borisjuk, N., Kishchenko, O., Eliby, S., Schramm, C., Anderson, P., Jatayev, S., Kurishbayev, A., Shavrukov, Y. (2019): Genetic modification for wheat improvement: from transgenesis to genome editing. – BioMed Research International. https://doi.org/10.1155/2019/6216304.
[22] Bratic, A. M., Majic-Dragana, B., Miljus-Dukic, J. D., Jovanovic, Z. S., Maksimovic, V. R. (2007): In planta transformation in buckwheat (*Fagopyrum esculentum* Moench.). – Archives of Biological Sciences 59: 135-138.
[23] Brunecky, R., Selig, M. J., Vinzant, T. B., Himmel, M. E., Lee, D., Blaylock, M. J., Decker, S. R. (2011): In planta expression of A. cellulolyticus Cel5A endocellulase reduces cell wall recalcitrance in tobacco and maize. – Biotechnology for Biofuels 4: 1-10.
[24] Camargo, C. P., Vaughan, C. E. (1973): Effect of seed vigor on field performance and yield of grain sorghum (*Sorghum bicolor* L.). – Proceedings of the Association of Official Seed Analytics 6: 135-147.
[25] Cheng, M., Fry, J. E., Pang, S., Zhou, H., Hironaka, C. M., Duncan, D. R., Conner, T. W., Wan, Y. (1997): Genetic transformation of wheat mediated by *Agrobacterium tumefaciens*. – Plant Physiology 115: 971-980.
[26] Cheng, M., Hu, T., Layton, J., Liu, C. N., Fry, J. (2003): Desiccation of plant tissues post-*Agrobacterium tumefaciens* infection enhances T-DNA delivery and increases stable transformation efficiency in wheat. – In Vitro Cellular & Developmental Biology - Plant 39: 595–604.
[27] Cushman, J. C., Bohnert, H. J. (2000): Genomic approach to plant stress tolerance. – Current Opinion in Plant Biology 3: 117-124.
[28] Dong, B., Liu, M. (2005): Integrated evaluation to high yield and water saving of winter wheat in north China. – Agrifood Research Reports 68: 11-18.
[29] Errabii, T., Gandonou, C. B., Essalmani, H., Abrini, J., Idaomar, M., Skali-Senhaji, N. (2006): Growth, proline and ion accumulation in sugarcane callus cultures under drought-induced osmotic stress and its subsequent relief. – African Journal of Biotechnology 5: 1488-1493.
[30] Fahliani, R. A., Assad, M. T. (2005): Evaluation of three physiological traits for selecting drought. – Journal of Agricultural Science and Technology 7: 81-87.
[31] Farooq, M., Aziz, T., Rehman, H. U., Rehman, A. U., Cheema, S. A. (2011): Evaluating surface drying and re-drying for wheat seed priming with polyamines: effects on emergence, early seedling growth and starch metabolism. – Acta Physiologiae Plantarum 33: 1707-1713.
[32] Filippou, P., Bouchagier, P., Skotti, E., Fotopoulos, V. (2014): Proline and reactive oxygen/nitrogen species metabolism is involved in the tolerant response of the invasive plant species Ailanthus altissima to drought and salinity. – Environmental and Experimental Botany 97: 1-10.

http://www.aloki.hu ● ISSN 1589 1623 (Print) ● ISSN 1785 0037 (Online)
DOI: http://dx.doi.org/10.15666/aeer/1802_19992024

[33] Fischer, K. S., Wood, G. (1981): Breeding and selection for drought tolerance in tropical maize. – Proc. Symp. on Principles and Methods in Crop Improvement for Drought Resistance with Emphasis on Rice, IRRI, Philippines.
[34] Fisher, R. A., Maurer, R. (1978): Drought resistance in spring wheat cultivars. I. grain yield response. – Australian Journal of Agricultural Research 29: 897-907.
[35] Hare, P. D., Cress, W. A., Staden, J. V. (1999): Proline synthesis and degradation: a model system for elucidating stress-related signal transduction. – Journal of Experimental Botany 50: 413-434.
[36] Hassan, U. A., Ogunlela, V. B., Sinha, T. D. (1987): Agronomic performance of wheat (*Triticum aestivum* L.) as influenced by moisture stress at various growth stages and seeding rate. – Journal of Agronomy and Crop Science 158: 172-180.
[37] He, Y., Jones, H. D., Chen, S. C., Chen, X. M., Wang, D. W., Li, K. X., Wang, D. S., Xia, L. Q. (2010): *Agrobacterium tumefaciens*-mediated transformation of durum wheat (*Triticum turgidum* L. var. durum, c.v. Stewart) with improved efficiency. – Journal of Experimental Botany 61: 1567-1581.
[38] Ishaq, W., Memon, S. Q. (2016): Roles of women in agriculture: a case study of rural Lahore, Pakistan. – Journal of Rural Development and Agriculture 1: 1-11.
[39] Jain, A. K., Basha, S. M., Holbrook, C. C. (2001): Identification of drought responsive transcripts in peanut (*Arachis hypogaea* L.). – Electronic Journal of Biotechnology 4: 1-9.
[40] Jan, S. A., Bibi, N., Shinwari, Z. K., Rabbani, M. A., Sana Ullah, Qadir, A., Khan, N. (2017): Impact of salt, drought, heat and frost stresses on morpho-biochemical and physiological properties of *Brassica* crops: an updated review. – Journal of Rural Development and Agriculture 2: 1-10.
[41] Jones, H. D. (2005): Wheat transformation: current technology and applications to gain development and composition. – Journal of Cereal Science 41: 137-147.
[42] Kasuga, M., Liu, Q., Miura, S., Yamaguchi-Shinozaki, K., Shinozaki, K. (1999): Improving plant drought, salt, and freezing tolerance by gene transfer of a single stress-inducible transcription factor. – Nature Biotechnology 17: 287-291.
[43] Keyvan, S. (2010): The effects of drought stress on yield, relative water content, proline, soluble carbohydrates and chlorophyll of bread wheat cultivars. – Journal of Animal and Plant Sciences 8: 1051-1060.
[44] Khan, A. S., Allah, S. U., Sadique, S. (2010): Genetic variability and correlation among seedling traits of wheat (*Triticum aestivum* L.) under water stress. – International Journal of Agriculture and Biology 12: 247-250.
[45] Khan, S., Anwar, S., Yu, S., Sun, M., Yang, Z., Gao, Z. (2019): Development of drought-tolerant transgenic wheat: achievements and limitations. – International Journal of Molecular Biology 20: 1-18. DOI: 10.3390/ijms20133350.
[46] Kumar, R. R., Karajol, K., Naik, G. R. (2011): Effect of polyethylene glycol induced water stress on physiological and biochemical responses in Pigeonpea (*Cajanus cajan* L. Millsp.). – Recent Research in Science and Technology 3: 148-152.
[47] Marcotte, W. R., Russel, S. H., Quatrano, R. S. (1989): Abscisic acid response sequences from *Em* gene of wheat. – Plant Cell 1: 969-976.
[48] Mehmood, K., Arshad, M., Ali, G. M., Razzaq, A. (2013): Tissue culture responses of some wheat (*Triticum aestivum* L.) cultivars grown in Pakistan. – Pakistan Journal of Botany 45: 545-549.
[49] Mehmood, K., Arshad, M., Ali, S., Qayyum, M., Ali, G. M. (2016): Comparative study of tissue culture response of some selected basmati rice cultivars of Pakistan. – Journal of Rural Development and Agriculture 1: 30-38.
[50] Moaveni, P. (2011): Effect of water deficit stress on some physiological traits of wheat (*Triticum aestivum*). – Agricultural Science Research Journal 1: 64-68.
[51] Moussa, H. R., Abdel-Aziz, S. M. (2008): Comparative response of drought tolerant and drought sensitive maize genotypes to water stress. – Australian Journal of Crop Science 1: 31-36.

http://www.aloki.hu ● ISSN 1589 1623 (Print) ● ISSN 1785 0037 (Online)
DOI: http://dx.doi.org/10.15666/aeer/1802_19992024

[52] Mowla, S. B., Thomson, J. A., Farrant, J. M., Mundree, S. G. (2002): A novel stressinducible antioxidant enzyme identified from the resurrection plant *Xerophyta viscosa* Baker. – Planta 215: 716-726.
[53] Mujtaba, S. M., Ali, M., Ashraf, M. Y., Khanzada, B., Farhan, S. M., Shirazi, M. U., Khan, M. A., Shereen, A., Mumtaz, S. (2007): Physiological responses of wheat (*Triticum aestivum* L.) genotypes under water stress conditions at seedling stage. – Pakistan Journal of Botany 39: 2575-2579.
[54] Murray, M. G., Thomson, W. F. (1980: Rapid isolation of high molecular weight plant DNA. – Nucleic Acids Research 8: 4321-4325.
[55] Oh, S. J., Song, S. I., Kim, Y. S., Jang, H. J., Kim, S. Y., Kim, M., Kim, Y. K., Nahm, B. H., Kim, J. K. (2005): Arabidopsis CBF3/DREB1A and ABF3 in Transgenic Rice Increased Tolerance to Abiotic Stress without Stunting Growth. – Plant Physiology 138: 341-351.
[56] Parameshwarappa, S. G., Salimath, P. M. (2007): Field screening of chickpea genotypes for drought resistance. – Karnataka Journal of Agricultural Sciences 21: 113-114.
[57] Pellegrineschi, A., Reynolds, M., Pacheco, M., Brito, R. M., Almeraya, R., Shinozaki, K. Y., Hoisington, D. (2004): Stress-induced expression in wheat of the *Arabidopsis thaliana DREB1A* gene delays water stress symptoms under greenhouse condition. – Genome 47: 493-500.
[58] Prasad, P. V. V., Pisipati, S. R., Momcilovic, I., Ristic, Z. (2011): Independent and combined effects of high temperature and drought stress during grain filling on plant yield and chloroplast EF-Tu expression in spring wheat. – Journal of Agronomy and Crop Science 197: 430-441.
[59] Qayyum, A., Razzaq, A., Ahmad, M., Jenks, M. A. (2011): Water stress causes differential effects on germination indices, total soluble sugar and proline content in wheat (*Triticum aestivum* L.) genotypes. – African Journal of Biotechnology 10: 14038-14045.
[60] Rab, M. A., Sultan, F., Hui, L., Yang, L. J., Xian, Z. H. (2012): Assessment of drought tolerance of some *Triticum* Species through physiological indices. – Czech Journal of Genetics and Plant Breeding 48: 178-184.
[61] Rao, K. S., Sreevathsa, R., Pinakee, D., Sharma, D., Keshamma, E., Kumar, M. U. (2008): *In planta* transformation of pigeon pea: a method to overcome recalcitrancy of the crop to regeneration *in vitro*. – Physiology and Molecular Biology of Plants 14: 321-328.
[62] Raziuddin, Swati, Z. A., Bakht, J., Farhatullah, Ullah, N., Shafi, M., Akmal, M., Hassan, G. (2010): *In situ* assessment of morpho-physiological response of wheat (*Triticum aestivum* L.) genotypes to drought. – Pakistan Journal of Botany 42: 3183-3195.
[63] Razzaq, A., Yan-min, Z., Fan, Y., Yan-Jie, Y., He, Z., Zhi-ying, M., Hai-bo, W. (2005): *In planta* transformation of wheat apical meristem: a preliminary study. – Acta Agriculturae Boreali Sinica 20: 17-22.
[64] Ritchie, S. W., Nguyan, H. T., Holaday, A. S. (1990): Leaf water content and gas exchange parameters of two wheat genotypes differing in drought resistance. – Crop Science 30: 105-111.
[65] Rong-Hua, L. I., Pei-Guo, G., Baum, M., Grando, S., Ceccarelli, S. (2006): Evaluation of chlorophyll content and fluorescence parameters as indicators of drought tolerance in barley. – Agricultural Sciences in China 5: 751-757.
[66] Saidi, A., Ookawa, T., Motobayashi, T., Hirasawa, T. (2008): Effects of soil moisture conditions before heading on growth of wheat plants under drought conditions in the ripening stage: insufficient soil moisture conditions before heading render wheat plants more resistant to drought during ripening. – Plant Production Science 11: 403-414.
[67] Seki, M., Narusaka, M., Abe, H., Kasuga, M., Yamaguchi-Shinozaki, K., Carninci, P., Hayashizaki, Y., Shinozaki, K. (2001): Monitoring the expression pattern of 1300 *Arabidopsis* genes under drought and cold stresses by using a full-length cDNA microarray. – Plant Cell 13: 61-72.

http://www.aloki.hu ● ISSN 1589 1623 (Print) ● ISSN 1785 0037 (Online)
DOI: http://dx.doi.org/10.15666/aeer/1802_19992024

[68] Shah, S. H., Ali, S., Jan, S. A., Din, J., Ali, G. M. (2015): Piercing and incubation method of *in planta* transformation producing stable transgenic plants by overexpressing *DREB1A* gene in tomato (*Solanum lycopersicum* Mill.). – Plant Cell, Tissue and Organ Culture 120: 1139-1157.
[69] Sieling, K., Christen, O., Richter-Harder, H., Hanus, H. (1994): Effects of temporary water stress after anthesis on grain yield and yield components in different tiller categories of two spring wheat varieties. – Journal of Agronomy and Crop Science 173: 32-40.
[70] Song-Ping, H., Hua, Y., Gui-Hua, Z., Hong-Yan, L., Guo-Lan, L., Han-Wei, M., Run, C., Ming-Shou, L., Li-Jun, L. (2007): Relationship between coleoptile length and drought resistance and their QTL mapping in rice. – Rice Science 14: 13-20.
[71] Stoyanov, Z. (2005): Effects of water stress on leaf water relations of young bean plants. – Journal of Central European Agriculture 6: 5-14.
[72] Strange, K., Yancey, P. H. (1994): Compatible and Counteracting Solutes. –In: Strange, K. (ed.) Cellular and Molecular Physiology of Cell Volume Regulation. CRC Press, Boca Raton, FL, pp. 81-109.
[73] Valifard, M., Moradshahi, A., Kholdebarin, B. (2012): Biochemical and physiological responses of two wheat (*Triticum aestivum* L.) cultivars to drought stress applied at seedling stage. – Journal of Agricultural Science and Technology 14: 1567-1578.
[74] Wu, H., Sparks, C., Amoah, B., Jones, H. D. (2003): Factors influencing successful *Agrobacterium tumefaciens*-mediated genetic transformation of wheat. – Plant Cell Reports 21: 659-668.
[75] Xue, Q., Zhu, Z., Musick, J. T., Stewart, B. A., Dusek, D. A. (2003): Root growth and water uptake in winter wheat under deficit irrigation. – Plant and Soil 257: 151-161.
[76] Yao, Q., Cong, L., Chang, J. L., Li, K. X., Yang, G. X., He, G. Y. (2006): Low copy number gene transfer and stable expression in a commercial wheat cultivar via particle bombardment. – Journal of Experimental Botany 57: 3737-3746.
[77] Yenchon, S., Te-chato, S. (2012): Effect of bacteria density, inoculation and co-cultivation period on *Agrobacterium tumefaciens* mediated transformation of oil palm embryogenic callus. – Journal of Agricultural Technology 8: 1485-1496.
[78] Yin, Z., Plder, W., Malepszy, S. (2004): Transgene inheritance in plants. – Journal of Applied Genetics 45: 127-144.
[79] Zhang, J. Y., Broeckling, C. D., Blancaflor, E. B., Sledge, M. K., Sumner, L. W., Wang, Z. Y. (2005): Over expression of *WXP1*, A putative *Medicago truncatula* AP2 domain-containing transcription factor gene, increases cuticular wax accumulation and enhances drought tolerance in transgenic alfalfa (*Medicago sativa*). – Plant Journal 42: 689-695.
[80] Zhu, J. K. (2001): Plant salt tolerance. – Trends in Plant Science 6: 66-71.

http://www.aloki.hu ● ISSN 1589 1623 (Print) ● ISSN 1785 0037 (Online)
DOI: http://dx.doi.org/10.15666/aeer/1802_19992024

PHYTOSOCIOLOGICAL STUDIES ON THE STEPPE COMMUNITIES OF NATURAL PASTURES IN ŞANLIURFA, UPPER MESOPOTAMIA, TURKEY

CEVHERI, C.[1*] – ASLAN, M.[2] – ATAMOV, V.[3]

[1]*Department of Biology, Faculty of Science and Art, Harran University, Şanlıurfa, Turkey*

[2]*Faculty of Education, Harran University, Şanlıurfa, Turkey*

[3]*Department of Biology, Faculty of Science and Art, Recep Tayyip Erdoğan University, Rize, Turkey*

**Corresponding author*
e-mail: ccevheri@harran.edu.tr; phone: +90-414-318-3566

(Received 28th May 2019; accepted 28th Nov 2019)

Abstract. This phytosociological study was carried out in the steppe of Fatik Mountains in Sanliurfa, between the years 2002-2005. At the end of this study, it was underlined that the dominant vegetation type was steppe in the region and different steppe associations were determined. These were also; *Festuco callieri–Teucrietum poliae* ass. nova, *Astragalo strictifolii–Salvietum sclarea* ass. nova, *Phlomido bruguieri–Thymbretum spicatae* ass. nova, *Asphodelo aestivum–Teucrietum poliae* ass. nova, *Cynodo dactyloni–Bromoetum danthoniae* ass. nova, and *Prosopo farctae–Avenetum erianthae* ass. nova. During the floristic surveys, 153 taxa belonging to 26 families and 107 genera were identified. *Poaceae* with 31 taxa (20.3%), *Asteraceae* with 24 taxa (15.7%), *Fabaceae* with 22 (14.4%), and *Apiaceae* with 13 taxa (8.5%) were the richest families.
Keywords: *steppe vegetation, grazing, ecosystems, characteristic species, association*

Introduction

Turkey is located at the intersection of two important gene centers namely the Mediterranean and Near East and has the ninth highest biodiversity among terrestrial countries. Natural species of most cereals cultivated for human consumption grow on steppe ecosystems (Ture and Bocuk, 2007).

Fatik Mountain, located at the southwestern part of Şanlıurfa, was selected as the research area since it has a peculiar steppe vegetation and has been paid less attention so far as "Adıgüzel and Aytac, 2001" mentioned earlier. The studied area is in the C7 square according to grid system adopted by Davis (1988). Phytogeographically located in the Irano–Turanian Floristic Region, extending between the longitudes of 37.2 North and 37.3 and between the latitudes of 38.6 and 38.7 East (Anonymous, 1995).

The central, eastern and southeastern parts of Turkey belong phytogeographically to the Irano–Turanian region (Zohary, 1973). The Irano–Turanian region is separated into two parts the West and the East Irano–Turanian subregions. There are three provinces in Turkey belonging to the West Irano–Turanian subregion namely; Central Anatolian, Irano–Anatolian and the Mesopotamian provinces. According to this classification, Southeast Anatolia is located in the Mesopotamian province of the West Irano–Turanian subregion (Zohary, 1973).

According to Flora of Davis (Davis 1965-1985; Davis et al.; 1988; Güner et al., 2000) some researchers among them Kotschy, Sintenis, Davis, and Zohary have visited and

http://www.aloki.hu ● ISSN 1589 1623 (Print) ● ISSN 1785 0037 (Online)
DOI: http://dx.doi.org/10.15666/aeer/1802_20252041

gathered plant specimens from Şanlıurfa by Baytop (2003). Some floristic and taxonomic studies were carried out in and around Southeast Anatolia (Kaynak and Ketenoğlu, 1980; Malyer, 1981-1983; Kaynak, 1987-1989a, b; Yıldırımlı, 1992-1994; Yıldız and Aktoklu, 1996; Ertekin and Saya, 1997; Ertekin, 2002; Adıgüzel and Aytac, 2001; Aslan and Turkmen, 2001-2003; Turkmen et al., 2002; Akan et al., 2005; Aydoğdu and Akan, 2005). But there has been no vegetational research data except for a study carried out by Zohary (1973). In addition, Southeast Anatolia is one of the most little known or unknown regions of Turkey (Davis, 1965-1985; Çırpıcı, 1987; Donner, 1990).

In the region, the natural areas are used as pastures like in all arid countries. Artificial pasture culture has not been demanded yet. It has been stated that it contains wheat, beans in pastures in arid regions and includes drought-resistant different vegetation types and other herbaceous plants such as Savanne, Praerie, Steppe, Maguis, Phyrgana. (Gençkan, 1983). This understanding and using of pastures are applied in Şanlıurfa on large scale, like in the most of regions of Turkey. In this region the open places which are out of using, belong to state, like slopes, stony, rocky places, stream beds, hills etc. (Çullu et al., 2002). Şanlıurfa is one of little researched region in Turkey (Aslan, 2015). It has 724.529 ha of area. 263.507 ha of this area is used as natural pastures. In the region, the pastures have the poorest plant cover (10-15%) in Turkey. 0.82 ha of area is divided for each cow. In the past years there have been significant changes in the diversity of plants in this area due to random overgrazing and in some years fires (steppe fires) due to the abundance of animals. But, when the pastures of the region are taken into consideration it is necessary to divide 4 ha area for each cow. This shows that the pastures are used five times excessively. Excessive and irregular using have caused succession and degradation. The primary vegetation has transformed to secondary vegetation and converting towards semi-desert ecosytem (Atamov et al., 2004).

The characteristic vegetation type is steppe in this region (Atamov et al., 2004). The threat factors are excessive grazing and transforming of natural pastures to agricultural areas. Because of increased industrial activities, urbanization, tourism activities, creating new agricultural areas, mining activities, using agricultural methods and overgrazing, the natural structures of steppe ecosystems have been getting destroyed (Ture and Bocuk, 2007). 74 taxa are under threat and of these 10 taxa on Karacadağ, 13 taxa in Ceylanpınar are endemic (Özhatay et al., 2003; Aslan, 2018). In Şanlıurfa, the steppe vegetation is dominant because of ecological, geographical and antropogenic factors. Usually, animals eat legumes, grasses and similar crops, which are fresh and delicious for a period of one year. However, the perennial shrub, smelly and prickly plants are not preferred.

Under effects of topographic and edafic factors, different steppe vegetation types are found in the region. In this steppe, wheats are dominant and different plants can be found, which have life forms like geophytes, camephytes, cryptophytes, hemicryptohytes and terophytes. In some districts, some remains of forest and rare old trees are found. In addition, the efemeres which grow rapidly and complete their life cycles in short time after spring and autumn rains are present in the vegetation.

The constant plants are perennial herbs, shrubs and trees that are seen rarely (Atamov et al., 2007). But, the efemeres are found and affect quality of fodder plants and yields positively.

In the region, watery agriculture has been made for years. Agricultural method applied to irrigation in semi-arid and arid regions depending on the characteristics of the plant sown or to obtain higher yields. Since these areas are not natural areas, weed yield

http://www.aloki.hu ● ISSN 1589 1623 (Print) ● ISSN 1785 0037 (Online)
DOI: http://dx.doi.org/10.15666/aeer/1802_20252041

is considerably reduced due to the excess number of animals. Holophytic areas have risen 394%. The agriculture of wheat and cotton have been stopped in some places because of salinity and these areas have been used as pastures for the last 15 years (Çullu et al., 2002).

Materials and methods

The city Şanlıurfa in Southeast of Anatolia is between 37° 49' 12" – 40° 10' 00" East meridian and 36° 41' 28" – 37° 55' 50" North parallel. In Şanlıurfa the uneven areas are at percentage of 60.4%, mountains 22%, plains 16.3% and plateaus 1.3%. Harran plain, covering the study area, is one of the most important agricultural areas of Turkey and located between 36°47' and 39°15' east longitude and 36°40' and 37°41' north latitude within the borders of the province of Şanlıurfa in Southeastern Anatolian region. The most important plains are named Harran, Suruç, Viranşehir, stayed on south part of Şanlıurfa. Ceylanpınar plain are stayed on southwest. In addition, Halfeti, Hilvan and Bozova plains have large areas. The average altitude is 375 m. The lowest plain is Harran plain. Viranşehir plain is at east, Suruç plain is at west of Harran plain. It is 141 535 ha (Anonymous, 1995) (*Figs. 1, 2* and *3*).

Floristic and phytosociologic research studies were carried out between the years 2000-2005 at Karacadağ, Tektek, Fatik, Kaşmer, Nemrut, Kalecik mountains and Direkli Hills where are used as natural pastures. Regular geobotanical trips were organized. Plant specimens were collected and preserved according to the herbarium techniques. These were identified with the help of "Flora of Turkey and the East Aegean Islands" (Davis, 1965-1985, 1988; Güner et al., 2000) and other relevant publications (Akman et al., 2001) as well as the flora of Syria, Iraq and Iran. In addition, the plants of Birecik Dam lake area and halophytic plants in Akçakale were gathered and classified (Ertekin and Saya, 1997; Ertekin, 2002; Adıgüzel and Aytac, 2001; Aslan, 2002; Aslan and Türkmen, 2001-2003; Kaya, 2002; Atamov et al., 2004; Akan et al., 2005; Aydın, 2003; Aydoğdu and Akan, 2005; Ayalp, 2005; Atamov et al., 2005).

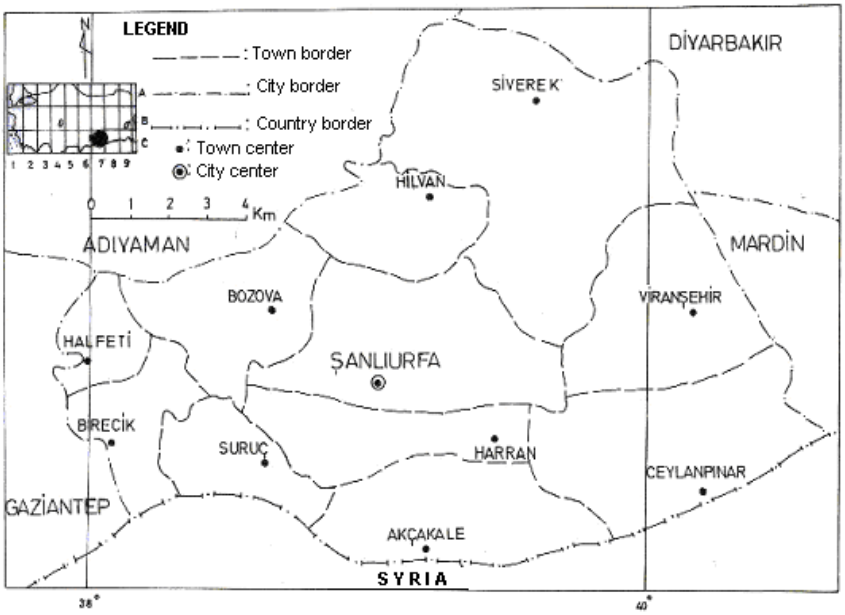

Figure 1. *Location of the study area in Turkey*

http://www.aloki.hu ● ISSN 1589 1623 (Print) ● ISSN 1785 0037 (Online)
DOI: http://dx.doi.org/10.15666/aeer/1802_20252041

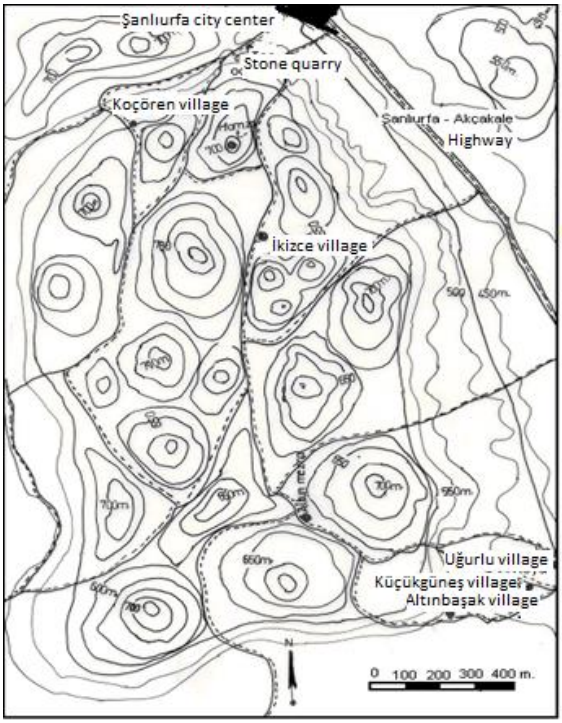

Figure 2. *The map of Fatik Mountains*

Figure 3. *A photo of the research area*

Braun-Blanquet's (1964) method was used for the naming of phytosociological plant groups. Plants were sampled twice a month during certain vegetation periods and plant samples were taken to identify the plants and examine the necessary materials.) These plants have been protected in the Herbarium of Harran University. The climatic data were taken from the Sanliurfa Meteorology Station and has been evaluated according to these data. Approximately 500 g. soil samples were taken from 5 cm under the soil in the research areas in spring, summer and autumn. The soil samples were dried naturally and analysis of them were made by the Ministry of Agriculture and the Rural Affairs General Directorate of Rural Services Sanliurfa Research Institute.

http://www.aloki.hu ● ISSN 1589 1623 (Print) ● ISSN 1785 0037 (Online)
DOI: http://dx.doi.org/10.15666/aeer/1802_20252041

Results and discussion

As it is seen in *Figure 4* and *Table 1,* the climate in Şanlıurfa is arid from June to October in a long period. In this period, most annual plants die. Only perennial herbs, shrubs and trees are alive. Semiarid Mediterranean climate occurs in research area. According to Emberger the precipitation–temperature coefficient (Q) is 42.94 (Akman, 1990). Annual mean temperature is 18.7 °C. The maximum mean temperature (M) is 46.8 °C, in July. The minimum mean temperature (m) is -6.8 °C, in February. Annual rainfall is about 457.8 mm (Anonymous, 2001) and the seasonal precipitation regime is winter, spring, autumn and summer. This is the first variant of the East Mediterranean precipitation regime. The ombrothermic diagram shows dry and rainy periods (*Fig. 4*).

Table 1. *The bioclimate and fall regime of Sanliurfa*

Altitude (m)	P (mm)	M (°C)	M (°C)	Q	PE	S	Fall regime	Bioclimate
547	457.8	46.8	-6.8	42.94	7.2	0.18	W.Sp.A.Su	Semi-arid, cold in winter

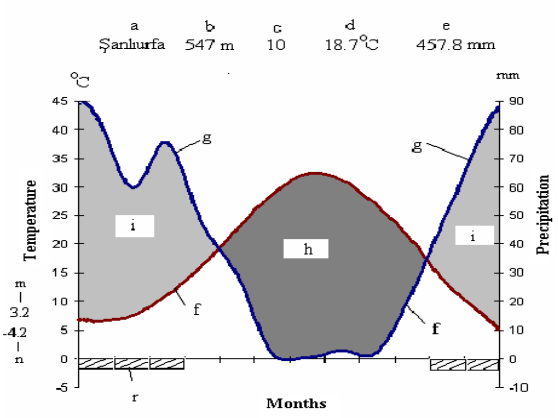

Figure 4. *The climatic diagram of Şanlıurfa.* ***a:*** *Meteorology station;* ***b:*** *The elevation of the Meteorology station (m);* ***c:*** *The year of temperature and precipitation;* ***d:*** *The mean annual temperature (°C);* ***e:*** *The mean annual precipitation (mm);* ***f:*** *The curved line of temperature;* ***g:*** *The curved line of precipitation;* ***h:*** *Arid season;* ***i:*** *Humid season;* ***m:*** *The least mean temperature of the most cold month (°C);* ***n:*** *Absolute minimum temperature (°C);* ***r:*** *Probable frosty month*

In the different plant associations in the steppe vegetation, the avarage productivity changes between 1.0-7.0 kg m^{-2}. Excessive aridity and temperature have caused decreasing productivity and quality of fodder plants in pastures. From the end of autumn to the middle of spring, the efemeres grow and these plants increase the quality and productivity of fodders by 2-3 times. At the end, yield of natural pastures, number of fodder plant species and their populations have been reduced day to day because of excessive and unconscious grazing, migration, negative habitat conditions like aridity and temperature. The plants which have prickle, etheric oils, latex, poison, bitter and fluff have spread out. Excessive grazing has caused the transforming of the primary steppe to secondary and then semi-desert to desert vegetation.

In most of the places in this area, the covering degree of the flora is 40-50%. And this is the characteristic property of half-desert and desert type associations. The flora

http://www.aloki.hu ● ISSN 1589 1623 (Print) ● ISSN 1785 0037 (Online)
DOI: http://dx.doi.org/10.15666/aeer/1802_20252041

has generally made up of a single layer and the average height of the grass covering is 10-20 cm.

On the contrary, the number of plants which are not eaten by animals have been increased. Thus, the primary steppe vegetation has been transformed to secondary and it is seen that the succession has been transformed to semi-desert conditions.

Immigration is widespread in this region and emigrants migrate from East Anatolia to use pastures for grazing. Thousands of sheep destroy the all immature and senile groups of plants. The yield of pastures has been decreased. This situation has caused transforming from steppe to desertation.

In the flora of Şanlıurfa, 71 families, 798 taxa belonging to 342 genera have been determined (Atamov et al., 2004). 135 of these plants were monocotyledonaes, 663 were dicotyledonaes.

The number of plants belonging to *Poaceae* family were more than others in spite of having less species (56) than *Fabaceae* (101). The dominant taxa which spread out in naturel pastures were as follows: *Bromus japonicus* Thunb. subsp. *japonicus, B. squarrosus* L., *B. sterilis* L., *B. tectorum* L., *Avena sterilis* L. subsp. *sterilis*, *Aegilops triuncialis* L. subsp. *triuncialis, A. neglecta* Req. ex Bertol, *Festuca callieri* (Hackel ex St. – Yves) F. Markgraf subsp. *callieri*, *Hordeum murinum* L. *subsp. glaucum* (Steudel) Tzvelev.

Some plants belonging to *Fabaceae,* have fodder quality. Most of them are used as fodders. These were as follows; *Astragalus onobrychis* L., *A. aleppicus* Boiss., *A. immarginatus* Labm., *A. dactylocarpus* Boiss., *Medicago rigidula* (L.) var. *rigidula, Onobrychis caput-galli* (L.) Lam. *O. crista-galli* (L.) Lam. *O. galegifolia* Boiss. *O. kotschyana* Fenzl. *Trifolium scabrum* L., *T. speciosum* Willd., *T. dasyurum C.* Presl, *T. angustifolium L.* var *intermedium, T. boisseri* Guss. ex Boiss., *T. meironense* Zoh., *T. campestre* Schreb., *Trigonella monspeliaca* L., *T. mesopotamica* Hub. Mor., *Vicia mollis* Boiss., *Coronilla orientalis* Miller var. *orientalis, C. scorpioides* (L.) Koch, *Hedysarum varium* Willd.

In the research area, 153 taxa belonging to 26 families and 107 genera were identified. *Poaceae* with 31 taxa (20.3%), *Asteraceae* with 24 taxa (15.7%), *Fabaceae* with 22 (14.4%), and *Apiaceae* with 13 taxa (8.5%) were the richest families.

Braun-Blanquet's (1964) method was used for the naming of phytosociological plant groups.

32 sample parcels were evaluated and 6 new associations and their upper categories are as follows:

Astragalo–Bromotea Quezel 1973
Astragalo–Bromotalia Quezel 1973
Agropyro–Stachyon Quezel 1973
1. *Festuco callieri–Teucrietum poliae* ass. ova
Onobrychido armenae–Thymetalia leucostomi Akman, Ketenoglu Quezel 1984
2. *Astragalo strictifolii–Salvietum sclarea* ass. nova
3. *Phlomido bruguieri–Thymbretum spicatae* ass. nova
4. *Asphodelo aestivum–Teucrietum poliae* ass. nova
5. *Cynodo dactyloni–Bromoetum danthoniae* ass. nova
6. *Prosopo farctae–Avenetum erianthae* ass. nova

http://www.aloki.hu ● ISSN 1589 1623 (Print) ● ISSN 1785 0037 (Online)
DOI: http://dx.doi.org/10.15666/aeer/1802_20252041

Festuco callieri–Teucrietum poliae ass. nova

There were no trees and shrubs in its structure. Only grass layer was present and covering was 40-80%. The length was between 10 and 35 cm (*Table 2*).

Festuco callieri–Teucrietum poliae association was spreading out where the calcereous main rock, gravelled and small pit areas. According to chemical and physical properties of soils where the association was spreading out homogenous, pH was between 7.0 and 7.71, the rate of lime ($CaCO_3$) was 3.8%, phosphorus (P_2O_5) was 5.2-5.3 kg dec^{-1}; potassium (K_2O) was 118.8-308.8 kg dec^{-1} and organic component was 2.17-2.48% (*Table 3*).

Table 2. *Festuco callieri–Teucrietum poliumae ass. nova. Thypus: Sample Parcel 62*

Sample parcel No	**12**	**23**	**34**	**35**	**37**	**41**	**42**	**46**	**48**	**50**	Frequency
Square size (m^2)	50	50	50	50	50	50	50	50	50	50	
Altitude (m)	500	478	530	540	570	510	515	530	535	550	
Gradient (%)	20	30	30	35	30	25	30	35	30	25	
Direction	N	NW	NW	N	N	N	N	N	N	NW	
Length of cover (cm)	10	25	20	17	20	22	20	25	25	20	
Number of species	21	21	20	16	17	18	18	15	16	17	
Cover (%)	60	55	55	60	65	65	60	60	60	65	
Characteristic species of Association											
Festuca callieri	22	22	+2	+2	+1	22	22	33	22	11	V
Teucrium polium	–	22	+1	11	11	1	33	33	+1	11	IV
Trifolium tomentosum	+2	+2	+1	+2	+2	.	.	.	.	.	III
Characteristic species of Allians *Festuca–Teucrion*											
Phleum phleoides	+1	+2	+2	+2	.	.	.	+2	+2	+2	III
Phlomis bruguieri	+2	+2	+2	+2	+2	+2	+2	+1	.	.	III
Eryngium creticum	+1	+2	+2	.	.	+2	+1	.	.	.	II
Characteristic species of Ordo *Daphno–Festucetalia*											
Thymbra spicata var. *spicata*	22	22	22	11	11	+2	+2	+2	.	.	III
Lolium rigidum	+2	+2	.	.	.	+2	+1	+1	+1	+1	II
Hordeum murinum subsp. *glaucum*	+2	.	.	+2	+2	+2	+2	+2	+2	.	III
Characteristic species of Classis *Daphno–Festucetea*											
Salvia sclarea	.	.	.	+2	+2	+2	+2	+2	+2	+1	II
Teucrium polium	+2	+1	+2	+2	+2	.	.	.	.	.	II
Scutellaria tomentosa	+2	+1	+2	.	.	.	.	.	+2	+2	II
Aegilops cylindirica	+2	+2	+1	+1	+1	+1	+1	.	.	.	II
Participants											
Allium flavum subsp. *tauricum* var. *tauricum*	+2	+2	+2	+2	+2	+2	+2	+2	+2	+2	III
Avena sterilis subsp. *sterilis*	+1	+1	.	.	.	+2	+2	+2	+2	+1	II
Euphorbia denticulata	+1	+1	+1	+1	+1	.	.	.	.	+1	I
Tordylium syriacum	.	.	.	.	.	+1	+2	+2	+2	+1	I
Erodium cicutarium subsp. *cicutarium*	+1	+1	+1	.	.	.	.	.	.	.	I
Cichorium glandulosum	.	.	.	.	+1	+1	+2	+2	.	.	I
Crepis reuterana subsp. *reuterana*	.	.	.	.	.	.	.	+1	+1	+1	I
Gagea luteoides	.	+1	.	.	.	.	.	.	.	.	I

http://www.aloki.hu ● ISSN 1589 1623 (Print) ● ISSN 1785 0037 (Online)
DOI: http://dx.doi.org/10.15666/aeer/1802_20252041

Thlaspi perfoliatum	+1	+1	+1	+1	.	.	.	.	.	.	I
Muscari comosum	.	.	.	.	.	.	+1	+1	+1	.	I
Scandix pecten–veneris	+1	.	.	.	.	.	+1	.	.	+1	I
Lappula barbata	.	.	.	.	+1	.	.	.	.	.	I
Cynosurus echinatus	.	+1	.	.	.	.	.	.	.	.	I
Torilis tenella	+1	+1	.	.	.	.	.	.	+1	.	I
Hypecoum imberbe	.	.	+1	.	.	.	.	.	.	+1	I
Senecio vulgaris	.	.	.	.	.	+1	.	.	.	.	I
Anthemis haussknechtii	.	.	.	.	+1	+1	+1	.	.	+1	I
Gypsophila antari	+1	+2	+2	+2	.	.	.	+1	.	.	II
Medicago minima var. *minima*	+1	+1	+2	+2	+2	.	.	.	+2	+2	II
Echinops microcephalus	.	.	+1	.	.	.	.	.	.	.	I
Centaurea solstitialis subsp. *solstitialis*	+1	.	.	.	.	.	.	.	.	.	I
Hypecoum pendulum	.	.	.	.	.	.	.	.	+1	+1	I
Torilis leptophylla	.	.	+2	+1	+1	+1	+1	.	.	.	I

Table 3. *Chemical characteristics of the soil of the research area*

Location	Deepth (cm)	Saturation with water (%)	Total salt (%)	pH	$CaCO_3$ (%)	P_2O_5	K_2O	Organic mass (%)
Ugurlu Village	0-20	77	0.071	7.70	3.8	5.3	118.8	2.48
Kocoren Village	0-20	77	0.060	7.71	3.8	5.2	308.8	2.17
Ikizce Village	0-20	68	0.073	7.28	2.6	4.9	179.2	1.44
Altun Village	0-20	66	0.098	7.42	6.8	4.5	108	2.35

The characteristic species of the association were *Festuca callieri* subsp. *callieri*, *Teucrium polium*. Each species are the elements of Irano–Turanian phytogeographic region.

Classis: *Daphno–Festucetea* Quezel 1964

Ordo: *Daphno–Festucetalia* Quezel1964

Alliance: *Festuca–Teucrion* ass. nova

Asphodelo aestivi–Teucrietum poliae ass. nova

The characteristic species of the association were *Asphodelus aestivus* and *Teucrium polium*. This association was at the north part of the Fatik Mountains and at the environs of Stone quarry. 10 sample areas were used. The gradient was 35-40%, The length was between 600 and 700 m (*Table 4*).

Table 4. *Asphodelo aestivi–Teucrietum poliae ass. nova. Thypus: Sample Parsel 63*

Sample parcel No	60	61	62	67	70	73	77	79	81	82	
Square size (m^2)	50	50	50	50	50	50	50	50	50	50	Frequency
Altitude (m)	531	535	500	510	515	520	530	505	500	517	
Gradient (%)	30	20	25	25	30	30	35	30	35	35	
Direction	W	W	W	W	NW	NW	NW	NW	NW	W	

http://www.aloki.hu ● ISSN 1589 1623 (Print) ● ISSN 1785 0037 (Online)
DOI: http://dx.doi.org/10.15666/aeer/1802_20252041

Length of cover (cm)	20	25	20	20	25	15	20	25	20	30	
Number of species	14	13	11	8	12	13	13	10	11	11	
Cover (%)	55	50	45	55	50	55	60	50	40	45	
Characteristic species of Association											
Astragalus strictifolius	11	+2	+2	11	11	12	22	22	22	+2	V
Teucrium polium	+2	22	22	22	11	.	.	11	+2	+2	VI
Asphodelus aestivus	12	33	33	.	.	+2	+2	.	.	.	III
Characteristic species of Allians *Agropyro–Stachyon*											
Euphorbia denticulata	+1	.	+1	.	+1	.	+2	+2	+2	.	III
Centaurea solstitialis subsp. *solstitialis*	.	+2	.	.	+2	+2	.	.	.	+1	II
Bromus japonicus subsp. *japonicus*	+1	+2	.	.	33	+1	+2	+1	.	.	III
Characteristic species of Ordo *Astragalo–Bromotalia*											
Astragalus lamarckii	11	+2	+2	22	22	11	11	11	+2	+2	IV
Bromus danthoniae	+2	+2	+1	+1	.	.	.	+1	+1	+2	III
Scutellaria tomentosa	+1	+1	.	.	.	.	+2	+1	+1	+1	II
Characteristic species of Classis *Astragalo–Bromotea*											
Arrhenatherum kotschyi	+2	+2	.	.	+2	+2	.	.	+1	11	II
Phlomis kurdica	+2	.	.	+2	+1	+1	.	+1	.	.	II
Gypsophila antari	+1	.	+1	.	.	.	+1	.	.	.	I
Stipa holosericea	.	.	.	+1	+2	+2	+2	+2	.	.	II
Participants											
Poa bulbosa	+1	+1	+2	+2	+	+1	+2	+2	+2	+2	II
Trifolium speciosum	.	.	+2	.	+2	+2	+1	.	.	+2	II
Torilis arvensis	+1	+1	+1	.	.	.	.	+1	+2	+1	II
Anthemis haussknechtii	+1	+1	+1	.	.	.	+1	.	.	.	I
Lolium rigidum	.	.	.	+1	+1	+2	+2	.	+2	.	I
Capparis spinosa	.	.	.	.	.	+1	+1	.	.	.	I
Convolvulus arvensis	.	.	.	.	+1	+2	.	.	.	.	I

The association contain one layer composed of grass and average length was between 20 and 30 cm. The plant cover was changing between 40 and 60%.

Classis: *Astragalo–Bromotea* Quezel 1973

Ordo: *Astragalo–Bromotalia* Quezel 1973

Alliance: *Agropyro–Stachyon* Quezel 1973

This association was spreading out on the calcereous main rock, and gravelled and small pit areas. According to chemical and physical properties of soils, pH was: 7.28-7.71, the rate of lime ($CaCO_3$) was 3.8%, phosphorus (P_2O_5) was 5.2 kg/dec.; potassium (K_2O) was 118.8 kg/dec. and organic component was 2.48%. (*Table 3*). The yield of pasture was low, between 0.5 and 1.0 ha^{-1}, because of excessive grazing. 20 taxa were determined.

Cynodo dactyloni–Brometum danthoniae ass. nova

The characteristic species of the association were *Cynodon dactylon* and *Bromus danthoni*. It was defined in stream beds and depressed places on the southwest of İkizce village at Fatik mountains. The gradient was low (5-10%), and the altitude was between

http://www.aloki.hu ● ISSN 1589 1623 (Print) ● ISSN 1785 0037 (Online)
DOI: http://dx.doi.org/10.15666/aeer/1802_20252041

600 and 700 m. 10 sample parcels were used. This association composed of only grass layer and the average length was between 10 and 20 cm., covering was 60–65% and taxon number was poor (between 7 and 13) (*Table 5*).

Classis: *Astragalo–Bromotea* Quezel 1973

Ordo: *Astragalo–Bromotalia* Quezel 1973

Alliance: *Agropyro–Stachyon* Quezel 1973

This association was spread out at red-brown soils. According to chemical and physical properties of soils; pH was: 7.42, the rate of lime ($CaCO_3$) was 6.8%, phosphorus (P_2O_5) was 4.5 kg dec^{-1}; potassium (K_2O) was 108.0 kg dec^{-1}. and organic component was found as 2.35% (*Table 3*). The yield of pasture was 1.0 ha^{-1}

The association Cynodo datyloni–Brometum danthoniae is composed of 27 taxa Table 5).

Table 5. *Cynodo dactyloni–Bromoetum danthoniae ass. nova. Thypus: Sample Parcel 64*

Sample parcel No	******	**63**	**64**	**69**	**71**	**74**	**75**	**76**	**78**	**80**	Frequency
Square size (m^2)	50	50	50	50	50	50	50	50	50	50	
Altitude (m)	470	485	480	485	490	485	480	458	500	505	
Gradient (%)	10	20	25	15	20	25	15	20	25	20	
Direction	NE	NE	NE	NE	NE	N	N	N	NE	NE	
Length of cover (cm)	15	15	10	10	15	15	10	15	10	20	
Number of species	13	13	13	12	13	8	12	12	7	10	
Cover (%)	65	60	65	65	60	60	65	55	55	65	
Characteristic species of Association											
Cynodon dactylon	.	+2	22	33	33	22	23	23	+2	+2	V
Bromus danthoniae	+1	+2	+1	+2	+2	11	11	22	11	12	IV
Bromus japonicus	+2	+1	+2	11	11	11	+2	.	.	.	III
Characteristic species of Allians *Agropyro–Stachyon*											
Avena eriantha	+1	+1	+1	+2	+2	+2	+2	.	.	.	III
Eryngium creticum	+1	.	+1	.	+1	.	.	+1	+1	+1	II
Cichorium glandulosum	.	.	.	+1	.	.	.	+1	.	+1	I
Characteristic species of Ordo *Astragalo–Bromotalia*											
Astragalus lamarckii	.	.	+2	+1	+1	+2	+2	+2	+2	+2	III
Bromus rubens	+2	+2	+2	.	.	.	+1	+1	.	.	II
Euphorbia characias subsp. *wullfenii*	.	.	.	+1	+1	+1	.	.	.	.	I
Characteristic species of Classis *Astragalo–Bromotea*											
Aegilops cylindirica	+2	+2	.	.	.	.	.	+1	+2	.	II
Hordeum bulbosum	.	.	+1	+2	+2	.	.	.	.	+2	I
Ziziphora capitata	+1	+1	+1	+2	.	.	.	.	.	.	I
Scrophularia canina subsp. *bicolor*	+1	+1	.	.	.	.	+1	.	.	.	I
Participants											
Scandix pecten–veneris	.	.	.	+1	+1	+1	+2	+2	+2	+2	III
Verbascum kotschyi	.	+1	+1	.	.	.	.	.	.	+1	I
Centaurea consanguinea	.	.	+1	.	.	.	+1	+1	+1	.	I
Veronica beccabunga subsp. *beccabunga*	+1	+1	.	.	+1	.	.	.	.	.	I
Ranunculus arvensis	11	+1	+2	+2	+2	+1	.	.	.	.	II
Secale sylvestris	.	.	.	.	.	.	+1	+1	+1	.	I

http://www.aloki.hu ● ISSN 1589 1623 (Print) ● ISSN 1785 0037 (Online)
DOI: http://dx.doi.org/10.15666/aeer/1802_20252041

Allium flavum subsp. *tauricum* var. *tauricum*	+1	+1	.	.	.	.	.	.	.	+1	I
Senecio vulgaris	.	.	.	.	.	.	+1	+1	.	.	I
Crepis reuterana subsp. *reuterana*	+1	.	.	.	+1	.	.	.	.	+1	I
Trifolium tomentosum	.	.	.	.	.	.	.	.	+1	.	I
Hypecoum pendulum	.	.	.	+1	+2	+2	.	.	.	.	I
Avena sterilis subsp. *sterilis*	+1	+1	.	.	.	.	.	.	.	+1	I
Hypericum capitatum var. capitatum	.	.	.	.	.	.	+1	.	.	.	I

Phlomido bruguieri–Thymbretum spicatae ass. nova

Phlomis bruguieri and *Thymbra spicata* subsp. *Spicata* were the characteristic species of this association. It was spread out on the south part of the Fatik mountain, between Ikizce village and Altun mezra village. The gradient was 15-30% and the altitude was between 610 and 850 m (*Table 6*).

The association contained only one layer like the others, grass layer. The average length was 12-25 cm and rate of covering was 50-60% (*Table 6*).

Classis: *Astragalo–Bromotea* Quezel 1973

Ordo: *Onobrychido armenae–Thymetalia leucostomi* Akman, Ketenoğlu Quezel 1984

Alliance: *Phlomido armeniaceae–Astragalion microcephali* Akman, Ketenoğlu Quezel 1986

It was spreading out at red-brown soils. According to chemical and physical properties of soils, pH was: 7.70, the rate of lime ($CaCO_3$) was 3.8%, phosphorus (P_2O_5) was 5.3 kg dec^{-1}; potassium (K_2O) was 118.8 kg dec^{-1} and organic component was found as 2.48% (*Table 3*). The yield of pasture was 1.0-1.5 ha^{-1} 29 taxa were determined from this association (*Table 6*).

Table 6. *Phlomido bruguieri–Thymbretum spicatae ass. nova Thypus: Sample Parcel 17*

Sample parcel No	**10**	**13**	**14**	**15**	**17**	**19**	**21**	**22**	**28**	**30**	**33**	**65**	**66**	Frequency
Square size (m^2)	50	50	50	50	50	50	50	50	50	50	50	50	50	
Altitude (m)	610	605	707	710	715	720	725	810	815	750	820	822	815	
Gradient (%)	20	15	25	20	25	35	30	20	20	25	30	30	30	
Direction	SE	S	S	S	S	SE	SE	SE	SE	SE	SE	SE	S	
Length of cover (cm)	25	20	20	25	20	20	25	20	25	20	20	20	25	
Number of species	12	12	10	11	15	9	9	9	12	7	9	9	7	
Cover (%)	50	55	55	60	60	60	65	55	55	50	50	60	55	
Characteristic species of Association														
Phlomis bruguieri	+2	+2	22	22	11	11	22	22	11	+2	+2	+2	+1	V
Thymbra spicata	+2	+2	+2	+1	+1	11	11	11	+2	+2	+1	+1	+2	IV
Characteristic species of Allians *Phlomido armeniaceae–Astragalion microcephali*														
Hordeum murinum subsp. *glaucum*	+2	+2	22	22	11	11	11	+1	+2	+2	22	11	11	IV
Phleum phleoides	+1	+2	+2	+2	+2	.	.	.	.	.	+2	.	.	III
Teucrium parviflorum	+2	.	.	.	+2	.	.	.	+2	.	.	.	.	II
Euphorbia characias subsp. *wullfenii*	.	.	.	.	.	.	+2	+2	.	.	+2	.	.	I

http://www.aloki.hu ● ISSN 1589 1623 (Print) ● ISSN 1785 0037 (Online)
DOI: http://dx.doi.org/10.15666/aeer/1802_20252041

Characteristic species of Ordo *Onobrychido armenae–Thymetalia leucostomi*														
Onobrychis caput-galli	+2	+2	+1	+2	+2	+2	+2	+2	+2	.	.	+2	+2	IV
Bromus scoparius	.	+2	+2	+2	+1	+1	+1	+1	+1	+2	+2	+1	.	III
Medicago rigidula	+1	+1	.	.	.	.	.	.	+1	+1	.	.	.	I
Characteristic species of Classis *Astragalo–Bromotea*														
Bromus japonicus	.	+2	+2	+2	+1	+1	+1	+2	+2	+2	+2	+2	+2	III
Satureja hortensis	+1	+1	+1	+2	+2	+2	.	.	.	.	.	.	+2	II
Scabiosa calocephala	+1	+1	+1	+2	+2	.	.	.	.	.	+2	.	.	II
Participants														
Hypecoum imberbe	.	.	.	.	+1	.	.	.	.	.	.	.	.	I
Torilis tenella	.	.	.	.	.	.	+1	.	.	.	.	.	.	I
Xanthium strumarium subsp. *strumarium*	.	.	.	.	.	.	.	+1	.	.	.	+1	.	I
Cynosurus echinatus	+1	.	.	.	.	+1	.	.	.	.	.	.	.	I
Eremopyrum bonaepartis subsp. *bonaepartis*	.	+1	.	.	+1	.	.	.	.	.	.	.	.	I
Urginea maritima	.	.	.	.	.	.	.	.	.		+1	.	.	I
Secale sylvestris	.	.	.	.	.	.	.	.	.	.	.	+1	.	I
Gagea luteoides	+2	.	.	.	.	.	.	.	.	.	.	.	.	I
Trfolium stellatum	.	.	.	.	+1	.	.	.	.	.	.	.	.	I
Crepis reuterana subsp. *reuterana*	.	.	.	.	.	.	+1	.	.	.	.	.	.	I
Sedum caespitosum	.	.	+1	.	.	.	.	.	.	.	.	.	+1	I
Echinops microcephalus	.	.	.	.	+1	.	.	+1	+1	.	.	.	.	I
Eryngium creticum	+1	.	.	+1	.	.	.	.	+1	.		.	.	I
Capsella bursa-pastoris	.	.	.	.	.	+1	.	.	.	+1	.	.	.	I
Thlaspi perfoliatum	+1	+1	.	+1	.	.	.	.	.	.	.	.	.	I
Velezia rigida	.	.	.	.	.	.	.	.	.	.	+1	.	.	I

Prosopo farctae–Avenetum erianthae ass. nova

The characteristic species were *Prosopis farcta, Avena eriantha* and *Bromus scoparius*. It was determined from the Northwest of Küçük Güneş, Aşağı Güneş and Yukarı Güneş villages of Fatik Mountain at 450-500 m altitudes.

The association composed of only grass layer except *Prosopis farcta,* the average length was between 15 and 30 cm and the covering was between 50 and 65%. The number of taxon was between 12 and 18 (*Table 7*).

Classis: *Astragalo–Bromotea* Quezel 1973

Ordo: *Astragalo–Bromotalia* Quezel 1973

Alliance: *Prosopo–Bromuon* ass. nova

This association was spreading out at red-brown soils. According to chemical and physical properties of soils, pH was: 7.28, the rate of lime ($CaCO_3$) was 2.6%, phosphorus (P_2O_5) was 4.9 kg dec^{-1}; potassium (K_2O) was 179.2 kg dec^{-1} and organic component was measured as 1.44% (*Table 3*). The yield of pasture was 1.0-1.5 ha^{-1} 26 taxa were determined (*Table 7*).

http://www.aloki.hu ● ISSN 1589 1623 (Print) ● ISSN 1785 0037 (Online)
DOI: http://dx.doi.org/10.15666/aeer/1802_20252041

Table 7. *Prosopio farctae–Avenetum erianthae ass. nova Thypus: Sample Parcel 9*

Sample parcel No	**2**	**5**	**6**	**8**	**9**	**11**	**12**	**16**	**18**	**20**	**25**	**26**	**27**	Frequency
Square size (m^2)	50	50	50	50	50	50	50	50	50	50	50	50	50	
Altitude (m)	450	455	460	470	475	480	485	490	495	500	505	510	515	
Gradient (%)	10	15	10	10	10	10	15	15	15	10	10	10	15	
Direction	E	E	E	SE	SE	SE	SE	SE	SE	SE	SE	SE	SE	
Length of cover (cm)	25	20	20	25	30	15	15	25	15	15	25	25	20	
Number of species	18	13	12	13	13	12	12	13	13	12	13	13	14	
Cover (%)	55	50	55	50	50	45	50	60	55	50	45	50	50	
Characteristic species of Association														
Prosopis farcta	+2	+2	33	33	22	22	11	11	11	22	22	33	33	V
Bromus scoparius	+1	+1	+2	.	.	22	22	+2	+2	+1	+1	+2	22	IV
Avena eriantha	+2	+2	22	22	22	+2	+2	+2	+2	+2	+2	.	+1	IV
*Characteristic species of Allians Prosopo–Bromuon****														
Phlomis bruguieri	+2	+2	+2	+2	+2	+1	+1	+2	+2	+2	+2	+2	+2	III
Hordeum murinum subsp. *glaucum*	+1	+1	+2	+2	11	11	11	11	11	+1	+1	.	.	III
Salvia sclarea	+1	.	.	.	+1	+1	+1	+2	+2	+2	+2	.	.	II
Characteristic species of Ordo *Astragalo–Bromotalia*														
Astragalus lamarckii	+1	+2	+2	+2	+2	+2	+2	+2	.	.	+2	.	.	II
Bromus japonicus	+1	+1	11	+2	+1	.	.	.	+1	+2	.	+1	12	II
Juncus articulatum	+1	+1	+1	22	22	22	22	.	.	.	11	11	.	III
Characteristic species of Classis *Astragalo–Bromotea*														
Phleum phleoides	+2	+2	+2	+2	+1	+1	+1	+2	+2	+1	+1	+1	+1	II
Phlomis bruguieri	+2	+2	.	.	+2	+2	.	.	+2	+2	+2	.	.	II
Cichorium glandulosum	+1	.	+1	+1	.	.	.	+1	+1	+1	.	.	.	I
Participants														
Althea officinalis	+1	+1	+1	+1	+1	.	+2	+2	+2	.	.	.	.	II
Verbascum kotschyi	.	.	.	+1	+2	+2	+1	+1	+1	.	.	+1	+1	II
Linum pubescens subsp. *pubescens*	+1	.	.	+1	.	.	.	.	.	.	+1	.	.	I
Euphorbia szovitsii var. *szovitsii*	.	.	.	.	.	.	.	.	+1	+1	+1	.	.	I
Eryngium campestre	.	+1	+1	.	.	.	.	.	.	.	.	.	+1	I
Hypericum capitatum var. *capitatum*	+1	.	.	.	.	.	.	+1	.	.	.	+1	.	I
Trifolium tomentosum	.	.	.	.	+1	.	.	.	.	.	.	+1	.	I
Hordeum bulbosum	.	.	.	.	.	.	+1	.	.	.	.	.	+1	I
Aegilops cylindirica	.	.	.	+1	.	+1	.	.	.	.	.	+1	.	I
Torilis arvensis	.	.	.	.	.	.	.	.	.	+1	.	.	.	I
Carduus pycnocephalus subsp. *albidus*	+1	.	.	.	.	.	.	.	.	.	+1	.	+1	I
Anthemis haussknechtii	.	+1	.	.	.	.	.	.	.	.	.	+1	+1	I
Erodium cicutarium subsp. *cicutarium*	+1	.	.	.	.	.	.	.	.	.	.	+1	+1	I
Lappula barbata	.	.	+1	.	.	.	.	+1	.	.	.	+1	+1	I
Secale sylvestre	.	.	.	+1	.	.	.	.	.	.	.	.	+1	I

http://www.aloki.hu ● ISSN 1589 1623 (Print) ● ISSN 1785 0037 (Online)
DOI: http://dx.doi.org/10.15666/aeer/1802_20252041

Astragalo strictifolii–Salvietum sclarea ass. nova

Astragalus strictifolius var. *strictifolius* and *Salvia sclarea* were the characteristic taxa of this association. It was determined between Fatik and Ikizce villages at northeast direction. The altitude was 600-750 m and the gradient was between 20 and 35%. The association composed of only grass layer except *Astragalus strictifolius* var. *strictifolius*. The average length was between 20 and 25 cm and the covering was between 50 and 65%. The number of taxon was between 10 and 18 (*Table 8*).

Classis: *Astragalo–Bromote* Quezel 1973

Ordo: *Astragalo–Bromotalia* Quezel 1973

Alliance: *Agropyro–Stachyon* Quezel 1973

This association was spreading out at the red-brown soils on the arid stone. According to chemical and physical properties of soils, pH was: 7.42, the rate of lime ($CaCO_3$) was 6.8%, phosphorus (P_2O_5) was 4.5 kg dec^{-1}; potassium (K_2O) was 108.0 kg dec^{-1} and organic component was measured as 2.35% (*Table 3*). The yield of dry grass was between 300 and 400 g m^{-2} 35 taxa were determined (*Table 8*).

Table 8. *Astragalo strictifolii–Salvietum sclarea ass. nova Thypus: Sample Parcel 36*

Sample parcel No	**1**	**3**	**4**	**36**	**38**	**44**	**45**	**47**	**49**	**51**	**52**	**54**	**58**	Frequency
Altitude (m)	50	50	50	50	50	50	50	50	50	50	50	50	50	
Gradient (%)	510	520	530	540	550	555	557	560	565	567	570	571	572	
Direction	30	35	20	20	25	30	30	35	35	30	35	30	25	
Length of cover (cm)	SE	SE	SE	S	S	S	SW	SW	SW	S	S	S	S	
Number of species	25	20	20	25	30	35	35	30	30	25	30	25	25	
Cover (%)	13	12	15	16	16	13	13	9	12	10	15	12	12	
Altitude (m)	50	55	55	60	65	60	60	55	55	60	60	60	50	
Characteristic species of Association														
Astragalus strictifolius var. *strictifolius*	12	12	22	+1	+1	22	+1	+2	22	22	22	11	11	IV
Salvia sclarea	12	.	12	11	+1	+1	+2	+2	11	22	+2	+2	11	IV
Characteristic species of *Allians Agropyro Stachyon*														
Thymbra spicata	.	.	+2	22	33	+2	+2	+2	+2	22	22	11	11	IV
Phlomis kurdica	+2	+2	+2	+2	+2	.	.	.	.	.	+2	+2	.	III
Euphorbia characias subsp. *wullfenii*	.	.	+2	+2	+2	+2	+2	.	.	.	.	.	+2	II
Stipa holosericea	.	.	.	.	.	.	.	.	+2	+2	+2	.	.	II
Characteristic species of Ordo *Astragalo–Bromotalia*														
Festuca callieri subsp. *callieri*	+2	+2	+2	+2	+2	+2	.	.	.	.	.	.	.	II
Astragalus lamarckii	22	+2	+2	22	22	.	.	.	22	11	11	22	11	IV
Phlomis ssp.	+2	+2	+2	.	.	.	+2	+2	+2	.	+2	.	.	III
Characteristic species of Classis *Astragalo–Bromotea*														
Eryngium creticum	.	.	+2	+2	+2	+2	+2	.	.	+2	+2	.	+2	III
Teucrium polium	+2	+2	.	.	+2	+2	+2	+2	.	.	.	.	.	II
Trifolium speciosum	.	.	.	+2	+2	+2	.	.	.	.	+2	+2	+2	II
Ranunculus arvensis	+2	.	+2	.	.	.	+1	+1	+1	+1	.	.	.	I

http://www.aloki.hu ● ISSN 1589 1623 (Print) ● ISSN 1785 0037 (Online)
DOI: http://dx.doi.org/10.15666/aeer/1802_20252041

	Participants													
Eminium rauwolffii var. *rauwolffii*	+2	+2	+2	+2	+2	+2	+2	+1	+1	+1	.	.	+2	III
Muscari comosum	+2	+2	+2	.	.	.	.	.	.	+1	+1	+1	.	II
Gagea luteoides	+2	+2	+2	+1	+2	+2	+2	.	.	.	.	+1	+1	III
Erodium cicutarium subsp. *cicutarium*	.	.	.	.	+1	+2	.	.	+1	+1	+1	.	.	I
Achillea vermicularis	.	.	.	.	.	.	.	+2	.	.	.	.	.	I
Eryngium campestre	.	.	.	+1	+2	+2	+1	.	.	.	.	.	.	I
Capsella bursa-pastoris	.	.	.	.	.	.	.	.	.	.	+1	+1	+1	I
Avena sterilis subsp. *sterilis*	+2	+1	+1	+2	+1	.	.	.	+2	.	.	.	.	I
Echinaria capitata	+1	+1	.	.	.	.	.	.	.	.	.	+1	+1	I
Althea officinalis	.	.	.	+2	.	.	+1	.	.	.	.	.	+2	I
Veronica beccabunga subsp. *beccabunga*	.	+1	.	.	.	.	.	.	.	.	+1	+1	+1	I
Vulpia persica	.	.	.	.	.	+1	+1	.	.	.	.	.	.	I
Bromus japonicus	.	.	.	+1	.	.	.	.	+1	+1	+1	.	.	I
Eremopyrum bonaepartis subsp. *bonaepartis*	.	.	.	.	.	.	+2	.	.	.	+2	.	.	I
Convolvulus arvensis	.	.	+2	.	.	.	.	.	.	.	.	.	+1	I
Cichorium glandulosum	.	.	.	.	.	+1	.	.	.	.	.	.		I
Linum pubescens	.	.	.	+1	.	.	.	+1	+1	.	.	.		I
Aegilops cylindirica	+2	.	.	.	+2	.	.	.	.	.	.	.	.	I
Xanthium strumarium subsp. *strumarium*	.	+1	.	.	.	.	.	+1	.	.	+1	.	.	I

Conclusion

In the region, due to excessive and uncontrolled grazing, steppe vegetation has turned into secondary vegetation rather than semi-desert and desert-type vegetation. Therefore, these areas should be controlled and over-grazing should be prevented. In natural pastures, the value of the forage plant and the most suitable pasture capacity should be determined. The productivity of pastures is related to the composition of plant species and habitat factors (Braun-Blanquet, 1964). Morphological structures and ecological habitat forms are one of the most important subjects that should be studied in pasture research projects.

First, the quality and quantity of a pasture should be examined. In the region, plant sociological characteristics of the dominant steppe vegetation change during the seasons. The efemers change the productivity and quality of the pastures. In pastures, forage crops have been reduced due to overgrazing, others spread if inedible to animals. These areas have been abandoned for agriculture and have become barren due to overgrazing. In the future research of these areas, controlled pasture stocking should be carried out together with controlled irrigation for the formation of productive pastures, and even pasture forage crops suitable for barren areas should be selected and trials should be conducted in the area. National and regional pasture management plans should continue to be implemented effectively, sustainable productivity must be ensured and these areas should be put back into service of Turkish livestock.

http://www.aloki.hu ● ISSN 1589 1623 (Print) ● ISSN 1785 0037 (Online)
DOI: http://dx.doi.org/10.15666/aeer/1802_20252041

REFERENCES

[1] Adıgüzel, N., Aytaç, Z. (2001): Flora of Ceylanpınar State Farm (Şanlıurfa-Turkey). – Fl Medit 11: 333-361.
[2] Akan, H., Kaya, Ö. F., Eker, I., Cevheri, C. (2005): The Flora of Kaşmer Mountain, Sanliurfa, Turkey. – Turk. J. Bot. 29: 1-20.
[3] Akman, Y. (1990): Climate and Bioclimate. – Palme Publications, Ankara.
[4] Akman, Y., Ketenoglu, O., Geven, F. (2001): Vegetation Ecology and Research Methods. – Ankara University Publications No: 9, Ankara.
[5] Anonymous (1995): Şanlıurfa Province Land Asset. – T. C. General Directorate of Rural Services Directorate Publications, Ankara.
[6] Anonymous (2001): Meteorological Bulletin. – T. C. State Meteorological Service General Directorate No: A-09: 27-29, Ankara.
[7] Aslan, M. (2002): Birecik Dam Lake area plants, hazard classes and conservation. – PhD Thesis, Cukurova University, Institute of Science and Technology, Adana.
[8] Aslan, M. (2015): Succession of steppe areas after fire in the Gap Region of Turkey. – Bangladesh J. Bot. 44(4): 489-497.
[9] Aslan, M. (2018): Habitats change in Ceylanpınar State's farm and the dangerous classes of plants (Şanlıurfa-Turkey). – International Journal of Science and Research (IJSR) 7(11): 1766-1772.
[10] Aslan, M., Türkmen, N. (2001): New floristic records for C7 grid square. – Herb Systematic Botanic Journal 8(2): 69-73.
[11] Aslan, M., Türkmen, N. (2003): New floristic records for squares C6 and C7 from Turkey. – Herb Systematic Botanic Journal 10(2): 163-168.
[12] Atamov, V., Cevheri, C., Parmaksız, A. (2004): Şanlıurfa Natural Rangeland Forage Bitkileri. – National Biology Congress XVII: 120, Adana, Turkey.
[13] Atamov, V., Yavuz, M., Cevheri, C., Parmaksız, A., Çen, O., Çetin, E. (2005): "Halophytes and Halophidıcation In Harran Plain (ŞANLIURFA)". – Biosalina Agriculture & High Salinity Tolerance, 9-14 January 2005, Muğla, Turkey.
[14] Atamov, V., Aslan, M., Cevheri, C., Cetin, E. (2007): Contribution to the flora of Fatik Mountain. – Asian J. Plant Sci. 6(1): 1-11.
[15] Ayalp, G. (2005): Flora and vegetation of Mezra Town. – Master Thesis, Harran University Institute of Science and Technology, Şanlıurfa.
[16] Aydın, N. (2003): Masted Hills flora. – Master Thesis. Harran University Institute of Science and Technology, Şanlıurfa.
[17] Aydoğdu, M., Akan, H. (2005): The flora of Kalecik Mountain, Şanlıurfa-Turkey. – Turk. J. Bot. 29: 155-174.
[18] Baytop, A. (2003): History of Botanical Studies in Turkey. – Çetin Printing, İstambul.
[19] Braun-Blanquet, J. (1964): Pflanzensoziologie. Dritte Aufl. – Springer Verlag, Wien.
[20] Çırpıcı, A. (1987): The studies on the flora and vegetation of Turkey. – Turk. J. Bot. 11(2): 217-232.
[21] Çullu, M., Almaca, A., Sahin, Y., Aydemir, S. (2002): Application of GIS monitoring soil salinization in The Harran Plain. – International Conference on Sustainable Land Use and Management, Şanlıurfa, Turkey, pp. 326-333.
[22] Davis, P. H. (ed). (1965-1985): Flora of Turkey and the East Aegean Islands. Vol. 1-9. – Edinburgh University Press, Edinburgh.
[23] Davis, P. H. (1988): Flora of Turkey and the East Aegean Islands. Vol. 10. – Edinburgh University Press, Edinburgh.
[24] Donner, J. (1990): Distribution Maps to P. H. Davis "Flora of Turkey, 1-10". – Linzer Biol. Beitr. 22(2): 381-515.
[25] Ertekin, S. (2002): Karacadağ Plant Diversity Book. – Sustainable Rural and Urban Development Association Publication, Diyarbakır.

http://www.aloki.hu ● ISSN 1589 1623 (Print) ● ISSN 1785 0037 (Online)
DOI: http://dx.doi.org/10.15666/aeer/1802_20252041

[26] Ertekin, S., Saya, Ö. (1997): New floristic records for the various grid squares from the Fabaceae. – Tr J of Botany 21: 187-189.
[27] Gençkan, M. (1983): Agriculture of Forage Crops. – Ege University Printing House, Bornova, Izmir.
[28] Güner, A., Özhatay, N., Ekim, T., Baser, K. H. C. (2000): Flora of Turkey and East Aegean Islands. Vol. 11. – Edinburgh University Press, Edinburgh.
[29] Kaya, F. Ö (2002): Flora of Tektek Mountains (Sanliurfa). – Master Thesis, Harran University Institute of Science and Technology, Sanliurfa.
[30] Kaynak, G. (1987): New record for some squares in flora of Turkey. – Nature TU Bot. Magazine 11(2): 118-123.
[31] Kaynak, G. (1989a): Contribution to the flora of Karacadağ (Urfa and Diyarbakır Provinces. – Nature TU Bot. Magazine 13(3): 376-397.
[32] Kaynak, G. (1989b): Ecological and chorological investigations on the ferns of Diyarbakir and surrounding provinces. – Nature TU Bot. Magazine 13(3): 437-451.
[33] Kaynak, G., Ketenoğlu, O. (1980): New fern specimens in South East Anatolian Region. – Ist Univ Science Faculty Mec Series B 45: 199-202.
[34] Malyer, H. (1981): A chorological study on the geophytes of the Iridaceae family of the Diyarbakır region. – Nature Science Journal Basic B 6: 17-20.
[35] Malyer, H. (1983): Chorological and ecological investigations on geophytes of Liliaceae and Iridaceae families in Karacadağ (between Diyarbakır and Urfa). – Nature Science Journal Basic, Series C 7(3): 279-288.
[36] Özhatay, N., Byfield, A., Atay, S. (2003): Turkey's Important Plant Alanları. – WWF-Turkey Natural Life Protection Foundation, Istanbul.
[37] Ture, C., Bocuk, H. (2007): An investigation on the diversity, distribution and conservation of Poaceae species growing naturally in Eskisehir province (Central Anatolia–Turkey). – Pak. J. Bot 39(4): 1055-1070.
[38] Türkmen, N., Aslan, M., Düzenli, A. (2002): New records for the various squares in the flora of Turkey. – Journal of Herb Systematic Botany 9(2): 63-68.
[39] Yıldırımlı, Ş. (1992): Distribution of new plant to Turkey from various squares. – Nature TU Bot Derg 16: 207-214.
[40] Yıldırımlı, Ş. (1994): From Turkey Brassicaceae (Cruciferae) were from New Floris squares for the various family Kayıtlar. – T J of Botany 18: 389-392.
[41] Yıldız, B., Aktoklu, E. (1996): New floristic records from C7 square (Malatya-Adıyaman). – Tr J of Botany 20: 207-211.
[42] Zohary, M. (1973): Geobotanical Foundations in the Middle East. Vol. 1-2. – Gustav Fischer Verlag, Stuttgart.

http://www.aloki.hu ● ISSN 1589 1623 (Print) ● ISSN 1785 0037 (Online)
DOI: http://dx.doi.org/10.15666/aeer/1802_20252041

ESTIMATION OF MORPHOLOGICAL AND MOLECULAR DIVERSITY OF SEVENTY-TWO ADVANCED PAKISTANI COTTON GENOTYPES USING SIMPLE SEQUENCE REPEATS

SHOUKAT, S.[1*] – ANWAR, M.[1*] – ALI, S.[1] – BEGUM, S.[1] – AQEEL, M.[1] – ZIA, M. A.[1] – SHAH, S. H.[2] – ALI, G. M.[1]

[1]*National Institute for Genomics and Advanced Biotechnology (NIGAB), National Agricultural Research Centre (NARC), Islamabad, Pakistan*

[2]*Department of Agricultural Sciences, Allama Iqbal Open University, Islamabad, Pakistan*

[*]*Corresponding authors*
e-mail: f_shehla@yahoo.com; muhammadanwar1964@gmail.com

(Received 25th Mar 2019; accepted 16th Jul 2019)

Abstract. Genetic diversity is the base of biological polymorphism and also the basic part of biological diversity. Significant role is played by genetic diversity and paternity of germplasm in cotton breeding. Genetic diversity in representative sets of advanced cotton genotypes was studied at molecular level employing polymorphic simple sequence repeats. Of seventy-two advanced cotton genotypes, thirty microsatellites primer pairs were studied, 29 showed to be polymorphic. DNA markers amplified fragments of 100 to 300 bp in size. The polymorphism information contents ranged between 0.76 and 0.99. Cluster analysis clearly grouped the 72 genotypes into seven groups A, B, C, D, E, F, G based on Nei's coefficient similarity matrix. Group B was found to be the most genetically distinct group when compared to other groups. However, group B had most of the candidates of under observed genotypes. This study exposed two major clusters of cotton cultivars and recognized the cotton genotypes which were genetically different. These results can be used as reference and baseline information to other researchers/breeders. The resolution to the genetic associations of these cotton accessions could be improved by increasing the number of more mapped markers.
Keywords: *cotton, genetic diversity, SSR markers, Pakistan, Gossypium, genome wide characterization*

Introduction

Man has been refining the domestication of crop plants by giving selection emphasis to the traits that suit to his agro-ecological and socioeconomic needs. Like many other crops, selection preference has been made for the improvement of the different traits in cotton. The process is being continued for centuries that has resulted in cultivars far different from the wild types in particular habitat and potential. During the last 30 years, Excessive breeding emphasis has led to some sort of genetic uniformity among the currently cultivated high yielding varieties and advanced lines (Van Becelaere et al., 2005). There is no precise knowledge of extent of exploitable variability beyond simple inherited traits during breeding of improved crop traits. Also it is not clear yet that what extent the different breeding strategies have been facilitating to broaden or narrow the genetic diversity in the breeding nurseries of cotton. Cotton belongs to Gossypieae tribe of the Malvaceae family. The main area for its cultivation is tropical as well as subtropical regions. Cotton genus Gossypium consists of almost 50 species that is contributing in making it the largest species in the Gossypieae tribe (Ashokkumar et al., 2011).

Cotton crop has great importance in agriculture, industry and trade in continents like Africa, Asia and South America. The cotton genus Gossypium has always been attracting the scientists' attention (Puspito et al., 2015). As far as the commercial

http://www.aloki.hu ● ISSN 1589 1623 (Print) ● ISSN1785 0037 (Online)
DOI: http://dx.doi.org/10.15666/aeer/1802_20432056

species of cotton are concerned, the *G. hirsutum* accounts for greater than 90% of world production, *G. barbadense* accounts for 3-4%, *G. arboreum* and *G. herbaceum* together accounts for 2%. By using selective breeding and hybridization of the above mentioned species many varieties of cotton have been developed. Humans use cotton as a source of natural fiber. However, cotton is also known as an oilseed crop and it is also the protein source for animals feed. Most of the cotton fiber is found in white color but it may also be found in brown, green and some mixing of these colors naturally (Chapagain et al., 2006). Above and beyond cotton fiber, edible oil is also extracted from cotton seeds. Cotton raw material is also used in poultry and livestock feed (Moiana et al., 2012). Cotton is being produced in many countries of the world, but China, US, India and Pakistan are producing two third of the global production (Ehsan et al., 2013).

In developed as well as developing countries, cotton is the cash crop (Puspito et al., 2015). The credit of being the oldest seed known so far goes to cotton seed. As far as Pakistan is concerned, the cotton is known as cash crop and its fiber is known as "White Gold" (Ahmad, 2018). The cropped area of cotton in Pakistan is about 2961 thousand hectares. In Pakistan, increase in cotton bales' production has been observed to the last years i.e. 14.98 million bales against 12.8 million bales (Economic Survey, 2014-15). In Indus Valley it has been cultivated since 3500 BC. In Balochistan it is cultivated near Bolan Pass (Li et al., 2008). Old-style variety identification technology using the old test and method involves rising plants to maturity and evaluating various phenotypic features which differentiate individual plants. It is difficult to collect morphological data because of environmental influence on morphological characters and also the time factor; other limitation includes explicit differentiation of genotypes (Rana et al., 2007).

Cultivated species of cotton are showing low level of genetic diversity as indicated by previous research. Due to lack of genetic diversity, cotton cultivars with stress resistance, improved yield and quality potential are in great danger (Li et al., 2008). It has been observed that genetic diversity is decreasing in breeding programs. This decrease in genetic diversity is leading to decline in yield improvement through crop breeding, since diversity is essential for selection (Rana et al., 2007). Orthodox breeding techniques are insufficient to explain the multifaceted traits. The choice of markers used for the estimation of diversity is of great alternative now a days as it gives alternatives to variety selection in the initial phase of breeding approach. The marker assisted selection is used to identify the superior parents in a cross. The advantage of this technique is to reduce the time and costs required for development of novel accessions (Bukhari, 2014). Genomics have come into being by doing advances in DNA marker technology. DNA repeats that comprise two to five nucleotide core units are known as simple sequence repeats (SSR) that are short and uncertain repetitive DNA sequences (Dongre et al, 2005). SSR markers have the advantage of being a PCR based marker, co-dominant, multi allelic, genetic marker system (Ullah et al., 2012). DNA markers (SSRs) have been used widely for the genetic diversity analysis as well as identification researches. Just because of high polymorphism rates, SSR markers are highly informative. This marker system is cheap to analyze when compared with other marker system. SSR regions are dispersed all over the genomes (Varshney et al., 2005). By using molecular markers, genetic diversity of cotton can excellently be estimated and this type of study offers beneficial information on the selection of parents in the expansion of cotton varieties and crossbreeds as well (Wu et al., 2006; Ullah et al., 2012). Fewer studies have been reported so far in Pakistani cotton germplasm. So this study was designed by keeping in view the importance of DNA markers to study

http://www.aloki.hu ● ISSN 1589 1623 (Print) ● ISSN1785 0037 (Online)
DOI: http://dx.doi.org/10.15666/aeer/1802_20432056

diversity among local cotton advanced lines, the genetic variability and estimation of relatedness and to illustrate genotypes with diverse fingerprints of selected advance cotton genotypes using SSR markers.

Materials and methods

The present research was conducted in National Institute for Genomics and Advanced Biotechnology (NIGAB), National Agricultural Research Center (NARC), Islamabad to estimate the genetic diversity among 72 Pakistani advanced cotton lines using thirty simple sequence repeats (SSR) markers. The seeds of 72 advanced cotton genotypes were acquired from National Coordinated Varietal Trial (NCVT), Pakistan Central Cotton Committee (PCCC) at NIGAB, NARC (*Table 1*). The 72 advanced cotton lines were categorized into two populations 1 and 2 based on unweighted pair group method with arithmetic mean (UPGMA). Thirty SSR primer pairs were selected for genotyping (*Table 2*). The Cotton Marker Database (CMD; http:// www.cottongen.org) was explored to select primers. All the markers were selected by reviewing the literature. Only those markers were selected which were polymorphic in others cotton genome.

Table 1. *List of National Coordinated Varietal Trial (NCVT) accessions*

S. No.	Genotypes	S. No.	Genotypes	S. No.	Genotypes	S. No	Genotypes
1	NCVT 1601 (Bahar-07)	19	NCVT 1619 (MNH-1016)	37	NCVT 1637 (GS-Ali-1)	55	NCVT 1655 (Weal-AG-Gold)
2	NCVT 1602 (Deebal)	20	NCVT 1620 (PB-896)	38	NCVT 1638 (GH-Hammad)	56	NCVT 1656 (Weal-AG-Shahkar)
3	NCVT 1603 (NIAB-878-B)	21	NCVT 1621 (NIAB-545)	39	NCVT 1639 (MNS-992)	57	NCVT 1657 (Weal-AG-1606)
4	NCVT 1604 (FH-152)	22	NCVT 1622 (BS-15)	40	NCVT 1640 (CIM-602 (S-1)	58	NCVT 1658 (Tahafuz-5)
5	NCVT 1605 (FH-142 (S-2)	23	NCVT 1623 (RH-668)	41	NCVT 1641 (QM-IUB-65)	59	NCVT 1659 (BH-201)
6	NCVT 1606 (Cyto-179)	24	NCVT 1624 (Eagle-2)	42	NCVT 1642 (NIA-86)	60	NCVT 1660 (Thakkar-808)
7	NCVT 1607 (Cyto-313)	25	NCVT 1625 (TH-20)	43	NCVT 1643 (RH-667)	61	NCVT 1661 (GS-Ali-5)
8	NCVT 1608 (CEMB-88*)	26	NCVT 1626 (IR-NIBGE_9)	44	NCVT 1644 (NS-181)	62	NCVT 1662 (Tarzan-5)
9	NCVT 1609 (FH-326)	27	NCVT 1627 (NIAB-1048)	45	NCVT 1645 (CIM-610)	63	NCVT 1663 (CIM-602 (S-1)
10	NCVT 1610 (CIM-632)	28	NCVT 1628 (Sahara-Buraq)	46	NCVT 1646 (FH-142 (S-2))	64	NCVT 1664 (Sitara-15)
11	NCVT 1611 (CRIS-543)	29	NCVT 1629 (RH-662)	47	NCVT 1647 (MPS-29)	65	NCVT 1665 (SAU-1)
12	NCVT 1612 (BPC-11)	30	NCVT 1630 (Bakhtawar-1)	48	NCVT 1648 (MPS-61)	66	NCVT 1666 (SLH-12)
13	NCVT 1613 (Crystal-12)	31	NCVT 1631 (Zakariya-1)	49	NCVT 1649 (CRIS-600)	67	NCVT 1667 (NIAB-Bt-2)
14	NCVT 1614 (BPC-10)	32	NCVT 1632 (CIM-573 (S)	50	NCVT 1650 (FH-Kehkashan)	68	NCVT 1668 (Shaheen-1)
15	NCVT 1615 (Thakkar-214)	33	NCVT 1633 (CEMB-55-S)	51	NCVT 1651 (VH-Gulzar)	69	NCVT 1669 (Tipu-1)
16	NCVT 1616 (IR_NIBGE-8)	34	NCVT 1634 (FH-142 (S-2)	52	NCVT 1652 (CIM-625)	70	NCVT 1670 (Sitara-14)
17	NCVT 1617 (CIM-602 (S-1)	35	NCVT 1635 (Saim-32)	53	NCVT 1653 (Tahafuz-7)	71	NCVT 1671 (VH-363)
18	NCVT 1618 (NIAB-444)	36	NCVT 1636 (Tipu-2)	54	NCVT 1654 (Suncrop-4)	72	NCVT 1672 (GH-Mubarak)

http://www.aloki.hu ● ISSN 1589 1623 (Print) ● ISSN1785 0037 (Online)
DOI: http://dx.doi.org/10.15666/aeer/1802_20432056

Table 2. *List of markers with anealing temperature, band size, number of allele per locus and expected/ observed heterozygosity*

	Marker List	Sequence 5'….3'	Annealing temp. C^{o}	Band size (bp)	Repeat motif	Expected heterozygosity	Observed heterozygosity	No. of alleles	PIC value
1	BNL 1551	F: CGCAAGCCACCTGTAAAAC R: TCGAATTTTCTCTCTCTCTCTCTCT	62	195	(AG)22	0.28	0	2	0.99
2	BNL 1053	F: AGGGTCTGTCATGGTTGGAG R: CATGCATGCGTACGTGTGTA	60	190	(AC)16	0.48	0	2	0.97
3	BNL1414	F: AAAAACCCCTTTCCATCCAT R: GGGTGTCCTTCCCAAAAATT	62	180	(AG)16	0.46	0	2	0.98
4	BNL 1672	F: TGGATTTGTCCCTCTGTGTG R: AACCAACTTTTCCAACACCG	62	200	(AG)14	0.49	0	2	0.97
5	BNL 2634	F: AACAACATTGAAAGTCGGGG R: CCCAGCTGCTTATTGGTTTC	62	200	(AG)11	0.43	0	2	0.97
6	BNL 3031	F: AGGCTGACCCTTTAAGGAGC R: AACCAACTTTTCCAACACCG	61	160	(AG)27	0.61	0	3	0.98
7	BNL 3089	F: TCGAACTTAACAAAAGAGAGAGAGA R: AAATCCGGATTCAGCAATACTT	62	150	(AG)10	0.62	0	3	0.97
8	BNL 3255	F: GACAGTCAAACAGAACAGATATGC R: TTACACGACTTGTTCCCACG	62	215	(GC)6AT(AC)14	0.6	0	4	0.99
9	BNL 3649	F: GCAAAAACGAGTTGACCCAT R: CCTGGTTTTCAAGCCTGTTC	55	200	(TC)20	0.59	0	3	0.99
10	BNL 4108	F: TCCACCATTCCCGTAAATGT R: TGGCCAAGTCATTAGGCTTT	55	150	(GA)31	0.61	0	3	0.99
11	CIR 122	F: AATGTGGGCTGATACG R: CAGACACAATCCACAAAG	43	-	(TG)16	0.59	0	1	1
12	CIR 133	F: TAGCCATTCTCACCCA R: AGGCAGTCAGAGTCAAAG	55	112	(TG)11	0.58	0	3	0.99
13	CIR 148	F: CTAATCTTTGGATTCTACCC R: TCCAAGCCCAGATAAGT	55	190	(TG)8	0.6	0	3	0.99
14	CIR 203	F: AGTTCAAGGGCACAAA R: ATCTCCAAGTCCCACC	41	200	(TG)11(N)1(TG)5	0.6	0	3	0.99
15	CIR 246	F: TTAGGGTTTAGTTGAATGG R: ATGAACACACGCACG	55	200	(TG)6	0.62	0	3	0.93
16	CIR 253	F: CCAACCAAGAAACCAG R: GTAAGCATGGGCATTT	43	205	(TC)15(N)8(AC)5(N)7(CA)8	0.48	0	2	0.99

http://www.aloki.hu ● ISSN 1589 1623 (Print) ● ISSN1785 0037 (Online)
DOI: http://dx.doi.org/10.15666/aeer/1802_20432056

	Marker List	Sequence 5'….3'	Annealing temp. C^o	Band size (bp)	Repeat motif	Expected heterozygosity	Observed heterozygosity	No. of alleles	PIC value
17	CIR 320	F: CCTCCATAAACCCTCTT R: TCACATACGAAGACAACC	45	200	(T)9(N)2(TG)8	0.56	0	3	0.99
18	CIR 364	F: ACTTTCATTTCGTGTGGT R: TGTTCATGCTTGTATCGT	45	100	(AC)10	0.59	0	3	0.70
19	CIR 376	F: ATACACAAGTCATTCACACA R: TGACTATGACACGAGTGG	49	200	(CA)15	0.62	0	3	0.97
20	CIR 393	F: GACCACACAGACAGACAA R: TCCACAACCAAACTAACA	58	200	(TG)7(T)9	0.62	0	3	0.84
21	JESPER 0065	F: CCACCCAATTTAAGAAGAAATTG R: GGTTAGTTGTATTAGGGTCGTTG	58	190	(GAA)25	0.62	0	3	0.92
22	JESPER 0092	F: GGGACCTCTATTGAATAGCTGGAG R: CTCTTGGCATCATTAGTTCCTGG	67	300	(GAA)23	0.1	0	2	0.99
23	JESPER 0101	F: CCAAGTCAAGGTGAGTTATATG R: GCTCTTTGTTACTGAAATGGG	57	190	(TA)3(GT)15	0.57	0	3	0.99
24	JESPER 0114	F: GATTTAAGGTCTTTGATCCG R: CAAGGGTTAGTAGGTGTGTATAC	51	105	(GT)12	0.62	0	3	0.98
25	JESPER -0135	F: CAAAACCATCATCACTCTCAAG R: CGAGAGCCCACTAACAGAAAAG	57	100	(CT)11	0.52	0	3	0.99
	JESPER 0152	F: GATGCACCAGATCCTTTTATTAG R: GGTACATCGGAATCACAGTG	59	250	(GAA)50	0.53	0	3	0.99
27	JESPER 0153	F: GATTACCTTCATAGGCCACTG R: GAAAACATGAGCATCCTGTG	57	150	(CTA)18	0.22	0	2	0.76
28	JESPER 0220	F: CGAGGAAGAAATGAGGTTGG R: CTAAGAACCAACATGTGAGACC	55	160	(GA)20	0.61	0	3	0.99
29	JESPER 0251	F: CAACTAGAATGATAAGACAC R: CTTTAAGTACGTATGCATC	49	100	(CA)15	0.61	0	3	0.80
30	JESPER 0300	F: CGCATCACAAACCAAACAC R: CGGAAAATGATGATGATGAAGAAG	51	210	(CTT)5(CAT)6	0.62	0	3	0.96

PIC denotes polymorphism information content

http://www.aloki.hu ● ISSN 1589 1623 (Print) ● ISSN1785 0037 (Online)
DOI: http://dx.doi.org/10.15666/aeer/1802_20432056

Experiment 1: Morphological characterization of cotton

Cotton seeds of each genotype were sown in the field using Randomized Complete Block Design (RCBD) with four replications under natural environmental conditions. Recommended cultural practices were adopted to grow the crop. Experimental layout was designed in four replications i.e. four rows for each line and in each row 20 plants were maintained. Plant to plant and row to row distances were maintained as 30 cm and 75 cm, respectively. Following traits were evaluated on 180 days after sowing. The data on plant height were recorded on five randomly selected plants using meter rod. Each plant was measured from soil to top of the main stem at crop maturity. Internodal distance was measured from one node to the other node on the same stem. Data on number of bolls per plant were recorded on five randomly selected plants by counting the number of bolls on each selected plant. Data on number of branches per plant were collected on five randomly selected plants by counting the number of branches of each selected plant. Data on boll weight were recorded on five randomly selected plants using weighing balance. Data on plant type were recorded whether they were conical or bushy type. Data on yield per plant were also recorded. The data recorded on each trait were subjected to analysis of variance (ANOVA) by using Minitab 16 software. Tukey's Test was applied to access the significance among the mean differences.

Experiment 2: Molecular characterization of cotton on the basis of SSR markers

Cotton seeds of each genotype were sown in the field of NIGAB at NARC, Islamabad using RCBD with three replications under natural environmental conditions. Recommended cultural practices were adopted to grow the crop. Young leaf tissue was collected from all the genotypes for DNA extraction. DNA extraction was carried out as per the procedure described by (Doyle et al., 1987). DNA was checked by measuring absorbance on nano-spectrophotometer. Purity was investigated by the absorbance ratios; 230/260 while concentration at 1 optical density. Polymerase chain reaction (PCR) amplification was performed in an automatic Applied Bio Systems Thermal Cycler (Veriti 96 well) at 94ºC for 5 min, afterward 35 cycles each containing of three phases: one phase of denaturation at 94ºC for 40 sec, one phase of annealing at specified temperature for each primer pair (*Table 2*) for 40 sec and an extension phase for 1 min at 72ºC followed by final extension of 10 min at 72ºC. On 1.5% agarose gel stained with ethidium bromide, amplified products was electrophoresed at 80 V for 45 min and then visualized by means of gel documentation system (Alpha Innotech).

DNA amplifications with each SSR primer were repeated three times to guarantee reproducibility. In three separate amplifications for each primer, bands were considered reproducible and scorable only after careful observation and comparison. Scoring was made on visualizing the bands. Each DNA fragment was transformed into binary character matrices i.e. 1 for presence, 0 for absence. The band size was determined using the software available with gel documentation system. The Minitab 16 was used to build dendrogram for cluster analysis. Sub population statistics, AMOVA, number of allele per locus and expected/observed heterozygosity was calculated using R language citation (locus_table, mlg, nei.dist and plot_poppr_msn) via poppr-package.

http://www.aloki.hu ● ISSN 1589 1623 (Print) ● ISSN1785 0037 (Online)
DOI: http://dx.doi.org/10.15666/aeer/1802_20432056

Results

Experiment 1: Morphological characterization of cotton

Grand mean of each trait have been shown in *Table 3*. Highly significant results were observed at P<0.05 among 72 NCVT lines of cotton germplasm for five traits i.e. plant height (cm), internodal distance (cm), number of bolls, total number of branches and boll weight (*Table 4*). The NCVT 1624 was the tallest (138.43 cm), while genotype NCVT 1668 produced the shortest (44.09 cm) plants. Highly significant differences were also observed within 72 NCVT lines of cotton germplasm. The NCVT 1630 showed minimum internodal distance (1.4 cm), while genotype NCVT 1624 produced the maximum internodal distance (4.76 cm). Highly significant differences were also observed within 72 NCVT lines of cotton germplasm for this trait as depicted in *Table 4*. The NCVT 1624 showed maximum number of bolls (59) per plant, while genotype NCVT 1651 produced the minimum (2) number of bolls per plant. Non-significant differences were observed among seventy-two NCVT lines of cotton germplasm regarding their number of branches per plant (*Table 4*). However, NVCT 1634 showed maximum number of branches per plant (26), while genotype NCVT 1609 produced the minimum (4) number of branches per plant.

Table 3. *Grand means of six traits in 72 cotton varieties with standard error at 0.05 confidence level*

	Plant height (cm)	Internodal distance (cm)	No. of bolls per plant	Total no. of branches	Boll weight/5	Yield per plant (g)
Grand total of mean of all varieties	76.61^{a}	2.88^{d}	18.08^{c}	13.62^{c}	3.67^{d}	64.95^{b}
Alpha	0.05	0.05	0.05	0/05	0.05	0.05
SE	7.69	0.30	4.85	4.86	0.06	4.49

SE: Standard error; a, b, c and d: Grouping by lettering to each accession according to Tukey's test of significance

Table 4. *ANOVA for five trait of Pakistani cotton germplasm at p = 0.05*

Source of variance	Degree of freedom	Plant height (cm)	Internodal distance	Number of branches per plant	No of boll per plant	Boll weight (g)
Replication	3	535.7	0.07	97.89	109.36	0.021
Genotypes	71**	1432.6**	1.68**	$130.3^{n.s}$	286.9**	1.82**
Error	141	177.6	0.28	71.10	70.85	0.01

**= highly significant; $^{n.s}$ = non-significant

Experiment 2: Molecular characterization of cotton

A total of 30 primers consisting of di, tri, tetra and penta nucleotide repeat motifs were used for initial screening with 6 genotypes, namely NCVT 1601, NCVT 1602, NCVT 1603, NCVT 1604, NCVT 1605 and NCVT 1606 were used for PCR amplification using all the 30 primers. Out of these, one primer gave no amplification, while rest of twenty-nine primers gave clear band patterns, and subsequently used to analyze the entire set of 72 genotypes. Thirty simple sequence repeats (SSRs) belonging to BNL, CIR and JESPER series were used to analyze genetic diversity among 72 cotton varieties. Out of these, six markers i.e. BNL 1551, BNL 3089, BNL 1672, BNL

http://www.aloki.hu ● ISSN 1589 1623 (Print) ● ISSN1785 0037 (Online)
DOI: http://dx.doi.org/10.15666/aeer/1802_20432056

2634, BNL 3031 and BNL1414 contained (AG)n repeat motif, CIR 246, CIR 133, CIR 148 and CIR 122 primer contained (TG)n repeat motif, JESPER 0065, JESPER 0152 and JESPER 0092 primers contained (GAA)n repeat motif, CIR 376 and JESPER 0251 primer contained (CA)n repeat motif, BNL 1053 and CIR 364 primers contained (AC)n motif, BNL 4108 and JESPER 0220 primers contained (GA)n repeat motif and BNL 3649 primer contained (TC)n repeat motif,. Apart from these, JESPER 0153 primer contained (CTA)18, JESPER 0135 primer contained (CT)11, JESPER 0114 primer contained (GT)12, JESPER 0101 primer contained (TA)3(GT)15, CIR 393 primer contained (TG)7(T)9, CIR 320 primer contained (T)9(N)2(TG)8, CIR 253 primer contained (TC)15(N)8(AC)5(N) 7(CA)8, CIR 203 primer contained (TG)11(N)1(TG)5, BNL 3255 primer contained (GC)6AT(AC)14 repeat motifs (*Table 2*).

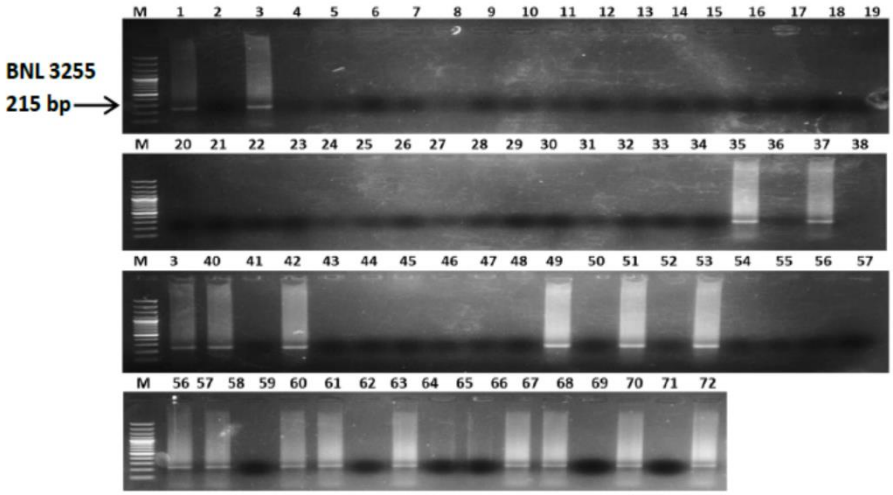

Figure 1. *BNL 3255 representative gel picture, 1-72 genotypes, 100bp ladder DNA, band size of 215 bp*

Out of thirty markers, twenty-nine markers were reproducible. These twenty-nine DNA markers amplified fragments of 100 to 300 bp in size through SSR profiling. On the basis of amplification percentage, markers were categorized into three groups. Sixteen markers i.e. BNL 1551, BNL 1414, BNL 3031, BNL 3255 (*Figure 1*), BNL 3649, BNL 4108, CIR 133, CIR 148, CIR 203, CIR 253, CIR320, JESPER 0092, JESPER 0101, JESPER 0135, JESPER 0152, JESPER 0220 gave low amplification (0-35%). Nine markers that are BNL 1053, BNL 1672, BNL 2634, BNL3089, CIR 246, CIR276, JESPER 0065, JESPER 0114, JESPER 0300 gave average amplification (36-60%). Four markers i.e. CIR 393, JESPER 0251, JESPER 0153, CIR 364 gave high amplification rate that was above 60% while one marker CIR 122 gave no result in any of the accession. The 72 advanced cotton lines were categorized into two populations 1 and 2 based on UPGMA. The population 1 contains 30 genotypes and population 2 was comprised of 42 genotypes.

The Nei's coefficient of similarity was used to construct the cluster diagram (*Figure 2*). All the genotypes were categorized into seven groups A, B, C, D, E, F, G based on Nei's coefficient. Group B was found to be the most genetically distinct/ dissimilar group when compared to other groups. However, group B have most of the candidates of under observed genotypes. Conversely group D, E and F, G have

http://www.aloki.hu ● ISSN 1589 1623 (Print) ● ISSN1785 0037 (Online)
DOI: http://dx.doi.org/10.15666/aeer/1802_20432056

similarity index of 1.3. The *Figure 3* shows significant population differentiation at all levels given that the observed data does not fall within the distribution expected from the permutation. The expected and observed heterozygosity is listed in *Table 2* along with the number of alleles per locus for each primer along with their polymorphism information content. The greatest number of allele observed was 4 and minimum number of allele per locus is 1 as depicted by population genetics. *Table 5* shows the variation within samples, between samples and population. Here, F value is -35.49, and p-value is very high in case of variation within samples. In other words, the variation within samples means and among different groups variation is much larger than the variation of allele presence within each group, at p-value is less than 0.01.

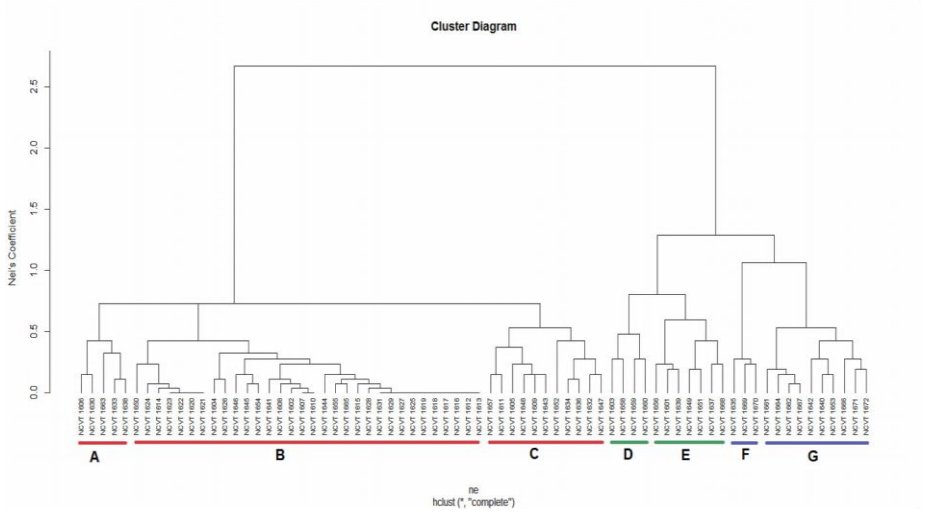

Figure 2. *Cluster dendrogram based on Nei's coefficient for two populations (Pop 1 indicates population 1 and Pop 2 indicates population 2)*

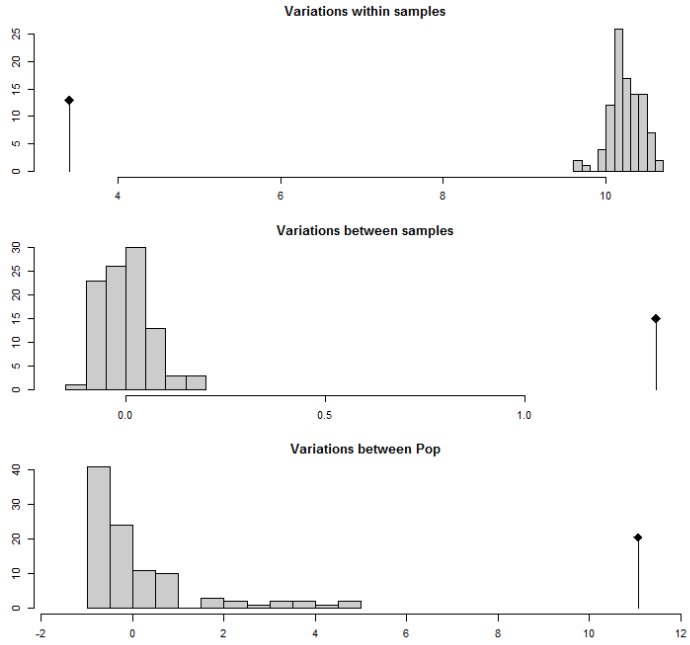

Figure 3. *AMOVA to check variations within samples, between samples and population*

http://www.aloki.hu ● ISSN 1589 1623 (Print) ● ISSN1785 0037 (Online)
DOI: http://dx.doi.org/10.15666/aeer/1802_20432056

Table 5. *AMOVA test to check variation within samples, between samples and population*

	Test	Obs	Std. Obs	Alter	P-value
1	Variations within samples	3.411277	-35.494080	Less	0.01
2	Variations between samples	1.328667	21.379898	Greater	0.01
3	Variations between Pop	11.063446	8.363728	Greater	0.01

Population Genetics parameters i.e. MLG multilocus genotypes showed that the genotypic richness is indeed higher in population 2 than that of population 1 when considering equal sample sizes with the standard error of 1.76 in both poulation. Diversity measures incorporate both genotypic richness and abundance. There are three measures of genotypic diversity employed by poppr used for statistical analysis, the Shannon-Wiener index (H), Stoddart and Taylor's index (G), and Simpson's index (lambda). Graphical representation of two population with respect to H, G, Lambda and E.5 constants are depicted in *Figure 4*. In our study, comparing the diversity of pop1 to pop 2 shows that H is greater for pop 1 (3.40 vs. 2.80), but G is also greater (30.0 vs. 9.0). Thus, our expectation that diversity is lower for population 1 than that of population 2 is accepted in the case of H, which is likely due to the sensitivity of the Shannon-Wiener index to genotypic richness in the even sample sizes, and rejected in the case of G *Figure 4*.

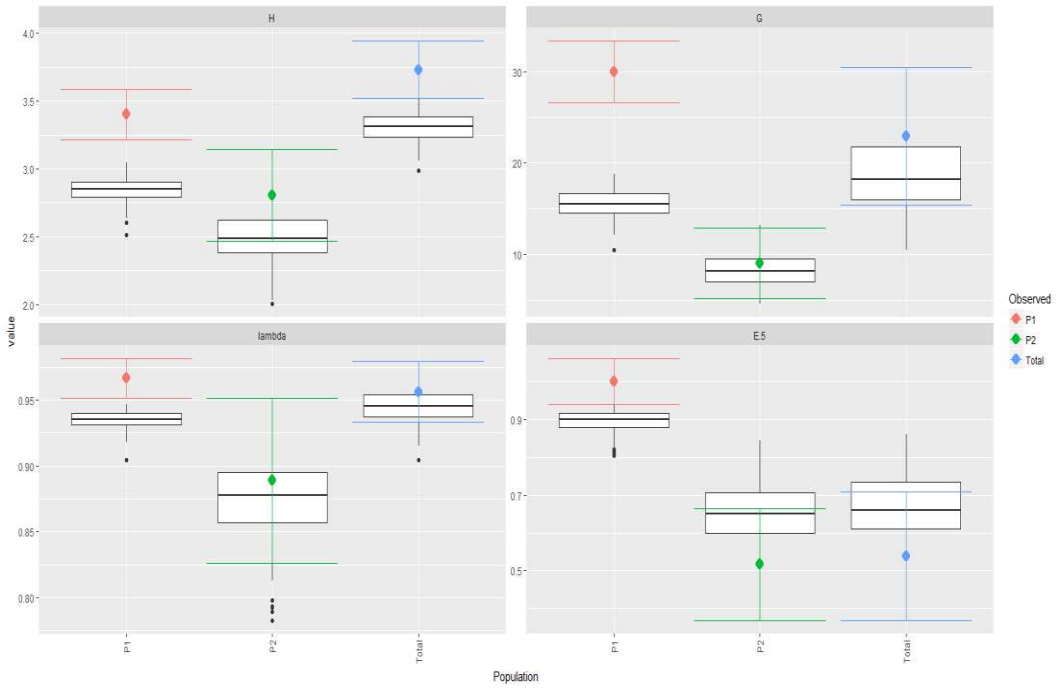

Figure 4. *Graphical representation of two populations with respect to H, G, Lambda and E.5 constants*

Evenness is a measure of the distribution of genotype abundances, wherein a population with equally abundant genotypes yields a value equal to 1 and a population dominated by a single genotype is closer to zero. In our study, the pop 1 has E.5 = 1.00 and the population 2 has E.5 = 0.516 (*Figure 4*). This indicates that the MLGs observed

http://www.aloki.hu ● ISSN 1589 1623 (Print) ● ISSN1785 0037 (Online)
DOI: http://dx.doi.org/10.15666/aeer/1802_20432056

in the population 1 are closer to equal abundance than those of population 2 (*Figure 4*). Indeed, when we look at a distribution of the MLGs for each population type it shows there are many more unique locus in population 1 as compared to the population 2 *Figure 5*.

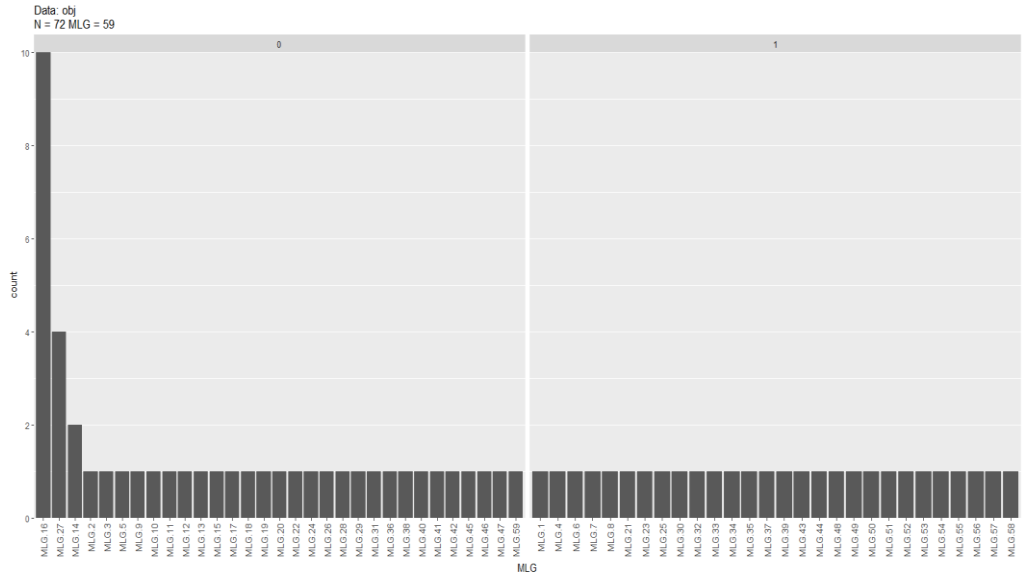

Figure 5. *Bootstrap analysis for MLG calculation against two populations*

Discussion

For characterization of any germplasm first step is to examine the material morphologically (Bidinger et al., 2009; Shen et al., 2017). All plant breeders still understand the value of enhancing plant genetic level by breeding available genetic variability. The results from different crops suggested that genetic diversity is very significant in breeding (Smartt, 1990; Reddy et al., 2005; Rasul et al., 2007). In this research the dendrogram clearly indicates two main clusters. The two groups A and B with the least value of 0% similarity were observed. The band sizes that obtained through SSR primer pairs were matched with the sizes of bands described in literature (Nguyen et al., 2004; Han et al., 2006). The scoring was based on bivariate as 1 is for presence and 0 is for absence. With respect to primer, the frequencies of scored bands or alleles were calculated (Upadhyaya et al., 2001).

Similar loci identified for every marker were assessed by scoring pattern. Twenty-nine (96.6%) out of the 30 SSR markers were evaluated and the results showed monomorphic fragments through the 72 varieties. Thus, the results are representing homogeneity of the cotton genome (Lacape et al., 2006). In sampled genome, SSR markers exhibited significant amount of variation on the basis of monomorphic bands as one genotype is giving the band, while the same band is absent in the other genotype (Fu, 2006). As far as polymorphism is concerned, no polymorphism was noticed among the experimental genotypes. This was expected from previous diversity analyses (Iqbal et al., 1997; Lacape et al., 2006). Irregularities among cultivar clustering on the basis of morphological and marker based dendrogram is just because of the markers that were not trait specific used for this study (Zhang et al., 2005). However, the SSR markers are depicting the genetic diversity to great extent. Inconsistencies between genotypes

http://www.aloki.hu ● ISSN 1589 1623 (Print) ● ISSN1785 0037 (Online)
DOI: http://dx.doi.org/10.15666/aeer/1802_20432056

clustering and known parentage should not be surprising for these cotton genotypes with such a narrow genetic base (Iqbal et al., 1997; Zhang et al., 2005).

The limited sample size of the genome of cotton exposed by only 29 SSR markers may subsidize to this type of variations (Fu, 2006). There is still need of using more mapped markers across the experimental genotypes that will progress the resolution to the genetic associations of these cotton varieties. On the other hand, the genetic relatedness estimated by this study still exhibit a beneficial direction for cotton breeding. This data is more helpful than that of other techniques used for parental selection and old-style pedigree analysis (Bowman et al., 1996). The values of similarity among cotton germplasm can change if more cotton varieties along with the experimental genotypes or varieties are evaluated or more markers applied. Also, the findings specify the distinctiveness, but not necessarily the relatedness of varieties (Fu, 2006). Regardless of some restrictions, the relative measure of genetic distinctiveness stated here offers useful information for selecting specific germplasm with diverse genetic background for a cotton-breeding program (Fu et al., 2007).

It has been observed that the current study is applicable in many ways. Like, considering polymorphism, the diversity among these cotton cultivars was less suggesting that the range of diversity for preservation of germplasm and breeding in future should be broadened. For selecting diverse plants for cotton breeding, the findings on genetic distinctiveness are beneficial. As this study exposed two major clusters of cotton cultivars and recognized the cotton cultivars which were genetically different. The classification of cotton varieties by the use of SSR primer pairs provides significant information to considerate the genetic diversity of top Pakistani cotton germplasm and to expand the cotton breeding program. It also gives a useful guide for selecting particular germplasm with diverse genetic background.

Conclusion

Relatively low genetic diversity has been revealed by this SSR analysis among experimental Pakistani cotton cultivars. Unique cotton cultivar was identified using the morphological analysis eagle 2 i.e. NCVT 1624. Molecular characterization depicted the homogeneity of the under study cotton genome as monomorphic bands were observed, while polymorphism was detected across the experimental genome via 29 markers. To conserve the elite cotton germplasm and developing future cotton breeding programs in Pakistan, these findings are useful. On the other hand, the genetic associations that have been estimated exhibit a beneficial direction for cotton breeding. It is recommended that more mapped markers across the genome should be used in future research that would improve the resolution to the genetic relationships as well as associations of the experimental cotton accessions. Regular assessment of National Cotton Varietal Trial should be carried out in order to update the diversity level of national cotton germplasm for cotton breeders.

REFERENCES

[1] Ahmad, I. (2018): Future of Bt cotton in Asia. – Pakissan.com. [cited 17 April 2018]. Retrieved from http://pakissan.com/english/ advisory/biotechnology/ future.of.bt.cotton.in.asia.shtml.

[2] Ashokkumar, K., Ravikesavan, R. (2011): Morphological diversity and per se

http://www.aloki.hu ● ISSN 1589 1623 (Print) ● ISSN1785 0037 (Online)
DOI: http://dx.doi.org/10.15666/aeer/1802_20432056

performance in upland cotton (*Gossypium hirsutum* L.). – Journal of Agricultural Science 3(2): 107-113.

[3] Bidinger, F. R., Yadav, O. P. (2009): Biomass heterosis as the basis for grain and stover yield heterosis in arid zone pearl millet (*Pennisetum glaucum* (L.) R. Br.) hybrids. – Crop Science 49(1): 107-112.

[4] Bowman, D., May, O., Calhoun, D. (1996): Genetic base of upland cotton cultivars released between 1970 and 1990. – Crop Science 36(3): 577-581.

[5] Bukhari, S. (2014): Studies on genetic diversity of cotton using RAPD markers. – Pure and Applied Biology 3(3): 95-100.

[6] Chapagain, A., Hoekstra, A., Savenije, H., Gautam, R. (2006): The water footprint of cotton consumption: An assessment of the impact of worldwide consumption of cotton products on the water resources in the cotton producing countries. – Ecological Economics 60(1): 186-203.

[7] Dongre, A., Parkhi, V. (2005): Identification of cotton hybrid through the combination of PCR based RAPD, ISSR and microsatellite markers. – Journal of Plant Biochemistry and Biotechnology 14(1): 53-55.

[8] Doyle, J., Doyle, L. (1987): Isolation of plant DNA from fresh tissue. – Focus 12(1): 13-15.

[9] Economic Survey (2014-15): Retrieved from http://finance.gov.pk/ survey/chapters_15/Highlights.pdf [Accessed 12 Jun. 2019].

[10] Ehsan, B., Haque, M., Younas, T., Shaheen, T., Huma, S., Sattar, S., Idrees, S., Iqbal, Z. (2013): Assessment of genomic diversity of cotton (*Gossypium hirsutum*) genotypes using simple sequence repeats markers through genetic analysis software. – International Journal of Agriculture & Biology 15(2): 968-972.

[11] Fu, Y. (2006): Redundancy and distinctness in flax germplasm as revealed by RAPD dissimilarity. – Plant Genetic Resources 4(2): 117-124.

[12] Fu, Y., Peterson, G., Morrison, M. (2007): Genetic diversity of Canadian soybean cultivars and exotic germplasm revealed by simple sequence repeat markers. – Crop Science 47(5): 1947-1954.

[13] Han, Z., Wang, C., Song, X., Guo, W., Gou, J., Li, C., Chen, X., Zhang, T. (2006): Characteristics, development and mapping of *Gossypium hirsutum* derived EST-SSRs in allotetraploid cotton. – Theoretical and Applied Genetics 112(3): 430-439.

[14] Iqbal, M., Aziz, N., Saeed, N., Zafar, Y., Malik, K. (1997): Genetic diversity evaluation of some elite cotton varieties by RAPD analysis. – Theoretical and Applied Genetics 94(1): 139-144.

[15] Lacape, J., Dessauw, D., Rajab, M., Noyer, J., Hau, B. (2006): Microsatellite diversity in tetraploid Gossypium germplasm: Assembling a highly informative genotyping set of cotton SSRs. – Molecular Breeding 19(1): 45-58.

[16] Li, Z., Wang, X., Zhang, Y., Zhang, G., Wu, L., Chi, J., Ma, Z. (2008): Assessment of genetic diversity in glandless cotton germplasm resources by using agronomic traits and molecular markers. – Frontiers of Agriculture in China 2(3): 245-252.

[17] Moiana, L. D., Vidigal Filho, P. S., Gonçalves-Vidigal, M. C., Lacanallo, G. F., Galvan, M. Z., de Carvalho, L. P., Maleia, M. P., Pacheco, C. M., Ribeiro, T., Neto, H. Z., Coimbra, G. K. (2012): Genetic diversity and population structure of cotton (*Gossypium hirsutum* L. race latifolium H.) using microsatellite markers. – African Journal of Biotechnology 11(54): 11640-11647.

[18] Nguyen, T., Giband, M., Brottier, P., Risterucci, A., Lacape, J. (2004): Wide coverage of the tetraploid cotton genome using newly developed microsatellite markers. – Theoretical and Applied Genetics 109(1): 167-175.

[19] Puspito, A., Rao, A., Hafeez, M., Iqbal, M., Bajwa, K., Ali, Q., Rashid, B., Abbas, M., Latif, A., Shahid, A., Nasir, I., Husnain, T. (2015): Transformation and evaluation of *Cry1Ac+Cry2A* and *GT*gene in *Gossypium hirsutum* L. – Frontiers in Plant Science, doi: 10.3389/fpls.2015.00943.

http://www.aloki.hu ● ISSN 1589 1623 (Print) ● ISSN1785 0037 (Online)
DOI: http://dx.doi.org/10.15666/aeer/1802_20432056

[20] Rana, M., Singh, S., Bhat, K. (2007): RAPD, STMS and ISSR markers for genetic diversity and hybrid seed purity testing in cotton. – Seed Science and Technology 35(3): 709-721
[21] Rasul, M., Hiramatsu, M., Okubo, H. (2007): Genetic relatedness (diversity) and cultivar identification by randomly amplified polymorphic DNA (RAPD) markers in teasle gourd (*Momordica dioica* Roxb.). – Scientia Horticulturae 111(3): 271-279.
[22] Reddy, L., Upadhyaya, H., Gowda, C., Singh, S. (2005): Development of core collection in pigeon pea [*Cajanus cajan* (L.) Millspaugh] using geographic and qualitative morphological descriptors. – Genetic Resources and Crop Evolution 52(8): 1049-1056.
[23] Shen, Z., Duan, J., Ma, L. (2017): Genetic diversity of *Xanthoceras sorbifolium* bunge germplasm using morphological traits and microsatellite molecular markers. – PLOS ONE 12(6): e0177577. https://doi.org/10.1371/journal. pone.0177577.
[24] Smartt, J. (1990): Grain legumes: evolution and genetic resources. – Cambridge University Press, p. 333.
[25] Ullah, I., Iram, A., Iqbal, M., Nawaz, M., Hasni, S., Jamil, S. (2012): Genetic diversity analysis of Bt cotton genotypes in Pakistan using simple sequence repeat markers. – Genetics and Molecular Research 11(1): 597-605.
[26] Upadhyaya, H., Ortiz, R. (2001): A mini core subset for capturing diversity and promoting utilization of chickpea genetic resources in crop improvement. – Theoretical and Applied Genetics 102(8): 1292-1298.
[27] Van Becelaere, G., Lubbers, E., Paterson, A., Chee, P. (2005): Pedigree- vs. DNA marker-based genetic similarity estimates in cotton. – Crop Science 45(6): 2281-2287.
[28] Varshney, R., Graner, A., Sorrells, M. (2005): Genic microsatellite markers in plants: features and applications. – Trends in Biotechnology 23(1): 48-55.
[29] Wu, Y., Machado, A., White, R., Llewellyn, D., Dennis, E. (2006): Expression profiling identifies genes expressed early during lint fiber initiation in cotton. – Plant and Cell Physiology 47(1): 107-127.
[30] Zhang, J., Lu, Y., Cantrell, R., Hughs, E. (2005): Molecular marker diversity and field performance in commercial cotton cultivars evaluated in the Southwestern USA. – Crop Science 45(4): 1483-1490.

http://www.aloki.hu ● ISSN 1589 1623 (Print) ● ISSN1785 0037 (Online)
DOI: http://dx.doi.org/10.15666/aeer/1802_20432056

GROWTH AND SURVIVAL OF MULTIPURPOSE SPECIES; ASSESSING BILLION TREE AFFORESTATION PROJECT (BTAP), THE BONN CHALLENGE INITIATIVE

ULLAH, I.[1*] – SALEEM, A.[1] – ANSARI, L.[1] – ALI, N.[2] – AHMAD, N.[1] – DAR, N. M.[3] – DIN, N. U.[3]

[1]Department of Forestry and Range Management, University of Arid Agriculture, Rawalpindi, Pakistan
(e-mail/phone: naveedahmad795@gmail.com/+92-332-903-3553 – N. Ahmad; +92-333-582-2202 – A. Saleem, +92-332-549-8460 – L. Ansari)

[2]Forest Education Division, Pakistan Forest Institute, Peshawar, Pakistan
(e-mail/phone: foresternizar@gmail.com/+92-334-969-6981 – A. Nizar)

[3]Institute of Geo-information and Earth Observation, University of Arid Agriculture, Rawalpindi, Pakistan
(e-mail: mnadeemdar2454@gmail.com – M. N. Dar; noorsmk321@gmail.com – N. U. Din)

**Corresponding author*
e-mail: irfanwazir577@gmail.com; phone: +92-335-928-0782

(Received 11th Nov 2018; accepted 8th Mar 2019)

Abstract. In context of Bonn Challenge commitment, Pakistan has implemented Billion Tree Afforestation Project (BTAP), the initiative of forest restoration and afforestation. The current research was a pilot one which evaluated the success of plantation and assessed growth performance and survival rate. A total of 115 sample plots (0.07 ha size) were laid out in 17 randomly selected sites extended over 1982 ha. Further, Sentinel-2 images were used to derive vegetation indices and regressed indices values with volume and survival percentage. Results showed that all plantation sites showed good performance in terms of survival rate (above 80%). Highest growth performance was exhibited by *Eucalyptus camaldulensis* which mean height was1.297 (m) and the lowest was of Deodar 0.35 (m). Among Sentinel-2 indices, Transformed Normalized Vegetation Index (TNDVI) has the highest value of R^2 of 0.425 whereas in case of survival percentage, Normalized Difference Vegetation Index (NDVI) has the highest value of R^2 of 0.859. Stepwise regression model showed that relationship between NDVI and volume was strongly significant compared to other indices. NDVI differencing of Landsat-8 2013 image and Sentinel-2 2018 image showed that in NDVI range were increased from 0.68 to 0.85, thus showed mosaic restoration and afforestation activities of BTAP.
Keywords: *Sentinel-2, vegetation indices, forest restoration, Landsat-8, Eucalyptus camaldulensis*

Introduction

Forests are among those ecosystems on earth that not only provide services to mankind but its biological, ecological and environmental services are manifold (Trumbore et al., 2015; Mori, 2017). Forests are of immense socioeconomic importance as a source of timber, pulpwood for paper making, fuel, and many non-wood products. Globally, forested region has been diminished for last 25 years from almost 31.6 to 30.6% from 1990 to 2015 respectively (FAO, 2015). Globally, about one to two billion hectares land degradation was identified by Global Partnership on Forest Landscape Restoration (Pistorius et al., 2017). Restoration of deforested areas and degraded areas can play significant role in environmental change mitigation (Guerra-De la Cruz and Galicia, 2017), conservation of biodiversity (Zwiener et al., 2017; Alves-Pinto et al., 2017) and yielding products and services that support local people's livelihoods (Ulian

http://www.aloki.hu ● ISSN 1589 1623 (Print) ● ISSN 1785 0037 (Online)
DOI: http://dx.doi.org/10.15666/aeer/1802_20572072

et al., 2017). Reducing Emission from deforestation and Forest Degradation (REDD+) is a globally accepted climate change mitigation initiative that primarily focused on emission reduction and ensuring forest conservation, sustainable forest management and enhancement of carbon stocks (Kelly, 2018; Hein et al., 2018; Bos et al., 2017). REDD+ can only be possible when afforestation, reforestation and plantation activities are supported and encouraged at local and regional scales (Kuemmerle et al., 2017).

The Bonn Challenge launched in 2011, is a global initiative of large-scale afforestation, reforestation and plantation programs to increase global forest stocks (De Jong et al., 2017). The Bonn Challenge not only further strengthens the present objectives of Global Partnership on Forest Landscape Restoration (GPFLR) but also provide opportunities for REDD+ and Convention on Biological Diversity (CBD) Aichi targets (Pistorius et al., 2017; Pistorius and Freiberg, 2014). Under the Bonn Challenge, different countries including Argentina, Colombia, Costa Rica, Ecuador, Ethiopia, Ghana, India, Madagascar, Mexico, Mozambique, Niger, Peru, Rwanda, Uganda, US Forest Service and Pakistan (Khyber Pukhtunkhwa) have committed large scale afforestation, plantations and restoration of forests (IUCN, 2018). The Bonn Challenge is committed to reforest and reclaim the degraded forests of about 150 million ha by 2020 and will approach to hit the target of 350 million ha till 2030 under New York Declaration on Forest Climate Summit (Pistorius and Freiberg, 2014; Climate Summit, 2014). The 150 million ha target will bring many benefits including about 84$ billion per year to national economies and the restored forests will have capacity of 1 $GtCO_2e$ per year sequestration (FAO, 2016). Among Bonn Challenge members, the US Forest Service has committed 15 million ha by 2020, the highest compared to other members. US Forest Service has restored about 12.3 million ha of degraded forests or land (IUCN, 2018). Recently, nine countries (Tunisia, Turkey, Iran, Morocco, Lebanon, Algeria, Portugal, Spain and France) have endorsed Agadir Commitment to strengthen Forest and Landscape Restoration (FLR) mechanism so as arrive at Bonn Challenge Commitment (FAO FLRM, 2017). The Bonn Challenge also ensure implementation of many globally agreed commitments by climate change bodies such as United Nations Framework on Climate Change (UNFCCC), Convention on Biological Biodiversity (CBD), United Nation Convention to Combat Desertification (UNCCD) and United Nations conservation programs (Asner et al., 2017).

In the context of Bonn Challenge, the Khyber Pukhtunkhwa (KPK) province of Pakistan, situated in northern part of the country, has started massive tree plantation and restoration programs of degraded forests in June 2015. KPK government has committed 0.35 million ha of forests restoration and afforestation by 2020. The potential benefits will include 120 million USD and 0.04 $GtCO_2$ sequestrations by 2020 (Laestadius et al., 2015). Pakistan is a forest deficit country with total land area of 88.43 million ha; with total forest area of 4.60 million forest and forest plantations which are equivalent to 5.23% of the total land area (Bukhari and Bajwa, 2012). About 40% of country forests are located in Khyber Pakhtunkhwa (KPK) province of Pakistan. The KPK province has diverse geo-ecological formation including many forest and vegetation types, ranging from at 250 m above mean sea level in the south to 7708 m high in the North. Around 20.25 of the area is forested with trees of fluctuating thickness and, and nine major vegetation type. Adding Alpine pastures to it makes almost one-third (28.98%) of the province under forest ecosystem. Almost same proportion of land (30.08%) is under agriculture (including orchards). Another 10.67% of the area is under rangelands (Go KP, 2016). Previously various forestry-based conservation and development projects

http://www.aloki.hu ● ISSN 1589 1623 (Print) ● ISSN 1785 0037 (Online)
DOI: http://dx.doi.org/10.15666/aeer/1802_20572072

have been completed in the past in Khyber Pukhtunkhwa, with the collaboration of provincial forest department, national government institution and international organizations. Some of the more famous projects include Malakand Social Forestry Project, Siran Forest Development Project and Kalam Integrated Development Project (Ahmed and Mahmood, 1998).

BTAP has been driven by present KP Government's dream of Green Growth which binds in the necessities to develop approaches towards sustainable forestry in Khyber Pukhtunkhwa. The project aimed to generate green jobs, gender equality and empowerment, also preserving Pakistan's forest resource while parallel addressing to the worldwide issue of environmental change (Go KP, 2015). The provincial forest department has initiated this project with primary targets to plan, support, design methodologies and launch sustainable forestry in KP through local communities' participation and to promote forestry-based employments. The project has been implemented in two phases; Phase-I in 2014-15 while Phase-II implementation was done in 2015-2017. The main targets of the project were establishment of departmental and private nurseries, closure within forests (fencing an area within forest for restoration purpose), plantation on communal and private lands, reclamation or rehabilitation of bad sites, reclamation of saline and waterlogged areas, roadside, canal side and railway side plantations and generating employment opportunities at local level (WWF, 2017). The project activities were monitored by third party, the World Wide Fund for Nature Pakistan (WWF-Pakistan). WWF-Pakistan has published phase wise monitoring reports and found that the project activities were successful (WWF, 2017, 2016).

Previously different researches reported growth and survival of different species as an indicator of plantation success (Leslie et al., 2018; Varghese et al., 2017; Yamada et al., 2016; Rawat et al., 2017; Edo et al., 2017). Pistorius et al. (2017) studied various opportunities, comparative cost and benefits of Forest Landscape Restoration (FLR) in Ethiopia under the Bonn Challenge and reported that FLR comprises mainly of five major components namely participatory forest management, degraded land restoration, afforestation on regional scale, woodland improvement and forest-based value chain investments. Rubilar et al. (2018) reported that productivity and sustainability in intensively managed plantations can be maintained through controlled genetic, environmental and silvicultural interactions. Binkley et al. (2017) examined growth and survival of *Eucalyptus camaldulensis* at different plantation sites along gradient at 36 locations. Sabastian et al. (2018) reported plantations success depends upon soil and slope as growth parameters such as diameter growth respond differently to these factors. Poersch et al. (2017) analyzed the growth of different *Eucalyptus camaldulensis* species and its relation with variables to identify differences in growth pattern, the study found the height growth was strongly affected by minimum temperature. Da Silva et al. (2010) estimated the carbon sequestration potential of road side planted *Eucalyptus camaldulensis* and considered the specie good for road side afforestation.

In large unreachable areas use of remote sensing is a cost-effective method of collecting data and provides an alternative source of data for extrapolating and estimating forest variables (Franklin et al., 2003). The data obtained can be quickly updated and compared with existing data, and the method can be easily incorporated with geographical information systems. These techniques have been effectively combined in many studies and factually noteworthy relationships between the spectral values (computed via Landsat satellite sensors) and field-estimated variables have been accounted for diameter at breast height, age and total height (Donoghue et al., 2004),

http://www.aloki.hu ● ISSN 1589 1623 (Print) ● ISSN 1785 0037 (Online)
DOI: http://dx.doi.org/10.15666/aeer/1802_20572072

volume (Poulain et al., 2010) and biomass (Ali et al., 2018). Secondly, Sentinel-2 is a state of the art sensor launched on 23 June 2015 by the European Space Agency (ESA). Contrasted with Landsat-8, Sentinel-2 imagery at high spatial resolution (10 m), this is expected to provide more accurate results (Rembold et al., 2015; Ali et al., 2018) and offering the capacity to detect small changes in vegetation. Sentinel-2 mission is a land observing star grouping of two indistinguishable satellites (Sentinel-2A and Sentinel-2B) that convey high resolution optical imagery. The framework gives a worldwide inclusion of the Earth's territory surface and is described by its high temporal frequency of ten days, which makes it suitable for temporal vegetation assessment. Keeping the unprecedented success of BTAP it is essential to evaluate the different interventions of the project; in this context the current study was designed. The main objectives of the study was to assess the overall survival rate, growth rate and to evaluate and compare growth performance of different tree species raised under the BTAP in district Dir lower Khyber Pukhtunkhwa, Pakistan. Further, the aim of the present study was to look at the connection between an arrangement of field-estimated factors and spectral data obtained by the Landsat-8 OLI (Operational Land Imager) sensor and Senetinel-2 image.

Materials and methods

Study area

In North Western part of Khyber Pakhtunkhwa province, District Dir lower is located and is spread over an area of 1583 km^2 (*Fig. 1*). The state lies most on the Panjkora River, which start in the mountainous area of Hindu Kush and join the Swat River close Chakdara. Apart from small areas in the south-west, Dir is a rocky, mountainous zone with peaks getting higher to 55,000 m (16,000 ft) in the north-east and 3,000 m (9,800 ft) along the watersheds, with Swat toward the east and Afghanistan and chitral toward the west and north. The topography of the district Dir Lower is dominated my mountains and hills which are part of the ranges/branches of southern Hindukush with the highest peaks in the northern part of Dir. The significant valleys of District Dir Lower include: Maidan, Jandool, Timargara, Samarbagh and Asband. District dir lower has the population of 1,435,917 according to the 2017 census report. The considered population of Dir Lower was 1.0937.091 in 2015 with same growth among the 1981 and 1998 census, i.e. 3.42% per annum (Population Census Organization, 2017).

Forest inventory

Stratified random sampling technique was adopted for the selection of sample plots within plantation sites. Sites were selected randomly from the list plantation provided by project management unit of Billion Tree Afforestation Project Office, Peshawar, Khyber Pukhtunkhwa. The total number of sampling plots was 115 in 17 different plantation sites keeping in view time and available resources. The detail of the sites, number and distribution of sample plots has been explained in *Table 1*. Sampling intensity is the sampled area divided by total area of plantation site and multiplied by 100. Sampling intensity has changed from site to site because of different area, species composition, accessibility and time limitation. The number of plots was calculated by dividing total area divide by plot size and multiplying it with sampling intensity. Field data collection was conduct from 25th September 2017 to 13th October 2017. Altogether, 115 circular plots every one of surface area 1000 m^2 was set up. The plots were geo

http://www.aloki.hu ● ISSN 1589 1623 (Print) ● ISSN 1785 0037 (Online)
DOI: http://dx.doi.org/10.15666/aeer/1802_20572072

referenced in respect to a reference in respect to a reference frame work (WGS 84 Datum/UTM zone 43N). Sub meter GNSS receiver GPS was used in collecting plot data. Data was collected from 115 circular sample plots having 15 m radius while considering slope correction with the help of measuring tape and reference points. The number of sample plots varies with the area of plantation sites as per sampling. For the collection of data measuring tape is used along with Sunnto Clinometer. The total number of plants as per 10 feet by 10 feet spacing was 1076 plants in 0.07 ha plot size. Due to time shortage, we measure height and girth of 20% ± 5 plants randomly in each sample plot and note it in the prescribed inventory forms. Then next plot location was assigned keeping in view 200 m plot to plot distance and particular angular measurement. Measurements were conducted with great care as accuracy of assessment of growth performance depends upon these variables. As the plantation was raised in three phases as per BTAP activities, but my study only conclude the data of one phase which phase II measurement of species growth was assessed by measuring two attributes; girth and height and age of the plantation. Height and girth are considered best indicators of growth performance comparatively. The height of trees was found according to the formula in *Equation 1* (WWF, 2016):

$$H = (\tan\theta \times d) + a \quad \text{(Eq.1)}$$

where:
H = Total height of tree in meter
θ = angle of tree to the top of the tree from observers' eyes
d = distance between the tree base and the observer in meter
a = Observer eye height in meter

Moreover, for survival rate pit density was counted as per departmental procedure and then it was up scaled to per hectare. The Pit density is the number of pits per unit area as explained in *Equation 2* (WWF, 2016). It is an important indicator for assessing the success of a plantation program. Pit density was calculated for ten sampled sites with 10 feet × 10 feet spacing which results in 1075 plants per hectares.

$$N = \frac{D \div 3.28^2}{A} \quad \text{(Eq.2)}$$

where:
N is the number of pits per hectare
D is the distance between two plants in feet
A is the area in square meters

Survival rate of plantation is the most important indicator for assessing the success or failure of plantation. The pit density and empty pits data was used to determine the survival rate of the plantation. Survival rate depends how much out of the total sowed seed or planted plants survived and will likely to become healthy plants in future (*Eq. 3;* WWF, 2016). The less number of empty pits the greater survival percentage for the particular site. Plot wise survival rates was up scaled to site wise survival rate by using pit density data and plantation areas.

$$S_p = \frac{N_s}{N_t} \times 100 \quad \text{(Eq.3)}$$

http://www.aloki.hu ● ISSN 1589 1623 (Print) ● ISSN 1785 0037 (Online)
DOI: http://dx.doi.org/10.15666/aeer/1802_20572072

where
S_p is the survival percentage
N_e is the number of empty pits per hectare
N_t is the number of total pits per hectare

All the enumerated plants were arranged by species name, number of trees per plot and site to know the species composition of all sampled plantation sites. Further, besides sampling planted in the pits, natural regeneration also plays out in the plantation areas. Natural regeneration was also observed during sampling in each site. Regeneration enumeration was divided into two categories, one having less than 9 inches height (not established) and other having more than 9 inches height (established). The site wise natural regeneration was also calculated as per collected data from sampled sites.

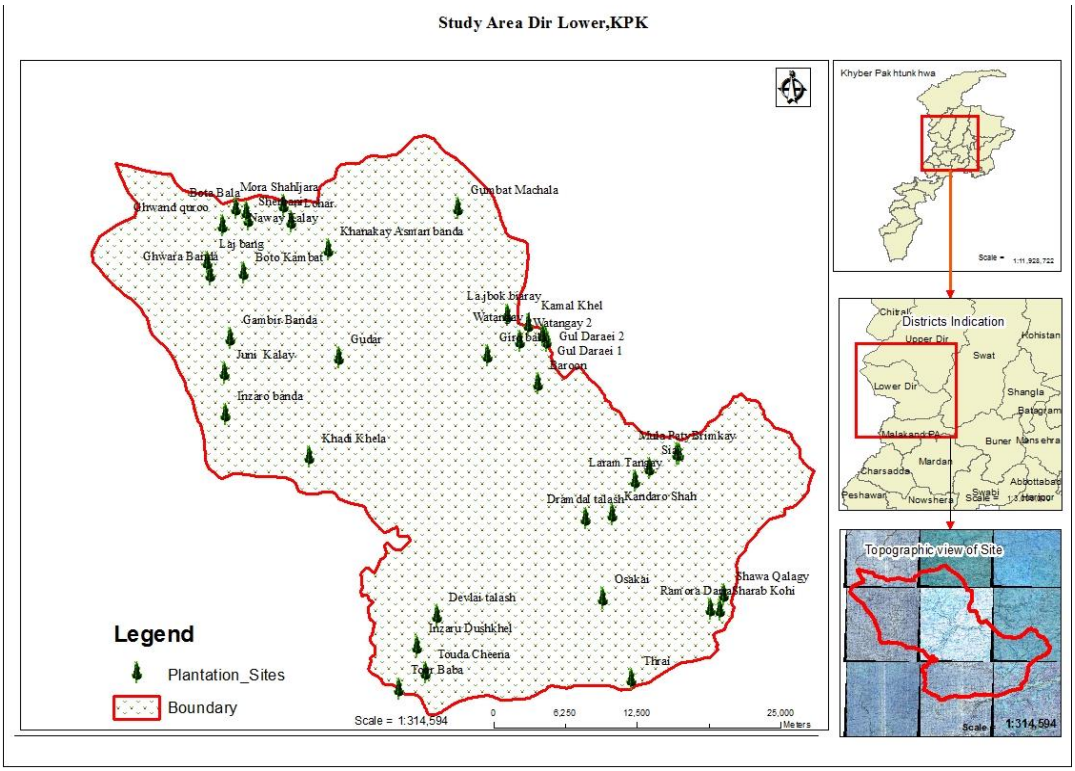

Figure 1. *Map of study area*

Remote sensing

The Landsat-8 Operational Land Imager (OLI) sensor image of in the study was acquired from the USGS Earth Explorer (http://earthexplorer.usgs.gov/). The image was acquired at the same time as the field sampling was carried out at the start of afforestation programs (January, 2014). The image was acquired as level L1T (i.e., they were geometrically rectified with ground control points). Landsat-8 image was carefully preprocessed by radiometric correction, topographic and dark object subtraction methods in ENVI 5.3. The Digital levels (DL) of each band were changed over to surface reflectance by perusing the model parameters and the geometrical attributes incorporated into the image metadata. Band 1 to 7 (B1, B2, B3, B4, B5, B6 and B7) of Landsat-8 OLI were used in the present study. The Sentinel-2 image was acquired from Copernicus Open

http://www.aloki.hu ● ISSN 1589 1623 (Print) ● ISSN 1785 0037 (Online)
DOI: http://dx.doi.org/10.15666/aeer/1802_20572072

Access Hub (https://scihub.copernicus.eu/). The Sentinel product was named as S2_MSI_Level-1C with processing Level-1C. Product bands ranged from 443 to 2190 nm with Band 2, 3, 4 and 8 in 10 m, Band 5, 6, 7, 8A, 11 and 12 in 20 m and Band 1, 9 and 10 in 60 m. Sentinel-2 image was corrected for atmospheric effects by applying the Sen2Cor version 2.2.1 software (Main-Knorn et al., 2015). The atmospheric correction transforms the Top-of Atmosphere level 1C product to Bottom-of Atmosphere atmospheric and terrain corrected product (level 2A) and its usability are described by Vuolo et al. (2016). A number of vegetation indexes and other derived parameters (Normalized difference vegetation index, *NDVI*; Modified soil adjusted vegetation index, M*SAVI*; Perpendicular Vegetation Index (PVI), Difference Vegetation Index (DVI), Transformed Normalized Difference Vegetation Index *(TNDVI)* were computed from the atmospherically and topographically corrected image bands and then included in the volume estimation models for evaluation as possible regress or variables.

Statistical analysis

Scatter plots were generated to analyze the relationship between volume (m^3) and individual indices (NDVI, MSAVI, PVI, DVI, TNDVI). Correlation and regression analysis (simple and stepwise models) were performed between volume (m^3) and spectral indices. Different models were established (linear, polynomial, power, logarithmic and exponential). Coefficient of determination (R^2) was calculated for each model with the level of significance ($P \leq 0.05$). As a result, model fulfilling the condition of highest value of R^2, was selected for effective biomass estimation and generation of biomass map as well.

Results

Pit density

Pit density of all these plantation sites have been summarized in *Table 1*. The total area of sampled sites was 1980 ha and total numbers of pits were 2107789 with 1065 (Average) number of pits per hectare. The highest pit density was found at Lram Tngaeishah village with 1086 pits per hectare while Inzrudushkhl kmalkhel the lowest number of pits with 1022 pits per hectare. As per third party monitoring of BTAP, WWF reported that total plantation on areas in the study area was 1998.6 ha and total number of plants was 2150493 with10 by 10 feet average plant to plants spacing (WWF, 2017). *Table 1* also showed plot wise Information about survival rate of all sampled sites. Almost all of the sampled plantation sites showed better survival percentage i.e. above 70%. As per plot level measurements, the highest survival percentage was observed at Shrbkohy Ramoradra with 91% whereas the lowest survival percentage was at Gambirghwara Banda area with 72%. The comparatively high rate of survival is probably due to choice of species i.e. most of the plantations consist of Chir and *Eucalyptus* which shows very high survival rate in especially Eucalyptus shows high resistance for survival in harsh conditions and secondly due to intensive care provided by the department. Regarding site wise survival rates, the Shrbkohy Ramoradra showed the highest success rate with 91% survival percentage while Gambirghwara Banda showed the lowest success rate among the sampled sites with 72% survival. The BTAP monitoring (WWF, 2017) also reported that in northern circle of project area, the highest survival rate was found of Upper Dir 93.8% in compared to

http://www.aloki.hu ● ISSN 1589 1623 (Print) ● ISSN 1785 0037 (Online)
DOI: http://dx.doi.org/10.15666/aeer/1802_20572072

other forest divisions while the rest were 90, 84.75, 82.97, 82.5, 81.5, 78, and 67 of Dirkohistan, Lower Dir, Swat, Buner, Kalam, Malakand and Alupri respectively. Yamada et al. (2016) conducted a study about the growth and survival of different tree species planted to renovate biodiversity at river side's and within Palm Plantations. Survival rates of 351 seedlings were above 90% during 3 years after planting. Rawat et al. (2017) evaluated multipurpose trees raised in three villages (Jaminikhal, Manjgaon, Hadiya) in India for biodiversity conservation and degraded lands restoration. After four years of plantation, survival rates were 96.6%, 90.3% and 71.1% for Jaminikhal, Manjgaon, Hadiya respectively. Poersch et al. (2017) reported survival rate of 96.43% for *Eucalyptus camaldulenis* in 12 months.

Table 1. *Detail of plantation sites, total number of pits, empty pits and survival rate*

Name of plantation site	Area (ha)	No of sample plots	Average pits per ha	Total no. of pits	Pits in plots	Empty pits/plot	Empty (ha)	Total empty pits	Survival rate (%)
Oskaei touda chena	180	10	1054	189720	74	14	171	36000	81
Lram Tngaeishah	73	5	1086	79278	76	9	129	9417	88
Sia Brimkpaty	128	7	1034	132352	72	9	129	16512	88
TorbabaTharei	83	5	1065	88395	74	13	186	15438	83
Shrbkohy Ramoradra	44	3	1082	47608	75	9	129	5676	91
Juni kalay	114	7	1067	121638	74	17	244	27816	77
Laj Bang Sherbani	64	4	1056	67584	73	18	1314	84096	75
Lohar khadi shah	88	5	1070	94160	75	12	172	15136	84
Botabala kambat	197	11	1067	210199	74	15	215	42355	80
Gambirghwara Banda	184	10	1072	197248	76	21	300	55200	72
Ghwnd Quro Ghudar	110	6	1079	118690	76	13	186	20460	83
Bagh Maidan	**123**	8	1081	132963	77	15	215	26445	81
Baroon sairtormang	113	7	1075	121475	76	18	258	29154	76
Devilai talash	195	11	1084	211380	76	15	215	41925	81
Inzrudushkhl kmalkhel	111	6	1022	113442	71	9	129	14319	87
Watangy Gumbtmachla	92	5	1058	97336	74	11	158	14536	85
Gul Daraei	81	5	1041	84321	73	10	143	11583	86
TOTAL	1980	**115**		**2107789**					

Growth rate of different species

The growth performance of different species is given in *Table 2*. Highest growth performance was exhibited *Eucalyptus camaldulensis*. *Eucalyptus camaldulensis* attained an average height of 1.29 m. This high growth was due to very good conditions of the sites where *Eucalyptus camaldulensis* has been planted. On the other hand, the

http://www.aloki.hu ● ISSN 1589 1623 (Print) ● ISSN 1785 0037 (Online)
DOI: http://dx.doi.org/10.15666/aeer/1802_20572072

remaining species have the average height growth of, 1.12, 0.96, 0.85, 0.79, 0.76, 0.58, 0.54, 0.45, 0.44, 0.44, 0.36 and 0.35 m of Robinia, Willow, Ailanthus, Shisham, Bakain, Chir*, Persian Pine,* Ippleipple, Walnut, Kail, Phulaei and deodar respectively. Data on growth performance of different tee species at different sites were also recorded to determine variation in growth at different sites. Leslie et al. (2018) studied growth functions for *Eucalyptus camaldulensis*, where *Eucalyptus camaldulensis* trees have attained height (m) of 0.5, 1.4, 1.5 and 2 m in 5, 14 and 29 respectively and overall mean height of 10.6 m in 5.5 years. Varghese et al. (2017) studied growth and wood properties of *Eucalyptus camaldulensis* raised from local seed sources and clones, the study reported that plants grow from local sources grow faster than clones. Poersch et al. (2017) evaluated monthly diameter and height growth of *Eucalyptus camaldulensis* during 12 months, diameter increment was recorded form 3.35 cm to 10.27 cm and height increment was recorded from 2.15 to 6.56 cm.

Table 2. *Detail of species utilized in plantation sites along with their age, DBH, height and volume (n = 115)*

Species	Age (month)	Dia (cm) mean	Height (m) mean	Volume (m^3) mean
Pinus roxburghii	17	4.15	0.59	0.0326
Eucalyptus camaldulensis	17	5.29	1.30	0.0540
Robinia pseudoacacia	17	4.18	1.12	0.0281
Pinus gerardiana	17	3.17	0.54	0.0024
Cedrus deodara	17	2.75	0.35	0.0008
Acacia modesta	17	2.	0.37	0.0005
Dalbergia sissoo	17	4	0.79	0.0032
Juglans regia	17	2.21	0.45	0.0005
Pinus wallichiana	17	2.75	0.44	0.0005
Salix tetrasperma	17	3.2	0.96	0.0015
Ailanthus altissima	17	3.5	0.85	0.0018
Leucaena leucocephela	17	2.3	0.46	0.0002
Melia azedarach	17	3.2	0.76	0.0006

Relationship between volume (m^3) and Sentinel-2 spectral indices

Different vegetation indices were assessed for their correlation with volume (m^3). Results obtained for different regression models for each index are shown in *Figure 2*. Among these indices TNDVI and NDVI has the highest value of R^2 of 0.425, followed by MSAVI with $R^2$0.41. Similarly, applying various regression models (linear, polynomial, power, logarithmic and exponential) the values of R2 change as per data behavior and model assumptions. Vafaei et al. (2018) reported that integration of Sentinel-2A with ALOS-2 PALSAR-2 can enhance vegetation estimation with greater accuracy. Among these two estimations of Sentinel-2A was more accurate. Adan (2017) reported that indices computed from Sentinel-2A have better potential to estimate biomass in contrast to vegetation indices of other sensors.

http://www.aloki.hu ● ISSN 1589 1623 (Print) ● ISSN 1785 0037 (Online)
DOI: http://dx.doi.org/10.15666/aeer/1802_20572072

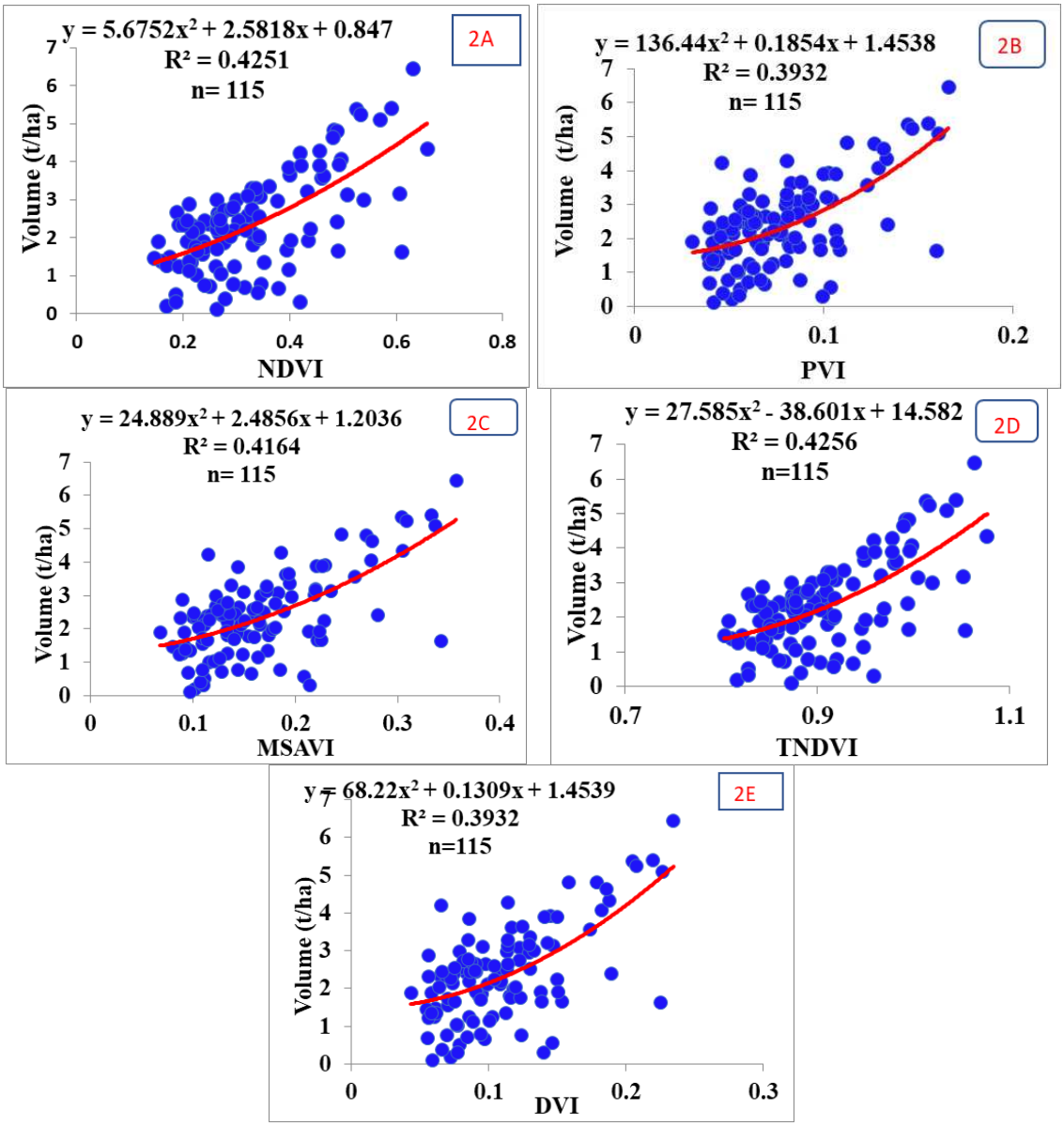

Figure 2. *Scatterplots of spectral indices and volume (t/ha); where NDVI, PVI, MSAVI, TNDVI, DVI were shown by Figure 2a, b, c, d and e respectively*

Relationship between survival percentage and Sentinel-2 spectral indices

Different vegetation indices were assessed for their correlation with survival percentage. Results obtained for different regression models for each index are shown in *Figure 3*. Among these indices NDVI has the highest value of R^2 of 0.859, followed by SAVI and DVI with 0.65 and 0.566 respectively. Similarly, applying various regression models (linear, polynomial, power, logarithmic and exponential) the values of R2 change as per data behavior and model assumptions.

Stepwise regression model

The stepwise Regression Model showed that NDVI was the best predictor for volume mapping at BTAP plantation sites. NDVI map was relatively the best to map

http://www.aloki.hu ● ISSN 1589 1623 (Print) ● ISSN 1785 0037 (Online)
DOI: http://dx.doi.org/10.15666/aeer/1802_20572072

biomass among other indices. *Table 3* depicted that the relationship of NDVI and volume was strongly significant while the rest of the indices (TNDVI, MSAVI, DVI, PVI) was not significant under stepwise criteria (Probability-of-F-to-enter < = .050 and Probability-of-F-to-remove > = .100). The correlation matrix showed that NDVI has the highest correlation followed by TANDVI and MASVI with R^2 values of 0.648, 0.645 and 0.637 respectively.

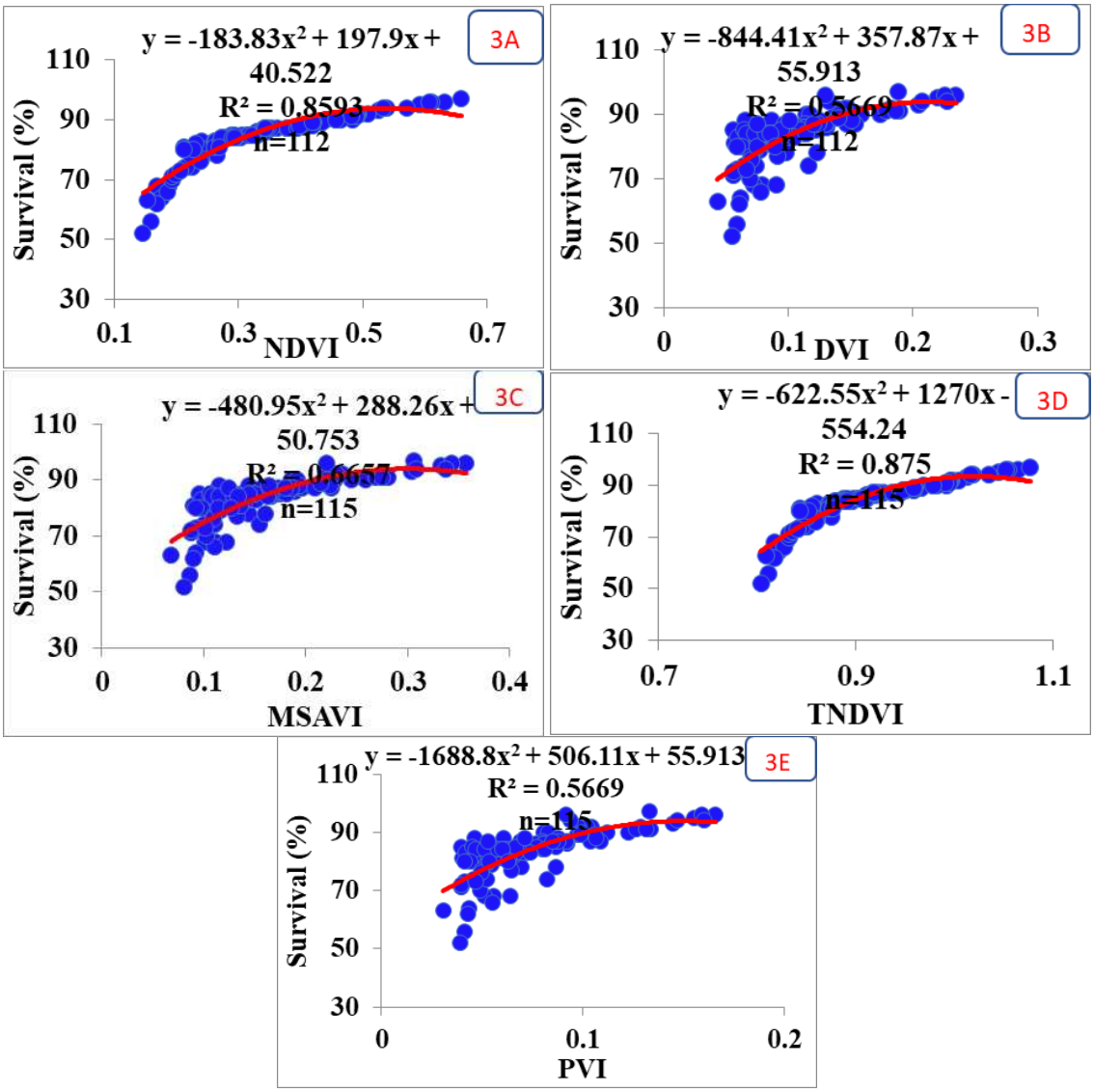

Figure 3. *Scatterplots of spectral indices and survival rate (t/ha); Where NDVI, PVI, MSAVI, TNDVI, DVI were shown by Figures 2a, b, 3c, d and e, respectively*

Whereas the overall R^2 of model was 0.420 with standard error of 0.949. Volume map of the plantation sites was produced using raster calculator in ArcGIS 10. Further, NDVI differencing showed that in NDVI range was from -0.65 to 0.68 in 2013 and the upper limit (value) was increased to 0.85 in 2018. Thus showed mosaic restoration and afforestation activities of BTAP. The lower sub-images of *Figure 4* compared same plantation sites before and after the project activities which showed substantial increase

http://www.aloki.hu ● ISSN 1589 1623 (Print) ● ISSN 1785 0037 (Online)
DOI: http://dx.doi.org/10.15666/aeer/1802_20572072

in the vegetation cover from 2013 to 2018. Thus it can be concluded that BTAP activities were efficiently managed and supervised by the department. WWF (2016, 2017) and World Economic Forum (2017) reported that project activities were successful and meet its Bonn Challenge commitment by the end of 2017.

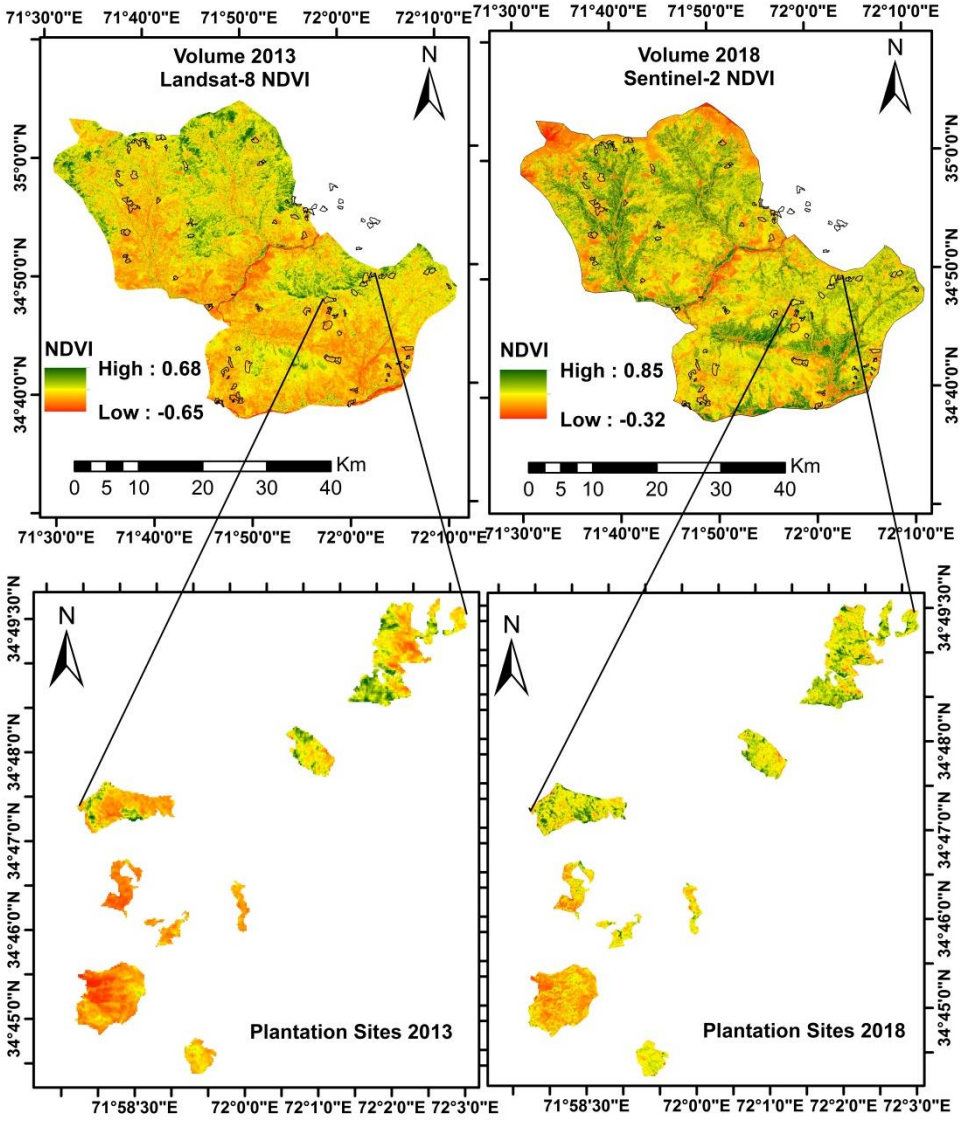

Figure 4. *Comparison of plantation sites before and after plantation (n = 115)*

Table 3. *Sentinel-2 stepwise regression (P ≤ 0.05, n = 115)*

Sentinel-2 stepwise regression-variables entered/removed			
Variables entered	**Variables removed**	**Sig**	**Method/decision**
NDVI		0.000	Stepwise (Criteria: Probability-of-F-to-enter < = .050, Probability-of-F-to-remove > = .100).
	TNDVI	0.296	
	DVI	0.151	
	PVI	0.151	
	MSAVI	0.138	

http://www.aloki.hu ● ISSN 1589 1623 (Print) ● ISSN 1785 0037 (Online)
DOI: http://dx.doi.org/10.15666/aeer/1802_20572072

Correlations							Regression Summary	
	Biomass	**TNDVI**	**DVI**	**PVI**	**MSAVI**	**NDVI**	R	0.648
Volume	1.000						R square	0.420
TNDVI	.645	1.000					Adjusted R square	0.415
DVI	.614	.866	1.000				Std. error	0.949
PVI	.614	.866	0.993	1.000			F-value	81.052
MSAVI	.637	.915	.993	.993	1.000`		Sig	0.000
NDVI	.648	.999	.869	.869	.918	1.000		
Model equation Volume (m^3/ha) = 6.840*NDVI + 0.138								

Conclusion

The present research evaluated the BTAP success by survival rate and growth performance of major multipurpose species raised in 15 randomly selected sites of Dir lower Forest division. The overall survival rate and growth performance of plantations was found satisfactory. However, the share of *Eucalyptus camaldulensis* is more than other species which needs to be balanced in the future plantations. Pit density is found bit lesser than the required 10 feet by10 feet spacing and in few sites it was 10 x 11 space i.e.1065 pits per hectare observed. Highest growth performance was exhibited *Eucalyptus camaldulensis*. *Eucalyptus camaldulensis* attained an average height of 1.29 m. This high growth was due to very good conditions of the sites where *Eucalyptus camaldulensis* has been planted. On the other hand, the remaining species have the average height growth of,1.12, 0.96, 0.85, 0.79, 0.76, 0.58, 0.54, 0.45, 0.44, 0.44, 0.36 and 0.35 m of Robinia, Willow, Ailanthus, Shisham, Bakain, Chir*, Persian Pine,* Ippleipple, Walnut, Kail, Phulaei and deodar respectively. Data on growth performance of different tee species at different sites were also recorded to determine variation in growth at different sites. Correlation between mean height (m) and mean diameter (cm) for all species was good and showed the overall data behavior shows good growth at present stage. If proper monitoring and management is continued for coming years, then these plantation will become fully established and contribute to successful implementation of Forest Landscape Restoration (FLR) under the Bonn Challenge commitment. To achieve future implementation and monitoring, based on the data collected during the field survey, personal observations of the researcher and interaction with staff of Forest Department and members of local community, some recommendation were suggested. There is a need to repeat such studies in the future to assess and monitor the survival rate and growth performance of plantations raised under BTAP. Due to shortage of time this study could not cover all the sites where plantations were raised. It is therefore advisable to conduct assessment of plantations in the sites not covered under the present study. It is also recommended to investigate the impacts of BTAP Plantations on ecological systems such as biodiversity, hydrological patterns and carbon sequestration after 5-10 years to ascertain the impacts on the ecosystem.

We also exhibit that using the free of charge Landsat-8 and Sentinel-2 data and open source software is a possible alternative achieving assure results for BTAP plantation spatial and temporal monitoring. The study suggested that Sentinel-2A product has considerable potential to estimate biomass and map forest areas. The Sentinel-2A item

http://www.aloki.hu ● ISSN 1589 1623 (Print) ● ISSN 1785 0037 (Online)
DOI: http://dx.doi.org/10.15666/aeer/1802_20572072

has nearly substantial spatial inclusion and high goals to perform proficiently for estimation of biomass than other open source sensors information items.

REFERENCES

[1] Adan, M. S. (2017): Integrating Sentinel-2A derived indices and terrestrial laser scanner to estimate above ground biomass/carbon in Ayer Hitam tropical forest, Malaysia. – Master of Science, University of Twente, The Netherlands.

[2] Ahmed, J., Mahmood, F. (1998): Changing Perspective on Forest Policy. Policy That Works for FORESTS and people. Pakistan Country Case Study. – IUCN, Islamabad.

[3] Ali, A., Ullah, S., Bushra, S., Ahmad, N., Ali, A. and Khan, M. A. (2018): Quantifying forest carbon stocks by integrating satellite images and forest inventory data. – Austrian Journal of Forest Science 135(2): 93-117.

[4] Alves-Pinto, H. N., Latawiec, A. E., Strassburg, B. B., Barros, F. S., Sansevero, J. B., Iribarrem, A., Crouzeilles, R., Lemgruber, L., Rangel, M. C., Silva, A. C. (2017): Reconciling rural development and ecological restoration: strategies and policy recommendations for the Brazilian Atlantic Forest. – Land Use Policy 60: 419-426.

[5] Asner, G. P., Martin, R. E., Tupayachi, R., Llactayo, W. (2017): Conservation assessment of the Peruvian Andes and Amazon based on mapped forest functional diversity. – Biological Conservation 210: 80-88.

[6] Binkley, D., Campoe, O. C., Alvares, C., Carneiro, R. L., Cegatta, Í., Stape, J. L. (2017): The interactions of climate, spacing and genetics on clonal Eucalyptus plantations across Brazil and Uruguay. – Forest Ecology and Management 405: 271-283.

[7] Bos, A. B., Duchelle, A. E., Angelsen, A., Avitabile, V., De Sy, V., Herold, M., Joseph, S., De Sassi, C., Sills, E. O., Sunderlin, W. D., Wunder, S. (2017): Comparing methods for assessing the effectiveness of subnational REDD+ initiatives. – Environmental Research Letters 12(7): 074007.

[8] Bukhari, S. S. B., Bajwa, G. A. (2012): Development of National Response Strategy to Combat Impacts of Climate Change on Forest of Pakistan. – Pakistan Forest Institute, Peshawar.

[9] Da Silva, A. M., Braga Alves, C., Alves, S. H. (2010): Roadside vegetation: estimation and potential for carbon sequestration. – iForest-Biogeosciences and Forestry 3(5): 124.

[10] De Jong, W., Galloway, G., Katila, P., Pacheco, P. (2017): Forestry discourses and forest based development - an introduction to the Special Issue. – International Forestry Review 19(1): 1-9.

[11] Donoghue, D. N. M., Watt, P. J., Cox, N. J., Dunford, R. W., Wilson, J., Stables, S., Smith, S. (2004): An evaluation of the use of satellite data for monitoring early development of young Sitka spruce plantation forest growth. – Forestry 77(5): 383-396.

[12] Edo, G. Y., Gebremedihn, G. K., Woldsenbet, A. F., Guta, K. K. (2017): Growth performance of some multipurpose tree species around the homesteads in Gimbo district, Southwestern Ethiopia. – Agriculture, Forestry and Fisheries 6(1): 1-5. DOI: 10.11648/j.aff.20170601.11.

[13] FAO FLRM (2017): The Forest and Landscape Restoration Mechanism, Countries commit to support achievement of the Bonn Challenge and SDG15 in new Mediterranean dynamic. – http://www.fao.org/in-action/forest-landscape-restoration-mechanism/news-and-events/news-detail/en/c/878735/. Accessed on February 17, 2018.

[14] FAO (2015): Global Forest Resources Assessment. – FAO Forestry Research Paper 163, Rome. http://www.fao.org/3/a-i4808e.pdf. Accessed on February 20, 2018.

[15] FAO (2016): Food and Agricultural Organization and Bonn Challenge – http://www.fao.org/fileadmin/user_upload/rap/Asia-Pacific_Forestry_Week/doc/Stream_5/ST5_24Feb_SaintLaurent_FLR_IUCN.pdf. Accessed on February 10, 2018.

http://www.aloki.hu ● ISSN 1589 1623 (Print) ● ISSN 1785 0037 (Online)
DOI: http://dx.doi.org/10.15666/aeer/1802_20572072

[16] Franklin, S. E., Hall, R. J., Smith, L., Gerylo, G. R. (2003): Discrimination of conifer height, age and crown closure classes using Landsat-5 TM imagery in the Canadian Northwest Territories. – International Journal of Remote Sensing 24(9): 1823-1834.
[17] Go, K. P. (2015): Revised PC-1 for Billion Trees Tsunami Afforestation Project in Khyber Pakhtunkhwa. – Department of Forestry, Environment & Wildlife Govt. of Khyber Pakhtunkhwa. http://103.240.220.71/btt/repos/files/2015/12/PC1-Phase1.pdf. Accessed on February 13, 2018.
[18] Go, K. P. (2016): Khyber Pakhtunkhwa Biodiversity Strategy & Action Plan – http://www.devconsult.pk/wp-content/uploads/2016/06/KP-Biodiversity-Strategy-Action-Plan-2016-Final-Draft.pdf. Accessed on February 05, 2018.
[19] Galicia, L. (2017): Tropical and highland temperate forest plantations in Mexico: pathways for climate change mitigation and ecosystem services delivery. – Forests 8(12): 489.
[20] Hein, J., Guarin, A., Frommé, E., Pauw, P. (2018): Deforestation and the Paris climate agreement: an assessment of REDD+ in the national climate action plans. – Forest Policy and Economics 90: 7-11.
[21] IUCN Forests (n.d.): The US Forest Service on tracing their Bonn Challenge Pledge. – https://infoflr.org/news-media/us-forest-service-tracking-their-bonn-challenge-pledge. Accessed on February 17, 2018.
[22] Kelly, A. C. (2018): Improving REDD+ (Reducing Emissions from Deforestation and Forest Degradation) Programs. – Doctoral Dissertation, University of Washington.
[23] Kuemmerle, T., Altrichter, M., Baldi, G., Cabido, M., Camino, M., Cuellar, E., Cuellar, R. L., Decarre, J., Díaz, S., Gasparri, I., Gavier-Pizarro, G. (2017): Forest conservation: remember Gran Chaco. – Science 355(6324): 465-465.
[24] Laestadius, L., Buckingham, K., Maginnis, S., Saint-Laurent, C. (2015): Before Bonn and beyond: the history and future of forest landscape restoration. – Unasylva 66(245): 11.
[25] Leslie, A. D., Mencuccini, M., Perks, M. P. (2018): Preliminary growth functions for Eucalyptus gunnii in the UK. – Biomass and Bioenergy108: 464-469.
[26] Main-Knorn, M., Pflug, B., Debaecker, V., Louis, J. (2015): Calibration and validation plan for the L2a processor and products of the Sentinel-2 mission. – International Archives of the Photogrammetry, Remote Sensing & Spatial Information Sciences 40: 1249-1255.
[27] Mori, A. S. (2017): Biodiversity and ecosystem services in forests: management and restoration founded on ecological theory. – Journal of Applied Ecology 54(1): 7-11.
[28] Pistorius, T., Freiberg, H. (2014): From target to implementation: perspectives for the international governance of forest landscape restoration. – Forests 5(3): 482-497.
[29] Pistorius, T., Carodenuto, S., Wathum, G. (2017): Implementing forest landscape restoration in Ethiopia. – Forests 8(3): 61.
[30] Poersch, N. L., FrançaFilho, L. R. T., Miguel, E. P., da Cruz, G. H. M., Francisquette, K. L., Cavalheiro, S. B. (2017): Influence of climate variables in the initial growth of Corymbiacitriodora and different species of eucalyptus. – Bioscience Journal 33(6).
[31] Population Census Report (2017): Lower DirBlockwise profile. – http://www.pbscensus.gov.pk/sites/default/files/bwpsr/kp/LOWER%20DIR_BLOCKWISE.pdf.
[32] Poulain, M., Peña, M., Schmidt, A., Schmidt, H., Schulte, A. (2010): Relationships between forest variables and remote sensing data in a Nothofaguspumilio forest. – Geocarto International 25(1): 25-43.
[33] Rawat, L. S., Maikhuri, R. K., Dhyani, D., Bahuguna, Y. M., Pharswan, D. S. (2017): Ecological restoration of village common degraded land through participatory approach for biodiversity conservation and socio-economic development in Indian Himalayan Region. – ActaEcologicaSinica 37(4): 240-252.
[34] Rembold, F., Leonardi, U., Ng, W. T., Gadain, H., Meroni, M., Atzberger, C. (2015): October. Mapping Areas Invaded by Prosopis Juliflora in Somaliland on Landsat 8

http://www.aloki.hu ● ISSN 1589 1623 (Print) ● ISSN 1785 0037 (Online)
DOI: http://dx.doi.org/10.15666/aeer/1802_20572072

Imagery. – In: Neale, C. M. U., Maltese, A. (eds.) Remote Sensing for Agriculture, Ecosystems, and Hydrology XVII. Vol. 9637: 963723. International Society for Optics and Photonics, Bellingham.

[35] Rubilar, R. A., Allen, H. L., Fox, T. R., Cook, R. L., Albaugh, T. J., Campoe, O. C. (2018): Advances in silviculture of intensively managed plantations. – Current Forestry Reports 4(1): 23-34.

[36] Sabastian, G. E., Kanowski, P., Williams, E., Roshetko, J. M. (2018): Tree diameter performance in relation to site quality in smallholder timber production systems in Gunungkidul, Indonesia. – Agroforestry Systems 92(1): 103-115.

[37] Trumbore, S., Brando, P., Hartmann, H. (2015): Forest health and global change. – Science 349(6250): 814-818.

[38] Ulian, T., Sacandé, M., Hudson, A., Mattana, E. (2017): Conservation of indigenous plants to support community livelihoods: the MGU–Useful Plants Project. – Journal of Environmental Planning and Management 60(4): 668-683.

[39] UN Climate Summit (2014): New York Declaration on Forests. – http://www.un.org/climatechange/summit/wp-content/uploads/sites/2/2014/07/New-York-Declaration-on-Forest-%E2%80%93-Action-Statement-and-Action-Plan.pdf. Accessed on January 17, 2018.

[40] Vafaei, S., Soosani, J., Adeli, K., Fadaei, H., Naghavi, H., Pham, T., Tien Bui, D. (2018): Improving accuracy estimation of forest aboveground biomass based on incorporation of ALOS-2 PALSAR-2 and Sentinel-2A imagery and machine learning: a case study of the Hyrcanian forest area (Iran). – Remote Sensing 10(2): 172.

[41] Varghese, M., Harwood, C. E., Bush, D. J., Baltunis, B., Kamalakannan, R., Suraj, P. G., Hegde, D., Meder, R. (2017): Growth and wood properties of natural provenances, local seed sources and clones of Eucalyptus camaldulensis in southern India: implications for breeding and deployment. – New Forests 48(1): 67-82.

[42] Vuolo, F., Żółtak, M., Pipitone, C., Zappa, L., Wenng, H., Immitzer, M., Weiss, M., Baret, F., Atzberger, C. (2016): Data service platform for Sentinel-2 surface reflectance and value-added products: system use and examples. – Remote Sensing 8(11): 938.

[43] WEF-World Economic Forum (2017): Social Innovation. Environmental and Natural Resource Security. – https://www.weforum.org/agenda/2018/07/pakistan-s-billion-tree-tsunami-is-astonishing/. Accessed on October 30, 2018.

[44] WWF (2016): Third Party Monitoring of The Billion Trees Afforestation Project in Khyber Pakhtunkhwa Pakistan, World Wide Fund for Nature Pakistan. – http://103.240.220.71/btt/third-party-monitoring-report-of-billion-trees-project-by-wwf-pakistan/bttap-third-party-monitoring-report-final-version-9-final/. Accessed on February 05, 2018.

[45] WWF (2017): Third Party Monitoring of The Billion Trees Afforestation Project in Khyber Pakhtunkhwa Pakistan, World Wide Fund for Nature Pakistan. – http://103.240.220.71/btt/repos/files/2018/02/THIRD-PARTY-MONITORING-OF-THE-BTAP-PHASE-2-Part-2.pdf. Accessed on February 10, 2018.

[46] Yamada, T., Watanabe, K., Okuda, T., Sugimoto, T., Azlin, Y. N. (2016): Growth and survival of trees planted in an oil palm plantation: implications for restoration of biodiversity. – Journal of Tropical Forest Science 28(1): 97-105.

[47] Zwiener, V. P., Padial, A. A., Marques, M. C., Faleiro, F. V., Loyola, R., Peterson, A. T. (2017): Planning for conservation and restoration under climate and land use change in the Brazilian Atlantic Forest. – Diversity and Distributions 23(8): 955-966.

http://www.aloki.hu ● ISSN 1589 1623 (Print) ● ISSN 1785 0037 (Online)
DOI: http://dx.doi.org/10.15666/aeer/1802_20572072

DETERMINATION OF NOISE POLLUTION IN THE HUDAVENDIGAR URBAN PARK OF BURSA, TURKEY

YALILI KILIC, M.* – ABUS, M. N.

Bursa Uludag University, Faculty of Engineering, Department of Environmental Engineering, 16059 Bursa, Turkey

**Corresponding author*
e-mail: myalili@uludag.edu.tr; phone: +90-224-294-2117; fax: +90-224-294-2635

(Received 5th Mar 2019; accepted 25th Nov 2019)

Abstract. Noise is one of the health and environmental problems of our age, and it is an undesirable phenomenon that annoys people. Increasing and uncontrolled noise creates physical, physiological and psychological problems, chasing people away from urban life and leading them back to nature. Since the urban parks, which are one of the places to relax, are intensely preferred by people, the noise here should be controlled. In this study, to determine the noise level of the Hudavendigar Urban Park located in the district of Nilufer, Bursa, Turkey, where the transportation routes are intense, measurements were performed, and the results were statistically interpreted. Measurements were carried out at 6 locations selected across the park, in summer, and winter, morning, lunch and evening hours, on weekdays and weekends. In this study, the noise sources indoor and outdoor of the park were determined, and the regions which exceed the limit values given in the Regulation on the Assessment and Management of Environmental Noise were confirmed. As a result of the study, the differences in noise measurements were significant in the summer and winter periods of the Hudavendigar Urban Park according to the statistical analysis.
Keywords: *noise measurements, noise pollution, recreation area, statistical analysis, urban park, Turkey*

Introduction

The effects of noise on the environment and people have increased by technology, industry and transportation. The noise defined as an unpleasant, unwelcome, uncomfortable acoustic phenomenon has become an environmental problem that needs to be controlled (Şerefhanoğlu, 1991; Aydın and Ateş, 1997).

Today, the effects of noise on the environment and human beings can not be estimated. Temporary or permanent hearing loss occurs in people exposed to prolonged and intense noise. Lower levels of noise make it difficult for people to have mutual communication, cause stress, and insomnia, and hamper human peace and prevent them from working efficiently (Balcı, 1994). With a noisy life, the factors that wear people up and down are increasing. There is a society in which noise resistance and tolerance are increasingly reduced.

Despite the diversity of the effects of noise on human, the limit values related to noise levels and disturbances are given in *Table 1* (Donoghue, 2004; Aslan and Yıldız, 2017).

The effect of noise on human beings is not only addressed by the high levels of noise, but also by its frequency (Rosenberg, 1991). The level of effect varies according to the duration, severity, frequency of the noise, whether it is continuous or intermittent. Also, the health and age of people exposed to noise cause differences in the degree of influence (Aydın and Ateş, 1997).

Although the term environmental noise generally used for sources outside the structures, noise sources commonly found in the interior environment of the buildings

http://www.aloki.hu ● ISSN 1589 1623 (Print) ● ISSN1785 0037 (Online)
DOI: http://dx.doi.org/10.15666/aeer/1802_20732085

and various places. In-building noise sources are particular noises that affect fewer people and can often be prevented with good external insulation (Kurra, 2009; Belek, 2017). Because the external noise sources affect a broader human population, the measures should be at the national level to minimize the noise generated by these sources.

Table 1. *Noise levels and disturbances (Donoghue, 2004)*

Degree	Noise Level dB(A)	Disturbances
1	30-65	Confusion, discomfort, anger, anger, sleep disorder and concentration disorder
2	65-90	Physiological reactions increased blood pressure, acceleration of heartbeat and respiration, decreased pressure in brain fluid, sudden reflexes
3	90-120	Increased physiological reactions, headaches
4	120	Permanent damage to the inner ear, disturbance of balance
5	140	Serious brain destruction

For this purpose, the Regulation on the Assessment and Management of Environmental Noise (RAMEN) No: 27601, dated 04.06.2010 (Anonymous, 2010), has begun to address noise control at the national level. Also, noise action plans, auxiliary guidelines, and informative publications are prepared by different institutions (Anonymous, 2004, 2011, 2012).

Noise measurements are essential in noise control. Generally, these measurements are performed to check if the environmental noise is within the required limit values or to avoid a negative effect on human (Belek, 2017). The studies on noise pollution have been widely used to determine noise levels from highway traffic (Karadayı, 2001; Aktürk et al., 2003a; Çetin, 2010; Ilgar, 2012; Delikanlı et al., 2014; Sharma et al., 2014; Kalıpçı, 2017), rail systems (Aktürk et al., 2003b; Neitzel et al., 2009; Kablan, 2012; Oruç, 2017) and machinery in some industrial plants (Şahin, 2003; Sakarya, 2016), or to address the effects of noise on human health (Singh and Davar, 2004; Özbıçakçı et al., 2012; Tür, 2016).

There are very few studies on noise pollution in urban parks in the literature (Zannin et al., 2006; Szeremeta and Zannin, 2009; Bayramoğlu et al., 2014; Özer, 2014, 2015, 2017). However, urban parks located within the areas where people can relax in nature by moving away from urban life, are significant for the peace of human life. To control and prevent noise occurring in these areas, the number of studies related to noise pollution should increase.

In this study, noise measurements were carried out at 6 points determined in the Hudavendigar Urban Park in the Nilufer district of Bursa province in the summer and winter periods, and the measurement results were evaluated statistically. The noise sources inside and outside the park were determined, and the regions exceeding and approaching the limit values were specified in the RAMEN.

Materials and Method

Hudavendigar Urban Park created on both sides of the Nilufer Stream of Bursa city in Turkey, is the largest urban park in the city, which has an area of approximately 510 thousand m^2. The measurements were carried out to determine the noise level in the park, which is in the center of the city and in an area with high access roads.

http://www.aloki.hu ● ISSN 1589 1623 (Print) ● ISSN1785 0037 (Online)
DOI: http://dx.doi.org/10.15666/aeer/1802_20732085

In the study, firstly the methods of noise pollution studies were investigated (Bayramoğlu et al., 2014; Özer, 2014, 2015), and sensitive points in terms of noise were determined by looking at the map of the park. When determining the points, parking entrance and exit points, parking lot, proximity to motor traffic, tennis courts and football fields were taken into consideration. These points are shown on the map (*Figure 1*) by giving measurement numbers, the coordinates of the measurement points are given in *Table 2*.

Figure 1. *Display of measurement points on the map (Anonymous, 2018a)*

Table 2. *The coordinates of measurement points (Anonymous, 2018b)*

Measurement points	Measurement coordinates	
	x	y
1	670544.22	4452165.38
2	670212.43	4452358.63
3	670012.58	4452166.61
4	670026.68	4451687.42
5	670499.32	4451918.18
6	670403.56	4452005.65

The noise measurements were made at determined points on Monday and Thursday on weekdays and Saturday or Sunday, at the weekend, in the morning, lunch and evening times, in October, November, December in 2016 and July, August, September

http://www.aloki.hu ● ISSN 1589 1623 (Print) ● ISSN1785 0037 (Online)
DOI: http://dx.doi.org/10.15666/aeer/1802_20732085

in 2017. The measurements were carried out in three minute periods on sunny days when the weather was rainless and windless. The measurement hours are 08:00-09:00 a.m., 12:00-1:00 p.m. and 5:00-6:00 p.m. according to the overtime start-end hours, and people may prefer to go to the park.

The noise measurements were taken from a height of 1.2 meters to a location at a 45-degree angle, close to the traffic roads that limit the parking areas and from the middle of the parking area (Göksu and Karabulut, 2014). It was taken to measure at least 1.5 m away from the noise reflective surfaces, such as trees, walls, and buildings in order not to cause the noise to be reflected and cause the actual noise to taken incorrectly. All subsequent measurements were taken from the same points and positions, the first measurement conditions (same point, same height, same direction, same time, etc.) were not changed (Morgül and Dal, 2012). Average air temperature, humidity and wind speed at the time of measurement are recorded.

The sound meter (EXTECH 407738, Massachusetts, USA) was used to determine the noise level in this study. The measurements are in the maximum equivalent noise level (Leqmax) and are in the A-weighted volume (dBA) unit. In this context, the 90 values from the single point of the park, a total of 540 values from 6 points were determined and Leq, which is the equivalent noise level, is translated according to *formula 1*.

$$Leq = 10\ Log 1/10 \sum_{i=1}^{n} 10^{Li/10} \quad \text{(Eq.1)}$$

where,

- Leq : Equivalent noise level (dBA).
- n : Number of noise measurements.
- Li : Noise level in measurement.

Thus, for a total of 27 hours in the park, 30 days measurements were made. These values were subjected to oneway variance analysis in a general linear model by using JMP 7 (SAS Inst. Inc., NC, USA) software, and their importance status was examined. Means were compared with LSD test by using MStatC software. The reasons for the values were evaluated and discussed according to the RAMEN.

Results and Discussions

This study was carried out on the determination of noise pollution in the Hudavendigar Urban Park located in Nilufer district of Bursa, Turkey. The noise measurements of the park were carried out in successive winter and summer periods. A comparison of minimum, maximum and average values for the summer and winter periods was performed at 6 points determined in the park and the number of measurements exceeding 65 dBA which is the limit in RAMEN were given in *Table 3*. The variance analysis results were given in *Table 4*. The differences between seasons, measurement points and measurement time were significant statistically during the study period ($P<0.01$). But the variation within measurement days was not significant ($P>0.05$). Noise levels in the park evaluated according to the noise-sensitive areas in the RAMEN Appendix VII, and 245 of the total 540 measurements were found to exceed the limit value of 65 dBA during the day. The regional, seasonal and temporal changes of noise measurements in Hudavendigar Urban Park and the possible sources of noise levels are discussed in detail in the following sections.

http://www.aloki.hu ● ISSN 1589 1623 (Print) ● ISSN1785 0037 (Online)
DOI: http://dx.doi.org/10.15666/aeer/1802_20732085

The average noise level of the Hudavendigar Urban Park was determined as 64.63 dBA. The average noise levels in other studies are 66.62 dBA in Yüzüncüyıl Park in Erzurum (Özer, 2017), 67.69 dBA in Aziziye Park (Özer, 2014), 60.07 dBA in Yakutiye Park (Özer, 2015), 63.74 dBA in Meydan Park in Trabzon and 64.67 dBA in Fatih Park (Bayramoğlu et al., 2014). These results show that the average noise levels in urban parks are close to each other.

Table 3. *Comparison of descriptive statistics and limit values for summer and winter measurements of determined points*

Point	Winter measurements				Summer measurements			
	Min (dBA)	Max (dBA)	Average (dBA)	Number of measurements exceeding 65 dBA	Min (dBA)	Max (dBA)	Average (dBA)	Number of measurements exceeding 65 dBA
1	60.8	90.8	71.7	43	65.7	86.6	74.3	45
2	58.8	84.3	67.6	30	51.9	78.6	61.0	11
3	49.9	74.5	59.0	6	51.0	87.8	64.9	22
4	47.0	62.8	54.7	0	52.4	74.4	61.2	14
5	49.9	83.7	68.0	31	50.0	85.0	74.0	43
6	46.7	69.4	58.2	4	49.0	77.8	61.0	12

Table 4. *Variance analysis table for all parameters*

Source	DF	Sum of Squares	Mean Square	F Ratio	Prob > F
Season	1	1008.6	1008.6	13.0672	<0.0003*
Points	5	17112.015	3422.4	71.88	<0.0001*
Time	2	1598.561	799.28	10.485	<0.0001*
Day	14	598.93	42.787	0.5356	0.9124

*P<0.05 level is significant

Regional Variations of Noise Measurements

The 1st point is the most used area of Hudavendigar Urban Park's entrance-exit gates. At the same time, it looks at Dikkaldırım Street, where there is heavy traffic. The measured values were higher than the park average for winter and summer measurements because the park is an entrance-exit zone, and due to high number of people-related mobility and the proximity to the street. The measured values at this point of the park have generally increased as a result of vehicles. Traffic lights around the measuring points increased the car stop-start, while the noise of the horns increased in parallel with the traffic during the pedestrian crossing and the work hours. The road traffic noise in Bursa had become a significant problem in a study conducted by Karadayı (2001). This result supports the conclusion that the traffic noise around Hudavendigar Urban Park also increases the noise level in the park. As a result of the 1st point measurements, the maximum value was 90.8 dBA, and 88 out of 90 measurements exceeded 65 dBA.

The selected point 2 is on the walking path of Hudavendigar Urban Park, located in the vicinity of the bridge where Nilufer River is lowered from a certain height and is close to the intersection of Dikkaldırım Street, where the traffic of motor vehicles is much. While noise levels increased overall at all points during the summer period, there were decreases in the noise levels at the 2nd point, and the measurement results which exceeded the RAMEN limit value of 65 dBA. Because the water level of the river is low

http://www.aloki.hu ● ISSN 1589 1623 (Print) ● ISSN1785 0037 (Online)
DOI: http://dx.doi.org/10.15666/aeer/1802_20732085

in this area and the intersection works during the winter months increased the noise in this period. The maximum noise level of the 2nd point was 84.3 dBA, and 41 of 90 measurements exceeded 65 dBA, which is the limit value of RAMEN.

The 3rd point located in the western part of the Hudavendigar Urban Park, where the football fields and the children's playground are densely populated. With the increase in the use of football fields and children's playground at this point in the summer, especially at noon and evening times, the noise levels increased more than 10 dBA on average according to winter. As a result of the measurements at point 3, the maximum value was 87.8 dBA, and 28 out of the 90 measurements exceeded 65 dBA, which is the limit value of RAMEN.

Nilufer River flows around the 4th point of the park, and there are picnic areas, benches, tennis courts and one watchtower. Because the tennis games took place in the closed area in winter, there were no sound levels to create unrest. However, in the summer period, the level of noise increased when the tennis was played on open courts. Especially in the winter period, the value above 65 dBA which is the RAMEN limit value is not read, in summer period the value above 65 dBA is recited 14 times. While the maximum noise level was 87.8 dBA, it was that 14 out of the 90 measurements in total exceeded 65 dBA.

There are children's amusement parks, basketball courts and kiosks around the 5th point, which is overlooking the entrance and exit doors of the park and Bent Street. The measured values are very close to or exceeded the limit value because this point is a park entrance and exit zone, and due to the high number of people-related mobility, closeness to the street and the presence of children's amusement parks, basketball fields and kiosks. The maximum noise level was 85.0 dBA, and 74 of the total 90 measurements made at this point were found to exceed 65 dBA, which is the limit value of RAMEN.

There is a large tea garden, restaurant and lake around the 6th point selected in the center of the park. Due to the preference of closed areas during winter, the results are generally below the limit values. However, with the warm weather, the preference of the tea garden and the open spaces of the restaurant, the opening of loud music in the tea gardens and the choice of kayak trips on the lake increased, the noise levels increased towards the evening hours. As a result of the measurements at point 6, the maximum value was 77.8 dBA, and 16 out of 90 measurements exceed the limit value of 65 dBA in the RAMEN.

When the results of the noise measurement values at 6 points in the park were examined, the differences between these values was statistically significant (*Table 5*). According to these results, the highest noise level was at the 1st point during the study. The 1st point of the noise measurements in Hudavendigar Urban Park is the most used area of the entrance-exit gates and at the same time looking at the Dikkaldırım Street where the traffic is heavy, explains why the highest noise values were obtained at this point.

Table 5. *Variation of noise levels among measurement points*

Points	Min (dBA)	Average** (dBA)	Median (dBA)	Max (dBA)	Standard deviation	Standard error	$LSD_{0.05}$ Value
1	60.80	73.00[a]	72.30	90.80	5.24	0.55	
2	51.90	64.26[b]	63.75	84.30	6.94	0.73	2.94
3	49.90	61.96[bc]	60.30	87.80	8.81	0.93	

http://www.aloki.hu ● ISSN 1589 1623 (Print) ● ISSN1785 0037 (Online)
DOI: http://dx.doi.org/10.15666/aeer/1802_20732085

4	47.00	57.97[d]	56.65	74.40	6.04	0.63	
5	49.90	71.05[a]	72.75	85.00	7.25	0.76	
6	46.70	59.41[cd]	58.85	77.80	6.58	0.69	

[**]P<0.0001 level is significant, [a-d] Means in a column with different superscripts significantly differ.

Seasonal Variations of Noise Measurements

There were differences in noise measurements of Hudavendigar Urban Park, in the summer and winter periods. The noise sources inside and outside the park for summer and winter periods caused the differences. The maximum noise levels for the summer and winter measurements of 6 points determined in Hudavendigar Urban Park are shown in *Figure 2*.

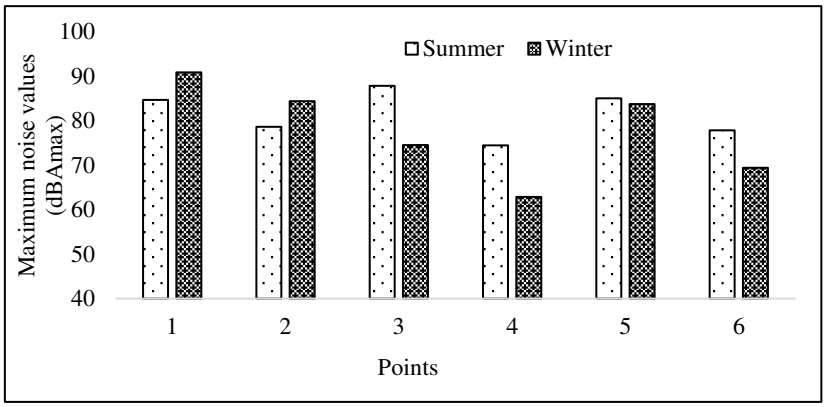

Figure 2. *Maximum noise levels according to the points in summer and winter measurements*

In the winter measurements of the Hudavendigar Urban Park, traffic-related noise has come to the fore. Since sports and recreation activities are carried out in closed areas, noise caused by these activities has remained passive according to non-park noise sources. 110 out of 270 measurements carried out during the winter period exceeded 65 dBA which is the limit value of RAMEN.

With the increase in the use of sports and recreation activities in summer, the noise levels caused by these activities increased significantly compared to winter. Traffic-induced noise levels are close to winter measurements. 135 out of 270 measurements carried out during the summer period were over 65 dBA, the limit of RAMEN. According to the statistical evaluation of winter and summer measurements, the difference between the measurement values of the two seasons was significant (*Table 6*).

Table 6. *Variation of noise levels among seasons*

Season	Min (dBA)	Average** (dBA)	Median (dBA)	Max (dBA)	Standard deviation	Standard error	$LSD_{0.05}$ Value
Winter	46.70	63.24[b]	62.90	90.80	8.43	0.51	4.22
Summer	49.00	65.98[a]	66.60	87.80	9.12	0.56	

[**]P<0.0001 level is significant, [a-b] Means in a column with different superscripts significantly differ.

http://www.aloki.hu ● ISSN 1589 1623 (Print) ● ISSN1785 0037 (Online)
DOI: http://dx.doi.org/10.15666/aeer/1802_20732085

In a study on the determination of noise pollution caused by traffic and recreational use in Çorlu city, noise levels were higher in winter than in other periods. It is thought that the population density in the region and accordingly the number of vehicles are not to decrease by winter holidays etc. (Ünver, 2008). In the Hudavendigar Urban Park, while the noise levels were higher in the regions close to the transportation roads during the winter months, it was observed that there were lower levels in park areas in winter when compared to the summer season. In a study conducted in Düzce city, the noise values of the park areas in summer were higher than in winter (Yerli and Demir, 2015). The results show that the parking areas are used more intensively in summer than in winter, and similar results also considered for Hudavendigar Urban Park.

Temporal Changes of Noise Measurements

In summer and winter measurements, there are more traffic and vehicle-related noise increases in the morning times during the week, and there is an increase in noise levels due to the active use of sports and recreation areas in the lunch and evening times during the weekend.

Noise levels according to morning, noon and evening hours

The maximum noise levels of 6 points determined in Hudavendigar Urban Park in the morning, noon, and evening times during the winter and summer periods are shown in *Figure 3*.

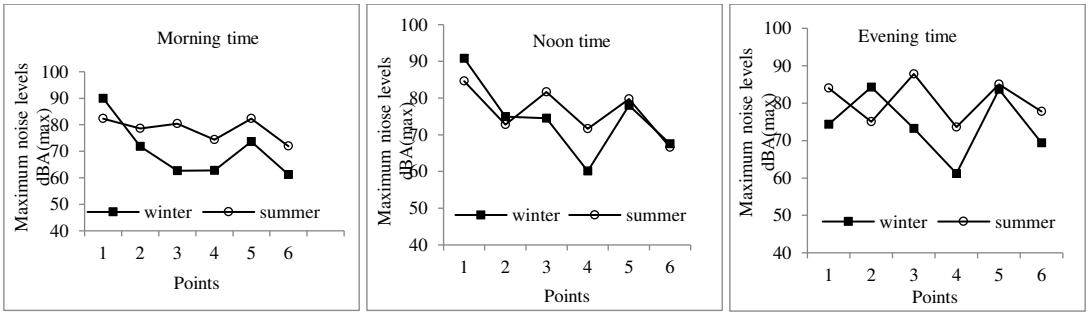

Figure 3. *Maximum noise levels of winter and summer periods according to morning, noon and evening hours*

In the morning measurements, the maximum value was at the 1st point with 90 dBA. Since the morning measurement time interval is the time for people going to work by their vehicles, significant traffic density has been observed mainly on the streets near the 1st and 5th points and high noise levels have been read at these points.

The maximum value was 90.8 dBA and 84.6 dBA at the 1st point in the winter and summer periods, respectively. There were substantial differences in noise levels between the 3rd and 4th points at noontime because children's playgrounds at these points and activities such as football and tennis are preferable at noon during the summer.

The maximum value of the park points in the evening hours was 87.8 dBA at the 3rd point in the summer period. In the summer period, noise levels increased due to the active use of sports and recreation areas. The differences between the measurement

http://www.aloki.hu ● ISSN 1589 1623 (Print) ● ISSN1785 0037 (Online)
DOI: http://dx.doi.org/10.15666/aeer/1802_20732085

times of noise values were significant according to statistical analysis (P <0.0001) (*Table 7*).

The highest noise value was measured as 68.75 dBA in the evening at the Yüzüncü Yıl Park in Erzurum (Özer, 2017), in another study conducted in Aziziye Park (Özer, 2014), the highest noise value in the evening time was read as 69 dBA, the highest noise value in Yakutiye Park (Özer, 2015) was determined as 64.29 dBA in the evening. In Hudavendigar Urban Park, the highest noise value was 77.4 dBA in the evening time. In a study conducted in the Düzce city of Turkey, the parking areas were used more intensively and until late hours in the summer than in winter. The noise levels in day and evening in summer are higher than in winter months (Yerli and Demir, 2015). A similar situation exists for Hudavendigar Urban Park.

Table 7. *Variation of noise levels among measured times*

Hours	Min (dBA)	Average** (dBA)	Median (dBA)	Max (dBA)	Standard deviation	Standard error	$LSD_{0.05}$ Value
Morning	46.70	62.41[b]	60.55	90.00	9.22	0.69	
Noon	49.00	64.81[a]	65.00	90.80	8.94	0.67	2.00
Evening	50.20	66.61[a]	66.90	87.80	7.99	0.59	

**P<0.0001 level is significant, [a-b] Means in a column with different superscripts significantly differ.

Noise levels of weekday and weekend

The change in the levels of weekday and weekend noise measurements of 6 points in the Hudavendigar Urban Park in the winter and summer periods are shown in *Figure 4*.

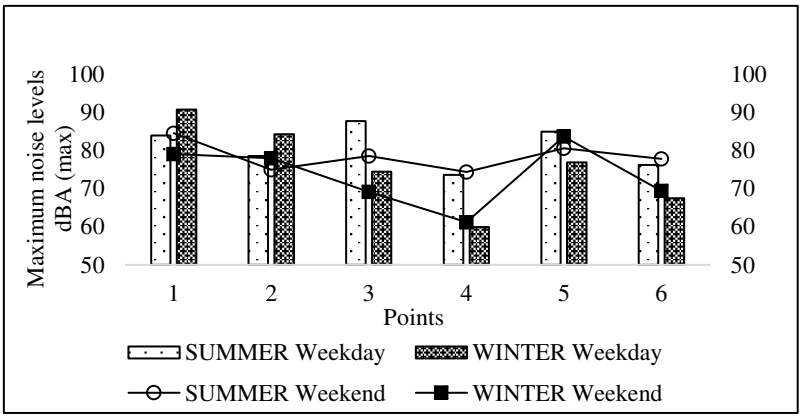

Figure 4. *Maximum noise values during weekdays and weekends in winter and summer periods*

As seen in *Figure 4*, there is a general increase in noise levels according to the winter period measurements in the weekday values of the summer period. There are increases in the summer period noise levels due to more summer activities in the park. Due to the intersection work carried out in the north of the park during the weekdays in the winter period, both the equipment used and the traffic generated caused an increase in noise levels at points 1 and 2.

http://www.aloki.hu ● ISSN 1589 1623 (Print) ● ISSN1785 0037 (Online)
DOI: http://dx.doi.org/10.15666/aeer/1802_20732085

There is an increase in summer measurements at weekends. It is thought to be because in-park activities are carried out in open areas and people prefer to use the park in hot weather.

Conclusions

In this study, measurements were made to determine the noise level in the Hudavendigar Urban Park, located in the Nilufer district of Bursa, which is an important recreation area for the urban population. These measurements were carried out for a total of 30 days during the summer and winter periods, including morning, lunch and evening hours. Observations and statistical data interpreted the measurement results. It was determined that the sensitive points exceed the limit values specified in the RAMEN and approach the limit values, and the points with noise differences have been associated with the purposes of the park. The findings of the measurements are summarized below:

- The traffic noise was prominent in the winter period measurements of the Hudavendigar Urban Park. Since sports and recreation activities are carried out in closed areas, noise caused by these activities is passive according to non-park noise sources. The 110 of 270 measurements exceeded 65 dBA, which is the limit value of RAMEN. In winter measurements, the highest value was 90.8 $dBA_{(max)}$ at the 1st point in November.
- With the increase in the use of sport and recreation activities in the park in summer, the noise levels caused by these activities have increased significantly compared to winter measurements. Traffic-induced noise levels are close to winter measurements, and 135 out of 270 measurements exceeded 65 dBA. In summer measurements, the highest value was 84.6 $dBA_{(max)}$ at the 1st point in noontime in July.
- In summer and winter measurements, traffic and vehicle noise increased throughout the park in the morning, and noise levels increased due to active use of sports and recreation areas especially at noon and evening hours during the summer. In the morning and noon measurements, the highest values were read in the summer and winter periods at the 1st point, while the highest winter values in the evening measurements were at the 5th point and the highest summer value at the 1st point. The highest values of the morning hours are 82.3 dBA (max) in summer and 90 dBA (max) in winter, the highest values of noon are 84.6 dBA (max) in summer and 90.8 dBA (max) in winter, the highest values of the evening hours were 85 dBA (max) in summer and 84.3 dBA (max) in winter.
- The noise levels during the weekdays in the summer period showed a general increase compared to the winter period. This increase is due to the more use of activities in the park in summer. In winter measurements, the high values in points 1 and 2 are affected by the intersection study in the north of the park and the traffic. The highest noise measurement value on weekdays was read at 90.8 $dBA_{(max)}$ at noon in November at the 1st point in winter.
- On the other hand, there is an increase in the summer measurements. Because in-park activities are carried out in open areas, and people prefer the park more in hot weather. The highest value of the weekend was read as 84.6 $dBA_{(max)}$ at noon in July at the 1st point in summer.

As a result of this study, which was carried out to determine noise pollution in urban parks in Bursa, the differences in noise measurements in summer and winter periods in

http://www.aloki.hu ● ISSN 1589 1623 (Print) ● ISSN1785 0037 (Online)
DOI: http://dx.doi.org/10.15666/aeer/1802_20732085

Hudavendigar Urban Park were observed. It was interpreted as a result of the measurements that the vehicle traffic around the park increased the noise level in the winter period, and the intensive use of the activities in the park increased the noise level, especially in the summer. It was concluded that it would be beneficial to take various measures by focusing on the noise-enhancing factors in the park to prevent people coming to the urban park to relax from these levels and not to exceed the RAMEN limit value.

Acknowledgements. The authors would like to thank Assoc. Prof. Ilker Kilic for his statistical evaluation of the manuscript.

REFERENCES

[1] Aktürk, N., Akdemir, O., Üzkurt, İ. (2003a): Environmental noise caused by traffic lights timing and traffic volume (Trafik ışık sürelerinin neden olduğu çevresel taşıt gürültüsü). – Journal of the Faculty Engineering and Architecture of Gazi University 18(1): 71-87.

[2] Aktürk, N., Toprak, R., Asiloğulları, E. (2003b): Environmental noise caused by rapid rail transit systems (Hızlı raylı ulaşım sistem kaynaklı çevresel gürültü). – Journal of the Faculty Engineering and Architecture of Gazi University 18(3): 15-25.

[3] Anonymous (2004): https://webdosya.csb.gov.tr/db/ced/icerikler/turk-yecevreatlas--20180514084340.pdf. Date of access October 16, 2018.

[4] Anonymous (2010): https://www.mevzuat.gov.tr/Metin.Aspx?MevzuatKod=7.5.14012&MevzuatIliski=0&sourceXmlSearch=%C3%A7evresel. Date of access October 16, 2018.

[5] Anonymous (2011): https://webdosya.csb.gov.tr/db/cygm/icerikler/cevresel-gurultu-olcum-ve-degerlend-rme-klavuzu-20180209145104.pdf. Date of access October 16, 2018.

[6] Anonymous (2012): http://megep.meb.gov.tr/mte_program_modul/moduller_pdf/G%C3%BCr%C3%BClt%C3%BCn%C3%BCn%20Etkileri.pdf. Date of access October 16, 2018.

[7] Anonymous (2018a): https://www.google.com/maps/@40.2007089,29.0015165,874m/data=!3m1!1e3?hl=tr-TR. Date of access April 2, 2018.

[8] Anonymous (2018b): https://www.google.com/earth/versions/#earth-pro. Date of access December 28, 2018.

[9] Aslan, Ş., Yıldız, S. (2017): Noise assessment of water and wastewater treatment plants (Atıksu ve içme suyu arıtma tesisinde gürültü kirliliği değerlendirmesi). – Cumhuriyet Science Journal 38-4: 798-812.

[10] Aydın, M. E., Ateş, N. (1997): Traffic noise in Konya and some proposals (Konya'da trafik gürültüsü ve bazı öneriler). – Pamukkale University Journal of Engineering Sciences 3(3): 447-456.

[11] Balcı, A. N. (1994): Bir çevre kirlenmesi sorunu olarak gürültü (in Turkish). – İstanbul Üniversitesi Orman Fakültesi Dergisi 44(3-4): 15-34.

[12] Bayramoğlu, E., Özdemir Işık, B., Demirel, Ö. (2014): The effect of noise pollution on city parks and proposed solutions: case of Urban Trabzon (Gürültü kirliliğinin kent parklarına etkisi ve çözüm önerileri: trabzon kenti örneği). – Inonu University Journal of Art and Design 4(9): 35-42.

[13] Belek, C. (2017): A research and a case study on the effect of environmental noise on accommodation facilities (Çevresel gürültünün konaklama tesislerine olan etkisi üzerine bir araştırma ve bir örneklem). – MSc. Thesis, Graduate School of Natural and Applied Sciences, Gazi University, Ankara.

http://www.aloki.hu ● ISSN 1589 1623 (Print) ● ISSN1785 0037 (Online)
DOI: http://dx.doi.org/10.15666/aeer/1802_20732085

[14] Çetin, F. (2010): Traffic noise pollution map of Denizli province (Denizli ili trafik gürültü kirliliği haritası). – MSc. Thesis, Health Sciences Institute, Celal Bayar University, Manisa.
[15] Delikanlı, N. E., Yücedağ, C., Kapdı, A. (2014): A preliminary study on noise pollution from vehicle traffic in Bartın City (Bartın kentinde araç trafiğinden kaynaklı gürültü kirliliği üzerine bir ön çalışma). – Journal of Engineering and Technological Sciences 2: 21-40.
[16] Donoghue, A. M. (2004): Occupational health hazards in mining: an overview. – Occupational Medicine 54: 283-289.
[17] Göksu, G., Karabulut, M. (2014): Kahramanmaraş şehir merkezinde gürültü kirliliğinin değerlendirilmesi (in Turkish). – Coğrafyacılar Derneği Uluslararası Kongresi, Muğla, 859-866.
[18] Ilgar, R. (2012): A preliminary study noise pollution source for urban vehicle traffic in Çanakkale. – Zeitschrift für die Welt der Türken 4(1): 253-267.
[19] Kablan, A. (2012): Noise pollution at railways and disposal methods, evaluation of the related legislation (Demiryollarında gürültü kirliliği ve bertaraf yöntemleri, ilgili mevzuatın değerlendirilmesi). – MSc. Thesis, Graduate School of Natural and Applied Sciences, Bahçeşehir University, İstanbul.
[20] Kalıpçı, E. (2017): Spatial analysis of traffic related noise pollution in the center of Avanos District (Avanos ilçe merkezinde trafik kaynaklı gürültü kirliliğinin mekansal analizi). – Nevşehir Journal of Science and Technology 6(1): 20-29.
[21] Karadayı, S. (2001): Preparation of Bursa's noise map resulted by traffic (Bursa İli'nin trafik kaynaklı gürültü haritasının hazırlanması). – MSc. Thesis, Graduate School of Natural and Applied Sciences, Sakarya University, Sakarya.
[22] Kurra, S. (2009): Çevre Gürültüsü ve Yönetimi I-II-III (in Turkish). – İstanbul Bahçeşehir Üniversitesi Yayınları, İstanbul.
[23] Morgül, Ö. K., Dal, H. (2012): A preliminary study on noise pollution of sakarya province city centre (Sakarya ili şehir merkezinin gürültü kirliliği üzerine bir ön çalışma). – Sakarya University Journal of Science 16(2): 83-91.
[24] Neitzel, R., Gershon, R. M., Zeltser, M., Canton, A., Akram, M. (2009): Noise levels associated with New York City's mass transit systems. – American Journal of Public Health 99(8): 1393-1399.
[25] Oruç, K. Ş. (2017): Environmental Noise Pollution Caused by Speed Train (Hızlı trenin neden olduğu çevresel gürültü kirliliği). – MSc. Thesis, Gazi University, Graduate School of Natural and Applied Sciences, Ankara.
[26] Özbıçakçı, Ş., Çapık, C., Aydoğdu Gördes, N., Ersin, F., Kıssal, A. (2012): Assesment of noise level and hearing conservation in a school community (Bir Okul Toplumunda Gürültü Düzeyi Tanılaması ve Duyarlılık Eğitimi). – Education and Science 37(165): 238-245.
[27] Özer, S. (2014): Determination of noise pollution in urban parks of Erzurum: in the case of Aziziye Park (Erzurum kent parklarındaki gürültü kirliğinin belirlenmesi: aziziye parkı örneğinde). – Journal of Adnan Menderes University Agricultural Faculty 11(2): 7-11.
[28] Özer, S. (2015): Noise level in the parks in the city centres; the sample of Yakutiye Park (Kent Merkezlerindeki Parklarda Gürültü Düzeyi: Yakutiye Parkı Örneğinde). – Journal of the Institute Science and Technology 5(3): 43-48.
[29] Özer, S. (2017): Present situation analysis of noise pollution in city parks of Erzurum in the sample of Yüzüncüyıl Park (Erzurum Kenti Yüzüncüyıl Parkı Örneğinde Kent Parklarındaki Gürültü Kirliğinin Mevcut Durum Analizi). – Alınteri Journal of Agricultural Sciences 32(1): 39-44.
[30] Rosenberg, J. (1991): Jets over Labrador and Quebec: noise effects on human health. – Canadian Medical Association Journal 144(7): 869-875.

http://www.aloki.hu ● ISSN 1589 1623 (Print) ● ISSN1785 0037 (Online)
DOI: http://dx.doi.org/10.15666/aeer/1802_20732085

[31] Sakarya, E. (2016): Effects of noise on working life and noise analysis in a construction site (Gürültünün çalışma hayatına etkileri ve bir inşaat şantiyesinde gürültü analiz çalışması). – MSc. Thesis, Health Sciences Institute, Üsküdar University, İstanbul.
[32] Sharma, A., Bodhe, G. L., Schimak, G. (2014): Development of a traffic noise prediction model for an urban environment. – Noise and Health 16(68): 63-67.
[33] Singh, N., Davar, S. C. (2004): Noise Pollution-Sources, Effects and Control. – Journal of Human Ecology 16(3): 181-187.
[34] Szeremeta, B., Zannin, P. H. T. (2009): Analysis and evaluation of soundscapes in public parks through interviews and measurement of noise. – Science of the Total Environment 407: 6143-6149.
[35] Şahin, E. (2003): Noise control techniques-a case study (Gürültü kontrol yöntemleri-bir uygulama). – Journal of the Faculty of Engineering and Architecture of Gazi University 18(4): 67-80.
[36] Şerefhanoğlu, M. (1991): Gürültü ile Savaşımda Temel İlkeler ve İnsan Etkeni (in Turkish). – Noise Symposium, Konya, 1-6.
[37] Tür, M. B. (2016): The effect of noise on blood pressure and sleep in health workers (Sağlık çalışanlarında gürültünün kan basıncı ve uyku üzerine etkisi). – MSc. Thesis, Health Sciences Institute, Dokuz Eylül University, İzmir.
[38] Ünver, E. (2008): Determination of noise pollution due to traffic and recreation: a case study of Çorlu (Trafik ve rekreasyonel kullanım kaynaklı gürültü kirliliğinin belirlenmesi: çorlu örneği). – MSc. Thesis, Graduate School of Natural and Applied Sciences, Namık Kemal University, Tekirdağ.
[39] Yerli, Ö., Demir, Z. (2015): An investigation of the noise differences in the settlement areas of Düzce (Düzce kenti yerleşim bölgelerindeki gürültü farklarının incelenmesi). – Erciyes University Journal of the Institute of Science and Technology 31(1): 32-42.
[40] Zannin, P. H. T., Ferreira, A. M. C., Szeremetta, B. (2006): Evaluation of Noise Pollution in Urban Parks. – Environmental Monitoring and Assessment 118: 423-433.

http://www.aloki.hu ● ISSN 1589 1623 (Print) ● ISSN1785 0037 (Online)
DOI: http://dx.doi.org/10.15666/aeer/1802_20732085

CONNECTIONIST MODELLING FOR ANTHROPOGENIC GREENHOUSE GASES (GHG) EMISSIONS IN URBAN ENVIRONMENTS

AL-HARBI, M.[1*] – BIN SHAMS, M.[2] – ALHAJRI, I.[3]

[1]*Department of Environmental Technology Management, College of Life Sciences, Kuwait University, P.O. Box 5969, Safat 13060, Kuwait*

[2]*Department of Chemical Engineering, University of Bahrain, P.O. Box 32038, Isa Town, Kingdom of Bahrain*

[3]*Department of Chemical Engineering, College of Technological Studies, P.O. Box 42325, Shuwaikh 70654, Kuwait*

[*]*Corresponding author*
e-mail: dr.meshari@ku.edu.kw

(Received 11th May 2019; accepted 4th Dec 2019)

Abstract. Global warming induced by greenhouse gases (GHGs) is already a reality and will continue to increase resulting in a severe climate change. The aim of the paper is twofold. First, to investigate the GHGs emissions between the year of 2004 and 2016 in four major urban cities, representing the residential band of Kuwait. Results showed a clear steady yearly increase in GHGs emissions, with more emissions in summer compared to winter, possibly due to the high consumption rate of fossil fuel for cooling purposes and traffic activities. Results also revealed a diurnal variation in GHGs emissions, plausibly attributed to the combined effects of busy traffic hours as well as respiration by the living organisms and/or from soils. A second objective in this paper is, to develop a reliable connectionist models such as neural networks for predicting GHGs emissions. Radial basis function (RBF) network due to its known approximation capabilities, localization of its transfer functions and its efficient training algorithms, showed a superior performance in predicting GHGs emissions. Parity and time series plots of the predicted concentrations against the observed concentrations demonstrated the appropriateness of connectionist modelling as a fast and precise tool for monitoring and forecasting the GHGs emissions.
Keywords: *GHGs trend, CO_2 and CH_4 emissions, artificial neural network, radial basis function, model performance*

Introduction

The threat of global warming induced by human-driven emissions of carbon dioxide (CO_2), methane (CH_4), and other greenhouse gases, as well as land-use changes, has become a reality acknowledged by billions of people. Although it is established that 57% of man-made CO_2 emissions can be removed by the biosphere and oceans (Walsh et al., 2017), the level of atmospheric CO_2 has increased progressively through the years as a result of human activities, including deforestation, combustion of fossil fuels, and power generation (Balch et al., 2016; Sterman et al., 2018). Methane atmospheric concentrations have increased by almost 150% since pre-industrial times, which corresponds to a radiative force of $0.48 Wm^{-2}$ (Jędrysek et al., 2015). Based on current trends, extreme events such as temperature extremes, heat waves, and heavy rains are likely to increase in both frequency and intensity. This will eventually induce a rise in Earth's temperature, including its seas.

http://www.aloki.hu ● ISSN 1589 1623 (Print) ● ISSN1785 0037 (Online)
DOI: http://dx.doi.org/10.15666/aeer/1802_20872107

Continuous monitoring of global warming-induced emissions has become an urgent step in mitigating and managing such emissions. Several attempts have been made to monitor the changes of atmospheric CO_2 and CH_4 in different regions around the world. As for 2016 (WDCGG, 2018), CO_2 records were reported as follows: Italy (427.6 ppm), Poland (427.7 ppm), Korea (416.3 ppm), Hungary (410 ppm), and Hong Kong (408 ppm). In India (region of Ahmedabad), CO_2 concentrations varied between 382 and 609 ppm with the annual average of 413 ± 13 ppm during the period of November 2013 to May 2015 (Chandra et al., 2016). In Pakistan, a significant increase in CO_2 concentration was noted from January 2010 (390 ppm) to December 2015 (400 ppm), leading to an increase of 1.75 ppm/year (Mahmood et al., 2016). Similar observations were also reported in South Korea (Shim et al., 2018). CH_4 trend was also investigated in different cities over the world and results revealed a steady increase with a range of 1.95 to 2.10 ppm as of the year of 2016 (WDCGG, 2018). Tracking the trend of GHGs at least during the past three decades, it reveals an increase in the level of greenhouse gases (GHGs) worldwide.

Thus, it is imperative to develop novel and better techniques to estimate concentrations of global warming-induced gases like CO_2 and CH_4. Several approaches have been suggested to model and forecast atmospheric gases. These include for example the atmospheric dispersion model (Loh et al., 2008), statistical regression models that determine the underlying relationship between a set of input data (predictors) and targets (predictands) (Mason and Baddour, 2008), and artificial neural network- based models (ANN) to predict future pollutant concentrations (Ozcan et al., 2006; Kunt et al., 2016; Zhang and Ding, 2017). Notably, ANN has shown promising results and gained more attention in recent years due to its superiority in modelling nonlinear correlations between input and output variables (Amoura et al., 2011; Nezhad et al., 2011; Zhang et al., 2016; Parvizi et al., 2018). ANN has numerous advantages over traditional phenomenological or semi–empirical models. One is its rapid information processing and ability to develop the mapping of input and output variables (Guclu and Dursun, 2010). Other features include the ANN's higher accuracy in predictions over other types of models (Noor et al., 2018) and its ability to handle huge and complex systems within many interrelated parameters (Tahboub et al., 2016).

Due the powerful, accurate, and fast prediction algorithm, ANN models have been used to forecast different pollutant concentrations (Wu et al., 2011) on numerous time scales with acceptable results. Hassan and Dong (2018) predicted the tropospheric ozone (O_3) concentrations using ANN as a function of meteorological conditions and several air quality parameters. Sahin et al. (2004) used the multi-layer perception neural network (MLP-NN) model to predict the daily level of carbon monoxide (CO) in Turkey (Istanbul) using meteorological parameters as predicators. Pawul and Sliwka (2016) applied ANN to predict the concentrations of benzene, CO, and nitrogen oxides (NOx). Elminir and Abdel-Galil (2006) modeled particulate matter (PM_{10}), CO, and nitrogen dioxide (NO_2) based on different climatological variables in Egypt. Rahimi (2017) applied MLP-NN to predict NO_2 in Tabriz, Iran. Several other researchers have used NN techniques to forecast pollutant concentrations (Kurt and Oktay, 2010; Elangasinghe et al., 2014; Russo et al., 2015; Zhao et al., 2018) and the consensus is that an NN can be a useful tool for predicting atmospheric pollutants.

The aim of the present study is twofold. Firstly, to provide a descriptive picture of the current and the trend of GHG's emission in four representative urban areas in Kuwait. Secondly and most importantly, to develop practical, robust, and effective neural networks that forecast the concentration of GHG, specifically, CO_2 and CH_4 emissions in

http://www.aloki.hu ● ISSN 1589 1623 (Print) ● ISSN1785 0037 (Online)
DOI: http://dx.doi.org/10.15666/aeer/1802_20872107

Kuwait. In order to accomplish this, the hourly, daily, seasonal, and yearly records of CO_2 and CH_4 emissions along with their meteorological conditions for the 13-year period were statistically investigated in four major urban cities, representing the residential band of Kuwait. Throughout the investigation, several combinations of artificial neural network (ANN) structures and types, including linear (L), multilayer perception (MLP), and radial basis function (RBF) networks, were tested and optimal models were selected. The neural networks were trained until the network training error achieved the specified acceptable error. The developed NN models in this study yielded feasible, reliable, and efficient prediction of CO_2 and CH_4 concentrations.

Methodology

Study areas

Kuwait is situated in western Asia, between latitudes 28°30'and 30°5' North and longitudes 46°33' and 48°30' East, with a total area of 17,818 km^2. It is bounded by Saudi Arabia in the south and southwest and with Iraq in north and northwest. The total population of Kuwait as of 2018 is about 4.56 million; of whom 1.38 million Kuwaitis and 3.18 million are expatriates. Kuwait's economy is heavily reliant on oil exports through its three refineries, namely Mina Al-Ahmadi (MAA), Mina Abdullah (MAB) and Mina Shuaiba (SHU). These three refineries with a total capacity of 936,000 bpd produce of a variety of refining products to fulfil the international client's needs. Fossil fuels combustion of and fugitive emissions release from oil and gas operations are most prevailing sources of GHG emissions in Kuwait. In this study, to gain overall picture about the trend of GHG in Kuwait, four representative urban areas spatially distributed along the residential band in Kuwait, were selected. These urban areas are Ali Sabah Al-Salem (far-south), Al-Riqqa (South-middle), Mansouriya (Middle), and Al-Jarha (far north), see *Figure 1*. Ali Sabah Al-Salem area is the last inhabited city in the south of Kuwait toward the borders with Saudi Arabia. It is next to highest capacity oil refineries (Mina Al-Ahamdi and Mina Abdullah) in the country. It is also adjacent to several small to large petrochemical industries. This city is surrounded from east by express highway (No.30) and by express highway (No.40) in west, which afterward merges together in one road (No.40) leading to Saudi Arabia borders. The residential area of Al-Riqqa is surrounded by numbers of residential areas in south, north, and west. In east, it is overlooking express highway (No.30) that extends from downtown of Kuwait to borders with Saudi Arabia. In south, it is also proximate to oil refineries (Mina Al-Ahamdi and Mina Abdullah). Al-Riqqa is adjacent to various small to middle scale commercial and industrial areas (e.g. car mechanics). Mansouriya residential area is located in the middle of Kuwait City with a total population of 8992. Mansouriya is typical residential area surrounded with a network of roads in north, south, and east. In west, it is facing express highways No. 40 which cross most of residential areas and connect the city center with south border of Kuwait. The city is few kilometers from numerous commercial buildings and famous traditional shopping centers. In North-West of Mansouriya, there are quite numbers of small-medium industrial business. Al-Jarha city is located in north-west of Kuwait City and it is one of the largest cities in Kuwait with total inhabitants of about 484,502 residents. It is surrounded by numerous emission sources such as Al-Jarha wastewater treatment, desalination and power plans, and different scales of industrial and commercial shops. Numbers of express highway pass through the city include 6^{th} ring

http://www.aloki.hu ● ISSN 1589 1623 (Print) ● ISSN1785 0037 (Online)
DOI: http://dx.doi.org/10.15666/aeer/1802_20872107

road, highway 80 that connects the city to Abdali on the Iraqi border and highway No.70 that links the city to Kuwait border with Saudi Arabia.

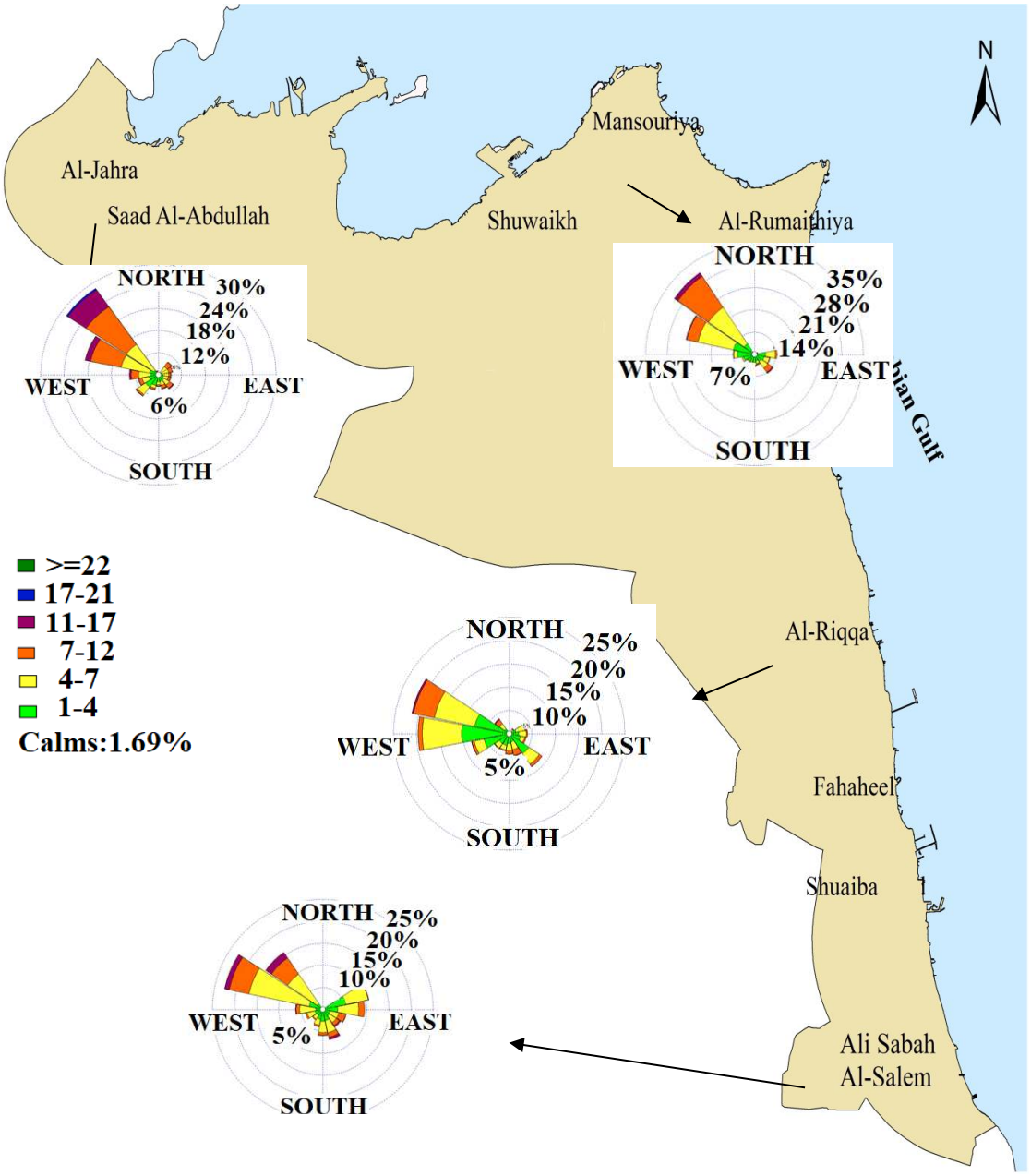

Figure 1. *Selected monitoring sites for quantifying and modeling of Greenhouse gases (GHGs) emissions*

Meteorological conditions

Kuwait is characterized by a desert-type environment and hot climate. Kuwait is experienced sharply by two distinct seasons; summer which last from May to October and winter which extends from November to April. Kuwait is typically arid with very hot summers, with average temperatures vary from 42 to 46°C. In winter, the weather is usually mild to relatively cold with temperatures from time to time even falling below

http://www.aloki.hu ● ISSN 1589 1623 (Print) ● ISSN1785 0037 (Online)
DOI: http://dx.doi.org/10.15666/aeer/1802_20872107

4°C. Dust storms and high concentration of particulate matter (PM) are prevailing characteristic of summer in Kuwait. Humidity is a unique feature of Kuwait climate, starts mid-August and last over September. Over at least the past two decades, relative humidity (RH) ranged from 47.5 and 49.5%, with mean yearly maxima varying from 84 to 95%. From one year to other, RH level could exceed 95%, which is ascribed to high seawater temperatures coincident with tropospheric temperature inversions.

Figure 1 shows wind rose plots for residential areas of Ali Sabah Al-Salem, Al-Riqqa, Mansouriya, and Al-Jarha, for the year of 2016. It is apparent that the prevailing wind directions were strongly northwest winds (~25-33% of time) and mild south to southeasterly winds (~23-28% of time). The average wind speeds (*Table 1*) varied from 2.5± 0.4 m/s to 3.8± 0.5 m/s in summer and between 1.6 ± 0.23 m/s and 2.9 ± 0.22 m/s in winter. In terms of seasonal variation, there is no marked variation in the wind direction throughout the year (*Table 1*).

Table 1. *Descriptive statistics of greenhouse gases (GHG) and climate conditions*

	Summer					Winter				
Ali Sabah Al-Salem	**Min.**	**Mean**	**SD**	**Max.**	**C.V**	**Min.**	**Mean**	**SD**	**Max.**	**C.V**
CO_2 (ppm)	388	428	17	435	0.04	382	412	9.6	420	0.02
CH_4 (ppm)	1.82	2.15	0.12	2.6	0.06	1.80	2.10	0.22	2.35	0.1
Temperature (ºC)	25.5	34.6	4.6	38.5	0.13	12.7	18	5	27.6	0.3
RH	26.6	29.4	2.1	32.7	0.07	26.3	42	14.6	61.4	0.4
Wind speed (m/s)	2.6	2.95	0.4	3.6	0.12	2.26	2.5	0.16	2.72	0.1
Wind direction (Deg.)	45	200.8	92	335	0.44	52	219	87	331	0.40
Al-Riqqa	**Min.**	**Mean**	**SD**	**Max.**	**C.V**	**Min.**	**Mean**	**SD**	**Max.**	**C.V**
CO_2 (ppm)	402	430	12	440	0.03	410	418	24.6	467	0.06
CH_4 (ppm)	1.83	2.25	0.2	2.70	0.1	1.79	2.11	0.21	2.50	0.01
Temperature (ºC)	27.3	37	5	41	0.13	14.8	19.5	5.2	30	0.3
RH	16	23	5.6	33	0.3	28.7	42.6	6.5	48.3	0.2
Wind speed (m/s)	2.03	2.5	0.4	3.14	0.14	1.32	1.65	0.23	1.97	0.1
Wind direction (Deg.)	42	223	76	322	0.34	42	218	70	316	0.32
Mansouriya	**Min.**	**Mean**	**SD**	**Max.**	**C.V**	**Min.**	**Mean**	**SD**	**Max.**	**C.V**
CO_2 (ppm)	394	429	16	429	0.04	385	417	27	431	0.06
CH_4 (ppm)	1.92	2.20	0.1	2.21	0.05	1.98	2.0	0.12	2.36	0.05
Temperature (ºC)	28.7	37.6	4.5	41.6	0.12	16.2	20.8	5.14	31	0.3
RH	29.7	35.1	4.2	42.5	0.12	43.7	56	7.8	67	0.1
Wind speed (m/s)	2.3	2.7	0.34	3.4	0.13	2.1	2.3	0.2	2.5	0.05
Wind direction (Deg.)	69	242	80	324	0.33	67	241	79	324	0.33
Al-Jarha	**Min.**	**Mean**	**SD**	**Max.**	**C.V**	**Min.**	**Mean**	**SD**	**Max.**	**C.V**
CO_2 (ppm)	387	398	3.5	410	0.01	380	390	7.2	399	0.02
CH_4 (ppm)	1.80	1.92	0.08	1.98	0.04	1.77	1.87	0.02	1.93	0.01
Temperature (ºC)	27	35.8	4.5	39.8	0.12	13.7	18.5	5.1	28.7	0.3
RH	7.85	12.61	4.7	21	0.4	20.3	32	7.06	42	0.22
Wind speed (m/s)	3.3	3.8	0.5	4.6	0.13	2.53	2.90	0.22	3.25	0.08
Wind direction (Deg.)	15	238	88	353	0.37	15	232	86	353	0.37

http://www.aloki.hu ● ISSN 1589 1623 (Print) ● ISSN1785 0037 (Online)
DOI: http://dx.doi.org/10.15666/aeer/1802_20872107

Data collection and analysis

The dataset for CO_2 and CH_4 were provided by Air Pollution Monitoring Division of the Kuwait Environment Public Authority (KUEPA). The monitoring stations were placed at Ali Sabah Al-Salem (28.957°N 48.154°E), Al-Riqqa (29.146°N 48.107°E), Mansouriya (29.358°N 47.993 °E), and Al-Jarha (29.3366°N 47.6755°E) and they are equipped with a state-of-art sampling devices and analyzers approved by US-EPA with accuracy of 98-99%. The CO_2 and CH_4 emission were measured using a CO_2/ CH_4/H_2O analyzer (Picarro G1301, US) whereas meteorological conditions such as relative humidity, wind speed, wind direction, and temperature were concurrently monitored using mobile monitoring station (Thermo Scientific, USA). Air probe was approximately between 10-15 m above sea level in all urban cities investigated. Measurements were taken at hourly intervals, which resulted in 8760 per year for each CO_2 and CH_4, with a total of 113,880 data points for each CO_2 and CH_4 for the entire period of 13 years (2004-2016). To study the diurnal cycle, the average concentration at each hour (0-23 hrs) was calculated in each urban area for the entire study period. As for seasonal variations, data were split into two prevailing seasons in Kuwait, summer and winter.

Statistical analysis

Descriptive statistical analyses were performed to demonstrate the overall picture of the CO_2 and CH_4 emissions and their corresponding meteorological conditions. Pearson's correlation (R) analysis and one-way analysis of variance (ANOVA) are used to determine whether there are any statistically significant differences between the means of data set with p value < 0.05. All statistical analyses, neural network modellings and model qualification were made using statistical software package (STATISTICA, StatSoft, USA) and R, version R 3.5.1.

Artificial neural network modeling (connectionist modelling)

Significant number of literature have shown different applications of neural networks for solving different types of problems, most of which can be broadly classified into classification, function approximation or prediction problems. The proficiency of neural networks is attributed to its ability to detect patterns and relationships in the data provided to them during the calibration or training phase. Generally, neural networks are classified according to (a) the network topology e.g. feed forward and recurrent architectures, (b) the network transfer function e.g. sigmoid, radial basis (c) the network learning algorithms e.g. supervised or unsupervised learnings (Karray and De Silva, 2004). The neural network architecture is depicted in *Fig. 2*. Parallel and distributed processing units called neurons or nodes are arranged within three layers, namely, input, hidden and output layers. Each neuron in the input layers is connected to the adjacent layer in the hidden layer through connection weights. Similarly, each neuron in the hidden layer is connected to the adjacent hidden layer or to the output layer through connection weights. In fact, these weights are the model parameters to be estimated using the input/output training sets. The output of each neuron is weighted, summed and passed to nonlinear transformation e.g. sigmoid function. For a chosen network's topology and transfer function, the neural network modelling is reduced to the problem of estimating the connection weights among the neurons such that a certain measure of the mismatch between the observed and predicted values is minimized. More specifically, the cumulative error E_c to be minimized may be given as:

http://www.aloki.hu ● ISSN 1589 1623 (Print) ● ISSN1785 0037 (Online)
DOI: http://dx.doi.org/10.15666/aeer/1802_20872107

$$E_c = \frac{1}{2}\sum_{k=1}^{n}\sum_{i=1}^{q}\left(t_i(k) - o_i(k)\right)^2 \quad \text{(Eq.1)}$$

where n is the total number of training points, q is the total number of neurons at the output layer, t_i is the target value and $o_i(k)$ is the network's output from the k^{th} neutron for the i^{th} training point. Accordingly, the optimization problem of the neural network can be formulated as:

$$\min_{\mathbf{w}} E_c = \min_{\mathbf{w}} \frac{1}{2}\sum_{k=1}^{n}\sum_{i=1}^{q}\left(t_i(k) - o_i(k)\right)^2 \quad \text{(Eq.2)}$$

where the vector w contains the network weights between all the neurons of the network. In the present study, two feed forward architectures, namely multilayer perceptron network (MLP) and the radial basis function network (RBFN) have been considered to predict CO_2 and CH_4 concentrations in 4 urban cities in the state of Kuwait (*Fig. 2*).

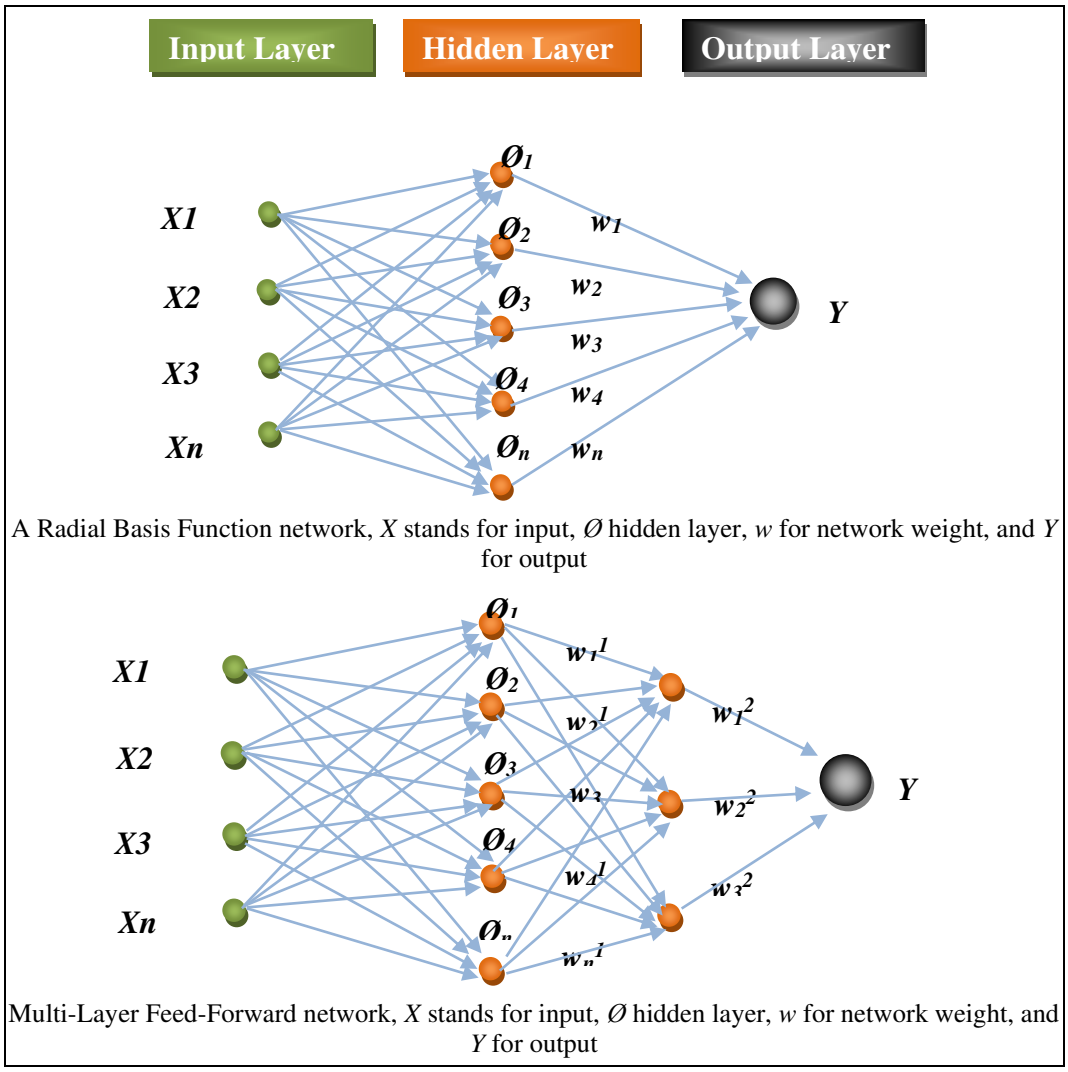

Figure 2. *Architecture of developed artificial neural network (ANN) models*

http://www.aloki.hu ● ISSN 1589 1623 (Print) ● ISSN1785 0037 (Online)
DOI: http://dx.doi.org/10.15666/aeer/1802_20872107

Both, MLP and RBFN are examples of feed forward network with different prediction capabilities (Karray and De Silva, 2004). MLP uses global transfer function such as sigmoid function

$$\text{sigmoid}(x) = \frac{1}{1+\exp(-x)} \quad \text{(Eq.3)}$$

whereas RBFN uses local basis functions such as Gaussian kernel

$$g_i(\mathbf{x}) = \exp\left(\frac{\|\mathbf{x}-\mathbf{v}_i\|^2}{2\sigma_i^2}\right) \quad \text{(Eq.4)}$$

where x is the input vector and v is the center of the radial basis function g_i and σ_i is the width/scaling parameter. While MLP uses back propagation algorithm (supervised learning) to estimate the network weights, RBFN use a two-stage training strategy. In the first stage, the parameters of the radial basis function (v and σ_i) are estimated using unsupervised learning e.g. *k*-means method, while in the second stage the network weights are estimated using gradient methods. A remarkable feature of the RBFN is that the weight between the input and the hidden layers are all equal to one and only the weights between the hidden and the output layer are to be estimated. In the current work, a total of 8,640 hourly concentration readings of CO_2 and CH_4 and their corresponding climatological variables, namely; ambient air temperature, relative humidity, wind speed, and wind direction, were used as input to build the ANN model. About 60% of the total data was used to train the network, 20% was used as a validation set, and the remaining 20% was used as test data. In testing step, the networks have one output, either CO_2 or CH_4 concentration. Training and testing data are normalized before presenting them to the networks. Normalization is an important pre-processing step, in particular, when the input and output variables of the network are of different order of magnitude as can be seen from *Table 1*. Although some rules of thumbs exist for selecting the number of hidden layers and the number of neurons, in practice, the appropriate number is determined through trial and error until certain error criterion is satisfied. There are several advantages of neural networks against other empirical modelling techniques. More importantly is the filtering capacity of neural networks. The reason of the latter is that no single node solely responsible of correlating a certain input to a specific output, but all the nodes contribute differently to the correlation structure extracted from in the input-output pattern presented to the network during the training phase (Baughman and Liu, 1995). On the contrary, for other regression techniques, if one of the variables is missing or very noisy, the model will likely give inaccurate result because each variable is associated with a unique parameter or weight. On the other hand, neural networks suffer from several limitations. The main disadvantage of neural networks is the necessity of large amount of training data. The latter is insignificant if large amount of historical data is available. Another disadvantage of neural networks is that the estimated weights are suboptimal solution, that is, no global solution can be guaranteed. One way to tackle the sub-optimality problem is to reinitiate the weights of the network several times during the training phase until stable weights are obtained.

http://www.aloki.hu ● ISSN 1589 1623 (Print) ● ISSN1785 0037 (Online)
DOI: http://dx.doi.org/10.15666/aeer/1802_20872107

Statistical performance indices

To evaluate the performance of all artificial neural network (ANN) models, commonly used statistical performance indices suggested by the US EPA, such as mean absolute error (MAE), root mean square error (RMSE), and fractional bias (FB) were used (Riswadkar and Kumar, 1994; Patel and Kumar, 1998; Kumar et al., 2006). The MAE is used to measure the closeness of predicted and observed values. In general, the smaller the MAE values, the smaller the difference between the predicted results and the actual data and the better the prediction performance of the network model.

$$\mathrm{MAE} = \frac{1}{\mathrm{n}} \sum_{\mathrm{i}=1}^{\mathrm{n}} \left| \mathrm{P_i} - \mathrm{O_i} \right| \qquad \text{(Eq.5)}$$

With respect to an acceptable model, RMSE values should be small and the RMSE should approach zero in an ideal model. RMSE is commonly used as a measure of the overall model performance:

$$RMSE = \sqrt{\frac{1}{n} \sum_{i=1}^{n} (P_i - O_i)^2} \qquad \text{(Eq.6)}$$

Fractional bias, a non-dimensional factor, is a measure of the difference between the average observed and the average predicted values and is written in symbolic form as:

$$FB = \frac{(\bar{O} - \bar{P})}{0.5(\bar{O} + \bar{P})} \qquad \text{(Eq.7)}$$

The FB parameter varies between -0.5 and +0.5 and a perfect model has an FB value of zero. FB>0 indicates an underestimate in predicted concentrations while FB<0 indicates an overestimate. In equation 5-7, n is the number of data points, P is the predicted data point, and O is the observed data point.

Results and discussion

Trend of GHG emissions in the ambient atmosphere

To gain better insight into the development of GHG emissions in the ambient atmosphere in Kuwait, the yearly mean concentrations for the period of 13 years (2004-2016) were statistically assessed in four representative urban cities (Ali Sabah Al-Salem, Al-Riqqa, Mansouriya, and Al-Jarha), as shown in *Figure 1*. CO_2 yearly mean concentrations in this study were plotted with those measured at the Mauna Loa Observatory in Hawaii for sake of comparison with the world CO_2 trend (*Figure 3a*). Over the period 2004 to 2016, there were considerable increases in the GHG emissions in the urban cities in Kuwait. CO_2 level varies between 342±18 ppm (Ali Sabah Al-Salem) and 350±13 ppm (Al-Jarha) in 2004. The CO_2 concentrations (*Figure 3a*) have shown an upward trend since 2004, with an 11% to 25% increase in 2016 in all urban cities. Prior to 2015, the CO_2 emissions quantified through monitoring networks in urban cities in

http://www.aloki.hu ● ISSN 1589 1623 (Print) ● ISSN1785 0037 (Online)
DOI: http://dx.doi.org/10.15666/aeer/1802_20872107

Kuwait were below those observed at Mauna Loa site (*Figure 3a*). In 2016, the CO_2 emission ranged from 394 ± 10 ppm to 425 ± 14, exceeded CO_2 emissions reported at the Mauna Loa site (404.21 ppm). In terms of CO_2 variation over the years, one-way analysis of variance (ANOVA) showed significant differences (p<0.05) among the urban cities.

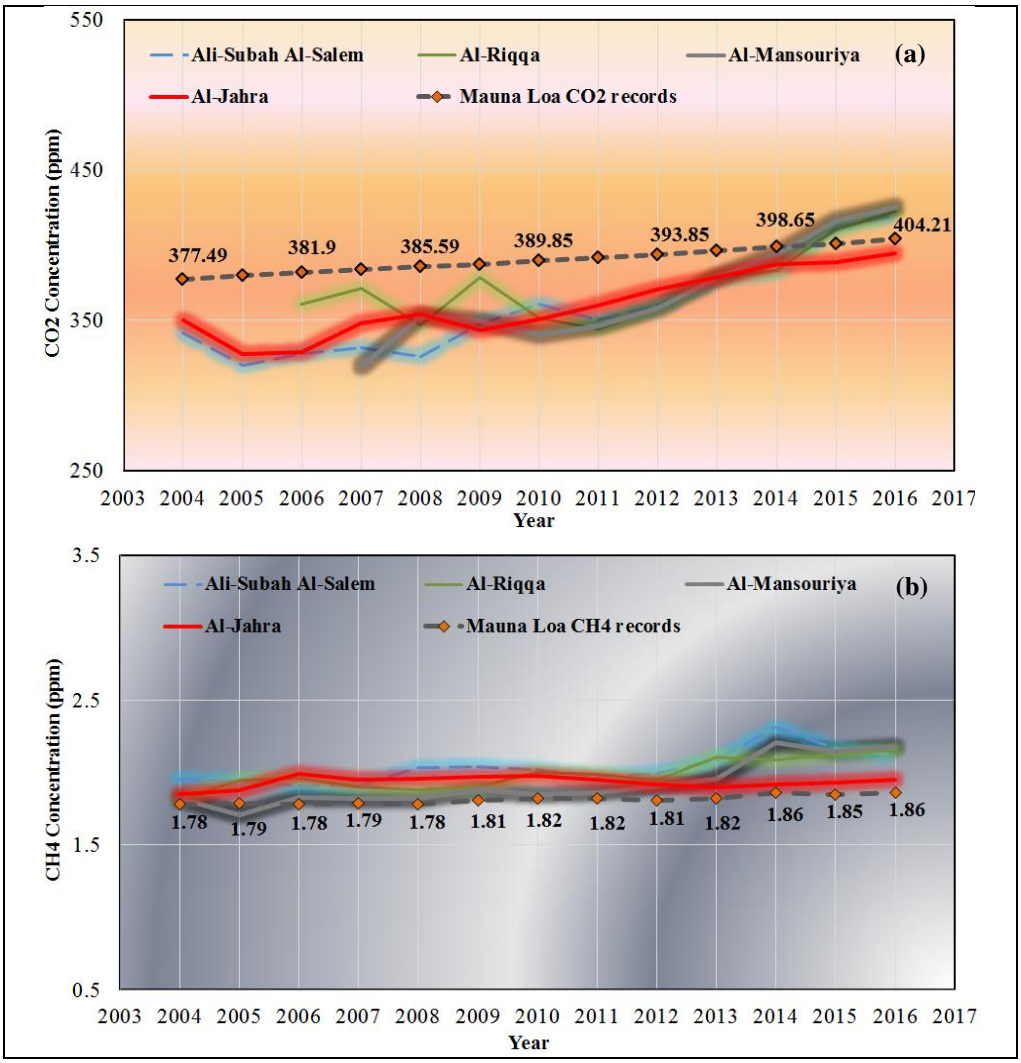

Figure 3. *Yearly trend of (a) CO_2 and (b) CH_4 concentrations in urban areas in Kuwait*

In comparison with other countries in the world, CO_2 levels in this study for the year of 2016 were compared with CO_2 reported in the same year by The World Data Centre for Greenhouse Gases (WDCGG, 2018). The average yearly CO_2 emission in Kuwait was 415.6 ppm, which is lower than those obtained in Poland (427.7 ppm), and Italy (427.6 ppm) and similar to those found in Korea (416.3 ppm), Hungary (410 ppm), Hong Kong (408 ppm), and USA (408 ppm), and higher than those reported in UK (404.6 ppm), Canada (404.5 ppm), Australia (400.8 ppm), and New Zealand (400.6 ppm).

The burning of fossil fuels (oil, gas and coal) for various activities such as transportation, electricity and heat supply, and water treatment is the main source of CO_2 emission in the atmosphere. The magnitude of CO_2 emissions is linked to the carbon content of the fuel as for instance oil and coal has approximately 25% and 40% more

http://www.aloki.hu ● ISSN 1589 1623 (Print) ● ISSN1785 0037 (Online)
DOI: http://dx.doi.org/10.15666/aeer/1802_20872107

carbon content than natural gas, respectively. The extent of CO_2 in the atmosphere is the result of balance of the fluxes between the oceans, the biosphere and the atmosphere. CO_2 circulates from and to the atmosphere via direct absorption/release phenomenon, respiration of plants and the decomposition of organic-matter in soil, and absorption of CO_2 through photosynthesis. To limit the level of atmospheric CO_2 emission, burning of fossil fuels pattern and energy mix should be highly considered.

CH_4 is the second crucial GHG with global warming potential (GWP) of 28 times greater than CO_2 over a 100-year time horizon (IPCC, 2013). It was reported that CH_4 is responsible for about 17% of rise in the total radiative forcing as results of long-lived GHG in the atmosphere during the period of 1750-2016 (WMO, 2017). CH_4 trend, in same urban areas and years span to those of CO_2, was also investigated in Kuwait and results are presented in *Figure 3b*. CH_4 concentrations varied between 1.82±0.09 to 1.94±0.1 ppm in all tested urban areas in Kuwait in 2004. Since 2004, CH_4 concentrations have increased by 100-360 ppb by the end of 2016, with varying rates in the tested urban areas, corresponding to an average range of increase of 8-27 ppb yr^{-1}. It is imperative to note that most CH_4 concentrations observed in all four urban areas exceeded Mauna Loa levels during 2004-2016 (*Figure 3b*). However, the average yearly CH_4 concentration in this study (2.10±0.10 ppm) in the year of 2016 was consistent with CH_4 records reported in other countries in 2016 (WDCGG, 2018) such as Italy (2.00 ppm), Hungary (1.97 ppm), Viet Nam (1.95 ppm), USA (1.97 ppm), and Canada (1.97 ppm). Methane is released to the atmosphere by anthropogenic sources including production and consumption of fossil fuel, biomass burning, and landfills and by natural processes such as wetlands and termites. Conversely, CH_4 level decreases in the atmosphere due to its reaction with hydroxyl radical (OH), persist for about 10 years. Despite the fact that CH_4 is a potent GHG, its influence is comparatively short-lived.

Seasonal and diurnal variation

GHG concentrations were compared in summer and winter, as these are the prevailing season in Kuwait, to learn more about seasonal variability. For the sake of brevity, the comparison in GHG concentrations was limited to 2016. Descriptive statistics of CO_2 and CH_4 concentrations, as well as climate conditions such as temperature, RH, wind speed, and wind direction, during summer and winter for four urban cities are listed in *Table 1*. In summer, the highest mean value of CO_2 emission was 430 ± 12 ppm and found in Al-Riqqa and the lowest value (398 ± 3.5 ppm(was observed in Al-Jahra. In winter, the highest mean value of CO_2 emission was 418 ± 24.6 ppm and observed in Al-Riqqa while the lowest mean value (390 ± 7.2ppm) was found in Al-Jahra. Maximum concentrations of CO_2 (summer = 440 ppm; winter = 467 ppm) were measured in Al-Riqqa while minimum concentrations (summer = 387 ppm; winter = 380 ppm) were found in Al-Jahra. One-way analysis of variance (ANOVA) demonstrated a significant difference ($p<0.05$) between summer and winter in all urban areas in this study. A seasonal variation of CO_2 is obvious in all the urban cities in this study with an overall higher level of CO_2 in summer than winter. This finding is consistent with reported CO_2 in major urban areas (Ghauri et al., 2007; Bergeron and Strachan, 2011). The high CO_2 level in summer is presumably due to the consumption rate of fossil fuel for cooling purposes (e.g., air conditioning) and traffic activities. The temperature in summer reaches 50°C in Kuwait and the air conditioning is in use all day in houses, government buildings, and businesses in the private sector. Increased CO_2 concentration is not restricted to local sources; it can also come from long-range transport from distant source areas.

http://www.aloki.hu ● ISSN 1589 1623 (Print) ● ISSN1785 0037 (Online)
DOI: http://dx.doi.org/10.15666/aeer/1802_20872107

The level of CH_4 in summer and winter was also investigated (*Table 1*). Similar observations to those of CO_2 were reported. The mean concentrations of CH_4 were between 1.92 ± 0.08 ppm and 2.25 ± 0.20 ppm in summer and from 1.87 ± 0.2 ppm and 2.11 ± 0.2 ppm in winter. The highest mean concentration of CH_4 was observed in Al-Riqqa during the summer and winter while the lowest values were found in Al-Jahra. Maximum CH_4 records in summer (2.70 ppm) and in winter (2.50 ppm) were also found in Al-Riqqa. Seasonal differences in all urban cities were statistically significant (ANOVA, $P<0.05$). CH_4 levels in this study exhibited higher levels in summer than in winter in all monitored urban areas (*Table 1*). Such observations were consistent with those reported in different parts of the worlds (Sikar and Scala, 2004; Ito et al., 2005; Ghauri et al., 2007; Satar et al., 2016).

Diurnal variation

Diurnal cycles of GHG emission in the four urban areas for the entire year of 2016 are plotted in *Figure 4a,b* to understand their short-term variability. CO_2 diurnal pattern (*Figure 4a*) in all tested urban localities were almost similar, but vary with magnitudes according to ANOVA analysis ($p<0.05$).

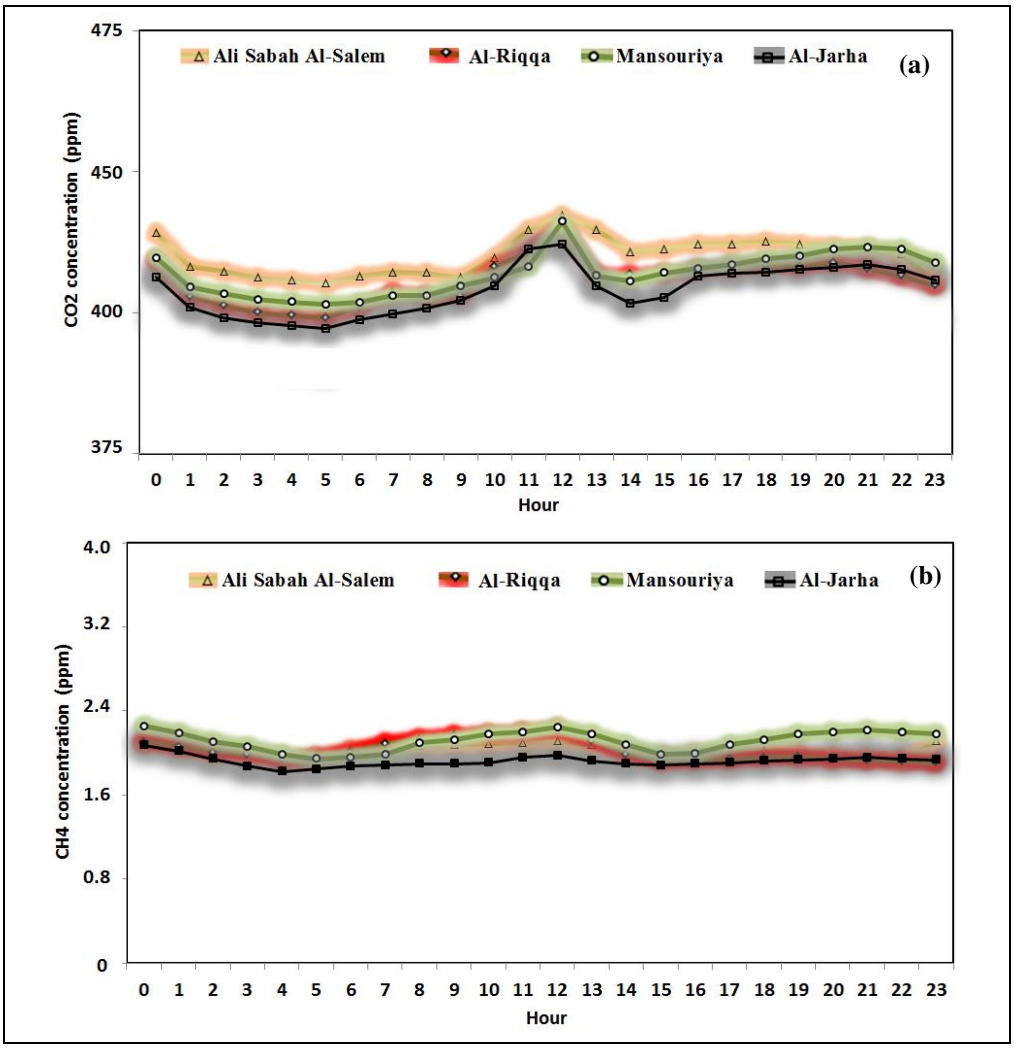

Figure 4. *Diurnal variations of (a) CO_2 and (b) CH_4 concentrations in urban areas in Kuwait*

http://www.aloki.hu ● ISSN 1589 1623 (Print) ● ISSN1785 0037 (Online)
DOI: http://dx.doi.org/10.15666/aeer/1802_20872107

As shown in *Figure 4a*, the increased CO_2 records were observed during three intermittent intervals of day along the entire year; one at near midnight (around 12 am); another at noon time (around 12 pm), and the last between 4 pm and 9 pm. In the latter two periods, high CO_2 levels could be ascribed to busy traffic hours in this study, which is consistent with other urban areas with strong anthropogenic activities, such as vehicular emissions as a result of burning fossil fuels (Aikawa et al., 1995; Takahashi et al., 2002; Gratani and Varone, 2005). While increased level of CO_2 at near midnight (around 12 am) could be possibly attributed to the combined effects of respiration by the living organism and/or from soils, the minimum levels occurred at the night/morning transition between 3 am and 5 am is likely due to decreases anthropogenic CO_2 emissions. Another decrease in CO_2 was observed in the afternoon, which can be attributed to photosynthetic activities (Spittlehouse and Ripley, 1977; Baez et al., 1988; Nasrallah et al., 2003) and the expansion of the mixing height (Aikawa et al., 1995). The CH_4 diurnal cycle was also investigated and the results are shown in *Figure 4b*. The CH_4 diurnal pattern was similar to those observed with CO_2, which implies that both CO_2 and CH_4 have common emission sources. Diurnal results in this study are consistent with other similar studies (Smith et al., 2002; Aikawa et al., 2006; Satar et al., 2016).

Modeling of GHG using artificial neural network (ANN) models

The forecasting of GHG (mainly CO_2 and CH_4) trends has received significant attention in recent years. The International Energy Agency (IEA) reported that 71% of energy-related GHG emissions were attributable to urban areas and it is assumed to grow by 5% by 2030 (IEA, 2008). As mention in methodology section, the number of hidden layers as well as the number of neurons within the hidden layers is usually determined by trial and error. A number of trials were carried out to determine the optimal number of hidden layers, number of neurons in the hidden layers, learning rate, and the learning algorithm. Among several ANN architectures evaluated, five cases are selected and listed in *Table 2*. For the MLP, sigmoidal functions were used whereas Gaussian functions were used for RBF based networks. In searching for the best network weights, conjugate gradient descent was used for MLP. On the other hand, and since two-stage training phase is used for RBF networks, *k*-mean centering and the pseudo-inverse (singular value decomposition) algorithm were used to determine the radial basis functions' parameters and the output layers' weights, respectively. In addition, two positive constants have to be set during the networks learning phase, namely the learning rate and the momentum coefficient. The latter become important especially for networks with large number of inputs-outputs and complex architecture. The rule of the learning rate is to regulate the rate at which the weights are adjusted while the momentum coefficient is a surplus that is added to the adjusted weights to speed up the training. The latter are important to avoid trapping in local minima and an unstable learning (Baughman and Liu, 1995). After several trials, the learning rate and the momentum was set to 0.5 and 0.7, respectively. The observed and predicted values of CO_2 and CH_4 concentrations for the best five models are presented in *Figures 5 and 6*, respectively. Among these five optimal models for each urban area, the best model was selected based on a low value of error mean, absolute error mean, and standard deviation ratio and high correlation coefficients (r). These performance indices differently demonstrate the association between observed and predicted concentration values of CO_2 and CH_4 as predicted by the ANN model as shown in *Table 2*. The higher correlation coefficient showed that the predicted CO_2 and CH_4 concentration values using the ANN model are in good agreement with the observed CO_2

http://www.aloki.hu ● ISSN 1589 1623 (Print) ● ISSN1785 0037 (Online)
DOI: http://dx.doi.org/10.15666/aeer/1802_20872107

and CH_4 concentrations as shown in *Table 2*. The correlation coefficients (r) of the parity plots of the selected optimal models for CO_2 were 0.76, 0.81, 0.72, and 0.73 for areas Ali Sabah Al-Salem, Al-Riqqa, Mansouriya, and Al-Jarha, respectively. For CH_4, the correlation coefficients were 0.77, 0.66, 0.72, and 0.96 for areas Ali Sabah Al-Salem, Al-Riqqa, Mansouriya, and Al-Jarha, respectively. It is worth highlighting that all the optimal models for CO_2 and CH_4 were radial basis function (RBF) network models for all urban cities investigated. The RBF network has shown great promise in this sort of problem due to several of its features, including its very good functional approximation capabilities (Park and Sandberg, 1991), which arise naturally as regularized solutions of ill-posed problems (Poggio and Girosi, 1990) and are utilized well in the theory of interpolation (Powell, 1987). In addition to these features, the intrinsic structure of the RBF network allows learning in stages, which leads to a reduction in training time. This has indeed resulted in the widespread use of RBF networks in numerous practical problems.

Table 2. *Selected ANN models for predictions CO_2 and CH_4 concentrations in the four urban cities*

	CO_2					**CH_4**				
Ali Sabah Al-Salem	**M1**	**M2**	**M3**	**M4**	**M5**	**M1**	**M2**	**M3**	**M4**	**M5**
Error Mean	0.80	0.64	-0.36	-0.61	-0.52	-0.012	-0.017	-0.017	-0.013	-0.003
Error S.D.	18.2	17.9	17.7	15.2	15.3	0.15	0.17	0.18	0.17	0.16
Abs E. Mean	14.8	14.7	14.3	10.92	10.94	0.11	0.13	0.13	0.12	0.12
S.D. Ratio	0.86	0.85	0.84	0.72	0.72	0.71	0.84	0.83	0.80	0.76
Correlation	0.56	0.58	0.60	0.74	0.76	0.77	0.60	0.61	0.68	0.69
Hidden	0	5	6	11	22	34	0	0	3	4
M. Type	L	MLP	MLP	RBF	RBF	RBF	L	L	MLP	MLP
Al-Riqqa	**M1**	**M2**	**M3**	**M4**	**M5**	**M1**	**M2**	**M3**	**M4**	**M5**
Error Mean	0.94	1.06	1.37	1.14	1.26	-0.003	-0.001	-0.003	0.009	-0.006
Error S.D.	22.2	17.3	18.2	17.2	16.4	0.308	0.345	0.345	0.336	0.322
Abs E. Mean	17.15	12.23	14.19	13.06	11.94	0.245	0.279	0.278	0.255	0.250
S.D. Ratio	0.94	0.72	0.76	0.72	0.69	0.841	0.942	0.941	0.915	0.877
Correlation	0.41	0.75	0.70	0.75	0.81	0.66	0.40	0.40	0.50	0.55
Hidden	0	4	5	11	22	34	0	0	5	6
M. Type	L	MLP	MLP	RBF	RBF	RBF	L	L	MLP	MLP
Mansouriya	**M1**	**M2**	**M3**	**M4**	**M5**	**M1**	**M2**	**M3**	**M4**	**M5**
Error Mean	0.87	-1.29	-1.11	0.11	-0.17	-0.01	0.00	0.00	-0.02	-0.01
Error S.D.	27.40	25.32	25.45	23.34	22.55	0.16	0.18	0.18	0.19	0.16
Abs E. Mean	21.26	20.57	20.44	17.75	17.06	0.12	0.14	0.14	0.14	0.12
S.D. Ratio	0.92	0.85	0.85	0.78	0.76	0.75	0.83	0.83	0.86	0.77
Correlation	0.50	0.58	0.58	0.67	0.72	0.72	0.61	0.61	0.56	0.70
Hidden	0	1	3	22	34	34	0	0	1	4
M. Type	L	MLP	MLP	RBF	RBF	RBF	L	L	MLP	MLP
Al-Jarha	**M1**	**M2**	**M3**	**M4**	**M5**	**M1**	**M2**	**M3**	**M4**	**M5**
Error Mean	-0.92	-0.60	0.26	0.19	-0.88	-0.001	0.030	0.031	-0.003	0.024
Error S.D.	7.29	6.91	7.10	7.72	6.71	0.10	0.42	0.42	0.10	0.42
Abs E. Mean	5.61	5.00	5.37	6.01	5.05	0.07	0.21	0.21	0.08	0.17
S.D. Ratio	0.89	0.85	0.87	0.94	0.82	0.24	1.01	1.00	0.25	1.01
Correlation	0.57	0.62	0.55	0.39	0.73	0.96	0.30	0.27	0.96	0.2
Hidden	0	6	34	22	3	34	0	0	1	4
M. Type	L	MLP	RBF	MLP	RBF	RBF	L	L	MLP	MLP

* M1-M5 stands for models' number, L: Linear, MLP: multilayer perception, and RBF: radial basis function

http://www.aloki.hu ● ISSN 1589 1623 (Print) ● ISSN1785 0037 (Online)
DOI: http://dx.doi.org/10.15666/aeer/1802_20872107

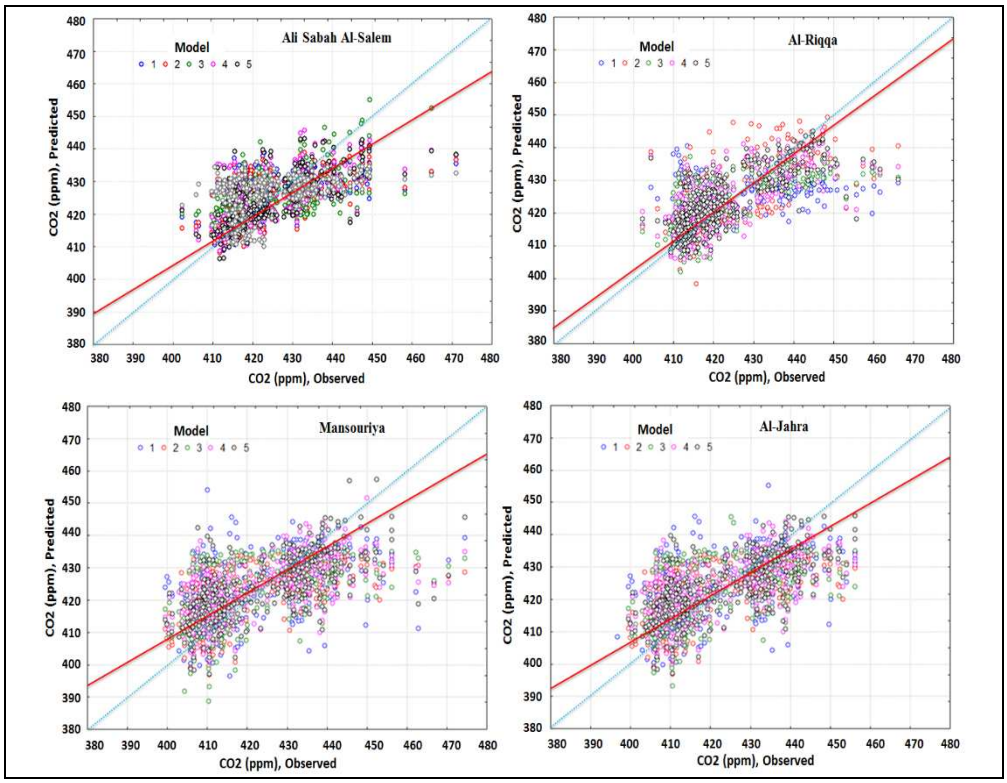

Figure 5. *Comparisons between the observed and predicted daily CO_2 emissions at all sites in 2016. The dashed line is the 1:1 line, and the solid line is the best-fit line*

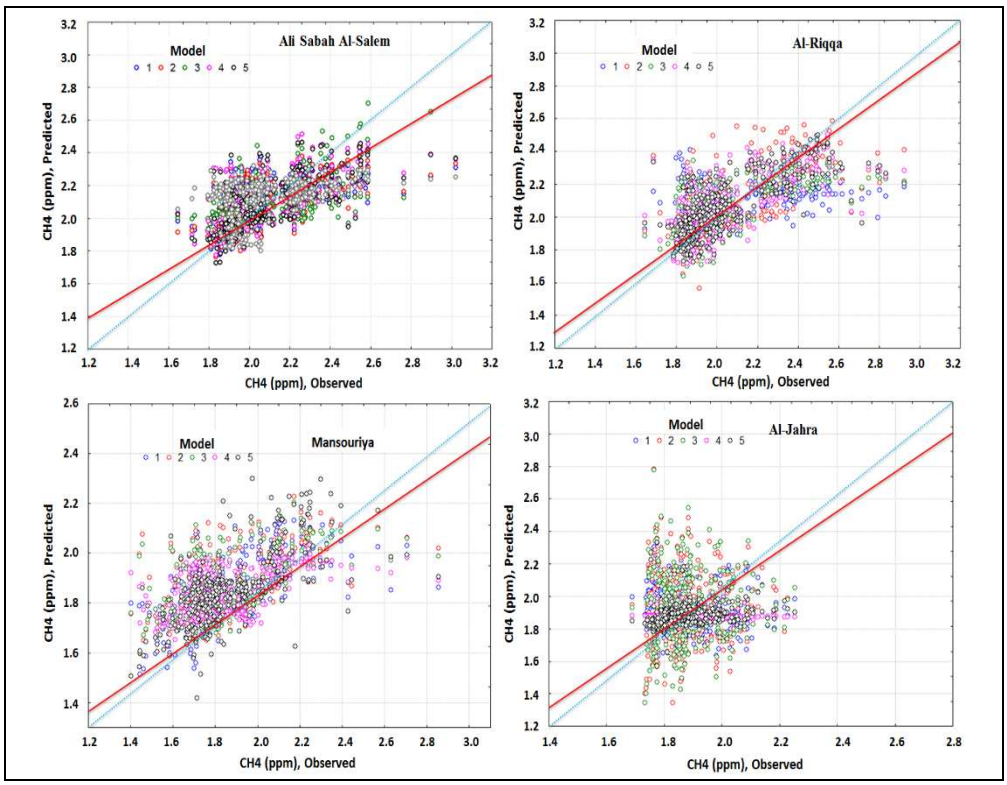

Figure 6. *Comparisons between the observed and predicted daily CH_4 emissions at all sites in 2016. The dashed line is the 1:1 line, and the solid line is the best-fit line*

http://www.aloki.hu ● ISSN 1589 1623 (Print) ● ISSN1785 0037 (Online)
DOI: http://dx.doi.org/10.15666/aeer/1802_20872107

To further check the accuracy of the developed model, a time series plot of the predicted versus the observed for CO_2 and CH_4 is shown in *Figures 7 and 8*. The performance statistics, MAE, RMSE, and FB, of the selected optimal ANN for the four urban areas for CO_2 and CH_4 are given in *Table 3*. The MAE ranged between 5.4 and 15.8 ppm and RMSE varied from 6.9 to 15.5 ppm for CO_2 in all tested urban areas. It is imperative to note that the slightly higher numbers of RMSE in the modeling of CO_2 are due to squaring the errors that tends to heavily weight statistical outliers and therefore a large RMSE may result even though errors may be small and fairly satisfactory elsewhere. Another important point to note is that the annual mean concentration of CO_2 varied between 394 and 425 ppm in the four tested urban areas and, therefore, performance statistics values, differences between the observed and the predicted, listed above represent 1.5% to 4.4% of the total concentrations, which can be deemed acceptable. Concerning CH_4, the MAE values were between 0.11 and 0.21 ppm and RMSE ranged from 0.1 to 0.31 ppm for all tested urban areas. FB was also calculated to test whether predicted values were underestimated (FB>0) or overestimated (FB<0). The FB values for CO_2 and CH_4 approach zero (-0.001 to -0.008 for CO_2 versus -0.001 to -0.04 for CH_4). Overall, the statistical performance indicators reveal that ANN models can estimate CO_2 and CH_4 concentrations in urban areas for the given data set with decent accuracy. To the best knowledge of the authors, there is no nonlinear predictive models that were used in Kuwait to monitor the concentrations levels of CH_4 and CO_2 in the atmosphere. These forecasting models would be beneficial for concerned authorities for planning and proposing environmental legislations to monitor and limit the levels of GHG in Kuwait.

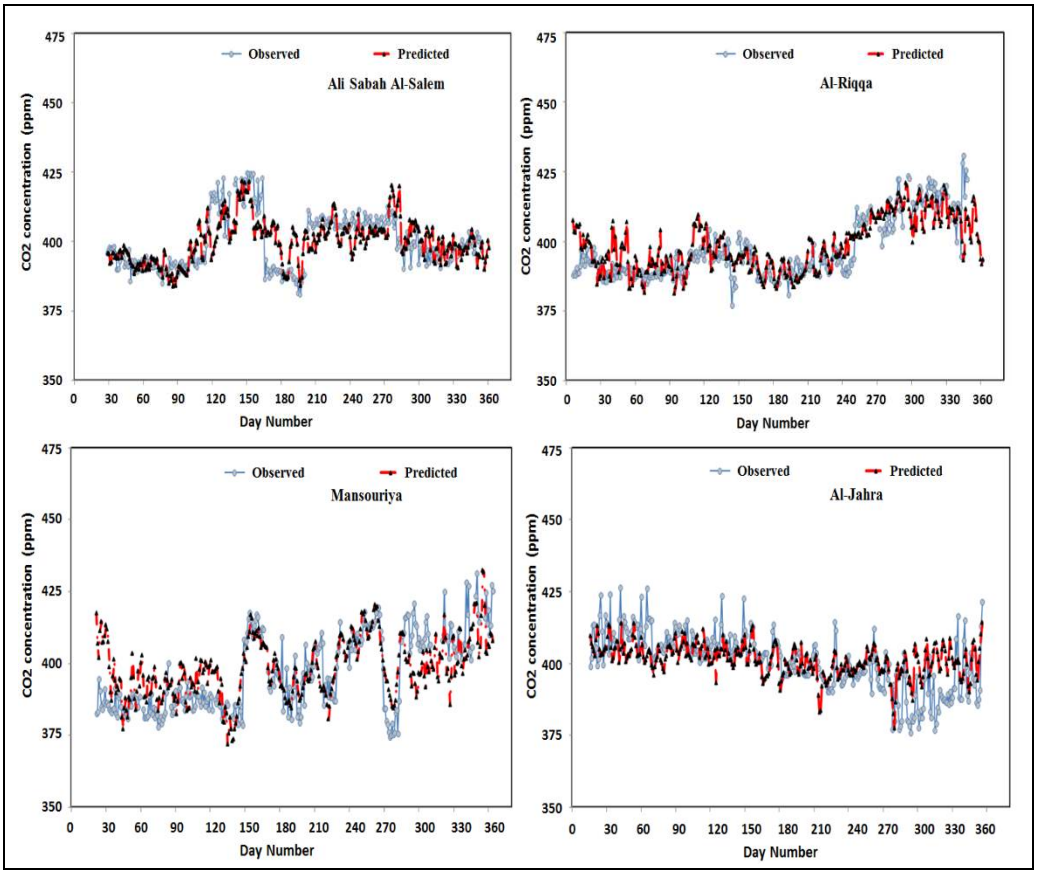

Figure 7. *Daily time series of observed and predicted concentration of CO_2 in four urban cities*

http://www.aloki.hu ● ISSN 1589 1623 (Print) ● ISSN1785 0037 (Online)
DOI: http://dx.doi.org/10.15666/aeer/1802_20872107

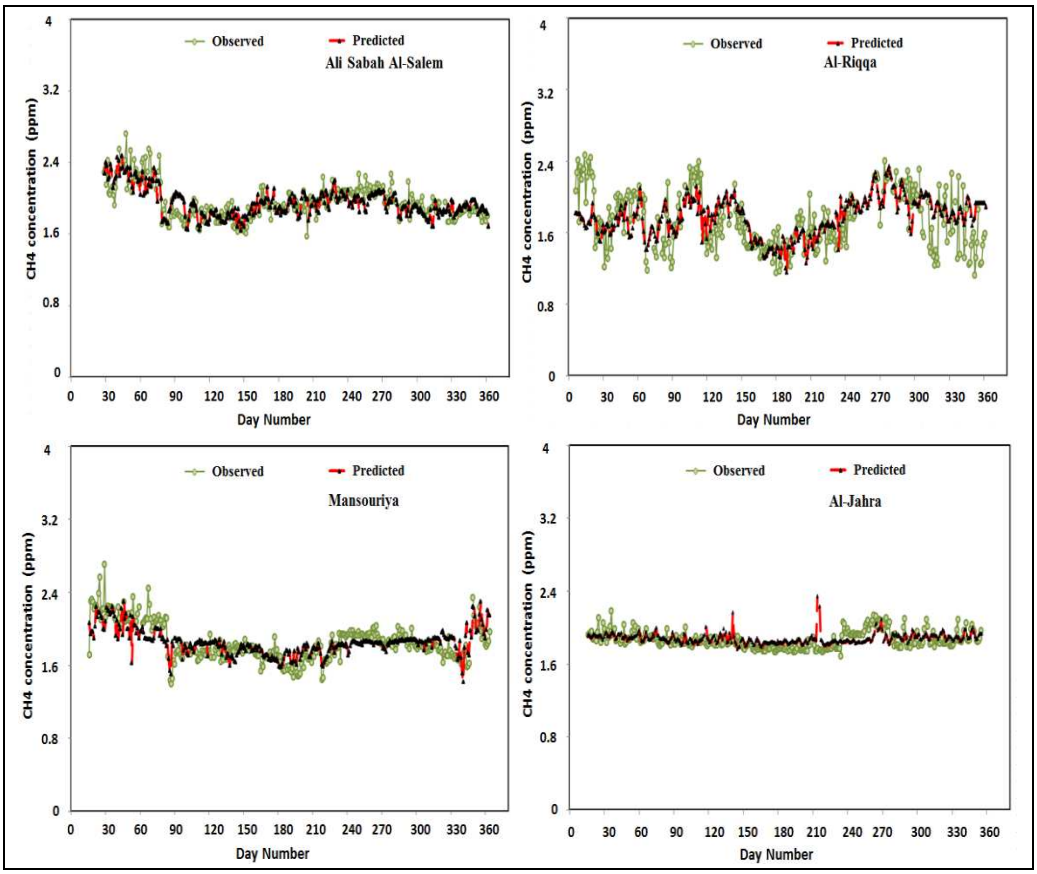

Figure 8. *Daily time series of observed and predicted concentration of CH_4 in four urban cities*

Table 3. *Performance statistical indicators in ppm*

Gases	Statistical indicators	Ali Sabah Al-Salem	Al-Riqqa	Mansouriya	Al-Jarha
CO_2	MAE	11.9	11.2	15.8	5.4
	RMSE	15.5	14.3	19.6	6.9
	FB	-0.002	-0.007	-0.008	-0.001
CH_4	MAE	0.17	0.21	0.11	0.12
	RMSE	0.26	0.31	0.1	0.1
	FB	-0.01	-0.04	-0.001	-0.003

Conclusions

In the present work, GHG emission for 13-year period was investigated in hourly, daily, seasonal, and yearly basis to gain overall picture about the trend of GHG emissions in Kuwait. Records confirmed year-year rising pattern in GHG emissions, higher levels in summer than in winter, due to enormous burning of fossil fuel for cooling purposes and traffic activities. Elevated levels of GHG emissions were observed both at noon and between 4 pm and 9 pm probably ascribed to busy traffic hours while during midnight are likely due to the combined effects of respiration by the living organism and/or from soils. Subsequently and most importantly, the capabilities of multiple linear regression and two types of neural networks, MLP and RBFN for forecasting GHG emissions have been investigated. Among the developed models and based on different statistical

http://www.aloki.hu ● ISSN 1589 1623 (Print) ● ISSN1785 0037 (Online)
DOI: http://dx.doi.org/10.15666/aeer/1802_20872107

performance indices, RBF models outperformed the multiple linear regression and MLP in all urban cities investigated. The RBF exhibited high performance in predicting GHG due to several reasons including its precise functional approximation capabilities and its intrinsic structure that permits learning in stages, which leads to a decrease in training time. This indeed explains the popularity use of RBF networks in numerous practical problems. This study and similar studies would be used as a control tool by government and decision makers for formulation of climate change policies in urban cities compatible with international standpoints.

Acknowledgement. The authors would like to thank Kuwait University and Kuwait Environment Public Authority (KUEPA) for their assitance in data measurments and for continuous support.

REFERENCES

[1] Aikawa, M., Yoshikawa, M., Tomida, M., Aotsuka, F., Haraguchi, H. (1995): Continuous monitoring of the carbon dioxide concentration in the urban atmosphere of Nagoya, 1991-1993. – Analytical Sciences 11: 357-362.

[2] Aikawa, M., Hiraki, T., Eiho, J. (2006): Vertical atmospheric structure estimated by heat island intensity and temporal variations of methane concentrations in ambient air in an urban area in Japan. – Atmospheric Environment 40(23): 4308-4315.

[3] Amoura, K., Wira, P., Djennoune, S. (2011): A state-space neural network for modeling dynamical nonlinear systems. – NCTA 2011 - Proceedings of the International Conference on Neural Computation Theory and Applications: 369-376.

[4] Baez, A., Reyes, M., Rosas, I., Mosiño, P. (1988): CO2 concentrations in the highly polluted atmosphere of Mexico City. – Atmosfera 1: 87-98.

[5] Balch, J., Nagy, R., Archibald, S., Bowman, D., Moritz, M., Roos, C., Scott, A., Williamson, G. (2016): Global combustion: the connection between fossil fuel and biomass burning emissions (1997-2010). – Philos Trans R Soc Lond B Biol Sci 371: 1696-1706.

[6] Baughman, D., Liu, Y. (1995): Neural networks in bioprocessing and chemical engineering. – Academic Press, Inc. USA.

[7] Bergeron, O., Strachan, I. (2011): CO_2 sources and sinks in urban and suburban areas of a northern mid-latitude city. – Atmospheric Environment 45: 1564-1573.

[8] Chandra, N., Lal, S., Venkataramani, S., Patra, P., Sheel, V. (2016): Temporal variations of atmospheric CO_2 and CO at Ahmedabad in western India. – Atmos. Chem. Phys. 16: 6153-6173.

[9] Elangasinghe, M., Singhal, N., Dirks, K., Salmond, J. (2014): Development of an ANN–based air pollution forecasting system with explicit knowledge through sensitivity analysis. – Atmos. Pollut. Res. 5: 696-708.

[10] Elminir, H., Abdel-Galil, H. (2006): Estimation of air pollutants concentrations from meteorological parameters using artificial neural network. – Journal of electrical engineering 57(2): 105-110.

[11] Ghauri, B., Lodhi, A., Mansha, M. (2007): Development of baseline (air quality) data in Pakistan. – Environmental Monitoring Assessment 127: 237-252.

[12] Gratani, L., Varone, L. (2005): Daily and seasonal variation of CO2 in the city of Rome in relationship with the traffic volume. – Atmospheric Environment 39: 2619-2624.

[13] Guclu, D., Dursun, S. (2010): Artificial neural network modelling of a large-scale wastewater treatment plant operation. – Bioprocess Biosyst Eng 33: 1051-1058.

[14] Hassan, M., Dong, Z. (2018): Analysis of Tropospheric Ozone by Artificial Neural Network Approach in Beijing. – Journal of Geoscience and Environment Protection 6: 8-17.

http://www.aloki.hu ● ISSN 1589 1623 (Print) ● ISSN1785 0037 (Online)
DOI: http://dx.doi.org/10.15666/aeer/1802_20872107

[15] International Energy Agency (IEA) (2008): World Energy Outlook 2008. – IEA, Paris, 569 pages.
[16] Intergovernmental Panel on Climate Change (IPCC) (2013): The Physical Science Basis. – In: Stocker, T. F., Qin, D., Plattner, G. K., Tignor, M., Allen, S. K., Boschung, J., Nauels, A., Xia, Y., Bex, V., Midgley, P. M. (eds.) Contribution of Working Group I to the Fifth Assessment Report of the Intergovernmental Panel on Climate Change. Cambridge University Press, Cambridge, United Kingdom and New York, NY, USA, 2013.
[17] Ito, A., Saigusa, N., Murayama, S., Yamamoto, S. (2005): Modeling of gross and net carbon dioxide exchange over a cool-temperate deciduous broad-leaved forest in Japan: Analysis of seasonal and interannual change. – Agricultural and Forest Meteorology 134(1-4): 122-134.
[18] Jędrysek, M., Halas, S., Pieńkos, T. (2015): Carbon Isotopic Composition of Early diagenetic Methane: Variations With Sediments Depth. – Annales UMCS, Physica 69: 29-52.
[19] Karray, F., De Silva, C. (2004): Soft Computing and Intelligent Systems Design. – Addison-Wesley Longman, Inc. UK.
[20] Kumar, A., Dixit, S., Varadarajan, C., Vijayan, A., Masuraha, A. (2006): Evaluation of the AERMOD dispersion model as a function of atmospheric stability for an urban area. – Environmental Progress 25: 141-151.
[21] Kunt, F., Ayturan, Z., Dursun, S. (2016): Used Some Modelling Applications in Air Pollution Estimates. – J. Int. Environmental Application & Science 11: 418-425.
[22] Kurt, A., Oktay, A. (2010): Forecasting air pollutant indicator levels with geographic models 3 days in advance using neural networks. – Expert Systems with Applications 37: 7986-7992.
[23] Loh, Z., Chen, D., Bai, M., Naylor, T., Griffith, D., Hill, J., Denmead, T., McGinn, S., Edis, R. (2008): Measurement of greenhouse gas emissions from Australian feedlot beef production using open-path spectroscopy and atmospheric dispersion modelling. – Aust J Exp Agric 48: 244-247.
[24] Mahmood, I., Iqbal, M., Shahzad, M., Waqas, A., Atique, L. (2016): Spatiotemporal Monitoring of CO_2 and CH_4 over Pakistan Using Atmospheric Infrared Sounder (AIRS). – Int Lett Nat Sci. 58: 35-41.
[25] Mason, S., Baddour, O. (2008): Statistical Modelling. – Troccoli, A., Harrison, M., Anderson, D. L. T., Mason, S. J. (eds.) Seasonal Climate: Forecasting and Managing Risk. NATO Science Series 82, Springer, Dordrecht.
[26] Nasrallah, H., Balling, R., Madi, S., Al Ansari, C. (2003): Temporal variations in atmospheric CO_2 concentration in Kuwait City, Kuwait with comparison to Phoenix, Arizona, USA. – Environmental Pollution 121: 301-305.
[27] Nezhad, A., Mousavi, S., Aghahoseini, S. (2011): Development of an artificial neural network model to predict CO_2 minimum miscibility pressure. – NAFTA 62: 105-108.
[28] Noor, C., Mamat, R., Ahmed, A. (2018): Comparative Study of Artificial NeutralNetwork and Mathematical modelon Marine Diesel Engine Performance Prediction. – International Journal of Innovative Computing, Information and Control 14: 959-969.
[29] Ozcan, H., Ucan, O., Sahin, U., Borat, M., Bayat. C. (2006): Artificial neural network modeling of methane emissions at Istanbul Kemerburgaz-Odayeri Landfill Site. – Journal of Scienfitic and Industrial Research 65: 128-134.
[30] Park, J., Sandberg, I. (1991): Universal approximation using radial basis function networks. – Neural Computation 3(2): 246-257.
[31] Parvizi, B., Khanlarkhani, A., Palizdar, A. (2018): Nonlinear predictive control based on artificial neural network model for pilot reformer plant: Approach for ratio control. – Bulgarian Chemical Communications 50: 286-293.
[32] Patel, V., Kumar, A. (1998): Evaluation of three air dispersion models: ISCST2, ISCLT2 and SCREEN2 for mercury emissions in an urban area. – Environmental Monitoring and Assessment 53: 259-277.

http://www.aloki.hu ● ISSN 1589 1623 (Print) ● ISSN1785 0037 (Online)
DOI: http://dx.doi.org/10.15666/aeer/1802_20872107

[33] Pawul, M., Śliwka, M. (2016): Application of Artificial Neutral Networks for Prediction of Air Pollution levels in Environmental Monitoring. – Journal of Ecological Engineering 17: 190-196.
[34] Poggio, T., Girosi, F. (1990): Networks for approximation and learning. – Proc. IEEE 78(9): 1481-1497.
[35] Powell, M. (1987): Radial basis function for multivariate interpolation. – In: Mason, J. C., Cox, M. G. (eds.) A review algorithms for the approximation of functions and data. Clarendon, Oxford, UK.
[36] Rahimi, A. (2017): Short-term prediction of NO2 and NOx concentrations using multilayer perceptron neural network: a case study of Tabriz, Iran. – Ecol Process 6(4): 1-9.
[37] Riswadkar, R., Kumar, A. (1994): Evaluation of the industrial source complex short-term model in a large-scale multiple source region for different stability classes. – Environmental Monitoring and Assessment 33: 19-32.
[38] Russo, A., Lind, P., Raischel, F., Trigo, R., Mendes, M. (2015): Neural network forecast of daily pollution concentration using optimal meteorological data at synoptic and local scales. – Atmos. Pollut. Res. 6: 540-549.
[39] Sahin, U., Ucan, O., Soyhan, B., Bayat, C. (2004): Modeling of CO distribution in Istanbul using artificial neural network. – Fresen. Environ Bull. 13: 839-845.
[40] Satar, E., Berhanu, T., Brunner, D., Henne, S., Leuenberger, M. (2016): Continuous CO2/CH4/CO measurements (2012–2014) at Beromünster tall tower station in Switzerland. – Biogeosciences 13: 2623-2635.
[41] Shim, C., Han, J., Henze, D., Yoon, T. (2018): Identifying local anthropogenic CO2 emissions with satellite retrievals: a case study in South Korea. – International Journal of Remote Sensing. DOI: 10.1080/01431161.2018.1523585.
[42] Sikar, E., La Scala, N. (2004): Methane and Carbon Dioxide Seasonal Cycles at Urban Brazilian Inland Sites. – Journal of Atmospheric Chemistry 47(2): 101-106.
[43] Smith, F., Elliott, S., Blake, D., Rowland, F. (2002): Spatiotemporal variation of methane and other trace hydrocarbon concentrations in the Valley of Mexico. – Environmental Science & Policy 5: 449-461.
[44] Spittlehouse, D., Ripley, E. (1977): Carbon dioxide concentrations over a native grassland in Saskatchewan. – Tellus 29: 54-65.
[45] Sterman, J. D., Siegel, L., Rooney-Varga, J. N. (2018): Does replacing coal with wood lower CO2 emissions? Dynamic life cycle analysis of wood bioenergy. – Environ. Res. Lett. 13:015007.
[46] Tahboub, K. K., Barghash, M., Arafeh, M., Ghazal, O. (2016): An ANN-GA Framework for Optimal Engine Modeling. – Mathematical Problems in Engineering 2016:6180758.
[47] Takahashi, H., Konohira, E., Hiyama, T., Minami, M., Nakamura, T., Yoshida, N. (2002): Diurnal variation of CO2 concentration, δ14C and δ13C in an urban forest: estimate of the anthropogenic and biogenic contributions. – Tellus 54B: 97-109.
[48] The World Data Centre for Greenhouse Gases (WDCGG) (2018): https://gaw.kishou.go.jp /search. (Accessed in 16/12/2018).
[49] Walsh, B., Ciais, P., Janssens, I., Pen˜uelas, J., Riahi, K., Rydzak, F., Vuuren, D. P., Obersteiner, M. (2017): Pathways for balancing CO2 emissions and sinks. – Nat. Commun. 8(14856): 1-12.
[50] World Meteorological Organization (WMO) (2017): WMO Greenhouse Gas Bulletin No.13. – https://library.wmo.int/doc_num.php?explnum_id=4022.
[51] Wu, S., Feng, Q., Du, Y., Li, X. (2011): Artificial neural network models for daily PM10 air pollution index prediction in the urban area of Wuhan. – China. Environ. Eng. Sci. 28: 357-363.
[52] Zhang, J., Feng, Q., Wang, S., Zhang, X., Wang, S. (2016): Estimation of CO2–brine interfacial tension using an artificial neural network. – J. of Supercritical Fluids 107: 31-37.

http://www.aloki.hu ● ISSN 1589 1623 (Print) ● ISSN1785 0037 (Online)
DOI: http://dx.doi.org/10.15666/aeer/1802_20872107

[53] Zhang, J., Ding, W. (2017): Prediction of Air Pollutants Concentration Based on an Extreme Learning Machine: The Case of Hong Kong. – Int J Environ Res Public Health 14(114): 1-19.
[54] Zhao, H., Wang, Y., Song, J., Gao, G. (2018): The pollutant concentration prediction model of NNP-BPNN based on the INI algorithm, AW method and neighbor-PCA. – Journal of Ambient Intelligence and Humanized Computing. https://doi.org/10.1007/s12652-018-0837-9.

http://www.aloki.hu ● ISSN 1589 1623 (Print) ● ISSN1785 0037 (Online)
DOI: http://dx.doi.org/10.15666/aeer/1802_20872107

GROUND BEETLES (COLEOPTERA: CARABIDAE) FOUND IN CONVENTIONAL POTATO CULTIVATIONS (*SOLANUM TUBEROSUM* L.) IN THE SUBCARPATHIAN REGION

CZERNIAKOWSKI, Z. W. – OLBRYCHT, T. – KONIECZNA, K.*

Uniwersity of Rzeszów, Faculty of Biology and Agriculture, Department of Agroecology Ćwiklińskiej 1, 35-601 Rzeszów, Poland

**Corresponding author*
e-mail: vespillo1@gmail.com; phone: +48-607-434-673

(Received 24th Jul 2019; accepted 8th Jan 2020)

Abstract. The aim of this research was to identify the species composition and quantitative and qualitative structure of ground beetles inhabiting conventional potato cultivations. The study was conducted over the 2008 and 2011-2013 period in eleven localities in the Subcarpathian region (*Podkarpacie*). Beetles were captured using Barber pitfall traps. A total of 7406 beetles were caught, which were classified in 29 genera and 54 species. Small zoophages proved to be the most numerously represented trophic group, whereas the species that were caught as greatest numbers at the study sites were as follows: *Harpalus rufipes*, *Pterostichus melanarius*, and *Poecilus cupreus*. The obtained results demonstrate that anthropogenic factors affect both the trophic structure of ground beetle populations and their habitat preferences. At the same time, species with wide ecological tolerance and lower susceptibility to anthropogenic pressure were promoted. It was also shown that the maintenance and appropriate management of diverse biocoenoses in agricultural space contribute to increased diversity of Carabidae found in agrarian areas.
Keywords: *carabids, cropping, species diversity, SE Poland*

Introduction

Beetles of the ground beetle family (Carabidae) are an important group of animals found in agrocenoses. Among them, omnivorous or partially herbivorous species can be distinguished (Clark et al., 1993; Kromp, 1999), but in the majority of cases representatives of Carabidae belong to non-specialized zoophages, thus being a factor regulating the numbers of some herbivorous species (Thiele, 1977). These active predators feed on both invertebrates (Mollusca) and phytophagous representatives of different taxa of the class Insecta (Coleoptera: in particular, Chrysomelidae, Lepidoptera, and Hemiptera, including Aphididae and Thysanoptera) (Wiltshire and Hughes, 2000; Sunderland, 2002; Schmidt et al., 2003).

The lack of food specialization of zoophagous carabids is manifested both in the wide species spectrum for potential victims and in the possibility of hunting different pests at different developmental stages (pre-imagoes and imagoes). At the same time, it should be noted that herbivorous carabids (obviously excluding phytophagous species that cause economic damage) can reduce weed density from 60 to 80% during one growing season (Ward et al., 2011). Therefore, we can consider Carabidae to be particularly valuable organisms in the aspect of controlling pests of cultivated plants.

For growing potato (*Solanum tuberosum* L.), the most dangerous pest is the Colorado potato beetle (*Leptinotarsa decemlineata* Say). Under field conditions, natural enemies can contribute to weakening a Colorado potato beetle population by 23–78% by destroying eggs, young larvae, and adult beetles (Karg, 1976; Sosnowska et al., 2009). The most important Carabidae species that are mentioned as predators significantly

http://www.aloki.hu ● ISSN 1589 1623 (Print) ● ISSN 1785 0037 (Online)
DOI: http://dx.doi.org/10.15666/aeer/1802_21092128

reducing Colorado potato beetle numbers include *Pterostichus melanarius* (Ill.), *Poecilus cupreus* (L.), and *Harpalus rufipes* (De Geer) (Koval, 1999; Oberholzer and Frank, 2003). Observations on the carabid fauna of potato cultivations have been conducted, among others, in Latvia (Bukejs, 2009), Russia (Cinītis, 1962; Koval and Guseva, 2008), Russia, Moldova, and Ukraine (Koval, 2012), Finland (Kinnunen and Tiainen, 1999), Austria (Kromp, 1990; Traugott, 1998; Juen et al., 2003), and Romania (Varvara, 2010). In the United States, such observations have been conducted, among others, by Zhang et al. (1998), Werling and Gratton (2008), and Rondon et al. (2013).

In Poland such research has been carried out predominantly in the northern and western parts of the country, in the following Voivodeships: Zachodniopomorskie (Fedorko, 1983), Warmińsko-Mazurskie (Kosewska et al., 2008), Wielkopolskie (Nijak, 2005; Kosewska and Nijak, 2012; Nijak et al., 2014), Dolnośląskie (Jasiński et al., 2015), and Świętokrzyskie (Huruk, 2006). The studies regarding the ground beetle fauna inhabiting potato cultivation s in south-eastern Poland that have been published thus far are only fragmentary (Szewkienicz and Olbrycht, 2012; Konieczna et al., 2015). Therefore, this publication presents more detailed results of a study on the species composition, quantitative structure, and ecological characteristics of ground beetles inhabiting conventional potato cultivation s in this region for the first time.

Material and Methods

Study sites

Observations on the species composition and numbers of ground beetles (Col., Carabidae) were conducted in eleven localities of south-eastern Poland during the 2008 and 2011-2013 growing seasons (*Fig. 1*). The study area comprised conventional potato (*Solanum tuberosum* L.) cultivations and the research covered thirteen sites. Samples collected in 2008 related to the sites in: Cierpisz, Olimpów, and Przeworsk. In Słonne, the selected site was investigated in 2011. Samples collected from potato cultivations in two growing seasons (2012-2013) related to the sites in Pakoszówka and Wiśniowa. In 2013 the sites in the following localities were studied: Drohojów, Kosina, Olszynka, Równia, and Wacławice.

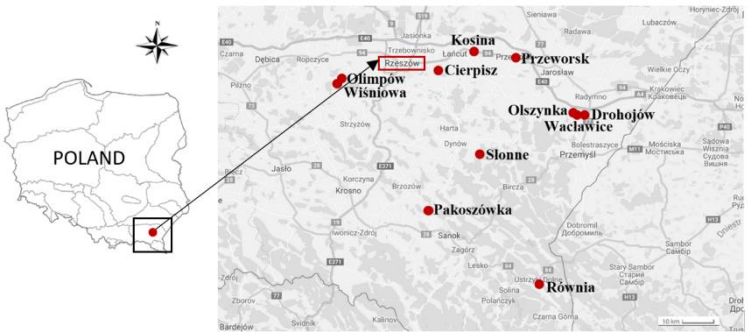

Figure 1. *Location of study sites (the authors' own figure based on www.lepidoptera.eu/utm)*

In a large majority of cases, potato cultivations where observations were conducted were surrounded by diverse habitats. Apart from intensively agriculturally used areas, such as cultivation fields, areas with lower agronomic pressure (meadows and pastures)

http://www.aloki.hu ● ISSN 1589 1623 (Print) ● ISSN 1785 0037 (Online)
DOI: http://dx.doi.org/10.15666/aeer/1802_21092128

and wooded areas (field trees and shrubs, forests) can be distinguished among them. The description of biocenoses adjacent to the potato cultivation s and areas of the study sites (in ares) are shown in *Table 1*, whereas the geographical characteristics, soil quality classes as well as a list of potato cultivars and cultivation protection products used in their cultivation are presented in *Table 2*.

Table 1. *Areas of the study sites (in ares) and characteristics of biocenoses adjacent to potato cultivations at study sites*

Site No.	Location	Year	Area [ares]	Adjacent habitats
1	Cierpisz	2008	25	oats cultivations, forest
2	Olimpów	2008	30	cereal cultivations, tree stands
3	Przeworsk	2008	30	wheat cultivations, meadow
4	Słonne	2011	12	agriculturally used areas, shrub stands, forest, meadow
5	Pakoszówka	2012	20	agriculturally used areas, meadow
6	Wiśniowa	2012	15	agriculturally used areas, forest, meadow
7	Drohojów	2013	51	meadows, tree stands, river
8	Kosina	2013	50	maize, rye and wheat cultivations
9	Olszynka	2013	70	oilseed rape and potato cultivations
10	Pakoszówka	2013	19	pastures, tree stands
11	Równia	2013	15	shrub stands, pastures, meadow, stream, ponds
12	Wacławice	2013	60	cereal cultivations, walnut plantation, forest
13	Wiśniowa	2013	20	forest, meadows, cultivation fields

Table 2. *Geographical characteristics, soil quality classes as well as a list of potato cultivars and cultivation protection products used in their cultivation at study sites*

Study site No. / GPS coordinates / variety / soil classification		Fertilizing and crop protection products *
1	N:50º9’33”, E:21º42’54” Bila / IV b	thiamethoxam 250 g/kg (25%), MCPA-300 g/l + dikamba-40 g/l, ammonium sulphate (28N)
2	N:50o0’20”, E:21o46’2” Atol, Ibis / n. d.	metribuzin, mancozeb 680 g/kg + cymoxanil 45 g/kg, imidacloprid
3	N:50º4’23”, E:22 º30’25” Balbina / II and III	acetamiprid, metalaxyl-M 3,8% + mancozeb 64%
4	N:49º47’39”, E:22º20’2” Atol i Irys / IV and V	deltamethrin, metalaxyl-M + mancozeb, acetamiprid
5	N:49 º37’44”, E:22º5’46” n. d. / III	deltamethrin
6	N:49º99’52”, E:21º75’42” Atol / III	metaflumizone
7	N:49º53’26”, E:22º47’00” Inova / III a	glyphosate, potassium mineral fertilizer 60% K, ammonium phosphate, nitrogen mineral fertilizer 27% N, linuron + clomazone, rimsulfuron, propamocarb hydrochloride + fenamidone, multi-component foliar fertilizer (N, MgO, B, Cu, Fe, Mn, Mo, Zn), tiaclopryd + deltamethrin, mandipropamid
8	N:50º5’5”, E:22º21’33” Żagiel, Denar / III	foliar fertilizer (N, P, K, S), linuron, quizalofop-P-ethyl, thiamethoxam, mancozeb + cymoxanil, metalaxyl-M + mancozeb
9	N:49º53’33”, E:22º45’4” Tajfun / n. d.	metribuzin, quizalofop-P-ethyl, metalaxyl-M + mancozeb, propamocarb hydrochloride + fenamidone, mandipropamid
10	N:49 º37’21”, E:22º6’3” Jelly N /III	multi-component fertilizer (N, P, K, Mg, B, Fe, Mn, Zn), nitrogen fertilizer
11	N:49º24’8”, E:22º35’9” n. d. / IV and V	MCPA, deltamethrin
12	N:49º53’15”, E:22º44’10” Denar / II and III	ammonium sulphate 32%N, foliar fertilizer (N, P, Mg, K, S), metribuzin, propamocarb + fenamidone, propamocarb hydrochloride + fluopicolide, thiacloprid + deltametrina
13	N:49º59’43”, E:21º45’15” Atol / III	metaflumizone

*- the names of active substances are given; n.d.- no data

http://www.aloki.hu ● ISSN 1589 1623 (Print) ● ISSN 1785 0037 (Online)
DOI: http://dx.doi.org/10.15666/aeer/1802_21092128

Catching of ground beetles

At each site, two Barber pitfall traps were set up at a distance of 2 m from each other. The pitfall traps were made of plastic containers placed flush with the ground level and filled with preserving fluid (25% ethylene glycol solution) to 1/3 of their volume. At individual sites, the traps were emptied every 2 weeks throughout the entire growing season of potato (starting from the last 10 days of April and ending in the first 10 days of September).

Nomenclature and Statistical Analyses

Identification of ground beetles was made using a study by Hurka (1996). The systematics of Carabidae followed a publication by Stachowiak (2008). The dominance structure (D) was described adopting the following classes: eudominants D5 (> 10% of individuals of an assemblage), dominants D4 (5.1–10%), subdominants D3 (2.1–5%), recedents D2 (1.1–2%), and subrecedents D1 (< 1%) (Trojan, 1980). The diversity indices used to analyze beetle assemblages were as follows: Margalef's species richness diversity index (d) (Trojan, 1998), Simpson's dominance index (λ), Shannon's species diversity index (H'_{ln}), and also Pielou's evenness index (J') (Magurran, 2004). The ecological and zoogeographical characteristics of carabids were described based on a study by Huruk and Barševskis (2014).

To determine similarities between the assemblages of beetles captured at individual sites, cluster analysis applying the Ward agglomeration method was used, in which the Euclidean distance was accepted as a measure of similarity. The obtained results were statistically analyzed using Statistica v.12 and Excel 2016 software.

Results

During the study conducted, a total of 7406 beetles were caught, representing 29 genera and classified in 54 species. The number of individuals and species caught as well as the indicators describing biodiversity at individual sites are collected in *Table 3*, whereas the dominance structure (D) of ground beetles at individual sites is shown in *Table 4*. The total numbers (N) and overall dominance (D) as well as the ecological and zoogeographical characteristics of species caught are presented in *Table 5*.

Table 3. *Number of individuals and species as well as indices describing the biodiversity of Carabidae caught at individual sites*

	Site												
	1	**2**	**3**	**4**	**5**	**6**	**7**	**8**	**9**	**10**	**11**	**12**	**13**
Year	2008	2008	2008	2011	2012	2012	2013	2013	2013	2013	2013	2013	2013
Number of species	15	18	15	16	13	14	12	14	11	13	14	21	18
Number of specimens	836	692	59	688	517	309	545	734	254	396	684	1272	420
Margalef index (d)	4.79	5.99	7.91	5.29	4.42	5.22	4.02	4.54	4.16	4.62	4.59	6,44	6.48
Simpson index (λ)	0.58	0.15	0.12	0.41	0.38	0.25	0.55	0.32	0.50	0.29	0.28	0.47	0.25
Shannon index ($H'l_n$)	1.03	2.19	2.37	1.26	1.26	1.72	0.94	1.45	1.12	1.56	1.66	1.28	1.75
Pielou index (J')	0.38	0.76	0.88	0.45	0.49	0.65	0.38	0.55	0.47	0.61	0.63	0.42	0.61

Total	Number of species	Number of specimens	Margalef index (d)	Simpson index (λ)	Shannon index ($H'l_n$)	Pielou index (J')
	54	7406	13.7	0.24	1.94	0.49

http://www.aloki.hu ● ISSN 1589 1623 (Print) ● ISSN 1785 0037 (Online)
DOI: http://dx.doi.org/10.15666/aeer/1802_21092128

Table 4. *Results of analysing of dominance stucture of Carabidae caught at individual sites*

Site	Class of dominance [D]				
	D5	**D4**	**D3**	**D2**	**D1**
1	*P.cup*	*H.ruf*	*P.ver, P.lep, C.err, A.sig*	*B.qua*	*C. fus, A. sex, A. bin, N. bre, M. lam, M. pro, A. par, D. hal*
2	*P.mel, H.ruf, M.lam, C.fus*	*P.cup, M.pro*	-	*A.sig, C.gra, T.qud, C. fos*	*C. err, A. mue, A. ple, C. can, P. nig, A. dor, A. flav*
3	*M.lam, B.qua, P.mel, H.ruf, C.amb*	*B.cep, C.fos, D.hal*	*D.glo, M.lam*	*A.bin, H.gri, P.cup, P.ver, P.vrn*	-
4	*H.ruf, P.mel*	*P.ver*	*P.nig*	*A.aul*	*C. gra, C. fus, C. cor, N. bre, A. sch, S. viv, C. ulr, C. lin, C. con, C. vio, C. car*
5	*H.ruf, P.cup*	-	*P.mel, P.nig, C.fus*	*C. vio*	*N. bre, P. ver, C. nit, C. gra, C. can, H. aff, P. ovo*
6	*H.ruf, P.cup*	*P.mel, C.gra, D.hal, C.fus*	-	*C.can*	*A. sig, N. bre, P. nig, C. ulr, C. viol, A. bin, A. mue*
7	*H.ruf, P.mel*	-	*C.ulr, D.hal, C.nit*	-	*C. ger, C. cor, P. ver, A. par, P. nig, S. viv, A. aul*
8	*P.mel, H.ruf, P.cup*	-	*C.gra*	*C.fus, A.sig*	*P. nig, D. hal, H. aff, P. vrn, A. mue, C. can, C. nit, S. pum*
9	*H.ruf, P.mel*	*D.hal*	*P.cup, P.nig*	*C.fus*	*B. qua, C. can, A. sig, H. aff, A. dor*
10	*P.cup, H.ruf, P.mel*	*C.fus*	*P.ver, B.qua*	*C.vio*	*N. bre, P. atr, C. cor, D. hal, M. lam, P. ant*
11	*P.cup, C.can, P.mel*	*H.ruf, P.ver*	-	*A.sex, P.ver, A.mue, C.nit*	*A. bin, C. cor, L. ass, C. gra, P. ant*
12	*H.ruf, P.mel*	*D.hal, P.cup*	-	*C.can, C.ulr*	*C. fus, C. gra, C. arc, A. sex, C. ger, B. cep, A. sig, P. obl, A. mue, C. nit, C. lin, P. nig, A. par, H. aff, H. lat*
13	*H.ruf, P.cup, C.fus*	*P.mel, D.hal*	*A.mue*	*A.sig, C.gra*	*C. can, B. qua, C. hyb, C. fos, C. col, M. lam, P. ver, A. dor, A. ple, Z. ten*

S - study site; Name of species: *N. bre- Nebria brevicollis, C. hyb- Cicindela hybrida, C. ger- Cylindera germanica, C. gra- Carabus granulatus, C. arc- Carabus arcensis, C. ulr- Carabus ulrichii, C. con- Carabus convexus, C. can- Carabus cancellatus, C. lin- Carabus linnei, C. vio- Carabus violaceus, C. cor- Carabus coriaceus, C. car- Cychrus caraboides, C. fos- Clivinia fossor, C. col- Clivinia collaris, D. glo- Dyschirus globosus, B. cep- Broscus cephalotes, T. qud- Trechus qudristriatus, A. fla- Asaphidion flavipes, M. lam- Metallina lampros, M. pro- Metallina properans, B. qua- Bembidion quadrimaculatum, P. atr- Patrobus atrorufus, A. bin- Anisodactylus binotatus, A. sig- Anisodactylus signatus, H. ruf- Harpalus rufipes, H. gri- Harpalus griseus, H. aff- Harpalus affinis, H. lat- Harpalus latus, A. par- Acupalpus parvulus, P. lep- Poecilus lepidus, P. cup- Poecilus cupreus, P. ver- Poecilus versicolor, P. vrn- Pterostichus vernalis, P. obl- Pterostichus oblongopuctatus, P. nig- Pterostichus niger, P. mel- Pterostichus melanarius, P.ant- Pterostichus anthracinus, P. ovo- Pterostichus ovoideus, A. par- Abax parallelus, A. sch- Abax schueppeli rendschmidtii, S. pum- Stomis pumicatus, C. fus- Calathus fuscipes, C. err- Calathus erratus, C. amb- Calathus ambiguus, D. hal- Dolichus halensis, S. viv- Synuchus vivalis, A. mue- Agonum muelleri, A. sex- Agonum sexpunctatum, L. ass- Limodromus assimilis, A. dor- Anchomenus dorsalis, A. ple- Amara plebeja, A. aul- Amara aulica, C. nit- Chlaeniellus nitidulus, Z. ten- Zabrus tenebrioides.*

D [%] - Dominance: D5 - eudominants, D4 - dominants, D3 - subdominants, D2 - recedents, D1 – subrecedents

http://www.aloki.hu ● ISSN 1589 1623 (Print) ● ISSN 1785 0037 (Online)
DOI: http://dx.doi.org/10.15666/aeer/1802_21092128

Table 5. *Total number of individuals and species, overall dominance (D), and ecological characteristics of Carabdae caught at all sites*

Species	N	D [%]		I	II	III	IV	V
Nebria brevicollis (F.)	13	0.18	D1	F	Sz	H	A	EM
Cicindela hybrida L.	1	0.01	D1	Oa	Lz	X	S	Esyb
Cylindera germanica (L.)	8	0.11	D1	Oa	Lz	H	S	P
Carabus granulatus L.	74	1.00	D1	OaF	Lz	H	S	Esyb
Carabus arcensis HERBST	7	0.09	D1	F	Lz	H	S	P
Carabus ulrichii GERMAR	31	0.42	D1	Oa	Lz	Mh	A	E
Carabus convexus F.	1	0.01	D1	OaF	Lz	Mh	S	Esyb
Carabus cancellatus ILL.	176	2.38	D3	Oa	Lz	Mh	S	Esyb
Carabus linnei (PANZ.)	4	0.05	D1	R	Lz	H	A	GEpl
Carabus violaceus (L.)	14	0.19	D1	F	Lz	Mh	S	P
Carabus coriaceus L.	12	0.16	D1	F	Lz	Mh	A	E
Cychrus caraboides L.	1	0.01	D1	F	Lz	H	S	Ea
Clivinia fossor (L.)	12	0.16	D1	Oa	Sz	H	S	H
Clivinia collaris (HERBST)	1	0.01	D1	Oa	Sz	H	S	P
Dyschirus globosus (HERBST)	2	0.03	D1	OaF	Sz	H	S	P
Broscus cephalotes (L.)	7	0.09	D1	Syn	Sz	Mh	A	Esyb
Trechus qudristriatus (SCHRANK)	10	0.14	D1	Oa	Sz	Mh	S	P
Asaphidion flavipes (L.)	1	0.01	D1	Oa	Sz	Mh	S	P
Metallina lampros (HERBST)	85	1.15	D2	Oa	Sz	Mh	S	P
Metallina properans (HERBST)	70	0.95	D1	Oa	Sz	H	S	P
Bembidion quadrimaculatum (L.)	73	0.99	D1	Oa	Sz	Mh	A	H
Patrobus atrorufus (STROM.)	3	0.04	D1	OaF	Sz	H	A	Esyb
Anisodactylus binotatus (F.)	9	0.12	D1	Oa	Sz	H	S	P
Anisodactylus signatus (PANZ.)	55	0.74	D1	F	Sz	Mh	S	EM
Harpalus rufipes (DE GEER)	2943	39.74	D5	Oa	Hz	Mh	A	P
Harpalus griseus (PANZ.)	1	0.01	D1	Oa	Hz	X	A	P
Harpalus affinis (SCHRANK)	9	0.12	D1	Oa	Hz	X	S	P
Harpalus latus (L.)	1	0.01	D1	Oa	Hz	Mh	A	P
Acupalpus parvulus (STURM)	1	0.01	D1	Oa	Sz	H	A	P
Poecilus lepidus (LESKE)	37	0.50	D1	Oa	Sz	Mh	A	Esyb
Poecilus cupreus (L.)	1742	23.52	D5	OaF	Sz	Mh	S	P
Poecilus versicolor (STURM)	111	1.50	D2	Oa	Sz	Mh	S	Esyb
Pterostichus vernalis (PANZ.)	52	0.70	D1	R	Sz	H	S	P
Pterostichus oblongopuctatus (F.)	3	0.04	D1	F	Sz	Mh	S	P
Pterostichus niger (SCHALL.)	61	0.82	D1	F	Lz	Mh	S	Esyb
Pterostichus melanarius (ILL.)	1211	16.35	D5	Oa	Lz	Mh	A	Esyb
Pterostichus anthracinus (ILL.)	2	0.03	D1	R	Sz	H	S	P
Pterostichus ovoideus (STURM)	1	0.01	D1	R	Sz	H	A	P
Abax parallelus (DUFT.)	6	0.08	D1	F	Sz	Mh	S	E
Abax schueppeli rendschmidtii (GERM.)	3	0.04	D1	F	Sz	Mh	S	GEpl
Stomis pumicatus (PANZ.)	1	0.01	D1	OaF	Sz	H	S	EM
Calathus fuscipes GOEZE	220	2.97	D3	OaF	Sz	Mh	A	P
Calathus erratus (C.R. SAHLB.)	34	0.46	D1	OaF	Sz	Mh	A	P
Calathus ambiguus (PAYK.)	6	0.08	D1	Oa	Sz	Mh	A	P
Dolichus halensis (SCHALL.)	177	2.39	D3	Oa	Sz	Mh	S	P
Synuchus vivalis (ILL.)	4	0.05	D1	OaF	Sz	Mh	A	Esyb
Agonum muelleri (HERBST)	39	0.53	D1	OaF	Sz	Mh	S	H
Agonum sexpunctatum (L.)	22	0.30	D1	F	Sz	Mh	S	P
Limodromus assimilis (PAYK.)	2	0.03	D1	F	Sz	H	S	P
Anchomenus dorsalis (PONT.)	4	0.05	D1	OaF	Sz	Mh	S	P
Amara plebeja (GYLL.)	6	0.08	D1	Oa	Hz	Mh	S	P
Amara aulica (PANZ.)	13	0.18	D1	Oa	Hz	H	S	P
Chlaeniellus nitidulus (SCHRANK)	23	0.31	D1	R	Sz	H	A	E
Zabrus tenebrioides (GOEZE)	1	0.01	D1	Oa	Hz	Mh	A	P

I- Habitat: F- forest, Oa- open area, OaF- open area and forest, R- riparian, Syn- synanthropic; II- Trophic categories: Lz- large zoophage, Sz- small zoophage. Hz- hemizoophage; III- Moisture preferences: H- hygrophilous, Mh- mesohygrophilous, X- xerophilous; IV- Breeding preferences: A- autumn breeder, S- spring breeder; V- Zoogeographical elements: E- European, Ea-Euro-Arctic, Esyb- Eyro-Siberian, EM- Euro-Mediterranean, GEPL- European Forest Province [montane], H- Holarctic, P- Palearctic. D [%]- Dominance: D5- eudominants, D4- dominants, D3- subdominants, D2- recedents, D1- subrecedents

http://www.aloki.hu ● ISSN 1589 1623 (Print) ● ISSN 1785 0037 (Online)
DOI: http://dx.doi.org/10.15666/aeer/1802_21092128

In terms of total numbers, *H. rufipes*, *P. cupreus*, and *P. melanarius* were species found in greatest numbers. At individual sites, these species also occurred in large numbers, but only *H. rufipes* was recorded at all study sites. The highest number of species was found at site 12 (21 taxa). At the same time, it was the site where the highest number of individuals was recorded (1272 exx.). The lowest number of species (11) was found at site 9, while as regards the number of individuals – at site 3 (59 exx.).

Overall, four dominance classes were distinguished, with the highest percentage of the least numerous class, i.e. subrecedents (D1) (46 species, more than 85% of the entire assemblage).

The recedent class (D2) was represented by 2 species that accounted for 3.7% of the total number. Three species (5.6%) were classified both in the eudominant (D5) and subdominant (D3) classes. The dominant class (D4), however, was not recorded. A slightly different dominance structure was observed at individual sites. Among all study areas, all dominance classes were only found at five of them (sites 1, 4, 9, 10, and 13), but still with a distinct proportion of subrecedents. The degree of dominance reached the highest value at site 1 (λ=0.58) (*Fig. 2a-b*, *Tables 4* and *5*).

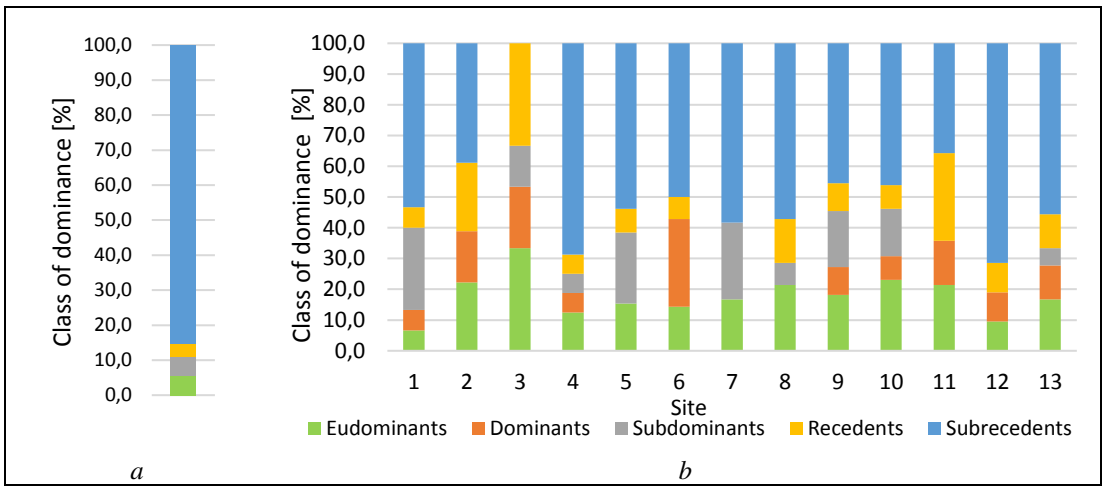

Figure 2a-b. *Overall percentage of particular dominance classes of Carabidae (a) and at individual sites (b)*

Forest, open area, open area and forest, riparian and synanthropic species were found to be present in the Carabidae assemblage. Open area species constituted the dominant group and they accounted for 46.3% of the entire assemblage, whereas their percentage at individual sites ranged 31.3-73.3%. The group of forest species was second ranking and their percentage was 22.2% of the total number. At individual sites, however, it was the third ranking category with an average percentage of 19%. A comparable proportion was determined for open area and forest species. Overall, they made up 20.4%, whereas the average for the study areas was 23.5%. Riparian species constituted 9.3% of the entire assemblage, while synanthropic species were least numerous. In this category, only *Broscus cephalotes* (L.) with a percentage of 1.9%. The above-mentioned five habitat categories were only found at one site (no. 12). At the other sites, the number of distinguished categories was 3 (sites 1, 2, and 13) or 4 (sites 3, 4, 5, 6, 7, 8, 9, 10, and 11) (*Fig. 3a-b*, *Table 5*).

http://www.aloki.hu ● ISSN 1589 1623 (Print) ● ISSN 1785 0037 (Online)
DOI: http://dx.doi.org/10.15666/aeer/1802_21092128

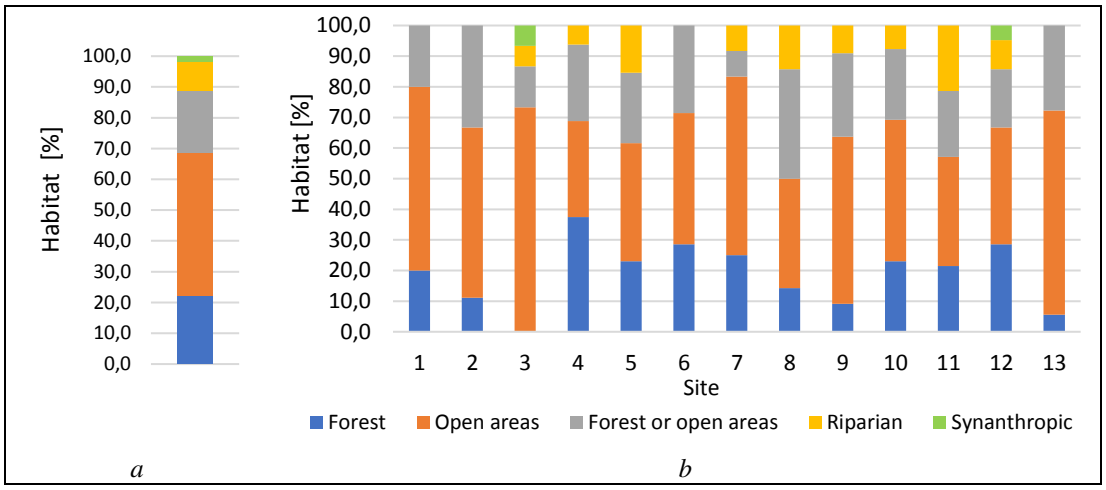

Figure 3a-b. *Overall percentage of habitat categories of Carabidae (a) and at individual sites (b)*

The analysis of the trophic structure showed three components to be present. Small zoophages were represented in largest numbers both in total terms and at individual sites. Overall, their percentage was 63%, whereas for the study sites the average percentage of this trophic group was 55.9%. Small zoophages were the second ranking class in terms of numbers only at two sites (4 and 9). Large zoophages, in turn, were found at 12 sites, with visible fluctuations in their numbers, similarly to the previous group. Their total percentage was 24.1%. At site 1, no species belonging to this trophic group were found. Hemizoophages were least numerous, accounting for 13% of all species. In quantitative terms, they occurred in greatest numbers at site 9 (*Fig. 4a-b*, *Table 5*).

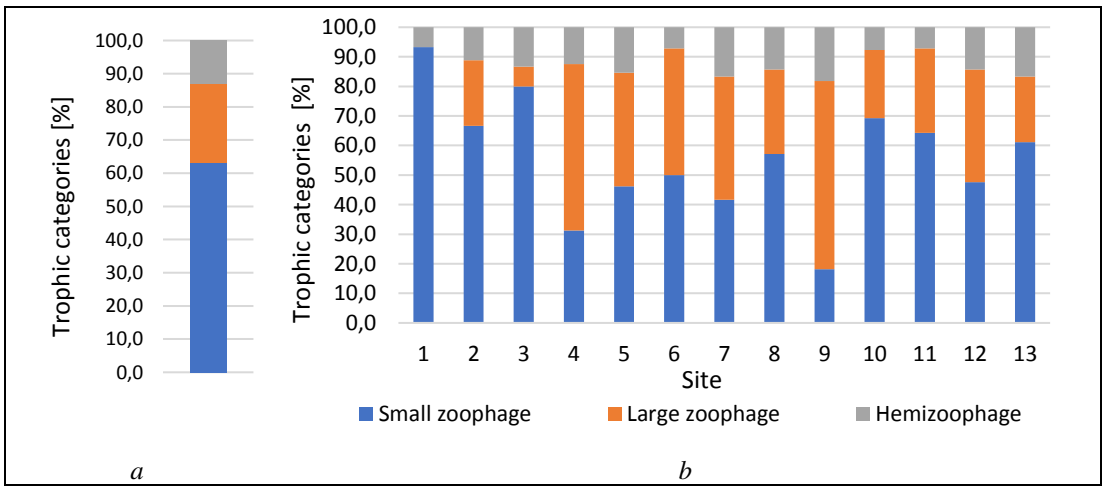

Figure 4a-b. *Overall percentage of particular trophic categories of Carabidae (a) and at individual sites (b)*

As far as moisture preferences are concerned, three types were distinguished. Species found in large numbers in habitats of diverse nature in terms of moisture, i.e. mesohygrophiles, constituted the largest group. Their percentage in the entire assemblage was 57.4%. At individual sites, this percentage ranged between 57.1% (site 11) and 90.9%

http://www.aloki.hu ● ISSN 1589 1623 (Print) ● ISSN 1785 0037 (Online)
DOI: http://dx.doi.org/10.15666/aeer/1802_21092128

(site 9) (on average 72.2%). Fewer hygrophilous species, that is, associated with strongly moist and wet environments, were found. They accounted for 37% of all carabids identified. At individual sites, in turn, the average percentage of this group was 24.6%. They occurred in greatest numbers at site 11 where their percentage was 42.9%. The only site where hygrophilous species were not observed to be present was site 9. Xerophiles, i.e. dry-loving species preferring environments with low humidity and strong insolation, were the last and at the same time least numerous group. Overall, they accounted for 5.6% of all species found, but at individual sites their percentage contribution was lower, averaging 3.1%. Xerophilous species were recorded at six sites (3, 5, 8, 9, 12, and 13); among them, site 9 was found to have the highest percentage (9.1%) (*Fig. 5a-b*, *Table 5*).

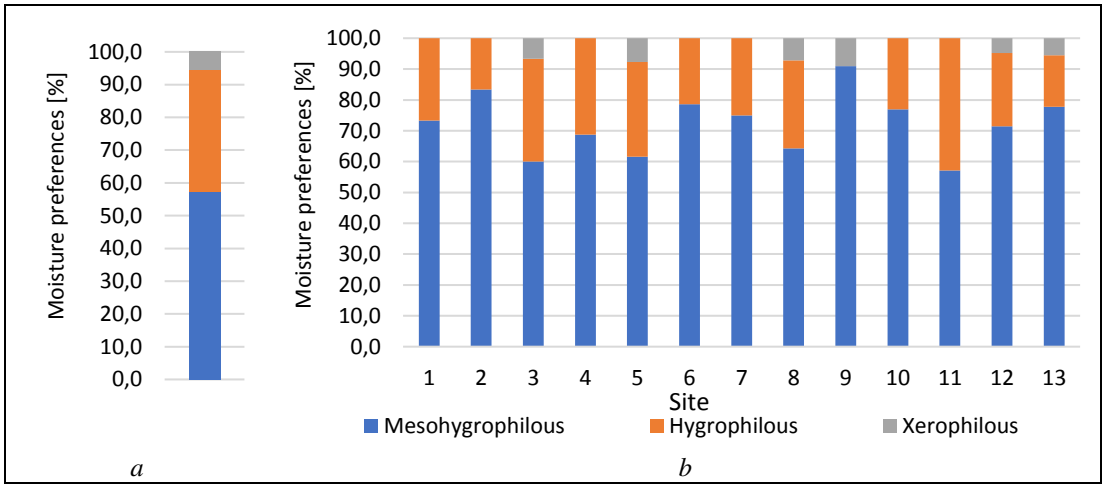

Figure 5a-b. *Overall percentage of particular moisture preferences of Carabidae (a) and at individual sites (b)*

In the assemblage of Carabidae caught, two breeding types were distinguished: species overwintering in the form of imago, i.e. spring breeders, and species being autumn breeders, that is, overwintering at the pre-imaginal stage. Spring breeding was found in 63% of ground beetles identified, while for individual sites the percentage of this category ranged from 46.2% to 72.2%, with an average value of 60.8%. The proportion of autumn breeders was lower, with their overall percentage standing at 37%. The lowest percentage of autumn breeding species was recorded at two sites: 2 and 13 (27.8% at either of them). Site 10, on the other hand, was observed to have the highest percentage of this ecological category, which was 53.8% of individuals collected at this site (*Fig. 6a-b*, *Table 5*).

The carabid fauna comprised seven zoogeographical elements. Overall, Palearctic species were most numerous, accounting for 55.6% of species found. Euro-Siberian species had a lower percentage: 20.4%. The other elements were represented by a much lower number of species: European (7.4%), Holarctic and Mediterranean (5.6%), montane European Forest Province (3.7%), and Euro-Arctic (1.9%). Palearctic and Euro-Siberian species were found at all sites. *Cychrus caraboides* L., as the only representative of the Euro-Arctic element, was only found at site 4 (1.9% of all species) (*Fig. 7c*). At the same time, this site and site 12 were shown to exhibit the greatest variation in ground beetles in terms of range (6 elements). Sites 3 and 7 were least chorologically varied as only 3 elements of this ecological category were recorded there (*Fig. 8a-b*, *Table 5*).

http://www.aloki.hu ● ISSN 1589 1623 (Print) ● ISSN 1785 0037 (Online)
DOI: http://dx.doi.org/10.15666/aeer/1802_21092128

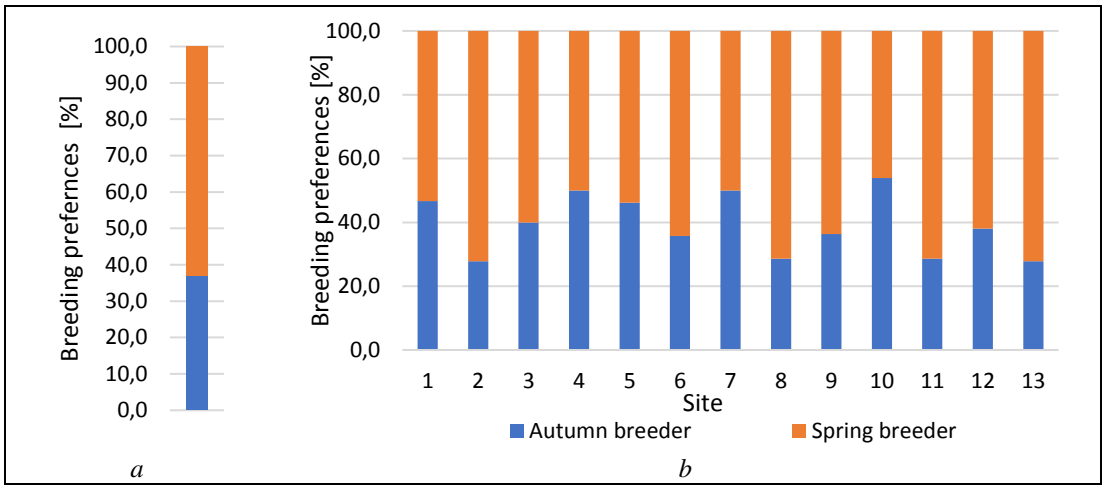

Figure 6a-b. *Overall percentage of particular breeding preferences of Carabidae (a) and at individual sites (b)*

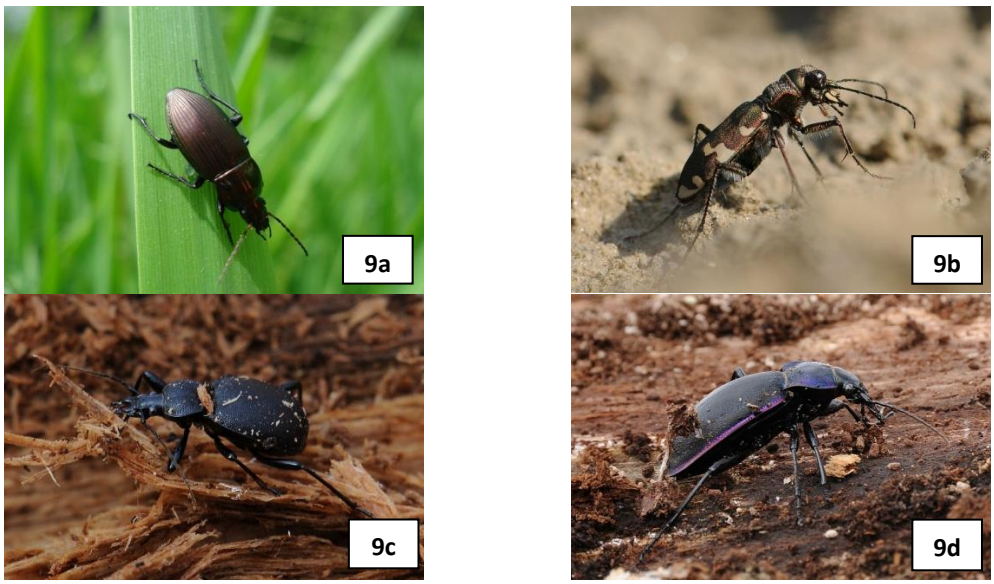

Figure 7a-d. *Representatives of different ecological groups of zoophagous Carabidae caught in potato cultivations at selected sites in Subcarpathian Voivodeship: (a) Poecilus cupreus (L.) – representative of the eudominant class (D5), open and wooded area species; (b) Cicindela hybrida L. – xerophile, open area species; (c) Cychrus caraboides L.– representative of the Euro-Arctic element, forest species; (d) Carabus violaceus (L.)– representative of the subrecedent class, forest species (photo by T. Olbrycht)*

In overall terms, the assemblage's diversity indices were as follows, respectively: Shannon's species diversity H'_{ln} = 1.94, while Pielou's evenness J' = 0.49. The values of the above-mentioned indices at individual sites differed from the total value. The species diversity index (d) reached the highest value at site 3 (d = 7.91), whereas the lowest one at site 7 (d = 4.02). The other biodiversity indices also had the minimum and maximum values, respectively, at the same sites: H'_{ln}= 2.37 (the highest value at site 3), H'_{ln} = 0.94

http://www.aloki.hu ● ISSN 1589 1623 (Print) ● ISSN 1785 0037 (Online)
DOI: http://dx.doi.org/10.15666/aeer/1802_21092128

(the lowest value at site 7), J' = 0.88 (the highest value at site 3), J' = 0.38 (the lowest value at sites 1 and 7). The Simpson dominance index (λ) was 0.24.

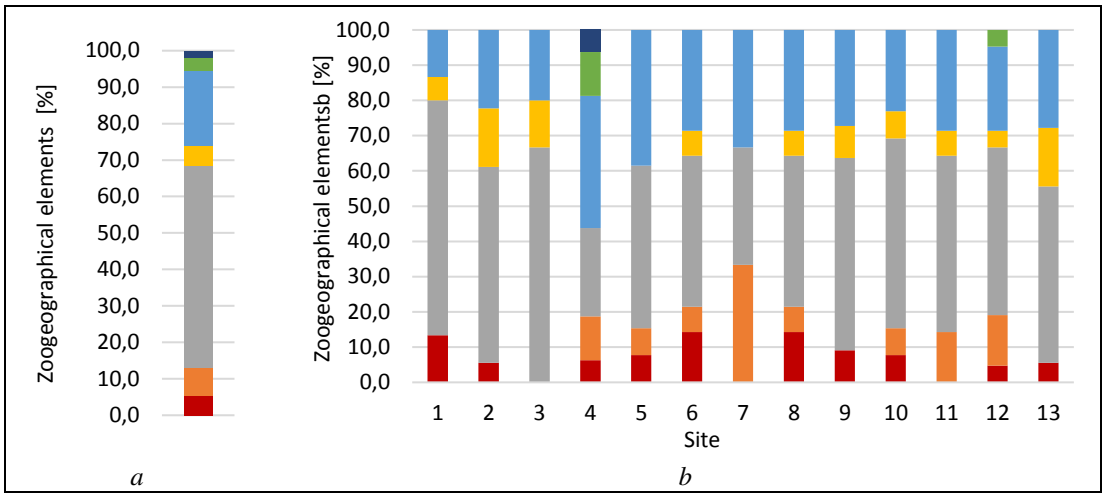

Figure 8a-b. *Overall percentage of zoogeographical elements of Carabidae (a) and at individual sites (b)*

The analysis of similarities between the Carabidae assemblages caught at individual sites revealed that sites 6 and 13 as well as sites 4 and 7 were most similar to each other in terms of beetles inhabiting them. Site 12 occupied a separate position in the dendrogram (*Fig. 9*).

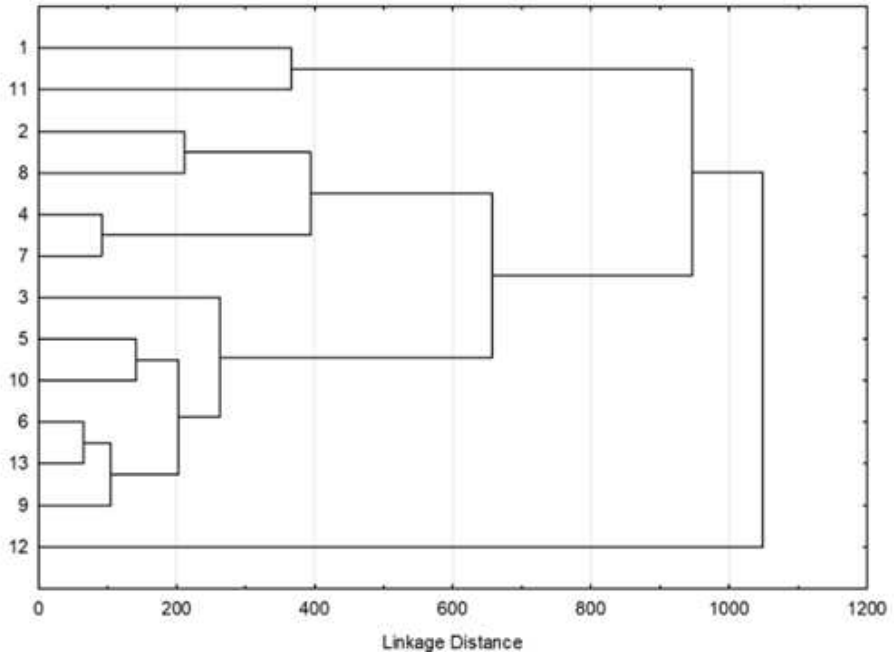

Figure 9. *Dendrogram of faunistic similarity of Carabidae inhabiting potato cultivations at selected sites in Subcarpathian Voivodeship. Cluster analysis by the Ward method, the Euclidean distance as a measure of similarity*

http://www.aloki.hu ● ISSN 1589 1623 (Print) ● ISSN 1785 0037 (Online)
DOI: http://dx.doi.org/10.15666/aeer/1802_21092128

Discussion

According to the research by Basedow et al. (1976) and Thiele (1977), in one-year studies 20-35 species are found in the qualitative structure of ground beetles of cultivation fields in Central Europe. 54 Carabidae species were recorded in the cross-sectional study of potato cultivations in the Subcarpathian region, while the average number of species per site was 15. The highest number of species was shown at site 12 (21 species identified). The number of beetles caught is dependent not only on environmental factors (temperature, humidity, climate) and the adopted research methodology (number of traps, study period), but in the case of agricultural ecosystems also on the type of cultivations, application of cultivation protection products, soil type, and adjacent biocenoses (Thiele, 1977; Aleksandrowicz, 2002; Bale et al., 2002; Huruk, 2002, 2006; Irmler, 2003; Kosewska and Nijak, 2012; Nijak et al., 2013).

The number of Carabidae species captured in potato cultivations varies. Compared to other publications, Koval (2012) showed a very large number of ground beetle taxa - 171 species. However, it is worth noting that this study, designed to determine the adaptation of Carabidae as zoophages feeding on *Leptinotarsa decemlineata*, was conducted within the area of nine regions in three countries (Russia, Ukraine, and Moldova) and covered a nearly 30-year study period. Another review publication reports a much lower number of species than in the study by Koval (2012), but almost twice higher than in the case of one- or two-year observations. In Latvia Bukejs et al. (2009) revealed 59 ground beetle species. This review included studies from the period 1960-2009. On the other hand, studies conducted over a shorter period of time present different results. A four-year study on the species composition of ground beetles of potato cultivations differing in soil type which was conducted in Russia showed a total of 58 taxa, out of which the number of species identified ranged from 26 to 34 depending on the site. In turn, a two-year study carried out in Latvia revealed a total of 44 Carabidae species (34 species in the first year of the study, 38 – in the second one) (Bukejs, 2009). As far as the number of species is concerned, similar results were obtained by Juen et al. (2003) in Austria. These authors recorded 46 imaginal species and 25 species at the larval stage. In Austria research was also conducted by Kromp (1990) and Traugott (1998) and the study results were also similar in their case. Kromp (1990) demonstrated a total of 48 species, whereas Traugott (1998) - 49. A smaller number of species was reported by Nijak et al. (2013) who described 39 taxa, Nijak et al. (2014) - 34 species, Kinnunen and Tiainen (1999) - 35 species, whereas Kosewska and Nijak (2012) - 32 species. A one-year study was also done by Jasiński et al. (2015) who found 11 (the first site) and 7 (the second site) species under organic farming system.

The most frequently occurring species (D5-eudominants) in the Subcarpathian region were *H. rufipes*, *P. cupreus*, and *P. melanarius,* which are components of epigeic Carabidae fauna commonly found in cultivation fields (Thiele, 1977). *H. rufipes* was a species that occurred most frequently at individual sites. At most of the sites, this species constituted the eudominant class (D5) and was classified as dominant (D4) only at two sites (1 and 11). It also proved to be the most numerous in other authors' studies (Juen et al., 2003; Kosewska et al., 2008; Kosewska and Nijak, 2012; Nijak et al., 2014).

Poecilus cupreus was the second most numerous Carabidae species in this study investigating the Subcarpathian region. This species occurred at 11 sites (it was not found at sites 4 and 7). Nevertheless, the numbers of this beetle in an agricultural ecosystem vary. In the study by Bukejs (2009), it was the most numerous species (whereas *H. rufipes* was a subrecedent). In the research of Kosewska and Nijak (2012), it achieved the

http://www.aloki.hu ● ISSN 1589 1623 (Print) ● ISSN 1785 0037 (Online)
DOI: http://dx.doi.org/10.15666/aeer/1802_21092128

subdominant status in integrated farming, whereas in organic farming - the subrecedent status. Under organic potato cultivation, in turn, Jasiński et al. (2015) showed this species to be an eudominant (D5) at site I, while at site II it was not found. In the study by Kosewska et al. (2008), *P. cupreus* was a dominant, whereas in the study by Traugott (1998), in turn, it proved to be an eudominant.

Similarly to *P. cupreus*, *P. melanarius* was a species that occurred in very large numbers both in the Subcarpathian region and in Austria (Traugott, 1998; Juen et al., 2003). It proved to be dominant (D4) or subdominant (D3) at locations in western Poland (Kosewska and Nijak, 2012), whereas in Latvia a subrecedent (D1) (Bukejs, 2009). In the present study, this species occurred at 12 sites where it constituted the eudominant (D5) or dominant (D4) class. Its numbers were lower only at one site (no. 5) where it was classified as a subdominant (D3). But it was not found at site 1.

A characteristic feature of the distribution of dominance of carabids inhabiting cultivation fields is the presence of a small number of dominant species with a very large proportion of individuals and a larger number of common species but represented by low numbers of individuals (Baranová et al., 2013). We see a very clear confirmation of this finding in the structure of Carabidae occurring at site no. 12. The analysis of the dendrogram (*Fig. 9*) revealed that this site stood out most in relation to the other study sites. In quantitative terms, the following eudominant species prevailed: *H. rufipes* and *P. melanarius*, which accounted for 77.9% of the assemblage (991 individuals). But in qualitative terms, this class accounted for 9.5%, similarly to dominants and subdominants (either of these classes was represented by two species). The recedent class was not found, whereas subrecedents were the most numerous class (71.4% of the assemblage, 15 species).

As reported by Czechowski (1981), agronomic practices used in cultivation fields promote the occurrence of open area species. The obtained study results confirm this dependence since nearly a half of species recorded are grouped in this ecological class (49% of individuals). Open area and forest species (ecotone ones) as well as forest species constituted the second ranking class, in terms of numbers, accounting for 23.5% and 19%, respectively. The presence of these species in the agrarian structure results from the presence of dendroflora in agricultural landscape and the migration capacity of ground beetles that seek both shelter and food in biocoenoses adjacent to cultivations (Krzysztofiak, 2001). Riparian species were less numerous (7.6%), while synanthropic species, which were represented only by one species – *B. cephalotes* (1.9% of the total number), were least numerous.

Trophism is another important factor used to analyze the carabidofauna structure. Both in qualitative and quantitative terms, zoophages were predominant in the entire carabid assemblage (47 species, 87% of the total number). The proportion of hemizoophages was small (7 species, 13% of the total number). However, the proportion of zoophagous species was not even as small zoophages were predominant (34 species, 63% of the total number). At site 1, no large zoophages were found at all, whereas small zoophages accounted for 93.3% of the assemblage. In turn, a high predominance of large zoophages was observed at two sites (4 - 56.3%, and 9 – 63.6%). The dominance of large zoophages is a very beneficial phenomenon, evidencing good condition of an environment (Szyszko, 1997). The dominance, both quantitative and qualitative, of predatory species is important from the ecological point of view because it may provide environmental resistance since zoophagous carabids reduce significantly the number of phytophagous species that threaten agricultural cultivation plantations (Koval, 1999; Aleksandrowicz, 2004).

http://www.aloki.hu ● ISSN 1589 1623 (Print) ● ISSN 1785 0037 (Online)
DOI: http://dx.doi.org/10.15666/aeer/1802_21092128

Nonetheless, the prevailing tendency towards a higher number of small zoophages is a typical phenomenon, characteristic of habitats that are subjected to adverse impacts of external factors; an increase in this tendency causes the numbers of hemizoophages to grow (Pałosz, 1995; Leśniak, 1997). Worth noting is also the fact that out of the total number of 13 species of large zoophages, 8 of them were beetles of the genus *Carabus*. It is a satisfactory result because in the research of other authors this number is usually lower. Juen et al. (2003) showed 3 species, both Bukejs (2009) and Jasiński et al. (2015) found 2 species, whereas Kinnunen and Tiainen (1999) only 1. Kosewska and Nijak (2012), in turn, did not demonstrate any species belonging to this genus. Varvara (2010) recorded a higher number of species of the genus *Carabus* occurring in potato cultivations. 11 species were described but this study covered a larger area (5 regions) and a longer study period (18 years).

It is also worth noting the fact that 3 species belonging to the genus *Carabus* caught in these studies are protected in Poland (*C. ulrichii* Germar, *C. convexus* F., and *C. coriaceus* Ill.). It was surprising to record two riparian species: *Pterostichus ovoideus* (Sturm) and *Carabus linnei* (Panz.). Both species were found in investigations of agrocenoses but not in potato cultivations (Konieczna et al., 2015). In a study by Szewkienicz and Olbrycht (2012), however, *P. ovoideus* was found in organic potato cultivation in the Subcarpathian region.

The analysis of moisture preferences showed mesohygrophilous species to have a dominant proportion (57.4%), with a much lower percentage of hygrophilous species, strictly associated with wet biocenoses (37%). According to Thiele (1977), the predominance of mesohygrophilous species is typical for European agroecosystems. Only 3 species, *Cicindela hybrida* L., *Harpalus griseus* (Panz.), and *H. affinis* (Schrank), represented dry-loving (xerophilous) species (5.56%).

The beetles caught were also characterized in terms of their breeding preferences. In the studied material, spring breeding species were predominant (63% of the assemblage - 34 species), whereas autumn breeding was represented by 20 species (37% of the assemblage). Similar results were obtained by Borowski et al. (1996) who indicated this breeding preference as characteristic of Carabidae occurring at sites where cultivation protection products are used. The variation in phenology is confirmed by the difference in the catch rate of individual species since the largest numbers and fluctuations were observed in spring and summer months.

Palearctic (55.6% of the total number) and Euro-Siberian (20.4% of the total number) species predominated in the studied material. As reported by Czechowski (1981) and Huruk (2006), these are zoogeographical elements characteristic of cultivation fields. Wide range spectra are characteristic of species occurring in environments subjected to greater pressure of external factors. Natural or semi-natural habitats, on the other hand, favor the occurrence of species with narrower zoogeographical ranges (Leśniak, 1997; Huruk et al., 2014). *C. caraboides* was such a species, the only representative of the Euro-Arctic element which was only found at one site (no. 4).

Species diversity is an important indicator describing a Carabidae assemblage (Nijak et al., 2013). The total value of H'_{ln}=1.94 and the values obtained at individual sites (H'_{ln} ranging 0.94-2.37) are comparable with results obtained by other authors: H'_{ln} =2.108 (Kosewska et al., 2008), H'_{ln} =1.98 and H'_{ln} =2.38 (Kosewska and Nijak, 2012), H'_{ln} =2.17 and H'_{ln} =1.58 (Jasiński et al., 2015). A higher value of this index characterizes assemblages with a quite good internal structure (species distribution), though not very numerous. The highest value of this indicator was observed at site 3, which was

http://www.aloki.hu ● ISSN 1589 1623 (Print) ● ISSN 1785 0037 (Online)
DOI: http://dx.doi.org/10.15666/aeer/1802_21092128

characterized by the lowest number of individuals (59) and a medium number of species (15). The Pielou evenness index (J') represents the equal distribution of individuals among all species. The total value of this index in the carabid assemblage was J'=0.49, which could have been due to a large (dominant) proportion of rare species. In turn, at site 3 where the subrecedent class was not observed, the value of this index was highest among all sites studied (J'=0.88). Another indicator used to analyze the Carabidae assemblage was the degree of species dominance (λ). This parameter assigns a lower weight to the occurrence of rare species, paying greater attention to common species, and takes on higher values in communities dominated by one or several species. The highest value of this index was recorded at site 1 (λ=0.58) where only one eudominant (*P. cupreus*) was found; its contribution to the assemblage was 633 individuals (75.7% of the assemblage). The lower the value of this index, the more equal distribution of individuals among species. The lowest values of λ were observed at two sites: 3 (λ=0.12) and 2 (λ=0.15). Not all dominance classes were found at these sites but the proportions of individual species recorded there were relatively equal. Huruk (2006) obtained similar results, which was related to the dominant contribution of one species. The sites that were characterized by the highest value of the dominance index, that is, they were dominated by one or two species, exhibited the lowest values of the diversity indices: site 1 (λ=0.58; H'_{ln} =1.03) and site 2 (λ=0.55; H'_{ln}=0.94) (*Fig. 10*).

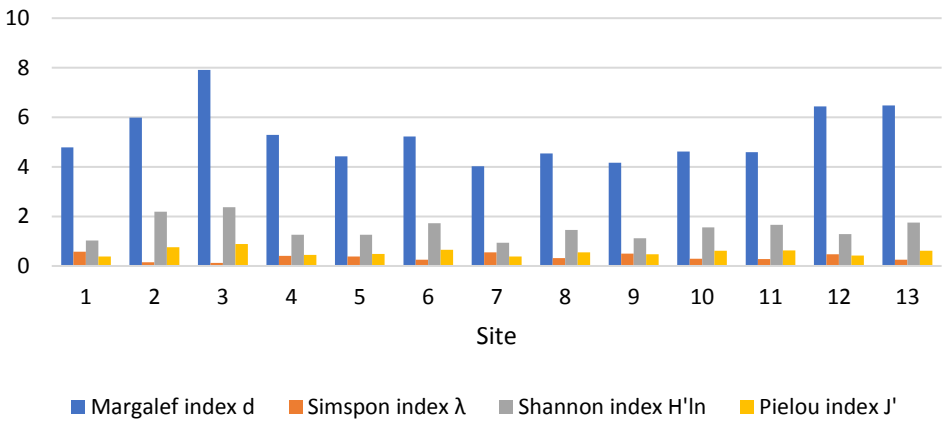

Figure 10. *Indices of α-diversity: species diversity of Margalef (d), Shannon (H'_{ln}), Simpson concentrate of dominance (λ) and Pielou's Evennes (J')*

Application of cultivation protection products can be another factor determining the qualitative and quantitative structure of ground beetles. In the studied material, samples were only taken from sites subjected to various agronomic practices. Due to the fact that no comparative observations were conducted based on control samples (i.e. without application of insecticides, for instance), one cannot determine the direct effect of anthropogenic factors on the occurrence of beetles.

As evidenced by research, changes in agricultural practices beneficially affecting the diversity of Carabidae include, among others, reduced use of pesticides and organic farming (Andresen and Eltun, 2002; Koss et al., 2005), but also changes in cultivation practices (Andersen, 2003) and reduced herbicide application (Thorbek and Bilde, 2004). The effect of insecticides (deltamethrin) was investigated by Kaczmarek (1992) and Aleksandrowicz (2002) who showed chemical treatments to adversely influence

http://www.aloki.hu ● ISSN 1589 1623 (Print) ● ISSN 1785 0037 (Online)
DOI: http://dx.doi.org/10.15666/aeer/1802_21092128

assemblages of ground beetles. Intensively cultivated potato plantations create adverse habitat conditions for most carabids (Werling and Gratton, 2008).

Nonetheless, not always does the impact of agronomic practices on the Carabidae structure cause a decrease in biodiversity. The studies by Kosewska et al. (2013) and Nijak et al. (2013) revealed that chemical protection in integrated potato cultivation does not affect adversely the preservation of the diversity of ground beetles. On the other hand, Kosewska et al. (2014) demonstrated that integrated cultivation protection can contribute to increased diversity of Carabidae. Insecticide application was not shown to have an adverse effect, but herbicide and fungicide application proved to have a significant impact on the structure of ground beetles.

Habitat factors, such as adjacent biocenoses, are an important element affecting the occurrence of Carabidae in cultivation fields. As demonstrated by Weibull et al. (2003), the vicinity of diverse biocoenoses has a major importance for the preservation of biodiversity of ground beetles in conventional cultivations. In most cases, the investigated cultivation sites in the Subcarpathian region were characterized by substantially diverse natural landscape in the form of bordering or adjacent field trees and shrubs, meadows, and forests. Among the study areas, only sites 8 and 9 bordered exclusively with agriculturally used areas. Potato cultivations located in the surroundings of low diversity habitats were characterized by the occurrence of a smaller number of both beetle species and individuals. Site 9 where the lowest number of species and a relatively low number of individuals were recorded was surrounded by cultivations of another potato cultivar and oilseed rape cultivations. In turn, the number of species and individuals was observed to increase at site 8 that also bordered with agricultural cultivations. This could have been associated with the type of the adjacent cultivation. The fields bordering with this site were sown with maize, rye, and wheat. Unlike potato cultivations, monocotyledonous cultivations are characterized by a high and dense canopy. Agronomic practices essentially involve soil preparation before seeding and harvest itself; these factors create more favorable living conditions for Carabidae than in the case of root cultivations, which is confirmed by the research conducted by Kinnunen and Tiainen (1999), Kosewska et al. (2008), Gailis and Turka (2014), and Jasiński et al. (2015). Potential microclimatic conditions prevailing not only in cultivation fields, but also in biocoenoses adjacent to them, influence the distribution of species of different moisture preferences. Dry-loving species were found in 6 cultivations studied and among them the highest percentage was shown at site 9. The presence of xerophiles can be explained, among others, by the similarity to bordering habitats (also potato cultivations), their low diversity (oilseed rape cultivations), and also more intense sun exposure. No moisture-loving species were observed there. In turn, among all study areas the highest proportion of moisture-loving species was observed at site 9 whose surroundings were most strongly diversified compared to the other sites, in particular in terms of moisture (shrubs, pastures, a meadow, a stream, ponds).

Moreover, the sites where the present study was carried out were characterized by agricultural production conducted in small-area farms which differ from large-area plantations (the largest potato cultivationping area – 70 ares). The mosaic agricultural landscape specific for the Subcarpathian region promotes the preservation of biodiversity. Comparative studies of the Carabidae species composition and numbers of individuals occurring in cultivation fields and adjacent areas indicate that edge habitats are of essential importance in agroecosystems. Such habitats are generally characterized by a smaller number of recorded individuals and a higher number of identified species

http://www.aloki.hu ● ISSN 1589 1623 (Print) ● ISSN 1785 0037 (Online)
DOI: http://dx.doi.org/10.15666/aeer/1802_21092128

(Thienemann's rule). Conscious shaping of agricultural landscape by preserving marginal habitats, field margins, and tree stands promotes the maintenance of biodiversity in an agro-ecosystem (Twardowski and Pastuszko, 2008; Szafranek and Woszczyk, 2012; Konieczna et al., 2015).

Conclusions

The following most frequently occurring species: *H. rufipes*, *P. melanarius*, and *P. cupresus*, can be considered to be typical for agriculturally used areas, including potato cultivations. These are species with wide ecological tolerance and lower susceptibility to anthropogenic pressure.

On the basis of the results obtained, it cannot be said that the intensity of chemical treatments related to potato protection affects the number and biodiversity of ground beetles.

On the other hand, the structure of neighboring arable fields and the presence of forest and midfield afforestations plays an important role. In this mean the maintenance and appropriate management of diverse biocoenoses in agricultural space contribute to increase diversity Carabidae in agrarian areas.

To better understand the impact of the agricultural environment on the structure of Carabidae, it would be necessary to analyze both the impact of individual environmental factors as well as the impact of the use of individual fertilizing and crop protection products. This type of research should be carried out under controlled conditions (controlled and examined samples) and outside production farms (experimental plots).

Acknowledgements. The authors would like to thank Mesdames Paulina Żuk, Alicja Szczepańska, Kinga Ochał, Anna Wrona, Aneta Kapałowska, Katarzyna Kolebuk, Monika Kubas, Aneta Kapałowska, Alicja Szczepańska, Barbara Zyma, Małgorzata Żądło, and Anna Tokarczyk as well as Mr. Jarosław Kot for their participation in field work.

REFERENCES

[1] Aleksandrowicz, O. (2002): Influence of Decis spraying on the community structure and species composition of beetles (Insecta: Coleoptera) on a potato field. – Baltic Journal of Coleopterology 2(2): 145-153.

[2] Aleksandrowicz, O. P. (2004): Ground beetles (Carabidae). – In: Bogdanowicz, W., Chudziak, I., Pilipiuk, I., Skibińska, E. (eds.) Fauna Polski – Charakterystyka i Wykaz Gatunków. Muzeum i Instytut Zoologii PAN, Warszawa. (in Polish).

[3] Andersen, A., Eltun, R. (2002): Long-term developments in the carabid and staphylinid (Col., Carabidae and Staphylinidae) fauna during conversion from conventional to biological farming. – Journal of Applied Ecology 124: 51-56.

[4] Andersen, A. (2003): Long-term experiments with reduced tillage in spring cereals. II. Effects on pests and beneţcial Insects. – Cultivation Protection 22: 147-152.

[5] Bale, J. S., Masters, G. J., Hodkinson, I. D., Awmack, C., Bezemer, T. M., Brown, V. K., Butterfield, J., Buse, A., Coulson, J. C., Farrar, J., Good, J. E. G., Harrington, R., Hartley, S., Jones, T. H., Lindroth, R. L., Press, M. C., Symioudis, I., Waltt, A. D., Whittaker, J. B. (2002): Herbivory in global climate change research: direct effects of rising temperature on insect herbivores. – Global Change Biology 8(1): 1-16.

http://www.aloki.hu ● ISSN 1589 1623 (Print) ● ISSN 1785 0037 (Online)
DOI: http://dx.doi.org/10.15666/aeer/1802_21092128

[6] Baranová, B., Fazekašová, D., Jászay, T., Manko, P. (2013): Ground beetle (Coleoptera: Carabidae) community of arable land with different cultivations. – Folis faunistica Slovaca 18(1): 21-29.
[7] Basedow, T., Borg, Å., de Clercq, R., Nijveldt, W., Scherney, F. (1976): Studies on the occurence of Carabidae in European wheat fields. – Entomophaga 21(1): 59-72. (in German).
[8] Borowski, J., Łęgowski, D., Mazur, S., Perliński, S., Skłodowski, J., Smoleński, M. (1996): Impact of the nun moth control treatments on some groups of forest epigeic arthropods. – Proc. Int. Conf. „Intefrated management of forest Lymantriidae". March. 27–29. 1996. Warsaw–Sękocin (Poland): 149-186.
[9] Bukejs, A., Petrova, V., Jankevica, L., Volkov, D. (2009): Carabid beetles (Coleoptera: Carabidae) of Latvian agrocenoses: review. – Acta Biologica Universitatis Daugavpiliensis 9(1): 79-88.
[10] Cinītis, R. (1962): Carabid beetles in agrobiocenosis of potato field. – Latvijas Entomologs 5: 25-28. (in Russian).
[11] Clark, M., Luna, J. M., Stone, N. D., Youngman, R. R. (1993): Habitat preference of generalist predators in reduced-tillage corn. – Journal of Economic Entomology 28: 404-416.
[12] Czechowski, W. (1981): Ground beetles (Carabidae, Coleoptera). – Fragmenta faunistica 10(12): 193-216. (in Polish).
[13] Fedorko, J. (1983): The dominance and species diversity structure of ground beetles (Col., Carabidae) in potato fields in Bonin near Koszalin. – Biuletyn Instytutu Ziemniaka 30: 117-126. (in Polish).
[14] Gailis, J., Turka, I. (2014): The diversity and structure of ground beetles (Coleoptera: Carabidae) assemblages in differently managed winter wheat fields. – Baltic Jornal of Coleopterology 14(1): 33-46.
[15] Hůrka, K. (1996): Carabidae of the Czech and Slowak Republics. – Kabourek, Zlin.
[16] Huruk, S. (2002): The carabid beetles (Coleoptera, Carabidae) in annual field crops on podsolic soils. – Rocznik Świętokrzyski. Seria B. Nauki Przyrodnicze 28: 39-52. (in Polish).
[17] Huruk, S. (2006): Comparison of structure of carabid (Coleoptera: Carabidae) communities of hay meadows and adjacent cultivated fields. – Entomological News 25(1): 9-23. (in Polish).
[18] Huruk, S., Barševskis, A. (2014): Characterisation of ground beetles (Carabidae, Coleoptera) of the Holy Cross Mountains. – Wydawnictwo Emporium, Kielce. (in Polish).
[19] Huruk, S., Huruk, A., Barševskis, A., Wróbel, G., Bochenek, W. (2014): Carabidae (Coleoptera) selected forest environments inhabiting the area of the Integrated Natural Environment Monitoring Station in Szymbark. – Proceedings of ECOpole 8(1): 161-172.
[20] Irmler, U. (2003): The spatial and temporal pattern of carabidbeetles on arable fields in northern Germany (Schleswig-Holstein) and their value as ecological indicators. – Agriculture, Ecosystems & Environment 98: 231-256.
[21] Jasiński, M., Twardowski, M., Tendziagolska, E. (2015): Organic cultivations as reservoir for beneficial epigeal arthropods. – Journal of Research and Applications in Agricultural Engineering 60(30): 125-130.
[22] Juen, A., Steinbergen, K. H., Traugott, M. (2003): Seasonal change in species composition and size distribution of epigeic predators in a small field. – Entomol Gener 26(4): 259-275.
[23] Kaczmarek, S. (1992): The influence of "Decis 2.5 EC" on Carabidae potato crop. – Polish Journal of Entomology 61(3-4): 125-129. (in Polish).
[24] Karg, I. (1976): Colorado beetle in agrocenoses of the Central Wielkopolska. – Polish Ecological Studies 2: 63-86.
[25] Kinnunen, H., Tiainen, J. (1999): Carabid distribution in a farmland mosaic: the effect of patch type and location. – Annales Zoologici Fennici 36(3): 149-158.

http://www.aloki.hu ● ISSN 1589 1623 (Print) ● ISSN 1785 0037 (Online)
DOI: http://dx.doi.org/10.15666/aeer/1802_21092128

[26] Konieczna, K., Olbrycht, T., Wojciechowicz-Żytko, E., Wilk, E. (2015): Effect of agrotechnical measures on the abundance of ground beetles (Coleoptera, Carabidae) in selected cultivations. – Episteme 26(2): 337-315. (in Polish).
[27] Kosewska, A., Nietupski, M., Laszczak-Dawid, A., Ciepielewska, D. (2008): Assemblages of epigeic carabid beetles (Col. Carabidae) in some agricultural biocenoses. – Progress in Plant Protection/ Postępy w Ochronie Roślin 48(4): 1304-1308.
[28] Kosewska, A., Nijak, K. (2012): Structure analysis of carabid beetles (Col., Carabidae) assemblages in integrated and organic potato management. Short communictaion. – Biuletyn Instytutu Hodowli i Aklimatyzacji Roślin 265: 157-164.
[29] Koss, A. M., Jensen, A. S., Schreiber, A., Pike, K. S., Snyder, W. E. (2005): Comparison of predator and pest communities in Washington potato fields treated with broadspectrum, selective, or organic insecticides. – Environmental Entomology 34: 87-95.
[30] Koval, A. G. (1999): Contribution to the knowledge of carabids (Coleoptera, Carabidae) preying on Colorado potato beetles in the potato files in Transcarpathians. – Entomological reviews 78(3): 527-536.
[31] Koval, A. G., Guseva, O. G. (2008): Structure of the Ground Beetle (Coleoptera, Carabidae) Complexes in Potato Field Agrocenoses on Different Soils in Northwestern Russia. – Entomological Review 88(3): 269-276.
[32] Koval, A. G. (2012): Studies of Adaptation of Carabid Beetles (Coleoptera, Carabidae) to Feeding on the Colorado Potato Beetle, *Leptinotarsa decemlineata* Say (Coleoptera, Chrysomelidae) in Agrocenoses of Potato and Other Cultivations. – Entomological Review 92(6): 633-641.
[33] Kromp, B. (1990): Carabid beetles (Coleoptera, Carabidae) as bioindicators in biological and conventional farming in Austrian potato fields. – Biology and Fertility of Soils 9: 182-187.
[34] Kromp, B. (1999): Carabid beetles in sustainable agriculture: a review on pest control efficency, cultivation impacts and enhancement. – Agriculture, Ecosystems and Environment 74(1-3): 187-228.
[35] Krzysztofiak, L. (2001): Ground beetles (Col., Carabidae) of the Wigry National Park. – Rocz. Augustowsko – Suwalski. Rocz. 1: 55-65. (in Polish).
[36] Leśniak, A. (1997): Methods of analysis of ground beetle (Col., Carabidae) assemblages in zooindication of ecological processes. – Evaluation of forest ecosystems by zooindication methods. Warszawa: Wyd SGGW: 29-41.
[37] Magurran, A. E. (2004): Measuring Biological Diversity. – Oxford: Blackwell Publishing Company.
[38] Nijak, K. (2005): Carabidae in sugar beet and potato cultivations. – Progress in Plant Protection / Postępy ochr. Roślin 45(2): 950-953. (in Polish).
[39] Nijak, K., Kosewska, A., Kordan, B. (2013): Comparison of carabid beetles (Col., Carabidae) assemblages in integrated and organic potato management. – Progress in Plant Protection / Postępy ochr. Roślin 53(1): 64-69. (in Polish).
[40] Nijak, K., Kosewska, A., Topa, E. (2014): Influence of plant protection on ground beetles (Col., Carabidae) assemblages in potato cultivations. – Zagadnienia Doradztwa Rolniczego 1(75): 66-74. (in Polish).
[41] Oberholzer, F., Frank, T. (2003): Predation by the Carabid beetles *Pterostichus melanarius* and *Poecilus cupreus* on Slugs and Slug eggs. – Biocontr. Sci. And Technology 1: 99-110.
[42] Pałosz, T. (1995): Intensive technologies in agriculture in relation to the ground beetle fauna. – Ochrony Roślin 39(5): 8. (in Polish).
[43] Rondon, S., Pantoja, A., Hagerty, A., Horneck, A. D. (2013): Ground beetle (Coleoptera: Carabidae) populations in commercial organic and conventional potato production. – Florida Entomologist 96(4): 1492-1499.
[44] Schmidt, M. H., Lauer, A., Purtauf, T., Thies, C., Schaefer, M., Tscharntke, T. (2003): Relative Importance of Predators and Parasitoids for Cereal Aphid Control. – Biological Sciences 270(1527): 1905-1909.

http://www.aloki.hu ● ISSN 1589 1623 (Print) ● ISSN 1785 0037 (Online)
DOI: http://dx.doi.org/10.15666/aeer/1802_21092128

[45] Sosnowska, D., Pruszyński, S., Lipa, J. (2009): Development of methods and insecticides for control of Colorado potato beetle (*Leptinotarsa decemlineata* Say). – Progress in Plant Protection / Postępy ochr. Roślin 49(2): 565-576. (in Polish).
[46] Stachowiak, M. (2008): Systematic review of ground beetles of Poland (Coleoptera, Carabidae). – http://www.entomo.pl/coleoptera/carabidae/index.php.[dostęp: 09.03.2019].
[47] Sunderland, K. D. (2002): Invertebrate pest control by carabids. – In: Holland, J. M. (ed.) The Agroecology of Carabid Beetles. Intercept, Andover, UK.
[48] Szafranek, P., Woszczyk, K. (2012): Diversity and abundance of ground beetles (oleoptera: Carabidae) occurring on red beet (*Beta vulgaris* L.) cultivated under conventional and organic systems. – Nowości Warzywnicze/Vegetable Cultivations News 54-55: 107-112. (in Polish).
[49] Szewkienicz, A., Olbrycht, T. (2012): Ecological potato culture as a refuge of ground beetles (Col., Carabidae). – Zeszyty Naukowe PTIE i PTG Oddział w Rzeszowie 15: 95-100. (in Polish).
[50] Szyszko, J. (1997): Carabids as an efficient indicator of the quality and functioning of forest ecosystems useful in forestry management. Evaluation of forest ecosystems by zooindication methods. – Warszawa: Wyd SGGW: 42-60.
[51] Thiele, H. U. (1977): Carabid beetles in their environments – a study on habitat selection by adaptations in physiology and behavior. – Springer-Verlag, New York.
[52] Thienemann, A. (1920): The basics of biocenotics and Monard faunistic principles. – Festschrift Zschokke Basel 4: 1-14. (in German).
[53] Thorbek, P., Bilde, T. (2004): Reduced numbers of generalist arthropod predators after cultivation management. – Journal of Applied Ecology 41: 526-538.
[54] Traugott, M. (1998): Larval and adult species composition, phenology and life cycles of carabid beetles (Coleoptera: Carabidae) in an organic potato field. – European Journal of Soil Biology 34(4): 189-197.
[55] Trojan, P. (1980): Ecology. – Wyd. IV. PWN, Warszawa. (in Polish).
[56] Trojan, P. (1998): New prospects for entofaunistic studies. – Entomol News 17 Supl.: 137-155. (in Polish, English abstract).
[57] Twardowski, J. P., Pastuszko, K. (2008): Field margins in winter wheat agrocenosis as reservoirs of beneficial ground beetles (Col., Carabidae). – Journal of Research and Applications in Agricultural Engineering 53(4): 123-127. (in Polish).
[58] Varvara, M. (2010): The genus Carabus (Coleoptera: Carabidae) in somne potato cops from Romania, 1978-1999. – Muzeul Olteniei Craiova. Oltenia. Studii şi comunicşri. Ştiinţele Naturii 26(2): 137-146.
[59] Ward, M. J., Ryan, M. R., Curran, W. S., Barbercheck, M. E., Mortensen, D. A. (2011): Cover cultivations and disturbance influence activity-density of weed seed predators *Amara aenea* and *Harpalus pensylvanicus* (Coleoptera: Carabidae). – Weed Science 59: 76-81.
[60] Weibull, A. C., Östman, Ö., Granqvist, Å. (2003): Species richness in agroecosystems: the effect of landscape, habitat and farm management. – Biodiversity and Conservation 12: 1335-1355.
[61] Werling, B. P., Gratton, C. (2008): Influence of field margins and landscape context on ground beetle diversity in Wisconsin (USA) potato fields. – Agriculture, Ecosystems and Environment 128: 104-108.
[62] Wiltshire, C. W., Hughes, L. (2000): Spatial Dynamics of Predation by Carabid Beetles on Slugs. – Journal of Animal Ecology 69(3): 367-379.
[63] Zhang, J., Drummond, F., Liebman, M. (1998): Effect of cultivation habitat and potato management practices on the population abundance of adult *Harpalus rufipes* (Coleoptera: Carabidae) in Maine. – Journal of Agricultural Entomology 15(1): 63-74.

http://www.aloki.hu ● ISSN 1589 1623 (Print) ● ISSN 1785 0037 (Online)
DOI: http://dx.doi.org/10.15666/aeer/1802_21092128

PHYSIOLOGICAL AND PHYTOCHEMICAL RESPONSES OF BABY SPINACH (*SPINACIA OLERACEA* L.) CULTIVARS TO COMBINED NPKS NUTRITION AND *BACILLUS SUBTILIS* BD233 INOCULATION USING LC-MS

THEKA-KUTUMELA, M. P.[1] – KANU, S. A.[1] – ARAYA, H. T.[2] – SEDIBE, M. M.[3] – MUDAU, F. N.[1*]

[1]*Department of Agriculture and Animal Health, College of Agriculture and Environmental Sciences, University of South Africa, Private Bag X6, Florida 1710, South Africa*

[2]*Agriculture Research Council, Vegetable and Ornamental Plant Institute, Private Bag X293, Pretoria 0001, South Africa*

[3]*Department of Agriculture, Central University of Technology, Free State, Private Bag X20539, Bloemfontein 9301, South Africa*

[*]*Corresponding author*
e-mail: thekamp@unisa.ac.za

(Received 30th Aug 2019; accepted 25th Nov 2019)

Abstract. Baby spinach (*Spinacia oleracea* L.) is grown for its nutritional benefits, edible leaves and medicinal purpose. The use of crop amendments such as inoculation with plant growth-promoting bacteria (PGPB) together with fertilizers for crop cultivation is more sustainable as it reduces the excessive use of fertilizers and increases crop yield. The aim of this study was to evaluate the physiological and phytochemical response of baby spinach cultivars to different levels of Nitrogen, Phosphorus, Potassium and Sulphur (NPKS) nutrition, amended with *Bacillus subtilis* strain BD233 inoculation. A factorial field experiment with treatments arranged in a randomized complete block design (RCBD) was carried out. The results showed that NPKS fertilization significantly affected the total biomass of baby spinach but not *B. subtilis* (BD233) inoculation and cultivar or their interaction. The level of chlorophyll varied between cultivars ranging from 19.96 ± 1.62^{b} mg/m^2 and 24.79 ± 1.98^{a} mg/m^2, however, no significant differences occurred in stomatal conductance among the three cultivars. However, significant difference was observed on compounds among cultivars with NPKS fertilizer application in most identified compounds such as patuletin-3-glucosyl-(1-6)[apiosyl(1-2)]-glucoside, spinacetin-3-glucosyl-(1-6)[apiosyl(1-2)]-glucoside, (S)-Malate and N-Acetyl-D-tryptophan. Therefore, the study recommends that fertilizer at 22N:22P:30K:5S kg/ha and 33N:33P:45K:7S kg/ha amended with *B. subtilis* inoculation be considered when cultivating baby spinach.

Keywords: *chlorophyll content, green leafy vegetables, multivariate analysis, Plant Growth Promoting Bacteria (PGPB), stomatal conductance*

Introduction

Baby spinach (*Spinacia oleracea* L.) is grown for its nutritional benefits, edible leaves and medicinal purpose (Schrader and Mayberry, 2003; Kerr, 2014; Mudau et al., 2015). It is extensively cultivated in Europe due to favorable conditions and high demand (Kerr, 2014). In South Africa, baby spinach is available to consumers as a fresh, salad mix and as a frozen and canned product (Zikalala et al., 2016). Its growing popularity led to baby spinach being grown worldwide. However, essential nutrients and phytochemical concentrations of baby spinach are affected by climatic conditions, agronomic practices and postharvest factors such as stage of harvesting (Kalt, 2005; Bergquist, 2006), cultivars (Masufi et al., 2019), storage temperature and time (Bergquist, 2006).

http://www.aloki.hu ● ISSN 1589 1623 (Print) ● ISSN 1785 0037 (Online)
DOI: http://dx.doi.org/10.15666/aeer/1802_21292140

The production of plants requires an accurate supply of nutrients whilst a slight variation in nutrient balance may have a negative effect on crop growth and nutrition status (Sedibe and Allemann, 2012). The availability of nitrogen, phosphorus and potassium in soils during production are essential to improve growth and vegetable quality (King et al., 2008). However, sustainable and proper use of synthetic chemical fertilizer is essential. Using improved production practices and technologies enhances crop growth (Shine and Guruprasad, 2012) and these techniques mitigate the effect of poor growing conditions including nutrient imbalance (Sedibe, 2012). The use of crop amendments together with fertilizers is more sustainable as it reduces excessive use of fertilizer (Diacono and Montemurro, 2010). These amendments respond differently from that of fertilizers, in as much as it only influences plant vigour (Yakhin et al., 2016).

The use of plant growth promoting bacteria (PGPB) in crop amendments is gaining popularity (Diacono and Montemurro, 2010). Inoculation with *Bacillus* strains showed increase in vegetative growth of crops (Pupathy and Radziah, 2015; Çakmakçi et al., 2007), however, their effect on chemical composition has not been well documented. *Bacillus* strains are among the most commonly used phosphate solubilizers and have been reported to increase phosphorus uptake (García-López and Delgado, 2016) there by improving plant growth and is less toxic to human and widely exists in soils (Wu et al., 2016). The aim of this study was to evaluate the effect of combined Nitrogen, Phosphorus, Potassium and Sulphur (NPKS) fertilization at different levels on physiological and phytochemical composition of baby spinach cultivars amended with *Bacillus subtilis* BD233.

Materials and Methods

Experimental site

The study was conducted at Agricultural Research Council - Vegetable and Ornamental Plant Institute (ARC-VOPI) in Roodeplaat farm, situated in the sourish mix of bushveld, 25 km north of central Pretoria, KwaMhlanga (R573) road; GPS coordinates: 25,56S;28,35E (Gauteng province, South Africa). The area is a relatively cool subtropical climate with summer rainfall and cold, dry winter.

Bacterial strain and preparation

Bacillus subtilis strain BD233 was obtained from the Agricultural Research Council-Plant Protection Research Institute (ARC-PPRI) in Pretoria, South Africa. *Bacillus subtilis* strain BD233 were cultured using a LB agar plates after incubation under dark conditions at 28°C for 24 h. The bacterial cells were harvested from LB agar plates into liquid LB media to yield 8.547x109 colony forming units (cfu) mL^{-1} determined by serial dilution with plate counts (Zhang et al., 2008). Baby spinach cv. Anna, Edna and Ohio seeds were surface decontaminated by washing in 0.35% (v/v) sodium hypochlorite and stirred for 5 min. The used sodium hypochlorite solution was discarded, and decontaminated seeds were washed three times with distilled water. Seeds were then left to dry under the laminar flow prior to planting in seedling trays filled with compost growth medium on 9 January 2016. Germination took place 7 days after planting and seedlings were transplanted after 3 weeks when the plants had 4 leaves each.

http://www.aloki.hu ● ISSN 1589 1623 (Print) ● ISSN 1785 0037 (Online)
DOI: http://dx.doi.org/10.15666/aeer/1802_21292140

Experimental design and layout

The experiment was a 5x2 factorial arranged in a randomized complete block design (RCBD) with three replicates. Five NPKS fertilizer ratios consisted of 0 (0:0:0:0 kg/ha), 25% (11:11:15:2 kg/ha), 50% (22:22:30:5 kg/ha), 75% (33:33:45:7 kg/ha) and 100% (45:45:60:10 kg/ha) of the recommended fertilizer application for baby spinach (Nemadodzi et al., 2017) and *Bacillus subtilis* strain BD233 amendments (zero *B. subtilis* (B-) and *B. subtilis* (B+) application) to three cultivars of baby spinach (Anna, Edna and Ohio) were evaluated.

Experimental plot size (2.2x2.2 m^2) used consisted of in-row and interrow spacing of 20 cm and 10 cm, respectively. Fertilizers were applied a week after transplanting followed by inoculation with 100 ml of *Bacillus subtilis* strain BD233 LB per plant a week after fertilizer application. Lime ammonium nitrate (28% N kg/ha) was applied as the N fertiliser source, phosphorus was supplied in the form of superphosphate (83% P kg/ha), potassium was supplied in the form of potassium chloride (50% K kg/ha) and sulphur was applied in the form of gypsum (17% S kg/ha). Irrigation was based on the soil moisture conditions for a period of 2.5 h per irrigation using sprinkler irrigation and weeds were removed manually by hands.

Physiological parameters

Plants were harvested at 35 days after planting and washed with running water. Chlorophyll content, upper-leaf stomatal and lower-leaf stomatal conductance and total biomass (fresh mass and dry mass) were measured on three baby spinach cultivars namely, Anna, Edna and Ohio. Chlorophyll content was measured using Spad 502 Chlorophyll Meter (Minolta Camera Co. Ltd., Japan) a non-destructive method on healthy mature leaves with homogeneous green colour. Stomatal conductance was measured between 11:00 to 13:00 using SC-1 Leaf Porometer instrument (Decagon Devices USA). Leaf porometer determine stomatal conductance using the actual vapour flux from the leaf through the stomata. At harvesting, freshly harvested material of baby spinach was oven dried at 45ºC for 24 h (Bashan et al., 2017). Both fress mass and dry mass were weight to determine the total biomass.

Ultra High Performance Liquid Chromatography–Mass Spectrometer (UHPLC-MS) solvent extraction and preparation

Mature leaves of baby spinach were harvested, and oven dried at 45ºC for 24 h before grounded into a fine powder using a pestle and mortar and stored in airtight tubes in an 80°C refrigerator. Thereafter, about 50 mg of ground leaves were weighed subsequent extraction using 15 ml methanol-water. The mixture was sonicated for 20 min at room temperature and centrifuged at 1300 rpm for 15 min. The mixture was filtered through 0.45 µm syringe filters and the supernatant (1 ml) was transferred into 2 ml amber glass vials for UHPLC-MS analysis (Mncwangi et al., 2014).

UHPLC-MS analysis

The method described by Mncwangi et al. (2014) was adopted with minor changes. The UHPLC analysis was performed on a Waters Acquity Ultra-High-Performance Liquid Chromatography system with PDA detector (Waters, Milford, MA, USA). UHPLC separation was achieved on a UHPLC Ultra C18 column (100 mm × 2.1 mm, i.d., 5-µm particle size, Restek) maintained at 35°C. The mobile phase consisted of 0.1%

http://www.aloki.hu ● ISSN 1589 1623 (Print) ● ISSN 1785 0037 (Online)
DOI: http://dx.doi.org/10.15666/aeer/1802_21292140

formic acid in water (solvent A) and LC-MS grade methanol (solvent B) at a flow rate of 0.3 ml/min. The gradient elution was applied as follows: 85% A: 15% B to 65% A: 35% B in 4 min, thereafter, changed to 50%: 50% in two min, to 20% A: 80% B in 1 min, maintaining for 1 min and back to an initial ratio in 0.5 min. The analysis time was 9 min. Samples were introduced into the mobile phase with an injection volume of 1.0 µl (full-loop injection) for samples and 2.0 µl for reference standards. The UHPLC system was interfaced with a Xevo G2QTof MS (Waters, USA). The following mass spectrometry operating conditions were applied: source – ESI negative mode; capillary voltage – 3 kW; cone voltage 30 V; calibration – sodium formate; lock spray – leucine enkaphalin and scan mass range – at 200–1500m/z.

Statistical analysis

Analysis of variance (ANOVA) data of agronomic parameters was conducted using Statistica version 10.0 and all-pairwise comparison tests were performed to detect differences among means at a significance level of $p \leq 0.05$. Significant means were separated using the Duncan Multiple Range Test. UHPLC-MS data was processed by XCMS version 3.5.1 (2016) and analysis of variance across metabolites treatment means was performed using SAS statistical package version 20. The chemometric analysis was performed using the MetaboAnalyst 3.0. (2017). Partial Least Squares - Discriminant Analysis (PLS-DA) was performed to identify compounds responsible for differentiation among cultivars and treatments. Compounds were identified using the Compass data analysis 4.3 and annotated by MetFrag version 2.1. (2010).

Results and Discussion

Physiological parameters

This study evaluated the effect of different levels of NPKS fertilization, on some physiological parameters (chlorophyll content, stomatal conductance and total biomass) of three baby spinach cultivars amended with *B. subtilis*. The results showed significant varietal differences in baby spinach's response to the treatments. Among the three cultivars, cv, Edna had the highest chlorophyll content (24±1.84 mg/m^2) and stomatal conductance (27.24±1.84 and 10.03±0.96 m^2/smol^{-1} upper and lower, respectively) compared to cv. Ohio with the lowest values (*Table 1*). The differences in baby spinach could be attributed to the genotypic predisposition of the cultivars tested in this study. The findings of the present study are consistent with the findings of Makus (2013) who reported differences in chlorophyll content of spinach cultivars, Samish and Lazio, grown under the same soil type treated with sulphur. Singh et al. (2014) also reported differences in chlorophyll content among cultivars, Siberian kale and Japanese kale.

There was a significant difference observed in the upper and lower stomatal conductance among the three cultivars, with cultivar Edna having the highest upper stomatal conductance and lower stomatal conductance (*Table 1*). The findings of the current study concured with the findings of Khan et al. (2009), who reported a high significant decrease in stomatal conductance of mustard cv. SS2 than Pusa Jai Kisan with increasing NaCl concentration. The results also indicated that cultivar type had no effect on the total biomass of baby spinach, ranging from 0.31g to 0.40 g. The results correlated with the findings by Masufi et al. (2019) who reported no significant difference on baby spinach cultivar ohio, guitar F1, Lazio F1, monstrous, viroflay and dash.

http://www.aloki.hu ● ISSN 1589 1623 (Print) ● ISSN 1785 0037 (Online)
DOI: http://dx.doi.org/10.15666/aeer/1802_21292140

Table 1. *Effect of NPKS nutrition and Bacillus subtilis strain BD233 inoculation on the physiology of three baby spinach cultivars*

Treatment	Total biomass /plant (g)	Chlorophyll content (mg/m^2)	Stomatal conductance (Upper) ($m^2/smol^{-1}$)	Stomatal conductance (Lower) ($m^2/smol^{-1}$)
Fertilization (NPKS)				
0% (0:0:0:0)	0.10 ± 0.01^{c}	7.85 ± 1.17^{e}	15.80 ± 1.32^{a}	17.74 ± 1.07^{a}
25% (11:11:15:2 kg/ha)	0.17 ± 0.01^{c}	18.67 ± 1.49^{d}	9.07 ± 1.33^{b}	7.93 ± 0.62^{b}
50% (22:22:30:5 kg/ha)	0.29 ± 0.04^{b}	26.55 ± 1.94^{c}	5.52 ± 0.75^{c}	4.92 ± 0.61^{bc}
75% (33:33:45:7 kg/ha)	0.54 ± 0.06^{a}	31.14 ± 1.81^{b}	4.53 ± 0.64^{c}	6.20 ± 0.93^{bc}
100% (45:45:60:10 kg/ha)	0.60 ± 0.07^{a}	35.77 ± 1.56^{a}	3.32 ± 0.51^{c}	6.84 ± 00.97^{c}
***B. subtilis* (B) inoculation**				
B-	0.32 ± 0.03^{a}	23.91 ± 1.55^{a}	7.22 ± 0.71^{a}	8.18 ± 0.72^{a}
B+	0.36 ± 0.04^{a}	24.08 ± 1.49^{a}	8.08 ± 0.89^{a}	9.27 ± 0.86^{a}
Cultivar (C)				
Anna	0.31 ± 0.04^{a}	24.79 ± 1.98^{a}	7.13 ± 0.92^{b}	8.38 ± 0.88^{b}
Edna	0.32 ± 0.04^{a}	27.24 ± 1.84^{a}	8.83 ± 0.80^{a}	10.03 ± 0.96^{a}
Ohio	0.40 ± 0.06^{a}	19.96 ± 1.62^{b}	6.99 ± 0.91^{b}	7.77 ± 0.74^{b}
Cultivar x *B*				
Anna x B-	0.28 ± 0.06^{a}	24.66 ± 3.02^{ab}	7.60 ± 1.45^{ab}	7.79 ± 1.17^{b}
Anna x B+	0.33 ± 0.05^{a}	24.92 ± 2.63^{ab}	6.66 ± 1.16^{ab}	8.96 ± 1.35^{ab}
Edna x B-	0.35 ± 0.06^{a}	26.06 ± 2.58^{ab}	9.04 ± 1.16^{a}	9.64 ± 1.18^{ab}
Edna x B+	0.28 ± 0.06^{a}	28.43 ± 2.66^{a}	8.62 ± 1.75^{a}	10.42 ± 1.55^{a}
Ohio x B-	0.44 ± 0.09^{a}	21.04 ± 2.42^{bc}	5.01 ± 0.89^{b}	7.11 ± 1.35^{b}
Ohio x B+	0.36 ± 0.07^{a}	18.89 ± 2.16^{c}	8.97 ± 1.66^{a}	8.43 ± 1.60^{b}
F-Statistics				
NPKS	20.64^{***}	53.32^{***}	27.24^{***}	25.52^{***}
B. subtilis (B)	0.70^{ns}	0.02^{ns}	1.01^{ns}	1.65^{ns}
Cultivar (C)	1.88^{ns}	10.04^{***}	1.88^{**}	2.53^{**}
C x B	0.90^{ns}	1.93^{*}	3.25^{*}	1.03^{*}
NPKS x B	1.32^{ns}	1.87^{ns}	0.88^{ns}	0.92^{ns}
NPKS x B x V	0.48^{ns}	0.86^{ns}	1.05^{ns}	9.96^{ns}

Values (M±S.E.) followed by similar letters in a column are significantly different at * $p\leq0.05$, ** $p\leq0.001$, ***$p\leq0.0001$ and ^{ns} = not significant. B- =Zero inoculation with Bacillus subtilis strain BD233, B+= inoculation with Bacillus subtilis strain BD233

In this study, different levels of NPKS fertilization significantly affected the measured physiological parameters. Baby spinach treated with a higher dose of fertilizer had higher chlorophyll content compared to control and in general, there was a steady increase in chlorophyll content with increase in NPKS fertilization level (*Table 1*). Similar trend was observed by Pramanik and Bera (2013), who reported gradual increase in total chlorophyll content of hybrid rice with increasing nitrogen levels from zero to 200 kg ha^{-1}. These results confirm that nitrogen is important in the formation of chlorophyll molecules (Gairola et al., 2009). However, in contrast, the increase in NPKS fertilization caused decreases in the stomatal conductance. The stomatal conductance of the control plant (0.10 ± 0.01 $m^2/smol^{-1}$ (upper) and 17.74 ± 1.07 $m^2/smol^{-1}$ (lower)) was the highest compared to the other treatments (*Table 1*). In agreement with results of the study, Nemadodzi et al. (2017), reported similar findings in chlorophyll content and stomatal conductance with the application of NPK fertilization at a ratio of 45:45:60 on baby spinach. The NPKS fertilization level significanly ($p<0.001$) affected the total biomass of baby spinach. In general, plant dry biomas increased with increases in the level of fertilization. However, the current study for plants fertilized with the highest NPKS level 45:45:60:10 kg/ha had the highest total biomass (0.60 g) compared to control. The results are in agreement with the findings of Nemadodzi et al. (2017) who reported that N and P fertilization significantly

http://www.aloki.hu ● ISSN 1589 1623 (Print) ● ISSN 1785 0037 (Online)
DOI: http://dx.doi.org/10.15666/aeer/1802_21292140

affected both the leaf fresh and dry weights in their study. The results contradicted by the findings of Boroujerdnia and Ansari (2007) who reported an increase in dry weight of romaine lettuce with an increase in N levels from 60 kg/ha to 180 kg/ha. Furthermore, Singh et al. (2004) conducted a study on the effect of NPK fertilizers on the growth of basil where it was found that fertilizer application at 75:40:40 kg/ha significantly increased the dry weight over the control of basil. In okra, no significant difference was reported in dry weight with increasing NPK fertilizers from 10 to 13 grams (Gloria et al. 2017).

From the results obtained in this study, it was evident that *Bacillus subtilis* (BD233) amendments influenced the chlorophyll content of baby spinach. *Bacillus subtilis* (BD233) had a significant ($p \leq 0.05$) effect on the chlorophyll content of baby spinach, however, there was no significant differences in stomatal conductance (*Table 1*). These results concurred with findings of Turan et al. (2014) who assessed the effect of *B. subtilis* on cabbage seedling growth and observed an increase in chlorophyll content compared to the control. Elsewhere, Ekinci et al. (2014) also found similar findings on cauliflower transplants grown under greenhouse conditions. Anjum et al. (2007) reported that an increase in leaf chlorophyll content stimulate plant growth. The stomatal conductance was not affected by the application of *Bacillus subtilis* BD 233, these findings accorded well with those of Porcel et al. (2014) who reported no effect on stomatal conductance when inoculation with *Bacillus* strain on tomato plants. The results also showed that *Bacillus subtilis* (BD233) exhibited no effect on the total biomass of baby spinach cultivars, the results concurred with the findings of Canbolat et al. (2006) who observed none statistical difference between bacterial inoculation and P fertilizer in terms of dry weight of barley seedling.

The interaction of cultivar and *B. subtilis* (BD233) was significant for the chlorophyll content and stomatal conductance of baby spinach. In addition, cv. Edna amended with *Bacillus subtilis* (BD233) had higher chlorophyll content (28.43±2.66 mg/m^2) and stomatal conductance (9.04±1.75 and 10.42±1.55 m^2/smol^{-1} for upper and lower, respectively) compared to the other cultivars with or without amendment with the bacteria (*Table 1*).

Phytochemical response

There has been a lack of a considerable research report on metabolites response of baby spinach to *Bacillus subtilis* BD 233 and different levels of NPKS using an untargeted approach. Thus, MS/MS was carried out to identify compounds and their differences with respect to the response of three selected baby spinach cultivars to the different treatments employed in this study. The results of this study demonstrated a wide range of compounds which included the patuletin-3-glucosyl-(1-6)[apiosyl(1-2)]-glucoside (m/z 787, Rt. 5.39), spinacetin-3-glucosyl-(1-6)[apiosyl(1-2)]-glucoside (m/z 801, Rt. 5.94), spinacetin-3-(2¢¢-feroylglucosyl)(1-6)[apiosyl(1-2)]-glucoside (m/z 977, Rt. 6.40), and (S)-Malate (m/z 133, Rt. 0.86). Baby spinach metabolites showed significant differences in response to cultivar and NPKS fertilization. Cultivar Ohio exhibited high concentration in most compound which were slightly significant when compared to cv. Anna and Edna (*Table 2a,b*). However, there were no significant differences in cultivar on compound suvorexant (m/z 449, Rt 6.20), 4-(beta-D-Glucopyranosyloxy)-2-hydroxy-6-pentadecylbenzoic acid (m/z 525, Rt 6.84) and (S)-malate (m/z 133, Rt 0.86). Among the compounds identified, *B. subtilis* inoculation and the interaction of NPKS fertilization with *B. subtilis* only had a slight significant difference ($p \leq 0.05$) on compound 2-(1-hydroxyethyl thiamine diphosphate (2-)) (m/z 465, Rt 5.20) (*Table 2a,b*). Similar compounds were previously reported by Bergquist et al. (2005), who observed a relatively stable total flavonoid content during normal retail storage conditions.

http://www.aloki.hu ● ISSN 1589 1623 (Print) ● ISSN 1785 0037 (Online)
DOI: http://dx.doi.org/10.15666/aeer/1802_21292140

Table 2a. *Concentration mean of compounds identified from three selected baby spinach cultivars with different levels of NPKS nutrition and Bacillus subtilis BD 233inoculation*

	Parameters						
	A	**B**	**C**	**D**	**E**	**F**	**G**
Mass(m/z)	**272**	**191**	**465**	**787**	**245**	**801**	**449**
RT (min)	**0.61**	**1.06**	**5.20**	**5.39**	**5.55**	**5.94**	**6.20**
Treatment							
NPKS							
0	73501^{a}	12176^{a}	311216^{b}	263265^{c}	356533^{c}	8414^{c}	82772^{b}
25	78459^{a}	53902^{a}	567483^{a}	881780^{a}	751495^{a}	14160^{a}	238209^{a}
50	72290^{ab}	44023^{a}	541828^{a}	679078^{ab}	809106^{ab}	12896^{a}	227119^{a}
75	62129^{ab}	38556^{a}	497287^{a}	591637^{b}	1012062^{b}	11930^{ab}	275271^{a}
100	55789^{b}	30516^{a}	478447^{a}	514456^{b}	926952^{b}	9424^{bc}	251944^{a}
Bacillus (B)							
B-	67010^{a}	38193^{a}	476703^{a}	631791^{a}	834954^{a}	11693^{a}	230982^{a}
B+	20570^{a}	41900^{a}	542397^{b}	654665^{a}	854248^{a}	12085^{a}	246132^{a}
Cultivar (C)							
Anna	58797^{a}	20288^{c}	461177^{b}	307612^{b}	735737^{b}	9669^{b}	201460^{a}
Edna	16491^{b}	62754^{a}	454200^{b}	305791^{b}	1062855^{b}	2869^{b}	273492^{a}
Ohio	82351^{b}	33700^{b}	603385^{a}	1259710^{a}	716530^{a}	15898^{a}	234115^{a}
NPKS x *B*							
0B-	58678^{a}	10562^{a}	273789^{d}	101151^{a}	394371^{a}	6232^{a}	78827^{a}
0B+	103149^{a}	15402^{a}	386071^{bc}	587494^{a}	280857^{a}	12776^{a}	90662^{a}
25B-	26898^{a}	53140^{a}	133162^{a}	609444^{a}	219078^{a}	4560^{a}	54750^{a}
25B+	17801^{a}	54665^{a}	206216^{ab}	620400^{a}	286249^{a}	2610^{a}	44251^{a}
50B-	17665^{a}	40268^{a}	81409^{abc}	446177^{a}	154596^{a}	3447^{a}	38595^{a}
50B+	25565^{a}	47779^{a}	86643^{abc}	546529^{a}	923148^{a}	3270^{a}	57034^{a}
75B-	17234^{a}	40833^{a}	71578^{abc}	494673^{a}	1078629^{a}	4471^{a}	34130^{a}
75B+	15195^{a}	36279^{a}	60887^{bc}	46292^{a}	945495^{a}	1788^{a}	35513^{a}
100B-	49501^{a}	27739^{a}	157851^{c}	545039^{a}	874736^{a}	4867^{a}	86260^{a}
100B+	62077^{a}	33293^{a}	136191^{bc}	555642^{a}	979168^{a}	5835^{a}	41873^{a}
NPKS x C							
0 Anna	-58678^{a}	10562^{i}	273789e	47384^{a}	394371^{a}	3062^{a}	78827^{a}
0 Edna	-	-	-	-	-	-	-
0 Ohio	103149^{a}	15402^{hi}	386071de	587494^{a}	280857^{a}	12776^{a}	90662^{a}
25 Anna	56685^{a}	23222^{fgh}	576210^{abc}	462357^{a}	531907^{a}	13748^{a}	214035^{a}
25 Edna	66298^{a}	80818^{a}	432702^{cde}	418615^{a}	951707^{a}	11205^{a}	266270^{a}
25 Ohio	99329^{a}	39259^{cd}	698772^{a}	1512713^{a}	639119^{a}	17279^{a}	219817^{a}
50 Anna	64382^{a}	25897^{efgh}	539804^{abcd}	380142^{a}	680569^{a}	10987^{a}	200745^{a}
50 Edna	64344^{a}	69863^{a}	477731^{bcd}	371036^{a}	1017338^{a}	11556^{a}	257992^{a}
50 Ohio	88142^{a}	36311^{cde}	607951^{ab}	1286054^{a}	729410^{a}	16143^{a}	222622^{a}
75 Anna	53114^{a}	19430^{ghi}	479974^{bcd}	327347^{a}	967246^{a}	10897^{a}	254232^{a}
75 Edna	57808^{a}	53379^{b}	474858^{bcd}	267365^{a}	1196505^{a}	9603^{a}	299310^{a}
75 Ohio	74292^{a}	34372^{cdef}	538308^{abcd}	1195195^{a}	815120^{a}	15615^{a}	261001^{a}
100 Anna	58591^{a}	18719^{ghi}	404631de	246138^{a}	889870^{a}	7108^{a}	217627^{a}
100 Edna	50580^{bc}	44786^{d}	431720^{cde}	147549^{a}	1080244^{a}	6174^{a}	265747^{a}
100 Ohio	58197^{defg}	28043^{d}	538308^{ab}	1149680^{a}	810743^{a}	14989^{a}	272456^{a}
F-value							
NPKS	0.05	0.0001	0.01	0.01	0.0001	0.01	0.0001
B	0.78	0.21	0.05	0.90	1.00	0.75	0.51
C	0.01	0.0001	0.0001	0.0001	0.0001	0.0001	0.05
NPKS x B	0.12	0.32	0.05	0.31	0.06	0.26	0.23
NPKS x C	0.46	0.008	0.31	0.93	0.91	0.72	0.91
B x C	0.37	0.37	0.87	0.33	0.26	0.64	0.50
NPKS x B x	0.46	0.42	0.22	0.94	0.90	0.85	0.24

A) 5-(Pentafluoro-lambda~6~-sulfanyl)-2H-benzimidazole-2-thione, **B)** (2S,3R)-2,3-Dihydroxy-5-oxohexanedioate, **C)** 2-(1-hydroxyethyl thiamine diphosphate (2-), **D)** Patuletin-3-glucosyl-(1-6) [apiosyl (1-2)]-glucoside, **E)** N-Acetyl-D-tryptophan, **F)** Spinacetin-3-glucosyl-(1-6) [apiosyl (1-2)]-glucoside, **G)** Suvorexant

http://www.aloki.hu ● ISSN 1589 1623 (Print) ● ISSN 1785 0037 (Online)
DOI: http://dx.doi.org/10.15666/aeer/1802_21292140

Table 2b. *Concentration mean of compounds identified from three selected baby spinach cultivars with different levels of NPKS nutrition and Bacillus subtilis BD233 inoculation*

	Parameters						
	H	**I**	**J**	**K**	**L**	**M**	**N**
Mass(m/z)	**977**	**525**	**133**	**429**	**675**	**96**	**837**
RT (min)	**6.40**	**6.84**	**0.86**	**7.40**	**7.40**	**0.70**	**7.02**
Treatment							
NPKS							
0	767784^{ab}	452420^{a}	5284^{a}	5214^{b}	4965^{a}	10374^{a}	1896^{b}
25	857838^{a}	324722^{a}	4612^{ab}	9008^{a}	2415^{b}	7370^{b}	2978^{a}
50	702175^{b}	411397^{a}	3813^{b}	4632^{b}	2239^{b}	3057^{bc}	2080^{b}
75	643453^{bc}	478901^{a}	2797^{c}	6010^{b}	2136^{b}	1244^{cd}	2058^{b}
100	517751^{c}	449850^{a}	2877^{c}	4488^{b}	2076^{b}	1456^{d}	1727^{b}
Bacillus (B)							
B-	672596^{a}	428948^{a}	3615^{a}	5223^{a}	2445^{a}	5934^{a}	2198^{a}
B+	698819^{a}	407322^{a}	3642^{a}	6780^{a}	2309^{a}	6227^{a}	2186^{a}
Cultivar (C)							
Anna	51961^{b}	371454^{a}	3682^{a}	2840^{b}	2570^{a}	7921^{a}	1757^{b}
Edna	528361^{b}	441268^{a}	3184^{a}	6965^{a}	2181^{a}	5612^{b}	2381^{a}
Ohio	980733^{a}	434503^{a}	4028^{a}	7630^{a}	2416^{a}	5008^{b}	2366^{a}
NPKS x *B*							
0B-	640602^{a}	383143^{a}	5591^{a}	2774^{a}	5271^{a}	10369^{a}	1710^{ef}
0B+	1022148^{a}	590975^{a}	4671^{a}	10092^{a}	4352^{a}	10383^{a}	2267^{cd}
25B-	860826^{a}	195521^{a}	4467^{a}	8921^{a}	2429^{a}	5720^{a}	1533^{a}
25B+	854851^{a}	107535^{abc}	4757^{a}	9095^{a}	2401^{a}	9020^{a}	1920^{ab}
50B-	703846^{a}	230787^{a}	4019^{a}	3244^{a}	2248^{a}	7109^{a}	2170^{cde}
50B+	700503^{a}	144074^{a}	2747^{a}	5040^{a}	2034^{a}	6476^{a}	1990^{cdef}
75B-	671590^{a}	245275^{a}	297368^{a}	671590^{a}	441871^{a}	5285^{a}	2393^{bc}
75B+	615316^{a}	127589^{ab}	2847^{a}	6981^{a}	2237^{a}	4232^{a}	1724^{def}
100B-	464786^{a}	151048^{ab}	2570^{a}	4502^{a}	2127^{a}	4146^{a}	1533^{f}
100B+	570716^{a}	82293^{a}	3183^{a}	4475^{a}	2025^{a}	4489^{a}	1920^{cdef}
NPKS x C							
0 Anna	640602de	383143^{a}	5591^{a}	2774^{a}	5271^{a}	10369^{a}	1710d^{efg}
0 Edna	-	-	-	-	-	-	-
0 Ohio	1022148^{ab}	590975^{a}	4671^{a}	10092^{a}	4352^{a}	10383^{a}	226^{bcd}
25 Anna	728881^{cd}	126845^{a}	6152^{a}	7628^{a}	2299^{a}	12150^{a}	2955^{a}
25 Edna	635646de	260222^{a}	3457^{a}	6683a	2352^{a}	8245^{a}	2839^{a}
25 Ohio	1131614^{a}	468372^{a}	5150^{a}	11884^{a}	2524^{a}	4583^{a}	3126^{a}
50 Anna	542803^{def}	350176^{a}	3285^{a}	614^{a}	2245^{a}	9910^{a}	1575^{fg}
50 Edna	575829de	469323^{a}	3319^{a}	7154^{a}	2124^{a}	4968^{a}	2609^{abc}
50 Ohio	987892^{ab}	414691^{a}	4836^{a}	6127^{a}	2349^{a}	5500^{a}	2056^{cdef}
75 Anna	485793^{ef}	489069^{a}	2605^{a}	3381^{a}	2051^{a}	4829^{a}	1402^{g}
75 Edna	526041^{def}	489069^{a}	3056^{a}	8330^{a}	2065^{a}	4982^{a}	2551^{abc}
75 Ohio	908462^{bc}	354418^{a}	2617^{a}	5084^{a}	2287^{a}	4426^{a}	1935^{defg}
100 Anna	356676^{f}	420981^{a}	2696^{a}	2298^{a}	2069^{a}	4914^{a}	1629^{efg}
100 Edna	349687^{f}	475623^{a}	2866^{a}	5423^{a}	2167^{a}	3750^{a}	1369^{g}
100 Ohio	846890^{bc}	452945^{a}	3069^{a}	5744^{a}	1992^{a}	4288^{a}	2182^{cde}
F-value							
NPKS	0.0001	0.20	0.001	0.0001	0.05	0.0001	0.0001
B	0.68	0.65	0.90	0.47	0.90	0.47	0.82
C	0.02	0.43	0.93	0.01	0.93	0.01	0.002
NPKS x B	0.43	0.25	0.95	0.18	0.95	0.18	0.01
NPKS x C	0.00	0.16	1.00	0.09	1.01	0.09	0.05`
B x C	0.36	0.44	0.91	0.98	0.91	0.98	0.80
NPKS x B x	0.87	0.34	1.01	0.78	1.00	0.79	0.57

H) Spinacetin-3-(2¢¢-feroylglucosyl) (1-6) [apiosyl(1-2)]-glucoside, **I)** 4-(beta-D-Glucopyranosyloxy)-2-hydroxy-6-pentadecylbenzoic acid, **J)** S)-Malate, **K)** 4-[3-(Benzyloxy)-1-(beta-D-glucopyranosyloxy) prosody] butanoic acid, **L)** Diethyl ({4-(6-oxo-7,11-diazatricyclo [7.3.1.0~2,7~] trideca-2,4-dien-11-yl)-3-[(3,4,5-trimethoxybenzoyl) amino] benzoyl} amino) malonate, **M)** 3-$l^ {1}-oxidanyl-4,5-didehydroisothiazole, **N)** 5-[(2-{[2-Acetamido-2-deoxy-3-O-(beta-D-galactopyranosyl)-alpha-D-galactopyranosyl] oxy} ethyl) carbamoyl]-2-[6-(dimethylamino)-3-(dimethyliminio)-3H-xanthen-9-yl] benzoa

http://www.aloki.hu ● ISSN 1589 1623 (Print) ● ISSN 1785 0037 (Online)
DOI: http://dx.doi.org/10.15666/aeer/1802_21292140

N-Acetyl-D-tryptophan (m/z 245, Rt. 5.55) was reported by Okazaki et al. (2009) on spinach leaves when treated by altering the ratio of NH_4^+/NO_3^- in the culture solution. However, 5-[(2-{[2-Acetamido-2-deoxy-3-O-(beta-D-galactopyranosyl)-alpha-D-galactopyranosyl] oxy} ethyl) carbamoyl]-2-[6-(dimethylamino)-3-(dimethyliminio)-3H-xanthen-9-yl] benzoate (m/z 837, Rt. 7.02), 5-(Pentafluoro-lambda~6~-sulfanyl)-2H-benzimidazole-2-thione (m/z 272, Rt. 0.61), (2S,3R)-2,3-Dihydroxy-5-oxohexanedioate (m/z 191, Rt. 1.06), 2-(1-hydroxyethyl)thiamine diphosphate(2-) (m/z 465, Rt. 5.20), suvorexant (m/z 449, Rt. 6.20), 4-(beta-D-Glucopyranosyloxy)-2-hydroxy-6-pentadecylbenzoic acid (m/z 525, Rt. 6.84), 1-(5''-Phosphoribosyl)-5-amino-4-imidazolecarboxamide (m/z 337, Rt. 5.84), Diacetylacteoside (m/z 707, Rt. 6.98),5,7-Dihydroxy-2-(4-hydroxy-3,5-dimethoxyphenyl)-4-oxo-4H-chromen-3-yl-beta-D-erythro-hexopyranosiduronic acid (m/z 521, Rt. 7.09), 2-(3,4-Dihydroxyphenyl)-5,7-dihydroxy-6-methoxy-4-oxo-4H-chromen-3-yl 6-O-acetyl-beta-D-erythro-hexopyranoside (m/z 535, Rt. 7.34), Narirutin (m/z 579, Rt. 5.60), 4-[3-(Benzyloxy)-1-(beta-D-glucopyranosyloxy)propoxy]butanoic acid (m/z 429, Rt. 7.40), 4-[(Nitrooxy)methyl]benzyl N-{(5Z)-7-[(1R,2R,3R,5S)-3,5-dihydroxy-2-{(1E,3R)-3-hydroxy-4-[3-(trifluoromethyl)phenoxy]-1-buten-1-yl}cyclopentyl]-5-heptenoyl}glycinate (m/z 679, Rt. 6.71), were not identified in previous studies on baby spinach.

PLS-DA score plot was used to assess the significance of class discrimination (*Fig. 1A,B*). The supervised comparison of baby spinach treated with different levels of fertilizers and *Bacillus subtilis* BD233 revealed distinct grouping among the control, 33N:33P:45K:7S kg/ha and 45N:45P:60K:10S kg/ha. The first component of the data was effective in separating the control from samples treated with fertilizers. Most of the fertilizer treated samples are on the left side of the plot and samples treated with fertilizers and *B. subtilis* on the right side of the plot (*Fig. 1A,B*).

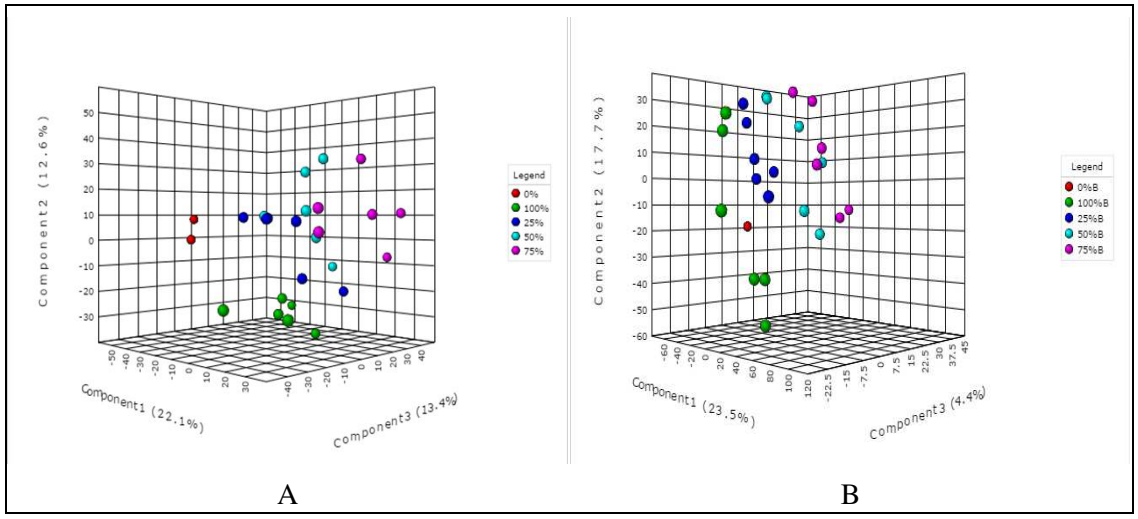

Figure 1. *Partial Least Squares - Discriminant Analysis (PLS-DA) 3D scores plot from LC-MS for baby spinach treated with different rates of fertilizers and Bacillus subtilis BD233. 0%=0N:0P:0K:0S kg/ha, 25% =11N:11P:15K:2S kg/ha, 50% =22N:22P:30K:5S kg/ha, 75% =33N:33P:45K:7S kg/ha, 100% =45N:45P:60K:10S kg/ha and B= Bacillus subtilis BD233*

http://www.aloki.hu ● ISSN 1589 1623 (Print) ● ISSN 1785 0037 (Online)
DOI: http://dx.doi.org/10.15666/aeer/1802_21292140

Conclusion

The current study showed evidence of differences in the chlorophyll content of the baby spinach cv. Anna, Edna and Ohio with the same treatments, however, no differences observed in stomatal conductance and total biomass among the three cultivars. Inoculation with *B. subtilis* also yielded the same results where no significant differences were observed in chlorophyll content, stomatal conductance and total biomass. Fertilizer application at 33N:33P:45K:7S kg/ha and 45N:45P:60K:10S kg/ha influenced the physiological parameters when compared to the control of the study. The results confirmed that plants treated with 11N:11P:15K:2S kg/ha and 22N:22P:30K:5S kg/ha baby spinach cv. Ohio is rich in flavonoids such as patuletin-3-glucosyl-(1-6)[apiosyl(1-2)]-glucoside (m/z 787, Rt. 5.39), spinacetin-3-glucosyl-(1-6)[apiosyl(1-2)]-glucoside (m/z 801, Rt. 5.94) and spinacetin-3-(2¢¢-feroylglucosyl)(1-6)[apiosyl(1-2)]-glucoside (m/z 977, Rt. 6.40), which have the potential protective response against cancer and heart diseases and also their antioxidative properties. Meanwhile, baby spinach cv. Anna, Edna and Ohio were found to be highly concentrated with amino acids such as (S)-Malate (m/z 133, Rt. 0.86) when no treatment applied, 2-(1-hydroxyethyl)thiamine diphosphate(2-) (m/z 465, Rt. 5.20) in all fertilizer application levels except the control, N-Acetyl-D-tryptophan (m/z 245, Rt. 5.55) when treated with 11N:11P:15K:2S kg/ha and Diethyl ({4-(6-oxo-7,11-diazatricyclo[7.3.1.0~2,7~]trideca-2,4-dien-11-yl)-3-[(3,4,5 trimethoxybenzoyl) amino] benzoyl} amino) malonate (m/z 675, Rt. 7.40) when no treatment applied, which are essential for tissue growth and repair, as well to assist in muscle building. There was a significant difference in the compounds among cultivars and NPKS fertilization. The study recommends that fertilizer at 22N:22P:30K:5S kg/ha and 33N:33P:45K:7S kg/ha amended with *B. subtilis* inoculation be considered when cultivating baby spinach. However, the metabolite profiling of baby spinach needs further investigation to determine the influence of *B. subtilis* application and levels of NPKS on flavor characterization.

Acknowledgements. The authors would like to thank SAKATA for providing seeds for the experiment and NRF (Grant No: 100503) for providing funds for this study.

Conflict of interests. The authors declared that there is no conflict of interests regarding the publication of this paper.

REFERENCES

[1] Anjum, M. A., Sajjad, M. R., Akhtar, N., Qureshi, M. A., Iqbal, A., Jami, A. R. (2007): Response of cotton to plant growth promoting rhizobacteria (PGPR) under different levels of nitrogen. – Journal of Agricultural Research 45: 135-143.

[2] Bashan, Y., Huang, P., Kloepper, J. W., de-Bashan, L. (2017): A proposal for avoiding fresh-weight measurements when reporting the effect of plant growth-promoting (rhizo) bacteria on growth promotion of plants. – Biology and Fertility of Soils 53: 1-2.

[3] Bergquist, S. A. M., Gertsson, U. E., Knuthsen, P., Olsson, M. E. (2005): Flavonoids in Baby spinach (*Spinacia oleracea* L.): Changes during Plant Growth and Storage. – Journal of Agricultural and Food Chemistry 53: 9459-9464.

[4] Bergquist, S. (2006): Bioactive compounds in baby spinach (*Spinacia oleracea* L.) effects of pre- and postharvest factors. – Journal of the Science of Food and Agriculture 86: 346-355.

http://www.aloki.hu ● ISSN 1589 1623 (Print) ● ISSN 1785 0037 (Online)
DOI: http://dx.doi.org/10.15666/aeer/1802_21292140

[5] Boroujerdnia, M., Ansari, N. A. (2007): Effect of different levels of nitrogen fertilizer and cultivars on growth, yield and yield components of romaine lettuce (*Lactuca sativa* L.). – Middle Eastern and Russian Journal of Plant Science and Biotechnology 1(2): 47-53.
[6] Çakmakçi, R., Erat, M., Erdogan, Ü., Dönmez, M. F. (2007): The influence of plant growth-promoting rhizobacteria on growth and enzyme activities in wheat and spinach plants. – Journal of Plant Nutrition and Soil Science 170: 288-295.
[7] Canbolat, M. Y., Bilen, S., Çakmakçı, R., Şahin, F., Aydın, A. (2006): Effect of plant growth-promoting bacteria and soil compaction on barley seedling growth, nutrient uptake, soil properties and rhizosphere microflora. – Biology and Fertility of Soils 42: 350-357.
[8] Diacono, M., Montemurro, F. (2010): Long-term effects of organic amendments on soil fertility. A review. – Agronomy for Sustainable Development 30: 401-422.
[9] Ekinci, M., Turan, M., Yildirim, E., Güneú, A., Kotan, R., Dursun, A. (2014): Effect of plant growth promoting rhizobacteria on growth, nutrient, organic acid, amino acid and hormone content of cauliflower (*Brassica oleracea* L. var. Botrytis) transplants. – Acta Sci Pol Hortorum Cultus 13(6): 71-85.
[10] Gairola, S., Umar, S., Suryapani, S. (2009): Nitrate accumulation, growth and leaf quality of spinach beet (*Beta vulgaris* Linn.) as affected by NPK fertilization with special reference to potassium. – Indian Journal of Science and Technology 2: 35-40.
[11] García-López, A. M., Delgado, A. (2016): Effect of *Bacillus subtilis* on phosphorus uptake by cucumber as affected by iron oxides and the solubility of the phosphorus source. – Agricultural and Food Science 25: 216-224.
[12] Gloria, P. M., Ibrahim, I. I., Zwalnan, D. N., Jameela, A., Henry, U. I. (2017): Effect of different levels of NPK fertilizer on the growth and yield of okra (Abelmoschus esculentus L.). – Int J Adv Acad Res. Sciences, Technology & Engineering 3(1): 1-8.
[13] Kalt, W. (2005): Effects of production and processing factors on major fruit and vegetable antioxidants. – Journal of food science 70: 11-19.
[14] Kerr, B. (2014): What is Spinach? – Farmer's Weekly, March 2014 Issue, South Africa.
[15] Khan, N. A., Nazar, R., Anjum, N. A. (2009): Growth, photosynthesis and antioxidant metabolism in mustard (*Brassica juncea* L.) cultivars differing in ATP-sulfurylase activity under salinity stress. – Scientia Horticulturae 122: 455-460.
[16] King, S., Davis, A., Perkins-Velazie, P., Helms, A., Stein, L. (2008): Effects of mineral nutrition on carotenoid content in spinach. – HortScience 43: 1246.
[17] Makus, D. J. (2013): Spinach leaf quality and yield is improved by supplemental gypsum application in two soil type in semi-arid South Texas. – Subtropical Plant Science 65: 24-30.
[18] Masufi, N. M., Mudau, A. R., Araya, H. T., Mudau, F. N. (2019): The developmental growth and quality assessment of five selected cultivars of baby spinach grown in the north of Pretoria, Gauteng Province, South Africa. – South African Journal of Plant and Soil (In press).
[19] Mncwangi, N. P., Viljoen, A. M., Zhao, J., Vermaak, I., Chen, W., Khan, I. (2014): What the devil is in your phytomedicine? Exploring species substitution in Harpagophytum through chemometric modeling of 1H-NMR and UHPLC-MS datasets. – Phytochemistry 106: 104-115.
[20] Mudau, A. R., Nkomo, M., Soundy, P., Araya, H. T., Ngezimana, W., Mudau, F. N. (2015): Influence of post-harvest storage temperature and duration on quality of baby spinach. – HortTechnology 25: 665-670.
[21] Nemadodzi, L. E., Araya, H., Nkomo, M., Ngezima, W., Mudau, F. N. (2017): Nitrogen, phosphorus, and potassium effects on the physiology and biomass yield of baby spinach (*Spinacia oleracea* L.). – Journal of Plant Nutrition 40(14): 2033-2044.
[22] Okazaki, K., Oka, N., Shinano, T., Osaki, M., Takebe, M. (2009): Metabolite profiling of spinach (*Spinacea oleracea* L.) leaves by altering the ration of NH4+/NO3- in the culture solution. – Soil Science and Plant Nutrition 55: 496-504.

http://www.aloki.hu ● ISSN 1589 1623 (Print) ● ISSN 1785 0037 (Online)
DOI: http://dx.doi.org/10.15666/aeer/1802_21292140

[23] Porcel, R., Zamarreño, A. M., García-Mina, J. M., Aroca, R. (2014): Involvement of plant endogenous ABA in *Bacillus megaterium* PGPR activity in tomato plants. – BMC Plant Biology 14: 36.
[24] Pramanik, K., Bera, A. K. (2013): Effect of seedling age and nitrogen fertilizer on growth, chlorophyll content, yield and economics of hybrid rice (*Oryza sativa* L.). – Journal of Agronomy and Plant Production 4(5): 3489-3499.
[25] Pupathy, U. T., Radziah, O. (2015): Growth response of corn to nitrogen-fixing bacteria enriched compost. – Asian Journal of Crop Science 7: 72-80.
[26] Schrader, W., Mayberry, K. S. (2003): Beet and Swiss chard production in California. – University of California, ANR Publication 8096.
[27] Sedibe, M. M. (2012): Yield and quality response of hydroponically grown rose geranium (*Pelargonium* Sp.) to changes in the nutrient solution and shading. – Doctoral Thesis (Soil, Crop and Climate Sciences), University of the Free State.
[28] Sedibe, M. M., Allemann, J. (2012): Yield and quality response of rose geranium (*Pelargonium* Sp.) to sulphur and phosphorus application. – South African Journal of Plant and Soil 29: 151-156.
[29] Shine, M. B., Guruprasad, K. N. (2012): Impact of pre-sowing magnetic field exposure of seeds to stationary magnetic field on growth, reactive oxygen species and photosynthesis of maize under field conditions. – Acta Physiologiae Plantarum 34: 255-265.
[30] Singh, K., Singh, P. P., Beg, S. U., Kumar, D., Patra, D. D. (2004): Effect of NPK fertilizers on growth, oil yield and quality of French basil (*Ocimum basilicum* L.). – Journal of Spices Aromatic Crops 13(1): 52-54.
[31] Singh, D. B., Ahmed, N., Singh, S. R., Mir, K. A., Lal, S. (2014): Variation in chlorophyll and carotenoid contents in kale (*Brassica oleracea*) as influenced by cultivars and harvesting dates. – Indian Journal of Agricultural Sciences 84(10): 1178-81.
[32] Turan, M., Ekinci, M., Yildirim, E., Güneş, A., Karagöz, K., Kotan, R., Dursun, A. (2014): Plant growth-promoting rhizobacteria improved growth, nutrient, and hormone content of cabbage (*Brassica oleracea*) seedlings. – Turkish Journal of Agriculture and Forestry 38: 327-333.
[33] Wu, Y. N., Feng, Y. L., Paré, P. W., Chen, Y. L., Xu, R., Wu, S., Wang, S. M., Zhao, Q., Li, H. R., Wang, Y. Q., Zhang, J. L. (2016): Beneficial soil microbe promotes seed germination, plant growth and photosynthesis in herbal crop *Codonopsis pilosula*. – Crop and Pasture Science 67(1): 91-98.
[34] Yakhin, O. I., Lubyanov, A. A., Yakhin, I. A. (2016): Biostimulants in agrotechnologies: problems, solutions, outlook. – Agrochemical Her 1: 15-21. Available online at: http://www.agrochemv.ru/en/nomer/2016/1; http://elibrary.ru/item.asp?id=25940647 (Accessed 16 March 2019).
[35] Zhang, H., Xie, X., Kim, M. S., Kornyeyev, D. A., Holaday, S., Paré, P. W. (2008): Soil bacteria augment Arabidopsis photosynthesis by decreasing glucose sensing and abscisic acid levels in plants. – The Plant Journal 56: 264-273.
[36] Zikalala, B. O., Nkomo, M., Araya, H., Ngezimana, W., Mudau, F. N. (2016): Nutritional quality of baby spinach (*Spinacia oleracea* L.) as affected by nitrogen, phosphorus and potassium fertilisation. – South African Journal of Plant and Soil 34(2): 79-86.

http://www.aloki.hu ● ISSN 1589 1623 (Print) ● ISSN 1785 0037 (Online)
DOI: http://dx.doi.org/10.15666/aeer/1802_21292140

EVALUATING DIFFERENT MODELS USED FOR PREDICTING THE INDOOR MICROCLIMATIC PARAMETERS OF A GREENHOUSE

ELANCHEZHIAN, A. – BASAK, J. K. – PARK, J. – KHAN, F. – OKYERE, F. G. – LEE, Y. – BHUJEL, A. – LEE, D. – SIHALATH, T. – KIM, H. T.*

Department of Bio-systems Engineering, Gyeongsang National University, Institute of Agriculture & Life Science, Jinju 52828, South Korea

**Corresponding author*
e-mail: bioani@gnu.ac.kr; phone: +82-55-772-1896; fax +82-55-772-1899

(Received 9th Sep 2019; accepted 25th Nov 2019)

Abstract. A robust adaptive model to predict and to control the greenhouse microclimatic condition is pivotal for better crop production and growth. The current research assesses the use of multiple linear regression (MLR), autoregressive integrated moving average (ARIMA), and multi-layered perceptron (MLR) for predicting indoor microclimate greenhouse, located in South Korea. The data were collected from the local weather station and regional weather station data named M1 (local weather station data combined with the regional weather station data), M2 (regional weather station data), and M3 (local weather station data), which were used as the input variables for the prediction. Four dependent variables were predicted (two temperature variables and two humidity variables) by each of the models using M1, M2, and M3 data sets. Performances of the models were evaluated with the coefficient of determination (R^2), the root mean square error (RMSE), the mean square error (MSE), and the mean absolute error (MAE). The simulation results showed that the prediction by the MLP model was highly correlated to the measured data with less RMSE, MSE, and MAE. Besides, seasonal based analysis results reinforce that the MLP performs a better simulation in different environmental conditions. Moreover, the M1 data were propitious for better performance than other data sets, which specifically improves the accuracy of the simulation results for humidity predictions. The present study developed a simple and powerful MLP model to predict the microclimate of the greenhouse, which may integrate into greenhouse controller devices through cloud technology in the future.
Keywords: *ARIMA, greenhouse, indoor microclimate, MLP, MLR, model comparison*

Introduction

Currently, one of the major challenges in worldwide agricultural productivity is climate change. Reducing food hunger is becoming an immense challenge due to the abnormal increase in the world population. Adopting precision farming methodologies such as greenhouse farming technology protect from the vulnerability of agriculture production (Kurt et al., 2017). From the last few decades, precision farming methodologies have boosted agriculture production due to the emergence in advanced technologies such as sensors, actuators and microprocessors, IoT based greenhouse systems, and big data analytics. In recent years, production in greenhouses has become more popular than ever before. The global smart greenhouse market is estimated to grow from 680.3 million in 2016 to 1.31 billion USD by 2022 (Leonetti, 2018). The key factors driving the smart greenhouse market include; improving the indoor farming space, vegetation on farmer preferences, high demand for quality, favorable government regulations, etc. The indoor microclimatic parameters such as temperature and humidity is an essential aspect of controlling the crop interaction with the environment. Enhancing microclimatic conditions in a greenhouse leads to improve crop quality and quantity of

http://www.aloki.hu ● ISSN 1589 1623 (Print) ● ISSN 1785 0037 (Online)
DOI: http://dx.doi.org/10.15666/aeer/1802_21412161

production since these crop properties directly influenced by the microclimate parameters (Santosh et al., 2017). Therefore, considering control of temperature and humidity is essential when a farmer plans to start planting in greenhouse facilities.

A robust, adaptive, and accurate model is essential to predict the indoor temperature and humidity of the greenhouse to develop an ideal control strategy for a greenhouse microclimate (Luan et al., 2011). Various static and dynamic models have been developed to predict and control microclimatic conditions in earlier studies (Lu and Viljanen, 2009; He and Ma, 2010; He et al., 2014; Shi et al., 2018). Most often, substantial studies carried out regression models, time series models, computer intelligence approaches, and hybrid approaches to predict the short term as well as long-term time series based variables (Cheng and Ni-Bin, 2011). A comprehensive performance assessment of the different prediction models helps to develop an ideal control strategy for greenhouse microclimate (Uchida and Pieters, 2004). The current study is hypothesised to make a comparative study between the performance of the physical models and the computational models. Likewise, the foremost objective of this study is to evaluate the performance of the physical model (multiple linear regression (MLR)), the time series forecast model (autoregressive integrated moving average (ARIMA)) and the computational model (multi-layered perceptron (MLR) with back propagation-BB training algorithm) with limited input variables. Numerous studies considered the outdoor environmental parameters along with indoor parameters such as soil temperature, plant phenotypes, and ventilation as accessible input variables for predicting the indoor microclimate of a greenhouse (Lu and Viljanen, 2009; He and Ma, 2010). However, the present study performs the prediction of greenhouse microclimate using a minimum number of input variables. For the data collection, most of the researches established a specific local weather station rather than the regional weather station to model the indoor climate of a greenhouse (Behrang et al., 2010; Singh and Tiwari, 2017), besides various studies consider the regional weather stations data for their greenhouse indoor climate modeling (Liu et al., 2018; Shi et al., 2018). The other objective of the current study is to predict microclimate using local weather station (near to the greenhouse) environmental parameters as well as the regional weather station data from the zonal weather station.

Literature review

Regression models are more often developed and applied for prediction in fields such as greenhouse microclimate, energy consumption, heat transfer, meteorological forecast, business forecast, and others (Feinberg and Genethliou, 2005). Generally, MLR model performances include the incorporation of deterministic influences, stochastic influences, and exogenous influences. Researchers considered standard errors as the dominant central point for evaluating regression models. Taki et al. (2016) utilized an MLR model to predict the temperature, humidity, soil temperature, and soil moisture level of a greenhouse in Iran. That study proves that the regression model is capable of making accurate predictions with minimal root mean square error (RMSE) and a higher coefficient of determination (R^2). Likewise, several studies that employed MLR techniques for their predictions (Davis, 2003; Zhao and Xue, 2010).

Most climatic-based variables follow a series type of wave correlated to time so that the time series forecast models could contribute to series based predictions. Moving average, exponential smoothing, and autoregressive integrated moving average (ARIMA) are frequently used techniques in prediction, which performed by past observations; ARIMA is more prevalent among time-series predictions (Khashei and Bijari, 2011).

http://www.aloki.hu ● ISSN 1589 1623 (Print) ● ISSN 1785 0037 (Online)
DOI: http://dx.doi.org/10.15666/aeer/1802_21412161

Hasni et al. (2010) designed an ARIMA model to predict the temperature flow of a greenhouse. In that study, various time series models were utilized and stimulated to predict the greenhouse temperature from 11 days of data. That literature concluded that the ARIMA models could efficiently produce a better forecast for long seasonal time series with high frequency. However, these models could not provide an exact forecast, which could be considered as a supplemental tool for environmental planning and decision-making for a seasonal based prediction.

In recent years, the development of advanced software technologies creates a platform to govern and analyze big data using a computational approach, which includes; artificial neural networks (ANN), convolutional neural networks (CNN), etc. ANN model is a robust computational method for classifying flow data, which may perform well for solving non-linear problems using their inner-parallel architecture (Atia and El-madany, 2017). Capabilities such as self-adaptive strategy, data-driven, extract the relationship between the inputs and outputs of a process, etc. makes ANN-based modeling as valuable and attractive for non-linear data predictions (Neshat et al., 2011). ANN models used with several algorithms including; multilayer perceptron (MLP), Support Vector Machine (SVM), backpropagation (BP), etc. which are included with or without various transfer functions. The performance of the models differs according to the description of the problem, target data, and processing time. MLP algorithm is popular among ANN models to solve various aspects of microclimatic prediction problems (Dombayci and Gölcü, 2009; Taki et al., 2015; Leopold et al., 2016). Since the MLR models have the capability to self-learn during the training, most of the studies are successful and statistically significant in terms of various error checking methods such as RMSE, Mean absolute error (MAE), and mean squared error (MSE).

Though there were performance tests between regression and ANN models in several researchers, most of the comparative studies have been carried out between the physical models and ANN models or else time series models and ANN (Taki et al., 2015, 2016; Hande et al., 2016; Nury et al., 2017). For instance, Taki et al. (2016) study made a comparison between the dynamic model and MLP model to predict the air temperature and roof temperature of a greenhouse and his literature concluded that the performance of MLP (ANN) model was better than the other models based on the small RMSE and mean absolute percentage error (MAPE). Mehdi et al. (2013) carried out a study about the accuracy of the prediction model between ANN, adaptive neuro-fuzzy inference system (ANFIS), and regression model and concluded that the MLR models are better in terms of simple and straightforward statistical methods then ANN. The efficiency of any model improved by the addition of more relevant input variables along with normalization. The current study used limited input details with non-preprocessed data.

Materials and Methods

Experimental site, materials and data collection

The study was conducted in a greenhouse facility, which maintained by the smart farm research center of Gyeongsang National University, South Korea, with GPS coordinates N35°09′09″, E128°05′44.99″ (Google earth). A flat arch-shaped, 2-layer polyethylene covering with 0.1 mm and 0.075 mm thickness patched, UV-Resistant greenhouse was used for this research. The dimensions of the greenhouse are shown in *Figure 1* with more details. The greenhouse was entirely operated by a UBN Farmlink™ v 3.0 (South Korea) farm management technology that collects and stores the data from the sensor node. A

http://www.aloki.hu ● ISSN 1589 1623 (Print) ● ISSN 1785 0037 (Online)
DOI: http://dx.doi.org/10.15666/aeer/1802_21412161

wireless sensor node, which shown in *Figure 2* was utilized to record the temperature and humidity data. In this research, two sets of temperature, humidity sensors were placed in the front and backside of the greenhouse which is displayed in *Figure 1*. The control system of the experimental site has three major parts that are the network controller, actuator, and wireless sensor nodes. All the electronic devices and data loggers were calibrated to minimize the device errors before the starting time of the experiment.

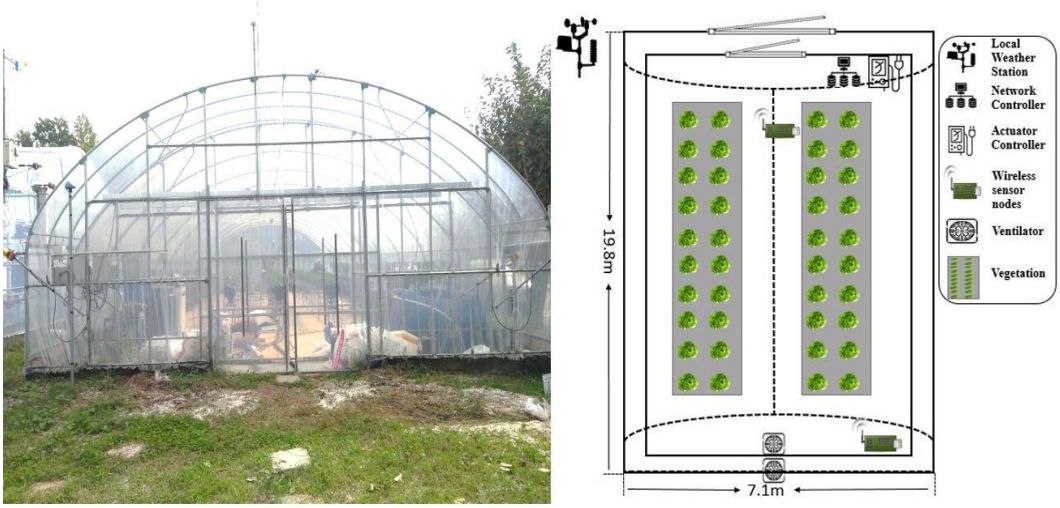

Figure 1. *Image of the experimental greenhouse and layout of the experimental setup*

Figure 2. *Images of local weather station, network controller with the data logger, wireless sensor nodes used in the experimental site*

A weather station which is contiguous to the greenhouse (Campbell Scientific, United States) comprising a data logger (LoggerNet 4.0) displayed in *Figure 2*, managed the acquisition of local weather data. The data collected from the local weather station was considered as 1st outdoor parameter. The regional weather data for the above-mentioned coordinates were collected from the Korea meteorological administration office, Seoul, South Korea. That data considered as 2nd outdoor parameter. The present study used both regional weather station data as well as local weather station data for prediction. This

http://www.aloki.hu ● ISSN 1589 1623 (Print) ● ISSN 1785 0037 (Online)
DOI: http://dx.doi.org/10.15666/aeer/1802_21412161

outdoor parameter 1 and 2 were considered as independent parameters, while indoor temperature and humidity were used as dependent variables for the entire prediction model. Temperature, humidity, temperature - humidity index, and solar radiation intensity data are considered input data sets for this experiment. The data loggers record data every 10 min interval in the period between April 2018 to January 2019; 70% of the data were used for training, and 30% used for validation. South Korea has four distinct seasons, which are spring (March-May), summer (June-August), autumn (September-November) and winter (December-February). During the summer period and autumn period the strawberry plants were grown on the experimental greenhouse. Since there is no particular climatic season for rainy or monsoon in the current region, the rainy days were considered based on the regional metrological report. Also, there are no simultaneous rainy days during this both period, so that 5 different days of every season from the validation data sets were considered as the rainy period data sets to find the performance of the model during that particular period. In June (2018), 5 days was selected as a rainy (for summer season) data (from 11^{th}–15^{th}). During that period the average air temperature was 21.8°C (19°C-27°C) and the average rainfall of the month was 70.42 mm. For the rainy days model validation in the winter season was considered from November (1^{st}–5^{th}). During that period the average rainfall of the month was 32.9 mm, and the average temperature was 10.9°C (8.3°C-12°C). All neural network models used for this study were designed by using MATLAB (R2018b (Version 9.5), Mathworks, USA) software. Likewise, all other statistical analysis works were done with IBM SPSS Statistics (version 26, IBM, USA) and OriginPro (version 9.0, Originlab, USA) software packages.

Prediction models

Multiple linear regression (MLR) model

Regression models develop the relationship between the dependent and independent or response variables involved in the process. Factors such as designing simplicity, comparatively accuracy, and a less amount of input data make the regression model as accessible tools for prediction. The functions of MLR can express by the following (*Equation 1*),

$$Y = \beta_0 + \beta_1 X_1 + \beta_2 X_2 + \cdots + \beta n X n + \varepsilon \quad \text{(Eq.1)}$$

where Y is the response variable (temperature or humidity), β_0, β_1, β_2… β_n - are regression coefficients estimated based on a record of observations, ε refers to the residual (Braun et al., 2014).

Time series model (ARIMA)

The autoregressive integrated moving average model (ARIMA) is the most preferred model in recent times used to forecast metrological parameters, especially in the short-term forecasting area (Murat et al., 2018). The combination of autoregressive (AR) model (p), moving average (MA) model (q) called ARIMA (p, d, q), which is a generalized random walk model. First, the time series is d-differenced to render it stationary. If d =0, the observations are modeled directly, and if d = 1, the differences between consecutive observations are modeled (Patel et al., 2014).

AR (p) is the relationship between the observation and number of lagged information, which can be expressed by *Equation 2*,

http://www.aloki.hu ● ISSN 1589 1623 (Print) ● ISSN 1785 0037 (Online)
DOI: http://dx.doi.org/10.15666/aeer/1802_21412161

$$X_t = C + \sum_{i=1}^{p} \emptyset_i x_{t-1} + \varepsilon_t \quad \text{(Eq.2)}$$

where X_t is the autoregressive operator of order p, C is the constant, ϕ_i refers to the parameter of the model, x_t is the value that observed at t, and ε_t stands for random error. The MA (q) model calculates the dependency between an observation and a residual error from a moving average model applied to lag observations. The moving average mathematically expressed by *Equation 3*,

$$X_t = \varepsilon_t + \sum_{i=1}^{q} \theta_i \varepsilon_{t-i} \quad \text{(Eq.3)}$$

where X_t is the autoregressive operator of order q, θ_i is the parameter of the model, ε_t is the error term. The combination of the autoregressive and moving average model that expressed in terms of (*Equation 4*),

$$Y_t = c + \sum_{i=1}^{p} \phi_i y_{t-i} + \sum_{j=1}^{q} \theta_j \varepsilon_{t-j} \quad \text{(Eq.4)}$$

where Y_t is the predicted value, c is the constant, ϕ_i is the coefficient determined by AR, and θ_i is the determined coefficient of the MA model. The ARIMA model was used as a prediction model to predict the indoor temperature and humidity for the greenhouse.

Multilayered perceptron algorithm

Multilayered perceptron is one of the commonly used feed-forward layered networks due to its low complexity and its ability to solve the nonlinear criteria. In general, the neural network model is included with various learning adaption techniques. Apart from the input, hidden, and output layer elements, the weights, and bias are the vital elements involved in the process of output layer calculation (Taki et al., 2016). The weights are calculated using the following *Equation 5*,

$$Y_j = \sum_{i-1}^{n} w_{ij} I_i + \beta_j \quad \text{(Eq.5)}$$

where Y_j is the weight values, I_i is the input variables, w_{ij} is the weight between input parameters, and neuron j and β_j is the bias. The structure of the network explained in *Figure 3*.

Next, an activation function is used to generate the output of neurons that is decided according to weight values. Different types of activation functions including log, hyperbolic, exponential, and sigmoid can be used in MLP. The most popular activation function to solve the nonlinear function is sigmoid (Taki et al., 2016), so that the current study used sigmoid as the transfer function of the MLP. The sigmoid transfer function is expressed by *Equation 6*,

http://www.aloki.hu ● ISSN 1589 1623 (Print) ● ISSN 1785 0037 (Online)
DOI: http://dx.doi.org/10.15666/aeer/1802_21412161

$$f(\theta) = \frac{1}{1 + e^{-\theta}} \quad \text{(Eq.6)}$$

Once each neuron and the transfer functions are calculated, the final output layer which is expressed by the following *Equation 7*,

$$y_k = \sum_{i=1}^{n} w_{kj} f_i + \beta_k \quad \text{(Eq.7)}$$

The next essential framework for performing any ANN model is training the network. The feed-forward back-propagation network undergoes supervised training, with a finite number of pattern pairs consisting of an input pattern and a desired or target output pattern (Taki et al., 2016). Since the back-propagation technique minimizes the cost error function, it is commonly used for training algorithms for MLP. For this study, MLP with the feed forward-back propagation model network was designed in the MATLAB software with various transfer functions and adaption techniques. The single hidden layer including a sufficient number of neurons is capable of predicting non-linear variables with the desired output. Based on past studies, the single-layered MLR with random combinational neuron models were used in these studies.

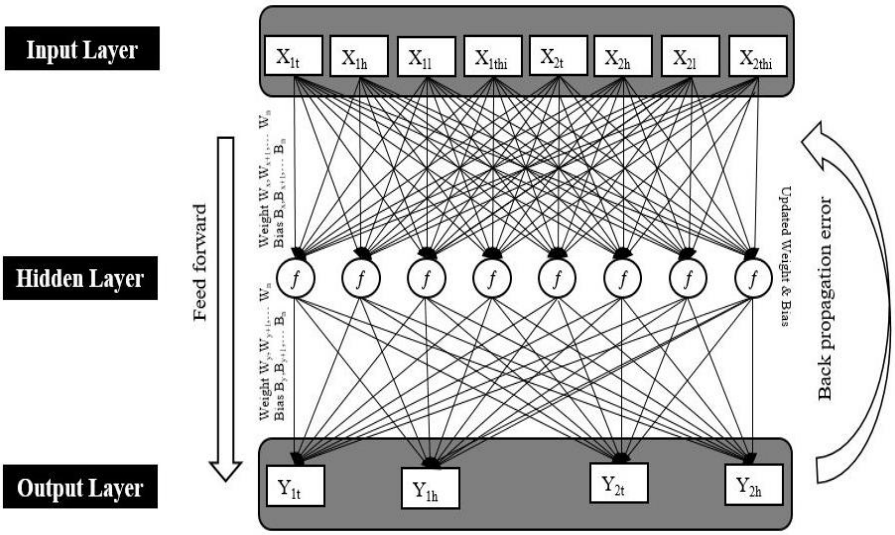

Figure 3. *Structure of the MLP with the function of feedforward and backpropagation method*

Input and output parameter modeling

The data were collected from the local weather station and regional weather station data named M1 (local weather station data combined with the regional weather station data), M2 (regional weather station data), and M3 (local weather station data), which were used as the input variables for the prediction. Four dependent variables were predicted (two temperature variables and two humidity variables) by each of the models using M1, M2, and M3 data sets. The comprehensive explanation of the models, as shown in *Table 1*. These same mixed models used for all of the modeling techniques that are used for the evaluation in this examination.

http://www.aloki.hu ● ISSN 1589 1623 (Print) ● ISSN 1785 0037 (Online)
DOI: http://dx.doi.org/10.15666/aeer/1802_21412161

Table 1. *Input and output variables of M1, M2, and M3*

Model	Input variables	Output variables
M1	Regional weather station temperature (X_{1t}), Regional weather station humidity (X_{1h}), Regional weather station solar intensity (X_{1l}), Regional weather station temperature-humidity index (X_{1thi}), Local weather station temperature (X_{2t}), Local weather station humidity (X_{2h}), Local weather station solar intensity (X_{2l}), Local weather station temperature-humidity index (X_{2thi})	Indoor temperature (front) (Y_{1t}), Indoor humidity (front) (Y_{1h}), Indoor temperature (back) (Y_{2t}), Indoor humidity (back) (Y_{2h})
M2	(X_{1t},X_{1h},X_{1l},X_{1thi})	(Y_{1t},Y_{1h}) &(Y_{2t},Y_{2h})
M3	(X_{2t},X_{2h},X_{2l},X_{2thi})	(Y_{1t},Y_{1h}) &(Y_{2t},Y_{2h})

Model evaluation criteria

Various statistical indicators were used to evaluate the prediction model. The coefficient of determination can well measure the degree of proximity between the actual data and the predicted values. For a comprehensive evaluation, the results of the models were analyzed by the coefficient of determination (R^2), the root mean square error (RMSE), the mean square error (MSE) and the mean absolute error (MAE) (Lu and Viljanen, 2009). R^2, MAE, RMSE, and MSE can be expressed by the following equations (*Equations 8-11*),

$$R^2 = 1 - \frac{\sum_{i=1}^{n}(y_i - p_i)^2}{\sum_{i=1}^{n}(y_i - \frac{1}{n}\sum_{i=1}^{n} y_i)^2} \quad \text{(Eq.8)}$$

$$RMSE = \sqrt{\frac{\sum_{i=1}^{n}(y_i - p_i)^2}{n}} \quad \text{(Eq.9)}$$

$$MSE = \frac{\sum_{i=1}^{n}(y_i - p_i)^2}{n} \quad \text{(Eq.10)}$$

$$MAE = \frac{\sum_{i=1}^{n}|y_i - p_i|}{n} \quad \text{(Eq.11)}$$

Results and discussion

MLR model results

The indoor temperature and humidity data were predicted using MLR. As mentioned earlier, stepwise and feed-forward methods were used during the time of testing. Even though the feed-forward method performs very similar to the stepwise approach, the stepwise approach outperforms in predicting the temperature as well as the humidity variables. The overall better performance of the MLR was with M1 in terms of R^2 value, and the evaluation results showed in *Table 2*. MLR prediction has the coefficient of determination 0.955 in M1, while M3 has 0.952. The least value, which was from M2

http://www.aloki.hu ● ISSN 1589 1623 (Print) ● ISSN 1785 0037 (Online)
DOI: http://dx.doi.org/10.15666/aeer/1802_21412161

with 0.708 with is 74% lesser than the higher prediction value. Importantly, MAE was similar in M1 (stepwise) and M3 (both stepwise and feed-forward), which resemble the maximum capacity of both the model. The prediction accuracy of M1 for Y_{2t} lower than the M1 (R^2=0.953) when compared to M3, but MSE and RMSE were lower in M3, which cannot be ignorable. All three models were predicted the Y_{2t} lesser than the Y_{1t}. Both M1 and M3 performs well for predicting the temperature variables in MLR modeling with less error with statistical substantiation.

Table 2. *Performance of the MLR analysis*

Predicted variable	Model	R^2	MAE	MSE	RMSE
Y_{1t}	**M1**	0.955	1.23	2.21	1.48
	M2	0.708	2.36	9.29	3.04
	M3	0.952	1.24	2.21	1.48
Y_{2t}	**M1**	0.953	1.21	2.16	1.47
	M2	0.682	2.41	9.80	3.13
	M3	0.950	1.18	2.04	1.42
Y_{1h}	**M1**	0.832	6.12	57.66	7.59
	M2	0.544	8.74	159.56	12.63
	M3	0.823	8.44	122.85	11.08
Y_{2h}	**M1**	0.824	6.85	72.66	8.52
	M2	0.524	9.73	201.48	14.1
	M3	0.812	10.0	167.36	12.93

In the case of humidity prediction, the results were clearly announcing the M1 predictions are better than the other two in terms of all model evaluation criteria. The overall performance ranking of the models for humidity prediction results was the same as the temperature prediction ranking of the models, accordingly M1, M3, and M2 (least). The difference between the highest and lowest performance was 71% in Y_{1h} prediction modeling in terms of R^2. Overall, the maximum R^2 of Y_{1h} was 0.832, which was obtained in M1 with MAE =6.12 and RMSE =7.59. In Y_{2h} prediction, MAE and RMSE were high in both M3 and M2, unlike temperature prediction, especially in M2. More detailed prediction curve, as shown in *Figure 4*. However, the following key points were observed during MLR model evaluation,

- Even though the M1 and M3 performance was similar, M1 successfully helps to make predictions better than the M3.
- Unlike the prediction of temperature variables, the prediction of the humidity variables is less in terms of correlation and evaluation. The detailed results of the MLR models are shown in *Table 2*.

ARIMA model results

The mixed autoregressive and moving average (ARIMA) model prediction performance results shown in *Table 3*. The better performance of predicting Y_{1t} with M1 has R^2=0.959, MAE=0.9, and RMSE=1.16, followed by M3 (R^2=0.95). Even though both M1 and M3 have a similar coefficient of determination but MAE and RMSE were high in M3. Y_{2t} resembled the pattern of Y_{1t} prediction, MAE and RMSE were higher in M1 than the M3. Anywhere of the model, M2 does not over 70% in terms of R^2 value for both temperature and humidity variable predictions also MSE, and RMSE was very high from the other two models. Since this experiment uses the moving average model, the model

http://www.aloki.hu ● ISSN 1589 1623 (Print) ● ISSN 1785 0037 (Online)
DOI: http://dx.doi.org/10.15666/aeer/1802_21412161

fits according to the different percentile of the full data set. From the observations, temperature variables fit was the same in all percentile, whereas humidity fit was low at the initial time, and gradually it increases and after 50 percentile. For instance, Y_{1h}'s R^2 was 0.818 in 5 percentile, and it gradually increases up to 70 percentile and its reach to the maximum best fit by the model 0.838. Not only R^2, MAE, and RMSE also been adjusted after percentile of data changes. For M1 obtained Y_{2h} prediction bet fit with 0.821 followed by M3 with 0.796. However, this model was performed well against temperature prediction; nevertheless, humidity predictions have low efficient performance.

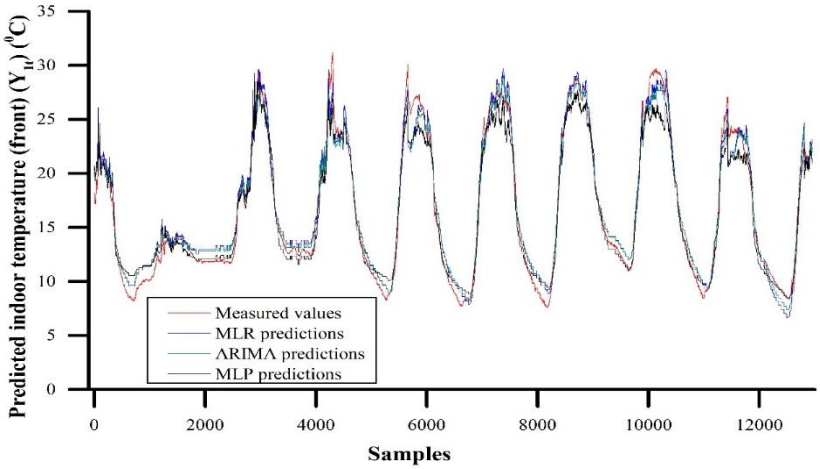

Figure 4. *Comparison of actual data and predicted indoor temperature (front) (Y_{1t}) by MLR, ARIMA and MLP models*

Table 3. *Performance of the time series model analysis*

Prediction variable	Model	R^2	MAE	MSE	RMSE
Y_{1t}	**M1**	0.959	0.90	1.35	1.16
	M2	0.665	2.68	11.20	3.34
	M3	0.958	0.92	1.41	1.19
Y_{2t}	**M1**	0.953	0.92	1.45	1.20
	M2	0.641	2.69	11.20	3.34
	M3	0.952	0.94	1.50	1.22
Y_{1h}	**M1**	0.838	5.90	54.96	7.41
	M2	0.656	8.30	116.76	10.80
	M3	0.818	6.16	61.77	7.86
Y_{2h}	**M1**	0.821	6.75	73.97	8.60
	M2	0.631	9.43	152.22	12.33
	M3	0.796	7.25	83.92	9.16

MLP model results

A multilayered perceptron feed-forward network with a back-propagation training algorithm was developed to predict the desired variables. The back propagation-training algorithm based on the Levenberg-Marquardt (LM) was used to simulate the prediction with more optimization. The transfer function used for this MLP was sigmoid since the desirable variables follow the sigmoid pattern. Still, there is a lack of detailed information

http://www.aloki.hu ● ISSN 1589 1623 (Print) ● ISSN 1785 0037 (Online)
DOI: http://dx.doi.org/10.15666/aeer/1802_21412161

regards fixing the hidden neurons, and this examination used random increasing neurons that start from minimum elements. All the random neuron combination results were referred to as *Table 4*. The training algorithm randomly generated bias and weight during this examination. For Y_{1t} prediction, M3 (5 neurons) has the highest performance that is with R^2=0.9793; MAE=0.85; RMSE =1.21 followed by the M3 (15 neurons). In M3 prediction, most of the validation gives better results than the M1 model in terms of R^2. All combinations of M3 have more than 0.96 R^2 values, whereas M1 result from 0.91 to 0.97. The highest evaluation criteria results obtained by M1 was with 20 neurons. Results of Y_{2t} resemble the same pattern as Y_{1t}; M3 model performs a higher than the M1. The top prediction of Y_{2t} variable in terms of R^2 = 0.974 obtained in M3 (30 neurons) with MAE=1.04; nevertheless, M1 prediction has the lowest MAE and RMSE values (MAE=0.95; RMSE=1.3; R^2=0.966) which could not negligible while consider for modeling. The least performance from the M2 models, which are extremely lower when compared to the other two models. Therefore overall performance shows that the M3 has a high R^2, and M1 has a lower number of error values.

Table 4. *Performance of the MLP model analysis with various neuron combinations*

Prediction variable	Model	Hidden neurons	R^2	MAE	MSE	RMSE
Y_{1t}	M1	**20**	0.9732	0.90	1.64	1.28
		25	0.9681	0.94	1.61	1.27
		30	0.9674	0.93	1.47	1.21
	M2	**35**	0.6698	4.79	31.97	5.65
		45	0.7574	3.75	20.75	4.55
		20	0.972	1.05	1.93	1.39
	M3	**5**	0.9793	0.85	1.47	1.21
		45	0.9764	0.95	1.72	1.31
		50	0.9756	1.15	2.21	1.48
Y_{2t}	M1	**30**	0.9609	0.96	1.84	1.35
		35	0.966	0.95	1.71	1.30
		40	0.961	0.97	1.84	1.35
	M2	**5**	0.7125	4.86	33.29	5.77
		20	0.6065	5.18	38.54	6.20
		50	0.6267	4.53	29.77	5.45
	M3	**30**	0.974	1.04	1.92	1.32
		35	0.97	1.00	1.96	1.40
		40	0.966	1.12	2.32	1.52
Y_{1h}	M1	**5**	0.9093	4.72	39.73	6.30
		10	0.7822	8.36	128.30	11.32
		35	0.8592	6.40	80.35	8.96
	M2	**15**	0.5072	14.54	461.44	21.48
		20	0.4131	16.67	516.20	22.72
		45	0.664	13.86	362.69	19.04
	M3	**5**	0.8574	6.88	81.39	9.02
		15	0.8316	6.87	79.90	8.93
		20	0.8375	7.23	88.88	9.42
Y_{2h}	M1	**5**	0.8151	7.66	119.88	10.94
		10	0.8116	7.956	124.39	11.15
		40	0.8154	7.876	121.02	11.00
	M2	**25**	0.4383	17.19	465.99	21.58
		40	0.5048	16.05	421.49	20.53
		45	0.5498	15.47	422.62	20.50
	M3	**5**	0.804	7.98	123.02	11.09
		40	0.771	9.18	202.47	14.22
		45	0.802	8.76	130.24	11.41

http://www.aloki.hu ● ISSN 1589 1623 (Print) ● ISSN 1785 0037 (Online)
DOI: http://dx.doi.org/10.15666/aeer/1802_21412161

For Y_{1h} predictions, M1 (5 neurons) has the highest R^2 (0.9093) among all other combinations with lower error values MAE=4.72 and RMSE=6.30 followed by 35 neurons set (R^2=0.8592; MAE =6.40; RMSE =8.96) in M1. The top prediction of M3 obtained from 40-neuron combination, but the error values higher than the second and third highest predicted combinations. Prediction results for the Y_{2h} have the highest in M1 (40 neurons) in terms of R^2 was 0.8154, whereas 5 neuron prediction has the lowest MAE=7.66 also it has the least RMSE value. Other than the 5, 10 and 40 neuron combinations, all M1 combinations were performed poor in terms of correlation and determination. The overall results of this model explain that neurons not linearly related to the performance. Maximum iteration was observed during both testing, and cross-validation period was 1000, whereas 400 iteration was the minimum. During the time of making the neuron combination randomly, other neurons combinations also have been tested, for instance, in between to the 5-10 combinations indiscriminately 6 or 7 also used to avoid the lesser accuracy. However, the random test results were not accurate than the highest prediction so that the random combination results not shown in *Table 4*.

Compression between MLR, ARIMA and MLP models

Previous studies prove that traditional statistical models are potential tools for predicting the environmental parameters in a more precise manner (Mehdi et al., 2013); also, several studies developed a high accurate computational model for the prediction (Taki et al., 2015; Shi et al., 2018). According to this results the highest accuracy of predicted values Y_{1t} for MLR, ARIMA and MLP accordingly 0.955; 1.23; 2.21; 1.48 (R^2; MAE; MSE; RMSE), 0.959; 0.90; 1.35; 1.16 and 0.9793; 0.85; 1.47; 1.21. For the Y_{1t} prediction, the MLP model has a higher R^2 and MSE, whereas ARIMA performed well in terms of RMSE and the MAE. MLR has two methods that are stepwise and feed-forward, and MLP has varied the combination of neurons. So according to the variable Y_{1t} MLP model prediction with 5-neuron combination doing the best performance in this examination. Y_{2t} best predictions in MLR, ARIMA and MLP model as follows 0.954; 1.20; 2.14; 1.46 (R^2; MAE; MSE; RMSE), 0.952; 0.94; 1.50; 1.22 and 0.974; 1.04; 1.92; 1.32. Even though R^2 is higher in the MLP model, ARIMA has the lower MAE, MSE and RMSE values that could not be ignored. Unlike temperature prediction, all three models have some limitations while simulating the humidity variables. M1 and M3 performed well during the temperature prediction in any prediction model, whereas for the humidity predictions, M1 help to improve the accuracy of each model. Most of the time, the highest number neurons combination fails to predict the humidity during MLP simulations and their error values were high when the neurons increased. The performance of MLP was 0.9093; 4.72; 39.73; 6.30 (R^2; MAE; MSE; RMSE), other than this model, no other model has no closer output to this model. 0.832; 6.12; 57.66; 7.59 was the performance of M1 in MLR and 0.838; 5.9; 54.96; 7.41 was obtained by the ARIMA. In between the 1000-2000 samples, all the models predicted beyond the limit and at these values impacted most in prediction. All these model performance graphs were displayed in *Figures 4-7*.

In Y_{2h} predictions MLR model performs better than the other models with the 0.824; 6.85; 72.66; 8.52 (R^2; MAE; MSE; RMSE) followed by the MLP 0.8154; 7.87; 121.02; 11.00. The predicted value graph shown in *Figure 7*, particularly at some point in time, the humidity value reached the maximum level, in that cases other than the MLR does not predict the changes. While observing the curves, MLP follows the same pattern but predicted more than the actual peak times. The overall performance of the MLP model

http://www.aloki.hu ● ISSN 1589 1623 (Print) ● ISSN 1785 0037 (Online)
DOI: http://dx.doi.org/10.15666/aeer/1802_21412161

was better than the other models except for Y_{2h} predictions in terms of R^2 and error values. The validation results with the post-regression model fit in the sense of R^2 shown in *Figure 8*, though Y_{2t} has some distinguished data scattering, Y_{1t} and Y_{2t} measured data were not much distributed, and it lies on the same level. The effects of non-normalized real-time data visible in evidence of Y_{1h} and Y_{2h} regression from *Figure 8*. From the analysis, error validation, and R^2, the MLP performs higher than the other models used in this literature.

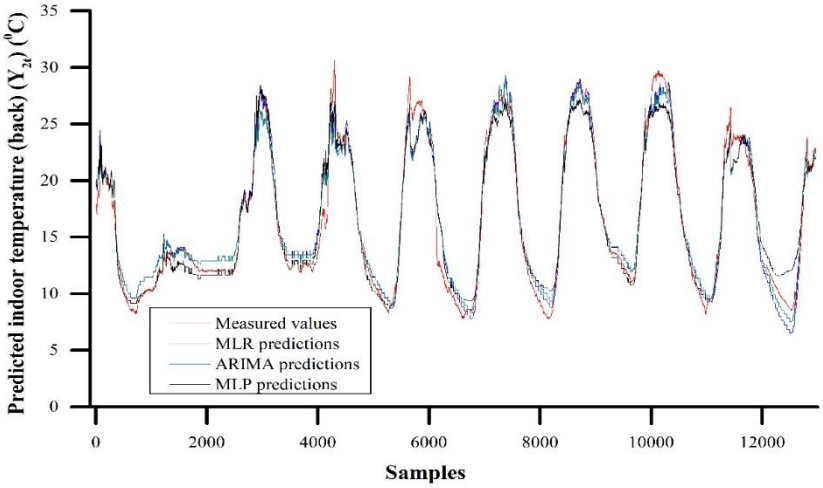

Figure 5. *Comparison of actual data and predicted indoor temperature (back) (Y_{2t}) by MLR, ARIMA and MLP models*

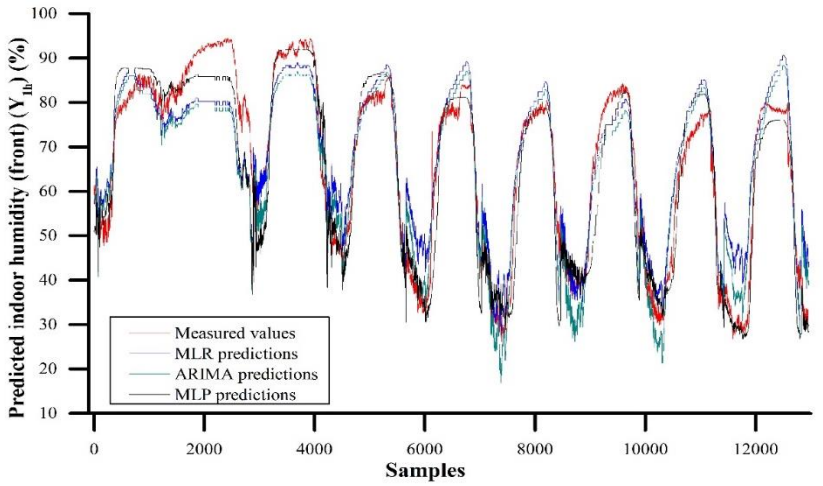

Figure 6. *Comparison of actual data and predicted indoor humidity (front) (Y_{1h}) by MLR, ARIMA and MLP models*

Seasonal based appraisal

According to the model evaluation results, the authentic resulted models were subjected to the seasonal based intensive test. The predicted data sets were separated according to the four seasons, and the results were appraised with the same evaluation criteria which are used for the whole year data sets. From the seasonal based analysis

http://www.aloki.hu ● ISSN 1589 1623 (Print) ● ISSN 1785 0037 (Online)
DOI: http://dx.doi.org/10.15666/aeer/1802_21412161

results during the spring period, for Y_{1t} prediction the MLP model outperformed (R^2; MAE; MSE; RMSE: 0.9589; 0.971; 1.765; 1.328) followed by the ARIMA (0.948; 1.111; 2.378; 1.542). In Y_{2t} predictions, the ARIMA performed better R^2 (0.8858) than the MLR (0.8768) model, based on the other criteria (MAE; MSE; RMSE) the MLR model have the lower mean error values (1.067; 2.23; 1.494) than the ARIMA model (1.34; 2.981; 1.726). In terms of R^2 values the ARIMA model followed by the MLP model (0.8814). For the Y_{1h} variable MLP performed better prediction (R^2=0.8447) which was followed by the ARIMA (R^2=0.7989). MLP has the highest R^2 (0.7843) for Y_{2h} among all models. Likewise, for all four seasons the most of MLP prediction has a good correlation with the measured temperature variables (autumn season R^2 for MLP (Y_{1t}=0.9589), summer season R^2 (Y_{1t}=0.8143; Y_{2t}=0.829), winter season R^2 (Y_{1t}=0.8432; Y_{2t}=0.8372)). Even though, in spring season Y_{2t} prediction performed well in ARIMA (R^2=0.8858; MAE=1.348; RMSE=1.726) followed by MLP (R^2=0.8814; MAE=1.215; RMSE=1.653) in terms of MAE and RMS values the MLR has the lower errors (R^2=0.8768; MAE=1.067; RMSE=1.494). Apart from spring season Y_{2t} prediction MLP outperformed in temperature prediction followed by ARIMA.

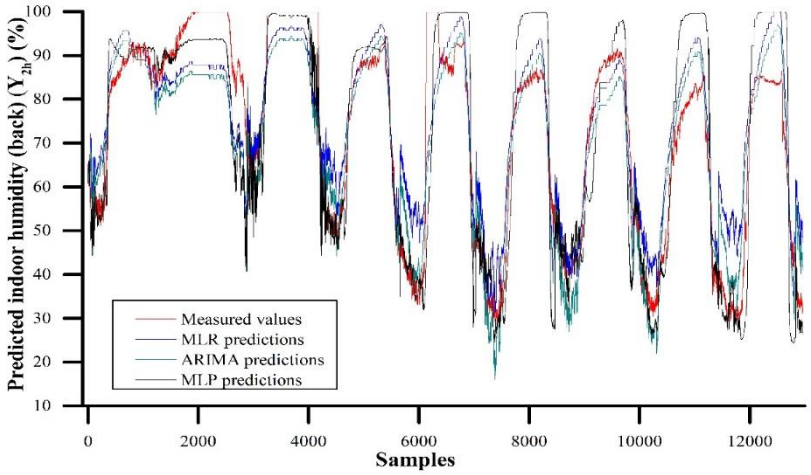

Figure 7. *Comparison of actual data and predicted indoor humidity (back) (Y_{2h}) by MLR, ARIMA, and MLP models*

Unlike temperature predicted data, the humidity predicted variables relationship with measured values was uncertain in MLR and ARIMA. The pattern of humidity prediction results resembles the prediction model results. In all the four seasons, MLP achieved better results (spring season results for MLP (Y_{1h}: R^2=0.8447; MAE=4.568; RMSE=6.378; Y_{2h}: R^2=0.7843; MAE=5.136; RMSE=7.539), summer season results (Y_{1h}: R^2=0.845; MAE=5.150; RMSE=7.187; Y_{2h}: R^2=0.7026; MAE=7.052; RMSE=9.588), autumn season results (Y_{1h}: R^2=0.9040; MAE=4.827; RMSE=6.446; Y_{2h}: R^2=0.8764; MAE=6.935; RMSE=9.045) winter season results (Y_{1h}: R^2=0.631; MAE=4.202; RMSE=4.930; Y_{2h}: R^2=0.471; MAE=5.976; RMSE=7.868)). Even though, the MEA and RMSE values were less when compared with total prediction model results, the R^2 values are less in seasonal based analysis. Especially in the winter season humidity prediction performed less among the all seasons. Moreover the prediction accuracy was higher than the overall all prediction during the autumn season. The coefficient of

http://www.aloki.hu ● ISSN 1589 1623 (Print) ● ISSN 1785 0037 (Online)
DOI: http://dx.doi.org/10.15666/aeer/1802_21412161

determination values displayed in the *Figure 9* to understand the model prediction accuracy in a comparative manner.

The cumulative validation results of all the three models for the rainy days in winter and summer displayed in *Figure 10*. Among these rainy days' validation, the winter season prediction was better in MLP for temperature and humidity data (Y_{1t}: R^2=0.8773; MAE=0.351; RMSE=0.488; Y_{2t}: R^2=0.7475; MAE=0.940; RMSE=1.000; Y_{1h}: R^2=0.9062; MAE=1.475; RMSE=2.919; Y_{2h}: R^2=0.7413; MAE=6.852; RMSE 6.976) followed by the ARIMA model performed better than MLR. When compared to the entire winter season results the rainy days' prediction has better R^2 values especially for the humidity variables. The humidity predictions were more reliable in MLR models when compared to other models. Even though the ARIMA model has a higher R^2 (Y_{1t}=0.8071; Y_{2t}=0.763) then the MLR (Y_{1t}=0.7927; Y_{2t}=0.7603) model in Y_{1t} and Y_{2t} predictions, the MAE and RMSE were less in MLR (Y_{1t} ; MAE=0.812; RMSE=1.143: Y_{2t} ; MAE=1.320; RMSE=1.863) than ARIMA (Y_{1t} ; MAE=0.868; RMSE=1.251: Y_{2t} ; MAE=1.526; RMSE=2.085). Apart from that, the overall MLP predictions were surpassed than other models.

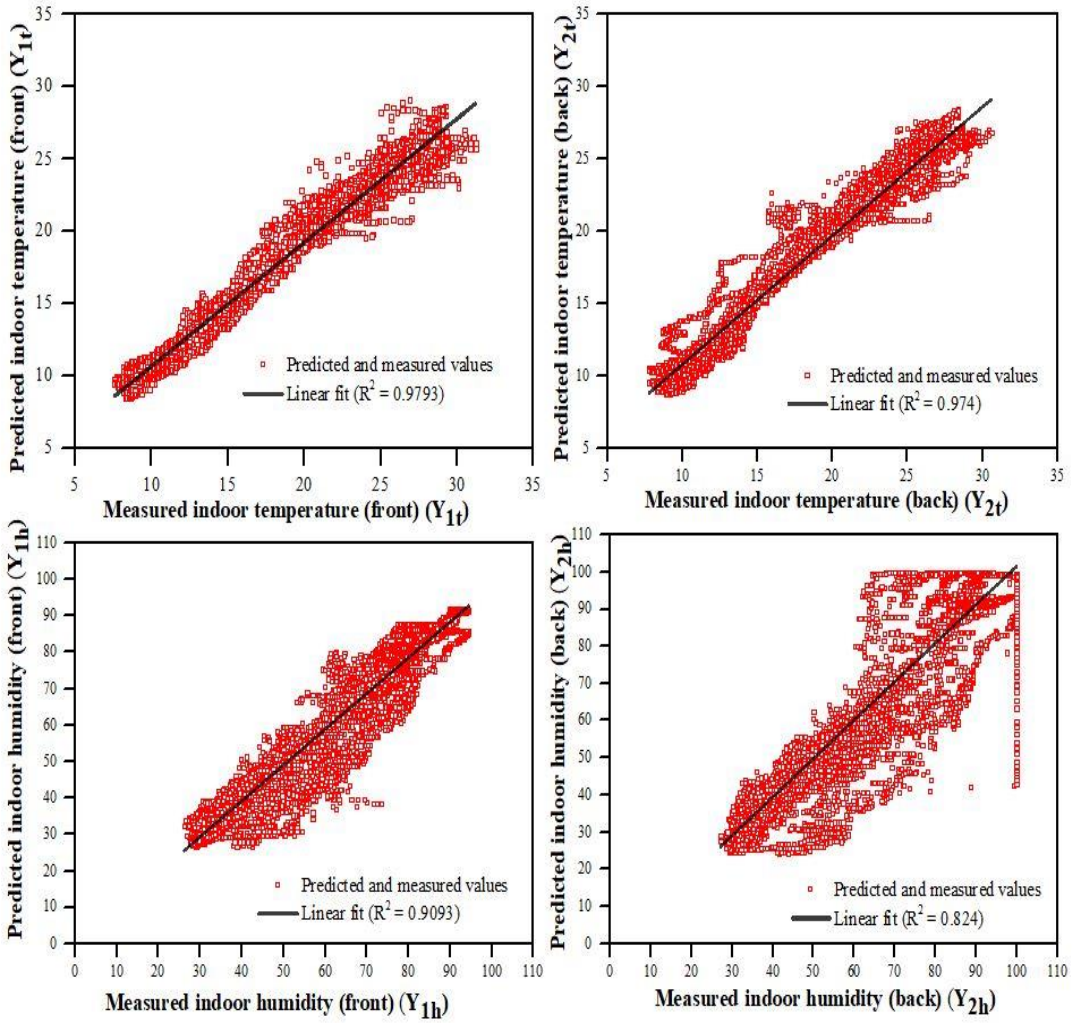

Figure 8. *Post-Regression results between predicted data and measured data of the MLP model (Y_{1t}, Y_{2t}, Y_{1h}, and Y_{2h})*

http://www.aloki.hu ● ISSN 1589 1623 (Print) ● ISSN 1785 0037 (Online)
DOI: http://dx.doi.org/10.15666/aeer/1802_21412161

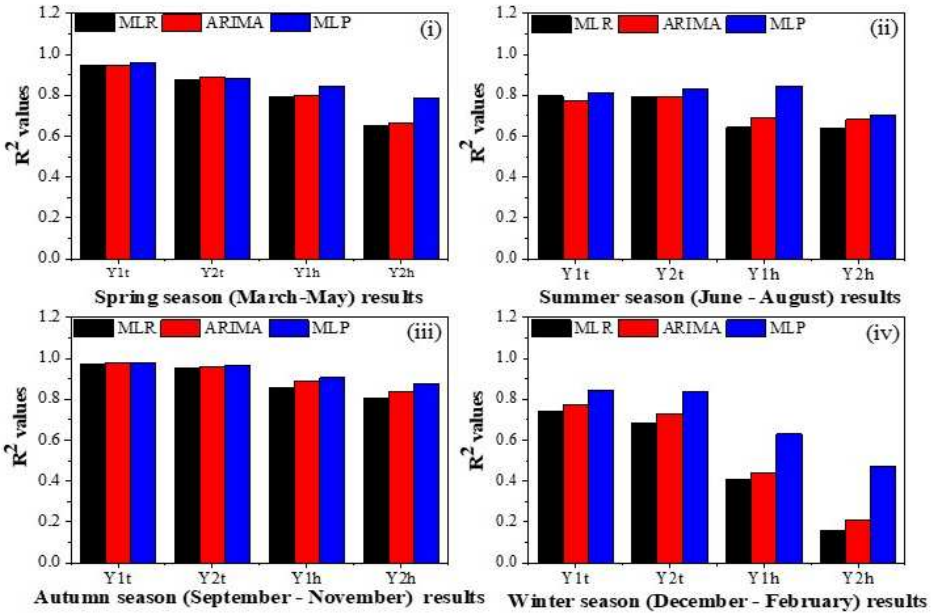

Figure 9. *The coefficient of determination (R^2) between measured and predicted values of all three models for (i) Spring season, (ii) Summer season, (iii) Autumn season, and (iv) Winter season*

Discussion

Prediction model

The present study predicted the temperature and humidity of a greenhouse with different approaches. The MLR models are simple and easy to handle; likewise the MLR predicts the temperature variables similar to the other models. Apart from the temperature variables, the MLP (computational model) performs better than the other models. It seems that the scenario of extrapolating beyond the range of the data, regression models face limitations to perform well; it decreases the model reliability. Though several studies developed a prediction model for greenhouse temperature prediction (Lu and Viljanen, 2009), the indoor humidity prediction with neural network models are lacking in literature due to its more complicated mechanism involved that depends on thermal behaviors or temperature prediction. Leopold et al. (2016) developed a neural network model to predict the indoor temperature and humidity with the Indoor temperature (R^2=0.970) and indoor humidity (R^2=0.694). The current study MLP model performed better than the literature mentioned above, in both temperature 1 (R^2=0.9793), temperature 2 (R^2=0.974), humidity 1 (R^2=0.9093) and humidity 2 (R^2=0.8154) prediction. However, the previous study used more input parameters with a large number of parameters; our model performed well with less number of input variables. Previous studies used different input factors to train their model for the highest accuracy, since the variables may affect by the indoor micro-climatic condition such as wind speed, solar radiation, soil moisture, rainfall, etc. (Lu and Viljanen, 2009; Choab et al., 2019). For instance, Taki et al. (2015) predicted the greenhouse indoor room temperature from 9 input parameters, and that study has the R^2 of 0.9941, which is higher than the current study (R^2=0.9793). However, the complexity of the prediction model increased if there are several input parameters while comparing it to our model is simpler than his model. Besides, his study conducted only on indoor

http://www.aloki.hu ● ISSN 1589 1623 (Print) ● ISSN 1785 0037 (Online)
DOI: http://dx.doi.org/10.15666/aeer/1802_21412161

temperature, not on indoor humidity. Preparation of data sets, preprocessing and normalizing the input data techniques are involved in mapping the data linearly over a specific range that increases the accuracy of the model. Particularly in models that used with neurons, the activation function can be performed within the limited range of values so that normalized data which ranges from [0, 1] can able to produce meaningful results during the neural network performance (Jayalakshmi and Santhakumaran, 2011; Taki et al., 2015). For instance, Shi et al. (2018) study designed a model for prediction of indoor temperature and relative humidity based on the cloud database by using a back-propagation neural network model. Unlike current literature, that model used improved techniques to train the network. However, that model accuracy was higher than our study (indoor temperature R^2=0.974 and indoor humidity R^2=0.917), the authors have mentioned that the preprocessing of the data during the training time increases the complexity of the model and the simulation time though the accuracy is improved. Our current model has no such kind of limitations including the training and stimulation time since the input variables were limited. This research has done with the aim that not only concluded with robustness and capability of various prediction model; also the extension of this research is to implement the high accuracy model in real-time control devices for the greenhouse control strategy. The current research prompted to analyze without modifying the data that was collected from cloud and sensors so that the entire study utilizes the actual data as the input to train the model also the model validation also conducted in the real-time datasheet. The strawberry plants were grown in the greenhouse during the time of the experiment, and it may affect the humidity very much. Rather than the temperature, humidity can easily be affected by many ways like change in rain amount and ventilation rate of the greenhouse, which are unfortunately not included as input parameters in this research, such limitation predicted both two indoor humidity parameters as a challenging factor (Lu and Viljanen, 2009). The deviation between the affected data and predicted data for especially in humidity prediction is inevitable, which needs attention while these models implement in real-time. When compared to the MLR and ARIMA, MLP learns the distribution of the data in a short period. The seasonal based analysis affirms that the MLP has surpassed performance than other models. Even though the country located in the temperate zone in geographical aspects, the wider temperature difference between summer and winter (much precipitation also occurs during both seasons) made the predictions as an intricate methodology. So that a quickly adaptable algorithm can able to fulfill the short time predictions as the desired manner. Most importantly, while talking about real-time implementation, predicting time is also a decisive factor. This current study MLP model performs quickly than the other models since the input parameters are well formulated.

Input variable model

By comparing M1, M2, and M3 models after post prediction analysis, most of the time M1 (local weather station data combined with the regional weather station data) helps to get more accuracy. During the time of temperature prediction (Y_{1t} and Y_{2t}), M3 performs better among the models used for this research. For instance, during the Y_{1t} prediction, best performance of M3 0.64% higher than the M1's best performance by R^2 comparison and 0.83% higher during Y_{2t} predictions. For Y_{1h} prediction, the M1's highest performance 6.05% higher than the M3's best performance and 1.48% higher during Y_{2h} prediction in terms of R^2 values. While comparing the MAE and RMSE value, during the time of Y_{1h}, M1 has 31% of lesser MAE and 34% of less RMSE values than the M3 model

http://www.aloki.hu ● ISSN 1589 1623 (Print) ● ISSN 1785 0037 (Online)
DOI: http://dx.doi.org/10.15666/aeer/1802_21412161

also in Y_{2h} prediction M1 has 31% of lesser MAE and 30% less RMSE than M3. Since the eccentricity between the predicted values and measured values, especially in cases of humidity predictions, these deviations unable to ignored or negligible. The individual performance of the regional weather station data is not up to the mark in this indoor microclimatic prediction, and it performs well if combined with local weather station data. The foremost point of every forecast is to obtain the maximum accuracy prediction so that the addition of regional weather station data has driven the model to higher performance than the normal one, though it was without undergoing any modified with optimized statistical methods such as normalization and sampling.

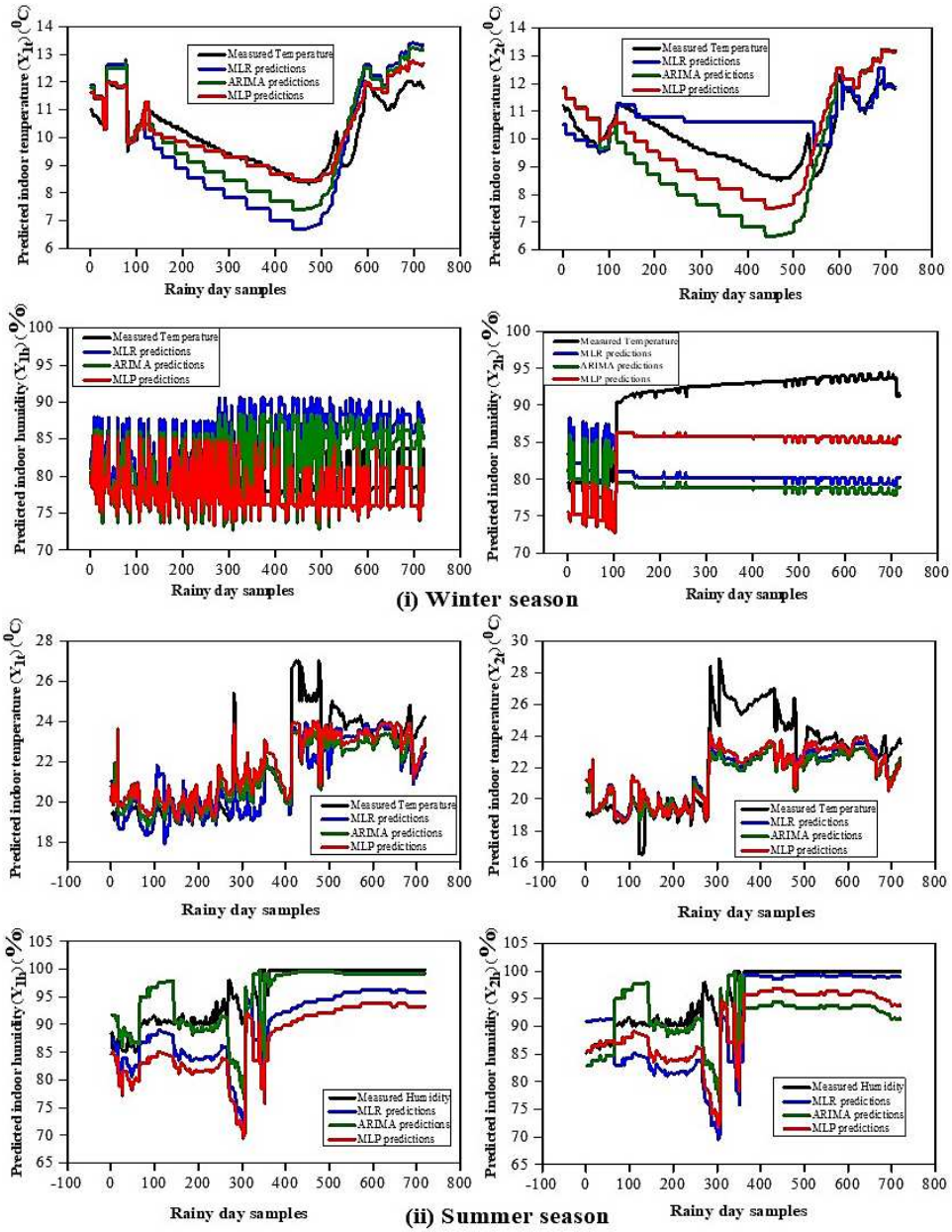

Figure 10. *Comparison of measured data and predicted Indoor temperature (front) (Y_{1t}), Indoor temperature (back) (Y_{2t}), Indoor humidity (front) (Y_{1h}), Indoor humidity (back) (Y_{2h}) by MLR, ARIMA, and MLP models for (i) Rainy days sample in winter season, (ii) Rainy days sample in summer season*

http://www.aloki.hu ● ISSN 1589 1623 (Print) ● ISSN 1785 0037 (Online)
DOI: http://dx.doi.org/10.15666/aeer/1802_21412161

Conclusion

By mimicking the plant behavior according to the environmental growing conditions, the growers can produce better plants and save energy as well. With the use of the temperature controllers, humidification, and de-humidification control capabilities resulting in production of stronger and healthier plants. The current research presents a comparison between physical, time series model, and computational models to select the best method to predict the two indoor temperature parameters and two indoor humidity parameters for a greenhouse from external weather parameters. Also, predicting the indoor parameters with local weather station data and regional weather station data. According to the results, this study concluded with the following salient points,

[1] The results of performance evaluations showed that the regression model and the ARIMA model has incompetent results in particular for humidity predictions and should improve mathematic-experimental equations related to this parameter. For real-time implementation of this model, a fine-tuning and optimization required to strengthen the efficiency of the model.

[2] Either in the physical model or computational model, the addition of regional weather data as input for the prediction model that can increase the accuracy prediction value. Whereas the data addition produces desired output when using the other local weather parameters input data set nevertheless it is less performable when used as an individual input data set.

[3] The MLP (with BB training) model performed surpass then other models for the non-linear variables of greenhouse microclimate. According to the R^2, MAE, RMSE, and MSE evaluations proofing that the superiority in prediction with the MLP model. For the real-time implementation, time consumption for learning and prediction as well needs to consider as one of the primary parameters, which could be possible by the MLP model.

[4] The present study developed a less complicated and fast learning MLP model, which is compatible with the online method, such as cloud-based modeling. In the future, the current model can be integrated into the computer through cloud technology in greenhouse controller devices to achieve better efficiency.

[5] By following this same methodology can develop models to predict soil temperature, soil moisture level, fuel consumption for heating and humidification, and CO_2 emission in the greenhouses. It is possible to use the same try to collect some suitable data related to the above-mentioned parameters and investigate these features. Modeling soil temperature, soil moisture level, fuel consumption for heating and humidification, and CO_2 emission would create more opportunities to utilize the advanced technologies for agriculture and modeling for better crop yield as well as a healthier environment for plants.

Acknowledgements. This research was supported by Korea Institute of Planning and Evaluation for Technology in Food, Agriculture and Forestry (IPET) through Agriculture, Food and Rural Affairs Research Center Support Program, funded by Ministry of Agriculture, Food and Rural Affairs (MAFRA) (Project No. 717001-7).

http://www.aloki.hu ● ISSN 1589 1623 (Print) ● ISSN 1785 0037 (Online)
DOI: http://dx.doi.org/10.15666/aeer/1802_21412161

REFERENCES

[1] Atia, D. M., El-madany, H. T. (2017): Analysis and design of greenhouse temperature control using adaptive neuro-fuzzy inference system. – Journal of Electrical Systems and Information Technology 4(1): 34-48.
[2] Behrang, M., Assareh, E., Ghanbarzadeh, A., Noghrehabadi, A. (2010): The potential of different artificial neural network (ANN) techniques in daily global solar radiation modeling based on meteorological data. – Solar Energy 84: 1468-1480.
[3] Braun, M. R., Altan, H., Beck, S. B. M. (2014): Using regression analysis to predict the future energy consumption of a supermarket in the UK. – Applied Energy 130: 305-313.
[4] Cheng, Q., Ni-Bin, C. (2011): System dynamics modeling for municipal water demand estimation in an urban region under uncertain economic impacts. – Journal of Environmental Management 92(6): 1628-1641.
[5] Choab, N., Allouhi, A., Maakoul, A. E., Kousksou,T., Saadeddine, S., Jamil, A. (2019): Review on greenhouse microclimate and application: Design parameters, thermal modeling and simulation, climate controlling technologies. – Solar Energy 191: 109-137.
[6] Davis, W. Y. (2003): Water Demand Forecast Methodology for California Water Planning Areas e Work Plan and Model Review. – In: Research Report. California Bay Delta Authority CA, USA.
[7] Dombayci, Ö., Gölcü, M. (2009): Daily means ambient temperature prediction using artificial neural network method: A case study of Turkey. – Renewable Energy 34: 1158-1161.
[8] Feinberg, E. A., Genethliou, D. (2005): Load Forecasting. – Applied Mathematics for Power Systems: 269-275.
[9] Hande, K., Sedat, B., Adil, A. (2016): A modeling study with an artificial neural network: Developing estimation models for the tomato plant leaf area. – Turkish Journal of Agriculture and Forestry 40: 203-212.
[10] Hasni, A., chikr Elmezouar, Z., Belkacem, D., Boulard, T. (2011): Applying Time Series Analysis Model to Temperature Data in Greenhouses. – Sensors and Transducers 126: 119-124.
[11] He, F., Ma, C. (2010): Modeling greenhouse air humidity by means of artificial neural network and principal component analysis. – Computers and Electronics in Agriculture 71: 9-23.
[12] He, X., Guan, H., Zhang, X., Simmons, C. T. (2014): A wavelet-based multiple linear regression model for forecasting monthly rainfall. – International Journal of Climatology 34: 1898-1912.
[13] Jayalakshmi, T., Santhakumaran, A. (2011): Statistical normalization and back propagation for classification. – International Journal Computer Theory Engineering 3: 89-93.
[14] Khashei, M., Bijari, M. (2011): A novel hybridization of artificial neural networks and ARIMA models for time series forecasting. – Applied Soft Computing 11: 2664-2675.
[15] Kurt, B., Bruce, T. (2017): Future food-production systems: vertical farming and controlled-environment agriculture. – Sustainability Science Practice and Policy 13(1): 13-26.
[16] Leonetti, A. (2018): By 2022, Smart Greenhouse Market to gain $1.31 Bn. – Journal of Green Engineering: 110.
[17] Leopold, M., Pierre, M., Alexis, K. (2016): Application of artificial neural network for predicting hourly indoor air temperature and relative humidity in modern building in humid region. – Energy and Buildings 121: 32-42.
[18] Liu, X., Zhang, C., Liu, P., Yan, M., Wang, B., Zhang, J., Higgs, R. (2018): Application of Temperature Prediction Based on Neural Network in Intrusion Detection of IoT. – Security and Communication Networks: 1-10.

http://www.aloki.hu ● ISSN 1589 1623 (Print) ● ISSN 1785 0037 (Online)
DOI: http://dx.doi.org/10.15666/aeer/1802_21412161

[19] Lu, T., Viljanen, M. (2009): Prediction of indoor temperature and relative humidity using neural network models: model comparison. – Neural Computing and Applications 18(4): 345-357.
[20] Luan, X., Shi, P., Liu, F. (2011): Robust adaptive control for greenhouse climate using neural networks. – International Journal of Robust and Nonlinear Control 21: 815-826.
[21] Mehdi, R., Hossein, T., Yazdi, A. A., Sabahattin, I., Latif, K. (2013): Flood flow forecasting using ANN, ANFIS and regression models. – Neural Computing and Applications 25(1): 25-37.
[22] Murat, M., Malinowska, I., Gos, M., Krzyszczak, J. (2018): Forecasting daily meteorological time series using ARIMA and regression models. – International Agrophysics 32: 253-264.
[23] Neshat, N., Mahlooji, H., Kazemi, A. (2011): An enhanced neural network model for predictive control of granule quality characteristics. – Scientia Iranica 18(3): 722-730.
[24] Nury, A. H., Hasan, K., Alam, J. B. (2017): Comparative study of wavelet-ARIMA and wavelet-ANN models for temperature time series data in northeastern Bangladesh. – Journal of King Saud University, Science 29(1): 47-61.
[25] Patel, D. P., Patel, M. M., Patel, D. R. (2014): Implementation of ARIMA model to predict Rain Attenuation for KU-band 12 Ghz Frequency. – IOSR Journal of Electronics and Communication Engineering 9(1): 83-87.
[26] Santosh, D. T., Tiwari, K. N., Singh, V. K., Raja Gopala Reddy, A. (2017): Micro Climate Control in Greenhouse. – International Journal of Current Microbiology and Applied Sciences 6(3): 1730-1742.
[27] Shi, X., Lu, W., Zhao, Y., Qin, P. (2018): Prediction of Indoor Temperature and Relative Humidity Based on Cloud Database by Using an Improved BP Neural Network in Chongqing. – IEEE Access 6: 30559-30566.
[28] Singh, V. K., Tiwari, K. N. (2017): Prediction of greenhouse micro-climate using artificial neural network. – Applied Ecology and Environmental Research 15: 767-778.
[29] Taki, M., Ajabshirchi, Y., Ranjbar, F., Rohani, A., Matloobi, M. (2015): Heat transfer and MLP Neural Network models to predict inside environment variables and energy lost in a semi-solar greenhouse. – Energy and Buildings 110: 314-329.
[30] Taki, M., Yahya, A., Faramarz, R., Mansour, M. (2016): Application of neural networks and multiple regression models in greenhouse climate estimation. – Agricultural Engineering International: The CIGR e-journal 18: 29-43.
[31] Uchida Fraus, H., Pieters, J. G. (2004): Modelling greenhouse temperature using system identification by means of neural networks. – Neurocomputing 56: 423-428.
[32] Zhao, T., Xue, H. (2010): Regression Analysis and Indoor Air Temperature Model of Greenhouse in Northern Dry and Cold Regions. – IFIP Advances in Information and Communication Technology 345: 252-258.

http://www.aloki.hu ● ISSN 1589 1623 (Print) ● ISSN 1785 0037 (Online)
DOI: http://dx.doi.org/10.15666/aeer/1802_21412161

SIMULATIONS OF WATER CYCLE IN THE SOIL-CROP SYSTEM: MODEL IMPROVEMENT AND VALIDATION

ZHANG, K. F.[1] – LI, C.[1] – HU, Z. F.[2*] – HUANG, S. Q.[1] – CHEN, J. S.[3] – MA, X. F.[3]

[1]*Ningbo Institute of Technology, Zhejiang University, Ningbo 315100, China*
(phone: +86-574-8813-0254; fax: +86-574-8813-0283)

[2]*Design and Research Institute of Environmental Protection Sciences of Zhejiang Province, Hangzhou 310007, China*

[3]*Ningbo Haitong Times Agricultural Co. Ltd, Cixi, Zhejiang Provice, China*

**Corresponding author*
e-mail: huzhengfeng2003@outlook.com

(Received 15th Sep 2019; accepted 8th Jan 2020)

Abstract. Accurate estimation of soil water dynamics, soil evaporation and crop transpiration are of great importance to make the best use of water in agriculture. In this study, the EU-Rotate_N model, which had been widely used for water and nitrogen dynamics for vegetables crops, was improved and evaluated for its capacity of simulating soil water movement under the condition of relatively high groundwater table. Rigorous validation of the newly modified model against data from two experiments on lettuce and tomato revealed that the simulated values of soil water content at various depths during crop growth were much better than those computed with the original model, compared with the measured values. The calculated statistical indices of the Nash–Sutcliffe model efficiency coefficient and the model agreement index were 0.556 and 0.808, respectively, for the Lettuce experiment, while the corresponding figures were 0.750 and 0.938 for the Tomato experiment. This indicates that the improvement of EU-Rotate_N model was a success, and the modified model could be used in crop production for water and nitrogen management more widely. Finally, the further improvement of the model to enhance its accuracy of predicting soil water dynamics was discussed.
Keywords: *soil water dynamics, EU-Rotate_N model, agricultural water management, SPAC system, agro-hydrological modelling*

Introduction

Soil moisture is a key variable for understanding hydrological process in the vadose zone. Agricultural and irrigation management practices largely depend on a timely and accurate characterization of temporal and spatial soil moisture dynamics in the root zone because of the impact of soil moisture on the production and health status of crops and salinization (Vereecken et al., 2008; Greenwood et al., 2010; Dogan et al., 2019). Additionally, soil moisture also plays a major role in the organization of natural ecosystems and biodiversity.

Mathematical models are powerful tools to estimate water and nutrients requirement of crops, which is essential information required to devise best farming practices in agriculture. The simulations of agricultural systems for water and nutrient cycles have increased drastically over the last two decades, in line with the development of more powerful hardware and software, and use-friendly interfaces, see reviews by Cannavo et al. (2008) and Kumar et al. (2013). Accurate modeling of water movement is crucially important for agro-hydrological models. Numerous studies on simulating water movement in the soil-crop system have been proposed for various crops grown under

http://www.aloki.hu ● ISSN 1589 1623 (Print) ● ISSN 1785 0037 (Online)
DOI: http://dx.doi.org/10.15666/aeer/1802_21632177

diverse conditions (Ahuja et al., 1993; Brisson et al., 1998; Shaffer and Brodahl, 1998; Šimunek et al., 1999; Rahn et al., 2010; Zhang et al., 2010; Sun et al., 2012; Kumar et al., 2013; Sun et al., 2013; Wang et al., 2013; Mohammad et al., 2014; Karandish and Šimůnek, 2018; Landl et al., 2019). Amongst these models, there were two approaches in simulating water dynamics in the soil. On the one hand, the mechanistic models described the movement of water in the soil by the Darcy's law, and the basic flow equation was solved numerically, as shown in RZQM (Ahuja et al., 1993) and Hydrus-2D (Šimunek et al., 1999) models. On the other hand, empirical approaches were used for soil water movement in agro-hydrological models such as STICS (Brisson et al., 1998), NLEAP (Shaffer and Brodahl, 1998), N_ABLE (Greenwood, 2001) and EU-Rotate_N (Rahn et al., 2010) models. In the empirical approaches the soil was divided into several layers, each with a specific water storage capacity according to the soil texture or its physical properties. Water entering a particular soil layer was stored until the moisture level reached field capacity, with water above this limit draining to the lower adjacent layer, at a rate varying among models. Soil water content at field capacity played a determinant role in the transport of water in the empirical approaches.

Since the algorithms used in the empirical approaches are fairly simple and parameters are relatively limited and easily available, empirical approaches are still widely used in agro-hydrological models for predicting soil water movement (Greenwood, 2001; Zhang et al., 2007, 2009; Pedersen et al., 2010). The EU-Rotate_N model (Rahn et al., 2010), which was developed recently with a similar approach for soil water movement, has shown encouraging results in simulating various crops on different sites under diverse climate conditions (Doltra and Muñoz, 2010; Guo et al., 2010; Rahn et al., 2010; Sun et al., 2013; Soto et al., 2014). Guo et al. (2010) concluded that the EU-Rotate_N model, which was initially designed for the use in European outdoor field conditions, could be applied in typical greenhouse in China without major modifications. Sun et al. (2013) calibrated and validated the EU-Rotate_N model for greenhouse tomato, and found the simulated values of soil water content were in good agreement with measured data. Similar results were also reported in the study by Soto et al. (2014). However, the experiments in the above studies on different crops were conducted under the condition of low groundwater table as the EU-Rotate_N model was originally designed for, and no reports were available on the accuracy of the simulated soil water content for crops grown under the relatively high groundwater table.

The main purposes of this study were twofold: (1) to modify the algorithm for soil water movement in the EU-Rotate_N model to enable it for crops grown under different groundwater conditions, and (2) to evaluate the modified model against data from two field experiments on lettuce and tomato conducted under relatively high groundwater condition.

Materials and methods

Improvements of the EU-Rotate_N model

EU-Rotate_N model was originally designed for simulating water and nitrogen dynamics in the soil-crop system for crop rotations (Rahn et al., 2010). The modules for crop growth and nitrogen requirement were identical with those in N_ABLE (Greenwood, 2001), which was well validated over a wide range of crops. The modules for soil water movement were newly developed. A cascade approach for soil water flow was employed. The algorithm for such an approach was simple, but did not work well

http://www.aloki.hu ● ISSN 1589 1623 (Print) ● ISSN 1785 0037 (Online)
DOI: http://dx.doi.org/10.15666/aeer/1802_21632177

universally. For the situations of relatively high groundwater table, modification of the algorithm is essentially required.

In the original EU-Rotate_N model, the soil was divided into 5 cm layers, and a capacity-based algorithm was used to calculate downwards water movement between soil layers (Rahn et al., 2010). In this approach, at any layer, the excessive water above field capacity (θ_{FC}) drained to the layer below, provided that the soil in that layer was not saturated. The amount of water that drains on a given day, Dr_i (mm), was limited by a drainage coefficient, C_{dr}, which accounted for the effect of the soil hydraulic conductivity (Doltra and Muñoz, 2010), i.e.:

$$Dr_i = \begin{cases} C_{dr}(\theta_i - \theta_{FCi})T_i & \theta_i > \theta_{FCi} \\ 0 & otherwise \end{cases} \quad \text{(Eq.1)}$$

where θ_i (cm^3 cm^{-3}) represents soil water content of the layer i, θ_{FCi} (cm^3 cm^{-3}) is the water content at field capacity, and T_i (mm) is the thickness of the soil layer. The drainage coefficient C_{dr} is calculated using the following equation:

$$C_{dri} = (\theta_{si} - \theta_{FCi}) / \theta_{si} \quad \text{(Eq.2)}$$

in which θ_{si} (cm^3 cm^{-3}) is the soil water content at saturation in the layer i.

It has been demonstrated that the above algorithm performed well in predicting soil water content under the condition of deep groundwater table (Wang et al., 2013; Doltra and Muñoz, 2010; Guo et al., 2010; Soto et al., 2014). However, when the groundwater table is relatively high, drainage may not occur in some part of the computational domain. Also, in the event of soil water content in a layer is smaller than that in the layer below for a given soil, no drainage would happen either. Therefore, in order for the model to deal with such situations, alterations of the algorithm for soil water movement of the model are required. In this study, we proposed the following algorithm for computing soil water drainage. The total amount of water drainage between soil layers, for a given soil layer i, was assumed to be the sum of the excessive water above saturation, Dr_{i1}, and the drained water induced by soil water content between field capacity and saturation, Dr_{i2}, i.e.

$$Dr_i = Dr_{i1} + Dr_{i2} \quad \text{(Eq.3)}$$

where Dr_{i1} (mm) is the excessive water above saturation, Dr_{i2} is the drainage amount caused by soil water above field capacity.

$$Dr_{i1} = \begin{cases} (Dr_{i-1}/T_i + \theta_i - \theta_{si})T_i & Dr_{i-1}/T_i + \theta_i - \theta_{si} > 0 \\ 0 & otherwise \end{cases} \quad \text{(Eq.4)}$$

where Dr_{i-1} (mm) is the drainage amount from the soil layer above *i-1*.

The equation for calculating Dr_{i2} (mm) is given below:

http://www.aloki.hu ● ISSN 1589 1623 (Print) ● ISSN 1785 0037 (Online)
DOI: http://dx.doi.org/10.15666/aeer/1802_21632177

$$Dr_{i2} = \begin{cases} C_{dr}(\theta_{si} - \theta_{FCi})T_i & Dr_{i1} > 0 \\ C_{dr}(Dr_{i-1}/T_i + \theta_i - \theta_{FC})T_i & Dr_{i-1}/T_i + \theta_i > \theta_{FC_i} \text{ and } \theta_i + Dr_{i-1}/T_i > \theta_{i+1} \\ 0 & otherwise \end{cases} \quad \text{(Eq.5)}$$

where θ_{i+1} is the soil water content in the layer below $i + 1$.

Experiments

The experiments on lettuce (Lactuca sativa L.) and tomato (S. lycopersicum) were carried out on the farm of Haitong Times Agricultural Co Ltd, Cixi, Ningbo, Zhejiang province, in eastern China (121.50°E, 30.11°N). The location is 7 km away from the seaside. The soil in the farm is silty loam, with fairly uniform distribution in the profile. The soil physical properties are shown in *Table 1*.

Table 1. *Soil physical properties in the experimental site*

Soil layer (cm)	Texture (-)	Sand (%)	Silt (%)	Clay (%)	Bulk density (g cm^{-3})
0-20	*Silty loam*	48.5	46.8	4.7	1.19
> 20	*Silty loam*	49.1	46.5	4.4	1.45

A fully randomized method was used in the experimental design. The field was divided into 7 experimental plots. The plots for the Tomato experiment were 6 m × 30 m, and the size for the Lettuce experiment was 6 m x 10 m. Lettuce was sowed on 3 June 2014 and harvested on 31 July 2014, while tomato was transplanted on 23 April 2014 and harvested on 15 August 2014. Lettuce was broadcast sowed, having an averaged plant population of 70 plants m^{-2}. Tomato plants were spaced at 30 cm within the row and 60 cm between rows. No irrigation was applied during the experiments, except for a small amount of irrigation in the seedling stage to help plants to develop. Fertiliser management was in accordance with local farming practice which was used for growing the same crops in the farm over the years. Pests control was carried out by conventional pesticides, when it was required. Weeds were managed manually.

Soil volumetric water content was measured with the SM100 sensors (Spectrum Technologies, Inc., Aurora, IL, USA). The SM100 sensors were positioned at the 10, 30, 50 cm depths in both the Lettuce and the Tomato experiments (unfortunately the sensors at the 30 cm depth did not function properly in the Tomato experiment). Since the measurements of soil water content in the soil profile were used for testing the model, it was not necessary to collect data from the depths too close to each other. The selection of soil depths with 20 cm intervals for sensors in this study was according to common practice for similar crop experiments. Sensors were installed in the soil horizontally. Prior to the installations, the SM100 sensors were calibrated using soil pillars with difference water content in the lab according to the product's manual. The volumetric water content data were recorded every 30 min on a Watchdog 1400 data logger (Spectrum Technologies, Inc., Aurora, IL, USA).

Daily air temperature and relative humidity were provided by a local weather station. Solar radiation was automatically measured and recorded every 30 min with a pyranometer (Mod. TBQ-2, JinZhou Sunshine Meteorological Science Co., Liaoning, China). Since the model uses a daily time step, the frequency of every 30 min for

http://www.aloki.hu ● ISSN 1589 1623 (Print) ● ISSN 1785 0037 (Online)
DOI: http://dx.doi.org/10.15666/aeer/1802_21632177

collecting solar radiation was considered sufficient enough. Rainfall was measured and recorded by Watchdog Data-Logging Rain Gauge (Spectrum Technologies, Inc.). Both solar radiation and rainfall were collected at the weather station installed on the experimental site. The observation of groundwater table was carried out in a well which was dig in the experimental field. The measured values of daily mean air temperature, relative humidity, rainfall and solar radiation are shown in *Figure 1*.

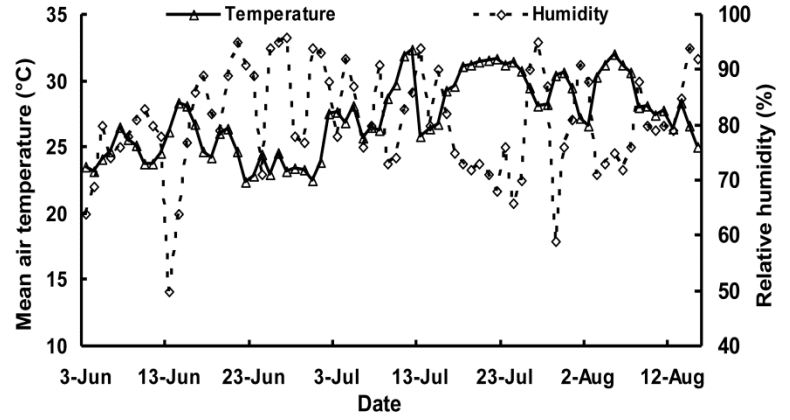

(a)

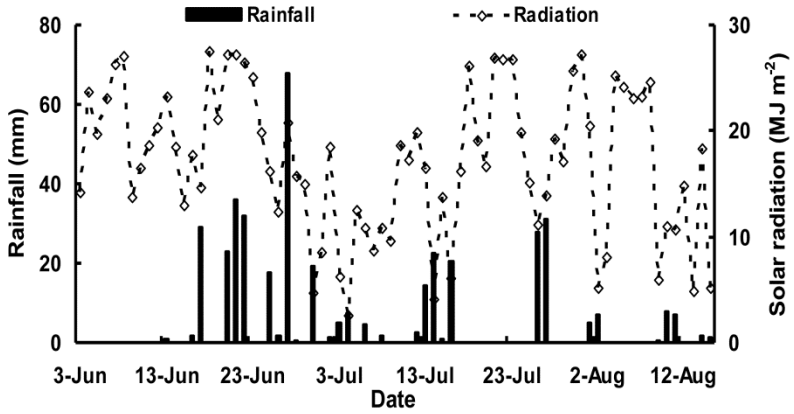

(b)

Figure 1. *Measured daily mean air temperature and relative humidity (a), solar radiation and rainfall (b) during the experiments*

Preparation of model run

Model parameterization

The parameters required to run the modified EU-Rotate_N model were the same as those for the original model listed in Rahn et al. (2010). Basically, the data from soil, crop and weather were required in the simulations. In this study, the model was used for modeling water dynamics in the soil-crop system, and therefore the data given below were only for this purpose.

http://www.aloki.hu ● ISSN 1589 1623 (Print) ● ISSN 1785 0037 (Online)
DOI: http://dx.doi.org/10.15666/aeer/1802_21632177

The required soil data were fairly simple and limited, including characteristic soil water content at saturation, field capacity and the permanent wilting point. Such a dataset was obtained by applying the Saxton and Rawles' (2006) approach to the measured soil physical properties. Saxton and Rawles' (2006) proposed a set of pedotransfer functions for estimating characteristic soil water content and soil moisture-tension relationships for various types of soils. The derived equations were based on soil texture and soil particle distribution (Saxton et al., 1986), and have been used extensively in previous studies for determining characteristic soil water content and soil hydraulic functions (Fry et al., 2014; Nyeko, 2015).

Crop data used in the EU-Rotate_N model were the dates of crop planting/sowing and harvest, and the durations of the various crop growth stages and their associated dual coefficients for potential soil evaporation and crop transpiration. The durations of the initial, development, middle and late stages for the crop were calculated according to the proportionalities over the entire growth period given in the FAO56 (Allen et al., 1998) for a given crop. Also, the corresponding values of crop coefficient were taken from the FAO56. Thus, on any day during growth the values of potential evaporation and transpiration could be calculated, given the reference evapotranspiration ETo was known. The detailed procedure for calculating ETo was given elsewhere (Allen et al., 1998).

Weather data were mainly used for estimating daily ETo. The weather variables, including daily air temperature, relative humidity, solar radiation, wind speed and rainfall, were all measured in the way described above, and were used directly in the simulations.

Computational domain and boundary conditions

The calculated soil depth in the EU-Rotate_N model was fixed to 200 cm (Rahn et al., 2010, 2007). The soil column was evenly divided into 40 layers with a thickness of 5 cm each layer. The model operated on a daily basis. The upper boundary condition in both experiments was set as atmospheric, i.e. the top soil layer subject to rainfall and evaporation. The lower boundary was specified as the soil below the 70 cm depth in saturation based on the observations. The time of the first measurements and the measured values of soil water content along the profile were used as the starting point and the initial conditions of the simulations.

Model evaluation

To evaluate the ability of the modified model to predict the values of temporal and spatial soil water content, statistical analyses were carried out using the indices of the Nash–Sutcliffe model efficiency coefficient (*NSE*) (Nash and Sutcliffe, 1970), the root of the mean squared errors (*RMSE*) and the model agreement index (*d*) (Willmott, 1981). These indices were used extensively in assessing hydrological models in previous studies.

$$NSE = 1 - \frac{\sum_{i=1}^{n} (Y - Y')^2}{\sum_{i=1}^{n} (Y - \overline{Y'})^2} \quad \text{(Eq.6)}$$

http://www.aloki.hu ● ISSN 1589 1623 (Print) ● ISSN 1785 0037 (Online)
DOI: http://dx.doi.org/10.15666/aeer/1802_21632177

$$d = 1 - \frac{\sum_{i=1}^{n}(Y - Y')^2}{\sum_{i=1}^{n}(|Y - \overline{Y'}| + |Y' - \overline{Y'}|)^2} \quad \text{(Eq.7)}$$

$$RMSE = \sqrt{\frac{1}{n}\sum_{i=1}^{n}(Y - Y')^2} \quad \text{(Eq.8)}$$

where n is the total number of samples, Y and Y' are the simulated and measured values, respectively, and $\overline{Y'}$ is the average of the measured values. For a perfect match between simulation and measurement, both *NSE* and *d* are equal to 1, and *RMSE* is 0.

Results and discussion

For the evaluation of the modified model, both the original and modified models were first run against the same measured data collected from the experiments on lettuce and tomato. The simulated results were then compared to make an objective assessment of the performance of the modified model.

Overall evaluation of the modified model

The overall comparison of temporal and spatial soil water content between simulation and measurement for both Lettuce and Tomato experiments is shown in *Figure 2*, and the quantitative statistical results are listed in *Table 2*. In both experiments, the simulated values are highly correlated with the measured values (*Fig. 2*). The gradient of the best fitted lines is approximately 1 and the intercept is close to 0. The regressions of the simulated values against the measured values give a high R^2 value greater than 0.61. The calculated values of *NSF* and *d* are greater than 0.56 and 0.81, respectively, while the *RMSE* value is smaller than 0.027 cm^3 cm^{-3}. The calculation of *NSF*, *d* and *RMSE* values were also carried out for the simulated results from the original model. The calculated *RMSE* were 0.038 and 0.036 cm^3 cm^{-3} for lettuce and tomato, respectively, greater than those from the modified model (*Table 2*). The values of *NSF* were -1.838 for lettuce and 0.562 for tomato, much worse than those from the modified model. This was especially true for the Lettuce experiment where *NSF* value even went to negative, indicating that the original model was unable to make reasonable predictions. All these indices suggest that the original model performed poorly and the modified EU-Rotate_N model was capable of re-producing measurements of soil water content fairly well. This proves that the improvement of the model was essential and successful.

Detailed comparisons of soil water content between the measured and simulated values with the modified EU-Rotate_N model at various depths in both experiments during crop growth were carried out (*Figs. 3* and *4*). Also shown in the graphs were the simulated results of soil water content from the original EU-Rotate_N model. It is evident that the simulated results from the modified model were far better than those from the original model, compared with the measured values. Not only did the modified model produce the same variation patterns in soil water content, but also the values were in good agreement with the measurements throughout the growing periods. The

http://www.aloki.hu ● ISSN 1589 1623 (Print) ● ISSN 1785 0037 (Online)
DOI: http://dx.doi.org/10.15666/aeer/1802_21632177

original model, on the other hand, failed to produce the results comparable with the measurements. The discrepancies between the measurement and simulation with the original model increased with time, especially at the deeper depths. The principal reasons for the discrepancies were due to the inability of the original model to handle the lower boundary condition of soil at saturation and the inappropriate algorithm for downwards water flow between soil layers. Clearly, *Figs. 3* and *4* demonstrated that the modification of the model was essential to simulate the crops in the present experiments. The work carried out in this study was a significant improvement of the original model to extend its use for modeling water dynamics in the soil-crop system under more diverse conditions.

Table 2. *Statistical indices of the simulated results of soil water content*

Experiment	*RMSE* (cm^3 cm^{-3})	*NSE* (-)	*d* (-)
Lettuce	0.024	0.556	0.808
Tomato	0.027	0.750	0.938

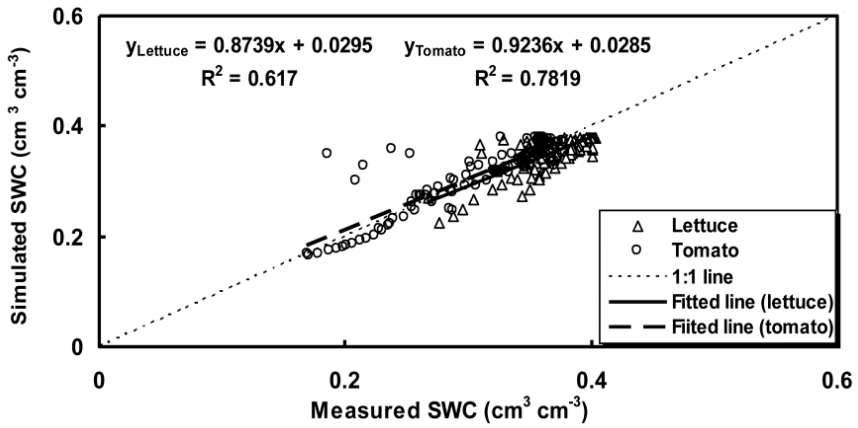

Figure 2. *Overall comparison of soil water content (SWC) between simulation and measurement.*

In the Lettuce experiment soil water content remained high and fairly constant at the 30 cm and 50 cm depth, except for the beginning and towards the end of the experiment (*Fig. 3*). This could be attributed to the fact that during the most period of the experiment the amount of rainwater exceeded the crop evapotranspirational demand. Over the experiment the cumulative rainfall reached as high as 367.6 mm. At the 50 cm depth, the soil was near its saturation throughout the experiment caused by combined effects of excessive rainfall, high groundwater table and the short rooting depth of the crop. Marked changes in soil water content at the 10 cm depth were observed and simulated in the Tomato experiment (*Fig. 4*). Soil water content decreased steadily at the beginning of the experiment due to the dry spell during the period. Big increase in soil water content occurred during the heavy rain period between 16th June to 30th June when an increase of 0.18 cm^3 cm^{-3} was recorded and 0.19 cm^3 cm^{-3} was simulated. High and fairly constant soil water content during 1st July to 10th July was observed for the reason explained in the Lettuce experiment. At the later stages of the experiment there

http://www.aloki.hu ● ISSN 1589 1623 (Print) ● ISSN 1785 0037 (Online)
DOI: http://dx.doi.org/10.15666/aeer/1802_21632177

were 3 dry-wet cycles which coincided with the rain pattern (*Fig. 1*). The changes in simulated soil water content at the 50 cm depth were small, in good agreement with the measurements (*Fig. 4*).

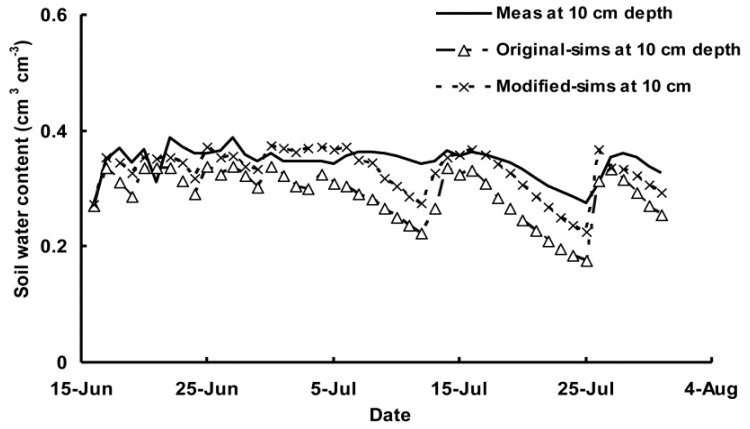

(a)

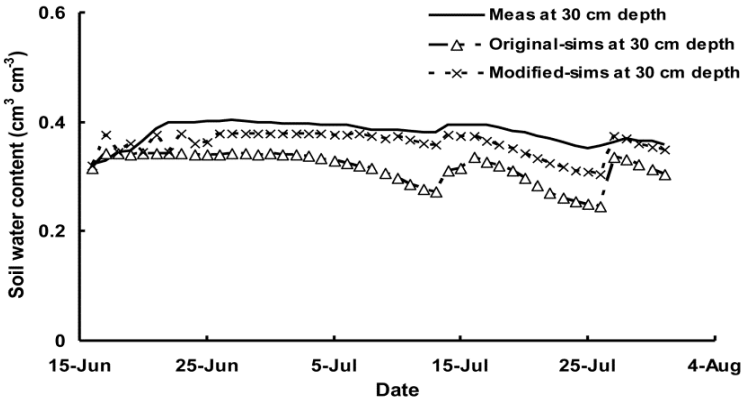

(b)

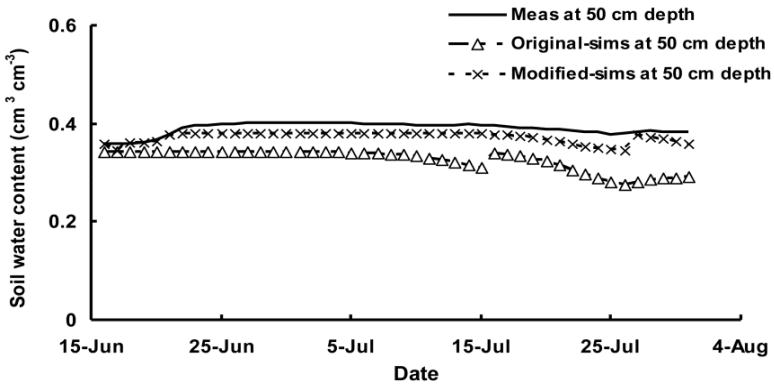

(c)

Figure 3. *Detailed comparison soil water content at the depths of 10 cm (a), 30 cm (b) and 50 cm (c) between simulation and measurement in the Lettuce experiment*

http://www.aloki.hu ● ISSN 1589 1623 (Print) ● ISSN 1785 0037 (Online)
DOI: http://dx.doi.org/10.15666/aeer/1802_21632177

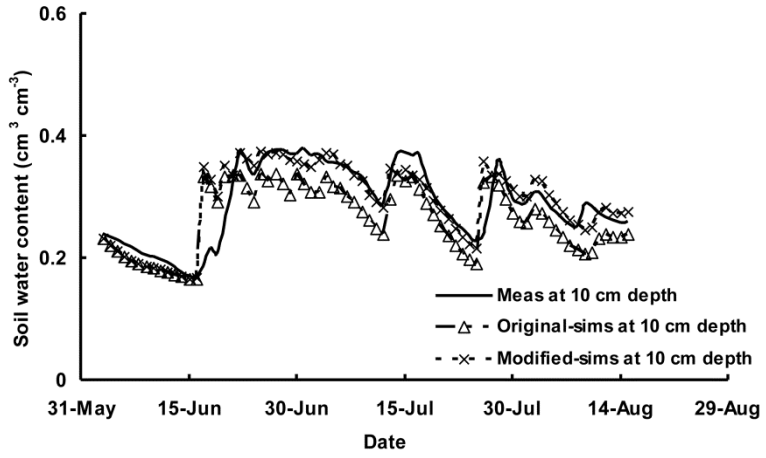

(a)

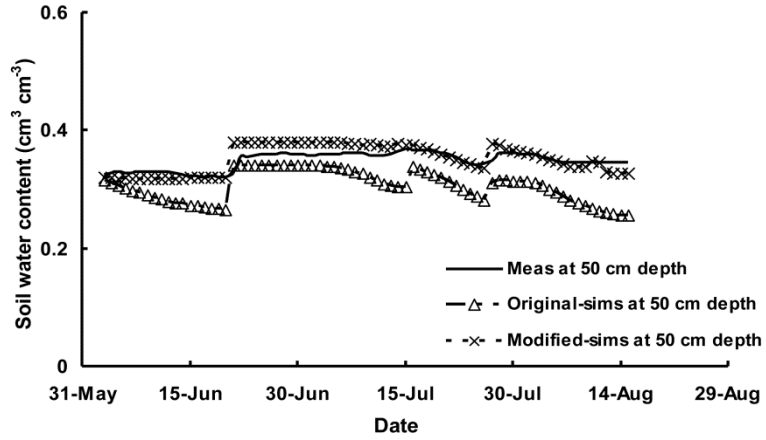

(b)

Figure 4. *Detailed comparison soil water content at the depths of 10 cm (a) and 50 cm (b) between simulation and measurement in the Tomato experiment*

The simulated soil evaporation and crop transpiration

Figure 5 shows the cumulative simulated soil evaporation and crop transpiration during growth, together with the cumulative rainfall. In both experiments, the simulated seasonal evapotranspiration approximately equaled the potential value, suggesting that the crop demand for water for the maximum growth was basically met. This was primarily down to the fact that the experiments were carried out in the fairly wet season. The cumulative seasonal potential evapotranspiration were 188.8 mm and 251.8 mm for the Lettuce and Tomato experiments, respectively, far less than the cumulative rainfall of 367.6 mm and 398.5 mm in the same periods. This indicates that the crop evapotranspiration was mainly met by the rainfall, not so much by the initially stored soil water. High soil evaporation occurred at the early crop development stage (*Fig. 5*). At this stage the ground cover was less intense and thus the evaporation demand was larger. Contrary to soil evaporation, the big crop transpiration happened when the crop

http://www.aloki.hu ● ISSN 1589 1623 (Print) ● ISSN 1785 0037 (Online)
DOI: http://dx.doi.org/10.15666/aeer/1802_21632177

was at its mid-season and later development stage. It should be pointed out that due to the combined effects of lack of rainfall (*Fig. 1b*) and the dry soil on the surface (*Fig. 4a*), soil evaporation was neglectable before 16th June in the Tomato experiment even when the crop was small (*Fig. 5b*).

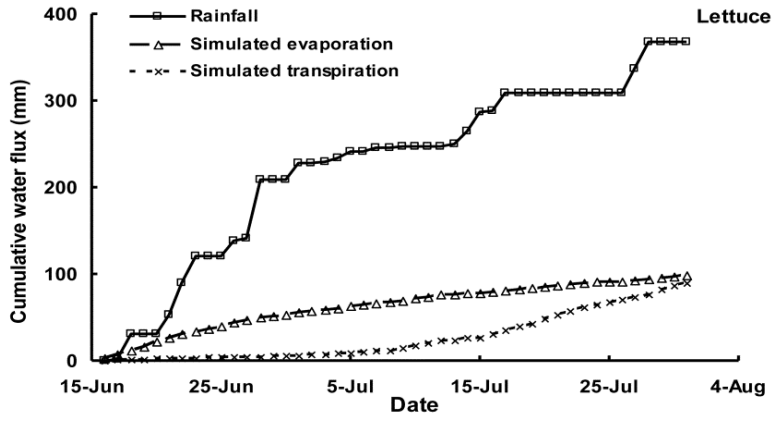

(a)

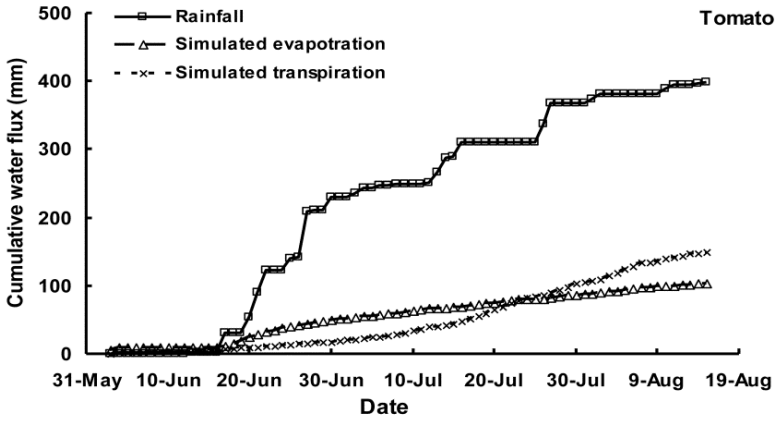

(b)

Figure 5. *Cumulative rainfall, simulated evaporation and transpiration in the Lettuce experiment (a) and in the Tomato experiment (b)*

Crop water uptake from the rooting depth

It is interesting to quantify the proportions of crop transpiration made by roots in various part of the rooting depth. There have been reports that each quarter of the rooting depth from the surface accounted for about 40%, 30%, 20% and 10% of the total water uptake (Molz and Remson, 1970; Kumar et al., 2013). In both experiments in this study the potential crop transpiration was all basically met (*Fig. 5*), indicating that roots in the various parts of the root zone absorbed the assigned amount of potential transpiration. Since the assignment of potential transpiration was according to the root distribution in the soil profile, the proportion of water uptake in each rooting depth was equal to that of the root distribution. In the EU-Rotate_N model, root distribution was

http://www.aloki.hu ● ISSN 1589 1623 (Print) ● ISSN 1785 0037 (Online)
DOI: http://dx.doi.org/10.15666/aeer/1802_21632177

normalized in the soil in the manner of $\int_0^1 e^{-\alpha z} dz$ with α being the shape parameter controlling root distribution, z being 0 at the surface and 1 at the bottom of the root zone (Rahn et al., 2010). α was parameterized to be 2 for both lettuce and tomato in the model. This worked out that each quarter of rooting depth from the upmost contributed about 46%, 28%, 17% and 10% of the total water uptake, respectively, in agreement with the experimental evidence by Molz and Remson (1970) and Kumar et al. (2013). The EU-Rotate_N model is a generic model for water and nitrogen management in crop production, and has up-to-data been parameterized for a wide range of crops (Rahn et al., 2010). For all the crops in the model the shape parameter α varies from 1.5 to 3. *Table 3* shows the proportions of roots in each quarter of the normalized rooting depth calculated from different shape parameter values. Broadly they are in reasonable ranges.

Table 3. *Proportion of roots in each quarter of the normalised rooting depth*

α[a]	(0~1/4) RD[b]	(1/4~1/2) RD	(1/2~3/4) RD	(3/4~1) RD
1.5	0.40	0.28	0.19	0.13
2	0.46	0.28	0.17	0.10
3	0.56	0.26	0.12	0.06

[a]α represents shape parameter controlling root distribution
[b]RD represents the normalised rooting depth (0~1)

Drainage coefficient

A capacity-based algorithm with a single drainage coefficient was used in each soil layer in the simulations of soil water movement in the EU-Rotate_N model. The biggest advantage of such an algorithm is its simplicity, and the values of characteristic soil water content are relatively easier to obtain, compared with the soil hydraulic parameters describing soil water retention and conductivity curves. In this study the drainage coefficient was calculated with *Equation 2,* and the results appeared to be encouraging, as shown in other previous studies (Doltra and Muñoz, 2010; Soto et al., 2014). However, *Equation 2* might not be universally held due to the complexity of the soil, and the EU-Rotate_N model treated the drainage coefficient as an optional model input (Rahn et al., 2010). If possible, the model users should calibrate this parameter to get better results.

The numerical simulations of soil water movement using the Richards' equation are more accurate, and normally involved in complicated numerical schemes such as the finite element method (FEM) and finite difference method (FDM). Recently there was a simplified numerical scheme, named Integrated Richards Equation (IRE) method, proposed and tested in the soil-crop system for water cycle (Yang et al., 2009). This scheme, based on the work by Boone and Wetzel (1996) and Lee and Abriola (1999), applied a simple and explicit FDM approach on each soil layer with a small time step. It has been demonstrated that with a time step of 0.001 d the IRE method could produce the simulated results as accurately as those from FEM. Since the IRE method employed an algorithm similar with that from the capacity-based method, the procedures for modeling water dynamics in the soil-crop system with the basic flow equation were greatly simplified. Such an approach could be utilized in the EU-Rotate_N model in the future so that the model could be more flexible in using different approaches for the simulations of soil water movement.

http://www.aloki.hu ● ISSN 1589 1623 (Print) ● ISSN 1785 0037 (Online)
DOI: http://dx.doi.org/10.15666/aeer/1802_21632177

Conclusions

A simple and effective algorithm has been proposed and tested in this study to simulate soil water movement for the EU-Rotate_N model. The simulated values of soil water content at various depths agreed fairly well with the measurements gathered from two experiments on crops with different rooting depth. Compared with the original model, the modified model with the new algorithm for soil water dynamics has greatly enhanced the accuracy of predicted soil water content. This suggests that the modification of the model was successful, and the model could be used more widely for water management in crop production.

Acknowledgements. The authors wish to acknowledge the financial support from National Natural Science Foundation of China (51379187), National Natural Science Foundation of Zhejiang Province (LY17E090001), and Ningbo Science and Technology Bureau, China (2016C10057).

REFERENCES

[1] Ahuja, L. R., DeCoursey, D. G., Barnes, B. B., Rojas, K. W. (1993): Characteristics of macropore transport studied with the ARS root zone water quality model. – Transactions of the ASAE 36(2): 369-380.

[2] Allen, R. G., Pereira, L. S., Raes, D., Smith, M. (1998): Crop Evapotranspiration-Guidelines for Computing Crop Water Requirements. – FAO, Irrigation and Drainage Paper No. 56. United Nations Food and Agriculture Organization, Rome, Italy.

[3] Boone, A., Wetzel, P. J. (1996): Issues related to low resolution modeling of soil moisture: experience with the PLACE model. – Global and Planetary Change 13: 161-181.

[4] Brisson, N., Mary, B., Ripoche, D., Jeuffroy, M. H., Ruget, F. et al. (1998): STICS: a generic model for the simulation of crops and their water nitrogen balances. I. Theory and parameterization applied to wheat and corn. – Agronomie 18: 311-346.

[5] Cannavo, P., Recous, S., Parnaudeau, V., Reau, R. (2008): Modelling N dynamics to assess environmental impacts of cropped soils. – Advances in Agronomy 97: 131-174.

[6] Doltra, J., Muñoz, P. (2010): Simulating nitrate leaching from a fertigated crop rotation in a Mediterranean climate using the EU-Rotate_N and Hydrus-2D models. – Agricultural Water Management 97: 277-285.

[7] Fry, E. L., Manning, P., Power, S. A. (2014): Ecosystem functions are resistant to extreme changes to rainfall regimes in a mesotrophic grassland. – Plant and Soil 381: 351-365.

[8] Greenwood, D. J. (2001): Modelling N-response of field vegetable crops grown under diverse conditions with N_ABLE: a review. – Journal of Plant Nutrition 24: 1799-1815.

[9] Greenwood, D. J., Zhang, K., Hilton, H., Thompson, A. (2010): Opportunities for improving irrigation efficiency with quantitative models, soil water sensors and wireless technology. – Journal of Agricultural Science 148: 1-16.

[10] Guo, R., Nendel, C., Rahn, C., Jiang, C. G., Chen, Q. (2010): Tracking nitrogen losses in a greenhouse crop rotation experiment in North China using the EU-Rotate_N simulation model. – Environmental Pollution 158(6): 2218-2229.

[11] Karandish, F., Šimůnek, J. (2018): A comparison of the HYDRUS (2D/3D) and SALTMED models to investigate the influence of various water-saving irrigation strategies on the maize water footprint. – Agricultural Water Management 213: 809-820.

[12] Kumar, R., Jat. M. K., Shankar, V. (2013): Evaluation of modeling of water ecohydrologic dynamics in soil-root system. – Ecological Modelling 269: 51-60.

http://www.aloki.hu ● ISSN 1589 1623 (Print) ● ISSN 1785 0037 (Online)
DOI: http://dx.doi.org/10.15666/aeer/1802_21632177

[13] Landl, M., Schnepf, A., Uteau, D., Peth, S., Athmann, M., Kautz, T., Perkons, U., Vereecken, H., Vanderborght, J. (2019): Modeling the impact of biopores on root growth and root water uptake. – Vadose Zone Journal 18: 180196.
[14] Lee, D. H., Abriola, L. M. (1999): Use of the Richards equation in land surface parameterizations. – Journal of Geophysical Research 104: 27519-2.
[15] Mohammad, N., EI-Nesr, A., Alazba, A., Šimunek, J. (2014): HYDRUS simulations of the effects of dual-drip subsurface irrigation and a physical barrier on water movement and solute transport in soils. – Irrigation Science 32(2): 111-125.
[16] Molz, F. J., Remson, L. (1970): Extraction term models of water soil moisture use by transpiring plants. – Water Resources Research 6(5): 1346-1356.
[17] Nash, J. E., Sutcliffe, J. V. (1970): River flow forecasting through conceptual models. Part 1: A discussion of principles. – Journal of Hydrology 10: 282-290.
[18] Nyeko, M. (2015): Hydrologic modelling of data scarce basin with SWAT model: capabilities and limitations. – Water Resources Management 29(1): 81-94.
[19] Pedersen, A., Zhang, K., Thorup-Kristensen, K., Jensen, L. S. (2010): Modelling diverse root density dynamics and deep nitrogen uptake - a simple approach. – Plant and Soil 326: 493-510.
[20] Rahn, C. R., Zhang, K., Lillywhite, R. D., Ramos, C., De Paz, J. M. et al. (2007): Development of a model based decision support system to optimize nitrogen use in horticultural crop rotations across Europe-EU-Rotate_N. – Final Scientific Report QLK5-2002-01100, Wellesbourne.
[21] Rahn, C. R., Zhang, K., Lillywhite, R. D., Ramos, C., De Paz, J. M. et al. (2010): A European Decision Support System, EU-Rotate_N to predict environment and economic consequences of the management of nitrogen fertilizer in crop rotations. – European Journal of Horticultural Science 75(1): 20-32.
[22] Saxton, K. E., Rawls, W. J. (2006): Soil water characteristic estimate by texture and organic matter for hydrologic solutions. – Soil Science Society of America Journal 70: 1596-1578.
[23] Saxton, K. E., Rawls, W. J., Romberger, J. S., Papendick, R. I. (1986): Estimating generalized soil water characteristics from texture. – Soil Science Society of America Journal 50: 1031-1035.
[24] Shaffer, M. J., Brodahl, M. K. (1998): Rule-based management for simulation in agricultural decision support systems. – Computers and Electronics in Agriculture 21: 135-152.
[25] Šimunek, J., Šejna, M., van Genuchten, M. T. (1999): The HYDRUS-2D Software Package for Simulating Two-Dimensional Movement of Water, Heat, and Multiple Solutes in Variably Saturated Media. Version 2.0. IGWMC-TPS-53. – International Ground Water Modeling Center, Colorado School of Mines, Golden, CO.
[26] Soto, F., Gallardo, M., Giménez, C., Peña-Fleitas, T., Thompson, R. B. (2014): Simulation of tomato growth, water and N dynamics using the EU-Rotate_N model in Mediterranean greenhouse with drip irrigation and fertigation. – Agricultural Water Management 132: 46-59.
[27] Sun, Y., Hu, K. L., Zhang, K. F., Jiang, L. H., Xu, Y. (2012): Simulation of nitrogen fate for greenhouse cucumber grown under different water and fertilizer management using the EU-Rotate_N model. – Agricultural Water Management 112: 21-32.
[28] Sun, Y., Hu, K. L., Fan, Z. B., Wei, Y. P., Lin, S., Wang, J. G. (2013): Simulating the fate of nitrogen and optimizing water and nitrogen management of greenhouse tomato in North China using the EU-Rotate_N model. – Agricultural Water Management 128: 72-84.
[29] Dogan, Y., Togay, N., Togay, Y. (2019): Determining irrigation scheduling and different manure sources of yield and nutrient content on maize (*Zea May*s L.) cultivation. – Applied Ecology and Environmental Research 17(2): 1559-1570.

http://www.aloki.hu ● ISSN 1589 1623 (Print) ● ISSN 1785 0037 (Online)
DOI: http://dx.doi.org/10.15666/aeer/1802_21632177

[30] Vereecken, H., Huisman, J. A., Bogena, H., Vanderborght, J., Vrugt, J. A., Hopmans, J. W. (2008): On the value of soil moisture measurements in vadose zone hydrology: a review. – Water Resources Research 44: 1-21.
[31] Wang, H., Gao, J. E., Zhang, S. L., Zhang, M. J., Li, X. H. (2013): Modeling the impact of soil and water conservation on surface and ground water based on the SCS and visual modflow. – Plos One 8(11): e79103.
[32] Willmott, C. J. (1981): On the validation of model. – Physical Geography 2: 184-194.
[33] Yang, D., Zhang, T., Zhang, K., Greenwood, D. J., Hammond, J., White, P. J. (2009): An easily implemented agro-hydrological procedure with dynamic root simulation for water transfer in the crop-soil system: validation and application. – Journal of Hydrology 370: 177-190.
[34] Zhang, K., Greenwood, D. J., White, P. J., Burns, I. G. (2007): A dynamic model for the combined effects of N, P and K fertilizers on yield and mineral composition: description and experimental test. – Plant and Soil 298: 81-98.
[35] Zhang, K., Yang, D., Greenwood, D. J., Rahn, C. R., Thorup-Kristenseen, K. (2009): Development and critical evaluation of a generic 2-D agro-hydrological model (SMCR_N) for the responses of crop yield and nitrogen composition to nitrogen fertilizer. – Agriculture Ecosystems and Environment 132: 160-172.
[36] Zhang, K., Greenwood, D. J., Spracklen, W. P., Rahn, C. R., Hammond, J. P. et al. (2010): A universal agro-hydrological model for water and nitrogen cycles in the soil-crop system SMCR_N: critical update and further validation. – Agricultural Water Management 97: 1411-1422.

http://www.aloki.hu ● ISSN 1589 1623 (Print) ● ISSN 1785 0037 (Online)
DOI: http://dx.doi.org/10.15666/aeer/1802_21632177

DIATOM ASSEMBLAGES IN SURFACE SEDIMENTS AND THEIR REFLECTION ON THE WATER MIGRATION PATHWAY FROM THE INSHORE WATERS OF WESTERN BOHAI BAY, CHINA

LI, Y.[1] – FANG, J.[1*] – TIAN, L. Z.[2,3*] – WANG, F.[2,3] – CHEN, Y. S.[2,3]

[1]*School of Geography and Environmental Science, Tianjin Normal University 300387 Tianjin, China*

[2]*Tianjin Centre, China Geological Survey, 300170 Tianjin, China*

[3]*Key Laboratory of Coast Geo-environment, China Geological Survey, 300000 Tianjin, China*

[*]*Corresponding authors*
e-mail: jq19066818jingxi@163.com (Fang, J.); lzrd1682340q@163.com (Tian, L. Z.)

(Received 17th Sep 2019; accepted 8th Jan 2020)

Abstract. One hundred and twenty-six surface diatom samples were analysed to investigate the characteristics of their assemblages and the seawater migration pathway from the inshore waters of the western Bohai Bay. For this task we used correspondence analysis (CA) and discussed the seawater pathway according to the distribution of freshwater diatoms and their abundance. Result shows that a total of 49 species and 32 genera are identified, of which *Cosinodiscus excentricus*, *Cosinodiscus radiatus*, *Actinocyclus normanii* and *Cyclotella stylorums* are the dominant species. The study area is divided into four diatom combination zones. The freshwater diatoms are regularly distributed in the study area and range from 0.48%-13.13%. In the waters south of the Duliujian River estuary, the proportion of freshwater diatoms decreases from south to north, indicating that the water currents tend to move in the same direction. In the southeastern sea area of the Lingang Economic Zone, due to land reclamation and hydrodynamic condition changes, freshwater diatoms are deposited. In the bay north of the Haihe River estuary, coastal currents are characterized by a clockwise circulation.
Keywords: *surface diatom, CA analysis, pathway of currents, sedimentary environment*

Introduction

Bohai Bay is located on the west bank of the Bohai Sea and is a typical semi-closed bay slope; thus, the water exchange capacity is inadequate. After many coastal rivers merge into the inshore waters of the western Bohai Bay, terrigenous sediments have trouble moving to the middle of the Bohai Sea or to the open sea. The coastal land reclamation project along the Bohai Bay has affected the hydrodynamic conditions and ecological environment of the coastal waters (Tu et al., 2017). Four hundred and thirty-two species of plankton have been identified in the Bohai Sea, of which diatoms are the dominant species (Li and Tao, 2000). Diatoms are sensitive to environmental changes and are affected by temperature, salinity, eutrophication, and fluid dynamics (Hendey and Part, 1964; Leroy et al., 2018). Many scholars have studied the ecological and geographical distribution of diatom species and their relationship with the sedimentary environment, but the characteristics of surface diatoms and the formation of diatom combinations vary between regions (Karpuz and Schrader, 1990; Cunningham and Leventer, 1998; Artemova, 2018).

Worldwide, research on surface diatoms in seas has been extensive. Cárdenasa et al. (2019) studied the way diatoms, bulk sediment composition and geochemical proxies

http://www.aloki.hu ● ISSN 1589 1623 (Print) ● ISSN1785 0037 (Online)
DOI: http://dx.doi.org/10.15666/aeer/1802_21792196

respond to oceanic domains and polar to subpolar frontal systems in surface sediments across the Drake Passage. Results show the relevance concerning the composition of surface sediments and ocean productivity, terrigenous input, the intensity of ocean currents, and ice proximity. Weckström and Juggins (2006) explored the relationship between surface sediment diatom assemblages and 15 environmental variables for providing potential means for quality assessments of coastal waters in the Gulf of Finland. In the Canary region, Modern diatom and C_{org} distribution patterns were investigated to quantitatively determine the influence of coastal upwelling and Saharan dust on the flux of sedimentary components (Nave et al., 2001). Hay et al. (2003) used the distribution patterns of diatom microflora in the Effingham Inlet off the west coast of Vancouver Island to determine the impact of coastal oceans on the interior of the Effingham Inlet Fjord. Perez et al. (2018) researched environmental gradients associated with the freshwater input and oceanic water intrusion of the Río de la Plata estuary (RdlP), and assessed diatom species distribution in surface sediment samples related to such environmental gradients. Researchers also investigated the distribution and combination of diatom in the surface sediments of the South China Sea and revealed the sedimentary environment and hydrodynamic changes in the sea; diatom combination are of great significance for tracking water currents and water masses (Ran and Jiang, 2005; Wu et al., 2013). Chen et al. (2019) determined the variation of the distribution of diatoms in surface sediments on the inner shelf of the East China Sea affected by season and typhoon. As for the East China Sea and the Yellow Sea, diatom combinations, as well as their impact on the environment have also been studied (Chen et al., 2000; Wang et al., 2001, 2009). However, at present, most diatom research concerning the Bohai Bay involves sea areas of >10 m isobaths (Shang et al., 2006; Liu et al., 2015). As for the inshore waters of the western Bohai Bay, Shang et al. (2012) studied surface sedimentary diatoms in the intertidal zone and adjacent sea areas, revealing that salinity and depth are essential factors controlling the distribution of diatoms.

Due to the low proportion of freshwater diatoms in Bohai Bay, the study of surface diatoms in that area has mainly concentrated on saltwater and brackish water diatoms, while few studies have been performed on freshwater diatoms (Chen et al., 2014; Xu et al., 2017; Pan et al., 2019). On the western coast of the Bohai Bay, many rivers are developing, thus freshwater diatoms inhabiting freshwater systems are often carried into the sea by those rivers, moving under the influence of tide and currents. The Bohai Bay is Semi-closed, and thus, the freshwater diatoms entering the sea impacts on the diatom species in the sea.

In recent years, large-scale coastal land reclamation projects along the Bohai Bay have changed the original coastline and affected the distribution of diatoms in the sea. Therefore, 126 surface samples were collected from the inshore waters of the western Bohai Bay for diatom identification and analysis. We analysed the characteristics of diatom combinations using correspondence analysis (CA) in the study sea area. Besides, we discussed the seawater pathway in the inshore waters of the western Bohai Bay according to the distribution of freshwater diatoms and their abundance.

Study area

The study area is located in the inshore waters of the western Bohai Bay, China (*Fig. 1*). The water depth ranges from 1 to 10 m in the isobath. Seabed topography tiltes from east to west and the slope is relatively low and flat. There are four types of sediments in the area, including sand, silty sand, sandy silt, and clay silt. The distribution of silt is the most extensive. The particle size has a distribution trend that gradually tapers from north to south and from inshore to offshore (Institute of Marine

http://www.aloki.hu ● ISSN 1589 1623 (Print) ● ISSN1785 0037 (Online)
DOI: http://dx.doi.org/10.15666/aeer/1802_21792196

Geology, Institute of Oceanology, Chinese Academy of Sciences, 1985; Tian et al., 2010; Ding et al., 2019). As a semi-closed inland sea, water temperature, salinity, and other factors are mainly affected by season and freshwater injections (Institute of Marine Geology, Institute of Oceanology, Chinese Academy of Sciences, 1985). The hydrodynamics in the sea are mainly affected by tides, currents, and waves. The current is affected by the warm Yellow Sea current, and the coastal current (Zhao et al., 1995). The study area is adjacent to the lowland plains, and the elevation is generally below 3 m. There are many rivers on the plains that terminate in the sea. From north to south, such rivers include the Jian River, the Jiyun River, the Chaobaixin River, the Yongdingxin River, the Haihe River, the Duliujian River, the Ziyaxin River, and the Shibei River. Most of those rivers are seasonal or sewage rivers, carrying sediment into the sea, and thus, providing a source of sediment. In recent years, land reclamation on the west coast of the Bohai Bay has destroyed the original natural coastline (Wang et al., 2010), which has complicated the current and tide in the region.

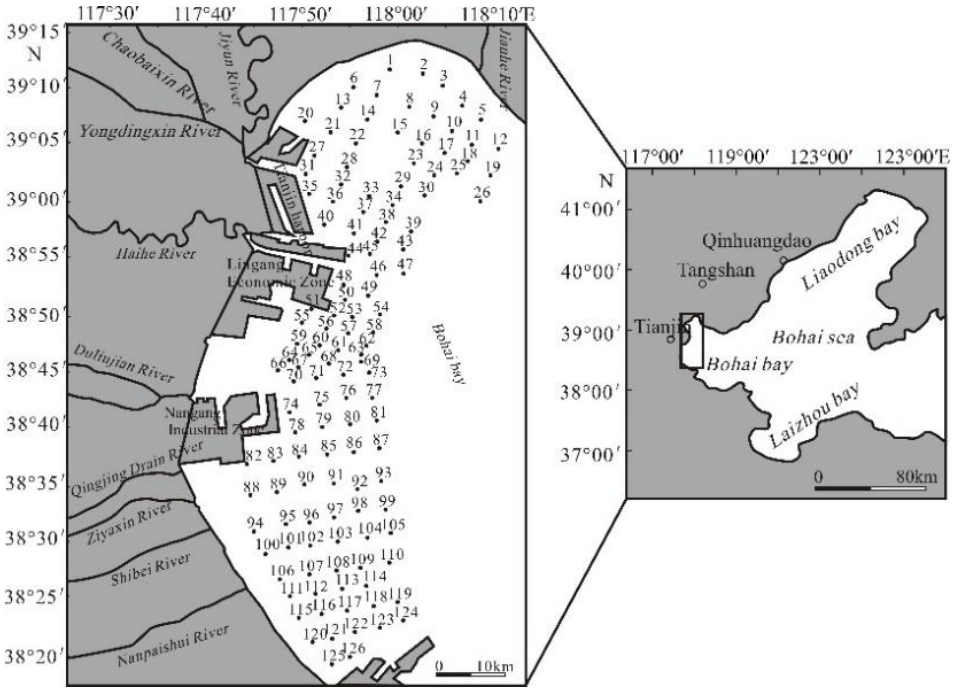

Figure 1. *Sampling sites in the inshore waters of the western Bohai Bay*

Materials and methods

One hundred and twenty-six surface diatom samples were obtained by the Tianjin Center of the China Geological Survey in August 2017 from the inshore waters of the western Bohai Bay (38°21'N- 39°10"N, 117°39'" E-118°11 'E) (*Fig. 1*). Samples were taken with grab or box corer. The top sediments were prepared for diatom analysis according to Renberg (1990) and Smol et al. (2001). Preparation was proceeded as follows: 1 g dry sample was weighed into a 250 mL flask and treated with 10% HCl overnight to remove carbonates. Then, samples were treated with 30% H_2O_2 for 24 h to remove organic material. Next, flasks were incubated with 250 mL distilled water for 24 h to disperse the clay material. The supernatant was then decanted after at least 24 h. The above steps were repeated 3-4 times. Subsequently, samples were adjusted to a

http://www.aloki.hu ● ISSN 1589 1623 (Print) ● ISSN1785 0037 (Online)
DOI: http://dx.doi.org/10.15666/aeer/1802_21792196

volume of 50 mL, and 0.5 mL of the solution was dripped onto a coverslip on a hot plate. After drying, the coverslip was placed on a glass slide coated with a neutral balsam to prepare diatom flakes. Approximately 3–4 flakes were generated per sample. Counting was performed with a Nikon 53-1 Nikon optical microscope at 400x magnification and photographed with a Nikon imaging system. For surface sediments, at least 500 diatom valves were enumerated. The absolute abundance of diatoms per station was calculated.

CA was used to analyse the characteristics of diatom assemblages using canoco4.5 software. Due to the low abundance of some diatom species, species appeared in at least two sediment samples and had a proportion of more than 1% in at least one sample were selected for analysis (Bennion, 1994; Hall and Smol, 2010).

Results

Diatom identification

One hundred and twenty-six surface sediment samples were analysed from the study area. A total of 49 species and varieties of diatoms from 32 genera are identified (*Fig. 2*). Saltwater diatoms mainly include *Cosinodiscus excentricus* and *Cosinodiscus radiates*, but also include *Actinocyclus normanii*, *Dictyocha fibula*, *Cyclotella striata*, *Cyclotella stylorum*, *Thalassiosira nizschioides*, *Paralla sulcata*, *Trachyneis aspera*, *Actinoptychus senarius*, *Surirella fluminensis*, *Triceratium favus*, *Eucampia Zoodiacus*, *Nitzschia kerguelensis* and *Navicula clementis*. Brackish water diatoms are mainly *Diploneis bombus* and *Nitzschia granulata*, but also include *Auliscus caelatus*, *Diploneis suborbicularis*, *Diploneis smithii*, *Nitzschia compressa*, *Rhaphoneis surirella*, *Rhaphoneis amphicero*, *Trybliоptychus cocconeiformi*, *Rhopalodia gibberula*, *Grammatophora macilenta*, *Opephora martyi*, *Navicula marina*, *Actinoptychus annulatus*, *Rhizosolenia imbricate*, *Nitzschia lorenziana* and *Dimeregramma minor*. Freshwater diatoms are found in low abundance in 93 stations, including *Achnanthes hauckiana*, *Synedra tabulata*, *Epithemia adanata*, *Pleurosigma normanii*, *Pinnularia nobils*, *Hantzschia amphioxys*, *Navicula radiosa*, *Nitzschia gracilis*, *Gomphonema tumidum*, *Melosira granulata*, *Nizschia amplectems*, *Synedra ulna*, *Nitzschia palea*, *Rhopalodia gibba*, *Ellerbeckia arenaria*, *Eunotia valida* and *Gyrosigma acuminatum*.

The dominant diatom species that can reflect the characteristics of the community, and control the community structure were determined according to the formula of Shen and Shi (2002), shown as *Formula (1)*:

$$Y=n_1*f_1/N \quad \text{(Eq.1)}$$

where n_i is the number of individuals of all species, f_i is the frequency of a given species in each sample, and N is the total number of individuals counted for each sample. A Y value > 0.02 indicates a dominant species.

According to the calculations, four dominant species are found, and all of which are saltwater species, including *Cosinodiscus excentricus*, *Cosinodiscus radiatus*, *Actinocyclus normanii* and *Cyclotella stylorums*. Among those species, *Cyclotella stylorums* is a dominant species from the Duliujian River estuary to the Nanpaishui River estuary, whereas its abundance in other sea areas is low.

http://www.aloki.hu ● ISSN 1589 1623 (Print) ● ISSN1785 0037 (Online)
DOI: http://dx.doi.org/10.15666/aeer/1802_21792196

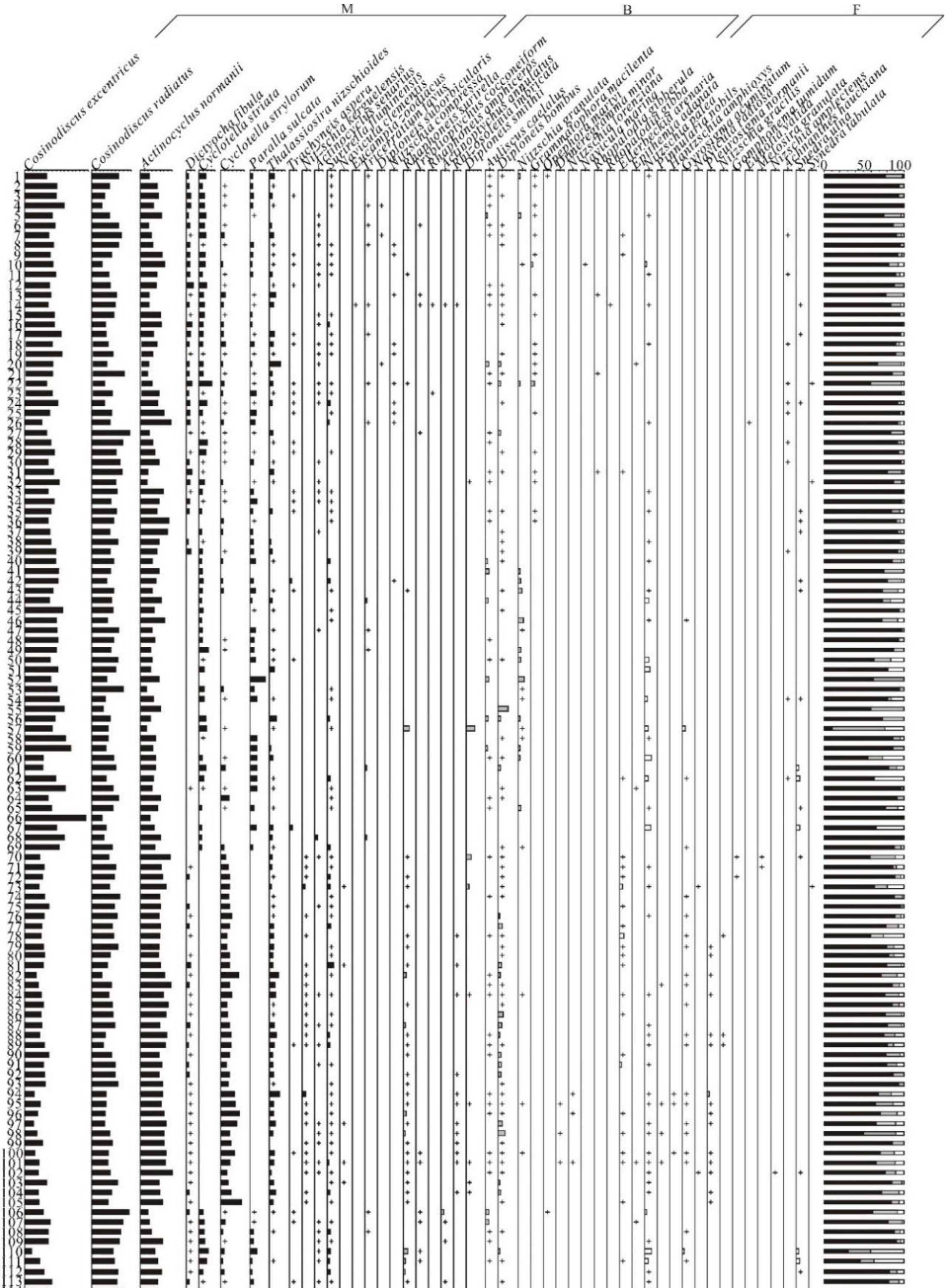

Figure 2. *Species of diatoms in the study area*

http://www.aloki.hu ● ISSN 1589 1623 (Print) ● ISSN1785 0037 (Online)
DOI: http://dx.doi.org/10.15666/aeer/1802_21792196

The distribution of diatoms

The distribution profiles were plotted using ARCGIS (ARCGIS version 10.2) according to the diatoms abundance, percentage of saltwater, brackish, and freshwater species at each station (*Fig. 3*).

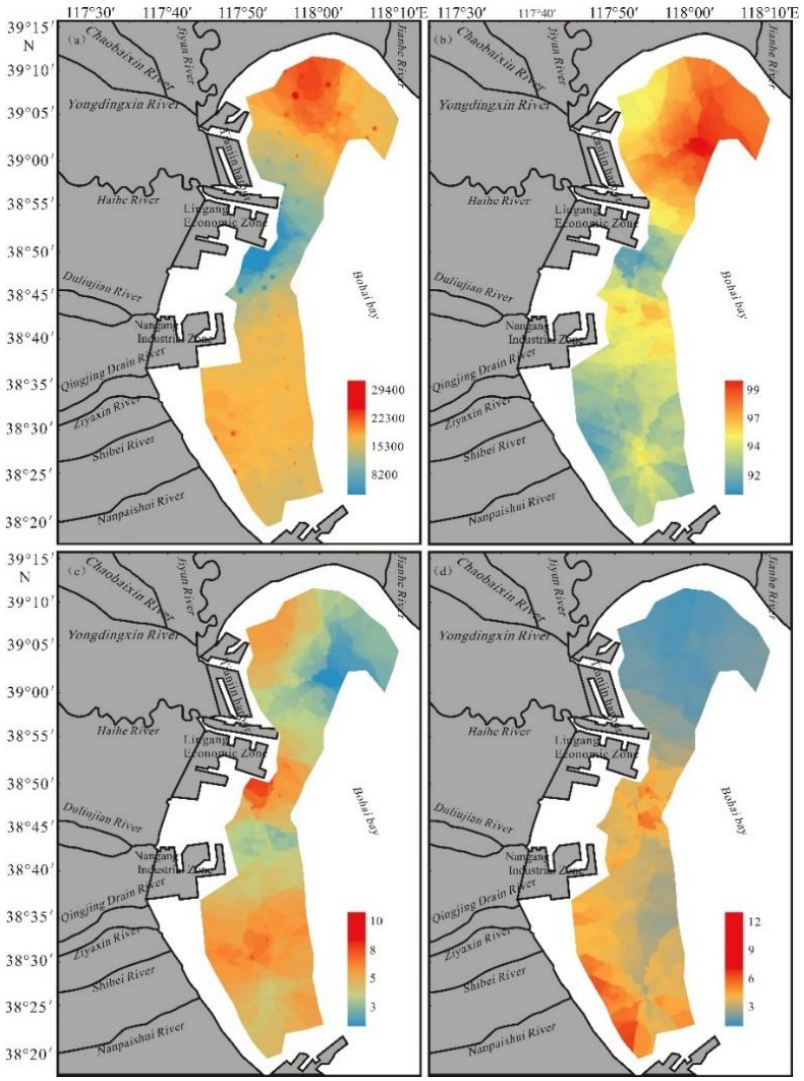

Figure 3. *The distribution of saltwater, brackish water, freshwater species and Diatom abundance in the study area (a- Diatom abundance; b- content of saltwater diatoms; c- content of brackish water diatoms; d- content of freshwater diatoms)*

The abundance of diatoms in the study area ranges from 800 to 30,600 /g, with an average of 12,979 /g. The diatoms in the bay north of the Haihe River estuary are the most abundant. Among the sample sites, the abundance of diatoms at stations 1–3, 6–8, 13–16, 18–19 and 21–22 on the northwest shore reach 15,800–30,600 /g, which is higher than the average of the study area. Diatoms are second most abundant in the sea south of the Duliujian River estuary at 7,000–21,000/g. Diatom abundance in the sea

http://www.aloki.hu ● ISSN 1589 1623 (Print) ● ISSN1785 0037 (Online)
DOI: http://dx.doi.org/10.15666/aeer/1802_21792196

between the Haihe River Estuary and the Duliujian River estuary is the lowest, with a range of 800-20,300/g.

Saltwater diatoms are distributed throughout the study area and have the highest proportion, with a proportion of 72.73% to 100.00%. Saltwater diatoms have the highest proportion in the bay north of the Haihe River estuary, and the proportion from shore to sea direction increases. The proportion of saltwater diatoms in the sea south of the Haihe River estuary is lower than that in the bay north of the Haihe River estuary. Among the sea south of the Haihe River estuary, the stations in the waters adjacent to the Nangang Industrial Zone (stations 64, 71–72, 74–77, 79–81 and 83–87) have a high proportion of saltwater diatoms, ranging from 92.86% to 98.84%. The proportion of saltwater diatoms in other stations is varied and ranges from 72.73% to 100.00%.

The proportion of brackish water diatoms is 0.00%-19.70% in the study sea area. In the bay north of the Haihe River estuary, the proportion of brackish water diatoms tends to decrease from the shore to the sea. The proportion of brackish water diatoms in the western coastal waters of the bay (at stations 1, 6, 13, 14, 20, 21, 22, 27, 31, 32, and 35) is relatively high compared to the inner bay, with a proportion of 3.05%–12.37%. The brackish water diatom proportion at the stations in the inner bay (stations 7–9, 11, 15–18, 23–26, 28, 30, 33–34, and 36-39) is low, ranging from 0% to 1.98%. In the sea south of the Haihe River estuary, the proportion of brackish water diatoms is relatively high in the southeastern sea area of the Lingang Economic Zone (stations 49, 50, 52, 55–57, 59–60, 65 and 70) and the sea south of the Nangang Industrial Zone, compared to the waters adjacent to the Nangang Industrial Zone, ranging from 3.77% to 19.7%. The proportion of brackish water diatoms in the waters adjacent to the Nangang Industrial Zone (stations 66, 67, 68, 71, 75 and 80) is relatively small, ranging from 0% to 1.89%.

The proportion of freshwater diatoms is 0.00%-13.13% in the study sea area. Freshwater diatoms are mainly distributed in the sea south of the Haihe River estuary, with a ratio of 0% to 13.13%, and the proportion decreases from the shore to the sea. The proportion of freshwater diatoms in the sea south of the Shibei River estuary (stations 94-95, 97–98, 100–102, 106, 110–112, 115–117, 119, 122 and 125-126) is the highest, reaching 2.22%–13.13%. Additionally, within that region, the proportion of freshwater diatoms shows a trend of initial decreases and subsequent increases from the shore to the sea. The freshwater diatom proportion in the sea area north of the Shibei River estuary decreased. The proportion of freshwater diatoms in the bay north of the Haihe River estuary is lowest, ranging from 0% to 2.14%. No freshwater diatoms are found at stations 15, 16, 23, 29 and 34 in the inner bay.

Discussion

Characteristics of diatom assemblages

CA was used to analyse the characteristics of diatom assemblages. In the scatter plot of the main taxa in the CA (*Fig. 4*), the locational distribution of diatom species reflects the composition of the major diatom species. The closer the location of the distribution of species in the figure, the closer the relationship between diatom species. The *Fig. 4* shows that the main diatom species are divided into four groups. Group I is the dominant species of diatoms, including *Cosinodiscus excentricus*, *Cosinodiscus radiatus*, *Actinocyclus normanii*, *Actinocyclus senarius* and *Surirella fluminensis.* The freshwater species, *Synedra ulna* and *Nitzschia palea* are also distributed throughout the study area. Group II is mainly brackish water diatoms, including *Grammatophora macilenta*, *Diploneis suborbicularis*, *Nitzschia compressa*, *Trybliоptychus*

http://www.aloki.hu ● ISSN 1589 1623 (Print) ● ISSN1785 0037 (Online)
DOI: http://dx.doi.org/10.15666/aeer/1802_21792196

cocconeiformi, *Rhopalodia gibberula*, *Actinoptychus annulatus* and *Auliscus caelatus*, as well as the saltwater diatoms, *Dictyocha fibula*, *Triceratium favus* and *Epithemia adanata*. Group III includes *Cyclotella striata*, *Trachyneis aspera* and *Paralla sulcata*, as well as the brackish water species, *Nitzschia granulata*, and the freshwater species, *Achnanthes hauckiana*. Group IV is mainly saltwater diatoms, including *Cyclotella stylorum*, *Thalassiosira nizschioides*, *Synedra tabulata*, *Ellerbeckia arenaria*, *Gyrosigma acuminatum*, *Nitzschia kerguelensis*, *Navicula clementis*, *Pleurosigma normanii*, *Navicula radiosa* and *Surirella fluminensis*, as well as the brackish water species, *Diploneis smithii*, *Rhaphoneis surirella*, *Diploneis Bombus* and *Rhizosolenia imbricata*.

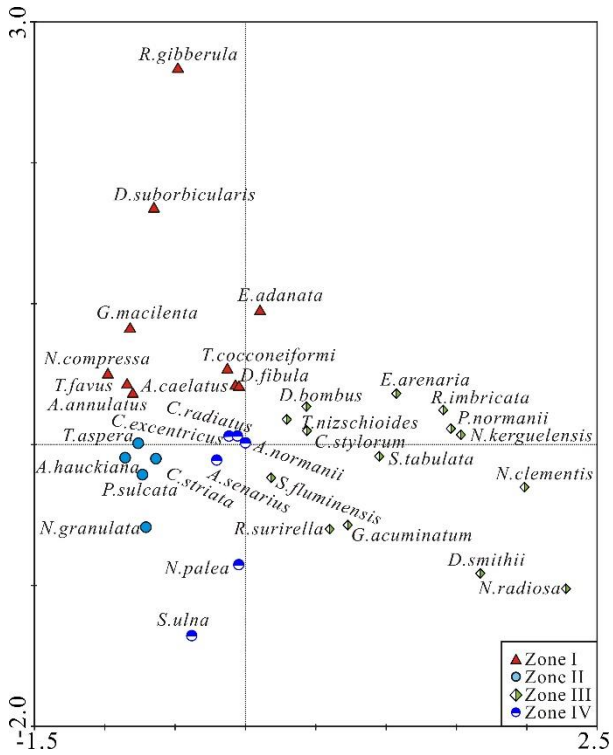

Figure 4. *Scatter diagram of CA main taxa*

Corresponding to the CA scatter diagram of diatom station (*Fig. 5a*), stations containing similar diatom species are distributed in adjacent locations. Therefore, the study area is divided into four diatom combination zone, according to the diatom combination division *(Fig. 5b*). Zone I includes stations 1–32, 34–35 and 38–39. Zone II includes stations 33, 36–37, 40–63 and 65–69. Zone III includes stations 64 and 70-105. Zone IV includes stations 106-126.

Zone I is distributed in the bay north of the Haihe River estuary. The abundance of diatoms in Zone I is 6500-30600 /g, and the average abundance is 15417 /g. *Cosinodiscus excentricus-Cosinodiscus radiates-Actinocyclus normanii* is the dominant diatom combination, with a proportion of 79.67%. The proportion of saltwater diatoms is 86.60%–99.48%, and the average proportion is 96.44%.Among the main saltwater species, *Cyclotella striata*, *Cyclotella stylorum*, *Triceratium favus* and *Paralla sulcate* are inner Bay indicator species (Kazuo and Kiyoshi, 1990; Chiba and Sawai, 2014),

http://www.aloki.hu ● ISSN 1589 1623 (Print) ● ISSN1785 0037 (Online)
DOI: http://dx.doi.org/10.15666/aeer/1802_21792196

with a proportion of 9.47%. *Dictyocha fibula* is seawater muddy intertidal indicator species (Kazuo and Kiyoshi, 1990; Chiba and Sawai, 2014), *Thalassiosira nizschioides* and *Actinocyclus senarius* are pelagic indicator species in the ocean (Kazuo and Kiyoshi, 1990; Chiba and Sawai, 2014), with a proportion of 2.94%. The proportion of brackish water diatoms is 0%-12.30%, with an average proportion of 2.92%. Among the main brackish water species, *Rhaphoneis surirella*, *Auliscus caelalus* and *Opephora martyi* are seawater sandy intertidal indicators species (Kazuo and Kiyoshi, 1990; Chiba and Sawai, 2014), with a proportion of 0.78%, *Diploneis bombus* is seawater muddy intertidal indicator species, with a proportion of 0.72%. *Trybliоptychus cocconeiformi* is indicator species of the seaweed field (Kazuo and Kiyoshi, 1990; Chiba and Sawai, 2014), with a proportion of 0.11%. Freshwater diatoms are found in the sea along the Yongdingxin River estuary and the Jian River estuary, ranging from 0.50% to 2.14%. The main diatom species are *Achnanthes hauckiana*, *Synedra ulna* and *Nitzschia palea*. Among those species, *Achnanthes hauckiana* often appeares in the estuary, coastal waters, and land lakes (Hartley, 1996). *Synedra ulna* lives in eutrophic environments with a salinity of less than 2% (Chiba and Sawai, 2014). *Nitzschia palea* can survive in highly polluted and highly corrosive waters (Kosugi, 1988). *Synedra tabulate, Ellerbeckia arenaria, Rhopalodia gibba, Eunotia valida and Epithemia adanata* are also found at individual stations. Among those species, *Eunotia valida* lives in oligotrophic environments (Fontana et al., 2014).

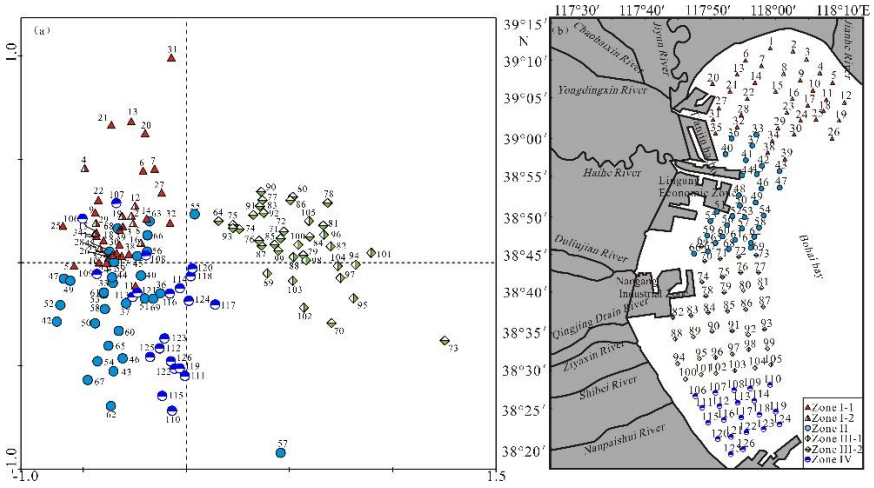

Figure 5. *CA scatter diagram of diatom station and diatom combination zone in the study area (a: CA scatter diagram of diatom station; b: diatom combination zone)*

The freshwater diatom proportion in the sea along the Yongdingxin River estuary is 0.56%-1.53%, with a decreasing trend from south to north. The freshwater diatom proportion in the sea along the Jian River Estuary is 0.50%–2.14%, with a decreasing trend from north to south. A total of 36 diatom species are found in zone I, with the most diversity and abundance in the four diatom combination zones. Because the tidal energy in the northwestern part of the bay is weak, and the barrier effect of the Luan River delta in eastern weakens the energy of the current (Pei et al., 2009). Thus, zone I is abundant in diatoms due to the suitable environment for their survival. According to the proportion of freshwater diatoms, zone I is divided into two sub-zones (I-1 zone and

http://www.aloki.hu ● ISSN 1589 1623 (Print) ● ISSN1785 0037 (Online)
DOI: http://dx.doi.org/10.15666/aeer/1802_21792196

I-2 zone). The I-1 zone includes the sea along the Yongdingxin River estuary (stations 1, 6–7, 13–14, 20–22, 27–28, 31–32, 35 and 38–39) and the sea along the Jian River estuary (stations 5, 9–11, 17–18, 24–26 and 30). The proportion of saltwater diatoms in zone I-1 is relatively low, but the proportion of brackish water species is high. In the sea along the Yongdingxin River estuary, the proportion of brackish water diatoms is 0.68%-12.37%, and the average proportion is 4.60%, which is much higher than the average value of zone I. Freshwater diatoms are found in the zone I-1. Due to the influence of the two rivers entering the sea, the maritime nature of area I-1 is weak, and is influenced by the action of the river. Xu et al. (2008) found that there is a low-salt sea area near the intersection of the Yonghexin River and the Jiyun River. The lowest salinity value is 27.21‰ (Xu et al., 2008), which is consistent with the trend in diatom species in zone I-1.

Zone I-2 is distributed in the inner bay (stations 2–4, 8, 12, 15–16, 19, 23, 29 and 34). The proportion of saltwater diatoms in zone I-2 is the highest in the overall study area, and no freshwater diatoms are found. Therefore, zone I-1 is an intertidal zone that is relatively strongly influenced by rivers, while zone I-2 is an inner bay that is not affected by rivers.

Zone II is mainly distributed in the sea between the Haihe River estuary and the Jian River estuary. The abundance of diatoms is the smallest, ranging from 800 to 21,000 /g, with an average abundance of 7,359 /g. *Cosinodiscus excentricus-Cosinodiscus radiates-Actinocyclus normanii* is the dominant diatom combination, with a proportion of 81.74%. The proportion of saltwater diatoms is 72.73%-100.00%, and the average proportion is 93.69%, which is lower than that in Zone I. The main saltwater diatoms include the inner bay indicator species (*Cyclotella striata*, *Cyclotella stylorum*, *Triceratium favus* and *Paralla sulcata*), with a proportion of 9.11%, and the pelagic indicator species (*Thalassiosira nizschioides*), with a proportion of 1.41%. The proportion of brackish water diatoms is 0%–19.7%, and the average proportion is 3.90%, which is higher than that in zone I. The main brackish water diatoms include the seawater muddy intertidal indicator species (*Diploneis bombus*, *Nitzschia granulata* and *Diploneis smithii*), with a proportion of 0.97%, and seawater sandy intertidal indicator species (*Rhaphoneis surirella*, *Auliscus caelalus*), with a proportion of 0.76%. The proportion of freshwater diatoms ranges from 0% to 11.50%, which are distributed throughout stations 33, 36–37, 40, 42–44, 46, 50-51, 54, 57–58, 60–63, 65, 67 and 69. The main freshwater diatoms are *Synedra ulna*, *Achnanthes hauckiana*, *Melosira granulate* and *Gomphonema tumidum*. A small amount of *Epithemia adanata* and *Ellerbeckia arenaria* is also discovered. The proportion of freshwater diatoms in stations 50–51, 54, 57, 60, 62, and 67 reachs 7.68%, which is higher than the average value in zone II.

Since 1967, the Duliujian River has contained a moisture barrier in the downstream estuary, causing serious silting of the river under the water barrier, and resulting in very low annual runoff, which has weakened the river's energy transfer to the sea. Thus, the impact of the Duliujian River on the proportion of freshwater diatoms in zone II is negligible. The sediments in zone II are mainly affected by the Haihe River (Tian et al., 2010; Han et al., 2011). Freshwater diatoms entering the sea are deposited by waves and tides, which are the main reasons for the high proportion of freshwater diatoms. Zone II is the least abundant zone among the three diatom combination zones, with a total of 24 species of diatoms found in zone II. Under the influence of the Haihe River, the salinity of the sea area is lower than that of the surrounding sea area. At the same time, the wave and tidal action of the sea area is dominated by hydrodynamic forces, and the sediments entering the sea are formed fine sand deposits during repeated waves and tides (Pei et al., 2010). Under complex hydrodynamic conditions, diatoms are not easy to preserve

http://www.aloki.hu ● ISSN 1589 1623 (Print) ● ISSN1785 0037 (Online)
DOI: http://dx.doi.org/10.15666/aeer/1802_21792196

due to their friction with coarse particles, which is also the reason for the lowest abundance of diatoms in zone II. Therefore, zone II is an intertidal zone that is affected by rivers and tides.

Zone III is distributed in the sea between the Duliujian River estuary and the Nanpaishui River estuary. The abundance of diatoms is 10400-21000 /g, and the average abundance is 15005 /g. *Cosinodiscus excentricus-Cosinodiscus radiates-Actinocyclus normanii-Cyclotella stylorum* is a dominant diatom combination, with a proportion of 84.82%. The proportion of saltwater diatoms is 72.73%-100%, and the average proportion is 93.69%. The main saltwater diatoms include seawater muddy intertidal indicator species (*Dictyocha fibula*), which have a proportion of 4.67%, and pelagic indicator species (*Thalassiosira nizschioides* and *Actinocyclus senarius*), which have a proportion of 4.39%. The proportion of brackish water diatoms is 0.58%–12.35%, and the average proportion is 4.46%. The main saltwater diatoms include seawater muddy intertidal indicator species (*Diploneis bombus*, *Nitzschia granulata*, *Diploneis smithii* and *Nitzschia lorenziana*), with a proportion of 2.67%, seawater sandy intertidal indicator species (*Rhaphoneis surirella*, *Auliscus caelalus* and *Dimeregramma minor*), with a proportion of 1.48%, and the indicator species of the seaweed field (*Trybliоptychus cocconeiformi*), with a proportion of 0.03%. The proportion of freshwater diatoms ranges from 0.58% to 7.69% and is distributed in stations 70–91, 94–98 and 100–105. Freshwater diatoms in zone III are the most diverse of the four combination zones, reaching 14 species. Additionally, the species of freshwater diatoms change, compared to the zone I and zone II. The main freshwater diatoms are *Nitzschia palea*, *Ellerbeckia arenaria*, *Gyrosigma acuminatum* and *Pleurosigma normanii*. Among those species, *Ellerbeckia arenaria* lives in eutrophic conditions (Fontana et al., 2014) and *Gyrosigma acuminatum* often lives in marsh environments (Chiba and Sawai, 2014; Chen, 2016). *Pinnularia nobils* lives in lakes with salinities of less than 2‰ (Zhang et al., 2012). *Hantzschia amphioxys* are freshwater species that live in alkaline environments (Kazuo and Kiyoshi, 1990; Kashima, 1992), and *Gomphonema tumidum* lives in swamp wetlands (Kazuo and Kiyoshi, 1990; Chiba and Sawai, 2014). *Melosira granulate* lives in eutrophic lakes (Jin, 1982; Kazuo and Kiyoshi, 1990; Kashima, 1992), while *Nizschia amplectems* lives in alkaline marsh wetlands (Kazuo and Kiyoshi, 1990; Kashima, 1992). Few *Synedra tabulate*, *Epithemia adanata* and *Synedra ulna* are found at individual stations.

According to the analysis of diatom combinations, zone III is divided into two sub-regions (regions III-1 and III-2). Zone III-1 includes stations 82, 88–89, 94–98 and 100–105, and locates along the Qingjing drain estuary, the Ziyaxin River estuary and the Shibei River estuary. The proportion of saltwater diatoms in Zone III-1 are the lowest in the study area, ranging from 84.57% to 95.52%. The proportion of brackish water diatoms and freshwater species is relatively high compared to zone III-2, with a proportion of 2.05%–12.35% and 0.75%–4.82%, respectively. Due to the influence of many rivers entering the sea, zone III-1 is strongly influenced by rivers, causing intense mixing of saltwater and freshwater. Thus, there is a low salinity sea area (Xu et al., 2008). Zone III-2 includes stations 64, 70–81, 83–87, 90–93 and 99, and is weakly affected by the river. The proportion of diatoms in saltwater in zone III-2 is higher than that in zone III-1, ranging from 86.89% to 98.84%. The proportion of brackish water diatoms and freshwater diatoms decreases compared to zone III-1, with proportions of 0.58%–9.84% and 0%–7.69%, respectively. Therefore, zone III-1 is an intertidal zone that is strongly affected by rivers. Zone III-2 is a subtidal zone that is weakly affected by rivers.

Zone IV is located in the sea south of the Nanpaishui River estuary and the zone includes stations 106–126. The abundance of diatoms is 7000-20600 /g, and the average

http://www.aloki.hu ● ISSN 1589 1623 (Print) ● ISSN1785 0037 (Online)
DOI: http://dx.doi.org/10.15666/aeer/1802_21792196

abundance is 13795 /g. *Cosinodiscus excentricus-Cosinodiscus radiates-Actinocyclus normanii* is a dominant diatom combination, with a proportion of 74.81%. The proportion of saltwater diatoms is 78.79%–97.14%, and the average proportion is 91.91%. The main saltwater diatoms include the inner bay indicator species (*Cyclotella striata*, *Cyclotella stylorum* and *Paralla sulcata*), with a proportion of 10.51%, pelagic indicator species in the ocean (*Thalassiosira nizschioides* and *Actinocyclus senarius*), with a proportion of 2.97%, and seawater muddy intertidal indicator species (*Dictyocha fibula*), with a proportion of 1.09%. The proportion of brackish water diatoms is 1.48%–9.48%, and the average proportion is 4.37%, which is similar to that in zone III. The main brackish water diatoms include seawater sandy intertidal indicator species (*Rhaphoneis surirella* and *Auliscus caelalus*), with a proportion of 3.03%, and seawater muddy intertidal indicator species (*Diploneis bombus*), with a proportion of 0.79%. The freshwater diatoms in the zone IV accounte for the largest proportion, ranging from 0.65% to 13.17%, and are distributed in stations 106–117, 119–123, 125 and 126. Freshwater diatoms mainly include *Synedra ulna*, *Nitzschia palea* and *Gyrosigma acuminatum*. Few *Ellerbeckia arenaria*, *Pleurosigma normanii* and *Epithemia adanata* are found at some of the stations. After freshwater diatoms enter the sea under the action of the river, a portion of freshwater diatoms are transported offshore by the inertia of the river, and another portion of freshwater diatoms migrate northward under the influence of coastal currents. We find that the proportion of saltwater diatoms in zone IV have a trend of increasing first and then decreasing from the coastal sea to the offshore. However, freshwater diatoms show the opposite trend. In the offshore (stations 108, 109, 110, 119 and 122-123), the proportion of freshwater diatoms increases, ranging from 1.14% to 13.13%, which are more than the coastal sea (stations 107, 118 and 120-121), ranging from 0%-1.55%. However, the species of freshwater diatoms in the offshore sea are similar to the species of freshwater diatoms in the nearshore sea. In addition to normal tidal hydrodynamics, the sea area is also affected by wind and waves on the shore (Pei et al., 2009), which is the reason for the changing trend of freshwater and saltwater diatoms. Therefore, zone IV is an intertidal-subtidal zone strongly affected by rivers.

The main diatom species and sedimentary environments in the study area are summarized in *Table 1*.

The function of freshwater diatoms in the seawater flow pathway

The distribution of freshwater diatoms is consistent with the diatom combination zones. The proportion of freshwater diatoms is the highest in zone IV, and the southern part of zone III (94–98, 100–117, 119–123, 125 and 126), ranging from 0.65% to 13.13%. Under the influence of the river that flows into the sea, freshwater diatoms, such as *Synedra ulna*, *Nitzschia palea*, *Ellerbeckia arenaria*, *Gyrosigma acuminatum*, *Pleurosigma normanii*, *Pinnularia nobils*, *Hantzschia amphioxys* and *Nizschia amplectems* enter the sea. After freshwater diatoms enter the sea, some diatoms are transported offshore by the inertia of the river, and form a sedimentary trend perpendicular to the coastline, while another portion of the freshwater diatom move northward under the action of the current.

http://www.aloki.hu ● ISSN 1589 1623 (Print) ● ISSN1785 0037 (Online)
DOI: http://dx.doi.org/10.15666/aeer/1802_21792196

Table 1. *Dominant diatom assemblages, proportion of freshwater diatoms and deposition environment in study area*

Zone station	Salt, brackish and freshwater species /%	Main diatoms assemblages /%	Freshwater diatoms /%	Deposition environment
I-1	95.62 3.46 1.10	*Cosinodiscus excentricus* (33.15),*Cosinodiscus radiates* (27.30),*Actinocyclus normanii* (18.09),*Cyclotella striata* (5.19),*Dictyocha fibula* (3.14)	*Nitzschia palea* (0.40), *Achnanthes hauckiana* (0.30), *Synedra ulna* (0.12)	intertidal zone relatively strongly influenced by rivers
I-2	98.31 1.69 0	*Cosinodiscus excentricus* (38.49),*Cosinodiscus radiate* (22.89),*Actinocyclus normanii* (20.85),*Cyclotella striata* (4.44),*Dictyocha fibula* (3.47)	not found	inner bay not affected by rivers
II	93.69 3.90 3.86	*Cosinodiscus excentricus* (39.89),*Cosinodiscus radiates* (23.27),*Actinocyclus normanii* (18.58),*Cyclotella striata* (3.47),*Nitzschia granulata* (1.57)	*Nitzschia palea* (2.49), *Synedra ulna* (0.86), *Achnanthes hauckiana* (0.14)	intertidal zone affected by rivers and tides
III-1	91.36 5.58 3.06	*Actinocyclus normanii* (28.56),*Cosinodiscus radiates* (19.63),*Cosinodiscus excentricus* (19.08),*Cyclotella stylorum* (13.94),*Thalassiosira nizschioides* (5.32)	*Pleurosigma normanii* (0.93), *Gyrosigma acuminatum* (0.72), *Nitzschia palea* (0.60)	intertidal zone very strongly affected by rivers
III-2	94.22 3.78 2.49	*Actinocyclus normanii* (27.58),*Cosinodiscus radiates* (26.95),*Cosinodiscus excentricus* (22.90),*Cyclotella stylorum* (9.83),*Thalassiosira nizschioides* (3.04)	*Ellerbeckia arenaria* (1.26), *Gyrosigma acuminatum* (0.31), *Nitzschia palea* (0.28)	subtidal zone weakly affected by rivers
IV	91.91 4.37 4.12	*Actinocyclus normanii* (27.54),*Cosinodiscus radiates* (26.12),*Cosinodiscus excentricus* (21.15),*Cyclotella striata* (5.24),*Cyclotella stylorum* (2.82)	*Nitzschia palea* (2.51), *Synedra ulna* (1.05), *Gyrosigma acuminatum* (0.44)	intertidal-subtidal zone strongly affected by rivers

The proportion of freshwater diatoms in the central and northern stations of zone III (74-91) decrease, ranging from 0.58% to 7.69%. Compared with the southern sea, the proportion of *Nitzschia palea*, *Ellerbeckia arenaria*, *Gyrosigma acuminatum*, and *Pleurosigma normanii* are decreased, while *Synedra ulna* is not observed in the sea. The proportion of freshwater diatoms in zone II (stations 40, 42–44, 46, 50–51, 54, 57–58, 60–63, 65, 67 and 69–73) increases, ranging from 0.48% to 11.5%. The species of freshwater diatoms in zone II have changed, compared to zone III and zone IV; *Pleurosigma normanii* is not observed in the sea, while *Melosira granulate, Gomphonema tumidum*, and *Synedra ulna*, albeit in low proportions. The proportion of the freshwater diatoms, *Nitzschia palea*, *Ellerbeckia arenaria*, and *Gyrosigma acuminatum* increases, especially in stations 50–51, 54, 57, 60, 62, and 67, reachs 7.68%, which is higher than the regional average in Zone II.

Since 1967, the Duliujian River has contained a moisture barrier in the downstream estuary, causing serious silting of the river under the gate, and resulting in very small annual runoffs, and a weakening the river's water flow to the sea. Thus, the impact of the Duliujian River on the proportion of freshwater diatoms in zone II is negligible. The increase in freshwater diatom proportion in zone II is mainly affected by the land reclamation project along the Haihe River estuary. Due to the construction of the Lingang Economic Zone, the hydrodynamic conditions in the sea near the Haihe River

http://www.aloki.hu ● ISSN 1589 1623 (Print) ● ISSN1785 0037 (Online)
DOI: http://dx.doi.org/10.15666/aeer/1802_21792196

estuary have been changed. At high tide, the flow rate in the southeastern side of the Lingang Economic Zone increased due to local flow, while during ebb tides, the flow rate in the southeastern side of the Lingang Economic Zone is reduced significantly. Therefore, sediments from the Haihe River are deposited, causing changes in the substrate (Nie and Tao, 2008). Also, due to the impact of the reclamation project on coastal currents, the deposition of freshwater diatoms increased in zone II. The freshwater diatoms in zone I are distributed in the sea along the Yongdingxin River Estuary and the Jian River Estuary. The main diatom species are *Achnanthes hauckiana*, *Synedra ulna*, *Nitzschia palea* and *Ellerbeckia arenaria*. Freshwater diatoms in the sea along the Yongdingxin River estuary (stations 1, 7, 14, 20, 22, 27–28, 31–32, 35 and 38–39) ranges from 0.56% to 1.53%, and shows a downward trend from south to north. The freshwater diatom proportion in the sea along the Jian River Estuary (stations 5, 9–11, 17–18, 24–26 and 30) is 0.50%–2.14%. The diatom species are similar to those in the waters along the Yongdingxin River estuary, and shows a decreasing trend in proportion from north to south.

In summary, the changes in the proportion of freshwater diatoms indicated the flow of seawater in the study area (*Figure 6*). In the summer, the current flows from south to north in the sea south of the Diujian River estuary. Due to the influence of the Haihe River flowing into the sea and the influence of the land reclamation project on the tide and currents from the Duliujian River estuary to the Haihe River estuary, the hydrodynamic conditions of the sea have changed. In the bay north of the Haihe River estuary, the current flows from south to north along the west coast, then the coastal current flows along the north coast, and then flows to the southeast, a clockwise water current is formed.

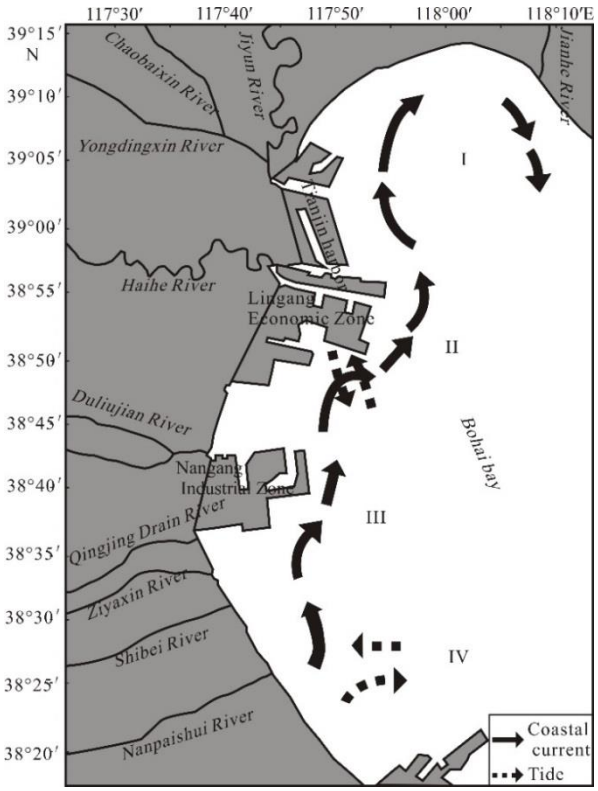

Figure 6. *Freshwater diatom moving direction*

http://www.aloki.hu ● ISSN 1589 1623 (Print) ● ISSN1785 0037 (Online)
DOI: http://dx.doi.org/10.15666/aeer/1802_21792196

Conclusions

According to the diatom combinations of surface sediments in the inshore waters of the western Bohai Bay and the distribution of freshwater diatoms, the following results and conclusions are obtained:

(1) A total of 49 species and varieties of diatoms from 32 genera are identified in the study area. Four dominant species are found, and all of which are saltwater species, including *Cosinodiscus excentricus*, *Cosinodiscus radiatus*, *Actinocyclus normanii* and *Cyclotella stylorums*. Diatom abundance in the bay north of the Haihe River estuary is the highest, while diatom abundance in the sea south of the Duliujian River estuary is the second. Diatom abundance in the sea between the Haihe River Estuary and the Duliujian River estuary is the lowest and is affected by the flow of the Haihe River, as well as tides.

(2) All 126 stations are dominated by saltwater diatoms. Saltwater diatoms have the highest proportion in the bay north of the Haihe River estuary. The proportion of saltwater diatoms in the sea south of the Haihe River estuary is lower than that in the bay north of the Haihe River estuary. The brackish water diatoms are mainly distributed in the Yongdingxin River estuary, the sea southeast of the Lingang Economic Zone and the sea south of the Nangang Industrial Zone. In the bay north of the Haihe River estuary, the proportion of brackish water diatoms tend to decrease from the shore to the sea. Freshwater diatoms are found at 93 stations with a proportion of 0.48%, and are regularly distributed in the study area.

(3) According to the diatom combination analyses, the study area is divided into four sedimentary areas. Zone I is distributed in the bay north of the Haihe River estuary and is divided into an intertidal zone (I-1 zone), which is strongly influenced by rivers, and the Inner Bay zone (I-2 zone), which is not affected by rivers. Zone II is distributed in the sea between the Haihe River estuary and Duliujian River estuary. It is an intertidal zone affected by the Haihe River, tides, and tidal currents. Zone III is distributed in the sea between the Duliujian River estuary and the Nanpaishui River estuary. It is divided into the intertidal zone (III-1), which is strongly influenced by rivers, and the subtidal zone (III-2), which is weakly affected by rivers. Zone IV is distributed in the sea south of the Nanpaishui River estuary. It is an intertidal-tidal zone that is strongly influenced by rivers.

(4) Trends in the distribution and abundance of freshwater diatoms in the inshore waters of the western Bohai Bay indicates that the land reclamation project on the west coast of the Bohai Bay affects the tide and water current, which changes the sediment transport direction. In the summer, the currents move from south to north in the sea south of the Haihe River estuary. The construction of the Lingang Economic Zone has changed the hydrodynamic conditions of the local waters, causing the rivers to enter the sea form sedimentary areas in the southeastern waters of the Lingang Economic Zone. In the bay north of the Haihe River estuary, a clockwise water current is formed.

（5）In this paper, we discussed the diatoms assemblage and the seawater flow pathway in summer. In future research we will investigate about whether the diatom assemblage changes with the season and freshwater could reflect the seawater flow pathway in winter.

Acknowledgements. This research was financially supported by the China geological survey program (DD20189506) and Tianjin Natural Science Foundation (18JCYBJC91100).

http://www.aloki.hu ● ISSN 1589 1623 (Print) ● ISSN1785 0037 (Online)
DOI: http://dx.doi.org/10.15666/aeer/1802_21792196

REFERENCES

[1] Artemova, A. V., Sattarova, V. V., Vasilenko, Y. P. (2018): Distribution of diatoms and geochemical features of holocene sediments from the Kuril Basin (Sea of Okhotsk). – Deep Sea Research Part II: Topical Studies in Oceanography 154: 10-23.

[2] Bennion, H. (1994): A diatom-phosphorus transfer function for shallow, eutrophic ponds in southeast England. – In: Mortensen, E., Jeppesen, E., Sondergaard, M., Kamp Nielsen, L. (eds.) Nutrient Dynamics and Biological Structure in Shallow Freshwater and Brackish Lakes: 391-410. Springer, Dordrecht.

[3] Cárdenas, P., Lange, C. B., Vernet, M., Esper, O., Srain, B., Vorrath, M. E., Ehrhardt, S., Müller, J., Kuhn, G., Arz, H. W., Lembke-Jene, L., Lamy, F. (2019): Biogeochemical proxies and diatoms in surface sediments across the Drake Passage reflect oceanic domains and frontal systems in the region. – Progress in Oceanography 174: 72-88.

[4] Chen, H. Y., Huh, C. A., Chang, N. Y., Chen, J. C. (2000): Sources and Distribution of Heavy Metals in East China Sea Surface Sediments. – Chemistry & Ecology 17(3): 227-238.

[5] Chen, M., Chen, C., Lan, B. B., Lan, D. Z., Qi, H. S. (2014): Diatom Assemblages and Distribution in Coastal Surface Sediments in the China Sea (Bohai Sea and Huanghai Sea). – Transactions of Oceanology and Limnology 33(2): 183-190.

[6] Chen, H. (2016): Sediment Diatom in Fresh Water. – Chemical Industry Press, Beijing.

[7] Chen, M., Li, Y. H., Qi, H. S., Wang, L., Zhang, A. M., Shen, L. N., Fang, Q. (2019): The influence of season and Typhoon Morakot on the distribution of diatoms in surface sediments on the inner shelf of the East China Sea. – Marine Micropaleontology 146: 59-74.

[8] Chiba, T., Sawai, Y. (2014): Reexamination and updating of diatom species for paleoenvironmental reconstructions. – Diatom 30 (Supplement): 14-30.

[9] Cunningham, W. L., Leventer, A. (1998): Diatom assemblages in surface sediments of the Ross Sea: relationship to present oceanographic conditions. – Antarctic Science 10(2): 134-146.

[10] Ding, X. G., Ye, S. Y., Laws, E. A., Mozdzer, T. J., Yuan, H. M., Zhao, G. M., Yang, S. X., He, L., Wang, J. (2019): The concentration distribution and pollution assessment of heavy metals in surface sediments of the Bohai Bay, China. – Marine pollution bulletin 149: 110497.

[11] Fontana, L., Albuquerque, A. L. S., Brenner, M., Bonotto, D. M., Sabaris, T. P., Pires, M. A., Cotrim, M. E., Bicudo, D. C. (2014): The eutrophication history of a tropical water supply reservoir in Brazil. – Journal of Paleolimnology 51(1): 29-43.

[12] Hall, R. I., Smol, J. P. (2010): A weighted-averaging regression and calibration model for inferring total phosphorus concentration from diatoms in British Columbia (Canada) lakes. – Freshwater Biology 27(3): 417-434.

[13] Han, Z. Z., Zhang, J. Q., Zou, H., Yi, W. H., Li, M. (2011): Characteristics and Provenance of Clay Mineral Assemblage of Sediments from the Northern Part of the Bohai Bay. – Periodical of Ocean University of China (Natural Science Edition) 41(11): 95-102.

[14] Hartley, B. (1996): An Atlas of British Diatoms. – Biopress, Bristol.

[15] Hay, M. B., Pienitz, R., Thomson, R. E. (2003): Distribution of diatom surface sediment assemblages within Effingham Inlet, a temperate fjord on the west coast of Vancouver Island (Canada). – Marine Micropaleontology 48(3-4): 291-320.

[16] Hendey, N. I., Part, V. (1964): Bacillariophyceae (Diatoms in an introductory account of the smaller algae of British coastal waters. – Fishery investigation Series, IV London, 317.

http://www.aloki.hu ● ISSN 1589 1623 (Print) ● ISSN1785 0037 (Online)
DOI: http://dx.doi.org/10.15666/aeer/1802_21792196

[17] Institute of Marine Geology, Institute of Oceanology, Chinese Academy of Sciences (1985): Bohai Geology. – Science Press, Beijing.
[18] Jin, D. X. (1982): Marine benthic diatoms in China (upper). – Shanghai Scientific & Technical Publishers, Shanghai.
[19] Karpuz, N. K., Schrader, H. (1990): Surface sediment diatom distribution and Holocene paleotemperature variations in the Greenland, Iceland and Norwegian Sea. – Paleoceanography 5(4): 557-580.
[20] Kashima, K. (1992): Catalog of Holocene diatom fossil part 1, Tokoro Plain, Hokkaido, North Japan. – The Geological Research Reports of Kyushu University, College of General Education 29: 1-36.
[21] Kazuo, A., Kiyoshi, F. (1990): Paleo-Environmental History and Sea-Level Records Based on the Diatom Assemblages in the Middle Part of the Arakawa Lowland, Central Japan. – The Quaternary Research 29(5): 427-437.
[22] Kosugi, M. (1988): Classification of living diatom assemblages as the indicator of environments, and its application to reconstruction of paleoenvironments. – The Quaternary Research (Daiyonki-Kenkyu) 27(1): 1-20.
[23] Leroy, S. A. G., Chalie, F., Wesselingh, F. P., Sanjani, M. S., Lahijani, H. A. K., Athersuch, J., Struck, U., Plunkett, G., Reimer, P. J., Habibi, P., Kabiri, K., Haghani, S., Naderi-Beni, A., Arpe, K. (2018): Multi-proxy indicators in a Pontocaspian system: a depth transect of surface sediment in the SE Caspian Sea. – Geologica Belgica 21: 143-165.
[24] Li, Q. X., Tao, J. H. (2000): Studies on Ecological Characteristics of Phytoplankton in the Waters Near Tianjin. – Journal of Tianjin University 4: 464-469.
[25] Liu, D., Liu, L., Di, B., Wang, Y. J., Wang, Y. N. (2015): Paleoenvironmental analyses of surface sediments from the Bohai Sea, China, using diatoms and silicoflagellates. – Marine Micropaleontology 114: 46-54.
[26] Nave, S., Freitas, P., Abrantes, F. (2001): Coastal upwelling in the Canary Island region: spatial variability reflected by the surface sediment diatom record. – Marine Micropaleontology 42(1): 1-23.
[27] Nie, H. T., Tao, J. H. (2008): Impact of coastal exploitation on the eco-environment of Bohai Bay. – The Ocean Engineering 26(3): 44-50.
[28] Pan, L., Fang, J., Tian, L. Z., Wang, F. (2019): Water Migration Pathway Based on Freshwater Diatoms in Sea Area Adjacent to the Nangang Industrial Zone of Tianjin. – Journal of Coastal Research 93(sp1): 232-240.
[29] Pei, Y. D., Wang, Y. S., Fan, C. F., Wang, F., Tian, L. Z., Shang, Z. W., Che, J. Y., Wang, H. (2009): The surface sediment types and distribution of Tianjin intertidal zone, China. – Geological Bulletin of China 7: 915-922.
[30] Pei, Y. D., Tian, L. Z., Wang, F., Wang, H. (2010): Causation of the Fine Sandy Intertidal Zone on the West Coast of Bohai Bay. – Geological Survey and Research 3: 180-184.
[31] Perez, L., Brugnoli, E., Muniz, P., Sunesen, I., Sar, E. A., Crisci, C., Cuña, C., García-Rodríguez, F. (2018): Diatom assemblages from surface sediments of the Río de la Plata estuary, Uruguay. – New Zealand journal of marine and freshwater research 52(3): 383-397.
[32] Ran, L., Jiang, H. (2005): Distributions of the surface sediment diatoms from the South China Sea and their palaeoceanographic significance. – Acta Micropalaeontologica Sinica 22(1): 97-106.
[33] Renberg, I. (1990): A procedure for preparing large sets of diatom slides from sediment cores. – Journal of Paleolimnology 4(1): 87-90.
[34] Shang, Z. W., Wang, H., Che, J. Y., Tian, L. Z., Pei, Y. D., Fan, C. F., Wang, F., Liu, Z. G. (2006): Diatom assemblages in the surface sediments of Bohai Bay. – Marine Geology & Quaternary Geology 26(5): 21-26.

http://www.aloki.hu ● ISSN 1589 1623 (Print) ● ISSN1785 0037 (Online)
DOI: http://dx.doi.org/10.15666/aeer/1802_21792196

[35] Shang, Z. W., Tian, L. Z., Wang, H., Li, J. F. (2012): Diatom assemblages from surficial sediments in north-central Bohai Bay and their implications for environments. – Geology in China 39(4): 1099-1107.
[36] Shen, G. Y., Shi, B. Z. (2002): Marine ecology. – Science Press, Beijing.
[37] Smol, J. P., Birks, H. J., Last, W. M. (2001): Tracking environmental change using lake sediments. – Springer Netherlands, Berlin.
[38] Tian, L. Z., Geng, Y., Pei, Y. D., Shang, Z. W., Wang, F., Fan, C. F., Wang, H. (2010): The grain-size characteristics and sediment mixing pattern of surface sediment from the western Bohai Bay, China. – Geological Bulletin of China 29(5): 668-674.
[39] Tian, L. Z., Pei, Y. D., Shang, Z. W., Wang, F., Wang, H. (2010): Elements Characteristics of the Suspended Component in Surface Sediments from the West Bohai Bay and the Provenance Implication. – Marine Geology &Quaternary Geology 1: 9-15.
[40] Tu, J., Bai, Y. C., Xu, H. Y. (2017): Change of Coastline and Tidal Current Caused by Boahi Bay Reclamation Project. – Port Engineering Technology 8(4): 1-4.
[41] Wang, K. F., Jiang, H., Zhi, C. Y., Tao, M. H., Wang, H. G. (2001): Study on the relationship between diatom assemblage in surface sediments and the environment in the east China sea. – Acta Micropalaeontologica Sinica 18: 379-384.
[42] Wang, W., Li, A. C., Xu, F. J., Huang, P., Li, Y. (2009): Distribution of surface sediments and sedimentary environment in the North Yellow Sea. – Oceanologia et Limnologia Sinica/Hai Yang Yu Hu Chao 40(5): 525-531.
[43] Wang, H., Shang, Z. W., Li, J. F., Pei, Y. D., Wang, F., Tian, L. Z., Fan, C. F., Sheng, J. J., Chen, Y. S., Liu, H. M. (2010): Holocene shoreline changes and marine impacts on the muddy coast, western Bohai Bay, China. – Geological Bulletin of China 29(5): 627-640.
[44] Weckström, K., Juggins, S. (2006): Coastal diatom-environment relationships from the Gulf of Finland, Baltic sea. – Journal of Phycology 42(1): 21-35.
[45] Wu, R., Gao, Y. H., Fang, Q., Chen, C. P., Lan, B. B., Sun, L., Lan, D. Z. (2013): Diatom assemblages in surface sediments from the South China Sea as environmental indicators. – Chinese Journal of Oceanology and Limnology 31(1): 31-45.
[46] Xu, H. F., Jiang, B., Wu, H. (2008): China's offshore marine comprehensive adjustment and evaluation (908 special). – Tianjin 908 special physical ocean survey report.
[47] Xu, S. S., Di, B. P., Wang, Y. J., Liu, D. Y., Wang, X. D. (2017): Spatial distribution of benthic diatom in the typical intertidal zones in China. – Acta Oceanologica Sinica 39(6): 95-113.
[48] Zhang, C. J., Zhang, W. Y., Fan, R., Gao, D. (2012): Early diagenesis impacting C/N and organic isotopic compositions in the lacustrince sediments. – Journal of Earth Environment 3(4): 1005-1012.
[49] Zhao, B. R., Zhuang, G. W., Cao, D. M., Lei, F. H. (1995): Circulation tidal residual currents and their effects on the sedimentions in the Bohai Bay. – Oceanologia et Limnologia sinica 26(5): 466-473.

http://www.aloki.hu ● ISSN 1589 1623 (Print) ● ISSN1785 0037 (Online)
DOI: http://dx.doi.org/10.15666/aeer/1802_21792196

THE COOLING EFFECT OF AN URBAN LAKE LANDSCAPE ON THE URBAN HEAT ISLAND: A CASE STUDY IN JINAN, CHINA

YANG, S. J.[1,2*] – RAN, G. P.[3] – ZHANG, W.[1] – WANG, Z. H.[2]

[1]*School of Environment Science and Spatial Informatics, China University of Mining and Technology, China*

[2]*College of Geography and Environment, Shandong Normal University, Jinan, China*

[3]*Information and Technology Centre, Jinan meteorological bureau, Jinan, China*

[*]*Corresponding author*
e-mail: sdnugps@qq.com

(Received 26th Sep 2019; accepted 21st Jan 2020)

Abstract. The fact that open water contributes to lowering air temperature is well known in urban landscape planning. Water bodies have been used as tools to reduce the urban heat island effect (UHI). However, the extent to which a water body propagates the cooling effect from the lakeshore is still largely unknown. This study aimed to (1) provide evidence for cooling air temperature on the surrounding urban lakeshore; (2) verify the effect of different land covers surrounding the lakeshore on lowering air temperature; and (3) determine the cooling effects at different distances from the different lakeside areas. Based on urban weather station data and on measured data from Daming lake, Jinan, China, the analytic results reveal significant cooling adjacent to the lakeshore with an average cooling of nearly 1℃ from July to August. Following the air temperature drop, the cooling effect becomes increasingly weaker, reaching the lowest value of 0.3℃ in October. Vegetated area causes more of a cooling effect than permeable or impermeable surface. However, the cooling difference between permeable surface and impermeable surface was less significant. At all measuring sites, the cooling level at a horizontal distance of 40 m from the lakeshore was less than 0.6℃.
Keywords: *urbanization, temperature monitoring, water bodies, cooling effect, vegetated landscapes*

Introduction

Over the past twenty years, urbanization and industrialization have been accelerating in developing countries. Although urbanization and industrialization improves the living-standards of urban inhabitants, these changes bring a series of environmental problems, such as the urban heat island effect, air pollution, and industrial waste (Rizwan et al., 2008; Sun and Chen, 2012; Singh et al., 2017; Li et al., 2018). The urban heat island (UHI) is an increasingly serious problem in many countries. The so-called UHI is simply defined as a metropolitan area that has a warmer near-surface air temperature than its surrounding rural areas (Unwin, 1980; Chang et al., 2007; Su et al., 2012). Aside from the UHI effect on temperature, the UHI has other negative impacts on weather and climate, air pollution, health and welfare, and energy consumption (Rosenfeld et al., 1995).

Water bodies, such as lakes, rivers, ponds, and streams, have the potential to lower surface temperature through continuous evaporation, particularly on sunny days when more water can be absorbed by the air. Each gram of evaporating water absorbs 2500 J and reduces the surface temperature very effectively (Grinzato et al., 2002). In urban landscape planning and design, water bodies are prominent features. They play the dominant role in urban development as well (Ding and Cao, 2004; Cai et al., 2018; Dai

http://www.aloki.hu ● ISSN 1589 1623 (Print) ● ISSN1785 0037 (Online)
DOI: http://dx.doi.org/10.15666/aeer/1802_21972211

et al., 2019). Additionally, urban water bodies are one of the important units of urban ecological systems at the scale of the entire city (Ding and Cao, 2004; Li et al., 2008; Gober et al., 2009; Xu et al., 2010). There have been numerous studies aimed at confirming the effects of water bodies on the UHI in the past few decades, and the data sources to measure urban heat island effect mainly include remotely sensed thermal infrared (TIR) data, in situ data and moving observation data. In recent years, TIR data have been widely employed to retrieve land surface temperature (LST) (Weng, 2009; Guillevic et al., 2014; Li et al., 2014). Sun and Chen (2012) explored the intensity and efficiency of cooling effects of urban water bodies in Beijing city, the LST data were extracted from ASTER images of August 8, 2007, the result showed the mean cooling intensity and efficiency was 0.54 °C/hm and 1.76 °C/hm/ha, respectively. Gupta et al. (2019) found that average temperature drop of 7.51°C and 3.12°C is observed during summer and winter, respectively for three years near the Sukhna Lake in Chandigarh city. However, most of the studies on the impacts of rivers on the UHI are confined to the scale of urban river segment. Moreover, the data were collected by conducting an on-site measurement. Murakawa et al. (1991) reported that the drop in the air temperature above the Ota River, Hiroshima, Japan, reached 5℃ on sunny days in the warmer seasons and that the cooling effect propagated a few hundred meters horizontally and more than eighty meters vertically. Another study based along the River Don, Sheffield, UK, demonstrated that the average cooling effect over the river reached nearly 1℃ when the ambient temperature exceeded 20℃ (Hathway and Sharples, 2012). The above studies are based on microclimatic conditions of an urban river. In addition, limited published studies exist on the cooling effect of water bodies at the urban scale. In the desert city of Phoenix, United States, Gober et al. (2009) found that an increasingly irrigated landscaping lowered night-time temperatures in the urban core. Two other studies revealed that the UHI effect was influenced by the surface area of urban water bodies and their geometry (Sun and Chen, 2012; Oláh, 2012). Additionally, in the city of Dongguan, China, research showed that a negative linear relationship exists between water surface area and decreasing ambient temperature at the spatial scale of 500 m x 500 m cells (Li et al., 2008). However, an analysis of a network of hobby-meteorological observations in the Netherlands showed that an open water surface area brought a significant increase of the 95 percentile of the UHI (Steeneveld et al., 2014).

Because most studies focusing on the relationship between the UHI and water bodies are limited to a river or a few rivers (Gober et al., 2009; Hathway and Sharples, 2012; Du et al., 2016), the literature on the role of a lake or pond in mitigating the UHI is limited. In comparison to a river, the different effect of a lake on mitigating the UHI is evident in many ways. For example, a river usually flows at a certain speed, while a lake is generally still. Compared with the heat absorbed by a river flowing downstream, the processes of heat absorption and emission from a lake's surface occur at nearly the same site. In addition, a lake usually occupies a larger area than a river in a specific block area of a city. As evaporation causes heat absorption from the ambient environment, it leads to a drop of the lake's surface temperature. Therefore, a lake may have a greater potential to moderate the UHI effect than a river in a city. In the planning and design of an urban lake, the designer should therefore not only pay attention to landscape forms and landscape aesthetics but also put more focus on their design's effect on the urban thermal environment, especially the landscape surface effect. Different landscape surfaces have different abilities to reduce the UHI effect. Vegetation and trees can provide shading and cooling through evapotranspiration, as the solar radiation intensity in tree shade is nearly

http://www.aloki.hu ● ISSN 1589 1623 (Print) ● ISSN1785 0037 (Online)
DOI: http://dx.doi.org/10.15666/aeer/1802_21972211

10% of the radiation in the open air (Givoni et al., 2003). Conversely, an artificial surface, such as concrete and asphalt, absorbs more heat during the day and release it into the ambient environment, resulting in an increase in the ambient temperature. Therefore, the planner and designer should put some emphasis on the rationality of the land cover.

Although the work discussed above has shown the effectiveness of urban water bodies in mitigating the UHI, the research does not give direct evidence of lowering the ambient temperature in a complex surrounding environment. Furthermore, the efforts of previous researchers are concentrated on how water bodies affect the variation of the surrounding air temperature through evaporation. They do not consider the effect of land cover on the lakeshore and the propagation of cooling from the lake into the ambient environment. Thus, a study evaluating the microclimate effect of a lake on moderating the UHI is necessary. This study will focus specifically on the urban lake because a natural lake or an artificial lake can provide many ecological benefits; it can store fresh water and clean water, recharge groundwater, protect biological diversity, control flooding, and regulate climate (Han, 2006). Thus, the functions of climate regulation that arise from an urban lake should be considered by the urban planner and designer. Meanwhile, it is important to provide the evidence of the potential that urban lakes have to lower air temperature and the extent to which different adjacent land covers affect and propagate cooling. The objectives of this study include (1) providing the evidence for cooling air temperature on the surrounding lakeshore; (2) verifying the effect of different land covers of the surrounding lakeshore on lowering air temperature; and (3) determining the cooling effects at different distances from the different banks of the lake.

Methods

Study area

The study area is situated in Daming lake Park, Jinan, China. Daming lake is a natural lake and the largest lake in Jinan city. The park covers 104 ha, including the water surface area (58 ha) and the land area (46 ha). This lake is shallow, ranging in depth from 1 m to 3.5 m (Wang et al., 2010). The water of four springs converges in the lake through three main water inlets that are situated at the southeast, south, and west bank of the lake. The lake water flows into the Xiaoqing River from the northern water gate and a water outlet. The lakeshore is fringed with shrubs, trees and grass on the ring shape of the lake, and the paved road and the bridges are the main connections between pavilions, the ancestral hall, and other buildings (*Fig. 1a,b*). The temperature difference, which resulted from the UHI of Jinan city, reached approximately 0.56℃ during the day and nearly 2℃ at night in July 2007, whereas the difference rose to nearly 1℃ during the daytime and up to 2.74℃ at night-time in October 2007 (Ran et al., 2010).

Description of measurement sites

Three automatic urban weather stations (UWS1, UWS2 and UWS3) were selected to evaluate the cooling effect of the waterfront of Daming lake. All of the UWS surrounding the study area were situated on the second ring road in the city. The maximum distance from a UWS to the centre of Daming lake was 2.5 km, and the minimum distance was 1.4 km (*Fig. 2*). The GPS coordinates of three UWS are shown in *Table 1*. The sites of the UWS were in built-up areas. Two of them were located in the open square, where the UWS instrument (ZQZ-A, Suzhou, China) was installed adjacent to several trees at a

http://www.aloki.hu ● ISSN 1589 1623 (Print) ● ISSN1785 0037 (Online)
DOI: http://dx.doi.org/10.15666/aeer/1802_21972211

height of 1.5 m above the grass lawn. The weather data provided by the instruments included air temperature, relative humidity, atmospheric pressure, wind speed, wind direction, and precipitation. The other UWS was sited on the green roof of a 5-storey building. Its instrument (ZQZ-A, Suzhou, China) was installed at the same height above the green roof to monitor air temperature and precipitation. Weather data were recorded hourly when the instrument worked properly. Additionally, all of the instruments were calibrated every year. Because the altitudes of the three sites were from 36.8 m to 39.0 m, and the altitude of the Daming lake water surface is 23.9 m, the height difference between the three UWS sites and Daming lake was too slight to take into account a lapse rate.

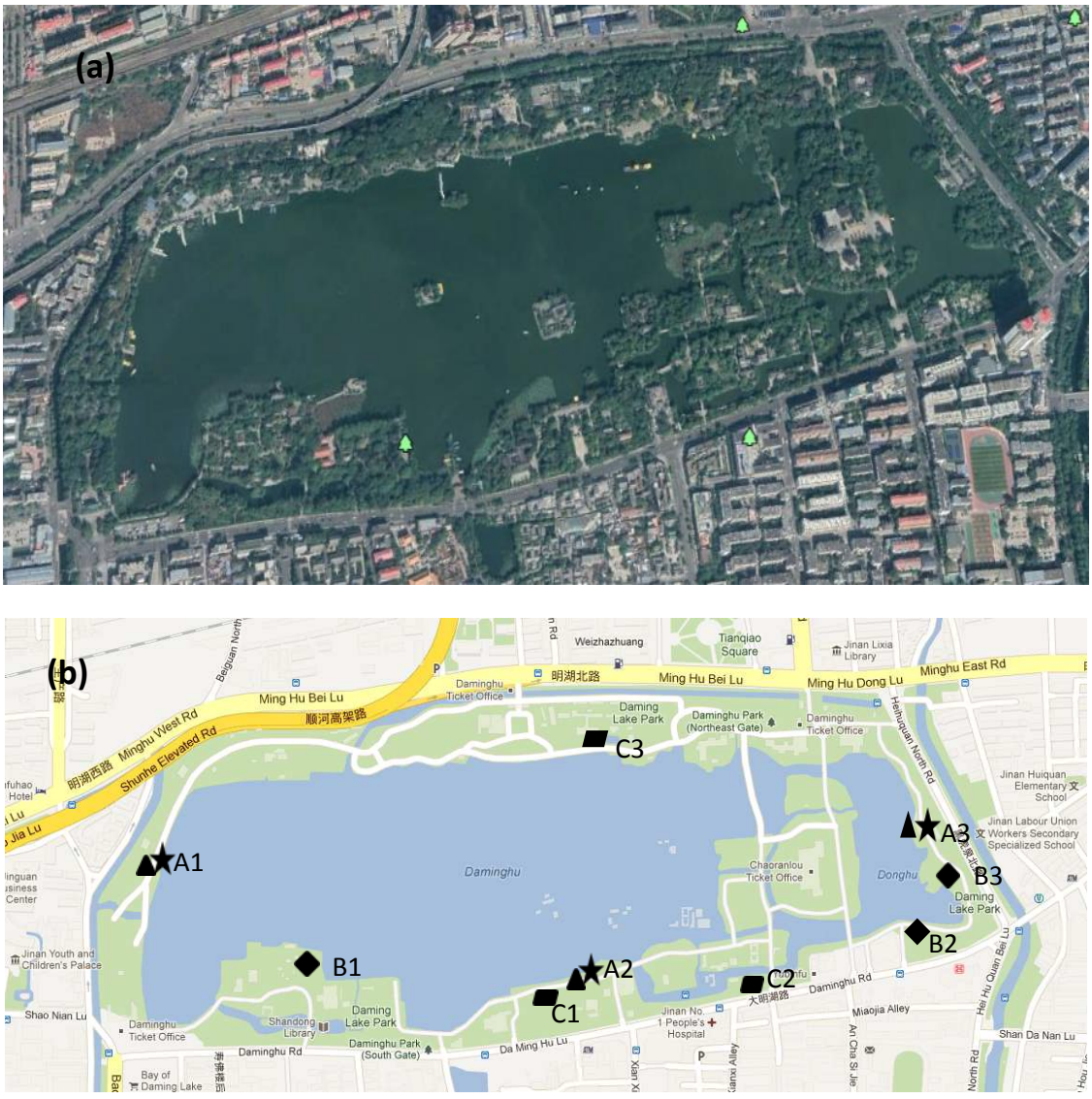

Figure 1. *Remote sensing image (a) and map (b) of Daming Lake (Map source: Google maps).*
▲ *a triangle represents the location of a measurement site*
★ *a pentagram represents the lakeshore area covered by vegetation*
◆ *a diamond represents the lakeshore area occupied by permeable paving*
▰ *a parallelogram represents the lakeshore area occupied by impermeable paving*

http://www.aloki.hu ● ISSN 1589 1623 (Print) ● ISSN1785 0037 (Online)
DOI: http://dx.doi.org/10.15666/aeer/1802_21972211

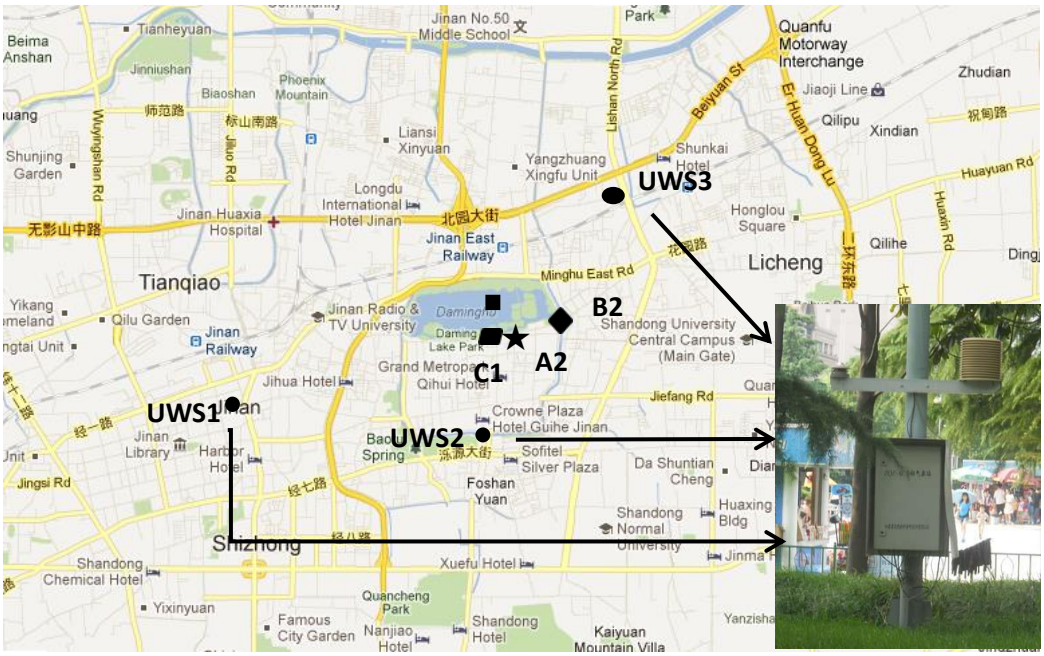

Figure 2. *Locations of weather stations and Daming Lake in Jinan City (Map source: Google maps).*
a square represents the location of Daming lake
★ represents the lakeshore A2 covered by vegetation
represents the lakeshore C1 occupied by impermeable paving
◆ represents the lakeshore B2 occupied by permeable paving
● represents the location of an automatic weather station

Table 1. *Measure sites and GPS coordinates in study area*

Sample Name	GPS coordinates		Sample Name	GPS coordinates	
	Latitude	Longitude		Latitude	Longitude
UWS1	36.664522°	116.993835°	B1	36.672819°	117.016575°
UWS2	36.660341°	117.015332°	B2	36.673743°	117.028641°
UWS3	36.687529°	117.942916°	B3	36.674896°	117.029581°
A1	36.674946°	117.011271°	C1	36.672806°	117.019918°
A2	36.672953°	117.020875°	C2	36.672504°	117.024482°
A3	36.675917°	117.028288°	C3	36.677002°	117.020313°

To assess the cooling effect of the lake, three sites (*Fig. 1*) on Daming lake located at the west, south and east bank of the lake were chosen. The conditions of the three measurement sites were similar to those at the UWS in all respects. The GPS coordinates of measure sites are shown in *Table 1*. A type of measurement sites was adjacent to several trees that had some grass and shrub cover. Images of the sites are shown in *Fig. 3-A2*, land surface of B type is permeable, and C type is impermeable. Their images are also shown in *Fig. 3-B2* and *Fig. 3-C1*, respectively.

To estimate the propagation of the cooling effect from the lakeshore to the ambient environment, nine research sites composed of three types of land covers were selected. These land covers (*Fig. 3*) included (1) vegetation, mainly covered by green grass and

http://www.aloki.hu ● ISSN 1589 1623 (Print) ● ISSN1785 0037 (Online)
DOI: http://dx.doi.org/10.15666/aeer/1802_21972211

shrubs; (2) permeable paving, paved by holey concrete brick; and (3) impermeable paving, constructed by impermeable concrete brick. Site A1 was located on the western lakeshore, where concrete brick was paved at a distance of 1-2 m from the lake bank. Green grass and shrubs were planted adjacent to the brick far from the lakeshore; the planted area was approximately 20 m×30 m. Sites A2 and A3 were similar in all respects, with green grass, shrubs and trees planted at a distance of approximately 30 m from the lakeshore. A concrete road approximately 3 m wide passes through the green area at a distance of approximately 15 m from the lakeshore. Sites B1 and B2 were smaller scale areas of approximately 15 m×20 m, with willows and other trees at heights of approximately 4 m around them. For site B3, its scale is smaller than that of the two sites B1 and B2, occupying an area of approximately 4 m×15 m with trees and shrubs surrounding it. Sites C1, C2 and C3 were adjacent to the lakeshore. Site C1 was located at the southern gate of Daming lake; it was an open square with a decorated archway and several trees. Site C2 was located at an open place with an area of approximately 30 m×20 m. Site C3 was located at the north bank of the lake, was fringed with several trees, and contained impermeable concrete brick extending to approximately 30 m from the waterfront.

Figure 3. *Images of every site type: a) vegetational site, b) permeable site, and c) impermeable site*

Survey methods

Measurements of air temperature, water temperature and relative humidity were conducted from July to October in 2012, survey times of air temperature and water temperature at the lakeshore focused on 9:00-21:00, and the time of measurement at different lakeshore forms was from 10:00 to 22:00. Measurements of air temperature and water temperature were taken with mercury thermometers (Wuqiang Thermometer Company, Hengshui, China). This thermometer has an accuracy of ±0.1℃ between 0℃ and 50℃ and a resolution of 0.1℃. All of the instruments were calibrated before the surveying period. Measurement campaigns were carried out in the periods of 21-26th July, 15-17th August, 13-16th September and 13-18th October. In the course of temperature measurement, mercury thermometers were shielded with a simple instrument shelter. Air temperature at the lakeshore was recorded 4 times per day (9:00, 13:00, 17:00, and 21:00), and surveying campaigns at different lakeshore forms were performed 4 times per day (10:00, 14:00, 18:00 and 22:00) at 10 m intervals from the lake edge to 40 m away. Water temperature was measured hourly from 9:00 to 21:00. When the surveyor stood at the bank, the mercury thermometer was placed 0.1 m vertically below the water surface. During September and October in Jinan, the prevailing winds were mostly from the northwest to west directions. Wind speed usually ranged from 0 to 3 m/s, so special days

http://www.aloki.hu ● ISSN 1589 1623 (Print) ● ISSN1785 0037 (Online)
DOI: http://dx.doi.org/10.15666/aeer/1802_21972211

in autumn were chosen when wind speed slowed below 1.0 m/s. For evaluating the role of the lake water body and lakeshore form in mitigating the UHI, the surveyor spent more than two minutes to accurately measure temperature at every site. The measurement location was 1.5 m above the ground.

The paired-samples *T*-test was applied for a significance level $\alpha = 0.05$. Thus, if a *p-value* was computed to be less than 0.05, then the temperature difference would be considered statistically significant. The statistical significance (*p*), *t*-statistic (*t*), and degrees of freedom (*df*) are found in the latter data analysis. The effect size (*r*) based on Pearson's correlation is used to measure the strength of the relationship between measuring the lakeshore air temperature and the UWS's.

Results

Role of the urban lake in mitigating the UHI

Part of the purpose of this paper is to assess the cooling effect of the lake, and therefore, we chose the study period between 21st July and 18th October. To estimate the temperature difference between the urban weather stations and the lakeshore, the measuring sites were selected for their vegetation cover. As such, the measuring conditions of urban weather stations (UWS1, UWS2 and UWS3) were similar to that of the lakeshore. The sites of the lakeshore are referred to as A1, A2 and A3, and the temperature differences between the urban weather stations and the lakeshore based on the measurement periods are calculated using:

$$\Delta T_i = T_i - T_{UWS} \quad \text{(Eq.1)}$$

where T_{UWS} is the mean temperature from the three urban weather stations, the index *i* is the reference for the individual lakeshore (A1, A2 or A3), and T_i is the arithmetical mean value of the monitoring data at the same measuring time for every monitoring period. A negative value of ΔT_i indicates cooling adjacent to the lake in comparison to the urban weather stations. *Fig. 4a-d* shows the value of ΔT_i for different time periods at different sites adjacent to the lake. All of the monitored air temperatures are lower than the air temperature at the urban weather stations.

The air temperature varied from 22.7℃ to 30.9℃ during the measuring period in July and varied from 23.1℃ to 31.7℃ in August, compared with a variation from 17.8℃ to 27.6℃ in September and from 14.1℃ to 20.1℃ in October. The temperature difference at different measuring times for one day in July and August is illustrated in *Fig. 4a-b*. During most hours of the day, it was lightly cloudy and the wind velocity varied from 0.3 ms^{-1} to 0.7 ms^{-1}. Analysing the temperature differences at different times, the mean of temperature difference was 1.0℃ and 1.2℃, respectively. The cooling effect was more significant in August than July. At the same time, the highest temperature difference at 9:00 was approximately equal between July (-1.9 to -1.1℃) and August (-1.8 to -1.1℃), and the lowest temperature at 21:00 in July was -0.7 to -0.3℃, compared with August (-0.6 to -0.4℃). Furthermore, temperature differences were also influenced by the measuring location in two periods: in July, the lowest temperature difference was recorded at site A2, where the mean of the temperature difference was 0.7℃, and the highest temperature difference was recorded at site A1, where the mean of the temperature difference reached 1.2℃. The paired-samples T-test result shows the value

http://www.aloki.hu ● ISSN 1589 1623 (Print) ● ISSN1785 0037 (Online)
DOI: http://dx.doi.org/10.15666/aeer/1802_21972211

of t, df, p and r, t (119) =3.50, p<0.05, and r=0.81. Similarly, in August, the level of cooling is lowest at site A2, where the mean of the temperature difference is 0.8℃, while site A1 presents the highest level of cooling, where the mean of the temperature difference is 1.2℃ (t (119) =3.49, p<0.05, r=0.74).

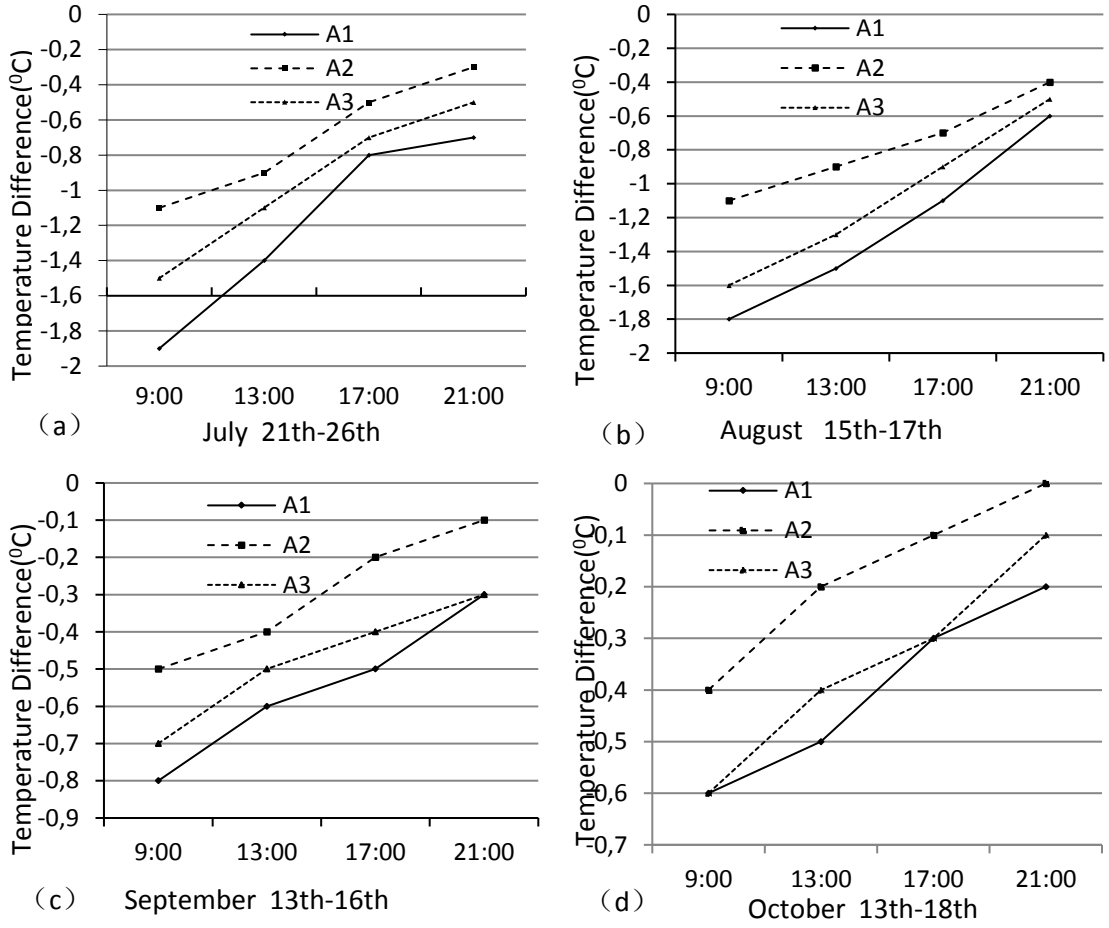

Figure 4. *Temperature differences for different sites at different periods, ΔT is the mean of the temperature differences in each measuring period*

Fig. 4c-d shows the temperature difference at different measuring times for one day in September and October. Calm conditions (0.4-1.0 ms^{-1}) were encountered in the two monitoring sessions, and light cloudiness was observed for the two periods. Likewise, the variation of the temperature difference is similar to that discussed above, so similar conclusions can be derived from the two periods. However, the mean of the temperature difference is 0.4℃ and 0.3℃, respectively, in September and October, so the cooling effect is less significant in these two periods than in the former two. The highest temperature difference arises at 9:00 (-0.8 to -0.5℃ and 0.6 to 0.4℃ in September and October, respectively) and the lowest at 21:00 (-0.3 to -0.1℃ and 0.2-0℃). In September, the lowest temperature difference also arises at site A2, where the mean of the temperature difference is just 0.3℃, and the highest temperature difference is at site A1, where the mean of the temperature difference reached 0.6℃ (t (119) =2.07, p<0.05, r=0.89). In October, the lowest temperature difference is recorded at site A2, where the mean of the

http://www.aloki.hu ● ISSN 1589 1623 (Print) ● ISSN1785 0037 (Online)
DOI: http://dx.doi.org/10.15666/aeer/1802_21972211

temperature difference is 0.2℃, and the highest temperature difference is calculated at A1, where the mean of the temperature difference is up to 0.4℃ (t (119) =1.12, p>0.05, r=0.90).

The average temperature difference is calculated from the measured data from the three lakeside measurement points (A1, A2 and A3) at 4 different times per day during the study period. The temperature difference between the lakeside sites and the urban weather stations for different observation times is illustrated in *Fig. 5*.

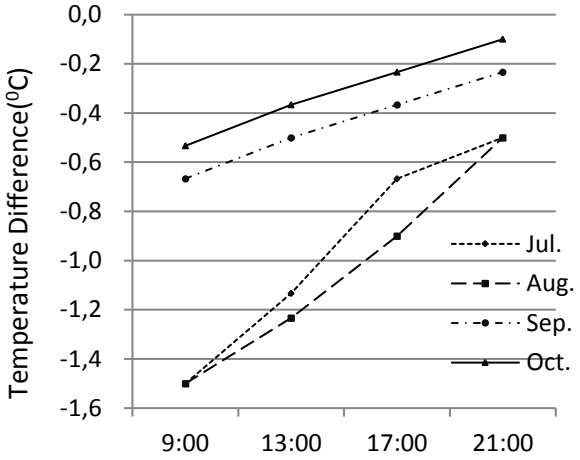

Figure 5. *Temperature differences at different time periods; ΔT is the mean of the temperature differences at the measuring times in each month*

The cooling effect is more significant in July and August than in September and October. The highest levels of cooling are shown in August, and the level of cooling in July is close to that in August, wherein the mean temperature difference is just 0.2℃ lower in August than July. Likewise, the cooling effect is no more significant in September than in October. The mean temperature difference is just 0.1℃ lower in September than in October.

The paired-samples *T-test* is applied to determine if temperature differences are significant among the four month. In terms of the statistics, the p value between July and August is 0.922, which is greater than the α level (α =0.05), so we fail to reject H_0. That is, there is insufficient evidence to claim that the temperature difference may be different from each other in the two month. Similarly, the statistical results show that the temperature differences are insignificant in September and October. However, the statistical result suggests that the temperature difference between August and September is significant, where the p value is less than 0.05. The full statistical results are shown in *Table 2*.

Table 2. *The paired-samples T-test for paired comparisons from July to October*

Pair	M	Std. D	t	df	P
Jul. – Aug.	0.04	3.90	0.10	119	0.92
Aug. –Sep.	-0.55	3.10	-1.93	119	0.05
Sep. – Oct.	-0.14	2.14	-0.70	119	0.48

M is for the temperature difference between the two months. Also shown is the standard deviation (Std. D), the t statistic (t), the degrees of freedom (df), and the two-tailed significance (P)

http://www.aloki.hu ● ISSN 1589 1623 (Print) ● ISSN1785 0037 (Online)
DOI: http://dx.doi.org/10.15666/aeer/1802_21972211

Effect of different lakeshore forms on the UHI

The cooling from the lake varies with the different forms of the lake bank, as illustrated in *Fig. 6*, with greater cooling found at the vegetated site and with less cooling at the impermeable site. Furthermore, a higher ambient air temperature contributes to greater cooling from July to October. The air temperature is higher in August than in the other measuring months, and the cooling effect is the most significant. Three type of urban forms (A is a vegetated site, B is a permeable site and C is an impermeable site) are adjacent to the lakeshore. At the A sites in August, the mean temperature difference reached 1.6℃ at 10:00. At the same time, the average temperature difference was just 0.8℃ and 0.6℃, respectively, at the B sites and C sites. Moreover, the level of cooling fell from 10:00 to 22:00. Similarly, a difference in the cooling effect derived from the different lakeshore forms was found in the other measuring months, but the difference of cooling was insignificant between B and C. By October, the difference of 0.03℃ between B and C is negligible.

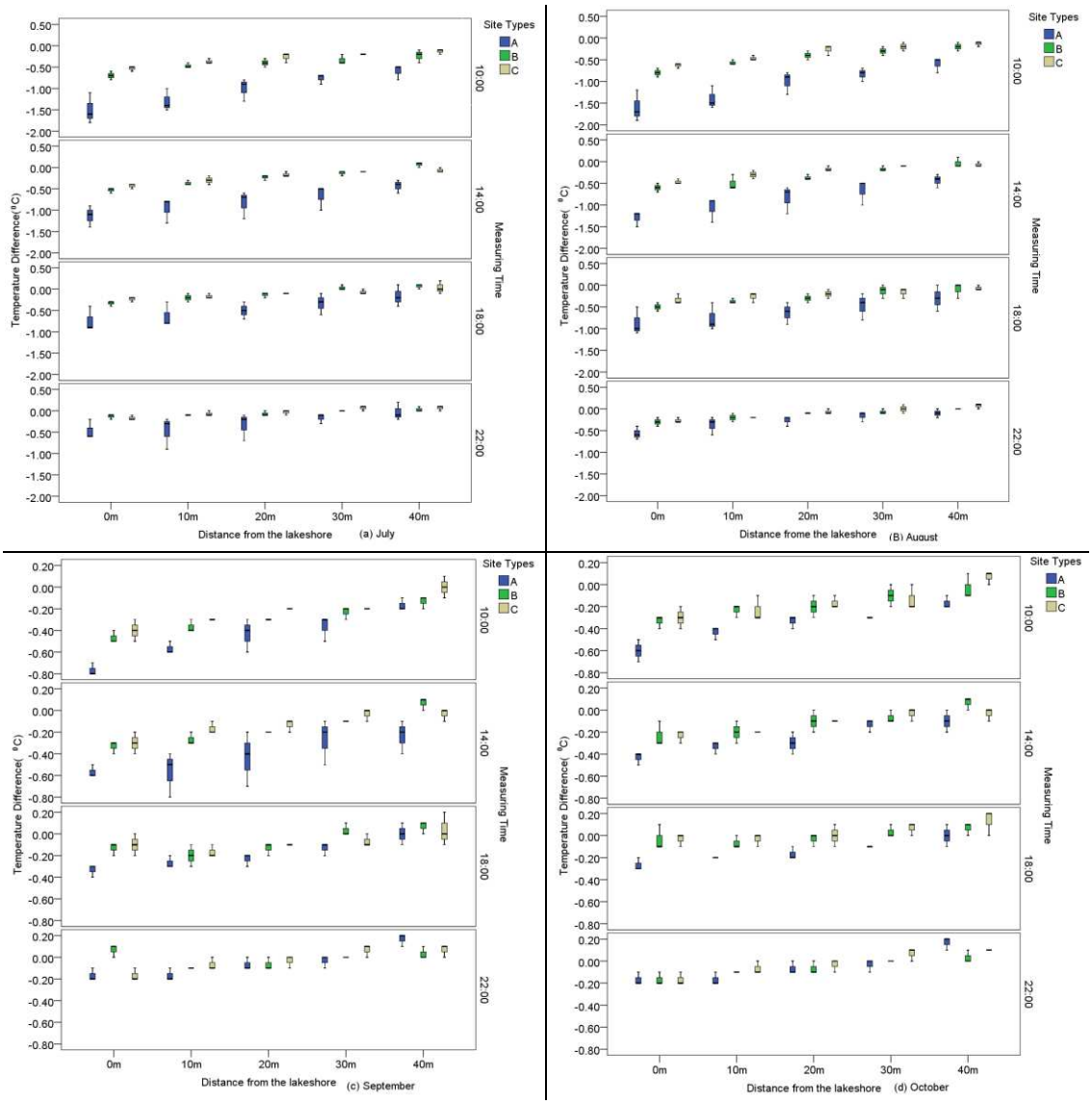

Figure 6. *Temperature differences at different distances from July to October, A represents the vegetated site, B represents the permeable site, and C represents the impermeable site*

http://www.aloki.hu ● ISSN 1589 1623 (Print) ● ISSN1785 0037 (Online)
DOI: http://dx.doi.org/10.15666/aeer/1802_21972211

Effect of distance from the water body on the UHI

The distance from the lake bank has significant effects on cooling. *Fig. 6* presents the variation in cooling across the different distances. Longer distances from the lakeshore are responsible for less cooling from July to October. At all measuring sites, the level of cooling 40 m from the lakeshore is less than 0.6℃, and there is little variation depending on the form of the lake bank in warmer months. For example, the temperature difference of A, B and C is just 0.6℃, 0.2℃ and 0.1℃, respectively, at 10:00 in August. However, the variation caused by lakeshore land cover can be ignored at 22:00 in October because each of the temperature differences of the three land covers is close to 0℃. Overall, the results indicate that vegetated sites next to the lake bank increase the cooling level. That is, the cooling effect is more significant at A sites than at B and C sites. *Fig. 6a-d* shows the average ΔT for each measuring time when combining the four periods, with values shown separately for the sites from 0 m to 40 m adjacent to the lakeshore. Very high levels of cooling are shown at the sites adjacent to the lakeshore, which reduce moving away from the lakeshore. The same trend of a cooling drop is observed from the morning to the night.

Discussion

Effect of the water body on cooling

Site A1 was located on the western lakeshore. Because concrete brick was paved at a distance of 1-2 m from the lake bank and the measuring location was 1.5 m above the water body adjacent to the lakeshore, there was no vegetation on the ground below the measuring location. Both site A2 and site A3 were also adjacent to the water body, and the measuring conditions of the two sites were similar to each other. The two measuring location were also 1.5 m above the water surface, but each of the grounds below the two measuring locations was filled with vegetation. The results above show that the cooling effect at A1 is more significant than that at the other two sites. However, the fact that vegetated land cover relieves urban heat is well known, so the result above also shows that the vegetated lakeshore form (A type) plays a greater role in lowering air temperature compared with the permeable sites and the impermeable sites. Why is the cooling effect at A1 the most significant? At the same time, the level of cooling is more significant at site A3 than at site A2. The difference in the cooling effect among the three measuring sites may relate to water temperature. Analysing the data on water temperature, the water temperatures at site A1 and site A3 are lower than that at site A2, especially in the early morning. In fact, cool spring water flows into the inlets of the lake, and A2 is further away from the water inlet compared with A1 and A3. *Fig. 7* shows the variation of the average water temperature at A1, A2 and A3 in August. Water temperature increases from 9:00 to 16:00, and it then declines in the latter measuring time intervals. The difference between the air temperature at the UWS and the water temperature rises from 9:00 to 13:00, and it then falls continually. The variation of the difference is out of sync with the cooling level, which suggests that other factors are also responsible for the cooling level.

Effect of climatic condition on cooling

Under the conditions of the same temperature interval, the level of cooling in July and August is more significant than that in September and October. Furthermore, there is a distinct cooling difference at different measuring times of the same month. *Fig. 8* shows

http://www.aloki.hu ● ISSN 1589 1623 (Print) ● ISSN1785 0037 (Online)
DOI: http://dx.doi.org/10.15666/aeer/1802_21972211

the variation of temperature differences in similar temperature conditions. The air temperature varied from 14.1 to 31.7℃ in the whole research period. With the maximum temperature difference of nearly 18℃, the interval of 2℃ is chosen in the statistical analysis. In the interval of 14-16℃, the mean of the air temperature at both 9:00 and 21:00 in October belongs to this interval, but the cooling effect at the two measuring times differs from 0.5 to 0.1℃. Furthermore, the difference in the cooling effect from 9:00 in July and 9:00 in August to 21:00 in July and 13:00 in September is more significant, from 1.5 to 0.5℃. However, the contribution to cooling at 21:00 in September and 17:00 in October is approximately equivalent in the interval of 16-18℃. Similar results are found at 13:00 in July and August in the interval of 30-32℃. These analyses suggest that other factors aside from the air temperature, such as solar light intensity, wind speed and water temperature, may have great influences on cooling. Research over the past two decades has shown significant correlations between temperature difference and these factors (Hathway and Sharples, 2012; Zhao et al., 2014; Li et al., 2014).

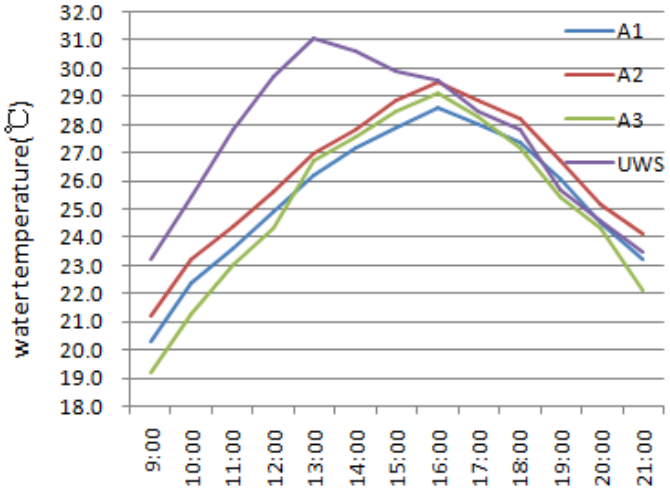

Figure 7. *Variation of the average water temperature at A1, A2 and A3 in August compared with the average air temperature of the UWS*

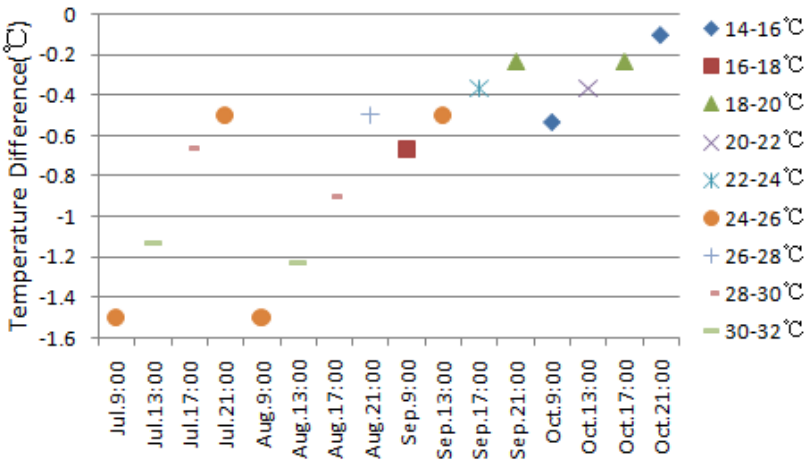

Figure 8. *The comparison of the temperature difference at different times during the entire study period. The right legend symbols represent different temperature conditions*

http://www.aloki.hu ● ISSN 1589 1623 (Print) ● ISSN1785 0037 (Online)
DOI: http://dx.doi.org/10.15666/aeer/1802_21972211

Advantages and limitations of the study

Numerous research have examined cooling effect of water bodies on the urban heat islands. this study employed the data from meteorological stations and field observation to evaluate the role of water bodies to mitigate urban heat islands during the two seasons. Hathway and Sharples (2012) found the cool island effect becomes more obvious during a spring/summer period as the temperature rose, and this conclusion was consistent with this paper and Xu et al. (2010), but we found that landscape type near lakeshore had different impact on cooling effect. Compared with data from meteorological stations and field observation, remote sensing images can provide more information on land use as well as retrieve land surface temperatures in larger areas. Many literature have showed the water bodies and adjacent landscape forms have important effect on land surface temperatures (Weng, 2009; Sun and Chen, 2012; Li et al., 2013; Kong et al., 2014; Cai et al., 2018). Although remote sensing images can retrieve land surface temperatures on a large scale, remote sensing images obtained are at a fixed time at a certain interval. In future studies, we will use field observation and remote sensing data to combine to analyse the cooling effect of water bodies.

Conclusions

In this study in Jinan, the statistical results show, first, that the urban lake plays a considerable role on cooling the air temperature around the lake bank. Second, the lakeshore type and distance from the lake bank have a significant effect on the level of cooling.

The analytic results reveal significant cooling adjacent to the lakeshore, with an average cooling of nearly 1℃ from July to August. Following the drop in air temperature, the effect of cooling increasingly weakened, and the level of cooling of 0.3℃ in October was less significant than that in July and August. The average temperature difference of the entire period tended to reach the maximum in the mornings, with cooling at the lake bank varying from 1.9℃ to 0.4℃ depending on the different lakeshore types and different months. Furthermore, the level of cooling declined from 9:00 to 21:00 each day. The results also show that highly vegetated lakeshores play a more significant role on cooling air temperatures than those lakeshores consisting of permeable or impermeable materials. Therefore, in the planning and design of an urban lake, the designers should not only focus on landscape forms and landscape aesthetics but also pay more attention to their effect on the urban thermal environment, especially the landscape surface effect. However, the results of this research were based on measurement data from only one urban lake for two seasons, and the research was conducted for only one metropolitan area. Future studies across metropolitan areas under different climatic conditions that combine measurement data with thermal infrared imaging would be desirable to confirm and refine these findings.

Acknowledgements. This work was funded by the National Natural Science Foundation of China (Project Number 41271116) and the Public Science Research Program of Surveying, Mapping and Geoinformation (Project Number 201412016). The authors would like to thank the editor and the anonymous reviewers for their helpful comments and suggestions.

http://www.aloki.hu ● ISSN 1589 1623 (Print) ● ISSN1785 0037 (Online)
DOI: http://dx.doi.org/10.15666/aeer/1802_21972211

REFERENCES

[1] Cai, Z., Han, G., Chen, M. (2018): Do water bodies play an important role in the relationship between urban form and land surface temperature? – Sustainable Cities and Society 39: 487-498.
[2] Chang, C. R., Li, M. H., Chang, S. D. (2007): A preliminary study on the local cool-island intensity of Taipei city parks. – Landscape and Urban Planning 80: 386-395.
[3] Dai, Z., Guldmann, J. M., Hu, Y. (2019): Thermal impacts of greenery, water, and impervious structures in Beijing's Olympic area: A spatial regression approach. – Ecological Indicators 97: 77-88.
[4] Ding, S., Cao, X. (2004): Landscape Pattern Dynamics of Water Body in Kaifeng City since the End of the Qing Dynasty (ADl898-2002). – Acta Geographica Sinica 59: 956-963.
[5] Du, H., Song, X., Jiang, H., Kan, Z., Wang, Z., Cai, Y. (2016): Research on the cooling island effects of water body: A case study of Shanghai, China. – Ecological Indicators 67: 31-38.
[6] Givoni, B., Noguchi, M., Saaroni, H., Pochter, O., Yaacov, Y., Feller, N., Becker, S. (2003): Outdoor comfort research issues. – Energy and Buildings 35: 77-86.
[7] Gober, P., Brazel, A., Quay, R., Myint, S., Grossman-Clarke, S., Miller, A., Rossi, S. (2009): Using Watered Landscapes to Manipulate Urban Heat Island Effects: How Much Water Will It Take to Cool Phoenix? – Journal of the American Planning Association 76: 109-121.
[8] Grinzato, E., Bison, P. G., Marinetti, S. (2002): Monitoring of ancient buildings by the thermal method. – Journal of Cultural Heritage 3: 21-29.
[9] Guillevic, P. C., Biard, J. C., Hulley, G. C., Privette, J. L., Hook, S. J., Olioso, A., Göttsche, F. M., Radocinski, R., Román, M. O., Yu, Y., Csiszar, I. (2014): Validation of Land Surface Temperature products derived from the Visible Infrared Imaging Radiometer Suite (VIIRS) using ground-based and heritage satellite measurements. – Remote Sensing of Environment 154: 19-37.
[10] Gupta, N., Mathew, A., Khandelwal, S. (2019): Analysis of cooling effect of water bodies on land surface temperature in nearby region: A case study of Ahmedabad and Chandigarh cities in India. – The Egyptian Journal of Remote Sensing and Space Science 22: 81-93.
[11] Han, Z. (2006): Functions of urban lake and the effect of lake restoration on surrounding environment. – Environment 12-13.
[12] Hathway, E. A., Sharples, S. (2012): The interaction of rivers and urban form in mitigating the Urban Heat Island effect: A UK case study. – Building and Environment 58: 14-22.
[13] Kong, F., Yin, H., James, P., Hutyra, L. R., He, H. S. (2014): Effects of spatial pattern of greenspace on urban cooling in a large metropolitan area of eastern China. – Landscape and Urban Planning 128: 35-47.
[14] Li, D., Ai, B., Li, X. (2008): Urban Water Body Alleviating Heat Island Effect Based on RS and GIS: A Case Study of Dongguan City. – Tropical Geography 28: 414-418.
[15] Li, Z. L., Tang, B. H., Wu, H., Ren, H., Yan, G., Wan, Z., Trigo, I. F., Sobrino, J. A. (2013): Satellite-derived land surface temperature: Current status and perspectives. – Remote Sensing of Environment 131: 14-37.
[16] Li, D., Bou Zeid, E., Oppenheimer, M. (2014): The effectiveness of cool and green roofs as urban heat island mitigation strategies. – Environmental Research Letters 9: 16.
[17] Li, G., Zhang, X., Mirzaei, P. A., Zhang, J., Zhao, Z. (2018): Urban heat island effect of a typical valley city in China: Responds to the global warming and rapid urbanization. – Sustainable Cities and Society 38: 736-745.
[18] Murakawa, S., Sekine, T., Narita, K.-i., Nishina, D. (1991): Study of the effects of a river on the thermal environment in an urban area. – Energy and Buildings 16: 993-1001.
[19] Oláh, A. B. (2012): The possibilities of decreasing the urban heat island. – Applied Ecology and Environmental Research 10: 173-183.
[20] Ran, G., Hu, P., Zhang, N., Chen, X., Hu, X. (2010): Analysis of Urban Heat Island Effect

http://www.aloki.hu ● ISSN 1589 1623 (Print) ● ISSN1785 0037 (Online)
DOI: http://dx.doi.org/10.15666/aeer/1802_21972211

in Jinan. – Meteorological Science and Technology 38: 97-101.
[21] Rizwan, A. M., Dennis, L. Y. C., Liu, C. (2008): A review on the generation, determination and mitigation of Urban Heat Island. – Journal of Environmental Sciences 20: 120-128.
[22] Rosenfeld, A. H., Akbari, H., Bretz, S., Fishman, B. L., Kurn, D. M., Sailor, D., Taha, H. (1995): Mitigation of urban heat islands: materials, utility programs, updates. – Energy and Buildings 22: 255-265.
[23] Singh, P., Kikon, N., Verma, P. (2017): Impact of land use change and urbanization on urban heat island in Lucknow city, Central India. A remote sensing based estimate. – Sustainable Cities and Society 32: 100-114.
[24] Steeneveld, G. J., Koopmans, S., Heusinkveld, B. G., Theeuwes, N. E. (2014): Refreshing the role of open water surfaces on mitigating the maximum urban heat island effect. – Landscape and Urban Planning 121: 92-96.
[25] Su, Y. F., Foody, G. M., Cheng, K.-S. (2012): Spatial non-stationarity in the relationships between land cover and surface temperature in an urban heat island and its impacts on thermally sensitive populations. – Landscape and Urban Planning 107: 172-180.
[26] Sun, R., Chen, L. (2012): How can urban water bodies be designed for climate adaptation? – Landscape and Urban Planning 105: 27-33.
[27] Unwin, D. J. (1980): The synoptic climatology of Birmingham's urban heat island, 1965-74. – Weather 35: 43-50.
[28] Wang, X., Wang, B., Li, X. (2010): Analysis and Assessment on Main Nutritious Elements from Inner and Exterior Contamination in Daming Lake. – Journal of University of Jinan (Science and Technology): 262-267.
[29] Weng, Q. (2009): Thermal infrared remote sensing for urban climate and environmental studies: Methods, applications, and trends. – ISPRS Journal of Photogrammetry and Remote Sensing 64: 335-344.
[30] Xu, J., Wei, Q., Huang, X., Zhu, X., Li, G. (2010): Evaluation of human thermal comfort near urban waterbody during summer. – Building and Environment 45: 1072-1080.
[31] Zhao, L., Lee, X., Smith, R. B., Oleson, K. (2014): Strong contributions of local background climate to urban heat islands. – Nature 511: 216-219.

http://www.aloki.hu ● ISSN 1589 1623 (Print) ● ISSN1785 0037 (Online)
DOI: http://dx.doi.org/10.15666/aeer/1802_21972211

PROPAGATION OF *MAGNOLIA BIONDII* PAMP THROUGH STEM CUTTINGS USING EXOGENOUS HORMONES

KHAN, M. A.[1] – WANG, Y.[1] – UDDIN, S.[3] – MUHAMMAD, B.[1]–BADSHAH, M. T.[4] – KHAN, D.[5] – MUNEER, M. A.[2]– MUNIR, M. Z.[3] –JIA, Z. K.[1*]

[1]*Ministry of Education Key Laboratory of Silviculture and Conservation, Beijing Forestry University, Beijing 100083, China*

[2]*College of Grassland Science, Beijing Forestry University, Beijing 100083, China*

[3]*College of Biological Sciences and Technology, Beijing Forestry University, Beijing 100083, China*

[4]*Research Center of Forest Management Engineering of National Forestry and Grassland Administration, Beijing Forestry University, Beijing 100083, China*

[5]*College of Forestry, Beijing Forestry University, Beijing 100083, China*

**Corresponding author*
e-mail: jiazk@bjfu.edu.cn; phone: +86-10-6233-7098

(Received 30th Sep 2019; accepted 8th Jan 2020)

Abstract. The effects of exogenous hormones were optimized with different morphological characteristics of cuttings (cuttings from the different crown position, cuttings length and cuttings soaking time) for rooting in successive experiments to enhance the efficiency of vegetative propagation of *Magnolia biondii* Pamp. For this purpose, a series of experiments were conducted in a greenhouse. Application of exogenous hormones at different concentrations significantly affected the rooting of *Magnolia biondii* Pamp cuttings, we found that Indole-3-butyric acid (IBA) at 750 mg/L resulted in the highest rooting rate (78.89%). 750 mg/L IBA was further applied in all other experiments. Stem cuttings collected from the lower position of the plant crown showed higher rooting rate (79.67%) than upper and middle position. Hence, IBA 750 mg/L and cuttings collected from the lower position of the crown were further evaluated under different soaking times (60, 120, 240, 360 min) and found that 120 min soaking time significantly affected the rooting and achieved the highest rooting rate of 80.67%. In the last step of optimization of key factors that affect the propagation of *Magnolia biondii* Pamp, we checked the effect of cutting length by applying all the previously determined factors (IBA 750 mg/L, lower crown position, 120 min). We found longer cuttings (21-25 cm) gave the highest rooting rate (83.11%) rather than short cuttings. Hence, we found that optimal method includes IBA 750 mg/L, the lower part of the crown, 120 min of soaking time, and longer cuttings for vegetative propagation of *Magnolia biondii* Pamp to produce high-quality planting stock material.
Keywords: *Magnolia biondii Pamp, vegetative propagation, exogenous hormones, crown position, soaking time, cuttings length*

Introduction

Magnolia biondii Pamp belonging to family Magnoliaceae, is a deciduous and popular ornamental species distributed in northern China (Coombes, 2014). This species was discovered and introduced to the western hemisphere more than 70 years ago (Coombes, 2014). Its flowering time is from late winter to early spring before leaf growth and blooms single at the top of the branches, each flower has three sepals and six petals which shaped like spoons showing purplish-red color on the base and whitish on the rest of the part. Leaves of *Magnolia biondii* Pamp are unifoliate alternate, the leaf

http://www.aloki.hu ● ISSN 1589 1623 (Print) ● ISSN 1785 0037 (Online)
DOI: http://dx.doi.org/10.15666/aeer/1802_22132229

blade is oblong-lanceolate or ovate-lanceolate glabrous on both sides. It grows up to 12 m and shows the best performance in sandy and loamy soil on above 600 m elevation.

Great differences in the rooting ability of cuttings exist among species and cultivars (Kester et al., 1990). Stem cuttings of some cultivars root so readily that the simplest facilities and care give high rooting percentages (Kester et al., 1990). On the other hand, cuttings of many cultivars or species have yet to be rooted (Kester et al., 1990). Cuttings of some difficult cultivars can be rooted only if specific influencing factors are taken into consideration and if the cultivars are maintained at the optimum condition (Kester et al., 1990). All the species neither propagate easily nor do they respond similarly to a single method of propagation (Kester et al., 1990). There is a lack of suitable propagation method for *Magnolia biondii* Pamp species on large scale through stem cuttings, but there are some published reports available in *Magnolia biondii* Pamp species (Zhang et al., 2003; Wang et al., 2017). However, these studies did not demonstrate a proper protocol for its propagation. So, we here optimized a complete propagation scheme for *Magnolia biondii* Pamp species.

On the other hand, the propagation method with stem cuttings is recommended for quicker establishment faster production (Kester et al., 1990). Adventitious rooting is a critical step in vegetative propagation because cutting do not form roots or they form poor quality root system (Villacorta-Martín et al., 2015). The formation of adventitious roots in mini-cuttings includes the formation of meristematic cells niches (i.e., initial cells and/or target cells), which are dependent on external and internal factors (Dettmer et al., 2009; Papp and Plath, 2011). Reproduction through cuttings is reproduction made by use of a piece taken from the stem, root, or leaf of a plant, cuttings are put in suitable environmental conditions and are forced to form roots (Sevik and Turhan, 2015). Adventitious roots are distinct from lateral roots in that they are formed from any tissue that is not a root, such as leaves and stems, naturally or in response to altered growth environments (Bellini et al., 2014; Geiss et al., 2009). Adventitious rooting is an essential step in the vegetative propagation of economically important horticultural and woody species (Geiss et al., 2009); therefore, it is very important to enhance their growth by using different plant growth regulators.

All classes of exogenous hormones auxin, cytokinin, gibberellin, ethylene, and abscisic acid, and ancillary compounds such as growth retardants/inhibitors, polyamines, and phenolics influence root initiation either directly or indirectly (Davis and Haissig, 1990). Exogenous hormones are commonly used in plant propagation methods to enhance the root development, number, and quality of roots. Generally, a high or low concentration of exogenous hormones supplemented in the propagation method could promote or inhibit cell growth. In several species, rooting competence has been associated with the presence of inductive factors such as exogenous hormones. Auxin and gibberellin particularly IBA, NAA, IAA, and GGR_6 have been reported to induce rooting in many of the plant species with varied success. The response of different exogenous hormones to percent success varied from species to species, changing physiological and environmental conditions. Most of the researchers have reported IBA and NAA as better growth regulators than others for inducing rooting in cuttings due to their stable nature. During the propagation through cuttings, there are some other factors that affect the rooting like environmental conditions, age of stock, rooting media, and concentration of exogenous hormones (Kester et al., 1990). Among

http://www.aloki.hu ● ISSN 1589 1623 (Print) ● ISSN 1785 0037 (Online)
DOI: http://dx.doi.org/10.15666/aeer/1802_22132229

all these factors, the concentration of exogenous hormones contributes significantly towards successful propagation.

Rooting ability of different plant species through stem cuttings can also be affected by the several factors such as the crown position of the parent plant, length of the cuttings and soaking time of the cuttings into the exogenous hormones (Kester et al., 1990; Leakey, 1983; Azamal and Mohinder, 2000; Elhaak et al., 2015). However, cuttings characteristics and these factors on the induction of rooting varies from species to species (Harrison-Murray and Knight, 1997). So, it imperative to include the characteristics of the cutting for the effective clonal propagation of plants (Luz et al., 2007; Lekha and Lalji, 2010).

Propagation through cuttings needs more concentration and scientific knowledge. Propagator need to keep thorough records of procedures and the seasonal condition of plant materials and conduct small tests to achieve optimum success for their particular propagation system (Dirr, 1989). Treatment of the cuttings with exogenous hormones, the size of the cuttings, humidity and bottom heat is desirable for rapid rooting. Cuttings must be taken from nutritionally healthy stock plants (Davies Jr, 1988). The propagation material for hardwood cuttings should be collected from healthy, fairly vigorous stock plants growing in full sunlight (Kester et al., 1990). All these factors and substances cannot be used without scientific knowledge, experiments and proper research. For this purpose and to give a proper scheme and scientific method to propagate *Magnolia biondii* Pamp, different experiments in the greenhouse and in the laboratory have been done. Despite being so special ornamental and medicinal features, this species got no attention for its propagation and research. *Magnolia Biondii* Pamp has not yet any published reports that demonstrate the potential for successful propagation.

The objectives of our study were to evaluate the effects of exogenous hormone type; soaking time on the rooting success; effect of the position of the stock plant crown and length of cuttings; and establish a proper cutting propagation scheme for *Magnolia biondii* Pamp to produce more elite clone plants.

Materials and methods

Plant material and experiment site

The plant material of *Magnolia biondii* Pamp cuttings were obtained from the seven-years-old mother plants located at the Silviculture test station of Beijing Forestry University at Jiufeng, Beijing in late June. The experiment was conducted in the greenhouse (temperature: 20-30 °C, relative humidity: about 80%) located near the test station in 2018-2019. The geographical coordinates of the test station are 40.3054" N and 116.05045" E (*Fig. 1*). This area has temperate humid monsoon climate zone with hot, variable rainy summers and dry cold winters. The average annual temperature is 12.5 °C with an accumulating temperature of 42 °C, and the number of annual sunshine hours is 2662 h.

Experiment-1: effect of exogenous hormones on the rooting

A complete randomized block design was set using six different concentrations (250, 500, 750, 1000, 1250, and 1500 mg/L) of four different plant growth regulators (GGR_6, NAA, IBA, IAA) along with water-treated control group (0 mg/L) with each plant growth

http://www.aloki.hu ● ISSN 1589 1623 (Print) ● ISSN 1785 0037 (Online)
DOI: http://dx.doi.org/10.15666/aeer/1802_22132229

regulator. A total of 28 treatments were performed in each replication and the experiment was replicated three times. The layout of the experiment was as follows (*Fig. 2*).

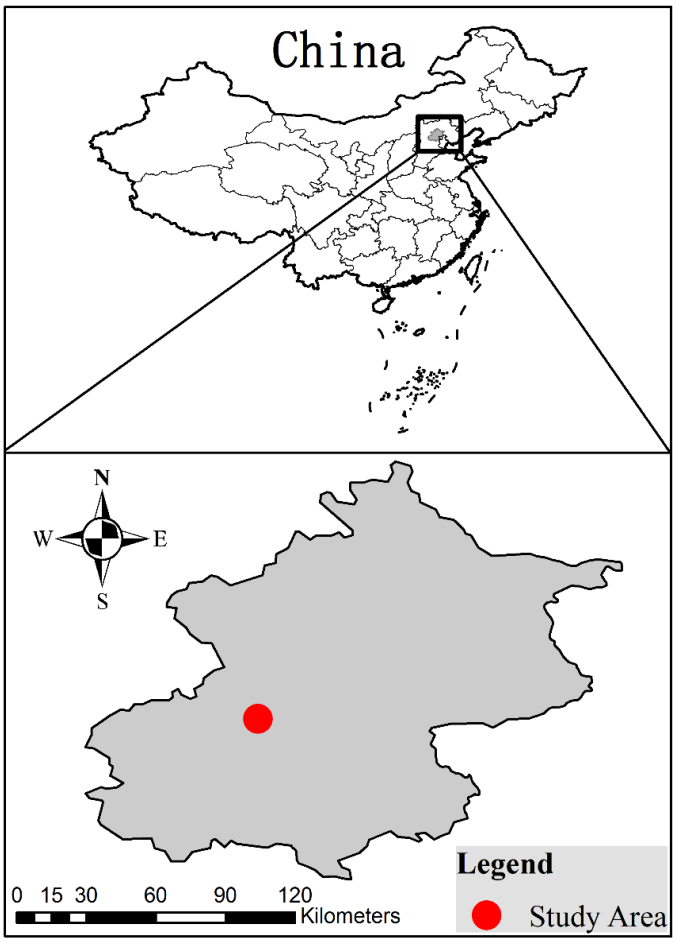

Figure 1. *Red point in the map shows the study area; Silviculture Test Station of Beijing Forestry University, Jiufeng Beijing, China*

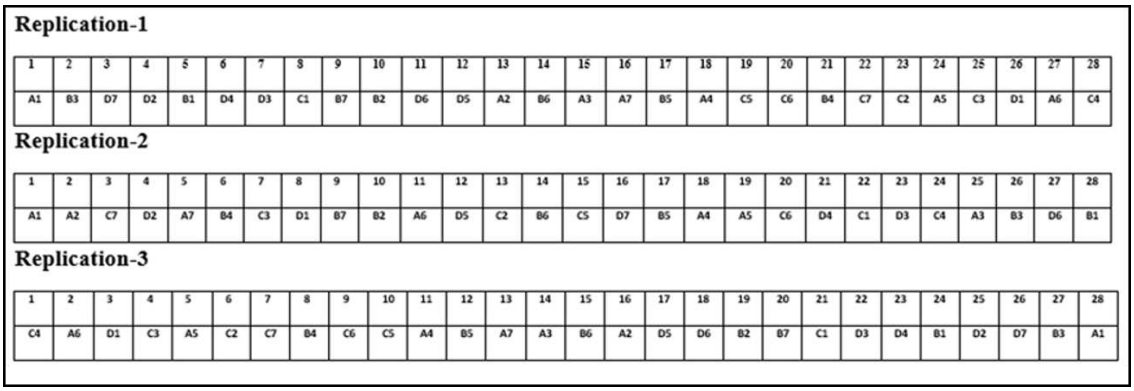

Figure 2. *Here A represents GGR_6, B represents NAA, C represents IBA, and D represents IAA. 1-7 represents different concentrations of plant growth regulator in which 1 represents 0 mg/L (control), 2 represents 250 mg/L, 3 represents 500 mg/L, 4 represents 750 mg/L, 5 represents 1000 mg/L, 6 represents 1250 mg/L and 7 represents 1500 mg/L*

http://www.aloki.hu ● ISSN 1589 1623 (Print) ● ISSN 1785 0037 (Online)
DOI: http://dx.doi.org/10.15666/aeer/1802_22132229

Culture of *Magnolia biondii* Pamp stems cuttings were established in the greenhouse. The environment of the greenhouse was uniform and did not cause errors in the results of each block. The soil beds consisted of the river sand. The length and width of the soil bed were 6 × 1.5 m and depth was 15 cm. Before shifting the treated cuttings into the beds, the rooting media was fully disinfected by 0.2% potassium permanganate solution (fungicide). The soil was pulverized and misted well. Softwood branches were brought from the mother trees in the morning and converted into the desired stem cuttings. The prepared cuttings were washed under running tap water several times and then shifted into the carbendazim solution for 15 min to disinfect before sticking in the soil. Exogenous hormones concentrations were prepared and cuttings were kept into the concentrations for 30 min and then cuttings were implanted into the soil according to the proposed experimental design. Cuttings were irrigated through a misting shower system.

Experiment-2: Effect of stem cuttings collected from the different positions of the tree crown

This experiment was conducted to check the effect of the crown position of the stock plant on the rooting. For this experiment shoots for the preparation of cuttings were collected from three different crown positions (upper, middle, lower). These cuttings were treated with IBA 750 mg/L (selected from experiment-1). Thirty cuttings per treatment were used and the experiment was repeated three times.

Experiment-3: Effect of soaking time of the cuttings into the exogenous hormone

In this experiment, we evaluated the effect of soaking time of cuttings into the IBA 750 mg/L with the lower crown position that was selected in the first and second experiments respectively. Prepared cuttings were soaked for four different time periods i.e., 60 min, 120 min, 240 min and 360 min. Thirty cuttings per treatment were prepared and the experiment was replicated three times.

Experiment-4: Effect of cuttings size on the rooting

In this experiment, four classes of stem cuttings length were prepared to select the best cutting length for the propagation of *Magnolia biondii* Pamp. Four different classes of cuttings i.e., 5-10 cm, 11-15 cm, 16–20 cm and 21-25 cm were prepared from the lower crown position and soaked into IBA 750 mg/L for 120 min. Thirty cuttings per treatment were used and the experiment was repeated three times.

Analytical measurements

After the completion of experiments, cuttings were carefully uprooted and rinsed with the water. First of all, the number of roots of each cutting was measured by counting. The rooting rate was measured by *Equation 1:*

$$Rooting\ rate = \frac{Number\ of\ rooted\ cuttings}{Total\ number\ of\ cuttings} \times 100 \qquad \text{(Eq.1)}$$

For the measurement of total root length, root diameter, and root volume, roots were scanned and these scanned images were further analyzed with WinRHIZO Pro 2013a software to measure aforesaid root parameters.

http://www.aloki.hu ● ISSN 1589 1623 (Print) ● ISSN 1785 0037 (Online)
DOI: http://dx.doi.org/10.15666/aeer/1802_22132229

Statistical analysis

Experiments were performed by following Complete Randomized Block Design (CRBD). Data were analysed using Analysis of Variance (ANOVA) method and least significant difference test ($LSD_{0.05}$) by using IBM SPSS Statistics v20. Graphs were prepared using Origin Pro 2018 software.

Results

Effect of exogenous hormones on the rooting

The macro propagation methods play an important role in the improvement of many plant species and have been discovered for the propagation of many valuable species, particularly the ornamental, aesthetical, rare and endangered species (Jamir et al., 2016). Propagation system through stem cuttings can be a significant step in vegetative propagation. This is the first research-based report which established a scientific method for the proliferation of roots from the stem cuttings of *Magnolia biondii* Pamp using different exogenous hormones.

The rooting rate was determined in term of rooting percentage. In this study, it was found that among different exogenous hormones, IBA with its different concentrations has a more obvious trend. With the increase in the concentration of IBA rooting rate increased and reached to its peak value and then decreased continuously with the increase in concentration. It showed the highest rooting rate at the concentration of 750 mg/L about 78% in comparison with other exogenous hormones i.e., GGR_6, NAA, IAA and control. Statistically significant differences ($F(6, 14) = 11.5$, $p = 0.0001$)) were found for IBA. While, GGR_6, NAA, and IAA also revealed the highest rooting rate at 750 mg/L (34%), 1000 mg/L (63%), and 1250 mg/L (43%) respectively. Moreover, there were also found statistically significant differences for all these exogenous hormones among different concentrations. Compared to all other exogenous hormones and their concentrations, GGR_6 performed very low rooting rate. IAA performed better than GGR_6, but with comparison to NAA and IBA, IAA has a very low rooting rate. So, IBA 750 mg/L comparatively performed best than other exogenous hormones (*Table 1*).

Table 1. *Effect of exogenous hormones on the rooting rate*

Conc. (mg/L)	GGR_6	NAA	IBA	IAA
0	24.44 ± 2.60^{ab}	25.56 ± 0.88^{d}	32.22 ± 1.45^{e}	17.78 ± 0.33^{b}
250	30.00 ± 1.15^{ab}	47.78 ± 0.88^{bc}	50.00 ± 1.53^{cd}	30.00 ± 1.53^{ab}
500	24.44 ± 0.88^{ab}	44.44 ± 1.20^{c}	56.67 ± 2.08^{bc}	35.56 ± 4.18^{ab}
750	34.44 ± 0.88^{a}	61.11 ± 1.20^{a}	78.89 ± 1.45^{a}	36.67 ± 3.51^{ab}
1000	18.89 ± 0.33^{bc}	63.33 ± 0.58^{a}	67.78 ± 1.33^{ab}	42.22 ± 1.67^{a}
1250	8.89 ± 0.88^{c}	56.67 ± 0.58^{ab}	50.00 ± 1.00^{cd}	43.33 ± 0.58^{a}
1500	7.78 ± 0.33^{c}	43.33 ± 1.15^{c}	38.89 ± 0.67^{de}	27.78 ± 0.67^{ab}

Values followed by the same letters show non-significant differences while different letters show significant differences ($LSD_{0.05}$) for each hormone at different concentrations. Data are mean ± SE

Different plant growth regulators resulted in significant differences in the mean number of roots per cutting. The number of roots was significantly ($P < 0.05$) effected

http://www.aloki.hu ● ISSN 1589 1623 (Print) ● ISSN 1785 0037 (Online)
DOI: http://dx.doi.org/10.15666/aeer/1802_22132229

by exogenous hormones. IBA 750 mg/L had the highest number of roots (20 pcs) which significantly differed with its other concentrations, control, and other exogenous hormones. Cuttings treated with the different concentrations of NAA had also significant ($F (6, 14) = 17.9$, $p = 0.0000$) ($P < 0.05$)) results. NAA 750 mg/L and NAA 1000 mg/L showed non-significant results i.e. 12 pcs and 11 pcs respectively but, they were significantly higher than its control (2 pcs). IAA did not show good results compared to IBA and NAA. IAA 1000 mg/L had the highest number of roots (5 pcs) compared to its other concentrations. Generally, GGR_6 had a very low mean number of roots. The highest mean number of roots within the GGR_6 concentrations were found at 750 mg/L (3 pcs) which did not have a much difference compared to its control (*Fig. 3a*).

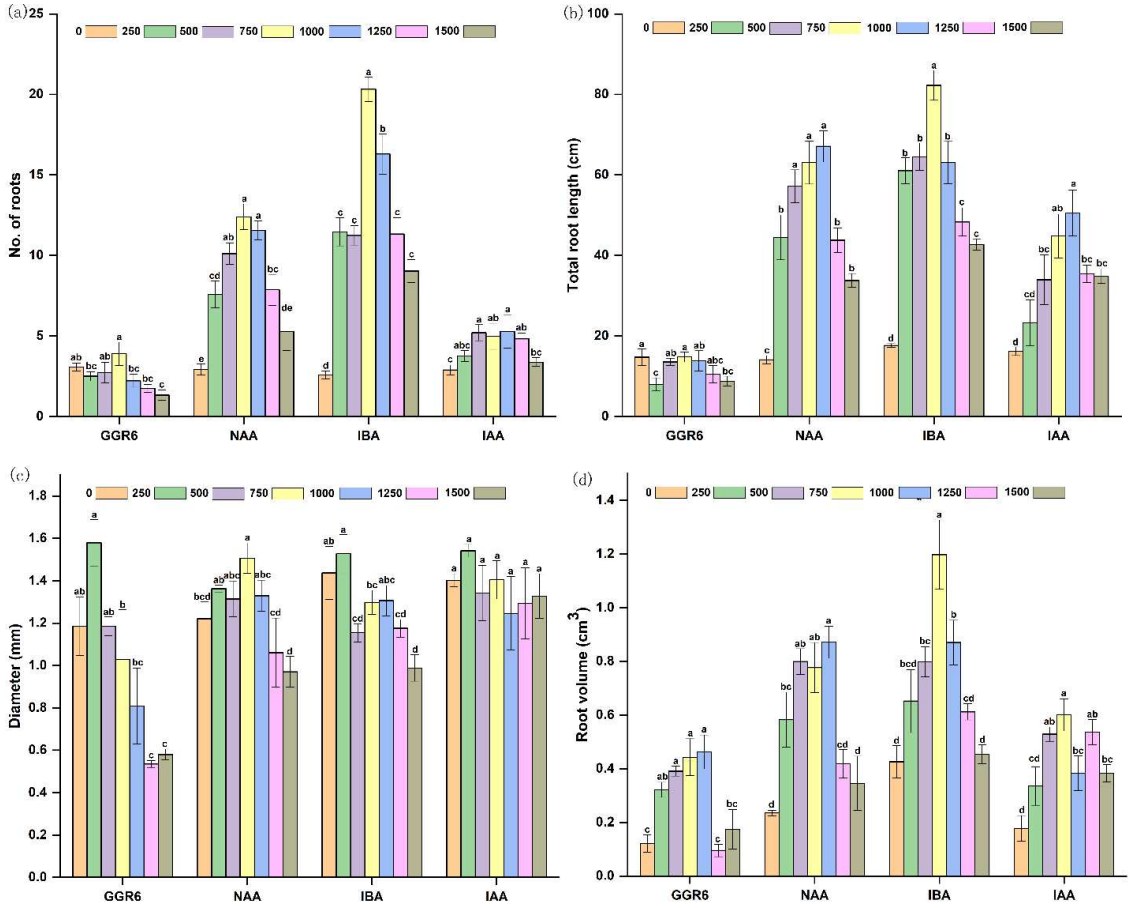

Figure 3. *Effect of different plant growth regulators on (a) the average number of roots per cutting; (b) mean total root length per cutting; (c) mean root diameter per cutting; (d) mean root volume per cutting at different exogenous hormones and their different concentrations. Alphabets on the top of each bar showing the $LSD_{0.05}$ difference. The same letters show the non-significant differences, while the different letters show the significant differences between different concentrations for each exogenous hormone*

One-way analysis of variance ANOVA indicated that mean total root length was significantly influenced by exogenous hormone application. Maximum mean total root length was found in IBA 750 mg/L (82 cm) which was significantly ($F (6, 14) = 38$, $p = 0.0000$) higher than control. Total root length in IBA increased continuously and

http://www.aloki.hu ● ISSN 1589 1623 (Print) ● ISSN 1785 0037 (Online)
DOI: http://dx.doi.org/10.15666/aeer/1802_22132229

reached its peak at 750 mg/L and then decreased. NAA had also an obvious trend, as it increased continuously and reached its peak at 1000 mg/L with 67 cm mean total root length and then decreased. IAA significantly showed higher mean total root length at 1000 mg/L (50 cm) compared to control (16 cm). Among all four plant growth regulator types, GGR_6 showed very low root length. Results showed that GGR_6 had similar mean total root length to its control at 750 mg/L (*Fig. 3b*).

Root diameter was observed almost the same in all treatments. Among all exogenous hormone types, GGR_6 at 250 mg/L showed highest mean root diameter (1.57 mm) and indicated the significant results ($(F (6, 14) = 7.98, p = 0.0007)$). GGR_6 at 500 mg/L showed significantly same mean root diameter (1.18 mm) to its control and then continuously decreased and reached to 0.53 mm at 1250 mg/L concentration. NAA 750 mg/L showed the highest mean root diameter (1.5 mm) among its all concentrations and control. IBA 250 mg/L significantly showed 1.5 mm mean root diameter. IBA 1500 mg/L significantly showed the lowest root diameter (0.98 mm). According to ANOVA, IAA showed non-significant results. IAA 250 mg/L showed a 1.54 mm root diameter which was non-significant to all its concentrations and control (*Fig. 3c*).

The application of plant growth regulators triggered and enhanced the root volume. Among all PGRs and their concentrations, IBA showed significant trend because IBA at 750 mg/L significantly ($(F (6, 14) = 10.8, p = 0.0001)$) showed highest mean root volume (1.19 cm^3) compared to all other exogenous hormone concentrations and its control group. Mean root volume trend was not obvious in NAA application because increasing and decreasing trend was found. NAA at 1000 mg/L showed maximum root volume (0.87 cm^3). IAA showed highest root volume at 750 mg/L (0.6 cm^3) which was not higher than IBA and NAA applications. IAA 1000 mg/L and 1500 mg/L showed non-significant results. GGR_6 showed low root volume compared to all other exogenous hormone applications. GGR_6 at 1000 mg/L showed the highest mean root volume (0.46 cm^3) which was non-significant to 750 and 500 mg/L concentrations. Lowest mean root volume was found in 1250 mg/L (0.09 cm^3) which was non-significant to its control application (*Fig. 3d*).

Principal component analysis

For the screening and evaluation of exogenous hormones and to provide a comprehensive analysis, the principal component analysis was performed on the first experiment. The variance and variance cumulative rate of each component is shown in *Table 2*. SPSS extracted two components along with their eigenvalues. The cumulative contribution of the two principal components is 94.387%.

Table 2. *Variance cumulative contribution rate of each composition*

Components	Initial Eigenvalue			Extracted sum square		
	Total	Variance (%)	Accumulation (%)	Total	Variance (%)	Accumulation (%)
1	3.880	77.609	77.609	3.880	77.609	77.609
2	0.839	16.778	94.387	0.839	16.778	94.387
3	0.126	2.529	96.916			
4	0.086	1.730	98.645			
5	0.068	1.355	100.000			

http://www.aloki.hu ● ISSN 1589 1623 (Print) ● ISSN 1785 0037 (Online)
DOI: http://dx.doi.org/10.15666/aeer/1802_22132229

Two principal component expressions and the formulas of the comprehensive scoring are sorted out as follows:

$$C1 = 0.0965\,X1 + 0.0958\,X2 + 0.0954\,X3 + 0.0471\,X4 + 0.948\,X5 \quad \text{(Eq.2)}$$

$$C2 = -0.032\,X1 - 1.20\,X2 - 0.2X3 + 0.881\,X4 - 0.083\,X5 \quad \text{(Eq.3)}$$

$$C = \frac{\lambda_1 C_1 + \lambda_2 C_2}{\lambda_1 + \lambda_2} \quad \text{(Eq.4)}$$

Among the formulas given above, C_1 indicates the main component 1 score while C_2 indicates the main component 2 score. C indicates the comprehensive score and X_1 to X_5 indicates rooting rate, total root length, number of roots, root diameter and root volume respectively. λ_1 and λ_2 indicate the variance of main component 1 and main component 2 respectively and it is known from *Table 5* that $\lambda_1 = 77.609$ and $\lambda_2 = 16.778$.

The five rooting parameters values are substituted into *Equations 2, 3* and *4*. The score and ranking of each treatment are listed in *Table 3*. According to the comprehensive ranking among four exogenous hormone treatments, the application of IBA to propagate *Magnolia biondii* Pamp has a better overall effect, especially at the concentration of 750 mg/L.

Table 3. *Principal component scores and comprehensive scores of each process*

	C1	C2	C	Rank
IBA 750	2.671	-0.217	2.158	1
IBA 1000	1.668	0.001	1.372	2
NAA 1000	1.338	0.223	1.140	3
NAA 750	1.076	0.913	1.047	4
IBA 500	1.251	-0.463	0.946	5
IBA 250	0.689	1.019	0.748	6
NAA 500	0.788	0.202	0.684	7
IBA 1250	0.746	-0.336	0.553	8
NAA 250	0.252	0.535	0.302	9
NAA 1250	0.453	-0.638	0.259	10
IAA 750	-0.082	0.758	0.067	11
IBA 1500	0.352	-1.002	0.111	12
IAA 1000	-0.009	0.132	0.016	13
IAA 1250	-0.098	0.370	-0.015	14
IAA 500	-0.249	0.535	-0.110	15
NAA 1500	-0.038	-0.908	-0.192	16
IAA 1500	-0.601	0.530	-0.400	17
IAA 250	-0.909	1.409	-0.497	18
IBA 0	-0.853	1.045	-0.515	19
GGR 750	-0.442	-0.610	-0.472	20
GGR 250	-1.230	1.643	-0.719	21
GGR 500	-0.848	0.037	-0.691	22
NAA 0	-0.999	0.187	-0.788	23
IAA 0	-1.283	0.888	-0.897	24
GGR 1000	-0.594	-1.460	-0.748	25
GGR 0	-1.086	0.049	-0.885	26
GGR 1500	-0.991	-2.329	-1.229	27
GGR 1250	-0.972	-2.514	-1.246	28

http://www.aloki.hu ● ISSN 1589 1623 (Print) ● ISSN 1785 0037 (Online)
DOI: http://dx.doi.org/10.15666/aeer/1802_22132229

Stem cuttings collected from the different positions of the tree crown

Analysis of variance indicated that cuttings collected from different position of the tree crown significantly affected all rooting parameters. All the rooting parameters either continuously increased or continuously decreased according to the position of the tree crown. The highest rooting rate was achieved with the cuttings collected from the lower part of the tree crown. *Table 4* depicted that rooting rate varied from 19.0% (upper position) to 79.67% (lower position), whereas the number of roots ranged from 1.73 to 22 roots from the upper part to the lower part of the tree crown respectively. Total root length also significantly increased from upper position to middle and then highest total root length (113.67 cm) was found in the lower position of the tree crown. Root diameter showed significantly different results from all other rooting parameters. Maximum mean root diameter (1.41 mm) was achieved in the upper position of the tree crown while lowest mean root diameter (1.03 mm) was found in the lower position of the tree crown, and significant results were achieved ($F (2, 6) = 11.1$, $p = 0.0096$). Root volume showed an obvious trend, increased from upper position to the lower position of the crown. It showed the mean root volume of 0.28 cm^3 at the upper position and 1.08 cm^3 at the lower position of the crown.

Table 4. *The effects of the cuttings taken from different positions of the trees on the rooting*

Tree crown	RR (%)	NR (pcs)	TRL (cm)	RD (mm)	RV (cm^3)
Upper	19.00 ± 1.52^{c}	1.73 ± 0.27^{c}	17.40 ± 1.28^{c}	1.41 ± 0.05^{a}	0.28 ± 0.03^{b}
Middle	63.33 ± 0.66^{b}	11.12 ± 1.17^{b}	74.87 ± 2.94^{b}	1.11 ± 0.07^{b}	0.90 ± 0.13^{a}
Lower	79.67 ± 2.33^{a}	22.04 ± 1.65^{a}	113.67 ± 4.93^{a}	1.03 ± 0.04^{b}	1.08 ± 0.02^{a}

Values followed by the same letters show non-significant differences while different letters show significant differences ($LSD_{0.05}$) for each rooting parameter at different crown position. RR indicates the rooting rate, NR number of roots, TRL total root length, RD root diameter, and RV indicates root volume. Data are mean ± SE

Effect of cuttings immersion time into the exogenous hormone

The rooting rate varied significantly between different immersion time periods of cuttings into the exogenous hormone ($P < 0.05$, ANOVA) (*Table 5*). Maximum rooting rate (80.67%) was achieved in the cuttings treated with IBA 750 mg/L for 120 min, while the minimum rooting rate was found 62.67% for 360 min. Cuttings treated for 60 min also yielded 77.33% rooting which is non-significant to 120 min treatment. The maximum number of roots were found in the cuttings treated for 120 min (27.21 roots), while the minimum number of roots were found in the cuttings treated for 360 min (15.47 roots). Total root length, root diameter, and root volume had no significant differences for different immersion time.

The effect of different cuttings length on the rooting

In this study, four-length classes of the cuttings were used to check their effect on the rooting. Our results revealed that the length of the cuttings significantly affected the rooting rate, number of roots, total root length and root volume, while no significant effect was found in root diameter (*Table 6*). Direct relation was found between the length of the cuttings and rooting rate. Maximum rooting rate (83.11%) was found in the cuttings having 21-25 cm length while the minimum rooting rate was found in 5-

http://www.aloki.hu ● ISSN 1589 1623 (Print) ● ISSN 1785 0037 (Online)
DOI: http://dx.doi.org/10.15666/aeer/1802_22132229

10 cm long cuttings (49.33%). Cuttings of class length 21-25 cm produced the highest number of roots (29.67), while the lowest number of roots were found in 5-10 cm length class cuttings (8.83). The highest total root length and root volume were also found in the longer cuttings (21-25 cm). In case of root diameter, non-significant results were found ($F(3, 8) = 1.30$, $p = 0.34$)). Maximum root diameter (1.26 mm) was found in the cuttings having the length of 11-15 cm while minimum root diameter (1.06 mm) was found in 16-20 cm long cuttings.

Table 5. *The effect of different time of immersion of the cuttings into the exogenous hormone on the rooting*

Time (min)	RR (%)	NR (pcs)	TRL (cm)	RD (mm)	RV (cm3)
60	77.33 ± 2.90^{a}	24.52 ± 0.86^{a}	116.85 ± 1.16^{a}	1.24 ± 0.09^{a}	1.15 ± 0.10^{a}
120	80.67 ± 2.33^{a}	27.21 ± 0.99^{a}	111.58 ± 4.61^{a}	1.19 ± 0.09^{a}	1.21 ± 0.23^{a}
240	73.33 ± 4.80^{ab}	26.73 ± 3.57^{a}	109.77 ± 2.63^{a}	1.12 ± 0.08^{a}	0.99 ± 0.06^{a}
360	62.67 ± 5.36^{b}	15.47 ± 1.42^{b}	106.71 ± 5.28^{a}	1.15 ± 0.04^{a}	1.02 ± 0.23^{a}

Values followed by the same letters show non-significant differences while different letters show significant differences ($LSD_{0.05}$) for each rooting parameter at different immersion times. RR indicates the rooting rate, NR number of roots, TRL total root length, RD root diameter, and RV indicates root volume. Data are mean ± SE

Table 6. *The effect of different lengths of the cuttings on the rooting*

Cutting length (cm)	RR (%)	NR (pcs)	TRL (cm)	RD (mm)	RV (cm3)
5-10	49.33 ± 2.60^{c}	8.83 ± 1.60^{c}	35.24 ± 1.93^{d}	1.10 ± 0.10^{a}	0.71 ± 0.05^{b}
11-15	55.81 ± 2.94^{c}	12.21 ± 1.50^{c}	73.94 ± 1.68^{c}	1.26 ± 0.02^{a}	1.20 ± 0.12^{a}
16-20	68.22 ± 2.61^{b}	19.00 ± 1.92^{b}	86.51 ± 1.87^{b}	1.06 ± 0.09^{a}	1.09 ± 0.09^{a}
21-25	83.11 ± 1.73^{a}	29.67 ± 0.88^{a}	108.99 ± 5.87^{a}	1.14 ± 0.06^{a}	1.21 ± 0.04^{a}

Values followed by the same letters show non-significant differences while different letters show significant differences ($LSD_{0.05}$) for each rooting parameter at different cutting lengths. RR indicates the rooting rate, NR number of roots, TRL total root length, RD root diameter, and RV indicates root volume. Data are means ± SE

Discussion

Adventitious rooting responses differently to different plant growth regulators. The previous findings also showed that exogenous hormones applications have apparent effects on rooting rate (Zhang et al., 2017; Sevik and Guney, 2013). The process of adventitious rooting is influenced by the number of internal and external factors (Kester et al., 1990; Kumar et al., 2009). Among the internal factors, the most important role is explained by the phytohormones, especially the auxins. These phytohormones cause the cells to change their elasticity, and as result cells absorb more water and energy that leads to more cell division. Therefore, it is generally accepted that auxins have a key role in the process of root initiation (Štefančič et al., 2005).

Among the different exogenous hormones such as GGR_6, NAA, IBA, and IAA are known to accelerate the rooting parameters in vegetative propagation through cuttings (Gehlot et al., 2014; Ibrahim et al., 2015). Therefore, in our study, we found the distinct differences in rooting rate, number of roots, total root length, root diameter and root volume due to different exogenous hormones application in the rooting of *Magnolia*

http://www.aloki.hu ● ISSN 1589 1623 (Print) ● ISSN 1785 0037 (Online)
DOI: http://dx.doi.org/10.15666/aeer/1802_22132229

biondii Pamp cuttings. It was also found that cuttings treated with IBA treatment induce early and better root initiation. Therefore, the maximum rooting rate and number of roots were found at 750 mg/L concentration of IBA. The exogenous application of IBA has been reported to enhance cell division and to speed up the translocation and movement of carbohydrates and nutrients to the base of stem cuttings and enhances root growth (Kester et al., 1990; Aminah et al., 1995; OuYang et al., 2015b). These findings are also supported by the previous findings of Kester et al., 1990 that also found similar results in many herbaceous perennial crops. Similarly, in other plant species such as *Lippia javanica* L. (Soundy et al., 2008) and *V. paradoxa* and *C.F. Gaerth* (Akakpo et al., 2014), highest rooting was attained when stem cuttings were treated with IBA. In the case of total root length, we also found that cuttings of *Magnolia biondii* Pamp treated with IBA 750 mg/L showed improved root length and it might be because of early cells differentiation and elongation. Moreover, exogenous application of hormones initiates the synthesis of structural enzyme protein in the formation of the adventitious root leading to increase the root length through the acidification process (Kaushik, 2017). Similar conclusions were found by Sharma (2014) in Marigold, Swamy et al. (2002) in *Grewia optiva* and *Robinia pseudoacacia*, Grewal et al. (2005) *Dendranthema grandiflora* cv. Snowball and Singh et al. (2013) in Night Jasmine. Root diameter and volume are also an important factor for the development of a newly developed seedling to keep its root system stronger to reach its climax stage during the early development. Therefore, application of exogenous hormones helps the plants to develop stronger and thicker roots during the early developmental stage.

In the literature, auxins were found better to develop more thick roots and as a result, the root diameter is increased (Bhatt and Tomar, 2011). We also found the prominent effects of auxins (NAA, IBA, IAA) and gibberellin (GGR_6), but compared to auxins, the gibberellin (GGR_6) had a relatively better effect in the root diameter (Liu et al., 2005). Because the gibberellins are the third most commonly used plant hormones with a share of 17%. The most commonly used commercial gibberellin is GGR_6. It is mostly used for increasing the height of a plant or flower yield (Kumlay and Eryigit, 2011), but in our study GGR_6 significantly affected the root diameter compared to auxin group of hormones and to the control, that is consistent with the results provided by Liu et al. (2013) that GGR_6 treated cuttings had higher root diameter values than other exogenous hormones. While, in the case of root volume, IBA had a significant effect on the cuttings. The root volume is also one of the essential parameters used for the evaluation of root morphology. Root volume reflects the quality of root growth, larger the volume of the root, more the developed root system will be (Jie, 2012). Exogenous hormones application plays a vital role in the rooting of the different plant species. Many studies have shown that exogenous application of hormones results in the increased initiation of lateral roots (Chhun et al., 2003). The effect of hormones on rooting and plant development have been discussed in several studies, for example, Kesari et al. (2009) studied the effect of IBA, NAA and IAA on the rooting of *Pongamia pinnata* and found the maximum rooting rate in IBA treated cuttings. Similarly, Tchinda et al. (2013) conducted a series of experiments by using NAA and IBA for the propagation of *Ricinodendron heudelotti Baill* species. Sevik and Güney (2013) also studied the rooting potential of Melissa officinalis L. species through stem cuttings using IAA, NAA, IBA, and GA_3. Thus, these studies showed that, in general, the exogenous hormones have an effect on rooting and their results are in conformity with the results of our study. We found that through the whole experiment, cuttings treated with

http://www.aloki.hu ● ISSN 1589 1623 (Print) ● ISSN 1785 0037 (Online)
DOI: http://dx.doi.org/10.15666/aeer/1802_22132229

exogenous hormones respond significantly towards the percent rooting. The differential response of the stem cuttings on various exogenous hormones has been ascribed to the chemical nature of the hormones and the mode of concentrations (Das, 2006). Our results were not impressive in all other hormone types other than IBA. Kester et al., 1990, mentioned that IBA could be used for general use because it is non-toxic to plants over varied concentrations than other auxins. To some extent, NAA also performed well compared to GGR_6 and IAA. This reveals that application of GGR_6 and IAA exhibits poor root ability and are unable to respond well in *Magnolia biondii* Pamp. Poor development of roots inhibits the success of vegetative propagation via stem cuttings (De Klerk, 2002). It was also found that, with the increase in exogenous hormone application, rooting also increased and then after reaching its peak value, it decreased with increase in concentration. Kester et al., 1990 mentioned that the higher concentration of exogenous hormones deters the initiation and elongation of roots and stimulates plant cell to produce ethylene.

After the successful screening of best hormone and its best concentration (IBA-750) for the rooting then it was combined with other factors for the optimization of successful propagation treatments the best results of rooting in *Magnolia biondii* Pamp cuttings. In this regard, first of all, we investigated how the time of soaking improved the rooting. We found that increasing the time of soaking (120 min) of cuttings into IBA 750 mg/L significantly increased the rooting and affected the rooting morphological characteristics of *Magnolia biondii* Pamp. Different time of soaking of the cuttings into the IBA significantly affected the rooting and it had various impacts on the morphological characteristics of *Magnolia biondii* Pamp cuttings which are in agreement with the finding of Panwar et al. (1999) and OuYang et al. (2015a), who studied the effect of exogenous hormones, length of the stem cuttings, and soaking time of the cuttings on the rooting of Norway spruce. Application of IBA 750 mg/L for 120 min significantly increased rooting rate, number of roots and root volume, while 60 min application enhanced total root length and root diameter. Maximum time application i.e. 360 min did not have good results which are in agreement to the previous results, who mentioned for Rosa species that, cuttings immersed for 360 min in IBA concentrations inhibited the rooting. Different environmental factors can influence and there can be variability in the results when cuttings are immersed for a long time period (Kester et al., 1990).

Cuttings of *Magnolia biondii* Pamp treated with IBA-750, and the best time of soaking was further evaluated to get the best results of rooting. We selected the three positions of the crown i.e., upper, middle and lower. Because the differences existed between the position of the crown on the donor plant for rooting percentage and other parameters (Fishel et al., 2003). We found that maximum rooting percentage was observed in the cuttings taken from the lower part of the crown. Similar results were found during the rooting process of *jack pine* when the cuttings were collected from the lower position of the crown, they significantly rooted more than the middle and upper position of the crown (Browne et al., 1996). Browne et al. (1996) studied that plant crown position play an important role in the rooting process, lower crown to the middle position of the crown typically show higher rooting frequency than the upper position of the crown. It has been extensively studied that cutting size can often be attributed to the origin of cuttings within and between shoots, and to its position within the stock plant (Leakey, 2004). In most of the tree species, rooting ability of cuttings has been reported to increase from the basal part of the tree crown that attributed to the accumulation of

http://www.aloki.hu ● ISSN 1589 1623 (Print) ● ISSN 1785 0037 (Online)
DOI: http://dx.doi.org/10.15666/aeer/1802_22132229

carbohydrates (Kester et al., 1990). The effect of crown position on rooting may be caused by the variation in the physiological status of cuttings on stock plants (Kester et al., 1990).

Furthermore, we investigated how the length of the cuttings can be more effective in the propagation of *Magnolia biondii* Pamp species. So, for this purpose, we explored the IBA-750 with the best time of soaking and crown position to evaluate the effect of cuttings length on the rooting. In our study, significant rooting results were obtained for longer cuttings (21-25 cm). Longer cuttings rooted at a higher percentage than shorter cuttings and similar results were found in Ayous (Triplochiton scleroxylon) (Leakey, 1983; Leakey and Mohammed, 1985). The effectiveness of rooting by longer cuttings can be explained by different factors. The first factor is that the level of endogenous Auxins and other rooting-inducing factors may be lower in shorter cuttings, which leads to the reduced rooting percentage or the absence of rotting in shorter cuttings (Palanisamy and Kumar, 1997). The second factor is that longer cuttings store more carbohydrates (Tchoundjeu and Leakey, 1996), the carbohydrates of sugars (soluble carbohydrates) and storage carbohydrates (starches or insoluble carbohydrates) are important to rooting as building blocks of complex macromolecules, structural elements, and energy sources (Sturve, 1981; Haissig, 1984, 1986). So, these cuttings use the stored carbohydrates in root regeneration (Kester et al., 1990).

Conclusion

A protocol for vegetative propagation of *Magnolia biondii* Pamp was optimized with subsequent development of plants using stem cuttings as source material. The stem cuttings pretreated with exogenous hormone IBA 750 mg/L, time of soaking for 120 min, the position of the parent plant crown (lower position) and longer cuttings of 21-25 cm significantly affected on the rooting in the greenhouse conditions. This optimized protocol can ease to propagate *Magnolia biondii* Pamp and can be used to develop healthier and more profuse root system for the propagation and more clone plants. Further studies can be carried out in-depth by using morpho-anatomical studies and antioxidant activities to provide a more effective and feasible method of propagation for *Magnolia biondii* Pamp species.

Acknowledgments. This research was financially supported by the Special Fund for Forest Scientific Research in the Public Welfare under grant no. 201504704.

REFERENCES

[1] Akakpo, D. B., Amissah, N., Yeboah, J., et al. (2014): Effect of indole 3-butyric acid and media type on adventitious root formation in sheanut tree (Vitellaria paradoxa CF Gaertn.) stem cuttings. – American Journal of Plant Sciences 5: 313.

[2] Aminah, H., Dick, J. M., Leakey, R., et al. (1995): Effect of indole butyric acid (IBA) on stem cuttings of Shorea leprosula. – Forest Ecology and Management 72: 199-206.

[3] Azamal, H., Mohinder, P. (2000): Analytical studies on the effects of interaction with respect to position, season and auxin on adventitious root formation in stem cuttings of mature teak (Tectona grandis Linn. f.). – Annals of Forestry 8: 253-261.

[4] Bellini, C., Pacurar, D. I., Perrone, I. (2014): Adventitious roots and lateral roots: similarities and differences. – Annual Review of Plant Biology 65: 639-666.

http://www.aloki.hu ● ISSN 1589 1623 (Print) ● ISSN 1785 0037 (Online)
DOI: http://dx.doi.org/10.15666/aeer/1802_22132229

[5] Bhatt, B. B., Tomar, Y. (2011): Effect of IBA and growing conditions on vegetative performance of Citrus aurantifolia (Swingle) cuttings. – Journal of Hill Agriculture 2: 98-101.
[6] Browne, R., Davidson, C., Gobin, S. M. (1996): Effects of crown position and plant age on rooting of jack pine long shoot cuttings. – Tree Planters' Notes 47: 100-104.
[7] Chhun, T., Taketa, S., Tsurumi, S., et al. (2003): The effects of auxin on lateral root initiation and root gravitropism in a lateral rootless mutant Lrt1 of rice (Oryza sativa L.). – Plant Growth Regulation 39: 161-170.
[8] Coombes, A. J. (2014): The Book of Leaves: A Leaf-by-Leaf Guide to Six Hundred of the World's Great Trees. – University of Chicago Press, Chicago.
[9] Das, N. (2006): Propagation prospects of dye yielding plant, Rhinacanthus nasutus (Linn.) Kurz. – Natural Product Radiance 5(1): 42-43
[10] Davies Jr., F. (1988): Influence of nutrition and carbohydrates on rooting of cuttings. – Comb. Proc. Int. Plant. Propag. Soc. 432-437.
[11] Davis, T., Haissig, B. (1990): Chemical control of adventitious root formation in cuttings. – Quarterly-PGRSA 18:1-17.
[12] De Klerk, G.-J. (2002): Rooting of microcuttings: theory and practice. – In Vitro Cellular & Developmental Biology-Plant 38: 415-422.
[13] Dettmer, J., Elo, A., Helariutta, Y. (2009): Hormone interactions during vascular development. – Plant Molecular Biology 69: 347.
[14] Dirr, M. A. (1989): Rooting response of Photinia × fraseri Dress 'Birmingham' to 25 carrier and carrier plus IBA formulations. – Journal of Environmental Horticulture 7: 158-160.
[15] Elhaak, M., Matter, M., Zayed, M., et al. (2015): Propagation principles in using indole-3-butyric acid for rooting rosemary stem cuttings. – Journal of Horticulture. DOI: 10.4172/2376-0354.1000121.
[16] Fishel, D., Zaczek, J., Preece, J. (2003): Positional influence on rooting of shoots forced from the main bole of swamp white oak and northern red oak. – Canadian Journal of Forest Research 33: 705-711.
[17] Gehlot, A., Gupta, R. K., Tripathi, A., et al. (2014): Vegetative propagation of Azadirachta indica: effect of auxin and rooting media on adventitious root induction in mini-cuttings. – Advances in Forestry Science 1: 1-9.
[18] Geiss, G., Gutierrez, L., Bellini, C. (2009): Adventitious root formation: new insights and perspectives. – Annual Plant Reviews 37: 127-156.
[19] Grewal, H., Kumar, R., Chauhan, R. (2005): Effect of IB A and N AA on rooting in chrysanthemum (Dendrantlwma grandiflora Tzevlev) terminal cuttings. – Journal of Ornamental Horticulture 8: 230-232.
[20] Haissig, B. E. (1984): Carbohydrate accumulation and partitioning in Pinus banksiana seedlings and seedling cuttings. – Physiologia Plantarum 61: 13-19.
[21] Haissig, B. E. (1986): Metabolic Processes in Adventitious Rooting of Cuttings. – In: Jackson, M. B. (ed.) New Root Formation in Plants and Cuttings. Springer, Dordrecht, pp. 141-189.
[22] Harrison-Murray, R., Knight, L. (1997): New Approaches to Optimising Environments for Rooting Cuttings. – Combined Proceedings-International Plant Propagators Society. Univ Washington, Int Plant Propagation Soc, pp. 206-210.
[23] Ibrahim, M., Mohamed, M., Khalid, K. (2015): Effect of plant growth regulators on the rooting of lemon verbena cutting. – Journal of Materials and Environmental Science 6: 28-33.
[24] Jamir, S. L., Deb, C. R., Jamir, N. S. (2016): Macropropagation and production of clonal planting materials of Panax pseudoginseng Wall. – Open Journal of Forestry 6: 135.
[25] Jie, J. (2012): Effects of IBA and 6-BA on the Growth of Roots and Aboveground Branches of Transplanted. – Nanjing Agricultural University, Nanjing.

http://www.aloki.hu ● ISSN 1589 1623 (Print) ● ISSN 1785 0037 (Online)
DOI: http://dx.doi.org/10.15666/aeer/1802_22132229

[26] Kaushik, S. (2017): Effect of IBA and NAA and Their Combination on Rooting in Stem Cuttings of African Marigold (Tagetes erecta L.) CV. Pusa Narangi Gainda. – Indira Gandhi Krishi Vishwavidhyalaya, Raipur.
[27] Kesari, V., Krishnamachari, A., Rangan, L. (2009): Effect of auxins on adventitious rooting from stem cuttings of candidate plus tree Pongamia pinnata (L.), a potential biodiesel plant. – Trees 23: 597-604.
[28] Kester, D., Davies, F., Hartmann, H. (1990): Plant Propagation: Principles and Practices. – Prentice-Hall, India.
[29] Kumar, B., Lakshman, K., Jayaveera, K., et al. (2009): Estimation of rutin and quercetin in Terminalia chebula by HPLC. – Asian Journal of Research in Chemistry 2: 388-389.
[30] Kumlay, A., Eryigit, T. (2011): Growth and development regulators in plants: plant hormones. – Igdır University Journal of the Institute of Science and Technology 1: 47-56.
[31] Leakey, R. (1983): Stockplant factors affecting root initiation in cuttings of Triplochiton scleroxylon K. Schum., an indigenous hardwood of West Africa. – Journal of Horticultural Science 58: 277-290.
[32] Leakey, R., Mohammed, H. (1985): The effects of stem length on root initiation in sequential single-node cuttings of Triplochiton scleroxylon K. Schum. – Journal of Horticultural Science 60: 431-437.
[33] Leakey, R. R. (2004): Physiology of Vegetative Reproduction. – Academic Press Cambridge, MA.
[34] Lekha, G., Lalji, S. (2010): Study of factors influencing vegetative propagation of Jatropha curcas. – Indian Forester 136: 1637-1648.
[35] Liu, G.-F., Song, X.-B., Xu, Y.-H., et al. (2005): A study on role of GGR6 in seedling-raising of Taxus chinensis var. mairei. – Forest Research-Chinese Academy of Forestry 18: 730.
[36] Liu, K.-C., Yu, Y.-P., Wang, L.-H., et al. (2013): Effects of three plant growth regulators on the root growth of Erythrophleum fordii. – Northern Horticulture 5.
[37] Luz, P. B. d., Paiva, P. D. d. O., Landgraf. P. R. C. (2007): Influence of different types of stem cuttings and substrates on the asexual reproduction of hydrangea (Hydrangea macrophylla) (Thunb.). – Ser. Ciência e Agrotecnologia 31: 699-703.
[38] OuYang, F., Junhui, W., Li, Y. (2015a) Effects of cutting size and exogenous hormone treatment on rooting of shoot cuttings in Norway spruce [Picea abies (L.) Karst.]. – New Forests 46: 91-105.
[39] OuYang, F., Wang, J., Li, Y. (2015b) Effects of cutting size and exogenous hormone treatment on rooting of shoot cuttings in Norway spruce [Picea abies (L.) Karst.]. – New Forests 46: 91-105.
[40] Palanisamy, K., Kumar, P. (1997): Effect of position, size of cuttings and environmental factors on adventitious rooting in neem (Azadirachta indica A. Juss). – Forest Ecology and Management 98: 277-280.
[41] Panwar, R., Gupta, A., Yamdagni, R., et al. (1999): Effect of growth regulators on the rooting of cuttings of Bougainvillea cv. Thimma. – Haryana Agric Univ J Res 29: 11-17.
[42] Papp, B., Plath, K. (2011): Reprogramming to pluripotency: stepwise resetting of the epigenetic landscape. – Cell Research 21: 486.
[43] Sevik, H., Guney, K. (2013): Effects of IAA, IBA, NAA, and GA3 on rooting and morphological features of Melissa officinalis L. stem cuttings. – The Scientific World Journal. https://doi.org/10.1155/2013/909507.
[44] Sevik, H., Turhan, H. (2015): Effects of IBA (indole butiric acide) on rooting and newly stem to Turkish lili (Lilium martagon L.) onion. – ICONSETE Conference Austria Proceedings Book, Vienna.
[45] Sharma, R. (2014): Study on the Effect of Auxins on Rooting, Growth and Flowering of African Marigold (Tagetes Erecta L.) Propagated Through Stem Cuttings. – Indira Gandhi Krishi Vishwavidyalaya, Raipur.

http://www.aloki.hu ● ISSN 1589 1623 (Print) ● ISSN 1785 0037 (Online)
DOI: http://dx.doi.org/10.15666/aeer/1802_22132229

[46] Singh, K., Rawat, V., Rawat, J., et al. (2013): Effect of IBA and NAA concentrations on rooting in stem cuttings of night queen (Cestrum nocturnum L) under sub-tropical valley conditions. – HortFlora Research Spectrum 2: 81-83.
[47] Soundy, P., Mpati, K. W., du Toit, E. S., et al. (2008): Influence of cutting position, medium, hormone and season on rooting of fever tea (Lippia javanica L.) stem cuttings. – Medicinal and Aromatic Plant Science and Biotechnology 2: 114-116.
[48] Štefančič, M., Štampar, F., Osterc, G. (2005): Influence of IAA and IBA on root development and quality of Prunus' GiSelA 5'leafy cuttings. – HortScience 40: 2052-2055.
[49] Sturve, D. (1981): The relation between carbohydrates, nitrogen and rooting of stem cuttings. – The Plant Propagator 27: 6-7.
[50] Swamy, S., Puri, S., Singh, A. (2002): Effect of auxins (IBA and NAA) and season on rooting of juvenile and mature hardwood cuttings of Robinia pseudoacacia and Grewia optiva. – New Forests 23: 143-157.
[51] Tchinda, N., Messi, H., Fotso, et al. (2013): Improving propagation methods of Ricinodendron heudelotti Baill. from cuttings. – South African Journal of Botany 88: 3-9.
[52] Tchoundjeu, Z., Leakey, R. (1996): Vegetative propagation of African mahogany: effects of auxin, node position, leaf area and cutting length. – New Forests 11: 125-136.
[53] Villacorta-Martín, C., Sánchez-García, A. B., Villanova, J., et al. (2015): Gene expression profiling during adventitious root formation in carnation stem cuttings. – BMC Genomics 16: 789.
[54] Wang, Q., Weijian, F., Shen, Y. (2017): Three kinds of magnolia full light cutting propagation technology. – Seed 36(3): 128-129.
[55] Zhang H., Charles, R. Z., Wang, J. (2003): Magnolia and Wangchun Yulan all-light spray twig cutting test. – Shaanxi Forestry Science and Technology 4: 22-23.
[56] Zhang, W., Fan, J., Tan, Q., et al. (2017): The effects of exogenous hormones on rooting process and the activities of key enzymes of Malus hupehensis stem cuttings. – PloS One 12: e0172320.

http://www.aloki.hu ● ISSN 1589 1623 (Print) ● ISSN 1785 0037 (Online)
DOI: http://dx.doi.org/10.15666/aeer/1802_22132229

ASSESSMENT OF TREE BIOMASS CARBON STOCK OF A SUBTROPICAL SCRUB FOREST, SOAN VALLEY PAKISTAN

GHAFOOR, G. Z.* – SHARIF, F. – KHAN, A. U. – SHAHZAD, L. – HAYYAT, M. U.

Sustainable Development Study Center, Government College University Lahore, Pakistan (email/phone:faizasharif@gcu.edu.pk/+92-321-4000-818; akeco1111@gmail.com/+92-300-8481-460; lailashahzad@gcu.edu.pk/+92-322-7878-517; umerenv@yahoo.com/+92-321-4032-300)

**Corresponding author*
e-mail: zareen.sdsc@gmail.com; phone+92-343-4624-022

(Received 7th Oct 2019; accepted 4th Dec 2019)

Abstract. In Pakistan the lack of development for local allometric equations has led to the use of simple generic volume equations which may generate errors in forest carbon estimates. This research was designed to quantify tree carbon stock and check the robustness of the existing models against local allometric models.The study was conducted in Hayat-ul-Mir subtropical scrub forest in Pakistan comprising of a bi-climax community of *Acacia modesta* Linn. and *Olea ferruginea* Royle.Tree measurements were taken in 47 plots of 0.04 ha and biomass carbon estimates were made using local allometric, existing generic pantropical model and i-Tree Eco tool.No significant difference in biomass carbon (ton/ha) was found between local (8.53) and pantropical models (8.68) for *A. modesta* and between the three models for *O. ferruginea* (10.92, 11.91 and 11.87 for local allometric, pantropical model and i-Tree Eco, respectively). All models fitted data well ($p< 0.001$), whereas the pantropical model incorporating three biophysical variables better predicted biomass and was found more robust for both species based on AIC, BIC, RMSE and R^2 adj. values. In the absence of local models, the pantropical model can provide better biomass estimates for deciduous and evergreen subtropical species to report carbon stock.
Keywords: *Allometry, volume, i-Tree Eco, pantropical, REDD+*

Introduction

Biomass carbon stock assessment is highly sensitive to the choice of adopted method due to differences in the biophysical factors incorporated into the model (van Breugel et al., 2011). Forest biomass carbon is partitioned mainly into aboveground (including stem, branches, and leaves) and belowground parts (including both fine and coarseroots) accounting for approximately 50% of the total biomass of the tree (Basuki et al., 2009; Yuen et al., 2016). For biomass estimation, various techniques are common ranging from site specific or locally developed to generic allometric/regression models and remote sensing techniques (Basuki et al., 2009; van Breugel et al., 2011). The most accurate and direct method of biomass quantification employs the use of destructive or semidestructive sampling in which fresh and oven dry weight of all components or parts of a tree is analytically determined by harvesting subsample of plants from sample plots. The results obtained give a precise estimate of the biomass carbon in a small sample area, and this technique is being used to develop site or species specific (local) regression models for the landscape based biomass estimations (Basuki et al., 2009; Yuen et al., 2016). The destructive harvest is often limited due to variable topography, environmental and financial constraints (Goussanou et al., 2016; Djomo and Chimi, 2017). To overcome this limitation researchers have devised non-destructive volume and allometric equations to estimate individual tree biomass, for which biomass carbon as a fraction is calculated (Philip, 1994; Yuen et al., 2016; Stas et al., 2017).

http://www.aloki.hu ● ISSN 1589 1623 (Print) ●ISSN1785 0037 (Online)
DOI: http://dx.doi.org/10.15666/aeer/1802_22312245

Allometry finds a mathematical explanation of how structural variables are related to biomass. This mathematical explanation or model is obtained by regressing total individual biomass of tree or its components against biophysical variables i.e. diameter at breast height (DBH), tree height and wood density (Chave et al., 2014; Yuen et al., 2016). Although generic allometric equations are considered applicable to wide range of species in diverse landscapes, but between the regions trees present different allometric relationships for biophysical variables depending on the environmental conditions such as climate and soil type. This requires the generic allometric models to be calibrated with local (site or species specific) allometries which gives a more precise estimate of tree carbon stock (Vieilledent et al., 2012). By this pre-calibration, the utility of generic models to wide range of environmental conditions and species increases when local biomass models are not available. Vieilledent et al. (2012) after a destructive sampling of 481 trees in Madagascar, developed local allometric equations and compared them with generic pantropical relations developed by Brown (1997) and Chave et al. (2005). The comparison showed that in the absence of local equations, the generic model proposed by Chave et al. (2005) based on height (Ht), DBH and wood density (WD) of tree species produced more accurate biomass estimates than other generic models considering only DBH or combination of DBH and WD.

The accuracy of the forest carbon estimates thus lies in the robustness of the allometric model adopted and also depends on the relationship between biophysical variables incorporated as predictors in the model (Gulzar et al., 2014). For instance, tree volume equations developed by foresters may relyon a geometric relationship of Ht, DBH and tree form factor and applies biomass expansion factoror species specific WD to estimate tree biomass (Philip, 1994; Nizami, 2012). While the generic or pantropical models are developed considering the climate of the region along with biophysical factors and also apply regression coefficients in determining tree biomass (Chave et al., 2014). Biomass estimations made through any of these methods can later be extrapolated to the whole forest or landscape scale level (Nizami, 2014).

A number of tools have also been developed to estimate tree biomass and carbon storage in urban and natural forest such as Carbon OnLine Estimator (COLE), U.S. Forest Carbon Calculation Tool (CCT), Center for Urban Forestry Research (CUFR) Tree Carbon Calculator (CTCC) and i-Treetools (Aguaron and McPherson, 2012; Nowak et al., 2013; Russo et al., 2014). i-Tree Eco, developed by the USDA Forest Service and Cooperators, is derived from the UFORE (Urban FORest Effects) and has widely been used to estimate the magnitude and monetary value of many of the ecosystem services provided by urban forests, including carbon storage and sequestration using the plot based or complete inventory data of forest. The use of meteorological data by i-Tree Eco as a baseline gives a better estimate of ecosystem services (Nowak et al., 2008). i-Tree Eco computes dry weight biomass, carbon storage and sequestration by applying species/genus/family specific allometric equations or average of hardwood/conifer equations using either DBH, a combination of DBH and Ht or Ht of the tree and crown characteristics (Nowak et al., 2013).

In order to implement REDD+ targets (Reducing Emissions from Deforestation and Forest Degradation) to reduce global greehouse gas emissions (Terakunpisut et al., 2007), it is mandatory for Pakistan to report its forest carbon stock and GHG emissions from other sectors in accordance with UNFCCC protocols. For this purpose, only a few allometric models have been developed in Pakistan for the estimation of biomass of individual tree components (stem, branches, twigs, leaves and root) or stem volume estimation (Nizami,

http://www.aloki.hu ● ISSN 1589 1623 (Print) ●ISSN1785 0037 (Online)
DOI: http://dx.doi.org/10.15666/aeer/1802_22312245

2014; Shaheen et al., 2016). Whereas, most of the studies have reported biomass estimates using volume relationships (Nizami et al., 2009; Nizami, 2012; Ahmad et al., 2014; Shaheen et al., 2016) which are now less recommended due to its limitations of incorporating fixed tree form factor and limited utility for closed canopy forests (Chave et al., 2005). No literature was found to the best of our knowledge using i-Tree Eco tool or on validation of generic allometric models to estimate tree carbon stock in Pakistan.

This study was conducted on the Hayat-ul-Mir (HM) Scrub forest, Soan Valley Pakistan to estimate tree biomass carbon stock. The forest is documented in detail by Parker (1915) and Champion et al. (1965) as cited by Khan et al. (2013). The vegetation type of scrub forest comprises of dry subtropical broad leaved deciduous and evergreen species covering a totalarea of 1.3 million hectares. The forest extends in the foothills and lowerslope of Himalayas, in the salt range, Kala-Chitta, and Sulaiman range. At suitable elevations, the forest is also seen throughout the country merging upward with sub-tropical pine and temperate forest and downward with tropical thorn forest. The dominant community of the scrub forest comprise of *Acacia modesta* (Linn.) Wall., *Olea ferruginea* Royle, *Tecoma undulata,* and *Pistacia integerima* however shrub cover is contributed by *Dodonea viscosa, Justica adhatoda, Zizyphus spp.* And *Nannorrhops ritchieana.* The local population benefits from the forest to fulfill its needs for fodder, fuelwood, timber and herbal medicines (Khan and Ahmad, 2015).

A number of studies have been conducted in Pakistan estimating tree biomass of different forest ecosystems. Nizami et al. (2009) has reported biomass carbon stock of sub-tropical pine forest in Lehterar and Ghoragali forest subdivisions in Murree hills using simple volume relationship. In another study by Nizami (2012), volume based biomass carbon estimates have been reported for sub-tropical pine forest, Kherimurat scrub and Sohawa forests comprising of vegetation stock of *Pinus roxburghii*, *Acacia modesta* and *Olea ferruginea*. Shaheen et al. (2016) have reported volume based and species specific allometric relationships for forest carbon stocka ssessment in subtropical Himalayan forest in Kashmir comprising a mixed vegetation of *Acacia spp*., *O. cuspidata*, *P. roxburghii, Punica gratum, Ficus spp., Broussonetia papyrifera, Melia azedarach, Mallotus philippensis* and *Delbergia sisso*. Other studies have reported biomass estimates of *Delbergia sisso* and *Picea smithiana* by destructive harvest in Daphar irrigated plantation in Punjab province and Kumrat valley in Khyber Pakhtun Khawa Province in Pakistan, respectively (Ahmad et al., 2014; Gulzar et al., 2014). In all of these studies, tree biomass was estimated from generic volume equations which are now less recommended for carbon accounting (Chave et al., 2005).

Current study was designed to 1) estimate tree biomass and carbon storage of *Acacia modesta* and *Olea ferruginea* in HM scrub forest and 2) to compare locally developed allometric equations to the existing models to evaluate their robustness and applicability for subtropical forest in Pakistan. It was hypothesized that increase in the number of biophysical factors in biomass model gives a better estimate of forest carbon stock.

Materials and Methods

Site description

The study was conducted in HM Scrub Reserve forest (32.54^{o} N and 72.31^{o} E) covering an area of 1646 ha in Soan Valley, district Khushab of Punjab province, Pakistan. Most of the hills in the valley have an average height between 400 to 1000 m and the highest point in the range i.e. Sakesar lies at a height of 1527 m. The forest

http://www.aloki.hu ● ISSN 1589 1623 (Print) ●ISSN1785 0037 (Online)
DOI: http://dx.doi.org/10.15666/aeer/1802_22312245

classified as arid receives annual precipitation of 600 mm which falls mostly during the monsoon (July to September), with an average annual temperature of 24°C (minimum temperature 1°C in January and an average maximum temperature of 36°C in June) making the area hot and dry with frequent droughts during summer and frost in winter (Ahmed, 2013; Khan et al., 2013). The forest has a dominant vegetation stock of two climax (mosaic) species i.e. *A. modesta* (deciduous) and *O. ferruginea* (evergreen), however a rich understory of other species such as *Justicia adhatoda, Buxus sp.*, *Dodonaea viscosa* and other shrubs are present at different elevations in the forest (Ahmed, 2013). The invasion of exotic *Prosopis juliflora* species was also seen at some locations in the HM forest (*Fig. A1*).

Field data collection

For the non-destructive estimation of tree biomass carbon, 47 plots of 20 m × 20 m (0.04 ha) were taken in the forest (*Fig. 1*, *Table A1*) during November 2017 to December 2018. To estimate the tree above ground biomass (AGB), tree dendrometric variables such as Diameter at Breast Height (DBH) and the total height (Ht) of the tree was measured following UNFCCC protocols. For multi stem trees (which forked below 1.3 m height), the individual diameter of each stem was recorded, summed the DBH squares and their square root was taken (*Eq.1*) producing a single value of DBH for a tree. Tree basal area was computed using equation below (*Eq.2*) (Nizami, 2012).

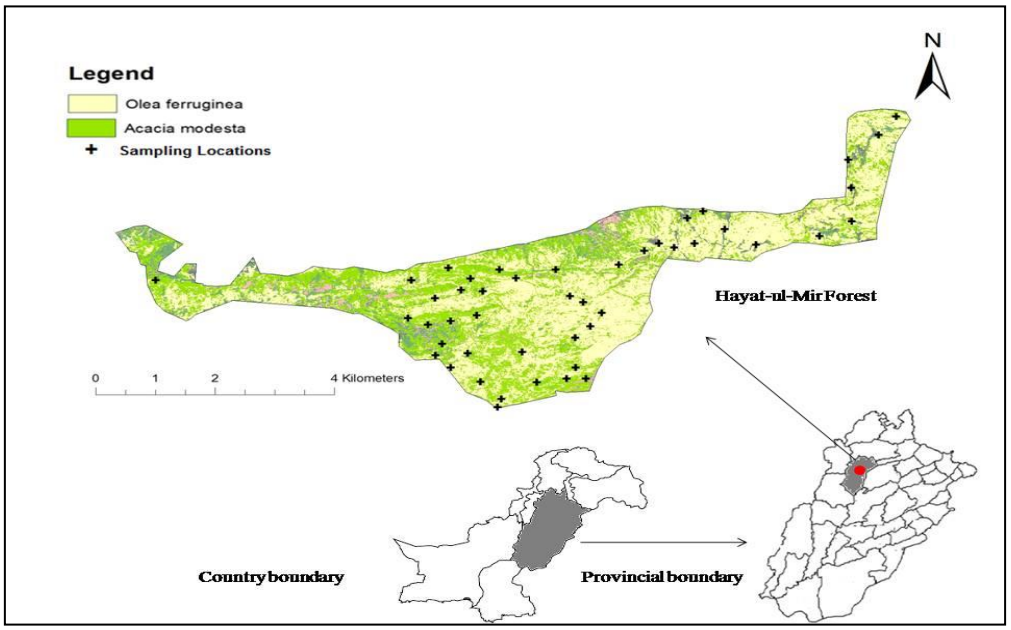

Figure 1.*Spatial distribution of sampling plots taken in the HM forest*

$$DBH = sqrt[DBH_1^2 + DBH_2^2 + \ldots DBH_n^2] \quad \text{(Eq.1)}$$

$$\text{Basal Area} = \pi/4 \times DBH^2 \quad \text{(Eq.2)}$$

The estimation of AGB of *A. modesta* and *O. ferruginea* in HM Reserve Forest was carried out using locally developed volume allometric equations which were considered

http://www.aloki.hu ● ISSN 1589 1623 (Print) ●ISSN1785 0037 (Online)
DOI: http://dx.doi.org/10.15666/aeer/1802_22312245

as a benchmark to check the robustness of other two existing biomass estimation methods (non-destructive) for subtropical forest in cases when local equations are not available. This study is first of its kind to refine and caliberate existing generic biomass models against locally developed models for accurate carbon accounting under REDD+ in Pakistan and for other forests in subtropical region.

AGB estimation using locally developed volume equations

Local harvest based volume allometric equations (Pakistan Forest Institute, 1993) were used to estimate total volume of *A. modesta* (*Eq.3*) and *O. ferruginea* (*Eq.4*);

$$ln\text{TV} = -9.35092 + 0.36032\ ln\text{H} + 2.22653 ln\text{D} \quad \text{(Eq.3)}$$

$$ln\text{TV} = -9.3826 + 0.56528 ln\text{H} + 2.09297 ln\text{D} \quad \text{(Eq.4)}$$

Where TV is the total tree volume, *ln* is the natural logarithm, H is height and D is Diameter at Breast Height. These equations were used to compute individual tree volume of bi-climax community at HM forest which was later multiplied with species specific wood density (Philip, 1994; Nizami, 2012) adopted from World Agroforestry Database (Pearson and Brown 1932) to compute aboveground biomass (AGB).

AGB estimation using generic pantropical biomass allometric equation

The generic pantropical biomass allometric equation (Model 4 from Chave et al., 2014) was used to regress AGB of *A. modesta* and *O. ferruginea* against the product of height (m), DBH (cm) and species specific wood density (gcm^{-3}). This model (based on harvest data from 58 sites across tropics with variable vegetation and climatic conditions) is a revised and improved version of Chave et al. (2005) and was selected as it performs well across forest types in pantropical bioclimatic conditions (*Eq.5*). The model is reported with slightly high variance and mean percent bias when compared with local models but no detectable effect of environmental factors or region on AGB considering height, DBH and wood density as covariates.The previous version (Chave et al., 2005) of this model has been evaluated by Kebede and Soromessa (2018) for *O. europea* L. sub sp. *cuspidata* (synonym *O. ferruginea*) in Ethiopia where allometric equations were developed through semi-destructive harvest and were compared with species specific and generic allometric models. This model has also been previously documented for *O. europea* by Tesfaye et al. (2016) and Muhati et al. (2018).

$$AGB_{est}\ (kg) = 0.0673 \times (\rho D^2 H)^{0.976} \quad \text{(Eq.5)}$$

From the AGB_{est} obtained through local (*Eqs.3 and 4*) and generic allometric equations (*Eq.5*), belowground biomass (BGB) was calculated as 26% of the AGB (Nowak et al., 2008). The AGB and BGB were summed across individuals of both species and total tree biomass (TB) was converted into total tree biomass carbon (TBC) by multiplying with IPCC default factor of 0.50 as carbon accounts for 50% of the total biomass.

Calculation of carbon storage through i-Tree Eco tool

i-Tree Eco (v6.0) tool was used to estimate tree biomass and carbon stored in bi-climax community (*A. modesta* & *O. ferruginea*) of HM forest. For this purpose, hourly annual

http://www.aloki.hu ● ISSN 1589 1623 (Print) ●ISSN1785 0037 (Online)
DOI: http://dx.doi.org/10.15666/aeer/1802_22312245

metrological data and field measurements of DBH, crown height, total tree height and crown light exposure (CLE) data was input into the tool to quantify total tree dry weight and carbon storage using species specific allometric equation. Crown light exposure was estimated considering number of sides of the crown exposed to sunlight following Bechtold (2003). The total tree (above and belowground) carbon in *A. modesta* and *O. ferruginea* was calculated using equation form 1 in the tool database (*Eq.6*).

$$\text{Carbon Storage} = \exp((A + B * \log(\text{Variable}) + (\text{Mean Squared Error}/2)/2 \quad \text{(Eq.6)}$$

where A and B are coefficients and Variable is DBH (*A. modesta*) or DBH & Height (*O. ferruginea*). The total tree dry weight biomass (including 26% of the belowground biomass) was converted to carbon stock by multiplying with a factor of 0.5 (Nowak et al., 2013). This tool was selected for being a novel approach which has not yet been used for tree species in Pakistan and also it additionally quantifies other ecosystem services along with biomass estimates.

The plot based (0.04 ha) biomass estimates were up-scaled to hectare level using an appropriate area based conversion factor and both existing methods were evaluated against locally developed equations to choose the best fit model for carbon stock assessment of the subtropical forests in Pakistan.

Data analysis

For data analysis, SPSS v.19 (Statistical Package for Social Sciences) was used. Independent sample *t*-test was performed to evaluate statistical relationship between biophysical factors (dendrometric factors) of the surveyed population of both species. Mean and standard errors of biomass and carbon estimates were computed to compare for the variation in estimates made by each method. Multiple comparisons were made using Repeated Measures ANOVA and Bonferroni statistics was used to find the significant differences in carbon storage estimates made by each method used in this study. Multiple linear and logistic regression analyses were also run to choose the best fit model based on their relative performance considering TB as dependent and biophysical factors (DBH, Ht, & WD) as independent variables (*Eq.7*).

$$Y = a + b_1X_1 + b_2X_2 + ...b_nX_n \quad \text{(Eq.7)}$$

In the equation above Y refers to the dependent variable, a is the Y-intercept, b_1 through b_n corresponds to regression coefficients and X represents independent variable(s). Goodness of fit statistics was considered for a model which had high value of R^2-adj., lowest AIC (Aikaike Information criteria), BIC (Beysian Information Criteria), RMSE (Root Mean Square Error) and p *value* ≤ 0.05. AIC and BIC were estimated by equations below (*Eq.8 and Eq.9*) where k = number of estimated parameters in the model and L = maximized likelihood function of the estimated model.

$$AIC = 2k - 2\ln(L) \quad \text{(Eq.8)}$$

$$BIC = \ln(n)k - 2\ln(L) \quad \text{(Eq.9)}$$

http://www.aloki.hu ● ISSN 1589 1623 (Print) ●ISSN1785 0037 (Online)
DOI: http://dx.doi.org/10.15666/aeer/1802_22312245

Results

Structural summary of the forest

In the HM forest, a total population of 399 trees (135 trees of *A. modesta* and 264 trees of *O. ferruginea*) was recorded in 47 survey plots (0.04 ha). Forest dendrometric characteristics have been presented in *Table 1*. *O. ferruginea* had higher tree density per hectare (150 trees/ha) than *A. modesta* (82 trees/ha). There was a significant difference in tree height ($t = 3.76$, $df = 397$, $p < 0.001$), DBH ($t = 3.11$, $df = 397$, $p < 0.01$) and basal area ($t = 3.14$, $df = 397$, $p < 0.05$) of both species but not in case of tree volume ($t = -0.251$, $df = 83$, $p = 0.802$) with highest mean DBH (20.69 ± 0.8 cm) and height (5.94 ± 0.1 m) recorded for *A. modesta* and basal area (4.46 ± 0.6 m^2/ha) and tree volume (17.10 ± 2.4 m^3/ha) recorded for *O. ferruginea* in the survey plots.

Table 1. *Dendrometric characteristics of the Hayat-ul-Mir Forest*

Species	Trees/ha	Height (m)	DBH (cm)	Basal area (m^2/ha)	Tree volume (m^3/ha)
		M ± SE	***M ± SE***	***M ± SE***	***M ± SE***
A. modesta	82	5.94 ± 0.1***	20.69 ± 0.8**	3.44 ± 0.4	16.22 ± 2.6
O. ferruginea	150	5.15 ± 0.1	17.78 ± 0.4	4.46 ± 0.6*	17.10 ± 2.4

***p < 0.001, **p < 0.01, *p < 0.05

Tree biomass and carbon storage

Both methods of biomass estimation used in this study produced comparable estimates for both species when evaluated against locally developed equations. On plot scale the TB and TBC of sampled population presented in *Table 2* shows that the generic allometric equation of Chave et al. (2014) produced slightly higher (70.88 ton and 35.44 ton) while i-Tree Ecotool produced lower (58.77 ton and 29.38 ton) TB and TBC estimates compared to the species specific local equations for bi-climax community (67.12 ton and 33.56 ton).

Table 2. *Total tree biomass and carbon storage in survey plots*

Species	**Tree biomass** (ton)			**Tree biomass carbon** (ton)		
	Local Eq.	**Chave et al. (2014)**	**i-TreeEco**	**Local Eq.**	**Chave et al. (2014)**	**i-Tree Eco**
A. modesta	28.66	28.96	16.97	14.33	14.48	8.48
O. ferruginea	38.45	41.92	41.80	19.22	20.96	20.90
Total	67.12	70.88	58.77	33.56	35.44	29.38

Figure 2 illustrates the mean of TB and TBC of both species of scrub forest estimated using the selected methods. It can be seen from figure below that i-Tree Eco produced lower TB and TBC estimates (10.34 ton/ha and 5.17 ton/ha) than generic pantropical allometric equation (17.36 ton/ha and 8.68 ton/ha) and local (17.06 ton/ha and 8.53 ton/ha) allometric equations when evaluated for *A. modesta*. However, in case of *O. ferruginea* both existing methods produced comparable but slightly higher estimates than local equation.

Repeated measures ANOVA with Greenhouse-Geisser correction showed that mean TB and TBC significantly differed between the methods for *A. modesta* ($F(1.536, 205.78) =$

http://www.aloki.hu ● ISSN 1589 1623 (Print) ●ISSN1785 0037 (Online)
DOI: http://dx.doi.org/10.15666/aeer/1802_22312245

31.22, p = 0.000) but not for *O. ferruginea* (F(1.429, 375.78) = 2.162, p = 0.132). For *A. modesta*, Post hoc test using Bonferroni correction revealed that the TB and TBC estimates of generic pantropical allometric equation of Chave et al. (2014) were not significantly different from the estimates of local equation (p = 1.000) but differed significantly in case of i-Tree Eco (p = 0.000) as shown in *Figure 2*.

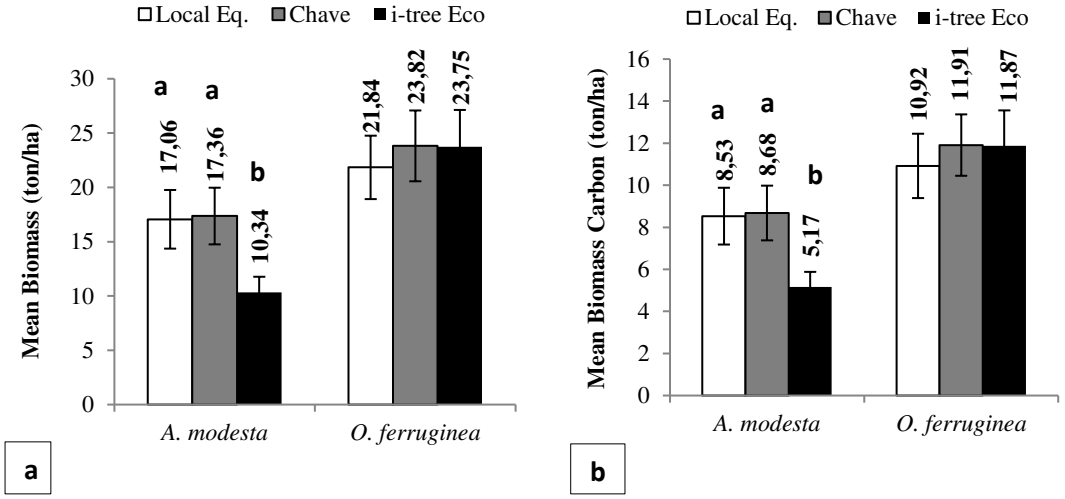

Figure 2.*Mean of (a) total biomass (TB) and (b) total biomass carbon (TBC) calculated using three different methods (bars with similar letters are not significantly different at p ≥ 0.05)*

Model assessment

The results of multiple linear regression analysis (*Table 3*) showed that the covariate DBH was statistically significant (p < 0.001) in all models for both species but height was not statistically significant in the local equations and i-Tree Eco (for *O. ferruginea* only). In case of both species, all of the models were good fit at p <0.001 but highest R^2-adj. (0.802), lowest AIC, BIC and RMSE were reported by generic pantropical allometric model of Chave et al. (2014) for *A. modesta*. However, for *O. ferruginea* the highest R^2-adj. (0.809) and lowest RMSE (0.093) were reported by local equation and lowest AIC and BIC by Chave et al. (2014).

Table 3.*Goodness of fit statistics of regression models for the prediction of TB across both species in the HM forest*

Models	Selection Criteria				Biophysical variables
	AIC	BIC	R^2 adj.	RMSE	
Acacia modesta					
Local Equation	1402	2455	0.792***	0.186	DBH***, H
Chave et al. (2014)	1379	2399	0.802***	0.138	DBH***, H*
i-Tree Eco tool	2060	2803	0.738***	0.193	DBH***
Olea ferruginea					
Local Equation	4179	8013	0.809***	0.093	DBH***, H
Chave et al. (2014)	4057	7809	0.802***	0.104	DBH***, H***
i-Tree Eco tool	4253	8174	0.752***	0.137	DBH***, H

*** p < 0.001, * p < 0.05, AIC = Akaike Information Criteria, BIC = Beysian Information Criteria, RMSE = Root Mean Square Error

http://www.aloki.hu ● ISSN 1589 1623 (Print) ●ISSN1785 0037 (Online)
DOI: http://dx.doi.org/10.15666/aeer/1802_22312245

Discussion

This study provides a comparison of methods that can be used to predict the biomass carbon stock of subtropical forests in Pakistan. In this study both existing models compared against the locally developed equations showed goodness of fit statistics at $p < 0.001$. The individual significance of biophysical variables (DBH & Ht) in predicting TB was also assessed through regression analysis. In case of both species, the generic allometric model of Chave et al. (2014) was found better predicting TB considering both DBH and Ht. There was an insignificant relationship of height with TB showing that i-Tree Eco was predicting TB using DBH only suggesting utility of this tool to predict TB if height data is not available for these two species. i-Tree Eco provides a range of dataset of species specific allometric equations for many other species across diverse climatic range. The locally developed allometric equation for *A. modesta* and *O. ferruginea* also showed similar relation with DBH ($p < 0.001$) and tree height ($p = 0.793$ and $p = 0.104$, respectively) suggesting the relative importance of inclusion of individual biophysical variables in the local model.

Goodness of fit statistics of the models used in this study was evaluated on the basis of multiple criteria. Any model which had high value of R^2 adj., lowest AIC, BIC and RMSE was considered best model in predicting TB of bi-climax community of the HM forest. In case of this study, when compared to the locally developed allometric equations, the lowest AIC and BIC was found for the generic pantropical allometric model of Chave et al. (2014) for both species. This model also reported high value of R^2 adj. When evaluated for *A. modesta* but only slightly less than local equation for *O. ferruginea*. This generic model has originally been developed by taking harvest dataset of multiple species across the tropical region (Chave et al., 2014) and its evaluation in this study confirms its robustness and reliability for the forest carbon stock assessment in the subtropical region of Pakistan as well. Results of this study are consistent to the findings of Kebede and Soromessa (2018), reporting goodness of fit statistics of four species specific allometric equations for *O. europea* sub sp. *cuspidata* (synonym of *O. ferruginea*) at $p < 0.001$ and found a strong correlation of AGB with DBH and height but insignificant relation with wood density. Similarly these results are also consistent to the findings of Vieiledent et al. (2012) who reported generic models of Chave et al. (2005) as more reliable and producing less bias for TBC estimates of tropical forests when compared with other generic models.

Among the biomass and carbon estimates, the post hoc test showed no significant difference between the estimates made with local equation and generic allometric equation of Chave et al. (2014) when compared for *A. modesta*, but i-Tree Eco significantly underestimated the TB and TBC. Reasons for this underestimation might be because i-Tree Eco considered DBH only for *A. modesta* in its equation form 1 and also it computes the weight of wood only in TBC estimates for the deciduous tree species (Nowak et al., 2008). i-Tree Eco relying on DBH only did not perform well with low R^2 adj. and high RMSE and AIC compared to the local and pantropical models. Similar results have been reported by Ruiz-Peinado et al. (2012), Huy et al. (2016) and Djomo and Chimi (2017) stating that inclusion of two (DBH & Ht) or three covariates (DBH, Ht & WD) in allometric models better predict biomass than models with DBH only as covariate. From this analysis it can be inferred that in the absence of local allometric equations or restriction in doing destructive harvest to accurately measure the TBC, the pantropical model of Chave et al. (2014) can be used as an alternative to better

http://www.aloki.hu ● ISSN 1589 1623 (Print) ●ISSN1785 0037 (Online)
DOI: http://dx.doi.org/10.15666/aeer/1802_22312245

predict the TBC relying on the field measurements of DBH, height and wood density in subtropical forest.

In case of *O. ferruginea*, the post hoc test showed no significant difference in the means of TBC estimated with local equation and other two existing models. The analysis suggests that both existing models accurately estimated TBC for subtropical scrub forest compared to the local model and can be considered as equal candidate models in predicting TBC if the local equations are not available. In such case it could be advantageous to select the pantropical equation of Chave et al. (2014) than i-Tree Eco considering their relative values of AIC, BIC and R^2 adj.

Most of the biomass estimates in Pakistan are made using generic volume equation of Philip (1994) which draws simple geometric relationship between the basal area (*Eq. 2*), height (H) and form factor (F) multiplied with species specific wood density (ρ) of tree ($AGB = \rho \times [BA \times F \times H$). This model was developed by foresters and is now seldom used in carbon accounting as it assumes fixed form factor and also cannot predict biomass if height data is not available in close canopy forests (Chave et al., 2005). A comparison of biomass estimates of this study has been made with other studies conducted on sub-tropical forests in Pakistan (*Table 4*). The TB estimates of *A. modesta* made using local allometric equation in this study are comparable to the findings of Nizami (2010, 2012) made through Philip (1994) in Kherimurat and Sohawa scrub forests in Pakistan. The species specific allometric equation used by Shaheen et al. (2016) underestimated the TB of *A. modesta* (12.7 t/ha) in the mixed forest at two sites in the Muzaffarabad District, Pakistan compared to the findings of this study. In case of *O. ferruginea* the TB was overestimated (approx. Four times) with volume equation (Philip, 1994) in Shaheen et al. (2016) than current study. The difference in the estimates might be due to the incorporation of differentset of biophysical variables in species specific, generic allometric and simple volume equations in both studies. Other reasons for the difference in the estimates might be related to the tree density, topographic and climatic differences as the subtropical forest in Muzaffarabad district is at a higher elevation, has low temperature and receives higher rainfall than the HM forest as summarized in *Table 4*. Located at the foothills of lesser Himalaya the subtropical forest in Muzaffarabad district is also under anthropogenic threats (not a protected forest) and the local population rely heavily on forest for its needs related to timber, food, fodder and fuelwood resulting in under reporting of actual tree biomass and carbon (Shaheen et al., 2016).

i-TreeEco has widely been used for the estimation of carbon storage and sequestration in urban forests across the United States and European countries. To the best of our knowledge none of the study citing i-Tree Eco for reporting carbon storage of tree species from Pakistan was found in the literature. The tool calculates carbon storage and sequestration using allometric equations based on natural forest-grown North American tree species and socan fairly be used for both natural and urban forests (Nowak et al., 2013; Russo et al., 2014). Results of this study (for *A. modesta*) are consistent to the findings of Russo et al. (2014) who compared the allometric equation against i-Tree Eco and CUFR Tree Carbon Calculator (CTCC) and reported the highest carbon storage value with the allometric equation (179.14 ton), followed by CTCC (140.15 ton) and lowest by i-Tree Eco (134.89 ton) in Bolzano's urban forest, Italy. Results of present study for *O. ferruginea* are contrary to the Aguaron and McPherson (2012) who compared four sets of allometric equations i.e. i-Tree Eco, i-Tree Street, CTCC and Urban General Equations and calculated CO_2 storage of Sacramento's urban forest.

http://www.aloki.hu ● ISSN 1589 1623 (Print) ●ISSN1785 0037 (Online)
DOI: http://dx.doi.org/10.15666/aeer/1802_22312245

Table 4.*Comparison of biomass estimates of HM forest and other subtropical forests in Pakistan*

Reference (Forest type)	**Study site**	**Elevation (m)**	**Legal status**	**Climate**		***Acaciamodesta***				***Oleaferruginea***			
				Temp. (ºC)	**Av. Rainfall (mm/yr)**	**Trees/ha**	**TB estimation method (t/ha)**			**Trees/ha**	**TB estimationmethod (t/ha)**		
							Volume eq.	**Allometric eq.**	**i-Tree Eco**		**Volume eq.**	**Allometric eq.**	**i-Tree Eco**
Current study (Subtropical scrub)	Hayat-ul-Mir	457-1067	Reserved forest	24 (Av.)	800	74	17	17.4	10.3	152	21.8	23.8	23.8
Nizami (2010, 2012) (Subtropical scrub)	Kherimurat	348	Protected forest	38 (Max) 15 (Min)	750-780	197	15			94	35.7		
	Sohawa		Protected forest			179	15			56	25.3		
Shaheen et al. (2016) (Subtropical scrub)	Muzaffarabad District	800-1300	NA	20 (Av.)	1511	NA		12.7		620	68.9		

NA = Not available

http://www.aloki.hu ● ISSN 1589 1623 (Print) ●ISSN1785 0037 (Online)
DOI: http://dx.doi.org/10.15666/aeer/1802_22312245

The study reported highest estimates by i-Tree Streets (6.41 Mt) and CTCC (6.4 Mt) followed by urban general equations (5.1 Mt) and lowest estimates by i-Tree Eco (4.9 Mt). In both above mentioned studies i-Tree Eco produced the lowest estimates than other methods because in both studies AGB estimates were reduced by applying a correction factor of 0.80 before computing total tree dry weight. i-Tree Eco is designed on the basis of forest grown trees so this correction factor is applied to the open grown trees as they produce less aboveground biomass than forest grown trees (Aguaron and McPherson, 2012; Nowak et al., 2013; Russo et al., 2014). The latest version of i-Tree Eco however considers crown light exposure (CLE) in place of landuse and applies this correction factor to trees with 4 or 5 CLE. This might be one reason for differences in the estimates of HM carbon stock and other studies.

All of the methods used in this study have produced comparable results with relatively minor mean differences which might have arisen from the variation in the input of tree biophysical factors and/or values of coefficients used in allometric equations evaluated in this study. Findings of Huy et al. (2016) also reported dissimilar values of coefficients of allometric equations as one reason for the variation in AGB estimates of broadleaf evergreen forests in Vietnam.

Conclusion

Reporting and implementation of REDD+ targets in Pakistan requires accurate assessment of forest biomass carbon through reliable methods. This study conducted in the HM forest reported high tree density and biomass of *O. ferruginea* but at lower DBH and height than *A. modesta*. The study provides first evidence of applicability of existing generic biomass allometric models in the subtropical forest in Pakistan. All of the models used in this study fitted data well but among them the models considering both height and DBH as covariates better predicted total biomass than other (DBH only) based on R^2 adj., RMSE, AIC and BIC values. For *O. ferruginea* both existing models accurately predicted TB when compared to the local equation while in case of *A. modesta* significant underestimation of TB was reported by i-Tree Eco (DBH only model for this species). Considering the multiple criteria (AIC, BIC, R^2 adj. and RMSE) to evaluate the good fit statistics of the existing models against the local equations, the generic pantropical model of Chave et al. (2014) was found better predicting TB suggesting its wide applicability and robustness for both deciduous and evergreen species while i-Tree Eco for evergreen species only in subtropical forests in the absence of local allometric equations. The analysis done in this study is helpful in selecting an appropriate biomass model for subtropical region to report carbon stock changes under REDD+. The study suggests that local and generic subtropical models considering the additional effect of other factors like crown area, site characteristics and forest type must be developed and caliberated for more precise accounting of national carbon stock.

Acknowledgements. Authors are thankful to the Higher Education Commission of Pakistan for providing funds (Project No. 3867) to conduct this research and to the officials from Forest Department of Naushehra, District Khushab Pakistan for helping in the field survey.

http://www.aloki.hu ● ISSN 1589 1623 (Print) ●ISSN1785 0037 (Online)
DOI: http://dx.doi.org/10.15666/aeer/1802_22312245

REFERENCES

[1] Aguaron, E., McPherson, E.G. (2012): Comparison of methods for estimating carbon dioxide storage by Sacramento's urban forest. – Carbon Sequestration in Urban Ecosystems: 43-71. Springer, Dordrecht. 10.1007/978-94-007-2366-5_3.

[2] Ahmad, S., Ahmad, A., Nizami, S.M. (2014): Assessment of biomass expansion factor of *Piceasmithiana* (Wall) Boiss. – International Journal of Scientific and Engineering Research 5: 1232-1239.

[3] Ahmed, F. (2013): Vegetation Description of three Scrub Forests of Salt Range. – FUUAST Journal of Biology 3: 157.

[4] Basuki, T.M., Van Laake, P.E., Skidmore, A.K., Hussin, Y.A. (2009): Allometric equations for estimating the above-ground biomass in tropical lowland Dipterocarp forests. – Forest Ecology and Management 257: 1684-1694. 10.1016/j.foreco.2009.01.027.

[5] Bechtold, W. A. (2003): Crown position and light exposure classification — An alternative to field-assigned crown class. – Northern Journal of Applied Forestry 20(4): 154-160.

[6] Brown, S. (1997): Estimating biomass and biomass change of tropical forests: A primer. – FAO Forestry Paper 134.

[7] Champion, H.G., Seth, S.K., Khattak, G.M. (1965): Forest Types of Pakistan. – Pakistan Forest Institute, Peshawar.

[8] Chave, J., Andalo, C., Brown, S., Cairns, M.A., Chambers, J.Q., Eamus, D., Folster, H., Fromard, F., Higuchi, N., Kira, T., Lescure, J.P. (2005): Tree allometry and improved estimation of carbon stocks and balance in tropical forests. – Oecologia 145: 87-99. 10.1007/s00442-005-0100-x.

[9] Chave, J., Réjou-Méchain, M., Búrquez, A., Chidumayo, E., Colgan, M.S., Delitti, W.B., Duque, A., Eid, T., Fearnside, P.M., Goodman, R.C., Henry, M. (2014): Improved allometric models to estimate the aboveground biomass of tropical trees. – Global Change Biology 20: 3177-3190. 10.1111/gcb.12629.

[10] Djomo, A.N., Chimi, C.D. (2017): Tree allometric equations for estimation of above, below and total biomass in a tropical moist forest: Case study with application to remote sensing. – Forest Ecology and Management 391: 184-193.

[11] Goussanou, C.A., Guendehou, S., Assogbadjo, A.E., Kaire, M., Sinsin, B., Cuni-Sanchez, A.(2016): Specific and generic stem biomass and volume models of tree species in a West African tropical semi-deciduous forest. – Silva Fennica 50(2):1474. http://dx.doi. org/10.14214/sf.1474.

[12] Gulzar, S., Nizami, S.M., Saleem, A., Mirza, S.N., Mahmood, T. (2014): Allometric relationships for predicting the biomass in Dalbergia sissoo roxb. plantation in Punjab, Pakistan. – Pakistan Journal of Agriculture Science 51: 525-529.

[13] Huy, B., Poudel, K.P., Temesgen, H. (2016): Aboveground biomass equations for evergreen broadleaf forests in South Central Coastal ecoregion of Viet Nam: Selection of eco-regional or pantropical models. – Forest Ecology and Management 376: 276-283. 10.1016/j.foreco.2016.06.031.

[14] Kebede, B., Soromessa, T. (2018): Allometric equations for aboveground biomass estimation of Olea europaea L. subsp. cuspidata in Mana Angetu Forest. – Ecosystem Health and Sustainability 4(1): 1-12. 10.1080/20964129.2018.1433951.

[15] Khan, A.U., Ahmad, F., Sharif, F. (2013): Rapid ranking method for prioritizing restoration by evaluating human influences on the status of scrub forest: A case study. – Pakistan Journal of Botany 45(1): 11-16.

[16] Khan, A.U., Ahmad, F. (2015): Establishing links between wood trading, grazing and mining activities with the underlying trends of continuous decline of natural scrub forest cover in the Soan Valley. – FUUAST Journal of Biology 5(1): 55-62.

[17] Muhati, G.L., Olago, D., Olaka, L. (2018): Quantification of carbon stocks in Mount Marsabit Forest Reserve, a sub-humid montane forest in northern Kenya under anthropogenic disturbance. – Global Ecology and Conservation 14: e00383. 10.1016/j.gecco.2018.e00383.

http://www.aloki.hu ● ISSN 1589 1623 (Print) ●ISSN1785 0037 (Online)
DOI: http://dx.doi.org/10.15666/aeer/1802_22312245

[18] Nizami, S.M., Mirza, S.N., Livesley, S., Arndt, S., Fox, J.C., Khan, I.A., Mahmood, T. (2009): Estimating carbon stocks in sub-tropical pine (*Pinus roxburghii*) forests of Pakistan. – Pakistan Journal of Agriculture Science 46: 266-270.
[19] Nizami, S.M. (2010): Estimation of carbon stocks in subtropical managed and unmanaged forests of Pakistan. – Ph. D thesis. Arid Agriculture University, Rawalpindi, Pakistan.
[20] Nizami, S.M. (2012): The inventory of the carbon stocks in sub tropical forests of Pakistan for reporting under Kyoto Protocol. – Journal of Forestry Research 23: 377-384. 10.1007/s11676-012-0273-1.
[21] Nizami, S. M. (2014): Status of tree volume calculation and development of allometric equations in Pakistan. – International Journal of Scientific & Engineering Research 5: 441-446.
[22] Nowak, D.J., Crane, D.E., Stevens, J.C., Hoehn, R.E., Walton, J.T., Bond, J. (2008): A ground-based method of assessing urban forest structure and ecosystem services. – Aboriculture & Urban Forestry 34: 347-358.
[23] Nowak, D.J., Greenfield, E.J., Hoehn, R.E., Lapoint, E. (2013): Carbon storage and sequestration by trees in urban and community areas of the United States. – Environmental Pollution 178: 229-236. 10.1016/j.envpol.2013.03.019.
[24] Pakistan Forest Institute. (1993): Revised volume tables of tree species growing on the farmlands in NWFP. – Forestry Research Division. Forest Mensuration Branch, Pakistan Forest Institute.
[25] Parker, R.N. (1915): A Forest Flora for the Punjab with Hazara and Delhi. – Lahore Government Printing Press West Pakistan.
[26] Pearson, R.S., Brown, H.P. (1932): Commercial timbers of India.Their distribution, supplies, anatomical structure, physical and mechanical properties and uses. – Nature 132: 727-728.
[27] Philip, M.S. (1994): Measuring trees and forests. – 2nd ed. Wallingford: CAB international.
[28] Ruiz-Peinado, R., Montero, G., del Rio, M. (2012): Biomass models to estimate carbon stocks for hardwood tree species. – Forest Systems 21(1): 42-52.
[29] Russo, A., Escobedo, F.J., Timilsina, N., Schmitt, A.O., Varela, S., Zerbe, S. (2014): Assessing urban tree carbon storage and sequestration in Bolzano, Italy. – International Journal of Biodiversity Science and Ecosystem Service Management 10: 54-70. 10.1080/21513732.2013.873822.
[30] Shaheen, H., Khan, R.W.A., Hussain, K., Ullah, T.S., Nasir, M., Mehmood, A. (2016): Carbon stocks assessment in subtropical forest types of Kashmir Himalayas. – Pakistan Journal Botany 48: 2351-2357.
[31] Stas, S.M., Rutishauser, E., Chave, J., Anten, N.P., Laumonier, Y. (2017): Estimating the aboveground biomass in an old secondary forest on limestone in the Moluccas, Indonesia: Comparing locally developed versus existing allometric models. – Forest Ecology Management 389: 27-34. 10.1016/j.foreco.2016.12.010.
[32] Terakunpisut, J., Gajaseni, N., Ruankawe, N. (2007): Carbon sequestration potential in aboveground biomass of Thong PhaPhum national forest, Thailand. – Applied Ecology And Environmental Research 5(2): 93-102.
[33] Tesfaye, M.A., Bravo-Oviedo, A., Bravo, F., Ruiz-Peinado, R. (2016): Aboveground biomass equations for sustainable production of fuelwood in a native dry tropical afro-montane forest of Ethiopia. – Annals of Forest Science 73(2): 411-423. 10.1007/s13595-015-0533-2.
[34] van Breugel, M., Ransijn, J., Craven, D., Bongers, F., Hall, J.S. (2011): Estimating carbon stock in secondary forests: decisions and uncertainties associated with allometric biomass models. – Forest Ecology and Management 262: 1648-1657.
[35] Vieilledent, G., Vaudry, R., Andriamanohisoa, S.F., Rakotonarivo, O.S., Randrianasolo, H.Z., Razafindrabe, H.N., Rakotoarivony, B., Rasamoelina, M. (2012): A universal approach to estimate biomass and carbon stock in tropical forests using generic allometric models. – Ecological Applications 22: 572-583.
[36] Yuen, J.Q., Fung, T., Ziegler, A.D. (2016): Review of allometric equations for major land covers in SE Asia: uncertainty and implications for above-and below-ground carbon estimates. – Forest Ecology and Management 360: 323-340. 10.1016/j.foreco.2015.09.016.

http://www.aloki.hu ● ISSN 1589 1623 (Print) ●ISSN1785 0037 (Online)
DOI: http://dx.doi.org/10.15666/aeer/1802_22312245

APPENDIX

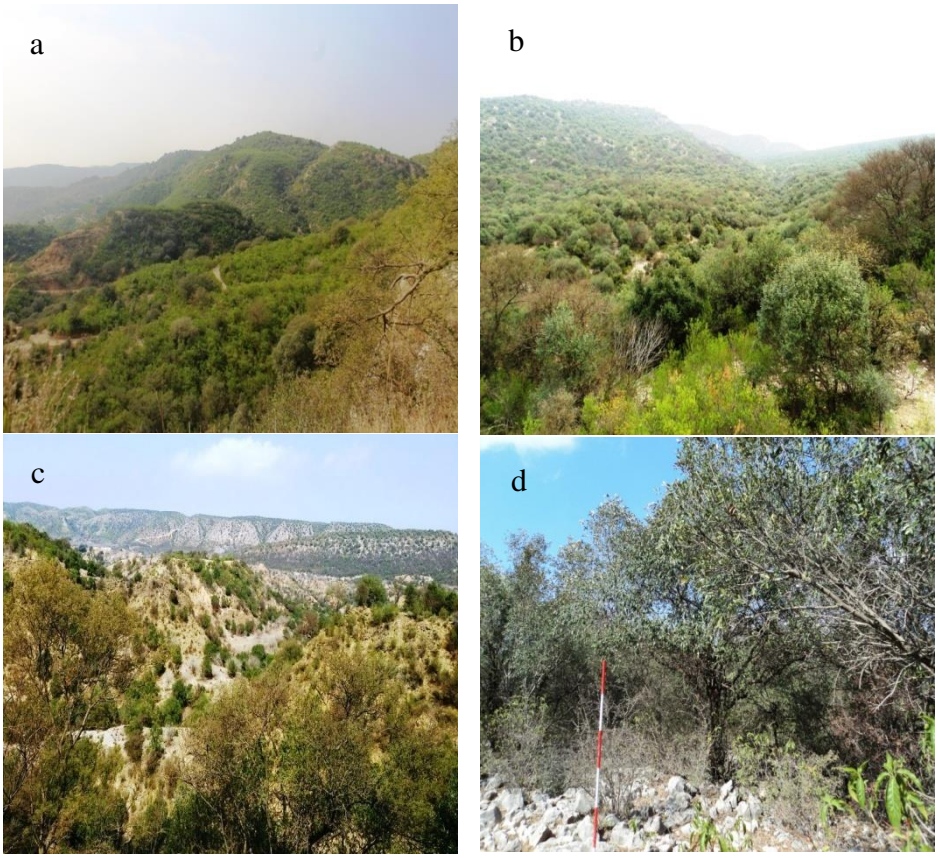

Figure A1. *(a to c) Dense co-occurring bi-climax community of A. modesta and O. ferruginea with shrub cover in the HM forest, (d) Setting up of sampling plots for biomass estimation*

Table A1. *GPS coordinates and altitude of sampling plots*

Coordinates	Altitude (m)	Coordinates	Altitude (m)	Coordinates	Altitude (m)
32.54378N, 72.24603E	853	32.52299N, 72.29811E	806	32.54058N, 72.28813E	818
32.54378N, 72.28457E	895	32.52590N, 72.30344E	806	32.53712N, 72.28403E	801
32.54590N, 72.29012E	860	32.52658N, 72.30799E	823	32.53595N, 72.28708E	782
32.54565N, 72.29782E	889	32.52653N, 72.31088E	834	32.53663N, 72.29047E	788
32.54565N, 72.30630E	916	32.52851N, 72.30931E	835	32.53762N, 72.29443E	816
32.54650N, 72.31582E	964	32.53119N, 72.30129E	800	32.53912N, 72.29766E	815
32.54880N, 72.31965E	1011	32.53097N, 72.29304E	795	32.54180N, 72.29531E	822
32.55020N, 72.32185E	1017	32.53261N, 72.28919E	756	32.57238N, 72.35765E	865
32.54950N, 72.32417E	984	32.54402N, 72.29347E	835	32.56917N, 72.35498E	813
32.55020N, 72.32721E	952	32.54409N, 72.30031E	861	32.56480N, 72.35040E	833
32.55463N,72.32618E	895	32.54099N, 72.30845E	826	32.55992N, 72.35088E	757
32.55580N, 72.32853E	975	32.53990N, 72.31048E	834	32.55402N, 72.35090E	620
32.53060N, 72.28817E	768	32.53807N, 72.31328E	842	32.55147N, 72.34605E	721
32.52850N, 72.29045E	779	32.53571N, 72.31151E	835	32.5500N, 72.336530E	885
32.52599N, 72.29499E	802	32.53370N, 72.30923E	823	32.55265N, 72.33180E	909
32.52153N, 72.29754E	788	32.54207N, 72.29202E	848		

http://www.aloki.hu ● ISSN 1589 1623 (Print) ●ISSN1785 0037 (Online)
DOI: http://dx.doi.org/10.15666/aeer/1802_22312245

DEVELOPING THE NEW MULTI RUST RESISTANT BREAD WHEAT CULTIVAR "MAAROOF" FOR THE IRRIGATED AND RAIN-FED ZONES OF IRAQ

AL-MAAROOF, E.[1*] – SALEH, R.[1] – MAHMOOD, H.[1] – NEFEL, A.[2] – ABDULRAHMAN, N.[3]

[1]*College of Agricultural Sciences Engineering, University of Sulaimani, Iraq*

[2]*Ministry of Science and Technology, Iraq*

[3]*Ministry of Agriculture and Water Resources, IKR, Iraq*

[*]*Corresponding author*
e-mail: ealmaaroof@yahoo.com; emad.ghalib@univsul.edu.iq

(Received 10th Oct 2019; accepted 30th Jan 2020)

Abstract. Following the designation of R-30 as a source of resistance to the three rusts; it was successfully introduced in a breeding program with Tamuz 2 using the pedigree method in 1997. The progenies of three successive generations (F3-F5) were screened for resistance to the three rusts under artificial inoculation conditions at the adult plant stage in Twaitha. Out of 135 hybrid lines, 12 promising lines were selected. The selected lines were introduced in a comprehensive evaluation test for yield potential and response to rusts and bunt diseases in different locations. As a result, the promising line "63" was selected due to its high grain yield in the presence and absence of rusts and bunt diseases. Yield potential of the genotype is 10-19% higher than that of the local commercial cultivars Araz and Tamuz 2. Maaroof was registered and released as a new cultivar with high yield potential and multi resistance to rusts and bunt diseases by the National Committee of Registration and Release of Agricultural Cultivars/Iraqi ministry of agriculture. There was a great emphasis on multiplication and delivery of the seeds to farmers. Yield potential of Maaroof on farm-scale was 3750 and 4750 kg/ha under rain-fed and irrigated conditions respectively.
Keywords: *Triticum aestivum, host resistance, wheat rusts, new genotypes, Iraq*

Introduction

Wheat (*Triticum aestivum* L.) is one of the most essential and strategic cereal crops for the majority of the world's population. It is the most critical staple food for about two billion people (36% of the world population). Worldwide, wheat provides nearly 55% of the carbohydrates and 20% of the food calories consumed globally (FAOSTAT, 2018). Wheat production area's in Iraq is divided into rain-fed and irrigated zones. Rain-fed areas are mainly in the north including Kurdistan region. An estimated 3.0 million tons of wheat were harvested in 2018, with a 14% reduction from 2017 production and 20% from the past five-year average, largely due to unfavorable environmental conditions. Nearly the same amount of wheat had been purchased by mid-August 2018 (FAO, 2018). In 2015, USDA projected that Iraq would continue to experience a long-term shortfall in wheat production and that it would need to import 3.8 million tons in 2015-16, followed by larger quantities each year after. By 2024-25, it projected that Iraq would require 4.9 million tons of wheat imports annually (USDA, 2015).

Biotic and abiotic stress particularly drought and salinity, are the leading causes of losses in wheat production. Many diseases can attack wheat, mainly caused by fungi, bacteria, and viruses. Yellow, brown and black stem rust diseases incited by the fungi *Puccinia striiformis* f. sp *tritici*, *P. triticina* and *P. graminis* f sp. *tritici* respectively are the most critical grain yield-limiting factor of wheat in Iraq followed by common bunt

http://www.aloki.hu ● ISSN 1589 1623 (Print) ● ISSN1785 0037 (Online)
DOI: http://dx.doi.org/10.15666/aeer/1802_22472258

disease; *Tilletia tritici* and *T. laevis* (Al-Maaroof et al., 2001, 2005, 2012). Yield losses due to the three rusts on wheat cultivars vary from 10 to 70% depending on the levels of resistance, stage of the crop at disease onset, pathogen races and, the environmental conditions (Al-Maaroof et al., 2001; Al-Maaroof and Nori, 2018).

Breeding for disease resistance is the most sustainable strategy to reduce yield losses, and also it is an environmentally safe approach to control the diseases (Line and Chen, 1995; Singh and Trethowan, 2007). Great importance is given to improve disease resistance in wheat using different breeding programs in Iraq (Ibrahim et al., 1993a,b). Several resistant and high yielding wheat cultivars were released in the nineteens (NCFRRAV, 2014). Successive release of the resistant cultivars participated in reducing grain yield losses caused by rust (Al-Maaroof et al., 2001, 2005, 2012). With the introduction of the resistant varieties new virulence's and races of rust pathogens also develop due to mutation or genetic recombination's that have contributed in switching resistance of these varieties (Al-Maaroof et al., 2003, 2005, 2010, 2012). Therefore, breeding for resistance to rust diseases and developing new resistant cultivars having higher yield potential became the main target in all wheat breeding programs and considered as the most economical and effective way to eliminate the use of fungicides and reducing crop losses caused by the disease (Singh et al., 2004).

The present study represents a long term breeding program for developing a new multi-resistant bread wheat cultivar "Maaroof" with different levels of resistance to brown, yellow, stem rust and common but diseases.

Material and Methods

Following designation of R-30 as a source of multiple resistance to the three rusts among hundreds of genotypes that was previously tested to rust diseases for five consecutive season under artificial inoculation conditions with the prevalent dominant races of the pathogens in different environmental conditions in Iraq (Al-Maaroof et al., 2002); it has successfully introduced in a breeding program with the promising local cultivar Tamuz 2 using the pedigree method in 1997. The progenies of three successive generations (F3-F5) were screened to the three rusts under artificial inoculation conditions at the adult plant stage in Twaitha research experimental station. The test variants were planted in a single 2-meter long, 30 cm apart. The highly susceptible cultivars Morocco and SaberBeg were used as spreaders. One hundred thirty-five hybrid lines were evaluated based on their desired agricultural characteristics, drought tolerance and resistance to rust and common bunt diseases in observation and preliminary comparative experiments with the parents under both irrigated and rain-fed conditions (Pessarakli, 2011). The best 12 selected genotypes were introduced in small scale yield trial conducted at Latifia and Bakrajo experimental stations in 6 rows plot of 4.0 m length spaced at 30 cm along with the local checks in RCBD with three replicates. Comprehensive evaluation test for grain yield potential, grain quality and response to the three rusts and bunt diseases were promoted in multi locations and agro-system in Large scale yield trial tests using RCBD with three replications in 16 rowed plots of 6.0 m length spaced at 30 cm. The recommended agricultural practices were adopted to raise a satisfactory crop as per ministry of agriculture (MOA) standards.

Artificial inoculations with a mixture of field collection of the three rust prevalent virulence's were carried out during March in each location using aqueous uredospore suspension to which two drops of Tween-20 were added to break the surface tension.

http://www.aloki.hu ● ISSN 1589 1623 (Print) ● ISSN1785 0037 (Online)
DOI: http://dx.doi.org/10.15666/aeer/1802_22472258

Seeds of each genotype were artificially inoculated with a bulk population of *T. tritici*, *T. laevis* and *T. intermedia* teliospores collected from different locations in the previous season at a rate of 0.5 g/100 g seeds. Inoculated seeds were mechanically mixed for 15 minutes by shaker at 80 rpm/minute (Gotes, 1996). Each genotype was planted by hand at a depth of 5 cm in two 1.5 m rows (5 g seed/line) spaced 30 cm between lines and 60 cm between treatments at Twaitha, Baghdad (Irrigated) and Talefar, Nineveh (Rain-fed).

Disease scoring for the three rusts was recorded as infection type on each genotype (Stakman et al., 1962; Lewllen et al., 1967) and disease severity as percent infection on the plants according to the modified Cobb's Scale (Peterson et al., 1948). Coefficient of Infection (CI) was calculated by multiplying the response value with the intensity of infection in percent (Roelfs et al., 1992). Infection percent of each genotype to common bunt disease was calculated at dough stage by counting the number of healthy and infected spike per each meter according to Dodov and Todorova (1974) modified method.

During the coordinated evaluation, data on agronomic traits including plant height, flag leaf area, stem width, spike length and awn length were recorded from ten random plants in each experimental unit; yield component traits including number of spike per square meter, spike weight, thousand grain weight, number of grain per each spike, grain weight per each spike were calculated from 50 randomly selected spikes from each plot at dough stage; grain yield was calculated by random harvesting of plant spikes in one meter square from the center of each plot at dough stage when the grain moisture was 14% (Bell and Fischer, 1994); disease resistance, quality attributes, and agronomical manipulations were also recorded (AACC, 2000; Salman and Mahdi, 2005). All the data were statistically analyzed at p=0.05 significant levels using the method of analyses of variance (ANOVA). Least significant differences at 5% level were used to compare the mean of traits.

The high yielding resistant promising genotypes were sent for registration and release by the ministry of agriculture. Great emphasis was done on multiplication of high-grade seed of the new cultivar "Maaroof" then delivering them to the farmers.

Results and Discussion

Results of screening (R-30/Tamuz2) hybrid variants to the three kind of rusts and common bunt diseases under artificial inoculation conditions at the adult plant stage and some other agronomic traits are represented in *Table 1*. In general, out of 135 tested variants; 18 resistant and 43 moderately resistant were identified to brown, yellow and stem rust diseases either alone or in combinations, while 38 genotypes out yielded their parents and 31 variants characterized with earliness on their parents. Eleven variants continued in their resistance to brown rust through the study period, while 8 and 5 variants explored resistant reaction to yellow and stem rust diseases, respectively. Moderately resistance reaction was diagnosed in 26, 19 and, 5 variants to brown, yellow and stem rust diseases, respectively. Common bunt disease resistance was identified in 5 resistant and 18 moderately resistant variants, respectively. Thirty-three and 65 variants were resistant and moderately resistant to lodging, while six variants only showed drought tolerance. Selection of the variants for further studies were carried out based on their resistance to the target disease alone or in combination accompanied with yield and yield components with other agronomic traits, where number of selected resistant and moderately resistant variants reached to 9, 12, 8, 14, 17 and 5 in brown rust, yellow rust,

http://www.aloki.hu ● ISSN 1589 1623 (Print) ● ISSN1785 0037 (Online)
DOI: http://dx.doi.org/10.15666/aeer/1802_22472258

stem rust, common bunt, lodging, and drought tolerance tests. Among the selected variants, the best 12 genotypes were introduced in small yield trails.

Table 1. *Host reaction of (R-30/Tamuz 2) hybrid variants to Yellow, brown stem rusts and common bunt diseases and some other related agricultural traits during 2001 to 2003 at Twaitha and Telafar experimental stations, Iraq*

Target Traits	Host Reaction*				Earliness	Out Yielded	No. of selected variants
	R	MR	MS	S			
BROWN RUST	11	26	18	80	31	38	9
YELLOW RUST	8	19	32	76	31	38	12
STEM RUST	5	13	26	93	31	38	8
COMMON BUNT	5	17	-	113	31	38	14
LODGING	33	65	27	8	31	38	17
DROUGT TOLERANCE	6	18	63	48	31	38	5

*: R, resistant; MR, moderately resistant; MS, moderately susceptible; S, susceptible

The results of *Table 2* show that the average grain yield and yield components of the selected (R-30/Tamuz 2) hybrid variants compared to the local cultivar during three successive seasons 2004-2006 at Latifia; indicating that there is a clear superiority of 1-14% in the mean of grains yield of the selected genotypes on Tamuz 2. The advantage was attributed mainly to improving grain filling rate by 37% in the best variant and 10% increase in plant tillering trait (number of ears per square meter).

Table 2. *Grain yield and yield component performance of the selected (R-30/Tamoz 2) hybrid variants comparing with the local cultivar in micro trials at Latifia and Jaderiah experimental station, Baghdad, Iraq during 2004-06*

Trait	Season	Genotype													LSD
		Tam. 2	2	10	13	20	23	32	33	61	63	76	84	113	0.05
PLANT HEIGHT (cm)	2004	94.6	100.1	98.9	91.0	107.5	105.2	88.6	110.3	96.0	101.5	108.5	98.4	94.3	4.5
	2005	86.3	97.2	95.4	87.6	95.3	100.7	92.4	99.3	94.8	97.9	101.2	88.5	89.5	N.S
	2006	92.1	98.2	95.6	88.2	103.4	103.5	90.6	107.4	91.0	105.6	105.3	96.4	88.5	3.6
	Mean	91.0	98.5	93.3	88.9	102.1	103.1	90.5	105.6	93.9	101.7	105.0	94.4	90.7	4.1
NUMBER OF SPIKE /m^2	2004	306.2	310.6	314.6	365.4	325.6	331.5	321.5	335.5	306.0	327.8	326.6	365.0	305.0	15.1
	2005	315.3	291.4	338.1	331.6	305.5	326.7	350.2	316.8	333.4	339.2	316.7	336.3	312.7	19.3
	2006	310.7	327.5	313.5	330.0	311.0	306.5	330.4	326.0	302.5	356.3	312.7	315.3	303.6	17.9
	Mean	310.7	309.8	322.0	342.3	314.0	321.6	334.0	326.1	313.9	341.1	318.6	338.8	307.1	17.4
GRAIN WEIGHT /SPIKE (g)	2004	2.19	2.25	2.16	2.23	2.23	2.17	1.97	2.45	2.07	2.26	2.35	2.13	1.87	N.S
	2005	2.08	2.17	2.25	2.34	2.47	2.26	2.10	2.60	2.17	2.32	2.14	2.35	2.10	0.18
	2006	2.14	2.22	2.12	2.17	2.32	2.30	1.84	2.35	1.98	2.35	2.21	2.30	1.80	0.21
	Mean	2.13	2.21	2.17	2.25	2.34	2.24	1.97	2.46	2.07	2.31	2.23	2.26	1.92	0.20
NUMBER OF GRAINS /SPIKE	2004	56.9	55.3	45.6	52.6	53.2	55.7	46.7	52.0	46.3	49.6	54.5	44.1	51.0	3.5
	2005	54.5	57.4	43.8	55.7	55.4	56.9	50.3	54.5	47.8	53.5	58.3	59.3	55.4	3.1
	2006	53.2	53.5	46.1	55.0	53.5	57.4	47.2	53.4	45.6	56.7	55.1	53.2	50.5	3.0
	Mean	54.8	55.4	45.1	45.4	54.0	56.7	48.0	53.3	46.5	53.2	55.9	52.2	52.3	3.2
1000 GRAIN WEIGHT (g)	2004	37.56	44.33	45.72	39.70	45.33	44.75	39.32	54.02	43.11	56.95	41.60	41.03	38.50	2.5
	2005	39.14	45.60	47.10	43.43	47.12	45.02	40.53	56.50	45.63	51.37	43.21	42.61	40.63	1.9
	2006	40.15	43.59	44.54	41.59	47.84	43.90	38.61	53.41	41.52	52.43	47.10	42.42	35.71	2.3
	Mean	38.95	44.53	45.82	41.54	46.73	44.42	39.42	54.61	43.42	53.55	43.90	42.02	38.27	2.2
GRAIN YIELD/M^2 (g/m^2)	2004	501.4	538.2	585.6	515.4	595.2	567.3	509.0	589.7	497.0	537.0	489.5	585.1	465.7	27.1
	2005	487.5	514.0	554.3	523.5	524.0	535.0	489.5	518.6	503.2	609.6	513.6	554.8	495.3	35.5
	2006	503.2	465.6	523.8	506.3	553.6	529.6	510.0	473.3	501.2	542.4	524.7	560.6	483.7	31.7
	Mean	497.4	529.3	554.5	515.0	557.6	544.0	502.6	527.2	500.3	563.0	509.3	566.8	481.6	31.4

http://www.aloki.hu ● ISSN 1589 1623 (Print) ● ISSN1785 0037 (Online)
DOI: http://dx.doi.org/10.15666/aeer/1802_22472258

Variance analysis of the data indicates the presence of significant differences among the genotypes in the mean of grain yield. Variant 84 out yielded all other genotypes with 566.8 g/m^2 and significantly surpassed most of the other variants including the local cultivar followed by variant no.63 that produce 563.0 g/m^2, while the lowest grain yields were created by the local check and variant no.113 with 497.4 and 481.6 g/m^2, respectively. The high yield potential in genotype 84 is mainly attributed to the high number of spike per meter square (338.8), while in genotype 63 is due to the top grain weight and the number of spike per meter square (53.55 and 341.1).

Number of spike per unit area, number of grain per spike and grain weight are the principle grain yield component of wheat (Al-Eseel, 1998). Each character separately or in combination with each other can increase or decrease grain yield in wheat. Grain yield is a complex character that depends on a large number of environmental, morphological, and physiological factors (Alam et al., 2007). High significant differences in grain yield components among the genotypes indicate the role of hybridization as a breeding method to induce wide genetic variations in the second generation, which has assisted in selecting the promising genotypes in the segregated generations (Baktash, 2001).

Table 3 data represent grain yield and yield components of the selected (R-30/Tamuz 2) genotype compared to the common local cultivar during three successive seasons 2009-2011 under Bakrajo experimental station representing rain-fed cultivation system; Variance analysis of the data indicates the presence of significant differences among the tested genotypes in the mean of grain weight per each spike, the maximum value of grain weight was detected in genotype 84 (1.97 g) which was significantly surpassed all other genotypes followed by genotype 63 (1.93 g), while the lowest value of spike grains weight was recorded in genotype 10 (1.61 g). Significant differences were detected in the effect of the genotypes in thousand-grain weight; the highest value (42.32 g) was recorded in genotype 33, which was significantly surpassed all other genotypes except genotype 63. Results also showed significant differences among the genotypes in the number of grains per spike; the highest value of this trait (56.8) was detected in genotype 84, which was significantly surpassed all other genotypes followed by genotype 63, while the lowest grain number of spikes were produced by genotype 23 (*Table 3*).

Number of grains per spike is one of the crucial components of yield. That's why any change in this value will directly affect the grain yield of the cultivar (Rajaram et al., 1996). Many biotic and abiotic factors can reduce the grain number per spike; also, the higher seed rate can result from low grains in the spike (Al-Maaroof et al., 2001).

Genotype 63 significantly surpassed all the tested genotypes in the number of spikes per meter square by producing 587.3 spike per meter square followed by genotype 84, while the lowest spike number per unit area was produced by genotype 10 (434.5) (*Table 3*).

The number of spikes per unit area depends on the genotype and environment and strongly influenced by seed rate and plant density, high temperature enhances fast development of the plant and low tillers production (Loveras et al., 2004).

Significant differences also detected among the genotypes in the mean of grain yield. Genotype 63 out yielded over all other genotypes with 399.1 g/m^2 and significantly surpassed all other genotypes except genotype 84, while the lowest grain yields were produced by genotypes 83 with 326.6 g/m^2. The lesser grain yield production of the genotypes in 2010 compared with 2009 and 2011 is mainly due to the unfavorable environmental conditions and the severe epidemic of yellow rust in 2010 (Al-Maaroof et al., 2012).

http://www.aloki.hu ● ISSN 1589 1623 (Print) ● ISSN1785 0037 (Online)
DOI: http://dx.doi.org/10.15666/aeer/1802_22472258

Table 3. *Grain yield and yield component performance of the selected (R-30/Tamoz2) hybrid variants comparing with the local cultivar in micro trials at Bakrajo experimental station, Sulaimania, Iraq during 2009-11*

Trait	Season	Genotypes								LSD 0.05
		Aras	10	20	23	33	63	83	84	
PLANT HEIGHT (cm)	2009	87.3	85.6	94.2	90.5	94.2	86.3	81.4	87.4	3.5
	2010	103.7	98.6	112.3	103.3	109.3	102.7	105.3	102.0	4.3
	2011	83.7	85.3	89.4	81.5	85.4	84.7	85.3	84.7	3.6
	Mean	91.6	89.9	98.7	91.8	96.3	91.2	90.7	91.4	3.7
NUMBER OF SPIKE /m^2	2009	527.3	476.5	475.9	481.7	495.5	589.6	478.4	551.0	17.4
	2010	516.1	453.4	473.2	516.5	526.9	612.8	486.7	536.1	15.2
	2011	507.3	373.5	414.0	456.6	513.0	559.5	362.7	554.3	15.3
	Mean	516.9	434.5	454.4	484.9	511.8	587.3	442.6	547.1	16.1
GRAIN WEIGHT /SPIKE (g)	2009	1.85	1.78	1.90	1.93	2.03	1.93	1.85	2.15	0.16
	2010	1.73	1.65	1.86	1.91	1.93	2.06	1.71	2.16	0.15
	2011	1.60	1.41	1.53	1.32	1.46	1.67	1.36	1.59	0.18
	Mean	1.73	1.61	1.76	1.72	1.81	1.88	1.64	1.97	0.17
NUMBER OF GRAINS /SPIKE	2009	51.8	50.6	54.21	48.6	50.1	56.8	50.5	55.7	2.9
	2010	41.4	42.9	45.8	41.9	43.0	47.5	42.3	49.1	2.7
	2011	48.7	46.1	48.5	43.3	41.4	54.5	45.1	58.2	3.1
	Mean	47.3	46.5	49.5	44.6	45.0	52.9	46.0	54.3	3.0
1000 GRAIN WEIGHT (g)	2009	39.65	41.34	43.55	40.35	48.42	45.75	41.50	40.03	2.1
	2010	38.31	37.10	38.63	46.31	46.70	44.80	39.21	38.56	1.9
	2011	33.70	29.30	27.90	31.33	31.83	32.35	27.21	26.81	1.7
	Mean	37.22	36.08	36,69	39.33	42.32	40.91	35.97	35.13	1.8
GRAIN YIELD/M^2 (g/m^2)	2009	328.3	344.2	398.1	352.7	371.5	385.5	330.3	360.9	23.5
	2010	236.7	244.3	305.6	285.0	318.6	369.3	265.5	354.8	19.3
	2011	418.2	385.6	418.0	389.3	426.3	442.5	384.0	409.3	25.6
	Mean	327.7	358.0	373.9	342.3	372.1	399.1	326.6	375.0	23.4

The high yield potential of genotype 63 is mainly attributed to the higher number of spike per meter square (587.3), while in genotype 84 was due to the higher number of grains per spike and number of spike per meter square (54.3 and 447.1, respectively).

Based on the above data and information concerning the performance of the tested genotypes and their response to the main wheat diseases under different environmental conditions, Genotype 63 was candidate to the large scale yield trail and multi-location test with the dominant local wheat cultivars in each location and nominated for registration and release under the name of "Maaroof".

Macro wheat yield trial results at Bakrajo experimental station (*Table 4*) shows that grain yield of Maaroof ranged from 3878.5 to 4548.7 kg ha^{-1} as compared to cv. Aras and Tamuz 2 in 2012 and 2013 for which grain yields ranged from 3454.2 to 3975.6 and 3696.8 to 4346.3 kg ha^{-1}, respectively. The new cultivar Maaroof out yielded both local cultivars by 12.3-14.4% in Aras and 4.7-12.2% in Tamuz 2 in 2012 and 2013, respectively.

The mean high yield potential of Maaroof (4213.6 kg ha^{-1}) is mainly attributed to the high number of spike per meter square (601.2) which is significantly surpassed the mean of the same trait in Aras and Tamuz 2 by 5.3 and 14.5%, respectively. Tamuz 2 significantly surpassed Maaroof and Aras in the mean number of grain per spike by 7.5% and 14%, respectively, while Aras significantly surpassed Tamuz 2 in the mean number of spike per meter square by 8.7% (*Table 4*).

http://www.aloki.hu ● ISSN 1589 1623 (Print) ● ISSN1785 0037 (Online)
DOI: http://dx.doi.org/10.15666/aeer/1802_22472258

Table 4. *Grain yield and yield component performance of Maaroof as compared with the local cultivars in macro yield trials at Bakrajo, Sulaimania, Iraq during 2012-13*

Traits	Season	Cultivar			LSD 0.05
		Aras	Tamuz	Maaroof	
GRAIN WEIGHT /SPIKE (g)	2012	1.54	1.88	1.71	0.14
	2013	1.63	2.06	1.83	0.17
	Mean	1.59	1.97	1.77	0.15
1000 GRAIN WEIGHT (g)	2012	32.41	33.41	32.70	0.85
	2013	33.30	37.35	33.81	1.31
	Mean	32.86	35.38	33.26	1.13
NUMBER OF GRAINS /SPIKE	2012	50.5	59.1	54.2	1.82
	2013	54.3	60.4	56.5	2.35
	Mean	52.4	59.75	55.4	2.10
NUMBER OF SPIKE /m^2	2012	557.3	513.4	589.1	23.15
	2013	584.6	536.9	613.2	26.30
	Mean	571.0	525.2	601.2	24.63
GRAIN YIELD/M^2 (g/m^2)	2012	3454.2	3696.8	3878.5	135.4
	2013	3975.6	4346.3	4548.7	156.1
	Mean	3714.9	4021.5	4213.6	145.3

Multi-location comparison of the new cultivar "Maaroof" with the predominant check cultivar for grain yield in 7 locations with different agro-ecological zones representing the main wheat production area's across Iraq is given in *Table 5*. Results revealed that Maaroof gave 14.3% higher grain yield than the check cultivar Aras on the bases of 5 locations and 6.3% and on Tamuz 2 on the bases of four locations. Grain yield increase of Maaroof ranged from 1.5-42.6% on Aras and 1.5 to 6.3% on Tamuz 2 based on the locations. No significant differences were obtained in the grain of Maaroof and Adana in four locations except in Erbil where Adana out-yielded Maaroof by 6.3%.

Table 5. *Grain yield performance of Maaroof compared with the local wheat cultivars at multi-location yield trials during 2014-2015*

Location	Grain yield (kg ha^{-1})				LSD 0.05
	Aras	Tamuz	Adana	Maaroof	
SULAIMANI	3567.4	3754.3	3883.1	3943.5	183.6
DOHUK	4025.1	---	4050.0	4065.1	N.S
ERBIL	2891.5	---	3180.6	2979.3	198.5
KALAR	3153.0	---	3650.1	3585.2	203.0
DIALA	---	4548.6	---	5060.7	316.5
WASIT	---	4165.5	---	4465.0	276.4
NINEVEH	2307.4	3122.8	---	3291.5	235.8
MEAN	3189.9	3897.8	3690.9	3912.9	-

Differences in genotype performance in different locations clearly state the interaction between the genotype and environment in each location as it is indicated in earlier studies (Annicchiarico, 2002).

Table 6 results represent a wide range of host reaction between the tested bread wheat cultivars with the natural populations of *P. striiformis, P. graminis* f.sp *tritici* and *P. triticina* pathogens started from high resistance reaction in Maaroof to high susceptibility in SaberBeg and Adana. Maaroof explored multiple resistance reaction to yellow and stem rust diseases and moderately resistance to brown rust diseases during the

http://www.aloki.hu ● ISSN 1589 1623 (Print) ● ISSN1785 0037 (Online)
DOI: http://dx.doi.org/10.15666/aeer/1802_22472258

severe Epidemics of the diseases through the study period. While all the local cultivars showed moderately susceptible to highly susceptible response to yellow and brown rust diseases, and only susceptible to highly susceptible response to stem rust disease. Furthermore, high significant differences between the tested cultivars in coefficient of infection value (C.I), the highest amount of C.I was recorded in Saber Beg and Maxipak to yellow rust (10.02 and 81.3, respectively), and brown rust disease (9.70 and 9.25) respectively, while to stem rust detected in SaberBeg and Adana (8.87 and 8.79, respectively). The new cultivar Maaroof showed the lowest C.I value to the three rust diseases. Maaroof significantly decreased the coefficient of infection value to yellow rust by 95-99%, Stem rust by 97-98% and brown rust by 90-95% as compared with the commercial wheat cultivars.

Table 6. *Mean coefficient of infection value (CI) and infection type (IT) of Maaroof to yellow, brown and black stem rust diseases as compared with the local wheat cultivars during the epidemic of each disease during 2010 to 2014*

Cultivar	Yellow Rust		Stem Rust		Brown Rust		Mean	
	IT[1]	CI[2]	IT	CI	IT	CI	IT	CI
SABERBEG	HS	100.0 10.02[3]	HS	78.3 8.87	HS	93.5 9.70	HS	90.6 9.54
ARAS	S	77.5 8.83	S	63.3 7.99	S	56.4 7.54	S	65.7 8.14
MAXIPAK	S	81.3 9.04	S	76.0 8.75	S	85.0 9.25	S	80.8 9.02
TAMUZ 2	MSS	56.0 7.52	S	53.7 7.36	S	60.3 7.80	MSS	56.7 7.56
ADANA	MS	30.5 5.57	HS	76.7 8.79	MSS	43.0 6.60	MSHS	50.1 7.11
MAAROOF	R	0.9 1.18	R	1.1 1.26	MR	4.3 2.55	RMR	2.7 1.79
LSD 0.05		1.23		0.85		0.91		0.99

1. IT: Infection Type, R= Resistant, MR= Moderately Resistant, MS= Moderately Susceptible, S= Susceptible, HS= Highly Susceptible (Stakman et al., 1962).
2. Coefficient of infection (CI): calculated by multiplying the Disease severity (DS)value with Infection Type (IT) (Roelfs et al., 1992).
3. Data transformed using Arcsine Transformation Formula for analysis purpose

The coefficient of infection value facilitates the statistical ranking or comparison between the genotypes with different responses to the disease. It is adding two separate factors in a single value results in nearly equal coefficient but from different disease score. The differences in the genetic background of resistance reflect the differences in the infection type toward the disease. The infection type in some cultivars may be changed by time due to the appearance of new virulences in the pathogen population. Some cultivar may stay resistant to many years, but after a period it will be susceptible. Al-Maaroof et al. (1995) mentioned Tamuz 2 was resistant at the time of release in 1992 while later on became susceptible. An unknown gene identified to confer resistance to Tamuz 2 (Al-Maaroof et al., 2005). The ability of the pathogen to change itself and its virulence and appearance of more aggressive pathogen might happen by the sexual reproduction, combination or crossing methods and other mechanisms. Hence, it is essential to study the pathogen population annually to recognize the new virulence's that may come from different countries mainly the disease is airborne, which make it very difficult to control, and it may overcome resistance of some cultivars after release

http://www.aloki.hu ● ISSN 1589 1623 (Print) ● ISSN1785 0037 (Online)
DOI: http://dx.doi.org/10.15666/aeer/1802_22472258

according to boom and bust cycle (Roelfs et al., 1992). Possessing more resistant genes in one cultivar increased the time of resistance stability, and decrease the probability of developing new virulence's (Messmer et al., 2000; Marasas et al., 2001). Based on this fact, we started our breeding program to improve resistance level in Tamuz 2.

Recently, many new virulence's and races were detected in Iraq that can attack most of the local wheat cultivars, such as Yr27 in *P. striiformis* population and race TKKTF and TTTTF in *P. graminis* populations (Al-Maaroof et al., 2015; Al-Maaroof, 2017).

The new promising genotype "Maaroof" was a candidate for registration and release as a new wheat cultivar for irrigated and rain-fed area's in Iraq due to its higher grain yield potential over the local commercial cultivars in the presence and absence of rust diseases. Mean coefficient infection of the cultivar was 0, 1.2, and 4.3 to yellow, stem, and brown rust diseases, respectively. It was also moderately resistant to common bunt, leaf blotch diseases, and tolerant to drought (*Table 7*). Molecular marker analysis of Maaroof using twelve SSR markers indicated the presence of the known resistant genes *Lr24* and *Lr46* to leaf rust disease, *Yr29* to yellow rust disease and *Sr22*, *Sr36* and *Sr46* to stem rust disease. Presence of some other unknown resistant genes as well probably will participate in conferring the multiple resistance to this cultivar against the three rust diseases at the adult plant stage. Yield potential of the new cultivar "Maaroof" was 10-19% higher than Araz and Tamuz 2. Grain yield potential of Maaroof on farm-scale ranged from 3750 and 4750 kg/ha under rain-fed and irrigated conditions, respectively. Most of the agronomic traits, qualitative and quantitative characteristics of the new bread wheat cultivar "Maaroof" presented in *Table 7* which indicates that Maaroof has shown good suitability for industrial and product making as well. It possesses higher value for other quality traits like protein content (15%), hectoliter weight (79.1), Specific loaf volume (cm^3/g) (2.37) that fall in the category of good quality according to the grain quality standers (AACC, 2000). Physiochemical, rheological, and baking characteristics of Maaroof is also confirmed in earlier studies (Sabir and Al-Maaroof, 2018).

Table 7. *Some agronomic traits, qualitative and quantitative characteristics of the new bread wheat cultivar "Maaroof"*

Agronomic traits		**Grain yield & quality**		**Biotic & abiotic Resistance**	
PLANT HEIGHT(cm)	100-115	1000 GRAIN WEIGHT (g)	40-43	BROWN RUST	MR
SPIKE LENGTH (cm)	11-12	No. OF GRAINS/ SPIKE	48-58	YELLOW RUST	R
AWN LENGTH (cm)	6 -7	No. OF SPIKE /m^2	450-500	STEM RUST	R
SHAPE OF AIR	Fusiform	GRAIN YIELD (kg/ha)	4500-5000	COMMON BUNT	MR
FLOWERING TIME (d)	110-115	PPROTEIN %	15.0	LEAF BLOTCH	MR
MATURITY TIME(d)	135-145	WET GLUTEN %	42.0	DROUGHT	T
FLAG LEAF AREA (cm^2)	40 -52	FLOUR EXTRACTION %	81.0	LODGING	R
GRAIN SIZE & SHAPE	Large ovoid	HECTOLETER WEIGHT (kg/hl)	79.1	SALANITY	MT
STEM WIDTH (mm)	4 -4.5	SPECIFIC LOAF VOLUME (cm^3/g)	2.37	SHUTTERING	R

Great emphasis was carried out by college of agricultural sciences at University of Sulaimani on multiplication and delivering high-grade seeds of "Maaroof" to the farmers as a strategy to increase wheat yield potential and decrease the risk of biotic and abiotic stress to secure food in Iraq.

http://www.aloki.hu ● ISSN 1589 1623 (Print) ● ISSN1785 0037 (Online)
DOI: http://dx.doi.org/10.15666/aeer/1802_22472258

Conclusions

The long term breeding program efforts led to the development of the new promising wheat cultivar Maaroof which was registered and released by the national committee of registration and release of agricultural cultivars/Iraqi ministry of agriculture according to order no. 40 dated 30th October, 2014 as a new cultivar with high yield potential under irrigated and rain-fed conditions coupled with multi-resistance to the three kinds of rusts and bunt diseases and has better quality traits.

The new variety may provide an excellent choice to the farmers in different agro-ecological zones of Iraq to increase wheat yield under low inputs and stress conditions. Furthermore, it can help in reducing the pollution risk of pesticide application in Iraq.

Acknowledgments. The first author is highly appreciable to the International Center for Agricultural Research in the Dry Areas (ICARDA) for providing seeds of the resistant sources to rust diseases, Ministry of Science and Technology (MOST) for funding the initial stage of the program, and College of Agricultural Sciences, Sulaimani University for their continuous support to the project of high grade seed production of the new promising wheat cultivar and delivering it to farmers.

REFERENCES

[1] AACC. (2000): Methods of the American Association of Cereal Chemistry. – Am. Assoc. Cereal Chem. Inc., St. Paul, Minnesota, 2000.

[2] Alam, M. Z., Haider, S. A., Paul, N. K. (2007): Yield and yield components of Barely (*Hordeum vulgaris* L.) cultivars in relation to nitrogen. – Fertilizer of Applied Research 3: 1022-1026.

[3] Al-Eseel, A. S. (1998): Genotypic and Phenotypic Correlations and Path Coefficients for Agronomy Characters in Bread Wheat (*Triticum aestivum* L.). – PhD Dissertation. Agri. Coll. Univ. of Baghdad. pp: 107.

[4] Al-Maaroof, E. M. (2017): Identification of physiological races of *Puccinia graminis* f. sp. *tritici* in Iraq. – Journal of Wheat Research 9: 47-53.

[5] Al-Maaroof, E. M., Ahmed, M. Y., Hussein, W. U. (2003): Virulence of wheat yellow rust disease in Iraq. – Iraqi J. of Biol. 13: 1-10.

[6] Al-Maaroof, E. M., Hadwan, H. A., Mohamed, L. O., Naser, A. H., Abdul Razak, A. M., Naser, H. M., Ali, S., Fattah, S., Rasheed, N., Laize, M., Naif, R., Tufeek, K. (2012): Serious outbreak of wheat stripe rust disease in Iraq. – Journal of University of Duhok 15: 358-369.

[7] Al-Maaroof, E. M., Hovmoler, M., Ali, R. M., Mohamed, H. A., Naser, A., Mohammed, L. O. (2015): Detection of Yr27 virulence in *Puccinia striiformis* f.sp. *tritici* population on wheat in Iraq. – Journal of wheat research 7: 39-47.

[8] Al-Maaroof, E. M., Ibrahim, I. F., Aboud, A. R. (2001): Effect of leaf rust disease (*Puccinia recondita* Rob ex Desm *tritici*) on different wheat cultivars and genotypes in Iraq. – Dirasat Journal for Agriculture Science 28: 111-120.

[9] Al-Maaroof, E. M., Ibrahim, I. F., Al-Janabi, A. A. (1995): Host reaction of some wheat cultivars with *Puccinia recondita* Rob. ex Desm. f. sp. *tritic*i in Iraq. – Arab Journal of Plant Protection 13: 86-88.

[10] Al-Maaroof, E. M., Latif, M. M., Said, H. A., Aboud, A. R. (2002): Detecting the effective resistant genes to leaf rust disease *Puccinia recondita* Rob ex Desm *tritici* on wheat in Iraq. – Arab Journal of Plant Protection 20: 118-125.

[11] Al-Maaroof, E. M., Naser, A. H., Naser, H. M., Mohammed, L. O. (2010): New virulence of *Puccinia striiformis* f.sp. *trittici* on wheat in Iraq. – Proceedings of the Borlaug Global

http://www.aloki.hu ● ISSN 1589 1623 (Print) ● ISSN1785 0037 (Online)
DOI: http://dx.doi.org/10.15666/aeer/1802_22472258

Rust initiative 2010 Technical work shop (BGRI), 30 May-4 June, 2010, St., Petersburg, Russia, 82p.
[12] Al-Maaroof, E. M., Nori, A. M. (2018): Yellow rust development on different wheat genotypes. – Journal of Zankoy Sulaimani Part-A, Special issue: 177-188.
[13] Al-Maaroof, E. M., Singh, R. P., Huerta, J., Rattu, A. (2005): Resistance of some Iraqi bread wheat cultivars to *Puccinia triticina*. – Phytopatholgia Mediterrania 44: 247-255.
[14] Annicchiarico, P. (2002): Genotype x environment interaction-challenges and opportunities for plant breeding and cultivar recommendations. – FAO Plant Production and Protection. Paper 174, Rome.
[15] Baktash, F. Y. (2001): Improvement bread wheat by pure line selection. – Iraqi Journal of Agricultural Sciences 32(3): 87-92.
[16] Bell, M. A., Fischer, R. A. (1994): Guide to plant and crop sampling; Measurements and observations for agronomic and physiological research in small grain cereals. – Wheat special report no. 32. Mexico, D.F.: CIMMYT.
[17] Dodov, D., Todorova, V. (1974): Physiological specialization of common bunt of wheat (*Tilletia leaves* and *T. tritici*) in Bulgaria. – Academic of Science 25: 181-197.
[18] FAO. (2018): Global information and early warning system on food and agriculture. – "Iraq: GIEWS Country Brief." March 2016.
[19] FAOSTAT. (2018): World food and agriculture, statistical pocket book 2018. – Food and Agriculture Organization of the United Nations, Rome 254p.
[20] Goates, B. J. (1996): Common bunt and dwarf bunt. – In: Wilcoxon, R. D., Saari, E. E. (eds.) Bunt and smut diseases of wheat: concepts and methods of disease management. CIMMYT, Mexico D.F., pp 12-25.
[21] Ibrahim, I. F., Al-Maaroof, E. M., Al-Ubaidi, M. O., Al-Janabi, K. K., Al-Janabi, A. A. (1993a): Induction of a new Iraqi wheat cultivar by gamma rays. Rachis. – Barley & Wheat Newsletter 12: 28-35.
[22] Ibrahim, I. F., Al-Ubaidi, M. O., Al-Maaroof, E. M., Al-Janabi, A. A., Al-Janabi, K. K., Ali, A. H. (1993b): Induced new wheat cultivar by gamma irradiation. – Proceedings of the Workshop on Technology Transfer in the Production of Cereals and Legumes. Sep., 20-22, 1993, pp 47-54. Mosul, Iraq.
[23] Lewellen, R. T., Sharp, E., Hehn, E. R. (1967): Major and Minor genes in wheat for resistance of *Puccinia striiformis* and their response to temperature changes. – Canadian Journal of Botany 45: 2155-2172.
[24] Line, R. F., Chen, X. (1995): Success in breeding for and managing durable resistance to wheat rusts. – Plant Disease 79(12): 1254-1255.
[25] Loveras, J., Manent, J., Viudas, J., Lopez, A., Santiveri, P. (2004): Seeding rate influence on yield and yield component of irrigated winter wheat in a Mediterranean climate. – Agronomy Journal 96: 1258-1265.
[26] Marasas, C. N., Smale, M., Singh, R. P., Pingali, P. (2001): The global economic impact of nonspecific leaf rust resistance in modern CIMMYT derived spring bread wheat: a preliminary report. – CIMMYT. http: www cmmyt.org /research/wheat/index htm.
[27] Messmer, M. M., Seyfarth, R., Keller, M., Schachermayr, G., Winzeler, M., Zanetti, N., Feuillet, C., Keller, B. (2000): Genetic analysis of durable leaf rust resistance in winter wheat. – Theoretical Applied Genetics 100: 419-431.
[28] NCFRRAV. (2014): Agricultural Cultivars and Hybrids Database. – National Committee for Registration and Release of Agricultural Varieties/Iraqi Ministry of Agriculture.
[29] Pessarakli, M. (2011): Handbook of plant and crop stress. – CRC Press London, 1195p.
[30] Rajaram, S., Braun, H., Van Gingle, M. (1996): CIMMYT, Approach to breed for drought tolerance. – Euphytica 92: 147-153.
[31] Roelfs, A. P., Singh, R. P., Saari, E. E. (1992): Rust disease of wheat, Concepts methods of disease management. – Mexico, D.F, CIMMYT. P81(1992).

http://www.aloki.hu ● ISSN 1589 1623 (Print) ● ISSN1785 0037 (Online)
DOI: http://dx.doi.org/10.15666/aeer/1802_22472258

[32] Sabir, D. A., Al-Maaroof, E. M. (2018): Evaluation of physiochemical, rheological and baking characteristics of some wheat genotypes and cultivars. – Proceedings of the LACC4 & IGW, 11-17 -03-2018, Mexico City, Mexico.
[33] Salman, R. M., Mahdi, A. S. (2005): Selection new promising lines of bread wheat. – The Iraqi Journal of Agricultural Sciences 36(5): 67-74.
[34] Singh, R. P., Duvillier, E., Huerta-Espino, J. (2004): Virulence to yellow rust resistance gene Yr27. – In: A new threat to stable wheat production in Asia. (Abs.). Second Regional yellow rust conference for CWANA; Islamabad, Pakistan, 22–26 March, 2004.
[35] Singh, R. P., Trethowan, R. (2007): Breeding spring bread wheat for irrigated and rain-fed production systems of the developing world. – In: Kang, M., Priyadarshan, P. M. (eds.) Breeding major food staples. Blackwell Publishing, Iowa, USA, pp 109-140.
[36] Stakman, E. C., Stewart, D. M., Loegering, W. Q. (1962): Identification of physiologic races of *Puccinia graminis var. tritici*. – U.S. Agriculture Research Service, E–617(rev), USA, 53p.
[37] USDA. (2015): Long-Term Projections Report. – OCE- 2015-1, 97pp.

http://www.aloki.hu ● ISSN 1589 1623 (Print) ● ISSN1785 0037 (Online)
DOI: http://dx.doi.org/10.15666/aeer/1802_22472258

EFFECTS OF SLURRY AND SOIL CONDITIONERS ON THE YIELD, PROTEIN AND ASH CONTENT IN ITALIAN RYEGRASS (*LOLIUM MULTIFLORUM* LAM)

WIŚNIEWSKA-KADŻAJAN, B.* – JANKOWSKI, K.

Institute of Agriculture and Horticulture, University of Natural Sciences and Humanities in Siedlce, B. Prusa 14, 08-110 Siedlce, Poland
(phone: +48-25-643-1320)

**Corresponding author*
e-mail: beata.wisniewska-kadzajan@uph.edu.pl

(Received 17th Oct 2019; accepted 23rd Jan 2020)

Abstract. The purpose of this research was to determine the effect of slurry applied on its own and supplemented with mineral fertilizers or soil conditioners (UGmax and Humus Active) on the yield of *Lolium multiflorum* and on its total protein and crude ash contents. The research was conducted on the basis of a two-year (2016-2017) field experiment in which *Lolium multiflorum* forage grass of the Dukat variety was used. For the two growing seasons the highest average yield of the grass was obtained from plots with slurry application and mineral fertilizers. However, interaction of slurry with soil conditioners resulted in a lower yield compared to the plot where slurry was used on its own. The highest total protein content was obtained to *Lolium multiflorum* treated with slurry supplemented with mineral fertilizers. The highest crude ash content (an average across growing seasons and treatments) was recorded in the biomass of the third harvest, with the lowest amount recorded in the first.
Keywords: *fertilization, feed value, forage grasses*

Introduction

The primary nutrient that determines forage quality is protein. According to Brzóska and Śliwiński (2011) total protein is made up of true protein and non-protein nitrogen compounds. Kukułka and Kozłowski (2004) point out that the share of true protein in grass biomass is 80-95% of total protein, while non-protein nitrogen compounds constitute the other 5-20%. The content of this nutrient in forage is affected to the highest degree by the level of nitrogen fertiliser. However, the amount of nitrogen doses mainly increases the content of non-protein nitrogen in plants. For this reason, with intensive nitrogen application the share of true protein might be reduced by up to 50-60%.

According to Falkowski et al. (2000), total protein content in grass also depends on the species and even on the variety, habitat fertility with the level of nitrogen, the development stage of the plant, the weather, and the harvest.

In addition to total protein, crude ash content is equally important from the point deleted of plant nutritional value (Kitczak et al., 2011). Forage mineral content is dependent on the species composition, the stage of plant development during harvest, and on weather conditions. Chemical elements required by animals in large quantities are potassium, phosphorus, magnesium, and calcium. Equally important but absorbed in small quantities are microelement such as copper, zinc, or manganese (Falkowski et al., 2000).

http://www.aloki.hu ● ISSN 1589 1623 (Print) ● ISSN 1785 0037 (Online)
DOI: http://dx.doi.org/10.15666/aeer/1802_22592268

The research was aimed at assessing the yield of *Lolium multiforum* biomass, as well as the content of total protein and crude ash as a result of slurry applied on its own and supplemented with soil conditioners or NPK mineral fertilisers.

Supplementing the slurry with biopreparations was supposed to show how it will affect the amount of biomass obtained as well as the content of protein and ash components in it. In addition, the experiment was to assess whether the addition of biological preparations to liquid manure is able to balance complementary mineral fertilization.

Materials and methods

The research was carried out on the basis of a two-year (2016-2017) field experiment established at the experimental facility of the University of Natural and Sciences and Humanities in Siedlce, with three replications and random layouts. The area of an experimental plot was 4.5 m^2 (1.5 x 3.0 m).

The main experimental factor tested in the research was slurry used separately and supplemented with NPK mineral fertilizers or soil conditioners with the commercial names of UGmax and Humus Active. The following research units were set up: (1) control (no treatment); (2) slurry; (3) slurry + UGmax; (4) slurry + Humus Active; (5) slurry + NPK.

The effect of slurry, soil conditioners, and mineral fertilisers was tested on the forage grass of the *Lolium multiflorum* species of the Dukat variety. It was sown in autumn 2015 at the sowing standard of 18 kg ha^{-1}. Slurry from dairy cows was used as natural fertiliser. It was applied each year in a total dose of 30 m^3 ha^{-1} divided into three equal parts used before each growth cycle.

Slurry had dry matter concentration of 10%, with a narrow ratio of C:N (8:1), while the concentration of selected macronutrients was as follows (g kg^{-1} DM): N-33.0, P_2O_5-16.0, K_2O-16, MgO-10.0 and Ca-21.0. Soil conditioners, according to the Institute of Soil Science and Plant Cultivation in Puławy, Poland, improve soil properties. Their composition is shown in *Table 1*.

Table 1. *Composition of soil conditioners*

Soil conditioner	Macronutrients (g kg^{-1})						Micronutrients (mg kg^{-1})				Microorganism and others
	N	P	K	Ca	Mg	Na	Mn	Fe	Zn	Cu	
UGmax	1.2	0.2	2.9	-	0.1	0.2	0.3	-	-	-	Lactic acid bacteria, photosynthetic bacteria, Azotobacter, Pseudomonas, yeast, actinomycetes
Humus Active	0.2	1.3	4.6	3.0	0.5	-	15	500	3	1	Permanent active humus with beneficial microorganisms

Soil conditioners were used annually before the first growth cycle at doses recommended by the manufacturer, i.e. UGmax (Ecodarpol company) at 0.6 L ha^{-1} and Humus Active (Bogdan company) at 50 L ha^{-1}. The addition of biologicals slurry was supposed to increase the use of manure nutrients by reducing losses, especially nitrogen. In addition, both biopreparations alleviate the symptoms of drought. Mineral nitrogen-

http://www.aloki.hu ● ISSN 1589 1623 (Print) ● ISSN 1785 0037 (Online)
DOI: http://dx.doi.org/10.15666/aeer/1802_22592268

phosphate-potassium fertilisers (NPK) were used in the following doses: N – 100, P (P_2O_5) – 80, K (K_2O) – 120 kg ha^{-1}. Mineral nitrogen fertilizers were used in the form of ammonium nitrate (NH_4NO_3), phosphorus in the form of triple granular superphosphate ($Ca(H_2PO_4)_2$) and potassium in the form of potassium salt (KCl). Phosphorus was applied once a year before the first growth cycle, whereas nitrogen and potassium doses were divided into three equal parts: the first before the start of vegetation, the second and third before the second and third growth cycles.

The experiment was set up on the soil with granulometric composition of loamy sand, the order of anthropogenic soils, the type of culture earth soil, and the subtype of hortisole (Polish Soil Classification, 2011). Chemical analysis of the soil found that carbon concentration in organic compounds (C_{org}) was 14.50 g kg^{-1} DM, with total nitrogen of 1.36 g kg^{-1} DM. The ratio of C:N was 10.6:1, and the pH value was 6.7. The concentration of absorbable forms of phosphorus (170.00 mg kg^{-1} DM) and magnesium (84.00 mg kg^{-1} DM) was high, with moderate concentration of potassium (114.00 mg kg^{-1} DM).

Hydrothermal conditions were determined on the basis of meteorological data from the Hydrological and Meteorological Station in Siedlce. In order to measure temporal variability of weather conditions and their effects on plant growth and development Sielianinov's hydrothermal coefficient (*Table 2*) was determined (Bac et al., 1993). It was calculated using the monthly sum of atmospheric precipitation (P) and the monthly sum of average daily air temperatures (Σt), applying the formula: $K = P/0.1\ \Sigma t$ (Skowera and Puła, 2004).

Table 2. *The value of Sielianinov's hydrothermal coefficient (K) in the growing seasons*

Year	Month						
	April	**May**	**June**	**July**	**August**	**September**	**October**
2015	1.36	1.87	1.64	0.59	1.92	0.64	0.12
2016	1.22	2.63	0.87	1.08	0.18	1.46	1.94
2017	2.88	1.15	1.08	0.45	0.96	1.92	1.90

$K \leq 0.4$ extremely dry (ed), $0.4 < K \leq 0.7$ severely dry (sd), $0.7 < K \leq 1.0$ dry (d), $1.0 < K \leq 1.3$ moderately dry (md), $1.3 < K \leq 1.6$ optimal (o), $1.6 < K \leq 2.0$ moderately wet (mw), $2.0 < K \leq 2.5$ wet (w), $2.5 < K \leq 3.0$ severely wet (sw), $K > 3.0$ extremely wet (ew)

The optimal value of this coefficient was the range of $1.3 < K \leq 1.6$ (Skowera and Puła, 2004). In the first year (2016) the optimum thermal and humidity conditions occurred only in the month of September, with severely wet May, while June, July, and August, the most important months for plant growth and development of plants, were dry, moderately dry, and extremely dry. In the second year of the experiment the period from May to August ranged from moderately dry to severely dry, and the optimum conditions were not recorded during any month of the growing season.

During the two-year experiment in each growing season three harvests of grass were collected. Immediately after each harvest fresh matter was weighed, and a sample of 0.5 kg was collected to determine the yield of dry matter and to perform chemical analyses. The yield of dry matter was determined with the drying method. Total protein and crude ash content was measured with the near-infrared spectroscopy method (LSDS), using the LSDFlex N-500 with the ready-to-use INGOT calibration for dry forage. The

http://www.aloki.hu ● ISSN 1589 1623 (Print) ● ISSN 1785 0037 (Online)
DOI: http://dx.doi.org/10.15666/aeer/1802_22592268

method is described in detail in the Polish standard of PN-EN ISO 12099:2010 and in the literature (Burns et al., 2010; Reddersen et al., 2012).

Analysis of variance for a three-factor experiment was used to process the results statistically. The significance of the effect of various treatments on the value of the tested traits was checked with the Fisher-Snedecor F test. The statistical program of Statistica 6.0-2001 was used for calculations.

Results

Dry matter yields (*Table 3*) of *Lolium multiflorum* showed a significant variation depending on the treatment applied and the harvest. In the first and second year the highest yield, 12,40 and 12.90 Mg ha^{-1}, respectively, was obtained from the plot where slurry was supplemented with NPK fertilisers. The lowest biomass yield was on the control plot (8.70 in the first and 9.50 Mg ha^{-1} in the second year.

In the first and second year the highest yield, 12,40 and 12.90 Mg ha^{-1}, respectively, was obtained from the plot where slurry was supplemented with NPK fertilisers. The lowest biomass yield was on the control plot (8.70 in the first and 9.50 Mg ha^{-1} in the second year. The addition of soil conditioners to slurry did not significantly increase the biomass of the grass compared with plots treated with slurry only. In the first year of the research the biomass yield on the plot treated with slurry and the Humus Active soil conditioner was lower than on the plot with slurry applied on its own. In the second year, plants responded with a lower yield to both of the soil conditioners added to slurry.

Table 3. *Dry matter yield of Lolium multiflorum (Mg ha^{-1})*

Growing season (B)	**Harvest (C)**	**Treatments (A)**					**Means**
		O	**S**	**S + UGmax**	**S + HA**	**S + NPK**	
2016	I	3.10	4.20	4.30	4.10	4.50	4.04
	II	2.90	3.50	3.50	3.80	4.40	3.62
	III	2.70	3.80	4.00	2.30	3.50	3.26
	Total	8.70	11.50	11.80	10.20	12.40	10.9
2017	I	3.60	4.50	4.30	4.40	4.70	4.30
	II	3.10	3.50	3.80	4.00	4.20	3.72
	III	2.80	4.30	2.40	2.60	4.00	3.22
	Total	9.50	12.30	10.50	11.00	12.90	11.24
Means across growing seasons		9.10	11.90	11.15	10.60	12.65	11.07
Means across harvests							
I		3.35	4.35	4.30	4.25	4.66	4.17
II		3.00	3.50	3.65	3.90	4.30	3.67
III		2.75	4.05	3.20	2.45	3.75	3.24
$LSD_{0.05}$ for:	A = 0.75	B = NS		C = 0.49			
	A/B = NS*	B/A = NS		A/C = NS			
	C/A = NS	B/C = NS		C/B = NS			

*not significant

http://www.aloki.hu ● ISSN 1589 1623 (Print) ● ISSN 1785 0037 (Online)
DOI: http://dx.doi.org/10.15666/aeer/1802_22592268

The amount of biomass in individual harvests, as an average for treatments, was the largest in the first one (4.04 and 4.30 Mg ha^{-1}), but the smallest in the third (3.26 and 3.22 Mg ha^{-1}). The biomass yield (average for years) was significantly higher only on the plot where slurry was supplemented with mineral NPK (12.65 Mg ha^{-1}) than in plants where slurry was applied on its own (11.90 Mg ha^{-1}).

The total protein content in grass dry matter (*Table 4*) was significantly differentiated across treatments and growing seasons. The largest average protein content was in plants treated with slurry supplemented with mineral NPK; in the first year it was 162.8 g kg^{-1} DM, in the second 163.4 g kg^{-1} DM. The smallest average protein content of *Lolium multiflorum* was recorded on control: 128.4 g kg^{-1} in the first and 129.4 g kg^{-1} in the second year of the experiment.

The addition of soil conditioners to slurry did not have a more favourable effect on protein content than the effect of slurry applied on its own. The mean protein content in plants treated with soil conditioners and slurry was lower than on plots treated with slurry only. Mean (across years and treatments) protein content decreased in consecutive harvests, and it was the largest in the first (155.4 g kg^{-1}) and the smallest in the third (145.9 g kg^{-1}).

Table 4. *Protein concentration in Lolium multiflorum dry matter (g kg^{-1})*

Growing season (B)	Harvest (C)	Treatments (A)					Means
		O	S	S + UGmax	S + HA	S + NPK	
2016	I	135.6	167.1	153.8	152.5	163.9	154.6
	II	123.8	156.3	162.5	158.7	169.5	154.2
	III	125.7	149.8	136.9	146.8	154.9	142.8
	Means	128.4	157.7	151.1	152.7	162.8	150.5
2017	I	132.5	168.2	160.1	168.7	168.1	159.5
	II	130.4	159.4	148.4	151.4	164.6	150.8
	III	125.4	158.6	159.2	154.9	157.6	151.1
	Means	129.4	162.1	155.9	158.3	163.4	153.6
Means across growing seasons		128.9	159.9	153.5	155.5	163.1	152.1
Means across harvests							
I		134.1	167.4	167.0	160.1	166.0	158.9
II		127.1	157.9	155.5	155.1	167.1	152.5
III		125.6	154.2	148.1	150.9	156.3	147.0
$LSD_{0.05}$ for:	A = 9.43	B = 6.19	C = NS				
	A/B = NS	B/A = NS	A/C = NS				
	C/A = NS	B/C = NS	C/B = NS				

Another ingredient in assessing feed quality is crude ash. Crude ash content in *Lolium multiflorum* dry matter (*Table 5*) significantly varied in both years. In the first year of research, the largest accumulation of crude ash (107.3 g kg^{-1}) was recorded in the biomass of the grass treated with slurry only. In the second year, on average, the most crude ash was on plots with slurry and mineral fertilizers (119.5 g kg^{-1}).

The smallest crude ash content in the first year of research was in plants treated with slurry and NPK (102.3 g kg^{-1}), and in the second on the control plot (102.7 g kg^{-1}).

http://www.aloki.hu ● ISSN 1589 1623 (Print) ● ISSN 1785 0037 (Online)
DOI: http://dx.doi.org/10.15666/aeer/1802_22592268

Across harvests, in the first year the largest ash content was recorded in the biomass of the third one (113.3 g kg^{-1}) and in the second one (114.4 g kg^{-1}), with the lowest amount in the first harvest of the first year (97.3 g kg) and in third one in the second year (107.9 g kg). Crude ash content, the average of years and harvests, was the smallest on the control plot (103.6 g kg^{-1}) and the largest in plants treated with slurry and mineral fertilizers (110.9 g kg^{-1}).

Table 5. *Crude ash concentration in Lolium multiflorum dry matter (g kg^{-1})*

Growing season (B)	Harvest (C)	Treatments (A)					Means
		O	S	S + UGmax	S + HA	S + NPK	
2016	I	97.6	95.5	98.9	92.3	102.3	97.3
	II	103.7	102.6	99.7	105.6	99.9	102.3
	III	112.1	123.9	111.6	114.5	104.6	113.3
	Means	104.5	107.3	103.4	104.1	102.3	104.3
2017	I	89.5	110.1	119.8	115.6	129.4	112.9
	II	103.5	116.8	115.7	116.2	119.7	114.4
	III	115.0	110.8	100.6	103.8	109.3	107.9
	Means	102.7	112.6	112.0	111.9	119.5	111.7
Means across growing seasons		103.6	109.9	107.7	108.0	110.9	108.0
Means across harvests							
I		93.6	102.8	109.4	103.9	115.9	105.1
II		103.6	109.7	107.7	110.9	109.8	108.3
III		113.6	117.4	106.1	109.2	106.9	110.6
$LSD_{0.05}$ for:	A = NS	B = 7.02	C = NS				
	A/B = NS	B/A = NS	A/C = NS				
	C/A = NS	B/C = 9.94	C/B = 12.3				

Discussion

Due to the fact that *Lolium multiflorum* is a short-term grass it can be used for alternating grassland. Studies have shown that its yields ranges from 9.10 to 12.65 Mg ha^{-1}. According to Jankowski et al. (2008) *Lolium multiflorum* is a high-productivity species. This is also confirmed by the study of Borowiecki (2002a, b), according to who the *Lolium multiflorum* yield can range from 9 to 12 Mg ha^{-1}.

In the present studies the best results in the form of increased biomass of the grass (an average across years and harvests) were recorded on plots where slurry was supplemented with mineral fertilizers. Olszewska (2008) points out that the yield is the basic criterion for assessing treatment effectiveness. A yield increase as a response to natural fertilizer applied to grassland was also recorded by Barszczewski et al. (2011). The present studies showed that slurry supplemented with soil conditioners increased the amount of biomass of the grass, and it was 16-20% greater than on the control plot, while slurry supplement with NPK fertilizers increased the yield by 40%.

According to Kryszak et al. (2012) as well as Jankowska-Huflejt (2012) periodic shortage of water reduces the yield of meadow plants below their potential.

http://www.aloki.hu ● ISSN 1589 1623 (Print) ● ISSN 1785 0037 (Online)
DOI: http://dx.doi.org/10.15666/aeer/1802_22592268

In the first year (2016) the optimum thermal and humidity conditions were only in the month of September, with severely wet May, while June, July and August, which are the most significant months for the growth and development of plants, were dry, moderately dry, and extremely dry. In the second year of the experiment (2017), the period from May to August ranged from dry to very dry, and the optimum conditions were not recorded during any month of the growing season.

The optimum total protein content is very important from the point of view of grass nutritional value. According to Grygierzec (2012) the lowest protein content in forage, necessary for the proper digestion process, should ranged from 150 to 170 g kg^{-1} DM. In contrast, according to Jankowska-Huflejt et al. (2011), *Lolium multiflorum* biomass should contain about 115 g kg^{-1} DM. In the present experiment protein content was within the limits of 128.9 to 163.1 g kg^{-1} DM, and it was undoubtedly the nitrogen introduced in the form of slurry and mineral fertilizer that increased it.

Kotlarz et al. (2010) as well as Kasperczyk (2004) confirm that the level of nitrogen fertilizer determines total protein content in forage. Many authors (Ciepiela, 2004; Jankowska et al., 2008; Szkutnik et al., 2012) point out that total protein content is not always increased in proportion to the applied nitrogen fertilizer. A lower total protein content in dry matter may be due to the high yield potential of the species and it can be caused by dilution of the content of this ingredient in the higher amount of biomass.

In the present experiment protein content in biomass depends on the harvest from which it originates. The dependence of the harvest impact on total protein content in grass was confirmed in the studies of Łyszczarz (2003) and Tonn et al. (2013). According to Juszczyk and Rękorajski (2007) the components of crude ash are chemical elements whose adequate quantity in forage is necessary for the normal growth and development of animal organisms, while excessive content (above 150 g kg^{-1} DM) may result from contamination of plant material with soil (Nazaruk et al., 2009).

Throughout the research crude ash content in *Lolium multiflorum* ranged from 89.5 g·kg^{-1} to 123.9 g kg^{-1} and did not exceed the above value, which shows the purity of the plant material analysed. Kotlarz et al. (2010) and Grzelak and Bocian (2009) point out that low content of crude ash of 40 g kg^{-1} DM in the forage may be related to low concentration of minerals in the soil and to species composition of the forage.

In the present experiment, the analysis of the content of this parameter clearly showed a significant effect of slurry application in comparison with the control plot. An increase in crude ash in meadow forage as a result of natural fertiliser application was also noted by Jankowska-Huflejt and Wróbel (2010); Barszczewski et al. (2010) as well as Wróbel et al. (2013).

In the present experiment in the first year crude ash content in *Lolium perenne* increased in subsequent harvests (from 97.3 to 113.3 g kg^{-1}). In the second year a reverse trend was recorded. Barszczewski et al. (2010) found that ash content in meadow plants varied depending on harvest time.

The obtained test results clearly show that the supplementary use of biopreparations did not affect the increase of the grass grown or the protein content in it compared to the facilities where the slurry itself was used. Only the addition to the slurry of mineral fertilization improved the value of these parameters in relation to the operation of the slurry itself.

http://www.aloki.hu ● ISSN 1589 1623 (Print) ● ISSN 1785 0037 (Online)
DOI: http://dx.doi.org/10.15666/aeer/1802_22592268

Conclusions

1. The dry matter yield of *Lolium multiflorum* significant varied across treatments and harvests. In both years of the research the highest yield of the grass was on the plot treated with slurry and mineral fertilizers, and the interaction of slurry with soil conditioners resulted in a decrease in the yield compared to the slurry-only plot.
2. Total protein content in *Lolium multiflorum* forage was significantly dependent on the treatment and growing season. The largest total protein content was recorded in biomass from the plot where slurry was applied together with mineral fertilizers, but this was not significantly different from plants treated with slurry only.
3. The growing season had a significant impact on crude ash content in the grass. The greatest amount of ash (on average from growing seasons and treatments) was recorded in *Lolium multiflorum* of the third harvest, while the least crude ash in the first one.
4. The obtained research results showed a beneficial effect of the slurry interaction only with mineral fertilization, while the interaction with biopreparations did not bring the expected effects. The most likely cause could be adverse hydrothermal conditions in both growing seasons of the crop. Therefore, the assessment of the interaction of slurry with biopreparations requires further research.

REFERENCES

[1] Bac, S., Koźmiński, C., Rojek, M. (1993): Agrometeorology. – State Publishing House, Warsaw, pp. 32-33 (in Polish).
[2] Barszczewski, J., Wróbel, B., Jankowska-Huflejt, H. (2011): Economic effect of permanent meadow spreading with the meadow limb. – Water - Environment - Rural Areas 3(35): 21-37 (in Polish).
[3] Barszczewski, J., Wróbel, B., Jankowska-Huflejt, H., Mendra, M. (2010): Impact of various fertilization methods on meadow sward and the quality of silage obtained. – Scientific Notebooks of the College of Agribusiness in Łomża 46: 7-16 (in Polish).
[4] Borowiecki, J. (2002a): Productivity of papilionaceous plants and their mixtures with grasses. – Puławski Diary 130/I: 57-63 (in Polish).
[5] Borowiecki, J. (2002b): Yielding of Festulolium cultivar Felopa in single-species sowing and mixtures with cocksfoot. – Puławski Diary 131: 49-58 (in Polish).
[6] Brzóska, F., Śliwiński, B. (2011): Quality of roughage for feeding ruminants and methods of its assessment. Vol. II. Methods for analyzing and assessing the nutritional value of roughage. – Zootechnical News XLIX(4): 57-68 (in Polish).
[7] Burns, G. A., Gilliland, T. J., McGilloway, D. A., O'donovan, M., Lewis, E., Blount, N., O'Kely, P. (2010): Using LSDS to predict composition characteristics of Lolium perenne L. cultivars. – Advances in Animal Biosciences 1: 321-321.
[8] Ciepiela, A. G. (2004): Reaction of Selected Grass Species to Nitrogen Fertilization Used in Urea Solution and in Ammonium Nitrate. – Scientific Dissertation No. 76. AP, Siedlce (in Polish).
[9] Falkowski, M., Kukułka, I., Kozłowski, S. (2000): Chemical Properties of Meadow Plants. – UP, Poznań (in Polish).

http://www.aloki.hu ● ISSN 1589 1623 (Print) ● ISSN 1785 0037 (Online)
DOI: http://dx.doi.org/10.15666/aeer/1802_22592268

[10] Grygierzec, B. (2012): Content of basic nutrients and fiber fractions in hay from extensively used communities of Alopecuretum pratensis and Holcetum lanati. – Grassland in Poland 15: 53-65 (in Polish).
[11] Grzelak, M., Bocian, T. (2009): Nutritional value of green fodder and hay from ecological meadows. – Journal of Research and Applications in Agricultural 54(3): 86-90.
[12] Jankowska, J., Ciepiela, A. G., Kolczarek, R., Jankowski, K. (2008): Impact of the type of mineral fertilizer and nitrogen dose on yield and nutritional value of permanent meadow sward. – Puławski Diary 147: 125-138 (in Polish).
[13] Jankowska-Huflejt, H. (2012): Durability and forage value of grass mixtures and their varieties as well as small-seeded papilionaceous plants selected for mowing use in organic farming. – Journal of Research and Applications in Agricultural 57(3): 172-178 (in Polish).
[14] Jankowska-Huflejt, H., Wróbel, B. (2010): Assessment of the impact of manure fertilization on the nutritional value of meadow sward and its suitability for ensiling. – Institute of Technology and Life Sciences in Falenty 133-136 (in Polish).
[15] Jankowska-Huflejt, H., Wróbel, B., Barszczewski, J., Domański, P. J. (2011): Mowing Use of Meadows on Organic Farms. – In: Węglarzy, K., Czubała, A. (eds.) Guide of the Organic Farmer. Śląski, Grodziec, pp. 70-110 (in Polish).
[16] Jankowski, K., Jodełka, J., Ciepiela, G. A., Kolczarek, R. (2008): Grasslands. – AP, Siedlce, pp. 32-35 (in Polish).
[17] Juszczyk, S., Rękorajski, M. (2007): Direct costs of meadow and grazing feed on dairy farms of the Łódź province. – Annals of Agricultural Sciences 94(2): 35-45.
[18] Kasperczyk, M. (2004: Yielding of mountain meadow depending on the course of meteorological conditions. – Acta Agrophysica 3(2): 263-269 (in Polish).
[19] Kitczak, T., Malinowski, R., Czyż, H. (2011): Content of macro- and microelements in soils and sward of grassland located on the Wrzosowska Bay. – Grassland in Poland 14: 51-61 (in Polish).
[20] Kotlarz, A., Stankiewicz, S., Biel, W. (2010): Botanical and chemical composition of hay from a semi-natural meadow and its nutritional value for horses. – Acta Sci. Pol., Zootechnica 9(4): 119-128 (in Polish).
[21] Kryszak, A., Klarzyńska, A., Kryszak, J., Strychalska, A., Maćkowiak, Ł. (2012): Influence of variability of ryegrass meadow soil conditions on their natural and utilization values. – Not. Bot. Horti. Agrobo. 40(1): 163-169.
[22] Kukułka, J., Kozłowski, S. (2004): Chemical Properties of Meadow Plants. – In: Rogalski, M. (ed.) Grassland. Kurpisz, Poznań, pp. 80-111.
[23] Łyszczarz, R. (2003): Impact of the harvest date on selected features of two varieties of cocksfoot. – Bulletin of the Institute of Plant Breeding and Acclimatization 225: 139-149.
[24] Nazaruk, M., Jankowska-Huflejt, H., Wróbel, B. (2009): Evaluation of feed nutritional value from permanent pasture on the ecological farms studied. – Water - Environment - Rural Areas 1(25): 61-76 (in Polish).
[25] Olszewska, M. (2008): Leaf greenness (SPAD) and yield of Festulolium braunia (K. Richt.) A. Camus grown in mixtures with legumes depending on multiple nitrogen rates. – Polish Journal of Natural Sciences 23(2): 310-325.
[26] Reddersen, B., Fricke, T., Wachendorf, M. (2012): Influence of LSDS - method on the calibration of N-, ash- and NDF-content of grassland hay and silage. Grassland - a European Resource? – EGF, Grassland Sciences in Europe 17: 385-387.
[27] Skowera, B., Puła, J. (2004): Extreme pluvirothermic conditions in spring in Poland in 1971-2000. – Acta Agrophysica 3(1): 171-177 (in Polish).
[28] Systematics of Polish Soils (2011): Polish soil classification. – Annals of Soil Science 62(3) (in Polish).

http://www.aloki.hu ● ISSN 1589 1623 (Print) ● ISSN 1785 0037 (Online)
DOI: http://dx.doi.org/10.15666/aeer/1802_22592268

[29] Szkutnik, J., Kacorzyk, P., Szewczyk, W. (2012): Change in total protein content and raw fiber depending on the level of fertilization and the development phase of grasses. – Grassland in Poland 15: 185-191 (in Polish).
[30] Tonn, B., Bienvenu, C., Isselstein, J. (2013): Assessing quantity and quality of grazed forage on multi-species swards. The role of grasslands in a green future. – EGF, Grassland Sciences in Europe 18: 82-84.
[31] Wróbel, B., Zielińska, K. J., Fabiszewska, A. U. (2013): Impact of bovine manure fertilization on the quality of sward and its suitability for ensilage. – Problems of Agricultural Engineering 2(80): 151-164 (in Polish).

http://www.aloki.hu ● ISSN 1589 1623 (Print) ● ISSN 1785 0037 (Online)
DOI: http://dx.doi.org/10.15666/aeer/1802_22592268

GENETIC STRUCTURE OF HONEY BEE (*APIS MELLIFERA* LINNAEUS, 1758) SUBSPECIES BASED ON tRNA^{leu}-COX2 AND ND5 REGIONS OF mtDNA

TOZKAR, C. Ö.

Yüzüncü Yıl University, Faculty of Agriculture, Department of Agricultural Biotechnology
Van, Turkey
(e-mail: tozkar@gmail.com)

(Received 17th Oct 2019; accepted 5th Feb 2020)

Abstract. Diversity of ecological conditions in Anatolia enables many species to adapt to different environments. Thus Turkey is inhabited by various strains of *A.m. mellifera* Linnaeus, 1978*; A.m. mellifera carnica, A.m. mellifera anatoliaca, A.m. mellifera caucasica, A.m. mellifera syriaca,* and *A.m. mellifera meda*. Analysis of mtDNA variants is a widely used tool to determine the phylogenetic relationships at the species and subspecies levels. In this study sequencing results of tRNA^{leu}-COX2 and ND5 gene segments of mtDNA were presented in comparison with some previously published mitochondrial haplotypes. According to the UPGMA dendogram and estimates of evolutionary distances, divergence among the subspecies and ecotypes were not verified strongly. Reproductive isolation barriers could be uneffective and lead to the exchange of the genetic materials between the populations. Intensive care should be taken while managing the colonies of different subspecies in bee yards. Degradation of biodiversity of honey bee subspecies through hybridization was also reported at wider geographic areas rather than small breeding units in some studies. Broad ranges of isolated colonies of subspecies should be established with proper selection studies to reduce the hazards of migratory beekeeping activities. Succesful management practices are needed through better beekeeping technologies and beekeeper training programmes to prevent the homogenization of the genetic structure of different subspecies and to conserve honey bee diversity.
Keywords: *hybridization, gene introgression, phylogenetic analysis, artificial sympatry, biodiversity*

Introduction

The natural dispersion areas of *A. mellifera* L. include Central Asia, Europe, Near East and sub-Saharan Africa and the species has also been introduced to East and Southeast Asia, Australia and the Americas (Ruttner, 1988). At least 29 subspecies of *A. mellifera* have been acknowledged and seperated into four main lineages based on their morphometric, genetic, ecological, physiological, and behavioral features (Han et al., 2012).

A. m. capensis, *A. m. intermissa*, *A. m. litorea*, *A. m. monticola*, *A. m. sahariensis* and *A. m. scutellata* are African subspecies from north and south Sahara belonging to mtDNA group A (2) mainly *A. m. mellifera* and some *A. m. iberiensis* are the subspecies of western and northern European populations of group M (3) group C is composed of southeastern European and northern and eastern Mediterranean populations, containing *A. m. carnica*, *A. m. ligustica*, Turkish and Georgian *A. m. caucasica*, *A. m.* meda and Turkish *A. m. anatoliaca*; and (4) group O includes *A. m. syriaca*, and perhaps other subspecies from Turkey and the Middle East and the last group is Y from the east African country of Ethiopia. Divergence among some subspecies within each lineage was also recognized (Ruttner, 1988; Arias and Sheppard, 1996; Franck et al., 2000).

Although it was not possible to distinguish the classes C and O by sequencing and restriction analysis, they were classified as C (Arias and Sheppard, 1996). Group O verification was performed by examination of mitochondrial DNA and analysis of

http://www.aloki.hu ● ISSN 1589 1623 (Print) ● ISSN1785 0037 (Online)
DOI: http://dx.doi.org/10.15666/aeer/1802_22692284

microsatellites (Arias and Sheppard, 1996; Franck et al., 2000; Palmer et al., 2000). Anatolian ecological diversity helps adaptive species to evolve in various environments. Thus Turkey hosts five subspecies of *A. mellifera; A. mellifera carnica, A. mellifera anatoliaca, A. mellifera caucasica, A. mellifera syriaca,* and *A. mellifera meda* (Ruttner, 1988). No other country today has so many different breeds of honey bee. Most of the geographical regions of Turkey is comprised of *A. m. anatoliaca* except for the northeastern part where *A. m. caucasica* dominates and *A. m. meda* exists in the southeastern part of the country. Thrace region of European Turkey is inhabited by *A. m. carnica* (Palmer et al., 2000), while the southern part of the country near Hatay is occupied by *A. m. syriaca* (Kandemir et al., 2000).

It is understood that morphological characteristics are vulnerable to the effects of selection and environmental changes, therefore they are not accurate and adequate to reconstruct phylogenetic relationships. The variation of mtDNA can be used as an additional and more reliable genetic marker for both classification and phylogenetic analysis of honey bee subspecies (Avise et al., 1987; Franck et al., 2000).

Honey bee lineages can be discerned by sequence analyses of the mitochondrial DNA (mtDNA) region between the cytochrome oxidase subunits I and II genes (CoxI–CoxII intergenic region). Throughout population genetics studies, evolutionary lineages and groups of subspecies can be distinguished by differences throughout length and sequence within the mitochondrial genome of honey bees (Garnery et al., 1992; Franck et al., 2000; Palmer et al., 2000). Numerous mitochondrial regions, such as 16s rDNA (Marino et al., 2002b; Bouga et al., 2005; Kekeçoğlu et al., 2009), ND2 (Arias and Sheppard, 1996), ND5 (Bouga et al., 2005; Martimianakis et al., 2011), cytochrome C oxidase I (COI or Cox1) (Bouga et al., 2005; Martimianakis et al., 2011), and the tRNAleu-COII region (COI-COII intergenic region) (Garnery et al., 1992; Franck et al., 2000; Palmer et al., 2000; Susnik et al., 2004; Munoz et al., 2009; Özdil et al., 2009a,b) have been studied to determine honey bee subspecies' diversity and phylogenetic relationships. tRNA^{leu}-COX2 intergenic region is a noncoding region found between a leucine tRNA gene and the cytochrome oxidase II gene and variation in this region may help to distinguish some mitochondrial haplotypes (Canovas et al., 2008).

The objective of this research was to find out the genetic structure and phylogenetic relationships of five *A. mellifera* subspecies and ecotypes of Turkey through direct sequencing of tRNA^{leu}-COX2 and ND5 mitochondrial regions with the comparison of reference mtDNA haplotypes that were published in previous studies.

Materials and methods

Sampling and DNA isolation

Subspecies and ecotypes were taken from their native habitats representing different regions of Turkey and then the colonies were located in a common garden at Middle East Technical University campus in the centre of Ankara. Subspecies were categorized according to their origin and distinguishable morphological characteristics prior to DNA isolation. Workers were collected in 95% ethanol and air-dried prior to the extraction. Four samples from each of the subspecies were used for DNA extraction. The extraction of DNA from thorax tissue by Qiagen DNeasy® Blood & Tissue Kit (www.quiagen.com).

The quantity of eluted DNAs was checked by Nanodrop ND-1000 (Thermo Fisher Scientific, Inc. Wilmington, Delaware, USA). By loading 2 ul of each sample, the

http://www.aloki.hu ● ISSN 1589 1623 (Print) ● ISSN1785 0037 (Online)
DOI: http://dx.doi.org/10.15666/aeer/1802_22692284

absorbance ratios of A260/280 and A260/230 were measured and DNA concentrations were quantified in ng/ul. To examine the phylogenetic relationships between the subspecies, E2-H2 primer pairs were used to amplify tRNA^{leu}-COX2 intergenic region and ND5 primer pairs were used to amplify ND-5 mitochondrial region. The sequence for forward primer, E2 was 5'-GGC AGA ATA AGT GCA TTG-3', and the reverse primer, H2 was 5'-CAA TAT CAT TGA TGA CC-3' whereas the sequence for ND5_F was 5'-TCG AAA TGA ATA GGA TAC AG-3' and ND5_R was 5'-GGT TGA GAT GGT TTA GGA TT -3'.

PCR was run in a total volume 30 µl of the following reaction mixture: 10 mM of each primer 3 µl of 10X reaction buffer with $MgCl_2$, 2mM of dNTP mix, 2 u of Tag polymerase, 20 ng DNA. For E2-H2 primer pair, the following reaction profile was used: initial denaturation at 94°C for 5 min, followed by 35 cycles of; 94°C for 45 sec, 48°C for 45 sec, 62°C for 2 min, and final elongation step of 20 min at 65°C. For ND5 primer pair, initial denaturation 94°C for 4 min, 35 cycles of 94°C for 1 min, annealing at 50°C (ND5) for 1 min, and extension at 72°C for 2 min, followed by a final extension step at 72°C for 15 min.

The amplified products obtained were next electrophoresed on 1.5% agarose gel to verify the size of the fragment length of 520 bp for tRNA^{leu}-COX2 intergenic region and 721 bp for ND5 mitochondrial region. PCR products were subsequently purified with QIAquick PCR purification kit (QIAgen) and directly sequenced with E2 and ND5-F sequencing primers commercially by Macrogen (Rockville, MD, USA).

Statistical details of the phylogenetic analysis

For the phylogenetic analysis, DNA sequences from this study and additional reference sequences from Genbank were trimmed and aligned using Clustal W (Thompson and Higgins, 1994). The resulting sequences were organized and compared with the published mitochondrial tRNA^{leu}-COX2 intergenic region and ND5 sequences available in Genbank. The sequences obtained in this study were deposited to Genbank with accession numbers MN701721 to MN701744 for ND5 region and MN701745 to MN701763 for tRNA^{leu}-COX2 region.

BLAST searches of the international sequence database (NCBI [National Center for Biotechnology Information] BLASTN search [http://www.ncbi.nlm.nih.gov/]) were used to include the sequences of the outgroup and the sequences of species most closely related subspecies to to the analysis. Phylogenetic and molecular evolutionary analyses were conducted using MEGA version 6 (Tamura et al., 2013).

UPGMA dendogram was built and estimates of evolutionary divergence between sequences were calculated using the same software. The analytical formulas and the bootstrap approach used to measure standart estimation errors. Comparisons were done nucleotide-by-nucleotide (Nei and Kumar, 2000).

Results

Relationships between the subspecies within tRNA^{leu}-COX2 intergenic region

Fragment length was 520 bp for tRNA^{leu}-COX2 intergenic region (*Fig. 1*). tRNA^{leu}-COX2 region within the samples of this study consisted of 2 variable sites, 2 parsimony informative sites and conserved region was 493 bp. According to the dendogram based on the statistical analysis of sequencing results of tRNA^{leu}-COX2

http://www.aloki.hu ● ISSN 1589 1623 (Print) ● ISSN1785 0037 (Online)
DOI: http://dx.doi.org/10.15666/aeer/1802_22692284

intergenic region (*Fig. 2*), Mugla and Yigilca ecotypes were grouped with *A. mellifera* haplotype C12 (FJ037777), *A. m. anatoliaca* C1g (FJ357804), *A. mellifera* haplotype C2d (JQ977701) and *A. m. anatoliaca clone* 5973 (AY618912) and they were closer to *A. m. anatoliaca* C1e (FJ357802) with a branch length of 0.001.

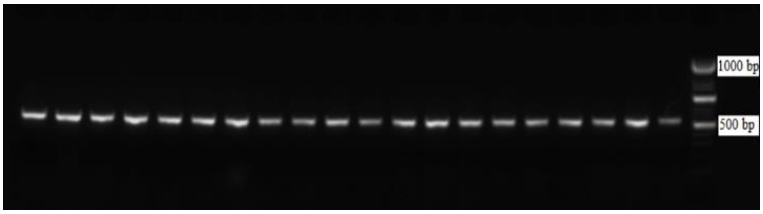

Figure 1. *The amplified PCR products of tRNAleu-COX2 intergenic region of mitochondrial DNA. (Bands represent A. m. anatoliaca-Mugla-1-2-3-4; A. m. caucasica 1-2-3-4; A. m. carnica 1-2-3-4; A. m. anatoliaca-Yigilca 1-2-3-4; A. m. syriaca 1-2-3-4, respectively)*

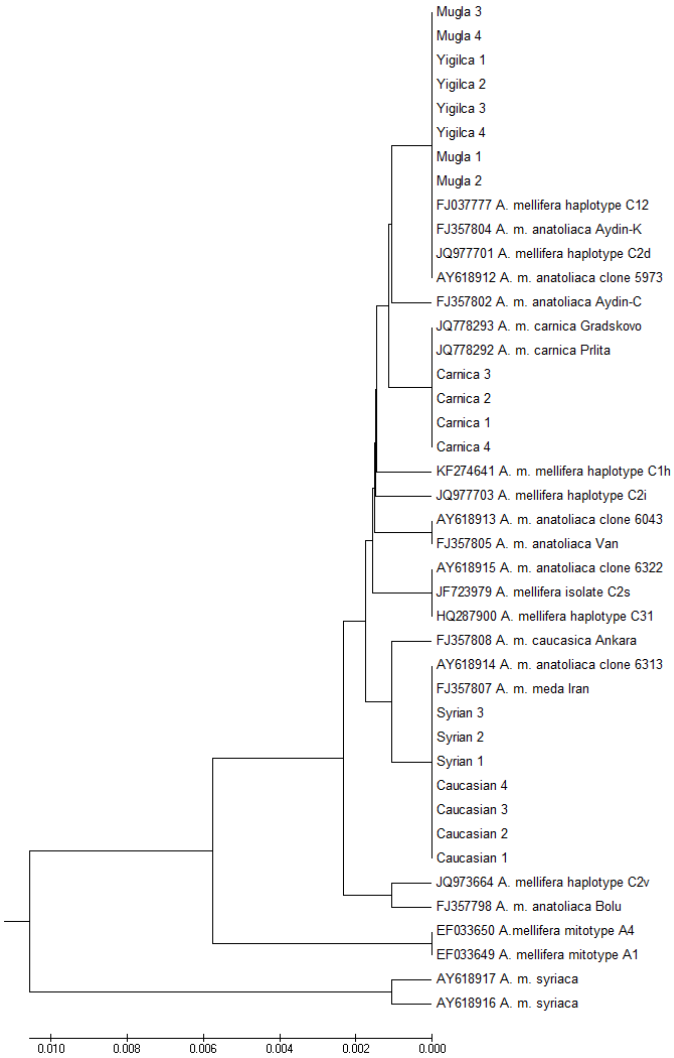

Figure 2. *The phylogenetic tree based on tRNA^{leu}-COX2 intergenic region. The evolutionary history was inferred using the UPGMA method. Samples of this study were labeled as Mugla 1-2-3-4; Yigilca 1-2-3-4; Carnica 1-2-3-4; Syrian 1-2-3; Caucasian 1-2-3-4*

http://www.aloki.hu ● ISSN 1589 1623 (Print) ● ISSN1785 0037 (Online)
DOI: http://dx.doi.org/10.15666/aeer/1802_22692284

Table 1. *Estimates of evolutionary divergence between sequences of tRNA^{leu}-COX2 intergenic region (left). Identification of the numbers respresenting the nucleotide sequences were given (right). (Samples of this study were represented by numbers 24, 25, 26, 27, 28)*

	1	2	3	4	5	6	7	8	9	10	11	12	13	14	15	16	17	18	19	20	21	22	23	24	25	26	27	28		
[1]																													[1]	#KF274641_*A. m. mellifera*_haplotype_C1h
[2]	1.00																												[2]	#AY618912_*A. m. anatoliaca*_clone_5973
[3]	10.00	9.00																											[3]	#AY618917_*A. m. syriaca*
[4]	11.00	10.00	1.00																										[4]	#AY618916_*A. m. syriaca*
[5]	2.00	1.00	10.00	11.00																									[5]	#AY618915_*A. m. anatoliaca*_clone_6322
[6]	2.00	1.00	10.00	11.00	2.00																								[6]	#AY618914_*A. m. anatoliaca*_clone_6313
[7]	2.00	1.00	10.00	11.00	2.00	2.00																							[7]	#AY618913_*A. m. anatoliaca*_clone_6043
[8]	2.00	1.00	8.00	9.00	2.00	2.00	2.00																						[8]	#JQ973664_*A. mellifera*_haplotype_C2v
[9]	2.00	1.00	10.00	11.00	2.00	2.00	2.00	2.00																					[9]	#JQ977703_*A. mellifera*_haplotype_C2i
[10]	1.00	0.00	9.00	10.00	1.00	1.00	1.00	1.00	1.00																				[10]	#JQ977701_*A. mellifera*_haplotype_C2d
[11]	2.00	1.00	8.00	9.00	2.00	2.00	2.00	2.00	2.00	1.00																			[11]	#JQ778293_*A. m. carnica*_Gradskovo
[12]	2.00	1.00	8.00	9.00	2.00	2.00	2.00	2.00	2.00	1.00	0.00																		[12]	#JQ778292_*A. m. carnica*_Prlita
[13]	2.00	1.00	10.00	11.00	0.00	2.00	2.00	2.00	2.00	1.00	2.00	2.00																	[13]	#JF723979_*A. mellifera*_isolate_C2s
[14]	2.00	1.00	10.00	11.00	0.00	2.00	2.00	2.00	2.00	1.00	2.00	2.00	0.00																[14]	#HQ287900_*A. mellifera*_haplotype_C31
[15]	2.00	1.00	10.00	11.00	2.00	0.00	2.00	2.00	2.00	1.00	2.00	2.00	2.00	2.00															[15]	#FJ357807_*A. m. meda*_Iran
[16]	3.00	2.00	11.00	12.00	3.00	1.00	3.00	3.00	3.00	2.00	3.00	3.00	3.00	3.00	1.00														[16]	#FJ357808_*A. m. caucasica*_Ankara
[17]	2.00	1.00	10.00	11.00	2.00	2.00	0.00	2.00	2.00	1.00	2.00	2.00	2.00	2.00	2.00	3.00													[17]	#FJ357805_*A. m. anatoliaca*_Van
[18]	1.00	0.00	9.00	10.00	1.00	1.00	1.00	1.00	1.00	0.00	1.00	1.00	1.00	1.00	1.00	2.00	1.00												[18]	#FJ357804_*A. m. anatoliaca*_Aydin-K

http://www.aloki.hu ● ISSN 1589 1623 (Print) ● ISSN1785 0037 (Online)
DOI: http://dx.doi.org/10.15666/aeer/1802_22692284

	1	2	3	4	5	6	7	8	9	10	11	12	13	14	15	16	17	18	19	20	21	22	23	24	25	26	27	28		
[19]	2.00	1.00	10.00	11.00	2.00	2.00	2.00	2.00	2.00	1.00	2.00	2.00	2.00	2.00	2.00	3.00	2.00	1.00											[19]	#FJ357802_*A. m. anatoliaca*_Aydin-C
[20]	3.00	2.00	9.00	10.00	3.00	3.00	3.00	1.00	3.00	2.00	3.00	3.00	3.00	3.00	3.00	4.00	3.00	2.00	3.00										[20]	#FJ357798_*A. m. anatoliaca*_Bolu
[21]	1.00	0.00	9.00	10.00	1.00	1.00	1.00	1.00	1.00	0.00	1.00	1.00	1.00	1.00	1.00	2.00	1.00	0.00	1.00	2.00									[21]	#FJ037777_*A. mellifera*_haplotype_C12
[22]	4.00	5.00	8.00	9.00	6.00	6.00	6.00	6.00	6.00	5.00	4.00	4.00	6.00	6.00	6.00	7.00	6.00	5.00	6.00	7.00	5.00								[22]	#EF033650_*A. mellifera*_mitotype_A4
[23]	4.00	5.00	8.00	9.00	6.00	6.00	6.00	6.00	6.00	5.00	4.00	4.00	6.00	6.00	6.00	7.00	6.00	5.00	6.00	7.00	5.00	0.00							[23]	#EF033649_*A. mellifera*_mitotype_A1
[24]	2.00	1.00	10.00	11.00	2.00	0.00	2.00	2.00	2.00	1.00	2.00	2.00	2.00	2.00	0.00	1.00	2.00	1.00	2.00	3.00	1.00	6.00	6.00						[24]	#Syriaca samples
[25]	2.00	1.00	8.00	9.00	2.00	2.00	2.00	2.00	2.00	1.00	0.00	0.00	2.00	2.00	2.00	3.00	2.00	1.00	2.00	3.00	1.00	4.00	4.00	2.00					[25]	#Carnica samples
[26]	1.00	0.00	9.00	10.00	1.00	1.00	1.00	1.00	1.00	0.00	1.00	1.00	1.00	1.00	1.00	2.00	1.00	0.00	1.00	2.00	0.00	5.00	5.00	1.00	1.00				[26]	#Mugla samples
[27]	1.00	0.00	9.00	10.00	1.00	1.00	1.00	1.00	1.00	0.00	1.00	1.00	1.00	1.00	1.00	2.00	1.00	0.00	1.00	2.00	0.00	5.00	5.00	1.00	1.00	0.00			[27]	#Yigilca samples
[28]	2.00	1.00	10.00	11.00	2.00	0.00	2.00	2.00	2.00	1.00	2.00	2.00	2.00	2.00	0.00	1.00	2.00	1.00	2.00	3.00	1.00	6.00	6.00	0.00	2.00	1.00	1.00		[28]	#Caucasica samples

http://www.aloki.hu ● ISSN 1589 1623 (Print) ● ISSN1785 0037 (Online)
DOI: http://dx.doi.org/10.15666/aeer/1802_22692284

Samples of Carnica subspecies clustered with two *A. m. carnica* breeding lines (JQ778293) and JQ778292 with 69% bootstrap value. Because they have C→T transition at position 354. They also showed close proximity to *A. m. anatoliaca* (FJ357802) and *A. m. mellifera* haplotype C1h (KF274641) and *A. mellifera* haplotype C2i (JQ977703) with a distance of 0.001.

Samples of Syrian and Caucasian subspecies were grouped within the same branch with *A. m. anatoliaca* clone 6313 (AY618914) and *A. m. meda* (FJ357807) with a bootstrap value of 66% because they all have A→T transversion at site 158. They were also closely related to *A. m. caucasica* (FJ357808) with a branch length of 0.001. *A. m. caucasica* (FJ357808) included additional C→T transition at site 362.

A. m. anatoliaca clone 6043 (AY618913), *A. m. anatoliaca* (FJ357805) *A. m. anatoliaca* clone 6322 (AY618915), *A. mellifera* isolate C2s (JF723979), *A. mellifera* haplotype C31 (HQ287900) were clustered together apart from the samples of this study with the branch length of 0.002 (*Fig. 2*). *A. m. syriaca* (AY618917), *A. m. syriaca* (AY618916) and *A. mellifera* mitotype A4 (EF033650) and *A. mellifera* mitotype A1 (EF033649) formed separate branches distant from the remaining groups with 74% and 62% bootstrap values.

According to nucleotide number of differences model, pairwise differences between Yigilca and Mugla ecotypes were 0.00. These ecotypes differed from the other subspecies with a distance value of 1.00. Pairwise distance between Syrian and Caucasian subspecies were also 0.00 and a dissimilarity was observed between this group and Carnica subspecies with a magnitude of 2.00. *A. m. meda* (FJ357807) which was clustered with Syrian and Caucasian samples, was distant from Carnica subspecies with a pairwise distance of 2.00 and dissimilar to Mugla and Yigilca ecotypes with a pairwise distance of 1.00 (*Table 1*).

A. m. anatoliaca (FJ357805) Van and *A. m. anatoliaca* (FJ357802) Aydin-C shared the same distance of 1.00 to Mugla-Yigilca group and the distance of 2.00 to Carnica, Syriaca and Caucasian samples. *A. m. anatoliaca* (FJ357804) Aydin-Kusadasi showed pairwise difference of 1.00 with Carnica, Syrian and Caucasian samples while this haplotype indicated similarity with Mugla and Yigilca ecotypes (pairwise distance = 0.00). The distance between *A. m anatoliaca* (FJ357798) Bolu and Mugla-Yigilca group was 2.00 while this haplotype was more distant from Carnica, Syriaca and Caucasian samples with a magnitude of 3.00 (*Table 1*). The branching pattern had a bootstrap value of 81% for UPGMA method.

Relationships between the subspecies within ND5 region

The amplified PCR product of NADH dehydrogenase subunit 5 (ND5) gene was 721 bp (*Fig. 3*). The dendogram based on the phylogenetic analysis of sequencing data for NADH dehydrogenase subunit 5 (ND5) gene, the samples included to this study did not reveal any genetic divergence and they were grouped in the same branch with *Apis mellifera* ND5 gene haplotype 3 (GU060468), *Apis mellifera* ND5 gene haplotype 1 (JN410833) and haplotype 5 (JN410837) and did not show much difference from *Apis mellifera* ND5 gene haplotype 2 (JN410834), haplotype 3 (JN410835), haplotype 4 (JN410836), haplotype 1 (GU060466), haplotype 2 (GU060467), haplotype 3 (GU060468), haplotype 4 (GU060469), haplotype 6 (GU060471) and haplotype 7 (GU060472) with a bootstrap value of 66% (*Fig. 4*). They indicated a pairwise difference of 0.01 with haplotype 8 (GU060473).

http://www.aloki.hu ● ISSN 1589 1623 (Print) ● ISSN1785 0037 (Online)
DOI: http://dx.doi.org/10.15666/aeer/1802_22692284

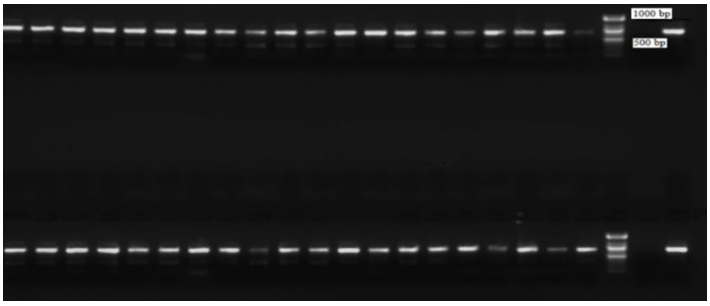

Figure 3. *The amplified PCR products of NADH dehydrogenase subunit 5 (ND5) gene of mıtochondrial DNA (Bands represented A.m. anatoliaca-Mugla-1-2-3-4; A.m. caucasica 1-2-3-4; A.m. carnica 1-2-3-4; A.m. anatoliaca-Yigilca 1-2-3-4; A.m. syriaca 1-2-3-4, respectively)*

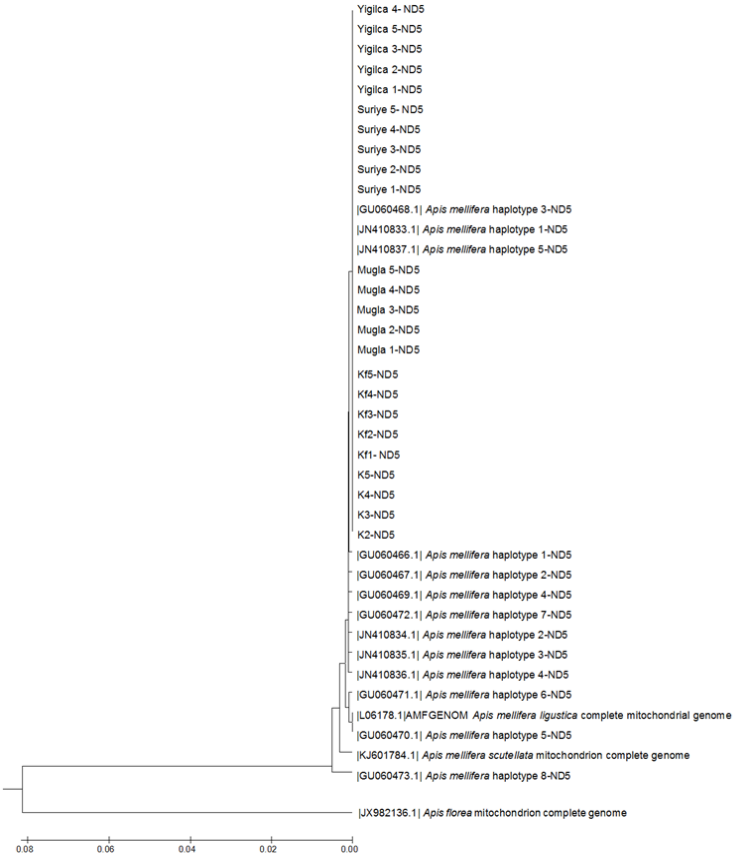

Figure 4. *The phylogenetic tree based on NADH dehydrogenase subunit 5 (ND5) gene. The evolutionary history was inferred using the UPGMA method. A.m. syriaca samples of the study were labeled as Suriye (1 to 5), A.m. caucasica samples as Kf (1 to 5), A.m. carnica samples as K (2 to 5), A.m. anatoliaca as Mugla ecotype (1 to 5) and A.m. anatoliaca as Yigilca ecotype (1 to 5)*

Only Yigilca ecotype was different from ND5 haplotype 5 (GU060470) and *Apis mellifera liguistica* ND5 segment (L06178) with a pairwise value of 0.01. All of the samples were distant from *Apis mellifera scutellata* ND5 gene (KJ601784) with a magnitude of 0.01 and from *Apis mellifera florea* ND5 gene JX982136 with a magnitude of 0.014 (*Table 2*).

http://www.aloki.hu ● ISSN 1589 1623 (Print) ● ISSN1785 0037 (Online)
DOI: http://dx.doi.org/10.15666/aeer/1802_22692284

Table 2. *Estimates of evolutionary divergence between sequences of ND5 gene (left). Identification of the numbers representing the nucleotide sequences were given (right). (Samples of this study were represented by numbers 1, 2, 3, 4, 5)*

	1	2	3	4	5	6	7	8	9	10	11	12	13	14	15	16	17	18	19	20	21		
[1]																						[1]	#Carniolan samples
[2]	0.00																					[2]	#Caucasica samples
[3]	0.00	0.00																				[3]	#Mugla samples
[4]	0.00	0.00	0.00																			[4]	#Syrian samples
[5]	0.00	0.00	0.00	0.00																		[5]	#Yigilca samples
[6]	0.00	0.00	0.00	0.00	0.00																	[6]	#GU060466_*Apis mellifera*_haplotype_1
[7]	0.00	0.00	0.00	0.00	0.00	0.00																[7]	#GU060467_*Apis mellifera*__haplotype_2
[8]	0.00	0.00	0.00	0.00	0.00	0.00	0.00															[8]	#GU060468_*Apis mellifera*_haplotype_3
[9]	0.00	0.00	0.00	0.00	0.00	0.00	0.00	0.00														[9]	#GU060469_*Apis mellifera*_haplotype_4
[10]	0.00	0.00	0.00	0.00	0.01	0.01	0.01	0.00	0.01													[10]	#GU060470_*Apis mellifera*_haplotype_5
[11]	0.00	0.00	0.00	0.00	0.00	0.00	0.00	0.00	0.00	0.00												[11]	#GU060471_*Apis mellifera*_haplotype_6
[12]	0.00	0.00	0.00	0.00	0.00	0.00	0.00	0.00	0.00	0.01	0.00											[12]	#GU060472_*Apis mellifera*_haplotype_7
[13]	0.01	0.01	0.01	0.01	0.01	0.01	0.01	0.01	0.01	0.01	0.01	0.01										[13]	#GU060473_*Apis mellifera*_haplotype_8
[14]	0.00	0.00	0.00	0.00	0.00	0.00	0.00	0.00	0.00	0.00	0.00	0.00	0.01									[14]	#JN410833_*Apis mellifera*_haplotype_1
[15]	0.00	0.00	0.00	0.00	0.00	0.00	0.00	0.00	0.00	0.01	0.00	0.00	0.01	0.00								[15]	#JN410834_*Apis mellifera*_haplotype_2
[16]	0.00	0.00	0.00	0.00	0.00	0.00	0.00	0.00	0.00	0.01	0.00	0.00	0.01	0.00	0.00							[16]	#JN410835_*Apis mellifera*_haplotype_3
[17]	0.00	0.00	0.00	0.00	0.00	0.00	0.00	0.00	0.00	0.01	0.00	0.00	0.01	0.00	0.00	0.00						[17]	#JN410836_*Apis mellifera*_haplotype_4
[18]	0.00	0.00	0.00	0.00	0.00	0.00	0.00	0.00	0.00	0.00	0.00	0.00	0.01	0.00	0.00	0.00	0.00					[18]	#JN410837_*Apis mellifera*_haplotype_5
[19]	0.14	0.14	0.14	0.14	0.14	0.14	0.14	0.14	0.14	0.14	0.14	0.14	0.13	0.14	0.14	0.14	0.14	0.14				[19]	#JX982136_*Apis_florea*
[20]	0.01	0.01	0.01	0.01	0.01	0.00	0.01	0.01	0.01	0.01	0.01	0.01	0.01	0.01	0.01	0.01	0.01	0.01	0.14			[20]	#KJ601784_*Apis_mellifera_scutellata*
[21]	0.00	0.00	0.00	0.00	0.01	0.01	0.01	0.00	0.01	0.00	0.00	0.01	0.01	0.00	0.01	0.01	0.01	0.00	0.14	0.01		[21]	#LO6178_*Apis_mellifera_ligustica*

http://www.aloki.hu ● ISSN 1589 1623 (Print) ● ISSN1785 0037 (Online)
DOI: http://dx.doi.org/10.15666/aeer/1802_22692284

Discussion

Relationships between the subspecies

In this study the genetic relationships of the subspecies was revealed by direct sequencing of mtDNA based on tRNA^{leu}-COX2 and ND5 genes. Fragment lengths can be determined with certainty but the identities of many of the mitochondrial haplotypes can't be specified by RFLP patterns alone. Genetic variation can be established with greater sensitivity of DNA sequencing.

For systematic and population biology, the mtDNA that is maternally inherited without recombination is a pivotal tool. DNA sequence data analysis can be performed in a simple phylogenetic context, making mitochondrial data advantageous over morphometric data. Sometimes there may be differences between morphometric and mitochondrial data sets, when previously isolated populations of honey bees come into contact through human transportation or range expansion and mtDNA haplotypes may be introgressed into new populations as a result of mating (Palmer, 2000). While mtDNA's uniparental inheritance appears to be a downside, it retains an notable source of data by preserving information on queen and queen lines that shed light on the history and phylogeography of *A. mellifera*. However, the mitochondrial genes are interrelated and the evolution of different regions of the mitochondrial genome at different rates leads to incompatible phylogenetic and phylogeographical patterns (Henriques et al., 2019).

Subspecies of C evolutionary lineage pinpoints a short sequence with a lack of length variability. Mitochondrial haplotypes can be discriminated via single nucleotide polymorphisms (Franck et al., 2000; Sušnik et al., 2004). Thus conservative mtDNA regions are more convenient than length polymorphisms to identify molecular variation within C lineage subspecies. The analysis of tRNA^{leu}-COX2 intergenic region indicated identical genetic information for Mugla and Yigilca sharing similarity with *A. mellifera* haplotype C2d (JQ977701) which was also frequent in *A. m. macedonica* Greek populations and observed in *A. m. carnica* Crotian subpopulations which meaned that these two ecotypes also carried mixed genetic information of different subspecies aside from *A. m. anatoliaca*. Mugla and Yigilca honey bees are ecotypes of *A. m. anatoliaca* thus they mostly shared similarity with *A. m. anatoliaca* haplotypes such as *A. m. anatoliaca* clone 5973 (AY618912), *A. m. anatoliaca* (FJ357804) from Aydin-Kusadasi. These ecotypes were also closer to *A. m. anatoliaca* haplotype C1e (FJ357802) from the center of Aydin which were studied by Özdil et al. (2009b). tRNAleu-COX2 region of Mugla and Yigilca ecotypes also carried *A. mellifera* haplotype C12 (FJ037777). In the study of Solorzano et al. (2009), *A. mellifera* haplotype C12 was the most prevalent mitotype acknowledged as basal ancestral mitotype and it corresponded for 47% of the *Apis mellifera* 'C' lineage samples and was found in 13 of the 22 sampled locations including Aegean (Mugla, Izmir), Black Sea (Yigilca, Giresun), Marmara (Kirklareli, Canakkale, Bursa), Mediterrenean (Hatay) regions.

Microsatellite analysis of honey bees from Turkey (Bodur et al., 2007) indicated that Kirklareli region had the lowest levels of gene flow but mtDNA results of Solorzano et al. (2009) did not support the genetic distinctiveness of this region because all sampled colonies consisted of mitotype C12. It was also concluded by Palmer et al. (2000) and Kandemir et al. (2006) that Thrace populations were not divergent from Anatolian

http://www.aloki.hu ● ISSN 1589 1623 (Print) ● ISSN1785 0037 (Online)
DOI: http://dx.doi.org/10.15666/aeer/1802_22692284

populations. In the current study, Carnica samples branched out separately away from C12 mitotype with a pairwise distance of 1.00. According to Solorzano et al. (2009), the incompatibility between mitochondrial and nuclear markers may reflect the maternal inheritance of mitochondrial DNA, and nuclear markers might be representing the polyandrous matings of queens with genetically distinct drones that makes the population in this region diverse. Samples of Carnica subspecies clustered with two *A. m. carnica* breeding lines JQ778293 and JQ778292 from Eastern Serbia. They also showed close proximity to *A. m. anatoliaca* from Aydin and *A. m. mellifera* haplotype C1h of German honey bee and *A. mellifera* haplotype C2i from Eastern Serbia which could result from human and biological influences that mix populations and compromise their purity.

Samples of Syrian and Caucasian subspecies were grouped within the same branch with *A. m. anatoliaca* clone 6313. This clone (TrDra-2 haplotype) was found to be widely distributed in Eastern Anatolia and also observed in Black Sea (7.09%), Mediterrenean (5.48%), Marmara (7.50%), Central Anatolia (3.92%) and Aegean (3.03%) regions (Kandemir et al., 2006). Syrian and Caucasian subspecies also shared the same branch with *A. m. meda* (FJ357807) and were closer to *A. m. caucasica* (FJ357808). The former was C2g haplotype from Iran and the latter was C2h from Ankara- Kazan (Özdil et al., 2009b). C2h haplotype from Ankara-Kazan were found to be similar to published sequences of *A. m. caucasica* (Garnery et al., 1992). Honey bee populations spreading along the northern coast from Kırklareli to Artvin were stated to be *A. m. anatoliaca* or an ecotype of it (Kandemir et al., 2000; Kekeçoğlu, 2007; Kekeçoğlu and Soysal, 2010; Çakmak et al., 2014). According to the results of Kambur and Kekeçoğlu (2018), *A. m. caucasica* was not found in each province of northeast of Turkey because of beekeeping activities. This resemblance of Caucasian subspecies to other subspecies could be attributed to the widespread use of Caucasian bees by many beekeepers in different provinces. The existence of close relationship between these subspecies (Syriaca and Caucasica) and a variety of haplotypes is coherent with the hypothesis that Anatolian zone is close to the origin of the speciation *of Apis mellifera* (Ruttner, 1988).

A. m. anatoliaca clone 6043 (AY618913), *A. m. anatoliaca* C2a haplotype from Van (Özdil et al., 2009b), *A. m. anatoliaca* clone 6322 (AY618915*)*, *A. mellifera* isolate C2s haplotype from Spain (JF723979) were clustered together apart from the samples of this study. The frequency of haplotype *A. m. anatoliaca* clone 6043 (TrDra-1) ascended from east to west in Turkey, the highest frequency was discovered in Thrace and with the lowest in northeastern Anatolia where *A. m. caucasica* prevailed. *A. m. anatoliaca* clone 6322- TrDra-3 haplotype which accounted for C2b (Franck et al., 2000) was identified in eastern Anatolia, Ardahan and Van (Kandemir et al., 2006).

A. m anatoliaca haplotype C1a from Bolu (Özdil et al., 2009b) and *A. mellifera* haplotype C2v from Romania were clustered together and genetically distinct from Mugla-Yigilca ecotypes as well as Caucasica, Carnica and Syrian subpecies by demonstrating more distance.

In the study of Kandemir et al. (2006), TrDra-4 haplotype (AY618916) which was detected in one province (Kastamonu) on the Black Sea coast and corresponds to C2a. *A. m. carnica* haplotype of Franck et al. (2000) was submitted as *A. m. syriaca* clone 6783 to the Genebank. In the same study, TrDra-5 haplotype (AY618917) was also submitted as *A. m. syriaca* clone 6800 to the Genbank. These clones as well as *A. mellifera* mitotypes A1 and A4 were far from Syrian and other samples of the

http://www.aloki.hu ● ISSN 1589 1623 (Print) ● ISSN1785 0037 (Online)
DOI: http://dx.doi.org/10.15666/aeer/1802_22692284

subspecies included in this study with a particular branching pattern. *A. mellifera* mitotypes A1 and A4 from Brazil and Uruguay also clustered apart from the other haplotypes included in the mtDNA analysis.

Conspicuous differences were not detected between honey bee subspecies and ecotypes in tRNA^{leu}-COX2 region in this study. Henriques et al. (2019) concluded in their study that care should be taken with regard to the results of analysis of tRNA^{leu}-COX2 region and this may not be a suitable marker for detecting relationships between honey bee colonies. The large numbers of indels and duplications of large fragments and homoplasy in this region reduce the accuracy of this region in relation to the capturing of maternal history.

Relative to other mitochondrial regions, the ND5 region was studied less at population level. According to the analysis of mitochondrial NADH dehydrogenase subunit 5 (ND5) gene, the samples of this study belonged to the same clade with *Apis mellifera* ND5 gene haplotype 3 (GU060468), *Apis mellifera* ND5 gene haplotype 1 (JN410833) and haplotype 5 (JN410837). In the study about phylogenetic relationships among *A. mellifera* subspecies depended on sequencing of mtDNA segments, ND5 haplotype 3 (GU060468) was monitored in *A. m. carnica* (Martimianakis et al., 2011). ND5 haplotype 1 (JN410833) was Anatolian haplotype captured in the samples from Konya-Sızma and haplotype 5 (JN410837) was found in honey bees from the South-East part of Turkey where mostly inhabited by *A. m. meda* (Özdil and İlhan, 2012).

NADH dehydrogenase subunit 5 (ND5) gene segments of our samples also did not point out any discrepancy from *Apis mellifera* ND5 gene haplotype 2 (JN410834-from Antalya and Konya), haplotype 3 (JN410835-widely distributed Anatolian haplotype among samples of Balıkesir, Bolu-Yığılca, and Konya), haplotype 4 (JN410836-Caucasian haplotype from Ardahan and Ankara) within the study of Özdil and İlhan (2012). In that study, the races couldn't be seperated from each other according to the NJ dendogram based on ND5 sequences, because they belonged to East European (C) lineage.

Our samples also did not differ from ND5 haplotypes of some other races such as haplotype 1 (GU060466) of *A. m. anatoliaca* (Bartin), *A. m. meda* (Osmaniye), *A. m. carnica*; haplotype 2 of *A. m. ligustica* (GU060467); haplotype 4 of *A. m. cecropia* (GU060469); haplotype 6 (GU060471) and haplotype 7 (GU060472) of *A. m. adami* (Martimianakis et al., 2011). Overall, a common branching pattern of the honey bee subspecies and ecotypes of this study with *A. m. anatoliaca*, *A. m. meda*, *A. m. carnica, A. m. ligustica* ND5 haplotypes of the other studies presented a coherent result by revealing the close relations at the species and subspecies level. It is known that the pattern typical of *A. m. carnica/A. m. ligustica* is considered to prevail across Turkey (97.9%) (Kandemir et al., 2006). It is not surprising to observe similarity to *A. m. ligustica* haplotype because its adaptability to various climatic conditions makes it a favored species to export globally. Consequently, the introduction of this species has usually been the main cause of genetic changes in local species (De la Rùa et al., 1998; Garnery et al., 1998a,b). Appearance of *A. m. meda* and *A. m. ligustica* in the same cluster was also congruent with the finding about the similarity between *A. m. meda* (Iranian) and *A. m. ligustica* (Italian) based on several characters of morphology and behavior (Ruttner et al., 1988). Settar (1983) showed that honey bee subspecies in Aegean region were transitional populations between *A. m. caucasica* and *A. m. ligustica*. In another study showing the haplotypes obtained in honey bee populations of Thrace region, some of the samples with variation were found to have *A. m. caucasica*

http://www.aloki.hu ● ISSN 1589 1623 (Print) ● ISSN1785 0037 (Online)
DOI: http://dx.doi.org/10.15666/aeer/1802_22692284

origin and hybridization between Caucasian/Anatolian and Carniolan/Macedonian haplotypes was detected. The reasons for this situation is thought to be the intense introduction of Caucasian queen bees and migratory beekeeping activities (Ünal and Özdil, 2018). Also some studies proved that there were mixed populations of *A. m. syriaca* and *A. m. meda* in both southeast and the eastern parts of Turkey (Palmer et al., 2000; Kandemir et al., 2000).

According to the study of Kambur and Kekeçoğlu (2018), the groups representing the Aegean and Marmara regions coincided and intertwined with the provinces representing the Eastern Anatolia. Those results indicated that bee biodiversity was significantly affected by commercial queen use activities.

Turkey is at the crossroads between Europe, Asia and the Middle East with a wide variety of climates and habitats. There are many subspecies and ecotypes of honey bees within these ranges such as *A. m. anatoliaca, A. m. caucasica, A. m. meda,* and *A. m. syriaca* as described by Ruttner (1988). Honey bees have been able to adapt to a variety of ecological environments including three phytogeographic regions; Euro-Syberian; Mediterranean; and Irano-Turanian where several honey bee ecotypes appeared with many morphological, biochemical, physiological, and behavioural adaptations. Widespread migratory beekeeping activities and the demand of exporting and establishing Caucasian bees (*A. m. caucasica*) in new locations contribute to transplantation and mixing of populations impacting the integrity of the ecotypes and the geographical variations among them.

Conclusion

Molecular data on mitochondrial DNA (mtDNA) tRNA^{leu}-COX2 and ND5 sequences inferred that all the subspecies and ecotypes in this study were not so diverse genetically. There is a possibility that reproductive isolation couldn't be achieved and gene introgression could have occured between them because of the close proximity of the colonies in the bee yard or in the past, the genetic structure of the colonies could have already mixed and exchanged in their native habitats from where they were originated and sampled. Phylogenetic analysis of this study would be more effective and strong if sample size was increased by including more colonies of the subspecies. Degradation of honey bee biodiversity in some locations of Turkey were reported previously by many studies. Overlapping of samples representing subspecies from different regions could mean that honey bee biodiversity could not maintain its current status and the use of commercial queen bee has significantly affected the biodiversity of honey bee in Turkey. Each of the subsepecies has its own unique behavioral and morphometric characteristics that make them well suited to their local environments, but hybridization and modification of the existing genetic pool among local bees can appear through fragmentation of land resources via urbanization, uncontrolled reproduction, the introduction of queen bees from other mtDNA lines and the preferences of the beekeepers to use different breeds for high yield (Güler, 2010). Thus local honey bee subspecies and ecotypes may lose their novel characteristics. Due to their social nature of the honey bees at the individual and colonial reproduction level, the distribution of mitochondrial markers are affected and diversified by commercial breeding and migratory beekeeping activities. Identification and protection of natural honey bee gene resources is vital for the development of beekeeping. Conventional methods are not not suitable to define the hybrids and not sufficient to prevent gene

http://www.aloki.hu ● ISSN 1589 1623 (Print) ● ISSN1785 0037 (Online)
DOI: http://dx.doi.org/10.15666/aeer/1802_22692284

flow among subspecies. Thus identification of hybrids must be enhanced to improve conservation management. Also next-generation sequencing of bee transcriptomes and genomes will extend the number of genes and data and provide new approaches to resolve phylogenetic relationships. Pure breeding populations are also a major instrument for an improved conservation management. Detailed beekeeping information of different regions needs to be collected systematically before making future conservation programmes. The mechanisms of hybridization and mating distances may assist protection of honey bee subspecies. Apicultural researches about identifying and improving local genetic lines must be encouraged and granted. Beekeeping policies must be regulated to minimize human induced artificial sympatry of honey bee populations. Conservation of honey bee biodiversity is a very necessary step to preserve the biological equilibrium in ecological environment, to meet the agricultural demands of humans and to benefit from production potentials in breeding and hybridization studies in the future.

Acknowledgements. The laboratory work was financially supported by the USDA-ARS Bee Research Laboratory. I especially would like to thank Dr. Jay D. Evans for his support about the research.

REFERENCES

[1] Arias, M. C., Sheppard, W. S. (1996): Molecular phylogenetics of honey bee subspecies (*Apis mellifera* L.) inferred from mitochondrial DNA sequence. – Mol Phylogenet Evol 5: 557-566.

[2] Avise, J. C., Arnold, J., Ball, R. M., Bermingham, E., Lamb, T., Neigel, J. E., Reeb, C. A., Saunders, N. C. (1987): Intraspecific phylogeography: the mitochondrial DNA bridge between population genetics and systematics. – Ann Rev Ecol Syst 18: 489-522.

[3] Bodur, C., Kence, M., Kence, A. (2007): Genetic structure of honey bee, *Apis mellifera* L. (Hymenoptera: Apidae) populations of Turkey inferred from microsatellite analysis. – J Apic Res 46: 50-6.

[4] Bouga, M., Harizanis, P. C., Kilias, G., Alahiotis, S. (2005): Genetic divergence and phylogenetic relationships of honey bee *Apis mellifera* (Hymenoptera: Apidae) populations from Greece and Cyprus using PCR-RFLP analysis of three mtDNA segments. – Apidologie 36: 335-344.

[5] Cánovas, F., De la Rúa, P., Serrano, J., Galián, J. (2008): Geographical patterns of mitochondrial DNA variation in *Apis mellifera iberiensis* (Hymenoptera: Apidae). – J Zool Syst Evol Res 46: 24-30.

[6] Çakmak, İ., Fuchs, S., Çakmak, S. S., Koca, A. Ö., Nentchev, P., Kandemir, İ. (2014): Morphometric analysis of honeybees ditributed in northern Turkey along the black sea coast. – Uludağ Arıcılık Dergisi 14(2): 59-68.

[7] De la Rua, P., Hernandez-Garcia, R., Pedersen, B. V., Galian, J., Serrano, J. (2004): Molecular diversity of honeybee *Apis mellifera iberica* L. (Hymenoptera: Apidae) from western Andalusia. – Archiv Zootec 53: 195-203.

[8] Franck, P., Garnery, L., Solignac, M., Cornuet, J. M. (2000): Molecular confirmation of a fourth lineage in honeybees from the near east. – Apidologie 31: 167-180.

[9] Garnery, L., Cornuet, J. M., Solignac, M. (1992): Evolutionary history of the honey bee *Apis mellifera* inferred from mitochondrial DNA analysis. – Mol Ecol 1: 145-154.

[10] Garnery, L., Franck, P., Baudry, E., Vautrin, D., Cornuet, J. M., Solignac, M. (1998a): Genetic diversity of the west European honey bee (*Apis mellifera mellifera* and *A. m. iberica*). Mitochondrial DNA. – Genet Sel Evol 30 (Suppl. 1): S31-S47.

http://www.aloki.hu ● ISSN 1589 1623 (Print) ● ISSN1785 0037 (Online)
DOI: http://dx.doi.org/10.15666/aeer/1802_22692284

[11] Garnery, L., Franck, P., Baudry, E., Vautrin, D., Cornuet, J. M., Solignac, M. (1998b): Genetic diversity of the west European honey bee (*Apis mellifera mellifera* and *A. m. iberica*) II. Microsatellite loci. – Genetics Selection Evolution 30(Suppl. 1): S49-S74. http://dx.doi.org/10.1051/gse:19980703.
[12] Güler, A. (2010): A morphometric model for determining the effect of commercial queen bee usage on the native honeybee (*Apis mellifera* L.) population in a Turkish province. – Apidologie 41(1): 622-635.
[13] Hall, H. G., Smith, D. R. (1991): Distinguishing African and European honeybee matrilines using amplified mitochondrial DNA. – Proc Natl Acad Sci 88: 4548-4552.
[14] Han, F., Wallberg, A., Webster, M. T. (2012): From where did the Western honeybee (*Apis mellifera*) originate? – Ecol evol 2(8): 1949-57.
[15] Henriques, D., Chávez-Galarza, J., Quaresma, A., Neves, C. J., Lopes, A. R., Costa, C., Costa, F. O., Rufino, J., Pinto, M. A. (2019): From the popular tRNA^{leu}-COX2 intergenic region to the mitogenome: insights from diverse honey bee populations of Europe and North Africa. – Apidologie 50(2): 215-229. doi:10.1007/s13592-019-00632-9.
[16] Kambur, M., Kekeçoğlu, M. (2018): The loss of genetic diversity on native Turkish honey bee (*Apis mellifera* L.) subspecies (Türkiye bal arısı (*Apis mellifera* L.) alttürlerinde genetik çeşitlilik kaybı). – Anadolu Tarım Bilimleri Dergisi 33(1): 73-84. DOI: 10.7161/omuanajas.337798.
[17] Kambur, M., Kekeçoğlu, M. (2018): The current situation of Turkey Honey Bee (*Apis mellifera* L.). – Biodiversity and Conservation 11(1): 105-119. DOI: 10.13140/RG.2.2.12203.54568.
[18] Kandemir, İ., Kence, M., Kence, A. (2000): Genetic and morphometric variation in honeybee (*Apis mellifera*) populations of Turkey. – Apidologie 31: 343-356.
[19] Kandemir, I., Kence, M., Sheppard, W. S., Kence, A. (2006): Mitochondrial DNA variation in honey bee (*Apis mellifera* L.) populations from Turkey. – Journal of Apicultural Research and Bee World 45(1): 33-38.
[20] Kekeçoğlu, M. (2007): Türkiye Balarılarının mtDNA ve Bazı Morfolojik Özellikleri Bakımından Karşılaştırılmasına Yönelik Bir Araştırma. – Doktora tezi, Namık Kemal Üniversitesi Zootekni Bölümü, 148s, Tekirdağ.
[21] Kekeçoğlu, M., Bouga, M., Soysal, M. I., Harizanis, P. (2009): Genetic divergence and phylogenetic relationships of honey bee populations from Turkey using PCR-RFLP's analysis of two mtDNA segments. – Bulgarian J Agric Sci 15: 589-597.
[22] Kekeçoğlu, M., Soysal, M. İ. (2010): Genetic Diversity Of Bee Ecotypes in Turkey and evidence for geographical differences. – Romanian Biotechnological Letters 15(5): 5646-5653.
[23] Marino, A., Sabatini, A. G., Carpana, E., Mantovani, B. (2002b): Analysis of mitochondrial genes NDH2, CO1 and 16S for the characterization of *Apis mellifera* populations. – Insects Soc Life 4: 87-92.
[24] Martimianakis, S., Klossa-Kilia, E., Bouga, M., Kilias, G. (2011): Phylogenetic relationships of Greek *Apis mellifera* subspecies based on sequencing of mtDNA segments (COI and ND5). – J Apicult Res 50: 42-50.
[25] Muñoz, I., Dall'Olio, R., Lodesani, M., De la Rúa, P. (2009): Population genetic structure of coastal Croatian honey bees (*Apis mellifera carnica*). – Apidologie 40: 617-626.
[26] Nei, M., Kumar, S. (2000): Molecular Evolution and Phylogenetics. – Oxford University Press, New York.
[27] Özdil, F., Yildiz, M. A., Hall, H. G. (2009a): Molecular characterization of Turkish honey bee populations (*Apis mellifera* L.) inferred from mitochondrial DNA RFLP and sequence results. – Apidologie 40: 570-576.
[28] Özdil, F., Fakhri, B., Meydan, H., Yildiz, M. A., Hall, H. G. (2009b): Mitochondrial DNA variation in the CoxI-CoxII intergenic region among Turkish and Iranian honey bees (*Apis mellifera* L.). – Biochem Genet 47: 717-721.

http://www.aloki.hu ● ISSN 1589 1623 (Print) ● ISSN1785 0037 (Online)
DOI: http://dx.doi.org/10.15666/aeer/1802_22692284

[29] Özdil, F., İlhan, F. (2012): Genetic Divergence of Turkish *Apis mellifera* Subspecies Based on Sequencing of ND5 Mitochondrial Segment. – Sociobiology 59(1): 225-234.
[30] Palmer, M. R., Smith, D. R., Kaftanoglu, O. (2000): Turkish honey bees: genetic variation and evidence for a fourth lineage of *Apis mellifera* mtDNA. – J Hered 91: 42-46.
[31] Ruttner, F. (1988): Biogeography and Taxonomy of Honey bees. – Springer-Verlag, Berlin, 284p.
[32] Settar, A. (1983): Ege Bölgesi Arı Tipleri Ve Gezginci Arıcılık Üzerine Arastırmalar. – Doktora tezi. Ege Zirai Arastırma Enstitüsü, 129s, İzmir.
[33] Solorzano, C. D., Szalanski, A. L., Kence, M., McKern, J. A., Austin, J. W., Kence, A. (2009): Phylogeography and population genetics of honey bees (*Apis mellifera* L.) from Turkey based on COI–COII sequence data. – Sociobiology 53: 237-246.
[34] Sušnik, S., Kozmus, P., Poklukar, J., Meglić, V. (2004): Molecular characterisation of indigenous *Apis mellifera carnica* in Slovenia. – Apidologie 35: 623-636.
[35] Tamura, K., Stecher, G., Peterson, D., Filipski, A., Kumar, S. (2013): MEGA6: molecular evolutionary genetics analysis version 6.0. – Mol Biol Evol 30: 2725-2729.
[36] Thompson, J. D., Higgins, T. J. (1994): Clustal W. improving the sensitivity of progressive multiple sequence alignment through sequence weighting, positions specific gap penalties and weight matrix choice. – Nucleic Acids Res 22: 4673-4680.
[37] Ünal, G., Özdil, F. (2018): Genetic characterization of Thrace honey bee populations of Turkey: restriction and sequencing of inter cytochrome C oxidase I-II (CoxI-CoxII) genes. – Journal of Apicultural Research 57(2): 213-218. https://doi.org/10.1080/00218839.2018.1426347.

http://www.aloki.hu ● ISSN 1589 1623 (Print) ● ISSN1785 0037 (Online)
DOI: http://dx.doi.org/10.15666/aeer/1802_22692284

IN VITRO SHOOT REGENERATION OF A *CENTAUREA AMAENA* BOISS. & BALANSA – A CRITICALLY ENDANGERED AND ENDEMIC PLANT

UZUN, S.[1*] – EKINCI, E.[1] – ÖZKATAN, H.[1] – ATASAGUN, B.[2*]

[1]*Department of Field Crops, Agricultural Faculty, Erciyes University, 38039 Kayseri, Turkey*

[2]*Yeşilhisar Vocational School, The University of Kayseri, 38800 Kayseri, Turkey*

**Corresponding author*
e-mail: saticocu@yahoo.com; phone: +90-352-621-7939/38675; fax: +90-352-621-7989

(Received 18th Oct 2019; accepted 30th Jan 2020)

Abstract. This study was conducted to investigate in vitro regeneration potential of *Centaurea amaena*, a critically endangered and an endemic plant in Turkey. For this purpose, cotyledon, leaf and cotyledon node explants were cultured in Murashige and Skoog (MS) media supplemented with different concentrations of 6-benzylaminopurine (BAP; 1-4 mg L^{-1}), thidiazuron (TDZ; 0.3-1.2 mg L^{-1}) or *meta*-Topolin (*m*T; 0.5-4 mg L^{-1}) with or without 0.5 mg L^{-1} α-naphthalene acetic acid (NAA). In axillary shoot regeneration experiments from cotyledon node explants, the greatest number of shoots per explant (9.975) was obtained from 4 mg L^{-1} *m*T-containing MS media, which yielded a shoot regeneration frequency of 70.83%. In indirect organogenesis experiments, the greatest number of shoots per explant in cotyledons (4.152 shoots/explant with the shoot regeneration frequency of 55.00%) was obtained from 1 mg L^{-1} *m*T-containing media and the greatest number of shoots per explant in leaves (4.132 shoots/explant with the shoot regeneration frequency of 50.00%) was obtained from 4 mg L^{-1} *m*T-containing media. Only callus induction was observed in TDZ-containing media or combinations of TDZ concentrations with NAA. About 50.00% root formation was achieved from half-strength MS medium containing 2.0 mg L^{-1} indole-3-butyric acid.
Keywords: *axillary shoot regeneration, BAP, mT, organogenesis, TDZ*

Introduction

Centaurea amaena Boiss. & Balansa belonging to the *Phalolepis* section of the Compositae family is classified as CR B2ab (i,iii) based on IUCN criteria (Atasagun et al., 2013; Atasagun and Aksoy, 2018). The species occurs over the stony slopes of Yılanlı Mountain, located between 38° 38' - 38° 41' N longitudes and 35° 30' - 35° 35' S latitudes to the west of Kayseri, Turkey and naturally grows in arid environments at altitudes of between 1.170-2.300 m (Atasagun and Aksoy, 2018). The species exists in two localities in Kayseri with distribution area of about 0.55 km^2. Number of individuals was identified by Atasagun and Aksoy (2018) as 5672. Atasagun and Aksoy (2018) indicated that the species had a quite isolated distribution between Erciyes and Yılanlı mountains of Kayseri; it was an endemic species under the threat of extinction mostly because of anthropogenic effects, animal grazing, stone quarry activities, Erciyes Mountain master plan, negative impacts of seasonal conditions based on altitude of spread zones, use of plant seeds by *Oxycarenus sp.* of Heteroptera suborder as nutrient and all these issues reduced formation of new individuals and negatively influenced the growth and development of the population.

C. amaena is rich in phenolics and flavonoids, thus has a strong antioxidant activity. Plants can be used as raw and processed food preservers and natural additives in

http://www.aloki.hu ● ISSN 1589 1623 (Print) ● ISSN 1785 0037 (Online)
DOI: http://dx.doi.org/10.15666/aeer/1802_22852293

pharmaceuticals, alternative medicine and natural treatment (Albayrak et al., 2017). *C. amaena* is under the threat of extinction and thus urgent measures should be taken to prevent extinction and for propagation of the species. Conservation is the effective storage of the diversity in the gene pool until its actual or potential use, and the introduction of this genetic diversity into the use of humanity. There are two primary conservation systems including in situ and ex situ conservation (Şehirali et al., 2015). In situ conservation means preservation of natural resources in their own habitats. However, ex situ conservation has become the most common practice for the conservation of plant genetic sources (Şehirali et al., 2015). Within the scope of ex situ conservation, in vitro tissue culture techniques are used. In recent years, several endangered and endemic species have been propagated and preserved from quite small quantity of plant material through these techniques without any significant impacts on wild populations (Erdağ and Emek, 2005a, b).

In previous studies, successful in vitro regeneration of *Centaurea* species were achieved from leaf, hypocotyl, cotyledon, node, soot tips, inflorescence stem parts-like explants with the aid of different cytokinin and auxin sources (Mallon et al., 2010; Aydoğan and Erdağ, 2015; Atalay and Erişen, 2017; Türkoğlu et al., 2018). In the different studies related to *Centaurea* species, the most commonly used cytokinins were BAP, kinetin, zeatin, TDZ and N6-(2-isopentyl) adenine (2-iP). Generally, BAP has been reported as the most efficient source of cytokinins for in vitro propagation of *Centaurea* species (Cuenca and Amo-Marco, 2000; Curkovic-Perica, 2003; Mallon et al., 2010; Atalay and Erişen, 2017). While the lowest response was obtained from zeatin, 2-iP and kinetin-containing media in *C. ultreiae* and from TDZ and kinetin-containing media in *C. lycaonica*, the use of kinetin was successful in *C. paui* (Cuenca et al., 1999) and *C. tchihatcheffii* (Ozel et al., 2006). In recent years, meta-topolin has been used to promote in vitro shoot regeneration as an alternative cytokinin source (Dimitrova et al., 2016). The use of *m*T as a cytokinin source in *Centaurea* species have not been reported before and there are no studies about in vitro regeneration of *Centaurea amaena*. Therefore, this study was conducted to produce an efficient in vitro regeneration method for *Centaurea amaena* and the effectiveness of BAP, TDZ and *m*T as a source of cytokinins was examined.

Materials and methods

Plant material and achene sterilization

Centaurea amaena Boiss & Balansa was used as the plant material of the present study. Mature seeds of the species were collected in limited numbers from the natural habitat, Yılanlı Mountain (Kayseri-Turkey), and seeds were preserved at +4 °C for later uses in further analyses. All experimental procedures were conducted at Tissue Culture Laboratory of Field Crops Department at Erciyes University Agricultural Faculty. Sterile distilled water and 50% diluted H_2SO_4 were used for surface sterilization of the seeds. Seeds were initially kept in this solution for a minute, rinsed through sterile distilled water, kept again in 50% diluted commercial bleach (ACE) in a magnetic stirrer for 10 min and finally rinsed through sterile distilled water three times and were germinated in sterile petri dishes with MSO media containing MS mineral salt and vitamins, 3% sucrose and 0.7% agar. About 15-20 seeds were placed into each magenta vessel (Sigma-Aldrich, 77 × 77 × 97).

http://www.aloki.hu ● ISSN 1589 1623 (Print) ● ISSN 1785 0037 (Online)
DOI: http://dx.doi.org/10.15666/aeer/1802_22852293

Indirect organogenesis

The cotyledon obtained from 2-weeks-old seedlings and leaves from about 1-month-old seedlings were used as explants for indirect organogenesis. Explants were cultured in MSO media containing different concentrations of TDZ (0.3-1.2 mg/l), BAP (1-4 mg L^{-1}) or *m*T (0.5-4 mg L^{-1}) alone or in combination with NAA (0.5 mg L^{-1}). About 7-8 weeks after the initiation of culture processes, callus induction ratio (%), shoot regeneration frequency (%) and number of shoots per explant were determined (*Fig. 1A*).

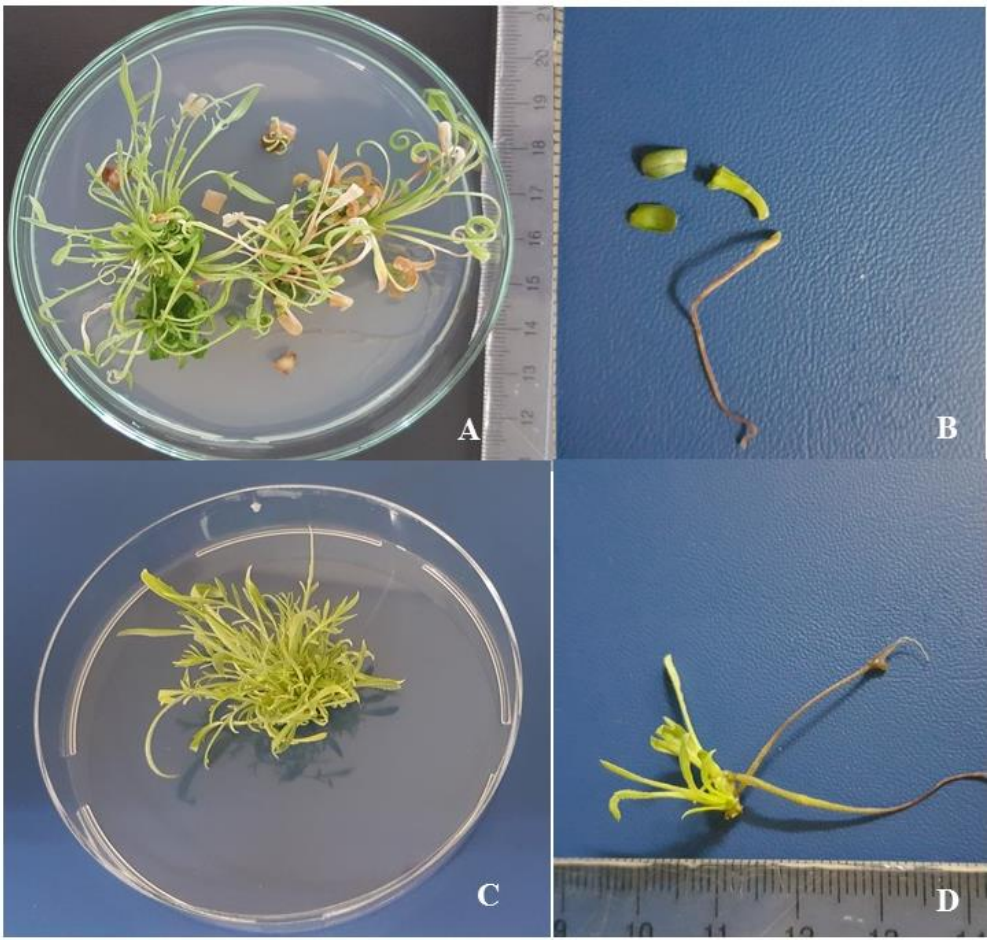

Figure 1. *In vitro propagation and rooting of Centaurea amaena. A - Indirect organogenesis from cotyledon explant on MSO medium supplemented with 4 mg L^{-1} mT, B - Isolation of cotyledon node explant, C - Axillary shoot regeneration form cotyledon node explant on MSO medium supplemented with 4 mg L^{-1} mT, D - Root formation of Centaurea amaena*

Axillary shoot regeneration

Cotyledon node explants were isolated from the plantlets about 15-20 days after initiation of germination processes and were cultured in Magenta Vessels with MSO media containing different concentrations of TDZ (0.3-1.2 mg L^{-1}), BAP (1-4 mg L^{-1}) or *m*T (0.5-4 mg L^{-1}) with or without 0.5 mg L^{-1} NAA (*Fig. 1B-C*). About 7-8 weeks after the initiation of culture processes, shoot regeneration frequency and number of shoots per explant parameters were determined.

http://www.aloki.hu ● ISSN 1589 1623 (Print) ● ISSN 1785 0037 (Online)
DOI: http://dx.doi.org/10.15666/aeer/1802_22852293

Rooting

Regenerated shoots were rooted in half-strength MS media containing 0.5, 1 or 2 mg L^{-1} IBA, 3% sucrose, solidified with 0.7% agar (*Fig. 1D*).

Experimental conditions

Entire sterile processes were conducted in a sterile cabin with a hepa-filter and horizontal air flow. Before the initiation of the sterile processes, the cabin was whipped with 96% ethyl alcohol, the cabin was then left open for 20 min and sterilized under UV light. All tools, equipment, distilled water and growth media used in this study were sterilized in an autoclave under standard conditions (1.2 atm pressure, 121 °C temperature, 20 min). Growth medium pH values were arranged as between 5.5-5.8 before agar supplementation. All cultures were grown under 16:8 light:dark photoperiod, 22 ± 2 °C temperature and 3000 lux light intensity.

Data analysis

Experiments were conducted at completely randomized design with 4 replications. Each replication had 6 (for cotyledon node) or 10 (leaf and cotyledon) explants. Before variance analysis, percentiles were subjected to "arcsine" transformation. Variance analysis was performed with SPSS software. Means were compared with the aid of Duncan's multiple range test.

Results and discussion

Indirect organogenesis

For plant regeneration through organogenesis in *C. amaena,* cotyledon and leaves taken from the plantlets obtained from sterile seeds were cultured in 20 different media containing different concentrations of BAP, TDZ or *m*T alone or in combination with NAA. About 7-8 weeks after the initiation of culture processes, callus induction ratio, shoot regeneration frequency and number of shoots per explant were determined. Callus induction ratios varied between 50 - 100%. While type of explant did not have any significant effects on callus induction ratios, PGR (plant growth regulator) concentrations and combinations had significant effects on callus induction ratios ($P < 0.01$). While the greatest callus induction ratios were obtained from BAP, BAP-NAA, *m*T-NAA, TDZ and TDZ-NAA-containing treatments, the lowest callus induction ratios were obtained from only *m*T-containing treatments (*Fig. 2*). Similarly, Atalay and Erişen (2017) also indicated that callus induction ratios in *Centaurea lycaonica* varied with the PGRs and reported high ratios for BAP-NAA and TDZ-NAA combinations. Researchers also identified differences in callus morphology of *C. lycaonica* based on PGR type and combinations.

PGRs and PGR × explant interactions had significant effects on shoot regeneration ratios and number of shoots per explant. Shoot regeneration frequencies varied between 0.00-57.50% in cotyledon explants and between 0.00-62.50% in leaf explant (*Table 1*). In both types of explants, callus induction was observed but shoot regeneration was not observed in TDZ-containing media. Similarly, Atalay and Erişen (2017) in *Centaurea lycaonica* and Aydoğan and Erdağ (2015) in *Centaurea zeybekii*, reported callus induction but no shoot regeneration in TDZ-containing media. In addition, Kazeroonian

http://www.aloki.hu ● ISSN 1589 1623 (Print) ● ISSN 1785 0037 (Online)
DOI: http://dx.doi.org/10.15666/aeer/1802_22852293

et al. (2018) indicated that type of cytokinin affected shoot regeneration and TDZ promoted callus induction rather than shoot regeneration in *Chrysanthemum morifolium* petiole explant. Dewir et al. (2018) reported that TDZ may result in various anomalies including inhibition of shoot proliferation, shoot elongation, etc., and indicated low TDZ concentrations, pulse treatment or short-duration TDZ treatments as efficient strategies to eliminate such anomalies. However, TDZ was also indicated as a strong synthetic cytokinin-like substance for shoot regeneration in several plant species (Erişen et al., 2011; Yorgancılar and Erişen, 2011; Uzun et al., 2014).

Table 1. *Effects of PGRs on adventitious shoot regeneration from cotyledon and leaf explants of Centaurea amaena*

PGRs	Shoot regeneration frequency (%)		Number of shoots per explant	
	Cotyledon	Leaf	Cotyledon	Leaf
1 mg L^{-1} BAP	40.00 ab*	40.00 bcd*	2.427 ef*	1.775 gh*
2 mg L^{-1} BAP	30.00 bc	50.00 ab	3.125 cd	3.997 ab
4 mg L^{-1} BAP	22.50 cd	47.50 ab	1.825 f	3.082 cd
1 mg L^{-1} BAP + 0.5 mg L^{-1} NAA	45.00 ab	62.50 a	2.052 f	3.930 ab
2 mg L^{-1} BAP + 0.5 mg L^{-1} NAA	25.00 cd	42.50 a-d	1.125 g	2.770 c-f
4 mg L^{-1} BAP + 0.5 mg L^{-1} NAA	15.00 d	45.00 abc	1.042 g	2.875 cde
0.5 mg L^{-1} *m*T	40.00 ab	47.50 ab	3.265 bcd	1.415 h
1 mg L^{-1} *m*T	55.00 a	27.50 cd	4.152 a	3.375 bc
2 mg L^{-1} *m*T	37.50 ab	25.00 d	3.227 cd	2.832 cde
4 mg L^{-1} *m*T	55.00 a	50.00 ab	3.965a	4.132 a
0.5 mg L^{-1} *m*T + 0.5 mg L^{-1} NAA	55.00 a	25.00 d	2.902 de	2.290 efg
1 mg L^{-1} *m*T + 0.5 mg L^{-1} NAA	57.50 a	55.00ab	3.927 ab	3.117 cd
2 mg L^{-1} *m*T + 0.5 mg L^{-1} NAA	40.00 ab	27.50 cd	3.970 a	2.082 fgh
4 mg L^{-1} *m*T + 0.5 mg L^{-1} NAA	47.50 ab	57.50 ab	3.657 abc	2.392 d-g
0.3 mg L^{-1} TDZ	0 e	0 e	0 h	0 ı
0.6 mg L^{-1} TDZ	0 e	0 e	0 h	0 ı
1.2 mg L^{-1} TDZ	0 e	0 e	0 h	0 ı
0.3 mg L^{-1} TDZ + 0.5 mg L^{-1} NAA	0 e	0 e	0 h	0 ı
0.6 mg L^{-1} TDZ + 0.5 mg L^{-1} NAA	0 e	0 e	0 h	0 ı
1.2 mg L^{-1} TDZ + 0.5 mg L^{-1} NAA	0 e	0 e	0 h	0 ı

*Values within a column followed by different letters are significantly different at 0.05 significance level using Duncan's multiple range test

The greatest numbers of shoots per explant were obtained from 1 mg L^{-1} *m*T, 4 mg L^{-1} *m*T, 1-2 or 4 mg L^{-1} *m*T + 0.5 mg L^{-1} NAA treatments in cotyledon explants and from 4 mg L^{-1} *m*T, 2 mg L^{-1} BAP and 1 mg L^{-1} BAP + 0.5 mg L^{-1} NAA treatments in leaf explants (*Table 1*). Optimum PGR type and concentration varied with explant type. Similarly, Erişen et al. (2011) reported differences in shoot regeneration of explants based on PGR concentrations and combinations in *Astragalus cariensis*. Success of a culture is influenced by type and concentration of applied cytokinin since cytokinin uptake, transport and metabolism varied with the plant species and cytokinin interacted with endogenous cytokinin of the explants (Magyar-Tabori et al., 2010).

http://www.aloki.hu ● ISSN 1589 1623 (Print) ● ISSN 1785 0037 (Online)
DOI: http://dx.doi.org/10.15666/aeer/1802_22852293

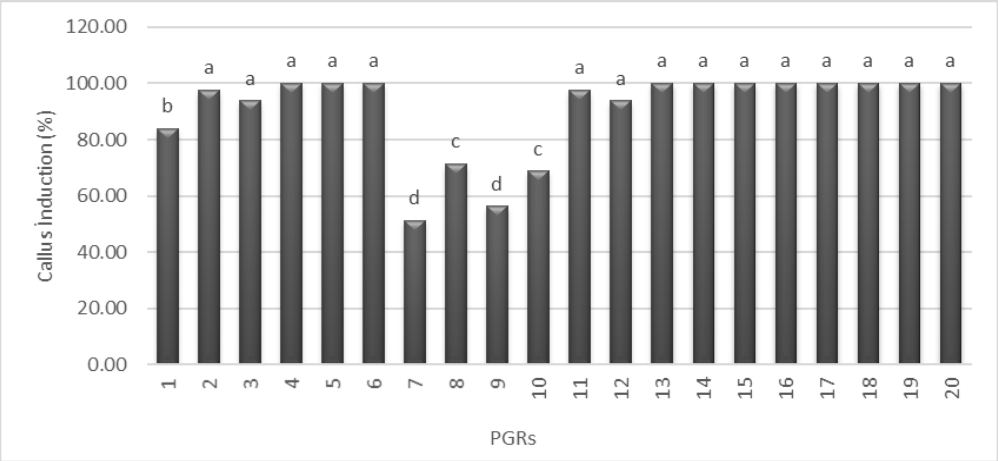

Figure 2. *Effects of different PGR concentrations and combinations on callus induction ratios. *Values within a column followed by different letters are significantly different at 0.05 significance level using Duncan's multiple range test.* ***1:*** *1 mg L^{-1} BAP;* ***2:*** *2 mg L^{-1} BAP;* ***3:*** *4 mg L^{-1} B AP;* ***4:*** *1 mg L^{-1} BAP + 0.5 mg L^{-1} NAA;* ***5:*** *2 mg L^{-1} BAP + 0.5 mg L^{-1} NAA,* ***6:*** *4 mg L^{-1} BAP + 0.5 mg L^{-1} NAA,* ***7:*** *0.5 mg L^{-1} mT;* ***8:*** *1 mg L^{-1} mT;* ***9:*** *2 mg L^{-1} mT;* ***10:*** *4 mg L^{-1} mT;* ***11:*** *0.5 mg L^{-1} mT + 0.5 mg L^{-1} NAA;* ***12:*** *1 mg L^{-1} mT + 0.5 mg L^{-1} NAA;* ***13:*** *2 mg L^{-1} mT + 0.5 mg L^{-1} NAA;* ***14:*** *4 mg L^{-1} mT + 0.5 mg L^{-1} NAA;* ***15:*** *0.3 mg L^{-1} TDZ;* ***16:*** *0.6 mg L^{-1} TDZ;* ***17:*** *1.2 mg L^{-1} TDZ;* ***18:*** *0.3 mg L^{-1} TDZ + 0.5 mg L^{-1} NAA;* ***19:*** *0.6 mg L^{-1} TDZ + 0.5 mg L^{-1} NAA;* ***20:****1.2 mg L^{-1} TDZ + 0.5 mg L^{-1} NAA*

Axillary shoot regeneration

PGRs had significant effects on shoot regeneration frequency and number of shoots per explant ($P < 0.01$). Shoot regeneration frequency of cotyledon node explants varied between 12.50-87.50% and the greatest shoot regeneration frequency was obtained from BAP, BAP-NAA, *m*T and *m*T-NAA treatments (*Table* 2). The greatest number of shoots per explant (9.975 shoots) was obtained from 4 mg L^{-1} *m*T treatment and followed by 2 mg L^{-1} *m*T and 0.5-1 mg L^{-1} *m*T. Only *m*T-containing media had greater number of shoots per explant than BAP and TDZ-containing media. When the BAP-containing media were assessed in themselves, it was observed that the greatest number of shoots per explant (3.582 shoots) was obtained from 2 mg L^{-1} BAP treatment. BAP was also indicated as an appropriate cytokinin for axillary shoot regeneration in shoot apices of *Centaurea ultreia* (Mallon et al., 2010) and node explants of *Centaurea lycaonica* (Atalay and Erişen, 2017). Similarly, in present study, BAP-containing media were found to be more efficient than TDZ, however just *m*T-containing media were identified as the most efficient for axillary shoot regeneration from cotyledon node. There were not any studies in literature about the use of *m*T as a source of cytokinin in *Centaurea* species, but it was reported in studies on cassava, pelargonium and sweet basil that *m*T improved in vitro shoot proliferation and shoot quality (Wojtania, 2010; Köszeghi et al., 2014; Chauhan and Taylor, 2018). Fajinmi et al. (2014) demonstrated *m*T as a quite active and an alternative cytokinin to BAP and other cytokinins for shoot regeneration in shoot tip explant of *Coleonema album*. Such an efficiency of *m*T is mostly attributed to chemical structure allowing production of O-glucoside metabolites from hydroxyl group of side chain of *m*T and rapid translocation of it in plant tissues (Fajinmi et al., 2014). In only *m*T-containing media, number of shoots per explant increased with increasing *m*T doses. Dimitrova et al. (2016) also reported increasing

http://www.aloki.hu ● ISSN 1589 1623 (Print) ● ISSN 1785 0037 (Online)
DOI: http://dx.doi.org/10.15666/aeer/1802_22852293

regenerations with increasing *m*T doses in *Pyrus communis*. As compared to only *m*T-containing media, number of shoots per explant decreased in *m*T-NAA combinations. But contrary to present findings, *m*T-NAA combinations increased the number of shoots per explant in *Coleonema album* and *Huernia hystrix* (Fajinmi et al., 2014; Amoo and Van Staden, 2013). Such differences were mainly attributed to synergic, antagonistic and additional interactions between auxins and cytokinin based on plant species and type of tissue (Coenen and Lomax, 1997).

Table 2. *Effects of PGRs on axillary shoot regeneration form cotyledon node explant of Centaurea amaena*

PGRs	Shoot regeneration frequency (%)	Number of shoots per explant
1 mg L^{-1} BAP	87.50 a*	2.867 ef*
2 mg L^{-1} BAP	87.50 ab	3.582 de
4 mg L^{-1} BAP	83.33 abc	2.445 f
1 mg L^{-1} BAP + 0.5 mg L^{-1} NAA	83.33 abc	3.000 ef
2 mg L^{-1} BAP + 0.5 mg L^{-1} NAA	83.33 abc	2.750 f
4 mg L^{-1} BAP + 0.5 mg L^{-1} NAA	87.50 a	2.685 f
0.5 mg L^{-1} *m*T	87.50 ab	5.375 c
1 mg L^{-1} *m*T	87.50 ab	5.165 c
2 mg L^{-1} *m*T	83.33 ab	6.250 b
4 mg L^{-1} *m*T	70.83 a-d	9.975 a
0.5 mg L^{-1} *m*T + 0.5 mg L^{-1} NAA	66.66 b-e	2.750 f
1 mg L^{-1} *m*T + 0.5 mg L^{-1} NAA	74.99 abc	4.137 d
2 mg L^{-1} *m*T + 0.5 mg L^{-1} NAA	83.33 abc	2.750 f
4 m mg L^{-1} *m*T + 0.5 mg L^{-1} NAA	58.33 cde	3.000 ef
0.3 mg L^{-1} TDZ	29.17 fg	0.875 g
0.6 mg L^{-1} l TDZ	37.49 ef	1.375 g
1.2 mg L^{-1} TDZ	41.67 def	1.083 g
0.3 mg L^{-1} TDZ + 0.5 mg L^{-1} NAA	12.50 g	0.750 g
0.6 mg L^{-1} TDZ + 0.5 mg L^{-1} NAA	12.50 g	0.750 g
1.2 mg L^{-1} + 0.5 mg L^{-1} NAA	25.00 fg	0.833 g

*Values within a column followed by different letters are significantly different at 0.05 significance level using Duncan's multiple range test

Rooting

Regenerated shoots were rooted in ½ MS media containing 0.5, 1 or 2 mg L^{-1} IBA. About 5-6 weeks after the initiation of culture processes, percentage of root-forming shoots were respectively identified as 33.33, 38.89 and 50.00%. IBA was also identified as an available auxin for promotion of rooting of regenerated shoots in *Centaurea rupestris* and *Centaurea arifolia* species (Curkovic-Perica, 2003; Yüzbaşıoğlu et al., 2012).

Conclusions

The primary target of the present study was to investigate regeneration potential of *Centaurea amaena*. In present experiments, 4 shoots per explant were obtained from

http://www.aloki.hu ● ISSN 1589 1623 (Print) ● ISSN 1785 0037 (Online)
DOI: http://dx.doi.org/10.15666/aeer/1802_22852293

cotyledons and leaves and 10 shoots per explant were obtained from the cotyledon nodes of *C. amaena*. It was concluded based on present findings that *m*T and BAP were efficient cytokinins for in vitro regeneration of *C. amaena*. Regenerated shoots were rooted in half-strength MS medium supplemented with IBA. A simple and efficient propagation procedure was developed in this study for the critically endangered species *C. amaena*. This procedure could be useful for the in situ and ex situ conservation of this valuable genetic source. However, the genetic stability of regenerated plants must be verified using molecular markers in further studies.

Acknowledgements. This study was supported by the Scientific Research Foundation of Erciyes University (Project Number: FYL-2016-6308). This paper has been prepared from Master's Thesis of Özge EKİNCİ.

REFERENCES

[1] Albayrak, S., Atasagun, B., Aksoy, A. (2017): Comparison of phenolic components and biological activities of two *Centaurea* sp. obtained by three extraction techniques. – Asian Pacific Journal of Tropical Medicine 10(6): 599-606.

[2] Amoo, S. O., Van Staden, J. (2013): Influence of plant growth regulators on shoot proliferation and secondary metabolite production in micropropagated Huernia *hystrix*. – Plant Cell, Tissue and Organ Culture (PCTOC) 112(2): 249-256.

[3] Atalay, E., Erisen, S. (2017): High frequency regeneration of critically endangered endemic plant *Centaurea lycaonica.* – Fresenius Environmental Bulletin 26(11): 6356-6363.

[4] Atasagun, B., Aksoy, A. (2018): Autecology and conservation biology of *Centaurea amaena* (Asteraceae). – JAPS Journal of Animal & Plant Sciences 28(1).

[5] Atasagun, B., Aksoy, A., Martin, E., Uzun, O. (2013): Morphological, anatomical, palynological, karyological and autecological characters of *Centaurea amaena* Boiss. & Balansa [Sect. Phalolepis (Centaurea/Asteraceae)]. – Plant Systematics and Evolution 299(9): 1761-1767. DOI: 10.1007/s00606-013-0831-9.

[6] Aydoğan, S. K., Erdağ, B. (2015): Callus induction and adventitious shoot regeneration of *Centura zeybekii* endangered endemic plant. – Nevşehir Bilim ve Teknoloji Dergisi, 4(2): 1-8.

[7] Chauhan, R. D., Taylor, N. J. (2018): Meta-topolin stimulates de novo shoot organogenesis and plant regeneration in cassava. – Plant Cell, Tissue and Organ Culture (PCTOC) 132(1): 219-224. DOI: 10.1007/s11240-017-1315-3.

[8] Coenen, C., Lomax, T. L. (1997): Auxin–cytokinin interactions in higher plants: old problems and new tools. – Trends in plant science 2(9): 351-356.

[9] Cuenca, S., Amo-Marco, J.B. (2000): In vitro propagation of Centaurea spachii from inflorescence stems. –Plant Growth Regulation 30: 99-103.

[10] Cuenca, S., Amo-Marco, J.B., Parra, R. (1999). Micropropagation from inflorescence stems of the Spanish endemic plant Centaurea paui Loscos ex Willk. (Compositae). – Plant Cell Reports 18: 674-679.

[11] Curkovic-Perica, M. (2003): In vitro propagation of *Centaurea rupestris* L. – Acta Biologica Cracoviensia Series Botanica 45(2): 127-130.

[12] Dewir, Y. H., Naidoo, Y., da Silva, J. A. T. (2018): Thidiazuron-induced abnormalities in plant tissue cultures. – Plant Cell Reports 37(11): 1451-1470. https://doi.org/10.1007/s00299-018-2326-1.

http://www.aloki.hu ● ISSN 1589 1623 (Print) ● ISSN 1785 0037 (Online)
DOI: http://dx.doi.org/10.15666/aeer/1802_22852293

[13] Dimitrova, N., Nacheva, L., Berova, M. (2016): Effect of meta-topolin on the shoot multiplication of pear rootstock OHF-333 (*Pyrus communis* L.). – Hortorum Cultus— Acta Scientiarum Polonorum 15: 43-53.
[14] Erdağ, B., Emek, Y. (2005a): In vitro adventitious shoot regeneration of *Liquidambar orientalis* Miller. – Journal of Biological Sciences 5(6): 805-808.
[15] Erdağ, B., Emek, Y. (2005b): In vitro micropropagation of *Anthemis xylopoda* O. Schwarz, a critically endangered species from Turkey. – Pakistan Journal of Biological Sciences 8(5): 691-695.
[16] Erişen, S., Atalay, E., Yorgancilar, M. (2011): The effect of thidiazuron on the in vitro shoot development of endemic *Astragalus cariensis* in Turkey. – Turkish Journal of Botany 35(5): 521-526. DOI: 10.3906/bot-1009-74.
[17] Fajinmi, O. O., Amoo, S. O., Finnie, J. F., Van Staden, J. (2014): Optimization of in vitro propagation *of Coleonema album*, a highly utilized medicinal and ornamental plant. – South African Journal of Botany 94: 9-13. http://dx.doi.org/10.1016/j.sajb.2014.05.006.
[18] Kazeroonian, R., Mousavi, A., Jari, S. K., Tohidfar, M. (2018): Factors Influencing in Vitro Organogenesis of *Chrysanthemum morifolium* cv.'Resomee Splendid'. – Iranian Journal of Biotechnology 16(2): 133-139. DOI: 10.21859/ijb.1454.
[19] Köszeghi, S., Bereczki, C., Balog, A., Benedek, K. (2014). Comparing the effects of benzyladenine and meta-Topolin on sweet basil (*Ocimum basilicum*) micropropagation. – Notulae Scientia Biologicae 6(4): 422-427. DOI: 10.1583/nsb649464.
[20] Magyar-Tabori, K., Dobranszki, J., da Silva, J. A. T., Bulley, S. M., Hudak, I. (2010): The role of cytokinins in shoot organogenesis in apple. – Plant Cell, Tissue and Organ Culture (PCTOC) 101(3): 251-267. DOI: 10.1007/s11240-010-9696-6.
[21] Mallon, R., Rodriguez-Oubina, J., Gonzalez, M. L. (2010): In vitro propagation of the endangered plant *Centaurea ultreiae*: assessment of genetic stability by cytological studies, flow cytometry and RAPD analysis. – Plant Cell, Tissue and Organ Culture (PCTOC) 101(1): 31-39. DOI: 10.1007/s11240-009-9659-y.
[22] Ozel, C. A., Khawar, K. M., Mirici, S., Ozcan, S., Arslan, O. (2006). Factors affecting in vitro plant regeneration of the critically endangered Mediterranean knapweed (*Centaurea tchihatcheffii* Fisch et. Mey). – Naturwissenschaften 93(10): 511-517. DOI: 10.1007/s00114-006-0139-5.
[23] Şehirali, S., Özgen, M., Karagöz, A., Sürek, M., Adak, S., Güvenç, İ., Tan, A., Burak, M., Kaymak, Ç. (2015): Bitki Genetik Kaynaklarının Korunma ve Kullanımı. – http://www.zmo.org.tr/resimler/ekler/7e8e17134dd7083_ek.pdf (erişim tarihi: 25.08.2015).
[24] Türkoğlu, N., Özdemir, F.A., Keskin, N., Khawar, K.M. (2018): Efficient protocol for multiple micro-shoot regenetation from endanger, endemic and ornamental plant Centaurea fenzlii Reichardt. Fresenius Environmental Bulletin 27(2): 1076-1080.
[25] Uzun, S., İlbaş, A. İ., İpek, A., Arslan, N., Barpete, S. (2014): Efficient in vitro plant regeneration from immature embryos of endemic *Iris sari* and *I. schachtii*. – Turk J Agric For 38: 348-353. DOI: 10.3906/tar-1306-47.
[26] Wojtania, A. (2010): Effect of meta-topolin in vitro propagation of cultivars. – Acta Societatis Botanicorum Poloniae, 79(2), 101-106.
[27] Yorgancilar, M., Erisen, S. (2011): The effect of thidiazuron (TDZ) on shoot regeneration of *Astragalus schizopterus*. – Journal of Animal and Plant Sciences 21(3): 519-524.
[28] Yüzbaşıoğlu, E., Dalyan, E., Bona, M., Öz, G. (2012): In vitro propagation of endemic plant *Centaurea arifola* Boiss. Taxa. – IUFS Journal of Biology 71(2): 121-127.

http://www.aloki.hu ● ISSN 1589 1623 (Print) ● ISSN 1785 0037 (Online)
DOI: http://dx.doi.org/10.15666/aeer/1802_22852293

THE DISTRIBUTION AND DIVERSITY OF BUTTERFLIES (LEPIDOPTERA: RHOPALOCERA) IN VARIOUS URBAN FORESTS IN NORTH MINAHASA REGENCY, NORTH SULAWESI PROVINCE, INDONESIA

KONERI, R.[1*] – MAABUAT, P. V.[1] – NANGOY, M.-J.[2]

[1]*Department of Biology, Sam Ratulangi University, Campus Sam Ratulangi University Street, Bahu, Manado, North Sulawesi, 95115, Indonesia*
(phone: +62-813-4027-5276)

[2]*Department of Animal Production, Sam Ratulangi University, Campus Sam Ratulangi University Street, Bahu, Manado, North Sulawesi 95115, Indonesia*
(phone: +62-812-4239-9445)

**Corresponding author*
e-mail: ronicaniago@unsrat.ac.id

(Received 20th Oct 2019; accepted 23rd Jan 2020)

Abstract. The establishment of urban forests are the way to reduce the impact of urban development on biodiversity. This study aimed to analyze the distribution and diversity of butterflies in various urban forests in North Minahasa Regency, North Sulawesi, Indonesia. Butterfly sampling was conducted in four urban forests. The sampling employed the sweeping technique following a the transect line. The results obtained included as many as 5 families of butterfly, consisting of 56 species and 985 individuals. Using the distribution pattern of butterfly species based on the Morisita index, 52 species were found classified as aggregate. The highest species diversity was found in the Kuwil City Forest. Diversity of butterfly species was negatively correlated with air temperature, light intensity, and wind speed. According to the similarity index of the butterfly species community, it was found that the Kaki Dian City Forest, Kenangan City Forest, and Kuwil City Forest shared a high similarity, while the Talise City Forest did not share many similarities with the other urban forests. The diversity of butterflies in urban forests was influenced by the surrounding area, the complexity of the composition of vegetation structures, water availability, and abiotic environmental factors.
Keyword: *aggregate, environmental, Morisita, sweeping technique, vegetation structures*

Introduction

Developing facilities and infrastructure in urban environments can support the activities of local dwellers and will improve the economy of the urban area, but urban development and human activity can also cause environmental quality to decline. This is because the urban area is filled with built-up area, while many green open spaces have been converted into areas of offices, settlements, trade, industry, ports, airports, and other urban infrastructure (Kusmana, 2015). Land-use change in urban areas raises various environmental problems and can affect and threaten the existence of biotic communities within it (Azahra et al., 2016). Land-use change can also have an impact on biodiversity (Bergerot et al., 2011; Lee et al., 2015).

Plants and animals that live in urban ecosystems often experience local extinction due to loss of habitat, habitat degradation, and fragmentation (McKinney, 2002; Clarket et al., 2007). Some studies reported that species composition and species abundance, such as bird abundance (Motegi and Yanai, 2005; Rubèn and Ian, 2009), ant abundance

http://www.aloki.hu ● ISSN 1589 1623 (Print) ● ISSN 1785 0037 (Online)
DOI: http://dx.doi.org/10.15666/aeer/1802_22952314

(Lee and Kwon, 2013), and butterfly abundance (Bergerot et al., 2011; Lee and Kwon, 2012), are lower in urban areas than in rural areas.

The establishment of urban forests is one of the efforts to reduce the impact of urban land-use change on biodiversity. According to Law No. 63 of 2002, urban forests serve to improve and maintain the microclimate and aesthetic value, absorb water, create a balance and harmony of the physical environment of the city, and support the preservation of biodiversity. Urban forests also have potential as a means of conserving biodiversity, including the butterfly community (Azahra et al., 2016).

Butterflies that live in urban ecosystems have a very important role in maintaining biodiversity. Adult butterflies help pollinate flowering plants so that the natural propagation process of plants can occur (Borror et al., 1992; Speight et al., 1999; Plona, 2002; Perveen and Haroon, 2015). Butterflies can also be used as bioindicators of environmental change because they are easily surveyed, quickly react to changes in the environment, and have high mobility and preferences for certain habitats (Lee et al., 2014; Dennies et al., 2017). Butterflies are also easily recognizable both taxonomically and ecologically (Kim et al., 2012).

Most butterfly species are cosmopolitan so that they can be found in various types of habitats, from forest to urban areas, and in various environmental conditions (Braby, 2004; Koh and Sodhi, 2004). The biggest threat to the survival of butterflies is humans. The beauty of colorful butterfly wings attracts people's attention and interest to collect them. Land conversion, tree felling, housing development, pollution, and the use of insecticides and herbicides contribute to the extinction of butterflies. Butterflies lose their host plant and lack food due to these environmental changes (Handayani et al., 2015; Thangjam et al., 2018).

Urban forest as one of the butterfly habitats in urban areas has a high conservation value, but on the other hand, the environmental disturbance that occurs indicates the causes of various changes in the environmental conditions of the urban forest that have an impact on the communities in it, including the butterfly community. Thus, habitat protection is very important to support the survival of butterflies. The existence of urban forests in North Minahasa Regency can be an effort to preserve biodiversity, one of which is butterflies.

The existence and availability of data regarding the distribution and diversity of butterflies in urban forests in North Minahasa have a crucial meaning in the initial steps of conservation of butterfly species in urban areas. Research on butterflies in urban forests in North Minahasa Regency has never been conducted before, so there are no detailed and published data on the distribution and diversity of butterflies. Considering the important role of butterflies in an ecosystem, research on the distribution and diversity of butterflies in various urban forests in North Minahasa Regency needs to be conducted. This study aims to analyze the distribution and diversity of butterflies (Lepidoptera: Rhopalocera) in various urban forests in North Minahasa Regency, North Sulawesi Province.

Materials and methods

Study area and types of urban forests

This research was conducted from May 2019 to August 2019. Sampling locations were four urban forests, namely, Kuwil City Forest, Talise City Forest, Kenangan City Forest, and Kaki Dian City Forest, in North Minahasa Regency, North Sulawesi

http://www.aloki.hu ● ISSN 1589 1623 (Print) ● ISSN 1785 0037 (Online)
DOI: http://dx.doi.org/10.15666/aeer/1802_22952314

Province, Indonesia (*Fig. 1*). The locations of this research were four urban forests in North Minahasa Regency. The selection of locations was based on city forests that have been commissioned through North Minahasa District Regulation Number 2 of 2012 concerning urban forests.

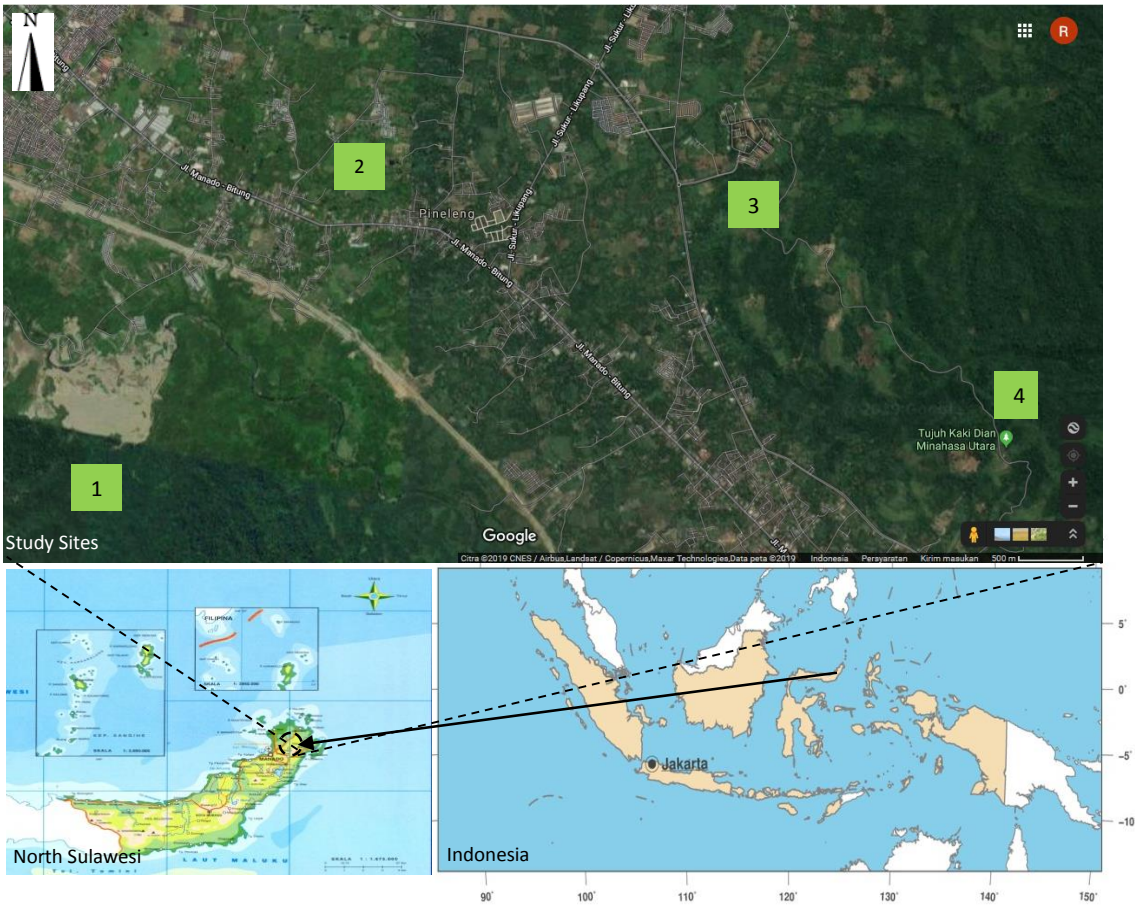

Figure 1. *Map of the study area in North Minahasa Regency (1. Kuwil City Forest, 2. Talise City Forest, 3. Kenangan City Forest, 4. Kaki Dian City Forest)*

Descriptions of the four urban forests are as follows:

1. Kaki Dian City Forest, which is located in Airmadidi Urban Village in the Mount Klabat forest area and covers an area of ± 37 Ha. The forest types that surround this urban forest are secondary forests and primary forests in protected forest areas. Vegetation cover is dominated by tall trees with medium diameter. The plant species found were dominated by species from the family Moraceae (genus Ficus) and Anacardiaceae, followed by species from the family Euphorbiaceae (*Fig. 2a, b*). The coordinates of the sampling points in the Kaki Dian City Forest were transect 1 N: 01°26'12.49" E: 124°59'32.46", transect 2 N: 01°26'12.72 E: 124°59; 34.58; transect 3 N: 01°26'18.25" E: 124°59'32.66, and transect 4 N: 01°26'00.69" E: 124°59'40.35". The air temperature in this urban forest ranged from 28.0 to 31.6 °C, humidity ranged from 61 to 67.0%, light intensity ranged from 599.0 to 725.0 lux, wind speed

http://www.aloki.hu ● ISSN 1589 1623 (Print) ● ISSN 1785 0037 (Online)
DOI: http://dx.doi.org/10.15666/aeer/1802_22952314

ranged from 0 m/s to 0.8 m/s, with altitudes between 553 masl and 654 masl (*Table 1*).

2. Kenangan City Forest, which is located in the area of the North Minahasa Regency Government office, covering an area of ± 15 ha. The area around Kenangan City forest is office center and plantation land. Vegetation that covers this urban forest consists of a collection of trees that were intentionally planted and native trees at that location (*Fig. 2c, d*). The coordinates of sampling in the Kenangan City Forest were transect 1 N: 01°27'23.17" E: 124°58'27.04", transect 2 N: 01°27'23.17" E: 124°58'27.04", transect 3 N: 01°27'23.20", E: 124°58'27.04", and transect 4 N: 01°27'23.20", E: 124°58'27.04". The air temperature in this urban forest ranged from 31.3 to 32.6 °C, humidity ranged from 58.0 to 61.5%, light intensity ranged from 789.0 to 955 lux, while wind speed ranged from 1.0 to 1.9 m/s with altitudes between 295 to 372 m asl (*Table 1*).
3. Kuwil City Forest, which is located in Kuwil Village, Kalawat District, covering an area of ± 43 Ha. The area around this urban forest is plantation land and settlements (*Fig. 2e, f*). The sampling coordinates of the Kuwil City Forest were transect 1 N: 01°26'17.80" E: 124°55'61.67", transect 2 N: 01°26'14.77" E: 124°55'28.94", transect 3 N: 01°26'12.76" E: 124°55'32.10, and transect 4 N: 01°26'12.49" E: 124°55'53.16". The air temperature in this urban forest ranged from 28.5 to 29.6 °C, humidity ranged between 74.0 and 75.0%, intensity light ranged from 548.0 to 722.0 lux, wind speed ranged from 0 to 0.1 m/s with altitude between 95 and 119 m asl (*Table 1*).
4. Talise City Forest, which is located in Kolongan Village, Kalawat District, covering an area of ± 6 Ha. The area around this urban forest is fish ponds, plantations, and settlements (*Fig. 2g, h*). The sampling coordinates of the Talise City Forest were transect 1 N: 01°27'36.43" E: 124°56'27.70", transect 2 N: 01°27'34.01" E: 124°56'29.09", transect 3 N: 01°27'30.96" E: 124°56'22.42", and transect 4 N: 01°27'29.04" E: 124°56'24.21". The temperature of the city forest ranged from 32.2 to 33.0 °C, humidity ranged from 46.5 to 50.0%, the light intensity ranged from 850 to 962.5 lux, with altitudes between 147 and 166 m asl (*Table 1*).

Figure 2. *Some photos of sampling site: Kaki Dian City Forest (a, b), Kenangan City Forest (c, d), Kuwil City Forest (e f), Talise City Forest (g, h)*

http://www.aloki.hu ● ISSN 1589 1623 (Print) ● ISSN 1785 0037 (Online)
DOI: http://dx.doi.org/10.15666/aeer/1802_22952314

Sampling and identification of butterfly samples

Sampling employed the purposive random sampling method. In each type of urban forest, four transect lines were made with a length of 300 m each. Sampling was conducted along the transect line using butterfly net (sweep net). Butterfly sampling was conducted for 4 days every month for 4 months. Sampling was performed every month for four months. Sampling was done monthly for 4 months. Butterfly sampling for 4 months was quite representative and can provide information about the diversity of butterflies in urban forests of North Minahasa Regency. This is because those four months were during dry season when the weather conditions were sunny. Those conditions were very suitable for butterflies to live. During this period, most of nectar-rich plants began to flower, thus providing butterflies food sources and supporting the life and breeding of butterflies"

Table 1. *The environmental factor in four urban forests in North Minahasa Regency*

Urban forest	Transect	Environmental factors				
		Temperature (°C)	Humidity (%)	Light (Lux)	Wind (m/s)	Altitude (M asl)
Kaki Dian	1	28.00	61.00	599.00	0.80	591.00
Kaki Dian	2	31.60	65.00	648.00	0.50	597.00
Kaki Dian	3	30.00	67.00	725.00	0.50	654.00
Kaki Dian	4	31.50	65.00	648.00	0.00	553.00
Average ± St dev		30.28 ± 1.68	64.50 ± 2.52	655.0 ± 57.07	0.45 ± 0.33	598.75 ± 41.67
Kenangan	1	31.30	58.00	824.00	1.45	295.00
Kenangan	2	32.00	58.67	789.00	1.87	295.00
Kenangan	3	32.60	61.50	859.00	1.35	325.00
Kenangan	4	32.00	60.00	955.00	1.00	372.00
Average ± St dev		31.98 ± 0.53	59.54 ± 1.55	856.75 ± 71.46	1.42 ± 0.36	321 ± 36.36
Kuwil	1	29.00	75.00	548.00	0.10	97.00
Kuwil	2	28.50	75.00	559.00	0.20	95.00
Kuwil	3	29.50	74.00	722.00	0.00	106.00
Kuwil	4	29.60	75.00	620.00	0.10	119.00
Average ± St dev		29.15 ± 0.51	74.75 ± 0.50	612.25 ± 79.73	0.10 ± 0.08	104.25 ± 10.94
Talise	1	33.00	46.50	887.00	1.45	152.00
Talise	2	32.50	50.00	850.00	1.80	153.00
Talise	3	32.15	48.00	942.00	2.00	166.00
Talise	4	32.95	49.50	962.00	1.40	147.00
Average ± St dev		32.65 ± 0.40	40.50 ± 1.58	910.25 ± 51.18	1.66 ± 0.29	154.50 ± 8.10

Samples were taken at 08.00-14.00 Central Indonesia Time (GMT + 8). The collection of butterfly samples was conducted during the day, because butterflies are active only during the day. Only one specimen per species was collected. If the same species was accidentally caught, the butterfly would be released.

The process of identifying specimens used identification books. The identification books used were Butterflies of the South East Asian Island, Part I Papilionidae, Part II Pieridae-Danaidae, Part III Satyridae-Lybytheidae, Part IV Nympalidae (I), Part V

http://www.aloki.hu ● ISSN 1589 1623 (Print) ● ISSN 1785 0037 (Online)
DOI: http://dx.doi.org/10.15666/aeer/1802_22952314

Nympalidae (II) (Tsukada and Nishiyama, 1981, 1982a, b; 1985, 1991), Insects of the Mount Halimun National Park in the Western Part of Java (Amir et al., 2003), Practical Guide of Butterflies in the Bogor Botanical Garden (Peggie and Amir, 2006), Agricultural Entomology (Jumar, 2000).

In taking samples, environmental factors were also measured. Environmental factors included air temperature and humidity, which were measured using a Thermohygrometer (Deko 637 Thermo-hygrometer), wind speed, which was measured using Anemometer, and light intensity, which was measured using a Lux meter (Lutron LM8010 Type K). Meanwhile, the altitude and coordinates were determined using the Global Positioning System (Garmin GPSMAP 78s).

Data analysis

Analysis of observational data included the distribution of butterfly species, species diversity, correlation between species diversity and environmental factors, and similarity index of butterfly species between urban forests. The distribution of butterfly species was calculated using the Morisita index according to Krebs (1999):

$$\text{Morisita Index (Id)} = n\left(\frac{\sum X^2 - N}{N\,(N-1)}\right) \quad \text{(Eq.1)}$$

Annotation: Id: Morisita disperse index; n: number of plots; x: number of individuals per plot; $\sum X^2$ = sum of squares of all species for each plot; N: total number of individuals with the following conditions: Id = 1 distribution pattern is classified as random (random), Id > 1 distribution pattern is classified as aggregate, and Id < 1 distribution pattern is classified as uniform.

Species diversity was calculated using the species richness index, species diversity index, and species evenness index. Species richness was calculated using the Margalef richness index (R1) with the formula:

$$\text{RI} = \frac{S-1}{LogN} \quad \text{(Eq.2)}$$

Annotation: RI: Richness Index, S: Number of species (n1, n2, n3, ...), N: total individuals in sampling. According to Magurgan (1988), the criteria used to interpret richness were: RI < 3.5: low species richness, RI = 3.5-5: moderate species richness, RI > 5: high species richness.

The species diversity index was calculated using the Shannon-Wiener index (Ludwig and Reynold, 1988):

$$H' = -\sum_{i=1}^{s}(P_i \ln P_i) \quad \text{(Eq.3)}$$

Annotation: Pi = ni/N; H'ː Shannon-Wiener diversity index, ni: number of individuals per species; N: number of individuals of all species. The criteria used to interpret the species diversity index, according to Magurran (1988), were: H' < 1.5: low diversity, H' = 1.5-3.5: moderate diversity, H' > 3.5: high diversity.

Meanwhile, species evenness employed Shannon evenness index (E) (Magurran, 2004):

http://www.aloki.hu ● ISSN 1589 1623 (Print) ● ISSN 1785 0037 (Online)
DOI: http://dx.doi.org/10.15666/aeer/1802_22952314

$$E = \frac{H'}{\ln S} \quad \text{(Eq.4)}$$

Annotation: E: evenness index, H': Shannon-Wiener diversity index, S: number of species (n1, n2, n3, ...). Magguran (1988) stated that the criteria used to interpret evenness were: E' < 0.3: low evenness, E' 0.3 - 0.6 : moderate evenness, E' > 0.6: high evenness.

Furthermore, species dominance (D) was calculated by Simpson index to determine the level of dominance of certain species of butterflies in a community (Magurran, 1988). The formula used to calculate dominance was:

$$D = \Sigma (ni/N)^2 \quad \text{(Eq.5)}$$

Annotation D: dominance index, ni: number of individuals of k-I species, N: total number of individuals. Indicators of the dominance index are if D = 0.00-0.50, it means the dominance is low. If 0.50 < D < 0.75, it indicates moderate dominance. Whereas, 0.75 < D < 1.0 shows high dominance.

To determine the relationship between species diversity (species richness index, species diversity index, species evenness index, and species dominance index) and environmental factors (air temperature, air humidity, light intensity, wind speed and altitude), Spearman rank correlation was performed. Correlation test used the Statistica program version 6 (Stat Soft, 2001).

To find out the similarity of butterfly communities between urban forests, Sørensen similarity index was used and the data used were the presence and absence of butterfly species (Magurran, 1988). The index was calculated using Biodiv 97, which is a macro software on Excel (Shahabuddin et al., 2005). Dissimilarity value (1-Sørensen index) was used to make two-dimensional ordination of all samples using multidimensional scaling (MDS) and dendrogram (Schulze and Fiedler, 1998). The similarity of butterfly communities between urban forests was calculated based on the Sørensen similarity index. The data used were data on species and species abundance of each habitat type (Cheng, 2004).

Sørensen dissimilarity matrix was then used to create MDS (Multidimensional Scaling) and dendrogram of butterfly species similarity. Multidimensional Scaling (MDS) was used to describe similarities or distances of some observed objects. The result of MDS analysis was a two-dimensional mapping of the objects of observation. MDS arranged the location of the observation objects so that it had the right placement on a two-dimensional map based on the similarity or dissimilarity matrix that has been inputted. After the two-dimensional map was obtained, the distance of the objects of observation could be seen (Hair et al., 1998 and Cheng, 2004). Dimensions functioned to describe the relative position between objects. The similarity of butterfly communities between urban forest locations based on the distances depicted in the two-dimensional graph (MDS) was analyzed using Statistica for Windows 6 (StatSoft, 2001).

In addition to using MDS, the similarity of butterfly communities between urban forests was also tested by cluster analysis (Krebs,1999; Ludwig and Reynold, 1988). Cluster analysis of each community was arranged hierarchically in the form of a dendrogram. Dendrograms were created using the Statistica for Windows 6 (StatSoft, 2001). Clustering employed the unweighted pair group method with arithmetic mean (UPGMA) and Euclidean distance (Lewis, 2001).

http://www.aloki.hu ● ISSN 1589 1623 (Print) ● ISSN 1785 0037 (Online)
DOI: http://dx.doi.org/10.15666/aeer/1802_22952314

Results

Distribution of butterfly species

In four urban forests, 2 butterfly species distribution patterns based on the Morisita index were found. They are aggregate and uniform distribution patterns. Meanwhile, random distribution pattern was not found. Pattern of aggregate distribution was found in 52 species, while 4 species showed uniform distribution. Butterflies from the family Nymphalidae were found as many as 28 species and included in aggregate distribution pattern, while 2 species, namely, *Elymnias hicetas* and *Lamasia lyncides* were classified as uniform distribution. Butterflies from the family Papilionidae were obtained as many as 9 species and had a pattern of aggregate distribution, while one species, namely *Papilio demoleus*, had a regular distribution. The butterflies of the family Hesperiidae were found as many as one species with aggregate distribution and one species with uniform distribution, while all species from the family Pieridae and the family Lycaenidae were found to have aggregate distribution pattern (*Table 2*).

Structure and composition of butterfly species

The butterflies found during the study were 5 families, consisting of 56 species and 985 individuals. The butterfly families found were Nymphalidae, Papilionidae, Pieridae, Lycaenidae and Hesperiidae. The family with the most number of species (30 species) and individuals (57.26%) was Nymphalidae, followed by Papilionidae, while the family that had the least number was Hesperiidae with 2 species and 8 individuals (*Table 3*).

Butterfly species of *Parthenos sylvia salentia* were the most common species found during the study, with a percentage of 12.93%, followed by *Troides helena* and *Ideopsis vitrea oenopsis* as many as 73 individuals (7.41%) (*Fig. 3*). The fewest species found were *Elymnias hicetas*, *Lamasia lyncides*, *Papilio demoleus*, and *Taractrocera luzonensis*, each found as many as one individual (0.10%) (*Table 3*).

Based on the type of urban forest, as many as 7 species of butterflies could be found in all urban forests. The only butterflies that were found in the Kaki Dian City Forest and not found in other urban forests were 7 species, while the species *Euploea eupator* was only found in the Kenangan City Forest. Five species were only found in the Kuwil City forest and were not found in other urban forests, while the *Euthalia amanda* and *Arhopala acetes* species were only found in the Kuwil City Forest (*Table 3*).

The highest abundance of butterfly species was found in the Kuwil City Forest, as many as 295 individuals (29.95%), then followed by the Kaki Dian City Forest, which had an abundance of 282 individuals (28.63%). The urban forest that had the least number of individuals was the Kenangan City Forest with a total of 175 individuals (17.77%) (*Table 3*).

The number of butterfly families found in the Kuwil City forest, Kenangan City Forest, and Talise City Forest was 5 families, while in the Kaki Dian City Forest was only 4 families. Nymphalidae was predominantly found in all types of urban forest and was most commonly found in the Kuwil City Forest and Talise City Forest (*Fig. 4*).

Diversity of butterfly species

The highest abundance and the highest evenness index of butterfly species was found in the Kuwil City Forest, while the lowest abundance and the lowest evenness index was in the Kenangan City Forest. The highest richness index and diversity index of

http://www.aloki.hu ● ISSN 1589 1623 (Print) ● ISSN 1785 0037 (Online)
DOI: http://dx.doi.org/10.15666/aeer/1802_22952314

species (H') were also found in the Kuwil City Forest, while the lowest richness index and diversity index of species were in Talise City Forest (*Fig. 5*).

Table 2. *Distribution patterns of butterfly species in four urban forests in North Minahasa Regency, North Sulawesi*

Famili/Species	N	$\sum x^2$	$(\sum x^2 - N)$	N(N-1)	Id	Distribution
Nymphalidae						
Parthenos sylvia salentia	122	6532	6410	14762	1.74	Aggregate
Idiopsis vitrea oenopsis	73	2161	2088	5256	1.59	Aggregate
Junonia hedonia intermedia	63	1055	992	3906	1.02	Aggregate
Idiopsis juventa tontoliensis	60	2072	2012	3540	2.27	Aggregate
Idea blanchardii	28	520	492	756	2.60	Aggregate
Ypthima loryma	26	370	344	650	2.12	Aggregate
Lasippa neriphus tawayana	25	323	298	600	1.99	Aggregate
Mycalesis horsfieldi	15	113	98	210	1.87	Aggregate
Danaus ismare alba	14	148	134	182	2.95	Aggregate
Doleschallia polybete celebensis	13	109	96	156	2.46	Aggregate
Euploea algea	12	50	38	132	1.15	Aggregate
Parantica cleona luciplena	12	90	78	132	2.36	Aggregate
Eupleoa eupator	11	121	110	110	4.00	Aggregate
Ypthima nynias	11	65	54	110	1.96	Aggregate
Neptis ida	10	54	44	90	1.96	Aggregate
Pareronia tritaea	9	81	72	72	4.00	Aggregate
Mycalesis janarda	8	50	42	56	3.00	Aggregate
Cyrestis strigata	6	18	12	30	1.60	Aggregate
Danaus genutia	6	36	30	30	4.00	Aggregate
Euthalia aconthea	6	20	14	30	1.87	Aggregate
Faunis menado	6	36	30	30	4.00	Aggregate
Yoma sabina	6	26	20	30	2.67	Aggregate
Euplea leucostictos westwoodi	5	25	20	20	4.00	Aggregate
Mycalesis nicotia	5	25	20	20	4.00	Aggregate
Cyrestis paulinus	3	9	6	6	4.00	Aggregate
Parantica menadensis	3	5	2	6	1.33	Aggregate
Euthalia amanda	2	4	2	2	4.00	Aggregate
Moduza lycone	2	4	2	2	4.00	Aggregate
Elymnias hicetas	1	1	-3	12	-0.25	Uniform
Lamasia lyncides	1	1	-3	12	-0.25	Uniform
Papilonidae						
Troides helena	73	2277	2204	5256	1.68	Aggregate
Papilio gigon	34	438	404	1122	1.44	Aggregate
Papilio ascalaphus	23	201	178	506	1.41	Aggregate
Pachliopta polyphonthes	14	108	94	182	2.07	Aggregate
Graphium meyeri	11	51	40	110	1.45	Aggregate
Graphium agamemnon	6	18	12	30	1.60	Aggregate
Papilio blumei	4	16	12	12	4.00	Aggregate
Papilio polytes	4	16	12	12	4.00	Aggregate
Papilio sataspes	2	4	2	2	4.00	Aggregate
Papilio demoleus	1	1	-3	12	-0.25	Uniform
Pieridae						
Catopsilia pomona flava	60	1254	1194	3540	1.35	Aggregate
Hebomia glaucippe celebensis	17	201	184	272	2.71	Aggregate
Catopsilia scylla asema	16	104	88	240	1.47	Aggregate
Eurema tominia	6	20	14	30	1.87	Aggregate
Appias zarinda	5	13	8	20	1.60	Aggregate
Lycaenidae						
Jamides celeno	34	534	500	1122	1.78	Aggregate
Euchrysops cnejus	24	210	186	552	1.35	Aggregate
Jamides alecto	23	201	178	506	1.41	Aggregate
Nadacuba berenice	17	289	272	272	4.00	Aggregate
Miletus leos	14	70	56	182	1.23	Aggregate
Acytolepsis puspa	13	85	72	156	1.85	Aggregate
Lampides boeticus	7	21	14	42	1.33	Aggregate
Tajuria mantra	3	9	6	6	4.00	Aggregate
Arhopala acetes	2	4	2	2	4.00	Aggregate
Hesperiidae						
Potanthus omaha	7	25	18	42	1.71	Aggregate
Taractrocera luzonensis	1	1	-3	12	-0.25	Uniform

N: total number of individuals, x: number of individuals per plot; $\sum^{X^2}$ = sum of squares of all species for each plot; N: total number of individuals Id: Morisita disperse index)

http://www.aloki.hu ● ISSN 1589 1623 (Print) ● ISSN 1785 0037 (Online)
DOI: http://dx.doi.org/10.15666/aeer/1802_22952314

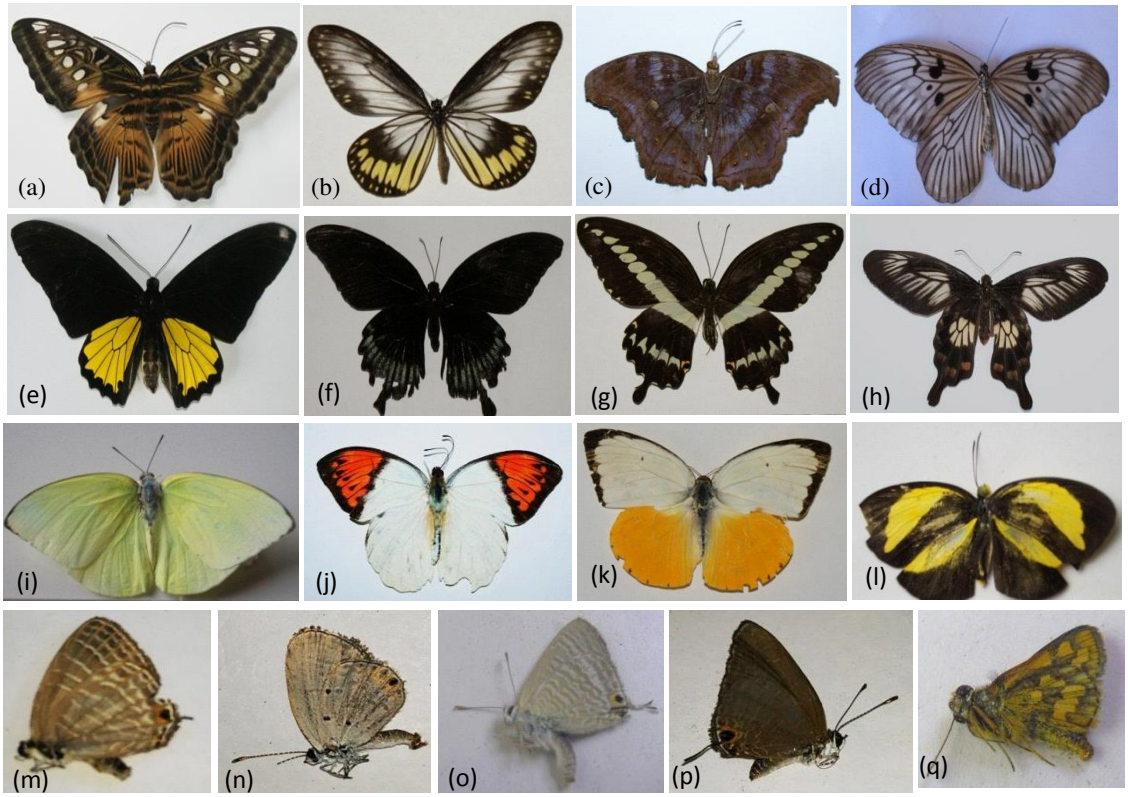

Figure 3. *Several species of butterflies in four urban forests in North Minahasa Regency. Nymphlidae: (a) Clipper (P. sylvia), (b) Blanchard's wood nymph (I. vitrea oenopsis), (c) rown pansy (J. hedonia intermedia, (d) Tree nymph (I. blanchardii). Papilionidae: (e) Common birdwing (T. helena), (f) Sulawesi blue mormon (P. ascalaphus), (g) Cream-banded Swallotail (P. gigon) (h). Pachliopta polyphontes). Pieridae: (i) Lemon emigrant (C. pamona flava), (j) Great orange-tip (H. glaucippe celebensis), (k) Orange emigrant (C. scylla asema), (l) Grass yellows (E. tominia). Lycaenidae: (m) Common Cerulean (J. celeno), (n) gram blue (E. cnejus), (o) Metallic cerulean (J. electo), (p) Rounded six-line blue (N. berenice). Hesperiidae: (q) Lesser dart (P. omaha)*

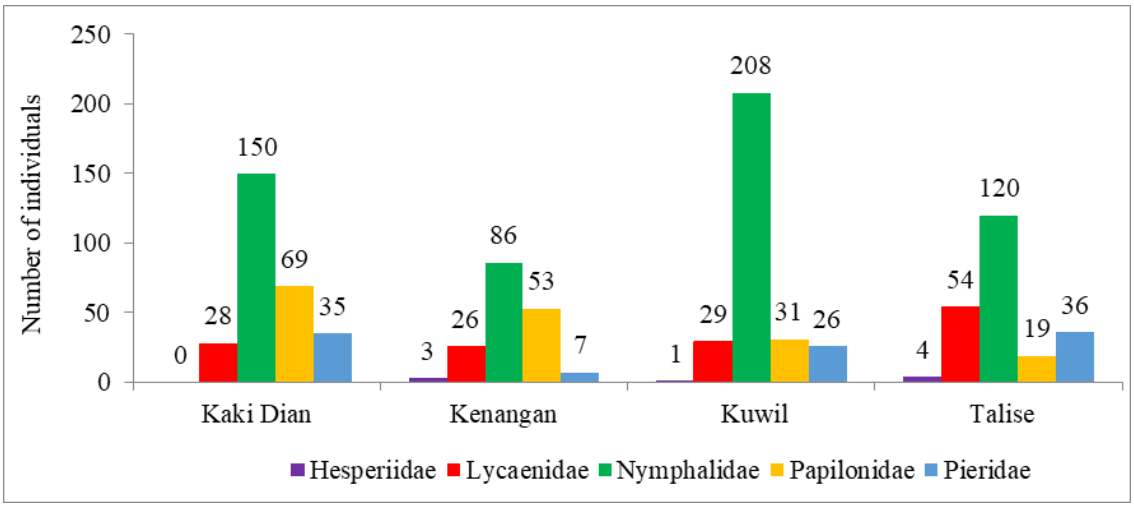

Figure 4. *Abundance of family butterflies found in four urban forests at North Minahasa, North Sulawesi*

http://www.aloki.hu ● ISSN 1589 1623 (Print) ● ISSN 1785 0037 (Online)
DOI: http://dx.doi.org/10.15666/aeer/1802_22952314

Table 3. *Number of family, species and individuals found in four urban forest in North Minahasa Regency, North Sulawesi*

Family/ species	Urban Forest/ Number of individuals				∑	%
	Kaki Dian	Kenagan	Kuwil	Talise		
Nymphalidae						
Parthenos sylvia salentia	12	0	42	68	122	12.39
Idiopsis vitrea oenopsis	28	36	9	0	73	7.41
Junonia hedonia intermedia	15	11	15	22	63	6.40
Idiopsis juventa tontoliensis	44	6	10	0	60	6.09
Idea blanchardii	6	0	22	0	28	2.84
Ypthima loryma	0	0	17	9	26	2.64
Lasippa neriphus tawayana	3	5	17	0	25	2.54
Mycalesis horsfieldi	0	10	3	2	15	1.52
Danaus ismare alba	2	0	12	0	14	1.42
Doleschallia polybete celebensis	0	0	3	10	13	1.32
Euploea algea	6	2	3	1	12	1.22
Parantica cleona luciplena	3	0	9	0	12	1.22
Euploea eupator	0	11	0	0	11	1.12
Ypthima nynias	0	0	7	4	11	1.12
Neptis ida	7	1	2	0	10	1.02
Pareronia tritaea	0	0	9	0	9	0.91
Mycalesis janarda	0	1	7	0	8	0.81
Cyrestis strigata	1	1	4	0	6	0.61
Yoma sabina	5	1	0	0	6	0.61
Danaus genutia	6	0	0	0	6	0.61
Euthalia aconthea	0	0	4	2	6	0.61
Faunis menado	6	0	0	0	6	0.61
Euploea leucostictos westwoodi	0	0	5	0	5	0.51
Mycalesis nicotia	0	0	5	0	5	0.51
Parantica menadensis	2	1	0	0	3	0.30
Cyrestis paulinus	0	0	3	0	3	0.30
Euthalia amanda	0	0	0	2	2	0.20
Moduza lycone	2	0	0	0	2	0.20
Elymnias hicetas	1	0	0	0	1	0.10
Lamasia lyncides	1	0	0	0	1	0.10
Papilionidae						
Troides helena	36	31	2	4	73	7.41
Papilio ascalaphus	0	11	4	8	23	2.34
Papilio gigon	7	8	18	1	34	3.45
Pachliopta polyphonthes	10	2	2	0	14	1.42
Graphium mayeri	5	1	5	0	11	1.12
Graphium agamemnon	3	0	0	3	6	0.61
Papilio blumei	4	0	0	0	4	0.41
Papilio demoleus	0	0	0	1	1	0.10
Papilio polytes	4	0	0	0	4	0.41
Papilio sataspes	0	0	0	2	2	0.20
Pieridae						
Catopsilia pomona flava	18	5	8	29	60	6.09
Hebomia glaucippe celebensis	2	0	14	1	17	1.73
Catopsilia scylla asema	8	0	2	6	16	1.62
Eurema tominia	4	2	0	0	6	0.61
Appias zarinda	3	0	2	0	5	0.51
Lycaenidae						
Jamides celeno	4	3	5	22	34	3.45
Euchrysops cnejus	11	2	2	9	24	2.44
Jamides alecto	0	11	8	4	23	2.34
Nadacuba berenice	0	0	0	17	17	1.73
Miletus leos	3	6	5	0	14	1.42
Acytolepsis puspa	6	0	7	0	13	1.32
Lampides boeticus	1	4	2	0	7	0.71
Tajuria mantra	3	0	0	0	3	0.30
Arhopala acetes	0	0	0	2	2	0.20
Hesperiidae						
Potanthus omaha	0	3	0	4	7	0.71
Taractrocera luzonensis	0	0	1	0	1	0.10
Total	**282**	**175**	**295**	**233**	**985**	**100.00**

http://www.aloki.hu ● ISSN 1589 1623 (Print) ● ISSN 1785 0037 (Online)
DOI: http://dx.doi.org/10.15666/aeer/1802_22952314

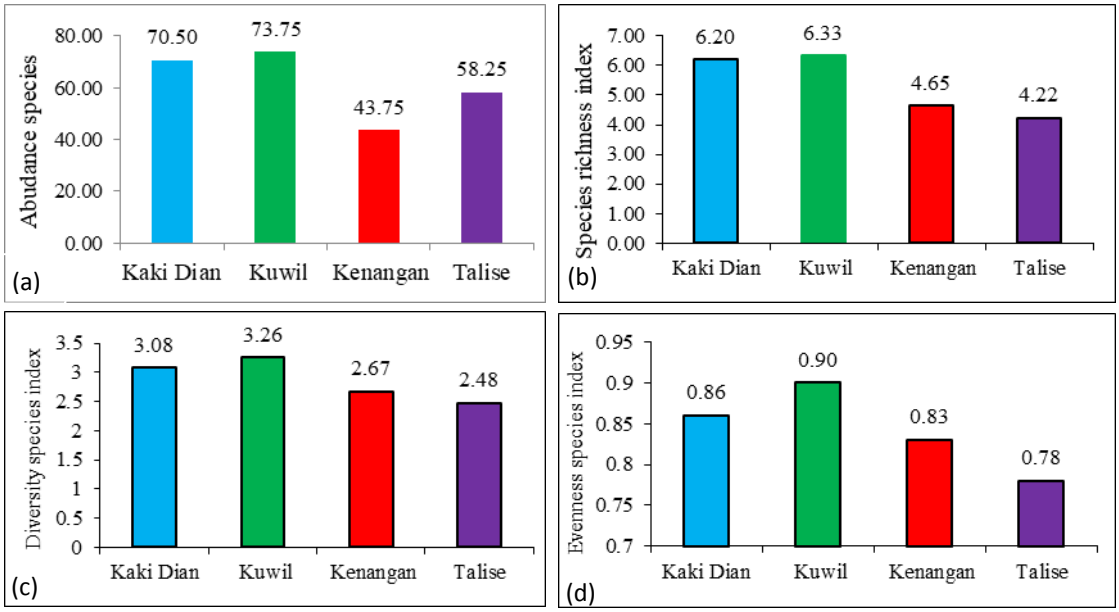

Figure 5. *The influence of urban forests types on (a) abundance, (b) richness (c) diversity and (d) evenness spescies index in North Minahasa, North Sulawesi*

Based on the categories, it was found that the species richness indices in the Kaki Dian City Forests and Kuwil City Forests were classified as high (S > 5), while the species richness indices in the Kenangan City Forest and Talise City Forest were classified as moderate (S: 3.5-5). The diversity index of butterfly species in the four urban forests was categorized as moderate (H: 1.5-3.5). Meanwhile, the evenness index of butterfly species was categorized as high because the index was greater than 0.6.

Index of species dominance

The highest dominance index of butterfly species was found in the Talise City Forest, while the lowest dominance index was in the Kuwil City Forest (*Fig. 6*). Based on the dominance index category, it was found that species dominance in the four urban forests was classified as low dominance (D < 0.5). This showed that no dominant butterfly species was found in the four urban forests.

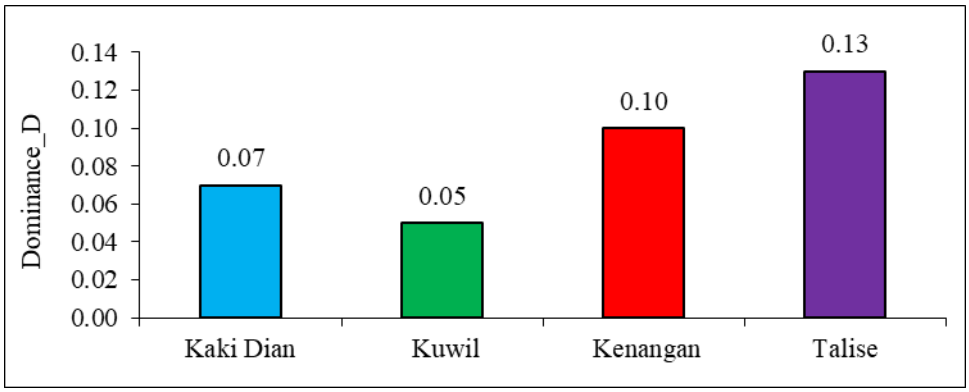

Figure 6. *Index of species dominance in four urban forests North Minahasa, North Sulawesi*

http://www.aloki.hu ● ISSN 1589 1623 (Print) ● ISSN 1785 0037 (Online)
DOI: http://dx.doi.org/10.15666/aeer/1802_22952314

Correlation between species diversity and environmental factors

Correlation of butterfly species diversity with environmental factors showed that there was a negative correlation of species abundance, richness index, diversity index, and species evenness index with air temperature, light intensity, and wind speed (*Table 4*). The correlation of species abundance, richness index, diversity index, and evenness index of species with air humidity was positive. Dominance index was positively correlated with air temperature, light intensity, wind speed and altitude, while dominance index and air humidity showed a negative correlation (*Table 4*).

Table 4. *Correlation of butterfly species diversity with environmental factors in four urban forests North Minahasa, North Sulawesi*

Variable	Air temperature	Air humidity	Light intensity	Wind velocity	Altitude
Abundance	-0.31	0.41	-0.42	-0.56*	0.04
Richness indexes	-0.36	0.48	-0.47	-0.45	0.20
Diversity indexes	-0.55*	0.57*	-0.66*	-0.59*	-0.01
Evenness indexes	-0.60*	0.46	-0.64*	-0.46	-0.23
Dominance indexes	0.56*	-0.47	0.67*	0.52*	0.07

*Marked correlations are significant at p < .05000. N = 16 (Casewise deletion of missing data)

The similarity of the butterfly community in the urban forests

Analysis of the similarity of the butterfly community in the urban forests using MDS showed that the objects of observation, which were Kota Dian City Forest, Kenangan City Forest, and Kuwil City Forest, had a relatively close distance, while Talise City Forest had a distant point, compared to other urban forests (*Fig. 7a*). The dendrogram results from the dissimilarity matrix resulted in the Kaki Dian City Forest, the Kenangan City Forest, and the Kuwil City Forest forming one group, while the Talise City Forest separated (*Fig. 7b*).

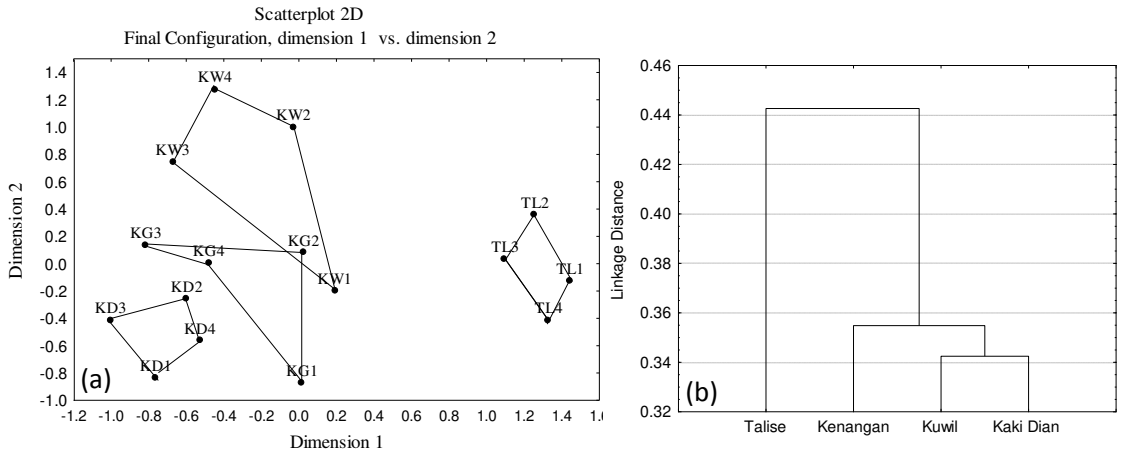

Figure 7. *Multidimensional Scaling (a), and dendrogram (b) about butterfly community similarity among urban forests in North Minahasa, North Sulawesi Utara (KD: Kaki Dian City Forest, KG: Kenangan City Forest, KW: Kuwil City Forest, TL: Talise City Forest)*

http://www.aloki.hu ● ISSN 1589 1623 (Print) ● ISSN 1785 0037 (Online)
DOI: http://dx.doi.org/10.15666/aeer/1802_22952314

Discussion

The number of butterfly species found in four urban forest in Minahasa Regency, North Sulawesi Province, only reached 0.28% of the 20,000 species of butterflies in the world (Alarape, et al., 2015), 2.80% of about 2,000 species butterflies found in Indonesia (Peggie, 2014), and 10.19% of the 557 species of butterflies spread across Sulawesi Island (Vane-Wright and de Jong, 2003). The number of butterfly species found in this research was higher than the number of butterflies found in some butterfly diversity studies in other urban forests. Alfida et al. (2016) obtained 18 species of butterflies in Banda Aceh City Forest. Rahayu and Basukriadi (2012) found 43 species of butterflies in Sabki City Forest in Jambi City. Oktavianti (2019) found 22 species of butterflies in Pontianak City Forest, while Kumar and Rana (2018) reported 30 species of butterflies found in fragmented urban forests in Lucknow, India.

The distribution of butterfly species in four urban forests in North Minahasa Regency, in general, was classified as aggregate distribution. Aggregate distribution pattern is generally found in insects, because of their tendency to aggregate, gathering from various degrees representing the most common characteristics. D'Abrera (1990) reported that butterflies migrated in large numbers (in groups) to a certain direction to find a place that provides enough food for larval development. The aggregation of individual organisms of a population results from responding to changes in daily or seasonal weather and responding to differences in local habitat conditions (Odum, 1996).

The dominant butterfly family found in all forests was Nymphalidae. This result was similar to the results of several studies, including studies by Ramesh et al. (2010), Boonvanno et al. (2000), Sutra et al. (2012), and Koneri and Nangoy (2019). The high abundance of butterflies from the family Nymphalidae was due to the abundant number of individuals from the family throughout the world and their high ability to live. According to Vane-Wright and de Jong (2003), compared to other families, Nymphalidae is a butterfly family with the largest number of species in the world, which is about 6,500 species consisting of 13 sub-families. The butterflies from this family are generally cosmopolitan in nature.

Nymphalidae also has a tendency to be polyphage. Their polyphage nature enables Nymphalidae to be able to meet its food needs even though the main host plants are not available (Lestari et al., 2015). Sreekumar and Balakrishnan (2001) reported that many members of the family Nymphalidae are polyphage. This means that if their main host plants are not available, the butterfly can still use other plants that are suitable for feeding its larvae. Different types of flowering and host plants will invite different types of butterflies to nectar or lay eggs on the suitable host. According to Peggie and Amir (2006), the feed source of the Nymphalidae family is plants from the families Fabaceae, Annonaceae, Asteraceae, and Poaceae.

The family Nymphalidae is easily found all year round. This is because these insects are generalist. Some species of Nymphalidae do not depend on the existence of flower nectar alone. Those species are able to obtain food sources from rotten fruit and urine of other animals (Sarma et al., 2012).

Hesperiidae was a butterfly family with the fewest species and individuals found. This was because this family is small in body size and prefers moist and shady places such as forest areas. In this study, butterflies from the family Hesperiidae were found in all locations of urban forests except in the Kaki Dian City Forest. According to Amir and Kahono (2008), Hesperiidae is usually crepuscular, that is, it is active before night

http://www.aloki.hu ● ISSN 1589 1623 (Print) ● ISSN 1785 0037 (Online)
DOI: http://dx.doi.org/10.15666/aeer/1802_22952314

or when the light is dim. Observation of butterflies in this research was carried out since morning (7:00 pm) until late afternoon (3:00 pm). This condition caused very few encounters with butterflies from the family Hesperiidae.

Parthenos sylvia salentia species had the highest abundance compared to other species. The butterfly species is included in the family Nymphalidae. This species is found in tropical rain forests, usually around rivers. During the observation, many species were found near river basins in the Kuwil City Forest.

The next species of butterfly that had a high abundance was *Troides helena,* which belongs to the family Papilionidae. *Troides helena* is included as species protected by Government Regulation No. 7 of 1999, Decree of the Minister of Agriculture No.576/Kpts/Um/8/1980, and Decree of the Minister of Agriculture No.716/Kpts/Um1/0/1980. The species is also included in Appendix II of CITES (Convention of International Trade in Endangered Species). This means that the species is currently not included in the endangered category, but has the possibility of being endangered if the trade of the species is not regulated (Soeharto and Mardiastuti, 2003). *Troides helena* are poached for sale because of their beauty and scarcity (Noerdjito and Aswari, 2003; Nurjannah, 2010).

Differences in abundance, richness index, diversity index, and evenness index of butterfly species in four urban forests were greatly influenced by the area of urban forests and the complexity of the composition of vegetation structures making up the urban forest. The Kuwil City Forest was the location with the highest species diversity, while the lowest species diversity was in the Talise City Forest. The Kuwil City Forest is the location with the largest area (±46 ha), compared to the Kaki Dian City Forest (±37 ha), the Kenangan City Forest (±15 ha), and the Talise City Forest (±6 ha), and according to the theory of island biogeography, area is directly proportional to the diversity of species. The large size of an island will support an increase in the population size of the butterfly species due to the availability of food sources and habitats (MacArthur and Wilson, 1967). Island biogeography can be applied to fragmentation of urban forest landscapes as a model of how “islands” as small habitats can adversely affect the biodiversity of their natural habitat (Harris, 1984). Urban forest is considered an “island” in the form of habitat area that is surrounded by other areas that are not suitable for the life of species, such as residential land, offices, and plantations that are intensively processed.

The diversity of butterfly species in urban forests is also influenced by the availability of feed plants and is closely related to physical environmental factors, such as soil, water, temperature, sunlight, and biological factors that include vegetation and other animals. The distribution and abundance of plants as a source of larval feed was one of the factors that had a major influence on the survival of butterfly larvae. Nectar-producing plants also greatly affect the survival of butterflies, because the main food of butterfly is flower nectar. The more liquid nectar is available, the more butterflies come to visit the place. In the Kuwil forest habitat, there are many nectar-producing plants, such as oranges (Rutaceae), soursop (*Annona muricata*), durian (*Durio zibethinus*), gmelina (*Gmelina arborea*), Ficus sp, mango (*Mangifera indica*), *Mussaenda frondosa*, *Calliandra calothyrsus*, *Clerodendrum paniculatum*, *Ageratum conyzoides*, and *Lantana camara*. More diverse vegetation in a habitat has the potential for greater availability of feed for butterflies, compared to less diverse vegetation does (Rahayuningsih, 2012).

http://www.aloki.hu ● ISSN 1589 1623 (Print) ● ISSN 1785 0037 (Online)
DOI: http://dx.doi.org/10.15666/aeer/1802_22952314

Another factor affecting the diversity of butterflies in urban forests in North Minahasa Regency was the availability of water. Urban forest where water flow can be found was the Kuwil City Forest and this urban forest provides a source of water for the surrounding community. The availability of water sources affects the existence of a type of butterfly, because butterflies like river banks (Amir et al., 2003). Butterflies come to the wet area to get water. Besides needing energy from their food, adult butterflies also need water in their life. Observations in the Kuwil City Forest showed that the source of water that was often visited by butterflies was sandy river banks. Glassberg (2001) argued that most species of butterflies, especially male butterflies, aggregated in moist sand or soil to absorb mineral salts and water. This behavior is called "puddling". The salt will be transferred to the female butterfly during the mating process as additional nutrient for the eggs.

Environmental factors in urban forests, such as air temperature, humidity, light intensity, and wind speed affect the diversity of butterfly species. According to Sharma and Joshi (2009), the structural complexity of habitat and vegetation diversity, including the influences of physical-chemical factors, such as air temperature, air humidity, and light intensity, was correlated with the diversity of insect species. The test results showed that species diversity was negatively correlated with air temperature, light intensity, and wind speed, whereas species diversity and wind speed was positively correlated.

Air temperature was very influential on the diversity of butterflies because these insects are poikilothermic, which means that their body temperature will increase or decrease following the temperature of the surrounding environment (Sihombing, 2002). Each butterfly species has different adaptability to temperature and humidity changes in their habitat. The temperature that can support the life of a butterfly ranges between 16 and 42 °C (Scoot, 1986), while the optimal temperature for butterflies is around 28-35 °C (Watanabe and Imoto, 2003). Based on temperature measurements in the four urban forests, it was found that the temperature in each urban forest could still support butterfly activity.

Furthermore, humidity is a very important climate factor. The correlation test found that the higher the relative humidity in an urban forest was, the higher the diversity of butterfly species in the urban forest became. Humidity can affect the breeding, growth, development, and activeness of insects. The ability of butterfly species to survive in the humidity of the surrounding air is different for each species and for each developmental stage. Air humidity can also affect the growth of host plants and indirectly affect the diversity of butterfly species (Efendi, 2009).

Light intensity influenced the diversity of butterflies. If the intensity of light was higher, the diversity of butterfly species would decrease. This was because the high light intensity caused the air temperature to rise and humidity to drop outside the range of air conditions required by a butterfly. Increased air temperature will accelerate the evaporation of body fluids and endanger the life of a butterfly. Low air humidity will affect butterflies that are large and wide-winged because the greater surface area of the body will increase the evaporation of body fluids. High light intensity also caused the volume of nectar secretions in flowers to decrease (Efendi, 2009).

Meanwhile, wind speed was negatively correlated with the diversity of butterfly species, which meant that if the wind speed got higher, the diversity of butterfly species would decrease. The results of wind speed measurements found that the lowest wind speed was in the Kuwil City Forest. Low wind speeds caused a high diversity of

http://www.aloki.hu ● ISSN 1589 1623 (Print) ● ISSN 1785 0037 (Online)
DOI: http://dx.doi.org/10.15666/aeer/1802_22952314

butterflies in this urban forest. High wind speed will damage the wings of butterflies, especially butterflies with broad and fragile wings, such as some species of the family Papilionidae and the family Nymphalidae, which will not last long in these conditions.

The similarity index of butterfly species between urban forests showed that the composition of butterfly species in the Kaki Dian City Forest, Kenangan City Forest, and Kuwil City Forest had many similarities, while the composition of butterfly species in the Talise City Forest did not share many similarities with the other urban forests. Species similarity between habitats is influenced by habitat characteristics, especially those characteristics related to plants as food, a place to take shelter from predator attacks, host plants to carry out their life cycle, playgrounds, and physical environmental factors, such as the presence of water flow, humidity, and weather conditions.

Conclusion

In general, the distribution of the butterfly species found (52 species) have a flocking pattern (aggregate). The butterfly species found consist of 5 families, comprising 56 species and 985 individuals. Butterfly species with the highest abundance is *Parthenos silva salentia* (29.93%). Family with the largest number of individuals is Nymphalidae (57.26%). The diversity of butterfly species which includes abundance, evenness index, richness index and the index of the highest species diversity was found in the urban forest of Kuwil. The highest domination index of butterfly species was found in the urban forest of Talise. The diversity of butterfly species is negatively correlated with air temperature, light intensity and wind speed. From the butterfly species community similarity index of urban forests, it is found that urban forests of Kaki Dian, Kenangan and Kuwil have a high similarity compared to the urban forest of Talise.

The results of this study recommend that further research on the types of plants that serve as food plants and hosts of butterflies should be done. The research period should include other seasons. It is expected that the Forestry Department of North Minahasa consider the diversity of butterflies in the management of urban forests by maintaining the habitat stability of urban forests. Habitat stability can sustain the butterfly conservation, especially *Troides Helena* butterflies which are protected and included in Appendix II of CITES (*Convention of International Trade in Endangered Species*).

Acknowledgements. The author would like to thank the rector of the Sam Ratulangi University, Manado, for funding this research through the scheme of *Riset Dasar Unggulan Unsrat* (RDUU) with the contract number: SP DIPA - 042.01.2.400959/2019 dated 5 December 2018.

REFERENCES

[1] Alarape, A. A., Omifolaji, J. K., Mwansat, G. S. (2015): Butterfly species diversity and abundance in University of Ibadan Botanical Garden, Nigeria. – Open Journal of Ecology 5: 352-360.

[2] Alfida, A., Hanum, U., Eliyanti, E. (2016): Butterflies (Rhopalocera) in urban forests are in BNI Banda Aceh. – Journal Biotik 4: 117-127.

[3] Amir, M., Kahono, S. (2008): Butterflies (Lepidoptera). – In: Amir, M., Kahono, S. (eds.) Insects in Halimun Mountain National Park West Region. JICA, Jakarta.

http://www.aloki.hu ● ISSN 1589 1623 (Print) ● ISSN 1785 0037 (Online)
DOI: http://dx.doi.org/10.15666/aeer/1802_22952314

[4] Amir, M., Noerdjito, W. A., Kahono, K. (2003): Butterflies (Lepidoptera). – In: Amir, M., Kahono, S. (eds.) Insects in Halimun Mountain National Park West Region. JICA, Jakarta.
[5] Azahra, S. D., Masyud, B., Farikhah, N. (2016): Comparison of butterfly communities in various types, characteristics, and environmental disturbance of urban forests. – Media Konservasi 21: 108-115.
[6] Bergerot, B., Fontaine, B., Julliard, R., Baguette, M. (2011): Landscape variables impact the structure and composition of butterfly assemblages along an urbanization gradient. – Landscape Ecology 26: 83-94.
[7] Boonvanno, K., Watanasit, S., Permkam, S. (2000): Butterfly diversity at ton Nga-Chang wildlife sanctuary, Songkhla Province, Southern Thailand. – Sci Asia 26: 105-110.
[8] Borror, D. J., Triplehorn, C. A., Johnson, N. F. (1992): Introduction to Insect Lessons. – UGM Press, Yogyakarta.
[9] Braby, M. F. (2004): The Complete Field Guide to Butterflies of Australia. – CSIRO Publishing, Collinwood.
[10] Cheng, C. (2004): Statistical approaches on discriminating spatial variation of species diversity. – Botanical Bulletin of Academia Sinica 45: 339-346.
[11] Clark, P. J., Reed, J. M., Chew, F. S. (2007): Effects of urbanization on butterfly species richness, guild structure, and rarity. – Urban Ecosystem 10: 321-337.
[12] D'abrera, B. (1990: Butterflies of the Australian Region. 3rd Ed. – Hill House, Melbourne and London.
[13] Dennis, E. B., Mogan, B. J. T., Roy, D. B., Brereton, T. M. (2017): Urban indicators for UK butterflies. – Ecology Indicators 76: 184-193.
[14] Efendi, M. A. (2009): Diversity of butterflies (Lepidoptera: Ditrysia) in "Corridor Forest", Gunung Halimun-Salak National Park, West Java. – Thesis, School of Post Graduate Studies of Bogor Agricultural University, Bogor.
[15] Glassberg, J. (2001): Butterflies through Binocular the West: A Field Guide to the Butterflies of Western North America. – Oxford University Press, New York.
[16] Hair, J. F. J., Anderson, R. E., Tatham, R. L., Black, W. C. (1998): Multivariate Data Analysis. 5th ed. – Prentice-Hall International, USA.
[17] Handayani, S. A., Bachri, K. S., Ismail, T., Sukmawati, Jasmin, E. I., Shagir, K. Y. (2015): Diversity of Butterly in Bantimurung Bulusaraung National Park. – In: Balai, T. N. (ed.) Bantimurung Bulusaraung. Maros, Sulawesi Selatan.
[18] Harris, L. D. (1984): The Fragmented Forest: Island Biogeography Theory and the Preservation of Biotic Diversity. – University of Chicago Press, Chicago, Illinois.
[19] Jumar (2000): Agricultural Entomology. – Rineka Cipta, Jakarta.
[20] Kim, S. S., Lee, C. M., Kwon, T. S., Joo, H. Z., Sung, J. H. (2012): Korean Butterfly Atlas 1996-2011. – Research Note 461, Korea Forest Research Institute, Korea Disabled Human Good Life Pub. Co, Seoul (in Korean).
[21] Koh, L. P., Sodhi, N. S. (2004): Importance of reserves, fragments, and park for butterfly conservation in a tropical urban landscape. – Ecological Applications 14: 1695-1708.
[22] Koneri, R., Nangoy, M. J. (2019): Butterfly community structure and diversity in Sangihe Islands, North, Sulawesi, Indonesia. – Applied Ecology and Environmental Research 17: 2501-2517.
[23] Krebs, C. J. (1999): Ecological Methodology. Second Ed. – Addison-Wesley, Menlo Park.
[24] Kumar, A., Rana, S. S. (2018): Species diversity and community structure of butterfly in urban forest fragments at Lucknow. – Indian Journal of Applied and Natural Science 10: 1276-1280.
[25] Kusmana, C. (2015): Keanekaragaman hayati (biodiversitas) sebagai elemen kunci ekosistem kota hijau. – Prosiding Seminar Nasional Masyarakat Biodiveritas Indonesia 1: 1747-175.

http://www.aloki.hu ● ISSN 1589 1623 (Print) ● ISSN 1785 0037 (Online)
DOI: http://dx.doi.org/10.15666/aeer/1802_22952314

[26] Lee, C. M., Kwon, T. S. (2012): Characterization of the butterfly community of a fragmented urban forest, Hongneung Forest. – Korean Journal Applied Entomology 51: 317-323.
[27] Lee, C. M., Kwon, T. S. (2013): Community structure, species diversity of insects (ants, ground beetle), and forest health in the Hongneung Forest. – Journal Korean for Society 102: 97-106.
[28] Lee, C. M., Kwon, T. S., Kim, S. S., Sohn, J. D., Lee, B.W. (2014): Effects of forest degradation on butterfly communities in the Gwangneung forest. – Entomology Science 17: 293-301.
[29] Lee, C. M., Park, J. W., Kwon, T. S., Kim, S. S., Ryu, J. W., Jung, S. J., Lee, S. K. (2015): Diversity and density of butterfly communities in urban green areas: an analytical approach using GIS. – Zoological Studies 54: 4: 1-12.
[30] Lestari, D. F., Putri, R. D. A., Ridwan, M., Purwaningsih, A. D. (2015): Butterfly diversity (Insect: Lepidoptera) at Alas Bromo Tourism Wana. – BKPH North Lawu, Karanganyar.
[31] Lewis, T. O. (2001): Effect of experimental selective logging on tropical butterflies. – Conservation Biology 15(2): 389-400.
[32] Ludwig, J. A., Reynolds, J. F. (1988): Statistical Ecology. A Primer on Methods and Computing. – John Wiley and Sons, New York.
[33] MacArthur, R. H., Wilson, E. O. (1967): The Theory of Island Biogeography. – Princeton University Press, Princeton, NJ.
[34] Magurran, A. E. (1988): Ecological Diversity and Its Measurements. – Croom Helm Limited, London.
[35] Magurran, A. E. (2004): Measuring Biological Diversity. – Wiley-Blackwell, Malden.
[36] MCKinney, M. L. (2002): Urbanization, biodiversity, and conservation. – BioScience 52: 883-890.
[37] Motegi, N., Yanai, S. (2005): A study on the characteristics of bird distribution in rooftop vegetation in Tokyo Ward. – Jpn Inst Landscape Architecture 68: 597-600.
[38] Noerdjito, W. A., Aswari, P. (2003): Methods of Surveying and Monitoring Animal Populations: 4th Series: Papilionidae Butterflies. – Center for Biological Research and Development, LIPI, Bogor.
[39] Nurjanah, S. T. (2010): Biology of *Troides helena helena* dan *Troides helena hephaestus* (Papilionidae) in captivity. – Thesis, Bogor Agricultural University, Bogor.
[40] Odum, E. P. (1996): Basics of Ecology. 3th Ed. – Gadjah Mada University Press, Yogyakarta.
[41] Oktaviani, W., Rifanjani, S., Ardian, H. (2019): Diversity of butterflies species (Ordo: Lepidoptera) in Urban forests in Pontianak City. – Jurnal Hutan Lestari 7: 79-85.
[42] Peggie, D., Amir, M. (2006): Practical Guide to the Butterflies of Bogor Botanic Garden. – Pusat Penelitian biologi, LIPI, Cibinong, Indonesia.
[43] Peggie, D. (2014): Butterflies. – Pandu Aksara Publishing, Jakarta.
[44] Plona, M. B. (2002): Butterfly Monitoring Report. – Cuyahoga Valley National. http://www.nps.gov/cuva/management/rm/02butterflies.htm.
[45] Preeven, F. K., Haroon, F. P. (2015): Checklist of Butterfly (Insecta: Lepidoptera) Fauna of Tehsil Tangi, Khyber Pakhtunkhwan, Pakistan. – Department of Zoology, Shaheed Benazir Bhutto University, Khyber Pakhtunkhwan, Pakistan.
[46] Rahayu, S. E., Basukriadi, A. (2012): Abundance and diversity of butterfly species (Lepidoptera; Rhopalocera) in various habitat types in the Muhammad Sabki Urban Forest, Jambi City. – Biospecies 5: 40-48.
[47] Rahayuningsih, M., Oqtafiana, R., Priyono, B. (2012): Diversity of butterfly species in the superfamily Papilionoidae at Banyuwindu Hamlet, Limbangan Village, Limbangan District, Kendal Regency. – Journal MIPA 35: 11-20.
[48] Ramesh, T., Hussain, K. J., Selvanayagam, M., Satpathy, K. K., Prasad, M. V. R. (2010): Pattern of diversity, abundance and habitat associations of butterfly communities in

http://www.aloki.hu ● ISSN 1589 1623 (Print) ● ISSN 1785 0037 (Online)
DOI: http://dx.doi.org/10.15666/aeer/1802_22952314

heterogeneous landscape of the Department of Atomic Energy (DAE) Campus at Kalpakkam, South India. – International Journal of Biodiversity and Conservation 2: 75-85.
[49] Rubèn, O. A., Ian, M. F. (2009): Living in the big city: effects of urban land-use on bird community structure, diversity, and composition. – Landscape Urban Plan 90: 189-195.
[50] Sarma, K., Kumar, A., Devi, A., Mazumdar, K., Krishna, M., Mudoi, P., Das, N. (2012): Diversity and habitat association of butterfly species in Foothills of Itanagar, Arunchal Pradesh. – Zoology 1: 67-77.
[51] Schulze, C. H., Fiedler, K. (1998): Habitat preferences and flight activity of Morphinae butterflies in a Bornean rain forest, with a note on sound production by adult Zeuxidia (Lepidoptera: Nymphalidae). – Malayan Biology 8: 800-809.
[52] Scott, J. (1986): The Butterflies of North America: A Natural History and Field Guide. – Oxford University Press, USA.
[53] Shahabuddin, Schulze, C. H., Tscharnke, T. (2005): Changes of dung beetle communities from rainforests towards agroforestry systems and annual cultures in Sulawesi (Indonesia). – Biodiversity and Conservation 14: 863-877.
[54] Sharma, G., Joshi, P. G. (2009): Diversity of butterflies (Lepidoptera: Insecta) from Dholbaha dam (Distt. Hoshiarpur) in Punjab Shivalik, India. – Biological Forum an International Journal 1(2): 11-14.
[55] Sihombing, D. T. H. (2002): Hope Animals I: Introduction to Agriculture Science and Cultivation Technology. – Pustaka Wirausaha Muda, Bogor.
[56] Soeharto, T., Mardiastuti, A. (2003): Implementation of Convention CITES at Jakarta: Indonesia. – JICA, PLC, London.
[57] Speight, M. R., Hunter, M. D., Watt, A. D. (1999): Ecology of Insects: Concepts and Applications. – Blackwell Science, London.
[58] Sreekumar, P. G., Balakrishnan, M. (2001): Habitat and altitude preferences of butterflies in Aralam Wildlife Sanctuary, Kerala. – Journal Tropical Ecology 42: 277-281.
[59] Stat Soft (2001): Stastistica for Windows, 6.0. – Statsoft Inc. Tulsa, Oklohoma.
[60] Sutra, N. S. M., Dahelmi, S., Siti, S. (2012): Butterflies species (Rhopalocera) in Tanjung Balai Karimun, Kabupaten Karimun Regency, Riau Islands. – Jurnal Biologi Univ. Andalas 1: 35-44.
[61] Thangjam, R., Kadam, V., Hemochandra, I., Ramalaxmi, V., Krishna, D. G., Patnaik, L. (2018): Studies on the diversity and abundance of butterfly in and around CUTM, Paralakhemundi campus, Odisha (India). – Journal of Entomology and Zoology Studies 6: 2484-2491.
[62] Tsukada, E., Nishiyama, Y. (1981): Butterflies of the South East Asian Island, Part II Pieridae-Danaidae. – Palapa Co. Ltd., Minatok-Tokyo.
[63] Tsukada, E., Nishiyama, Y. (1982a): Butterflies of the South East Asian Island, Part I Papilionidae. – Palapa Co. Ltd., Minatok-Tokyo.
[64] Tsukada, E., Nishiyama, Y. (1982b): Butterflies of the South East Asian Island, Part III Satyridae-Lybytheidae. – Palapa Co. Ltd., Minatok-Tokyo.
[65] Tsukada, E., Nishiyama, Y. (1985): Butterflies of the South East Asian Island, Part IV Nympalidae (I). – Palapa Co. Ltd., Minatok-Tokyo.
[66] Tsukada, E., Nishiyama, Y. (1991): Butterflies of the South East Asian Island, Part V Nympalidae (II). – Palapa Co. Ltd., Minatok-Tokyo.
[67] Vane-Wright, R. I., de Jong, R. (2003): The butterflies of Sulawesi: annotated checklist for a critical island fauna. – Zoologische Verhandelingen 343: 3-267.
[68] Watanabe, M., Imoto, T. (2003): Thermoregulation and flying habits of the Japanese sulfur butterfly *Colias erate* (Lepidoptera: Pieridae) in an open habitat. – Entomology Science 6: 111-118.

http://www.aloki.hu ● ISSN 1589 1623 (Print) ● ISSN 1785 0037 (Online)
DOI: http://dx.doi.org/10.15666/aeer/1802_22952314

THE PHYSIOLOGICAL AND DNA DAMAGE RESPONSE OF IN THE LICHEN *HYPOGYMNIA PHYSODES* TO UV AND HEAVY METAL STRESS

HAMUTOĞLU, R.[1] – DERICI, M. K.[2] – ARAS, E. S.[3] – ASLAN, A.[4,5] – CANSARAN-DUMAN, D.[6*]

[1]*Histology and Embryology Department, Faculty of Medicine, Cumhuriyet University, Sivas, Turkey*

[2]*Medical Pharmacology Department, Faculty of Medicine, Kırıkkale University, Kırıkkale, Turkey*

[3]*Biology Department, Faculty of Science, Ankara University, Ankara, Turkey*

[4]*Department of Biology, Faculty of Arts and Science, Kyrgyz-Turkish Manas University, Bishkek, Kryrgyzstan*

[5]*Department of Pharmacology, Faculty of Pharmacy, Yüzüncü Yıl University, Van, Turkey*

[6]*Biotechnology Institute, Ankara University, Ankara, Turkey*

**Corresponding author*
e-mail: dcansaran@yahoo.com; phone: +90-312-596-1032/2563

(Received 24th Oct 2019; accepted 21st Jan 2020)

Abstract. This work aims to determine the response of *Hypogymnia physodes* (L.) Nyl. (hooded tube lichen) collected in an unpolluted site (Yenice Forest in Karabük, Turkey) to stress conditions. In the present study, the effect of exposure to different heavy metals (Cd^{+2}, Pb^{+2}, and Cr^{+6}) for different durations and UV radiations dosages on lichen was examined at the physiological and molecular levels. The effects of stress conditions were determined in the case of different parameters concerning heavy metal, protein, chlorophyll, and carotenoid contents and changes in the DNA profiles. According to the results obtained that exposure to heavy metals and UV radiations leads to a physiological response in a concentration and dose-dependent manner through differences in chlorophyll, protein content in heavy metals and UV treated lichen specimen. Furthermore, changes in RAPD assay and DNA methylation analysis showed that homologous nucleotide sequences in the genome from untreated and stress conditions treated lichen specimen showed different band patterns and methylation under heavy metals and UV stress. The results determined that lichen specimen suggest as a possible bioindicator able to measure the biological effects of heavy metal pollution and damage to UV radiation.
Keywords: *lichen, UV radiations, metal uptake, chlorophyll content, DNA alteration*

Introduction

Due to population and rapid economic growth and urbanization, air pollution creates a major threat both to the environment and living organisms in the world. Environmental Protection Agency (EPA) has reported that some pollutants are poisonous, and inhaling them, in particular, can rapidly increase problems in human health (Cheloni et al., 2014; Mateos et al., 2018). Environmental pollution caused by heavy metals is one of the most serious problems at a global extent (Pescott et al., 2015; Ares et al., 2017). Among all heavy metals, cadmium (Cd^{+2}), chromium (Cr^{+3} and Cr^{+6}) and lead (Pb^{+2}), in particular, cause an ever-increasing international concern. The excessive Cr^{+6}, Cd^{+2} and Pb^{+2} concentrations in contaminated areas can give rise to a

http://www.aloki.hu ● ISSN 1589 1623 (Print) ● ISSN 1785 0037 (Online)
DOI: http://dx.doi.org/10.15666/aeer/1802_23152338

variety of problems, which is metal toxicity to mainly humans and animals (Frohnmeyer and Staiger, 2003). Another main problem in ecotoxicology is the damage of the stratospheric ozone layer due to anthropogenic activities, which results in increased UV radiation on the surface of the Earth and causes damage to the biological system (Singh et al., 2012). Pollutants and UV radiation interrupt metabolic activities at the cellular level and damage biological molecules such as proteins and nucleic acids (Pourrut et al., 2011).

In contrast to organic pollutants, heavy metals cannot be degraded through any known biological processes (Brown et al., 2005), and thus, there remains an urgent need for remediation of contaminated areas by environmentally friendly technology. An appropriate and cost-effective method to remove pollutants and UV radiation from the environment is needed. Biological methods, instead of physical and chemical methods, enable to direct assessment of environmental stressors. Thus, information obtained from biological data can be allowed to determinate the environmental impact of global problems on biological organisms. The solution to many global problems, such as bioremediation of toxic chemicals in the environment and decreasing the effect of UV radiation will require further research on cellular and molecular biology with biological organisms (Bah et al., 2011). For instance, *Typha angustifolia* shows protein changes when exposed to Cr^{+6}, Cd^{+2} and Pb^{+2} heavy metals. Results of the study suggest that abiotic stress, such as heavy metal, temperature, drought and salt stress, induces changes in protein expression level in plants (Cho and Seo, 2005; Pandey et al., 2005). The liverwort (*Lunularia cruciate*) has been used to evaluate the effect of heavy metals on the cellular levels, including changes in the mRNA level (Basile et al., 2005). Lichen species have used to determinate the response of physiological and molecular mechanisms in stress conditions in recent years (Aras et al., 2010; Cansaran-Duman, 2011; Matos et al., 2015). Due to lichen species lack protective cuticle and roots, they can adsorb all metals directly from contaminated areas and ability to absorb in high quantity heavy metals in contaminated areas are usually used as model organisms for various purposes by the environmental area.

Damage to DNA may generate mutations, altered bases and strand breaks (Shugart and Theodorakis, 1994), and afterward, to carcinogenesis, teratogenesis and health disorders (Kurelec, 1993). Some researchers have reported that positively charged metal ions can react with negatively charged oxygen atoms located in both chains of the DNA in phosphate groups (Anastassopoulou, 2003). The DNA damage generated by environmental stress sources has been shown with various studies conducted in our laboratory (Cansaran-Duman et al., 2011; Cansaran and Aras, 2014; Vardar et al., 2014).

In recent years, some studies have shown that low UVB fluence rate is the cause of cellular changes in higher plants (Brown et al., 2005; Brown and Jenkins, 2008). It has been demonstrated that low UVB fluence rate responses involve specific receptors and appear to be photoregulatory. The changes caused by UV radiation on plant development, morphology and physiology have been observed in several studies (Mackerness, 2000; Frohnmeyer and Staiger, 2003; Jenkins, 2009; Hideg et al., 2013). Generally, energy-rich UV radiation gives rise to the formation of free radicals that damage DNA, proteins, and the damage of photosynthetic pigments (Hideg et al., 2013).

This study aimed to understand, predict and expand the knowledge of the possible biological response of *Hypogymnia physodes* lichen specimen to different types and

http://www.aloki.hu ● ISSN 1589 1623 (Print) ● ISSN 1785 0037 (Online)
DOI: http://dx.doi.org/10.15666/aeer/1802_23152338

exposure periods of both UV and heavy metal solutions on cellular organization and physiological responses by examining bioaccumulation performance. Firstly, we evaluated heavy metal contents, chlorophyll (chl-a, chl-b, total chl, and carotenoids) and protein content in response to different heavy metal accumulation and UV radiations exposure to lichen specimen. Secondly, RAPD and MSAP-AFLP techniques were examined in *H. physodes* for possible changes in the DNA exposed to different heavy metal solutions and UV radiations. Although the capacity of heavy metal accumulation on lichen specimen has been extensively studied, only a few studies to date have shown that lichen specimen exposes to UV radiations at molecular and biochemical levels and heavy metal accumulation. This is the first manuscript examining methyl profiles in lichen specimen. Thus, this study will provide a better understanding of the molecular mechanisms of cellular protection against different stress factors on lichen species.

Materials and methods

Lichen sample and stress treatment

All procedures were carried out at Ankara University Department of Biology Molecular Systematic Laboratory and Ankara University Biotechnology Institute Central Laboratory, Ankara, Turkey. *Hypogymnia physodes* lichen specimen was selected as suitable bioindicators due to it has a large thallus surface. The lichen specimen was obtained from the unpolluted area of Yenice Forest, Karabük, Turkey in 2011 (41°10'N, 32°23'E). The sample collected from Yenice Forest was firstly washed and stored at appropriate conditions (4 °C) for a few days and sprayed distilled water. Then, the lichen specimen was sprayed constantly with distilled water in the laboratory. The sample was kept at room temperature for 2-3 h. During the treatments, thallus was placed in a climate chamber at 15 °C, exposure a photosynthetic photon flux density (PPFD) of 75 μmol m^2 s^{-1} and a 16 h photoperiod. All analytical procedures were carried out at least three replicates (n = 3).

Two different stress treatments (exposure to heavy metals and UV radiations) were applied in the study. A schematic representation of stress treatments in lichen specimen was shown in *Figure 1*. *H. physodes* was subjected to Pb^{+2}, Cd^{+2} and Cr^{+6} (30, 60 and 120 mg/L) heavy metal stress for different time periods (0.5, 1, 2, 6, 18, 24, 48 and 72 h). In brief, the stock solutions of Cd^{+2}, Pb^{+2} and Cr^{+6} (200 mg/L) were prepared by dissolving a weighed quantity in deionized water. In this study, the required concentrations were prepared from the stock solution with dilution. Lichen thallus (10 g weight) was immersed for an incubation period of 0.5, 1, 2, 6, 18, 24, 48 and 72 h. The lichen specimen was studied with three unexposed samples. The procedure followed for UV exposure; thallus sample placed in a petri dish was exposed to UV radiations at different doses of 4, 8, 12, 20 and 40 j/cm^2 (352 nm, 50 Hz, 0.60 Amps) by using dose-meter at 25 °C. Irradiation chamber BS-03 (Dr. Gröbel UV-Electronic GmbH) and dosemeter were used to lichen for determining to expose to UV radiations (UVA, UVB, UVC, daylight, UVA + UVB, UVA + day light) ratios. The control (non-stressed) group was analyzed with molecular markers and was indicated as a 'control sample'. Negative control was also used to determine the presence of any contamination.

Determination of heavy metals concentration

http://www.aloki.hu ● ISSN 1589 1623 (Print) ● ISSN 1785 0037 (Online)
DOI: http://dx.doi.org/10.15666/aeer/1802_23152338

The determination of heavy metal contents was performed from the previous study of Cansaran-Duman (2011). Lichen sample exposed to Cd^{+2} and Pb^{+2} heavy metals was collected at different time intervals. The sample was dried at 90 °C for 9 h and mineralization using HNO_3 and H_2O_2 (2:1, v/v) under ultrasonication. The set of standard calibration curves with good linear regression and better relative standard deviations were achieved for Cd^{+2} and Pb^{+2} metals in *H. physodes*. Cd^{+2} and Pb^{+2} concentrations of lichen sample were analyzed using Flame Atomic Absorption Spectroscopy (FAAS; Instrument PM Avarta, GBC Scientific Equipment, Australia). Standard reference material, CRM 482 Lichen (*P. furfuracea*), was used in the study to determine whether within range of the recommended values. The measured recovery % ± SD for Cd^{+2} and Pb^{+2} in the added CRM 482 reference material were 98 ± 7, 99 ± 6, 98 ± 3, respectively. The recovery was about 100% for Cd^{+2} and Pb^{+2} in the lichen sample, and the results with the CRD 482 material suggested that sample preparation and analyses were accurate. The conventional spectrophotometric method of Cr^{+6} was analyzed via 1.5–diphenylcarbazide measured at 540 nm in acid solution (APHA, 1985).

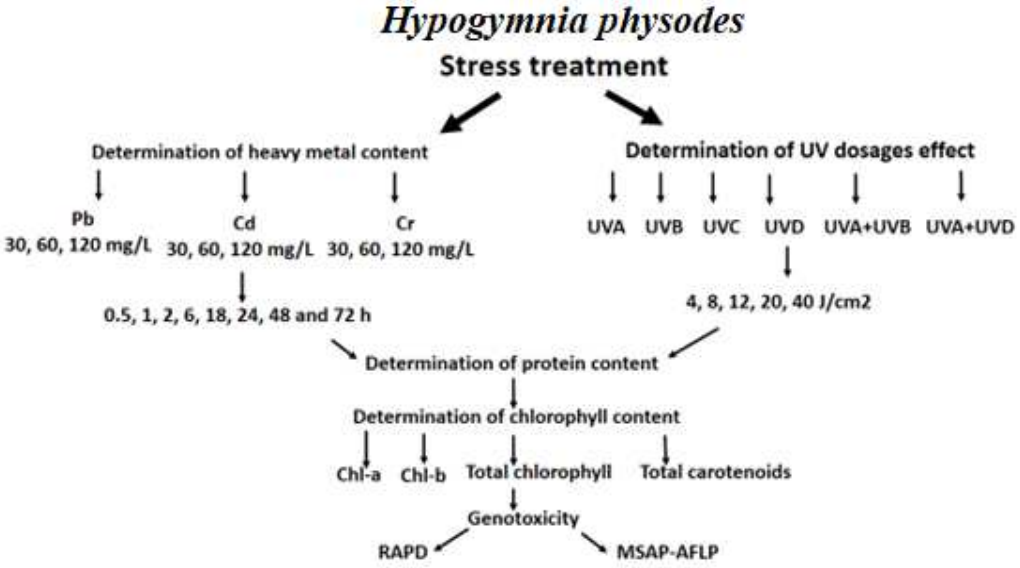

Figure 1. *A schematic representation of the treatments in Hypogymnia physodes lichen specimen. In this study evaluated three different metal stress treatments (Pb^{+2}, Cd^{+2} and Cr^{+6}) for eight different time periods (0.5, 1, 2, 6, 18, 24, 48 and 72 h) and in five different UV doses (4, 8, 12, 20, 40 J/cm^2 for UVA, UVB, UVC, daylight, UVA + UVB, UVA + daylight) in lichen sample. Also, the genotoxic effect of heavy metals and UV radiations was investigated for lichen specimen by RAPD and DNA methylation analysis*

Determination of total soluble protein content

Lichen specimen was homogenized (1:1, w/v) with 0.2 M phosphate buffer (pH 7.0). The obtained homogenate was centrifuged at 27.000 × *g* for 20 min. The supernatant was removed after centrifugation period. The total soluble protein content was determined according to the Bradford method (Bradford, 1976), using bovine serum albumin (BSA) standard. The experiments were repeated three times (n = 3).

http://www.aloki.hu ● ISSN 1589 1623 (Print) ● ISSN 1785 0037 (Online)
DOI: http://dx.doi.org/10.15666/aeer/1802_23152338

Determination of chlorophyll contents

Unexposed lichen sample was immersed in distilled water for 5 min to obtain photosynthetic activity. Lichen specimen was exposed to Cd^{+2}, Pb^{+2}, and Cr^{+6} heavy metal solution and different UV radiations, and the chlorophyll content were determined by taking samples from this sample exposed to stress at certain time intervals (*Fig. 1*). Contents of chlorophyll a, chlorophyll b, total chlorophyll, chlorophyll a/b, and total carotenoids were spectrophotometrically determined (Metzner et al., 1965). Briefly, a 40-60 mg lichen sample was kept within 3 ml of dimethylsulfoxide (DMSO) for 1 h at 65 °C in the dark. Lichen sample kept in the dark for 1 h was centrifuged at 12000 *g* for 10 min at 20 °C. The supernatant was transferred to a fresh tube, and then, spectrophotometric measurements were taken at wavelengths of 644 (chl-a), 663 (chl-b), 452 (total chl) and 470 nm (Chls) (Ronen and Galun, 1984; Wellburn, 1994). This process was performed triplicate (n = 3). Each analysis was replicated three times.

Genomic DNA extraction and RAPD assay

H. physodes was exposed to Pb^{+2}, Cd^{+2} and Cr^{+6} (30, 60 and 120 mg/L) heavy metal stress for different periods (0.5, 1, 2, 6, 18, 24, 48 and 72 h), UV radiations and DNA of the lichen sample was extracted (*Fig. 1*). DNA extraction was performed according to the protocol defined by Aras and Cansaran (2006). Concentration and purity of the DNA extracted are measured at OD 260 and with a 260 nm/280 nm absorbance ratio by nanodrop (NanoDrop ND-1000 Spectrophotometer, Thermo Scientific, Wilmington, USA), respectively.

Primer screening for RAPD analysis was performed using 10 primers. The six of the ten primers amplified clear and reproducible bands in heavy metal stress and UV stress, respectively. PCR components were determined as follows; 200 ng genomic DNA, 2.5 µL 10X reaction buffer, 3.0 mM $MgCl_2$, 20 mM dNTPs, 0.3 mM primer, and 0.5 unit of Taq polymerase (Promega, Madison, USA), and ddH_2O was added to the final volume of 25 µL. Negative controls were used in all PCR reactions. The PCR program operated with the following steps: 95 °C for 30 s for denaturation, 36 °C for 1 min at 35 cycles for annealing step, 72 °C for 2 min for extension and a final extension at 72 °C for 10 min. PCR products were loaded on 1.5% agarose gels and run at 80 V for 4 h.

MSAP-AFLP analysis

In the MSAP-AFLP analysis was used OPC10 primer which is one of the primers giving sharp bands during RAPD analysis. The genomic DNA (200 ng) of the two stress exposed samples were separately digested with *Eco*R I/*Msp* I and *Eco*R I/*Hpa* II restriction enzymes at 37 °C for 2.0 h. Subsequently, the digested aliquot was ligated to specific adopters for examined restriction enzymes because it was applied to avoid reconstruction of restriction sites one for *Eco*R I sticky ends and other for *Msp* I or *Hpa* II sticky ends, at 20 °C for 90 min. The ligated DNA was diluted with Tris-EDTA buffer, and then the diluted products were amplified using different combinations of *Eco*R I and *Msp* I or *Hpa* II primer each with three selective nucleotides at 5′ and 3′, respectively. MSAP-AFLP analyses were conducted following the method described by Mastan et al. (2012). Briefly, selective amplifications were performed at 65 °C temperature for the first cycle, the annealing temperature was successively reduced by 0.7 °C for the other 11 subsequent cycles. The remaining 23 from 45 cycles were run at 56 °C annealing temperature. After the formamide dye added PCR product, the

http://www.aloki.hu ● ISSN 1589 1623 (Print) ● ISSN 1785 0037 (Online)
DOI: http://dx.doi.org/10.15666/aeer/1802_23152338

electrophoresis assay was run. The gels were stained with silver nitrate and scanned (Bassam et al., 1991). To test the reproducibility of the AFLP-PCR, the experiments were repeated at least twice for each primer, faint bands were not involved in this study.

Statistical analysis

The results of heavy metal content, ratio of UV radiation and total soluble protein content of the lichen specimen were evaluated by multifactor analysis of variance (univariate ANOVA) or Student's t-test followed by posthoc Tukey test as appropriate (SPSS for Windows version 11.0) to display the effects of both stress sources on the exposed lichen.

Chlorophyll a, b, total chlorophyll and carotenoids were calculated by the following equations by Shakoor et al. (2014). The experiments were repeated three times (n = 3) and then evaluated with multifactor analysis of variance (ANOVA).

Estimation of profiling scoring and data analyses for RAPD assay

The RAPD analysis of the results was evaluated by considering the number of bands, which appear in the control (non-stressed) sample. Polymorphism calculated in RAPD profiles included the disappearance and appearance bands when compared with the non-stressed sample (Atienzar et al., 1999; Liu et al., 2005). Each polymorphic DNA band on the gel was treated as an individual locus and scored for their presence (1) or absence (0). Genomic template stability (GTS%) was calculated as followed by Atienzar et al. (1999). Changes in RAPD patterns were evaluated as decreases in GTS, compare with the number of RAPD profiles exposed to a different stress condition, and profiles obtained from the control samples.

Estimation of profiling scoring and data analyses for methylation analyses

MSAP data analysis was scored reproducible bands. All the amplified bands obtained from the MSAP-AFLP analysis were divided into four methylation types based on the presence or absence of groups as indicated by Li et al. (2009). According to this classification, the bands indicating each methylation type (I, II, III, and IV) were counted and placed in their location in *Table 1*.

The percentage of methylation was evaluated as the number of methylated bands × 100 by dividing the total number of bands. The percentage of methylation polymorphism was calculated using the formula (=number of polymorphic methylated bands×100/number of methylated bands).

Table 1. *Methylation types created by the cutting ability of HPAII and MspI restriction enzymes*

Methylation type	Methylation pattern	HpaII	MspI
Type I	CCGG CCGG GGCC GGCC	Active	Active
Type II	CCGG GGCC	Active	Inactive
Type III	CCGG GGCC	Inactive	Active
Type IV	CCGG GGCC	Inactive	Inactive

http://www.aloki.hu ● ISSN 1589 1623 (Print) ● ISSN 1785 0037 (Online)
DOI: http://dx.doi.org/10.15666/aeer/1802_23152338

Results

We analyzed *H. physodes* lichen specimen for three different metal stress treatments were applied (Pb^{+2}, Cd^{+2} and Cr^{+6}) in three different doses (30, 60 and 120 mg/L) for eight different periods (0.5, 1, 2, 6, 18, 24, 48 and 72 h). The same concerns exposure to UV radiations on lichen specimen examined six combinations of UV radiations (UVA, UVB, UVC, daylight, UVA + UVB, UVA + daylight) with five different doses of 4, 8, 12, 20 and 40 j/cm^2. Subsequently, in the analyzed sample, heavy metal, total soluble protein, chlorophyll a, chlorophyll b, total chlorophyll, and total carotenoids contents were measured (*Fig. 1*). The changes of DNA profile exposed to different heavy metals and UV radiations determined RAPD and DNA methylation analysis assays.

Determination of heavy metal contents in lichen specimen

The 30 mg/L Cd^{+2} metal absorption by *H. physodes* was very fast and optimum equilibrium was reached at 30 min ($P < 0.05$) (*Fig. 2; Table 2*). *H. physodes* was found to have an optimum absorption rate of 70.5% after 30 mg/L Pb^{+2} applications in 72 h ($P < 0.05$). It was noticed that 60 mg/L Cr^{+6} exposure significantly reduced (79.9%) heavy metal content in *H. physodes* (47.8 mg/L) in 72 h when compared to unexposed sample (59.8 mg/L) ($P < 0.05$). The highest absorption efficiency (94.2%) was obtained at 120 mg/L Cr^{+6} for 72 h in *H. physodes* lichen specimen ($P < 0.05$).

The highest absorption efficiency was achieved as about 92.2%, 95.1% and 95.5% using 30, 60 and 120 mg/L Cr^{+6} for 18 h, respectively. According to the results of 30, 60 and 120 mg/L Pb^{+2} application in lichen specimen, the absorption capacity percentage decreased from 43.4% to 34.5% as *H. physodes* was applied to 30 mg/L Pb^{+2} for 24 h. 60 mg/L Pb^{+2} heavy metal absorption decreased from 58.1% for 24 h in *H. physodes*. At 120 mg/L Pb^{+2}, the absorption efficiency was found to be low in *H. physodes* (59.2%) for 24 h ($P < 0.05$).

The optimum absorption capacity against 30, 60 and 120 mg/L Cd^{+2} heavy metal stress was found as 43.8% for 30 min, 63.3% for 12 h and 57.5% for 6 h in *H. physodes*, respectively ($P < 0.05$).

Table 2. *30 mg/L Cd^{+2} content of Hypogymnia physodes lichen specimen with ANOVA (Same letters in a column indicate the absence of significant differences at $P < 0.05$ by ANOVA)*

Samples	N	Mean	Std. deviation	Std. error	95% confidence interval for mean		Min	Max
					Lower bound	Upper bound		
Control	3	29.7000-	.10000	.05774	29.4516	29.9484	29.60	29.80
30 min	3	12.9000	.20000	.11547	12.4032	13.3968	12.70	13.10
1 h	3	11.6000	.10000	.05774	11.3516	11.8484	11.50	11.70
2 h	3	12.1000	.10000	.05774	11.8516	12.3484	12.00	12.20
6 h	3	11.8000	.30000	.17321	11.0548	12.5452	11.50	12.10
18 h	3	11.2000	.20000	.11547	10.7032	11.6968	11.00	11.40
24 h	3	10.9000	.20000	.11547	10.4032	11.3968	10.70	11.10
48 h	3	10.9000	.40000	.23094	9.9063	11.8937	10.50	11.30
72 h	3	10.9000	.30000	.17321	10.1548	11.6452	10.60	11.20
Total	27	13.5556	5.85526	1.12685	11.2393	15.8718	10.50	29.80
	Sum of	**df**	**Mean**	**F**	**Sig.**			

http://www.aloki.hu ● ISSN 1589 1623 (Print) ● ISSN 1785 0037 (Online)
DOI: http://dx.doi.org/10.15666/aeer/1802_23152338

	squares		square		
Between groups	890.407	8	111.301	2044.301	.000
Within groups	.980	18	.054		
Total	891.387	26			

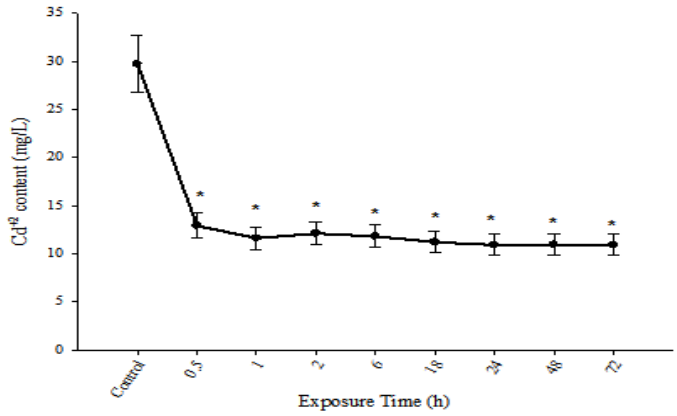

Figure 2. *The time-concentration curve of Cd^{+2} content of the stock solution that exposed to Hypogymnia physodes. (* = statistically different from control (P < 0.05) Cd^{+2} removal by H. physodes at initial Cd^{+2} concentration for 72 h*

Determination of protein content in lichen specimen

Effect of heavy metals on protein content

Protein content decreased with the increase in the concentration of heavy metals in *H. physodes* at the examined time range (30 min–72 h). Maximum protein content in *H. physodes* was increased for 30 mg/L Cr^{+6} and 30 mg/L Cd^{+2} until 30 min; however, there was a significant decrease in protein content afterward (from 60 min to 72 h) ($P < 0.05$). Protein content of lichen specimen was also significantly increased at both heavy metal stress levels (60 mg/L Cr^{+6} and Cd^{+2} heavy metals) for 30 min ($P < 0.05$). Protein content of *H. physodes* decreased all concentrations of Pb^{+2} stress when compared with the unexposed sample. The results of this study showed that the protein content of lichen specimen significantly decreased ($P < 0.05$) by 120 mg/L concentration of Cr^{+6} (*Table 3*) and Cd^{+2} at 1 h after treatment (0.023 mg/L, respectively). However, the protein content of *H. physodes* significantly decreased by 120 mg/L Pb^{+2} exposure for 1 h when compared with the unexposed lichen sample (20.73 and 19.23, 19.9 and 18.32 mg/L, respectively) ($P < 0.05$). Protein content significantly decreased after from 2 to 72 h exposure to 120 mg/L Pb^{+2}.

Effect of UV radiations on protein content

The protein content of *H. physodes* significantly decreased at 40 j/cm^2 among the other four UV radiations. Exposure to 40 j/cm^2 UVA + UVB radiations, protein content significantly decreased by 28% in *H. physodes* ($P < 0.05$), similarly after the 4, 8, 12 and 20 j/cm^2 UV radiations exposure decreased protein content of *H. physodes*. The lowest UVB radiation (4 j/cm^2) exposure was recorded as 0.0470 mg/L protein content and the highest UV radiations exposure (40 j/cm^2) was measured as 0.0157 mg/L protein content in *H. physodes* when compared to unexposed sample (0.0505 mg/L) ($P < 0.05$).

http://www.aloki.hu ● ISSN 1589 1623 (Print) ● ISSN 1785 0037 (Online)
DOI: http://dx.doi.org/10.15666/aeer/1802_23152338

Determination of chlorophyll content

Effect of heavy metals on chlorophyll-a content

The results of the study showed that the chl-a content was significantly decreased by 30, 60 and 120 mg/L concentration of Cr^{+6}, Pb^{+2} and Cd^{+2} after 2 h exposure (15.42 and 14.46, 14.55 and 11.49 mg g^{-1}, respectively) ($P < 0.05$). 120 mg/L Cr^{+6} exposure for 2 h significantly decreased the chl-a content of *H. physodes* by 18% (0.404 mg g^{-1}) ($P < 0.05$).

Table 3. *Protein content of exposing to 120 mg/L Cr^{+6} of Hypogymnia physodes lichen specimen with ANOVA (Same letters in a column indicate the absence of significant differences at $P < 0.05$ by ANOVA)*

Samples	N	Mean	Std. deviation	Std. error	95% confidence interval for mean		Min	Max
					Lower bound	Upper bound		
Control	3	.0176289	.00003006	.00001736	.0175542	.0177035	.01760	.01766
30 min	3	.017689	.00002009	.00001160	.0178190	.0179188	.01785	.01789
1 h	3	.0231703	.00002001	.00001155	.0231206	.0232200	.02315	.02319
2 h	3	.0145604	.00006000	.00003464	.0144114	.0147095	.01450	.01462
6 h	3	.0101416	.00004010	.00002315	.0100420	.0102413	.01010	.01018
18 h	3	.0132290	.00003005	.00001735	.0131543	.0133036	.01320	.01326
24 h	3	.0116093	.00001008	.00000582	.0115842	.0116343	.01160	.01162
48 h	3	.0097306	.00003002	.00001733	.0096560	.0098051	.00970	.00976
72 h	3	.0124985	.00007005	.00004044	.0123245	.0126725	.01243	.01257
Total	27	.0144930	.00418853	.00080608	.0128361	.0161500	.00970	.02319

	Sum of squares	df	Mean square	F	Sig.
Between groups	.000	8	.000	37374.901	.000
Within groups	.000	18	.000		
Total	.000	26			

Effect of UV radiations on chlorophyll-a content

In UV radiations exposure, chl-a content of the unexposed sample of *H. physodes* was determined as 2.300 mg g^{-1}. In terms of the applied stress level among all UV radiations types (UVA, UVB, UVC, daylight, UVA + daylight, UVA + UVB), the highest increase was observed at 40 j/cm^2 ($p<0.05$). After the implementation of 40 j/cm^2 UVA + UVB radiations level, the highest chl-a content increase (10.760 mg g^{-1}) was observed about 5 fold when compared to the unexposed sample (2.300 mg g^{-1}) ($p<0.05$). In contrast, exposure to UVA radiation alone at a dose of 40 j/cm^2 increased the amount of the lowest chl-a (2.742 mg g^{-1}) ($p<0.05$).

http://www.aloki.hu ● ISSN 1589 1623 (Print) ● ISSN 1785 0037 (Online)
DOI: http://dx.doi.org/10.15666/aeer/1802_23152338

Effect of heavy metals on chlorophyll-b content

This study was determined the changes in chlorophyll-b content after exposure to heavy metals and UV radiations compared to the unexposed sample. The results of the study showed that chl-b content of *H. physodes* unexposed sample (1.518 mg g^{-1}) significantly decreased with 30, 60 and 120 mg/L concentration of Cr^{+6}, Pb^{+2} and Cd^{+2} after 48 h treatment ($P < 0.05$). After 30, 60 and 120 mg/L Pb^{+2} treatments, the highest decrease rate at all concentrations when compared to the unexposed specimen was determined as 0.013, 0.209 and 0.057 mg g^{-1}, respectively ($p<0.05$).

Effect of UV radiations on chlorophyll-b content

H. physodes lichen specimen was observed 1.629, 2.873, 2.659, 2.229, 2.033 and 2.853 mg g^{-1} chl-b content exposed to 8 j/cm^2 UVA, UVB, UVC, daylight, UVA + UVB, UVA + day light when compared to the unexposed sample (1.518 mg g^{-1}), respectively.

Effect of heavy metals on total chlorophyll content

Total chlorophyll content in the unexposed sample in *H. physodes* was observed as 3.818 mg g^{-1}. The optimum result of total chlorophyll content in *H. physodes* was obtained at three heavy metal exposures (Cr^{+6}, Pb^{+2}, and Cd^{+2}) and concentrations (30, 60 and 120 mg/L) after a 60 min treatment. The highest decrease rates of Cr^{+6} heavy metal among all concentrations were observed as 0.857, 1.130 and 0.583 mg g^{-1} in *H. physodes* lichen specimen, respectively ($P < 0.05$).

Effect of UV radiations on total chlorophyll content

Total chlorophyll content of *H. physodes* was observed as 4.341 and 5.394 mg g^{-1} expose to 8 j/cm^2 UVA + day light radiations. The highest content of total chlorophyll was determined as 14.923, 12.989, 12.159 and 16.010 mg g^{-1} after exposure to 20 j/cm^2 UVB, UVC, UVA + daylight, and UVA + UVB radiations, respectively ($p<0.05$). Especially, after the 20 j/cm^2 UVA + UVB radiations treatment, the maximum decrease of total chlorophyll content (16.010 mg g^{-1}) was observed in *H. physodes*, when compared to the unexposed sample (3.818 mg g^{-1}) ($P < 0.05$).

Effect of heavy metals on the ratio of chlorophyll a/b

Variations in the ratio of chlorophyll a/b were caused by increasing lichen metal content. The ratio of chlorophyll a/b in *H. physodes* exposed to 30, 60 and 120 ppm Cr^{+6} heavy metal stress showed a significant decrease after 30 min of all three heavy metal treatments ($p<0.05$). Exposed to 30 ppm Cd^{+2} and Pb^{+2} heavy metal stress in *H. physodes* lichen specimen, the treatments showed a marked increase in the ratio of chlorophyll a/b (86.02 mg g^{-1}) as a result of 18 and 24 h, respectively ($p<0.05$). After treatments, the ratio is gradually decreasing towards the lowest level.

Effect of UV radiations on the ratio of chlorophyll a/b

An increase in the ratio of chlorophyll a/b was observed after 4 j/cm^2 treatment in *H. physodes* lichen specimen exposed to UVB radiation.

http://www.aloki.hu ● ISSN 1589 1623 (Print) ● ISSN 1785 0037 (Online)
DOI: http://dx.doi.org/10.15666/aeer/1802_23152338

Determination of total carotenoid content

Effect of heavy metals on total carotenoid content

The content of total carotenoid in the control sample of *H. physodes* was observed as 0.092 mg g^{-1}. The optimum time of after all heavy metal exposure was determined at 18 h. All examined heavy metal concentrations (30, 60 and 120 mg/L) significantly decreased total carotenoid contents in *H. physodes* when compared to unexposed sample ($P < 0.05$). The maximum change in total carotenoid content was observed as 0.056 mg g^{-1} after 18 h 120 mg/L Cd^{+2} treatment in *H. physodes* ($P < 0.05$).

Effect of UV radiations on total carotenoid content

Total carotenoid content of lichen specimen was founded a decrease expose to all UV radiations when compared to the control sample. The maximum change in total carotenoid contents was determined after 12 j/cm^2 expose to UV radiations ($P < 0.05$). The highest decrease after 12 j/cm^2 treatment was observed after UVA + UVB radiations exposure (0.070 mg g^{-1}) in *H. physodes* ($P < 0.05$).

Determination of heavy metals and UV radiations on RAPD profiles in Hypogymnia physodes

A representative example of the results obtained by RAPD analysis is shown in *Figure 3*. The concentrations measured for the DNA samples were approximately in the range of 1285–2012 ng/µl for all heavy metals and 964–2077 ng/µl for all UV radiations exposures at 260 nm/280 nm ratios between 1.64–1.97 and 1.54–1.99, respectively.

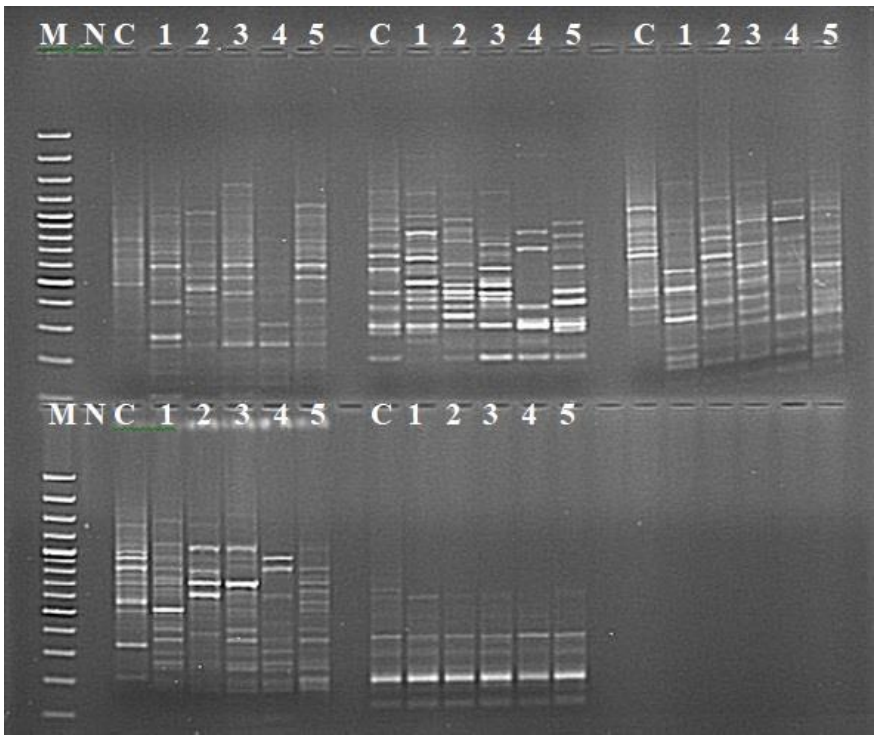

Figure 3. *The results of RAPD-PCR treating at UVB radiation in Hypogymnia physodes (top-left OPC02, top-center OPC04; top-right TubeA05, lower-left OPC07, lower-center OPC10*

http://www.aloki.hu ● ISSN 1589 1623 (Print) ● ISSN 1785 0037 (Online)
DOI: http://dx.doi.org/10.15666/aeer/1802_23152338

primers). (M: Marker; N: Negative control; C: Control sample (non-stressed sample); 1: 4 j/cm^2; 2: 8 j/cm^2; 3: 12 j/cm^2; 4: 20 j/cm^2; 5: 40 j/cm^2)

In RAPD analyses, some of the primers displayed significant differences in band patterns formed by loss of normal bands and appearance of new bands in the treated heavy metals and UV radiation exposure in comparison to the untreated sample profiles. The highest number of appearance and disappearance of new bands was observed at 30 mg/L Cd^{+2} concentrations with ten primers. Most of the new band appearances/disappearances were shown in Cd^{+2} contaminations (33 bands) observed in 30 mg/L Cd^{+2} contaminations. The lowest band appearances/disappearances were determined in Cd^{+2} (8 bands) and Pb^{+2} (8 bands) exposure to 30 min. The highest band appearances/disappearances in different UV radiation exposures were shown at 40 j/cm^2 exposure (42 bands).

As an analysis of the samples applied Cd^{+2} heavy metal in *H. physodes*, the highest genomic template stability (GTS%) value occurred after exposure to Cd^{+2} heavy metal stress at 72 h in all concentrations (30, 60 and 120 mg/L). 30, 60 and 120 mg/L Cd^{+2} treatment resulted in the highest GTS value of 91.1%, 85.5% and 86.6%, respectively. The lowest GTS value occurred after exposure to Cd^{+2} at 2 h in all concentrations. The lowest GTS value (63.3%, 64.4% and 70.0%) was obtained in the 30, 60 and 120 mg/L Cd^{+2} heavy metal treatment, respectively. According to this, the highest and lowest band variations were observed at 30, 60 and 120 mg/L Cd^{+2} concentrations at 2 h and 72 h, respectively. In terms of Cr^{+6} stress in *H. physodes* lichen specimen, the highest and the lowest GTS values were detected at 48 h of 30 mg/L (88.5%) and 72 h of 60 mg/L (90.6%) and 72 h of 120 mg/L (90.6%), respectively. The lowest GTS value was obtained at 30 min and 18 h in the 30 mg/L Cr^{+6} (69.7%), 2 h in the 60 mg/L Cr^{+6} (70.8%) and 1 h in 120 mg/L Cr^{+6} (78.1%). In terms of Pb^{+2} stresses in *H. physodes*, the highest GTS value was observed after exposure to Pb^{+2} at 72 h in all concentrations. 30, 60 and 120 mg/L Pb^{+2} treatments resulted in the highest GTS values of 93.0%, 93.0% and 91.3%, respectively. The lowest GTS values were obtained at 30 min, 2 h and 6 h in 30 mg/L (82.6%), 30 min at 60 mg/L (78.2%) and 30 min at 120 mg/L (80.8%) Pb^{+2} treatments.

In terms of UVA radiation stress in *H. physodes* lichen specimen, the highest GTS value (87.8%) was observed after exposure to 4 j/cm^2 UVA radiation. The lowest GTS value (76.5%) was obtained at 40 j/cm^2 UVA radiation. As regards UVA and daylight stress in *H. physodes*, the highest GTS value (88.6%) was observed after exposure to 4 j/cm^2 UVA and daylight radiations. The lowest GTS value (80.86%) was obtained at 12 j/cm^2 UVA and daylight radiations. Despite UVC stress in *H. physodes*, the highest GTS value (92.1%) was observed exposed to 4 j/cm^2 UVC radiation and the lowest GTS value (76.5%) was determined at 40 j/cm^2 UVC radiation. In terms of daylight stress in *H. physodes*, the highest GTS value (89.67%) was realized exposed to 8 j/cm^2 daylight radiation but the lowest GTS value (84.78%) was obtained at 40 j/cm^2 daylight radiation.

When all UV radiations and UVB exposure were compared, maximum changes of UV exposure were determined in UVB radiation in *H. physodes*. The significant changes were determined, such as appearances of some new bands or the disappearance of bands when compared to the control. A maximum of 28 bands disappeared among the exposed *H. physodes* with 40 j/cm^2, while in 20 j/cm^2, a maximum of 13 new bands appeared in *H. physodes* exposed to UVB radiation (*Table 4*). Also, the results showing the most variation among the different heavy metal (Cd^{+2}, Cr^{+6}, Pb^{+2}) and time arrival

http://www.aloki.hu ● ISSN 1589 1623 (Print) ● ISSN 1785 0037 (Online)
DOI: http://dx.doi.org/10.15666/aeer/1802_23152338

(0.5, 1, 2, 6, 18, 24, 48 and 72 h) combinations applied to the *H. physodes* lichen species are given in *Table 5*. *H. physodes* lichen specimen for three different UV treatments were applied (UVA, UVB, UVC, UVD, UVA + UVB, UVA + UVD) in five different doses (4, 8, 12, 20 and 40 j/cm^2). The results showing the most variation among the UV radiations and doses combinations applied to the *H. physodes* lichen species are given in *Table 6*. The highest GTS value (88.4%) was observed exposed to 4 j/cm^2 UVB radiation (*Table 7*). The lowest GTS value (73.18%) was obtained at 40 j/cm^2 UVB radiation (*Table 7*). Regarding UVA and UVB stress in *H. physodes*, the highest GTS value (84.3%) was observed exposed to 4 j/cm^2 UVA and UVB radiations. The lowest GTS value (63.4%) was obtained at 40 j/cm^2 UVA and UVB radiations.

Table 4. *Varying band-number using OPC01, OPC02, OPC04, OPC07, OPC10 and TubeA05 primers as a result of UVB radiation samples in Hypogymnia physodes*

Primers	**C**	**4 j UVB**		**8 j UVB**		**12 j UVB**		**20 j UVB**		**40 j UVB**	
		a	**b**	**a**	**b**	**a**	**b**	**a**	**b**	**a**	**b**
OPC 01	23	1	3	1	1	0	3	2	4	2	4
OPC 02	23	2	0	3	2	4	2	3	3	1	3
OPC 04	23	0	0	0	2	0	3	4	3	3	7
OPC 07	23	1	4	2	3	1	3	1	7	0	4
OPC 10	23	2	0	1	2	2	2	1	2	2	6
Tube A05	23	0	3	0	1	2	4	2	0	1	4
138		6	10	7	11	9	17	13	19	9	28
a + b		16		18		26		32		37	

a + b = The total number of band alternations, C = control sample = non-stressed sample

Table 5. *H. physodes lichen specimen for three different metal stress treatments were applied (Pb^{+2}, Cd^{+2}, and Cr^{+6}) in three different doses (30, 60 and 120 mg/L) for eight different periods (0.5, 1, 2, 6, 18, 24, 48 and 72 h). The results showing the most variation among the different heavy metal (Cd^{+2}, Cr^{+6}, Pb^{+2}) and time arrival (0.5, 1, 2, 6, 18, 24, 48 and 72 h) combinations applied to the H. physodes lichen species are given*

Primers	**30 ppm Cd^{+2}**		**60 ppm Cd^{+2}**		**120 ppm Cd^{+2}**		**30 ppm Cr^{+6}**		**60 ppm Cr^{+6}**		**120 ppm Cr^{+6}**		**30 ppm Pb^{+2}**		**60 ppm Pb^{+2}**		**120 ppm Pb^{+2}**		**T**
	TB	**a+b (2 h)**	**TB**	**a+b (2 h)**	**TB**	**a+b (2 h)**	**TB**	**a+b (6 h)**	**TB**	**a+b (2 h)**	**TB**	**a+b (1 h)**	**TB**	**a+b (30 min)**	**TB**	**a+b (30 min)**	**TB**	**a+b (30 min)**	
OPC 01 OPC 02 OPC 04 OPC 07 OPC 10 TubeA05	90	33	90	32	90	27	96	30	96	28	96	21	115	20	115	25	115	22	RAPD
Methylation types (MT)	**TB**	**a+b MTII**	**TB**	**a+b MTII**	**TB**	**a+b MTI**	**TB**	**a+b**	**TB**	**a+b MTII**	**TB**	**a+b**	**TB**	**a+b**	**TB**	**a+b MTII**	**TB**	**a+b**	
Type I Type II Type III Type IV	413	213	413	314	413	351	357	81	357	87	357	98	456	127	456	149	456	181	MSAP-AFLP

a + b = The total number of band alternations, TB = Total band (non-stressed sample = control sample), T = Technic, MT = Methylation types

http://www.aloki.hu ● ISSN 1589 1623 (Print) ● ISSN 1785 0037 (Online)
DOI: http://dx.doi.org/10.15666/aeer/1802_23152338

Methylation DNA and polymorphism in examined lichen specimen to different levels of stress condition

Band alterations in heavy metals and UV radiations exposure were compared with respect to the untreated control samples. 413 to 691 bands were produced in the untreated sample, and 217 bands with an average of 11 per primer were obtained in the MSAP-AFLP analysis. The total number of band alterations (a + b) was 117 bands for the Cd^{+2} heavy metal and lichen specimen stressed with UVB (*Fig. 4*).

Table 6. *H. physodes lichen specimen for three different UV treatments were applied (UVA, UVB, UVC, UVD, UVA + UVB, UVA + UVD) in five different doses (4, 8, 12, 20 and 40 j/cm^2). The results showing the most variation among the UV radiation and dose combinations applied to the H. physodes lichen species are given*

Primers	UVA		UVB		UVC		UVD		UVA+UVB		UVA+UVD		T
	TB	a+b (40 J)	TB	a+b (40 J)	TB	a+b (40 J)	TB	a+b (40 J)	TB	a+b (40 J)	TB	a+b (12 J)	
OPC 01 OPC 02 OPC 04 OPC 07 OPC 10 Tube A05	115	27	138	37	115	27	115	28	115	42	115	22	RAPD
Methylation types	**TB**	**a+b MTII**	**TB**	**a+b MTII**	**TB**	**a+b MTI**	**TB**	**a+b**	**TB**	**a+b MTII**	**TB**	**a+b**	
Type I Type II Type III Type IV	691	117	691	451	691	141	691	92	691	381	691	204	MSAP-AFLP

a + b = The total number of band alternations, TB = Total band (non-stressed sample = control sample), T = Technic, MT = Methylation types

Table 7. *The rates of GTS values using UVB radiation in Hypogymnia physodes lichen specimen*

Samples-UVB	Rates of GTS (%)
4 j/cm^2	88.40
8 j/cm^2	86.95
12 j/cm^2	81.15
20 j/cm^2	76.81
40 j/cm^2	73.18

The highest rate of methylation was obtained with Type-2 primer (28.9%) and Type-3 (59.3%) primers in the Cd^{+2} heavy metal (*Table 5*) and *H. physodes* lichen specimen stressed with UVB radiation (*Table 6*). The highest rate of changes was observed in the *H. physodes* exposed to heavy metal stress for 6 h and UVB radiation stress for 12 and

http://www.aloki.hu ● ISSN 1589 1623 (Print) ● ISSN 1785 0037 (Online)
DOI: http://dx.doi.org/10.15666/aeer/1802_23152338

24 h. When the results of the MSAP - AFLP analysis were evaluated based on the methylation types in the heavy metal stressed samples, the maximum level of methylation (33.3%) was observed in Type II, and the lowest level of methylation (63.3%) was seen in Type III. Type II methylation was not observed for the first 6 h and then, occurred at a rate of 34.3% at 12 h and 24 h. The rate of Type II methylation (34.3%) remained the same until the end of 12 h and completely disappeared at 24 h in Cr^{+6} heavy metal exposure in *H. physodes*.

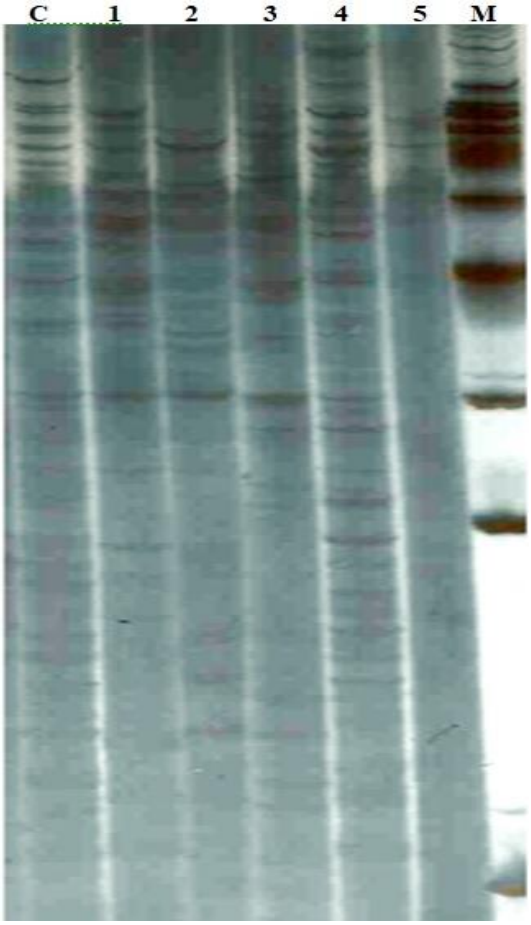

Figure 4. *AFLP profiles generated by Type II metilation from Hypogymnia physodes exposed to UVB radiation. (C: Control sample (non-stressed sample); 1: 4 j/cm^2; 2: 8 j/cm^2; 3: 12 j/cm^2; 4: 20 j/cm^2; 5: 40 j/cm^2; M: Marker)*

Discussion

In our study were applied increasing Cr^{+6}, Pb^{+2} and Cd^{+2} heavy metal concentrations and UV radiations in different doses in *H. physodes* lichen specimen. Heavy metal accumulation capacities, total protein content and chlorophyll parameters constituted against stress were determined in lichen specimen. In addition, the genotoxic effect generated by heavy metals and UV radiations was investigated with RAPD and MSAP - AFLP techniques at a molecular level (*Fig. 1*). This is the first evaluation of the changes in DNA methylation and polymorphism in methylated DNA in lichen specimen under heavy metals and UV radiations stress.

Gill et al. (2015) have shown that the toxic effects of Cr^{+6} heavy metal are observed in four different cultivars of *Brassica napus* L. The study determined plant growth and

http://www.aloki.hu ● ISSN 1589 1623 (Print) ● ISSN 1785 0037 (Online)
DOI: http://dx.doi.org/10.15666/aeer/1802_23152338

biomass ratio changed to exposure to Cr^{+6} concentrations. After Cr^{+6} application, the effect of Malondialdehyde (MDA) and Reactive oxygen species (ROS) increased, which could be an indication of cell damage in the plant. According to the results of our study also found that *H. physodes* lichen specimen was more accumulate in Cd^{+2} and Cr^{+6} heavy metals when compared to Pb^{+2} ($P < 0.05$). In our study, the damage caused by heavy metal application to lichen specimen may be due to the effects of ROS and MDA.

In another study, Fernandez et al. (1992) have indicated that fly ash, tending to be close to the source, is normally associated with the coarse fraction. This study has reported more storage Cr capacity of the samples collected around 5 km from the iron-steel factory. They have also stated that particularly *H. physodes* and *Evernia prunastri* have similar Cr accumulation ratio. Aslan et al. (2006) have reported that *H. physodes* shows high levels of Ca, Ti, Fe and Ba heavy metal accumulation collected from Ordu, province of Turkey. In our study results revealed that *H. physodes* lichen specimen showed to accumulate all heavy metals at a significant level ($P < 0.05$). Koroleva and Revunkov (2017) investigated to create a database of trace elements concentrations in the sample of the epiphytic lichen *Hypogymnia physodes* and to identify the spatial patterns of iron, manganese, nickel, cadmium, silver, lead, strontium, rubidium, and calcium in the Kaliningrad region. They stated that the lichen specimen accumulates microelements more intensively in the west of the Kaliningrad region than in its continental part, which is also due not only to a higher level of urbanization of the territory but also to the region's climatic features. Zulaini et al. (2019) investigated the accumulation of heavy metals on two types of epiphytic lichens, *Parmotrema tinctorum* and *Usnea diffracta*. They stated that *P. tinctorum* can be positively compared to *U. diffracta* for identifying the levels of heavy metals, due to the higher capability to accumulate heavy metals without affecting the internal structure. These lichen species positively responded to the heavy metal accumulation levels. Branquinho et al. (1997) have shown that they were able to determine and quantify the cellular location of Cu in lichens. They have been expected to regulate the extracellular uptake, time or concentration from conventional kinetic studies with other organisms and heavy metals. *Usnea* sp. were most sensitive to Cu uptake compare with other lichen species, since physiological changes occurred for lower supplied Cu concentrations than *R. fastigiata*. It seems that lichen specimen can accumulate much more metal elements than it needs and that accumulation is capable of high tolerance in our study. Thanks to these properties, lichens are defined as the best monitor-indicator organisms that can be used to display atmospheric heavy metal pollution (Abas et al., 2019; Benitez et al., 2019; Ramic et al., 2019). Li et al. (2009) have demonstrated comparative effects of Cd^{+2} and Pb^{+2} on biochemical response and DNA damage in the earthworm *Eisenia fetida* (Annelida, Oligochaeta). The evaluation of DNA damage in earthworms used the comet assay. As a result, it was the aim of the study to determine more detailed information on the effects of heavy metals on earthworms' organisms. When the results of our study and that of Liu et al.'s are compared, both studies clearly show that both of the examined biological organisms were affected by all heavy metal treatments. This study determined that selecting lichen specimen was important for accumulating heavy metals. As a result of this study, *H. physodes* lichen specimen could serve as biomarkers for environmental pollution. It can be used to a novel organism as an environmentally friendly and cost-effective technology for remediation of polluted sites.

http://www.aloki.hu ● ISSN 1589 1623 (Print) ● ISSN 1785 0037 (Online)
DOI: http://dx.doi.org/10.15666/aeer/1802_23152338

Doğan and Saygıdeğer (2009) have investigated some morphological and physiological changes in *Ceratophyllum demersum* L. at different concentrations of Cd^{+2} (0, 0.01, 0.1 and 1 ml/L) effect in 96 h. They have stated that total soluble sugar and protein content are reduced by the application of Cd^{+2}. Although the amount of protein showed a decrease when compared to the controls, there was no significant correlation between protein content and heavy metals. The reason for the decrease in protein content in plants is often caused by the inhibition of protein synthesis or proteolysis triggered by ROS produced by oxidative stress. Duman et al. (2010) have investigated the biological response against Cr^{+6} heavy metal in *Ceratophyllum demersum* L. Cr accumulation, plant growth, lipid peroxidation, ion escape, photosynthetic pigmentation, protein and proline content have been investigated depending on concentration changes. They have stated a statistically significant difference between 1 mM Cr^{+6} treatment and 5-10 mM Cr^{+6} treatments. In our study, the decrease in total protein in lichen specimen was observed when compared with 60 and 120 mg/L Pb^{+2}, Cr^{+6} and Cd^{+2} heavy metals ($p<0.05$). Particularly, Cd^{+2} and Cr^{+6} heavy metals constitute a high level of damage to protein content when compared with other examined parameters in *H. physodes* ($p<0.05$). In brief, the amount of protein in lichen specimen decreased at a statistically significant level after all heavy metals application ($P < 0.05$). Our study results revealed that the respond of heavy metal stress was similar to the protein content of other study results. We evaluated the change in the protein content of *H. physodes* lichen sample exposure to UV stress. Our study results also demonstrated that total protein content in *H. physodes* lichen specimen applied with UV radiations showed an opposite relation with all samples. Reduction in total protein content was observed depending on the application dose of UVA, UVB, UVC, daylight, UVA + daylight, and UVA + UVB radiations when compared to the unexposed sample. A decrease in protein content of lichen specimen was determined up to 12 j UV dose, but further UV doses were not detected changes of protein content in lichen specimen. For this reason, lichen specimen may have a certain level of tolerance. It is very important to evaluate the protein relationship with the response given to stress conditions. Protein molecules play a significant role in the determination of mainly heavy metal stress and UV radiations exposure. If further protein-related works like proteome studies it may be used in a biomarker for environmental pollution.

A study conducted has shown the physiological change generated at a cellular extent as a result of the exposure of *Cladonia arbuscular* and *Peltigera rufescens* lichen species to mercury (Hg) (Pisani et al., 2011). The results of this study have put forward that photosynthetic pigments are sensitive to $HgCl_2$ in both species. Chl-a, -b, and carotenoids content significantly decreased in *C. arbuscula* subsp. *mitis* but only Chl-a and carotenoids significantly decreased in *P. rufescens* (Pisani et al., 2011). Chettri et al. (1998) were hypothesized that Cu was responsible for the reduced chlorophyll content of lichens growing in mining areas in which Cu, Zn, and Pb were present in the soil. Therefore, they were examined the effect of Cu, Zn, and Pb, individually and in combination, on the respective thallus metal content of the lichens *C. convoluta* and *C. rangiformis*, and the subsequent effect on chlorophyll content. They found that increasing lichen Cu content [up to 1600 μg g^{-1} dry weight (DW)] had no effect on the total chlorophyll content of *C. rangiformis*, whereas Cu concentrations exceeding 175 μg g^{-1} DW caused a decrease in total chlorophyll content in *C. convoluta*, which was 40% at 1560 μg Cu g^{-1} DW. As a result, the Cu effects on chlorophyll were reduced in the presence of Pb and Zn in both lichens, but to a lesser extent in *C. rangiformis*.

http://www.aloki.hu ● ISSN 1589 1623 (Print) ● ISSN 1785 0037 (Online)
DOI: http://dx.doi.org/10.15666/aeer/1802_23152338

Metal cations appeared to be ionically bound within the cell wall in an exchangeable form with binding affinities of Pb > Cu > Zn. Similarly, Karakoti et al. (2014) found that Pb, Cu, Fe, and Cr have little effect on chlorophyll degradation in lichen *Pyxine cocoes*. Monnet et al. (2001) have observed an increase of chl-a content after applied with 10 mg/L heavy metal stress for 8 days, but then the content of chl-a decreased in ryegrass (*Lolium perenne*). Casano et al. (2015) reported that the proportion of cell walls is important for the capacity to immobilize extracellular Pb^{+2} from the photobiont layer. Therefore, the external cell wall could help to decrease the deleterious effects of Pb on chlorophyll content in a short time (24 h) exposure. Gurbanov and Unal (2018) revealed that Pb^{+2} exposure diminished the total nucleic acid quantity, which could be an important parameter for the elucidation of heavy metal tolerance mechanisms in lichens. Similarly, we observed that the contents of chl-a, chl-b and total chl in *H. physodes* were highest decreased after applied with 30 mg/L Cr^{+6}, Pb^{+2} and Cd^{+2} heavy metal concentration ($P < 0.05$). The contents of the same parameters in *H. physodes* were also significantly decreased after applied with all other 60 and 120 mg/L Pb^{+2} and Cd^{+2} concentrations ($P < 0.05$). Spectrophotometric measures were conducted to determine the carotenoid amount in *H. physodes* applied different heavy metal concentrations and UV radiations. There was a significant decrease in carotenoid amounts after exposed to 8 j/cm^2 all UV radiations in *H. physodes* ($P < 0.05$). In this study, we found that the application of heavy metals and UV exposure prevents loss of chlorophyll and carotenoid. UVA and UVB radiations together have more harmful effects, although *H. pyhsodes* may have shown quite a tolerance. Similarly, *H. pyhsodes* have been deposited at higher rate heavy metals.

Chettri et al. (1998) have indicated that the ratio of chlorophyll a/b is more sensitive to changes in the content of the lichen. They determined a marked decrease in the ratio of chlorophyll a/b, from 3.0 to 0.4 for *C. convoluta* and from 3.2 to 0.8 for *C. rangiformis*, occurred when the thallus Cu content exceeded 175 and 200 mg g^{-1} DW, respectively. Similarly, we found that there is a significant decrease with increasing treatments the ratio of chlorophyll a/b content in *H. physodes*. Larsson et al (2009) reported that the ratio of chlorophyll a/b ratio increased with increasing UVB radiation in *Xantoria aureola* lichen species at 21 °C degrees. We also found that after 4 j/cm^2 treatments, the ratio of chlorophyll a/b increase with increasing UVB radiation.

Heavy metal and UV stress toxicity have been extensively described in physiological, cellular and molecular biological aspects in the literature. The development of several PCR based techniques provides many advantages in the analysis of genetic toxicology. PCR based technique is simple, fast and capable of detecting point mutations and also a temporary alteration of DNA. Many studies have displayed that molecular technique may potentially form to detect DNA damage and mutational events in cells of different organisms. Genotoxic pollutants in the environment continue to grow rapidly, thereby stressing the need for rapid monitoring of genotoxicity in lichen species. Lichens can be used for this purpose due to the best biomonitor organism. The RAPD band profile generated after exposure to Cr^{+6}, Cd^{+2} and Pb^{+2} heavy metals in the lichen specimen was determined with the RAPD profile of the controls, differences of band number were detected. Cansaran-Duman et al. (2011) have determined the genotoxic contamination in the *Evernia prunastri* lichen species with the RAPD analyses. Körpe-Aksoy and Aras (2010) have studied eggplant seeds in a controlled setting applied to Cu^{+2} metal stress in different concentrations. The results showed that the changes in the GTS rates of the seeds that developed in different Cu^{+2}

http://www.aloki.hu ● ISSN 1589 1623 (Print) ● ISSN 1785 0037 (Online)
DOI: http://dx.doi.org/10.15666/aeer/1802_23152338

concentrations could be determined by generating RAPD profiles. This study significantly determined the maximum change of band intensities. The highest number of bands that appeared and disappeared was observed in the *H. physodes* lichen sample for UVB exposure. Especially, different changes in GTS rates (%) were shown in lichen specimen. Monitoring of various environmental stresses induced genotoxic effect directly on genomic DNA by RAPD analysis is mainly associated with unexposed sample and lichen treated with different stresses conditions. The changes in physiological and biochemical parameters such as shoot–root length, photosynthetic pigment contents, and antioxidative enzyme level support genomic template stability (Atienzar et al., 1999).

DNA methylation has been shown as a significant indicator of epigenetic and mutagenic effects and it causes differential gene expression, cell differentiation, chromatin inactivation and carcinogenesis in eukaryotic organisms (Xu et al., 2000; Mastan et al., 2012). The epigenetic organization of plant development can be used in production as much as an adaptation to stress since gene expression can be affected by the structure of the chromatin related to the epigenetic organization (Mirouze and Paszkowski, 2011). The level of the presence of methylcytosine can be determined with multiple approaches in many terms since there is a very appropriate technique to determine the methylation rate in the genome (Rein et al., 1997). MSAP-AFLP is a very potent technique to study the genome methylation status. The use of MSAP-AFLP assay has been useful in the detection of the tolerance level toward different environmental stresses. Therefore, biochemical and physiological assays are not enough to obtain deeper insight into the lichen stress response to biotic or abiotic stresses. In the present study, assessment of changes in DNA methylation by MSAP-AFLP in lichen specimen subjected to heavy metals and UV exposures. *H. physodes* thallus 69% methylation was determined in heavy metal stress. Similarly, 58% polymorphism was showed in methylated DNA from *H. physodes* on both stresses. According to the MSAP analysis, compared control with all stress treated; lichen specimen showed different patterns of methylation under heavy metals and UV radiations stress. In comparison to salt-untreated plants, Lu et al. (2007) have detected an increase of total methylated bands in plants exposed to 50-200 mM salt. In our study, as a result of the MSAP - AFLP analyses conducted in lichen specimen exposed to different heavy metals (Cr^{+6}, Pb^{+2}, and Cd^{+2}) and UV radiations (UVA, UVB, UVC, daylight, UVA + UVB, and UVA + daylight) stresses, serious changes of methylation were observed (*Fig. 4*).

Several studies published for determining the genotoxicity by DNA molecular markers of heavy metals exposure in cryptogams and algae so far. Sorrentino et al. (2017) were investigated by ISSR molecular markers in moss *Sphagnum palustre* for determining metal-induced genotoxicity. As a result of their study, both Cd and Pb salts showed a genotoxic effect with a dose-dependent trend. At concentration > 10^{-5} Cd also induced a general toxic effect in *S. palustre*, leading to chlorophyll degradation and moss death. The 12 primers used for the analysis provided a total of 169 reproducible bands, ten of which gave polymorphisms (appearance/disappearance of bands), indicating a clear genotoxic effect induced by the metals (Sorrentino et al., 2017). In our study, some primers showed significant differences in band patterns formed by loss of normal bands and appearance of new bands in the treated heavy metals and UV radiation exposure in comparison to the untreated sample profiles. We determined a total of 138 bands using six primers to evaluate UVB radiation samples in *H. physodes*.

http://www.aloki.hu ● ISSN 1589 1623 (Print) ● ISSN 1785 0037 (Online)
DOI: http://dx.doi.org/10.15666/aeer/1802_23152338

Both *Sphagnum palustre* moss and *H. physodes* lichen species could be used as bioindicator organisms for genotoxicity.

The study evaluated the genotoxicity of MnONP in *Physcomitrella patens* a model plant system utilized for epigenetic alterations (Ghosh et al., 2018). DNA methylation pattern at the level of single cells was examined by the methylation-sensitive comet assay with HpaII and MspI. MnONP incited DNA hypomethylation in *P. patens* gametophores exposed with 20 μg/mL MnONP concentration. In this study, the highest rate of methylation was obtained in *H. physodes* lichen specimen stressed with UV exposure with Type-2 primer (28.9%).

Compared with the RAPD and MSAP - AFLP analyses, the rate of change in the methylation model in lichen sample applied with heavy metal stress showed more diversity than sample applied with different UV radiations. While sample applied with heavy metal stress had a higher GTS rate in RAPD, GTS rate was determined to decrease based on the increasing UV radiations. The effect of UV stress on DNA stability was found to be higher than heavy metal stress in lichen specimen. The stability of the methylation model applied with heavy metal stress was thought to be less than UV stress in terms of epigenetics.

Conclusion

In the present study, we examined physiological and DNA damage indicator capacity of lichen specimen that has different features than other organisms. Certain organisms, such as lichens, may have properties such as being more tolerant to some pollutants than other organisms in contaminated areas or being able to accumulate the pollutant factor. These properties of organisms are used to provide qualitative information about the level of pollution in their environment. Therefore, it should be possible to make a correlation between observing and measuring the changes in the organism and the sources of the pollutant, pollution and the intensity of the pollution. This study was shown that the use of lichen specimen could eliminate the contaminants that cause environmental pollution. Detailed presentation of possible changes generated in the DNA structure and the presentation of contamination at a molecular level were ensured with our study enriched with molecular techniques. Therefore, the effect of UV stress on lichen DNA stability was thought to be greater than genetically heavy metals. The results indicated that *H. physodes* has great potential to be used in phytoremediation exercises. In addition to the properties of this lichen, the literature data has proved their antibacterial and antioxidant activity as well as cancer cell cytotoxicity and inhibitory effects on enzymes (Song et al., 2014; Mitrovic et al., 2015; Studzinska-Sroka and Zarabska-Bozjewicz, 2019). Finally, it was possible to observe the strong mechanisms of *H. physodes* lichen specimen against stressors such as heavy metals and UV radiation, allowing it to persist under highly stressful conditions. In future studies, the investigation of the biosorption capacity to accumulate different heavy metal tolerant lichen species in laboratory work still need further research. Determination of the biological response of lichens against toxic chemicals could be useful for the treatment of wastewater with lichens. These and similar studies will contribute to the identification of DNA markers.

http://www.aloki.hu ● ISSN 1589 1623 (Print) ● ISSN 1785 0037 (Online)
DOI: http://dx.doi.org/10.15666/aeer/1802_23152338

Acknowledgments. We thank TUBITAK (The Scientific and Technical Research Council of Turkey), Project no. 112T004 and Ankara University Project Manager, Project no. 13L4240004 for the financial support.

REFERENCES

[1] Abas, A., Sulaiman, N., Adnan, N. R., Aziz, S. A., Nawang, N. (2019): Using lichen (*Dirinaria* sp.) as bio-indicator for airborne heavy metal at selected industrial areas in Malaysia. – Environment Asia 12(3): 85-90.

[2] Anastassopoulou, J. (2003): Metal–DNA interactions. – Journal of Molecular Structure 651: 19-26.

[3] APHA (1985): Standard Methods for the Examination of Water and Wastewater. 16th Ed. – American Public Health Association, Washington DC.

[4] Aras, S., Cansaran-Duman, D. (2006): Isolation of DNA for sequence analysis from herbarium material of some lichen species. – Turkish Journal of Botany 30: 449-453.

[5] Aras, S., Kanlıtepe, Ç., Cansaran-Duman, D., Halıcı, M. G., Beyaztaş, T. (2010): Assesment of air pollution genotoxicity by molecular markers in the exposed samples of *Pseudevernia furfuracea* (L.) Zopf in the Province of Kayseri (Central Anatolia). – Journal of Environmental Monitoring 12: 536-543.

[6] Ares, Á., Itouga, M., Kato, Y., Sakakibara, H. (2017): Differential metal tolerance and accumulation patterns of Cd, Cu, Pb and Zn in the liverwort *Marchantia polymorpha* L. – Bulletin of Environmental Contamination and Toxicology 100: 444-450.

[7] Aslan, A., Budak, G., Tıraşoğlu, E., Karabulut, A. (2006): Determination of elements in some lichens growing in Giresun and Ordu province (Turkey) using energy dispersive X-ray fluorescence spectrometry. – Journal of Quantitative Spectroscopy and Radiative Transfer 97: 10-19.

[8] Atienzar, F. A., Conradi, M., Evenden, A. J., Jha, A. N., Depledge, M. H. (1999): Qualitative assessment of genotoxicity using random amplified polymorphic DNA: comparison of genomic template stability with key fitness parameters in *Daphnia magna* exposed to benzo[a]pyrene. – Environmental Toxicology and Chemistry 18: 2275-2282.

[9] Bah, A. M., Dai, H., Zhao, J., Sun, H., Cao, F., Zhang, G., Wu, F. (2011): Effects of cadmium, chromium and lead on growth, metal uptake and antioxidative capacity in *Typha angustifolia*. – Biological Trace Element Research 142: 77-92.

[10] Basile, A., Di Nuzzo, R. A., Capasso, C., Sorbo, S., Capasso, A., Carginale, V. (2005): Effect of cadmium on gene expression in the liverwort *Lunularia cruciata*. – Gene 356: 153-159.

[11] Bassam, B. J., Caetano-Anolles, G., Gresshoff, P. M. (1991): Fast and sensitive silver staining of DNA in polyacrylamide gels. – Analytical Biochemistry 195: 80-83.

[12] Benitez, A., Medina, J., Vasquez, C., Loaiza, T., Luzuriaga, Y., Calva, J. (2019): Lichens and bromeliads as bioindicators of heavy metal deposition in Ecuador. – Diversity 11: 28.

[13] Bradford, M. M. (1976): A rapid and sensitive method for the quantitation of microgram quantities of protein utilizing the principle of protein-dye binding. – Analytical Biochemistry 72: 248-254.

[14] Branquinho, C., Brown, H. D., Catarino, F. (1997): The cellular location of Cu in lichens and its effect on membrane integrity and chlorophyll fluorescence. – Environmental and Experimental Botany 38: 165-179.

[15] Brown, B. A., Jenkins, G. I. (2008): UV-B signaling pathways with different fluence-rate response profiles are distinguished in mature Arabidopsis leaf tissue by requirement for UVR8, HY5, and HYH. – Plant Physiology 146: 576-588.

[16] Brown, B. A., Cloix, C., Jiang, G. H., Kaiserli, E., Herzyk, P., Kliebenstein, D. J., Jenkins, G. I. (2005): UV-B-specific signaling component orchestrates plant UV

http://www.aloki.hu ● ISSN 1589 1623 (Print) ● ISSN 1785 0037 (Online)
DOI: http://dx.doi.org/10.15666/aeer/1802_23152338

protection. – Proceedings of the National Academy Science of the United States of America 102: 18225-18230.

[17] Cansaran-Duman, D. (2011): Study on accumulation ability of two lichen species (*Hypogymnia physodes* (L.) Nyl and *Usnea hirta* (L.) Weber ex F. H. Wigg) at iron-steel factory site, Turkey. – Journal of Environmental Biology 32: 839-844.

[18] Cansaran-Duman, D., Aras, S. (2014): Alternative Biosorbent for Biosorption: Lichens - A Review. – In: Ahmed, E. (ed.) Phytoremediation. Springer, UK.

[19] Cansaran-Duman, D., Beyaztaş, T., Atakol, O., Aras, S. (2011): Assessment of the air pollution genotoxicity by RAPD in *Evernia prunastri* L. Ach. province of iron-steel factory in Karabük, Turkey. – Journal of Environmental Sciences 23: 1171-1178.

[20] Casano, L. M., Braga, M. R., Alvarez, R., del Campo, E. M., Barreno, E. (2015): Differences in the cell walls and extracellular polymers of the two Trebouxia microalgae coexisting in the lichen *Ramalina Farinacea* are consistent with their distinct capacity to immobilize extracellular Pb. – Plant Science 236: 195-204.

[21] Cheloni, G., Cosio, C., Slaveykova, V. I. (2014): Antagonistic and synergistic effects of light irradiation on the effects of copper on *Chlamydomonas reinhardtii*. – Aquatic Toxicology 155: 275-282.

[22] Chettri, M. K., Cook, C. M., Vardaka, E., Sawidis, T., Lanaras, T. (1998): The effect of Cu, Zn and Pb on the chlorphyll content of the lichens *Cladonia convolute* and *Cladonia rangiformis*. – Environmental and Experimental Botany 39: 1-10.

[23] Cho, U. H., Seo, N. H. (2005): Oxidative stress in *Arabidopsis thaliana* exposed to cadmium is due to hydrogen peroxide accumulation. – Plant Science 168: 113-120.

[24] Doğan, M., Saygıdeğer, S. D. (2009): Effect of lead toxicity on aquatic macrophyte Elodea canadensis Michx. – Bulletin of Environmental Contamination and Toxicology 83: 249-254.

[25] Duman, F., Şahan, S., Ceylan, A., Koca, F. D. (2010): Cr^{+6}'ya maruz bırakılmış *Ceratophyllum demersum* L.'nin biyolojik cevabı. – Süleyman Demirel Üniversitesi Journal of Science 5: 163-171 (in Turkish).

[26] Fernandez, M. A., Martinez, L., Segarra, M., Garcia, J. C., Espiell, F. (1992): Behavior of heavy metals in the combustion gases of urban waste incinerators. – Environmental Science and Technology 26(5): 1040-1047.

[27] Frohnmeyer, H., Staiger, D. (2003): Ultraviolet-B radiation-mediated responses in plants. – Plant Physiology 133: 1420-1428.

[28] Ghosh, I., Sadhu, A., Moriyasu, Y., Bandyopadhyay, M., Mukherjee, A. (2018): Manganese oxide nanoparticles induce genotoxicity and DNA hypomethylation in the moss *Physcomitrella patens.* – Mutation Research/Genetic Toxicology and Environmental Mutanegenis. https://doi.org/10.1016/j.mrgentox.2018.12.006.

[29] Gill, R. A., Zang, L., Ali, B., Farooq, M. A., Cui, P., Yang, S., Ali, S., Zhou, W. (2015): Chromium induced physio-chemical and ultrastructural changes in four cultivars of *Brassica napus* L. – Chemosphere 120: 154-164.

[30] Gurbanov, R., Unal, D. (2018): The biomolecular alterations in C*ladonia convoluta* in response to lead exposure. – Spectroscopy Letters 51(10): 563-570.

[31] Hideg, E., Jansen, M. A. K., Strid, A. (2013): UV-B exposure, ROS, and stress: inseparable companions or loosely linked associates? – Trends in Plant Science 18: 107-115.

[32] Jenkins, G. I. (2009): Signal transduction in response to UV-B radiation. – Annual Review of Plant Biology 60: 407-431.

[33] Karakoti, N., Bajpai, R., Upreti, D. K., Mishra, G. K., Srivastava, A., Nayaka, S. (2014): Effect of metal content on chlorophyll fluorescence and chlorophyll degradation in lichen Pyxine cocoes (Sw.) Nyl.: a case study from Uttar Pradesh, India. – Environmental Earth Sciences 71: 2177-2183.

[34] Koroleva, Y., Revunkov, V. (2017): Air pollution monitoring in the South-East Baltic using the epiphytic lichen *Hypogymnia physodes*. – Atmosphere 8: 119.

http://www.aloki.hu ● ISSN 1589 1623 (Print) ● ISSN 1785 0037 (Online)
DOI: http://dx.doi.org/10.15666/aeer/1802_23152338

[35] Körpe-Aksoy, D., Aras, S. (2010): Evaluation of copper stress on eggplant (*Solanum melongena* L.) seedlings at molecular and population levels using various biomarkers. – Mutation Research 719: 29-34.
[36] Kurelec, B. (1993): The genotoxic diseases syndrome. – Marine Environmental Research 35: 341-348.
[37] Larsson, P., Vecerova, K., Cempirkova, H., Solhaug, K. A. (200): Does UV-B influence biomass growth in lichens deficient in sun-screening pigments? – Environmental and Experimental Botany 67: 215-227.
[38] Li, M., Liu, Z., Xu, Y., Cui, Y., Li, D., Kong, Z. (2009): Comparative effects of Cd and Pb^{+2} on biochemical response on DNA damage in the earthworm *Eisenia foetida* (Annelida, Oligochaeta). – Chemosphere 74: 621-625.
[39] Liu, W., Li, P. J., Qi, X. M., Zhou, Q. X., Zheng, L., Sun, T. H., Yang, Y. S. (2005): DNA changes in barley (*Hordeum vulgare*) seedlings induced by cadmium pollution using RAPD analysis. – Chemosphere 61: 158-167.
[40] Lu, G. Y., Wu, X. M., Chen, B. Y., Gao, G. Z., Xu, K. (2007): Evaluation of genetic and epigenetic modification in rapeseed (*Brassica napus*) induced by salt stress. – Journal of Integrative Plant Biology 49: 1599-1607.
[41] Mackerness, S. A. H. (2000): Plant responses to ultraviolet-B (UV-B: 280–320 nm) stress: what are the key regulators? – Plant Growth Regulation 32: 27-39.
[42] Mastan, S. G., Rathore, M. S., Bhatt, V. D., Yadav, P., Chikara, J. (2012): Assessment of changes in DNA methylation by methylation-sensitive amplification polymorphism in *Jatropha curcas* L. subjected to salinity stress. – Gene 508: 125-129.
[43] Mateos, A. C., Amarillo, A. C., Carreras, H. A., González, C. M. (2018): Land use and air quality in urban environments: human health risk assessment due to inhalation of airborne particles. – Environmental Research 161: 370-380.
[44] Matos, P., Pinho, P., Aragon, G., Martinez, I., Nunes, A., Soares, A. M. V. M., Branquinho, C. (2015): Lichen traits responding to aridity. – Journal of Ecology 103: 451-458.
[45] Metzner, H., Rau, H., Senger, H. (1965): Untersuchungen zur Synchronisierbarkeit einzelner Pigment-Mangelmutanten von *Chlorella*. – Planta 65: 186 (in German).
[46] Mirouze, M., Paszkowski, J. (2011): Epigenetic contribution to stress adaptation in plants. – Current Opinion in Plant Biology 14: 267-274.
[47] Mitrovic, T. L., Stamenkovic, S. M., Cvetkovic, V. J., Radulovic, N. S., Mladenovic, M. Z., Stankovic, M. S., Topuzovic, M. D., Radojevic, I. D., Stefanovic, O. D., Vasic, S. M., Comic, L. R., Seklic, D. S., Obradovic, A. D., Markovic, S. D. (2015): Contribution to the knowledge of the chemical composition and biological activity of the lichens *Cladonia foliacea* Huds. (Wild.) and *Hypogymnia physodes* (L.). – Oxidation Communication 38: 2016-2032.
[48] Monnet, F., Vaillant, N., Vernay, P., Coudret, A., Sallanon, H., Hitmi, A. (2001): Relationship between PSII activity, CO_2 fixation, and Zn, Mn and Mg contents of *Lolium perenne* under zinc stress. – Journal of Plant Physiology 158: 1137-1144.
[49] Pandey, V., Dixit, V., Shyam, R. (2005): Antioxidative responses in relation to growth of mustard (*Brassica juncea* cv. Pusa Jai Kisan) plants exposed to hexavalent chromium. – Chemosphere 61: 40-47.
[50] Pescott, O. L., Simkin, J. M., August, T. A., Randle, Z., Dore, A. J., Botham, M. S. (2015): Air pollution and its effects on lichens, bryophytes, and lichen-feeding Lepidoptera: Review and evidence from biological records. – Biological Journal of the Linnean Society 115: 611-635.
[51] Pisani, T., Munzi, S., Paoli, L., Backor, M., Kovácik, J., Piovar, J., Loppi, S. (2011): Physiological effects of mercury in the lichens *Cladonia arbuscula* subsp. Mitis (Sandst.) Ruoss and *Peltigera rufescens* (Weiss) Humb. – Chemosphere 82: 1030-1037.

http://www.aloki.hu ● ISSN 1589 1623 (Print) ● ISSN 1785 0037 (Online)
DOI: http://dx.doi.org/10.15666/aeer/1802_23152338

[52] Pourrut, B., Jean, S., Silvestre, J., Pinelli, E. (2011): Lead-induced DNA damages in *Vicia fabia* root cells: potential involvement of oxidative stress. – Mutation Research-Genetic Toxicology and Environmental Mutagenesis 726: 123-128.
[53] Ramić, E., Huremović, J., Muhić‐Šarac, T., Đug, S., Žero, S., Olovčić, A. (2019): Biomonitoring of air pollution in Bosnia and Herzegovina using epiphytic lichen *Hypogymnia physodes*. – Bulletin of Environmental Contamination and Toxicology 102: 763-769.
[54] Rein, T., Zorbas, H., De Pamphilis, M. L. (1997): Active mammalian replication origins are associated with a high-density cluster of mCpG dinucleotides. – Molecular Cell Biology 17: 416-426.
[55] Ronen, R., Galun, M. (1984): Pigment extraction from lichens with dimethyl sulfoxide (DMSO) and estimation of chlorophyll degradation. – Environmental and Experimental Botany 24: 239-245.
[56] Shakoor, M. B., Ali, S., Hameed, A., Farid, M., Hussain, S., Yasmeen, T., Najeeb, U., Bharwana, S. A., Abbasi, G. H. (2014): Citric acid improves lead (pb) phytoextraction in brassica napus L. by mitigating pb-induced morphological and biochemical damages. – Ecotoxicology and Environmental Safety 109: 38-47.
[57] Shugart, L., Theodorakis, C. (1994): Environmental genotoxicity: probing the underlying mechanisms. – Environmental Health Perspective 102: 13-17.
[58] Singh, V. P., Srivastava, P. K., Prasad, S. M. (2012): Differential effect of UV-B radiation on growth, oxidative stress and ascorbate-glutathione cycle in two cyanobacteria under copper toxicity. – Plant Physiology and Biochemistry 61: 61-70.
[59] Song, Y., Sun, H., Zhang, A., Yan, G., Han, Y., Wang, X. (2014): Plant-derived natural products as leads to anti-cancer drugs. – Journal of Medicinal Plant and Herbal Therapy Research 2: 6-15.
[60] Sorrentino, M. C., Capozzi, F., Giordano, S., Spagnuolo, V. (2017): Genotoxic effect of Pb and Cd on in vitro cultures of *Sphagnum palustre*: an evaluation by ISSR markers. – Chemosphere 181: 208-215.
[61] Studzinska-Sroka, E., Zarabska-Bozjewicz, D. (2019): *Hypogymnia physodes*–A lichen with interesting medicinal potential and ecological properties. – Journal of Herbal Medicine. https://doi.org/10.1016/j.hermed.2019.100287.
[62] Vardar, Ç., Başaran, E., Cansaran-Duman, D., Aras, S. (2014): Assessment of air pollution genotoxicity in the province of Kayseri (Central Anatolia) by using *Pseudevernia furfuracea* (L.) Zopf and AFLP markers. – Mutation Research/Genetic Toxicology and Environmental Mutagenesis 759: 43-50.
[63] Wellburn, A. R. (1994): The spectral determination of chlorophylls a and b, as well as total carotenoids, using various solvents with spectrophotometers of different resolution. – Journal of Plant Physiology 144: 307-313.
[64] Xu, M., Li, X., Korban, S. S. (2000): AFLP based detection of DNA methylation. – Plant Molecular Biology Reporter 18: 361-368.
[65] Zulaini, A. A. M., Muhammad, N., Asman, S., Hashim, N. H., Jusoh, S., Abas, A., Jusof, H., Din, L. (2019): Evaluation of transplanted lichens, *Parmotrema tinctorum* and *Usnea diffracta* as bioindicator on heavy metals accumulation in southern peninsular Malaysia. – Journal of Sustainability Science and Management 14(4): 1-13.

http://www.aloki.hu ● ISSN 1589 1623 (Print) ● ISSN 1785 0037 (Online)
DOI: http://dx.doi.org/10.15666/aeer/1802_23152338

DEVELOPMENT OF *IN VITRO* STERILIZATION PROTOCOL FOR DO-1 (*Prunus domestica*) ROOTSTOCK

UGUR, R.

East Mediterranean Transitional Zone Agricultural Research Institute, Hacimustafa Mah. Gazi Mustafa Kemal Bulvari No: 122 (Adana Yolu Uzeri 5. Km) Onikisubat/Kahramanmaras, Turkey (e-mail: remzibey@hotmail.com; phone: +90-536-925-9915, +90-344-237-6020; fax: +90-344-237-7196)

(Received 30th Oct 2019; accepted 30th Jan 2020)

Abstract. Commercial companies have focused on clonal rootstocks free of diseases and been propagated through tissue culture for fruit seedling production lately to obtain products with higher quality and quantity. Two important stages in tissue culture are surface sterilization and *in vitro* culturing of the explants to be micro-propagated. Because *prunus* varieties which sources of explants are grown on open lands, contamination risk is higher. This study has been conducted to minimize the contamination of DO1 (*Prunus domestica*) explants by microorganisms as *prunus* rootstock for micropropagation. Several concentrations and application durations of 4 different sterilization agents ($HgCl_2$, NaClO, H2O2, and AgNO3) have been applied on the axillary buds taken from the rootstock for surface sterilization. Then, the explants have been transferred to MS nutrient media and the number of the aseptic explants was determined. Shoot and leaf regeneration have been observed on the aseptic explants 40 days after the application. While the highest aseptic explant rate (91%) was achieved with 2% NaClO application in 15 minutes, the lowest aseptic explant rate (23.33%) was achieved with 0.5% $HgCl_2$ application in ten days. Finally, the lowest contamination rate was observed in NaClO applications (18.34%) and the highest contamination rate was observed in $HgCl_2$ applications among the sterilization agents.
Keywords: *in vitro, micropropagation, prunus, rootstock, sterilization*

Introduction

Turkey is among the leading fruit producers in the world with 226.783 ha of plantation area and 2.138.393 tons of apricot, plum, peach-nectarine and almond production (FAO, 2019). These fruits are produced in different regions of the country with different climatic conditions. This situation affects the production stability of these fruit species. Therefore, the usage of suitable clonal rootstock compatible with the soil conditions of the region is very important. Recently, high quality genotypes which have been tolerant to diseases and pests, compatible with scion, adaptable to different climatic conditions, positive effect yield and fruit quality of fruit varieties have been selected as rootstock and propagated clonally in the modern horticulture (Beckman and Lung, 2003; Nimbolkar et al., 2016; Suranyi et al., 2019). Generally, clonal production through vegetative ways in rootstock improvement and rootstock production are made by cuttings and tissue culture. High numbers of plants having the same genetic structure can be produced in a quick way free of diseases and viruses during micropropagation using tissue culture. Propagation by cutting, one of classical production methods, is dependent on seasons, whereas production *in vitro* conditions is constantly possible in all season with proper explants and sub-cultural applications (Wolella, 2017). Micropropagation has become important quality criteria in terms of obtaining healthier and homogenous plants in improvement of *Prunus* rootstock breeding studies (Martinez-Gomez et al., 2005). Micropropagation techniques are commonly used in many *Prunus* species; apricot (Reighard et al., 1990; Perez-Tornero et al., 1999), almond (Ainsley et al., 2001; Choudhary et al., 2015), peach (Bhansali et al., 1990; Declerck and Karbon, 1996; Felek et al., 2015), cherry (Matt and Jehle, 2005;

http://www.aloki.hu ● ISSN 1589 1623 (Print) ● ISSN1785 0037 (Online)
DOI: http://dx.doi.org/10.15666/aeer/1802_23392349

Ružić and Vujović, 2008; Zarei et al., 2013) and in certain *Prunus* hybrid rootstocks (Tsipouridis and Thomidis, 2003; Felipe, 2009; Dejampour et al., 2011; Canlı and Demir, 2014). Sterilization is important *in vitro* tissue culture such as tools, equipment and nutrient medium. And besides surface sterilization of the explants, seeds, bulbs, leaves, stems, shoots, etc. taken *in vivo* such as fields, greenhouses, gardens, etc. are important (Babaoğlu et al., 2002). Obtaining aseptic explant is the first stage of tissue culture. It is also for viability of the explants taken into *in vitro* culture following surface sterilization. Microbial contamination is a serious problem in micropropagation. It causes significant number of plant losses in micropropagation (Da Silva and Kulus, 2014). Minimization of the losses are crucial for sustainability of the study (Nazary and Aghaye, 2012). Especially fungus, bacteria, viruses and yeasts cause microorganism contaminations *in vitro* culture (Omamor et al., 2007; Altan et al., 2010; Da Silva et al., 2016; Hesami et al., 2018). They cause decaying such as white, yellow and pink colonies of the nutrient medium. Another factor is which fungi are transmitted by either explant source or from the air. They may also cover the nutrient media with their grey micelles. Many researchers suggested that the main damage of these microorganisms should be defined as their nutritional competition with the explant on the medium (Nazary and Aghaye, 2012; Da Silva et al., 2016). Many activities occur during this process; slow growth of explants, necrosis formed on tissues, reduction on tissue regeneration and rooting, and their results can be disruptions leading to explant death (Mihaljevic et al., 2013). For the solution of these problems, an appropriate surface sterilization method, which varies according to the plants among the species, should be determined. Even different concentrations of chemical agents, impacts of application times within the same varieties of a single species influence the success of the surface sterilization. There are some other factors that affect performance; such as season of taking the explant, density and type of the microorganisms on the same explants but in different places (Bhojwani and Razdan, 2005; Eed et al., 2010).

Various commercial bleaches including sodium hypochlorite (NaClO), calcium hypochlorite ($Ca(ClO)_2$) and ethanol (C_2H_6O) are densely used for surface sterilization of the explants *in vitro* culture in many plant species. Besides, the chemical agents such as mercury chloride ($HgCl_2$), hydrogen peroxide (H_2O_2) and silver nitrate ($AgNO_3$) are used as disinfectants (Andreu and Marin, 2005; Arab et al., 2014). In addition, some pretreatments are carried out according to contamination, size and type of plant material prior to sterilization with chemicals. If the explant is big in size, generally the plant material is first washed under the tap water and kept in alcohol for several seconds (1 to 30 seconds) for sterilization of the plant material, which is followed by the actual surface sterilization. In case of an explant with an indented surface, 2 to 4 drops of Tween 20 may be dripped into the sterilization solution in order to benefit from diffuser and adhesive characteristics of such substance for the purpose of increasing effectiveness of the surface sterilization solution. Despite the chemical agents used in surface sterilization during *in vitro* culture studies, the establishment of the right protocol specific to using the plant material is the most important step of a successful study (Papafotiu and Martini, 2009).

There are no universal sterilization agents and nutrient medium for *in vitro* culture because rootstocks are genetically specific with regard to different components of the medium. Whereas MS (Murashige and Skoog, 1962) has been proved to be most suitable medium for successful explant development of stone fruits (almond, apricot and peach). Thus, the objective of this study was to develop on effective sterilization protocol for *in vitro* clonal prunus rootstock DO-1 (*P. domestica*). In this study, the axillary bud explants

http://www.aloki.hu ● ISSN 1589 1623 (Print) ● ISSN1785 0037 (Online)
DOI: http://dx.doi.org/10.15666/aeer/1802_23392349

of DO-1 (*P. domestica*) clonal rootstock which was obtained through selection breeding program which was treated with different concentrations of four chemical agents ($HgCl_2$, NaClO, H_2O_2 and $AgNO_3$) in different time durations as well as the most favorable sterilization protocol were studied. As a result of the study, the surface sterilization protocol at the lowest contamination level and giving the least damage to the explants of DO-1 (*P. domestica*) rootstock cultures *in vitro* was obtained.

Materials and Methods

This study was carried out at the Plant Tissue Culture Laboratory of Eastern Mediterranean Transitional Zone Agricultural Research Institute, Kahramanmaras / Turkey, on April and May 2018. The study material consisted of young and healthy shoots at a length of 20 to 25 cm, which contained 10-15 buds on them, were grown in greenhouse and obtained from DO-1 (*P. domestica*) rootstock improved by Eastern Mediterranean Transitional Zone Agricultural Research Institute. The shoots were taken from the mother plant and the leaves on the shoots were cut and brought to the preliminary preparation room of the laboratory in a container full of water before taking into *in vitro* culture. The factors that dust and waste of insects which negative effect on sterilization application exist on the shoots were cleaned out with sterile water. Then, such shoots were cut at a length of 2.5 – 3.5 cm in such a way to contain one bud on each of them and the obtained explants were brought into sterile cabin in order to perform surface sterilization procedures. The explants were kept in 70% alcohol for a duration of 30 seconds in the sterile cabin as a pretreatment procedure before application of the chemical agents to be used in surface sterilization. Later on, they were rinsed with distillate water for three times in order to avoid the caustic effect of the alcohol.

When ethanol application was completed, explants were kept in solutions, which were prepared at different concentrations of 4 different sterilization agents as shown in *Table 1* for different periods. During this period, the bottle was shaken slightly in order to increase the effect of the solution on the explant surface. At the end of the awaiting duration, the sterilization solution at each application was poured down and the explants were rinsed for 3 times in sterile pure water (*Figure 1*).

Covered with roughing filter paper petri dishes were used for sterilization for a duration of 20 minutes at 121ºC at the autoclave. When surface sterilization was completed, excess water of the explants was taken with these petri dishes. After taking the first water of the explants, they were transferred to another petri and the cap of the petri was left half open in order to let it lose the water drops and the humidity on the explants. In addition, each tools used for surface sterilization (bottles, petri dishes, forceps, bistouries and the bottles full of water) were exposed to sterilization at the autoclave at 121ºC for a duration of 20 minutes. Before the autoclave process; the forceps and the bistouries were wrapped with aluminum folio and left in refrigerator bags, the caps of the bottles were strapped with autoclave band and the petri dishes were placed in autoclave bags. In addition, the forceps and the bistouries used in the sterile cabin were kept in the sterilizer in the cabin; and they were used during the study repeatedly through treatment with alcohol.

During all applications the damaged parts of the tissues as well as all the irregular and unnecessary parts were removed by the help of forceps and bistouries. The explants at the length of 2 cm and containing one bud on each of them were planted in the nutrient media

http://www.aloki.hu ● ISSN 1589 1623 (Print) ● ISSN1785 0037 (Online)
DOI: http://dx.doi.org/10.15666/aeer/1802_23392349

in such a way to keep the leaf stalks at the upper part with an angle at an amount of 45° to the nutrient media.

Table 1. *Chemicals used in surface sterilization applications and their application durations*

Treatments	Chemical agents	Application Combinations	
		Concentrations (% wv^{-1})	Durations (minute)
T1	$HgCl_2$ (Mercuric (II) chloride)	0.1	15
T2	$HgCl_2$ (Mercuric (II) chloride)	0.5	10
T3	$HgCl_2$ (Mercuric (II) chloride)	1.0	5
T4	NaClO (Sodium hypochlorite)	1.0	30
T5	NaClO (Sodium hypochlorite)	1.5	20
T6	NaClO (Sodium hypochlorite)	2.0	15
T7	H_2O_2 (Hydrogen peroxide)	20.0	30
T8	H_2O_2 (Hydrogen peroxide)	30.0	20
T9	H_2O_2 (Hydrogen peroxide)	40.0	10
T10	$AgNO_3$ (Silver nitrate)	0.5	30
T11	$AgNO_3$ (Silver nitrate)	1.0	20
T12	$AgNO_3$ (Silver nitrate)	1.5	10

Figure 1. *Stages of application with different chemical agents for surface sterilization to the explants*

MS (Murashige and Skoog, 1962) nutrient media supplemented with 0.5 mg/l BAP in combination with 0.1 mg/l of IBA was used for regeneration of the explants *in vitro* tissue culture. pH was adjusted to 5.6 to 5.8 with 1 N NaOH or 1 N HCI and then 30 $g.L^{-1}$ sucrose and 8 $g.L^{-1}$ agar were added into the MS medium. After addition and dissolution of agar, the nutrient media were sterilized at the autoclave at 121°C at 1.2 atmospheric pressure for a duration of 15 minutes. Clear glass bottles of 350 ml containing MS medium of 65 ml were used as culture containers. Each bottle was labeled with tags of different colors having different sterilization application information on them. All *in vitro* culture conditions were incubated at climate chamber at 16/8 light/dark photoperiod adjusted to 40 µmol m^{-2} s^{-1} light density, 25 ± 2°C temperature and 70-80% humidity (*Figure 2*).

In all different sterilization application, 15 bottles of 350 ml were placed in the testing area randomly. Sterilization data were completed in 28 days, once in 7 days. The shoot and leaf growth data were taken after 40 days for the vivid explants and the effect of different sterilization methods were investigated for plant growth *in vitro* culture. The shoot growth was measured as the length of the shoots at the end of 28-days duration. Then such data were interpreted as percentage.

http://www.aloki.hu ● ISSN 1589 1623 (Print) ● ISSN1785 0037 (Online)
DOI: http://dx.doi.org/10.15666/aeer/1802_23392349

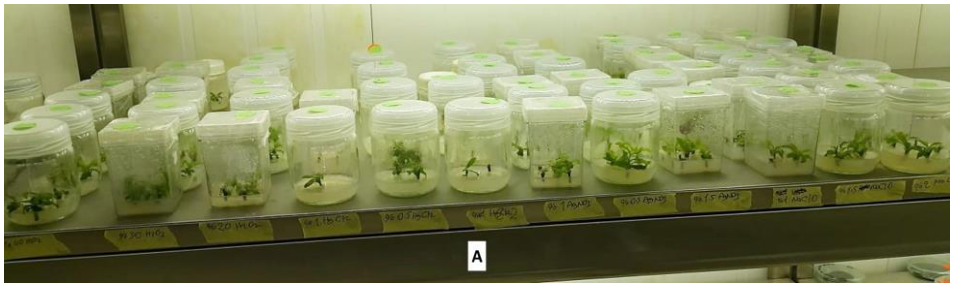

Figure 2. *An image from the climate chamber, where the explants, whose sterilization procedures have been completed, are incubated*

Data of percentage of survived explant, proliferation and shoot length, average number of leaf were analyzed by analysis of variance (ANOVA) in a completely randomized experimental design by SAS computer software (version 7.1). Significant different between means were assessed by Low Significant Different test (LSD, P≤0.05)

Result and Discussion

Table 2 shows the percentage of aseptic explant percentage at the end of applications on DO-1 (*P. domestica*) rootstock taken under *in vitro* culture through application of different doses and durations of four different chemical agents. The variations arising from the effects of different chemicals on surface sterilization may also be seen on *Table 2*.

Table 2. *Aseptic explant amount at the end of application different chemical agents (%)*

Treatments	Chemical agents	Application Combinations		Application Mean (%)	Chemical Mean (%)
		Concentrations (% wv^{-1})	Durations (minute)		
T1	$HgCl_2$	0.1	15	26.66^{d}	27.77^{c}
T2	$HgCl_2$	0.5	10	23.33^{d}	
T3	$HgCl_2$	1.0	5	33.33^{d}	
T4	NaClO	1.0	30	88.66^{a}	81.66^{a}
T5	NaClO	1.5	20	65.33^{bc}	
T6	NaClO	2.0	15	91.00^{a}	
T7	H_2O_2	20.0	30	70.00^{bc}	67.77^{b}
T8	H_2O_2	30.0	20	60.00^{bc}	
T9	H_2O_2	40.0	10	73.33^{b}	
T10	$AgNO_3$	0.5	30	61.33^{bc}	60.44^{b}
T11	$AgNO_3$	1.0	20	64.33^{bc}	
T12	$AgNO_3$	1.5	10	55.66^{c}	
LSD $_{chemical}$: 8.69**				LSD $_{application}$: 7.51*	

F** indicate P ≤ 0.01 and F* indicate P ≤ 0.05 significance level. Distinct letters in the fifth and sixth columns indicate significant differences according to LSD's test (P ≤ 0.05)

As a result, the differences among the aseptic explants obtained from application of the chemical agents) were observed to be significant at a level of 1%. It was observed that the highest aseptic explant rate was 81.66% for NaClO (sodium hypochlorite) and followed by H_2O_2 (Hydrogen peroxide) and $AgNO_3$ (silver nitrate) as 67.77% and 60.44%,

http://www.aloki.hu ● ISSN 1589 1623 (Print) ● ISSN1785 0037 (Online)
DOI: http://dx.doi.org/10.15666/aeer/1802_23392349

respectively. The lowest aseptic explant rate was obtained from $HgCl_2$ (Mercury chloride) application as 27.77%. Unlike to our study, Thakur et al. (2016) indicated that HgCl was a better disinfectant than NaClO during the surface sterilization stage of *in vitro* propagation of the explants (axillary buds) taken from Gisela-5 rootstock. However, it was observed in many studies that Ethanol, NaClO and Tween 20 prevent growth of bacteria and fungus when they are used as disinfectant *in vitro* culture. Even very little amounts of sodium hypochlorite ensure significant decrease in microbial population and it is rather effective disinfectant known as bacteria killer (Odutayo et al., 2007; Eed et al., 2010).

It was observed that the differences between the aseptic explant rates at interactions of application with different chemical agents for different durations were statistically important. The highest aseptic explant rates were obtained from application of 2% NaClO for a duration of 15 minutes with 91.00% and 30 minutes 88.66%; and the lowest explant rates were obtained from application of 0.5% $HgCl_2$ for a duration of 10 minutes and application of 0.1% $HgCl_2$ for a duration of 10 minutes with 23.32% and 15 minutes with 26.66%, respectively.

When distribution of application combination interactions with chemical agents evaluated, the highest aseptic explant rates of the plants displayed a distribution between 60 and 70% while mercuric (II) chloride applications remained at very low levels (23 to 33%). Mihaljević et al. (2013) used different sterilization agents (NaClO, $Ca(ClO)_2$, DICA, $HgCl_2$, $AgNO_3$, H_2O_2) for surface sterilization on the axillary buds of sour cherry plant in *in vitro* propagation. The best result was indicated to be achieved from application of 1% $AgNO_3$ for a duration of 20 minutes (96.67% healthy and 3.3% contaminated bud explants). Similar to our study, the second best surviving explants obtained from 1-3% NaClO application for surface sterilization with 80%.

Table 3 shows the shoot growth [shoot length (mm)] data for the explants *in vitro* incubation after a duration of about 1 month in order to monitor the effect of four different surface sterilization agent on regeneration of the aseptic explants came from DO-1 (*P. domestica*) rootstock following *in vitro* culture.

Table 3. *Shoot lengths of aseptic explants after application different chemical agents (mm)*

Treatments	Chemical agents	Application Combinations		Application Mean (mm)	Chemical Mean (mm)
		Concentrations (% wv^{-1})	Durations (minute)		
T1	$HgCl_2$	0.1	15	7.60^{bc}	
T2	$HgCl_2$	0.5	10	8.00^{bc}	8.31
T3	$HgCl_2$	1.0	5	9.33^{abc}	
T4	NaClO	1.0	30	9.23^{abc}	
T5	NaClO	1.5	20	6.56^{c}	8.65
T6	NaClO	2.0	15	10.16^{ab}	
T7	H_2O_2	20.0	30	10.23^{ab}	
T8	H_2O_2	30.0	20	8.50^{abc}	9.86
T9	H_2O_2	40.0	10	10.86^{a}	
T10	$AgNO_3$	0.5	30	6.66^{c}	
T11	$AgNO_3$	1.0	20	11.16^{a}	9.34
T12	$AgNO_3$	1.5	10	10.20^{ab}	
LSD $_{chemical}$: NS				LSD $_{application}$: 1.42*	

F** indicate P ≤ 0.01 and F* indicate P ≤ 0.05 significance level. Distinct letters in the fifth and sixth columns indicate significant differences according to LSD's test (P ≤ 0.05)

It was observed that the differences among the shoot lengths of the sterile explants according to the applied chemical were not statistically important. According to *Table 3*,

http://www.aloki.hu ● ISSN 1589 1623 (Print) ● ISSN1785 0037 (Online)
DOI: http://dx.doi.org/10.15666/aeer/1802_23392349

the highest shoot value was obtained for the explants, which were applied H_2O_2 (9.86 mm); and followed by $AgNO_3$, NaClO $HgCl_2$, and applications with 9.34 mm, 8.65 mm and 8.31 mm, respectively. The results indicate that the lowest shoot length was obtained from $HgCl_2$ application with 8.31 mm.

The highest shoot length value was observed for application of 1% $AgNO_3$ for a duration of 20 minutes (11.16 mm) and for application of 2% H_2O_2 for a duration of 15 minutes (10.86 mm) and that such interactions occurred in a way to take place in the same group statistically. The lowest shoot length values were observed as 6.56 mm for interaction of application of 1.5% NaClO for a duration of 20 minutes and as 7.60 mm for application of 0.1% $HgCl_2$ for a duration of 15 minutes.

Table 4 shows the number of leaves developed on the shoots after application of shoot surface sterilization with four different sterilization chemicals on DO-1 (*P. domestica*) rootstock. It was observed that the differences among the values of the numbers of leaves were not statistically different. As it may also be seen on the table, the highest number of leaves was obtained from H_2O_2 application as 6.54 leaves; followed by NaClO, $AgNO_3$ and $HgCl_2$ applications as 6.35, 5.92 and 5.30 leaves, respectively.

Table 4. *Average leaf numbers of the explants survived after application different chemical agents (per/explant)*

Treatments	Chemical agents	Application combinations		Application mean	Chemical mean
		Concentrations (% wv^{-1})	Durations (minute)		
T1	$HgCl_2$	0.1	15	4.56	
T2	$HgCl_2$	0.5	10	5.33	5.30
T3	$HgCl_2$	1.0	5	6.00	
T4	NaClO	1.0	30	6.93	
T5	NaClO	1.5	20	6.30	6.35
T6	NaClO	2.0	15	5.83	
T7	H_2O_2	20.0	30	6.23	
T8	H_2O_2	30.0	20	6.66	6.54
T9	H_2O_2	40.0	10	6.73	
T10	$AgNO_3$	0.5	30	4.46	
T11	$AgNO_3$	1.0	20	6.86	5.92
T12	$AgNO_3$	1.5	10	6.43	
$LSD_{chemical}$: NS				$LSD_{application}$: NS	

F^{**} indicate $P \leq 0.01$ and F^{*} indicate $P \leq 0.05$ significance level. Distinct letters in the fifth and sixth columns indicate significant differences according to LSD's test ($P \leq 0.05$)

The highest number of leaves was observed at interaction of 1% NaClO application for a duration of 30 minutes as 6.93 leaves and 1% $AgNO_3$ application for a duration of 20 minutes as 6.86 leaves. On the other hand, the lowest number of leaves was observed on the aseptic explants obtained at the interaction of 0.5% $AgNO_3$ application for a duration of 30 minutes as 4.46 leaves and 0.1% $HgCl_2$ application for a duration of 15 minutes as 4.56 leaves.

It was reported that the explants obtained from the buds of the shoots, which have completed their development, gave better results (Naghmouchi et al., 2008). Our study showed that when the explants were taken from *in vitro* culture, the season was important for the success of the surface sterilization. And especially spring season affected *in vitro* regeneration positively as the shoots taken in spring are active. It was reported that *in vitro* culturing time of the explants to be taken from woody plants (cherry rootstocks) was very

http://www.aloki.hu ● ISSN 1589 1623 (Print) ● ISSN1785 0037 (Online)
DOI: http://dx.doi.org/10.15666/aeer/1802_23392349

important in terms of contaminations and that contamination was less especially in spring months and that development was faster (Fidancı et al., 2008).

Another factor affecting the shooting speed of the explants of DO-1 (*P. domestica*) rootstocks (exposed to different chemical agents) is whether the caustic effect of the chemical agent is high or not as well as the duration of keeping the explants in such chemicals. It was observed that the explants (67.77% aseptic) exposed to H_2O_2 application are distinguished for their shoot lengths and leaf numbers. And also the caustic effect of NaClO chemical, which gave the highest value of 81.66% in terms of aseptic plants, was higher and hence lower values were obtained in regeneration of the shoots.

Conclusion

Surface sterilization is first stage of *in vitro* culture and it is important for healthy and fast growth. In order to achieve this, the proper chemical agent for surface sterilization and the application duration of the chemical agent have to be determined according to some criteria; such as explant taking time of the species and varieties to be taken into *in vitro* culture, the texture of the explants (indented, puberulent, spinous, waxy, etc.) and types of the explants (leaf, stem, bud, etc.) (Mihaljevic et al., 2013; Nongalleima et al., 2014). The method, which would avoid contamination and give the least damage to the explant, has to be determined in order to avoid loss of time for the rootstocks that has to be produced *in vitro* mass micropropagation. It is necessary to achieve maximum level of regeneration speed of the explants to be source in the future.

In this study, a protocol for surface sterilization of clonal rootstock DO-1 (*P. domestica*) was developed using axillary bud explant. During sterilization protocol investigation, the highest significant survival value (91%) was recorded when disinfected with T6 (2% NaClO for 15 min). The induction, regeneration and proliferation of this explants were depending on the application combination and duration times of chemical agents that were used. The length of newly shoot varied with application chemical agents and duration times. The best length of shoot was obtained on T11 (1% $AgNO_3$ for 20 min) treatments. Whereas no differences were found between the number of leaf values of explants. Therefore, treatments of T6 (2% NaClO for 15 min) is recommended for true type and disease free plants of DO-1 (*P. domestica*).

The results of the study showed that $HgCl_2$, which has an extremely toxic effect, gave negative results in surface sterilization of plant explant in our *in vitro* studies. Although the best surface sterilization results were obtained with NaClO, the use of H_2O_2 and $AgNO_3$ also yielded positive results (*Figure 3*).

Figure 3. *Development of the aseptic plants at the incubation medium after application of different chemical agents at surface sterilization*

http://www.aloki.hu ● ISSN 1589 1623 (Print) ● ISSN1785 0037 (Online)
DOI: http://dx.doi.org/10.15666/aeer/1802_23392349

REFERENCES

[1] Ainsley, J., Hammerschlag, A. F., Bertozzi, T., Graham, G. C., Sedgley, M. (2001): Regeneration of almond from immature seed cotyledons. – Plant Cell, Tissue and Organ Culture 67: 221-226.

[2] Altan, F., Bürün, B., Sahin, N. (2010): Fungal contaminants observed during micropropagation of Lilium candidum L. and the effect of chemotherapeutic substances applied after sterilization. – African Journal Biotechnology 9: 991-995.

[3] Andreu, P., Marin, J. A. (2005): In vitro culture establishment and multiplication of the Prunus rootstock 'Adesoto 101' (*P. insititia* L.) as affected by the type of propagation of the donor plant and by the culture medium composition. – Scientia Horticulturae 106: 258-262.

[4] Arab, M. M., Yadollahi, A., Mazinani-Hossaini, M., Bagheri, S. (2014): Effects of antimicrobial activity of silver nanoparticles on in vitro establishment of G N15 (hybrid of almond X peach) rootstock. – Journal of Engineering and Biotechnology 12: 103-110.

[5] Babaoglu, M., Yorgancilar, M., Akbudak, M. A. (2002): Doku Kültürü: Basic Laboratory Techniques. – Selcuk University Foundation Publications, Konya.

[6] Beckman, T. G., Lang, G. A. (2003): Rootstock Breeding for Stone Fruits. XXVI IHC – Genetics and Breeding of Tree Fruits and Nuts. – Acta Horticulture 622: 531-551.

[7] Bhansali, R. R., Driver, J. A., Durzan, D. J. (1990): Rapid multiplication of adventitious somatic embryos in peach and secondary embryogenesis. – Plant Cell Report 9: 280-284.

[8] Bhojwani, S. S., Razdan, M. K. (2005): Plant Tissue Culture: Theory and Practice. – Elsevier, New Delhi, India: 30-35.

[9] Canli, F. A., Demir, F. (2014): *In vitro* multiplication and rooting of 'F12-1' (*Prunus avium* L.) and 'Ma x ma 14' (*Prunus mahaleb L.* × *P. avium L.*) rootstocks. – Indian Journal of Horticulture 71: 145-150.

[10] Choudhary, R., Chaudhury, R., Malik, S., Sharma, K. (2015): An efficient regeneration and rapid micropropagation protocol for Almond using dormant axillary buds as explants. – Indian Journal Experimental Biology 53: 462-467.

[11] Da Silva, J. A. T., Kulus, D. (2014): Chrysanthemum biotechnology: discoveries from the recent literature. – Folia Horticulture 26: 67-77.

[12] Da Silva, J. A. T., Kulus, D., Zhang, X., Zeng, S., Ma, G., Piqueras, A. (2016): Disinfection of explants for saffron (*Crocus sativus*) tissue culture. – Environmental Experimental Biology 14: 183-198.

[13] Declerck, V., Korban, S. S. (1996): Influence of growth regulators and carbon source on callus induction, growth and morphogenesis from leaf tissues of peach (*Prunus persica* L. Batsch). – Journal Horticultural Science 71(1): 49-55.

[14] Dejampour, J., Majidi, I., Khosravi, S., Farhadi, S., Shadmehr, A. (2011): *In Vitro* Propagation of HS314 Rootstock (*Prunus amygdalus x P. persica*). – HortScience 46(6): 928-931.

[15] Eed, A. M., Reddy, A. S., Reddy, K. M., Silva, J. A. T., Reddy, V. P., Beghum, H., Venkatsubbaiah, P. Y. (2010): Effects of Antibiotic and Fungucides on the *in vitro* Production of *Citrus limonia* Osbeck Nodal Segment and Shoot Type Explants. – Asian and Australasian Journal of Plant Science and Biotechnology 4(1): 66-70.

[16] FAO. (2019): Food and Agricultural Organization. 20 June 2019. – http://www.fao.org/faostat/en/#data/QC.

[17] Felek, W., Mekibib, F., Admassu, B. (2015): Optimization of explant surface sterilization condition for field grown peach (*Prunus persica* L. Batsch Cv. Garnem) intended for in vitro culture. – African Journal of Biotechnology 14(8): 654-660.

[18] Felipe, A. J. (2009): 'Felinem', 'Garnem' and 'Monegro' almond x peach hybrid rootstocks. – HortScience 44(1): 196-197.

http://www.aloki.hu ● ISSN 1589 1623 (Print) ● ISSN1785 0037 (Online)
DOI: http://dx.doi.org/10.15666/aeer/1802_23392349

[19] Fidanci, A., Burak, M., Erenoglu, B., Akcay, M. E. (2008): Determination of i*n vitro* propagation techniques for some clonal cherry rootstocks. – Acta Horticulture 795: 409-412.
[20] Hesami, M., Naderi, R., Yoosefzadeh-Najafabadi, M. (2018): Optimizing sterilization conditions and growth regulator effects on in vitro shoot regeneration through direct organogenesis in *Chenopodium quinoa*. – BioTechnologia 99: 49-57.
[21] Martinez-Gomez, P., Sanchez-Perez, R., Rubio, M., Dicenta, F., Gradziel, T. M., Sozzi, G. O. (2005): Application of recent biotechnologies to *Prunus* tree crop genetic improvement. – Ciencia e Investigación Agraria 32(2): 55-126.
[22] Matt, A., Jehle, J. A. (2005): *In vitro* plant regeneration from leaves and internode sections of sweet cherry cultivars (*Prunus avium* L.). – Plant Cell Reports 24: 468-476.
[23] Mihaljević, I., Dugalić, K., Tomaš, V., Viljevac, M., Pranjić, A., Čmelik, Z., Puškar, B., Jurković, Z. (2013): *In vıtro* sterilization procedures for micropropagation of 'OBLAČINSKA' Sour Cherry. – Journal of Agricultural Sciences 58: 117-126.
[24] Murashige, T., Skoog, F. (1962): A revised medium for rapid growth and bioassays with tobacco tissue cultures. – Physiology of Plant 15: 473-497.
[25] Naghmouchi, S., Khouja, M. L., Rejep, M. N., Boussaid, M. (2008): Effect or growth regulators and eksplant origin on *in vitro* propagation of *Ceratonia siliqua* L. Via cuttings. – Biotechnologie Agronomie Societe Environment 12(3): 251-258.
[26] Nazary, R., Aghaye, M. (2012): Micropropagation of GF 677 Rootstock. – Journal Agricultural Science 4(5): 131-138.
[27] Nimbolkar, P. K., Shiva, B., Rai, A. K. (2016): Rootstock breeding for abiotic stress tolerance in fruit crops. – International Journal of Agriculture, Environment and Biotechnology 9(3): 375-380.
[28] Nongalleima, K., Dikash Singh, T., Amitabha, D., Deb, L., Sunitibala Devi, H. (2014): Optimization of surface sterilization protocol, induction of axillary shoots regeneration in Zingiber zerumbet (L.) Sm. as affected by season. – Biological Rhythm Reserach 45: 317-324.
[29] Odutayo, O. I., Amusa, N. A., Okutade, O. O., Ogunsanwo, Y. R. (2007): Sources of microbial contamination in tissue culture laboratories in southwestern Nigeria. – African Journal Agricultura 2: 067-072.
[30] Omamor, I. B., Amusa, N. A., Eke, C. R., Ezia, E. L. (2007): Fungal contamination of the oil palm tissue culture in Nigerian institute for Oil Palm Research (NIFOR). – African Journal Agriculture 2(10): 534-537.
[31] Papafotiu, M., Martini, A. N. (2009): Effects of season and sterilization method on response of *Malasorbus florentina* Browies (Rosacea) buds in vitro culture. – Acta Horticulturae 813: 503-508.
[32] Perez-Tornero, D., Egea, J., Van Oostende, A., Burgos, L. (1999): Assessment of factors affecting adventitious regeneration from *in vitro* cultured leaves of apricot. – Plant Science 158: 61-70.
[33] Reighard, G. L., Cain, D. W., Newall Jr., W. C. (1990): Rooting and survival potential of hardwood cuttings of 406 species, cultivars, and hybrids of *Prunus*. – HortScience 25(5): 517-518.
[34] Ružić, D. V., Vujović, T. (2008): The effects of cytokinin types and their concentration on *in vitro* multiplication of sweet cherry cv. Lapins (*Prunus avium* L.). – Horticultural Science 35: 12-21.
[35] Suranyi, D. (2019): Evaluation of introduced plum varieties under extreme climatic conditions. – International Journal of Horticultural Science 25(1-2): 7-10.
[36] Tsipouridis, C., Thomidis, T. (2003): Methods to improve the *in vitro* culture of GF677 (peach × almond) peach rootstock. – New Zealand Journal of Crop and Horticultural Science 31: 361-364.
[37] Wolella, E. K. (2017): Surface sterilization and *in vitro* propagation of *Prunus domestica L. cv. Stanley* using axillary buds as explants. – Journal of Biotech Research 8: 18-26.

http://www.aloki.hu ● ISSN 1589 1623 (Print) ● ISSN1785 0037 (Online)
DOI: http://dx.doi.org/10.15666/aeer/1802_23392349

[38] Zarei, M., Garoosi, G., Nezami, E., Hosseini, R., Ahmadi, J. (2013): The effect of medium, carbon source, light spectrum and style treatment of auxin on shoot and root regeneration of 'Gisela 6' rootstock. – Journal of Cell & Tissue Culture 4: 169-185.

http://www.aloki.hu ● ISSN 1589 1623 (Print) ● ISSN1785 0037 (Online)
DOI: http://dx.doi.org/10.15666/aeer/1802_23392349

MOLECULAR IDENTIFICATION OF COTTON WHITEFLY *BEMISIA TABACI* GENN. (HEMIPTERA: ALEYRODIDAE) POPULATIONS OF TURKEY BASED ON MITOCHONDRIAL CYTOCHROME OXIDASE SUBUNIT I

DAĞLI, F.[1*] – YÜKSELBABA, U.[1] – İKTEN, C.[1] – TOPAKÇI, N.[2] – GÖÇMEN, H.[1,3]

[1]*Department of Plant Protection, Faculty of Agriculture, Akdeniz University, 07059 Antalya, Turkey*

[2]*Vocational School of Technical Science, Akdeniz University, 07059 Antalya, Turkey*

[3]*Department of Plant Protection, Faculty of Agriculture, Kyrgyz-Turkish Manas University, 720044 Bishkek, Kyrgyzstan*

**Corresponding author*
e-mail: fdagli@akdeniz.edu.tr; phone: +90-242-310-2426; fax: +90-242-310-2479

(Received 31st Oct 2019; accepted 30th Jan 2020)

Abstract. The cotton whitefly (*Bemisia tabaci* Genn.) is a major pest of cultivated plants in tropical and subtropical regions. In this study, the genetic diversity between populations and various biotypes of *B. tabaci* collected from Hatay, Adana, İçel, Antalya, Muğla, Aydın and Denizli provinces of Turkey were investigated using mitochondrial cytochrome oxidase subunit 1 (mtCOI) sequences. Thirty-two nucleotide variations were found in a 617 bp mtCOI sequence of the among the populations studied. Phylogenetic analysis divided the *B. tabaci* populations of Turkey into two groups clustering around the main Middle East-Asia Minor 1(MEAM1) and Mediterranean (MED) groups, (i.e. the so-called B and Q biotypes respectively). Mediterranean species were also divided into two subgroups. The populations from Aydin and Denizli provinces identified as the Qw haplotype were closely related to populations of Greece, whereas the remaining samples were identified as the Qe haplotype. This study indicated that the biotype status of the *B. tabaci* populations might have changed from year to year depending on several factors, such as insecticide resistance, host plant preferences, and climate niches to understand the factors causing changes in the biotype structure, pest populations should be monitored, and surveys must be conducted at regular intervals.
Keywords: *whitefly, biotype, MEAM1, Mediterranean, genetic variability*

Introduction

Bemisia tabaci (Genn.) is one of the most important pests of industrial plants, vegetables and cotton in tropical and subtropical regions (Brown et al., 1995). The pest was initially identified in Greece in 1889, and it has been responsible for several outbreaks in cotton. Although, its history dates back to 1928, the exact timeframe over which *B. tabaci* has caused damage to plants cultivated in Turkey is unknown (Göçmen and Özgür, 1990).

Bemisia tabaci has been reported to contain various biotypes that are morphologically indistinguishable from each other but differ according to their host sequences, fecundity, insecticide resistance and virus carrying ability (Bedford et al., 1994). Studies have shown that these biotypes can be genetically distinguished from each other using molecular methods (Frohlich et al., 1999; Bedford et al., 1994; Costa and Brown, 1991).

http://www.aloki.hu ● ISSN 1589 1623 (Print) ● ISSN 1785 0037 (Online)
DOI: http://dx.doi.org/10.15666/aeer/1802_23512361

In terms of qualitative and quantitative characteristics, the *B. tabaci* biotypes have been differentiated based on protein (Costa and Brown, 1991; Brown et al., 1995) and nucleotide polymorphisms using random amplified polymorphic DNA (RAPD) markers (Gawell and Barlett, 1993; Lima et al., 2002; Moya et al., 2001), amplified fragment length polymorphism (AFLP) markers (Cervera et al., 2000), restriction fragment length polymorphism (RFLP) markers (Abdullahi et al., 2004), ribosomal ITS1 sequences (De Barro, 2000) and microsatellites (De Barro, 2005; Valle et al., 2013). Furthermore, biotypes can be separated by analysing gene sequences isolated from the mitochondrial DNA (mtDNA) (Frohlich et al., 1999). Currently, because of the limitations of some molecular techniques, mtCOI gene is proposed for identification of several species within the *B. tabaci* complex (Dinsdale et al., 2010). Hitherto, *B. tabaci* has been reported to form a complex comprised of at least 24 different species that cannot be separated morphologically from each other (Dinsdale et al., 2010; De Barro et al., 2011).

The diversity of *B. tabaci* biotypes in Turkey has been investigated before. Bedford et al. (1994) reported the *B. tabaci* populations as the M biotype. Göçmen and Devran (2002) studied the genetic structures of eight *B. tabaci* populations collected from Antalya with the AFLP technique and found 2 groups in relation to their hosts. Ulusoy et al. (2002) reported the presence of the B biotype in the *B. tabaci* populations in Turkey. Göçmen et al. (2004) also predicted that the B, Q and M biotypes were found in Turkey using RAPD markers. In another study Bayhan et al. (2006) reported that the *B. tabaci* populations collected from Adana, Mersin and Hatay provinces were the B biotype based on analysis of the same single gene region for all the mtCOI sequences. Karut et al. (2012) carried out a survey on pests collected from cucumber, cotton, eggplant and soybean in the 2008-2009 production seasons in the Balcalı district of Adana and reported that the *B. tabaci* populations belonged to the B and Q biotypes, with the Q biotype being the most dominant. In 2015, southwestern populations of *B. tabaci* collected from cotton fields were also studied (Karut et al., 2017). According to the above findings, to date studies have been restricted to the eastern provinces of Turkey, and there is a need to determine the distribution of whitefly biotypes in Turkey using mtCOI sequences.

In this study, *B. tabaci* populations were sampled from various cultivated plants during 2005 and 2006 from different provinces of Turkey and identified as biotypes based on the sequence analysis of mtCOI regions. The purpose of the study was to determine the species/biotype structure and genetic diversity of the *B. tabaci* populations in Turkey. Furthermore, phylogenetic analysis was conducted to clarify the relationships among *B. tabaci* populations in Turkey.

Materials and methods

Adult *B. tabaci* samples were collected from cultivated plants in the Hatay, Adana, İçel, Antalya, Muğla, Aydın and Denizli provinces of Turkey (*Table 1; Fig. 1*). At least 100 individual adults were collected from each location using a mouth aspirator and stored in 96% alcohol for DNA isolation.

DNA extraction

Total DNA was isolated from the *B. tabaci* adults by using Omega DNA isolation kit (EZNA SQ Tissue DNA Kit, D5040-02) according to the manufacturer's instructions. The DNA was precipitated in isopropanol, kept at 20 °C overnight and then dissolved in 30 µl of distilled water.

http://www.aloki.hu ● ISSN 1589 1623 (Print) ● ISSN 1785 0037 (Online)
DOI: http://dx.doi.org/10.15666/aeer/1802_23512361

To identify the biotypes of the collected whitefly samples, a combination of the C1-J-2195(Primer A) and L2-N-3014 (Primer B) primer sets designed by Frohlich et al. (1999) was used to amplify a fragment of the mtCOI gene region (*Table 2*).

Table 1. *Sampling locations and host plants of the Bemisia tabaci*

Location	Host	Sampling date	GenBank accession numbers
HATAY			
Kırıkhan-Hassa	Cucumber	03.09.2005	MK360004
Samandağ	Eggplant	03.09.2005	MK360005
ADANA			
Mihmandar	Cotton and soybean	02.09.2005	MK360006
Mustafabeyli	Cucumber	02.09.2005	MK360007
MERSİN (İÇEL)			
Mahmutağa (Tarsus)	Eggplant	04.09.2005	MK360008
Gümüşkum	Eggplant	04.09.2005	MK360009
Ovacık (Silifke)	Eggplant	04.09.2005	MK360010
Melleç (Anamur)	Nightshade	01.09.2005	MK360011
ANTALYA			
Yurtpınar (Aksu)	Eggplant	30.09.2005	MK360012
Kampus (Uncalı-city center)	Cotton	28.11.2005	MK360013
Konaklı (Alanya)	Eggplant	30.09.2005	MK360014
Çobanlı (Gazipaşa)	Cucumber	30.09.2005	MK360015
Demirtaş (Alanya)	Eggplant	30.09.2005	MK360016
Kumluca (Mavikent)	Pepper	05.07.2006	MK360017
Demre	Pepper	05.07.2006	MK360018
MUĞLA			
Kınık	Cotton	17.08.2006	MK360019
Fethiye-Çalış	Eggplant	18.08.2006	MK360020
Ortaca	Cucumber	18.08.2006	MK360021
AYDIN			
Koçarlı	Cotton	18.08.2006	MK360022
DENİZLİ			
Beylerbeyi	Cotton	19.08.2006	MK360023

Table 2. *Primer sequences used in the amplification of the mtCOI gene region (Frohlich et al., 1999)*

Primer name	Primer sequence	Fragment size (bp)
Primer A (Forward)	5’ TTGATTTTTTGGTCATCCAGAAGT 3’	~ 800 bp
Primer B (Reverse)	5’ TCCAATGCACTAATCTGCCATATTA 3’	---------
Primer C (Forward)	5’ATAGCAGTGAGGCTGGAAAA 3’	760 bp
Primer D (Forward)	5’ GGGTATAATTTATGCTATA 3’	720 bp

Each PCR reaction was performed in a total volume of 12.5 µl containing 0.2 mM dNTPs (Larova), 2.5 mM of each primer (Biomer), 0.5 units of *Taq* DNA Polymerase

http://www.aloki.hu ● ISSN 1589 1623 (Print) ● ISSN 1785 0037 (Online)
DOI: http://dx.doi.org/10.15666/aeer/1802_23512361

(Bioron), 1.25 µl of reaction buffer solution, 4 mM $MgCl_2$ and 1 µl of DNA, as described by Frohlich et al. (1999).

Polymerase chain reaction (PCR) was carried out using the following cycling parameters: an initial denaturation step at 94 °C for 2 min, and 30 cycles of a denaturation step at 94 °C for 45 s, an annealing step at 48 °C for 45 s and an extension step at 72 °C 45 s. The amplified products were separated and visualized on a 1% agarose gel containing 10 mg/l of ethidium-bromide. Amplification products of approximately 800 bp in length were re-amplified with the primers B and C (*Table 2*) using the same PCR conditions used for the nested PCR amplifications when the amplicon yield was not sufficient for direct Sanger sequencing of the initial PCR products.

Single-band PCR products with the expected fragment size (760 bp) were stored at -20 °C for sequencing. Three different PCR products derived from different individuals from each population were sequenced with the B and Q biotype control samples obtained from Dr. A. R. Horowitz.

The amplicons were subjected to DNA sequencing using the capillary Sanger sequencing platform and the Beckman 8000 CEQ Genetic Analysis System according to the manufacturer's instructions with the exception of the reaction volume which was 10 µl instead of 20 µl. Since better and clear electropherogram signals were obtained from the forward primer D than for forward primer C in the initial tests, the sequencing reactions were carried out in both directions using forward primer D and reverse primer B.

Phylogenetic analysis

The raw fluorescence data were analysed with the 'Beckman Sequence Analysis' program. The obtained sequences were manually confirmed and edited, and the sequence of each individual sample was finalized. The determination of biotype structure of the cotton whitefly populations in Turkey and phylogenetic analyses were conducted as outlined in Boykin and De Barro (2014) with curated global dataset of mtCOI sequences of Bemisia tabaci species (Boykin et al., 2017). The sequences were aligned using Clustal W implemented in the MEGAX software (Kumar et al., 2018), and the phylogenetic analysis was performed using the MEGA X program with the Kimura two-parameter model and Neighbor- Joining method with 1000 bootstrap iterations. The genetic distances were calculated using Maximum Composite Likelihood Option of MEGAX.

Results

All whitefly samples yielded a band with an expected fragment size of ~760 bp using the indicated primer pair (*Table 2*) to amplify the mtCOI fragment. The sequences were trimmed to a length of 617 bp and aligned with the CLUSTAL W program. The alignment results indicated a lack of variation among samples derived from the same populations. Samples from the same population were identified as having the same mtCOI sequences (single haplotype) and therefore were considered as homogeneous.

In contrast to the lack of variation within populations, a total of thirty-two nucleotides variants were detected in the 617 bp sequence of the analysed region among populations. All of the variable nucleotide positions involved a single base substitution with the exception of one position at which the B, Qw and Qe haplotypes had the T, A,

http://www.aloki.hu ● ISSN 1589 1623 (Print) ● ISSN 1785 0037 (Online)
DOI: http://dx.doi.org/10.15666/aeer/1802_23512361

and C nucleotides, respectively. Furthermore, nucleotide bases in variable positions were not independent of each other. In other words, the nature of the variation at any nucleotide position in the mtCOI gene was related to the structure of the other changes. Therefore, the thirty-two different nucleotide polymorphisms identified in the studied populations did not result in thirty- two different haplotypes. Indeed, only three different haplotype groups were present in all tested individuals (*Fig. 1*). Among all haplotypes, the average nucleotide frequencies were A = 0.255, T = 0.431, G = 0.185 and C = 0.128. Hence, in light of these nucleotide values, the T + A and C + G base ratios reflected the rich A + T composition typically found in the genes of insect mitochondrial genes.

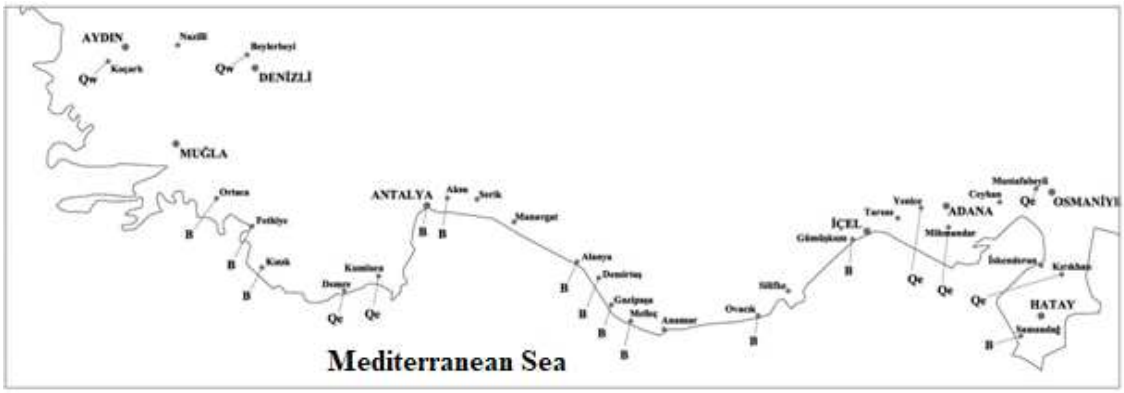

Figure 1. *The geographical distribution of the Bemisia tabaci biotypes in Turkey*

The Neighbor- Joining phylogenetic tree demonstrated that the cotton whitefly populations from Turkey were grouped into three different clusters (*Fig. 2*). When these populations were examined in relation to curated global dataset, they were grouped into two different biotypes commonly known worldwide as the B and Q biotypes which belong to the Middle East-Asia Minor 1 and Mediterranean species, respectively. Of the 20 populations analyzed eleven clustered with the B biotype in the same haplotype group (*Fig. 2*). Although the remaining nine populations were clustered with the Q biotype, the two populations collected from the Aydın-Denizli provinces (western Turkey) slightly differed from the other 7 population having Q biotype (*Fig. 2*). These two Q haplotypes were categorized with those present in Syria and Cyprus under the newly designated Qe haplotype, and the others were clustered with those present in Greece and Turkey/Aydın and Denizli province under the Qw haplotype to clearly delineate them (*Fig. 2*).

When the genetic distances of the three clusters of the Turkish populations were analyzed, they were observed to be less related to the other main group because they clustered under the main Mediterranean and MEAM1 group (*Fig. 2*). Accordingly, while the distance between the reference B biotype and Qe was 0.050, its distance to Qw was 0.055 and the genetic distance between Qe and Qw haplotypes was only 0.010. In contrast, the distances of the Turkish populations to the other world biotypes varied between 0.231 and 0.252 (*Fig. 2*). No nucleotide polymorphism was identified among all 11 Turkish populations of the B biotype. Similarly, no nucleotide polymorphism was found among the seven Qe haplotype populations or between the two Qw haplotype populations.

http://www.aloki.hu ● ISSN 1589 1623 (Print) ● ISSN 1785 0037 (Online)
DOI: http://dx.doi.org/10.15666/aeer/1802_23512361

Figure 2. *Two parts of the phylogenetic tree generated by the MEGAX Phylogenetic Analysis Program under the Neigbour Joining with 1000 Bootstrap values using the mtCOI sequences of the curated global dataset and cotton whitefly samples collected from different geographical regions of Turkey. A: whitefly samples from Turkey clustered within Mediterranean species, B: whitefly samples from Turkey clustered within MEAM1 species (complete tree was added as supplementary file). *Populations used in this study*

http://www.aloki.hu ● ISSN 1589 1623 (Print) ● ISSN 1785 0037 (Online)
DOI: http://dx.doi.org/10.15666/aeer/1802_23512361

Discussion

The mtCOI gene region sequence was first used by Frohlich et al. (1999) to determine the biotypes of whitefly populations from different parts of the world. They were identified about 240 polymorphic nucleotides in their study. However, in our study, only 32 polymorphic nucleotides were detected. Similarly, Horowitz et al. (2003) reported limited polymorphism levels in populations collected from narrow geographical regions like our findings. Although the polymorphism level recorded in this study was low compared to that of the global populations, the mtCOI sequence information both provided sufficient data about the cotton whitefly populations in Turkey and allowed us to determine the biotypes in different regions of the country. When the geographical distribution of these biotypes was analysed, the emergence of the certain biotypes was observed intermittently rather than in a structure of spread and infestation into a geographical region. For instance, whereas the B biotype was prevalent in the Hatay/Samandağı region, the Q biotype was found in the Kırıkhan region (*Fig. 1*). Similarly, whereas the B biotype was present in the eastern region of Antalya, the Q biotype was found in the western region of the province; moreover, the B biotype was observed as the dominant population in Muğla province, which is geographically close to Antalya (*Fig. 1*).

In the current study, investigation of the biotype distribution in Turkey found that the B biotype was intermittently present in three geographical regions. The biotype could either have been introduced into Turkey from various locations and thus was still been undergoing the spreading process or could have been introduced into Turkey from only one location and not yet replaced the Q biotype in some regions. Another scenario was that the B biotype became the prevalent biotype after its introduction into Turkey, but the Q biotype started to dominate the B biotype in various geographical regions, as was observed recently. For instance, the Q biotype was identified several years after the B biotype was identified in Spain (Guirao et al., 1997). Later the Q biotype prevailed in some regions, whereas the B and Q biotypes survived together in others (Simón et al., 1999). In surveys conducted in these regions, only the Q biotype was detected (Simón et al., 2007).

In a study conducted between 2000 and 2002 in the Adana, Mersin and Hatay provinces of Turkey, the B biotype was the sole biotype present in these regions. Additionally, nucleotide polymorphisms were reported to be at a very low level among the B biotype populations which were highly homogeneous (Bayhan et al., 2006). The homogeneity of the B biotype reported by Bayhan et al. (2006) was in accordance with our findings because all populations in this study were clustered around the B biotype with 100% nucleotide sequence similarity. Since the GenBank accession numbers of the B biotypes reported by Bayhan et al. (2006) were not provided, we could not make a direct comparison between those sequences and the sequences generated in this study. The B biotype was also identified in Mersin province in 2004 (Topakçı and Göçmen, 2018). In another study carried out in the Mersin and Antakya provinces, whitefly samples collected from cucumbers, beans and tomatoes between 2007 and 2009, were identified as the B biotype (Erdoğan et al., 2011). These two studies clearly proved that the B biotype was the dominant biotype in these provinces.

In 1985, the whitefly specimens collected from cotton plants in Adana were named 'TC' and were reported to present very similar mtCOI nucleotide profiles to the Q biotype (Bedford et al., 1994). The Q biotype was determined to be rife in our study among samples collected from the Adana and Hatay regions. In this region, the presence

http://www.aloki.hu ● ISSN 1589 1623 (Print) ● ISSN 1785 0037 (Online)
DOI: http://dx.doi.org/10.15666/aeer/1802_23512361

of the Q biotype in the 2004 samples came to the forefront. (Topakçı and Göçmen, 2018). In addition, we have observed that this trend to continued based on samplings from among the regions. Also Karut et al. (2012) reported in their study performed in Adana that four of the 18 samples collected from cucumbers, cotton, eggplants and soya in 2008 and in only one of the 13 samples collected from the same plant species in 2009 were identified as be the B biotype; hence, the remaining samples were the Q biotype. During the 2006–2011 (except for the 2010) period, the majority of the whitefly population collected from cotton plants in Adana were identified as the Q biotype within the Mediterranean group (Karut et al., 2014).

Based on the above findings, the Q biotype may have been the local biotype in the past and then lost its dominance due to an aggressive B biotype within the region. In reference to Bayhan et al. (2006) we can speculate that the B biotype was dominant in the region and continues to spread. However, this trend has changed after 2005, when the Q biotype has started to replace the B biotype in Adana and Hatay provinces. As demonstrated in this study, the Q biotype may be in the process of becoming the dominant biotype. In a similar study, Chu et al. (2010) reported the presence of the Q (MED) biotype in the Shandong District of China: the B biotype was the dominant biotype until 2005, but the Q biotype became the dominant biotype within three years. Similar data were reported for populations in Spain; after introduction of the B biotype in the country, the Q biotype regained its dominance over the B biotype for a period of time (Brown et al., 2000; Simón et al., 2007). In another study, the Q biotype was reported to have become dominant in many regions of China partly by occupying the B biotype regions (Teng et al., 2010).

In the present study, whitefly populations collected on vegetables and cotton from Antalya province between 2005 and 2006 were identified as the B and Q biotypes. Both the B and Q biotypes were found in Antalya in 2005 (Topakçı and Göçmen, 2018). However, Erdoğan et al. (2011) reported that only the B biotype was collected from tomatoes and eggplants in Antalya province during the 2007-2009 period. Similarly, only the B biotype was reported from different districts of Antalya province in 2011 (Yükselbaba and Göçmen, 2012).

The populations collected from Aydın and Denizli provinces (Qw) were clustered within the same subgroup showed one-to-one similarity to the Greece Q biotype, and the populations collected from Adana, Hatay and Antalya provinces (Qe) were clustered within the same subgroup with the Syria and Cyprus samples. Similar findings were reported about the species and subgroups of *B. tabaci* populations collected from southwestern cotton fields in 2015 (Karut et al., 2017). In one study, the Q biotypes clustered into two subgroups under the Mediterranean main group (Dinsdale et al., 2010). The population from Turkey used by Dinsdale et al. (2010), was found to have the same evolutionary relationship with the Qe biotypes used in this study. It was observed that the samples collected from Spain, Greece and other European countries were clustered into the same subgroup of the Mediterranean main group, hence, our data are in agreement with the above-mentioned information after clarification of the Q biotype into Qe and Qw haplotypes.

The intra-population variations in all the three biotypes found in Turkey are at the zero level in terms of mtCOI. For this reason, predicting which of these populations appeared earlier in our country is impossible. However, a collected and known sample was established to show a close relationship to the Q biotype; this sample is regarded as the oldest record for our country. Based on the literature, the B biotype was first

http://www.aloki.hu ● ISSN 1589 1623 (Print) ● ISSN 1785 0037 (Online)
DOI: http://dx.doi.org/10.15666/aeer/1802_23512361

described between 1988 and 1989 in the USA, whereas the Q biotype was first described in Spain in 1997. However, the origin of both biotypes is known to be the Mediterranean. For this reason, the likelihood of the B biotype existing in our country before 1985 is at least as high as that of the Q biotype. Answering this question will only be possible if more variations of each biotype are investigated and revealed. For this goal, investigating these biotypes with different fingerprinting methods is a useful approach. When geographically distributed biotypes are examined, the transition zone between the B and Q biotypes will probably be the transition zone between Tarsus and Mersin from Q to B, whereas Central Antalya is likely to be a re-transition zone from B to Q.

Conclusion

Studies needs to be conducted in these regions to provide detailed information about gene exchange between the biotypes or the evolution of the biotypes into dominant species in different geographic regions. In addition, testing whitefly samples taken at regular intervals every year will be useful for monitoring how the biotypes are distributed in our southern regions, where agriculture is heavily concentrated.

Acknowledgements. We thank the TÜBİTAK for their contribution to the TOVAG-104O312 project.

Conflict of interests. The authors declare that they have no conflict of interests.

REFERENCES

[1] Abdullahi, I., Winter, S., Atiri, G. I., Thottappilly, G. (2003): Molecular characterization of whitefly, *Bemisia tabaci* (Hemiptera: Aleyrodidae) populations infesting cassava. – Bulletin of Entomological Research 93(2): 97-106.

[2] Bayhan, E., Ulusoy, M., Brown, J. K. (2006): Host range, distribution and natural enemies of *Bemisia tabaci* B bi*otype* (Homoptera:Aleyrodidae) in Turkey. – Journal of Pest Science 79: 233-240.

[3] Bedford, I. D., Briddon, R. W., Brown, J. K., Rosell, R., Markham, P. G. (1994): Geminivirus transmission and biological characterisation of *Bemisia tabaci* (Gennadius) biotypes from different geographic regions. – Annals of Applied Biology 125: 311-325.

[4] Boykin, L. M., De Barro, P. J. (2014): A practical guide to identifying members of the *Bemisia tabaci* species complex: and other morphologically identical species. – Frontiers in Ecology and Evolution 2(45) doi.org/10.3389/fevo.2014.00045.

[5] Boykin, L. M., Savill, A., De Barro, P. (2017): Updated mtCOI reference dataset for the *Bemisia tabaci* species complex F1000. – Research 6: 1835 (DOI: 10.12688/f1000research.12858.1).

[6] Brown, J. K. (2000): Molecular markers for the identification and global tracking of whitefly vector-Begomovirus complexes. – Virus Res. 71(1-2): 233-260.

[7] Brown, J. K., Coats, S. A., Bedford, I. D., Marcham, P. G., Bird, J., Frohlich, D. R. (1995): Characterization and distribution of esterase electromorphs in the whitefly, *Bemisia tabaci* (Genn.) (Homoptera:Aleyrodidae). – Biochemical Genetics 33(7/8): 205-214.

[8] Cervera, M. T., Cabezas, J. A., Simón, B., Martinez-Zapater, J. M., Beitia, F., Cenis, J. L. (2000): Genetic relationships among biotypes of *Bemisia tabaci* (Hemiptera:Aleyrodidae) based on AFLP analysis. – Bulletin of Entomological Research 90: 391-396.

http://www.aloki.hu ● ISSN 1589 1623 (Print) ● ISSN 1785 0037 (Online)
DOI: http://dx.doi.org/10.15666/aeer/1802_23512361

[9] Chu, D., Wan, F. H., Zhang, Y. J., Brown, J. K. (2010): Change in the biotype composition of Bemisia tabaci in Shandong Province of China from 2005 to 2008. – Environmental Entomology 39: 1028-1036.
[10] Costa, H. S., Brown, J. K. (1991): Variation in biological characteristics and esterase patterns among populations of Bemisia tabaci and the association of one population with silverleaf symptom induction. – Entomologia Experimentalis et Applicata 61: 211-219.
[11] De Barro, P. J. (2005): Genetic structure of the whitefly Bemisia tabaci in the Asia-Pasific region revealed using microsatellite markers. – Molecular Ecology 14: 3695-3718.
[12] De Barro, P. J., Driver, F., Trueman, J. W. H., Curran, J. (2000): Phylogenetic relationships of world populations of *Bemisia tabaci* (Gennadius) using ribosomal ITS1. – Molecular Phylogenetics and Evolution 16(1): 29-36.
[13] De Barro, P. J., Liu, S. S., Boykin, L. M., Dinsdale, A. B. (2011): *Bemisia tabaci*: a statement of species status. – Annual Review of Entomology 56: 1-19.
[14] Dinsdale, A., Cook, L., Riginos, C., Buckley, Y. M., De Barro, P. (2010): Refined global analysis of *Bemisia tabaci* (Hemiptera: Sternorrhyncha: Aleyrodoidea: Aleyrodidae) mitochondrial cytochrome oxidase 1 to identify species level genetic boundaries. – Annals of the Entomological Society of America 103(2): 196-208.
[15] Erdoğan, C., Velioğlu, A. S., Gürkan, M. O., Moores, G. D., Denholm, I. (2011): Determination of *Trialeurodes vaporariorum* (Westw.) and *Bemisia tabaci* (Genn.) (Hemiptera:Aleyrodidae) species collected from greenhouses by using polyacrylamide gel electrophoresis. – Bitki Koruma Bülteni 51(4): 373-385 (in Turkish with English abstract).
[16] Frohlich, D. R., Torres-Jerez, I., Bedford, I. D., Markham, P. G., Brown, J. K. (1999): A phylogeographical analysis of the *Bemisia tabaci* species complex based on mitochondrial DNA markers. – Molecular Ecology 8: 1683-1691.
[17] Gawell, N. J., Barlett, A. C. (1993): Characterization of differences between whiteflies using RAPD-PCR. – Insect Molecular Biology 2(1): 33-38.
[18] Göçmen, H., Devran, Z. (2002): Determination of genetic variation in populations of *Bemisia tabaci* in Antalya. – Turkish Journal of Agriculture and Forestry 26: 211-216.
[19] Göçmen, H., Özgür, A. F. (1990): Migration of cotton whitefly *Bemisia tabaci* (Genn.) (Homoptera:Aleyrodidae) between various host plants and its population changes (in Turkish). – Çukurova University, Institute of Natural and Applied Science, Journal of Science and Engineering 4(3): 115-129.
[20] Göçmen, H., İkten, C., Göçmen, M., Devran, Z., Topakçı, N. (2004): The research on genetic variations of cotton white fly *Bemisia tabaci* (Genn.) (Homoptera; Aleyrodidae). – Proceedings of the First Plant Protection Congress of Turkey, 8-10 September 2004, Samsun, Turkey.
[21] Guirao, P., Beitia, F., Cenis, J. L. (1997): Biotype determination of Spanish populations of *Bemisia tabaci* (Hemiptera:Aleyrodidae). – Bulletin of Entomological Research 87: 587-593.
[22] Horowitz, A. R., Denholm, I., Gorman, K., Cenis, J. L., Kontsedalov, S., Ishaaya, I. (2003): Biotype Q of *Bemisia tabaci* identified in Israel. – Phytoparasitica 31(1): 1-5.
[23] Karut, K., Malik, A. A. Y., Kazak, C., Kamberoğlu, M. A., Ulusoy, M. R. (2012): Determination of biotypes of *Bemisia tabaci* Gennadius 1889 (Hemiptera: Aleyrodidae) on different host plant in Adana (Balcalı) by using two different molecular methods. – Turkish Journal of Entomology 36: 93-100 (in Turkish with English abstract).
[24] Karut, K., Kaydan, M. B., Castle, S. J., Kazak, C., Ulusoy, M. R. (2014): Study on species composition of *Bemisia tabaci* (Gennadius, 1889) (Hemiptera: Aleyrodidae) on cotton in Çukurova plain, Turkey. – Turkish Journal of Entomology 38(1): 43-50.
[25] Karut, K., Karaca, M. M., Döker, İ., Kazak, C. (2017): Analysis of Species, Subgroups, and Endosymbionts of *Bemisia tabaci* (Hemiptera: Aleyrodidae) From Southwestern Cotton Fields in Turkey. – Environmental Entomology. DOI: 10.1093/ee/nvx093.

http://www.aloki.hu ● ISSN 1589 1623 (Print) ● ISSN 1785 0037 (Online)
DOI: http://dx.doi.org/10.15666/aeer/1802_23512361

[26] Kumar, S., Stecher, G., Li, M., Knyaz, C., Tamura, K. (2018): MEGA X: Molecular Evolutionary Genetics Analysis across computing platforms. – Molecular Biology and Evolution 35: 1547-1549.
[27] Lima, L. H. C., Campos, L., Moretzsohn, M. C., Navia, D., De Oliveira, M. R. V. (2002): Genetic diversity of *Bemisia tabaci* (Genn.) populations in Brazil revealed by RAPD markers. – Genetic and Molecular Biology 25(2): 217-223.
[28] Moya, A., Guirao, P., Cifuentes, D., Beitias, F., Cenis, J. L. (2001): Genetic diversity of Iberian populations of *Bemisia tabaci* (Hemiptera:Aleyrodidae) based on RAPD- PCR. – Molecular Ecology 10: 891-897.
[29] Simón, B., Moriones, E., Soria, C., Beitia, F., Bosco, D., Cenis, J. L. (1999): Variación genética de poblaciones de *Bemisia tabaci* (Gennadius) en la cuenca del Mediterráneo occidental. – Proc. Congreso Nacional de Entomología Aplicada. Aguadulce, Spain, Nov 8-12.
[30] Simón, B., Cenis, J. L., De La Rúa, P. (2007): Distribution patterns of the Q and B biotypes of *Bemisia tabaci* in the Mediterranean Basin based on microsatellite variation. – Entomologia Experimentalis et Applicata 124(3): 327–336.
[31] Teng, X., Wan, F. H., Chu, D. (2010): *Bemisia tabaci* biotype Q dominates other biotypes across China. – Florida Entomologist 93(3): 363-368.
[32] Topakçı, N., Göçmen, H. (2018): A research on the determination of molecular genetic characteristics of some *Bemisia tabaci* (Genn.) (Hemiptera:Aleyrodidae) populations. – Fresenius Environmental Bulletin 2: 1095-1103.
[33] Ulusoy, R., Brown, J. K., Bayhan, E. (2002): The B biotype of *Bemisia tabaci* now established in European whitefly studies. – Network Newsletter 13(5): 4.
[34] Valle, G. E., Lourenção, A. L., Zucchi, M. I., Pinheiro, J. B., De Abreu, A. G. (2013): Population variability of *Bemisia tabaci* (Genn.) in different hosts. – Genetics and Molecular Research 12(4): 4615-4624.
[35] Yükselbaba, U., İkten, C., Göçmen, H. (2012): Determination of the biotypes of *Bemisia tabaci* (Gennadius) (Hemiptera: Aleyrodidae) populations from Antalya Province of Turkey by sequence analysis of mitochondrial cytochrome oxidase I (mtCOI) gene region. – *QBOL-EPPO* Conf-DNA Barcoding and Diagnostic Methods for Plant Pests, 21-25 May, Haarlem, Holland.

http://www.aloki.hu ● ISSN 1589 1623 (Print) ● ISSN 1785 0037 (Online)
DOI: http://dx.doi.org/10.15666/aeer/1802_23512361

DETECTION OF A NEGATIVE BIOMARKER FOR AMEBIASIS (*ENTAMOEBA HISTOLYTICA*) IN THE HUMAN GUT MYCOBIOME

ABULJADAYEL, D.[1] – ATEF, A.[1] – AL-MATARY, M.[1] – EDRIS, S.[1,2,3] – AL-QUWAIE, D. A. H.[4] – ALSUBHI, N. H.[4] – AL-HINDI, R. R.[1] – SABIR, J. S. M.[1] – HALL, N.[1,5] – BAHIELDIN, A.[1,2*]

[1]*Department of Biological Sciences, Faculty of Science, King Abdulaziz University (KAU), P.O. Box 80141, Jeddah 21589, Saudi Arabia*

[2]*Department of Genetics, Faculty of Agriculture, Ain Shams University, Cairo, Egypt*

[3]*Princess Al-Jawhara Al-Brahim Centre of Excellence in Research of Hereditary Disorders (PACER-HD), Faculty of Medicine, King Abdulaziz University (KAU), Jeddah, Saudi Arabia*

[4]*Department of Biological Sciences, Rabigh College of Science and Arts, King Abdulaziz University (KAU), Rabigh, Saudi Arabia*

[5]*The Genome Analysis Center, Norwich Research Park, Norwich NR4 7UH, UK*

**Corresponding author*
e-mail: abmahmed@kau.edu.sa

(Received 8th Nov 2019; accepted 12th Feb 2020)

Abstract. Amebiasis caused by *Entamoeba histolytica* parasite is among the worst gut diseases worldwide. The study involved detection of gut mycobiome signature of the infected subjects in a trial to improve ability to diagnose and treat this disease. The results indicated that diversity of samples slightly changed due to infection. Dendrogram indicated that the most common phyla in the human gut are Ascomycota, Basidiomycota and Zygomycota. Species *Pichia kudriavzevii*, *Candida glabrata*, *Saccharomyces cerevisiae* of phylum Ascomycota and *Rhodotorula mucilaginosa* of phylum Basidiomycota were found highly OTU abundant. Weighted unifrac diversity distances resulted in complete separation of the two groups. Differential abundance analysis indicated that four phyla, six families, nine genera and ten species showed considerable changes in gut mycobiome signatures within and among groups. Unclassified species of genus *Malassezia* (phylum Basidiomycota) showed high abundance in infected subjects as compared to healthy subjects, while families Saccharomycetaceae and Trichocomaceae, genus *Saccharomyces* and species *S. cerevisiae* showed opposite results. Linear discriminant analysis effect size (LEFSE) indicated that family Saccharomycetaceae, of which *S. cerevisiae* is a downstream taxon, can be a negative biomarker for amebiasis. In conclusion, the study provides new insights into possible use of *Saccharomyces* as a probiotic against amebiasis.
Keywords: *encystation, yeast, Crabtree effect, oxidative stress, chitin formation*

Introduction

Entamoeba histolytica parasite is among the most common causes of death worldwide (WHO, 1997). It is estimated that around 50-100 million people are infected with the disease each year. Infection can be symptomatic (dysentery or amoebic colitis) or asymptomatic, and can also be invasive (amoebic liver abscess) (Stanley, 2003; Ximénez et al., 2009; Lozano et al., 2010; Verkerke et al., 2012). Furthermore, amoebae can cause abscess in the brain, pericarditis in the heart or pleuropulmonary disease in the lung (Stanley, 2003). Infection is usually drug-treated (Ali and Nozaki, 2007), however, in severe cases surgical intervention might be necessary (Ishida et al., 2003;

http://www.aloki.hu ● ISSN 1589 1623 (Print) ● ISSN 1785 0037 (Online)
DOI: http://dx.doi.org/10.15666/aeer/1802_23632394

Gupta et al., 2009). Amebiasis is proven to be mainly associated with water supplies contaminated with human feces resulting in 50,000-100,000 deaths reported annually, which make this protozoan parasite a significant cause of death worldwide (WHO, 1997; Soares et al., 2019).

E. histolytica parasite is transmitted via the ingestion of water contaminated with cysts. After excystation, the *Entamoeba* trophozoite divides and colonizes the colon, then, eventually produces new cysts that are excreted into the environment (Ali and Nozaki, 2007). Two major processes are crucial for the existence and cycling of these two forms of *Entamoeba*. They are encystation and trophozoite adhesion to human cells. If one of the two processes is impaired, then, existence or life cycling of the parasite will be in jeopardy. Encystation requires a number of processes including Gal-lectin production and chitin metabolism (Mi-ichi et al., 2016). Chitin in the cyst wall comprises of two chitin synthases (Chs), one of which is unique (EhCHS-1) to *Entamoeba*, while the other (EhCHS-2) resembles those in insects, fungi and nematodes (Van Dellen et al., 2006). Adhesion of trophozoites to human cells is the main event of subsequent cytopathogenic activities, contact-mediated cytolysis and phagocytosis, intestinal colonization and invasion (Eaton et al., 1970; Trissl et al., 1978; Ravdin et al., 1980; Mi-ichi et al., 2016). Phagocytosis is a mandatory process for survival of this organism, while blocking this process results in the inhibition of its proliferation and loss of pathogenicity (Hirata et al., 2007; Iyer et al., 2019). Other process for survival of *Entamoeba* is the modifications in the structure of transmembrane proteins that makes the parasite unidentified, thus, helps in escaping the host immune system (Khomkhum et al., 2019).

The human gut ecosystem contains a microbiome representing the three domains of life, with fungi—the mycobiome—predominates gut Eukarya (Rajilic-Stojanovic et al., 2007; Scanlan and Marchesi, 2008). The gut microbiome is presumed sterile at birth and the primary route for microbes to enter the gastrointestinal (GI) tract occurs via ingestion (Penders et al., 2006) of which Saccharomycetalean yeasts are the first fungi detected in the infant gut (Bliss et al., 2008). The exact relationship of host gut and its ecosystem, comprising prokaryotes, fungi, viruses and parasites, is extremely obscure (Hugon et al., 2017). The composition of the different microbiomes of the human body reflects health and disease parameters (Moyes and Naglik, 2012; Wang et al., 2014; Gouba and Drancourt, 2015; Mukherjee et al., 2015; Richard et al., 2015). Thus, studying the gut microbiota of *Entamoeba*-infected subjects might help in improving our understanding of these parameters that help in diagnosing and treating the disease more efficiently.

Although human mycobiomes have received little attention compared with bacteriomes, a number of recent articles have evidenced the importance of this organ in the whole body (Cui et al., 2013; Huffnagle and Noverr, 2013; Seed, 2014; Underhill and Iliev, 2014), especially in the gut (Ianiro et al., 2014; Kirschner et al., 2015; Suhr and Hallen-Adams, 2015). Therefore, the present study was planned to address the possible influence of human gut mycobiome on the occurrence and level of *Entamoeba* infection. The study also attempted to detect new biomarkers linked to amebiasis.

Materials and methods

Recruitment of participants and sample collection

Samples have been collected during summer 2019 from dysentery-infected subjects in four hospitals in Jeddah, KAU. An ethical approval (no. A00451) was issued by the Ministry of Health, Saudi Arabia following the regulation of the General Administration

http://www.aloki.hu ● ISSN 1589 1623 (Print) ● ISSN 1785 0037 (Online)
DOI: http://dx.doi.org/10.15666/aeer/1802_23632394

for Research and Studies at the Ministry of Health (registration no. 1195437) and the National Committee for Medical and Biological Ethics (registration no. H-02-J-002). Consent forms were filled by healthy and infected subjects or their relatives at sampling time. Patient's fecal samples were diagnosed by microscopic examination and positive samples were kept in iSWAB-TM Microbiome©2016 (Mawi DNA Technologies LLC. USA/Canada) to ensure the integrity of DNA required for deep sequencing. Genomic DNA was extracted using the QIAamp® DNA Mini kit (Qiagen®51306; Hilden, North Rhine-Westphalia, Germany) according to the manufacturer's instructions. DNA purity was evaluated via A260/A280 ratio using NanoDrop 7000 Spectrophotometer (Thermo Fisher Scientific, Waltham, MA, USA), and DNA integrity was checked by 1% agarose gel electrophoresis. PCR amplification of the V5-V7 region of 18S rRNA gene was performed using the universal primers SSU0817F (forward) 5′-TTAGCATGGAATAATRRAATAGGA -3′ and SSU1196R (reverse) 5′-TCTGGACCTGGTGAGTTTCC -3′. The PCR program was: initial denaturation at 95 °C for 5 min; 25 cycles of denaturation at 95 °C for 30 s, annealing at 56 °C for 30 s, and extension at 72 °C for 40 s; and final extension of 72 °C for 10 min. Amplicons were run on agarose gel (1.2%). Based on PCR results, original high-quality DNAs were shipped to Beijing Genome Institute (BGI) in China for library construction and deep sequencing on Illumina Miseq platform to recover ≥ 300 bp pair-ended reads of the V5-V7 region of 18S rRNA gene.

18S dataset processing and statistics

The ends of each read were overlapped to generate high-quality, full-length reads. The resulted sequencing data will eventually be deposited in the European Nucleotide Archive (ENA) (https://www.ebi.ac.uk/ena/submit/sra/#studies). The raw data were pre-processed to get clean data by in-house procedure as the following: (1) truncation of sequence reads not having an average quality of 20 over a 25 bp sliding window based on the Phred algorithm (Ewing and Green, 1998), (2) removal of trimmed reads having less than 75% of their original length, as well as its paired read; (3) removal of reads contaminated by adapter (default parameter: 15 bases overlapped by reads and adapter with maximal 3 bases mismatch allowed); (4) removal of reads with ambiguous base (N base), and its paired reads; and (5) removal of reads with low complexity (default: reads with 10 consecutive same base). The consensus sequence was generated by FLASH (Fast Length Adjustment of Short reads, v1.2.11; Magoc and Salzberg, 2011) in case the two paired-end reads overlapped with the following parameters: (1) minimal overlapping length: 15 bp; (2) mismatching ratio of overlapped region: < = 0.1; and (3) paired end reads without overlaps were removed.

Then, tags were clustered to OTU (Operational Taxonomic Unit) by scripts of software USEARCH (v7.0.1090; Edgar, 2010; http://drive5.com/usearch/manual/uparse_pipeline.html) as the following: (1) the tags were clustered into OTU with a 97% threshold by using UPARSE (Edgar, 2013), and the OTU unique representative sequences were obtained; (2) *de novo* chimeras were filtered out by using UCHIME (v4.2.40, Edgar et al., 2011); and (3) all tags were mapped to each OTU representative sequences using USEARCH GLOBAL. Then, the tags number of each OTU in each sample was summarized in OTU abundance table. OTU representative sequences were taxonomically classified using Ribosomal Database Project (RDP) Classifier (v.2.2; Cole et al., 2014), using 0.6 confidence values as cutoff. Silva (default) V119 database was used for species annotation (Quast et al., 2013).

http://www.aloki.hu ● ISSN 1589 1623 (Print) ● ISSN 1785 0037 (Online)
DOI: http://dx.doi.org/10.15666/aeer/1802_23632394

OTUs were filtered as the following: (1) unassigned OTUs were removed; and (2) OTUs not assigned to the target species were removed. Then, filtered tags were clustered into OTUs to be used in downstream processing.

Alpha diversity was addressed by Shannon and Simpson indices. Both parameters were calculated by Mothur (v1.31.2; Schloss et al., 2009), and the corresponding boxplot of alpha diversity and rarefaction curve were drawn by software R (v3.1.1; https://cran.r-project.org/bin/windows/base/old/3.1.1/). Drawing rarefaction curve was based on calculating OTU numbers of the extracted tags (in multiples of 500), then, detecting the maximum depth (no. reads) permitted to retain all samples in the dataset. Sequences were extracted randomly according to the minimum sequence number for all samples, and the extracted sequences formed a new 'OTU table biom' file.

The representative sequences were aligned against the Silva core set (Silva_108_core_aligned_seqs) using PyNAST (Caporaso et al., 2010b) by 'align_seqs.py'. Then, a representative OTU phylogenetic tree was constructed using the QIIME (v1.80, Caporaso et al., 2010b) built-in scripts including the fast-tree method for tree construction. The tags with the highest abundance of each genus was chosen as the corresponding genus representative sequences, and genus level phylogenetic tree was obtained by the same way of OTU phylogenetic tree. Then, the phylogeny tree was imaged by software R (v3.1.1).

Venn diagram was drawn by Venn program of software R (v3.1.1), while differences in the relative abundances of taxa at the phylum, genus and species levels were analyzed using Metastats (Paulson et al., 2011). Benjamini–Hochberg false discovery rate (FDR) correction (Benjamini and Hochberg, 1995) was used to correct for multiple hypothesis testing where applicable.

Heat maps were generated using the package 'gplots' of software R (v3.1.1). The used distance algorithm is 'euclidean' and the clustering method is 'complete'. At phylum level, all species were used to draw the heat map and taxa of which abundance is less than 0.5% in all samples were classified as 'others'. To minimize the differences degree of the relative abundance value, the values were all log transformed.

To detect the beta diversity within and between groups, the weighted and unweighted UniFrac distances were calculated (Lozupone et al., 2011) and plotted *via* principal coordinate analysis (PCoA) using package 'ade4' of software R (v3.1.1). UniFrac uses the system evolution information to compare the composition of community species between samples. The results can be used as a measure of beta diversity. It takes into account the distance of evolution between species, and the higher the index values, the greater the differences between samples or groups. The UniFrac is divided into weighted UniFrac and unweighted UniFrac of which the weighted UniFrac considers the abundance of sequences, while unweighted UniFrac puts more emphasis on species presence or absence.

Linear discriminant analysis (or LDA) Effect Size (LEFSE) was done to determine the features (organisms, clades, operational taxonomic units, genes, or functions) explaining the differences between the two groups of subjects by coupling standard tests for statistical significance in addition to the tests encoding biological consistency and effect relevance as described (Abarenkov et al., 2010). In the LEFse tree, different colors indicate different groups. Colored node (red) indicates an important microbe biomarker in either group and the biomarker name lists in the upper right corner of the tree. The yellow nodes represent the biomarkers, which do not show any importance in either group.

http://www.aloki.hu ● ISSN 1589 1623 (Print) ● ISSN 1785 0037 (Online)
DOI: http://dx.doi.org/10.15666/aeer/1802_23632394

Results

Statistics of gut 18S rRNA sequence datasets

Illumina MiSeq was used in analyzing a number of two healthy subjects as well as nine patients proved via microscopic examination to be infected with *Entamoeba*. The statistical analysis of gut mycobiome was done for the 11 gut mycobiome samples based on the 18S rRNA as shown in *Table 1*. The average sequence length per read was 296 bp across different samples ranging from 293 to 299 bp. Average percentages of N base and low-quality reads were as little as 0.097% and 0.00%, respectively. A total of 9,086,626 raw sequence reads were generated across subjects with an average of 1,514,437 reads per sample. While, a total of 9,050,377 clean sequence reads were generated across subjects with an average read number of 822,762 per sample. Average percentage of data utilization was as high as 99.61% (*Table 1*). The data in *Figure 1* indicates that the average number of clean reads is 791,462 across healthy subjects, while 829,717 across patients. The highest value of clean reads was given to patient 5 or P5 (1,127,017), while the lowest was given to P1 (692,848) (*Table 1*; *Fig. 1*).

Table 1. *Statistics of data generated from deep sequencing for healthy and Entamoeba-infected individuals*

Sample ID	Reads length (bp)	Raw data (Mbp)	N base (%)	Low quality (%)	Clean data (Mbp)	Raw reads	Clean reads	Read utilization (%)
H1	294:298	470.19	0.098	0	469.07	794239	792348	99.76
H2	294:297	469.35	0.096	0	467.23	794155	790575	99.55
P1	294:296	409.75	0.094	0	408.78	694500	692848	99.76
P2	293:299	473.51	0.098	0	472.17	799844	797581	99.72
P3	293:298	435.56	0.094	0	434.65	736986	735454	99.79
P4	293:297	506.06	0.099	0	504.42	857721	854957	99.68
P5	295:299	673.04	0.097	0	669.45	1133058	1127017	99.47
P6	295:298	421.7	0.100	0	419.55	711138	707511	99.49
P7	295:297	550.46	0.096	0	546.63	929832	923365	99.3
P8	295:296	446.04	0.099	0	444.03	754715	751321	99.55
P9	294:299	522.1	0.096	0	520.3	880435	877400	99.66

A total of 8,776,506 tag-linked sequences were generated across subjects with an average number of 783,091 sequences across healthy subjects and 801,147 sequences across patients (*Fig. 1*). The highest value of tag-linked sequences was given to patient P5 (1,061,387), while the lowest was given to P1 (685,566) (*Table 1*; *Fig. 1*), with an average connect percentage of 97.16%. These sequence tags were assigned to 146 eukaryotic OTUs (operational taxonomic units) across samples with an average of 60,113 sequence tags per OTU. The results for the number of observed species (S_{obs}) or number of OTUs indicated a summation of 698 OTUs for the 11 samples with an average of about 63 OTUs per sample ranging from 47 (P6) to 82 (P4) OTUs and averages of 60 and about 64 OTUs for healthy subjects and patients, respectively (*Fig. 1*). Number of OTUs in relation to relative abundance of OTUs for different healthy subjects (H) and *Entamoeba*-infected patients (P) is shown in *Figure A1* in the *Appendix*. The results in this figure complement those of *Figure 1* as P4 showed the highest number and abundance of OTUs, while P6 showed the lowest.

http://www.aloki.hu ● ISSN 1589 1623 (Print) ● ISSN 1785 0037 (Online)
DOI: http://dx.doi.org/10.15666/aeer/1802_23632394

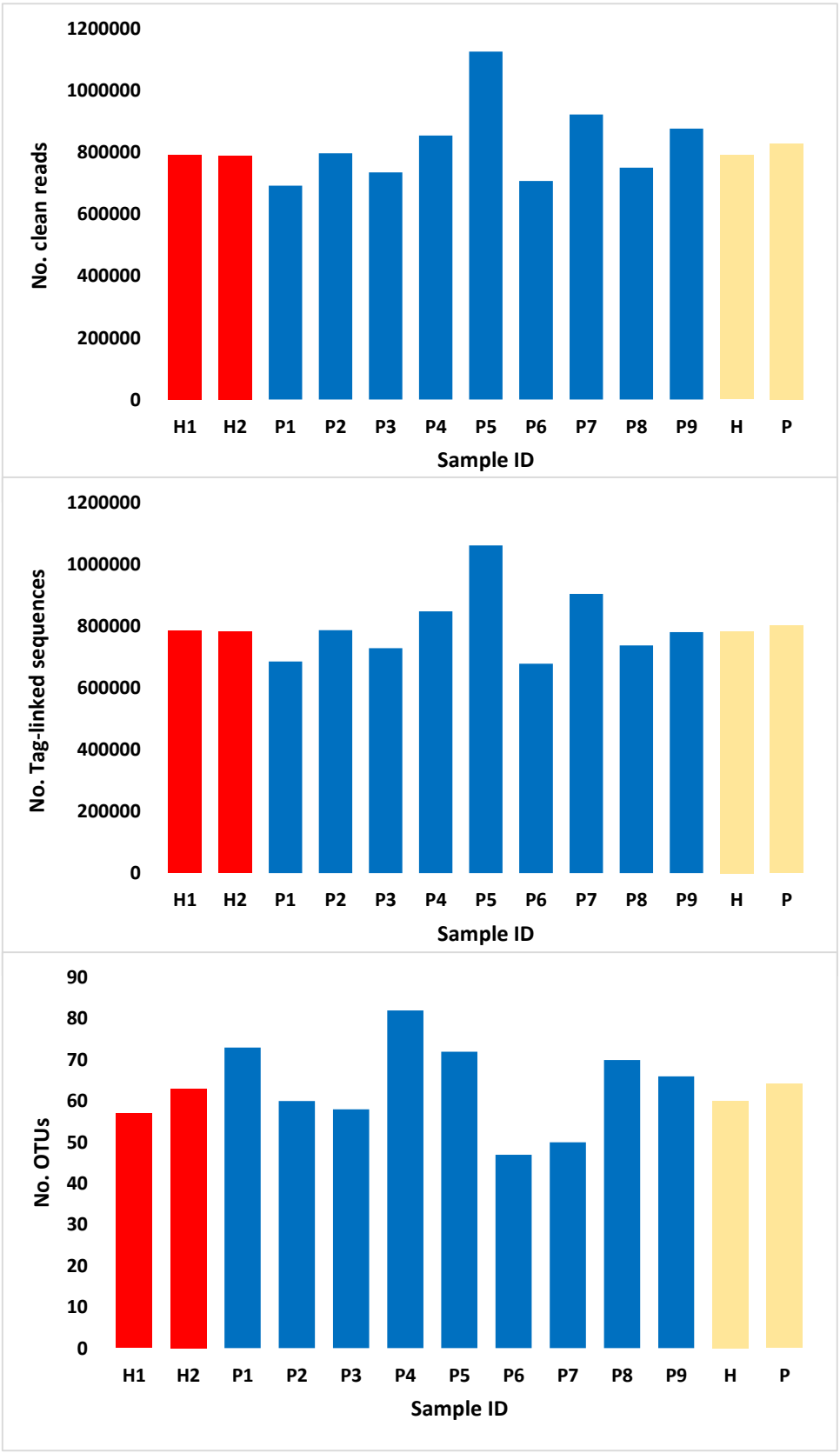

Figure 1. *Comparison between numbers of clean reads, tag-linked sequences and no. OTUs among and across healthy individuals (H) and Entamoeba-infected patients (P). Healthy = red, Infected = blue, Mean = beige*

http://www.aloki.hu ● ISSN 1589 1623 (Print) ● ISSN 1785 0037 (Online)
DOI: http://dx.doi.org/10.15666/aeer/1802_23632394

Diversity and rarefaction curve analysis

Alpha diversity analysis, as Shannon and Simpson indices, was applied to detect complexity among species and the deviation due to the disease. Shannon and Simpson values reflect the species diversity of the community at both richness and evenness levels. But Shannon index poses more weight on sequence richness, while Simpson index poses more weight on evenness. With the same species richness, the greater the species evenness, the greater the community diversity. Trend of values for the two measures likely to be opposite. The results in *Figure 2* exactly aligned with the latter statement as subject with high richness shows low evenness and vice versa. Subjects with the highest richness and lowest evenness are P2 followed by P9, while those with the lowest richness and highest evenness are P3 followed by P7 (*Fig. 2*). Overall, the results indicated that alpha diversity slightly changed due to the infection indicating an influence of the parasite on the type and intensity of the other eukaryotic microbes hosted in the gut.

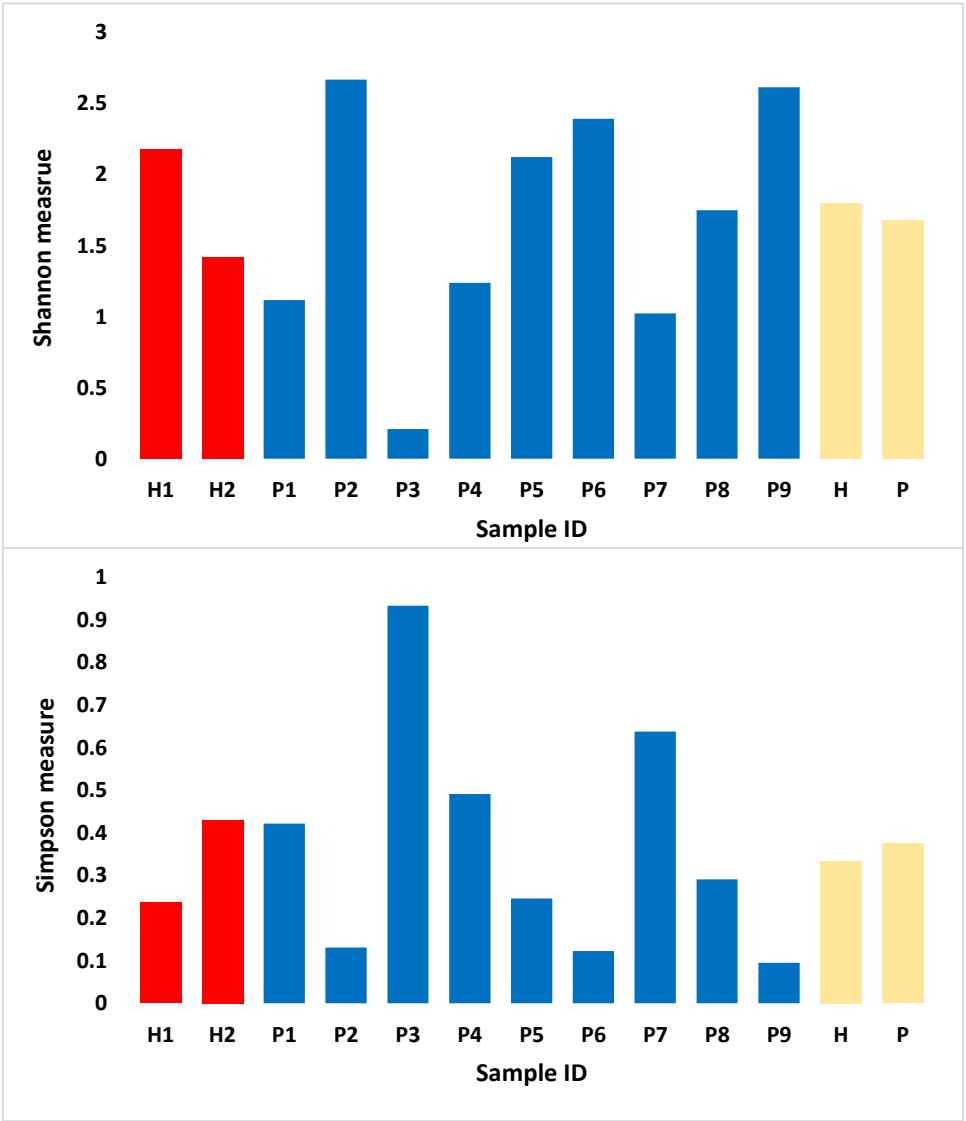

Figure 2. *Alpha diversity measures among and across healthy (H) and Entamoeba-infected (P) individuals to describe sample or group richness (Shannon index) and evenness (Simpson index). Healthy = red, Infected = blue, Mean = beige*

http://www.aloki.hu ● ISSN 1589 1623 (Print) ● ISSN 1785 0037 (Online)
DOI: http://dx.doi.org/10.15666/aeer/1802_23632394

Principal Coordinate Analysis (PCoA) was used in order to address the differences of OTU composition in different samples and groups. PCoA summarizes factors that are responsible for this difference. When similarity between two groups is high, then, the two groups are closely located. Based on the OTU abundance information, the relative abundance of each OTU in each sample and group was calculated, thus the PCoA of OTUs was plotted (*Fig. 3*). The PCoA plot completely showed a similar tendency in the distances within and between groups. The diversity of healthy subjects was localized in the positive directions of PCoA 1 (PC1) and PC2, while diversity of patients was higher towards the negative direction of PC2, and distributed evenly in the PC1 direction. These results indicated that the gut mycobiome signatures of the two groups differed due to amebiasis.

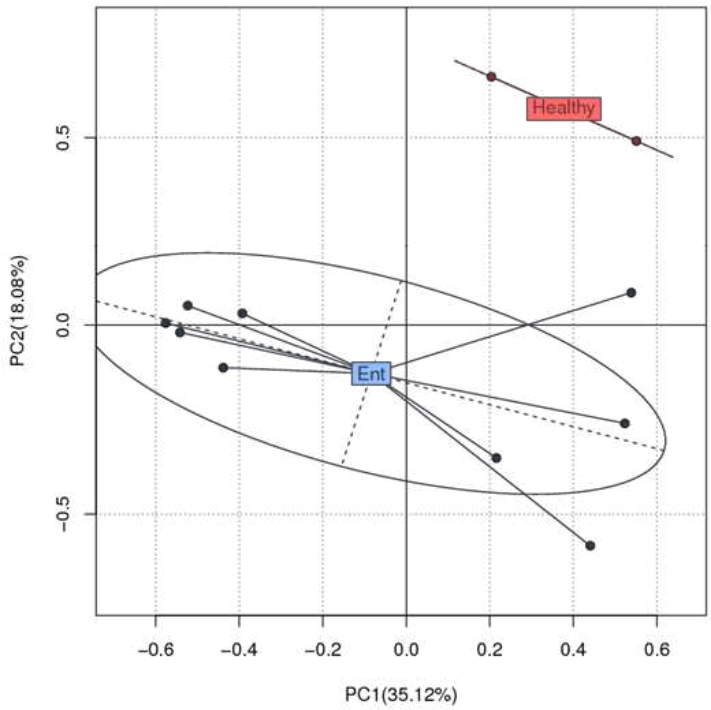

Figure 3. *PCoA based on OTU abundance of different samples. Blue box indicates samples of Entamoeba-infected patients, while red box indicates samples of healthy individuals. X-axis is the first principal coordinate and Y-axis is the second. Number in brackets represents contributions of PCoAs to differences among samples. A dot represents each sample, and different colors represent different groups. Healthy = red, Infected = blue*

Rarefaction curves based on stacked number of OTUs and number of observed species were drawn (*Fig. 4*). Stacked number of OTUs were analyzed, as rarefaction measures, in order to describe the maximum depth permitted to retain all samples in the dataset for studying taxonomic relative abundance and to evaluate if produced data is enough to cover all species in the microbial community. The point where a stacked value of a given sample approaches dropping or moving downwards (indicated by arrow in the figure) indicates the sealing at which further analysis that holds homogeneity in the datasets can be done. The more the curve continues to climb with increasing sequencing reads, the higher the complexity in samples, i.e., there still be species uncovered by the sequencing data. The rarefaction measures indicated that the

http://www.aloki.hu ● ISSN 1589 1623 (Print) ● ISSN 1785 0037 (Online)
DOI: http://dx.doi.org/10.15666/aeer/1802_23632394

maximum number of sequence reads to be used for further analysis of taxonomy abundance is as high as ~667,000 (*Fig. 4*).

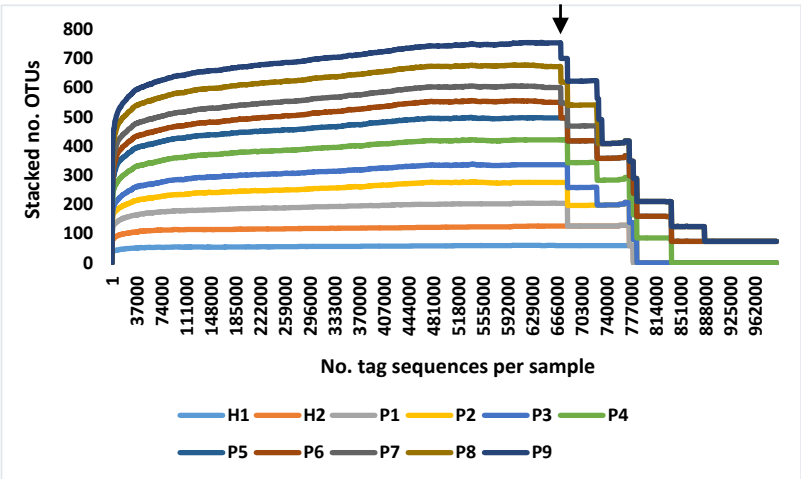

Figure 4. *Stacked number of OTU tags as rarefaction measures to describe the maximum depth permitted to retain all samples in the dataset for studying taxonomic relative abundance. The arrow indicates the suitable sample size for analyzing taxonomy abundance (~660,000 sequence reads) for healthy individuals (H) and Entamoeba-infected patients (P)*

Description of gut microbiome signatures

Description of observed species detected from OTU annotation is shown in *Table A1* (see electronic appendix). Phylogenetic tree describing taxonomic groups of oral microbiomes at the phyla and genera levels are shown in *Figure 5* and organized in *Table 2*. A phylogenetic tree is a branching diagram showing the inferred evolutionary relationships among various biological taxa based upon similarities and differences in their physical or genetic characteristics. The evolution distance between taxa is closer if the branch length is shorter. Besides the taxa composition and abundance analysis, phylogenetic tree could further clarify the species evolution relationships. The results expectedly indicated that the most common phyla in the gut are Ascomycota (11 genera), Basidiomycota (nine genera) and Zygomycota (two genera).

Six genera of Ascomycota belong to family Saccharomycetaceae, while the rest belong to separate families. The nine genera of Basidiomycota belong to nine different families, while the two genera of Zygomycota belong to the family Mucoraceae (*Table 2*). Family information of one genus of Basidiomycota namely *Tilletiopsis* is not available. Abundance of individual OTUs across samples was also studied in which OTUs with number of sequences over 100,000 were considered highly abundant (*Fig. 6*). This criterion was met for a number of 18 out of the 146 OTUs (*Table A2; Fig. 6*). These selected OTUs are OTU1-OTU15, OTU86, OTU109 and OTU130. Description of these selected highly abundant OTUs in terms of taxonomy of their phyla, genera and/or species is shown in *Table A1*. After removal of 12 non-fungal OTUs (OTU2, OTU7, OTU9-OTU15, OTU86, OTU109 and OTU130), the results indicated that the highly abundant OTUs belong to *Pichia kudriavzevii* (OTU3), *Candida glabrata* (OTU4), *Saccharomyces cerevisiae* (OTU5) and OTU6 of phylum Ascomycota and *Rhodotorula mucilaginosa* of phylum Basidiomycota.

http://www.aloki.hu ● ISSN 1589 1623 (Print) ● ISSN 1785 0037 (Online)
DOI: http://dx.doi.org/10.15666/aeer/1802_23632394

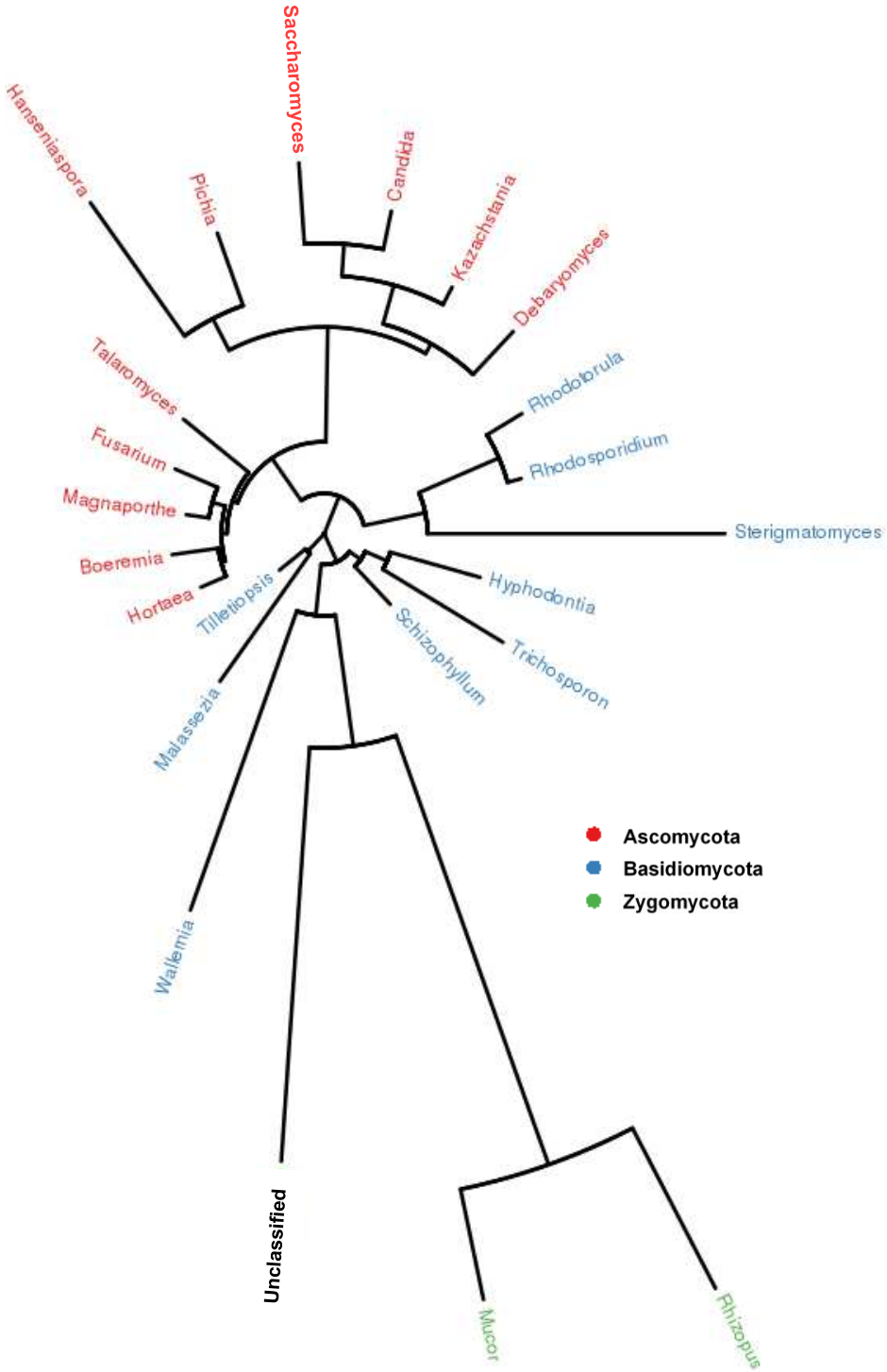

Figure 5. *Genus level phylogenetic tree of gut mycobiome across healthy individuals and Entamoeba-infected patients. Genera with the same color belong to the same phylum*

Venn diagram indicated the existence of 71 common OTUs in both groups (*Fig. 7*; *Table A3*). The number of OTUs uniquely found in healthy subjects was 11, reduced to eight after removal of non-fungal taxa representing the taxonomic groups of the phyla

http://www.aloki.hu ● ISSN 1589 1623 (Print) ● ISSN 1785 0037 (Online)
DOI: http://dx.doi.org/10.15666/aeer/1802_23632394

Ascomycota (5), Basidiomycota (2) and Zygomycota (1). The main taxa of Ascomycota are *Pichia kluyveri*, *Candida sake* and *Xylariales* spp., while those of Basidiomycota are *Malassezia obtusa* and unclassified genera of family Cystofilobasidiaceae and that of Zygomycota is *Rhizopus oryzae*. The number of OTUs uniquely found in healthy subjects was 64, reduced to 36 after removal of non-fungal taxa representing the taxonomic groups of the phyla Ascomycota (27), Basidiomycota (8) and Zygomycota (1).

The main taxa of Ascomycota are *Hortaea werneckii*, *Talaromyces purpurogenus*, *Debaryomyces hansenii*, *Kazachstania servazzii*, unclassified genera of the family Plectosphaerellaceae, *Hemibeltrania* sp. CL12WA, while those of Basidiomycota are *Schizophyllum radiatum*, *Hyphodontia rimosissima*, *Malassezia* spp., *Malassezia pachydermatis*, *Trichosporon coremiiforme*, *Rhodosporidium toruloides*, *Wallemia* spp. and that of Zygomycota is *Mucor racemosus*. None of these unique markers was consistent in either group in terms of existence as well as abundance. A larger number of samples might be required in order to reach a certain conclusion before we decide which of them can be considered as a biomarker for amebiasis.

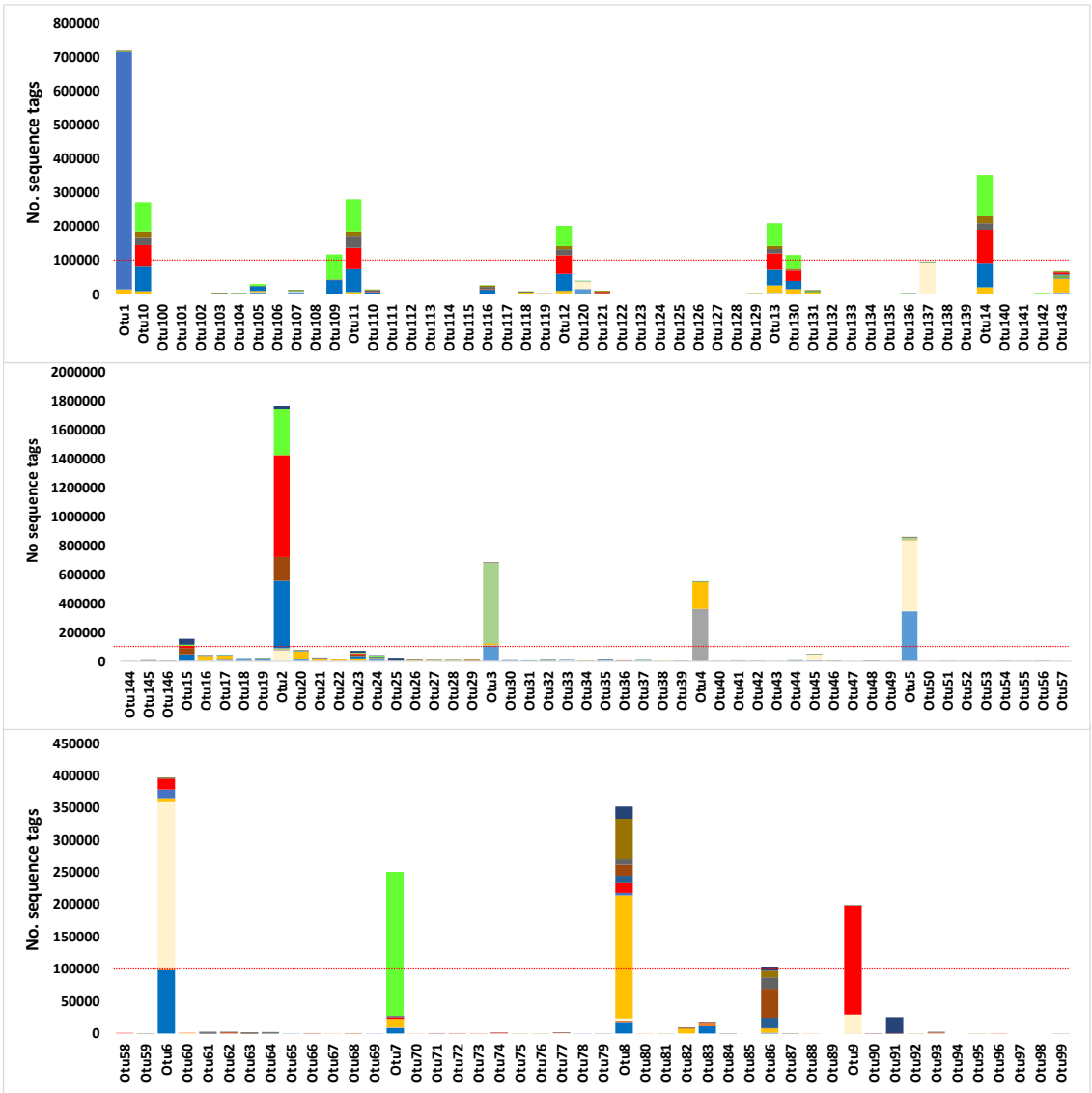

Figure 6. *Stacked OTU abundance across healthy individuals and Entamoeba-infected patients*

http://www.aloki.hu ● ISSN 1589 1623 (Print) ● ISSN 1785 0037 (Online)
DOI: http://dx.doi.org/10.15666/aeer/1802_23632394

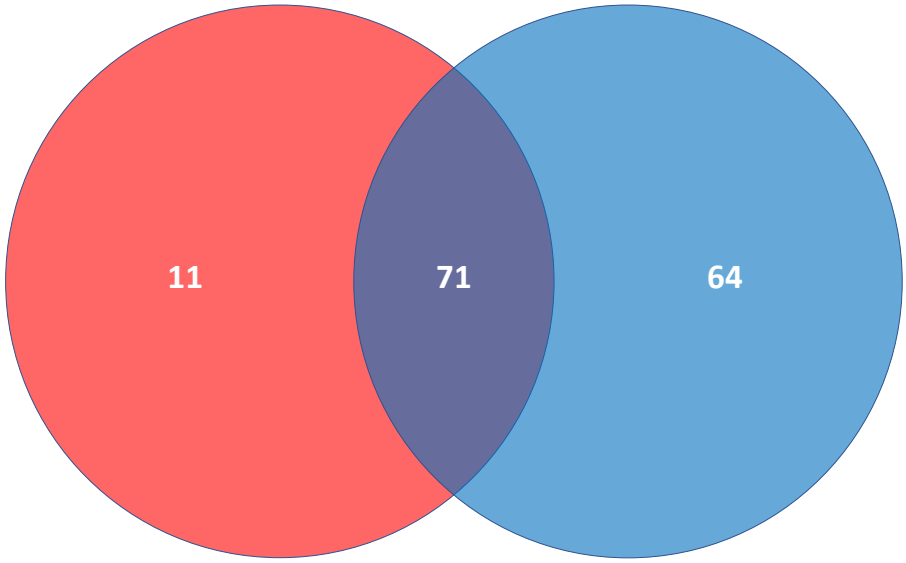

Figure 7. *Venn diagram describing the unique (11 for healthy individuals and 64 Entamoeba-infected patients) and shared OTUs (71) between the two groups of samples. The OTUs of different groups are shown in Table A3 and description of these OTUs is shown on Tables A1 and A2. Healthy = red, Infected = blue*

Table 2. *Taxonomy of gut mycobiome across healthy individuals and Entamoeba-infected patients*

Phylum	Family	Genus
Ascomycota	Didymellaceae	*Boeremia*
	Saccharomycetaceae	*Kazachstania*
		Candida
		Saccharomyces
		Debaryomyces
		Hanseniaspora
		Pichia
	Nectriaceae	*Fusarium*
	Teratosphaeriaceae	*Hortaea*
	Magnaporthaceae	*Magnaporthe*
	Trichocomaceae	*Talaromyces*
Basidiomycota	Hymenochaetaceae	*Hyphodontia*
	Sporidiobolaceae	*Rhodotorula*
	Ustilaginaceae	*Rhodosporidium*
	Schizophyllaceae	*Schizophyllum*
	Agaricostilbaceae	*Sterigmatomyces*
	N/A	*Tilletiopsis*
	Wallemiaceae	*Wallemia*
	Malasseziaceae	*Malassezia*
	Trichosporonaceae	*Trichosporon*
Zygomycota	Mucoraceae	*Mucor*
		Rhizopus

http://www.aloki.hu ● ISSN 1589 1623 (Print) ● ISSN 1785 0037 (Online)
DOI: http://dx.doi.org/10.15666/aeer/1802_23632394

The analysis of weighted and unweighted unifrac diversity distances, as a beta diversity measures, describing the overall structures of gut mycobiomes of different healthy (H) and infected (P) subjects is shown in *Figure 8*. As indicated earlier, the weighted diversity considers the abundance of the different OTUs, while unweighted diversity considers presence or absence of a given OTU. *Figure 8* indicates that analysis based on weighted unifrac diversity distances successfully resulted in complete separation between the two groups, e.g., healthy subjects (H) and *Entamoeba*-infected patients (P). However, analysis based on unweighted unifrac diversity distances resulted in no separation between the two groups although a large number of group-specific OTUs was recovered. As indicated above, these unique or group-specific OTUs were not consistently shown in all subjects of the group. Thus, no particular gut mycobiome signature was detected for either group. As this inconsistency was shown for all unique OTUs, analysis was not able to make a complete discrimination between the two groups based on the unique OTUs.

The results shown in *Figure A2,* displaying the beta diversity heat maps of weighted and unweighted unifrac diversity distances between the two groups supports the latter conclusions. A heat map is a graphical representation of data where the subject distance values contained in a matrix are represented as colors. *Figure A2* also indicated that P4 followed by P1 are the most divergent within the infected subjects (P). Gut mycobiome signature of P1 was shown to be the closest to the signatures of the two healthy subjects. However, the most closely related infected subjects in terms of gut mycobiome signatures are P5, P6, P7 and P10. The differential signatures among infected subjects might reflect the differential severity of the disease.

Differential abundance of microbes due to amebiasis

Differential abundance of microbes of different healthy (H) and infected (P) subjects was studied at the phylum, family, genus and species levels (*Fig. 9, 10, 11* and *12,* respectively). The results indicated that a number of four phyla, six families, nine genera and ten species showed considerable changes in gut mycobiome signatures within and among groups. The phyla Ascomycota and Basidiomycota were consistently shown in all subjects, albeit different in abundance, while Chytridiomycota and Cnidaria were only shown with relatively low abundances, in a single subject, e.g., P2 and H2, respectively. Therefore, no conclusions can be taken for the latter two phyla in terms of relative abundance (*Fig. 9*). The results at the family level indicated consistency in two out of the six families, e.g., Saccharomycetaceae and Trichocomaceae (*Fig. 10*). The two families belong to phylum Ascomycota. The results at the genus level indicated consistency in three out of the nine genera, e.g., *Candida* spp., *Malassezia* spp. and *Saccharomyces* spp. (*Fig. 11*). The first two genera were relatively highly abundant in the infected subjects as compared with the healthy subjects. Opposite conclusion was reached for the third genus, e.g., *Saccharomyces* spp., where it was relatively highly abundant in the healthy subjects as compared with the infected subjects (*Fig. 11*). The results at the species level indicated consistency in only one, e.g., *Saccharomyces cerevisiae*, out of the ten species (*Fig. 12*). Accordingly, it was decided to further analyze the results of the Ascomycota at the phylum level, Saccharomycetaceae and Trichocomaceae at the family level, *Malassezia* spp. and *Saccharomyces* spp. at the genus level and *Saccharomyces cerevisiae* at the species level (*Figs. 13* and *14*).

http://www.aloki.hu ● ISSN 1589 1623 (Print) ● ISSN 1785 0037 (Online)
DOI: http://dx.doi.org/10.15666/aeer/1802_23632394

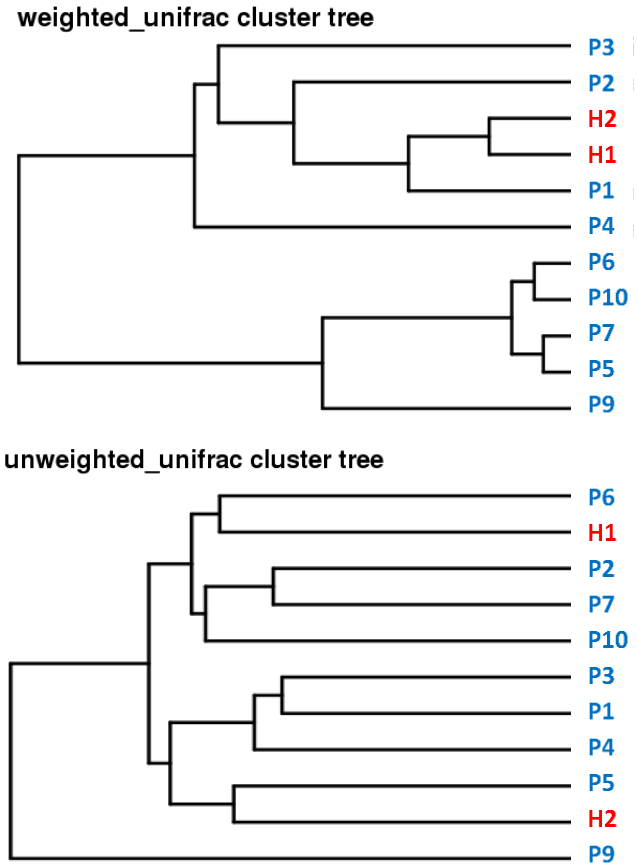

Figure 8. *Dendrogram trees describing the weighted and unweighted unifrac diversity distances among healthy individuals (H) and Entamoeba-infected patients (P). Healthy = red, Infected = blue*

Among these taxa, unclassified species of the genus *Malassezia* belonging to phylum Basidiomycota showed high abundance in infected subjects as compared with healthy subjects (*Fig. 13*), while the rest of taxa belonging to phylum Ascomycota showed opposite results (*Fig. 14*).

Linear discriminant analysis (or LDA) effect size (LEFSE) is a software that determines the entire features (organisms, clades, operational taxonomic units, genes, or functions) likely explaining differences among groups. Such features were determined by coupling standard tests for statistical significance with additional tests encoding biological consistency and effect relevance. In the present study, LEFSE was based on determining the features in the different taxa in order to detect the ones that can conclusively be considered as biomarkers for amebiasis. The analysis shown in *Figure 15* indicated that the family Saccharomycetaceae, of which *Saccharomyces cerevisiae* is a downstream taxon, is the only taxon meeting the standard criteria set of the analysis. Interestingly, there is no particular OTU specific to this family, however, the most consistent OTU with this result, e.g., OTU107, belongs to the genus *Saccharomyces*, also a downstream taxon (*Table A4*). This taxon, referring to OTU107, along with its downstream species, referring to OTU5, share a negative biomarker of amebiasis (*Fig. 15*). This result supports that generated when studying the relative abundance at the phylum, family, genus and species levels. Considering the richness of

http://www.aloki.hu ● ISSN 1589 1623 (Print) ● ISSN 1785 0037 (Online)
DOI: http://dx.doi.org/10.15666/aeer/1802_23632394

the two OTUs (*Table A2*), we claim that OTU5, referring to *Saccharomyces cerevisiae*, is more appropriate as the new negative biomarker for amebiasis.

Discussion

Preliminary detection of the gut diseases usually involves microscopic observation with the fecal samples. Although this approach is not sensitive, it remains to be the gold standard utilized in almost all parasitological diagnostic laboratories (McHardy et al., 2014). Drawbacks of this approach arise when only few eggs exist in samples, thus, other methods such as serology-based, e.g., ELISA (Ungar, 1990), might be a better alternative. More recently, molecular approaches have been used as a promising tool for differentiating and detecting stool parasites (Tavares et al., 2011), with the first molecular study to detect mycobiome signatures published in 2008 (Scanlan and Marchesi, 2008).

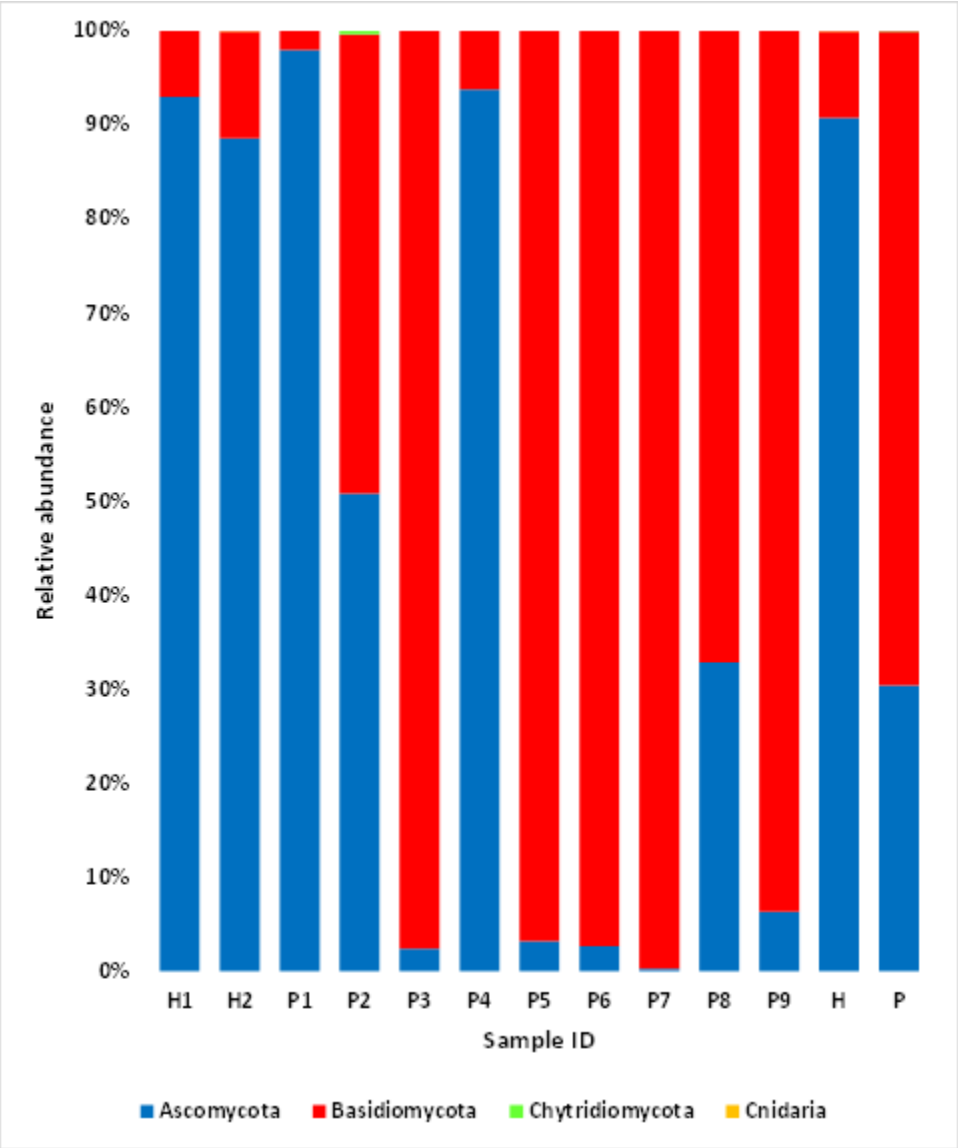

Figure 9. *Relative abundance at the phylum level as measured by Metastats at the sample and group levels for healthy individuals (H) and Entamoeba-infected patients (P)*

http://www.aloki.hu ● ISSN 1589 1623 (Print) ● ISSN 1785 0037 (Online)
DOI: http://dx.doi.org/10.15666/aeer/1802_23632394

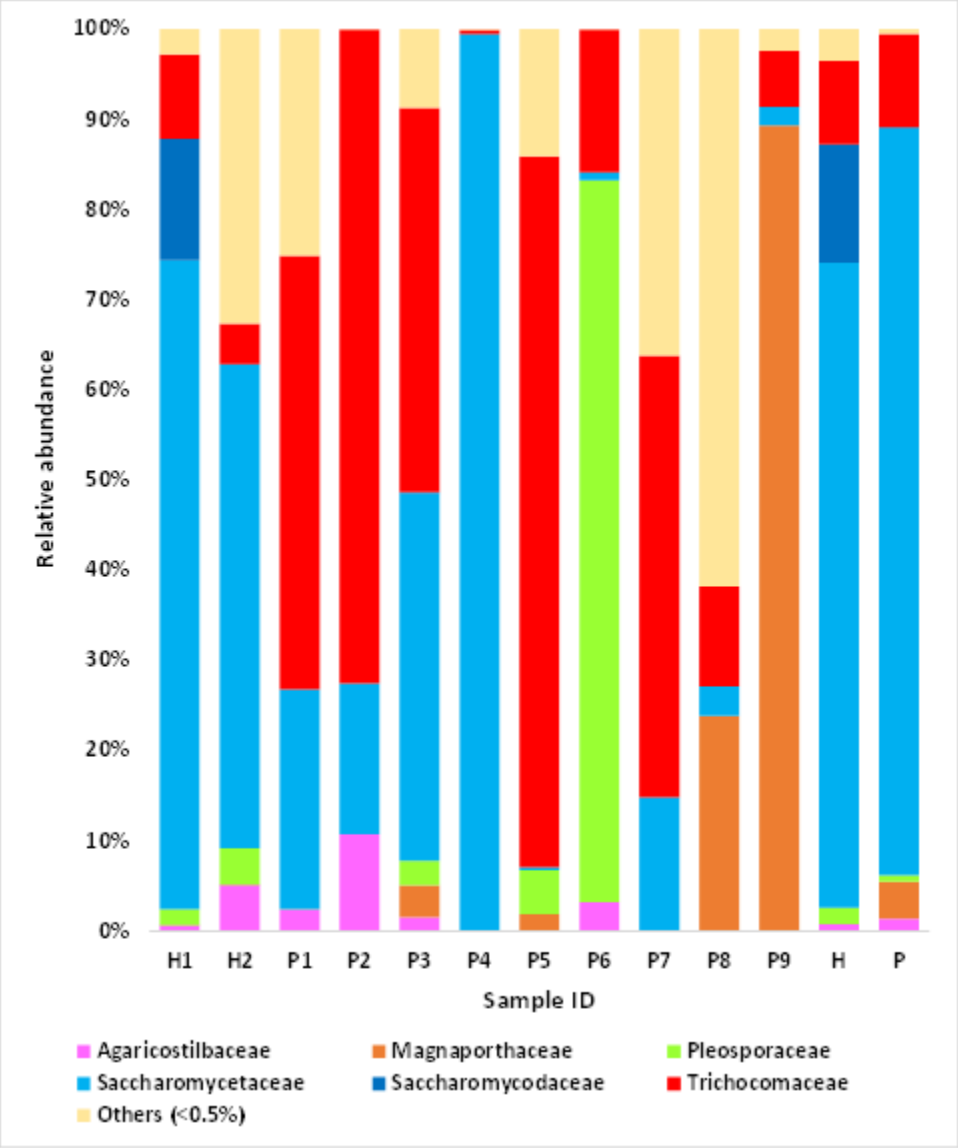

Figure 10. *Relative abundance at the family level as measured by Metastats at the sample and group levels for healthy individuals (H) and Entamoeba-infected patients (P)*

Nowadays, next generation sequencing (NGS) has proven to be the ideal approach in detecting the microbiome signatures and providing an accurate figures of microbe intensity (Stensvold et al., 2010). Such high-throughput technologies are employed in detecting microbiome signatures in different human organs in relation to disease status, e.g., amebiasis (Gao et al., 2017; Jo et al., 2017). The approach is based on the use of 16S ribosomal RNA (rRNA) gene for bacteriome, while 18S or ITS (internal transcribed spacer) for fungal microbiome or mycobiome (Belda-Ferre et al., 2012; Ahn et al., 2015; Johansson et al., 2016; Zhou et al., 2016). Although, internal transcribed spacer (ITS) seems to be more appropriate than 18S rDNA for analyzing human gut mycobiome at the level of clades and species (Hamad et al., 2016), it still difficult to use it in making a proper fungal metagenomic analysis due to the absence of a well-established or rich fungal ITS database for OTU annotation (Tang et al., 2015).

http://www.aloki.hu ● ISSN 1589 1623 (Print) ● ISSN 1785 0037 (Online)
DOI: http://dx.doi.org/10.15666/aeer/1802_23632394

There were two major issues to be considered before we approach analyzing mycobiome. The first is concerned with the influence of diet at the harvest time and the second is concerned with the lack of a database specific for mycobiome at the species level. The preliminary observation made during the analysis was the presence of a large number of non-fungal OTUs at the species level, while none at the levels of the phylum, family or genus (*Figs. 9–12*).

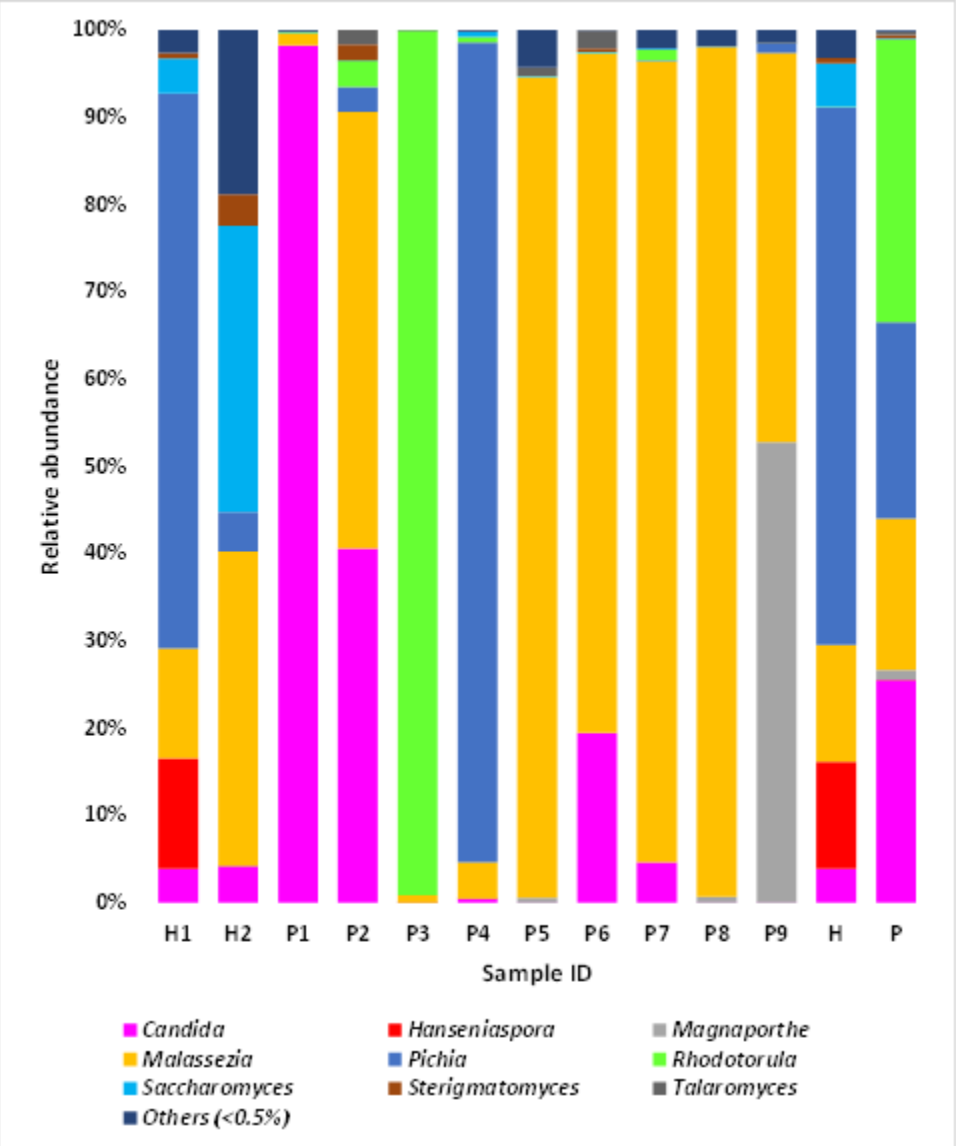

Figure 11. *Relative abundance at the genus level as measured by Metastats at the sample and group levels for healthy individuals (H) and Entamoeba-infected patients (P)*

This indicates that the data recovered at the species level requires further removal of non-fungal OTUs in order to get accurate figure of the relative abundance at the species level. *Figure 16* indicates the comparison of relative abundance of mycobiomes of the two healthy subjects at the species level before and after removal of non-fungal species. The latter are four plant species namely *Oryza sativa* (rice), *Triticum aestivum* (bread wheat), *Sesamum indicum* (sesame) and *Prunus mume* (Japanese apricot). As shown in

http://www.aloki.hu ● ISSN 1589 1623 (Print) ● ISSN 1785 0037 (Online)
DOI: http://dx.doi.org/10.15666/aeer/1802_23632394

the figure, fungal species showed a more accurate results for their relative abundance after correcting the data (*Fig. 16*). The datasets of OTU taxonomy also required further removal of uncharacterized fungi. In addition, OTUs for a single species, genus, family, order or phylum were merged to avoid redundancy in the taxon and getting a better estimate of its relative abundance, thus, can give a better estimate of the mycobiome signature of the *Entamoeba*-infected subject. The corrected number of OTUs became 46 out of the total 146 OTUs recovered after the initial annotation step. A recent study discussed the influence of diet and the environmental factors to gut mycobiome composition, and indicated that gut mycobiome is less stable than the bacteriome, and is subject to the two factors, thus, usually changes from day to day and over time (Hallen-Adams and Suhr, 2017). David et al. (2014) further indicated that dietary-induced changes in the gut microbiome rely on the type of food consumed (either plant- or animal-based). Hugon et al. (2017) indicated that bacterial composition responds to nutrient availability, while fungal composition appears to be driven by food colonization. The latter evidences were fully supported by gut mycobiome analysis of the present study.

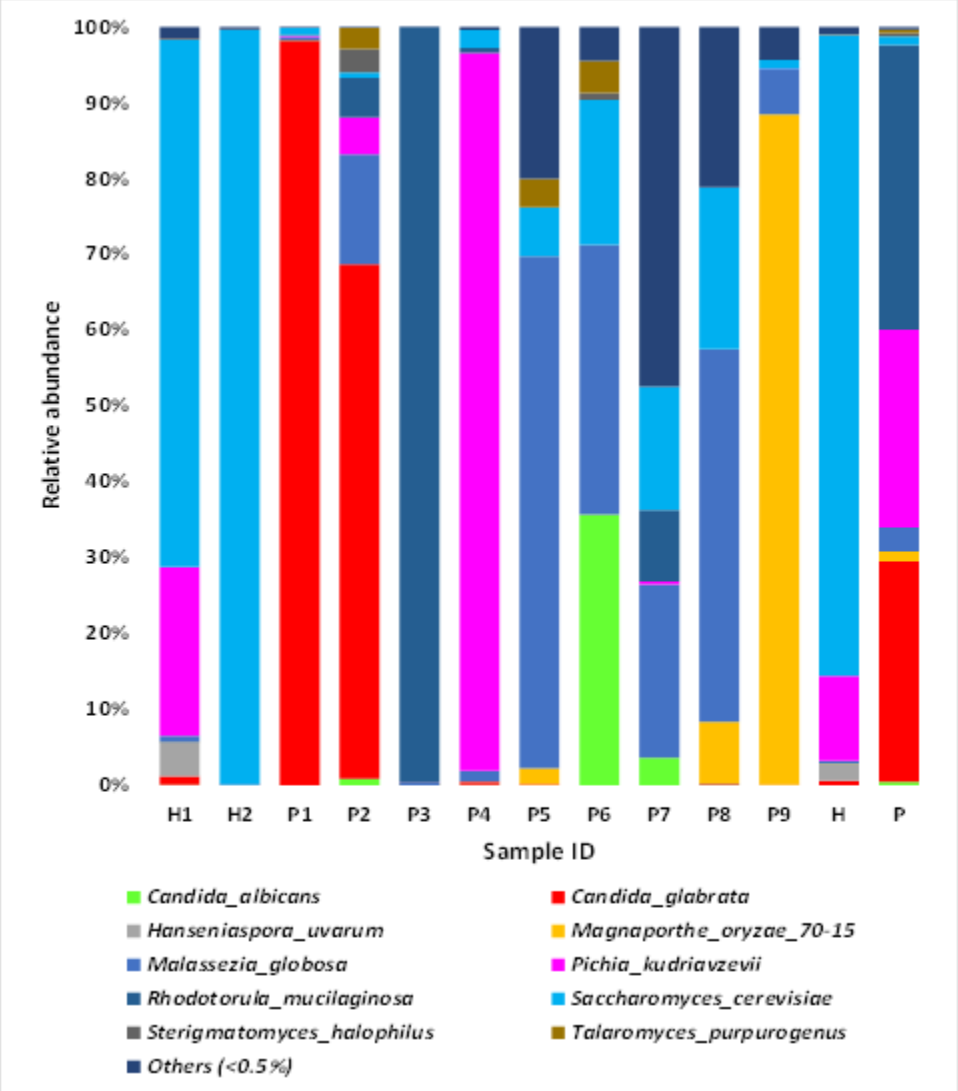

Figure 12. *Relative abundance at the species level as measured by Metastats at the sample and group levels for healthy individuals (H) and Entamoeba-infected patients (P)*

http://www.aloki.hu ● ISSN 1589 1623 (Print) ● ISSN 1785 0037 (Online)
DOI: http://dx.doi.org/10.15666/aeer/1802_23632394

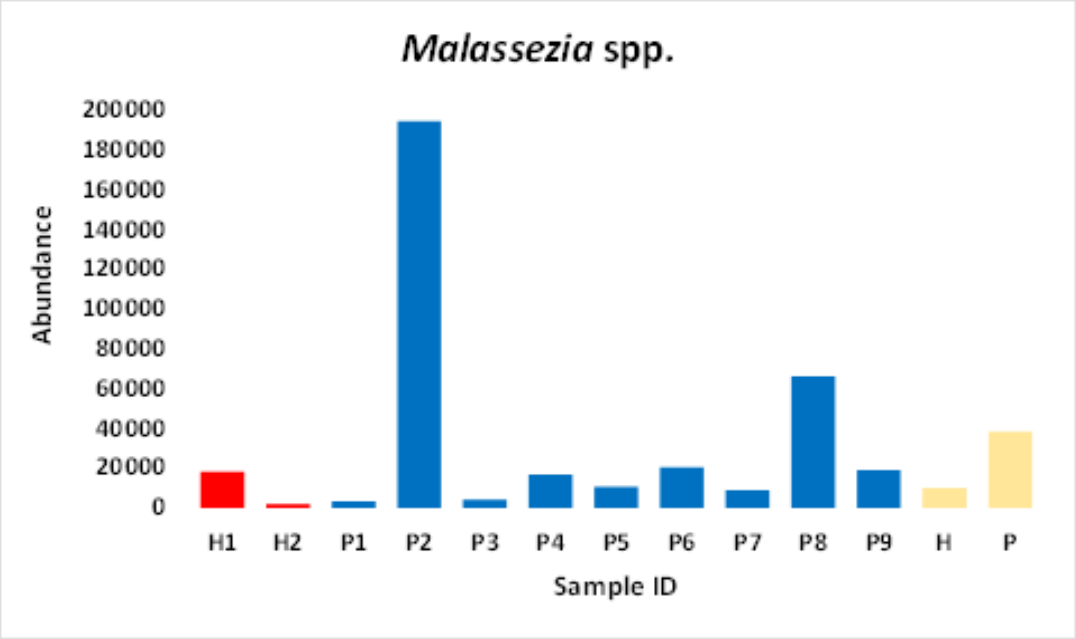

Figure 13. *High abundance of the unassigned species of the genus Malassezia spp. within or across Entamoeba-infected patients (P) as compared with healthy individuals (H)*

Based on recent molecular phylogenetic classification, the taxonomy of human gut eukaryotes includes the five major groups of Amoebozoa, Opisthokonta (including fungi), Excavata, Sar and Archaeplastida (Adl et al., 2012; Hamad et al., 2016). Fungal species, including yeasts and filamentous fungi, are considered as the most abundant group of eukaryotes in the human gut. It is likely that most fungi species represent some sort of food contamination (Rajilic-Stojanovic and de Vos, 2014), thus, their role in the human gut microbiota remains unclear. While, eukaryotic parasites, e.g., protozoa and helminths, exist in the human gut in lower abundance (Rajilic-Stojanovic and de Vos, 2014). Gut mycobiome was proven to be comprised of the four major phyla of Ascomycota, Basidiomycota, Zygomycota and Microsporidia (Moran et al., 2012; Rajilic-Stojanovic and de Vos, 2014). In the present study, only the first three phyla were detected in the mycobiomes of healthy and infected subjects (*Table 2*). Other reports indicated that gut mycobiota in healthy subjects mainly comprises Ascomycota and Basidiomycota as the most abundant phyla, and the *Candida*, *Saccharomyces* and *Malassezia* and as the most abundant genera (Ott et al., 2008; Moran et al., 2012; Hoffmann et al., 2013; Rajilic-Stojanovic and de Vos, 2014; Nash et al., 2017). The results of the present study completely align with those of the latter reports. We also found that two species of *Candida* as well as *Saccharomyces cerevisiae*, followed by *Malassezia globosa* and *Pichia kudriavzevii* are the most dominating species across subjects (*Fig. 12*). The latter species are natural, asymptomatic fungi of the human microbiome, but can become opportunistic pathogens under specific circumstances and cause candidiasis or gut microbial dysbiosis (Vogel et al., 2007; Saleh et al., 2011; Rajilic-Stojanovic and de Vos, 2014). Several other species belonging to genera *Penicillium* and *Aspergillus* have also been detected in GI tract in many researches (Scanlan and Marchesi, 2008; Gouba et al., 2013, 2014). None of the two species was detected across subject in the present study.

http://www.aloki.hu ● ISSN 1589 1623 (Print) ● ISSN 1785 0037 (Online)
DOI: http://dx.doi.org/10.15666/aeer/1802_23632394

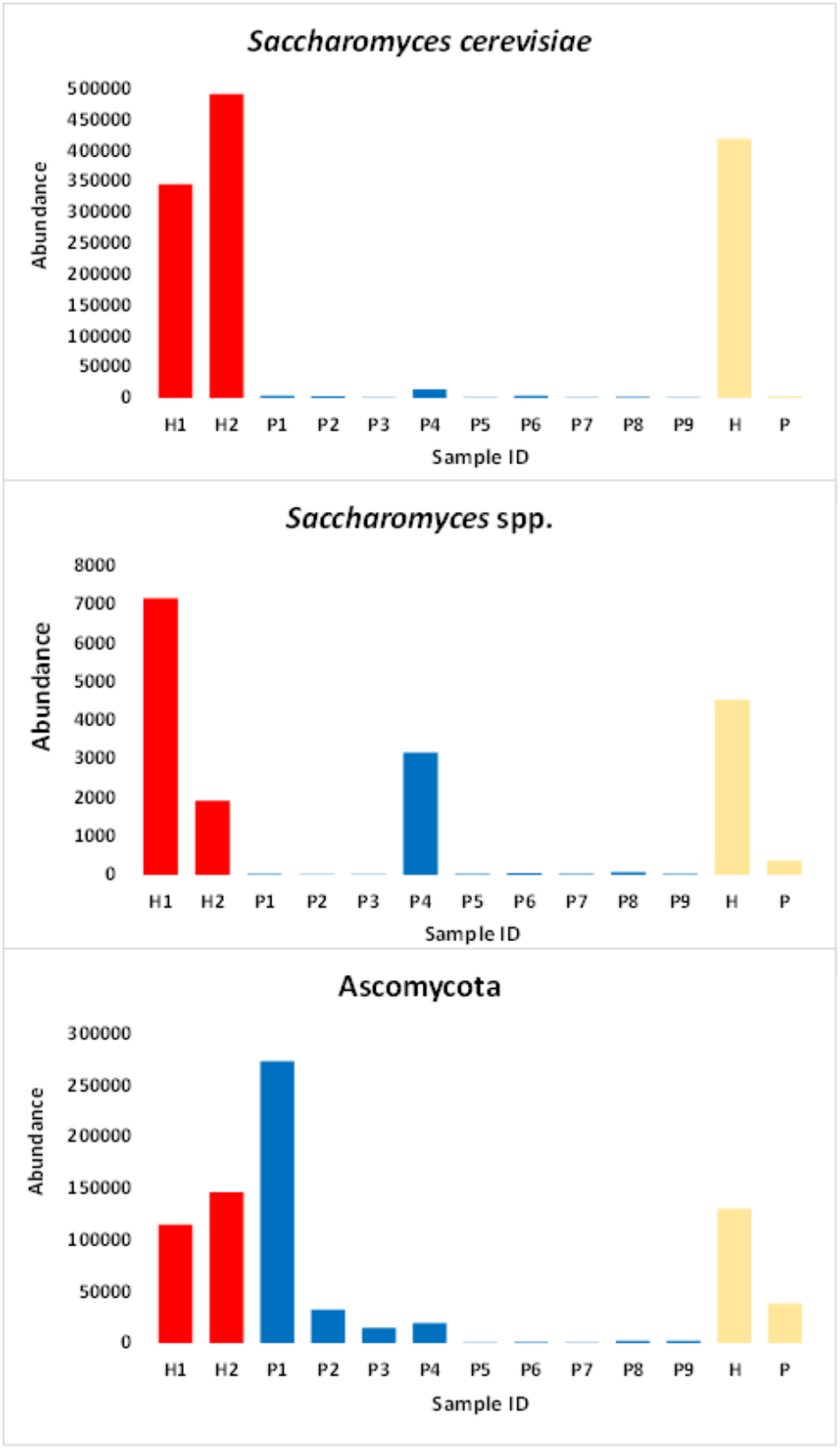

Figure 14. *Low abundance of Saccharomyces cerevisiae, unassigned species of Sccharomyces spp. along with their phylum Ascomycota as well as member of the family Trycocomaceae within or across Entamoeba-infected patients (P) as compared with healthy individuals (H). Healthy = red, Infected = blue, Mean = beige*

http://www.aloki.hu ● ISSN 1589 1623 (Print) ● ISSN 1785 0037 (Online)
DOI: http://dx.doi.org/10.15666/aeer/1802_23632394

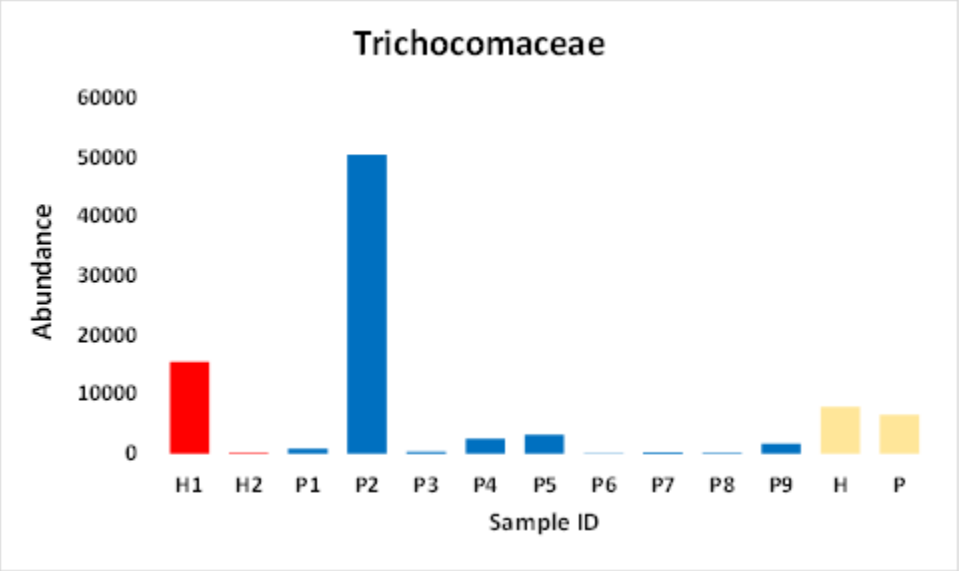

Figure 14. *Continued*

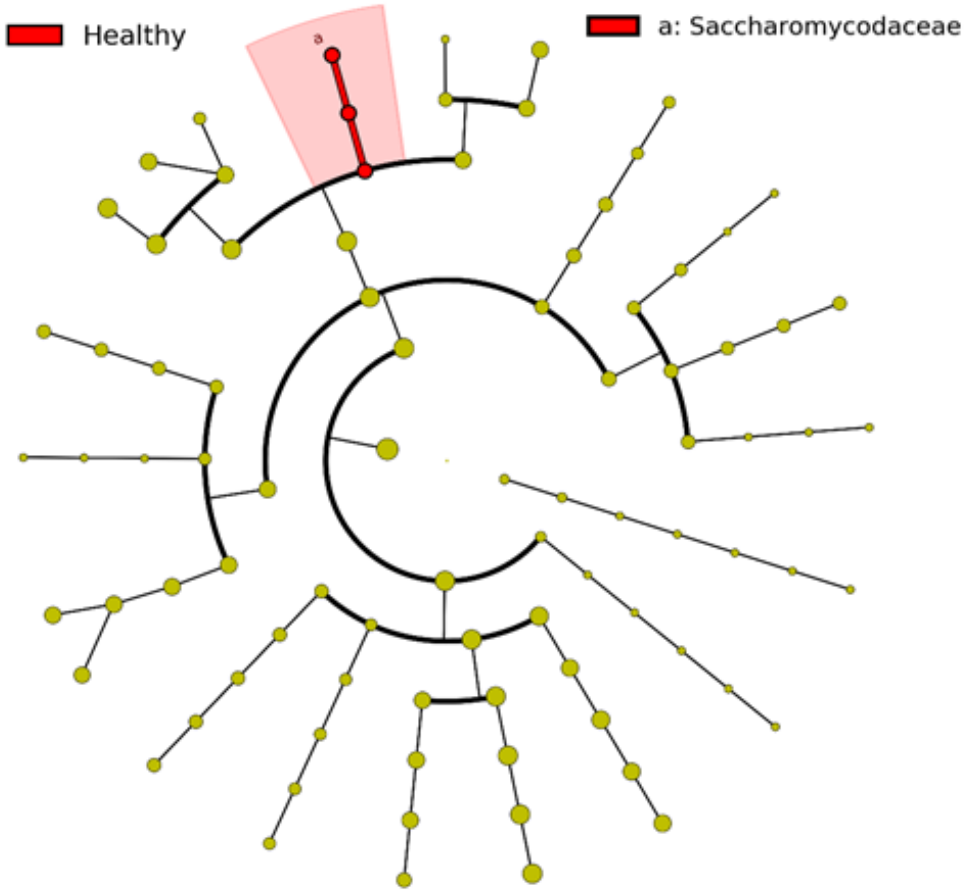

Figure 15. *LEFse cladogram describing a negative biomarkers for amebiasis. The new important microbe biomarker in the healthy group and the biomark name are listed in the upper right corner. The yellow notes represent the other biomarker which do not show any importance in either groups for healthy individuals (H) or Entamoeba-infected patients (P)*

http://www.aloki.hu ● ISSN 1589 1623 (Print) ● ISSN 1785 0037 (Online)
DOI: http://dx.doi.org/10.15666/aeer/1802_23632394

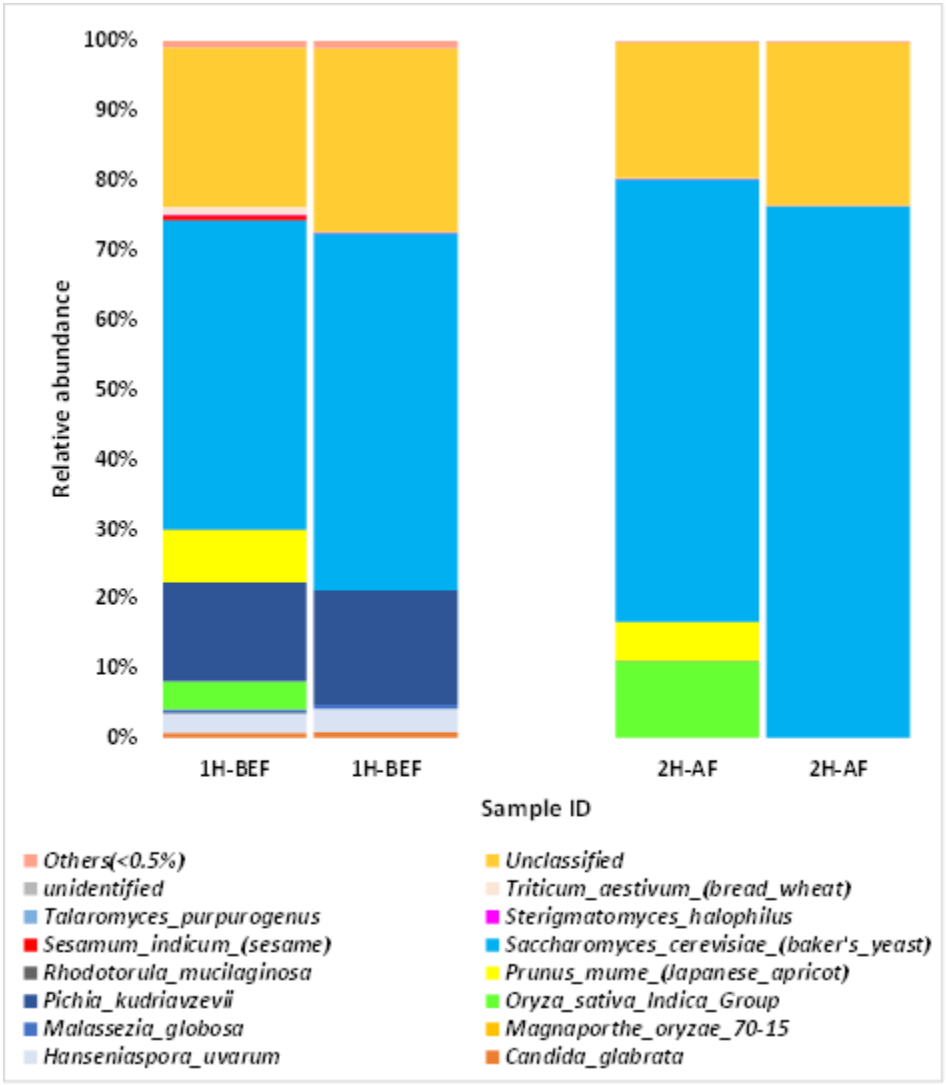

Figure 16. *Differential relative abundance of the two healthy subjects (H) before (BEF) and after (AF) removal of non-fungal information. Description of OTUs for mycobiome species is shown in Table A4*

Species of the genus *Malassezia* are well-known for the inability to synthesize their own lipids, thus, they are completely dependent on their host for nutritional needs (Gupta et al., 2004). In the present study, abundance of this genus increased in mycobiomes of the infected subjects. In other words, there is a positive relationship in the present study in the abundances of *Malassezia* and *Entamoeba histolytica*. Upon infection, *E. histolytica* was reported to exploit lipids and carbohydrates present in the colonic environment (Thibeaux et al., 2013). This indicates that lipids are available for other microbes. Therefore, there is a possibility that *E. hystolytica* be indicative of lipids available for *Malassezia* (*Fig. 17*). The latter conclusion might require further experimentation and support as genes involved in lipids metabolism were recently reported to be upregulated under growth stress in the study of RNA-Seq data of *Entamoeba* (Naiyer et al., 2019b). Expectedly, the known niche for this genus is the skin that is rich of adipose cells, while, surprisingly, it was reported in significant abundance in the gut (Gouba et al., 2013; Cano et al., 2014; Suhr et al., 2016).

http://www.aloki.hu ● ISSN 1589 1623 (Print) ● ISSN 1785 0037 (Online)
DOI: http://dx.doi.org/10.15666/aeer/1802_23632394

Therefore, there should be other resources of lipids for this genus in the gut. There are two other groups of fungi of the phylum Ascomycota that reported to colonize the healthy human GI tract although gut is not their primary colonizer (Hugon et al., 2017). They are *Cladosporium* and yeasts of the family Dipodascaceae (e.g., *Geotrichum* and *Galactomyces*). Several evidences suggest that the majority of the fungi in GI tract are indigenous (Iliev et al., 2012; Dollive et al., 2013). Family Trichocomaceae also belongs to phylum Ascomycota and includes species *Aspergillus nidulans*, an ascomycetous fungus that is used extensively for studying processes in fungi. This species was proven to be closely related to the *S. cerevisiae* (Class: Hemiascomycetes) in several biological processes, but little is known about the family it derived from (https://www.sciencedirect.com/topics/agricultural-and-biological-sciences/trichocomaceae).

The dimorphic yeast *S. cerevisiae* is widely distributed in the environment and considered commensal upon being colonized in the gut, however, it can occasionally cause superficial and systemic infections (Byron et al., 1995; Munoz et al., 2005; De Llanos et al., 2006). This species is detected frequently in human fecal samples and abundance is directly associated with food ingestion prior to sampling (Scanlan and Marchesi, 2008). The ability of this species to grow at 37 °C makes it likely contributes to gut microbial ecology (Hugon et al., 2017). The potential for *S. cerevisiae* to persist and respond to the gut environment does not support their possible role in the gut, as its preferred niche is the open environmental (soil, air, plant matter). More recently, an article documented a protective role of *S. cerevisiae* inflammatory disorders (Jiang et al., 2017), while other article showed that *S. cerevisiae* reduces bacterial growth and colonization, and inhibits the adhesion of enterotoxigenic *E. coli* (ETEC) (Roussel et al., 2018). The gut mycobiome analysis in the present study indicated that *S. cerevisiae* proved to be a negative biomarker of amebiasis. At the relative abundance level, *S. cerevisiae* was shown to dominate in gut mycobiomes of the healthy subject. There are two possible speculations that can be reached based on the relative abundance of this species. The first is that the high abundance of *S. cerevisiae* might block the growth/spread of *E. histolytica* trophozoites by different possible ways, thus *S. cerevisiae* dominates in the healthy subjects. The second is that *E. histolytica* might propagate due to the low abundance of *S. cerevisiae*, thus, *E. histolytica* might dominate in the infected subjects. We speculate that the two species cross-talk via a number of processes basically relied on glucose level as well as growth condition (aerobic or anaerobic) in the gut, besides, the possible occurrence of oxidative stresses (*Fig. 17*).

Chitin formation is a process made by trophozoite during encystation. Chitin in the cyst wall of *E. histolytica* is synthesized by two chitin synthases, one of which is unique to it (EhCHS-1) and the other is analogue to those of insects, fungi and nematodes (EhCHS-2) (Tellam et al., 2000; Roncero, 2002; Ruiz-Herrera, 2002). In *S. cerevisiae*, chitin is produced by three specialized chitin synthases (Chs1p, Chs2p and Chs3p) (Bulawa, 1993; Choi and Cabib, 1994; Henar Valdivieso, 1999; Roncero, 2002). The first enzyme functions during cytokinesis, while the second makes the chitin in the primary septum and the third makes the bulk of cellular chitin. Yeasts transformed with the unique EhCHS-1 was proven to be functional and chitin was detected in their cells. Action of this enzyme seems to be extracellular towards the cell walls, thus, we speculate that yeast cells might compete with trophozoite for the use of the amoebic enzyme (EhCHS-1), which eventually retards the spread of the parasite by inhibiting the encystation process.

http://www.aloki.hu ● ISSN 1589 1623 (Print) ● ISSN 1785 0037 (Online)
DOI: http://dx.doi.org/10.15666/aeer/1802_23632394

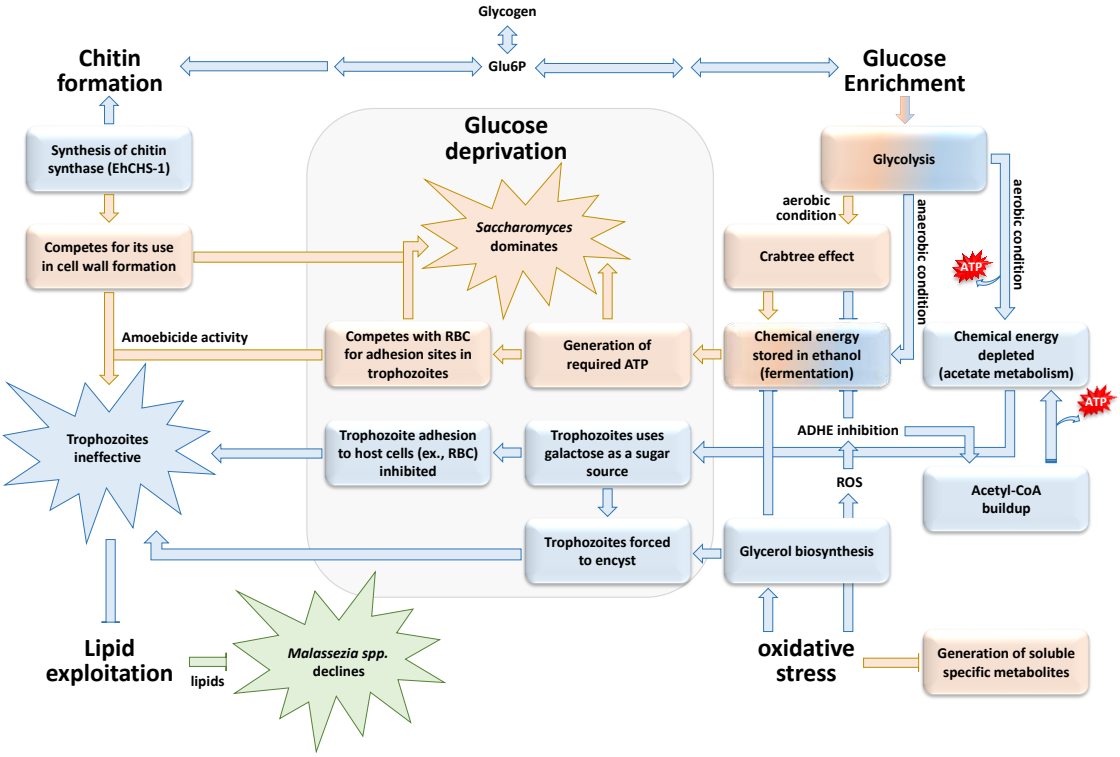

Figure 17. *Roles of the new negative biomarker for amebiasis, e.g., Saccharomyces cerevisiae. Main influence of the biomarker possibly occurs in relation to availability of glucose in the gut and/or during cell wall formation of Entamoeba histolytica. Abundance of Malassezia spp. is based on the availability of lipids proposed to be provided by E. histolytica. Cross-talking among the three taxa involves five major conditions/actions, e.g., glucose enrichment, glucose deprivation, oxidative stress, chitin formation and lipid exploitation. Processes or actions related to S. cerevisiae are shown in pink, while those of E. histolytica and Malassezia spp. are shown in light blue and light green, respectively*

It is well-established that glucose in the human gut perform four different destinations in amoebic cells (*Fig. 18*). They are glycolysis, chitin formation, fermentation and acetate biosynthesis. The first two destinations and the last two destination are very much connected by a number of redux reactions. The direction of the different reactions is dependent on the conditions at which parasite is facing, e.g., glucose level, oxygen presence, oxidative stress, etc. Glucose-6-phosphate (Glu6P) is considered as the main substrate lying upstream redux reactions of these four destinations (*Figs. 17* and *18*). Under the low level of glucose and anaerobic condition, it was reported earlier that adhesion of trophozoites to red blood cells (RBCs) were inhibited (López-Revilla and Cano-Mansera, 1982). The authors indicated that adhesion is dependent on amoebal cytoskeleton and affinity of both amoebal and RBC surface receptors. Another analysis on the effects of *Saccharomyces* on cecal amebiasis in rats indicated that the numbers of diseased rats and the severity of the infection were significantly reduced by the yeast treatment (Rigothier et al., 1990). A more recent report justified the inhibition of adhesion of trophozoite to RBCs as it indicated that pretreatment of amoebae with live yeast led to a significant reduction in the percentage of adhesion (Rigothier et al., 1994). The authors indicated that substances produced by *Saccharomyces* might compete with red blood cells, as an amoebicide, for adhesion

http://www.aloki.hu ● ISSN 1589 1623 (Print) ● ISSN 1785 0037 (Online)
DOI: http://dx.doi.org/10.15666/aeer/1802_23632394

sites of the trophozoite (*Fig. 17*). Other reports indicated that the reptilian parasite *Entamoeba invadens* was induced to encyst under osmotic shock, glucose deprivation, or both (Vazquezdelara-Cisneros and Arroyo-Begovich, 1984; Avron et al., 1986; Sanchez et al., 1994; Van Dellen et al., 2006). Un-organized encystation threatens trophozoite's life or it can be a reason for the inefficiency of trophozoite to cause further action in the human body (*Fig. 17*). On the other hand, *Saccharomyces* will not suffer from glucose deprivation as it can consult its saved energy in ethanol that was synthesized by fermentation and use it for regular metabolic processes rather than being forced to make irregular metabolic processes.

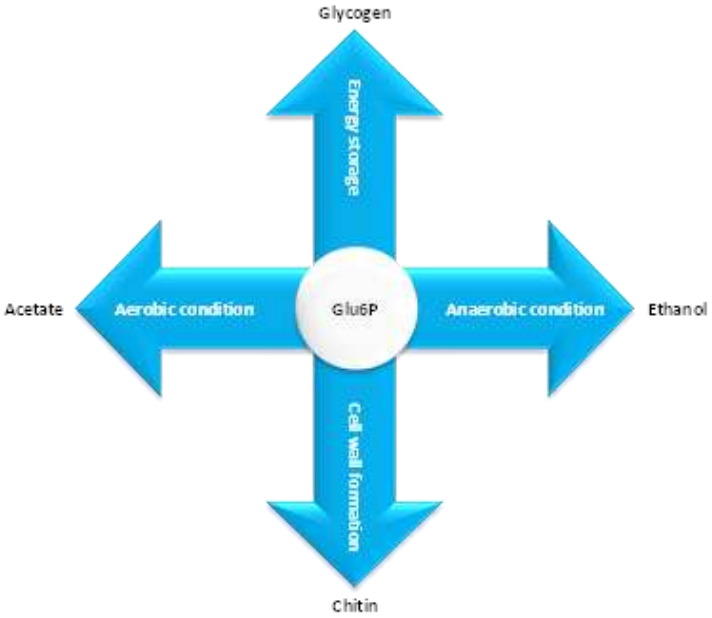

Figure 18. *Four different destinations for glucose metabolism of which Glu6P is the core molecule upstream several redox reaction based on the condition at which parasite is facing*

As a response to glucose deprivation in the human gut, trophozoite has to utilize another source of carbon such as galactose. Frederick and Petri (2005) indicated that adhesion of the trophozoites to colonic mucins and host cells occurs mainly through the abundant galactose-binding lectin on the surface of the cells, however, this adhesion is almost completely inhibited by β-D-galactose (*Fig. 17*). We speculate that utilization of galactose as a carbon source due to glucose deprivation will negatively affect the trophozoite efficiency. On the other hand, *S. cerevisiae* simply transports galactose into the cell, when glucose level is low, by galactose permease enzyme to be converted to glucose-6-phosphate (Glu-6P) that drive the reaction normally towards glycolysis (Bro et al., 2005). More recently, Naiyer et al. (2019a) indicated that aspartate might be used as energy source by *Entamoeba* under glucose deprivation due to the regulation of the gene encoding aspartate aminotransferase. Galactose was also recently reported to act in inhibiting the formation of neutrophil extracellular traps (NET) that traps trophozoites, thus, makes trophozoites invisible by host neutrophil (Fonseca et al., 2019).

Husain et al. (2012) indicated that oxidative stress also resulted in reduced level of glycolysis and ethanol production and the redirection of metabolic flux towards glycerol production and chitin biosynthesis. Reduction of glycolysis and ethanol levels indicate

http://www.aloki.hu ● ISSN 1589 1623 (Print) ● ISSN 1785 0037 (Online)
DOI: http://dx.doi.org/10.15666/aeer/1802_23632394

the reduced stored energy required for trophozoite actions and the promotion of chitin biosynthesis can stimulate the trophozoites to encyst, thus, further retard their actions. In addition, oxidative stress induces the production of reactive oxygen species (ROS). The latter inhibits the bifunctional aldehyde/alcohol dehydrogenase (ADHE) enzyme, important during ethanol production (Nozaki and Bhattacharya, 2015), thus, results in the buildup of Acetyl CoA that is the intermediate step towards acetate metabolism and depletion of energy. Chitin biosynthesis is a further response to oxidative stress. As indicated earlier, this process enforces trophozoites to encyst, thus, no further action is taken by the microbe in the gut. *Saccharomyces boulardii* has previously been used effectively to treat rotavirus (RV) diarrhea in human enterocytes by preventing RV-induced oxidative stress (Buccigrossi et al., 2014). The study was repeated in an organ culture model using human intestinal biopsies, and results indicated that *Saccharomyces* produces soluble metabolites that prevent oxidative stress in human intestine (*Fig. 17*). Interestingly, Naiyer et al. (2019a) indicated that genes upregulated during encystation include phospholipase D as well as genes involved in meiotic division such as *MND1*, *Hop2* and *Rad52*. Meiosis was not proven in *Entamoeba*, however, earlier reports indicated the occurrence of homologous recombination (Singh et al., 2013).

Glucose is known to be converted into pyruvate through glycolysis, a metabolic pathway employed in nearly all organisms (Berg et al., 2002). In the downstream reactions, pyruvate is further degraded either through the respiration or the fermentation pathway. The first is a pathway to release or exhaust ATP, while the second is a pathway to store ATP. Under conditions of glucose enrichment, trophozoites mainly perform fermentation under anaerobic condition, while acetate biosynthesis under aerobic condition (Nozaki and Bhattacharya, 2015). Aerobic condition is accompanied by the presence of oxygen. It was reported that trophozoites produce 75% ethanol and 25% acetate under anaerobic condition, while opposite ratios under aerobic condition. The latter ratios indicate that trophozoites cannot save appropriate amount of stored energy at the form of ATP via fermentation under aerobic or oxidative stress condition (*Fig. 17*). On the other hand, some yeast species such as *S. cerevisiae* use fermentation even in the presence of oxygen, albeit glucose concentration is sufficiently high. Such *Saccharomyces* species are able to choose the proper destination for glycolysis (respiration or fermentation) under high glucose levels and aerobic conditions, a property related to Crabtree effect (Crabtree, 1929; De Deken, 1966; Postma and Verduyn, 1989; Van Urk et al., 1990; Pfeiffer and Morley, 2014), of which the direction choices are based on cell's requirement for energy. This phenomenon indicates that excess sugar availability promotes cells to ferment it rather than going through respiration or oxidative phosphorylation. Reasons for this phenomenon includes the limited membrane space that harbors the enzymes involved in oxidative phosphorylation (Hagman et al., 2013).

Conclusion

The main goal of the present study is the detection of gut mycobiome signature of *E. histolytica*-infected patients in a trial to improve our ability to diagnose and treat the disease. We suggest that the results on the discovery of new negative biomarker for amebiasis can provide new insights into the possible use of *Saccharomyces* in the future as a probiotic to treat diarrhea and downstream severity of the disease. The latter conclusion requires further experimentation way before we decide to use yeasts as a treatment in the market place.

http://www.aloki.hu ● ISSN 1589 1623 (Print) ● ISSN 1785 0037 (Online)
DOI: http://dx.doi.org/10.15666/aeer/1802_23632394

REFERENCES

[1] Abarenkov, K., Nilsson, R. H., Larsson, K.- H., et al. (2010): The UNITE database for molecular identification of fungi-recent updates and future perspectives. – New Phytol. 186: 281-285.
[2] Adl, S. M., Simpson, A. G., Lane, C. E., et al. (2012): The revised classification of eukaryotes. – J. Eukaryot. Microbiol. 59: 429-493.
[3] Ahn, J., Yang, L., Paster, B. J., et al. (2015): Oral microbiome profiles: 16S rRNA pyrosequencing and microarray assay comparison. – PLoS ONE 6: e22788.
[4] Ali, V., Nozaki, T. (2007): Current therapeutics, their problems, and sulfur-containing-amino-acid metabolism as a novel target against infections by 'amitochondriate' protozoan parasites. – Clin. Microbiol. Rev. 20: 164-187.
[5] Avron, B., Stolarsky, T., Chayen, A., Mirelman, D. (1986): Encystation of *Entamoeba invadens* IP-1 is induced by lowering the osmotic pressure and depletion of nutrients from the medium. – J. Protozool. 33: 522-525.
[6] Belda-Ferre, P., Alcaraz, L. D., Cabrera-Rubio, R., et al. (2012): The oral metagenome in health and disease. – ISME J. 6: 46-56.
[7] Benjamini, Y., Hochberg, Y. (1995): Controlling the false discovery rate: a practical and powerful approach to multiple testing. – J. Royal Stat. Soc. (Series B) 57: 289-300.
[8] Berg, A. H., Combs, T. P., Scherer, P. E. (2002): ACRP30/adiponectin: an adipokine regulating glucose and lipid metabolism. – Trends Endocrinol. Metab. 13: 84-89.
[9] Bliss, J. M., Basavegowda, K. P., Watson, W. J., et al. (2008): Vertical and horizontal transmission of *Candida albicans* in very low birth weight infants using DNA fingerprinting techniques. – Pediatr. Infect. Dis. J. 27: 231-235.
[10] Bro, C., Knudsen, S., Regenberg, B., et al. (2005): Improvement of galactose uptake in *Saccharomyces cerevisiae* through overexpression of phosphoglucomutase: example of transcript analysis as a tool in inverse metabolic engineering. – Appl. Environ. Microbiol. 71: 6465-6472.
[11] Buccigrossi, V., Laudiero, G., Russo, C., et al. (2014): Chloride secretion induced by rotavirus is oxidative stress-dependent and inhibited by *Saccharomyces boulardii* in human enterocytes. – PLoS ONE 9: e99830.
[12] Bulawa, C. E. (1993): Genetics and molecular biology of chitin synthesis in fungi. – Annu. Rev. Microbiol. 47: 505-534.
[13] Byron, J. K., Clemons, K. V., McCusker, J. H., et al. (1995): Pathogenicity of *Saccharomyces cerevisiae* in complement factor five-deficient mice. – Infect. Immun. 63: 478-485.
[14] Cano, R. J., Rivera-Perez, J., Toranzos, G. A., et al. (2014): Paleomicrobiology: revealing fecal microbiomes of ancient indigenous cultures. – PLoS ONE 9: e106833.
[15] Caporaso, J. G., Bittinger, K., Bushman, F. D., et al. (2010a): PyNAST: a flexible tool for aligning sequences to a template alignment. – Bioinformatics 26: 266-267.
[16] Caporaso, J. G., Justin, K., Jesse, S. (2010b): QIIME allows analysis of high-throughput community sequencing data. – Nature Methods 7: 335-336.
[17] Choi, W. J., Cabib, E. (1994): The use of divalent cations and pH for the determination of specific yeast chitin synthetases. – Anal. Biochem. 219: 368-372.
[18] Cole, J. R., Wang, Q., Fish, J. A., et al. (2014): Ribosomal Database Project: data and tools for high throughput rRNA analysis. – Nucleic Acids Res. 42: D633-D642.
[19] Crabtree, H. G. (1929): Observations on the carbohydrate metabolism of tumours. – Biochem. J. 23: 536-545.
[20] Cui, L., Morris, A., Ghedin, E. (2013): The human mycobiome in health and disease. – Genome Med. 5: 63.
[21] David, L. A., Maurice, C. F., Carmody, R. N., et al. (2014): Diet rapidly and reproducibly alters the human gut microbiome. – Nature 505: 559-563.

http://www.aloki.hu ● ISSN 1589 1623 (Print) ● ISSN 1785 0037 (Online)
DOI: http://dx.doi.org/10.15666/aeer/1802_23632394

[22] De Deken, R. H. (1966): The Crabtree effect: a regulatory system in yeast. – J. Gen. Microbiol. 44: 149-156.
[23] De Llanos, R., Querol, A., Pemán, J., et al. (2006): Food and probiotic strains from the *Saccharomyces cerevisiae* species as a possible origin of human systemic infections. – Int. J. Food Microbiol. 110: 286-290.
[24] Dollive, S., Chen, Y.- Y., Grunberg, S., et al. (2013): Fungi of the murine gut: episodic variation and proliferation during antibiotic treatment. – PLoS ONE 8: e71806.
[25] Eaton, R. D. P., Meerovitch, E., Costerton, J. W. (1970): The functional morphology of pathogenicity in *Entamoeba histolytica*. – Ann. Trop. Med. Parasitol. 64: 299-304.
[26] Edgar, R. C. (2010): Search and clustering orders of magnitude faster than BLAST. – Bioinformatics 26: 2460-2461.
[27] Edgar, R. C. (2013): UPARSE: highly accurate OTU sequences from microbial amplicon reads. – Nature Methods 10: 996-998.
[28] Edgar, R. C., Haas, B. J., Clemente, J. C., et al. (2011): UCHIME improves sensitivity and speed of chimera detection. – Bioinformatics 27: 2194-2200.
[29] Ewing, B., Green, P. (1998): Base-calling of automated sequencer traces using Phred. II. Error probabilities. – Genome Res. 8: 186-194.
[30] Fonseca, Z., Uribe-Querol, E., Díaz-Godínez, C., et al. (2019): Pathogenic *Entamoeba histolytica*, but not *Entamoeba dispar*, induce neutrophil extracellular trap (NET) formation. – J. Leukoc. Biol. 105: 1167-1181.
[31] Frederick, J. R., Petri Jr., W. A. (2005): Roles for the galactose-/N-acetylgalactosamine-binding lectin of *Entamoeba* in parasite virulence and differentiation. – Glycobiol. 15: 53R-59R.
[32] Gao, R., Gao, Z., Huang, L., et al. (2017): Gut microbiota and colorectal cancer. – Eur. J. Clin. Microbiol. Infect. Dis. 36: 757-769.
[33] Gouba, N., Drancourt, M. (2015): Digestive tract mycobiota: a source of infection. – Med. Mal. Infect. 45: 9-16.
[34] Gouba, N., Raoult, D., Drancourt, M. (2013): Plant and fungal diversity in gut microbiota as revealed by molecular and culture investigations. – PLoS ONE 8: e59474.
[35] Gouba, N., Raoult, D., Drancourt, M. (2014): Eukaryote culturomics of the gut reveals new species. – PloS ONE 9: e106994.
[36] Gupta, A. K., Batra, R., Bluhm, R., et al. (2004): Skin diseases associated with *Malassezia* species. – J. Am. Acad. Dermatol. 51: 785-98.
[37] Gupta, S. S., Singh, O., Shukla, S., Raj, M. K. (2009): Acute fulminant necrotizing amoebic colitis: a rare and fatal complication of amoebiasis: a case report. – Cases J. 2: 6557.
[38] Hagman, A., Sall, T., Compagno, C., Piskur, J. (2013): Yeast "Make-accumulate-consume" life strategy evolved as a multi-step process that predates the whole genome duplication. – PloS ONE 8: e68734.
[39] Hallen-Adams, H. E., Suhr, M. J. (2017): Fungi in the healthy human gastrointestinal tract. – Virulence 8: 352-358.
[40] Hamad, I., Raoult, D., Bittar, F. (2016): Repertory of eukaryotes (eukaryome) in the human gastrointestinal tract: taxonomy and detection methods. – Parasite Immunol. 38: 12-36.
[41] Henar Valdivieso, M., Duran, A., Roncero, C. (1999): Chitin synthases in yeast and fungi. – EXS 87: 55-69.
[42] Hirata, K. K., Que, X., Melendez-Lopez, et al. (2007): A phagocytosis mutant of *Entamoeba histolytica* is less virulent due to deficient proteinase expression and release. – Exp. Parasitol. 115: 192-199.
[43] Hoffmann, C., Dollive, S., Grunberg, S., et al. (2013): Archaea and fungi of the human gut microbiome: correlations with diet and bacterial residents. – PLoS ONE 8: e66019.
[44] Huffnagle, G., Noverr, M. (2013): The emerging world of the fungal microbiome. – Trends Microbiol. 21: 334-341.
[45] Hugon, P., Lagier, J.- C., Colson, P., et al. (2017): Repertoire of human gut microbes. – Micro. Pathog. 106: 103-112.

http://www.aloki.hu ● ISSN 1589 1623 (Print) ● ISSN 1785 0037 (Online)
DOI: http://dx.doi.org/10.15666/aeer/1802_23632394

[46] Husain, A., Sato, D., Jeelani, G., et al. (2012): Dramatic increase in glycerol biosynthesis upon oxidative stress in the anaerobic protozoan parasite *Entamoeba histolytica.* – PLoS Negl. Trop. Dis. 6: e1831.
[47] Ianiro, G., Bruno, G., Lopetuso, L., et al. (2014): Role of yeasts in healthy and impaired gut microbiota: the gut mycome. – Curr. Phar. Des. 20: 4565-4569.
[48] Iliev, I. D., Funari, V. A., Taylor, K. D., et al. (2012): Interactions between commensal fungi and the C-type lectin receptor Dectin-1 influence colitis. – Science 336: 1314-1317.
[49] Ishida, H. Inokuma, S., Murata, N., et al. (2003): Fulminant amoebic colitis with perforation successfully treated by staged surgery: a case report. – J. Gastroenterol. 38: 92-96.
[50] Iyer, L. R., Verma, A. K., Paul, J., et al. (2019): Phagocytosis of gut bacteria by *Entamoeba histolytica.* – Front. Cell. Infect. Microbiol. 9: Article 34.
[51] Jiang, T. T., Shao, T.- Y., Ang, W. G., et al. (2017): Commensal fungi recapitulate the protective benefits of intestinal bacteria. – Cell Host Microbe 22: 809-816.
[52] Jo, J. H., Kennedy, E. A., Kong, H. H. (2017): Topographical and physiological differences of the skin microbiome in health and diseases. – Virulence 8: 324-333.
[53] Johansson, I., Witkowska, E., Kaveh, B., et al. (2016): The microbiome in populations with a low and high prevalence of caries. – J. Dent. Res. 95: 80-86.
[54] Khomkhum, N., Leetachewa, S., Pawestri, A. R., et al. (2019): Host-antibody inductivity of virulent *Entamoeba histolytica* and non-virulent *Entamoeba moshkovskii* in a mouse model. – Parasites & Vectors 12: Article 101.
[55] Kirschner, R., Hsu, T., Tuan, N. N., et al. (2015): Characterization of fungal and bacterial components in gut/fecal microbiome. – Curr. Drug. Metab. 16: 272-283.
[56] López-Revilla, R., Cano-Mansera, R. (1982): Adhesion of *Entamoeba histolytica* trophozoites to human erythrocytes. – Infect. Immun. 37: 281-285.
[57] Lozano, R., Naghavi, M., Foreman, K., et al. (2012): Global and regional mortality from 235 causes of death for 20 age groups in 1990 and 2010: a systematic analysis for the Global Burden of Disease Study 2010. – Lancet 380: 2095-2128.
[58] Lozupone, C., Lladser, M. E., Knights, D., et al. (2011): UniFrac: an effective distance metric for microbial community comparison. – ISME J. 5: 169-172.
[59] Magoc, T., Salzberg, S. (2011): FLASH: fast length adjustment of short reads to improve genome assemblies. – Bioinformatics 27: 2957-63.
[60] McHardy, I. H., Wu, M. R., Shimizu-Cohen, R., et al. (2014): Detection of intestinal protozoa in the clinical laboratory. – J. Clin. Microbiol. 52: 712-720.
[61] Mi-Ichi, F., Yoshida, H., Hamano, S. (2016): *Entamoeba* Encystation: new targets to prevent the transmission of amebiasis. – PLOS Pathog. 12: e1005845.
[62] Moran, G., Coleman, D., Sullivan, D. (2012): An Introduction to the Medically Important Candida Species. – In: Calderone, R. A., Clancy, C. J. (eds.) Candida and Candidiasis. 2nd Ed. ASM Press, Washington, DC, pp. 11-25.
[63] Moyes, D. L., Naglik, J. R. (2012): The mycobiome: influencing IBD severity. – Cell Host Microbe 11: 551-552.
[64] Mukherjee, P. K., Sendid, B., Hoarau, G., et al. (2015): Mycobiota in gastrointestinal diseases. – Nat. Rev. Gastroenterol. Hepatol. 12: 77-87.
[65] Munoz, P., Bouza, E., Cuenca-Estrella, M., et al. (2005): *Saccharomyces cerevisiae* fungemia: an emerging infectious disease. – Clin. Infect. Dis. 40: 1625-1634.
[66] Naiyer, S., Bhattacharya, A., Bhattacharya, S. (2019a): Advances in *Entamoeba histolytica* biology through transcriptomic analysis. – Front. Microbiol. 10: Article 1921.
[67] Naiyer, S., Kaur, D., Ahamad, et al. (2019b): Transcriptomic analysis reveals novel downstream regulatory motifs and highly transcribed virulence factor genes of *Entamoeba histolytica*. – BMC Genomics 20: 206.
[68] Nash, A. K., Auchtung, T. A., Wong, M. C., et al. (2017): The gut mycobiome of the human microbiome project healthy cohort. – Microbiome 5: 153.

http://www.aloki.hu ● ISSN 1589 1623 (Print) ● ISSN 1785 0037 (Online)
DOI: http://dx.doi.org/10.15666/aeer/1802_23632394

[69] Nozaki, T., Bhattacharya, A. (2015): Amebiasis: Biology and Pathogenesis of *Entamoeba*. – Springer, Japan.
[70] Ott, S. J., Kühbacher, T., Musfeldt, M., et al. (2008): Fungi and inflammatory bowel diseases: alterations of composition and diversity. – Scand. J. Gastrol. 43: 831-841.
[71] Paulson, J. N., Pop, M., Bravo, H. C. (2011): Metastats: an improved statistical method for analysis of metagenomic data. – Genome Biol. 12(Suppl 1): P17.
[72] Penders, J., Thijs, C., Vink, C., et al. (2006): Factors influencing the composition of the intestinal microbiota in early infancy. – Pediatrics 118: 511-521.
[73] Pfeiffer, T., Morley, A. (2014): An evolutionary perspective on the Crabtree effect. – Front. Mol. Biosci. Article 17.
[74] Postma, E., Verduyn, C. (1989): Enzymic analysis of the Crabtree effect in glucose-limited chemostat cultures of *Saccharomyces cerevisiae*. – Appl. Environ. Microbiol. 55: 468-477.
[75] Quast, C., Pruesse, E., Yilmaz, P., et al. (2013): The SILVA ribosomal RNA gene database project: improved data processing and web-based tools. – Nucl. Acids Res. 41: D590-D596.
[76] Rajilic-Stojanovic, M., de Vos, W. M. (2014): The first 1000 cultured species of the human gastrointestinal microbiota. – FEMS Microbiol. Rev. 38: 996-1047.
[77] Rajilic-Stojanovic, M., Smidt, H., de Vos, W. M. (2007): Diversity of the human gastrointestinal tract microbiota revisited. – Environ. Microbiol. 9: 2125-2136.
[78] Ravdin, J. I., Croft, B. Y., Guerrant, R. L. (1980): Cytopathogenic mechanisms of *Entamoeba histolytica*. – J. Exp. Med. 152: 377-390.
[79] Richard, M. L., Lamas, B., Liguori, G., et al. (2015): Gut fungal microbiota: the Yin and Yang of inflammatory bowel disease. – Inflamm. Bowel Dis. 21: 656-665.
[80] Rigothier, M. C., Maccario, J., Vuong, P. N., Gayral, P. (1990): Effects of *Saccharomyces boulardii* yeast on trophozoites of *Entamoeba histolytica in vitro* and in cecal amebiasis in young rats. – Ann. Parasitol. Hum. Comp. 65: 51-60.
[81] Rigothier, M. C., Maccario, J., Gayral, P. (1994): Inhibitory activity of *saccharomyces* yeasts on the adhesion of *Entamoeba histolytica* trophozoites to human erythrocytes in vitro. – Parasitol. Res. 80: 10-15.
[82] Roncero, C. (2002): The genetic complexity of chitin synthesis in fungi. – Curr. Genet. 41: 367-378.
[83] Roussel, C., Sivignon, A., de Vallée, A., et al. (2018): Anti-infectious properties of the probiotic *Saccharomyces cerevisiae* CNCM I-3856 on enterotoxigenic *E. coli* (ETEC) strain H10407. – Appl. Microbiol. Biotechnol. 102: 6175-6189.
[84] Ruiz-Herrera, J., Gonzalez-Prieto, J. M., Ruiz-Medrano, R. (2002): Evolution and phylogenetic relationships of chitin synthases from yeasts and fungi. – FEMS Yeast Res. 1: 247-356.
[85] Saleh, H. A., Moawad, A. A., El-Hariri, M., Refai, M. K. (2011): Prevalence of yeasts in human, animals and soil sample at El-Fayoum Governorate in Egypt. – Int. J. Microbiol. Res. 2: 233-239.
[86] Sanchez, L., Enea, V., Eichinger, D. (1994): Identification of a developmentally regulated transcript expressed during encystation of *Entamoeba invadens*. – Mol. Biochem. Parasitol. 67: 125-135.
[87] Scanlan, P. D., Marchesi, J. R. (2008): Micro-eukaryotic diversity of the human distal gut microbiota: qualitative assessment using culture-dependent and independent analysis of feces. – ISMA J. 2: 1183-1193.
[88] Schloss, P. D., Westcott, S. L., Ryabin, T., et al. (2009): Introducing mothur: open-source, platform-independent, community-supported software for describing and comparing microbial communities. – Appl. Environ. Microbiol. 75: 7537-7541.
[89] Seed, P. C. (2014): The human mycobiome. – Cold Spring Harb. Perspect. Med. 5: a019810.
[90] Singh, N., Bhattacharya, S., Paul, J. (2011): *Entamoeba invadens*: dynamics of DNA synthesis during differentiation from trophozoite to cyst. – Exp. Parasitol. 127: 329-333.

http://www.aloki.hu ● ISSN 1589 1623 (Print) ● ISSN 1785 0037 (Online)
DOI: http://dx.doi.org/10.15666/aeer/1802_23632394

[91] Stensvold, C. R., Smith, H. V., Nagel, R., et al. (2010): Eradication of *Blastocystis* carriage with antimicrobials: reality or delusion? – J Clin Gastroenterol 44: 85-90.
[92] Soares, N. M., Azevedo, H. C., Pacheco, F. T. F., et al. (2019): A cross-sectional study of *Entamoeba histolytica/dispar/moshkovskii* complex in Salvador, Bahia, Brazil. – BioMed Res. Intl. Article ID 7523670.
[93] Stanley, S. L. (2003): Amebiasis. – Lancet 361: 1025-1034.
[94] Suhr, M. J., Hallen-Adams, H. E. (2015): The human gut mycobiome: pitfalls and potentials - a mycologist's perspective. – Mycologia 107: 1057-1073.
[95] Suhr, M. J., Banjara, N., Hallen-Adams, H. E. (2016): Sequence-based methods for detecting and evaluating the human gut mycobiome. – Lett. Appl. Microbiol. 62: 209-215.
[96] Tang, J., Iliev, I. D., Brown, J., et al. (2015): Mycobiome: approaches to analysis of intestinal fungi. – J. Immunol. Methods 421: 112-121.
[97] Tavares, R. G., Staggemeier, R., Borges, A. L. P. (2011): Molecular techniques for the study and diagnosis of parasite infection. – The Journal of Venomous Animals and Toxins including Tropical Diseases 17: 239-248.
[98] Tellam, R. L., Vuocolo, T., Johnson, S. E., et al. (2000): Insect chitin synthase cDNA sequence, gene organization and expression. – Eur. J. Biochem. RD 267: 6025-6043.
[99] Thibeaux, R., Weber, C., Hon, C.- C., et al. (2013): Identification of the virulence landscape essential for *Entamoeba histolytica* invasion of the human colon. – PLoS Pathog. 9: e1003824.
[100] Trissl, D., Martinez-Palomo, A., de la Torre, M., et al. (1978): Surface properties of *Entamoeba*: increased rates of human erythrocyte phagocytosis in pathogenic strains. – J. Exp. Med. 148: 1137-1145.
[101] Underhill, D., Iliev, I. (2014): The mycobiota: interactions between commensal fungi and the host immune system. – Nat. Rev. Immunol. 14: 405-416.
[102] Ungar, B. L. (1990): Enzyme-linked immunoassay for detection of *Cryptosporidium* antigens in fecal specimens. – J. Clin. Microbiol. 28: 2491-2495.
[103] Van Dellen, L., Bulik, D. A., Specht, C. A., et al. (2006): Heterologous expression of an *Entamoeba histolytica* chitin synthase in *Saccharomyces cerevisiae*. – Eukaryotic Cell 5: 203-206.
[104] Van Urk, H., Voll, W. S., Scheffers, W. A., Van Dijken, J. P. (1990): Transient-state analysis of metabolic fluxes in Crabtree-positive and Crabtree-negative yeasts. – Appl. Environ. Microbiol. 56: 281-287.
[105] Vazquezdelara-Cisneros, L. G., Arroyo-Begovich, A. (1984): Induction of encystation of *Entamoeba invadens* by removal of glucose from the culture medium. – J. Parasitol. 70: 629-633.
[106] Verkerke, H. P., Petri, W. A., Marie, C. S. (2012): The dynamic interdependence of amebiasis, innate immunity, and undernutrition. – Semin. Immunopathol. 34: 771-785.
[107] Vogel, C., Rogerson, A., Schatz, S., et al. (2007): Prevalence of yeasts in beach sand at three bathing beaches in South Florida. – Water Res. 41: 1915-1920.
[108] Wang, Z. K., Yang, Y. S., Stefka, A. T., et al. (2014): Review article: fungal microbiota and digestive diseases. – Aliment Pharmacol. Ther. 39: 751-766.
[109] WHO, PAHO, UNESCO (1997): Report: A Consultation with Experts on Amoebiasis. – WHO, Geneva; PAHO, Washington; UNESCO, Paris.
[110] Ximénez, C., Morán, P., Rojas, L., et al. (2009): Reassessment of the epidemiology of amebiasis: state of the art. – Infect. Genet. Evol. 9: 1023-1032.
[111] Zhou, J., Jiang, N., Wang, S., et al. (2016): Exploration of human salivary microbiomes-insights into the novel characteristics of microbial community structure in caries and caries-free subjects. – PLoS ONE 11: e0147039.

http://www.aloki.hu ● ISSN 1589 1623 (Print) ● ISSN 1785 0037 (Online)
DOI: http://dx.doi.org/10.15666/aeer/1802_23632394

APPENDIX

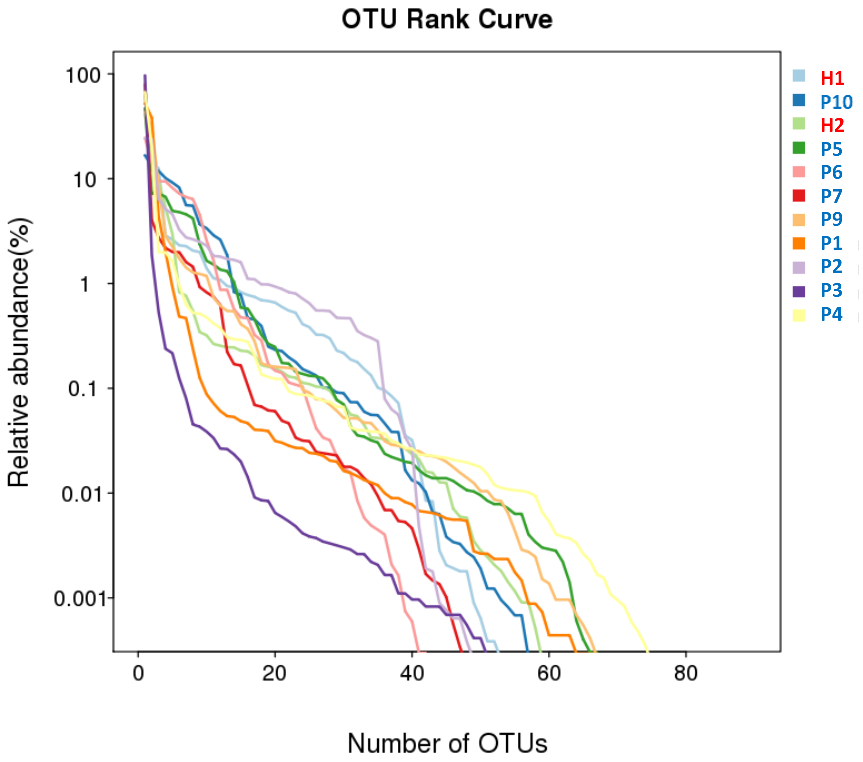

Figure A1. *Number of OTUs in relation to relative abundance of OTUs for different healthy individuals (H) and Entamoeba-infected patients (P)*

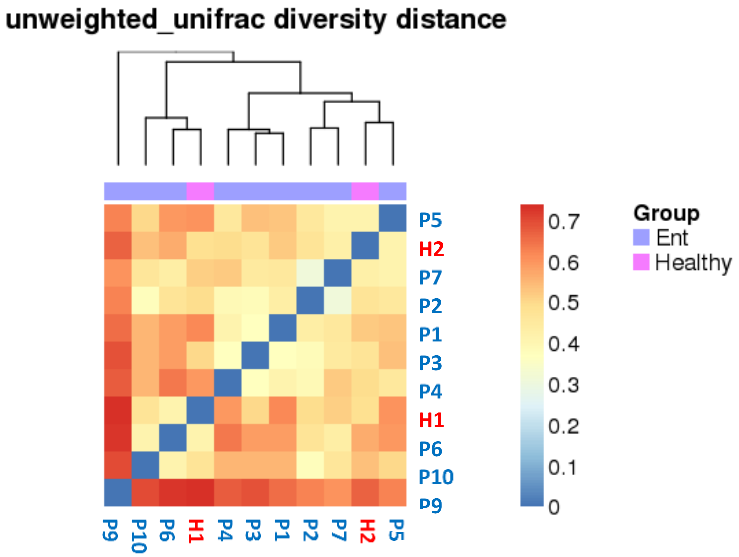

Figure A2. *Beta diversity heat map describing weighted and unweighted unifrac diversity distances for different healthy individuals (H) and Entamoeba-infected patients (P)*

Tables A1–A4: *See electronic appendix*

http://www.aloki.hu ● ISSN 1589 1623 (Print) ● ISSN 1785 0037 (Online)
DOI: http://dx.doi.org/10.15666/aeer/1802_23632394

CHANGES IN EXTREME TEMPERATURE EVENTS AND THEIR RELATIONSHIPS WITH THE EL NIÑO-SOUTHERN OSCILLATION IN THE WEI RIVER BASIN, CHINA

YAN, D. F.[1] – JIANG, R. G.[1,2*] – XIE, J. C.[1*] – ZHAO, Y.[3] – LIANG, J. C.[1] – WANG, Y. P.[1]

[1]*State Key Laboratory of Eco-hydraulics in Northwest Arid Region of China, Xi'an University of Technology, Xi'an 710048, China*

[2]*Department of Geography, National University of Singapore, Kent Ridge 117570, Singapore*

[3]*State Key Laboratory of Simulation and Regulation of Water Cycle in River Basin, China Institute of Water Resources and Hydropower Research, Beijing 100038, China*

[*]*Corresponding authors*
e-mail: jrengui@163.com; jcxie@xaut.edu.cn

(Received 12th Nov 2019; accepted 12th Feb 2020)

Abstract. Extreme temperature indices (ETIs) are used to assess extreme temperature events, to further reveal possible climate impacts of El Niño-Southern Oscillation (ENSO) on temperature extremes. The primary objective of this paper is to investigate the spatial and temporal variability of ETIs, and further examine the linear and nonlinear relationships between ETIs and two ENSO anomalies including the Niño 3.4 and Southern Oscillation Index (SOI) between 1969 and 2016 in the Wei River Basin (WRB) of China. The trends of ETIs were analyzed using Mann-Kendall test and cloud model, and the relationships between ENSO and ETIs were quantified using correlation and wavelet analysis. Results showed that the ETIs had increased from 1969 to 2016. Most of the stations exhibited similar trends for each ETIs except diurnal temperature range (DTR). The trend of minimum temperature (Tmin) was larger than that of maximum temperature (Tmax). Meanwhile, the variability of Tmin in the south of WRB was more stable than in other regions. Niño 3.4 was mainly positively correlated with PC1 of ETIs, and vice versa for SOI. The results help to understand the changes in extreme temperature events and their relationships with climate anomalies, which can provide scientific references for the water resource management of the watershed.
Keywords: *extreme temperature events, linear and nonlinear relationships, cross wavelet analysis, trend analysis, cloud model, Wei River Basin*

Introduction

According to the fifth Assessment Report (AR5) of Intergovernmental Panel on Climate Change (IPCC), surface air temperature had increased for past several decades, especially since 1850. In addition to the conclusive multi-decadal warming, the global average surface temperature showed obvious inter-decadal and inter-annual variations (IPCC, 2014). The frequency and magnitude of extreme climate events had significantly increased around the world (Utsumi et al., 2011; Sun et al., 2016). Therefore, it is of great significance to understand and reveal the trends and possible climate change impacts of extreme climate events.

The increasing frequency of extreme climate events has caused severe socioeconomic losses, which has garnered widespread attention (Zhang et al., 2008; Farajzadeh et al., 2015; Ruml et al., 2017). Many previous studies mainly focused on the extreme circumstances of climate change, including the causes, intensity and frequency. For example, Jiang et al. (2019b) investigated the trends of extreme

http://www.aloki.hu ● ISSN 1589 1623 (Print) ● ISSN 1785 0037 (Online)
DOI: http://dx.doi.org/10.15666/aeer/1802_23952412

precipitation indices (EPIs) for the period of 1969-2016 in the Wei River Basin (WRB). The results found that El Niño-Southern Oscillation (ENSO) exerted great impacts on the extreme precipitation events. Liu et al. (2018) analyzed the spatial-temporal change patterns of maximum and minimum temperature in the WRB. The results found that solar activity and large-scale atmospheric circulation have stronger influences on annual Tmin than annual Tmax. Tong et al. (2019) found that extreme temperature indices (ETIs) have significantly increased but the EPIs did not show significant changes in the Inner Mongolia.

Previous studies mainly investigated the spatiotemporal changes of extreme climate indices and obtained some results (Menang, 2017; Xiao et al., 2017; Agnihotri et al., 2018). However, few studies focused on the extreme climate events especially extreme temperature events in the WRB, which is the largest tributary of the Yellow River of China (Liu et al., 2017). Based on observed daily temperature data, this paper assessed the spatial and temporal variability of extreme temperature events using fourteen ETIs for the period of 1969-2016 in the WRB. The principal component analysis (PCA), Pearson's correlation, wavelet coherence and phase difference were used to explore the linear and nonlinear relationships between ETIs and typical large-scale global climate anomalies. This paper is organized as follows: material and methods are provided in the Section 2, followed by results and discussion in the Section 3, and conclusions in the Section 4.

Material and methods

Study area

The WRB is located between 33.68°N-37.39°N latitude and 103.94°W-110.03°W longitude, with basin area nearly 135,000 km^2. It originates from Gansu province, and flows through Ningxia Hui autonomous region and Shaanxi province from west to east, with length of 818 km, as shown in *Figure 1*. It can be divided into five sub-basins including the upstream, midstream and downstream of the WRB, Jing River Basin (JRB) and Beiluo River Basin (BRB). The upstream of WRB rises from the Qin Mountains with a length of 430 km. The midstream flows from Linjiacun to Xiwanyang, with length about 180 km. The downstream flows into the Yellow River from Xianyang, with length about 208 km. The JRB originates in the eastern foot of Liupan Mountain (Jiang et al., 2019b).

Due to the diversity of geological, geographical and climatic conditions, the climate of the WRB has obvious seasonal characteristics (Zou et al., 2017). The average temperature in summer is about 25°C, and below 0°C in winter. The WRB is a grain production and important economic zone in the northwest of China, especially after the establishment of Guanzhong-Tianshui Economic Zone (Chang et al., 2015). However, the climate of the WRB varied from region to region, and many extreme climate events happened in the history (Jiang et al., 2013, 2015).

Climate data

Daily temperature data from 34 meteorological stations that were downloaded from China Meteorological Administration (http://data.cma.cn/), covering the period from January 1st, 1969 to December 31st, 2016, were used to calculate the ETIs. The temperature data have passed strict quality control, the missing data and unreasonable

http://www.aloki.hu ● ISSN 1589 1623 (Print) ● ISSN 1785 0037 (Online)
DOI: http://dx.doi.org/10.15666/aeer/1802_23952412

data were carefully checked. The standard deviation exceeding 3 times was defined as the out-of-bound value, compared with the records of adjacent stations through manual inspection, reasonable reservation and unreasonable treatment according to absence. Two anomalies including Niño 3.4 and SOI were used as ENSO indices. The Niño 3.4 data was downloaded from Earth System Research Laboratory of National Oceanic and Atmospheric Administration (NOAA) at http://www.esrl.noaa.gov/. The SOI was downloaded from website at https://crudata.uea.ac.uk/cru/data/soi/.

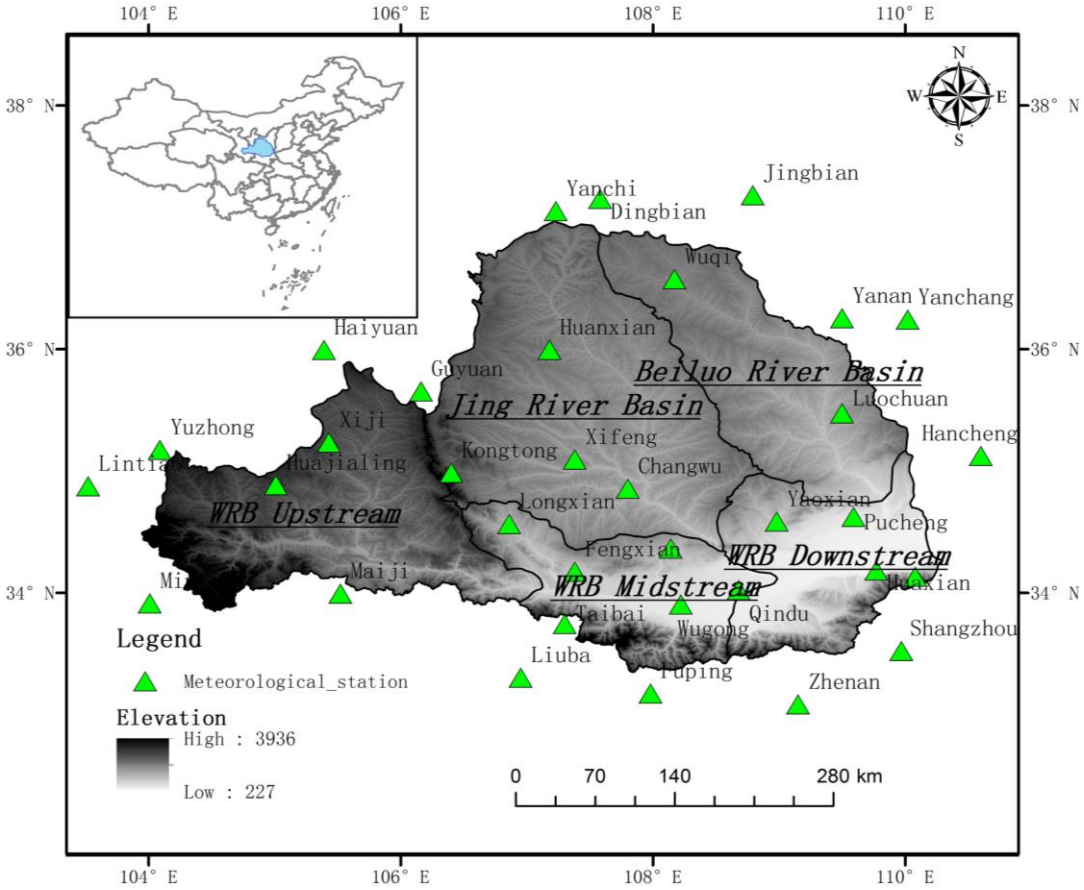

Figure 1. *Locations of the WRB and meteorological stations*

Definition and calculation of ETIs

Fourteen ETIs were defined to identify the extreme temperature events in this paper. The details of ETIs are shown in *Table 1*. These indices identify the changes of temperature in different aspects including intensity, duration and percentile, which have been widely used in previous studies (Popov et al., 2018; Jiang et al., 2017; Sun et al., 2018; Jiang et al., 2019a). A R based software named RClimDex was used to calculated the ETIs. RClimDex was based on a powerful and freely available statistical package R which runs under both Windows and Unix/Linux. It has a friendly graphical user interface and provides simple quality control process on the input daily temperature data, which has been widely used after it was developed (Almazroui et al., 2014; Jiang et al., 2018). More details of extreme climate indices and RClimDex can refer to the website at http://etccdi.pacificclimate.org/software.shtml.

http://www.aloki.hu ● ISSN 1589 1623 (Print) ● ISSN 1785 0037 (Online)
DOI: http://dx.doi.org/10.15666/aeer/1802_23952412

Table 1. *Details of 14 ETIs used in the study*

Acronym	ETIs	Definitions	Units
FD0	Frost days	Annual count when daily minimum (TN) < 0°C	Days
SU25	Summer days	Annual count when daily maximum (TX) > 25°C	Days
ID0	Ice days	Annual count when TX < 0°C	Days
GSL	Growing season Length	Annual count between first span of at least 6 days with daily mean temperature (TG) > 5°C and first span after July 1 of 6 days with TG < 5°C	Days
TN10p	Cool nights	Percentage of days when TN < 10th percentile	% of Days
TX10p	Cool days	Percentage of days when TX < 10th percentile	% of Days
TN90p	Warm nights	Percentage of days when TN > 90th percentile	% of Days
TX90p	Warm days	Percentage of days when TX > 90th percentile	% of Days
WSDI	Warm spell duration indicator	Annual count of days with at least 6 consecutive days when TX > 90th percentile	Days
CSDI	Cold spell duration indicator	Annual count of days with at least 6 consecutive days when TN < 10th percentile	Days
DTR	Diurnal temperature range	Monthly mean difference between TX and TN	°C
TR20	Tropical nights	Annual count when TN > 20°C	Days
Tmax	Annual maximum temperature	Annual maximum temperature	°C
Tmin	Annual minimum temperature	Annual minimum temperature	°C

Research methodology

Non-parametric Mann-Kendall test

The non-parametric Mann-Kendall test, recommended by the World Meteorological Organization, which has been widely used to estimate the trends of time series, was used to examine the trends of the ETIs (Mann, 1945; Kendall, 1975; Du et al., 2015).

For a data series $X = \{x_1, x_2, ..., x_n\}$, the statistic *S* is calculated by *Equation 1*.

$$S = \sum_{i=1}^{n-1} \sum_{j=i+1}^{n} \mathrm{sgn}(x_j - x_i) \quad \text{(Eq.1)}$$

where

$$\mathrm{sgn}(x_j - x_i) = \begin{cases} 1, x_j - x_i > 0 \\ 0, x_j - x_i = 0 \\ -1, x_j - x_i < 0 \end{cases} \quad \text{(Eq.2)}$$

The variance *V* is calculated using by *Equation 3*.

$$V = \frac{n(n-1)(2n+5)}{18} \quad \text{(Eq.3)}$$

http://www.aloki.hu ● ISSN 1589 1623 (Print) ● ISSN 1785 0037 (Online)
DOI: http://dx.doi.org/10.15666/aeer/1802_23952412

where n is the length of the data sequences, and Mann-Kendall' Z is calculated by *Equation 4*.

$$Z = \begin{cases} (S-1)/\sqrt{V}, S > 0 \\ 0, S = 0 \\ (S-1)/\sqrt{V}, S < 0 \end{cases} \quad \text{(Eq.4)}$$

The value of Z indicates the trend of series. $Z>0$ means positive trend, and vice versa for $Z<0$. Two significance levels including 1% and 5% were used to detect the statistically significant trends of ETIs.

Wavelet coherence and phase difference

Wavelet coherence (WTC) can be used to measure the part of local correlation between two data series in time and frequency domain. The wavelet transform of data series X and Y were $W_n^X(S)$ and $W_n^Y(S)$. The wavelet coherence defined by Torrence and Webster was given as follows:

$$R_n^2(s) = \frac{\left|S\left\langle s^{-1}W_n^{XY}(s)\right\rangle\right|^2}{S\left\langle s^{-1}\left|W_n^X(s)\right|^2\right\rangle S\left\langle s^{-1}\left|W_n^Y(s)\right|^2\right\rangle} \quad \text{(Eq.5)}$$

where $R_n^2(s) \in [0,1]$, and $W_n^{XY}(s) = W_n^X(s) \times W_n^Y(s)$.

The smoothing operator S of $W_n^{XY}(s)$ in numerator and wavelet power spectrum in denominator is given as follows:

$$S(W) = S_{scale}(S_{time}(W(s,t))) \quad \text{(Eq.6)}$$

$$S(W)\big|_s = (W(t,s)c_1 e^{-(t^2/2s^2)})\big|_s \quad \text{(Eq.7)}$$

$$S(W)\big|_n = (W(t,s)c_2 \Pi(0.6s))\big|_n \quad \text{(Eq.8)}$$

where S_{scale} indicates smoothing along the wavelet scale axis and S_{time} denotes smoothing in time, C_1 and C_2 are the normalized constants, Π is the rectangle function. The wavelet phase difference is given as follows:

$$\phi_n(s) = \tan^{-1}\left(\Im\left\{\left\langle s^{-1}W_n^{XY}(s)\right\rangle\right\} / \Re\left\{\left\langle s^{-1}W_n^{XY}(s)\right\rangle\right\}\right) \quad \text{(Eq.9)}$$

where $\Im\{\ldots\}$ and $\Re\{\ldots\}$ are the imaginary and real part of wavelet spectra, respectively. More details of WTC can be found at previous studies (Torrence and Compo, 1998; Grinsted et al., 2004).

http://www.aloki.hu ● ISSN 1589 1623 (Print) ● ISSN 1785 0037 (Online)
DOI: http://dx.doi.org/10.15666/aeer/1802_23952412

Normal Cloud model

The cloud model is mainly used to reveal the uncertain transformation between qualitative concept and quantitative instance (Li et al., 2009; Qin et al., 2011; Wang et al., 2014). It has been widely used in many fields such as data mining, pattern recognition. (Li et al., 1998; Grecu and Krajewski, 2000; Zhou et al., 2015). The cloud model uses three indicators to represent its characteristics: 1) Expectation (Ex), is the expectation of cloud droplets in domain space division, 2) Entropy (En), is a measure of qualitative concept uncertainty, which is determined by the randomness and fuzziness of concepts, 3) Hyper-Entropy (He), is the entropy of entropy. More details of normal cloud model can be found in previous studies (Li et al., 2009; Qin et al., 2011).

Let U be the universe of discourse and $\tilde{A}$ be a qualitative concept in U. If $x \in U$ is a random instantiation of concept $\tilde{A}$, which satisfies $x \sim N(Ex, En'^2)$, $En' \sim N(En, He^2)$, and the certainty degree of x belong to concept $\tilde{A}$ satisfies.

$$y = e^{-\frac{(x-Ex)^2}{2(En')^2}} \quad \text{(Eq.10)}$$

Then the distribution of x in the universe U is called as a normal cloud.

Principal component analysis

As a frequently-used statistical method, the PCA obtain different orthogonal principal components by reducing the dimension of multivariate data series, and explain most of the variability of original data series through a certain number of principal components. The leading principal component (PC1) was used as a substitution for each ETIs (Singh, 2006; Jiang et al., 2014).

Results and discussion

Change patterns of ETIs in the WRB

Trends of each ETIs were analyzed using non-parametric Mann-Kendall test. The trends were classified into seven categories including positive, statistically significant positive (5% & 1%), stationary, negative, statistically significant negative (5% & 1%), to provide more knowledge of the change characteristics of the ETIs.

The trends of 14 ETIs are shown in *Table 2*, which demonstrate the proportions of positive, stationary and negative trends of 14 ETIs in 34 stations, respectively.

Figure 2 shows the spatial distributions of trends in 14 ETIs for 34 meteorological stations for the period of 1969-2016 in the WRB. All fourteen ETIs except DTR were significantly increasing trends dominated. Eight ETIs including Tmax, Tmin, SU25, TR20, TN90P, TX90P, WSDI and GSL showed increasing trends for most of the stations. Other six ETIs showed decreasing trends.

http://www.aloki.hu ● ISSN 1589 1623 (Print) ● ISSN 1785 0037 (Online)
DOI: http://dx.doi.org/10.15666/aeer/1802_23952412

Table 2. *Trends of 14 ETIs (%)*

ETIs	Positive trend	SS (5%)	SS (1%)	Negative trend	SS (5%)	SS (1%)	Stationary trend
Tmax	94.12%	17.65%	5.88%	5.88%	0.00%	0.00%	0.00%
Tmin	82.35%	2.94%	14.71%	17.65%	0.00%	0.00%	0.00%
FD0	0.00%	0.00%	0.00%	100.00%	2.94%	91.18%	0.00%
ID0	0.00%	0.00%	0.00%	100.00%	38.24%	47.06%	0.00%
SU25	100.00%	32.35%	50.00%	0.00%	0.00%	0.00%	0.00%
TR20	91.18%	17.65%	38.24%	2.94%	0.00%	0.00%	5.88%
TN10P	2.94%	0.00%	0.00%	94.12%	2.94%	88.24%	0.00%
TX10P	0.00%	0.00%	0.00%	100.00%	8.82%	91.18%	0.00%
TN90P	100.00%	5.88%	94.12%	0.00%	0.00%	0.00%	0.00%
TX90P	100.00%	17.65%	79.41%	0.00%	0.00%	0.00%	0.00%
WSDI	100.00%	5.88%	0.00%	0.00%	0.00%	0.00%	0.00%
CSDI	2.94%	0.00%	0.00%	94.12%	14.71%	0.00%	2.94%
DTR	47.06%	5.88%	8.82%	52.94%	0.00%	14.71%	0.00%
GSL	100.00%	11.76%	79.41%	0.00%	0.00%	0.00%	0.00%

*SS denote statistically significant trends at 5% or 1%, respectively

Among 34 stations, only Changwu and Yanchi station showed downward trends in Tmax, which are located at the north and south of the JRB, respectively. Other stations showed upward trends. Three stations including Fengxiang and Wugong stations in the WRB midstream, and Luochuan station in the middle of the BRB, had significant increasing trends. Compared with Tmax, six stations had decreasing trends in Tmin. The trends of FD0 and ID0 in 34 stations were similar, with mainly downward trends dominated, and more than 90% of the stations had statistically significant decreasing trends at 5% significance level for FD0. Compared with the upward trends of SU25 for all stations, one station showed decreasing trend and two stations showed stationary trends for TR20. It is worth noting that TR20 in Minxian and Huajialing were all stationary. TX10P and TN10P showed downward trends for almost 34 stations. However, TX90P and TN90P showed upward trends. The trends of WSDI and CSDI were mainly opposite. The CSDI showed upward trends in all stations, but only several stations were statistically significant at 5% significance level for the period of 1969-2016.

Spatial distributions of Tmax and Tmin

In this study, the natural neighborhood method was used to interpolate three primary numerical characteristics in the WRB, and details are shown in *Figure 3*. Generally, three numerical characteristics have obvious and irregular spatial distributions. *Figure 3a* shows that the Tmax ranges from 25.29°C to 39.08°C, and the western WRB is lower than other regions. *Figure 3b* shows that the Tmin ranges from -23.50°C to -8.53°C, but the northern WRB is lower than that in the Guanzhong Plain. *Figure 3c* shows that the entropy values in the north and centre of the WRB are lower than those in the south and west, which indicates that the change in the north is more stable. *Figure 3d* show that the change of Tmin entropy is greater than the annual maximum. It can be concluded that the change of Tmin is more stable in the south-central region near the Qinling Mountains, but it is unstable in the north.

http://www.aloki.hu ● ISSN 1589 1623 (Print) ● ISSN 1785 0037 (Online)
DOI: http://dx.doi.org/10.15666/aeer/1802_23952412

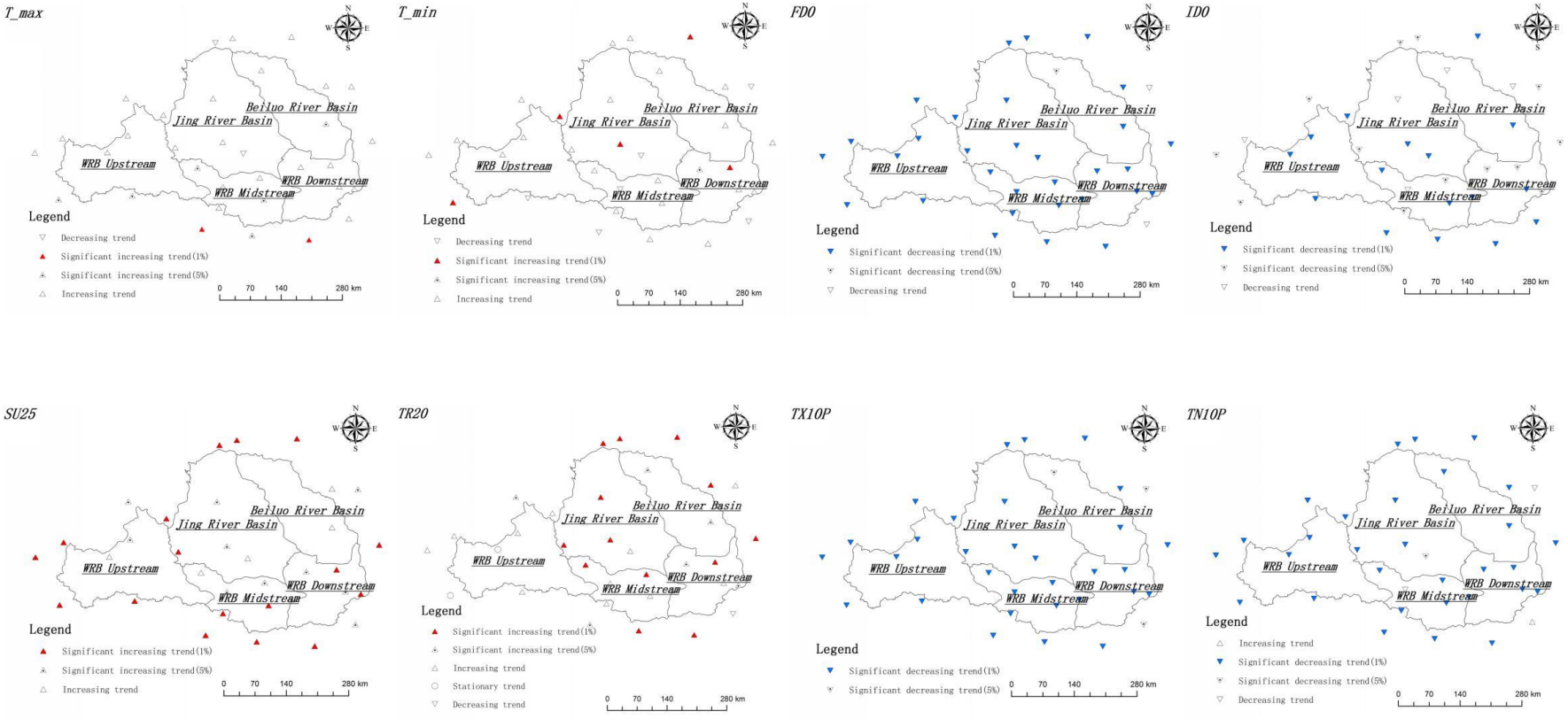

http://www.aloki.hu ● ISSN 1589 1623 (Print) ● ISSN 1785 0037 (Online)
DOI: http://dx.doi.org/10.15666/aeer/1802_23952412

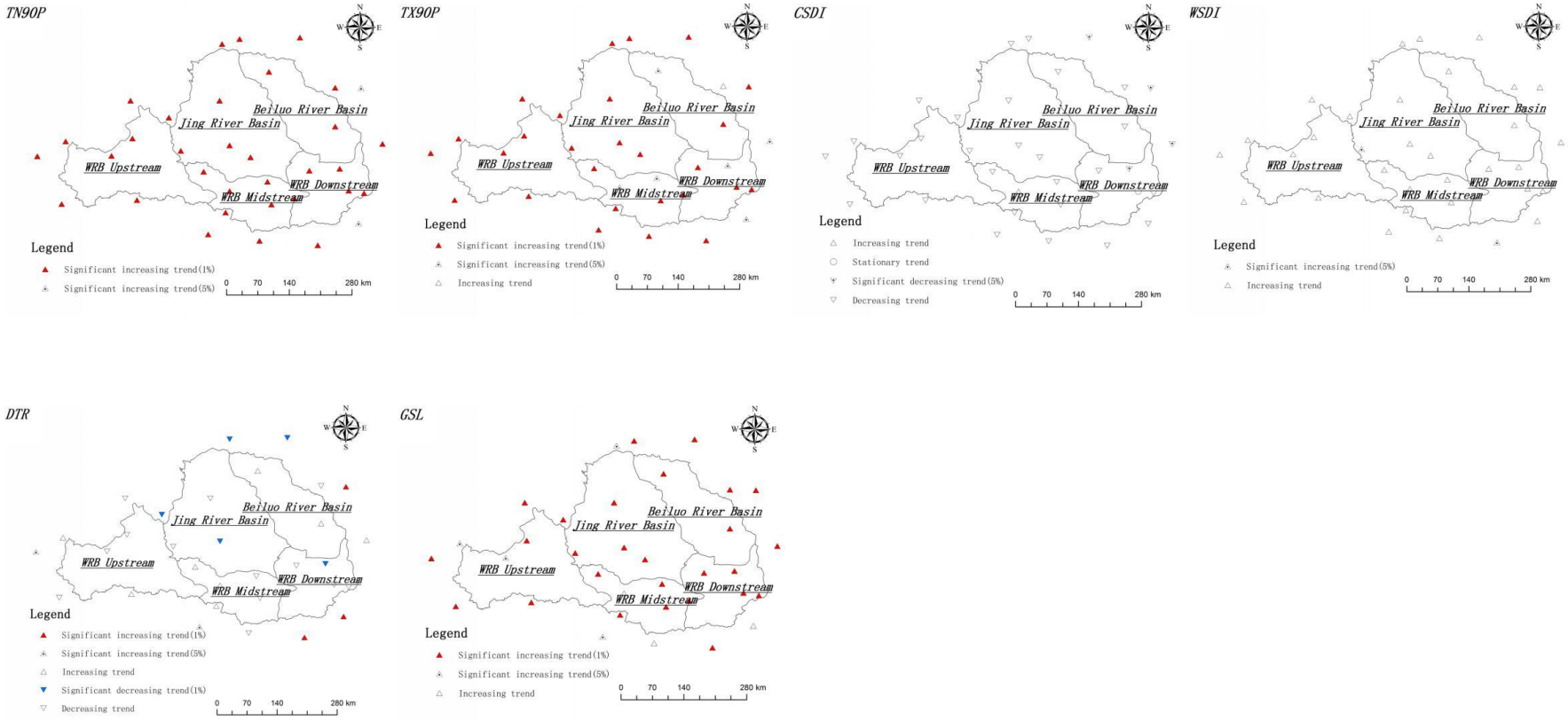

Figure 2. *Spatial distributions of trends of 14 ETIs: (a)Tmax, (b)Tmin, (c)FD0, (d)ID0, (e)SU25, (f)TR20, (g)TN10P, (h)TX10P, (i)TN90P, (j)TX90P, (k)CSDI, (l)WSDI, (m)DTR, (n)GSL*

http://www.aloki.hu ● ISSN 1589 1623 (Print) ● ISSN 1785 0037 (Online)
DOI: http://dx.doi.org/10.15666/aeer/1802_23952412

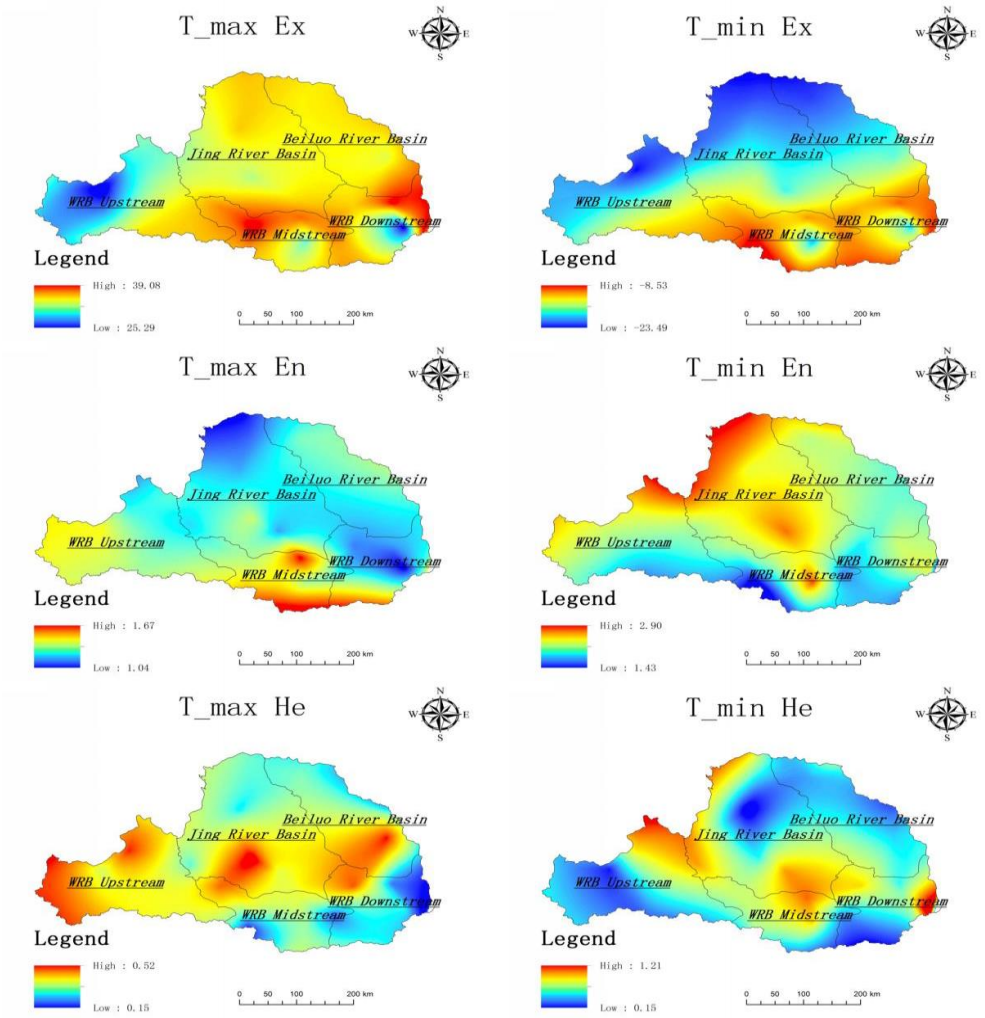

Figure 3. *Spatial distributions of three numerical characteristics in the WRB. (a)Ex of Tmax, (b)Ex of Tmin, (c)En of Tmax, (d)En of Tmin, (e)He of Tmax, (f)He of Tmin*

Ex indicates average values of Tmax and Tmin. *En* is used to react the instability of Tmax and Tmin sequences. The entropy value of Tmin is larger than that of Tmax, which indicates that the Tmin in the WRB is more unstable and scattered than that of Tmax. The standard deviations of them are calculated to further verify that the Tmin series is more uneven and unstable.

He represents the dispersion of entropy, and the larger the hyper entropy, the more the instability. Similar with entropy, the super entropy of Tmin is larger than that of Tmax, which indicates that the Tmin is more nonuniform the Tmax. In general, the Tmin variation has higher dispersion and instability than the Tmax variation in the WRB. Guanzhong Plain is the main grain production area in Shaanxi province. Annual minimum temperature changes have a negative impact on grain production. Therefore, the local government should scientifically prevent and adopt appropriate strategies to deal with this phenomenon.

The results show that generally the ETIs have similar trends for different stations, which are increasing trends dominated, as shown in *Table 2* and *Figure 2*. The cold extreme indices such as FD0 and ID0 have significant negative trends, and the warm

http://www.aloki.hu ● ISSN 1589 1623 (Print) ● ISSN 1785 0037 (Online)
DOI: http://dx.doi.org/10.15666/aeer/1802_23952412

extreme indices have significant positive trends. Changes in these indices indicate that extreme temperature events had mainly increased from 1969 to 2016, which is mainly consistent with previous results. For example, Zhou et al. (2011) founded that the numbers of frost days and ice days were significantly reduced in mainland China. Shi et al. (2018) found that the TR20, SU25, TX90P and TN90P had increased, but the FD0, ID0, TX10P and TN10P had decreased. The results showed that Tmax and Tmin of the JRB located in the Loess Plateau, have higher instability compared with other areas of the WRB. The results are consistent with Liu et al. (2018) who explored the maximum and minimum temperature variation in the WRB. The results found that solar activity and large-scale atmospheric circulation have stronger influences on annual Tmin than annual Tmax.

Correlation between ETIs and typical climate anomalies

PCA was used to extract the PC1 of each ETIs before correlation analysis between ETIs and two typical large-scale global climate anomalies including Niño 3.4 and SOI, because the PC1 of each ETIs represented the largest proportion of total variability.

Table 3 shows the correlation coefficients between each ETIs. The results show that PC1 of FD0 was negatively correlated with TN90P (ρ=-0.87). FD0 showed decreasing trends in 34 stations, but TN90P showed increasing trends. Thus, PC1 of FD0 and TN90P showed negative correlation. It is worth noting that there has positive correlations between typical warm temperature extremes including TX90P, TN90P, SU25, TR20 and WSDI. Similarly, there has positive correlations between typical cold temperature extremes including TN10P, TX10P, FD0, ID0 and CSDI, indicating that the warm ETIs are generally correlated with the cold ETIs. DTR and GSL also have positive correlations with warm ETIs and negative correlations with cold ETIs, except that the DTR is positively correlated with TN10P.

Table 3. *Cross correlation coefficients between different ETIs*

ETIs	FD0	ID0	TMAX	TMIN	SU25	TR20	TN10P	TX10P	TN90P	TX90P	WSDI	CSDI	DTR	GSL
FD0	1	0.42*	-0.11	-0.15	-0.55*	-0.45*	0.77*	0.63*	-0.87*	-0.64*	-0.39*	0.31*	-0.35	-0.85*
ID0		1	-0.19	-0.46*	-0.30*	-0.32*	0.60*	0.68*	-0.49*	-0.51*	-0.40*	0.48*	-0.38*	-0.35*
TMAX			1	0.25	0.47*	0.44*	-0.16*	-0.45*	0.37*	0.40*	0.35*	-0.18	0.39*	0.14
TMIN				1	0.22	0.13	-0.27	-0.37*	0.25	0.29*	0.26	-0.43*	0.24	0.12
SU25					1	0.56*	-0.45*	-0.66*	0.67*	0.76*	0.51*	-0.28	0.60*	0.50*
TR20						1	-0.61*	-0.57*	0.62*	0.48*	0.33*	-0.30*	0.19	0.43*
TN10P							1	0.70*	-0.74*	-0.46*	-0.25	0.63*	0.07	-0.64*
TX10P								1	-0.65*	-0.54*	-0.35*	0.50*	-0.46*	-0.61*
TN90P									1	0.81*	0.48*	-0.33*	0.19	0.77*
TX90P										1	0.77*	-0.28	0.62*	0.66*
WSDI											1	-0.13	0.51*	0.33*
CSDI												1	-0.18	-0.35*
DTR													1	0.24
GSL														1

- indicates statistically significant at 5% significant level

http://www.aloki.hu ● ISSN 1589 1623 (Print) ● ISSN 1785 0037 (Online)
DOI: http://dx.doi.org/10.15666/aeer/1802_23952412

Figure 4 shows the correlation coefficients between ETIs and Niño 3.4, SOI. In general, all cold ETIs except TN10P are negatively correlated with Niño 3.4 and positively correlated with SOI, and all warm ETIs are positively correlated with SOI and negatively correlated with Niño 3.4, except TN90P, which indicated that Niño 3.4 had negative impacts on the cold EITs and positive impacts on the warm ETIs, and vice versa for SOI. Among the cold ETIs, ρ between ID0 and two typical climate anomalies was the strongest. In case of the warm ETIs, TX90P and WSDI was more strongly correlated with Niño 3.4 and SOI than other ETIs. Therefore, four ETIs including TN10P, TX10P, TN90P and TX90P were selected to analysis the nonlinear relationships between Niño 3.4 and SOI using wavelet analysis in the following section.

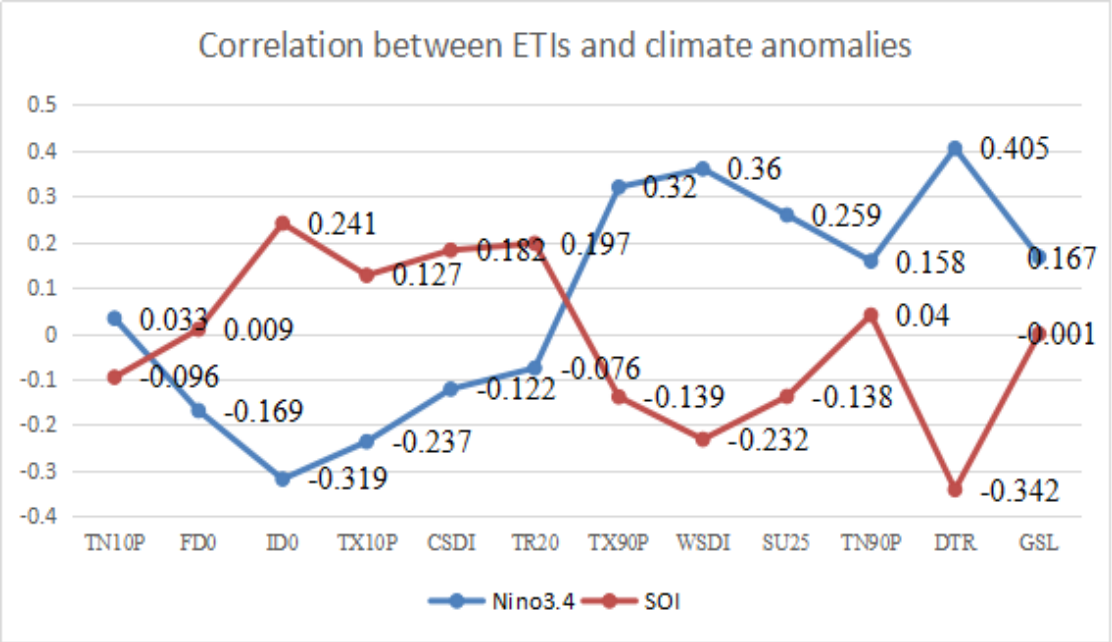

Figure 4. *Pearson's correlation coefficients between ETIs and Niño 3.4, SOI*

Wavelet analysis between ETIs and SOI

Figure 5a shows the wavelet coherence and phase difference between SOI and PC1 of TN10P. The results show that there is a 0-3 years cycle during 1969-1975 with negative correlations, a 2-4 years cycle after 2005 with a -90° phase difference and an 8-12 years cycle during 1970-1988 with a 45° phase difference. A 3 year cycle during 1995-2000 with a -90° phase difference and a 6 years cycle during 1994-1996 with negative correlations are also detected. *Figure 5b* shows wavelet coherence and phase difference between SOI and PC1 of TX10P. The results indicate that there is a 0-4 years cycle during 1995-2000, and the coherence was in-phase dominated. *Figure 5c* shows the wavelet coherence and phase difference between SOI and PC1 of TN90P. There is a 2-4 years cycle during 1990-2000, and the phase difference was 45°. The WTC analysis between SOI and PC1 of TX90P is shown in *Figure 5d*. There have a 3-6 years cycle during 1969-2016 and a 0-3 years cycle during 1985-1990, both of the coherence were dominated by anti-phase.

http://www.aloki.hu ● ISSN 1589 1623 (Print) ● ISSN 1785 0037 (Online)
DOI: http://dx.doi.org/10.15666/aeer/1802_23952412

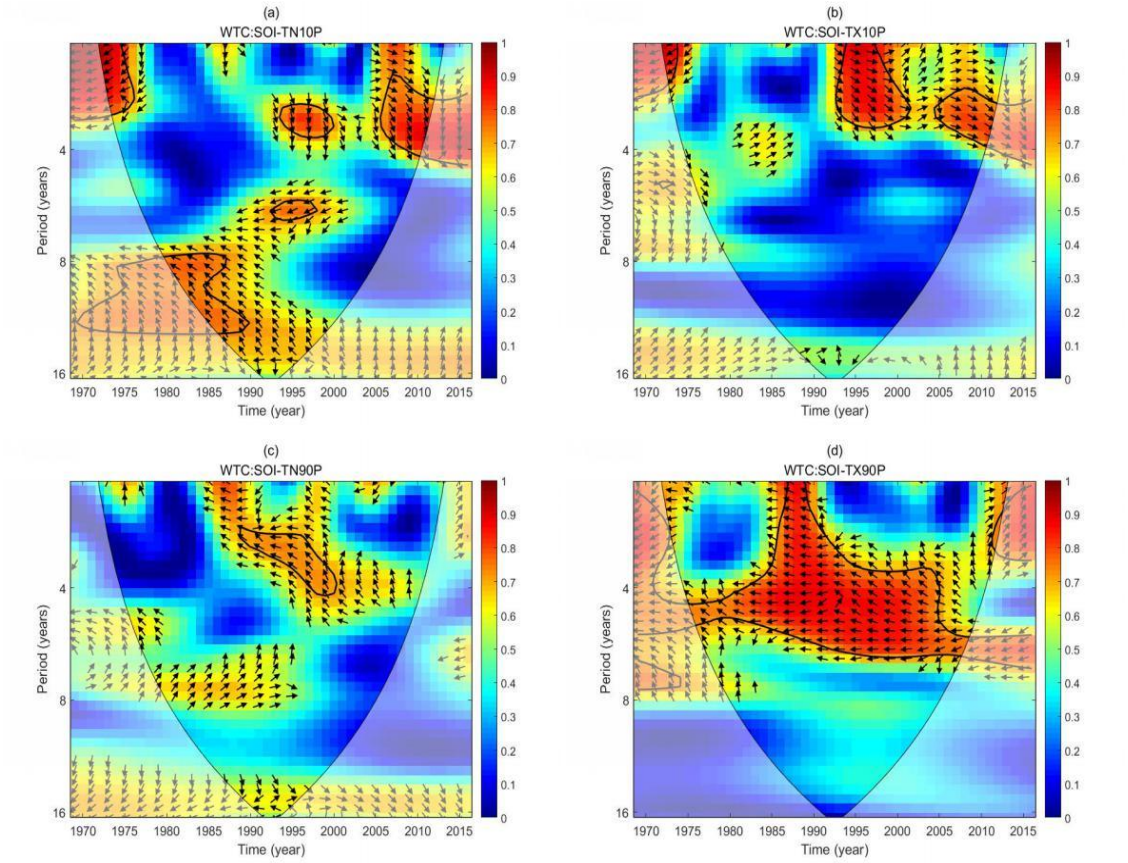

Figure 5. *WTC between SOI and PC1 of typical ETIs: (a)TN10P, (b)TX10P, (c)TN90P, (d)TX90P during 1969-2016*

Wavelet analysis between ETIs and Niño 3.4

Figure 6a shows the wavelet coherence and phase difference between Niño 3.4 and PC1 of TN10P. The results show that PC1 of TN10P is positively correlated with Niño 3.4, with a signal of 6-7 years during 1993-2003 and a 0-3 years signal during 1969-1977, it is noteworthy that half of the area are outside the cone of influence (COI), which need to be interpreted in cautious. The results also show that the Niño 3.4 leads PC1 of TN10P a quarter cycle, with a signal of 3 years during 1995-2000 and a 0-4 years signal during 2005-2016. The results also show the Niño 3.4 lags PC1 of TN10P a quarter cycle with a 12 years signal during 1970-1988, but most of the area are outside the COI. *Figure 6b* shows the wavelet coherence and phase difference between Niño 3.4 and PC1 of TX10P. There has a 2-year cycle during 1995-2000, and the phase difference was 45°. There are also statistically significant negative correlations with a 4 years cycle during 1983-1985. *Figure 6c* shows the wavelet coherence and phase difference between Niño 3.4 and PC1 of TN90P. There has a 4-year cycle during 1999-2005, and the phase difference was -90°. The WTC analysis between Niño 3.4 and PC1 of TX90P is shown in *Figure 6d*. The results show that PC1 of TX90P is positively correlated with Niño 3.4, with a signal of 4-6 years during 1980-2005 and a 0-4 years cycle during 1988-1990.

To reveal the change mechanism and potential influencing factors of ETIs in the WRB, we further investigate the teleconnections between typical ETIs and climate

http://www.aloki.hu ● ISSN 1589 1623 (Print) ● ISSN 1785 0037 (Online)
DOI: http://dx.doi.org/10.15666/aeer/1802_23952412

anomalies including Niño 3.4 and SOI. The results show that the correlation between ETIs and global climate anomalies is intricate, which vary in both time and frequency. However, the results of correlation between PC1 of ETIs and Niño 3.4, SOI (as shown in *Figure 4*) are consistent with the phase difference in *Figure 5* and *Figure 6*. Take TN10P and TX10p for examples, we found that the PC1 of TN10P and SOI are negatively correlated in *Figure 4*, and their phase differences are anti-phase, similarly, TX10P and SOI are positively correlated with each other and their phase differences are in-phase. The teleconnections between ETIs and ENSO indicated that the extreme temperature events might be predicted using large-scale climate anomalies as potential predictors. Previous studies have shown that the negative correlation between rainfall and SOI in the Loess Plateau is significant on the high time-frequency scale (Wang et al., 2019). However, the effects of atmospheric circulation patterns on regional temperature have been studied by many previous studies, such as Pacific Decadal Oscillation (PDO) (Newman et al., 2016; Zhang et al., 2018; Geng et al., 2019), Pacific/ North American (PNA) (Ning and Bradley, 2016), North Atlantic Oscillation (NAO) (Pokorna and Huth, 2015; Wang et al., 2017) and Arctic Oscillation (AO) (Otomi et al., 2013; Park and Ahn, 2016). Therefore, it should be better to include more global climate anomalies to predict the extreme temperature events based on their strong relationships (Loikith and Broccoli, 2012; Grotjahn et al., 2016).

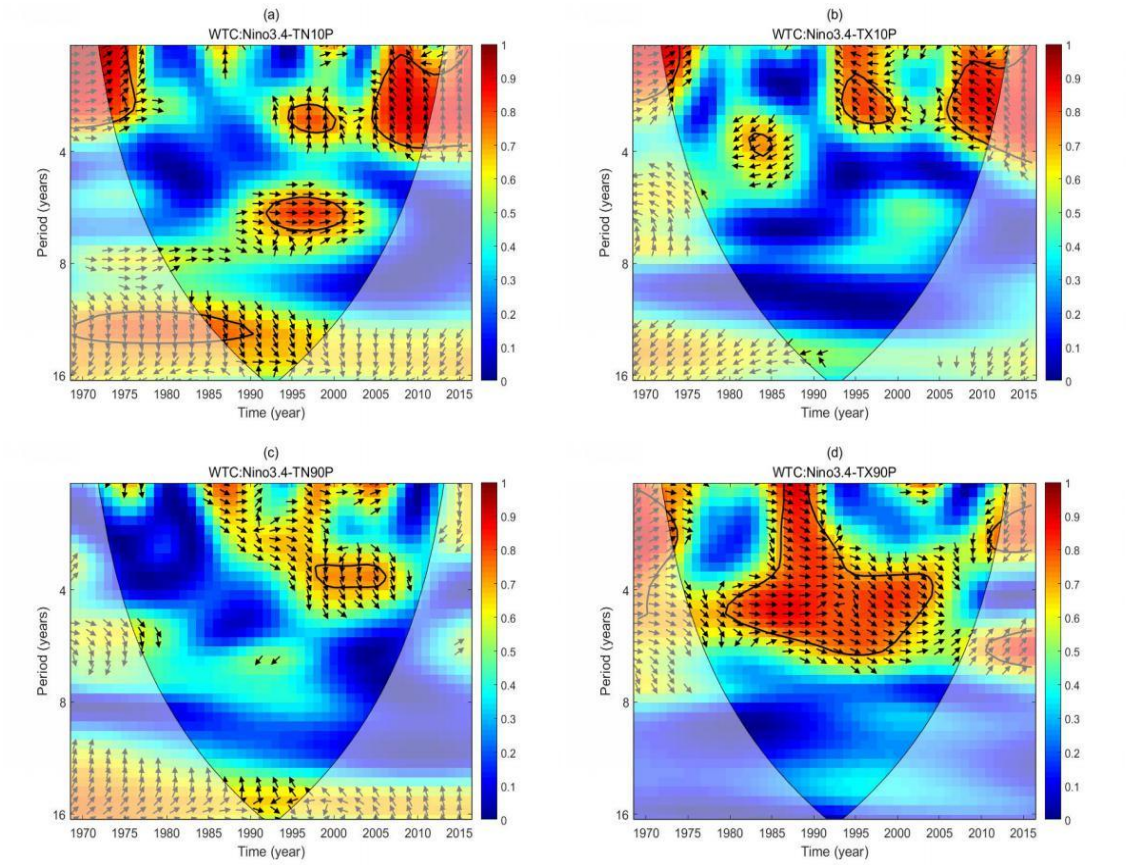

Figure 6. *WTC between Niño 3.4 and PC1 of typical ETIs: (a)TN10P, (b)TX10P, (c)TN90P, (d)TX90P during 1969-2016*

http://www.aloki.hu ● ISSN 1589 1623 (Print) ● ISSN 1785 0037 (Online)
DOI: http://dx.doi.org/10.15666/aeer/1802_23952412

Conclusions

In this paper, fourteen ETIs were used to evaluate the extreme temperature events. The temporal and spatial variability of ETIs were analyzed using non-parametric Mann-Kendall test method during 1969-2016 in the WRB. To reveal the potential relationships between extreme temperature change and atmospheric circulation factors, Niño 3.4 and SOI were used to investigated their linear and nonlinear relationships with ETIs. The main conclusions are summarized as follows:

In general, ETIs exhibited similar variability for different stations. Eight ETIs including Tmax, Tmin, SU25, TR20, TN90P, TX90P, WSDI and GSL showed mainly increasing trends, and five ETIs including FD0, ID0, TN10P, TX10P and CSDI showed mainly negative trends. Using cloud model of Tmax and Tmin, the results showed that the geographical location has an important influence on the spatial variability of *En*, *Ex* and *He*. Tmax, Tmin and *Ex* in the middle and lower reaches are higher than the JRB and BRB, which might be caused by the rapid urbanization of Guanzhong Plain and the urban heat island effect. *En* and *He* in the middle reaches are higher, which indicates that the Guanzhong Plain is more uneven and stable than other regions, which may be due to the influence of human activities and the difference of solar activities in different regions.

Two climate anomalies including Niño 3.4 and SOI had similar wavelet coherence and phase difference with PC1 of four ETIs. The inter-decadal oscillation between Niño 3.4 (SOI) and TN10P was found at about 12 years cycle. The results of phase difference between ETIs and SOI, Niño 3.4 are mainly opposite, positive with SOI, and negative with Niño 3.4, which are consistent with the results of Pearson's correlation (*Figure 4*). It is noteworthy that the oscillations between ETIs and climate anomalies need to be interpreted in cautious because of the limited data series.

The results of this study provide a reliable estimation of extreme temperature events, which provide references for water resource management and climate planning in the WRB. In particular, the potential impacts between large-scale climate anomalies and extreme temperature events provide some scientific basis and ideas for using large-scale climate anomalies to estimate the occurrence of regional extreme temperature events. The future work will focus on the prediction of extreme climate events using multiple global climate anomalies.

Acknowledgements. This study was partly supported by National Key Research and Development Program of China (2016YFC0401408), National Natural Science Foundation of China (51679188, 51509201 and 51979221), Natural Science Basic Research Plan in Shaanxi Province of China (Grant No. 2018JM5031). Daily temperature data can be downloaded from the China Meteorological Administration at http://data.cma.cn/. The SOI data can be downloaded from https://crudata.uea.ac.uk/cru/data/soi/. ENSO data were obtained from the Earth System Research Laboratory of NOAA, which can be downloaded from https://www.esrl.noaa.gov/psd/data/correlation/nina34.data/. RClimDex used to calculate the ETIs can be downloaded at http://etccdi.pacificclimate.org/software.shtml.

REFERENCES

[1] Agnihotri, I., Punia, M. P., Sharma, J. R. (2018): Assessment of spatial variations in temperature and precipitation extremes in west-flowing river basin of Kutch, Saurashtra and Marwar, India. – Current Science 114(2): 322-328.

http://www.aloki.hu ● ISSN 1589 1623 (Print) ● ISSN 1785 0037 (Online)
DOI: http://dx.doi.org/10.15666/aeer/1802_23952412

[2] Almazroui, M., Islam, M. N., Dambul, R., Jones, P. D. (2014): Trends of temperature extremes in Saudi Arabia. – International Journal of Climatology 34: 808-826.
[3] Chang, J. X., Wang, Y. M., Istanbulluoglu, E., Bai, T., Huang, Q., Yang, D. W., Huang, S. Z. (2015): Impact of climate change and human activities on runoff in the Weihe River Basin, China. – Quaternary International 380: 169-179.
[4] Du, S. Q., Gu, H. H., Wen, J. H., Chen, K., Van Rompaey, A. (2015): Detecting Flood Variations in Shanghai over 1949-2009 with Mann-Kendall Tests and a Newspaper-Based Database. – Water-Sui 7(5): 1808-1824.
[5] Farajzadeh, M., Oji, R., Cannon, A. J., Ghavidel, Y., Bavani, A. M. (2015): An evaluation of single-site statistical downscaling techniques in terms of indices of climate extremes for the Midwest of Iran. – Theoretical and Applied Climatology 120(1-2): 377-390.
[6] Geng, T., Yang, Y., Wu, L. X. (2019): On the Mechanisms of Pacific Decadal Oscillation Modulation in a Warming Climate. – Journal of Climate 32(5): 1443-1459.
[7] Grecu, M., Krajewski, W. F. (2000): Rainfall forecasting using variational assimilation of radar data in numerical cloud models. – Advances in Water Resources 24(2): 213-224.
[8] Grinsted, A., Moore, J. C., Jevrejeva, S. (2004): Application of the cross wavelet transform and wavelet coherence to geophysical time series. – Nonlinear Processes in Geophysics 11: 561-566.
[9] Grotjahn, R., Black, R., Leung, R., Wehner, M. F., Barlow, M., Bosilovich, M., Gershunov, A., Gutowski, W. J., Gyakum, J. R., Katz, R. W., Lee, Y.-Y., Lim, Y.-K., Prabhat (2016): North American extreme temperature events and related large scale meteorological patterns: a review of statistical methods, dynamics, modeling, and trends. – Climate Dynamics 46(3-4): 1151-1184.
[10] Huang, S. Z., Chang, J. X., Huang, Q., Chen, Y. T. (2014): Spatio-temporal Changes and Frequency Analysis of Drought in the Wei River Basin, China. – Water Resources Management 28(10): 3095-3110.
[11] Huang, S. Z., Hou, B. B., Chang, J. X., Huang, Q., Chen, Y. T. (2015): Spatial-temporal change in precipitation patterns based on the cloud model across the Wei River Basin, China. – Theoretical and Applied Climatology 120(1-2): 391-401.
[12] Intergovernmental Panel on Climate Change (IPCC). (2014): Climate Change 2014: Synthesis Report. – Contribution of Working Groups I, II and III to the Fifth Assessment Report of the Intergovernmental Panel on Climate Change. IPCC: Geneva, Switzerland.
[13] Jiang, R. G., Xie, J. C., Li, J. X. (2013): Application of World Wind on hydrologic monitoring and simulation in Shaanxi province, China. – Disaster Advances 6: 33-47.
[14] Jiang, R. G., Gan, T. Y., Xie, J. C., Wang, N. (2014): Spatiotemporal variability of Alberta's seasonal precipitation, their teleconnection with large-scale climate anomalies and sea surface temperature. – International Journal of Climatology 34(9): 2899-2917.
[15] Jiang, R. G., Xie, J. C., He, H. L., Luo, J. G., Zhu, J. W. (2015): Use of four drought indices for evaluating drought characteristics under climate change in Shaanxi, China: 1951-2012. – Natural Hazards 75(3): 2885-2903.
[16] Jiang, R. G., Xie J. C., Zhao Y., He H. L., He G. H. (2017): Spatiotemporal variability of extreme precipitation in Shaanxi province under climate change. –Theoretical and Applied Climatology, 130, 831-845.
[17] Jiang, R. G., Yu, X., Xie, J. C., Zhao, Y., Li, F. W., Yang, M. X. (2018): Recent changes in daily climate extremes in a serious water shortage metropolitan region, a case study in Jing-Jin-Ji of China. – Theoretical and Applied Climatology 134: 565-584.
[18] Jiang, R. G., Wang Y. P. , Xie J. C., Zhao Y., Li F. W, Wang X. J. (2019a): Multiscale characteristics of Jing-Jin-Ji's seasonal precipitation and their teleconnection with large-scale climate indices. –Theoretical and Applied Climatology 137(1-2):1495-1513.
[19] Jiang, R. G., Wang, Y. P., Xie, J. C., Zhao, Y., Li, F. W., Wang, X. J. (2019b): Assessment of extreme precipitation events and their teleconnections to El Nino Southern

http://www.aloki.hu ● ISSN 1589 1623 (Print) ● ISSN 1785 0037 (Online)
DOI: http://dx.doi.org/10.15666/aeer/1802_23952412

Oscillation, a case study in the Wei River Basin of China. – Atmospheric Research 218: 372-384.
[20] Kendall, M. G. (1975): Rank Correlation Measures. – Charles Griffin: London, UK.
[21] Li, D. Y., Han, J. W., Shi, X. M., Chung Chan, M. (1998): Knowledge representation and discovery based on linguistic atoms. – Knowledge-Based Systems 10(7): 431-440.
[22] Li, D. Y., Liu, C. Y., Gan, W. Y. (2009): A New Cognitive Model: Cloud Model. – International Journal of Intelligent Systems 24(3): 357-375.
[23] Liu, S. Y., Huang, S. Z., Huang, Q., Xie, Y. Y., Leng, G. Y., Luan, J. K., Song, X. Y., Wei, X., Li, X. Y. (2017): Identification of the non-stationarity of extreme precipitation events and correlations with large-scale ocean-atmospheric circulation patterns: A case study in the Wei River Basin, China. – Journal of Hydrology 548: 184-195.
[24] Liu, S. Y., Huang, S. Z., Xie, Y. Y., Huang, Q., Leng, G. Y., Hou, B. B., Zhang, Y., Wei, X. (2018): Spatial-temporal changes of maximum and minimum temperatures in the Wei River Basin, China: Changing patterns, causes and implications. – Atmospheric Research 204: 1-11.
[25] Loikith, P. C., Broccoli, A. J. (2012): Characteristics of Observed Atmospheric Circulation Patterns Associated with Temperature Extremes over North America. – Journal of Climate 25(20): 7266-7281.
[26] Mann, H. B. (1945): Non-parametric test against trend. – Econometrica 13: 245-259.
[27] Menang, K. P. (2017): Climate extreme indices derived from observed daily precipitation and temperature data over Cameroon: the need for further assessments. – Meteorological Applications 24(2): 167-171.
[28] Newman, M., Alexander, M. A., Ault, T. R., Cobb, K. M., Deser, C., Di Lorenzo, E., Mantua, N. J., Miller, A. J., Minobe, S., Nakamura, H., Schneider, N., Vimont, D. J., Phillips, A. S., Scott, J. D., Smith, C. A. (2016): The Pacific Decadal Oscillation, Revisited. – Journal of Climate 29(12): 4399-4427.
[29] Ning, L., Bradley, R. S. (2016): NAO and PNA influences on winter temperature and precipitation over the eastern United States in CMIP5 GCMs. – Climate Dynamics 46(3-4): 1257-1276.
[30] Otomi, Y., Tachibana, Y., Nakamura, T. (2013): A possible cause of the AO polarity reversal from winter to summer in 2010 and its relation to hemispheric extreme summer weather. – Climate Dynamics 40(7-8): 1939-1947.
[31] Park, H. J., Ahn, J. B. (2016): Combined effect of the Arctic Oscillation and the Western Pacific pattern on East Asia winter temperature. – Climate Dynamics 46(9-10): 3205-3221.
[32] Pokorna, L., Huth, R. (2015): Climate impacts of the NAO are sensitive to how the NAO is defined. – Theoretical and Applied Climatology 119(3-4): 639-652.
[33] Popov, T., Gnjato, S., Trbic, G., Ivanisevic, M. (2018): Recent Trends in Extreme Temperature Indices in Bosnia and Herzegovina. – Carpathian Journal of Earth and Environmental Sciences 13(1): 211-224.
[34] Qin, K., Xu, K., Liu, F. L., Li, D. Y. (2011): Image segmentation based on histogram analysis utilizing the cloud model. – Computer & Mathematics with Applications 62(7): 2824-2833.
[35] Ruml, M., Gregoric, E., Vujadinovic, M., Radovanovic, S., Matovic, G., Vukovic, A., Pacuca, V., Stojfcic, D. (2017): Observed changes of temperature extremes in Serbia over the period 1961-2010. – Atmospheric Research 183: 26-41.
[36] Shi, J., Cui, L. L., Ma, Y., Du, H. Q., Wen, K. M. (2018): Trends in temperature extremes and their association with circulation patterns in China during 1961-2015. – Atmospheric Research 212: 259-272.
[37] Singh, C. V. (2006): Pattern characteristics of Indian monsoon rainfall using principal component analysis (PCA). – Atmospheric Research 79(3): 317-326.

http://www.aloki.hu ● ISSN 1589 1623 (Print) ● ISSN 1785 0037 (Online)
DOI: http://dx.doi.org/10.15666/aeer/1802_23952412

[38] Sun, W. Y., Mu, X. M., Song, X. Y., Wu, D., Cheng, A. F., Qiu, B. (2016): Changes in extreme temperature and precipitation events in the Loess Plateau (China) during 1960-2013 under global warming. – Atmospheric Research 168: 33-48.
[39] Sun, P., Zhang, Q., Yao, R., Singh, V. P., Song, C. Q. (2018): Spatiotemporal Patterns of Extreme Temperature across the Huai River Basin, China, during 1961-2014, and Regional Responses to Global Changes. – Sustainability 10(4): 1-21.
[40] Tong, S. Q., Li, X. Q., Zhang, J. Q., Bao, Y. H., Bao, Y. B., Na, L., Si, A. L. (2019): Spatial and temporal variability in extreme temperature and precipitation events in Inner Mongolia (China) during 1960-2017. – Science of the Total Environment 649: 75-89.
[41] Torrence, C., Compo, G. P. (1998): A practical guide to wavelet analysis. – Bulletin of the American Meteorological Society 79: 61-78.
[42] Utsumi, N., Seto, S., Kanae, S., Maeda, E. E., Oki, T. (2011): Does higher surface temperature intensify extreme precipitation? – Geophysical Research Letter 38.
[43] Wang, G. Y., Xu, C. L., Li, D. Y. (2014): Generic normal cloud model. – Information Sciences 280: 1-15.
[44] Wang, X. F., Li, J. P., Sun, C., Liu, T. (2017): NAO and its relationship with the Northern Hemisphere mean surface temperature in CMIP5 simulations. – Journal of Geophysical Research-Atmosphere 122(8): 4202-4227.
[45] Wang, X. H., Wang, B. T., Xu, X. Y. (2019): Effects of large-scale climate anomalies on trends in seasonal precipitation over the Loess Plateau of China from 1961 to 2016. – Ecol Indic 2019: 107.
[46] Xiao, M. Z., Zhang, Q., Singh, V. P. (2017): Spatiotemporal variations of extreme precipitation regimes during 1961-2010 and possible teleconnections with climate indices across China. – International Journal of Climatology 37(1): 468-479.
[47] Zhang, F., Gao, H., Cui, X. (2008): Frequency of extreme high temperature days in China, 1961-2003. – Weather 63(2): 46-49.
[48] Zhang, Y., Xie, S. P., Kosaka, Y., Yang, J. C. (2018): Pacific Decadal Oscillation: Tropical Pacific Forcing versus Internal Variability. – Journal of Climate 31(20): 8265-8279.
[49] Zhou, Y. Q., Ren, G. Y. (2011): Change in extreme temperature event frequency over mainland China, 1961-2008. – Climate Research 50(2-3): 125-139.
[50] Zhou, Q., Wang, W., Pang, Y., Zhou, Z. Y., Luo, H. P. (2015): Temporal and spatial distribution characteristics of water resources in Guangdong Province based on a cloud model. – Water Science and Engineering 8(4): 263-272.
[51] Zou, L., Xia, J., She, D. X. (2017): Drought Characteristic Analysis Based on an Improved PDSI in the Wei River Basin of China. – Water 9(3): 178.

http://www.aloki.hu ● ISSN 1589 1623 (Print) ● ISSN 1785 0037 (Online)
DOI: http://dx.doi.org/10.15666/aeer/1802_23952412

GENETIC AND CHEMICAL VARIATION OF *SERIPHIDIUM QUETTENSE* AN ENDEMIC TAXA OF TWO MOUNTAINOUS REGIONS OF QUETTA, PAKISTAN

SAEED, S.[1*] – AHMED, A.[1] – LAGHARI, S. K.[1] – ALI, G. M.[2] – BEGUM, S.[2]

[1]*Department of Botany, University of Balochistan, Quetta, Pakistan*
(phone: +92-81-921-1264)

[2]*National Institute of Genomics and Advanced Biotechnology (NIGAB), NARC, Islamabad, Pakistan*

[*]*Corresponding author*
e-mail: shazia_botany@yahoo.com

(Received 12th Nov 2019; accepted 30th Jan 2020)

Abstract. *Serriphidium quettense* of the Asteraceae family is endemic to Balochistan, Pakistan. It has been used in traditional medicine for treating gastrointestinal diseases; while also having germicidal and antibacterial properties. However, no molecular and chemical characterization was demarcated earlier. Thus this study aimed to depict the genetic variability in two mountainous populations by molecular markers. Genetic variability assessment was carried out by polymorphic bands analysis to generate a dendrogram based on Sequential Agglomerative Hierarchical and Non-overlapping (SAHN) algorithm by Unweighted Pair Group Method of Arithmetic (UPGMA) means by using Numerical Taxonomy and Multivariate Analysis System (NTSYS) Pc version 2.01 for Cluster analysis. Chemical characterization was done by evaluating Total Phenolic Content (TPC) and flavonoids. A total of 68 amplified loci with 30 polymorphic were found with an average of 11.3 and 45% polymorphism. Cluster dendrogram based on similarity coefficient ranged from 0.285 to 0.785. Chemical vaiation was assesed by Agglomerative Hierarchical Clustering (AHC) based on dissimilarity matrix as indicated by two main clusters. Cluster 1 was represented by two sub clusters exhibited more chemical variation with in Zargoon population. Overall results obtained exhibited the diverse pattern of genetic and chemical variation. In conclusion, molecular marker profiling together with phytochemical variation of total phenolic and flavonoid content in all accessions of *S. quettense* and impact of ecological diversity on genetic and chemical variation can be used as base line study. Furthermore, implementation of conservation strategies of this endemic medicinal plant is highly recommended.
Keywords: *cluster analysis, agglomerative hierarchical clustering, morphological, chemical and genetic characterization*

Introduction

S. quettense (Podlech) Ling, Bull. of Asteraceae is an important medicinal plant with different medicinal and ornamental uses. Locally it is known as Jir in Brahvi and Terkhasperah in Pashtu. This species is endemic to Balochistan and utilized abundantly by local communities and grazed by livestock. The genus *Seriphidium* is a moderate-sized genus comprising of 135 species, distributed in Europe, and temperate Asia, a few species in N. America. Ethno medicinally used for various digestive problems (Anon, 2003; Durrani et al., 2003) also exhibited significant antibacterial activities (Kakar et al. 2012). This shrub provides forage to small ruminants when other range species produce limited dry matter particularly under drought conditions. Likewise, this shrub provides many benefits to humans and animals including feed for livestock and wildlife, erosion control and industrial products. High density of survived seedlings of *S. quettense* was found under plant canopies. Maximum established

http://www.aloki.hu ● ISSN 1589 1623 (Print) ● ISSN1785 0037 (Online)
DOI: http://dx.doi.org/10.15666/aeer/1802_24132423

seedlings were observed in the vicinity of adult conspecific plants. High survival rate of *S. quettense* may be due to low autumn precipitation that probably strengthen the seedlings and enable them to survive in winter season (Gul et al., 2007). Morphological markers (similar to leaf shape, plant height, color etc.) are one of the earliest markers utilized in the calculation of genetic variation. Still they are not abundantly unique and informational for the reason that the several chromosome character in the distinctive environments reasons extensive fluctuation of phenotypic qualities in individuals (Shinwari, 2011). Genetic marker is the arrangement of gene or DNA through recognized vicinity upon chromosomes and related to a unique gene or character; it may be defined as a version that can appear because of evolution or alternation of nucleotide in the genomic arrangement that may be discovered (Srivatsava and Nidhi, 2009). Molecular marker based on DNA is helping in development of beneficial plant species. DNA markers are over dependable since the phylogenetic data being exclusive and independent of age for every species, physiologic surroundings and environmental aspect (Kalpana et al., 2004). Based on PCR mostly molecular indicators RAPD is usually a conventional approach in the distinct floras (Mahmood et al., 2011; Kayani et al., 2011). PCR approach is probably the most competitive accessible DNA built techniques used for recording dissimilarities among cultivars inside species (Lakshmikumaran and Bhatia, 1998). Random amplified polymorphic DNA (RAPD) and Inter Simple Sequence Repeat (ISSR) markers were used as combined marker system for genetic variability of wild taxa (Saeed et al., 2017).

In this view, the present study was conducted to assess the genetic variability in two mountainous populations of *S. quettense* from Quetta valley Balochistan, Pakistan represented by six accessions through morphological, molecular and phytochemical profiling.

Materials and Methods

Site Selection

Two mountainous ranges of Quetta were selected for plant collection Zarghoon mountain range (3,578 masl) of high hills, steep slopes and narrow valleys and Hazarganji Chiltan National Park mountain range from 1600-3300 m asl (*Figure 1* and *Table 1*).

Figure 1. *Map of Quetta illustrating two study sites with geographical coordinates from which the examined populations of selected plants were sampled (Source: CAMEOS 2013)*

http://www.aloki.hu ● ISSN 1589 1623 (Print) ● ISSN1785 0037 (Online)
DOI: http://dx.doi.org/10.15666/aeer/1802_24132423

Table 1. *Geographical coordinates of study sites*

S. No.	Sampling sites	Site Code	Latitude (N)	Longitude (E)	Elevation (m)
Site 1	Zarghoon (ZR)	B.1	30.21	67.12	2200
		B.2	31.05	67.18	2830
		B.3	31.22	68.01	3200
Site 2	Hazarganji (HG)	C.1	30.21	66.54	1700
		C.2	30.07	65.55	2100
		C.3	30.15	66.07	2600

Plant Material

Plants were sampled during (2012-2014) from six different locations from two mountainous ranges and identified. Five replicate samples were collected from each sampling site. The voucher specimens were submitted to herbarium of Botany department, University of Balochistan Quetta for future references. Fresh and young leaves were collected and stored at ultra-low freezer at NIGAB, NARC Islamabad.

DNA Extraction and Purification

Total genomic DNA was extracted from young and fresh leaves samples of selected plants by CTAB (Cetyl Trimethyl Ammonium Bromide) method as described by Doyle and Doyle (1987) with few modifications (Saeed et al., 2015). The whole procedures including modifications are as follows:

Two to three leaves of plant material were grinded with the help of pestle and mortar, by adding 1 ml of preheated (65ºC) 2x CTAB buffer (100 mM Tris HCl (pH 8.0), 20 m Methylene Diamine Tetra Acetic acid (EDTA) with pH 8.0, 1.4 M sodium chloride (NaCl) and 1.5% mercaptoethanol. The homogenized leaf tissues were transferred to 1.5 ml eppendorf tubes and incubated at 65ºC for half an hour. An equal volume of chloroform/ isoamyl alcohol was added and the tubes were inverted gently 5–10 times, followed by centrifugation at 10,000 rpm for 10 min. After centrifugation, supernatant was transferred to a new eppendorf tube. Phenol is prepared and used as Phenol:Chloroform :Iso-amyalcohol (P:C:I) (25:24:1,v/v) to the samples to deprotenized the mixture double washed with Chloroform:Isoamyalcohol (C:I) (24:1, v/v). DNA was precipitated by adding an equal volume of 100% cold isopropanol. The DNA pellets were washed with 70% cold ethanol. The pellets were air dried and resuspended in the mixture of 40–50 µl 0.1x TE buffer. RNase were incubated at 37ºC for 30 min to remove RNA contamination and purified DNA samples were stored at -20ºC for further use. The quality of DNA was checked on a 1% agarose gel prepared in 0.5x TAE (Tris–acetate-EDTA) buffer. 1% Agarose gel stained with ethidium bromide was used to observe purified DNA along with DNA standard (50, 100 ng conc.) at 100 to 120 V for 35 min. The estimation of DNA concentration in a given samples was further checked on Biospec-Nano (230v) at ratio of 260/280 nm and values were recorded. The DNA was diluted by adding 5 µl DNA to 95 µl ddH_2O for downstream processes.

Molecular Markers Selection

For the first time for *S.quettense*10-mer RAPD (Operon USA) and 18-mer ISSR were purchased from gene link USA (*Tables 2* and *3*).

http://www.aloki.hu ● ISSN 1589 1623 (Print) ● ISSN1785 0037 (Online)
DOI: http://dx.doi.org/10.15666/aeer/1802_24132423

Table 2. *List of RAPD markers used for molecular characterization of S. quettense*

S. No.	Primer Name	Sequence (5'-3')
1	OPA-01	5'CAGGCCCTTC3'
2	OPA-02	5'TGCCGAGCTG3'
3	OPA-03	5'AGTCAGCCAC3'
4	OPA-04	5'AATCGGGCTG3'
5	OPA-05	5'AGGGGTCTTG3'
6	OPA-06	5'GGTCCCTGAC3'
7	OPA-07	5'GAAACGGGTG3'
8	OPA-08	5'GTGACGTAGG3'
9	OPA-09	5'GGGTAACGCC3'
10	OPA-10	5'GTGATCGCAG3'
11	OPB-01	5'GTTTCGCTCC3'
12	OPB-02	5'TGATCCCTGG3'
13	OPB-03	5'CATCCCCCTG3'
14	OPB-04	5'GGACTGGAGT3'
15	OPB-05	5'TGCGCCCTTC3'
16	OPB-06	5'TGCTCTGCCC3'
17	OPB-07	5'GGTGACGCAG3'
18	OPB-08	5'GTCCACACGG3'
19	OPB-09	5'TGGGGGACTC3'
20	OPB-10	5'CTGCTGGGAC3'

Table 3. *List of ISSR primers used for molecular characterization of S. quettense*

S. No.	Name	Sequence (5'-3')
1	UBC804	CTCTCTCTCTCTCTCTA
2	UBC806	CACACACACACACACAT
3	UBC807	AGAGAGAGAGAGAGAGT
4	UBC808	AGAGAGAGAGAGAGAGC
5	UBC810	GAGAGAGAGAGAGAGAT
6	UBC811	GAGAGAGAGAGAGAGAC
7	UBC851	GTGTGTGTGTGTGTGTYG
8	UBC852	TCTCTCTCTCTCTCTCRA
9	UBC853	TCTCTCTCTCTCTCTCRT
10	UBC854	TCTCTCTCTCTCTCTCRG

PCR Reaction

The PCR reaction for amplification was carried out in total 20 µl volume. The PCR master mix was prepared that containing, 3 mM $MgCl_2$, 1X PCR buffer, 0.2 mM dNTPs mix, 20 pmol primers, 0.01% gelatin, 1U/rxn Dream *Taq* DNA polymerase and 25 ng DNA template DNA. PCR amplification was performed using Applied Biosystems 96 well (USA), thermal cycler. For RAPD primers, PCR was programmed as mentioned below in table with initial denaturation at 94ºC for 3 min and then 36 cycles with denaturation at 94ºC for 1 min, annealing temperature at 36ºC for 1 min, extension step at 72ºC for 2 minutes and final extension for 5 minutes at 72ºC. For ISSR primers, PCR was programmed as; initial denaturation at 94ºC for 3 min and then 40 cycles with denaturation at 94ºC for 1 min, annealing temperature 56ºC for 1 min, extension step at 72ºC for 2 minutes followed by an additional final extension for 5 minutes at 72ºC (Abbas et al., 2015). Then amplified products were checked by electrophoresis in 1.8% agarose gels containing ethidium bromide (0.5µg / ml) in 1X TAE buffer. And product

http://www.aloki.hu ● ISSN 1589 1623 (Print) ● ISSN1785 0037 (Online)
DOI: http://dx.doi.org/10.15666/aeer/1802_24132423

was visualized by Gel documentation system under UV light and the size of markers were estimated by comparing to the standard ladder (100 bp BIORON 0.2 mg/ml) in the gel.

Phytochemical Variation of PSMs

Flavonoids

For flavonoids estimation, method described by Ordonez et al. (2006) was used. Take 0.5 ml sample, equal volume of 2% $AlCl_3$ ethanol solution was added and incubated at room temperature for 1 h. A yellow color indicated the presence of flavonoids. After 1 h, the absorbance was measured at 420 nm with the help of spectrophotometer. Total flavonoids contents was calculated as quercetin (mg/g) equivalent equation ($Y=0.0255x$, $R^2=0.9812$) where x is the absorbance and Y is the quercetin equivalent.

Total Phenolic Content (TPC)

Total Phenolic Contents (TPC) was measured by the method of Slinkard and Singleton (1977). An aliquot of the extract was mixed with 5 ml Folin–Ciocalteu reagent (FCR) reagent (previously diluted with water 1:10 v/v) and 4 ml of sodium carbonate (7%). The tubes were vortex for 15 seconds and were allowed to stand for 30 minutes at 40ºC for color development. Absorbance was then measured at 765 nm. Total phenolic contents were expressed as mg/g tannic acid equivalent equation ($Y=0.1216x$, $R^2=0.9365$) where x is the absorbance and Y is the quercetin equivalent.

Statistical Analysis

The amplified bands were scored as 1 (present) and 0 (absent). RAPD and ISSR data were clustered and dendrograms based on similarity matrices were calculated by using Sequential Agglomerative Hierarchical and Non-overlapping (SAHN) algorithm by "Unweighted Pair Group Method with Arithmetic Mean" (UPGMA) through Numerical Taxonomy System (NTSYS) pc 2.10j (Rohlf, 1998). Plant secondary metabolites (PSMs) were analyzed statistically by using XLSTAT version (2007). Clustering were also generated based on dissimilarity matrices by using Agglomerative Hierarchical Clustering (AHC). Data were statistically studied by "Analysis of Variance" (ANOVA) differences in Phytochemical TPC and Flavonoids Significance level ($P<0.05$, $P<0.01$ and $P<0.001$) was generated among the samples of different study sites by one way ANOVA.

Results and Discussion

This is the first comprehensive report of this endemic species *S. quettense* on morphological, chemical and molecular characterization from two mountainous regions of Quetta, Balochistan.

Morphological Diversity

Morphologically *S. quettense* is a complex species difficult to distinguish from the genus Artemisia life form is Perennial. Height of this shrub may range from 30-40 cm. Habit of shrub is woody below and upright branches are herbaceous aromatic. Stem

http://www.aloki.hu ● ISSN 1589 1623 (Print) ● ISSN1785 0037 (Online)
DOI: http://dx.doi.org/10.15666/aeer/1802_24132423

color vary from green to grayish green covered with densely whitish hair sometimes lack hair. Surface also varies from smooth to finely sulcate. Leaves are punctate-glandular, covered by greyish green to whitish hair. Leaf lamina is orbiculate. Upper leaves are sessile. Middle stem leaves are similar to lower but auriculate. Inflorescence based on panicles of 3-4 cm. Capitula numerous, homogamous, sessile, erect. Phyllaries green. Corolla reddish tinged to yellow. Cypsela are 0.8 mm long mostly brown in colour (*Table 4*). Present study revealed significant correlation of altitude and morphology of plants. That may be due to the differences of temperature, light intensity, change in soil properties, wind intensity or change in humidity. Earlier reported findings suggest the possibility of adaptation and variation in morphology of the plants due to change in any situations (Hovanden and Schoor, 2003). Plants can also change their morphological characters in harsh climate or weather. They were also capable to alter their characteristics in response to any biotic factors (Stenstrom et al., 2002). Earlier results revealed reduced size of *Mimulis primuloide* along low altitude that may be due to a higher competition at low altitude. Findings also explored low temperature at high-altitude resulted reduced plant size while increased size at intermediate altitude. Similarly, higher altitude decrease in growth of buds, shorter leaves length and less production of leaves (Tiwari et al., 2013).

Table 4. *Morphological Characteristics of S. quettense from Zarghoon and Hazraganji*

Sites	Stem colour	Stem surface	Shoot length	Leaf colour	Middle leaf length	Leaf lamina	Inflorescence
B.1	Green	Finely sulcate	25 cm	Green	3 cm	Orbiculate, uper sesile	Many Capitula.
B.2	Greish green	Slightly sulcate	26 cm	Green	2.5 cm	Orbiculate, uper sesile	Many sessile
B.3	Green	Slightly sulcate	30 cm	Green	2.9 cm	Orbiculate, uper sesile	Many Capitula.
C.1	Grey	Finely sulcate	28 cm	Silver green	3 cm	Orbiculate, uper sesile	Many sessile
C.2	Greish green	Smooth	27 cm	Green	3 cm	Orbiculate, uper sesile	Many sessile
C.3	Light green	Sulcate	28 cm	Silver green	2 cm	Orbiculate, to auriolat	Many Capitula.

Genetic Diversity

This is the first comprehensive report on molecular characterization and impact of ecosystem diversity on genetic diversity and chemical variation of *S. quettense*. DNA isolation was carried out without using Liquid Nitrogen. A modified protocol of Doyle and Doyle (1987) was used to extract DNA. This protocol gave a DNA with a sufficient quality to PCR reaction. This plant is also rich in polyphenolic compounds. Out of four tested ISSR and ten-mer RAPD primers on six accessions of two *S. quettense* populations, 2 ISSR and four RAPD primers exhibited polymorphic bands. (*Table 5* shows the banding pattern attained from specific primers). Combined ISSR and RAPD data revealed that total 68 loci are amplified and 30 of them were polymorphic with (44% polymorphism). Band size for ISSR ranged from 300 to 1500 bp and RAPD primers ranged from 150 to 1000 bp with an average of 11.3 bands per primer (*Figure 2*). Genetic similarity matrix was produced on the basis of combined ISSR and RAPD markers using genetic similarity coefficient. Results revealed that genetic

http://www.aloki.hu ● ISSN 1589 1623 (Print) ● ISSN1785 0037 (Online)
DOI: http://dx.doi.org/10.15666/aeer/1802_24132423

similarity value ranged from 0.285 to 0.785 between populations B.3 and B2. Characterized the closely related population. Mean genetic similarity also calculated as 0.53 the highest degree of genetic similarity occurred between B3 and B2 0.785 of ZR populations depicted low genetic variability within population. In contrast, lowest genetic similarity coefficient of 0.285 was found between B2 (ZR) and C3 (HG) populations, indicating high genetic variability between two mountainous sites. Overall the study revealed that in *S. quettense* genetic variability is 53% among all comparables (*Table 6*). Cluster analysis exhibited the UPGMA generated dendrogram by six accessions from two populations (*Figure 3*) showed exactly two clusters comprising of B2 B3 closely related with in ZR range and C3 cluster HG population further divided into C3, C1,and C2 clusters whereas B1 (ZR) accession also clustered with C2 indicated a different variation pattern. Morphologically *S. quettense* is a complex species difficult to distinguish from the genus Artemisia. Previously Nazar and Mahmood (2011) reported 68% polymorphism in some species of Artemisia from Rawalakot, Pakistan. Similar type of study was carried out by Hasan et al. (2009) using RAPD markers for evaluating genetic diversity of *A. capillaris* between two populations and has reported low genetic variability within the population. Whereas in present project 44% polymorphism is observed in *S. quettense*, representing less genetic diversity in isolated populations. This may also be because of over exploitation, uprooting of this significant endemic taxon due to its medicinal value and considered as a good source of fodder for livestock. Additionally, in the vicinity of the study area local communities depend mainly on many wild shrubs including *S. quettense* as a source of fuel for cooking and other purposes.

Table 5. *Primers analyses and number of DNA polymorphic bands produced*

S. No	Primers	TB	NPB	%PB
1	OPB-6	12	6	50
2	OPB-8	10	4	40
3	OPA-7	10	4	40
4	OPA-9	12	4	33
5	ISSR-1	12	6	50
6	ISSR-2	12	6	50
	TOTAL	68	30	44

T_A (°C) (annealing temperature), TB (Total bands), NPB (Number of polymorphic bands), *%PB*, percentage of polymorphism

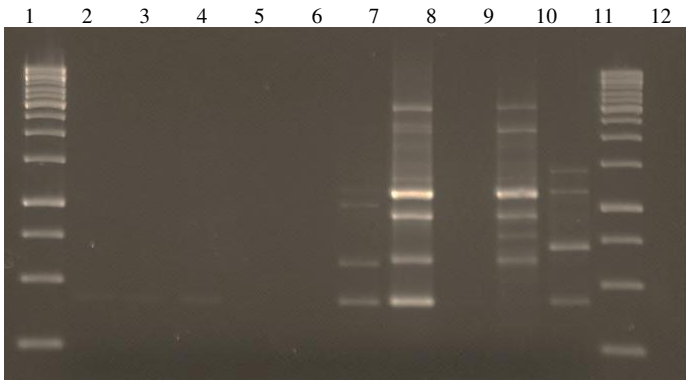

Figure 2. *PCR amplification of S. quettense of RAPD OPB-6 population from lane 2-11. With 100 bp marker lane 1 and 12*

http://www.aloki.hu ● ISSN 1589 1623 (Print) ● ISSN1785 0037 (Online)
DOI: http://dx.doi.org/10.15666/aeer/1802_24132423

Table 6. *Genetics similarity matrix of S. quettense based on combined RAPD and ISSR data*

	B.1	B.2	B.3	C.1	C.2	C.3
B.1	1					
B.2	0.642	1				
B.3	0.571	0.785	1			
C.1	0.571	0.357	0.285	1		
C.2	0.714	0.5	0.428	0.571	1	
C.3	0.5	0.285	0.5	0.357	0.642	1

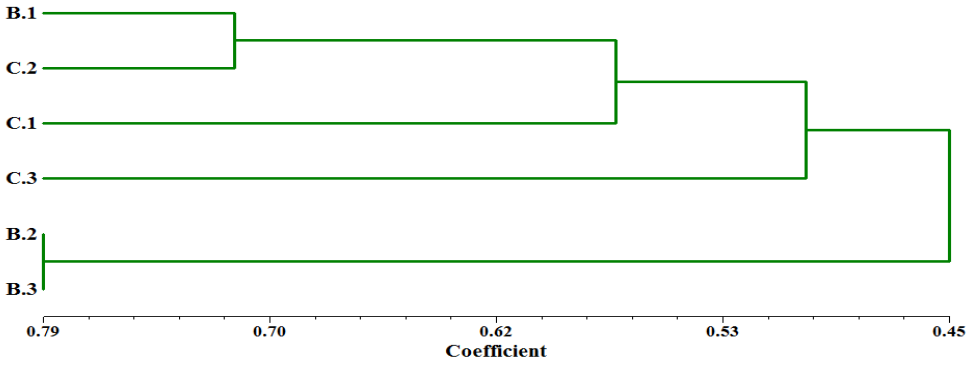

Figure 3. *NTSYS- dendrogram of cluster analysis based on data generated from RAPD and ISSR among S. quettense populations (Listed in Table 2)*

Chemical Variation

The results of Chemical variation estimated between and within population. TPC ranged from 42 mg/g to 47 mg/g within population B (Zarghoon) and 48 mg/g to 51 within population C (Hazarganji) Among the population B and C it varies from 42 to 51 mg/g general linear model ANOVA indicated that the significante diffrence P=0.03 at significant level P<0.05 (*Table 7, Figure 4*). Flavonoids also varies within and among the populations it ranges from 110 mg/g to 113 mg/g within population B (Zarghoon) and 92 to 96 mg/g within population C (Hazarganji). Among the populations it ranges from 92 to 113 mg/g ANOVA shows it is highly significant P=0.000 at significant level P<0.001 (*Table 8*). Chemical vaiation is assesed by Agglomerativ hierarchical clustering (AHC) based on dissimilarity matrix indicated two main clusters. Cluster 1 represented by two sub clusters exhibited more chemical variation with in Zargoon population (*Figure 5*).

Table 7. *Overall Mean ± SD of TPC and Flavonoid mong different population of S. quettense*

Area Code	Phenolics	Flavonoids
B	44.8±2.3	112±1.7
C	49.8±1.4	94.6±2.1

Geographical location is the major element that may causes differences in natural climatic condition. Earlier reported research (Malencic et al., 2007) explains with the recorded climatic data that the agricultural practices of various geographical zones are

http://www.aloki.hu ● ISSN 1589 1623 (Print) ● ISSN1785 0037 (Online)
DOI: http://dx.doi.org/10.15666/aeer/1802_24132423

incorporating by seasonal and climatic variation. Geographical locations also have an impact on phenolic contents. The phenolic contents are also under the impact of biotic and abiotic stresses. Higher temperature inhibited the expression of flavonoid pathway genes and resulted in lower phenolic accumulation (Yamane et al., 2006; Cohen et al., 2008, 2012). The findings of this project demarcated the Total Phenolic Content (TPC) and flavonoids variation maximum among population supported by similar results that high diversity in quantities of chemical compounds was found among populations (Bottin et al., 2007). On the other hand, the mechanism behind chemical variations is still need to be studied within and among species (Pichersky and Gang, 2000). There are other factors, in addition to genetic and environmental factors that affect the chemical diversity and need to be explored (Kumar et al., 2009). Therefore, future detailed greenhouse studies are suggested to assess correlations between genetic and chemical diversities.

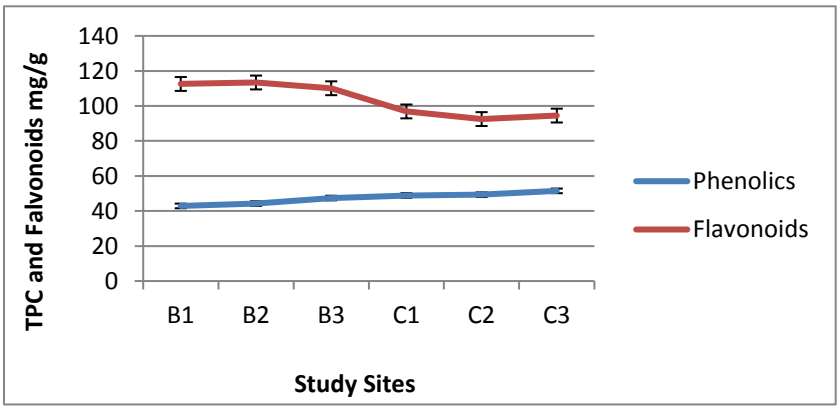

Figure 4. *Pehnolics and Flavonoid variation with standard error bars among study sites*

Table 8. *Analysis of Variance of TPC and Flavonids among different population of S. quettense*

	TPC	**Flavonoids**
F-Value	10.32	117.83
P-Value	0.03	0.000
Significance level	*	***

Significance level *,**,*** at p<0.05, p<0.01, p<0.001 respectively

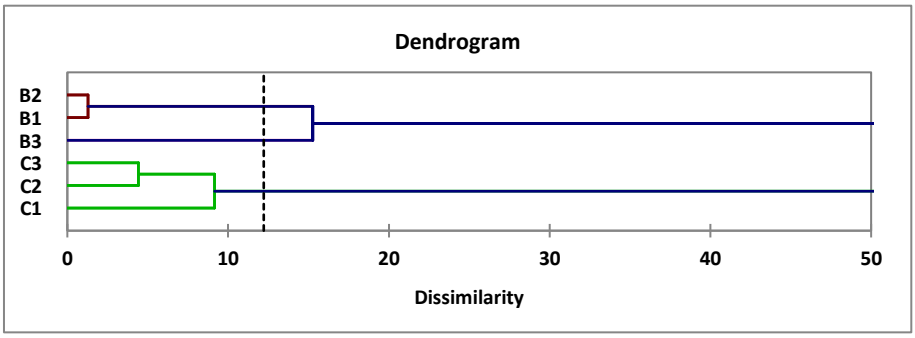

Figure 5. *Dendrogram estimating genetic distance among S. quettense populations based on TPC and Flavonoids*

http://www.aloki.hu ● ISSN 1589 1623 (Print) ● ISSN1785 0037 (Online)
DOI: http://dx.doi.org/10.15666/aeer/1802_24132423

Conclusion

Based on our findings, it was concluded that there is an impact of ecological consequences on morphological, genetic diversity and phytochemical composition of *S. quettense*. Due to fragmented habitat and anthropogenic effects, diversity within population found to be less than between populations. Though semi-conserved and conserved regions of Zarghoon range and Hazarganji Chiltan National park still retained genetic diversity within populations, however, sustainable management plans are to be implemented. It has also been concluded that the assessment and conservation of genetic diversity through molecular markers is essential that could be used as a key to conserve genetic variability and assess environmental changes on allelic frequency. Furthermore, implementation of conservation strategies for such an important wild endemic taxa is highly recommended.

REFERENCES

[1] Abbas, G., Hameed, A., Rizwan, M., Ahsan, M., Asghar, M. J., Iqbal, N. (2015): Genetic Confirmation of Mungbean (*Vigna radiata*) and Mashbean (*Vigna mungo*) Interspecific Recombinants using Molecular Markers. – Frontiers in Plant Science 6: 1107.

[2] Anonymous. (2003): 1998 District Census Report of Karak. – Publication Census Organization, Statistics Division, Government of Pakistan, Islamabad.

[3] Bottin, L., Isnard, C., Lagrange, A., Bouvet, J. M. (2007): Comparative molecular and phytochemical study of the tree species *Santalum austrocaledonicum* (Santalaceae) distributed in the New-Caledonian Archipelago. – Chemistry and Biodiversity 4: 1541-1556.

[4] Cohen, S. D., Tarara, J. M., Kennedy, J. A. (2008): Assessing the impact of temperature on grape phenolic metabolism. – Analytica Chimica Acta 621: 57-67.

[5] Cohen, S. D., Tarara, J. M., Gambetta, G. A., Matthews, M. A., Kennedy, J. A. (2012): Impact of diurnal temperature variation on grape berry development, proanthocyanidin accumulation, and the expression of flavonoid pathway genes. – Journal of Experimental Botany 63: 2655-2665.

[6] Doyle, J. J., Doyle, J. L. (1987): A rapid DNA isolation procedure for small quantities of fresh leaf material. – Phytochemical Bulletin 19(1): 11-15.

[7] Durrani, M. J., Malik, A. M., Hussain, F. (2003): Folk Medicinal plants of Nushki, District Chaghi, Pakistan. – Journal of Science and Technology 27(1-2): 45-52.

[8] Gul, S., Ahmad, S., Achakzai, A. K. K., Islam, M. (2007): Impact of microhabitat on survival of *Seriphidium quettense* seedlings. – Pak. J. Bot 39(5): 1717-1724.

[9] Hasan, S. M. Z., Shafie, M. S. B., Shah, R. M. (2009): Analysis of Random Amplified polymorphic DNA (RAPD) of Artemisia Capillaris (Worm Wood Capillary) in East Coast of Peninsular Malaysia. – World Applied Sciences Journal 6(7): 976-986.

[10] Hovanden, M. J., Vander, S. J. K. (2003): Nature Vs nurture in the leaf morphology of southern beech, *Nothofagus cunninghamii* (Nothofagaceae). – New Phytologist 161: 585-594.

[11] Kakar, S. A., Tareen, R. B., Kakar, M. A., Jabeen, H., Kakar, S. R., Al-Kahraman, Y. M. S. A., Shafee, M. (2012): Screening of antibacterial activity of four medicinal plants of Balochistan Pakistan. – Pakistan Journal of Botany 44(S): 245-250.

[12] Kalpana, J., Warude, P. C., Bhushan, P. (2004): Molecular markers in herbal drug technology. – Current science 87(2): 159-165.

[13] Kayani, W. K., Majid, S. A., Mahmood, T., Saqlan, S. M. N., Waheed, A. (2011): Effect of temperature Stress on polyphenol oxidase activity in grains of some Wheat cultivars. – Pakistan Journal of Botany 43: 1011-1020.

http://www.aloki.hu ● ISSN 1589 1623 (Print) ● ISSN1785 0037 (Online)
DOI: http://dx.doi.org/10.15666/aeer/1802_24132423

[14] Kumar, J., Verma, V., Goyal, A., Shahi, A. K., Sparoo, R., Sangwan, R. S., Qazi, G. N. (2009): Genetic diversity analysis in *Cymbopogon* species using DNA markers. – Plant Omics Journal 2: 20-29.
[15] Lakshmikumaran, M., Bhatia, S. (1998): DNA fingerprinting of medicinal plants. – In: Debry, B. (ed.) Intellectual Property Rights. Rajiv Gandhi Institute for Contemporary studies B.R. Publishing Corporation, Delhi. pp. 293-331.
[16] Mahmood, T., Siddiqua, A., Rasheed, A., Nazar, N. (2011): Evaluation of genetic diversity in different Pakistani wheat land races. – Pakistan Journal of Botany 43(2): 1233-1239.
[17] Malencic, D., Popovic, M., Miladinovic, J. (2007): Phenolic content and antioxidant properties of soyabean (*Glycine max* (L) meer.) seeds. – Molecules 12: 576-581.
[18] Nazar, N., Mahmood, T. (2011): Morphological and molecular characterization of selected Artemisia species from Rawalakot, Azad Jammu and Kashmir. – Acta Physiology of Plant 33: 625-633.
[19] Ordonez, A. A. L., Gomez, J. D., Vattuone, M. A., Isla, M. I. (2006): Antioxidant activities of *Sechiumedule* (Jacq). – Food Chemistry 97: 452-458.
[20] Pichersky, E., Gang, D. R. (2000): Genetics and biochemistry of secondary metabolites in plants: an evolutionary perspective. – Trends in plant Science 5: 439-445.
[21] Rohlf, J. (1998): NTSYSpc numerical taxonomy and multivariate analysis system version 2.0 User Guide F. – Department of Ecology and Evolution State University of New York Stony Brook, NY 11794-5245.
[22] Shinwari, Z. K., Sultan, S., Mehmood, T. (2011): Molecular and Morphological characterization of selected *Mentha* species. – Pakistan Journal of Botany 43(3): 1433-1436.
[23] Slinkard, K., Singleton, V. L. (1977): Total phenol analyses: automation and comparison with manual methods. – American Journal for Enology and Viticulture 28: 49-55.
[24] Srivatsava, S., Nidhi, M. (2009): Genetic markers- A cutting edge technology in herbal drug research. – Journal of Chemical and Pharmaceutical Research 1(1): 1-18.
[25] Stenstrom, A., Jonsdottir, I. S., Augner, M. (2002): Genetic and environmental effects on morphology in clonal sedges in the Eurasian arctic. – American Journal of Botany 89: 1410-1421.
[26] Tiwari, S. P., Kumar, P., Yadav, D., Chauhan, D. K. (2013): Comparative morphological, epidermal and anatomical studies of *Pinus roxburghii* needles at different altitudes in the North-West Indian Himalayas. – Turkish Journal of Botany 37: 65-73.
[27] Williams, J. G. K., Kubelik, A. R. K., Livak, T., Rafalski, J. A., Tingey, S. V. (1990): DNA polymorphisms amplified by arbitrary primers are useful as genetic markers. – Nucleic Acids Research 18: 6531-6539.
[28] Yamane, T., Jeong, S. T., Goto-Yamamoto, N., Koshita, Y., Kobayashi, S. (2006): Effects of temperature on anthocyanin biosynthesis in grape berry skins. – American Journal for Enology and Viticulture 57: 54-59.

http://www.aloki.hu ● ISSN 1589 1623 (Print) ● ISSN1785 0037 (Online)
DOI: http://dx.doi.org/10.15666/aeer/1802_24132423

PHYTOCHEMICAL SCREENING, ISOLATION OF COUMARINS AND EXAMINING BIOACTIVITY OF *PRANGOS PLATYCHLAENA* BOISS. PLANT IN IRAQ

RAHMAN, J. K.[1*] – JAFF, D. M. A.[2] – BASAR, N.[3] – KUTHI, N. A.[3] – YAQUBU, R.[4]

[1]*Department of Environmental Sciences, College of Science, University of Salahaddin-Erbil, Kurdistan Region, Iraq*

[2]*Department of Biology, College of Education, University of Salahaddin-Erbil, Kurdistan Region, Iraq*

[3]*Department of Chemistry, Faculty of Science, University Teknology Malaysia, 81310 Johor Bahru, Malaysia*

[4]*Department of Chemistry, Federal College of Education (FCE), Okene P. M .B. 1062, Kogi State, Nigeria*

**Corresponding author*
e-mail: jwanbio9@gmail.com

(Received 17th Nov 2019; accepted 30th Jan 2020)

Abstract. The *Prangos platychlaena* Boiss. a wild plant belonging to the *Apiaceae* family, is a native plant of Kurdistan-Iraq. The roots, leaves, stem and flowers of the plant were collected in the Halgurd mountain of the Kurdistan region of Iraq, and extracted by petroleum ether, ethanol and water to obtain the crude extracts. Our results showed that the plant contains different phytochemicals that are distributed unequally in different parts. The chromatography technique was used for the isolation and purification of three coumarins (5,8-dimethoxy psoralen, 5-methoxy psoralen and 8-methoxy psoralen) from the parts of the flower, all compounds are new among the Prangos species. The extracts of different plant parts and isolated compounds showed anti-oxidant and anti-microbial activities against pathogenic bacteria and yeasts. These findings suggested that this plant, specially their leaves and flowers can be used for the treatment of some diseases in the future.
Keywords: *antioxidant, Erbil, bacteria, yeast, psoralen*

Introduction

Kurdistan region of Iraq is well known for the diversity of wild plants and their natural products, which have been used for a long time by its habitants as traditional medicine, fodder and for other purposes (Hamad et al., 2017). The current task is to identify the chemical compounds of the plant, facilitating its use in new medicines and may be assumed as therapies for treating many diseases with few side effects (Moradi et al., 2016). *Apiaceae* family in this aspect is regarded as one of the most important families, with its different plant species. The genus of Prangos belongs to the family of *Apiaceae*, having thirty species distributed from the Mediterranean to central Asia, seven species of them which are distributed in the Kurdistan region of Iraq, which are *P. platychlaena Boiss., P. ferulacea* (L.), *P. uloptera* DC., *P. asperula* Boiss., *P. pabularia* Lindl., *P. peucedanifolia* Fenz, and *P. carymbosa* Boiss. (Ghazanfar and Edmondson, 2013). *Prangos platychlaena* Boiss. is a perennial plant, length can reach up to 1-1.5 m. This plant is found naturally growing in the mountain of Kurdistan region, it contains

http://www.aloki.hu ● ISSN 1589 1623 (Print) ● ISSN 1785 0037 (Online)
DOI: http://dx.doi.org/10.15666/aeer/1802_24252443

different quantities of phytochemical compounds that have important roles in the biological activities and medicinal values of this plant.

Terpenoids in the plant may contribute against the microbial activity (Irfan et al., 2014), the alkaloid used to fight the oral intoxication (Matsuura and Fett-Neto, 2015), phenol compounds are considerably antimicrobial and the sources of antioxidants properties (Mariem et al., 2014) flavonoides and saponin compounds participate in antiviral, anti-inflammation, antioxidation and antimicrobial activities (Juca et al., 2018) (Desai et al., 2009) and tannines polyphenolic compounds are able to reduce the number of worm in the digestive tract of goat or sheep and also have great roles in the other biological activities (Wina et al., 2010). Based on the available literature the root, leaves, stem and flowers of *P. platychlaena* Bioss. has not been subjected to any investigation of this type. This is the first research performed on this species. As part of this study on the chemical constituents and their bioactivity of a different plant part of *P. platychlaena Boiss*. Thus, the work will concentrate on the chemical constituents, antioxidant and antimicrobial activities of the different plant parts.

Materials and methods

Plant collection

The different plant parts of *P. platychlaena* Boiss. were collected during June-July 2017 from the Halgurd mountain in the Kurdistan region of Iraq and shown in *Figure 1,* at the altitude of 2170 m, Dr. Abdulah Shukur, a plant taxonomist at the department of biology, College of Education/Salahaddin University, was helping for the identification of this plant.

Figure 1. *The whole plant of P. platychlaena Boiss.*

http://www.aloki.hu ● ISSN 1589 1623 (Print) ● ISSN 1785 0037 (Online)
DOI: http://dx.doi.org/10.15666/aeer/1802_24252443

Maceration extraction

The different plant parts of the *P. platychlaena* Boiss. were collected, cleaned and shed dried at room temperature near 38 °C to constant weight and ground by grinders slowly. Dry powder of each plant part was extracted by using a solvent, with increasing polarity in the order of petroleum ether, ethanol and distilled water for three days at room temperature. The extract solution was concentrated using a rotary evaporator to obtain the crude extract.

Phytochemicals screening in different plant part of Prangos platychlaena Boiss.

Detection of terpenoid

In the test tube, a 5 ml stock solution of extract was mixed with 2 ml chloroform followed by 2 ml concentrated H_2SO_4. A reddish brown coloration has suggested the presence of terpenoids (Mujeeb et al., 2014).

Test for alkaloid

To 10 ml of the extract solution, 0.4 ml of HCl (1%) was added to a solution, followed by 6 drops of Dragendroff reagent, the brownish-red precipitate indicated the presence of alkaloids (Mujeeb et al., 2014).

Phenol detection test

Lead acetate test: Two drops of lead acetate solution (10%) was added to 2 ml of plant extract solution. The formation of a bulky white precipitate showed the presence of phenolic compounds (Singh and Bag, 2013).

Detection of flavonoid (Alkaline reagent)

In this test, two drops of diluted NaOH (10%) solution were added to the stock solution of the plant (2 ml), an intense yellow coloration showed the presence of flavonoid compounds (Hossain et al., 2013).

Detection of saponin

In this test, 10 ml of the plant extraction solution was taken in the test tube. It was shaken vigorously by hand for 2 min, the formation of stable foam indicated the presence of saponins (Mandal et al., 2013).

Tannin detection test

Two drops of $FeCl_3$ (1%) were added to the plant extract solution, the blue-black or blue- green coloration appeared as an indicator for the presence of tannin (Bankole et al., 2016)**.**

Isolation and identification of compounds in P. platychlaena Boiss.

General procedure

Normal extraction technique was applied to the dried powder of flower *P. platychlaena Boiss.* in the laboratory of the Chemistry Department of University Technology of Malaysia. Vacuum liquid chromatography (VLC) was performed using

http://www.aloki.hu ● ISSN 1589 1623 (Print) ● ISSN 1785 0037 (Online)
DOI: http://dx.doi.org/10.15666/aeer/1802_24252443

silica gel 60 (230-400 mesh), and gravity column chromatography (CC) was carried out using Merck silica gel 60(70-230 mesh). Silica gel aluminum sheets (Merck Kieselgel 60 F254,0.20 mm) were used for Thin layer chromatography (TLC) analysis of crude extract, fraction and isolation of pure compounds. Spots on TLC were observed under UV light at 254 nm and 365 nm, followed by spraying vanillin sulphuric acid reagent and heating at 120 °C on a hot plate for 5 min. Infrared (IR) spectra were measured using the Perkin Elmer series 1600 FT-IR spectrophotometer with a KBr pellet for a solid sample. Melting points were measured using a hot stage Leica Gallen apparatus with a microscope and were uncorrected. Nuclear Magnetic Resonance (NMR) Bruker Advance 400 Spectrometer (400/100 MHZ) was used to measure ^{1}H, ^{13}C and correlation spectroscopy (COSY) spectra by using Deuterated chloroform-d as a solvent. Mass spectral data were obtained using Gas Chromatography (GC) and Bruker Mass Spectroscopy (MS) services at the Department of Chemistry, National University of Singapore, Singapore.

5, 8- Dimethoxy psoralen (Isopimpinellin) (1)

The petroleum ether crude extract of the flower of *P. platychlaena Boiss.* (6.0 g) was subjected to silica gel VLC (285.0 g, column size:14.0 × 11.0 cm), the solvent system: n-hexane, n-hexane –chloroform, chloroform-ethyl acetate, acetone (100%) and methanol (100%) in order of increasing polarity to give 13 fractions, each fraction was subjected to TLC analysis. Finally, the single (colorless) spot showed indicated Isopimpinellin.

5-Methoxy psoralen (2)

The petroleum ether extract was partitionated from ethanol extract (2.85 g) of *P. platychlaena Boiss.* The flower was subjected to silica gel VLC column, eluted with n-hexane: chloroform: ethyl acetate: methanol: acetone in step gradient to give thirteen fractions. The fraction 4, fraction 5 and fraction 7 were selected and mixed for further purification by silica gel column chromatography, the single (colorless) spot showed indicated 5-Methoxy psoralen**.**

8-Methoxy psoralen (3)

The extract of diethyl ether (1.41 g) of *P. platychlaena* Boiss. flower was subjected to silica gel VLC, the solvent system: n-hexane, n-hexane –chloroform, chloroform-ethyl acetate, acetone and methanol in order of increasing polarity to give thirteen fractions. The 2nd fraction was used for further purification by silica gel column chromatography, the single (colorless) spot showed indicated 8-Methoxy psoralen.

Bioactivity of different plant parts of P. platychlaena Boiss.

1. Antioxidant activity (DPPH assay)

The antioxidant activity (A%) of the sample was assayed according to the method described by Giweli et al. (2012). The standard DPPH (2,2-diphenylpicrylhydrazyl) assay was carried out using 96 –well sterile micro plates. DPPH solution (0.04%) in methanol was prepared, the stock solution of the samples was prepared in methanol. 200 µL of the stock solution of sample was added to the first column and the rest of the wells were filled with 100 µL of methanol, next, 100 µL content of the first well was

http://www.aloki.hu ● ISSN 1589 1623 (Print) ● ISSN 1785 0037 (Online)
DOI: http://dx.doi.org/10.15666/aeer/1802_24252443

transferred into the next well of the same raw of the microplate, this procedure was repeated for the following well of the same row to obtain a serial dilution of extraction. 100 µL DPPH solution was added to all well except for the blank well, while methanol (100 µL) and 100 µL DPPH solution was added to the control well. The plate was shaken for mixing the solution and incubated for 30 min in the dark at room temperature. The absorbance value of each well was measured at a wavelength of 517 nm, using a microplate reader. Ascorbic acid was used as a positive control, the DPPH radical scavenging activity at different concentrations was calculated by the following equation employed by Ahmed et al. (2015).

$$\% A = A_c - A_s / A_c \times 100 \quad \text{(Eq.1)}$$

where, %A is the percentage of antioxidant activity, A_c is the absorbance of the control and A_s is the absorbance of the sample. The lower absorbance of the reaction mixture indicated a higher free radical scavenging activity and the color of the reaction change from violet to yellow color. The IC_{50} value (mg/ml) was the concentration of the sample required to scavenge 50% of the DPPH free radical.

2. Antimicrobial activity of P. platychlaena Boiss.

Microbial strain

The in vitro antimicrobial activities of the extract and pure compound were carried out by using pathogenic bacteria such as *Pseudomonas aeruginosa* ATCC 9027, clinical *Pseudomonas aeruginosa*, *Staphylococcus aureus* ATCC 6538P, and clinical *Staphylococcus aureus*. The clinical pathogen bacteria isolated from humans were obtained from the Media Diagnostic Health Center in Erbil. While pathogenic yeast such as *Candida albicans*, and *Candida parapsilosis* were obtained from the Biology Department, College of Science, University of Salahadden-Erbil, Iraq. The yeasts were isolated from humans and identified by Dr. Hero Muhammed Ismael.

Culture media and activation of microbial strain

The medium of the Sabouraud Dextrose broth and Mueller-Hinton broth were used for the cultivation of fungi and bacteria, respectively. The inocula were prepared by transferring several single colonies of microbes into a sterile broth media and mixed together, then incubated at 37^0 C for overnight. Inoculum of the culture solution was adjusted to the McFarland scale 0.5 and confirmed by spectrophotometrical reading at 580 nm (Ginovyan et al., 2017).

Evaluation of antimicrobial activities

Antimicrobial activities of the extracts and pure compounds were assessed by the Microdilution method according to previous methods (Bacha et al., 2016; Silva et al., 2011), this was used for determining the minimum Inhibitory Concentration (MIC) of the *P. platychlaena* Boiss. The assay was carried out in 96-well sterile micro plates, then, 100 µl of nutrient broth was added to each well of the microplate. The first well was filled with 100 µl of the sample, prepared at a concentration of mg/ml. Next, by transferring 100 µl content from the first well into the next well of the same row of the microplate, after mixing the content of the well, this procedure was repeated for the

http://www.aloki.hu ● ISSN 1589 1623 (Print) ● ISSN 1785 0037 (Online)
DOI: http://dx.doi.org/10.15666/aeer/1802_24252443

following well of the same row to obtain serial dilution, in this case, the concentration of the sample will decrease. While pure dimethyl sulfoxide and broth media were used as a negative control, whereas Ketoconazol (antifungal) and Ciprofloxacin (antibacterial) were considered as references. For each well a microbial suspension of the working solution was inoculated. The absorbance for each well was measured at 630 nm before incubation time; by using ELISA microplate reader, the microplate was incubated at 37 °C for 24 h for the growth of microbes. The absorbance was re-measured after incubation time to compare with the initial measurement. The MIC was calculated at the break point concentrations by comparing the absorbance before and after incubation time.

Statistical analysis

The antioxidant and antimicrobial activity of *P. platychlaena* Boiss. were statistically analyzed using the Kruskal- Wallis test and Dunn's multiple comparison test by Graph Pad-Prism version 7. All results arranged as mean ± SE for each property and *P* value less than 0.05 considered as statistically significant differences among them.

Result and discussion

According to the available literature, this is the first study on the phytochemical contents and bioactivity of the *P. platychlaena* Boiss.

Phytochemical screenings in different plant part of P. platychlaena Boiss.

Due to the fact that plant extracts usually occur as a combination of various types of phytochemicals and bioactive compounds with different polarities, their separation still remains a big demand for the process of isolation, identification and characterization of active compounds.

Qualitative chemical analysis was conducted by using petroleum ether, ethanol and water extract of roots, leaves, stem and flowers of the *P. platychlaena* Boiss. The data revealed the presence of terpenoids, alkaloids, polyphenols, flavonoids, saponins and tannins as major phytochemical groups and the results designated as (+) for the presence and (-) for absence of phytochemicals (*Table 1*). The results showed the diversity of phytochemical distribution in the *P. platychlaena* Boiss. plant parts.

Isolation and purification of compounds in P. platychlaena Boiss.

The structures of the isolated compounds (5,8 dimethoxy psoralen, 5-Methoxy psoralen and 8-Methoxy psoralen) from flower *P. platychlaena*, were determined by using IR, ^{1}H-NMR, ^{13}C-NMR, COSY, GC and MS spectrum.

5,8-dimethoxy psoralen (1)

Pale-yellow solid with m.p. 117.05 °C, R_f: 0.3 in petroleum ether: chloroform (3:2). IR υ_{max} (ATR) cm^{-1}: 1718 (C = O), 1593 (C = C), 1478 (C = C), 1170 (C-O), 1092 (C-O). GC: major peak at t_R 29.06 min. MS (EIMS): *m/z* 246 (87%) $[M]^+$ ($C_{13}H_{10}O_5$), 231 (100%), 203 (19%), 188 (23%), 175 (22%), 160 (16%), 147 (13%), 132 (5%), 119 (4%), 104 (9%), 76 (12%). ^{1}H-NMR (400 MHz, $CDCl_3$): 4.19 (s, 2 x OCH_3), 6.32 (d, J = 10.0 Hz, H-3), 7.02 (d, J = 2.4 Hz, H-3'), 7.65 (d, J = 2.4 Hz, H-2'), 8.16 (d,

http://www.aloki.hu ● ISSN 1589 1623 (Print) ● ISSN 1785 0037 (Online)
DOI: http://dx.doi.org/10.15666/aeer/1802_24252443

J = 10.0 Hz, H-4). ^{13}C-NMR (300 MHz, $CDCl_3$): 60.8 (8-OCH_3), 61.9 (5-OCH_3), 105.2 (C-3'), 107.7 (C-10), 112.9 (C-3), 114.9 (C-6), 128.2 (C-8), 139.6 (C-4), 143.8 (C-9), 144.5 (C-5), 145.2 (C-2'), 149.9 (C-7), 160.7 (C = O) (*Figures A1–A6*) (Dincel et al., 2013).

Table 1. *Qualitative phytochemical analysis of various extracts of different plant parts of Prangos platychlaena Boiss.*

Extracts	Plant parts	Ter.	Alk.	Phe.	Fla.	Sap.	Tan.
Petroleum ether	Root	+	-	+	-	-	-
	Leaves	+	-	+	-	-	-
	Stem (front)	+	-	+	-	-	-
	Flowers	+	-	+	-	-	-
Ethanol	Root	-	+	-	+	-	-
	Leaves	-	+	+	+	-	+
	Stem (front)	-	+	-	+	-	-
	Flowers	-	+	+	+	-	+
Water	Root	-	-	+	-	+	-
	Leaves	-	-	+	+	+	+
	Stem (front)	-	-	+	+	+	-
	Flowers	-	-	+	+	+	+

-: Absent, +: Present, Terpeniod: Ter, Alkaloid: Alk, Phenol: phe, Flavonoid: Fla, Saponin: Sap, Tannin: Tan.

5-Methoxy psoralen (2)

White crystals with m.p. 185 °C. R_f :0.5 in petroleum ether: chloroform (3:2). IR υ_{max} (ATR) cm^{-1} 1727 (C = O), 1624 (C = C), 1606 (C = C), 1580 (C = C), 1468 (C = C), 1155 (C-O), 1076 (C-O). GC: single peak at t_R 26.61 min. MS (EIMS): *m/z* 216 (100%) $[M]^+$ ($C_{12}H_8O_4$), 201 (31%), 188 (13%), 173 (65%), 145 (20%), 89 (38%). ^{1}H-NMR (400 MHz, $CDCl_3$): 4.28 (s, OCH_3), 6.30 (d, *J* = 13.2 Hz, H-3), 7.03 (d, *J* = 3.2 Hz, H-3'), 7.27 (s, H-5), 7.61 (d, *J* = 3.2 Hz, H-2'), 8.17 (d, *J* = 13.2 Hz, H-4). ^{13}C-NMR (300 MHz, $CDCl_3$): 60.2 (5-OCH_3), 105.1 (C-3'), 106.4 (C-10), 112.6 (C-6), 112.6 (C-3), 139.4 (C-4), 145.0 (C-2'), 149.6 (C-5), 152.8 (C-9), 158.5 (C-7), 161.4 (C = O) (*Figures A6–A12*) (Dincel et al., 2013).

8-Methoxy psoralen (3)

White crystals with m.p. 140 °C**.** R_f 0.4 in petroleum ether: chloroform (3:2) IR (ATR) cm^{-1} 1704 (C = O), 1617 (C = C), 1583 (C = C), 1454 (C = C), 1150 (C-O), 1023 (C-O). GC: single peak at t_R 26.88 min. MS (EIMS): *m/z* 216 (100%) $[M]^+$ ($C_{12}H_8O_4$) 201 (30%), 188 (9%), 173 (62%), 145 (41%), 89 (17%). ^{1}H-NMR (400 MHz, $CDCl_3$): 4.31 (s, OCH_3), 6.38 (d, *J* = 12.8 Hz, H-3), 6.8 (d, *J* = 2.8 Hz, H-3'), 7.37 (s, H-5), 7.70 (d, *J* = 2.8 Hz, H-2'), 7.78 (d, *J* = 12.8 Hz, H-4). ^{13}C-NMR (300 MHz, $CDCl_3$): 61.3 (8-OCH_3), 106.7 (C-3'), 112.9 (C-5), 114.8 (C-3), 116.6 (C-10), 126.0 (C-6), 132.8 (C-8), 143.1 (C-9), 144.5 (C-4), 146.8 (C-2'), 147.6 (C-7), 160.6 (C = O) (*Figures A12–18*) (Dincel et al., 2013; Luz et al., 2015).

http://www.aloki.hu ● ISSN 1589 1623 (Print) ● ISSN 1785 0037 (Online)
DOI: http://dx.doi.org/10.15666/aeer/1802_24252443

Bioactivity of Prangos platychlaena Boiss. extract of different parts

Antioxidant content

Table 2 showed the antioxidant activity of the *P. platychlaena* Boiss. extracts, which were analyzed using the DPPH free radical scavenging method. The total antioxidant activity of the *P. platychlaena* Boiss. extracts increased with an increased concentration of the sample. The low value of IC_{50} shows the high antioxidant content. A significant difference ($P < 0.05$) was noted among the antioxidant activities of the plant parts in different solvents. It has been shown that the IC_{50} of the petroleum ether extract of *P. platychlaena* Boiss. root, leaves, stem and flower were (1.02 ± 0.04, 0.68 ± 0.01, 0.70 ± 0.03 and 0.19 ± 0.01 mg/ml) respectively, and the significant differences were increasing between root and flower parts. It was observed that petroleum ether extract of the flower of *P. platychlaena* Boiss. has higher antioxidant activity than the other parts. The activity effectiveness can be classified as follows: flower > leaves > stem > root. As well as, the IC_{50} of the ethanol extraction for root, leaves, stem and flower were (1.16 ± 0.12, 0.61 ± 0.01, 1.12 ± 0.19 and 0.67 ± 0.01 mg/ml), respectively, and the statistical analysis showed that the significant increasing of the results was present between the root and leaves parts. The data reported that extraction of the leaf parts of *P. platychlaena* Boiss. showed higher antioxidant potential than the other parts, this activity can be classified as: leaves > flowers > stem > root. While, the IC_{50} value of the water extractions of different plant part (root, leaves, stem and flower) were (1.13 ± 0.14, 0.84 ± 0.02, 0.83 ± 0.01, 0.54 ± 0.02 mg/ml), respectively, also the antioxidant values between root and flower parts were significantly increasing. This finding indicated that the flower part has a higher antioxidant potential than the other parts, this activity can be classified as: flowers > stem > leaves > root. These results showed that the plant extracts inhibited the DPPH radical but in different manners, the variation observed among the plant part extracts, may be depending on the plant part and their growth stages, and unequal distribution of the polyphenols and flavonoids which have important roles in antioxidant activities (Sylvie et al., 2014).

Table 2. *Antioxidant content (IC_{50}) of different plant parts of P. platychlaena Boiss.*

Extracts	Plant parts	IC_{50} (mg/g)
Petroleum ether	Root	$1.02 \pm 0.04^{*}$
	Leaf	0.68 ± 0.01
	Stem	0.7 ± 0.03
	Flower	$0.19 \pm 0.01^{*}$
Ethanol	Root	$1.16 \pm 0.12^{*}$
	Leaf	$0.61 \pm 0.01^{*}$
	Stem	1.12 ± 0.19
	Flower	0.67 ± 0.01
Distilled water	Root	$1.13 \pm 0.14^{*}$
	Leaf	0.84 ± 0.02
	Stem	0.83 ± 0.01
	Flower	$0.54 \pm 0.02^{*}$

Values are mean ± SD, Symbol *: it means significantly with data caring the same symbol in the same extract

http://www.aloki.hu ● ISSN 1589 1623 (Print) ● ISSN 1785 0037 (Online)
DOI: http://dx.doi.org/10.15666/aeer/1802_24252443

Antimicrobial activities of P. platychlaena Boiss.

The antimicrobial activity of the plant extracts was implemented against *Staphylococcus aureus* ATCC 6538P, clinical *Staphylococcus aureus, Pseudomonas aeruginosa* ATCC 9027, clinical *Pseudomonas aeruginosa*, *Candida albicans*, and *Candida parapsilosis* were studied by using the microdilution method and their potency was assessed by the corresponding MIC value, and the results are shown in *Tables 3* and 4. The petroleum ether extracts of *P. platychlaena* Boiss. for leaves showed higher activities against *S. aureus* ATCC 6538P, clinical *S. aureus*, clinical *P. aeruginosa, C. albicans,* and *C. parapsilosis*, with the lowest MIC values of 0.23, 1.16, 1.33, 0.74 and 0.87 mg/ml, respectively, these values were significantly higher than those of other parts of plant.

Table 3. *Antibacterial activities of different plant parts of P. platychlaena Boiss.*

Samples		**Plant parts**	**MIC (mg/ml)**			
			***S. aureus* ATCC6538P**	***S. aureus***	***P. aeruginosa* ATCC 9027**	***P. aeruginosa***
Extracts	Petroleum ether	Root	0.83 ± 0.20	2.66 ± 0.16	1.41 ± 0.08	5 ± 0.00*
		Leaves	0.23 ± 0.03*	1.16 ± 0.08*	1.16 ± 0.08	1.33 ± 0.08*
		Stem	0.86 ± 0.13	2.66 ± 0.16	1.23 ± 0.01	4.16 ± 0.83
		Flowers	1.16 ± 0.08*	4.33 ± 0.66*	1.21 ± 0.11	4.66 ± 0.33
	Ethanol	Root	1.66 ± 0.41	10.0 ± 0.0*	1.33 ± 0.08	8.33 ± 1.66
		Leaves	2.16 ± 0.16	10 ± 0.0**	4.16 ± 0.83*	4.5 ± 0.28*
		Stem	2.66 ± 0.166*	10 ± 0.0*	10.0 ± 0.66**	10.67 ± 0.66*
		Flowers	1.04 ± 0.20*	2.66 ± 0.1*,**,***	1.16 ± 0.08*,**	8.33 ± 1.66
	Water	Root	> 10	> 10	> 10	> 10
		Leaves	> 10	> 10	> 10	> 10
		Stem	> 10	> 10	> 10	> 10
		Flowers	> 10	> 10	> 10	> 10
5,8- dimethoxy psoralen			1.33 ± 0.16	1.43 ± 0.29	2.5 ± 0.5	3.16 ± 0.44
Ciprofloxacin			1.0 ± 0.28	1.66 ± 0.33	1.0 ± 0.28	2.33 ± 0.33

Values are mean ± S D, Symbol *, **, ***: it means significantly with data carrying the same symbol in the same extracts and in the same pathogen

While the activity of flower ethanol extraction showed more activity against *S. aureus* ATCC 6538P, clinical *S. aureus, P. aeruginosa* ATCC 9027, *C. albicans*, and *C. parapsilosis* with the lowest MIC values of 1.04, 2.66, 1.16, 4.5, 2.5 and 3.36 mg/ml, respectively. The statistical analysis showed significant differences among the ethanol extractions of different plant parts. Whereas, the MIC values of the water extracts of different plant parts against the pathogen bacteria and yeasts were more than 10 mg/ml. The statistical analysis showed that the extraction of different plant parts of the *P. platychlaena* Boiss. have significant differences ($p<0.05$) against the *S. aureus* ATCC 6538P, clinical *S. aureus, P. aeruginosa* ATCC 9027, clinical *P. aeruginosa*, *C. albicans*, and *C. parapsilosis*.

http://www.aloki.hu ● ISSN 1589 1623 (Print) ● ISSN 1785 0037 (Online)
DOI: http://dx.doi.org/10.15666/aeer/1802_24252443

Table 4. *Anti-yeast activities of the different plant parts of Prangos platychlaena Boiss.*

Samples		Plant parts	MIC (mg/ml)	
			Candida albicans	***Candida parapsilosis***
Extracts	Petroleum ether	Root	1.70 ± 0.56	6.66 ± 1.66**
		Leaves	0.74 ± 0.12*	0.87 ± 0.12*,**
		Stem	4.16 ± 0.83*	5.83 ± 2.12*
		Flowers	2.16 ± 0.16	2.03 ± 0.41
	Ethanol	Root	4.14 ± 0.83	4.66 ± 0.33
		Leaves	8.33 ± 1.6*	8.33 ± 1.66*
		Stem	10.67 ± 0.66**	10 ± 0.0**
		Flowers	2.5 ± 0.83*,**	3.36 ± 0.13*,**
	Water	Root	<10	<10
		Leaves	<10	<10
		Stem	<10	<10
		Flower	<10	<10
5,8- dimethoxy psoralen			1.33 ± 0.16	2.0 ± 0.5
Ketoconazol			1.33 ± 0.16	2.0 ± 0.5

Values are mean ± SD, Symbol *,**: it means significantly with data carrying the same symbol in the same extracts and in the same pathogen

While, the MIC values of the compound 5,8- dimethoxy psoralen for both strain *S. aureus* were 1.33 and 1.43 mg/ml and for both strains of *P. aeruginosa* were 2.5 and 3.16 mg/ml, respectively, our result disagreed with those findings of Mbah et al. (2010), that concluded the 5,8- dimethoxy psoralen does not have antibacterial activities against pathogen bacteria. As well as, MIC values of the 5,8- dimethoxy psoralen for both *C. albicans* and *C. parapsilosis* were 1.33 and 2.0 mg/ml, respectively. We have not more amount of 5-Methoxy psoralen and 8-Methoxy psoralen for microbial activities. Whereas, the MIC values of Ciprofloxacin for both strains of *S. aureus* were 1.0 and 1.66, and also for both strains of *P. aeruginosa* were 1.0 and 2.33 mg/ml, respectively. While, the MIC values of Ketoconazol for *C. albicans*, and *C. parapsilosis* were 1.33 and 2.0 mg/ml, respectively. Also, when all MIC values of the extraction compared to both Ciprofloxacin and Ketoconazol, showed the extracts of this plant were close or better than antimicrobial references. All data obtained in this work, indicated that the clinical pathogen microbes are more tolerant than standard microbes that might be due to the presence of indigenous compounds resistant against the plant extracts (Mahendra et al., 2016). According to literature have not scientific research about the antimicrobial activities of *P. platychlaena* but the essential oils from the fruits of *P. ferulacea* showed antibacterial activity against *Staphylococus aureus, Eschrechia coli* and *Pseudomonas aeruginosa* (Massumia et al., 2007). Other studies revealed the methanol extract of *P. acaulis* root has potent antibacterial activity against *Streptococcus mutan* (Nosrati et al., 2018). Generally, the variation in antimicrobial activities of *P. platychlaena* Boiss. might be due to the variation in the distributions of phytochemical compounds and the quantity of phytochemicals in each of root, leaves, stem and flowers of this plant. The petroleum ether extraction for the leaves and the flower ethanol extracts of the *P.*

http://www.aloki.hu ● ISSN 1589 1623 (Print) ● ISSN 1785 0037 (Online)
DOI: http://dx.doi.org/10.15666/aeer/1802_24252443

platychlaena Boiss. showed higher toxicity towards both bacteria and yeasts than extracts of other parts, this may be due to the presences of some compounds detected in our study, such as terpenoid, alkaloid, phenol, flavonoid, saponin and tannin, while other parts have less antimicrobial activities that may be due to the containing of less amount of the phytochemicals. The pure compound 5,8- dimethoxy psoralen, was an active compound isolated from *P. platychlaena* Boiss. having potential activity to inhibit the growth of bacteria and yeast pathogen. The differences in the susceptibility of both bacteria and yeast strains used in this work to the phytochemical compounds, may be attributed to the variation in the penetration rates of the phytochemicals through the cell wall, and cytoplasmic membrane of those organisms, one of the important properties of most compounds is causing the partition of the lipids of cell membrane of microbes and leakage of the cell contents leads to the damage of the intracellular structure of microbes (de Lira Mota et al., 2012) (Murbach Teles Andrade et al., 2013). According to literature have not scientific research about antioxidant activites of this species but in the previous years other studies conducted on other species of the same genus (Çoruh et al., 2007) have shown *Prangos ferulacea* Lindl. extracts have antioxidant properties with IC_{50} value of 0.24 mg/ml. As well as, it has been reported (Ahmed et al., 2011) that the water extracts of *Prangos ferulacea, P. heyniae*, *P. meliocarpoides* var. *meliocarpoides*, and *P. uechtritzii* display low antioxidant activities than the methanol extract of Prangos species. Also, slight antioxidant activity was observed in the fruit of *Prangos ferulacea* (L.) (Cesur et al., 2017).

Conclusion

This is the first study performed on the extract of *Prangos platychlaena* Boiss. The results revealed the presence of terpenoids, alkaloids, polyphenols, flavonoids, saponins and tannins as major phytochemical groups distributed in different plant parts of *P. platychlaena*. As well as, the three compounds (5,8 dimethoxy psoralen, 5-Methoxy psoralen and 8-Methoxy psoralen) were isolated and purified from flowers of *P. platychlaena* Boiss. and recorded for the first time in this species. The extracts and isolated compounds of this plant have shown antioxidant and antimicrobial activities against common bacteria and yeast pathogen. In conclusion, more studies are necessary to isolate and purify the active compounds and to use their antimicrobial, anti-inflammation and anticancer activities and more studies are required on the toxicology and pharmacology of crude extracts of this plant, the safety of isolated compounds should be assessed before clinical progression.

Acknowledgments. The authors thank Dr. Abdullah Shukur from the Biology department, College of Education, University of Salahadden, for helping in the identification of plant species.

Conflict of interests. The authors declare no conflict of interests.

REFERENCES

[1] Ahmed, D., Khan, M. M., Saeed, R. (2015): Comparative analysis of phenolics, flavonoids, and antioxidant and antibacterial potential of methanolic, hexanic and aqueous extracts from Adiantum caudatum leaves. – Antioxidants (Basel) 4(2): 394-409.

http://www.aloki.hu ● ISSN 1589 1623 (Print) ● ISSN 1785 0037 (Online)
DOI: http://dx.doi.org/10.15666/aeer/1802_24252443

[2] Ahmed, J., Guvenc, A., Kucukboyaci, N., Baldemir, A., Coskun, M. (2011): Total phenolic contents and antioxidant activities of Prangos Lindl. (Umbelliferae) species growing in Konya province (Turkey). – Turkish Journal of Biology 35: 353-360.
[3] Bacha, K., Tariku, Y., Gebreyesus, F., Zerihun, S., Mohammed, A., Weiland-Brauer, N., Schmitz, R. A., Mulat, M. (2016): Antimicrobial and anti-Quorum sensing activities of selected medicinal plants of Ethiopia: implication for development of potent antimicrobial agents. – BMC Microbiology 16(1): 1-9.
[4] Bankole, A. E., Adekunle, A. A., Sowemimo, A. A., Umebese, C. E., Abiodun, O., Gbotosho, G. O. (2016): Phytochemical screening and in vivo antimalarial activity of extracts from three medicinal plants used in malaria treatment in Nigeria. – Parasitol Res 115(1): 299-305.
[5] Cesur, C., Coşge Şenkal, B., Yaman, C., Uskutoğlu, T., Koç, M. (2017): Antioxidant activity of fruit extracts of Prangos ferulacea (L.) Lindl. from Turkey. – Journal of the Institute of Science and Technology 7(4): 249-256.
[6] Çoruh, N., Celep, A. G. S. d. l., Özgökçe, F. (2007): Antioxidant properties of Prangos ferulacea (L.) Lindl., Chaerophyllum macropodum Boiss. and Heracleum persicum Desf. from Apiaceae family used as food in Eastern Anatolia and their inhibitory effects on glutathione-S-transferase. – Food Chemistry 100(3): 1237-1242.
[7] de Lira Mota, K. S., de Oliveira Pereira, F., de Oliveira, W. A., Lima, I. O., de Oliveira Lima, E. (2012): Antifungal activity of Thymus vulgaris L. essential oil and its constituent phytochemicals against Rhizopus oryzae: interaction with ergosterol. – Molecules 17(12): 14418-14433.
[8] Desai, S. D., Desai, D. G., Kaur, H. (2009): Saponins and their biological activities. – Pharma Times 41(3): 13-16.
[9] Dincel, D., Hatipoglu, S. D., Goren, A. C., Tocu, G. (2013): Anticholinesterase furocoumarins from Heracleum platytaenium, an endemic species to Idea mountains. – Turkish Journal of Chemistry 37: 675-683.
[10] Ghazanfar, S. A., Edmondson, J. R. (2013): Flora of Iraq. – National Herbarium of Iraq of the Ministry of Agriculture, Baghdad 5(2): 109-220.
[11] Ginovyan, M., Petrosyan, M., Trchounian, A. (2017): Antimicrobial activity of some plant materials used in Armenian traditional medicine. – BMC Complementary and Alternative Medicine 17(1): 1-9.
[12] Giweli, A., Dzamic, A. M., Sokovic, M., Ristic, M. S., Marin, P. D. (2012): Antimicrobial and antioxidant activities of essential oils of Satureja thymbra growing wild in Libya. – Molecules 17(5): 4836-4850.
[13] Hamad, R., Balzter, H., Kolo, K. (2017): Multi-criteria assessment of land cover dynamic changes in Halgurd Sakran national park (HSNP), Kurdistan region of Iraq, using remote sensing and GIS. – Land 6(1): 1-17.
[14] Hossain, M. A., Al-Raqmi, K. A. S., Al-Mijizy, Z. H., Weli, A. M., Al-Riyami, Q. (2013): Study of total phenol, flavonoids contents and phytochemical screening of various leaves crude extracts of locally grown Thymus vulgaris. – Asian Pacific Journal of Tropical Biomedicine 3(9): 705-710.
[15] Irfan, M., Ahmed, S., Sharma, M. (2014): Antimicrobial activity of terpenoids from Sphaeranthus indicus. L. – Asian Journal of Plant Science and Research 4(1): 1-16.
[16] Juca, M. M., Filho, F. M. S. C., Almeida, J. C. d., Mesquita, D. d. S., Barriga, J. R. d. M., Dias, K. C. F., Barbosa, T. M., Vasconcelos, L. C., Leal, L. K. A. M., Ribeiro, J. e. E., Vasconcelos, S. M. M. (2018): Flavonoids: biological activities and therapeutic potential. – Natural Product Research 16: 1-14.
[17] Luz, R. F., Vieira, I. J. C., Braz-Filho, R., Moreira, V. F. (2015): 13C-NMR Data from coumarins from Moraceae family. – American Journal of Analytical Chemistry 6(11): 851-866.

http://www.aloki.hu ● ISSN 1589 1623 (Print) ● ISSN 1785 0037 (Online)
DOI: http://dx.doi.org/10.15666/aeer/1802_24252443

[18] Mahendra, A. D., Tirtodiharjo, K., Kusuma, I. T. D. (2016): The pattern of bacteria and its resistance on adult sepsis patient at Dr. Moewardi general hospital, Indonesia. – Archives of Clinical Microbiology 7(5): 1-6.
[19] Mandal, S., Patra, A., Samanta, A., Roy, S., Mandal, A., Mahapatra, T. D., Pradhan, S., Das, K., Nandi, D. K. (2013): Analysis of phytochemical profile of Terminalia arjuna bark extract with antioxidative and antimicrobial properties. – Asian Pacific Journal of Tropical Biomedicine 3(12): 960-966.
[20] Mariem, S., Hanen, F., Inès, J., Mejdi, S., Riadh, K. (2014): Phenolic profile, biological activities and fraction analysis of the medicinal halophyte Retama raetam. – South African Journal of Botany 94: 114-121.
[21] Massumia, M. A., Fazelib, M. R., Alavic, S. H. R., Ajanid, Y. (2007): Chemical constituents and antibacterial activity of essential oil of Prangos ferulacea (L.) Lindl. Fruits. – Iranian Journal of Pharmaceutical Sciences 3: 171-176.
[22] Matsuura, H. N., Fett-Neto, A. G. (2015): Plant Alkaloids: Main Features, Toxicity, and Mechanisms of Action. – In: Gopalakrishnakone, P., Carlini, C., Ligabue-Braun, R. (eds.) Plant Toxins. Toxinology. Springer, Dordrecht.
[23] Mbah, J. A., Gatsing, D., M. N., Efange, S. (2010): Antibacterial agents from the seeds of Peucedanum zenkeri L. (Umbelliferae). – Pakistan Journal of Medical Sciences 26(2): 314-318.
[24] Moradi, M.-T., Rafieian-Kopaei, M., Karimi, A. (2016): A review study on the effect of Iranian herbal medicines against in vitro replication of herpes simplex virus. – Avicenna Journal Phytomedicine 5(6): 506-515.
[25] Mujeeb, F., Bajpai, P., Pathak, N. (2014): Phytochemical evaluation, antimicrobial activity, and determination of bioactive components from leaves of Aegle marmelos. – BioMed Research International. https://doi.org/10.1155/2014/497606.
[26] Murbach Teles Andrade, B. F., Nunes Barbosa, L., da Silva Probst, I., Fernandes Júnior, A. (2013): Antimicrobial activity of essential oils. – Journal of Essential Oil Research 26(1): 34-40.
[27] Nosrati, M., Behbahani, M., Mohabatkar, H., Shakeran, z. (2018): Antibacterial and antibiofilm activities of Prangos acaulis Bornm. extract against Streptococcus mutans: an in silico and in vitro study. – Journal of Herbmed Pharmacology 7(3): 176-184.
[28] Silva, S. M., Abe, S. Y., Murakami, F. S., Frensch, G., Marques, F. A., Nakashima, a. T. (2011): Essential oils from different plant parts of eucalyptus cinerea F. Muell. ex Benth. (Myrtaceae) as a Source of 1,8-Cineole and their bioactivities. – Pharmaceuticals 4: 1535-1550.
[29] Singh, K. L., Bag, G. C. (2013): Phytochemical analysis and determination of total phenolics content in water extracts of three species of hedychium. – International Journal of PharmTech Research 5: 1516-1521.
[30] Sylvie, D. D., Anatole, P. C., Cabral, B. P., Veronique, P. B. (2014): Comparison of in vitro antioxidant properties of extracts from three plants used for medical purpose in Cameroon: Acalypha racemosa, Garcinia lucida and Hymenocardia lyrata. – Asian Pacific Journal of Tropical Biomedicine 4: 625-632.
[31] Wina, E., I. W. R., S., Tangendjaja, B. (2010): Biological activity of tannins from Acacia mangium bark extracted by different solvents. – Media Peternakan 33(2): 103-107.

http://www.aloki.hu ● ISSN 1589 1623 (Print) ● ISSN 1785 0037 (Online)
DOI: http://dx.doi.org/10.15666/aeer/1802_24252443

APPENDIX

Figure A1. *IR spectrum of 5,8 dimethoxy psoralen (isopimpinellin)*

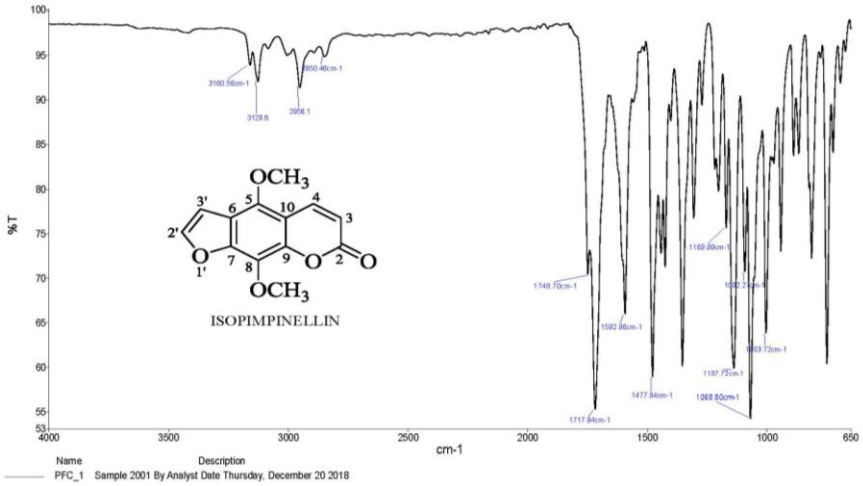

Figure A2. *^{13}C-NMR spectrum of 5,8 dimethoxy psoralen (isopimpinellin)*

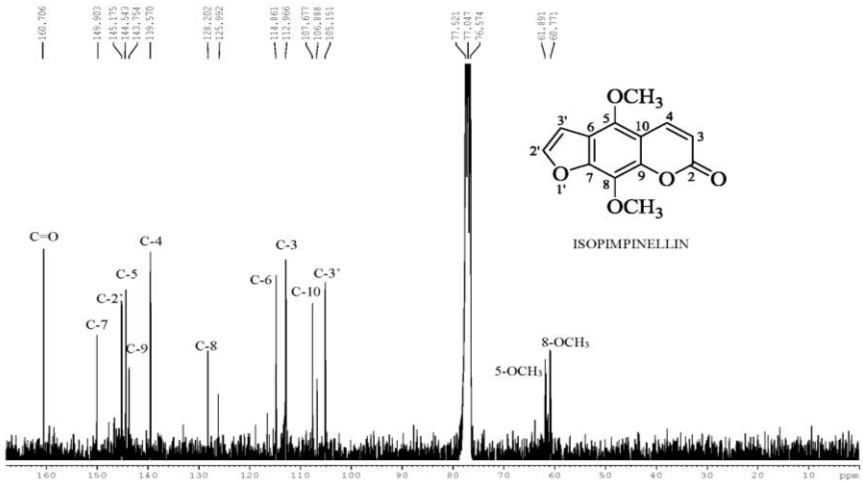

Figure A3. *^{1}H-NMR spectrum of 5,8 dimethoxy psoralen (isopimpinellin)*

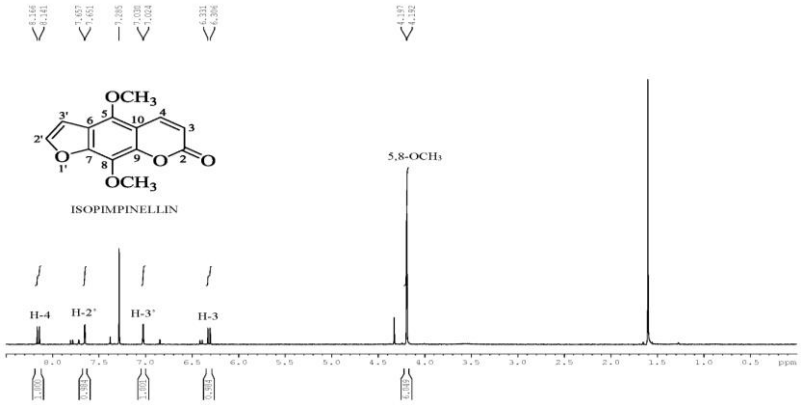

APPLIED ECOLOGY AND ENVIRONMENTAL RESEARCH 18(2):2425-2443.
http://www.aloki.hu ● ISSN 1589 1623 (Print) ● ISSN 1785 0037 (Online)
DOI: http://dx.doi.org/10.15666/aeer/1802_24252443

Figure A4. *COSY spectrum of 5,8 di methoxy psoralen (isopimpinellin)*

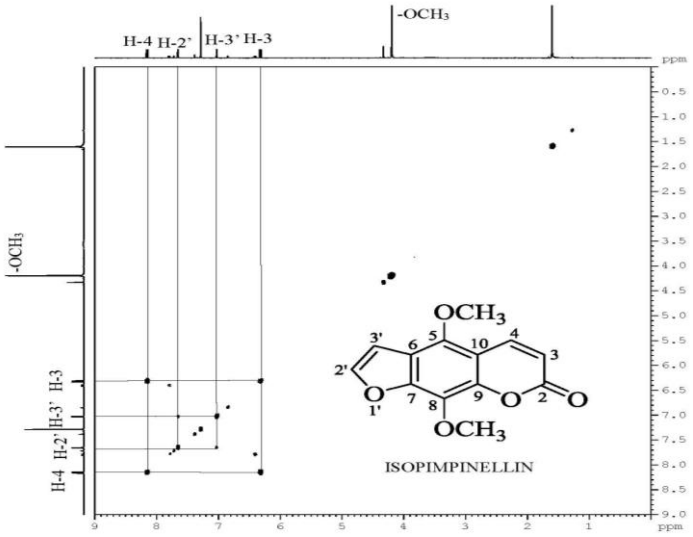

Figure A5. *GC spectrum of 5,8 dimethoxy psoralen (isopimpinellin)*

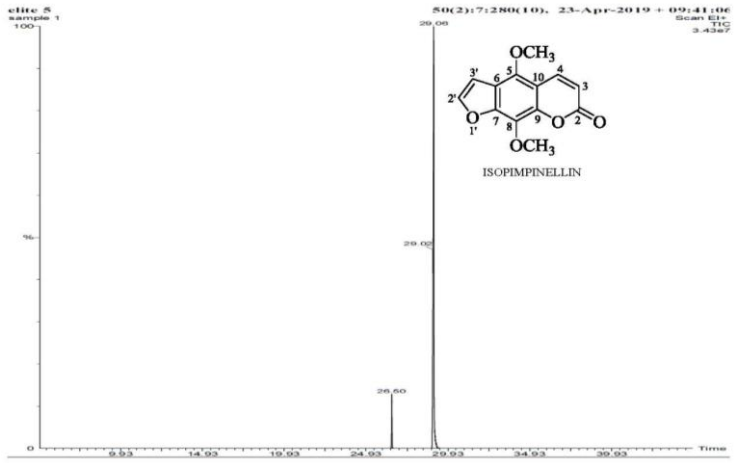

Figure A6. *MS spectrum of 5,8 dimethoxy psoralen (isopimpinellin)*

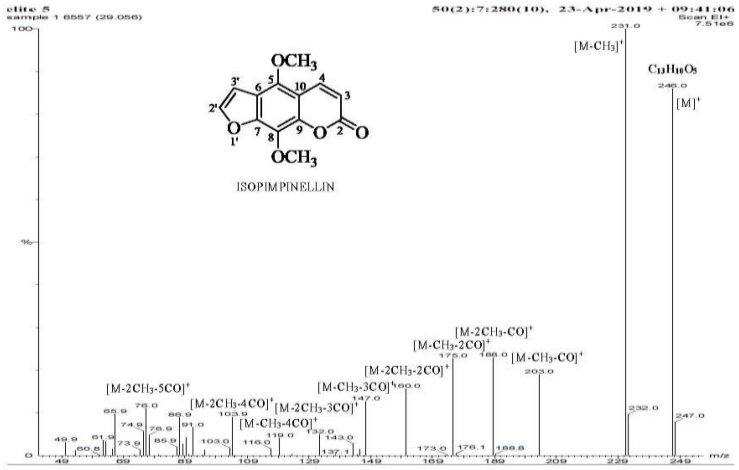

http://www.aloki.hu ● ISSN 1589 1623 (Print) ● ISSN 1785 0037 (Online)
DOI: http://dx.doi.org/10.15666/aeer/1802_24252443

Figure A7. *IR spectrum of 5-methoxy psoralen*

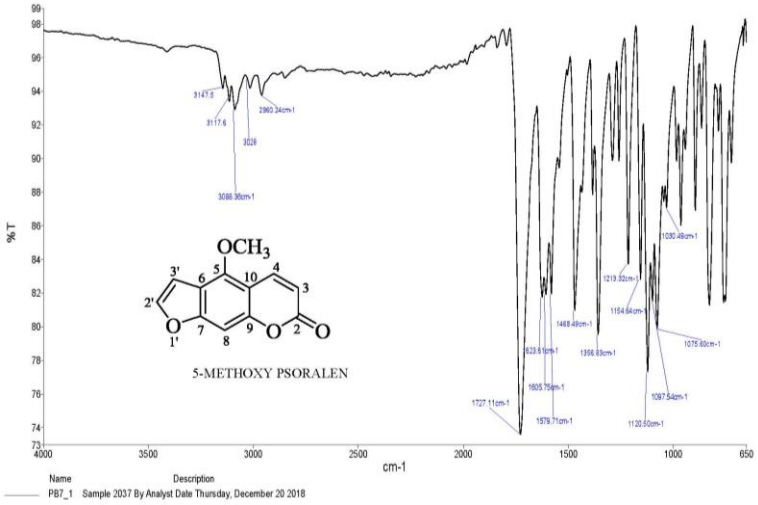

Figure A8. *^{1}H-NMR spectrum of 5-methoxy psoralen*

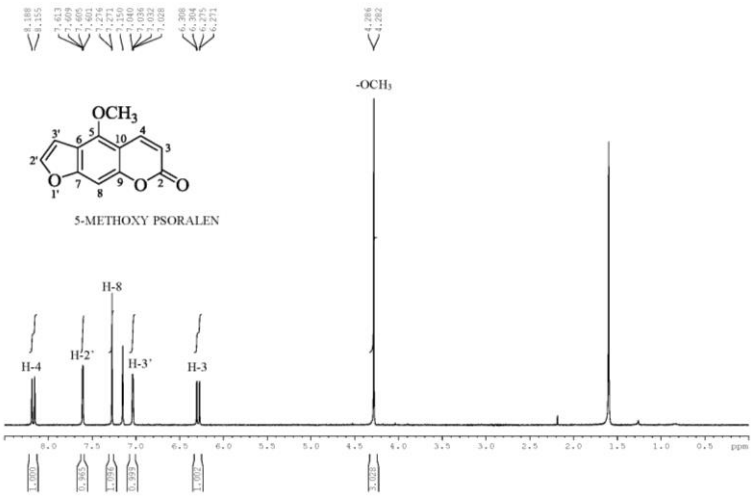

Figure A9. *^{13}C-NMR spectrum of 5-methoxy psoralen*

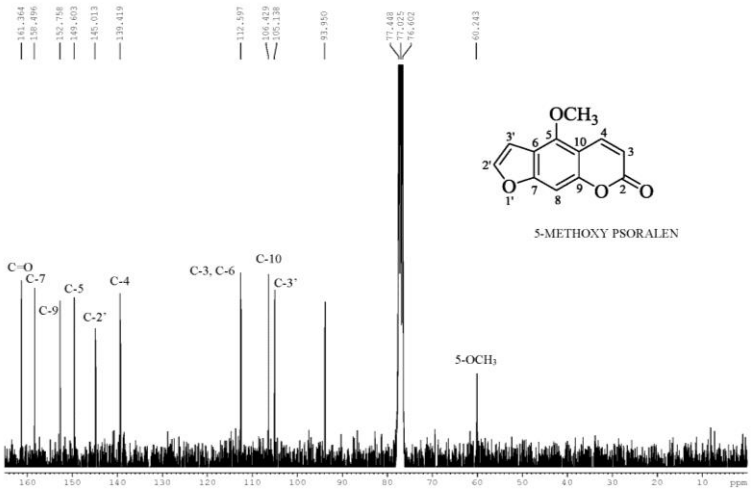

http://www.aloki.hu ● ISSN 1589 1623 (Print) ● ISSN 1785 0037 (Online)
DOI: http://dx.doi.org/10.15666/aeer/1802_24252443

Figure A10. *COSY spectrum of 5-methoxy psoralen*

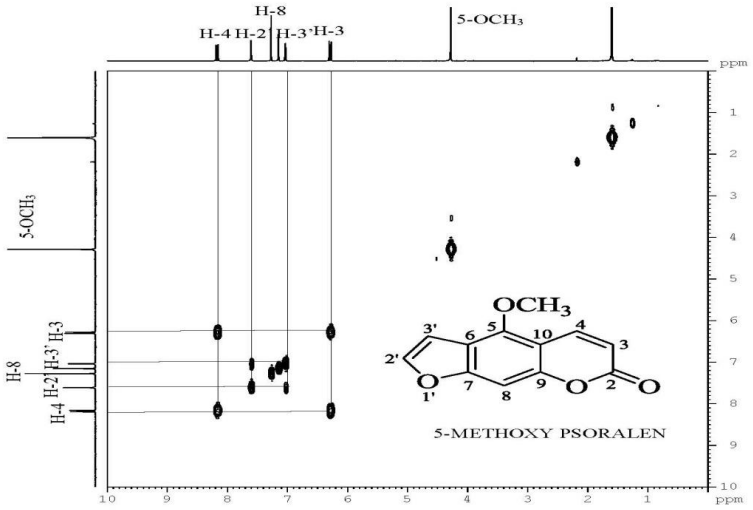

Figure A11. *GC spectrum of 5-methoxy psoralen*

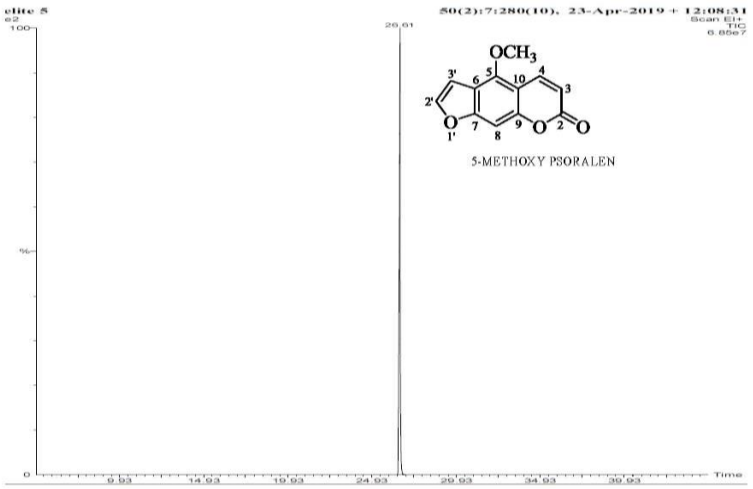

Figure A12. *MS spectrum of 5-methoxy psoralen*

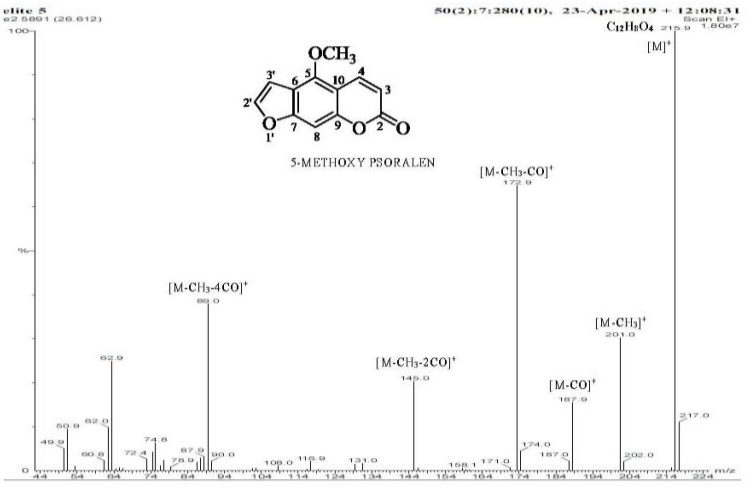

http://www.aloki.hu ● ISSN 1589 1623 (Print) ● ISSN 1785 0037 (Online)
DOI: http://dx.doi.org/10.15666/aeer/1802_24252443

Figure A13. *IR spectrum of 8-methoxy psoralen*

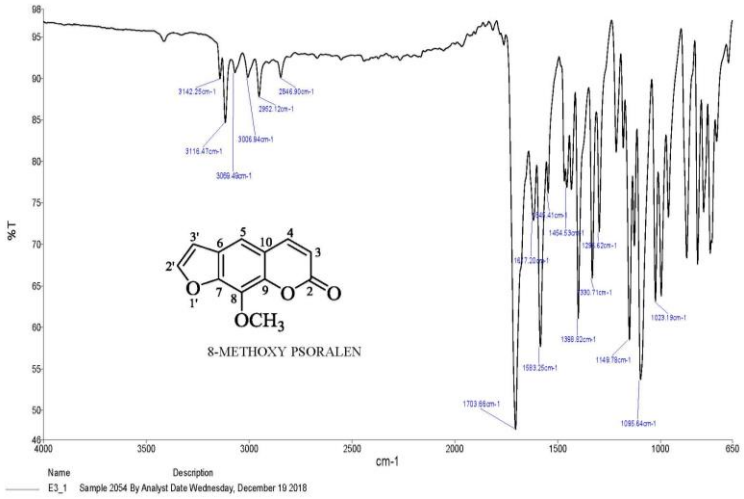

Figure A14. *^{1}H-NMR spectrum of 8-methoxy psoralen*

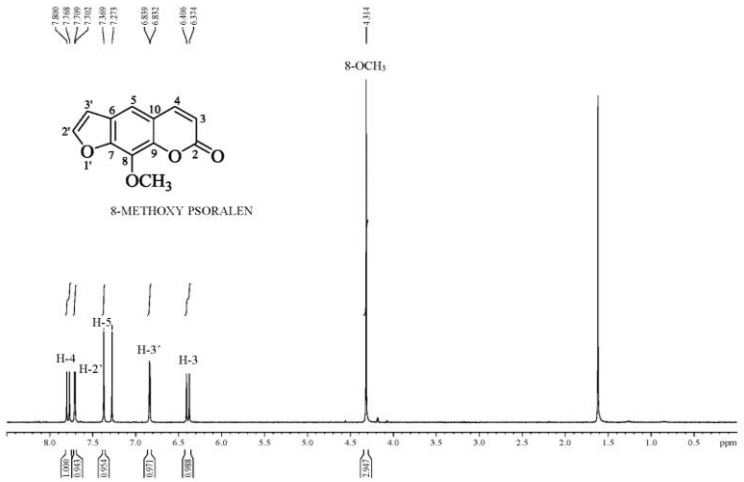

Figure A15. *^{13}C-NMR spectrum of 8-methoxy psoralen*

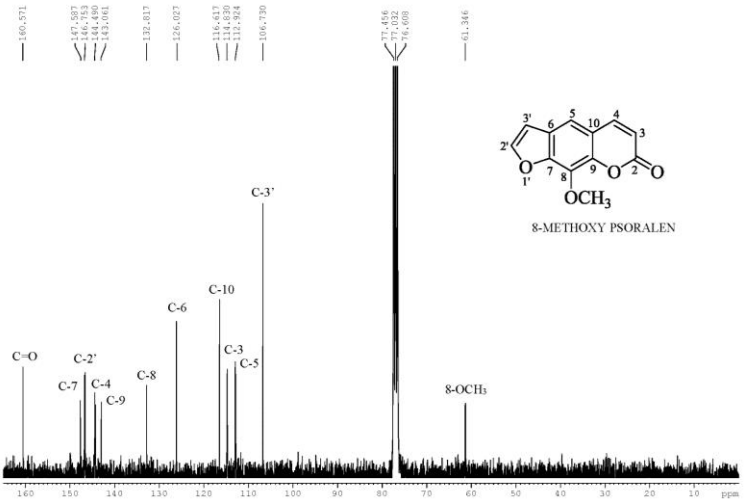

http://www.aloki.hu ● ISSN 1589 1623 (Print) ● ISSN 1785 0037 (Online)
DOI: http://dx.doi.org/10.15666/aeer/1802_24252443

Figure A16. *COSY spectrum of 8-methoxy psoralen*

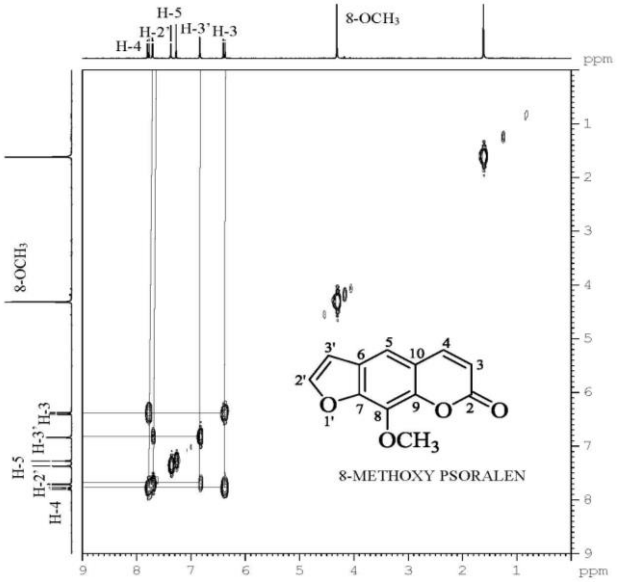

Figure A17. *GC spectrum of 8-methoxy psoralen*

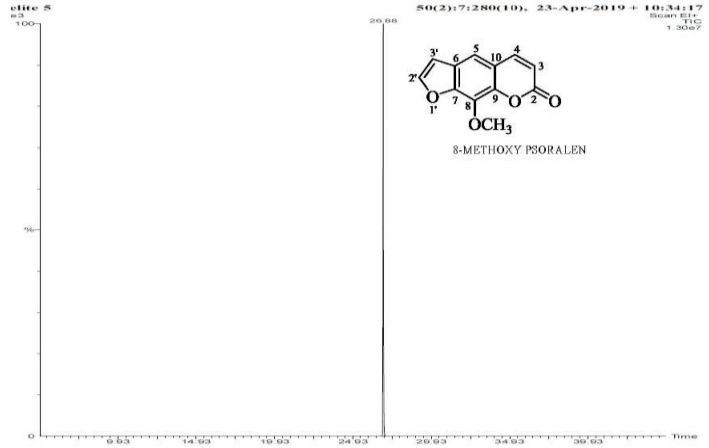

Figure A18. *MS spectrum of 8-methoxy psoralen*

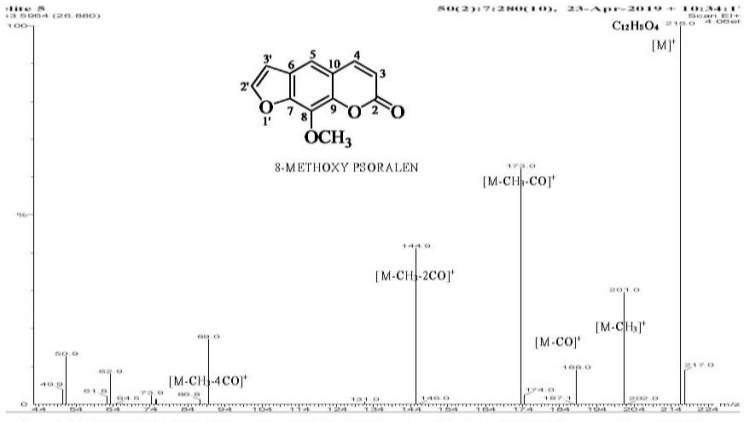

Appendix (1): IR , H-NMR, ^{13}C –NMR , COSY correlation (H-H), GC and MSS spectrum of Isopimpinellin, 5-Methoxy psoralen and 8-Methoxy psoralen respectively.

http://www.aloki.hu ● ISSN 1589 1623 (Print) ● ISSN 1785 0037 (Online)
DOI: http://dx.doi.org/10.15666/aeer/1802_24252443

ECOLOGICAL DISTRIBUTION, MORPHOLOGICAL AND MOLECULAR CHARACTERIZATION OF ZYGOPHYLLACEAE FROM DIVERSE ECOLOGICAL ZONES OF BALOCHISTAN, PAKISTAN

AHMED, A.[1*] – HAMEED, A.[2] – SAEED, S.[1]

[1]*Department of Botany, University of Balochistan, Quetta 87300, Pakistan (phone: +92-81-921-1264)*

[2]*Nuclear Institutes for Agriculture and Biology (NIAB), Fasialabad 38000, Pakistan*

[*]*Corresponding author*
e-mail: aliaahmed_botany@yahoo.com

(Received 20th Nov 2019; accepted 30th Jan 2020)

Abstract. The study was aimed to characterize and document the wild plants of Zygophyllaceae in arid and semi-arid regions of Balochistan. The morphology, ecology and molecular characteristics and taxonomic implications of many taxa were subject to analysis. The field survey was carried out during 2017-18 in the diverse elevation zones of Balochistan selected due to the presence of the highest number of Zygophyllaceae in these regions. Morphological and molecular characterization was carried out by using, agglomerative hierarchical clustering and Principal Component Analysis. A total of 17 plants of Zygophyllaceae were documented from Sibi, Mashkaf, Noshki, Naal, Dalbandeen, Punjgur, Hingol National Park, Bella, Uthal and Quetta region. Commonly distributed taxa were *Peganum hermala* and *Tribulus terrestris*. Furthermore, seven species of *Fagonia*, five species of *Tribulus* and four species of *Zygophyllum* were also assessed. The present study documents and contributes detailed significant information of naturally occurring medicinal plants of Zygophyllaceae from diverse remote zones of Balochistan. It also provides a base line for identification of controversial taxa on morphological and molecular basis. Especially the data provided may further be utilized for novel drug development. Furthermore, the ecological distribution may be useful in management of conservation of endangered and endemic taxa.
Keywords: *Fagonia, Tribulus, Zygophyllum, Peganum, arid and semi-arid zones, PCA, AHC*

Introduction

Balochistan is the largest province comprising 44% of the total area of Pakistan. Geographical region comprised of arid to semi-arid structure ranging from cool temperate to coastal tropics. The diverse ecological conditions have an impact on the diversity of flora found. Local communities utilize wild plants as folk medicines in large amount. Selected areas are blessed by botanical diversity and endemism. Diverse taxa of the region include herbs, shrubs, and trees including evergreen Juniper forest. Aromatic, non-aromatic flowering and non-flowering plants contributes in more than sixteen hundred wild plant species. Total of 44 species are endemic to the Balochistan (Saeed et al., 2014).

The Zygophyllaceae consists of diverse habits of wild flora including succulents, herbs, undershrub, shrubs and small trees. The habitat of these plants is predominantly desert or saline areas of temperate and tropical regions around the globe (Beier et al., 2003; Bellstedt et al., 2008). *Tribulus, Fagonia, Zygophyllum* and *Peganum* considered being the main genera. Folk medicinal System is a precious resource, hence utilized as potent safe drugs (Hussain and Sher, 1998). Many members of the family are being used ethno medicinally for centuries in folk medicines. Taxa like *Peganum hermala, Fagonia indica, F. ovalifolia, F. bruguieri, Tribulus terrestris, T. longipetalus* etc traditionally used by local communities to cure fever, cough, inflammation of organs, gonorrhea, obesity, urinary tract infection (UTI) etc.

http://www.aloki.hu ● ISSN 1589 1623 (Print) ● ISSN1785 0037 (Online)
DOI: http://dx.doi.org/10.15666/aeer/1802_24452462

(unpublished data). Many medicinal plants extract constituted various types of chemicals, each have a property to control a variety of biological and pharmacological activities such as antimicrobial, anti-parasitic, anti-diabetic, antioxidant, anti-inflammatory and anticholinesterase. These chemicals may have a combined effect in controlling various diseases (Rates, 2001; Houghton et al., 2007).

For proper identification and standardization of crude drugs, accurate anatomical and morphological description is necessary, and this description must take into account all the diagnostic features. The evaluation of crude drug involves a number of methods such as organoleptic, microscopic, chemical, physiological and biological. Organoleptic evaluation includes shape, size, odor, taste, texture, and color of crude drug along with external marking. On the basis of gross morphology, drugs may be grouped as leaves, bark, root, rhizome, and so forth. Microscopic features such as spines, trichomes, spores, and epidermal structures may be examined which are used as diagnostic features in the identification of plant drugs (Fransworth and Soejarto, 1988; Fazal et al., 2013). As the selected plants are medicinally important and utilized in folk medicine system, their authentication is essential on morphological and molecular basis that may be utilized for novel drug discovery as a future prospect.

During the past few decades, the theoretical framework of population genetics and empirical data gathered with the help of molecular genetic methods have been widely used in conservation biology. Given a haploid nature and a low frequency of genetic recombination, molecular markers of organelle DNA have long been used for phylogenetic reconstruction at various taxonomic levels, conservation genetics, and assessing the migratory routes of species (Nite-Kang and Yong, 2014; Yong and Nite-Kang, 2015).

Molecular marker system used to assess genetic variability within and among populations. Several marker systems were being used for genetic diversity analysis. Randomly Amplified Polymorphic DNA (RAPD) markers are appropriate for DNA fingerprinting of unknown sequences and they are rapid and easy to assess, (Kernodle et al., 1993). The Inter Simple Sequence Repeat (ISSR) did not need prior sequence and was less vulnerable (Adams et al., 2003). Universal Rice Primer (URP) markers were first time used by Kang et al. (2002). These are repeated chains that were extracted of genome bank of the rice of local Korea. URP markers with suitable PCR condition, produce high polymorphs. Additionally, it has been proved that these markers are useful tools for genetic analysis in between and within species (Rashmi et al., 2008; Abbas et al., 2015). Combined marker system used to assess genetic diversity within and among the population of different wild plants which were not sequenced earlier (Saeed et al., 2015, 2017).

In this view the present study was designed to provide comprehensive information about the medicinally important and highly controversial taxa of Zygophyllaceae used in folklore from different ecological zones of Balochistan, based on morphological and molecular characterization.

Material and Methods

Study Sites

The field survey was carried out during 2017-18 in various regions viz., Quetta valley, Sibi, Mashkaf, Noshki, Naal, Dalbandeen, Punjgur, Hingol National Park, Bella and Uthal. These areas of Balochistan were selected due to the presence of high number of taxa of Zygophyllaceae (*Figure 1*).

http://www.aloki.hu ● ISSN 1589 1623 (Print) ● ISSN1785 0037 (Online)
DOI: http://dx.doi.org/10.15666/aeer/1802_24452462

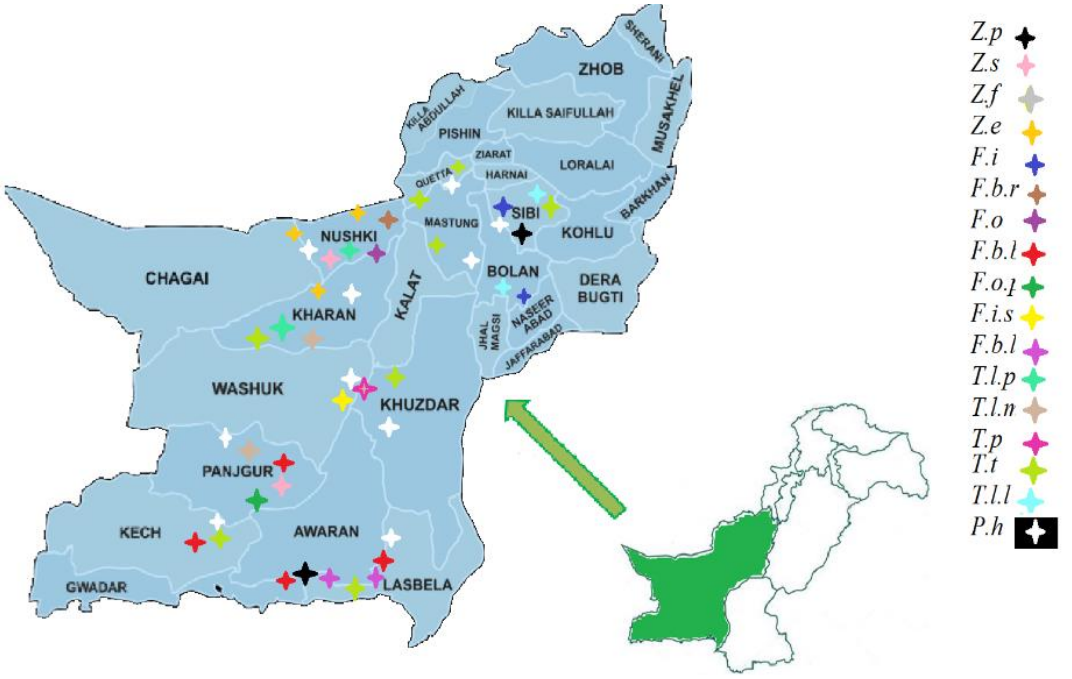

Figure 1. *Map of Balochistan (Pakistan) illustrating the sampling site areas with geographical coordinates*

Morphological Analysis

Total 58 characters were observed during the morphological analysis. Qualitative and Quantitative morphological characters were appraised and subjected to Principal Component Analysis (PCA) and Agglomerative Hierarchical Clustering (AHC).

Molecular Analysis

This study was carried out using three different marker systems namely, RAPD, ISSR and URP's (*Table 1*). Combined markers RAPD, ISSR and URP were used to amplify for cluster analysis.

DNA Extraction

Genomic DNA was isolated by using CTAB (Cetyl Trimethyl Ammonium Bromide) Doyle and Doyle (1987). Quantified on a spectrophotometer at 260 nm and Checked DNA Quality on 0.8% gel by electrophoreses.

PCR Amplification

PCR reaction for amplification was carried out. Total 20 µl volume reaction was prepared. Enzynomics 2X TOPsimple DyeMIX-nTaq, Master Mix was used. PCR mixture contains 5 µl Master Mix (2X), 0.4 µl Primer (5 pmol/ µl), 4 µl DNA template (0.1 ng/µl). PCR amplification was performed using thermal cycler (Applied Biosystems 96 well USA). For RAPD primers, PCR was performed with initial denaturation at 94ºC for 4 min, Denaturation 94ºC for 4 min and then 36 cycles with annealing temperature 33ºC for 1 min, extension step at 72ºC for 2 minutes. An additional extension step for 7 minutes at 72ºC in the final cycle was also added. For

http://www.aloki.hu ● ISSN 1589 1623 (Print) ● ISSN1785 0037 (Online)
DOI: http://dx.doi.org/10.15666/aeer/1802_24452462

URP primers, cycles increased to 40. ISSR primers performed 40 cycles. The amplified products were checked by electrophoresis in 1.8% agarose gels. Gel stained with ethidium bromide (0.5 µg / ml) in 1X TAE buffer. The product was visualized by Gel documentation under UV light and the size of markers were estimated by comparing to the standard ladder (100 bp BIORON 0.2 mg/ml) in the gel.

Table 1. *List of primers includes name of primers, and sequence of the primers used in the study*

S. No.	Primer Name	Sequence (5'-3')
	RAPD	
1	OPA-01	CAGGCCCTTC
2	OPA-02	TGCCGAGCTG
3	OPA-03	AGTCAGCCAC
4	OPA-04	AATCGGGCTG
5	OPA-07	GAAACGGGTG
6	OPA-09	GGGTAACGCC
7	OPC-19	GTTGCCAGCC
8	OPC-26	CACGTTATCGCA
9	OPD-13	GGGGTGACGA
10	OPD-20	ACCCGGTCAC
11	OPD-69	CGCTCCAAAT
12	OPF-21	AGCAACAATC
13	OPF-22	AAGATCAAAGAC
14	OPG-04	AGCGTGTCTG
15	OPG-09	CTGACGTCAC
16	OPG-13	CTCTCCGCCA
17	OPH-02	TCGGACGTGA
18	OPH-04	GGAAGTCGCC
19	OPP-03	CTGATACGCC
20	OPT-02	GGAGAGACTC
21	OPT-05	GGGTTTGGCA
22	OPU-03	CTATGCCGAC
23	OPW-04	CAGAAGCGGA
24	OPX-17	GACACGGACC
25	OPAJ-20	ACACGTGGTC
26	S-03	AGCGGGGTCA
27	S-05	GGTCAACCCT
28	S-11	GAGGCGCTGC
29	S-23	CGGCCACCGT
30	UBC-181	ATGACGACGG
31	UBC-194	AGGACGTGCC
32	UBC-733	GGGAAGGGAG
	URPS	
01	URP-25F	GATGTGTTCTTGGAGCCTGT
02	URP-1F	ATCCAAGGTCCGAGACAACC
03	URP-2R	CCCAGCAACTGATCGCACAC
04	URP-17R	AATGTGGGCAAGCTGGTGGT
	ISSR	
01	INC-6	CGCGATAGATAGATAGATA
02	INC-7	GACGATAGATAGATAGATA
03	INC-8	AGACAGACAGACAGACGC
04	INC-14	CTCCTCCTCCTCCTCTT
05	INC-16	TCTCTCTCTCTCTCTCA

http://www.aloki.hu ● ISSN 1589 1623 (Print) ● ISSN1785 0037 (Online)
DOI: http://dx.doi.org/10.15666/aeer/1802_24452462

Gel Analysis by Software

Then amplified products were checked by electrophoresis in 1.5% agarose gels in 1X TAE buffer. Further gel was stained in ethidium bromide. The product was visualized by Gel documentation system under UV light and the size of markers was estimated by 100-1500 bp DNA ladder (RTU) containing orange G & xylene cyanol FF tracking dyes in the gel. Gel analysis was carried out by using UVI-Soft UVI-Band Map. Similarity coefficients Nie & Li (Dice) were performed by UPGMA. Dendrogram generated based on homology.

Results

In this project seventeen wild species of Zygophyllaceae were reported from diverse and remote ecological zones of Balochistan including endemic taxa (*Figure 2*). Voucher specimen of all collected species was submitted in www.openherbarium.edu. Geographical coordinates of these plants at their existing habitats were recorded and the Phenology (flowering period) of the taxa was also recorded (*Table 2*).

Table 2. *Geographical coordinates, soil type and phenology of selected Taxa of Zygophyllaceae*

S. No	Plant Name	Plant code	Voucher No.	Locality	Elevation (meter above sea level)	Soil type	Phenology (Flowering Period)
1	*Z. propinquum*	*Z.p*	QUETTA000208	Hingol National Park, Mushkaf, Sibi	100-350	Sandy, common carnonishius saline sandy loam soil	March -April
2	*Z. simplex*	Z.s	QUETTA000218	Panjgur, Noshki	950-990	Sandy Rocks	March -April
3	*Z. fabago*	Z.f	QUETTA000090	Quetta	1650-1700	Sandy loam	July-Aug
4	*Z. eurypterum*	Z.e	QUETTA000157	Noshki, Dalbandeen, Kharan	990-1000	Sandy rock	March-April
5	*F. indica*	F.i	QUETTA000207	Mushkaf, Sibi	100-200	Sandy	Feb-Aug
6	*F. bruguieri* var *rechingeri*	F.b.r	QUETTA000222	Noshki (Stone)	990-1000	Sandy rock	March-May
7	*F. oliveri*	F.o	QUETTA000221	Noshki (Janglat area)	1000	Sand	March-May
8	*F. bruguieri* var. *bruguieri*	F.b.b	QUETTA000220	Panjgur, Uthal, Hingol National Park, Turbat	970	Sand	February-April
9	*F. ovalifolia* var. *pakistanica*	F.o.p	QUETTA000219	Panjgur	980	Sandy stones	March-April
10	*F. indica* var. *scheweinfurthii*	F.i.s	QUETTA000223	Naal	1200	Sandy Rock	April-September
11	*F. bruguieri* var *laxa*	F.b.l	QUETTA000224	Uthal, Hingol National Park	0-150	Sandy Rock	February-April
12	*T. longipetalus* subsp. *pterophorus*	T.l.p	QUETTA000215	Noshki	993	Sandy rock	March-May
13	*T. longipetalus* subsp. *macropterus*	T.l.m	QUETTA000216	Panjgur, Kharan	970	Sand	February-May.
14	*T. pentandrus*	T.p	QUETTA000217	Naal	1200	Sandy Rock	February-August.
15	*T. terrestris*	T.t	QUETTA000085	Bella, Punjgur, Noshki, Sibi, Hingol National Park, Quetta	100-1650	Sand	April-October
16	*T. longipetalus* subsp. *longipetalus*	T.l.l	QUETTA000209	Mushkaf, Sibi	130-150	Sand	March-October
17	*P. hermala*	P.h	QUETTA000002	Uthal, Khuzdar, Bella, Punjgur, Noshki, Kharan, Sibi, Hingol National Park, Naal, Quetta	100-1700	Sand	April- August.

http://www.aloki.hu ● ISSN 1589 1623 (Print) ● ISSN1785 0037 (Online)
DOI: http://dx.doi.org/10.15666/aeer/1802_24452462

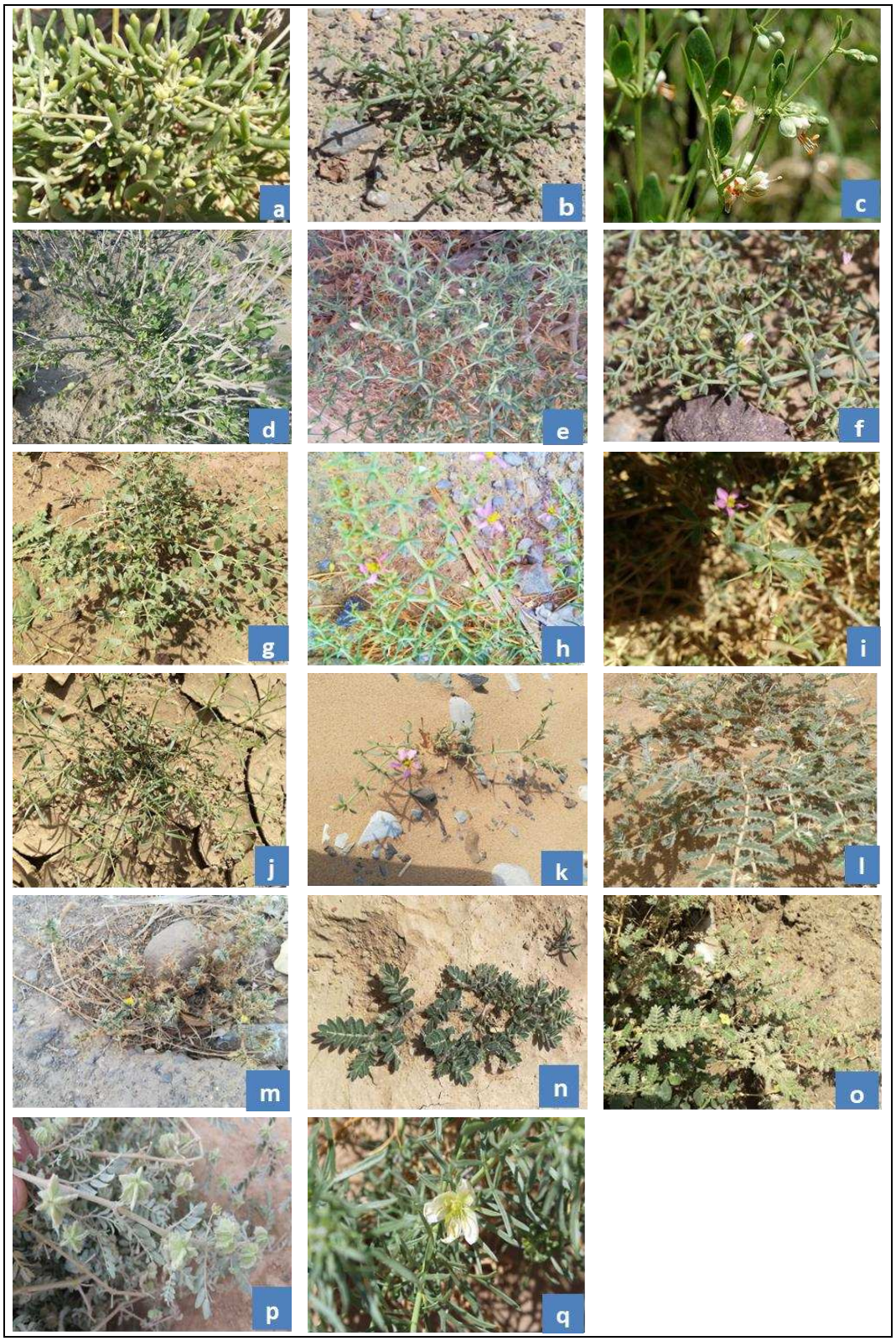

Figure 2. *Plants at their habitat* **a)** *Z. propinquum,* **b)** *Z. simplex,* **c)** *Z. fabago,* ***d)*** *Z. eurypterum,* **e)** *F. indica,* **f)** *F. bruguieri* var *rechingeri,* **g)** *F. oliveri,* **h)** *F. bruguieri* var. *bruguieri,* **i)** *F. ovalifolia* var. *pakistanica,* **j)** *F. indica* var. *scheweinfurthii,* **k)** *F. bruguieri* var *laxa,* **l)** *T. longipetlus* sub.sp. *pterophorus,* **m)** *T. longipetalous* sub.sp. *macropterus,* **n)** *T. pentandrus,* **o)** *T. terrestris,* **p)** *T. longipetalus* sub.sp *longipetlus,* **q)** *P. hermala*

http://www.aloki.hu ● ISSN 1589 1623 (Print) ● ISSN1785 0037 (Online)
DOI: http://dx.doi.org/10.15666/aeer/1802_24452462

Morphological Analyses

Morphological evaluation of 17 taxa of Zygophyllaceae found in study area was carried out by total of fifty-nine morphological characters. Out of which thirty-one were qualitatively measured and twenty-eight were quantitative characters.

Qualitative Analyses

Life cycle

Studied taxa exhibited different life cycles. All the taxa of *Tribulus* were annual except the *T. pentandrus* was biannual. Perennial taxa were *P. hermala*, *Z. fabago, Z. propinquum, Z. eurypterum* and *F. bruguieri* var. *laxa. F. indica* var. *schweinfurthii* and *F. indica* were annual herbs all other taxa of *Fagonia* were Bi-annual.

Plant nature

Plant nature varied in all studied species of Zygophyllaceae. *T. longipetalus* subsp. *pterophorus* and *T. longipetalus* subsp. *macropterus* were prostrate-erect. *T. longipetalus* subsp. *longipetalus, T. terrestris, T. pentandrus, F. bruguieri* var. *rechingeri, F. bruguieri* var. *bruguieri* were prostrate in nature. *Z. simplex* was the only taxa having sub-erect plant nature. *F. ovalifolia* subsp. *pakistanica* was unique in nature i.e. Procumbent. *F. indica* var. *schweinfurthii* was ascending in nature. *F. indica* was decumbent and *F. olivieri* was sub-prostrate. All remaining were erect in nature.

Plant surface

Plant surface of *T. longipetalus* subsp. *macropterus* and *T. pentandrus* were densely hairy while *T. longipetalus* subsp. *longipetalus, T. terrestris* and *Z. propinquum* were sparsely hairy. *F. bruguieri* var. *laxa* was sparsely glandular whereas *F. indica* var. *schweinfurthii, F. olivieri* and *F. bruguieri* var *bruguieri* were glandular. Other taxa had glabrous plant surface.

Hair shapes

Hair shapes of *T. longipetalus* subsp. *pterophorus, T. longipetalus* subsp. *macropterus*, *T. longipetalus* subsp. *longipetalus*, *T. terrestris*, *T. pentandrus, Z. propinquum* and *F. ovalifolia* subsp. *pakistanica* were glandular.

Trichome stalk

In most of the taxa trichome stalk were absent while present only in all genera of *Tribulus.*

Stem nature

Nature of the stem varies from woody to herbaceous in selected taxa of Zygophyllaceae. *Z. eurypterum* was characterized in woody stem nature. All genera of *Tribulus, P. hermala* and *Z. simplex* were having herbaceous stem. The stem in all genera of *Fagonia* were woody at the base.

http://www.aloki.hu ● ISSN 1589 1623 (Print) ● ISSN1785 0037 (Online)
DOI: http://dx.doi.org/10.15666/aeer/1802_24452462

Stem outline shape

Significant variations were found in stem outline shape of different taxa of Zygophyllaceae. *T. terrestris, T. pentandrus, P. hermala* and *Z. propinquum* were terete outline shape of stem. *Z. fabago*, *Z. simplex* and *Z. eurypterum* were striate. *F. indica* var. *schweinfurthii* and *F. indica* were terete and striate, while all other were quadrangular.

Stipule

Stipule was present in selected taxa of Zygophyllacae. Nature of stipule varies within the selected taxa. Stipule of *T. pentandrus* was bristles while other four genera of *Tribulus* and *Z. eurypterum* were foliaceous. Stipule nature of *P. hermala* was also bristles. *Z. fabago, Z. propinquum* and *Z. simplex* stipule were scarious and all the *Fagonia* species have spinescent stipule nature.

Leaves/leaflets arrangement

Leaves/leaflets arrangements were alternate in *T. longipetalus* subsp. *pterophorus* and *F. indica* var. *schweinfurthii,* whereas all other taxa were having opposite Leaves/leaflets arrangements.

Leaf-blade\leaflets

Leaf-blade\leaflets of all the studied taxa of *Tribulus* were in paired while other taxa leaves were not paired.

Leaf structure

Variation was found in leaf structure of studied taxa. Leave of *T. longipetalus* subsp. *pterophorus* was paripinnat abruptly. Leave structure of *T. longipetalus* subsp. *macropterus, T. longipetalus* subsp. *longipetalus, T. terrestris, T. pentandrus, Z. propinquum* and *Z. fabago* were bifoliate. *P. hermala and Z. eurypterum* leaves were found simple. *Z. simplex* leaves succulent. *F. bruguieri* var. *laxa* leaves was trifoliate below and unifoliate above. All other taxa of *Fagonia* were had unifoliate leaf structure.

Leaf petiole

Leaf petiole showed variation among all selected taxa. *Z. fabago, Z. propinquum, Z. eurypterum, F. ovalifolia* subsp. *pakistanica, F. bruguieri* var. *bruguieri, F. bruguieri* var. *laxa, F. indica* var. *schweinfurthii, F. indica* and *F. olivieri* were petiolate. *T. terrestris* was sub-sessile while other taxa were sessile.

Leaf\leaflet shape

Leaf\leaflet shape also showed variation in all studied taxa. *T. terrestris* had ovate shape. *T. longipetalus* subsp. *pterophorus, T. longipetalus* subsp. *macropterus, T. longipetalus* subsp. *longipetalus, T. pentandrus* and *Z. simplex* shape were oblong. *Z. propinquum* was semi-cylindrical. *P. hermala, F. bruguieri* var. *rechingeri, F. olivieri* and *F. bruguieri* var. *bruguieri* were found in lanceolate shape. *F. indica* was ovoid, *F. indica* var. *schweinfurthii* was trifoliate, *F. bruguieri* var. *laxa* was linear lanceolate, and *F. ovalifolia* subsp. *pakistanica* was oblanceolate shape leaflets.

http://www.aloki.hu ● ISSN 1589 1623 (Print) ● ISSN1785 0037 (Online)
DOI: http://dx.doi.org/10.15666/aeer/1802_24452462

Leaf apex

Leaf apex of *P. hermala, F. indica var schweinfurthii* and all taxa of *Tribulus* were acute. *Z. fabago* was oval apex. *Z. propinquum* and *Z. simplex* had obtuse apex. *Z. eurypterum* was found with spathulate, *F. ovalifolia* sub sp *pakistanica* was minutely mucronate. *F. bruguieri* var. *rechingeri, F. bruguieri* var. *bruguieri, F. bruguieri* var. *laxa, F. indica* and *F. olivi*eri had mucronate apex.

Sepal shape

Shape of sepal of *F. bruguieri* var. *rechingeri, F. bruguieri* var. *laxa* and all species of *Tribulus* were lanceolate. *P. hermala* had linear sepal shape. *Z. simplex* was elliptic-oblong, *F. olivieri* was oblong. Whereas ovate sepal shape were found in *F. indica, F. indica* var. *schweinfurthii*, *F. bruguieri* var. *bruguieri*, *F. ovalifolia* subsp. *pakistanica*, *Z. propinquum, Z. fabago* and *Z. eurypterum.*

Sepal apex

Sepal apex was obtuse in *Z. fabago* and *Z. propinquum,* retuse in *Z. eurypterum* and acute in all remaining taxa.

Sepal surface

Sepal surface varies from glabrous to hairy. Sepal surface of *T. longipetalus* subsp. *longipetalus* was sparsely hairy. *F. ovalifolia* subsp. *pakistanica*, *F. indica* and *F. olivieri* had glandular sepal surface. *T. longipetalus* subsp. *pterophorus, T. longipetalous* subsp. *macropterus, T. terrestris, T. pentandrus* and *F. indica* var. *schweinfurthii* were having hairy sepal surface. While all other remaining taxa sepal were having glabrous surface.

Sepal and petal persistence at fruit maturity

Sepal in *T. longipetalus* subsp. *pterophorus*, *T. longipetalus* subsp. *macropterus*, *T. longipetalus* subsp. *longipetalus, T. terrestris¸ T. pentandrus, P. hermala, Z. propinquum, Z. simplex, F. bruguieri* var. *rechingeri, F. bruguieri* var. *laxa* and *F. indica* were persistent at the time of maturity. While in other taxa it was not persistent. Petals in all the studied taxa were not persistence at the time of fruit maturity.

Petal shape

Petal shape varies in these studied taxa. Obovate shape of petal was found in *T. longipetalus* subsp. *pterophorus, T. longipetalus* subsp. *macropterus, T. longipetalus* subsp. *longipetalus, T. terrestris, Z. fabago, Z. eurypterum, F. ovalifolia* subsp. *pakistanica* and *F. indica* var. *schweinfurthii. T. pentandrus* and *P. hermala* were oblong. *Z. propinquum, Z. simplex, F. bruguieri* var. *rechingeri, F. bruguieri* var. *bruguieri, F. bruguieri* var. *laxa, F. indica* and *F. olivieri* were spathulate.

Petal colour

Petal colour of all studied taxa showed variation. Petals of *P. hermala, Z. propinquum* and *Z. simplex* were yellowish white. Petal of *Z. fabago* was yellowish above orange at the base and *Z. eurypterum* was pale white. *F. ovalifolia* subsp. *pakistanica* and *F. bruguieri* var *bruguieri* were light pink in colour. *F. bruguieri* var. *rechingeri* was

http://www.aloki.hu ● ISSN 1589 1623 (Print) ● ISSN1785 0037 (Online)
DOI: http://dx.doi.org/10.15666/aeer/1802_24452462

purple, *F. bruguieri* var. *laxa* was pale pink *F. indica* var. *schweinfurthii* pinkish purple and *F. olivieri* was pinkish white. Petals of all species of *Tribulus* were yellow in colour.

Petal apex

Retuse petal apex was found in *Z. fabago.* In *Z. propinquum* it was reported spathulate/margin serrate. *Z. simplex* was having serrate margin apex. The apex of petal *T. longipetalus* subsp. *pterophorus, T. longipetalus* subsp. *macropterus, T. longipetalus* subsp. *longipetalus* and *T. terrestris* were clawed. While in remaining taxa obtuse petal apex were found.

Ovary surface

Ovary surface was hairy in all selected species of *Tribulus* and as well as all selected species of *Fagonia*. While the surface glabrous in *P. hermala* and all selected species of *Zygophyllum*.

Fruit type

Fruit type of *T. longipetalus* subsp. *pterophorus, T. longipetalus* subsp. *macropterus, T. longipetalus* subsp. *longipetalus* and *T. terrestris* were schizocarpic. Fruit of *Z. eurypterum* was capsule oblong-sherical. Loculicidal capsule type of fruits was found in all the other remaining taxa.

Fruit surface

Fruit surface in *P. hermala, Z. fabago, Z. propinquum* and *Z. eurypterum* were glabrous. *Z. simplex* fruit surface was regulose. While all the other studied fruits type surface was Hairy to sparsely hairy.

Fruit shape

Fruit shapes vary in all selected studied taxa of Zygophyllacae. Shape of fruits in all species of *Fagonia* was pyramidate and not winged. *Z. eurypterum* was oblong-spherical and winged. *Z. simplex* fruit shape was oblong and not winged. *Z. propinquum* fruit was oblong pyramidate and not winged. *Z. fabago* was oblong-cylindric and not winged. Fruit shape of *P. hermala* was found trigonous and not winged. *T. terrestris* was also not winged and sub spherical. All other four species were winged and discoid.

Seed shape

Seed shape in all species of *Tribulus* and *P. hermala* were triangular. *Z. eurypterum* seed shape was reniform. *Z. fabago, Z. propinquum* and *Z. simplex* was oblong/compressed. Seed shape of *F. indica* var. *schweinfurthii, F. indica* and *F. olivieri* was broadly oblong. While oblong shape type of seeds were reported in three species of *Fagoina* i.e *F. ovalifolia* subsp. *pakistanica, F. bruguieri* var. *bruguieri* and *F. bruguieri* var. *rechingeri.* However seeds of *F. bruguieri* var. *laxa* were obovoid.

Quantitative Analysis of Morphological Characters

Morphological characterization was also performed on the basis twenty-eight quantitative characters in seventeen species of Zygophyllaceae. Quantitative characters were further subjected to analyses through Principle component analyses (PCA).

http://www.aloki.hu ● ISSN 1589 1623 (Print) ● ISSN1785 0037 (Online)
DOI: http://dx.doi.org/10.15666/aeer/1802_24452462

Principle Component Analyses (PCA)

Eigenvalues

Out of 16 principal components (PCs), three viz. PC-1, PC-II, PC-III, PC-IV, PC-V and PC-VI had Eigen values >1 and contributed for 89.41% of total cumulative variability among different species (*Table 3*). The contribution of PC-I towards variability was highest (35.96%), PC-II contributed (15.42%), PC-III showed (13.72%) variability, PC-IV gives (13.28%), PC-V and PC-VI (6.05% and 4.92%) variability, respectively.

Table 3. *Eigenvalues of Principle component analyses*

	F1	F2	F3	F4	F5	F6
Eigenvalue	10.069	4.319	3.843	3.719	1.707	1.379
Variability (%)	35.960	15.424	13.725	13.281	6.095	4.924
Cumulative %	35.960	51.384	65.109	78.390	84.485	89.409

The PC-I showed 17 positive factor loadings (*Figure 3*) for Plant length, Petiole, Flower pedicle, Sepal length, Sepal width, Petal length, Petal width, Stamens number, Filament length, Style number, Style length, Stem internode, leaf length, leaf width, Fruit length, Fruit width, Fruit wings size, Fruit pedicel, Seed length, Seed width. PC-II indicated 15 positive factor loading for stipule width, Leaf-blade\leaflets no, flower pedicle, sepal length, Petal length, Petal width, Sepal No, Stamens number, Style number, Fruit width, Fruit wings size, Mericarp edge no, Fruit pedicel, Seed length. Quantitative characters which contributed 17 positive factor loadings towards PC-III were Plant length, Stipule width, Leaf-blade\leaflets no, Petiole, Sepal width, Petal No, Filament length, Style number, Stem internode, leaf width, Fruit length, Fruit width, Fruit wings size, Mericarp edge no, Number of fruit locules, Seed Length, Seed width. Plant length, Stipule width, Leaf-blade\leaflets no. leaflet petiole size, Petiole size, Sepal length, Petal length, Petal No, Sepal No, Stamens number, Filament length, Style number, Style length, Stem internode, leaf length, leaf width, Mericarp edge no, Number of fruit locules, Fruit pedicel were contributed 20 positive factor loadings towards PC-IV. 19 positive factor loadings towards PC-V were Plant length, Stipule length, Leaf-blade\leaflets no, leaflet petiole size, Petiole size, Flower pedicle, Sepal length, Sepal width, Petal width, Petal No, Sepal No, Filament length, Style length, Stem internode, leaf width, Fruit length, Fruit width, Fruit wings size, Mericarp edge no., and PC-VI included 17 positive factor loadings Plant length, Stipule length, Leaf-blade\leaflets no, leaflet petiole size, Petiole size, Flower pedicle, Sepal length, Petal length, Petal width, Stamens number, Style number, Fruit length, Fruit width, Number of fruit locules, Fruit pedicel, Seed size Length, Seed width.

Cluster Analysis

Clustering of studied taxa based on quantitative characters only is presented in (*Figure 4*). Cluster analysis grouped all taxa into 3 clusters which are further divided as Cluster-I comprised T.l.p, Cluster-II comprised of 15 taxa which are further divided into sub clusters a & b. Cluster a comprised of P.h and Z.s. Cluster b further divided into c & d. Cluster c comprised of Z.e. Cluser d have two more groups e and f. Cluster e comprised of T.t. Z.p. Z.f. T.l.m and T.l.l. while cluster f comprised of all *Fagonia* species. Cluster-III comprised of T.p.

http://www.aloki.hu ● ISSN 1589 1623 (Print) ● ISSN1785 0037 (Online)
DOI: http://dx.doi.org/10.15666/aeer/1802_24452462

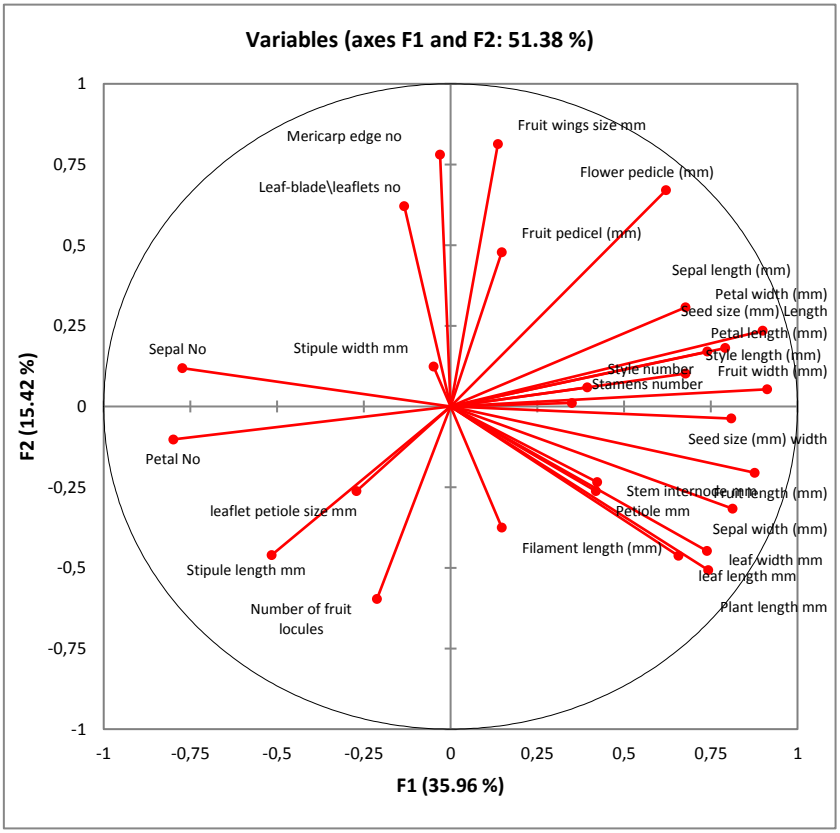

Figure 3. *Correlations chart of 17 taxa of Zygophyllaceae plotted according to the first two principal components, obtained from morphological and quantitative traits*

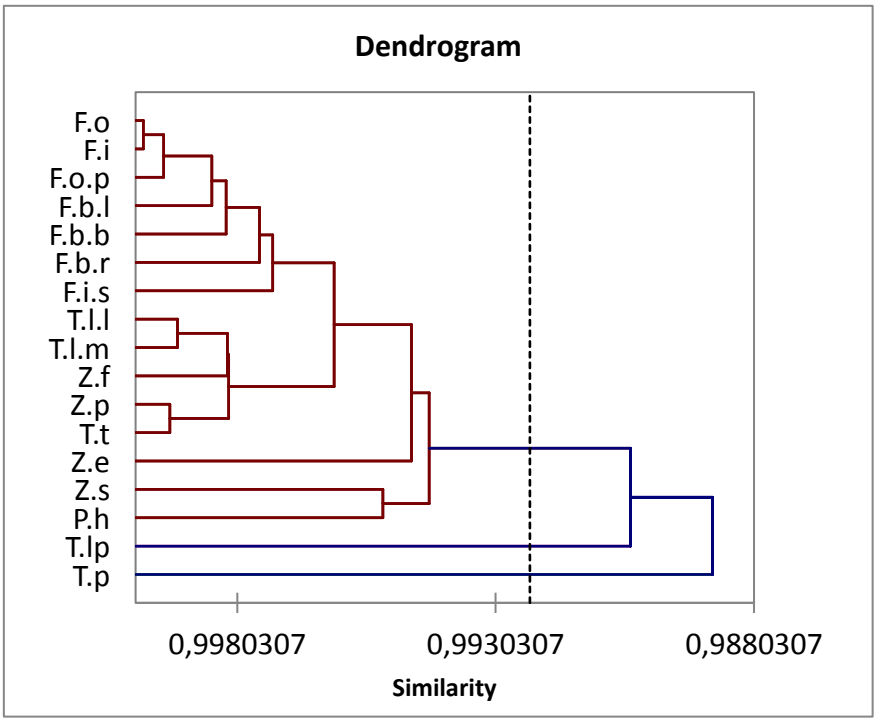

Figure 4. *Tree diagram based on 28 quantitative characters in all selected taxa of Zygophyllaceae*

http://www.aloki.hu ● ISSN 1589 1623 (Print) ● ISSN1785 0037 (Online)
DOI: http://dx.doi.org/10.15666/aeer/1802_24452462

Molecular Characterization

Using different molecular markers may target different regions of genome and could help in removing errors for the detection of polymorphism. Out of forty-one tested primers, thirty two RAPD and five ISSR revealed polymorphism, and exhibited reproducible bands among all selected taxa of Zygophyllaceae. The URP's did not give amplification in selected taxa. These taxa were not characterized earlier by different markers combination so this study would give the amended pattern of genetic variation.

Dendrogram based on molecular data grouped all genera into three main clusters A, B and C (*Figure 5*). Cluster A grouped into four sub-clusters a,b,c,d. Cluster a comprised of three species i.e *T. longipetalus* subsp. *longipetalus*, *T. longipetalus* subsp. *pterophorus* and *T. longipetalus* subsp. *macropterus*. Cluster b comprised of four species i.e *P. hermala*, *Z. simplex*, *Z. propinquum* and *Z. fabago*. Cluster c comprised of *F. olivieri*, *F. bruguieri* var. *rechingeri*, *F. bruguieri* var. *bruguieri.* Cluster comprised of *T. terrestris* and *T. pentandrus*. Cluster B having sub-clusters f and e contained *Z. eurypterum*, *F. indica*, and *F. indica* var. *schweinfurthii* while on cluster C *F. bruguieri* var. *laxa* collected from Uthal (Zero point) and Hingol National Park both plants were identified with same species showing interspecific diversity that may be due to change in elevation.

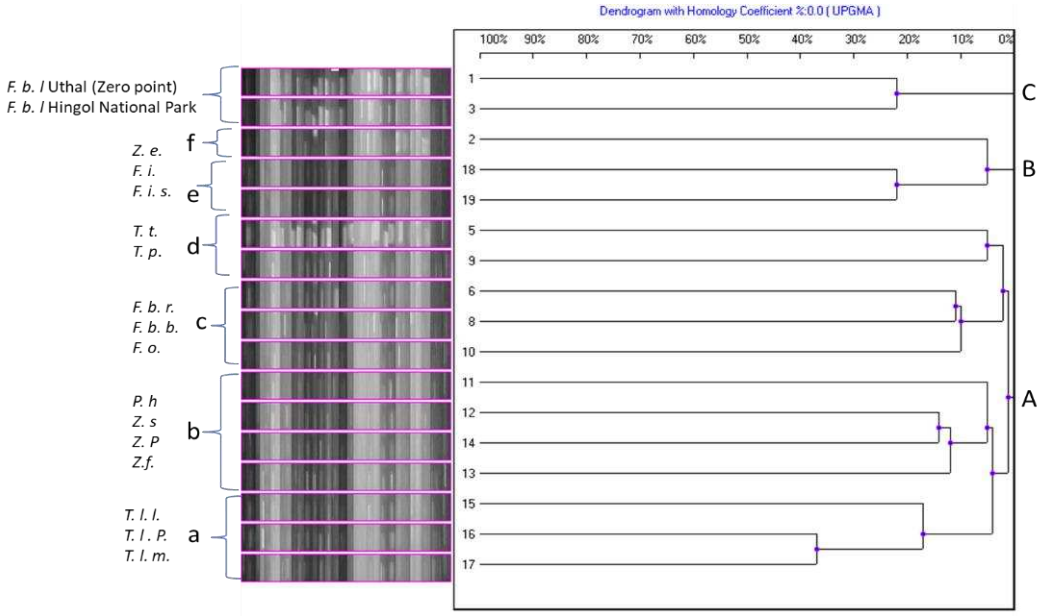

Figure 5. *Cluster analysis UPGMA based on Homology Coefficient among taxa of Zygophyllaceae generated by combined tested markers*

Discussion

Ecological Distribution

The species of Zygophyllaceae are widely distributed in scattered populations usually at diverse ecological zones from low to high elevations in Balochistan Pakistan. Earlier reported by Ghafoor (1974) that the plants are widespread in tropical, subtropical and warm temperate, often in drier areas and represented by 8 genera and 22 species. The present study revealed that *P. hermala* is widely distributed in all studied

http://www.aloki.hu ● ISSN 1589 1623 (Print) ● ISSN1785 0037 (Online)
DOI: http://dx.doi.org/10.15666/aeer/1802_24452462

sites. From high-elevation to low-elevation zones, High elevation includes Quetta, Naal, Noshki, Low elevation includes Uthal, Hingol National Park, Mushkaf, Sibi. Environmental conditions play a key role in determining the distribution and functional distinctiveness of the species occupying a particular region (Ricklefs and Latham, 1992; Noman et al., 2012). Previously, few ethnobotanical and phytochemical studies of Zygophyllaceae were reported from Balochistan by Tareen et al. (2010), Perveen and Qaiser (2008), Zaidi and Crow (2005) and Manzoor et al. (2017). *F. ovalifolia* subsp. *pakistanica* is the Endemic species to Pakistan collected from Panjgur (Ghafoor, 1974). *F. bruguieri* was earlier reported from Johan and Kalat area of Balochistan by Goodman and Ghafoor (1992) whereas in present study three sub.species of *F. bruguieri* i.e. *F. bruguieri* var. *rechingeri* from Noshki sandy Rocks, *F. bruguieri* var. *bruguieri* were collected from Panjgur, *F. bruguieri* var. *laxa* were found from Hingol National Park and Uthal. *F. indica* var. *schweinfurthii* were collected from Naal. *F. indica* were collected from Mushkaf earlier reported in plant biodiversity of Dureji in southern Balochistan Province by Perveen and Qaiser (2008). *F. olivieri* were collected from Noshki, Near Janglat area, *T. terrestris* were collected from Quetta, Mushkaf, Lasbella and Noshki earlier Goodman and Ghafoor (1992) reported from Kalat and Khuzdar. *T. longipetalus* subsp. *pterophorus* were collected from Noshki. *T. longipetalus* subsp. *macropterus* from Panjgur, *T. longipetalus* subsp. *longipetalus* from Sibi and Mushkaf, *T. pentandrus* were collected from Naal area. *Z. fabago* were found from Quetta earlier also reported by Zaidi and Crow (2005) from Quetta. *Z. eurypterum* from Dalbandeen and Noshki Goodman and Ghafoor (1992) earlier reported from Mastung, Naal and Kharan. *Z. simplex* collected from Punjgur, Naal and Noshki. *Z. propinquum* were found in Hingol National Park and Mushkaf earlier work has been done on *Z. propinquum* from Dureji in Southern Balochistan by Perveen and Qaiser (2008). Manzoor et al. (2017) also collected *Z. propinquum* from Hub District Balochistan. It was observed that the studied sites most dominated plants were succulents, often xerophytic and spiny as the area were mostly deserted. The areas have dry and warm climatic conditions, with low rate of precipitations.

Morphological Characterization

Morphological characters play an important role identification and documentation of the taxa. Earlier different studies were conducted explaining morphological identification of different taxa. Pollen morphology of the family has also been examined by Perveen and Qaiser (2006). Sheahan and Cutler (1993) investigated the vegetative anatomy of 37 species in 19 genera of Zygophyllaceae. In present study based on 57 morphological characters were recorded to study the interspecific relationships between taxa present in Balochistan, Pakistan. Plants of Zygophyllaceae reported earlier for its great medicinal importance so the morphological characterization leads towards the validation of taxa used in folk medicines. The results of cluster and principal component analysis revealed that all collected species of *Fagonia* form a well-distinguished group earlier also reported by Kadry (2012). *Fagonia* species indicated the *F.o* and *F.i* closely related and clustered with *F.o.p. F.b.l, F.b.r, F.i.s*. *Tribulus* genus was also reported from the region. Previously El-Hadidi (1975, 1977) classified the species of *Tribulus*. Mohamed (2006) studied seed morphology, proteins and Iso-enzymes in *Tribulus*. Kadry (2012) also characterized different species of *Tribulus*. In present study *T.p* clustered separately. Its closed group was *T.l.p*. while *T.l.l* and *T.l.m* were clusterd together. Its closed group was *T.t.* Van Zyl (2000) presented morphological analysis of

http://www.aloki.hu ● ISSN 1589 1623 (Print) ● ISSN1785 0037 (Online)
DOI: http://dx.doi.org/10.15666/aeer/1802_24452462

the genus Zygophyllum in South Africa. Kadry (2012) also characterized different species of Zygophyllum. *Z.p*. grouped with *Z.f, Z.e* grouped separately, may be because of its diverse habit, plant height and woody stem. *Z.s* grouped with *P.h*. In some previous reports, *Peganum* was placed in a distinct family (Takhtajan, 1969; El Hadidi, 1975). However, Takhtajan (1980) and El Hadidi and Fayed (1995) placed it in Zygophyllaceae. Kadry (2012) grouped *Peganum* with species of Zygophyllaceae as in present study. Shamso et al. (2013) concluded *Zygophyllum* and *Fagonia* linked in one group based on many characters.

Molecular Characterization

The molecular analysis confirmed the characterization of different genus of Zygophyllaceae. Earlier characterizations with in different genera of Zygophyllacae have been reported from many regions of the world. Al-Arjany et al. (2014) worked on molecular diversity among three genera of Zygophyllaceae they displayed the genetic relationships between *Zygophyllum*, *Tribulus* and *Fagonia* species. Their work is in agreement with the present work here we also included *Peganum* with these three genera. All species of *Fagonia* has different pattern as they give amplification on very different pattern. To the knowledge of the authors no earlier work has been reported on the characterization of *Fagoina* species. Bakatoushi and Ahmed (2017) represented the genetic diversity in different wild populations of *Peganum* from desert of Egypt. Molecular analysis of present data of *Fagonia* exhibited no amplification in two species by the selected markers that may be due to varying base pair patterns. Similar findings were earlier reported by Al-arjany et al. (2014). Thus these two species need to be studied with additional diverse molecular markers. As the *F. ovalifolia* var. *pakistanica* is the endemic taxa of the region no earlier report has been found. No molecular characterization data on *Peganum* has been reported earlier from the region. Patil et al. (2014) characterized three species of *Tribulus*. Hammad and Qari (2010) worked on twelve populations of *Zygophyllum* and explained the genetic diversity. Wu et al. (2015) characterized different species of Zygophyllaceae. Few reports also explained the molecular characterization of Zygophyllaceae by Godoy-Bürki et al. (2018) and Kadry (2012). Finding of present study is in agreement with earlier reported work. Molecular characterization plays an important role in characterization of taxa at inter specific and infraspecific level. As these important plants used in folk medicines their authentication is very important. Furthermore, molecular characterization for evaluating genetic diversity has widely been used in conservation biology.

Conclusion and Recommendations

The selected zones of Balochistan have diverse distribution of different genera of Zygophyllaceae. These plants are well adapted in suitable habitats and soil types of these regions. Enormous morphological and molecular markers provide a better understanding in authentication of some controversial taxa that could further be exploited for a novel drug discovery. Furthermore, the unsustainable utilization of these taxa may cause a serious decline. It is thus recommended that conservation strategies must be implemented including cultivation techniques of theses significant medicinal plants to fulfill the needs of local and International herbal market.

http://www.aloki.hu ● ISSN 1589 1623 (Print) ● ISSN1785 0037 (Online)
DOI: http://dx.doi.org/10.15666/aeer/1802_24452462

Acknowledgements. This research project was supported by Higher Education Commission under Start-up Research Grant Program (No. 21-1978/SRGP/R&D/HEC/2018).

REFERENCES

[1] Abbas, G., Hameed, A., Rizwan, M., Ahsan, M., Asghar, M. J., Iqbal, N. (2015): Genetic Confirmation of Mungbean (Vignaradiata) and Mashbean (Vignamungo) Interspecific Recombinants using Molecular Markers. – Front. Plant Sci. 6: 1107.

[2] Adams, P. A., Schwarzbach, A. E., Naresh, P. R. (2003): The concordance of terpenoid, ISSR and RAPD markers, and ITS sequence data sets among genotypes: an example from Juniperus. – Bioch. Sys. and Eco. 31: 375-387.

[3] Al-Arjany, K. M., Bukhari, N. A. W., Ibrahim, M. M. (2014): Molecular diversity among three genera of Zygophyllaceae. – Conference Proceedings ICABEE. 1-6.

[4] Beier, B. A., Chase, M. W., Thulin, M. (2003): Phylogenetic relationships and taxomony of subfamily Zygophylloideae (Zygophyllaceae) based on molecular and morphological data. – Plant Systematics and Evolution 240: 11-39.

[5] Bellstedt, D. U., Van Zyl, L., Marais, E. M., Bytebier, B. L. G., De Villiers, C. A., Makwarela, A. M., Dreyer, L. L. (2008): Phylogenetic relationships, character evolution and biogeography of southern African members of genus *Zygophyllum* (Zygophyllaceae) based on three plastid regions. – Molecular Phylogenetics and Evolution 47: 932-949.

[6] Doyle, J. J., Doyle, J. L. (1987): A rapid DNA isolation procedure for small quantities of fresh leaf material. – Phytochemical bulletin 19: 11-15.

[7] El-Bakatoushi, R., Ahmed, D. G. A. (2017): Evaluation of genetic diversity in wild populations of *Peganum harmala* L., a medicinal plant. – Journal of Genetic Engineering and Biotechnology 16(1): 143-151.

[8] El-Hadidi, M. N. (1975): Zygophyllaceae in Africa. – Boissieria 24: 317-323.

[9] El-Hadidi, M. N. (1977): Two new Zygophyllum species from Arabia. – Publication of Cairo University Herbarium 7/8: 327-331.

[10] El-Hadidi, M. N., Fayed, A. A. (1995): Materials for an Excursion Flora of Egypt. – Taeckholmia 15: 40-53.

[11] Fazal, H., Ahmad, N., Abbasi, B. H. (2013): Identification, Characterization, and Palynology of High-Valued Medicinal Plants. – The Scientific World Journal Vol. 2013, 9 pages.

[12] Fransworth, N. R., Soejarto, D. D. (1988): Global importance of medicinal plants. – In: Akerele, O., Heywood, V., Synge, H. (eds.) The Conservation of Medicinal Plants. Proceedings of an international consultation, pp. 25-51.

[13] Ghafoor, A. (1974): *Zygophyllaceae*. – In: Nasir, E., Ali, S. I. (eds.) Flora of Pakistan. Pakistan: Karachi University, 1-35.

[14] Godoy-Bürki, A. C., Acosta, J. M., Aagesen, L. (2018): Phylogenetic relationships within the New World subfamily Larreoideae (Zygophyllaceae) confirm polyphyly of the disjunct genus Bulnesia. – Systematics and Biodiversity 16(5): 453-468.

[15] Goodman, S. M., Ghafoor, A. (1992): The Ethnobotany of southern Balochistan, Pakistan, with particular reference to medicinal plants. – Publication/Field museum of natural history.

[16] Hammad, I., Qari, S. H. (2010): Genetic diversity among *Zygophyllum* (Zygophyllaceae) populations based on RAPD analysis. – Genetics and Molecular Research 9(4): 2412-2420.

[17] Houghton, P., Howes, M. J., Lee, C., Steventon, G. (2007): Uses and abuses of in vitro tests in ethnopharmacology: visualizing an elephant. – Journal of Ethnopharmacology 110(3): 391-400.

http://www.aloki.hu ● ISSN 1589 1623 (Print) ● ISSN1785 0037 (Online)
DOI: http://dx.doi.org/10.15666/aeer/1802_24452462

[18] Hussain, F., Sher, H. (1998): In-situ protection management and conservation of some important medicinal plants of District Swat. Proc. National Seminar on Medicinal Plants of Pakistan. – PGRI, NARC-IUCN Islamabad December 2-3.
[19] Kadry, N. A. K. (2012): A numerical taxonomic study of the family Zygophyllaceae from Egypt. – Acta Botanica Brasilica 26(1): 165-180.
[20] Kang, H. W., Park, D. S., Park, Y. J., You, C. H., Lee, B. M., Eun, M. Y., Go, S. J. (2002): Printing of diverse genomes using PCR with universal rice primers generated from repetitive sequence of Korean weedy rice. – Mol. Cells. 13(2): 72-81.
[21] Kernodle, S. P., Cannon, R. E., Scandalios, J. G. (1993): Concentration of primer and template qualitatively affects product in random amplified polymorphic DNA-PCR. – Biotechniques 14: 362-364.
[22] Manzoor, S., Hameed, A., Khan, M. A., Gul, B. (2017): Seed germination ecology of a medicinal halophyte Zygophyllum propinquum: responses to abiotic factors. – Flora 233: 163-170.
[23] Mohammed, A. H. (2006): Taxonomic Significance of Seed Proteins and Iso-enzymes in *Tribulus* (Zygophyllaceae). – International Journal of Agriculture & Biology 8(5): 573-575.
[24] Nite-Kang, F., Yong, J. N. (2014): The chemistry and biological activities of natural products from Northern African plant families: from Aloaceae to Cupressaceae. – RSC Advances 106(4): 61975-61991.
[25] Noman, A., Hameed, M., Ali, Q., Aqeel, M. (2012): Foliar tissue architectural diversity among three species of genus Hibiscus for better adaptability under industrial environment. – International Journal of Environmental Sciences 2(4): 2212-2222.
[26] Patil, B., Harisha, C. R., Parmar, N., Save, A. (2014): Variants of *Tribulus* species – a scientific study through DNA RAPD molecular characterization. – Indian Journal of Pharmaceutical and Biological Research 2(4): 15-19.
[27] Perveen, A., Qaiser, M. (2008): Pollen flora of Pakistan-XLIX. Zygophyllaceae. – Pakistan Journal of Botany 38(2): 225-232.
[28] Rashmi, A., Sharma, V., Lalit, L. (2008): Molecular characterization of Chaetomium species using URP-PCR. – Genetics and Molecular Bio. 4: 946-943.
[29] Rates, S. M. K. (2001): Plants as source of drugs. – Toxicon 39(5): 603-613.
[30] Ricklefs, R. E., Latham, R. E. (1992): Intercontinental correlation of geographical ranges suggests stasis in ecological traits of relict genera of temperate perennial herbs. – American Naturalist 139: 1305-1321.
[31] Saeed, S., Barozai, M. Y. K., Ahmed, A., Shah, S. H. (2014): Impact of altitude on soil physical and chemical properties in Sra Ghurgai (Takatu mountain range) Quetta, Balochistan. – International Journal of Scientific & Engineering Research 5(3): 730-735.
[32] Saeed, S., Barozai, M. Y. K., Ahmed, A., Tareen, R. B., Ali, G. M., Shehzad, S., Begum, S. (2015): Genetic diversity of Ephedra procera from high altitudes of Quetta valley, Balochistan using RAPD and ISSR. – Pak. J. Weed Sci. Res. 21(2): 163-172.
[33] Saeed, S., Barozai, M. Y. K., Ahmed, A., Tareen, R. B., Begum, S., Ali, G. M. (2017): Impact of Ecological Diversity On Genetic And Phytochemical Variation Injuniperus Excelsa From High Elevation Zones Of Quetta Valley, Pakistan. – Pak. J. Bot. 49(1): 201-206.
[34] Shamso, M., Rabei, S., Hamdy, R. (2013): Identification keys and numerical studies of Zygophyllaceae (*S. Str.*) and allied families in Egypt. – Assiut University Journal of Botany 42(2): 79-106.
[35] Sheahan, M. C., Cutler, D. F. (1993): Contributions of vegetative anatomy to the systematics of Zygophyllaceae R.Br. – Botanical Journal of the Linnean Society 113(3): 227-262.
[36] Takhtajan, A. (1969): Flowering plants: origin and dispersal. – Edinburgh, Oliver and Boyd.

http://www.aloki.hu ● ISSN 1589 1623 (Print) ● ISSN1785 0037 (Online)
DOI: http://dx.doi.org/10.15666/aeer/1802_24452462

[37] Takhtajan, A. (1980): Outline of the classification of the flowering plants (Magnoliophyta). – Botanical Review 46: 225-359.
[38] Tareen, R. B., Bibi, T., Khan, M. A., Ahmad, M., Zafar, M., Hina, S. (2010): Indigenous knowledge of folk medicine by the women of Kalat and Khuzdar regions of Balochistan, Pakistan. – Pakistan Journal of Botany 42(3): 1465-1485.
[39] Van Zyl, L. (2000): A Systematic Revision of *Zygophyllum* in the Southern African Region. – Ph.D. thesis, University of Stellenbosch.
[40] Wu, S. D., Lin, L., Li, H. L., Yu, S. X., Zhang, L. J., Wang, W. (2015): Evolution of Asian Interior Arid-Zone Biota: Evidence from the Diversification of Asian Zygophyllum (Zygophyllaceae). – PLoS ONE 10(9): e0138697.
[41] Yong, J. N., Nite-Kang, F. (2015): The chemistry and biological activities of natural products from Northern African plant families: from Ebenaceae to Solanaceae. – RSC Advances 34(5): 26580-26595.
[42] Zaidi, M. A., Crow, S. A. Jr. (2005): Biologically active traditional medicinal herbs from Balochistan, Pakistan. – Journal of Ethnopharmacology 96: 331-334.

http://www.aloki.hu ● ISSN 1589 1623 (Print) ● ISSN1785 0037 (Online)
DOI: http://dx.doi.org/10.15666/aeer/1802_24452462

PROPAGATION TECHNIQUES AND THEIR EFFICACY RATE IN *PROSOPIS CINERARIA* (L) DRUCE – A MULTIPURPOSE TREE OF CHOLISTAN DESERT, PAKISTAN

RAFAY, M.[1*] – ALI, M. Y.[1] – ABDULLAH, M.[3] – MALIK, Z.[4] – RIAZ, U.[1] – ABID, M.[1] – FAROOQI, M. A.[2] – AKHTAR, S.[2]

[1]*Department of Forestry, Range and Wildlife Management, The Islamia University of Bahawalpur, Bahawalpur, Pakistan*

[2]*Department of Entomology, The Islamia University of Bahawalpur, Bahawalpur, Pakistan*

[3]*Cholistan Institute of Desert Studies, The Islamia University of Bahawalpur, Bahawalpur, Pakistan*

[4]*Department of Soil Science, The Islamia University Bahawalpur, Bahawalpur, Pakistan*

**Corresponding author*
e-mail: Rafay@iub.edu.pk

(Received 18th Apr 2018; accepted 20th Sep 2018)

Abstract. The present work is an effort to determine the best and easiest method of producing plant of *Prosopis cineraria* from branch cutting. The root initiating hormones IBA were used for vegetative propagation of *Prosopis cineraria.* The results of this research well help in reducing the size of shoot being used in vegetative propagation. It will also reduce the plant genotypic variability and will help to ensure increased germination percentage by determining the best dose of root initiating hormones and different cutting sizes. Sprouting percentage is very important to predict the behavior of the tree if any species is to be propagated by asexual method of shoot cutting. Overall 15.24 cm cutting at open air was found best (2.38 C) in all the treatments, but it sprouted maximum in growth regulator IBA (3.71 A). Production of more number of leaves is also an important factor in determining the fodder value of the plant. Under the individual factor highest number of leaves (4.21 A) was produced by the 15.24 cm cuttings with IBA and least was produced by the 5.08 cm cutting in open air. The number of leaves produce was higher in 10.16 cm cuttings with (3.44 A) in polythene sheet compared to open air. Plant height showed its peak value (2.21 A) in 15.24 cm cutting with provided IBA and least height (1.23 C) was noted in 15.24 cm cutting without growth regulator. The second peak value was observed (1.78 B) in 5.08 cm cutting followed by (1.75 B) in 10.16 cm cutting. Root length indicated its peak value (2.18 A) in 15.24 cm cutting with provided IBA and least height (1.19 B) was noted in 15.24 cm cutting.
Keywords: *variability, vegetative, growth regulator, IBA, sprouting*

Introduction

Prosopis cineraria (L.) belongs to the (Family Fabaceaea) which is extraordinary versatile tree species of Cholistan Desert. This tree is locally called Jhand which holds the vital place in rural bargain in the southern region of the Punjab, Pakistan. The genus *Prosopis* contains about 44 species of shrubs and trees scattered mainly in the dry regions of the Southwest part of Asia, Africa and generally America from the western North America to Patagonia (Liu et al., 2012; Puri and Kumar, 1995). Therefore all the parts of this tree are useful, it is also known as "wonder tree" and "king of desert". It is a small, irregularly forked and thorny tree which is about 5-10 m in height. It has uneven, thick and grey bark with the deep gaps. Roots are very bottomless; the tap root of *P. cineraria* may enter perpendicularly nearly about 20 m or more (Mahoney, 1990; Preek et al., 2015). *Prosopis cineraria* are an imperative member of the arid, semiarid

http://www.aloki.hu ● ISSN 1589 1623 (Print) ● ISSN 1785 0037 (Online)
DOI: http://dx.doi.org/10.15666/aeer/1802_24632474

environments of the sub-tropical and tropical area around the world (Sushant et al., 2010). Maximum species of the *Prosopis* originate in the Americas, and the only four species of *Prosopis*is arising outside the America, in region like Southwest Asia and Africa (Atalano et al., 2008).

In Pakistan this species *is* found wildly and well adopted to the semiarid and arid condition of the Pakistan may be due to their well-developed and extensive tap root system, which reaches nearly to the length of 20 m habitually reaching out to the ground resources of the water (Gehlot et al., 2008). It becomes an important factor of the desert Ecosystem in the Pakistan as the biomass producer and as leguminous tree which enriches the desert soil, fixes atmospheric nitrogen and offers a green coverage. It donates to ecological constancy of the region and providing the wide support to human beings, nutrient deficient soils and the livestock (Chaudhry and Castle 2011). Furthermore, this plant species also provide remaining fuel wood for cooking and the heating in utmost households and restoration of despoiled lands in the arid and semiarid areas (Oduor and Githiomi 2013). All the closely related species of *Prosopis* keeps the similar morphology and their identification can be difficult, especially in the absence of fruit and flowers. In adding, the environment can have wide ranging effects on plant form, growth and leaf characteristics (Pasiecznik et al., 2001), and closely related species of *Prosopis* are known to crossbreed readily (Hunziker et al., 1986; Chaudhry, 2011).

Prosopis cineraria are one of the highly valued plant in the native system of medicine. It is also known to possess antibacterial, anthelmintic antifungal, anticancer antiviral and many other pharmacological qualities (Malik and Kalidhar, 2007). *Prosopis cineraria* an evergreen or nearly so, it forms an open crown and has thick, uneven grey bark with profound gaps (Rajesh et al., 2012). Its slim, glabrous and armed branches with prickles of 3-4 cm length, that is slightly compacted, straight and scattered. Flower is in the form of axillary spines with 7-11 cm length, either lonely or in terminal panicles. Flowers have yellow corolla, attracting a bulk of insects including great number of *Apis florae* and various other wild bees in December and April months (Gorain et al., 2012). It possesses bipinnately compound leaves, alternate in organization. The leaflets are 15–18 pairs, and designed rectangle with an entire margin, apiculate apex, obtuse base, glabrous surface, reticulate venation, petiolate, and the petiole is 0.5-4 cm long. The typical leaf size is 2.5 cm (length) and 1 cm (breadth). Morphologically, fresh leaves are green in colour, and are odorless with a bitter palatability (Dharani et al., 2011). The general phenological phase of Jhand, mainly flowering and fruiting will be in May-June of summer season. New leaf formation due to high protein content during end of summer (June-August) guarantees the availability of fodder to the livestock in severe summer period (Raj and Hooda, 1994; Chaudhry and Castle 2011). Their wood is valuable for making cart, house construction and agricultural tools (Gupta et al., 1998; Preek et al., 2015).

Existing shrinkage of forest area is due to some obvious factors. Clearing of forest for cultivation of farm crops and for fuel wood are among major factors. Our forest department, despite of their tiresome efforts are ineffective to raise the forest area even by 1% (FAO 2004). At this stage Pakistan is capable in forest resource even to meet growing local demand of wood. Pakistan is an agrarian country; the existing forests cover is only 4.8% of its area. This is very low as compared to desired ratio of 25% which is declared for sustained economic development and to encounter the wood demand of a country. The use of cutting is the best vital method for reproducing new

http://www.aloki.hu ● ISSN 1589 1623 (Print) ● ISSN 1785 0037 (Online)
DOI: http://dx.doi.org/10.15666/aeer/1802_24632474

plants. During the favourable situation cutting any isolated plant part that for rebirth will produce new plant similar to the parent plant (Singh et al., 2015). In this situation agro-forestry is best solution where the forest land cannot increase. In this way we can not only produce extra amount of wood to meet our domestic demands but can also complete the goals of exports for our valued wood product. It has been estimated that of our 10% farmland area can be brought under agro forestry without destroying of our farm crops.

In our land just about concerning 330 million timber standing throughout the entire farmland with the standing up with the amount of 70 million m^3 (Qurashi, 1998; Kaushik and Kumar, 2003; FAO 2004). The vegetative reproduction has been one response. The capability to harness bigger genetic characters through the asexual reproduction is being observed in various forest tree development plans. This method of reproduction is fast becoming a very vital nursery controlling tool because of reduced time requirement for cutting of larger trees to root and grow (Hudson, 1997; Singh et al., 2007). The present work is best and easiest method to determine the method of producing plant of *Prosopis cineraria* from branch cutting. The root initiating hormones IBA were used for asexual propagation of *Prosopis cineraria.* The results of this research will play an important role in reducing the size of shoot being used in asexual propagation and it will also reducing the plant genotypic variability and will help to ensure increased germination percentage by determining the finest amount of root initiating hormones. The research was conducted to check the propagation potential in shoot cuttings of *Prosopis cineraria* collected from various locations in Cholistan desert. To check the individual effects at various concentrations of growth hormone like IBA in inducing the root formation in *Prosopis cineraria* cuttings. To relate the propagation potential of various sizes of cuttings as a growing stocks.

Materials and methods

The research work was carried out in the nursery area, Department of Forestry, Range and Wildlife Management, The Islamia University of Bahawalpur during the last week February in 2015. The site is located at the latitude 36°-26”N and longitude of 73°-06”E. Altitude of site is 184.4 m. Different sized cuttings of *Prosopis cineraria* were collected from a healthy tree of *Prosopis cineraria* from the various locations of Cholistan desert.

Collection of plant samples

Selection of tree was done on following phenotypic qualities.

(1) The age of tree should be between 20-25 years. (2) The plant which is selected should be disease free, with leaves and branches. (3) The selected plant should have more and straight bole. Approximately one year old branches of thumb thickness were selected.

Size of cutting

Cutting of three sizes i.e. 5.08 cm, 10.16 cm and 15.24 cm were prepared. While preparing, the cuttings were taken to avoid that the bark may not get damaged. Flush cutting was done to avoid the peeling away of the bark. A slanting cut was given on the upper end of cutting to avoid fungal attack. The cuttings were dipped in bleach solution carefully prepared at a ratio of 1: 4 in water. Cuttings were planting in polythene bags

http://www.aloki.hu ● ISSN 1589 1623 (Print) ● ISSN 1785 0037 (Online)
DOI: http://dx.doi.org/10.15666/aeer/1802_24632474

(6 cm × 18 cm). These polythene bag were filled with silt, sand and clay in equal ratio, which acted as the rooted medium.

Application of IBA

Treating with root initiating hormone, the root initiating hormones, Indole butyric acid (IBA) were used in 4000 ppm. Basal 1/3 portion of cutting were dipped in the root initiating hormone solution for 16 h (Ram et al., 2013).

Data collection

Three parameters were studied along with their interaction. Following six treatments were applied to different cuttings. Only 15.24 cm cuttings were applied to the root initiating hormones, Indole butyric acid (IBA) in open air to check its effect on different growth parameters. Cuttings of different sizes 5.08 cm and 10.16 cm in pen air and under Polythene sheet were used. Cuttings were observed daily but the measurement were taken after every 7 days interval. The last reading was taken after sixty days. Data on Sprouting percentage, Number of leaves, Plant height and Root length were recorded during experiment.

Statistical analysis

Experiment was carried out according to CRD (Complete randomized design) (Steel et al., 1997).

Results and discussion

The present work was an effort to determine the best and easiest method of producing plants of *Prosopis cineraria* from branch cuttings. The root initiating hormone lndole butyric acid was applied on the branch cuttings of *Prosopis cineraria*. This research was an effort to reduce the size of shoot being used in vegetative propagation. This method reduces the plant genotypic variability.

Sprouting percentage

Sprouting percentage always plays an important role for a good future crop. If there is more sprouting it means the cultural practices you are doing and planting material used is satisfactory. Environmental conditions are also important for good sprouting. High sprouting percentage is the primary requirement for a good nursery business. Sprouting percentage is very important to predict the behaviour of the tree if any species is to be propagated by asexual method of shoot cutting. Good sprouting percentage is a perquisite for a healthy future crop stand. Analysis of variance for the sprouting per outing are given *Table 1* and the comparison of means for the factors like cutting size and Growth hormones are given in *Table 1* and overall sprouting % age given in *Table 1*. From the results of the sprouting percentage it is clear that 15.24 cm cutting under growth regulator IBA gave the best result with sprouting. Overall 15.24 cm cutting at open air was found best (2.38 C) in all the treatments as shown in *Table 1* but it sprouted maximum in growth regulator IBA (3.71 A) as shown in *Table 1*. 10.16 cm cuttings were also good (3.12 B) in polythene sheet as shown in *Table 1,* but showed less sprouting than 15.24 cm. 5.08 cm cutting showed good sprouting in polythene and

http://www.aloki.hu ● ISSN 1589 1623 (Print) ● ISSN 1785 0037 (Online)
DOI: http://dx.doi.org/10.15666/aeer/1802_24632474

it was even lower in open air as shown in (*fig. 1*). Our findings are in the line of Ngo Mpeck et al. (2003), Wang et al. (1997) and Edson et al. (1991). Cuttings were observed very carefully and after 30 days sprouting percentage was calculated by (Mebrahtu and Hanover 1990).

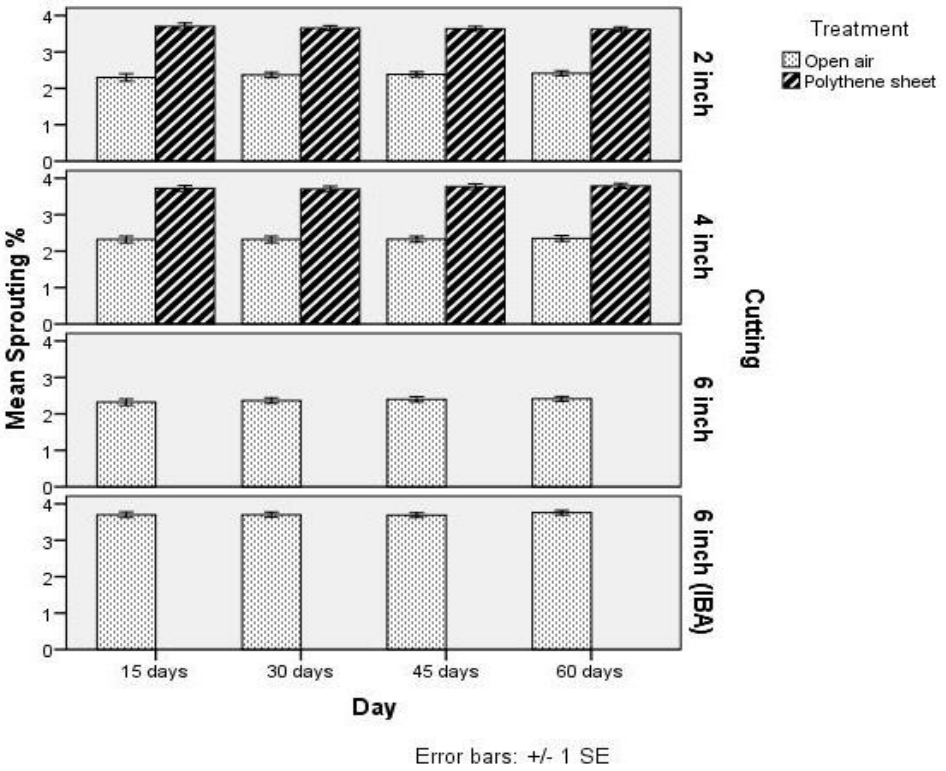

Figure 1. *Sprouting percentage as affected by different cutting sizes*

Table 1. *Comparison between open air and polythene sheets regarding number of leaves, sprouting percentage, height (cm) and root length (cm) for overall data*

Parameter	Treatment	N	Mean	SD	SE	t-value	Prob
No. of leaves	Open air	1005	3.04	0.958	0.030	-19.37**	0.000
	Polythene sheet	571	3.93	0.684	0.029		
Sprouting %	Open air	1005	2.77	0.857	0.027	-22.81**	0.000
	Polythene sheet	571	3.70	0.611	0.026		
Height (cm)	Open air	1005	1.51	0.516	0.016	-30.72**	0.000
	Polythene sheet	571	2.22	0.253	0.011		
Root length (cm)	Open air	1005	1.50	0.497	0.016	-30.68**	0.000
	Polythene sheet	571	2.16	0.166	0.007		

** = highly significant (P < 0.01); N = number of observations; SD = standard deviation; SE = standard error

Number of leaves

The number of leaves is important for the good growth of plants, if a plant has more leaves it means the plant will utilize the sunlight in a more efficient way and the plant

http://www.aloki.hu ● ISSN 1589 1623 (Print) ● ISSN 1785 0037 (Online)
DOI: http://dx.doi.org/10.15666/aeer/1802_24632474

overall will be healthy. Number of leaves also determines the growth of plants at nursery stage. The plant having more leaves are more vigorous in their growth and are stable than the plants having less number of leaves. Production of more number of leaves is also an important factor in determining the fodder value of the plant (Rafay et al., 2013). After 15 days under the individual factor highest number of leaves (4.21) was produced by the 15.24 cm cuttings with IBA as shown in *Figure 2* and least was produced by the 5.08 cm cuttings in open air. Number of leave was produce (3.44) more in 10.16 cm cutting in polythene sheet as compared to open air as shown in *Table 1*. Different scientists observed that 15.24 cm cuttings growth is better and produce more number of leaves in plastic tunnels (Pomper et al., 2002). After 30, 45 and 60 days highest numbers of leaves were produces by the 15.24 cm cutting as shown in *Figure 2* with growth hormone IBA in open air and the least number of leaves were produced by the 5.08 cm cutting in open air. In 10.16 cm cutting number of leaves are more as compared to 5.08 cm cutting in polythene sheet. Other scientists observed that under plastic sheets 15.24 cm cutting showed better growth and produce more number of leaves (Rafay et al., 2013).

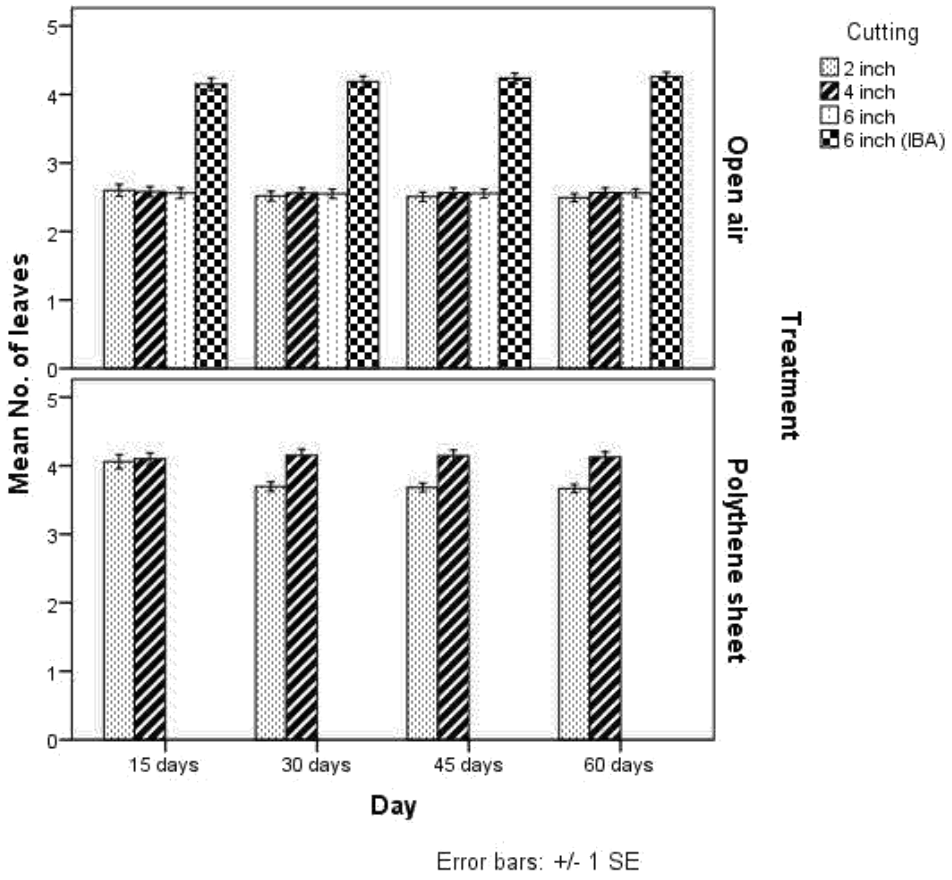

Figure 2. *Mean comparison of leaves in different cutting size*

Plant height (cm)

Plant height is measured in order to determine the total length of the plant (Root and Shoot). Plant height in open air after fifteen days showed its peak value (2.20 A) in 15.24 cm cutting with provided IBA and least height (1.23 C) was noted in 15.24 cm

http://www.aloki.hu ● ISSN 1589 1623 (Print) ● ISSN 1785 0037 (Online)
DOI: http://dx.doi.org/10.15666/aeer/1802_24632474

cutting without growth regulator. Second peak value (1.19 B) in 5.08 cm cutting followed by (1.19 B) in 10.16 cm cutting. Plant height in polythene sheet after fifteen days showed its peak value (2.20 A) in 10.16 cm cutting and least height (1.20 A) was noted in 5.08 cm cutting. 10.16 cm cutting was noted to be highly significant as given in *Figure 3*. Plant height in open air after thirty days showed its peak value (2.20 A) in 15.24 cm cutting with provided IBA and least height (1.19 B) was noted in 10.16 cm cutting. Second peak value (1.22 B) in 15.24 cm cutting without growth regulator followed by (1.20 B) in 5.08 cm cutting. Plant height in polythene sheet after thirty days showed its peak value (2.22 A) in 5.08 cm cutting and least height (2.20 A) was noted in 10.16 cm cutting. 5.08 cm cutting was noted to be highly significant as given in *Table 1*. Plant height in open air after forty five days showed its peak value (1.52 A) in 15.24 cm cutting with provided IBA and least height (1.19 B) was noted in 10.16 cm cutting. Second peak value (1.23 B) in 15.24 cm cutting without growth regulator followed by (1.22 B) in 5.08 cm cutting. Plant height in polythene sheet after forty five days showed its peak value (2.25 A) in 5.08 cm cutting and least height (2.19 A) was noted in 10.16 cm cutting. In these factors the factor A of 5.08 cm cutting was noted to be highly significant as given in *Table 1*. Plant height in open air after sixty days showed its peak value (2.21 A) in 15.24 cm cutting with provided IBA and least height (1.21 B) was noted in 10.16 cm cutting. Second peak value (1.25 B) in 15.24 cm cutting without growth regulator as well as (1.25 B) in 5.08 cm cutting. In these factors the factor A was found to be highly significant as given in *Table 1*. Plant height in polythene sheet after sixty days showed its peak value (2.26 A) in 5.08 cm cutting and least height (2.20 A) was noted in 10.16 cm cutting. 5.08 cm cuttings were noted to be highly significant as given in *Table 1* (*Figs. 4* and *5*).

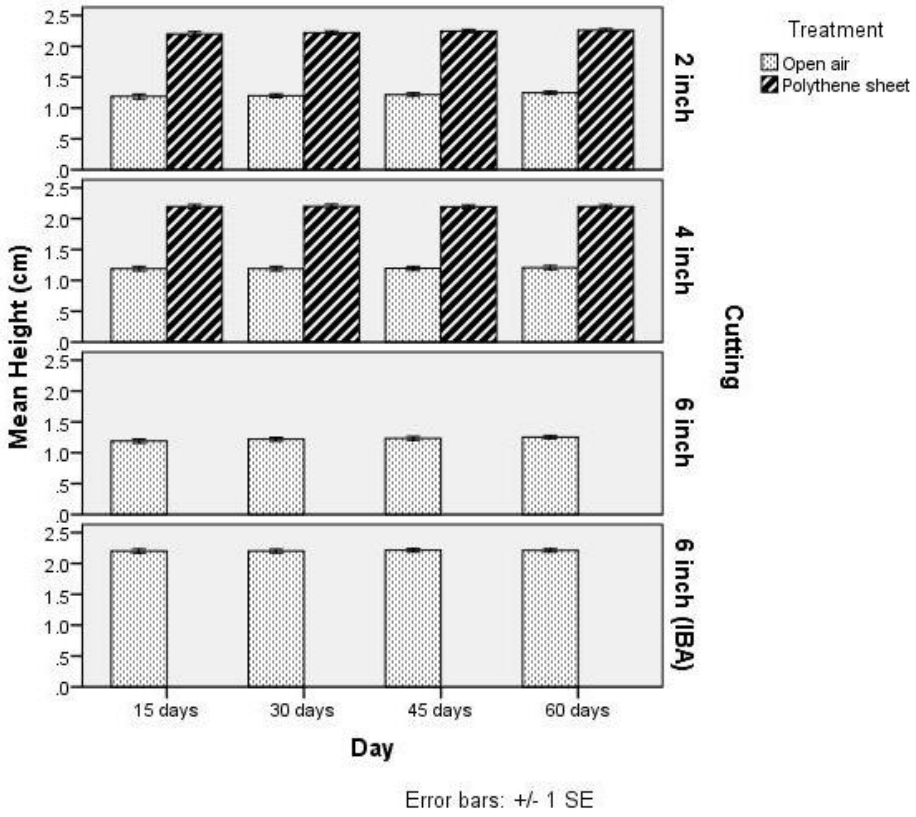

Figure 3. *Height affected by different cutting sizes*

http://www.aloki.hu ● ISSN 1589 1623 (Print) ● ISSN 1785 0037 (Online)
DOI: http://dx.doi.org/10.15666/aeer/1802_24632474

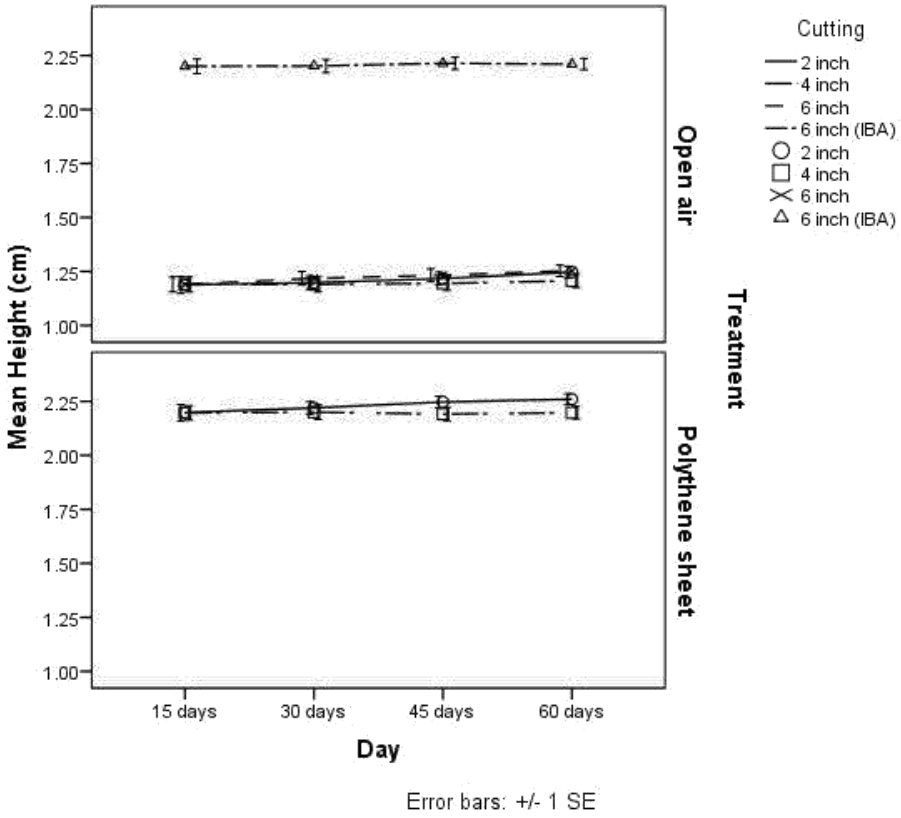

Figure 4. *Height in open air and polythene sheet*

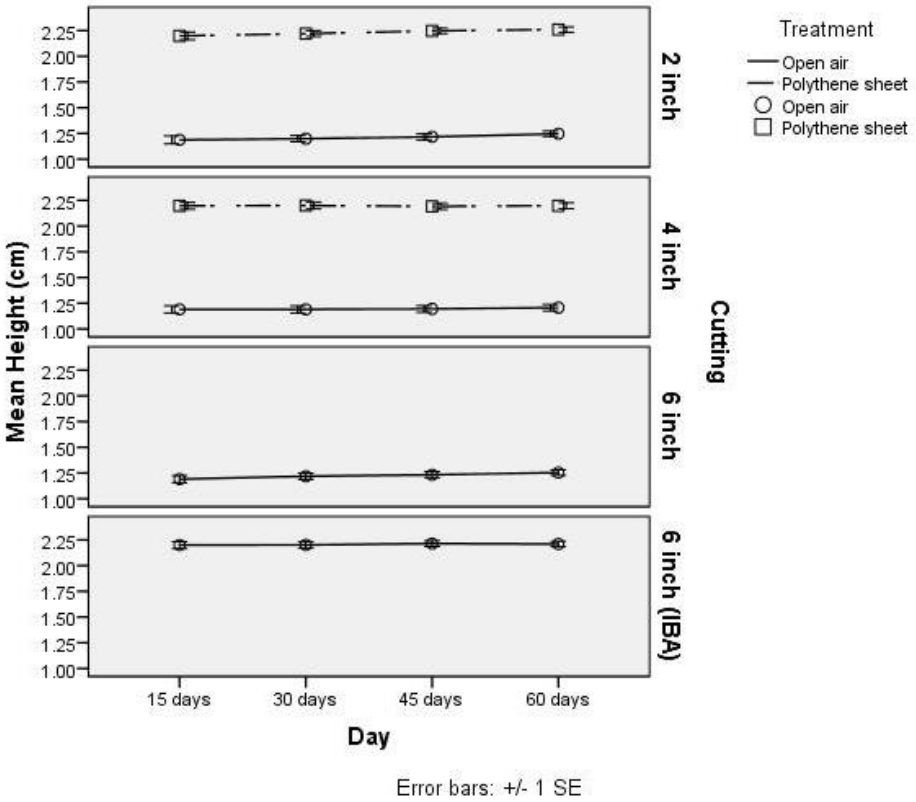

Figure 5. *Height affected by different cutting size*

http://www.aloki.hu ● ISSN 1589 1623 (Print) ● ISSN 1785 0037 (Online)
DOI: http://dx.doi.org/10.15666/aeer/1802_24632474

Root length (cm)

Root is the basic organ, which plays a vital role in the plant development. Roots not only provide anchorage to the plant but also absorb important nutrients which are essential for the growth of the plant. A root goes deeper into the soil and explores the soil mass for more and more nutrients. Root length determines the growth of the plant. The plants having healthy and more vigorous roots are healthier than those with weak root system. Good plant root system developed at the early stages of plat growth is the prerequisite for the good survival percentage of the crop. Analysis of variance for the root length in open air taken after 15 days and mean comparison of 5% level of significant is given in the *Table 1*. Analysis of variance for the root length in polythene sheets taken after 15 days and mean comparison of 5% level of significant is given in the *Table 1*. Root Length in open air after fifteen days showed its peak value (2.14 A) in 15.24 cm cutting with provided IBA and least height (1.19 B) was noted in 5.08 cm cutting as shown in *Table 1*. After that (1.20 B) value was recorded in 10.16 cm cutting as well as in 15.24 cm cutting without growth regulator. Root Length in polythene sheet after fifteen days showed its peak value (2.14 A) in 10.16 cm cutting and least height (2.14 A) was noted in 5.08 cm cutting (*Fig. 6*).

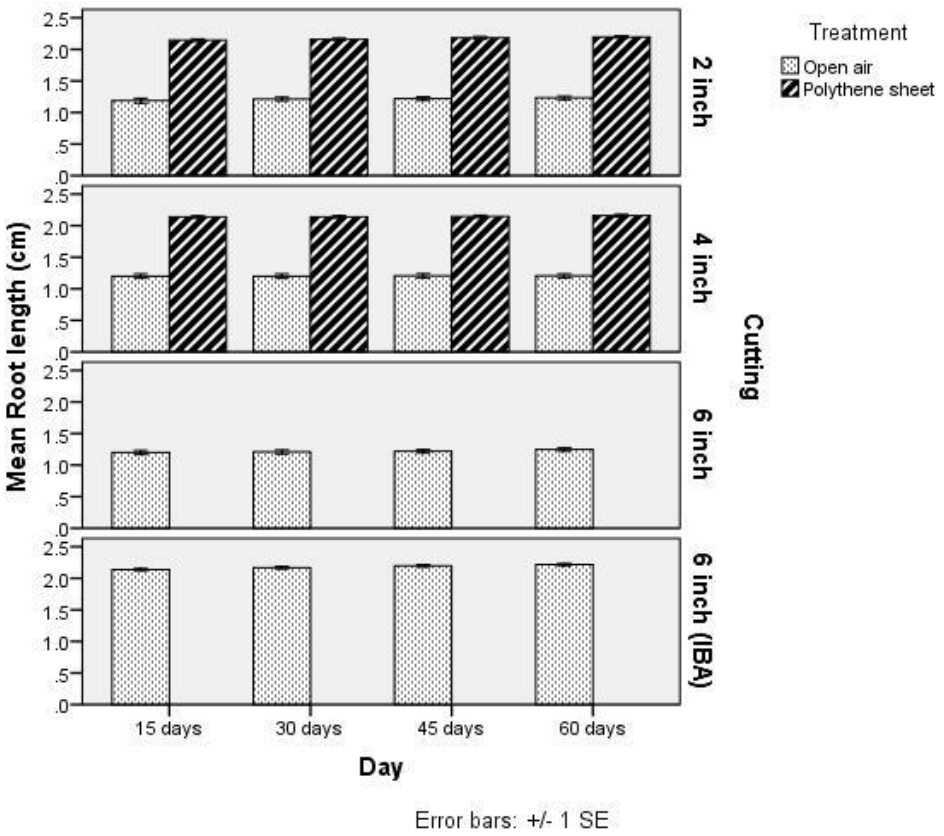

Figure 6. *Root length in open air and polythene sheet*

Analysis of variance for the root length in open air taken after thirty days and mean comparison of 5% level of significant is given in *Table 1*. Analysis of variance for the root length in polythene sheets taken after thirty days and mean comparison of 5% level of significant is given in *Table 1*. Root Length in open air after thirty days showed its

http://www.aloki.hu ● ISSN 1589 1623 (Print) ● ISSN 1785 0037 (Online)
DOI: http://dx.doi.org/10.15666/aeer/1802_24632474

peak value (2.17 A) in 15.24 cm cutting with provided IBA and least height (1.20 B) was noted in 10.16 cm cutting. After that (1.21 B) value was recorded in 5.08 cm cutting as well as in 15.24 cm cutting without growth regulator. Root Length in polythene sheet after thirty days showed its peak value (2.16 A) in 5.08 cm cutting and least height (2.14 A) was noted in 10.16 cm cutting. Analysis of variance for the root length in polythene sheets taken after forty five day and mean comparison of 5% level of significant is given in *Table 1*. Root Length in open air after forty five days showed its peak value (2.20 A) in 15.24 cm cutting with provided IBA and least height (1.21 B) was noted in 10.16 cm cutting. After that (1.22 B) value was recorded in 5.08 cm cutting as well as in 15.24 cm cutting without growth regulator. Root Length in polythene sheet after forty five days showed its peak value (2.18 A) in 5.08 cm cutting and least height (2.14 A) was noted in 10.16 cm cuttings. Root Length in open air after sixty days showed its peak value (2.22 A) in 15.24 cm cutting with provided IBA and least height (1.21 B) was noted in 10.16 cm cutting. After that (1.25 B) value was recorded in 15.24 cm cutting without growth regulator followed by (1.23) in 5.08 cm cutting. Root Length in polythene sheet after sixty days showed its peak value (2.20 A) in 5.08 cm cutting and least height (2.16 A) was noted in 10.16 cm cutting. Jhand is a desert tree species and it is a difficult species to root unlike *Teerminalia chebula* which sprouted after 30 days (Jose and thomas 1998). Best rooting was observed in IAA, which is in contradiction with the other scientists who found IBA, the most effective auxin (Palanisamy et al., 1998; Reddy et al., 1998; Hee et al., 1997; McGuigan et al., 1996; Wang et al., 1997).

Conclusions

Indole Butyric Acid (IBA) was used to determine the different parameter including the sprouting percentage, number of leaves, plant height and root length. In open air experiment, 15.24 cm cuttings showed excellent results. Maximum number of leaves during air experiment by using 15.24 cm cuttings were 4.21 A. similarly sprouting was maximum at 3.71 A in open air. Best height was obtained from 15.24 cm cuttings with 2.21 A. Root length at 2.18 A for 15.24 cm cuttings were maximum. During open air experiment it was observed that numbers of leaves were reduced with the reduction in cutting size. While under polythene sheet at 3.44 A maximum number of leaves was produced by using 10.16 cm cuttings. Maximum heights were obtained from 15.24 cm cuttings with 2.21 A. minimum height was shown from 15.24 cm cuttings without regulator. So these treatments showed best result for maximum growth, sprouting, heights and number of leaves of *Prosopis cineraria*. We can get desired plant by applying these conditions on our nursery to ensure better results in future.

REFERENCES

[1] Atalano, S., Vilardi, J., Tosto, D., Saidman, B. (2008): Molecular phylogeny and diversification history of *Prosopis* (Fabaceae: Mimosoideae). – Biological Journal of the Linnean Society 93(3): 621-640.

[2] Chaudhry, Q., Castle, L. (2011). Food applications of nanotechnologies: an overview of opportunities and challenges for developing countries. Trends in Food Science & Technology, 22(11), 595-603.

http://www.aloki.hu ● ISSN 1589 1623 (Print) ● ISSN 1785 0037 (Online)
DOI: http://dx.doi.org/10.15666/aeer/1802_24632474

[3] Chaudhry, P. (2011). *Prosopis cineraria* (L) Druce: A life line tree species of the Thar Desert in danger.
[4] Dharani, B., Sumathi, S., Sivaprabha, J., Padma, P. R. (2011): In vitro antioxidant potential of *Prosopis cineraria* leaves. – J. Nat. Prod. Plant Resource 1(3): 26-32.
[5] Edson Jhon, L., Wenny David, L., Lauren, F. (1991): Propagation of western larch by stem cutting. – Western Journal of Applied Forestry 6(2): 115-125.
[6] FAO (2004): Introduction. National forest products Statistics, Pakistan. – http//www.fao.org./DOCREP/005AC778E15.html.
[7] Gehlot, P., Bohra, N. K., Purohit, D. K. (2008): Endophytic mycoflora of inner bark of *Prosopis cineraria* - a key stone tree species of Indian desert. – American-Eurasian Journal of Botany 1(1): 1-4.
[8] Gorain, M., Charan, S. K., Ahmed, S. I. (2012): Role of insect bees in the pollination of *Prosopis cineraria* (L.) Druce (Leguminosae, Subfamily Mimosideae) in Rajasthan. – Advances in Applied Science Research 3(6): 3448-3451.
[9] Gupta, G. N., Singh, G., Kachwaha, G. R. (1998): Performance of *Prosopis cineraria* and associated crops under varying spacing regimes in the arid zone of India. – Agr. Sys. 40: 149-157.
[10] Hee, H. B., Young, J. H., Young, K. J. (1997): In vitro propagation of *Ficus benjimana* by shoot tip culture. – Journal of Korean Society for Horticultural Sciences 38(3): 315-319.
[11] Hudson, K. (1997): Overview of Cutting Propagation. – FY 614, 3/7/97. University of Auburn, Auburn, AL.
[12] Hunziker, J., Saidman, B. O., Naranjo, C. A., Palacios, R. A., Poggio, L., Burghardt, A. D. (1986): Hybridization and genetic variation of Argentine species of *Prosopis.* – Forest Ecology and Management 16: 301-315.
[13] Jose, P., Thomas, A. J. (1998): An account of the vegetative propagation in *Terminalia chebula* Retz. – Indian forester 124(5): 357-359.
[14] Kaushik, N., Kumar, V. (2003): Khejri (Prosopis cineraria)-based agroforestry system for arid Haryana, India. – Journal of Arid Environments 55(3): 433-440.
[15] Liu, Y., Singh, D. and Nair, M. G. (2012): Pods of Khejri (Prosopis cineraria) consumed as a vegetable showed functional food properties. – Journal of Functional Foods 4(1): 116-121.
[16] Mahoney, D. (1990): Trees of Somalia - A Field Guide for Development Workers. – Oxfam/HDRA, Oxford, pp. 133-136.
[17] Malik, A., Kalidhar, S. B. (2007): Phytochemical investigation of Prosopis cineraria L. (Druce) leaves. – Indian Journal of Pharmaceutical Science 69: 576-578.
[18] McGuigan, P. J., Blazich, F. A., & Ranney, T. G. (1996). Propagation of Quercus myrsinifolia and Quercus canbyi by stem cuttings. Journal of Environmental Horticulture, 14(4), 217-220.
[19] Mebrahtu, T., Hanover, J. W. (1990): The effect of root cutting size on the time of sprouting of Black Locust. – Nitrogen Fixing Trees Research Report 8: 156-158.
[20] Mpeck, M.-L., Tchoundjeu, Z., Asaah, E (2003): Vegetative propagation of *Pausinystalia johemble* k. Schum. By leafy stem cuttings. – Propagation of ornamental plants 3(2): 11-18.
[21] Oduor, N. M., Githiomi, J. K. (2013) Fuel-wood energy properties of Prosopis juliflora and Prosopis pallida grown in Baringo District, Kenya. – African Journal of Agricultural Research 8(21): 2476-2481.
[22] Palanisamy, K., Ansari, S. A., Kuma, P., Gupta, B. (1998): Adventitious root in shoot cuttings of *Azadirachta indica* and *Pogamia pinnata*. – New Forest 16(1) 81-88.
[23] Pasiecznik, N. M., Felker, P., Harris, P. J., Harsh, L., Cruz, G., Tewari, J. C., ... & Maldonado, L. J. (2001). The' *Prosopis juliflora'*-'Prosopis pallida'complex: a monograph (Vol. 172). Coventry: HDRA.

http://www.aloki.hu ● ISSN 1589 1623 (Print) ● ISSN 1785 0037 (Online)
DOI: http://dx.doi.org/10.15666/aeer/1802_24632474

[24] Pomper, K. W., Layne, D. R., Jones, S. C. (2002): Incidence Irradiance and cupric hydroxide container treatment effects on early growth and development of container Grown Pawpaw seedling. – J. Amer. Soc. Hort. Sca. 127(1): 13-19.
[25] Preek, A. K., Garg, S., Kuma, M. (2015): Prosopis cineraria: a gift of nature for pharmacy. – Int. J. Pharma Sci. Res. 6(6): 958-964.
[26] Puri, S., Kumar A. (1995): Establishment of *Prosopis cineraria* (L.) Druce in the hot deserts of India. – New forests 9: 21-33.
[27] Qurashi Masood, A. A. (1998): Basic of Forestry and Allied Sciences. Vol. 1. – Department of Forestry, University of Agriculture Faisalabad.
[28] Rafay, M., Khan, R. A., Yaqoob, S., Ahmad, M. (2013): Nutritional evaluation of major range grasses from Cholistan Desert. – Pakistan Journal of Nutrition 12: 23-29.
[29] Raj, B., Hooda, M. S. (1994): Studies on phenology and breeding system of *Jand* (*Prosopis cineraria* (L.) Druce). – Crop Res. 7(3): 473-478.
[30] Rajesh., K., Verma, K. S., Chaturvedi, O. P., Alam, N. M. (2012): Leaf litter decomposition and nutrient dynamics in four multipurpose tree species. – Range Management and agroforestry 33(1): 20-27.
[31] Ram, Newaj ., Dhyani, S., Badre, K., Ajit, A., Rajendra, P., Handa, A. K., Upendra, K., Shikha, N. (2013): Long term effect of root management practices on rooting pattern in *Dalbergia sissoo* and grain yield of mustard under agrisilviculture system. – Range Management and Agro Forestry 34(1): 47-50.
[32] Reddy, P. S. A., Rajasekhar, G., Gopal, R. (1998): Vegetative propagation of *Acacia concinna* DC by stem cutting. – Indian forester 124(3): 264-266.
[33] Singh, G., Mutha, S., Bala, N. (2007): Effect of tree density on productivity of a Prosopis cineraria agroforestry system in North Western India. – Journal of Arid Environments 70(1): 152-163.
[34] Singh, Y. P., Vijay, D., Malaviya, D. R. (2015): Effect of cutting management on seed yield and quality attributes of tetraploid berseem. – Range Management and Agro Forestry 36(1): 47-51.
[35] Steel, R. G. D., Torrie, J. H., Dickey, D. A. (1997): Principles and Procedures of Statistics: A Biometrical Approach. 3rd Ed. – McGraw Hill, New York, pp. 400-428.
[36] Sushant, S., Rajdavinder, K., Soodan, A. S. (2010): Morphology of diaspores of some range grasses of Punjab. – Range Management and Agroforestry 31(1): 52-58.
[37] Wang, X., Wang, J., Wang, Y., Dong, X., Chang, G., Cui, Z., Wang, X. S., Wang, Y. C., Dong, X. G., Chang, G. S., Cui, Z. L. (1997): Effect of cutting length on rooting and growth of two year old plants of *Larixka empferi* in nursery. – Forest Research 10(6): 659-662.

http://www.aloki.hu ● ISSN 1589 1623 (Print) ● ISSN 1785 0037 (Online)
DOI: http://dx.doi.org/10.15666/aeer/1802_24632474

EVALUATION OF SOME MEDICINAL PLANT EXTRACTS FOR THEIR NEMATICIDAL PROPERTIES AGAINST ROOT-KNOT NEMATODE, *MELOIDOGYNE INCOGNITA*

HUMAIRA[1*] – SHAD, A. A.[1] – MUHAMMAD, D.[2] – SHAH, H. U.[1]

[1]*Department of Agricultural Chemistry, Faculty of Nutrition Sciences, The University of Agriculture Peshawar, Pakistan*

[2]*Department of Soil and Environmental Sciences, Faculty of Crop Production Sciences, The University of Agriculture Peshawar, Pakistan*

[*]*Corresponding author*
e-mail: aminses@yahoo.com

(Received 9th Aug 2018; accepted 31st Oct 2019)

Abstract. Nematicidal activities of some plant extracts were assayed against *Meloidogyne incognita.*. Six different medicinal plants were collected from Swat valley of Pakistan. Plants were moderately washed with tap water in order to remove various impurities like dust, dirt and adhering materials. The plants were shade dried and powdered. Aqueous Methanolic extraction of the dried powdered samples were carried out through cold percolation technique followed by removal of the solvent using vacuum rotary evaporator under controlled temperature. The methanolic crude extracts were further fractionated using different polarity solvents n-hexane, chloroform, ethyl acetate, and n-butanol. Methanolic extracts were screened for egg hatchability and nematicidal activity against second stage juveniles of *M. j incognita.* in the laboratory under the microscope. The nematode eggs and juveniles were exposed 24, 48 and 72 hrs in different concentrations (10, 100, 1000 ppm) of plant extracts. The plant extracts of *Acacia modesta* (roots), *Segeratia thea* (leaves), and *Celtis caucasic* (aerial part) exhibited highly promising mortality of more than 60% after 72 hrs exposure. There was a gradual decrease in egg hatching with increase in extract concentration of *Acacia modesta* (roots), *Segeratia thea* (leaves), and *Celtis caucasic* (aerial part) were found to be the most effective in reducing egg hatching. Larval mortality were strongly influenced by concentration of extract, plant species and duration of period.
Keywords: *Segeratia thea, methanolic extraction, larval mortality, Acacia modesta, juveniles*

Introduction

Root-knot nematode, *Meladogyne incognita.* is one of the major plant- parasitic nematodes adversely affecting the quantity and quality of the major crops. Plant parasitic nematodes are the main pathogens on most food crops and without adequate control cause loss of yield and quality. Yield losses due to plant parasitic nematodes have been reported to be $100 billion worldwide annually (Sasser and Freckman, 1987). Root-knot nematodes (*Meloidogyne* species) infect almost all types of plants and cause considerable damage (Adekunle and Akinlua, 2007). Root knot nematode larvae infect plant root causing the development of root knot galls that affect the plant's photosynthetic process and nutrient uptake (Eisenback and Triantaphyllous, 1991).

Nematodes are difficult to control because of their high rate of reproduction and wide host range, while females are capable of producing up to one thousand eggs/female (Natarajan et al., 2006). Plant–parasitic nematodes are documented as the causes of serious yield losses on a wide range of crops (Javad et al., 2006). Current study shows that *M. incognita.* is the species which cause serious problem in various agricultural crops.

http://www.aloki.hu ● ISSN 1589 1623 (Print) ● ISSN1785 0037 (Online)
DOI: http://dx.doi.org/10.15666/aeer/1802_24752482

Although chemical nematicides hold major role in nematode control but it is expensive and is economically viable only for high value crops and create a potential hazard to the environment and human health (Tsay et al., 2004). This issue has stimulated research on nematode management through natural products with nematicidal activity such as root exudates, plant volatile compounds (Linford et al., 1938), endophytic bacteria (Vetrivelkalai et al., 2010) and plant extracts (Muniasamy et al., 2010; Pavaraj et al., 2010). A wide variety of plant species, representing 57 families have been shown to exhibit nematicidal compounds (Sukul, 1992), which includes isothiocynates, thiophenics glycosides, alkaloids, phenolics and fatty acids (Gommers, 1973). Nematicidal phytochemicals are generally safe for the human health and environment (Chitwood, 2002). Hence, the present study has been carried out to evaluate some plant extracts for their nematicidal properties against root-knot nematode *M. incognita.*.

Material and methods

Several hundred plants wildly grow in Swat valley and adjacent areas. Due to their socioeconomic, agricultural and pharmacological potential they are very popular in the native people. *Debregeasia saeneb* aerial part (stem + leaves), *Celtis caucasica* aerial part (stem + leaves), *Acacia modesta* (roots & bark), *Segeretia thea* (leaves), *Isodon rugosus* (roots), *Buxus papillosa* (leaves + stem + roots) were used in the study. The plants samples were collected from different regions of district Swat and district Upper Dir (*Figure 1*). The collected species were moderately washed with tap water to remove various impurities like dust, dirt and adhering materials. Then were shade dried until complete dryness of the plant material was achieved. The dried samples were grinded by using electrical grinder. The powdered samples were extracted in aqueous methanol followed by removal of the solvent using vacuum rotary evaporator under controlled temperature.

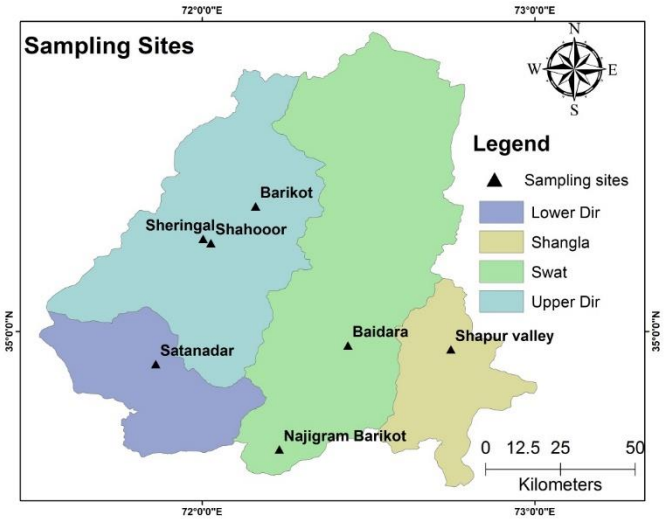

Figure 1. *Map of the sampling sites*

The methanolic crude extracts were further fractionated using different polarity solvents n-hexane, chloroform, ethyl acetate, and n-butanol in separating funnel. The

http://www.aloki.hu ● ISSN 1589 1623 (Print) ● ISSN1785 0037 (Online)
DOI: http://dx.doi.org/10.15666/aeer/1802_24752482

crude extracts and their respective fractions were then dissolved in 5% aqueous DMSO to prepare stock solution. Different concentrations of plant extracts (10, 100, 1000 ppm) were prepared from the stock solution using 5% aqueous DMSO. For obtaining of egg masses and larvae pure culture of *M. incognita.* were collected from the roots of infected *Red duranta* plant. Plant roots were washed well to remove soil and debris. Then infected roots were cut into 2-3 cm pieces. Root pieces were placed in a blender. Enough water was added to cover the roots and blended for 15 –20 sec at low speed. The suspension was poured through the sieves 25 µm, 36 µm, 63 µm, 100 µm. The top sieve (100 µm mesh) was used to retain debris, washed with tap running water.

Eggs on the 500 mesh sieve are gentle washed under a slow stream of cold tap water. The eggs were collected from the 500 mesh sieve into a beaker. The egg suspension was brought to a known volume to determine the number of eggs per millilitre. 1 ml of the egg suspension was used in counting plate with the plant extract and was kept at room temperature for 24, 48 and 72 hrs for egg hatchability test. The nematodes eggs were exposed to 10, 100 and 1000 ppm of each plant extract for 24, 48 and 72 hrs. Four plant extracts exhibited highly promising mortality rates of more than 60% after 72 hrs of exposure ($P<0.05$).

Rest of the egg suspension was stored in saline solution in refrigerator. For the juveniles study the freshly extracted egg suspension was kept in incubator at 24°C for 4 days to let the eggs hatched and get the second stage juveniles. Effect on egg hatching was evaluated on mature uniform size eggs of *M. incognita.* were suspended in the extract, 5% aqueous DMSO (control) and nemacur (nematicide) replicated three times in counting plates. The counting plates were kept at room temperature. Observations were recorded on number of eggs hatched after 24, 48, 72 hrs. For effect of % mortality freshly hatched J_2 of *M. incognita.* were placed in each dilutions and control, replicated three times in counting plates. The plates were kept at room temperature. Mortality of larvae was calculated as a percent of total larvae suspended (Cayrol et al., 1989).

$$\% \text{ egg hatching} = \text{No. of hatched eggs} / \text{Total No. of eggs} \times 100$$

$$\% \text{ Mortality} = \text{No. of dead juveniles} / \text{Total No. of juveniles} \times 100$$

Statistical analysis

All the data were analysed using 2-way factorial experimental design at 5% level of significance, using statistical package Statistix. The letters showing a, b and c with the mean values shows that the means are significantly different from each other.

Results and Discussions

% Egg Hatchability of Plant Methanolic Crude Extracts

A gradual decrease was observed in egg hatching with increase in plant extract concentration (*Table 1*). Abdalla et al. (2008) reported that methanol and hexane extracts of the 27 samples were screened for nematicidal activity against second stage juveniles of *M. incognita* in the laboratory. The present study revealed that plant extracts of *Acacia modesta* (roots), *Segeratia thea* (leaves), *Isodon rugosus* (roots), *Celtis caucasica* (arial part) were found to be most effective in reducing % egg

http://www.aloki.hu ● ISSN 1589 1623 (Print) ● ISSN1785 0037 (Online)
DOI: http://dx.doi.org/10.15666/aeer/1802_24752482

hatching. Plant extracts of *Boxus papillosa* (leaves, stem and roots), *Acacia modesta* (bark) and *Debregeasea saeneb* proved to be less effective against *M. incognita*.

Table 1. *Effect of different concentrations of plant crude extracts on %egg hatchability in the root-knot nematode, Meloidogyne incognita*

Plants	Exposure time hours	% of egg hatching at different dilutions (ppm) of plant extract		
		10	**100**	**1000**
***Acacia modesta* (roots)**	24	54.38	31.23	20.80
	48	51.36	20.10	14.53
	72	24.30	15.23	8.30
		43.35a	**22.19b**	**14.54c**
***Acacia modesta* (bark)**	24	43.73	27.76	22.2
	48	38.13	25.03	15.93
	72	29.80	22.20	8.30
		37.22a	**25.00b**	**15.54c**
***Segeretia thea* (leaves)**	24	86.07	23.57	20.8
	48	18.03	11.07	8.30
	72	14.53	8.30	6.23
		39.54a	**14.31b**	**11.77b**
***Isodon rugosus* (roots)**	24	40.23	33.3	18.7
	48	33.3	25.66	14.53
	72	29.13	23.26	9.70
		34.22a	**27.41b**	**14.31c**
***Buxus papillosa* (leaves)**	24	77.76	68.73	44.40
	48	61.76	49.30	27.76
	72	51.36	26.36	19.40
		63.63a	**48.13b**	**30.52c**
Buxus papillosa (stem)	24	58.30	42.33	27.06
	48	52.76	37.46	25.66
	72	44.40	33.96	23.56
		51.82a	**37.92b**	**25.43c**
Buxus papillosa (roots)	24	88.16	77.06	67.96
	48	77.66	67.33	47.23
	72	66.63	54.83	39.50
		77.48a	**66.41b**	**51.56c**
***Debregeasia saeneb* (aerial part)**	24	75.00	48.46	31.13
	48	63.16	38.13	21.50
	72	57.63	34.83	20.10
		65.26a	**40.47b**	**24.24c**
***Celtis caucasica* (aerial part)**	24	44.43	38.86	29.13
	48	33.26	27.73	20.80
	72	24.96	17.33	10.36
		34.22a	**27.97b**	**20.10b**

% Mortality of Plants Methanolic Crude Extracts

The methanolic crude extracts of *Acacia modesta* (Roots), *Segeratia thea* (leaves), *Isodon rugosus* (roots) and *Celtis caucasica* (aerial part) exhibited mortality more than 50% after 72 hrs exposures (*Table 2*). Pavaraj et al. (2012) observed the plant extracts effect on egg hatching of nematode and mortality of the second stage juveniles of *M. incognita in vitro* after 24, 48 and 72 hrs of exposure. Similar results were observed in the current work from crude extracts of *Segeratia thea* (leaves) and *Celtis caucasica* (aerial part) exhibited 74.5 and 87.3% of larval mortality, while undiluted root extracts of *Acacia modesta* and *Isodon rugosus* exhibited 69 and 54% of larval mortality each at 1000 ppm concentration after 72 hrs of exposure, respectively. Egg hatching inhibition

http://www.aloki.hu ● ISSN 1589 1623 (Print) ● ISSN1785 0037 (Online)
DOI: http://dx.doi.org/10.15666/aeer/1802_24752482

and larval mortality decreased with decrease in the concentration of the extracts. Juvenile mortality increased parallel to an increased time of exposure. The potential of using plant extracts in controlling plant parasitic nematodes has been shown by several authors (Adegbite and Adesiyan, 2005; Opareke et al., 2005; Orisajo et al., 2007; Abbasi et al., 2008). Extracts from *Segeratia thea* and *Celtis caucasica* were the most toxic compared to other plant extracts (*Table 2*). The nematicidal effect of the tested crude extracts may probably be because of higher content of certain oxygenated compounds which are considered to possess lipophilic properties that allow them to dissolve the cytoplasmic membranes of nematode cells and their functional groups interfering with enzyme protein structure (Knoblock et al., 1989).

Table 2. *Effect of different concentrations of plant Methanolic crude extracts on larval mortality in the root-knot nematode, Meloidogyne incognita*

Plants	**Exposure time hours**	**% mortality of juveniles at different concentration (ppm) of plant extract**		
		10	100	1000
***Acacia modesta* (roots)**	24	2.1	16.49	28.48
	48	3.2	31.17	56.34
	72	7.31	53.46	69.43
		4.20 c	**33.70 b**	**51.42 a**
***Acacia modesta* (bark)**	24	11	6.95	16.70
	48	14	21	27
	72	21	33	41.33
		15.33 c	**20.31 b**	**28.34 a**
***Segeretia thea* (leaves)**	24	2.33	21.1	47.55
	48	13.33	25.56	54.41
	72	17.45	34.61	74.54
		11.04 c	**27.09 b**	**58.83 a**
***Isodon rugosus* (roots)**	24	3.2	6.89	13.37
	48	15.22	21	24.27
	72	31	44	54.11
		16.47 c	**23.96 b**	**30.58 a**
***Buxus papillosa* (leaves)**	24	1.2	24.14	6.35
	48	7.52	23.11	26.55
	72	10.33	27.32	36.52
		6.35 b	**24.85 a**	**23.14 a**
***Buxus papillosa* (stem)**	24	1.3	11	13.16
	48	3.46	21	26.73
	72	13.6	31	46.36
		6.12 c	**21 b**	**28.75 a**
***Buxus papillosa* (roots)**	24	4.36	7.58	24
	48	11	21.66	27
	72	15.22	35.44	51
		10.19 c	**21.56 b**	**34 a**
***Debregeasia saeneb* (aerial part)**	24	3.33	11	23
	48	6.52	16.22	34
	72	12.1	25.22	44
		7.31 c	**17.48 b**	**33.66 a**
***Celtis caucasica* (aerial part)**	24	2.4	21	41
	48	11	31.23	67.62
	72	21	41.54	87.37
		11.46 c	**31.25 b**	**65.33 a**

In *Acacia modesta* (roots) among all the four fractions the chloroform and ethyl acetate fractions exhibited highly mortality rates of 68.13 and 70%, respectively after 72 hours exposure (*Table 3*). In *Segeretia thea* (leaves) the chloroform and ethyl acetate

http://www.aloki.hu ● ISSN 1589 1623 (Print) ● ISSN1785 0037 (Online)
DOI: http://dx.doi.org/10.15666/aeer/1802_24752482

fractions exhibit high mortality rates of 74.14 and 75.16%, respectively after 72 hours exposure (*Table 4*). *Celtis caucasica* (aerial part) fractions caused larval mortality at the rate of n-hexane 84, chloroform 86, and ethyl acetate 88% after 72 hours of exposure at 1000 ppm (*Table 5*). While *Isodon rugosus* (roots) ethylacetate fraction showed highly mortality rates of juveniles at 55% after 72 hours exposure time at 1000 ppm concentration (*Table 6*). All the means regarding concentration level were significantly different among each plant extract. The nematicidal effect of ethyl acetate and chloroform fractions are may be due to the presence of nematicidal compounds isothiocynates, thiophenics glycosides, alkaloids, phenolics and fatty acids (Gommers, 1973).

Table 3. *Effect of different concentrations of different polarity fractions of Acacia modesta (roots) on larval mortality of the root-knot nematode, Meloidogyne incognita*

***Acacia modesta* (roots)**	**Exposure time hours**	**% mortality of juveniles at different dilutions (ppm) of plant extract**		
		10	**100**	**1000**
n- hexane fraction	24	1.2	13.6	22.66
	48	2.13	20.56	42.43
	72	3.73	39.96	53.56
		2.35c	**24.71b**	**39.55a**
Chloroform fraction	24	2.50	15.93	27.2
	48	3.60	31.23	55.23
	72	7.06	42.96	68.13
		4.40c	**30.04b**	**50.18a**
Ethyl acetate fraction	24	3.2	17.13	28.48
	48	4.3	33.43	57.4
	72	7.86	54.6	70.15
		5.12c	**35.05b**	**52.01a**
n- butanol fraction	24	1.63	14.76	25.06
	48	2.20	30.28	54.16
	72	5.63	51.76	64.6
		3.15c	**32.27b**	**47.94a**

Table 4. *Effect of different concentrations of different polarity fractions of Segeratia thea (leaves) on larval mortality of the root-knot nematode, Meloidogyne incognita*

***Segeratia thea* (leaves)**	**Exposure time hours**	**% mortality of juveniles at different dilutions (ppm) of plant extract**		
		10	**100**	**1000**
n- hexane fraction	24	1.26	14.63	41.93
	48	10.56	23.3	48.83
	72	13.6	27.5	66.7
		8.47c	**21.81b**	**52.48a**
Chloroform fraction	24	2.16	19.16	46.0
	48	12.26	24.3	53.36
	72	16.53		74.13
		10.32c	**25.62b**	**57.85a**
Ethyl acetate fraction	24	2.53	22.33	48
	48	14.36	26.13	54.9
	72	18.16	35.06	75.16
		11.68c	**27.84b**	**59.35a**
n-butanol fraction	24	1.66	20.3	46.56
	48	12.53	24.4	53.56
	72	16.4	33.16	72.00
		10.2 c	**25.95 b**	**57.37 a**

http://www.aloki.hu ● ISSN 1589 1623 (Print) ● ISSN1785 0037 (Online)
DOI: http://dx.doi.org/10.15666/aeer/1802_24752482

Table 5. *Effect of different concentrations of different polarity fractions Celtis caucasica (aerial part) on larval mortality of the root-knot nematode, Meloidogyne incognita*

Celtis caucasica **(aerial part)**	**Exposure time hours**	**% mortality of juveniles at different dilutions (ppm) of plant extract**		
		10	**100**	**1000**
n- hexane fraction	24	2.16	19	35.66
	48	9	29.5	65.36
	72	18.33	39.8	84.86
		9.83c	**29.43b**	**61.96a**
Chloroform fraction	24	2.23	19.2	40
	48	10.26	29.5	66.36
	72	20.4	40.83	86.26
		10.96c	**29.84b**	**64.21a**
Ethyl acetate fraction	24	2.53	22.5	41.5
	48	12	31.73	68.00
	72	21.66	41.00	88.13
		12.06c	**32.01b**	**65.87a**
n- butanol fraction	24	2.1	19.63	37
	48	9	30	65.33
	72	17	40.23	85.4
		9.36c	**29.95b**	**62.57a**

Table 6. *Effect of different concentrations of different polarity fractions of Isodon rugosus (roots) on larval mortality of the root-knot nematode, Meloidogyne incognita*

Isodon rugosus **(roots)**	**Exposure time hours**	**% mortality of juveniles at different dilutions (ppm) of plant extract**		
		10	**100**	**1000**
n- hexane fraction	24	1.67	4.7	10.33
	48	13.33	19.0	21.0
	72	26.50	36.33	4
		13.83c	**20.01b**	**26.11a**
Chloroform fraction	24	1.86	5.66	12.00
	48	14.33	19	21.66
	72	31.33	42	49.66
		15.84c	**22.22b**	**27.77a**
Ethyl acetate fraction	24	3.06	6.08	14
	48	14.16	20	25
	72	30	43.83	55
		15.74	**23.30**	**31.33**
n- butanol fraction	24	2.63	5.73	11.13
	48	12.66	16.66	21
	72	26	37.66	46
		13.76c	**20.02b**	**26.04a**

REFERENCES

[1] Abbasi, W. M., Ahmed, N., Zaki, J. M., Shaukat, S. S. (2008): Effect of *Barleria acanthoides* Vahl. on root-knot nematode infection and growth of infected okra and brinjal plants. – Pakistan Journal of Botany 40(5): 2193-2198.

[2] Abdalla, E. M., Woon, L. D., Chan, P. J., Bin, Y. H., Yul, C. H. (2008): Evaluation of various plant extracts for their nematicidal efficacies against juveniles of *Meloidogyne incognita*. – Journal of Asia-Pasific Entomology 11(2): 99-102.

[3] Adegbite, A. A., Adesiyan, S. O. (2005): Root extracts of plants to control root-knot Nematode on edible soybean. – World Journal of Agricultural Sciences 1(1): 18-21.

http://www.aloki.hu ● ISSN 1589 1623 (Print) ● ISSN1785 0037 (Online)
DOI: http://dx.doi.org/10.15666/aeer/1802_24752482

[4] Adekunle, O. K., Akinlua, A. (2007): Nematicidal effects of *Leucaena leucocephala* and *Gliricidia sepium* extracts on *Meloidogyne incognita* infecting okra. – J. Agri. Sci. 52(1): 53-63.
[5] Caryrol, J. C., Djian, C., Pijarowski, I. (1989): Studies on the nematicidal properties of the culture filtrate of the nematophagous fungus *Paecilomyces lilacinus*. – Rev. Nematol. 12: 331-336.
[6] Chitwood, D. J. (2002): Phytochemical based strategies for nematode control. – Annual Review of Phytopathology 40: 221-249.
[7] Eisenback, J. D., Triantaphyllous, H. H. (1991): Root knot nematode *Meloidogyne* species and races. – In: Nickle, W. R. (ed.) Manual of Agriculture Nematology. Marcel Dekker, Inc. New York, pp. 281-286.
[8] Gommers, F. J. (1973): Nematicidal principles in Compositae. – Mededelingen Landbouwhogeschool, Wageningen, The Netherlands 17: 71-73.
[9] Javad, N., Gowmen, S. R., Ulhaq, M. I., Abdullah, K., Shahina, F. (2006): Systemic and persistent effect of neem (*Azardirachta indica*) formulations against root knot nematodes, *Meloidogyne javanica* and their storage life. – Crop Protection 26: 911-916.
[10] Knoblock, K., Weis, K., Wergent, R. (1989): Mechanism of antimicrobial activity of essential oils. – Proceedings of 37th Annual Congress Medicine Plant Research (ACMPR'89), Braunisweig, pp. 5-9.
[11] Linford, M. B., Yap, F., Oliveira, J. M. (1938): Reduction of soil population of root-knot nematode during decomposition of organic matter. – Soil Science 45: 127-142.
[12] Muniasamy, S., Pavaraj, M., Rajan, M. K. (2010): Efficacy of the fruit extract of *Citrullus colocynthis* (L.) on the root-knot nematode *Meloidogyne incognita* infecting *Vigna ungiculata* (L.). – Journal of Biopesticides 3(1): 309-312.
[13] Natarajan, N., Cork, A., Boomathi, N., Pandi, R., Velavan, S., Dhaskshanamoorthy, G. (2006): Cold aqueous extracts of African marigold, *Tagetes erecta* for control tomato root-knot nematode. – Meloidogyne incognita Crop Protection 25: 1210-1213.
[14] Opareke, A. M., Dike, M. C., Amatobi, C. I. (2005): Field evaluation of extracts of five Nigerian species for control of post flowering insect pest of cowpea, *Vignaunguiculata* (L.) Walp. – Plant Protection Science 41: 14-20.
[15] Orisajo, S. B., Okeniyi, M. O., Fademi, O. A., Dongo, L. N. (2007): Nematicidal effects of water extracts of *Acalypha ciliate*, *Jatropha gosssypifolia, Azadiractha indica* and *Allium ascalonicum* on *Meloidogyne incognita* infection on cacao seedlings. – Journal of Research in Biosciences 3(3): 49-53.
[16] Pavaraj, M., Karthikairaj, K., Rajan, M. K. (2010): Effect of leaf extract of *Ageratum conyzoides* on the biochemical profile of blackgram *Vigna mungo* infected by root-knot nematode, *Meloidogyne incognita*. – Journal of Biopesticides 3(1): 313-316.
[17] Pavaraj, M., Bakavathiappan, G., Baskaran, S. (2012): Evaluation of some plant extracts for their nematicidal properties against root-knot nematode, Meloidogyne incognita. – JBiopest 5 (Supplimentary): 106-110.
[18] Sasser, J. N., Freckman, D. W. (1987): A world perspective on nematology. The role of society. – In: Veech, J. A., Dickerson, D. W. (eds.) Vistas in Nematology. Hyattsville. Society of Nemat. pp. 7-14.
[19] Sukul, N. C. (1992): Plant antagonistic to plant parasitic nematodes. – Indian Review of Life Sciences 12: 23-52.
[20] Tsay, T. T., Wu, T. S., Lin, Y. Y. (2004): Evaluation of asteraceae plant for control of *Meloidogyne incognita*. – Journal of Nematology 36: 36-41.
[21] Vetrivelkalai, P., Sivakumar, M., Jonathan, E. I. (2010): Biocontrol potential of endophytic bacteria on *Meloidogyne incognita* and its effect on plant growth in bhendi. – Journal of Biopesticides 3(2): 452-457.

http://www.aloki.hu ● ISSN 1589 1623 (Print) ● ISSN1785 0037 (Online)
DOI: http://dx.doi.org/10.15666/aeer/1802_24752482

THE TRANSFORMATION OF ECOSYSTEMS OF THE ILI RIVER DELTA (KAZAKHSTAN) UNDER THE FLOW REGULATION AND CLIMATE CHANGE

MUKHITDINOV, A.[1] – NURTAZIN, S.[2] – ALIMOVA, S.[2] – ABLAIKHANOVA, N.[2] – YESSIMSIITOVA, Z.[2] – SALMURZAULY, R.[2*] – MARGULAN, I.[2] – MIRASBEK, Y.[2]

[1]*Satbayev Kazakh National Technical University, Almaty, Kazakhstan*

[2]*Al-Farabi Kazakh National University, Almaty, Kazakhstan*

**Corresponding author*
e-mail: zhanat_2006@mail.ru

(Received 9th Dec 2018; accepted 8th Jan 2020)

Abstract. This paper presents the results of a study on the main reasons for the transformation of wetland ecosystems in the Delta of the Ili River in the period of 1979-2014. The study results are shown based on the analysis of multi-temporal satellite data Landsat, dynamics of hydrological regime of the river Ili, climate conditions and features of economic activities of the local community, as well as fieldwork in the study region. Analysis of area changes of main types of hydromorphic and semi-hydromorphic ecosystems of Delta river Ili in high and medium on water discharge in the following (1979, 1993, 2000, 2010, and 2015) years. Increasing water consumption in China and in Kazakhstan part of the Ili-Balkhash basin due to the development of the agrarian and municipal sectors of economy especially in China, significantly exceed increasing flow of Ili River, caused by regional warming in the catchment part of Ili River Basin. The global warming has intensified the degradation of glaciers in mountain catchment areas of Ili River, this in the near future threatens with a decline in river flow and as a consequence lead to the deterioration of delta ecosystems and the desiccation of lake Balkhash similarly to the ecological disaster of the Aral Sea. Analysis of long-term (from 1970 to 2013) climatic data from three meteorological stations demonstrated a trend of the regional increase of average annual air temperature by 1.4 °C and decreasing of average annual precipitation by 10 mm. These factors also contribute to the transformation process of hydromorphic ecosystems.
Keywords: *Ili-Balkhash basin, Ili Delta, hydrology, ecosystem transformation, climate warming and anthropogenic pressure*

Introduction

The processes of landscape degradation in river deltas in connection with regulation of runoff, in recent years has given more consideration (Hajdarov, 1968; Magasheva, 1977; Plisak, 1981; Starodubtsev et al., 1978). Similar works were carried out during the filling of Kapchagai reservoir from 1969 to1989 on the middle stream of river Ili, which provides nearly 80% of the water inflow into the largest inland water body in Kazakhstan - Lake Balkhash (Evstifeev et al., ND; Sovolova and Zhelnova, 1984; Plisak and Ogar, 1985). Ili is the most abounding in water river of South-East Kazakhstan. More than 3 million people live in the basin, and over many years a large industrial and agricultural complex was formed, which occupies an important place in the socio-economic life of the country.

The lower reaches of river Ili from Kapshagai ravine to the estuary, lies in the western part of the Balkhash flat depression. Modern Ili Delta geomorphologically enters into its composition and covers an area about 8000 km^2, as well as it is currently the largest River Delta in Central Asia. The Delta is represented as mosaics of zonal-

http://www.aloki.hu ● ISSN 1589 1623 (Print) ● ISSN 1785 0037 (Online)
DOI: http://dx.doi.org/10.15666/aeer/1802_24832498

desert and intrazonal-floodplain-lowland hydromorphic biocenoses. This latter is distinguished by high biological productivity and cenotic biodiversity in the delta that are crucial for the conservation of some rare and endangered species and populations of animals and plants, as well as the unique wetland ecosystems (Jensen et al., 1987; Frazier et al., 2003). Ili Delta and the southern part of Lake Balkhash were declared as wetlands of international importance and included in the list of the Ramsar Convention in February 2012 (Du et al., 2014).

Since the 1970s, due to a sharp increase in water consumption and construction of reservoirs in Kazakhstan, and then in the Chinese part of the River Ili Basin, the runoff was significantly reduced in the lower reaches. This led to a sharp deterioration of water cut of floodplain and wetland areas and aridization of hydromorphic landscapes with the expansion of zonal, desert-like ecosystems (Tso and Mather, 2009). Quite a large number of articles are published on the threatening ecological situation in the Ili-Balkash basin, which is a reminder to the well-known catastrophe of the Aral region (Kanika et al., 2013; Congalton and Green, 1999; Neasset, 1996; Cherednichenko et al., 2010). However, volume of standard observations that were conducted previously was sharply reduced in 1990s, in particular, part of weather stations and gauging stations has been closed and field scientific studies are almost stopped (Vilesov et al., 2006). Currently, it is very little data on the current environmental state of the Basin in general and the modern Delta of the Ili River. In view of this, the aim of the study that had been done in 2008-2015, was to examine the main trends in the transformation of wetland ecosystems of the Ili River in relation to the regulation of river flow, regional climate changes, and anthropogenic impacts on the delta biocenoses.

Methods

The methods and multi-temporal remote sensing data were used in this study taking into account the large area of the Ili River Delta. Multi-temporal comparative analysis of biocenoses and classification of main studied biocenoses were based on the Landsat series: Multispectral Scanner (MMS); Thematic Mapper (TM); Plus Enhanced Thematic Mapper (ETM+) and Operational Land Imager (OLI), which are widely used in the world in the investigations of wetlands and delta ecosystems (Burlibaev et al., 2004, 2011). The time interval of used satellite images based on the changes of Ili Delta over the past 36 years due to fluctuations of average annual runoff from the relatively water-short years (1979, 1993, 2015) to an average water year (2000) and abnormally high 2010. These satellite images are in open access (http://earthexplorer.usgs.gov) *Table 1*. In selecting of satellite images all standard quality criteria (minimum cloudiness, image clarity and comprehensive coverage of the study area) was taken into account, as well as date of images, which were focused on the full-flowing months: June and July. In addition to remote data a complex fieldwork was carried out in 2008-2015 and during the fieldwork data were collected on land cover, features of terrestrial and aquatic landscapes on 382 representative points from different types of biocenoses.

Data from the gauging station “The tract Kapshagay” which is located on 37 km below the Kapshagai hydropower plant (44° 7’ 48.21” N; 76°59’ 12.98” E) and gauging station 164 which located in 164 km further upstream of Kapshagai hydropower plant (43°51’ 20.00” N; 79°11’ 53.38” E) were used to analyze dynamics of hydrological regime of the lower reaches of the Ili River for the period of 1950 to 2013.

http://www.aloki.hu ● ISSN 1589 1623 (Print) ● ISSN 1785 0037 (Online)
DOI: http://dx.doi.org/10.15666/aeer/1802_24832498

Apart from runoff, the fluctuations of weather conditions also have a significant impact to the delta. An analysis of average annual fluctuations of air temperature and precipitation for the period of 1970-2012 was made based on the data of the weather stations Aul-4 and Kuigan, which located in the Delta (*Fig. 1*). Long-term runoff and climate data were purchased from the National Hydrometeorological Service "Kazhydromet". Influence of various forms of economic and human activities to the delta ecosystem were also taken into account.

Table 1. *Information on the used satellite images*

Identification image number	Date	Shooting scene of Landsat path/row (WRS)	Name of the SC
LM21630291979171AAA05	20.06.1979	163/29	Landsat 2 MMS
LM21630281979171AAA05	20.06.1979	163/28	Landsat 2 MMS
LT51510291993161ISP00	10.06.1993	151/29	Landsat 5 TM
LT51510281993161ISP00	10.06.1993	151/28	Landsat 5 TM
LE71510292000157SGS00	05.06.2000	151/29	Landsat 7 ETM +
LE71510282000157SGS00	05.06.2000	151/28	Landsat 7 ETM +
LT51510291993161ISP00	10.06.2010	151/29	Landsat 5 TM
LT51510281993161ISP00	10.06.2010	151/28	Landsat 5 TM
LC81510292015190LGN00	09.07.2015	151/29	Landsat 8 OLI
LC81510282015190LGN00	09.07.2015	151/28	Landsat 8 OLI

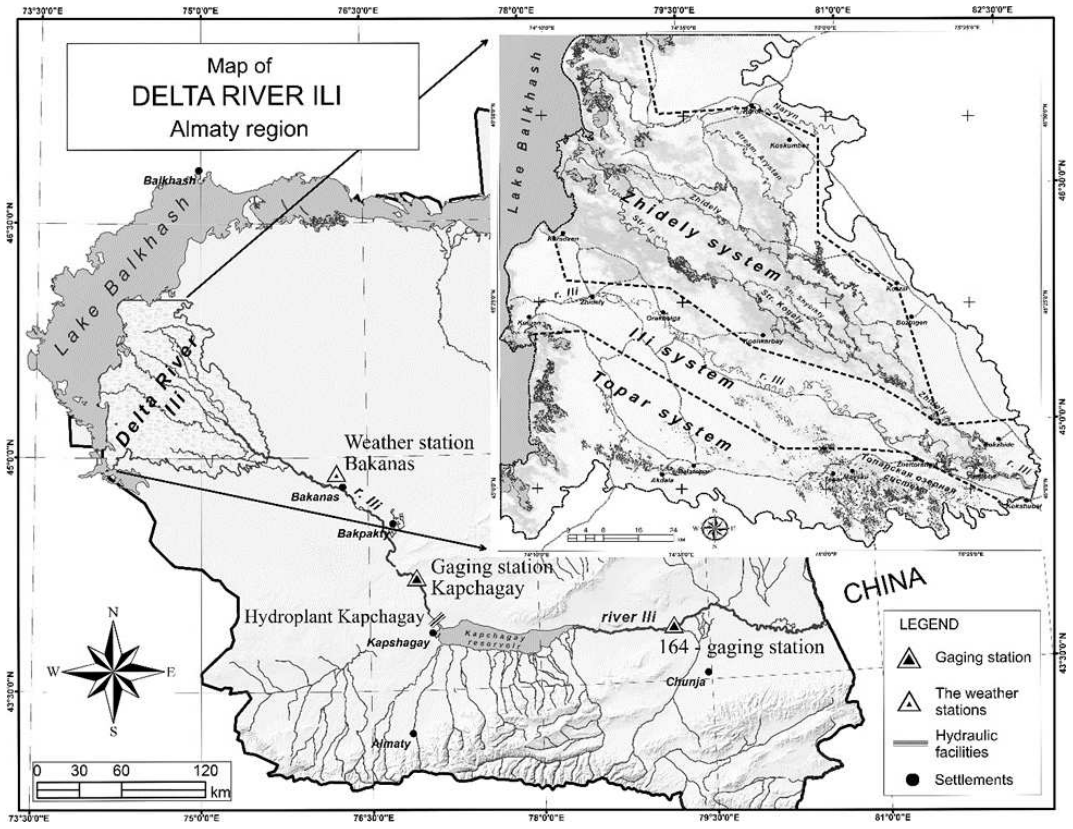

Figure 1. *Map of the study region*

http://www.aloki.hu ● ISSN 1589 1623 (Print) ● ISSN 1785 0037 (Online)
DOI: http://dx.doi.org/10.15666/aeer/1802_24832498

Preprocessing satellite data

To eliminate the radiometric, geometric and atmospheric distortions, all used satellite images have passed preliminary processing in accordance with conventional methods of Remote Sensing (Starodubtsev and Truskavetskij, 2007). The spatial resolution of images was unified to 30 m. As single geographic coordinate system the Universal Transverse Mercator (UTM) was used.

Classification

Classification of hydromorphic and semi-hydromorphic ecosystems were carried out by using algorithm-supervised classification «Maximum Likelihood» as the most reliable and widely used algorithm for classifying the environment (Kanika et al., 2013; Hajdarov, 1963). For improving results and minimizing errors of classification ecosystems in 1979-1993 soil cover and geobotanical maps of 1981-1985 were used. For visual adjustment of boundaries of anthropogenic objects as ancillary data high-resolution satellite images on Google Earth mode were used.

Accuracy of the classification

The accuracy of classification of ecosystems was estimated based on multinomial algorithm, known under the name «confusion matrix». Matrix differences is a static analysis, which uses cross-tabs to display the degree of difference between the classes obtained by supervised classification and a set of field data in reference points, which carry a more accurate information (Congalton and Green, 1999). Thus, the overall accuracy and accuracy of "producer" and "user" classification results of multi images from 1979 to 2014 (*Table 2*) have been calculated. Final accuracy of the derived class has been assessed by the Kappa coefficient, which is calculated by:

$$K = \frac{N\sum_{i=1}^{n} x_{ii} - \sum_{i=1}^{r} x_{i+}x_{+i}}{N^2 - \sum_{i=1}^{r} x_{i+}\, x_{+i}}$$

where x_{ii}- is the diagonal elements of the matrix's errors; x_i + - is the total number of pixels in line; $x + i$ – is the total number of pixels on the column; N- is the total number of pixels in the matrix; n - is the number of classes (Neasset, 1996).

Table 2. *Classifications reliability of satellite images*

Ecosystems	1979		1993		2000		2010		2015	
	Production accuracy	**Custom accuracy**	**Production accuracy**	**Custom accuracy**	**Production accuracy**	**Custom accuracy**	**Production accuracy**	**Custom accuracy**	**Production accuracy**	**Custom accuracy**
Grassland	91.32	82.17	96.33	92.47	92.33	84.61	95.11	96.6	94.59	93.49
Reed	91.85	98.4	93.76	98.78	91.85	99.18	97.32	97.07	93.76	96.46
Aquatic	99.27	84.5	98.75	95.02	99.4	91.68	89.87	88.17	99.6	90.71
Total accuracy	91.65		95.86		93.88		95.49		94.67	
The Kappa coefficient (K)	0.89		0.93		0.90		0.92		0.90	

http://www.aloki.hu ● ISSN 1589 1623 (Print) ● ISSN 1785 0037 (Online)
DOI: http://dx.doi.org/10.15666/aeer/1802_24832498

Results and discussion

The dynamics of hydrological regime and weather conditions in Ili River Delta 1950-2013

Since the 1970s there have been a trend in the reduction of average annual runoff of river Ili, primarily because of intensive building of irrigation systems and hydropower objects, both in China and in the Kazakh part of the Ili-Balkhash basin. It is known that due to the location of the main catchment area and hydrological regime, Ili River has a predominantly glacier-snow feeding. The riverhead of Ili is located at an altitude over 4000 m in the Tien-Shan mountain and numerous tributaries that considerably influence hydrological regime also have large catchment areas in mountains Zailiyskiy and Zhetysuskiy Alatau.

The annual runoff of Ili River before the building of Kapchagay hydropower plant was observed based on long-term data for the period of 1950-1969: spring flood in April-May, with an average monthly runoff of 455 m^3/s; three-month summer flood with an average monthly runoff 900 m^3/s and seven-month autumn and winter low-water period with an average monthly runoff of 321 m^3/s. Maximum monthly average runoff was observed about 950 m^3/s in July during the most intensive melting the of snowfields and glaciers (*Fig. 2*). Runoff begins to decline in September due to decrease in air temperature. Runoff begins to decline in September due to decrease in air temperature. Precipitation of the autumn period had no significant effect on volume runoff of Ili River and slump of runoff continued. Minimal value of runoff of the described period was around 200 m^3/s. and observed in winter months.

On average for the period of 1950-1969, the annual value of flow of Ili River from China to Kazakhstan was 12.47 km^3 with an average runoff of 395.42 m^3/s on the gauging station Dubyn. On the gauging station of Kapchagay it was increased until 14.9 km^3 with an average runoff of 473/516 m^3/s at expense of water inflow from Kazakhstan part of the Ili-Balkash basin. A significant reduction of Ili River runoff occurred from 1969, caused by the filling of Kapchagay reservoir since September 1969 and by increased water consumption due to irrigation in China and Kazakhstan. Before the building of hydropower plant the annual average runoff was 516 m^3/s, during the filling time (1970-1987) of Kapchagay reservoir it decreased by 28.2% to 370.2 m^3/s. At the same time, in the gauging station "164" the annual average runoff of Ili River was equal to 442 m^3/s. After the 1970s, the water runoff in the lower stream of river Ili never surpassed the runoff of the middle stream (*Fig. 3*).

The hydrological and atmospheric thermal conditions in the lower reaches of the river including the delta also changed dramatically with the beginning of the filling of Kapshagay reservoir. In seventeen years, there was a sharp more than 48% reduction of summer runoff and increased winter month runoff by 28% (*Fig. 2*). Winter floods have arisen that were not peculiar to Ili River, conditioned by increasing of water releases due to growth of energy needs during the cold season. Therefore, in winter the waves with a height up to 0.5 m from the Kapshagay power plant reached the upper reaches of the delta that caused ice drift, congestion and numerous spillages, which adversely affected biocenoses, especially the fauna. Despite the artificial discharges in May, spring floods did not achieve the scale of the former natural runoff of Ili River (*Fig. 2*).

In the following twenty-five years (1988-2013) in the same Kapshagay gauging station the annual average runoff of the Ili River has increased again to 466 m^3/s however, without attaining the previous amount (*Fig. 2*). The dramatic reasons of increasing runoff

http://www.aloki.hu ● ISSN 1589 1623 (Print) ● ISSN 1785 0037 (Online)
DOI: http://dx.doi.org/10.15666/aeer/1802_24832498

to 47.6-60 m^3/s are the result of regional warming. By results of investigation of glaciers from 1955 to 2004, the area of glacier systems of Kazakhstan part of Ili River Basin has decreased by 38.5%, from 926.13 to 570.15 km^2 (Vilesov et al., 2006). At the same time, due to the profound social and economic transformations in the 1990s and 2000s, the area of irrigated agriculture and water consumption have been reduced overall at the Kazakhstan part of the Ili-Balkhash basin (Burlibaev et al., 2011).

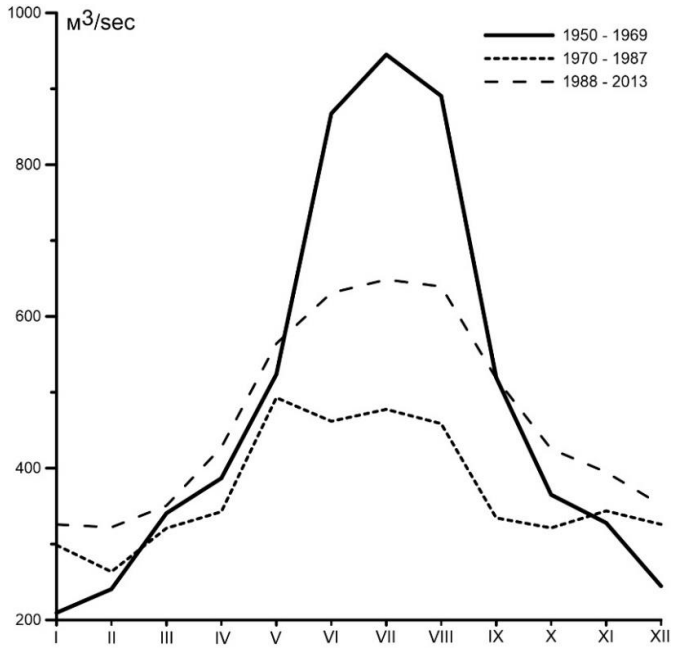

Figure 2. *Monthly average runoff before building Kapchagay hydroplant 1950 -1969; during the filling time 1970-1987; after filling of Kapchagay reservoir 1988-2013; according to Kapchagai gauging station*

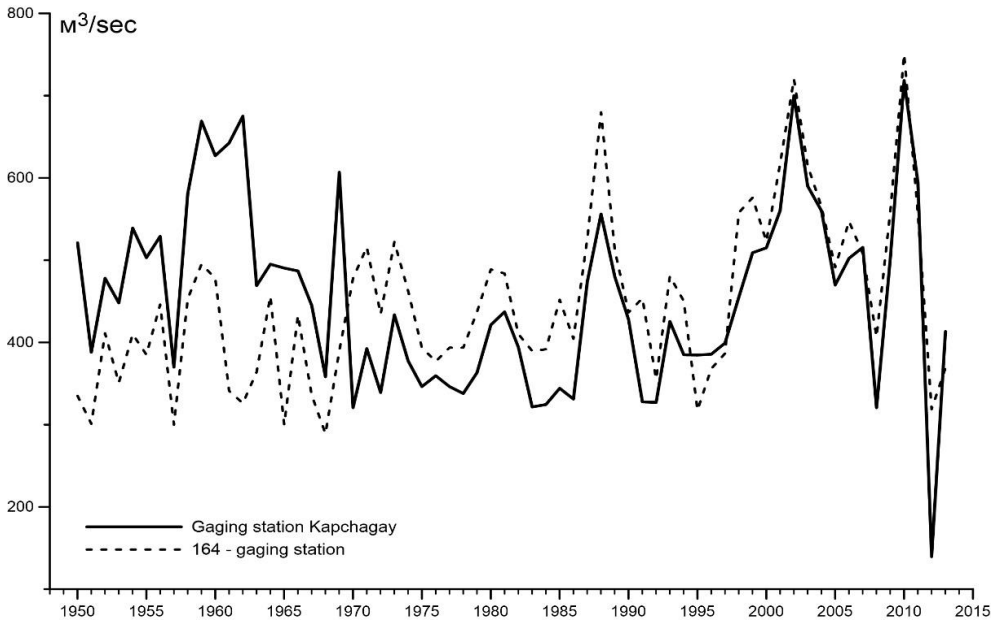

Figure 3. *Combined schedule of annual runoff of average annual water content of Ile River in alignment of gauging station Kapshagai and gauging station 164 (1950-2013)*

http://www.aloki.hu ● ISSN 1589 1623 (Print) ● ISSN 1785 0037 (Online)
DOI: http://dx.doi.org/10.15666/aeer/1802_24832498

An intensive construction of hydro-economic facilities in the Ili River Basin is accompanied by increasing water losses due to evaporation and filtration. After filling the Kapshagay reservoir 1.5-2.3 km^3 of water was lost annually for evaporation and filtration. In lower and middle reaches of the Ili River with the Kapshagay reservoir a series of large irrigation massifs were activated causing large water losses in Shengeldy, Akdaly, Kerbulak and Karoi. Besides, unjustifiably high water consumption caused by the imperfection of irrigation systems with an efficiency coefficient of 0.59 (Burlibaev et al., 2004) and, in our opinion, cultivation of hydrophilous crops as rice and alfalfa was an unfortunate choice.

Thus, area of irrigated lands at 1986 in the Ili River Basin in Kazakhstan's part was 369.6 thousand ha, and by 2000 it was reduced until 299.2 thousand ha due to radical social and economic collision in Kazakhstan. In contrast, water consumption in the Chinese part of the basin increasing rapidly, where large hydraulic works had been built and continued to be built for intensively developing industrial and agricultural sectors, as well as a growing population of Xinjiang Uygur Autonomous Region (Burlibaev et al., 2004).

Analysis of satellite images shows the area of irrigated land on the Chinese side has reached 465 500 ha already in 2007 and the annual water withdrawal from the Ili River in China has increased from 1.4 to 4.0 km^3 (Starodubtsev and Truskavetskij, 2007). In the coming years active construction of water facilities in the Chinese part of the Ili River basin will continue, and this creates a serious problem of water scarcity, desertification of ecosystems in the South-East of Kazakhstan and, as a consequence, water sharing between China and Kazakhstan at government level.

The climate-geographical conditions and soil characteristics of much of the Kazakh part of the Ili River Basin refers to the northern deserts and semi-deserts and historically used as natural pastures for livestock and in particular for irrigated agriculture. Location of the delta in the center of Eurasia determines the continental climate with large daily temperature range and seasonal temperature. The highest average monthly air temperature is 25-27 °C observed in July, with an absolute maximum of 44-46 °C; the lowest average monthly temperature is -13-15 °C observed in January, with an absolute minimum of - 45 °C.

The amount of positive annual temperatures above 10 °C reaches to 3500 °C that is the cause of high evaporation around 1000 mm/year in the delta area and Balkhash Lake and extra-arid climate. The average annual precipitation in the delta during 1970-2012 was little less than 160 mm/year, with a range of 80-260 mm/year that is about 13% of total evaporation. According to our data in the summer, the humidity can vary between 25 and 30% in the course of day and content of moisture in the soils at depth of 12-24 cm can vary between 1-2%. Hence, hydrological regime of the Ili River has a determinative importance on the state of intrazonal hydromorphic biocenosis of delta and the conservation of Balkhash Lake.

The negative anthropogenic impacts on the delta biocenoses

The lower reaches of the Ili River from the Kapshagai gorge to estuary occupies the western part of the Balkhash flat depression with an area of more than 20 000 km^2 (Hajdarov, 1968). Geomorphologically situated in the lower reaches the modern Ili Delta it covers an area about 7,000 km^2. On the top of the modern delta, about 120 km from the shore of Balkhash Lake, Ili River divides into many deltaic channels, which form three major hydrographic systems: Toparsky, Ilisky and Zhidelinsky (*Fig. 1*). Each

http://www.aloki.hu ● ISSN 1589 1623 (Print) ● ISSN 1785 0037 (Online)
DOI: http://dx.doi.org/10.15666/aeer/1802_24832498

of them, in its turn divides into smaller channels. Large part of the delta occupies the vast depressions between channels bounded by hilly sands that are flooding forming a shallow lakes and marshes.

Flat relief of the Balkhash depression and granulometric soil structure: light clay loams, loamy sands, fine-grained sands, as well as significant fluctuations of water content of the Ili River caused the variability of hydrographic system: some of the streams and channels are silting and disappear, others are increasing and new ones appear.

The system of lakes and swamps of deltaic territories are also very dynamic. The study area of the Ili Delta varies with the largest species and cenotic diversity in the region, with the presence of fertile land, rich natural pastures and hayfields, with an extensive hydrographic network of lakes, canals and sleeves with commercial fish fauna and bird colonies. It has been under intense economic use from the beginning of the formation of the modern delta over the years. This has led to a violation of the integrity of plant communities and caused great damage to the rich fauna of the region. With regard to vegetation this is reflected in a simplified structure of the communities, in impoverishment of their species composition, in reducing or complete disappearance of the most valuable indigenous species, in increasing the number and biomass of secondary species (including fault indicators, etc.), in reducing the role of perennial species and in increasing the specific value of annual plants. Negative processes are caused by unsystematic livestock grazing, uncontrolled burning of low productivity grass and last year's reed beds, as well as by cutting riparian and saxaul forest during harvesting for the winter. The number of livestock in the delta area reached 101.7 thousand units, sheep and goats account for - 50.8%, cattle - 38.4%, and horses - 10.8%. Negative delta transformation of biocenosis are particularly strongly expressed in the vicinity of settlements, livestock sheds on distant pastures and close to water bodies. Restoration of vegetation in desert is going slowly, due to the harsh climate, soil poverty, poor water content and high salinity of groundwater. Therefore, floristic diversity is reduced now almost on the entire territory, and for its restoration requires different phytomeliorative events. Vertebrate fauna of the region has about 345 species, that includes 33 rare and endangered animals, which are also under threat from poaching, habitat degradation, disturbance growth at the moment. The load on the ecosystem of the delta from huge number of tourists, hunters and fishermen on private cars, motorcycles and water transport is practically not regulated, especially those that are heavily influencing on floodplain, riparian and wetland biocenoses and vertebrate fauna as well.

Pollution of surface water and terrestrial ecosystems by various pollutants, household, industrial, agricultural effluents and emissions are increasing. Violation of hydrological and hydrochemical regime of the Ili River has a particularly devastating impact on the floodplain and deltaic wetland ecosystems.

Regional climate change in the study region from 1970-2013

Precipitation regime in the study area has been considered with 2 meteorological stations for the period of 1971-2013. In the annual course precipitation maximum occurs in spring months (April-May) and secondary maximum was observed in the fall. The minimum amount of precipitation falls in August and September, as well as in January and February across the study area. In general, rainfall throughout the year dominates in the warm period. Taking into account high evaporation in the delta region, long-term fluctuations in average precipitation sums cannot play a decisive role. An analysis of the

http://www.aloki.hu ● ISSN 1589 1623 (Print) ● ISSN 1785 0037 (Online)
DOI: http://dx.doi.org/10.15666/aeer/1802_24832498

linear trend in temporary course of annual precipitation sums and precipitation sums for warm and cold periods on both considered meteorological stations have shown weak trends. The maximum positive value 1.5 mm/10 years of the linear trend coefficient had been observed at Bakanas meteorological station. The character of changes in precipitation during the warm period of the year roughly corresponds to the annual. A negative trend (minus 1.2 mm/10 years) was noted in Bakanas. In the cold season there is a weak positive trend (3-6 mm/10 years) or sometimes it is not possible to observe them at all.

At the same time, the main volume of the Ili River flow is formed by precipitations in the catchment part of the basin, which is situated in the mountains at an altitude of over 2,000 m, where the average annual rainfall is equal to 900-1100 mm. For example, 2010 was an abnormally high-water year for the Ili River, according to Shymbulak (2300 m. above sea level) and Myn Zhylki (3100 m above sea level) meteorological stations, which are located in the valley Maloalmatinskoe in Zailiysky Alatau, that fell on 50% of precipitation more than the average annual rainfall for the period 2000-2009.

An analysis of the linear trend in temporary course of annual precipitation shows that despite the great variability of precipitation from year to year in considered period (1971-2013) trends are expressed weakly, but in general, the average annual amount of precipitation decreased to 10 mm according to Bakanas and Kuigan weather stations for 44 years (*Fig. 4*).

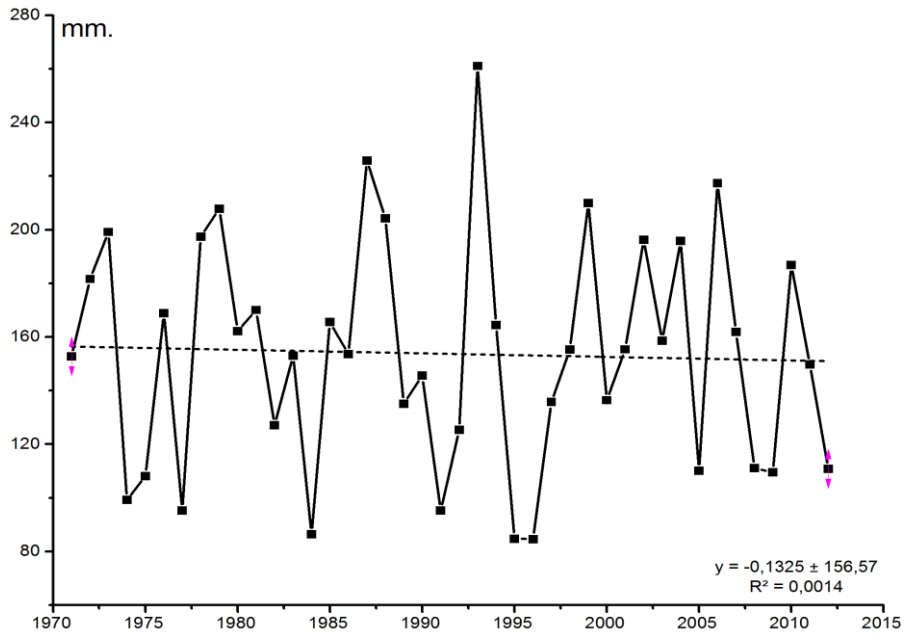

Figure 4. *Average annual amount of precipitation in Bakanas and Kuigan meteorological stations*

The main characteristics of temperature regime are average annual and average monthly air temperature, as well as absolute maximum and absolute minimum. Deviations of the actual temperature from its long-term average (norm) give an idea about temperature variation. Long-term data (1970-2013) on the air temperature provided by Bakanas and Kuigan weather stations (*Fig. 5*) were the source material for the study.

http://www.aloki.hu ● ISSN 1589 1623 (Print) ● ISSN 1785 0037 (Online)
DOI: http://dx.doi.org/10.15666/aeer/1802_24832498

The annual course that is ordinary for a continental climate, when the warmest month is July and the coldest - January, is typical for the whole territory. The average monthly air temperature can vary significantly from year to year. Therefore, in addition to the monthly values in the description of the climatic conditions it is important to have data on their variability. The highest interannual variability is possessed by the winter months, and the smallest by the summer months. So the long-term average air temperature in January may vary from -7.3 °C to -14.6 °C, and in July from 23.8 °C to 26.0 °C. Variability of air temperature fluctuates during the winter months from 3.7 °C to 5.1 °C, and in the summer months from 1.0 °C to 1.5 °C.

Temperatures of warm period of the year, especially in the summer are fairly stable, and its interannual variability is minimal in comparison with other months of the year. The absolute maximum of temperature was recorded in Kuigan meteorological station (46 °C) in 1983, and at Bakanas meteorological station (45 °C) in 1997. The absolute minimum of air temperature was observed in 1969 and amounted minus 43 °C in Bakanas and (minus 41 °C) in Kuygan. The daily amplitude, that is the difference between the daily maximum and minimum of temperature gives an idea of the weather variability. Its highest values are confined to the warm period (April-September) and constitute 13.1-19.3 °C (Bakanas), and the lowest - in winter (December-February) – are 8.2-12.2 °C (Bakanas). The daily amplitude in clear weather is much greater than in cloudy. In the high water year 2010 the average monthly air temperature for January-September was near normal in the study area, almost all the months were warm, with the exception of February and July. January was very warm and the average monthly air temperature at all stations was above the long term average 3.8-4.3 °C. February was abnormally cold with temperatures below the long term average 1.6-4.3 °C and in July air temperature was 23.7-24.4 °C, so that was lower by 1.1-1.3 °C than the average of long term average values. The air temperature in other months fluctuated within normal limits. An analysis of factual material on the air temperature and precipitation for 2010 and 2011 have shown that the positive trend in the annual air temperature and in annual precipitation sum, that identified material for many years (1971-2008) is preserved (*Fig. 5*).

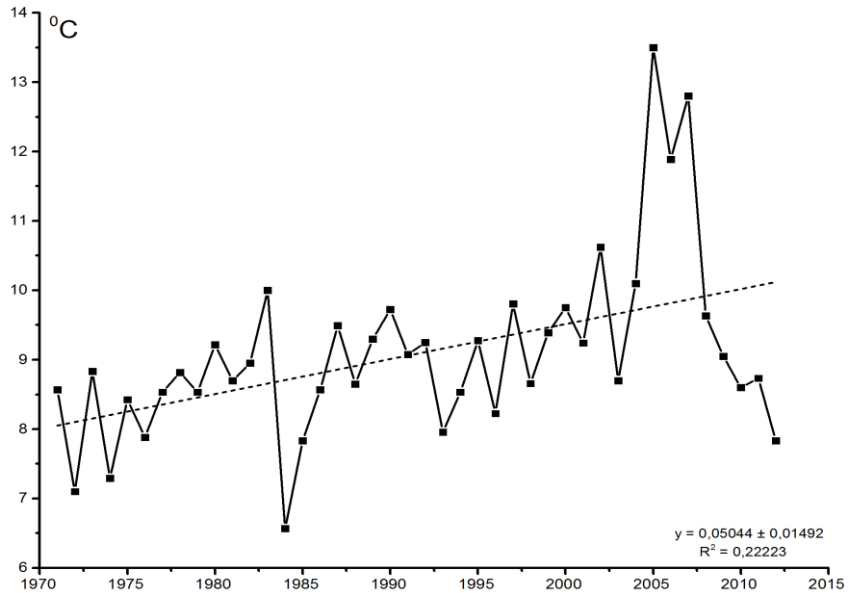

Figure 5. *The graph of long-term dynamics of average annual temperature at Bakanas meteorological station*

http://www.aloki.hu ● ISSN 1589 1623 (Print) ● ISSN 1785 0037 (Online)
DOI: http://dx.doi.org/10.15666/aeer/1802_24832498

Monitoring of Ili Delta for 1979-2015 on satellite images

Reducing the average annual runoff in lower reaches of the Ili River from 472 m^3/s (1948-1969) to 361 m^3/s (1970-1986) and the lowering of water level by 1-1.5 m, as well as changes in the natural hydrological regime of water releases by Kapshagai hydropower plant significantly worsened the flooding of the delta region of the river. Additionally, it was the reason for the drying of many flowing and stagnant lakes, reducing the area of reed massifs, salinization of soils and desertification of shores. Thus, these negative processes extend from the least watered peripheral part of the delta, which is adjacent to the coast of the Balkhash, to its top.

To identify the features of the dynamics of intra-zonal ecosystems depending on the water content of the river in different years, areas of hydromorphic ecosystems (meadows, reed, aquatic) were defined in dry years (1979, 1993, 2015), in a year with average water flow (2000) and in a year abnormally abounding in water (2010). As the analysis of satellite images show, significant amplitude of fluctuations of the delta watering have caused corresponding dynamic changes in the area of hydromorphic ecosystems, the total area and the relation between them have varied in a wide range (*Table 3*). Specially marked dynamics in changing the wetland area attracts attention. So according to Hydroproject the total delta area of the Ili River was 7740 km^2 in 1948, and 841 km^2 of them accounted for an open water surface of delta lakes and ducts (Hajdarov, 1963). And 50 years later, in 2000 lakes and ducts area on the basis of our data, has decreased by 36% and amounted to 540 km^2. However, after 2010 the abnormally high-water year the open water of lakes and ducts enormously increased, reaching 1177.7 km^2.

Table 3. *Areal ratio of hydromorphic Ili Delta ecosystems (km^2)*

Date of space images	1979		1993		2000		2010		2015	
	1978	1979	1998	1993	1999	2000	2009	2010	2014	2015
The average annual water content on of Ili River at "Tract Kapchagai" gauging station	337.9	363.2	327.1	425.5	509.0	515.0	503.0	718.5	220.0	No available data
Aquatic ecosystems	438.0		393.7		540.4		1177.7		539.9	
Grassland ecosystems	1767.6		1148.7		1153.1		1340.6		1895.6	
Reed ecosystems	1771.0		1669.2		2630.9		3027.3		2430.0	
The total area of hydromorphic ecosystems	3538.6		2817.9		3784		4367.9		4325.6	

The study of the temporal dynamics of the transformation of the delta ecosystems by satellite images revealed the following changes (*Fig. 6*):

1979

Analysis of satellite imagery that was made during the filling of Kapchagai reservoir showed pronounced negative changes of hydromorphic and semi-hydromorphic ecosystems. Low water period in lower reaches of the Ili River continued from 1970 to 1986. This caused desiccation of the major large delta lakes of the Zhideli system: Blue, White and Kaldayakskoe with a total area of 11; 3.5 and 45 km^2, respectively. Most ducts of the Zhideli system has been lost. Zhideli duct and its secondary ducts on the right side, such as Shybykty, Kertyubel, Zhalasar, Ketpenkaldy and partially Arystan

http://www.aloki.hu ● ISSN 1589 1623 (Print) ● ISSN 1785 0037 (Online)
DOI: http://dx.doi.org/10.15666/aeer/1802_24832498

ducts that feed the eastern part of the delta and their surrounding hydromorphic ecosystems strongly have become shallow. Unique Topar lake system has undergone a massive transformation and drying, where the water content of major ducts such as Topar I (Suminka) and Topar II did not exceed 1.4% of the Ili River flow. This is explained by a weak elaboration of Topar riverbed and its great fragmentedness due passive follow to local relief. The total water surface area of the Topar system was 120 km^2 in 1979, that is 220 km^2 less than in 1948. There has also been drying up of lakes and Topar side ducts such as Balatopar, Kishpa, Aksyir, Koktal that filled inter-ridge depressions before.

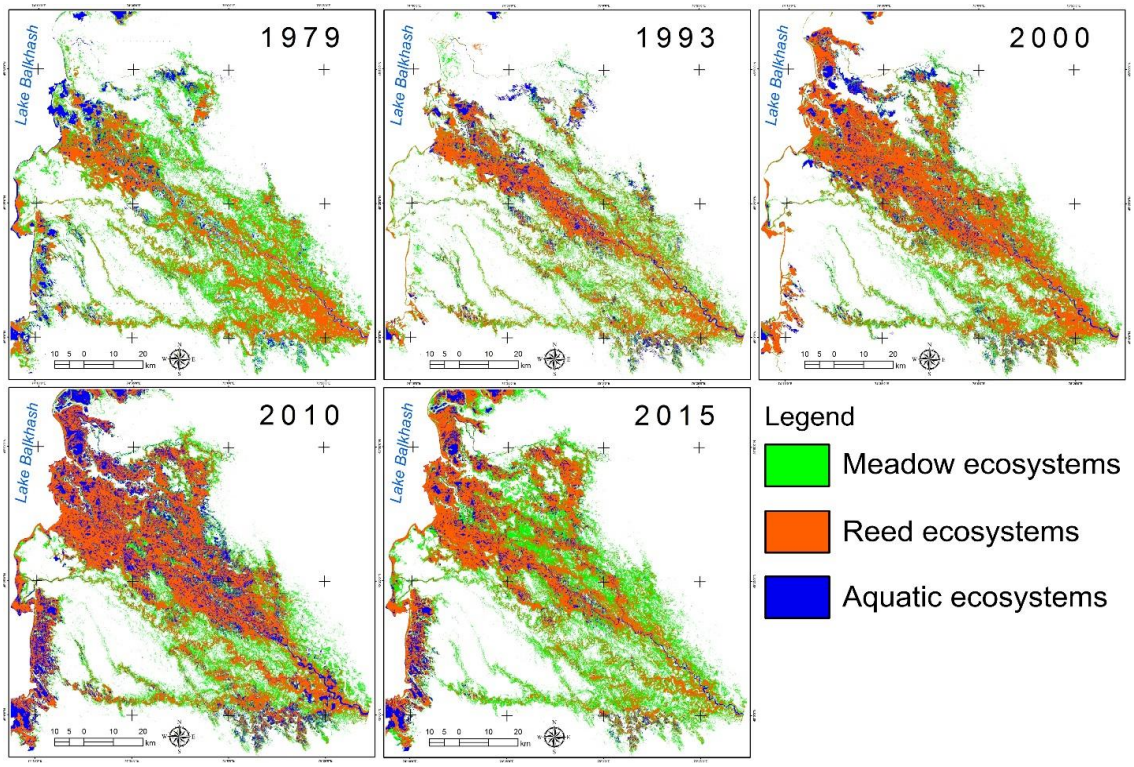

Figure 6. *Dynamics of area change of major ecosystems in the Ili Delta in 1979-2015*

1993

Despite the sharp decrease the area of irrigated land in the Kazakh part of the Ili basin in the 1990s there was a three-year water shortage during 1990-1992. The average water flow rate was 327.4 m^3/s and this led to sharp deterioration of general status and reducing the area of hydromorphic and semi-hydromorphic ecosystems for 720 km^2 in comparison with 1979. Such a sharp drop in runoff in lower reaches of the Ili River is explained by artificial changes in the hydrological regime by the Kapshagai hydropower plant. As a result, the level of the reservoir has increased by 23.5 cm during the period of 1990-1993, and the water surface area has increased from 1150 km^2 to 1244 km^2.

The sharp decline in the average annual runoff in lower reaches of the Ili River from 503 m^3/s to 327.4 m^3/s and the reduction of the level of Balkhash Lake by 25 cm from the nominal level 341.30 m occurred. This has led to the drying up of the aquatic, particularly coastal ecosystems and to the subsequent large-scale desertification of the Ili Delta's hydromorphic and semihydromorphic ecosystems, which is clearly observed

http://www.aloki.hu ● ISSN 1589 1623 (Print) ● ISSN 1785 0037 (Online)
DOI: http://dx.doi.org/10.15666/aeer/1802_24832498

in the picture in 1993. It should be highlighted that the total disappearance of lake systems - former bays of Balkhash Lake, were previously a part of the Topar system. The largest of them are Semizkol, Akkol, Bogatoe and Abishkol with the total area of 39.4 km^2, which had links with Aksiyr ducts from the Topar system in the 40-ies of the last century. Reducing the level of Balkhash Lake as in 1979 has led to the drying up of the major lakes of Zhideli System such as - Sinee, Beloe, Kaldayakskoe and Nauryzbaevskoe. Moreover, it has led to extended arm of large bays Majtán and Balakashkan, which penetrated into the delta for 10-15 km. Desertification of hydromorphic and semi-hydromorphic biocenoses took place on the periphery of the Zhideli system, especially in the eastern part. In the full-flowing years the lake, such as Erimbay dominated by flowing, where the runoff is carried out during the whole year.

2000

The annual average runoff of Ili River increased from 360 m³/s up to 430 m³/s in the period from 1993 to 2000. This has led to the expansion of the area of hydromorphic ecosystems, including reed community and meadow-bog cenoses in the northern periphery of the Zhideli system. Thus, the runoff increase on 19.5% has increased the area of hydromorphic and semi-hydromorphic ecosystem to 966 km^2. The proportion of aquatic ecosystem is also increased to 146.7 km^2 due to flooding and restoration of large deltaic lakes - Sinee, Beloe and Nauryzbaevskoe, which had dried during the period of 1979-1993.

At the same time, further drying processes and increase in the areas of desertification occurred in the Topar system. Increasing the level of Balkhash Lake to the mark of 341.54 m above sea level is not particularly wag on coastal lake systems (Semizkol, Akkol, Bogatoe and Abishkol), which are mainly recharged by groundwater inflow from the Balkhash.

2010

The average runoff of the Ili further increased and reached 538.6 m³ in the period of 2001-2010. The record for 2010 and the last 60 years of water content observing notices difference, because the water content reached 718.5 m³/s. This led to a significant increase in the area of all hydromorphic ecosystems, especially in the central and peripheral parts of the Zhidelinsk system and in a lesser degree, the first time after the 60s, in the Ili duct system where flooding phenomenon was detected. Appreciable growth of hydromorphic biocenosis was also observed at the head of the most abounding Topar system, where the total water surface area was 284 km², where the total water surface area was 284 km² not reaching the index in 1948, it achieved only 63 km².

In 2010, in the Ili River basin three waves of flood occurred - winter 411 m³/s (from October to February), spring 739 m³/s (from March to May), summer 1155 m³/s (from June to September), which is typical for a river with glacial feeding. Due to the significant increase in the water content of the River Ili and its tributaries, in many areas of the lower reaches, in the delta, spills and floods formed, which significantly changed the water regime and environmental conditions in aquatic and semi-aquatic ecosystems of the territory.

http://www.aloki.hu ● ISSN 1589 1623 (Print) ● ISSN 1785 0037 (Online)
DOI: http://dx.doi.org/10.15666/aeer/1802_24832498

2015

Since the 12th May 2014 the Ili River runoff on the Kazakh-Chinese border sharply fell, from 291 m³/s to 90 m³/s. The level of water in the Kapchagai reservoir decreased by 113 cm. Throughout the more than a century of instrumental hydrological observations of such flow reduction.

This caused a sharp reduction in the area of reed communities of the Zhideli system, firstly in the place of head part. In the middle and in the peripheral part the reed plant communities were preserved. In the Topar system drying of meadow and marsh phytocenoses was observed. Drying processes spread from the head of the Delta to the periphery, to the north direction. Based on an analysis of satellite images, it can be concluded desertification processes in most parts of the delta, particularly in the central regions of the Zhidelinsk system was expressed. Compared with 2010 semi-hydromorphic ecosystem area decreased by 555 km² and reed area by 597 km², which shows the extent of ongoing desertification processes. Reduction of aquatic ecosystems is observed at the head of the delta, where significant drying of large lakes occurred (*Table 4*).

Table 4. *Change of area ratio in Zhideli system delta lakes*

Year	Lake name					
	Siniy	**Belyiy**	**Kaldayakskie**	**Nauryizbaevskoe**	**Asaubay**	**Kokol**
2010	10.84	2.52	38.51	8.68	9.22	17.87
2015	9.32	2.18	17.08	3.58	5.27	8.19

Conclusion

In summary, it is supposed that the main anthropogenic factors that have a significant, often negative, impact on intrazonal half and hydromorphic ecosystems downstream of the Ili River include:

1. Regulation of water flow and decrease in water availability considering Ili River and its tributaries in China and Kazakhstan, in spite of the total increase in river flow due to degradation of glaciers in mountainous areas of the catchment basin of Ili.
2. Economic activities of the local population, as well as leisure travelers, hikers, hunters, fishermen, etc., adversely affecting the landscape, flora, plant communities, fauna and habitats of animals.
3. There is an urgent need to develop and implement a program of rational use of water resources of Ili-Balkash basin, including the modernization of irrigation systems, as well as the introduction of drought-resistant agricultural crops, water-saving technologies in the industrial and utilities sector.
4. Pollution of surface and ground water and terrestrial ecosystems with various pollutants, household, industrial and agricultural effluent sand emissions.
5. Related to the global and regional climate changes that lead to a marked increase in the average annual air temperature and reduction the number of drop-down in the region of precipitation, increase desertification process.

All of these factors which are strong and continuously increasing under human impacts since the early 70s and make less noticeable climatic changes, put unique

http://www.aloki.hu ● ISSN 1589 1623 (Print) ● ISSN 1785 0037 (Online)
DOI: http://dx.doi.org/10.15666/aeer/1802_24832498

ecosystems of the lower reaches of the Ili River, including its delta and Lake Balkhash, in a position that is more and more difficult to resolve causing to face the ecological crisis very reminiscent of the Aral Sea catastrophe. Naturally, the importance of each of these factors varies for different types of ecosystems. Anthropogenic factors are less effecting to the desert biocenosis remote from populated areas and water bodies. Because of the extra arid climate, they are not used for commercial purposes and are not visited by tourists. Their condition is determined mainly by climatic geographical features of the territory, whereas state hydromorphic delta ecosystems depends mainly on the factors of human nature.

At the same time, the state of soil and vegetation, especially wetlands, mainly determined by the water content of the Ili, and the condition of the animal world, especially commercial species of vertebrate fauna, by environmental services. Considering the continuously growing water demand, both in the Kazakh and especially in the Chinese part of the Ili basin, one should expect a significant further reduction of the hydromorphic ecosystems deltaic areas. The hydrographic Zhideli-Kogalinsk network system has the best prospects for the partial preservation of the unique intrazonal ecosystems.

Solving the problem of maintaining the water content in the lower reaches of the Ili River at an acceptable level is impossible without intergovernmental agreement between China and the RK on water allocation and a cardinal restructuring of irrigation and water distribution systems.

REFERENCES

[1] Burlibaev, M. Z., Volchek, A. A., Kalinin, M. J. (2004): Gidrometricheskie imerenija i gidrogeologicheskie raschety dlja vodohoz jajstvennyh tselej. – Kaganat, Almaty.

[2] Burlibaev, M. Z., Dostaj, Z. D., Mirhashimov, I., Nikolaenko, A. J. (2011): Sovremennoe sostojanie hozjajstvennoj dejatel'nosti v Ile-Balhashskom bassejne. Integrirovannoe upravlenie vodnymi resursami v Ile-Balkashskom bassejne. – UNDP, Almaty, pp. 3-16.

[3] Cherednichenko, A. V. (2010): Izmenenie klimata Kazahstana i vozmozhnosti adaptatsii za schet dostupnyh vodozapasov oblachnosti. – Ilim, Bishkek.

[4] Congalton, R. G., Green, K. (1999): Assessing the Accuracy of Remotely Sensed Data: Principles and Practices. – Lewis, Boca Raton, FL.

[5] Du, Z., Linghu, B., Ling, F., Li, W., Tian, W., Wang, H. (2014): Analysis of Landsat-8 OLI imagery for land surface water mapping. – Remote Sensing Letters 5(7): 672-681.

[6] Evstifeev, J. G., Egrohin, O. G., Nasyrov, R. M. (ND): Pochvennaja karta Semirech'ja. M:500 000 TOO. – Kazakh Scientific research institute of soil study and crops named after U Uspanov.

[7] Frazier, P., Page, K., Louis, J., Briggs, S., Robertson, A. I. (2003): Relating wetland inundation to river flow using Landsat TM data. – International Journal of Remote Sensing 24: 3755-3770.

[8] Hajdarov, R. M. (1963): Gidrologicheskij ocherk. V kng. – In: Lomonovicha, M. I. (ed.) Ilijskaja dolina, ee priroda i resursy / AN Kaz. SSR. Pod obsch. Izd-vo Akad. nauk KazSSR, Alma-Ata, pp. 238-249.

[9] Hajdarov, R. M. (1968): Dinamika del'ty r. Ili. – Trudy GGI, Vyp. 160: 180-221.

[10] Jensen, J. R., Ramsay, E. W., Mackey, H. E., Christensen, E. J., Sharitz, R. P. (1987): Inland wetland change detection using aircraft MSS data. – Photogrammetric Engineering and Remote Sensing 53: 521-529.

http://www.aloki.hu ● ISSN 1589 1623 (Print) ● ISSN 1785 0037 (Online)
DOI: http://dx.doi.org/10.15666/aeer/1802_24832498

[11] Kanika, K., Anil, K. G., Rhythm, G. (2013): A comparative study of supervised image classification algorithms for satellite images. – International Journal of Electrical, Electronics and Data Communication 1(10): 10-16.
[12] Magasheva, R. (1977): Meliorativnye uslovija sovremennoj del'ty reki Ili i ih izmenenija v svjazi s zaregulirovaniem stoka Kapchagajskim vodohranilischem. – Avtoref. kand. dis., Alma-Ata.
[13] Neasset, E. (1996): Use of the weighted Kappa coefficient in classification error assessment of thematic maps. – International Journal of Geographical Information Systems 10(5): 591-603.
[14] Plisak, R. P. (1981): Izmenenie rastitel'nosti del'ty reki Ili pri zaregulirovanii stoka. – Nauka, Alma-Ata.
[15] Plisak, R. P., Ogar, N. P. (1985): Karta rastitel'nosti sovremennoj del'ty r. Ili. M 1:300 000. M. edition.
[16] Sovolova, N. P., Zhelnova, N. I. (1984): Karta kormovyh ugodij Balhaschskogo rajona Alma-Atinskoj rajona Alma-Atinskoj oblasti KazSSR. M. 1:300 000. Karta sostavlena po materialam polevogo obsledovanija v 1981 g. – MSH SSR Institute, Kazgiprozem.
[17] Starodubtsev, V. M., Truskavetskij, S. R. (2007): Degradatsija pochv del'tah rek.– Problemy osvoenija pustyn 2: 26-29.
[18] Starodubtsev, V. M., Nekrasova, T. F., Popov, J. M. (1978): Aridizatsija pochv del'tovyh ravnin Juzhnogo Kazahstana v svjazi s zaregulirovaniem rechnogo stoka. – Vodnye resursy 5: 14-23.
[19] Tso, B., Mather, P, M. (2009): Classification Methods for Remotely Sensed Data. 2nd Ed. Chaps. 2-3. – Taylor and Francis Group, USA.
[20] Vilesov, E. N., Gorbunov, A. P., Morozova, V. N., Severskij, E. V. (2006): Degradatsija ledenenija i kriogenez na sovremennyh morenah severnogo Tjan'-Shanja. – Kriosfera Zemli 1: 69-73.

http://www.aloki.hu ● ISSN 1589 1623 (Print) ● ISSN 1785 0037 (Online)
DOI: http://dx.doi.org/10.15666/aeer/1802_24832498

ALGAE-BASED HEAVY METAL REMEDIATION IN ACID MINE DRAINAGE: A REVIEW

MANG, K. C. – NTUSHELO, K.*

Department of Agriculture and Animal Health, University of South Africa, Pretoria, South Africa (e-mail: kaluchimdimang@yahoo.com; phone: +27-748-366-063)

**Corresponding author*
e-mail: ntushk@unisa.ac.za; phone: +27-789-027-944

(Received 28th May 2019; accepted 11th Oct 2019)

Abstract. The production of acid mine drainage (AMD) is among the factors responsible for much of the degradation of water and soil resources and the disruption of biodiversity in the environment. Several studies have shown that organisms (either macro or micro) present at sites contaminated with AMD have the potential to bioaccumulate heavy metals and hence stimulate their application in bioremediation processes. Algal strains are not an exception to those organisms found in AMD. This review was aimed at examining the heavy metal remediation of AMD using algae, remediation properties of algae and different algal-based methods used in heavy metal remediation of AMD. Algal strains such as *Spirulina* sp., *Chlorella* spp., *Scenedesmus* spp., *Cladophora* spp., *Oscillatoria* spp., *Anabaena* spp. and *Phaeodactylum tricornutum* act as "hyper-accumulators" and "hyper-adsorbents" with a high selectivity for different elements from AMD. However, algae-based methods of abating AMD are not the ultimate solution to the problem and there is room for more studies. The current study suggests further attention to phycoremediation individually and synergistically with sulphate-reducing bacteria.
Keywords: *bioremediation, hyperaccumulation, phycoremediation, phytoremediation, sulphate-reducing bacteria*

Abbreviations: AMD: acid mine drainage, HRAP: high-rate algal ponds, SRB: sulphate-reducing bacteria, ATS: algal turf scrubber, PIMR: pipe inserted microalgae reactor

Introduction

Industrialisation has brought immense development and economic improvement to most countries of the world. Despite the positive impact of industrialization, it also has negative effects on the environment and biodiversity. Acid mine drainage (AMD) is one of the negative consequences of industrialisation. The mining of gold (Au), copper (Cu), nickel (Ni) and other minerals are associated with AMD, which may have adverse effects on human and animal health as well as the environment (Azapagic, 2004). Conventional approaches to remediation and other active and passive technologies have been adopted to neutralise the threat of AMD. However, they have been found to have many drawbacks, including high cost of application and further and unforeseen environmental damage. The option of using green technologies in remediating AMD has been researched and applied in many countries, and offers much promise for a cleaner and safer environment (Galiulin and Galiulina, 2003, 2008; Koptsik et al., 2014; Cunningham and Ow, 1996; Nowack et al., 2006; Prasad and Freitas, 2003). These green technologies involve, among others, the use of algae that offer solutions without causing any adverse effects on the environment.

The process of using macro- and microalgae to remediate AMD and other contaminated environments is termed phycoremediation. Kalin et al. (2006) state that the use of algae as decontaminating agents provides some advantages, including low costs of operation, easy manipulation, lack of pollution, relatively simple recovery of

http://www.aloki.hu ● ISSN 1589 1623 (Print) ● ISSN 1785 0037 (Online)
DOI: http://dx.doi.org/10.15666/aeer/1802_24992512

the metal contaminants for recycling and not constituting a source of secondary waste. The accumulated heavy metals can be recovered after the growth of algae in the contaminated environment by separating the algal biomass from the water. The separated algal biomass is dried and the heavy metals are recovered by converting the heavy metals into oxides or other recoverable salts. In addition, the separated algal biomass can either be sequestered or stored for future purposes or disposed of in municipal waste landfills to reduce its environmental footprint (Edmundson and Wilkie, 2013).

Compared to the conventional method of remediation, phycoremediation has been shown to be less costly, less energy consuming and with no generation of sludge (Ghosh and Singh, 2005; Abdel-Raouf et al., 2012). In phycoremediation, macro- or microalgae are used for the removal or biotransformation of pollutants from wastewater (Ahmad et al., 2013). Algae of the genera *Chlorella*, *Chlamydomonas*, *Spirulina*, *Scendesmus*, *Nostoc* and *Oscillatoria* have been used in wastewater treatment over the last few decades (Dubey et al., 2011; Sharma and Khan, 2013). It was assumed that microalgae are versatile in converting contaminants into a non-hazardous material, making the treated water fit for reuse or discharge into receiving water bodies (Rao et al., 2011). Algae-based treatment can be used in combination with secondary treatment where microorganisms work in symbiosis with algae cells for effective treatment.

The remediation of AMD by using algae has been the focus of many studies since the ability of algae to adsorb and actively transport heavy metals through the cellular tissues was identified (Stevens et al., 2001; Malik, 2004; Das et al., 2009; Mehta and Gaur, 2005). The transported heavy metals can be intracellularly immobilized by metal-binding peptides found in the vacuoles of the cells and stored in the cytoplasm through the synthesis of polyphosphate bodies (Pawlik-Skowrońska, 2001; Priya et al., 2014). Nishikawa et al. (2003) point out that algal cells are composed of electron-dense bodies made up of polyphosphate that are capable of accumulating metals and protecting algal cells from metal toxicity. Irrespective of the ability of algae to remediate water contaminated by heavy metal, the species of algae prospected to be used in bioremediation of heavy metals in AMD must be able to tolerate highly concentrated mixtures of distinct heavy metals. In this review, heavy metal remediation of AMD is examined. In addition, the heavy metal remedial properties of algae and the different methods involving algal strains in heavy metal remediation of AMD are reviewed. Topics under discussion include remediation properties of algae and an overview of different algal-based methods used in heavy metal remediation of AMD.

Heavy metal remediation of acid mine drainage using algal strains

Intense mining leads to the production of AMD, which has detrimental effects on the environment – hence the need to control and possibly manage the waste and acidic water produced by mines. Conventional treatment methods have been widely researched and applied in the remediation of AMD (Gazea et al., 1996; Robinson and Robb, 1995; Ghosh and Singh, 2005; Abdel-Raouf et al., 2012). A medium-sized mining operation may spend over US$70 000 annually on the cost of lime alone, making conventional treatment methods expensive (Gazea et al., 1996; Robinson and Robb, 1995; Ghosh and Singh, 2005; Abdel-Raouf et al., 2012).

Harris and Ramelow (1990) point out that research has been done on the use of algal strains in bioremediation but the main focus has been the metal ion accumulation

http://www.aloki.hu ● ISSN 1589 1623 (Print) ● ISSN 1785 0037 (Online)
DOI: http://dx.doi.org/10.15666/aeer/1802_24992512

abilities of some algae species from solutions. McKnight and Morel (1980) report that complex metal ions forming chelatins and polysaccharides produced in algae strains have been extensively studied to enhance the knowledge of heavy metal remediation by algae. Shiraiwa et al. (1993) discovered the ability of certain strains of algae to increase the alkalinity of the medium as a by-product of their inorganic carbon accumulating mechanism. However, the use of this alkaline production by algae in precipitation of metals in AMD has not been widely reported.

Some researchers have shown that direct treatment of AMD with an algal culture has a short period of effectiveness and the sustainability of this direct treatment is poor (Wallace et al., 1997; Boshoff et al., 1996). Cu, lead (Pb) and zinc (Zn) are toxic to algal species such as *Spirulina* sp. when the accumulated concentrations of these metals exceed 7 μmol/g (Payne et al., 1999). Van Hille et al. (1999) developed a system that separates the growing culture of algae from the untreated effluent to help solve the problem of heavy metal toxicity in *Spirulina* sp. The system combines the principles of passive treatment with simple, low-cost reactors associated with active treatment methods. Furthermore, Van Hille et al. (1999) utilized the alkalinity produced by the alga *Spirulina* sp. in a continuous system and found that the alkaline environment elicited by the algal strain enhanced heavy metal precipitation. According to their findings, the primary treatment process consistently removed between 80 and 95% of Zn (7.16 mg/l), over 99% of iron (Fe) (98.9 mg/l) and Pb (2.35 mg/l) within 14 days. Van Hille et al. (1999) further discovered that the combination of the primary and secondary treatments enhanced the removal of over 95% of all metals tested as well as a 90% reduction in sulphate concentration.

Recently, Oberholster et al. (2018) grew *Microspora tumidula*, *Oedogonium crassum* and *Klebsormidium klebsii* previously established by Oberholster et al. (2014) under laboratory conditions for 192 h to determine their bioaccumulation of sulphur (S) and other important algal growth elements such as calcium (Ca), magnesium (Mg) and phosphorus (P) from AMD water and treatment constructed wetland water in the vicinity of the Boesman Spruit (stream) near the town of Carolina in the Ermelo coalfield in South Africa at different pH values. They observed that *Microspora tumidula* showed the highest bioaccumulation of S and P at a pH of 5 and *Oedogonium crassum* showed the highest bioaccumulation of Ca and Mg at a pH of 7. The accumulation efficiency of Mg by all three macroalgal species increased significantly with an increase in the pH. *Oedogonium crassum* and *Klebsormidium klebsii* showed very little increase in chlorophyll A (mg g^{-1} fw) and ash-free dry weight (mg g^{-1} AFDW) when compared to the species *M. tumidula* at all four pH ranges. In conclusion, their study established *Microspora tumidula* as a good candidate for use in a biological hybrid system for treating sulphur-rich AMD.

Remediation properties of algal biomass

The removal of heavy metals and sulphates by algae is believed to be very flexible and depends on the type of metal, the taxon of the alga and the age of material to be removed (Novis and Harding, 2007). Studies have shown that the removal of heavy metals and other contaminants by algae is influenced by seasons (Elbaz-Poulichet et al., 2000; Brake et al., 2004). The seasons influence the availability of light and temperature range, and this can in turn affect the rate of bioremediation by algae because of their sensitivity to light intensity and temperature.

http://www.aloki.hu ● ISSN 1589 1623 (Print) ● ISSN 1785 0037 (Online)
DOI: http://dx.doi.org/10.15666/aeer/1802_24992512

The common mechanisms used by algae in the remediation process are absorbency and adsorbency. Heavy metal remediation is dependent on the species of algae. The algae feed on the nutrient elements during the process of heavy metal removal and there is an increase in their biomass. Some of these heavy metals adhere to the surface of algae (adsorbency) and others are taken up into the inner cells (absorbency) of the algae. An aqueous solution is required by algae in the removal of a low concentration of metal ions and the bioaccumulation of these metals in their cells (Afkar et al., 2010; Chen et al., 2012; Kumar and Gaur, 2011; Mehta and Gaur, 2005). The heavy metals are bioaccumulated in the cell vacuoles, intercellular spaces and cell wall (Afkar et al., 2010; Chen et al., 2012; Kumar and Gaur, 2011; Mehta and Gaur, 2005), as shown in *Figure 1*. Vymazal (1984) observed that *Cladophora glomerata* and *Oedogonium rivulare* are among the species used to continuously remove cobalt (Co), Ni, Pb, cadmium (Cd), manganese (Mn), Fe, chromium (Cr) and Cu from wastewater. The ability and extent of heavy metal removal by algae is believed to vary from strain to strain (Al-Shwafi and Rushdi, 2008). Mehta and Gaur (2005) discovered that dead algae biomass adsorbs more heavy metals than living ones. Pawlik-Skowrońska (2001) observed that the freshwater algae *Stigeoclonium* spp. can thrive well and effectively remove Zn in mining water containing a high concentration of Zn.

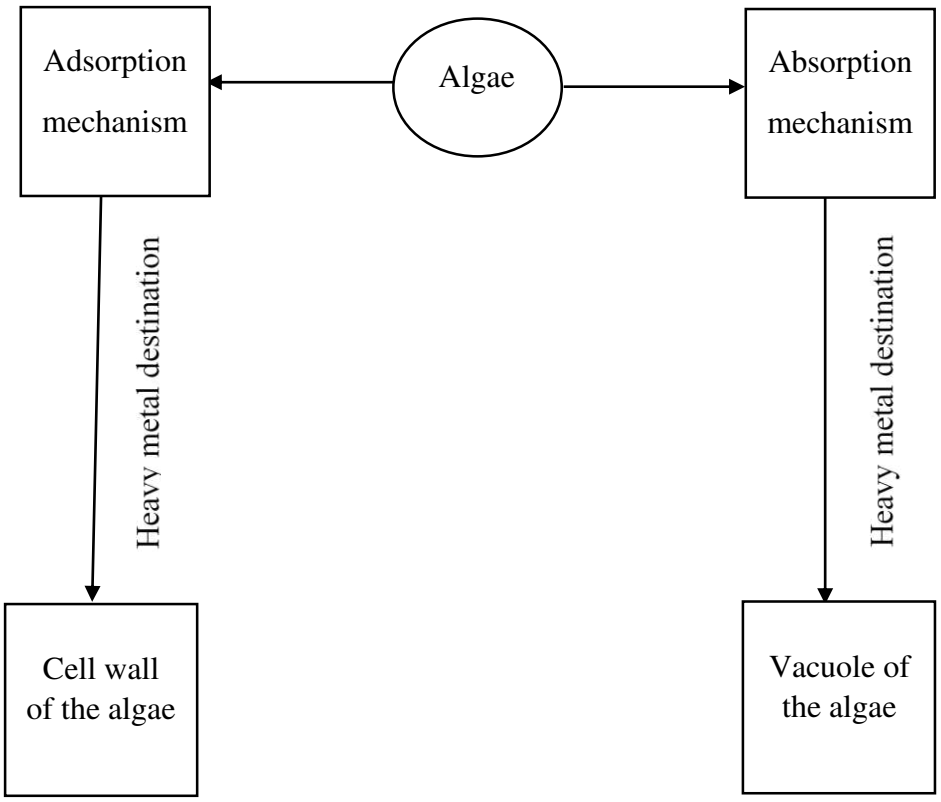

Figure 1. *Mechanisms of heavy metal remediation and their destination in algae*

Living algae accumulate trace metals intracellularly through active biological transport (Ajjabi and Chouba, 2009; Kiran and Thanasekaran, 2011). The synergic activity of different types of algae, along with their multilayer cell walls, makes them a suitable adsorbent for heavy metals (Bilal et al., 2013; Gupta et al., 2015; Wang and

http://www.aloki.hu ● ISSN 1589 1623 (Print) ● ISSN 1785 0037 (Online)
DOI: http://dx.doi.org/10.15666/aeer/1802_24992512

Chen, 2009). Algae can survive in both fresh and marine brackish waters and are among the most commonly found photosynthetic eukaryotes (Ioannis and Kyzas, 2015). Bishnoi and Pant (2004) discovered that Spirogyra algal species were able to remove Cu (II) with an efficiency of 58 to 85% at an initial concentration of 20 mg/l after 30 min. Furthermore, Pavasant et al. (2006) found that *Caulerpa lentillifera* (a dried green macroalga) was also effective in the removal of multiple metals in an aqueous solution through adsorbency. Other algae such as the brown alga *Turbinaria ornate* and the green alga *Ulothrix zonata* were also found to be very effective adsorbents in the removal of heavy metals (Nuhoglu et al., 2002; Vijayaraghavan and Prabu, 2006; Djati et al., 2016). Regarding the tolerance of *Ulothrix* sp. LAFIC 010 (Chlorophyta) for a high concentration of metals from ACD in Brazil, Massocato et al. (2018) found that the algae accumulated Mn and Ni in their cell walls and vacuole respectively.

Microbial sulphate reduction generates alkalinity and this promotes the bioremediation of acid mine drainage through the formation of metal sulphides that allows for the precipitation of metals from the solution. Acid mine drainage environments are known to be deficient of natural carbon (Koschorreck, 2008), and the addition of suitable carbon sources promotes the activity of sulphate-reducing bacteria (SRB) (Zhang et al., 2017). For SRB to survive and for their better growth, nutrients such as yeast extract and tryptone are absolutely necessary (Zhang et al., 2017). Kiran et al. (2017) state that the most studied bioremediation for heavy metals removal is based on SRB which cause metal sulphide precipitation and hence the removal of the metals from the contaminated environment. The use of SRB to remove heavy metals was successful on a large scale for heavy metal removal at low pH values, stable sludge, very low operating costs and minimal energy consumption. Based on this, SRB could provide an on-site alternative treatment method for AMD; however, they may not be suitable for sites with low temperatures such as those in extreme winter conditions (Sheoran et al., 2010).

The use of SRB for the remediation of the contaminated environment has the weakness of long residence times that can last for weeks. Furthermore, a constant supply of organic substrates and the use of large steel bioreactors are required for them to be effective (White et al., 1997; Sheoran et al., 2010). SRB also require time to grow and reach the critical population growth level to work effectively. This can be a cost of remediation. However, the greatest advantage of using SRB to remediate the environment is their ability to remove both metals and sulphates simultaneously. This is not common when the traditional chemical remediation process is used (Kiran et al., 2017).

Overview of remediation methods of acid mine drainage using algal strains

Various policies, regulations and standards have been suggested in many countries to prevent the threat of AMD to human health and the environment, to reduce the concentrations of the pollutants and to develop cost-effective technologies that will enhance AMD remediation (Fan, 1996). This is due to the challenge that AMD has imposed on most countries of the world (Nriagu and Pacyna, 1988). The conventional treatment methods which are based on either separation (such as precipitation, adsorption and filtration) or reaction have shown many weaknesses, such as low removal capacity, lack of selectivity and intolerance to organic substances.

http://www.aloki.hu ● ISSN 1589 1623 (Print) ● ISSN 1785 0037 (Online)
DOI: http://dx.doi.org/10.15666/aeer/1802_24992512

The high-rate algal pond (HRAP) system is believed to be the most frequently used method for remediating AMD (Oswald, 1998; Mehrabadi et al., 2015). In addition, the algal turf scrubber (ATS) was also developed to remediate AMD and polluted groundwater. The ATS method involves the application of suspended biomass of cyanobacteria such as S*pirulina, Oscillatoria, Anabaena* or consortia of species or common green algae species such as *Chlorella, Scenedesmus, Cladophora* (Craggs et al., 1996; Adey et al., 1996). These methods were found to be effective in the removal of heavy metals and organic compounds such as chlorinated and aromatic organic compounds to acceptable levels in AMD or any other industrial wastewater (Craggs et al., 1996; Adey et al., 1996).

Toumi et al. (2000) reported that the HRAP has a higher removal rate per unit volume per day. Tested on urban polluted water with lower ion concentrations of Zn, Cu and Pb, the HRAP was found to be 10 times more efficient in removing Cu compared to the waste stabilization pond system. Furthermore, high pH values enhanced metal precipitation and effective algal photosynthesis. Rose et al. (1998) reported the formation of a patent ATS formed from a combination of HRAP and SRB. This process involves the direct addition of AMD into HRAP with a high pH value to enhance the precipitation of heavy metals, followed by the recovering of HRAP biomass which is used as a carbon source for SRB (Perales-Vela et al., 2006). However, these methods had challenges in maintaining a dynamic equilibrium between algae net oxygen production, bacterial respiration due to low light penetration, rich microalgal biomass, climate conditions and proper mixing (Fallowfield and Garret, 1985).

Phillips et al. (1995) suggest non-agitated algal ponds as a remedy for the challenges faced with constructed wetland technologies in enhancing the effective removal of Mn and stability of a neutralizing pH. They show that consortia of algae and cyanobacteria can reduce Mn concentrations effectively to an environmentally safe level. The work done by Perales-Vela et al. (2006) also shows that Mn can be removed through biomass adsorption, high pH precipitation and immobilization. All these findings provide a promising future for the treatment of AMD and wastewaters through algae bioremediation.

Dinardo et al. (1991) state that the history of the ability of aquatic plants to remove heavy metals efficiently from contaminated AMD water dates back to 1973. Since then, several algae strains have been successfully used in the removal of heavy metals from AMD or wastewater but most of the work was completed during a batch process in which microalgal species were grown. Wang et al. (2016) state that algae can produce oxygen at a lower cost and also be effective in phycoremediation.

Algae play an essential role in the bioaccumulation of heavy metals in wetland remediation of AMD. Zagury et al. (2007) state that this role of algae makes it possible to design passive bioreactor systems for the remediation of AMD. A passive bioreactor system is based on a similar principle as a large activated carbon filter where AMD comes into the surface area, percolates through a specially constructed barrier layer and exits the system from below. The major components of this bioreactor, especially the initial stage, include algae. *Spirulina* spp. was discovered to be useful in remediating AMD because they were able to absorb various heavy metals rapidly through direct contact with the AMD effluent stream and reached saturation within 30 min (Van Hille et al., 1999; Balaji et al., 2014). Furthermore, it was observed that *Spirulina* spp. exhibited toxicity after the period of saturation but continued to generate an alkaline environment capable of reducing the acidity of AMD through the production of

http://www.aloki.hu ● ISSN 1589 1623 (Print) ● ISSN 1785 0037 (Online)
DOI: http://dx.doi.org/10.15666/aeer/1802_24992512

inorganic bicarbonate salts. Species of both micro- and macroalgae have been identified as useful in phycoremediation. A *Chlorella* strain that was capable of sustaining growth at 11.24 mg of Cd^{2+}/l was analysed in a marine screen and was found to have a removal efficiency of 65% when exposed to an amount of 5.62 mg of Cd^{2+}/l (Matsunaga et al., 1999). Furthermore, *Chlorella* and *Scenedesmus* strains were analysed in a batch process at 20 mg Cr^{6+}/l and were found to have removal efficiencies of 48% and 31% respectively (Travieso et al., 1999).

Algal biomass was observed to accumulate heavy metals in the work done by Freitas et al. (2011) on the biosorption of heavy metals by algal species in AMD from coal mining in Brazil. They further observed that the algal biomass' capabilities to absorb the heavy metals were Fe > Al > Ca > Mg > Zn > Mn > Cu in all the sampling sites. Algal genera such as *Microspora, Eunotia, Euglena, Mougeotia* and *Frustulia* survived in the AMD environment and *Microspora* was the most dominant (Freitas et al., 2011). A hybrid system comprising a pipe inserted microalgae reactor (PIMR) and an active treatment unit for the removal of Fe from AMD was used by Park et al. (2013) to study the removal of heavy metals by algal species. Fe can hinder the growth of algae and lipid formations which can limit the ability of algal biomass to remove heavy metals in AMD, hence the need to remove the element in the hybrid system. Furthermore, in the study carried out by Park et al. (2013), *Nephroselmis* sp. was observed to be effective in removing heavy metals and had a strong tendency to grow with pre-treated AMD. Based on the ability of the algal species to grow well and also remove heavy metals, PIMR was suggested to be more effective in removing heavy metals and enhancing the growth of algal species. PIMR was found to be more protective than HRAP and SRB in protecting the algal species against environmental contaminants. However, the HRAP system has more treatment capacity and heavy metal removal than the PIMR system.

At least 14 algal species and their ability to take up heavy metal contaminants from AMD and other pollution sources were reviewed by Ben and Baghour (2013), and were found to hyperaccumulate or hyperabsorb heavy metals with high selectivity for different metals. Furthermore, the results of a few studies regarding the use of some microalgae species for AMD bioremediation were compiled by Das et al. (2009). The removal efficiencies of heavy metals and sulphates which are the main contaminants in AMD, operating conditions and the growth methods used to achieve the results, and the effectiveness and possibility of algae technology for AMD bioremediation are contained in *Table 1*. Cu, Zn, Fe, Pb, Ni, Mn and sulphates, under a known pH range, can be removed by microalgae. This knowledge about microalgae enhances the possibility of modifying phycoremediation of the algal biomass to suit specific pollutant conditions, alongside both uptake limits and specificity through genetic engineering of algal species.

Since the early 1990s, passive water treatment systems where algae remove heavy metals from AMD or other contaminated wastewater as a common component have been used. Although the algal biomass has been proven to be efficient in removing both organic and inorganic pollutants, there is a need for more studies to explore its full potential with the development of innovative technologies. Such innovative technologies could include gene modification technology. This technology involves identifying specific genes responsible for producing metal-chelating proteins and enhancing this capability in algal strains.

http://www.aloki.hu ● ISSN 1589 1623 (Print) ● ISSN 1785 0037 (Online)
DOI: http://dx.doi.org/10.15666/aeer/1802_24992512

Table 1. *Summary of the use of some algal species in acid mine drainage bioremediation (adapted from Das et al., 2009)*

Algal strains	Remediation role	Achieved results	Growth method	Reference
Blue-green algae – cyanobacterial mat		Removal of 2.59 g of Mn/day/m^2	Oxidation pond	Phillips et al. (1995)
Spirulina sp.	Metal adsorption, re-alkalization, nutrient for SRB (dead biomass)	(i) Removal of Fe (up to 100%), Zn (86-98%), Cu (38-76%), Pb (40-78%) at retention time of 10 days (ii) Rise of pH from 3 to 8.5 for a biomass loading of 3 mg/mL chlorophyll A	HRAP (high-rate algal pond)	Rose et al. (1998)
Spirulina sp.	Alkalinity generation and metal precipitation	(i) pH rise from 1.8 to 8.18 (ii) Reduction of sulphates (SO_4) 89%, Fe 99%, Pb 95%, Zn 93%, Cu 94%	Bench scale anaerobic digester, primary and secondary treatment	Van Hille et al. (1999)
Mixed algal population	Soluble EPS as carbon source for SRB	Up to 57% of sulphates (SO_4) and 52% COD removal by mixed SRB	HRAP	Molwantwa et al. (2000)
Eunotia exigua and *Pinnularia obscura*	Primary production	Chlorophyll A (Chl A) Content 52-72 mg/m^2	Mining lake	Koschorreck et al. (2002)
Spirulina spp.	Dead biomass as nutrient for SRB	150 mg SO_4 removal/g algal biomass/day	Bench scale anaerobic upflow reactor	Boshoff et al. (2004)
Blue-green algae (predominantly *Oscillatoria* spp.) – microbial consortium	SO_4 removal, metal precipitation by consortium	(i) pH increase from 2.93 to 6.78 (ii) Reduction of SO_4 29%, Fe 95%, Pb 88%, Zn 86%, Cu 97%, Co 83%, Ni 62%, Mn 45%.	Bench scale test cell	Sheoran and Bhandari (2005)
Chlorella ellipsoidea	Bioremediation potential		In-situ test using limnocorrals	EPA (2005)
Eunotia exigua and *Chlamydomonas* sp.	Enhance primary production, thereby SRB growth	Reduction of Fe from 14 mg/L to 0.2 mg/L and SO_4 from 344 mg/L to 124 mg/L	Microcosm experiment	Fyson et al. (2006)
Ulothrix spp.	Metal absorption	Absorption of Cu 3500 mg/L and As 500 mg/L	AMD, Sar Cheshmeh copper mine	Orandi et al. (2007)

http://www.aloki.hu ● ISSN 1589 1623 (Print) ● ISSN 1785 0037 (Online)
DOI: http://dx.doi.org/10.15666/aeer/1802_24992512

The knowledge of the use of algae and their ability to remove heavy metals is widely accepted and growing fast. However, significant contributions are yet to be made in light of the success of passive systems used in the remediation of AMD. Many researchers have focused on the production of biofuel or biodiesel from algal sources. This has taken the attention of most researchers away from the potential value of algae in phycoremediation which presents a promising solution in AMD remediation. Das et al. (2009) encourage the use of *Lepocinclis* sp. and *Klebsormidium* sp. in the treatment of AMD because they showed promising features in terms of their growth and distribution. Furthermore, the use of a consortium of algae and fungi has been encouraged, either used individually or as a group, as they offer the advantage of working in symbiosis and synergy. However, this consortium of algae and fungi could bring the challenges of high heavy metal concentrations, acidity, low availability of organic carbon and phosphates because these factors affect the growth of both organisms. This can be a setback to the success of using this consortium of algae and fungi in treating AMD because it contains high levels of heavy metals with a very low pH.

Conclusion

Many studies have indicated the effectiveness of phycoremediation of AMD and its potential for future applications, as shown in this current review. It is also evident from this review that passive systems involving the use of algal biomass have achieved commendable results; however, they are not the ultimate solution to the problem of AMD. Consequently, there is a need for further studies on effective remediation of AMD to provide more solutions to the environmental problem caused by this scourge. It is believed that each AMD tailing site has unique chemical characteristics and compositions that require a unique way of remediation.

Therefore, a conclusive study will require evaluation of various algae species, their removal mechanisms and growth, pH, temperature, residence time and flow rate of the AMD to enhance the success of AMD remediation using algae species. Some algae species are known as extremophiles because they can thrive well in unusual and extreme environmental conditions. As a result, there is a need to study in detail their adaptability to be used in phycoremediation processes, especially for AMD. However, algae as sources of oxygen have some weaknesses such as their unpredictable response to a complex changing environment or wastewater when compared to conventional wastewater treatment plants. Furthermore, the opacity of the medium, solar radiation, rise of nutrients, temperature, season and ecological succession, and other major environmental factors are not easily understood and require careful monitoring to ensure the success of the process.

This current review suggests that more studies should be done on different aspects of phycoremediation and SRB approaches, and possibly a combination of the two approaches in the remediation of AMD. This should range from identifying and developing simple, effective physical barrier materials to advanced genetic research suitable for AMD.

Acknowledgements. The authors are grateful to the Agricultural Research Council and University of South Africa Climate Change Collaboration Centre for funding.

http://www.aloki.hu ● ISSN 1589 1623 (Print) ● ISSN 1785 0037 (Online)
DOI: http://dx.doi.org/10.15666/aeer/1802_24992512

REFERENCES

[1] Abdel-Raouf, N., Al-Homaidan, A. A., Ibraheem, I. B. M. (2012): Microalgae and wastewater treatment. – Saudi Journal of Biological Sciences 19: 257-275.

[2] Adey, W. H., Luckett, C., Smith, M. (1996): Purification of industrially contaminated groundwaters using controlled ecosystems. – Ecological Engineering 7(3): 191-212.

[3] Afkar, A., Ababna, H., Fathi, A. A. (2010): Toxicological response of the green alga *Chlorella vulgar* to some heavy metals. – American Journal of Environmental Science 6: 230-237.

[4] Ahmad, F., Khan, A. U., Yasar, A. (2013): Comparative phycoremediation of sewage water by various species of algae. – Proceedings of the Pakistan Academy of Science 50: 131-139.

[5] Ajjabi, L. C., Chouba, L. (2009): Biosorption of Cu^{2+} and Zn^{2+} from aqueous solutions by dried marine green macroalga *Chaetomorpha linum*. – Journal of Environmental Management 90: 3485-3489.

[6] Al-Shwafi, N. A., Rushdi, A. I. (2008): Heavy metal concentrations in marine green brown and red seaweeds from coastal waters of Yemen, the Gulf of Aden. – Environmental Geology 55: 653-660.

[7] Azapagic, A. (2004): Developing a framework for sustainable development indicators for the mining and minerals industry. – Journal of Cleaner Production 12(6): 639-662.

[8] Balaji, S., Kalaivani, T., Rajasekaran, C. (2014): Biosorption of zinc and nickel and its effect on growth of different *Spirulina* strains. – CLEAN - Soil, Air, Water 42(4): 507-512.

[9] Ben, C. K., Baghour, M. (2013): The role of algae in phytoremediation of heavy metals: a review. – Journal of Material and Environmental Science 4: 873-880.

[10] Bilal, M., Shah, J. A., Ashfaq, T., Gardazi, S. M. H., Tahir, A. A., Pervez, A., Haroon, H., Mahmood, Q. (2013): Waste biomass adsorbents for copper removal from industrial wastewater—a review. – Journal of Hazardous Materials 263: 322-333.

[11] Bishnoi, N. R., Pant, A. (2004): Biosorption of copper from aqueous solution using algal biomass. – Journal of Scientific and Industrial Research 113: 813-816.

[12] Boshoff, G. A., Duncan, J. R., Rose, P. D. (1996): An algal-bacterial integrated ponding system for the treatment of mine drainage waters. – Journal of Applied Phycology 8: 442.

[13] Boshoff, G. A., Duncan, J. R., Rose, P. D. (2004): The use of micro-algal biomass as a carbon source for biological sulphate reducing systems. – Water Research 38: 2659-2666.

[14] Brake, S. S., Hasiotis, S. T., Dannely, H. K. (2004): Diatoms in acid mine drainage and their role in the formation of iron-rich stromatolites. – Geomicrobiology Journal 21: 331-340.

[15] Chen, C., Chang, H., Kao, P., Pan, J., Chang, J. (2012): Biosorption of cadmium by CO_2-fixing microalga *Scenedesmus obliquus* CNW-N. – Bioresource Technology 105: 74-80.

[16] Craggs, R. J., Adey, W. H., Jenson, K. R., St. John, M. S., Green, G. F., Oswald, W. J. (1996): Phosphorous removal from wastewater using and algal turf scrubber. – Water Science Technology 33: 191-198.

[17] Cunningham, S. D., Ow, D. W. (1996): Promises and prospects of phytoremediation. – Plant Physiology 110: 715-719.

[18] Das, B. K., Roy, A., Koschorreck, M., Mandal, S. M., Potthoff, K. W., Bhattachary, J. (2009): Occurrence and role of algae and fungi in acid mine drainage environment with special reference to metals and sulfate immobilization. – Water Research 43: 883-894.

[19] Dinardo, O., Kondos, P. D., MacKinnon, D. J., McCready, R. G. L., Riveros, P. A., Skaff, M. (1991): Study on Metals Recovery/Recycling from Acid Mine Drainage. – Phase IA: Literature Survey, for MEND Treatment Committee.

[20] Djati, U. H., Tan, K. X. D., Choong, Z. Y. D., Yu, J. J., Ong, J. J., Lim, Z. B. (2016): Biosorption of heavy metal by algae biomass in surface water. – Journal of Environmental Protection 7: 1547-1560.

http://www.aloki.hu ● ISSN 1589 1623 (Print) ● ISSN 1785 0037 (Online)
DOI: http://dx.doi.org/10.15666/aeer/1802_24992512

[21] Dubey, S. K., Dubey, J., Mehra, S., Tiwari, P., Bishwas, A. J. (2011): Potential use of cyanobacteria species in bioremediation of industrial effluent. – African Journal of Biotechnology 10: 1125-1132.
[22] Edmundson, S. J., Wilkie, A. C. (2013): Landfill leachate – a water and nutrient resource for algae-based biofuels. – Environmental Technology 34: 1849-1857.
[23] Elbaz-Poulichet, F., Dupuy, C., Cruzado, A., Velasqaez, Z., Achterberg, E. P., Braungardt, C. B. (2000): Influence of sorption process by iron oxides and algae fixation on arsenic and phosphate cycle in an acidic estuary (Tinto River, Spain). – Water Research 34: 3222-3230.
[24] Environmental Protection Agency (EPA) (2005): Algal Bioremediation of the Berkeley Pit Lake System: An In-Situ Test Using Limnocorrals. – EPA, Washington.
[25] Fallowfield, H. J., Garret, M. K. (1985): The photosynthetic treatment of pig slurry in temperate climatic conditions: a pilot plant study. – Agricultural Wastes 12: 111-136.
[26] Fan, A. M. (1996): Assessment of Metals in Drinking Water with Specific References to Lead and Arsenic. – In: Chang, L. W. (ed.) Toxicology of Heavy Metals. CRC Press Inc., Boca Raton, FL, pp. 39-53.
[27] Freitas, A. P. P., Schneider, I. A. H., Schwartzbold, A. (2011): Biosorption of heavy metals by algal communities in water streams affected by the acid mine drainage in the coal-mining region of Santa Catarina state, Brazil. – Mineral Engineering 24: 1215-1218.
[28] Fyson, A., Nixdorf, B., Kalin, M. (2006): The acidic lignite pit lakes of Germany – microcosm experiment on acidity removal through controlled eutrophication. – Ecological Engineering 28: 288-295.
[29] Galiulin, R. V., Galiulina, R. A. (2003): Phytoextraction of heavy metals from contaminated soils. – Agrokhimiya 3: 77-85.
[30] Galiulin, R. V., Galiulina, R. A. (2008): Soil purification from heavy metals with the help of plants. – Vestnik Rossiiskoi Akademii Meditsinskikh Nauk 78: 247-249.
[31] Gazea, B., Adam, K., Kontopoulos, A. (1996): A review of passive systems for the treatment of acid mine drainage. – Minerals Engineering 9: 23-42.
[32] Ghosh, M., Singh, S. P. (2005): A review of phycoremediation of heavy metals and utilization of its by- products. – Asian Journal on Energy and Environment 6: 214-231.
[33] Gupta, V. K., Nayak, A., Agarwal, S. (2015): Bioadsorbents for remediation of heavy metals: current status and their future prospects. – Environmental Engineering Research 20: 1-18.
[34] Harris, P. O., Ramelow, G. J. (1990): Binding of metal ions by particulate biomass derived from *Chlorella vulgaris* and *Scenedesmus quadricauda*. – Environmental Science and Technology 24: 220-228.
[35] Ioannis, A., George, Z. K. (2015): Progress in batch biosorption of heavy metals onto algae. – Journal of Molecular Liquids 209: 77-86.
[36] Kalin, M., Fyson, A., Wheeler, W. N. (2006): The chemistry of conventional and alternative treatment systems for the neutralization of acid mine drainage. – Science of the Total Environment 366: 395-408.
[37] Kiran, B., Thanasekaran, K. (2011): Copper biosorption on *Lyngbya putealis*: application of response surface methodology (RSM). – International Biodeterioration and Biodegradation 65: 840-845.
[38] Kiran, M. G., Pakshirajan, K., Das, G. (2017): Heavy metal removal from multicomponent system by sulfate reducing bacteria: mechanism and cell surface characterization. – Journal of Hazardous Materials 324: 62-70.
[39] Koptsik, G. N., Koptsik, S. V., Smirnova, I. E. (2014): Efficiency of remediation of technogenic barrens around the Pechenganikel works in the Kola subarctic. – European Journal of Soil Science 47: 519-528.
[40] Koschorreck, M. (2008): Microbial sulphate reduction at a low pH. – FEMS Microbiology Ecology 64: 329-342.

http://www.aloki.hu ● ISSN 1589 1623 (Print) ● ISSN 1785 0037 (Online)
DOI: http://dx.doi.org/10.15666/aeer/1802_24992512

[41] Koschorreck, M., Frommichen, R., Herzsprung, P., Tittel, J., Wendt-Potthoff, K. (2002): Function of straw for in situ remediation of acidic mining lakes. – Water, Air and Soil Pollution 2: 97-109.
[42] Kumar, D., Gaur, J. P. (2011): Metal biosorption by two cyanobacterial mats in relation to pH, biomass concentration, pre-treatment and reuse. – Bioresource Technology 102: 2529-2535.
[43] Malik, A. (2004): Metal bioremediation through growing cells. – Environment International 30: 261-278.
[44] Massocato, T. F., Ramos, J. C., Bascuñan, V. L. F., Simioni, C., Röriga, L. R., Bonomi, B. J. (2018): Tolerance of *Ulothrix* sp. LAFIC 010 (Chlorophyta) against high concentration of metals from acid mine drainage. – Ecotoxicology and Environmental Safety 157: 227-234.
[45] Matsunaga, T., Takeyama, H., Nakao, T., Yamazawa, A. (1999): Screening of marine microalgae for bioremediation of cadmium polluted seawater. – Journal of Biotechnology 70: 33-38.
[46] McKnight, D. M., Morel, F. M. M. (1980): Copper complexation by siderophores from filamentous blue–green algae. – Limnology and Oceanography 25: 62-71.
[47] Mehrabadi, A., Craggs, R., Farid, M. M. (2015): Wastewater treatment high rate algal ponds (WWT HRAP) for low-cost biofuel production. – Bioresource Technology 184: 202-214.
[48] Mehta, S. K., Gaur, J. P. (2005): Use of algae for removing heavy metal ions from wastewater: progress and prospects. – Critical Reviews in Biotechnology 25: 113-152.
[49] Molwantwa, J. B., Molipane, N. P., Rose, P. D. (2000): Biological sulphate reduction utilizing algal extracellular products as a carbon source. – WISA 2000 Biennial Conference, Sun City, South Africa.
[50] Nishikawa, K., Yamakoshi, Y., Uemura, I., Tominaga, N. (2003): Ultrastructural changes in *Chlamydomonas acidophila* (Chlorophyta) induced by heavy metals and polyphosphate metabolism. – FEMS Microbiology Ecology 44: 253-259.
[51] Novis, P. M., Harding, J. S. (2007): Extreme Acidophiles: Freshwater Algae Associated with Acid Mine Drainage. – In: Seckbach, J. (Ed.), Algae and Cyanobacteria in Extreme Environment. Springer, Dordrecht, pp. 443-463.
[52] Nowack, E., Schulin, R., Robinson, B. H. (2006): Critical assessment of chelant-enhanced metal phytoextraction. – Environmental Science and Technology 40: 5225-5232.
[53] Nriagu, J. O., Pacyna, J. M. (1988): Quantitative assessment of worldwide contamination of air, water and soils by trace metals. – Nature 333: 134-139.
[54] Nuhoglu, Y., Malkoc, E., Gürses, A., Canpolat, N. (2002): The removal of Cu (II) from aqueous solutions by *Ulothrix zonata*. – Bioresource Technology 85: 331-333.
[55] Oberholster, P. J., Genthe, B., Cheng, P., Botha, A-M. (2014): The potential of selected macroalgal species for treatment of AMD at different pH ranges in temperate regions. – Water Resources 60: 82-92.
[56] Oberholster, P. J., Cheng, P., Botha, A-M., Philip, H., Liesl, H. (2018): Assessment of selected macroalgae for use in a biological hybrid system for treating sulphur in acid mine drainage (AMD). – Journal of Applied Phycology 30: 1361-1370.
[57] Orandi, S., Yaghubpur, A., Sahraei, H. (2007): Influence of AMD on aquatic life at Sar Cheshmeh copper mine. Abstract. – Goldschmidt Conference, Cologne, Germany.
[58] Oswald, W. J. (1988): Micro-algae and Waste-Water Treatment. – In: Borowitzka, M. A., Borowitzka, L. J. (eds.) Micro-algal Biotechnology. Cambridge University Press, Cambridge, pp. 305-328.
[59] Park, Y. T., Lee, H., Yun, H., Song, K., Yeom, S., Choi, J. (2013): Removal of metal from acid mine drainage using a hybrid system, including a pipes inserted microalgae reactor. –Bioresource Technology 150: 242-248.

http://www.aloki.hu ● ISSN 1589 1623 (Print) ● ISSN 1785 0037 (Online)
DOI: http://dx.doi.org/10.15666/aeer/1802_24992512

[60] Pavasant, P., Apiratikul, R., Sungkhum, V., Suthiparinyanont, P., Wattanachira, S., Marhaba, T. F. (2006): Biosorption of Cu^{2+}, Cd^{2+}, Pb^{2+}, and Zn^{2+} using dried marine green macroalga *Caulerpa lentillifera*. – Bioresource Technology 97: 2321-2329.
[61] Pawlik-Skowrońska, B. (2001): Phytochelatin production in freshwater algae *Stigeoclonium* in response to heavy metals contained in mining water: effects of some environmental factors. – Aquatic Toxicology 52: 241-249.
[62] Payne, R. A., Van Hille, R. P., Duncan, J. R. (1999): The effect of toxic heavy metals on the alga *Spirulina* sp. – Proceedings of the Biannual Conference of the Water Institute of South Africa, Cape Town, South Africa.
[63] Perales-Vela, H. V., Peña-Castro, J. M., Cañizares-Villanueva, R. O. (2006): Heavy metal detoxification in eukaryotic microalgae. – Chemosphere 64: 1-10.
[64] Phillips, P., Bender, J., Simms, R., Rodriguez-Eaton, S., Britt, C. (1995): Manganese removal from acid coal-mine drainage by a pond containing green algae and microbial mat. – Water Science and Technology 31: 161-170.
[65] Prasad, M. N. V., Freitas, H. M. O. (2003): Metal hyperaccumulation in plants — biodiversity prospecting for phytoremediation technology. – Electronic Journal of Biotechnology 6: 285-321.
[66] Priya, M., Gurung, N., Mukherjee, K., Bose, S. (2014): Microalgae in removal of heavy metal and organic pollutants from soil. – Microbial Biodegradation and Bioremediation. https://doi.org/10.1016/B978-0-12-800021-2.00023-6.
[67] Rao, P. H., Kumar, R. R., Raghavan, B. G., Subramanian, V. V., Sivasubramanian, V. (2011): Application of phycoremediation technology in the treatment of wastewater from a leather processing chemical manufacturing facility. – Water SA 37: 7-14.
[68] Robinson, J. D. F., Robb, G. A. (1995): Methods for the control and treatment of acid mine drainage. – Coal International 152-156.
[69] Rose, P. D., Boshoff, G. A., Van Hille, R. P., Wallace, L. C. M., Dunn, K. M., Duncan, J. R. (1998): An integrated algal sulphate reducing high rate ponding process for the treatment of acid mine drainage wastewaters. – Biodegradation 9: 247-257.
[70] Sharma, G. K., Khan, S. A. (2013): Bioremediation of sewage wastewater using selective algae for manure production. – International Journal of Environmental Engineering and Management 4: 573-580.
[71] Sheoran, A. S., Bhandari, S. (2005): Treatment of mine water by a microbial mat: bench scale experiments. – Mine Water and the Environment 24: 38-42.
[72] Sheoran, A. S., Sheoran, V., Choudhary, R. P. (2010): Bioremediation of acid-rock drainage by sulphate-reducing prokaryotes: a review. – Minerals Engineering 23: 1073-1100.
[73] Shiraiwa, Y., Goyal, A., Tolbert, N. E. (1993): Alkalization of the medium by unicellular green algae during uptake of dissolved inorganic carbon. – Plant Cell Physiology 34: 649-657.
[74] Stevens, A. E., McCarthy, B. C., Vis, M. L. (2001): Metal content of *Klebsormidium*-dominated (Chlorophyta) algal mats from acid mine drainage waters in south-eastern Ohio. –Journal of the Torrey Botanical Society 226-233.
[75] Toumi, A., Nejmeddine, A., El-Hamouri, B. (2000): Heavy metal removal in waste stabilisation ponds and high rate ponds. – Water, Science and Technology 42: 17-21.
[76] Travieso, L., Cañizares, R. O., Borja, R., Benitez, F., Domínguez, A. R., Dupeyrón, R., Valiente, V. (1999): Heavy metal removal by microalgae. – Bulletin of Environment Contamination and Toxicology 62: 144-151.
[77] Van Hille, R. P., Boshoff, G. A., Rose, P. D., Duncan, J. R. (1999): A continuous process for the biological treatment of heavy metal contaminated acid mine water. – Resources, Conservation and Recycling 27: 157-167.
[78] Vijayaraghavan, K., Prabu, D. (2006): Potential of *Sargassum wightii* biomass for copper (II) removal from aqueous solutions: application of different mathematical models to batch and continuous biosorption data. – Journal of Hazardous Materials 137: 558-564.

http://www.aloki.hu ● ISSN 1589 1623 (Print) ● ISSN 1785 0037 (Online)
DOI: http://dx.doi.org/10.15666/aeer/1802_24992512

[79] Vymazal, J. (1984): Short term uptake of heavy metals by periphyton algae. – Hydrobiologia 119: 171-179.
[80] Wallace, L. C. M., van Hille, R. P., Boshoff, G. A., Rose, P. D., Duncan, J. R. (1997): Bioremediation of acidic mine effluent by an algal based system. – Proceedings Biotechnology SA, Grahamstown.
[81] Wang, J., Chen, C. (2009): Biosorbents for heavy metals removal and their future. – Biotechnology Advances 27: 195-226.
[82] Wang, Y., Ho, S. H., Cheng, C. L., Guo, W. Q., Nagarajan, D., Ren, N. Q., Lee, D. J., Chang, J. S. (2016): Perspectives on the feasibility of using microalgae for industrial wastewater treatment. – Bioresource Technology 222: 485-497.
[83] White, C., Sayer, J. A., Gadd, G. M. (1997): Microbial solubilization and immobilization of toxic metals: key biogeochemical processes for treatment of contamination. – FEMS Microbiology Reviews 20: 503-516.
[84] Zagury, G. J., Neculita, C., Bussière, B. (2007): Passive treatment of acid mine drainage in bioreactors: short review, applications and research needs. – OttawaGeo 2007: 1439-1446.
[85] Zhang, M., Xingyu, L., Yibin, L., Guangyuan, W., Zining, W., Jiankang, W. (2017): Microbial community and metabolic pathway succession driven by changed nutrient inputs in tailings: effects of different nutrients on tailing remediation. – Scientific Reports 7(1): 1-10.

http://www.aloki.hu ● ISSN 1589 1623 (Print) ● ISSN 1785 0037 (Online)
DOI: http://dx.doi.org/10.15666/aeer/1802_24992512

HYDROGEOLOGICAL CHARACTERIZATION AND REGIONAL GROUNDWATER CIRCULATION USING GIS AND MODFLOW MODELS: A CASE STUDY FROM KURUKTAG REGION, NORTHWEST CHINA

ZHENG, J. M.* – XIE, F.

Northwest Institute of Nuclear Technology, Xi'an, 710024, China

**Corresponding author*
e-mail: 13899012052@163.com

(Received 24th Jun 2019; accepted 25th Oct 2019)

Abstract. In order to realize the evaluation of hazardous chemicals disposal sites in the Kuluktag region of Xinjiang, China, this paper conducted a numerical simulation study of the circulation of groundwater in the carrier of nuclide migration. Based on the hydrogeological survey in the field, a hydrogeological conceptual model of regional groundwater flow and a three-dimensional numerical model of regional groundwater flow were established. The finite difference method was applied to obtain the flow velocity and characteristics of groundwater under various scenarios. By analyzing the sensitivity of the structure of water-containing medium and its parameters, this paper aims to explore the impact of the uncertainty of precipitation, water-containing medium structure and its parameters on the flow velocity and direction of regional groundwater, simulate the change of flow velocity and direction of groundwater in the study area, and predict the groundwater circulation rules in the long run measured in the unit of 10,000 years.
Keywords: *Kuruktag, hydrogeological conditions, groundwater circulation model, nuclide migration, numerical simulation*

Introduction

As groundwater is the carrier of nuclides migration, the quantitative evaluation of groundwater flow and migration of nuclide in underground complex geological bodies is critical to the evaluation and selection of disposal sites. Research and discovery on hydrogeology, groundwater circulation and nuclides migration evaluation is one of the hottest research topics on disposal site evaluation (Kolbe et al., 2016; Post et al., 2019; Cao et al., 2016; Tatti et al., 2019; Zhou et al., 2013; Jiang et al., 2018).

In recent decades, numerical simulation has been carried out extensively to analyze groundwater flow in various areas. Kihm et al. (2007) predicted the relationship between groundwater flow and land deformation using three-dimensional numerical simulation. Blessent et al. (2011) conducted fluid flow and solute transport model in discretely-fractured crystalline bedrock for nuclear-fuel site. Tatti et al. (2019) built numerical model of the contaminated low permeability layers based on groundwater Circulation Wells. Pétré et al. (2019) analyzed the regional groundwater flow system of the transboundary Milk River Aquifer using numerical modeling. Mengistu et al. (2019) employed the numerical simulation to evaluate groundwater monitoring network of the Moab Khutsong deep gold mine.

This article makes full use of existing data, including geological, hydrogeological, groundwater dynamic data and satellite imagery, combined with field hydrogeological surveys to analyze regional hydrogeological conditions and groundwater distribution characteristics, including aquifer media system structure, boundary conditions, characteristics of groundwater flow field, hydraulic connection between different water-bearing units, and characteristics of groundwater recharge and discharge (Chang et al., 2001).

http://www.aloki.hu ● ISSN 1589 1623 (Print) ● ISSN 1785 0037 (Online)
DOI: http://dx.doi.org/10.15666/aeer/1802_25132538

According to the survey of stratigraphic lithology in combination with the analysis of groundwater dynamic field, geological structure and hydrogeology in the Kuruktag region of Xinjiang, the model of regional groundwater circulation is established, and the numerical model of three-dimensional groundwater flow is constructed to obtain the parameters related to the aquifer system. Based on the existing research results and risk assessment experience at home and abroad (Kendall, 1998; Singleton et al., 2005), the groundwater flow numerical model is used to simulate the spatial and temporal distribution characteristics of groundwater flow under various scenarios, and the influence of the uncertainty of geological medium structure and parameters on groundwater flow is studied and explored. The variation rules of regional groundwater flow under long-term scale could be predicted through the mechanism and pattern of groundwater flow.

(1) We use GIS (Geographic Information System) technology to integrate a large number of regional scale data (including geology, topography, spring location, and well information) into hydrogeological information data. The method not only accurately describes the hydrogeological conditions of the study area, improving the data management and efficiency, but also provides necessary data to support the establishment of regional groundwater models.

(2) Due to the large-scale work area and the difficulties determining hydrogeological boundaries, SRTM DEM (the digital elevation model) data is used for hydrological space analysis, that is, the extraction of digital river network and the division of the drainage basin, so as to grasp the boundary of the whole basin. On the basis of hydrological analysis, the model boundary is determined according to the hydrogeological conditions, flow conditions and replenishment relationship of the work area.

(3) According to the stratigraphic age and lithology, the regional groundwater permeability coefficient is divided. At the same time, considering the strong heterogeneity of the work area, the faults are separately characterized in the model to analyze the impact of faults on groundwater flow.

(4) We aimed to establish a regional groundwater flow model by MODFLOW (Visual MODFLOW 2000 software), and correct the model through the measured groundwater water level so that the regional groundwater model can reflect the real groundwater flow field more accurately.

Hydrogeology introduction

Natural geographical conditions

Topography

The western part of the work area is Bosten Lake by an altitude of about 1,050 m, and the eastern part gradually becomes mountainous. On the north side of the east is the Qoltag Mountains, and on the south side is the Kuruktag Mountain interspersed with the mountain basins. The eastern part of the work area is mainly the Nanhu Gobi. The north side of the work area is the Turpan Basin, and the south faces the Lop Nurdriedbasin. Lop Nur, the lowest plutonium in the Tarim Basin, is a modern dried-up salt lake with an area of 10,350 km^2. Its outer zone is the vast Taklimakan Desert in the west; the eastern part is the Beishan and the Aqike Valley; the alluvial fan and dune of the Altun Mountains is in the south, and the low hills of Kuruktag in the north. There are large areas of Yadan or wind-eroded mounds and terraces in the north, west and east of Lop Nur. Lop Nur is an endless salt-desert plain with a slope of only 0.04%. The surface presents different forms of salt crust, which often exhibits micro-topography such as ploughing land and cracks.

http://www.aloki.hu ● ISSN 1589 1623 (Print) ● ISSN 1785 0037 (Online)
DOI: http://dx.doi.org/10.15666/aeer/1802_25132538

The salt crust is hard and sharp, and the height of the undulation varies from 10 to 60 cm approximately (Xia, 2007). The surface elevation of the work area is shown in *Figure 1*.

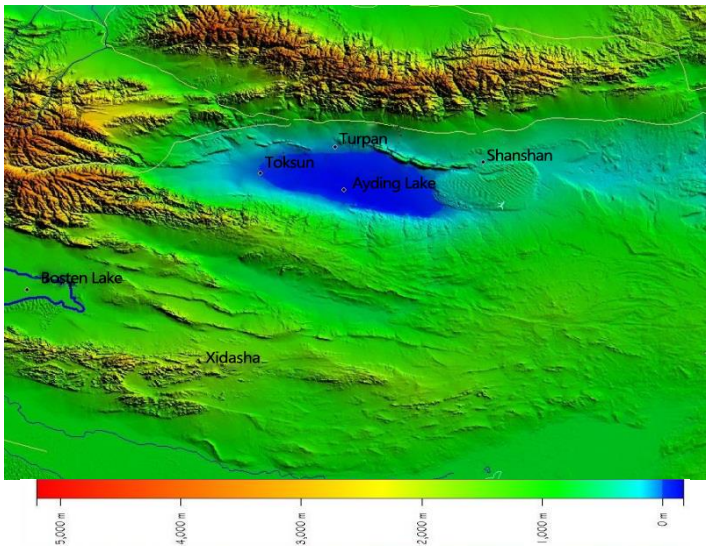

Figure 1. *Work area elevation*

Meteorology and hydrology

The work area belongs to the arid area of the northwest inland. The average annual precipitation is less than 60 mm, and the most rainfall is concentrated in the summer. The average annual precipitation of Kumish and Tokson in the west of the work area is 61.6 mm and 9.2 mm; 26.3 mm of Shanshan and 56.9 mm of Hami in the north; 47.8 mm of Ruoqiang and 42.9 mm of Milan in the south.

Lop Nur in the south-central part of the work area is located at the lowest recess in the eastern end of the Tarim Basin and surrounded by mountains to the north, east and south of the typical continental arid climate, which means that the region considered to be dry. For example, the average annual precipitation of Tieqianlike is less than 20 mm, however the annual average evaporation is up to 2,600 mm with 10.6 °C as the annual average temperature and 26.7 °C of the average temperature in July, -9.5 °C in January. There is a lot of wind in the area, and the prevailing wind direction is NE (SDIC Xinjiang Lop Nur Potash Co. Ltd, 2006).

Geological introduction

The northern part of the work area is the Turpan-Hami Basin. The Turpan-Hami Basin is an intermountain basin in the eastern section of the Tianshan fold mountain range. It is a Mesozoic and Cenozoic sedimentary basin that occurred and developed on the basis of the returning slanting slope of the Hercynian period. The layer thickness is 5,000-6,000 m with the maximum of 8,700 m. The southern part of the basin is about 2000 m above sea level. They are composed of Upper Paleozoic volcanic rocks, volcanic clastic rocks and rammed rocks. The pier uplift divides the Turpan-Hami basin into east and west Quaternary sedimentary basins, and the western part is the Turpan Basin, with an area of about 21,000 km^2. The structural pattern of the Tu-ha Basin is shown in *Figure 2* (Chen, 1993).

http://www.aloki.hu ● ISSN 1589 1623 (Print) ● ISSN 1785 0037 (Online)
DOI: http://dx.doi.org/10.15666/aeer/1802_25132538

The central and western part of the work area is the Kuruktag region, and the structure of the area is shown in *Figure 3*. Most of the Sinian and Paleozoic caprocks were constructed with carbonate platforms and clastic rocks. The total thickness is up to 8,000 m, and the maximum thickness reaches 14,000-15,000 m. When the Tertiary continental clastic sediments are developed, the thickness of the caprock is greatly reduced to only 100-200 m. Due to the different neotectonic movements, the geomorphology of the area is in a relatively young development stage, especially in the northwest, where many high and steep mountains are formed. There is a clear topographical difference between the area and the north of the CazelTaga (geosyncline) and the Tarim Basin (Lot) in the south (Chen, 1966; Feng et al., 1994).

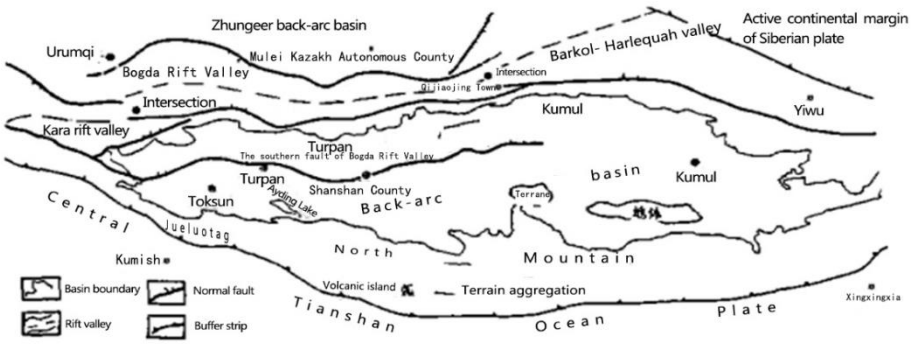

Figure 2. *Tectonic framework of the Tu-ha basin and its adjacent area*

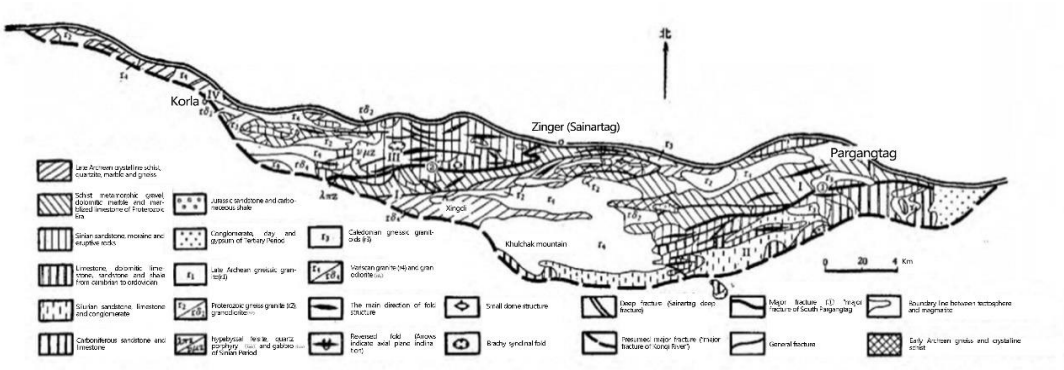

Figure 3. *Tectonic sketch of the Kuruktag*

Stratum

The Paleozoic and pre-Paleozoic clastic rocks, magmatic rocks and carbonate rocks are widely distributed in the Kuruktag Mountains. There are thin Quaternary loose stratums distributed in the piedmont strips and local inter-mountain basins. The Tertiary clastic rocks are mainly distributed in the denudation platform and the inter-mountain depression in the northeastern part of the Lop Nur Basin. The formation is generally gentle, and the lithology is mainly mudstone, sandy mudstone, sandstone and glutenite. The Quaternary loose sediments are mainly distributed in the lake basin and its surrounding low-lying areas. The thicker Quaternary alluvial sand and gravel stratums are distributed in the sloping plains of the Altun Mountains in the south and the Aqike Valley in the east.

http://www.aloki.hu ● ISSN 1589 1623 (Print) ● ISSN 1785 0037 (Online)
DOI: http://dx.doi.org/10.15666/aeer/1802_25132538

Tectonics

(1) Fracture

There are three lithospheric faults within the work area, and two shell faults, and more general faults. According to its distribution direction, it can be roughly divided into three groups: the north-north-east fault, the near east-west fault and the north-east-east fault, among which the north-east-east fault is the most developed. The near east-west basal-type fault developed in the Altun Mountains is mostly spread in a sleek shape in a large scale. The main compresso-shearing structure with water-resistance controls the boundary between the bedrock mountain and the basin. The northwestward fault constitutes a conjugated fault zone, which develops in the Kuruktag, Beishan and Aqike Valleys (The Second Hydrogeology Engineering Geology Brigade of Xinjiang Geology and Minerals Bureau, 2003). It extends far with a large scale, and it is regarded as left-handed compresso-shearing, which controls the northern boundary of the dried-up Lop Nur salt lake. Across the dried-up Lop Nur salt lake, the fault divide it into several units, and along the fault the spring points are distributed (Shi et al., 2017).

(2) Fold

There is a large number of folds in diverse forms mainly developed in the Kuruktag and Beishan areas. Among them, the large-scale Beishan fold belt with complex folds is generally north-east-east and north-eastward directed. The fold belt in Kuruktag region is small and omnidirectional in axial direction. In the red clay castle in Luobei, there is a new generation of anticline development.

(3) Joint fissures

In the Kuruktag and Beishan areas, there are common joint fissures in the rock, and the dense belts are mostly distributed on both sides of the fault. The development of joint fissures in brittle rocks such as limestone and granite are significantly higher than those of soft rocks.

Regional hydrogeological conditions

Division of groundwater systems

Based on the viewpoint of groundwater system theory, the complete groundwater migration space with relatively independent recharge, runoff and excretion is divided into six groundwater first-level systems in the region, and then according to aquifer characteristics, recharge conditions, hydrodynamic characteristics and groundwater quality, characteristics, several secondary systems (sub-zones) can be divided (Lei et al., 2019).

Regional groundwater circulation characteristics

Atmospheric precipitation in the mountainous area is transformed into bedrock fissure water and surface water in the Altun Mountains and Kuruktag and Beishan. Part of the bedrock fissure water is transferred to deep circulation water to the deep subsurface, and the other part along the valley or the front of the mountain to replenish surface water as spring. The surface water flows out of the mountain, passing and then enters the Altun Mountains and Kuruktag and the sloped gravel plains of the Beishan

http://www.aloki.hu ● ISSN 1589 1623 (Print) ● ISSN 1785 0037 (Online)
DOI: http://dx.doi.org/10.15666/aeer/1802_25132538

Mountain and the front edge of the mountain depressions are turned into springs along the faults and then converted into surface water. It is supplied in the form of lateral replenishment to the Acoch Valley, the Peacock River Delta and the Tarim River Delta alluvial plain, and then to the Lop Nur Lake Plain (Shao et al., 2017). In this migration process, it is excreted by water surface evaporation, phreatic evaporation, plant transpiration and artificial mining. In the vertical direction, the groundwater system is relatively stable and moves upwards and downwards. The water alternates in a mixed type, and the middle and deep layer confined water heads are relatively more. High, the shallow confined water is replenished through faults or relative water-repellent layers, and the shallow confined water is replenished for diving. During this process, the groundwater forms a dynamic equilibrium and the property of water changes from HCO_3-Ca•Mg to SO_4. • Cl-Ca•Na, which eventually becomes Cl-Na; in the vertical direction, it also changes from SO_4-Ca•Mg to SO_4•Cl-Ca•Na, eventually it becomes Cl-Na, and then after long-term evaporation and concentration, a highly mineralized potassium-rich brine is formed (Jiao et al., 2004; Liu et al., 1999; Lei et al., 2019; Wang, 2016).

Simulation analysis of regional groundwater flow patterns

Due to the development of today's groundwater modelling technology and the rapid improvement of computer technology, groundwater numerical model has become an important tool for quantitative study of groundwater movement rules, and plays an increasingly important role in solving specific hydrogeological problems. So far, only through the model, can data from different methods (such as geophysical exploration, drilling, surveying, monitoring, remote sensing, etc.) be put into a unified system for data integration and management, and whether there is any existing contradiction between them. If there is some prior understanding of hydrogeology, it can be analyzed by means of modelling whether the data is consistent with our understanding, which is extremely essential. In the process of comprehensive processing of hydrogeological data by modelling, the sufficient and absent hydrogeological information can be found respectively, which leads to the further exploration of the lacking information. Therefore, the model is also an important means to help deploy further field surveys, and place limited investment on the situations in need of data. We have many assumptions about the flow, excretion, and recharge of groundwater. An effective way to test whether these assumptions are correct is to put the hypothesis into the model and compare the results of the model with the reliable measured results. In this way, we can understand more about hydrogeological conditions.

Groundwater flow is a complex geological process, which means that we cannot directly observe where the groundwater flows to, how fast the water flows, and the spatial variation of aquifer hydrogeological parameters. To comprehend the spatial distribution of groundwater in the ground, the characteristics of groundwater flow and its dynamics over time, scientists have conducted a large number of field surveys and studies in order to master the distribution characteristics and rules of groundwater flow in time and space. Nevertheless, this scientific problem still cannot reach a satisfactory solution for a long time. One of the main reasons is the heterogeneity of the aquifer structure and the uncertainty of its parameters. Because people can only analyze and study aquifer systems based on limited geological and hydrogeological

http://www.aloki.hu ● ISSN 1589 1623 (Print) ● ISSN 1785 0037 (Online)
DOI: http://dx.doi.org/10.15666/aeer/1802_25132538

exploration data. The hydrogeological community has been seeking for a theory and method that can more reasonably describe the distribution of aquifer system parameters. Therefore, the use of numerical model of three-dimensional groundwater flow to describe the spatial variation characteristics of aquifer structure and groundwater flow rules is the current research trend in the field of hydrogeology.

This paper focuses on the simulation analysis of the groundwater flow pattern in the work area, so as to take in the mode and flow characteristics of regional groundwater circulation.

Mathematical models and numerical methods

The numerical method has the rules of groundwater flow that can be characterized by complex hydrogeological conditions, artificial activity conditions, irregular boundary conditions, and a series of time variables. After the 1970s, with the development and popularization of computers, numerical methods have been successfully used to simulate groundwater movement and groundwater resource evaluation. The previous numerical simulation research and application of groundwater flow has two distinct features: first, most models discuss numerical algorithms and computational formats, and the processing of boundary conditions is too simple and often insufficient. Many models use artificial boundaries. Whether the artificial boundary selection is reasonable or not will affect the flow pattern of groundwater. The artificial boundary is not a problem in the simulation process. The local parameters can be adjusted to make the calculated value and the measured value reach the expected target. When forecasting, the hydraulic head of the original artificial boundary is generally not given and can only be treated as a known boundary. Second, most studies rely on the two-dimensional model, although in recent years, the use of three-dimensional model has increased, but in practice, few three-dimensional models are adopted with few vertical stratifications in the model. More models use idealized research fields and units (rectangular domain regular hexahedron), depending on the aquifer as a horizontal layer. The calculation unit is too idealized and the aquifer is horizontally layered, which is far from the actual distance, bringing about difficulties to reasonably characterize the actual spatial structure changes of the aquifer (Xue et al., 2018).

In this paper, the three-dimensional finite difference model is used to simulate groundwater flow, and the spatial and temporal distribution characteristics of regional groundwater flow are analyzed, and the influencing factors are studied and analyzed.

Mathematical model of three-dimensional groundwater flow

According to the three-dimensional hydrogeological conceptual model of groundwater flow, the unsteady three-dimensional mathematical model of groundwater flow in the regional aquifer system can be described as follows:

$$\frac{\partial}{\partial x}\left(Kxx\frac{\partial H}{\partial x}\right)+\frac{\partial}{\partial y}\left(Kyy\frac{\partial H}{\partial y}\right)+\frac{\partial}{\partial z}\left(Kzz\frac{\partial H}{\partial z}\right)=\mu s\frac{\partial H}{\partial t}+W \quad (x,y,z)\in D \quad \text{(Eq.1)}$$

Initial conditions:

$$H(x,y,z,0)=H_0(x,y,z) \quad \text{(Eq.2)}$$

http://www.aloki.hu ● ISSN 1589 1623 (Print) ● ISSN 1785 0037 (Online)
DOI: http://dx.doi.org/10.15666/aeer/1802_25132538

Boundary conditions:

$$\begin{aligned} &H(x,y,z,t)|_{\Gamma 1} = H(x,y,z) \\ &H(x,y,z,t)|_{\Gamma 2-1} = Z \\ &Kzz\frac{\partial H}{\partial z}|_{\Gamma 2-1} = \varepsilon' - \mu_d \frac{\partial H}{\partial t}|_{\Gamma 2-1} \\ &Kzz\frac{\partial H}{\partial z}|_{\Gamma 2-2} = 0 \end{aligned} \quad \text{(Eq.3)}$$

where: xyz - Cartesian axis; t - time; H - known hydraulic heads; *KxxKyyKzz* - the main permeability coefficient in the direction of the coordinate axis; μs - specific storage; μ_d - gravity specific storage; W - the flow rate per unit volume of the well, taking a negative sign when pumping; $\Gamma 1$ - the Dirichlet boundary; $\Gamma 2-1$ - the boundary of the phreatic surface; $\Gamma 2-2$ - zero flow boundary; ε' - recharge amount of precipitation infiltration.

Numerical methods

The basic idea of the finite difference method is to replace the continuous vadose zone with a set of finite discrete points in the Vadose zone, as well as replacing the derivative approximated by the difference quotient at the discrete point, and condition the differential equation and its solution as an unknown function. The approximation of the discrete points is an algebraic equation of unknown quantity, and then the difference equation is solved, and then the approximation of the solution of the differential equation at discrete points is obtained.

The method is based on a continuity equation for groundwater flow according to which, the differences between the water flows into and out of a computing element is equal to the change in the water storage capacity of the unit.

The groundwater continuity equation can be expressed as:

$$\sum Q_i = SS \cdot \Delta h \cdot \Delta v \quad \text{(Eq.4)}$$

where: Q_i - the amount of water flowing into or out of the calculation unit per unit time; SS - the storativity of the aquifer; Δh - changes of the hydraulic head per unit time; Δv - the volume of the computing element.

After the Vadose zone is split and separated, the computing element can be determined according to the continuity equation and the Darcy formula:

$$\begin{aligned} &\sum Q_i = SS \cdot \Delta h \cdot \Delta v \\ &Q = K \cdot \omega \cdot \frac{h}{L} \end{aligned} \quad \text{(Eq.5)}$$

http://www.aloki.hu ● ISSN 1589 1623 (Print) ● ISSN 1785 0037 (Online)
DOI: http://dx.doi.org/10.15666/aeer/1802_25132538

The flow into the unit (i, j, k) by the computing element (i, j-1, k) in the row direction can be obtained as:

$$q_{i,j-1/2,k} = KR_{i,j-1/2,k}\Delta c_i \Delta v_k \frac{(h_{i,j-1,k} - h_{i,j,k})}{\Delta r_{j-1/2}} \quad \text{(Eq.6)}$$

where: $q_{i,j-1/2,k}$ - the flow through the interface between the grid points (i, j, k) and (i, j-1, k) ($L^3\ T^{-1}$); $KR_{i,j-1/2,k}$ - the permeability coefficient (LT^{-1}) between the grid point (i, j, k) and (i, j-1, k); $\Delta c_i \Delta v_k$ - cross-sectional area (L^2); $h_{i,j-1/2,k}$ - the value of the hydraulic head at the grid point (i, j-1, k); $h_{i,j,k}$ - the value of the hydraulic head at the grid point (i, j, k); $\Delta r_{j-1/2}$ - the distance (L) between the grid point (i, j, k) and (i, j-1, k).

Groundwater flow through the other five interfaces can be analogized. For example, the groundwater flow rate from the grid point (i, j + 1, k) to (i, j, k) in the row direction is:

$$q_{i,j+1/2,k} = KR_{i,j+1/2,k}\Delta c_i \Delta v_k \frac{(h_{i,j+1,k} - h_{i,j,k})}{\Delta r_{j+1/2}} \quad \text{(Eq.7)}$$

Similarly, it can be concluded in turn:

$$q_{i+1/2,j,k} = KC_{i+1/2,j,k}\Delta r_j \Delta v_k \frac{(h_{i+1,j,k} - h_{i,j,k})}{\Delta c_{i+1/2}} \quad \text{(Eq.8)}$$

$$q_{i-1/2,j,k} = KC_{i-1/2,j,k}\Delta r_j \Delta v_k \frac{(h_{i-1,j,k} - h_{i,j,k})}{\Delta c_{i-1/2}} \quad \text{(Eq.9)}$$

$$q_{i,j,k+1/2} = KV_{i,j,k+1/2}\Delta r_j \Delta c_i \frac{(h_{i,j,k+1} - h_{i,j,k})}{\Delta v_{k+1/2}} \quad \text{(Eq.10)}$$

$$q_{i,j,k-1/2} = KV_{i,j,k-1/2}\Delta r_j \Delta c_i \frac{(h_{i,j,k-1} - h_{i,j,k})}{\Delta v_{k-1/2}} \quad \text{(Eq.11)}$$

The above formula shows the groundwater flow through the six interfaces of the computing element (i, j, k), and the grid spacing and the permeability coefficient are combined into one variable as the hydraulic conductivity coefficient:

$$CR_{i,j-1/2,k} = KR_{i,j-1/2,k}\Delta c_i \Delta v_k / \Delta r_{j-1/2} \quad \text{(Eq.12)}$$

Applying the hydraulic conductivity to *Equations 6* to *11,* it can be concluded that:

$$q_{i,j-1/2,k} = CR_{i,j-1/2,k}(h_{i,j-1,k} - h_{i,j,k}) \quad \text{(Eq.13)}$$

http://www.aloki.hu ● ISSN 1589 1623 (Print) ● ISSN 1785 0037 (Online)
DOI: http://dx.doi.org/10.15666/aeer/1802_25132538

$$q_{i,j+1/2,k} = CR_{i,j+1/2,k}\left(h_{i,j+1,k} - h_{i,j,k}\right) \quad \text{(Eq.14)}$$

$$q_{i-1/2,j,k} = CC_{i-1/2,j,k}\left(h_{i-1,j,k} - h_{i,j,k}\right) \quad \text{(Eq.15)}$$

$$q_{i+1/2,j,k} = CC_{i+1/2,j,k}\left(h_{i+1,j,k} - h_{i,j,k}\right) \quad \text{(Eq.16)}$$

$$q_{i,j,k-1/2} = CV_{i,j,k-1/2}\left(h_{i,j,k-1} - h_{i,j,k}\right) \quad \text{(Eq.17)}$$

$$q_{i,j,k+1/2} = CV_{i,j,k+1/2}\left(h_{i,j,k+1} - h_{i,j,k}\right) \quad \text{(Eq.18)}$$

These formulas are used to calculate the groundwater flow inflows from the six boundary faces of the unit (i, j, k). In addition, the effects of other various external sources and sinks on the calculation unit, such as rivers, ditches, production wells, and injection wells, evapotranspiration, etc. need to be considered. The quantity of these sources and sinks into the unit can be calculated by a formula:

$$a_{i,j,k,n} = p_{i,j,k,n}h_{i,j,k} + q_{i,j,k,n} \quad \text{(Eq.19)}$$

where: $a_{i,j,k,n}$ - the replenishment of the nth external source pair calculation unit (i, j, k) (L3 T-1); $q_{i,j,k,n}$, $p_{i,j,k,n}$ - constant, the unit is (L2 T-1), (L3 T-1).

Considering the six adjacent grid points of the calculation unit and all the sources and sinks contained in the unit, the continuity equation (*Eq. 4*) can be calculated as:

$$\begin{aligned} &q_{i,j-1/2,k} + q_{i,j+1/2,k} + q_{i-1/2,j,k} + q_{i+1/2,j,k} + q_{i,j,k-1/2} + q_{i,j,k+1/2} + \sum_{n=1}^{N} a_{i,j,k,n} \\ &= SS_{i,j,k}\frac{\Delta h_{i,j,k}}{\Delta t}\Delta r_i \Delta c_j \Delta v_k \end{aligned} \quad \text{(Eq.20)}$$

where: $SS_{i,j,k}$ - the storativity of the computing element (L^{-1}); $\frac{\Delta h_{i,j,k}}{\Delta t}$ - a differential approximation of the partial derivative of the hydraulic head for time; $\Delta r_i \Delta c_j \Delta v_k$ - the volume of computing element (L^3).

Substituting *Equations 13–18* and *19* into *Equation 20* yields:

$$\begin{aligned} &CR_{i,j-1/2,k}\left(h_{i,j-1,k} - h_{i,j,k}\right) + CR_{i,j+1/2,k}\left(h_{i,j+1,k} - h_{i,j,k}\right) + CC_{i-1/2,j,k}\left(h_{i-1,j,k} - h_{i,j,k}\right) + \\ &CC_{i+1/2,j,k}\left(h_{i+1,j,k} - h_{i,j,k}\right) + CV_{i,j,k-1/2}\left(h_{i,j,k-1} - h_{i,j,k}\right) + CV_{i,j,k+1/2}\left(h_{i,j,k+1} - h_{i,j,k}\right) + \\ &P_{i,j,k,n}h_{i,j,k} + Q_{i,j,k,n} = SS_{i,j,k}\frac{\Delta h_{i,j,k}}{\Delta t}\Delta r_i \Delta c_j \Delta v_k \end{aligned} \quad \text{(Eq.21)}$$

The partial derivative of the hydraulic head to time is approximated by the difference quotient:

http://www.aloki.hu ● ISSN 1589 1623 (Print) ● ISSN 1785 0037 (Online)
DOI: http://dx.doi.org/10.15666/aeer/1802_25132538

$$\frac{\Delta h_{i,j,k}}{\Delta t} \approx \frac{h_{i,j,k}^{m} - h_{i,j,k}^{m-1}}{t_m - t_{m-1}}$$

Then all the flows are based on the end time t_m of a certain time period, then *Equation 21* becomes:

$$CR_{i,j-1/2,k}\left(h_{i,j-1,k}^{m} - h_{i,j,k}^{m}\right) + CR_{i,j+1/2,k}\left(h_{i,j+1,k}^{m} - h_{i,j,k}^{m}\right) + CC_{i-1/2,j,k}\left(h_{i-1,j,k}^{m} - h_{i,j,k}^{m}\right) +$$
$$CC_{i+1/2,j,k}\left(h_{i+1,j,k}^{m} - h_{i,j,k}^{m}\right) + CV_{i,j,k-1/2}\left(h_{i,j,k-1}^{m} - h_{i,j,k}^{m}\right) + CV_{i,j,k+1/2}\left(h_{i,j,k+1}^{m} - h_{i,j,k}^{m}\right) +$$
$$P_{i,j,k,n}h_{i,j,k}^{m} + Q_{i,j,k,n} = SS_{i,j,k}\frac{h_{i,j,k}^{m} - h_{i,j,k}^{m-1}}{t_m - t_{m-1}}\Delta r_i \Delta c_j \Delta v_k \qquad \text{(Eq.22)}$$

The above equations are iteratively solved. At the beginning, the unknown computing element to each hydraulic head is assigned to the initial head or the estimated head, and the result of each iteration is used for the next calculation.

According to the difference equation, the matrix form of the system of equations can be concluded:

$$[\mathrm{A}]\{\mathrm{h}\} = [\mathrm{q}]$$

where: [A] - the coefficient matrix of the hydraulic head; - the requested matrix of the hydraulic head; [q] - All absolute terms and known terms contained in each equation.

In MODFLOW, the coefficient matrix and the right term are gradually established by each software package. Finally, MODFLOW solves by iteration based on these two matrices.

Software for realizing numerical simulation of 3D flow

Visual MODFLOW 2000 software was used to build a finite difference model for groundwater flow and particle migration in this workspace. Visual MODFLOW is the most complete and user-friendly 3D groundwater flow and contaminant transport simulation software for practical applications. This complete integrated software combines MODFLOW, MODPATH and MT3D with an intuitive and powerful graphical user interface to easily determine the size of the simulation area, select parameter units, set model parameters and boundary conditions, and run model simulations (MT3D, MODFLOW, and MODPATH), correcting the model and visualize the model mesh, inputting parameters and results in the form of sections and plans.

Regional groundwater flow modelling

Model boundary

On the account of the large-scale work area and the difficulties of hydrogeological boundary to be determined, first, the SRTM DEM data is used for hydrological space analysis, digital river network extraction and watershed division, so as to have a brief knowledge of the boundary in terms of the whole basin. The DEM elevation map of the work area is shown in *Figure 1*.

http://www.aloki.hu ● ISSN 1589 1623 (Print) ● ISSN 1785 0037 (Online)
DOI: http://dx.doi.org/10.15666/aeer/1802_25132538

SRTM is the abbreviation of The Shuttle Radar Topography Mission, which was completed in February 2000. Most of its data is located between 60° north latitude and 56° south latitude, covering 80% of the continent. SRTM includes two resolutions: SRTM1, only covering the continental United States with a resolution of 1 s of arc; SRTM3, with global coverage and a resolution of 3 s of arc. Due to the areas without data in SRTM DEM database, the CGIAR-CSI SRTM3, the SRTM DEM product processed by CIAT (International Tropical Agriculture Center) can also be used, which has released the latest V3 version recently with two formats named as arc-formatted ASCII and GeoTIFF. The CGIAR-CSI SRTM3 DEM in GeoTIFF format downloaded from CIAT, which is referred to as SRTM3 DEM, is used in this study. The SRTM3 elevation reference is the geoid of the EGM96 and the planar reference is WGS84. SRTM3 has an accuracy of 3 s arc, which divides the area of 1 square degree into 1,200 × 1,200 small areas, each small area is 3 s (90 m × 90 m) in size, and each small area has a value representing the elevation of the center of the area. The SRTM3 DEM data is equivalent to 1:250,000 scale map data. The 3D perspective of the work area is shown in *Figure 4*.

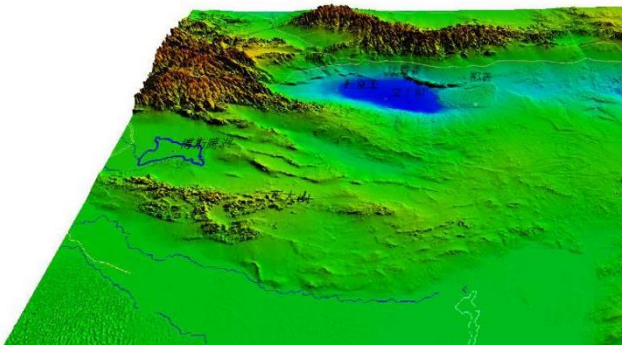

Figure 4. *Three-dimensional view of the work area*

Hydrological analysis is an important aspect of DEM data applications. The use of DEM to generate catchment basins and water flow networks to analyze surface water flow conditions is an important application as well as the great significance for comprehension of the shape of the Earth's surface. The main content of surface hydrological analysis based on DEM is to use hydrological analysis tools to extract the flow direction, the cumulative amount of flow, the length of water flow, the river network (including the classification of river networks, etc.) of the surface water runoff model, and the division of the watershed in the work area. By extracting these basic hydrological factors and basic hydrological analysis, the process of water flowing can be redisplayed on the surface of the DEM, contributing to the hydrological analysis process eventually.

The hydrological analysis mainly constitutes the direction of surface water flow in the region and the possible surface watersheds in each basin. Therefore, the analysis core is placed on the extraction of river networks and the division of watersheds.

The basic flow of extracting digital river network and watershed based on DEM data is as follows (Wang et al., 2018):

(1) DEM data preprocessing. Before extracting the digital river network of the watershed by using DEM data, the data is supposed to be preprocessed to eliminate the

http://www.aloki.hu ● ISSN 1589 1623 (Print) ● ISSN 1785 0037 (Online)
DOI: http://dx.doi.org/10.15666/aeer/1802_25132538

invalid data area existing in the DEM. In addition, since the DEM data itself often has a lot of depressions and plane ground, as a result, the DEM data such as the determination of the DEM data and the filling of the depression and the lifting of the ground must be pre-processed, after the valid DEM data is available in order to obtain effective DEM data for river network water extraction.

(2) The grid flow direction is determined. After the pre-processed valid DEM data is in hand, the flow direction of each raster in the data can be determined. The method of judging the flow direction mainly includes a multi-flow method and a single flow method. As specified, the single flow method is so simple and convenient that it can be extensively used, among which D8 is the most widely used one. The D8 method assumes that there are only eight possible flow directions in the water flow in a single grid, that means, the water flow will flow into the eight adjacent grids. It uses the steepest slope method to determine the direction of the water flow, that is to calculate the distance weight difference between the center grid and each adjacent grid (i.e., the grid center point drop divide the distance between the gridcenter points) on the 3 × 3 DEM grid, the grid with the largest distance drop is the outflow grid of the center grid, which is the flow direction of the center grid.

(3) Determination of the water flow accumulation matrix. Based on the determined water flow direction data, the upstream water supply area range of each grid unit is accumulated, which means to determine the specific upstream grids flow direction to be cumulatively directed to the grid unit.

(4) Drainage networks extraction. Set the catchment area threshold to the flow accumulating grid according to the threshold value, then the river network grid network map of the area can be obtained to generate a digital drainage network.

(5) Watershed division. The drainage basin collects all kinds of precipitation divided by watersheds. It determines all the grids that are interconnected and in the same basin by analyzing the water flow direction data. The first step of determination of the drainage basin is to determine the location of the outlet at the edge of the analysis window that is to say, in the division of the drainage basin, the outlets of all drainage basins are at the edge of the analysis window. When the location of the water outlet is determined, the determination of the collection area of the drainage basin is similar to that of the contribution area of the depression, equal to the location of all upstream grids flowing into the outlet.

After the GIS hydrological space analysis, the river network and watershed model of the work area can be obtained, as shown in *Figure 5*.

It is better to build the regional groundwater model with the natural hydrogeological boundaries as far as possible from a holistic perspective. It is assumed that the watershed at the surface drainage basin is also a ground watershed, so the surface watershed of the drainage basin obtained by hydrological space analysis is treated as a groundwater watershed with a zero flux boundary. However, due to the asymmetry of precipitation recharge and topography, the watershed of surface water and surface water is inconsistent, but the impact on groundwater simulation in large areas is acceptable.

Based on the analysis results, the model boundaries are generalized as follows:

- West Bosten Lake is a type of head boundary.
- The eastern part is the lateral replenishment boundary, defined as the Neumann boundary.
- The northern part of Aidin Lake is defined as Dirichlet head boundary.
- Southern Lop Nur is the evaporation boundary.

http://www.aloki.hu ● ISSN 1589 1623 (Print) ● ISSN 1785 0037 (Online)
DOI: http://dx.doi.org/10.15666/aeer/1802_25132538

- The other boundary is the flux boundary.
- The vertical top boundary of is the phreatic boundary, and the model is divided to the surface, directly accepting the recharge of atmospheric precipitation and evaporation and drainage, leading to a definition as the flux boundary in the form of source and sink items in the model.
- The vertical bottom boundary is the Neumann confining boundary (zero flux boundary).

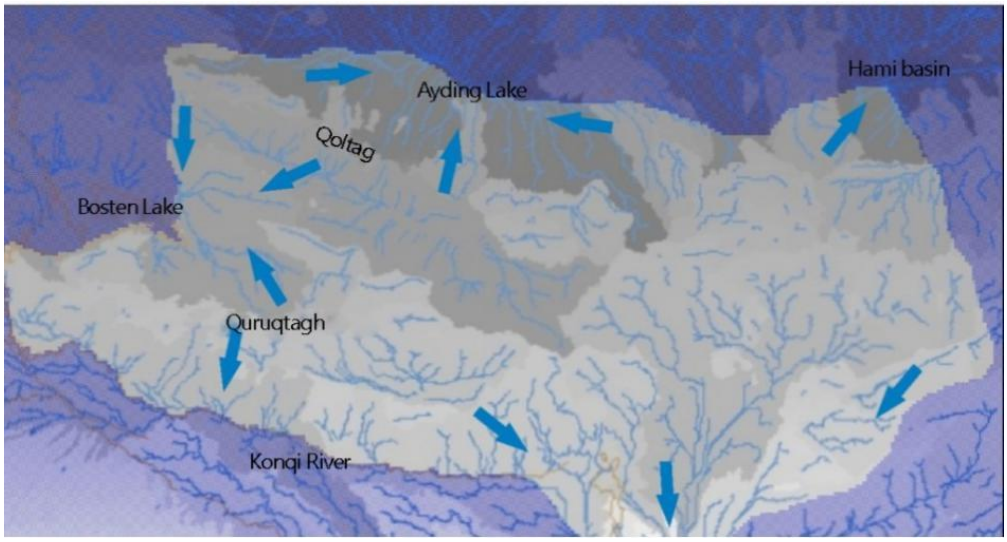

Figure 5. *Work area hydrological space analysis results*

Model splitting

The work area is divided by a rectangular hexahedron (the upper and lower planes are not necessarily parallel).

The model is discretely divided into 160 rows and 285 columns, each of which has a length and width of 2 km (*Fig. 6*). The vertical model is divided into three layers, each of which has a constant thickness. The thickness of the three layers is 0-1,000 m, 1,000-1,800 m, 1,800-2,600 m from the top to the bottom, and each layer is not horizontally distributed. The vertical division into three layers is the most simplified way of performing three-dimensional numerical simulation. As the geological survey of the work area is deepened, it will be continuously improved to accurately describe the spatial distribution of the aquifer. The bottom of the model is 2,600 m below the surface of the submerged surface. It is assumed that the groundwater is mainly horizontally flowing at this depth.

The total model is split into 136,800 units in total, of which 79,356 are effective and 57,444 are invalid ones.

Aiming at solving the problem of insufficient terrain data of large-area model, SRTM DEM data is used to establish groundwater space model, and high-precision surface elevation characterization can effectively improve the calculation accuracy of groundwater model phreatic evaporation.

http://www.aloki.hu ● ISSN 1589 1623 (Print) ● ISSN 1785 0037 (Online)
DOI: http://dx.doi.org/10.15666/aeer/1802_25132538

Parameter partitioning

(1) Horizontal permeability coefficient

The horizontal permeability coefficient division is mainly conducted according to the 1:2.5 million scale geological map of the working area, as shown in *Figure 7*, mainly considering the dominant hydrogeological features, including granite, shale, clasticrocks, Quaternary sediments, etc. It is divided into different coefficient partitions and reflected in the model to obtain a heterogeneous parameter model. The consideration of heterogeneous characteristics is more in line with the actual hydrogeological conditions and can better reflect the groundwater flow conditions in the area.

It could be reduced to three parameter partitions: high permeability performance partition (K1), medium permeability performance partition (K2), and low permeability performance partition (K3). The permeability coefficient parameter partitioning is discontinuous, and each partition contains several units in the model, as shown in *Figure 8*.

According to the research results of the permeability coefficient of the predecessors in the work area (see *Table 1*), combined with the characteristics of the regional groundwater model, the basic values of the three partition permeability coefficients are defined in *Table 2*.

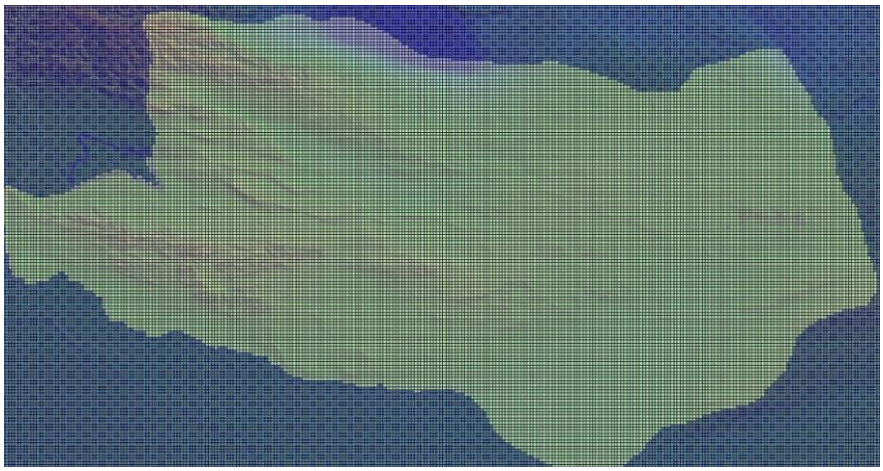

A Plane split diagram

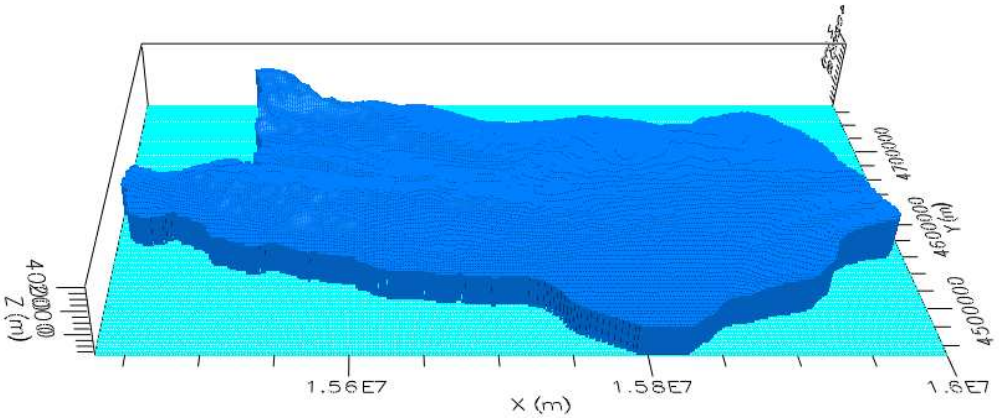

B Stereoscopic view

Figure 6. *Model split diagram*

http://www.aloki.hu ● ISSN 1589 1623 (Print) ● ISSN 1785 0037 (Online)
DOI: http://dx.doi.org/10.15666/aeer/1802_25132538

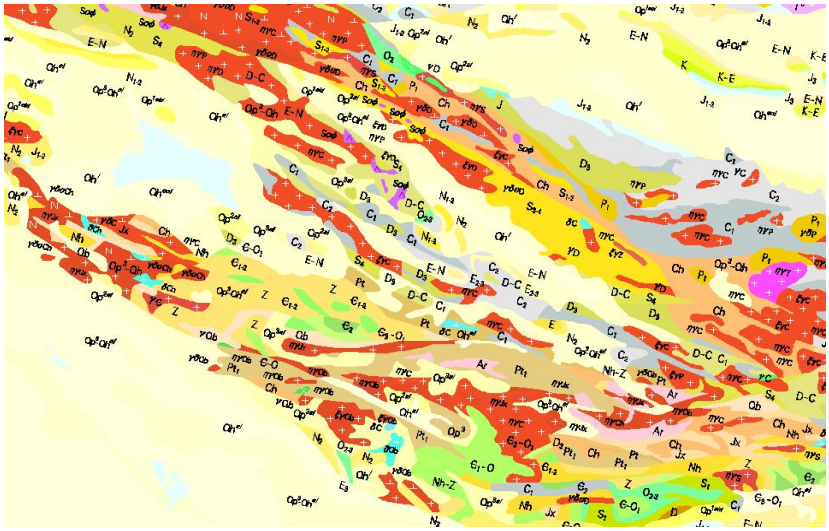

Figure 7. *Geological map of work area*

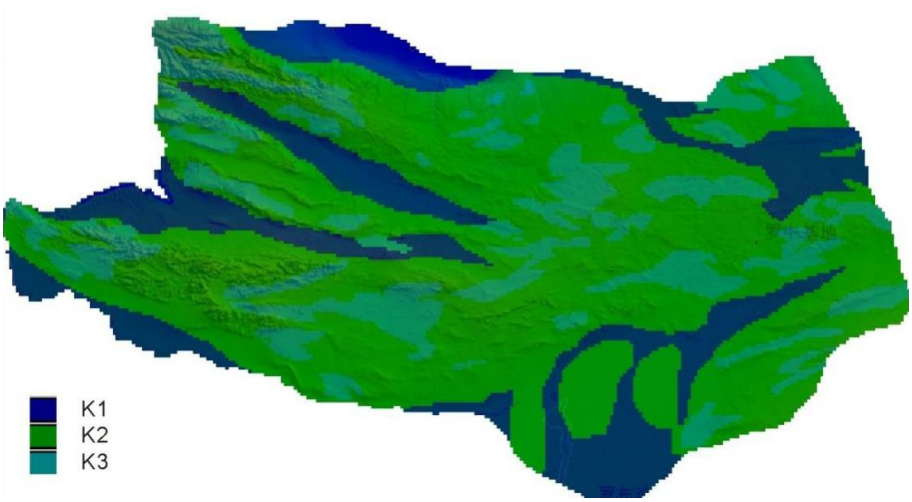

Figure 8. *Horizontal permeability coefficient partition map*

Table 1. *Permeability coefficient of work area*

Groundwater location and type	Permeability coefficient value (m/d)
Peacock river alluvial delta pore water	0.14–5.73
Aqike valley unit	0.621–4.49
Luobei concave ground pores and intercrystalline pore water	0.5–80
Lop Nur dry salt lake pores and intercrystalline pore water	< 1.0

Table 2. *Partition values of each permeability coefficient of the model*

Partition	Permeability coefficient value (m/d)
K1 High permeability performance partition	2.0
K2 Medium permeability performance division	0.26
K3 Low permeability performance zone	0.004

http://www.aloki.hu ● ISSN 1589 1623 (Print) ● ISSN 1785 0037 (Online)
DOI: http://dx.doi.org/10.15666/aeer/1802_25132538

The permeability coefficient values for each partition will be scaled up or down during multiple scenario simulations to analyze the uncertainty of the parameters.

(2) Vertical permeability coefficient

The vertical permeability coefficient partition is consistent with the horizontal permeability coefficient partition. According to the geological conditions and empirical values of the working area, the ratio of the vertical permeability coefficient to the horizontal permeability coefficient in the model is 0.25, and the trial calculation is carried out in the model.

(3) Precipitation

The average annual precipitation of the working area is shown in *Table 3,* and the precipitation parameters can be divided according to different regions.

Table 3. *Annual average precipitation statistics of the work area*

Area	Statistical time period	Annual average precipitation (mm)
Milan	2,004-2,005	42.9
Lop Nur Town	2,005	29.3
Kumish	2,001-2,005	61.6
Toksun	2,001-2,005	9.2
Yan Shan	2,001-2,005	29.3
Hami	2,001-2,005	56.9
Qarkilik	2,001-2,005	47.8

According to the "95" national key scientific and technological research project, the effective precipitation infiltration rate of the Hexi Corridor area (climate condition which is similar to that of the Lop Nur area) is 30-50%. Depended on the previous research results, the infiltration recharge of atmospheric precipitation in different depths of Luobei depression is shown in *Table 4*.

Table 4. *Recharge of atmospheric precipitation infiltration in different depths of Luobei depression*

Groundwater depth (m)	1.0-1.5 m	1.5-2.0 m	> 2.0 m
Rainfall infiltration coefficient	0.235	0.15	0.11

According to different rainfall infiltration coefficient and precipitation, the rainfall infiltration in each region can be obtained.

Calculation formula:

$$Q\ drop = A \bullet \beta$$

where: Q drop - atmospheric precipitation infiltration recharge (10^4 m^3/a); A - year effective precipitation; B - effective precipitation infiltration coefficient.

The effective precipitation infiltration in each region can be determined by model identification.

http://www.aloki.hu ● ISSN 1589 1623 (Print) ● ISSN 1785 0037 (Online)
DOI: http://dx.doi.org/10.15666/aeer/1802_25132538

(4) Evaporation

See *Table 5* for the phreatic evaporation coefficient of in different regions of the work area. See *Table 6* for the phreatic evaporation in different areas.

Table 5. *List of different buried depth underground water coefficients in different regions*

Area	Buried depth							
	0.5 m	**1.0 m**	**1.5 m**	**2.0 m**	**2.5 m**	**3.0 m**	**3.5 m**	**4.0 m**
Yumen Station	0.174	0.116	0.060	0.047	0.028	0.019	0.015	0.009
Turpan Station	0.253	0.149		0.051				0.021
Gunke Station	0.164	0.112	0.076	0.050	0.040	0.028		0.014

Table 6. *List of underground water evaporation in each region*

Area	Evaporation (mm)
Aqike Valley	2,500
Yumen Town	2,511.9
Turpan	2,837.8
Gunke	2,700

Regarding the formula of the evaporation law of diving, we use the empirical formula (index formula) obtained in the article Study on water transport and equilibrium factors of the aeration zone in the middle reaches of the Heihe River in Gansu Province (internal data from Second Hydrogeological Institute of Gansu Province, 1995):

$$\varepsilon = \varepsilon_0 \cdot e^{-bD}$$

where: ε - diving evaporation intensity; ε_0 - water surface evaporation intensity; D - diving depth; b - Experience factor (related to soil quality), determined by model identification.

Numerical simulation and correction of regional groundwater flow

Due to the large scope of the work area in remote areas in the northwest, the researches on hydrogeological work area are relatively less, so there is a lack of dynamic data required for the simulation of groundwater unsteady flow, such as long-term water level observation data, monthly precipitation, monthly evaporation, etc., so the use of multi-year average data in the study for stable flow simulation, focusing on the characteristics of the water cycle in the work area.

Stable flow simulation

On the strength of average data of multiple years, the permeability coefficient is taken as a basic combination for steady flow numerical simulation. The simulation results are shown in *Figure 9*.

There are multiple groundwater flow systems in the area by the regional groundwater flow field. In the vicinity of the Turpan Basin in the northern part of the work area,

http://www.aloki.hu ● ISSN 1589 1623 (Print) ● ISSN 1785 0037 (Online)
DOI: http://dx.doi.org/10.15666/aeer/1802_25132538

groundwater mainly flows from the Qoltag Mountain and the eastern side of the basin to the Aiding Lake; the southwestern side of the Qoltag Mountain and the northwest side of the Kuruktag are collected from the Bosten Lake; the groundwater in the south of Kuruktag mainly flows along the Peacock River to Lop Nur; the groundwater in the northeastern part of the working area flows from the west and south to the sand lake in the Hami Basin; the eastern part of the working area receives the lateral recharge of the downstream of the Shule River and flows to Lop Nur (Zhu et al., 2001).

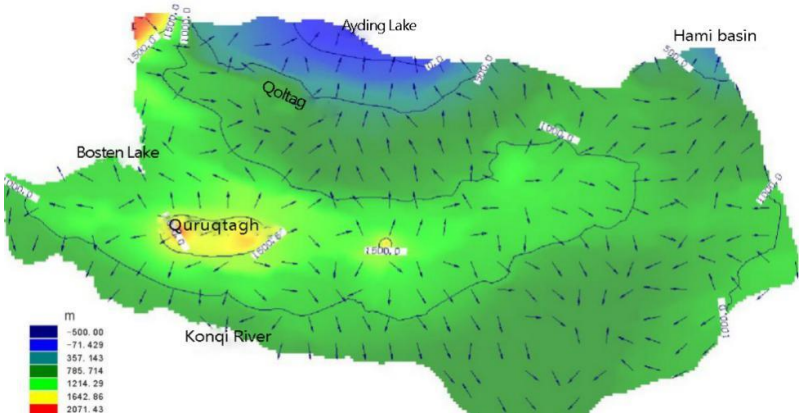

Figure 9. *Basic model steady flow field*

Model adjustment

Due to the lack of water level observation data in the working area, the groundwater heads formed by interpolation of some measured groundwater data in the area are compared with the simulated preliminary flow field, and the differences are analyzed. The parameters in the model are then adjusted according to the hydrogeological conditions of different locations. The adjusted and simulated flow field and the measured value interpolated flow field are shown in *Figure 10*.

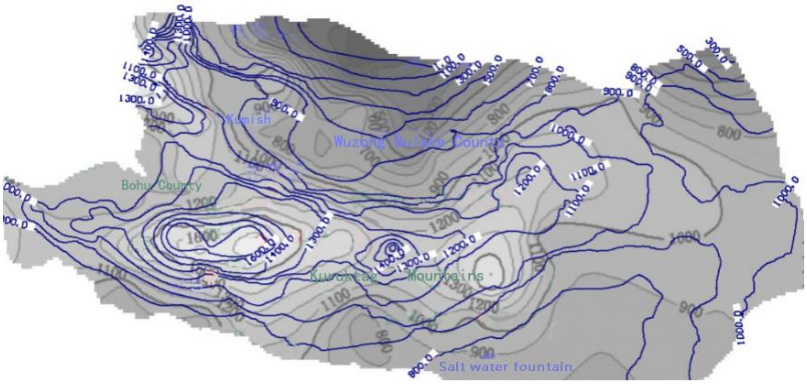

Figure 10. *Comparison of measured and simulated groundwater level contours (blue line-analog value, black-measured value)*

It can be seen from *Figure 10* that the simulated flow field is consistent with the measured flow field as a whole, but there are certain differences in some parts mainly resulting from the following reasons:

http://www.aloki.hu ● ISSN 1589 1623 (Print) ● ISSN 1785 0037 (Online)
DOI: http://dx.doi.org/10.15666/aeer/1802_25132538

(1) Insufficient measured groundwater level data causes local distortion of the interpolation flow field, which cannot fully represent the real groundwater flow field. The work area is over 100,000 km^2, but there are only a few dozen groundwater data for interpolation, especially in the eastern part of the work area, with fewer interpolation points. Taking the northern part of Dongshuiquan as an example, there is a high water point in the measured interpolation flow field, but in fact it is not the highest point of the surrounding elevation, and there is no other water supply, just because there are no other interpolation points nearby.

(2) On the account of large working area but less relevant geological and hydrogeological information, the model based on the water quantity information cannot completely simulate the local and detailed groundwater flow characteristics in the area. The lack of basic data in the work area, the characterization of geological structures and the treatment of source and sink items such as precipitation and evaporation are not able to reach high standards, giving rise to the lack of ability to characterize small cycles in local areas such as small basins in the mountains.

Although there is a lack of local details and precision, the model initially depicts the unaffected characteristics of groundwater flow with the overall regional perspectives which can support the analysis of regional groundwater circulation.

Multi-scenario particle tracer simulation analysis

In order to analyze the particle migration in key areas of the work area, the MODPATH software was used to simulate the particle tracing under multiple scenarios with comprehensive consideration of the uncertainty of the parameters.

MODPATH is a convection transmission simulation software that can acquire groundwater model and simulation result data from MODFLOW and calculate the particle migration trajectory. MODPATH uses a semi-analytical solution for particle tracking to calculate groundwater migration routes and flowing time. The method assumes that the velocity components in each direction of each grid cell vary linearly in their own coordinate direction, allowing us to get an analytical expression that describes the streamlines within the grid cell. Given any initial position of the mass point in the cell, the coordinates of other points on the streamline within the cell and the time interval between the groundwater masses passing through the two points can be calculated.

Through the graphical interaction interface of MODPATH, the user can use the mouse to click to set the particle point and demonstrate of the particle migration. Most particle migration simulation software requires post-processing to get the route and time visualization results, however it can be calculated and displayed simultaneously on the MODPATH. MODPATH also provides a variety of data display functions for any selected model layer and time step, such as displaying the water head contour, the drop contour, and the flow rate and direction.

It is assumed that the nuclide is the ideal particle, that is to say, the program module can be used to conveniently simulate the migration trajectory of the nuclide particle under different scenarios without consideration of the reaction of the nuclide-water-rock.

According to the research geological map, three large-area granite areas located in the eastern and central parts of the work area were selected for particle tracing simulation. The position of the tracer particles is shown in *Figure 11*. In the central region of each granite zone, 20 particles were placed on a circumference with a radius of 5 km. The particles in the simulation are shown in green and the migration trajectory is shown in red.

http://www.aloki.hu ● ISSN 1589 1623 (Print) ● ISSN 1785 0037 (Online)
DOI: http://dx.doi.org/10.15666/aeer/1802_25132538

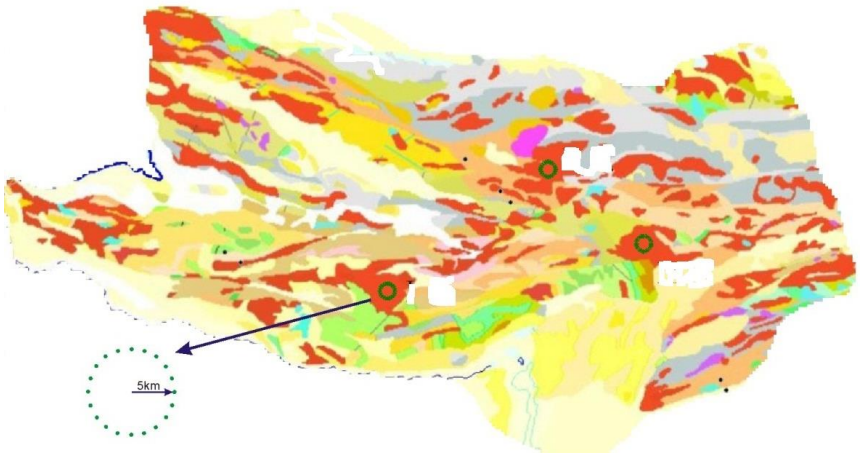

Figure 11. *Tracer particle position map*

Basic scenario

This scenario uses a combination of permeability coefficient and rainfall parameters as a basic scenario for the migration simulation of tracer particles. A simulation of 10,000 years was carried out, and the results of particle tracing are shown in *Figure 12*.

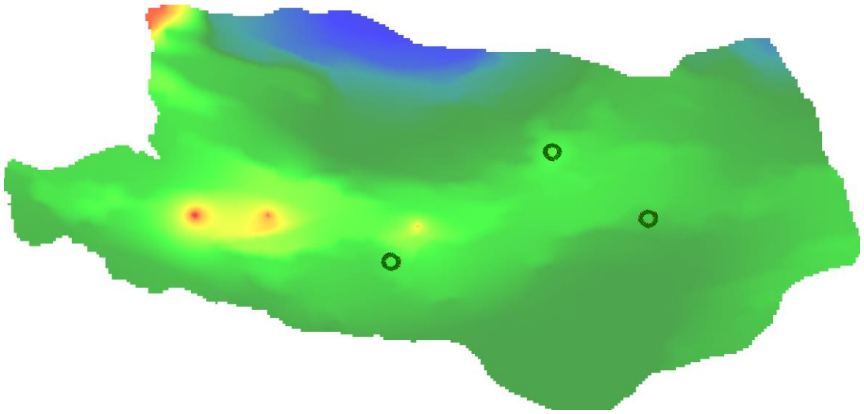

Particle migration trajectory in 10,000 years

Figure 12. *Basic scenario particle migration simulation results*

Scenario 1

Scenario 1 considers the change trends of particle migration when doubling the permeability coefficient of granite. The partition values of the permeability coefficient used are shown in *Table 7,* and the simulation is carried out for 10,000 years. The results of particle tracing are shown in *Figure 13*.

Table 7. *Scenario 1 permeability coefficient partition value*

Partition	Permeability coefficient value (m/d)
K1 High permeability performance partition	2.0
K2 Medium permeability performance partition	0.26
K3 Low Permeability performance partition	0.008

http://www.aloki.hu ● ISSN 1589 1623 (Print) ● ISSN 1785 0037 (Online)
DOI: http://dx.doi.org/10.15666/aeer/1802_25132538

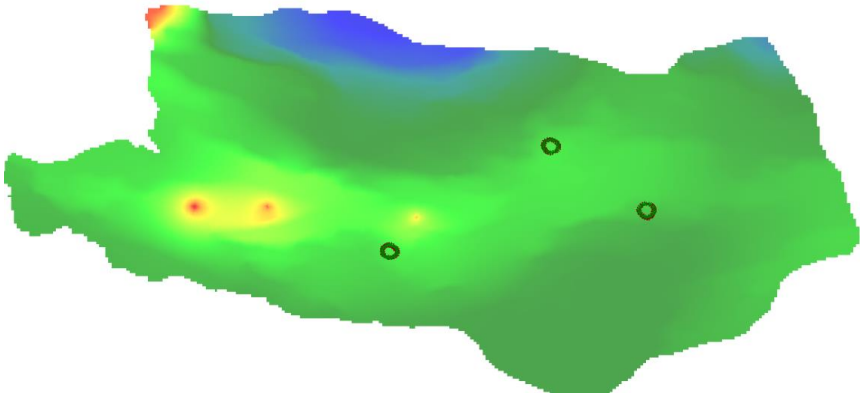

Particle migration trajectory in 10,000 years

Figure 13. *Scenario 1 particle migration simulation results*

Scenario 2

Scenario 2 considers the variation trends of particle migration when the permeability coefficient of granite is reduced to half. The partition values of the permeability coefficient used are shown in *Table 8*, and the simulation is performed for 10,000 years. The results of particle tracing are shown in *Figure 14*.

Table 8. *Scenario 2 permeability coefficient partition value*

Partition	Permeability coefficient value (m/d)
K1 High permeability performance partition	2.0
K2 Medium permeability performance partition	0.26
K3 Low permeability performance partition	0.002

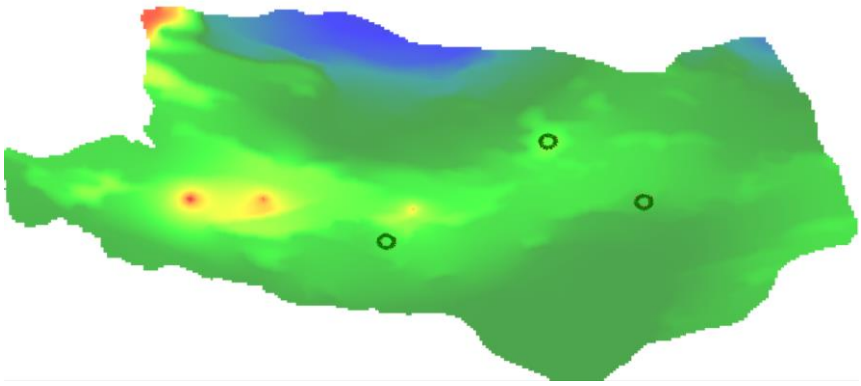

Particle migration trajectory in 10,000 years

Figure 14. *Scenario 2 particle migration simulation results*

Scenario 3

Scenario 3 considers the trends of particle migration change when the precipitation is doubled, and simulates it for 10,000 years. The results of particle tracing are shown in *Figure 15*.

http://www.aloki.hu ● ISSN 1589 1623 (Print) ● ISSN 1785 0037 (Online)
DOI: http://dx.doi.org/10.15666/aeer/1802_25132538

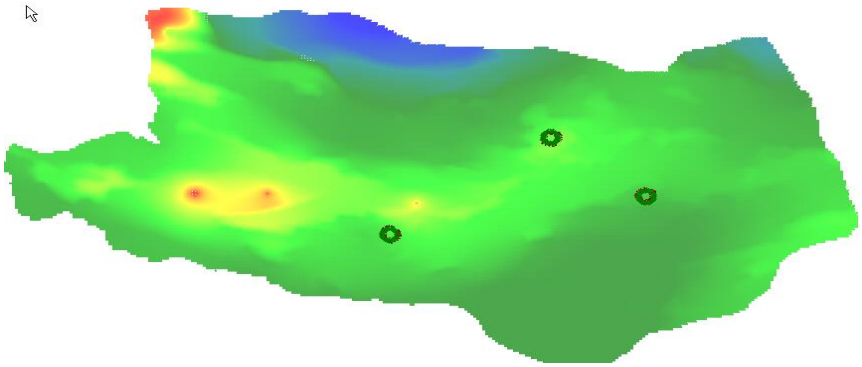

Particle migration trajectory in 10,000 years

Figure 15. *Scenario 3 particle migration simulation results*

Scenario 4

Scenario 4 considers the trends of particle migration change when the precipitation is half reduced, and simulates for 10,000 years respectively. The results of particle tracing are shown in *Figure 16*.

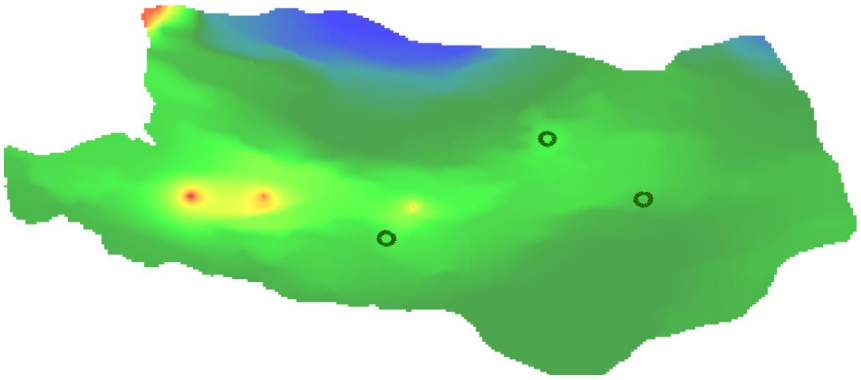

Particle migration trajectory in 10,000 years

Figure 16. *Scenario 4 particle migration simulation results*

Conclusion

By analyzing the hydrogeological conditions of the Kuruktag region in Xinjiang, including the structure and boundary conditions of the aquifer system, the characteristics of the groundwater flow field, the hydraulic connection between different water-bearing units, and the relation between groundwater and surface water, the characteristics of the groundwater recharge and discharge, etc. are analyzed from the perspective of groundwater dynamics.

By adopting the combination of groundwater dynamics and field hydrogeological surveys and analyzing the hydrogeological conditions in the work area, the hydrogeological conditions are relatively simple, focusing on weakly water-bearing, low-permeability, slow flow rate, and relatively closed areas. Based on the above preparations, the simulation study of regional groundwater flow can be carried out, besides, the variation rules of regional groundwater flow under long-term scale is able to be predicted.

http://www.aloki.hu ● ISSN 1589 1623 (Print) ● ISSN 1785 0037 (Online)
DOI: http://dx.doi.org/10.15666/aeer/1802_25132538

Owing to the insufficient basic data and high uncertainty of large-scale model, the simulation of the groundwater flow of the model under multiple conditions and multiple scenarios by means of multi-scenario analysis. The study mainly considers the influence of permeability coefficient, precipitation change and fault on groundwater flow. Additionally, the particle tracing simulation is performed in three granite areas located in the eastern and central parts of the work area with six scenarios carried out by MODPATH to figure out the trajectories of nuclide migration in varied periods, reflecting the influencing factors and regularity of groundwater flow change and nuclide migration.

In order to comprehensively analyze and evaluate the particle migration conditions in multiple scenarios, the particle migration trajectories of the four scenarios are superimposed by 10,000 years of migration time respectively. The results of particle tracing are shown in *Figure 17*.

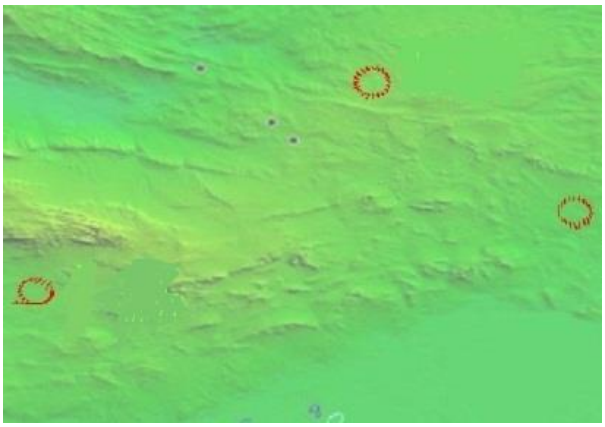

Superimposed particle migration trajectories in 10,000 years (4 scenarios)

Figure 17. *Comprehensive analysis of particle migration simulation in four scenarios*

From the above superposition results, the trends of particle migration in each simulation period can be analyzed as follows: The migration of particles in the three regions is not large in 10,000 years, mainly moving along the direction of groundwater flow, and the migration length is 2 to 5 km.

With the help of comprehensive analysis of particle motion in three regions under different scenarios in different periods, from the perspective of hydrogeology, the following conclusions can be drawn: the particle motion changes little under various scenarios, and the groundwater flow is stable subject to external conditions. The interference is small, the groundwater flow rate is relatively slow, and the particle migration speed is small.

Recommendations for future studies: (1) Due to scarce monitoring data of groundwater level, the interpolation of flow field would be distorted, which cannot represent the real flow field. To further correct the results of numerical simulation, the monitoring data of groundwater level should be enriched, and more hydrological drill holes are proposed to be set. (2) As the carrier of underground nuclide migration, groundwater should be defined as the circulation process. Numerical simulation of groundwater circulation is suggested to be conducted in the area with abundant monitoring data. Taking the petrological and hydrological conditions into consideration, the long-term groundwater circulation is able to be predicted.

http://www.aloki.hu ● ISSN 1589 1623 (Print) ● ISSN 1785 0037 (Online)
DOI: http://dx.doi.org/10.15666/aeer/1802_25132538

REFERENCES

[1] Blessent, D., Therrien, R., Gable, C. W. (2011): Large-scale numerical simulation of groundwater flow and solute transport in discretely-fractured crystalline bedrock. – Advances in Water Resources 34(12): 1539-1552.
[2] Cao, G., Han, D., Currell, M. J., Zheng, C. (2016): Revised conceptualization of the North China Basin groundwater flow system: groundwater age, heat and flow simulations. – Journal of Asian Earth Sciences 127: 119-136.
[3] Chang, Z., Qi, W., Zhao, Z., Chen, X. (2001): Application of Isotope Techniques in Groundwater Exploration in Lop Nur Region. – Xinjiang Geology 19(3).
[4] Chen, M. (1993): Tectonic Style of the Turpan-Hami Basin. – Petroleum Exploration and Development 20(5): 1-7.
[5] Chen, Z. (1966): A brief history of the geological development of Kuruktag and the basic characteristics of geological structures. – Geological Review 24(3): 171-180.
[6] Second Hydrogeological Institute of Gansu Province (1995): Study on water transport and equilibrium factors of the aeration zone in the middle reaches of the Heihe River in Gansu Province. 1995: 23.
[7] Feng, X., Zhao, R., Li, J. (1994): Preliminary study on seismic geology in the Turpan Basin. – Inland Earthquake 8(2): 97-108.
[8] Jiang, Z., Xu, T., Owen, D. D. R., Jia, X., Feng, B., Zhang, Y. (2018): Geothermal fluid circulation in the Guide Basin of the northeastern Tibetan Plateau: isotopic analysis and numerical modeling. – Geothermics 71: 234-244.
[9] Jiao, P., Wang, Y., Liu, C. (2004): The strontium isotope characteristics and its geological significance of the salt lake brine in Lop Nur, Xinjiang. – Nuclear Technology 27(9): 710-715.
[10] Kendall, C. (1998): Tracing Nitrogen Sources and Cycling in Catchments. – In: Kendall, C., McDonnel, J. J. (eds.) Isotope Tracers in Catchment Hydrology. Elsevier, Amsterdam, pp. 534-569.
[11] Kihm, J.-H., Kim, J.-M., Song, S.-H., Lee, G.-S. (2007): Three-dimensional numerical simulation of fully coupled groundwater flow and land deformation due to groundwater pumping in an unsaturated fluvial aquifer system. – Journal of Hydrology 335(1): 1-14.
[12] Kolbe, T., Marçais, J., Thomas, Z., Abbott, B. W., de Dreuzy, J., Rousseau-Gueutin, P., Aquilina, L., Labasque, T., Pinay, G. (2016): Coupling 3D groundwater modeling with CFC-based age dating to classify local groundwater circulation in an unconfined crystalline aquifer. – Journal of Hydrology 543: 31-46.
[13] Lei, X., Liu, B., Quan, J., Wang, H. (2019): Review of the interactive relation between surface water and groundwater. – China Rural Water and Hydropower 19(5): 1-5.
[14] Liu, C., Wang, Y., Jiao, P. (1999): Hydrogen, oxygen, sulfur, isotope geochemistry and source of ore-forming minerals in Lop Nur salt lake, Xinjiang. – Deposit Geology 18(3): 268-275.
[15] Mengistu, H. A., Demlie, M. B., Abiye, T. A., Xu, Y., Kanyerere, T. (2019): Conceptual hydrogeological and numerical groundwater flow modelling around the Moab Khutsong deep gold mine, South Africa. – Groundwater for Sustainable Development 100266.
[16] Pétré, M.-A., Rivera, A., Lefebvre, R. (2019): Numerical modeling of a regional groundwater flow system to assess groundwater storage loss, capture and sustainable exploitation of the transboundary Milk River Aquifer (Canada - USA). – Journal of Hydrology 575: 656-670.
[17] Post, V. E. A., Galvis, S. C., Sinclair, P. J., Werner, A. D. (2019): Evaluation of management scenarios for potable water supply using script-based numerical groundwater models of a freshwater lens. – Journal of Hydrology 571: 843-855.
[18] SDIC Xinjiang Lop Nur Potash Co., Ltd. (2006): Detailed Report on the Potash Deposit of Luobei Depression in Ruoqiang County, Xinjiang. – SDIC Xinjiang Lop Nur Potash Co., Ltd., Bayingolin.

http://www.aloki.hu ● ISSN 1589 1623 (Print) ● ISSN 1785 0037 (Online)
DOI: http://dx.doi.org/10.15666/aeer/1802_25132538

[19] Shao, J., Li, Y., Hou, G., Wang, W., Zeng, L., Duan, L. (2017): Characteristics of groundwater circulation and evolution in Ili valley of Xinjiang. – Arid Zone Research 34(1): 20-25.
[20] Shi, K., Liu, B., Liu, H., Liu, J., Pan, W. (2017): Neoproterozoictectono-sedimentary evolution in Quruqtagh area, NE Tarim Basin, Xinjiang, China. – Earth Science Frontiers 24(01): 298-307.
[21] Singleton, M. J., Wood, K. N., Conrad, M. E., Depaolo, D. J., Dresel, P. E. (2005): Tracking sources of unsaturated zone and groundwater nitrate contamination using nitrogen and oxygen stable isotopes at the Hanford Site, Washington. – Environmental Science Technology 39: 3563-3570.
[22] Tatti, F., Papini, M. P., Torretta, V., Mancini, G., Boni, M. R., Viotti, P. (2019): Experimental and numerical evaluation of groundwater circulation wells as a remediation technology for persistent, low permeability contaminant source zones. – Journal of Contaminant Hydrology 222: 89-100.
[23] The Second Hydrogeology Engineering Geology Brigade of Xinjiang Geology and Minerals Bureau (2003): Hydrogeology and Geological Survey of Water Supply in Potash Mine of Lop Nur, Xinjiang. – Hydrogeology and Geological Survey Report of the Aqike Valley.
[24] Wang, J., Zhang, H., Zhang, G., Wu, F., Lei, K. (2018): Development and application of groundwater numerical simulation methods. – Environment and development 18(6): 103-106.
[25] Wang, K. (2016): Analysis of groundwater formation and occurrence conditions in Korla Region, Xinjiang. –Groundwater 38(6): 253-254.
[26] Xia, X. (2007): China Lop Nur. – Science Press, Beijing.
[27] Xue, L., Wei, Q., Wei, G. (2018): Coupled simulation of surface water and groundwater in the main stream of Tarim River. – Journal of Hohai University (Natural Sciences) 47(3): 196-201.
[28] Zhou, X., Gao, Q., Chen, X., Yao, M., Zhao, X. (2013): Numerically simulating the thermal behaviors in groundwater wells of groundwater heat pump. – Energy 61: 240-247.
[29] Zhu, W., Ma, R., Hu, D., Xu, M. (2001): Tectonic contact relationships between Qoltag Mountain and Turpan-Hami basin in Xinjiang. – Geotectonica et Metallogenia 25(2): 128-135.

http://www.aloki.hu ● ISSN 1589 1623 (Print) ● ISSN 1785 0037 (Online)
DOI: http://dx.doi.org/10.15666/aeer/1802_25132538

THE EFFECT OF PHOSPHORUS AND ZINC DOSES ON YIELD AND YIELD COMPONENTS OF BEANS (*PHASEOLUS VULGARIS* L.) IN VAN-GEVAŞ, TURKEY

BİLDİRİCİ, N.[1*] – ORAL, E.[2]

[1]*Yüzüncü Yıl University, Gevaş Vocational School of Higher Education, Department of Plant and Animal Production, Gevaş, Van, Turkey*

[2]*Department of Field Crops, Faculty of Agriculture, Yüzüncü Yıl University, 65080 Van, Turkey*

[*]*Corresponding author*
(e-mail: numanbildirici@gmail.com; phone: +90-539-427-3208)

(Received 25th Jun 2019; accepted 25th Oct 2019)

Abstract. This research was carried out in Van-Gevaş in 2015 and 2016 with three replications according to the Divided Parcel Trial Design that was divided into random blocks. The experiment involved 2 bean varieties (Aras-98 and Seker-90) x 4 phosphorus dose (0.0, 40.0, 60.0 and 80.0 kg ha^{-1}) x 4 zinc dose (0.0, 10.0, 25.0 and 50.0 kg ha^{-1}) x 3 repetition = 72 parcels were planned and examined. In the experiment, 4 different phosphorus (P) doses were applied to the subparcels as TSP (P2O5) fertilizer. and to gold sub-parcels 4 different zinc (Zn) doses were applied as zinc sulfate (ZnS04.7H20) fertilizer. Two bean varieties used in the study on the effect of phosphorus and zinc doses on plant height (cm), the number of pods per plant (units of plant^{-1}), number of branches (plant^{-1}), seed yield (kg ha^{-1}), harvest index (%) and the effect of protein (%) on grain was also investigated. According to the results obtained in 2015 and 2016, the highest grain yield was obtained from Sugar-90 beans. In the first year, the highest grain yield was obtained from 3380.00 kg ha^{-1} and 40.0 kg ha^{-1} phosphorus and 10.0 kg ha^{-1} zinc, while in the second year 4250.70 kg ha^{-1} was obtained in the same phosphorus and zinc dose. As a result, it has been determined that due to degradation in the phosphorus balance in soil, the efficiency of utilization of zinc in plants affects the yield and quality characteristics.
Keywords: *bean, number pods, interaction, grain yield*

Introduction

For many thousands of years, legume grains have had a very important place in human nutrition. In cases where animal proteins cannot be provided in suffiecient amount, the deficiencies are met from these plants (Adak, 2014). These plants are rich in vitamins and also minerals such as iron, phosphorus, calcium and potassium, as well as dietary fibers (Pekşen and Artık, 2005). It form in nutrition programs together with cereals a very good group (McPhee and Muehlbauer, 2002). Especially together with high lysin content, cholesterol rates are very low. In human nutrition, edible grain legumes contain 22% of proteins and 7% of carbohydrates. 18-31.6% of the leguminous protein is an important and inexpensive source for solving nutritional problems in the body (Adak et al., 2010; Altunkaynak, 2018). In terms of cultivation and production in the world, this is an important genus in the family of beans. Dry and fresh consumption is common. Around 29 million hectares of land is cultivated in the world. The total production amount is 23 million tons and the yield per hectare is 8000.00 kg (FAO, 2015). In our country, bean cultivation area is 848 thousand ha, 220 thousand tons production and 2590.00 kg ha^{-1} yield is obtained (TÜİK, 2018).

Cultivation, irrigation, fertilization and harvesting are very important in bean production. Fertilization has an important place in these cultural applications. The fact that they fix the free nitrogen of air due to the rhizobium bacteria found in the roots of

http://www.aloki.hu ● ISSN 1589 1623 (Print) ● ISSN1785 0037 (Online)
DOI: http://dx.doi.org/10.15666/aeer/1802_25392553

legumes reduces their need for nitrogenous fertilizers. In this case, in the case of deficiencies such as phosphorus and zinc, it increases the importance of the nutritional elements affecting other yield parameters, in particular efficiency. In terms of legumes, phosphorus is an important macro element. This need must be eliminated by fertilization with sowing (Togay and Anlarsal, 2008). The greatest benefit of phosphorous fertilizers is the increase in the quality of the grain and the availability of nitrogen by increasing nodulation and nitrogenase activity (Arıoğlu, 1989).

Another important plant nutrient is zinc, while various enzymes operating in the plant are the building blocks of some hormones in tissue development, the deficiency of zinc leads to the decrease of tryptophan hormone level and protein synthesis is disrupted. In addition, free amino acid accumulation in plants adversely affects grain quality (Yalçın and Usta, 1990).

The height of elements such as phosphorus and zinc in the soil does not always mean that they will be taken and used by plants. In soil, pH, salinity and the amount of other elements are important factors affecting plants. As a result, deficiencies in plants cause significant reductions in yield and quality (Togay and Anlarsal, 2008).

With this study, it was aimed to determine the effect of phosphorus and zinc fertilizers on yield and yield components of beans grown in our region, and as well as to investigate the interactions between P and Zn micronutrients.

Materials and Methods

The research was conducted in Van-Gevaş District (38.2978° N, 43.1055° E) between the years of 2015-2016 (*Figure 1*). In the experiment, two bean varieties (Aras-98 and Şeker-90) were used as plant material. The varieties are registered at the East Anatolian Agricultural Research Institute are white and coarse in color (Şehriali, 1988). Climate data for the years of research and the average for many years are given in *Table 1*.

Figure 1. *Place of trial (Van-Gevaş)*

The total amount of precipitation during the period from May to September in 2015, when the experiment was conducted, was 43.6 mm. In 2016, it was observed that this amount was more than 2015 with 73.3 mm. The average temperature was 18.5°C in the

http://www.aloki.hu ● ISSN 1589 1623 (Print) ● ISSN1785 0037 (Online)
DOI: http://dx.doi.org/10.15666/aeer/1802_25392553

first year. This value was measured as 17.9°C in the second year of the experiment. The average humidity was lower in the first year (42.4%) than in the second year (50.5%).

Table 1. *Experimental climate data**

Months	2015 year					2016 year				
	Temperature (°C)			Cover. Moisture (%)	Rains (mm)	Temperature (°C)			Cover. Moisture (%)	Rains (mm)
	Min	Max	Avg.			Min	Max	Ave.		
May	8.6	27.5	14.4	54.7	31.6	6.5	24.3	13.6	62.3	48.7
June	13.0	34.1	18.1	39.0	11.2	12.0	34.5	18.0	56.0	15.0
July	18.0	37.9	21.7	39.2	-	17.3	37.2	20.7	46.7	3.2
August	17.1	36.4	21.5	38.7	0.8	17.5	35.9	21.1	42.0	1.8
September	13.8	32.0	16.9	40.4	-	13.4	30.4	16.2	45.3	4.6
Average	14.1	33.6	18.5	42.4	-	13.3	32.5	17.9	50.5	-
Total					43.6					73.3

* Van Regional Directorate of Meteorology Records, 2017

Soil samples were taken from the 0-20 cm depth of the soils belonging to the experimental site and analyzed physically and chemically (*Table 2*).

Table 2. *Some chemical properties of experimental soils at a depth of 0-30 cm**

Years	Texture	Total Salt	pH	Calcanty	Available K (K_2O)	Available P (P_2O_5)	Organic matter	Available Zn
		(%)		(%)	(kg da^{-1})	(kg da^{-1})	(%)	(kg da^{-1})
2015	Sandy-Loam-Clay	0.044	7.6	8.06	51.3	2.76	2.32	0.286(Poor)
2016	Sandy-Loam-Clay	0.039	7.5	8.72	42.0	3.58	2.57	0.311(Poor)

*Van Commodity Exchange was conducted in soil analysis laboratories, 2015

The experimental soils are slightly alkaline and the organic matter levels are moderate. It was found that the soil was low in lime, poor in phosphorus and zinc and rich in potassium.

The research was established according to the experimental design of Divided Parcels Divided into Randomized Blocks with 3 replications. The trial area, which was driven deeply in the last spring, was completed in April with a second surface version and disc harrow. Seed planting was carried out in the first week of May, in 5 rows per parcel. The distance between the rows in the parcels was 40 cm. The area of a parcel was 2.0 m x 4.0 m = 8 m². In the study, the varieties in the main parcels were Aras-98 and Seker-90, phosphorus (18-19% P_2O_5) doses in sub-parcels and zinc (Zn) sulphate doses ($ZnS0_4.7H_20$) were applied to the six parcels in the same test design. The amount of seed to be taken into the parcel was determined to be 45 seeds per m^2 21% Ammonium Sulphate $(NH4)_2SO_4$ fertilizer was placed in the soil with 20.00 kg of pure nitrogen per hectare evenly to each parcel. Trial parcels; 1 The first foliation period, 2 with branching, 1 before flowering, 1 flowering period, and 1 bean binding period in including was irrigated 6 times in total. (Engin, 1989). In this study, the effect of increasing Zinc (Zn) and Phosphorus (P) doses on plant height, number of pods per plant, grain yield, harvest index (Harvest index = Grain / Plant stalk ratio), thousand seed weight and protein ratio in two bean varieties were investigated. In the study, two bean varieties were treated in 4 different doses (0.0, 10.0, 25.0, 50.0 kg ha^{-1}) in the form of Zinc $ZnSO_4.7H_2O$ and in 4 different doses (0.0 (control), 40.0, 60.0, 80.0, kg ha^{-1}) in the form of phosphorus P_2O_5. Each row of 5 parcels on each side of each row and 50 cm within the row of plants in the row

http://www.aloki.hu ● ISSN 1589 1623 (Print) ● ISSN1785 0037 (Online)
DOI: http://dx.doi.org/10.15666/aeer/1802_25392553

as the edge of the effect was excluded from the observation (Ceylan and Sepetoğlu, 1979). All observations were made on an area of 1.2 m x 3 m = 3.6 m². The data obtained after trial in terms of yield and yield components were used in determining the differences of split parcel design with the variance analysis method. In the determination of different groups Duncan (5%) multiple comparison test was utilized with Costata and Mstatc software (Düzgüneş et al., 1987).

Results

Plant Height (cm)

According to the data obtained at the end of the research in 2015, the interactions of year, variety, phosphorus, zinc doses, variety x phosphorus, variety x zinc, variety x phosphorus and variety x phosphorus x zinc doses were significant and phosphorus x zinc interactions were not statistically significant. In 2016, other differences between plant height averages were significant (*Table 3*).

Table 3. *Bean varieties in the groups and averages related to the height of the plant**

		2015 Zn Doses						**2016** Zn Doses					
Variety	P Dose	Zn0	Zn1	Zn2	Zn3	Ç x P. Ave.	Ç. Ave.	Zn0	Zn1	Zn2	Zn3	Ç x P. Ave.	Ç. Ave.
Ç1	P0	42.90qr	47.13l	41.68s	49.12ij	45.20D		61.29	65.89	63.05	67.24	64.36A	
	P1	43.78pq	45.00no	52.04g	47.27kl	47.02C		60.56	66.12	66.47	65.74	64.71A	
	P2	45.90mn	55.50bc	52.79fg	44.78op	49.74B	46.68B	70.96	76.93	64.47	69.76	70.53A	65.12A
	P3	42.02rs	46.64lm	45.40no	45.02no	44.77D		60.40	57.80	63.69	61.58	60.86B	
ÇxZn Ave.		43.65B	48.57A	47.98A	46.54A			63.30AB	66.68A	64.42A	66.08A		
	P Dose	Zn0	Zn1	Zn2	Zn3	Ç x P. Ave.	Ç. Ave.	Zn0	Zn1	Zn2	Zn3	Ç x P. Ave.	Ç. Ave.
Ç2	P0	53.10ef	58.28a	54.05de	50.88h	50.07B		55.57	57.24	53.08	58.77	56.16B	
	P1	48.85j	50.97h	48.32jk	50.03jk	49.54B		52.86	54.95	58.88	59.94	56.66B	
	P2	52.45fg	54.86cd	56.22b	54.98cd	54.62A	50.93A	66.46	65.70	62.33	65.95	65.11A	60.04B
	P3	52.90fg	52.17fg	42.87qr	50.02hi	49.49B		69.72	54.53	59.94	64.79	62.24AB	
ÇxZn Ave.		51.82B	54.07A	50.36C	51.48B			61.15B	58.10B	58.56B	62.36A		
Zn Ave.		47.73B	51.32A	49.17A	49.01A			60.26C	60.69BC	62.05B	67.82A		
Yıl Ave.		48.80B						62.58A					
	P Dose	Zn0	Zn1	Zn2	Zn3	P Ave.		Zn0	Zn1	Zn2	Zn3	P Ave.	
P x Zn	P0	48.00	52.70	47.86	50.00	49.64A		58.43j	61.56gh	58.06j	63.00e	60.26B	
	P1	46.31	47.98	50.18	48.65	48.28B		56.71k	60.53i	62.67ef	62.84e	60.68B	
	P2	49.17	55.18	54.50	49.88	52.18A		68.71b	71.31a	63.40e	67.85bc	67.81A	
	P3	47.46	49.40	44.13	47.52	47.12B		65.06d	56.16k	61.81fg	63.18e	61.55B	
C.V (%)		5.29						4.14					

*The difference between the averages indicated with the same letters is not significant at 5%; C.V-Coefficient of variation. Zn- Zinc Dose; Ç1- Aras-98; Ç2-Sugar-90; P-Phosphorus doses; Ave.-Average; Z x Zn- Variety x Zinc Dose Interaction; P x Zn- Phosphorus x Zinc Doses Interaction

According to the data obtained at the end of the experiment; In 2015 and 2016, the average plant height was 46.68-65.12 cm with Aras-98 cultivar, while the Sugar-90 variety was higher with 50.93- 60.04 cm. The plant height values obtained from the Seker-90 variety in both years of the experiment were found to be higher than that of the Aras-98 variety (*Table 3*).

According to the data obtained, average plant height values obtained from different phosphorus doses ranged from 54.62-44.77 cm in 2015 and from 70.53-56.16 cm in 2016. In

http://www.aloki.hu ● ISSN 1589 1623 (Print) ● ISSN1785 0037 (Online)
DOI: http://dx.doi.org/10.15666/aeer/1802_25392553

the first year of the experiment, the highest plant height (54.62 cm) was obtained in Sugar-90 from 60 kg ha^{-1} phosphorus dose. The lowest plant height value was determined at a dose of 0 (control) applied to Aras-98 cultivar with 45.20 cm. In 2016, the plant height average values ranged from 56.16 to 70.53 cm. The highest plant height values (70.53 cm) were obtained from 60.00 kg ha^{-1} phosphorus dose applied to Aras-98 cultivar, 56.16 cm with the lowest value was obtained from parcels belonging to sugar-90 cultivar of not phosphorous.

As shown in *Table 2*, plant height average values obtained from different zinc doses changed between 51.32-47.73 cm in 2015 and 67.82-60.26 cm in 2016. In the first year of the experiment, the highest plant height value was obtained from Sugar-90 varieties with 54.07 cm and 25.00 kg ha^{-1} zinc. The lowest value was determined in Aras-98 cultivar, which does not apply zinc dose, which is measured as 43.65 cm.

The highest plant height (56.22 cm) value in the first year in terms of zinc x phosphorus doses applied in the research; It was obtained from 25.00 kg ha^{-1} zinc x 60.00 kg ha^{-1} phosphorus dose applied to Sugar-90 bean variety, and the lowest value was obtained from the P3 phosphorus dose and non-zinc parcels with 42.02 cm (*Table 3*).

Number of Pods (number / plant)

As seen in *Table 4*, there were differences in the number of pods in the experiment. In the first year of the experiment on the average number of pods; Interactions between year, variety, zinc doses, type x phosphorus and phosphorus x zinc dose interactions were significant, some x phosphorus x zinc doses were considered statistically insignificant. In the second year of the experiment, cultivar, zinc, phosphorus, Zn x P, Ç x Zn and Ç x Zn x P interactions were found statistically significant.

Table 4. *Averages and formed groups on number of pods in bean varieties**

		2015 Zn Doses						**2016** Zn Doses					
Variety	P Dose	Zn0	Zn1	Zn2	Zn3	Ç x P. Ave.	Ç. Ave.	Zn0	Zn1	Zn2	Zn3	Ç x P. Ave.	Ç. Ave.
Ç1	P0	7.38	9.31	10.30	10.64	9.40BC		10.46o	12.53klm	13.18ijk	14.04gh	12.55	
	P1	9.20	10.85	11.22	11.70	10.74A		12.66jkl	15.21de	13.34hij	12.00lmn	13.30	
	P2	9.11	10.75	12.87	10.48	10.80A	10.23A	15.61cd	16.58b	16.02bc	15.55cd	15.94	14.35A
	P3	8.18	12.19	10.27	9.26	9.97AB		13.88ghi	15.19de	18.04a	15.45cde	15.64	
ÇxZn Ave.		8.46	10.77	11.16	10.52			13.15D	14.87AB	15.14A	14.26BC		
	P Dose	Zn0	Zn1	Zn2	Zn3	Ç x P. Ave.	Ç. Ave.	Zn0	Zn1	Zn2	Zn3	Ç x P.Ave.	Ç. Ave.
Ç2	P0	7.28	9.32	8.81	7.94	8.11D		9.37p	8.09q	10.45o	10.33o	9.56	
	P1	7.75	9.59	10.39	10.19	9.48BC		11.77n	10.70o	14.36fg	12.64jkl	12.36	
	P2	8.16	11.11	8.66	8.30	9.05CD	8.75B	11.64n	14.83ef	15.25de	11.80mn	13.38	12.48B
	P3	6.94	10.57	7.06	7.88	8.15D		11.85mn	16.31b	15.42cde	14.96def	14.63	
ÇxZn Ave.		7.53	10.14	8.73	8.57			11.15E	12.48E	13.87C	12.43D		
Zn Ave.		7.99C	10.45A	9.94A	9.54B			12.15C	13.67B	14.50A	13.34B		
Yıl Ave.		9.48B						13.41A					
	P Dose	Zn0	Zn1	Zn2	Zn3	P Ave.		Zn0	Zn1	Zn2	Zn3	P Ave.	
P x Zn	P0	7.33g	9.31cd	9.55bc	9.29cd	8.87B		9.91h	10.31h	11.81g	12.18fg	11.05C	
	P1	8.47def	10.22ab	11.05a	10.94a	10.17A		12.21efg	12.95de	13.85c	12.32efg	12.83B	
	P2	8.63def	10.93a	10.76a	9.39bcd	9.92AB		13.62cd	15.70b	15.63b	13.67c	14.65A	
	P3	7.70fg	10.45a	8.66cde	8.57def	8.84B		12.86f	15.75b	16.73a	15.20b	15.13A	
C.V (%)		10.36						6.93					

*The difference between the averages indicated with the same letters is not significant at 5%; C.V-Coefficient of variation. Zn- Zinc Dose; Ç1- Aras-98; Ç2-Sugar-90; P-Phosphorus doses; Ave.-Average; Z x Zn- Variety x Zinc Dose Interaction; P x Zn- Phosphorus x Zinc Doses Interaction

http://www.aloki.hu ● ISSN 1589 1623 (Print) ● ISSN1785 0037 (Online)
DOI: http://dx.doi.org/10.15666/aeer/1802_25392553

The average number of pods obtained at the end of the study was 9.48 in the first year and 13.41 in the second year. According to the results, the average number of pods per year was determined to be 10.21-14.35 in Seker-98 cultivar and 8.75-12.45 in Sugar-90 cultivar, respectively (*Table 4*). According to the data obtained, the interaction of the first year varieties x phosphorus doses on the average number of pods was statistically significant and the second year was insignificant. The highest number of pods was obtained from Aras-98 bean varieties with 10.8 pieces at 60.0 kg ha^{-1} phosphorus dose, while the lowest value was obtained from 00.0 kg ha^{-1} phosphorus dose in Sugar-90 cultivar with 8.11 pieces. According to these results, it was seen that increased phosphorus doses increased the number of pods in the plant up to a certain point. According to the data obtained at the end of the study, it was observed that the correlation was statistically significant on the average number of pods per day. The highest number of pods was obtained from 10.00 kg ha^{-1} zinc and 40.00 kg ha^{-1} phosphorus application per decare with 11.05 pcs in the first year. The lowest value was obtained with 0.33 doses of both fertilizer doses. The highest number of pods obtained in the second year of the experiment was obtained from 16.73 number pods of 60.00 kg ha^{-1} phosphorus and 10.00 kg ha^{-1} zinc dose. The lowest value was found in 9 doses with 9.91 pieces (*Table 4*). According to the data obtained in the second year of the experiment, the interactions between the number of phosphorus x zinc doses considering the average number of pods were statistically significant and the first year was insignificant. The highest average number of pods was 18.04 and was obtained from 60.00 kg ha^{-1} phosphorus and 10.00 kg ha^{-1} zinc dose applied to Aras-98 bean cultivar. The lowest value was measured in the control parcel with Sugar-90 cultivar with 9.37 units (*Table 4*).

Number of Branches (pieces / plant)

In the study carried out in 2015-16 years, year, variety, phosphorus doses, variety x phosphorus doses and phosphorus x zinc doses interactions were found statistically significant considering the average number of branches in bean varieties in the first year. In the second year of the experiment, the effect of varieties on the average number of pods was found statistically significant (*Table 5*).

According to the results obtained in the experiment, the average number of branches in the first year was 4.33 and in the second year it was 5.24. The number of branches among the varieties were obtained from Aras-98 variety with 4.78-5.78 units, respectively. Sugar-90 varieties (3.88-4.70) branching was detected in a lower number (*Table 5*).

According to the results obtained, the first year on the number of branches was statistically significant and the second year was insignificant. According to the results obtained from the experiment, the highest average number of branches was obtained from the 40.00 kg ha^{-1} phosphorus dose applied to the Aras-98 variety. The lowest value was obtained from the control (0 dose) of Sugar-90 variety with 3.59.

As seen in *Table 5*, the effect of P x Zn interaction on the average number of branches was found significant ($p<0.01$). The highest average number of branches was obtained from 4.67 pieces and 40.00 kg ha^{-1} phosphorus x10.00 kg ha^{-1} zinc dose. The lowest value (3.89) was measured in the application of 60.00 kg ha^{-1} phosphorus x 25.00 kg ha^{-1} zinc dose.

http://www.aloki.hu ● ISSN 1589 1623 (Print) ● ISSN1785 0037 (Online)
DOI: http://dx.doi.org/10.15666/aeer/1802_25392553

Table 5. *Groups and averages of the number of branches in bean varieties**

		2015 Zn Doses						**2016** Zn Doses					
Variety	P Dose	Zn0	Zn1	Zn2	Zn3	Ç x P. Ave.	Ç. Ave.	Zn0	Zn1	Zn2	Zn3	Ç x P. Ave.	Ç. Ave.
Ç1	P0	4.41	4.58	4.74	4.54	4.56B		5.77	5.53	5.76	5.41	5.62	
	P1	4.59	4.87	4.76	4.43	4.66AB	4.78A	5.45	5.67	5.94	5.65	5.67	
	P2	4.89	5.20	4.98	4.66	4.93A		6.06	5.77	5.79	5.72	5.83	5.78A
	P3	4.78	4.98	5.12	4.40	4.82AB		6.03	6.03	6.23	5.82	6.02	
ÇxZn Ave.		4.66	4.90	4.90	4.50			5.81	5.75	5.93	5.65		
	P Dose	Zn0	Zn1	Zn2	Zn3	Ç x P. Ave.	Ç. Ave.	Zn0	Zn1	Zn2	Zn3	Ç x P. Ave.	Ç. Ave.
Ç2	P0	3.66	3.29	3.95	3.48	3.59D		4.55	4.06	4.56	4.49	4.41	
	P1	3.93	3.64	3.74	3.74	3.76CD		4.70	4.98	4.88	4.60	4.79	
	P2	4.08	4.15	3.98	3.92	4.03B	3.88B	4.84	5.11	5.06	4.73	4.93	4.70B
	P3	3.70	3.74	3.96	3.39	3.70CD		4.60	4.58	5.01	4.56	4.68	
ÇxZn Ave.		3.84	3.70	3.90	3.63			4.67	4.68	4.87	4.59		
Zn Ave.		4.25	4.30	4.40	4.06			5.24	5.21	5.40	5.12		
Yıl Ave.		4.33B						5.24 A					
	P Dose	Zn0	Zn1	Zn2	Zn3	P Ave.		Zn0	Zn1	Zn2	Zn3	P Ave.	
P x Zn	P0	4.03defg	3.93fg	4.34bcd	4.01efg	4.07B		5.16	4.79	5.16	4.95	5.01	
	P1	4.26bcde	4.25bcdef	4.25bcdef	4.08cdef	4.21AB		5.07	5.32	5.41	5.12	5.23	
	P2	4.48ab	4.67a	4.48ab	4.29bcde	4.48A		5.45	5.44	5.42	5.22	5.38	
	P3	4.24bcdef	4.36bc	4.51ab	3.89g	4.25AB		5.31	5.30	5.62	5.19	5.35	
C.V (%)		5.36						6.42					

*The difference between the averages indicated with the same letters is not significant at 5%; C.V-Coefficient of variation. Zn- Zinc Dose; Ç1- Aras-98; Ç2-Sugar-90; P-Phosphorus doses; Ave.-Average; Z x Zn- Variety x Zinc Dose Interaction; P x Zn- Phosphorus x Zinc Doses Interaction

Harvest Index (%)

In the study conducted between 2015-16 years; It was statistically determined that other factors other than the varieties on the harvest index of zinc x phosphorus fertilizer application were insignificant (*Table 6*).

According to the results obtained in the study, the harvest index was found to be 41.89-41.91% in the Aras-98 variety and 45.67-46.18 % in the Ç2 (Şeker-90). In this study; phosphorus and zinc fertilizer doses were not found to be very effective on the harvest index. Harvest index = Grain / Plant stalk ratio is calculated with the formula.

Grain Yield (kg ha^{-1})

In 2015 and 2016, the effect on average grain yield of different phosphorus and zinc doses in dry bean varieties year, variety, phosphorus, zinc, variety x phosphorus, variety x zinc, phosphorus x zinc and cultivar x phosphorus x zinc interactions were found statistically significant (*Table 7*). The mean grain yields obtained at the end of the experiment were 2320.71 kg ha^{-1} in the first year and 2518.90 kg ha^{-1} in the second year.

According to the data, the average grain yield of Aras-98 bean varieties was 1449.80-2174.40 kg ha^{-1} in years, and in Sugar-90 variety 2308.70-2863.00 kg ha^{-1} (Das et al., 2005) in the study carried out in Erzurum. The yield of Yakutiye-98 and Aras-98 varieties were determined as 1842.00 and 1944.00 kg ha^{-1}, respectively. The effect of

http://www.aloki.hu ● ISSN 1589 1623 (Print) ● ISSN1785 0037 (Online)
DOI: http://dx.doi.org/10.15666/aeer/1802_25392553

phosphorous fertilizer on average grain yield in beans was found statistically significant. The highest grain yield in both years of the experiment was obtained from a dose of 60.00 kg ha^{-1} phosphorus in Sugar-90 cultivar with 2465.10-3468.50 kg ha^{-1}, respectively. The lowest value is determined as 1209.80-2000.00 kg ha^{-1} in parcels with no fertilizer (*Table 7*). In parallel with the increasing phosphorus doses, the average grain yield of the varieties was increased up to 60.00 kg ha^{-1} phosphorus dose and the yields of grain decreased.

Table 6. *Groups and averages of harvest index in bean varieties**

		2015 Zn Doses						**2016** Zn Doses					
Variety	P Dose	Zn0	Zn1	Zn2	Zn3	Ç x P. Ave.	Ç. Ave.	Zn0	Zn1	Zn2	Zn3	Ç x P.Ave.	Ç. Ave.
Ç1	P0	40.56	43.06	42.11	41.81	42.17		39.38	38.38	41.89	41.80	40.36	
	P1	41.64	43.16	44.84	40.39	42.74		38.96	44.49	41.55	41.73	41.68	
	P2	42.49	40.24	41.92	39.17	42.55	41.89B	40.18	43.15	40.37	41.08	41.19	41.19B
	P3	43.98	44.50	41.34	39.42	40.20		40.41	41.25	40.63	42.66	41.23	
ÇxZn Ave.		42.17	42.74	42.55	40.20			39.73	41.81	41.11	41.81		
	P Dose	Zn0	Zn1	Zn2	Zn3	Ç x P. Ave.	Ç. Ave.	Zn0	Zn1	Zn2	Zn3	Ç x P.Ave.	Ç. Ave.
Ç2	P0	41.42	46.17	48.01	47.31	43.12		44.71	45.87	47.47	43.81	45.46	
	P1	43.31	48.18	47.73	48.39	47.43		44.88	46.40	49.69	45.23	46.55	
	P2	48.34	47.63	44.78	42.30	46.47	45.67A	42.92	47.87	48.27	49.45	47.20	46.18A
	P3	47.74	45.34	47.02	43.25	45.31		45.45	45.89	45.16	45.88	45.59	
ÇxZn Ave.		45.20	46.83	46.89	45.31			44.49	46.50	47.65	46.09		
Zn Ave.		43.68	44.78	44.72	42.75			42.11	41.16	44.37	43.95		
Yıl Ave.		43.79						43.65					
	P Dose	Zn0	Zn1	Zn2	Zn3	P Ave.		Zn0	Zn1	Zn2	Zn3	P Ave.	
P x Zn	P0	40.99	44.62	45.06	44.56	43.80		42.04	42.12	44.68	42.80	43.91	
	P1	42.48	45.67	46.29	44.39	44.70		41.92	45.44	45.62	43.48	44.11	
	P2	45.42	43.94	43.35	40.74	43.36		41.55	45.51	44.32	45.26	44.16	
	P3	45.86	44.92	44.18	41.34	44.07		42.93	43.57	42.89	44.27	43.41	
C.V (%)		5.32						4.91					

*The difference between the averages indicated with the same letters is not significant at 5%. ; C.V-Coefficient of variation. Zn- Zinc Dose; Ç1- Aras-98; Ç2-Sugar-90; P-Phosphorus doses; Ave.-Average; Z x Zn- Variety x Zinc Dose Interaction; P x Zn- Phosphorus x Zinc Doses Interaction

As shown in *Table 7*, the effect of zinc doses on average grain yields in bean varieties was found significant. The highest grain yields obtained from the experiment were obtained from the application of 2340.00-4416.60 kg ha^{-1} and 25.00 kg ha^{-1} zinc dose in Sugar-90 bean cultivar by years. The highest grain yields obtained from the experiment were obtained from the application of 2340.00-4416.60 kg ha^{-1} and 25.00 kg ha^{-1} zinc dose in Sugar-90 bean cultivar by years.

The effect of phosphorus and zinc on the average grain yield in beans was found significant ($p<0.01$). The highest average grain yield was obtained in 2548.80-3304.80 kg ha^{-1} and 60 kg ha^{-1} phosphorus and 25.00 kg ha^{-1} zinc in both years of the experiment. The lowest value was obtained from the fertilizer-free parcels with 1425.50 kg ha^{-1} in the first year and from the parcel applied 40.00 kg ha^{-1} phosphorus in the second year (*Table 7*).

The effect of phosphorus and zinc fertilizer doses on mean grain evolution was found statistically significant. The highest average grain yield was obtained from the Sugar-90

http://www.aloki.hu ● ISSN 1589 1623 (Print) ● ISSN1785 0037 (Online)
DOI: http://dx.doi.org/10.15666/aeer/1802_25392553

cultivar in both years of the experiment with 3380.00-4257.00 kg ha^{-1} and 40.00 kg ha-1 phosphorus (P2) x 10.00 kg ha^{-1} zinc (Zn) respectively, the lowest values were 1014.50-1484.70 kg ha^{-1} Aras-98 cultivars were obtained from fertilizer applications (*Table 7*).

Table 7. *Groups and averages of grain yield in bean varieties**

		2015						**2016**					
		Zn Doses						Zn Doses					
Variety	P Dose	Zn0	Zn1	Zn2	Zn3	Ç x P. Ave.	Ç. Ave.	Zn0	Zn1	Zn2	Zn3	Ç x P. Ave.	Ç. Ave.
Ç1	P0	101.45w	127.49j	128.00j	127.00j	120.98E		148.47z	229.98s	167.22z	255.70n	200.34CD	
	P1	138.34s	145.76h	146.76gh	147.76gh	144.65CD		203.70x	242.42p	215.04v	222.68u	220.96C	
	P2	148.22qh	167.50e	171.77n	169.70e	164.31C	144.98B	212.70v	229.30st	235.26r	193.96y	217.80C	217.44B
	P3	139.33i	151.20f	156.40f	153.00f	149.98CD		251.66o	227.06t	238.32q	206.34w	230.84BC	
Ç x Zn Ave.		131.84C	147.98B	150.73A	149.38B			204.13E	232.19 D	213.96D	219.67D		
	P Dose	Zn0	Zn1	Zn2	Zn3	Ç x P. Ave.	Ç. Ave.	Zn0	Zn1	Zn2	Zn3	Ç x P. Ave.	Ç. Ave.
Ç2	P0	127.49j	127.20j	318.58c	318.20c	222.86B		286.59k	305.47h	352.90c	239.62q	221.14BC	
	P1	146.76gh	146.00h	336.48a	336.40a	241.60A		192.63y	320.40e	326.07d	278.23m	279.33B	
	P2	150.25fg	169.77e	338.00a	328.03b	246.51A	230.87A	307.63g	370.79b	425.70a	283.30l	346.85A	286.30A
	P3	135.20i	151.20f	282.75d	281.00d	212.53B		284.14l	314.06f	301.97i	291.39j	297.89AB	
Ç x Zn Ave.		139.92B	148.54B	318.95A	315.90A			267.74C	327.68B	351.66A	273.13C		
Zn Ave.		135.88C	148.26B	234.84A	232.64A			235.93C	279.93A	282.81A	246.40B		
Year Ave.		232.71 B						251.89 A					
	P Dose	Zn0	Zn1	Zn2	Zn3	P Ave.		Zn0	Zn1	Zn2	Zn3	P Ave.	
P x Zn	P0	114.47m	127.34l	223.29d	222.60de	171.92C		217.53j	267.72e	260.06e	247.66h	248.24B	
	P1	142.55j	145.88ij	241.62c	242.08c	193.03A		198.16k	281.41c	270.55d	250.45g	250.14B	
	P2	149.23hi	168.63g	254.88a	248.86b	205.40A		260.16f	300.04b	330.48a	238.63i	282.32A	
	P3	137.26k	151.20h	219.57ef	217.00f	181.25B		267.90e	270.56d	270.14d	248.86gh	264.36B	
C.V (%)		7.01						4.83					

*The difference between the averages indicated with the same letters is not significant at 5%; C.V-Coefficient of variation. Zn- Zinc Dose; Ç1- Aras-98; Ç2-Sugar-90; P-Phosphorus doses; Ave.-Average; Z x Zn- Variety x Zinc Dose Interaction; P x Zn- Phosphorus x Zinc Doses Interaction

Crude Protein Content (%)

At the end of the study, it was found that the effects of type x zinc and phosphorus x zinc doses on the crude protein content were statistically significant. As of years, the protein ratio was obtained from Seker-90 variety with 22.48-12.08%, respectively. Lower crude protein ratios were obtained from Aras-98 variety (22.45-22.04%) (*Table 8*).

The effect of different zinc doses on average crude protein ratios was found statistically significant in every two years when seen in *Table 8*. The highest crude protein content (24.20-23.96%) was obtained from Sugar-90 bean cultivars of 25.00 kg ha^{-1} zinc fertilizer while the lowest values (20.95-21.79%) were obtained from the fertilizer application of the same type.

The effect of phosphorus doses on the average crude protein ratio was found significant ($p < 0.01$). The highest values were obtained from 23.56 to 23.26% crude protein ratios and 60.00 kg ha^{-1} phosphorus dose in 2015-2016. The lowest value was

http://www.aloki.hu ● ISSN 1589 1623 (Print) ● ISSN1785 0037 (Online)
DOI: http://dx.doi.org/10.15666/aeer/1802_25392553

found in the first year without fertilizer with a rate of 21.23% and with a rate of 80.00 kg ha^{-1} phosphorus with 21.98% in the second year (*Table 8*).

Table 8. *Groups and averages of crude protein ratios in bean varieties**

		2015 Zn Doses						**2016** Zn Doses					
Variety	P Dose	Zn0	Zn1	Zn2	Zn3	Ç x P. Ave.	Ç. Ave.	Zn0	Zn1	Zn2	Zn3	Ç x P. Ave.	Ç. Ave.
Ç1	P0	21.05	20.33	21.75	20.74	20.97		21.22	21.77	21.66	21.22	21.46	
	P1	21.92	23.00	23.55	21.70	22.54		22.92	23.43	24.24	23.23	23.45	
	P2	23.10	24.19	24.71	23.47	23.86	22.45A	22.14	22.24	22.98	22.06	22.35	22.04B
	P3	21.89	22.47	23.45	22.45	22.56		20.90	21.77	21.10	19.84	20.90	
Ç x Zn Ave.		21.99C	22.49B	23.36A	22.09B			21.79B	22.30B	22.49B	21.58BC		
	P Dose	Zn0	Zn1	Zn2	Zn3	Ç x P. Ave.	Ç. Ave.	Zn0	Zn1	Zn2	Zn3	Ç x P. Ave.	Ç. Ave.
Ç2	P0	20.07	20.99	23.66	21.32	21.51		20.85	23.93	24.62	23.38	23.19	
	P1	20.94	21.87	24.54	22.20	22.38		20.80	23.55	24.57	23.37	23.07	
	P2	21.32	23.25	24.93	23.25	23.18	22.48	20.59	23.33	24.35	23.75	23.00	23.08A
	P3	21.48	23.40	23.67	22.81	22.84		22.91	23.60	22.33	23.45	23.07	
Ç x Zn Ave..		20.95C	22.37B	24.20A	22.39B			21.28C	23.60AB	23.96A	23.48B		
Zn Ave.		21.47	22.43	23.78	22.42			21.53BC	22.95AB	23.22A	22.53C		
Year Ave.		22.46						22.56					
	P Dose	Zn0	Zn1	Zn2	Zn3	P Ave.		Zn0	Zn1	Zn2	Zn3	P Ave.	
P x Zn	P0	20.56	20.66	22.70	21.03	21.23B		21.03	22.85	23.14	22.30	22.33B	
	P1	21.43	22.43	24.04	21.95	22.46AB		21.86	23.49	24.40	23.30	23.26A	
	P2	22.21	23.72	24.82	23.36	23.52A		21.36	22.78	23.66	22.90	22.67B	
	P3	21.68	22.93	23.56	22.63	22.70A		21.90	22.68	21.71	21.64	21.98C	
C.V (%)		5.43						5.16					

*The difference between the averages indicated with the same letters is not significant at 5%; C.V-Coefficient of variation. Zn- Zinc Dose; Ç1- Aras-98; Ç2-Sugar-90; P-Phosphorus doses; Ave.-Average; Z x Zn- Variety x Zinc Dose Interaction; P x Zn- Phosphorus x Zinc Doses Interaction

Discussion

These results of plant height values in the second year were significantly higher than the first year. In the first trial year, due to lack of precipitation, the decrease in the plant output and the decrease in the time between the output and the maturation caused the plant height values to decrease. This difference is thought to be caused by the climate in terms of plant height values (Elkoca and Kantar, 2003). This difference between years is thought to be due to the effect of climate factors as well as phosphorus fertilizer applied. It is stated that phosphorus, like nitrogen, increases the root, stem length, seed production, seed quality and resistance to diseases (Marschner, 1995; Hussein and Alva, 2014). Many research studies (Shrotriya, 1998; Bokhtiar and Sakurai, 2005; Pholsen and Sormsungnoen, 2005; Bayu et al., 2006; Barros et al., 2007; Alatürk, 2012) on fertilization obtained similar results as this study. In similar studies, increased fertilization of leguminous crops indicated that zinc fertilization increased plant height (Sing and Saxena, 1986; Togay and Anlarsal, 2008). In the second year of the experiment, the interaction effect between doses was statistically insignificant. In similar studies Tisdale and Nelson (1966), reported that phosphorous fertilizers added to phosphorous-rich soils make it difficult for the plants to uptake other nutrients, especially zinc, resulting in zinc deficiency in the plants grown in these parcels.

http://www.aloki.hu ● ISSN 1589 1623 (Print) ● ISSN1785 0037 (Online)
DOI: http://dx.doi.org/10.15666/aeer/1802_25392553

Similarly, Bayraktar (1966) also stated that when excess phosphorus is present in the soil or when more phosphorus is supplied to the plant, excess phosphorus prevents the extraction of 67 micro elements such as zinc and iron.

In a similar study conducted by Elkoca and Kantar (2004), the number of pods ranged from 3.5-4.2, indicating that this feature showed a wide variation according to the types and lines. Legumes in plants are the most effective group of phosphorus in the soil (Altın et al., 2005; Batıca et al., 2017). Turunko and Mohammed (2014), in Ethiopia's Arbe Minch agricultural enterprise using Red Wolaita varieties; 5 different doses of phosphorus (00.00, 10.00, 20.00, 30.00, 40.00 kg ha^{-1}) growth, dry matter and yield components were investigated. As a result, the most suitable phosphorus fertilizer dose was 20.00 kg ha^{-1}. In another similar study, it was noted that the leaf area of beans increased significantly with the increase of phosphorus dose from 25.00 kg ha-^{1} to 75.00 kg ha^{-1} (Veeresh, 2003). According to these results, increasing doses of phosphorus in low zinc doses caused increases in the number of pods up to a certain point. Lonergan et al. (1982) obtained higher yields than plants in low Zn and high P conditions. In contrast, an antagonist effect also occured, resulting in reduced yields (Ozanne, 1980). As the reason for these results; Besides to the environment and genotype, high doses of phosphorous fertilizers are thought to result in yield losses due to reduced zinc uptake (Ozanne, 1980).

Unlike nitrogenous fertilizers, the effect of phosphorus fertilizers remains limited on the number of branches depending on the environment and genetic structure. It is thought that this difference in average number of branches due to years is due to insufficient quantity and distribution of rainfall in the first year as well as genetic factors (Elkoca and Kantar, 2003). Like the number of pods, the number of branches also show a very wide variation depending on the variety and lines (Elkoca and Kantar, 2004). In spite of increasing doses of phosphorus, it is thought that zinc use efficiency and number of branches decrease (Ozanne, 1980).

In the studies conducted by some researchers, it has been observed that these effects vary widely. It is thought that this difference is caused by environment, genotype and cultural practices. Gangwar and Singh (1986) showed in their study, that the rate of harvest index of zinc fertilizers increased the maximum rate of foliar applied fertilizers. Azad et al. (1993), reported that zinc fertilizers increased the rate of harvest index up to a certain dose and then decreased. In this study, it is observed that zinc fertilizer increased the ratio of harvest index by 15.00 and 30.00 kg ha^{-1} and then it started to decrease.

Climate factors are undoubtedly the most important factors in determining the fate of agricultural production. It is thought that this difference between years is mainly due to the fact that the precipitation amount (43.6 mm) and distribution in the first year is lower and insufficient compared to the second year (73.33 mm) (*Table 1*). The balance of soil water in beans is very sensitive to flowering period. Fluctuations in this period are reported to cause 20% yield losses in yields (Elkoca and Kantar, 2003). In the second year fertilizer doses were used more effectively with rainfall in the development periods of the plant. In the first year, the average temperature were recorded higher than in the second year, especially in flowering and pollination periods of the plant in other developmental according to the periods.

The grain yield in beans is dependent on other genetic-based variations, particularly earliness in various environmental conditions (Dreyer and Wielpütz, 1998). Similar studies have shown that phosphorus promotes flowering and pod formation in the plant

http://www.aloki.hu ● ISSN 1589 1623 (Print) ● ISSN1785 0037 (Online)
DOI: http://dx.doi.org/10.15666/aeer/1802_25392553

(Araújo et al., 2000). In the experiment, it can be said that the difference between the first year and the second year zinc doses was due to the fact that the phosphorus in the first year inhibited the uptake of zinc more than in the second year. In the second year, it is thought that the climate is more suitable and fertilizers may be taken more uniformly (Toğay and Anlarsal, 2007). In many studies, it has been reported that phosphorus and zinc fertilizers are used together and that the efficiency of phosphorus zinc decreases the efficiency and quality decreases (Ozanne, 1980; Lonergan et al., 1982). In a similar study, it was reported that environmental and genetic factors were effective on the average grain yield in lentils (Islam et al., 1989).

Many previous studies have shown that the protein content of beans varies between 17.40% and 28.00%. It has been reported that bacterial applications, especially nitrogen fertilization, increase this rate (Tajini et al., 2012; Bulut, 2013; Özturan and Akman, 2017). The effect of zinc fertilizer on crude protein content was found to be important due to environmental and genotypic factors. Similar results were obtained in other studies conducted on legumes (Toğay and Anlarsal, 2008). Zinc is an active element in biochemical events and has a biological interaction. When used in combination with phosphorus, a decrease in the uptake by plants occurs. The most important element limiting the use efficiency of zinc by plants is phosphorus. Especially in the case of phosphorus poor soils, where the need for excess phosphorus is met, the use of zinc decreases. Disruptions in phosphorus and zinc balance in the plant cause disruptions in the cell and some parts of the cell (Das et al., 2005; Khorgamy and Farnis, 2009; Salimpour et al., 2010).

Conclusion

In this study carried out in Van-Gevaş, the effect of different phosphorus and zinc doses on the yield and yield components of dry bean varieties were investigated. Although these factors have changed over the years, they have provided important information about yield and yield components. The results of the decrease in zinc utilization efficiency in high phosphorus doses have emerged in yield and quality parameters. Especially in our city where zinc deficiency is seen too much, and especially before planting other plants, soil analysis should be conducted before planting. In view of these results, phosphorus fertilization should be done between 10.00-30.00 kg ha^{-1} zinc and 20.00-80.00 kg ha^{-1}. The grain yield which is close to Turkey's on average or above on a yearly basis may be interrelated with zinc and phosphorus deficiency in the soil, which is thought to reduce the yield and quality losses.

REFERENCES

[1] Adak, M. S., Güler, M., Kayan, N. (2010): Possibilities to increase the production of edible legumes. – Türkiye Ziraat Mühendisliği VII. Teknik Kongresi, Ankara: 329-341. (in Turkish).

[2] Adak, M. S. (2014): The importance of edible beans in Turkey, production and monitoring policies. – Tarım ve Mühendislik 103: 24-30. (in Turkish).

[3] Alatürk, F. (2012): The effects of fertilization on yield and chemical composition of Çanakkale province and pastures. – Master's Thesis, Çanakkale Onsekiz Mart

http://www.aloki.hu ● ISSN 1589 1623 (Print) ● ISSN1785 0037 (Online)
DOI: http://dx.doi.org/10.15666/aeer/1802_25392553

Üniversitesi, Fen Bilimleri Enstitüsü. Tarla Bitkileri Anabilim Dalı, Çanakkale. (in Turkish).
[4] Altın, M., Gökkuş, A., Koç, A. (2005): Breeding of meadow pasture plants. – TKB, TÜGEM, Çayır-Mera Yem Bitkileri ve Havza Geliştirme Daire Başkanlığı, Ankara, 468p. (in Turkish).
[5] Altunkaynak, Ö. A. (2018): Effects of different nitrogen doses and bacterial vaccination on grain yield and yield characteristics in bean (*Phaseolus vulgaris* L.). – Selcuk Üniversitesi Fen Bilimleri Enstitüsü, Yüksek Lisans Tezi, 35p. Konya. (in Turkish).
[6] Araújo, A. P., Teixeira, M. G., De Almeida, D. L. (2000): Growth and yield of common bean cultivars at two soil phosporus leves under biological nitrogen fixation. – Pesg. Agropec. Bras. 35(4).
[7] Arıoğlu, H. (1989): Yağ bitkileri (Soya ve Yerfıstığı). – Çukurova Üni. Ziraat Fak. Ders Kitabı, No.35.
[8] Azad, A. S., Manchada, J. S., Gill, A. S., Bains, S. S. (1993): Effect of zinc application on grain yield, yield components and nutrient content of lentil. – Lens Newsletter 20(2): 30-33.
[9] Barros, I., Gaiser, T., Lange, F. M., Römheld, V. (2007): Mineral nutrition and water usepatterns of a maize/cowpea ıntercrop on a highly acidic soil of the tropic semiarid. – Field Crops Research 101: 26-36.
[10] Batıca, M., Alatürk, F., Gökkuş, A. (2017): The effect of fertilization on the yield and some Properties of chewing gum (*Cyamopsis tetragonoloba* L. Taub.). – Türk Tarım ve Doğa Bilimleri Dergisi 4(1): 79-87. (in Turkish).
[11] Bayraktar, K. (1966): Vegetable growing. – Ege Üniversitesi Ziraat Fakültesi Yayınları 1: 144-160.
[12] Bayu, W., Rethman, N. F. G., Hammes, P. S., Alemu, G. (2006): Effects of farmyard manure and ınorganic fertilizers on sorghum growth, yield, and nitrogen use in a Semi-Arid Area of Ethiopia. – Journal of Plant Nutrition 29: 391-407.
[13] Bokhtiar, S. M., Sakurai, K. (2005): Effect of application of inorganic and organic fertilizers on growth, yield and quality of sugarcane. – Sugar Tech. 7: 35-37.
[14] Bulut, N. (2013): Effect of organic fertilizers on yield and yield components in bean (*Phaseolus vulgaris* L.) in grafted ungrafted conditions. – Yüzüncü Yıl Üniversitesi, Fen Bilimleri Enstitüsü (Yüksek Lisans), Van, 47. (in Turkish).
[15] Ceylan, A., Sepetoğlu, H. (1979): Lentil (*Lens culinaris Medic*.) Sowing Frequency Research. – E.Ü. Ziraat Fak. Dergisi, Cilt: 25(2). (in Turkish).
[16] Das, K., Dang, R., Shivananda, T. N., Sur, P. (2005): Interaction between phosphorus and zinc on the biomass yield and yield attributes of the medicinal plant stevia (*Stevia rebaudiana*). – Science World Journal 5: 390-395.
[17] Dreyer, S., Wielpütz, J. (1998): Cultivar trials with bush beans. – Gemüse (München) 34(6): 359-361.
[18] Düzgüneş, O., Kesici, T., Koyuncu, O., Gürbüz, F. (1987): Research and experiment methods. – A.Ü. Ziraat Fakültesi Yayınları: 1021 Ders Kitabı: 295. S.381. (in Turkish).
[19] Elkoca, E., Kantar, F. (2003): Determination of early and high yield bean (*Phaseolus vulgaris* L.) genotypes suitable for Erzurum ecological conditions. – Atatürk Üniversitesi Ziraat Fakültesi Dergisi 35(4): 137-142.
[20] Elkoca, E., Kantar, F. (2004): Erzurum ekolojik koşullarına uygun erkenci ve yüksek verimli kuru fasulye (*Phaseolus vulgaris* L.) genotiplerinin belirlenmesi. – Atatürk Üniversitesi Ziraat Fakültesi Dergisi 35(3-4): 137-142.
[21] Engin, M. (1989): Yemeklik dane baklagiller. – Ç.Ü. Ziraat Fakültesi Yayınları, Ders Kitabı: 110. ÇÜ Basımevi Adana.
[22] FAO. (2015): Tarımsal İstatistikler. – http://faostat3.fao.org/browse/Q/QC/E. (Erişim Tarihi: 13.05.2019).
[23] Gangwar, K. S., Singh, N. P. (1986): Effect of zinc application on yield and quality of lentil (*Lens culinaris* Medic.). – Legume Research 11(1): 11-14.

http://www.aloki.hu ● ISSN 1589 1623 (Print) ● ISSN1785 0037 (Online)
DOI: http://dx.doi.org/10.15666/aeer/1802_25392553

[24] Hussein, M. M., Alva, A. K. (2014): Growth, yield and water use efficiency of forage sorghum as affected by NPK fertilizer and deficit irrigation. – American Journal of Plant Sciences 5: 2134-2140.
[25] Islam, M. S., Bhuriya, M. S., Mich, M. G. (1989): Effect of zinc on lentil yield and yield components. – Lens Newsletter 16(1): 30-32.
[26] Khorgamy, A., Farnia, A. (2009): Effect of phosphorus and zinc fertilisation on yield and yield components of chick pea cultivars. – African Crop Science Conference Proceedings 9: 205-208.
[27] Loneragan, J. F., Grunes, D. L., Welch, R. M., Aduayi, E. A., Tengah, A., Lazar, V. A., Cary, E. E. (1982): Phosphorus accumulation and toxicity in leaves in relation to zinc supply. – Soil Science Soc. Am. J. 46: 345-352.
[28] McPhee, K. E., Muehlbauer, F. J. (2002): Improving the nutritional value of cool season food legumes. – Journal of Crop Production 5(1-2): 191-211.
[29] Olsen, S. R., Dean, L. A. (1965): Phosphorus of sail analysis. Part. 2. – Agıon. 9. Amer. Sac. of Agr. Inc. Publisher. Madison, Wisconsin U. S. A.
[30] Ozanne, P. G. (1980): Phosphate nutrition of plants - a general treatise. – American Society of Agronomy: 559-589.
[31] Özturan Akman, Y. (2017): Rhizobium and mycorrhiza applications of beans (*Phaseolus)vulgaris* L.) on grain yield and some agricultural characteristics. – Ondokuz Mayıs Üniversitesi, Fen Bilimleri Enstitüsü (Yüksek Lisans), Samsun, 155. (in Turkish).
[32] Pekşen, E., Artık, C. (2005): Anti-besinsel maddeler ve yemeklik tane baklagillerin besleyici değerleri. – Ondokuz Mayıs Üniversitesi Ziraat Fakültesi Dergisi 20(2): 110-120.
[33] Salimpour, S., Khavazi, K., Nadian, H., Besharati, H., Miransari, M. (2010): Enhancingphosphorous availability to canola (*Brassica napus* L.) using P solubilizing and sulfur oxidizing bacteria. – Australian Journal of Crop Science 4(5): 330-334.
[34] Shrotriya, G. C. (1998): Balanced fertilizer-India experience. – Proceedings of Symposium on Plant Nutrition Management for Sustainable Agricultural Growth, NFDC, 8-10 December 1997, Islamabad.
[35] Sing, K. N., Bali, A. S., Ganai, B. A., Hasan, B. (1994): Optimum Spacing and Seed Rate for Lentil (*Lens culinaris* Medic.) in Casmir. – Indian Journal of Agricultural Sciences 64(6): 392-393.
[36] Singh, N. P., Saxena, M. C. (1986): Response of Lentil to Phosphorus and Zinc Application. – Lens Newsletter 13(2): 27-28.
[37] Şehirali, S. (1988): Legumes, edible. – A.Ü. Ziraat Fakültesi Yayınları, 1089, Ders Kitabı 314. (in Turkish).
[38] Tajini, F., Trabelsi, M., Drevon, J. (2012): Combined inoculation with glomusintraradices and rhizobium tropici CIAT 899 increases phosphorus use efficiency for symbiotic nitrogen fixation in common bean (*Phaseolus vulgaris* L.). – Saudi Journal of Biological Sciences 19: 157-163.
[39] Tisdale, S. L., Nelson, W. L. (1966): Soil Fertility and fertilizers. – Second edition. The MacmlHan Cd: Collier·MacmiUan Ltd, London. S: 239, 340.
[40] Togay, Y., Anlarsal, A. E. (2008): Different doses of zinc and phosphorus lentils (*Lens culinaris* Medic.) and its effect on yield components. – Yüzüncü Yıl Üniversitesi, Ziraat Fakültesi, Tarım Bilimleri Dergisi (J. Agric. Sci.) 18(1): 49-59. (in Turkish).
[41] TÜİK. (2018): Tarımsal İstatistikler. – http://www.tuik.gov.tr/PreTablo.do?alt_id=1001: (Erişim Tarihi: 13.05.2019).
[42] Turuko, M., Mohammed, A. (2014): Effect of different phosphorus fertilizer rates on growth, dry matter yield and yield components of common bean (*Phaseolus vulgaris* L.). – World Journal of Agricultural Research 2(3): 88-92.
[43] Veeresh, N. K. (2003): Response of French bean (*Phaseolus vulgaris* L.) to fertilizer levels in northern transitional zone of Karnataka. – M.Sc. Thesis, University of Agriculture Science Dharwad (India).

http://www.aloki.hu ● ISSN 1589 1623 (Print) ● ISSN1785 0037 (Online)
DOI: http://dx.doi.org/10.15666/aeer/1802_25392553

[44] Yalçın, S. R., Usta, S. (1990): The effect of zinc application on the development of corn plant and zinc, iron, manganese and copper scopes. – A.Ü. Ziraat Fakültesi Yıllığı 41(1-2): 195-204. (in Turkish).

http://www.aloki.hu ● ISSN 1589 1623 (Print) ● ISSN1785 0037 (Online)
DOI: http://dx.doi.org/10.15666/aeer/1802_25392553

EFFECT OF NPK AND HUMIC ACID ON GROWTH, FLOWERING AND CHEMICAL COMPOSITION OF (BLUE SAKE) *ERANTHEUMUM PULCHELLUM* ANDREWS PLANT

NOFAL, E. M. S.[1] – MENESI, F. A.[1] – EL-BABLY, S. Z.[2] – ABD EL RAHMAN, M.[2]

[1]*Hort. Dept., Fac. Agric., Kafr ELSheikh Univ., Kafr El-Sheik, Egypt*

[2]*Sakha Exper. Stat., Hort. Res. Inst., Kafr El-Sheik, Egypt*

**Corresponding author*
e-mail: ahmed.ebad@rocketmail.com

(Received 8th Jul 2019; accepted 23rd Jan 2020)

Abstract. In this study the treatments were carried out as follows: Control; Full dose of NPK containing 6 g ammonium sulphate (20.5%N) + 4 g calcium super phosphate(15.5%P_2O_5) + 3 g potassium sulphate (48.5%K_2O) to 8 kg soil in the pot; Half NPK dose; Half NPK dose + 50 ppm (HA); Half NPK dose + 100 ppm(H.A.); Half NPK dose + 150 ppm (H.A.); as well as (H.A.) at 50,100 and 150 ppm. The obtained results showed that most treatments resulted significantly taller plants, higher branch and leaf plural, wider leaf area compared to control with $^1/_2$ NPK + 150 ppm (H.A.) treatment providing the best results as this treatment gave also the high significant. Additionally, this treatment caused significantly the earliest flowering with the longest flower stem, widest flower diameter, number of flowers per plant as well as the heaviest fresh and dry weight of flowers. Most treatments gave significantly higher total chlorophyll in the leaves than the control with the superiority of the treatment of $^1/_2$ NPK + 150 ppm (H.A.) followed by the treatment of NPK alone with non-significant differences in between. N ratio in the leaves significantly increased over control in most treatments and especially for the treatment of $^1/_2$ NPK + 150 ppm (H.A.). P ratio in the leaves were significantly the highest as a result of the NPK treatment with no other additives. While the highest K ratio resulted from the treatment of either 100 or150 ppm (H.A.) without significant differences in between. However, the treatment of ½ NPK + 150 ppm (H.A.) is recommended to obtain high quality plants.
Keywords: *potassium humate; N, P and K fertilization; chemical fertilization; Erantheumum pulchellum*

Introduction

Chemical fertilization provides nutrients optimal for plant growth and development. The essential nutrients in the fertilizers are nitrogen, phosphorous and potassium (NPK). The most important major nutrient is nitrogen (N) which partakes in many compounds in the plant such as amino acids, proteins, chlorophylls, hormones, alkaloids and enzymes. Phosphorus (P) partakes in phospholipids, DNA, RNA and metabolism of fats. Potassium (K) regulates water condition within the plant cell and water loss by transpiration as a catalyst and condensing agent of complex substances through its active properties (Devlin, 1975) and potassium has a main role in plant metabolism such as photosynthesis, translocation of photosynthates, water relation as well as enzyme activation. Although, potassium is not a constituent of any plant structures or compounds, but it plays a part in many important regulatory roles in the plant, i.e. osmo-regulation process, regulation of plant stomata and water use, translocation of sugars and formation of carbohydrates, energy status of the plant, the regulation of enzyme activities, protein synthesis and many other processes needed to sustain plant growth and reproduction (Hasio and Lauchli, 1986).

http://www.aloki.hu ● ISSN 1589 1623 (Print) ● ISSN 1785 0037 (Online)
DOI: http://dx.doi.org/10.15666/aeer/1802_25552567

Humic acid (HA), called humin materials widely consists of a part of soil organic matter (65-70%) (Stott and Martin, 1990). It is a potential natural resource that can be utilized to increase growth, nutrient availability and yield (Sharif et al., 2002). It has direct and indirect effects on plant growth due to roles of humic acid (Pal and Biswas, 2005). Humic acid treatments improve soil aggregation, structure, water permeability, air conditioning, fertility, moisture-holding capacity. It constitutes a stable fraction of carbon (C), thus regulating the carbon cycle and releasing of nutrients, including N, P and S (Stevenson,1994) and improving nutrients uptake and hormonal effects (Nikbakht et al., 2008).

Erantheumum pulchellum Andrews (syn Daedalacanthus nervosum R) blue sake

The 7.5 to 15.3 cm-long flower spikes are borne above the large, rounded and prominently veined leaves. Leaves are large, dark green, simple, opposite and leaf blade length arrives 5 to 10 cm. Fruit shape is oval and its length is less than 12.5 cm. It is used in flower beds. It is popular with gardeners because of the spikes of flowers that are bright gentian blue - an unusual color in the tropics (Edward, 1999) as illustrated in *Figure 1*.

Figure 1. *Erantheumum pulchellum Andrews plant*

http://www.aloki.hu ● ISSN 1589 1623 (Print) ● ISSN 1785 0037 (Online)
DOI: http://dx.doi.org/10.15666/aeer/1802_25552567

The aim of this work was to study the effect of (NPK) nitrogen, phosphorus and potassium and humic acid (HA) on the growth, flowering and chemical composition of the plant and try to obtain the synergistic effect of HA to partly replace the risk of pollution to environments by chemical fertilization. Hence there was no need for the treatment of NPK (full dose) + HA.

Martials and methods

A series of pot experiments in the open field were conducted during 2014/2015 and 2015/2016 seasons in Hort. Dept., Agric. Fac., Kafr El-Sheik Univ. Egypt. The site is located at 31°07 N latitude and 30°57 E longitude with an elevation of about 6 m above mean sea level. The climatic conditions of the study area are provided in *Table 1*.

Table 1. *Monthly air temperature (Max., Min. and Mean °C), relative humidity (RH %), at the experimental site during the two growing seasons of 2014/2015 and 2015/2016. (Source Sakha Agricultural Research Station, Kafr El-Sheikh Governorate, Egypt)*

Season	2014/2015				2015/2016			
Month	Air Temp			RH%	Air Temp			RH%
	Max	Min	Mean		Max	Min	Mean	
September	32.49	20.76	26.58	69.89	34.6	22.8	28.7	64.6
October	29.75	18.75	24.25	67.16	22.9	20.06	21.75	67.1
November	24.3	13.79	19.04	74.15	24.4	14.42	19.41	75.6
December	22.27	9.72	16.00	76.05	19.7	8.36	14.03	77.9
January	18.79	6.46	12.63	74.6	18.4	6.35	12.38	74.05
February	19.01	7.69	13.35	74.8	22.58	9.35	15.96	69.05
Mars	22.69	11.69	17.19	70.6	25.5	11.6	18.55	69.9
April	25.64	13.7	19.67	63.4	30.03	18.62	24.33	61.7
May	30.19	18.79	24.49	61.7	30.04	22.8	26.42	58.4
June	30.85	21.4	26.13	65	33.6	26.3	29.95	61.15
July	33.0	22.4	27.7	70.0	33.7	26.1	29.9	69.75
Augustus	35.1	25.0	30.05	67.8	33.6	26.0	29.8	70.3

The aim was to study the effect of N, P and K fertilization and humic acid foliar spray on the growth, flowering and chemical composition of a local variety of *Eranthemum pullchellum* Vahl R.BR. The cuttings of one-year-old plants of 10 cm length were planted in 20 cm diameter clay pots filled with about 8 kg clayey soil as one plant/pot commencing on the 1st September till September of the next year. The plants were treated as follows: 1-Control, 2-Full dose of NPK containiing 6 g ammonium sulphate (20.5% N) + 4g calcium super phosphate (15.5%P2O5) + 3 g potassium sulphate (48.5% K2O), 3-Half NPK dose, 4- Half NPK dose + 50 ppm humic acid (HA), 5- Half NPK dose + 100 ppm humic acid (HA), 6- Half NPK dose + 150 ppm humic acid (HA), 7- 50 ppm humic acid (HA), 8- 100 ppm humic acid (HA) and 9- 150 ppm humic acid (HA). The treatments were replicated three times involving 9 plants in a complete randomized design. NPK fertilizer was drench-applied as calcium super phosphate at preparing the soil, while N and K were monthly applied after one month from planting. HA was foliar applied monthly after one month from planting as the

http://www.aloki.hu ● ISSN 1589 1623 (Print) ● ISSN 1785 0037 (Online)
DOI: http://dx.doi.org/10.15666/aeer/1802_25552567

plants were run-off sprayed. The watering was every three days at summer and weekly in winter. The following data were recorded after one year, plant height (cm), number of branches, number of leaves/plant, leaf area as mean of 3 leaves in the middle part of the plant (cm^2) by using CI-202 portable laser leaf area meter (cidb10-science) made in USA, WWW.CID-INC.COM, fresh and dry weights of vegetative parts per plant (g), root length of the longest root (cm), fresh and dry weight of the roots per plant (g) after removing soil by water, flowering date (days) as the first flower showed color on the plant, number of flowers per plant, diameters of flower (cm), fresh and dry weights of flowers/plant (g) and flower stem length (cm). As for chemical composition total chlorophyll in leaf of the middle part of the plant was carried out according to Minolta chlorophyll method SPAD-SO (Yadava, 1986). Nitrogen% was determined by modified micro Kjeldahle method as described by Black (1983)

Phosphorus was determined colorimetrically as the method described by King (1951) while, potassium was estimated using the flame photometer according to Jackson (1967). Means of treatments were compared by Duncan' s multiple range test (Duncan, 1955) at a level of 5% probability according to Sendecor and Cochran (1980).

Results

Effect of treatments of NPK and humic acid on vegetative growth, flowering and chemical composition parameters of the plants

A. Vegetative growth, plant height, No. branches, No. leaves and leaf area

Data presented in *Table 2* showed that in most cases treatments of NPK and humic acid significantly increased plant height and gave more branches than the control in both seasons. The significantly tallest plants and highest number of branches in the first season resulted from the treatment of $^1/_2$ NPK + 150 ppm humic acid. In the second season, this treatment extended the simulative effect in addition to the treatment of NPK alone without significant differences in between.

The same table revealed that most treatments gave significantly more leaf number and widest leaf area per plant compared to control in the two seasons with the superiority of treatment of $^1/_2$ NPK + 150 ppm humic acid in both seasons. In the second season, this treatment was partaken with the treatment of $^1/_2$ NPK + 100 ppm humic acid (HA) and NPK alone without significant differences.

B. Fresh and dry weight of vegetative parts

Data presented in *Table 3* revealed that most treatments gave significantly heavier fresh and dry weights than control in the two seasons. The significantly heaviest fresh and dry weight in the first season resulted from the treatment of $^1/_2$ NPK + 150 ppm humic acid (HA). In the second season, this resulted from the treatment of NPK and the treatment of $^1/_2$ NPK + 150 ppm humic acid (HA) without significant differences.

C. Root parameters

Data of the root length No. roots/plant fresh and dry weight of roots are presented in *Table 4*. Data exhibited that most treatments significantly increased root length over control in the first season as the significantly longest roots and highest roots number/plant resulted from the treatment of $^1/_2$ NPK + 150 ppm humic acid (HA)

http://www.aloki.hu ● ISSN 1589 1623 (Print) ● ISSN 1785 0037 (Online)
DOI: http://dx.doi.org/10.15666/aeer/1802_25552567

followed by the treatments of $^1/_2$ NPK + 50 ppm humic acid (HA), treatment of $^1/_2$ NPK + 100 ppm humic acid (HA) without significant differences. In the second season, all treatments significantly increased root length when compared to the control and the significantly longest roots resulted from the treatment of $^1/_2$ NPK + 150 ppm humic acid (HA) followed by the treatment of NPK alone without significant differences.

Table 2. *Effect of NPK and humic acid treatments on some vegetative growth characters of Erantheumum pulchellum Andrews in two seasons*

Treatments	Plant height (cm)	No. of branches/plant	No. of leaves/plant	Leaf area (cm^2)
1st season				
Control	65.00 e	1.00 b	27.00 d	53.30 d
NPK	119.67 c	2.00 a	68.00 b	70.00 c
$^1/_2$ NPK	104.00 d	1.67 ab	58.00 b	51.73 d
$^1/_2$ NPK + 50 ppm humic acid (HA)	109.00 d	1.67 ab	62.00 b	55.70 d
$^1/_2$ NPK + 100 ppm humic acid (HA)	131.67 b	2.00 a	68.00 b	90.30 b
$^1/_2$ NPK + 150 ppm humic acid (HA)	159.00 a	2.00 a	89.00 a	120.70 a
50 ppm humic acid (HA)	68.33 e	1.00 b	47.00 c	41.93 d
100 ppm humic acid (HA)	70.33 e	1.33 ab	42.67 c	48.06 d
150 ppm humic acid (HA)	73.67 e	1.67 ab	29.33 d	44.80 d
Mean	100.07	1.60	54.62	64.09
2nd season				
Control	68.00 d	1.33 b	17.00 d	63.83 cd
NPK	103.67 a	2.00 ab	95.00 a	112.63 a
$^1/_2$ NPK	88.00 c	1.67 b	54.67 b	84.16 b
$^1/_2$ NPK + 50 ppm humic acid (HA)	94.00 bc	3.00 a	62.33 b	107.26 a
$^1/_2$ NPK + 100 ppm humic acid (HA)	99.00 ab	3.00 a	95.00 a	98.63 a
$^1/_2$ NPK + 150 ppm humic acid (HA)	107.33 a	1.67 b	108.67 a	108.57 a
50 ppm humic acid (HA)	73.33 d	1.00 b	35.00 c	77.70 bc
100 ppm humic acid (HA)	71.33 d	1.67 b	26.67 cd	59.40 d
150 ppm humic acid (HA)	67.00 d	1.67 b	16.67 d	74.70 bc
Mean	85.74	1. 88	56.77	87.43

Means within a column having the same letters are not significantly different according to Duncan's multiple range test

Data showed clearly that most treatments gave significantly heavier fresh and dry weight of roots than the control in both seasons. The significantly heaviest value of roots weight resulted from the treatment of $^1/_2$ NPK + 150 ppm humic acid (HA), followed with non- significant differences by the treatment of NPK alone. The results were similar in the second season but the significantly highest value resulted from the treatment of NPK alone followed with non-significant differences by the treatment of ½ NPK + 150 ppm humic acid (HA).

http://www.aloki.hu ● ISSN 1589 1623 (Print) ● ISSN 1785 0037 (Online)
DOI: http://dx.doi.org/10.15666/aeer/1802_25552567

Table 3. *Effect of NPK and humic acid (HA) treatments on fresh and dry weights of vegetative parts of Erantheumum pulchellum Andrews in two seasons*

Treatments	Fresh weight of vegetative plant parts (g)	Dry weight of vegetative plant parts (g)
1st season		
Control	36.00 f	24.83 d
NPK	99.33 bc	51.50 a
1/2 NPK	86.33 cd	42.67 b
1/2 NPK + 50 ppm humic acid	88.00 cd	43.30 b
1/2 NPK + 100 ppm humic acid	115.67 b	43.70 b
1/2 NPK + 150 ppm humic acid	244.67 a	56.50 a
50 ppm humic acid	67.33 de	36.23 bc
100 ppm humic acid	56.00 ef	31.40 cd
150 ppm humic acid	35.67 f	26.50 d
Mean	92.11	39.62
2nd season		
Control	25.77 d	16.13 f
NPK	130.93 a	48.23 c
1/2 NPK	60.63 c	38.30 d
1/2 NPK + 50 ppm humic acid	64.93 c	29.00 e
1/2 NPK + 100 ppm humic acid	100.00 b	60.83 b
1/2 NPK + 150 ppm humic acid	126.40 a	74.17 a
50 ppm humic acid	26.73 d	15.87 f
100 ppm humic acid	22.67 de	13.00 f
150 ppm humic acid	16.47 e	8.00 g
Mean	63.83	33.72

Means within a column having the same letters are not significantly different according to Duncan's multiple range test

D. Flowering characters

Data presented in *Table 5* showed that the precocity of flowering in both seasons was for the treatment of 1/2 NPK + 150 ppm humic acid (HA) followed by NPK alone with non-significant differences. The previous promotive effect of these treatments was extended to the other flowering parameters. The stimulatory effect of NPK on flowering is well known as nitrogen is a main constituent of chlorophyll leading to effective characteristic as flower stem length, flower diameter, number of flowers per plant and fresh and dry weights of flower registering the significantly highest values when compared to control and other treatments. A few exceptions were gained for the treatment of 1/2 NPK + 100 ppm humic acid giving values close to the previous treatments in the criteria of fresh and dry weights of flower.

E. Chemical composition of plants

Data of the effect of NPK treatment and humic acid on total chlorophyll, nitrogen, phosphorus and potassium ratio are presented in *Table 6,* as revealed the significantly highest values of total chlorophyll resulted from the treatment of ½ NPK + 150 ppm

http://www.aloki.hu ● ISSN 1589 1623 (Print) ● ISSN 1785 0037 (Online)
DOI: http://dx.doi.org/10.15666/aeer/1802_25552567

humic acid (HA) followed by the treatment of NPK alone. with non- significant differences. It is apparent that most treatments of either NPK + humic acid or NPK alone increased total chlorophyll in the leaves of plant over control in both seasons. The superiority was for the treatments of 1/2 NPK + 150 ppm humic acid followed by the other treatments of NPK alone or with humic acid with non-significant differences in most cases.

Table 4. *Effect of NPK and humic acid treatments on some rooting characters and fresh and dry weight roots of Erantheumum pulchellum Andrews in two seasons*

Treatments	Root length (cm)	No. of roots plant	Fresh weight of roots (g)	Dry weight of roots (g)
1st season				
Control	20.67 c	16.33 e	14.33 cd	3.83 c
NPK	22.00 bc	22.33 cd	22.33 ab	5.03 b
1/2 NPK	21.33 c	19.00 de	12.00 de	3.00 d
1/2 NPK + 50 ppm humic acid (HA)	28.67 ab	24.67 c	18.33 bc	4.60 b
1/2 NPK + 100 ppm humic acid (HA)	26.67 ab	29.33 b	19.00 bc	5.03 b
1/2 NPK + 150 ppm humic acid (HA)	32.67 a	40.00 a	24.67 a	6.17 a
50 ppm humic acid (HA)	26.67 ab	17.00 e	11.16 de	3.06 d
100 ppm humic acid (HA)	25.00 bc	17.00 e	8.47 e	3.16 cd
150 ppm humic acid (HA)	25.00 bc	15.33 e	10.16 de	2.80 d
Mean	25.40	22.33	15.60	4.07
2nd season				
Control	17.33 f	15.67 c	13.27 d	3.04 c
NPK	44.67 a	35.33 a	34.30 a	7.83 a
1/2 NPK	33.33 bc	29.67 b	24.33 c	5.60 b
1/2 NPK + 50 ppm humic acid (HA)	35.00 bc	33.33 b	27.83 b	6.17 b
1/2 NPK + 100 ppm humic acid (HA)	35.67 b	32.67 b	25.60 bc	5.23 b
1/2 NPK + 150 ppm humic acid (HA)	45.00 a	32.00 b	32.73 a	7.80 a
50 ppm humic acid (HA)	29.67 cd	14.33 c	11.33 d	2.60 c
100 ppm humic acid (HA)	26.33 de	13.33 c	10.33 d	2.77 c
150 ppm humic acid (HA)	24.00 e	15.00 c	10.17 d	2.57 c
Mean	32.33	27.93	21.09	4.89

Means within a column having the same letters are not significantly different according to Duncan's multiple range test

The results presented in *Table 6* showed that most treatments gave significantly higher N percentage than control in both seasons. The utmost highest values resulted from the treatments of NPK alone and 1/2 NPK + 150 ppm humic acid (HA) with non-significant differences in between. A somewhat similar trend was obtained for phosphorus percentage (P%) with an exception for the treatment of 1/2 NPK + 100 ppm humic acid giving values which non- significantly differ from the treatment of either NPK alone or 1/2 NPK + 150 ppm humic acid.

For potassium percentage (K %) a similar trend was obtained. but the treatment of 1/2 NPK + 100 ppm humic acid gave a value which did not differ from the treatments of NPK alone and 1/2 NPK + 150 ppm humic acid.

http://www.aloki.hu ● ISSN 1589 1623 (Print) ● ISSN 1785 0037 (Online)
DOI: http://dx.doi.org/10.15666/aeer/1802_25552567

Table 5. *Effect of NPK and humic acid treatments on some flowering characters and their fresh and dry weights of Erantheumum pulchellum Andrews in two seasons*

Treatments	No of days to first flower	Flower stem length (cm)	Flower diameter (cm)	No. of flowers/plant	Fresh weight of flowers (g)	Dry weight of flowers (g)
Control	311.00 a	4.03 e	4.07 ef	10.00 d	1.61 d	1.10 e
NPK	258.33 d	5.90 b	6.57 a	13. 67 c	2.20 c	1.46 c
1/2 NPK	272.67 c	4.87 d	5.13 c	11. 67 cd	1.87 cd	1.21 de
1/2 NPK + 50 ppm humic acid (HA)	274.66 c	5.00 d	5.43 bc	13.33 c	2.14 c	1.40 cd
1/2 NPK + 100 ppm humic acid (HA)	268.67 c	5.23 c	5.73 b	17.00 b	2.74 b	1.72 b
1/2 NPK + 150 ppm humic acid (HA)	249.33 d	6.53 a	6.53 a	22. 00 a	3.54 a	2.24 a
50 ppm humic acid (HA)	294.00 b	3.90 e	4.63 d	12.33 cd	1.99 cd	1.06 e
100 ppm humic acid (HA)	277.00 c	3.87 e	4.20 e	11.33 cd	1.82 cd	1.01 e
150 ppm humic acid (HA)	273.67 c	3.80 e	3.80 f	10.00 d	1.61 d	1.03 e
Mean	275.48	4.79	5.12	13.48	2.17	1.36
2nd season						
Control	292.3 a	4.50 e	4.33 e	10.33 ef	1.56 fg	1.34 d
NPK	264.3 c	6.10 b	7.07 a	22.33 ab	3.43 b	2.59 a
1/2 NPK	258.7 cd	4.77 de	5.73 c	22.33 ab	2.38 d	1.99 c
1/2 NPK + 50 ppm humic acid (HA)	257.0 cd	5.07 cd	6.03 bc	18.00 c	2.70 c	2.14 bc
1/2 NPK + 100 ppm humic acid (HA)	255.3 d	5.30 c	6.27 b	20. 67 b	3.42 b	2.10 bc
1/2 NPK + 150 ppm humic acid (HA)	244.7 e	6.70 a	7.17 a	23.33 a	3.72 a	2.37 ab
50 ppm humic acid	275.3 b	4.33 ef	4.80 d	12.67 e	1.96 e	1.04 d
100 ppm humic acid	290.6 a	4.03 f	4.60 de	11.00 ef	1.71 f	1.04 d
150 ppm humic acid	280.3 b	3.93 f	4.50 de	9.33 f	1.45 g	1.07 d
Mean	268.7	5.00	5.61	15.89	2.48	1.74

Means within a column having the same letters are not significantly different according to Duncan's multiple range test

Discussion

The aforementioned results showed that the treatment of 1/2 NPK + 150 ppm humic acid gave the best vegetative growth characters in both seasons followed by the treatment of NPK alone in a few cases. This may be due to the synergistic effect of NPK and humic acid. Nitrogen stimulates stronger green growth, which provides healthy stems and leaves. Phosphorus is a vital nutrient involved in stimulating and enhancing bud development. Potassium plays a main role in plant metabolism as well as enzymes activation for formation of carbohydrate, energy status of the plants, which strengthen the stem. This coincides with the results of El Sallami (2002) on *Chorisia speciosa, Leucaena leucocephala* and *Prosopis juliflora*, and El-Naggar and El-Nasharty (2009) on amaryllis and Dubey et al. (2017) who mentioned that NPK fertilization treatments significantly increased plant height, number of leaves and suckers per plant. For humic acid, it helps in improving respiration in the growing medium and increasing the water holding capacity (Dorer and Paecock, 1997) in addition to the production of hormone-like activities that improved photosynthesis, phosphorylation, protein synthesis and various enzymatic reactions. However, it reduces inputs of chemical fertilization and minimizes environmental risks (Koreish et al., 2004). It supplies soil with carbon, microbes, increases cell membrane permeability, respiration, photosynthesis, oxygen and phosphorus uptake and helps chelation, and

http://www.aloki.hu ● ISSN 1589 1623 (Print) ● ISSN 1785 0037 (Online)
DOI: http://dx.doi.org/10.15666/aeer/1802_25552567

improves the effects of mineral fertilizers (Henry, 2011). Atiyeh et al. (2002) reported that the combined application of humic acid and macronutrients helps to transport vital sugars through plant membranes, promotes cell division, cell wall formation, and acts as an enzyme activation in protein.

Table 6. *Effect of NPK and humic acid treatments on chemical composition of Erantheumum pulchellum Andrews leaves in two seasons*

Treatments	Total chlorophyll (SPAD)	Nitrogen (%)	Phosphorus (%)	Potassium (%)
1st season				
Control	31.50 c	3.68 c	0.48 d	1.29 c
NPK	50.67 ab	6.01 a	0.77 ab	1.96 a
1/2 NPK	45.83 b	4.67 b	0.45 d	1.64 b
1/2 NPK + 50 ppm humic acid (HA)	51.33 ab	4.78 b	0.50 cd	1.72 ab
1/2 NPK + 100 ppm humic acid (HA)	51.63 ab	5.13 ab	0.66 bc	1.88 ab
1/2 NPK + 150 ppm humic acid (HA)	56.83 a	5.90 a	0.92 a	1.93 a
50 ppm humic acid (HA)	33.50 c	3.67 c	0.35 d	1.19 cd
100 ppm humic acid (HA)	26.10 c	3.44 c	0.45 d	1.27 c
150 ppm humic acid (HA)	26.53 c	3.26 c	0.53 cd	0.99 d
Mean	41.54	4.50	0.57	1.54
2nd season				
Control	32.30 c	4.02 de	0.41 f	1.05 c
NPK	52.60 a	5.89 ab	0.91 ab	1.38 b
1/2 NPK	47.17 b	4.38 de	0.54 e	1.17 bc
1/2 NPK + 50 ppm humic acid (HA)	46.97 b	4.78 cd	0.73 c	1.30 b
1/2 NPK + 100 ppm humic acid (HA)	48.87 b	5.48 bc	0.83 b	1.87 a
1/2 NPK + 150 ppm humic acid (HA)	53.20 a	6.30 a	1.00 a	1.93 a
50 ppm humic acid (HA)	33.87 c	3.68 e	0.65 cd	1.14 bc
100 ppm humic acid (HA)	32.87 c	2.86 f	0.55 de	1.10 c
150 ppm humic acid (HA)	26.80 d	1.40 g	0.47 ef	1.08 c
Mean	41.63	4.31	0.68	1.22

Means within a column having the same letters are not significantly different according to Duncan's multiple range test

Stimulatory effect of the treatment 1/2 NPK + 150 ppm humic acid followed in some cases by NPK alone on the fresh and dry weight of the plant is a reflection of the better growth attributes mentioned before. It is well known that nitrogen forms about 40-50% of dry matter of the plant. Phosphorus has a vital role in photosynthesis and respiration while potassium plays a very important role in regulation of photosynthesis, respiratory rate and increases protein synthesis (Csirzinsky, 1999). This coincides with the results of Hendawy (2008) on *Plantago arenaria* and Sakr et al. (2018) on *Pelargonium graveolens.*

Regarding the promotive effect of humic acid, it affects growth through producing hormone analogues or growth regulators (Albayrak and Camas, 2005). Moreover, Sathiyabama and Selvakumari (2001) mentioned that application of 10 kg/ha humic acid, along with 75% of the recommended NPK dose was found to significantly influence production of green matter of Amaranthus.

http://www.aloki.hu ● ISSN 1589 1623 (Print) ● ISSN 1785 0037 (Online)
DOI: http://dx.doi.org/10.15666/aeer/1802_25552567

The mentioned results, concluded that the rooting parameters (root length, root number and fresh and dry weighs of roots) significantly responded to the treatment of $^1/_2$ NPK + 100 ppm humic acid and then in a few cases to the treatment NPK alone. This is explained in the view that nitrogen stimulates vegetative growth, which reflects on better root growth. Root stimulating fertilizers are often higher in phosphorus as it helps strengthen young roots and give them a strong start (Ayemi et al., 2017). As for humic acid which includes microorganisms capable of producing plant growth regulators such as auxins, gibberellins, cytokinins, etc. and also buffers the hydrogen ion (pH) concentration of the soil as attained by several workers as Mohammad Ipour et al. (2013) on pot marigold and Boogar et al. (2014) on *Petunia hybrida.*

The stimulatory effect of NPK on flowering was well known as nitrogen is a main constituent of chlorophyll leading to effective photosynthesis process with more carbohydrates necessary for flowering. Phosphorus is the element most responsible for stimulating stronger bud and flower development (Ayemi et al., 2017) and potassium is vital to several areas of plant growth as photosynthesis and metabolism, etc. including drought tolerance, disease resistance, stem strength, improved texture, colour and photosynthesis. Ahmed et al. (2010) reported that NPK treatments increased number of flowers per plant, fresh and dry weights of flower reached maximum with 15:20:10 NPK application in African marigold and 15:10:10 in French marigold. Similarly, were the results of EL-Naggar et al. (2016) on *Anthurium andreanum* and Ayemi et al. (2017) who demonstrated that Gerbera cv Ruby Red responded to NPK fertilization treatments in terms of number of flowers per plant, days to first flower appearance, flower diameter, stalk length and diameter and vase life of flowers.

The simulative effects of humic acid on plant growth was previously discussed and are supported by the findings of Dudley et al. (2004) on *Zinnia elegans* (Memon et al., 2014) on *Petunia multiflora*. As for the synergistic effect of humic acid due to partitioning of NPK with it, Ibrahim et al. (2014) mentioned that the significantly highest values of enhanced growth, flowering and quality of wild garlic plants, resulted from the treatment of 2 ml humic acid + 1 g/pot NPK (10:10:10).

Briefly it is a must to maximize from the synergistic effect of humic acid to reduce the risk of chemical minerals on environment as well as their high costs from the economical point of view as the treatment of $^1/_2$ NPK + 150 ppm humic acid seems to be the best in this concern. Moreover, the application of humic acid alone gave close values or even less than control in all studied characters as failed to compensate the effect of NPK at anyhow.

This is logical since nitrogen is a main constituent of chlorophyll molecule and has a great role to form protein, which affects forming of chlorophyll. Also, phosphorus is vital in photosynthesis and respiration. Potassium affects many functions in plant like regulating photosynthesis, respiratory rate and increases protein synthesis by Hasio and Lauchi (1986).

The data in *Table 6* were in agreement with the findings of the synergistic effects of humic acid due to its beneficial effects associated with elevated tissue concentration of macronutrients. This was attained by Boogar et al. (2014) on *Petunia hybrida L* and Ibrahim et al. (2014) on *Tulbaghiavi oleracea* L and Sakr et al. (2018) on *Pelargonium graveolens*.

The results were a reflection of the promotive effect of NPK and humic acid on the various vegetative, rooting and chlorophyll characters leading to more accumulation of dry matter in the leaves. These results were confirmed by the findings of Darwish

http://www.aloki.hu ● ISSN 1589 1623 (Print) ● ISSN 1785 0037 (Online)
DOI: http://dx.doi.org/10.15666/aeer/1802_25552567

(2008) on *Casuarina glauca* and Sayed et al. (2010) on *Vinca rosea* c.v Major who indicated that all NPK treatments increased the leaf content of chlorophyll a and b and N, P and K %.

Humic acid helps the soil to retain the nutrients making plants healthier and less susceptible to insect and disease problems (Henry, 2011). These results were supported by those of Ibrahim et al. (2014) on *Tulbaghiavi oleracea* L. who mentioned that application of humic acid at 9 cm/l as soil drench increased chlorophyll (a) and (b), content, N, P and K% in the leaves compared to untreated plants.

Conclusion

From the aforementioned results, it is recommended to fertilize the *Erantheumum pulchellum* plant with half dose of NPK (3 g ammonium sulphat 2 g calcium super phosphate + 1.5 g potassium sulphat) plus spraying plants with 150 ppm humic acid for each/pot to minimize the risk of the pollution due to chemical fertilization. Calcium super phosphate should be applied at preparing of the soil while N and K as well as spraying humic acid should be applied monthly during the growing season to obtain the high quality vegetative, rooting and flowering characteristics of the plants.

REFERENCES

[1] Ahmed I., Asif, M., Amjad, A., Ahmed, S. (2010): Fertilization enhances growth, yield, and xanthophyll contents of marigold. – Turk J Agric. For. 35: 641-648.

[2] Albayrak, S., Camas, N. (2005): Effects of different levels and application times of humic acid and leaf yield and yield components of forage turnip (*Brassica rapa* L.). – J. Agron. 4: 130-133.

[3] Atiyeh, R. M., Edwards, C. A., Metzger, J. D., Lee, S., Arancon, N. Q. (2002): The influence of humic acids derived from earth worm processed organic wastes on plant growth. – Bioresour. Technol. 84: 7-14.

[4] Ayemi, T. J., Sing, D., Fatmi, U. (2017): Effect of NPK on plant growth, flower quality and yield of Gerbera (*Gerbera jamesonii* L.) cv. Ruby Red under. naturally ventilated polyhouse condition. – International Journal of Current Microbiology and Applied Sciences 6(8): 1049-1056.

[5] Black, C. A. (1983): Method of Soil Analysis. A Part 1 and 2. – Soil Sci. Soc Amer. Inc., Madison, WI.

[6] Boogar, A. R., Ebrahim, S., Abolfazl, G. (2014): Effect of humic acid application on qualitative characteristic and micronutrient status in *Petunia hybrida* L. – Bull. Env. Pharmacol. Life Sci. 3(9): 15-19.

[7] Csirzinsky, A. A. (1999): Yield response of herbs to N and K in sand in multiple harvests. – J Herbs, Spices and Medic. Plants. 6(4): 11-22.

[8] Darwish, M. A. (2008): Effect of biofertilizers, NPK and humic acid on growth and chemical composition of *Casuarina glauca* Sieber seedlings. – J. Product Dev. 13(3): 507-522.

[9] Devlin, R. M. (1975): Plant Physiology. – Affiliated East West Press, New Delhi, pp. 159-205.

[10] Dorer, S. P., Paecock, C. H. (1997): The effect of humate and organic fertilizer on establishment and nutrition of creeping bentgrass putting greens. – Inter. Turfgrass Soc. Res. J. 8: 437-443.

[11] Dubey, A. K., Singh, D., Rajput, P. S., Kumar, Y., Verma, A. K., Chandraker, S. K. (2017): Effect of NPK on plant growth, yield and quality of Capsicum (*Capsicum annum*

http://www.aloki.hu ● ISSN 1589 1623 (Print) ● ISSN 1785 0037 (Online)
DOI: http://dx.doi.org/10.15666/aeer/1802_25552567

L.) c. v. Swarna under shade net condition. – International Journal of Current Microbiology and Applied Sciences 6(3): 1085-1091.
[12] Dudley, J. B., Pertuit, A. J., Toler, J. E. (2004): Leonardite influences zinnia and marigold growth. – Hort Sci. 39(2): 251-255.
[13] Duncan, D. B. (1955): Multiple Range and Multiple F-Test. – Biometrics 11: 1-42.
[14] Edward F. G. (1999): One of a Series of the Environmental Horticulture Department. – Florida Cooperative Extension Service, Institute of Food and Agricultural Sci, Univ of Florida.
[15] El-Naggar, A. H., El-Nasharty, A. B. (2009): Effect of growing media and mineral fertilization on growth, flowering, bulbs productivity and chemical constituents of *Hippeastrum vittatum*. – American-Eurasian J. Agric. and Environ. Sci. 6(3): 360-371.
[16] El-Naggar, A. H., Naglaa, E. M., El-Naggar, A. A. (2016): Effect of mineral and bio-fertilization on vegetative growth and flowering of *Anthurium andreanum* L. plants under greenhouse conditions. – J. Alex. Sci. Exch. 37(1): 1-9.
[17] El-Sallami, I. H. (2002): Seedling response of some ornamental trees to soil type and NPK fertilization. – Assuit. J. Agric. Sci. 33(3): 49-83.
[18] Hasio, T. C., Lauchli, A. (1986): A Role of Potassium in Plant-Water Relations. – In: Tinker, P. B. A. (ed.) Advances in Plant Nutrition. Vol. 2. Praeger Sci, New York, pp. 281-311.
[19] Hendawy, S. F. (2008): Comparative study of organic and mineral fertilization on *Plantago arenaria* plant. – J. App. Sci. Res. 4(5): 500-506.
[20] Henry, T. (2011): Spring is a true re-constructionist. – J&L Garden Center's News. http://jlgardencenter.com/news/11/15.
[21] Ibrahim, H. E., Abdel-Moniem, A., El-Foly, S. A. (2014): Effect of some fertilization treatments on growth, flowering and chemical composition of wild garlic (*Tulbaghia violavea* L.) plant. – J. Biol. Chem. Environ. Sci. 9(4): 165-180.
[22] Jackson, M. L. (1967): Soil Chemical Analysis. – Prentice Hall, Inc., Englewood Cliffs.
[23] King, E. J. (1951): Micro Analysis in Medical Biochemistry. 2nd Ed. – Churchill, London.
[24] Koreish, E. A., El-Fayoumy, M. E., Ramadan, H. M., Mohamed, W. H. (2004): Interaction effect of organic and mineral fertilization on faba bean and wheat productivity in calcareous soils. – Alex. J. Agric. Res. 2: 101-114.
[25] Memon, S. A., Baloch, M. H., Baloch, R. A. (2014): Influence of humic acid and macronutrients (MgSO4 + S) application on growth and yield of petunia (*Petunia multiflora*). – Journal of Agricultural Technology 10(6): 1501-1516.
[26] Mohammadipour, E., Golchin, A., Mohammadi, J., Negahdar, N., Zarchini, M. (2013): Effect of humic acid on yield and quality of pot marigold (*Calendula officinalis L.*). – Ann. Biolog. Res. 3(11): 5095-5098.
[27] Nikbakht, A., Kafi, M., Babalar, M., Xia, Y. P., Luo, A., Etemadi, N. (2008): Effect of humic acid on plant growth, nutrient uptake, and postharvest life of gerbera. – Journal of Plant Nutrition 31: 2155-2167.
[28] Pal, A. L., Biswas, B. (2005): Response of fertilizer on the growth and yield of tuberose (*Polianthes tuberosa*) cv. Calcutta Single in the plants of West Bengal. – Inter Academicia 9(1): 33-36.
[29] Sakr, W. R. A., El-Sayed, A. A., Hammouda, A. M., Saad El Deen, F. S. A. (2018): Effect of NPK, Aloe gel and Moringa extracts on geranium plants. – Journal of Horticultural Science & Ornamental Plants 10(1): 1-16.
[30] Sathiyabama, K., Selvakumari, G. (2001): Effect of humic acid on growth, yield and nutrition of Amaranthus. – South-Indian-Hort. 49: 155-156.
[31] Sayed, B. A., Samira, S. A., Shahin, S. M. (2010): Response of *Vinca rosea* cv. Major plant to chemical and biofertilization treatments. – J Biol. Chem Environ. Sci. 5(4): 25-38.

http://www.aloki.hu ● ISSN 1589 1623 (Print) ● ISSN 1785 0037 (Online)
DOI: http://dx.doi.org/10.15666/aeer/1802_25552567

[32] Sharif, M., Khattak, R. A., Sarir, M. S. (2002): Effect of different levels of lignitic coal derived humic acid on growth of maize plants. – Communic Soil Sci and Plant Analy 33: 3567-3580.
[33] Sendecor, G. W., Cochran, W. G. (1980): Statistical Methods. 6th Ed. – Iowa State Univ. Press, Ames, IA.
[34] Stevenson, F. J. (1994): Humus Chemistry: Genesis, Composition, Reactions. – Wiley, New York.
[35] Stott, D. E., Martin, J. P. (1990): Synthesis and Degradation of Natural and Synthetic Humic Material in Soils. – In: MacCarthy, P., Clapp, C. E., Malcolm, R. L., Bloom, P. R. Humic Substances in Soil and Crop Sciences: Selected Readings. SSSA, Madison, WI, pp. 37-64.
[36] Yadava, U. L. (1986): A rapid and nondestructive method to determine chlorophyll in intact leaves. – Hort. Sci. 21(6): 1449-1450.

http://www.aloki.hu ● ISSN 1589 1623 (Print) ● ISSN 1785 0037 (Online)
DOI: http://dx.doi.org/10.15666/aeer/1802_25552567

THE HEAVY METAL ADSORPTION CAPACITY OF STALK BIOCHAR IN AN AQUEOUS PHASE

LU, N.[1,2,3,4,5] – HAN, J. C.[2,3,4,5*] – WEI, Y.[1,2,3,4,5] – LI, G.[1,2,3,4,5] – SUN, Y. Y.[1,2,3,4,5]

[2]*Shaanxi Key Laboratory of Land Consolidation, Xi'an city, Shaanxi province 710061, China*

[1]*Shaanxi Provincial Land Engineering Construction Group Co. Ltd., Xi'an city, Shaanxi province 710075, China*

[3]*Key Laboratory of Degraded and Unused Land Consolidation Engineering, the Ministry of Natural Resources, Xi'an 710075, China*

[4]*Institute of Land Engineering and Technology, Shaanxi Provincial Land Engineering Construction Group Co. Ltd., Xi'an 710075, China*

[5]*Shaanxi Provincial Land Consolidation Engineering Technology Research Center, Xi'an 710075, China*

[*]*Corresponding author*
e-mail: hanjc_sxdj@126.com; phone: +86-(029)-8662-5019

(Received 12th Jul 2019; accepted 12th Feb 2020)

Abstract. Several heavy metal ions including chromium(II), nickel(II), copper(II), zinc(II), cadmium(II), and lead(II) have gained attention due to their common occurrence in recent years. At medium-high temperatures, rice plant stalk (*Oryza sativa* L.) biochar, cassava stalk (*Manihot esculenta Crantz*) biochar and reed stalk (*Phragmites Trin.*) biochar automatically undergo pyrolysis, and the resulting biochar can be used as an adsorbent of heavy metal ions. While maintaining the pH and temperature of the solution and the dosages of biochar, the adsorption capacity of heavy metal ions in biochar under different treatment times (1 h, 6 h, 12 h, 24 h, 48 h, 72 h, and 96 h) were assessed. The physical and chemical characterization of the biochar was also performed. In this article, biochars produced from two common grain crop stalk (rice plant and cassava) and cash crop stalk (reed) were estimated as potential adsorbents for the removal of heavy metal ions from the contaminated solution.
Keywords: *agricultural residues, stalk biochar, heavy metal solution, removal efficiency, potential adsorbent*

Introduction

Biochar products are obtained by the pyrolysis of biomass energy materials under high temperatures (300-900°C) in environments with limited oxygen content (Ahmad et al., 2012), and have been used in agricultural soil improvement. Depending on the porous structure, biochar can be considered anadsorbent and water-retaining admixture material. A large amount of material from agricultural production and industrial processing can be used as biochar raw stock due to its abundance and low cost (Inyang et al., 2016). In the harvest season especially, many agricultural residues are produced, such as rice, wheat, corn and peanut. Processing abundant biomass into biochar by pyrolysis in anaerobic conditions not only greatly reduces the volume, but also improves the value (Abdelhadi et al., 2017). Typical biological carbon has high cation exchange ability (CEC) and alkalinity. With increasing biological soil activity, biochar improves soil properties, ultimately giving potential to increase agricultural yield (Chun et al., 2004). Biochar may also affect the bioavailability of heavy metals in soil and the accumulation of heavy metals in soil-grown plants. However, previous studies have not shed much light on the

http://www.aloki.hu ● ISSN 1589 1623 (Print) ● ISSN 1785 0037 (Online)
DOI: http://dx.doi.org/10.15666/aeer/1802_25692579

effects of biocarbon on heavy metals in soil (Chen et al., 2011). Unlike most biodegradable organic and inorganic pollutants, heavy metals cannot be biodegraded and accumulated through the food chain (Inyang et al., 2016). In recent years, more attention has been paid to biological carbon, because of its role in ecological restoration, such as carbon sequestration, soil fertility improvement and soil restoration. Recent literature provides evidence that it has the ability to hold organic and inorganic pollutants in soil (Inyang et al., 2016). Therefore, biochar is considered to be a new type of remediation agent that can help to repair heavy metal soil pollution (Liu and Zhang, 2009).

Water is an important part of human ecological environments. Human health is harmed by the contamination of drinking water, agricultural products, and aquatic products with heavy metals. Owing to the characterization of heavy metal pollutants as being non-degradable, cumulative, and potentially harmful, heavy metal pollution of water has attracted more attention. In light of research results for the application of biochar, multi-aperture, specific surface area, cationic exchange ability, high stability, and other characteristics were considered. Biochar use as an adsorbent material for metal contaminated water treatment has important application prospects (Meng et al., 2014). Researchers found that biochars produced by anaerobic digestion had higher adsorption capacity to heavy metals (Inyang et al., 2011, 2012). Cellulosic biomass waste from agricultural and forestry production are usually used as the raw materials for biochar processing (Keiluweit and Kleber, 2009).

In China, reed is a common cash crop that is often used as the raw material for paper production. Owing to the ability of adsorption and enrichment of heavy metals, reed could be used for wastewater treatment and as a landscape plant in constructed wetlands (Hou et al., 2016). Cassava and rice are common food crops and the residues account for a large proportion of agricultural waste in tropical areas (Deng et al., 2014; Huang et al., 2018). Biochar production from these three stalk materials has been reported (Huang et al., 2017; Edhirej et al., 2017; Li et al., 2018). Therefore, this paper mainly compared the different adsorption capacities of heavy metals by biochars using rice plant stalk, cassava stalk, and reed stalk as raw materials for biochar. The aims of this study were: (1) to examine the physical and chemical characteristics of biochars, (2) to examine the surface and pore characterization of biochars, and (3) to examine their adsorption capacity of common heavy metals.

Materials and methods

Biochar preparation and characterization

The biochars that were texted were made of rice plant stalk, cassava stalk, and reed stalk material. The raw materials used in this study were collected in Fuping County, China. The sorption ability of the biochar was enhanced by pulverization prior to pyrolysis (Tong et al., 2011). In order to do this, the stalk were initially cut to 25 mm pieces with an electronic chipper and then these were cut in a 5 mm cross-cutting mill. The material was dried at 60°C for constant weight before pyrolysis (Sevilla and Fuertes, 2009). Studies have shown that when the carbonization temperature reaches 500°C, the carbon yield biomass is essentially stable (Bridgwater, 2007). Thus, all biochar from this study was produced at a temperature of 550°C for 4 h. Only the small particles that passed through a 0.5 mm sieve were used in the experiments described below.

Ash content was determined by combusting the biochar at 750°C for 6 h in open crucibles on a dry weight basis (105°C for 18 h under argon). A CHN elemental analyzer

http://www.aloki.hu ● ISSN 1589 1623 (Print) ● ISSN 1785 0037 (Online)
DOI: http://dx.doi.org/10.15666/aeer/1802_25692579

(Flash EA 1112, Thermo Finnigan) was used to determine the carbon (C), hydrogen (H), and nitrogen (N) contents of all biochars. Oxygen content was calculated according to *Eq. 1*. Elemental composition was measured in duplicate, and in this paper, the averaged data was used for analysis. Biochar SEM images were obtained by FEI Q45 scanning electron microscop (FEI, USA). The pH of the biochar was measured in a 1:10 ratio of biochar suspension in deionized water. To determine the concentrations of heavy metals in the biochar, each of the 0.1 g of biochar samples was dissolved in 3 mL of HNO_3 (65%), 9 mL of HCl (37%), and digested for 1 h. The digestion solution was poured into 50 mL flask and diluted with deionised water to reach the tick mark (Pundytė et al., 2011; Baltrėnaitė et al., 2016). The concentrations of heavy metals in the solution were determined by ICP-MS (Agilent 7700e, USA).

Metal adsorption experiments

All chemical reagents were of analytical grade. Heavy metal solution (10 mg/L) of Cd, Cr, Pb, Cu, Zn, Ni was prepared. The mixed solutions made to have a pH 7.0±0.1 which was adjusted by the addition of nitric acid or sodium hydroxide solutions. For adsorption efficiency investigation, 50 ml centrifuge tubes were filled with a heavy metal solution into which 0.01 M $CaCl_2$ and 0.2 g/L NaN_3 were added to maintain a constant ionic strength and to inhibit microbial activities. 0.5 g of biochar per sample were added to the test solutions. Other scholars who studied the equilibrium adsorption time in similar biochars found the time to be around 24 h (Deng et al., 2014; Huang et al., 2018). In order to compare the adsorption effects of the three kinds of biochar, the experimental adsorption time was set to 1 h, 6 h, 12 h, 24 h, 48 h, 72 h, and 96 h. Heavy metals mixed without biochar and biochar with the addition of double distilled water were used as blank controls. All tubes were agitated in the dark at 180 rpm at 25°C. After the adsorption completed, samples were centrifuged for 10 min at 5000 rpm, and the supernatant was then filtered through a 0.45 μm membrane. The removed amount was determined by measuring concentration differences of heavy metals before and after the adsorption experiment (Hou et al., 2016).

Evaluation method

Oxygen content of biochar was calculated according to *Eq. 1*.

$$O = 100 - (C + H + N + \text{ash}) \quad \text{(Eq.1)}$$

where O is the oxygen content of the biochar; C, H and N are the carbon, hydrogen, and nitrogen contents of the biochar, respectively; ash is the ash content of the biochar.

Data processing

The adsorption capacity of biochar (q_t) was calculated by *Eq. 2*:

$$q_t = \frac{(C_{i0} - C_{if}) \times V_0}{m_f} \quad \text{(Eq.2)}$$

http://www.aloki.hu ● ISSN 1589 1623 (Print) ● ISSN 1785 0037 (Online)
DOI: http://dx.doi.org/10.15666/aeer/1802_25692579

where C_{i0} and C_{if} are the initial and final concentrations of the tested solution ($mg \cdot L^{-1}$), respectively; V_0 is the volume of the tested solution volume (ml); m_j (g) is the weight of the biochar; j refers to the different biochars.

Data analysis

ANOVA test was performed at 95% level using SPSS 22 (IBM SPSS Statistics, Version 22) which tested for the significance of the differences between treatments.

Results and Discussion

Characterization of the biochars

The physicochemical properties of the three different biochars are shown in *Table 1*. We found that all the biochars were alkaline (pH > 10). This observed higher pH of the three biochars is an indication that they may have potential to ameliorate and neutralize soil acidity, which can be an important component in the mobility of heavy metals. The ash content of rice plant stalk (40.00%) was higher than that of cassava stalk (9.85%) and reed stalk (15.75%). The ash content of the three biochars is consistent with the productivity trend, rice plant stalk (43.19%), cassava stalk (23.13%) and reed stalk (24.27%), respectively. Ash is made up of solid inorganic substances, which are the residual mineral elements that remain after burning the stalk material, such as sodium, potassium, calcium, magnesium, phosphorus, and iron. The ash content shows the selective absorption and accumulation of minerals by different plants. Higher ash content indicates that rice plant can absorb more mineral elements, which creates favorable conditions for biochar to absorb heavy metals. The productivity of the three biochars are 43.19%, 23.13% and 24.27%, respectively. The productivity of biochars is consistent with the ash content.

Table 1. *Physicochemical characteristics of the three different biochars*

Physicochemical characteristics	Biochar		
	Reed stalk	***Cassava stalk***	***Rice stalk***
pH	10.55	10.24	10.94
Conductivity ($\mu S \cdot cm^{-1}$)	677	1313	911
TC (%)	65.82±14.62	59.12±10.81	39.23±5.28
Ash content (%)	15.75±0.36	9.85±0.42	40.00±2.08
Productivity (%)	28.53±2.57	31.05±1.69	41.71±0.61
C (%)	61.93±0.98	64.30±0.32	41.05±0.44
H (%)	1.65±0.07	1.61±0.05	1.12±0.02
N (%)	0.73±0.09	1.53±0.11	1.36±0.09
S (%)	0.69±0.27	0.50±0.17	0.35±0.02
O (%)	19.94±0.97	22.71±0.41	16.47±0.49
C/N	85.07±10.13	42.13±2.87	30.15±1.96
H/C	0.027±0.001	0.025±0.001	0.027±0.000
O/C	0.32±0.02	0.35±0.01	0.40±0.02
(N+O)/C	0.33±0.02	0.38±0.01	0.43±0.02

Chemical composition of the three biochars is shown in *Table 1*. Rice stalk biochar contained lower concentrations of C, H, O, and S than cassava stalk and reed stalk biochar. This might be related to the different cellulose content of each feedstock.

http://www.aloki.hu ● ISSN 1589 1623 (Print) ● ISSN 1785 0037 (Online)
DOI: http://dx.doi.org/10.15666/aeer/1802_25692579

Previous study found that the C content was higher in hardwood than stover (Park et al., 2016). The lignin content in the raw material biomass directly affects the total carbon content of the biochar. While the N content of reed stalk was the least (0.73%), it was probably related to the accumulation of N in plants. In addition, the higher content of hydrogen and oxygen for cassava stalk and reed stalk revealed that more activated sites were available and stable carbon-oxygen complexes existed on the surface of cassava stalk and reed stalk as opposed to rice plant stalk (Guerrero et al., 2005; Tong et al., 2011). The degree of carbonization can be described by the molar H/C ratio, where H is primarily associated with plant organic matter (Tong et al., 2011). Compared to activated carbon (AC) with H/C ratios of 0.12 and 0.256 (Chen et al., 2011; Xu and Zhao, 2013), the observed H/C ratios of 0.027, 0.025, and 0.027 for rice stalk biochar, cassava stalk biochar and reed stalk biochar, respectively, indicate that these biochars are strongly carbonized and are consistent with high amounts of aromatization.

These low H/C ratios suggest that the biochars contain low amount of organic plant residues. The molar oxygen to carbon (O/C) ratio of biochar has been used as a surrogate for surface hydrophilicity since it is indicative of polar-group content, most likely derived from carbohydrates. Based on this assumption, rice plant stalk (0.4) is likely to be more hydrophilic than cassava stalk biochar (0.35) and reed stalk biochar (0.32), as it has a higher O/C ratio. (N+O)/C ratios of rice stalk biochar, cassava stalk biochar and reed stalk biochar were 0.43, 0.38 and 0.33, respectively. The lower O/C and (N+O)/C ratios indicated an increase in aromaticity and a reduction in polarity. Hydrophobic carbon can provide more sorption domains for HOCs (Teixidó et al., 2011; Yang et al., 2011). Different plant types affect the reduction of mass (Keiluweit and Kleber, 2009). The reduction in biomass weight of cassava stalk and reed stalk are more than that of rice stalk. The weight of dry rice stalk biomass, cassava stalk, and reed stalk decreased 2.32, 4.32, and 4.12 times during the production of biochar, respectively.

For rice stalk biochar, ash content and TC had a significant effect at 95% level ($p < 0.05$), C and (N+O)/C had a significant effect at 95% level ($p < 0.05$). For cassava stalk biochar, ash content led to a significant increase in N and C/N. N and C/N had a significant effect at 95% level ($p < 0.001$) and O/C and (N+O)/C had a significant effect at 95% level ($p < 0.05$). For reed stalk biochar, C and O had a significant effect at 95% level ($p < 0.001$), and C and (N+O)/C had a significant effect at 95% level ($p < 0.05$). C and O/C had a significant effect at 95% level ($p < 0.001$), and O and (N+O)/C had a significant effect at 95% level ($p < 0.05$). The O and O/C of the three biochars were all significantly correlated at 95% level ($p < 0.05$).

Surface characterization

Scanning electron microscope images (*Fig. 1*) indicated that three biochar samples consisted of small 1–20 μm diameter pores. The pores of cassava stalk biochar were larger than that of rice stalk biochar. And the pores of reed stalk biochar were the smallest. SEM imaging showed that heat-treated stalk retained its original stalk pores structure.

The strong sorption ability of biochars may be attributed to their surface properties, which is inherited from the feedstock materials. Obvious microporous structures were observed after carbonization of the three substances. The average pore size of the rice biochar was the smallest (1.0 μm–4.2 μm) followed by reed stalk biochar (3.5 μm-4.4 μm), and cassava stalk biochar (7.0 μm–20.0 μm). Within the same field of vision, the pore arrangement of cassava stalk biochar was more compact and the reed stalk biochar had the least number of pores.

http://www.aloki.hu ● ISSN 1589 1623 (Print) ● ISSN 1785 0037 (Online)
DOI: http://dx.doi.org/10.15666/aeer/1802_25692579

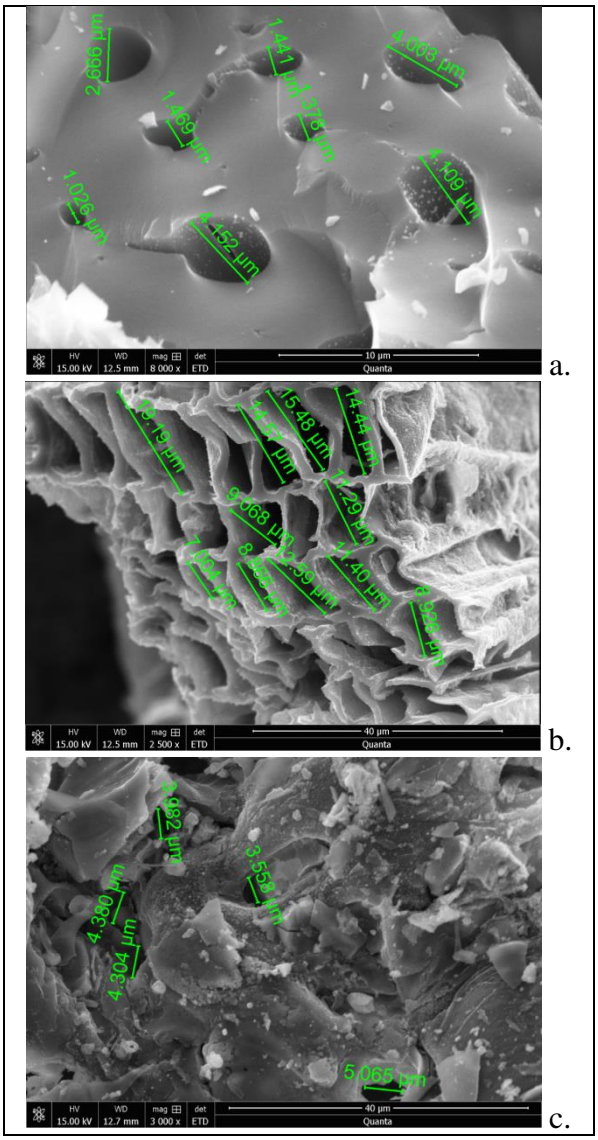

Figure 1. *Scanning electron microscope images of biochar (a. reed stalk biochar, b. Cassava stalk biochar, c. rice stalk biochar)*

Capacity of heavy metal adsorption for three biochars

The capacity of adsorpion of heavy metals q_t (*Eq. 2.*) by three types of biochar is shown in *Fig. 2*. The temperature, pH, dosage of biochar were kept the same. Within the entire experimental adsorption time range, the amount of heavy metal adsorption of the three biochars all showed an increasing trend with the increase in adsorption time. During the entire adsorption process, cassava stalk biochar had the largest cumulative adsorption of heavy metals. When the adsorption time was at 1 h, the reed stalk biochar had a stronger adsorption capacity for various heavy metals than the rice stalk biochar. At other adsorption times, the cumulative adsorption of various heavy metals by rice stalk biochar was higher than that of reed stalk biochar. There are some differences in the adsorption capacity of the three biochars for each of the different heavy metals. For example, cassava stalk biochar had stronger adsorption capacity for Cr, Cu, and Pb than the other two biochars. Their adsorption amounts accounted for 49.17%, 70.56%, and 65.27% of the

http://www.aloki.hu ● ISSN 1589 1623 (Print) ● ISSN 1785 0037 (Online)
DOI: http://dx.doi.org/10.15666/aeer/1802_25692579

total adsorption of the three heavy metals, respectively. Rice stalk biochar showed good adsorption capacity for Zn, and its adsorption amount accounted for 51.67% of the total adsorption. The final adsorption amount of rice stalk biochar for Ni and Cd was higher than that of cassava stalk biochar. However, the contribution of cassava stalk and rice stalk biochar to the adsorption of Ni and Cd was not much different. For example, rice stalk biochar adsorption contribution rates of Ni and Cd were 36.66% and 36.69%, respectively, and cassava stalk biochar adsorption contribution rates of Ni and Cd were 34.81% and 35.64%, respectively.

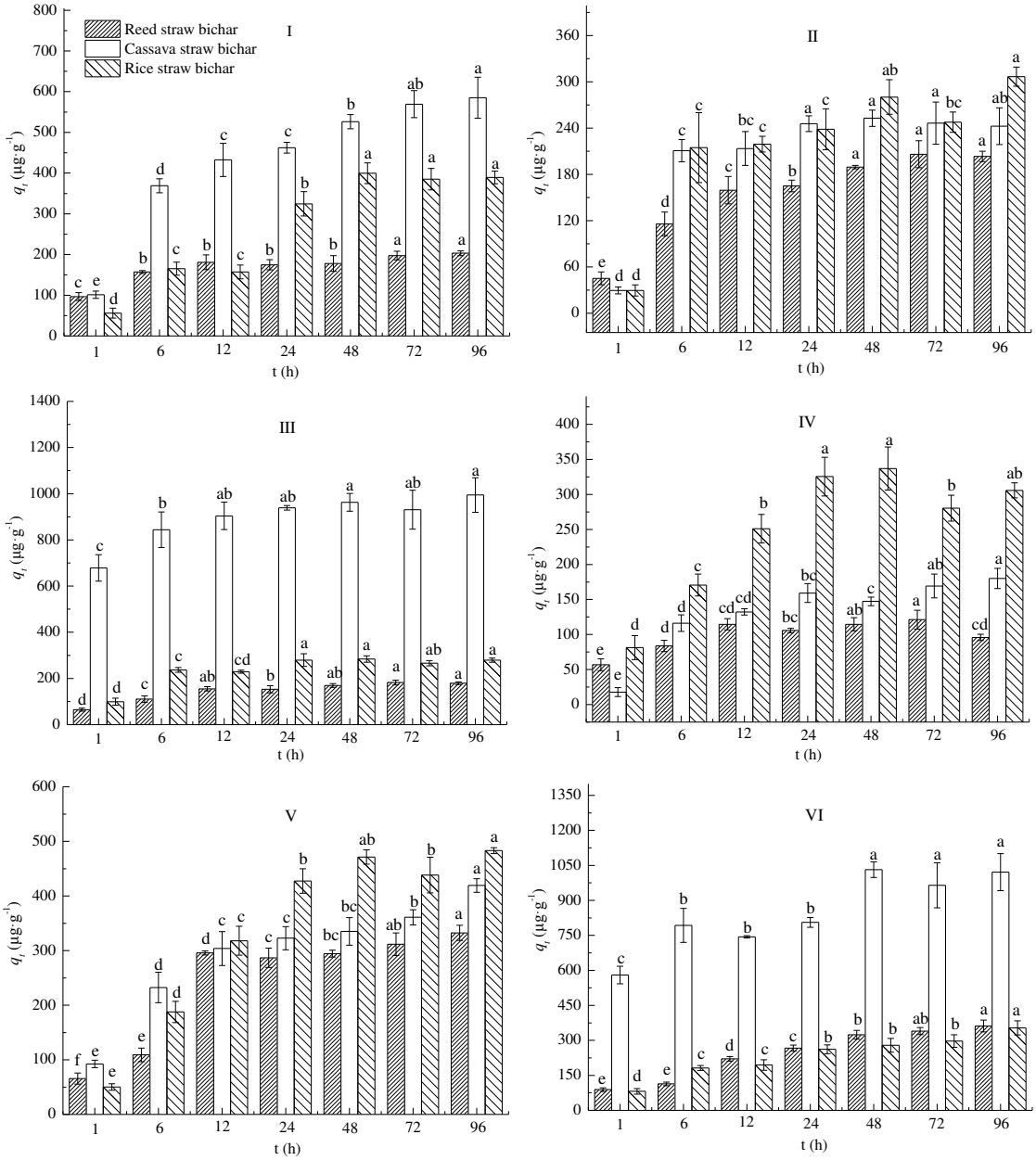

Figure 2. *Effect of biochar concentration on heavy metal adsorption efficiency for three different biochars. I, II, III, IV, V, and VI represent Cr, Ni, Cu, Zn, Cd, and Pb, respectively. Bars indicate standard errors. Lowercase letters indicate significant differences in heavy metal adsorption capacity of the same biochar at different adsorption times ($p < 0.05$)*

http://www.aloki.hu ● ISSN 1589 1623 (Print) ● ISSN 1785 0037 (Online)
DOI: http://dx.doi.org/10.15666/aeer/1802_25692579

As the contact time increased, available adsorption sites became occupied, followed by an increase in adsorption capacity of heavy metals and a decrease in adsorption efficiency. Research has shown that biochars with higher O content and more acidic surface sites have higher CECs (Harvey et al., 2011). High carbonization temperatures (> 400°C) also promote the formation of graphene structures in biochars, which favor electrostatic attraction sorption mechanisms (Keiluweit and Kleber, 2009). High temperature pyrolysis can remove aliphatic groups and form surface functional groups that have strong adsorption ability, increasing the adsorption and fixation strength of biochar for heavy metal ions.

The correlation analysis of the adsorption test data shows that when the adsorption time does not exceed 6 h, the amount of Cr, Zn, and Cu adsorbed by the biochar of reed stems and the amount of Ni, Cu, Zn, and Pb adsorbed by the biochar of cassava stalks was significantly related to the adsorption time ($p < 0.05$). When the adsorption time did not exceed 12 h, the amounts of Cr and Cd adsorbed by cassava stalk biochar and Zn and Cd by rice stalk biochar were significantly related to the adsorption time ($p < 0.05$). When the adsorption time was at 24 h, the amount of Cd adsorbed by reed stalk biochar increased significantly with the increase in the adsorption time ($p < 0.05$). When the adsorption time was less than 48 h, the adsorption amount of Ni and Pb by reed stem biochar was positively correlated with the adsorption time ($p < 0.05$).

In addition, there are some other notable adsorption phenomena. Within 6-48 h, the adsorption amount and adsorption time of Cr by reed stem biochar was not significant ($p > 0.05$), and the adsorption amount of Zn within this adsorption time range was not significant ($p > 0.05$). The adsorption amount of Cr at 72 h and 96 h was significantly correlated with adsorption amount at 48 h ($p < 0.05$), but there was no correlation between the adsorption amount at 72 h and 96 h ($p > 0.05$). The result shows that the adsorption amount of Cr by reed stalk biochar falls within 6 h of adsorption time, and the adsorption amount increases rapidly with adsorption time. The adsorption amount from 6-48 h does not increase or increases very slowly with the adsorption time. Once a certain adsorption amount was reached, the adsorption amount stabilized itself from the time points of 72-96 h.

The adsorption of Ni (II) and Zn (IV) by cassava stalk biochar was not significant at 6 h and 12 h ($p > 0.05$). The adsorption amount of these two heavy metals did not increase during this adsorption time. Ni (II) adsorption increased at 12 h and 24 h ($p < 0.05$), but stabilized at 24-96 h. The adsorption amount of Zn (IV) increased from 12 h to 48 h ($p < 0.05$) and the adsorption amount was stable after 48 h. The adsorption amount of Cu (III) gradually stabilized after 12 h. The adsorption amount of Pb (VI) stabilized from 6 h to 24 h, increased from 24 h to 48 h, and then stabilized again.

Based on the above analysis, cassava stalk biochar and rice stalk biochar can achieve high adsorption efficiency for six heavy metals in a relatively short time (that is, an adsorption time less than 12 h). The adsorption of the heavy metal Cd (V) by reed stalk biochar reached its highest level within 24 h of adsorption time, but its final adsorption amount was lower than that of cassava stalk biochar and rice stalk biochar. The reed stalk biochar adsorbed heavy metals Ni (II) and Pb (VI) only after 48 h, and the final adsorption of Ni (II) was lower than that of rice stalk and cassava stalk biochar. The final Pb (VI) adsorption amount by reed stalk biochar was basically the same as that of rice stalk, indicating that compared with cassava stalk biochar and rice stalk biochar, reed stalk biochar has poor adsorption capacity and poor adsorption strength for these six heavy

http://www.aloki.hu ● ISSN 1589 1623 (Print) ● ISSN 1785 0037 (Online)
DOI: http://dx.doi.org/10.15666/aeer/1802_25692579

metals. For reed stalk biochar, it may take longer to adsorb the same amount of heavy metals as the other two biochar types in this study.

Higher quantities of biochar minerals are produced at higher temperature ranges (350-600℃). Most of the biochar minerals produced at high temperatures are insoluble and are slowly released during the adsorption process, forming precipitate with heavy metals (Inyang et al., 2011). Higher specific surface area and pore volume can physically adsorb heavy metal ions on the surface of biochar and in its pores. The surface of biochar is often negatively charged and can attract positively charged metal ions (Patra et al., 2017).

The three biochar raw materials used in this study were primary stalk residues from agricultural and forestry production. In China, a large amount of agricultural and forestry production residues provide feasibility for biochar production. Biocharing technology not only efficiently treats biomass waste, but also produces by-products such as biochar and bio-oil which both have a higher utilization value.

Studies have shown that adding a certain amount of biochar to heavy metal contaminated soils usually has the effect of improving pH in acidic soils, increasing soil nutrient content and its effectiveness. Biochar can increase the pH of acidic soil by increasing the alkaline saturation of the soil, reducing aluminum levels, thereby reducing the transportable forms of heavy metal ions (Zhao et al., 2015). Adding biochar can increase soil available P, available K, organic matter, total N, total P, and total K to different degrees. First, biochar contains mineral nutrients such as N, P, K, etc., which can be directly applied to soils in order to increase soil nutrient content (Yuan et al., 2011). Second, biochar can also significantly increase the available content of major cations such as K, Mg, and Ca in the soil, provide essential nutrients for plant growth, and improve soil nutrient effectiveness (Lehmann et al., 2003). Third, the strong adsorption and structural characteristics of biochar have a retention effect on water-soluble nutrients in the soil, effectively reducing soil nutrient leaching-loss, slowly and continuously releasing nutrients, and enhancing effective soil nutrient content (Angst and Sohi, 2012). In summary, the application of stalk-based biochar in the restoration of contaminated land is very significant. Not only is the biomass waste used efficiently, but it can also achieve carbon sequestration, improve soil structure and soil fertility.

Conclusions

Excellent removal of heavy metals from soil results from the advantageous physical and chemical characteristics of biochar. Due to the fact that heavy metal removal mechanisms vary with respect to different biochars and metal contaminants, the interest in understanding adsorption processes and the removal efficiency of various pollutants by different types of biochar has increased in recent years. For certain heavy metals, the suitable biochar repairer is different. For Cu, Pb, and Cr, cassava stalk biochar should be chosen as the adsorbent. For Zn, rice stalk biochar is more suitable for treatment, because of the stability of the heavy metal adsorption efficiency. For Ni and Cd, cassava stalk biochar and rice stalk biochar are more suitable as adsorbents than reed biochar.

The soil system is more complex than just a mixed solution of heavy metals. In this experiment, we initially obtained the heavy metal ion adsorption effect for different types of biochar under different adsorption time conditions. The types of biochar with specific adsorption capacity for different heavy metals were summarized. The simulation and calculation of heavy metal chemical conversion processes, heavy metal ion infiltration,

http://www.aloki.hu ● ISSN 1589 1623 (Print) ● ISSN 1785 0037 (Online)
DOI: http://dx.doi.org/10.15666/aeer/1802_25692579

and diffusion processes in the soil solution will be carried out in the future. The application of biochar for the remediation of contaminated land will soon become an effective treatment rapidly used across the world.

Acknowledgements. Financial support were provided by the Fund Project of Shaanxi Key Laboratory of Land Consolidation (2019-JC04, 2018-JC16, and 2019-JC05), and the Research Project of Shaanxi Provincial Land Engineering Construction Group in China (DJNY2019-18).

REFERENCES

[1] Abdelhadi, S. O., Dosoretz, C. G., Rytwo, G., Gerchman, Y., Azaizeh, H. (2017): Production of biochar from olive mill solid waste for heavy metal removal. – Bioresource Technology 244: 759-767.
[2] Ahmad, M., Lee, S. S., Dou, X., Mohan, D., Sung, J. K., Yang, J. E., Ok, Y. S. (2012): Effects of pyrolysis temperature on soybean stover and peanut shell-derived biochar properties and TCE adsorption in water. – Bioresource technology 118: 536-544.
[3] Angst, T. E., Sohi, S. P. (2013): Establishing release dynamics for plant nutrients from biochar. – Gcb Bioenergy 5(2): 221-226.
[4] Baltrėnaitė, E., Baltrėnas, P., Lietuvninkas, A. (2016): Contamination Features of Ecosystem Components in a Forested Surrounding Environment. – The Sustainable Role of the Tree in Environmental Protection Technologies. Springer International Publishing: Cham. 29-80.
[5] Bridgwater, T. (2007): Biomass pyrolysis. – Biomass and Bioenergy 31(4): 7-18.
[6] Chen, X., Chen, G., Chen, L., Chen, Y., Lehmann, J., McBride, M. B., Hay, A. G. (2011): Adsorption of copper and zinc by biochars produced from pyrolysis of hardwood and corn straw in aqueous solution. – Bioresource technology 102(19): 8877-8884.
[7] Chun, Y., Sheng, G., Chiou, C. T., Xing, B. S. (2004): Compositions and Sorptive Properties of Crop Residue-Derived Chars. – Environmental Science & Technology 38(17): 4649-4655.
[8] Deng, H., Yu, H., Chen, M., Ge, C. (2014): Sorption of atrazine in tropical soil by biochar prepared from cassava waste. – BioResources 9(4): 6627-6643.
[9] Edhirej, A., Sapuan, S. M., Jawaid, M., Zahari, N. I. (2017): Cassava: Its polymer, fiber, composite, and application. – Polymer Composites 38(3): 555-570.
[10] Guerrero, M., Ruiz, M. P., Alzueta, M. U., Bilbao, R., Millera, A. (2005): Pyrolysis of eucalyptus at different heating rates: studies of char characterization and oxidative reactivity. – Journal of Analytical and Applied Pyrolysis 74(1-2): 307-314.
[11] Harvey, O. R., Herbert, B. E., Rhue, R. D., Kuo, L. J. (2011): Metal interactions at the biochar-water interface: energetics and structure-sorption relationships elucidated by flow adsorption microcalorimetry. – Environmental science & technology 45(13): 5550-5556.
[12] Hou, J., Huang, L., Yang, Z., Zhao, Y., Deng, C., Chen, Y., Li, X. (2016): Adsorption of ammonium on biochar prepared from giant reed. – Environmental Science and Pollution Research 23(19): 19107-19115.
[13] Huang, D., Liu, L., Zeng, G., Xu, P., Huang, C., Deng, L., Wang, R., Wan, J. (2017): The effects of rice straw biochar on indigenous microbial community and enzymes activity in heavy metal-contaminated sediment. – Chemosphere 174: 545-553.
[14] Huang, P., Ge, C., Feng, D., Yu, H., Luo, J., Li, J., Strong, P. J., Sarmah, A. K., Bolan, N. S., Wang, H. (2018): Effects of metal ions and pH on ofloxacin sorption to cassava residue-derived biochar. – Science of the Total Environment 616: 1384-1391.
[15] Inyang, M. D., Gao, B., Ding, W. C., Pullammanappallil, P., Zimmerman, A. R., Cao, X. D. (2011): Enhanced lead sorption by biochar derived from anaerobically digested sugarcane bagasse. – Separation Science and Technology 46(12): 1950-1956.

http://www.aloki.hu ● ISSN 1589 1623 (Print) ● ISSN 1785 0037 (Online)
DOI: http://dx.doi.org/10.15666/aeer/1802_25692579

[16] Inyang, M. D., Gao, B., Yao, Y., Xue, Y., Zimmerman, A. R., Pullammanappallil, P., Cao, X. (2012): Removal of heavy metals from aqueous solution by biochars derived from anaerobically digested biomass. – Bioresource Technology 110: 50-56.
[17] Inyang, M. I., Gao, B., Yao, Y., Xue, Y., Zimmerman, A., Mosa, A., Pullammanappallil, P., Ok, Y. S., Cao, X. (2016): A review of biochar as a low-cost adsorbent for aqueous heavy metal removal. – Critical Reviews in Environmental Science and Technology 46(4): 406-433.
[18] Keiluweit, M., Kleber, M. (2009): Molecular-Level Interactions in Soils and Sediments: The Role of Aromatic π-Systems. – Environmental Science & Technology 43(10): 3421-3429.
[19] Lehmann, J., da Silva, J. P., Steiner, C., Nehls, T., Zech, W., Glaser, B. (2003): Nutrient availability and leaching in an archaeological Anthrosol and a Ferralsol of the Central Amazon basin: fertilizer, manure and charcoal amendments. – Plant and soil 249(2): 343-357.
[20] Li, Y., Zhang, Y., Wang, G., Li, S., Han, R., Wei, W. (2018): Reed biochar supported hydroxyapatite nanocomposite: Characterization and reactivity for methylene blue removal from aqueous media. – Journal of Molecular Liquids 263: 53-63.
[21] Liu, Z., Zhang, F. S. (2009): Removal of lead from water using biochars prepared from hydrothermal liquefaction of biomass. – Journal of Hazardous Materials 167(1): 933-939.
[22] Meng, J., Feng, X., Dai, Z., Liu, X., Wu, J., Xu, J. (2014): Adsorption characteristics of Cu(II) from aqueous solution onto biochar derived from swine manure. – Environmental Science and Pollution Research 21(11): 7035-7046.
[23] Park, J. H., Cho, J. S., Ok, Y. S., Kim, S. H., Heo, J. S., Delaune, R. D., Seo, D. C. (2016): Comparison of single and competitive metal adsorption by pepper stem biochar. – Archives of Agronomy & Soil Science 62(5): 617-632.
[24] Patra, J. M., Panda, S. S., Dhal, N. K. (2017): Biochar as a low-cost adsorbent for heavy metal removal: A review. – International Journal of Research in Biosciences 6(1): 1-7.
[25] Pundytė, N., Baltrėnaitė, E., Pereira, P., Paliulis, D. (2011): Anthropogenic effects on heavy metals and macronutrients accumulation in soil and wood of Pinus sylvestris L. – Journal of Environmental Engineering and Landscape Management 19(1): 34-43.
[26] Sevilla, M., Fuertes, A. B. (2009): Chemical and structural properties of carbonaceous products obtained by hydrothermal carbonization of saccharides. – Chemistry 15(16): 4195-4203.
[27] Teixidó, M., Pignatello, J. J., Beltrán, J. L., Granados, M., Peccia, J. (2011): Speciation of the ionizable antibiotic sulfamethazine on black carbon (biochar). – Environmental science & technology 45(23): 10020-10027.
[28] Tong, X. J., Li, J. Y., Yuan, J. H., Xu, R. K. (2011): Adsorption of Cu(II) by biochars generated from three crop straws. – Chemical Engineering Journal 172(2): 828-834.
[29] Xu, R. K., Zhao, A. Z. (2013): Effect of biochars on adsorption of Cu(II), Pb(II) and Cd(II) by three variable charge soils from southern China. – Environmental Science and Pollution Research 20(12): 8491-8501.
[30] Yang, Y., Shu, L., Wang, X., Xing, B., Tao, S. (2011): Impact of de-ashing humic acid and humin on organic matter structural properties and sorption mechanisms of phenanthrene. – Environmental science & technology 45(9): 3996-4002.
[31] Yuan, J. H., Xu, R. K., Zhang, H. (2011): The forms of alkalis in the biochar produced from crop residues at different temperatures. – Bioresource technology 102(3): 3488-3497.
[32] Zhao, R., Jiang, D., Coles, N., Wu, J. (2015): Effects of biochar on the acidity of a loamy clay soil under different incubation conditions. – Journal of soils and sediments 15(9): 1919-1926.

http://www.aloki.hu ● ISSN 1589 1623 (Print) ● ISSN 1785 0037 (Online)
DOI: http://dx.doi.org/10.15666/aeer/1802_25692579

THE EFFECTS OF COPPER-ZINC INTERACTIONS ON YIELD AND YIELD COMPONENTS IN SOILLESS GROWN BEANS (*PHASEOLUS VULGARIS* L.)

BİLDİRİCİ, N.

Yüzüncü Yıl University, Gevaş Vocational School of Higher Education, Department of Plant and Animal Production, Gevaş, Van, Turkey
(e-mail: numanbildirici@gmail.com; phone: +90-539-427-3208)

(Received 23rd Jul 2019; accepted 12th Feb 2020)

Abstract. This research was conducted under the ecological conditions of Van-Gevaş, Turkey in 2015 and 2016 in three replications according to the Random Parcel Trial Pattern. This study is a flowerpotting trial investigating the effects of copper (Cu) and zinc (Zn) doses applied in increasing amounts to the bean plant grown in the hydroponic system. Four different copper doses (0-200-400-800 mg Cu kg^{-1}) and four different zinc doses (0-2.5-5.0-10.0 mg Zn kg^{-1}) were applied. This study was conducted in drybean varieties on different doses and interactions of Cu and Zn; characteristics such as plant height, number of pods in the plant, number of branches, grain yield in the plant, harvest index and protein ratio were examined. According to the results of the research, while the of 400 mg kg^{-1} Cu and 5.0 mg kg^{-1} Zn dose applied to Yakutiye-98 variety in the first year increased the seed yield (36.32 g $plant^{-1}$) in the plant; in the second year, 200 mg kg^{-1} Cu applied to Yakutiye-98 variety and 5.0 mg kg^{-1} Zn increased the yield (28.45 g $plant^{-1}$). In general copper-zinc interaction; Co-administration of Cu and Zn doses led to increases in yield and yield parameters of bean varieties compared to the separate administration of these doses and was found statistically significant at 1% level.
Keywords: *dry beans, hydroponics, copper, zinc, fertilizer, grain yield*

Introduction

High content of protein in the composition of grains between 22-30% is sufficient by carbohydrates; bean is an important legume plant as it is rich in potassium, calcium, magnesium and phosphorus and also has various vitamins. It is in the first place among legumes in terms of cultivation and production in the world. Dry and fresh consumption of bean is very common. Around 29 million hectares of land is cultivated in the world. The total production is 23 million tons and the yield per hectare is 800 kg (FAO, 2017). In Turkey, bean cultivation area is 848 thousand ha, 220 thousand tons of production and 2590.00 kg ha^{-1} yield is obtained (TUİK, 2018).

As the world population increases rapidly, food consumption is increasing accordingly. This brings about an urgent need for increasing the production together with the need for vegetable protein sources. In order to increase production in existing agricultural areas, grain yield per unit area should be increased. For this reason, it is very important to apply the macro and micro nutrients in sufficient doses considering the interactions with each other as well as technical agricultural practices.

Copper (Cu) and zinc (Zn) are absolutely essential micro nutrients for plants. However, although it is necessary for the life of living things, high doses cause toxic effects on plants and other living things. Although high concentrations of Cu and Zn is toxic, they are part of molecules that play a key role in photo-synthetic electron transport and enzyme activation (Raven et al., 1999).

Copper is a micro nutrient in plants and it is required for respiration, protein synthesis and chlorophyll production. Indeed, it is very effective in protein and carbohydrate

http://www.aloki.hu ● ISSN 1589 1623 (Print) ● ISSN1785 0037 (Online)
DOI: http://dx.doi.org/10.15666/aeer/1802_25812598

metabolism. It is an important trace element due to its role in carbohydrate and lipid metabolism through influencing enzyme activity in plants (Kacar and Katkat, 2006). Activation and electron transfer of many oxidase enzymes are carried out by copper (Cu). In particular, the role of copper in the symbiotic nitrogen fixation in legume plants as the subject to this study is important (McCauley et al., 2009). In addition, Cu is an effective element in plant resistance against fungal diseases and in controlling plant moisture (Plaster, 1992).

Copper is present in the soil attached to organic materials, manganese (Mn) and iron (Fe) oxides. As a matter of fact, copper deficiency can be seen in soils rich in organic matter and ready pit soils containing more than 50% organic matter because organic matter holds copper very strongly. In addition, silicates contain copper, which changes and dissolves in weak amounts. Washing of sandy soils also causes copper deficiency. In the absence of copper in the young leaves of plants, chlorosis necrosis such as jaundice is seen, development is stunted, maturation is late and sometimes due to the excess color matter the coffee color symptoms are detected. However, in copper deficiency, plants are particularly vulnerable to fungal diseases caused by fungi. Carbohydrate content in Cu deficiency is very low in the plant. In addition, it was found that the nodule formation in legume plants was interrupted and a small amount of N was fixed (McCauley et al., 2009; Bolat and Kara, 2017).

Copper concentration in clean soils that are not polluted in nature varies between 2-40 ppm, while in dirty soils this value can increase up to 1000 ppm (Sönmez et al., 2006a). Toxic effects occur when the amount of copper in the soil is high and it is difficult for plants to take iron up. Therefore, symptoms of chlorosis appear to be iron deficiency. Another disadvantage of the excess copper in plants is the slowdown of root and shoot development. Also, it's excess in the soil affects the uptake of molybdenum negatively (Bolat and Kara, 2017).

If the amount of copper (Cu) in the dry matter weight of the plant is more than 15-30 mg Cu kg^{-1} toxic effects occur. Copper toxicity in the plant generally occurs in the root region and causes some degradation of the plant's physiological properties such as protein synthesis, photosynthesis, respiration, ion exchange and cell membrane structure (Sossé et al., 2004).

Heavy metal pollution is generally seen in soils with physical, chemical and biological degradation. Copper pollution is caused by natural disasters such as earthquakes, volcanic eruptions and floods as well as anthropogenic activities such as industrial, urban, mining and pesticide use in agriculture and the use of sewage wastes as fertilizers (Karaca and Turgay, 2012; Dağhan and Öztürk, 2015). It is known that copper fertilizers, copper-containing fungicides and pesticides are used more and more widely than necessary in recent years especially against the fungal factors that are defective in agricultural areas. As a matter of fact, it has been reported that Cu content is close to the critical toxicity limit in the Mediterranean Region soils of Turkey and Cu content is above the critical limit in 8% of greenhouse soils (Kaplan, 1999).

Zinc (Zn) plays a role in the metabolism of certain hormones such as auxin, which provides the formation of shoots, and it is also important for the activity of various enzymes that occur in the plant (Marschner, 1997; Kaya et al., 2018). Zinc is one of the micro nutrients that is essential for plants in small amounts.The effect of zinc in plants is similar to magnesium (Mg) and manganese (Mn). Zinc enzyme activation is directly effective in the formation of product quantity and quality due to its effect on photosynthesis, respiration and biological membrane stability (Rout and Das, 2003). At the same time, zinc which acts on

http://www.aloki.hu ● ISSN 1589 1623 (Print) ● ISSN1785 0037 (Online)
DOI: http://dx.doi.org/10.15666/aeer/1802_25812598

nitrogen (N) metabolism in plants, is effect in the formating of starch and ripening of seed (McCauley et al., 2009).

Zinc is present in the soil in the form of oxides in silicate minerals, bonded to clay minerals or in combination with organic matter. While the Zn concentration in the soil varies between 10-300 ppm, it is reported that the Zn concentration that can be taken by plants varies between 3.6-5.5 ppm (Öktüren Asri and Sönmez, 2006). Zinc toxicity in plants generally occurs above 400 ppm. Root and shoot growth of plants exposed to zinc toxicity weakens, roots become thin, young leaves curl and signs of chlorosis appear. In addition, cell growth and elongation are interrupted, cell organelles are broken down and chlorophyll synthesis is reduced (Rout and Das, 2003; Öktüren Asri and Sönmez, 2006). The zinc in the soil occurs in complex compounds that do not dissolve in time. This bonding of zinc (Zn) also affects the high soil pH. In contrast, the solubility of zinc compounds increases as the soil gains an acidic character. Zinc poisoning due to excess zinc in the soil is a very rare condition in plants. Likewise, the zinc content of plants grown in soils close to mineral deposits can be quite high. When the Zn concentration is high, the root and leaf growth of the plant is significantly weakened. In addition, the nitrogen, phosphorus and iron uptake rate of the plant decreases (Bolat and Kara, 2017).

Zinc deficiency is generally found in soils with high alkaline pH and alkaline plants with high basic character (Marschner, 1997; Bolat and Kara, 2017). In Zn deficiency, carbohydrate, protein and auxin metabolism is damaged due to the decrease in enzyme activity. The most obvious symptom of zinc deficiency in plants is a dwarf development and small leaf formation caused by deterioration of auxin metabolism and especially decrease in IAA synthesis (Kacar and Katkat, 2006; Kaya et al., 2018). In addition, chlorose-like necrosis appear between the veins of the leaves. The veins of such leaves may be green, the color of the parts between the veins are yellowish green, yellow or white. Leaf formation in plants decreases, leaves become sparse, top shoots die and early foliage is seen (Plaster, 1992).

It is reported that the amount of tryptophan in zinc deficiency in legume plants is decreased, protein synthesis is stopped and the quality of the product is adversely affected due to the accumulation of free amino acids (Yalçın and Usta, 1990; Toğay and Anlarsal, 2008).

Zinc deficiency not only limits crop yield but also lowers product quality. As a matter of fact, the lack of zinc in agricultural areas is quite common in recent years. Because, 30% of agricultural land in the world 83%, if in Turkey; It has been determined by studies that it contains less than 0.5 ppm Zn and it is reported that zinc deficiency is at significant levels in agricultural areas (Yağmur and Aydın, 2013).

In this study, the effect of increasing Cu and Zn doses and different dose application interactions on yield and yield characteristics of bean cultivars, a legume plant, was investigated. Bildirici et al. (2016) conducted different researches on the effect of heavy metals on beans in Van and its soils. They determined the relationships between some growth parameters and micro nutrients (Zn, Cu, Mn, Mg, Pb, Co, Cd and Fe). In line with this information; The aim of this study was to investigate the effects of copper (Cu) and zinc (Zn) nutrients and their interactions on the yield and yield components of bean plants grown hydroponically in the unheated greenhouse of Gevaş Vocational School of Yüzüncü Yıl University.

http://www.aloki.hu ● ISSN 1589 1623 (Print) ● ISSN1785 0037 (Online)
DOI: http://dx.doi.org/10.15666/aeer/1802_25812598

Materials and Methods

This research was conducted in Turkey's Van province in 2015 and 2016 in three replications according to the Random Parcel Trial Pattern. The trial was carried out with hydroponic system in the un-heated greenhouse of Yüzüncü Yıl University in Gevaş District of Van. In the experiment, Göynük-98(Ç1) and Yakutiye-98(Ç2) bean varieties registered in 1998 were used as plant material. These varieties are among Turkey's proprietary 12 varieties of beans. It is white and coarse colored and registered to Eastern Anatolia Agricultural Research Institute (Şehirali, 1988).

Cocopeat, which is rich in organic matter, was preferred as soil material in order to see the effects of copper (Cu) and zinc (Zn) doses applied to bean cultivars. Its properties and nutrient content are given in *Table 1*.

Table 1. *Some physical and chemical properties of Cocopeat**

Soil Properties	Values
pH	5.5-6.5
Cation exchange capacity (meq/100g)	64-130
Electrical transmission (EC)	0.5-1.0 mS/cm
Compression ratio	5:1
Color	Light brown-dark brown
Appearance	Short fiber and granular
Fiber	25%
Fiber length	3-30 mm
Particle size	0.1-9 mm
Water holding capacity	9 times dry weight
Total porosity	96%
Composition (% by dry weight)	
Organic matter	94-98
Organic carbon	45-50
Lignin	65-70
Cellulose	20-30
N	0.30
K2O	0.90
P2O5	0.05
CaO	0.40
C : N rate	80 : 1

*Gül, 2008

The micro nutrients subject to the study are copper (Cu) and zinc (Zn). $CuSO_4 \cdot 5H_2O$ copper sulfate as Cu source; $ZnSO_4 \cdot 7H_2O$ zinc sulfate solution was applied homogeneously to the pots before sowing (Eren and Mert, 2016). Cu and Zn doses applied in the experiment were determined by taking into consideration the averages and upper limits reported by Lindsay (1978).

The research was established with randomized plot design with 3 replications. Before sowing the pots; 4 different levels of copper dose [0 mg kg^{-1} (Cu1), 200 mg kg^{-1} (Cu2), 400 mg kg^{-1} (Cu3), 800 mg kg^{-1} (Cu4)] in copper sulfate ($CuSO_4 \cdot 5H_2O$) format and 4 different levels of zinc dose [0 mg kg^{-1} (Zn1), 2.5 mg kg^{-1} (Zn2), 5.0 mg kg^{-1} (Zn3), 10.0 mg kg^{-1} (Zn4)] in zinc sulfate ($ZnSO_4 \cdot 7H_2O$) were determined. The main reason for the high application of copper doses is the widespread use of Cu-containing pesticides, especially in agricultural pesticides. In addition to this, to observe the possible effects of copper toxicity and the effects of copper-zinc interactions on beans

http://www.aloki.hu ● ISSN 1589 1623 (Print) ● ISSN1785 0037 (Online)
DOI: http://dx.doi.org/10.15666/aeer/1802_25812598

due to the increase in the use of sewage residues such as sewage sludge as fertilizer in plant production. The experiment subjects consisted of 2 bean varieties and 4 different application doses for each element.

In this study, 540 g of cocopeat was placed in 3 liter pots with a diameter of 16.5 cm and a depth of 19.0 cm. In the experiment, seed sowing process was made 1 week after the copper application for the incubation of the copper given to the pots. Bean varieties seeds were sowed in the first year on 07.05.2015 and the second year on 10.05.2016 with one plant per flowerpot. Irrigation and fertilization of the test pots were carried out evenly and homogeneously after the exit. In the research, the macro and micro basic nutrients required by the plant were prepared as separate solutions (Buttaro et al., 2012; Di Lorenzo et al., 2013). In the preparation of the nutrient solution, Tangolar et al.'s work (2017) on the soilless culture system was used. The applied nutrient solution mixture was prepared in 150 ppm nitrogen (N) as NH_4NO_3; 20 ppm phosphorus (P) as H_3PO_4; 100 ppm potassium (K) as K_2SO_4; 15 ppm magnesium (Mg) as $MgSO_4$; 10 ppm sulfur (S) sulphate in the form of compounds; 5 ppm iron (Fe) as Fe-EDDHA; 3 ppm manganese (Mn) as $MnSO_4$ format; It was formed of three different solutions in 0.4 ppm boron (B) as H_3BO_3 and 0.05 ppm molybdenum (Mo) as $NH_4Mo_7O_{24}.4H_2O$. The plants were periodically fertilized once a week by introducing these three nutrient mixtures into the system. In both years of the study, the application of nutrient solution was started when the plants had 4-5 leaves and 1.0 mL of plant^{-1} from macro nutrient solution and 0.5 mL of plant^{-1} from micro nutrient solution were applied. The pH value of the deionized water used in this study was determined as 7.45 and electrical conductivity as 0.667.

In the experiment, harvesting was carried out on 4 October in 2015 and on 22 September in 2016 based on the physiological yellow maturity of the beans. The plants were harvested after 120-130 days of ripening period and the following characteristics were examined in comparison of the applications;

Plant height (cm), number of pods (number of plant^{-1}), number of branches (number of plant^{-1}), grain yield in the plant (g plant^{-1}), harvest index (%) and protein content (%) characteristics were measured (Yağmur and Aydın, 2013; Tangolar et al., 2017).

In the study, randomized experiment design variance analysis method was used in statistical evaluation of the effects of different doses of Cu and Zn applications on yield and yield components of plant and interactions of nutrient concentrations. In determining different groups; Duncan's (5%) Multiple Comparison Test (Düzgüneş et al., 1987), Costat and Mstatc package programs were used.

Results

Plant height (cm)

According to the data obtained at the end of the research, in year 2015, varieties, copper (Cu) doses and varieties x copper (Cu) interactions were significant; zinc (Zn), cultivar x zinc (Zn), copper x zinc and Ç x Cu x Zn interactions were statistically insignificant. In 2016, except for cultivar x copper (Cu) and Cultivar x Cu x Zn interactions, other differences between plant averages were significant (*Table 2*).

As shown in *Table 2*, the average plant height in 2015 and 2016 was obtained as higher in Göynük-98 (Ç1) cultivar (with 50.82-44.86 cm), compared to Yakutiye-98 (Ç2) cultivar. The average plant height values obtained from different copper doses in the experiment varied between 53.08-45.14 cm in 2015 and 46.19-41.39 cm in 2016.

http://www.aloki.hu ● ISSN 1589 1623 (Print) ● ISSN1785 0037 (Online)
DOI: http://dx.doi.org/10.15666/aeer/1802_25812598

Table 2. *Bean varieties in the groups and averages related to the height of the plant (cm)**

		2015						2016					
		Zn Doses						Zn Doses					
Variety	**Cu Doses**	**Zn1**	**Zn2**	**Zn3**	**Zn4**	**Ç x Cu. Ave.**	**Ç. Ave.**	**Zn1**	**Zn2**	**Zn3**	**Zn4**	**Ç x Cu. Ave.**	**Ç. Ave.**
Ç1	**Cu1**	47.64	44.60	49.02	50.44	47.92ABC		44.14	41.43	41.19	38.80	41.39	
	Cu2	52.00	51.58	54.49	52.18	52.56AB		46.62	45.07	50.74	40.97	45.85	
	Cu3	52.50	55.10	51.87	52.83	53.08A	50.82	46.95	42.75	50.97	44.09	46.19	44.86A
	Cu4	48.14	49.16	53.71	47.90	49.73ABC		46.90	43.48	51.15	42.54	46.02	
ÇxZn Ave.		50.07	50.11	52.27	50.84			46.15B	43.18C	48.51A	41.60D		
	Cu Doses	**Zn1**	**Zn2**	**Zn3**	**Zn4**	**Ç x Cu. Ave.**	**Ç. Ave.**	**Zn1**	**Zn2**	**Zn3**	**Zn4**	**Ç x Cu. Ave.**	**Ç. Ave.**
Ç2	**Cu1**	45.42	42.81	46.64	47.50	45.59C		45.24	44.85	42.54	43.96	44.15	
	Cu2	47.57	45.66	44.36	47.54	46.28BC		44.23	46.52	45.21	45.07	45.26	
	Cu3	45.14	48.13	46.82	44.78	46.22BC	45.80	42.89	47.11	46.27	46.80	45.77	44.63B
	Cu4	45.01	45.78	45.57	44.19	45.14C		40.78	45.78	40.35	46.41	43.34	
ÇxZn Ave.		45.79	45.60	45.85	46.00			43.29B	46.07A	43.59B	45.56A		
Zn Ave.		47.93	47.85	49.06	48.42			44.72B	44.61BC	46.05A	45.56C		
Yıl Ave.		48.31A						45.41 B					
		Zn1	**Zn2**	**Zn3**	**Zn4**	**Cu Ave.**		**Zn1**	**Zn2**	**Zn3**	**Zn4**	**Cu Ave..**	
Cu x Zn	**Cu1**	45.42	42.81	46.64	47.50	46.75B		44.69bc	43.14c	41.87d	41.38d	42.77B	
	Cu2	47.57	45.66	44.36	47.54	49.42A		45.43b	45.80b	47.98ab	43.02c	45.55A	
	Cu3	45.14	48.13	46.82	44.78	49.65A		44.92bc	44.93bc	48.62a	45.45b	45.98A	
	Cu4	45.01	45.78	45.57	44.19	47.43B		43.84c	44.63bc	45.75b	44.48bc	44.67A	
LSD $_{0.05}$		1.51						1.24					
C.V (%)		5.43						4.72					

*The difference between the averages indicated by the same letters is not significant at 5% level. Cu: Copper Dose, Zn: Zinc Dose, Ç1: Göynük-98, Ç2: Yakutiye-98, Avg.: Average, ÇxCu: Variety x Copper Dose Interaction, Ç x Zn: Variety x Zinc Dose Interaction, Cu x Zn: Copper x Zinc Dose Interaction

According to the results of the research, the plant height in the averages of in 2015 and 2016 and both year averages was obtained from the applications of 400 mg kg^{-1} Cu3 applied, respectively to Göynük-98 variety with 53.08-46.19 cm.

In the first year of the experiment, the lowest plant height was determined as 45.14 cm with 800 mg kg^{-1} Cu4 dose applied to Yakutiye-98 cultivar. In the second year, the low plant height was 41.39 cm and it was obtained from Göynük-98 variety without copper application.

It was determined that the plant height value was higher in plots with 5.0 mg kg^{-1} zinc dose applied to Göynük-98 cultivar (52.27-48.51 cm) in both years of the experiment. The shortest plant length was measured in Yakutiye-98 cultivar, where a dosage of 41.60 cm and 2.5 mg kg^{-1} zinc was applied. In similar studies on legumes, they reported that increased zinc fertilization increased plant height (Togay and Anlarsal, 2008).

In terms of zinc x copper doses applied in the study, the interaction effect between the doses in 2015 was found to be statistically insignificant. In 2016, the effect of the interaction between 5.0 mg kg^{-1} zinc dose and 800 mg kg^{-1} copper doses applied to Göynük-98 bean variety was found to be statistically significant in terms of plant height (51.15 cm) (*Table 2*).

It is known in the studies on legumes that increasing doses of zinc fertilization increases the plant height to a certain extent. However, this difference between years is

http://www.aloki.hu ● ISSN 1589 1623 (Print) ● ISSN1785 0037 (Online)
DOI: http://dx.doi.org/10.15666/aeer/1802_25812598

thought to be due to the effect of climate factors as well as the usefulness of copper applied. As a matter of fact, the expected benefit from fertilizing in terms of yield and quality in crop production depends on the application of the right fertilizer source at the right time, with the right methods and appropriate quantities.

Number of pods (pieces / plant)

According to the results of the experiment, there was a difference between the number of pods between the years. On average number of pods in 2015 copper and zinc doses, varieties x copper and varieties x zinc dose interactions were significant, varieties, copper x zinc and varieties x copper x zinc interactions were statistically insignificant. In 2016, varieties, copper, zinc, copper x zinc interactions were found to be statistically significant.

The average number of pods obtained as a result of the research was counted as 14.12 in the first year and 9.31 in the second year. According to the results obtained, the average number of pods in years for Göynük-98 variety, was respectively, 14.04-9.93 in the other varieties of Yakutiye-98 variety was determined as 14.20-8.71 (*Table 3*).

Table 3. *Averages and formed groups on number of pods in bean varieties (pieces / plant)**

		2015						2016					
		Zn Doses						Zn Doses					
Variety	**Cu Doses**	**Zn1**	**Zn2**	**Zn3**	**Zn4**	**Ç x Cu. Ave.**	**Ç. Ave.**	**Zn1**	**Zn2**	**Zn3**	**Zn4**	**Ç x Cu. Ave.**	**Ç. Ave.**
Ç1	**Cu1**	10.46	12.66	15.61	13.88	13.15AB		8.08	9.18	8.81	8.96	8.76	
	Cu2	12.53	15.21	14.71	15.15	14.40AB		8.81	9.73	10.03	12.55	10.28	
	Cu3	13.18	13.34	15.35	15.48	14.34AB	14.04	10.01	10.34	11.62	10.27	10.55	9.93A
	Cu4	14.04	12.00	15.55	15.45	14.26AB		10.28	11.30	10.02	8.80	10.10	
ÇxZn Ave.		12.55D	13.30C	15.31A	14.99B			9.30B	10.13A	10.12A	10.15A		
	Cu Doses	**Zn1**	**Zn2**	**Zn3**	**Zn4**	**Ç x Cu. Ave.**	**Ç. Ave.**	**Zn1**	**Zn2**	**Zn3**	**Zn4**	**Ç x Cu. Ave.**	**Ç. Ave.**
Ç2	**Cu1**	11.80	12.67	14.24	11.57	12.57B		7.77	8.25	7.96	7.05	7.76	
	Cu2	14.76	12.12	15.25	16.57	14.68AB		9.12	8.79	10.07	10.12	9.52	
	Cu3	16.58	14.78	17.37	16.47	16.30A	14.20	8.29	10.95	9.28	7.71	9.06	8.71B
	Cu4	13.91	11.96	13.79	13.34	13.25AB		7.74	9.88	8.39	7.93	8.48	
ÇxZn Ave.		14.26B	12.88C	15.16A	14.49B			8.23B	9.47A	8.93AB	8.19B		
Zn Ave.		13.41B	13.09B	15.23A	14.74A			8.76B	9.80A	9.52AB	9.17B		
Yıl Ave.		14.12A						9.31 B					
		Zn1	**Zn2**	**Zn3**	**Zn4**	**Cu Ave.**		**Zn1**	**Zn2**	**Zn3**	**Zn4**	**Cu Ave.**	
Cu x Zn	**Cu1**	11.13	12.67	14.93	12.73	12.86D		7.93d	8.72cd	8.39cd	8.01d	8.26B	
	Cu2	13.65	13.67	14.98	15.86	14.54B		8.97cd	9.26bc	10.05b	11.34a	9.91A	
	Cu3	14.88	14.06	16.36	15.98	15.32A		9.15bc	10.63ab	10.45ab	8.99c	9.80A	
	Cu4	13.98	11.98	14.67	14.40	13.76C		9.01c	10.59ab	9.21bc	8.35cd	9.29A	
LSD $_{0.05}$		0.80						0.73					
C.V (%)		9.88						13.64					

*The difference between the averages indicated by the same letters is not significant at 5% level. Cu: Copper Dose, Zn: Zinc Dose, Ç1: Göynük-98, Ç2: Yakutiye-98, Avg.: Average, ÇxCu: Variety x Copper Dose Interaction, Ç x Zn: Variety x Zinc Dose Interaction, Cu x Zn: Copper x Zinc Dose Interaction

According to the data obtained, the interaction of varieties x copper doses in the first year was statistically significant and the second year was insignificant on the average

http://www.aloki.hu ● ISSN 1589 1623 (Print) ● ISSN1785 0037 (Online)
DOI: http://dx.doi.org/10.15666/aeer/1802_25812598

number of pods. The highest number of broad beans was obtained from Yakutiye-98 bean cultivars with 16.30 doses of 400 mg kg^{-1} Cu3, and the lowest value was obtained from 0 mg Cu kg^{-1} Cu1 control dose in Yakutiye-98 cultivars with 12.57 units. According to these results, increasing doses of copper increased the number of pods per plant up to a certain point and then decreased.

In the study, the interaction of copper x zinc doses on the average number of pods was found statistically insignificant in the first year and significant in the second year. The highest number of pods was obtained in the first year with 16.36 units of 400 mg Cu kg^{-1} Cu3 and 5.0 mg Zn kg^{-1} Zn3. The lowest value was obtained from 0 doses of both application doses with 11.13 units (*Table 3*). In the second year of the experiment, the highest number of pods was obtained from 11.34 units of 200 mg Cu kg^{-1} Cu2 and 10.0 mg Zn kg^{-1} Zn4. The lowest value was determined in doses of 7.93 with 0 (*Table 3*). According to these results, increased zinc doses at low copper doses increased the number of pods per plant. It is known that where copper and zinc fertilizer are used together, copper x zinc decreases the efficiency of use and causes decrease in yield and quality.

Number of branches (pieces / plant)

In 2015, it was found that the number of branches, beans, zinc doses, varieties x zinc doses and copper x zinc doses interactions on the average number of branches were statistically significant. In the second year of the experiment, the effect of all application doses and interactions on the average number of branches in bean cultivars was found to be statistically insignificant (*Table 4*).

Table 4. *Groups and averages of the number of branches in bean varieties (pieces / plant)**

		2015						2016					
		Zn Doses						Zn Doses					
Variety	**Cu Doses**	**Zn1**	**Zn2**	**Zn3**	**Zn4**	**Ç x Cu. Ave.**	**Ç. Ave.**	**Zn1**	**Zn2**	**Zn3**	**Zn4**	**Ç x Cu. Ave.**	**Ç. Ave**
Ç1	**Cu1**	6.27	5.98	6.37	5.11	5.93		4.79	4.32	4.86	4.99	4.74	
	Cu2	4.77	6.59	6.65	6.42	6.11		5.41	4.58	4.64	4.10	4.68	
	Cu3	5.12	5.35	5.60	6.33	5.60	5.83B	4.65	4.14	4.26	4.66	4.43	4.58
	Cu4	5.96	5.74	6.14	4.94	5.70		4.49	4.10	4.79	4.53	4.48	
ÇxZn Ave.		5.53D	5.92B	6.19A	5.70C			4.84	4.29	4.64	4.57		
	Cu Doses	**Zn1**	**Zn2**	**Zn3**	**Zn4**	**Ç x Cu. Ave.**	**Ç. Ave.**	**Zn1**	**Zn2**	**Zn3**	**Zn4**	**Ç x Cu. Ave.**	**Ç. Ave.**
Ç2	**Cu1**	7.10	7.74	7.55	6.95	7.34		4.83	4.54	4.84	4.75	4.74	
	Cu2	6.03	7.20	6.05	7.64	6.73		4.93	5.18	5.22	5.41	5.19	
	Cu3	6.52	8.67	6.45	7.42	7.27	7.12A	5.27	5.32	4.96	4.18	4.93	4.80
	Cu4	6.99	7.63	7.30	6.74	7.17		4.55	4.37	4.36	4.16	4.36	
ÇxZn Ave.		6.66C	7.81A	6.84C	7.19B			4.90	4.84	4.85	4.63		
Zn Ave.		6.10C	6.86A	6.51AB	6.44BC			4.87	4.57	4.74	4.60		
Yıl Ave.		6.48A						4.69B					
		Zn1	**Zn2**	**Zn3**	**Zn4**	**Cu Ave.**		**Zn1**	**Zn2**	**Zn3**	**Zn4**	**Cu Ave.**	
Cu x Zn	**Cu1**	6.69b	6.86ab	6.96ab	6.03cd	6.63b		4.81	4.43	4.85	4.87	4.74	
	Cu2	5.40de	6.90ab	6.35c	7.03a	6.42b		5.17	4.88	4.93	4.76	4.93	
	Cu3	5.82d	7.01a	6.03cd	6.88ab	6.43b		4.96	4.73	4.61	4.42	4.68	
	Cu4	6.48b	6.69b	6.72ab	5.84d	6.43b		4.52	4.24	4.58	4.35	4.42	
LSD $_{0.05}$		0.40						0.34					
C.V (%)		10.79						13.01					

*The difference between the averages indicated by the same letters is not significant at 5% level. Cu: Copper Dose, Zn: Zinc Dose, Ç1: Göynük-98, Ç2: Yakutiye-98, Avg.: Average, ÇxCu: Variety x Copper Dose Interaction, Ç x Zn: Variety x Zinc Dose Interaction, Cu x Zn: Copper x Zinc Dose Interaction

http://www.aloki.hu ● ISSN 1589 1623 (Print) ● ISSN1785 0037 (Online)
DOI: http://dx.doi.org/10.15666/aeer/1802_25812598

According to the results obtained in the experiment, the average number of branches was 6.48 in the first year and 4.69 in the second year. The number of branches among the bean varieties was obtained from 5.83-4.58 plant^{-1} and Göynük-98 varieties, respectively. In the Yakutiye-98 variety, a higher number (7.12-4.80) of branching was detected (*Table 4*). According to the results obtained on the average number of branches in the first year Ç x Zn interaction was statistically significant, the second year was found to be insignificant. According to the results obtained from the experiment, the highest average branch number was obtained from 2.5 mg kg^{-1} Zn2 dose applied to Yakutiye-98 cultivar. The lowest value was obtained from the control (0 dose) application of Göynük-98 variety with 5.53 units (*Table 4*).

As shown in *Table 4*, the effect of Cu x Zn interaction on the mean number of branches was significant ($p<0.01$). The highest average number of branches was obtained from 7.03 Zn4 dose of 200 mg kg^{-1} Cu2 x 10.0 mg kg^{-1}. The lowest value was measured with 5.40 units of 200 mg kg^{-1} Cu2 x 0 mg kg^{-1} Zn1 control dose.

Harvest index (%)

It was determined that the factors other than cultivars, copper doses, varieties x copper dose interactions were insignificant on the harvest index of bean cultivars in 2015.

In 2016, the effect of varieties, copper and zinc doses, cultivar x zinc and Ç x Cu x Zn interactions on harvest index averages were found to be statistically significant (*Table 5*).

Table 5. *Groups and averages of harvest index in bean varieties(%)**

		2015						2016					
		Zn Doses						Zn Doses					
Variety	**Cu Doses**	**Zn1**	**Zn2**	**Zn3**	**Zn4**	**Ç x Cu Ave.**	**Ç. Ave.**	**Zn1**	**Zn2**	**Zn3**	**Zn4**	**Ç x Cu Ave.**	**Ç. Ave.**
Ç1	**Cu1**	34.51	37.12	39.39	36.18	36.80C		37.51cd	37.90c	38.22c	39.40bc	38.26	
	Cu2	40.65	39.54	40.54	43.40	41.03A		38.52c	42.49a	41.90ab	40.66b	40.89	
	Cu3	40.28	41.69	40.56	40.70	40.81B	38.83B	39.76bc	41.26ab	39.66bc	39.07bc	39.94	39.38B
	Cu4	39.21	35.60	37.27	34.59	36.67C		34.85e	40.58b	41.64ab	36.61d	38.42	
ÇxZn Ave.		38.66	38.49	39.44	38.72			37.66C	40.56A	40.36A	38.94B		
	Cu Doses	**Zn1**	**Zn2**	**Zn3**	**Zn4**	**Ç x Cu. Ave.**	**Ç. Ave.**	**Zn1**	**Zn2**	**Zn3**	**Zn4**	**Ç x Cu. Ave.**	**Ç. Ave.**
Ç2	**Cu1**	44.25	42.44	43.68	42.04	43.10C		41.73cd	44.37b	43.18	42.79c	43.02	
	Cu2	48.03	40.92	45.44	45.21	44.90A		45.20ab	44.08b	44.57b	45.99ab	44.96	
	Cu3	44.72	42.43	45.39	43.34	43.97B	44.03A	45.51ab	43.46bc	46.56a	46.52a	45.51	44.07A
	Cu4	43.24	46.42	47.05	39.94	44.16AB		43.30bc	42.60c	41.97cd	43.30bc	42.79	
ÇxZn Ave.		45.06	43.05	45.39	42.63			43.94B	43.63B	44.07A	44.65A		
Zn Ave.		41.86	40.77	42.42	40.68			40.80B	42.09A	42.21A	41.79AB		
Yıl Ave.		41.43A						41.72B					
		Zn1	**Zn2**	**Zn3**	**Zn4**	**Cu Ave.**		**Zn1**	**Zn2**	**Zn3**	**Zn4**	**Cu Ave.**	
Cu x Zn	**Cu1**	39.38	39.78	41.54	39.11	39.95B		39.62	41.14	40.70	41.10	40.64B	
	Cu2	44.34	40.23	42.99	44.31	42.97A		41.86	43.29	43.24	43.33	42.93A	
	Cu3	42.50	42.06	42.98	42.02	42.39A		42.64	42.36	43.11	42.80	42.73A	
	Cu4	41.23	41.01	42.16	37.27	40.42B		39.08	41.59	41.81	39.96	40.61B	
LSD $_{0.05}$		1.53						1.02					
C.V (%)		6.42						4.26					

*The difference between the averages indicated by the same letters is not significant at 5% level. Cu: Copper Dose, Zn: Zinc Dose, Ç1: Göynük-98, Ç2: Yakutiye-98, Avg.: Average, ÇxCu: Variety x Copper Dose Interaction, Ç x Zn: Variety x Zinc Dose Interaction, Cu x Zn: Copper x Zinc Dose Interaction

http://www.aloki.hu ● ISSN 1589 1623 (Print) ● ISSN1785 0037 (Online)
DOI: http://dx.doi.org/10.15666/aeer/1802_25812598

According to the results obtained at the end of the research, harvest index was found to be 38.83-39.38% in Ç1 (Göynük-98) and 44.03-44.07% in Ç2 (Yakutiye-98). In this research, the highest harvest index average was obtained from Ç2 according to the results of both years. It is thought that this difference, which occurred a little between the years, is due to environmental factors, genotype and cultural practices.

In the study, average harvest index values obtained from different copper doses applications varied between 42.97-39.95% in 2015 and 42.93-40.6% in 2016 (*Table 5*). According to the results of the study, the highest harvest index in 2015 and 2016 and the average of both years was obtained from 200 mg kg^{-1} Cu2 dose applied to Ç2 (Yakutiye-98) with 44.90-45.51%, respectively. In the first year of the experiment, the lowest harvest index value was found to be 800 mg Cu kg^{-1} Cu4 administered to Ç1 with 36.67%. In the second year, the lowest harvest index was obtained from the parcel without copper applied to Ç1 with 38.26%. Eren and Mert (2016) investigated the effect of increasing Cu applications on the growth and development of plants and found that the lowest plant dry weight of the plants was 2.28 g $plant^{-1}$ and 800 mg Cu kg^{-1} application and control application.

As it can be seen in *Table 5*, zinc (Zn) and Ç x Zn dose interactions on the average harvest index were found to be statistically insignificant and significant in the second year. According to the results obtained from the experiment, the highest harvest index was obtained from the dose of 5.0 mg kg^{-1} Zn3 applied to Ç2 (Yakutiye-98) with 42.21%. The lowest value was obtained from control (0 dose) application of Ç1 (Göynük-98) with 37.66% (*Table 5*). In the study, it was observed that increasing the dose of Çx Zn increased the harvest index up to a certain point. Taban and Alpaslan (1996) from the soil to the corn plant; in a similar study by applying 0, 2.5, 5.0 and 10.0 mg Zn kg^{-1}, the highest increase in dry weight (67.3% increase) was obtained from the dose of 5.0 mg Zn kg^{-1} applied to flowerpot-1 with 14.96 g.

According to the results, the effect of cultivars x Cu x Zn interactions on the harvest index was statistically insignificant in the first year and was significant in the second year. The average harvest index values were 34.51-48.03% in 2015 and 34.85-46.56% in 2016 (*Table 5*). In the second year, the highest harvest index was obtained from interaction of doses of 400 mg Cu kg^{-1} Cu3 x 5.0 mg Zn kg^{-1} Zn3 applied to Yakutiye-98 cultivar with 46.56% (Z2 x Cu3 x Zn3). The lowest value of 34.85% Göynük-98 variety was obtained from the application of 800 mg kg^{-1} Cu4 x Zn1 control (0 dose) (*Table 5*).

Grain yield in the plant (g / plant)

On the average seed yield in bean plant of different phosphorus and zinc doses in 2015 and 2016 research years; cultivar, copper, zinc, cultivar x copper, cultivar x zinc, copper x zinc and cultivar x copper x zinc interactions were found to be statistically significant (*Table 6*). Average seed yields in per plant obtained at the end of the experiment were measured as 23.49 g $plant^{-1}$ in the first year and 18.72 g $plant^{-1}$ in the second year.

According to the results, average seed yield of Göynük-98 bean cultivar was 19.35-16.87 g $plant^{-1}$ over the years, while it was 27.63-20.58 g $plant^{-1}$ in Yakutiye-98 cultivar. Düzdemir and Akdağ (2001) in their study; reported that the mean seed yield in the plant was between 10.20-27.40 g $plant^{-1}$. In the study of by Bildirici and Baran (2018) in under the ecological conditions of Van-Gevaş, the seed yields of Akman-98 and Göynük-98 varieties were determined as 9.82-13.44 g $plant^{-1}$, respectively. Seed

http://www.aloki.hu ● ISSN 1589 1623 (Print) ● ISSN1785 0037 (Online)
DOI: http://dx.doi.org/10.15666/aeer/1802_25812598

yield in beans shows dependence on other genetic-based variations, especially earliness in different environmental conditions.

Table 6. *Groups and averages of grain yield in bean varieties (g /plant)**

		2015						2016					
		Zn Doses						Zn Doses					
Variety	**Cu Dose**	**Zn1**	**Zn2**	**Zn3**	**Zn4**	**Ç x Cu Ave.**	**Ç. Ave.**	**Zn1**	**Zn2**	**Zn3**	**Zn4**	**Ç x Cu Ave.**	**Ç. Ave.**
Ç1	**Cu1**	12.02fg	19.15bc	18.65bc	21.54ab	17.84D		15.97c	18.45ab	14.65cd	17.15bc	16.55B	
	Cu2	20.17b	22.40a	21.57ab	19.83b	21.00A		17.92b	18.94ab	19.38a	19.50a	18.93A	
	Cu3	17.02cd	17.00cd	21.11ab	22.58a	19.43B	19.35B	18.50ab	19.58a	17.90b	17.19bc	18.30A	16.87B
	Cu4	21.43ab	18.19c	18.18c	18.76bc	19.14C		13.62d	18.24ab	12.07de	10.85ef	13.69C	
Ç x Zn Ave.		17.66 D	19.20 C	19.88 B	20.68 A			16.50 B	18.79 A	16.00 C	16.17 C		
	Cu Dose	**Zn1**	**Zn2**	**Zn3**	**Zn4**	**Ç x Cu Ave.**	**Ç. Ave.**	**Zn1**	**Zn2**	**Zn3**	**Zn4**	**Ç x Cu Ave.**	**Ç. Ave.**
Ç2	**Cu1**	21.51f	19.35g	27.24de	23.65de	260.13B		12.18cd	16.19bc	20.74b	21.94ab	17.76C	
	Cu2	28.12d	30.94b	33.83ab	31.27ab	343.93A		17.86bc	24.33ab	28.45a	24.69a	23.83A	
	Cu3	29.36c	29.21c	36.32a	31.11c	342.19A	27.63A	13.88c	26.06a	20.28ab	20.28b	20.63B	20.58A
	Cu4	22.69f	23.61ef	25.01e	24.51de	269.64B		16.47bc	21.80ab	22.08b	22.08ab	20.09B	
Ç x Zn Ave.		25.42	25.78	30.61	28.73			15.10	22.09	22.87	22.25		
Zn Ave.		21.54C	22.48B	25.24A	24.71A			15.80C	20.45A	19.43AB	19.21B		
Year Ave.		23.49						18.72					
		Zn1	**Zn2**	**Zn3**	**Zn4**	**Cu Ave.**		**Zn1**	**Zn2**	**Zn3**	**Zn4**	**Cu Ave.**	
Cu x Zn	**Cu1**	16.76fg	19.25f	22.94cd	20.74c	20.74D		14.08e	17.32cd	17.69cd	19.55bc	17.16C	
	Cu2	24.15c	26.67b	27.71ab	27.71b	26.13A		17.89cd	21.64ab	23.92a	22.10ab	21.39A	
	Cu3	23.19cd	23.10cd	28.72a	28.72b	25.27B		16.19d	22.82a	20.09b	18.74c	19.46B	
	Cu4	22.06d	20.90de	21.60d	21.60cd	21.83C		15.05de	20.02b	16.03d	16.47d	16.89C	
LSD $_{0.05}$		8.27						11.62					
C.V (%)		5.56						9.79					

*The difference between the averages indicated by the same letters is not significant at 5% level. Cu: Copper Dose, Zn: Zinc Dose, Ç1: Göynük-98, Ç2: Yakutiye-98, Avg.: Average, ÇxCu: Variety x Copper Dose Interaction, Ç x Zn: Variety x Zinc Dose Interaction, Cu x Zn: Copper x Zinc Dose Interaction

The effects of copper fertilizer on average seed yield in the plant of beans were found to be statistically significant. The highest seed yield was obtained from the doses of 31.27-23.83 g plant^{-1} and 200 mg kg^{-1} Cu2 in Yakutiye-98 cultivars in both years of the experiment. The lowest value for years 17.84-13.69 g plant^{-1} and 0 fertilizer dose of copper and copper (800 mg kg^{-1} Cu4) dose was determined in the parcels applied (*Table 6*). As seen in *Table 6*, the effect of zinc doses on average seed yields of bean cultivars was found to be significant. Average highest seed yields obtained in the experiment over the years for Yakutiye-98 bean cultivar 30.61-22.87 g plant^{-1} and 5.0 mg Zn kg^{-1} Zn3 dose was obtained from the application. The lowest yield values (25.42-15.10 g plant^{-1}) in 0 zinc dose (Zn1) was measured in Göynük-98 bean cultivar.

The effect of copper and zinc doses on the average seed yield of beans was significant ($p< 0.01$). The highest average seed yield in both years of the study was obtained from 28.72-23.92 g plant^{-1}, 200-400 mg kg^{-1} copper and 5.0 mg kg^{-1} Zn3 zinc, respectively. The lowest yield value in two years 16.76-14.08 g plant^{-1}, respectively with 0 copper and zinc fertilizer dose was obtained from parcels (*Table 6*). The effect of copper and zinc fertilizer doses on average seed yield of bean cultivars was found to be statistically significant in both years. The highest average seed yield was obtained from

http://www.aloki.hu ● ISSN 1589 1623 (Print) ● ISSN1785 0037 (Online)
DOI: http://dx.doi.org/10.15666/aeer/1802_25812598

Yakutiye-98 cultivar in 36.32-28.45 g plant^{-1} and 400 mg kg^{-1} Copper (Cu3) x 5.0 mg kg^{-1} Zinc (Zn3) application in two years. Low values 12.01-10.85 g plant^{-1} were obtained from Ç1 (Göynük-98) variety, in the cases of 0 dose and 800 mg kg^{-1} copper-zinc dose (Cu4 x Zn4) applications (*Table 6*).

Crude protein content (%)

As a result of the research, the interactions of the varieties, varieties x zinc, varieties x copper doses and copper x zinc doses were found to be statistically significant on the crude protein content of the grains obtained. Protein ratio by years are as follows: while Göynük-98 variety was obtained with 21.93-22.01%, 22.06-21.45% protein ratios were obtained from Yakutiye-98 variety (*Table 7*).

Table 7. *Groups and averages of crude protein ratios in bean varieties(%)**

		2015						2016					
		Zn Doses						Zn Doses					
Variety	**Cu Doses**	**Zn1**	**Zn2**	**Zn3**	**Zn4**	**Ç x Cu. Ave.**	**Ç. Ave.**	**Zn1**	**Zn2**	**Zn3**	**Zn4**	**Ç x Cu. Ave.**	**Ç. Ave.**
Ç1	**Cu1**	19.74	22.89	22.94	20.43	21.50		20.75	22.87	22.56	20.41	21.65	
	Cu2	21.29	22.48	24.16	20.92	22.21		22.66	22.45	23.35	21.05	22.38	
	Cu3	20.36	23.55	23.06	22.75	22.43	21.93	20.71	23.52	22.61	22.74	22.40	22.01A
	Cu4	20.50	21.83	22.82	21.23	21.60		20.72	21.86	22.44	21.47	21.62	
ÇxZn Ave.		20.47D	22.69B	23.25A	21.33C			21.21B	22.68A	22.74A	21.42B		
	Cu Doses	**Zn1**	**Zn2**	**Zn3**	**Zn4**	**Ç x Cu. Ave.**	**Ç. Ave.**	**Zn1**	**Zn2**	**Zn3**	**Zn4**	**Ç x Cu. Ave.**	**Ç. Ave.**
Ç2	**Cu1**	21.99	22.88	22.62	21.15	22.16		20.99	22.04	22.25	22.03	21.83	
	Cu2	21.81	22.68	22.14	22.43	22.27		21.76	21.93	21.76	22.21	21.92	
	Cu3	20.75	21.64	22.79	23.67	22.21	22.06	20.63	21.64	21.61	21.37	21.31	21.45B
	Cu4	20.41	21.26	21.93	22.84	21.61		20.40	20.37	20.81	21.43	20.75	
ÇxZn Ave.		21.24B	22.12A	22.37A	22.52A			20.95B	21.50A	21.61A	21.76A		
Zn Ave.		20.86C	22.40AB	22.81A	21.93B			21.08C	22.09AB	22.17A	21.59BC		
Yıl Ave.		22.00						21.73					
		Zn1	**Zn2**	**Zn3**	**Zn4**	**Cu Ave.**		**Zn1**	**Zn2**	**Zn3**	**Zn4**	**Cu Ave.**	
Cu x Zn	**Cu1**	20.87bc	22.89ab	22.78ab	20.79bc	21.83AB		20.87	22.46	22.41	21.22	21.74AB	
	Cu2	21.55b	22.58ab	23.15a	21.68b	22.24A		22.21	22.19	22.56	21.63	22.15A	
	Cu3	20.56bc	22.60ab	22.93ab	23.21a	22.32A		20.67	22.58	22.11	22.06	21.85A	
	Cu4	20.46bc	21.55b	22.38ab	22.04ab	21.60B		20.56	21.12	21.63	21.45	21.19B	
LSD $_{0.05}$		0.51						0.54					
C.V (%)		4.02						4.34					

*The difference between the averages indicated by the same letters is not significant at 5% level. Cu: Copper Dose, Zn: Zinc Dose, Ç1: Göynük-98, Ç2: Yakutiye-98, Avg.: Average, ÇxCu: Variety x Copper Dose Interaction, Ç x Zn: Variety x Zinc Dose Interaction, Cu x Zn: Copper x Zinc Dose Interaction

The effect of different zinc doses on protein ratios in beans was found to be statistically significant in both years. The highest crude protein content by years with 5.0 mg Zn kg^{-1} was obtained from Göynük-98 bean cultivar with 23.25-22.74%, the lowest values were obtained from 0 dose application of 20.47-20.95%.

As shown in *Table 7*, the effect of copper doses on average crude protein ratios in beans was significant in 2015-16 ($p < 0.05$). The highest crude protein content was obtained from 200-400 mg kg^{-1} copper applications with 22.15-22.32%. The lowest value was found to be 800 mg Cu kg^{-1} copper (Cu4) with 21.19-21.60% (*Table 7*).

http://www.aloki.hu ● ISSN 1589 1623 (Print) ● ISSN1785 0037 (Online)
DOI: http://dx.doi.org/10.15666/aeer/1802_25812598

Discussion

In addition, plant height values were lower in both cultivars in the second year than in the first year. According to the first year of the experiment, due to the high average temperature and the lack of moisture due to the decrease in the time from the output to ripening caused the plant height values to decrease. It is thought that this difference is caused by climate in terms of plant height values between years (Elkoca and Kantar, 2004). It is thought that this difference between the years is due to the effect of climate factors as well as the usefulness of the applied copper. Çopur and Sarı (2012) in the study of the effect of $CuSO_4.5H_2O$ on the growth of cucumber seedlings concluded that applications are significant in terms of seedling length. Seedling height of 9.53 cm of the highest seedlings with copper sulfate 4000 + 4000 mg / l were detected in the application. Zengin and Munzuroğlu (2004) investigated the effects of mercury, copper, cadmium and lead on the amount of growth hormone cytokine in bean seedlings. In their study, control seedlings and seedlings grown in 0.1, 0.2 and 0.3 mM $CuCl_2$ solutions were measured the cytokine content of 1.83x10-7, 4.42x10-7, 3.77x10-7, 3.66x10-7 and 3.55x10-7 M, respectively. They stated that growth is supported up to a point, increasing the dose of copper decreases the cytokinin level of the seedlings and this situation occurs due to increase in copper concentration. These results are consistent with our findings.

Yağmur and Aydın (2013) applied 10, 20 and 30 mg Zn kg-1 (ZnSO4.7H2O) in the soil and in addition 0.1%, 0.2% and 0.3% ZnSO4.7H2O solution to the leaves in lettuce cultivation. The highest plant height (22.25 cm and 21.10 cm) was obtained from applications of 20 mg kg-1 zinc to the soil and 0.2% zinc to the leaves. The results obtained support our study.

Elkoca and Kantar (2004), in a similar study conducted by the number of pods between 3.5-4.2 on this variety showed a wide variation according to the variety and lines. Sönmez et al. (2006b) applied 1000 and 2000 mg Cu kg^{-1} yield in tomatoes grown in the greenhouse yield, fruit number, dry root weight and plant height were reported to decrease with the amount of Cu in the soil. This study supports our findings. In a similar study Yağmur and Aydın (2013) applied Zn in the form of 0.1%, 0.2% and 0.3% $ZnSO_4.7H_2O$ solution from the leaf in addition to 10, 20 and 30 mg Zn kg^{-1} ($ZnSO_4.7H_2O$) doses. As a result of the research, they were obtained the highest plant height (22.25 cm and 21.10 cm) by applying 20 mg kg^{-1} zinc to the soil and 0.2% Zinc dose to the leaf. The results obtained from these studies are in parallel with the findings of our research.

It is thought that this difference in average number of branches over the years is due to the differences in the amount of humidity and temperature in the greenhouse as well as genetic factors (Elkoca and Kantar, 2004). Babagil et al. (2011) stated that they measured the maximum number of branches in 3.1 beans-1 and Yakutiye-98 cultivars in their study with 6 bean cultivars under Erzurum conditions. Kumar et al. (1993) reported that zinc doses applied to the soil between 0 and 5 kg da^{-1} increase the yield and decrease at the next doses. Similar results have been obtained in many studies (Azad et al., 1993; Yağmur and Aydın, 2013). Unlike nitrogenous fertilizers, the effect of micro nutrients on the number of branches depends on the environment and genetic structure. In the study, increasing dose of Cu x Zn increased the number of pods per plant up to a certain point. Wang et al. (2016) in a similar study conducted in China on Indian beans; reported that Cu and Zn interactions applied at low concentrations in the soil caused a slight increase in the growth of the plant, whereas high concentrations

http://www.aloki.hu ● ISSN 1589 1623 (Print) ● ISSN1785 0037 (Online)
DOI: http://dx.doi.org/10.15666/aeer/1802_25812598

showed a significant decrease in plants height and biomass. We can assume that the interaction of Cu and Zn is clear. Zn, Cd and Cu interactions related to the similar results have been reported about the interactions (Chizzola and Mitteregger, 2005; Chaoui et al., 2017).

Gangwar and Singh (1986), in their studies of zinc fertilizer increases the rate of harvest index rate has been reported that the maximum rate is taken from the applied foliar fertilizer. Azad et al. (1993) reported that zinc fertilizers increased the harvest index rate up to a certain dose and then decreased. In this study, it was observed that zinc fertilizer increased the harvest index rate up to 2.5 and 5.0 mg Zn kg^{-1} and then started to decrease. MacFarlane and Burchett (2002), in their study applied an increasing doses from 100 μg Cu g^{-1} to 400 μg Cu g^{-1} reported a reduction in total plant biomass and a decline in root growth. Therefore, similar results were obtained in this study as in many fertilization studies (Pholsen and Sormsungnoen, 2005; Barros et al., 2007). According to some other studies, it has been reported that the green parts and grain contents of wheat plant increase with Zn application and this increase varies according to varieties (Helaloğlu et al., 1997). Many of these studies support our findings.

It is known that there is an antagonistic effect between Cu and Zn ions (Aktaş, 1991; Chizzola and Mitteregger, 2005). Wang et al. (2016) stated that Cu and Zn interactions applied at low concentrations in the soil caused a slight increase in the growth of the plant, whereas a significant decrease in plant height and biomass was observed in high concentrations. The most important factor in determining fate of crop production is undoubtedly the growing conditions and climate factors. It is thought that this difference between years is mainly due to the fact that the average temperature and distribution in the first year(21.3 ^{o}C) is higher compared to the second year (17.90 ^{o}C). In addition, the bean is very sensitive to the water balance in the soil during the flowering period. It has been reported that fluctuations in this period cause 20% yield losses in grain yield. In the first year of the research, the average temperature has been identified to be higher than the second year, especially during the flowering and pollination periods (Elkoca and Kantar, 2004). Seed yield in bean plants shows dependence on earliness of different environmental conditions in genetic variations. In the study, it was observed that the average seed yield of varieties increased up to 200 mg kg^{-1} copper dose in parallel with the increasing copper doses, and it caused decreases in seed yield in subsequent doses (Wang et al., 2016). Sönmez et al. (2006b) 1000 and 2000 mg Cu kg^{-1} applied to the soil in greenhouse grown tomatoes; reported that yield, fruit number, dry root weight and plant height decreased with high Cu doses such as. This study supports our findings. It is estimated that the difference between the first and second year zinc doses of the study is due to the fact that copper inhibits the zinc uptake more than the second year.

In the first year, it is estimated that fertilizers are used more beneficially due to the favorable conditions of the average temperature and climate (Taban et al., 1997; Toğay and Anlarsal, 2008). In studies where copper and zinc fertilizer are used together, it is known that copper x zinc increases the efficiency of use, decreases soil pH, increases total N and P intake and has a positive effect on yield and quality (Sönmez et al., 2006a). In this study, it has been found that increasing doses of Ç x Cu x Zn increases the seed yield up to a certain point (Wang et al., 2016). Sonmez et al. (2006a) found that the effect of Cu applications on soil, which Zn contents was increased by 5% was significant. This study in bean is in agreement with the results of many researchers.

http://www.aloki.hu ● ISSN 1589 1623 (Print) ● ISSN1785 0037 (Online)
DOI: http://dx.doi.org/10.15666/aeer/1802_25812598

In many studies, it has been determined that the protein content of bean grains varies between 17.40% and 28.00% according to the varieties and applications. It was stated that bacterial applications, especially nitrogen fertilization, increased this rate (Tajini et al., 2012). The effect of zinc fertilizer on crude protein content was found to be important depending on environmental and genotypic factors. Similar results have been obtained in other studies conducted on legume plants (Toğay and Anlarsal, 2008). Zinc is an active element in biochemical processes as well as has a biological interaction. When zinc (Zn^{++}) is used together with copper (Cu^{++}), an increase in uptake occurs by plants (Sönmez et al., 2006a; Wang et al., 2016). According to some other studies; Leaf and soil zinc sulphate applications to watermelon, grapes, wheat, lentils, spinach have been found to have a positive effect on quality components yield, yield components of different crop plants, vegetative growth and development (Kaya et al., 20018).

Conclusion

In this study carried out as a greenhouse experiment in Van-Gevaş ecological conditions, the effect of different copper-zinc dose and applications and interactions on the yield and yield characteristics of dry bean cultivars grown in soilless systems were investigated. Although these factors have changed over the years, they have provided important information in terms of yield and yield components. The use of zinc at increasing copper doses and the decrease in efficacy and it has been seen decline in yield and quality parameters too. Soil analysis should be done before sowing in culture plants, especially legumes, in our province where zinc deficiency is seen too much. Based on these results, in case of deficiency, copper fertilization between 2.5-5.0 mg Zn kg^{-1} zinc and 200-400 mg Cu kg^{-1} can be performed. It is known that copper zinc increases usage efficiency, decreases soil pH, increases total N and intake P contents, and has a positive effect on yield and quality. However, it should not be ignored that it may have toxic effects in overuse. In general, the interaction of copper-zinc concentrations examined did not reach the degree of toxic effect in the plant.

As a result, co-administration of copper-zinc interactions, 400 mg kg^{-1} Cu and 5.0 mg kg^{-1} Zn doses resulted in an increase in yield and yield parameters in bean compared to the separate administration of these doses and was found to be statistically significant at 1% level. It is thought that this study will contribute to the new studies to reduce the yield and quality losses that may occur due to Zn deficiency, Cu excess or interactions in agricultural soils.

REFERENCES

[1] Aktaş, M. (1991): Plant Nutrition and Soil Fertility. – AÜ Faculty of Agriculture Publications: 1202, Textbook: 347, Ankara, 345 p.

[2] Azad, A. S., Manchada, J. S., Gill, A. S., Bains, S. S. (1993): Effect of Zinc Application on Glrain Yield, Yield Components and Nutrient Content of Lentil. – Lens Newsletter 20(2): 30-33.

[3] Babagil, G., Tozlu, E., Dizikısa, T. (2011): Determination of Yield and Yield Components of Some Haricot Bean (*Phaseolus vulgaris* L.) Genotypes Grown in Erzincan and Hınıs Ecological Conditions. – Atatürk University Journal of the Faculty of Agr. Sci 42(1): 11-17.

http://www.aloki.hu ● ISSN 1589 1623 (Print) ● ISSN1785 0037 (Online)
DOI: http://dx.doi.org/10.15666/aeer/1802_25812598

[4] Barros, I., Gaiser, T., Lange, F. M., Römheld, V. (2007): Mineral nutrition and water use patterns of a maize/cowpea ıntercrop on a highly acidic soil of the tropic semiarid. – Field Crops Research 101: 26-36.
[5] Bildirici, N., Demir, C., Demir, H. (2016): Effects of Heavy Metals on Bean Plant. – Int. Environmental Application & Sci. 11(3): 267-269.
[6] Bildirici, N., Baran, İ. (2018): Determine of Yield and Yield Components of Some Dry Bean (*Phaseolus vulgaris* L.) Varieties and One Local Ahlat Population in The Van-Gevaş Ecological Conditions. – International Journal of Research In Agricultural and Food Sciences 10(1): 2311-2476.
[7] Bolat, İ., Kara, Ö. (2017): Plant Nutrients: Sources, Functions, Deficiencies and Excesses. – Bartin Orman Fakültesi Dergisi 19(1): 218-228. (in Turkish).
[8] Buttaro, D., Serio, F., Santamaria, P. (2012): Soilless greenhouse production of table grape under Mediterranean conditions. – Journal of Food, Agriculture & Environment 10(2): 641-645.
[9] Chaoui, A., Ghorbal, M. H., Ferjani, E. (2017): Effects of cadmium-zinc interactions on hydroponically grown bean (*Phaseolus vulgaris* L.). – Plant Science 126(1997): 21-28.
[10] Chizzola, R., Mitteregger, U. S. (2005): Cadmium and zinc interactions in trace element accumulation in chamomile. – J. Plant Nutr 28(8): 1383-1396.
[11] Çopur, H., Sarı, N. (2012): The effects of paclobutrazole and copper sulphate applications on seedling growth in greenhouse cucumber seedlings. – J. Agric. Fac. ÇÜ 27(1): 1-12.
[12] Dağhan, H., Öztürk, M. (2015): Soil pollution in Turkey and remediation methods. – In: Hakeem, K. R., Sabir, M., Ozturk, M., Mermut, A. (eds.) Soil Remediation and Plants: Prospects and Challenges. September 2015, Academic Press, Elsevier, New York, pp. 287-312.
[13] Di Lorenzo, R., Pisciotta, A., Santamaria, P., Scariot, V. (2013): From soil to soilless in horticulture: Quality and typicity. – Italian Journal of Agronomy 8(4): 255-260.
[14] Düzdemir, O., Akdağ, C. (2001): Türkiye Kuru Fasulye (*Phaseolus vulgaris* L.) Gen Kaynaklarının Karakterizasyonu: 2. Verim ve Diğer Bazı Özellikleri. – GOÜ Ziraat Fakültesi Dergisi 18(1): 101-105.
[15] Düzgüneş, O., Kesici, T., Koyuncu, O., Gürbüz, F. (1987): Research and Experimental Methods. – AÜ Faculty of Agriculture Publications: 1021, Textbook: 295, S.381.
[16] Elkoca, E., Kantar, F. (2003): Determination of early and high yield dry bean (*Phaseolus vulgaris* L.) genotypes suitable for erzurum ecological conditions. – Atatürk Univ. Journal of Agriculture Sci 35(3-4): 137-142.
[17] Eren, A., Mert, M. (2016): Investigation of table grape cultivation in soilless culture system. – Turkey Agricultural Research Journal 4(1): 50-58.
[18] FAO. (2017): Agricultural Statistics. – http://faostat3.fao.org/browse/Q/QC/E (13.05.2019).
[19] Gangwar, K. S., Singh, N. P. (1986): Effect of Zinc Application on Yield and Quality of Lentil (*Lens culinaris* Medic.). – Legume Research 11(1): 11-14.
[20] Gül, A. (2008): Soilless Agriculture. – Hasad Publishing, İstanbul, 135p.
[21] Helaloğlu, C., Torun, B., Tolay, İ., Çakmak, İ. (1997): Reactions of various wheat genotypes to zinc fertilization in Harran plain irrigated conditions and selection of zinc deficiency resistant genotypes. – I. National Zinc Congress, May 12-16, 1997, Eskisehir, Journal of Bartin Faculty of Forestry 19(1): 218-228.
[22] Kacar, B., Katkat, V. (2006): Plant nutrition. – Nobel Publication, Number: 849.
[23] Kaplan, M. (1999): Accumulation of Copper in Soils and Leaves of Tomato Plants in Greenhouses in Turkey. – Journal of Plant Nutrition 22(2): 237-244.
[24] Karaca, A., Turgay, O. C. (2012): Soil pollution. – Journal of Soil Science and Plant Nutrition 1(1): 13-19.
[25] Kaya, Y., Zengin, M., Yılmaz, F. G., Gezgin, S. (2018): Effects of gibberellic acid and zinc applications on yield and yield components of lettuce. – SÜ J Agr Food Sci 32(3): 373-380.

http://www.aloki.hu ● ISSN 1589 1623 (Print) ● ISSN1785 0037 (Online)
DOI: http://dx.doi.org/10.15666/aeer/1802_25812598

[26] Kumar, P., Agarwal, J. P., Chandra, S. (1993): Effect of inoculation, nitrogen and phosphorus fertilization on growth and yield of lentil. – Lens newsletter 20(1): 57-59.
[27] Lindsay, W. L., Norvell, W. A. (1978): Development of a DTPA soil test for zinc, iron, manganese, and copper. – Soil Science Society of America Journal 42: 421-428.
[28] MacFarlane, G. R., Burchett, M. D. (2002): Toxicity, growth and accumulation relationships of copper, lead and zinc in grey mangrove Avicennia marina (Forsk.) Vierh. – Marine Environmental Research 54(1): 65-84.
[29] Marschner, H. (1997): Minereal Nutrition of Higher Plants. – Institute of Plant Nutrition, University of Hohenheim. Academic Press, Inc., Sandiego, CA 9210, Germany, 889p.
[30] McCauley, A., Jones, C., Jacobsen, J. (2009): Nutrient Management. – Nutrient management module 9 Montana State University Extension Service 4449-9: 1-16.
[31] Öktüren Asri, F., Sönmez, S. (2007): The Effect of Heavy Metal Toxicity on Plant Metabolism. – Derim 23(2): 36-45.
[32] Pholsen, S., Sormsungnoen, N. (2005): Effects of nitrogen and potassium rates and planting distances on growth, yield and fodder quality of a forage sorghum (*Sorghum bicolor* L.). – Pakistan Journal of Biological Sciences 7: 1793-1800.
[33] Plaster, E. J. (1992): Soil Science and Management. – 2nd Edition, Delmar Publishers Inc., Albany, New York, USA.
[34] Raven, J. A., Evans, M. C. W., Korb, R. E. (1999): The role of trace metals in photosynthetic electron transport in O2-evolving organisms. – Photosynth. Res. 60(2-3): 111-149.
[35] Rout, G. R., Das, P. (2003): Effect of metal toxicity on plant growth and metabolism: I. Zinc. – Agronomie 23: 3-11.
[36] Sönmez, S., Kaplan, M., Sönmez, N. K., Kaya, H. (2006a): The effect of copper applications from soil on soil pH and plant nutrient contents. – J. Mediterranean Agricultural Sciences 19(1): 151-158.
[37] Sönmez, S., Kaplan, M., Sönmez, N. K., Kaya, H., Uz, İ. (2006b): High level of copper application to soil and leaves reduce the growth and yield of tomato plants. – Sci. Agric. (Piracicaba, Braz.) 63(3): 213-218.
[38] Sossé, B. A., Genet, P., Dunand-Vinit, F., Toussaint, L. M., Epron, D., Badot, P. M. (2004): Effect of copper on growth in cucumber plants (*Cucumis sativus*) and its relationships with carbonhydrate accumulation and changes in ion contents. – Plant Science 166: 1213-1218.
[39] Şehirali, S. (1988): Yemeklik Tane Baklagiller. – AÜ Ziraat Fakültesi Yayınları 1089, Ders Kitabı: 314.
[40] Taban, S., Alpaslan, M. (1996): Effect of Zinc Fertilization on Zinc, Iron, Copper, Manganese and Chlorophyll Content of Corn Plant. – Pamukkale University, Journal of Engineering Sciences 2(1): 69-73.
[41] Taban, S., Alpaslan, M., Güneş, A., Aktaş, M., Erdal, İ., Eyüboğlu, H., Baran, İ. (1997): The effect of zinc applied in different forms on yield and biological usefulness of wheat in wheat plant. – I. National Zinc Congress, May 12-16, 1997, Eskisehir.
[42] Tajini, F., Trabelsi, M., Drevon, J. (2012): Combined Inoculation with Glomus Intraradices and Rhizobium tropici CIAT 899 Increases Phosphorus Use Efficiency for Symbiotic Nitrogen Fixation in Common Bean (*Phaseolus vulgaris* L.). – Saudi Journal of Biological Sciences 19: 157-163.
[43] Tangolar, S., Tangolar, S., Alkan Torun, A., Tarım, G., Ada, M. (2017): Investigation of table grape cultivation in soilless culture system. – Journal of Turkey Agricultural Research 4(2): 163-170.
[44] Togay, Y., Anlarsal, A. E. (2008): Effect of different doses of zinc and phosphorus on yield and yield components in lentil (*Lens culinaris* Medic.). – Yüzüncü Yıl University, Journal of Agricultural Sciences 18(1): 49-59.
[45] TUİK. (2018): Agricultural Statistics. – http://www. tuik.gov.tr/PreTablo.do?alt_id= 1001 (13.05.2019).

http://www.aloki.hu ● ISSN 1589 1623 (Print) ● ISSN1785 0037 (Online)
DOI: http://dx.doi.org/10.15666/aeer/1802_25812598

[46] Wang, S., Zhao, Y., Guo, J., Zhou, L. (2016): Effects of Cd, Cu and Zn on *Ricinus communis* L. Growth in single element or co-contaminated soils: Pot experiments. – Ecological Engineering 90: 347-351.
[47] Yağmur, B., Aydın, Ş. (2013): The Effects of Zinc and Soil Applications on the Development of Lettuce (*Lactuca sativa* L.) and Some Mineral Substance Coverage. – Anadolu, J. of AARI. 23(2): 36-43. (in Turkish with English Abstract).
[48] Yalçın, S. R., Usta, S. (1990): The effect of zinc application on the development of corn plant and zinc, iron, manganese and copper scopes. – AÜ Faculty of Agriculture Yearbook 41(1-2): 195-204.
[49] Zengin, F. K., Munzuroğlu, Ö. (2004): Effects of lead (Pb++) and copper (Cu++) on the growth of root, shoot and leaf of bean (*Phaseolus vulgaris* L.) seedlings. – Gazi Universty Journal of Science 17(3): 1-10.

http://www.aloki.hu ● ISSN 1589 1623 (Print) ● ISSN1785 0037 (Online)
DOI: http://dx.doi.org/10.15666/aeer/1802_25812598

EFFECTS OF SALINE CONDITIONS ON POLYPHENOL AND PROTEIN CONTENT AND PHOTOSYNTHETIC RESPONSE OF DIFFERENT OLIVE (*OLEA EUROPAEA* L.) CULTIVARS

DEMIR, S.[1] – CETINKAYA, H.[2*]

[1]*Graduate School of Natural and Applied Sciences, Kilis 7 Aralık University, Kilis, Turkey*

[2]*Department of Horticulture, Faculty of Agriculture, Kilis 7 Aralık University, Kilis, Turkey*

[*]*Corresponding author*
e-mail: hcetinkaya67@gmail.com; phone: +90-348-814-2666/7214

(Received 24th Jul 2019; accepted 15th Nov 2019)

Abstract. Physiological responses of plants against biotic and abiotic stresses limit plant cultivation. The present study was designed to investigate the changes in polyphenol and protein content and photosynthetic response in different olive cultivars under influence of saline conditions. For this, the effects of different sodium chloride (NaCl) salinity levels (0, 75, and 150 mM) on physiological and biochemical parameters of *Olea europaea* L. cultivars (Gemlik, Kilis Yaglık, and Nizip Yaglık) were investigated. The highest total chlorophyll content was obtained under 75 mM salinity level while the lowest one was determined under 150 mM salinity. With respect to the cultivars, the highest chlorophyll content was found in Kilis Yaglık cv. whereas the lowest value was obtained from Gemlik. However, flavonoid content was determined to be highest under 150 mM but lowest under 75 mM salinity level. Regarding cultivars, total flavonoid content was ascertained for Gemlik cv. while it was lowest for Kilis Yaglık cv. Accordingly, it can be deduced that salinity decreased the chlorophyll content and cultivars showed different reactions against salinity and its doses. In addition, it influenced total phenolic and protein content in small quantities except for flavonoids which were differently synthesized against salinity levels.
Keywords: *Gemlik, Kilis Yaglık, Nizip Yaglık, olive cultivar, salt stress, phenolic content, flavonoid content*

Introduction

Historically, plants have been extensively used for medicinal, nutritional, flavoring, cosmetic and industrial purposes. Of those plants, *Olea europaea* L. belonging to the *Oleaceae* family is one of the most widely grown fruit crops in the countries of the Mediterranean basin and Turkey is one of the important producer and stakeholders of olive and olive oils. Origin and homeland of olive tree is considered to be the eastern Mediterranean Basin, Syria, central Mesopotamia and Anatolia. The existence of a large number of native wild olive trees in Anatolia reinforces this theory. Archaeological studies revealed that olives were cultivated and evolved in the Mediterranean Basin about 6000-7000 years ago and it then moved on and spread initially in the Aegean, later on in the central and western Mediterranean, and from there it spread to the other places (Ozkaya et al., 2009; Zohary et al., 2012; Breton et al., 2012; Kostelenos and Kiritsakis, 2017). *Olea europaea* L. has many cultivars and genotypes widely distributed in the southern parts of Turkey near Syrian border which is a semi-arid part. In this region, it is possible to see the sub-varieties and rich biological diversity of the species. The cultivars (cv. Gemlik, Kilis Yaglık and Nizip Yaglık) herein are the most commonly cultivated olive tree in this part.

Stress in plant cultivation is defined a number of regressions resulting in low yield and decline plant growth due to abiotic stress (salinity, drought, nutrient deficiencies or excesses, heavy metals, low and high temperatures, air pollution, radiation) and biotic

http://www.aloki.hu ● ISSN 1589 1623 (Print) ● ISSN1785 0037 (Online)
DOI: http://dx.doi.org/10.15666/aeer/1802_25992610

stress (bacteria, fungus, viruses etc. and pests). Drought and salinity are the most important abiotic stress factors that limit agricultural production in the world. Approximately 45% of the world's agricultural land is constantly exposed to drought stress, while about 6% of the world's surface is suffering from salinity (Asraf and Foolad, 2007). Salinity is one of the important environmental abiotic stresses that adversely affect plant growth, yield, quality and soil fertility (Ozturk et al., 2004; Debez et al., 2004; Zehtab-Salmasi, 2008). Under natural climatic conditions, plants are routinely subjected to the environmental conditions, which affect plants growth, development and subsequently or consequently primary or secondary metabolite contents but the effects depend on the type, duration and magnitude of abiotic or biotic factors. Plants in general have given various biochemical and physiological responses to the biotic or abiotic stress (Bray et al., 2000). Physiology and biochemistry of plants such as photosynthesis, protein synthesis and energy and lipid metabolism are affected by salinity and that may result growth inhibition, fading or death of plants (Hamouda et al., 2015; Ahmad et al., 2016). Results such as toxicity, deterioration in mineral metabolism, consequently decline in productivity and yield can be observed in the biochemical and physiological processes of plants due to detrimental effects of high salinity. However, plant behavior can change with respect to the secondary metabolite synthesis, production, secretion, and storage during onset and development of salt stress or drought stress (Khalid and Da Silva, 2010; Ozkan and Kulak, 2013). Irrigation with saline water may effect growth of plants. In salinity exposed plants a significant reduction of shoot elongation and Na accumulation, an enhancement of cells area and a thickening of epidermis, cuticle, hypodermis and outer mesocarp were observed. These alterations could be considered that plant protection against stress factors. So it must be applied a proper irrigation management with saline water for fruit production and olive tree quality (Moretti et al., 2018).

In some areas it is important to estimate the effects of irrigation-induced salinity on olive oil phytochemicals and bioactivities because of irrigation with recycled wastewater or salty groundwater. Effect of saline water irrigation on tree physiological parameters in different olive varieties at various salinity levels have been examined by many researchers. In this context, they have examined tree growth, fruit and oil yield, tree nutritional status, oil content and fruit characteristics, mechanisms of salt tolerance in olives and differences among cultivars in these studies (Chartzoulakis et al., 2006; Melgar et al., 2009; Ben-Gal, 2011; Kchaou et al., 2013; Moretti et al., 2018; Trabelsi et al., 2019; Tietel et al., 2019). Olive trees are able to resist water and salt stresses. Decreasing in total chlorophyll content, leaf water potential and photosynthetic gas exchange are observed in rainfed olive trees during drought. But half of their photosynthetic activity of olive leaves are permanently lost during to drought without irrigation and after being exposed to severe water or salt stress, they are unable to recover their whole photosynthetic capacity. However, they were not able to totally recover their physiological performance after re-watering (Tabelsi et al., 2019).

Leaves and roots of different pistachio rootstocks have given different physiological responces to salinity. Therefore, improving salt-tolerant genotypes are important for cultivation (Akbari et al., 2018).

Phenolic compounds are synthesized in plants via the shikimic acid metabolic pathway and endogenously controlled process during developmental differentiation. But their biosynthesis can be regulated by exogenous and stress factors such as light, temperature, drought, salinity, cold etc. (Crozier et al., 2006; Waśkiewicz et al., 2013).

http://www.aloki.hu ● ISSN 1589 1623 (Print) ● ISSN1785 0037 (Online)
DOI: http://dx.doi.org/10.15666/aeer/1802_25992610

Phenolic compounds play an important role in scavenging free radicals and protect plants against the damaging effects of reactive oxygen species due to salt and drought stresses (Petridis et al., 2012; Waskiewicz et al., 2013). On the other hand salt stress has effects on the lipid and phytochemicals and it has increased polyphenol contents of olive oil. The increased levels of polyphenols in response to increasing salinity level show that exposure to salinity probably due to stress response to high salt levels. Polyphenol augmentation of olive oil was previously reported in response to various tree stress conditions involving, e.g., water, salinity, and drought (Artajo et al., 2006; Ben Ahmet et al., 2012; Tietel et al., 2019).

Southeast part of Turkey has major agricultural areas for crop production. Most of these crops are grown under dry conditions. With the development of irrigation systems, irrigation has become widespread in this region in recent years. Salinity problems arise with the irrigation of the orchards. Pistachios and olives are the most grown crops in this region. Kilis Yaglik, Nizip Yaglik and Gemlik olives are widely grown olive cultivars. Thus, present study was designed to investigate the alterations in polyphenol and protein content and photosynthetic response in three important and widely cultivated olive cultivars in response to the saline conditions.

Material and Methods

Plant material

The study was conducted with three cultivars of olive common in the study region (Kilis, Turkey), namely Gemlik, Kilis Yaglık and Nizip Yaglık.

Growth conditions and salt treatment

The present study was carried out according to the method with slight modifications (Demiral et al., 2011) differing with cultivars and stress exposure time. In the study, three olive cultivars (Gemlik, Kilis Yaglık and Nizip Yaglık) were used. The experiment was conducted using irrigation water with 2 different salinity levels (75 and 150 mM). The salinity levels were adjusted by the addition of appropriate amounts of NaCl to half-strength Hoagland's solution. The experiments were conducted in pots and arranged as a factorial, using a randomized complete design with three replications and one plant per pot. The seedlings were grown for one month using half-strength Hoagland's solution before the application of saline solutions to the plants were subjected. Experiments were conducted in a greenhouse with a 14-hour photoperiod and lasted 4 months (August-December). Mean temperature and relative humidity were 26-30^{o}C during day and 16-20^{o}C at night, 60%, respectively. All plants were irrigated twice week with half-strength Hoagland solution. Before the flowering period, uniform sized leaves were detached from the same plant parts and immediately stored -80^{o}C until analysis. The soil mixture was included with soil: peat: perlite (3:1:1).

Preparation of extracts

The air-dried and finely powdered leaves of olive cultivars (5 g) were stirred with 100 ml of pure methanol for 30 min, respectively. Extraction was carried out using maceration at room temperature for 24 h followed by filtration through Whatman No.4 filter paper. The extracts were then concentrated in vacuo at 40^{o}C using a Rotary evaporator. Then the extracts were preserved in sealed vials at 4^{o}C until further analysis.

http://www.aloki.hu ● ISSN 1589 1623 (Print) ● ISSN1785 0037 (Online)
DOI: http://dx.doi.org/10.15666/aeer/1802_25992610

Photosynthetic pigment and total protein determination

The contents of chlorophyll a, chlorophyll b and total chlorophyll a + b in the leaves were determined, according to the method of Arnon (1949). Protein content in the crude extracts was determined after TCA precipitation according to the method of Bradford (1976), using bovine serum albumin (BSA) as a standard. The measurements were done using three replicates corresponding to the five samples for each replicate.

Determination of total phenolic content

Total phenolic content was determined according to the Folin-Ciocalteu reagent method (Singleton et al., 1999). The amount of total phenol was calculated as mg/g (Gallic Acid Equivalents) from calibration curve of Gallic acid standard solution (R^2=0.9993). An aliquot of each sample (0.1 ml) was diluted to 1 ml with distilled water. Briefly, 0.5 ml of Folin-Ciocalteu reagent (1:1 v/v) and 1.5 ml of 20% (w/v) sodium carbonate were added to the diluted sample solution, and the mixture was then vortexed and allowed to stand for 2 hours at room temperature for color development. The volume was completed to 10 ml with distilled water and their absorbance was measured at 765 nm (Evolution 201 UV-Visible Spectrophotometer).

Determination of total flavonoid content

The flavonoid content was determined by aluminum chloride method using quercetine as a reference compound (Kumaran and Karunakaran, 2006). This method based on the formation of a complex flavonoid-aluminum. The amount of total flavonoid was calculated from calibration curve of quercetine standard solution (R^2=0.9815). 1ml of olive leaf extracts or standards catechol solution (500 µg/ml) was added to 4 ml distilled water and 0.3 ml of 5% $NaNO_2$ was added. After 5 minutes, 0.3 ml of 10 % $AlCl_3$ was added. After 6 min, 2 mL of 1 mol L- NaOH was added and final total volume was completed to 10 mL with distilled water. Afterwards the absorbance of the mixture was measured at 510 nm.

Statistical analysis

Three replications were used for each treatment. Data were expressed as mean. The experiments were arranged as a split plot design with three MSTAT-C statistical program was used to determine statistical significance levels and the differences between individual averages were considered to be statistically important at $p<0.01$. Herein, one-way variance analysis followed by post-hoc tests of Duncan and regression analysis was performed to determine the differences between the cultivars and applied doses of salt.

Results

Photosynthetic pigment content

Leaf chlorophyll a, chlorophyll b, and total chlorophyll content in relation to salt stress effects are collectively represented in *Table 1* and *Table 2*. Determination of chlorophyll content in plants is an important indicator for photosynthesis capacity. The effects of different concentration of saline conditions on photosynthetic pigments were statistically significant ($P\leq0.01$). There were also statistically significant differences

http://www.aloki.hu ● ISSN 1589 1623 (Print) ● ISSN1785 0037 (Online)
DOI: http://dx.doi.org/10.15666/aeer/1802_25992610

associated with different olive cultivars and concentration levels of sodium chloride (P≤0.01). The highest content of photosynthetic pigments was determined in 75 mM whereas the lowest content was ascertained in 150 mM NaCl concentration. Chlorophyll a content was the highest at 75 mM concentration in Nizip Yaglık cultivar, the lowest at Gemlik cultivar control group. Chlorophyll b content was the highest at 75 mM concentration in Kilis Yaglık cultivar, the lowest at 150 mM concentration in Gemlik cultivar.

Table 1. *Chlorophyll a, chlorophyll b, and total chlorophyll content of olive cultivars leaves at different NaCl concentration*

	NaCl (mM)	Chlorophyll a				Chlorophyll b				Total Chlorophyll			
		I	II	III	Ave.	I	II	III	Ave.	I	II	III	Ave.
Gemlik	**0**	2.53	3.06	3.59	**3.060 h**	1.04	1.57	2.10	**1.547 ff**	1.57	4.10	4.63	**5.155**
	75	2.99	3.52	4.05	**3.520 f**	1.15	1.68	2.21	**1.682 ee**	1.68	4.67	5.20	**5.730**
	150	2.18	2.71	3.24	**2.708 ı**	0.93	1.46	1.98	**1.455 gg**	1.46	3.63	4.16	**4.692**
Kilis Yaglık	**0**	4.16	4.75	5.35	**4.753 d**	1.55	2.15	2.74	**2.148 cc**	2.15	6.30	6.90	**7.495**
	75	4.37	4.97	5.56	**4.967 b**	1.69	2.29	2.88	**2.288 aa**	2.29	6.66	7.25	**7.850**
	150	4.24	4.84	5.43	**4.837 c**	1.57	2.16	2.76	**2.161 bc**	2.16	6.40	7.00	**7.592**
Nizip Yaglık	**0**	3.53	4.10	4.68	**4.102 e**	1.22	1.80	2.37	**1.796 dd**	1.80	4.32	4.90	**5.470**
	75	4.56	5.13	5.71	**5.133 a**	1.65	2.23	2.80	**2.227 ab**	2.23	6.79	7.36	**7.931**
	150	2.68	3.25	3.83	**3.253 g**	0.90	1.47	2.05	**1.474 fc**	1.47	4.15	4.73	**5.299**

Means in the same column by the same letter are not significantly different to the test of Duncan (α=0.01)

Table 2. *Relationship between salinity and chlorophyll content in olive cultivar leaves*

CV	IV	DV	RE	DC (R^2)	CC (r)
Gemlik	**Salinity**	Chlorophyll a	y=-0.0023x+3.272	0.187	-0.432
		Chlorophyll b	y=-0.0006x+1.6073	0.162	-0.403
		Chlorophyll (a+b)	y=-0.0031x+4.8948	0.198	-0.445
Kilis Yaglık	**Salinity**	Chlorophyll a	y=0.0006x+4.8103	0.152	0.389
		Chlorophyll b	y=9E-05x+2.1925	0.007	0.084
		Chlorophyll (a+b)	y=-0.0038x+7.1123	0.373	-0.611
Nizip Yaglık	**Salinity**	Chlorophyll a	y=-0.0057x+4.5872	0.203	-0.451
		Chlorophyll b	y=-0.0021x+1.9933	0.182	-0.426
		Chlorophyll (a+b)	y=-0.0011x+5.7458	0.003	-0.058

CV: Cultivars; IV: Independent variable; DV: Dependent variable; RE: Regression equation; DC: Determination coefficient; CC: Correlation coefficient

Polyphenol and protein content

In the current study, the effects of different NaCl concentration did not elicit any statistical significant changes in relation to the cv. Gemlik, Nizip Yaglık and Kilis Yaglık but total flavonoids were differently influenced with salt application (*Table 3* and *Table 4*). Even different salt concentration did not induce any statistically significant differences associated with total phenolic content; the highest total phenolic content was ascertained in 150 mM for both cv. Nizip Yaglık. Total flavonoid content decreased with increasing salt concentration in cv. Gemlik. The effects of salt concentration and cultivars were statistically significant in terms of flavonoid content.

http://www.aloki.hu ● ISSN 1589 1623 (Print) ● ISSN1785 0037 (Online)
DOI: http://dx.doi.org/10.15666/aeer/1802_25992610

Flavonoid content increased an all cultivars with salt stress. The difference concerned with respect to the concentration was statistically significant at $p< 0.01$. The highest content was determined at 150 mM concentration.

Table 3. *Polyphenol and protein content of olive cultivars leaves at different NaCl concentration*

Olive cultivars	NaCl (mM)	Total phenolics (mg/g GAE)				Total flavonoid (mg/g QE)				Protein content (%)			
		I	II	III	Ave.	I	II	III	Ave.	I	II	III	Ave.
Gemlik	**0**	217.8	206.7	233.8	219.4	53.47	53.39	53.16	53.30 **bb**	0.031	0.032	0.031	0.031
	75	219.6	218.7	222.9	220.4	53.86	49.43	51.14	51.48 **bc**	0.059	0.059	0.059	0.059
	150	216.3	229.5	233.4	226.4	50.68	50.36	50.21	50.42 **cc**	0.038	0.024	0.031	0.031
Kilis Yaglık	**0**	224.6	231.1	218.8	224.6	35.77	36.16	35.46	35.80 **gg**	0.019	0.029	0.023	0.024
	75	224.4	213.1	211.9	216.5	37.25	37.25	37.40	37.30 **fg**	0.057	0.067	0.062	0.062
	150	232.0	229.8	230.2	230.6	43.30	42.21	42.80	42.77 **ee**	0.025	0.024	0.024	0.024
Nizip Yaglık	**0**	229.2	221.4	229.6	226.7	46.64	46.72	46.17	46.51 **dd**	0.017	0.015	0.016	0.016
	75	221.3	222.0	223.4	222.2	39.34	39.34	39.50	39.39 **ff**	0.006	0.008	0.007	0.027
	150	221.3	228.4	219.6	223.1	57.63	58.49	55.47	57.18 **aa**	0.005	0.003	0.004	0.024

Means in the same column by the same letter are not significantly different to the test of Duncan (α=0.01)

Table 4. *Relationship between salinity and protein, total phenolic and flavonoid content in olive cultivar leaves*

CV	IV	DV	RE	DC (R^2)	CC (r)
Gemlik	**Salinity**	Total phenolic	y=0.0465x+218.57	0.85	0.924
		Total flavonoid	y=-0.0192x+53.173	0.98	-0.989
		Protein content	y=-4E-20x+0.0403	3E-32	0.000
Kilis Yaglık	**Salinity**	Total phenolic	y=0.04012x+220.91	0.178	0.422
		Total flavonoid	y=0.0465x+35.138	0.902	0.950
		Protein content	y=-1E-20x+0.0267	3E-32	0.000
Nizip Yaglık	**Salinity**	Total phenolic	y=-0.024x+225.81	0.5714	-0.756
		Total flavonoid	y=0.0711x+42.358	0.355	0.596
		Protein content	y= 5E-05x+0.0183	0.495	0.703

CV: Cultivars; IV: Independent variable; DV: Dependent variable; RE: Regression equation; DC: Determination coefficient; CC: Correlation coefficient

Effects of cultivars and salinity concentration

The effects of different NaCl concentration and cultivars on chlorophyll a, chlorophyll b, total chlorophyll, polyphenol and protein content in olive leaves are shown *Table 5*. Cultivars have given different response to salinity. While there was no statistical difference between the total phenol and protein contents, total chlorophyll, chlorophyll a and b content and total flavonoid content were significant. Accordingly, the highest total chlorophyll, chlorophyll a and chlorophyll b content were observed in Kilis Yaglık cultivar and lowest in Gemlik cultivar. In terms of total flavonoid content, Gemlik cultivar was the highest and Kilis Yaglık cultivar was the lowest content. According to the results, while Gemlik was the most and Kilis Yaglık the least affected

http://www.aloki.hu ● ISSN 1589 1623 (Print) ● ISSN1785 0037 (Online)
DOI: http://dx.doi.org/10.15666/aeer/1802_25992610

cultivar to salinity. The high flavonoid in the Gemlik cultivaris due to the fact that the cultivar has developed a defense mechanism against salinity.

When the salt concentrations were evaluated, no statistically significant difference was observed between the total phenol and protein contents, but total chlorophyll, chlorophyll a and b content and total flavonoid content were found to be significant. Accordingly, the highest total chlorophyll, chlorophyll a and chlorophyll b content were observed at 75 mM and the lowest 150 mM concentrations. In terms of total flavonoid content, the highest content was determined at 150 mM and the lowest 75 mM concentrations. Consequently, the effect of salt stress was most at 150 mM concentration. As in cultivars, the high content of total flavonoid at 150 mM shows the effect of the dose level.

Table 5. *The effects of different NaCl concentration and cultivars on Chl a, Chl b, total Chl, polyphenol and protein content in olive leaves*

		Chl a	Chl b	Total Chl	Total Phenolic (mg/g GAE)	Total Flavanoid (mg/g QE)	Protein Content (%)
CULTIVARS	**Gemlik**	3.096 **c**	1.561 **c**	4.663 **c**	222.06	51.74 **a**	0.040
	Kilis Yaglık	4.852 **a**	2.199 **a**	6.827 **a**	223.98	38.62 **c**	0.037
	Nizip Yaglık	4.163 **b**	1.832 **b**	5.660 **b**	224.01	47.70 **b**	0.023
NaCl (mM)	**0**	3.972 **b**	1.830 **b**	5.474 **b**	223.65	45.22 **b**	0.024
	75	4.540 **a**	2.066 **a**	6.604 **a**	219.69	42.72 **c**	0.049
	150	3.599 **c**	1.697 **c**	5.073 **b**	226.71	50.13 **a**	0.026

Discussion

Cultivars have given different response to salinity in the study. The highest total chlorophyll, chlorophyll a and chlorophyll b content were observed in Kilis Yaglık cultivar and lowest in Gemlik cultivar. It is concluded that Kilis Yaglık variety is more resistant to salt than others. Olives give some physiological and biochemical responces to salinity such as decreasing photosynthesis, stomatal and mesophyll conductance, leaf starch, Rubisco carboxylation rate, actual PSII efficiency etc. (Munns, 1993; Ben Ahmed et al., 2008; Mousavi et al., 2008; Tattini and Traversi, 2009; Remorini et al., 2009). Growth inhibition is a common effect of salinity but in olive tree mechanism of salt effects are prevention of salt translocation, decreasing its transport (Tattini, 1994; Tabatabaei, 2006; Cimato et al., 2010). In the recent studies, physiological, epigenetic, genetic regulation, water status, biochemical and molecular mechanism in olive cultivars under salt stress have been examined and revealed (Abdallah et al., 2018; Trabelsi et al., 2019; Mousavi et al., 2019).

Physiological parameters like Na accumulation in shoots, decrease in shoot elongation, reduction of maximum photosynthetic efficiency to NaCl treated plants demonstrate that treated plants perceive the stress (Loreto et al., 2003; Kchaou et al., 2013; Koubouris et al., 2015).

Leaf chlorophyll (a, b) and total chlorophyll content in various olive cultivars were reported to decline when exposed to the saline conditions (Atia, 2002; Melgar et al., 2008; Shaheen et al., 2011). Halophyte plants demonstrate more protective mechanisms against salt stress concerned with chlorophyll content. Salt at higher concentration in apoplast of cells leads to the ionic toxicity, cellular disequilibrium and hyper osmolality

http://www.aloki.hu ● ISSN 1589 1623 (Print) ● ISSN1785 0037 (Online)
DOI: http://dx.doi.org/10.15666/aeer/1802_25992610

and as a result, induction of oxidative stress by increasing formation of reactive oxygen species which causes chlorophyll degradation (Sevengor et al., 2011).

High salt concentrations bring about many problems in the plant cell. These stages are water stress, damages caused by ion toxicity due to high concentration of Na and Cl ions in the cell and degradation of Ca and K ions in the cell as a result of Na and Cl accumulation (Marschner, 1995; Borsani et al., 2003; Xue and Liu, 2008). High salt concentrations negatively affect parameters such as green parts, root development, water use efficiency and root/stem ratio and K/Na and Ca/Na ratios were found higher in salt resistant plant species (Grewal, 2010).

Differences in salt tolerance are reported among olive tree cultivars. Salinity reduces photosynthesis and stomatal conductance more in salt tolerant than in salt sensitive cultivars according to gas exchange measurement (Tattini et al., 1997). Most of these cultivars such as Manzanillo, Chemlali, Arbequina, Mission, Leccino, Koroneiki, Mastoidis, Frantoio, Cipressino, Allora and Zard response to salinity by decreasing stomatal conductance and photosynthesis (Chartzoulakis et al., 2006; Tabatabaei, 2006; Ben Ahmed et al., 2008; Mousavi et al., 2008; Melgar et al., 2008, 2009; Remorini et al., 2009; Tattini and Traversi, 2009; Tattini et al., 2009; Kchaou et al., 2010). Chétoui variety is moderately sensitive to both drought and salt stress, although it has greater ability to tolerate water depletion. The most significant changes were observed under the salinity stress condition. Under both stress conditions, a greater growth reduction observed due to reduction of all photosynthetic parameters like the integrity of photosystem II and leaf nitrogen content (Abdallah et al., 2018).

Phenolic compound are essential indicators in determination of olive quality. Olive leaves phenolic compounds are significantly influenced by many factors such as genetic factor, harvest time, color, and age (Ranalli et al., 2006). Phenolic components are significant elements in struggle against abiotic and biotic stress factors (Ruiz and Romero, 2001). Phenolic compound biosynthesis and accumulation was stimulated in response to the abiotic and biotic stress factors (Naczk and Shahidi, 2004). However, studies on different species and genotypes have also shown that there may be decreases in total phenolic content with increasing stress factors. Flavonoid content increased and then lipid peroxidation decreased and a negative correlation was reported between lipid peroxidation and flavonoid content under saline conditions (Chutipaijit et al., 2009). Flavonoids have been reported to increase the plant's ability to tolerate stress through affecting physiological performance (Chutipaijit et al., 2009).

It has been reported that the increase in salt doses may affect the amount of free amino acids, although it may lead to reductions in total protein content. Increased acidic and alkaline protease activity increases the amount of free amino acids and provides resistance to stress conditions (Parida et al., 2004).

Conclusion

As a result, the amount of chlorophyll in the leaves of the olive cultivars decreased with salt stress. Cultivars demonstrated different responses in relation to the salt stress and chlorophyll content. Moreover, while the salt application did not elicit any significant change in terms of total phenolic content, total flavonoid content increased with increasing salt stress. With respect to growth parameters the highest total chlorophyll, chlorophyll a and chlorophyll b content were observed in Kilis Yaglık cultivar and lowest in Gemlik cultivar. It is concluded that Kilis Yaglık variety is more

http://www.aloki.hu ● ISSN 1589 1623 (Print) ● ISSN1785 0037 (Online)
DOI: http://dx.doi.org/10.15666/aeer/1802_25992610

resistant to salt than others and Gemlik was the most and Kilis Yaglık the least affected cultivar to salinity. The high flavonoid in the Gemlik is due to the fact that the cultivar has developed a defense mechanism against salinity.

According to the findings of the study, the salt conditions affected the crops at different doses. In addition, the responses of cultivars have been different against salt concentration. Cultivars may develop a defense mechanism against saline conditions through biosynthesizing polyphenols in different amounts. However, chlorophyll content was adversely influenced and consequently, photosynthesis yield is expected to decline under saline conditions.

For further studies, to discriminate the cultivars for their response, enzymatic antioxidant systems of the plants and responsive responses proteins or genes can be revealed. In addition, the results should be compared with the multi-successive year field studies.

Acknowledgement. The current study was a part of MSc thesis "Defense Strategy of Some Olive Cultivars against Salt Stress" written by Sekvan Demir.

REFERENCES

[1] Abdallah, M. B., Trupiano, D., Polzella, A., De Zio, E., Sassi, M., Scaloni, A., Scippa, G. S. (2018): Unraveling physiological, biochemical and molecular mechanisms involved in olive (*Olea europaea* L. cv. Chétoui) tolerance to drought and salt stresses. – Journal of Plant Physiology 220: 83-95.

[2] Ahmad, P., Latef, A. A. A., Hashem, A., Abd-Allah, E. F., Gucel, S., Tran, L-S. P. (2016): Nitric oxide mitigates salt stress by regulating levels of osmolytes and antioxidant enzymes in chickpea. – Front Plant Sci 7: 347.

[3] Akbari, M., Mahna, N., Ramesh, K., Bandehagh, A., Mazzuca, S. (2018): Ion homeostasis, osmoregulation, and physiological changes in the roots and leaves of pistachio rootstocks in response to salinity. – Protoplasma 255(5): 1349-1362.

[4] Arnon, D. I. (1949): Copper enzymes in isolated chloroplasts, polyphenoxidase in *Beta vulgaris*. – Plant Physiology 24: 1-15.

[5] Artajo, L. S., Romero, M. P., Tovar, M. J., Motilva, M. J. (2006): Effect of irrigation applied to olive trees (*Olea europaea* L.) on phenolic compound transfer during olive oil extraction. – Eur J Lipid Sci Technol 108: 19-27.

[6] Asraf, M., Foolad, M. R. (2007): Roles of Glycine Betaine and Proline in Improving Plant Abiotic Stress Resistance. – Envionmental and Experimental Botany 59: 206-216.

[7] Atia, S. A. (2002): Study on growth of olive plants under salt stress. – PhD thesis, Cairo University, Egypt: 129.

[8] Ben Ahmed, C., Ben Rouina, B., Boukhris, M. (2008): Changes in water relations, photosynthetic activity and proline accumulation in one-year-old trees (*Olea europaea* L. cv. Chemlali) in response to NaCl salinity. – Acta Physiologiae Plantarum 30: 553-560.

[9] Ben Ahmed, C., Magdich, S., Ben Rouina, B., Boukhris, M., Ben Abdullah, F. (2012): Saline water irrigation effects on soil salinity distribution and some physiological responses of field grown Chemlali olive. – J. Environmental Management 113: 538-544.

[10] Ben-Gal, A. (2011): Salinity and olive: from physiological responses to orchard management. – Israel Journal of Plant Sciences 59: 15-28.

[11] Borsani, O., Valpuesta, V., Botella, M. A. (2003): Developing Salt Tolerant Plants in A New Century: A Molecular Biology Approach. – Plant Cell, Tissue and Organ Culture 73: 101-115.

http://www.aloki.hu ● ISSN 1589 1623 (Print) ● ISSN1785 0037 (Online)
DOI: http://dx.doi.org/10.15666/aeer/1802_25992610

[12] Bradford, M. M. (1976): A rapid and sensitive method for the quantitation of microgram quantities of protein utilizing the principle of protein-dye binding. – Analytical Biochemistry 72: 248-254.
[13] Bray, E., Bailey-Serres, J., Weretilnyk, E. (2000): Responses to Abiotik Stresses. – In: Buchanan, B. B., Gruissem, W., Jones, R. L. (eds.) Biochemistry and Moleculer Biology of Plants. Chapter 22, Amer Soc Plant Physiol., Rockrille MD.
[14] Breton, C. M., Warnock, P., Bernille, A. J. (2012): Origin and history of the olive. – In: Innocento, M. (ed.) Olive germplasm. TECH, Rijeka, Croatia: 3-22.
[15] Chartzoulakis, K., Psarras, G., Vemmos, S., Loupassaki, M., Bertaki, M. (2006): Response of two olive cultivars to salt stress and potassium supplement. – Journal of Plant Nutrition 29: 2063-2078.
[16] Chutipaijit, S., Cha-um, S., Sompornpailin, K. (2009): Differential accumulations of proline and flavonoids in indica rice varieties against salinity. – Pakistan Journal of Botany 41: 2497-2506.
[17] Cimato, A., Castelli, S., Tattini, M., Traversi, M. L. (2010): An ecophysiological analysis of salinity tolerance in olive. – Environmental and Experimental Botany 68: 214-221.
[18] Crozier, A., Jaganath, I. B., Cliford, M. N. (2006): Phenols, polyphenols and tannins: An overview. – In: Crozier, A., Clifford, M. N., Ashihaea, H. (eds.) Plant Secondary Metabolites. Oxford, Blackwell, pp: 1-24.
[19] Debez, A., Hamed, K., Grignon, B., Abdelly, C. (2004): Salinity effects on germination, growth and seed production of the halophyte *Cakile maritima*. – Plant and Soil 262: 179-189.
[20] Demiral, M. A., Aktas Uygun, D., Uygun, M., Kasirga, E., Karagozler, A. A. (2011): Biochemical response of *Olea europaea* cv. Gemlik to short-term salt stress. – Turkish Journal of Biology 35: 433-442.
[21] Grewal, H. S. (2010): Water uptake, water use efficiency, plant growth and ionic balance of wheat, barley, canola and chickpea plants on a sodic vertosol with variable subsoil NaCl salinity. – Agricultural Water Management 97(1): 148-156.
[22] Hamouda, I., Badri, M., Mejri, M., Cruz, C., Siddique, K., Hessini, K. (2015): Salt tolerance of Beta macrocarpa is associated with efficient osmotic adjustment and increased apoplastic water content. – Plant Biology 18: 369-375.
[23] Kchaou, H., Larbi, A., Gargouri, K., Chaieb, M., Morales, F., Msallem, M. (2010): Assessment of tolerance to NaCl salinity of five olive cultivars, based on growth characteristics and Na+ and Cl− exclusion mechanisms. – Sci. Horticulture 124: 306-315.
[24] Kchaou, H., Larbi, A., Chaieb, M., Sagardoy, R., Msallem, M., Morales, F. (2013): Genotypic differentiation in the stomatal response to salinity and contrasting photosynthetic and photoprotection responses in five olive (*Olea europaea* L.) cultivars. – Scientia Horticulturae 160: 129-138.
[25] Khalid, A. K., Da Silva, J. A. T. (2010): Yield, essential oil and pigment content of *Calendula officinalis* L. flower heads cultivated under salt stress conditions. – Scientia Horticulturae 126: 297-305.
[26] Kostelenos, G., Kiritsakis, A. (2017): Olive tree history and evolution. – In: Shahidi, F., Kiritsakis, A. (eds.) Olives and Olive Oil as Functional Foods: Bioactivity, Chemistry and Processing. John Wiley & Sons, Ltd., pp: 1-12.
[27] Koubouris, G. C., Tzortzakis, N., Kourgialas, N. N., Darioti, M., Metzidakis, I. (2015): Growth, photosynthesis and pollen performance in saline water treated olive plants under high temperature. – International Journal of Plant Biology 6: 28-32
[28] Kumaran, A., Karunakaran, R. J. (2006): Antioxidant and free radical scavenging activity of an aqueous extract of *Coleus aromaticus*. – Food Chemistry 97: 109-114.
[29] Loreto, F., Centritto, M., Chartzoulakis, K. (2003): Photosynthetic limitations in olive cultivars with different sensitivity to salt stress. – Plant Cell Environment 26: 595-601.
[30] Marschner, H. (1995): Mineral Nutrition of Higher Plants. – Academic Press, pp: 657-680.

http://www.aloki.hu ● ISSN 1589 1623 (Print) ● ISSN1785 0037 (Online)
DOI: http://dx.doi.org/10.15666/aeer/1802_25992610

[31] Melgar, J. C., Syvertsen, J. P., García-Sánchez, F. (2008): Can elevated CO_2 improve salt tolerance in olive tree? – Journal Plant Physiology 165: 631-640.
[32] Melgar, J. C., Mohamed, Y., Serrano, N., García-Galavís, P. A., Navarro, C., Parra, M. A., Fernández-Escobar, R. (2009): Long term responses of olive trees to salinity. – Agricultural Water Management 96(7): 1105-1113.
[33] Moretti, S., Francini, A., Minnocci, A., Sebastiani, L. (2018): Does salinity modify anatomy and biochemistry of *Olea europaea* L. fruit during ripening? – Scientia Horticulturae 228: 33-40.
[34] Mousavi, A., Lessani, H., Babalar, M., Talaei, A. R., Fallahi, E. (2008): Influence of salinity on chlorophyll, leaf water potential, total soluble sugars, and mineral nutrients in two young olive cultivars. – Journal of Plant Nutrition 31: 1906-1916.
[35] Mousavi, S., Regni, L., Bocchini, M., Mariotti, R., Cultrera, N. G. M., Mancuso, S., Googlani, J., Chakerolhosseini, M. R., Guerrero, C., Albertini, E., Baldoni, L., Proietti, P. (2019): Physiological, epigenetic and genetic regulation in some olive cultivars under salt stress. – Scientific reports 9(1): 1093. doi:10.1038/s41598-018-37496-5.
[36] Munns, R. (1993): Physiological processes limiting plant growth in saline soils: some dogmas and hypotheses. – Plant Cell Environment 16: 15-24.
[37] Naczk, M., Shahidi, F. (2004): Extraction and analysis of phenolic in food. – Journal of Chromatography A 1054: 95-111.
[38] Ozkan, A., Kulak, M. (2013): Effects of water stress on growth, oil yield, fatty acid composition, and mineral content of *Sesamum indicum*. – The Journal of Animal and Plant Sciences 23: 1686-1690.
[39] Özkaya, M. T., Ergülen, E., Ülger, S., Özilbey, N. (2009): Molecular characterization of some selected wild olive (*Olea oleaster* L.) ecotypes grown in Turkey. – Journal of Agricultural Sciences 15: 14-19.
[40] Ozturk, A., Unlukara, A., İpek, A., Gurbuz, B. (2004): Effect of salt stress and water deficit on plant growth and essential oil content of lemon balm (*Melisa officinalis* L.). – Pakistan Journal of Botany 36: 787-792.
[41] Parida, A. K., Das, A. B., Mittra, B., Mohanty, P. (2004): Salt-stress induced alterations in protein profile and protease activity in the mangrove Bruguiera parviflora. – Verlag der Zeitschrift für Naturforschung 59c: 408-414.
[42] Petridis, A., Therios, I., Samouris, G., Tananaki, C. (2012): Salinityinduced changes in phenolic compounds in leaves and roots of four olive cultivars (*Olea europaea* L.) and their relationship to antioxidant activity. – Environ. Exp. Botany 79: 37-43.
[43] Ranalli, A., Contento, S., Lucera, L., Di Febo, M., Marchegiani, D., Di Fonzo, V. (2006): Factors affecting the contents of iridoid oleuropein in olive leaves (*Olea europaea* L.). – Journal of Agricultural and Food Chemistry 54: 434-440.
[44] Remorini, D., Melgar, J. C., Guidi, L., Degl'Innocenti, E., Castelli, S., Traversi, M. L., Massai, R., Tattini, M. (2009): Interaction effects of root-zone salinity and solar irradiance on the physiology and biochemistry of *Olea europaea*. – Environmental and Experimental Botany 65: 210-219.
[45] Ruiz, J. M., Romero, L. (2001): Bioactivity of the phenolic compounds in higher plants. – In: Rahman, A. (ed.) Studies in Natural Products Chemistry 25(F): 651-681.
[46] Sevengor, S., Yasar, F., Kusvuran, S., Ellialtıoglu, S. (2011): The effect of salt stress on growth, chlorophyll content, lipid peroxidation and antioxidative enzymes of pumpkin seedling. – African Journal of Agricultural Research 6: 4920-4924.
[47] Shaheen, M. A., Hegazi, A. A., Hmmam, I. S. A. (2011): Effect of salinity treatments on vegetative characteristics and leaves chemical content of transplant of five olive cultivars. – Journal of Horticultural Science and Ornamental Plants 3: 143-151.
[48] Singleton, V. L., Orthofer, R., Lamuela-Raventós, R. M. (1999): Analysis of total phenols and other oxidation substrates and antioxidants by means of Folin-Ciocalteu reagent. – Methods in Enzymology 299: 152-178.

http://www.aloki.hu ● ISSN 1589 1623 (Print) ● ISSN1785 0037 (Online)
DOI: http://dx.doi.org/10.15666/aeer/1802_25992610

[49] Tabatabaei, S. J. (2006): Effects of salinity and N on the growth, photosynthesis and N status of olive (*Olea europaea* L.) trees. – Scientia. Horticulture 108: 432-438.
[50] Tattini, M. (1994): Ionic relations of aeroponically-grown olive genotypes during salt stress. – Plant Soil 161: 251-256.
[51] Tattini, M., Lombardini, L., Gucci, R. (1997): The effect of NaCl stress and relief on gas exchange properties of two olive cultivars differing in tolerance to salinity. – Plant and Soil 197(1): 87-93.
[52] Tattini, M., Traversi, M. L. (2009): On the mechanism of salt tolerance in olive (*Olea europaea* L.) under low-or high-Ca2+ supply.–Environmental and Exp. Botany 65:72-81.
[53] Tattini, M., Traversi, M. L., Castelli, S., Biricolti, S., Guidi, L., Massai, R. (2009): Contrasting response mechanisms to root-zone salinity in three co-occurring Mediterranean woody evergreens: a physiological and biochemical study. – Funct. Plant Biolology 36: 551-563.
[54] Tietel, Z., Dag, A., Yermiyahu, U., Zipori, I., Beiersdorf, I., Krispin, S., Ben-Gal, A. (2019): Irrigation-induced salinity affects olive oil quality and health-promoting properties. – Journal of the Science of Food and Agriculture 99(3): 1180-1189.
[55] Trabelsi, L., Gargouri, K., Hassena, A. B., Mbadra, C., Ghrab, M., Ncube, B., Van Staden, J., Gargouri, R. (2019): Impact of drought and salinity on olive water status and physiological performance in an arid climate. – Agricultural Water Management 213: 749-759.
[56] Waśkiewicz, A., Muzolf-Panek, M., Goliński, P. (2013): Phenolic content changes in plants under salt stress. – In: Ahmad, P., Azooz, M., Prasad, M. (eds.) Ecophysiology and Responses of Plants under Salt Stress. New York, Springer: 283-314.
[57] Xue, Y. F., Liu, Z. H. P. (2008): Antioxidant Enzymes and Physiological Characteristics in Two Jerusalem Artichoke Cultivars under Salt Stress. – Russian Journal of Plant Phy. 55(6): 776-781.
[58] Zehtab-Salmasi, S. (2008): Effect of salinity and temperature on the germination of dill (*Anethum graveolens* L.). – Plant Science Research 1: 27-29.
[59] Zohary, D., Hopf, M., Weiss, E. (2012): Domestication of plants in the old world. – 4th ed., Oxford University Press, New York.

http://www.aloki.hu ● ISSN 1589 1623 (Print) ● ISSN1785 0037 (Online)
DOI: http://dx.doi.org/10.15666/aeer/1802_25992610

MOLECULAR CHARACTERIZATION AND PRODUCTION OF BACTERIAL AMYLASES FROM SHAHDARA SPRING, PAKISTAN

AFRIDI, S.[1†] – ALI, N.[2,3†*] – NIAZ, M.[1] – HUSSAIN, S. I.[2] – FARMAN, F. U.[4] – KIM, B. C.[3*]

[1]*Department of Microbiology, Kohat University of Science & Technology (KUST), 26000 Kohat, Pakistan*

[2]*Department of Biotechnology and Genetic Engineering, Kohat University of Science & Technology (KUST), 26000 Kohat, Pakistan*

[3]*Division of Nano-Bioengineering, Incheon National University, Incheon 22012, Republic of Korea*

[4]*Department of Chemistry, Kohat University of Science & Technology (KUST), 26000 Kohat, Pakistan*

[†]*These authors have contributed equally to this work*

**Corresponding authors*
e-mail: nawabali_1857@yahoo.com, introbc@gmail.com

(Received 27th Jul 2019; accepted 30th Jan 2020)

Abstract. Microorganisms are the preferred source of enzyme applicable to a variety of industries, such as food, paper, detergent, and energy. In this study, amylase enzymes were explored for the first time in the springs of Shahdara, Islamabad, Pakistan. 22 out of 28 bacterial isolates showed amylase activity from which the three best amylase producing isolates (S5, S13, and S17) were selected for further studies. These isolates were identified as *Bacillus spp* and *Clostridium spp* using microscopic, biochemical, and molecular-based (16S rRNA) approaches. Phylogenetic analysis further revealed that strains (S5, S13, and S17) have 97% similarity with *Paraclostridium benzoelyticum, Bacillus subtilis,* and *Bacillus tequilensis,* respectively. The maximum amylase production of *Bacillus subtilis* and *Paraclostridium benzoelyticum* was observed at pH 5 and 55 °C whereas that of *Bacillus tequilensis* was at pH 8 and 55 °C. Similarly, the highest activity of amylases from each strain was found at 55 °C in common, but in different pH conditions (at pH 5 for *Paraclostridium benzoelyticum* and *Bacillus subtilis* and at pH 6-8 for *Bacillus tequilensis*). Our study represents that Shahdara springs have beneficial microbial reservoirs producing acidic and thermostable amylases, having great importance to various bio-industrial applications.
Keywords: *thermostable amylase, Shahdara springs, Bacillus spp, Clostridium spp, 16S rRNA gene sequencing*

Introduction

Microbial enzymes are preferred natural sources to animals and plants due to the ease of cultivation, shorter generation time, low cost, and feasibility for human consumption. Microorganisms, which synthesize the microbial enzymes, are found in different sources including extreme sites such as springs, salt mines, and deserts. Among them, springs are considered the best natural source of microbial enzymes. It provides suitable environments for various extremophiles including thermophiles, acidophiles, and alkaliphiles that produce extremophilic enzymes (Sen et al., 2010), which collectively have attracted researchers' attention (Ali et al., 2013; Tango and Islam, 2002). The

http://www.aloki.hu ● ISSN 1589 1623 (Print) ● ISSN 1785 0037 (Online)
DOI: http://dx.doi.org/10.15666/aeer/1802_26112620

extremophilic enzymes gathered from springs, in particular, have a great potential for many industrial applications because of their diversity and unique enzyme activity (Gopinath et al., 2017; Li et al., 2012; Singh et al., 2016).

Among these enzymes, amylases, which can be used to hydrolyze starch into dextrin and small polymers of glucose, are the most widely used enzymes in various industries, taking the first place in the global enzyme market (25-33%). Amylases have replaced acidic hydrolysis and chemical catalysts for starch degradation which is available in huge amounts in waste reservoirs (Sen et al., 2014). Amylases have many applications in the food and pharmaceutical industries such as production of fruit juices, bread making, glucose syrups and alcoholic beverages (Wajeeha et al., 2011). Amylases are generally classified into 1) endoamylases (α-amylases), 2) exoamylases (β-amylase, glucoamylase), and 3) debranching enzymes (pullulanase, isoamylase) based on their modes of action to generate glucose, maltose, malto-oligosaccharides, and dextrins (Kim and Toldrá, 2016; Suriya et al., 2016). Amylase enzymes have diverse bio-industrial applications which demand large scale exploration of these enzymes in extreme reservoirs (de Souza and de Oliveira Magalhaes, 2010; Parmar and Pandya, 2012; Patel et al., 2018). Pakistan is particularly gifted with a number of extremophilic environments. Several hot springs, salt mines, deserts, glaciers, marine brine pools, and hydrothermal vents are present in various localities of Pakistan e.g., novel strains producing hydrolytic enzymes were isolated from hot springs and salt mines in Pakistan (Roohi et al., 2012, 2014; Zahoor et al., 2016). We are still exploring different microbial reservoirs to characterize novel extremophilic enzymes from sources such as hot springs, glaciers, deserts, salt mines, and coal mines located at Pakistan. Although there are few reports regarding microbial explorations in these areas, there is still a lot of work needed to identify novel microbial sources of bio-industrial importance (Afridi et al., 2019; Ali et al., 2016; Shah et al., 2017). Here, we report new amylase producing bacterial strains taken from the Shahdara springs located in the hilly area of Margalla-Islamabad-Pakistan. The Shahdara springs have been explored for microbial flora, however, these springs have been rarely investigated for microbes producing enzymes. Total of 28 bacteria were primarily isolated from the Shahdara springs and screened for the amylase activity. The three best amylase producing bacteria were selected out of 22 amylase producers to check its growth and activity under different physical factors like pH and temperature.

Materials and methods

Specimen collection and enrichment of bacterial isolates

Freshwater samples (n = 25) were collected from different locations in the springs of Shahdara valley, Islamabad (31° 37’ 16.0068” N and 74° 16’ 56.5104” E) in 2018. Temperature and pH at the time of sampling collection was approximately 22ºC and 7-8, respectively. The samples in sterilized bottles were immediately transported to the microbiology laboratory of Kohat University of Science & Technology (KUST), Kohat and preserved at 4 °C until further use. The bacterial isolation was carried out through a standard serial dilution technique. Moreover, enrichment was done using 2 ml of bacterial culture into 10 ml of LB broth and incubated at temperatures 40, 50, 55 and 60 °C for 24 h. After that, 100 µl of samples were diluted and spread onto LB agar and nutrient agar. The plates were then incubated at temperatures 40, 50, 55, and 60 °C for 24 and 48 h. The bacterial isolates were further purified based on colonial morphology.

http://www.aloki.hu ● ISSN 1589 1623 (Print) ● ISSN 1785 0037 (Online)
DOI: http://dx.doi.org/10.15666/aeer/1802_26112620

Screening and identification of amylase producing bacteria

All the isolated colonies were further streaked on the spot method on a starch agar plate and were incubated at 37 °C for 24 h. The incubated plates were checked for amylase activity by adding 1% iodine and 2% potassium iodide solution. The isolate that survived and produced a clear zone around the colony was considered as an amylase producing bacteria. Bacterial isolates giving the largest clear zones were taken for further studies. The bacterial isolates were characterized according to the standard procedure based on morphological and biochemical tests for initial identification that were further identified by 16S rRNA gene sequencing (Sen et al., 2014). Therefore, for molecular identification, bacterial DNA was extracted using Gene Jet Genomic DNA Purification Kit. Genomic DNA samples were subjected to PCR for the amplification of the 16S rRNA gene using universal primers (5-GGAGGCAGCAGTAGGGAATA-3) and (3-TGACGGGCGGTGAGTACAAG-5). The PCR conditions were set as initial denaturation (94 °C for 6 min), followed by annealing temperature (56 °C for 40 s) and extension (72 °C for 50 s). The final extension was performed at 72 °C for 3 min for a total of 35 cycles. The PCR amplified product was sequenced using the commercial service of Advance Bioscience International (ABI). The sequence was BLAST searched on EZ-Biomedical server to get the exact nomenclature of the isolates. The phylogenetic tree was constructed with MEGA 6 using the neighbor-joining method with a bootstrap value of 1000.

Optimization of bacterial growth and amylase production

The selected amylase producing bacterial isolates were optimized by the following factors such as pH and temperature in liquid media. The liquid medium was contained of starch peptone (10 g/l each), yeast extract (20 g/l), KH_2PO_4 (0.10 g/l), $CaCl_2.2H_2O$ (0.10 g/l), $MgSO_4.7H_2O$ (0.50 g/l) and $FeSO_4.7H_2O$ (0.02 g/l) to evaluate amylase production. The effect of pH on bacterial growth and production was conducted in a flask containing the above liquid media by maintaining pH range of 3-11. While the effect of temperature was checked by incubating at different temperature ranges from 35, 45, 55, 65 and 75 °C. The turbidity of bacterial culture was measured by spectrophotometer at 540 nm as amylase produced.

Bernfeld (1995) method is used to determine the activity of amylase (Bernfeld, 1995). The assay was performed in a test tube using enzyme extract (1 ml), 0.05 M sodium phosphate buffer (1 ml) at pH 7.0 and 1% starch (1 ml). The mixture was then incubated at 55 °C for 15 min followed by the addition of 1 ml of DNS reagent to stop reaction. The optical density of color produced was reported by spectrophotometer at 540 nm using maltose as standard. One unit of enzyme was defined as the amount of enzyme requires releasing one µmol of reducing sugar per minute by applying the following formula reported in literature (Singh et al., 2015):

$$\text{Amylase Activity}(\text{IU/ml/min}) = \frac{\text{Activity of enzyme} \times 1000}{\text{Molecular weight of maltose} \times \text{Incubation time}}$$

Partial purification of amylase

Ammonium sulfate precipitation method was used to partially purify crude amylase enzyme. The precipitation mixture was centrifuged at 4000 rpm at 4 °C for 30 min. The supernatant was discarded and protein pellet was dissolved in 5 ml of phosphate buffer and store at 4 °C for further analysis.

http://www.aloki.hu ● ISSN 1589 1623 (Print) ● ISSN 1785 0037 (Online)
DOI: http://dx.doi.org/10.15666/aeer/1802_26112620

Electrophoretic amylase separation

The Laemmle method was used to determine the purity and molecular weight of partially purified amylase on 12% (w/v) Sodium dodecyl polyacrylamide gel electrophoresis (SDS-PAGE) under reducing conditions. The enzyme was taken in eppendorf tube and loading dye was added. The solution was mixed gently. Both were heated in a water bath for 5 min. The protein sample was loaded in each well along with standard protein ladder. The process was performed for 120 min at 120 V until the bromophenol blue reached to the bottom of the gel. Coomassie Brilliant blue solution was used to stain the gel for 30 min and the gel was de-stained for 2.5 h.

Characterization of partially purified amylase

The activity of amylase enzyme was determined using a buffer of different pH range from 3 to 11. Similarly, the temperature effect was studied by incubating at 35, 45, 55, 65, 75 °C and amylase activity was measured as per the assay procedure.

Statistical analysis

All assays were performed in triplicate (n = 3) and their means and standard errors were statistically analyzed using Graph Pad Prism Software.

Results

Isolation and screening of amylase producing isolates

In current study, total 28 bacterial isolates were isolated on the basis of their morphology using spread plate technique from Shahdara valley Islamabad, Pakistan. These isolates were further screened for their amylase activity on the basis of sizes of clear zones by applying 1% iodine solution using starch agar media. Among these, 22 isolates showed amylase activity ranged from a small to large zone around the bacterial colony (*Fig. 1A, B*). The amylase activities based on clear zones around the colonies are also reported in previous literature (Padhiar and Kommu, 2016). On the basis of their maximum amylase activity on specific conditions, the strains such as S5, S13, and S17 were selected to proceed further for onward characterization.

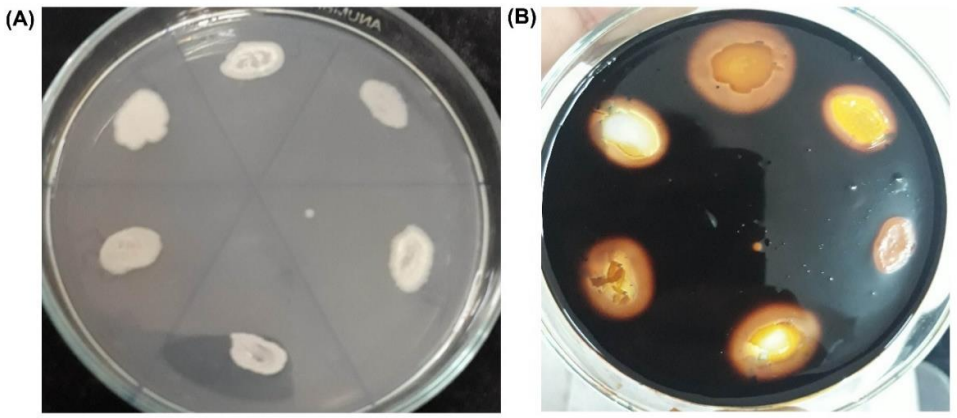

Figure 1. *Amylase activity test. (A) Bacterial zone before addition of iodine and potassium iodide solution. (B) clear zone around the colonies after addition of iodine and potassium iodide solution*

http://www.aloki.hu ● ISSN 1589 1623 (Print) ● ISSN 1785 0037 (Online)
DOI: http://dx.doi.org/10.15666/aeer/1802_26112620

Morphological and molecular identification of the selected isolates

The selected bacterial isolates were further subjected to gram staining and were observed as gram-positive rods and positive for spore staining. Based on their morphological and biochemical tests, the isolates were identified as *Bacillus* and *Clostridium spp* as described in *Table 1*. Moreover, 16S rRNA gene sequencing for these isolates revealed that the isolate S5, S13, and S17 have 97% similarity with *Paraclostridium benzoelyticum*, *Bacillus subtilis* and *Bacillus tequilensis* respectively using phylogenetic analysis (*Fig. 2A-C*).

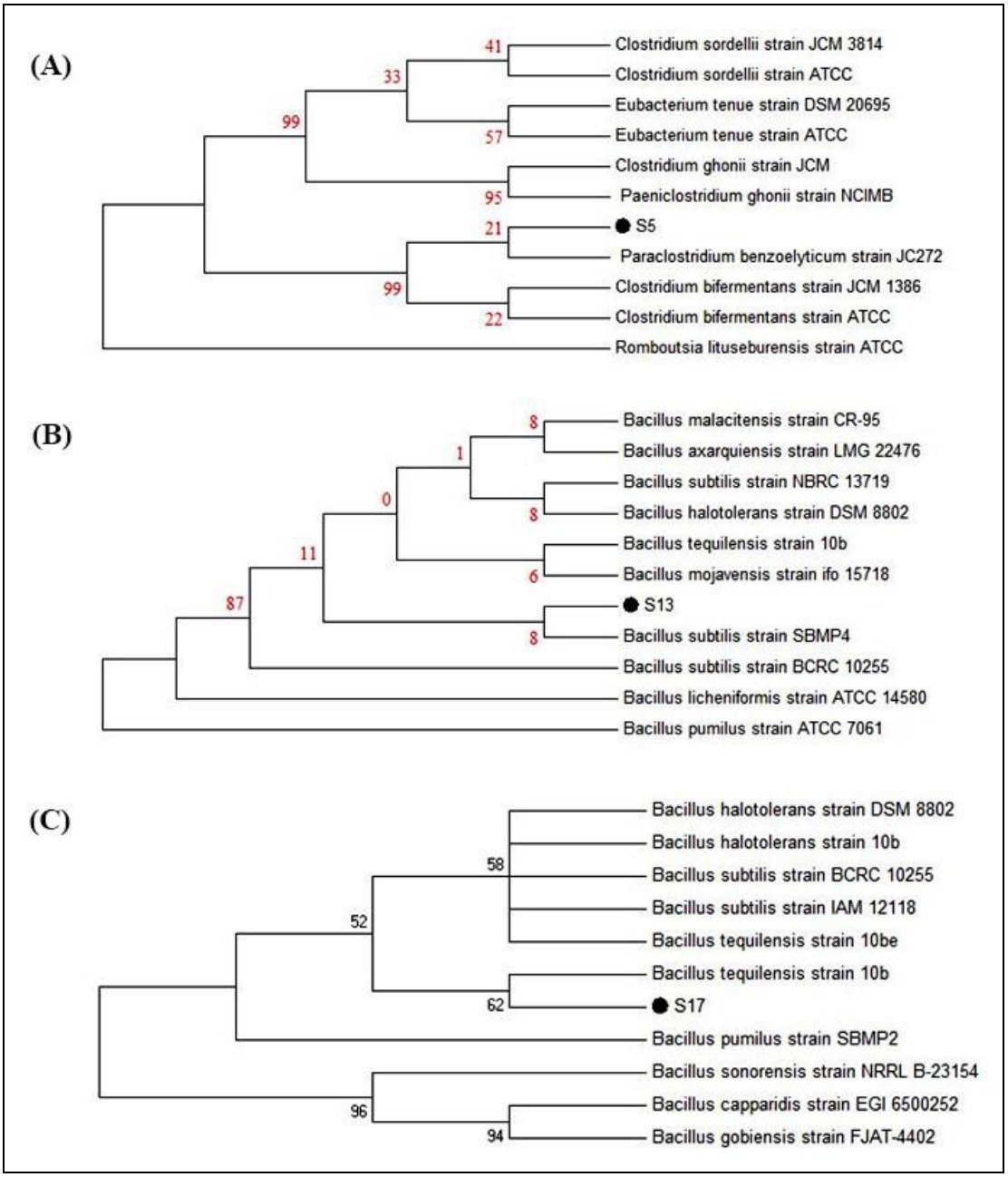

Figure 2. *Phylogenetic tree of isolates from Shahdara springs. (A-C) Phylogenetic tree showing the interrelationships of isolates of S5, S13 and S17 and their close relatives inferred from 16 S rRNA gene sequence. (Evolutionary analysis was conducted in MEGA 6. Scale bar = 0.005 changes per nucleotide position)*

http://www.aloki.hu ● ISSN 1589 1623 (Print) ● ISSN 1785 0037 (Online)
DOI: http://dx.doi.org/10.15666/aeer/1802_26112620

Table 1. *Tentative identification of the selected isolates (n = 3) on the basis of gram staining and different biochemical tests*

Variables	Strain 5	Strain 13	Strain 17
Morphology	Rods	Rods	Rods
Gram staining	+	+	+
Endspore staining	+	+	+
Oxidase	-	-	-
Glucose test	+	+	+
Urease test	+	+	+
Indole test	+	-	+
Citralase	+	+	+
Voges-Proskauer	-	-	-
Catalase	-	-	-
Identification	*Clostridium*	*Bacillus*	*Bacillus*

Analysis of bacterial growth and amylase production

The selected isolates were subjected to variable temperature and pH, in order to evaluate optimum bacterial growth as well as optimum amylase production. Among them, the *Paraclostridium benzoelyticum* strain S5 given the highest growth at pH 7 while the highest production of amylase at pH 5. The growth and production were also checked for *Bacillus subtilis* strain. It was observed that the maximum growth and optimum production of amylase enzyme were at the same pH, i.e. pH 5. However, *Bacillus tequilensis* showed the optimum growth at pH 6 and amylase production at pH 8. In addition, the temperature effect on the growth and production of all selected isolates were also checked. It was observed that the optimal temperature for growth of *Paraclostridium benzoelyticum* was 45 °C and obtained a maximum yield of amylase at 55 °C. However, for the *Bacillus subtilis* and *Bacillus tequilensis*, the optimum temperature of bacterial growth and yield was the same and reported as 55 °C (*Fig. 3A-F*).

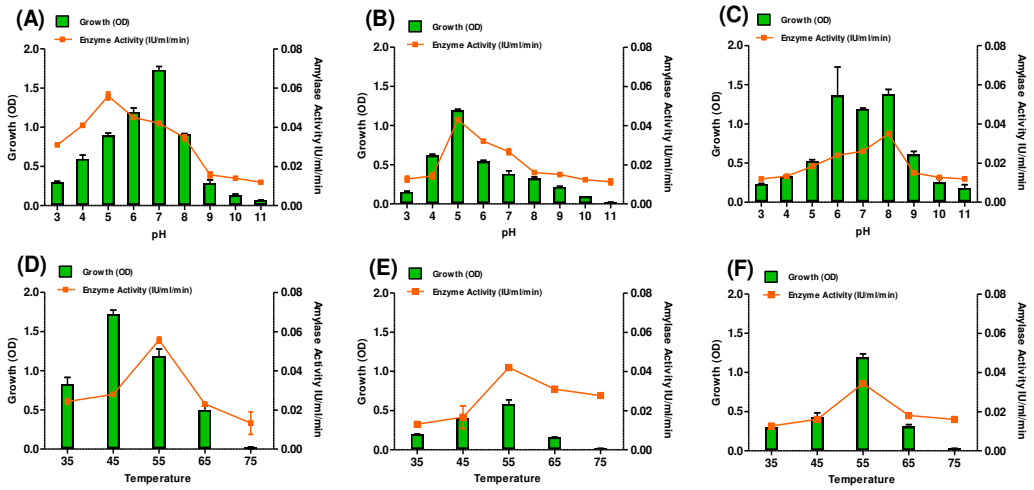

Figure 3. *Effect of pH and temperature on bacterial growth and amylase production. (A and D) growth and amylase production of isolate S5, (B and E) growth and amylase production of isolate S13, (C and F) growth and amylase production of isolate S17 at different pH and temperature*

http://www.aloki.hu ● ISSN 1589 1623 (Print) ● ISSN 1785 0037 (Online)
DOI: http://dx.doi.org/10.15666/aeer/1802_26112620

SDS-PAGE analysis and activity of amylase enzymes

Partial purification of amylase enzymes was performed using 80% saturation of ammonium sulfate. The pellet was separated by SDS PAGE and the amylase enzymes of the strain *Paraclostridium benzoelyticum* (S5), *Bacillus subtilis* (strain S13) and *Bacillus tequilensis* (S17) had the molecular weight of 35 kDa, 37 kDa, and 36 kDa, respectively (*Fig. 4*).

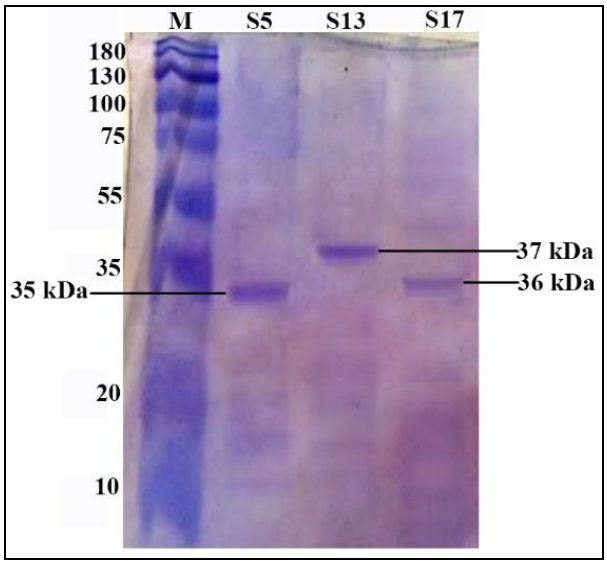

Figure 4. *SDS-PAGE analysis of partially purified amylase enzymes extracted from isolates S5, S13, and S17*

In order to find optimum conditions for amylase activity, the product of selected isolates was subjected to a gradient range of pH and temperature. The highest activity of amylase for both species *Paraclostridium benzoelyticum* strain (S5) and *Bacillus subtilis* strain (S13) was at pH 5. However, for *Bacillus tequilensis* strain (S17), the optimal pH for amylase activity was found in the ranges of pH 6-8. Moreover, the maximum amylolytic activity of all the three isolates was reported at the same temperature, i.e. 55 °C (*Fig. 5A, B*).

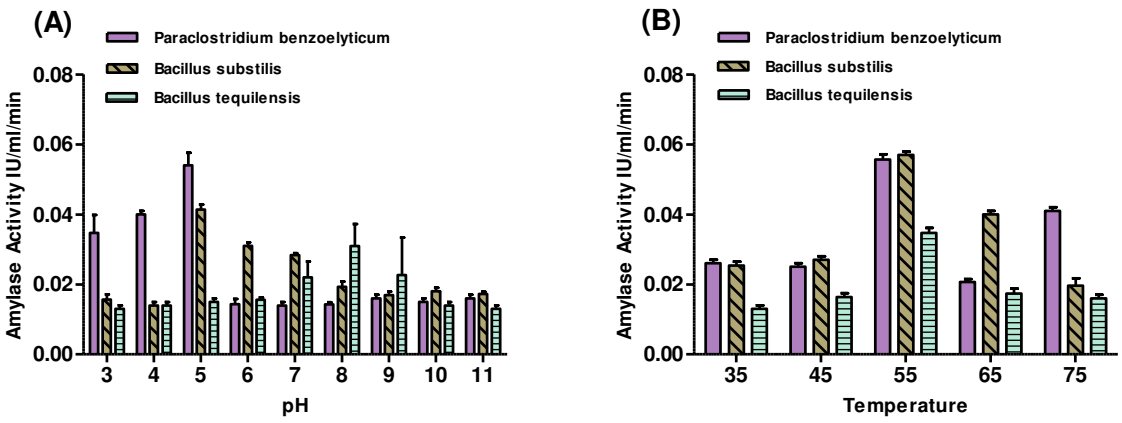

Figure 5. *Effect of pH and temperature on amylases activity of selected bacterial isolates. (A) pH effect on amylase activity, (B) temperature effect on amylase activity*

http://www.aloki.hu ● ISSN 1589 1623 (Print) ● ISSN 1785 0037 (Online)
DOI: http://dx.doi.org/10.15666/aeer/1802_26112620

Discussion

Amylases are the most widely used enzymes in different industries for manufacturing purposes. In the food industry, amylase enzymes play a significant and leading role in hydrolysis of starch into dextrins and small polymers of glucose. In addition, amylases are widely applicable to other industries such as textile and pulp (Gupta et al., 2003). Microbial sources, for examples, bacteria, and fungi, are the most preferred sources to harvest amylase enzymes due to the ease of cultivation, shorter generation time, smaller space requirements and efficient purification procedures (Burhan et al., 2003). In this study, the amylase producing bacterial isolates are explored for the first time in the rarely explored Shahdara springs, Pakistan. In total, 28 bacteria were isolated and among these, 22 bacterial isolates showed amylase activity ranged from small to large zone around the bacterial colony. Three best amylase producing strains, S5, S13, and S17, were selected for onward characterization based on their high amylase activity, in other words, starch degradation potentials, as depicted in *Figure 1A-B*. The morphological and biochemical characteristics revealed differences in bacterial diversity of Shahdara springs. 16 sRNA gene sequencing provided the precise identifications of microbes, revealing that the three selected strains S5, S13 and S17 are *Paraclostridium benzoelyticum, Bacillus subtilis* and *Bacillus tequilensis*, respectively. The amylase enzymes collected in the pellet after ammonium sulfate precipitation was separated by SDS PAGE and three bands of similar sizes ranging from 35 kDa to 37 kDa were obtained on the gel. The molecular sizes of the amylases in the literature varied mainly depending on the microbial sources from which enzymes were purified. We have reported the bacterial amylase from a different source such as salt mines of Karak, which had a molecular weight of 50 kDa (Shah et al., 2017).

Intriguingly, temperature and pH conditions for the highest bacterial growth did not always correspond to those of the highest amylase yield. The best bacterial growth and amylase yield of *Paraclostridium benzoelyticum* (S3) were at pH 7 and 5. *Bacillus tequilensis* (S17) also revealed the maximum growth and enzyme production at different pH values, 6 and 8. Similar results in the same species were reported by Khan and Gupta (2011) They reported the best growth and enzyme production of *Bacillus tequilensis* were achieved at pH 7 and 10, respectively (Khan and Gupta, 2011). However, the *Bacillus subtilis* (S13) showed the best growth and amylase production at the same pH 5 (*Fig. 3A-F*). In the previous work of our laboratory, the same condition for optimum growth and enzyme production of proteases produced by *Pseudomonas aeruginosa* strain collected from coal mines was reported (Afridi et al., 2019). Taken together, these results indicate that there is no direct relationship between the growth and production of enzymes.

In a similar fashion, the effect of temperature on amylase production and bacterial growth was evaluated as well. It is characterized that the *Bacillus subtilis* and *Bacillus tequilensis* strains have the maximum growth and enzyme production at the same temperature, 55 °C. However, *Paraclostridium benzoelyticum* strain grew well at 45 °C, whereas the optimum temperature for enzyme production was 55 °C (*Fig. 3A-F*). The amylase enzymes activity has also been reported for *Bacillus sp. WA21* at 55 °C which is supported here by our findings (Wajeeha et al., 2011).

Furthermore, the amylase activity of the three isolates was studied on various pH and temperature conditions. The two isolates, *Bacillus subtilis* (S5) and *Paraclostridium benzoelyticum* (S13), showed the highest amylase activity in the same conditions, pH 5 and 55 °C (*Fig. 5A, B*). This revealed the acidic and thermophilic nature of the amylase

http://www.aloki.hu ● ISSN 1589 1623 (Print) ● ISSN 1785 0037 (Online)
DOI: http://dx.doi.org/10.15666/aeer/1802_26112620

enzymes produced by these bacteria. The third isolate *Bacillus tequilensis* (S17) had the highest amylase activity at the same temperature, but the optimum pH was in a range of 6-8. These unique acid-stable and thermo-stable amylases can be used in unavoidable acidic and high temperature conditions frequently occurred in fermentation, food processing, and pharmaceutical manufacturing. Together, this study revealed that Shahdara springs are the rich source of microbial enzymes of diverse nature and of biotechnological importance.

Conclusion and future studies

In total, 22 amylase producing bacteria were isolated from the rarely explored Shahdara springs and the three best producers were identified and characterized as *Paraclostridium benzoelyticum* (S5), *Bacillus subtilis* (S13) and *Bacillus tequilensis* strain (S17). The two isolates *Paraclostridium benzoelyticum* (S5), and *Bacillus subtilis* (S13) have surprisingly revealed the same optimum conditions for amylase enzymes activity such as pH 5 and temperature 55 °C. This revealed the acidic and thermophilic nature of amylases produced by these isolates which can be of high importance at acidic and high temperature operational conditions in bio-industrial applications. On the basis of previous studies, it has been recommended that most of the springs located in Pakistan, possessed valuable bacterial flora that need to be explored for enzymes using metagenomics-based approaches for various bio-industrial applications.

Acknowledgements. The authors are grateful to the Higher Education Commission of Pakistan for financial support and the Department of Biotechnology and Genetic Engineering, Kohat University of Science and Technology for providing laboratory facilities to carry out the present research work. This work was also supported by *Research Assistance Program* (2019) in the Incheon National University.

Conflict of interests. All authors declared no conflict of interests, and also the funding body had no role in the experiment design, methodology or data interpretation.

REFERENCES

[1] Afridi, M. I., Ali, N., Memon, A. R., Qasim, M., Jamal, Q., Khattak, B., Adnan, M., Khan, S. N., Ullah, A., Younas, F., Ullah, F. (2019): Protease producing Pseudomonas aeruginosa strain (IBC-2) from coal mines of Orakzai Agency, Pakistan. – Appl Ecol Env Res. 17(3): 6081-6093.

[2] Ali, I., Kanhayuwa, L., Rachdawong, S., Rakshit, S. K. (2013): Identification, phylogenetic analysis and characterization of obligate halophilic fungi isolated from a man-made solar saltern in Phetchaburi province, Thailand. – Annals of Microbiology 63(3): 887-895.

[3] Ali, N., Ullah, N., Qasim, M., Rahman, H., Khan, S. N., Sadiq, A., Adnan, M. (2016): Molecular characterization and growth optimization of halo-tolerant protease producing Bacillus Subtilis Strain BLK-1.5 isolated from salt mines of Karak, Pakistan. – Extremophiles 20(4): 395-402.

[4] Bernfeld, P. (1995): Amylases α and β. – Meth. Enzymology. 1149-158.

[5] Burhan, A., Nisa, U., Gokhan, C., Omer, C., Ashabil, A., Osman, G. (2003): Enzymatic properties of a novel thermostable, thermophilic, alkaline and chelator resistant amylase from an alkaliphilic Bacillus sp. Isolate ANT-6. – Process Biochem. 38: 1397-1403.

[6] De Souza, P. M., De Oliveira Magalhaes, P. (2010): Application of microbial alpha-amylase in industry – a review. – Braz J Microbiol. 41(4): 850-61.

http://www.aloki.hu ● ISSN 1589 1623 (Print) ● ISSN 1785 0037 (Online)
DOI: http://dx.doi.org/10.15666/aeer/1802_26112620

[7] Gopinath, S. C., Anbu, P., Arshad, M. K., Lakshmipriya, T., Voon, C. H., Hashim, U., Chinni, S. V. (2017): Biotechnological processes in microbial amylase production. – Biomed Res Int. 20171272193.
[8] Gupta, R., Gigras, P., Mohapatra, H., Goswami, V. K., Chauhan, B. (2003): Microbial a-amylases: a biotechnological perspective. – Process Biochem. 00(00): 1-18.
[9] Khan, I., Gupta, P. J. V. (2011): Thermo-alkaliphilic halotolerant detergent compatible protease(s) of Bacillus tequilensis MTCC 9585. – Afr. J. Microbiol. Res. 5(23): 3968-3975.
[10] Kim, S.-K., Toldrá, F. (2016): Marine Enzymes Biotechnology: Production and Industrial Applications, Part II – Marine Organisms Producing Enzymes. – Academic Press, Cambridge, MA.
[11] Li, S., Yang, X., Yang, S., Zhu, M., Wang, X. (2012): Technology prospecting on enzymes: application, marketing and engineering. – Comput Struct Biotechnol J. 2e201209017.
[12] Padhiar, A. R., Kommu, S. (2016): Isolation, characterization and optimization of bacteria producing amylase. – Int. J. Adv. Res. Biol. Sci. 3(7): 1-7.
[13] Parmar, D., Pandya, A. (2012): Characterization of amylase producing bacterial strain. – Bull Environ Pharmacol Life Sci 1(6): 42-47.
[14] Patel, G., Patel, P., Patel, N. (2018): Purification and characterization of amylase produced by Halobacterium sp. GB24 isolated from marine National Park. – G. J. B. B. 7(3): 406-411.
[15] Roohi, A., Ahmed, I., Iqbal, M. M. J. (2012): Preliminary isolation and characterization of halotolerant and halophilic bacteria from salt mines of Karak, Pakistan. – Pak. J. Bot. 44(Special Issue March 2012): 365-370.
[16] Roohi, A., Ahmed, I., Khalid, N., Iqbal, M., Jamil, M. (2014): Isolation and phylogenetic identification of halotolerant/halophilic bacteria from the salt mines of Karak, Pakistan. – Int. J. Agric. Biol. 16(3): 564-570.
[17] Sen, S. K., Mohapatra, S. K., Satpathy, S., Rao, G. T. V. (2010): Characterization of hot water spring source isolated clones of bacteria and their industrial applicability. – Int J Chem Res. 2(1): 1-7.
[18] Sen, S. K., Raut, S., Satpathy, S., Rout, P. R., Bandyopadhyay, B., Das Mohapatra, P. K. (2014): Characterizing novel thermophilic amylase producing bacteria from Taptapani hot spring, Odisha, India. – Jundishapur J Microbiol. 7(12): e11800.
[19] Shah, W., Ali, N., Ahmad, S., Qasim, M., Rahman, H., Ullah, S., Ullah, F., Khattak, B., Khan, M. D. (2017): Molecular characterization and growth optimization of halo-tolerant amylase producing bacteria isolated from salt mines of Karak, Pakistan. – Pure Appl. Biol. 6(1): 385-393.
[20] Singh, R., Kumar, M., Mittal, A., Mehta, P. K. (2016): Microbial enzymes: industrial progress in 21st century. – 3 Biotech. 6(2): 174.
[21] Singh, V., Sharma, R., Sharma, P. (2015): Isolation, screening and optimization of amylase producing Bacillus sp. from soil. – Asian Pac. J. Health Sci. 2(3): 86-93.
[22] Suriya, J., Bharathiraja, S., Krishnan, M., Manivasagan, P., Kim, S. K. (2016): Marine microbial amylases: properties and applications. – Adv Food Nutr Res. 79161-177.
[23] Tango, M. S. A., Islam, M. R. (2002): Potential of extremophiles for biotechnological and petroleum applications. – Energy Sources 24(6): 543-559.
[24] Wajeeha, A., Asif, M., Rasool, S. A. (2011): Extracellular enzyme production by indigenous thermophilic bacteria: partial purification and characterization of α-amylase by bacillus sp. WA21. – Pak. J. Bot. 43(2): 1045-1052.
[25] Zahoor, S., Javed, M. M., Babarl, M. E. (2016): Characterization of a novel hydrolytic enzyme producing thermophilic bacterium isolated from the hot spring of Azad Kashmir-Pakistan. – Braz. Arch. Biol. Technol. 59: e16150662(1): 1-13.

http://www.aloki.hu ● ISSN 1589 1623 (Print) ● ISSN 1785 0037 (Online)
DOI: http://dx.doi.org/10.15666/aeer/1802_26112620

STABILITY ANALYSIS OF SEED YIELD OF ADVANCED CHICKPEA (*CICER ARIETINUM* L.) GENOTYPES UNDER TROPICAL AND SUBTROPICAL RAINFED REGIONS OF IRAN

HAJIVAND, A.[1] – ASGHARI, A.[1*] – KARIMIZADEH, R.[2] –
MOHAMMADDOUST-CHAMANABAD, H. R.[1] – ZEINALZADEH-TABRIZI, H.[3]

[1]*Department of Agronomy and Plant Breeding, Faculty of Agriculture and Natural Resources, University of Mohaghegh Ardabili, Ardabil, Iran*
(phone: +98-914-304-2117; fax: +98-453-351-3920)

[2]*Dryland Agricultural Research Institute, Agricultural Research, Education and Extension Organization (AREEO), Gachsaran, Iran*
(phone: +98-917-344-5107; fax: +98-743-234-3402)

[3]*Crops and Horticultural Science Research Department, Ardabil Agricultural and Natural Resources Research and Education Center (AREEO), Ardabil (Moghan), Iran*
(phone: +98-453-275-1013; fax: +98-453-275-1420)

[*]*Corresponding author*
e-mail: a_asghari@uma.ac.ir; phone: +98-914-304-2117; fax: +98-453-351-3920

(Received 1st Aug 2019; accepted 25th Nov 2019)

Abstract. Evaluation of compatibility and stability of cultivars under different environmental conditions is a particular interest in crop breeding programs. In order to evaluate the seed yield stability of advanced chickpea genotypes under tropical and subtropical rainfed areas of Iran, 18 advanced chickpea genotypes and two check varieties (Adel and Azad) were studied in terms of randomized complete block design (RCBD) with three replications in four locations including Gachsaran, Gonbad, Khorramabad and Ilam using GGE biplot analysis during three growing seasons (2014-2017). Results of GGE biplot analysis and which-won-where pattern revealed that the genotype G13 was the most stable genotype for Khorramabad, Gachsaran and Gonbad while it was genotype G12 for Ilam. According to average tester coordinate (ATC), the genotype G13 was the most stable one across average test environment. The genotype G13 was also determined as a stable and high yielding genotype among all investigated genotypes and environments. Based on the average yield and Shukla Stability Index, as well as the mean of yield to maximum or Superiority Index (SI), G12, G13 genotypes were superior to the other genotypes in all regions with warm climate and thus be recommended.
Keywords: *adaptation, environment, GGE biplot, interaction, promising line, superiority index*

Introduction

The chickpea (*Cicer arietinum* L.) is a self-pollinated, diploid, and annual plant (2x=2n=16). After peas and beans, it is the most important legume in the world (Varshney et al., 2013). The main countries producing chickpeas in the world are India, Pakistan, Turkey, Iran and Australia, respectively (Gan et al., 2005). The area under cultivation of chickpea in Iran is 650 thousand hectares and its annual production is about 350 thousand tons (Kanouni et al., 2016). Iran ranked seventh in the world for chickpea production after India, Australia, Turkey, Myanmar, Pakistan and Ethiopia (FAO, 2012). Farmers who grow chickpea need cultivars with high yields and maintain desirable qualities in a wide range of environmental conditions throughout the years (Zali et al., 2007; Tabrizi, 2012). The genotype by environment interaction (GEI) is the reaction of a variety to the changes in the environments (Yan et al., 2000). This interaction is

http://www.aloki.hu ● ISSN 1589 1623 (Print) ● ISSN 1785 0037 (Online)
DOI: http://dx.doi.org/10.15666/aeer/1802_26212636

important to plant breeding researchers and is one of the complexities of breeding programs for the preparation of a high-yielding and sustainable genotype (Yan et al., 2010; Karimizadeh et al., 2016). The GEI indicates a different sensitivity to environmental conditions, which means that the best genotype in an environment is not necessarily the best genotype in another environment (Farshadfar, 1998). Stability analysis is the most important method used to find out the nature of the GEI. Therefore, stable and compatible cultivars can be identified by using this analysis. Different methods have been proposed to investigate the GEI and the determination of stable genotypes, which include univariate and multivariate parametric and nonparametric methods (Dehghanpour et al., 2007; Mohammadi et al., 2012). The GGE biplot method is one of the multivariate methods for evaluating and interpreting the pattern response of cultivars, environments and their interaction (Gabriel, 1971). In the GGE biplot method, the effect of the genotype and the G×E are not separated and selection of cultivars with yield stability is based on both effects (Yan et al., 2000). What is important in assessing genotypes in different environments is that the environmental effect is very large in most cases, but not exploitable, thus eliminating the environmental impact of the data and focusing on the effects of genotype (G) and the G×E are important (Yan and Kang, 2002). Only effect of the genotype and the G×E are important to select the lines with stable yield. The main point is that the two mentioned effects should be considered together (Yan, 2001). The GGE biplot method examines these two effects graphically (Yan, 2001). This method has been identified to be useful and applicable by numerous researchers for different crops for analyzing regional test data. Employing the GGE biplot method for selecting suitable chickpea cultivars (Kanouni et al., 2007; Zali et al., 2007; Farshadfar et al., 2012, 2013; Mostafavi et al., 2013; Pourdad and Jamshidi-Moghaddam, 2013; Shiri and Bahrampour, 2015), canola (Zali et al., 2016; Jabbari et al., 2019; Kheybari et al., 2019), bread wheat (Omrani et al., 2017), lentil (Karimzadeh et al., 2013), durum wheat (Mohammadi et al., 2016; Karimzadeh et al., 2019) for Iranian germplasm has been reported.

The present study aimed to investigate the GEI using GGE biplot methodology in chickpea genotypes to obtain high yielding cultivars, which are adapted with climatic conditions in tropical and subtropical regions of Iran.

Materials and Methods

Description of the trials

The plant materials used in this study were 18 advanced chickpea lines with two local check varieties (Adel and Azad) grown for three years (2014-2017) at each of four different locations in Iran. Geographical characteristics and soil properties of the test environments are presented in *Table 1*. These plant materials used in national chickpea breeding program for rainfed areas of Iran are provided from the International Centre for Agricultural Research in the Dry Areas (ICARDA) chickpea international breeding program. Genotype names and their pedigrees are presented in *Table 2*.

Seed density for each genotype was 50 seed per m^2 and planting was done using experimental planter's machine. Sowing date of all experiments was November 15. Each plot consists of five plant rows, 6 m length with row space of 25 cm. Therefore, the size of each plot was 7 m^2. Fertilizers were applied 100 kg ha^{-1} of ammonium phosphate as triple super phosphate at planting time, and 35 kg of urea during field preparation. No disease was shown during growth period. Weed control and thinning of plants were done

http://www.aloki.hu ● ISSN 1589 1623 (Print) ● ISSN 1785 0037 (Online)
DOI: http://dx.doi.org/10.15666/aeer/1802_26212636

by hand during the experiments. To avoid the marginal effects, 25 cm from the beginning and end of the rows of each experimental plot was removed. Then 5 m^2 of each plot were harvested at physiological maturity of each genotype and finally seed yield of each plot was weighted. Weather data of the test site locations during the experiments are presented in *Table 3*.

Table 1. *Geographical characteristics and soil properties of the test environments*

Test environment name	Longitude and Latitude	Altitude (m)	Soil Texture	Soil Type	Annual Precipitation (mm)
Gachsaran	30 21 N 50 47 E	726	Silty Clay Loam	Regosols	455
Gonbad	55 18 N 37 17 E	45	Silty Clay Loam	Regosols	367
Ilam	33 36 N 46 36 E	1427	Clay Loam	Regosols	502
Khorramabad	33 48 N 48 35 E	1148	Silt-Loam	Regosols	433

Table 2. *The name, origin and code of the studied chickpea genotypes*

Name/Pedigree	Origin	Code
FLIP03-26C/3/98TH70/4/(FLIP93-210C/ FLIP87-8C)//S96086	ICARDA	G1
FLIP06-17C//2002TH 18/3/FLIP98-130C / FLIP98-120C	ICARDA	G2
FLIP06-39C//2002TH 37/3/S99520 / FLIP98-048C	ICARDA	G3
FLIP06-43C//2002TH 40/3/FLIP98-28C/ FLIP98-079C	ICARDA	G4
FLIP06-97C/4/2002TH 119/5/[(FLIP 98-64C/ FLIP98-47C)//Sel99ter85488] /3/ FLIP98-022C	ICARDA	G5
FLIP06-120C/3/2002TH 131/4/(ILWC 141/S85581)//FLIP98-130C	ICARDA	G6
FLIP07-201C/3/03TH-20/4/(S00784/FLIP97-28C)//ICCV2	ICARDA	G7
FLIP88-85C//85 TH143/3/ILC 629 / FLIP 82-144C	ICARDA	G8
FLIP06-59C//2002TH 76/3/S99858/FLIP 97-026C	ICARDA	G9
FLIP03-141C/3/00TH 51//FLIP98-52C/FLIP98-47C	ICARDA	G10
FLIP05-44C/3/2000TH 39//FLIP98-29C/S99001	ICARDA	G11
FLIP05-46C/3/2000TH 39//FLIP98-29C/S99001	ICARDA	G12
FLIP05-46C/3/2000TH 39/FLIP98-29C//S99001	ICARDA	G13
FLIP07-11C/3/03TH-138/FLIP98-130C//FLIP99-34C.	ICARDA	G14
FLIP07-33C/3/03TH-153/FLIP98-133C//FLIP98-117C	ICARDA	G15
FLIP08-14C/4/00TH95//(FLIP84-182C/FLIP91-138C)/3/ S99075	ICARDA	G16
FLIP08-58C/3/02TH3/FLIP 98- 28C // FLIP 97-102C	ICARDA	G17
FLIP03-31C/3/98TH18//S96114/FLIP 92-148C	ICARDA	G18
ADEL (99-66C) (check)	IRAN	G19
AZAD (check)	IRAN	G20

http://www.aloki.hu ● ISSN 1589 1623 (Print) ● ISSN 1785 0037 (Online)
DOI: http://dx.doi.org/10.15666/aeer/1802_26212636

Table 3. *Weather data of the test site locations*

		OCT			NOV			DEC			JAN		
		2014	**2015**	**2016**	**2014**	**2015**	**2016**	**2014**	**2015**	**2016**	**2015**	**2016**	**2017**
Precipitation (mm)	Gachsaran	7.4	0.0	0.0	31.1	81.7	3.4	107.9	57.5	78.6	5.5	139.4	4.0
	Gonbad	24.3	37.9	29.8	41.6	99.6	58.2	48.5	61.0	37.5	14.0	43.1	9.0
	Ilam	50.7	0.5	2.7	77.7	319.6	1.9	45.1	67.7	35.3	17.2	75.9	87.5
	Khorramabad	70.3	14.0	0.0	33.9	190.8	8.6	61.6	125.4	66.2	9.6	57.5	82.6
Average temperature (°C)	Gachsaran	25.5	27.3	24.8	17.5	18.3	20.4	17.8	13.2	14.1	11.9	11.2	14.5
	Gonbad	21.4	23.7	21.4	14.4	17.5	14.7	10.2	12.7	8.3	10.2	13.0	10.7
	Ilam	20.1	24.2	22.0	13.3	13.9	17.3	9.9	8.1	8.1	6.7	6.7	7.3
	Khorramabad	19.9	21.5	19.7	11.5	13.2	15.5	8.5	6.7	7.2	6.0	6.2	6.9
		FEB			**MAR**			**APR**			**MAY**			**JUN**		
		2015	**2016**	**2017**	**2015**	**2016**	**2017**	**2015**	**2016**	**2017**	**2015**	**2016**	**2017**	**2015**	**2016**	**2017**
Precipitation (mm)	Gachsaran	12.8	30.5	88.5	83.3	21.7	25.3	63.8	57.3	28.7	3.8	2.0	8.4	0.0	0.0	0.0
	Gonbad	40.9	49.4	94.6	76.9	52.1	35.6	25.1	65.1	37.2	8.0	27.8	30.4	0.1	42.8	0.3
	Ilam	18.7	56.9	102.3	59.2	53.0	74.7	58.9	138.6	93.8	7.5	25.6	10.7	0.1	0.0	0.0
	Khorramabad	34.0	30.6	101	52.9	63.9	44.3	51.4	244	80.8	12.6	17.2	32.8	0.0	0.0	0.0
Average temperature (°C)	Gachsaran	14.8	11.4	11.1	14.2	16.1	14.9	19.6	17.3	20.0	26.2	25.9	26.6	32.1	33.2	30.8
	Gonbad	10.2	12.9	9.3	9.2	16.0	14.9	14.8	16.7	18.0	20.7	25.1	24.4	28.8	26.8	27.1
	Ilam	9.3	7.0	4.9	9.3	12.0	10.2	16.1	12.9	14.0	19.8	20.4	21.1	28.3	28.5	26.2
	Khorramabad	9.3	6.2	4.2	9.3	11.5	9.4	13.5	11.7	14.1	20.0	19.7	20.1	26.1	21.3	24.5

http://www.aloki.hu ● ISSN 1589 1623 (Print) ● ISSN 1785 0037 (Online)
DOI: http://dx.doi.org/10.15666/aeer/1802_26212636

Statistical analysis

The experimental design in all locations was a randomized complete block design with four replicates. Outliers were firstly detected using Grubb's test (Grubbs, 1969) before variance analysis. Then the normality of seed yield data was checked by the Shapiro-Wilk test (Shapiro and Wilk, 1965). To test the uniformity of the variance of experimental errors, the Levene test (Leven, 1960) and Bartlett's test (Bartlett, 1937) were employed. Combined analysis was performed by SAS 9.1 software package. Graphical stability analysis was performed using GGE biplot software version 6.3 (Yan, 2001).

Model 1 based on singular value decomposition (SVD) of tester-centered data of the first two principal components was chosen to construct various biplots. This model is used for dataset in which all testers have the same unit, such as a genotype-by-environment table of a single trait like seed yield in this study.

The model is: $Yij - u - \beta j = gi1\ e1j + gi2\ e2j + \varepsilon ij$; where: Yij is the performance expected seed yield of genotype (entry) i in location (environment) j; μ is the overall mean of the observations; βj is the main effect of location j; g1i and e1j are the primary scores for the ith genotype in the jth environment, respectively; gi2 and e2j are the secondary scores for the ith genotype in the jth environment, respectively; and εij is the residual not explained by primary and secondary effects (Yan and Kang, 2002). Therefore, biplot in the GGE biplot model is generated by the simple dispersion of g1i and gi2 for genotypes and e1j and e2j for environments, via singular value decomposition, in accordance with the equation $Yij - \mu - \beta j = \lambda 1 \xi i1 \eta 1j + \lambda 2 \xi i2 \eta 2j + \varepsilon ij$, where λ1 and λ2 are the largest eigenvalues of the first and second principal components, PC1 and PC2, respectively; ξi1 and ξi2 are the eigenvalues of the ith genotype for PC1 and PC2, respectively; and η1j and η2j are the eigenvalues of the jth environment for PC1 and PC2, respectively (Yan and Kang, 2002).

Superiority Index (SI) was calculated using YREM which refers to "Yield relative to the maximum". The output is the average YREM of each genotype across environments. It is a [0,1] superiority index, the larger the value of a genotype the more superior it is (Yan, 1999).

Results and Discussion

Before combined analysis of data, the results of the Levene's Test (1.35^{ns}) and Bartlett's test (11.53^{ns}) to ensure the uniformity of the experimental errors in the test environments showed that there is a uniformity of error among the variances of the experimental errors. Therefore, combined analysis can be carried out. Combined analysis of variance showed that there was a significant difference between the genotypes in terms of seed yield at a probability level of 0.05. The G×E was also significant (*Table 4*). The significance of the G×Y×E indicated that the mean seed yield of chickpea genotypes was different across different locations. Therefore, stability analysis could be used to identify genotypes or stable genotypes. This model is suitable for a series of data that have the same units as the genotype table in the environment for a trait, such as the seed yield in this study.

Graphical analysis of chickpea genotypes by GGE biplot method showed that the first two components explained 62.5% of variations in seed yield in different environments. 32.9% of these variations belonged to the first component, and 29.6% belonged to the second component. According to Yan and Kang (2002), if GGE biplot methodology can

http://www.aloki.hu ● ISSN 1589 1623 (Print) ● ISSN 1785 0037 (Online)
DOI: http://dx.doi.org/10.15666/aeer/1802_26212636

explain at least 60% of the variance of the total data, it can be applicable and useful for evaluating mega environments.

Table 4. *Combined analysis of seed yield in chickpea genotypes across different environments*

S.O.V	Df	MS
Year (Y)	2	4816696.8^{ns}
Location (P)	3	68100256.5*
Y×P	6	13945279.2**
Error	24	403237.2
Genotypes (G)	19	251286.3*
G×Y	38	107198.9^{ns}
G×P	57	227210.2**
G×Y×P	114	106548.1**
Error	456	77917
Total	719	
CV%	19.38	

ns * and **: non-significant, significant at 5% and 1% probability level, respectively

Total variance percentages, as well as the percentage of the first and second components in Maqbool et al. (2015) study, were 98.61%, 87.67%, and 10.49%, respectively. In Kanouni et al. (2016), the values were, 66.43%, 43.09% and 23.34%, and in Usefi et al. (2017) they were 75%, 46%, and 29%, respectively. *Table 5* illustrates the variance values explained by genotype, environment, and G×E. Accordingly, 2.15% of the total variance, as explained by the first two components of the biplot analysis was related to the genotype (G), 92.02% was related to the environment (year and location), and 5.83% was related to the G×E. In Farshadfar et al. (2011) conducted on the stability of chickpea cultivars, 2.48% of the total variance was related to the genotype, 86.44% was related to the effect of the environment, and 11.08% was related to the G×E, which are with consistent with the results of the present research. Gauch and Zobel (1996) concluded that the large environment main effect, however, is not relevant to cultivar evaluation. Only G and G×E are relevant to cultivar evaluation. Therefore, for cultivar evaluation, it is essential to remove E from data and to focus on G and G×E. Thus, large environment main effect reported in this study was in accordance with previous studies. Another important point in cultivar evaluation and stability analysis is that G and G×E must be considered simultaneously to make any meaningful selection decisions (Yan and Kang, 2002).

Table 5. *Relative magnitude of the genotype, environment and their interaction based on two first components of biplot analysis*

S.O.V	SS	Percentage of total variance
Genotype (G)	1591434	2.15
Environment (E)	68097475	92.02
G×E	4317009	5.83
Total	74005918	

http://www.aloki.hu ● ISSN 1589 1623 (Print) ● ISSN 1785 0037 (Online)
DOI: http://dx.doi.org/10.15666/aeer/1802_26212636

Assessment of test environments showed that the highest seed yield was obtained in Khorramabad, and the lowest was in Gachsaran. Also, Gonbad has highest, and Khorramabad the lowest coefficient of environmental variations among testers. In terms of heritability of the test environments, Gonbad and Gachsaran have the highest values, indicating the power of differentiation of these regions in the discriminating of genotypes in terms of stability (*Table 6*).

Table 6. *Mean yield, heritability and coefficient of variations of the test environments*

Test environment name	Mean Yield (kg ha^{-1})	Standard Error	Heritability	CV (%)
Gachsaran	1029.065	115.891	0.668	11.26
Gonbad	1241.449	174.349	0.723	14.04
Ilam	1136.55	142.364	0.637	12.53
Khorramabad	2353.557	238.292	0.459	10.12

The heritability values reflect the variation detected among the genotypes, which will be greater when increase the environment discriminating ability (Cravero et al., 2010).

Fig. 1 shows a biplot graphical analysis and a which-won-where pattern of 20 genotypes of chickpea based on the mean seed yield in four environments examined. The visualization of the which-won-where pattern is important in multi-environmental data to study the possibility of having large environments in a region. The biplot polygon diagram is the best way to visualize the patterns of G×E and to correctly interpret a biplot (Yan and Tinker, 2006). Accordingly, G13 was the most stable one in Khorramabad and Gachsaran, and G12 was the highest yielding and most stable one for Ilam (*Fig. 1*). This conclusion can also be obtained from drawing specific biplots for each location (*Figs. 2, 3, 4, and 5*). In other words, the G13 in Khorramabad, Gachsaran and Gonbad, and G12 in Ilam have a specific adaptability to the locations.

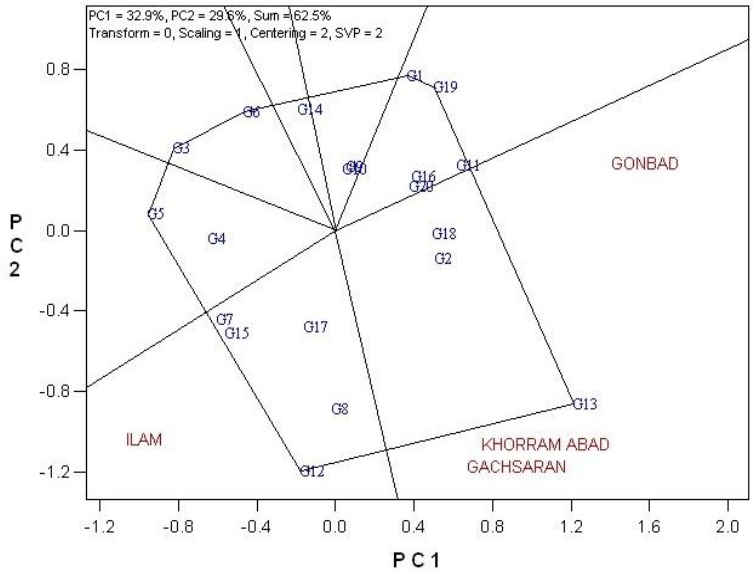

Figure 1. *Which-won-where pattern biplot based on seed yield of chickpea genotypes in different test environments*

http://www.aloki.hu ● ISSN 1589 1623 (Print) ● ISSN 1785 0037 (Online)
DOI: http://dx.doi.org/10.15666/aeer/1802_26212636

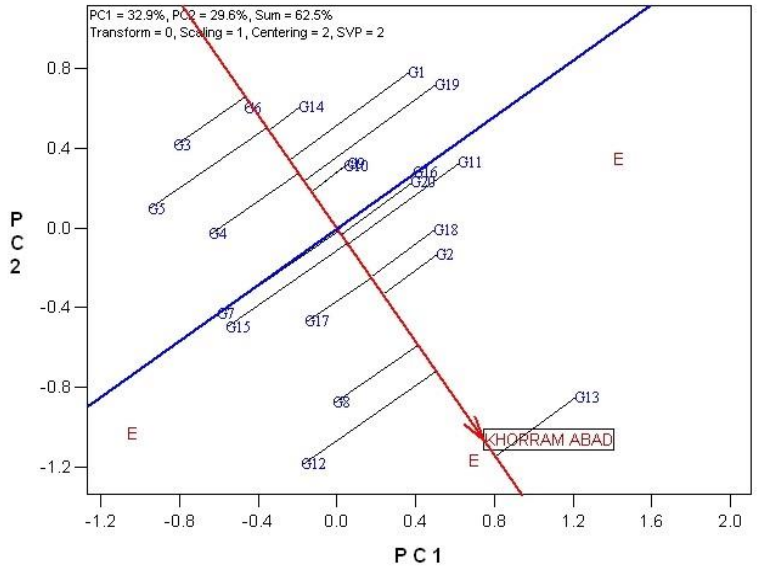

Figure 2. *Ranking of all genotypes and determination of specific adaptability in the Khorramabad test environment*

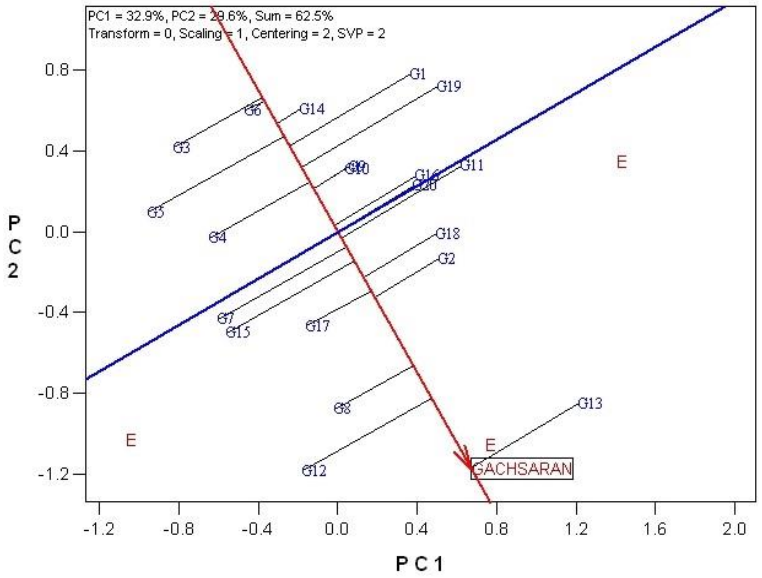

Figure 3. *Ranking of all genotypes and determination of specific adaptability in the Gachsaran test environment*

Also, genotype G5 at the left side of the biplot had the lowest seed yield and stability among the genotypes tested. In *Figs. 2, 3, and 4,* the red axis, indicates the mean yield of genotypes (G) and the perpendicular blue axis indicates the G×E. Thus, from the right side of the biplot to the left, the genotype yield decreases. The best genotype is a genotype that is inclined to the positive end of red axis and its vertical distance is shortest from this line. Genotypes with the shortest distance from the center have more stability (Yan and Kang, 2002).

http://www.aloki.hu ● ISSN 1589 1623 (Print) ● ISSN 1785 0037 (Online)
DOI: http://dx.doi.org/10.15666/aeer/1802_26212636

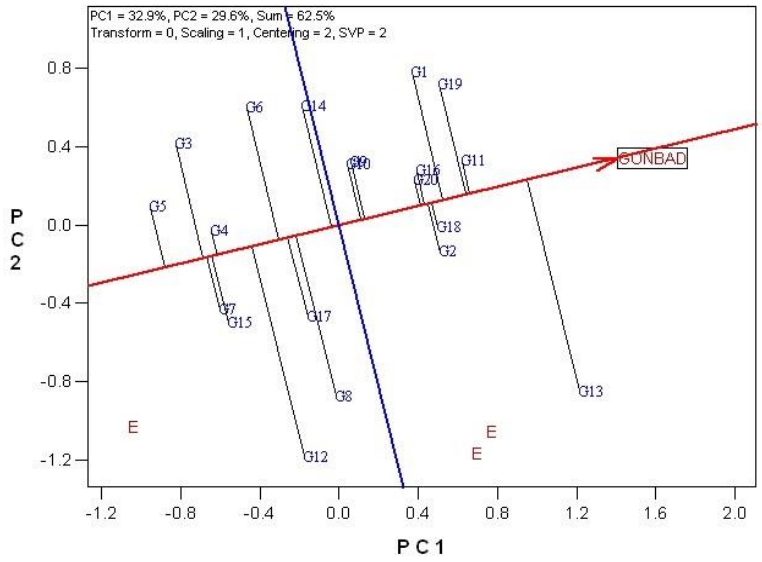

Figure 4. *Ranking of all genotypes and determination of specific adaptability in the Gonbad test environment*

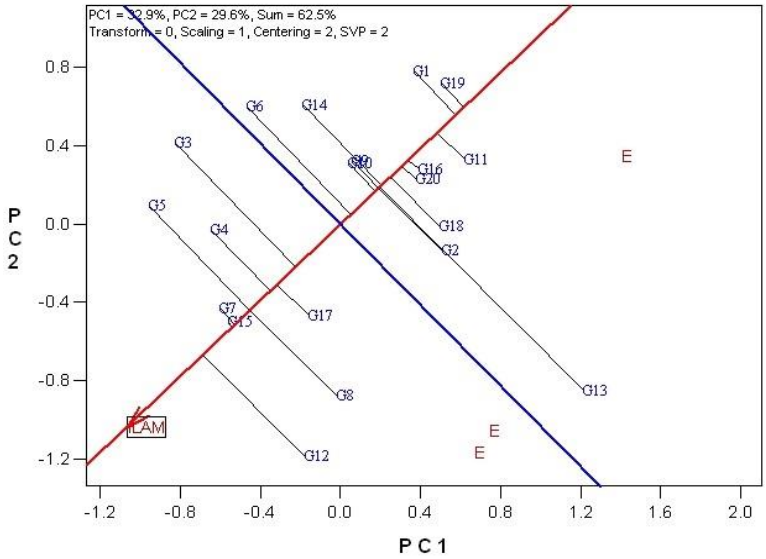

Figure 5. *Ranking of all genotypes and determination of specific adaptability in the Ilam test environment*

To examine the stability and yield of genotypes the Average Environment Coordination (AEC) was used (*Fig. 6*). In this biplot, the horizontal axis with an arrow moves from the origin of the coordinates (Yan et al., 2000). The images of genotypes on this axis represent approximately their yield. This axis is called the average environment axis. The results of the biplot (*Fig. 6*) showed that G13 was the most efficient and stable genotype in the average environment of all test environments. The vertical axis, originating from the coordinates of the past and perpendicular to the average environment axis indicates the G×E and determines the stability of the genotypes. How much vertical distance is highest from red line, represents unstable mean yield. One of the features of

http://www.aloki.hu ● ISSN 1589 1623 (Print) ● ISSN 1785 0037 (Online)
DOI: http://dx.doi.org/10.15666/aeer/1802_26212636

GGE biplot analysis is based on the analysis of the main components is genotype-based scaling, and using the same unit for both horizontal and vertical axes, which allows more accurate examination of genotypes. This feature can be used to show the average of genotype and stability simultaneously (Farshadfar et al., 2011). The common unit for the mean yield and stability allows both criteria of yield and stability can be combined and conceptualized into a single criterion. The display of average genotype and stability of genotypes can be possible through drawing an axis that passes through the biplot and the average environment (small red circle on the axis). The images of the signs of genotypes on this axis are estimations of their mean yield (Yan and Kang, 2002). The correlation coefficient between this ranking and the average genotype yield was 0.927, indicating an appropriate explanation of the average genotypes on the average environment axis. Direction of red arrow displays a higher average. The blue vertical axis provides an estimate of the interaction and stability of the genotypes, and distance from the source (the intersection with the red axis) is a criterion for the variability or instability of genotypes. Moreover, the vertical blue axis, perpendicular to the red axis, provides an estimate of the interaction and stability of the genotypes, and the distance from the origin, (the intersection with the red axis) is a criterion for variability or instability of genotypes.

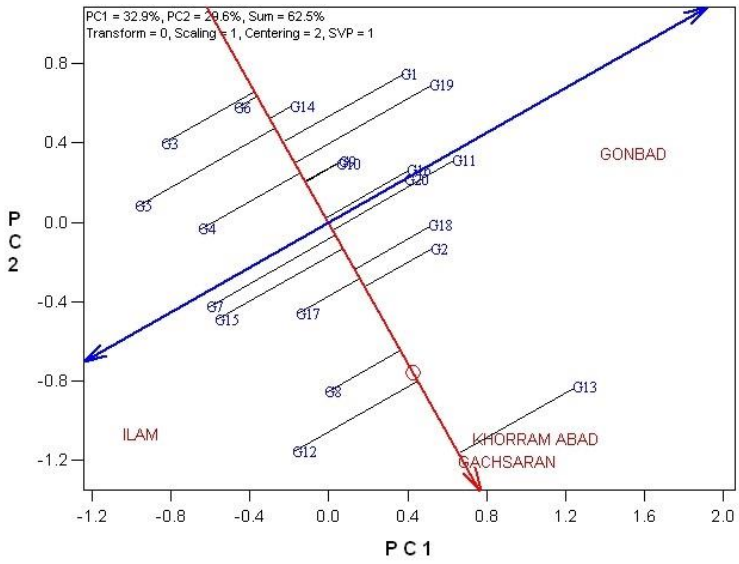

Figure 6. *Average Environment Coordination (AEC) of seed yield stability in chickpea genotypes using GGE biplot analysis in different test environments*

The stability criterion determined by the G×E is only useful when considered together with the mean yield (G) (Yan, 1999). For example, in *Fig. 6* it seems that G4 is more stable than G13 because it is less close to the average environment vector, but is not desirable because it has a much lower yield than G13. Kang (1993) and Yan (1999) concluded that stability is a non-dimensional value which displays a high-yield value better, but displays a low-yield value worse. Eskridge (1996) concluded that stability is less inherited than mean yield. Therefore, stability, along with the mean yield, are useful, and the GGE biplot methodology converts it to a benchmark that can be evaluated graphically (Yan et al., 2000).

http://www.aloki.hu ● ISSN 1589 1623 (Print) ● ISSN 1785 0037 (Online)
DOI: http://dx.doi.org/10.15666/aeer/1802_26212636

Fig. 7 shows the biplot of comparison different test environments with the ideal test environment, and vector display of the interaction between them based on the seed yield of the chickpea genotypes using the graphical GGE biplot analysis. For this purpose, the origin of the linear coordinates is connected to the point of the average environments and continues to the sides. The best environment is the environment that is closer to the center of the circles. Since the comparison of genotypes in this biplot is not indicated, they are shown with small circles. Based on this biplot, Gachsaran and Khorramabad regions had higher representation and differentiation than Gonbad and Ilam in terms of differentiation and discriminating of the genotypes. In fact, the length of each test environment estimates the standard deviation within each environment. The longer the test environment, the more power of differentiation and representativeness of that environment (Yan and Kang, 2002).

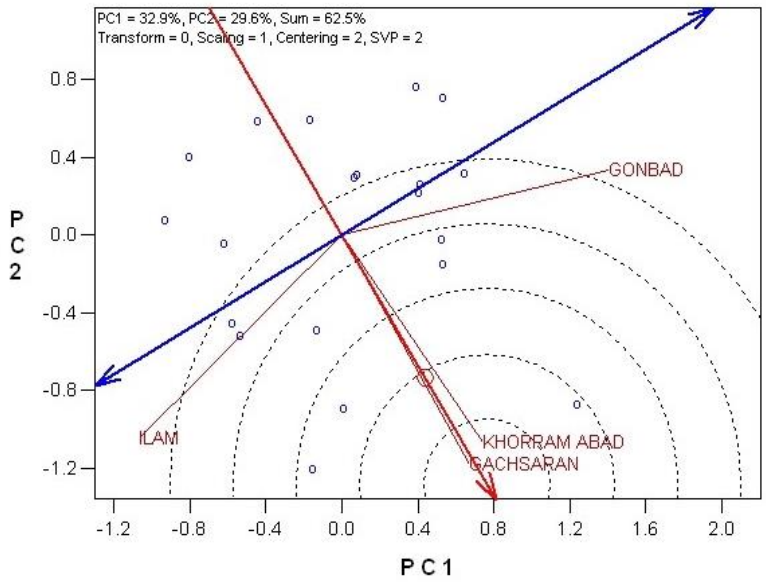

Figure 7. *Biplot for comparison environments with the ideal environment and vector display of the interaction between them based on seed yield of chickpea genotypes*

Table 7 shows the correlation coefficients between different environments. As *Table 7* illustrates, there is no significant positive correlation between each environment, in other words the effect of the year was different during the three years of the experiment. The GGE biplot method is also used to separate of similar environments from non-similar (Navabi et al., 2006).

Table 7. *Correlation coefficients among different test environments*

Location	Gachsaran	Gonbad	Ilam	Khorramabad
Gachsaran	1			
Gonbad	0.106	1		
Ilam	0.064	-0.281	1	
Khorramabad	0.176	0.100	0.023	1

http://www.aloki.hu ● ISSN 1589 1623 (Print) ● ISSN 1785 0037 (Online)
DOI: http://dx.doi.org/10.15666/aeer/1802_26212636

In fact, in the fitted model of GGE biplot, the cosine of the angle between any two environments approximates their correlation coefficient between them (Yan and Kang, 2002). In this study, Gachsaran and Khorramabad have a close angle between their vectors, therefore, they should be correlated. Indeed, the correlation coefficient between them is 0.176 because the model is not 100% fitted. Yan and Kang (2002) concluded that the cosine of the angles does not precisely translate into correlation coefficients, since the biplot does not explain all of the variation in a dataset.

Fig. 8 shows the biplot of comparison of all genotypes with the ideal genotype. The red circle on the red axis represents the ideal hypothetical genotype that has the highest yield and stability among all genotypes and environments. In practice, however, such a genotype does not exist, but the ranking of other genotypes is estimated based on this ideal genotype (Yan and Kang, 2002). Accordingly, G13 was identified as a stable and high yield genotype among all genotypes and environments (*Fig. 8*). The correlation coefficient was calculated between the average genotypes and their distance on the biplot as -0.903, indicating a proper explanation of the biplot of comparison of the genotypes with the ideal genotype. Moreover, the results of this biplot were consistent with the results of the biplot of the average environment (*Fig. 6*).

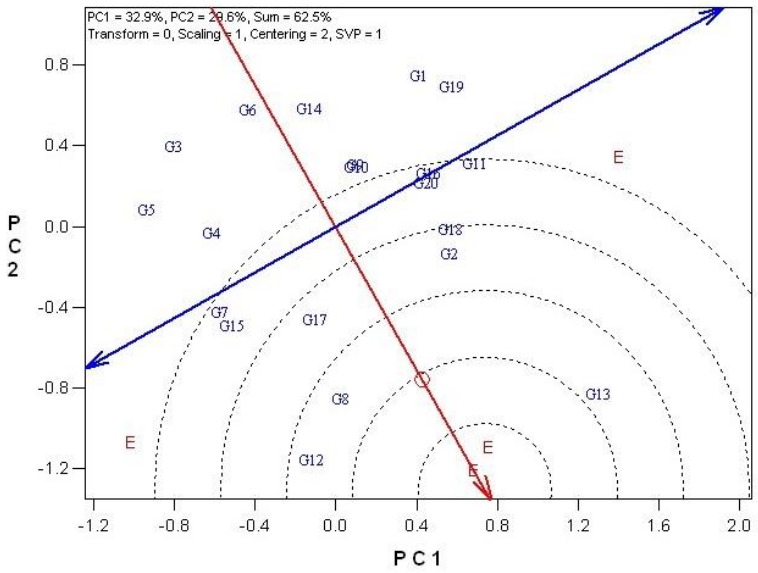

Figure 8. *Biplot drawn based on genotype-focused scaling for comparison of chickpea genotypes with an ideal genotype*

Fig. 9 shows the mean seed yield of chickpea genotypes versus the deviation of their stability (Shukla's Stability Index). Accordingly, genotypes G13 and G12 were superior to the other genotypes.

Fig. 10 displays the mean seed yield in relation with the maximum seed yield (YERM) or Superiority Index of seed yield of chickpea genotypes versus the deviation of the stability of the superiority index. Accordingly, genotypes G13 and G12 were superior to other genotypes in all regions of the study. This criterion, which was first suggested by Yan (1999), is a superiority index based on (0 and 1), so that the larger its value, the more stable its genotype.

http://www.aloki.hu ● ISSN 1589 1623 (Print) ● ISSN 1785 0037 (Online)
DOI: http://dx.doi.org/10.15666/aeer/1802_26212636

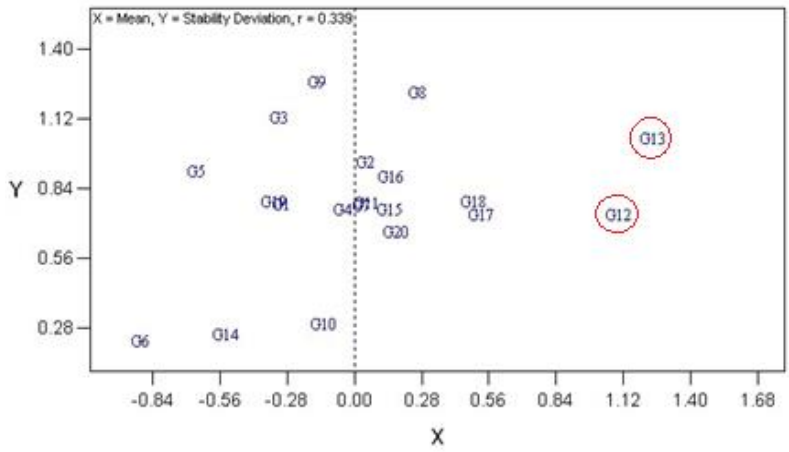

Figure 9. *Shukla's Stability Index and Mean yield in chickpea genotypes*

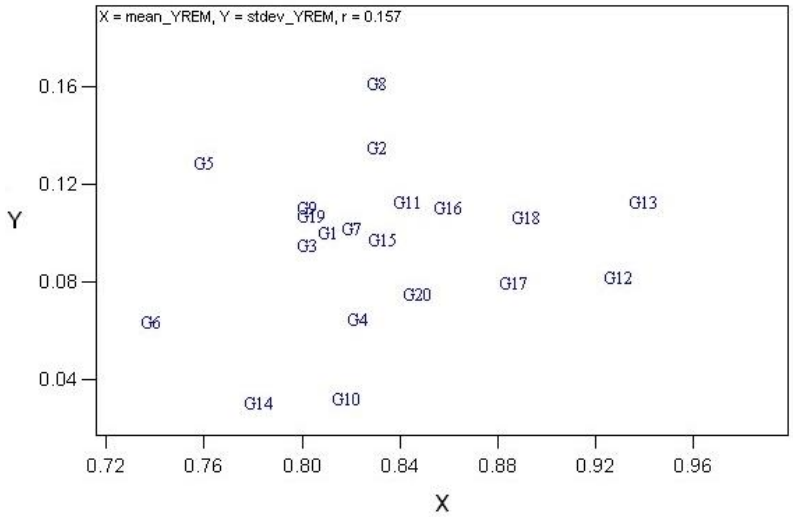

Figure 10. *Mean yield of superiority index for each chickpea genotype in all test environments*

Concurrent selection for yield and stability is one of the most important considerations in breeding plans (Yan and Kang, 2002). GGE biplot analysis with a user-friendly graphical interface can analyze different kinds of two-way data and provide a quick and complete understanding of the relationships between genotypes, environments, and their interactions. In this regard, the results of a study by Farshadfar (2011), investigating phenotypic stability evaluation in 17 chickpea genotypes in five research stations in Iran using the GGE biplot methodology, pointed up that the environment explained 86.44%; the genotype 2.48%; and the G×E 11.8% of the total variations of G + E + GE equation. The overall biplot analysis revealed three large environments from five research sites for chickpeas in Iran. Sabaghpour (2010) used GGE biplot in studying the stability of seed yield in 16 chickpea genotypes in autumn crop under rainfed conditions for three years. They also analyzed the two sites of Gachsaran and Gonbad separately and examined the interaction between year and location as well as genotype and year.

http://www.aloki.hu ● ISSN 1589 1623 (Print) ● ISSN 1785 0037 (Online)
DOI: http://dx.doi.org/10.15666/aeer/1802_26212636

Conclusion

One of the main subjects among plant breeders is to understand the concept of the relationship between crop yield and environment. Analysis of the G×E is one of the substantial issues in plant breeding, which is very important in the development and expansion of new cultivars. In this experiment, G×E of advanced chickpea genotypes in tropical and subtropical rainfed regions in Iran were investigated. The main effects of genotype and environment as well as the G×E were significant and the environment caused the most variations in seed yield. The highest mean seed yield of chickpea genotypes was observed in Khorramabad (2353.557 kg ha^{-1}) and the lowest was observed in Gachsaran (1029.065 kg ha^{-1}). GGE biplot analysis and which-won-where pattern of 20 genotypes showed that G13 was the most stable genotype for Khorramabad, Gonbad and Gachsaran, and G12 was the highest yielding and most stable and suitable genotype for Ilam. Based on the average environment coordinates, G13 was the highest yielding and most stable genotype in the average environment. Based on the biplot of comparison of all genotypes with the ideal genotype, G13 was identified as a stable and top-yielding genotype among all genotypes and environments. Based on the mean seed yield and Shukla's Stability Index, as well as the mean yield in relation with maximum or Superiority Index, G13 and G12 are superior and more stable than all other genotypes in the whole tropical regions in southern area of Iran; hence they are well recommended. Also, evaluation of the qualitative traits of the genotypes studied in this experiment can be recommended for future research.

Acknowledgements. The authors thank the Iranian Dryland Agricultural Research Institute for making available the plant materials, experimental locations and technical assistance.

REFERENCES

[1] Bartlett, M. S. (1937): Properties of sufficiency and statistical tests. – Proceedings of the Royal Society A 160: 268-282.
[2] Cravero, V., Espósito, M. A., Lopez-Anido, F., García, S. M., Cointry, E. (2010): Identification of an ideal test environment for asparagus evaluation by GGE-biplot analysis. – Australian Journal of Crop Science 4(4): 273-277.
[3] Dehghanpour, Z., Karimizadeh, R., Dehghani, H., Sabaghnia, N. (2007): Determination of adaptability and stability of seed yield in foreign earl maturity. – Iranian Journal of Agricultural Sciences 38: 249-257. (In Persian with English Abstract).
[4] Eskridge, K. (1996): Analysis of multiple environment trials using the probability of outperforming a check. – In: Kang, M. S., Gauch, H. (eds.) Genotype by environment interaction. CRC Press, NY, USA, pp. 273-307.
[5] FAO. (2012): Food and Agriculture Organization of the United Nations. – Rome, Italy.
[6] Farshadfar, E. (1998): Application of Biometrical Genetics in Plant Breeding. – Razi University. Kermansha, Iran.
[7] Farshadfar, E., Zali, H., Mohammadi, R. (2011): Evaluation of phenotypic stability in chickpea genotypes using GGEBiplot. – Annals Biology Research 2(6): 282-292.
[8] Farshadfar, E., Sabaghpour, S. H., Zali, H. (2012): Comparison of parametric and non-parametric stability statistics for selecting stable Chickpea (*Cicer arietinum* L.) genotypes under diverse environments. – Australian Journal of Crop Sciences 6(3): 514-524.
[9] Farshadfar, E., Rashidi, M., Jokar, M., Zali, H. (2013): GGE biplot analysis of genotype × environment interaction in chickpea genotypes. – Eur. Journal of Experimental Biology 3(1): 417-423.

http://www.aloki.hu ● ISSN 1589 1623 (Print) ● ISSN 1785 0037 (Online)
DOI: http://dx.doi.org/10.15666/aeer/1802_26212636

[10] Gabriel, K. R. (1971): The biplot graphic display of matrices with application to principal component analysis. – Biometrika 58: 453-467.
[11] Gan, Y. T., Siddique, K. H. M., MacLeod, W. J., Jayakunar, P. (2005): Management options of minimizing the damage by ascochyta blight (*Ascochyta rabiei*) in chickpea (*Cicer arietinum* L.). – Field Crops Research 97: 121-134.
[12] Gauch, H. G. Jr., Zobel, R. W. (1996): AMMI analysis of yield trials. – In: Kang, M. S., Gauch, H. G. Jr. (eds.) Genotype-by-environment interaction. CRC Press, Boca Raton, FL, pp. 85-122.
[13] Grubbs, F. E. (1969): Procedures for Detecting Outlying Observations in Samples. – Technometrics 11: 1-21.
[14] Jabbari, H., Zeinalzadeh-Tabrizi, H., Enayati-Shariatpanahi, M. (2019): Response of germination and seedling traits in different canola genotypes to soil moisture conditions using GGEBiplot method. – Iranian Journal of Seed Science and Technology. Doi:10.22034/ijsst.2019.124388.1245. (In press).
[15] Kang, M. S. (1993): Simultaneous selection for yield and stability in crop performance trials: Consequences for growers. – Journal of Agronomy 85(3): 754-757.
[16] Kanouni, H., Taleei, A. R., Khalily, M. (2007): Stability analysis of seed yield and one-hundred seeds weight in Desi type chickpea genotypes. – Seed and Plant Improvement Journal 23(3): 297-310. (In Persian).
[17] Kanouni, H., Farayedi, Y., Sabaghpour, S. H. (2016): Assessment of genotype × environment interaction effect on seed yield of chickpea (*Cicer arietinum* L.) lines under rainfed winter planting conditions. – Iranian Journal of Crop Sciences 18(1): 63-75. (In Persian).
[18] Karimizadeh, R., Mohammadi, M., Sabaghni, N., Mahmoodi, A. A., Roustami, B., Seyyedi, F., Akbari, F. (2013): GGE biplot analysis of yield stability in multi-environment trials of lentil genotypes under rainfed condition. – Notulae Scientia Biologicae 5(2): 256.
[19] Karimizadeh, R., Asghari, A., Chinipardaz, R., Sofalian, O., Ghaffari, A. (2016): Determining yield stability and model selection by AMMI method in rain-fed durum wheat genotypes. – Turkish Journal of Field Crops 21(2): 174-183.
[20] Karimizadeh, R., Asghari, A., Chinipardaz, R., Sofalian, O., Ghaffari, A., Shahbazi, K., Hosseinpour, T., Ghogog, H., Armion, M. (2019): Use of principal coordinate analysis for measuring GE interactions in rain-fed durum wheat genotypes. – Journal of Agriculture Sciences 25: 38-46.
[21] Kheybari, M., Saifzadeh, S., Shirani-Rad, A. H., Hadidi-Masouleh, E., Zakerin, H. R., Zeinalzadeh-Tabrizi, H. (2019): Determination of suitable planting date and stable genotype in cultivars and promising lines of rapeseed (*Brassica napus* L.) using GGE Biplot graphical analysis. – Applied Field Crops Research. (In press). Doi:10.22092/aj.2019.121709.1295.
[22] Levene, H. (1960): Robust testes for equality of variances. – In: Olkin, I. (ed.) Contributions to Probability and Statistics. Stanford Univ. Press, Palo Alto, CA, pp. 278-292.
[23] Maqbool, M. A., Aslam, M., Ali, H., Mahmud Shah, T., Atta, B. M. (2015): GGE biplot analysis based selection of superior Chickpea (*Cicer arietinum* L.) inbred lines under variable water environments. – Pakistan Journal of Botany 47(5): 1901-1908.
[24] Mohammadi, R., Armion, M., Zadhasan, E., Ahmadi, M. M., Sadeghzadeh Ahari, D. (2012): Genotype × environment interaction for grain yield of rainfed durum wheat using the GGE biplot model. – Seed and Plant Improvement Journal 28(3): 503-518. (In Persian).
[25] Mohammadi, M., Hosseinpour, T., Armion, M., Khanzadeh, H., Ghojogh, H. (2016): Analysis of genotype, environment and genotype × environment interaction in bread wheat genotypes using GGE biplot. – Agriculture Communications 4(3): 1-8.
[26] Mostafavi, K., Mohammadi, A., Khodarahmi, M., Zabet, M., Zare, M. (2013): Yield response of commercial canola cultivars to different locations using graphical GGE biplot method. – Iranian Journal of Agronomy Plant Breeding 8(4): 133-143. (In Persian).

http://www.aloki.hu ● ISSN 1589 1623 (Print) ● ISSN 1785 0037 (Online)
DOI: http://dx.doi.org/10.15666/aeer/1802_26212636

[27] Navabi, A., Yang, R., Helm, J., Spaner, D. M. (2006): Can spring wheat-growing mega environments in the northern Great Plains be dissected for representative locations or niche-adapted genotypes. – Journal of Crop Sciences 46: 1107-1116.
[28] Omrani, S., Mohammad Naji, A., Esmaeilzadeh-Moghaddam, M. (2017): Yield stability analysis of promising bread wheat lines in southern warm and dry agroclimatic zone of Iran using GGE biplot model. – Journal of Crop Breeding 23(9): 157-165. (In Persian).
[29] Pourdad, S. S., Jamshidmoghadam, M. (2013): Study on genotype × environment interaction through GGE biplot for seed yield in spring rapeseed (*Brassica napus* L.) in rain-fed condition. – Journal of Crop Breeding 5(12): 1-14. (In Persian).
[30] Sabaghpour, S. H., Pezeshkpour, P., Sarparast, R., Saeid, A., Safikhani, M., Hashembeigi, A., Karami, E. (2010): study of grain yield stability in chickpea (*Cicer arietinum* L.) genotypes in autumn planting in dryland conditions. – Seed and Plant Improvement Journal 26: 173-191. (In Persian).
[31] Shapiro, S. S., Wilk, M. B. (1965): An Analysis of Variance Test for Normality (Complete Samples). – Biometrika 52: 591-611.
[32] Shiri, M. R., Bahrampour, T. (2015): Genotype × environment interaction analysis using GGE biplot in grain maize (Zea mays L.) hybrids under different irrigation conditions. – Cereal Res 5(1): 83-94. (In Persian).
[33] Tabrizi, H. Z. (2012): Genotype by environment interaction and oil yield stability analysis of six sunflower cultivars in Khoy, Iran. – Advances in Environmental Biology 6: 227-231.
[34] Usefi, M., Dashti, H., Bihamta, M. R., Madah Hosseini, Sh. (2017): Analysis of genetic diversity in agronomic traits of chickpea (*Cicer arietinum* L.) genotypes using multivariate methods. – Iranian Journal of Field Crop Sciences 48: 567-578. (In Persian).
[35] Varshney, R. K., Song, C., Saxena, R. K., Azam, S., Yu, S., Sharpe, A. G. (2013): Draft genome sequence of chickpea (*Cicer arietinum* L.) provides a resource for trait improvement. – Nature Biotechnology 31: 240-246.
[36] Yan, W. (1999): A study on the methodology of cultivar evaluation based on yield trial data - with special reference to winter wheat in Ontario. – Ph.D Dissertation, University of Guelph, Guelph, Ontario, Canada.
[37] Yan, W., Hunt, L., Sheng, Q., Szlavnics, Z. (2000): Cultivar evaluation and mega-environment investigation based on the GGE biplot. – Journal of Crop Sciences 40(3): 597-605.
[38] Yan, W. (2001): GGEbiplot-a Windows application for graphical analysis of multi-environment trial data and other types of two-way data. – Journal of Agronomy 93(5): 1111-1118.
[39] Yan, W., Kang, M. S. (2002): GGE biplot analysis: A graphical tool for breeders, geneticists, and agronomists. – CRC press. Boca, Raton, FL.
[40] Yan, W., Tinker, N. A. (2006): Biplot analysis of multi-environment trial data: Principles and applications. – Canadian Journal Plant Sciences 86: 623-645.
[41] Yan, W., Fregeau-Reid, J., Pageau, D., Martin, R., Mitchell-Fetch, J., Etienne, M., Rowsell, J., Scott, P., Price, M., De Haan, B., Cummiskey, A., Lajeunesse, J., Durand, J., Sparry, E. (2010): Identifying essential test locations for oat breeding in eastern Canada. – Crop Sciences 50: 504-515.
[42] Zali, H., Sabaghpour, S., Farshadfar, E., Pezeshkpour, P., Safikhani, M., Sarparast, R., Hashembeigi, A. (2007): Stability analysis of yield in chickpea genotypes by additive main effects and multiplicative interaction (AMMI). – Journal of Crop Production 11(42): 173-180. (In Persian).
[43] Zali, H., Sofalian, O., Hasanloo, T., Asghari, A. (2016): AMMI and GGE biplot analysis of yield stability and drought tolerance in *Brassica napus* L. – Agricultural Communications 4(1): 1-8.

http://www.aloki.hu ● ISSN 1589 1623 (Print) ● ISSN 1785 0037 (Online)
DOI: http://dx.doi.org/10.15666/aeer/1802_26212636

EFFECT OF ORGANIC MATTER, BIO-FERTILIZERS AND MAGNETIC WATER ON THE VEGETATIVE GROWTH AND FLOWER QUALITY OF GLADIOLUS (*GLADIOLUS HYBRIDA* L.) VAR. CARTAGO

AHMMAD, C. A. – ABDULLATIF, S. A.*

University of Sulaimani, Kurdistan, Iraq

**Corresponding author*
e-mail: chnwr. ahmmad@univsul.edu.iq

(Received 5th Aug 2019; accepted 28th Nov 2019)

Abstract. The experiment was conducted to investigate the effects of poultry manure (without Poultry manure A_0, 2% poultry manureA_1 and 4% poultryA_2), bio-fertilizers (not inoculation corms by bacteria B_0, inoculation corms by bacteria *Azospirillum brasilense* B_1, and inoculation corms by *Bacillus subtilis* B_2) and type of irrigation (tap water C_1 and magnetic water treated by 500 gauss C_2) on cut flowers and vase life of Gladiolus flowers Cartago cultivar in two seasons (autumn 2016 and spring 2017) The field experiment was laid down in a factorial 2*3*3 in Split plot Randomized Complete Block Design (RCBD) with three replications and seven plants for each treatment. Results showed a significant increase in vegetative growth (Plant height, Leaf dry matter, Leaf chlorophyll intensity, N, P and K concentration in the leaves) and flower quality (number of days to flowering, anthocyanin concentration in petals (mg.100 g^{-1}), basal floral diameter and vase life), these due to effect of plants with 2% poultry manure, inoculation by bacteria and irrigation with magnetic water. Decreasing in vegetative and flowering characteristics was also observed, when Poultry manure was used at 4% rate and without inoculation by bacteria and irrigation by tap water. But the magnetic water reduced the negative effect.
Keywords: *Azospirillum, Bacillus, cut flower, soil media, irrigation*

Introduction

Gladiolus (*Gladiolus hybrida* L.) belonging to family Irridaceae, it is a monocotyledonous, perennial bulbous flowering plant (Manning and Goldblatt, 2008). are one of the most important flowering plants that are used worldwide for cut flowers production, as they rank among of the top ten best cut flowers due to their different shapes, dazzling colors, varying sizes and excellent vase life. There is a considerable demand in both domestic and export production (Ali et al., 2014). For an amount of 16 million dollars, 60 million gladiolus spikes were sold in the United States of America (Sajjad et al., 2014). The success of gladiolus cultivation depends on many factors like soil fertility, irrigation, planting time, planting density, plant protection, plant growth regulators and some chemicals, these may play major role towards increasing production and quality of gladiolus. But, biofertilzers have positive impact on availability of nutrients (Bhalla et al., 2006). Organic fertilizers including farmyard manure, and poultry manure, sheep manure may be used for the crop production as a substitute of the chemical fertilizer because the importance of the organic manures cannot be overlooked. In recent year organic matter as a suitable source of nutrients to the soil has been replaced by chemical fertilizers that positively affect both the chemical and physical properties of the soil such as soil structure (Bot and Benites, 2005).

The emphasis is now focused on the use biofertilizers like Azotobacter, Azospirillium and phosphate solubilizing bacteria (PSB). Species of Bacillus is known to promote plant growth. The principal mechanisms of growth promotion include production of growth

http://www.aloki.hu ● ISSN 1589 1623 (Print) ● ISSN 1785 0037 (Online)
DOI: http://dx.doi.org/10.15666/aeer/1802_26372655

stimulating phytohormones, solubilization and mobilization of phosphate, siderophore production, production of antibiotics, inhibition of plant ethylene synthesis, and induction of plant systemic resistance to pathogens (Gutiérrez-Mañero et al., 2001). Azospirillum is a symbiotic N-fixing bacterium. Azotobacter and Azospirillum fix atmospheric nitrogen when inoculated to plants, which help to save the application of N-fertilizers to an extent of 20-25 percent (Chaitra and Patil, 2007).

The magnetic water technology is wide studied subject throughout the world, especially in major countries like China, USA, and Australia (Hozayn and Qados, 2010). A magnetic field is an unpreventable environmental factor for plants in the soil. However, its impact on plant growth (Eşitken and Turan, 2004). Magnetic treatment results in changes in structure of the water, such as changes the formation of clustering structures from linear and ring hydrogen-bound chains of molecules, the magnetic interaction between these clustering structures and increasing polarization effects of water molecules (Pang and Deng, 2008). Magnetic fields have a positive effect on plant characteristics such as seed germination, seedling growth, agronomic traits and seed yield (Aladjadjiyan, 2002; Tahir and Karim, 2010).

The postharvest longevity of flowers has a critical importance in determining the value of the crop. Cut flowers are highly perishable commodities and are highly vulnerable to postharvest losses. It is estimated that nearly 70% of the potential lasting quality of cut flowers is pre-determined at harvest while postharvest factors influence 30% of the quality. In cut flower trade, it is very important to maintain freshness and original colors of flowers for the longer period, throughout the postharvest chain. Harvesting of flowers at an optimum stage of bud development (Kumari, 2014).

The aim of this study is to determine the effect of various amounts of poultry manure, bio-fertilizer and magnetic water processor on the growth characteristics and flower quality of gladiolus plants of the Cartago cultivar.

Materials and methods

The experiment sites

The experiment was conducted at the College of Agricultural Engineering Sciences, Sulaimani University, Kurdistan, Iraq in greenhouse for two seasons first period in 7th of October 2016 to May 2017 (autumn), second study in 5th of March 2017 to August 2017 (spring). The area is located at 35° 3214" N, 45° 2197" E, and an altitude of (743.40 M) above sea level, with GPS reading.

The experiment was conducted to investigate the effects of poultry manure, (A_0 without poultry manure, A_1 poultry manure at 2% of soil weight, A_2 poultry manure at 4% of soil weight), biofertilizers (B_0 without inoculation, B_1 inoculation by *Azospirillum brasilense*, B_2 inoculation by *Bacillus subtilis*) and water processor magnetic (C_1 irrigation by tap water, C_2 irrigation by magnetic water) and its impact on the vegetative and flower quality of *Gladiolus hybrida*. These treatments were randomized in a split plot design with three replicates, were irrigation types contributed as the main plots, while interaction of poultry manure and biofertilizers (A*B) were distributed in the sub plots.

The magnetic water treatment was conducted by passing the irrigation water through magnetic flux densities 500 Gauss. A local magnetic device is special magnets spaced a part and parallel to the length of water carrying copper pipe.

http://www.aloki.hu ● ISSN 1589 1623 (Print) ● ISSN 1785 0037 (Online)
DOI: http://dx.doi.org/10.15666/aeer/1802_26372655

Planting the corms

Planting the corms in the plastic bags (4 kg size) were filled from the soil agriculture consisting of the three levels, first was consisting of soil and Peatmoos in equal proportions. The second media was composed of the soil and Peatmoos in equal proportions plus poultry manure at 2% and the third level was consisting of soil and Peatmoss in equal proportions with 4% of poultry manure based on soil weight. Analysis of the physical and chemical properties of three soil media is shown in *Table 1.*

Table1. *The main physical and chemical properties of three soil media*

Soil properties	Units	Without poultry manure	2% poultry manure	4% poultry manure
Sand	%	34.40	30.40	32.40
Silt		34.00	32.00	46.00
Clay		31.60	37.60	21.60
Texture		Loam clay	Loamy clay	Loamy
EC	dsm^{-1}	2.52	1.70	2.91
pH		7.33	7.13	7.18
Cation				
Ca^{++}	mq/L	11.52	9.30	14.00
Mg^{++}		7.81	5.22	10.31
Na^{+}		6.22	2.31	4.34
K^{+}		1.14	1.03	1.11
Cl^{-}		17.50	12.50	20.32
$HCO3^{-}$		2.30	1.50	2.54
$CO3^{=}$		Nil	Nil	Nil
$SO4^{=}$		4.98	3.28	5.34
CaCO3	%	15.22	30.19	23.41
Organic matter	%	0.79	0.73	0.89
Available nitrogen	Mg. kg^{-1}	23.00	12.00	31.00
Available phosphorus		15.25	14.70	10.13
Soluble potassium		87.11	79.39	68.93

Data were analyzed in the Central Laboratories of College of Agriculture, University of Baghdad

Source of the corms

The corms of gladiolus var. Cartago were brought from the company of stoop flower bulbs in Holland. Healthy and uniform size 10-12 cm corms are divided in to three groups the first group dipped in the distillates water, second group were dipped in the solution which contain *Azospirillum brasilence* and the third group were dipped in the solution which contain *Bacillus subtilis* for half an hour and dried in shade for 30 min before planting.

Planting one corm in the plastic bags in 8 cm depth (Greving, 1987). Agricultural practices were carried out for all replications, such as weeding and hoeing the surface of the soil, in order to ventilate. Ventilation of the greenhouse was done by opening the doors and slots. Also, air cooler and heater were used to adjust the temperature in the greenhouse in both high and low temperature conditions. Atmospheric condition inside

http://www.aloki.hu ● ISSN 1589 1623 (Print) ● ISSN 1785 0037 (Online)
DOI: http://dx.doi.org/10.15666/aeer/1802_26372655

the greenhouse had been measured by recording maximum and minimum temperatures and relative humidity.

Experimental parameters

The experimental parameters are presented in *Table 2.*

Table 2. *Study parameters*

Parameters	Methods
Plant height (cm)	Measured from the soil surface to the end of the flower spike length
Leaf dry mater (%)	Dry matter (%) = $\frac{\text{dry weight of leaves}}{\text{fresh weight of leaves}} \times 100$
Chlorophyll (spad unit)	Portable chlorodhyll meter CCM-200 plus. OPTI-SCIENCES
Nitrogen concentration in leaves (%)	Micro-Kjeldahl (Page et al., 1982)
Phosphorus concentration in leaves (%)	Spectrophotometer at (882 ηm) wavelength (Olsen et al., 1982)
Potassium concentration in leaves (%)	Flame Photometer (Page et al., 1982)
Number of days for flowering (day)	We have counted the days from the first day of planting unit the first appearance of the basal floret's color
Anthocyanin concentration in flower petals (mg.100 g^{-1})	Spectrophotometer (Ranganna, 1977) method
Basal floral diameter (cm)	Digital caliper vernier
Vase life (day)	Measured by the number of days after harvesting the flower as until ¾ of the florets are wilted

Preparation of bacterial inoculants

Pure isolated bacteria were taken from the laboratories of the Agricultural Research Center- Baghdad- Zaafaraniyah associated to the ministry of Science and Technology, Iraq.

Inoculants corms by bacteria Azospirillum brasilense and Bacillus subtilis

- Preparation of 1 L of nutrient solution, 25 g of nutrient broth was dissolved in one litter of distilled water and sterilized by using autoclave with the pressure of 1.5 bar at temperature 121 °C for 15 min before adding bacteria.
- Adding 6 cm^3 of bacteria to the cultural media (liquid nutrient broth) and shaken for 15 min.
- Then the bacterial culture putted in an incubator at 28 °C for 72 h.
- After inoculation period 3 g of sugar and 2 g of Arabic gum were added to the bacteria suspension shake it for 30-60 min. The bacteria inoculants ready to use.

Description of the experiment

The field experiment was carried out based on the Split plot randomized complete block design (RCBD) with three replications and seven plants for each treatment. The data were analyzed by a computer program Statistical Analysis System (SAS) and the comparisons among means were carried out by the least significant difference (L.S.D) at $P \leq 0.05$ (*Table 2*).

http://www.aloki.hu ● ISSN 1589 1623 (Print) ● ISSN 1785 0037 (Online)
DOI: http://dx.doi.org/10.15666/aeer/1802_26372655

Results

Effect of poultry manure, bio-fertilizers and magnetic water and their interaction on the plant height (cm)

Table 3 illustrates that using A_1 treatment which is 2% of poultry manure has a significant effect on plant height 124.74 and 139.58 cm for autumn and spring respectively compared to control A_0 120.26 and 134.68 cm. In addition, it was noticed that plant height after using A_1 was significantly different as compared to using 4% of poultry manure A_2 98.38, 133.91 cm for both seasons respectively.

Regarding the inoculation of gladiolus corms with bacteria *Azospirillum brasilense* and *Bacillus subtilis*, the maximum plant height values are 116.89, 117.11 and 138.85, 137.15 cm in autumn and spring respectively. These results are significantly different from control B_0 (without inoculation by bacteria), which are 109.38 and 132.16 cm in both seasons. With regard to irrigation, using magnetic water C_2 significantly increases plant height 118.07, 138.08 cm as compared to C_1 which gave 110.85, 134.02 cm in autumn and spring season respectively. The significant effect of interaction of organic matter, bio-fertilizers, and magnetic water on plant height of gladiolus shown in the same table, the highest plants 132.88, 145.90 cm were achieved from $A_1B_1C_2$ for both seasons, respectively. While the lowest plant height 93.49 cm was noticed from $A_2B_0C_1$ in the autumn and 128.94 cm from $A_0B_0C_1$ in the spring.

Table 3. *Effect of poultry manure, bio-fertilizers and magnetic water and their interaction on the plant height (cm) in two seasons*

Autumn							Spring				
C	A	B_0	B_1	B_2	A*C	C	B_0	B_1	B_2	A*C	C
C_1	A_0	110.07	117.00	118.10	115.05	110.85	128.94	132.32	131.44	130.90	134.02
	A_1	112.00	122.67	126.00	120.22		131.73	142.67	139.09	137.83	
	A_2	93.49	99.95	98.40	97.28		131.68	133.33	135.00	133.33	
C_2	A_0	118.51	128.86	129.03	125.47	118.07	133.53	141.89	139.94	138.45	138.08
	A_1	124.59	132.88	130.27	129.25		137.11	145.90	140.96	141.33	
	A_2	97.64	99.95	100.86	99.48		130.00	137.00	136.44	134.48	
Interaction of C*B							Interaction of C*B				
C_1	105.19		113.21	114.17			130.78	136.11	135.18		
C_2	113.58		120.56	120.06			133.55	141.60	139.12		
Interaction of A*B					A		Interaction of A*B				A
A_0	114.29		122.93	123.57	120.26		131.23	137.11	135.69		134.68
A_1	118.29		127.78	128.14	124.74		134.42	144.29	140.03		139.58
A_2	95.57		99.95	99.63	98.38		130.83	135.17	135.72		133.91
B	109.38		116.89	117.11			132.16	138.85	137.15		
LSD 0.05											
A	B	C	A*B	A*C	B*C	A*B*C	A	B	C	A*B	A*C	B*C	A*B*C
3.53	3.53	2.88	7.99	6.15	12.57	9.22	3.91	3.91	3.19	6.81	5.67	5.65	9.45

A is poultry manure, A0 without poultry manure, A1 application of poultry manure at 2% of soil weight, A2 application of poultry manure at 4% of soil weight. B is bio-fertilizers, B1 is inoculation by bacteria *Azospirillum brasilense,* B2 is inoculation by bacteria *Bacillus subtilis,* C is type of irrigation, C1 is irrigation by tap water, C2 is irrigation by magnetic water

http://www.aloki.hu ● ISSN 1589 1623 (Print) ● ISSN 1785 0037 (Online)
DOI: http://dx.doi.org/10.15666/aeer/1802_26372655

Effect of poultry manure, bio-fertilizers and magnetic water and their interaction on leaf dry matter %

Table 4 shows that planting the corms in medium containing 2% of poultry manure A_1 has a significant effect on leaf dry matter. The highest value 24.54, 26.95% were found from A_1 for autumn and spring respectively, while the lowest value 20.84% was achieved from A_2 in the autumn and 22.71% was found from A_0 in spring. Inoculation of gladiolus corms with *Azospirillum brasilense* B_1 significantly affected the percentage of the leaf dry matter which were 22.94, 25.71% for both seasons. Also, the inoculation by *Bacillus subtilis* B_2, significantly affected the percentage of the leaf dry matter 23.57, 25.69% as compared to control B_0 20.50, 21.89% for both seasons respectively.

Table 4. *Effect of poultry manure, bio-fertilizers and magnetic water and their interaction on leaf dry matter % of Gladiolus in two seasons*

Autumn							Spring				
C	A	B_0	B_1	B_2	A*C	C	B_0	B_1	B_2	A*C	C
C_1	A_0	18.43	20.52	21.78	20.24	20.97	19.14	21.69	21.87	20.90	22.24
	A_1	22.12	23.87	24.17	23.39		21.77	25.51	27.56	24.94	
	A_2	17.79	19.89	20.12	19.26		17.90	22.63	22.09	20.87	
C_2	A_0	20.42	23.74	24.93	23.03	23.71	23.05	25.20	25.31	24.52	26.62
	A_1	23.71	26.13	27.20	25.68		26.09	30.46	30.32	28.96	
	A_2	20.51	23.52	23.20	22.41		23.39	28.78	26.99	26.39	
Interaction of B*C							Interaction of B*C				
C_1		19.45	21.43	22.02			19.60	23.28	23.84		
C_2		21.55	24.46	25.11			24.18	28.15	27.54		
Interaction of A*B					A		Interaction of A*B			A	
A_0		19.43	22.13	23.36	21.64		21.10	23.45	23.59	22.71	
A_1		22.92	25.00	25.69	24.54		23.93	27.99	28.94	26.95	
A_2		19.15	21.71	21.66	20.84		20.64	25.71	24.54	23.63	
B		20.50	22.94	23.57			21.89	25.71	25.69		

LSD 0.05													
A	B	C	A*B	A*C	B*C	A*B*C	A	B	C	A*B	A*C	B*C	A*B*C
1.16	1.15	0.94	2.65	2.07	2.25	3.08	2.06	2.06	1.68	4.39	3.24	3.27	5.24

A is poultry manure, A0 without poultry manure, A1 application of poultry manure at 2% of soil weight, A2 application of poultry manure at 4% of soil weight. B is bio-fertilizers, B1 is inoculation by bacteria *Azospirillum brasilense,* B2 is inoculation by bacteria *Bacillus subtilis,* C is type of irrigation, C1 is irrigation by tap water, C2 is irrigation by magnetic water

Irrigation by magnetic water C_2 has a significant effect on the leaf dry matter 23.71, 26.62%, while irrigation by tap water C_1 gave 20.97, 22.24% for both seasons, respectively. The significant effect of interaction of poultry manure, bio-fertilizers and magnetic water on leaf dry matter percentage in the autumn shown in the same table. The maximum leaf dry matter value 27.20% in autumn was found from $A_1B_2C_2$, while the minimum leaf dry matter value 17.79% was observed from $A_2B_0C_1$. However, the highest value in the spring (30.46%) was achieved from $A_1B_1C_2$ and the lowest value 17.90% was found from $A_2B_0C_1$.

http://www.aloki.hu ● ISSN 1589 1623 (Print) ● ISSN 1785 0037 (Online)
DOI: http://dx.doi.org/10.15666/aeer/1802_26372655

Effect of poultry manure, bio-fertilizers and magnetic water and their interaction on the leaf chlorophyll intensity (spad unit)

Table 5 shows the significant effect of using poultry manure on the leaf chlorophyll intensity of gladiolus plant var. Cartago. In both seasons, the maximum leaf chlorophyll intensity 58.18, 58.08 spad unit were noticed from A_1 treatment, while the minimum leaf chlorophyll intensity 50.53, 47.43 spad unit were achieved from A_2 treatment for both seasons respectively.

Table 5. *Effect of poultry manure, bio-fertilizers and magnetic water and their interaction on the leaf chlorophyll intensity (spad unit) of gladiolus in two seasons*

Autumn							Spring				
C	A	B_0	B_1	B_2	A*C	C	B_0	B_1	B_2	A*C	C
C_1	A_0	42.49	50.48	46.05	46.34	49.14	43.13	51.35	49.31	47.93	49.14
	A_1	47.49	59.98	54.35	53.94		48.96	60.92	55.95	55.28	
	A_2	42.20	50.71	48.52	47.14		40.91	49.24	42.47	44.21	
C_2	A_0	50.31	64.47	61.50	58.75	58.37	49.83	60.51	53.70	54.68	55.41
	A_1	57.02	68.83	61.42	62.42		55.42	67.71	59.50	60.88	
	A_2	50.25	58.16	53.36	53.92		46.81	58.16	47.05	50.67	
Interaction of B*C							Interaction of B*C				
C1		44.06	53.72	49.64			44.33	53.84	49.24		
C2		52.52	63.82	58.76			50.69	62.13	53.42		
Interaction of A*B					A		Interaction of A*B			A	
A_0		46.40	57.47	53.78	52.55		46.48	55.93	51.51	51.31	
A_1		52.25	64.41	57.89	58.18		52.19	64.31	57.73	58.08	
A_2		46.22	54.43	50.94	50.53		43.85	53.70	44.75	47.43	
B		48.29	58.77	54.20			47.51	57.98	51.33		
LSD 0.05							LSD 0.05				
A	B	C	A*B	A*C	B*C	A*B*C	A	B	C	A*B	A*C	B*C	A*B*C
4.05	4.05	3.31	8.93	6.76	6.76	10.05	2.42	2.42	1.97	5.56	5.44	5.44	5.74

A is poultry manure, A0 without poultry manure, A1 application of poultry manure at 2% of soil weight, A2 application of poultry manure at 4% of soil weight. B is bio-fertilizers, B1 is inoculation by bacteria *Azospirillum brasilense,* B2 is inoculation by bacteria *Bacillus subtilis,* C is type of irrigation, C1 is irrigation by tap water, C2 is irrigation by magnetic water

However, the significant effect of using *Azospirillum brasilense* B_1 noticed 58.77, 57.98 spad unit and *Bacillus subtilis* 54.20, 51.33, was found. These results were significantly differed from control B_0 as 48.29, 47.51 spad unit was obtained for both seasons respectively.

Irrigation by magnetic water caused increasing of leaf chlorophyll intensity by giving 58.37, 55.41 spad unit for C_2 as compared to C_1 which gave 49.14, 49.14 spad unit for both seasons respectively. The interaction of poultry manure, bio-fertilizers and magnetic water had a significant effect on the leaf chlorophyll intensity for both seasons as shown in the same table. The maximum value 68.83, 67.71 spad unit were found from $A_1B_1C_2$, while the minimum value 42.20, 40.91 spad unit were found from $A_2B_0C_1$.

http://www.aloki.hu ● ISSN 1589 1623 (Print) ● ISSN 1785 0037 (Online)
DOI: http://dx.doi.org/10.15666/aeer/1802_26372655

Effects of poultry manure, bio-fertilizers magnetic water and their interaction on the Nitrogen (%) in the leaves

Table 6 presents the results of application of poultry manure on the nitrogen content in gladiolus leaves and a statistical difference was found in both seasons. It can be noticed that poultry manure at 2% A_1 recorded highest value 2.52, 2.26%, on the other hand, lowest value 1.79, 1.76% were obtained from A_2 for two seasons respectively.

Table 6. *Effects of poultry manure, bio-fertilizers magnetic water and their interaction on the concentration of Nitrogen (%) in the leaves of Gladiolus in two seasons*

Autumn							**Spring**				
C	A	B_0	B_1	B_2	A*C	C	B_0	B_1	B_2	A*C	C
C1	A_0	1.55	2.00	1.63	1.72	1.83	1.32	1.84	1.54	1.57	1.62
	A_1	1.83	2.39	2.06	2.09		1.65	1.87	1.87	1.80	
	A_2	1.48	1.95	1.58	1.67		1.27	1.78	1.44	1.49	
C2	A_0	1.91	2.44	2.06	2.13	2.33	1.81	2.49	1.99	2.09	2.27
	A_1	2.49	3.63	2.72	2.95		2.39	3.40	2.34	2.71	
	A_2	1.82	2.06	1.89	1.92		1.83	2.43	1.78	2.01	
Interaction of B*C							Interaction of B*C				
C1		1.62	2.11	1.76			1.41	1.83	1.62		
C2		2.07	2.71	2.22			2.01	2.77	2.04		
Interaction of A*B					A		Interaction of A*B			A	
A_0		1.73	2.22	1.84	1.93		1.57	2.17	1.76	1.83	
A_1		2.16	3.01	2.39	2.52		2.02	2.64	2.11	2.26	
A_2		1.64	2.00	1.73	1.79		1.55	2.11	1.61	1.76	
B		1.84	2.41	1.99			1.71	2.31	1.83		
LSD 0.05											
A	B	C	A*B	A*C	B*C	A*B*C	A	B	C	A*B	A*C	B*C	A*B*C
0.24	0.24	0.20	0.53	0.40	0.40	0.60	0.24	0.24	0.2	0.57	0.43	0.43	0.61

A is poultry manure, A0 without poultry manure, A1 application of poultry manure at 2% of soil weight, A2 application of poultry manure at 4% of soil weight. B is bio-fertilizers, B1 is inoculation by bacteria *Azospirillum brasilense,* B2 is inoculation by bacteria *Bacillus subtilis,* C is type of irrigation, C1 is irrigation by tap water, C2 is irrigation by magnetic water

Inoculated corms with bio-fertilizers were affected significantly on concentration of nitrogen in leaves. The maximum nitrogen concentration 2.41, 2.31% were observed from B_1 treatment, while the minimum nitrogen concentration 1.84, 1.71% were noticed from B_0 for both seasons respectively. Moreover, the effect of irrigation by magnetic water on nitrogen content in leaves differences significantly was found in two seasons. The highest concentrations 2.33, 2.27% were observed from C_2, while the lowest concentrations of nitrogen 1.83, 1.62% were found from both C_1 for both seasons respectively.

The interaction between poultry manure, bio-fertilizers and magnetic water on the nitrogen content in gladiolus leaves was statistical difference in both seasons. The maximum values 3.63, 3.40% were achieved from $A_1B_1C_2$, while the minimum values 1.48, 1.27% were found in both $A_2B_0C_1$ respectively.

http://www.aloki.hu ● ISSN 1589 1623 (Print) ● ISSN 1785 0037 (Online)
DOI: http://dx.doi.org/10.15666/aeer/1802_26372655

Effect of poultry manure, bio-fertilizers, magnetic water and their interaction on the concentration of phosphorus (%) in the leaves

Table 7 gives the results of application of poultry manure on the phosphorus content in gladiolus leaves var. Cartago and a statistical difference was found in both seasons. The highest phosphorus concentrations 0.31, 0.28% were found from A_1, whereas the lowest phosphorus concentrations 0.20, 0.18% were observed from both A_2 respectively.

Table 7. *Effect of poultry manure, bio-fertilizers, magnetic water and their interaction on the concentration of phosphorus (%) in the leaves of Gladiolus in two seasons*

Autumn							Spring				
C	A	B_0	B_1	B_2	A*C	C	B_0	B_1	B_2	A*C	C
C1	A_0	0.20	0.22	0.27	0.23	0.22	0.17	0.19	0.24	0.20	0.20
	A_1	0.22	0.25	0.28	0.25		0.21	0.23	0.24	0.23	
	A_2	0.15	0.19	0.19	0.18		0.15	0.17	0.20	0.17	
C2	A_0	0.22	0.26	0.30	0.26	0.28	0.21	0.24	0.28	0.24	0.26
	A_1	0.30	0.37	0.44	0.37		0.28	0.33	0.39	0.33	
	A_2	0.19	0.26	0.20	0.22		0.16	0.21	0.22	0.20	
Interaction of B*C							Interaction of B*C				
C1		0.19	0.22	0.25			0.18	0.20	0.23		
C2		0.24	0.30	0.31			0.22	0.26	0.30		
Interaction of A*B					A		Interaction of A*B			A	
A_0		0.21	0.24	0.29	0.25		0.19	0.22	0.26	0.22	
A_1		0.26	0.31	0.36	0.31		0.24	0.28	0.32	0.28	
A_2		0.17	0.22	0.20	0.20		0.16	0.19	0.21	0.18	
B		0.21	0.26	0.28			0.20	0.23	0.26		
LSD 0.05							LSD 0.05				
A	B	C	A*B	A*C	B*C	A*B*C	A	B	C	A*B	A*C	B*C	A*B*C
0.02	0.02	0.01	0.06	0.05	0.05	0.05	0.03	0.03	0.03	0.07	0.06	0.06	0.09

A is poultry manure, A0 without poultry manure, A1 application of poultry manure at 2% of soil weight, A2 application of poultry manure at 4% of soil weight. B is bio-fertilizers, B1 is inoculation by bacteria *Azospirillum brasilense,* B2 is inoculation by bacteria *Bacillus subtilis,* C is type of irrigation, C1 is irrigation by tap water, C2 is irrigation by magnetic water

Inoculated corms with bio-fertilizers were affected significantly on phosphorus concentration in leaves. The maximum phosphorus concentrations 0.28, 0.26% were observed from B_2 inoculation, while the minimum phosphorus concentrations 0.21, 0.20% were achieved from control B_0 for both seasons respectively. Although the irrigation by magnetic water C_2 caused significant differences on phosphorus concentrations 0.28, 0.26%, as compared to tap water C_1 which gave 0.22, 0.20%.

The interaction between poultry manure, bio-fertilizers and magnetic water on the phosphorus content in gladiolus leaves was statistical difference in both seasons. The maximum values 0.44, 0.39% were observed from both $A_1B_2C_2$, whereas the minimum values 0.15, 0.15% were found from $A_2B_0C_1$.

http://www.aloki.hu ● ISSN 1589 1623 (Print) ● ISSN 1785 0037 (Online)
DOI: http://dx.doi.org/10.15666/aeer/1802_26372655

Effect of poultry manure, bio-fertilizers, magnetic water and their interaction on the concentration of potassium (%) in the leaves

The data in *Table 8* showed the maximum potassium concentrations due to application of poultry manure at 2% percentage A_1 which were 3.24, 2.95% significantly differed with A_2 resulted 2.55, 2.34% for both seasons respectively. However, the significant effect of bio-fertilizers was noticed with B_1 and B_2 in two seasons without significant differences between them. The highest potassium concentrations 3.19, 2.99% were found from both *Azospirrilum brasilense* B_1 followed by *Bacillus subtilis* B_2 which gave 2.92, 2.65% and the lowest potassium concentrations 2.28, 2.12% were resulted from two control B_0 respectively.

Irrigation by magnetic water resulted increasing of potassium concentrations by giving 3.21, 2.92% for C_2 as compared to C_1 which gave 2.37, 2.25% for both seasons respectively.

The interaction between poultry manure, bio-fertilizers and magnetic water on the potassium content in gladiolus leaves was statistical difference in both seasons. The highest concentrations 4.19, 3.81% were achieved from $A_1B_1C_2$, while the lowest concentration 1.83, 1.83% was noticed from both treatments $A_2B_0C_1$.

Table 8. *Effect of poultry manure, bio-fertilizers, magnetic water and their interaction on the concentration of potassium (%) in the leaves of Gladiolus in two seasons*

Autumn							**Spring**				
C	A	B_0	B_1	B_2	A*C	C	B_0	B_1	B_2	A*C	C
C1	A_0	2.01	2.48	2.23	2.24	2.37	1.95	2.44	2.14	2.17	2.25
	A_1	2.35	3.40	2.81	2.85		2.23	3.11	2.64	2.66	
	A_2	1.83	2.18	2.09	2.03		1.83	2.03	1.91	1.92	
C2	A_0	2.46	3.23	3.09	2.93	3.21	2.06	3.29	2.95	2.77	2.92
	A_1	2.92	4.19	3.77	3.63		2.69	3.81	3.23	3.24	
	A_2	2.11	3.62	3.50	3.08		1.99	3.26	3.01	2.75	
Interaction of B*C							Interaction of B*C				
C1		2.06	2.69	2.38			2.00	2.53	2.23		
C2		2.50	3.68	3.45			2.25	3.45	3.06		
Interaction of A*B					A		Interaction of A*B			A	
A_0		2.24	2.86	2.66	2.59		2.00	2.87	2.55	2.47	
A_1		2.64	3.80	3.29	3.24		2.46	3.46	2.93	2.95	
A_2		1.97	2.90	2.80	2.55		1.91	2.64	2.46	2.34	
B		2.28	3.19	2.92			2.12	2.99	2.65		

LSD 0.05													
A	B	C	A*B	A*C	B*C	A*B*C	A	B	C	A*B	A*C	B*C	A*B*C
0.32	0.32	0.26	0.77	0.59	0.59	0.80	0.41	0.41	0.33	0.80	0.64	0.64	1.01

A is poultry manure, A0 without poultry manure, A1 application of poultry manure at 2% of soil weight, A2 application of poultry manure at 4% of soil weight. B is bio-fertilizers, B1 is inoculation by bacteria *Azospirillum brasilense,* B2 is inoculation by bacteria *Bacillus subtilis,* C is type of irrigation, C1 is irrigation by tap water, C2 is irrigation by magnetic water.

http://www.aloki.hu ● ISSN 1589 1623 (Print) ● ISSN 1785 0037 (Online)
DOI: http://dx.doi.org/10.15666/aeer/1802_26372655

Effect of poultry manure, bio-fertilizers, magnetic water and their interaction on the number of the days for flowering of Gladiolus

Table 9 shows that the numbers of the days required for flowering for gladiolus var. Cartago were affected significantly by application of poultry manure. The use of A_1 resulted of decreasing of the number of the days for flowering 123.95, 84.89 significantly as compared to A_2 treatment which flowered after 132.93, 89.19 days for both seasons, respectively. However, the lowest number of the days for flowering affected by inoculations with both bacteria B_1 125.55, 85.25 days and B_2 128.28, 85.99 days as compared to control 130.37, 89.96 days for two seasons, respectively.

Irrigation by magnetic water caused decreasing of the number of the days for flowering by giving 125.63, 85.33 days for C_2 as compared to C_1 which gave 130.50, 88.81 days for two seasons, respectively.

However, the interaction between poultry manure, bio-fertilizers and magnetic water on the number of the days for flowering was found to be significant. In the autumn the minimum numbers of the days required for flowering 120.73, 120.96, 120.99 days were found from $A_1B_0C_2$, $A_1B_1C_2$, $A_1B_2C_2$ without any significant differences between them, while all of them differed significantly with control $A_0B_0C_1$ 139.18 days. However, in the spring the lowest number of the days required for flowering 82.11, 83.72 days were obtained from $A_1B_1C_2$ and $A_1B_2C_2$, while the highest number of the days required for flowering 93.83 days was achieved from $A_0B_0C_1$.

Table 9. *Effect of poultry manure, bio-fertilizers, magnetic water and their interaction on the number of the days for flowering of Gladiolus in two seasons*

Autumn							**Spring**				
C	A	B_0	B_1	B_2	A*C	C	B_0	B_1	B_2	A*C	C
C_1	A_0	139.18	118.30	133.85	130.44	130.50	93.83	87.44	86.28	89.18	88.81
	A_1	129.10	127.32	124.61	127.01		88.72	84.89	83.22	85.61	
	A_2	134.47	132.32	135.33	134.04		93.89	88.33	92.67	91.63	
C_2	A_0	127.27	122.67	122.67	124.20	125.63	88.21	83.22	83.77	85.07	85.33
	A_1	120.73	120.96	120.99	120.89		86.66	82.11	83.72	84.16	
	A_2	131.48	131.72	132.23	131.81		88.44	85.53	86.27	86.75	
Interaction of B*C							Interaction of B*C				
C_1		134.25	132.64	131.26			92.15	86.89	87.39		
C_2		126.49	125.12	125.30			87.77	83.62	84.59		
Interaction of A*B					A		Interaction of A*B			A	
A_0		133.22	120.49	128.26	127.32		91.02	85.33	85.03	87.13	
A_1		124.92	124.14	122.80	123.95		87.69	83.50	83.47	84.89	
A_2		132.98	132.02	133.78	132.93		91.16	86.93	89.47	89.19	
B		130.37	125.55	128.28			89.96	85.25	85.99		
LSD 0.05							LSD 0.05				
A	B	C	A*B	A*C	B*C	A*B*C	A	B	C	A*B	A*C	B*C	A*B*C
1.23	1.23	1.01	5.86	2.21	4.93	3.01	1.69	1.69	1.38	3.64	3.09	2.96	4.03

A is poultry manure, A0 without poultry manure, A1 application of poultry manure at 2% of soil weight, A2 application of poultry manure at 4% of soil weight. B is bio-fertilizers, B1 is inoculation by bacteria *Azospirillum brasilense,* B2 is inoculation by bacteria *Bacillus subtilis,* C is type of irrigation, C1 is irrigation by tap water, C2 is irrigation by magnetic water

http://www.aloki.hu ● ISSN 1589 1623 (Print) ● ISSN 1785 0037 (Online)
DOI: http://dx.doi.org/10.15666/aeer/1802_26372655

Effect poultry manure, of bio-fertilizers, magnetic water and their interaction on the anthocyanin concentration in flower petals (mg.100 g^{-1}) of gladiolus

Table 10 explains that poultry manure applications A had significant effect on the anthocyanin concentration in flower petals of gladiolus var. Cartago. The highest concentrations 21.99, 19.27 mg. 100 g^{-1} were found from A_1, whereas the lowest concentrations 15.93, 13.40 mg. 100 g^{-1} were obtained from A_2 for both seasons respectively.

Table 10. *Effect poultry manure, of bio-fertilizers, magnetic water and their interaction on the anthocyanin concentration in flower petals (mg.100 g^{-1}) of gladiolus in two seasons*

Autumn							Spring				
C	A	B_0	B_1	B_2	A*C	C	B_0	B_1	B_2	A*C	C
C_1	A_0	14.96	16.60	20.87	17.48	17.90	11.62	11.77	12.36	11.92	13.12
	A_1	18.82	21.73	23. 49	21.35		14.57	16.38	19.17	16.70	
	A_2	13.94	15.58	15.09	14.87		9.46	10.93	11.84	10.74	
C_2	A_0	16.56	19.19	20.86	18.87	19.50	15.23	19.78	21.81	18.94	18.94
	A_1	20.26	22.10	25.53	22.63		18.58	22.17	24.76	21.83	
	A_2	16.34	17.60	17.03	16.99		13.65	17.29	17.24	16.06	
Interaction of B*C							Interaction of B*C				
C_1		15.90	17.97	19.82			11.88	13.03	14.46		
C_2		17.72	19.63	21.15			15.82	19.75	21.27		
Interaction of A*B					A		Interaction of A*B			A	
A_0		15.76	17.89	20.87	17.93		13.42	15.78	17.09	15.43	
A_1		19.54	21.92	24.51	21.99		16.57	19.28	21.97	19.27	
A_2		15.14	16.59	16.06	15.93		11.55	14.11	14.54	13.40	
B		16.81	18.80	20.48			13.85	16.39	17.87		
LSD 0.05							LSD 0.05				
A	B	C	A*B	A*C	B*C	A*B*C	A	B	C	A*B	A*C	B*C	A*B*C
1.20	1.2	0.97	2.26	2.24	3.11	3.05	1.82	1.82	1.49	4.88	2.96	2.96	4.53

A is poultry manure, A0 without poultry manure, A1 application of poultry manure at 2% of soil weight, A2 application of poultry manure at 4% of soil weight. B is bio-fertilizers, B1 is inoculation by bacteria *Azospirillum brasilense,* B2 is inoculation by bacteria *Bacillus subtilis,* C is type of irrigation, C1 is irrigation by tap water, C2 is irrigation by magnetic water

Also, the significant effect of bio-fertilizers on anthocyanin concentration in flower petals was shown in the same table. In the autumn the maximum value 20.48 mg. 100 g^{-1} due to inoculation by B_2, while the minimum value 16.81 mg. 100 g^{-1} was found from control. In the spring there were not significant differences between inoculations of $B_1$and B_2 which gave 16.39, 17.87 mg. 100 g^{-1} whereas both of them differed significantly with control 13.85 mg.100 g^{-1}.

Irrigation by magnetic water C_2 caused increasing of anthocyanin concentration in flower petals which gave 19.50, 18.94 mg.100 g^{-1} as compared to irrigation by tap water C_1 which achieved 17.90, 13.12 mg.100 g^{-1} for both seasons, respectively.

However, the interaction between poultry manure, bio-fertilizers and magnetic water on the anthocyanin concentration in flower petals had significant differences. In the autumn the highest concentration 25.53 mg.100 g^{-1} was noticed from $A_1B_2C_2$ followed

http://www.aloki.hu ● ISSN 1589 1623 (Print) ● ISSN 1785 0037 (Online)
DOI: http://dx.doi.org/10.15666/aeer/1802_26372655

by $A_1B_2C_1$ which gave 23.49 mg.100g^{-1}, while the lowest concentration 13.94 mg.100g^{-1} was achieved from $A_2B_0C_1$. Also, the interaction of three study factor affected significantly in the spring, the maximum concentration 24.76 mg.100 g^{-1} was found from $A_1B_2C_2$ followed by $A_1B_1C_2$ which gave 22.17 mg.100 g^{-1} while the minimum concentration 9.46 17 mg.100 g^{-1} was obtained from $A_2B_0C_1$.

Effect of poultry manure, bio-fertilizers, magnetic water and their interaction on the basal floral diameter (cm) of gladiolus

Results shown in *Table 11* indicates that the application of A_1 gave highest values in two seasons 12.16, 10.44 cm were noticed from both A_1, while the lowest values 8.76, 8.86 cm were obtained from both A_2 respectively. Moreover, the floral diameter was affected significantly by inoculations the corms by B_1 and B_2. The maximum floral diameter 11.33, 10.32 cm were found from B_1 followed by B_2 which gave 11.09, 9.97 cm those two treatments varied significantly with both control 9.07, 8.23 cm for two seasons respectively.

The irrigation by C_2 caused increasing in floral diameter in two seasons by giving 11.01, 10.17 cm were found from C_2 as compared to C_1 which gave 9.89, 8.84 cm respectively. However, the interaction between poultry manure, bio-fertilizers and magnetic water gave statistical differences on lower floral diameter. The highest values in the autumn 13.73, 13.54, 13.01 cm were obtained from $A_1B_2C_2$, $A_1B_1C_2$, $A_1B_2C_1$, while the lowest value 7.58 cm was noticed from $A_2B_0C_1$. In the spring the maximum floral diameter 12.19, 11.99 cm were obtained from $A_1B_1C_2$, $A_1B_2C_2$, whereas the minimum floral diameter 6.96 cm was found from $A_2B_0C_1$.

Table 11. *Effect of poultry manure, bio-fertilizers, magnetic water and their interaction on the basal floral diameter (cm) of gladiolus in two seasons in two seasons*

Autumn							Spring				
C	A	B_0	B_1	B_2	A*C	C	B_0	B_1	B_2	A*C	C
C_1	A_0	8.34	10.54	10.29	9.72	9.89	7.88	9.02	8.37	8.42	8.84
	A_1	9.76	12.03	13.01	11.60		8.80	10.01	10.47	9.76	
	A_2	7.58	9.34	8.13	8.35		6.96	9.10	8.92	8.33	
C_2	A_0	9.97	12.11	12.17	11.42	11.01	8.27	11.28	10.47	10.01	10.17
	A_1	10.89	13.54	13.73	12.72		9.16	12.19	11.99	11.11	
	A_2	7.88	10.39	9.20	9.16		8.30	10.30	9.58	9.39	
Interaction of B*C							Interaction of B*C				
C_1		8.56	10.64	10.48			7.88	9.38	9.25		
C_2		9.58	12.01	11.70			8.58	11.26	10.68		
Interaction of A*B					A		Interaction of A*B			A	
A_0		9.16	11.33	11.23	10.57		8.07	10.15	9.42	9.21	
A_1		10.33	12.79	13.37	12.16		8.98	11.10	11.23	10.44	
A_2		7.73	9.87	8.67	8.76		7.63	9.70	9.25	8.86	
B		9.07	11.33	11.09			8.23	10.32	9.97		

LSD 0.05														
A	B	C	A*B	A*C	B*C	A*B*C	A	B	C	A*B	A*C	B*C	A*B*C
1.02	1.02	0.84	1.79	1.68	1.68	2.54	0.98	0.98	0.80	1.77	1.39	1.39	2.36

A is poultry manure, A0 without poultry manure, A1 application of poultry manure at 2% of soil weight, A2 application of poultry manure at 4% of soil weight. B is bio-fertilizers, B1 is inoculation by bacteria *Azospirillum brasilense,* B2 is inoculation by bacteria *Bacillus subtilis,* C is type of irrigation, C1 is irrigation by tap water, C2 is irrigation by magnetic water

http://www.aloki.hu ● ISSN 1589 1623 (Print) ● ISSN 1785 0037 (Online)
DOI: http://dx.doi.org/10.15666/aeer/1802_26372655

Effect of poultry manure, bio-fertilizers, magnetic water and their interaction on the vase life (day) in magnetic water of gladiolus

The effect of poultry manure on the number of the days for vase life of gladiolus var. Cartago is shown in *Table 12*. The highest number of the days 12.12, 9.83 day were noticed from A_1 application for both seasons, while the lowest number of the day 8.88 day in the autumn was obtained from A_2 application and 8.18 day in the spring was noticed from A_0.

However, the inoculation of gladiolus corms with bio-fertilizers significantly affected flowers vase life. The highest vase lives 11.04, 10.45 days were obtained with B_2, B_1 inoculation in the autumn respectively, whereas the lowest vase life 8.85 day was found from B_0. In the spring the highest vase lives 9.62, 9.54 days were found from B_1, B_2, while the lowest vase lives 7.66 days was achieved from B_0. The irrigation by magnetic water caused increasing of vase life significantly. The 11.05, 9.35 day achieved from C_2 as compared to C_1 which gave 9.17, 8.53 day for both seasons, respectively.

Table 12. *Effect of poultry manure, bio-fertilizers, magnetic water and their interaction on the vase life (day) in magnetic water of gladiolus in two seasons*

Autumn							Spring				
C	A	B_0	B_1	B_2	A*C	C	B_0	B_1	B_2	A*C	C
C_1	A_0	7.13	8.42	9.90	8.48	9.17	6.99	8.17	8.53	7.90	8.53
	A_1	9.62	11.22	11.85	10.90		7.50	9.89	9.55	8.98	
	A_2	6.58	8.66	9.11	8.12		7.41	9.22	9.50	8.71	
C_2	A_0	8.97	10.15	11.44	10.19	11.05	7.44	9.28	8.66	8.46	9.35
	A_1	11.89	13.89	14.22	13.33		9.11	11.39	11.55	10.68	
	A_2	8.89	10.33	9.67	9.63		7.52	9.77	9.44	8.91	
Interaction of B*C							Interaction of B*C				
C_1		7.78	9.43	10.29			7.30	9.09	9.19		
C_2		9.92	11.46	11.78			8.02	10.15	9.88		
Interaction of A*B					A		Interaction of A*B			A	
A_0		8.05	9.29	10.67	9.34		7.22	8.73	8.60	8.18	
A_1		10.76	12.55	13.03	12.12		8.31	10.64	10.55	9.83	
A_2		7.73	9.49	9.39	8.88		7.47	9.50	9.47	8.81	
B		8.85	10.45	11.04			7.66	9.62	9.54		

LSD 0.05													
A	B	C	A*B	A*C	B*C	A*B*C	A	B	C	A*B	A*C	B*C	A*B*C
0.56	0.56	0.45	1.55	1.22	1.22	1.39	0.65	0.65	0.53	1.22	1.12	1.12	1.60

A is poultry manure, A0 without poultry manure, A1 application of poultry manure at 2% of soil weight, A2 application of poultry manure at 4% of soil weight. B is bio-fertilizers, B1 is inoculation by bacteria Azospirillum brasilense, B2 is inoculation by bacteria Bacillus subtilis, C is type of irrigation, C1 is irrigation by tap water, C2 is irrigation by magnetic water

However, the interaction between A, B and C gave statistical differences on vase life in both seasons. The highest vase life 14.22, 11.55 days were found from $A_1B_2C_2$ followed by $A_1B_1C_2$ which amounted 13.89, 11.39 days for both seasons respectively, while the lowest vase life 6.58day was recorded from $A_2B_0C_1$ for autumn season, and 6.99 day was noticed from $A_0B_0C_1$ for spring season.

http://www.aloki.hu ● ISSN 1589 1623 (Print) ● ISSN 1785 0037 (Online)
DOI: http://dx.doi.org/10.15666/aeer/1802_26372655

Discussion

The reason for the difference of plant height in autumn and spring seasons *Table 3* might be that clay percentage in soil media A_1 is 37.6 compared to soil media A_2 is 21.6 as it is shown in *Table 1*. This effect may be attributed to the physical properties of some ions adhere on the clay soil particles (Mazhar, 2010).

Regarding the inoculation of gladiolus corms with bacteria *Azospirillum brasilense,* it gave the maximum plant height and there were not significant differences with inoculation by *Bacillus subtilis,* while both of them are different from treatment without bacteria. This result is similar to what was obtained by Ali et al. (2014) as they reported that the vegetative growth improved after the application of bacteria *Azospirillum*. Moreover, a significant difference in vegetative growth was observed after using Azotobacter and Phosphate Solubilizing Bacteria (PSB) on growth of gladiolus by Srivastava and Govil (2005). Using magnetic water can improve plant height as it increases the ability of soil to get rid of salt, and it helps to better assimilate nutrients in plants during vegetative growth.

In this study, dry matter percentage in Gladiolus leaves were significantly affected by the application of 2% poultry manure in soil media (*Table 4*). These results could be due to efficient nitrogen availability which led to the improvement of vegetative growth (Shah et al., 2016). Nitrogen as an essential component of protein, nucleic acid and many important substances like chlorophyll, which are required for vegetative growth and might be responsible for the increase in dry matter accumulation in leaves. The soil bacteria belonging to the genera *Bacillus* is more common. The major microbiological means by which insoluble phosphorus compounds are mobilized by the production of organic acids, accompanied by acidification of the medium. The organic and inorganic acids convert tricalcium phosphate to di- and monobasic phosphates with the net result of an enhanced availability of the element to the plant (Yazdani et al., 2009).

The magnetic field can increase ions mobility and ions uptake which leads to a better photo stimulation and growth (Pietruszewski, 1999). Moreover, magnetic field has the ability to change water properties. Thus, this results in the increase of chlorophyll content which leads to increase in fresh weight of leaves and might cause nutrient accumulation in the leaves.

Effects of the interaction $A_1B_1C_2$ on chlorophyll intensity might be due to effects of each factor on all vegetative growth characteristics of Gladiolus var. Cartago, and it was clearly compact with the high concentration of nitrogen in leaves for both seasons 3.63, 3.40% that is shown in *Table 6,* which had major role of increasing photochemical reduction. These results are close with findings of Al-Khazan et al. (2011) that noticed that photosynthetic pigment and nutrient content of *Simmondsia chinensis L.* enhanced when irrigated by magnetic water. Atak et al. (1997) suggested that the increase of photosynthetic pigments was due to an increase in cytokinin synthesis and this plays an important role on chloroplast development. Magnetic fields are known to induce biochemical changes and affect photo pigments (Dhawi and Al-Khayri, 2009).

Tables 6–8 illustrated that A_1 had significant effect on nutrient concentration in leaves of gladiolus. This may be due to poultry manure which is an excellent organic fertilizer, as it contains high nitrogen, phosphorus, potassium and other essential nutrients (Garg and Bahl, 2008). The addition of organic fertilizers gives the plant an opportunity to provide more efficiently in the nutrients needed by nitrogen that enters into the composition of a number of important organic compounds in the biological processes in

http://www.aloki.hu ● ISSN 1589 1623 (Print) ● ISSN 1785 0037 (Online)
DOI: http://dx.doi.org/10.15666/aeer/1802_26372655

the plant. It also involves into the synthesis of nucleic acids such as DNA, RNA and helps the building of important proteins that increase division and elongation of cells.

Although, the inoculation corms of Gladiolus var. Cartago by each *Azospirrilum brasilense* and *Bacillus subtilis* had significant differences in nutrient content in leaves as compared to treatment with control. These results are accordance with (Orhan et al., 2006) who investigated two Bacillus strains OSU-142 (N2-fixing) and M3 (N2-fixing and phosphate solubilizing) that were tested alone or in combinations on organically grown primo cane fruiting raspberry (cv. Heritage). It was found that bacterial treatment improves nutrient uptake and increase most nutrient element contents P, Ca, Fe, Mn and K in leaves.

Third factor that caused of increasing nutrient element concentration in leaves was irrigation by magnetic water. These results agree with findings of Al-Ma athidi (2006) who investigated the effect of magnetic water on *Gerbera jamessonii* which caused to increasing of nitrogen and magnesium availability in soil solution (Hashemabadi et al., 2015; Abdelaziz and Abdelrazig, 2014).

As indicated in *Tables 9–12,* treatment A_1 had significant effects on most flower characterizes (Number of the days for flowering, anthocyanin concentration in petals, basal floral diameter and vase life) of gladiolus var. Cartago. The results were on line with Jha (2011) findings that the farm yard manure10 t. ha^{-1} with 75% RDF gave significant effect on the reducing the number of the days for spike emergence of gladiolus cultivar candyam. In this study, the use of 4% did not have significant effects on the flower attributes which may be because of effects of high Electrical conductivity of A_2 which 2.91 was higher than A_1 1.70 which might be due to the presence of more salts in the poultry manure at the rate A_2 as shown in *Table 1*.

The bio-fertilizers inoculation gave significant effects on most flowering characterizes as compared to control. The data in *Table 9* indicated that the number of the days required to opening of basal floret was significantly reduced with the inoculation of *Azospirillum barasilense* and *Bacillus subtilis* in two seasons. These results were in close with findings of Singh (2009). The study was carried out to use bio-fertilizers in combination with nitrogen on growth and flowering of Gladiolus, to see the effect of Bacillus and Pseudomonas strains on growth and flowering of gladiolus cultivar American Beauty. Significant increase in spike length, and number of florets per spike and floret diameter was recorded under levels of nitrogen, bio-fertilizers, Bacillus, Pseudomonas strains and their combinations.

Moreover, irrigation by magnetic water caused improvements in flower quality. The reason for the positive effects of magnetized water could be due to the fact that the magnetic field is dependent on changes in the physical and chemical properties of water, including reducing surface tension, viscosity and water density, making it lighter and easier to absorb. The results were close with findings of Al-Maathidi (2006) in the study of using magnetized water on *Gerbera jamesonii.*

Regarding of vase life, the biofertilizers regulate nutrient uptake process and prolonged vase life phenomenon. Bekheta and Mahgoub (2005) concluded that the increase in nitrogen level lead to change in amino acids quantity and specific proteins in carnation plants. Plants treated with microbial inoculations showed more sugar contents.

http://www.aloki.hu ● ISSN 1589 1623 (Print) ● ISSN 1785 0037 (Online)
DOI: http://dx.doi.org/10.15666/aeer/1802_26372655

Conclusion

The study discusses that the poultry manure at the rate of 2% of soil weight improves vegetative growth of Gladiolus (*Gladiolus hybrida*) as well as flower characteristics. Moreover, inoculation by *Azospirillum brasilense* and *Bacillus subtilis* increases the plant height, chlorophyll intensity, N, P, K uptake and flower quality in autumn and spring seasons. Since the soils of Sulaimani farms are suffering from organic matter deficiency, application of animal residue as poultry manure is used as it improves organic matter content. Furthermore, using biofertilizer is safer than chemical fertilizer to decrease soil pollution, and it costs less. It is clear that the irrigation with magnetic water and using bacteria Azosperilum spp. can improve flower production and reduced salinity of the soil. It is recommended for future researches to study the different type of bacteria and mycorrhiza with organic matter.

REFERENCES

[1] Abdelaziz, E., Abdelrazig, A. (2014): Impact of magnetized water on elements contents in plants seeds. – International Journal of Scientific Research and Innovative Technology 1(4): 12-21.

[2] Al-Khazan, M., Abdullatif, B. M., Al-Assaf, N. (2011): Effects of magnetically treated water on water status, chlorophyll pigments and some elements content of Jojoba (Simmondsia chinensis L.) at different growth stages. – African Journal of Environmental Science and Technology 5(9): 722-731.

[3] Al-Maathidi, A. (2006): Effect of magnetic technology on some ornamental plants. – PhD. Thesis, College of Agriculture, University of Baghdad.

[4] Aladjadjiyan, A. (2002): Study of the influence of magnetic field on some biological characteristics of Zea mais. – Journal of Central European Agriculture 3(2): 89-94.

[5] Ali, A., Mehmood, T., Hussain, R., Bashir, A., Najam‐Ud‐Din, S., Ahmad, A. (2014): Investigation of biofertilizers influence on vegetative growth, flower quality, bulb yield and nutrient uptake in gladiolus (Gladiolus grandiflorus L.). – International Journal of Plant, Animal and Environmental Sciences 4(1): 94-99.

[6] Atak, Ç., Yurttaş, B., Yalçın, S., Mutlu, D., Rzakoulieva, A., Danilov, V. (1997): Effects of Magnetic Field on Soybean (Glycine Max. L. Merrill) Seeds. – Com JINR, Dubna.

[7] Bot, A., Benites, J. (2005): The Importance of Soil Organic Matter: Key to Drought-Resistant Soil and Sustained Food Production. – Food & Agriculture Org., Rome.

[8] Bekheta**,** M. A., Mahgoub, M. H. (2005): Application of kinetin and phenylalanine to improve flowering characters, vase life of cut flowers as well as vegetative growth and biochemical constituents of carnation plants. – Egypt Academic Journal Biological Science 20(6): 234-246.

[9] Bhalla, R., Kanwar, P., Dhiman, S. and Jain, R. (2006) 'Effect of biofertilizers and biostimulants on growth and flowering in gladiolus', *Journal of Ornamental Horticulture,* 9(4), pp. 248-252.

[10] Chaitra, R., Patil, V. (2007): Effect of integrated nutrient management on growth, yield and quality of China aster (Callistephus chinensis (L.) Nees). – Karnataka J. Agric. Sci. 20: 689-90.

[11] Dhawi, F., Al-Khayri, J. M. (2009): Magnetic fields induce changes in photosynthetic pigments content in date palm (Phoenix dactylifera L.) seedlings. – The Open Agriculture Journal 3(1).

http://www.aloki.hu ● ISSN 1589 1623 (Print) ● ISSN 1785 0037 (Online)
DOI: http://dx.doi.org/10.15666/aeer/1802_26372655

[12] Eşitken, A., Turan, M. (2004): Alternating magnetic field effects on yield and plant nutrient element composition of strawberry (Fragaria x ananassa cv. Camarosa). – Acta Agriculturae Scandinavica, Section B-Soil & Plant Science 54(3): 135-139.
[13] Garg, S., Bahl, G. (2008): Phosphorus availability to maize as influenced by organic manures and fertilizer P associated phosphatase activity in soils. – Bioresource Technology 99(13): 5773-5777.
[14] Greving, A. J. (1987): G87-852 Growing Gladiolus. – Historical Materials from University of Nebraska-Lincoln Extension.
[15] Gutiérrez-Mañero, F. J., Ramos-Solano, B., Probanza, A., Mehouachi, J., R Tadeo, F., Talon, M. (2001): The plant-growth-promoting rhizobacteria Bacillus pumilus and Bacillus licheniformis produce high amounts of physiologically active gibberellins. – Physiologia Plantarum 111(2): 206-211.
[16] Hashemabadi, D., Zaredost, F., Solimandarabi, M. J. (2015): The effect of magnetic water and irrigation intervals on the amount of the nutrient elements in soil and aerial parts of periwinkle (Catharanthus roseus L.). – Journal of Ornamental & Horticultural Plants 5(3).
[17] Hozayn, M., Qados, A. A. (2010): Magnetic water application for improving wheat (Triticum aestivum L.) crop production. – Agriculture and Biology Journal of North America 1(4): 677-682.
[18] Jackson, M. L. (1958): Soil Chemical Analysis. – Prentice-Hall, Englewood Cliffs, NJ.
[19] Jha, S. (2011): Studies on Integrated Nutrient Management in Gladiolus with Special Reference to Growth, Yield and Flowering Quality. – Indira Gandhi Krishi Vishwavidyalaya, Raipur.
[20] Kumari, M. (2014): Postharvest Studies in Chrysanthemum (Dendranthema grandiflorum L.). – Division of Floriculture and Landscaping, New Delhi.
[21] Manning, J., Goldblatt, P. (2008): The Iris Family: Natural History and Classification. – Timber Press, Portland, OR, pp. 91-93.
[22] Mazhar, Azza, A. M., Nahed, G., Abd El Aziz, E. El Habba (2010): Impact of different soil media on growth and chemical constituents of Jatropha curca L. seedlings growth under water regime. – Journal of American Science 6(8): 549-556.
[23] Olsen, S. R., Sommers, L. E. (1982): Phosphorus. – In: Page, A. L. (ed.) Methods of Soil Analysis. Part 2. Chemical and Microbiological Properties. 2nd Ed. Amer. Soc. of Agron. Inc. Soil. SOCOM, Madision, WI.
[24] Orhan, E., Esitken, A., Ercisli, S., Turan, M., Sahin, F. (2006): Effects of plant growth promoting rhizobacteria (PGPR) on yield, growth and nutrient contents in organically growing raspberry. – Scientia Horticulturae 111(1): 38-43.
[25] Page, A. L., Miller, R. H. Keeug, D. R. (1982): Methods of Soil Analysis. Part 2: Chemical and Microbiological Properties. – Amer. Soc. Agron., Madison, WI.
[26] Pang, X., Deng, B. (2008): Investigation of changes in properties of water under the action of a magnetic field. – Science in China Series G: Physics, Mechanics and Astronomy 51(11): 1621-1632.
[27] Pietruszewski, S. (1999): Influence of pre-sowing magnetic biostimulation on germination and yield of wheat. – International Agrophysics 13: 241-244.
[28] Ranganna, S. (1977): Manual Analysis of Fruit and Vegetable Products. Method II. – Tata McGraw-Hill Publishing Company Limited, New Delhi.
[29] Sajjad, Y., Jaskani, M. J., Ashraf, M. Y., Qasim, M., Ahmad, R. (2014): Response of morphological and physiological growth attributes to foliar application of plant growth regulators in gladiolus white prosperity. – Pak. J. Agri. Sci. 51(1): 123-129.
[30] Shah, S. T., Ghafoor, F., Khan, N., Sajid, M., ul Amin, N., Shah, Z., Bibi, S., Ahmad, T., ul Haq, F. (2016): Organic fertilizers affect the growth attributes of weeds and Swiss chard. – Pakistan Journal of Weed Science Research 22(3).
[31] Singh, Y. (2009): Studies on the use of biofertilizers in gladiolus. – PhD. Thesis, Agricultural University, Hisar.

http://www.aloki.hu ● ISSN 1589 1623 (Print) ● ISSN 1785 0037 (Online)
DOI: http://dx.doi.org/10.15666/aeer/1802_26372655

[32] Srivastava, R., Govil, M. (2005): Influence of biofertilizers on growth and flowering in gladiolus cv. American Beauty. – International Conference and Exhibition on Soilless Culture: ICESC 742: 183-188.

[33] Tahir, N. A.-R., Karim, H. F. H. (2010): Impact of magnetic application on the parameters related to growth of chickpea (Cicer arietinum L.). – Jordan Journal of Biological Sciences 3(4): 175-184.

[34] Yazdani, M., Bahmanyar, M. A., Pirdashti, H., Esmaili, M. A. (2009): Effect of phosphate microorganisms (PSM) and plant growth solubilization promoting rhizobacteria (PGPR) on yield and yield components of corn (Zea mays L.). – International Journal of Biological, Biomolecular, Agricultural, Food and Biotechnological Engineering 3(1).

http://www.aloki.hu ● ISSN 1589 1623 (Print) ● ISSN 1785 0037 (Online)
DOI: http://dx.doi.org/10.15666/aeer/1802_26372655

BIOSORPTION OF CADMIUM AND LEAD USING MICROALGAE *SPIRULINA SP.* ISOLATED FROM KOYA CITY (IRAQ)

ABDULKAREEM, P. M.[1*] – ANWER, S. S.[2]

[1]*Department of Biology, Health and Sciences Faculty, Koya University, Erbil, Iraq*

[2]*Department of Clinical Biochemistry, College of Health Sciences, Hawler Medical University, Erbil, Iraq*
(phone: +964-750-494-3730)

**Corresponding author*
e-mail: parween.mohsin@koyauniversity.org; phone: +964-750-441-2402

(Received 25th Aug 2019; accepted 8th Jan 2020)

Abstract. The alternative to the traditional method for heavy metal uptake is biosorption. The potential of *Spirulina sp.* for biosorption of waste effluent was examined. In this study, morphology and molecular features of microalgae *Spirulina sp.* isolated from Koya city were identified on. The rate of biosorption of cadmium (Cd^{+2}) and lead (Pb^{+2}) were studied by using a spectrophotometer. The optimum uptake for both metals Cd^{+2} and Pb^{+2} showed at low metal concentration of 100 mgl^{-1} 88.8% and 93.6%, respectively. *Spirulina sp.* showed the ability to remove metals at all pH values 38.1% and 85.8% for Cd^{+2} and 34.6% and 88.4% for the Pb^{+2} with maximum uptake at 30 °C 85.7% for Cd and Pb optimum uptake was 88.4%. Optimum removal showed at agitation rate 150 rpm 87.1) in Cd^{+2}, and Pb^{+2} optimum adsorption at 150 rpm was 89.9%. Both metals showed optimum adsorption at 1.5 g l^{-1} of algal biomass, Cd^{+2} removed 86.7%, and Pb^{+2} 89.2%. Pb^{+2} showed the best performance for metal biosorption.
Keywords: *metal uptake, algal biomass, temperature, agitation rate, pH*

Introduction

Microalgae include those chlorophyll-bearing organisms that are thalloid (Vashishta et al., 2002). Nearly 75% of algal species are microalgae that contribute 30-40% of oxygen to the atmosphere (Ponuswamy et al., 2013). They are the primary producers who switch water and carbon dioxide into carbohydrates and oxygen in the presence of the sun (Chisti, 2008). Microalgae biomass is often measured with a concentration of chlorophyll and can provide a useful index of potential production.

Cadmium (Cd^{+2}) is a chemical element that involves different machinery to induce its harmful effect on many biological activities in humans, animals, and various other organisms. In humans, the adverse effect of Cd^{+2} is not only limited to the kidney and bone, but it includes nearly every organ and tissue where it accumulates, which argues the need for public health measures aimed at reducing exposure. There are many ways in which this heavy metal can be suppressed in its activities, forming the prospect for reduced metal toxicity involving Cd^{+2} (Hogan, 2010; Sharma et al., 2015).

Lead (Pb^{+2}) is number two on the "Top 20 List" of toxic and hazardous substances of the ATSDR. Pb^{+2} accounts for the majority of pediatric heavy metal poisoning (Roberts, 1999). Pb^{+2} occurs in many forms worldwide in natural sources and is one of the most commonly and uniformly distributed trace metals (Jackson et al., 2005). Pb^{+2} creates several adverse effects in both males and females on the reproductive system. Common impacts shown in males involve decreased libido, unusual spermatogenesis (decreased motility and number), chromosomal harm, infertility, abnormal prostatic function, and

http://www.aloki.hu ● ISSN 1589 1623 (Print) ● ISSN 1785 0037 (Online)
DOI: http://dx.doi.org/10.15666/aeer/1802_26572668

serum testosterone alterations. Women, on the other hand are more prone to infertility, miscarriage, premature membrane rupture, pre-eclampsia, pregnancy hypertension, and premature delivery (Flora et al., 2011). Also, during gestation, the direct influence of Pb^{+2} on the developmental stages of the fetus was registered (Saleh et al., 2009; Flora et al., 2012). Hasson (2018) measured concentrations of some heavy metals in various imported and locally produced vegetable crops in Baghdad city, including root crops and the daily intake of four main heavy metals (Cd, Cu, Zn, and Pb) had been estimated, which revealed a high consumption of Cd^{+2} (310 and 372 μg per day) for imported and local vegetables that affect human health. Because of multiple anthropogenic activities, heavy metals are released into the fairway. Their therapy is of particular significance since heavy metals are non-biodegradable and cause environmental damage due to their poisoning to many crops, livestock, and microorganisms in the aquatic environment (Sadettin and Donmez, 2007; Kaplan, 2013; Salih et al., 2017). Traditional methods for the removal of dissolved heavy metal ions involve chemical precipitation, electrochemical treatment, chemical oxidation and reduction, ion exchange, filtration and evaporative recovery (Aksu et al., 2002). Biosorption of heavy metals by microalgae is generally a biphasic process involving adsorption by materials associated with extracellular cells, such as polysaccharides and cell wall components (Roy et al., 1993; Das et al., 2008).

Materials and methods

Sampling and cultivation

Microalgae sample was isolated along Taq-Taq river in Koya city during May-September 2018, Water samples were taken from a depth between 10 and 50 cm from the bottom (Prasad et al., 2013) and plated Blue-green 11 medium (BG11) as described by Allen (1968) and Oswaled (1988). The cultures were incubated at pH 7.8 and 28 ℃ under constant light 800Lx. Two weeks later, following the growth of colonies on the agar media, the colonies were removed with pasture micropipettes and gently blown into the liquid medium, then incubated at 28 ℃, 800 Lx, and pH 7.8.

Morphological and molecular identification of algae

After a 15-days single colony removed and examined under a light microscope for identification purposes based on their morphology as described by Prescott (1963), Desikachary (1968), Rippka (1988) and Holt et al. (1994). Further identification was performed by polymerase chain reaction (PCR) to confirm algal genera.

Extraction of DNA

Genomic DNA extraction was performed using a commercial extraction kit (Thermofisher, USA) according to the manufacture's instruction. DNA samples were then checked for their quantity and quality using Bio-photometer (Eppendorf, German).

PCR amplification and DNA sequencing

The targeted region of 16S rRNA of algae amplified by PCR using universal primers, forward primer A8F (5- AGAGTTTGATCCTGGCTCAG-3), and the reverse primer A1492R (5- TACGGCTACCTTGTTACGACTT- 3). Primers were previously used by

http://www.aloki.hu ● ISSN 1589 1623 (Print) ● ISSN 1785 0037 (Online)
DOI: http://dx.doi.org/10.15666/aeer/1802_26572668

Ponnuswamy et al. (2008). A total of 50 µl volume of the reaction mixture was prepared, which contained 40–55 ng DNA, 100 mM of each primer, 0.05 U/µl Taq DNA polymerase, 4 mM MgCl2, and 0.4 mM of each dNTP.

ABI 3130XL genetic analyzer (USA) was employed to find the order of the nucleotides of 16S rRNA for the algae sample. The PCR products were cut from the agarose gel and utilized as a base of DNA template for sequence-specific PCR amplification and sent for nucleotide sequencing analysis to the private medical genetic laboratory in Intergene Genetic Center, Ankara, Turkey.

Preparation of biomass

Spirulina sp. biomass initially dried from moisture on an aluminium tray, kept in the oven at 80 ℃ for 24 h, after cooling, this material was subjected to sieve analysis.

Chemicals

Cadmium nitrate tetrahydrate ($Cd(NO_3)_2 \bullet 4H_2O$) and lead nitrate ($Pb(NO_3)_2$) were used to prepare 1000 mg l^{-1} inventory metal ion solutions that were diluted to produce metal ion alternatives for adsorption. Before the microorganisms were mixed, the pH value of each metal solution was adapted with 1 mol l^{-1} NaOH to the appropriate value (Fan et al., 2008).

Batch experiments

Batch experiments were performed at different initial metal concentrations 100-500 mgl^{-1}, pH 6.5-8.5, temperature 20-40 ℃, agitation speed from zero-200 rpm, and biosorbent dosage 0.3-1.5 gl^{-1} according to Aksu (2005). The rate of biosorption was read using spectrophotometer at 540 nm for Cd^{+2} and 530 nm for the Pb^{+2}. Metal containing medium was used as blank (control medium contained both metals and solution without biosorbent to observe any reaction of the solution with metals). Each experiment was carried out in triplicate. The yield of biosorption was determined (*Eq. 1*) by the formula below (Blanco et al., 1999; Aksu, 2005):

$$Biosorption\ \% = (Co) - (C).100/Co \qquad \text{(Eq.1)}$$

C_o - Initial metal concentration, C - Final metal concentration.

Statistical analysis

The test results were statistically analyzed with a one-way variance analysis (ANOVA) followed by a Tukey post hoc test ($P \leq 0.5$) to assess significant differences between the experimental classes.

Results

Morphological and molecular identification of algal strain

After observation under the microscope at different magnifications and according to the guide of taxonomic, in the isolated and purified samples trichomes width without akinetic and heterocyst, cell length, pointed calyptras, type of coil and helix shape (*Fig.*

http://www.aloki.hu ● ISSN 1589 1623 (Print) ● ISSN 1785 0037 (Online)
DOI: http://dx.doi.org/10.15666/aeer/1802_26572668

1) were observed and identified as *Spirulina* according to Ciferri (1983), Rippka (1988), Tomasseli (1997) and Prasal et al. (2013).

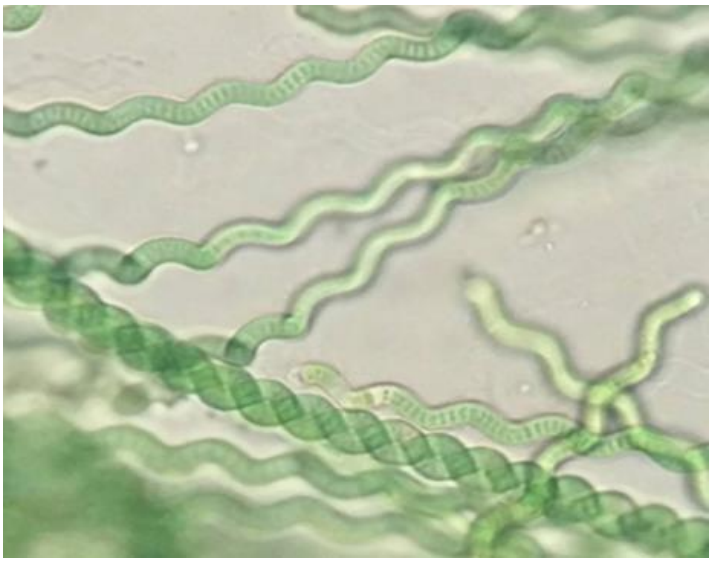

Figure 1. *Microscopic observation of Spirulina sp.*

By molecular examination, the sequence from 16S rDNA of algae specimen was made of 1200-1400 bp (amplified fragment was 1468 bp, also after testing some non-nucleotides were removed, linked to the character of the sequencing assessment) and then placed to BLAST compared to other stored algae sequence genus from the Gene Bank database. The primary sequence analysis using a universal primer of the observed specimen disclosed that algae from Koya city belong to the *Spirulina sp.* genus. Its rDNA conforms to the same rDNA sequence fragment symbol required at the Gene Bank in the National Center for Biotechnology Information (NCBI), pairwise analysis of the algae specimen is shown in *Figure 2.*

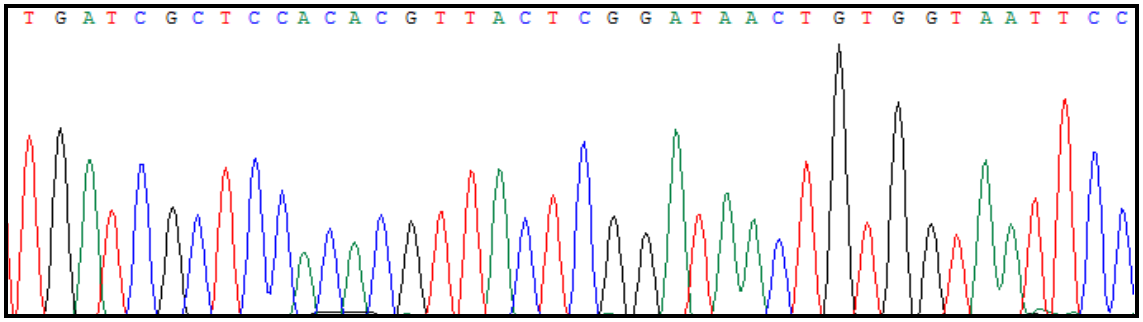

Figure 2. *The partial sequencing result of 16S rDNA of Spirulina sp.*

Effect of Cd and Pb concentrations on biosorption

Figures 3 and *4* showed the effect of initial metal ion concentration (Cd^{+2} and Pb^{+2}) ranging from (100-500 mg l^{-1}). Optimum removal showed during 15 h, and the rapid removal showed at hour 3; by increasing metal concentration, the biosorption process decreased. In the case of Cd^{+2}, the optimum adsorption (88.8%) was recorded at a

http://www.aloki.hu ● ISSN 1589 1623 (Print) ● ISSN 1785 0037 (Online)
DOI: http://dx.doi.org/10.15666/aeer/1802_26572668

concentration of 100 mg l^{-1}, while high removal of Pb^{+2} was (93.6%) at the same concentration. Increasing concentration of both metal ions led to a decline in adsorption, indicating saturation of all the binding sites on the algal surface. The result showed that there were no significant differences between heavy metal concentration with Cd^{+2} (*p*-value = 0.0936) and Pb^{+2} (*p*-value = 0.0981).

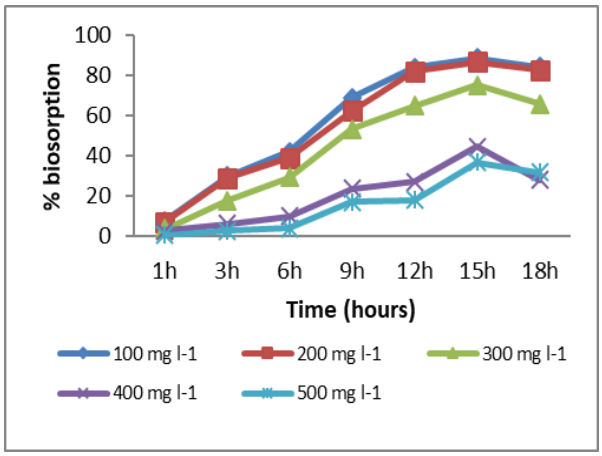

Figure 3. *Effect of metal Cd^{+2} concentration on biosorption process (pH 7, 35 °C, 100 rpm)*

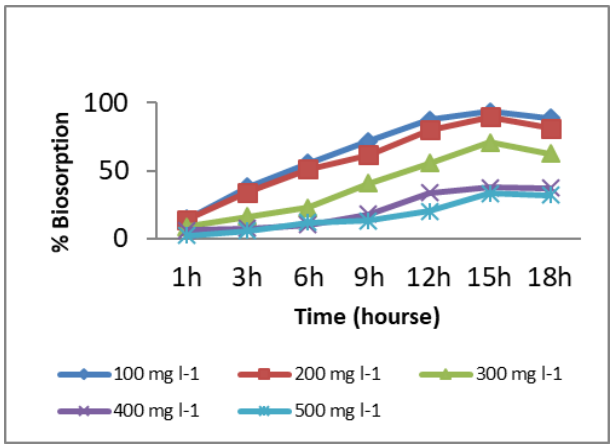

Figure 4. *Effect of metal Pb^{+2} concentration on biosorption process (pH 7, 35 °C, 100 rpm)*

Effect of pH on biosorption of Cd and Pb by Spirulina sp.

The pH is an important factor in biosorption processes. To find an appropriate pH for *Spirulina sp.* efficient heavy metal biosorption, studies were conducted at five distinct original pH values (6.5, 7, 7.5, 8, 8.5), *Spirulina sp.* showed ability to remove metals at all pH values 38.1% and 85.8% for Cd^{+2} and 34.6% and 88.4% for the Pb^{+2}. The Statistical analysis showed significant differences among pH and adsorption percentage of both Cd^{+2} and Pb^{+2} ions. A significant correlation had been recorded among pH degree change with both Cd^{+2} (*p*-value = 0.0039) and Pb^{+2} (*p*-value = 0.0065), which means with increasing pH, the adsorption percent increased, and the peak of adsorption percent was reached to 85.8 for Cd^{+2} and 88.4 for Pb^{+2} ion. The optimum removal showed at pH 8 (Cd^{+2} 85.8% and Pb^{+2} 88.4%) as shown in *Table 1*.

http://www.aloki.hu ● ISSN 1589 1623 (Print) ● ISSN 1785 0037 (Online)
DOI: http://dx.doi.org/10.15666/aeer/1802_26572668

Table 1. *Effect of pH on biosorption of Cd^{+2} and Pb^{+2} by Spirulina sp. 200 mg l^{-1}), 35 °C, 100 rpm*

pH	*Spirulina sp.* (Cd^{+2})			*Spirulina sp.* (Pb^{+2})		
	C_0(mg l^{-1})	CC_0(mg l^{-1})	%Adsorption	C_0(mg l^{-1})	CC_0(mg l^{-1})	%Adsorption
6.5	167.9	63.9	38.1	162.7	56.3	34.6
7	178.6	122.2	68.4	172.7	108.7	62.9
7.5	188.6	157.2	83.3	178.7	147.4	82.5
8	214.3	183.9	**85.8**	192	169.7	**88.4**
8.5	202.1	169.6	83.9	183.3	156.6	85.5

Effect of temperature on biosorption of Cd^{+2} and Pb^{+2} by Spirulina sp.

To find an appropriate temperature for *Spirulina sp.*'s on efficient heavy metal adsorption, studies were conducted at five distinct temperature values (20, 25, 30, 35, and 40 °C) as shown in *Figures 5* and *6*. Rapid removal showed in first hour at 20 °C. Optimum removal of Cd^{+2} showed at a temperature of 30 °C (85.7%), and for Pb^{+2}, optimum removal was (88.4%) at the same temperature. The effect of temperature showed significant differences among temperature and adsorption percentage of both Cd^{+2} and Pb^{+2} ions. Significant differences had been stated related to temperature change in both Cd^{+2} (p-value = 0.025) and Pb^{+2} (p-value = 0.0248) biosorption.

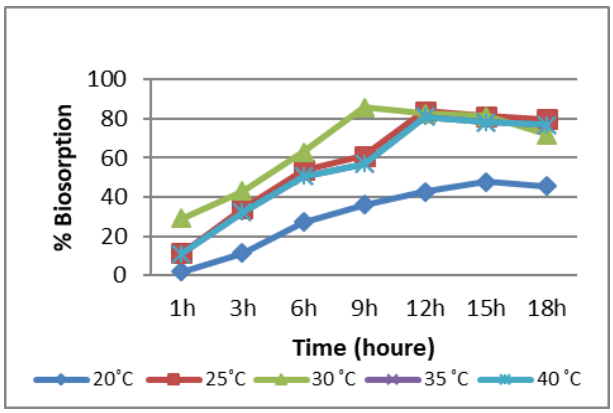

Figure 5. *Effect of temperature on Cd^{+2} adsorption C_0- 200 mg l^{-1}, pH 8, 100 rpm*

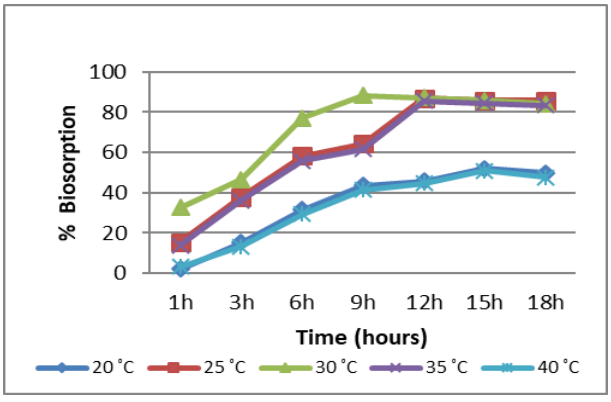

Figure 6. *Effect of temperature on Pb^{+2} adsorption by Spirulina sp. C_0- 200 mg l^{-1}, pH 8, 100 rpm*

http://www.aloki.hu ● ISSN 1589 1623 (Print) ● ISSN 1785 0037 (Online)
DOI: http://dx.doi.org/10.15666/aeer/1802_26572668

Effect of agitation rate (rpm) on biosorption of Cd^{+2} and Pb^{+2} by Spirulina sp.

The effect of agitation rate on Cd^{+2} and Pb^{+2} adsorption by *Spirulina sp.* is shown in *Table 2*. At equilibrium, metal uptake increases with an increase of agitation rate - rpm (unshaken to 150 rpm), and the optimum removal showed at rpm 150 (87.1%) in Cd^{+2} and Pb^{+2} showed optimum adsorption at 150 rpm (89.9%). The adsorption process decreased with 200 rpm. The *p*-value of Cd^{+2} (*p*-value = 0.469) and Pb^{+2} (*p*-value = 0.5031) that showed no significant correlation between rpm, in spite of increasing rpm, the adsorption percent of Cd^{+2} and Pb^{+2} ions were not changed significantly.

Table 2. *Effect of agitation rate on biosorption of Cd^{+2} and Pb^{+2} by Spirulina sp. (200 mg l^{-1} initial metal concentration (C_0), pH 8, 30 °C)*

Agitation rate	*Spirulina sp.* (Cd^{+2})			*Spirulina sp.* (Pb^{+2})		
	C_0(mg l^{-1})	CC_0(mg l^{-1})	%Adsorption	C_0(mg l^{-1})	CC_0(mg l^{-1})	%Adsorption
Unshaken (non-agitated)	122.1	26.1	21.3	186	59.0	31.7
50 rpm	127.9	76.5	59.8	197.3	102.6	52.0
100 rpm	141.4	119.6	84.6	208	179	86.1
150 rpm	146.4	124.6	**87.1**	212	185	**89.9**
200 rpm	132.1	106.0	80.3	204	174.3	85.5

Effect of algal biomass on biosorption of Cd^{+2} and Pb^{+2} by Spirulina sp.

The effect of biomass on Cd^{+2} and Pb^{+2} ion removal is indicated in *Figures 7* and *8*. At equilibrium, metal uptake increases with an increase in biomass from 0.3 to 1.5 g l^{-1}. Optimum removal showed during 6 h in a biomass of 1.5 g l^{-1}, rapid removal showed at 1 h in a biomass of 0.3 g ml^{-1}. Both metals showed optimum adsorption at 1.5 g l^{-1} of algal biosorbent 86.7%, of Cd^{+2} and 89.2% of Pb^{+2} were removed.

The result showed significant differences among algal biomass and adsorption percent of both Cd^{+2} and Pb^{+2} ions. The *p*-value for both Cd^{+2} (*p*-value = 0.0095) and Pb^{+2} (*p*-value = 0.0036), means with increasing of algal biomass, the adsorption percent increase and the peak of adsorption percent was reached to 86.7 for Cd^{+2} and 89.2 for Pb^{+2} ion.

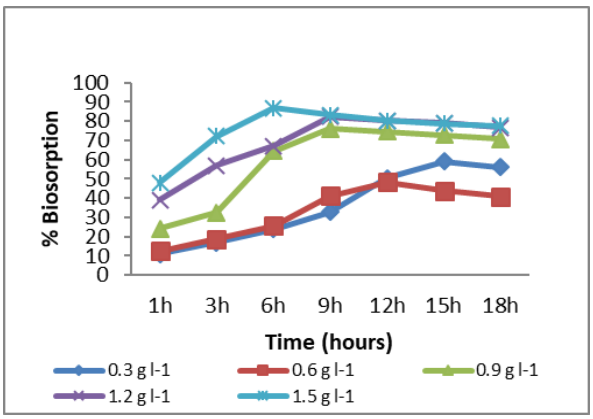

Figure 7. *Effect of biosorbent dosage on Cd^{+2} adsorption (200 mg l^{-1} initial metal concentration, pH 8, 30 °C, 150 rpm)*

http://www.aloki.hu ● ISSN 1589 1623 (Print) ● ISSN 1785 0037 (Online)
DOI: http://dx.doi.org/10.15666/aeer/1802_26572668

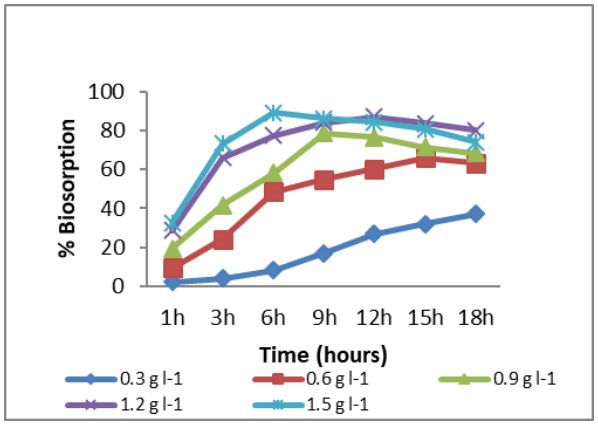

Figure 8. *Effect of biosorbent dosage on Pb^{+2} adsorption (200 mg l^{-1} initial metal concentration, pH 8, 30 °C, 150 rpm)*

Scanning electron microscopy (SEM) analysis

The biosorbent morphology, which is cell/filamentous algae-binding-Pb^{+2} and Cd^{+2}, was examined using SEM with 200x magnification to demonstrate the porous places of cell/filamentous algae as seen in (*Fig. 9a, b, c*) illustrate the efficient binding with Cd^{+2} and Pb^{+2}, respectively. However, in composites with a greater content of Cd^{+2} and Pb^{+2}, the particles are often abnormal in form and circular in the preparing of irregular surface, this distinctive shift in the analyzed SEM pictures highlights the existence of Cd^{+2}.

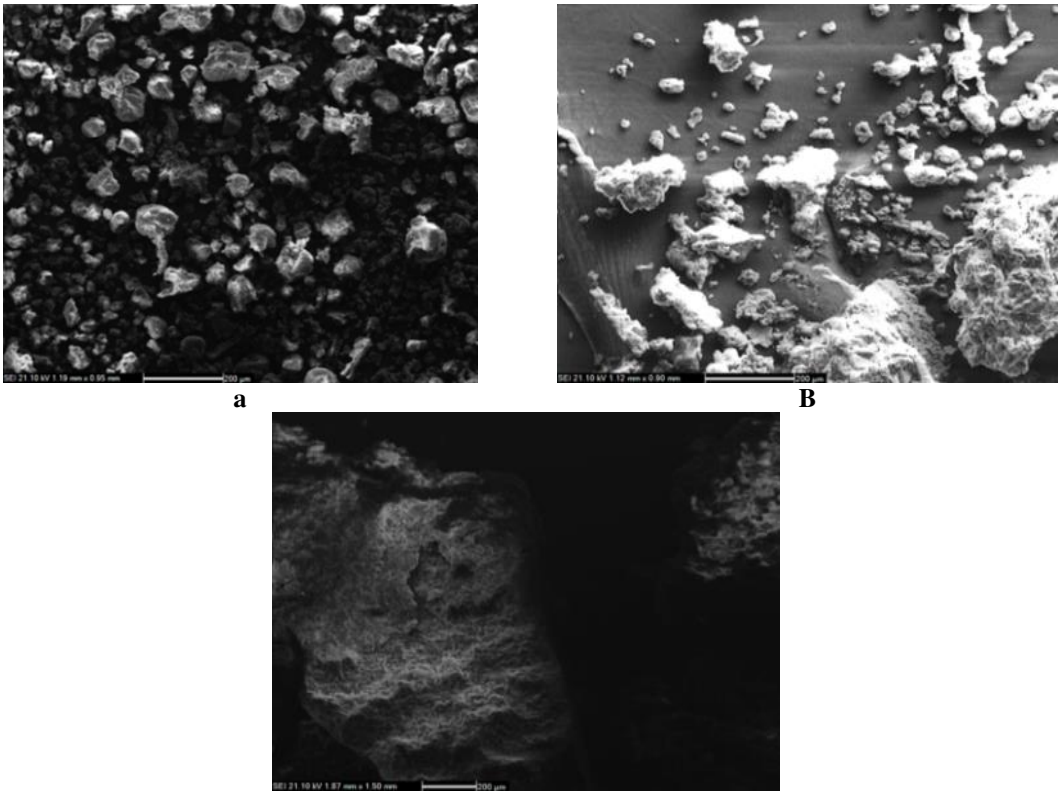

a **B**

C

Figure 9. *SEM image Spirulina (a) before adsorption, (c) and (c) binding Cd^{+2} and Pb^{+2} and on the cell/filamentous algae surface*

http://www.aloki.hu ● ISSN 1589 1623 (Print) ● ISSN 1785 0037 (Online)
DOI: http://dx.doi.org/10.15666/aeer/1802_26572668

Discussion

Isolated and purified microalgae strain observed under microscope and culture showed filamentous spiral-shaped microalgae that were identified as *Spirulina sp.* and the strain was confirmed by using molecular identification. The same characteristics showed by isolated *Spirulina* from (Koya city). In many cases, the selection of efficient organism is known to be essential tools in the successful treatment of wastewater effluents rich in toxic compounds such as Cd (II) and Pb (II) in textile industry effluents. Microalgae were proposed as perfect candidates for the wastewater treatment system. In the present research, *Spirulina* strain was used as biomass for Cd^{+2} and Pb^{+2} adsorption process under various initial metal concentrations, pH, biosorbent dosage, temperature, and agitation velocity. In the experiments, it was showed that there are different factors affecting the biosorption of heavy metals by *Spirulina sp.* The present results were in agreement with Gupta and Rastogi (2008), Kőnig-Péter et al. (2015). Al-Homaidan et al. (2015) and Palaniswamy and Veluchamy (2017). As shown in the results, Pb^{+2} biosorption was more prominent than Cd^{+2} biosorption. Similar results were obtained by Domínguez-Bocanegra et al. (2013), who reported that Pb^{+2} biosorption was more prominent than Cd^{+2} and nickel. By increasing the original metal concentration, the proportion of biosorption of metal ions reduced (*Figs. 3* and *4*) same result was obtained by Abdel-Aty et al. (2013).

The fast adsorption of the metals shows that the sorption method may be ionic where the acidic (anionic) dye molecules bind to the multiple strongly loaded organic functional groups present on the biomass surface (Gulnaz et al., 2004).

pH is one of the most significant parameters affecting original adsorption frequency and ability; the optimum pH was 8 (*Table 1*). This phenomenon is due to the nature of the chemical interaction of each heavy metal with algal cell walls. Hydrogen ion also functions as a bridging ligand between the cyanobacterial cell wall and the heavy metal molecules, and the results were in agreement with Abdel-Aty et al. (2013) who confirmed that the biosorption of Cd (II) and Pb (II) was increased with increasing the pH value and disagreed with Kőnig-Péter et al. (2015) who stated that the biosorption process was successful at pH 5–6 for Pb(II) and pH 4−6 for Cd(II) adsorption. Metals biosorption on *Spirulina sp.* has been researched at various temperatures of 20-40 ℃, and the optimum temperature for adsorption of metals showed at 30 ℃ and the lowest adsorption at 20 ℃ (*Figs. 5* and 6). However, temperature variation in comparisons had an important impact on the removal of Cd^{+2} and Pb^{+2} of *Spirulina sp.* The results of this investigation were in agreement with Donmez et al. (1999), Dhargalkar (2004) and Kőnig-Péter et al. (2015). To determine the impact of agitation velocity on metal adsorption, a series of studies at distinct agitation degrees (unagitated – 200 rpm) were conducted and shown in *Table 2* indicating that the degree of agitation positively affected the sorption process rise in agitation rate biosorption of metals improved optimum adsorption at 150 rpm with agitation levels greater than 200 rpm. This relates to the weakening interaction between the sorbent locations and the metal ion described by the Van-der Waals interaction Anwer and Abdullah (2017) when they study the effect of agitation rate on direct Blue nine adsorption using baker's yeast.

Figures 7 and *8* showed the effect of biosorbent dosage to remove heavy metal, Optimum removal showed in biomass 1.5 at 6 h, fast removal showed in biomass 0.3 at 1 h. By increasing biosorbent dosage adsorption of biomass increased due to increase in the region and the accessibility of more biosorption locations (Mane et al., 2007). After

http://www.aloki.hu ● ISSN 1589 1623 (Print) ● ISSN 1785 0037 (Online)
DOI: http://dx.doi.org/10.15666/aeer/1802_26572668

biosorption process ended the algal biomass accumulated and used for further study which was desorption experiments.

However, in composites with a higher content of Cd^{+2} and Pb^{+2}, the particles are mainly abnormal in form and circular in the preparation of a rougher surface, this distinctive shift in the analyses SEM pictures highlights the existence of Cd^{+2} and Pb^{+2} in the cell/filamentous algae surface this result is agreed with Salih et al. (2017).

Conclusion

Biosorption of heavy metals (Cd^{+2} and Pb^{+2}) increased by increasing biosorbent (*Spirulina sp*.). This study shows that isolated *Spirulina sp.* deserves attention as biosorbent, which can be utilized in the treatment of wastewater effluents containing heavy metals before the treatment, and the technique can be modified further to make it applicable on a large scale to clean up heavy metal contamination using dried biomass of *Spirulina* sp. In most of the studies that done previously by researchers spirulina cells were purchased in the dried form while in our research we isolated spirulina from different site of Koya city which was not conducted before, and cultured Spirulina sp. by using different parameters to obtain high rate of biomass in lab.

Acknowledgements. The authors would like to thank Salahaddin University-Erbil, College of Education and Koya University, for their support.

REFERENCES

[1] Abdel-Aty, A. M., Ammar, N. S., Ghafar, H. H. A., Ali, R. K. (2013): Biosorption of cadmium and lead from aqueous solution by fresh water alga Anabaena sphaerica biomass. – Journal of Advanced Research 4(4): 367-374.

[2] Aksu, Z. (2005): Application of biosorption for the removal of organic pollutants: a review. – Process Biochemistry 40(3-4): 997-1026.

[3] Aksu, Z., Gönen, F., Demircan, Z. (2002): Biosorption of chromium (VI) ions by Mowital® B30H resin immobilized activated sludge in a packed bed: comparison with granular activated carbon. – Process Biochemistry 38(2): 175-186.

[4] Al-Homaidan, A. A., Alabdullatif, J. A., Al-Hazzani, A. A., Al-Ghanayem, A. A., Alabbad, A. F. (2015): Adsorptive removal of cadmium ions by *Spirulina platensis* dry biomass. – Saudi Journal of Biological Sciences 22(6): 795-800.

[5] Allen, M. M., Stanier, R. Y. (1968): Growth and division of some unicellular blue-green algae. – Microbiology 51(2): 199-202.

[6] Anwer, S. S., Abdullah, B. A. (2017): Biosorption of Direct Blue9 using baker's yeast (*Saccharomyces cerevisiae*). – ZANCO Journal of Pure and Applied Sciences 28(6): 170-175.

[7] Blanco, A., Sanz, B., Llama, M. J., Serra, J. L. (1999): Biosorption of heavy metals to immobilised *Phormidium laminosum* biomass. – Journal of Biotechnology 69(2-3): 227-240.

[8] Chisti, Y. (2008): Biodiesel from microalgae beats bioethanol. – Trends in Biotechnology 26(3): 126-131.

[9] Ciferri, O. (1983): *Spirulina*, the edible micro-organism. – Microbiological Reviews 47: 551-578.

[10] Das, N., Vimala, R., Karthika, P. (2008): Biosorption of heavy metals - an overview. – Indian Journal Biotechnology 7: 159-169.

http://www.aloki.hu ● ISSN 1589 1623 (Print) ● ISSN 1785 0037 (Online)
DOI: http://dx.doi.org/10.15666/aeer/1802_26572668

[11] Desikachary, V. (1968): Cyanophyta, Chrococcales. – Academic Press, New York and London.
[12] Dhargalkar, V. K. (2004): Effect of different temperature regimes on the chlorophyll a concentration in four species of Antarctic macroalgae. – Seaweed Res. Util. 26: 237-243.
[13] Domínguez-Bocanegra, A., Torres-Muñoz, J., Aguilar López, R. (2013): Biosorption of cadmium (ii), lead (ii) and nickel (II) by *Spirulina maxima*. – International Journal of Sciences 2(2): 45-55.
[14] Dönmez, G. Ç., Elmaci, A., Obali, O., Öztürk, A., Çakmakçi, L. (1999): Isolation and abundance of unicellular Cyanobacteria from mosquito development sites. – Turkish Journal of Biology 23(4): 451-456.
[15] Fan, T., Liu, Y., Feng, B., Zeng, G., Yang, C., Zhou, M., Wang, X. (2008): Biosorption of cadmium (II), zinc (II) and lead (II) by *Penicillium simplicissimum*: isotherms, kinetics and thermodynamics. – Journal of Hazardous Materials 160(2-3): 655-661.
[16] Flora, G., Gupta, D., Tiwari, A. (2012): Toxicity of lead: a review with recent updates. – Interdisciplinary Toxicology 5(2): 47-58.
[17] Flora, S., Pachauri, V., Saxena, G. (2011): Arsenic, Cadmium and Lead. Reproductive and Developmental Toxicology. – Academic Press, New York, 415-438.
[18] Gulnaz, O., Kaya, A., Matyar, F., Arikan, B. (2004): Sorption of basic dyes from aqueous solution by activated sludge. – Journal of Hazardous Materials 108(3): 183-188.
[19] Gupta, V. K., Rastogi, A. (2008): Biosorption of lead from aqueous solutions by green algae *Spirogyra* species: kinetics and equilibrium studies. – Journal of Hazardous Materials 152(1): 407-414.
[20] Hasson, H. A. (2018): Heavy metals contamination for some imported and local vegetables. – Iraqi Journal of Agricultural Sciences 49(5): 794-802.
[21] Hogan, C. M. (2010): Encyclopedia of Earth. – National Council for Science and the Environment, Washington, DC.
[22] Holt, G., Rieg, R., Smeath, A., Staley, T., Williams, T. (1994): Berge's Manual of Determinative Bacteriology. 9th Ed. – LWW, Philadelphia, PA.
[23] Jackson, R. N., Baird, D., Els, S. (2005): The effect of the heavy metals lead (Pb 2+) and zinc (Zn 2+) on. – Water SA 31(1): 107-116.
[24] Kaplan, D. (2013): Absorption and Adsorption of Heavy Metals by Microalgae. – In: Richmond, A., Hu, Q. (eds.) Handbook of Microalgal Culture: Applied Phycology and Biotechnology. Wiley, Hoboken, NJ, pp. 602-611.
[25] Kőnig-Péter, A., Kilár, F., Felinger, A., Pernyeszi, T. (2015): Biosorption characteristics of *Spirulina* and *Chlorella* cells for the accumulation of heavy metals. – Journal of the Serbian Chemical Society 80(3): 407-419.
[26] Mane, V. S., Mall, I. D., Srivastava, V. C. (2007): Use of bagasse fly ash as an adsorbent for the removal of brilliant green dye from aqueous solution. – Dyes and Pigments 73(3): 269-278.
[27] Oswaled, W. (1988): Microalgae and Waste Water Treatment – In: Borowitizka, M. A., Borowitizka, L. J. (eds.) Microalgae Biotechnology. Cambridge University Press, Cambridge, pp. 305-328.
[28] Palaniswamy, R., Veluchamy, C. (2017): Biosorption of heavy metals by *Spirulina platensis* from electroplating industrial effluent. – Environ Sci Ind J 13(4): 139.
[29] Ponnuswamy, I., Soundararajan Madhavan, D., Shabudeen, S., Shoba, U. S. (2008): Isolation and identification of green microalgae for carbon sequestration and waste water treatment by using PCR studies. – International Journal of Engineering Science and Innovative Technology 2(5): 263-268.
[30] Ponnuswamy, I., Madhavan, S., Shabudeen, S. (2013): Isolation and characterization of green microalgae for carbon sequestration, waste water treatment and bio-fuel production. – International Journal of Bio-Science and Bio-Technology 5(2): 17-25.
[31] Prasad, R. N., Sanghamitra, K., Antonia, G. M., Juan, G. V., Benjamin, R. G., Luis, I. M. J., Guillermo, V. V. (2013): Isolation, identification and germplasm preservation of

http://www.aloki.hu ● ISSN 1589 1623 (Print) ● ISSN 1785 0037 (Online)
DOI: http://dx.doi.org/10.15666/aeer/1802_26572668

different native *Spirulina* species from Western Mexico. – American Journal of Plant Sciences 4: 65-71.

[32] Prescott, W. (1963): Algae of the Western Great Lakes Area. – Michigan State University, East Lansing, pp. 443-451.

[33] Rippka, R. (1988): Recognition and identification of cyanobacteria. – Methods in Enzymology 167: 28-67.

[34] Roberts, R. (1999): Metal Toxicity in Children. – In: Training Manual on Pediatric Environmental Health: Putting It into Practice. Children's Environmental Health Network, Emeryville, CA. http://www.cehn.org/cehn/trainingmanual/pdf/manualfull.pdf.

[35] Roy, D., Greenlaw, P. N., Shane, B. S. (1993): Adsorption of heavy metals by green algae and ground rice hulls. – Journal of Environmental Science and Health Part A 28(1): 37-50.

[36] Sadettin, S., Dönmez, G. (2007): Simultaneous bioaccumulation of reactive dye and chromium (VI) by using thermophil *Phormidium* sp. – Enzyme and Microbial Technology 41(1-2): 175-180.

[37] Saleh, H. A., El-Aziz, G. A., El-Fark, M. M., El-Gohary, M. (2009): Effect of maternal lead exposure on craniofacial ossification in rat fetuses and the role of antioxidant therapy. – Anatomia, Histologia, Embryologia 38(5): 392-399.

[38] Salih, S. J., Anwer, S. S., Faraj, R. H. (2017): a biosorption of mercury from wastewater using isolated *Aspergillus* Sp. modified 1, 10-phenanthroline: Hill Isotherm Model. – Science Journal of University of Zakho 5(4): 288-295.

[39] Sharma, H., Rawal, N., Mathew, B. B. (2015): The characteristics, toxicity and effects of cadmium. – International Journal of Nanotechnology and Nanoscience 3: 1-9.

[40] Tomaselli, L. (1997): Morphology, Ultrastructure and Taxonomy of Arthrospira (*Spirulina*) Maxima and Arthrospira (*Spirulina) Platensis*. – In: Vonshak, A. (ed.) *Spirulina Platensis* (Arthrospira): Physiology, Cell-Biology and Biotechnology. Taylor & Francis, London, pp. 1-16.

[41] Vashishta, B. R., Snha, A. K., Singh, V. P. (2002): Botany for Degree Students - Algae. Introduction to Algae. – S. Chand Publishing, New Delhi, pp. 1-30.

http://www.aloki.hu ● ISSN 1589 1623 (Print) ● ISSN 1785 0037 (Online)
DOI: http://dx.doi.org/10.15666/aeer/1802_26572668

CORRELATION BETWEEN LONG-TERM FERTILIZATION AND SOIL ENZYME ACTIVITY IN THE RHIZOSPHERE OF HALOPHYTES

CHEN, H. W.* – HUANG, L.

College of Life Science, Henan Institute of Science and Technology, Xinxiang 453003, China

**Corresponding author*
e-mail: chenhongwei1966@sina.cn

(Received 3rd Sep 2019; accepted 12th Feb 2020)

Abstract. In order to reveal the correlation between long-term different fertilization methods and soil enzyme activity in rhizosphere of halophytes, Salicornia salina was selected as the research object and cultured in root bags in coastal saline soil. The effects of plastic film mulching, non-plastic film mulching and non-fertilization on invertase, catalase and urease activities in rhizosphere soil of Salicornia salsa during its growth period were studied, while the effects of plastic film mulching and non-fertilization on the activities of invertase, catalase and urease in the rhizospheric soil of Salicornia salicornis were also investigated. Bacillus, Bacillus licheniformis, Bacillus amylolytica and compound microbial fertilizers had effects on the activities of three soil enzymes. The results showed that the activities of S-SC, S-CAT and S-UE could be promoted by mulching and that fertilization at any time, and the effect of mulching combined with fertilization was the best. Soil enzyme activity showed the same change pattern during the growth period of Salicornia salina. The highest activity of soil invertase and urease occurred at jointing stage, and the highest activity of soil catalase occurred at maturity stage. Compared to spraying treatment, adding compound microbial fertilizer could increase catalase activity by 6.3% and 4.0% at different stages, while adding Bacillus amyloliquefaciens microbial fertilizer, the activity of sucrase and urease increased by 20.7% and 18.6%, respectively, and 21.8% and 4.6%, respectively in different periods. In conclusion, the application of plastic film mulching combined with fertilization, inorganic fertilizer and microbial fertilizer can improve soil enzyme activity and soil fertility, and enhance the sustainable productivity of soil.
Keywords: *appropriate temperatures, phosphorus, potassium, microbial fertilizer*

Introduction

Soil is a living ecosystem, containing various soil enzymes. They play an important role in the process of soil material circulation, energy and nutrient transformation (Tang et al., 2016). The activity of soil enzymes is one of the biological indicators to characterize soil biological activity, soil fertility level and soil quality. Nature and environmental conditions are closely related, and are regarded as sensitive indicators of soil ecosystem change (Cunha et al., 2017). Soil enzymes are proteins that catalyze soil biochemical reactions, mainly from soil microorganisms and plant roots, and also from soil animals and plant residues (Cheng et al., 2016), which are one of the most active organic components in soil components. Plant rhizosphere is the place where plant roots grow and develop, absorb nutrients and metabolize. It is also an important interface between plant and soil environment (Nawaz et al., 2016). The effect of plant living roots on soil enzyme activities is reflected in two aspects. On the one hand, plant roots can secrete extracellular enzymes; on the other hand, they may also be root thorns. It stimulates the activity of soil microorganisms. It is more sensitive to the soil environment and more responsive to the soil environment. Rhizosphere is also the most active micro domain of soil chemical and biological properties, and its importance has been widely recognized. Soil enzyme activity,

http://www.aloki.hu ● ISSN 1589 1623 (Print) ● ISSN1785 0037 (Online)
DOI: http://dx.doi.org/10.15666/aeer/1802_26692685

as a quick-acting index to measure the rhizosphere micro-ecological environment, has been widely used in the study of soil ecological environment. Therefore, the study of soil enzyme activity is of great significance to the formation, evolution, and improvement of soil fertility and the material cycle process of soil ecosystem (Fan et al., 2016).

Soil invertase (S-SC), catalase (S-CAT) and soil urease (S-UE) activities play an important role in evaluating soil fertility. Among them, S-SC activity reflects the intensity of soil respiration and carbon transformation (Van et al., 2017), and has been widely used to characterize the intensity and direction of soil carbon cycle and biochemical activity. S-CAT is an indicator of aerobic microorganisms. It can effectively promote the decomposition of harmful substance hydrogen peroxide, which is related to the redox capacity of soil and the transformation rate of soil organic matter (Chen et al., 2018). The activity of S-UE represents the abundance of soil nitrogen and is closely related to the transformation of nitrogen in soil. Therefore, the activity of S-UE is commonly used to characterize soil nitrogen status (Liu et al., 2016). At present, there are a lot of reports about the effect of organic fertilizer on soil enzyme activity. Fertilizer application is the way to apply fertilizer to soil. The basic requirements of scientific fertilization methods are as follows: to apply fertilizer to the soil layer which is easy to absorb by the root system of the crop as far as possible, to improve the utilization rate of chemical fertilizer; to select the appropriate location and to reduce fertilizer fixation, volatilization and leaching. Fertilization methods vary with different crops, fertilization loss and fertilizer properties. The most commonly used methods are artificial spraying, acupoint application, rotation, radial fertilization and external fertilization. According to the planting mode of Salicornia salsa, artificial spraying and hole fertilization (Ma et al., 2016) were used in the fertilization process, and after fertilization, sowing was conducted. Microbial fertilizer is applied in the same hole as seed fertilizer. The mixed strains were Bacillus subtilis, Bacillus licheniformis and Bacillus amyloliquefaciens.

Halophyte is a kind of natural plant flora (Poeplau et al., 2016) which grows on saline soil with certain salt resistance. Phytoremediation on saline-alkali soil is a feasible method to solve the problem of saline-alkali land utilization. Therefore, the research on the phytoremediation of saline-alkali soil by plant rhizosphere has received extensive attention. The strong salt and barren tolerance of coastal halophytes may also be related to their rhizosphere soil enzymes. The rhizosphere soil enzymes of halophytes may be one of the most direct characteristics of coastal halophytes to rapidly absorb, utilize soil nutrients and adapt to saline environment (Zhao et al., 2016). The research of plant rhizosphere is very limited, especially the soil enzyme activities of these plants are seldom concerned. Studying the soil enzyme activities of coastal halophytes will help to protect the resources of Halophytes in these areas, and provide a theoretical basis for the restoration and utilization of these plants in coastal saline soil. Based on this, the correlation between long-term different fertilization methods and soil enzyme activities in rhizosphere of halophytes was studied. The activities and dynamic changes of S-SC, S-CAT and S-UE in rhizosphere of five fertilization treatments under artificial spraying and hole application during the growth period of halophyte Salicornia salina were mainly studied in order to clarify different microorganisms. The intrinsic relationship between fertilizer and soil enzyme activity provides theoretical basis for rational fertilization, soil improvement and seeking the best growth environment for stable and high yield of halophytes. In order to reveal the correlation between long-term different fertilization methods and soil enzyme activity in rhizosphere of halophytes, Salicornia salina was selected as the research object and cultured in root bags in coastal saline soil.

http://www.aloki.hu ● ISSN 1589 1623 (Print) ● ISSN1785 0037 (Online)
DOI: http://dx.doi.org/10.15666/aeer/1802_26692685

Materials and Methods

Halophytes and soils

Generally speaking, the basic conditions for plant growth are: moderate sunshine, air and water. The five essential elements of plant life are: sunlight, temperature, water, air and nourishment, which are the lifeline of plants. Temperature has a great influence on the growth and development of plants. Plants need different and appropriate temperatures in different growth periods and development stages; water is an important part of plants; oxygen, nitrogen and carbon dioxide in the air have a great impact on plant life; plants need a lot of nutrients, including carbon, hydrogen, oxygen, nitrogen, phosphorus, potassium, calcium, sulfur, magnesium, iron and other 10 kinds of elements. Air affects the lives of animals and plants. The photosynthesis of plants needs carbon monoxide, and the respiration of animals needs oxygen. Only under light conditions can plants carry out photosynthesis, produce organics and store energy every day. Light plays a decisive role in plant physiology and distribution. Some plants can grow well only under strong light, such as wheat, corn, etc.

Salicornia salina, a typical halophyte in northern coastal areas of China, was selected to adapt to the coastal saline soil environment. Salicornia salina is a salt-accumulating halophyte (Xu et al., 2017). Seeds of the tested plants were collected in the coastal area of Dagang, Tianjin, in October 2016. The coastal saline soil with natural distribution of halophytes was selected for the tested soil, and the basic properties of the soil were shown in *Table 1*.

Table 1. *Main properties of soils used*

Soil properties	Littoral rock and soil
PH value	8.52
w(Total salt) ($g \cdot kg^{-1}$)	12.72
w(CO_3^{2-})($g \cdot kg^{-1}$)	0.08
w(HCO^{3-})($g \cdot kg^{-1}$)	0.17
w(CI^-)($g \cdot kg^{-1}$)	7.15
w(SO_4^{2-})($g \cdot kg^{-1}$)	0.75
w(Na^+)($g \cdot kg^{-1}$)	2.63
w(K^+)($g \cdot kg^{-1}$)	1.50
w(Ca^{2+})($g \cdot kg^{-1}$)	1.49
w(Mg^{2+})($g \cdot kg^{-1}$)	0.20
w(Quick-actingN) ($mg \cdot kg^{-1}$)	30.18
w(Quick-actingP) ($mg \cdot kg^{-1}$)	12.63
w(Quick-actingK) ($mg \cdot kg^{-1}$)	384

Root bag culture and sample collection of plants

The experiment began on May 9, 2017. Firstly, the soil was collected, dried, crushed and fully blended, grinded over 0.2 mm sieve, and then added distilled water to the soil water content of 140 $g \cdot kg^{-1}$ for reserve. The potted root bag method was used to simulate the experiment (Gu et al., 2016). All the experiments were carried out in greenhouse. The nylon mesh yarn with 30 μm aperture was sealed with a plastic sealing machine to form a root bag with a diameter of 3 cm and a height of 15 cm. The root bags of Salicornia salicornis could not grow out. Each root bag was filled with 240 g of prepared soil (Chen et al., 2017). The same soil was also put into a basin with a height

http://www.aloki.hu ● ISSN 1589 1623 (Print) ● ISSN1785 0037 (Online)
DOI: http://dx.doi.org/10.15666/aeer/1802_26692685

of 40 cm and a diameter of 30 cm, and then one of the prepared root bags was buried in the center of the basin. Fifteen dew-white seeds of Salicornia salsa were planted in each root bag, and six seedlings were retained in each root bag after emergence. Water every 15 days during the growth period, and pour the same amount of distilled water 3 L for each treatment, and do not do any other treatment. After 100 days of plant growth, 12 pots with similar seedling emergence and growth were selected for sampling, i.e. 12 replicates. When all the roots of Salicornia salsa were observed to be fully filled with root bags, the soil below 2 cm in the root bags was taken as rhizosphere soil, and the soil samples were dried in shade to be tested.

Fertilizer for test and test design

There are three kinds of fertilization methods: film-covered fertilization (CF), film-covered non-fertilization (C), non-film-covered fertilization (F) (Gschwendtner et al., 2016), and non-mulching and non-fertilization (CK) as control. Samples were taken for 15, 30 and 45 days after treatment. There are 10 treatments in the fertilization process, and the different treatment schemes are shown in *Table 2*.

Table 2. *Test design scheme*

Serial number	Code	Handle	Consumption/ g
1	SCK	Manual application of chemical fertilizer	1.5
2	TCK	Point application of chemical fertilizer	1.5
3	SKC	Manual Spraying of Chemical Fertilizer + Microbial Fertilizer (Bacillus subtilis)	1.5+3.0
4	TKC	Point Application of Chemical Fertilizer + Microbial Fertilizer (Bacillus subtilis)	1.5+3.0
5	SDY	Manual fertilization + microbial fertilizer (Bacillus licheniformis)	1.5+3.0
6	TDY	Point Application of Chemical Fertilizer + Microbial Fertilizer (Bacillus licheniformis)	1.5+3.0
7	SJDF	Manual fertilization + microbial fertilizer (Bacillus amylolytica)	1.5+3.0
8	TJDF	Point Application of Chemical Fertilizer + Microbial Fertilizer (Bacillus amyloliquefaciens)	1.5+3.0
9	SFH	Manual Spraying of Chemical Fertilizer + Microbial Fertilizer (Compound Bacteria)	1.5+3.0
10	TFH	Point Application of Chemical Fertilizer + Microbial Fertilizer (Compound Bacteria)	1.5+3.0

According to the characteristics of rapid cooling and unstable temperature in saline soil area in the morning and evening, fertilization treatment was carried out in June 20, July 1 and July 10, respectively. The test chemical fertilizer was Stanley slow-release mixed fertilizer ($N:P_2O_5:K_2O$=26:12:10) (Liu et al., 2016). The microbial fertilizer was organic fertilizer plus 10% bacteria (bacteria 2×10^{10}cfu/g) and organic matter content was 40.857% (Li et al., 2017). The tested strains were Bacillus subtilis, Bacillus licheniformis and Bacillus amyloliquefaciens (Gong et al., 2017), which were preserved by the Biochemical Laboratory of Institute of Applied Chemistry, Shanxi University.

http://www.aloki.hu ● ISSN 1589 1623 (Print) ● ISSN1785 0037 (Online)
DOI: http://dx.doi.org/10.15666/aeer/1802_26692685

Artificial spraying

Artificial spraying is the way of evenly spreading fertilizer on the field (Duan and Liu, 2019), which belongs to topsoil fertilization and mainly meets the needs of shallow root distribution at seedling stage. This method is commonly used in the application of base fertilizer to uncultivated crops or in the topdressing of densely planted grain crops (Wang et al., 2018). Artificial spraying combined with soil tillage measures can increase the uniformity of soil and fertilizer mixing, which is conducive to the extension of crop roots and early absorption.

Point application

Point application can be made by opening hole fertilizer in the designated planting position or termination of the crop, or in the seedling stage, per plant or between two sides of the plant during the crop growth period (Zhou and Lin, 2016). Point fertilizer is usually 5-10 cm deep and covered with soil after application. Point application is a more centralized method of chemical fertilizer application, avoiding damage to the root system. Generally, less chemical fertilizer is applied, and the appropriate position and depth are maintained with the root system of crops. After fertilization, irrigation is combined before covering soil, and the effect of chemical fertilizer application is better.

Determination of nutrients and active enzymes in soil

Soil samples are used for the determination of various indicators after indoor shade drying. Soil nutrient determination methods: Kjeldahl method for total nitrogen, HCl-HF method for digestion of total phosphorus, anti-colorimetric method for molybdenum and antimony, alkali hydrolysis diffusion method for available nitrogen and Bray1 method for available phosphorus.

The activity of S-SC (soil sucrase) was determined by the colorimetric method using 3,5-Dinitrosalicylic acid as the chromogenic agent (Song et al., 2018). S-SC can enzymatically hydrolyze sucrose to produce glucose and fructose. The hydrolyzed sucrose can form colored compounds with 3,5-Dinitrosalicylic acid. The content of glucose can be determined by colorimetry. The activity of S-SC was expressed by the quality of soil glucose (mg) 1 g after 24 hours (Hicks et al., 2017).

The activity of S-CAT was determined by titration with 0.1 $mol \cdot L^{-1}$ KMnO4 using hydrogen peroxide as matrix, and the activity of S-CAT was expressed by the amount of 0.1 $mol \cdot L^{-1}$ KMnO4 consumed by 1 g of dry soil after 20 minutes of incubation.

The activity of S-UE (urease) was determined by urea residue method. S-UE can hydrolyze urea into ammonia, water and carbon dioxide. After incubating fresh soil and urea at 37℃ for 5 hours, the urea residue was determined and the activity of S-UE was estimated. The activity of S-UE was expressed by the mass (mg) of urea nitrogen reduction per unit time.

Data processing

Microsoft Excel 2016 and SPSS 22.0 were used to analyze the test data. The determination of s-ue (urease) activity by urea residue method is improved on the basis of research method: take 1 g soil (rhizosphere soil stored at -20℃) and add 9 ml sterile water, mix it with vortex, take 200 μl soil suspension respectively and add it into 50 ml sterilized medium (Ca-P, Fe-P and Al-P liquid medium), culture it in 160 r min^{-1} shaking bed at 30℃ for 9 days, and take 5 ml soil suspension every 1 day. After

http://www.aloki.hu ● ISSN 1589 1623 (Print) ● ISSN1785 0037 (Online)
DOI: http://dx.doi.org/10.15666/aeer/1802_26692685

centrifugation at 4000 r min^{-1} and 4℃ for 10 min, the supernatant was taken to determine the effective phosphorus content and pH. The treatment was repeated 3 times.

Results

Effects of different fertilization periods and modes on soil enzyme activities in the rhizosphere of Salicornia Salsa

In order to verify the effect and feasibility of the method in this paper, an experiment is set up for verification. The soil culture dish diagram of the experimental plant is shown in *Figure 1*.

Figure 1. *Dish chart of experimental plant soil*

Effects of different fertilization periods and modes on S-SC activity of Salicornia salsa rhizosphere

Table 3 describes the effects of different fertilization stages and modes on S-SC activity in the rhizosphere of Salicornia salina.

Table 3 showed that both fertilization and mulching methods were beneficial to the improvement of S-SC activity in Salicornia salina rhizosphere soil. The effect of film mulching combined with fertilization was the best, and the S-SC activity was significantly higher than that of non-film mulching and non-fertilization, showing significant difference. Among them, S-SC activity was the highest on June 20 when the fertilizer was applied with plastic film for 15 days. The S-SC activity of mulching treatment and fertilization treatment also increased, but the effect of the two treatments was different. The S-SC activity of mulching treatment was the highest at 15 days of sampling on July 1, and the S-SC activity of fertilization treatment was the highest at 45 days of sampling on July 1. Soil S-SC activity was also affected by different fertilization stages, which showed that the S-SC activity was the highest in the treatment on July 1. The S-SC activity of each treatment was higher in the 15-day sampling on June 20. The S-SC activity of each treatment was higher in the 45-day sampling on July 1. The S-SC activity of each treatment was higher in the 45-day sampling on July 10. The S-SC active phase of each treatment was the highest in the 45-day sampling on July 10.

http://www.aloki.hu ● ISSN 1589 1623 (Print) ● ISSN1785 0037 (Online)
DOI: http://dx.doi.org/10.15666/aeer/1802_26692685

Table 3. *Effects of different fertilization methods on soil S-SC activity under different fertilization time*

Fertilization time	Fertilization methods	S-SC activity in rhizosphere soil (U/g)		
		15d	30d	45d
20 June	CF	4.70±0.27a	2.02±0.30b	2.74±0.02ab
	C	2.50±0.06bcde	1.85±0.49bc	1.58±0.12c
	F	1.51±0.27de	1.92±0.18bc	1.87±0.08bc
	CK	1.12±0.14e	1.05±0.02de	1.13±0.10c
1 July	CF	3.35±1.57b	3.64±0.27a	3.73±1.05a
	C	3.22±2.02bc	1.81±0.32bc	2.70±0.85ab
	F	2.88±0.02bcd	2.18±0.08b	3.61±1.30a
	CK	1.64±0.01de	1.46±0.27cd	1.40±0.22c
10 July	CF	1.90±0.32cde	3.20±0.35a	3.37±0.41a
	C	1.36±0.09e	1.86±0.55bc	1.43±0.26c
	F	1.33±0.03e	1.01±0.02de	1.78±0.16bc
	CK	1.30±0.10e	0.92±0.09e	0.88±0.12c

Different lower-case letters in the same column in the table show significant differences at the level of 0.05, the same below

Effects of different fertilization periods and manners on S-CAT activity in rhizosphere of Salicornia salina

Table 4 describes the effects of different fertilization stages and modes on S-CAT activity in the rhizosphere of Salicornia salina.

Table 4. *Effects of different fertilization periods and manners on S-CAT activity in rhizosphere of Salicornia salina*

Fertilization time	Fertilization methods	S-CAT activity in rhizosphere soil (U/mL)		
		15d	30d	45d
20 June	CF	14.77±0.15a	10.13±0.25b	11.37±0.06a
	C	11.77±0.15b	8.13±0.15d	10.87±0.15b
	F	7.40±0.20e	9.30±0.36c	10.30±0.10c
	CK	7.23±0.06ef	7.76±0.60de	5.20±0.66g
1 July	CF	12.37±00.31b	10.37±0.42b	8.50±0.40d
	C	12.33±0.06b	9.83±0.50bc	6.87±0.25e
	F	10.40±0.50cd	9.87±0.06bc	6.70±0.20e
	CK	5.23±0.65g	7.67±0.25de	4.40±0.10h
10 July	CF	10.97±0.60c	14.13±0.25a	8.47±0.23d
	C	9.83±0.06d	7.33±0.32e	6.63±0.40e
	F	7.57±0.15e	7.57±0.12de	5.70±0.20f
	CK	6.77±0.42f	5.30±0.10f	4.00±0.20h

Table 4 shows that both fertilization and mulching methods are beneficial to the improvement of S-CAT activity in Salicornia salina rhizosphere soil. The effect of combined application of film mulching and fertilizer was the best, and the activity of S-CAT was significantly higher than that of non-film mulching and non-fertilization, showing a significant difference. The S-CAT activity was the highest on June 20 when the treatment of plastic film mulching fertilization was sampled for 15 days. The S-CAT activity of plastic film mulching treatment and fertilization treatment also increased, but

http://www.aloki.hu ● ISSN 1589 1623 (Print) ● ISSN1785 0037 (Online)
DOI: http://dx.doi.org/10.15666/aeer/1802_26692685

the effect of the two treatments was different. The S-CAT activity of the two treatments was the highest when they were sampled for 15 days on July 1. Different fertilization time also affected the activity of S-CAT, which was the highest in the treatment on July 1, and it was found that the activity of S-CAT was higher in the treatment on the 15th day of sampling.

Effects of different fertilization periods and manners on S-UE activity in rhizosphere of Salicornia salsa

Table 5 describes the effects of different fertilization periods and modes on S-UE activity in the rhizosphere of Salicornia salina.

Table 5. *Effects of different fertilization periods and manners on S-UE activity in rhizosphere of Salicornia salsa*

Fertilization time	Fertilization methods	S-UE activity in rhizosphere soil (U/g)		
		15d	30d	45d
20 June	CF	48.94±3.28b	37.71±0.85a	2293±1.55cde
	C	30.29±1.92d	24.08±1.24b	21.69±3.19de3
	F	34.59±3.39c	18.06±2.89bc	17.75±0.11fg
	CK	20.97±1.75ef	9.15±1.34d	12.91±0.87h
1 July	CF	75.77±0.40a	38.32±10.29a	33.34±0.46a
	C	22.95±1.70e	32.16±1.98a	30.01±3.31b
	F	34.76±0.06c	33.34±2.94a	24.81±0.06c
	CK	22.10±1.08ef	20.35±5.65bc	16.56±0.12g
10 July	CF	30.86±3.39cd	33.91±2.26a	23.10±0.69cd
	C	24.47±4.02e	24.70±1.19b	20.22±1.16ef
	F	28.94±1.47d	20.63±1.53bc	16.65±1.21g
	CK	18.20±2.60f	16.23±1.76c	11.80±1.26h

Table 5 shows that both fertilization and film mulching are beneficial to the improvement of S-UE activity in Salicornia rhizosphere soil. The effect of film mulching combined with fertilization was the best, and the S-UE activity was significantly higher than that of non-film mulching and non-fertilization, showing significant difference. The S-UE activity was the highest on July 1st when the film mulching treatment was taken for 15 days. The S-UE activity of mulching treatment and fertilization treatment also increased, but the effect of the two treatments was different. The S-UE activity of mulching treatment was the highest at 30 days of sampling on July 1, and the S-UE activity of fertilization treatment was the highest at 15 days of sampling on July 1. The activity of S-UE was also affected by different fertilization periods. The highest activity of S-UE was observed on July 1. At the same time, it was found that the activity of S-CAT was higher in different fertilization methods at different time.

Effects of point fertilization on soil enzyme activity

Effect of point fertilization on S-SC activity

Figure 2 depicts the effect of hole fertilization on S-SC activity under plastic film mulching. Different lower-case letters in the picture showed significant difference ($P < 0.05$), and the following is no longer repeated.

http://www.aloki.hu ● ISSN 1589 1623 (Print) ● ISSN1785 0037 (Online)
DOI: http://dx.doi.org/10.15666/aeer/1802_26692685

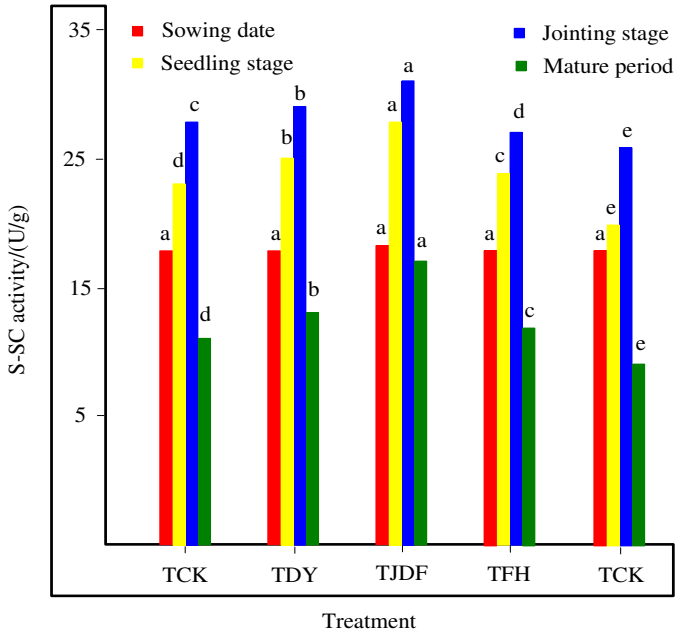

Figure 2. *Effects of point-based fertilization on S-SC activity*

Figure 2 shows that the S-SC activity of Salicornia salicornis showed the same change rule during its growth period, and reached the maximum at jointing stage, then decreased gradually. The activity of S-SC was higher than that of control, and TJDF had the greatest influence on S-SC activity. Compared with the single application of chemical fertilizer (TCK), the enzymatic activities of TJDF treatment increased by 41.9%, 20.7% and 68.0% at seedling stage, jointing stage and maturity stage, 15.1%, 8.7% and 16.6% in TKC treatment, 23.7%, 12.8% and 33.1% in TDY treatment, 17.3%, 4.1% and 23.2% in TFH treatment, respectively. It can be seen that the increase of S-SC activity can be promoted by applying microbial fertilizer. Among them, microbial fertilizer combined with chemical fertilizer (Bacillus amylolytica) has the most obvious effect, followed by microbial fertilizer combined with chemical fertilizer (Bacillus licheniformis).

Effects of point-based fertilization on S-CAT activity

Figure 3 depicts the effect of hole fertilization on S-CAT activity under plastic film mulching.

Figure 3 shows that the activity of S-CAT increases gradually during the growth period of Salicornia salsa. The highest value occurs in the mature stage. The fertilization treatments mainly based on hole application show that TFH treatment has the most significant effect on the activity of S-CAT. Compared with TCK, the activity of S-CAT increased by 7.6%, 9.0% and 6.3% at seedling stage, jointing stage and mature stage, respectively. Therefore, the application of microbial fertilizer can improve the activity of S-CAT, and the effect of microbial fertilizer combined with chemical fertilizer (compound bacteria) is the most obvious. Other fertilization treatments inhibited S-CAT activity.

http://www.aloki.hu ● ISSN 1589 1623 (Print) ● ISSN1785 0037 (Online)
DOI: http://dx.doi.org/10.15666/aeer/1802_26692685

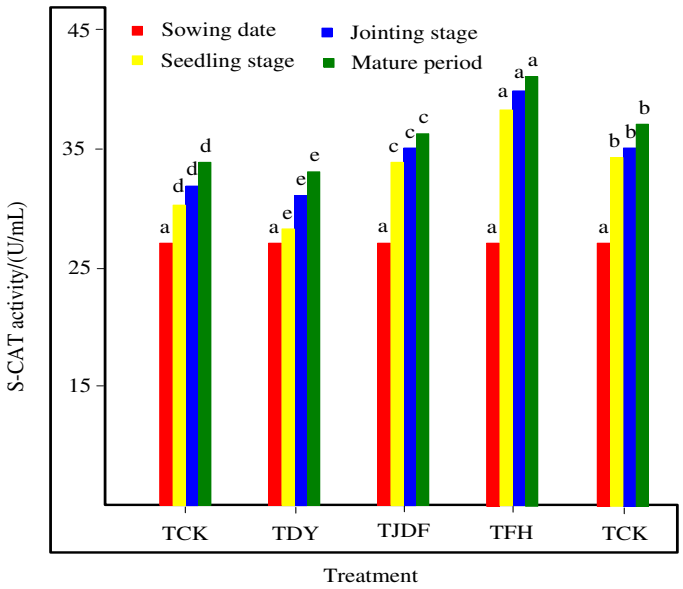

Figure 3. *Effects of point-based fertilization on S-CAT activity*

Effects of point fertilization on S-UE activity

Figure 4 depicts the effect of hole fertilization on S-UE activity under plastic film mulching.

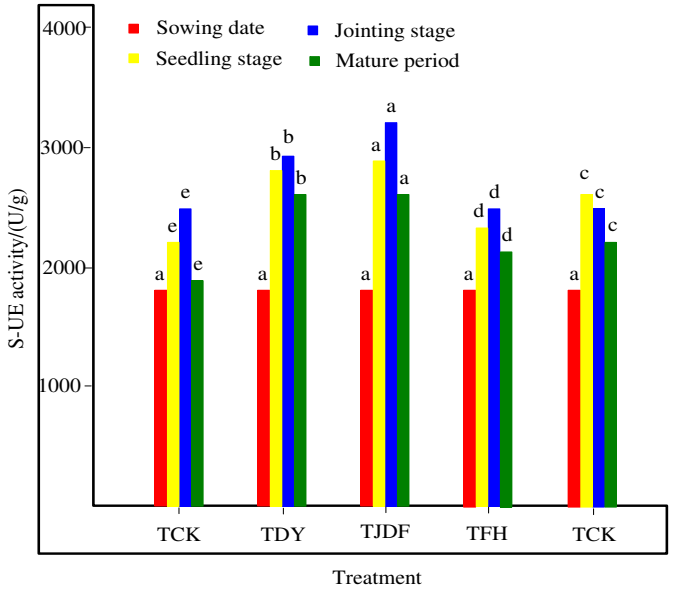

Figure 4. *Effects of point-based fertilization on S-UE activity*

Figure 4 shows that the activity of S-UE increases first and then decreases during the growth period of Salicornia salina, and reaches its peak at jointing stage. Among them, TJDF treatment had the greatest effect on S-UE activity, which increased by 15.8%, 30.4% and 21.8% at seedling stage, jointing stage and maturity stage, compared with

http://www.aloki.hu ● ISSN 1589 1623 (Print) ● ISSN1785 0037 (Online)
DOI: http://dx.doi.org/10.15666/aeer/1802_26692685

TCK alone, while TDY treatment increased by 12.7%, 19.7% and 19.9% respectively. Therefore, the increase of S-UE activity can be promoted by applying microbial fertilizer, the most significant effect is the combination of chemical fertilizer and microbial fertilizer (Bacillus amyloliquefaciens), followed by microbial fertilizer (Bacillus licheniformis).

Effects of fertilizer application on soil enzyme activities

Effects of spraying-based fertilization on S-SC activity

Figure 5 depicts the effect of spraying fertilization on S-SC activity under mulched fertilization.

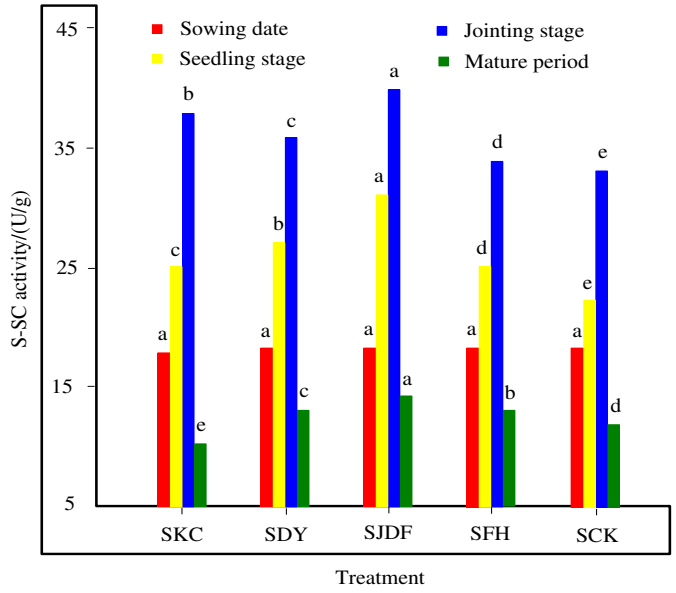

Figure 5. *Effects of spraying-based fertilization on S-SC enzyme activity*

From *Figure 5*, we can see that S-SC activity reached the highest level at jointing stage of Salicornia salsa under spraying mode, and then decreased gradually. Among them, SJDF treatment had the highest enzymatic activity, which increased by 37.4%, 18.6% and 22.9% at seedling stage, jointing stage and maturity stage, respectively, compared with SCK treatment; the enzymatic activity of SKC treatment increased by 11.6%, 12.5% and 2.5%, respectively; the enzymatic activity of SDY treatment increased by 19.3%, 6.9% and 14.8%, respectively; and the enzymatic activity of SFH treatment increased by 19.3%, 6.9% and 14.8%, respectively. They increased by 10.0%, 2.9% and 18.9%, respectively.

S-SC activity of Salicornia salina in seedling and jointing stage was lower than that in spraying mode, but there was no significant difference at maturity stage. During the growth period of Salicornia salsa, the fertilization methods were different, and the activity of Salicornia salicornis was different among different fertilization treatments. The activity of S-SC in seedling stage, jointing stage and ripening stage of Salicornia salsa under different fertilization methods were SJDF > SDY > SKC > SFH > SCK, SJDF > SKC > SDY > SFH > SCK, SJDF > SFH > SDY > SCK > SKC, while the activity of S-SC in seedling stage, jointing stage and ripening stage was

http://www.aloki.hu ● ISSN 1589 1623 (Print) ● ISSN1785 0037 (Online)
DOI: http://dx.doi.org/10.15666/aeer/1802_26692685

TJDF=TDY=TFH=TKC=TCK, TJDF=TDY=TKC=TFH=TCK and TJDF=TDY=TFH=TKC=TCK, respectively. Therefore, hole fertilization can promote the comprehensive utilization rate of fertilizer, benefit the absorption and utilization of nutrients by halophytes, and improve soil enzyme activity.

Effects of spraying-based fertilization on S-CAT activity

Figure 6 depicts the effect of spraying fertilization on S-CAT activity under Mulched fertilization.

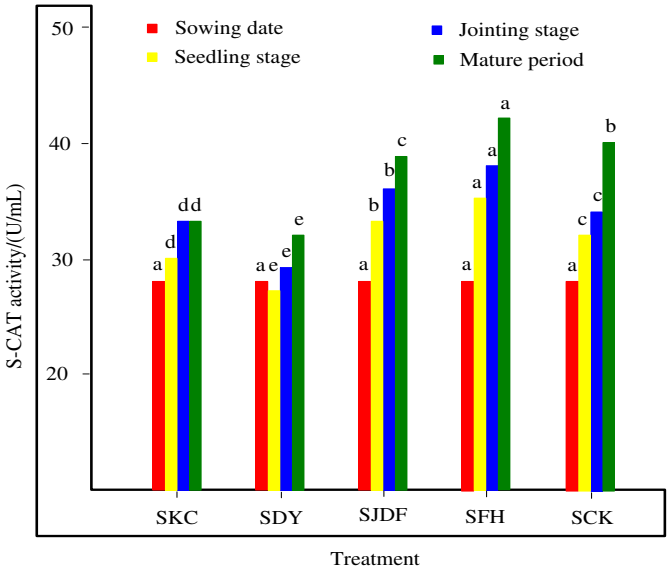

Figure 6. *Effects of spraying-based fertilization on S-CAT activity*

Figure 6 showed that the activity of S-CAT reached its peak at the ripening stage of Salicornia salsa under the spraying mode, and the activity of SFH treatment was the highest. Compared with SCK, the activity of SFH treatment increased by 9.5%, 10.5% and 4.0% at seedling stage, jointing stage and mature stage, respectively. The effect of other fertilization treatments on S-CAT activity was not obvious.

S-CAT activity was higher in seedling stage and jointing stage of Salicornia salsa than in spraying mode, but lower in ripening stage than in spraying mode. During the growth period of Salicornia salsa, there were some differences in S-CAT activity among different fertilization treatments. The activity of S-CAT at seedling stage, jointing stage and maturity stage of Salicornia salsa under different fertilization methods were SFH > SJDF > SCK > SKC > SDY, SFH > SJDF > SCK > SKC > SDY, SFH > SCK > SJDF > SKC > SDY, and the activity of S-CAT at seedling stage, jointing stage and maturity stage of Salicornia salicornis were TFH > TCK > TJDF > TKC > TDY, TFH>TCK>TJDF>TKC>TDY and TFH > TCK > TJDF > TKC > TDY. Therefore, hole fertilization can promote the utilization of fertilizer, benefit the absorption and utilization of nutrients by halophytes, and improve soil enzyme activity.

http://www.aloki.hu ● ISSN 1589 1623 (Print) ● ISSN1785 0037 (Online)
DOI: http://dx.doi.org/10.15666/aeer/1802_26692685

Effects of spraying-based fertilization on S-UE activity

Figure 7 depicts the effect of spraying fertilization on S-UE activity under Mulched fertilization.

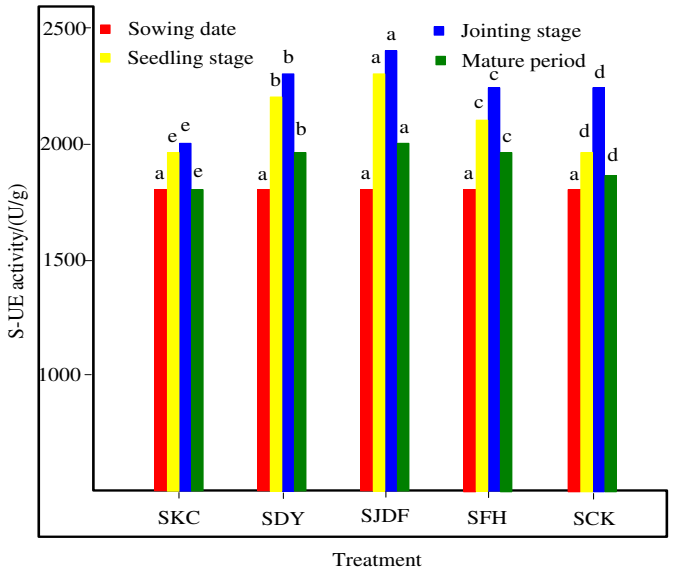

Figure 7. *Effects of spraying-based fertilization on S-UE activity*

Figure 7 shows that the peak value of S-UE activity occurs at elongation stage of Salicornia salsa under spraying mode. SJDF treatment has the greatest effect on S-UE activity. Compared with SCK, the activity of S-UE in SJDF treatment increased by 14.4%, 4.6% and 8.6% at seedling, elongation and maturity stages, respectively; SDY treatment increased by 12.0% and 2.0%, respectively; SFH treatment increased by 4.3%, 0.4% and 6.3%, respectively. The effect of SKC on S-UE activity was not obvious.

S-UE activity of Salicornia salsa was higher than that of Salicornia salicornis in the growth period. The activity of S-UE in the seedling stage, jointing stage and mature stage of Salicornia salicornis was JDF > SDY > SFH > SCK > SKC. Therefore, hole fertilization can promote the utilization of fertilizer, benefit the absorption and utilization of nutrients by halophytes, and improve soil enzyme activity.

Discussions

In this paper, the correlation between long-term different fertilization methods and soil enzyme activities in rhizosphere of halophytes was studied. The effects of different fertilization methods and different fertilization treatments on S-SC, S-CAT and S-UE enzymes in root soil during the development of Salicornia salicornis were studied. The results show that:

The activities of S-SC, S-CAT and S-UE could be promoted by mulching and fertilization at any time. Among them, film mulching combined with fertilization had the best effect, and the three enzymes activities of soil were the highest. This is because the saline soil is hot and dry in summer, and the temperature is high. Film mulching improves soil moisture and temperature, which is conducive to the absorption and

http://www.aloki.hu ● ISSN 1589 1623 (Print) ● ISSN1785 0037 (Online)
DOI: http://dx.doi.org/10.15666/aeer/1802_26692685

transformation of soil nutrients, thereby improving soil enzyme activity. The soil enzyme activities of plastic film mulching and fertilization treatments also increased, but the effects of the two treatments were different, which was due to the large fluctuation of temperature in the saline soil area in summer morning and evening. The soil enzyme activity was also affected by different fertilization time, and the soil enzyme activity was the highest when the soil enzyme was sampled on July 1.

The activities of S-SC and S-UE increased first and then decreased with time during the growth period of Salicornia salsa, and reached the highest level at jointing stage. During this period, Salicornia salicornis grew vigorously, its root system developed, and its nutrient demand increased, which stimulated the activities of S-SC and S-UE to increase rapidly to meet the growth needs of Salicornia salicornis. It was soil microbial activity. S-CAT activity gradually increased during the growth period of Salicornia salsa and reached its peak at maturity. Because of the maturity of Salicornia salicornis, the residue and litter of Salicornia salicornis increased in rhizosphere, which induced its activity to increase to oxidize and decompose hydrogen peroxide in soil.

From the effect of different fertilization treatments on soil enzyme activity, it can be seen that the combination of chemical fertilizer and starch-dissolving microbial fertilizer has the greatest influence on S-SC activity and S-UE activity, and the combination of chemical fertilizer and microbial fertilizer of compound bacteria has the greatest influence on S-CAT activity. The results showed that the combined application of chemical fertilizer and starch-dissolving microbial fertilizer could significantly enhance the activity of S-SC and S-UE, and the combined application of chemical fertilizer and microbial compound fertilizer could significantly enhance the activity of S-CAT, because the input of microbial fertilizer and inorganic fertilizer not only provided abundant energy for the soil, but also brought a large number of microorganisms into the soil, thus stimulated the energy metabolism of the soil. It can greatly improve soil enzyme activity. This is consistent with the research results of relevant scholars, so the combination of chemical fertilizer and microbial fertilizer can improve soil environment and soil enzyme activity.

The S-SC activity in the seedling stage and jointing stage of Salicornia salsa was lower than that in the spraying treatment, and the law of maturity was not obvious. This indicated that spraying fertilizer was beneficial to the early absorption of Salicornia salicornis root system, so the S-SC activity was higher in the seedling stage and jointing stage. The activity of S-CAT in the seedling and jointing stage was higher than that in the spraying treatment, and in the mature stage was lower than that in the spraying treatment. This indicated that the hole application was beneficial to reduce the toxic effect of hydrogen peroxide on Salicornia salicornis, which might be caused by root exudates, soil physical and chemical properties, soil environment and crop growth in different growth stages of Salicornia salicornis. As a result, S-UE activity was lower in spraying treatment than in hole application treatment during the growth period of Salicornia salsa, so hole application of chemical fertilizer could improve the effective utilization rate of nitrogen and promote the absorption and utilization of fertilizer by Salicornia salicornis. This may be due to the effects of Fertilization on soil nutrients, mineral elements, root metabolism and secretion activities. In order to reveal the effect of long-term different fertilization methods on the enzyme activity of halophyte rhizosphere soil, the halophyte was used as the research object to carry out the root bag culture on the coastal saline soil. The effects of mulching, non-mulching and no fertilization on the activities of invertase, catalase and urease in rhizosphere soil were

http://www.aloki.hu ● ISSN 1589 1623 (Print) ● ISSN1785 0037 (Online)
DOI: http://dx.doi.org/10.15666/aeer/1802_26692685

studied, and the effects of mulching and no fertilization on the activities of invertase in rhizosphere soil were also studied. Catalase and urease in rhizosphere soil of saline alkali soil were studied. Bacillus, Bacillus licheniformis, Bacillus amylolyticus and compound microbial fertilizer all affected the enzyme activities of the three soils. The results showed that mulching could promote the activities of S-SC, S-CAT and S-UE, and the effect of mulching and fertilization was the best at any time. The changes of soil enzyme activity were the same in the growth period. The activities of invertase and urease were the highest in jointing stage and catalase was the highest in mature stage. In conclusion, the application of plastic film mulching combined with fertilization, inorganic fertilizer and microbial fertilizer can improve soil enzyme activity, soil fertility and sustainable productivity.

Conclusions

In this paper, the relationship between long-term fertilization and soil enzyme activity in rhizosphere of halophytes was studied. A typical halophyte, Salicornia salina, was taken as the research object to study the soil enzyme activity in rhizosphere during the growth period of Salicornia salicornis under different fertilization methods and fertilization treatments. The results showed that the activities of S-SC, S-CAT and S-UE could be promoted by mulching and fertilization, and the effect of mulching combined with fertilization was the best. Different soil enzymatic activities showed different changes during the growth period of Salicornia salina. Soil invertase and soil urease activities showed a trend of increasing first and then decreasing, and soil catalase activity showed a trend of increasing gradually. There are some differences in soil invertase, catalase and urease activities under different fertilization treatments. The long-term application of organic fertilizer and chemical fertilizer can improve the content of soil organic matter, nitrogen and phosphorus nutrients, and enhance the activities of soil invertase, protease, pulse enzyme, phosphatase and catalase. In a certain control period, the transformation of soil available nitrogen and phosphorus is related to growth and development stage, soil enzyme activity and fertilization mode. Single application of chemical fertilizer is not conducive to the improvement of soil organic matter and nitrogen and phosphorus nutrients, and the enzyme activity of soil is also low. The relationship between fuel, feed and fertilizer in rural areas is quite contradictory. Crop straw is mainly used for fuel, feed and paper making. In fact, the residue in the soil every season is only crop stubble. Therefore, the long-term application of livestock manure and green manure in the medium and low yield soil is conducive to the increase of soil organic matter content and the enhancement of soil biological activity, and creates a good soil biochemical environment for the stable and high yield of crops.

Therefore, hole fertilization can improve the comprehensive utilization rate of fertilizer, promote the transformation and release of nutrients in soil, and benefit the growth and development of halophytes. Different fertilization treatments showed that microbial fertilizer combined with chemical fertilizer could improve soil environment, enhance soil enzyme activity, and provide favorable growth conditions for halophytes. Therefore, under the combination of plastic film mulching and fertilization, hole fertilization is the main treatment. Adding microbial fertilizer can improve soil enzyme activity, physical and chemical properties, and promote soil fertility level and sustainable production capacity. In the future research, we can study how to reduce the

http://www.aloki.hu ● ISSN 1589 1623 (Print) ● ISSN1785 0037 (Online)
DOI: http://dx.doi.org/10.15666/aeer/1802_26692685

transformation and release time of soil nutrients, and provide strong experimental data and theoretical reference for the research of soil enzyme activity.

Acknowledgements. National natural science foundation of China - Effects of different water and nitrogen treatments on soil microflora in wheat fields and their regulatory mechanisms (No. 51509085); Fund project for high-level talents of Henan University of Science and Technology: Study on the spatial distribution regulation mechanism of nitrogen compensation utilization in maize and soybean intercropping (No. 2015010).

REFERENCES

[1] Chen, J. F., Sun, H., Xia, Y., Cai, K. X., Liu, H. Y., Li, Y. Y., Guo, R. L., Hou, B., Feng, S., Jiang, X. X. (2017): Changes in Soil Enzyme Activity and Nutrient Content in Different Years of Continuous Cropping Tobacco Fields. – Asian Agricultural Research 9(5): 100-104.

[2] Chen, S., Zhu, Z. K., Yuan, H. Z. (2018): Dynamics of Rice Photosynthesized Carbon Input and Its Response to Nitrogen Fertilization at the Jointing Stage:13 C-CO2 Pulse-labeling. – Environmental Science 39(1): 331.

[3] Cheng, M., Peng, W., Kopittke, P. M. (2016): Cadmium accumulation is enhanced by ammonium compared to nitrate in two hyperaccumulators, without affecting speciation. – Journal of Experimental Botany 67(17): 5041-5050.

[4] Cunha, J. C., Ruiz, H. A., Silva, J. D. G. (2017): Phytoextraction Potential of Atriplex Nummularia Plants under Nitrogen and Phosphate Fertilization. – Communications in Soil Science & Plant Analysis 48(1): 20-36.

[5] Duan, P. P., Liu, L. (2019): Target Aspect Angle Estimation of SAR Images Based on Correlation Analysis. – Journal of China Academy of Electronics and Information Technology 14(1): 46-50.

[6] Fan, P., Chen, D., He, Y. (2016): Alleviating salt stress in tomato seedlings using Arthrobacter and Bacillus megaterium isolated from the rhizosphere of wild plants grown on saline-alkaline lands. – Int J Phytoremediation 18(11): 1113-1121.

[7] Gong, Z., Bao, G. Z., Li, Y. F. (2017): Physiological Response of Ryegrass Seedlings under Freezing-Thawing and Combined with NaHCO3 Stress. – Journal of Jilin University (Science Edition) 55(2): 451-457.

[8] Gschwendtner, S., Engel, M., Lueders, T. (2016): Nitrogen fertilization affects bacteria utilizing plant-derived carbon in the rhizosphere of beech seedlings. – Plant & Soil 407(1-2): 203-215.

[9] Gu, M. Y., Tang, G. M., Liu, H. L. (2016): Effects of cotton stalk biochar on microbial community structure and function of continuous cropping cotton rhizosphere soil in Xinjiang, China. – Ying Yong Sheng Tai Xue Bao 27(1): 173-181.

[10] Hicks Pries, C. E., Castanha, C., Porras, R. C., Torn, M. S. (2017): The whole-soil carbon flux in response to warming. – Science 355(6332): 1420.

[11] Li, H., Hu, J., Xu, K. (2017): Effect of storage period and enzyme activity on bioelectrical property of potato battery. – Chinese Journal of Power Sources 41(7): 1001-1003.

[12] Liu, H., Ruwan, D. U., Zhao, J. (2016): Effects of fertilization on enzyme activities and bacterial community structures in rhizosphere soil of flue-cured tobacco. – Tobacco Science & Technology 49(11): 1-6.

[13] Ma, Q., Ran, L., Hu, B. R. (2016): Temperature Dependency Characteristic of SiC MOSFET Static Performance Based on Comparative Analysis with Si IGBT. – Journal of Power Supply 14(6): 67-79.

http://www.aloki.hu ● ISSN 1589 1623 (Print) ● ISSN1785 0037 (Online)
DOI: http://dx.doi.org/10.15666/aeer/1802_26692685

[14] Nawaz, M. F., Bourrie, G., Gul, S. (2016): Exploring the dynamics of physico-chemical properties of soil waters in the rhizosphere of rice plants. – Pakistan Journal of Agricultural Sciences 51(2): 351-361.
[15] Poeplau, C., Bolinder, M. A., Kirchmann, H. (2016): Phosphorus fertilisation under nitrogen limitation can deplete soil carbon stocks – evidence from Swedish meta-replicated long-term field experiments. – Biogeosciences 13(19): 16527-16551.
[16] Song, W. L., Yu, Y., Wang, Z. (2018): Study on Temperature Field Uniformity Control in Micro Carbon Plant Cultivation System. – Computer Simulation 35(2): 205-210.
[17] Tang, X., Placella, S. A., Daydé, F. (2016): Phosphorus availability and microbial community in the rhizosphere of intercropped cereal and legume along a P-fertilizer gradient. – Plant & Soil 407(1-2): 119-134.
[18] Van Veen, B. K., Rutten, W. L. C., Wallinga, W. (2017): The Influence Of The Position Of The Active Fiber Relative To The Muscle Boundary In Computing Single Fiber Action Potentials. – Acta Biol Colomb 18(3): 449-464.
[19] Wang, T., Ma, Y. D., Xu, Y. D., Guo, S. J., Wang, W. Y., Han, X. H., Yang, G. H., Wang, X. J. (2018): Relationship between soil nutrients and enzyme activity in Robinia pseudoacacia plantation. – Chinese Journal of Ecology 37(7): 2083-2091.
[20] Xu, L., Yi, M., Yi, H. (2017): Manure and mineral fertilization change enzyme activity and bacterial community in millet rhizosphere soils. – World Journal of Microbiology & Biotechnology 34(1): 8.
[21] Zhao, S., Zhou, N., Zhao, Z. (2016): Estimation of endophytic bacterial diversity in root of halophytes in Northern Xinjiang by high throughput sequencing. – Acta Microbiologica Sinica 56(10): 1583-1594.
[22] Zhou, B., Lin, X. (2016): Design of wireless water-saving irrigation system for urban vegetation. – Automation & Instrumentation 4: 134-135.

http://www.aloki.hu ● ISSN 1589 1623 (Print) ● ISSN1785 0037 (Online)
DOI: http://dx.doi.org/10.15666/aeer/1802_26692685

STUDY ON SIGNAL INDUCED EXPRESSION OF COLD TOLERANCE IN EDIBLE LILY IN ALPINE ENVIRONMENT

TIAN, X. H.[1,2*] – XIE, J. M.[2] – YU, J. H.[2]

[1]*Department of Ecological and Environmental Engineering, Yangling Vocational & Technical College, Yangling 712100, China*

[2]*College of Horticulture, Gansu Agricultural University, Lanzhou 730070, China*

[*]*Corresponding author*
e-mail: txh_1214@126.com

(Received 3rd Sep 2019; accepted 12th Feb 2020)

Abstract. The objective of this experiment was to study the differentially expressed proteins and genes of edible lily in alpine environment, and to provide a better growth environment for edible lily. The edible lily of Heilongjiang Province, China, was selected as the object of the study. The samples were divided into two groups. The first group grew normally in the artificial climate box; the second group was treated at 4℃ for 16 hours after spraying with Abscisic Acid (ABA) hormone, and the second group included edible lily No. 1 and edible lily No. 2. The total protein of one leaf was extracted by the trichloroacetic acid-acetone method and the differential protein spots of edible lily were analyzed by DeCyder software. The leaf genes of two edible lilies were extracted based on cold-resistant gene primer design. The results showed that alpine environments could induce energy metabolism, fatty acid metabolism, photosynthesis and signal transduction of differential proteins in edible lily; exogenous ABA could promote Coscisic Rirna (COR) gene expression by activating transcription factors dependent on ABA signaling pathway, and to some extent, it promotes the expression of cold resistance genes in signal pathways independent of ABA, and improves the cold resistance of edible lily.
Keywords: *differentially expressed proteins and genes, Abscisic Acid, cold-resistant gene primer design, energy metabolism, fatty acid metabolism*

Introduction

Alpine environment is one of the main stress factors for lily growth processes. Alpine environment seriously damages Lily growth, even causing physiological imbalance of the whole lily, and bringing serious losses to production and ornamentation (Wei et al., 2017). Edible lilies are mainly distributed in the north temperate zone, the lowest temperature in winter can reach -35℃, but edible lilies can spend winter open field, adapt to the cold environment and continue to germinate and blossom in the next spring (Lu et al., 2017). In addition, they also have the ability to resist high temperature, drought and change soil salinity. However, with the deterioration of the ecological environment, the number of edible lilies has gradually decreased in recent years. Therefore, it is necessary to further protect the edible lily resources and explore the signal-induced expression of cold tolerance of Edible Lily in alpine environment. At present, there are many studies on Lily growth and yield in China. The results show that temperature and drought are the ecological factors restricting Lily regional distribution, abiotic stress directly affects Lily growth and development and yield, and even causes physiological imbalance of lily, which is the main reason for reducing Lily ornamental value (Templ et al., 2017).

The objective of this experiment was to study the differentially expressed proteins and genes of Edible Lily in alpine environment, and to provide a better growth environment for edible lily. In this paper, the differential protein analysis of edible lily and the effect of

http://www.aloki.hu ● ISSN 1589 1623 (Print) ● ISSN1785 0037 (Online)
DOI: http://dx.doi.org/10.15666/aeer/1802_26872701

exogenous Abscisic Acid (ABA) on cold resistance gene expression in alpine environment were used to study the differential protein and gene expression of edible lily induced by two cold tolerance signals. ABA is a signal factor of plants responding to external stresses. The content of endogenous ABA increases significantly during cold acclimation, indicating that external cold stress increases ABA levels in plants and ABA is involved in signal transduction. With the development of signal transduction pathway research, ABA has become a research hotspot. It can induce related genes in stress response, and make them up-regulated or down-regulated. The ecological balance and metabolic activity of lily were affected by external stress. The expression of differentially expressed genes and the changes of differentially expressed proteins indirectly reflected the physiological activities of lily during the same period. Lily resumed normal metabolism through self-repair and regulation. Therefore, the study of proteomics will further explore the signal transduction pathway of Lily in response to external stress. Edible lilies live in a low temperature environment. In order to adapt to cold conditions, the protein and gene expression in Lily cells will change in response to cold stress. Lily was induced by cold stress and ABA hormone. The differential proteins were identified and classified by protein spectrum identification technology. The effect of ABA on the regulation process of cold-resistant genes of edible lily under cold stress was clarified. The relationship between the changes of protein points in Lily and the adaptation of cold and low temperature environment was discussed. Inverse mechanism and further scientific basis were provided to complete the signal-induced expression of cold tolerance of Edible Lily in alpine environment.

Materials and methods

Materials

Lily was selected from Heilongjiang Province of China for food (the same bulb should be propagated with the same genotype). Sample treatment was divided into two groups: CK 0 h, i.e. the control plant grew normally in the artificial climate box; ABA + cold-treated 16 h, i.e. the lily was treated at 4℃ for 16 h after spraying ABA hormone. Sample 1 contained two kinds of Lily cultivars, edible lily 1 (10 lily leaves) and edible lily 2 (10 lily leaves), respectively. Sample 2 contained two kinds of Lily cultivars, edible lily 1 (10 lily leaves) and edible lily 2 (10 lily leaves). The mean minimum temperatures of two kinds of edible lilies collected in No. 2 Middle School were 4℃, 0℃, -10℃ and -25℃, respectively. When sampling, 50 lilies with the same growth were randomly selected, washed with distilled water, dried and cut into 0.5 cm segments. After mixing, the leaves were frozen in liquid nitrogen and stored in a refrigerator at -80℃. Then the edible lily leaves of Sample 1 were taken to extract protein. The leaves of Edible Lily in Sample 2 were taken to extract genes.

Main instruments for testing

The test instruments include: GE Amersham (USA), Second-dimension: Hofer SE600 (GE Amersham), Scanner: UMaxPowerlook 21 IOXL (GE Amersham). Leica DFC500 stereo microscope, BIO-RAD UV Gel imaging system, BIO-RAD SmartSpec Plus UV spectrophotometer, BeckMan Coulter Allegra 648 centrifuge, Illumina company's Solexa genome analyzer (Allegra), fluorescence quantitative analyzer, sterilizing pot, 54158 centrifuge, G-storm-482 PCR, TaiSite water bath pot, Microwave oven (*Figure 1*).

http://www.aloki.hu ● ISSN 1589 1623 (Print) ● ISSN1785 0037 (Online)
DOI: http://dx.doi.org/10.15666/aeer/1802_26872701

(a) Microscope (b)Spectrophotometer (c)Fluorescence quantitative analyzer

Figure 1. *Main instruments for testing*

Test reagent

The main reagents were solid phase pH gradient (IPG) tape (24 cm, pH 3-11), IPG buffer pH 3-11, and ammonium bicarbonate was purchased from Sigma Company. CHCA (Sigma No. 034K3707), Merck No. 1499230-935, Merck No. 56002262-009, Mass Standards Kit for the 4700 Proteomics Analyzer (AB SCIEX No. 4333604), concentrated sulfuric acid, onion ketone, acetic acid, acetic acid, beta-sparse ethanol, EASYspinPplant RNA rapid extraction kit of Adelai Company (RLT, RLT Plus, RW1, RW, RNase-free H20, PLANTaid, Genomic DNA Clearance Column and Collection Tube, RNase-free Adsorption Column and Collection Tube), Promega'sPolyATtract RNA Isolation System III with mAGnetic Stand BioTinyLated-Oligo (dT), 20×SSC M-MLV RTase Gene Synthesis Kit (5×1 st strand synthesis Buffers 5×2 st strand synthesis Buffer, dNTP Mixtures RNase Inhibitor Oligo (DT), Reverse Transcriptase (M-MLV) (200 U/mL), EcoDNA Polymerase I, E. DNA Li Gase Mixture, T4 DNA Polymerase, Tris-HCL (pH 7.6), MgCL2, DTT, ATP, T4 DNA Ligase, EDTA, SDS, phenol/chloroform/isoamyl alcohol (25:24::1).

Method

The study was conducted on edible lilies in the alpine environment. The main picking site is Gansu Province in China, located between 32°11'-42°57' north latitude and 92°13'-108°46' east longitude. The terrain of Gansu is narrow and long, and the landforms are complex and diverse. The mountains, plateaus, Pingchuan, river valleys, deserts, and Gobi are surrounded by mountains and mountains. The terrain slopes from southwest to northeast. Gansu is located at the intersection of the three plateaus of the Loess Plateau, the Qinghai-Tibet Plateau and the Inner Mongolia Plateau. The annual average temperature is 0-15°C. Taking edible lily in this area as a research example, the induced expression of lily cold tolerance signal in alpine environment was studied.

Extraction of total protein from edible lily leaves

Lily protein was extracted by trichloroacetic acid-acetone method (Shimo et al., 2017).

(1) Take a sample of about 1 g tissue, grind it with liquid nitrogen, add 45 mL TCA/acetone solution, stay overnight at -20℃, and centrifuge for 30 minutes to remove the supernatant.

(2) Add equal volume precooling acetone, centrifuge to remove supernatant, repeat this step until acetone is completely colorless; dry and precipitate at room temperature.

http://www.aloki.hu ● ISSN 1589 1623 (Print) ● ISSN1785 0037 (Online)
DOI: http://dx.doi.org/10.15666/aeer/1802_26872701

(3) 1.5 mL 2D pyrolysis solution was added to the dry powder of each group, and the supernatant was obtained by ice-bath ultrasonic cooling treatment (100 W, 10 s, 15 s interval, 10 times); 12 000 rpm, 4℃, 30 min.

(4) Quantitative: Bio-Rad protein assay reagent was used to quantify and stored at -80℃.

Identification of differentially expressed proteins in Edible Lily

The differential protein spots of edible lily (Liu et al., 2017) were analyzed by DeCyder software. The original mass spectrometry documents were retrieved by in-gel enzymatic hydrolysis, Ziptip desalination, mass spectrometry analysis and Mascot 2.2 software. The identified protein results (Donaldson et al., 2017) were obtained.

Primer design of cold resistance gene

Based on the existing data of DFCI Wheat Gene Index and NCBI, the primers with good performance (Ahmed et al., 2019) were designed using the conserved regions of each coding enzyme and cold-resistant gene as templates. Primers should be designed strictly according to the requirement of real-time quantitative reaction in order to obtain primers with high amplification efficiency and specificity. The primers of cold-resistant genes were designed according to the requirements of fluorescence quantitative PCR, as shown in *Table 1*.

Table 1. *Real-time quantitative PCR primers*

Gene	NCBI accession number	Primer type	Primer sequence 5' to 3'
CBFII−5.2	EF028753.1	Forward	AACATCACCTCACTCACCAGTCA
		Reverse	GTACTGGTCCATGGTGTTGCA
Wcor15	AB095006.1	Forward	ACGACGCTGCGGATGCTAC
		Reverse	CCTTGTCCGTGATGCCCTGT
WCS120	M93342.2	Forward	ATGGACACGCTGGAGTGAT
		Reverse	CTGTCCAGGCAGCTTATCCT
COR39	AFO58794.1	Forward	ATGCACACACTGGAATGACC
		Reverse	GTGCTGTCCAGGCAGCTT
CBFIVd-D22	EF028753.1	Forward	GAGCCAGAGCCACTTGTTCA
		Reverse	ACAAGATGCTACTGTGTTTCTCTCCAA
MYB80	AY625680.1	Forward	CAGATAGAGCAACACCTAA
		Reverse	AGAATGAATCACTAGAATCCT
Wabi5	AB193553.1	Forward	GCAGGCTTATACAATGGA
		Reverse	GAACTGATCCTTCATCTCA
Wrabl7	AF255053	Forward	TTTTACGGCGACAAGACTGAC
		Reverse	GGGGTATCCTTGGTGTACTGTG

Results

Extraction and quantification of protein from Edible Lily leaves

Using 2-D quant Kit to quantify the total protein of Sample 1 and accurately quantify the lily protein is the precondition for the follow-up study of differential proteome. SDS-PAGE single-dimensional electrophoresis was used to further verify the quantitative results. Quant Tool software analysis and visual observation showed that the results of protein display were more accurate, indicating that the quantitative results of these proteins can continue to be used in the follow-up study of differential proteins. The results of protein quantification are shown in *Table 2*.

http://www.aloki.hu ● ISSN 1589 1623 (Print) ● ISSN1785 0037 (Online)
DOI: http://dx.doi.org/10.15666/aeer/1802_26872701

Table 2. *Quantitative results of protein*

Sample	Concentration μg/μL	Total /μL
Sample 1	5.9	405
Sample 2	5.9	705

Identification of differentially expressed protein profiles in Edible Lily

In this study, 21 protein spots were selected and identified by MALDI-TOF mass spectrometry after two-dimensional electrophoresis analysis using imageMaster 2D Elite Platnum software. Finally, 20 proteins were obtained complete peptide fingerprints, and 19 proteins were successfully identified by searching MIPS database. The identification results are shown in *Table 3*.

Table 3. *Identification of Protein Points in Edible Lily Leaves under Low Temperature Stress by Mass Spectrometry*

Number	Protein Identification	Organism	Biological Process	Protein Score	PI/MW
J24	Late embryogenesis abundant protein	VitisVinifera	Response to abiotic stimulus; Transport; signal transduction	66	39220/5.14
K1	Photosystem I reaction center subunit II chloroplastic-like	Setariaitalica	Protein metabolic process; cell cycle; Generation of precursor metabolites and energy	296	29932.8/10.04
K2	Integrasetransposasefamily protein	Halorubrmalamnqense	Response to abioticstimulus; transport; signal transduction	71	22788.4/5.23
K3	Cytochrome b6-fcomplex iron-sulfur subunit	Zea mays	Generation of precursor metabolites and energy; biological process	214	24321.3/8.52
K4	Intracellular pathogenesis-related protein PR-107	Liliumlongiflorum	Response to stress; celldeath; transcripnal; signal transduction	97	16699.6/5.37
K5	ATP dependant RNA helicase	Chondruscrispus	Response to stress; response to abiotic stimulus; transpor	62	83477.9/8.9
K6	Ribulose-1 , 5-bisphosp hatecarboxylase / oxygenaselarge subunit	Dioscoreaschimperiana	Biosynthetic process; carbon hydrate metabolism; photosynthesis metabolic process	437	51125.6/6.44
K7	Zinc finger protein 51	Musmusculus	Metablicprocess; cellular process	69	86746.1/9.07
K8	Phosphoglycerate mutase 2, 3-bisphosphoglycerate-independent isoform	Theobroma cacao	Response to stress; biological process; carbonhydrate metablic process; catabolic process; Generation of precursor metabolites and energy	256	48133.4/5.9
K9	UPF0664 stress-induced protein C29B12. 11c-like	Brachypodiumdistachyon	Response to stress; response to abiotic stimulus; transport	83	22956.4/7.01
K10	Aconitatehydratase	pinuspinaster	Response to stress	213	40867.6/6.34
K11	S-adenosylmethionine synthase2	Populustrichocarpa	Generation of precursor metabolites and energy	546	43564.9/5.5
K12	Keratin cytoskeletal	Homo sapiens	Generation of precursor metabolites and energy	277	66184.1/8.15
K13	Protein translocase subunit secA	Cryptobacteriumcuryum	Carbonhydrate metablic process; catabolic process	75	105722.9/5.07
K14	Receptor-like protein kinase	Ricinuscommunis	Response to stress; Transcription; transport; signal transduction	275	21732.9/6.1
K15	Cytosolic malate dehydrogenase	Sugarcane mosaic virus	Carbonhydrate metallic process; catabolic process energy metalic	117	39790.3/5.7
K17	Actin protein	Lilium regale	Response to stress; Transcription; transport; signal transduction	147	41847.1/5.31
K18	Oxygen-evolving enhancer protein chloroplast	Arabidopsis thaliana	Generation of precursor metabolites and energy; photosynthesis	96	28231.3/8.67
K19	Conjugal transfer protein Tral	Escherichia coli	Transcription; transport; signal; transduction	80	188993.2/5.78
K20	peptide l-prolylcis-trans isomerase FKBP5-like	Oreochromisniloticus	response to stress; Transcription; transport; signal transduction	66	52267.3/8.69

http://www.aloki.hu ● ISSN 1589 1623 (Print) ● ISSN1785 0037 (Online)
DOI: http://dx.doi.org/10.15666/aeer/1802_26872701

Functional analysis of differentially expressed proteins in edible lily under different treatment conditions

Table 3 shows that a protein can participate in different biological processes and play different roles in response to external stresses. Four differentially expressed proteins are stress response related proteins. Three proteins are involved in signal transduction, four proteins are related to energy metabolism, three proteins are related to photosynthesis response, and the other three proteins may be involved in other biological processes. In this study, stress response related proteins, signal transduction proteins and energy metabolism proteins were introduced in detail.

Changes in expression of stress-related proteins

Four differentially expressed proteins are stress response-related proteins, namely J24:LEA synthetic protein; K2:transcriptase family protein; K9:stress-induced protein. The expression of PR-107 was significantly down-regulated, while the expression of other proteins was significantly up-regulated. Protein Point K4: Some results of mass spectrometry identification of cell disease resistance protein PR-107 are shown in *Figure 2*.

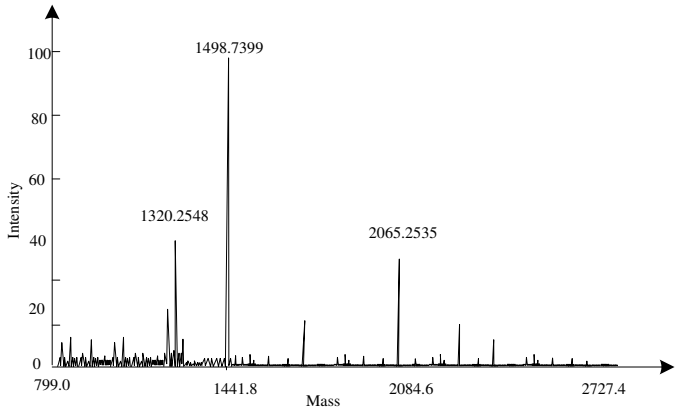

Figure 2. *Protein point K4 mass spectrometry identification partial results*

Participation in signal transduction proteins

In this study, three signal transduction related proteins were identified, namely K14: receptor protein kinase; K19: combined transporter; K20: peptide-prolylcis-trans isomerase. The expression of K14 and K19 protein was significantly up-regulated, but the abundance of the peptide-prolylcis-trans isomerase K20, which played a role in protein folding, was down-regulated under low temperature stress. K14: Some of the results of mass spectrometric identification of receptor protein kinases are shown in *Figure 3*.

Proteins involved in energy metabolism

In this study, four differentially expressed proteins, K5:ATP synthase; K6:ribose-1,5-diphosphate carboxylase/oxygenase subunit; K8:2,3-diphosphate glycerol mutase, were identified under the regulation of low temperature stress. The expression abundance of these three proteins was more than two times under cold stress and increased

http://www.aloki.hu ● ISSN 1589 1623 (Print) ● ISSN1785 0037 (Online)
DOI: http://dx.doi.org/10.15666/aeer/1802_26872701

significantly. K15 is malic deoxygenase, and its expression is significantly up-regulated. K6: Some results of the identification of ribose-1,5-diphosphate carboxylase / oxygenasemacrosubstrates are shown in *Figure 4*.

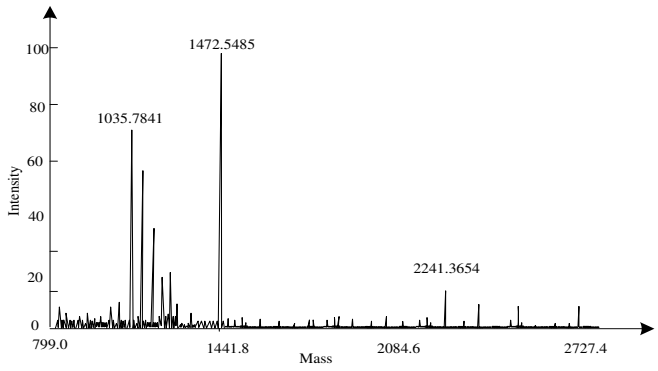

Figure 3. *Partial results of protein point K14 mass spectrometry identification*

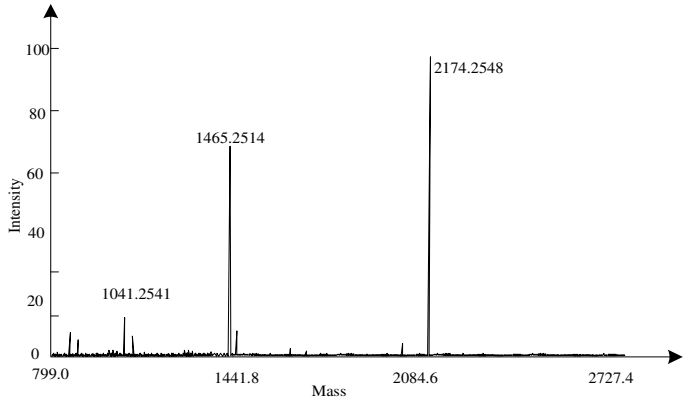

Figure 4. *Protein point K6 mass spectrometry identification partial results*

Effect of exogenous ABA on cold-resistant gene expression of Edible Lily in alpine environment

Effects of exogenous ABA on the expression of CBF and COR genes independent of ABA in edible lily under high and cold environment

The expression of TaCBFII-5.2 gene in leaf control group of two edible lily cultivars increased first and then decreased. The expression of TaCBFII-5.2 gene in leaf control group of edible lily cultivar No. 2 increased again at -25℃. The peak values above 0℃ were shown in *Figure 5a* and *Figure 5b*. Exogenous ABA treatment promoted the expression of TaCBFII-5.2 gene in the leaves of edible lily No. 1 and reached a significant level at temperatures above 0℃ ($P < 0.05$); in the leaves of edible lily No. 2, the expression of TaCBFII-5.2 gene in the ABA treatment group was higher than that in the control at 4℃, and reached a significant level ($P < 0.05$), but at temperatures below 0℃ and below. The expression of the gene in the ABA treatment group was lower than that in the control group, and the difference reached significant level at 0℃ and -25℃ ($P < 0.05$).

http://www.aloki.hu ● ISSN 1589 1623 (Print) ● ISSN1785 0037 (Online)
DOI: http://dx.doi.org/10.15666/aeer/1802_26872701

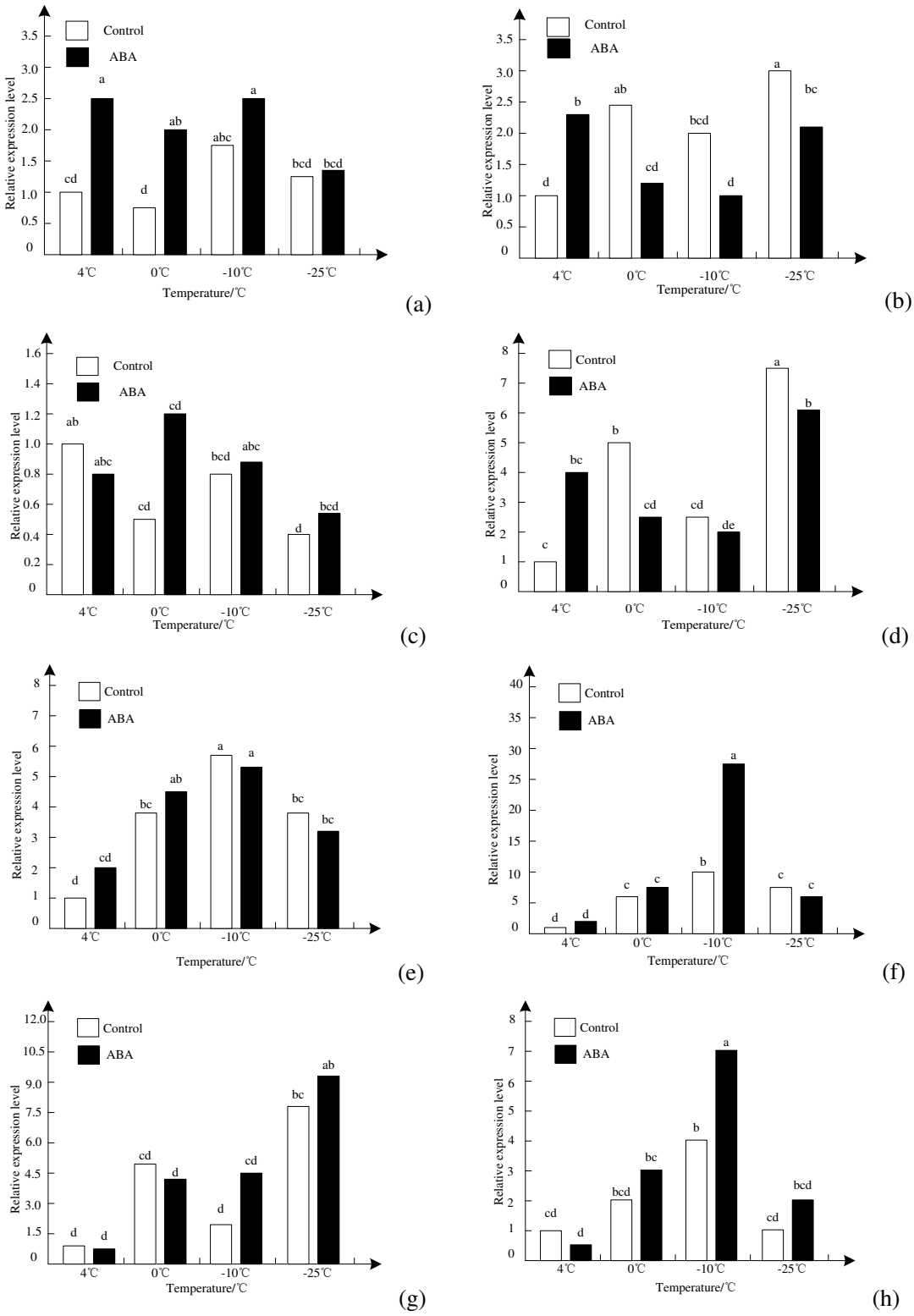

Figure 5. *Relative expressions of TaCBFII-5.2, TaWcorl5, TaWcs 120 and TaCOR39 in leaves of two edible lilies at low temperature during winter. There were significant differences in different letters of edible lily of the same cultivar ($p < 0.05$); TaCBFII-5.2, TaWcorl 5, TaWcs 120, TaCOR39 genes of edible lily No. 1 leaves were a, c, e and g respectively, and TaCBFII-5.2, TaWcorl 5, TaWcs 120 and TaCOR39 genes of edible lily No. 2 leaves were b, d, f and h, respectively*

http://www.aloki.hu ● ISSN 1589 1623 (Print) ● ISSN1785 0037 (Online)
DOI: http://dx.doi.org/10.15666/aeer/1802_26872701

The expression of TaWcorl15 gene in the leaf control group of edible lily No. 1 showed a downward and downward trend. As shown in *Figure 5c*, the expression of TaWcorl5 gene was inhibited by exogenous ABA at the initial stage of low temperature at 4℃, but the expression of TaWcorl5 gene was promoted after the temperature continued to decrease, but the difference was not significant. The expression of TaWcorl5 gene in the leaves of control group No. 3 showed a rising and falling trend. As shown in *Figure 5d*, exogenous ABA only promoted the expression of TaWcorl5 gene at 4℃ (< 0.05) in the early stage of low temperature, but inhibited the expression of TaWcorl5 gene at other temperatures, and reached a significant level at 0℃ (< 0.05) and -25℃ (< 0.05).

The expression of TaWcs 120 gene in the leaves of two lily cultivars increased first and then decreased. As shown in *Figure 5e* and *Figure 5f*, the expression of TaWcs 120 gene in the leaves of Lily cultivar No. 1 treated with ABA was higher than that in the control at temperatures above 0℃, while the expression of TaWcs 120 gene was inhibited at temperatures below 0℃, but the expression of TaWcs 120 gene was inhibited at temperatures below 0℃. At all temperatures, there was no significant difference between the two treatments. The expression of TaWcs 120 gene in the leaves of Lily No. 2 treated with ABA was higher than that in the control group at temperatures above -10℃, and reached a significant level at -10℃ ($P < 0.05$). The expression of TaWcs 120 gene in the leaves of Lily No. 2 treated with ABA was lower than that in the control group at late -25℃ ($P < 0.05$), but the difference between the two treatments was not significant.

The expression of TaCOR39 gene in leaves of two edible lily control groups increased first and then decreased, as shown in *Figure 5g* and *Figure 5h*. However, at the lowest temperature -25℃, the expression of the gene in the leaves of edible lily No. 1 increased to a peak. In the leaves of Lily cultivars, ABA inhibited the expression of TaCOR39 gene in the early stage of low temperature, and promoted the expression of TaCOR39 gene in the late stage of low temperature, but the difference between the two treatments was significant only at -10℃ ($P < 0.05$).

Effects of exogenous ABA on the expression of ABA-dependent transcription factor genes and COR genes in edible lilies in alpine environment

TaCBFIVd-D22, TaMYB80 and TaWabi5 are ABA-dependent transcription factors.

The expression of TaCBFIVd-D22 gene in the leaves of the control group showed a downward and downward trend. As shown in *Figure 6a*, exogenous ABA significantly inhibited the expression of TaCBFIVd-D22 gene at the initial stage of low temperature ($P < 0.05$), and increased the expression of TaCBFIVd-D22 gene at the lowest temperature, reaching a significant level at 0℃ and -10℃ (< 0.05). The expression of TaCBFIVd-D22 gene in the leaves of edible lily No. 2 increased as a whole. As shown in *Figure 6b*, exogenous ABA significantly promoted the expression of TaCBFIVd-D22 gene ($P < 0.05$) in the early stage of low temperature at 4℃, but inhibited the expression of TaCBFIVd-D22 gene when the temperature continued to decrease, reaching a significant level at 0 and -25℃ ($P < 0.05$).

The expression of TaMYB80 gene increased first and then decreased with the decrease of temperature in the control group. As shown in *Figure 6c and 6d*, exogenous ABA treatment promoted the expression of TaMYB80 gene in the leaves of edible lily No. 1. The difference between the two treatments was significant at low temperatures ($P < 0.05$). In edible lily No. 2 leaves, exogenous ABA significantly promoted the

http://www.aloki.hu ● ISSN 1589 1623 (Print) ● ISSN1785 0037 (Online)
DOI: http://dx.doi.org/10.15666/aeer/1802_26872701

expression of TaMYB80 gene only at 4℃ in the early stage of low temperature ($P < 0.05$), and inhibited the expression of TaMYB80 gene at other temperatures, especially at 0℃ and -25℃.

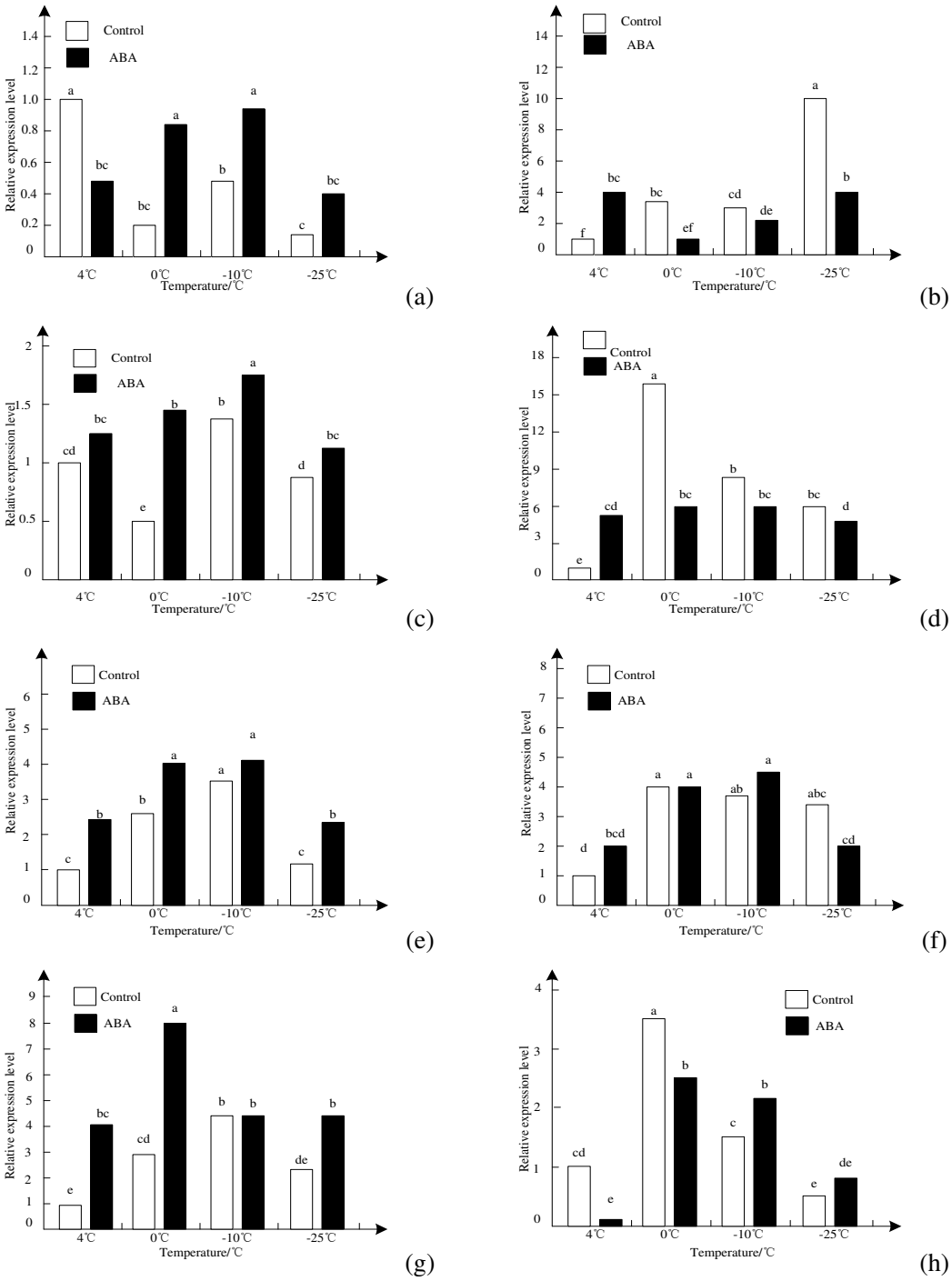

Figure 6. *Relative expressions of TaCBFIVd-D22, TaMYB80, TaWabi5 and TaWrabl7 in leaves of two edible lilies during winter. There were significant differences in different letters of edible lily of the same variety ($p < 0.05$); TaCBF1Vd-D22, TaMYB80, TaWabi5 and TaWrabl7 genes of edible lily No. 1 leaf were TaCBF1Vd-D22, TaMYB80, TaWabi5 and TaWrabl7 genes respectively; and b, d, f and h genes of edible lily No. 2 leaf were TaCBF1Vd-D22, TaMYB80, TaWabi5 and TaWra7 genes, respectively*

http://www.aloki.hu ● ISSN 1589 1623 (Print) ● ISSN1785 0037 (Online)
DOI: http://dx.doi.org/10.15666/aeer/1802_26872701

TaWabi5 belongs to the transcription factor of bZIP family. The expression of TaWabi5 gene in the leaves of two edible lily varieties increased first and then decreased. As shown in *Figure 6e and 6f*, exogenous ABA treatment promoted the expression of TaWabi5 gene in the leaves of edible lily No. 1. Except -10℃, the difference reached significant level ($P < 0.05$). In the leaves of edible lily No. 2, the expression of TaWabi5 gene reached a significant level ($P < 0.05$). Exogenous ABA promotes the expression of the gene at degree, but there is no significant difference between the two treatments, it inhibits the expression of the gene at the late stage of low temperature -25℃, and the difference is not significant.

TaWrabl7 belongs to ABA-dependent COR gene. The expression of TaWrabl7 gene in the leaves of two edible lilies increased first and then decreased, as shown in *Figure 6g and 6h*. In edible lily No. 1 leaves, exogenous ABA promoted the expression of TaWrabl7 gene, reaching a significant level ($P < 0.05$) except -10℃. In edible lily No. 2 leaves, exogenous ABA significantly inhibited the expression of TaWrabl7 gene at temperatures above 0℃, while temperature continued to decrease, and then promoted its expression at -10℃. In edible lily No. 2 leaves, exogenous ABA significantly inhibited the expression of TaWrabl7 gene. The difference was significant ($P < 0.05$).

Discussions

Functional analysis of differential proteins

Mass spectrometry analysis revealed that differential proteins were mainly involved in the balance of photosynthetic respiration, carbon, nitrogen, sulfur and energy metabolism, protein translation, protein processing, signal transduction, RNA processing and redox (Tang et al., 2017). In this study, differential proteomics of edible lily leaves under low temperature stress was studied. Twenty-one protein spots were selected and identified by MALDI-TOF mass spectrometry (Wu et al., 2018) after the analysis of protein spots with more than two-fold abundance in two-dimensional electrophoresis (2-DE) by using ImageMaster 2D Elite Platnum software. Finally, 20 proteins obtained complete skin fingerprints. These 19 proteins were successfully identified by searching the MIPS database. The identification results showed that they were involved in energy metabolism, fatty acid metabolism, photosynthesis and signal transduction. The possible physiological functions of these proteins in response to low temperature stress are discussed below.

Stress-related proteins

The Edible Lily will produce a series of proteins with protective function after being stressed by adversity. Late embryogenesis abundant proteins (LEA proteins) is one of the most important proteins (Li et al., 2017). LEA protein was first discovered in 1981. It can be enriched in the process of dehydration during the late stage of embryonic development and can improve the resistance of seeds to dehydration (He et al., 2019). Dehydration is a highly hydrophilic and molecular chaperone in the metabolic process of edible lily, which can stabilize the structure and properties of cell membranes, avoid protein denaturation caused by water shortage caused by low temperature stress, and reduce external damage to plants. A large number of studies have shown that cold stress can promote the accumulation of large amounts of LEA protein (Li et al., 2017) in plants. The expression level of LEA protein spots (J24) identified in this study was

http://www.aloki.hu ● ISSN 1589 1623 (Print) ● ISSN1785 0037 (Online)
DOI: http://dx.doi.org/10.15666/aeer/1802_26872701

significantly up-regulated, indicating that LEA protein played an important role in the resistance of edible lily to external stresses and reduced the damage of edible lily plants under low temperature stress. K2: transcriptase family protein; K4: cell disease resistance protein PR-107; K9: stress-induced protein, the expression of cell disease resistance protein (K4) was significantly down-regulated, and other protein expression was significantly up-regulated.

Signal transduction related proteins

When lily is stressed, plant cells receive signals, which are received by cell membrane sensors, and then transferred from cytoplasm to nucleus by a second signal molecule, such as catalytic protein kinase. In nucleus, protein kinase C and PPPC can induce Ca^{2+} and ABA pathways respectively to initiate signal transduction (Xu and Zhu, 2017). After opening the defense mechanism, it mainly includes physical structural adaptation, such as changes in lipid composition and extracellular metabolic activities, increased intercellular osmotic protective agents such as soluble sugar, proline, betaine, etc., and up-regulated synthesized antioxidants such as superoxide dismutase, pathogen defense, catalase, ascorbic acid reductase, recovery. The balance of complex biosynthesis and carbohydrate metabolism can improve the survival rate of Edible Lily in cold environment. When most signaling molecules bind to their receptors, they begin to regulate cellular behavior, including intracellular responses to metabolism, exercise, proliferation, survival and differentiation. Finally, the edible lilies were adapted to cold acclimation and resisted external stress (Jiang et al., 2017). In this study, an up-regulated protein, receptor protein kinase (K14, RLK), was identified as a signal-accepting receptor protein with a single transmembrane alpha-helix receptor. When plants respond to low temperature stress, the expression of receptor protein kinase is significantly up-regulated. It is speculated that it may be stimulated by external cold signals and participate in the process of signal transduction in cell membranes and intracellular membranes. It can transmit signals to the nucleus and inspire the expression and regulation of downstream genes. It is a series of physiological and biochemical sounds produced by plants cold stress (Yu et al., 2017). Studies have shown that active protein molecules have specific amino acid sequences and three-dimensional spatial structures, and the sequences of these genes are folded into proteins with specific structures and functions. The polypeptide prolinephthalidecis-trans isomerase CIS (K20) identified in this study has protein folding effect. It belongs to the chloroplast membrane protein, which can transmit cold signals in chloroplasts, and its expression changes directly lead to changes in the structure of chloroplast membrane.

Energy metabolism related proteins

Liu et al. (2017) showed in related research that proteins and enzymes play an important role in plant response to low temperature stress signal pathway, and the expression of genes related to these proteases are up-regulated or down-regulated. Proteins are involved in the primary and secondary metabolic processes of plants in response to stress, especially in osmotic regulators and soluble sugar soluble proteins (Liu et al., 2017). In plants, energy provides essential ATP for various life activities and intermediate metabolites for many metabolisms, so it is the basic metabolism of various life activities (Yu et al., 2018).

In this study, four differentially expressed proteins were identified, including protein points K6, K8 and K15, which play an important role in the tricuspid acid cycle and

http://www.aloki.hu ● ISSN 1589 1623 (Print) ● ISSN1785 0037 (Online)
DOI: http://dx.doi.org/10.15666/aeer/1802_26872701

participate in the glycolysis process of material and energy metabolism pathway. Protein point K5 is the key enzyme of oxidative phosphorylation. The increase of their expression level will promote the synthesis of downstream substances and provide essential substances and energy for edible lilies to cope with low temperature stress. At the same time, it can promote the changes of extracellular metabolic activities, restore the balance of biosynthesis and carbohydrate metabolism, and improve the survival rate in cold environment.

Effect of exogenous ABA on cold resistance gene expression

Exogenous ABA can regulate the synthesis of endogenous ABA. ABA plays an important role in ABA-dependent signal transduction pathway. Many studies have shown that ABA may activate bZIP transcription factors and regulate COR genes that depend on ABA. The activation regions of these COR genes contain ABREs. Other transcription factors such as MYC/MYB and CBF4 also play an important role in ABA-dependent stress signal transduction pathways (An et al., 2017). At present, many bZIP transcription factors, MYC/MYB transcription factor, CBF4 gene and ABA-dependent COR gene have been isolated and identified in Edible Lily and other plants. TaWabi5 gene is a bZIP transcription factor in edible lily, TaMYB80 is a MYC/MYB transcription factor in edible lily, TaCBF4 is an ABA-dependent CBF transcription factor in edible lily, and TaWrabl7 belongs to the ABA-dependent COR gene in Edible Lily (Chen et al., 2019). In this study, we found that exogenous ABA promoted the expression of TaCBF4 gene in leaves of edible lily No. 1 at the late stage of moderate and low temperatures, and exogenous ABA promoted the expression of TaMYB80, TaWabi5 and TaWrabl7 genes in leaves of edible lily No. 1, while exogenous ABA only promoted the expression of TaMYB80, TaWabi5 and TaWrabl7 genes in leaves of edible lily No. 2 at the early stage of low temperature at 0℃ or above The expression of these cold-resistant genes was inhibited when the temperature was lowered.

In ABA-independent signaling pathways, low temperature can promote the expression of CBF family transcription factors, while CBF transcription factors may cause the expression of many downstream COR genes to improve plant cold resistance. TaCBFlI-5.2 is a CBF/DREB transcription factor in edible lilies. This study found that in high-cold environment, at temperatures of -10℃ and above. Exogenous ABA promotes the expression of this gene (Lee et al., 2017). Exogenous ABA has no significant effect on the expression of COR gene independent of ABA in the leaves of two edible lilies.

Conclusions

In this paper, the differential protein of edible lily and the expression of cold-resistant gene of exogenous ABA in alpine environment were studied. The research results are as follows:

Differential protein of edible lily showed that differentially expressed protein participated in many life processes such as acceptance and transmission of stress signals, promotion of substance and energy metabolism, regulation of photosynthesis and respiration, and improved the ability of edible lily to resist external stress.

Exogenous ABA may promote COR gene expression by activating transcription factors that depend on ABA signaling pathway, and improve cold resistance of edible

http://www.aloki.hu ● ISSN 1589 1623 (Print) ● ISSN1785 0037 (Online)
DOI: http://dx.doi.org/10.15666/aeer/1802_26872701

lily. The results show that the effects of exogenous ABA on cold resistance genes in winter Edible Lily are inconsistent in alpine environment. The effect of exogenous ABA on cold resistance gene expression of edible lily may be enhanced by activating transcription factors that depend on ABA signaling pathway. The noise was more obvious in Edible Lily No. 1 than in Edible Lily No. 2. However, exogenous ABA also has some effects on cold-resistant genes in signal pathways independent of ABA, and can promote the expression of these genes to a certain extent. It can be seen that the effect of exogenous ABA on cold resistance gene expression of Edible Lily in high-cold environment is a complex process, and more mechanisms need to be further explored.

Acknowledgement. This work was supported by grants from the Key Research and Development Projects in China (No. 2016YFD0201005) and the Yang Ling College of Vocational Technology Natural Science Fund Project (No. A2017027).

REFERENCES

[1] Ahmed, B., Rizvi, A., Zaidi, A., Khana, M. S., Musarrat, J. (2019): Understanding the phyto-interaction of heavy metal oxide bulk and nanoparticles: evaluation of seed germination, growth, bioaccumulation, and metallothionein production. – RSC Advances 9(8): 4210-4225.

[2] An, D., Ma, Q., Wang, H., Yang, J., Zhou, W., Zhang, P. (2017): Cassava C-repeat binding factor 1 gene responds to low temperature and enhances cold tolerance when overexpressed in Arabidopsis and cassava. – Plant Molecular Biology 94(1): 109-124.

[3] Chen, X., Duan, X., Wang, S., Wu, W., Zhang, X. (2019): Virus-induced gene silencing (VIGS) for functional analysis of MYB80 gene involved in Solanum lycopersicum cold tolerance. – Protoplasma 256(2): 409-418.

[4] Donaldson, J., Madziva, M. T., Erlwanger, K. H. (2017): The effects of high-fat diets composed of different animal and vegetable fat sources on the health status and tissue lipid profiles of male, Japanese quail (Coturnix coturnix japonica). – Asian-Australasian Journal of Animal Sciences 30(5): 700-711.

[5] Jiang, R., Qi, L. D., Du, Y. Z., Li, Y. X. (2017): Thermotolerance and Heat-Shock Protein Gene Expression Patterns in Bemisia tabaci (Hemiptera: Aleyrodidae) Mediterranean in Relation to Developmental Stage. – Journal of Economic Entomology 110(5): 2190-2198.

[6] Li, R. Q., Yu, A., Bai, B., Xu, R., Ding, W. J. (2016): Potential Health and Ecological Risks of Accumulation of Cadmium, Lead and Mercury in Soil-Edible Lily Systems. – Food Science 12(6): 52-60.

[7] Li, L., Wang, F., Yan, P., Jing, W., Zhang, C., Kudla, J., Zhang, W. (2017): A phosphoinositide-specific phospholipase C pathway elicits stress-induced Ca2+ signals and confers salt tolerance to rice. – New Phytologist 214(3): 1172-1187.

[8] Li, Y., Song, Y., Xu, B., Xie, J., Zhang, D., Cooke, J. (2017): Poplar CBF1 functions specifically in an integrated cold regulatory network. – Tree Physiology 37(1): 98-115.

[9] Liu, F., Bai, S. E., Zhang, X. Z. (2017): Design and research of embedded wind power generation monitoring system. – Chinese Journal of Power Sources 41(5): 798-800.

[10] Liu, T., Meng, Q., Han, J. N. (2017): Interference Signal Separation of Computer Communication System Based on Neural Network. – Journal of Jilin University (Science Edition) 55(6): 1545-1551.

[11] Long, T. L., Yi, Y. J. (2014): Progress of the lowering blood lipid effect of medicinal and edible medicine. – Journal of Food Safety & Quality 41(16): 934-941.

http://www.aloki.hu ● ISSN 1589 1623 (Print) ● ISSN1785 0037 (Online)
DOI: http://dx.doi.org/10.15666/aeer/1802_26872701

[12] Lu, K. H., Weng, C. Y., Chen, W. C., Lee, Y. S. (2017): Ginseng essence, a medicinal and edible herbal formulation, ameliorates carbon tetrachloride-induced oxidative stress and liver injury in rats. – Journal of Ginseng Research 41(3): 316-325.
[13] Shang, Q., Yang, G., Wang, Y., Wu, X., Zhao, X., Hao, H., Li, Y., Xie, Z., Zhang, Y., Wang, R. (2016): Illumina-based analysis of the rhizosphere microbial communities associated with healthy and wilted Lanzhou lily (Lilium davidiivar.unicolor) plants grown in the field. – World Journal of Microbiology and Biotechnology 32(6): 95.
[14] Singh, H., Lily, M. K., Dangwal, K. (2015): Evaluation and comparison of polyphenols and bioactivities of wild edible fruits of North-West Himalaya, India. – Asian Pacific Journal of Tropical Disease 5(11): 888-893.
[15] Templ, B., Templ, M., Filzmoser, P., Lehoczky, A., Bakšienė, E., Fleck, S., Gregow, H., Hodzic, S., Kalvane, G., Kubin, E., Palm, V., Romanovskaja, D., Vucetic, V., Žust, A., Czúcz, B., NS-Pheno Team (2017): Phenological patterns of flowering across biogeographical regions of Europe. – International Journal of Biometeorology 61(7): 1347-1358.
[16] Wang, J. M., Ma, S. L., Li, W. Q., Wang, Q., Cao, H. Y., Gu, J. H., Lu, Y. M. (2016): Genetic variability and diversity of the main resources of lily assessed via phenotypic characters, pollen morphology, and ISSR markers. – Genetics and Molecular Research 15(2).
[17] Wu, Z., Liang, J., Wang, C., Zhao, X., Zhong, X., Cao, X., Li, G., He, J., Yi, M. (2018): Overexpression of lilyHsfA3s in Arabidopsis confers increased thermotolerance and salt sensitivity via alterations in proline catabolism. – Journal of Experimental Botany 69(8): 2005-2021.
[18] Xu, P. L., Zhu, Z. Q. (2017): Carrier signal injection-based sensorless control for permanent magnet synchronous machine drives with tolerance of signal processing delays. – IET Electric Power Applications 11(6): 1140-1149.
[19] Yu, H. Q., Han, N., Zhang, Y. Y., Tao, Y., Chen, L., Liu, Y. P., Zhou, S. F., Fu, F. L., Li, W. C. (2017): Cloning and characterization of vacuolar H + -pyrophosphatase gene (AnVP1) from Ammopiptanthus nanus and its heterologous expression enhances osmotic tolerance in yeast and Arabidopsis thaliana. – Plant Growth Regulation 81(3): 385-397.
[20] Yu, S., Huang, A., Jia, L., Gao, L., Feng, Y., Pemberton, E., Chen, C. (2018): OsNAC45 plays complex roles by mediating POD activity and the expression of development-related genes under various abiotic stresses in rice root. – Plant Growth Regulation 84(3): 519-531.

http://www.aloki.hu ● ISSN 1589 1623 (Print) ● ISSN1785 0037 (Online)
DOI: http://dx.doi.org/10.15666/aeer/1802_26872701

MOLECULAR MARKER ASSISTED HEAVY METAL RESISTANCE ANALYSIS OF PHYSIOLOGICAL GENES IN NATURAL PLANTS – TAKING RICE AS AN EXAMPLE

GAO, J.

Department of Life Sciences, Lvliang University, Lvliang 033001, China
(e-mail: gaojiaojiao2019@163.com)

(Received 3rd Sep 2019; accepted 12th Feb 2020)

Abstract. At present, heavy metal pollution seriously threatens the survival and development of natural plants, so it is necessary to use a molecular marker-assisted method to select natural plant physiological genes, select good breeding, and enhance the heavy metal resistance of natural plants. Heavy metal resistance of natural plants was studied, which heavy metal resistance of rice mainly included blast resistance and stripe blight resistance. To study rice blast resistance, improved SDS extraction method was used to extract rice DNA. The obtained DNA solution could be directly used as a template to start PCR amplification. In the study of resistance to stripe blight, the varieties of stripe blight and rice were used as resistance donor parents and resistance receptor parents. The resistance of hybrid plants was identified through hybridization and backcross marker-assisted selection. The results showed that molecular marker-assisted method could identify rice germplasm resources containing Pib gene. Among 18 BC2F3 lines carrying homozygous resistance genes, the disease grade index was 16.0 at the highest level and 0.45 at the lowest level. The resistance level to stripe blight belonged to resistant. The re-harvested Indica rice had better resistance to stripe blight, which could significantly enhance its heavy metal resistance.
Keywords: *molecular markers, natural plants, physiological genes, heavy metals, rice, stripe blight resistance*

Introduction

Heavy metal pollution is in the focus of attention for the world nowadays, mostly concerning the harmfulness of heavy metals to natural plants. Natural plants are the energy, temperature, humidity, light and fresh water obtained by photosynthesis from the sun are the basic needs of plant survival, rice is one of the natural plants. On the one hand, heavy metals are permanently released into the environment and can accumulate slowly in natural plants (Gherib et al., 2017); on the other hand, most heavy metals are not essential elements of natural plants. When the content of heavy metals reaches the tolerance level of a natural plant, excessive heavy metals can destroy the structural components of natural plants, thereby threatening the survival of natural plants. As people pay more attention to the hazards of heavy metals, the remediation technology of heavy metal contaminated soil emerges. Traditional remediation methods for heavy metals have their own defects (Huang et al., 2017). Measures such as guest soil, covering soil and passivator cost a lot but have little effect. At the same time, new pollutants may be introduced to cause more serious harm. Bioremediation technology has become the mainstream remediation technology (Wang et al., 2018a) because of its advantages of wide materials, low price, strong adsorption capacity and easy management. Nowadays, bioremediation technology is taking Rhizobium of leguminous plants as a new research trend to assist natural plants to resist heavy metal stress. Although the new repair methods can overcome most of the drawbacks of traditional repair methods, the research is still in its infancy. In terms of provenance, the

http://www.aloki.hu ● ISSN 1589 1623 (Print) ● ISSN 1785 0037 (Online)
DOI: http://dx.doi.org/10.15666/aeer/1802_27032718

Rhizobium of leguminous plants in natural growth state has little or no ability to assist natural plants in resisting heavy metal uptake, while the practical application effect of leguminous plants with high resistance obtained by gene technology is not clear (Kusch et al., 2016). Whether the community of rhizobia and natural plants has the ability to activate heavy metals in the surrounding environment is not clear; besides the heavy metals absorbed by natural plants, many new problems such as whether the residual heavy metals are harmful to human beings and the environment have not been solved (Liang et al., 2017). In addition, as a new land remediation method, resistant natural plants (organisms with high accumulation and low absorption) have attracted wide attention since 1950s. With the further study at molecular level, it has been found that not only the external characteristics of plants will change under the stress of heavy metals, but also the resistance genes in natural plants response to heavy metal stress by expressing transcriptional proteins. The mechanisms and models of these natural plants have been gradually explored and applied in variety breeding, food safety and land remediation (Shah et al., 2017). In a word, in recent years, the research on heavy metal-resistant natural plants mainly focuses on the screening and marking of resistance genes, analyzing the degree of heavy metal resistance in natural plants, screening out natural plants with strong heavy metal resistance, improving the heavy metal resistance of natural plants and improving the growth status of natural plants (Wang et al., 2018b).

Natural plant resistance refers to the ability of natural plants to adapt to adversity. The acquisition of resistant materials plays a key role in elucidating the whole biological resistance research (Wang et al., 2017). It has been found that natural plants can be identified as stress-resistant by observing their living conditions under stress. They have a wide range of sources, stable heredity, and can adapt to different environments through sexual and asexual reproduction. Therefore, they have become the most common experimental material in scientific research (Wang et al., 2016), which is currently used for research. The main heavy metal-tolerant plants are Rhodiola, centipede, ryegrass and cash crops such as rice and rye. As far as the tolerance of natural plants to heavy metals is concerned, natural plants of different families and genera show different abilities. Generally speaking, woody natural plants have the best tolerance to heavy metal stress (Danilova et al., 2016). Mench et al. studied the responses of common tobacco, yellow tobacco and maize to cadmium stress. The results showed that different natural plants had different tolerance to cadmium due to different physiological metabolism, and the resistance of tobacco was stronger than that of maize. Common tobacco has stronger cadmium resistance than yellow tobacco. Mench et al. also showed that there was a positive correlation between the cadmium stress intensity and heavy metal activation ability of these two tobacco species. Therefore, the heavy metal resistance of natural plants could be analyzed by observing the tolerance of different natural plants and varieties under different concentration gradients of heavy metal stress. However, this method takes a long time and can be used to analyze the heavy metal resistance of natural plants. The observation process is susceptible to the influence of external environment (Beohar et al., 2018). In view of the fact that rice blast strains cannot be shared among the major rice-producing regions in the world, it is difficult to identify the alleles of disease-resistant genes in different rice germplasm resources. With the emergence and rapid development of DNA molecular marker technology, marker-assisted selection technology has become an effective way to select disease-resistant genes correctly. However, the recombination rate between disease-resistant genes and molecular markers varies greatly in different populations, and the

http://www.aloki.hu ● ISSN 1589 1623 (Print) ● ISSN 1785 0037 (Online)
DOI: http://dx.doi.org/10.15666/aeer/1802_27032718

population constructed with molecular markers is often not a breeding material, which has certain limitations in practical application. In addition, because these molecular markers themselves are aimed only at genes, there may be unconnected situations in a large number of population breeding, leading to the failure of disease-resistant gene selection (Jimenez et al., 2016). Therefore, the best way is to use the disease-resistant gene sequence itself to establish the corresponding molecular markers, quickly and accurately analyze the genetic composition of individuals at the molecular level, so as to realize the direct selection of genotypes, molecular breeding, and obtain natural plants with strong resistance to heavy metals.

Heavy metal resistance of physiological genes of natural plants includes many kinds, and different kinds of heavy metal resistance of natural plants are different. Molecular marker assistant method can significantly improve the accuracy of predicting disease resistance and heavy metal toxicity, salt damage, drought resistance, dry resistance and heat resistance of natural plants. Taking rice as an example, the heavy metal resistance of rice was studied.

Materials and methods

Analysis of rice blast resistance

Test material

Choosing China as the experimental country, the tested rice materials were 122 parents or breeding intermediate materials of hybrid rice such as IRBLb-B, F-145-2 and 93-11, Shuhui 363, Shuhui 527 and D62B. IRBLb-B and F-145-2 were provided by Dr. Lei Cailin, Institute of Crop Science, Chinese Academy of Agricultural Sciences; 93-11 was an indica rice cultivar bred by Jiangsu Lixia River Institute of Agricultural Sciences. IRBLb-B and F-145-2 are monoclonal resistance Pib genetic materials bred by recurrent parents in Heigu, Lijiang New Regiment, while 93-11 does not contain Pib gene. Therefore, IRBLb-B and F-145-2 were used as resistant parents and 93-11 as susceptible parents.

The remaining 120 materials are parents or breeding intermediate materials of hybrid rice developed by Rice Research Institute of Sichuan Agricultural University in recent years. In March 2017, six hybrid combinations were prepared in Yangzhou with IRBLb-B and F-145-2 as female parents, Shuhui 363, Shuhui 527 and D62B as male parents. F1 was planted in Sichuan in the summer of the same year. In September 2017, 100 seeds of each F2 combination were selected for disease resistance test at the Rice Research Institute experimental site of Yangzhou Agricultural University.

Molecular marker-assisted selection

Firstly, Molecular marker-assisted selection (MAS) was used to link resistance genes, and DNA was extracted from resistance genes. The improved SDS method was used to extract DNA. Specific methods are as follows:

a) Take about the leaves of the tender green rice, cut them into grain-sized fragments and put them into a 2 ml centrifugal tube. Sprinkle liquid nitrogen into the tube and quickly smash it with plastic chopsticks (Hu et al., 2016).
b) 400 ml SDS buffer (1 M Tris-Hcl PH8.0, 0.5 M EDTA PH8.0, Nacl, SDS) was added to the tube, and the tube was heated for 30 min at 65 (?) C, during which

http://www.aloki.hu ● ISSN 1589 1623 (Print) ● ISSN 1785 0037 (Online)
DOI: http://dx.doi.org/10.15666/aeer/1802_27032718

three to four oscillations occurred, and the mixture of SDS in the tube blade was dark green.

c) Add 100 μl KAc (glacial acetic acid adjusts PH to 8.0 with NaOH) to the tube, mix evenly and insert the centrifugal tube into the ice cube, and rest for 30 min.
d) 600 μl chloroform isoamyl alcohol (24:1) was added to the tube. After homogeneous mixing, it was placed in the shaker and continued to oscillate for 30 min.
e) 8000 rpm was centrifuged for 10 min. The supernatant (about 400 l) was removed and put into 1.5 ml centrifugal tube.
f) Add 600 μl absolute ethanol which is pre-cooled at -20 ℃ and put it in the refrigerator at -20 ℃ for overnight.
g) 1200 rpm centrifugation for 15 min, discarding supernatant, visible at the bottom of the tube gray-white precipitation adherence.
h) Add 400 μl TE buffer (1M Tris-Hcl PH8.0, 0.5M EDTA), dissolve precipitation by oscillation, and keep the refrigerator in reserve at -20 ℃. The obtained DNA solution can be directly used as a template for PCR amplification.

PCR amplification

Polymerase chain reaction (PCR) amplification primers, using the Pib dominant molecular marker reported by Concetta, can specifically amplify the corresponding fragment sequence of the disease-resistant allele Pib. At the same time, using the sequenced indica rice variety 93-11 and the sequence corresponding to the Pib gene as the susceptible sequence, the polymorphism design of the disease-resistant gene Pib on the DNA sequence can specifically amplify (Salgaonkar et al., 2016). The name, sequence, location and expected size of the primers used for PCR amplification are shown in *Table 1*.

Table 1. *Primer names and sequences for PCR reactions*

Primer name	**PibdomF**	**PibdomR**	**Lys145F**	**Lys145R**
Order Sequence (5'-3')*	GAACAATGCCCAAA CTTGAGA	GGGACCACATGTCAGT GAGC	TGGGTGCCTCGGTAGTC AGT	GGGAAGCGGATCCTA GGTCT
Location	8669-8720*	9016-8996**	37285710-37285729***	37286477-37286458***
Expect size (bp)	365		803	

* represents the polymorphism of the disease-resistant gene Pib is shown below. ** represents the location of specific primer sequence in the Pib resistance gene. See GenBank accession No. AB013448 for details. *** represents the location of specific primer sequence in indica rice 93-11 corresponding to Pib gene

The primer sequence was synthesized by Yingjun Biotechnology Co., Ltd. The PCR reaction system was 25 μl, containing 2.5 μl 10×Buffer, 2.0 μl dNTP, 3.0 μl 4 $mol \cdot L^{-1}$ positive and reverse primers, 0.2 μl 4 $U \cdot \mu l^{-1}$ Taq enzyme, 3.0 μl 20 $ng \cdot \mu l^{-1}$ template DNA and 14.3 μl pure water. The procedure of PCR was as follows: pre-denaturation at 94 for 5 min, denaturation at 94 for 45 s, annealing at 55 for 45 s, extension at 72 for 1.5 min, and extension at 72 for 10 min. The amplified products were electrophoretic in 3% agarose gel, stained with ethidium bromide and photographed under ultraviolet light. When 122 parents or materials of hybrid rice and 600 F2 plants tested in early stage were detected by PCR, each sample was repeated three times.

http://www.aloki.hu ● ISSN 1589 1623 (Print) ● ISSN 1785 0037 (Online)
DOI: http://dx.doi.org/10.15666/aeer/1802_27032718

Gel preparation and electrophoresis

The PCR products were electrophoretic by 8% polyacrylamide amide non gel. The basic procedures were as follows:

1. Clean the glass plate with deionized water and wipe it with degreased cotton dipped in absolute ethanol.
2. Insert the glass plate into the plastic pad as required, and then seal the gap in the lower part of the school with 1% agar.
3. After agar solidification, about 35 ml of collocated propylene-clozamine solution, 25 μl TEMED, 150 μl AP, were injected into the glass panels, and the comb was inserted.
4. The comb was pulled out and poured into the 1×TBE electrophoretic buffer after 30 min of standing for gel coagulation. Clear the bubbles in the sample hole (Dong et al., 2019).
5. 2 μl 6×Loading Buffer was added to the amplified products of each tube of PCR. After mixing, 1.5 l sample was injected into the dot hole with a micro-sampler.
6. Connect the electrophoresis apparatus with the electrophoresis cell, adjust the voltage to 250 V, and electrophoresis for about 2 h.
7. After electrophoresis, remove the glass plate from the electrophoresis tank and remove the gel carefully.
8. Rinse the gel two times in the steamed water and transfer it to 0.1% $AgNO_3$ solution, then put it on the shaking table and shake 12 min to dye it.
9. Remove the gel and transfer it to the distilled water for two times, then pour into the chromogenic solution for color rendering.
10. Take out the gel and wrap it with fresh-keeping film and scan the results.

Preparation of bacterial solution and identification of resistance to rice scar

The strains resistant to Pib gene were 05-7 (ZA13), 05-12 (ZB13), 05-3 (ZB15), 05-30 (ZC15), 05-16 (ZD7), 05-23 (ZE3), 05-2 (ZF1), 05-11 (ZG1) and so on. 122 parents of hybrid rice and 600 F2 plants tested in early stage were identified by single inoculation. The rice genotype strains were 05-12 (ZB13) and 05-30 (ZC15). The tested strains were provided by Plant Protection Laboratory of Rice Research Institute of Sichuan Agricultural University. The strain culture and the preparation of bacterial solution were carried out according to the introduced methods. Rice blast resistance (Peng et al., 2017) was determined according to the international classification criteria for rice blast resistance evaluation. The evaluation classification criteria are shown in *Table 2*.

The resistance to rice blast was analyzed according to *Table 2*. The selected samples were identified for natural induced disease resistance in the field. The infected plants were found in the field, and the disease spot length was measured to identify the level of resistance to rice blast.

Resistance to rice stripe blight

Test material

The selected indica rice varieties were selected in the "Materials and methods" section.

http://www.aloki.hu ● ISSN 1589 1623 (Print) ● ISSN 1785 0037 (Online)
DOI: http://dx.doi.org/10.15666/aeer/1802_27032718

Table 2. *Evaluation and classification criteria*

Resistance level	Leaf plague standard	Standard of panicle neck plague
Resist (R)	0 leaf is disease-free	0 Disease-free panicle
	1 The leaf blade has brown spots and is smaller in diameter than 0.5 mm	1 Ear blast rate less than 1%
	2 Leaf blade has oval brown spot, diameter between 0.5-1 mm	3 Panicle blast rate 1% ≤ 5%
Medium anti- (MR)	3 The blade has an elliptical lesion, the center is off-white, the edge is brown, and the diameter is between 1 mm and 2 mm	
	4 The fusiform spot is between 1-2 mm and limited to two veins, and the damage area is less than 2%	
Moderate (MS)	5 Typical disease spot, damage area 3% ≤ 10%	5 The ear blast rate was 6%and 25%.
	6 Typical disease spot, damage area 11% ≤ 25%	
Susceptible (S)	7 Typical disease spot, damage area 25% ≤ 50%	7 Panicle blast rate 25% ≤ 50%
High sensitivity (HS)	8 Typical lesions, 51% 75% of the area	9 Ear blast rate 51% ≤ 100%
	9 All leaves withered to death	

Marker-assisted selection and backcross breeding

In the main season of 2017, indica rice was crossed with Dular in Yangzhou, and backcross combinations were made in Sichuan in the same winter. BC_1F_1 was sown in Sichuan in 2017 and molecular marker-assisted selection was initiated to screen plants carrying disease-resistant genes for further backcross with indica rice. In order to speed up the breeding generation and ensure the normal germination of hybrid seeds, the hybrid seeds were dried immediately after harvest, disinfected and germinated on the culture medium. BC_2F_1 seedlings were added to Sichuan in early November 2017, and BC_2F_1 plants carrying disease resistance genes were screened by molecular markers to continue backcrossing and harvesting self-crossing seeds (Chen et al., 2017). BC_3F_1 and BC_2F_2 seeds were planted in Sichuan in January 2017 after the seeds were harvested and dried, and the second season was planted. BC3F1 contains BC3F1, BC2F2, BC2F3. The plants carrying disease resistance genes were selected from BC_3F_1 and the seeds of BC_3F_1 and BC_2F_2 were harvested. BC_4F_1, BC_3F_2, BC_2F_3 and indica rice were sown in Sichuan in 2018. The disease resistance was identified and the important traits were investigated. According to the resistance and comprehensive traits, the good and the bad were selected and eliminated. Considering that the cytoplasm and backcross thicknesses of Indica Rice need to be preserved in the backcross progenies, indica rice is the female parent for each cross and backcross.

DNA extraction and molecular marker analysis DNA

The extraction method of DNA is the same as that of the above 2.1.3 section extraction method. After DNA extraction, PCR is amplified by molecular marker assisted, then glued and electrophoretic, and observed and read under ultraviolet lamp and BIORAD gel imager (Song, 2017). The band type assignment of parents is 1, Dular band type assignment is 3, F1' band type assignment is 2 and default band assignment is 0.

http://www.aloki.hu ● ISSN 1589 1623 (Print) ● ISSN 1785 0037 (Online)
DOI: http://dx.doi.org/10.15666/aeer/1802_27032718

Evaluation of disease resistance

Natural insecticidal inoculation was used for identification. When a large number of rice planthoppers migrated to the seedlings, they were treated three times a day to make the seedlings uniformly poisoned. Before transplanting, the incidence of rice plants was investigated. In this study, two criteria for disease resistance identification were used: one was the incidence of disease, i.e. the ratio of the number of plants with disease to the total number of plants; the other was the disease grade index. According to Washio's criteria for resistance identification, the plants were divided into six grades, namely *A*, *B*, *Bt*, *Cr*, *C* and *D*. The disease grade of each inoculated plant was investigated (Sun et al., 2018), and then according to the criteria, the disease grade index was divided into six grades. The following formula calculates the disease grade index of each strain according to the disease grade.

$$B_j = \frac{(100 \times A + 80 \times B + 60 \times Bt + 40 \times Cr + 20 \times C + 5 \times D)}{Z_z} \quad \text{(Eq.1)}$$

In the formula, *Bj* represents disease grade index. *Zz* tests the total number of seedlings. *A*, *B*, *Bt*, *Cr*, *C* and *D* in the formula are calculated by substituting the number of plants with different symptoms. The resistance of inoculated seedlings can be divided into resistance (R, 0-29), moderate resistance (MR, 30-39), moderate susceptibility (S, 40-69) and high susceptibility (HS, 70-100) according to disease grade index.

Character determination

BC_4F_1, BC_3F_2 and BC_2F_3 were planted in Sichuan in the season of 2018. The parents of indica rice were planted on May 10 and transplanted on June 10. BC_4F_1 plants were planted to the full, BC_3F_2 plants were planted to 50, BC_2F_3 plants were planted to 100, with a row spacing of 16.7 cm × 26.7 cm. After heading in late August, the heading date was recorded and harvested in time after maturity. The plant height, flag leaf length, leaf angle of flag leaf (angle between base of flag leaf and main stem), panicle length of main stem, total grain number of main stem panicle, panicle curvature (angle between neck node and apex of panicle and vertical axis of panicle), 1000 of homozygous disease-resistant plants detected in BC_4F_1 population and BC_3F_2 population were investigated at harvest time. Seven agronomic traits with high heritability such as grain weight (Li et al., 2017).

BC_2F_3 strains with homozygous resistance genes were observed and evaluated in detail from heading to maturity, and excellent strains were selected. After maturation, 20 BC_2F_3 strains were selected to investigate yield traits such as yield per plant, panicle number per plant, total grains per panicle, number of solid grains per panicle, seed setting rate and 1000-grain weight, and 5 of them were selected to investigate plant height, flag leaf length, flag leaf width, flag leaf angle, panicle-leaf difference (distance between spike tip of main stem and flag leaf tip), stem. The agronomic traits included basal diameter (stem diameter at 1 cm of the main stem of stripped leaf sheath), neck diameter (axis diameter at 1 cm above the neck node), ear length of the main stem, total grain number of the main stem ear, and ear curvature. The chalky grain rate and chalkiness of rice were measured by BC_2F_3 mature seeds. Starch viscosity spectrum was measured by 3-D RVA instrument produced by Newport Scientific Instrument Company, Australia.

http://www.aloki.hu ● ISSN 1589 1623 (Print) ● ISSN 1785 0037 (Online)
DOI: http://dx.doi.org/10.15666/aeer/1802_27032718

Results

Resistance analysis of rice blast

Anti-Pib gene spectrum

In order to verify the validity of molecular marker assisted resistance gene in this method, it is necessary to analyze whether Pib gene has any utilization value in disease resistance breeding. 16 near strains of IRBLb-B and F-145-2 were used to spray two near isogenic lines. The results of the analysis were shown in *Table 3,* using sham you 63, a common susceptible variety.

Table 3. *Analysis results*

Strain (race)	Rice material		
	IRBLb-B	F-145-2	Oil excellent63Shanyou63
05-7(A13)	R	R	S
56(A49)	R	R	S
04-25(A1)	S	R	S
04-15(A1)	S	R	S
04-1(A15)	R	R	S
05-12(B13)	R	R	S
05-3(B9)	S	S	S
04-27(B15)	S	R	S
04-10(B13)	R	R	S
05-29(B31)	R	S	S

R means disease resistance, S means disease susceptibility. Among the 10 tested strains, IRBLb-B and F-145-2 were resistant to 6 and 8 strains respectively, and the resistance frequencies were 60% and 80%, respectively. The difference of resistance frequencies between them was 20%. This indicated that Pib gene had good utilization value in disease resistance breeding, that is, the molecular marker of resistance genes in rice had strong validity

Pib molecular marker assisted selection of rice blast resistance breeding

In this paper, 600 F-2 strains derived from IRBLb-B and F-145-2 hybridization were amplified by using the molecular marker-assisted method. The amplification results are shown in *Table 4*.

From *Table 4,* 185 homozygous plants of Pib gene were screened out from 600 F2 plants. At the same time, 600 F2 plants were used as materials to investigate the relationship between Pib gene and disease resistance in the field. The results showed that all Pib homozygous and heterozygous plants were resistant to the disease, while all Pib-free plants were susceptible to the disease. The results showed that the existence of Pib gene was consistent with the field resistance and the Pib gene was dominant.

Application of Pib molecular markers in germplasm resources identification

As we all know, germplasm resources (including wild and domesticated species) play an important role in both production practice and scientific research. In order to verify the consistency of Pib gene molecular markers with blast resistance, 122 hybrid rice parents or materials were tested by single race inoculation with blast fungus strains

http://www.aloki.hu ● ISSN 1589 1623 (Print) ● ISSN 1785 0037 (Online)
DOI: http://dx.doi.org/10.15666/aeer/1802_27032718

05-12 (ZB13) and 05-30 (ZC15). The results of Pib molecular identification are shown in *Table 5*. At the same time, the parent material is the basis of cultivating new crop varieties. Two pairs of dominant molecular markers Pibdom and Lys 145 were used to detect 122 parents or materials of Hybrid Rice by PCR. The results of PCR amplification were shown in *Figure 1*.

Table 4. *Molecular test of Pib gene and its resistance to rice blast in the field*

Hybridized combination	Disease resistance response	Number of pure plants with Pib gene	Number of hybrid plants with Pib gene	Number of plants without Pib gene
IRBLb-B/D62B	R	28	46	0
IRBLb-B/D62B	S	0	0	26
IRBLb-B/Shuhui363	R	35	44	0
IRBLb-B/shuhui363	S	0	0	19
IRBLb-B/Shuhui527	R	36	40	0
IRBLb-B/shuhui527	S	0	0	24
F-145-2/D62B	R	27	45	0
F-145-2/D62B	S	0	0	28
F-145-2/Shuhui363	R	32	38	0
F-145-2/shuhui363	S	0	0	29
F-145-2/Shuhui527	R	27	41	0
F-145-2/shuhui527	S	0	0	32
Total		185	254	158

In the field resistance identification, 3 plants did not get results because of death

Table 5 shows that only 22 of 157 rice varieties contain the blast resistance gene Pib, while most varieties do not. The results showed that the molecular marker-assisted method could quickly and accurately identify rice germplasm resources containing Pib gene, and provide effective methods and scientific basis for selection of resistant parents in blast resistance breeding. At the same time, it can be seen from *Figure 1* that the dominant molecular marker Pidom can specifically amplify a fragment about 350 bp in size, and the dominant molecular marker Lys145 can specifically amplify a fragment about 800 bp in size. In *Figure 1,* it can be seen that only 7 parents or materials of 122 hybrid rice contain blast resistance. Pib gene was not found in other parents or materials of hybrid rice.

Table 5. *Molecular identification of Pib gene in rice varieties from different countries*

Whether the disease resistance gene Pib is present or not	Number of rice varieties	Representative rice varieties
Pib	22	Special Qing, Tetep, Kaly etal
No Pib	135	Short for Zhejiang Province 733, Japan clear, Wells etal

The existence of Pib gene is based on the amplification results of Pib dominant marker YL155/YL87 and susceptible allele Pib dominant marker YL155/YL87

http://www.aloki.hu ● ISSN 1589 1623 (Print) ● ISSN 1785 0037 (Online)
DOI: http://dx.doi.org/10.15666/aeer/1802_27032718

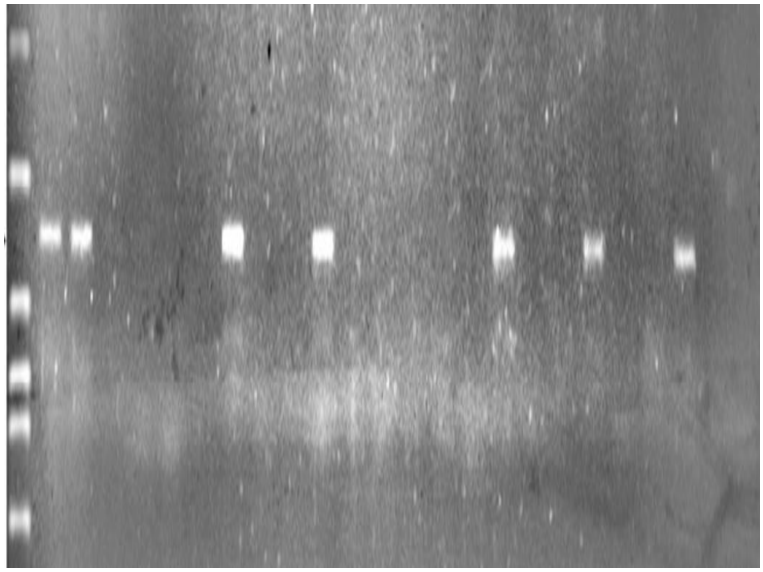

(a)

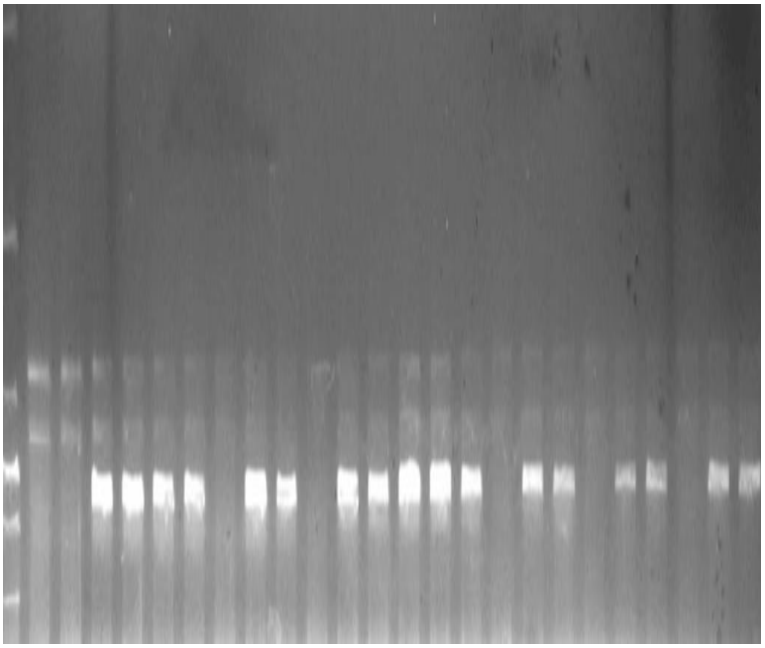

(b)

Figure 1. *Results of PCR amplification of resistance genes in different rice varieties. (a) PCR amplification products of dominant molecular marker pibdom for disease resistance isogenes. (b) Dominant molecular marker Lys145PCR amplification products of susceptible genes*

Resistance test of rice stripe blight

Molecular marker assisted effect

In order to verify the effect of molecular marker-assisted resistance to rice stripe blight, a practical test and analysis are needed. The results are shown in *Table 6* and *Figure 2*.

From *Table 6,* it can be seen that this method can better label the gene of rice stripe blight, and can accurately reflect the positive and reverse sequence of the gene and the

http://www.aloki.hu ● ISSN 1589 1623 (Print) ● ISSN 1785 0037 (Online)
DOI: http://dx.doi.org/10.15666/aeer/1802_27032718

location of the clone. At the same time, from *Figure 2,* it can be seen that most of the amplification results of BC_3F_1 are the same as those of all the selected individuals, which indicates that other rice bodies have the same amplification results. It also contains the stripe blight gene.

Table 6. *Analysis of marker results*

Tab	Forward sequence	Reverse sequence	Where the clone is located
STS11-19	ACGGTCGCTAGTATGTCCTG	CCTCGATAATGCACCTAAAT	AC135568
STS11-31	GGGCTTTCAACTCGTACTCTG	ATGAACTGCGGGTCCAATAA	AC136009
STS11-43	TAAGAAGGGCGAACAAAG	AACCACCGCTACCAAGAC	AC1332481
STS11-71	GGGTCCTGCCGAGATTTA	CCATCGTTGCCAGGTTAG	AC124151

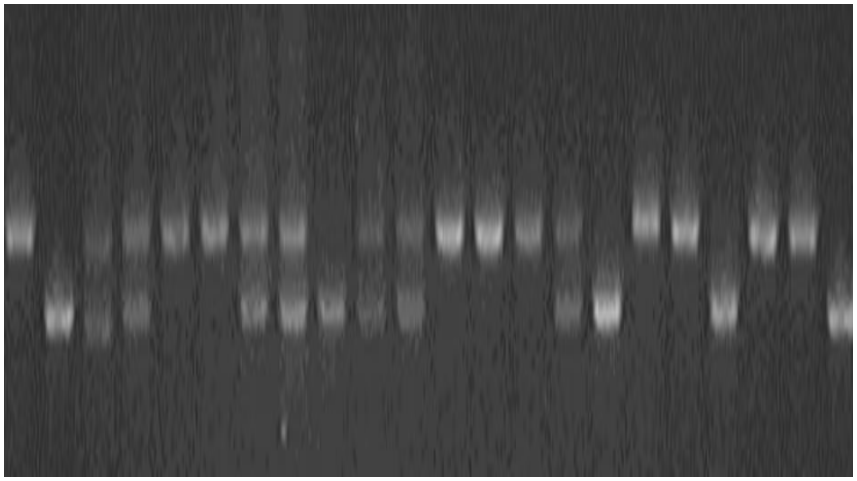

Figure 2. *Amplification results*

Molecular marker-assisted selection of backcross transfer stripe blight resistance genes

Marker-assisted selection (MAS) breeding was carried out according to the technical route. The acquisition of each backcross generation population and individual plant carrying disease-resistant genes was shown in *Table 7*.

Table 7. *Detection of disease resistance per plant*

For generations	Plant coefficient	Number of plants detected	Number of plants carrying resistance genes	B/A%
BC_1F_1	1	13	5	38.46
BC_2F_1	3	9	5	55.56
BC_3F_1	5	331	51	15.41
BC_4F_1	52	1297	407	31.38
BC_2F_2	4	139	17	12.23
BC_3F_2	51	1066	218	20.45

The BC_nF_1 population was detected as a hybrid plant with disease resistance gene, and the BC_nF_2 population was detected as a homozygous plant with disease resistance gene

http://www.aloki.hu ● ISSN 1589 1623 (Print) ● ISSN 1785 0037 (Online)
DOI: http://dx.doi.org/10.15666/aeer/1802_27032718

From *Table 7,* it can be seen that with the increase of backcross generations, backcross and inbred population gradually expanded. A total of 407 plants containing heterozygous resistance genes were obtained by BC_4F_1 and 218 plants containing homozygous resistance genes were obtained by BC_3F_2. It is hopeful to select new lines with good disease resistance from these offspring. After marking resistance genes by molecular marker-assisted method in this paper, the effect of selecting rice breeding is better.

Identification of resistance to stripe blight

The resistance of BC_2F_3 strains with homozygous resistance genes and their parents to natural insects was identified. The incidence and disease grade index of rice were investigated after the disease condition was stable. The results were shown in *Table 8*.

Table 8. *Results of the survey*

Strain number	Disease grade index	Plant incidence rate	Resistance level
E1	5.20	11	R
E2	0.45	2	R
E3	3.80	8	R
E4	0.61	2	R
E5	3.00	4	R
E6	16.00	31	R
E7	10.20	14	R
E8	8.80	12	R
E9	3.80	5	R
E10	10.00	14	R
E11	5.85	8	R
E12	3.61	6	R
E13	8.00	9	R
E14	6.80	9	R
E15	8.80	12	R
E16	10.90	16	R
E17	4.60	6	R
E18	10.60	15	R
CK	85.00	85	HS

From *Table 8,* it can be seen that the incidence rate of indica rice is 85%, the disease grade index is 85.0, and the resistance level belongs to high susceptibility. Among 18 BC_2F_3 lines carrying homozygous resistance genes, the highest disease grade index is only 16.0, and the lowest is 0.45. The resistance level to stripe blight belongs to resistance level, which indicates that the resistance level to stripe blight is assisted by molecular markers in this paper. Later, the re-harvested indica rice had better resistance to stripe blight.

Discussion

With the development of industrial and agricultural production, the discharge of three wastes, the exploitation and utilization of minerals, sewage irrigation and the use of pesticides, herbicides and fertilizers have seriously polluted the soil, water quality

http://www.aloki.hu ● ISSN 1589 1623 (Print) ● ISSN 1785 0037 (Online)
DOI: http://dx.doi.org/10.15666/aeer/1802_27032718

and atmosphere, resulting in environmental deterioration and causing immeasurable harm to society, economy and human beings. Excess heavy metals can hardly be eliminated once they enter the environment, especially in the soil. In addition, there is a trend of organic in the organism, so heavy metal pollution has a greater hazard. Through actual investigation and analysis, it is found that many heavy metals are essential trace elements for natural plants, and play a very important role in the growth and development of natural plants. However, when the amount of heavy metals in the environment exceeds the even-critical point, it will have a certain toxic effect on plants. In light of this, the lower processes in plants will be disordered, growth and development will be inhibited, and the heavy metals will change the genes in plants, leading to a variety of diseases in plants and eventually leading to plant death. Taking rice as an example, the main heavy metal resistance in rice was blast resistance and stripe blight resistance. Therefore, molecular marker-assisted method should be used to label rice blast resistance and stripe blight resistance, so as to shorten breeding years, improve the selection efficiency, enhance the heavy metal resistance of natural plants, and promote the growth and development of natural plants.

The significance of marker-assisted genes was found through the above studies. Molecular marker-assisted selection (MAS) is an important means of crop breeding, which uses molecular markers closely linked to target genes to select genotypes, and is not affected by environmental conditions. MAS can shorten breeding years and improve selection efficiency. However, the recombination rate between target traits and markers is different in different populations, and often the target traits are not breeding populations. Therefore, in practical application, the recombination rate of molecular markers and target traits for assisted selection must be low, so it is greatly limited. Therefore, the best way is to use the resistance gene itself to establish the corresponding molecular markers. Cloning of disease-resistant genes provides the possibility of establishing such markers. Wang established the molecular marker of Pi-ta gene based on the PI-ta gene which has been cloned. These markers were successfully applied to rice blast resistance assistant breeding. This kind of marker is defined as functional gene-assisted selection. The molecular marker of Pib gene mentioned in this paper is based on the disease-resistant gene Pib itself. It is of great significance to select target genes accurately by using these markers, to speed up the screening of resistant sources, to identify resistant genes and to breed rice varieties with high resistance (Li et al., 2017).

Studies on the marker-assisted gene of rice Pib show that previous scholars could only detect whether the material contained the disease-resistant gene Pib when using the dominant molecular marker Pibdom molecular detection, and could not directly determine the homozygous disease-resistant gene Pib material. If homozygous plants are to be selected, they need to be differentiated by several generations of field resistance identification, which is time-consuming and vulnerable to environmental impact without accurate results. In this paper, a set of molecular markers of resistance gene Pib itself was established by using dominant molecular markers Pibdom and Lys 145 for molecular detection. Combined with Yangzhou Jiadai, homozygous plants containing resistance gene Pib could be selected in F2 generation of hybrid isolation within one year, and the results were identical through field resistance identification. The results showed that the homozygous plants containing Pib gene could be selected quickly and accurately by using this set of molecular markers, which could simplify the complicated identification of resistance in the field. Most parents and combinations of

http://www.aloki.hu ● ISSN 1589 1623 (Print) ● ISSN 1785 0037 (Online)
DOI: http://dx.doi.org/10.15666/aeer/1802_27032718

hybrid rice currently used in production are not resistant to rice blast. Pib gene is a major disease resistance gene, which is a good choice in disease resistance breeding. By using these molecular markers, the blast resistance gene Pib can be quickly and accurately selected from numerous rice resources. The parents selected by this marker can transfer Pib resistance gene into rice varieties by conventional hybridization breeding method to produce resistance. At the same time, other resistance genes and Pib genes can be aggregated into the same fine varieties by MAS technology to produce durable resistance and to maintain the best varieties to the greatest extent. By using STS and SSR markers OSR20, OSR32, RM213, RM207 and RM262 closely linked to disease resistance genes, Chen Xuewei et al. tracked and screened rice blast resistance genes. Pi-d(t)1, Pib and Pi-ta2 were aggregated into G46B. In a relatively short time, relatively durable resistant strains of several physiological races were developed. Our laboratory is using this kind of molecular marker to polymerize Pib and Pi-ta multiple blast resistance genes, so as to further use Pib gene to breed persistent resistant varieties and lay the foundation for the ultimate goal of rice disease resistance breeding.

At the same time, the resistance of rice stripe blight was studied. It was found that this method could improve the resistance of rice stripe blight. It was found that Dular had strong resistance to stripe blight, but its agronomic morphology was not good. In practical application, because of rice hybridization, the characters of both donor and recipient are quite different, and they are severely separated in the lower generations of backcross, so it is difficult for the characters to return to the status of recipient parents. Fertility and character segregation still existed in the offspring of Indica Rice crossed with Dular to BC_4F_1 in this experiment. This needs to be solved by increasing the number of backcross to break the linkage between unfavorable trait genes and good trait genes, or by enlarging backcross population and increasing selection pressure. Indica rice is a semi-erect panicle variety. If the erect panicle-type indica rice varieties with resistance to stripe blight, such as Zhendao 88, Zhendao 99 and Xudao 3, were selected or bred in recent years as resistant donor parents, the speed of backcross improvement might be accelerated. Of course, this is only considered from improving the resistance of recipient parents by backcrossing, so that the comprehensive traits of offspring can be completely restored to the status of recipient parents. If we want to breed new varieties resistant to stripe blight, we need to increase the character differences between donor and recipient parents, which is more conducive to enriching variation and breeding varieties beyond recipient parents. If five BC_2F_3 lines of Indica Rice crossed with Dular were screened out in the experiment, their yield would be much higher than that of Indica rice. In conclusion, this method can significantly enhance the resistance to heavy metals and promote the healthy growth of rice after analyzing the marker-assisted heavy metal resistance of rice.

Conclusions

In order to enhance the heavy metal resistance of natural plants and improve the survival and development ability of natural plants, it is necessary to use molecular marker-assisted method to label heavy metal resistance genes of natural plants, select natural plants, accelerate the speed of crop improvement and improve the level of crop improvement. In this paper, rice was taken as an example for specific analysis. Through practical analysis, it was found that rice heavy metal resistance was mainly composed of blast resistance and stripe blight resistance. Molecular marker-assisted method was

http://www.aloki.hu ● ISSN 1589 1623 (Print) ● ISSN 1785 0037 (Online)
DOI: http://dx.doi.org/10.15666/aeer/1802_27032718

needed to label rice blast resistance genes and stripe blight resistance genes. Higher resistant rice was selected to improve rice quality. It was found that the molecular marker of rice resistance gene could retain the basic characteristics of rice and enhance the heavy metal resistance gene of rice, which plays a new role in production, and breeding new disease-resistant varieties. Due to the limited time, this paper only chooses rice as the research object, which has one-sidedness, so more natural plants need to be selected as the research object, which lays the foundation for the research of heavy metal resistance genes in natural plants.

Acknowledgements. This research was supported by Scientific and Technologial Innovation Programs of Higher Education Institutions in Shanxi (No. 2019L0943).

REFERENCES

[1] Beohar, A., Yadav, N., Vishvakarma, S. K. (2018): Analysis of trap-assisted tunnelling in asymmetrical underlap 3D-cylindrical GAA-TFET based on hetero-spacer engineering for improved device reliability. – Iet Micro & Nano Letters 12(12): 982-986.
[2] Chen, J. B., Chen, A. L. (2017): An improved active frequency offset island detection algorithm. – Journal of Power Supply 15(3): 140-147.
[3] Danilova, M. N., Kudryakova, N. V., Doroshenko, A. S. (2016): Molecular and physiological responses of Arabidopsis thaliana plants deficient in the genes responsible for ABA and cytokinin reception and metabolism to heat shock. – Russian Journal of Plant Physiology63(3): 308-318.
[4] Dong, M. A., Lu, H., Cai, S. (2019): Molecular mapping of stripe rust resistance gene YrH9017 in wheat - Psathyrostachys huashanica introgression line. – Journal of Integrative Agriculture 18(1): 112-118.
[5] Gherib, A., Djebaili, H., Bouchaala, L. (2017): Physiological and biochemical markers in the process of resistance and/or tolerance of heavy metals in the abandoned mining area of Sidi Kamber, Skikda, Algeria. – International Journal of Environmental Studies 74(2): 1-15.
[6] Hu, S. B., Zhou, Q., An, J. (2016): Cloning PIP genes in drought-tolerant vetiver grass and responses of transgenic VzPIP2;1 soybean plants to water stress. – Biologia Plantarum 60(4): 655-666.
[7] Huang, Z., Zhang, X., Jiang, S. (2017): Analysis of cold resistance and identification of SSR markers linked to cold resistance genes in Brassica rapa L. – Breeding Science 67(3): 213-220.
[8] Jimenez, F., Rojano-Delgado, A. M., Fernández, P. T. (2016): Physiological, biochemical and molecular characterization of an induced mutation conferring imidazolinone resistance in wheat. – Physiologia Plantarum 158(1): 2-10.
[9] Kusch, S., Pesch, L., Panstruga, R. (2016): Comprehensive phylogenetic analysis sheds light on the diversity and origin of the MLO family of integral membrane proteins. – Genome Biology & Evolution 8(3): 878-895.
[10] Li, J. Q., Sun, E. C., Wang, Z. (2017): Software definition wireless network - overview and prospect. – Journal of China Academy of Electronics and Information Technology 12(6): 570-578.
[11] Liang, B. Y., Peng, L. (2017): Molecular screening of blast resistance genes in rice germplasms resistant to Magnaporthe oryzae. – Rice Science 24(1): 41-47.
[12] Peng, P., Cheng, H. X., Chen, X. C. (2017): SOC estimation of lithium battery based on adaptive Kalman filter. – Chinese Journal of Power Sources 41(11): 35-38.

http://www.aloki.hu ● ISSN 1589 1623 (Print) ● ISSN 1785 0037 (Online)
DOI: http://dx.doi.org/10.15666/aeer/1802_27032718

[13] Salgaonkar, B. B., Das, D., Bragança, J. M. (2016): Resistance of extremely halophilic archaea to zinc and zinc oxide nanoparticles. – Applied Nanoscience 6(2): 251-258.
[14] Shah, L., Rehman, S., Ali, A. (2017): Genes responsible for powdery mildew resistance and improvement in wheat using molecular marker-assisted selection. – Journal of Plant Diseases & Protection125(7426): 1-14.
[15] Song, B. (2017): Research on construction technology and engineering management of water conservancy and hydropower project. – Automation & Instrumentation 63(10): 170-171.
[16] Sun, J. Y., Zhao, Y., Wang, S. G. (2018): Improvement of SIFT feature matching algorithm based on image gradient information enhancement. – Journal of Jilin University (Science Edition) 56(1): 82-88.
[17] Wang, P., Wang, L., Guo, J. (2016): Molecular mapping of a gene conferring resistance to Phytophthora capsici Leonian race 2 in pepper line PI201234 (Capsicum annuum L.). – Molecular Breeding36(6): 1-11.
[18] Wang, Y. P., Jia, J., Song, N. X. D. (2017): Dynamic simulation and experimental study of loader working device. – Computer Simulation 34(7): 184-187.
[19] Wang, Y. X., Hu, Y., Chen, B. H., Zhu, Y. F., Dawuda, M. M., Svetla, S. (2018a): Physiological mechanisms of resistance to cold stress associated with 10 elite apple rootstocks. – Journal of Integrative Agriculture 17(4), 857-866.
[20] Wang, Z. Z., Xie, J. Z., Li, G. (2018b): Molecular mapping of YrTZ2, a stripe rust resistance gene in wild emmer accession TZ-2 and its comparative analyses with Aegilops tauschii. – Journal of Integrative Agriculture 17(6): 1267-1275.

http://www.aloki.hu ● ISSN 1589 1623 (Print) ● ISSN 1785 0037 (Online)
DOI: http://dx.doi.org/10.15666/aeer/1802_27032718

THE SYNTHESIS MECHANISM OF CHLOROGENIC ACID IN LEAVES OF *EUCOMMIA ULMOIDES* OLIVER

MA, Y.[1] – LIU, Y.[1] – YANG, P.[1] – ZHANG, T.[1] – WU, Y.[2*]

[1]*School of Life Sciences, Henan University, Kaifeng 475004, China*

[2]*School of Pharmacy, Henan University, Kaifeng 475004, China*

**Corresponding author*
e-mail: wuyijun@henu.edu.cn

(Received 3rd Sep 2019; accepted 12th Feb 2020)

Abstract. This study revealed intraday variation of chlorogenic acid (CGA) and synthesis mechanism in leaves of *Eucommia ulmoides* Oliver by investigating relation of CGA content in leaves and the light intensity. CGA was quantified by High performance liquid chromatography (HPLC) with diode array detection (DAD). Illumination intensity was determined by portable photosynthesis system. It was shown that CGA content in leaves enhanced with the increase of light intensity and the highest point of CGA content in leaves got behind the highest point of illumination intensity. The fact that dark spots of blue formazan appeared in leaves which had been illuminated by sun light and were treated with nitroblue tetrazolium (NBT) showed that sunlight induces $O_2^{\cdot-}$ production in leaves. In addition, CGA possessed higher antioxidant activity and free radical scavenging activity in vitro experiment. DPPH radical scavenging activity was 2.43 ± 0.092 times of vitamin C equivalents (molar ratio), and ABTS radical cation scavenging activity was 3.61 ± 0.14 time of trolox equivalents (molar ratio), and reducing powers was 3.40 ± 0.11 times of vitamin C equivalents (molar ratio). In plant cells, free radicals produced by photo oxidation can damage the cells, and however, CGA can protect cells by eliminating free radicals. This may be the mechanism of the synthesis of chlorogenic acid in plants.
Keywords: *chlorogenic acid, Eucommia ulmoides Oliver, oxygen free radical*

Introduction

Eucommia ulmoides Oliver (*E. ulmoides*) is a traditional medicinal plant of China, and is also one of the main sources of chlorogenic acid (CGA). The pharmacological functions of CGA have been studied extensively. Potentially beneficial properties to human such as antimicrobial, antiinflammatory, antioxidant, anticancer, antiviral, hepatoprotective activities, antihypertension and protection against UV radiation have been attributed to CGA in vitro (Bhattacharyya et al., 2014; Chen et al., 2010; Shao et al., 2015). In plants, CGA performs anti-oxidant functions, and increased CGA accumulation is also associated with increased UV-protection (Cle et al., 2008; Doring and Petersen, 2014; Mudge et al., 2016). In this paper, the effect of illumination intensity on produce of CGA in leaves of *E. ulmoides* was investigated.

The quantitative determination methods of CGA have been reported, including gradient HPLC method, new flow injection chemiluminescent method, nano-LC-ESI mass spectrometry and electrochemical sensor (Hu et al., 2009; Santos et al., 2011; Wang et al., 2007; Zhang et al., 2007). However, a rapid, reliable and convenient determination of CGA is required. High performance liquid chromatography (HPLC) with diode array detection (DAD), more common and less costly, currently represents the most prevalent and reliable analytical method for the characterization of compounds, which need to be simultaneously acquired of chromatograms at any wavelength accompanied by the absorption spectrum of each eluted band and verified

http://www.aloki.hu ● ISSN 1589 1623 (Print) ● ISSN 1785 0037 (Online)
DOI: http://dx.doi.org/10.15666/aeer/1802_27192725

of separation quality with peak purity analysis (Huang et al., 2015; Luo et al., 2011; Sriseadka et al., 2012; Zeraik and Yariwake, 2010). Consequently, a normally manageable HPLC-DAD process was proposed in this research.

Materials and methods

Materials

Fresh leaves of *E. ulmoides* were obtained in campus of Henan University in summer and ground into dry powder, followed by sieving through 200 mesh screen to control the particle size.

Reagents

1,1-diphenyl-2-picrylhydrazyl (DPPH) and 2,2'-azinobis-(3-ethylbenzthiazoline- 6-sulphonate (ABTS) were purchased from Sigma Chemical Co. Trolox was purchased from MP Biomedicals. Nitroblue tetrazolium (NBT) and CGA were purchased from Bomei Biotechnology Co. Methanol was chromatographically reagent grade. All other chemicals used in this study were of analytical reagent grade.

Determination of sunlight intensity

Sunlight intensity and temperature of leaves were determined by portable photosynthetic apparatus (LI-6400XT, LICOR USA) in a clear day.

Determination of CGA in leaves

CGA in leaves was separated and quantified using a Waters HPLC (Milford, Massachusetts, USA) equipped with a Waters1525 pump, a Waters 2707 autosampler, and Waters diode array detector 2998. Breeze Software was used for the data processing. C18 column (Waters, 250 × 4.6 mm i.d., 5 μm particle size) was used to identify CGA. The chromatographic separation was operated with solvent A (MeOH) and B (water). The separated flavonoid peaks were identified by comparing the retention time of individual standards. The optimum procedure elution used in this study was as follows: a gradient of 70-30% A (0-15 min), 30-70% A (15-20 min). The samples were injected automatically (20.0 μL). The column and guard column were controled at 30 °C and a 1.0 mL min^{-1} flow rate was applied, and the CGA were scanned from 210 to 400 nm in HPLC.

O_2^- localization in situ

Fresh leaves from control (dark-treated leaves) and light-treated leaves were excised and immersed in a 0.1% solution of nitroblue tetrazolium (NBT) in 50 mM Kphosphate buffer (pH 6.4), containing 10 mM Na-azide, and were vacuum-infiltrated for 5-10 min and illuminated until appearance of dark spots, characteristic of blue formazan precipitates. Leaves were bleached by immersing in boiling ethanol (Romero-Puertas et al., 2004).

Analytical method of antioxidant capacity

The antioxidant capacity of CGA was determined by the Thermo Multiskan GO (Thermo Fisher Scientific Oy, Finland) (Shown as *Table 1*). The free radical scavenging

http://www.aloki.hu ● ISSN 1589 1623 (Print) ● ISSN 1785 0037 (Online)
DOI: http://dx.doi.org/10.15666/aeer/1802_27192725

activity was evaluated using the 2.2-diphenyl-1-picrylhydrazil (DPPH) assay and the absorbance values were measured at 518 nm and converted into the percent antioxidant activity (AA) using the following formula: AA% = [(absorbance of the control - absorbance of the sample) / absorbance of the control] × 100, The Vitamin C equivalents (VCEs) values of CGA were calculated from a linear regression of the AA of Vitamin C (VC, ascorbic acid); the scavenging activity against 2,2'-azino-bis(3-ethylbenzo thiazoline)-6-sulfonic acid (ABTS) radical cation was measured by the method that ABTS radical cation was produced directly by reacting ABTS solution with potassium persulfate and allowing the mixture to stand for 12-16 h in dark at the room temperature and prior to beginning the assay, and ABTS solution was diluted with methanol to an absorbance of at 734 nm, and then sample solution was added to ABTS solution and read at 734 nm after mixture and 30 min incubation at room temperature, and then The trolox equivalents (TEs) values of CGA were calculated from a linear regression of the AA of trolox equivalents; the determination of reducing powers of CGA was changed according to the method described by Ozsoy: 0.1 ml VC (20-100 μg/ml) and 0.1 ml CGA (20 μg/ml) were mixed with an equal volume of 0.2 M phosphate buffer (pH 6.6) and 1% potassium ferricyanide and then incubated at 50 °C for 20 min, and then 0.25 ml of 1% trichloroacetic acid was added to the mixture to stop the reaction, and then the mixture was centrifuged at 3000 g for 10 min, and the supernatant (0.25 ml) was mixed with 0.25 ml distilled water and 0.1% $FeCl_3$ (0.5 ml) and then the absorbance was measured at 700 nm, and the VCEs values of CGA were calculated from a linear regression of the AA of Vitamin C (Du et al., 2009; Dudonne et al., 2009; Ma et al., 2017; Ozsoy et al., 2008; Reis et al., 2015; Zengin et al., 2015).

Table 1. *Antioxidant capacity of chlorogenic acid (CGA)*

	VCEs (mass ratio)	**VCEs (molar ratio)**	**TEs (mass ratio)**	**TEs (molar ratio)**
DPPH radical scavenging activity	1.21±0.046	2.43±0.092	-	-
ABTS radical cation scavenging activity	-	-	2.55±0.099	3.61±0.14
Reducing powers	1.69±0.054	3.40±0.11	-	-

VCEs: vitamin C equivalents; TEs: trolox equivalents

Statistical analysis

Results were described as means ± standard deviation (SD) of three measurements. Statistical analysis was carried out using Student's t-test and significant difference was statistically considered at the level of $p < 0.05$.

Result and discussion

The CGA peaks were identified by their UV/DAD spectra due to their characteristic UV spectral pattern (Band I, λ max around 320 nm and Band II, λ max around 220 nm) in *Figure 1*. The absorption spectrum of each eluted band of leaves of *E. ulmoides* at any wavelength was consistent with that of CGA standard (*Fig. 1a* and *b*). Practically, UV/DAD scanning of herbal medicines without grinding makes CGA determination much more convenient.

http://www.aloki.hu ● ISSN 1589 1623 (Print) ● ISSN 1785 0037 (Online)
DOI: http://dx.doi.org/10.15666/aeer/1802_27192725

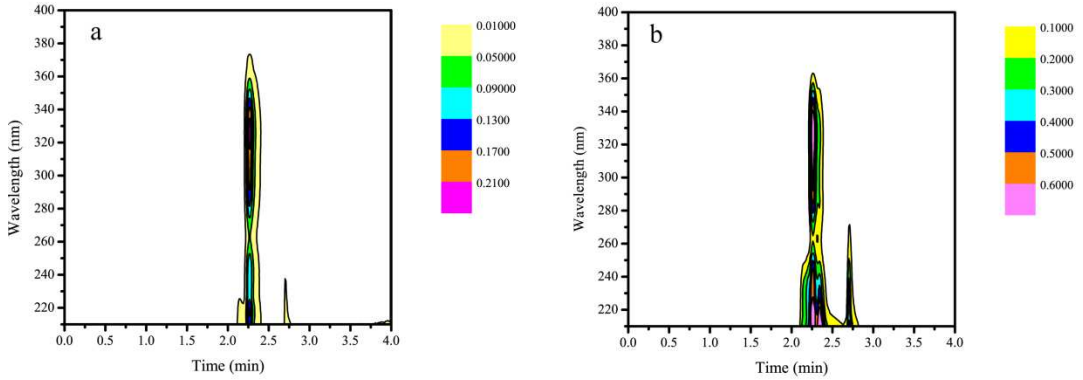

Figure 1. *HPLC-UV/DAD of chlorogenic acid (CGA). a: CGA standard, b: leaves of E. ulmoides*

Under clear day solar radiation condition, the change of CGA content in leaves of *E. ulmoides* with the illumination intensity was shown in *Figure 2*. The highest CGA content in leaves appeared at the decrease point of illumination intensity (14:00) but not the top of illumination intensity (12:00). And then CGA content in leaves dropped fast with illumination intensity after 14:00.

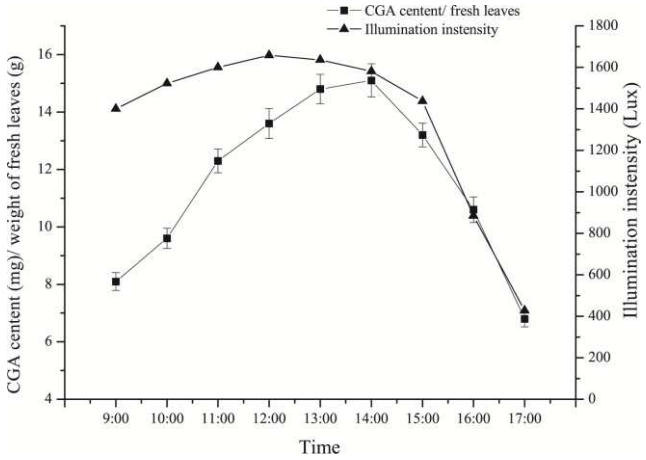

Figure 2. *Intraday variation of chlorogenic acid (CGA) content in leaves of E. ulmoides*

Fresh leaves of *E. ulmoides* had been illuminated by sun light and then were treated with nitroblue tetrazolium (NBT). In *Figure 3,* the dark spots of blue formazan appeared in leaves, while no dark spots appearing in the control (leaves in dark). This showed that sunlight induces $O_2^{\cdot-}$ production in leaves.

CGA performed higher antioxidant capacity: DPPH radical scavenging activity was 2.43 ± 0.092 times of VCEs (mmol/mmol), and ABTS radical cation scavenging activity was 3.61 ± 0.14 time of TEs (mmol/mmol), and reducing powers was 3.40 ± 0.11 times of VCEs (mmol/mmol).

In plant, reactive oxygen species (ROS) are involved in plant responses to various biotic and abiotic stresses (Ma et al., 2012; Wang et al., 2013; Qi et al., 2018). Plants requires light for photosynthesis, but absorption of too much light can lead to photo-oxidative damage to the photosynthetic apparatus, and then this phenomenon occurs due

http://www.aloki.hu ● ISSN 1589 1623 (Print) ● ISSN 1785 0037 (Online)
DOI: http://dx.doi.org/10.15666/aeer/1802_27192725

to imbalances which result from the overproduction of ROS (Chung et al., 2015; Ramabulana et al., 2016). However, accumulation of ROS can damage various cellular components such as proteins, nucleic acids, carbohydrates, and unsaturated lipids (Yu et al., 2018). Here, increased illumination intensity accelerated photooxidation reaction rate, which lead to enhancement of ROS level in cells. And then ROS heightened the content of CGA in the cell by increasing the expression of the genes related to the biosynthesis of CGA, which was completed over a period of time. Probably, this was why the top CGA content in leaves was late for a few hours than illumination intensity.

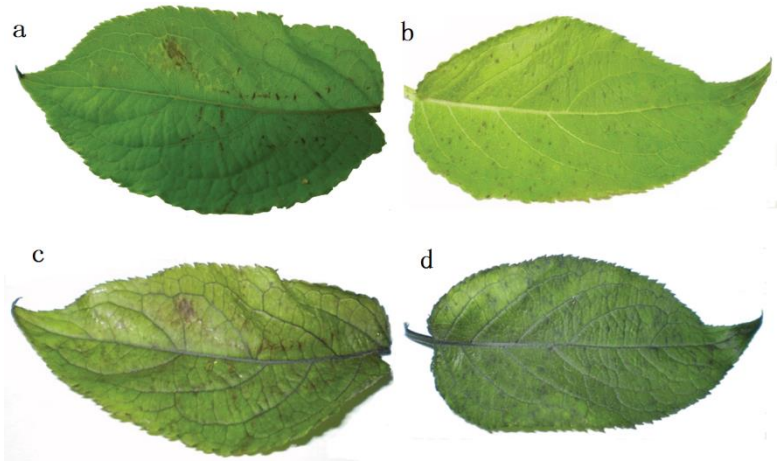

Figure 3. *$O_2^{\cdot-}$ localization in situ of fresh leaves of E. ulmoides. Control leaf and sample leaf illuminated by sun light were treated with NBT and then bleached by immersing in boiling ethanol; a: control leaf; b: sample leaf c: control leaf treated by boiling ethanol; d: sample leaf treated by boiling ethanol*

In plant cells, free radicals produced by photo oxidation can damage the cells, and however, CGA can eliminate free radicals, which can protect cells. This may be the mechanism of the synthesis of chlorogenic acid in plants.

Acknowledgements. The authors are grateful to Zhiqi Cao, Yuanlong Li and Zhen Yang for the preparation work of this study. Scientific Research Fund of Henan Provincial Education Department (12B180004).

REFERENCES

[1] Bhattacharyya, S., Majhi, S., Saha, B. P., Mukherjee, P. K. (2014): Chlorogenic acid-phospholipid complex improve protection against UVA induced oxidative stress. – Journal of Photochemistry and Photobiology B-Biology 130: 293-298.

[2] Chen, X. M., Sang, X. X., Li, S. H., Zhang, S. J., Bai, L. H. (2010): Studies on a chlorogenic acid-producing endophytic fungi isolated from Eucommia ulmoides Oliver. – Journal of Industrial Microbiology & Biotechnology 37(5): 447-454.

[3] Chung, V. C. H., Ho, R. S. T., Wu, X., Fung, D. H. Y., Lai, X., Wu, J. C. W., Wong, S. Y. S. (2015): Are meta-analyses of Chinese herbal medicine trials trustworthy and clinically applicable? A cross-sectional study. – Journal of Ethnopharmacology 162(0): 47-54.

http://www.aloki.hu ● ISSN 1589 1623 (Print) ● ISSN 1785 0037 (Online)
DOI: http://dx.doi.org/10.15666/aeer/1802_27192725

[4] Cle, C., Hill, L. M., Niggeweg, R., Martin, C. R., Guisez, Y., Prinsen, E., Jansen, M. A. K. (2008): Modulation of chlorogenic acid biosynthesis in Solanum lycopersicum; consequences for phenolic accumulation and UV-tolerance. – Phytochemistry 69(11): 2149-2156.
[5] Doring, A. S., Petersen, M. (2014): Production of caffeic, chlorogenic and rosmarinic acids in plants and suspension cultures of Glechoma hederacea. – Phytochemistry Letters 10: CXI-cxvii.
[6] Du, G., Li, M., Ma, F., Liang, D. (2009): Antioxidant capacity and the relationship with polyphenol and Vitamin C in Actinidia fruits. – Food Chemistry 113(2): 557-562.
[7] Dudonne, S., Vitrac, X., Coutiere, P., Woillez, M., Merillon, J.-M. (2009): Comparative study of antioxidant properties and total phenolic content of 30 plant extracts of industrial interest using DPPH, ABTS, FRAP, SOD, and ORAC assays. – Journal of Agricultural and Food Chemistry 57(5): 1768-1774.
[8] Hu, F. L., Deng, C. H., Liu, Y., Zhang, X. M. (2009): Quantitative determination of chlorogenic acid in Honeysuckle using microwave-assisted extraction followed by nano-LC-ESI mass spectrometry. – Talanta 77(4): 1299-1303.
[9] Huang, R. T., Lu, Y. F., Inbaraj, B. S., Chen, B. H. (2015): Determination of phenolic acids and flavonoids in Rhinacanthus nasutus (L.) Kurz by high-performance-liquid-chromatography with photodiode-array detection and tandem mass spectrometry. – Journal of Functional Foods 12(0): 498-508.
[10] Luo, C., Zou, X., Li, Y., Sun, C., Jiang, Y., Wu, Z. (2011): Determination of flavonoids in propolis-rich functional foods by reversed phase high performance liquid chromatography with diode array detection. – Food Chemistry 127(1): 314-320.
[11] Ma, L. Y., Zhang, H., Sun, L. R., Jiao, Y. H., Zhang, G. Z., Miao, C., Hao, F. S. (2012): NADPH oxidase AtrbohD and AtrbohF function in ROS-dependent regulation of Na+/K+homeostasis in Arabidopsis under salt stress. – Journal of Experimental Botany 63(1): 305-317.
[12] Ma, Y., Wu, Y., Yang, J., Liang, H., Shang, F. (2017): Flavonoids content and antioxidant activity of ethanol extracts of Osmanthus fragrans flowers. – Bangladesh Journal of Botany 46(3): 907-915.
[13] Mudge, E., Applequist, W. L., Finley, J., Lister, P., Townesmith, A. K., Walker, K. M., Brown, P. N. (2016): Variation of select flavonols and chlorogenic acid content of elderberry collected throughout the Eastern United States. – Journal of Food Composition and Analysis 47: 52-59.
[14] Ozsoy, N., Can, A., Yanardag, R., Akev, N. (2008): Antioxidant activity of Smilax excelsa L. leaf extracts. – Food Chemistry 110(3): 571-583.
[15] Qi, J. S., Song, C. P., Wang, B. S., Zhou, J. M., Kangasjarvi, J., Zhu, J. K., Gong, Z. Z. (2018): Reactive oxygen species signaling and stomatal movement in plant responses to drought stress and pathogen attack. – Journal of Integrative Plant Biology 60(9): 805-826.
[16] Ramabulana, T., Mavunda, R. D., Steenkamp, P. A., Piater, L. A., Dubery, I. A., Madala, N. E. (2016): Perturbation of pharmacologically relevant polyphenolic compounds in Moringa oleifera against photo-oxidative damages imposed by gamma radiation. – Journal of Photochemistry and Photobiology B-Biology 156: 79-86.
[17] Reis, L. C. B., Carneiro, L. M., Branco, C. R. C., Branco, A. (2015): Comparison of conventional microwave and focused microwave-assisted extraction to enhance the efficiency of the extraction of antioxidant flavonols from jocote pomace (Spondias purpurea L.). – Plant Foods for Human Nutrition 70(2): 160-169.
[18] Romero-Puertas, M. C., Rodriguez-Serrano, M., Corpas, F. J., Gomez, M., Del Rio, L. A., Sandalio, L. M. (2004): Cadmium-induced subcellular accumulation of O-2(.-) and H2O2 in pea leaves. – Plant Cell and Environment 27(9): 1122-1134.
[19] Santos, W. D. R., Santhiago, M., Yoshida, I. V. P., Kubota, L. T. (2011): Novel electrochemical sensor for the selective recognition of chlorogenic acid. – Analytica Chimica Acta 695(1-2): 44-50.

http://www.aloki.hu ● ISSN 1589 1623 (Print) ● ISSN 1785 0037 (Online)
DOI: http://dx.doi.org/10.15666/aeer/1802_27192725

[20] Shao, P., Zhang, J. F., Chen, X. X., Sun, P. L. (2015): Microwave-assisted extraction and purification of chlorogenic acid from by-products of Eucommia ulmoides Oliver and its potential anti-tumor activity. – Journal of Food Science and Technology-Mysore 52(8): 4925-4934.
[21] Sriseadka, T., Wongpornchai, S., Rayanakorn, M. (2012): Quantification of flavonoids in black rice by liquid chromatography-negative electrospray ionization tandem mass spectrometry. – Journal of Agricultural and Food Chemistry 60(47): 11723-11732.
[22] Wang, P. C., Du, Y. Y., Zhao, X. L., Miao, Y. C., Song, C. P. (2013): The MPK6-ERF6-ROS-responsive cis-acting element7/GCC box complex modulates oxidative gene transcription and the oxidative response in Arabidopsis. – Plant Physiology 161(3): 1392-1408.
[23] Wang, X. X., Wang, J. W., Yang, N. J. (2007): Chemiluminescent determination of chlorogenic acid in fruits. – Food Chemistry 102(1): 422-426.
[24] Yu, J. J., Zhang, Y. X., Liu, J. M., Wang, L., Liu, P. P., Yin, Z. P., Guo, S. Y., Ma, J., Lu, Z., Wang, T., She, Y. M., Miao, Y. C., Ma, L., Chen, S. X., Li, Y., Dai, S. J. (2018): Proteomic discovery of H2O2 response in roots and functional characterization of PutGLP gene from alkaligrass. – Planta 248(5): 1079-1099.
[25] Zengin, G., Uysal, S., Ceylan, R., Aktumsek, A. (2015): Phenolic constituent, antioxidative and tyrosinase inhibitory activity of Ornithogalum narbonense L. from Turkey: a phytochemical study. – Industrial Crops and Products 70: 1-6.
[26] Zeraik, M. L., Yariwake, J. H. (2010): Quantification of isoorientin and total flavonoids in Passiflora edulis fruit pulp by HPLC-UV/DAD. – Microchemical Journal 96(1): 86-91.
[27] Zhang, Q. L., Li, J., Wang, C., Sun, W., Zhang, Z. T., Cheng, W. M. (2007): A gradient HPLC method for the quality control of chlorogenic acid, linarin and luteolin in Flos Chrysanthemi Indici suppository. – Journal of Pharmaceutical and Biomedical Analysis 43(2): 753-757.

http://www.aloki.hu ● ISSN 1589 1623 (Print) ● ISSN 1785 0037 (Online)
DOI: http://dx.doi.org/10.15666/aeer/1802_27192725

ECOLOGICAL REMEDIATION OF PETROLEUM-CONTAMINATED SOIL BASED ON MICROBIAL DEGRADATION

WANG, C.[1] – LI, Z.[2*] – GENG, X.[1] – ZHANG, H.[1]

[1]*Department of Chemical Engineering and Safety, Binzhou University, Binzhou 256600, China*

[2]*School of Petroleum Engineering, China University of Petroleum, Qingdao 266580, China*

**Corresponding author*
e-mail: kerwin_11@163.com

(Received 3rd Sep 2019; accepted 12th Feb 2020)

Abstract. In the process of oil exploitation, refining, storage, transportation and use, due to the limitations of technological level and treatment technology, a large amount of petroleum-containing wastewater and waste residue are inevitably discharged into the soil, thus affecting the whole soil ecosystem. In this paper, an ecological remediation method for petroleum contaminated soil based on microbial degradation is proposed. The natural biodegradation of petroleum contaminants in soil is discussed. The types of degrading microorganisms and their degradation mechanisms for saturated hydrocarbons and aromatic hydrocarbons are introduced, and the chemical composition of petroleum and the number of microorganisms in the soil are analyzed. The effects of nutrients, oxygen supply, temperature, humidity and pH on the degradation efficiency of petroleum are studied, and the in-situ soil ecological remediation is carried out after the degradation of pollutants. Experiments show that the ecological remediation of petroleum contaminated soil based on microbial degradation can be more thorough in essence. This method has the advantages of requiring only a low time investment, being, low cost, simple and effective, and having a good remediation effect and no secondary pollution.
Keywords: *ecological remediation method, natural biodegradation, soil ecological remediation, degradation efficiency, chemical composition*

Introduction

Petroleum is a complex mixture of thousands of substances with different chemical properties, including saturated hydrocarbons, aromatic hydrocarbons, asphaltenes, resins and so on. Pollution and omission accidents in the process of oil exploitation, smelting, use and transportation, as well as the discharge of oily wastewater, sewage irrigation, volatilization of various petroleum products and falling of incomplete combustion materials, have caused a series of soil pollution problems. Especially the crude oil produced in the process of oil exploitation has become a significant source of mineral oil pollution in soil.

With the rapid development of the petroleum industry, the contamination of soil by petroleum pollutants is becoming more and more serious. Many studies have shown that some petroleum hydrocarbons have carcinogenic, teratogenic and mutagenic effects on humans and other mammals after they enter the animal body. It is difficult to remove petroleum hydrocarbons when they enter the soil, which will lead to changes in soil properties, even groundwater pollution and other major ecological crises. The serious pollution of soil will lead to the accumulation of some petroleum hydrocarbons in grain, affect its quality, and endanger human health through the food chain. Finding out how to effectively remediate petroleum contaminated soil has become a global environmental problem.

http://www.aloki.hu ● ISSN 1589 1623 (Print) ● ISSN 1785 0037 (Online)
DOI: http://dx.doi.org/10.15666/aeer/1802_27272746

(1) Rapid pyrolysis technology will be used to remediate the soil. The effects of remediation related to pyrolysis parameters, oil recovery rate and its possible formation pathway, as well as the physical and chemical properties of the remediated soil and its suitability for planting are systematically studied. However, this method cannot degrade petroleum pollutants and remediate soil very well, and there are some shortcomings such as troublesome process and time-consuming (Li et al., 2018).

(2) The technology of supersulphate bioaugmentation foam spray is put forward, and used to accomplish the purpose of removing total petroleum hydrocarbon (TPHS) from diesel petroleum contaminated soil. The penetration/unsaturated hydraulic conductivity of unsaturated soils increased with the use of foam remedies. The mixture of sulfate and surfactant solution penetrates the soil faster than peroxide, but it does not make the soil moisture and dryness to an average effect (Bajagain et al., 2018).

(3) Based on the distribution mechanism of cell temperature in soil, the energy efficiency and distribution mechanism of EKR process are proposed. To some extent, the transformation mechanism of Cr6 + and Cr3 + in EKR process is discussed. Through this transformation mechanism, the regularity of chromium fractionation in soil is obtained, so that the degradation of soil is optimized. Although it had the function of post-transformation distillation, it cannot make remediation of soil well (Fu et al., 2017).

In this paper, an ecological remediation method for petroleum contaminated soil based on microbial degradation is proposed. According to the way of microbial degradation, the essential remediation of petroleum contaminated soil is fundamentally carried out. This method has the advantages of simple, effective, time-consuming and good soil remediation.

Material and methods

Materials

Chemical reagents: $M_gSO_4 \cdot 7H_2O$, NH_4NO_3, $CaCl_2$, $FeCl_3$, KH_2PO_4, KCl, HCl, $C_4H_4KNaO_6$, $CHCl_3$, etc., which are all analytical pure.

Additives: chicken manure, chicken manure soil, etc.

The test site is located about 20 kilometers northwest of Daqing oil field, Heilongjiang Province, China (45°46′-46°55′N, 124°19′-125°12′E). For loess, the test depth is 0-15 cm, and the maximum thickness is 50 cm. There are 2-10 mm gravels in the soil. The wet bulk density of the soil is 1.821 g/cm^3. The natural water content is 9.18%. The pH is 8.4; the nitrate content is 55.3 mg/kg, and the oil background content is 1.3-4.6 mg/kg. The experimental water is local shallow groundwater with pH of 8.2 and TDS of 420.5 mg/L. The crude oil produced in the test site is 2400 m underground.

Testing glassware: 150 mL, 250 mL triangle bottle with plug, 125 mL, 1000 mL grinding fine-mouth reagent bottle, various types of bacteria culture tube, Petri dish, rubber plug, 2SL plastic barrel.

Main instruments: QZD-1 electromagnetic oscillator, KQ218 ultrasonic cleaner, biothermostat incubator, high-speed centrifuge, high-pressure steam sterilizer, sterile laboratory, biochemical incubator, shaker incubator, Leica biomicroscopy, 752N ultraviolet-visible grating spectrophotometer, pH meter (pHB-3), DDB-303A conductivity meter, electrothermal drying chamber and various glass instruments for chemical analysis, etc.

http://www.aloki.hu ● ISSN 1589 1623 (Print) ● ISSN 1785 0037 (Online)
DOI: http://dx.doi.org/10.15666/aeer/1802_27272746

Chemical analysis test methods: ultraviolet spectrophotometry is used for analysis of petroleum and NO_3, reagent colorimetry for NH_4, pHB-3 type of pH meter for pH testing, DDB-303A type of conductivity meter for calculation of TDS. Using the above experimental materials, chemical reagents were used to sample the oil-contaminated soil. *Figure 1* shows a sample of oil-contaminated soil.

Figure 1. *Oil contaminated soil samples*

The relevant data obtained are processed by SPASS18.0 statistical software, and the measured data are represented by $(\bar{x} \pm s)$, and the average values of multiple samples are compared by variance analysis method. When there are differences between groups, the average values of multiple samples between groups are pairwise. The average values of the corresponding samples in each comparison group are equal. The test is carried out by LSD-t. If the average value of the corresponding samples in each comparison group is not equal, the Dunnett-T3 test is used. $P > 0.05$ indicated that there was no significant difference.

Sources and hazards of petroleum contaminated soil

(1) Mode of production

Petroleum pollutants (Varjani et al., 2017) are products of oilfield development and petroleum processing. Every link of the petroleum industry may produce petroleum pollutants, of which drilling, oil recovery, transportation, emissions and accidents are the main links. Drilling wastewater and oil-bearing mud containing petroleum pollutants are produced during drilling in oilfields, mainly from oil pollution on flushing surface equipment, loss of drilling mud and leakage of mud circulation system. During the period of oil production, oil production wastewater will be discharged from normal production operation, well washing wastewater will be discharged from well washing, dewatering treatment of crude oil will produce wastewater, and overhaul of equipment will also produce oily wastewater. Accident pollution includes natural and human factors. Natural accidents include blowout and equipment failure. When vehicles are used for transportation, crude oil leakage is caused by traffic accidents caused by landslides, avalanches, floods and gales. Man-made accidents refer to the destruction of oil production equipment and pipelines caused by various man-made factors, and the pollution caused by the rollover of crude oil transport vehicles caused by man-made traffic accidents, etc. Investigations show that the oil content of most soils collected in the 100 m range around oil wells in Shengli and Daqing oilfields is higher than the national standard threshold (500 μg/g). In addition, oil sludge from oil tanks, sedimentation tanks, sewage tanks and sediment from oil transfer stations and combined stations in oilfields can also pollute the soil, causing the oil content in the soil to exceed the standard seriously.

http://www.aloki.hu ● ISSN 1589 1623 (Print) ● ISSN 1785 0037 (Online)
DOI: http://dx.doi.org/10.15666/aeer/1802_27272746

Harmful to soil ecological environment

Petroleum pollutants rank eighth among 48 hazardous wastes in China (Sharma et al., 2018). After petroleum pollutants are discharged into soil, soil structure is destroyed, soil permeability is affected, soil organic matter composition and structure are changed, and soil quality is reduced. Petroleum hydrocarbons accumulated in soil, mostly macromolecule compounds, form a layer of mucosa on plant roots, hinder root respiration and absorption, and even cause root decay. Petroleum pollutants often accumulate in the soil surface, and the soil surface is the most developed area of crop root system, so the degree of soil pollution directly affects the growth of crops. As oil contaminates the soil, it also causes pollutants to enter the grain, causing the accumulation and amplification of pollutants. It not only affects the quality of food, but also makes oil pollutants enter the food chain, endangering human health. In the process of infiltration into the soil, oil also diffuses along the surface, erodes the soil layer, makes it saline-alkali, asphalt, hardening, and migrates to the deep part of the soil under the action of gravity. Because of the strong viscosity of petroleum pollutants, they will form a small range of high concentration pollution in a short time.

Ecological remediation of petroleum contaminated soil based on microbial degradation

Bioremediation technology (Fruchter, 2017) is a new clean technology developed on the basis of biodegradation. It is the development of traditional biological treatment methods. Compared with physical and chemical remediation of contaminated soil, it has the advantages of low cost, no damage to the soil environment needed by plant growth, safe oxidation of pollutants, no secondary pollution, good treatment effect and simple operation. Bioremediation can accelerate the rate of natural biodegradation by optimizing environmental factors. It is an efficient, economical and ecologically affordable clean technology. At present, there are two main types of bioremediation technologies for petroleum hydrocarbon contaminated soil: one is microbial remediation technology, which can be divided into in situ bioremediation and heterotropic bioremediation according to the location of remediation; the other is phytoremediation.

In situ bioremediation and ectopic bioremediation technology

In situ treatment method is to treat contaminated soil in situ. During the treatment period, the soil is basically undisturbed. The most common method of in-situ treatment is to biodegrade the water saturated area of the soil. In addition to adding nutrients and oxygen sources (mostly hydrogen peroxide), microorganisms should be introduced to improve the biodegradability. Sometimes, a group of wells are dug in the contaminated area and injected directly into the appropriate solution, so that microorganisms in the water can be introduced into the soil. After some treatment, groundwater can be recovered and recycled, and soil amendment can be added before groundwater is recycled. It is impossible to remove most PAHs (polycyclic aromatic hydrocarbons) effectively by in situ treatment within a certain period of time, and this method has some limitations due to the influence of temperature and soil type. Ectopic bioremediation mainly includes field treatment, prefabricated bed treatment, composting treatment, bioreactor and anaerobic biological treatment.

http://www.aloki.hu ● ISSN 1589 1623 (Print) ● ISSN 1785 0037 (Online)
DOI: http://dx.doi.org/10.15666/aeer/1802_27272746

Field treatment method

In recent years, there have been many studies on Bio-treatment of petroleum hydrocarbon contamination (Jupp et al., 2017; Wu et al., 2017), among which soil tillage treatment is a common method for field treatment of soil contamination. Polluted wastes are applied to the soil, and the optimum values of oxygen, water and pH are maintained through fertilization, irrigation and lime addition. Tillage is carried out to improve soil ventilation and ensure the degradation of pollutants in polluted wastes and underlying soil layers. Most of the microorganisms used in the degradation process are indigenous microorganisms, but domesticated microorganisms need to be introduced to improve the effect.

Prefabricated bed method

The biggest drawback of soil tillage treatment in field treatment is that pollutants may migrate from the treatment area. The design of prefabricated bed can minimize the amount of pollutants migration because of its filtrate collection and emission control system. The bottom of the prefabricated bed is low permeability material, such as high-density polyethylene or clay. Contaminated soil is transferred to prefabricated bed, pH is adjusted through fertilization, irrigation, and sometimes microorganisms and surfactants are added to make it most suitable for pollutant degradation.

Piling treatment method

Soil piling treatment (Selvi et al., 2017) is to excavate contaminated soil from contaminated areas, prevent contaminants from spreading to groundwater or larger areas, transport it to a treated site (layout of seepage prevention bottom, ventilation pipelines, etc.) and pile it up to form a rising slope, and carry out biological treatment. Piling is a new alternative technology in bioremediation technology.

Bioreactor method

Bioreactor method (Ming et al., 2017) is to treat contaminated soil in a special reactor. Bioreactor is usually built on site or in a specific treatment area, usually in horizontal drum and elevator shape, with two types of gap and continuous. Because the reactor can completely mix the soil with microorganisms and other additives such as nutrients, surfactants and so on, and can control the degradation conditions well, the treatment speed is fast and the effect is good. The process of bioreactor treatment is as follows: firstly, the soil is dug out and mixed with water to form mud, and then transferred into the reactor. In order to improve the degradation rate, domesticated microorganisms are often isolated from the soil previously treated by the reactor and added to the soil prepared for treatment.

Anaerobic bioremediation method

Aerobic remediation technologies such as bio-layer, composting and soil slurry reactor have been developed for the remediation of petroleum hydrocarbon-contaminated soils. However, when some degrading bacteria are isolated, some degrading bacteria are accompanied by products with high ecological risk. Recent studies have shown that anaerobic microbial remediation technology characterized by anaerobic reductive dechlorination has great potential.

http://www.aloki.hu ● ISSN 1589 1623 (Print) ● ISSN 1785 0037 (Online)
DOI: http://dx.doi.org/10.15666/aeer/1802_27272746

Biodegradation of petroleum pollutants in soil

After petroleum pollutants enter the soil, they can be transformed and degraded through three natural ways: volatilization, autoxidation and degradation. The latter mainly includes biodegradation (Chandrangsu et al., 2017), photolysis and mechanical degradation, which is a very slow process. The ultimate fate of petroleum pollutants in the environment is that they are degraded by microorganisms, and thee photolysis is very small. When petroleum pollutants enter the environment, various microorganisms will participate in their biodegradation process. As nutrients, pollutants are absorbed and transformed into organic components in microorganisms or reproduced into new microorganisms. The rest is oxidized and decomposed into simple organic or inorganic substances such as methane, carbon dioxide and water by microorganisms. Petroleum pollutants are biodegraded by aerobic respiration, anaerobic respiration and fermentation after they enter the cell membrane of degrading microorganisms. In aerobic respiration, organic matter is oxidized to carbon dioxide, water and other final products, and the electron acceptor is atomic oxygen; in anaerobic respiration, other inorganic substances are used as electron acceptors, and organic matter is oxidized to methane, sulfate is reduced to sulfide, nitrate is reduced to N_2 or ammonia; the fermentation process does not depend on oxygen, but on the presence of oxygen. As electron acceptors, the final products are carbon dioxide, acetic acid, alcohol, propionate and so on. Generally, biodegradation of petroleum substances is mainly accomplished by aerobic degradation.

In soil, bacteria (Papale et al., 2017) are dominant decomposers, followed by fungi. Different petroleum degrading bacteria have different degrading ability for different hydrocarbons in pollutants. Most petroleum degrading bacteria can degrade only one or several hydrocarbons. Among them, long-chain n-alkanes in petroleum hydrocarbons can be utilized by most petroleum-degrading bacteria, while short-chain alkanes and aromatics can only be degraded by a few bacteria. The proportion of hydrocarbon-degrading bacteria in the total heterotrophic population varies greatly. So far, more than 200 kinds of hydrocarbon-degrading microorganisms have been known.

Biochemical principle of petroleum degradation by microorganisms

It is a very complicated process that petroleum pollutants are degraded by assimilation after they enter the cells of degrading microorganism (Barp et al., 2017). Under aerobic conditions, mainly under the catalysis of oxygenase, molecular oxygen is combined into the matrix to form oxygen-containing intermediates, and then converted into other substances. In the degradation of alkanes, one oxygen atom in O_2 is bound, while in the degradation of aromatics, two oxygen atoms are bound. Since petroleum is a mixture of hydrocarbons, the degradation of petroleum can only be accomplished by the interaction of various microorganisms.

When the degradation of petroleum pollutants by microorganisms are caused by intracellular enzymes, the whole process of microbial degradation can be divided into the following three steps:

(1) Compounds are adsorbed on the surface of microbial cell membrane, which is a dynamic equilibrium process.

(2) Compounds adsorbed on the surface of cell membrane enter the cell membrane (when the biomass is constant, the penetration rate of the compound to the cell membrane determines the amount of the compound penetrating the cell membrane).

http://www.aloki.hu ● ISSN 1589 1623 (Print) ● ISSN 1785 0037 (Online)
DOI: http://dx.doi.org/10.15666/aeer/1802_27272746

(3) Enzymatic reactions occur when compounds entering microbial cell membranes bind to degrading enzymes, which is a fast process. The metabolic pathways and mechanisms of microorganisms to different hydrocarbons in petroleum pollutants are different. The following are mainly discussed.

Biodegradation of saturated hydrocarbons in petroleum

Straight-chain alkanes: it is generally believed that saturated hydrocarbons (Pattison et al., 2018) are first oxidized to alcohols under the action of microorganisms, alcohols are oxidized to corresponding aldehydes under the action of dehydrogenase, and then oxidized to fatty acids through the action of aldehyde dehydrogenase. The oxidation pathways include single-end oxidation, double-end oxidation and sub-end oxidation. After converting to the corresponding fatty acids, one form of conversion is to directly undergo the subsequent β-oxidation sequence, i.e. to form carboxyl groups and to shed two carbon atoms; the other is to undergo the ω-hydroxylation of fatty acids to form ω-hydroxy fatty acids, which are then oxidized to dicarboxylic acids with the participation of non-specific hydroxylase, and finally experienced the final β-oxidation sequence. Fatty acids are degraded into acetyl coenzyme A by β-oxidation, which enters the tricarboxylic acid cycle, decomposes into CO_2 and H_2O and releases energy, or enters other biochemical processes. Alkanes can also be dehydrogenated directly to form olefins, which can be further oxidized to alcohols and aldehydes through enzymatic catalysis, and finally to fatty acids, which can be further decomposed according to the sequence of β-oxidation; or alkanes can be oxidized to alkyl hydrogen peroxide and then directly converted to fatty acids.

Branched alkanes: the degradation mechanism of branched alkanes by microorganisms is basically the same as that of straight alkanes. Compared with n-alkanes, the presence of branched chains increases the resistance of microbial oxidation and degradation. The main part of oxidation and decomposition occurs on the straight chain, and it is difficult to oxidize near the end of the side chain. The degradation of branched alkanes can be carried out through α-oxidation, ω-oxidation or β-base removal pathway. Generally speaking, the degradation rate of hydrocarbons with branched chain structure is slower than that of straight chain hydrocarbons with the same carbon number, because the branched chain of alkanes reduces the decomposition rate.

Naphthalene: Naphthalene accounts for a large proportion of petroleum fractions. Its biodegradation principle is similar to that of sub-terminal oxidation of alkanes. First, naphthenols are oxidized by mixed-function oxidase (hydroxylase), then dehydroketones are oxidized to esters, or fatty acids are formed by direct ring opening. Taking cyclohexane as an example, its biodegradation mechanism is as follows: cyclohexane is hydroxylated by oxidase to form cyclohexanol, which dehydrogenates to ketone, then oxidizes further. An oxygen atom inserts into the ring to form ester, ester opens, and hydroxyl at one end is oxidized to form aldehyde group, then oxidized to form carboxyl group, finally, dicarboxylic acid is further metabolized by β-oxidation.

Monocyclic aromatic benzene and short-chain alkylbenzene are metabolized to catechol and substituted catechol through the intermediate process of diol under the action of dehydrogenase and redox enzyme. The aerobic degradation of benzene is the formation of cis-dioxyl compounds by introducing two hydroxyl groups into the benzene ring, and then deoxidized to form catechol.

Catechol (Du et al., 2017) can be cleaved in two ways: between two hydroxyl groups; between hydroxyl carbon atoms and non-hydroxyl carbon atoms.

http://www.aloki.hu ● ISSN 1589 1623 (Print) ● ISSN 1785 0037 (Online)
DOI: http://dx.doi.org/10.15666/aeer/1802_27272746

There are two ways to degrade toluene, ethylbenzene and xylene: oxidation of methyl or ethyl groups on benzene rings to form carboxyl groups, then removal of carboxyl groups, and introduction of two hydroxyl groups to form catechol under the action of hydrogenase; direct oxidation of benzene rings to connect two hydroxyl groups, and further oxidation.

Polycyclic aromatic hydrocarbons (PAHs) are very difficult to degrade. The degree of degradation is related to the solubility of PAHs, the number of rings, the type of substituents, the position of substituents, the number of substituents and the properties of heterocyclic atoms. Biodegradation of polycyclic aromatic hydrocarbons (PAHs) begins with the progressive degradation of pyruvic acid and CO_2 by hydroxylation of the first ring, followed by the decomposition of the second ring in the same way. Prokaryotic and eukaryotic microorganisms have the ability to oxidize aromatic hydrocarbons, but the mechanisms of aromatic hydrocarbon oxidation by bacteria and fungi are different. Bacteria produce dioxygenase, which combines the two oxygen atoms of molecular oxygen with the substrate by the catalysis of dioxygenase to oxidize aromatic hydrocarbons into cis-structured diols, and cis-diols break the aromatic ring into catechols under the catalysis of another peroxidase. Fungi, on the other hand, can oxidize aromatic hydrocarbons to trans-dihydrodiphenols by catalysis of monooxygenase and cyclohydrolase. Different metabolic pathways have different intermediates, but the common intermediates are catechol, 2,5-dihydroxybenzoic acid and 3,4-dihydroxybenzoic acid. These metabolites are degraded through similar pathways, i.e. the breaking of carbon bonds. On the one hand, the metabolites can be utilized by microorganisms to synthesize cell components, on the other hand, they can also be oxidized to CO_2 and H_2O.

Influencing factors of microbial degradation of petroleum pollutants

Chemical composition and environmental factors of petroleum are the most significant factors affecting biodegradation in soil. Environmental factors include microbial species and quantity in soil, nutrient elements in soil, oxygen supply, temperature, humidity, pH value and so on.

Chemical composition of petroleum

The degradability of petroleum products varies with their composition. Petroleum compounds are mainly composed of saturated hydrocarbons, aromatics, nitrogen sulfur oxides and asphaltene. Petroleum compounds can be classified into thousands of chemical systems according to the length of carbon chain (Schmidbaur and Schier, 2017) and whether they form straight chain, branched chain, ring or aromatic hydrocarbon structure (Sinsabaugh et al., 2017). The degree of biodegradation of various hydrocarbons is different, and the degradation rate is mainly determined by the number of carbon and its functional groups. Among the components, saturated hydrocarbons are the most easily degraded, followed by aromatic compounds with lower molecular weight, while aromatic compounds, resins and asphaltenes with higher molecular weight are extremely difficult to degrade. Among saturated hydrocarbons, straight-chain alkanes are the most easily degraded, while branched-chain alkanes are more difficult to be degraded by microorganisms. The presence of branched-chain enhances the corrosion resistance of alkanes, and the more and larger the branched-chain is, the more difficult it is to be degraded by microorganisms. In aromatic

http://www.aloki.hu ● ISSN 1589 1623 (Print) ● ISSN 1785 0037 (Online)
DOI: http://dx.doi.org/10.15666/aeer/1802_27272746

hydrocarbons, dicyclic and tricyclic compounds are easily degraded. The degradation order of aromatic compounds generally decreases with the increase of aromatic rings and alkyl substituted side chains. The biodegradability of polycyclic aromatic hydrocarbons decreases in the following order: triaromatic steroids, yield series, phenanthrene series and naphthalene series. Cycloalkanes and aromatic hydrocarbons with more than four rings, or compounds containing tar and asphaltene components, have a slower biodegradation rate. A large number of these substances remain in the final products of biodegradation and become the main residual substances after degradation.

Generally, medium-length alkanes degrade rapidly, while longer-chain alkanes are not easy to degrade. Compounds with relative molecular weight more than 500 cannot be directly used as carbon source for microbial growth (Han and Currell, 2017). Generally speaking, C10-C22 compounds in alkanes and aromatics are the least toxic and most easily degraded. C1-C6 volatilizes rapidly, mainly in the form of gases in the environment, and short-chain hydrocarbons are degraded by a small number of microorganisms because of their relatively stable structure. Hydrocarbons above C22 are poorly water-soluble, usually in the form of gases. In the case of solid, the degradation of microorganisms is very limited; with the increase of relative molecular weight, the biodegradability decreases. Because of the difference of biological stability, the degree of biodegradability of petroleum components is very different, and the environment of microorganisms in the same polluted area is also quite different.

Microbial species and quantities

As the executor of petroleum biodegradation, the number and species of microorganisms are the important factors affecting the efficiency of petroleum biodegradation. Environmental conditions affect the biodegradation of organic pollutants (Lee et al., 2017), generally by affecting the activity of microorganisms. Different microorganisms have different ability to degrade petroleum hydrocarbons, and the same strain has different ability to utilize different hydrocarbons. In the petroleum contaminated soil environment, the more the number and species of petroleum-degrading microorganisms are, the faster the degradation rate is. Petroleum pollution can induce the growth of oil-degrading microbial population. The number of oil-degrading microbial population is less than 0.1% in non-oil-polluted areas, but the proportion and quantity of oil-degrading bacteria in the polluted areas have increased significantly. The more serious the pollution is, the more bacteria there are. The results show that the number of microorganisms is an important factor affecting the oil degradation efficiency. Within a certain range of oil concentration, the petroleum degradation efficiency of microorganisms is not affected by other factors.

Oxygen supply and nutrition in soil

Adequate oxygen content in soil has an important influence on degradation efficiency. The initial process of microbial degradation of petroleum pollutants is the oxidation of matrix by oxidase (Naafs et al., 2017). First of all, oxygen must be involved. That is, under the catalysis of oxygenase, oxygen is added into the matrix to form an intermediate product containing oxygen. In theory, the amount of oxygen required for degradation is about 3.5 times the mass of hydrocarbons. Under anaerobic conditions, although some microorganisms may react to degrade petroleum pollutants, it

http://www.aloki.hu ● ISSN 1589 1623 (Print) ● ISSN 1785 0037 (Online)
DOI: http://dx.doi.org/10.15666/aeer/1802_27272746

is much slower than that under aerobic conditions, and there are few kinds of microorganisms that can degrade hydrocarbons. Experiments show that under anaerobic conditions, the degradation rate of pollutants is less than 5% after 233 days, while under aerobic conditions, the degradation rate of some hydrocarbons is increased, and the degradation rate of some hydrocarbons is more than 20% after 14 days.

The most basic limiting factor for microbial growth is the lack of appropriate energy sources. There are at least 11 macronutrient and micronutrient elements (N, P, K, Na, S, Ca, Mg, Fe, Mn, Zn, Cu) necessary for microorganisms in the soil. These elements must maintain a certain amount, form and proportion in order to maintain the growth of aerobic bacteria. The other micronutrient elements necessary for several anaerobic bacteria include Ni and Co. Lack of nutrients inhibits microbial degradation of petroleum hydrocarbons. Most microorganisms are heterotrophic and use certain organic matter as energy source. In petroleum contaminated soils, organic carbon is usually high, while N and P are relatively deficient. If m(C):m(N):m(P) does not reach the required proportion of bacterial metabolism, the metabolic rate of bacteria will be limited, thus restricting the degradation of organic pollutants. Therefore, adjusting the proportion of essential nutrients is a necessary condition for the smooth degradation process. The results show that close to 100:10:1 is the most suitable ratio for hydrocarbon biodegradation.

Soil temperature

Soil temperature also affects degradation efficiency. Temperature can directly affect the growth, reproduction and metabolism of microorganisms, and the biochemical reaction accords with the general law of chemical reaction rate, that is, the higher the temperature is, the faster the reaction rate is. The results show that the effect of soil temperature (T) on the rate constant (k) of biological reaction is in accordance with the following relationship:

$$k = 3145\exp(-5233/T) \quad \text{(Eq.1)}$$

In the aerated zone, the half-lives of petroleum pollutants at 5 ℃, 10 ℃, 20 ℃ and 30 ℃ are 1499 d, 1075 d, 572 d and 317 d, respectively. The results show that microorganisms can degrade at -72 – -2 ℃; the number of microorganisms increases and the degradation rate increases with the increase of temperature at -10-0 ℃; the degradation rate of n-alkanes can be doubled at 20-30 ℃, and the degradation rate of heavy oil and light oil can be decreased by 50-60% and 0-40% respectively, when the temperature decreased from 20 to 10 ℃. Temperature affects the degradation of petroleum organisms mainly in the following two aspects: the effect of temperature on enzymes in microorganisms and the effect of temperature on petroleum properties.

The effect of temperature on enzymes in microorganisms: because microorganisms are accompanied by complex biochemical reactions in the process of degradation of organic substances, the biodegradation of these organic substances actually needs to be carried out under the catalysis of enzymes produced in microorganisms, and temperature is an important dominant factor in the kinetics of enzymatic reaction. The catalytic activity of each enzyme can only be brought into play within a certain temperature range, and beyond a certain temperature range, the activity of the enzyme will be inhibited or even cause the inactivation of the enzyme. The activity of microbial

http://www.aloki.hu ● ISSN 1589 1623 (Print) ● ISSN 1785 0037 (Online)
DOI: http://dx.doi.org/10.15666/aeer/1802_27272746

enzymes can be reduced by too low temperature, and the degradation rate of hydrocarbons can be accelerated and the maximum value can be achieved by increasing temperature. The appropriate temperature is generally 15-35 ℃. The toxicity of hydrocarbons will increase when the temperature is higher, which will affect the degradation and biological activity of hydrocarbons.

The influence of temperature on petroleum properties: temperature also affects the physical and chemical properties of petroleum, and ultimately affects the interaction between microorganisms and petroleum molecules, thus changing the process and rate of biodegradation. When the temperature is low, the membrane toxicity of hydrocarbons is small, the oil viscosity is high, the volatility decreases, the start-up of biodegradation lags behind, and the rate decreases. With the increase of temperature, the membrane toxicity of hydrocarbons increases, and the emulsification degree of oil increases. In addition, the microbial activity needs liquid water, so the degradation temperature should be at least above the freezing point of water (Wu et al., 2018).

Soil moisture and pH value

Water is an indispensable nutrient for microbial life activities. Microorganisms cannot survive without water, and let alone degrade petroleum pollutants. In addition, organic matter must be water-soluble in order to be utilized by microorganisms. Water is also closely related to redox potential and solubility of compounds. The results are important factors affecting petroleum degradation. Soil moisture varies in depth, soil moisture is too low, microorganisms cannot get enough water supply, cell activity is inhibited, and metabolic rate is reduced; but excessive soil moisture will hinder air permeability and oxygen supply. The results showed that the maximum soil water holding capacity is 25-85%, which is the most suitable time for microorganisms to survive, and the best soil water holding capacity is 30-90% for petroleum pollutants degradation.

Most heterotrophic bacteria and fungi which can degrade petroleum pollutants prefer neutral environment. The suitable pH value of many soil microorganisms is 6-8. Excessive or low pH value will affect the degradation ability of microorganisms. The optimum pH values of hydrocarbons and polynuclear aromatic hydrocarbons are 7.5, 7.5-7.8, respectively. The optimum pH values of most bacteria are slightly greater than 7. The degradation rate of petroleum in neutral soil is twice as fast as that in acidic soil (pH 4.5) or alkaline soil (pH 8.5).

Results

The main mechanism of microbial remediation technology is that petroleum hydrocarbons are directly involved in the biochemical reaction of microorganisms. The development and research of microbial remediation technology for degradation of contaminants in soil by metabolic process has attracted extensive attention of scholars at home and abroad. At present, more than 100 genera and 200 species of microorganisms are known to degrade hydrocarbons in petroleum. They belong to bacteria, actinomycetes, fungi, yeasts and algae. Geological microecology technology is a comprehensive remediation technology which makes full use of the optimization of in-situ microbial flora, supplemented by physical and chemical methods and combined with geological environment. In the past, most of the research materials reported are indoor studies. This study is carried out in situ soil remediation experiments in the field,

http://www.aloki.hu ● ISSN 1589 1623 (Print) ● ISSN 1785 0037 (Online)
DOI: http://dx.doi.org/10.15666/aeer/1802_27272746

and achieves good results, which provides technical support for the popularization and application of this technology, and has important practical significance.

Experimental steps

The crude oil obtained in the test area is used as carbon source (pollutant). The strains and flora of petroleum-degrading soil in the test area are selected and cultured in a large scale. According to the inoculum amount used in the test, sufficient bacterial liquid preparations are cultured, and a large number of bacterial flora for the test are grown through microscopic examination. According to the calculation, a certain amount of oil is evenly mixed into the surface layer of soil in the test area at a depth of 15 cm. The microorganisms that degrade petroleum compounds can be divided into bacteria, fungi and algae according to their biological types (as shown in *Table 1*).

Table 1. *Microbial composition of oil contaminated soil*

Soil sample	Germ		Fungus		Actinomyces	
	10^5CFU (g)	**Percentage composition (%)**	**10^3CFU (g)**	**Percentage composition (%)**	**10^3CFU (g)**	**Percentage composition (%)**
CK	33 ± 8b	94.25	3 ± 1c	0.08	176 ± 55a	5.10
PCS-1	297 ± 35a	98.88	27 ± 4a	0.08	9 ± 3b	0.03
PCS-2	193 ± 49a	99.92	12 ± 3b	0.08	3 ± 1b	0.02

According to the soil weight of the test layer in the test area, 4.3% chicken manure and 50% chicken manure are evenly mixed as additives. The amplified culture liquid is evenly inserted into the test area according to the 3% spray tillage, and then the nutrient solution of nitrogen, phosphorus, calcium, magnesium, sulphur and iron is adjusted uniformly according to the proportion of the medium. The water content of the soil layer is about 20% with the local groundwater regulation test. Agricultural plastic film is covered in the test area for heat preservation, moisturizing, rainproof and so on. Within a certain time interval, the sampling method is to take the sample with same depth soil (15 cm) at five different points in the shape of plum blossom in each area, and then mix it thoroughly and test it with 4-point sampling method. After sampling, the experimental layer of the tillage test area is aerated by the storm air and supplemented with a certain amount of water to ensure that the soil's water content in the test area is about 20%. The amount of petroleum added into the control area is basically the same as that in the experimental area, but not in the other areas, which is regarded as natural degradation. There is no substance added to the blank area as a monitoring sample. Three areas are sampled at the same time and tested components are petroleum content, pH, soil soluble salt, water content, NH_4, NO_3 and so on. At the same time, the surface temperature and soil temperature are monitored. After the completion of the test period, samples are taken from the lower part of the test layer in each district. The test results are shown in *Table 2.*

Experimental result

In this paper, Matlab simulation tool was used to simulate the oil content and removal rate of soil, the degradation rate of organic matter in oil pollution samples with different water content, the degradation rate of petroleum by microorganisms and the

http://www.aloki.hu ● ISSN 1589 1623 (Print) ● ISSN 1785 0037 (Online)
DOI: http://dx.doi.org/10.15666/aeer/1802_27272746

degradation characteristics of n-alkane in oily soil under the environment of Microsoft Windows XP operating system, Intel (R) Celeron (R) 2.6 GHz processor and 24 GB memory.

Removal rate of petroleum from soil

From *Table 2* it can be seen that the implementation of in-situ micro-ecological remediation technology for petroleum contaminated soil has certain effectiveness through field experiments. In the early stage of the experiment (0-7 d), the added optimum bacterial solution does not play a role. That is to say, when indoor optimum bacterial solution is applied in the field, it needs an adaptation period or a lagphase of bacteria. The optimum period of this experiment is about 7 days. Later, the proliferative phase (logarithmicphase) is entered. *Table 1* shows that the removal rate is over 80% after the 11th day of the experiment, that is, after the adaptation period. The sample is slightly higher because of the sampling location and heterogeneity. However, the removal rate is over 68% at the 16th day of the experiment, and 84.3% at the 32nd day of the experiment. The oil content of the soil in the control area does not change much, except that the two abnormal low values are less than 10%, which indicates that the degradation of oil in the soil is slow under natural conditions. The test data of 16 and 21 days of the two abnormal low values may be caused by the uneven oil content in the soil, and also reflects the heterogeneity and complexity of soil material composition. The blank area reflects the oil content in the soil without adding any substance, but in the later stage of the experiment, the oil content increases because of the adjacent of the test area and the control area, as well as the contamination of the area by rainfall and artificial sampling.

Table 2. *Testing results of changes of oil content and removal rate with time in soils of different areas*

Sampling date (month/day)	8/19	8/23	8/26	8/30	9/4	9/9	9/14	9/20
Number of test days	0 d	3 d	7 d	11 d	16 d	21 d	26 d	32 d
Test area	2302.0	1868.0	2335.0	422.6	731.0	516.0	557.8	364.0
Control area	2279.0	2442.0	2245.0	2122.0	1532.2	1855.2	2110.6	2120.2
Local area	4.6	18.2	4.5	0.95	5.75	29.55	45.55	159.0
Removal rate of test area/%	0	0	0	81.77	68.47	77.74	75.94	84.3

Controlling factors of geological microecological remediation technology

Geological microecology technology is an in-situ remediation technology which changes macro-environment by micro-effect. The key to the application of this technology is the combination and regulation of microorganisms and geological environment. The main controlling factors are improvement of temperature, water, oxygen, nutrient elements and geological environment.

(1) Regulation and control of soil temperature

Temperature is one of the important factors affecting the growth and survival of bacteria, and the activity intensity and biochemical function of bacteria are related to it. Excessive or low temperature can inhibit growth or cause bacterial death, and moderate

http://www.aloki.hu ● ISSN 1589 1623 (Print) ● ISSN 1785 0037 (Online)
DOI: http://dx.doi.org/10.15666/aeer/1802_27272746

temperature can accelerate the biochemical reaction rate in bacterial cells. Most of the microorganisms we used are mesophilic microorganisms (13-45 ℃), and the optimum growth temperature is 25-38 ℃. How to control the temperature is the key to the test effect. Therefore, agricultural plastic film is used for thermal insulation in the test area, and grass curtain is used to cover the night after September because of the obvious drop in temperature.

(2) Analysis of soil pH, water content, soluble salt, NH_4 and NO_3 content

Firstly, the effect of soil dryness and wetness on the degradation rate of oil pollution.

Under different water content conditions, the degradation characteristics of petroleum contaminated soil samples with 100 g/kg petroleum pollutant concentration by microorganisms are shown in *Figure 2*.

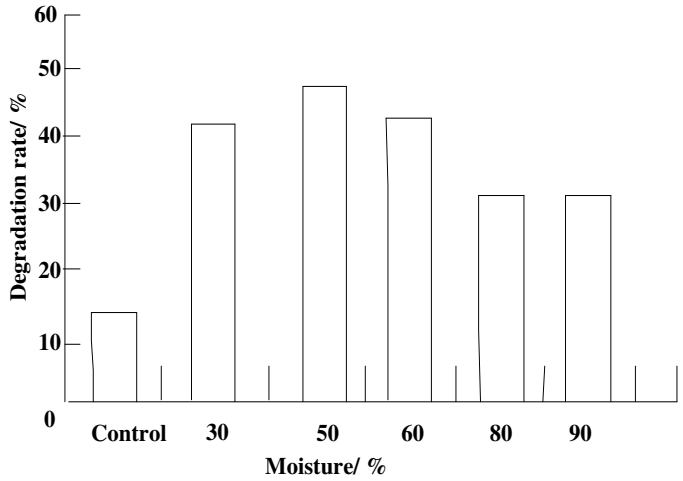

Figure 2. *Degradation rate of organic matter in oil pollution samples with different water contents by microorganisms*

Figure 2 shows that the water content of petroleum contaminated samples has a significant effect on the petroleum-degrading ability of oil-loving microorganisms. When the water content is less than 50%, the ability of microorganism to degrade petroleum increases with the increase of water content; however, when the water content is higher than 50%, the ability of microorganism to degrade petroleum begins to weaken gradually with the increase of water content. In fact, microorganisms in soil need water to maintain their basic metabolism. If the soil water content is too low, microorganisms will not get enough water supply, and cell activity will be inhibited, resulting in a decrease in its metabolic rate; while excessive soil moisture will hinder air permeability and oxygen supply. According to the conditions required for microbial activity, the degradation of petroleum hydrocarbons is more advantageous in the range of 30-80% of the maximum water holding capacity of soil. When the water content is less than 30% or more than 90%, the activity of petroleum hydrocarbon-degrading bacteria will be adversely affected. This phenomenon shows that the growth and reproduction of microorganisms need certain water conditions, and water is necessary for some enzymes of microorganisms; however, excessive water will prevent

http://www.aloki.hu ● ISSN 1589 1623 (Print) ● ISSN 1785 0037 (Online)
DOI: http://dx.doi.org/10.15666/aeer/1802_27272746

microorganisms from effectively contacting with oxygen, resulting in microbial hypoxia and inhibiting the ability of microorganisms to degrade petroleum.

Secondly, the effect of adding H_2O_2 on the degradation of petroleum pollution.

Microorganisms continuously consume dissolved oxygen in petroleum hydrocarbon degradation process, so that the concentration of dissolved oxygen decreases. In this study, H_2O_2 is added to the sample, which is decomposed to supplement the dissolved oxygen consumed by microorganisms. In order to maintain the dissolved oxygen in the sample, a certain amount of H_2O_2 is added every day. At the same time, because of the strong oxidation of hydrogen peroxide, if the amount of hydrogen peroxide is too high, it will inhibit the growth of microorganisms. Therefore, this study determines that the upper limit of adding H_2O_2 is 0.5 ml/d. In the process of experiment, under the best conditions of other factors, for the sample 1-4 containing 100 g/kg oil-polluted soil, 0.1 ml, 0.2 ml, 0.5 ml and 0.6 ml of H_2O_2 are added. And the degradation characteristics of petroleum contamination by microorganisms are shown in *Figure 3*.

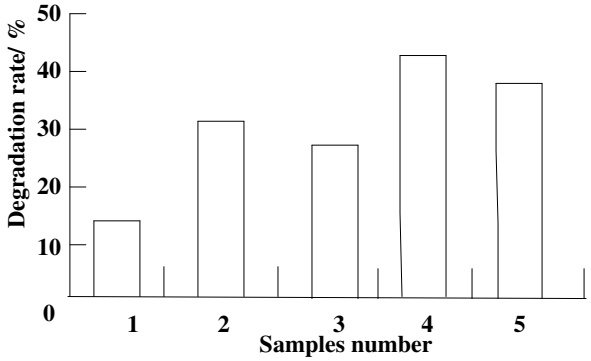

Figure 3. *Effects of microorganisms on petroleum degradation rate under different conditions of H_2O_2*

It can be seen that the influence of oxygen content on the ability of microorganisms to degrade petroleum is also relatively large. With the addition of H_2O_2, the activity of microorganisms is gradually strengthened and the degradation ability is gradually improved. When H_2O_2 is added to 12 ml in 24 days, the degradation efficiency reaches its maximum value. Moreover, it can be seen from the determination of microorganisms in oily soil that the number of living bacteria in test samples increases with the addition of H_2O_2, and the number of living bacteria in test samples increases gradually. Increase of the number of living bacteria will inevitably accelerate the degradation rate of petroleum pollutants. In addition, the pH value of slurry can be maintained stable without obvious change with the addition of H_2O_2. In the absence of electron acceptor, microbial oxidation of fatty acids is difficult and hydrocarbon contaminants cannot be completely oxidized, which results in the accumulation of some short-chain fatty acids in the test samples and the decrease of pH value. If sufficient electron acceptors are provided, microorganisms will completely oxidize hydrocarbons to CO_2 and H_2O, thus keeping the pH value of the sample stable. This is conducive to the growth and reproduction of microorganisms, enhancing their activity, and leading to the degradation of microorganisms more obvious.

Thirdly, the degradation characteristics of alkanes under different N/P ratios.

http://www.aloki.hu ● ISSN 1589 1623 (Print) ● ISSN 1785 0037 (Online)
DOI: http://dx.doi.org/10.15666/aeer/1802_27272746

Under different N/P ratios, the relative content of residual alkanes after degradation of petroleum contaminated samples with 100 g/kg contamination by microorganisms is shown in *Figures 4* and *5*. *Figures 4* and *5* show that the residual content of n-alkanes and iso-alkanes with various carbon numbers is the least when the ratio of N to P is 10:1 under different N/P ratios, while the residual amount of n-alkanes and iso-alkanes is higher under other N/P ratios. Quality can effectively enhance the degradation ability of microorganisms and promote oil-loving microorganisms to effectively degrade alkanes in petroleum. It also reflects that oil-loving microorganisms have a relatively balanced degradation of n-alkanes in the range of C16-C21, however, oil-loving microorganisms are selective for the consumption of isoparaffins in the range of C15-C20. The degradation rates of C16 isoprene, Pr and Ph are significantly lower than those of C15, C18 isoprene, Pr2 and MP isoalkanes. The characteristics of selective degradation show that Pr, Ph are difficult to degrade, and the stability of Pr and Ph can also be utilized, so that Pr and Ph are used as molecular markers for the degradation of petroleum pollutants.

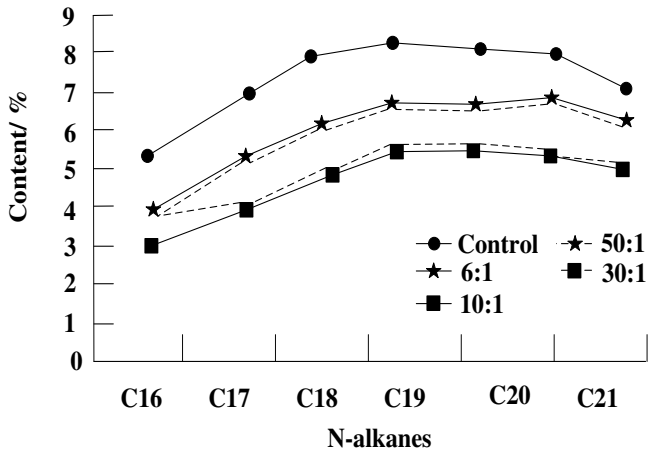

Figure 4. *Degradation characteristics of n-alkanes in oily soil under different nutrient conditions*

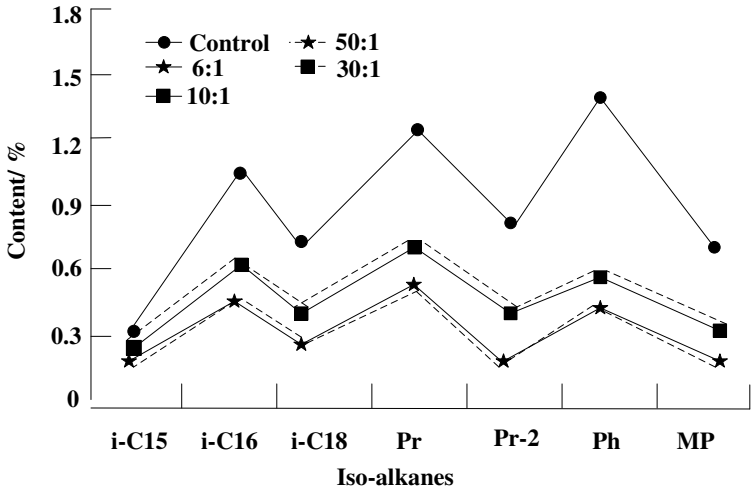

Figure 5. *Degradation characteristics of isoalkanes in oily soil under different nutrient conditions*

http://www.aloki.hu ● ISSN 1589 1623 (Print) ● ISSN 1785 0037 (Online)
DOI: http://dx.doi.org/10.15666/aeer/1802_27272746

The pH of the environment has a certain influence on the life activities of microorganisms. It can cause the change of cell membrane charge, affect the absorption of nutrients and the activity of enzymes, and change the availability of nutrients and the toxicity of harmful substances in the environment. The survival of each microorganism has a certain range of pH value and the optimum pH value. The optimum pH value of most bacteria is 6.5-7.5, and that of actinomycetes is 7.5-8.0. Fungi can grow and develop in a wide range of pH. For example, fungi can grow at pH below 3 and above 9, and the optimum is 5-6.

Effect of test process on lower soil in test area

Table 3 is to test the contents of oil, pH, water content, soluble salt, NH_4 and $N0_3$ in different depths of the lower part of the test area after the completion of the test. From the test results, it can be seen that the oil content in the lower part of the test layer does not increase significantly. Compared with the control and blank areas, it shows that the oil in the soil of the experimental layer has not diffused downward or has been degraded. From the contents of pH, water content, soluble salt, NH_4, NO_3, it can be seen that they are different from the control area and blank area. That is to say, some soluble nutrients such as nitrogen and phosphorus enter the lower soil layer with water. In the future, this kind of remediation work is of great significance to the requirements of water quantity and soluble nutrients and the adding methods.

Table 3. *Test for soil pH, water content and soluble salt, NH_4, NO_3 content changing with depth in each area after the experiment*

Different depths	Petroleum (mk/kg)	pH	Water content (%)	Soluble salt (Ms/cm)	NH_4 (mol/L)	NO_3 (g/cm^3)
Test area 20-25	61.9	7.8	14.04	821.5	70.0	246.4
30-35	102.2	8.0	15.27	612.0	5.0	242.7
45-50	87.7	8.0	17.78	504.0	3.0	242.6
Control area 20-25	30.15	8.5	13.06	97.0	1.5	24.2
30-35	58.31	8.4	13.51	96.5	1.5	22.2
45-50	76.45	8.4	14.67	123.0	1.5	18.4
Blank area 20-25	99.42	8.7	10.8	68.1	3.0	24.1
30-35	36.55	8.7	10.58	80.2	1.5	32.7
45-50	36.95	8.5	14.09	171.2	1.5	31.6

Discussion

Oxygen supply has become one of the important regulators in the process of bacterial degradation of petroleum pollution. The amount of oxygen supply can affect the activity of many enzymes and cell respiration in microbial cells, and control the growth of microorganisms and the ability to degrade petroleum pollution. Generally, 1.02 g petroleum per 3.5 g of oxidation is required, which can be degraded rapidly only under sufficient oxidation conditions. In this experiment, the supply of soil oxygen is regulated from four aspects. Firstly, the soil is fully tilled and the experimental layer is tilled after each sampling, which is fully mixed with the atmosphere. The second is to ensure that the tested soil has a certain water content and oxygen provided by water. In addition, chicken manure is used as an additive, which is not only cheap and easy to obtain, but also can supplement nutrients, and the soil of the experimental layer is improved to increase the fluffy and permeability, so that oxygen in the air is easy to

http://www.aloki.hu ● ISSN 1589 1623 (Print) ● ISSN 1785 0037 (Online)
DOI: http://dx.doi.org/10.15666/aeer/1802_27272746

enter. Finally, the added nutrients of NH_4O_3, KH_2PO_4, K_2HPO_4, NO_3, etc., not only increase the nitrogen source, but also the sources of oxygen.

Nutrient elements are the active components of microbial cells, enzymes, substance transport systems and the energy required to provide physiological activities. Microbial cells are mainly composed of C, H, O, N, P and so on, in which C and H come from petroleum pollutants. Oxygen comes from water and air and other regulated sources of oxygen. The trace elements of N and P as well as S, K, Ca, Mg and Fe need to be supplemented and regulated as nutrients, and chicken manure from local chicken farms is as additive to supplement other biotin and nutrients. *Table 2* shows the changes of soluble salts, NH_4 and NO_3 contents with the test process. It can be seen that the test area is supplemented various nutrient elements on August 21, reflecting the process of utilizing, degrading and transforming petroleum and various elements with the microbial activities in the test process. This process verifies that the nutrient elements added in the regulation and control of this experiment are appropriate. The control area and blank area reflect the natural content change, and the rainfall makes the content decrease.

Conclusions

(1) Based on the preliminary experimental study on in-situ microecological remediation of petroleum contaminated soils, the soil temperature, water, oxygen, nutrients and geological environmental factors in the test area are regulated by optimizing in-situ (indigenous) microbial flora and combining physical and chemical methods with geological environment. The experiment of degradation and remediation of man-made petroleum contaminants in soil shows that the average content of oil in soil is 2318.5 mg kg^{-1}. After 11-32 days of in-situ microecological remediation, the removal rate of petroleum in soil can reach 68.47-84.30%. The oil content of artificial filling in the soil of the control area does not change much, basically less than 10%, indicating that the degradation of oil in the soil is slow under natural conditions. The validity of geological microecological remediation technology for petroleum pollution remediation is verified, and the feasibility of its popularization and application is explored.

(2) It is concluded that the best season for using microecological restoration technology in this area should be from late June to early September every year, and soil temperature can be kept above 25 ℃ through regulation.

(3) It is proved that the nutrients added in the experiment and the improvement of soil environment are moderate, and the method is feasible.

The experimental process preliminarily verifies that the geo-microecological remediation technology is effective and feasible in the field in situ soil's oil pollution remediation experiment. It has the advantages of simple treatment method, low cost, good remediation effect, little environmental impact, no secondary pollution, and in situ remediation. Although it is an experimental study and needs to be improved for large-scale field restoration, it can be achieved through continuous efforts. It can not only effectively remediate soil, aeration zone and prevent and control oil pollution of groundwater in situ, but also increase soil fertility and improve soil environment. It is of great significance to remediate contaminated soil and increase crop production. It is also one of the effective methods to remediate and control oil pollution in large areas of soil fundamentally, having certain practical application value. In this paper, the ecological restoration of soil oil pollution is studied, but the application of the technology to the ecological restoration of heavy metal soil pollution is still to be verified.

http://www.aloki.hu ● ISSN 1589 1623 (Print) ● ISSN 1785 0037 (Online)
DOI: http://dx.doi.org/10.15666/aeer/1802_27272746

Acknowledgments. Binzhou University Doctoral Research Initiation Fee Project (2017Y15).

REFERENCES

[1] Bajagain, R., Lee, S., Jeong, S. W. (2018): Application of persulfate-oxidation foam spraying as a bioremediation pretreatment for diesel petroleum contaminated soil. – Chemosphere 67(23): 145-147.

[2] Barp, L., Biedermann, M., Grob, K., Blas-Y-Estrada, F., Nygaard, U. C., Alexander, J., Cravedi, J. P. (2017): Accumulation of mineral oil saturated hydrocarbons (MOSH) in female Fischer 344 rats: comparison with human data and consequences for risk assessment. – Science of the Total Environment 575(9): 1263-1278.

[3] Chandrangsu, P., Rensing, C., Helmann, J. D. (2017): Metal homeostasis and resistance in bacteria. – Nature Reviews Microbiology 15(23): 338.

[4] Du, S., Li, H., Li, W. (2017): Low-carbon supply policies and supply chain performance with carbon concerned demand. – Annals of Operations Research 255(34): 569-590.

[5] Fruchter, J. (2017): Peer reviewed: in-situ treatment of chromium-contaminated groundwater. – Environmental Science & Technology 36(9): 464A-472A.

[6] Fu, R., Wen, D., Xia, X., Zhang, W. (2017): Electrokinetic remediation of chromium (Cr)-contaminated soil with citric acid (CA) and polyaspartic acid (PASP) as electrolytes. – Chemical Engineering Journal 316(1): 601-608.

[7] Han, D., Currell, M. J. (2017): Persistent organic pollutants in China's surface water systems. – Science of the Total Environment 580(67): 602-625.

[8] Jupp, B. P., Fowler, S. W., Dobretsov, S., van der Wiele, H., Al-Ghafri, A. (2017): Assessment of heavy metal and petroleum hydrocarbon contamination in the Sultanate of Oman with emphasis on harbours, marinas, terminals and ports. – Marine Pollution Bulletin 121(134): 260-265.

[9] Lee, H. J., Lee, D. Y., Mariappan, M. M., Feliers, D., Ghosh-Choudhury, G., Abboud, H. E., Gorin, Y., Kasinath, B. S. (2017): Hydrogen sulfide inhibits high glucose-induced NADPH oxidase 4 expression and matrix increase by recruiting inducible nitric oxide synthase in kidney proximal tubular epithelial cells. – Journal of Biological Chemistry 2017, 292(3): 5665-5675.

[10] Li, D. C., Xu, W. F., Mu, Y., Yu, H. Q. (2018): Remediation of petroleum contaminated soil and simultaneous recovery of oil by fast pyrolysis. – Environmental Science & Technology 2018, 12(3): 7b03899.

[11] Ming, C., Qin, X., Zeng, G. (2017): Biodegradation of carbon nanotubes, graphene, and their derivatives. – Trends in Biotechnology 35: S0167779916302049.

[12] Naafs, B. D. A., Gallego-Sala, A. V., Inglis, G. N., et al. (2017): Refining the global branched glycerol dialkyl glycerol tetraether (brGDGT) soil temperature calibration. – Organic Geochemistry 106(9): 48-56.

[13] Papale, M., Giannarelli, S., Francesconi, S., Di Marco, G., Mikkonen, A., Conte, A., Rizzo, C., De Domenico, E., Michaud, L., Giudice, A. L. (2017): Enrichment, isolation and biodegradation potential of psychrotolerant polychlorinated-biphenyl degrading bacteria from the Kongsfjorden (Svalbard Islands, High Arctic Norway). – Marine Pollution Bulletin 114(78): 849.

[14] Pattison, D. I., Dean, R. T., Davies, M. J. (2018): Oxidation of DNA, proteins and lipids by DOPA, protein-bound DOPA, and related catechol(amine)s. – Toxicology 177(76): 23-37.

[15] Schmidbaur, H., Schier, A. (2017): Gold η2-coordination to unsaturated and aromatic hydrocarbons: the key step in gold-catalyzed organic transformations. – Organometallics 29(12): 4540-4561.

http://www.aloki.hu ● ISSN 1589 1623 (Print) ● ISSN 1785 0037 (Online)
DOI: http://dx.doi.org/10.15666/aeer/1802_27272746

[16] Selvi, M., Hariharan, G., Kannan, K. (2017): A reliable spectral method to reaction-diffusion equations in entrapped-cell photobioreactor packed with gel granules using Chebyshev wavelets. – Journal of Membrane Biology 250(1): 1-8.
[17] Sharma, B., Dangi, A. K., Shukla, P. (2018): Contemporary enzyme based technologies for bioremediation: a review. – Journal of Environmental Management 210(56): 10-22.
[18] Sinsabaugh, R. L., Moorhead, D. L., Xu, X., Litvak, M. E. (2017): Plant, microbial and ecosystem carbon use efficiencies interact to stabilize microbial growth as a fraction of gross primary production. – New Phytologist 214(89): 1518-1526.
[19] Varjani, S. J., Gnansounou, E., Pandey, A. (2017): Comprehensive review on toxicity of persistent organic pollutants from petroleum refinery waste and their degradation by microorganisms. – Chemosphere 188(4): 280-291.
[20] Wu, B., Rui, X. P., Li, Z. Z., Song, X. F. (2018): Simulation of forecasting for diffusion of groundwater contaminants in aeration zone. – Computer Simulation 35(04): 445-449.
[21] Wu, H., Lai, C., Zeng, G., Liang, J., Chen, J., Xu, J., Dai, J., Li, X., Liu, J., Chen, M., Lu, L., Hu, L., Wan, J. (2017): The interactions of composting and biochar and their implications for soil amendment and pollution remediation: a review. – Critical Reviews in Biotechnology 37(42): 754-764.

http://www.aloki.hu ● ISSN 1589 1623 (Print) ● ISSN 1785 0037 (Online)
DOI: http://dx.doi.org/10.15666/aeer/1802_27272746

SOLIDIFICASTION REMEDIATION METHOD FOR SOIL HEAVY METAL POLLUTION WHILE CONSIDERING ENVIRONMENTAL BEARING CAPACITY

LI, X.[1] – ZHAO, X.[1] – SHI, Z.[2*]

[1]*Marxist College, China University of Petroleum-Beijing, Beijing 102249, China*

[2]*Unit 93656 of People's Liberation Army of China, Beijing 101113, China*

**Corresponding author*
e-mail: 17791653486@163.com

(Received 3rd Sep 2019; accepted 12th Feb 2020)

Abstract. As heavy metal pollution in the soil is becoming more and more serious, a solidification remediation method considering environmental carrying capacity is proposed. Firstly, the index system for soil environmental carrying capacity is constructed to obtain an evaluation method and grade soil carrying capacity, in order to be able to take the evaluation results into account. According to the soil remediation standard, the method of solidification remediation is used to remediate the heavy metal pollution in soil. The method first measures the soil sample and adds water to the mixture based on the results of measurement; excavates the soil and sprinkles the mixture with water; mixes the mixture until the color and moisture are uniform; smoothes and regularly compacts the toppled soil to solidify the contaminated elements in the soil. In order to remedy the contaminated soil, the organic and inorganic pollutants in its solid phase are transferred into the liquid phase by ethylenediamine tetraacetic acid (EDTA) reagent. The experimental results show that the average reduction rate of soil contaminated elements is 95.86% after remediation by the proposed method, and this method can effectively remediate the various forms of heavy metal contaminated elements in soil.
Keywords: *evaluating indicator, comprehensive evaluation value, range standardization, data preprocessing, expert evaluation method*

Introduction

In recent decades, with the rapid development of China's industry, heavy metals have been widely used in production. However, with the adjustment of industrial structure and the implementation of policies such as "retreat into three" and "retreat to the city and enter the park", a large number of industrial and mining enterprises have been shut down and relocated. "Retreat into three" is the phenomenon that the original plant land is re planned as residential land. Many industrial enterprises in the old urban area move to the industrial park, suburb or development zone. This process is called "retreat to the city and enter the park". According to the data released by the State Environmental Protection Administration in 2013, from 2006 to 2012, there were nearly 100,000 industrial relocation sites in China (Matos et al., 2017). Due to the extensive environmental safety management model, the disorderly discharge or leakage of industrial wastewater and the stacking of metal slag, a large number of heavy metal contaminated sites have been produced, which has exerted tremendous pressure on the subsequent land development and utilization.

Land resources are the basic guarantee for human survival and development, sustainable utilization of ecological environment and regional economic construction. In recent years, with the rapid development of urbanization in China, there are many problems such as environmental pollution and shortage of resources. There is a "one more

http://www.aloki.hu ● ISSN 1589 1623 (Print) ● ISSN 1785 0037 (Online)
DOI: http://dx.doi.org/10.15666/aeer/1802_27472760

and three less" phenomenon: more land resources, less per capita, less high-quality arable land and less arable land reserve (Liu et al., 2018). Therefore, according to the regional population, economy, industry, agriculture, city, transportation, energy, environmental management, industrial environmental governance, urban environmental governance and other factors, this paper establishes a comprehensive evaluation model of environmental carrying capacity (Chen and Li, 2018) to evaluate the level of soil environmental carrying capacity in the region, which provides scientific basis for strengthening the scientific management of regional land resources, protecting the ecological environment, improving the productivity of regional soil cultivated land and ensuring human health.

Heavy metal pollution has the characteristics of wide pollution range, long duration, hidden pollution, and cannot be degraded by microorganisms. It directly or indirectly endangers human health and life (Tian et al., 2017). With the continuous transformation of regional economy and the constant adjustment of economic structure, enterprises located in urban areas began to "retreat to the city and enter the park". A number of enterprises with high pollution and low productivity are facing relocation, transformation or elimination. The polluted soil left behind must be repaired before it can be transferred and redeveloped.

The remediation of heavy metal contaminated soils has been a hot topic both at home and abroad. Wang et al. (2016) focuses on the application of remediation methods for heavy metal contaminated soil, but the remediation of heavy metal contaminated soil is not carried out under the premise of considering the environmental carrying capacity. Rutskii et al. (2017) only described the remediation of pollution elements Cu and Pb in detail, however, it does not show that the method adopted has the effect of remediation for most of the contaminated elements. Yang et al. (2016) uses a variety of chemical reagents to transfer organic and inorganic pollutants from the solid phase of contaminated soil to liquid phase fluid, but this process is only carried out once, and the data obtained from heavy metal pollution of soil are not accurate.

In this paper, physical, chemical and biological methods (Lü et al., 2017) are used to remediate heavy metal contaminated soils through the following ways: (1) reducing the concentration of heavy metals in soil by dilution; (2) changing the form of heavy metals to fix or passivate them, and reducing their mobility and bioavailability in the environment; (3) removal of heavy metals from soil. The domestic soil remediation industry is still in its infancy and growing stage. Most of the pilot projects are site pollution control in urban relocation plant areas. There are many cases of organic pollution remediation, few cases of heavy metal pollution remediation, and many heavy metal technologies are still in the laboratory research stage (Chen et al., 2017). Based on the index system of soil environmental carrying capacity, the evaluation method and grade of soil environmental carrying capacity are obtained, and the solidification remediation method of soil heavy metal pollution is studied considering the effect of environmental carrying capacity. This method first determines the soil sample and adds water to the mixture on the basis of the measured results; excavates the tested soil and sprays the mixed material with water; mixes the mixed soil until the color and moisture are uniform; smoothes the overturned soil, and regularly rolls the soil to make it uniform. Polluted elements in soil are solidified, organic and inorganic pollutants in the solid phase of contaminated soil are transferred to liquid phase fluids by chemical reagents to achieve the purpose of remediation of contaminated soil (Wang et al., 2016). According to the above analysis, the soil treated by this method has been significantly improved, and a variety of heavy metal pollution elements have been effectively repaired.

http://www.aloki.hu ● ISSN 1589 1623 (Print) ● ISSN 1785 0037 (Online)
DOI: http://dx.doi.org/10.15666/aeer/1802_27472760

Material and methods

Establishment of evaluation index system for soil environmental carrying capacity

In order to objectively, comprehensively and scientifically evaluate the status of soil carrying capacity, when studying and determining the evaluation index system of soil carrying capacity and its evaluation method, we should follow the scientific principles of selecting evaluation index, determining index weight, the scientific principle of calculating and synthesizing index, the dynamic principle of the change of soil carrying capacity in time and space, and the feasibility principle based on regional sustainable development (Rutskii et al., 2017).

According to the five principles of index selection, an index system for evaluating soil environmental carrying capacity in Liaoning province is established, with 522 indexes (Yang et al., 2016). Specific indexes are shown in *Table 1*.

Table 1. *Evaluation index system of soil environmental bearing capacity*

Project level	Factor layer	Index layer	Company
Pressure	Population economy	Population density	Ten thousand people/km^2
		Natural population growth rate	%
		Per capita GDP	Ten thousand yuan
		The proportion of output value of secondary industry	%
	Industry	Emission intensity of industrial smoke and dust	Tons/km^2
		Discharge intensity of industrial wastewater	10,000 tons/km^2
		Discharge intensity of industrial solid waste	10,000 tons/km^2
	Agriculture	Use strength of chemical fertilizer	10,000 tons/km^2
		Pesticide use intensity	Tons/km^2
	City	Domestic sewage discharge	10,000 m^3
		Domestic waste emissions	Ten thousand tons
	Transportation, energy	Ten thousand yuan GDP energy consumption	Ton standard coal
		Highway passenger transport intensity	Ten thousand people/km^2
	Environmental management	Proportion of environmental protection input to GDP	%
Response	Industrial environmental governance	Achievement rate of industrial wastewater discharge from key pollution sources	%
		Comprehensive utilization rate of industrial waste	%
	Urban environmental governance	Urban domestic sewage treatment rate	%
		Harmless treatment of municipal domestic waste	%

Evaluation method of bearing capacity

Select the data provided by Google dataset search dataset as the data source of the experiment. Google dataset search data set can be regarded as a one-stop data set, which contains massive data of different sizes and types from NASA, propublica and other sources. The data source is comprehensive, so the data set has strong

http://www.aloki.hu ● ISSN 1589 1623 (Print) ● ISSN 1785 0037 (Online)
DOI: http://dx.doi.org/10.15666/aeer/1802_27472760

application value. In this database, six datasets are selected as the experimental data. The datasets involve image and other fields, and contain 150000 kb different data groups. In order to facilitate evaluation, the above basic data is standardized by the range standardization method (Li et al., 2015), that is, the data is dimensionless and unified by an order of magnitude. Soil environmental assessment indexes are divided into favorable indexes and unfavorable indexes. According to the different types of indexes, standardized treatment is carried out according to the formula. Among them, the higher the favorable index is, the better the soil bearing capacity is, and the lower the unfavorable index is, the better the soil bearing capacity is (Wang et al., 2015).

$$P = \left(X_i - X_{\min}\right) / \left(X_{\max} - X_{\min}\right) \quad \text{(Eq.1)}$$

$$Q = 1 - \left(X_i - X_{\min}\right) / \left(X_{\max} - X_{\min}\right) \quad \text{(Eq.2)}$$

where P represents favorable index after standardization; Q represents the disadvantageous index after standardization; X_i represents the measured value of an index; $X_{\max}$ represents the maximum value in the statistical range of an index; $X_{\min}$ represents the minimum value in the statistical range of an index.

Because of the coexistence of quantitative index and qualitative index in the evaluation index of soil environmental carrying capacity (Liu et al., 2018), this paper uses expert evaluation method to determine the weight of each evaluation index. Five experts scored the importance of each indicator, obtained the scoring results, and calculated the average value of each indicator. According to the standardized results of *Equations 1* and *2*, the weight of each indicator is allocated after the implementation of inspection as shown in *Table 2*.

Computation of comprehensive evaluation value

The final comprehensive evaluation value is calculated by multiplying the dimensionless utility value of an index in the terminal index by the corresponding weight of the index to the target layer (Yu et al., 2015), which is expressed by the following formula:

$$Y = \sum_{i=1}^{n} X_i P_i \quad \text{(Eq.3)}$$

In the formula, Y is the total score of soil carrying capacity, P_i is the utility value of the i-th index and X_i is the weight of the i-th index to the target.

Criteria for evaluating soil environmental bearing capacity

According to the comprehensive score of soil carrying capacity of cities in the provincial capital city group, this study formulates five bearing capacity grades (Girsowicz et al., 2018), as shown in *Table 3*.

Based on the above assessment results of soil environmental carrying capacity and soil remediation standards, the following remediation schemes are adopted to remediate heavy metal pollution in soil.

http://www.aloki.hu ● ISSN 1589 1623 (Print) ● ISSN 1785 0037 (Online)
DOI: http://dx.doi.org/10.15666/aeer/1802_27472760

Table 2. *Weight distribution of index system*

Project level		Factor layer		Index Layer		Comprehensive weight
Pressure	0.554	Population economy	0.071	Population density	0.444	0.032
				Natural population growth rate	0.222	0.029
				Per capita GDP	0.222	0.029
				The proportion of output value of secondary industry	0.111	0.027
		Industry	0.424	Emission intensity of industrial smoke and dust	0.164	0.041
				Discharge intensity of industrial wastewater	0.297	0.054
				Discharge intensity of industrial solid waste	0.539	0.077
		Agriculture	0.134	Use strength of chemical fertilizer	0.5	0.04
				Pesticide use intensity	0.5	0.04
		City	0.239	Domestic sewage discharge	0.333	0.043
				Domestic waste emissions	0.667	0.062
		Transportation, energy	0.134	Ten thousand yuan GDP energy consumption	0.667	0.045
				Highway passenger transport intensity	0.333	0.035
		Environmental management	0.539	Proportion of environmental protection input to GDP	1	0.131
Response	0.446	Industrial environmental governance	0.297	Achievement rate of industrial wastewater discharge from key pollution sources	0.333	0.077
				Comprehensive utilization rate of industrial waste	0.667	0.089
		Urban environmental governance	0.164	Urban domestic sewage treatment rate	0.333	0.072
				Harmless treatment of municipal domestic waste	0.667	0.078

Table 3. *Criteria for evaluating soil environmental carrying capacity*

Interval value of soil bearing capacity	Grade of bearing capacity	Representation state
<0.2	Ⅰ	More weak bearing capacity
0.2-0.4	Ⅱ	Weak bearing capacity
0.4-0.6	Ⅲ	General bearing capacity
0.6-0.8	Ⅳ	Strong bearing capacity
>1.0	Ⅴ	More strong bearing capacity

Standards for soil remediation

Remediation standard

Secondary development of sites requiring remediation is carried out. Remediation criteria are selected according to different development projects. This paper mainly assumes that the secondary development project is commercial land. Then, after the

http://www.aloki.hu ● ISSN 1589 1623 (Print) ● ISSN 1785 0037 (Online)
DOI: http://dx.doi.org/10.15666/aeer/1802_27472760

demonstration of industry experts, the standard of site excavation and remediation is the commercial land standard in the secondary standard of Soil Environmental Quality Standard (GB 15618-2008) (Arenaslago et al., 2018), i.e. the standard values of C_r, C_u, N_i, P_b and Z_n are 800, 500, 200, 600 and 700 mg/kg, respectively.

Scheme of solidification remediation

The solidification method solidifies contaminated soil with solidifying agent, which reduces the mobility and bioavailability of contaminated molecules. The selection of solidifying agent is very important for the remediation of contaminated soil by solidification method.

Flow chart of solidification remediation process

Figure 1 is the flow chart of solidification remediation. It can be seen from the figure that: (1) the moisture content of the soil sample in the field is measured to determine the water content of the mixture; (2) earthwork excavation; (3) material distribution; (4) mixing: dry mixing for 3-4 times, and spraying water solution containing stabilizer on the mixture; mixing twice more carefully and turning the bottom "plain soil" up each time without loosening the underlying stratum; the mixture has uniform color without gray strips, ash and flower surface, no coarse and fine particle nests, and suitable moisture content; (5) shaping: preliminary scraping and shaping, straight line section from both sides to the center, return to scraping if necessary, pay attention to the flat seam.(6) rolling: Rolling requires following the paving closely with no wheel tracks, generally rolling first slow and then fast, first light and then heavy; (7) Maintenance; (8) Testing: testing dry density and moisture content, calculating whether the compaction coefficient meets the requirements (Yan et al., 2015).

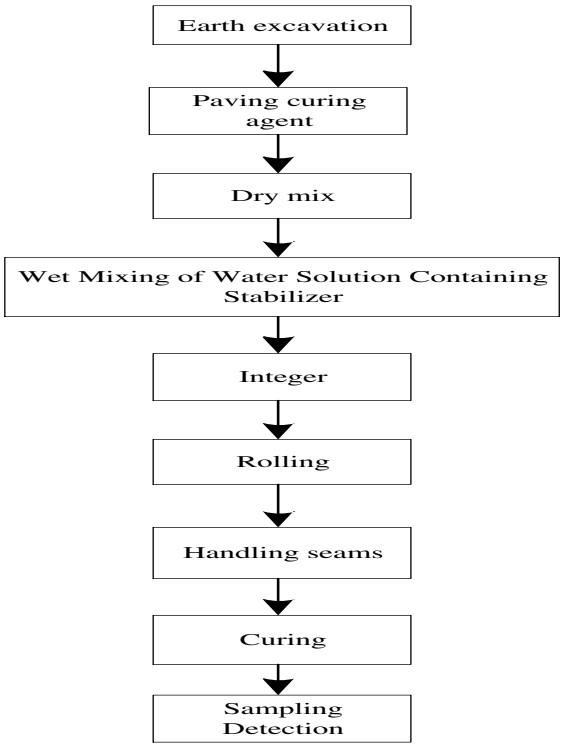

Figure 1. *Flow chart of solidification remediation*

http://www.aloki.hu ● ISSN 1589 1623 (Print) ● ISSN 1785 0037 (Online)
DOI: http://dx.doi.org/10.15666/aeer/1802_27472760

Content analysis of soil leaching solution for remediation

Leaching is the main way for harmful substances from solid waste to enter the environment (Li et al., 2017). Leaching experiment is a laboratory simulation of leaching process. Its purpose is to assess the environmental risk of different solid waste under different treatment environments and treatment modes. According to the current management needs and disposal methods of solid waste in China, in the standard experimental study, there are two hypothetical scenarios: non-standard landfill treatment of industrial solid waste, waste accumulation, land use of wastes after innocuous treatment (Xiao et al., 2017); 5% of industrial wastes or harmless wastes enter sanitary landfills and are combined with 95% of municipal wastes. In the first scenario, nitric acid sulfate solution is used as extractant to simulate this adverse environmental factor. In the second scenario, acetic acid buffer solution is used as extractant.

When sulfuric acid nitric acid solution is used as leaching agent, its acidity is helpful for metal leaching, but it has no buffer capacity, and the leaching amount of metal is very low. If the content of any hazardous substance in leaching liquor exceeds the standard value of leaching toxicity in "Hazardous Waste Identification Standard of Leaching Individual Identification" (GB5085.3-2007), it is determined that the solid waste is a hazardous waste with leaching toxicity characteristics.

When acetic acid buffer solution is used as leaching agent, the complexation effect on metal leaching is obvious, and the acidity of the system changes slightly after leaching (Ma et al., 2017), and the amount of metal leaching is very high.

These two extractants have their own advantages and disadvantages in remediation of heavy metal pollution in soil, but EDTA is often used as a leaching agent for heavy metal pollution in soil and as an amendment for the bioavailability of heavy metals in soil (Zhang, 2018). Soil elution is to transfer organic and inorganic pollutants in the solid phase of contaminated soil to liquid phase fluid by chemical reagents, so as to achieve the purpose of remediation of contaminated soil. In this paper, EDTA is used as soil eluent, and the hydrolysis stability is high in the range of high temperature and wider pH value.

Results

Analysis of remediation effect of different methods on heavy metal contaminated soil

In order to verify the best remediation effect of the proposed method for heavy metal contaminated soil, on the premise of sufficient soil environmental carrying capacity. The experiment was carried out under the hardware conditions of Intel core-m480i5cpu @ 2.67 GHz, 4 GB memory, 32-bit operating system and windows 7 version. And the simulation data set my sea is selected as the basic data set, and the data is analyzed by the online data anal ysis software MOA (an experimental tool for massive online analysis). The effects of chemical leaching, cement kiln co-disposal, phytoremediation (Bennabi et al., 2017) and the proposed method on remediation of heavy metal contaminated soil are compared, as shown in *Table 4*.

Table 4 shows that after the remediation of heavy metal contaminated soil by the proposed method, the content of various contaminated elements has been greatly reduced. The average reduction rate of the content of contaminated elements after remediation is 95.86%, which is higher than that of the contaminated elements removed by other methods.

http://www.aloki.hu ● ISSN 1589 1623 (Print) ● ISSN 1785 0037 (Online)
DOI: http://dx.doi.org/10.15666/aeer/1802_27472760

Table 4. *Comparison of reduction rates of contaminated elements after remediation of heavy metal contaminated soil*

Repair Technology	Reduction ratio of Cr content%	Reduction ratio of Cu content%	Reduction ratio of Ni content%	Reduction ratio of Pb content%	Reduction ratio of Zn content%
Chemical elution	83.22%	89.19%	88.33%	90.02%	87.54%
Co-disposal of cement kiln	88.49%	85.32%	86.13%	88.96%	81.23%
Phytoremediation	90.22%	91.32%	89.01%	88.39%	88.14%
The method in this paper	95.32%	97.19%	96.33%	94.56%	95.92%

In order to make the data comparison in *Table 4* more intuitive, a column chart is constructed to analyze the content of pollutant elements reduced by various methods, as shown in *Figure 2*.

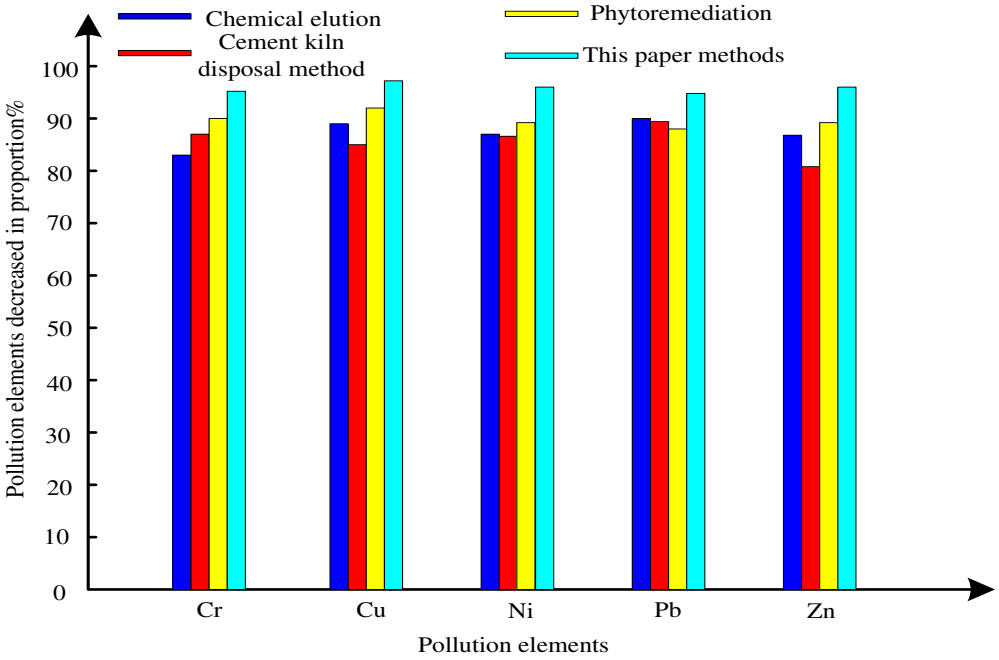

Figure 2. *Percentage decrease of various pollutant elements after remediation of heavy metal land pollution*

As can be seen intuitively in *Figure 2,* the method in this paper has the highest removal rate of various pollutant elements in all comparison methods, so the method in this paper has the best effect on remediation of heavy metal pollution in soil by considering environmental carrying capacity.

Morphological analysis of heavy metals removal

In order to verify the remarkable effect of DETA extractant on remediation of heavy metal pollution in soil, the morphological analysis model of heavy metal removal is constructed. The precipitation of 0.2 mol/L citric acid and 0.05 mol/L EDTA is analyzed after washing once and five times, respectively, in order to find out the mechanism of removing copper and nickel from soil by the eluent, as shown in *Table 5*.

http://www.aloki.hu ● ISSN 1589 1623 (Print) ● ISSN 1785 0037 (Online)
DOI: http://dx.doi.org/10.15666/aeer/1802_27472760

Table 5. *Morphological analysis of precipitation after elution*

Project		Cu			Ni		
		Content of each speciation in precipitation (mg/kg)	Removal rate of various forms (%)	Proportion of each form in removal amount (%)	Content of each speciation in precipitation (mg/kg)	Removal rate of various forms (%)	Proportion of each form in removal amount (%)
0.2 mol/L citric acid pickling once	Commutative state	56.2444	84.98	46.22	203.8444	86.89	84.33
	Carbonate state	8.4111	94.16	19.7	14.7667	77.69	3.21
	Iron ferocity	41.5556	67.42	12.49	15.786	32.54	0.48
	Organic state	43.6	39.29	4.1	11.4017	39.83	0.48
	Residual state	231.7556	34.18	17.48	860.9679	17.64	11.51
0.05 mol/L EDTA wash once	Commutative state	14.7222	96.07	47.89	129.3328	98.8	85.37
	Carbonate state	6.3324	96.27	20.89	8.5769	92.09	3.23
	Iron ferocity	27.5839	83.28	13.57	5.4433	38.2	0.52
	Organic state	29.7333	40.12	5.88	8.0667	41.05	0.51
	Residual state	210.9985	44.35	19.34	769.3831	26.4	14.62
0.2 mol/L citric acid pickling 5 times	Commutative state	6.9444	98.015	45.48	9.3367	99.4	82.06
	Carbonate state	2.0889	98.55	17.57	2.378	96.41	3.39
	Iron ferocity	16.3333	87.2	13.76	7.9613	65.98	0.82
	Organic state	30.1333	58.04	5.16	6.8083	64.07	0.64
	Residual state	206.4333	41.37	18.03	799.019	23.56	13.08
EDTA wash 5 times at 0.05 mol/L	Commutative state	3.0667	99.18	46.32	5.6252	99.83	84.83
	Carbonate state	2.0113	101.98	17.6	2.2698	96.57	3.49
	Iron ferocity	11.9778	94.34	14.42	6.302	70.43	0.85
	Organic state	20.9667	61.82	7.85	4.2667	68.65	0.65
	Residual state	183.3111	45.1	19.81	763.903	26.92	14.66

In *Table 5,* the removal rates of five forms of copper and nickel by citric acid and EDTA at one and five leaching times show that the removal rates are almost exchangeable> residual> carbonate-bound> iron-manganese oxide-bound> organic-bound, which are related to the content of the original forms of heavy metals in soil. The main forms of copper removal by citric acid and EDTA are exchangeable, carbonate-bound and iron-manganese oxide-bound and the removal rates are above 60%, while the removal rates of organic and residual states are generally low. The data in the observation table show that the removal rates of various forms of contaminated elements by citric acid are weaker than EDTA. Therefore, the removal rate of various forms of contaminated elements is very high by the proposed method.

Comparison of remediation techniques for different heavy metal contaminated elements

In order to verify the best effect of the proposed method on remediation of heavy metal contaminated soil, the heavy metal contaminated soil area in the suburb of a city is selected as the experimental area, the range value of soil environmental carrying capacity is 0.6-0.8, and the soil environmental grade is grade IV. Taking the carrying capacity as the consideration factor, chemical leaching method, cement kiln co-treatment method and phytoremediation and the method in this paper are used to make compare. *Table 6* is a comparative table of four methods.

As can be seen from *Table 6,* the proposed method has mature technology, the lowest cost of remediation, the highest efficiency of remediation, and little impact on the environment. Therefore, the effect of the proposed method on remediation of heavy metal pollution in soil is remarkable.

http://www.aloki.hu ● ISSN 1589 1623 (Print) ● ISSN 1785 0037 (Online)
DOI: http://dx.doi.org/10.15666/aeer/1802_27472760

Table 6. *Comparison of remediation methods for different heavy metal contaminated soils*

Repair technology	Technical maturity	Repair unit price	Repair efficiency	environmental effect	Advantage	Shortcoming
Chemical elution	More mature	2000-3000	Higher	Less	Disposable compound contaminated soil, safe operation	Not suitable for soils with high clay content
Co-disposal of cement kiln	Test phase	800-1000	Commonly	Less	Disposal cost is relatively low and operation is simple and safe	Limited by cement production and emission
Phytoremediation	Test phase	It depends	Low	Less	Polluted soils need not be excavated and the cost of disposal is low	Remediation takes a long time and plant screening is difficult
The method in this paper	More mature	500-800	High	Less	The disposal cost is low, the disposal quantity is large, the operation is simple and safe	No pollutants were removed from the soil

Analysis of soil remediation capacity and environmental bearing capacity

In order to verify that the proposed method can improve the soil environmental carrying capacity, the improvement of soil carrying capacity after remediation of heavy metal contaminated soils in mountainous, plain, plateau, basin and hilly areas is compared, as shown in *Figure 3*.

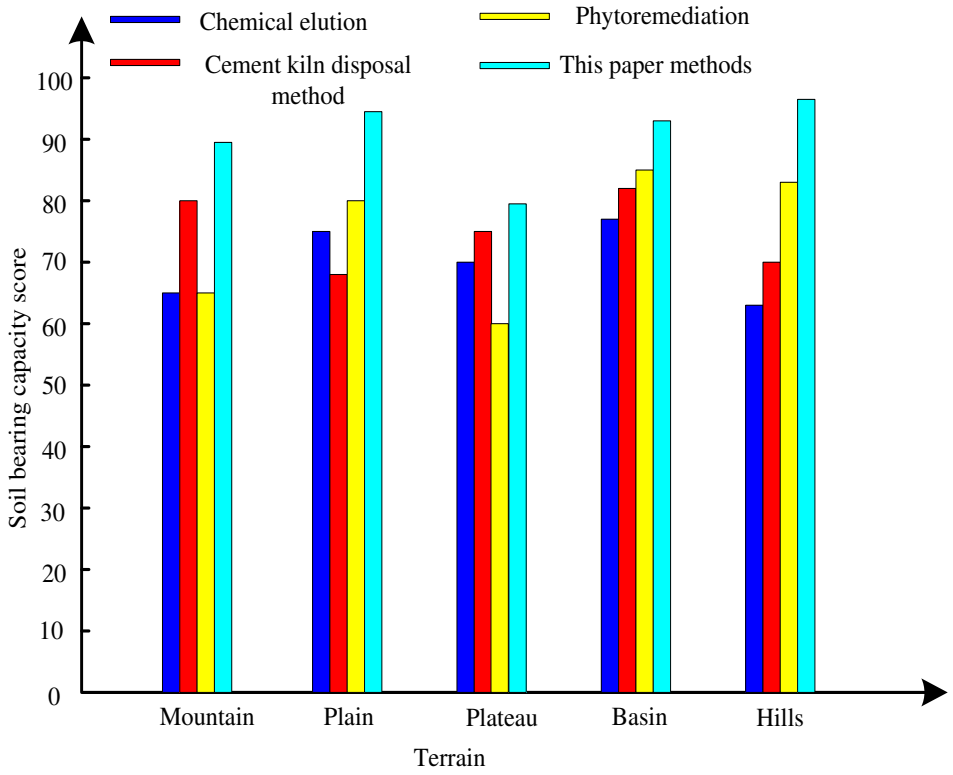

Figure 3. *Score of soil carrying capacity after remediation of heavy metal contaminated soil*

http://www.aloki.hu ● ISSN 1589 1623 (Print) ● ISSN 1785 0037 (Online)
DOI: http://dx.doi.org/10.15666/aeer/1802_27472760

The comparative results of soil remediation capacity of different methods are shown in *Table 7*.

Table 7. *Comparison of soil remediation capacity*

Terrain	Soil remediation capacity/m^3.s				Standard for element content of soil pollutants			
	Chemical elution	Cement kiln disposal method	Phytoremediation	The method in this paper	Chemical elution	Cement kiln disposal method	Phytoremediation	The method in this paper
A mountain country	15	12	13	24	Excessive content	The content is up to the standard	The content is up to the standard	The content is up to the standard
Plain	18	11	16	28	The content is up to the standard	Excessive content	The content is up to the standard	The content is up to the standard
Plateau	10	15	15	29	Excessive content	Excessive content	Excessive content	The content is up to the standard
Basin	20	17	15	31	Excessive content	Excessive content	The content is up to the standard	The content is up to the standard
Hill	20	16	12	33	The content is up to the standard	The content is up to the standard	Excessive content	The content is up to the standard

Remediation time and cost analysis of heavy metal contaminated soil

In order to verify that the proposed method can reduce the repair time-consuming and reduce the cost, the repair time and cost of the five topographies mentioned above are compared. The results are shown in *Table 8*.

Table 8. *Comparison of soil remediation time and cost*

Terrain	Repair time (days)				Repair cost (10,000 yuan)			
	Chemical elution	Cement kiln disposal method	Phytoremediation	The method in this paper	Chemical elution	Cement kiln disposal method	Phytoremediation	The method in this paper
A mountain country	1	1.5	1	0.5	1.3	1.2	1.4	0.9
Plain	0.5	1.5	1	0.5	1.5	1.6	1.6	1.1
Plateau	2.5	3	2.5	1	2.6	2.4	2.4	1.5
Basin	2	2.5	2	1	1.6	1.9	1.8	1.1
Hill	1.5	1.5	1.5	1	1.4	1.6	1.6	1.2

Analysis of the data in *Table 8* shows that the method in this paper has the shortest time and the lowest cost to repair the five topographies.

http://www.aloki.hu ● ISSN 1589 1623 (Print) ● ISSN 1785 0037 (Online)
DOI: http://dx.doi.org/10.15666/aeer/1802_27472760

Discussion

Heavy metal pollution refers to the fact that the content of heavy metals in soil is much higher than its background value, which leads to the deterioration of the original function of the soil. The main pollution in urban soils comes mainly from human activities. Heavy metal wastes are produced in heavy industries such as metal smelting and processing, fur and products processing, glass manufacturing, printing and dyeing, electronic component manufacturing and other light manufacturing industries, as well as in the process of garbage disposal in people's daily life and medical activities.

Based on the above-mentioned environment, this paper firstly constructs the index system of soil environmental carrying capacity and the standard of soil remediation, and uses the method of curing remediation to fix the heavy metal pollution in soil. According to the above experimental results, we can see that:

Figure 3 shows that when five topographies are restored by four different methods, only the proposed method can get the highest score of soil bearing capacity. Because of the sparse vegetation and serious soil erosion in the plateau area, it is more difficult to repair the heavy metal contaminated soil. Therefore, the land carrying capacity score of the proposed method in the plateau topographic area is only 80 points. *Table 7* shows that chemical leaching method, cement kiln treatment method and phytoremediation method are not effective in soil remediation, and the content of contaminated elements in the remediated soil still exceeds the standard, while the method in this paper has the highest remediation ability in all methods, and the content of contaminated elements in the remediated soil does not exceed the standard.

Through the analysis of the above data, it can be seen that the moire method effectively improves the traditional method, and can effectively repair various forms of heavy metal pollution elements in the soil.

Conclusions

The main characteristics of heavy metal pollution in urban soils are long duration, concealment, hysteresis and irreversibility. Based on the index system of soil environmental carrying capacity, the evaluation method and grade of soil carrying capacity are obtained, and the soil environmental carrying capacity is assessed. The evaluation results are taken into account and the technology of solidification and remediation is used to remediate urban heavy metal pollution. Metal contaminated soil makes the remediated soil have a certain strength, which is conducive to rational utilization and disposal in the subsequent commercial development. At the same time, EDTA leaching solution used in the proposed method can remove various forms of heavy metal contaminated elements very well. Using the proposed method to solidify and treat soil not only can control soil pollution, but also can play a solid role in the soil, making the foundation more solid. Therefore, the proposed method has the best effect on remediation of heavy metal contaminated soil.

Although the method in this paper is effective, more environmental factors should be considered, such as water, weather and so on. In the future, this paper will focus on the influence of these factors on the remediation of heavy metal pollution in soil.

Acknowledgments. 1. National Social Science Fund Major Project: "Translation and Research of Cutting-Edge Theories of Contemporary Western Narratology" (project number: 17ZDA281). 2. Beijing Social Science Fund Project: "From Analysis to Construction: A Corpus-Based Study on the Translation of *XI JINPING THE GOVERNANCE OF CHINA*" (project number: 18YYB010).

http://www.aloki.hu ● ISSN 1589 1623 (Print) ● ISSN 1785 0037 (Online)
DOI: http://dx.doi.org/10.15666/aeer/1802_27472760

REFERENCES

[1] Arenaslago, D., Santos, E. S., Carvalho, L. C., et al. (2018): Cistus monspeliensis L. as a potential species for remediation of soils with multielemental contamination under Mediterranean conditions. – Environmental Science & Pollution Research 25(7): 6443-6455.

[2] Bennabi, N., Menana, H., Charpentier, J. F., et al. (2017): Improving efficiency and emissions of small ships by the use of hybrid electrical propulsion. – Journal of Power Supply 15(2): 12-23.

[3] Chen, A. N., Wu, J. M., Xiao, H., et al. (2017): Rapid and uniform in-situ solidification of alumina suspension via a non-contamination DCC-HVCI method using MgO sintering additive as coagulating agent. – Ceramics International 43(13): 9926-9933.

[4] Chen, W., Li, H. (2018): Cost-effectiveness analysis for soil heavy metal pollution treatments. – Water Air & Soil Pollution 229(4): 126.

[5] Girsowicz, R., Koryachenko, O., Chen, S., et al. (2018): Impact of oil-spill contamination on a soil bacterial community: A 40-year history of remediation in the Arava Valley. – Soil & Sediment Contamination 27(3): 1-11.

[6] Li, M. X., Sun, S. J., Cui, P., et al. (2017): Effects of water environmental chemical characteristics on difference of phytoplankton community structure in Xianghai and Chagan Lake wetlands. – Journal of Jilin University (Science Edition) 55(3): 739-750.

[7] Li, Y. Q., Wang, H. Z., Zhang, J., et al. (2015): A feasibility study on co-processing of soil contaminated with heavy metals in cement kilns. – Applied Mechanics & Materials 768(8): 135-141.

[8] Liu, L., Li, W., Song, W., et al. (2018): Remediation techniques for heavy metal-contaminated soils: Principles and applicability. – Science of the Total Environment 633: 206-219.

[9] Lü, H. Y., Fei, Y., Wang, A. Q., et al. (2017): Effects and mechanisms of in-situ cement solidification/stabilization on a Pb-, Zn-, and Cd-contaminated site at Baiyin, China. – Huan Jing Ke Xue 38(9): 3897-3906.

[10] Ma, X. L., Gao, S., Zhou, Y. (2017): Development of anode materials for magnesium air battery. – Chinese Journal of Power Sources 41(2): 331-333.

[11] Matos, M. P. S. R., Correia, A. A. S., Rasteiro, M. G. (2017): Application of carbon nanotubes to immobilize heavy metals in contaminated soils. – Journal of Nanoparticle Research 19(4): 126.

[12] Rutskii, D. V., Gamanyuk, S. B., Zyuban, N. A., et al. (2017): Effect of liquid–solid pouring on the as-cast structure and the distribution of nonmetallic inclusions in a 24.2-t steel 38KhN3MFA ingot. – Russian Metallurgy 23(5): 376-383.

[13] Tian, L. I., Jiang, J. G., De-An, L. I., et al. (2017): Stabilization of vanadium deposit contaminated soil with liquid iron-based agents. – China Environmental Science 37(9): 3481-3488.

[14] Wang, F., Wang, H., Jin, F., et al. (2015): The performance of blended conventional and novel binders in the in-situ stabilisation/solidification of a contaminated site soil. – Journal of Hazardous Materials 285(285C): 46-52.

[15] Wang, P., Xue, Q., Li, J., et al. (2016): Effects of pH on leaching behavior of compacted cement solidified/stabilized lead contaminated soil. – Environmental Progress & Sustainable Energy 35(1): 149-155.

[16] Xiao, S. A., Wu, H., Wang, J. P., et al. (2017): Research on effectiveness evaluation of integrated electronic information system based on multi-level modeling. – Journal of China Academy of Electronics and Information Technology 12(3): 257-261.

[17] Xu, Y. K. (2018): From “third industry priority” to “value park”: transition and regression of Guangzhou industrial land use. – Planners 34(12): 54-62.

http://www.aloki.hu ● ISSN 1589 1623 (Print) ● ISSN 1785 0037 (Online)
DOI: http://dx.doi.org/10.15666/aeer/1802_27472760

[18] Yan, X., Sun, X., Jing, R., et al. (2015): Genetic diversity and association mapping of cadmium tolerance in bermudagrass [Cynodon dactylon (L.) Pers.]. – Plant & Soil 390(1-2): 307-321.
[19] Yang, P., Byrne, J. M., Li, H., et al. (2016): Evaluation of semi-arid arable soil heavy metal pollution by magnetic susceptibility in the Linfen basin of China. – Arid Soil Research & Remediation 30(3): 11.
[20] Yu, Q., Zhang, W., Yu, L., et al. (2015): Metal pollution in coastal sediments. – Current Pollution Reports 1(4): 203-219.
[21] Zhang, B. P. (2018): The 3d landscape pattern optimization index is simulated under big data analysis. – Computer Simulation 35(4): 214-217.

http://www.aloki.hu ● ISSN 1589 1623 (Print) ● ISSN 1785 0037 (Online)
DOI: http://dx.doi.org/10.15666/aeer/1802_27472760

APPENDIX

SPATIAL VARIABILITY IN GREENHOUSE GAS FLUXES FROM A TEMPERATE FRESHWATER MARSH IN CHINA: EFFECTS OF SOIL MOISTURE, ANIMAL ACTIVITIES AND LAND USE

BAO, T.[1, 2] – ZHU, R. B.[1*] – WANG, P.[1] – FANG, Z. Y.[1] – LI, B. K.[1] – GAO, Y. S.[1] – XU, H.[3]

S1. Study Area

The Shengjin Lake Wetland National Nature Reserve (116° 55′ E-117°15′ E, 30° 15′ N-30° 30′ N) is located at the junction of Dongzhi County and Guichi district in Anhui Province and in the Middle-Lower Yangtze Plain near the Yangtze River. The Shengjin Lake is an important flood storage/discharge reservoir and a natural fishing ground, and it is surrounded by diverse terrains with curving lakeshore lines. Topographically it can be divided into three parts: the upper lake, the middle lake and the lower lake. At present, there are 13 towns and 46 villages around the lake with total population of about 80,000 (Jiang et al., 2007). Most of the villagers depend on the cultivation of cotton and rice on the plain around the lake. Grazing livestocks in the lake marsh and fishery resource from the Shengjin Lake are also essential food sources for the local residents (Fox et al., 2013).

The Shengjin Lake Marsh (SLM) has similar hydrological and ecological features to other Chinese wetlands in mid-latitudinal area. The marsh around the lake has diverse vegetation types including *Artemisia lavandulaefolia DC*, *Artemisia scoparia Waldst* and *pinus massoniana* (Lu and Liu, 2011; Bernal and Mitsch, 2012; Yang et al. 2015). Human activities including the land use conversion and aquaculture, and natural disturbances have intensively affected the local environment (Yang et al., 2015). This marsh is a natural colony for over 100 species of migratory birds to overwinter and breed (Lu and Liu, 2011). The common species of waterbirds include bean goose *Anser fabialis*, greater white-fronted goose *Anser albifrons*, lesser white-fronted goose *Anser erythropus*, swan goose *Anser cygnoides* and tundra swan *Cygnus columbianus bewickii* (Zhang et al., 2015). Migrant birds play an important role in the nutrient cycling in the ecosystems, and their activities strongly influence the physical and chemical properties for the marsh soils, which might lead to be generally high in soil organic carbon, total nitrogen and total phosphorus levels (Lu and Liu, 2011; Zhu et al., 2014a, b). Overall the marsh has been experiencing human disturbance from the conversion of land use, and natural disturbance from waterbirds, drought and flooding (Lu and Liu, 2011).

S2. Investigation Sites and Experimental Design

(i) The upland marsh area: During the rain season in July 2013, the lake water level rose up to the highest, and the marsh was formed along the lakeshore. The total 14 stations (sj1-1 to sj1-14) for GHG flux observations were set up from the dry to waterlogged marsh areas along the lakeshore transect.

(ii) The lowland marsh area: A large flooded land area was exposed with the decrease in the lake water level during the dry season in December 2013. We selected a long transect from the upland to the lowland, and then to a small island along the lakeshore. The middle lowland was exposed only during the dry season in winter, and the upland and the island were both exposed areas throughout the year.

(iii) The marsh sites disturbed by animal activities and land use: Four disturbed areas including waterbird active area (BA), poultry active area (PA), landfill (LF) and farmland (FD), were identified as the observation areas for GHG fluxes. The waterbird active area was located near the transect. A great number of migrant birds flew to the lake marsh to live through the winter, and their guano could be seen everywhere in the exposed marsh. The poultry active area was located in the northwest of the marsh. A lot of geese and ducks often went into the area, and their fertile excreta deposited into the marsh soils. The ground surface in the poultry and waterbird active areas had sparse vegetation due to the tramp of the animals and the input of high nutrients from their excreta. The landfill was a bog with the soft peat and a large amount of garbage. The marsh exposed in summer was transformed into the farmland where winter wheat grew, resulting in soft soil texture and low soil moisture. Two repetitions were made at each station. The soil physiochemical properties at all the microsites were summarized in ***Table S1*** and ***Table S2***.

Table S1. *Soil physical and chemical properties at the upland marsh area.*

Marsh sites	pH	TOC (%)	TN (%)	TC (%)	TS (%)	NH_4^+-N ($\mu g\ g^{-1}$)	NO_3^-N ($\mu g\ g^{-1}$)	Mc (%)
Stations at wet site (SW)								
sj1-1	5.9	0.79±0.15	0.13±0.01	0.98±0.19	0.11±0.01	9.2±3.6	203.7±268.0	40
sj1-2	5.5	1.06±0.12	0.18±0.02	1.10±0.09	0.09±0.03	3.6±0.6	429.4±291.6	42
sj1-3	5.5	1.11±0.04	0.19±0.02	1.16±0.09	0.04±0.01	5.0±0.7	905.4±234.5	40
sj1-4	5.2	1.25±0.05	0.20±0.00	1.29±0.01	0.03±0.00	6.9±3.0	990.1±147.1	40
Mean	5.5±0.1a	1.05±0.10a	0.18±0.02a	1.13±0.06a	0.07±0.02a	6.2±1.2a	632.2±188.7ab	41±1a
Stations at mesic site (SM)								
sj1-5	6.1	1.28±0.03	0.20±0.01	1.36±0.03	0.03±0.00	9.6±0.7	727.0±404.4	28
sj1-6	5.7	1.25±0.13	0.20±0.01	1.32±0.12	0.02±0.00	1.8±2.6	1120.7±172.4	28
sj1-7	5.9	0.89±0.07	0.16±0.01	0.99±0.04	0.02±0.00	5.9±2.1	669.3±547.6	29
sj1-8	5.7	0.88±0.06	0.17±0.01	1.02±0.02	0.01±0.00	4.7±1.8	451.9±165.6	26
sj1-9	5.7	0.87±0.01	0.17±0.00	1.08±0.04	0.01±0.00	1.2±0.7	1736.7±1458.4	29

Mean	5.8±0.1a	1.03±0.09a	0.18±0.01a	1.15±0.08a	0.02±0.00b	4.6±1.5a	941.1±226.3b	28±1b
Stations at dry site (SD)								
sj1-10	5.8	0.96±0.05	0.16±0.00	1.06±0.05	0.01±0.00	6.3±0.9	839.3±450.4	26
sj1-11	5.8	1.47±0.19	0.21±0.01	1.64±0.21	0.02±0.00	5.2±2.1	735.1±140.4	20
sj1-12	5.6	1.32±0.07	0.20±0.01	1.45±0.03	0.01±0.00	4.7±1.7	968.8±440.3	19
Mean	5.7±0.1a	1.25±0.15a	0.19±0.02a	1.38±0.17a	0.01±0.00b	5.4±0.5a	847.7±67.6b	22±2c
Stations at paddy site (SP)								
sj1-13	5.9	1.41±0.06	0.18±0.01	1.56±0.06	0.01±0.00	21.5±3.1	85.2±60.1	39
sj1-14	5.7	1.33±0.09	0.18±0.00	1.41±0.07	0.01±0.00	9.0±2.7	210.9±64.1	29
Mean	5.8±0.1a	1.37±0.04a	0.18±0.00a	1.49±0.08a	0.01±0.00b	15.3±6.3b	148.1±62.9a	34±5d

Note: TOC, TN, TC, TS, Mc indicate total organic carbon, total nitrogen, total carbon, total sulfur and soil moisture respectively. The measured soil physical and chemical properties at the upland marsh transect sites with the same suffix letter (a, b, c or d) are not significantly different from one another (LSD, $P<0.05$).

Table S2. *Soil physical and chemical properties at the lowland marsh area and the marsh sites disturbed by animal activities and land use.*

Marsh sites	**TOC (%)**	**TN (%)**	**TC (%)**	**TS (%)**	**NH_4^+-N ($\mu g\ g^{-1}$)**	**NO_3^-N ($\mu g\ g^{-1}$)**	**Mc (%)**
Stations at the lowland marsh area							
Stations at dry site (WD)							
sj2-1	0.64±0.25	0.13±0.03	1.05±0.41	0.24±0.05	6.0±1.1	23.0±171.5	23
sj2-2	1.82±0.91	0.29±0.08	2.42±1.03	0.17±0.03	7.5±14.7	281.1±231.6	42
sj2-3	2.14±0.10	0.35±0.01	2.75±0.09	0.13±0.01	22.0±9.2	47.8±73.0	46
sj2-4	2.57±1.30	0.42±0.15	3.57±1.73	0.13±0.03	44.5±41.9	158.9±277.7	42
Mean	1.79±0.41ac	0.30±0.06ac	2.45±0.52ad	0.17±0.03d	20.0±8.9a	127.7±59.1a	38±5a
Stations at mesic site (WM)							
sj2-5	3.54±0.21	0.48±0.03	4.46±0.35	0.12±0.01	59.4±38.1	355.3±427.2	51
sj2-6	3.16±1.25	0.50±0.11	4.13±1.23	0.12±0.01	116.6±13.4	97.3±27.6	51
sj2-7	2.71±0.58	0.50±0.05	4.02±0.31	0.11±0.00	25.4±8.9	87.7±65.3	54
Mean	3.14±0.24a	0.49±0.01a	4.20±0.13b	0.12±0.00a	67.1±26.6bc	180.1±87.6a	52±1b
Stations at wet site (WW)							
sj2-8	2.93±0.40	0.46±0.01	4.27±0.09	0.09±0.00	49.3±33.0	108.0±45.0	55
sj2-9	3.21±0.10	0.49±0.02	4.49±0.27	0.08±0.01	65.9±1.6	154.0±39.9	59
sj2-10	1.04±0.24	0.23±0.01	1.69±0.10	0.05±0.00	5.8±1.4	712.5±310.6	55
Mean	2.39±0.68a	0.39±0.08ac	3.48±0.90ab	0.07±0.01ab	40.3±17.9ab	324.8±194.3a	56±1bd
Stations at dry island site (WI)							
sj2-11	3.51±0.15	0.53±0.01	4.66±0.06	0.09±0.01	22.3±15.2	27.8±25.3	45
sj2-12	1.23±0.03	0.24±0.02	1.70±0.05	0.04±0.00	9.6±2.3	27.2±34.4	20
sj2-13	1.96±0.44	0.28±0.04	2.44±0.54	0.05±0.00	22.2±4.1	27.3±34.6	20
sj2-14	1.49±0.38	0.25±0.03	2.07±0.48	0.04±0.00	19.5±7.0	7.8±15.4	17

Mean	2.05±0.51a	0.33±0.07ac	2.72±0.66abd	0.06±0.01b	18.4±3.0a	22.5±4.9a	26±7c
Stations at the marsh sites disturbed by animal activities and land use							
Stations at the landfill site (LF)							
sj2-15	9.10±1.31	1.10±0.10	10.62±1.10	0.18±0.2	123.3±13.4	784.4±685.9	73
sj2-16	11.16±0.02	1.46±0.15	13.37±0.06	0.19±0.04	53.8±36.8	1502.4±1282.7	68
Mean	10.13±1.03b	1.28±0.18b	12.00±1.38c	0.19±0.01d	88.6±34.8bc	1143.4±359.0a	71±3d
Stations at the poultry active site (PA)							
sj2-17	0.61±0.15	0.17±0.08	1.14±0.33	0.01±0.01	4.7±1.9	2474.0±127.9	19
sj2-18	0.58±0.09	0.16±0.02	1.10±0.23	0.02±0.01	3.4±2.7	2727.0±703.4	20
sj2-19	0.56±0.02	0.18±0.02	1.03±0.03	0.03±0.01	1.2±0.1	2273.3±246.2	20
sj2-20	1.22±0.46	0.33±0.06	2.00±0.42	0.07±0.00	2.8±3.9	4939.6±2381.2	26
Mean	0.74±0.16c	0.21±0.04c	1.32±0.23d	0.03±0.01bc	3.0±0.7a	3103.5±619.0b	21±2c
Stations at water bird active site (BA)							
sj2-21	2.04±0.05	0.41±0.01	2.76±0.05	0.09±0.00	36.2±3.0	1009.7±346.0	46
sj2-22	2.42±0.04	0.45±0.01	3.21±0.01	0.10±0.01	49.0±26.7	767.5±365.9	51
Mean	2.23±0.19ac	0.43±0.02ac	2.99±0.23abd	0.10±0.01ab	42.6±6.4abc	888.6±121.1a	49±3ab
Stations at farmland site (FD)							
sj2-23	1.92±0.24	0.39±0.03	2.84±0.19	0.09±0.01	107.3±4.0	628.1±185.5	43
sj2-24	1.23±0.12	0.27±0.01	1.81±0.19	0.06±0.00	72.2±1.0	1201.4±76.2	42
Mean	1.58±0.35ac	0.33±0.06ac	2.33±0.52abd	0.08±0.02ab	89.8±17.6c	914.8±286.7a	43±1ab

Note: TOC, TN, TC, TS, Mc indicate total organic carbon, total nitrogen, total carbon, total sulfur and soil moisture respectively. The measured soil physical and chemical properties at the upland marsh transect sites with the same suffix letter (a, b, c or d) are not significantly different from one another (LSD, $P<0.05$).

S3. Determination of GHG Concentrations and Flux Calculation

The CH_4 concentration was tested by gas chromatography (Shimadzu GC-12A, Japan) with flame ionization detector (FID), and the column and detector temperatures were 80 and 200 °C, respectively. The N_2, H_2 and air flow rates were 40 ml min^{-1}, 35 ml min^{-1} and 350 ml min^{-1}, respectively (Zhu et al., 2009a, b). The N_2O concentration was determined by the gas chromatography (GC-HP5890, USA) with the ^{63}Ni electron capture detector (ECD). The Ar-CH_4 (95:5) was used as the carrier gas, and the flow rate was 30 ml min^{-1}; the column and detector temperatures were 85 and 330 °C, respectively. The back flush time was 2.80 min and the volume of the sample injector is 1.7 ml (Chen et al., 2013). The CO_2 concentration was determined equipped with the gas chromatography (GC) with thermal conductivity detector (TCD) (Shimadzu GC-14B, Japan) and 80/100 mesh Chromosorb 102 column. The oven, injector and detector temperatures were 60, 100 and 60 °C, respectively. The carrier gas (H_2) had a flow rate of 80 ml min^{-1}. The variance coefficient for standard samples was within 0.2-0.5% in 24 h (Zhu et al., 2009a, b).

The GHG fluxes were calculated using a linear least squares fit to the four points in the time series (0, 10, 20, and 30 min during the time of chamber closure) of

concentrations with an average chamber temperature. The least squares regression lines "headspace GHG concentrations versus time" were first visually inspected for abrupt changes in the direction of the flux, resulting from disturbances such as the leakage of the chamber or disturbances of soils during sampling. The correlation coefficient R^2>0.95 for the linear regression was used as a quality check for the measurement. If the fluxes are low, the random error of the measurement can be larger than the change in GHG concentrations between two sampling points. Discarding these fluxes based on low R^2 values would lead to an overestimation of the overall fluxes. Some low GHG fluxes were included regardless of their R^2 value. For the gas fluxes, positive values indicate net emission to the atmosphere, and negative values indicate net uptake from the atmosphere.

REFERENCES

[1] Bernal, B., Mitsch, W.J. (2012): Comparing carbon sequestration in temperate freshwater wetland communities. – Glob. Chang. Biol. 18:1636-1647.

[2] Chen, Q.Q., Zhu, R.B., Xu, H. (2013): Spatial and temporal variations in CO_2, CH_4 and N_2O concentration in Ny-alesund, Svalbard. – Adv. Polar Sci. 25:150-160.

[3] Fox, A.D., Hearn, R.D., Cao, L., Cong, P.H., Wang, X., Zhang, Y., Dou, S.T., Shao, Z.F., Barter, M., Rees, E.C. (2013): Preliminary observations of diurnal feeding patterns of Swan Geese Anser cygnoides using two different habitats at Shengjin Lake, Anhui Province, China. – Wildfowl 58:20-30.

[4] Jiang, H.X., Xu, W.B., Qian, F.W., Chu, G.Z. (2007): Impact of habitat evolvement and human disturbance on wintering water birds in Shengjin Lake of Anhui Province, China. – Chinese J. Appl. Ecol. 18:1832-1836.

[5] Lu, Z.M., Liu, L. (2011): Investigation and analysis of Present Wetland Environmental Situation of Shengjin Lake. – J. Chizhou Coll. 6:80-83 (in Chinese).

[6] Yang, S.W., Dong, B., Liu, L.P., Sun, L., Sheng, S.W., Wang, Q., Peng, W.J., Wang, X., Zhang, Z.F., Zhao, J. (2015): Research on Vegetation Coverage Change in Sheng Jin Lake Wetland of Anhui Province. – Wetlands 35:677-682.

[7] Zhang, Y., Jia, Q., Prins, H.H.T. (2015): Effect of conservation efforts and ecological variables on waterbird population sizes in wetlands of the Yangtze River. – Sci. Rep. 5:17136.

[8] Zhu, R.B., Bao, T., Wang, Q., Xu, H., Liu, Y.S. (2014a): Summertime CO_2 fluxes and ecosystem respiration from marine animal colony tundra in maritime Antarctica. – Atmos. Environ. 98:190-201.

[9] Zhu, R.B., Liu, Y.S., Ma, E.D., Sun, J.J., Xu, H., Sun, L.G. (2009a): Greenhouse gas emissions from penguin guanos and ornithogenic soils in coastal Antarctica: effects of freezingethawing cycles. – Atmos. Environ. 43: 2336-2347.

[10] Zhu, R.B., Liu, Y.S., Ma, E.D., Sun, J.J., Xu, H., Sun, L.G. (2009b): Nutrient compositions and potential greenhouse gas production in penguin guano, ornithogenic soils and seal colony soils in coastal Antarctica. – Antarct. Sci. 21:427-438.

[11] Zhu, R.B., Ma, D.W., Xu, H. (2014b): Summertime N_2O, CH_4 and CO_2 exchanges from a tundra marsh and an upland tundra in maritime Antarctica. – Atmos. Environ. 83:269-281.

SPATIAL VARIABILITY IN GREENHOUSE GAS FLUXES OF A TEMPERATE FRESHWATER MARSH IN CHINA: EFFECTS OF SOIL MOISTURE, ANIMAL ACTIVITIES AND LAND USE

BAO, T.[1,2] – ZHU, R. B.[1*] – WANG, Q.[1] – FANG, Z. Y.[1] – LI, B. K.[1] – GAO, Y. S.[1] – XU, H.[3]

[1]*Anhui Province Key Laboratory of Polar Environment and Global Change, School of Earth and Space Sciences, University of Science and Technology of China, Hefei 230036, China*

[2]*Key Laboratory of Regional Climate-Environment for Temperate East Asia, Institute of Atmospheric Physics, Chinese Academy of Sciences, Beijing 100029, China*

[3]*State Key Laboratory of Soil and Sustainable Agriculture, Institute of Soil Science, Chinese Academy of Sciences, Nanjing 210008, China*

[*]*Corresponding author*
e-mail: zhurb@ustc.edu.cn; phone: +86-551-6360-6010; fax: +86-551-6360-6010

(Received 7th Sep 2019; accepted 4th Dec 2019)

Abstract. The greenhouse gas (CH_4, N_2O and CO_2) fluxes from Shengjin Lake Marsh (SLM) were *in situ* investigated at the undisturbed sites and the disturbed sites by animal colonization and human activities. Overall the CH_4 emissions from the wet sites were one order of magnitude higher than those from the mesic or dry sites, whereas higher N_2O emissions and net CO_2 uptake occurred at dry sites rather than at mesic and wet sites. Soil moisture was the predominant factor controlling the spatial variability in marsh CH_4 and N_2O fluxes and NEE at undisturbed sites. Mean CH_4 fluxes from migrating water bird and poultry active areas showed no statistically significant differences from the undisturbed sites, but their activities significantly increased N_2O emissions and decreased marsh CO_2 sink, with the highest N_2O fluxes (mean 49.5±11.9 μg N_2O m^{-2} h^{-1}) in poultry active areas. The conversion of the marsh into agricultural field and landfill did not significantly change CH_4 and N_2O fluxes, but significantly decreased CO_2 sink. Our results revealed that the accurate evaluation of GHG budget for the SLM and other similar temperate wetlands should involve soil water regimes, water bird colonization and human-induced influences.
Keywords: *CH_4 flux, N_2O flux, NEE, Shengjin Lake Marsh, temperate wetland*

Introduction

Atmospheric carbon dioxide (CO_2), methane (CH_4) and nitrous oxide (N_2O) are key radiatively active greenhouse gases (GHGs) (Ravishankara et al., 2009). Natural wetlands play a critical role in the global GHG budgets due to the storage of a large amount of carbon and nitrogen (Post et al., 1982), the high temperature sensitivity of microbial respiration, and nitrogen mineralization (Davidson and Janssens, 2006; Song et al., 2009). The wetlands are one of important sources for atmospheric GHGs (Jungkunst and Fiedler, 2007; Marani and Alvala, 2007; Song et al., 2009). For example, natural wetlands present the largest single CH_4 source, accounting for more than 75% of natural CH_4 source and more than 20% of the global CH_4 source (Kirschke et al., 2013). Global wetland ecosystems also contribute considerably to N_2O budget although sometimes the N_2O emissions from the wetlands are very low (Martikainen et al., 1993; Xu et al., 2008). Therefore, it is necessary to conduct the research about GHG fluxes from the wetlands in different climatic zones.

http://www.aloki.hu ● ISSN 1589 1623 (Print) ● ISSN1785 0037 (Online)
DOI: http://dx.doi.org/10.15666/aeer/1802_27612780

At present, net GHG fluxes have been extensively measured at a number of sites of global wetlands to better understand the relationships between GHG fluxes and environmental parameters (Jungkunst and Fiedler, 2007; Marani and Alvala, 2007; Song et al., 2009). China is home to the world's fourth largest wetland area (Wang et al., 2012), and *in situ* GHG flux observations have covered the wetlands in Northeast China (Ding et al., 2004; Ding and Cai, 2007; Song et al., 2009), the Tibetan Plateau (Chen et al., 2008; Song et al., 2015; Wei et al., 2015), Inner Mongolia (Duan et al., 2005; Wang et al., 2009), coastal salt marshes (Song and Liu, 2016), and the Middle-Lower Yangtze Floodplain (MLYP) wetlands including the freshwater marshes in Poyang Lake and Taihu Lake (Xing et al., 2005; Wang et al., 2006; Hu et al., 2016). Observations suggest that the wetlands showed the micro- and macro-scale spatial pattern of GHG release (Kato et al., 2011; Song and Liu, 2016; Wei and Wang, 2017), and soil physicochemical properties, soil microbial community structure, vegetation coverage and warming climate are important factors affecting wetland GHG fluxes (Johansson et al., 2006; Wei and Wang, 2017). The MLYP is characterized by dense human population and rapid economic development, which both impose unprecedented pressure on the wetland ecosystems, and has caused serious wetland degradation (Zhou et al., 2010). In addition, the MLYP wetland is an important wintering habitat and stopover site for migrating waterbirds on the East Asia-Australia Flyway (Fang et al., 2006). Environmental variables, animal colonization and human activities might lead to spatial variability in GHG emissions from the MLYP wetland. A better understanding of the spatial patterns in the GHG fluxes and their controlling factors is crucial to accurately estimate the regional and global GHG budgets from wetlands (Song et al., 2009; Kirschke et al., 2013; Wei and Wang, 2017). Nevertheless, the data about GHG fluxes are still lacking in the MLYP wetlands, and especially effects of animal colonization and human activities on GHG fluxes are highly neglected.

The Shengjin Lake Marsh (SLM), as a natural freshwater wetland, is located in the MLYP with temperate monsoon climate and an evident distinction between rainy and dry seasons in the precipitation. Part of the marsh is often converted into farmlands including paddy fields or wheat lands with the drawdown of water level. This marsh also provides an important natural colony for some migrant waterbirds to overwinter and breed, and a natural raising area for the poultry including ducks and gooses (Lu and Liu, 2011). The natural disturbances due to flood and drought, animal colonization and human activities have intensively affected the local environment (Yang et al., 2015). However, effects of these natural and anthropogenic factors on GHG fluxes to date have not been investigated in the SLM. During summer and winter in 2013, the SLM was selected as study area, and CH_4, N_2O and CO_2 fluxes were simultaneously observed at the upland and lowland marsh areas, and the marsh sites disturbed by animal colonization and land use. Our objectives were (1) to study spatial variability in GHG fluxes from the marsh; (2) to investigate the effects of soil moisture on GHG fluxes; (3) to examine the effects of animal activities and land use on GHG fluxes. This is an important attempt to reasonably evaluate the importance of soil moisture, animal activities and land use in the GHG budgets in the MLYP wetland.

http://www.aloki.hu ● ISSN 1589 1623 (Print) ● ISSN1785 0037 (Online)
DOI: http://dx.doi.org/10.15666/aeer/1802_27612780

Materials and methods

Study area

The Shengjin Lake Wetland National Nature Reserve (116° 55′ E-117°15′ E, 30° 15′ N-30° 30′ N) is located in the Middle-Lower Yangtze Plain (*Fig. 1*). The wetland covers an area of approximately 133 km^2 in the rain season and only 33 km^2 in the dry season. This area has a temperate monsoon climate with a hot and humid summer, and a cold and dry winter; its mean annual air temperature and precipitation is about 16.1°C and about 1600 mm, respectively (Xu et al., 2008). Topographically the Shengjin Lake can be divided into three parts: the upper lake, the middle lake and the lower lake. The marsh around the lake has diverse vegetation types including *Artemisia lavandulaefolia DC*, *Artemisia scoparia waldst* and *Pinus massoniana* (Lu and Liu, 2011; Yang et al., 2015). It is a natural colony for over 100 species of migratory birds to overwinter and breed (Lu and Liu, 2011). The common species of waterbirds include bean goose *Anser fabialis*, greater white-fronted goose *Anser albifrons*, lesser white-fronted goose *Anser erythropus*, swan goose *Anser cygnoides* and tundra swan *Cygnus columbianus bewickii* (Zhang et al., 2015). Overall the Shengjin Lake Marsh (SLM) has been experiencing the disturbance from human activities, poultry raising and natural disturbances from waterbirds, drought and flooding (Jiang et al., 2007; Lu and Liu, 2011; Fox et al., 2013).

More information was given in *S1 for Electronic Appendix*.

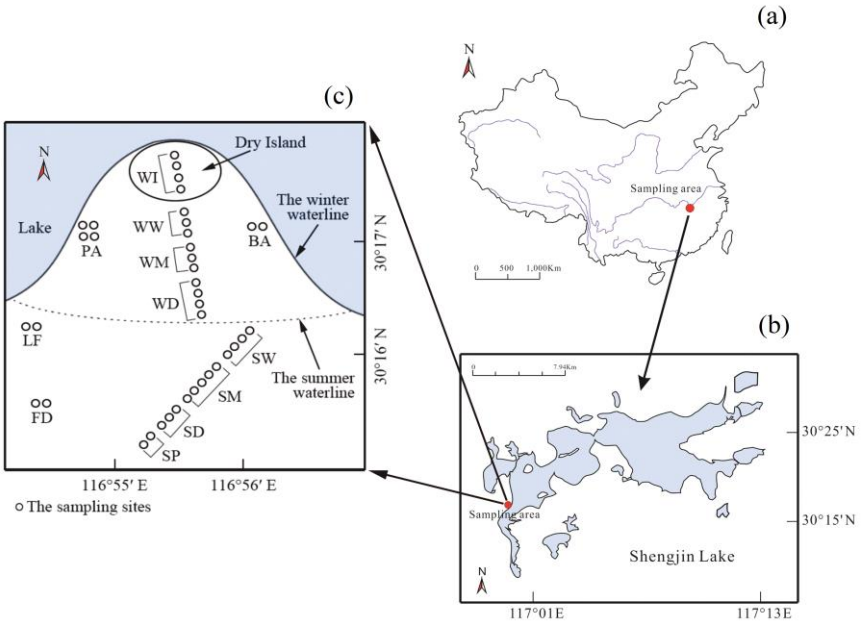

Figure 1. *(a) The red dot indicates location of the investigation area in China. (b) The topographic feature of Shengjin Lake and the red dot indicates location of the investigation area in Shengjin Lake. (c) The location of the investigation sites for the SLM in the summer and winter. SD, SM, SW and SP represent the dry, mesic and wet marsh sites, and paddy field sites in the summer, respectively; WD, WM, WW and WI represent the dry, mesic and wet marsh sites, and the island marsh sites, respectively, in the winter; BA, PA, LF and FD represents water bird active area, poultry active area, landfill and farmland, respectively. In the summer, the lake water level rose up to the highest, and the marsh formed along the summer waterline. In the winter, a large flooded land area was exposed with the decrease in the lake water level and the marsh formed along the winter waterline*

http://www.aloki.hu ● ISSN 1589 1623 (Print) ● ISSN1785 0037 (Online)
DOI: http://dx.doi.org/10.15666/aeer/1802_27612780

Investigation sites and experimental design

To test effects of soil moisture, waterbird colonization and human activities on the spatial variability in GHG fluxes from the SLM, a series of the flux observation sites were established within the following three areas located on the western shore of the upper lake as illustrated in *Fig. 1*:

(i) The upland marsh area: In summer, the lake water level rises up to the highest along the shore. In July 2013 (From July 1st to July 30th), a total of 14 stations (sj1-1 to sj1-14) for summer GHG flux observations were set up from the wet to dry marsh areas along a transect. These stations were further divided into four types of sites according to soil water regime: (a) wet site (SW), which were near the lake with almost no vegetation; (b) mesic site (SM) with few vegetation; (c) dry site (SD) with the extensive vegetation; and (d) paddy site (SP), which was located at the uppermost locality of the transect with changing water levels. Two repetitions of GHG flux measurements were made at each station.

(ii) The lowland marsh area: A large flooded land area was exposed in winter with the drawdown of water level. In December 2013 (From December 1st to December 30th), we selected a long transect from the upland to the lowland, and then to a small island along the shore. A total of 14 stations (sj2-1 to sj2-14) along the transect were set up for GHG flux measurements. These stations were divided into four types of sites as follows: (a) dry marsh site (WD); (b) mesic marsh site (WM); (c) wet marsh site (WW); (d) dry island marsh site (WI). Two repetitions were made at each station.

(iii) The marsh sites disturbed by animal activities and land use: In December 2013, a total of 10 stations were set up in the disturbed areas for GHG flux measurements. These stations were divided into four types of sites: waterbird active site (BA, two stations), poultry active site (PA, four stations), landfill (LF, two stations) and farmland (FD, two stations). Two repetitions were made at each station. In *Electronic Appendix*, more detailed information was given in *S2*, and soil physiochemical properties at all the stations were summarized in *Table S1* and *Table S2*.

In-situ GHG flux measurements

The GHG fluxes from all the stations were measured in the SLM during two sampling campaigns (July, 2013 in the summer, and December, 2013 in the winter) using a static chamber technique (Hutchinson and Mosier, 1981; Zhu et al., 2014a,b). Open-bottomed clear plexiglass chambers (50 cm×50 cm×50 cm) were placed on the PVC collars installed at the measurement sites. The collars enclosed an area of about 0.25 m^2 and were inserted into the soils to a depth of about 5 cm. The use of flux collars ensures that flux chambers are well sealed since the chambers fit into a water-filled notch in the collars. The average chamber height was 45 cm above the ground, which met the minimum required without influencing gas diffusion patterns under normal atmospheric pressure (Hutchinson and Mosier, 1981).

During gas flux measurements, upon enclosure of the cover chambers, headspace gas samples were collected at 0, 10, 20 and 30 min intervals with a double ended needle connected to pre-vacuated glass vials (18 mL) with butyl rubber septa. For each gas flux measurement, a total of four samples were withdrawn from each chamber after enclosure. Internal air temperature inside the chambers was simultaneously measured using a thermometer installed on the chamber. Ground temperature (GT) and soil moisture (Mc) were measured before and after the gas sampling. The order of

http://www.aloki.hu ● ISSN 1589 1623 (Print) ● ISSN1785 0037 (Online)
DOI: http://dx.doi.org/10.15666/aeer/1802_27612780

measurements was varied to ensure that the measuring time did not bias the results, resulting in two replicate measurements per station.

Net ecosystem exchange (NEE), defined as net ecosystem CO_2 flux under light conditions, was measured by the change in CO_2 concentrations in transparent chambers (Ström et al., 2007). In summer 2013, immediately following NEE measurements, ecosystem respiration (ER) was measured by the same procedure after darkening of the chamber covered by three layers of thick black cloth. Marsh ER includes soil and vegetation respiration, and photosynthesis was calculated as the difference between NEE and dark respiration (Ström et al., 2007).

Determination of GHG concentrations and flux calculation

The methods of analyzing GHG concentrations and flux calculation are described in detail in our previous papers (Zhu et al., 2014a,b; Bao et al., 2018a,b). In brief, N_2O, CH_4 and CO_2 concentrations were analyzed using gas chromatography equipped with a ^{63}Ni electron capture detector, a flame ionization detector and a thermal conductivity detector, respectively (GC-HP5890 II, USA; Shimadzu GC-12A, Japan; Shimadzu GC-14B, Japan). Net GHG fluxes were calculated using a linear least squares fit to four points in the time series of concentrations with an average chamber temperature. The least squares regression lines "headspace GHG concentrations versus time" were first visually inspected for abrupt changes in the direction of the flux, resulting from disturbances such as the leakage of the chamber or disturbances of soils during sampling. The correlation coefficient $R^2>0.95$ for linear regression was used as a quality check for the measurement. If the fluxes are low, the random error of the measurement can be larger than the change in GHG concentrations between two sampling points. Discarding these fluxes based on low R^2 values would lead to an overestimation of the overall fluxes. Some low fluxes were included regardless of their R^2 values. For the gas fluxes, positive values indicate net emission to the atmosphere, and negative values indicate net uptake from the atmosphere. More information was given in *S3 for Electronic Appendix*.

Environmental variables and general soil properties

Altogether 41 soil samples (3 samples were taken at each station except sj1-1 only 2 samples) in summer and 48 soil samples (2 samples were taken at each station) in winter were taken along with the same stations where GHG fluxes were measured. All the soil samples were air-dried, milled and screened using the 200 mesh sifter for the detection. Soil gravimetric moisture content (M_C) was determined by drying the soil at 105°C for 12 h. M_C was calculated as: M_C=the weight of the lost water/dry soil weight×100%. The pH was determined in distilled water and in 1M KCl solution (soil: solution ratio=1:3). Total organic carbon (TOC) was analyzed from the dry soil by the potassium dichromate volumetric method with an analytic error of 2.5%. Total carbon (TC), total nitrogen (TN) and total sulfur (TS) were determined using vario MACRO CHNS analyzer. The NH_4^+-N and NO_3^--N were determined by an ion-selective electrode method with an analytical error of <5.0%, and total phosphorus (TP) was determined by ultraviolet visible spectrometry (UV-2450, Shimadzu, Japan) with an analytical error of <2.0% (Zhu et al., 2009).

http://www.aloki.hu ● ISSN 1589 1623 (Print) ● ISSN1785 0037 (Online)
DOI: http://dx.doi.org/10.15666/aeer/1802_27612780

Statistical analysis

Microsoft Excel 2013 and SPSS 20.0 are used to make the statistical analysis of the data under the Windows 10 environment. For each station, we used standard error (SE) to estimate the uncertainty of the individual fluxes. The individual fluxes and their associated uncertainty were then averaged for each type of marsh site. All the data for GHG fluxes were expressed as mean ± SE. We used the coefficient of variance (CV) of those flux as a measure of intra-site spatial variability. The statistically significant differences between the means for each type of sites in the upland, lowland and disturbed marsh areas were tested using Fisher's Least Significant Difference (LSD, $P<0.05$) tests. We used the Principal Component Analysis (PCA) as a multivariate exploratory technique to explain the main factors affecting spatial variability in GHG emissions at the undisturbed and disturbed sites. To find factors causing spatial variability in the fluxes, the correlations of GHG fluxes with environmental variables were tested separately for all the types of sites using Spearman's rank order correlation. A univariate exponential function model (*Eq.1*) was fitted for the relationship between ER and soil temperature:

$$ER=\beta_0 e^{\beta_1 T} \quad \text{(Eq.1)}$$

where ER is ecosystem respiration (mg CO_2 m^{-2} h^{-1}), T is mean soil temperature (ºC), and β_0 and β_1 are the constants fitted with the least squares technique. The Q_{10} value was calculated as (*Eq.2*):

$$Q_{10}=e^{10\beta_1} \quad \text{(Eq.2)}$$

In all analyses where $p<0.05$, the factor tested and the relationship were considered statistically significant. Although our data might represent a rough estimate of GHG fluxes, we still used the GWP (Global Warming Potential) as a conversion factor to evaluate the impact of the SLM on the greenhouse effect. Based on a 100-year time frame, the GWPs of CH_4 and N_2O are, respectively, 25 and 298 times higher than that of CO_2 (Ravishankara et al., 2009). The net GWP were calculated by taking mass factors, 1 for CO_2, 25 for CH_4, and 298 for N_2O.

Results

Environmental variables in the marsh

The soils at the upland marsh transect were slightly acid with the pH of 5.2-6.1, and soil moisture decreased from the lowland to the upland marsh with the range of 17%-59% (*Table S1* and *Table S2*). Ground temperatures showed no significant differences between four types of sites in summer or in winter (*Fig. 2*). TC, TOC and TN levels in the soils showed no significant differences. The TC and TOC levels were very close to each other (average 1.24% and 1.13%), and they showed a significant correlation ($R=0.941$), indicating that soil carbon in the marsh mainly existed as organic carbon. Soil organic carbon content (average 2.62%) at the lowland marsh was almost twice higher than that at the upland marsh (average 1.13%). Soil NO_3^--N contents were one to two orders of magnitude higher than NH_4^+-N contents at upland or lowland

http://www.aloki.hu ● ISSN 1589 1623 (Print) ● ISSN1785 0037 (Online)
DOI: http://dx.doi.org/10.15666/aeer/1802_27612780

marsh transects. Soil NO_3^--N contents in landfill, poultry and waterbird active areas and farmland were evidently higher than those in non-disturbed marsh areas, and extremely high NO_3^--N occurred in poultry active soils (1143.4 μg g^{-1}). In addition, soil moisture showed evident differences with the range of 19%-73% between the types of marsh sites due to effects of animal activities and land use.

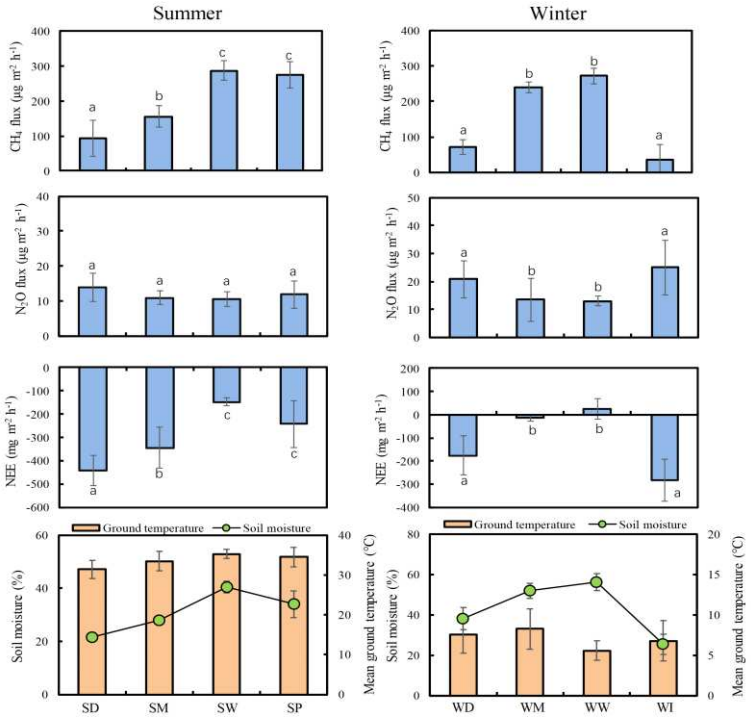

Figure 2. *Spatial variability in CH_4, N_2O and CO_2 fluxes from the SLM transects during the summer and winter. The given data are the mean values at each site in the marsh, and the vertical bars indicate standard errors of GHG fluxes. (a) In the summer, SD (n=6), SM (n=10), SW (n=8) and SP (n=4) represent the dry, mesic and wet marsh sites, and paddy field sites, respectively; (b) In the wintertime, WD (n=8), WM (n=6), WW (n=6) and WI (n=8) represent the dry, mesic and wet marsh sites, and the island marsh sites, respectively. The different lowercase letters (a, b, c) indicate statistically significant differences between the mean values (Fisher's LSD, $P < 0.05$)*

CH_4 fluxes

The wet marsh sites SW and WW showed strong CH_4 emissions with the mean fluxes of 287.3±51.1 μg CH_4 m^{-2} h^{-1}, and 271.2±21.1 μg CH_4 m^{-2} h^{-1}, respectively. Dry marsh sites SD and WD showed net weak CH_4 emissions with the mean rates of 93.9±27.8 μg CH_4 m^{-2} h^{-1} and 70.1±20.7 μg CH_4 m^{-2} h^{-1}, one order of magnitude lower than those from the mesic and wet sites, whereas the lowest CH_4 emission occurred at the dry island site WI (*Fig. 2*). The paddy site SP showed strong CH_4 emission (275.8±37.7 μg CH_4 m^{-2} h^{-1}), comparable to the sites SW and WW, but significantly higher than those at the sites SM and SD (*Table 1*). Overall the fluxes from waterbird active area (148.3±51.5 μg CH_4 m^{-2} h^{-1}) and landfill (98.8±28.9 μg CH_4 m^{-2} h^{-1}) were higher than those from poultry active area (64.4±44.3 μg CH_4 m^{-2} h^{-1}) and farmland (20.0±105.0 μg CH_4 m^{-2} h^{-1}) although their mean fluxes showed no statistical significant differences (*Fig. 3*).

http://www.aloki.hu ● ISSN 1589 1623 (Print) ● ISSN1785 0037 (Online)
DOI: http://dx.doi.org/10.15666/aeer/1802_27612780

Table 1. *Comparisons of CH_4, N_2O and CO_2 fluxes at the different types of sites in Shengjin Lake Marsh*

Marsh site types	CH_4 flux (μg CH_4 m^{-2} h^{-1})			N_2O flux (μg N_2O m^{-2} h^{-1})			NEE (mg CO_2 m^{-2} h^{-1})			ER (mg CO_2 m^{-2} h^{-1})		
	Range	Mean ± SE	CV (%)	Range	Mean ± SE	CV (%)	Range	Mean ± SE	CV (%)	Range	Mean ± SE	CV (%)
Summertime, July, 2013												
SW	152.0-773.0	287.3±51.1a	17.8	1.5-18.3	10.6±4.1a	38.7	-270.6-28.3	-148.5±65.0a	43.8	218.9-1531.9	694.2±420.1a	60.5
SM	10.2-399.8	155.9±31.5b	20.2	6.4-16.5	11.0±2.0a	18.2	-552.5 to -42.6	-345.9±88.1b	25.5	15.7-1132.9	674.9±210.8a	31.2
SD	62.6-149.3	93.9±27.8c	29.6	10.3-17.7	13.9±2.1a	15.1	-473.8 to -415.0	-443.6±17.0c	3.8	926.9-1305.5	1106.9±109.7b	9.9
SP	139.6-412.0	275.8±37.7a	13.7	8.1-15.7	11.9±3.8a	31.9	-472.2 to -12.8	-242.5±101.2a	41.7	887.2-1200.1	1043.7±156.5b	15.0
Comprehensive	10.2-773.0	197.3±205.5	104.2	1.5-18.3	11.6±4.9	42.2	-552.5-28.3	-295.7±192.9	65.2	15.7-1305.5	835.8±446.1	53.4
Wintertime, December, 2013												
WW	127.4-403.8	271.2±21.1b	7.8	10.2-16.2	13.0±1.7b	13.1	-406.0 to -104.2	-24.1±43.8b	1.8			
WM	212.3-265.5	240.3±15.4b	6.4	-1.8-21.9	13.4±7.6b	56.7	-39.4-8.5	-14.5±13.9b	96.0			
WD	20.9-110.5	70.1±20.7a	29.5	9.8-38.0	20.8±6.7a	32.2	-323.8-48.8	-176.1±84.2a	47.8			
WI	-35.5-104.8	36.4±40.5a	111.3	14.1-35.2	25.1±9.8a	39.0	-44.3-151.5	-284.7±90.1a	31.6			
Comprehensive	-35.5-403.8	108.3±191.1	176.5	-1.8-38.0	18.8±10.9	58.0	-406.0-151.5	-129.6±173.0	133.5			

The measured GHG fluxes at marsh site types with the same suffix letter (a, b or c) are not significantly different from one another (LSD, $P< 0.05$). Marsh ER was not observed in 2013 winter

http://www.aloki.hu ● ISSN 1589 1623 (Print) ● ISSN1785 0037 (Online)
DOI: http://dx.doi.org/10.15666/aeer/1802_27612780

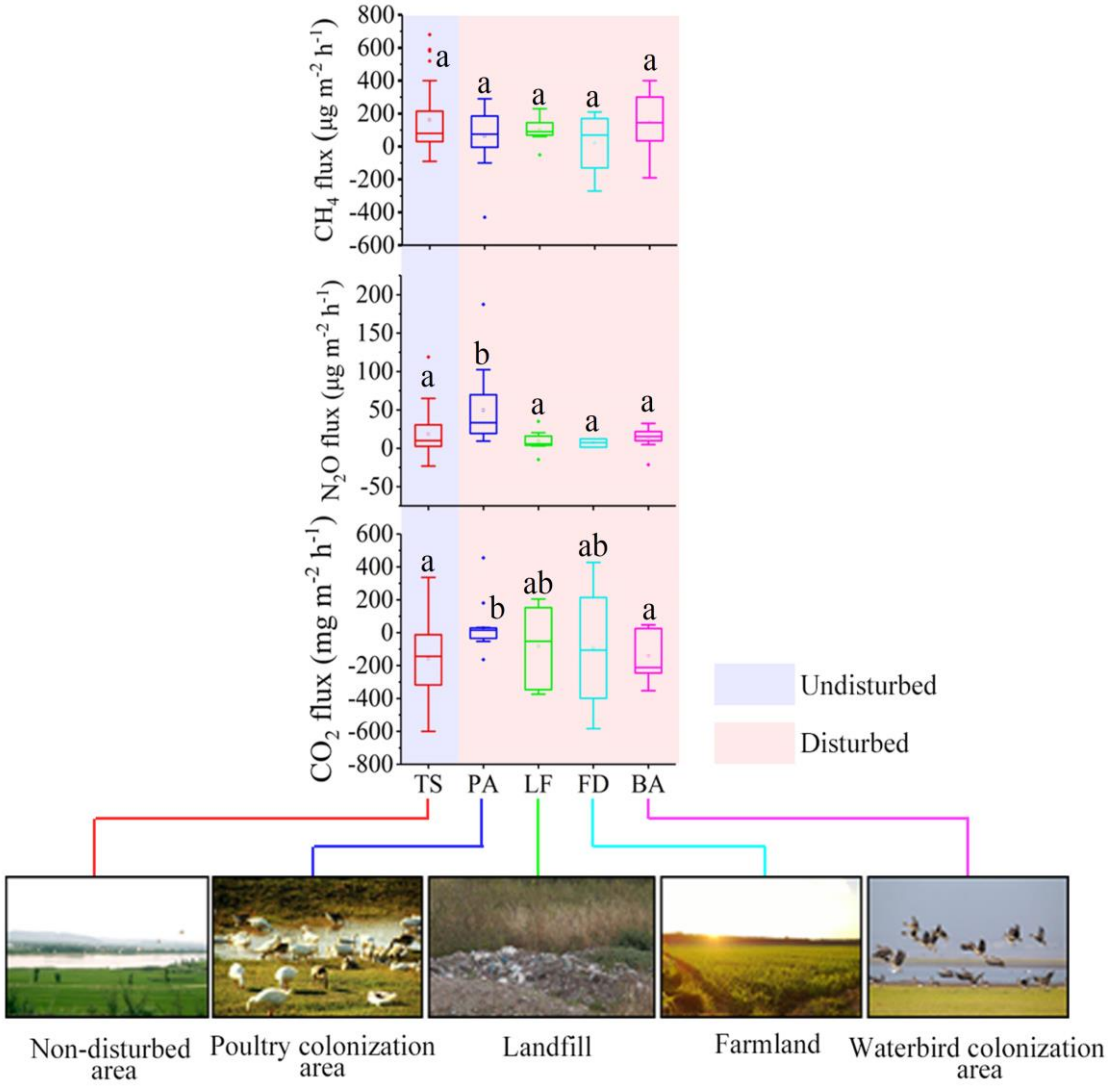

Figure 3. *Comparisons of CH_4, N_2O and CO_2 fluxes from different non-disturbed and disturbed marsh areas. TS (n=56), PA (n=8), LF (n=4), FD (n=4) and BA (n=4) represent non-disturbed site, poultry colonization area, landfill, farmland, and waterbird colonization area, respectively. The different lowercase letters (a, b) indicate statistically significant differences between the mean fluxes (Fisher's LSD, $P < 0.05$)*

The PCA analysis showed that the environmental variables in the first two components explained 71.0% and 87.2% of the cumulative variance of the CH_4 fluxes at the undisturbed and disturbed marsh sites, respectively, and soil moisture was the predominant factor affecting spatial variability in CH_4 emission (*Fig. 4*). The CH_4 fluxes showed a significant positive correlation with soil moisture at the undisturbed or disturbed marsh sites. When the data at all the observation sites were combined, CH_4 fluxes showed a strong positive correlation (P=0.000) with soil moisture (*Table 2*). The TN, NH_4^+–N did not significantly affect CH_4 emissions at the undisturbed sites, whereas they showed a significant positive correlation with CH_4 emissions at the disturbed marsh sites.

http://www.aloki.hu ● ISSN 1589 1623 (Print) ● ISSN1785 0037 (Online)
DOI: http://dx.doi.org/10.15666/aeer/1802_27612780

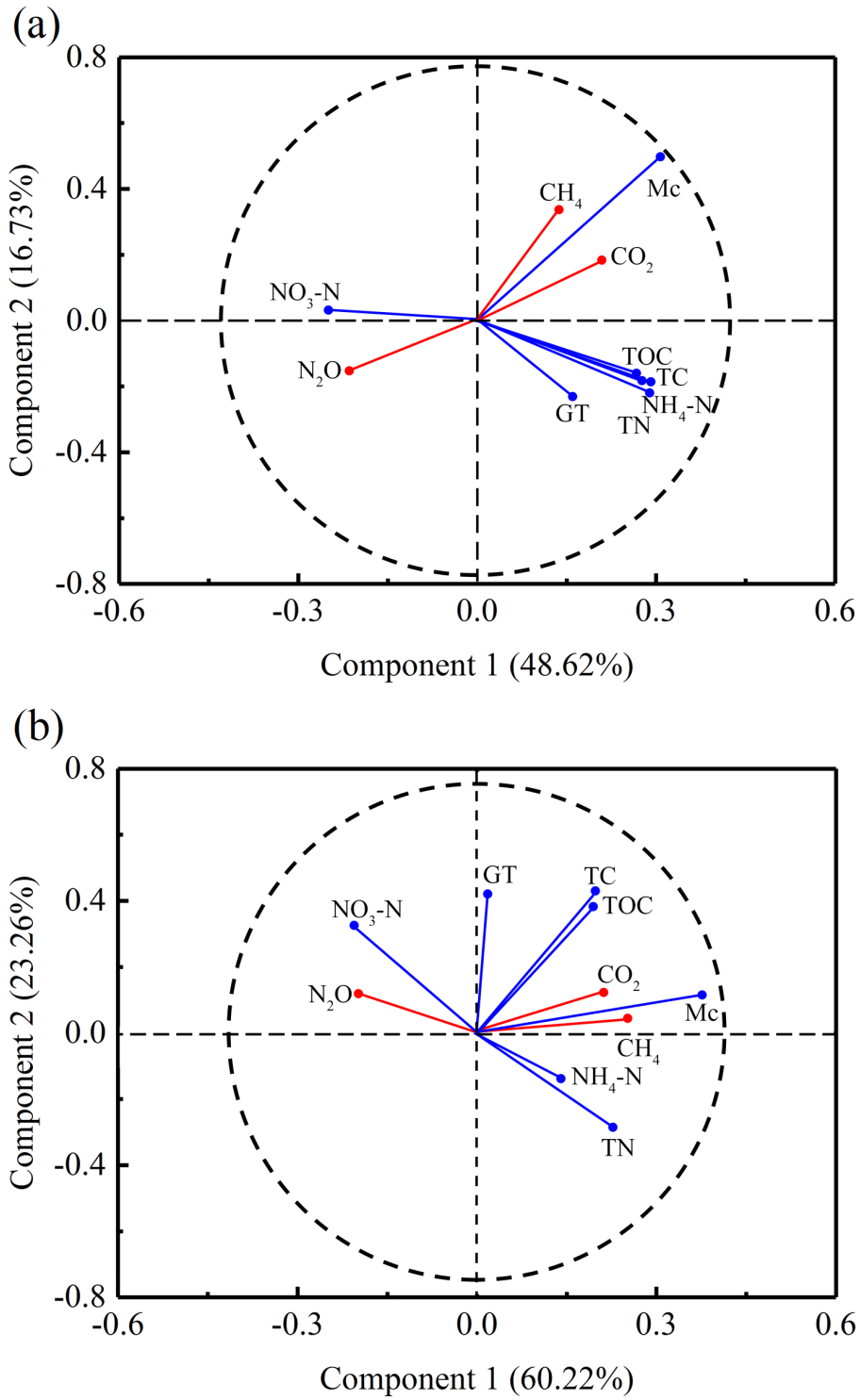

Figure 4. *Correlation bi-plot between GHG fluxes and environmental variables in non-disturbed (a) and disturbed (b) marsh areas based upon the standardized principal component analysis. The first two dimensions explained 65% and 83% of the variation for non-disturbed and disturbed marsh areas, respectively. Mc, TOC, TN, TC and GT indicate soil moisture, total organic carbon, total nitrogen, total carbon and ground temperature, respectively*

http://www.aloki.hu ● ISSN 1589 1623 (Print) ● ISSN1785 0037 (Online)
DOI: http://dx.doi.org/10.15666/aeer/1802_27612780

Table 2. *Correlations between marsh greenhouse gas fluxes and environmental parameters during the observation period. Significant statistics ($P < 0.05$) are highlighted in bold type*

	Undisturbed marsh sites (n=69)			**Disturbed marsh sites (n=20)**			**Overall (n=89)**		
	CH_4 Flux (μg CH_4 m^{-2} h^{-1})	**N_2O Flux (μg N_2O m^{-2} h^{-1})**	**CO_2 Flux (mg CO_2 m^{-2} h^{-1})**	**CH_4 Flux (μg CH_4 m^{-2} h^{-1})**	**N_2O Flux (μg N_2O m^{-2} h^{-1})**	**CO_2 Flux (mg CO_2 m^{-2} h^{-1})**	**CH_4 Flux (μg CH_4 m^{-2} h^{-1})**	**N_2O Flux (μg N_2O m^{-2} h^{-1})**	**CO_2 Flux (mg CO_2 m^{-2} h^{-1})**
Mc (%)	**0.449** **P=0.000**	**-0.656** **P=0.000**	**0.258** **P=0.032**	**0.556** **P=0.011**	**-0.578** **P=0.008**	**0.501** **P=0.025**	**0.641** **P=0.000**	**-0.704** **P=0.000**	**0.244** **P=0.021**
TOC (%)	0.053 P=0.664	-0.190 P=0.235	0.190 P=0.235	0.065 P=0.787	**-0.449** **P=0.047**	0.171 P=0.472	0.074 P=0.492	**-0.254** **P=0.038**	0.114 P=0.289
TN (%)	0.018 P=0.880	-0.124 P=0.439	0.091 P=0.456	**0.459** **P=0.042**	**-0.509** **P=0.022**	0.186 P=0.433	**0.313** **P=0.046**	**-0.244** **P=0.021**	0.124 P=0.439
TC (%)	0.036 P=0.825	-0.141 P=0.379	0.134 P=0.403	0.050 P=0.835	**-0.502** **P=0.024**	0.217 P=0.359	0.043 P=0.689	**-0.223** **P=0.036**	0.138 P=0.197
NH_4^+-N (μg g-1)	0.021 P=0.862	-0.128 P=0.283	0.124 P=0.439	**0.484** **P=0.031**	**-0.531** **P=0.016**	0.227 P=0.336	**0.224** **P=0.036**	**-0.313** **P=0.046**	0.206 P=0.196
NO_3^--N (μg g-1)	-0.025 P=0.841	**0.237** **P=0.049**	-0.128 P=0.293	-0.208 P=0.380	**0.752** **P=0.000**	-0.291 P=0.214	-0.089 P=0.581	**0.641** **P=0.000**	**-0.223** **P=0.036**
GT (°C)	0.010 P=0.948	-0.089 P=0.581	0.085 P=0.492	0.202 P=0.394	-0.186 P=0.433	0.057 P=0.812	0.124 P=0.439	-0.114 P=0.289	0.094 P=0.383

Undisturbed, disturbed sites indicate regular transect sites and the marsh sites disturbed by waterbird colonization and human activities, respectively. Mc, TOC, TN, TC and GT indicate soil moisture, total organic carbon, total nitrogen, total carbon and ground temperature, respectively

N_2O fluxes

The dry marsh sites SD and WD showed strong N_2O emissions with the mean fluxes of 13.9±2.1 μg N_2O m^{-2} h^{-1} and 20.8±6.7 μg N_2O m^{-2} h^{-1}, respectively, whereas the mesic sites SM and WM and wet sites SW and WW presented weak N_2O emissions (*Fig. 2*). The mean fluxes from SM (11.0±2.0 μg N_2O m^{-2} h^{-1}) and WM (13.4±7.6 μg N_2O m^{-2} h^{-1}) were comparable to those from SW (10.6 μg N_2O m^{-2} h^{-1}) and WW (13.0±1.7 μg N_2O m^{-2} h^{-1}). High emission (25.1±9.8 μg N_2O m^{-2} h^{-1}) occurred at the site WI, corresponding to the lowest soil moisture (*Fig. 2*). Overall the highest N_2O fluxes (mean 49.5±11.9 μg N_2O m^{-2} h^{-1}) and slightly enhanced fluxes (mean 14.1±3.9 μg N_2O m^{-2} h^{-1}) occurred in poultry and waterbird active areas, respectively (*Fig. 3*). The landfill site LF (mean 8.9±5.1 μg N_2O m^{-2} h^{-1}) and farmland site FD (mean 5.2±2.8 μg N_2O m^{-2} h^{-1}) showed relatively low N_2O fluxes, comparable to the undisturbed sites (mean 8.7±4.2 μg N_2O m^{-2} h^{-1}).

The PCA analysis showed that environmental variables in the first two components explained 72.2% and 87.9% of the cumulative variance of the N_2O fluxes at the undisturbed and disturbed marsh sites, respectively, and soil NO_3^--N contents and soil moisture were the predominant factors affecting spatial variability in N_2O emission (*Fig. 4*). The N_2O fluxes showed a significant negative correlation with soil moisture at the undisturbed or disturbed marsh sites. Almost no statistically significant correlations were obtained between N_2O fluxes and other environmental parameters at the undisturbed marsh sites. However, a strong positive correlation occurred between the fluxes and NO_3^--N contents at the disturbed sites, but the weak negative correlations between the fluxes and TOC, TN and NH_4^+-N (*Table 2*), indicating that animal-derived NO_3^-–N input significantly enhanced N_2O emissions from the SLM.

NEE and ER

NEE between dry, mesic and wet marsh sites showed a significant difference ($P<0.05$), and the maximum mean CO_2 uptake occurred at the dry sites SD and WI (-443.6±17.0 mg CO_2 m^{-2} h^{-1} and -284.7±90.1 mg CO_2 m^{-2} h^{-1}, respectively) (*Table 1*). The marsh experienced a net gain of CO_2 in the summer or in the winter (*Fig. 2*). Overall net CO_2 emission occurred in the poultry active area (29.1±33.2 mg CO_2 m^{-2} h^{-1}), whereas waterbird activity area (-140.0±41.9 mg CO_2 m^{-2} h^{-1}), landfill (-82.6±86.6 mg CO_2 m^{-2} h^{-1}) and farmland (-92.2±210.9 mg CO_2 m^{-2} h^{-1}) showed weak CO_2 uptake compared to the non-disturbed marsh areas (*Fig. 3*). The marsh NEE had a strong positive correlation with soil moisture at both the undisturbed and disturbed sites, and soil moisture played a more important role in explaining the spatial variability in net CO_2 fluxes (*Fig. 4* and *Table 2*).

The mean ER rate at the dry site (1106.9±109.7 mg CO_2 m^{-2} h^{-1}) was greatly higher than those at the mesic (674.9±210.8 mg CO_2 m^{-2} h^{-1}) and wet (694.2±420.1 mg CO_2 m^{-2} h^{-1}) sites (*Fig. 5a* and *Table 1*). Marsh ER showed a significant negative correlation with soil moisture ($P<0.05$). However, the pattern of ER appeared to follow soil temperature with a strong, positive exponential correlation ($R^2=0.57$, $P<0.05$) and the Q_{10} value of 8.7 (*Fig. 5b*). Summertime photosynthesis (Pg) rates at the dry, mesic, paddy and wet sites averaged 1550.4±126.7 mg CO_2 m^{-2} h^{-1}, 1020.4±202.8 mg CO_2 m^{-2} h^{-1}, 1286.2±386.2 mg CO_2 m^{-2} h^{-1} and 820.4±341.6 mg CO_2 m^{-2} h^{-1}, respectively, and showed a large spatial variability between the types of sites (CV=8.2%, 19.9%, 30.0% and 41.6%, respectively). The Pg rates at the dry marsh

http://www.aloki.hu ● ISSN 1589 1623 (Print) ● ISSN1785 0037 (Online)
DOI: http://dx.doi.org/10.15666/aeer/1802_27612780

(1550.4±126.7 mg CO_2 m^{-2} h^{-1}) and paddy sites (1286.2±386.2 mg CO_2 m^{-2} h^{-1}) were significantly higher than those at the mesic (1020.9.4±202.8 mg CO_2 m^{-2} h^{-1}) and wet marsh sites (820.4±341.6 mg CO_2 m^{-2} h^{-1}) (*Fig. 5a*).

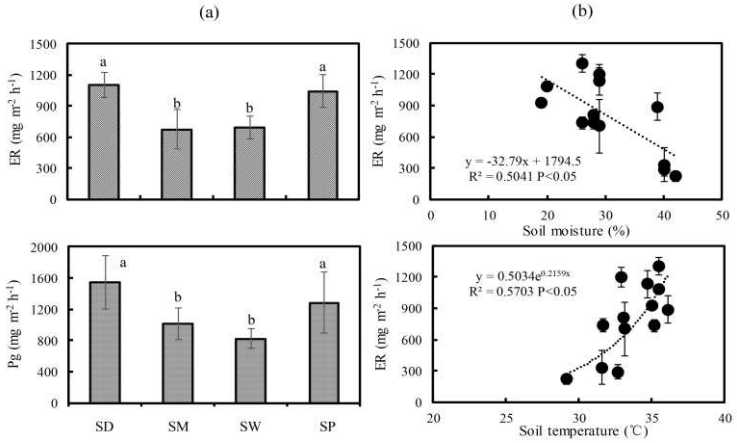

Figure 5. *(a) The ecosystem respiration rates (ER) and gross photosynthesis (Pg) from the marsh transect sites during the summertime. The different lowercase letters (a, b) indicate statistically significant differences between means (Fisher's LSD, P < 0.05); (b) The relationship between ER and soil moisture, soil temperature at the marsh transect sites. If the overall regression is significant at P<0.05, regression lines and r values are given*

Correlation between GHG fluxes and global warming potential

The N_2O and CH_4 fluxes from different types of marsh sites showed a significant negative correlation, i.e. so-called ''trade-off effect". The significant positive relationships occurred between CH_4 flux and ER, NEE, whereas N_2O fluxes showed a significant negative correlation with NEE (*Fig. 6*). The average CH_4 and N_2O fluxes are 178.8 μg m^{-2} h^{-1} (n=76) and 15.2 μg m^{-2} h^{-1} (n=76), respectively, and their fluxes are equivalent to 4.5 mg CO_2 m^{-2} h^{-1} and 4.5 mg CO_2 m^{-2} h^{-1}, respectively. However, net mean CO_2 flux from the marsh is -212.6 mg m^{-2} h^{-1}. A GWP-negative process strongly dominates when N_2O, CH_4 and CO_2 fluxes from the marsh are combined in terms of their relative GWPs. Overall the SLM is still a large "carbon sink".

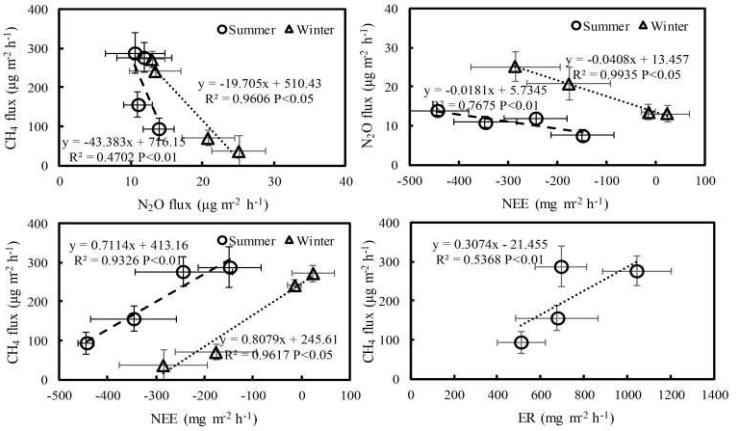

Figure 6. *Correlations between CH_4 flux, N_2O flux, NEE and ER from different types of marsh sites*

http://www.aloki.hu ● ISSN 1589 1623 (Print) ● ISSN1785 0037 (Online)
DOI: http://dx.doi.org/10.15666/aeer/1802_27612780

Discussion

Effects of soil moisture on spatial variations of GHG fluxes

Overall our statistical analyses showed soil temperatures and soil nutrient variables were not predominant factors affecting marsh CH_4 and CO_2 fluxes at the undisturbed sites (*Table 2*). Soil moisture (Mc) had a significant difference among the sites due to the drawdown of lake level and the differences in topography, slope and hydrology, which influenced the magnitudes and variations of GHG fluxes at spatial scale (Ding et al., 2002; Song et al., 2009). Mc showed a significant positive correlation with CH_4 fluxes and NEE, but a significant negative correlation with N_2O (*Fig. 4* and *Table 2*). This indicated that marsh soil moisture regulated spatial variability in marsh GHG fluxes. Soil water regime is widely recognized as the fundamental factor in regulating small-scale variation in CH_4 emissions from the wetlands, given water regime can directly affect the anaerobic condition, which is necessary for CH_4 production (Christensen et al., 2003; Wang et al., 2008; Wei and Wang, 2017), whereas low soil moisture make O_2 diffuse into soil to oxidize CH_4 into CO_2 (Song and Liu, 2016; Bao et al., 2018a). Therefore the decrease in soil moisture inhibited marsh CH_4 production. N_2O is an intermediate product of soil nitrification and denitrification processes, and soil moisture might have an important effect on N_2O production through its effects on nitrification and denitrification processes (Granli and Bockman, 1994). In this study, N_2O fluxes showed a significant positive correlation with soil NO_3^--N contents, indicating that denitrification might be the main process responsible for marsh N_2O emissions. Furthermore increasing soil moisture could cause high anaerobic condition and low O_2 availability, and most of N_2O can be reduced to N_2 via denitrification, which might cause the decrease in N_2O emissions from the wetlands (Kato et al., 2011; Zhu et al., 2014b; Bao et al., 2018b). The lowering of water table could increase the volume of modestly aerated soil, thus increased the proportion of N_2O production in either of nitrification and denitrification (Kato et al., 2011; Chen et al., 2013). The incomplete denitrification releases N_2O, which might be favorably produced in marsh soil at well-drained, aerated marsh sites (Granli and Bockman, 1994; Scaroni et al., 2014). Therefore higher N_2O emissions occurred at the dry marsh sites SD, WD and WI in the SLM.

On the other hand, the decrease in soil moisture might stimulate carbon sequestration in the marsh (*Fig. 2*). Stronger plant photosynthesis occurred at the site SD than SM and SW (*Fig. 5a*), which might be due to higher vegetation coverage at the dry upland marsh (Lu and Liu, 2011; Yang et al., 2015). Soil moisture directly affected the distribution of soil microbial communities and marsh vegetation, thus influenced ecosystem respiration (Llstedt et al., 2000). Previous studies indicated that the Pg rates were the highest in dry tundra marsh with smaller differences in net CO_2 exchange whereas the ER rates were limited, therefore the dry marsh showed much higher net CO_2 uptake (Dagg and Lafleur, 2011). In the SLM, the decrease in soil moisture stimulated ER rates instead of limiting ER (*Fig. 5b*). The increase in net CO_2 uptake at the dry marsh sites showed that plant photosynthesis might surpass ER with the drawdown of lake water level. Similarly, plant photosynthesis, rather than the mineralization of organic matter, played a more important role in net CO_2 flux at the dry marsh site (Del Giorgio et al., 1999; Huttunen et al., 2003). Therefore plant photosynthesis might dominate CO_2 exchange across air-soil interface in the SLM. In addition, a strong, positive exponential correlation between ER and soil temperature

http://www.aloki.hu ● ISSN 1589 1623 (Print) ● ISSN1785 0037 (Online)
DOI: http://dx.doi.org/10.15666/aeer/1802_27612780

showed a positive feedback of ER to current warming climate. Climate warming might decrease CO_2 sink through the increase in ER (Davidson and Janssens, 2006; Zhu et al., 2014a). The Q_{10} value of 8.7 in the SLM was much higher than the range (1.3-5.6) for different biomes of the world (Davidson and Janssens, 2006), indicating a greater temperature sensitivity to ER.

Effects of animal activity and land use on GHG fluxes

Overall the mean CH_4 fluxes from waterbird and poultry active areas showed no statistical significant differences ($p>0.05$) from the undisturbed sites (*Fig. 3*).The fluxes from waterbird (148.3±51.5 μg CH_4 m^{-2} h^{-1}) and poultry (64.4±44.3 μg CH_4 m^{-2} h^{-1}) active areas were lower than those from dairy cow feeding yards (358.3 μg CH_4 m^{-2} h^{-1}), dairy cow collecting yards (429.2 μg CH_4 m^{-2} h^{-1}), and pig loading areas (158.3 μg CH_4 m^{-2} h^{-1}) (Misselbrook et al., 2001), which might be related with low soil moisture, especially in poultry active area (Mc<30%, *Table S2*). Lower soil moisture might greatly increase marsh CH_4 consumption (Gulledge and Schimel, 1998). However, net CO_2 emission occurred in the poultry active area (29.1±33.2 mg CO_2 m^{-2} h^{-1}), whereas waterbird activity area showed weak CO_2 uptake compared to non-disturbed marsh areas, indicating that poultry activity could decrease marsh CO_2 sink, even convert a marsh site from CO_2 sink into a net source. Similar results also occurred in the tundra marsh disturbed by marine animal activities (Zhu et al., 2014a).

The N_2O fluxes from poultry (mean 49.5±11.9 μg N_2O m^{-2} h^{-1}) and waterbird (mean 14.1±3.9 μg N_2O m^{-2} h^{-1}) active areas were comparable to or even greater than those from the farm yards used by livestock (11.8-27.5 μg N_2O m^{-2} h^{-1}) (Misselbrook et al., 2001), and from some temperate extensive pastures or rangelands (0-26.6 μg N_2O m^{-2} h^{-1}) (Phillips et al., 2007), and those from heavily fertilized agricultural systems and tropical forests (23.6-83.3 μg N_2O m^{-2} h^{-1}), which are the two largest N_2O sources worldwide (Perez et al., 2001). Similar results also occurred in tundra marsh sites disturbed by seabird activities (13.3-57.4 μg N_2O m^{-2} h^{-1}) (Zhu et al., 2012, 2013). The high N_2O emissions from poultry or waterbird active areas might be modulated by soil physical and chemical processes associated with animal activities: continuous N input from animal excreta and animal tramp (Zhu et al., 2012). Significantly elevated NO_3^-–N concentrations occurred in animal-disturbed marsh soils as compared with undisturbed soils (*Table S2*). A strong positive correlation between N_2O fluxes and soil NO_3^-–N contents confirmed that animal-derived NO_3^-–N input had an important effect on spatial variability in N_2O fluxes (*Fig. 4* and *Table 2*). Therefore, animal activity and the deposition of their excreta significantly enhanced N_2O emissions in the SLM.

During the conversion of the marsh into paddy fields, human tillage and the rice plants with well-developed aerenchyma might lead to the increase in CH_4 emission (Cai et al., 1997). The plants with well-developed aerenchyma are important in determining net CH_4 fluxes from some wetlands (Bass et al., 2014; Bao et al., 2018b). However, net CH_4, N_2O and CO_2 fluxes from agricultural field site FD were comparable to the undisturbed sites (*Fig. 3*), indicating that the conversion of the marsh into agricultural fields did not significantly change GHG emissions. Landfill gas is mainly composed of CH_4 and CO_2, which is generated during decomposition of the solid waste (Sharma et al., 2011). The landfill did not change CH_4 and N_2O fluxes, and slightly decreased CO_2 uptake compared to non-disturbed marsh areas (*Fig. 3*). GHG fluxes from the landfill were lower than those reported from sanitary landfills (Bogner et al., 1995; Rinne et al., 2005; Kormi et al., 2017). Generally landfill GHG emission estimates are highly

http://www.aloki.hu ● ISSN 1589 1623 (Print) ● ISSN1785 0037 (Online)
DOI: http://dx.doi.org/10.15666/aeer/1802_27612780

uncertain because factors influencing gas emission and mitigation are site specific (Boeckx et al., 1996). Landfill GHG emissions can range over six orders of magnitudes (Lando et al., 2017). The ambient and soil moisture had an important effect on GHG production from the landfill (Rinne et al., 2005). During the study period, very high soil moisture (68%-73%, *Table S2*) might stimulate CH_4 and CO_2 emissions, but decrease N_2O production from the landfill (*Fig. 3*).

In summary, correlation analyses revealed that GHG fluxes from the disturbed marsh sites were involved in more complicated factors than from undisturbed sites (*Table 2*). Significant positive correlations ($p<0.05$) between net CH_4 and CO_2 fluxes and soil moisture, soil nutrients indicated that their fluxes might be modulated by soil physical and chemical processes associated with animal activities (Zhu et al., 2012, 2013). Negative correlations were generally observed between N_2O emissions and soil moisture, nutrient variables TOC, TC, TN and NH_4^+ at the disturbed sites and all the combined sites (*Fig. 4* and *Table 2*), which was different from some previous studies (Chen et al., 2011; Sun et al., 2014). One possible reason was related to the interaction of vegetation and microorganism (nitrifiers and denitrifiers) during N_2O production (Sun et al., 2014). N_2O production might be partly inhibited as the available N was significantly competed by both vegetations and microorganisms in *Artemisia lavandulaefolia DC* and *Artemisia scoparia waldst* community (Lu and Liu, 2011; Yang et al., 2015), which partly contributed to the difference in N_2O emissions at spatial scale. Overall the PCA analysis showed that soil moisture was the predominant factor affecting spatial variability in marsh GHGs fluxes from the undisturbed and disturbed sites in the SLM (*Fig. 4*). This preliminary study only provided short summertime or wintertime GHG fluxes from agricultural field or landfill in the SLM, and effects of animal activities and land use on marsh GHG emissions need to be further confirmed in the future.

Implication of marsh GHG evaluation

The SLM, as a typical natural freshwater wetland in the Middle-Lower Yangtze Plain, is involved in effects of complicated factors including environmental variables, human activities and waterbird colonization (Lu and Liu, 2011; Yang et al., 2015; Zhang et al., 2015). The coefficients of variance (CV) of CH_4, N_2O and CO_2 fluxes were relatively small (<100%) within the same type of sites. However, their fluxes showed significant differences among the sites, indicating that to assess the regional GHG budget precisely, measurements should be designed at fine scales and environmental heterogeneity should be considered in the marsh. In addition, the study area has a temperate monsoon climate with an evident distinction in precipitation between rainy and dry seasons. This could lead to soil moisture changes, dry-wet alternation and wetland extent dynamics, and cause the ‘‘trade-off effect” of N_2O and CH_4 fluxes and carbon sequestration in the marsh (Cai et al., 1997; Ding and Cai, 2007). Effects of soil moisture changes on ‘‘trade-off effect” of N_2O and CH_4 fluxes need to be used for accurate evaluation of net GWP in the SLM. In summary, there still remains a large uncertainty regarding the evaluation of GHG budgets in the SLM. The GHG budget evaluation for the SLM and other similar MLYP wetlands should be involved in soil water regimes, waterbird colonization and human-induced influences.

http://www.aloki.hu ● ISSN 1589 1623 (Print) ● ISSN1785 0037 (Online)
DOI: http://dx.doi.org/10.15666/aeer/1802_27612780

Conclusions

We revealed effects of soil moisture, animal activities and land use on GHG fluxes from the SLM based upon *in situ* flux measurements. Overall CH_4 emissions from the dry marsh sites were much lower than those from wet or mesic sites, vice versa for N_2O emissions and NEE. Soil moisture was the predominant factor controlling the spatial variability in marsh CH_4 and N_2O fluxes and NEE at undisturbed sites. Correlation analyses revealed that GHG fluxes from the disturbed marsh sites were involved in more complicated factors than from undisturbed sites. The mean CH_4 fluxes from waterbird and poultry active areas showed no statistically significant differences ($p>0.05$) from the undisturbed sites, but animal activities increased N_2O emissions, decreased marsh CO_2 sink, even convert into a net CO_2 source. The conversion of the marsh into agricultural field and landfill did not significantly change GHG emissions compared to non-disturbed marsh areas. To assess the regional GHG budget precisely, measurements should be designed at fine scales and environmental heterogeneity should be considered in the marsh. This study only provided short summertime and wintertime GHG fluxes, and long-term and high-frequency observations are needed to accurately quantify GHG budgets in the SLM. Continued investigations into the dynamics of GHG fluxes as well as mechanisms of GHG production in natural wetland, with an emphasis on temporal variation are essential in the future.

Acknowledgments. This work was supported by the National Natural Science Foundation of China (Grant No. 41576181; 41776190) and the Strategic Priority Research Program of Chinese Academy of Science (No. XDB40010200). The authors would like to thank three anonymous reviewers for their helpful comments.

REFERENCES

[1] Bao, T., Zhu, R., Li, X., Ye, W., Cheng, X. (2018a): Effects of multiple environmental variables on tundra ecosystem respiration in maritime Antarctica. – Scientific Reports 8(1): 12336.

[2] Bao, T., Zhu, R., Wang, P., Ye, W., Ma, D., Xu, H. (2018b): Potential effects of ultraviolet radiation reduction on tundra nitrous oxide and methane fluxes in maritime Antarctica. – Scientific Reports 8(1): 3716.

[3] Bass, A. M., O'Grady, D., Leblanc, M., Tweed, S., Nelson, P. N., Bird, M. I. (2014): Carbon Dioxide and Methane Emissions from a Wet-Dry Tropical Floodplain in Northern Australia. – Wetlands 34: 619-627.

[4] Boeckx, P., Van Cleemput, O., Villaralvo, I. D. A. (1996): Methane emission from a landfill and the methane oxidising capacity of its covering soil. – Soil Biology and Biochemistry 28: 1397-1405.

[5] Bogner, J., Spokas, K., Burton, E., Sweeney, R., Corona, V. (1995): Landfills as atmospheric methane sources and sinks. – Chemosphere 31: 4119-4130.

[6] Cai, Z. C., Xing, G. X., Yan, X. Y., Xu, H., Tsuruta, H., Yagi, K., Minami, K. (1997): Methane and nitrous oxide emissions from rice paddy fields as affected by nitrogen fertilisers and water management. – Plant and Soil 196: 7-14.

[7] Chen, H., Yao, S. P., Wu, N., Wang, Y. F., Luo, P., Tian, J. Q., Gao, Y. H., Sun, G. (2008): Determinants influencing seasonal variations of methane emissions from alpine wetlands in Zoige Plateau and their implications. – Journal of Geophysical Research: Atmosphere 113 (D12).

http://www.aloki.hu ● ISSN 1589 1623 (Print) ● ISSN1785 0037 (Online)
DOI: http://dx.doi.org/10.15666/aeer/1802_27612780

[8] Chen, H., Wu, N., Wang, Y. F., Gao, Y. H., Peng, C. H. (2011): Methane fluxes from alpine wetlands of Zoige Plateau in relation to water regime and vegetation under two scales. – Water Air and Soil Pollution 217: 173-183.
[9] Chen, Q. Q., Zhu, R. B., Xu, H. (2013): Spatial and temporal variations in CO_2, CH_4 and N_2O concentration in Ny-alesund, Svalbard. – Advance in Polar Science 25: 150-160.
[10] Christensen, T. R., Panikov, N., Mastepanov, M. (2003): Biotic controls on CO_2 and CH_4 exchange in wetlands-a closed environment study. – Biogeochemistry 64: 337-354.
[11] Dagg, J., Lafleur, P. (2011): Vegetation community, foliar nitrogen, and temperature effects on tundra CO_2 exchange across a soil moisture gradient. – Arctic Antarctic and Alpine Research 43: 189-197.
[12] Davidson, E. A., Janssens, I. A. (2006): Temperature sensitivity of soil carbon decomposition and feedbacks to climate change. – Nature 440: 165-173.
[13] Del Giorgio, P. A., Cole, J. J., Caraco, N. F., Peters, R. H. (1999): Linking planktonic biomass and metabolism to net gas fluxes in northern temperate lakes. – Ecology 80: 1422-1431.
[14] Ding, W. X., Cai, Z. C., Tsuruta, H. (2002): Effects of standing water depth on methane emissions from freshwater marshes in northeast China. – Atmospheric Environment 38: 181-188.
[15] Ding, W. X., Cai, Z. C., Tsuruta, H. (2004): Diel variation in methane emissions from the stands of Carex lasiocarpa and Deyeuxia angustifolia in a cool temperate freshwater marsh. – Atmospheric Environment 38: 181-188.
[16] Ding, W. X., Cai, Z. C. (2007): Methane emission from natural wetlands in China: Summary of years 1995-2004 studies. – Pedosphere 17: 475-486.
[17] Duan, X. N., Wang, X. K., Mu, Y. J., Ouyang, Z. Y. (2005): Seasonal and diurnal variations in methane emissions from Wuliangsu Lake in arid regions of China. – Atmospheric Environment 39: 4479-4487.
[18] Fang, J. Y., Wang, Z. H., Zhao, S. Q., Li, Y. K., Tang, Z. Y., Yu, D., Ni, L. Y., Liu, H. Z., Xie, P., Da, L. G., Li, Z. Q., Zheng, C. Y. (2006): Biodiversity changes in the lakes of the Central Yangtze. – Frontiers in Ecology and the Environment 4: 369-377.
[19] Fox, A. D., Hearn, R. D., Cao, L., Cong, P. H., Wang, X., Zhang, Y., Dou, S. T., Shao, Z. F., Barter, M., Rees, E. C. (2013): Preliminary observations of diurnal feeding patterns of Swan Geese Anser cygnoides using two different habitats at Shengjin Lake, Anhui Province, China. – Wildfowl 58: 20-30.
[20] Granli, T., Bockman, O. C. (1994): Nitrogen oxide from agriculture. – Norwegian Journal of Agricultural Sciences 12: 7-127.
[21] Gulledge, J., Schimel, J. P. (1998): Moisture control over atmospheric CH_4 consumption and CO_2 production in diverse Alaskan soils. – Soil Biology and Biochemistry 30: 1127-1132.
[22] Hu, Q. W., Cai, J. Y., Yao, B., Wu, Q., Wang, Y. Q., Wu, X. L. (2016): Plant-mediated methane and nitrous oxide fluxes from a *Carex* meadow in Poyang Lake during drawdown periods. – Plant and Soil 400: 367-380.
[23] Hutchinson, G. L., Mosier, A. R. (1981): Improved soil cover method for field measurement of nitrous oxide fluxes. – Soil Science Society of America Journal 45: 311-316.
[24] Huttunen, J. T., Alm, J., Liikanen, J. S., Larmola, T., Hannar, T., Sivola, J., Martikainen, P. J. (2003): Fluxes of methane, carbon dioxide and nitrous oxide in boreal lakes and potential anthropogenic effects on the aquatic greenhouse gas emissions. – Chemosphere 52: 609-621.
[25] Jiang, H. X., Xu, W. B., Qian, F. W., Chu, G. Z. (2007): Impact of habitat evolvement and human disturbance on wintering water birds in Shengjin Lake of Anhui Province, China. – Chinese Journal of Applied Ecology 18: 1832-1836.
[26] Johansson, T., Malmer, N., Crill, P. M., Mastepanov, M., Christensen, T. R. (2006): Decal vegetation changes in a northern peatland, greenhouse gas fluxes and net radiative forcing. – Global Change Biology 12: 2352-2369.
[27] Jungkunst, H. F., Fiedler, S. (2007): Latitudinal differentiated water table control of CO_2, CH_4 and N_2O fluxes from hydromorphic soils: feedbacks to climate change. – Global Change Biology 13: 2668-2683.

http://www.aloki.hu ● ISSN 1589 1623 (Print) ● ISSN1785 0037 (Online)
DOI: http://dx.doi.org/10.15666/aeer/1802_27612780

[28] Kato, T., Hirota, M., Tang, Y. H., Wada, E. (2011): Spatial variability of CH_4 and N_2O fluxes in alpine ecosystems on the Qinghai-Tibetan Plateau. – Atmospheric Environment 45: 5632-5639.
[29] Kirschke, S., Bousquet, P., Ciais, P. (2013): Three decades of global methane sources and sinks. – Nature Geoscience 6: 813-823.
[30] Kormi, T., Ali, N. B. H., Abichou, T., Green, R. (2017): Estimation of landfill methane emissions using stochastic search methods. – Atmospheric Pollution Research 8: 597-605.
[31] Lando, A. T., Nakayama, H., Shimaoka, T. (2017): Application of portable gas detector in point and scanning method to estimate spatial distribution of methane emission in landfill. – Waste Management 59: 255-266.
[32] Llstedt, U., Nordgren, A., Maimer, A. (2000): Optimum soil water for soil respiration before and after amendment with glucose in humid tropical acrisols and a boreal mor layer. – Soil Biology and Biochemistry 32: 1591-1599.
[33] Lu, Z. M., Liu, L. (2011): Investigation and analysis of Present Wetland Environmental Situation of Shengjin Lake. – Journal of Chizhou College 6: 80-83. (in Chinese).
[34] Marani, L., Alvala, P. C. (2007): Methane emissions from lakes and floodplains in Pantanal, Brazil. – Atmospheric Environment 41: 1627-1633.
[35] Martikainen, P., Nykänen, H., Crill, P., Silvola, J. (1993): Effect of a lowered water table on nitrous oxide fluxes from northern peatlands. – Nature 366: 51-53.
[36] Misselbrook, T. H., Webb, J., Chadwick, D. R., Ellis, S., Pain, B. F. (2001): Gaseous emissions from outdoor concrete yards used by livestock. – Atmospheric Environment 35: 5331-5338.
[37] Perez, T., Trumbore, S. E., Tyler, S. C., Matson, P. A., Ortiz-Monasterio, I., Rahn, T., Griffith, D. W. T. (2001): Identifying the agricultural imprint on the global N_2O budget using stable isotopes. – Journal of Geophysical Research 106: 9869-9878.
[38] Phillips, F. A., Leuning, R., Baigenta, R., Kelly, K. B., Denmead, O. T. (2007): Nitrous oxide flux measurements from an intensively managed irrigated pasture using micrometeorological techniques. – Agricultural and Forest Meteorology 143: 92-105.
[39] Post, W. M., Emanuel, W. R., Zinke, P. J., Stangenberger, A. G. (1982): Soil carbon pool and world life zones. – Nature 298: 156-159.
[40] Ravishankara, A. R., Daniel, J. S., Portmann, R. W. (2009): Nitrous oxide (N_2O): the dominant ozone-depleting substance emitted in the 21st century. – Science 326: 123-125.
[41] Rinne, J., Pihlatie, M., Lohila, A., Thum, T., Aurela, M., Tuovinen, J. P., Laurila, T., Vesala, T. (2005): Nitrous oxide emissions from a municipal landfill. – Environmental Science and Technology 39: 7790-7793.
[42] Scaroni, A. E., Ye, S. Y., Lindau, C. W., Nyman, J. A. (2014): Nitrous Oxide Emissions from Soils in Louisiana's Atchafalaya River Basin. – Wetlands 34: 545-554.
[43] Sharma, S. K., Choudhury, A., Sarkar, P. (2011): Greenhouse gas inventory estimates for India. – Current Science 101: 405-415.
[44] Song, C. C., Xu, X. F., Tian, H. Q., Wang, Y. Y. (2009): Ecosystem-atmosphere exchange of CH_4 and N_2O and ecosystem respiration in wetlands in the Sanjiang Plain, Northeastern China. – Global Change Biology 15: 692-705.
[45] Song, W. M., Wang, H., Wang, G. S., Chen, L. T., Jin, Z. N., Zhuang, Q. L., He, J. S. (2015): CH_4 emissions from an alpine wetland on the Tibetan Plateau: neglected but vital contribution of non-growing season. – Journal of Geophysical Research: Biogeoscience 120: 1475-1490.
[46] Ström, L., Christensen, T. R. (2007): Below ground carbon turnover and greenhouse gas exchanges in a sub-arctic wetland. – Soil Biology and Biochemistry 39: 1689-1698.
[47] Sun, Z. G., Wang, L. L., Mou, X. J., Jiang, H. H., Sun, W. L. (2014): Spatial and temporal variations of nitrous oxide flux between coastal marsh and the atmosphere in the Yellow River estuary of China. – Environmental Science and Pollution Research 21: 419-433.
[48] Wang, H. J., Lu, J. W., Wang, W. D., Yang, L. Y., Yin, C. Q. (2006): Methane fluxes from the littoral zone of hypereutrophic Tai Lake, China. – Journal of Geophysical Research: Atmosphere 111 (D17).

http://www.aloki.hu ● ISSN 1589 1623 (Print) ● ISSN1785 0037 (Online)
DOI: http://dx.doi.org/10.15666/aeer/1802_27612780

[49] Wang, W. Q., Zeng, C. S., Tong, C. (2008): Methane Production and Oxidation Capacities of Soil from the Reed Marsh of the Minjiang River Estuary. – Wetland Science 6: 60-68.
[50] Wang, Z. P., Song, Y., Gulledge, J., Yu, Q., Liu, H. S., Han, X. G. (2009): China's grazed temperate grasslands are a net source of atmospheric methane. – Atmospheric Environment 43: 2148-2153.
[51] Wang, Z. M., Wu, J. G., Madden, M., Mao, D. H. (2012): China's wetlands: conservation plans and policy impacts. – Ambio 41: 782-786.
[52] Wei, D., Xu, R., Tarchen, T., Dai, D. X., Wang, Y. S., Wang, Y. H. (2015): Revisiting the role of CH_4 emissions from alpine wetlands on the Tibetan Plateau: evidence from two in situ measurements at 4758 and 4320 m above sea level. – Journal of Geophysical Research: Biogeoscience 120: 1741-1750.
[53] Wei, D., Wang, X. D. (2017): Uncertainty and dynamics of natural wetland CH_4 release in China: Research status and priorities. – Atmospheric Environment 154: 95-105.
[54] Xing, Y. P., Xie, P., Yang, H., Ni, L. Y., Wang, Y. S., Rong, K. W. (2005): Methane and carbon dioxide fluxes from a shallow hypereutrophic subtropical lake in China. – Atmospheric Environment 39: 5532-5540.
[55] Xu, L. L., Xu, W. B., Zhou, Z. Z., Sun, Q. Y. (2008): Flora and vegetation in Shengjin Lake. – Journal of Wuhan Botanical Research 27: 264-270. (in Chinese).
[56] Yang, S. W., Dong, B., Liu, L. P., Sun, L., Sheng, S. W., Wang, Q., Peng, W. J., Wang, X., Zhang, Z. F., Zhao, J. (2015): Research on vegetation coverage change in Shengjin Lake Wetland of Anhui Province. – Wetlands 35: 677-682.
[57] Zhang, Y., Jia, Q., Prins, H. H. T. (2015): Effect of conservation efforts and ecological variables on waterbird population sizes in wetlands of the Yangtze River. – Scientific Reports 5: 17136.
[58] Zhou, B., Zhou, L. Z., Chen, J. Y., Cheng, Y. Q., Xu, W. B. (2010): Diurnal time activity budgets of wintering hooded cranes (*Grus monacha*) in Shengjin Lake, China. – Waterbirds 33: 110-115.
[59] Zhu, R. B., Liu, Y. S., Ma, E. D., Sun, J. J., Xu, H., Sun, L. G. (2009): Nutrient compositions and potential greenhouse gas production in penguin guano, ornithogenic soils and seal colony soils in coastal Antarctica. – Antarctic Science 21: 427-438.
[60] Zhu, R. B., Chen, Q. Q., Ding, W., Xu, H. (2012): Impact of seabird activity on nitrous oxide and methane fluxes from High Arctic tundra in Svalbard, Norway. – Journal of Geophysical Research 117: G04015.
[61] Zhu, R. B., Liu, Y. S., Xu, H., Ma, D. W., Jiang, S. (2013): Marine animals significantly increase tundra N_2O and CH_4 emissions in maritime Antarctica. – Journal of Geophysical Research: Biogeoscience 118: 1773-1792.
[62] Zhu, R. B., Bao, T., Wang, Q., Xu, H., Liu, Y. S. (2014a): Summertime CO_2 fluxes and ecosystem respiration from marine animal colony tundra in maritime Antarctica. – Atmospheric Environment 98: 190-201.
[63] Zhu, R. B., Ma, D. W., Xu, H. (2014b): Summertime N_2O, CH_4 and CO_2 exchanges from a tundra marsh and an upland tundra in maritime Antarctica. – Atmospheric Environment 83: 269-281.

APPENDIX

Electronic Appendix: The detailed information about investigation sites, experimental design and soil physiochemical properties at all the stations were summarized in the Appendix.

http://www.aloki.hu ● ISSN 1589 1623 (Print) ● ISSN1785 0037 (Online)
DOI: http://dx.doi.org/10.15666/aeer/1802_27612780

ECOLOGICAL STATUS OF SAND BINDER PLANT WHITE SAXAUL (*HALOXYLON PERSICUM*) AT THE MANAGED AREA OF AL-QASSIM, SAUDI ARABIA: PLANT ASSOCIATIONS AND POPULATION STRUCTURE

ELMEFREGY, M.[1*] – EL-SHEIKH, M. A.[1,2]

[1]*King Saud University, College of Science, Botany & Microbiology Department B.O. Box 2455, Riyadh 11451, Saudi Arabia*

[2]*Damanhour University, Faculty of Science, Botany & Microbiology Department, Damanhour, Egypt*

[*]*Corresponding author*
e-mail: melmefregy@outlook.com

(Received 8th Sep 2019; accepted 8th Jan 2020)

Abstract. *Haloxylon persicum* is a desert shrub with economic and ecological importance for arid zones in Saudi Arabia. It has a vital role in the protection of Unaizah and Buraidah, two large cities, and their surrounding from the dangerous mobile sand dunes and without it, the area could be covered by these dunes in a few years. The current study aims to analyze the floristic, vegetation structure and size structure of *H. persicum*. Eighteen stands were selected along the north and south of the study area with 20 m^2 each. At each stand, the vegetation inventory including plant species abundance percentage and size structure for *H. persicum* were estimated. Three plant associations; *H. persicum-Plantago boissieri*, *H. persicum-Stipagrostis plumose* and *H. persicum* were identified. Analysis of *H. persicum* size structure frequency was skewed towards medium size classes in all populations and the early life stages such as juvenile and the seedling recruitment was extremely limited. These results indicated that the populations of *H. persicum* are threatened by aridity and human impacts. Therefore, efforts are required to minimize uncontrolled exploitation. Finally, *in situ* and *ex situ* conservation of *H. persicum* populations are strongly recommended.
Keywords: *human impact, managed area, population demography, seedling recruitment, size structure*

Introduction

Sand dunes are one of the largest arid terrestrial ecosystems in Saudi, covering huge area of land surface (Reynolds et al., 2007). This sandy arid dry land is a fragile ecosystem component and one of the most sensitive areas to climate change and human activities, because the rare of rainfall and high evapotranspiration (Huang et al., 2015). Conversely, there are a lot of groundwater under these sand dunes due to the seeping of the rainfall water through the sand layers and stored against the evapotranspiration. These quantities of underground water are often an important water source for perennial plants and can be used for cultivation of farms (Cui and Shao, 2005; Naumburg et al., 2005; Imada et al., 2008). Moreover, the dynamics and the availability of the groundwater plays an important role in defining vegetation composition and distribution (Naumburg et al., 2005; Elmore et al., 2006), and in driving the vegetation dynamic and shifting the interactive balance between wooden species and herbaceous plants (Cooper et al., 2006; Holzapfel et al., 2006; McCluney et al., 2012). The unsustainable exploitation of groundwater associated with rapid population expansion and socio-economic development in these regions has aggravated the fluctuation of the groundwater table and influenced the availability of groundwater to desert shrub plants

http://www.aloki.hu ● ISSN 1589 1623 (Print) ● ISSN 1785 0037 (Online)
DOI: http://dx.doi.org/10.15666/aeer/1802_27812794

(Wang et al., 2011; Orellana et al., 2012). Declining or shifting the area of vegetation will decrease the diversity of plant associations and the stability of sand dunes this can consequently result in covering of the cities and productive farms by sands (Naumburg et al., 2005; Padilla and Pugnaire, 2007).

H. persicum is one of the most characteristic communities inhabit the Nafud habitat (flat sand seas with high sand dune) and characteristically occupies deep sand on the shoulders of sand dunes and shallow hollows of center Saudi (Schulz and Whitney, 1986). It nearly corresponds to the *Calligonum comosum* and *Artemisia monosperma* shrubland. *H. persicum* is an important plant for binding the mobile sand and shelter for many other plant associations which increasing the plant diversity (Brown and Porembski, 1998; El-Sheikh et al., 2010). Removal of *H. persicum* and *Calligonum comosum* for using as fuel and *Stipagrostis* by heavy gazing are common anthropogenic practices in Al-Qassim area. Therefore, people are managed this area at Unaizah from long time ago. Because, this managed area is the main reason for saving Unaizah and Buraydah cities and farms against the common dangerous sandy storms with strong mobile sand dunes. Without a dominant *H. persicum* and its associations, the area will be covered by mobile sand dunes in few years. However, there have been only few studies on the status of woody vegetation such as (Alatar et al., 2015). Therefore, understanding the mechanisms underlying the size, shape and dynamics of the geographic distributions of various species remains a key challenge (Pennisi, 2005; Gaston, 2009).

However, the present study aims to: 1- analysis the floristic and vegetation structure of managed area, 2- examine the status of *H. persicum* size structure if the population grow or decline after the long period of protection, and 3- analysis the ecological relations of *H. persicum* with edaphic and dominant anthropogenic factors.

Materials and methods

Study area

Al-Ghada managed area is located in Nafud Al-Shuqayyqah 'sandy arc'. It is located in the center of Al-Qassim area, south-west of Unaizah city and south of Wadi Al-Rumah valley between 43°-44° E 25°-26° N, lat. 630-724 meters above sea level (*Figure 1*). It is surrounded by sand dunes from the north and the west called the sands of Ghamis. The presence of *H. persicum* on the deep sand habitat, often in the form of low sand dune and extended to covering large area with low cover and it only scattered hummocks are to be seen in the landscape. There are associated few sub-shrubs, perennial grasses and annuals indicate a shallow ground water table fed by percolation.

According to the data of the meteorological station in Qassim region, the study area is located in the arid regions of Saudi Arabia. The climate is mildly moderate as the temperature reaches 20.0°C around the day during winter season and at night it is cold as the temperature drops to 6.0°C. Daytime temperatures reach up to 44°C and at night 27°C in the summer season.

Sample stands

A total of 18 stands in the north and south sector of the managed area were selected to covering all variations of habitats and vegetation structure. To analyze floristic and vegetation structure, in each stand plants were collected, identified and classified into

http://www.aloki.hu ● ISSN 1589 1623 (Print) ● ISSN 1785 0037 (Online)
DOI: http://dx.doi.org/10.15666/aeer/1802_27812794

their different life forms and chorotypes were recorded. Identification of plant species were conducted based on available references (Collenette, 1985, 1998, 1999; Chaudhary, 2001). Plant species cover were estimated in each stand as abundance percentage according to Kent (2012) and Canfield (1941).

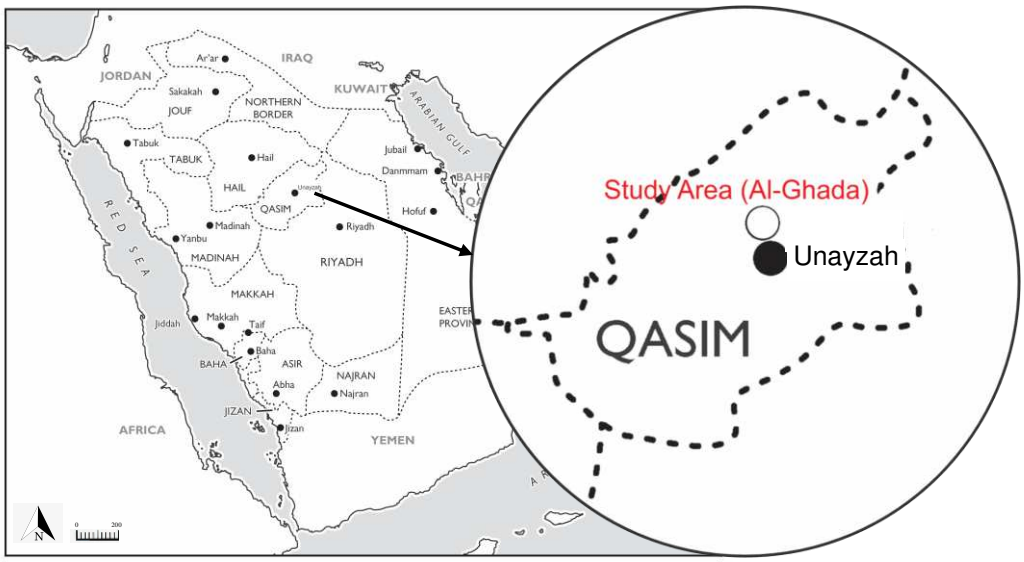

Figure 1. *A map showing the study in site at Unaizah area (Source: Ministry of Petroleum and Mineral Resources, Saudi Arabia)*

Soil analysis

Eighteen soil samples were collected; one from each stand from 0 - 50 cm depth. Soil texture (sand, silt and clay) was analyzed by Hydrometer method (Allen, 1989). The percentage of total organic matter was determined by loss of ignition of soil at 550°C for 2 hours. The prepared soil water extract (1:5) was used for further chemical analysis. Soil reaction (pH) measured by pH-meter and electrical conductivity (EC in mS cm^{-1}) was measured by conductivity -meter. The soil content of nutrient elements (N, P, K, Ca, Mg, Na and Fe) was estimated by using Inductively Coupled Plasma Optical Emission Spectrometry (ICP MSEOS 6000 Series, Thermo Fisher Scientific) method. All these methods are outlined in Allen (1989).

Data analysis

The numerical classification analysis TWINSPAN using two-way indicator species analysis (Hill, 1979b) were applied for plant species cover in 18 sample studied i.e matrix of 18 stand x 35 species cover values; and Detrended Correspondence Analysis (DCA) using DECORANA software (Hill, 1979a; ter Braak and Smilauer, 2002) was applied on the same data to obtain a graphical representation of the ecological structure of the vegetation groups identified using TWINSPAN. The second matrix of 18 stand X 35 species cover values X soil variables was using for detecting the correlations of the derived vegetation groups with environmental data, Canonical Correspondence Analysis, 'CCA', according to ter Braak and Smilauer (2002).

http://www.aloki.hu ● ISSN 1589 1623 (Print) ● ISSN 1785 0037 (Online)
DOI: http://dx.doi.org/10.15666/aeer/1802_27812794

Species richness of each vegetation group was calculated as the average number of species stand^{-1}. Simpson index following the equation $C = \sum_{i=1}^{s} p_i^2$ as an indicator for the relative dominance concentration and Shannon-Wiener index following the equation $\hat{H} = -\sum_{i=1}^{s} p_i \log p_i$ were calculated for each stand on the basis of the relative cover (pi) of *i*th species (Pielou, 1975; Magurran, 1988). The correlation between the ordination axes on one hand and soil variables on the other hand were estimated by Pearson's simple linear correlation coefficient (r). Moreover, the relations between species diversity indices and soil variables were tested. The variation in species diversity, soil variables and stand characters in relation to vegetation group was assessed by one-way analysis of variance SPSS 20.0 software, IBM, Chicago, IL.

Plant size structure analysis

The size of *H. persicum* individuals were counted by their height (H) and average crown diameter (D) were measured (based on 3-diameter measurements/individual) and their average of H and D were calculated in each stand. The size index H+D/2 was calculated (modified Crisp and Lange, 1976). This obtained value used for calculation the size frequency distribution category of *H. persicum*. The frequency of each category is calculated separately as a percentage frequency and drawing graphically. Density of *Haloxylon persicum* in the studied area was calculated as the number of individuals/ha. Finally, the mean and coefficient of variation of density, height, diameter, and size index of *H. persicum* were calculated.

Results

Floristic diversity

A total of 35 plant species belonging to 12 families were collected from the studies stands. The most represented families in the study area were Poaceae and Caryophyllaceae (21% each), Boraginaceae (18%) and Geraniaceae (7%). The most prominent life forms (*Figure 2a*) were annual herbs (61%), sub-shrubs (12%), annual grasses (9%), perennial herbs (6%), perennial grasses (6%) and shrubs (6%). The dominant chorotypes were the Saharo Arabian region represented by 12 species (41%) followed by the Mediterranean-Irano Turanian-Saharo Arabian (17%), the Saharo Arabian-Somali Masai (14%) and the Saharo Arabian-Irano Turanian (10%) (*Figure 2b*).

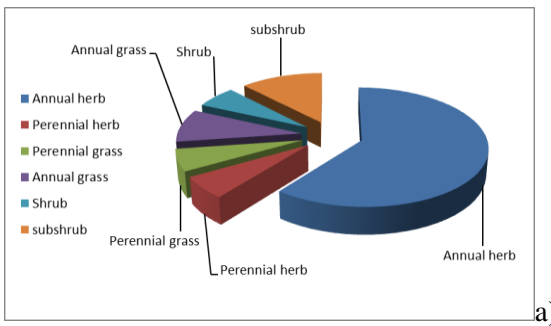

a)

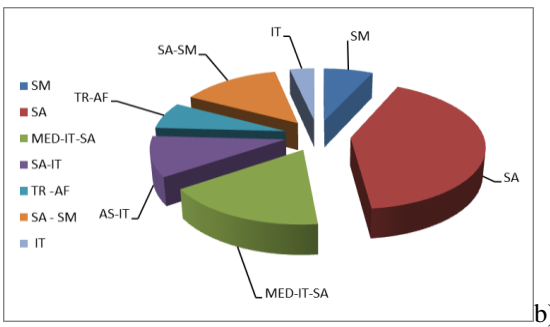

b)

Figure 2. *The represented a) life forms and different represented b) chorotypes in the study area. SA: Saharo-Arabian, MED: Mediterranean, IT: Irano Turanian, SM: Somali Masai, TR-AF: Tropical Africa*

http://www.aloki.hu ● ISSN 1589 1623 (Print) ● ISSN 1785 0037 (Online)
DOI: http://dx.doi.org/10.15666/aeer/1802_27812794

Multivariate analysis

The dataset formed in this study consisted of 18 studied stands and 35 species. TWINSPAN analysis of this dataset generated a dendrogram divided it into three vegetation groups (plant communities) at the second level. Characterization and nomination of these groups were assigned based on the dominant and subdominant species in each group as follows: vegetation group (VG) I: *H. persicum-Plantago boissieri*, VG II: *H. persicum- Stipagrostis plumosa*, VG III: *H. persicum*. Further CCA and DCA analysis confirmed the separation of these plant communities generated by TWINSPAN and reveals a great relationship between topographic aspects and environmental gradients in Ghada managed area (*Table 1* and *Figure 3a,b*). The association VG I: *H. persicum-Plantago boissieri* mostly inhabits on the north sector of managed area (75%) of total stands and the association II: *H. persicum- Stipagrostis plumosa* inhabits mostly on the south zone (57%) of total stands. On the other hand, the association III *H. persicum* is completely inhabited on the north sector of the managed area (*Table 2*).

Table 1. *Percentage frequency synoptic table*

Group No.			**VG I**	**VG II**	**VG III**
No. of relevés			**8**	**7**	**3**
% No. of releve in North sector			**75**	**43**	**100**
% No. of releve in South sector	**Life forms**	**Chorotype**	**25**	**57**	**0**
Haloxylon persicum	SH	IT	**100**	86	**100**
Schismus barbatus	AG	SA-IT	50	71	33
Eremobium lineare	AH	SA	63	71	33
Plantago boissieri	AH	SA	75	71	.
Stipagrostis plumosa	PG	SM	50	43	33
Bassia muricata	AH	SA	38	43	67
Neurada procumebens	AH	SA	38	43	.
Launaea capitata	AH	MED-IT-SA	25	29	33
Silene villosa	AH	MED-IT-SA	.	29	67
Moltkiopsis ciliata	SS	SM	38	14	67
Haloxylon salicornicum	SH	SA	25	43	33
Hypecoum littorale	AH	ME	.	14	33
Ifloga spicata	AH	MED-IT-SA	13	14	.
Salsola arabica	SS	SA	25	43	.
Paronychia arabica	AH	TR -AF	25	29	.
Polycarpaea repens	SS	SA	13	.	.
Gastrocotyle hispida	AH	SA-IT	.	29	.
Bassia eriophora	AH	SA-IT	13	.	.
Centropodia forsskalei	PG	SA	38	.	33
Cakile arabica	AH	SA	13	14	33
Astragalus schimperi	AH	SA	.	.	33
Stipa capensis	AH	SA-SM	.	.	.
Anthemis deserti	AH	SA	13	.	.
Senecio glaucus	AH	IT	13	.	.
Aristida adscensionis	PG	MED-IT-SA	13	.	.
Erodium laciniatum	AH	MED-IT-SA	13	14	67
Launaea mucronata	AH	SA-SM	13	.	.
Heliotropium digynum	SS	SA - SM	13	.	33
Gisekia pharnaceoides	AH	TR -AF	13	.	.
Cynomorium coccineum	PH	ME	13	.	.
Cutandia memphitica	AG	SA	13	14	33
Malva parviflora	AH	SA-SM	.	29	33
Monsonia nivea	AH	Med - IT	13	.	.

VG I: Haloxylon persicum-Plantago boissieri; VG II: Haloxylon persicum-Stipagrostis plumosa; VG III: Haloxylon persicum. Life forms are: AH: Annual Herbs, PH: Perennial Herbs, AG: Annual Grasses, Perennial Grasses, SH: Shrubs, SS: Sub-Shrubs. Chorotypes are: SA: Saharo-Arabian, MED: Mediterranean, IT: Irano Turanian, SM: Somali Masai, TR-AF: Tropical Africa

http://www.aloki.hu ● ISSN 1589 1623 (Print) ● ISSN 1785 0037 (Online)
DOI: http://dx.doi.org/10.15666/aeer/1802_27812794

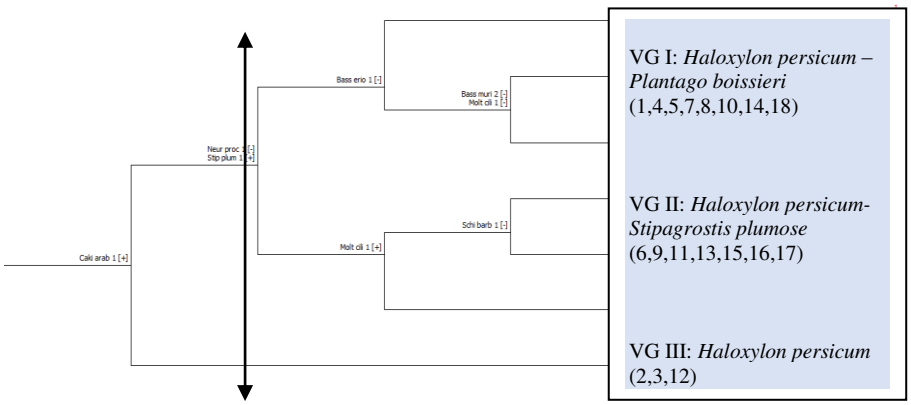

(a)

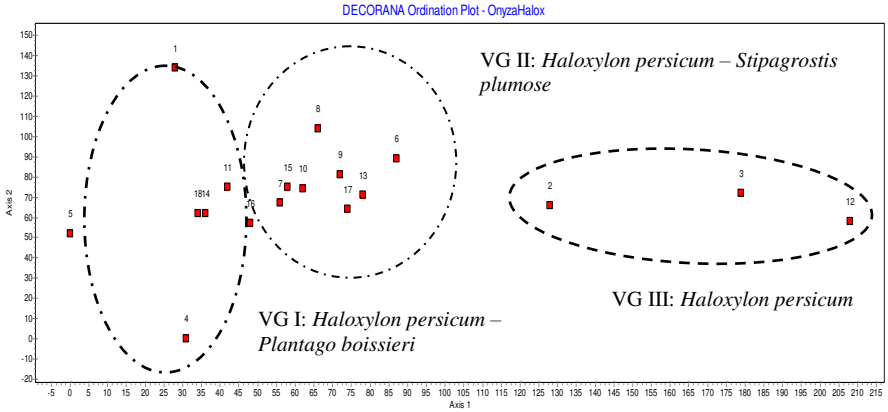

(b)

Figure 3. *Results of TWINISPAN classification of the dataset (35 species × 18 stands) (a) and DECORANA ordination of the same dataset by using the average values of three associations and sub-associations (b). In figure (a) numbers represent stands*

Table 2. *Inter set correlations of environmental variables with CCA axes*

N	NAME	AX1	AX2	AX3	AX4
	Diversity indices				
1	**Species number**	0.5721**	0.4329*	0.0456	-0.2412
2	**Species cover** (m 100m^{-1})	-0.0800	0.2491	0.6075	-0.4776
3	**Species richness** (sp. stand^{-1})	0.6515**	0.3991	-0.0210	-0.0508
4	**Evenness**	0.4389*	0.0932	0.7337	0.0680
5	**Shannon** (Ĥ)	0.6022**	0.2552	0.4411	-0.0745
6	**Simpson** (C)	-0.4804*	-0.1116	-0.6824	-0.0354
	Soil				
7	**pH**	-0.2246	0.1344	-0.1765	0.0461
8	**EC** (mS/cm^{-1})	-0.3477	-0.0158	-0.1733	-0.0041
	Bulk soil (%)				
9	**Sand**	0.3447	-0.1759	0.0713	0.0979
10	**Clay**	-0.3876	-0.0416	0.2336	-0.0722
11	**Silt**	-0.2357	0.2615	-0.2338	-0.0894
12	**Organic Matter** (%)	-0.1692	0.1328	-0.0858	0.1074
	Minerals (ppm)				
13	**Na**	-0.1728	-0.0220	-0.4835	0.0489
14	**Ca**	-0.3585	-0.0967	0.0856	-0.0386
15	**K**	-0.0725	0.0394	-0.2406	-0.0403
16	**Mn**	0.4216*	0.5596**	-0.3983	-0.0691
17	**Fe**	0.3755	0.5414**	-0.4583	-0.0618
18	**Mg**	-0.0066	0.1783	-0.2558	-0.1397
19	**N**	-0.1273	0.2075	-0.3100	0.0100
20	**P**	-0.2872	0.2147	-0.4901	0.0513

* Significant correlation P ≤ 0.05; ** Significant correlation P ≤ 0.01

http://www.aloki.hu ● ISSN 1589 1623 (Print) ● ISSN 1785 0037 (Online)
DOI: http://dx.doi.org/10.15666/aeer/1802_27812794

Correlation analysis

The relation between the environmental variables and ordination axes was done by CCA application (*Table 2* and *Figure* 4). The separation of stands along the AX-1 is affected positively by species number, richness, evenness, Mn and negatively by Simpson index (*Table 2* and *Figure 4a*). The species number, Mn and Fe are positively correlated with the AX-2. The distribution of *H. persicum* are located on the lower negative side of the AX-1 and correlated with EC, Na, Clay and Ca content (*Figure 4b*).

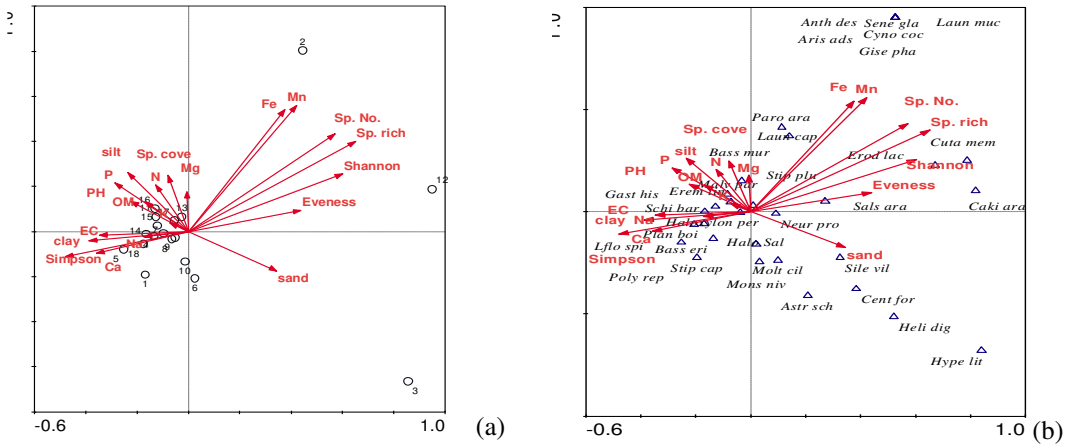

Figure 4. *CANOCO ordination biplot with environmental variables (arrows); 18 stands (a) represented by circles and 35 abundant species (b) represented by triangles with the first four letters of genus and three letters of species name. Fullanames of the abundant species are available in Table 1*

Species number and species richness are correlated positively by Fe and Mn and negatively by clay content. Species evenness and Shannon index are correlated positively by sand and negatively by silt, Na and P but the Simpson index are correlated vice versa by these element contents (*Table 3*).

Table 3. *Pearson's correlation coefficients between species diversity and soil characteristics*

Variable	Species no.	Species cover (m-100 m^{-1})	Species richness	Species evenness	Shannon index	Simpson index
Bulk soil (%)						
Sand	0.077	-0.172	0.215	0.368*	0.302*	-0.327*
Silt	0.112	0.139	-0.017	-0.392*	-0.220	0.314*
Clay	-0.369*	0.161	-0.469*	-0.186	-0.324	0.221
OM	-0.231	-0.241	-0.127	-0.018	-0.147	0.085
Soil						
pH	-0.255	-0.095	-0.251	-0.310	-0.329	0.282
EC (mS/cm)	-0.260	-0.086	-0.299	-0.413	-0.420	0.393
Minerals (ppm)						
K	0.036	-0.011	-0.007	-0.289	-0.183	0.233
Mg	0.218	0.079	0.126	-0.283	-0.089	0.199
Ca	-0.290	-0.059	-0.320	-0.207	-0.296	0.219
Fe	0.453*	0.016	0.427*	-0.167	0.105	0.115
Na	-0.183	-0.159	-0.191	-0.415*	-0.376*	0.414*
Mn	0.517**	0.025	0.501**	-0.060	0.209	0.009
N	0.108	-0.109	0.094	-0.256	-0.128	0.197
P	-0.117	-0.154	-0.136	-0.433*	-0.362*	0.417*

*: P≤0.05 and **: P≤0.01

http://www.aloki.hu ● ISSN 1589 1623 (Print) ● ISSN 1785 0037 (Online)
DOI: http://dx.doi.org/10.15666/aeer/1802_27812794

Soil-plant association characteristics

The association of VG I: *H. persicum-Plantago boissieri* had the high values of species cover, silt and clay and lower values sand, Fe and Mn content (*Table 4*). The association of VG II: *H. persicum- Stipagrostis plumosa* had the highest values of Simpson index, organic matter, pH, EC, K, Mg, Na, N, Fe and lower in species cover, species number, species richness, species evenness and Shannon index. On the other hand, the association of VG III *H. persicum* had the highest values of species number, richness, evenness, Shannon indices, sand, Fe, Mn and lower values of Simpson index, silt, clay, organic matter, pH, EC, K, Ca, Mg, Na, N and P content.

Table 4. *Mean ± standard deviation of diversity indices and Soil variables of different vegetation groups in the study area*

VG	VG I	VG II	VG III	Total	F-Value
Diversity indices					
Sp. no.	7.50±1.69	**6.71±1.25**	**11.00±4.00**	7.78±2.44	4.84*
Sp. cover m 100m^{-1}	**49.63±9.4**	**38.14±10.19**	39.67±27.74	43.5±13.98	1.471
Sp. rchness	1.67±0.43	**1.59±0.35**	**2.9±0.42**	1.85±0.62	12.63***
Sp. evenness	0.62±0.09	**0.51±0.09**	**0.83±0.12**	0.61±0.14	11.81***
Shannon Ĥ	0.54±0.09	**0.42±0.11**	**0.83±0.05**	0.54±0.17	20.82***
Simpson (C)	0.43±0.1	**0.57±0.12**	**0.17±0.1**	0.44±0.17	14.79***
Soil bulk (%)					
Sand	**84.75±3.2**	86.57±3.21	**88.67±2.31**	86.11±3.25	1.871
Silt	**7.75±2.49**	6.29±2.14	**5.33±2.31**	6.78±2.39	1.426
Clay	**7.50±1.41**	7.14±1.57	**6.00±0.00**	7.11±1.41	1.279
OM	7.88±5.13	**11.71±10.23**	**7.33±4.54**	9.28±7.36	0.604
Soil					
pH	7.85±0.1	**7.91±0.08**	**7.83±0.03**	7.87±0.09	1.383
EC (ms/cm)	0.11±0.03	**0.12±0.06**	**0.07±0.01**	0.1±0.04	1.597
Minerals (ppm)					
K	439.77±161.88	**668±530.31**	**397.41±76.14**	521.47±354.16	0.996
Ca	323.15±135.39	300.81±109.54	**212.41±18.44**	296.01±115.81	1.008
Mg	574.79±148.52	**686.73±272.83**	**573.57±126.21**	618.12±201	0.639
Fe	**155.99±74.62**	273.42±117.88	**309.26±176.95**	227.2±123.84	3.070
Na	74.57±14.13	**111.83±55.07**	**61.95±7.36**	86.96±39.95	2.831
Mn	**17.7±12.39**	28.84±14.92	**39.05±24.39**	25.59±16.65	2.324
N	4.25±1.75	**10.86±10.55**	**3.67±2.08**	6.72±7.25	2.114
P	106.57±29.24	**147.48±47.74**	**86.31±20.4**	119.1±42.43	3.700*

The plant associations identified after TWINSPAN are as the follows: VG I: Haloxylon persicum-Plantago boissieri; VG II: Haloxylon persicum-Stipagrostis plumosa; VG III: Haloxylon persicum. The higher and lower value are in bold. *: P≤0.05, **: P≤0.01, ***: P≤0.001

H. persicum size structure

The northern part of the studied area is characterized by high density number and lower values of plants' height, diameter, height/diameter ratio and size index as compared to the southern region of the studied area (*Table 5*).

The size structure of *H. persicum* individuals in the northern sector and in all over the study managed area showed an inversed-J shape approving that there is a growth of individuals toward the medium individuals which constitutes the highest percentage (*Figure 5*). On the other hand, the size structure frequency of *H. persicum* growing in the southern sector of the study area showed a bi-modal pattern of growth indicating

http://www.aloki.hu ● ISSN 1589 1623 (Print) ● ISSN 1785 0037 (Online)
DOI: http://dx.doi.org/10.15666/aeer/1802_27812794

that there is equal of juvenile and medium individuals age (*Figure 5c*). This could be considered as an indicator of dangers threatens the *H. persicum* individuals in the southern studied area.

Table 5. *Demographic analysis of Haloxylon persicum in the study area*

Sector	Density (ha)	Height (cm)	Diameter (cm)	H:D (cm)	Size index
North (1-12)	164.28	190.16 ± 82.94	210.25 ± 126.61	1.04 ± 0.38	200.21 ± 101.5
South (13-18)	137.84	250.95 ± 184.11	235.06 ± 136.81	1.08 ± 0.70	243.01 ± 144.8
Total Mean ± SD	301.86	207.48 ± 123.88	217.47 ± 129.88	1.05 ± 0.06	212.66 ± 117.1

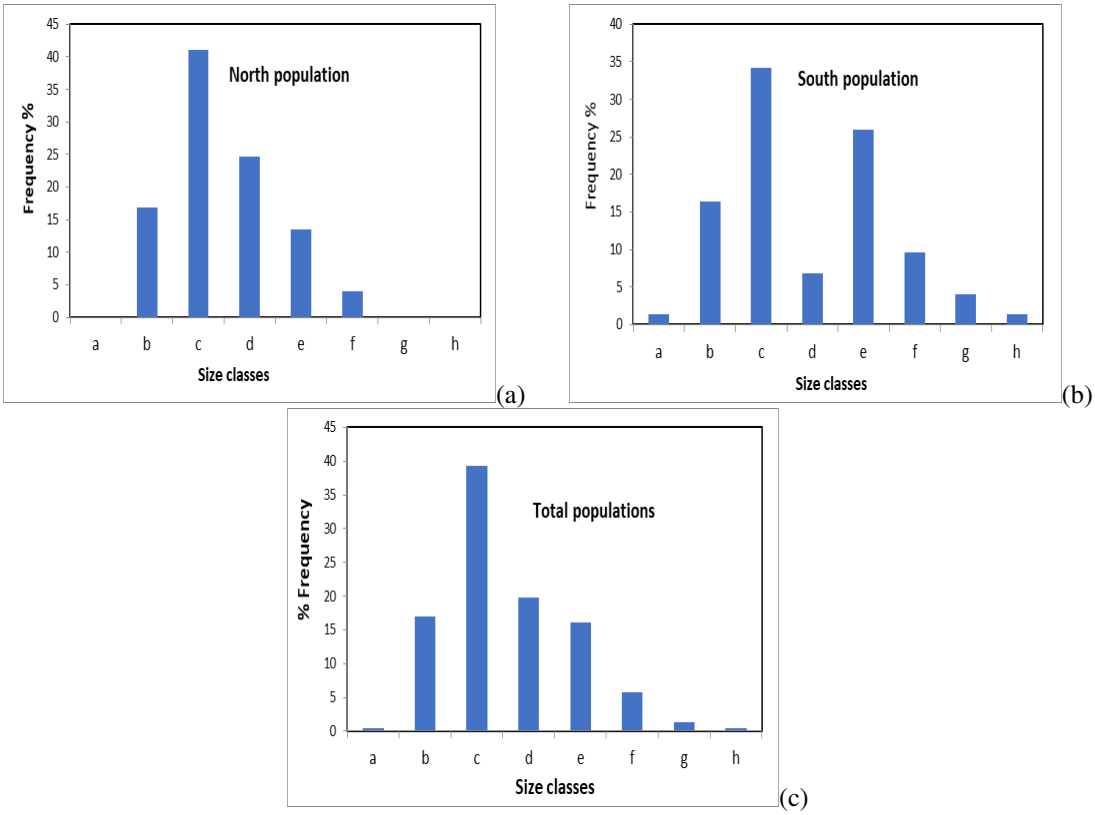

Figure 5. *The size-frequency distribution of the Haloxylon persicum in the study area. The size classes cm ind.-1 are: a<40, b: 41-100, c: 101-200, d: 201-300, e: 301-400, f: 401-500, g: 501-600 and h>600*

Discussion

Topography and land forms significantly influence the growth, existence and distribution of different plant life forms in arid and semi-arid regions (Kassas and Girgis, 1964; Zohary, 1973; Shaltout et al., 2010) such as the managed area of Unaizah; the studied area. The results obtained in this study indicated that the dominant life form in the study site is annual herbs. This dominance of annual herbs could be attributed to the abundance of water during rainy seasons which supporting the growth of such plants on these *H. persicum* Nabkhas. Moreover, these Nabkhas are considering as shelter for many therophytes because it is modified the soil substrates by retain with rainfall under soil surface (Schulz and Whitney, 1986; Shaltout and Mady, 1996; Hosni and Hegazy,

http://www.aloki.hu ● ISSN 1589 1623 (Print) ● ISSN 1785 0037 (Online)
DOI: http://dx.doi.org/10.15666/aeer/1802_27812794

1996; Shaltout et al., 2010). However, this water is adequate to support the growth of sub-shrubs e.g. *H. persicum*; therefore, the existence of such plants may be due to their adaptation to the harsh conditions exist in the study site (Alatar et al., 2012). The composition of vegetation life forms in the study area showed a typical pattern of the desert flora dominated by xerophytes and chamaephytes. The same pattern of vegetation was observed in different desert habitats among different parts of Saudi Arabia (Collenette, 1985, 1998, 1999; El-Demerdash et al., 1994; Chaudhary, 2001; Al-Turki and Al-Olayan, 2003; Fahmy and Hassan, 2005; El-Ghanim et al., 2010). In general, there is a great correlation between the plants' life forms and topography of their habitats (Kassas and Girgis, 1964; Zohary, 1973; Shaltout et al., 2010).

In study site, the dominant plant chorotype is the Saharo Arabian. The species of Saharo Arabian chorotype are distributed only along the central strip of Saudi Arabia and are more abundant in habitats providing protection and/or habitats characterized by more favorable micro-climate conditions (Zohary, 1973; Hegazy et al., 1998; El-Ghanim et al., 2010; Ghazanfar and Fisher, 2013). The central region of Saudi Arabia covers a wide range of bioclimatic zones and characterized by the existence of different habitats that supports several other chorotypes which were found in the study area beside the Saharo Arabian species e.g. the Mediterranean, Irano Turanian and Somali Masai. Furthermore, the Central region of Saudi Arabia covers the transition zone between these regions (Zohary, 1973; Mandaville, 1990; White and Léonard, 1990; Hegazy et al., 1998; Alfarhan, 1999; Ghazanfar and Osborne, 2010).

The three associations (VG) I: *Haloxylon persicum-Plantago boissieri*, VG II: *H. persicum-Stipagrostis plumosa*, VG III: *H. persicum* are comparable to the previous studies and represented the open sandy desert shrubland in center Saudi. This open shrubland is the most widespread community in An Nafud and corresponds to Vesey-Fitzgerald's (1957) 'central Arabian red sand vegetation' and the 'abal-'adhir sand shrubland described by Mandaville (1990). It is found near the mid-upper parts of dunes and also on undulating sheets of deep sand. Annual and perennial herbs are commonly associated with these communities of *H. persicum* Nabkhas such as *Plantago boissieri*, *Stipagrostis plumosa*, *Moltkiopsis ciliata, Monsonia heliotropoides*, *Stipa capensis, Centropodia fragilis* and *Cyperus conglomeratus* (Chaudhary, 1983). The distribution of plants and diversity are correlated with some edaphic factors, such as Mn, Fe EC, Na, clay and Ca content. Many authors stated that the climate, topography and habitat heterogeneity (John et al., 2007), seed and fruits dispersal (Svenning et al., 2008) and biotic interactions (Richards et al., 1997; Araújo and Guisan, 2006). However, determinants of species distributions vary on spatial and temporal scales. For instance, climate appears to be important at the landscape level and above (Davis and Shaw, 2001; Walther et al., 2002). Soil or topography dominates at landscape and local scales, hydrology at local scales, and dispersal functions at all scales (Angert and Schemske, 2005). Moreover, our finding indicated that the species diversity is positively correlated with soil content of soil Fe, Mn and sand content; and has a negative correlation with soil silt clay and Na content. Other studies reported the same pattern of correlation in desert habitats of Saudi Arabia (El-Demerdash et al., 1994; Abbadi and El-Sheikh, 2002; El-Sheikh et al., 2010, 2013, 2018).

The results obtained via the analysis of size structure and frequency of *H. persicum* plants in the studied area showed an inversed-J shape approving that there is a significant growth of these plants all over the protected area as the young individuals constitute the highest percentage. Similarly, the northern part of the studies area showed

http://www.aloki.hu ● ISSN 1589 1623 (Print) ● ISSN 1785 0037 (Online)
DOI: http://dx.doi.org/10.15666/aeer/1802_27812794

the inversed-J pattern of size structure percentages showing that juvenile and medium individuals of *H. persicum* plants represent the highest percentages among all the other age categories. On the other hand, frequency calculation of size structure of *H. persicum* plants growing in the southern part of the studied area showed a bi-modal pattern of growth indicating that there is a significant abundance of young individuals and old individuals as well in the similar area (El-Sheikh, 2013). This could be considered as an indicator of dangers threatens the *H. persicum* community in the studied area. The obtained result showed significant evidence that *H. persicum* plants in managed area of Unaizah goes under a great negative human impact threating their abundance in the studied area (El-Sheikh, 2005, 2013). Therefore, these plants should be protected via all available means. Over-grazing and wood cutting are considered among the main factors affecting the abundance of *H. persicum* plants. The removal of *H.* and *Calligonium* for fuel is widespread as it is long and clean burning.

Acknowledgements. This scientific paper contains studies and research results supported by King Abdulaziz City for Science and Technology grant no. (1-17-01-001-0032).

REFERENCES

[1] Abbadi, G. A., El-Sheikh, M. A. (2002): Vegetation analysis of Failaka Island (Kuwait). – Journal of Arid Environments 50: 153-165.
[2] Al-Turki, T., Al-Olayan, H. (2003): Contribution to the flora of Saudi Arabia: Hail region. – Saudi journal of biological sciences 10: 190-222.
[3] Alatar, A., El-Sheikh, M. A., Thomas, J. (2012): Vegetation analysis of Wadi Al-Jufair, a hyper-arid region in Najd, Saudi Arabia. – Saudi Journal of Biological Sciences 19: 43-54.
[4] Alatar, A. A., El-Sheikh, M. A. R., Thomas, J., Hegazy, A. K., El Adawy, H. A. (2015): Vegetation, Floristic Diversity, and Size-Classes of Acacia gerrardii in an Arid Wadi Ecosystem. – Arid Land Research and Management 29: 335-359.
[5] Alfarhan, A. (1999): A phytogeographical analysis of the floristic elements in Saudi Arabia. – Pakistan Journal of Biological Sciences (Pakistan) 2: 702-711.
[6] Allen, S. E. (1989): Chemical analysis of ecological materials. – Blackwell Scientific, Oxford.
[7] Angert, A. L., Schemske, D. W. (2005): The evolution of species' distributions: reciprocal transplants across the elevation ranges of Mimulus cardinalis and M. lewisii. – Evolution 59: 1671-84.
[8] Araújo, M. B., Guisan, A. (2006): Five (or so) challenges for species distribution modelling. – Journal of Biogeography 33: 1677-1688.
[9] Brown, G., Porembski, S. (1998): Flora and vegetational aspects of miniature dunes in a sand-depleted Haloxylon salicornicum community in the Kuwait desert. – Flora 193: 133-140.
[10] Canfield, R. H. (1941): Application of the Line Interception Method in Sampling Range Vegetation. – Journal of Forestry 39: 388-394.
[11] Chaudhary, S. A. (1983): Vegetation of the Great Nefud. – Journal of the Saudi Arabian Natural History Society 2: 2-7.
[12] Chaudhary, S. A. (2001): Flora of the Kingdom of Saudi Arabia. – Ministry of Agriculture and Water, Riyadh.
[13] Collenette, S. (1985): An illustrated guide to the flowers of Saudi Arabia. – Scorpion publishing Ltd, Riyadh.

http://www.aloki.hu ● ISSN 1589 1623 (Print) ● ISSN 1785 0037 (Online)
DOI: http://dx.doi.org/10.15666/aeer/1802_27812794

[14] Collenette, S. (1998): A Checklist of Botanical Species in Saudi Arabia. – International Asclepiad Society, West Sussex (UK).
[15] Collenette, S. (1999): Wildflowers of Saudi Arabia. – National Commission for Wildlife Conservation and Development (NCWCD), Riyadh.
[16] Cooper, D. J., Sanderson, J. S., Stannard, D. I., Groeneveld, D. P. (2006): Effects of long-term water table drawdown on evapotranspiration and vegetation in an arid region phreatophyte community. – Journal of Hydrology 325: 21-34.
[17] Crisp, M. D., Lange, R. T. (1976): Age Structure, Distribution and Survival under Grazing of the Arid-Zone Shrub Acacia burkittii. – Oikos 27: 86-92.
[18] Cui, Y., Shao, J. (2005): The Role of Ground Water in Arid/Semiarid Ecosystems, Northwest China. – Groundwater 43: 471-477.
[19] Davis, M. B., Shaw, R. G. (2001): Range Shifts and Adaptive Responses to Quaternary Climate Change. – Science 292: 673.
[20] El-Demerdash, M., Hegazy, A., Zilay, A. (1994): Distribution of the plant communities in Tihamah coastal plains of Jazan region, Saudi Arabia. – Vegetatio 112: 141-151.
[21] El-Ghanim, W. M., Hassan, L. M., Galal, T. M., Badr, A. (2010): Floristic composition and vegetation analysis in Hail region north of central Saudi Arabia. – Saudi Journal of Biological Sciences 17: 119-128.
[22] El-Sheikh, M. A. (2005): Plant succession on abandoned fields after 25 years of shifting cultivation in Assuit, Egypt. – Journal of Arid Environments 61: 461-481.
[23] El-Sheikh, M. A., Abbadi, G. A., Bianco, P. M. (2010): Vegetation ecology of phytogenic hillocks (nabkhas) in coastal habitats of Jal Az-Zor National Park, Kuwait: Role of patches and edaphic factors. – Flora-Morphology, Distribution, Functional Ecology of Plants 205: 832-840.
[24] El-Sheikh, M. A. (2013): Population structure of woody plants in the arid cloud forests of Dhofar, southern Oman. – Acta Botanica Croatica 72: 97-111.
[25] El-Sheikh, M. A., Thomas, J., Alatar, A. A., Hegazy, A. K., Abbady, G. A., Alfarhan, A. H., Okla, M. I. (2013): Vegetation of Thumamah Nature Park: a managed arid land site in Saudi Arabia. – Rendiconti Lincei 24: 349-367.
[26] El-Sheikh, M. A., Al-Oteiby, S. A., Alfarhan, A. H., Barcelo, D., Picó, Y., Alatar, A. A., Javed, S. B., Eid, E. M. (2018): Distribution of soil organic carbon in Wadi Al-Thulaima, Saudi Arabia: A hyper-arid habitat altered by wastewater reuse. – CATENA 170: 266-271.
[27] Elmore, A. J., Manning, S. J., Mustard, J. F., Craine, J. M. (2006): Decline in alkali meadow vegetation cover in California: the effects of groundwater extraction and drought. – Journal of Applied Ecology 43: 770-779.
[28] Fahmy, A., Hassan, L. (2005): Plant diversity of wadi el Ghayl, Aseer Mountains, Saudi Arabia. – Egyptian Journal of Desert Research 55: 39-52.
[29] Gaston, K. J. (2009): Geographic range limits: achieving synthesis. – Proceedings of the Royal Society B: Biological Sciences 276: 1395-1406.
[30] Ghazanfar, S. A., Osborne, J. (2010): Conservation through restoration: study of a degraded gravel plain in South Eastern Arabia. – Pakistan Journal of Botany 42: 193-204.
[31] Ghazanfar, S. A., Fisher, M. (2013): Vegetation of the Arabian peninsula. – Springer Science & Business Media, London.
[32] Hegazy, A. K., El-Demerdash, M. A., Hosni, H. A. (1998): Vegetation, species diversity and floristic relations along an altitudinal gradient in south-west Saudi Arabia. – Journal of Arid Environments 38: 3-13.
[33] Hill, M. O. (1979a): DECORANA: A FORTRAN Program for Detrended Correspondence Analysis and Reciprocal Averaging. – Section of Ecology and Systematics, Cornell University, NY.
[34] Hill, M. O. (1979b): TWINSPAN: A FORTRAN Program for Arranging Multivariate Data in an Ordered Two-way Table by Classification of the Individuals and Attributes. – Section of Ecology and Systematics, Cornell University, NY.

http://www.aloki.hu ● ISSN 1589 1623 (Print) ● ISSN 1785 0037 (Online)
DOI: http://dx.doi.org/10.15666/aeer/1802_27812794

[35] Holzapfel, C., Tielbörger, K., Parag, H. A., Kigel, J., Sternberg, M. (2006): Annual plant–shrub interactions along an aridity gradient. – Basic and Applied Ecology 7: 268-279.
[36] Hosni, H. A., Hegazy, A. K. (1996): Contribution to the flora of Asir, Saudi Arabia. – Candollea 51: 169-202.
[37] Huang, J., Yu, H., Guan, X., Wang, G., Guo, R. (2015): Accelerated dryland expansion under climate change. – Nature Climate Change 6: 166.
[38] Imada, S., Yamanaka, N., Tamai, S. (2008): Water table depth affects Populus alba fine root growth and whole plant biomass. – Functional Ecology 22: 1018-1026.
[39] John, R., Dalling, J. W., Harms, K. E., Yavitt, J. B., Stallard, R. F., Mirabello, M., Hubbell, S. P., Valencia, R., Navarrete, H., Vallejo, M., Foster, R. B. (2007): Soil nutrients influence spatial distributions of tropical tree species. – Proceedings of the National Academy of Sciences 104: 864.
[40] Kassas, M., Girgis, W. A. (1964): Habitat and Plant Communities in the Egyptian Desert: V. The Limestone Plateau. – Journal of Ecology 52: 107-119.
[41] Kent, M. (2012): Vegetation Description and Data Analysis: A Practical Approach. – John Wiley & Sons, Chichester.
[42] Magurran, A. E. (1988): Diversity indices and species abundance models. – In: Magurran, A. E. (ed.) Ecological Diversity and Its Measurement. Dordrecht: Springer Netherlands.
[43] Mandaville, J. P. (1990): Flora of Eastern Saudi Arabia. – Routledge, London.
[44] McCluney, K. E., Belnap, J., Collins, S. L., González, A. L., Hagen, E. M., Nathaniel Holland, J., Kotler, B. P., Maestre, F. T., Smith, S. D., Wolf, B. O. (2012): Shifting species interactions in terrestrial dryland ecosystems under altered water availability and climate change. – Biological Reviews 87: 563-582.
[45] Naumburg, E., Mata-gonzalez, R., Hunter, R. G., McLendon, T., Martin, D. W. (2005): Phreatophytic Vegetation and Groundwater Fluctuations: A Review of Current Research and Application of Ecosystem Response Modeling with an Emphasis on Great Basin Vegetation. – Environmental Management 35: 726-740.
[46] Orellana, F., Verma, P., Loheide II, S. P., Daly, E. (2012): Monitoring and modeling water-vegetation interactions in groundwater-dependent ecosystems. – Reviews of Geophysics 50: 1-24.
[47] Padilla, F. M., Pugnaire, F. I. (2007): Rooting depth and soil moisture control Mediterranean woody seedling survival during drought. – Functional Ecology 21: 489-495.
[48] Pennisi, E. (2005): Sky-High Experiments. – Science 309: 1314.
[49] Pielou, E. C. (1975): Ecological diversity. – Wiley, NY.
[50] Reynolds, J. F., Smith, D. M., Lambin, E. F., Turner II, B. L., Mortimore, M., Batterbury, S. P. J., Downing, T. E., Dowlatabadi, H., Fernandez, R. J., Herrick, J. E., Huber-Sannwald, E., Jiang, H., Leemans, R., Lynam, T., Maestre, F. T., Ayarza, M., Walker, B. (2007): Global desertification: building a science for dryland development. – Science 316: 847-851.
[51] Richards, C., Haro, R., Johnson, L., Host, G. (1997): Catchment and reach-scale properties as indicators of macroinvertebrate species traits. – Freshwater Biology 37: 219-230.
[52] Schulz, E., Whitney, J. (1986): Vegetation in north-central Saudi Arabia. – Journal of arid environments 10: 175-186.
[53] Shaltout, K. H., Mady, M. A. (1996): Analysis of raudhas vegetation in central Saudi Arabia. – Journal of Arid Environments 34: 441-454.
[54] Shaltout, K. H., Sheded, M. G., Salem, A. I. (2010): Vegetation spatial heterogeneity in a hyper arid Biosphere Reserve area in north Africa. – Acta Botanica Croatica 69: 31-46.
[55] Svenning, J.-C., Normand, S., Kageyama, M. (2008): Glacial refugia of temperate trees in Europe: insights from species distribution modelling. – Journal of Ecology 96: 1117-1127.

http://www.aloki.hu ● ISSN 1589 1623 (Print) ● ISSN 1785 0037 (Online)
DOI: http://dx.doi.org/10.15666/aeer/1802_27812794

[56] ter Braak, C. J. F., Smilauer, P. (2002): CANOCO Reference Manual and CanoDraw for Windows User's Guide: Software for Canonical Community Ordination (version 4.5). – Ithaca NY, USA: www.canoco.com.
[57] Walther, G.-R., Post, E., Convey, P., Menzel, A., Parmesan, C., Beebee, T. J. C., Fromentin, J.-M., Hoegh-Guldberg, O., Bairlein, F. (2002): Ecological responses to recent climate change. – Nature 416: 389-395.
[58] Wang, P., Zhang, Y., Yu, J., Fu, G., Ao, F. (2011): Vegetation dynamics induced by groundwater fluctuations in the lower Heihe River Basin, northwestern China. – Journal of Plant Ecology 4: 77-90.
[59] White, F., Léonard, J. (1990): Phytogeographical links between Africa and southwest Asia. – Flora et Vegetation Mundi 9: 229-246.
[60] Zohary, M. (1973): Geobotanical foundations of the Middle East. – Gustav Fischer Verlag, Stuttgart.

http://www.aloki.hu ● ISSN 1589 1623 (Print) ● ISSN 1785 0037 (Online)
DOI: http://dx.doi.org/10.15666/aeer/1802_27812794

DETERMINING THE CHEMICAL COMPOSITION AND NUTRITION QUALITY OF HUNGARIAN VETCH SILAGE (*VICIA PANNONICA* CRANTZ) MIXED WITH WHEAT (*TRITICUM AESTIVUM* L.) AND BARLEY (*HORDEUM VULGARE* L.) AT DIFFERENT RATES

TURAN, N.

Department of Field Crops, Faculty of Agriculture, Siirt University, Siirt, Turkey
(e-mail: nturan49@siirt.edu.tr; phone: +90-484-212-1111; fax: +90-484-223-1998)

(Received 23rd Sep 2019; accepted 30th Jan 2020)

Abstract. This research was carried out to determine the quality values of Hungarian vetch silage mixed with wheat and barley grown in winter under the ecological conditions of Eastern Anatolia region, Turkey in the 2017-2018 growing season. To determine the quality values and chemical composition of the silage mixtures obtained from the different of Hungarian vetch, wheat and barley it was prepared as three replications and filled in 2-L jars and then firmly suppressed and tightly closed so that they do not breathe. The mixture rates of Hungarian vetch (HV), wheat (W) and barley (B), their pure sowed were 80%, 60%, 40%, 20% of B + 20%, 40%, 60%, 80% of HV + 80%, 60%, 40%, 20% of W. Silage jars were opened after 60 days and pH value, acid detergent fiber (ADF), neutral detergent fiber (NDF), crude protein content and organic acid values and some macro element contents were measured. The values for ADF, NDF, digestible dry matter (DDM), dry matter intake (DMI), relative feed value (RFV), dry matter (DM), crude protein (CP) of silages were 28.57-41.65%, 29.69-59.05%, 56.45- 66.63%, 2.62-4.05%, 89.78-201.62%, 22.22-33.00%, 8.15-17.27%, respectively. At the same time, values of lactic acid (LA), acetic acid (AA), butyric acid (BA) and propionic acid (PA), calcium (Ca), phosphor (P) and potassium (K) were 1.50-1.94%, 0.33-0.71%, 0.27-0.76%, 0.02-0.08%; was 0.30-1.68%, 0.33-0.62%, 1.93-4.48%, respectively. According to these results, it can be proposed that silages achieved from the HV + B mixture have some superior properties for CP, ADF, NDF, RFV, Ca, P, and K compared with HV + W mixtures.
Keywords: *barley, chemical composition, Hungarian vetch, mixture rates, silage quality, wheat*

Introduction

Turkey's Eastern Anatolia region which it is cold and snowy in winter and hot and dry in summer has a significant potential for animal breeding. As similar to other regions, Turkey, the pasture areas at Eastern Anatolia Region have noticeably declined as a result of excessive and uncontrolled grazing and the quality of pasture have decreased to the lowest levels. Because of this degradation of the pastures, a major decrease has occurred in the production of quality roughage and a quality. For this reason, to fodder forage crop cultivation, diversity the forage crops, produce alternative fodder crops and obtain silage from different fodder plants are quite important to overcome these problems.

In recent years, a considerable increase in silage production has become in Turkey. More than 80% of the total silage produced is corn silage (Alcicek and Karaayvaz, 2003). Corn, a hot climatic plant, can be effective in good maintenance and sufficient water conditions. The planting of silage corn at eastern Anatolia region or similar ecological places can appositely be affected from short period of vegetation and even sometimes spring and autumn frost damages. Therefore, Hungarian vetch is more

http://www.aloki.hu ● ISSN 1589 1623 (Print) ● ISSN 1785 0037 (Online)
DOI: http://dx.doi.org/10.15666/aeer/1802_27952806

resistant to cold and drought in comparison with vetch species, which it is grown and harvested without watering.

It can be said that silages of Hungarian vetch + barley mixtures have higher nutrition properties, because these crops contain both protein and carbohydrate. Thus, Miller (1984) reported that silages mixtures were more productive and quality when compared with pure ones. Lithourgidis et al. (2011) reported that environmental sources in mixed cultivation can more effectively be used and that it obtained the higher yields compared with pure sowing ones. Similarly, Tuna and Orak (2007) stated that the protein/carbohydrate ratio is better for silages obtained from these mixtures. In another study (Tas, 2002) it was reported that there was a lodging rate rising with an increase development of Hungarian vetch and for this reason it can be suggested that Hungarian vetch sowed mixing by wheat or triticale in winter sowings is better. In a study which investigated the effect of grass pea (*Lathyrus sativus* L.) and barley (*Hordeum vulgare* L.) on silage properties in Diyarbakır conditions (Seydosoglu and Gelir, 2019) was detected that pH and DM of silages at 100% of Grass pea and 100% barley were 3.99-4.09 and 28.28-32.98%, respectively. Likewise, Saruhan et al. (2011) reported that DM, CP ratio and pH for mixtures of different levels of barley and birdsfoot trefol (20, 30, 40, 50, 60, 70% birdsfoot trefol + 80, 70, 60, 50, 40, 30% barley) in same conditions of Diyarbakir were, respectively, 28.08-32.60%, 10.08-12.20% and 4.76-5.11.

Also, Koc et al. (1997) conducted to determine effect of microbial additive use in silages achieved form mixtures vetch *(Vicia sativa* L.) with cereal in laboratory conditions. In the study, the DM, pH, CP, NH3-N, LA, AA, BA of the this silages were 32.00-35.00%; 3.70-3.65;11.15-10.01%; 3.03-2.75 g/kg DM; 2.48-2.83%; 0.40-0.40%; 0.10-0.05%, respectively, whereas these values showed an difference in field conditions (it were, respectively, 48.00-44.00%; 3.86-4.59; 11:37 to 11:49%; 1.57-1.73 g/kg DM; 3:36 to 3:16%; 0.63-0.42%; 0.00-0.05%). After the 56 days of silage harvested during flowering of vetch and at milk stage of barley, Polat et al. (1998) observed that pH, CP, LA and AA and ADF of the silages with control and Lactobacillus plantarum + Enterecoccus faecium groups were 4.40-4.37; 10.84-10.77%; 2.25-2.38%; 0.67-0.59%; 65.20-65.20%; 41.80-42.62%.

Aykan and Saruhan (2018) conducted to determine the ensiled ability of silages achieved mixing by in different rates of barley and pea intercrops forage plants. In that study, pH value, DM, ADF, NDF, CP of these silages were 3.90-4.12, 19.23-30.98%, 35.33-40.50%, 55.02-69.76%, 13.00-18.29%, respectively. The dry matter, CP, pH of silages obtained from different levels mixtures of white clover and barley were 27.53-31.38%, 10.17-13.63% and 5.05-5.34, respectively (Demirel et al., 2010). Bergen et al. (1991) reported that DM, pH, NDF ADF, LA and AA in the silages of wheat harvested at milk stage and dough stage after ensiling of 64 days were, respectively, 34.50-43.50%,4.00-4.10, 50.00-51.80%, 34.50-35.60%, 5.96-6.12%, 1.17-0.82%. In some studies on silage it was indicated that propionic acid content of silage varied to type of silage or mixture (Homan, 2016; Seydosoglu, 2018).

In this study, it was aimed to determine the contents of organic acid, composition of some nutrient matter and values with quality of silages obtained from mixture Hungarian vetch with barley and wheat at different levels of mixture and thus to detect the best mixture ones.

http://www.aloki.hu ● ISSN 1589 1623 (Print) ● ISSN 1785 0037 (Online)
DOI: http://dx.doi.org/10.15666/aeer/1802_27952806

Materials and methods

This research was carried out at Mus city located at the Eastern Anatolia region, Turkey in 2017-2018 growing season (*Fig. 1*). As barley and wheat, the sowing of Hungarian vetch was made in winter season (3 November 2017). As material of plant, we used the Hungarian vetch which it is the most cultivated plant in Mus, Syrena (wheat), and Tokak 157/37 (barley) varieties. These varieties used are resistant to cold and drought and are recommended to Southern Marmara, Northern Inner and Aegean, Thrace, Black Sea, Southeast and Eastern Anatolia, Central Anatolia as well as Mediterranean Regions.

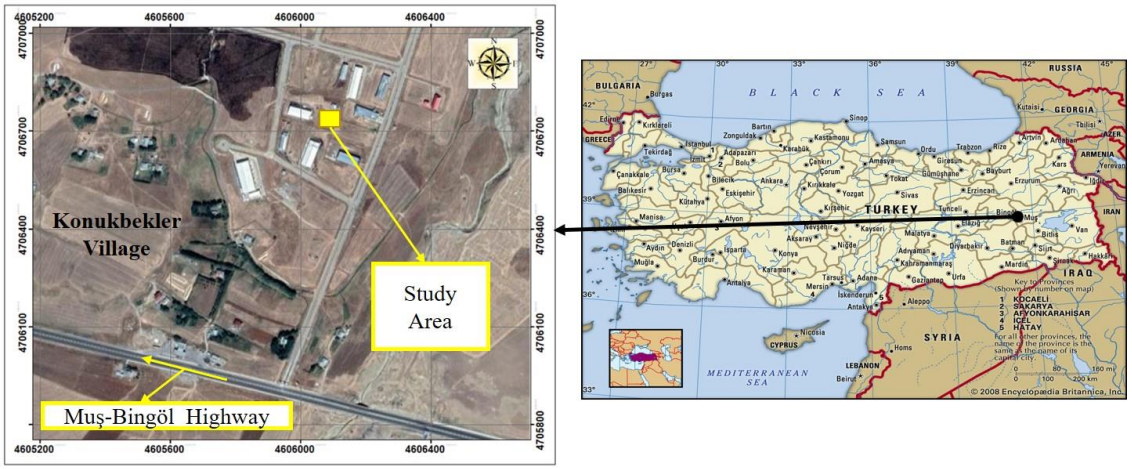

Figure 1. *Location map of the study area*

Each of these varieties was separately planted in 0.004 ha. 200 kg ha^{-1} of barley and wheat, and 100 kg ha^{-1} of Hungarian vetch were sowed. At the same time, 150 kg ha^{-1} of DAP fertilizer (27 kg ha^{-1} N, 69 ha^{-1} P) were applied to barley and wheat during sowing; whereas it was 100 kg ha^{-1} DAP (18 kg ha^{-1} N, ha^{-1} P) for Hungarian vetch.

Harvests were made in at full bloom for Hungarian vetch, at milking stage for barley and at heading stage for wheat (3 June 2018). The plots were separately simultaneously harvested with hand sickle. After the harvesting, material of silage was faded in the shade for 3-4 h and then cut into 0.5-1 cm dimensions with a silage harvester working with the tail shaft. After the chopping process, the materials were weighed on the sensitive scale according to the standardized rates.

The materials weighed were filled homogeneously and filled in 2-L plastic jars with 3 replications. The jars filled with silage materials are hand-tightened thoroughly. After the lid of the jars is closed tightly, they are wrapped with duct tape so that they do not breathe. It was then allowed to ferment into the dark environment for 60 days. At the end of this period, the maturing silages were opened and after the 4-5 cm part of the mouth of the jars were removed; the pH values were measured (Polan et al., 1998). After weighing 500 g of silage from each jar, it was dried to a constant weight for 48 h (AOAC, 1990) at 60 °C. After the dry weight of the silages was obtained, the samples were ground and prepared for analysis.

The content of crude protein (CP), calcium (Ca), magnesium (Mg), phosphor (P), potassium (K) content of silage, acid detergent fiber (ADF) and neutral detergent fiber (NDF) was determined with Near Infrared Reflectance Spectroscopy (NIRS), Near

http://www.aloki.hu ● ISSN 1589 1623 (Print) ● ISSN 1785 0037 (Online)
DOI: http://dx.doi.org/10.15666/aeer/1802_27952806

Infrared Analysis (NIR) by spectroscopic technique (Hoy et al., 2002), while organic acid ratios such as LA, AA, PA and BA were detected with HPLS (Canale et al., 1984).

The data obtained were analyzed to variance analysis by using JUMP program based on 5% and 1% of significance levels (SAS, 1998). The differences between the mean values were compared according to the LSD, multiple comparison tests (Gulumser et al., 2006). Digestible dry matter [DDM = 88.9 - (0.779 x ADF%)] and dry matter consumption (DMI = 120/NDF%) and relative feed value from DDM and DMI ratios [RFV = (DDM x DMI)] were calculated from formulation described by Van Dyke and Anderson (2000).

Climate characteristics of research area

The average rainfall for many years in Mus province was 745.02 mm, the relative humidity was 61.99%, and the temperature was 8.10 °C. In planting period which relative humidity in January was highest, the temperature was low and rainfall was high (*Table 1*).

Table 1. *Temperature, precipitation and relative humidity values of their search area*[*]

Months	Temperature (°C)		Precipitation (mm)		Relative humidity (%)	
	LYA[**]	**2017**	**LYA**[**]	**2017**	**LYA**[**]	**2017**
September	21.13	22.90	20.16	0.00	32.76	20.50
October	13.54	12.80	65.87	34.40	53.12	41.70
November	5.56	6.00	65.24	69.60	67.91	70.80
December	-1.62	1.30	99.36	33.30	80.23	75.40
Months	**LYA**[**]	**2018**	**LYA**[**]	**2018**	**LYA**[**]	**2018**
January	-5.25	0.50	113.30	84.00	82.09	76.40
February	-2.87	4.10	86.69	81.30	77.90	64.30
March	3.78	9.40	104.27	61.40	67.56	54.70
April	10.58	12.50	90.63	26.80	57.90	46.70
May	15.28	15.40	69.22	125.60	57.42	63.40
June	20.91	20.50	30.28	48.80	43.02	48.60
Total/Average	8.10	10.54	745.02	565.20	61.99	56.25

*Meteorological Service of Mus. **LYA: Long years' average (2009-2018)

The temperature was above the average temperature during the growing season for a long time. However, relative humidity and rainfall was lower than the average of long years. The experiment area was harvested without required irrigation.

Soil characteristics of research area

Soil analysis of the experiment area was made in the soil analysis laboratory of private Mus. According to results of soil analyses of the experiment area, it was neutral, calcareous, salt-free and organic matter was low and also, the amount of phosphor is poor and potassium is sufficient (*Table 2*).

Table 2. *Results of soil analysis of the search area*[*]

pH	Salt ds/m	Lime ($CaCO_3$) (%)	Organic matter (%)	P (P_2O_5) kg ha^{-1}	K (K_2O) ppm
7.02	0.02	1.58	1.14	26.30	209.99

*Soil analysis were conducted at the Special Mus Soil Analysis Laboratory (2017)

http://www.aloki.hu ● ISSN 1589 1623 (Print) ● ISSN 1785 0037 (Online)
DOI: http://dx.doi.org/10.15666/aeer/1802_27952806

Results and discussion

Content of ADF, NDF, DDM, DMI, RFV and DM

In the present study we found that there were significant differences in silage mixtures achieved Hungarian vetch, barley and wheat for ADF, NDF, DDM, DMI, RFV and DM ($P < 0.01$) (*Table 3*).

Table 3. *The mean values of silages for ADF, NDF, DDM, DMI, RFV and DM and groups*

Mixtures	ADF (%)	NDF (%)	DDM (%)	DMI (%)	RFV	DM (%)
100% H	31.71 ^{de}	29.69 ^{f}	64.19 ^{b}	4.05 ^{a}	201.62 ^{a}	22.11 ^{f}
100% B	28.57 ^{e}	32.91 ^{ef}	66.63 ^{a}	3.65 ^{bc}	188.66 ^{ab}	28.77 ^{c}
100% W	41.06 ^{ab}	59.05 ^{a}	56.91 ^{de}	2.03 ^{g}	89.78 ^{f}	33.00 ^{a}
80% HV+20% B	37.88 ^{bc}	30.87 ^{f}	59.39 ^{cd}	3.88 ^{ab}	178.98 ^{bc}	22.22 ^{f}
60% HV+40% B	37.60 ^{bc}	33.76 ^{de}	59.60 ^{cd}	3.55 ^{bc}	164.23 ^{cd}	21.78 ^{f}
40% HV+60% B	35.95 ^{c}	36.11 ^{de}	60.89 ^{c}	3.32 ^{cd}	156.91 ^{d}	23.55 ^{e}
20% HV+80% B	35.18 ^{cd}	37.81 ^{cd}	61.48 ^{bc}	3.17 ^{de}	151.40 ^{d}	24.88 ^{d}
80% HV+20% W	36.04 ^{c}	36.47 ^{de}	60.81 ^{c}	3.30 ^{cd}	155.90 ^{d}	23.55 ^{e}
60% HV+40% W	40.72 ^{ab}	42.19 ^{bc}	57.17 ^{de}	2.90 ^{ef}	129.19 ^{e}	29.33 ^{c}
40% HV+60% W	41.65 ^{a}	45.87 ^{b}	56.44 ^{e}	2.62 ^{f}	114.76 ^{e}	28.22 ^{c}
20% HV+80% W	41.65 ^{a}	46.14 ^{b}	56.45 ^{e}	2.60 ^{f}	113.80 ^{e}	31.33 ^{b}
Average	37.09	39.17	60.00	3.19	149.57	26.25
CV (%)	5.62	6.96	2.72	6.96	8.23	2.85
LSD	7.38**	9.65**	5.74**	0.77**	43.61**	2.64**

Values indicated by the same letters are not significantly different at the 5% level of significance, $^{**}P > 0.01$. ADF: acid detergent fiber; NDF: neutral detergent fiber; DDM: digestible dry matter; DMI: dry matter intake; RFV: Relative Feed Value; DM: Dry matter

ADF and NDF ratio

The rate of ADF of silages obtained from pure wheat and Hungarian vetch with wheat were higher than those of other mixture silages. Average ADF of these silages was 37.09%, though the ADF values ranged in 28.57-41.65%. According to the quality standards of legume, wheat and legume mixtures (Rohweder et al., 1978), ADF ratio of mixture silages obtained from wheat and Hungarian vetch (except 80% HV + 20% W) was in the 3 grade quality class (41-42%), whereas the silage obtained from barley and Hungarian vetch is in the 2 grade quality class (36-40%) for ADF. In the current study, while The ADF content of the pure barley silage is in the top-quality class, Hungarian vetch silage is in the 1st quality class. NDF ratios of mixture silages pure wheat silages with Hungarian vetch + wheat were higher than pure barley with Hungarian vetch + barley mixture silages. Average NDF of pure and mixture silages 39.17%, though the ADF values ranged in 29.69-59.05%. According to the quality standards of legume, wheat and legume mixtures (Rohweder et al., 1978), NDF of mixture silages obtained wheat with Hungarian vetch was in the 1st quality class (40-46%). Similarly, NDF of mixture silages achieved barley and Hungarian vetch was in the top-quality class (*Tables 3* and *4*).

There are many of studies on ADF and NDF rates of silage and findings of these studies Bergen et al. (1991) 34.50-35.60%; Aykan and Saruhan (2018) 35.33-40.50%;

http://www.aloki.hu ● ISSN 1589 1623 (Print) ● ISSN 1785 0037 (Online)
DOI: http://dx.doi.org/10.15666/aeer/1802_27952806

Polat et al. (1998) 41.80-42.62% have changed at regular intervals. At the same time, rates of NDF were indicated by Bergen et al. (1991) 50.00-51.80%; Aykan and Saruhan (2018) 55.02 - 69.76% and Polat et al. (1998) 65.20-65.20%.

Our findings for ADF and NDF in this study were different in some of the literature mentioned above. It is suggested that these differences between the findings can be resulted from the differences of plant species, periods, rations of mixture and ecological conditions.

Table 4. *Quality standards for legume, wheat and legume mixtures (Rohweder et al., 1978)*

Standard of quality	CP	ADF	NDF	DDM %	DMI % of BW	RFV
	% of DM					
Prime	> 19	<< 31	<< 40	> 65	> 3.0	> 151
1	17-19	31-35	40-46	62-65	3.0-2.6	151-125
2	14-16	36-40	47-53	58-61	2.5-2.3	124-103
3	11-13	41-42	54-60	56-57	2.2-2.0	102-87
4	8-10	43-45	61-65	53-55	1.9-1.8	86-75
5	<< 8	> 45	> 65	<< 53	<< 1.8	<< 75

DDM (digestibility dry matter) ratio

The mean DDM of the pure and mixture silages in this study was 60%. DDM was the highest in pure barley silage with 66.63%, whereas it was the lowest in mixture silages of 40% HV + 60% W (56.44%) and 20% HV + 80% W (56.45%) in the same group. The digestible dry matter (DDM) of pure barley silage was in the top-quality class, pure Hungarian vetch was in the first quality class and DDM of other pure and mixture silages were in the second quality class (58-61%) based on the quality class described by Rohweder et al. (1978) (*Tables 3* and *4*).

DMI (dry matter intake) ratio

The mean DMI for all silages studied were 3.19% and the highest DMI were observed from mixture silages of 100% HV (4.05%) and 80% HV + 20% B (3.88%), indicating that it is in the top-quality class based on the quality class described by Rohweder et al. (1978). The lowest DMI was observed in the pure wheat silage and it was in the 3nd quality class, whereas mixture silages of Hungarian vetch and wheat at different mixing levels 60% HV + 40% W, 40% HV + 60% W, 20% HV + 80% W were in the second quality class based on the quality class described by Rohweder et al. (1978) (*Tables 3* and *4*).

RFV (relative feed value)

In the present study the mean RFV of pure and mixture silages was 149.57. The highest RFV was founded at 100% HV (201.62) and 100% B (188.66) of silage in the same group and its quality class was the highest, while silage of pure wheat for RFV was in the 3rd quality class according to quality criteria's Rohweder et al. (1978). Additionally, we observed that RFV of silage obtained from Hungarian vetch + barley mixture was higher than Hungarian vetch + wheat silage ones and it was better quality based on classification on quality (*Tables 3* and *4*).

http://www.aloki.hu ● ISSN 1589 1623 (Print) ● ISSN 1785 0037 (Online)
DOI: http://dx.doi.org/10.15666/aeer/1802_27952806

DM (dry matter) ratio

In the present study, the mean DM of silages was 26.25%. The highest DM was achieved from pure wheat silages (33%), whereas it was the lowest pure and the mixtures containing high Hungarian vetch with barley [80% HV + 20% B (22.22%); 60% HV + 40% B (21.78%)]. Besides we detected that DM contains of mixture silages increase with increasing wheat.

The results of this study were different in findings reported in a several studies (Saruhan et al., 2011; Basaran et al., 2018; Aykan and Saruhan, 2018). These differences among studies mentioned above for DM of silage can be resulted from diverse harvesting periods or plant material of silage.

Mineral matters and crude protein content

In this present study, there were significant differences in calcium (Ca), potassium (K), phosphor (P) and crude protein (CP) contents of silages obtained from different mixture ratios of Hungarian vetch with barley and wheat ($P < 0.01$) except for magnesium (Mg) (*Table 5*).

Table 5. *The means of Ca, P, Mg, K and CP of mixture silages*

Mixtures	Ca (%)	P (%)	Mg (%)	K (%)	CP (%)
100% H	1.68 ^{a}	0.57 ^{ab}	0.26	3.63 ^{b}	17.27 ^{a}
100% B	0.88 ^{e}	0.62 ^{a}	0.12	4.48 ^{a}	9.83 ^{e}
100% W	0.30 ^{f}	0.33 ^{e}	0.23	4.47 ^{a}	8.15 ^{f}
80% HV + 20% B	1.44 ^{b}	0.54 ^{bc}	0.21	3.25 ^{bc}	16.39 ^{ab}
60% HV + 40% B	1.40 ^{b}	0.50 ^{c}	0.22	2.98 ^{bd}	16.56 ^{ab}
40% HV + 60% B	1.13 ^{cd}	0.50 ^{c}	0.21	2.96 ^{bd}	15.82 ^{ac}
20% HV + 80% B	0.98 ^{de}	0.58 ^{ab}	0.19	3.05 ^{bd}	15.96 ^{ab}
80% HV + 20% W	1.23 ^{bc}	0.49 ^{c}	0.22	2.90 ^{ce}	14.35 ^{c}
60% HV + 40% W	1.14 ^{cd}	0.41 ^{d}	0.21	2.39 ^{df}	12.68 ^{d}
40% HV + 60% W	0.96 ^{de}	0.38 ^{de}	0.19	2.22 ^{ef}	10.35 ^{e}
20% HV + 80% W	0.94 ^{de}	0.35 ^{de}	0.23	1.93 ^{f}	15.41 ^{bc}
Average	1.10	0.48	0.21	3.12	13.89
CV (%)	12.34	8.51	16.72	12.88	6.54
LSD	0.48**	0.15**	NS	1.41**	3.20**

Values indicated by the same letters are not significantly different at the 1% level of significance, **$P < 0.01$ significant, NS: No significant, Ca: Calcium, P: Phosphor, Mg: Magnesium, K: Potassium, CP: Crude protein

Average Ca, P, K contents of silages was 1.10%, 0.48%, and 3.12%, respectively. The highest Ca was in the Hungarian vetch silage (1.68%), but it was lowest in wheat silage (0.30%). While silages of pure barley and Hungarian vetch and 20% HV + 80% B had the most P content, it was the lowest in pure wheat silage. The highest K content was found in pure barley and wheat silage in the same group. However, it was the lowest in 20% HV + 80% W mixture silage (*Table 5*). These elements are quite important in animal nutrition and animal rates should be contained at levels of 0.21% P, 0.65% K, 0.31% Ca and 0.1% Mg (Kidambi et al., 1989).

http://www.aloki.hu ● ISSN 1589 1623 (Print) ● ISSN 1785 0037 (Online)
DOI: http://dx.doi.org/10.15666/aeer/1802_27952806

According to these findings, when the mineral content of silages is evaluated; the mean Ca (1.10%), P (0.48%), K (3.12%) contents are above the amounts required to be in the feed rates of cattle and therefore there is no feeding problem in terms of the mentioned nutrients. In order to determine the yield and the quality of the mixture silages of Grass pea and Oat and Barley, Basaran et al. (2018) conducted a study. In that study, the highest of K (2.89%), Ca (0.87%), P (0.30%) were founded in the mixture ratio of 80% HV + 20% B. We however, observed that our findings for these elements were higher than values reported by that study.

The CP values of silages analyzed were presented in *Table 5*. The average crude protein ranging from between 17.27% and 8.15% in silages studied was 0.89%. It was observed that the CP content of the pure Hungarian vetch and Hungarian vetch + barley silages was higher than the CP content of the Hungarian vetch + wheat mixture silages.

Although the CP of pure wheat and barley silage was low (8.15-9.83%, respectively), mixing of Hungarian vetch with wheat and barley improved the ratio of CP. The highest CP was obtained from pure Hungarian vetch (17.27%) or silages of different mixing rates such as 80% HV + 20% B (16.39%); 60% HV + 40% B (16.56%); 40% HV + 60% B (15.82%); 20% HV + 80% B (15.96%) (*Table 5*). We found that there are differences for silage CP between the results reported by various researchers such as Polat et al. (1998) (10.84-10.77%), Saruhan et al. (2011) (10.08-12.20%), Seydosoglu (2019) (12.10-18.75%), Aykan and Saruhan (2018) (13.00-18.29%), Demirel et al. (2010) (10.17-13.63%) and Polat et al. (1998) (10.84-10.77%). Generally, our findings for pure or mixture silage CP were in accordance with literature for CP. Differences observed can be resulted from harvest periods and different plant species.

pH and organic acid contents of silages

In the present study we observed that there were significant differences in the pH values and ratios of organic acids of the silages obtained from the mixture silages achieved Hungarian vetch and barley and wheat in different ratios ($P < 0.01$).

In this study, the pH values of the silages ranged from 3.76 to 4.08, with an average pH of 3.90. Indicating differences in rates of mixture with barley, pH values of mixture Hungarian vetch with wheat was higher than mixture Hungarian vetch with barley ones. The highest pH was obtained from Hungarian vetch and barley mixtures in the same group. These groups were 80% HV + 20% B (3.99%), 60% HV + 40% B (4.08%), 40% HV + 60% B (4.01%) and 20% HV + 80% B (3.99%).

Nonetheless, the pH of pure wheat silage was the lowest and also it was low in the other some groups such as 80% HV + 20% W (3.82%), 60% HV + 40% W (3.83%), 40% HV + 60% W (3.81%) and 20% HV + 80% W (3.81%). The authors reported that the most adequate of silage pH ranged from between 3.5 and 4.2. Our finding (3.76-4.08) for silage pH was in accordance with values of silage pH reported by these studies, showing that it was appropriate for nutrition quality (Kilic, 2006; Acikgoz et al., 2002; Aykan and Saruhan, 2018).

However, there were contrast with values of pH reported by Saruhan et al. (2011), Polat et al. (1998), Basaran et al. (2018), Demirel et al. (2010), Seydosoglu and Gelir (2019) and Bergen et al. (1991) and it was lower than in comparison with the results of these researches. The lactic acid (LA) values of the silages obtained mixed by at difference levels ranged from 1.50% to 1.94%, with an average pH of 1.69%. The highest LA was in the mixture group of 80% HV + 20% W (1.94%) and pure wheat

http://www.aloki.hu ● ISSN 1589 1623 (Print) ● ISSN 1785 0037 (Online)
DOI: http://dx.doi.org/10.15666/aeer/1802_27952806

(1.80%), whereas it was the lowest. In mixture silages of 60% HV + 40% B (1.50%) and 20% HV + 80% W (1.50%) in the same group.

The acetic acid (AA) values of the silages ranged from 0.31% to 0.71%, with an average pH of 0.49%. The highest AA of pure Hungarian vetch, pure wheat and mixture of 20% HV + 80% B were 0.71%, 0.65% and 0.66%, respectively. It was the lowest for mixture of 60% HV + 40% B (0.31%). The butyric acid (BA) values of the silages ranged from 0.27% to 0.76%, with an average pH of 0.47%. It was highest in the pure Hungarian vetch (0.73%) and mixture of 80% HV + 20% W (0.76%). The propionic acid (PA) values of the silages ranged from 0.02% to 0.08%, with an average pH of 0.06%. The highest of propionic acid (PA) was obtained from mixtures of 80% HV + 20% W and 60% HV + 40% W of silages (*Table 6*).

Table 6. *The means of pH, LA, AA, BA and PA of mixture silages*

Mixtures	pH	LA (%)	AA (%)	BA (%)	PA (%)
100% H	3.88 ^{ce}	1.70 ^{bc}	0.71 ^{a}	0.73 ^{a}	0.07 ^{bc}
100% B	3.90 ^{bd}	1.69 ^{bc}	0.56 ^{b}	0.47 ^{c}	0.08 ^{ab}
100% W	3.76 ^{e}	1.80 ^{ab}	0.65 ^{a}	0.35 ^{de}	0.02 ^{e}
80% HV + 20% B	3.99 ^{ab}	1.75 ^{b}	0.36 ^{eg}	0.52 ^{bc}	0.07 ^{ab}
60% HV + 40% B	4.08 ^{a}	1.50 ^{d}	0.31 ^{g}	0.27 ^{f}	0.07 ^{ab}
40% HV + 60% B	4.01 ^{ab}	1.59 ^{cd}	0.41 ^{de}	0.36 ^{d}	0.03 ^{e}
20% HV + 80% B	3.99 ^{ab}	1.71 ^{bc}	0.66 ^{a}	0.55 ^{b}	0.03 ^{e}
80% HV + 20% W	3.82 ^{de}	1.94 ^{a}	0.46 ^{cd}	0.76 ^{a}	0.08 ^{a}
60% HV + 40% W	3.83 ^{de}	1.69 ^{bc}	0.41 ^{df}	0.51 ^{bc}	0.08 ^{a}
40% HV + 60% W	3.81 ^{de}	1.67 ^{bc}	0.33 ^{fg}	0.30 ^{ef}	0.05 ^{d}
20% HV + 80% W	3.81 ^{de}	1.50 ^{d}	0.53 ^{bc}	0.36 ^{de}	0.06 ^{cd}
Average	3.90	1.69	0.49	0.47	0.06
CV (%)	1.71	4.67	9.27	8.02	13.65
LSD	0.23**	0.27**	0.16**	0.12**	0.02**

Values indicated by the same letters are not significantly different at the 1% level of significance, $^{**}P < 0.01$ significant, LA: lactic acid, AA: acetic acid, BA: butyric acid, PA: propionic acid.

According to some authors the butyric acid is not adequate for quality of silage and in general it has 0.1-0.6% of butyric acid (Woolford, 1984). By contrast, some researchers showed that there is a significant relationship between LA, AA and BA ratios with high quality of silage. According to these authors, LA ratio in these forages was above 2%, whereas AA ratio must be between 0.3-0.7% percent in type of these silages (McDonald et al., 1991; Alcicek and Ozkan, 1996). In this present study, it is observed that the LA ratio is lower than when compared with studies mentioned above, but ration of AA was normal. However, the amount of butyric acid was found to be higher than normal values in pure Hungarian vetch silage (0.73%) and in mixtures of 80% of Hungarian vetch + wheat silages (0.76%). However other groups of silages were normal for butyric acid (*Table 6*).

The insufficiency of homo-fermentative lactic acid bacteria (LAB) of the plant material used for silage leads to a delay in the decrease in pH. Because of the insufficiency of LAB, an increase in the loss of nutrients and a decrease in the consumption of silages occur (Woolford, 1984). Therefore, in order to increase the

http://www.aloki.hu ● ISSN 1589 1623 (Print) ● ISSN 1785 0037 (Online)
DOI: http://dx.doi.org/10.15666/aeer/1802_27952806

lactic acid content in silages consisting of Hungarian vetch + wheat or Hungarian vetch + barley mixture, it is recommended to use various additives like *Lactobacillus plantarum*, which are homo fermantative. On the contrary, Kung et al. (2003) reported that the main ingredient used for legume silage in the USA is bacterial inoculants.

In current study, the findings with organic acids were lower than the results reported by Seydosoglu (2018) (2.01-2.16%), Polat et al. (1998) (2.25-2.38%) and Bergen et al. (1991) (5.96-6.12%). However, our findings with AA, BA and PA showed differences in results reported by some authors (Bergen et al., 1991; Polat et al., 1998; Homan, 2016; Seydosoglu, 2018; Basaran et al., 2018).

Conclusion

In this present study it was conducted to determine the quality and chemical composition of the silage obtained by mixing Hungarian vetch with barley and wheat in different proportions, which they have same vegetation periods. At the same time, it was conducted to determine the quality and chemical composition of the silage obtained by mixing Hungarian vetch with barley and wheat in different proportions, which they have same vegetation periods. As a result, we observed that CP, Ca, P, K and RFV of Hungarian vetch + wheat silages were higher than compared other groups of silages. Similarly, when the proportion of Hungarian vetch in mixing was increased, it also leads to an increase of Ca, P, K and RFV, DM and LA ratios of these silages. However, ADF and NDF ratios were lower in Hungarian vetch + barley silages.

REFERENCES

[1] Acikgoz, E., Turgut, İ., Filya, İ. (2002): Silage Plants Growing and Silage Making. – Hasad Publishing, Istanbul (in Turkish).

[2] Alcicek, A., Karaayvaz, K. (2003): Use of corn silage in cattle feed. – Animalia 203: 68-76 (in Turkish).

[3] Alcicek, A., Ozkan, K. (1996): Determination of milk acid, acetic acid and butyric acid by distillation in silage feeds. – Ege University, Journal of Agricultura Faculty 33(2-3): 191-198 (in Turkish).

[4] AOAC (1990): Official Methods of Analysis of the Association of Official Analytical Chemists. 15th Ed. Vol. 1. – AOAC, Washington, DC.

[5] Aykan, Y., Saruhan, V. (2018): Determination of silage quality features of field pea (*Pisum sativum* L.) and barley (*Hordeum vulgare* L.) mixtures ensiling at different rates. – Dicle University, The Journal of Faculty of Veterinary Medicine 11(2): 64-70 (in Turkish).

[6] Basaran, U., Gulumser, E., Mut, H., Copur Dogrusoz, M. (2018): Determination of silage yield and quality of grasspea + cereal intercrops. – Turkish Journal of Agriculture - Food Science and Technology 6(9): 1237-1242 (in Turkish).

[7] Bergen, W. G., Byrem, T. M., Grand, A. L. (1991): Ensiling characteristics of whole-crop harvested at milk and dough stages. – J. Animal Sci. 69: 1766-1774.

[8] Canale, A., Valente, M. E., Ciotti, A. (1984): Determination of volatile carboxylic acids (C_1-C_{5i}) and lactic acid in aqueous acid extracts of silage by high performance liquid chromatography. – J. Sci. Food. Agric 35(11): 1178-1182.

[9] Demirel, R., Saruhan, V., Baran, M. S., Andic, N., Senturk Demirel, D. (2010): Determination of different ratios of Trifolium repens and Hordeum vulgare mixtures on silage quality. – YYU J. AGR. SCI. 20 (1): 26-31 (in Turkish).

http://www.aloki.hu ● ISSN 1589 1623 (Print) ● ISSN 1785 0037 (Online)
DOI: http://dx.doi.org/10.15666/aeer/1802_27952806

[10] Gulumser, A., Bozoglu, H., Peksen, E. (2006): Research and Testing Methods. – Ondokuz Mayis University, Faculty of Agriculture, Text Book (2. Press), Number: 48, Samsun.
[11] Homan, E. (2016): A study on determination of quality parameters of corn and soybean silages prepared with different mixing ratios. – MSc. Thesis. Yuzuncu Yil University, Institute of Natural and Applied Science, Van (in Turkish).
[12] Hoy, M. D., Moore, K. J., George, J. R., Brummer, E. C. (2002): Alfalfa yield and quality as influenced by establishment method. – Agronomy Journal 94:65-71.
[13] Kidambi, S. P., Matches, A. G., Gricgs, T. C. (1989): Variability for Ca, Mg, K, Cu, Zn and K/(Ca + Mg) ratio among 3 wheat grasses and sainfoin on the southern high plains. – Journal of Range Management 42: 316-322.
[14] Kilic, A. (2006): Determination of Quality in Forage. – Hasad Publishing, İstanbul (in Turkish).
[15] Koc, F., Ozduven, M. L., Yurtman, I. Y., Erman, S. M. (1997): A study on quality properties and use of microbial additives in vetch grain silage. – Hasad Journal 142: 34-36.
[16] Kung, L., J. R., Stokes, M. R., Lin, C. J. (2003): Silage Additives. – In: Allen, M. et al. (eds.) Silage Science and Technology. Argon. Monogr. 42. ASA. CSSA, Madison, WI, pp. 305-360.
[17] Lithourgidis, A. S., Dordas, C. A., Damalas, C. A., Vlachostergios, D. N. (2011): Annual intercrops: an alternative pathway or sustainable agriculture. – Australian Journal of Crop Science 5(4): 396-410.
[18] McDonald, P., Henderson, A. R., Heron, S. J. E. (1991): The Biochemistry of Silage. 2nd Ed. – Chalcombe Publications, Aberystwyth.
[19] Miller, D. A. (1984): Forage Crops. – McGraw-Hill Book Company, New York.
[20] Polan, C. E., Stieve, D., Garrett, J. (1998): Protein preservation and ruminal degradation of ensiled forage treated with heat, formic acid, ammonia or microbial inoculant. – Journal of Dairy Science 81: 765-776.
[21] Polat, C., Yurtman, I. Y., Koc, F., Coskuntuna, L., Ozduven, M. L. (1998): Use of microbial additives 1st and 2nd product effects on corn, vetch grain mixture, fermentation development and aerobic stability in sunflower silages. – Project Number: VHAG-1238, Tekirdag (in Turkish).
[22] Rohweder, D. A., Barnes, R. F., Jorgensen, N. (1978): Proposed hay grading standards based on laboratory analyses for evaluating quality. – Journal of Animal Science 47(3): 747-759.
[23] Saruhan, V., Demirel, R., Baran, M. S., Senturk Demirel, D. (2011): Determination of ensilage properties of different levels of Lotus corniculatus and Hordeum vulgare mixtures. – Anadolu J. Agr. Sci. 26(1): 40-45 (in Turkish).
[24] SAS (1982): User's Guide. – Statistical Analysis Systems. SAS, Cary, NC.
[25] Seydosoglu, S. (2018): Investigation of organic asic ratio of the effect of fodder pea (*Pisum sativum* L.) and barley (*Hordeum vulgare* L.) herbages mixed at different ratios. – Anatolia the 1st International Congress of Multidisciplinary Studies, 28-29 December, 893-898 (in Turkish).
[26] Seydosoglu, S. (2019): Investigation of the effect of fodder pea (*Pisum sativum* L.) and barley (*Hordeum vulgare* L.) herbages mixed at different rates on silage and feed quality. – Ege University, Journal of Agricultura Faculty 56 (3):297-302 (in Turkish).
[27] Seydosoglu, S., Gelir, G. (2019): A research on the silage properties of grass pea (*Lathrus sativus* L.) and barley (*Hordeum vulgare* L.) herbages mixed at different rates. – Igdir Univ. J. Inst. Sci. and Tech. 9(1): 397-406 (in Turkish).
[28] Tas, N. (2002): Determination of optimum mixture type, mixture rate and cutting time for vetch + wheat mixtures sown in spring and autumn under irrigated conditions. – PhD. Thesis. Ataturk University, Institute of Natural and Applied Science, The Department of Field Crops, Erzurum (in Turkish).

http://www.aloki.hu ● ISSN 1589 1623 (Print) ● ISSN 1785 0037 (Online)
DOI: http://dx.doi.org/10.15666/aeer/1802_27952806

[29] Tuna, C., Orak, A. (2007): The role of intercropping on yield potential of common vetch (*Vicia sativa* L.)/oat (*Avena sativa* L.) cultivated in pure stand and mixtures. – Journal of Agricultural and Biological Science 2 (2): 14-19.
[30] Van Dyke, N. J., Anderson, P. M. (2000): Interpreting a Forage Analysis. – Alabama Cooperative Extension, Circular ANR-890.
[31] Woolford, M. K. (1984): The Silage Ferment. – Grassland Research Institute, Hurley.

http://www.aloki.hu ● ISSN 1589 1623 (Print) ● ISSN 1785 0037 (Online)
DOI: http://dx.doi.org/10.15666/aeer/1802_27952806

THE INFLUENCE OF ORGANIC FERTILISER PROTOTYPES WITH THE *TRICHODERMA* ON THE SANITARY AND ENZYMATIC CONDITIONS OF SOIL AND THE YIELD OF SPINACH (*SPINACIA OLERACEA* L.)

WOLNA-MARUWKA, A.[1*] – NIEWIADOMSKA, A.[1] – GRZYB, A.[1] – PIECHOTA, T.[2] – SZCZECH, M.[3] – RYCHLIK, P.[4]

[1]*Department of General and Environmental Microbiology, Poznan University of Life Sciences, Szydłowska 50, 60-656 Poznan, Poland*

[2]*Department of Agronomy, Poznan University of Life Sciences, Dojazd 11, 60-656 Poznan, Poland*

[3]*Research Institute of Horticulture, Konstytucji 3 Maja 1/3, 96-100 Skierniewice, Poland*

[4]*Long Island Horticultural Research and Extension Center, Cornell University, 3059 Sound Ave Riverhead, NY 1190, USA*

[*]*Corresponding author*
e-mail: amaruwka@up.poznan.pl

(Received 13th Oct 2019; accepted 12th Feb 2020)

Abstract. A two-year study was conducted to find how mineral and organic fertilisation and *Trichoderma* sp. strains influenced the total count of molds, including *Fusarium*, *Alternaria* and *Trichoderma* genera, the biological index of fertility (BIF) and the yield of spinach (*Spinacia oleracea* L.). Eleven variants were used in a field experiment conducted on lessivè soil: a control sample, mineral fertilisation, organic fertilisation with manure and eight variants with tomato or onion waste composts. Some of them were inoculated with *Trichoderma atroviride* (T1) and/or *T. harzianum* (T2 and T3) isolates. The addition of manure resulted in the greatest increase in the total count of moulds in the soil. The highest BIF value was noted in the soil enriched with tomato compost and inoculated with both T1 and T2 strains. The count of *Fusarium* sp. was reduced the most in the soil fertilised with onion compost with the addition of T1 and T3 isolates. The greatest decrease in the count of *Alternaria* sp. was observed in the soil fertilised with compost inoculated with the T1 strain. The onion compost inoculated with *Trichoderma* T1 and T3 resulted in the highest yield of spinach, which was comparable to the one obtained after mineral fertilisation.
Keywords: *pathogens, molds, soil, biofertiliser, plant*

Introduction

Currently one of the main focuses in waste management and energy generation from biomass is to reduce the amount of plant waste produced and to reuse it properly, in accordance with the Regulation of the Minister of the Environment on Recycling R10 (Journal of Laws of 2015, item 132).

According to the data of the Central Statistical Office (Statistics Poland, 2018), the amount of waste generated in Poland increases every year and most of it is disposed of in landfills. In 2017 23 kg of biodegradable waste was generated per capita, whereas in 2010 it was 4.7 kg. According to Minelgaitė and Genovaitė (2019), Germany, Italy and the United Kingdom are leaders in the production of this waste, whereas Poland ranks eighth.

Directive 2008/98/EC of the European Parliament and of the Council of 19 November 2008 is the main act specifying general requirements concerning waste management. This

http://www.aloki.hu ● ISSN 1589 1623 (Print) ● ISSN1785 0037 (Online)
DOI: http://dx.doi.org/10.15666/aeer/1802_28072821

directive establishes a legal framework for handling waste within the community to protect the environment and human health by from the negative effects of waste generation and management. The current waste policy in the EU is a challenge for Poland because according to the Regulation of the Minister of the Environment of 25 May 2012 (Journal of Laws of 2012, item 676), by 2020 Poland will have to limit the amount of landfilled biodegradable waste to 35%.

Adequate handling of organic waste, by composting, for example enables disposal of troublesome material and acquisition of a high-quality fertiliser product, which can be reintroduced to the environment (Journal of Laws of 2015, item 132).

During the composting process the thermophilic phase, when the temperature reaches 60-70°C, guarantees effective hygienisation of the composted material, which is to be used as a carrier for moulds of the *Trichoderma* sp. genus entered into the soil, which are regarded as a biocontrol agent (López-Mondéjar et al., 2011; López-Bucio et al., 2015).

The Regulation of the Minister of Agriculture and Rural Development of 18 April 2013 (Journal of Laws of 2013, item 505) and Directive 2009/128/EC imposed the obligation to search for alternative methods of plant production so as to limit or completely eliminate chemical crop protection products and mineral fertilisers. Organic fertilisers inoculated with *Trichoderma* moulds, which are antagonistic to plant pathogens, seem to be an excellent solution (Smolińska et al., 2014; Wolna-Maruwka et al., 2017).

Mycoparasitism against plant pathogens is the most powerful biocontrol mechanism caused by filamentous fungi of the *Trichoderma* genus. According to John et al. (2010), Hermosa et al. (2011 and 2012), this phenomenon provides plants with biological protection against plant pathogens such as *Fusarium* sp., *Pythium* sp., *Alternaria* sp., *Verticillium* sp., *Colletotrichum* sp., *Rhizoctonia solani*, and *Botrytis cinerea*.

Trichoderma sp. also protect plants by producing substances which act as antibiotics. These are: gliotoxin, viridine, and peptide antibiotics (peptaibols): trichotoxins A and B, trichodecenins, trichocellins, trichorovins, alamentacins, trichorzianines A and B, trichorzins HA and MA, tricholongins BI and BII, longibrachins, trichocongins, atroviridins A-C, neoatroviridins A-D, sesquiterpenoids, isonitriles, polyketides, purine alkyls, as well as metabolites containing the isocyanide group (Wojtkowiak-Gębarowska, 2006).

According to Smolińska et al. (2014), Colla et al. (2015) and Druzhinina et al. (2011), the antagonism exhibited by *Trichoderma* moulds also involves competing with plant pathogens for the place of colonisation and nutrients, as well as modification of environmental conditions through acidification and production of siderophores.

Apart from that, research has proved that fungi of the *Trichoderma* genus are capable of inducing systemic immunity of plants. Secondary metabolites released by *Trichoderma* hyphae, e.g. enzymatic proteins, as well as components of the cell wall of plants and of these filamentous fungi are the substances inducing systemic immunity (Mathys et al., 2012).

The aim of the study was to assess the influence of composts inoculated with three *Trichoderma* strains on the sanitary condition of soil, measured with the count of potentially pathogenic moulds of the *Alternaria* and *Fusarium* genera. Apart from that, the soil activity and yield of spinach were measured.

The research assumption was that *Trichoderma* strains in combination with organic fertilisation had positive effect on the sanitary condition of soil and significantly

http://www.aloki.hu ● ISSN 1589 1623 (Print) ● ISSN1785 0037 (Online)
DOI: http://dx.doi.org/10.15666/aeer/1802_28072821

influenced the soil enzymatic activity, thus increasing the yield of crops. This treatment strictly follows the policy of integrated crop protection.

Currently the Polish market does not offer any organic fertilisers containing native Polish strains of *Trichoderma* sp. The development of an innovative fertiliser based on composted plant waste and isolates of *Trichoderma* fungi will promote the growth and development of plants. In consequence, it will result in development of the domestic and global biofertiliser management.

Material and methods

Experimental design

A two-year experiment (2013 and 2014) was located on a private farm in Lubosz, Commune of Kwilcz, Greater Poland Voivodeship, Poland.

The experiment was conducted on the following three *Trichoderma* isolates: *T. atroviride* (T1) and *T. harzianum* (T2 and T3), which were supplied by the Institute of Horticulture in Skierniewice, Poland. They were used for the inoculation of onion and tomato waste composts and then they were applied to the soil under spinach (*Spinacia oleracea* L.), Renegade F1.

The experimental composts were produced on a technical scale (in prisms with about 20 tonnes of input). Both the tomato waste compost and onion waste compost (mostly clusters, leaves, etc.) were mixed with wheat straw (about 10% added) and a small amount of pig manure (5%).

When the thermophilic phase finished (the prism temperature was about 25°C), the composts were inoculated with *Trichoderma* strains.

The output concentration of individual spores in the resulting suspension was measured by means of a haemocytometer under a light microscope (Zeiss). The following results were noted: strain T1 – $3.9 \cdot 10^8$, T2 – $2.3 \cdot 10^8$, T3 – $3.1 \cdot 10^8$ spores per 1 ml. The composts were inoculated with a suspension of conidial spores concentrated at 10^4 per g wet mass of compost. Therefore, after calculation each prism of the composted material was respectively inoculated with 512.01 ml of T1 strain spore suspension, 869.21 ml of T2 isolate, 645.16 ml of T3 strain, 690.60 ml of a T1+T2 mixture and 578.58 ml of a T1+T3 strain suspension. These conidial spore suspensions were mixed in 5 l of dechlorinated tap water and applied with a hand sprayer.

One month after the inoculation of the composts they were entered into the soil. The following amounts were applied: onion waste compost – 43 t ha^{-1} and tomato waste compost – 38 t ha^{-1}. Apart from the aforementioned composts, pig manure fertilisation (37 t ha^{-1}) and mineral fertilisation with nitrogen as urea (90 kg N ha^{-1}), with phosphorus as triple superphosphate (40 kg P ha^{-1}) and with potassium as potassium salt (182 kg Kha^{-1}) were also applied in the experiment. All organic fertilisers entered into the soil were equivalent to 170 kg N ha^{-1}.

The field research was conducted after harvest of winter burley, on typical haplic luvisols formed from light loamy sands, deposited in a shallow layer on light loam. The granulometric composition of the soil ranged from light clayey to strong sands deposited on light clays. Selected soil characteristics are shown in *Table 1*.

Experiment was designed as randomised complete block, with four replications and plot size 9.3 m^2 (6 x 1.55 m). Spinach, v. Renegade F1, were planted by means of a manual, precision seed drill Terradonis JP-1, with 25 seeds m^{-2}, at 40 cm row spacing. Planting was carried out of August 16, both years.

http://www.aloki.hu ● ISSN 1589 1623 (Print) ● ISSN1785 0037 (Online)
DOI: http://dx.doi.org/10.15666/aeer/1802_28072821

Table 1. *Chemical characteristics of the soil*

Pure components	Value (mg kg^{-1})
N	94.0
P	36.01
K	69.77
Mg	60.02
pH_{KCl}	5.8

Eleven fertiliser combinations were used in the experiment: 1 – control sample, no fertiliser, 2 – mineral fertiliser, 3 – manure, 4 – onion waste compost, 5 – onion waste compost inoculated with strain T1, 6 – onion waste compost inoculated with strain T3, 7 – onion waste compost inoculated with strains T1 and T3, 8 – tomato waste compost, 9 – tomato waste compost inoculated with strain T1, 10 – tomato waste compost inoculated with strain T2, 11 – tomato waste compost inoculated with strains T1 and T2.

Both in 2013 and 2014 soil samples for microbiological and biochemical analyses were collected at three periods (ten replications), according to the Polish standard PN - ISO 10381 – 2: 2007. Depending on the research year, the sample collection dates coincided with the pre-sowing phase (15, 16 July) – term I, crop emergence phase (8, 9 August) – term II and harvesting phase (3, 6 October) – term III.

At each term of analyses 20 representative soil samples weighing about 0.5 kg were collected with an Egner-Riehm soil stick from each experimental site at a depth of 0-20 cm. A collective sample was prepared in accordance with the recommendations of the Polish Standard: PN-ISO 10381-2: 2007. On collection the soil and plant samples were transported to the laboratory of the Department of General and Environmental Microbiology and the Department of Agronomy, Poznań University of Life Sciences for microbiological and enzymatic analyses and to estimate the spinach yield value.

Soil microorganisms

The total count of moulds as well as the counts of *Trichoderma* sp., *Alternaria* sp. and *Fusarium* sp. were measured in the experiments (in five replicates). The microorganisms were cultured with the plate method on solid substrates. Appropriate soil solutions were used and expressed as cfu g^{-1} DM of soil. The count of molds in the medium was measured according to the procedure developed by Martin (1950), with 3.5ml·l^{-1} rose bengal and 0.1g·l^{-1} aureomycin added. The plates were incubated for 6 days at a temperature of 25°C. The count of *Trichoderma* sp. was measured with the plate method, on a modified Martin's medium with 0.05g·l^{-1} chloramphenicol, 0.05g·l^{-1} streptomycin, 0.29g·l^{-1} metalaxyl and 0.01g·l^{-1} PCNB (pentachloronitrobenzene) added. The plates were exposed to visible light and incubated for 7 days at a temperature of 24°C. In order to confirm that *Trichoderma* sp. belonged taxonomically to the *Trichoderma harzianum* or *Trichoderma atroviride* species the fungal colonies were inoculated to a PDA substrate (Sigma Aldrich). They were initially identified with a microscope. Next, the identification was confirmed by means of fluorescent in situ hybridisation (FISH) (Amann et al., 1990) with 4% PFA (paraformaldehyde), 0.5% Triton solution, alcohol series (70%, 80%, 96%), 70% formamide solution and two probes, whose ends were marked with Cy3 marker (ACT CCC AAA CCC AAT GTG AA and ATA CCA AAC TGT TGC CTCGG) (Siddiquee et al., 2010).

http://www.aloki.hu ● ISSN 1589 1623 (Print) ● ISSN1785 0037 (Online)
DOI: http://dx.doi.org/10.15666/aeer/1802_28072821

In the experimental variants where the aforementioned *Trichoderma* sp. isolates were not applied, but native *Trichoderma* sp. strains were identified in the soil (e.g. in the control sample), only the counts of *Trichoderma harzianum* and *Trichoderma atroviride* were measured.

The count of *Fusarium* sp. was measured with the plate method, on a Komada medium (Komada, 1975) with 0.5g·l^{-1} ox bile, 0.05g·l^{-1} chloramphenicol, 0.3g·l^{-1} streptomycin, 1.0 g·l^{-1} borax and 1.0 g·l^{-1} PCNB (pentachloronitrobenzene) added. The plates were incubated for 14 days at a temperature of 24°C. The count of *Alternaria* sp. was measured on a medium developed by Hong and Pryor (2004). It was composed of 20% lactic acid, 0.005 g·l^{-1} botram (active ingredient: dichloran), 0.2 g·l^{-1} bayleton (active ingredient: triadimefon) and 0.3 g·l^{-1} streptomycin. The plates were incubated at a temperature of 24°C for 7 days. The fungal colonies were inoculated to a PDA substrate (Sigma Aldrich). Next, they were identified taxonomically on the basis of mycological keys (Gerlach and Nirenberg, 1982; Chełkowski, 1989; Chełkowski and Visconti, 1992; Domsch et al., 1993).

Soil enzymes

Spectrophotometry was used for biochemical analyses. The dehydrogenase activity (DHA) was measured according to the procedure developed by Thalmann (1968), with some minor modifications. The soil (1 g) with 2, 3, 5-triphenyltetrazolium chloride (TTC) was incubated for 24 h at 30°C, pH 7.4. Triphenylformazan (TPF) was produced, extracted with 96% ethanol and measured spectrophotometrically at 485 nm. The dehydrogenase activity was expressed as μmol TPF g^{-1} DM of soil 24 h^{-1}.

The catalyse activity (CAT) in the soil was measured by means of titration (Johnson and Temple, 1964). The soil with 0.3% H_2O_2 solution was incubated for 20 minutes. Next, 1.5 M H_2SO_4 was added. The resulting solution was titrated with 0.02 M $KMnO_4$. The catalyse activity was expressed as μmol H_2O_2 g^{-1} D.M. of soil min^{-1}.

The dehydrogenases and catalyse activity were measured to determine the soil BIF (Biological Index of Fertility) (*Eq.1*) (Stefanic et al., 1984):

$$BIF = (1.5\,DHA + 100\,k\,CAT) / 2 \qquad \text{(Eq.1)}$$

where k – the proportionality coefficient = 0.01.

Crops

The whole plant, aboveground biomass of spinach was harvested manually from two central rows in the plot for the yield measurement.

Statistical analysis

Statistica 12.0 software (StatSoft Inc., 2012) was used for statistical analyses. Two-way analysis of variance was used to determine the significance of variation in the count of groups of microorganisms and the soil enzymatic activity, depending on the soil combination and term of analysis. Homogeneous subsets of means were identified by means of Tukey´s test at a significance level of $p < 0.05$.

The second step of the diagnostic procedure involved stepwise regression to determine the optimal set of variables for a given characteristic of the microorganisms. The best

http://www.aloki.hu ● ISSN 1589 1623 (Print) ● ISSN1785 0037 (Online)
DOI: http://dx.doi.org/10.15666/aeer/1802_28072821

regression model was chosen on the basis of the highest F-value for the model and the significance of all the independent variables.

The relation between the count of microorganisms, soil enzymatic activity and the yield was illustrated by means of Principal Component Analysis (PCA).

Results and discussion

The analysis of the soil samples at the first term, i.e. before the application of the *Trichoderma* sp. strains, showed that these microorganisms were part of the natural, autochthonous soil microbiome (*Table 2*).

Table 2. *The count of Trichoderma sp. in the soil with the fertilisers at the three terms of analysis*

	Ist TERM	IInd TERM	IIIrd TERM
Control	0.00	5.38^{bc}	0.00
MIN	2.89^{a-c}	3.83^{a-c}	0.37^{a}
MAN	0.00	2.76^{a-c}	0.00
O	0.73^{ab}	1.88^{a-c}	0.00
O1	0.00	3.06^{a-c}	0.00
O3	0.00	1.9^{a-c}	0.00
O1+3	0.00	5.7^{c}	1.86^{a-c}
T	1.45^{a-c}	1.54^{a-c}	0.74^{ab}
T1	0.00	1.88^{a-c}	0.36^{a}
T2	0.00	1.94^{a-c}	0.00
T1+2	0.00	1.18^{a-c}	0.37^{a}

Explanation: The means followed by the same letters do not differ significantly at *p=0.05*; Combination: Control – no fertiliser, MIN – mineral fertiliser, MAN – manure, O – onion waste compost, O1 – onion waste compost inoculated with strain T1, O3 – onion waste compost inoculated with strain T3, O1+3 – onion waste compost inoculated with strains T1 and T3, T – tomato waste compost, T1 – tomato waste compost inoculated with strain T1, T2 – tomato waste compost inoculated with strain T2, T1+2 – tomato waste compost inoculated with strains T1 and T2; Terms: Ist – pre-sowing phase, IInd – crop emergence phase, IIIrd – harvesting phase

According to Smolińska et al. (2014), these microorganisms are commonly found in all soil types around the world. They usually occur on the surface of roots. Only few species can penetrate deeper. Apart from that, *Trichoderma* sp. can quickly colonise the substrate by competing with other microorganisms for the place of colonisation and nutrients. This situation was observed at the second term of analyses. It is most likely that the intensive growth of *Trichoderma* sp. in that period was caused by a change in the qualitative and quantitative composition of spinach root secretions, which acted as attractants (Vallance et al., 2011).

On harvesting the plants (the third term) the count of *Trichoderma* sp. decreased sharply or was totally reduced, especially in the control variant (without fertilisation). *Trichoderma* sp. were found only in the variant where the mineral fertiliser had been applied, in the one with onion compost inoculated with two strains and in three variants enriched with tomato compost. The highest, but statistically insignificant count of these microorganisms was noted in the soil with the onion compost inoculated with both the T1

http://www.aloki.hu ● ISSN 1589 1623 (Print) ● ISSN1785 0037 (Online)
DOI: http://dx.doi.org/10.15666/aeer/1802_28072821

and T3 strains (O1+3). The rapid, but in most cases statistically insignificant decrease or total reduction in the count of *Trichoderma* sp. in the experimental variants may have been caused by more intense proliferation of the total count of molds (*Fig. 1*). This may have resulted in the occurrence of species inhibiting the growth and development of *Trichoderma* sp.

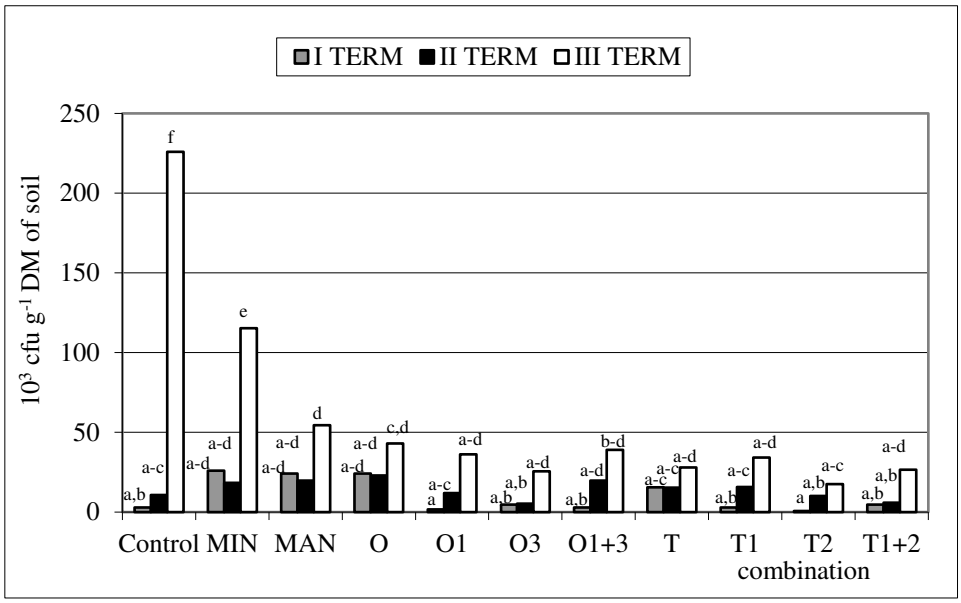

Figure 1. *Changes in the total count of molds in the soil. Explanation: The means followed by the same letters do not differ significantly at p=0.05; Combination: Control – no fertiliser, MIN – mineral fertiliser, MAN – manure, O – onion waste compost, O1 – onion waste compost inoculated with strain T1, O3 – onion waste compost inoculated with strain T3, O1+3 – onion waste compost inoculated with strains T1 and T3, T – tomato waste compost, T1 – tomato waste compost inoculated with strain T1, T2 – tomato waste compost inoculated with strain T2, T1+2 – tomato waste compost inoculated with strains T1 and T2; Terms: I^{st} – pre-sowing phase, II^{nd} – crop emergence phase, III^{rd} – harvesting phase*

According to Piegza et al. (2009), the fact that fungi of the *Trichoderma* genus exhibit poorer adaptation properties in vitro may be caused by their poorer ability to compete for nutrients and place of colonisation as well as their less abundant sporulation than some other species of fungi. Wawrzyniak and Waśkiewicz (2014) proved that some *Penicillium* species were capable of producing antibiotics and mycotoxins, e.g. ochratoxin A and citrinin, which inhibit the growth and development of other microorganisms, including *Trichoderma*.

The analysis of changes in the total count of molds during the experiment showed that the most intense colonisation of the soil with these microorganisms occurred particularly at the third term and at the second term of analyses and that it depended on the experimental variant (*Fig. 1*). There were statistically significant differences ($p = 0.05$) between the experimental variants in the count of moulds mainly at the plant harvesting phase. In comparison with the previous two terms the count of microorganisms increased significantly in the control and MIN treatments.

During the experiment the highest average count of these microorganisms was found in the control variant, while the lowest count was observed in the soil sample with the

http://www.aloki.hu ● ISSN 1589 1623 (Print) ● ISSN1785 0037 (Online)
DOI: http://dx.doi.org/10.15666/aeer/1802_28072821

tomato compost enriched with the T2 strain (T2 treatment). Wolna-Maruwka et al. (2016) conducted research on the influence of analogous experimental variants on the microbiological parameters of soil under a radish plantation. During the experiment the highest count of molds was found in the soil fertilised with manure, whereas the lowest count was observed in the variant where a mineral fertiliser had been applied. These observations clearly indicate that the count of these microorganisms in soil depends on various factors, i.e. the type of fertiliser, species of a plant and its phase of development (Baetz and Martinoia, 2014; Guo, 2019).

The sanitary analysis of the soil showed that, like in the case of *Trichoderma* sp., in most of the experimental variants the highest statistically significant counts of fungi of the *Alternaria* and *Fusarium* genera were noted at the phase of the plants' emergence (the second term) (*Figs. 2 and 3*), especially in the variants where the onion waste compost had been added. During the period under analysis the lowest, statistically insignificant increase in the count of these microorganisms in relation to the control variant was noted in the experimental variants enriched with the tomato compost.

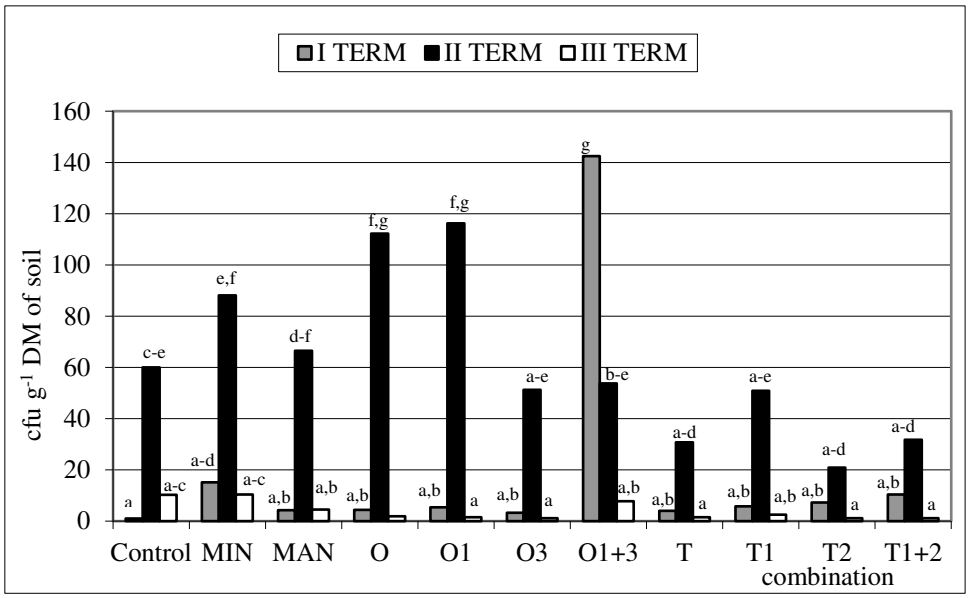

Figure 2. *Changes in the count of Fusarium sp. in the soil. Explanation: The means followed by the same letters do not differ significantly at p=0.05; Combination: Control – no fertiliser, MIN – mineral fertiliser, MAN – manure, O – onion waste compost, O1 – onion waste compost inoculated with strain T1, O3 – onion waste compost inoculated with strain T3, O1+3 – onion waste compost inoculated with strains T1 and T3, T – tomato waste compost, T1 – tomato waste compost inoculated with strain T1, T2 – tomato waste compost inoculated with strain T2, T1+2 – tomato waste compost inoculated with strains T1 and T2; Terms: Ist – pre-sowing phase, IInd – crop emergence phase, IIIrd – harvesting phase*

According to Utama et al. (2002), during the decomposition of plant residue contained in composts many different substances with strong biological properties (such as phenols, aldehydes, alcohols, essential oils, terpenes and acids) may be released and they may inhibit the development of soil microorganisms. As results from the study by Steinka and Kukułowicz (2008), caffeic acid, which can be found in tomato tissues, has strong antimicrobial properties.

http://www.aloki.hu ● ISSN 1589 1623 (Print) ● ISSN1785 0037 (Online)
DOI: http://dx.doi.org/10.15666/aeer/1802_28072821

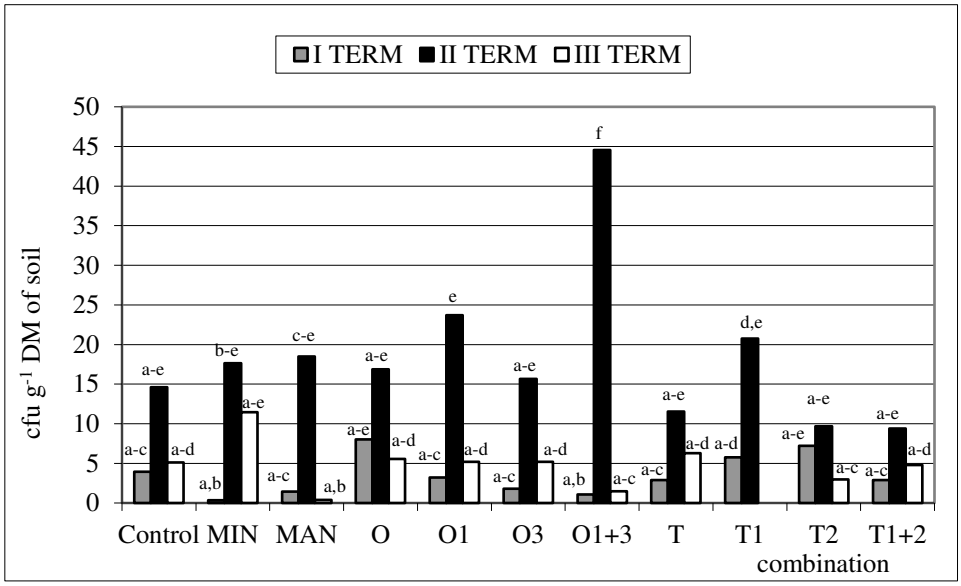

Figure 3. *Changes in the count of Alternaria sp. in the soil. Explanation: The means followed by the same letters do not differ significantly at p=0.05; Combination: Control – no fertiliser, MIN – mineral fertiliser, MAN – manure, O – onion waste compost, O1 – onion waste compost inoculated with strain T1, O3 – onion waste compost inoculated with strain T3, O1+3 – onion waste compost inoculated with strains T1 and T3, T – tomato waste compost, T1 – tomato waste compost inoculated with strain T1, T2 – tomato waste compost inoculated with strain T2, T1+2 – tomato waste compost inoculated with strains T1 and T2; Terms: Ist – pre-sowing phase, IInd – crop emergence phase, IIIrd – harvesting phase*

Poorer proliferation of *Alternaria* sp. and *Fusarium* sp. in the variants with the tomato waste compost was additionally intensified by the effect of the *Trichoderma* sp. strains (especially applied separately in the case of *Alternaria*). The phenomenon was illustrated by the regression curves (*Figs. 4 and 5*).

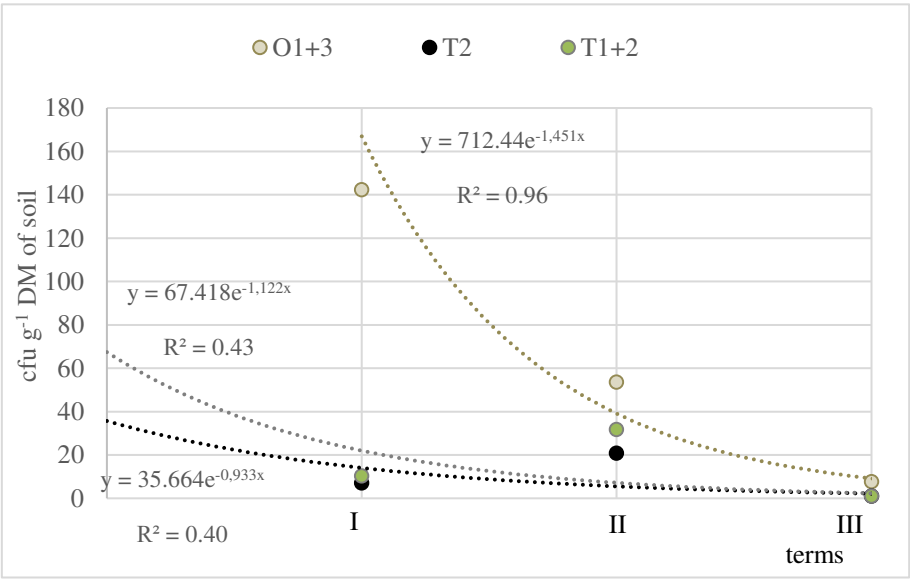

Figure 4. *The dynamics of changes in the count of Fusarium sp. during the experiment*

http://www.aloki.hu ● ISSN 1589 1623 (Print) ● ISSN1785 0037 (Online)
DOI: http://dx.doi.org/10.15666/aeer/1802_28072821

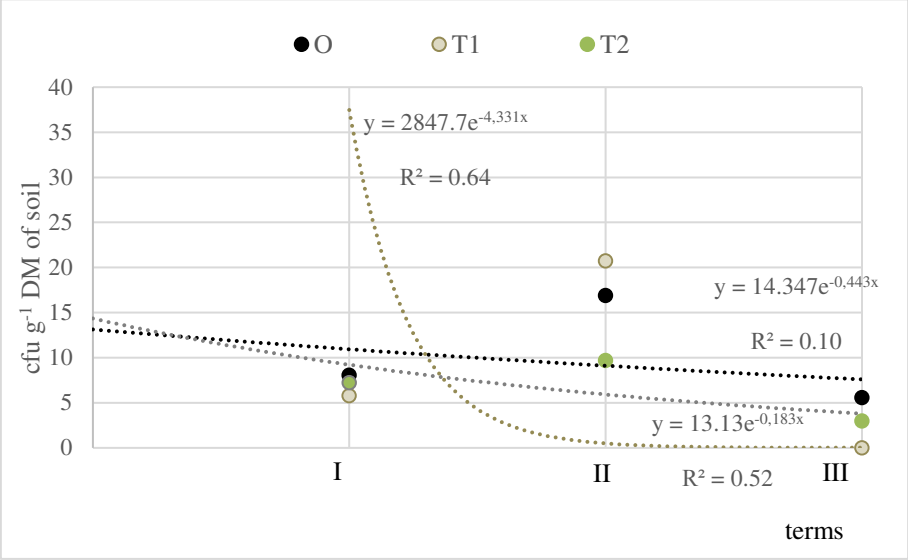

Figure 5. *The dynamics of changes in the count of Alternaria sp. during the experiment*

The comparison of the sanitary condition of the soil variants at the first term of analyses with the harvest phase (the third term) showed that the greatest statistically significant limitation of the development of *Fusarium* sp. took place in the variant enriched with the onion compost, additionally inoculated with two *Trichoderma* sp. strains – T1 and T3, and in the soil fertilised with the tomato compost, also with the addition of two isolates – T1 and T2 (statistically insignificant limitation at *p=0.05*). There was a statistically significant decrease in the count of *Alternaria* sp. in the soil where the tomato compost and T1 strain had been added and in the variant with the tomato compost and T2 strain (statistically insignificant limitation at *p=0.05*).

The analysis of changes in the activity of soil enzymes (BIF) during the study showed that the highest enzymatic activity occurred at the phase of spinach emergence (*Fig. 6*).

In most of the experimental variants (except the control and MIN treatments) these were statistically significant differences in comparison with the other two terms of analyses.

As results from the research conducted by Sasse et al. (2018) and Vallence et al. (2011), the composition of plant root secretions depends not only on the type of plant but also on the phase of its development. This finding explains the differences in the activity of soil enzymes. According to these authors, root secretions, which are rich in sugars, amino acids and vitamins, modify both the count of soil microorganisms and their activity. This fact was confirmed by the principal component analysis (*Fig. 7*), which showed a positive dependency between the enzyme activity and the counts of *Trichoderma* sp., *Fusarium* sp. and *Alternaria* sp.

In our experiment, at the second term of analyses the BIF reached the highest statistically significant values (in most cases they were statistically significant at *p=0.05*) in the soil samples enriched with manure (MAN) or various compost variants, especially in the ones based on tomato waste (T and T1+2). The BIF values were greater than at the other terms of analyses. This observation was in agreement with the findings of the study by Wolna-Maruwka et al. (2017). The soil sample with the mineral fertiliser (MIN) exhibited the lowest statistically insignificant enzymatic activity. According to

http://www.aloki.hu ● ISSN 1589 1623 (Print) ● ISSN1785 0037 (Online)
DOI: http://dx.doi.org/10.15666/aeer/1802_28072821

Acosta-Martinez and Tabatabai (2000), this phenomenon can be explained by the fact that although mineral fertilisation positively affects the physicochemical properties of soil, it may reduce its enzymatic activity due to the presence of easily absorbable forms of mineral compounds.

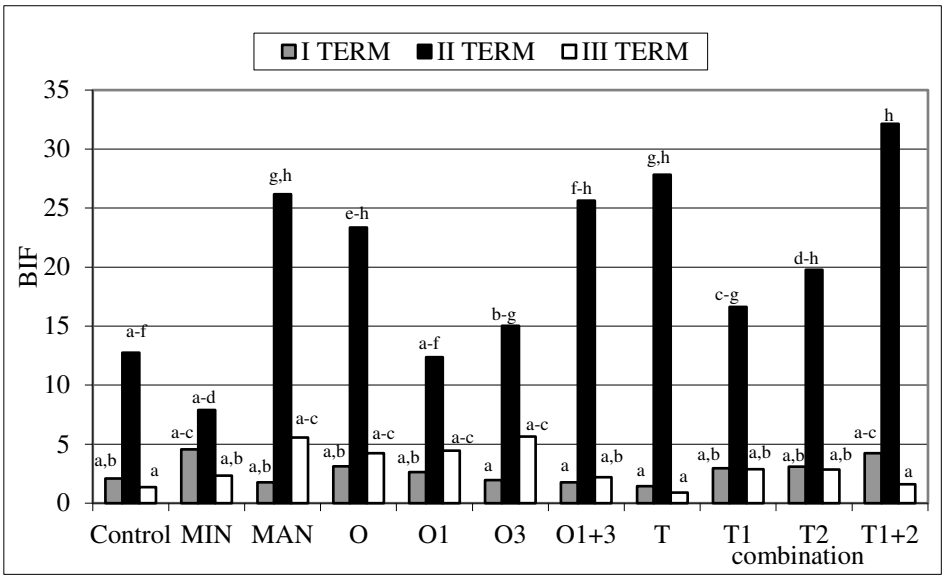

Figure 6. *Changes in the Biological Index of Fertility (BIF) in the soil. Explanation: The means followed by the same letters do not differ significantly at p=0.05; Combination: Control – no fertiliser, MIN – mineral fertiliser, MAN – manure, O – onion waste compost, O1 – onion waste compost inoculated with strain T1, O3 – onion waste compost inoculated with strain T3, O1+3 – onion waste compost inoculated with strains T1 and T3, T – tomato waste compost, T1 – tomato waste compost inoculated with strain T1, T2 – tomato waste compost inoculated with strain T2, T1+2 – tomato waste compost inoculated with strains T1 and T2; Terms: Ist – pre-sowing phase, IInd – crop emergence phase, IIIrd – harvesting phase*

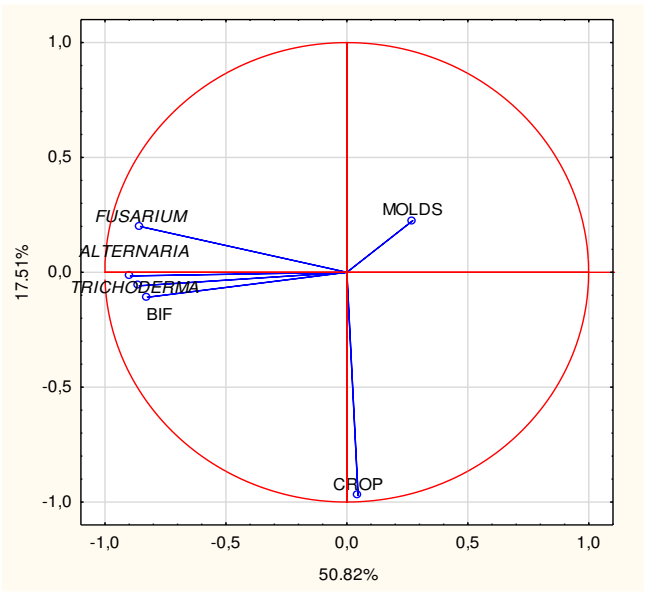

Figure 7. *Dependences between the number of groups of microorganisms and the enzymatic activity in the experimental soil combinations at the consecutive terms of analyses (PCA)*

http://www.aloki.hu ● ISSN 1589 1623 (Print) ● ISSN1785 0037 (Online)
DOI: http://dx.doi.org/10.15666/aeer/1802_28072821

At the harvest phase (the third term) the BIF dropped rapidly in all the experimental variants, especially in the ones enriched with the tomato compost. This decrease in the soil enzymatic activity was statistically significant at *p=0.05.*

The mineral fertilisation (MIN) resulted in the highest yield (8.89 $t \cdot ha^{-1}$) of the fresh mass of spinach (*Fig. 8*). However, the total yield of the fresh mass of spinach in the unfertilised control (7.09 $t \cdot ha^{-1}$), variant with manure (8.50 $t \cdot ha^{-1}$), the ones with the tomato waste compost, (T1, T2, T1+2 treatments), and the combination O1+3 did not differ significantly from the yield in the MIN variant application. The other types of onion waste composts (O, O1, O3) resulted in a statistically significant decrease in the yield in comparison with the MIN, O1+3, T1, T1+3 treatments, but did not differ from MAN, T, T2 and control variant.

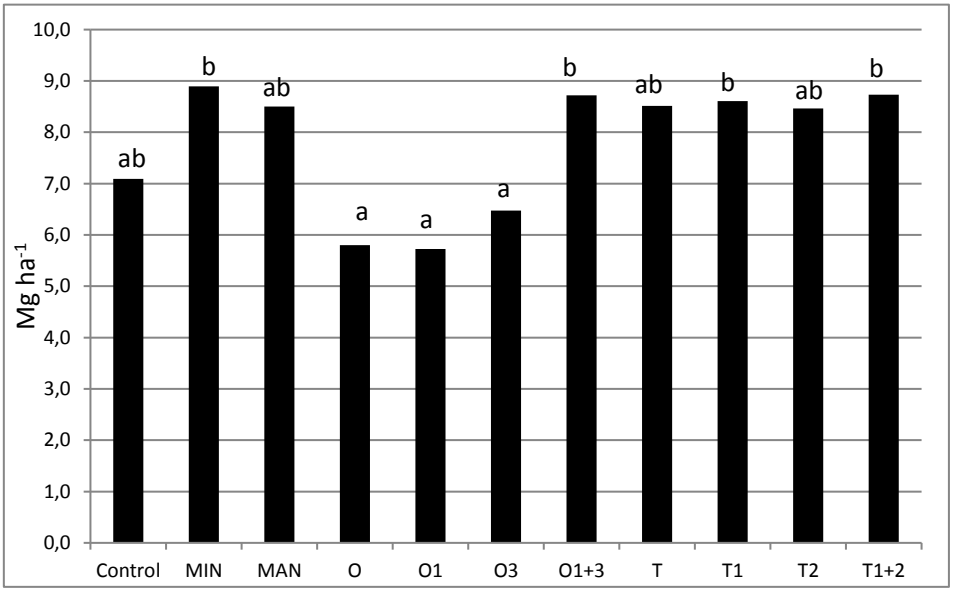

Figure 8. *The average yield of spinach leaves as affected by fertilisation between 2013 and 2014 (Mg ha^{-1}). Explanation: The means followed by the same letters do not differ significantly at p=0.05; Combination: Control – no fertiliser, MIN – mineral fertiliser, MAN – manure, O – onion waste compost, O1 – onion waste compost inoculated with strain T1, O3 – onion waste compost inoculated with strain T3, O1+3 – onion waste compost inoculated with strains T1 and T3, T – tomato waste compost, T1 – tomato waste compost inoculated with strain T1, T2 – tomato waste compost inoculated with strain T2, T1+2 – tomato waste compost inoculated with strains T1 and T2*

Organic fertilisers are a valuable source of nutrients because they contain all macro- and micronutrients that are necessary for plants and thus they minimise the risk of deficiency of any of them. Nitrogen is the component that usually determines the yield level. Its bioavailability in organic fertilisers is usually lower than in mineral fertilisers (Chambers et al., 2000).

The direct yield effect of solid organic fertilisers, including composts, is usually smaller than that of mineral fertilisers due to the wide C/N ratio and the slow release of nitrogen in mineral forms. In our experiment the same dose of nitrogen was used in all the composts and manure, but there were extreme differences in the effects. The yield in the variants with manure and tomato waste compost was equal to the yield after mineral fertilisation. However, in the sample fertilised with the onion waste compost the yield

http://www.aloki.hu ● ISSN 1589 1623 (Print) ● ISSN1785 0037 (Online)
DOI: http://dx.doi.org/10.15666/aeer/1802_28072821

decreased even below the level in the control variant. The situation improved significantly when a mixture of *Trichoderma* strains was applied into this compost. This fact lets us suppose that the composts matured at different rates, depending on their composition. The tomato waste became composted faster and gave a more mature compost, from which nutrients were released. The onion waste compost was still immature and the nutrients were not accessible to plants. Only when the two *Trichoderma* strains were added, maturation was accelerated and the availability of nutrients increased.

Apart from the direct yield effect, organic fertilisers significantly affect the content of humus. Humus deficiency is common in agricultural soils. It results in defective physical properties of soil, which can be improved only by applying large doses of organic matter (Piechota, 2005).

Conclusions

1. The phase of plants' development and the type of fertilisation significantly modified the microbiological and enzymatic condition of soil.
2. The application of manure resulted in the most intense proliferation of molds.
3. The most intense proliferation of *Trichoderma* sp. was observed in the soil enriched with the onion waste compost inoculated with the T1 and T3 strains.
4. The simultaneous application of the *Trichoderma* T1 and T3 strains into the onion waste compost provided the best protection of spinach against fungal pathogens of the *Fusarium* genus. The T1 isolate applied together with the tomato compost resulted in the most effective limitation of the development of *Alternaria* sp.
5. The onion compost inoculated simultaneously with the T1 and T3 strains gave the highest yield of spinach, which was comparable to the one obtained after mineral fertilisation.
6. The study proved that vegetable waste could be used as a carrier when applying *Trichoderma* sp. isolates into soil. It may increase the yield of crops and limit the development of some pathogens, but it is important to select the right strain of *Trichoderma* sp.
7. The research is strictly related with integrated crop and environment protection and provides huge prospects for organic waste management. Organic matter can be recovered as a valuable organic fertiliser and used as a carrier for selected *Trichoderma* sp. strains that exhibit antagonism to pathogens and promote the growth and development of plants.

Acknowledgements. The research was conducted as part of the project of the National Centre for Research and Development, No. UDA-POIG.01.03.01-00-129/09-09: 'Polish Strains of *Trichoderma* in Plant Protection and Organic Waste Handling'.

REFERENCES

[1] Acosta-Martinez, V., Tabatabai, M. A. (2000): Enzyme activities in a limed agricultural soil. – Biol. Fert. Soils 31: 85-91.

[2] Amann, R. I., Krumholz, L., Stahl, D. (1990): A Fluorescent-oligonucleotide probing of whole cells for determinative, phylogenetic, and environmental studies in microbiology. – J. Bacteriol. 172: 762-770.

http://www.aloki.hu ● ISSN 1589 1623 (Print) ● ISSN1785 0037 (Online)
DOI: http://dx.doi.org/10.15666/aeer/1802_28072821

[3] Baetz, U., Martinoia, E. (2014): Root exudates: the hidden part of plant defense. – Trends Plant Sci. 19: 90-98.
[4] Chambers, B. J., Smith, K. A., Pain, B. F. (2000): Strategies to encourage better use of nitrogen in animal manures. – Soil Use Manag. 16: 157-161.
[5] Chełkowski, J. (ed.) (1989): *Fusarium*, mycotoxins, taxonomy and pathogenicity; Topics in secondary metabolites. – Elsevier Science Publishers, Amsterdam, The Netherlands.
[6] Chełkowski, J., Visconti, A. (1992): *Alternaria*. Biology, plant diseases and metabolites. – Elsevier Science Publishers, Amsterdam, The Netherlands.
[7] Colla, G., Rouphael, Y., Di Mattia, E., El-Nakhel, C., Cardarelli, M. (2015): Coinoculation of *Glomus intraradices* and *Trichoderma atroviride* acts as abiostimulant to promote growth, yield and nutrient uptake of vegetable crops. – J. Sci. Food Agr. 95: 1706-1715.
[8] Directive 2008/98/EC of the European Parliament and of the Council of 19 November 2008 on waste and repealing certain Directives.
[9] Directive 2009/128/EC of the European Parliament and of the Council establishing a framework for Community action to achieve the sustainable use of pesticides. – Official Journal of the European Union L 309, 71, 24 November 2009.
[10] Domsch, K. H., Gams, W., Anderson, T. H. (1993): Compendium of soil fungi. – Academic Press, London.
[11] Druzhinina, I., Seidl-Seiboth, V., Herrera-Estrella, A., Horwitz, B., Kenerley, C. M., Monte, E. (2011): *Trichoderma*: the genomics of opportunistic success. – Nat. Rev. Microbiol. 9: 749-759.
[12] Gerlach, W., Nirenberg, H. (1982): The genus *Fusarium*-a pictorial atlas. – Mitteilungen aus der Biologischen Bundesanstalt für Land und Forstwirtschaft. Berlin-Dahlem.
[13] Guo, X. F. (2019): Diversity and community structure of fungi in the roots of machilus pauhoi in different age groups. – Appl. Ecol. Environ. Res. 17(2): 2073-2083.
[14] Hermosa, R., Botella, L., Keck, E., Jiménez, J. Á., Montero-Barrientos, M., Arbona, V. (2011): The overexpression in *Arabidopsis thaliana* of a *Trichoderma harzianum* gene that modulates glucosidase activity, andenhances tolerance to salt and osmotic stresses. – J. Plant Physiol. 168: 1295-1302.
[15] Hermosa, R., Viterbo, A., Chet, I., Monte, E. (2012): Plant beneficial effects of *Trichoderma* and its genes. – Microbiology 158: 1-25.
[16] Hong, S. G., Pryor, B. M. (2004): Development of selective media for the isolation and enumeration of Alternaria species from soil and plant debris. – Can. J. Microbiol. 50: 461-468.
[17] John, R. P., Tyagi, R. D., Brar, S. K., Pouleur, S., Surampalli, R. Y. (2010): Mycoparasitic *Trichoderma viride* as a biocontrol agent against *Fusariumo oxysporum* f. sp. *adzuki* and *Pythium arrhenomanes* and as a growth promoter of soybean. – Crop Prot. 29: 1452-1459.
[18] Johnson, J. L., Temple, K. L. (1964): Some Variables Affecting the Measurement of "Catalase Activity" in Soil 1. – Soil Sci. Soc. Am. J. 28: 207-209.
[19] Komada, H. (1975): Development of a selective medium for quantitative isolation of *Fusarium oxysporum* from natural soil. – Rev. Plant Prot. Res. 8: 114-124.
[20] López-Bucio, J., Pelagio-Flores, R., Herrera-Estrella, A. (2015): *Trichoderma* as biostimulant: exploiting the multilevel properties of a plant beneficial fungus. – Sci. Hortic. 196: 109-123.
[21] López-Mondéjar, R., Ros, M., Pascual, J. A. (2011): Mycoparasitism-related genes expression of *Trichoderma harzianum* isolates to evaluate their efficacy as biological control agent. – Biol. Control 56: 59-66.
[22] Martin, J. P. (1950): Use of acid, rose bengal and streptomycin in the plate method for estimating soil fungi. – Soil Sci. 69: 215-232.
[23] Mathys, J., De Cremer, K., Timmermans, P., Van Kerckhove, S., Lievens, B., Vanhaecke, M. (2012): Genome-wide characterization of ISR induced in Arabidopsis thaliana by *Trichoderma hamatum* T382 against *Botrytis cinerea* infection. – Front. Plant Sci. 3: 1-25.

http://www.aloki.hu ● ISSN 1589 1623 (Print) ● ISSN1785 0037 (Online)
DOI: http://dx.doi.org/10.15666/aeer/1802_28072821

[24] Minelgaitė, A., Genovaitė, L. (2019): Waste problem in European Union and its influence on waste management behaviours. – Sci. Total Environ. 667: 86-93.
[25] Piechota, T. (2005): Impact of long-term effects of plant succession and fertilization systems on the soil's physical properties. – Fragm. Agron. 2: 158-166.
[26] Piegza, M., Stolaś, J., Kancelista, A., Witkowska, D. (2009): Influence of *Trichoderma* strains on the growth of pathogenic moulds in biotic test on untypical carbon sources. – Acta Sci. Pol. Biotechnol. 8: 3-14.
[27] PN-ISO 10381-2:2007 Soil quality – Collecting Samples - Part 2: The rules of collection techniques.
[28] Regulation of the Minister of Agriculture and Rural Development on the Reduction of the Mass of Biodegradable Municipal Waste to Be Landfilled and the Method of Calculation of the Limits of This Mass of Waste, 25 May 2012. – Journal of Laws of 2012, item. 676.
[29] Regulation of the Minister of Agriculture and Rural Development on Integrated Crop Protection Requirements of 18 April 2013. – Journal of Laws of 2013, item 505.
[30] Regulation of the Minister of Agriculture and Rural Development on Recycling R10 of 20 January 2015. – Journal of Laws of 2015, item 132.
[31] Sasse, J., Martinoia, E., Northen, T. (2018): Feed your friends: do plant exudates shape the root microbiome? – Trends Plant Sci. 23: 25-41.
[32] Siddiquee, S., Yusof, N. A., Salleh, A. B., Tan, S. G., Bakar, F. A., Heng, L. Y. (2010): DNA hybridization based on *Trichoderma harzianum* gene probe immobilization on self-assembled monolayers on a modified gold electrode. – Sensors and Actuators B-Chem 147: 198-205.
[33] Smolińska, U., Kowalska, B., Kowalczyk, W., Szczech, M. (2014): The use of agro-industrial wastes as carriers of *Trichoderma* fungi in the parsley cultivation. – Sci. Hortic. 179: 1-8.
[34] Statistics Poland. (2018): Statistical analyses. – Municipal infrastructure in 2017 - Warsaw.
[35] Stefanic, G., Eliade, G., Chirnogeanu, I. (1984): Researches concerning a biological index of soil fertility. – 5. Symposium on Soil Biology, Feb 1981 Jassy (Romania).
[36] Steinka, I., Kukułowicz, A. (2008): The biostatic influence of plant pulp and solutions on *Staphylococci*. – Bromat. Chem. Toksykol. 2: 191-196.
[37] Thalmann, A. (1968): Zur methodik der bestimmung der dehydrogenase aktivität in boden mittels Triphenyltetrazoliumchlorid (TTC). – Landwirt Forsch 21: 249-258.
[38] Utama, I. M. S., Wills, R. B. H., Ben-Yehoshua, S., Kuek, C. (2002): In vitro efficacy of plant volatiles for inhibiting the growth of fruit and vegetable decay microorganisms. – J. Agric. Food Chem. 50: 6371-6377.
[39] Vallance, J., D´eniel, F., Le Floch, G., Gu´erin-Dubrana, L., Blancard, D., Rey, P. (2011): Pathogenic and beneficial microorganisms in soilless cultures. – Agron. Sustain. Dev. 31: 191-203.
[40] Wawrzyniak, J., Waśkiewicz, A. (2014): Ochratoxin A and citrinin production by *Penicillium verrucosum* on cereal solid substrates. – Food Addit. Contam. A. 31: 139-148.
[41] Wojtkowiak-Gębarowska, E. (2006): The Mechanisms of Controlling Soil Phytopathogens by Fungi of the *Trichoderma* Genus. – Postępy Mikrobiologii 45: 261-273.
[42] Wolna-Maruwka, A., Piechota, T., Kosicka-Dziechciarek, D., Szczech, M., Niewiadomska, A., Dach, J. (2016): A mycological analysis of soil fertilised with vegetable waste composts under a radish (*Raphanus sativus*) plantation. – J. Res. App. Agric. Eng. 61: 223-229.
[43] Wolna-Maruwka, A., Piechota, T., Dach, J., Szczech, M., Szczerbal, I., Niewiadomska, A., Budka, A., Gaj, R. (2017): The influence of *Trichoderma* on the phytosanitary status of soil and yield of red beets (*Beta vulgaris* L. *subsp. vulgaris*). – Pol. J. Environ. Stud. 26: 847-859.

http://www.aloki.hu ● ISSN 1589 1623 (Print) ● ISSN1785 0037 (Online)
DOI: http://dx.doi.org/10.15666/aeer/1802_28072821

PROBIOTIC-YEAST IMPROVES PERFORMANCE INDICATORS IN BROILER CHICKENS: EVIDENCE FROM META-ANALYSIS

OGBUEWU, I. P.[1*] – OKORO, V. M.[2] – MBAJIORGU, C. A.[1]

[1]*Department of Animal Agriculture and Animal Health, University of South Africa, Florida 1710, South Africa*

[2]*Department of Animal Science and Technology, Federal University of Technology, PMB 1526 Owerri, Nigeria*

**Corresponding author*
e-mail: ogbueip@unisa.ac.za, dr.ogbuewu@gmail.com

(Received 15th Oct 2019; accepted 8th Jan 2020)

Abstract. Antibiotics modulate gut microbiomes and enhance broiler chicken productivity. Nevertheless, their use in chicken nutrition has been linked to the spread of resistant strains of bacteria. Studies have shown that probiotic-yeast improves the productivity of broiler chickens. However, agreement has not been reached among investigators as to whether yeast improves the production indices of broiler chickens. The objective of this meta-analysis therefore was to determine the effect of yeast supplementation on feed consumption (FC), feed conversion ratio (FCR) and body weight gain (BWG) in broiler chicken using meta-analysis. The study focused on published primary studies comparing broiler chickens fed diet supplemented with yeast versus without yeast. Sixteen published primary studies were included in the meta-analysis. Results of pooled effects estimate revealed that yeast supplementation improved FCR ($p < 0.001$), BWG ($p < 0.001$) and reduced FC ($p < 0.001$) in broiler chickens. The results of sub-analysis indicated that broiler chickens that received yeast at < 10 g/kg diet had better performance than those that received yeast at 10 g/kg feed and > 10 g/kg feed. The chosen moderators were predictors of study effect observed in the meta-analysis. It is concluded that yeast can be used as a performance enhancer in broiler chickens instead of antibiotics.
Keyword: *beneficial microbes, meat-typed chickens, productivity, meta-analysis, meta-regression*

Introduction

Broiler chicken farming plays a vital part in supporting the livelihoods of most households in many parts of the world, because of its role as a source of animal protein. Incidentally, several households in developing nations, still regard poultry products as luxury (Adene and Oguntade, 2006). This has been attributed to the high cost of poultry products driven mainly by the elevated feed price, which led poultry nutritionist to search for feed additives with the potential to increase feed digestion and nutrient uptakes (Gadde et al., 2017). Antibiotics, one of such feed additives has been reported to modulate gut microbiomes, enhance feed efficiency, boost growth rate as well as deter the emergence of diseases in chickens (Costa et al., 2017). Regardless of the established positive actions of in feed antibiotics in boosting growth performance in chickens, their use has been tied to the proliferation of resilient strains of bacteria and meat with remnants of antibiotics (Kabir et al., 2004; Chen et al., 2017; Gadde et al., 2017) which is a threat to public health (Kabir et al., 2004; Piątkowska et al., 2012). Although, views are mixed on whether the use of antibiotics in poultry feed can transfer resistance genes from animals to humans (Gadde et al., 2017), consumers of poultry meat were increasingly concerned about the risk of continued use of antibiotics in animal feeds (Kabir et al., 2004; Piątkowska et al.,

http://www.aloki.hu ● ISSN 1589 1623 (Print) ● ISSN 1785 0037 (Online)
DOI: http://dx.doi.org/10.15666/aeer/1802_28232843

2012). This ugly development called for an investigation into the use of probiotics as an alternative to antibiotics in broiler nutrition (Ahmed et al., 2015; Gao et al., 2017; Ogbuewu et al., 2019).

Probiotics are living organisms that elicit positive health effects in animal and humans when included in the diet at the right proportions (FAO, 2016). The beneficial health property of probiotics can be ascribed to either its ability to modulate gut microbiomes or their direct nutritional effect (Saulnier, 2007; Shareef and Al-Dabbagh, 2009). Yeast (*Saccharomyces cerevisiae*), one of the commonly used probiotics in both human and animal food is a single-celled organism that measures about 3 to 4 microns in size. Yeast is rich in protein and amino acids (Gomes et al., 2014; Ogbuewu et al., 2019) as well as vitamin B complex and minerals (USDA, 2018). Chand et al. (2014) reported that yeast contains 93.00% dry matter, 1.00% ether extract, 44.40% crude protein, 2.70% crude fibre, 0.12% calcium and 1.40% phosphorus. Indisputably, the results of the production parameters of broiler chickens fed yeast supplemented diets in literature as reported by several authors were disaggregated and conflicting, hence calling for evidence synthesis. Evidently, there are several studies on the actions of yeast on broiler performance (Paryard and Mahmoudi, 2008; Ezema, 2013; Ahmed et al., 2015; Chen et al., 2017), and many have undoubtably shown that yeast enhance broiler chicken productivity (Ezema and Ugwu, 2014; Ogbuewu et al., 2019). Earlier reviews conducted to ascertain the beneficial effect of yeast on broiler chicken performance, however, were narrative, which is bias-friendly due to non-repeatability of the results and lacked the ability to manage large datasets. For example, Ezema and Ugwu (2014) did a narrative review of published studies of the effect of probiotic-yeast on broiler productivity and discovered that yeast improve growth rate and nutrient digestibility in chickens. Incongruity, a recent narrative review by Ogbuewu et al. (2019) found disparity on production data of broiler chickens fed yeast supplemented diets. The current study aims to use meta-analytical technique to identify and quantify several variables that affect the outcomes of the effect of probiotic yeast on the growth performance indices of broiler chickens.

Materials and methods

Selection guidelines and ethical approval

The main criteria for selecting the primary studies included in this meta-analysis were: randomized and controlled tests (RCTs) in diseased-free broiler chickens fed yeast supplemented diets. Studies were included if peer-reviewed and published in English. Study reported at least one of these growth performance indices (FC, FCR and BWG) and a dispersion metric such standard error (SE), standard deviation (SD) or 95% confidence interval (CI) for each effect size. This study was conducted at the University of South Africa during the months of June to September 2019. Literature search and data analysis were conducted in line with the guidelines of the University of South Africa Ethics Committee.

Data sources, extraction and data integrity

The investigators independently searched for articles in PubMed, Scopus and Google scholar databases from 1999 to 2017. Studies were panel-selected to guarantee the reliability of outcome of the meta-analysis, which relies on the validity of papers that

http://www.aloki.hu ● ISSN 1589 1623 (Print) ● ISSN 1785 0037 (Online)
DOI: http://dx.doi.org/10.15666/aeer/1802_28232843

make up the database. Yeast* and broiler chickens* were included in the search conditions. Articles were evaluated, and those that met the selection guidelines were selected. Information on the surname of the first author, the year the study was published, broiler breed, yeast supplementation level, duration of yeast supplementation, outcomes of interest (FC, FCR, BWG) and measures of variance (SE, SD or p-value) from the papers included in the meta-analysis are presented in the supplementary file. Most of the articles assessed did not report the yeast type used and the failure of the authors to obtain extra information from the corresponding author led to the removal of yeast type from the a priori selection criteria that an article must meet in order to be included in the meta-analysis. Furthermore, where the SD was not supplied, but can be estimated from SE, where it is reported using the method (Higgins and Deeks (2011).

Statistical analysis

Data analysis was performed in Open Meta-analyst for Ecology and Evolution (OpenMEE) software and forest plots were produced (Wallace et al., 2016). Continuous variable results (FC, BWG and FCR) were evaluated as the difference between the groups in yeast treatment and control with 95% CI. Q-statistic (DerSimonian and Laird, 1986) and I^2 – statistic; (Higgins et al., 2003) were used to calculate heterogeneity. Pooled effects estimate of the responses of broiler chickens to yeast supplementation were calculated using the DerSimonian and Laird (1986) random-effects model (REM). The REM selection is based on the premise that information used in the current study were not the same, therefore, the variance must be split into variance within and variance between studies plus sampling error (Borenstein et al., 2009).

For robustness of our results, we used sensitivity analysis which according to Lean et al. (2009) is used to assess the impacts of studies judged to be deviant or to have an undue influence on the analysis. This was accomplished by leaving one study each time the analysis was conducted. The influence graph shows the global impact without each study. The magnitude of the effect of yeast supplementation on broiler chicken productivity may be affected by several explanatory variables (moderators). The moderators considered in this study matched the factors we assumed to predict the association between yeast supplementation and broiler performance. In the subgroup analysis, the data were stratified using the following modifiers (study continent, study country, supplementation level, duration of supplementation and broiler breed used) thought to influence the physiological traits of broiler chickens fed probiotic yeast. Subgroup analysis was not performed when there are comparatively few studies (< 3 comparisons) in an individual stratum. The same variables used in the subgroup analysis were included as the modifier variables in the meta-regression (Dohoo et al., 2003). Meta-regression was used to examine whether the selected predictors (study continent, study country, yeast supplementation level, duration of yeast supplementation and breed of broiler used) explained any of the sources of heterogeneity.

Rosenberg's fail-safe number (Nfs) and funnel plots were used in this study to assess the existence of publication bias. Studies are said to have no publication bias when the funnel is inverted and symmetrical. Evidently, Jennions et al. (2013) have shown the robustness of meta-analysis results in the presence of publication bias regarded Nfs is greater than "5 (n = number of effect sizes) + 10". Forest plots (DerSimonian and Laird, 1986; IntHout et al., 2014) displayed the outcome of yeast intervention on broiler chicken productivity. Points to the left of the no effect line show a decline in the results

http://www.aloki.hu ● ISSN 1589 1623 (Print) ● ISSN 1785 0037 (Online)
DOI: http://dx.doi.org/10.15666/aeer/1802_28232843

of our parameters of interest, and the opposite demonstrates the reverse. The effect size is represented by individual square in the forest plot, while the upper and lower 95% CI for the effect size are the line that joined the square. According to Leah et al. (2009), the inverse of the effect size variance is shown by the weight of each study, whereas the square box size is equivalent to the inverse variance of the estimates with larger square boxes suggesting greater weight. The pooled effects estimate depicts the dotted line with the diamond at the bottom making up 95% CI. The pooled estimate was not significant when the diamond at the bottom is in contact with the no effect line (Koricheva et al., 2013). Effect sizes of approximately 0.2 and 0.5 are designated low and medium respectively, and large when they are more than 0.8.

Results

Overview of the articles included in the meta-analysis

The literature search in PubMed, Scopus and Google scholar produced 64 articles evaluating the productive indices of broiler chickens fed yeast supplemented diets (*Fig. 1*). A total of 25 articles were excluded from the analysis because they were reported in animal species other than broiler chickens. Six papers were removed from the study because they were narrative reviews, while five papers were excluded because they reported only the abstract. Five articles were excluded from the meta-analysis because of they were not randomized, and the control group was missing. Seven articles were not considered suitable for the analysis because they did not report any of the outcomes of interest. For the analysis of FC, 16 studies (with 4874 birds and 62 comparisons) representing 10 study countries drawn from three study continents met the eligibility criteria (*Table 1*). The publications used in the meta-analysis to assess the effect of yeast supplementation on FC in broiler chickens span 18 years with first study published in 1999 and the most current published in 2017 (*Table 1*). The FCR analysis included 15 studies containing 59 comparisons and 4874 birds conducted in 10 study countries drawn from 3 study continents (*Table 1*), while 13 studies comprising 49 comparisons and 3930 birds were included for the assessment of the effect of yeast on BWG in broiler chickens (*Table 1*). Of the all articles used in the meta-analysis to evaluate the effect of yeast on production indices of broiler chickens, the oldest study was published in 1999 and the most recent published in 2017. Most of the studies used Ross followed with Arbor acres. Yeast was added via the feed in the present meta-analysis.

Table 1. *Studies used to evaluate the effect of yeast-based diets on FC (g/bird), FCR and BWG (g/bird) of broiler chickens*

Study	Year	Sources of variation					NOB	Outcomes
		Study country	Study continent	SL (g/kg)	Broiler breeds	DS (d)		
Oyedeji et al.	2008	Nigeria	Africa	0, 0.2	Ross	28	80	FC, FCR, BWG
Al Mansour et al.	2011	Saudi Arabia	Asia	0, 1	Ross	21	120	FC, FCR
Al Mansour et al.	2011	Saudi Arabia	Asia	0, 1.25	Ross	21	120	FC, FCR
Al Mansour et al.	2011	Saudi Arabia	Asia	0, 1.5	Ross	21	120	FC, FCR, BWG
Al Mansour et al.	2011	Saudi Arabia	Asia	0, 1	Ross	42	120	FC, FCR
Al Mansour et al.	2011	Saudi Arabia	Asia	0, 1.25	Ross	42	120	FC, FCR
Al Mansour et al.	2011	Saudi Arabia	Asia	0, 1.5	Ross	42	120	FC, FCR
Njeru	2013	Kenya	Africa	0, 1.25	Arbor Acres	21	80	FC, FCR, BWG
Njeru	2013	Kenya	Africa	0, 0.63	Arbor Acres	42	80	FC, FCR, BWG

http://www.aloki.hu ● ISSN 1589 1623 (Print) ● ISSN 1785 0037 (Online)
DOI: http://dx.doi.org/10.15666/aeer/1802_28232843

El Fatah	1999	Sudan	Africa	0, 25	Ross	42	60	FC, FCR, BWG
El Fatah	1999	Sudan	Africa	0, 50	Ross	42	60	FC, FCR, BWG
El Fatah	1999	Sudan	Africa	0, 75	Ross	42	60	BWG
El Fatah	1999	Sudan	Africa	0, 100	Ross	42	60	FC, FCR, BWG
Mohamed et al.	2015	Sudan	Africa	0, 10	Hubbard	21	80	FC, FCR, BWG
Mohamed et al.	2015	Sudan	Africa	0, 20	Hubbard	21	80	FC, FCR, BWG
Mohamed et al.	2015	Sudan	Africa	0, 30	Hubbard	21	80	FC, FCR, BWG
Mohamed et al.	2015	Sudan	Africa	0, 10	Hubbard	42	80	FC, FCR, BWG
Mohamed et al.	2015	Sudan	Africa	0, 20	Hubbard	42	80	FC, FCR, BWG
Mohamed et al.	2015	Sudan	Africa	0, 30	Hubbard	42	80	FC, FCR, BWG
Chen et al.	2017	Taiwan	Asia	0, 2.5	Arbor Acres	21	120	FC, BWG
Chen et al.	2017	Taiwan	Asia	0, 2.5	Arbor Acres	35	120	FC, FCR, BWG
Aluwong et al.	2012	Nigeria	Africa	0, 15	Marshall	42	100	FC, FCR
Aluwong et al.	2012	Nigeria	Africa	0, 20	Marshall	42	100	FC, FCR
Osman	2006	Sudan	Africa	0, 0.2	Lohman	28	100	FC, FCR, BWG
Osman	2006	Sudan	Africa	0, 0.4	Lohman	28	100	FC, FCR, BWG
Osman	2006	Sudan	Africa	0, 0.6	Lohman	28	100	FC, FCR, BWG
Shareef and Al-Dabbagh	2009	Iraq	Asia	0, 5	Faobrow CD	21	40	FC, FCR, BWG
Shareef and Al-Dabbagh	2009	Iraq	Asia	0, 10	Faobrow CD	21	40	FC, FCR, BWG
Shareef and Al-Dabbagh	2009	Iraq	Asia	0, 15	Faobrow CD	21	40	FC, FCR, BWG
Shareef and Al-Dabbagh	2009	Iraq	Asia	0, 20	Faobrow CD	21	40	FC, FCR, BWG
Chand et al.	2014	Pakistan	Asia	0, 3.5	Hubbard	35	60	FC, FCR
Chand et al.	2014	Pakistan	Asia	0, 7	Hubbard	35	60	FC, FCR
Chand et al.	2014	Pakistan	Asia	0, 10.5	Hubbard	35	60	FC, FCR
Manal	2012	Egypt	Africa	0, 3	Arbor Acres	21	60	FC, FCR, BWG
Manal	2012	Egypt	Africa	0, 5	Arbor Acres	21	60	FC, FCR, BWG
Manal	2012	Egypt	Africa	0, 7	Arbor Acres	21	60	FC, FCR, BWG
Manal	2012	Egypt	Africa	0, 3	Arbor Acres	42	60	FC, FCR, BWG
Manal	2012	Egypt	Africa	0, 5	Arbor Acres	42	60	FC, FCR, BWG
Manal	2012	Egypt	Africa	0, 7	Arbor Acres	42	60	FC, FCR, BWG
Buba et al.	2016	Nigeria	Africa	0, 5	White Rose	28	102	FC, FCR, BWG
Buba et al.	2016	Nigeria	Africa	0, 10	White Rose	28	102	FC, FCR, BWG
Buba et al.	2016	Nigeria	Africa	0, 15	White Rose	28	102	FC, FCR, BWG
Buba et al.	2016	Nigeria	Africa	0, 20	White Rose	28	102	FC, FCR, BWG
Buba et al.	2016	Nigeria	Africa	0, 5	White Rose	56	102	FC, FCR, BWG
Buba et al.	2016	Nigeria	Africa	0, 10	White Rose	56	102	FC, FCR
Buba et al.	2016	Nigeria	Africa	0, 15	White Rose	56	102	FC, FCR, BWG
Buba et al.	2016	Nigeria	Africa	0, 20	White Rose	56	102	FC, FCR, BWG
Atul Shankar et al.	2017	India	Asia	0, 1	Cobb	42	144	FC, FCR, BWG
Atul Shankar et al.	2017	India	Asia	0, 1.5	Cobb	42	144	FC, FCR, BWG
Atul Shankar et al.	2017	India	Asia	0, 2	Cobb	42	144	FC, FCR, BWG
Yalçin et al.	2013	Turkey	Europe	0, 1	Ross	21	70	FC, FCR, BWG
Yalçin et al.	2013	Turkey	Europe	0, 2	Ross	21	70	FC, FCR, BWG
Yalçin et al.	2013	Turkey	Europe	0, 3	Ross	21	70	FC, FCR, BWG
Yalçin et al.	2013	Turkey	Europe	0, 4	Ross	21	70	FC, FCR, BWG
Yalçin et al.	2013	Turkey	Europe	0, 1	Ross	42	70	FC, FCR, BWG
Yalçin et al.	2013	Turkey	Europe	0, 2	Ross	42	70	FC, FCR, BWG
Yalçin et al.	2013	Turkey	Europe	0, 3	Ross	42	70	FC, FCR, BWG
Yalçin et al.	2013	Turkey	Europe	0, 4	Ross	42	70	FC, FCR, BWG
Mohamed et al.	2016	Sudan	Africa	0, 2.5	Ross	42	42	FC, FCR, BWG
Mohamed et al.	2016	Sudan	Africa	0, 5	Ross	42	42	FC, FCR, BWG
Mohamed et al.	2016	Sudan	Africa	0, 10	Ross	42	42	FC, FCR
Priya and Buba	2013	India	Asia	0, 5	Ross	36	100	FC
Priya and Buba	2013	India	Asia	0, 10	Ross	36	100	FC

DS – duration of supplementation; SL – supplementation level; NOB – number of birds

http://www.aloki.hu ● ISSN 1589 1623 (Print) ● ISSN 1785 0037 (Online)
DOI: http://dx.doi.org/10.15666/aeer/1802_28232843

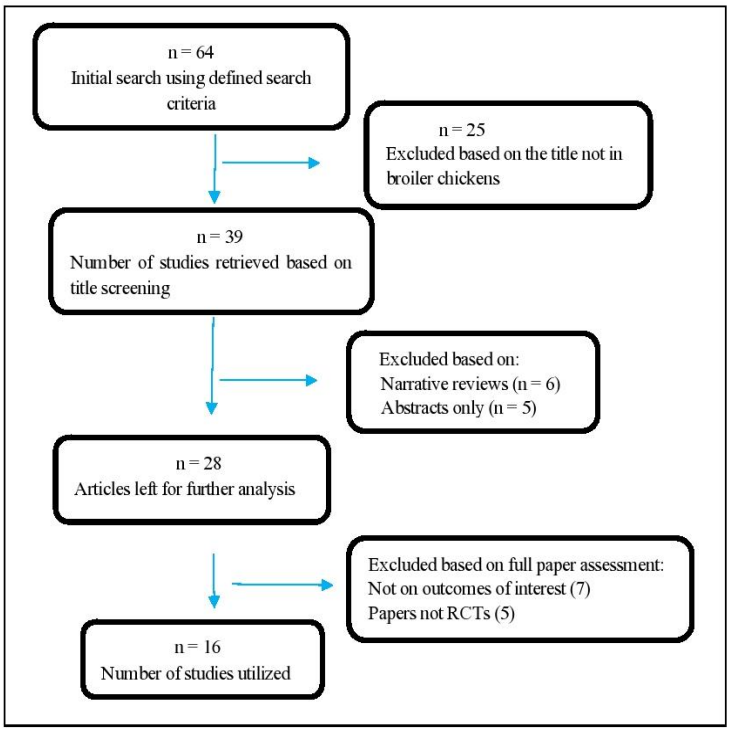

Figure 1. *Flow chart of articles used for the meta-analysis*

Feed consumption (FC)

The results of the overall effects estimate of yeast supplementation revealed that the incorporation of yeast in broiler diets reduced FC relative to broilers on control diet (d = -0.429, 95% CI: -0.606 to -0.253, I^2 = 89.59%, p < 0.001; *Fig. 2*). The temporal trends of the outcome of yeast supplementation on FC of broiler chickens are presented in *Figure 3*. The results of stratified subgroup analysis of the relationship between modifier variables and FC in broiler chickens are presented in *Table 2*. When the analysis was disaggregated, the results of the grand mean indicated that FC was significantly influenced by the explanatory variables (study continent, study country, duration of supplementation, supplementation level, broiler breed used; p < 0.001) following the removal of subgroup with one or two effect sizes. Disaggregation based on study continent, revealed that FC was not significantly reduced for studies performed in Africa, whereas studies conducted in Asia (p < 0.001) and Europe (p < 0.001) had significantly reduced FC. Results of the disaggregated studies of the effect of yeast on FC in broiler chickens based on study country showed that studies conducted in Pakistan, Egypt, India and Turkey were significantly different from zero (p < 0.001). Broiler chickens fed diet supplemented with yeast at < 10 g/kg feed had significantly reduced FC (p < 0.001). However, there was no association between FC and supplementation level (> 10 g/kg feed, p = 0.054;10 g/kg feed, p = 0.113, respectively). Stratified subgroup analysis results showed that FC was significantly reduced in broiler chickens fed yeast supplemented diet for 21 days (p = 0.001), 35 days (p = 0.038) and 42 days (p < 0.001), while FC in studies where broiler chickens were placed on yeast supplemented diets for 28 days (p = 0.340) and 56 days (p = 0.665) were not significant. Ross (p < 0.001), Arbor acres (p < 0.001) and Cobb (p < 0.001) had significantly decreased FC, whilst other breeds were not significant (p > 0.05).

http://www.aloki.hu ● ISSN 1589 1623 (Print) ● ISSN 1785 0037 (Online)
DOI: http://dx.doi.org/10.15666/aeer/1802_28232843

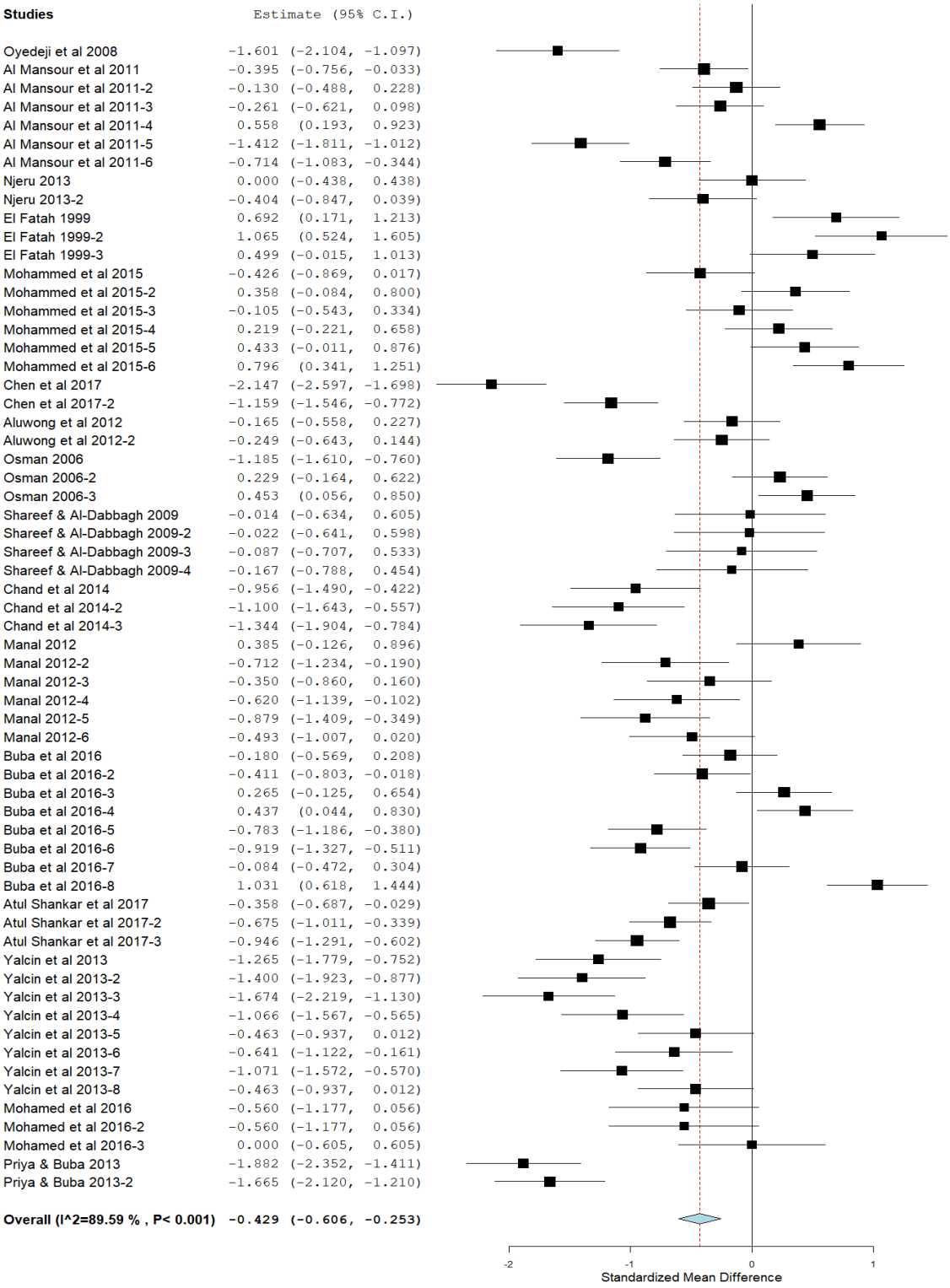

Figure 2. *Forest plot of the effect of yeast supplementation on feed consumption in broiler chickens. The points to the right of the no effect line shows an increase in the outcome of interest, and the opposite depicts the reverse. The effect size is represented by individual square in the forest plot, while the upper and lower 95% CI for the effect size are the line that joined the square*

http://www.aloki.hu ● ISSN 1589 1623 (Print) ● ISSN 1785 0037 (Online)
DOI: http://dx.doi.org/10.15666/aeer/1802_28232843

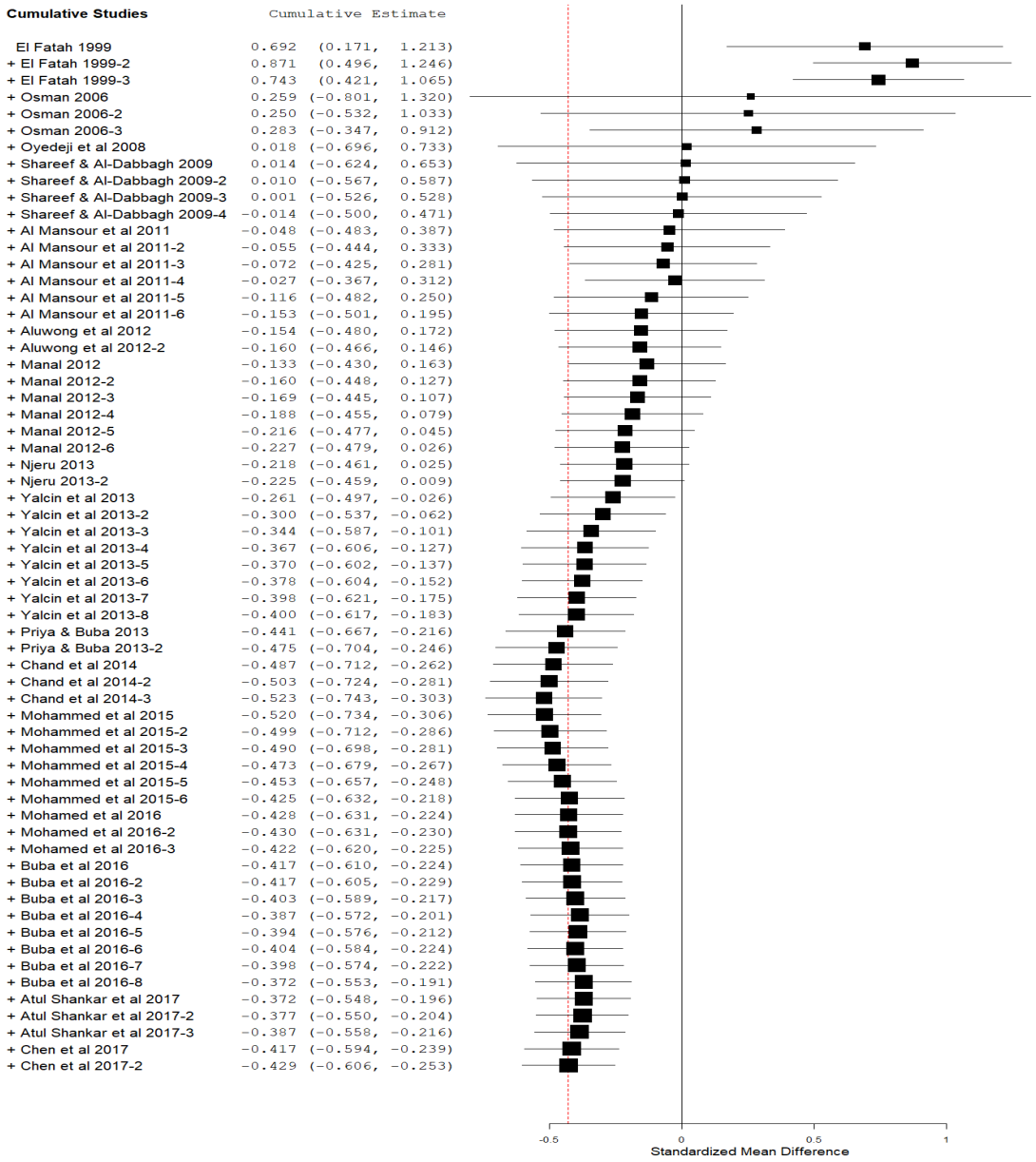

Figure 3. *Trends of FC in broilers fed yeast supplemented diets*

Feed conversion ratio (FCR)

The results of pooled effects estimation found a positive association between yeast supplementation and FCR in broiler chickens (d = -0.354, 95% CI: -0.517 to -0.190, I^2 = 87.27%, p < 0.001; *Fig. 4*). The temporal trends on the effect patterns of yeast supplementation on FCR in broiler chickens are shown in *Figure 5*. The results of the stratified analysis found an association between modifier variables and FCR in broiler chickens on yeast diet as presented in *Table 3*. Results of the stratified subgroup analysis revealed that FCR was positively influenced by the explanatory variables (study continent, p < 0.001; study country, p < 0.0001; duration of supplementation, p < 0.001; supplementation level, p < 0.001; broiler breed used, p < 0.001) when subgroup with one or two effect size(s) were removed from the analysis. Birds from

http://www.aloki.hu ● ISSN 1589 1623 (Print) ● ISSN 1785 0037 (Online)
DOI: http://dx.doi.org/10.15666/aeer/1802_28232843

studies undertaken in Europe ($p < 0.001$) and Asia ($p < 0.001$) had superior FCR compared to chickens from studies performed in Africa ($p = 0.296$). Stratified analysis results indicate that the FCR for studies performed in Pakistan, Egypt, Indian and Turkey differed significantly ($p < 0.001$). There was a correlation between FCR and duration of supplementation (21 days, $p = 0.002$; 35 days, $p < 0.001$; 42 days, $p = 0.038$), whereas no correlation exists between the FCR and the duration of supplementation (28 days, $p = 0.340$; 56 days, $p = 0.665$). Broiler chickens fed yeast supplemented diet at a level of > 10 g/kg feed ($p = 0.111$) and 10 g/kg feed ($p = 0.113$) had poor FCR, whilst those that received yeast supplemented diet at a level of < 10 g/kg feed ($p < 0.001$) had improved FCR. Ross ($p = 0.001$), Arbor acres ($p = 0.003$) and Cobb ($p < 0.001$) had significantly improved FCR relative to Hubbard ($p = 0.354$), Lohman ($p = 0.742$), Faobrow CD ($p = 0.648$) and White Rose ($p = 0.718$).

Table 2. *Relationship between moderators and FC in broiler chickens on yeast-based diets*

Subgroups	n	*d*	95% CI)	I^2 (%)	*p*-value
Study continent	62	-0.429	-0.606 to -0.253	88.59	< 0.001
Africa	34	-0.109	-0.313 to 0.095	85.61	0.296
Asia	20	-0.747	-1.052 to -0.443	90.14	< 0.001
Europe	8	-0.993	-1.301 to -0.685	66.94	< 0.001
Study country	58	-0.394	-0.571 to -0.217	88.80	< 0.001
Nigeria	11	-0.235	-0.662 to 0.152	90.09	0.233
Saudi Arabia	6	-0.389	-0.894 to 0.116	91.12	0.131
Sudan	15	0.131	-0.172 to 0.434	83.64	0.395
Iraq	4	-0.072	-0.382 to 0.238	0.00	0.648
Pakistan	3	-1.127	-1.442 to -0.812	0.00	< 0.001
Egypt	6	-0.442	-0.800 to -0.084	65.12	< 0.001
India	5	-1.086	-1.618 to -0.554	89.88	< 0.001
Turkey	8	-0.993	-1.301 to -0.685	88.80	< 0.001
DS (days)	60	-0.384	-0.555 to -0.213	88.25	< 0.001
21	19	-0.499	-0.808 to -0.191	87.41	< 0.001
28	8	-0.239	-0.731 to 0.253	91.43	0.340
35	4	-1.140	-1.384 to -0.896	0.00	0.038
42	25	-0.260	-0.506 to -0.015	86.78	< 0.001
56	4	-0.189	-1.047 to 0.669	94.49	0.665
SL (g/kg feed)	62	-0.429	-0.606 to -0.253	89.59	< 0.001
< 10	39	-0.684	-0.882 to -0.485	87.17	< 0.001
> 10	16	0.218	-0.051 to 0.487	81.94	0.054
10	7	-0.473	-0.955 to 0.008	86.56	0.113
Broiler breed used	60	-0.437	-0.620 to -0.254	89.90	< 0.001
Ross	23	-0.626	-0.952 to -0.300	91.20	< 0.001
Arbor Acres	10	-0.642	-1.084 to -0.201	83.32	< 0.001
Hubbard	9	-0.221	-0.689 to -0.246	88.63	0.354
Lohman	3	-0.165	-1.144 to -0.815	94.31	0.742
Faobrow CD	4	-0.072	-0.382 to 0.238	0.00	0.648
White Rose	8	-0.081	-0.519 to 0.358	89.76	0.718
Cobb	3	-0.657	-0.990 to -0.323	66.02	< 0.001

n – number of effect sizes; d – Hedges' d, CI – confidence interval, I^2 – heterogeneity

http://www.aloki.hu ● ISSN 1589 1623 (Print) ● ISSN 1785 0037 (Online)
DOI: http://dx.doi.org/10.15666/aeer/1802_28232843

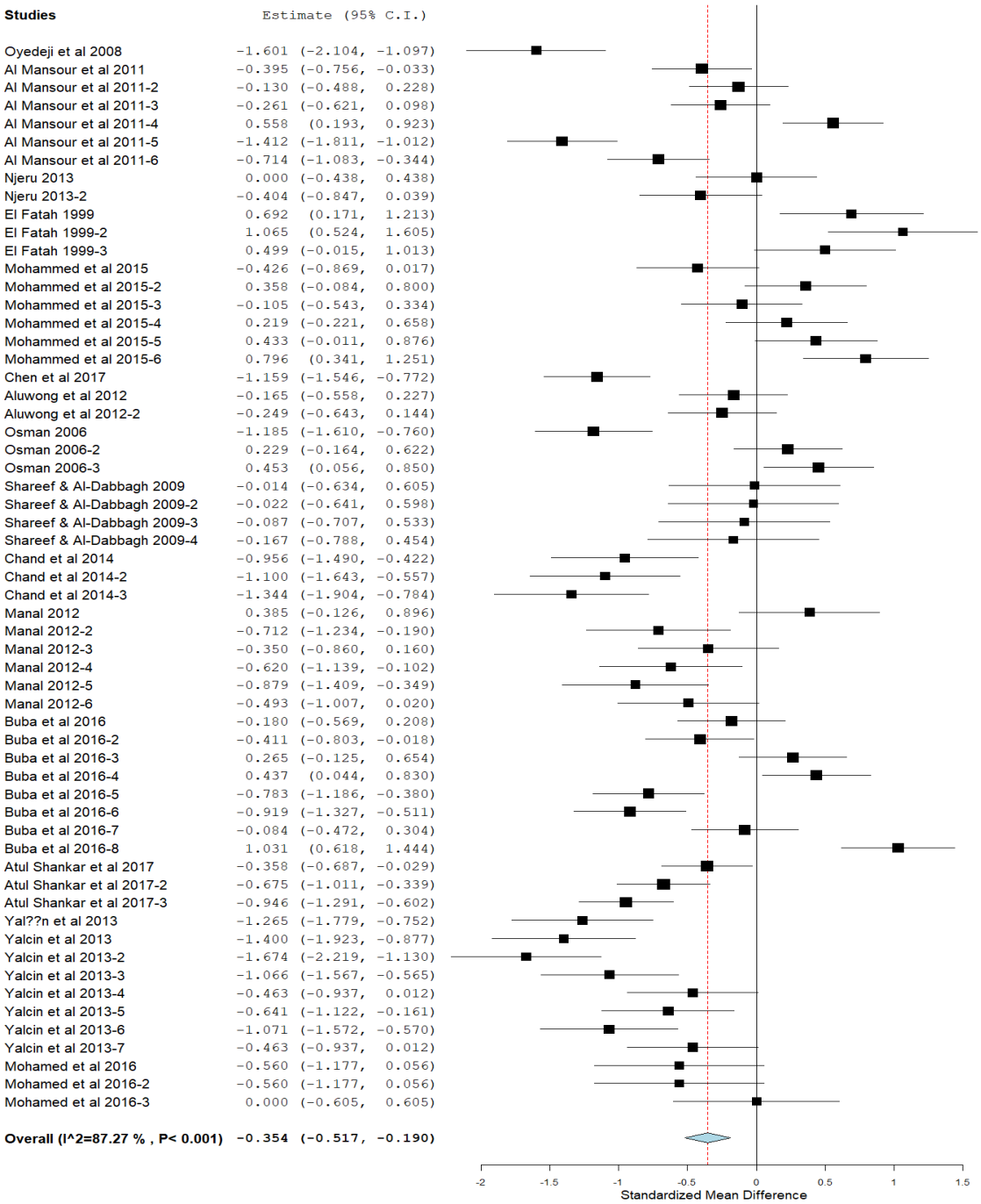

Figure 4. *Effect of probiotic-yeast supplementation on FCR of broiler chickens*

Body weight gain (BWG)

BWG was statistically increased from zero ($d = 0.310$, 95% CI: 0.130 to 0.491, $I^2 = 87.13\%$, $p < 0.001$; *Fig. 6*). The impact of yeast on BWG in broiler chickens in chronological order are shown in *Figure 7*. The results of the stratified subgroup analysis of the association between the explanatory variables and the BWG in broiler chickens are presented in *Table 4*. The mean effects estimate for the meta-analysis were 0.310, 0.325, 0.329, 0.310 and 0.310 for study continent ($p < 0.001$), study

http://www.aloki.hu ● ISSN 1589 1623 (Print) ● ISSN 1785 0037 (Online)
DOI: http://dx.doi.org/10.15666/aeer/1802_28232843

country (p = 0.001), duration of supplementation (p < 0.001), supplementation level (p < 0.001) and broiler breed used (p < 0.001), respectively, when the analysis was stratified. When the BWG analysis was disaggregated by study continent, studies conducted in Asia (p < 0.001) and Europe (p < 0.001) had improved BWG compared to those conducted in Africa. The results of BWG disaggregated by study country revealed that studies conducted in Iraq (p = 0.015), India (p = 0.019) and Turkey (p < 0.001) had statistically increased BWG following the removal of studies conducted in Saudi Arabia, Kenya and Taiwan that had less than 3 effect sizes. Studies conducted in Egypt, Sudan and Nigeria had similar values (Egypt: p = 0.556, Sudan: p = 0.728, Nigeria: p = 0.172). Broiler chickens from experiments that received yeast supplemented diets for 21 days (p < 0.001) had increased BWG, while those that received yeast supplemented diets for 42 days (p = 0.125) and 56 days (p = 0.983) were not significant. Studies that fed yeast for 35 days were removed from the analysis because they had less than 3 effect sizes. There was a significant positive association between BWG, and yeast supplementation level (< 10 g/kg feed, p < 0.001), whereas there was no significant association between BWG, and supplementation level (10 g/kg feed, p = 0.135; > 10 g/kg feed, p = 0.349). When BWG was disaggregated by breed of broiler used, Ross (p = 0.001), Faobrow CD (p = 0.015) and Cobb (p < 0.019) had significantly improved BWG.

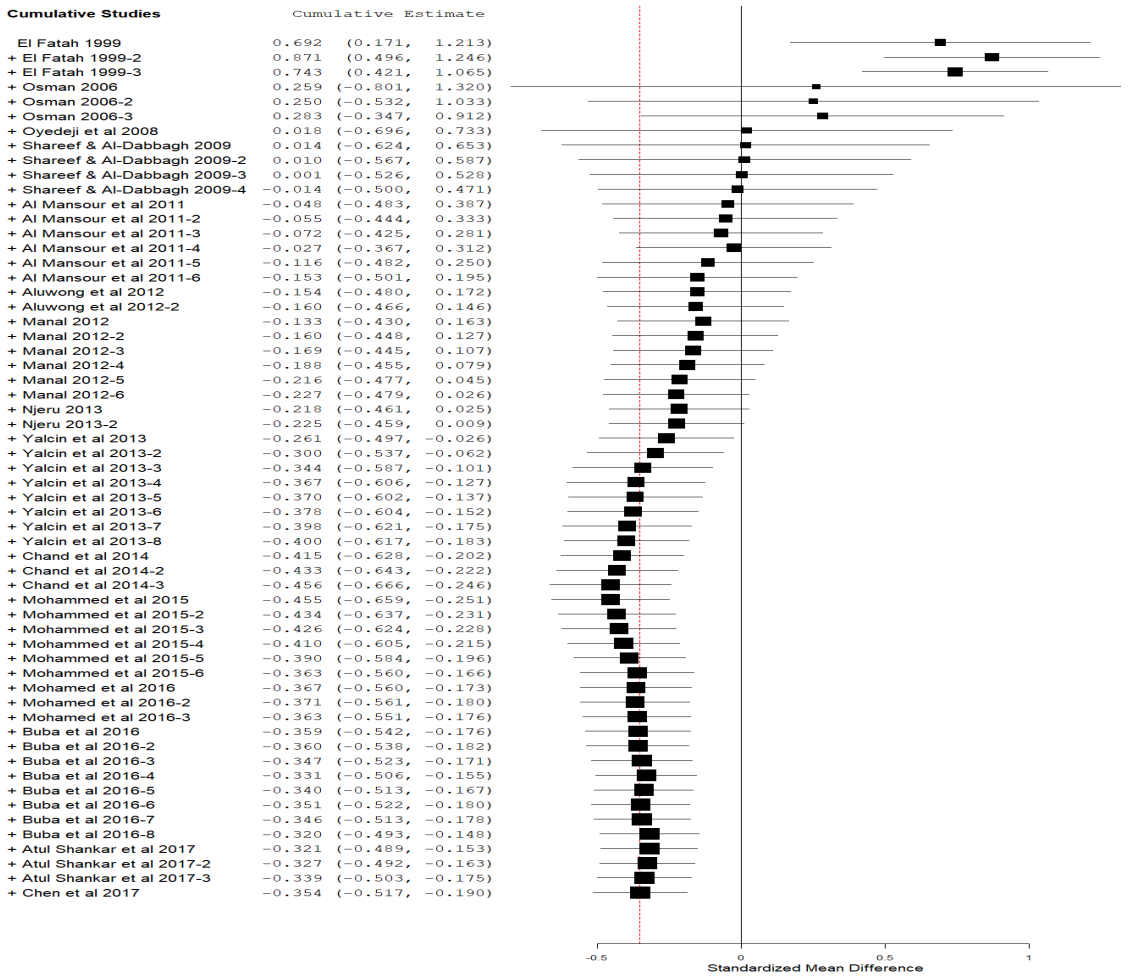

Figure 5. *Trends of FCR in broilers fed yeast supplemented diets*

http://www.aloki.hu ● ISSN 1589 1623 (Print) ● ISSN 1785 0037 (Online)
DOI: http://dx.doi.org/10.15666/aeer/1802_28232843

Table 3. *Association between moderators and FCR in broilers on yeast-based diets*

Subgroups	n	*d*	95% CI)	I^2 (%)	*p*-value
Study continent	59	-0.354	-0.517 to -0.190	87.27	< 0.001
Africa	34	-0.109	-0.313 to 0.095	85.61	0.296
Asia	17	-0.545	-0.806 to -0.285	84.32	< 0.001
Europe	8	-0.993	-1.301 to -0.685	66.94	< 0.001
Study country	56	-0.344	-0.513 to -0.175	87.37	< 0.001
Nigeria	11	-0.235	-0.662 to 0.152	90.09	0.233
Saudi Arabia	6	-0.389	-0.894 to 0.116	91.12	0.131
Sudan	15	0.131	-0.172 to 0.434	83.64	0.395
Iraq	4	-0.072	-0.382 to 0.238	0.00	0.648
Pakistan	3	-1.127	-1.442 to -0.812	0.00	< 0.001
Egypt	6	-0.442	-0.800 to -0.084	65.12	< 0.015
India	3	-0.657	-0.990 to -0.323	66.02	< 0.001
Turkey	8	-0.993	-1.301 to -0.685	88.80	< 0.001
DYS (days)	59	-0.354	-0.517 to -0.190	88.27	< 0.001
21	18	-0.404	-0.659 to -0.149	80.36	0.002
28	8	-0.239	-0.731 to 0.253	91.43	0.340
35	4	-1.140	-1.384 to -0.896	0.00	< 0.001
42	25	-0.260	-0.506 to -0.015	86.78	0.038
56	4	-0.189	-1.047 to 0.669	94.49	0.665
YSL (g/kg feed)	59	-0.354	-0.517 to -0.190	87.27	< 0.001
< 10	37	-0.610	-0.791 to -0.429	83.78	< 0.001
> 10	16	0.218	-0.051 to 0.487	81.94	0.111
10	6	-0.284	-0.633 to 0.065	69.57	0.113
Breeds of broiler used	57	-0.359	-0.529 to -0.189	87.68	< 0.001
Ross	21	-0.516	-0.833 to -0.199	89.77	0.01
Arbor Acres	9	-0.474	-0.790 to -0.159	74.20	0.003
Hubbard	9	-0.221	-0.689 to -0.246	88.63	0.354
Lohman	3	-0.165	-1.144 to -0.815	94.31	0.742
Faobrow CD	4	-0.072	-0.382 to 0.238	0.00	0.648
White Rose	8	-0.081	-0.519 to 0.358	89.76	0.718
Cobb	3	-0.657	-0.990 to -0.323	66.02	< 0.001

Analysis of heterogeneity and moderators

Data in *Table 5* presents the mixed effects meta-regression of the impact of yeast supplementation in broiler chicken performance. Forest plots of the 16 studies comprising 62 comparisons that evaluated the effect of yeast on FC in broilers provided evidence of significant heterogeneity (I^2-statistic = 89.59%, 95% CI: -0.606 to -0.253, $p < 0.001$, *Fig. 2*) and sensitivity analysis was not able to resolve the problem heterogeneity. Subgroup analysis did not remove the challenges of large heterogeneity among the studies included in the meta-analysis. Thus, the substantial heterogeneity continues, suggesting that these analyses cannot fix the problem of heterogeneity. Meta-regression, revealed that study continent ($Q_B = 19.9$, degree of freedom, $df = 2$, $p < 0.001$), study country ($Q_B = 44.87$, $df = 9$, $p < 0.001$), duration of supplementation

http://www.aloki.hu ● ISSN 1589 1623 (Print) ● ISSN 1785 0037 (Online)
DOI: http://dx.doi.org/10.15666/aeer/1802_28232843

(Q_B = 15.5, df = 5, p = 0.0084) and supplementation level (Q_B = 23.8, df = 2, p < 0.001) accounted for most the heterogeneity. Heterogeneity existed amongst the articles utilized in the analysis (FCR; I^2 = 87.27%, 95% CI: -0.517 to -0.190, p < 0.001, *Fig. 4* and BWG; I^2 = 87.13%, 95% CI: 0.130 to 0.491, p < 0.001, *Fig. 6*). Mixed effect meta-regression analysis revealed that study continent and yeast supplementation level were predictors of the study effect observed on FCR, whereas study continent, study country, supplementation level and broiler breed were predictors of study effects noticed on BWG results.

Table 4. *Relationship between moderators and BWG in broilers on yeast-based diets*

Subgroups	n	*d*	95% CI)	I^2 (%)	*p*-value
Study continent	49	0.310	0.133 to 0.487	86.51	< 0.001
Africa	31	0.167	-0.067 to 0.401	87.63	0.163
Asia	10	0.335	0.054 to 0.615	77.12	0.019
Europe	8	0.838	0.512 to 1.164	71.35	< 0.001
Study country	44	0.325	0.130 to 0.520	71.35	0.001
Nigeria	8	0.307	-0.314 to 0.748	89.49	0.172
Sudan	15	0.068	-0.315 to 0.451	89.76	0.728
Iraq	4	0.389	0.075 to 0.703	0.00	0.015
Egypt	6	0.147	-0.343 to 0.637	81.49	0.556
India	3	0.549	0.089 to 1.009	82.33	< 0.019
Turkey	8	0.838	0.512 to 1.164	71.35	< 0.001
DS (days)	48	0.329	0.147 to 0.510	86.36	< 0.001
21	17	0.555	0.243 to 0.867	83.62	0.003
28	8	0.322	-0.176 to 0.819	91.58	0.205
42	20	0.208	-0.058 to 0.473	84.73	0.125
56	3	-0.007	-0.673 to 0.658	88.34	0.983
SL (g/kg feed)	49	0.310	0.133 to 0.487	86.51	< 0.001
< 10	31	0.470	0.271 to -0.669	83.72	< 0.001
> 10	14	-0.134	-0.413 to 0.146	80.11	0.349
10	4	0.573	-0.179 to 1.325	89.79	0.135
Broiler breed used	49	0.310	0.133 to 0.487	86.51	< 0.001
Ross	16	0.651	0.342 to 0.960	83.53	0.001
Arbor Acres	10	0.145	-0.174 to 0.464	79.08	0.374
Hubbard	6	-0.173	-0.758 to 0.412	90.07	0.563
Lohman	3	0.027	-0.933 to 0.988	94.11	0.956
Faobrow CD	4	0.389	0.075 to 0.703	0.00	0.015
White Rose	7	0.182	-0.249 to 0.612	87.93	0.408
Cobb	3	0.549	0.089 to 1.009	88.51	0.019

Analysis of publication bias

The results of the funnel plot of the impact of yeast supplementation on the productivity of broiler chickens as shown in *Figure 8A-C* revealed that the plots were asymmetrical. However, the Rosenberg fail-safe number of 3138 (FC), 1913 (FCR) and 964 (BWG) which is more than 9, 6 and 4-folds, respectively above the threshold of 320

http://www.aloki.hu ● ISSN 1589 1623 (Print) ● ISSN 1785 0037 (Online)
DOI: http://dx.doi.org/10.15666/aeer/1802_28232843

(5 × 62 + 10), 305 (5 × 59 + 10) and 255 (5 × 49 + 10) is required to declare the mean effect size robust. Consequently, the existence of publication bias was not a problem in this study as comparatively large number of unpublished studies would be needed to alter the statistically significant effects.

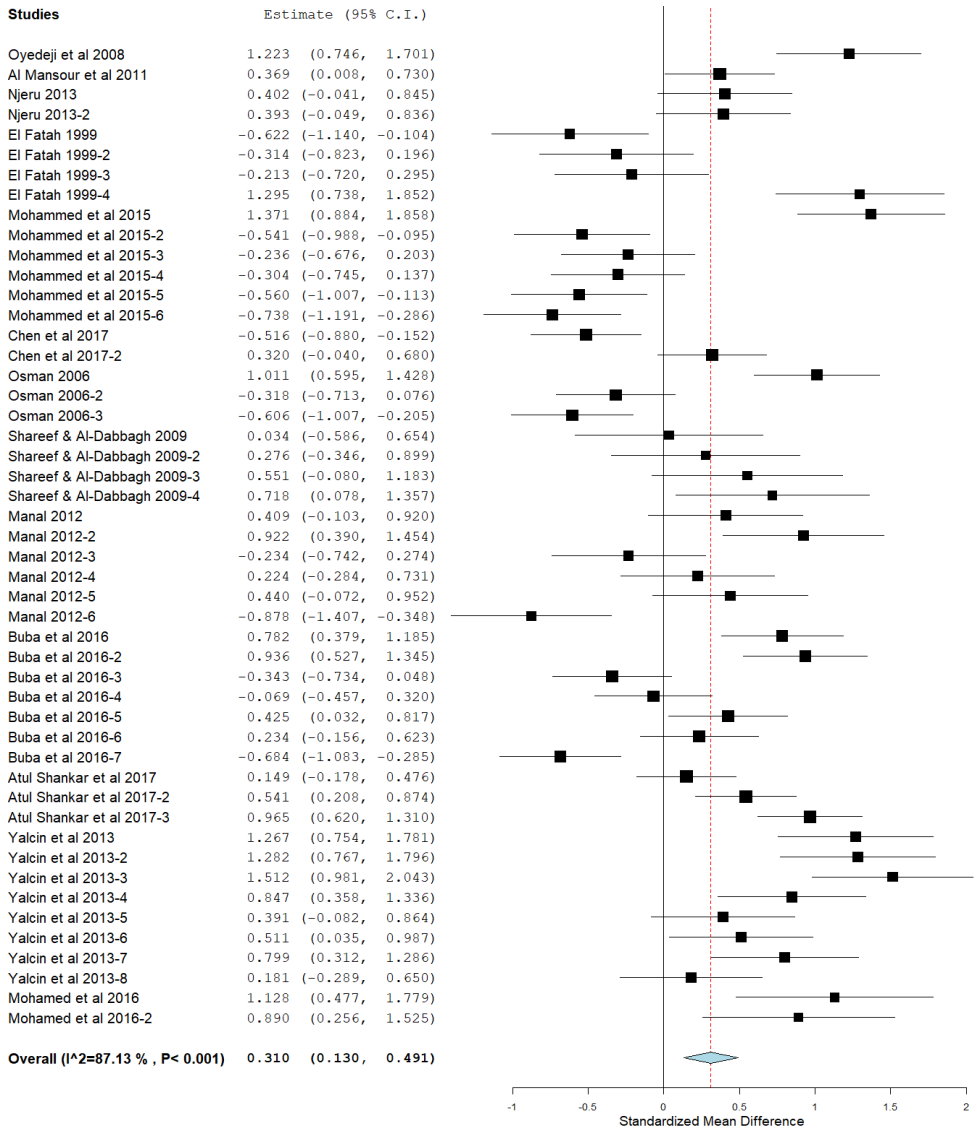

Figure 6. *Forest plot of the effects probiotic (yeast) supplementation on BWG of broiler chickens*

Discussion

Probiotic effect

In the last couple of years, the incorporation of small amounts of yeast in animal feed as a growth enhancing agent instead of antibiotics has received considerable attention (Ahmed et al., 2015; Gao et al., 2017; Ogbuewu et al., 2019). Basically, yeast is rich in essential nutrients and contains mannan oligosaccharides (MOS) that helps in the multiplication of beneficial microbes in the guts of broilers (Spring et al., 2000). The findings from the present meta-analysis of 16 RCTs representing 10 study countries

http://www.aloki.hu ● ISSN 1589 1623 (Print) ● ISSN 1785 0037 (Online)
DOI: http://dx.doi.org/10.15666/aeer/1802_28232843

drawn from three study continents indicated that broilers fed yeast supplemented diets had improved productive indices. This finding is consistent with the previous results of Hooge (2004) and Frizzo et al. (2011) who reported that probiotic (lactic acid bacteria) and actigen® (second-generation, yeast (*Saccharomyces cerevisiae* var. *boulardii*) cell wall product) supplementation improved BWG and FCR in broilers and calves, respectively. The enhanced FC, FCR and BWG recorded in the current meta-analysis could be partly ascribed to the direct nutritional effect of yeast that has been documented to increase productivity in broiler chickens (Hooge, 2004; Yalcin et al., 2013; Mohamed et al., 2016) and in calves (Frizzo et al., 2011). In addition, yeast has been recorded to improve the multiplication of helpful microbes in the intestines of chickens (Schneitz, 2005; Awad et al., 2006; Apata, 2008; Musa et al., 2009). It has also been documented that yeast activates the innate immune response of broilers (Haghighi et al., 2006; Apata, 2008; Musa et al., 2009); stimulates digestive enzyme production and activity (Yoon et al., 2004); and competes with pathogens for adhesion sites in the gut, thus preventing their multiplication in the intestine (Choudhari et al., 2008). The enhanced feed efficiency and the resultant increase in body weight gain is the ultimate result of probiotic intervention as reported by Bozkurt et al. (2009) in male broiler chickens fed MOS.

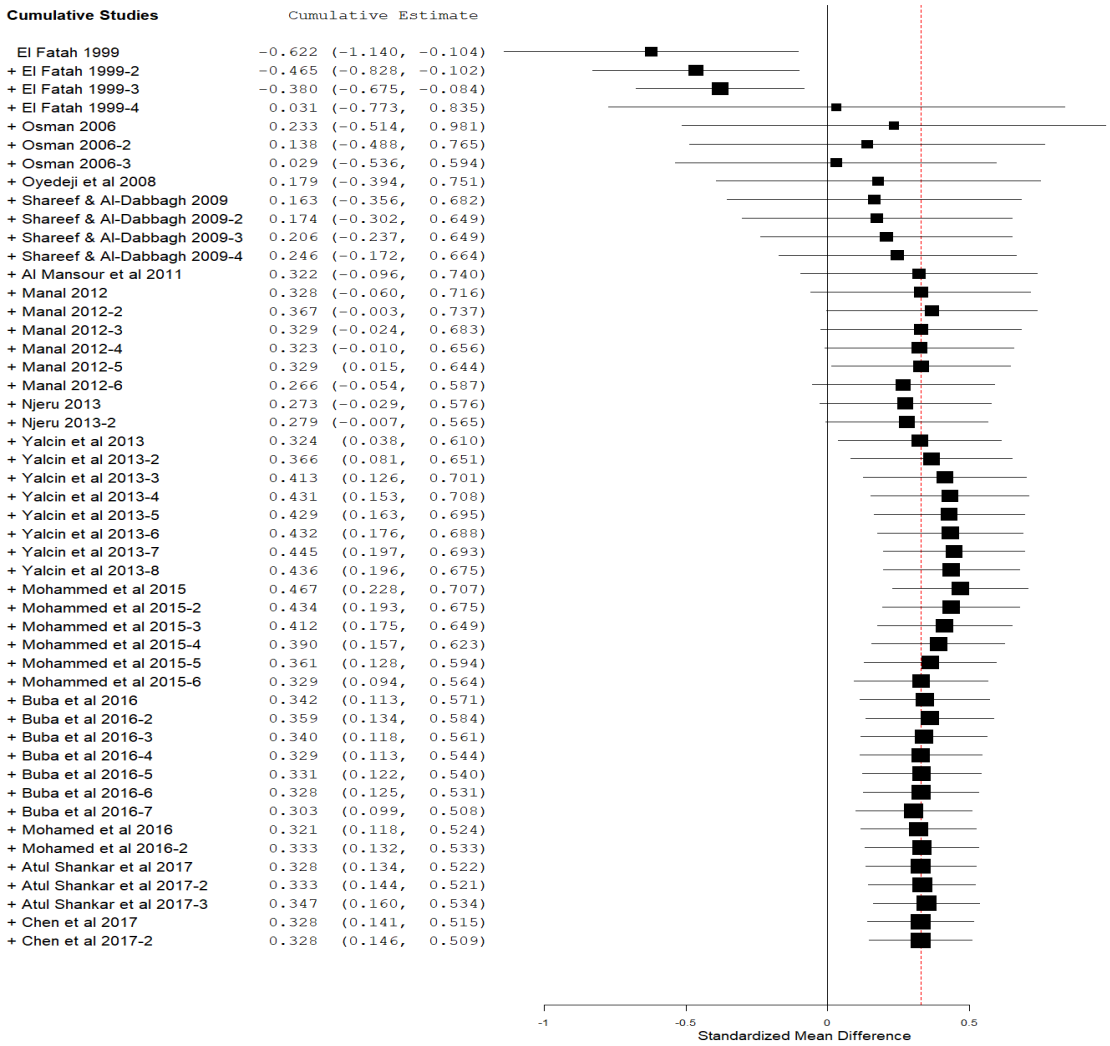

Figure 7. *Trends of BWG in broilers fed yeast supplemented diets*

http://www.aloki.hu ● ISSN 1589 1623 (Print) ● ISSN 1785 0037 (Online)
DOI: http://dx.doi.org/10.15666/aeer/1802_28232843

Table 5. *Summary of the random weighted meta-analysis for the explanatory variables that act as a modifier on the effects of yeast supplementation on productivity of broiler chickens*

Parameters	Moderators	QM	df	p-value	I^2 accounted
FC	Study continent	19.9	2	$p < 0.001$	25.61
	Study country	44.87	9	$p < 0.001$	41.20
	Duration of supplementation	15.5	5	$p = 0.0084$	16.42
	Supplementation level	23.8	2	$p < 0.001$	29.56
	Broiler breed used	7.04	7	$p = 0.425$	0.24
FCR	Study continent	7.80	2	$p = 0.0202$	12.63
	Study country	9.71	8	$p = 0.286$	4.24
	Duration of supplementation	2.41	4	$p = 0.66$	0.00
	Supplementation level	10.81	2	$p = 0.0045$	18.92
	Broiler breed used	10.8	6	$p = 0.094$	10.42
BWG	Study continent	7.76	2	$p = 0.021$	12.63
	Study country	9.71	8	$p = 0.286$	4.24
	Duration of supplementation	2.41	4	$p = 0.66$	0.00
	Supplementation level	10.8	2	$p = 0.0045$	18.92
	Broiler breed used	10.8	6	$p = 0.0944$	10.42

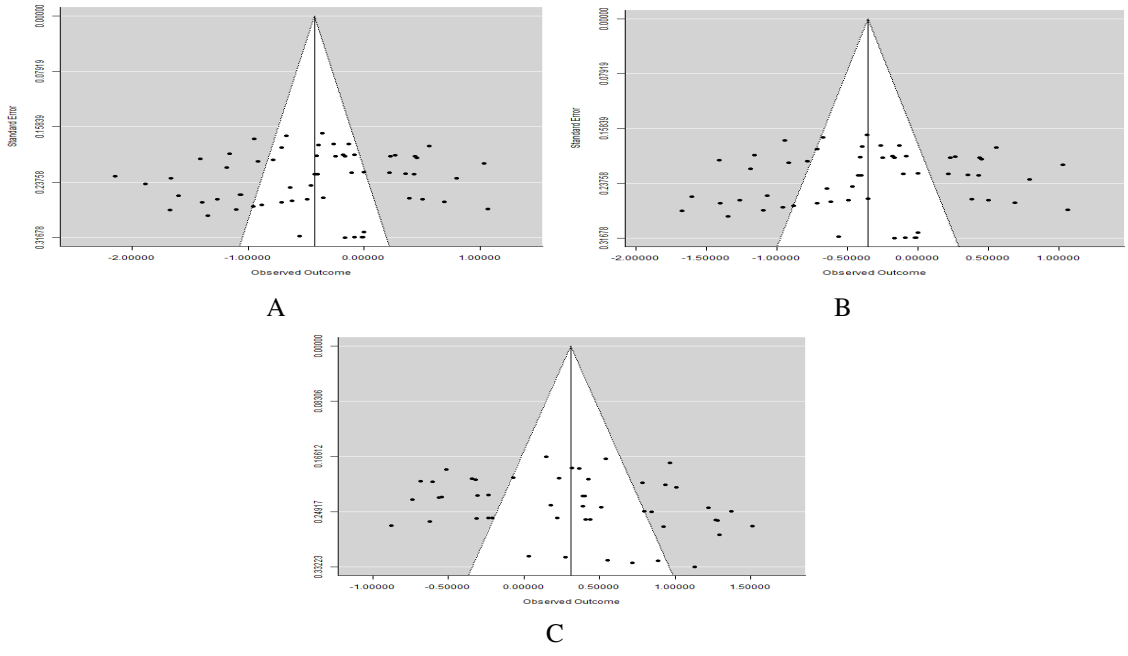

Figure 8. *Funnel plots of the effect of yeast on FC (A), FCR (B) and BWG (C) in broiler chickens*

Analysis of moderators

The current meta-analysis disclosed an important association between yeast supplementation in broilers and some elements of our selected explanatory variables. This revealed that the moderators chosen were responsible for the inconsistency of results reported in broiler chickens fed probiotic yeast supplemented diets. There is

http://www.aloki.hu ● ISSN 1589 1623 (Print) ● ISSN 1785 0037 (Online)
DOI: http://dx.doi.org/10.15666/aeer/1802_28232843

significant relationship between probiotic (yeast) supplementation and FC, FCR and BWG in broiler chickens for studies performed in Asian and Europe. However, studies undertaken in Europe found a bigger relationship (FC, $d = 0.993$; FCR, $d = 0.993$; BWG, $d = 0.838$) than those conducted in Asia. The effect of yeast on FC, FCR and BWG in broilers for studies conducted in Africa had no significant association. The observed disparity between the production indices of broiler chickens from studies undertaken in Africa and those performed in Europe and Asia can be partially attributed to differences in the environmental conditions of the three study continents. The environmental conditions hampering chicken performance and health include temperature, relative humidity, light and housing system (Elijah and Adedapo, 2006). Environmental temperatures have a negative impact on the survival and success of the broiler production. Broiler chickens are susceptible to environmental change because there is a narrow range of thermal conditions under which they can maintain a stable body temperature. However, no data was reported on the weather conditions of the study countries and continents as at the time the investigated was conducted. The failure of the authors of the study included in the meta-analysis to report the weather condition of the study region as at the time the study was carried out was the reason we could not identify the specific variables that might have been accountable for the differences in the productivity of broilers raised in Africa compared to those raised on the other two continents. The current meta-analysis also found that there was significant association effect of yeast on FC and FCR in broilers raised in Egypt, India, Pakistan, Iraq and turkey, whereas for BWG it was evident on studies undertaken in India, Iraq and Turkey. Yeast effect on FC and FCR was found in studies which lasted for 21, 35 and 42 days. However, there was no beneficial effect of yeast on studies that lasted 28 and 56 days. Enhancement in FC and FCR for studies that lasted for 21 days translates to an increase in body weight gain in broiler chickens. This indicate that study continent, study country, duration of supplementation are the limiting factors in several of the studies included in the meta-analysis. The level of yeast supplementation is a determinant in many studies and has led to differences in the outcomes reported by the various authors (Frizzo et al., 2011; Ezema and Ugwu, 2014). In this study, the beneficial activities of yeast on FC, FCR and BWG were shown in studies that fed diet supplemented with yeast at the rate of < 10 g/kg feed. The Ross and Cobb broiler type had enhanced FCR and BWG with less feed intake, whereas Arbor acre had enhanced FCR, which did not translate to increased body weight gain in the current meta-analysis.

Source of heterogeneity and publication bias

This meta-analysis included research conducted in several parts of the world. In this context, the generalization and validity of the conclusions reached are strong. Potential biases, however, such as publication bias and heterogeneity were evident in the present meta-analysis and this was anticipated as most of the studies were undertaken in 10 study countries drawn from 3 continents. Substantial heterogeneity was recorded, sensitivity and stratified analysis fail to fix the issue. Results of meta-regression analysis showed that explanatory variables (study continent, study country, duration of yeast supplementation, yeast supplementation level and breed of broiler used) accounted for most of the variations among the studies included in the meta-analysis. For FC, FCR and BWG, the Rosenberg Nfs is 3138, 964 and 1913 respectively, which is 9, 4 and 6 times higher the threshold of 320 ($5 \times 62 + 10$), 255 ($5 \times 49 + 10$) and 305 ($5 \times 59 + 10$) required to consider the mean effect size robust. Thus, publication bias was not an issue

http://www.aloki.hu ● ISSN 1589 1623 (Print) ● ISSN 1785 0037 (Online)
DOI: http://dx.doi.org/10.15666/aeer/1802_28232843

in the current meta-analysis since a relatively large number of unpublished studies would be required to alter significant impacts of yeast supplementation on broiler chicken productivity.

Conclusion

This meta-analysis provided baseline information on guidelines to standardize the experimental designs of future trials on the effect of probiotic-yeast supplementation on broiler chicken productivity. Results found that adding yeast to the broiler chicken diet at a level less than 10 g/kg feed improved the productivity of broiler chickens. There was also a significant association effect between probiotic-yeast and explanatory variables. These results will encourage feed producers, poultry nutritionists, and farmers to make informed choices about the use of yeast in broiler chicken diets as an alternative feed additive instead of antibiotics. More research is, however, needed to ascertain the effect of yeast supplementation on quality characteristics of broiler chicken meat using meta-analytical approach.

REFERENCES

[1] Adene, D. F., Oguntade, A. E. (2006): Poultry Sector Country Review. – FAO Animal Production and Health Division, Emergency Centre for Transboundary Animal Diseases Socio Economics, Production and Biodiversity Unit, Rome.

[2] Ahmed, M. E., Abbas, T. E., Abdlhag, M. A., Mukhtar, D. E. (2015): Effect of dietary yeast supplementation on performance, carcass characteristics and some metabolic responses of broilers. – Animal and Veterinary Science 3(5-1): 5-10.

[3] Al-Mansour, S., Al-Khalf, A., Al-Homidan, F. M. M. (2011): Feed efficiency and blood hematology of broilers chicks given a diet supplemented with yeast culture. – International Journal of Poultry Science 10(8): 603-607.

[4] Aluwong, T., Raji, M. A., Hassan, B. F., Kawu, M. U., Kobo, P. I., Ayo, J. O. (2012): Effect of different levels of supplemental yeast on performance indices and serum biochemistry of broiler chickens. – The Open Conference Proceeding Journal 3(Suppl 1-M7): 41-45.

[5] Apata, D. F. (2008): Growth performance, nutrient digestibility and immune response of broiler chicks fed diets supplemented with a culture of *Lactobacillus bulgaricus*. – Journal of Science Food and Agriculture 88: 1253-1258.

[6] Atul Shankar, K. P., Omprakash, A. V., Kirubakaran. J. J., Hudson, G. H. (2017): Effect of dietary yeast supplementation on the production performance of broilers. – International Journal of Advanced Biological Research 7(2): 222-228.

[7] Awad, W. A., Bohm, J., Razzazi-Fazeli, E., Ghareeb, K., Zentek, J. (2006): Effect of addition of a probiotic microorganism to broiler diets contaminated with deoxynivalenol on performance and histological alterations of intestinal villi of broiler chickens. – Poultry Science 85: 974-979.

[8] Borenstein, M., Hedges, L. V., Higgins, J. P. T., Rothstein, H. R. (2009): Introduction to Meta-analysis. – John-Wiley & Sons Ltd., Chichester, pp.17-125.

[9] Bozkurt, M., Kucukyilmaz, K., Cath, A. U., Cinar, M. (2009): Effect of dietary mannan oligosaccharide with or without oregano essential oil and hop extract supplementation on the performance and slaughter characteristics of male broilers. – South African Journal of Animal Science 39: 223-232.

[10] Buba, W., Olugbemi, T. S., Omage, J. J., Duru, S., Iyiola-Tunji, A. O. (2016): Performance of broiler chickens fed varying levels of baker's yeast (*Saccharomyces*

http://www.aloki.hu ● ISSN 1589 1623 (Print) ● ISSN 1785 0037 (Online)
DOI: http://dx.doi.org/10.15666/aeer/1802_28232843

cerevisiae) during the hot season in the northern guinea savannah of Nigeria. – Journal of Animal Production Research 28(1): 215-226.

[11] Chand, N., Ihsanuddin, A., Khan, R. U. (2014): Replacement of soybean meal with yeast single cell protein in broiler ration: the effect on performance traits. – Pakistan Journal of Zoology 46(6): 1753-1758.

[12] Chen, C. Y., Chen, S. W., Wang, H. T. (2017): Effect of supplementation of yeast with bacteriocin and Lactobacillus culture on growth performance, caecal fermentation, microbiota composition, and blood characteristics in broiler chickens. – Asian-Australasian Journal of Animal Science 3: 211-220.

[13] Choudhari, A., Shinde, S., Ramteke, B. N. (2008): Prebiotics and probiotics as health promoter. – Veterinary World 1: 59-61.

[14] Costa, M. C., Bessegatto, J. A., Alfieri, A. A., Weese, J. S., Filho, J. A. B., Oba, A. (2017): Different antibiotic growth promoters induce specific changes in the cecal microbiota membership of broiler chicken. – PLoS ONE 12(2).

[15] DerSimonian, R., Laird, N. (1986): Meta-analysis in clinical trials. – Controlled Clinical Trials 7: 177-188.

[16] Dohoo, I., Martin, W., Stryhn, H. (2003): Veterinary Epidemiologic Research. – AVC Inc., Prince Edward Island, Canada.

[17] El Fatah, S. F. A. (2003): Effect of various yeast levels on broiler performance. – M.Sc. Thesis, University of Khartoum.

[18] Elijah, O. A., Adedapo, A. (2006): The effect of climate on poultry productivity in Ilorin Kwara State, Nigeria. – International Journal of Poultry Science 5(11): 1061-1068.

[19] Ezema, C. (2013): Probiotics in animal production: a review. – Journal of Veterinary Medicine and Animal Health 5(11): 308-316.

[20] Ezema, C., Ugwu, C. C. (2014): Probiotic effects of *Saccharomyces cerevisiae* on nutrient digestibility and pH of the gastrointestinal tract of broilers. – Proceedings of the International Conference on Beneficial Microbes ICOBM2014: Microbes for the Benefits of Mankind, May 27-29, Parkroyal Penang Resort, Penang, Malaysia, A-3, pp 10-13.

[21] Food and Agriculture Organization of the United Nations (FAO) (2016): The FAO Action Plan on Antimicrobial Resistance 2016-2020. – Food and Agriculture Organization of the United Nations, Rome.

[22] Frizzo, L. S., Zbrun, M. V., Soto, L. P., Signorini, M. L. (2011): Effects of probiotics on growth performance in young calves: a meta-analysis of randomized controlled trials. – Animal Feed Science and Technology 169: 147-156.

[23] Gadde, U., Kim, W. H., Oh, S. T., Lillehoj, H. S. (2017): Alternatives to antibiotics for maximizing growth performance and feed efficiency in poultry: a review. – Animal Health Research Reviews 18(1): 26-45.

[24] Gao, P., Chen, M., Zheng, S., Wang, L., Huang, S., Xiaoquan, S., Xu, J., Zhang, H. (2017): Feed additive probiotics accelerate yet antibiotics delay intestinal microbiota maturation in broiler chicken. – Microbiome 5(91): 1-14.

[25] Gomes, L. C., Alcalde, C. R., Lima, L. R., Lima, L. S., Souza, R., Possamai, A. P. S. (2014): Nutritive value of diets containing inactive dry yeast for lactating Saanen goats. – Revista Brasileira de Zootecnia 43(1): 36-43.

[26] Haghighi, H. R., Gong, J., Gyles, C. L., Hayes, M. A., Zhou, H., Sanei, B., Chambers, J. R., Sharif, S. (2006): Probiotics stimulate the production of natural antibodies in chickens. – Clinical Vaccine Immunology 13: 975-980.

[27] Higgins, J., Thompson, S. G., Deeks, J. J., Altman, D. G. (2003): Measuring inconsistency in meta-analyses. – British Medical Journal 327: 557-560.

[28] Higgins, J. P. T., Deeks, J. J. (2011): Chapter 7: Selecting Studies and Collecting Data. – In: Higgins, J. P., Green, S. (eds.) Cochrane Handbook for Systematic Reviews of Interventions Version 5.1.0 (updated March 2011). The Cochrane Collaboration 2011. http://handbook.cochrane.org/ (accessed: 10th September 2019).

http://www.aloki.hu ● ISSN 1589 1623 (Print) ● ISSN 1785 0037 (Online)
DOI: http://dx.doi.org/10.15666/aeer/1802_28232843

[29] Hooge, D. M. (2004): Meta-analysis of broiler chicken pen trials evaluating dietary mannan oligosaccharide, 1993-2003. – International Journal of Poultry Science 3: 163-174.
[30] IntHout, J., Ioannidis, J. P., Borm, G. F. (2014): The Hartung-Knapp-Sidik-Jonkman method for random effects meta-analysis is straightforward and considerably outperforms the standard DerSimonian-Laird method. – BMC Medical Research Methodology 14: 25. doi: 10.1186/1471-2288-14-25.
[31] Jennions, M. D., Lortie, C. J., Rosenberg, M. S., Rothstein, H. R. (2013): Chapter 4: Publication and Related Bias. – In: Koricheva, J., Gurevitch, J., Mengersen, K. (eds.) Handbook of Meta-Analysis in Ecology and Evolution. Princeton University Press, Princeton, pp. 207-236.
[32] Kabir, J., Umoh, V. J., Audu-okoh, E., Umoh, J. U., Kwaga, J. K. P. (2004): Veterinary drug use in poultry farms and determination of antimicrobial drug residues in commercial eggs and slaughtered chicken in Kaduna State, Nigeria. – Food Control 15: 99-105.
[33] Koricheva, J., Gurevitch, J., Mengersen, K. (2013): Handbook of Meta-Analysis in Ecology and Evolution. – Princeton University Press, Princeton.
[34] Lean, I. J., Rabiee, A. R., Duffield, T. F., Dohoo, I. R. (2009): Invited review: use of meta-analysis in animal health and reproduction: methods and applications. – Journal of Dairy Science 92: 3545-3565.
[35] Manal, K. A. (2012): Effect of dietary yeast supplementation on broiler performance. – Egyptian Poultry Science 32(I): 95-106.
[36] Mohamed, E. A., Talha, E. A., Mojahid, A. A., Dafaalla, E. M. (2015): Effect of dietary yeast (*Saccharomyces cerevisiae*) supplementation on performance, carcass characteristics and some metabolic responses of broilers. – Animal and Veterinary Science 3(5-1): 5-10.
[37] Mohamed, S., Abdalla, A., Mukhtar, A. M. (2016): Effect of commercial (Y-MOS) yeast on performance and carcass characteristics of broiler chicks. – World Journal Pharmacy and Pharmaceutical Science 5(6): 168-179.
[38] Musa, H. H., Wu, S. L., Zhu, C. H., Seri, H. I., Zhu, G. O. (2009): The potential benefits of probiotics in animal production and health. – Journal Animal and Veterinary Advance 8: 313-321.
[39] Njeru, H. K. (2013): Effects of enzyme complex (Allzyme SSF) and yeast metabolites (Diamond V XPC) on performance, immune responses, gastrointestinal morphology and intestinal microbiota in broiler chicken (*Gallus domesticus*). – MSc. Thesis, University of Nairobi.
[40] Ogbuewu, I. P., Okoro, V. M., Mbajiorgu, E. F., Mbajiorgu, C. A. (2019): Yeast (*Saccharomyces cerevisiae*) and its effect on production indices of livestock and poultry - a review. – Comparative Clinical Pathology 51(2): 669-677.
[41] Osman, A. E. (2010): Effect of dietary supplementation of yeast (*Saccharomyces cerevisiae)* on performance and carcass characteristics of broiler chicks. – M.Sc. Thesis, University of Khartoum.
[42] Oyedeji, J. O., Ajayi, H. I., Egere, T. (2008): The effects of increasing levels of yeast culture (Levucel SB) in a high fibre diet on the performance and nutrient retention in broiler chicks. – Asian Journal Poultry Science 2(1): 53-57.
[43] Paryard, A., Mahmoudi, M. (2008): Effect of different levels of supplemental yeast (Saccharomyces cerevisiae) on performance, blood constituents and carcass characteristics of broiler chicks. – Journal of African Agricultural Research 3(12): 835-842.
[44] Piątkowska, M., Jedziniak, P., Żmudzki, J. (2012): Residues of veterinary medicinal products and coccidiostats in eggs: causes, control and results of surveillance program in Poland. – Polish Journal of Veterinary Science 15(4): 803-812.
[45] Priya, B. S., Babu, S. S. (2013): Effect of different levels of supplemental probiotics (*Saccharomyces cerevisiae*) on performance, haematology, biochemistry, microbiology,

http://www.aloki.hu ● ISSN 1589 1623 (Print) ● ISSN 1785 0037 (Online)
DOI: http://dx.doi.org/10.15666/aeer/1802_28232843

histopathology, storage stability and carcass yield of broiler chicken. – International Journal of Pharmaceutical and Biological Archives 4(1): 201-207.

[46] Saulnier, D. M. (2007): Identification of prebiotic fructooligosaccharide metabolism in Lactobacillus plantarum WCFS1 through microarrays. – Applied and Environmental Microbiology 73: 1753-1765.

[47] Schneitz, C. (2005): Competitive exclusion in poultry - 30 years of research. – Food Control 16: 657-667.

[48] Shareef, A. M., Al-Dabbagh, A. S. A. (2009): Effect of probiotic (*Saccharomyces cerevisiae*) on performance of broiler chicks. – Iraqi Journal of Veterinary Science 23(1): 23-29.

[49] Spring, P., Wenk, C., Dawson, K. A., Newman, K. E. (2000): The effects of dietary mannanoligosaccharides on caecal parameters and the concentrations of enteric bacteria in the ceca of Salmonella-challenged broiler chicks. – Poultry Science 79: 205-211.

[50] USDA (2018): National Nutrient Database for Standard Reference. Full Report (All Nutrients) 18375, Leavening Agents, Yeast, Baker's, Active Dry. – USDA, Washington.

[51] Wallace, B. C., Lajeunesse, M. J., Dietz, G., Dahabreh, I. J., Trikalinos, T. A., Schmid, C. H., Gurevitch, J. (2016): OpenMEE: intuitive, open-source software for meta-analysis in ecology and evolutionary biology. – Methods Ecology and Evolution 8: 941-947.

[52] Yalcın, S., Eser, H., Yalcın, S., Cengiz, S., Eltan, O. (2013): Effects of dietary yeast autolysate (*Saccharomyces cerevisiae*) on performance, carcass and gut characteristics, blood profile, and antibody production to sheep red blood cells in broilers. – Journal of Applied Poultry Research 22: 55-61.

[53] Yoon, C., Na, C. S., Park, J. H., Han, S. K., Nam, Y. M., Kwon, J. T. (2004): Effect of feeding multiple probiotics on performance and fecal noxious gas emission in broiler chicks. – Korean Journal of Poultry Science 3: 229-235.

http://www.aloki.hu ● ISSN 1589 1623 (Print) ● ISSN 1785 0037 (Online)
DOI: http://dx.doi.org/10.15666/aeer/1802_28232843

THE EFFECT OF NANO-BIOCHAR ON SOIL, WATER, AND NUTRIENT LOSS OF A SLOPING LAND WITH DIFFERENT VEGETATION COVERS ON LOESS PLATEAU OF CHINA

ZHOU, B. B.[1*] – CHEN, X. P.[1] – HENRY, L.[1,2]

[1]*State Key Laboratory of Eco-Hydraulic Engineering, Institute of Water Resources and Hydro-electric Engineering, Xi'an University of Technology, Xi'an 710048, China*

[2]*Department of Ecosystem Science and Management, Pennsylvania State University, State College, PA 16802, USA*

**Corresponding author*
e-mail: happyangle222@aliyun.com

(Received 21st Oct 2019; accepted 30th Jan 2020)

Abstract. Nano-biochar with unique characteristics compared to common biochar has been confirmed to promote soil physical properties. Highly weathered soils in arid and semi-arid areas are characterized by low soil nutrients and high erosion potential. This study evaluated the influences of nano-biochar made from oak tree branches on the soil, water, and nutrient conservation on a sloping land of the Chinese Loess Plateau. Five nano-biochar rates (0.0%, 0.1%, 0.5%, 0.7%, and 1.0% by mass, equal to 0 t/ha, 0.0263 t/ha, 0.131 t/ha, 0.184 t/ha, 0.268 t/ha) were applied in three bands with simulated rainfall plots (1.0 m in length, 1.0 m in width) with five different vegetation covers (bare, alfalfa, bean, *Caragana microphylla*, and corn). A simulated typical rainfall event of 90 mm h^{-1} was performed for all the treatments. Experimental results indicated that the initial runoff time was delayed with the increasing nano-biochar contents. Compared to the treatments with no biochar application, soil, water, and nutrient losses in runoff significantly decreased. The conservation effect of nano-biochar was the most significant in the alfalfa plot. Soil containing 0.7% nano-biochar (0.131 t/ha) with alfalfa planting mollusc. This study provides an effective method for soil water and nutrient conservation.
Keywords: *nano-biochar, soil and water loss control, nutrient loss and conservation, conservation value, vegetation cover*

Introduction

Semi-arid loess region of northwestern China has been suffering from severe soil erosion (up to 1000–15,000 t/km^2 per year) and nutrient loss (Shi et al., 2000; Chen et al., 2008), which is the primary cause of soil degradation and water pollution (Guo et al., 2013). In order to control the serious soil water erosion and nutrient loss, huge researches have been conducted since the end of 1950s (Huang et al., 2015). Over the years, China government has taken various conservation measures to solve this serious soil and water erosion, as well as nutrient loss problems, such as minimum tillage and no-tillage, Hedgerows, and straw mulch (Lin et al., 2009; Wang et al., 2017; Rahma et al., 2017). However, in practical terms, the effects were quite limited because of different perceived problems. Minimum tillage and no-tillage resulted in more weeds and lower yield than conventional tillage (Wozniak and Kwiatkowski, 2013; Beibei Zhou, et al., 2016). Hedgerows would also consume water, nutrient and sunlight which will reduce crop yields, besides the existence of hedgerows will also make tillage inconvenient (Sun et al., 2001). Straw mulch could be an adoptable method which could help with reducing soil and water runoff, as well as evaporation, but the straw will be washed away when the storm came (Peng et al., 2016; Li et al., 2017). Thus, to find an

http://www.aloki.hu ● ISSN 1589 1623 (Print) ● ISSN 1785 0037 (Online)
DOI: http://dx.doi.org/10.15666/aeer/1802_28452861

appropriate and effective method in controlling soil, water erosion and nutrient loss on the Loess Plateau remains an urgent task.

Moreover, soils in semi-arid loess region of northwestern China have high silt content, low organic matter content, and poor soil structure, which is difficult to overcome. The poor soil condition, combined with inappropriate land use, makes soil and nutrient loss very vulnerable to rainfall. Since the 1990s, kinds of soil amendments have been widely studied in order to control soil erosion and nutrient loss, such as polyacrylamides (PAM) and biochar (or black carbon) (Busscher et al., 2011; Wang et al., 2013). The PAM has been proved to control soil and water erosion for a long time, but PAM could also restrict infiltration which in turn accelerates runoff (Lu and Wang, 2016). The increased runoff will facilitate erosion in the downslope with villages that may turn out to be a big disaster. Besides, PAM belongs to water-soluble polyacrylamide and its limited capability in improving soil structures and quantity makes the PAM less feasible for soil and water conservation. Because of the high porosity and large inner surface area, biochar has been widely used to improve soil physical properties, especially soil water holding capacity since the 2000s (Hina et al., 2010; Herath et al., 2013; Li, 2017). Moreover, lots of studies have shown that biochar is promising to ameliorate soil physicochemical properties, improve nutrient utilization and crop yield (Laird et al., 2010; Mukherjee and Zimmerman, 2013). However, high biochar rate such as 40 to 50 tons per hectare is usually suggested (Cheng et al., 2015; Nguyen et al., 2010; Li et al., 2017). The high biochar rate together with its high mobility with storm runoff largely limits the biochar application.

Compared with common biochar, nano-biochar made of tree branches is also a carbon-rich product, which has similar properties as common biochar. Furthermore, due to the small size, nano-biochar could also achieve similar properties to nano material which have strong absorption. But little research has been done. The objective of this study was to examine the impact of nano-biochar applied into a sloping land on soil erosion, water runoff, as well as nutrient loss under five vegetation species on Loess Plateau of China using simulated rainfalls.

Materials and methods

Experimental site

The experiment was done at Liudaogou watershed (35°20’ − 40°100’N, 110°21’ − 110°23’E), which is located in the northern part of the Chinese Loess Plateau. The catchment is 6.89 km^2 and the elevations is between 1,081 and 1,274 m which belong to semi-arid area. The annual average temperature of the experiment site is 8.4 °C with the lowest temperature -9.7 °C in January and the highest temperature 23.7 °C in July. The annual mean rainfall is about 437 mm with the minimum rainfall of 109 mm and maximum rainfall of 891 mm. The underground water level is more than 20 m.

Experimental plots

In this study, five nano-biochar application rates (0.0%, 0.1%, 0.5%, 0.7%, and 1.0%, equal to 0 t/Ha, 0.0263 t/ha, 0.131 t/ha, 0.184 t/ha, 0.268 t/ha) and five vegetation types (i.e., bare, alfalfa, bean, *Caragana microphylla* and corn) were considered, so the total number of the treatments were 25, together with one plot in bared soil without

http://www.aloki.hu ● ISSN 1589 1623 (Print) ● ISSN 1785 0037 (Online)
DOI: http://dx.doi.org/10.15666/aeer/1802_28452861

nano-biochar which was used as the control. Each treatment was conducted in one plot with 1 m in length and 1 m in width.

To study how the nano-biochar affect the soil and nutrient loss, the nano-biochar was mixed well with soils and then applied in bands (5 cm wide, 200 cm long, and 5 cm thick) 5–10 cm under the surface. The bands were located at top, middle, and bottom of the plot shown in *Figure 1,* respectively. Before nano-biochar was applied into the plots, soils of top 10 cm in the band were removed. The nano-biochar was then mixed uniformly with half of the removed soils at a mass rate of 0.0% (control), 0.1, 0.5, 0.7, and 1.0% of nano-biochar, respectively, to make a 5 cm-thick soil nano-biochar mixture layer in the original position. Finally, the other half of the removed top soil was piled onto the soil nano-biochar mixture layer with its original bulk density. To minimize the possible influences by human disturbance, the mixtures-buried plots were sitting for four months before rainfall simulation experiments.

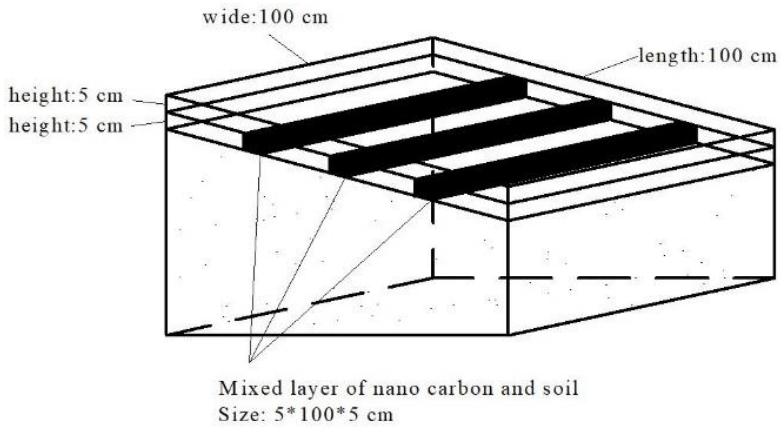

Figure 1. *The position of nano-biochar bands applied in the plot (1 m × 1 m)*

The plants were seeded 3 months before experiments. Before the rainfall experiment was conducted, vegetation was trimmed to similar vegetation coverage (*Table 1*). To reduce the disturbance due to agriculture, the vegetation specified above was planted in the plots and left undisturbed for a period of 4 m before simulated rainfall after NB was applied to the soil. *Caragana microphylla* and alfalfa were drill sown, with rows spaced 25 cm apart; corn and bean were bunch planted, with rows spaced 25 cm apart and individual plants were spaced 35 cm apart in each row. Planting and field management of vegetation were carried out according to local farming practices. Status of vegetation growth was taken before the simulated rainfall. Vegetative coverage of *Caragana microphylla* and corn was 45.93% and 42.39% on slope of plot area, respectively, which could represent the local general situation. The vegetation coverage was calculated with Matlab software. Each plot has an average slope of 152°.

Table 1. *Vegetation growth status in the experimental area*

Vegetation species	Height (cm)	Leaf area of a single plant (cm^2)	Vegetation coverage
Corn	84.3−93.9	163.2−201.5	41.4%
Bean	36.7−45.8	25.1−34.7	42.3%
Alfalfa	41.3−49.6	1.2−2.7	43.3%
Caragana microphylla	54.1−71.3	0.9−1.5	43.9%

http://www.aloki.hu ● ISSN 1589 1623 (Print) ● ISSN 1785 0037 (Online)
DOI: http://dx.doi.org/10.15666/aeer/1802_28452861

The physical and chemical characteristics of the experimental soil are shown in *Table 2*. The experimental soil was sandy textured which belonged to the Aeolian sandy soil (Hillel, 1982).

Table 2. *Physical and chemical properties of the experimental soil*

Clay (%)	Silt (%)	Sand (%)	Soil texture	Organic content (g kg^{-1})	pH
5.5	30.5	64.0	Sandy	3.5	6.2

Physical and chemical properties of nano-biochar

The nano-biochar applied in this experiment was provided by the Hainuo Nano Company (Shanghai, China) and produced by oak tree branches over 5-6 h at 500 ℃. The diameter of nano-biochar was less than 40 nm. Its physics-chemical properties are shown in *Table 3*.

Table 3. *Basic properties of the nano-biochar used in this study*

pH	Water content (kg kg^{-1})	Ash content (kg kg^{-1})	Bulk density (g cm^{-3})	Iodine sorption value (mg g^{-1})	BET* (m^2 g^{-1})
9.6	5%	60.0%	0.38	1,300	1,300

*BET refers to Brunauer, Emmett and Teller, which is a classical method to measure the specific area of particles

Rainfall simulation

The simulated rainfall experiments were conducted in the plots shown in *Figure 1* using a pinhole rainfall device invented by Zhou and Hu (2015) (*Fig. 2*) from June to September of 2016. The raindrops of 2.5 mm could be produced from the tubes of the simulated rainfall device 2.0 m above the plant canopy in experimental plots. The simulated rainfall intensity of this study was 90 mm h^{-1} (Chen and Zhou, et al., 2019), which is the average rainfall intensity in summer of the local. The simulated rainfall experiment will last for 40 min after the runoff occurred.

Before the simulated rainfall experiment, a mixed solution with 1.0 mol L^{-1} potassium bromide (KBr), 1.0 mol L^{-1} potassium nitrate (KNO_3), and 1.0 mol L^{-1} monopotassium phosphate (KH_2PQ_4) was sprayed on the soil surface. The application rate for each individual solution was 40 $g \cdot m^{-2}$. The water runoff and soil sediment will be collected at the low end of each plot. Once the water runoff started, the runoff samples (volume depending on time and the plot) will be collected with a plastic bottle every 3 min. All the samples were then transported in an ice box to the laboratory where samples will be analyzed immediately. The concentrations of NO_3^--N, K^+, PO_4^{-3}, together with the total solids (T_s, representing sediment) in runoff and soil sediment samples were measured by the ultraviolet spectrophotometric method, atomic absorption spectrophotometer HG-9602A, and standard methods, respectively (Bao, 2005).

After the first simulated rainfall experiment was finished, the plot was left for a period of time (depending the weather, mostly, it will usually be one month) until the soil water content measured by oven dry method dropped back to the status right before

http://www.aloki.hu ● ISSN 1589 1623 (Print) ● ISSN 1785 0037 (Online)
DOI: http://dx.doi.org/10.15666/aeer/1802_28452861

the first rainfall simulation. Then another replication of rainfall simulation was conducted in the same way.

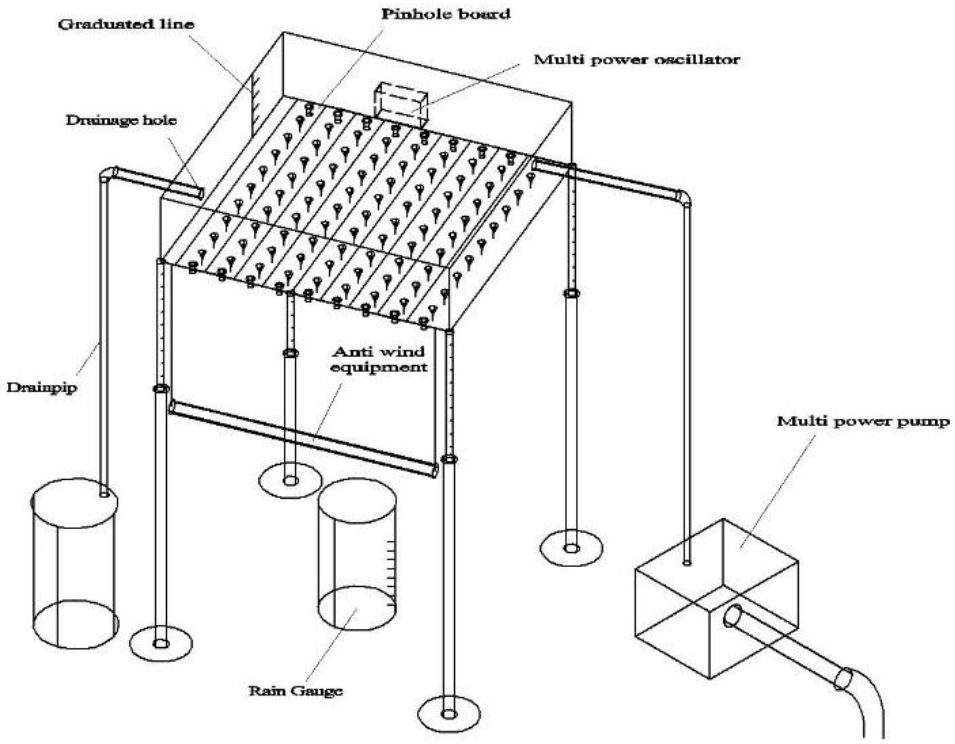

Figure 2. *Pinhole type simulated rainfall device for experiments on effect of rainfall on erosion on the Loess Plateau, China*

Conservation value (C_v) of soil, water, and nutrients for each treatment was calculated with the equation as follows (Kumar et al., 1992):

$$C_v = \left(1 - \frac{S_p}{S_0}\right) \times 100\% \quad \text{(Eq.1)}$$

where S_p, S_0 are the total amount of soil, water, or nutrient loss from the experimental plots and control plots, respectively.

Statistical analysis

Analysis of variance (ANOVA) method was used to determine the effect of nano-biochar contents and vegetation species on water runoff, soil erosion, as well as nutrient loss.

Results and discussion

Nano-biochar contents affect water runoff and soil erosion

Effect of nano-biochar contents on initial runoff time

In order to know the effect of nano-biochar on initial runoff time is one of the important parameters for characterizing runoff. The initial runoff time increased with

http://www.aloki.hu ● ISSN 1589 1623 (Print) ● ISSN 1785 0037 (Online)
DOI: http://dx.doi.org/10.15666/aeer/1802_28452861

an increase in nano-biochar contents (*Table 4*), indicating that the nano-biochar delayed the runoff generation. Infiltration excess overland flow is the main reason of runoff on the slope in the semi-arid loess region of China. Based on the laboratory experiment of Lv et al. (2016), the result indicated the nano-biochar applied 5 cm under the soil surface can increase the infiltration rate obviously. So in this study, the increased infiltration rate delayed the initial runoff time comparing to that in control plot. Moreover, the effect of nano-biochar on the initial runoff time was more pronounced when the nano-biochar content was larger than 0.5%. However, when nano-biochar content approached to 1.0%, the effect became weak (*Table 4*). Similar results were obtained by Sadeghi et al. (2016), of which it showed an effective impact of biochar application on delaying runoff time by 55% comparing to that in control experiment.

Table 4. *Effect of nano-biochar content on initial runoff time in minute*

Vegetation type	Nano-biochar content (%)				
	0 (control)	**0.1**	**0.5**	**0.7**	**1.0**
Bare (control)	5.2	5.5	8.0	7.5	8.4
Alfalfa	15.2	20.0	29.5	29.6	/
Bean	11.8	12.2	13.2	14.3	14.3
Caragana microphylla	13.1	13.3	13.9	14.1	14.5
Corn	12.0	12.8	13.2	13.4	13.4

"/" represents no runoff. The values in this table were average values

The initial runoff time in the plots with vegetation cover lagged behind as compared with the control plot (*Table 4*), indicating that vegetation also delayed the runoff time. The main reason is that the presence of the vegetation root could effectively prevents runoff, together with plant interception impact. As a result, vegetal cover provided sufficient time for infiltration and slowed down the runoff commence (Marques et al., 2007). Alfalfa followed by *Caragana microphylla* was the most efficient species to delay runoff, which was in agreement with a previous study (Wu et al., 2011). The dense vegetal cover and well-developed root of alfalfa and *Caragana microphylla* may contribute to the slower movement of simulated rainfall. Therefore, planting alfalfa and *Caragana microphylla* with band application of nano-biochar (≥0.5% or 0.488 t/ha) would be a good method to slow down the runoff on the sloping land in the study area.

Effect of nano-biochar content on water runoff and soil loss

Table 5 shows the amount of runoff and soil loss and associated C_v values of various vegetation species and nano-biochar contents averaged for two simulated rainfall events. The maximum amount of runoff and soil loss was obtained in the bare plot with no nano-biochar. With the increase of nano-biochar content, the runoff was reduced from 3,911 to 2,538 cm^3 and the soil loss (sediments) was reduced from 565 g to 239 g. No water runoff and soil loss were obtained in alfalfa plot with 1% of nano-biochar. The runoff amount was significantly reduced when nano-biochar amendments were used, and almost kept unchanged when the nano-biochar content was 0.7 – 1.0% (*Table 5*). The decreasing amount of soil loss also clearly confirmed the benefit of nano-

http://www.aloki.hu ● ISSN 1589 1623 (Print) ● ISSN 1785 0037 (Online)
DOI: http://dx.doi.org/10.15666/aeer/1802_28452861

biochar in improving field water holding capacity and conserving soil particles. Water runoff and soil erosion in vegetal plots with nano-biochar were generally reduced compared with the control plot which showed the maximum runoff. This was because vegetal cover slowed down water movement and rendered more time for infiltration thereby less runoff. Among plots with no nano-biochar, the alfalfa plot showed the minimum runoff (1,008 mL) and soil loss (58 g), with C_v values of 74.2% and 81.9%, respectively. This again indicated that alfalfa was the most efficient species in soil and water conservation especially when nano-biochar content was 1%, runoff was eliminated. *Caragana microphylla* was the second most efficient species showing C_v values of 48.7% and 54.1%, respectively, for runoff and soil loss.

Table 5. *Effect of nano-biochar content on runoff, soil loss, and associated conservation values (C_v)**

Vegetation species	Nano-biochar content (%)	Runoff amount (mL)	C_v for water (%)	Soil loss (g)	C_v for soil (%)
Bare (control)	0 (control)	3911.1	NA	565.0	NA
	0.1	3889.0	23.6	397.3	29.7
	0.5	3484.5	36.5	336.1	40.5
	0.7	3158.6	19.2	257.3	54.5
	1.0	2537.5	35.1	239.2	57.7
Alfalfa	0	1007.9	74.2	57.8	89.8
	0.1	875.6	77.6	77.1	86.4
	0.5	768.5	80.4	65.1	88.5
	0.7	617.6	84.2	22.2	96.1
	1.0	/	100.0	/	NA
Bean	0	2334.5	48.0	356.4	36.9
	0.1	2199.9	43.8	342.4	39.5
	0.5	2120.3	45.8	324.6	42.6
	0.7	1768.4	54.8	317.6	43.8
	1.0	1703.4	56.5	243.3	56.9
Caragana microphylla	0	2005.0	48.7	259.3	54.1
	0.1	1677.8	57.1	220.3	61.0
	0.5	1251.8	68.0	169.9	69.9
	0.7	1204.4	69.2	194.8	65.5
	1.0	1439.9	63.2	151.0	73.3
Corn	0	2555.3	34.7	348.6	38.3
	0.1	2637.9	32.6	289.9	48.7
	0.5	2119.3	45.8	259.9	54.0
	0.7	2311.8	40.9	246.8	56.3
	1.0	1913.1	51.1	204.8	63.8

"/" refers to no runoff. *All the data shown in *Table 5* are averaged values of two simulated rainfall events

The observed behavior has a much more good results comparing to the previous studies reported by Smetanová et al. (2013) who indicated that 10% biochar in mass

http://www.aloki.hu ● ISSN 1589 1623 (Print) ● ISSN 1785 0037 (Online)
DOI: http://dx.doi.org/10.15666/aeer/1802_28452861

could reduce runoff events by more than 40%. In this study, nano-biochar could reduce 0.57–43.5% runoff in bare land, 74.2%-100% runoff in alfalfa land, 40.3–87.0% runoff in bean land, 48.7–97.4% runoff in *Caragana microphylla* land, and 34.7–78.7% runoff in corn land. The significant effect of nano-biochar on reducing runoff production could be attributed to the strong water capacity of nano-biochar and increasing infiltration rate (Lv et al., 2016; Li et al., 2017).

Water drops triggered soil erosion and soil deposition at the outlet of bared plots (Srivastava and Singh, 2012). Artificial rain drops also broke soil clumps into finer particles, which made the soil easily be carried over by runoff. For all the plots with nano-biochar, however, the runoff was reduced due to the increased infiltration and absorption. The effect of reducing runoff was larger at a higher rate of nano-biochar application. For the vegetated plots, the vegetation intercepted water drops and formed local hindrance to free and fast movement of water. Besides, runoff always moved down the slope more strongly forming narrowing channels in the bared plots, whereas the vegetated plots reduced the free flow of runoff and therefore reduced soil loss. The vegetation roots and nano-biochar also bound soil firmly and prohibited soil moving along the slope. Corn did not have abundant roots. This may explain why corn was the least efficient species in reducing soil loss.

The ANOVA analysis indicated that both nano-biochar content and vegetation cover had significant ($p < 0.001$) effects on soil and water conservation (*Tables 6* and *7*). Based on the discussion above, planting alfalfa with application of nano-biochar at a rate of 0.5% would be an efficient and economic method to reduce water and soil loss on Loess Plateau of China.

Table 6. *Analysis of variance (ANOVA) for the effect of nano-biochar content and vegetation species on runoff and soil loss*

Source	Sum of squares	Degree of freedom	Mean sum of square	*F*-statistic	*p*-value
Runoff					
Nano-biochar	3.8E + 07	4	9.5E + 06	14.4	< 0.001
Vegetation	3.0E + 08	4	7.5E + 06	114.5	< 0.001
Error	1.1E + 07	16	6.6E + 06		
Total	3.5E + 08	49			
Soil loss					
Nano-biochar	2.5E + 04	4	6.3E + 03	8.7	< 0.001
Vegetation	1.7E + 05	4	4.2E + 04	58.2	< 0.001
Error	1.2E + 04	16	7.2E + 02		
Total	2.1E + 05	24			

Effect of nano-biochar content on nutrient loss

Effect of nano-biochar on nutrient loss in runoff

Loss of nutrients (i.e., NO_3^--N, K^+, PO_4^{-3}) in the runoff presented the same temporal trend for different treatments except for the control plot in the first 10 min (*Figs. 3–5*). Concentration of all three ions increased over time approximately in the first 10 min followed by a constant or slowly decreased nutrient concentration. The solute

http://www.aloki.hu ● ISSN 1589 1623 (Print) ● ISSN 1785 0037 (Online)
DOI: http://dx.doi.org/10.15666/aeer/1802_28452861

concentration in the runoff at the early stage was mainly caused by the raindrops and solute concentration in subsurface of the plot. Few minutes after the water runoff production, more solute will be found in the runoff which was transferred from the surface. In the control plot, however, the nutrient on the surface was washed downward directly as there were no nano-biochar or vegetation to prevent runoff. As such, concentration of nutrients in the runoff reached a relatively high values in a short time, and dropped quickly due to the fast attenuation of nutrients in the surface layer. The solute concentration in the runoff was controlled by diffusion from the soil at the later stage. This resulted in a stabilized concentration of solute in the runoff. The higher solute concentration in the soil usually led to more solute loss with runoff. But the runoff was reduced remarkably with application of nano-biochar, especially at rates greater than 0.5%. The nano-biochar was, therefore, confirmed to reduce the nutrient loss due of the reduction of runoff and strong absorption capacity.

Table 7. *Effect of nano-biochar on nutrient loss and conservation value (C_v) in runoff*

Vegetation species	NB content (%)	NO_3^--N loss (mg)	C_v for NO_3^-N (%)	P loss (mg)	C_v for P (%)	K loss (g)	C_v for K (%)
Bare	0	4.5	/	2.46	/	16.7	/
	0.1	2.5	44.1	1.62	33.8	10.8	35.4
	0.5	1.5	65.5	1.10	75.5	7.5	55.4
	0.7	1.6	63.3	1.44	68.0	9.9	40.8
	1	1.7	63.2	0.87	80.5	6.4	61.5
Caragana microphylla	0	1.8	59.3	0.93	79.2	4.23	74.7
	0.1	1.0	77.7	0.57	87.3	3.897	76.7
	0.5	0.8	83.2	0.53	88.2	3.76	77.5
	0.7	0.5	88.4	0.57	87.3	6.566	60.7
	1	0.7	85.4	1.13	74.9	6.539	60.9
Alfalfa	0	0.9	81.1	0.54	88.0	3.2	80.7
	0.1	0.6	87.7	0.31	93.2	2.5	85.3
	0.5	0.4	91.2	0.28	93.7	2.0	88.3
	0.7	0.3	92.7	0.20	95.5	1.6	90.5
	1	/	100.0	/	100.0	/	100.0
Bean	0	2.6	42.8	1.31	70.8	9.5	43.3
	0.1	1.8	58.9	0.99	78.0	7.5	55.1
	0.5	1.4	69.7	0.80	82.2	6.2	62.7
	0.7	1.0	78.7	0.52	88.4	4.9	70.5
	1	0.9	79.0	0.63	85.9	4.5	73.1
Corn	0	2.9	35.5	1.75	61.0	10.672	36.2
	0.1	2.0	54.8	1.28	71.5	8.478	49.3
	0.5	1.4	68.7	0.91	79.6	5.702	65.9
	0.7	1.4	69.6	0.79	82.4	5.781	65.4
	1	0.8	82.3	0.64	85.7	4.197	74.9

NB is short for nano-biochar

http://www.aloki.hu ● ISSN 1589 1623 (Print) ● ISSN 1785 0037 (Online)
DOI: http://dx.doi.org/10.15666/aeer/1802_28452861

The loss quantity of three ions varied greatly because of different chemical properties. As nitrate nitrogen is always lost through runoff and leaching, the amount of runoff would directly affect the quantity of nitrate nitrogen loss in runoff. From *Figures 3–5,* it could be found that in the initial 10 min, the nitrate nitrogen loss in runoff increased continuously in the soil surface after the simulated rainfall started. Subsequently, the nitrate nitrogen loss reduced gradually. As a result, the total nitrates loss at the initial time was about 4 times of that at the end of the experiment. The main reason is that at the beginning of runoff, the soil has a much higher clay particle which could absorb more nitrate nitrogen and more nitrate nitrogen was kept in soil water. So high nitrate contents could be obtained at the initial stage in runoff. With the reduce of nitrate nitrogen and the increase of mixed layer depth, nitrate was reduced gradually. Besides, the nitrate nitrogen loss was reduced obviously in the plots with nano-biochar, especially when the nano-biochar contents were 0.7% and 1.0%. The cumulative loss of nitrate nitrogen in the control treatment was much higher than that of others, which further indicating that the application of nano-biochar in soil could effectively reduce the loss of nitrate in the soil. Furthermore, the cumulative loss of nitrate in runoff was negatively correlated with increased nano-biochar contents. In bare, the runoff of each treatment with different nano-biochar reduced nitrite loss by 29.9–42.7%. With more nano-biochar was applied, more nitrate was kept in soil profile which could attribute to the excellent properties of nano-biochar, such as an enormous specific surface area, rich pore structure, and strong adsorption capacity (Deborah et al., 2011). As a result, can reduce the loss of nutrients by absorbing nutrient ions, preventing deep leaching from the surface soil.

Similar to nitrate nitrogen, at the initial time of the rainfall, more phosphorus was kept in soil water or be absorbed in soil particle, so the loss of phosphorus in runoff also first increased sharply in the initial 10 min (Vadas and Busch et al., 2015). The soil on Loess Plateau, has a poor structure, which prevent phosphorus from deep leaching but make phosphorus easily involved in runoff (Yan et al., 1999). As a result, the phosphorus loss tended to be stable. While with the increase of nano-biochar, the loss of phosphorus in runoff was also reduced.

Potassium was easily dissolved in soil water and runoff, so the potassium loss in runoff was much greater than that of other two nutrients for all the treatments (Poss et al., 2010). But the potassium loss also increased in the early 10 min and then became constant. Moreover, the effect became more significant at a higher rate of nano-biochar content.

In order to further analyze how nano-biochar affect nutrient loss, the nutrient loss and nutrient conservation values in runoff were calculated (*Table 8*). Nano-biochar effectively reduced the nutrient loss. With the increase of nano-biochar content, the nutrient loss was reduced and nutrient conservation value increased, especially when the nano-biochar content was 0.7% and 1.0%. Furthermore, nutrient conservation values of phosphorus, which is the main element to contribute to eutrophication, were much greater than those of nitrate nitrogen and potassium. The main reason was that the chemical interactions between phosphorus and clay minerals (Dutta, 2007; Tomer et al., 2007) largely reduced the mobility of phosphorus in soils except very sandy or organic soils. Most of the phosphorus was lost with the eroded soil particles. Vegetation species also affected the amount of nutrient loss in runoff (*Figs. 3–5; Table 8*). The bared plots showed the highest amount of nutrient loss in the surface runoff. Plots with alfalfa followed by *Caragana microphylla* showed the lowest amount of nutrient loss and highest nutrient conservation values. This indicated that nano-biochar application with planting alfalfa and *Caragana microphylla* had a positive influence in conserving nutrient.

http://www.aloki.hu ● ISSN 1589 1623 (Print) ● ISSN 1785 0037 (Online)
DOI: http://dx.doi.org/10.15666/aeer/1802_28452861

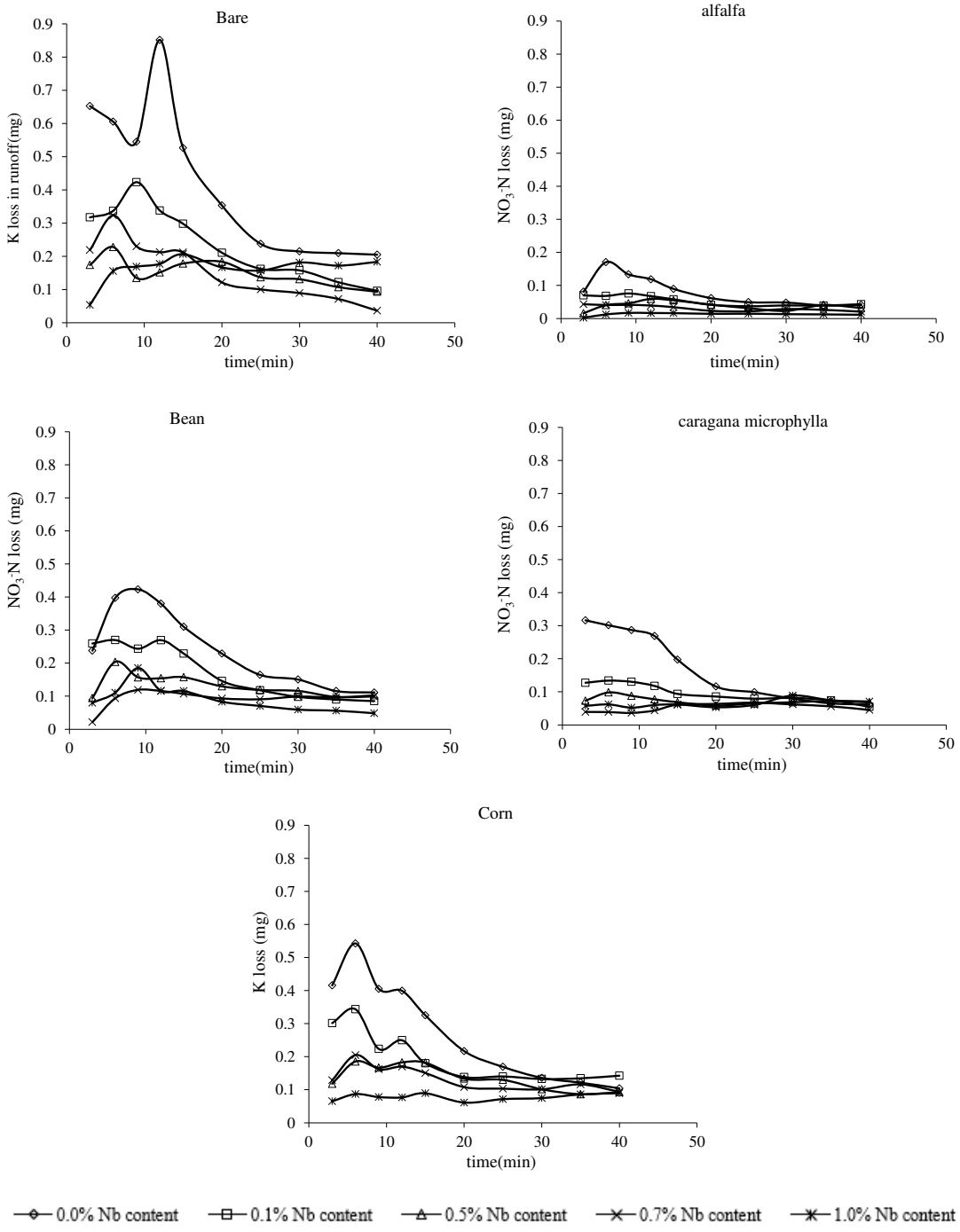

Figure 3. *Effect of nano-biochar on nutrient losses in runoff, showing the averaged nitrogen (N) mass loss as a function of time in two simulated rainfall events*

Effect of nano-biochar on nutrient loss in sediments

Nutrient loss not only occurred in runoff but also in sediments. The amounts of nutrient loss and nutrient conservation values in sediments are shown in *Tables 7* and *8*. Similar to the nutrient loss in runoff, nutrient loss in sediments was the greatest in the bared plots. The nutrient loss in sediments was reduced effectively with the increase of

http://www.aloki.hu ● ISSN 1589 1623 (Print) ● ISSN 1785 0037 (Online)
DOI: http://dx.doi.org/10.15666/aeer/1802_28452861

nano-biochar contents. The lowest nutrient loss was found in plots with nano-biochar contents of 0.7% and 1.0%. Nano-biochar delayed the initial runoff time and reduced the quantity of runoff hence soil loss by erosion. This resulted in less nutrient loss with sediment. Moreover, at the initial time, absorptive and dissolved nutrient was much higher, so nutrient loss in sediment was much higher. With further process of the simulated rainfall, more nutrient was washed away with soil particles. When the energy of soil adsorption and desorption was in a dynamic equilibrium, the nutrient contents in sediment tended to be stable. Besides, nutrient loss in sediments was less than that in runoff. The main reason was that nitrate nitrogen and potassium were hardly bound by soil particles and hence easily dissolved in the runoff. Moreover, phosphorus transport along slope was mainly controlled by water flow rather than by sediment movement (Osborne and Kovacic, 1993).

Table 8. *Effect of nano-biochar on nutrient loss and conservation values (C_v) in sediments*

Vegetation species	Nano biochar content (%)	NO_3-N loss (mg)	C_v for NO_3-N (%)	P los (mg)	C_v for P (%)	K loss (mg)	C_v for K (%)
Bare (control)	0	4.4	/	2.8	/	10.0	/
	0.1	2.5	44.0	1.8	33.8	6.5	35.4
	0.5	1.5	65.4	1.2	55.3	4.0	60.4
	0.7	1.6	63.3	1.6	41.8	4.5	55.4
	1	1.6	63.1	1.0	64.4	5.5	45.6
Caragana microphylla	0	2.5	42.6	1.5	46.9	5.7	43.3
	0.1	1.8	58.8	1.1	60.0	4.5	55.0
	0.5	1.3	69.7	0.9	67.6	3.7	62.7
	0.7	0.9	78.6	0.6	78.9	2.7	73.4
	1	0.9	79.0	0.7	74.2	2.4	76.3
Alfalfa	0	0.8	56.0	0.6	78.2	1.9	80.8
	0.1	0.5	67.7	0.3	87.6	1.4	85.8
	0.5	0.4	78.4	0.3	88.4	1.2	90.5
	0.7	0.3	92.9	0.2	91.6	1.0	90.5
	1	/	100.0	/	100.0	/	100.0
Bean	0	1.8	59.2	1.2	1.2	4.1	59.5
	0.1	1.0	77.9	0.9	0.9	3.0	69.8
	0.5	0.7	83.4	0.6	0.6	2.0	80.5
	0.7	0.5	88.4	0.6	0.6	1.7	83.1
	1	0.6	85.4	0.6	0.6	1.7	83.4
Corn	0	2.8	35.5	1.9	1.9	6.4	36.2
	0.1	2.0	54.7	1.4	1.4	4.7	53.2
	0.5	1.4	68.8	1.0	1.0	3.0	69.7
	0.7	1.3	69.7	0.9	0.9	3.0	69.8
	1	0.8	82.5	0.7	0.7	2.2	77.9

Re: NB is short for nano-biochar

http://www.aloki.hu ● ISSN 1589 1623 (Print) ● ISSN 1785 0037 (Online)
DOI: http://dx.doi.org/10.15666/aeer/1802_28452861

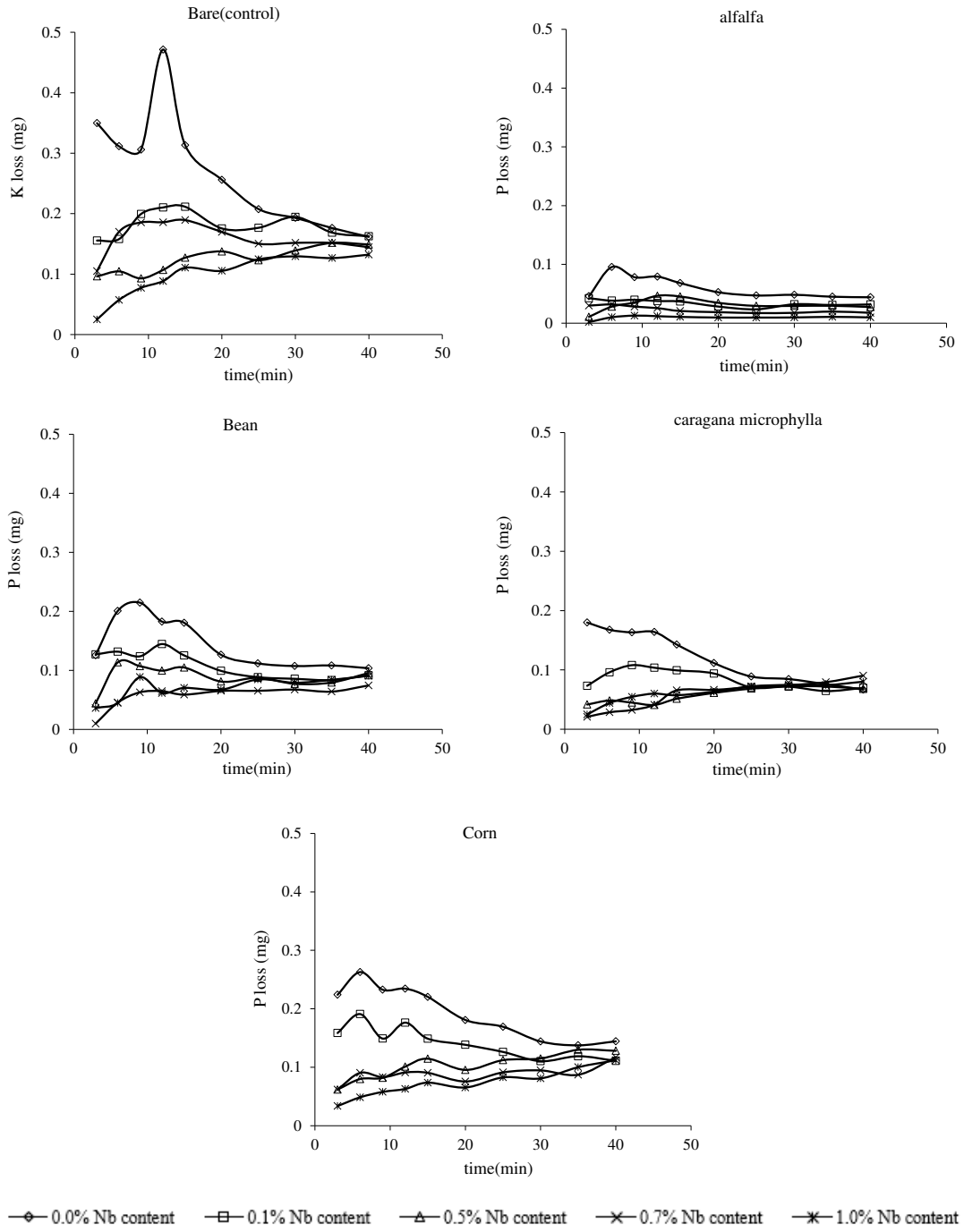

Figure 4. *Effect of nano-biochar on nutrient losses in runoff, showing the averaged phosphorus (P) mass loss as a function of time in two simulated rainfall events*

The nutrient loss in plots with vegetation was much smaller comparing to that in bare. The main reason for that is vegetal cover could reduce the energy of rain drops falling on the soil surface. This in turn reduced the amount of eroded soils that move down the slope. Besides these, plots with vegetation would accumulate more decayed leaves. Due to decomposition of humus, mollusk will always exist (such as earthworms) (Lipiec et al., 2015) which could loosen the soil and make it for air and water to reach

http://www.aloki.hu ● ISSN 1589 1623 (Print) ● ISSN 1785 0037 (Online)
DOI: http://dx.doi.org/10.15666/aeer/1802_28452861

the roots of plants. As a result, loose soil and good structure improved soil infiltration rate. Meanwhile, for bare land, due to the impact and erosion of rain drops, the soil structure was damaged, resulting in the reduction or blockage of soil surface pores, which will lead to a significant decrease in soil infiltration rate. Thus, the nutrient will be easily lost. Among all the vegetation species considered in this study, alfalfa was the most efficient species to reduce the nutrient loss in sediments.

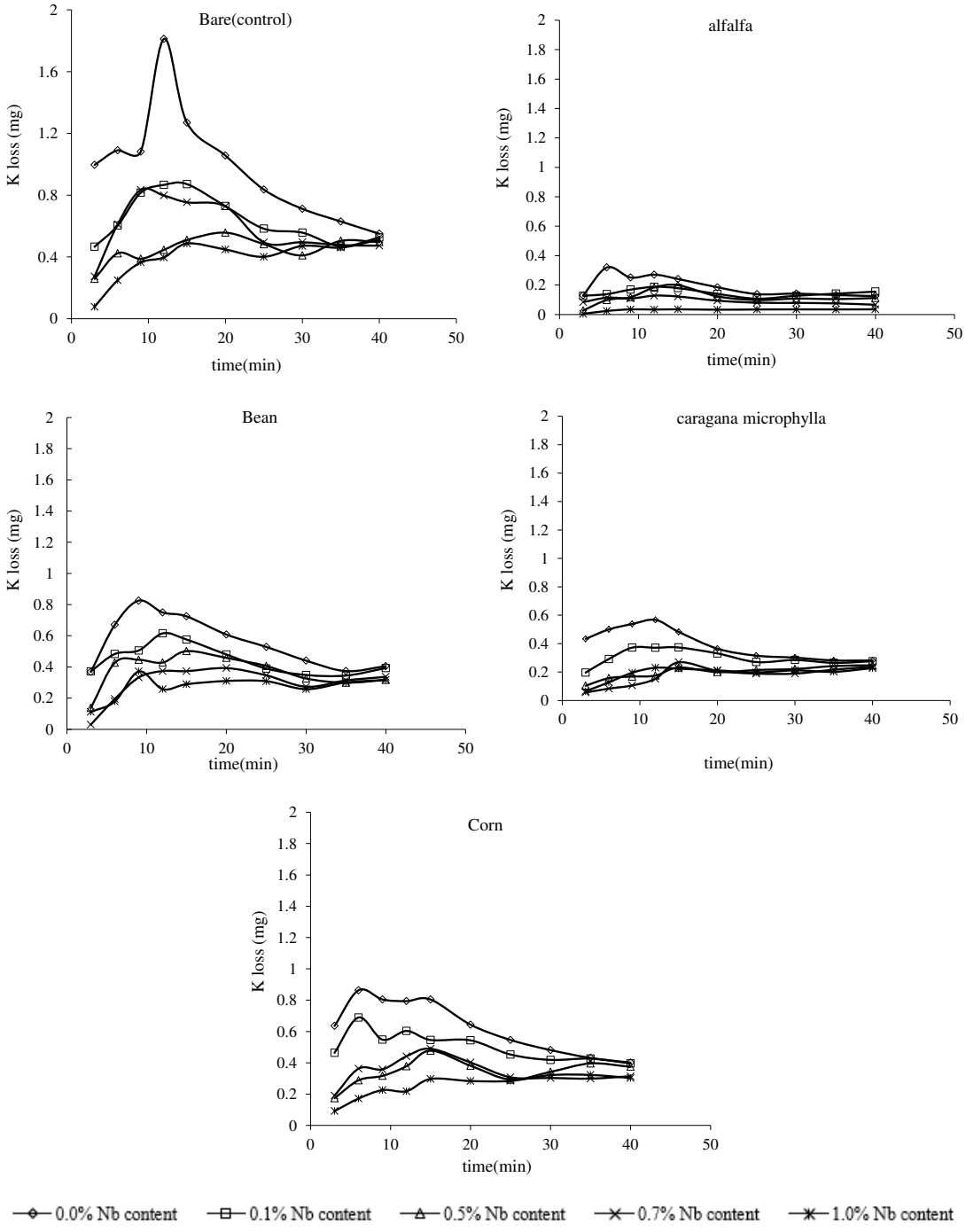

Figure 5. *Effect of nano-biochar on nutrient losses in runoff, showing the averaged potassium (K) mass lost as a function of time in two simulated rainfall events*

http://www.aloki.hu ● ISSN 1589 1623 (Print) ● ISSN 1785 0037 (Online)
DOI: http://dx.doi.org/10.15666/aeer/1802_28452861

In general, the nano-biochar and even biochar is still at its initial research stage, most of the experiment related to soil and water conservation are conducted in pot experiment with short period. So long-term experiments are still needed to know the effects of nano-biochar application to control soil and water control better, as well as nutrient loss. Additionally, Sadeghi et al. (2016) and Li et al. (2107) also found biochar particles in the runoff, which indicated that biochar will be runoff easily with rainfall. So, in order to use biochar effectively, straw covering, manure or polyacrylamide, et al., could be used to help with coherence of biochar-soil particles and to avoid floating away by runoff. But in our study, no nano-biochar was found in runoff and soil sediment which showed a superior property to biochar. Moreover, high biochar rate such as 40 to 50 tons per hectare is always needed, together with its high mobility with storm runoff largely limits the its application. However, further comprehensive studies are still needed to examine the stability of nano-biochar in a long time before large-scale application of nano-biochar was used as a new soil amendment.

Conclusion

This study showed a positive effect of nano-biochar on the conservation of soil, water, and nutrients. We found that nano-biochar addition of more than 0.5% (0.131 t/ha on a mass basis) could delay the initial generation of runoff as well as reduce the amount of water runoff, soil erosion, and nutrient loss in a sandy soil of semi-arid loess region of China. Nutrient loss in runoff and sediment significantly decreased with the increase of nano-biochar content in all the treatments. Alfalfa was the most efficient species to conserve soil, water, and nutrient. The two-way ANOVA indicated that nano-biochar content and vegetation species had significant influences on soil water and nutrient conservation. Therefore, planting alfalfa with 0.131 t/ha nano-biochar in a sloping land have positive effects on soil and water conservation in the loess area. In the Loess Plateau of China, the wide application of vegetation cover has great influence on the treatment of soil erosion, and the combined application of nano-biochar will promote the effect of which more positive.

Acknowledgements. The research was fouded by the National Natural Science Foundation of China (Grant Nos. 41977007,4180713 and 41830754), the Science and Technology Program of Shaanxi Province (Grant No. 2018slkj-06) and Research project of State Key Laboratory of Eco-hydraulics in Northwest Arid Region of China (2019KJCXTD-4andQJNY-2019-01).

REFERENCES

[1] Bao, S. D. (2005): Soil Agricultural Chemistry Analysis. – China Agriculture Press, Beijing.
[2] Busscher, W. J., Novak, J. M., Ahmedna, M. (2011): Physical effects of organic matter amendment of a southeastern US coastal loamy sand. – Soil Science 176: 661−667.
[3] Chen, H. S., Shao, M. G., Li, Y. Y. (2008): Soil desiccation in the Loess Plateau of China. – Geoderma 143: 91-100.
[4] Cheng, C. H., Lehmann, J., Thies, J. E., Burton, S. D. (2015): Stability of black carbon in soils across a climatic gradient. – Journal of Geophysical Research Biogeosciences 113: 50−55.

http://www.aloki.hu ● ISSN 1589 1623 (Print) ● ISSN 1785 0037 (Online)
DOI: http://dx.doi.org/10.15666/aeer/1802_28452861

[5] Deborah, A. B., Gwynn, R. J., Graig, A. S. (2011): Amending greenroof soil with biochar to affect runoff water quantity and quality. – Environmental Pollution 159: 2111-2118.
[6] Dutta, S., Mukhopadhyay, D. (2007): Dynamics of phosphorus sorption in some acid soils of West Bengal, India. – Asian Journal of Soil Science 2: 118-127.
[7] Guo, T. L., Wang, Q. J., Bai, W. J., Zhuang, J. (2013): Effect of land use on scouring flow hydraulics and transport of soil solute in erosion. – Journal of Hydrologic Engineering 18: 465-473.
[8] Herath, H. M. S. K., Camps-Arbestain, M., Hedley, M. (2013): Effect of biochar on soil physical properties in two contrasting soils, an Alfisol and an Andisol. – Geoderma 209-210: 188−197.
[9] Hillel, D. (1982): Introduction to Soil Physics. 5. Soil Water: Content and Potential. – Elsevier, Amsterdam, pp. 57-89.
[10] Hina, K., Bishop, P., Arbestain, M. C., Calvelo-Pereira, R., and Macia-Agullo, J. A., Hindmarsh, J., Hanly, J. A., Macias, F., Hedley, M. J. (2010): Producing biochars with enhanced surface activity through alkaline pretreatment of feedstocks. – Australian Journal of Soil Research 48: 606-617.
[11] Huang, Y. M., Liu, D., An, S. S. (2015): Effects of slope aspect on soil nitrogen and microbial properties in the Chinese Loess region. – Catena 125: 135-145.
[12] Kumar, R., Srivastava, N. K. (1992): Conservation efficiency of five common riparian weeds in movement of soil, water and phosphorus. – Journal of Applied Ecology 29: 734−744.
[13] Laird, D., Fleming, P., Wang, B. Q., Horton, R., Karlen, D. (2010): Biochar impact on nutrient leaching from a Midwestern agricultural soil. – Geoderma 158: 436-442.
[14] Li, B., Bi, Z. C., Xiong, Z. Q. (2017b): Dynamic responses of nitrous oxide emission and nitrogen use efficiency to nitrogen and biochar amendment in an intensified vegetable field in southeastern China. – Global Change Biology Bioenergy 9: 1-14.
[15] Li, Y. P., Jia, Z. K., Han, Q. F., Wang, C. S., Xie, Y. Z., Wei, H. S. (2017a): Effects of mulching straw at different rates on water use pattern and soil properties of dry-land wheat. – Agricultural Research in the Arid Areas 35: 217-229 (in Chinese with English abstract).
[16] Li, Z. G., Gu, C. M., Zhang, R. H., Ibrahim, M., Zhang, G. S., Wang, L., Zhang, R. Q., Chen, F., Liu, Y. (2017c): The benefic effect induced by biochar on soil erosion and nutrient loss of slopping land under natural rainfall conditions in central China. – Agricultural Water Management 185: 145-150.
[17] Lin, C. W., Tu, S. H., Huang, J. J., Chen, Y. B. (2009): The effect of plant hedgerows on the spatial distribution of soil erosion and soil fertility on sloping farmland in the purple-soil area of China. – Soil & Tillage Research 105: 307-312.
[18] Lipiec, J., Turski, M., Hajnos, M., Swieboda, R. (2015): Pore structure, stability and water repellency of earthworm casts and natural aggregates in loess soil. – Geoderma 243: 124-129.
[19] Lu, S. J., Wang, Z. L. (2016): Research progress of soil conditioner polyacrylamide. – Yellow River 38: 73-77 (in Chinese with English abstract).
[20] Lv, J. B., Zhou, B. B., Wang, Q. J. (2016): Influence of nano-biochar-soil layer applied subsurface on soil water movement. – Journal of Soil & Water Conservation 12: 15-21. (in Chinese with English abstract).
[21] María, J. M., Bienes, Ramón, B., Luis, J., Raquel, P. R. (2007): Effect of vegetal cover on runoff and soil erosion under light intensity events. Rainfall simulation over USLE plots. – Science of the Total Environment 378: 161-165.
[22] Mukherjee, A., Zimmerman, A. R. (2013): Organic carbon and nutrient release from a range of laboratory-produced; biochars and biochar-soil mixtures. – Geoderma 193: 122-130.

http://www.aloki.hu ● ISSN 1589 1623 (Print) ● ISSN 1785 0037 (Online)
DOI: http://dx.doi.org/10.15666/aeer/1802_28452861

[23] Nguyen, B. T., Lehmann, J., Hockaday, W. C., Joseph, S., Masiello, C. A. (2010): Temperature sensitivity of black carbon decomposition and oxidation. – Environmental Science & Technology 44: 3324−3331.
[24] Osborne, L. L., Kovacic, D. A. (1993): Riparian vegetated buffer strips in water-quality restoration and stream management. – Freshwater Biology 29: 243-258.
[25] Peng, X., Zhu, Q. H., Xie, Z. B., Darboux, F., Holden, N. M. (2016): The impact of manure, straw and biochar amendments on aggregation and erosion in a hillslope Ultisol. – Catena 138: 30-37.
[26] Poss, R., Fardeau, J. C., Saragonit, H., Quantin, P. (2010): Potassium release and fixation in Ferralsols (Oxisols) from Southern Togo. – European Journal of Soil Science 42: 649-660.
[27] Rahma, A. E., Wang, W., Tang, Z., Lei, T. W., Warrington, D. N., Zhao, J. (2017): Straw mulch can induce greater soil losses from loess slopes than no mulch under extreme rainfall conditions. – Agricultural & Forest Meteorology 232: 141-151.
[28] Sadeghi, S. H., Hazbavi, Z., Harchegani, M. K. (2016): Controllability of runoff and soil loss from small plots treated by vinasse-produced biochar. – Science of the Total Environment 541: 483-490.
[29] Shi, H., Shao, M. A. (2000): Soil and water loss from the Loess Plateau in China. – Journal of Arid Environments 45: 9-20.
[30] Smetanová, A., Dotterweich, M., Diehl, D. (2013): Influence of biochar and terra preta substrates on wettability and erodibility of soils. – Zeitschrift für Geomorphologie 57: 111-134.
[31] Srivastava, P., Singh, S. (2012): Conservation of soil, water and nutrients in surface runoff using riparian plant species. – Journal of Environmental Biology 33: 43-49.
[32] Sun, H., Tang, Y., Wang, C., He, Y. H. (2001): Contour hedgerow intercropping for exploitation and conservation of slope cropland in mountain areas. – Journal of Mountain Research 29: 125-129 (in Chinese with English abstract).
[33] Tomer, M. D., Moorman, T. B., Kovar, J. L., James, D. E., Burkart, M. R. (2007): Spatial patterns of sediment and phosphorus in a riparian buffer in western Iowa. – Journal of Soil & Water Conservation 62: 329-338.
[34] Vadas, P. A., Busch, D. L., Powell, J. M., Brink, G. E. (2015): Monitoring runoff from cattle-grazed pastures for a phosphorus loss quantification tool. – Agriculture Ecosystems & Environment 199: 124-131.
[35] Wang, C., Walter, M. T., Parlange, J. Y. (2013): Modeling simple experiments of biochar erosion from soil. – Journal of Hydrology 499: 140−145.
[36] Wang, L. H., Dalabay, N., Lu, P., Wu, F. Q. (2017): Effects of tillage practices and slope on runoff and erosion of soil from the Loess Plateau, China, subjected to simulated rainfall. – Soil & Tillage Research 166: 147-156.
[37] Wozniak, A., Kwiatkowski, C. (2013): Effect of long-term reduced tillage on yield and weeds of spring barley. – Journal of Agricultural Science & Technology 15: 1335-1342.
[38] Wu, S. F., Wu, P. T., Feng, H., Merkley, G. P. (2011): Effects of alfalfa coverage on runoff, erosion and hydraulic characteristics of overland flow on loess slope plots. – Frontiers of Environmental Science & Engineering in China 5: 76-83.
[39] Yan, W. J., Zhang, S. (1999): Loss and prediction of bio available phosphorus in surface runoff under simulated rainfall condition. – Environmental Chemistry 18: 497-506 (in Chinese with English abstract).
[40] Zhou, B. B., Hu, Z. C., Wang, Q. J. (2015): Pinhole type artificial field simulated rainfall device with anti-clogging. – China ZL2015100694924.

http://www.aloki.hu ● ISSN 1589 1623 (Print) ● ISSN 1785 0037 (Online)
DOI: http://dx.doi.org/10.15666/aeer/1802_28452861

THE EFFECTS OF NANO-BIOCHAR ON MAIZE GROWTH IN NORTHERN SHAANXI PROVINCE ON THE LOESS PLATEAU

YANG, Y.[1] – ZHOU, B.[1]* – HU, Z.[1] – LIN, H.[1,2]

[1]*State Key Laboratory of Eco-Hydraulics in Northwest Arid Region of China, Xi'an University of Technology, Xi'an 710048, China*

[2]*Department of Ecosystem Science and Management, The Pennsylvania State University, University Park PA 16802, USA*

**Corresponding author*
e-mail: happyangle222@aliyun.com

(Received 22nd Oct 2019; accepted 30th Jan 2020)

Abstract. Soil erosion and nutrient loss on the Loess Plateau cause severe desertification and land degradation, which results the loss of soil fertility and grain production. To improve soil quality and grain yield, nano-biochar was banded (5 cm in width, 5 cm in depth) into a plot (3 m × 3 m) in Shenmu County, in northern Shaanxi Province on Loess Plateau. The effects of different nano-biochar contents (0, 0.1%, 0.5%, 0.7%, 1% in mass) on soil moisture, nutrients, maize growth and yields, were analyzed. The result showed that with increased nano-biochar rates, soil bulk density also increased, and soil aggregates with particle size > 2mm increased from 0.69 to 37.12%. At the seedling and shooting stages, soil moisture content in the plots with nano-biochar were significantly higher than those in control. Nano-biochar slowed transport rate of nitrogen from the surface to deeper soil profile. At 0–10 cm soil depth, the amount of available potassium with nano-biochar applied was higher than those in control plot. The plots with higher nano-biochar content (0.7% and 1%) significantly increased the 1000-grain weight and yield of maize.
Keywords: *nano-biochar, growth parameters, 1000-grain weight, maize yields*

Introduction

Northern Shaanxi, China, is large and rich in natural resources. Changes in land use patterns and increasing population have resulted a decrease in the number of grain fields in this area. The remaining farmland is mainly located on slopes, but the plains are suitable for spring maize growth. Rainfall is the main source of water in this region. During the growing period, high rates of evaporation from soil occur due to high solar radiation intensity and high temperature. This results in insufficient water supply for spring maize growth. Previous studies have assessed how changes to management can improve the soil environment, and nutrient and water use efficiency, however, poor soil structure often impedes these efforts (Liu et al., 2012b; Manivasakan et al., 2013; Reese et al., 2014; Zhou et al., 2017, 2018). More research is needed to develop innovative strategies to improve fertilizer use by crops to increase crop yields, enhance plant use of nutrient, and minimize environmental damage.

As a soil amendment, biochar can be used to improve the utilization efficiency of chemical fertilizers and increasing grain yield. High rates (tons per hectare) are often applied, and because soil biochar may be lost via runoff, successfully using biochar to optimize fertilizer strategies may be unpractical. However, researchers have reported that after special treatment, biochar can become nano-biochar, which exists widely in soil-vegetation-atmosphere cycling. Due to the large specific surface and small particle size, nano-carbon is easily coupled with nutrient elements and soil microelements to become a

http://www.aloki.hu ● ISSN 1589 1623 (Print) ● ISSN 1785 0037 (Online)
DOI: http://dx.doi.org/10.15666/aeer/1802_28632877

high-efficiency fertilizer (Roy et al., 2000; Vacher et al., 2003; Mesarič et al., 2013; Guo et al., 2013). Zhou et al. (2018) proposed that nano-biochar could reduce nutrient loss from rainfall-induced erosion on loess slopes under different vegetation cover and concluded that nano-biochar significantly affected soil moisture movement in the Loess Plateau. Wang et al. (2016) found that fertilizer with nano-biochar can increase crop yield by 10% to 20%, while reducing the amount of fertilizer required by 30% to 50%.

The objectives of this experiment were to test how banding different nano-biochar concentrations (0, 0.1%, 0.5%, 0.7%, 1%) affected soil physical and chemical properties, growth characteristics and soil water, and fertilizer utilization efficiency of spring maize crop.

Materials and methods

Site description

The experiment was conducted in Liudaogou Village, Xigou Township, Shenmu County, Northern Shaanxi, China (longitude 110°21'–110°23'E, latitude 38°46'–38°51'N). The experimental site was 6.89 km^2 in area and situated in an ecologically fragile zone prone of water and wind erosion. The annual mean temperature is 8.4℃ with the lowest temperature in January and the highest in July. The annual average precipitation is 437.4 mm and varies from 108.6 to 819.1 mm. (Fu et al., 2015; Jia et al., 2013). The soil types in the basin include aeolian sandy soil and sandic entisols. Poor soil structure is causing serious soil erosion (Wang et al., 2015; Tan et al., 2016). The soil in the test plot is aeolian sandy soil, and the soil physical and chemical properties are shown in *Table 1*.

Experimental materials and crops

A local spring maize (the type of maize grown in the region was spring sowing, harvested in autumn, and the region grows only one season of maize so that it is spring maize) was selected in this study. The species of tested maize was Dafeng 30, which came from Shanxi Dafeng Seed Industry Co., Ltd. The tested nano-biochar was a black powder produced by Shanghai Hainuo Carbon Industry Co., Ltd. The nano-biochar diameter was 40 nm, and was carbon powder made of coconut shells, carbonized at high temperature, activated by water vapor and refined by ultrafine grinding at nanometer level. It had rich micropore structure, strong specific surface area and strong absorbability, which can load soil microbes and nutrients. The biochar had a pH of 9.6, a water content of ≤ 5 and volume density of 0.38 g/cm^3.

Experimental design

The experiment was performed from March 2016 to July 2018, which have three consecutive growing seasons. The plot size of 3 m × 3 m was allocated for each treatment. Different concentrations of nano-biochar (0, 0.1%, 0.5%, 0.7%, 1%) were banded at 5-10 cm under the soil surface.

The nano-biochar was added to the soil by removing the top 5 cm of soil, mixing the nano-biochar with soil at 5-10 cm depth, then replacing the previously removed top 5 cm of soil. To monitor the water content at different soil depths, five one-meter TRIME pipes were installed at the tested plot. A 3 m × 3 m protective net was arranged on the periphery of each test plot to prevent farm livestock and wild animals from interfering with the

http://www.aloki.hu ● ISSN 1589 1623 (Print) ● ISSN 1785 0037 (Online)
DOI: http://dx.doi.org/10.15666/aeer/1802_28632877

plots. The row width and the plant-to-plant distance were 50 cm and 25 cm. In replicates of two for each treatment, total of 10 experimental plots were established.

Table 1. *The soil physical and chemical properties of experimental field*

Soil	Particle content (%)			pH	$CaCO_3$ (%)	Organic matter ($g \cdot kg^{-1}$)	Total nitrogen ($g \cdot kg^{-1}$)	Total phosphorus ($g \cdot kg^{-1}$)
	Clay (<0.001 mm)	Silt (0.05-0.001 mm)	Sand (>0.05 mm)					
Aeolian sandy soil	15.70	37.47	46.83	8.0	4.31	5.32	0.82	0.61

The maize seeds were washed with 10% H_2O_2 for 30 min before sowing. After rinsing with water, the spring maize seeds were soaked in saturated calcium sulfate ($CaSO_4$) solution for 4 h, and were transferred to gauze soaked with saturated $CaSO_4$, covered with black plastic film at 25 ℃ to accelerate germination. The seeds were sowed after the radicals appeared. Before sowing, nitrogen fertilizer (N) 1.458 kg, phosphate fertilizer (P_2O_5) 0.874 kg, potassium fertilizer (K_2O) 0.874 kg were evenly applied in each plot. The field was irrigated before sowing but not after. The sowing depth was 3-5 cm.

Date collection and calculations

Initial and post-sowing soil nutrients throughout the experiment were measured. The soil moisture characteristic curve was determined by using the H–1400 pF soil moisture characteristic curve measurement system produced by Kokusan in Japan. The soil water stable aggregates were determined by a wet sieving apparatus (wet screening device) produced by Eijkelkamp in Netherlands. At different growth stages of maize (seedling stage; shooting stage; tasselling stage; filling stage; and maturation stage), the soil moisture content at different soil depths was measured. Five maize samples (roots, stems and leaves intact) were randomly selected to measure plant nutrients. Soil moisture evapotranspiration in the soil profile was measured by micro-lysimeter. At the same time, five points were randomly selected in each plot to collect soil samples. The plant N content was determined by the salicylic acid-zinc powder reduction method. The plant phosphorus content was measured by the molybdenum antimony colorimetric method. The plant potassium content was measured by flame photometer. The stem diameter and plant height of the crops was measured by caliper and ruler. After the crop was mature, its production was recorded according to the degranulation of the plot.

The result use Microsoft Excel, IBM Spss10.1 software and Origin function drawing software for statistical analysis, and charting of relevant parameters, single factor variance analysis for significance test (95% confidence interval).

Results and discussion

Effects of nano-biochar on the physical and chemical properties

Effects of nano-biochar on the soil water characteristic curves

The soil water characteristic curves of eolian sandy soil with different nano-biochar content are shown in *Figure 1*. *Figure 1* shows that under the same soil moisture content, the water suction increased with increasing nano-biochar contents. The soil moisture

http://www.aloki.hu ● ISSN 1589 1623 (Print) ● ISSN 1785 0037 (Online)
DOI: http://dx.doi.org/10.15666/aeer/1802_28632877

content in soil with higher nano-biochar contents was higher than in lower nano-biochar contents, and the control, at equivalent soil water suction. Similar results regarding nano-biochar effects on soil water capacity have been reported (Fan et al., 2014 and Han et al., 2010). This is because the addition of nano-biochar decreases the number of large pores and increases the number of small pores in the soil. When the suction is applied, the water in the small pores is less affected by the external suction compared with the large pores. The nano-biochar also has a large specific surface area, high surface energy, and a high water retention force. Therefore, nano-biochar has potential to promote root water absorption and improve the water retention of sandy soil.

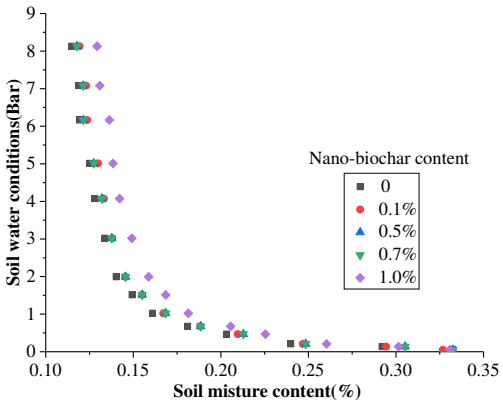

Figure 1. *The effect of different nano-biochar content on the soil water characteristics curve*

Effect of nano-biochar on soil water stable aggregates

The influence of nano-biochar application on soil water stable aggregates was determined and the results are presented in *Table 2*. From *Table 2* it was shown that with increases of nano-biochar content in soil, soil aggregates with particle sizes < 0.25 mm were reduced from 38.21 to 24.33%, while soil aggregates with particle size > 2 mm increased from 0.69 to 37.12%. The content of soil aggregates with particle size > 2 mm had the greatest increases with nano-biochar application, showing the ability of nano-biochar to improve soil aggregation. Nano-biochar mass contents of 0.7% and 1% had the greatest effects on improving soil water-stable aggregates. Different materials (e.g., minerals, organic matter) with various molecular sizes and chemical characteristics attach to nano-biochar surfaces, and this reduces the nano-biochar's surface area at a molecular scale, thus serving as the binding agents for the formation and stability of soil aggregates (Liang et al., 2006; Bossuyt et al., 2001). The nano-biochar enhanced the formation and stabilization of the soil macroaggregates, especially in sandy loam soil (Six et al., 2004; Liu et al., 2015).

Table 2. *The influence of nano-biochar content on the soil water stable aggregate*

Soil particle size analysis (mm)	**Nano-biochar content**				
	0	**0.10%**	**0.50%**	**0.70%**	**1%**
< 0.25	38.21%	33.38%	30.48%	26.47%	24.33%
0.25 ≤ d < 0.5	44.85%	40.52%	36.14%	31.53%	28.74%
0.5 ≤ d < 2	16.25%	12.96%	13.66%	11.16%	9.81%
> 2	0.69%	13.14%	19.72%	30.84%	37.12%

http://www.aloki.hu ● ISSN 1589 1623 (Print) ● ISSN 1785 0037 (Online)
DOI: http://dx.doi.org/10.15666/aeer/1802_28632877

Effects of nano-biochar on water and fertilizer utilization rates of maize

Effects of nano-biochar on soil moisture content in the soil profile

The effects of different nano-biochar concentrations on the soil moisture content is shown in *Figure 2*. From *Figure 2* it is shown that the soil moisture content amended with nano-biochar was significantly higher than in the control, especially in the maize seedling and shooting stages. Within 10 cm of the soil surface, the soil moisture content changed slightly, and it gradually increased with increasing soil depth. At soil depths of 10–30 cm, the soil moisture content increased rapidly. At soil depths of 30–35 cm, soil moisture content gradually stabilized. The surface soils had the lowest soil moisture content because they were affected by high rates of evapotranspiration. With increasing soil depth, the soil moisture content gradually increased. Ouyang et al. (2013) concluded that amending soil with biochar affected the shape of soil water retention curves. Itabari et al. (1993) and Shukla et al. (2012) found that below field capacity, higher soil moisture content in the 0–20 cm soil layer resulted in faster emergence of maize. Biochar added to soil reduces the number of macro-pores, increases the number of small pores and increases the water-holding capacity of the soil. Ahmed et al. (2018) indicated that biochar amended to soil at rates of 1% and 3% increased soil moisture content at field capacity. The results suggest that the application of nano-biochar to soil has potential to greatly improve the water-holding capacity of farmland which may increase the emergence rates of maize.

Effects of nano-biochar on soil nitrate

Optimal amounts of nitrogen fertilizer to maize crops can promote absorption and use of nitrogen, thereby increasing maize biomass and yield. At the seedling stage of spring maize, the horizontal and vertical distribution of roots is small, root hairs are fine, and root density is sparse. These root characteristics limit the uptake capacity of nitrogen from soil by maize. We observed that the difference between initial and after sowing measurements of soil nitrate were small, and the nitrate content was high (*Fig. 3*). During the shooting and tasselling stages, the growth and development rate of spring maize increased as the root system increased in size and density. Some of the nitrogen in the soil was absorbed by maize roots and some was transported to the deeper soil layers. These factors resulted in a decrease in soil nitrogen content and greater differences in nitrate between the initial and after sowing measurements. At the grain filling and maturation stages, the growth and development of maize was complete and the rate of nitrogen absorption decreased. The differences in nitrogen between filling and maturation stages were smaller than between the jointing and heading stages. Further analysis of *Figure 3* shows that the soil nitrate differences in the plots amended with nano-biochar at rates of 0.7% and 1% were smaller than the control group. At the advanced stages of spring maize growth, the differences in nitrate in the soil profile decreased as the nano-biochar contents increased. This indicated that under a consistent crop, the presence of nano-biochar decreases the rate of nitrogen transported to the deep soil (Albiter et al., 2010). Excessive nitrogen application causes the accumulation of nitrate in the soil and increases the risk of nitrate leaching (Zhang et al., 2010). Dempster et al. (2016) found that biochar application increased nitrate adsorption. Therefore, banding nano-biochar at 5–10 cm below the surface can inhibit nitrate leaching and increase nitrogen use efficiency in fertilized soils.

http://www.aloki.hu ● ISSN 1589 1623 (Print) ● ISSN 1785 0037 (Online)
DOI: http://dx.doi.org/10.15666/aeer/1802_28632877

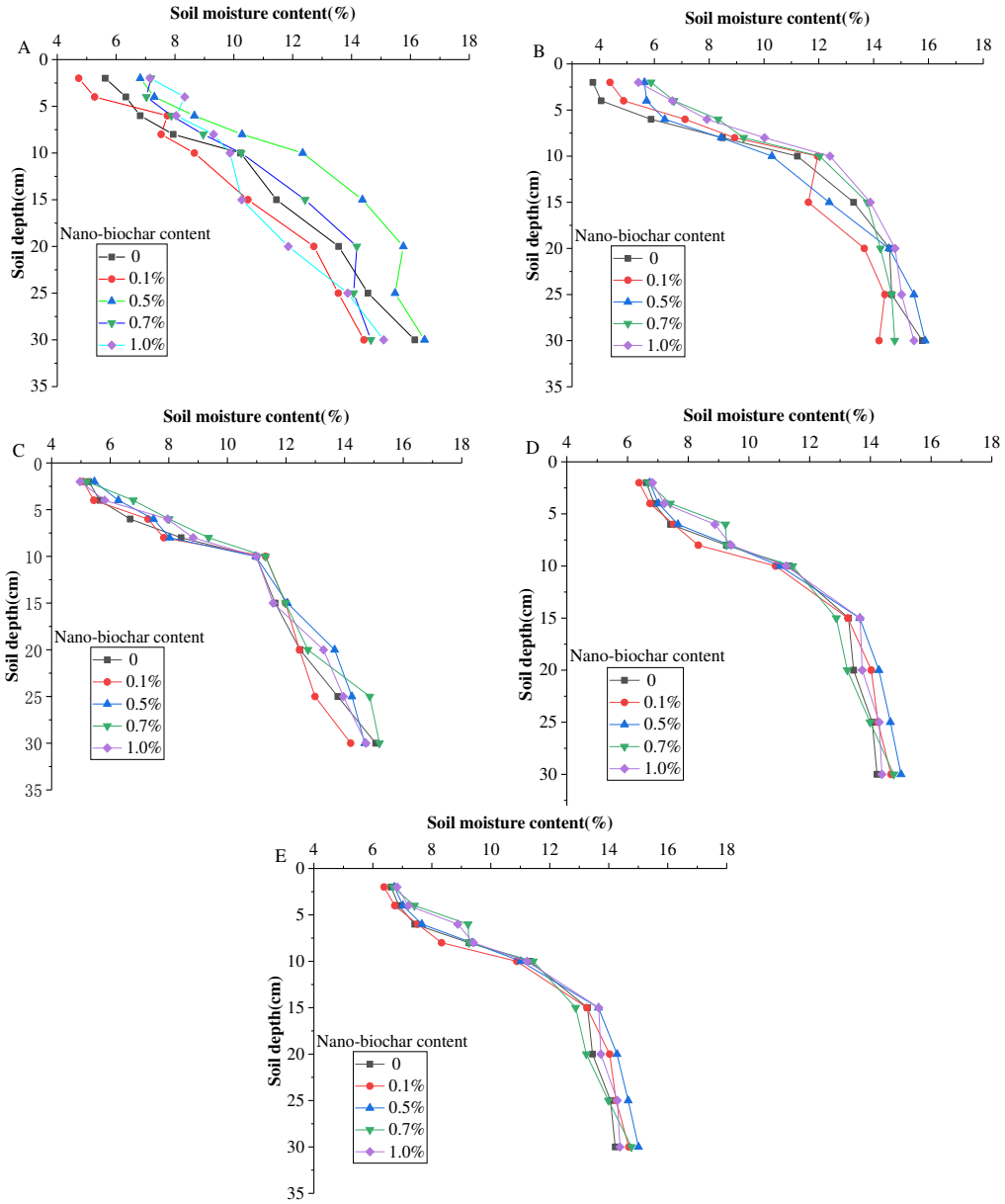

Figure 2. *The effect of different nano-biochar content on soil water content: (A) seedling stage; (B) shooting stage; (C) tasselling stage; (D) filling stage; (E) maturation stage*

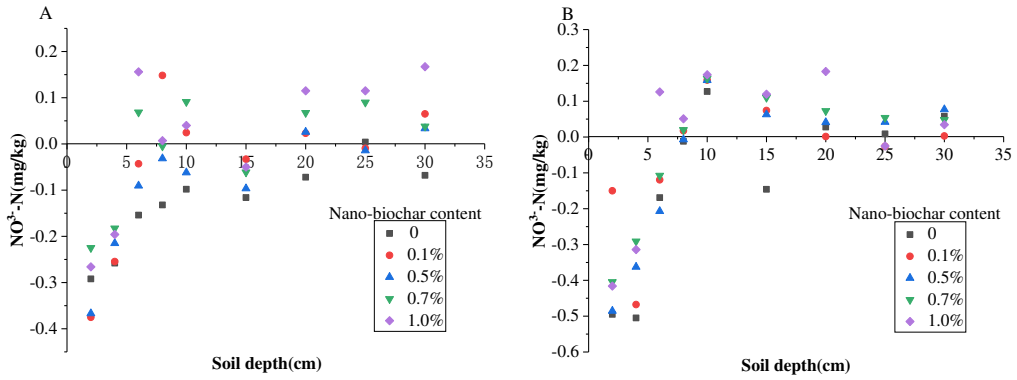

http://www.aloki.hu ● ISSN 1589 1623 (Print) ● ISSN 1785 0037 (Online)
DOI: http://dx.doi.org/10.15666/aeer/1802_28632877

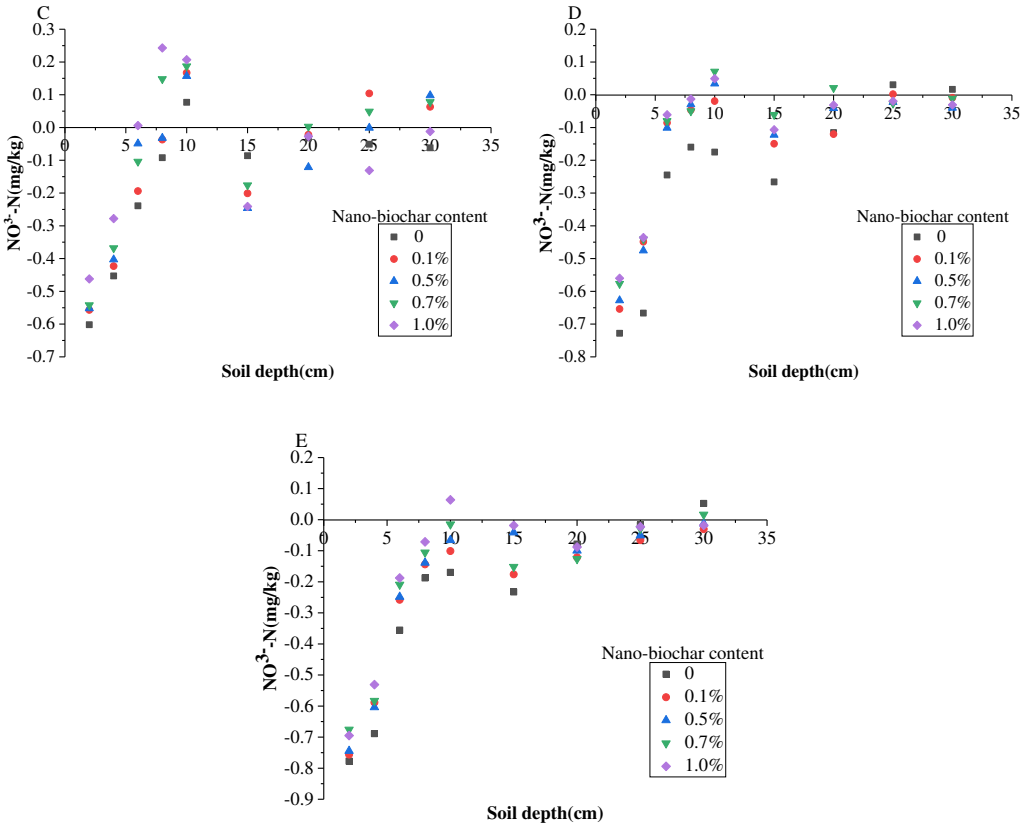

Figure 3. *The effect of different nano-biochar content of soil nitrate content: (A) seedling stage; (B) shooting stage; (C) tasselling stage; (D) filling stage; (E) maturation stage*

Nano-biochar effects on soil available potassium

The differences in potassium content in the soil profile at different growth stages of spring maize are shown in *Figure 4*. At 0–10 cm soil depth, the amount of available soil potassium in nano-biochar amended soil was higher than in the control. In the 5–10 cm soil layer, the average available potassium content in soil amended with nano-biochar at rates of 0.7% and 1% increased by 11.1% and 22.6% compared to the control, respectively, during the tasselling stage. During the early stages of spring maize growth, low amounts of potassium were absorbed by the plants. With the growth and development of spring maize, the uptake of potassium by plant roots gradually increased. At the filling and maturation stages, the growth of spring maize ended and the rate of potassium absorption decreased. Liu et al. (2012a) concluded that when nano-biochar was added to compost, plant-available Ca, K, P, and Na contents increased by a factor of 2.2, 2.5, 1.2, and 2.8, respectively. By increasing the availability of micro-nutrients like potassium in soil, nano-biochar can promote soil fertility (Dong, et al., 2016). When adsorption is poor, available potassium is highly mobile in the soil (Rens et al., 2018). The agglomeration of nano-biochars on soil particles increased the number of small soil pores thus inhibiting the longitudinal migration of potassium ions. This increases the residence time of the available potassium ions in the nano-biochar layer, and ensures high concentrations of potassium ions in the root layer. By doing so, this improves potassium use by spring maize.

http://www.aloki.hu ● ISSN 1589 1623 (Print) ● ISSN 1785 0037 (Online)
DOI: http://dx.doi.org/10.15666/aeer/1802_28632877

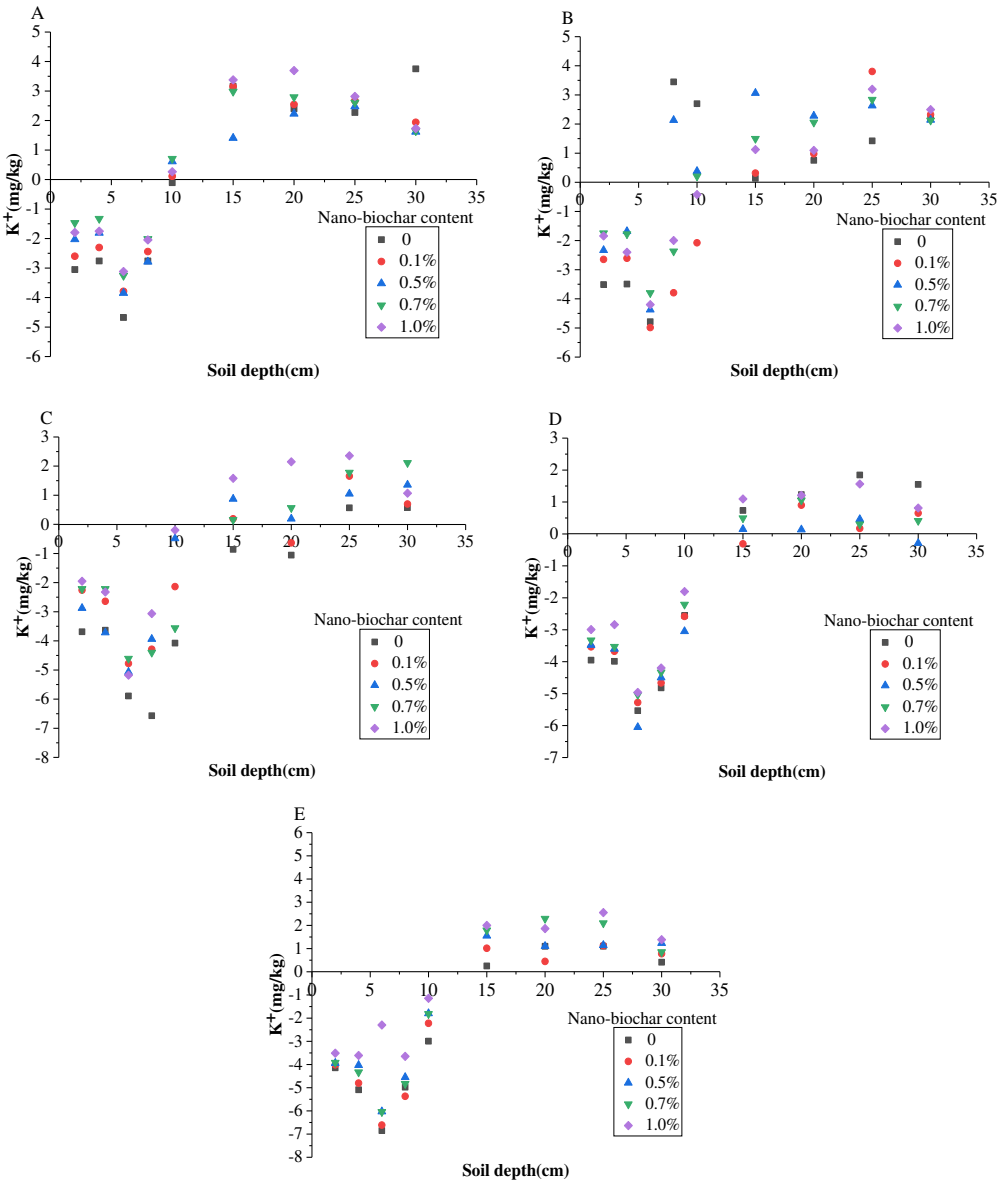

Figure 4. *The influence of nano-biochar content on soil potassium content: (A) seedling stage; (B) shooting stage; (C) tasselling stage; (D) filling stage;(E) maturation stage*

Nano-biochar effects on soil available phosphorus

The effects of nano-biochar content on soil available phosphorus in spring maize at different growth periods are shown in *Figure 5*. Available soil phosphorus concentrations of each treatment were lower in the measurements made after sowing than the initial measurements. There were few differences in soil phosphorus concentrations between each growth period. In the 0–5 cm soil depth, the differences in soil available phosphorus between the initial and after sowing measurements in nano-biochar amended soil were smaller than in the control group. The variation of the differences between the initial and after sowing soil concentrations decreased with increased nano-biochar concentrations. At 10–35 cm soil depth, available soil phosphorus variation was low, but the differences in available soil phosphorus initial

http://www.aloki.hu ● ISSN 1589 1623 (Print) ● ISSN 1785 0037 (Online)
DOI: http://dx.doi.org/10.15666/aeer/1802_28632877

and after sowing measurements in each treatment fluctuated greatly. This suggests that the ability of soil to maintain available phosphorus in the upper layers was greater when soil was banded with nano-biochar, and the ability to regulate available phosphorus in the soil below the carbon layer was limited. In soil, available phosphorus is easily adsorbed by soil particles; phosphorus has strong stability and weak mobility (Sharma et al., 2015; Petr et al., 2011). The soil available phosphorus contents increased with increasing amounts of applied biochar (Arif et al., 2017). Biochar amendments to degraded soils have been shown to improve crop yield and soil quality (Novak et al., 2009). Nano-biochar can significantly improve the inherent soil physical and chemical properties, increasing the proportion of large particles and reducing the soil porosity. A large amount of phosphorus was stabilized in the root zone where nano-biochar was banded because the phosphorus was absorbed to soil particles. This increased the content of phosphorus available for spring maize in the root zone.

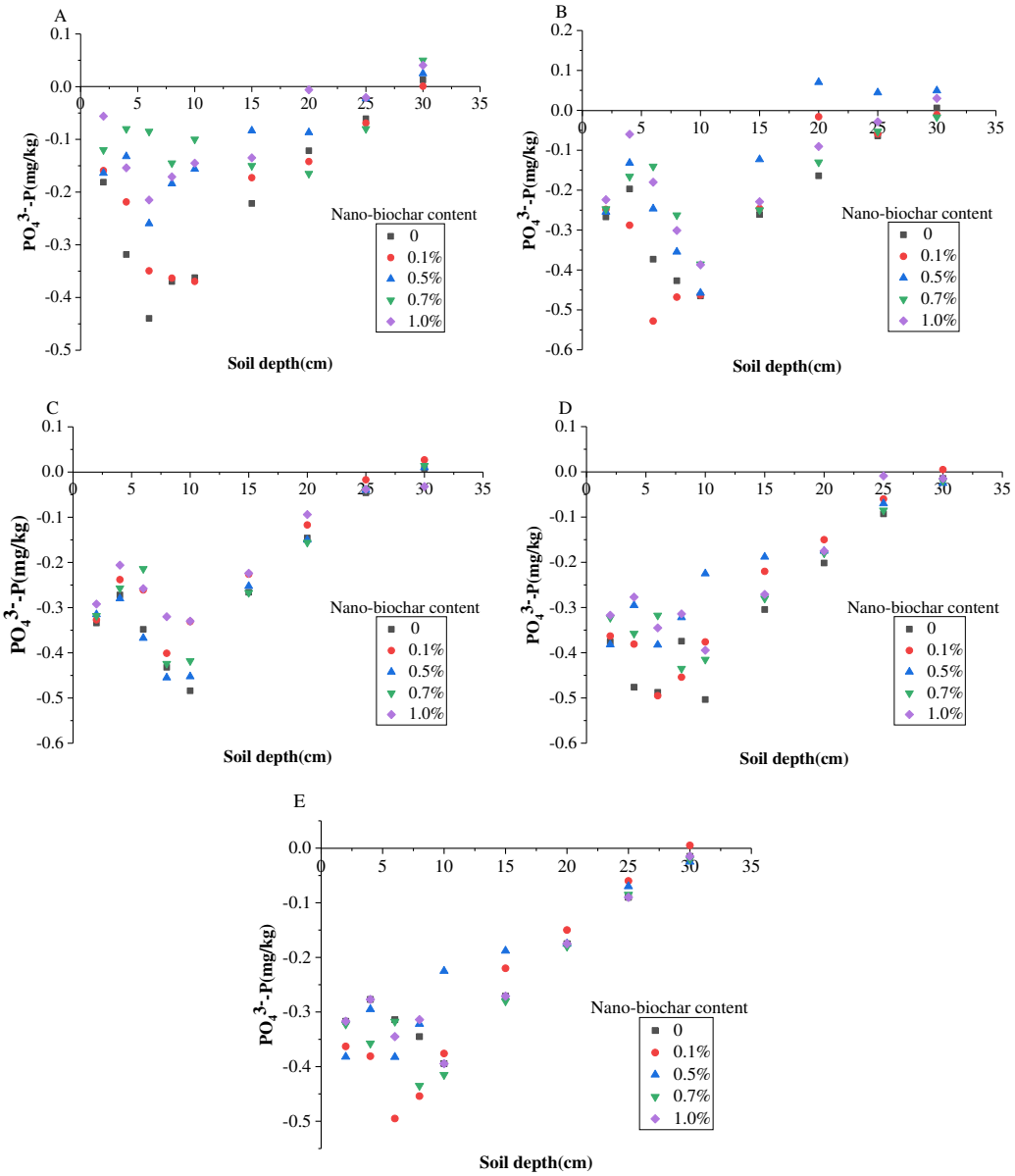

Figure 5. *The influence of nano-biochar on soil phosphorus content: (A) seedling stage; (B) shooting stage; (C) tasselling stage; (D) filling stage; (E) maturation stage*

http://www.aloki.hu ● ISSN 1589 1623 (Print) ● ISSN 1785 0037 (Online)
DOI: http://dx.doi.org/10.15666/aeer/1802_28632877

The effects of nano-biochar on growth traits of spring maize

The effects of nano-biochar on plant nutrients

The effects of nano-biochar content on spring maize root, stem, leaves and nutrients in each growth period are summarized in *Table 3*. As shown in *Table 3,* there is a significant correlation between each factor of different nano-biochar contents; the P-value < 0.01, indicating that each factor has a very significant effect on the test results. Visible, the application of nano-carbon in the soil has an important effect on maize growth. The roots, stems, leaves and other organs had the highest nutrient demand during the shooting stage. Nutrient uptake and accumulation rates in the shooting stage were higher than the tasselling, filling and maturation stages. After the shooting stage, the accumulation of nitrogen, phosphorus and potassium in spring maize plants gradually decreased. Adding nano-biochar to the soil resulted in strong adsorption of nano-biochar to soil nutrients which inhibited the vertical migration of nitrogen. This increased the plant nitrogen concentrations because it promoted nitrogen absorption from the soil by the spring maize, and then nitrogen was transported from the roots to other parts of the plant. Therefore, the spring maize in the nano-biochar amended plots had high concentrations of nitrogen.

Table 3. *The influence of nano-biochar content on spring maize nutrient content*

Growth stages	Nano-biochar content	Leaf (mg·kg^{-1})			Stem (mg·kg^{-1})			Root (mg·kg^{-1})		
		N	P	K	N	P	K	N	P	K
Shooting stage	0	23.21	1.66	30.54	26.88	1.85	36.22	18.37	1.36	38.48
	0.10%	23.28	1.69	30.88	26.84	1.93	36.28	18.41	1.33	38.41
	0.50%	23.44	1.72	31.23	27.01	2.01	36.71	18.62	1.34	38.56
	0.70%	23.65	1.75	31.58	27.12	2.05	36.88	18.77	1.41	39.13
	1%	23.58	1.81	31.94	27.23	2.13	37.04	19.16	1.45	39.44
	P-value	3.131×10^{-17}	2.9×10^{-12}	1.74×10^{-14}	3.14×10^{-18}	1.34×10^{-10}	1.68×10^{-16}	1.35×10^{-14}	6.29×10^{-12}	6.48×10^{-16}
Tasselling stage	0	17.06	1.47	23.66	21.54	1.55	28.42	14.21	1.28	27.53
	0.10%	17.03	1.42	23.78	21.06	1.47	27.86	14.26	1.26	27.56
	0.50%	17.15	1.39	24.15	22.13	1.53	28.19	14.98	1.24	27.68
	0.70%	17.88	1.61	24.26	22.41	1.6	29.21	14.73	1.32	27.43
	1%	18.13	1.65	24.37	22.68	1.63	29.48	15.09	1.38	28.11
	P-value	1.05×10^{-12}	2.16×10^{-9}	1.33×10^{-15}	1.17×10^{-12}	1.22×10^{-11}	1.97×10^{-13}	6.03×10^{-13}	2.11×10^{-11}	1.31×10^{-16}
Filling stage	0	12.9	1.28	19.18	15.63	1.34	21.14	10.04	1.16	22.58
	0.10%	12.74	1.17	19.21	15.77	1.36	21.25	10.82	1.05	22.54
	0.50%	12.86	1.31	19.28	15.86	1.38	21.36	10.66	1.18	22.87
	0.70%	13.15	1.32	19.33	16.14	1.4	21.77	11.15	1.22	23.14
	1%	13.23	1.38	19.45	16.47	1.47	22.06	11.33	1.26	23.65
	P-value	7.25×10^{-15}	2.99×10^{-10}	1.62×10^{-18}	6.57×10^{-14}	5.26×10^{-12}	1.94×10^{-14}	3.76×10^{-11}	7.85×10^{-10}	4.46×10^{-14}
Maturation stage	0	8.58	1.06	13.37	11.15	1.13	16.62	7.43	1.08	15.37
	0.10%	8.68	1.11	13.41	10.98	1.18	16.48	7.56	1.14	16.18
	0.50%	8.79	1.08	13.2	11.23	1.2	16.83	7.84	1.2	16.44
	0.70%	9.03	1.15	13.68	11.54	1.22	17.14	7.88	1.22	16.37
	1%	9.36	1.2	13.77	11.86	1.24	17.36	8.01	1.26	17.14
	P-value	4.18×10^{-12}	7.42×10^{-11}	1.48×10^{-14}	1.43×10^{-12}	4.63×10^{-12}	8.23×10^{-14}	1.54×10^{-12}	3.05×10^{-10}	9.37×10^{-12}

N = available nitrogen; P = available phosphorus; K = available potassium

The amount of phosphorus absorbed by spring maize plants was lower than that of nitrogen and potassium. Applying phosphate fertilizer to soil can result in the accumulation of high concentrations of phosphorus in surface soils which cannot be

http://www.aloki.hu ● ISSN 1589 1623 (Print) ● ISSN 1785 0037 (Online)
DOI: http://dx.doi.org/10.15666/aeer/1802_28632877

effectively converted into plant-available forms of phosphorus (Turtola et al., 1999). At different growth stages in nano-biochar amended soil, the phosphorus content of spring maize plants was higher than the control group, indicating nano-biochar can promote phosphorus leaching and the absorption of phosphorus by spring maize roots.

With strong mobility and water solubility of potassium ions in soil, its content is higher than nitrogen and phosphorus. This is why we observed that the accumulation of available potassium was larger than nitrogen and phosphorus in the plant during the growth period of spring maize. However, soil adsorption of potassium ions is poor, so water-soluble potassium ions tend to migrate downward into the soil. Following banding, the nano-biochar adsorbed potassium and the longitudinal migration rate of potassium in the soil decreased, which extended the retention time of potassium in the root soil layer of spring maize.

Spring maize biomass accumulation and yields are closely related to the accumulation of plant nutrients. After the jointing stage, the growth and development of spring maize organs accelerates, and the absorption and accumulation rate of nutrients also greatly increases (Qin et al., 2012). We noted the accumulation of plant nutrients increased continuously throughout the whole growth period. The soil nitrogen and potassium contents were highest at the filling stage, and the soil phosphorus content were highest at the maturation stage. Nutrient accumulation in the spring maize plants was the product of soil nutrient availability and plant biomass requirements. During the spring maize growth period, the nutrient content of crops tended to decline while the nutrient accumulation tended to increase.

Figure 6 summarizes the accumulation of nitrogen, phosphorus and potassium in spring maize plants for each nano-biochar treatment during each spring maize growth period. As shown in *Figure 6,* plant accumulation of nutrients increased rapidly after the shooting stage, the accumulation of nitrogen and potassium were highest at the filling stage, and the accumulation of phosphorus was highest at the maturation stage. In each growth stage, nano-biochar had a significant effect on the absorption of nutrients in spring maize, with the greatest accumulation of nutrients associated with 0.7% and 1% nano-biochar treatments.

The effects of nano-biochar on spring maize growth and yield

Table 4 shows the effects of nano-biochar contents on growth indicators of spring maize in every growth stage. As shown in *Table 4,* in the plots with higher nano-biochar content, the plant height, stem diameter and leaf area of spring maize (0.7% and 1%) were significantly higher than those in the control group in the same growth stage. Over the spring maize life-cycle, the plant height and leaf area increased, but the basal stem diameter first increased and then decreased. This was attributed to the vigorous growth of spring maize at the shooting stage when a large amount of water was absorbed by the roots and transported upward. During this time, spring maize was more inclined to radial development, which weakened the horizontal growth.

Table 5 shows the effects of nano-biochar content on maize yields. Based on *Table 5,* there was a significant correlation between the 1000-grain weight, yield and different nano-biochar contents; the P-value was less than 0.01, indicating that the application of nano-carbon in the soil has an important effect on maize yield. The plots with higher nano-biochar content (0.7% and 1%) had significantly greater 1000-grain weight and yield than the control. Compared with the control group, the yield of 0.7% and 1% nano-biochar treatment plots were 4.4% and 5.7% greater, respectively.

http://www.aloki.hu ● ISSN 1589 1623 (Print) ● ISSN 1785 0037 (Online)
DOI: http://dx.doi.org/10.15666/aeer/1802_28632877

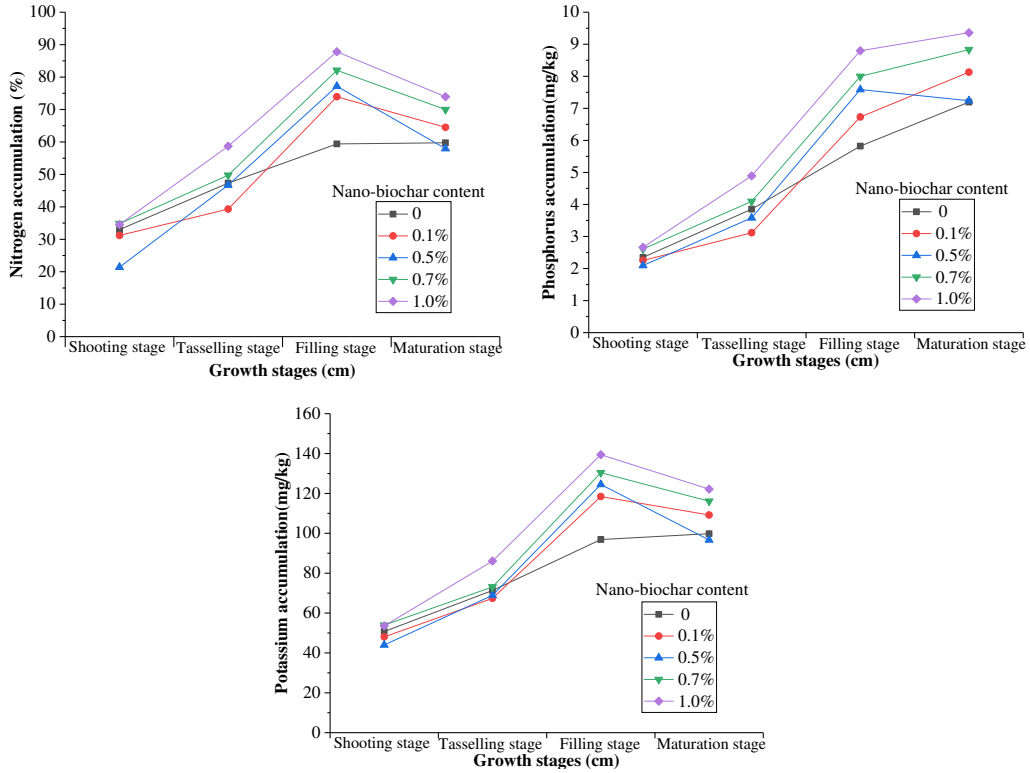

Figure 6. *The influence of nano-biochar contents on nutrient accumulation in spring maize*

Table 4. *The influence of nano-biochar content on spring maize growth indices*

Nano-biochar content	Measurement variables	Growth stages				
		Seedling stage	Shooting stage	Tasselling stage	Filling stage	Maturation stage
0	Plant height /cm	46.2±1.1b	90.3±2.2b	168.4±2.7c	188.4±5.4b	226.7±3.9a
	Stem diameter /cm	1.98±0.291b	3.62±0.155a	6.77±0.148b	7.04±0. 088b	6.83±0.236a
	Leaf area /cm^2	45.3±1.2b	882.4±11.4c	4654.8±21.3c	5763.9±23.1c	5614.2±38.2c
	Biomass /g	3.12±0.141c	21.7±3.52b	75.2±8.67b	221.6±17.33c	398.3±23.23c
0.1%	Plant height /cm	45.4±2.4b	92.3±3.2a	170.4±8.2b	190.5±7.3b	224.3±6.4b
	Stem diameter /cm	2.03±0. 208a	3.58±0. 232a	6.81±0. 313a	7.01±0. 283b	6.78±0.426b
	Leaf area /cm^2	47.1±3.0a	891.1±23.0b	4668.5±41.7b	5784.1±37.5b	5598.5±55.1c
	Biomass /g	3.21±0.523bc	20.8±2.031b	77.3±5.051b	225.9±9.142c	404.6±18.216c
0.5%	Plant height /cm	47.1±1.4a	92.4±3.3a	172.4±1.5b	193.3±2.6a	228.3±1.9a
	Stem diameter /cm	2.111±0. 152a	3.66±0. 206a	6.84±0. 236a	7.05±0. 218b	6.88±0.134a
	Leaf area /cm^2	47.5±1.5a	895.8±28.7b	4685.3±52.5b	5804.2±41.3b	5645.6±62.1b
	Biomass /g	3.44±0.116b	22.6±2.48a	76.8±5.73b	232.6±8.14b	415.6±14.74b
0.7%	Plant height /cm	46.8±1.9a	93.1±3.8a	173.9±5.9b	195.6±7.8a	231.7±7.2a
	Stem diameter /cm	2.08±0.217a	3.64±0. 276a	6.86±0. 259a	7.1±0. 393a	6.84±0.308a
	Leaf area /cm^2	48.2±3.0a	904.6±33.1b	4705.9±67.9b	5844.3±52.4a	5714.9±71.7a
	Biomass /g	3.73±0.033a	22.7±1.025a	80.1±3.032a	241.1±7.208a	421.8±6.316b
1%	Plant height /cm	48.6±2.1a	95.2±4.7a	176.4±6.4a	196.5±5.2a	233.7±8.7a
	Stem diameter /cm	2.15±0.203a	3.7±0. 337a	6.91±0. 361a	7.14±0. 644a	6.94±0.776a
	Leaf area /cm^2	49.9±3.2a	918.7±15.8a	4745.2±44.2a	5865.8±83.3a	5725.8±65.5a
	Biomass /g	3.8±0.119a	23.5±1.445a	81.4±4.628a	245.3±2.53a	430.4±8.97a

'±' = standard deviation. There is no significant difference at 0.05 level in the same column of data with the same letters (Duncan's method)

http://www.aloki.hu ● ISSN 1589 1623 (Print) ● ISSN 1785 0037 (Online)
DOI: http://dx.doi.org/10.15666/aeer/1802_28632877

Table 5. *The yield of spring maize in every plot*

Nano-biochar content	1000-grain weight (g)	Yield (kg·hm^{-2})
0	252.4	4836.25
0.1%	250.3	4853.18
0.5%	261.1	4908.68
0.7%	266.8	5047.42
1%	274.9	5112.88
p-value	9.55×10^{-12}	2.51×10^{-13}

Conclusion

The study tested different rates of nano-biochar application and analyzed the subsequent effects on physical and chemical properties of soil, soil water characteristics, fertilizer use and growth characteristics of spring maize in the field. The results indicated that banding nano-biochar in the root zone slightly increased soil bulk density. Amending soil with nano-biochar increased soil aggregates with the soil particle size > 2 mm from 0.69 to 37.12%, and nano-biochar application rates of 0.7% and 1% had the greatest effects on improving soil water-stable aggregates. The band of nano-biochar in the soil inhibited the movement of soil moisture to the deep soil and decreased evapotranspiration. It also improved nutrient retention and delayed the leaching of nitrogen, phosphorus and potassium in soil. Nano-biochar also prompted spring maize uptake of soil nutrients. Maize grown in soil amended with nano-biochar had significantly greater plant height, stem diameter and leaf area than those grown in soils without nano-biochar. The plot with the highest nano-biochar contents (0.7% and 1%) has the greatest 1000-grain weights and yields. Compared with the control group, the yields of 0.7% and 1% nano-biochar were increased by 4.4% and 5.7%, respectively. Nano-biochar has an obvious effect on soil improvement and crop growth, but its application is slightly complicated. In order to promote the large-scale popularization of this method on Loess Plateau, how to simplify the method is still the key problem we should consider.

Acknowledgments. This study was funded by the National Natural Science Foundation of China (41977007 ; 41830754 ; 41807131), Research project of State Key Laboratory of Eco-hydraulics in Northwest Arid Region of China (2019KJCXTD-4 ; QJNY-2019-01).

REFERENCES

[1] Ahmed, F., Arthur, E., Plauborg, F., et al. (2018): Biochar amendment of fluvio-glacial temperate sandy subsoil: effects on maize water uptake, growth and physiology. – Journal of Agronomy and Crop Science 204(2): 123-136.

[2] Albiter, M. A., Crooks, R. M., Zaera, F., et al. (2010): Adsorption of carbon monoxide on dendrimer-encapsulated platinum nanoparticles: liquid versus gas phase. – The Journal of Physical Chemistry Letters 1(1): 38-40.

[3] Arif, M., Ilyas, M., Riaz, M., et al. (2017): Biochar improves phosphorus use efficiency of organic-inorganic fertilizers, maize-wheat productivity and soil quality in a low fertility alkaline soil. – Field Crops Research 214: 25-37.

[4] Bossuyt, H., Denef, K., Six, J., et al. (2001): Influence of microbial populations and residue quality on aggregate stability. – Applied Soil Ecology 16(3): 195-208.

http://www.aloki.hu ● ISSN 1589 1623 (Print) ● ISSN 1785 0037 (Online)
DOI: http://dx.doi.org/10.15666/aeer/1802_28632877

[5] Dempster, D. N, Jones, D. L, Murphy, D. V. (2012): Clay and biochar amendments decreased inorganic but not dissolved organic nitrogen leaching in soil. – Soil Research 50(3): 216-221.
[6] Dong, X., Guan, T., Li, G., et al. (2016): Long-term effects of biochar amount on the content and composition of organic matter in soil aggregates under field conditions. – Journal of Soils and Sediments 16(5): 1481-1497.
[7] Fan, J., Yu, G., Wang, Q., et al. (2014): Mulching effects on water storage in soil and its depletion by alfalfa in the loess plateau of northwestern China. – Agricultural Water Management 138: 10-16.
[8] Fu, Z., Wang, Y., An, Z. (2015): Spatio-temporal characteristics of soil bulk density and saturated hydraulic conductivity at small watershed scale on loess plateau. – Transactions of the Chinese Society of Agricultural Engineering 31(13): 128-134 (in Chinese).
[9] Guo, Y., Li, Y., Zhu, T., Ye, M. (2013): Effects of concentration and adsorption product on the adsorption of SO_2 and NO on activated carbon. – Energy Fuels 27(1): 360-366.
[10] Han, F., Zheng, J., Hu, W., et al. (2010): Spatial variability and distribution of soil nutrients in a catchment of the loess plateau in china. – Acta Agriculturae Scandinavica, Section B - Plant Soil Science 60(1): 48-56.
[11] Itabari, J. K., Gregory, P. J., Jones, R. K. (1993): Effects of temperature, soil water status and depth of planting on germination and emergence of maize (Zea mays) adapted to semi-arid eastern Kenya. – Experimental Agriculture 29(3): 351-364.
[12] Jia, Y. H., Shao, M. A., Jia, X. X. (2013): Spatial pattern of soil moisture and its temporal stability within profiles on a loessial slope in northwestern China. – Journal of Hydrology 495: 150-161.
[13] Liang, B., Lehmann, J., Solomon, D., et al. (2006): Black carbon increases cation exchange capacity in soils. – Soil Science Society of America Journal 70(5): 1719.
[14] Liu, J., Schulz, H., Brandl, S., et al. (2012a): Short-term effect of biochar and compost on soil fertility and water status of a dystric cambisol in NE Germany under field conditions. – Journal of Plant Nutrition and Soil Science 175(5): 698-707.
[15] Liu, Y., Fu, B., Yihe Lü, et al. (2012b): Hydrological responses and soil erosion potential of abandoned cropland in the Loess Plateau, China. – Geomorphology 138(1): 0-414.
[16] Liu., Y. L., Zhou, B. B., Z., Wang, Q. J., et al. (2015): Effects of nano-carbon on water movement and solute transport in loessial soil. – Journal of Soil and Water Conservation 29(1): 21-25 (in Chinese).
[17] Manivasakan, P., Karunakaran, G., Yuvakkumar, R., et al. (2013): Effect of nanosilica and silicon sources on plant growth promoting rhizobacteria, soil nutrients and maize seed germination. – IET Nanobiotechnology 7(3): 70-77.
[18] Mesarič, T., Baweja, L., Drašler, B., et al. (2013): Effects of surface curvature and surface characteristics of carbon-based nanomaterials on the adsorption and activity of acetylcholinesterase. – Carbon 62: 222-232.
[19] Novak, J. M., Lima, I., Xing, B. S., et al. (2009): Characterization of designer biochar produced at different temperatures and their effects on a loamy sand. – Annals of Environmental Science 3: 195-206.
[20] Ouyang, L., Wang, F., Tang, J., et al. (2013): Effects of biochar amendment on soil aggregates and hydraulic properties. – Journal of Soil Science and Plant Nutrition 13(4): 991-1002.
[21] Petr, K., Bernd, S., Astrid, R., et al. (2011): Citramalic acid and salicylic acid in sugar beet root exudates solubilize soil phosphorus. – BMC Plant Biology 11(1): 121.
[22] Qin, X., Liu, K., Zhou, S. L. (2012): Studies on characteristics of nitrogen absorption and utilization under water-saving cultivation in winter wheat region of north china plain. – Journal of Agricultural Science Technology, pp. 96-101 (in Chinese).
[23] Reese, C. L., Clay, D. E., Clay, S. A., et al. (2014): Winter cover crops impact on corn production in semiarid regions. – Agronomy Journal 106(4): 1479-1488.

http://www.aloki.hu ● ISSN 1589 1623 (Print) ● ISSN 1785 0037 (Online)
DOI: http://dx.doi.org/10.15666/aeer/1802_28632877

[24] Rens, H., Bera, T., Alva, A. K. (2018): Effects of biochar and biosolid on adsorption of nitrogen, phosphorus, and potassium in two soils. – Water, Air, and Soil Pollution 229(8): 281. https://doi.org/10.1007/s11270-018-3925-8.
[25] Roy, J. L., Mcgill, W. B. (2000): Flexible conformation in organic matter coatings: an hypothesis about soil water repellency. – Canadian Journal of Soil Science 80(1): 143-152.
[26] Sharma, R., Bell, R. W., Wong, M. T. F. (2015): Phosphorus forms in soil solution and leachate of contrasting soil profiles and their implications for P mobility. – Journal of Soils and Sediments 15(4): 854-862.
[27] Shukla, J., Maldar, N. N., Sharon, M., et al. (2012): Synthesis of carbon nano material from different parts of maize using transition metal catalysts. – Der Chemica Sinica 1058-1070.
[28] Six, J., Bossuyt, H., Degryze, S., et al. (2004): A history of research on the link between (micro)aggregates, soil biota, and soil organic matter dynamics. – Soil and Tillage Research 79(1): 7-31.
[29] Tan, S., Zhou, B., Wang, Q. (2016): Effects of nanocarbon on the hydraulic parameters and the solute transport process for disturbed loessial soil. – Arabian Journal of Geosciences 9(1): 4.
[30] Turtola, E., Yli-Halla, M. (1999): Fate of phosphorus applied in slurry and mineral fertilizer: accumulation in soil and release into surface runoff water. – Nutrient Cycling in Agroecosystems 55(2): 165-174.
[31] Vacher, C. A., Loch, R. J., Raine, S. R., et al. (2003): Effect of polyacrylamide additions on infiltration and erosion of disturbed lands. – Australian Journal of Soil Research 41(8): 1509.
[32] Wang, Y., Hu, W., Zhu, Y., et al. (2015): Vertical distribution and temporal stability of soil water in 21-m profiles under different land uses on the Loess Plateau in China. – Journal of Hydrology 527: 543-554.
[33] Wang, Y., Han, Z., Zhang, Z., et al. (2016): Biochar application promote growth parameters of soybean and reduces the growth difference. – Communications in Soil Science and Plant Analysis 47(12): 1493-1502.
[34] Zhang, J. H., Liu, J. L., Zhang, J. B., et al. (2010): Effects of nitrogen application rates on translocation of dry matter and nitrogen utilization in rice and wheat. – Acta Agronomica Sinica 36(10): 1736-1742.
[35] Zhou, B. B., Chen, X. P., Lü, J., et al. (2017): Inhibiting effect of nano-carbon on rainfall erosion of different vegetation cover on loess slope land. – Transactions of the Chinese Society of Agricultural Engineering 33(2): 116-124 (in Chinese).
[36] Zhou, B. B., Chen, X. P., Wang, Q. J., et al. (2018): Effects of nano carbon on soil erosion and nutrient loss in a semi-arid loess region of Northwestern China. – International Journal of Agricultural Biological Engineering 11(1): 138-145.

http://www.aloki.hu ● ISSN 1589 1623 (Print) ● ISSN 1785 0037 (Online)
DOI: http://dx.doi.org/10.15666/aeer/1802_28632877

EFFECT OF NITROGEN FERTILIZER APPLICATION RATE ON NITRATE REDUCTASE ACTIVITY IN MAIZE

CHEN, H.* – HUANG, L.

College of Life Science, Henan Institute of Science and Technology, Xinxiang 453003, China

**Corresponding author*
e-mail: chenhongwei1966@sina.cn

(Received 26th Oct 2019; accepted 23rd Jan 2020)

Abstract. In this paper, the effect of nitrogen application on nitrate reductase activity of the Sidan 19 maize (*Zea mays* L.) cultivar was studied. The Sidan 19 maize is a medium maturity maize single variety, which is a hybrid of 44/4 (Huangzao4 improved line) as the female parent and Mo17 as the male parent. It has high average hectare yield, good early-onset, easy to catch seedlings and other excellent properties, so it was selected as a model plant. In order to study the effect of nitrogen application on the activity of nitrate reductase in maize, the method of this paper is to prepare nitrate reductase, extract corn leaves, add trichloroacetic acid solution to stop the enzyme reaction, and use standard curve method to determine the content of maize nitrate reductase. The experimental results show that: (1) N application rate of nitrate reductase activity (NRA) was N300 > N200 > N100 > N0. (2) NRA activity of maize leaves was the lowest at the seedling stage, the highest at heading stage, and then decreased. Under 15% pec-6000 drought stress, 72 mmol/L salt stress and 72 mmol/L Saline-alkali stress, nitrate reductase activity of maize leaves and roots was the highest. (3) Under the same amount of nitrogen application, the nitrate reductase activity of maize roots increased, and the nitrate reductase (NR) activity of leaves was higher than that of roots under the same stress effect. (4) Under the same amount of nitrogen application, the nitrate reductase activity of maize leaves was the highest. At nitrogen levels of N_0, $N_{0.1}$ and $N_{0.5}$, the activity of nitrate reductase enzymes in roots of each treatment from highest to lowest were sodium nitrate > urea > ammonium chloride. It showed that the activity of nitrate reductase increased with the increase of nitrogen application. The nitrate reductase activity of maize root was the highest at heading stage, and under low nitrogen condition.
Keywords: *single variety, model plant, trichloroacetic acid solution, standard curve method, heading stage*

Introduction

As the world's largest crop, maize is not only an important food crop, but also a feed and industrial raw material. It occupies an important position in the national economy (Zheng et al., 2018). Scientists have been working to increase their production and productivity in order to solve the food problem and the shortage of feed and industrial raw materials in China (Helmers et al., 2017). At present, with the increase of population, the expansion of animal husbandry and the shortage of energy, the total demand for crop production in the market are increasing day by day, and the demand for grain in China is increasing rigidly. At present, the number of cultivated lands in China is decreasing year by year, so improving the unit yield is one of the key measures to solve the food shortage (Russo et al., 2017). The increasing dependence of high-yielding varieties on chemical fertilizers, especially nitrogen fertilizers, has resulted in the increasing use of nitrogen fertilizers in China (Li et al., 2017). Excessive application of nitrogen fertilizer resulted in low efficiency of nitrogen fertilizer use in maize production in China, resulting in a large amount of nutrient loss to the environment and serious environmental problems (İlhan et al., 2018). How to improve the utilization rate of nitrogen fertilizer, reduce the loss of nitrogen fertilizer and the environmental

http://www.aloki.hu ● ISSN 1589 1623 (Print) ● ISSN 1785 0037 (Online)
DOI: http://dx.doi.org/10.15666/aeer/1802_28792894

pollution caused by the application of nitrogen fertilizer in maize under the current difficult conditions is a difficult problem to be solved urgently in the maize planting industry (Juárezhernández et al., 2017). Breeding and screening nitrogen-efficient maize varieties is one of the main ways to solve the problems of food shortage, shortage of arable land and environmental pollution (Zhang et al., 2017). It is the premise and basis for breeding maize varieties with high nitrogen efficiency to study the nitrogen uptake regularity and identify and excavate candidate genes for high nitrogen efficiency (Iqbal et al., 2017). Nitrate reductase, as an important inducible enzyme in nitrogen metabolism of maize, is the first rate-limiting enzyme in the process of nitrogen uptake and utilization. Nitrate reductase plays a key biological role in the process of efficient nitrogen utilization in maize (Kang et al., 2017).

In the process of plant growth and development, many biological metabolic reactions, such as N metabolism, are involved. N is one of the essential elements in plants. N is an important factor in plant metabolic system related to yield. Nitrate, ammonia and amino acid are the three main forms of nitrogen uptake by plants, and nitrate is the most important form of nitrogen uptake. When external nitrogen enters plants, ammonia, amino acids and amides are formed in turn, and then they participate in the biosynthesis of other living substances for plant growth, development and metabolism (Li, 2017). Nitrate reductase plays an important role in plant nitrogen uptake and development. As a key enzyme, nitrate reductase plays an important role in plant nitrogen uptake and assimilation. Its activity can directly reflect the status of plant nitrogen uptake and utilization (Liu et al., 2018). The results showed that nitrate reductase activity was affected by environmental factors such as water, nitrate concentration, light, carbon dioxide, molybdenum and temperature, and exogenous hormone analogues such as cytokinin, abscisic acid, indole-3-acetic acid, gibberellin and ethephon could affect nitrate reductase activity (Sui et al., 2017). Nitrate reductase was found in all tissues of maize, but its activity was the highest in maize leaves. Nitrate reductase activity has an important impact on the utilization of nitrate nitrogen, is an important basis for crop selection of nitrogen fertilizer, and is also one of the breeding indicators for crop nitrogen efficient utilization (Castillogodina et al., 2018). The main content of this paper is to study the effect of nitrogen application rate on nitrate reductase activity of maize, so as to improve crop yield, avoid nitrogen loss, promote the development of agricultural technology and promote the progress of agricultural economy. Therefore, it is necessary to study the effect of nitrogen application rate on nitrate reductase activity of maize.

Materials and methods

This study was carried out in the experimental site of Sichuan Agricultural University in 2019. The GPS coordinates are N29° 58′ 54.23″ north latitude and E102° 59′ 57.54″ east longitude. The experimental variety is Sidan 19, and the sowing time is July. The method of sowing or strip sowing is adopted, the temperature is 20 °C, the water is sufficient, and the time is 5-7 days. The nutrient content of the soil is shown in *Table 1*.

Effects of different amounts of pure ammonia fertilizer on nitrate reductase activity in maize

Fixed the amount of phosphorus and potassium, four nitrogen fertilizer treatments were set up in the experiment:

http://www.aloki.hu ● ISSN 1589 1623 (Print) ● ISSN 1785 0037 (Online)
DOI: http://dx.doi.org/10.15666/aeer/1802_28792894

(1) N0: no nitrogen fertilizer
(2) N100: 100 kg of pure nitrogen per hectare
(3) N200: 200 kg of pure nitrogen per hectare
(4) N300: 300 kg of pure nitrogen per hectare

The experiment was designed by random block design and repeated three times. The length of residential area is 5 m and the distance of 6 rows is 70 cm.

Table 1. *Nutrient content of soil*

Organic matter content	2.56%
Total nitrogen	0.134
Total phosphorus	0.064
Slowly available potassium	98
Hydrolyzable nitrogen	146.2
Available phosphorus	44.78
Available potassium	143.2
pH value	6.62

Effects of different proportion of nitrogen fertilizer applied by stages on nitrate reductase activity in maize

The total amount of chemical fertilizer application is fixed, which is pure N 370 mg/hm^2, pure P_2O_5 150 kg/hm^2 and pure K_2O 150 kg/hm^2. Nitrogen fertilizer is applied in stages according to different proportions, as detailed in *Table 2*.

Table 2. *Distribution ratio of nitrogen fertilizer in different growth periods*

Handle	Base fertilizer	Topdressing at jointing stage	Topdressing at silking stage
N1	370	0	0
N2	296	74	0
N3	296	37	37
N4	222	148	0
N5	222	111	37
N6	222	74	74

Nitrate reductase activity in leaves and roots was measured at seedling stage, jointing stage, trumpet mouth stage, booting stage, silking stage, filling stage and maturity stage (Ma et al., 2017). The top fully unfolded leaves were selected before silking, and the ear leaves were selected after silking (Han et al., 2018), and the roots were selected to be measured at a distance of more than 1 cm from the root tip.

Effects of nitrogen fertilizer application rate on nitrate reductase activity in maize under different stress environment

Formulas of simulated solutions for different stress treatments are shown in *Table 3*. After 48 h of stress treatment, physiological indexes were measured (Wang et al., 2018).

http://www.aloki.hu ● ISSN 1589 1623 (Print) ● ISSN 1785 0037 (Online)
DOI: http://dx.doi.org/10.15666/aeer/1802_28792894

Table 3. *Formulas of solutions for different stress treatments*

Stress treatment	Ratio of nitrogen fertilizer	Solution formulation	Solution J_c (MPa)	Solution pH
Drought stress	Application of pure nitrogen per hectare 100 kg	Hoaglangsolution + 15% PEC-6000 (Actual site conditions)	-0.363	6.8
		Hoaglangsolution + 15% PEC-6000 (Water culture experiment)		
Salt stress	Application of pure nitrogen per hectare 100 kg	Hoaglang solution + 72 mmol/L NaCl (Actual site conditions)	-0.363	6.7
		Hoaglang solution + 72 mmol/L NaCl (Water culture experiment)		
Saline-alkali stress	Application of pure nitrogen per hectare 100 kg	Hoaglangsolution + 72 mmol/L $NaHCO_3$ (Actual site conditions)	-0.363	8.9
		Hoaglangsolution + 72 mmol/L $NaHCO_3$ (Water culture experiment)		
Control (normal)	Application of pure nitrogen per hectare 100 kg	Hoaglangsolution (Hoaglangsolution + 72 mmol/L $NaHCO_3$)	-0.050	6.5
		Hoaglang solution (Water culture experiment)		

Effects of nitrogen fertilizer varieties and nitrogen fertilizer dosage on nitrate reductase activity in maize

The experimental settings are as shown in *Table 4*.

Table 4. *Effects of nitrogen fertilizer varieties and nitrogen fertilizer dosage on nitrate reductase activity in maize*

Nitrogen fertilizer varieties	Code name	Control level (g/kg)
Sodium nitrate	N_0	0.00
	$N_{0.1}$	0.61
	$N_{0.3}$	1.82
	$N_{0.5}$	3.04
Ammonium chloride	N_0	0.00
	$N_{0.1}$	0.38
	$N_{0.3}$	1.15
	$N_{0.5}$	1.91
Ammonium nitrate	N_0	0.00
	$N_{0.1}$	0.28
	$N_{0.3}$	0.86
	$N_{0.5}$	1.43
Urea	N_0	0.00
	$N_{0.1}$	0.22
	$N_{0.3}$	0.64
	$N_{0.5}$	1.07

http://www.aloki.hu ● ISSN 1589 1623 (Print) ● ISSN 1785 0037 (Online)
DOI: http://dx.doi.org/10.15666/aeer/1802_28792894

Method of determination

(1) Nitrate reductase production (Hwang et al., 2018) could be induced by adding 50 mmol/L KNO_3 or $NaNo_3$ to the water of maize seedlings one day before sampling.

(2) 0.5 g of maize leaves were weighed (three parts were cut into about 1 cm segments) and put into three triangular bottles, one of which was used as control, and the other two were used for enzyme activity determination (Song et al., 2017).

(3) Reaction: First add 1 mL 30% trichloroacetic acid solution to the control triangle bottle, then add 9 ml 0.1 moL/L KNO_3 solution to each triangle bottle. After mixing, put it into the dryer immediately, and exhaust for 30 min (during several times, air is injected, then vacuum is pumped to make the blade sink completely into the bottom of the bottle, and then react in 25-degree darkness for half an hour, respectively (Ahamed et al., 2017). 1 m 130% trichloroacetic acid was added to the determination bottle (except the control bottle) to terminate the enzyme reaction.

(4) Colorimetric determination: Shake each bottle for 2 min, take 2 mL reaction solution, add 1 mL sulfonamide, shake well, add 1 mL vinylamine, and then color in 35 water baths for 15 min, and then colorimetric 540 nm.

(5) Blank solution: 2 mL distilled water + 1 mL sulfonamide, the same as the sample solution for 15 min.

Nitrate reductase activity in maize was determined by standard curve method (Johansson et al., 2017). The content of NO_2^- ($\mu g/\mathrm{mL}$) was detected from the standard curve, and the activity of nitrate reductase in maize was expressed by the amount of NO_2^- produced per gram fresh weight per hour. The calculation method was as follows:

$$\text{Enzymatic activity} \quad \left[\mu g/(g\cdot h)\right]=\frac{(C_1-C_0)\times V_t}{FW\times t\times V_s} \qquad \text{(Eq.1)}$$

In the formula, C_0 and C_1 are the amount of NO_2^- obtained from the standard curve ball at the beginning of the test and in the course of the test respectively; V_t is the total volume of the reaction liquid; V_s is the sampling volume at the time of determination; FW is the fresh weight; t is the reaction time.

Results

In order to further verify the effect of nitrogen application rate on nitrate reductase activity of corn, relevant test experiments need to be carried out. The research content of this experiment is as follows: effect of pure nitrogen fertilizer application rate on nitrate reductase activity in maize at different growth stages, effects of different proportion of nitrogen fertilizer applied by stages on nitrate reductase activity in maize, effects of nitrogen fertilizer application rate on nitrate reductase activity in maize under different stress environment and effects of nitrogen fertilizer varieties and nitrogen fertilizer dosage on nitrate reductase activity in maize. The experimental environment is shown in *Figure 1.*

Effect of pure nitrogen fertilizer application rate on nitrate reductase activity in maize at different growth stages

After analyzing the effect of nitrogen fertilizer application rate on nitrate reductase activity in maize at different growth stages, the results are shown in *Figure 2*.

http://www.aloki.hu ● ISSN 1589 1623 (Print) ● ISSN 1785 0037 (Online)
DOI: http://dx.doi.org/10.15666/aeer/1802_28792894

Figure 1. *Experimental environment diagram*

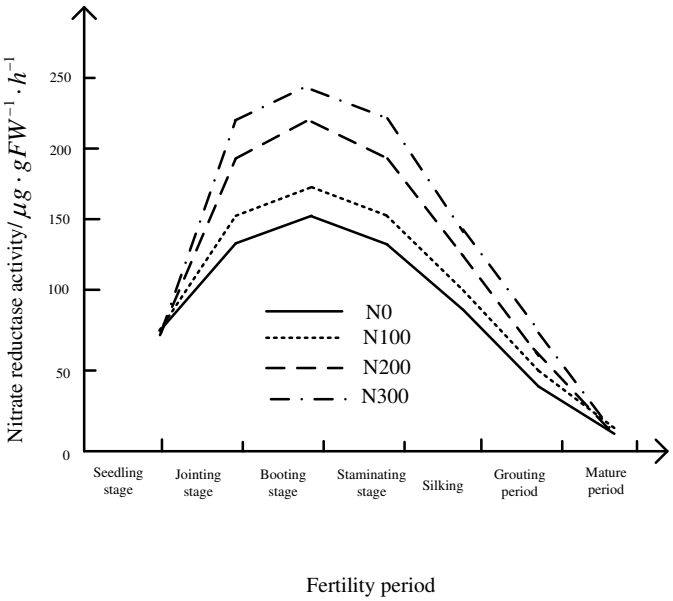

Figure 2. *Effects of nitrogen fertilizer application rate on nitrate reductase activity in maize at different growth stages*

The activity of nitrate reductase changed with the amount of nitrogen. The activity of nitrate reductase showed a single peak curve during the whole growth period. With the advancement of fertility process, it gradually increases and then decreases after reaching the peak. Nitrate reductase activity increased with the increase of nitrogen application (Yang et al., 2017). Nitrate reductase activity increased rapidly after jointing stage, reached its peak at booting stage, decreased gradually from booting stage to maturity stage, and decreased after heading stage.

After analyzing the effect of nitrogen application rate on nitrate reductase activity in ear leaves of maize during grain filling, the results are as shown in *Table 5*.

Table 5 shows that nitrate reductase activity in ear leaves of maize decreases gradually with the advance of grain filling, and increase with the increase of nitrogen nutrition level. From 7 to 49 days after silking, the activity of nitrate reductase was N300 > N200 > N100 > N0. With the increase of nitrogen fertilizer application rate, the nitrogen metabolism of maize maintained a high level at the later growth stage.

http://www.aloki.hu ● ISSN 1589 1623 (Print) ● ISSN 1785 0037 (Online)
DOI: http://dx.doi.org/10.15666/aeer/1802_28792894

Table 5. *Nitrate reductase activity in ear leaves of maize (silking in spite of spinning)*

Handle	Number of days after spinning (d)						
	7	**14**	**21**	**28**	**35**	**42**	**49**
N0	71.31	50.91	38.41	22.41	16.91	14.21	13.11
N100	82.41	62.41	51.31	35.61	22.81	19.91	18.21
N200	100.91	85.81	60.61	42.61	27.31	22.81	19.91
N300	116.71	90.21	69.91	52.21	34.81	27.61	21.41

Effects of different proportion of nitrogen fertilizer applied by stages on nitrate reductase activity in maize

(1) Effect of different proportion of nitrogen fertilizer on nitrate reductase activity in maize leaves

The effects of different proportion of nitrogen fertilizer on nitrate reductase activity in maize leaves were analyzed. The results are shown in *Figure 3*.

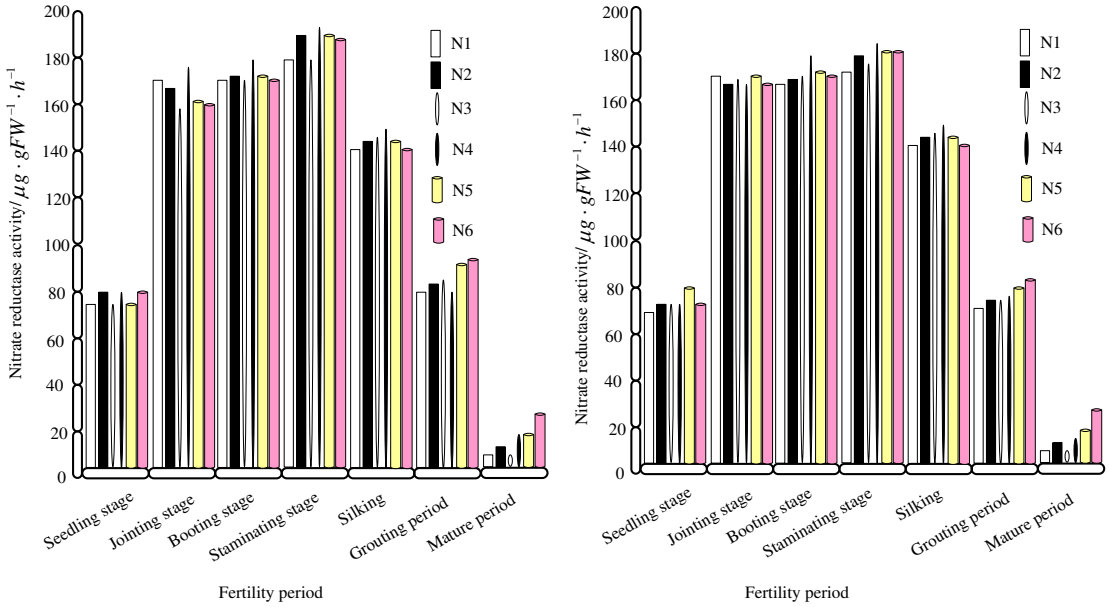

(a) 85 thousand/plant hm^2 (b) 95 thousand/plant hm^2

Figure 3. *Effects of different proportion of nitrogen fertilizer applied in stages on nitrate reductase activity in maize leaves*

Figure 3 shows that nitrate reductase activity is lower at seedling stage and reaches the maximum at male-drawing stage, then it shows a downward trend, and changes in a single peak curve during the whole growth period. Because the male-drawing stage is the key period for the morphological formation of maize reproductive organs, carbon and nitrogen metabolism is the most vigorous, and nitrate reductase activity is the highest in the male-drawing stage, so a large number of nitrates can be assimilated into leaves to meet the needs of crop growth and development.

Nitrate reductase activity changed with the application ratio of nitrogen fertilizer at different growth stages. Nitrate reductase activity of maize leaves treated with N6

http://www.aloki.hu ● ISSN 1589 1623 (Print) ● ISSN 1785 0037 (Online)
DOI: http://dx.doi.org/10.15666/aeer/1802_28792894

maintained higher activity of nitrate reductase than that of other treatments in the process of decreasing from silking stage (Chelladurai, 2017). Nitrogen metabolism in maize is an integral part of photosynthesis, which determines the accumulation of dry matter and has an important impact on yield.

By comparing the changes of nitrate reductase activity in maize leaves under two planting densities, it can be seen that the nitrate reductase activity of maize leaves under 85,000 thousand/plant hm^2 density and 95,000 thousand/plant hm^2 density had little difference at seedling and jointing stages, and the nitrate reductase activity under 85,000 thousand/plant hm^2 density began to be higher than 95,000 thousand/plant hm^2 from booting stage, indicating that the activity of nitrate reductase in the leaves of high-density planted maize was lower.

(2) The effect of different proportion of nitrogen fertilizer applied by stages on nitrate reductase activity in maize roots

After analyzing the effect of different proportion of nitrogen fertilizer on nitrate reductase activity in maize roots by stages, the results are shown in *Figure 4.*

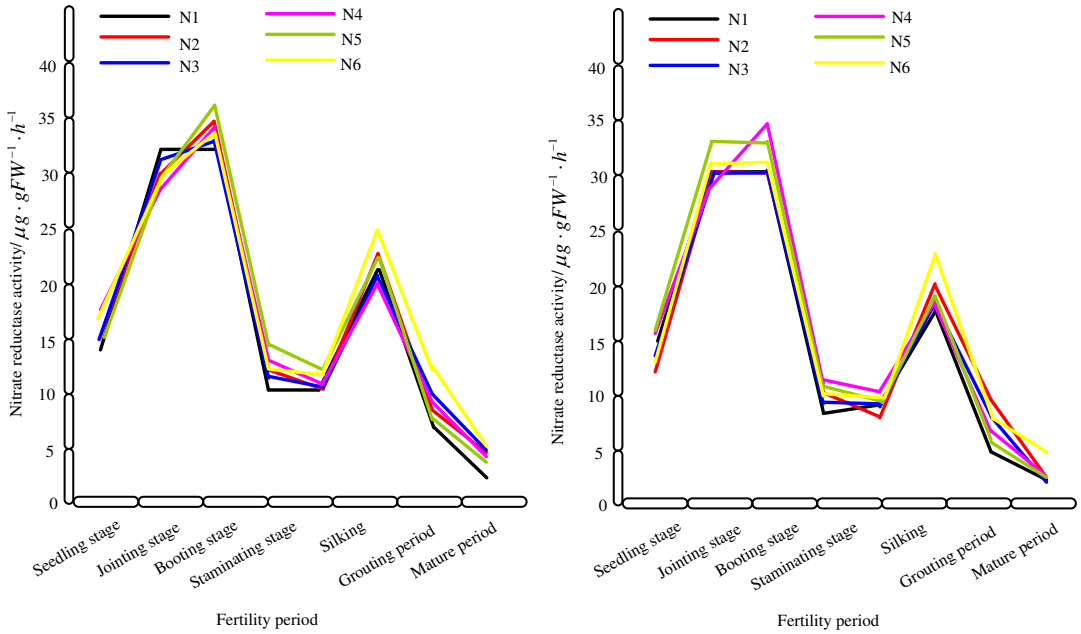

(a) 85 thousand /plant hm^2 (b) 95 thousand/plant hm^2

Figure 4. *Effects of different proportion of nitrogen fertilizer on nitrate reductase activity in maize roots*

From *Figure 4,* it can be seen that the nitrate reductase activity in roots changes in a bimodal curve with the development of the growth process. It is highest at booting stage, then decreases sharply, and begins to rise after silking stage, and then decreases after the second peak at grain filling stage.

Nitrate reductase activity in roots varied with the proportion of nitrogen fertilizer applied in different growth stages. Nitrate reductase activity was the highest in N4 treatment at booting stage.

Before booting stage, the nitrate reductase activity in maize roots had little difference between the two densities (Sarkar et al., 2017). From booting stage, the nitrate reductase

http://www.aloki.hu ● ISSN 1589 1623 (Print) ● ISSN 1785 0037 (Online)
DOI: http://dx.doi.org/10.15666/aeer/1802_28792894

activity of 85,000 thousand/plant hm^2 densities were higher than 95,000 thousand plant/hm^2.

Effects of nitrogen fertilizer application rate on nitrate reductase activity in maize under different stress environment

Nitrate Reductase (NR) is an important regulator and rate-limiting enzyme in plant nitrogen metabolism. NR plays an important role in plant growth and development, yield formation and protein content. NR activity is induced by substrates and is influenced by many other environmental factors. The effects of nitrogen application rate on nitrate reductase activity in maize under different stress environments, as shown in *Table 6*.

Table 6. *Effects of nitrogen fertilizer application rate on nitrate reductase activity in maize under different stress environments*

Stress treatment	NR activity/ $\mu g \cdot gFW^{-1} \cdot h^{-1}$		Activity ratio
	Root system	Blade	
Contrast	36.52 ± 3.10	106.22 ± 6.77	65.6
15% PEC-6000	37.70 ± 2.00	34.00 ± 4.99**	-9.8
72 mmol/L NaCl	61.96 ± 5.24**	38.93 ± 2.24**	-59.2
72 mmol/L	142.58 ± 8.40*	43.2 ± 3.00**	-230.0

* Activity ratio (%) = (leaf NR activity - root NR activity), leaf NR activity 100; ** t test reached a very significant level

Table 6 shows that the nitrate reductase activity of maize roots increases under different stress environments with a certain amount of nitrogen fertilizer. In 72 mmol/L saline-alkali stress environment, the increase of NR activity was 69.7% compared with the control, and the t test also reached a very significant level (Ramezani et al., 2017). In 15% PEC-6000 drought stress environment, the increase of NR activity was the smallest, which was 3.2% higher than the control, and t test was not significant. For comparison, we also measured the NR activity of maize seedling leaves under the same stress conditions as the root. As shown in *Table 6,* NR activity in leaves was higher than that in roots, reaching 106.22 $\mu g \cdot gFW^{-1} \cdot h^{-1}$, which was 2.9 times higher than that in roots. However, NR activity in leaves decreased significantly under different stress environments, and reached a significant level by t-test analysis compared with the control values. The NR activity ratios of roots treated with the same treatment were - 9.8% under drought stress, - 59.2% under salt stress and - 230.0% under salt stress, respectively. The results showed that leaf NR activity stress was greater than root NR activity stress under the same stress.

Effects of nitrogen fertilizer varieties and nitrogen fertilizer dosage on nitrate reductase activity in maize

(1) The effect of different nitrogen fertilizer varieties and dosage on nitrate reductase activity in maize leaves

Figure 5 is a comparative study of nitrate reductase activity in maize leaves under different nitrogen fertilizer varieties and nitrogen levels. The results showed that the

http://www.aloki.hu ● ISSN 1589 1623 (Print) ● ISSN 1785 0037 (Online)
DOI: http://dx.doi.org/10.15666/aeer/1802_28792894

variety and amount of nitrogen fertilizer had significant effects on the activity of nitrate reductase in maize leaves.

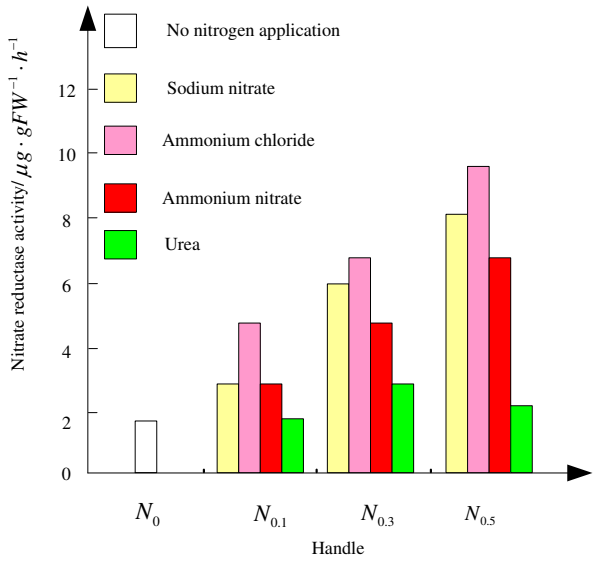

Figure 5. *Effects of different nitrogen fertilizer varieties and amounts on nitrate reductase activity in maize leaves*

Nitrogen fertilizer application could significantly increase the activity of nitrate reductase in maize leaves. The results showed that the nitrate reductase activity of maize leaves treated with sodium nitrate, ammonium chloride, ammonium nitrate and urea was higher than that of maize leaves without nitrogen application. The nitrate reductase activity of maize Treated with sodium nitrate increased significantly from $N_{0.1}$ to $N_{0.5}$, and increased 59.5%, 200.5% and 299.5% under three levels of nitrogen application compared with N_0, respectively. When the nitrogen supply level increased from N_0 to $N_{0.5}$, the nitric acid in leaves of maize Treated with ammonium chloride increased. The activity of nitrate reductase increased significantly with the increase of nitrogen application level. There was no significant difference in the activity of nitrate reductase between the treatments with ammonium nitrate application amount of N_0, $N_{0.1}$ and $N_{0.5}$, but the activity of nitrate reductase in leaves increased significantly with the further increase of nitrogen application amount of $N_{0.5}$. The activity of nitrate reductase in urea treatment was significantly higher than that in $N_{0.3}$ treatment. Compared with other nitrogen supply levels, the activity of nitrate reductase was 107.1%, 87.1% and 30.8% higher than that of N_0, $N_{0.1}$ and $N_{0.5}$, respectively. There was no significant difference in the activity of nitrate reductase between $N_{0.5}$ and $N_{0.1}$ levels.

Nitrogen fertilizer varieties also had a great influence on nitrate reductase activity. According to *Figure 5,* the difference of nitrate reductase activity in maize leaves treated with low-nitrogen $N_{0.1}$ was as follows: ammonium chloride > sodium nitrate > sodium nitrate > urea due to different varieties of nitrogen fertilizer. That is to say, when ammonium chloride was used as nitrogen source, the nitrate reductase activity of maize leaves was the highest, reaching 4.72 $\mu g \cdot gFW^{-1} \cdot h^{-1}$, and the value was 2.4 times of the control at this time. When urea was used as nitrogen source, the nitrate

http://www.aloki.hu ● ISSN 1589 1623 (Print) ● ISSN 1785 0037 (Online)
DOI: http://dx.doi.org/10.15666/aeer/1802_28792894

reductase activity of maize leaves was the lowest, only 1.86 $\mu g \cdot gFW^{-1} \cdot h^{-1}$, which was 1.1 times of the control. The nitrate reductase activity of maize leaves treated with medium nitrogen $N_{0.3}$ and high nitrogen $N_{0.5}$ were the highest with ammonium chloride and sodium nitrate as nitrogen sources. There was no significant difference in nitrate reductase activity between the two nitrogen fertilizer varieties, and the nitrate reductase activity of maize leaves treated with four nitrogen fertilizer varieties was the same under the same nitrogen application level.

It can be seen that the nitrate reductase activity of leaves treated with nitrogen fertilizer increased to varying degrees, regardless of which nitrogen fertilizer variety was used as nitrogen source.

(2) Effects of different nitrogen fertilizer varieties and amounts on nitrate reductase activity in maize roots.

The effects of different nitrogen fertilizer varieties and amounts on nitrate reductase activity in maize roots are shown in *Figure 6*.

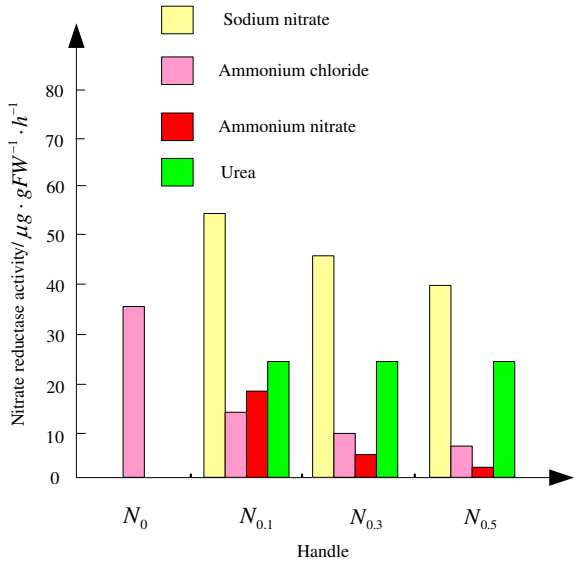

Figure 6. *Effects of different nitrogen fertilizer varieties and amounts on nitrate reductase activity in maize roots*

The results of *Figure 6* showed that the activity of nitrate reductase decreased with the increase of nitrogen fertilizer application. The nitrate reductase activity of roots treated with sodium nitrate increased in varying degrees compared with the control, while the nitrate reductase activity of roots treated with other three fertilizers was lower than that of the control. (1) Nitrate reductase activity was most affected by nitrogen application, which was significantly decreased under three levels of fertilization: $N_{0.1}$, $N_{0.3}$ and $N_{0.5}$; (2) Nitrate reductase activity in urea treatment was least sensitive to the amount of nitrogen application, and there was no significant difference among the four nitrogen treatments.

(3) The nitrate reductase activity of ammonium chloride and ammonium nitrate treatments was not significantly different under three levels of nitrogen application. The nitrate reductase activity of ammonium nitrate treatments of $N_{0.3}$ and $N_{0.5}$. were significantly lower than that of $N_{0.1}$.

http://www.aloki.hu ● ISSN 1589 1623 (Print) ● ISSN 1785 0037 (Online)
DOI: http://dx.doi.org/10.15666/aeer/1802_28792894

The difference of nitrate reductase activity in roots caused by different nitrogen fertilizers was as follows: at the same level of nitrogen application, the nitrate reductase activity in roots of different treatments was sodium nitrate > urea > ammonium chloride, ammonium nitrate, ammonium chloride and ammonium nitrate, but there was no significant difference between the nitrate and urea, and between the other two nitrogen fertilizer varieties.

According to the results of nitrate reductase activity in maize Leaves under different nitrogen fertilizer varieties and different amounts of nitrogen fertilizer, the nitrate reductase activity in leaves and roots of maize treated with urea as nitrogen source did not change much compared with the other three nitrogen sources, while the nitrate reductase activity in leaves treated with other three nitrogen sources were all in the same condition. The nitrate reductase activity of roots was the highest under high nitrogen and low nitrogen. Nitrate reductase activity in leaves and roots showed opposite trends in four fertilizers when nitrogen application increased.

Discussion

Combining with the research contents in this paper, the technical principles of improving the utilization rate of nitrogen fertilizer are discussed. The utilization rate of nitrogen fertilizer in China's agricultural production is low and its loss is great, and the effect of increasing production is far from being fully exerted. The potential of reducing the loss of nitrogen fertilizer, improving its utilization rate and increasing production effect is also great. According to the experimental analysis, under the condition of increasing application of pure nitrogen fertilizer, the nitrate reductase activity of maize increased gradually at the start-up stage and before, and decreased gradually at the beginning of endurance stage; different application proportion of nitrogen in each period will have an impact on the nitrate reductase activity of maize; under different stress environment, a certain amount of nitrogen is applied Under the same stress, the NR activity of leaves was higher than that of roots; the effect of nitrogen fertilizer on NR activity of leaves was the greatest. Following is a brief description of the relevant technical principles:

(1) Avoiding excessive accumulation of mineral nitrogen in soil as far as possible

Exchangeable ammonium and nitrate nitrogen in soil are not only available nitrogen that crops can absorb directly, but also the common source of various nitrogen loss processes. It is undoubtedly necessary to have a proper amount of available nitrogen in soil, but excessive nitrogen will increase the loss of nitrogen. Therefore, it is one of the important principles for effective application of nitrogen fertilizer to avoid its excessive presence in soil.

(2) The countermeasures for the main loss ways of nitrogen fertilizer

Due to the different environmental conditions of different soils and crops, the loss of nitrogen through different mechanisms and pathways and their proportion in total loss of nitrogen fertilizer are quite different, so the technology to reduce the loss of nitrogen fertilizer should also be different. However, there are some internal links between different ways of loss. Therefore, when taking one of the loss mechanisms and ways as

http://www.aloki.hu ● ISSN 1589 1623 (Print) ● ISSN 1785 0037 (Online)
DOI: http://dx.doi.org/10.15666/aeer/1802_28792894

the control object to formulate technical countermeasures, we should take into account its possible impact on other loss mechanisms and ways.

A. Reducing ammonia volatilization

Ammonia volatilization rate is a function of partial pressure of ammonia in surface water and wind speed above surface water. The former is also a function of $\left[NH_3+NH_4^+\right]-N$, pH and temperature of surface water. Therefore, reducing $\left[NH_3+NH_4^+\right]-N$ and pH in surface water after fertilization is the key technology to reduce ammonia volatilization. In addition, ammonia volatilization can be reduced by inhibiting the loss of ammonia from surface water of maize fields to the atmosphere.

For dry farming, these principles are basically applicable, but because there is no water layer in dry farming soil, the key to reducing ammonia volatilization loss is to try to apply ammonia fertilizer in a certain depth of soil layer to reduce the partial pressure of ammonia on the soil surface.

B. Inhibition of nitrification

Nitrification of ammonium not only produces a small amount of N_2O, but also forms nitrate nitrogen which is easy to pass through denitrification (also produces part of N_2O) and leaching loss. Therefore, for ammonium nitrogen fertilizer and ammonia fertilizer that can be formed, delaying or maintaining nitrification is one of the important ways to reduce losses, improve utilization rate and reduce environmental impact.

(3) Improving the ability of crops to absorb mineral nitrogen

There is a competition between the uptake of mineral nitrogen and the loss of nitrogen in crops. Therefore, eliminating all kinds of limiting factors affecting crop growth, such as lack of phosphorus and potassium, drought and flood, to improve the ability of crops to absorb mineral nitrogen, will help to improve the utilization rate of nitrogen fertilizer and reduce losses. In addition, in the period of vigorous crop growth, nitrogen fertilizer applied will be absorbed rapidly because of the strong absorption ability of root system, which is beneficial to reduce its loss; moreover, because of the high vegetation coverage on the ground, it is also helpful to reduce the wind speed across the soil (dry farming) or water surface, thus reducing ammonia volatilization.

In the process of this experiment, the experimental environment is in line with the actual measurement conditions, and the experimental data is accurate and reliable. Therefore, we can draw relevant conclusions through the experimental results, which has scientific guidance and statistical significance. The results showed that the nitrate reductase activity could be significantly increased by increasing nitrogen content. The amount of nitrogen should be controlled at the early stage of crop growth, and the top dressing should be focused at the vigorous stage of crop growth.

Conclusions

In order to deeply analyze the effect of nitrogen fertilizer application rate on nitrate reductase activity of maize, the effects of different application rates of pure ammonia fertilizer on nitrate reductase activity of maize, the effects of different proportions of nitrogen fertilizer applied in stages on nitrate reductase activity of maize, the effects of

http://www.aloki.hu ● ISSN 1589 1623 (Print) ● ISSN 1785 0037 (Online)
DOI: http://dx.doi.org/10.15666/aeer/1802_28792894

nitrogen fertilizer application rate on nitrate reductase activity of maize in different stress environments, and nitrogen fertilizer products were studied. The effects of seed and nitrogen fertilizer on nitrate reductase activity in maize were analyzed in four aspects. The results showed that:

Conclusion 1: Nitrate reductase activity tends to increase with the increase of nitrogen application. Nitrate reductase activity increases rapidly after jointing stage, peaks at booting stage, decreases gradually from booting stage to maturity stage, and decreases after heading stage.

Conclusion 2: Because the male-drawing stage is the key period for the morphological formation of maize reproductive organs, carbon and nitrogen metabolism is the most vigorous, and nitrate reductase activity is the highest in the male-drawing stage; nitrate reductase activity in roots varies with the proportion of nitrogen fertilizer applied in different growth stages. Nitrate reductase activity was the highest in N4 treatment at booting stage.

Conclusion 3: Nitrate reductase activity in maize roots increased under different stress environments and with a certain amount of nitrogen fertilizer.

Conclusion 4: Nitrate reductase activity of maize leaves was higher than that of maize leaves without nitrogen application. When ammonium chloride was used as nitrogen source, the nitrate reductase activity of maize leaves was the highest. When nitrogen source was urea, the nitrate activity of leaves and roots increased with the increase of nitrogen application. Compared with the other three nitrogen sources, the activity of nitrate reductase in maize leaves was the highest under high nitrogen conditions, and the activity of nitrate reductase in roots was the highest under low nitrogen conditions.

To study the effect of nitrogen application on nitrate reductase activity of maize is helpful to improve the quality and yield of maize, promote the economic development of our country, and improve the international status of our country. In order to further understand the effect of nitrogen application rate on nitrate reductase activity of maize, we can study the environmental temperature, soil moisture and other factors, so as to better realize the research of this part.

Acknowledgements. National Natural Science Foundation of China - Effects of different water and nitrogen treatments on soil microflora in wheat fields and their regulatory mechanisms (No. 51509085); Fund project for high-level talents of Henan University of Science and Technology: Study on the spatial distribution regulation mechanism of nitrogen compensation utilization in maize and soybean intercropping (No. 2015010).

REFERENCES

[1] Ahamed, A. J., Loganathan, K., Ananthakrishnan, S., Ahmed, J., Ashraf, M. A. (2017): Evaluation of graphical and multivariate statistical methods for classification and evaluation of groundwater in Alathur Block, Perambalur District, India. – Applied Ecology and Environmental Research 15(3): 105-116.

[2] Berber, M. R., Hafez, I. H. (2018): Synthesis of a new nitrate-fertilizer form with a controlled release behavior via an incorporation technique into a clay material. – Bulletin of Environmental Contamination and Toxicology 101(6): 751-757.

[3] Castillogodina, R. G., Foroughbakhchpournavab, R., Benavidesmendoza, A. (2018): Effect of selenium on elemental concentration and antioxidant enzymatic activity of tomato plants. – Journal of Agricultural Science 18(1): 233-244.

http://www.aloki.hu ● ISSN 1589 1623 (Print) ● ISSN 1785 0037 (Online)
DOI: http://dx.doi.org/10.15666/aeer/1802_28792894

[4] Chelladurai, G. (2017): Influence of diets on growth and biochemical parameters of Babylonia spirata. – Geology, Ecology, and Landscapes 1(3): 162-166.
[5] Han, T., Zhan, W., Gan, M. (2018): Phosphorylation of glutaminase by PKCε is essential for its enzymatic activity and critically contributes to tumorigenesis. – Cell Research 28(6): 655-669.
[6] Helmers, M. J., Zhou, X., Baker, J. L. (2017): Nitrogen loss on tile-drained Mollisols as affected by nitrogen application rate under continuous corn and corn-soybean rotation systems. – Canadian Journal of Soil Science 92(3): 493-499.
[7] Hwang, K. S., Yang, J. Y., Lee, J. (2018): A novel anti-melanogenic agent, KDZ-001, inhibits tyrosinase enzymatic activity. – Journal of Dermatological Science 89(2): 165-171.
[8] İlhan, Ö., Okyay, G., Ulaş, A. (2018): Coating of nonwovens with potassium nitrate containing carboxymethyl cellulose for efficient water and fertilizer management. – Cellulose 25(2): 1527-1538.
[9] Iqbal, S., Thierfelder, C., Khan, H. Z. (2017): Maximizing maize quality, productivity and profitability through a combined use of compost and nitrogen fertilizer in a semi-arid environment in Pakistan. – Nutrient Cycling in Agroecosystems 107(2): 197-213.
[10] Johansson, M., Lundh, Å., De, V. R. (2017): Composition and enzymatic activity in bulk milk from dairy farms with conventional or robotic milking systems. – Journal of Dairy Research 84(02): 154-158.
[11] Juárezhernández, E. O., Casadosvázquez, L. E., Bideshi, D. K. (2017): Role of the C-terminal and chitin insertion domains on enzymatic activity of endochitinase ChiA74 of Bacillus thuringiensis. – International Journal of Biological Macromolecules 102(2017): 52-59.
[12] Kang, J., Zhang, Y., Zhang, Z. Y. (2017): Preparation and performance of nano array composite electrodes for lithium battery. – Chinese Journal of Power Sources (12): 1701-1702.
[13] Li, D., Huang, Z. X., Lu, J. C. (2017): Research on the concept and mechanism of military information system based on cloud computing architecture. – Journal of China Academy of Electronics and Information Technology 12(4): 365-370.
[14] Li, R. T. (2017): Design and application of electrical automation system for intelligent building. – Automation & Instrumentation (5): 164-166.
[15] Liu, R., Siththanandan, V., Yang, Y. (2018): The enzymatic activity and cellular localization of drosophila myosin 7a is regulated by a novel binding protein. – Biophysical Journal 114(3): 210a-211a.
[16] Ma, Y. Y., Zhou, C., Li, Q. M. (2017): Simulation research on optimization of intrusion node information in network. – Computer Simulation 34(8): 315-318.
[17] Ramezani, M. R., Bavani, A. R. M., Jafari, M., Binesh, A. (2017): Evaluating gridded BIOME-BGC for simulating LAI at Kasilian watershed-Iran. – Geology, Ecology, and Landscapes 1(4): 225-231.
[18] Russo, T. A., Tully, K., Palm, C. (2017): Leaching losses from Kenyan maize cropland receiving different rates of nitrogen fertilizer. – Nutrient Cycling in Agroecosystems 108(2): 195-209.
[19] Sarkar, M. I. U., Islam, M. N., Jahan, A., Islam, A., Biswas, J. C. (2017): Rice straw as a source of potassium for wetland rice cultivation. – Geology, Ecology, and Landscapes 1(3): 184-189.
[20] Song, M. S., Rossi, J. J. (2017): Molecular mechanisms of Dicer: endonuclease and enzymatic activity. – Biochemical Journal 474(10): 1603-1618.
[21] Sui, C. H., Xu, Y. W., Yan, G. L. (2017): Preparation of a 76-Mer selenium-containing peptide with GPx and SOD double enzyme activity and its cell-penetrating effects. – Journal of Jilin University (Science Edition) 55(01): 168-174.

http://www.aloki.hu ● ISSN 1589 1623 (Print) ● ISSN 1785 0037 (Online)
DOI: http://dx.doi.org/10.15666/aeer/1802_28792894

[22] Wang, H., Li, P., Yu, D. (2018): Unraveling the enzymatic activity of oxygenated carbon nanotubes and their application in the treatment of bacterial infections. – Nano Letters 18(6): 3344-3351.
[23] Yang, X. P., Luo, N., Zong, Y. Y., Jia, Z. H., Liao, X. J. (2017): Quantum dots extraction coupled with high-performance liquid chromatography for the determination of polycyclic aromatic hydrocarbons in water. – Applied Ecology and Environmental Research 15(3): 171-186.
[24] Zhang, R., An, J. C., Hao, L. C. (2017): Influence of transformer magnetic saturation on low-voltage frequency converter driving high-voltage submersible motor system. – Journal of Power Supply 15(4): 162-167.
[25] Zheng, J., Mmari, W. N., Nishigaki, T. (2018): Nitrogen availability to maize as affected by fertilizer application and soil type in the Tanzanian highlands. – Nutrient Cycling in Agroecosystems 112(2): 1-17.

http://www.aloki.hu ● ISSN 1589 1623 (Print) ● ISSN 1785 0037 (Online)
DOI: http://dx.doi.org/10.15666/aeer/1802_28792894

EFFECTS OF DIFFERENT TILLAGE METHODS ON THE SOIL ENZYME ACTIVITY IN SORGHUM CULTIVATED LAND IN A HILLY ENVIRONMENT

WANG, A. P. – XUE, S. T. – DONG, Z. P. – DONG, Q.*

College of Agriculture, Shanxi Agricultural University, Taigu 030801, China

**Corresponding author*
e-mail: 13834833463@163.com

(Received 28th Oct 2019; accepted 12th Feb 2020)

Abstract. Through no tillage, deep ploughing, shallow ploughing + straw mulching and deep ploughing + straw mulching, sorghum planting experiments were carried out in hilly areas to study the effects of different tillage methods on soil enzyme activity. The acidity of Sorghum at jointing, flowering and harvesting stages was determined. The results showed that deep tillage and straw mulching could improve soil enzyme activities of sorghum. RS tillage improved soil invertase, acid phosphatase, polyphenol oxidase, catalase, soil urease, soil invertase and alkaline phosphatase activities in the whole growth period of sorghum, and the effects were relatively significant. There were differences between growth periods. At the jointing and flowering stages of sorghum, the protease activity of R and TS treatments was significant, and the activity of soil beta-glucosidase in T treatment was higher than that in RS treatment. Tillage can change the activity of sorghum soil enzymes and improve soil fertility in Hilly environments. Therefore, the method of Sorghum planting in hilly environment can be reasonably selected according to the growth demand of sorghum soil enzymes.
Keywords: *deep ploughing, straw mulch, growth period, protease, soil fertility*

Introduction

Sorghum (*Sorghum bicolor* (L.) Moench) is an annual herb of Gramineae. Its stalks are thicker and erect, basally with root sheaths glabrous or slightly white; leaf ligules dura mater, apex rounded. The ciliated panicles are loose at the edges, the main axis is bare, and the total stem is erect or slightly curved. Caryopsis convex on both sides, light red to reddish brown, 2.5-3 mm wide at ripening, apex slightly exposed. Spikelets with stalks are about 2.5 mm long, and linear to lanceolate, flowering and fruiting occurred in June-September. Soil enzymes activity refers to the ability of soil enzyme to catalyze material transformation (Jun et al., 2017). It is usually expressed by the amount of catalytic reaction products per unit of soil or the amount of residual substrates per unit of time. Domestic scholars have done a lot of research on Sorghum planting and growth: Bo (2016) showed that with the increase of planting density, the leaf area per plant of sorghum decreased, the ventilation and light transmission conditions deteriorated, and the ear, ear grain number and 1000-grain weight decreased, which was harmful to the development of sorghum. With the increase of planting density, the number of sorghum leaves did not change significantly. Zhang et al. (2016) studied the sweet sorghum 8 agronomic traits such as the simple correlation, plant height and spike length, section number, stem diameter, sugar content, significantly associated heading stage, plant height and yield of straw, stem length, node number were positively correlated, and straw yields were positively correlated, stem diameter and the grain yield was significantly positively related, and plant height and fresh weight, leaf area per plant were positively correlated,

http://www.aloki.hu ● ISSN 1589 1623 (Print) ● ISSN1785 0037 (Online)
DOI: http://dx.doi.org/10.15666/aeer/1802_28952908

were very significant positive correlation, and ear length were very significant negative correlation with thick stems.

Sorghum is the main raw material for liquor brewing. The traditional habit of planting sorghum in southeastern Sichuan is the dominant production area of waxy sorghum in China. The waxy sorghum planted under unique ecological conditions is the preferred raw material for famous liquor manufacturers in Sichuan, Guizhou and Chongqing provinces (Supriya et al., 2017). However, due to the wide range of hills, fewer flat dams, more slopes, small plots and small scale of concentrated production of Sorghum in southeastern Sichuan, some of them adopt the way of planting sorghum in hills. Sorghum planting in hilly environment is more common, the degree of mechanization is very low, the phenomenon of "old, chaotic and miscellaneous" varieties is serious, the cultivation techniques are relatively backward, the control of diseases and insect pests is not in place in time, the docking of production and demand is not keeping pace with other factors, resulting in higher relative cost and poor efficiency of Sorghum planting (Kosmambetova et al., 2017). Under the condition of market economy, sorghum producers should aim at pursuing the highest economic benefits.

Soil enzymes are the general term of enzymes existing in soil, and they are one of the components of soil (Feng et al., 2018). Soil enzyme activity includes not only the enzymes accumulated in the soil, but also the enzymes released from the proliferating microorganisms to the soil. It mainly comes from the cell secretions of animals, plant roots and microorganisms in the soil and the decomposition of residues. Soil enzymes are involved in the synthesis and decomposition of humus, hydrolysis and transformation of organic compounds, plant and animal residues and various redox reactions of organic and inorganic compounds in soil (Xu et al., 2017). These processes are closely related to the release and storage of various nutrient elements in soil, the formation and development of humus in soil, the structure and physical condition of soil. They participate in the whole process of the occurrence and development of soil and the formation and evolution of soil fertility. Therefore, soil enzyme activity directly affects soil fertility and indirectly affects Sorghum yield (Cao et al., 2016). It is a feasible way to optimize the yield of Sorghum in hilly environment from the perspective of improving soil enzyme activity. In this paper, a sorghum cultivation area in hilly environment was selected as the research area, and sorghum was cultivated by different tillage methods to study the effect of Tillage Methods on soil enzyme activity. In order to increase the yield of sorghum, we should improve the activity of soil enzymes and optimize the formation and evolution of soil fertility.

Materials and Methods

Experimental Design

The experimental area is located in the hilly area of 29°51', 106°27' and 244 m above sea level, with a subtropical monsoon humid climate. This is because there is a small difference in soil enzyme activity between flat land use patterns, while there is a large difference in soil microbial quantity in the hilly area with obvious characteristics. The average slope of the experimental area is between 10^{-6}~10^{-2} mol/L. The annual total solar radiation is 87,108 kJ·cm^{-2}, the annual total sunshine time is 1,276.7 hours, the annual average temperature is 18°C (≥ 10°C), the accumulated temperature is 5,979.5°C, the highest temperature in summer is about 40°C and the average rainfall is 1,133.7 mm. The

http://www.aloki.hu ● ISSN 1589 1623 (Print) ● ISSN1785 0037 (Online)
DOI: http://dx.doi.org/10.15666/aeer/1802_28952908

soil of the test plot is purple soil of dry land, with gentle slope and relatively uniform soil fertility. The cultivated soil in hilly environment is irrigated and silted soil with early cultivation and high maturity. Its thickness can reach 30-60 cm. The cultivation layer is light in texture and poor in water retention capacity. The volumetric heat capacity is generally 1-2.5 coke/$cm^3 \cdot ℃$. Moreover, due to the limiting factor of soil fertility level, the fertility level is quite different.

The experiment was started in April 2018. Four tillage treatments (no-tillage, deep tillage, shallow tillage + straw mulching, deep tillage + straw mulching) were set up. Each treatment set was repeated three times. The area of each treatment plot ranged from 12 to 24.75 hm^2 and was arranged in random blocks. In order to facilitate experimental recording and improve detection efficiency, the following four methods are set as follows: (1) No-tillage (T): no tillage of the land, plastic film was replaced until the experimental Jiedong; and (2) Deep tillage (TS): tillage 30 cm of cultivated land with subsoiling shovel after autumn harvest, and rotary tillage, mulching and sowing in spring. (3) Shallow tillage + straw mulching (R): Stalk-straw cutting and shallow harrow suppression-ploughing-shallow tillage-fertilization preparation-open-field drilling-weeding, pest control, treatment area 2.4 hm^{-2}, straw returning amount of 104 hm^{-2}. (4) Deep tillage + straw mulching (RS): Stalk-straw cutting and shallow harrowing to suppress, deep tillage-fertilization preparation-open field drilling-weeding, pest control during sorghum harvesting in the previous crop. The treatment area is 2.67 hm^{-2}, and the amount of straw returned to the field is about 114 kg hm^{-2}.

Sorghum was planted uniformly, sowing time was April 20, plant spacing was 20 cm, row spacing was 30 cm, and 7.2×10^4 plants/hm^2were planted. Unified fertilization measures were adopted. The fertilizers used were urea, diamine phosphate, calcium and potassium chloride. The amount of chemical fertilizer used in each treatment was uniformly N 180 kg/hm^2 and $P_2O_5$95-98 kg/hm^2 per year. Diamine iodate, calcium and potassium chloride were applied on the whole, urea 20%, jointing to heading 20%, heading to flowering 10%, and filling 50%. Irrigation for the whole growth period ranged from 34.1 to 36.3 m^3/hm^2. The fertilization, irrigation and management of sorghum cultivated land are the same in four different tillage modes of No-tillage, shallow tillage + straw mulching, deep tillage, deep tillage + straw mulching, which are different only in farming methods. Sorghum cultivation in the experimental area is shown in *Figure 1*.

Sample Collection and Indicator Determination

Sampling of soil samples

In 2018, root soil was collected during the jointing, flowering and harvesting periods of sorghum. During the collection, 2 cm of topsoil was taken, and 0-20 cm of root soil was taken for each plot according to the s-shaped sampling method. Soil enzyme activity is different in different areas. In order to ensure the accuracy of experimental data, it is necessary to control the consistent amount of experimental enzymes. Therefore, different plot sizes are needed, and the sampling points of each plot are 90, 80 and 70, respectively. After collecting at multiple points on each plot, the soil is evenly mixed. Some are packaged in sterile, self-sealing bags. They were immediately placed in an ice box and taken back to the lab. 4℃ refrigerator preservation, soil microbial diversity measurement. The other part of the soil was removed, dried and stored in a 2mm screen for the determination of soil enzyme activity and soil nutrient content.

http://www.aloki.hu ● ISSN 1589 1623 (Print) ● ISSN1785 0037 (Online)
DOI: http://dx.doi.org/10.15666/aeer/1802_28952908

(a) Sorghum planting coverage

(b) Mature sorghum

Figure 1. *Sorghum planting in hilly environment*

Method for determination of enzyme activity

Soil invertase activity (in terms of glucose quality, $mg \cdot g^{-1}$, 24h, 37°C) was determined by 3,5-Dinitrosalicylic acid colorimetry, soil acid phosphatase (in terms of phenol quality, $\mu mol \cdot g^{-1}$, 24h, 37°C) and soil polyphenol oxidase (in terms of purple gall quality, $mg \cdot g^{-1}$, 24h, 37°C) were extracted by Suzhou Keming Biotechnology Co., Ltd. Soil acid phosphatase (S-ACP) kit and soil polyphenol oxidase (PPO) kit (Pan et al., 2018); catalase activity was determined by potassium permanganate titration, expressed in milliliters of potassium permanganate consumed by 1 g of dry soil after 20 minutes; urease activity was determined by Indigo phenol colorimetry, and transformed into biogenic soil after 6 hours and 1 g of dry soil. The NH3-N milligram number was expressed; the activity of sucrase was determined by nitrosalicylic acid colorimetric method, expressed by the milligram number of glucose in 1 g of dry soil after 24 hours (Wen et al., 2017); the activity of alkaline phosphatase was determined by sodium phosphate colorimetric method; the activity of protease was determined by Indigo colorimetric method; and the activity of β-D-glucosidase was determined by B-D-glucosidase colorimetric method.

Microbial bacteria determination

The number of bacteria, actinomycetes and fungi were counted by dilution plate method.

http://www.aloki.hu ● ISSN 1589 1623 (Print) ● ISSN1785 0037 (Online)
DOI: http://dx.doi.org/10.15666/aeer/1802_28952908

Soil respiration measurement

Soil respiration flux was measured by Li-8100 soil carbon flux automatic measurement system. Seasonal variation was determined according to the main growth stages of summer sorghum. Fertilizer application and irrigation should be avoided, and the optimum period was about 15 days. Soil respiration was measured at different growth stages, from 8:00 to 20:00 (every 2 hours). It was required that the plastic film should be uncovered on the bare area of the respiratory chamber edge one day before each measurement to remove the accumulated CO_2 in the film. On the premise of not disturbing the soil and the PVC ring, the above-ground green plants were cut off from the roots and litter was removed from the circle one day before each determination (Zheng et al., 2017; Faust et al., 2018). In order to reduce the error of temperature to the test in the diurnal variation of respiration, we adopt the sequential measurement method to carry out the cyclic measurement. The flux value can also be automatically calculated by synchronous measurement of CO_2 volume fraction in the respiratory chamber, soil temperature, near-surface air temperature and air relative humidity (Wang et al., 2017).

Soil nutrient determination

Soil organic carbon: using chromic acid redox titration dilution method; total nitrogen: using semi-micro Kjeldahl method; quick-acting potassium: using Extraction Flame photometry; pH value using potentiometric method.

Data Processing

The experimental data were unified by Excel 2003, and then analyzed by SPSS 22.0 statistical analysis software for variance, correlation ($p < 0.05$), and significant difference ($p < 0.05$).

Results

Effects of Different Tillage Ways on Soil Enzyme Activities in Soil of Sorghum

Effects of different tillage methods on soil invertase activity in Sorghum

Soil invertase can hydrolyze sucrose into corresponding monosaccharides and be absorbed by the organism. Enzymatic products are closely related to the content of organic matter, nitrogen and phosphorus in soil, the number of microorganisms and the intensity of soil respiration (Moon et al., 2019). They are important indicators for evaluating soil fertility. *Table 1* shows that the invertase activity changes in different treatments are basically the same, that is, with the development of sorghum growth period, the invertase activity in rhizosphere soil of each treatment increased rapidly from jointing stage to flowering stage, and decreased rapidly at maturity stage. The activity of invertase in Sorghum soil was increased by different treatments at different growth stages, but the increment was different among different treatments. At jointing stage, there was significant difference between treatments and T treatment ($P < 0.05$), but there was no significant difference between them. At flowering stage, there was significant difference between RS treatment and T treatment ($P < 0.05$), and the activity of TS and TS treatment was significantly higher than that of T treatment ($P < 0.05$); at harvesting stage, the activity of RS and R was significantly higher than that of T and TS treatment ($P < 0.05$), and other treatments ($P < 0.05$). There was no significant

http://www.aloki.hu ● ISSN 1589 1623 (Print) ● ISSN1785 0037 (Online)
DOI: http://dx.doi.org/10.15666/aeer/1802_28952908

difference between them. The results showed that RS, R and TS treatments could improve the activity of transformation enzymes in Sorghum rhizosphere soil during the whole growth period, and RS treatment had the most significant effect.

Table 1. *Changes of invertase activity in Sorghum soil ($mg \cdot g^{-1}$)*

Handle	Jointing stage	Florescence	Harvest period
T	8.80±1.08b	58.55±6.07c	47.38±4.08b
TS	15.35±0.21a	79.35±0.95ab	68.63±9.35a
R	15.64±3.07a	78.03±5.71ab	57.14±0.29b
RS	16.70±0.61a	89.05±2.52a	78.02±0.17a

Different lowercase letters in the same column indicate significant difference in $P < 0.05$ level. The same below

Effects of different tillage methods on acid phosphatase activity in Sorghum soil

Soil acid phosphatase is a kind of enzymes that catalyze the mineralization of soil organic compounds. Its activity directly affects the decomposition and transformation of soil organic compounds and their bioavailability. It is an index to evaluate the direction and intensity of soil phosphorus biotransformation. *Table 2* shows that the activity of acid phosphatase in the rhizosphere of sorghum is higher at flowering and ripening stages. The activity of acid phosphatase in the rhizosphere of sorghum treated by RS, R and TS is higher than that of T during the whole growth period of sorghum (Xu et al., 2017). The activity of acid phosphatase in rhizosphere soil under RS treatment at flowering stage was significantly higher than that of other treatments ($P < 0.05$), but there was no significant difference between other treatments and control. The results showed that RS could significantly increase phosphatase activity in Sorghum rhizosphere soil at flowering stage, and R and TS could also increase phosphatase activity in Sorghum soil, but the effect was not significant compared with RS.

Table 2. *Changes of soil phosphatase activity in Sorghum ($\mu mol \cdot g^{-1}$)*

Handle	Jointing stage	Florescence	Harvest period
T	87.34±16.87a	97.20±3.44b	92.08±13.00a
TS	95.62±9.27a	102.40±10.77ab	108.32±14.47a
R	102.37±17.26a	109.53±1.85ab	108.08±26.07a
RS	103.25±14.00a	113.10±2.07a	112.81±23.66a

Effects of different tillage methods on polyphenol oxidase activity in Sorghum soil

Soil polyphenol oxidase mainly comes from the decomposition and release of soil biological, plant root exudates and animal and plant residues, catalyzing the oxidation of aromatic compounds into quinones, quinones react with soil proteins, amino acids, sugars, minerals and other substances to form organic matter and pigments, completing soil aromatic compounds recycling for soil environmental remediation. During sorghum growth period, the change trend of polyphenol oxidase activity in rhizosphere of different treatments was similar (Basak et al., 2018). The polyphenol oxidase activity increased rapidly from jointing stage to flowering stage, and then decreased rapidly at harvest stage (*Table 3*). At jointing stage and harvest stage, the activities of polyphenol oxidase in Sorghum soil treated with RS and R were significantly higher than those

http://www.aloki.hu ● ISSN 1589 1623 (Print) ● ISSN1785 0037 (Online)
DOI: http://dx.doi.org/10.15666/aeer/1802_28952908

treated with T ($P < 0.05$). At flowering stage, the activity of enzyme under RS and R treatment was higher than TS and T, but only the difference between RS and R reached significant level ($P < 0.05$). The results showed that RS and R could significantly increase the activity of polyphenol oxidase in Sorghum soil, while TS could improve the activity of polyphenol oxidase in Sorghum rhizosphere to a certain extent, but the effect was not significant.

Table 3. *Changes of polyphenol oxidase activity in Sorghum soils ($mg \cdot g^{-1}$)*

Handle	Jointing stage	Florescence	Harvest period
T	4.74±1.28d	5.07±1.33b	4.82±0.45d
TS	8.07±0.91ab	6.57±1.14c	5.20±3.27ab
R	6.83±0.49bc	9.10±1.38ab	7.04±1.72ab
RS	9.28±0.22a	11.47±0.26ab	9.12±0.86a

Effects of different tillage methods on catalase activity in Sorghum soil

Table 4 shows that the catalase activity of all treatments has the same trend during the growth period of sorghum. The catalase activity of all treatments is the highest at jointing stage, then decreases at flowering stage, while the catalase activity of treatments T, R and RS rises slightly at harvest stage. Different tillage treatments could increase the activity of soil catalase in different stages of sorghum. At jointing stage of sorghum, the activity of soil hydrogen peroxide changed from 1.54 to 1.66 mL/g (Kylili et al., 2018). Among them, the activity of hydrogen peroxide in RS treatment was higher than that in other treatments, reaching 1.66 mL/g, and there was no significant difference with other treatments. During the flowering stage of sorghum, the change of catalase activity in soil was 1.30-1.46 mL/g, and there was no significant difference among different tillage treatments. During sorghum harvest period, the change of soil catalase activity was 1.36-1.58 mL/g, and the order of soil catalase activity was RS > R > T > TS.

Table 4. *Changes of catalase activity in Sorghum soil ($mL \cdot g^{-1}$)*

Handle	Jointing stage	Florescence	Harvest period
T	1.54±0.02ab	1.30±0.01b	1.44±0.04b
TS	1.55±0.04ab	1.41±0.05b	1.36±0.04b
R	1.56±0.03ab	1.34±0.01b	1.58±0.05b
RS	1.66±0.03b	1.46±0.05b	1.59±0.06b

Effects of different tillage methods on soil urease activity in Sorghum

From *Table 5*, it can be seen that the trend of urease activity in different growth stages of sorghum is basically the same, and the peak value of urease activity is reached at flowering stage. Soil urease activity changed from 2.34 mg/g to 2.46 mg/g at jointing stage of sorghum, and there was no significant difference among different fertilization treatments. At the flowering stage of sorghum, the soil urease activity changed from 2.51 mg/g to 2.86 mg/g, and the activity of urease in RS treatment was the highest (Ye et al., 2017). The urease activity in each tillage treatment was RS > R > TS > T, and the difference between treatments was small. Soil urease activity changed from 2.05 mg/g to 2.32 mg/g during harvest period. The order of size and flowering time of all tillage treatments were the same. RS treatment was significantly higher than T treatment, with an increase of 13.1%.

http://www.aloki.hu ● ISSN 1589 1623 (Print) ● ISSN1785 0037 (Online)
DOI: http://dx.doi.org/10.15666/aeer/1802_28952908

Table 5. *Changes of catalase activity in Sorghum soil ($mg \cdot g^{-1}$)*

Handle	Jointing stage	Florescence	Harvest period
T	2.34±0.003b	2.51±0.08ab	2.05±0.13b
TS	2.34±0.121b	2.66±0.13b	2.10±0.10bc
R	2.37±0.06b	2.70±0.03b	2.13±0.04bc
RS	2.46±0.09b	2.86±0.06b	2.32±0.02c

Effects of different tillage methods on invertase activity in Sorghum soil

Table 6 shows that all tillage treatments can improve soil invertase activity at different stages of sorghum. The changes of soil invertase activity at jointing stage and harvest stage of sorghum are 15.03-25.55 mg/g and 15.60-34.42 mg/g, respectively. The activities of RS and TS in treatment are significantly higher than those in treatment T and R. At the flowering stage of sorghum, the change of soil sucrose activity was 21.14-34.3.7 mg/g, the order of size was RS > TS > R > T. Compared with T treatment, the increase of RS, TS and R were 62.58%, 38.55%, 21.71%, respectively. The soil enzyme activity of RS treatment was significantly higher than that of T treatment.

Table 6. *Changes of invertase activity in Sorghum soils ($mg \cdot g^{-1}$)*

Handle	Jointing stage	Florescence	Harvest period
T	15.03±1.07a	21.14±1.06a	15.60±3.16a
TS	22.82±1.47c	29.29±4.07c	34.42±4.31c
R	16.26±0.50b	25.73±1.76b	19.52±2.80b
RS	25.55±1.48c	34.37±1.86c	30.36±1.23c

Effects of different tillage methods on alkaline phosphatase activity in Sorghum soil

Table 7 shows that the change trend of alkaline phosphatase activity is basically the same in all growth stages of sorghum. The alkaline phosphatase activity is higher at jointing stage, slightly decreased at flowering stage, increased at harvest stage and reached the peak value. Soil alkaline phosphatase activity was increased by different tillage treatments. Soil alkaline phosphoric acid activity changed from 0.926 g/g to 1.205 mg/g in jointing stage of sorghum. The order of size was RS > TS > R > T. The activity of RS and TS in treatment was significantly higher than that in treatment T, and there was no significant difference between treatment R and treatment R. At the flowering stage of sorghum, soil alkaline phosphatase activity changed from 0.933 mg/g to 1.037 mg/g. The soil alkaline phosphatase activity of RS treatment was 1.037 mg/g significantly higher than that of T treatment, and there was no significant difference with other treatments. Soil alkaline phosphatase activity changed from 1.107 mg/g to 1.40 mg/g during sorghum harvest, and the order of size was RS > R > TS > T. Among them, RS treatment was significantly higher than T and TS treatment, and there was no significant difference between R treatment and RS treatment.

Table 7. *Alkaline phosphatase activity in Sorghum soil ($mg \cdot g^{-1}$)*

Handle	Jointing stage	Florescence	Harvest period
T	1.004±0.008ab	0.933±0.036ab	1.107±0.029ab
TS	1.064±0.013c	0.942±0.014ab	1.234±0.043bc
R	1.010±0.051bc	0.972±0.021ab	1.307±0.039cd
RS	1.104±0.021c	1.037±0.011b	1.400±0.020d

http://www.aloki.hu ● ISSN 1589 1623 (Print) ● ISSN1785 0037 (Online)
DOI: http://dx.doi.org/10.15666/aeer/1802_28952908

Effects of different tillage methods on soil protease andβ-glucosidase activities in Sorghum

Table 8 shows that there are significant differences in protease activity between different treatments at jointing and flowering stages. The effects of R and TS treatments are significant in the two growth stages, but not in the harvest stage. *Table 9* shows that the activity of soil beta-glucosidase is better in R treatment at different stages of sorghum growth and development, jointing stage and flowering stage, T > RS, harvest stage, T < RS.

Table 8. *Changes of soil protease activity in Sorghum ($mg \cdot g^{-1}$)*

Handle	Jointing stage	Florescence	Harvest period
T	43.23±1.48ab	20.45±1.20cd	22.01±1.62a
TS	13.05±3.64cd	20.73±0.27ab	21.40±0.17a
R	61.05±3.26ab	23.64±0.64bc	21.40±3.07a
RS	31.42±1.67cd	15.10±1.30cd	23.20±9.21a

Table 9. *Changes of soilβ-glucosidaseactivity in Sorghum ($mg \cdot g^{-1}$)*

Handle	Jointing stage	Florescence	Harvest period
T	52.82±1.26b	59.73±4.28a	35.84±0.59b
TS	46.53±2.02c	50.06±2.28b	29.21±4.00c
R	62.79±0.70a	60.02±2.33a	47.16±1.66a
RS	42.03±0.35d	57.00±1.77a	44.09±1.55a

Correlation Analysis

Analysis of correlation between soil microbial biomass and soil enzymes (invertase, phosphatase, polyphenol oxidase) activity

Soil enzymes are involved in various soil metabolic processes and energy transformation, and have a good correlation with the number of soil microorganisms. Pearson correlation analysis of soil microbial quantity and soil enzyme activity showed that there was a certain correlation between them (*Table 10*). Among them, bacteria were positively correlated with acid phosphatase, transformation and polyphenol oxidase; fungi were positively correlated with acid phosphatase and invertase, but not with polyphenol oxidation; actinomycetes were positively correlated with acid phosphatase, invertase and polyphenol oxidase.

Table 10. *Number of soil microorganisms and correlation coefficients of soil enzymes under different tillage patterns*

Content	Bacteria	Actinomyces	Fungus
Acid phosphatase	0.568**	0.908**	0.586**
Polyphenol oxidase	0.468**	0.699**	0.323
Invertase	0.603**	0.550**	0.757**

** indicates a significant correlation at P < 0.01 level and * a significant correlation at P < 0.05 level

Correlation between soil respiration rate and activities of soil enzymes (catalase, urease, invertase, alkaline phosphatase, protease, beta glucosidase) and soil nutrients

Soil respiration in this area varies significantly with different growth stages (*Figure 2*).

http://www.aloki.hu ● ISSN 1589 1623 (Print) ● ISSN1785 0037 (Online)
DOI: http://dx.doi.org/10.15666/aeer/1802_28952908

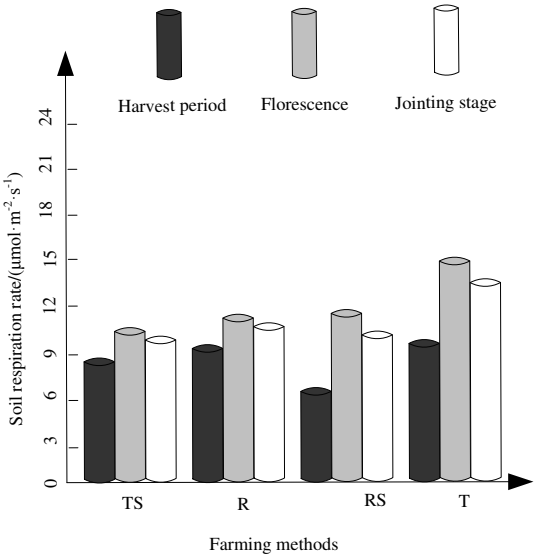

Figure 2. *Changes of soil respiration rate during Sorghum growth period under different tillage patterns*

In the figure above, T represents no-tillage, TS represents deep tillage, R represents shallow tillage + straw mulch, and RS represents deep tillage + straw mulch. It can be seen from figure 2 that soil respiration rates vary at different growing stages. The soil respiration rate at harvest stage was the lowest when RS method was adopted, with a value of 6.5 $mol \cdot m^{-2} \cdot s^{-1}$, and the soil respiration rate at elongation stage was also the lowest with a value of 9.8 $mol \cdot m^{-2} \cdot s^{-1}$. The soil respiration rate at flowering stage was the lowest when TS mode was adopted, and the value was 10.5 $mol \cdot m^{-2} \cdot s^{-1}$.

Soil nutrient content of Sorghum in hilly environment includes organic carbon, total nitrogen, available potassium and pH value. The change of soil organic carbon content during sorghum growth period is only listed in this paper as shown in *Figure 3*.

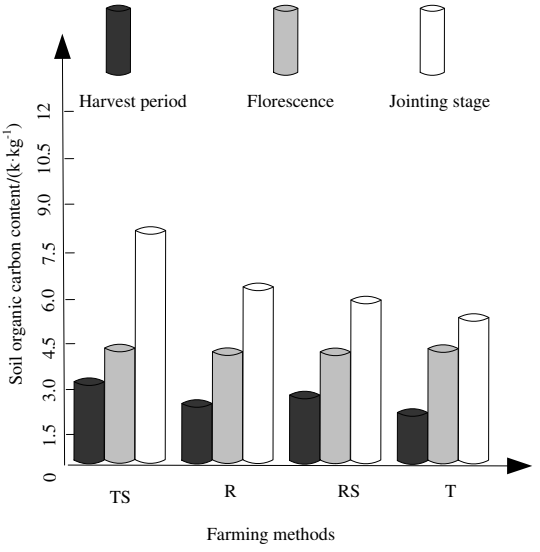

Figure 3. *Changes of soil organic carbon content in Sorghum growing period under different tillage patterns*

http://www.aloki.hu ● ISSN 1589 1623 (Print) ● ISSN1785 0037 (Online)
DOI: http://dx.doi.org/10.15666/aeer/1802_28952908

In the figure above, Trepresents no-tillage, TS represents deep tillage, R represents shallow tillage + straw mulch, and RS represents deep tillage + straw mulch. It can be seen from *Figure 3* that soil organic carbon content varies at different growing stages. The soil organic carbon content in the harvest period was the lowest when R method was adopted, and the value was $3.3k \cdot kg^{-1}$. The soil organic carbon content in jointing stage was the lowest when T method was adopted, and the value was $5.8k \cdot kg^{-1}$. The soil organic carbon content at flowering stage was the same in all four ways, and the value was $4.5k \cdot kg^{-1}$.

The results of correlation analysis between soil respiration and soil fertility factors showed that *(Table 11*) the correlation degree between soil nutrients was high, and the correlation among various indicators reached significant or extremely significant levels, which could be used to evaluate the soil fertility. The correlation analysis of soil enzyme activities showed that urease and other enzymes except protease reached a significant level, among which catalase, alkaline phosphatase andβ-glucosidase reached a very significant level ($p < 0.01$). There was a good correlation between soil respiration rate and other soil fertility indicators except alkaline acid enzyme, total nitrogen, available potassium and pH value, among which catalase, urease and invertase reached a very significant level ($p < 0.01$).

Table 11. *Relationships between soil respiration rate and soil enzyme activity and soil nutrients*

Content	Respiratory rate	Protease	Catalase	Alkaline phosphatase	Urease	Invertase	Beta-glucosidase	Organic carbon	Total nitrogen	Available potassium	PH value
Respiratory rate	1										
Protease	0.373*	1									
Catalase	-0.736**	-0.322*	1								
Alkaline phosphatase	-0.228	0.230	0.181	1							
Urease	-0.640**	0.001	0.421**	0.744**	1						
Invertase	0.428**	0.155	-0.507**	-0.048	-0.348*	1					
Beta-glucosidase	0.320*	0.304	-0.308	-0.327*	-0.580**	0.502**	1				
Organic carbon	0.387*	0.302	-0.286	-0.222	-0.461**	0.525**	0.585**	1			
Total nitrogen	0.305	-0.103	-0.204	-0.283	-0.383*	0.347*	0.404*	0.507**	1		
Available potassium	0.199	0.148	-0.270	-0.506**	-0.527**	0.627**	0.699**	0.602**		1	
pH value	-0.260	-0.204	0.300	0.483**	0.483**	-0.506**	-0.551**	-0.605**		-0.717**	1

Discussions

The total activity of soil enzymes can reflect the soil fertility to a certain extent. Material cycle and energy conversion in soil ecosystem are closely related to soil enzyme activity (Nannipieri et al., 2017). The results showed that different crop tillage, fertilization system and planting methods could cause changes in soil enzyme activity. In this study, we found that the activities of polyphenol oxidase, invertase and acid phosphatase in Sorghum rhizosphere soil were higher at flowering stage (Chen et al., 2016). The main reason is that the enzyme activity is affected by temperature and soil properties. When the soil temperature is low, the activity is weak, and when the soil

http://www.aloki.hu ● ISSN 1589 1623 (Print) ● ISSN1785 0037 (Online)
DOI: http://dx.doi.org/10.15666/aeer/1802_28952908

temperature is suitable, the enzyme activity increases. At harvest time, the microbial activity decreases, and the enzyme activity decreases at a certain level. At the same time, the results showed that deep tillage and straw mulching could improve soil enzyme activity in varying degrees, and the effect was most significant under both deep tillage and straw mulching (Sun et al., 2017). This is because straw mulching not only regulates soil temperature, but also has a greater impact on soil organic matter and available nutrients, and can increase the number of soil microorganisms, increase the substrate for microbial transformation, so soil enzyme activity will increase.

The results showed that the effects of different tillage methods on soil enzymes in Sorghum growth period were different. On the whole, straw mulching and deep tillage could significantly improve the activities of soil hydrogen peroxide and urease in Sorghum at different stages. However, there was no significant difference in soil catalase and urease activities among different tillage treatments, except TS, T and T treatments at jointing stage of catalase, which indicated that the activities of hydrogen peroxide and urease in sorghum were less affected by straw mulching and deep tillage. Deep tillage and straw mulching can improve soil acid and alcohol activity. The results showed that alkaline acidase activity of soil treated by deep tillage or straw mulching was higher than that treated by chemical fertilizer. Straw mulching played a key role. Straw mulching improved soil productivity, increased the activity of plants, animals and microorganisms in soil, promoted the secretion of extracellular enzymes and enhanced soil enzyme activity (Wang et al., 2018). Deep tillage or straw returning can improve soil invertase activity, which is similar to the conclusions reported in many literatures. The straw returned to the field also provided the substrate for soil enzymes, provided enough energy for microorganisms, and caused changes in soil enzyme activities (Gopalsamy et al., 2017).

The correlation between urease, alkaline phosphatase, sucrose alcohol, protein alcohol, catalase and beta-glucosidase and soil respiration rate were studied in this experiment to provide basis for improving soil enzyme activity. The results showed that there was a good correlation between soil respiration and soil enzyme activity (except alkaline phosphatase) (Chen, 2017). In addition, the effect of growth period on soil respiration rate should not be neglected. This study found that the respiration rate of Sorghum at jointing stage and before jointing stage was higher than that at flowering and harvesting stage. This may lead to a large loss of soil organic carbon and an increase in CO release from soils caused by early tillage and sowing, on the other hand, it may be caused by early irrigation. The increase of water content promoted root respiration and the activity of biological community, which enhanced soil respiration.

Conclusions

This study analyzed the soil enzyme activity of sorghum under different tillage methods at different growth stages. The activities of sucrase, acid phosphatase, polyphenol oxidase, catalase, soil urease, soil invertase and alkaline phosphatase in deep tillage and straw mulching were detected by colorimetry. Under tillage, shallow tillage + straw mulch and deep tillage, enzyme activity was significant. Protease activity was significantly different between treatments at jointing and flowering stages. In the two stages of growth, R treatment and TS treatment were effective. The activity of soil -glucosidase was better during the growth, jointing, flowering, ripening, harvesting and ripening of sorghum. Using li-8100 soil carbon flux automatic measurement system, it

http://www.aloki.hu ● ISSN 1589 1623 (Print) ● ISSN1785 0037 (Online)
DOI: http://dx.doi.org/10.15666/aeer/1802_28952908

was proved that soil microbial quantity was positively correlated with soil enzymes, bacteria and actinomycetes were positively correlated with acidity, invertase and polyoxygenase, and fungi were positively correlated with acid phosphatase and invertase. Choose deep tillage and straw mulching cultivation, therefore, to improve the soil microorganism quantity and activity, to the growth of sorghum in the hilly environment to build a good ecological environment, to keep the hilly ecosystem sustainable production capacity at the same time is important, then can be tested with different temperature experiment indexes such as, in order to promote the further development of this part.

REFERENCES

[1] Basak, B. B., Gajbhiye, N. A. (2018): Herbage yield and bioactive principle of senna as influenced by micronutrient application in soil. – Journal of Environmental Biology 39(1):43-49.

[2] Bo, T. (2016): Influence of Combined Soil Heavy Metal Pollution on Soil Enzyme Activity in the Pb–Zn Mining Area of Southern Shaanxi. – Journal of Computational & Theoretical Nanoscience 13(2):1147-1152.

[3] Cao, R., Wu, F. Z., Yang, W. Q., Xu, Z. F., Tani, B., Wang, B., Li, J., Chang, C. H. (2016): Effects of altitudes on soil microbial biomass and enzyme activity in alpine-gorge regions. – Ying Yong Sheng Tai Xue Bao 27(4):1257-1264.

[4] Chen, S. T., Sang, L., Zhang, X., Hu, Z. H. (2016): Effects of warming and straw application on soil respiration and enzyme activity in a winter wheat cropland. – Huanjing kexue 37(2):703-709.

[5] Chen, C. (2017):Safety evaluation of electromagnetic environment around electric vehicle during wireless charging. – Automation & Instrumentation232(02):11-13, 17.

[6] Faust, S., Kaiser, K., Wiedner, K., Glaser, B., Joergensen, R. G. (2018): Comparison of different methods for determining lignin concentration and quality in herbaceous and woody plant residues. – Plant and Soil 433(1-2):7-18.

[7] Feng, B. G.,Guo, P.,Li, L. H., Sun, Y., Chen, W. W. (2018): Effect of Nano-TiO_2 on Mass Ratio of Nitrate Nitrogen and Activity of Nitrate Reductase in Soil. – Journal of Jilin University (Science Edition) 56(06):1570-1576.

[8] Gopalsamy, A., Narayanan, A., Liu, S., Parikh, M. D., Kyne, R. E. Jr., Fadeyi, O., Tones, M. A., Cherry, J. J., Nabhan, J. F., LaRosa, G., Petersen, D. N., Menard, C., Foley, T. L., Noell, S., Ren, Y., Loria, P. M., Maglich-Goodwin, J., Rong, H., Jones, L. H. (2017): Design of potent mRNA decapping scavenger enzyme (DcpS) inhibitors with improved physicochemical properties to investigate the mechanism of therapeutic benefit in Spinal Muscular Atrophy (SMA). – Journal of Medicinal Chemistry 60(7):3094-3108.

[9] Jun, S. Y., Walker, A. M., Kim, H.,Ralph, J., Vermerris, W., Sattler, S. E., Kang, C. H. (2017): Enzyme activity and substrate specificity of the major cinnamyl alcohol dehydrogenases in sorghum. – Plant Physiology 174(4):2128.

[10] Kim, S., Li, G., Han, S. H.,Kim, H. J., Kim, C., Lee, S. T., Son, Y. (2018): Thinning affects microbial biomass without changing enzyme activity in the soil of PinusdensifloraSieb. etZucc. forests after 7 years. – Annals of Forest Science 75(1):13.

[11] Kosmambetova, G. R., Kalchuk, N. S., Didenko, O. Z., Strizhak, P. E. (2017): Comparative study of magnesia-supported highly-dispersed CuO solids prepared by different methods in CO oxidation. – Canadian Journal of Chemical Engineering 95(8):1510-1517.

[12] Kylili, A., Fokaides, P. A., Ioannides, A., Kalogirou, S. (2018): Environmental assessment of solar thermal systems for the industrial sector. – Journal of Cleaner Production 176:99-109.

http://www.aloki.hu ● ISSN 1589 1623 (Print) ● ISSN1785 0037 (Online)
DOI: http://dx.doi.org/10.15666/aeer/1802_28952908

[13] Moon, C., Ahn, Y., Lee, T., Hwang, Y. (2019): Importance of microbial adaptation for concentrate management in wastewater reuse process. – Energy & Environment 30(4):719-731.
[14] Nannipieri, P., Trasar-Cepeda, C., Dick, R. P. (2017): Soil enzyme activity: a brief history and biochemistry as a basis for appropriate interpretations and meta-analysis. – Biology & Fertility of Soils 54(5):11-19.
[15] Pan, Z., Baerson, S. R., Wang, M., Bajsa-Hirschel, J., Rimando, A. M., Wang, X., Nanayakkara, N. P. D., Noonan, B. P., Fromm, M. E., Dayan, F. E., Khan, I. A., Duke, S. O. (2018): A cytochrome P450 CYP71 enzyme expressed in Sorghum bicolor root hair cells participates in the biosynthesis of the benzoquinone allelochemicalsorgoleone. – New Phytologist 218(2):616.
[16] Sun, X., Shi, J., Ding, G. (2017): Effects of arbuscularmycorrhiza and drought stress on plant growth and mortality of forage sorghum. – Applied Soil Ecology 119(2017):384-391.
[17] Supriya, M., De, T., Christopher, R. (2017): Effect of temperature on lysosomal enzyme activity during preparation and storage of dried blood spots. – Journal of Clinical Laboratory Analysis 32(1): e22220.
[18] Wang, L.,Tang, P. W., Yan, W., Gao, X., Wang, E. (2017): Influence on power quality and electromagnetic environment to electric vehicle charging pile. – Journal of Power Supply 15(3):91-99.
[19] Wang, L., Ma, L., Sun, J., Zhang, Y., Zhou, Q., Wu, Z., He, F. (2018): Effects of different aquaculture methods for introduced bivalves (Hyriopsiscumingii) on seston removal and phosphorus balance at the water–sediment interface. – Journal of Freshwater Ecology 33(1):251-265.
[20] Wen, J., Liu, H., Xiao, S., Li, X., Fang, K., Zeng, M., Tang, Z., Cao, S., Li, F. (2017): Comparison of mid-term efficacy of spastic flatfoot in ambulant children with cerebral palsy by 2 different methods. – Medicine 96(22): e7044.
[21] Xu, Z. W., Yu, G. R., Zhang, X. Y., He, N. P., Wang, Q. F., Wang, S. Z., Wang, R. L., Zhao, N., Jia, Y. L., Wang, C. Y. (2017): Soil enzyme activity and stoichiometry in forest ecosystems along the North-South Transect in eastern China (NSTEC). – Soil Biology & Biochemistry 104(1):152-163.
[22] Ye, Y. Y., Luo, Y., Wang, Y., Lin, M., Xiang, P., Ashraf, M. A. (2017): Relation between diversity of phytoplankton and environmental factors in waters around Nanri Island. – Applied Ecology and Environmental Research 15(3):241-252.
[23] Zhang, M. Z., Niu, W. Q., Xu, J., Li, Y. (2016): Influences of micro-irrigation and subsoiling before planting on enzyme activity in soil rhizosphere and summer maize yield. – Chinese Journal of Applied Ecology 27(6):1925-1934.
[24] Zheng, H., Liu, Y., Zhang, J., Chen, Y., Yang, L., Li, H., Wang, L. (2017): Factors influencing soil enzyme activity in China's forest ecosystems. – Plant Ecology 219(1):31-44.

http://www.aloki.hu ● ISSN 1589 1623 (Print) ● ISSN1785 0037 (Online)
DOI: http://dx.doi.org/10.15666/aeer/1802_28952908

THE EFFECTS OF BOTANICAL OILS ON THE RED PALM WEEVIL, *RHYNCHOPHORUS FERRUGINEUS* OLIVIER (COLEOPTERA: CURCULIONIDAE)

REYAD, N. F.[1,2] – AL-GHAMDI, H. A.[1] – ABDEL-RAHEEM, M. A.[3*] – AL-SHAERI, M. A.[4]

[1]*Biology Department, College of Science, King Khalid University, Abha, Saudi Arabia*
(e-mail: dr.huda.gh@gmail.com; phone: +966-567-000-464)

[2]*Plant Protection Research Institute A. R. C. Dokki, Giza, Egypt*
(e-mail: drnagla@hotmail.com; phone: +966-559-206-370)

[3]*Pests & Plant Protection Department, Agricultural and Biological Research Division, National Research Centre, 33rd ElBohouth St., Dokki, Giza, Egypt*
(e-mail: abdelraheem_nrc@hotmail.com, abdelraheem_nrc@yahoo.com;
phone: +201-155-527-583, +201-009-580-797; Orcid.org/0000-0001-9240-064X)

[4]*Department of Biological Sciences, Faculty of Science, King Abdulaziz University, Jeddah, Saudi Arabia*
(e-mail: malshaere@kau.edu.sa; phone: +966-567-000-464)

[*]*Corresponding author*
e-mail: abdelraheem_nrc@hotmail.com

(Received 29th Oct 2019; accepted 12th Feb 2020)

Abstract. Date palm trees are liable to be attacked by many insect pests which cause serious damage to the different parts of tree. The most serious insect pest is the red palm weevil, *Rhynchophorus ferrugineus* (Oliver) (RPWs). To evaluate the impact of four botanical oils of *Melissa officinalis*, *Borago officinalis*, *Laurus nobilis* and *Carapichea ipecacuanha* on *R. ferrugineus*. 4 botanical oils were tested against newly emerged adults of *R. ferrugineus* for the purpose of investigating their insecticidal activity and effects on some biological aspects. Males of *R. ferrugineus* were more susceptible to the four botanical oils than females, followed by the immature larvae. The larvae showed different degrees of susceptibility to the four botanical oils. They showed the highest susceptibility to *C. ipecacuanha* and the lowest to *B. officinalis* oil at LC_{50} levels. Adult males and females were more susceptible to *C. ipecacuanha* and the least to *L. nobilis* oil at LC_{50} levels. The four tested oils disrupted some biological aspects of the insects. These oils remarkably reduced male and female longevity, female fecundity and hatchability of the laid eggs.
Keywords: *effects, botanical oils, Rhynchophorus ferrugineus, control*

Introduction

Date palm trees are liable to be attacked by a lot of insect pests. The most serious insect pest was the red palm weevil, *Rhynchophorus ferrugineus* (Oliver) (Saleh, 1992). Essential oils have high volatility and toxicity towards stored-grain pests and weevils (Regnault-Roger and Hamraoui, 1995; Regnault-Roger, 1997; Shaaya et al., 1997). Various chemical organic compounds have been isolated from plants; they include fixed oils, volatile oils and other plant constituents which expressed potential action against insect species. Extraction, isolation and identification of the fixed oils have been studied by Abdallah et al. (1986), Moustafa et al. (1986), Baraka and El-Hady (1993), Hussein and Shoukry (1997) and Shoukry-Karima (2003). El-Sayed et al. (1989) mentioned that maize oil and coconut oil used on *Callosobruchus maculatus* reduced their progeny.

http://www.aloki.hu ● ISSN 1589 1623 (Print) ● ISSN1785 0037 (Online)
DOI: http://dx.doi.org/10.15666/aeer/1802_29092919

Abdel-Kawy and Gharib (1991) stated that oils of cotton seeds, sesame and peanut showed efficiency in treatment of yellow meal corn against the rice weevil, *Sitophilus oryzae* (L.). Jood et al. (1993) used neem oil (*Azadirachta indica*), powders of neem leaf and neem kernel, *Citrus limon* leaf, *Allium sativum*, *Mentha spichata* leaf in wheat grains at levels of 1% and 2% (w/w) against larvae of *Trogoderma granarium* Everts and they found that neem products completely prevented damage by an introduced larval population. *C. macculatus*, adult emergence of was completely inhibited by castor oil, black seed oil and olive oil at concentration 1% for 30 days (Swidan, 1996; Ismail et al., 2014, 2016; Salem et al., 2016). Also, the essential oils were tested against many insect species (Bouda et al., 2001; Isikber et al., 2006). The volatile oils of *Boxus chinensis* against 10 days-old larvae of the *R. ferrugineus* showed toxicological and pathological effects (Abdullah, 2009; Ahmed et al., 2015). Huseyin et al. (2006) noticed that ethanolic extracts of some aerial parts of lamiaceae species showed high larvicidal activity after 24 hours and *M. officinalis* (Linn.) oil was the highest toxic against larvae of *Culex pipiens* Linn. Karahroodi-Zahra et al. (2011) using of six essential oils from *M. officinalis* (L.), *M. piperata* (L.), *P. sativum* (Hoffman), *L. angustifolia* (Mill.), *Z. clinopodioides* (Lam.), and *A. dracunculus* (L.), on eggs and first instar larvae of *P. interpunctella*, they found that *M. officinalis* recorded moderate ovicidal activity. Ben Jemâa et al. (2011) studied the chemical composition and the repellent activity of *Laurus nobilis* essential oil against 7-10 days old-adults of the cigarette beetle, *Lasioderma serricorne*. The repellent action was highly dependent upon oil concentration and exposure time and *L. nobilis* essential oil may have potential as a control agent against this beetle. The essential oil of *B. officinalis* (L.) showed good larvicidal potential after 48 hours of exposure period against *A. gambiae* (Kweka et al., 2012). Essential oil of *L. nobilis* showed strong fumigant toxicity against *T. granarium* larvae (Tayoub et al., 2012). The ability of the aggregation pheromone to capture more females than males RPWs in the traps which makes trapping a potential tool for managing *R. ferrugineus* (Lee et al., 2001; Khalaf et al., 2009; El-Bokl et al., 2015). Powder of four plants, *B. officinalis*; *M. piperta*; *Officinalis anisum*; *Eucalyptus glubulus* was tested by Farman-Khansaa (2009) on the red flour beetle, *Tribolium castaneum* and found that *M. piperta* had most repellent efficiency plant, followed by *O. anisum*, *E. glubulus*, while the lowest was *B. officinalis*. The plant oils, (fixed and volatile) seriously disrupted some biological aspects of *R. ferrugineus* (Oliver) (Ahmed et al., 2015). Essential oils from various plants have shown promise as sources for insecticides. Earlier attempts to explore the toxicity of plant derivatives against *R. ferrugineus* have been made by essential oils. Two natural insecticides, *Boxus chinensis* oil and precocene II topically against larvae, prepupae and adult of red palm weevil, *R. ferrugineus* and the larvae of the palm beetle, pseudophilus testsceous. They found that larvae of *R. ferrugineus* were less tolerant to *B. chinensis* oil and more tolerant to precocene II than palm beetle larvae (Nassar and Abdullah, 2005). Nemazal and ethanolic neem extracts have a considerable significant remedial efficacy altogether with an effective, repellency against *R. ferrugineus* infestations (Merghem and Mohamed, 2017). An artificial diet incorporated with Picrotoxin was proven to inhibit the growth activities and to reprogram the detoxification defense mechanism of red palm weevils. Picrotoxin, a natural plant neurotoxin, is an important addition in the list of red palm weevil controlling products. Future research should focus on various aspects including formulation, safety, and application in order to optimize the e_cacy of Picrotoxin for managing red palm weevil infestations (Hussain et al., 2019). In this

http://www.aloki.hu ● ISSN 1589 1623 (Print) ● ISSN1785 0037 (Online)
DOI: http://dx.doi.org/10.15666/aeer/1802_29092919

study, four botanical oils of *Melissa officinalis*, *Borago officinalis*, *Laurus nobilis* and *Carapichea ipecacuanha* were tested against newly emerged adult males and females of the red palm weevil, *R. ferrugineus* (Oliver) for investigating their insecticidal activity and effects on some biological aspects.

Materials and Methods

This study was carried out in Pests & Plant Protection Department, National Research Centre, Giza, Egypt and Biology Department, College of Science, King Khalid University, Abha, Saudi Arabia.

Mass rearing of R. ferrugineus

Adults of *Rhynchophorus ferrugineus* were obtained from coccons collected from infested date palm trees, incubated in plastic boxes (120 × 60 × 30 cm). These coccons were kept in wet toweling till adult emergence. The newly emerged adults were sexually differentiated and fed on small pieces of red palm core.

Used plants

The plants under investigation were originally obtained from international markets, identified, divided into two groups fixed and volatile oils, these plants are listed in *Table 1*.

Table 1. *Tested plants*

Group	Plants		Family name	Used parts
	Common name	Scientific name		
A Fixed oils	Lemon balm	*Melissa officinalis*	Lamiaceae	Leaf
	Borage	*Borago officinalis*	Boraginaceae	Leaf
B Volatile oils	Bay Laurel	*Laurus nobilis*	Lauraceae	Leaf & fruit
	Rio ipecac	*Carapichea ipecacuanha*	Rubiaceae	Root &leaf

Oils extraction

Extraction of fixed oils was performed from crushed and previously steam distilled plant parts of group A, where the dry powdered plants were macerated in petroleum ether (40/60) according to Harbourne (1984) and El-Sayed et al. (1989). The petroleum-ether extracts were filtered through anhydrous sodium sulphate. The solvent was removed by using rotary evaporator. The volatile oils were extracted from plants in group B, by using steam distillation technique according to the method of Anderson et al. (1980). Then oils were saturated with sodium chloride and extracted again with diethyl ether. The extracts were dried over anhydrous sodium sulphate and evaporated under reduced pressure by using rotary evaporator apparatus.

Methods of bioassay

The concentrations of the two groups of oils were prepared and added 0.1% tween to the fixed oil as an emulsifier. Pieces of date palm hearts were rinsed in each concentration for 20 seconds, and left to dry at room temperature. Treated pieces were

http://www.aloki.hu ● ISSN 1589 1623 (Print) ● ISSN1785 0037 (Online)
DOI: http://dx.doi.org/10.15666/aeer/1802_29092919

put separately in all replicates of pairs of newly emerged adults or 8 days-old larvae of the second generation. 100 (larvae, and adults) were used for each treatment, divided into 4 groups, each of 25 (larvae, and adults) were placed in Petri dishes, one individual/dish. For each concentration individuals of larvae were counted after 7 days and after 10 days for adults after treatments under laboratory conditions (30°C, 75 ± 5% R.H., and 12D : 12 L hrs.) to determine the % mortality.

Analysis of results

Toxicity lines were established and LC_{50} values were determined. The Toxicity lines were analyzed according to the method described by Finney (1952). The slope function and the relative potency of the tested oils were determined according to Sun (1950).

Results

Table 2 showed that the *C. ipecacuanha* was the highest toxic to the larvae (LC_{50}=1260.09 ppm), followed by *L. nobilis* oil (LC_{50}=2412.30) and then *B. officinals* (LC_{50}=2500.71 ppm). The relative potencies based on *C. ipecacuanha* were 1.20, 1.87 and 1.90 for *M. officinalis*, *B. officinalis* and *L. nobilis*, respectively. The relatively low values of slope functions revealed the homogenous response of the tested stages to the different concentrations of the tested oils.

Table 2. *Toxicity and the relative potency of the fixed oils and volatile oils on R. ferrugineus*

Botanical oil	**Tested plant**	**LC_{50} (ppm) (Confidence limits)**	**Slope function**	**Relative potency**
8 days-old larvae:				
Fixed oils	*Melissa officinalis*	1600.635 (1260.820-2010.140)	2.300	1.200
	Borago officinalis	2500.712 (2368.900-2652.556)	4.333	1.871
Volatile oils	*Laurus nobilis*	2412.300 (2288.700-2522.806)	5.233	1.900
	Carapichea ipecacuanha	1260.093 (1030.866-1510.820)	2.533	1
Adult females:				
Fixed oils	*Melissa officinalis*	1280.556 (1140.284-1460.300)	2.000	1.200
	Borago officinalis	1350.210 (1230.500-1500.239)	2.500	1.270
Volatile oils	*Laurus nobilis*	1880.763 (1778.800-2000.500)	4.400	1.755
	Carapichea ipecacuanha	1060.500 (960.800-1170.130)	2.457	1
Adult males:				
Fixed oils	*Melissa officinalis*	1130.75 (1023.744-1252.700)	2.320	1.290
	Borago officinalis	1248.155 (970.053-1515.300)	3.120	1.400
Volatile oils	*Laurus nobilis*	1750.645 (1440.210-2020.120)	4.400	2.000
	Carapichea ipecacuanha	870.721 (780.840-970.900)	2.111	1

http://www.aloki.hu ● ISSN 1589 1623 (Print) ● ISSN1785 0037 (Online)
DOI: http://dx.doi.org/10.15666/aeer/1802_29092919

Table 3 showed a highly significant decrease in both male and female longevity of *R. ferrugineus* when treated with the plant oils of *M. officinalis* and *B. officinalis* as fixed oils; *L. nobilis* and *C. ipecacuanha* as volatile oils. Also, the treatment with the tested plant oils of *M. officinalis*, *B. officinalis*, *C. ipecacuanha* and *L. nobilis* showed a high significant reduction on the fecundity. Hatching percentage of eggs laid by adult females treated with the all tested oils decreased significantly. The hatching percentages were 55.3±0.22% and 64.2±0.24% in case of treatment with *C. ipecacuanha*, and *L. nobilis* volatile oils, respectively. While the hatching percentages in case of treatment with the two fixed oils reached 58.8±0.3% in *M. officinalis* and 59.09±0.21% in *B. officinalis* oil.

Table 3. *Effect of (LC_{50}s) of plant oils on biological aspects of newly emerged adults of R. ferrugineus*

Treatment		LC_{50} (ppm)		Adult longevity (days) Mean ± S.E.		Fecundity (eggs/♀) Mean ± S.E.	(Eggs /♀/ day) Mean ± S.E.	Fertility (eggs/♀) Mean ± S.E.	Hatching percentage (%) Mean ± S.E.
		♂	♀	♂	♀				
Control		----------		140 ±3.10	130.23 ±3.08	148 ±2.20	2.40 ±0.02	135.13 ±0.42	89.70 ±1.3
Fixed oils	Lemon balm *(Melissa officinalis)*	1138	1288	75.2 ±4.33**	82.45 ±2.2**	95.20 ±2.80**	1.13 ±0.52**	56.0 ±1.83**	58.8 ±0.3**
	Borage (*Borago officinalis)*	1357	1368	92.0 ±4.52**	103.65 ±8.10**	120.0 ±1.79**	1.10 ±0.15**	72.30 ±1.66**	59.02 ±0.21**
Volatile oils	Bay leaf (*Laurus nobilis)*	1753	1880	102.57 ±3.2**	112.30 ±3.2**	134.65 ±3.33**	1.1± 0.02**	85.65 ±2.1**	64.2 ±0.24**
	Rio ipecac (*Carapichea ipecacuanha)*	875	1050	61.61 ±3.2**	68.0 ±6.16**	75.32 ±8.30**	1.12 ±0.11**	42.47 ±4.20**	55.3 ±0.22**

Without * Non significant (P>0.05). * Significant (P<0.05). ** highly significant (P<0.001)

Table 4 showed that, there was significant increase in larval duration in case of treatment with the volatile oils while statistical analysis of the decrease in the larval duration in case of treatment with the two fixed oils of *M. officinalis* and *B. officinalis* was not significant. Significant increase in prepupal and pupal durations occurred by the treatment with *C. ipecacuanha* as it reached 7.0±0.34 and 11.3±1. 2 days, respectively. While treatment with fixed oils of *M. officinalis* and *B. officinalis* decreased non significantly in the prepupal and pupal durations. High significant reduction in the pupation percentage of treated larvae reached 40.2±0.2% by *C. ipecacuanha*, 54.2±2.0% by *M. officinalis*, 60.2±1.2% by *B. officinalis*, and 60.2±2.2% by *L. nobilis*, while that, of control was 90.0±0.0%. The 8 days treatment of old-larvae with (LC_{50}) of plant oils (fixed oils and volatile oils) resulted in high significant reduction of adult emergence (%). Both male and female longevity also decreased significantly when treated by the two fixed oils and volatile oils and showed high significant decrease in their duration when treated with *C. ipecacuanha*. The tested plant oils had variable effects on fecundity of females emerged from treated larvae. The mean number of eggs deposited by a female decreased high significantly in case of treatment with *C. ipecacuanha* oil and was non-significant in case of treatment with *M. officinalis*,

http://www.aloki.hu ● ISSN 1589 1623 (Print) ● ISSN1785 0037 (Online)
DOI: http://dx.doi.org/10.15666/aeer/1802_29092919

B. officinalis and *L. nobilis*. Also, *Table 4* showed non-significant decrease in hatching (%) of eggs laid by females emerged from treated larvae except that, of *C. ipecacuanha*, which showed a significant decrease. It was clear that, the plant oils (both the fixed and volatile) seriously disrupted some biological aspects of *R. ferrugineus* (Oliver).

Table 4. *Effect of (LC_{50}s) of plant oils on different biological aspects of 8 days old larvae of R. ferrugineus*

Treatment		LC_{50} (ppm)	Larval duration (days) Mean ± S.E.	Pupal stage				Adult Longevity (days) Mean ± S.E.		Fecundity Mean ± S.E.	Hatching (%) Mean ± S.E.
				Prepupal Duration (days) Mean ±S.E.	Pupal Duration (days) Mean ±S.E.	Pupation (%)	Mean ± S.E.	♂	♀		
Control		------	44.65 ±2.30	5.0 ±0.2	8.22 ±0.32	90.0 ±0.0	84.0 ±0.2	140 ±2.2	132.32 ±3.2	150± 1.22	90.23 ±1.2
Fixed oils	*M. officinalis*	1600	37.2 ±1.6	3.6 ±0.3*	7.4 ±0.30	54.2 ±2.0**	54.22 ±3**	95.22 ±3.2**	108.2 ±2.2*	118.9 ±2.5*	77.8 ±0.62
	B. officinalis	2510	39.9 ±2.4	4.3 ±0.4	8.0 ±0.20	60.2 ±1.2**	61.9 ±0.4**	115.3 ±2.2*	120.9 ±1.7	135.8 ±2.5	83.8 ±0.2
Volatile Oils	*L. nobilis*	2420	55.5 ±2.0*	5.3 ±0.30	9.3 ±0.7	60.2 ±2.2**	64.5 ±2.3**	122.2 ±2.2*	124.9 ±2.2	140.0 ±2.5	85.3 ±0.2
	C. ipecacuanha	1260	65.0 ±2.0**	7.0 ±0.34*	11.3 ±1.2*	40.2 ±0.2**	50.2 ±1.1**	80.0 ±2.1**	85.0 ±3.5**	100.0 ±3.2 **	75.0 ±0.3*

Without * Non significant (P>0.05). * Significant (P<0.05). ** highly significant (P<0.001)

Discussion

Essential oils from many plants have become promising sources of insecticides. Several attempts to explore the toxicity of plant derivatives against *R. ferrugineus* have been made by by the use of essential oils. Nassar and Abdullah (2005) tested two natural insecticides, *Boxus chinensisoil* and precocene II topically against larvae, prepupae and adult of red palm weevil, *R. ferrugineus* and the larvae of the palm beetle, *pseudophilus testsceous*. They found that larvae of *R. ferrugineus* were less tolerant to *B. chinensis* oil and more tolerant to precocene II than palm beetle larvae. Huseyin et al. (2006) studied the larvicidal activity of ethanolic extracts of some arial parts of Lamiaceae species against *Culex pipiens* (Linn.). They found that all plant extracts had strong larvicidal activity after 24 hours exposure tests. *Melissa officinalis* (Linn.) oil showed the highest toxic activity. Abdullah (2009) tested the volatile oil of *Boxus chinensis* against 10-day old larvae of the red palm weevil, *R. ferrugineus*. He found that it had toxicological and pathological effects on *R. ferrugineus* larvae. The results of the current study, concerning the toxicity of the four botanical oils to the 8-day old larvae and adults of *R. ferrugineus*, showed that the (*C. ipecacuanha*) oil was superior to the other three oils of lemon palm (*M. officinalis*), Bay leaf (*L. nobilis*) and the borage (*B. officinalis*) oils, while Borage was the least toxic oil. The variation in the toxicological effects of the tested oils might be due to differences in their chemical composition as well as the variation in sensitivity and response to the various cells and

http://www.aloki.hu ● ISSN 1589 1623 (Print) ● ISSN1785 0037 (Online)
DOI: http://dx.doi.org/10.15666/aeer/1802_29092919

tissues. This might also depend on the amount of poison that reaches the site of action. Mostafa et al. (1995) mentioned that the volatile oils of some plants increased the activity of Malic Dehydrogenase Enzyme (MDE) and decreased the activity of (Malic Enzyme) (ME) in *Pectinophora gossypiella* and *Erias insulana* larvae. From the above mentioned data we concluded that the two fixed and the two volatile oils caused a similar significant decrease in both male and female longevities. This result is in line with findings of Andronikashvili and Reichmuth's study (2003) who concluded that the volatile oil of *L. nobilis* had high repellency effect towards adult of red flour beetle, *Tribolium castaneum* explaining its moderate insecticidal activity and reducing periods of male and female longevity. Similar results were obtained by Isikber et al. (2006). Farman-Khansaa (2009) investigated the repellent effect of powder of four plants; *B. officinalis*, *M. piperta*, *O. anisum* and *Eucaluptus glubulus* against the red flour beetles *Tribolium castanium*, reflecting the first essential reason of weevil longevities decrease, which is due to their high repellency. The same high repellency was recorded by Ben Jemâa et al. (2011) against adults of the cigarette beetle *Lasioderma serricorne*, and also led to decrease in adult longevity. Also Mohamad et al. (2011) studied the causes of attraction and repellency effect of some plants extracts from leaves and roots of Borago and Tages plant against the Southern cowpea weevil, *C. maculates* (Fab.). The results showed significant differences in attraction and repellency effect according to the kind of extracted plant and concentration. When repellency occurs, it refers to the major reason of dramatical weevil longevity decrease. The same result was achieved by the volatile oil and this is similar to the results obtained by Karahroodi-Zahra et al. (2009) who came to the concusion that the volatile oils of *M. officinalis* had a moderate repellency against adults of *P. interpunctella* reflecting the first essential reason of weevil longevities decrease. Furthermore, the present study revealed that both fixed and volatile oils caused a significant decrease in both male and female longevities. This result was confirmed by Andronikashvili and Reichmuth (2003) who illustrated that the volatile oil of *L. nobilis* had high repellency effect towards adult of red flour beetle, *T. Castaneum*. Similar results were obtained by Isikber et al. (2006). The present study revealed that, fixed oils remarkably decreased the average number of eggs deposited by treated females. This was confirmed by the findings of Schoonhoven (1978) and Shankaranarayana et al. (1979). Singh et al. (1978) mentioned that, groundnut oil prevented the emergence of progeny rather than affecting the oviposition of *C. maculates*. Abdel-Kawy and Gharib (1991) indicated that cotton seed oil, sesame, peanut and paraffin oils reduced the number of progeny in *Sitophilus oryzae*. Taheya and Al-Moagel (1993) indicated that tumeric extract reduced the khapra beetle F1 progeny, and interfered with its development. Regnault-Roger and Hamraoui (1995) showed that the volatile oils of *L. nobilis* could protect kidney beans by direct or delayed insecticidal effect through increased adult mortality and inhibition of beetle reproduction of *Acanthoscelides obtectus* (Say). Also, the authors of this study concluded that the treatments by fixed and volatile oils had a significant effect on the reproductive potential of *R. ferrugineus* (Oliver). The average number of eggs laid per female as well as hatching (%) was reduced significantly. Similar results related to the fecundity of other treated insects with volatile oils were obtained by several authors (Frik and Nazirov, 1981; Dongre and Rahalkar, 1982). Nassar (1995) stated that complete sterility of *Muscina stabulans* adult was achieved by larval treatment with some plant extracts and Hussein (1995) reported that treatment of the second larval instar of *Parasarcophaga aegyptiaca* with some volatile plant oils induced a remarkable

http://www.aloki.hu ● ISSN 1589 1623 (Print) ● ISSN1785 0037 (Online)
DOI: http://dx.doi.org/10.15666/aeer/1802_29092919

reduction in reproductive potential of developing adults. Shoukry-Karima (2003) stated that the tested plant volatile oils of Pipe rcubebae and Sativa officinalis had a high significant decrease effect on pupation percentage, adult emergence percentage, fecundity, fertility and hatchability of females emerged from treated larvae of *P. interpunctella*. In contrast, Singh et al. (1989) found that volatile oils extracted from *Callicarpa macrophylla* and *Zanthoxylum alatum* plant increased the fecundity of *S. oryzae* and *Sitophilus granarius*. Karahroodi-Zahra et al. (2011) referred to the great toxicity of the volatile essential oils of *M. officinalis* against the first instar larvae and eggs of *P. interpunctella* leading to significant decrease in the number of hatched eggs. Karahroodi-Zahra et al. (2008) investigated fumigant toxicity of the essential oil from *M. officinalis* L. against first instar larvae and eggs, of *P. interpunctella* (Hübner) showing moderate ovicidal and egg deterrence effect against this pest. Nassar and Abdullah (2001, 2005) recorded some pupal morphogenetic abnormalities of the red palm weevil resulting in incomplete adult eclusion due to the treatment with azadirachtin and *Boxus chinensis*. The same result was also reported by Bream et al. (2001). As most of the puparia failed to reach adults (aborted puparia).

Conclusion

The four tested oils disrupted some biological aspects of the tested insects. These oils remarkably reduced male and female longevity, female fecundity and hatchability of the laid eggs. In the future the authors will use it as Nano Particles against the insects to get more effects on the insects.

Acknowledgements. The authors extend their appreciation to the Deanship of Scientific Research at King Khalid University, Abha, KSA for funding this study through Research Groups Program under grant number (R.G.P.1/78/40).

Conflict of Interests. No conflict of interests associated with this work.

REFERENCES

[1] Abdallah, M. D., Kandil, M. A., Farag, A. A. (1986): Isolation and identification of biologically active compounds from extracts of Minteena, Barnoof and Ullaiq. – Bull. Entomol. Soc. Egypt. Econ. Ser. 15: 191-197.

[2] Abdel-Kawy, F. K., Gharib, O. H. (1991): Treatment with different oils for the control of rice weevil, *Sitophilus oryzae* (L.), in yellow meal corn. – Bull. Entomol. Soc. Egypt. Econ. Ser. 19: 115-119.

[3] Abdullah, M. A. R. (2009): Toxicological and histopathological studies of Boxus chinensis oil and precocene II on larvae of the red palm weevil, *Rhynchophorus ferrugineus* (Oliver) (Coleoptera: Curculionidae). – Egypt. Acad. J. biol. Sci. 2(2): 45-54.

[4] Ahmed, F. A., Hussein, K. T., Gad, M. I. (2015): Biological activity of four plant oils, against the red palm weevil, *Rhynchophorus ferrugineus* (Oliver), (Coleoptera: Curculionidae). – Journal of Bioscience and Applied Research 1(5): 213-222.

[5] Anderson, B. A., Holman, R. T., Lundgren, L., Stenhagen, G. (1980): Capillary gaschromatogrpahy of leaf volatiles. A possible aid to breeders for pest and disease resistance. – J. Agric. Food Chem. 28: 985-989.

[6] Andronikashvili, M., Reichmuth, C. (2003): Repellency and toxicity of essential oils from *Ocimum gratissimum* (Lamiaceae) and *Laurus nobilis* (Lauraceae) from Georgia against

http://www.aloki.hu ● ISSN 1589 1623 (Print) ● ISSN1785 0037 (Online)
DOI: http://dx.doi.org/10.15666/aeer/1802_29092919

the rust-red flour beetle (*Tribolium castaneum* Herbst) (Coleoptera: Tenebrionidae). – Advances in Stored Product Protect: 749-762.

[7] Baraka, D. M., El-Hady, A. F. (1993): Comparative study of seed lipid constitutents of four species of family Faraceae. – Egypt. J. App. Sci. 8(3): 44-49.

[8] Ben Jemâa, J. M., Tersim, N., Khouja, M. L. (2011): Composition and repellent efficacy of essential oil from *Laurus nobilis* against adults of the Cigarette Beetle *Lasioderma serricorne* (Coleoptera: Anobiidae). – Tunisian J. Plant Protect 6(1): 29-42.

[9] Bouda, H., Tapondjou, L. A., Fontem, D. A., Gumedzoe, M. Y. D. (2001): Effect of essential oils from leaves of *Ageratum conyzoides*, *Lantana camara* and *Chromolaena odorataon* on the mortality of *Sitophilus zeamais* (Coleoptera, Curculionidae). – J. Stored Prod. Res. 32(2): 153-164.

[10] Bream, A. S., Ghoneim, K. S., Tanani, M. A., Nassar, M. M. (2001): Respiratory metabolic risponsiveness, during the pupal stage of the red palm weevil to certain plant exeracts. – Med. Fac. Landbouww. Univ. Gent 66(2): 491-502.

[11] Dongre, T. K., Rahalkar, G. W. (1982): Effect of *Blumea eriantha* (Compositae) oil on reproduction in *Earias vittella* (F.). – Experientia 38(1): 98-99.

[12] El-Bokl, M. M., Sallam, A. M., Abdallah, G. A., Gabr, B. M., (2015): Efficay of aggregation pheromone in trapping red palm weevil (*Rhynchophorus ferrugenious* Olivier) infested Date palms in Damietta, Egypt. – Egypt. Acad. J. Biolog. Sci. 7(1): 51-59.

[13] El-Sayed, F. M. A., Etman, A. A., Abdel-Razik, M. (1989): Effectiveness of natural oils in protecting some stored products from two stored product pests. – Bull. Fac. Agric., Cairo Univ. 40(2): 409-418.

[14] Farman-Khansaa, S. (2009): The repellency effect of powder of many plants on red flour beetles *Tribolium castanium*. – Dialy Agric. Sci. J. 1(2): 18-24.

[15] Finney, D. J. (1952): Probit analysis: a statistical treatment of the sigmoid response curves. – 2nd ed. Cambridge Univ. Press.

[16] Frik, L. P., Nazirov, Z. N. (1981): Components of *Euphorbia jaxaritica* CF. – Chem. Abst. 95(9): 3467.

[17] Gujar, G. T., Mehrotra, K. N. (1983): Juvenilizing effect of azadirachtin on noctuid moth, *Sopodoptera litura* Fabr. – Indian J. Exp. Biol. 21: 292-293.

[18] Harborne, J. B. (1984): Phytochemical Methods. – Second Edition, pp 150-160. Chapman & Hall. London, New York.

[19] Huseyin, C., Ilker, C., Atila, Y., Mustafa, G. (2006): Larvicidal activity of some labiatae (Lamiaceae) plant extracts from Turkey. – Phytother Res. 20(12): 1088-1090.

[20] Hussain, A., Rizwan-ul-haq, M., Mohammed, A., Al-Ayedh, H. (2019): Lethality of Sesquiterpenes Reprogramming Red Palm Weevil Detoxification Mechanism for Natural Novel Biopesticide Development. – Molecules 24: 1648.

[21] Hussein, K. T. (1995): Effect of some plant extracts in the control of a non-biting Muscoid fly. – Ph.D. Thesis, Fac. Sci. Zag. Univ., Egypt.

[22] Hussein, K. T., Shoukry, I. F. (1997): Toxicological and histopathological studies of certain plant fixed oils on *Culex pipiens* larvae. – Ain Shams Sci. Bull. 35: 287-305.

[23] Isikber, A. A., Alma, M. H., Kanat, M., Karci, A. (2006): Fumigant toxicity of essential oils from *Laurus nobilis* and *Rosmarinus officinalis* against all life stages of *Tribolium confusum*. – Phytoparasitica 34(2): 167-177.

[24] Ismail, I. A., Farg, N. A., Abdel-Rahman, R. S., Abdel-Raheem, M. A., Radwan, H. M. (2014): Insecticidal activity of some plant extracts rich in coumarin against cowpea beetle, *Callosobruchus maculatus* (Fab.) (Coleoptera: Bruchidae). – Egyptian Journal of Biological Pest Control 24(2): 465-469.

[25] Ismail, I. A., Abdel-Rahman, R. S., Abdel-Raheem, M. A. (2016): Utilization of certain plant extracts and entomopathogenic fungi for controlling the black fig fly, *Lonchaea aristella* on fig trees. – International Journal of Chem Tech Research 9(4): 35-42.

http://www.aloki.hu ● ISSN 1589 1623 (Print) ● ISSN1785 0037 (Online)
DOI: http://dx.doi.org/10.15666/aeer/1802_29092919

[26] Jood, S., Kapoor, A. C., Singh, R. (1993): Evaluation of some plant parts against *Trogoderma granarium* Everts in stored wheat and their effect on nutritional composition and organoleptic characteristics of treated grains. – Int. J. Pest. Manag. 39(1): 93-98.
[27] Karahroodi-Zahra, R., Moharramipour, S., Farazmand, H., Karimzadeh-Esfahani, J. (2008): Effect of eighteen plant essential oils on nutritional indices of larvae *Plodia interpunctella* Hubner (Lep.: Pyralidae). – Entomol. J. Res. Islamic Azad Univ., Arak Branch 1(3): 209-219.
[28] Karahroodi-Zahra, R., Moharramipour, S., Rahbarpour, A. (2009): Original articles investigated repellency effect of some essential oils of 17 native medicinal plants on adults *Plodia interpunctella*. – American-Euras J. of Sustainable Agric. 3(2): 181-184.
[29] Karahroodi-Zahra, R., Moharramipour, S., Farazmand, H., Karimzadeh-Esfahani, J. (2011): Insecticidal effect of six native medicinal plants essential oil on Indian meal moth, *Plodia interpunctella* Hübner (Lep.: Pyralidae). – Munis Entomol and Zool. 6(1): 339-345.
[30] Khalaf, A. F. A., Hussein, K. T., Shoukry, K. K. (2009): Biocidal activity of two botanical volatile oils against the larvae of *Synthesiomyia nudiseta* (Wulp) (Diptera: Muscidae). – Egypt. Acad. J. Biol. Sci. 2(1): 89-101.
[31] Kweka, E. J., Senthilkumar, A., Venkatesalu, V. (2012): Toxicity of essential oil from Indian borage on the larvae of the African malaria vector mosquito, *Anopheles gambiae*. – Parasites & Vectors J. 277(5): 1-5.
[32] Lee, B. H., Choi, W. S., Lee, S. E., Park, B. S. (2001): Fumigant toxicity of essential oils and their constituent compounds towards the rice weevil, *Sitophilus oryzae* (L.). – Corp protection 20: 317-320.
[33] Merghem, A., Mohamed, A. (2017): Impact of Neem Extracts, *Azadirachta indica* A. Juss Induced against Red Palm Weevil, *Rhynchophorus ferrugineus* (Olivier) Attacking Date Palm Orchards in Egypt. – Egypt. Acad. J. Biolog. Sci. 9(2): 109-117.
[34] Mohamad, A. H., Obadi, A. K., Ramdan, F. M. (2011): Attraction, repellency and toxic effect of some plant extracts on the Southern cowpea weevil *Callosobruchus maculates* (Fab.) (Coleoptera: Bruchidae). – Tekrit Agric. Sci. J. 11(2): 204-209.
[35] Mostafa, Z. K., El-Sherif, L. S., Hewady, M. A. A. (1995): Effect of certain volatile plant oils on the activity of malate dehydrogenase and malic enzyme in *Pectinophora gossypiella* (Saun.) and *Earias insulana* (Boisd) larvae (Lepidoptera: Noctuidae). – J. Egypt. Ger. Soc. Zool. 17: 13-23.
[36] Moustafa, S. M., Kadry, H. A., El-Olemy, M. M., Bisher, M. M. (1986): Lipids, pigments and saponines of *Sansevieria cylindrica*, Bjor. – Bull. Pharm. Sci., Assuit. Univ. 9(1): 1.
[37] Nassar, M. I. (1995): The potential of some juvenoids precocenes and botanical extracts for the control of *Muscina stabulans* (Fallin). – Ph.D. Thesis, Fac. Sci. Cairo University, Egypt.
[38] Nassar, M. M., Abdullah, A. A. (2001): Evaluation of Azadirachtin for control of the red palm weevil *Rhynchophorus ferrugineus* (Oliver). – J. Egypt. Ger. Soc. Zool. Entomol. 36: 163-173.
[39] Nassar, M. I., Abdullah, A. M. (2005): Assessement of *Boxus chinensis* oil and Precocene II for the control of the red palm weevil, *Rhynchophorus ferrugineus* (Oliver) (Coleoptera-Curculionidae) and the palm beetle *Pseudophilus testsceous* (Gahan) (Coleoptera-Cerambycidae). – J. Entomol. 2(1): 1-8.
[40] Regnault-Roger, C., Hamraoui, A. (1995): Comparison of the insecticidal effects of water extracted and intact aromatic plants on *Acanthoscelides obtectus*, a bruchid beetle pest ofkidney beans. – Chemoecology 5: 1-5.
[41] Regnault-Roger, C. (1997): The potential of botanical essential oils for insect pest control. – Integrated Pest Management Reviews 2: 25-34.
[42] Saleh, M. R. A. (1992): Red palm weevil, *Rhynchophorus ferruginous* (Oliver) in the first record for Egypt and indeed the African continent list No: 10634 Africa collection. – International Institute of Entomol. 56 Queen5 gate. London, Sw., 75 JR.UK.

http://www.aloki.hu ● ISSN 1589 1623 (Print) ● ISSN1785 0037 (Online)
DOI: http://dx.doi.org/10.15666/aeer/1802_29092919

[43] Salem, S. A., Abd El-Salam, A. M. E., Abdel-Raheem, M. A., Farage, N. A., El-Hawary, F. M. (2016): Field studies to assess the efficiency of bio-extracts against the scourge of onion crops, *Thrips tabaci* Lindeman in Egypt. – Der Pharma Chemica 8(20): 74-77.
[44] Schoonhoven, A. V. (1978): Use of vegetable oils to protect stored beans from Bruchid attack. – J. Econ. Entomol. 71(2): 254-256.
[45] Shaaya, E., Kostjukovski, M., Eilberg, J., Sukprakarn, C. (1997): Plant oils as fumigants and contact insecticides for the control of stored-product insects. – J. Stored-Prod. Res. 33: 7-15.
[46] Shankaranarayana, K. H., Shivaramakrishnan, U. R., Ayyar, K. S., Sarma, P. A. (1979): Isolation of a compound from the barch of sandal *Santhalum album* (L.) and its activity against some lepidopterous and coleopterous insects. – J. Entomol. Res. 3(1): 116-118.
[47] Shoukry-Karima, K. (2003): Toxicological effects of botanical extracts against some stored product insects. – M.Sc. Thesis, Fac. Sci. Zagazig Univ.
[48] Singh, S. R., Luse, R. A., Leuschner, K., Nangju, D. (1978): Groundnut oil treatment for the control of *Callosobruchus maculatus* (F.). – J. Stored Prod. Res. 14(2-3): 77-80.
[49] Singh, D., Siddiqui, M. S., Sharma, S. (1989): Reproductive retardant and fumigant properties in essential oils against rice weevil (Coleoptera: Curculionidae) in stored wheat. – J. Econ. Entomol. 82(3): 227-233.
[50] Sun, Y. P. (1950): Toxicity index: an improved method of comparing the relative toxicity of insecticides. – J. Econ. Entomol. 43: 45-53.
[51] Swidan, M. H. (1996): Effectiveness of some vegetable oils in protecting blackeyed peas from the attack of cowpea weevils, *Callosobruchus maculates* F. (Coleoptera: Bruchidae). – J. Egypt. Ger. Soc. Zool. 19: 29-39.
[52] Taheya, S. M., Al-Moagel, N. H. (1993): Grain insect control agent from tumeric (*Curcuma longa* L.) rhizome extract. – J. Egypt. Ger. Soc. Zool. 12: 111-130.
[53] Tayoub, G., Odeh, A., Ghanem, I. (2012): Chemical composition and fumigation toxicity of *Laurus nobilis* L. and *Salvia officinalis* L. essential oils on larvae of khapra beetle (*Trogoderma granarium* Everts). – Herba Polonica 58(2): 26-37.

http://www.aloki.hu ● ISSN 1589 1623 (Print) ● ISSN1785 0037 (Online)
DOI: http://dx.doi.org/10.15666/aeer/1802_29092919

EFFECT OF HABITAT FACTORS AND PREDATOR DENSITY ON THE SPATIAL ABUNDANCE OF CAPE HARE (*LEPUS CAPENSIS*) IN THE KARAKORUM RANGE

ZAMAN, M.[1,2#] – RAKHA, B. A.[2#] – BAO, H.[1#] – VITEKERE, K.[1#] – JIANG, G.[1*]

[1]*Feline Research Center of National Forestry and Grassland Administration, College of Wildlife and Protected Areas, Northeast Forestry University,26 Hexing Road,Harbin 150040, China*

[2]*Department of Wildlife Management, Pir Mehr Ali Shah Arid Agriculture University, Rawalpindi 46300, Pakistan*

[#]*These authors contributed equally to this work.*

[*]*Corresponding author*
e-mail: jgshun@126.com; phone: +85-0451-82190-279

(Received 7th Nov 2019; accepted 12th Feb 2020)

Abstract. In fragmented landscapes, the accessibility of resources not only influences the spatial distribution of the predators themselves, but may similarly affect the abundance of their prey. We studied the influence of habitat dynamics and predator density on the spatial abundance of Cape hare (*Lepus capensis*) in the Karakorum Range in a 5700 km^2 area in Shigar valley during 2015–16 and 2017. We found that, seasonally the population density of Cape hare at deciduous forest plantation (site 3), was the highest and the lowest density of Cape hare was found in the closed to open herbaceous vegetation (site 1). Seasonally the detection probability and encounter rate were found the highest in the closed to open herbaceous vegetation (site 1), and detection probability was the lowest in the grassland and bare lands (site 2). In summer, we found a positive correlation between Cape hare and Red fox density in the deciduous forest plantation (site 3). In winter, a positive relationship between Cape hare and Red fox density were observed in the grassland and bare lands (site 2). Seasonally, the density of Cape hare were the highest recorded in the deciduous forest plantation (site 3) where the relative density of Red fox and encounter rate of active burrows were the lowest. In this economically poor study area, humans often retaliate against damages caused by local wildlife using guns. The conclusions are discussed in the perspective of predator –prey interaction and the implications for management and mitigation of human – wildlife conflicts are also considered.
Keywords: *distance samplings, habitat factors, human – wildlife conflict, predator – prey, seasonal estimation*

Introduction

Prey population density can fluctuate in responses to both lethal and non-lethal effects caused by predators (Preisser et al., 2005). In such habitats with the presence of predators, the prey is likely to be more alert, to lower the risk of being killed (Brown et al., 1999). For prey species, the decision of when and how to escape from a potential threat is a complex process that is subject to relations between numerous biotic and abiotic factors (Stankowich and Blumstein, 2005). Typically, herbivore behavior is divided into three main activity types: grazing, resting and moving (Arnold and Dudzinski, 1978). These activities have significant impacts within the landscape (both spatial and temporal distribution, and habitat and vegetation preference) (Lima, 1998). It has been shown that both natural predation and anthropogenic threats cause similar behaviors such as increased alertness in herbivores (Lima and Dill, 1990). These risk effects are negatively influence foraging efficiency (Møller, 2008).

http://www.aloki.hu ● ISSN 1589 1623 (Print) ● ISSN 1785 0037 (Online)
DOI: http://dx.doi.org/10.15666/aeer/1802_29212934

Predation risk effects are dependent on the body–size of prey like small (e.g. rodent) and medium–sized prey (e.g. lagomorph). Medium–sized prey in open habitat is able to run fast, and in dense habitats, prey are expected to persist due to the availability of refuge (Waggett and Buskey, 2007). Cape hare is a medium–sized herbivore and active at night time or day time as well as hares have adopted a very strong active anti–predator tactic; such as they can leap and immobile (Weterings et al., 2016). The predation risk on hare is increased as they cannot depend on a burrow system (Creel, 2011). The obtainability and quality of resources influences the size of animal home range (Macdonald, 1983), such that, in canids for example, a home range in a resource–rich area may be smaller than in a resource–poor area (e.g., 0.4 km^2 and > 40 km^2, respectively, Macdonald, 2004). Furthermore, den selection is influenced by prey availability in the corsac red fox (*Vulpes corsac*) (Murdoch et al., 2009), the Eurasian badger (*Meles meles*) and the red fox (Márton et al., 2016).

However, Red foxes prey on hares (Goszczyński and Wasilewski, 1992a), and utilize dens for birthing and rearing offspring ('breeding dens') and as resting sites outside the breeding periods ('non–breeding dens) (Meia and Weber, 1992). Predator and preys interaction in a landscape were demonstrated by Hearn et al. (1987), that decreasing in the survival rate of juvenile arctic hares (*Lepus arcticus*) in Newfoundland was predation by the red fox (*Vulpes vulpes*). Santilli et al. (2007) defined that high Red fox predation was related to the mortality of European hares (*Lepus europaeus*) in Italy. Furthermore, in Sweden, Artic hare (*Lepus timidus*) densities enhanced when Red foxes were controlled from two islands (Marcström et al., 1989). Additionally, when sarcoptic mange killed many Red foxes in Sweden during the late 1970s and 1980s, mountain hare populations increased and their cyclicity vanished, but decreased again when Red foxes recovered from the disease (Kauhala et al., 1999; Newman et al., 2002). The hunting bags manage for Red fox in the Norway during 1976–19, 86 decreased the population, in contrasts, the hare population has ultimately increased (Selås and Vik, 2006). Goszczyński and Wasilewski (1992b) reported positive correlation between Red fox and hare density in central Poland.

In northern Pakistan, Karakoram range is occupied by globally important wildlife species such as snow leopard (*Panthera uncia*) and Tibetan wolf (*Canis lepus*) of which prey on or competitively displace red foxes (Roberts, 2005; Raza et al., 2015; Zaman et al., 2019b). Locally, Red fox are also a main predator of small mammals (e.g, Indian Pika (*Ochotona roylei*)) (Schneider, 2001). Major factors affecting declining Red fox population involve retaliatory killing for wheat crop damage and local poultry damages, local perception of the Red fox as a pest species (Maheshwari, 2018). Major threats affecting the decrease of hare population has been explained (Smith et al., 2005) as agricultural practices and human activities (Reichlin et al., 2006).

Assessments of the proportions of wildlife populations are essential to various phases of conservation and wildlife monitoring (Thomas et al., 2006), and hare abundance ecologically performing a vital role to regulate and maintain predator density, such as Red fox (Schneider, 2001). Similarly, predators density affect on the abundance, daily activities and spaitial distribution of their prey (Gilg et al., 2003). If predators vanished from a landscape, prey species become 'naive' to the predator (Berger et al., 2001). However, population density of hare from the interaction with predator density in study sites yet is unstudied and such experiments under the human disturbance are lacking (Weston et al., 2012). Besides the clear gap in the knowledge, the aims of the study were: 1), to determine a relationship between hare density and Red fox density, with the underlying hypothesis that hare density would be expected to be lower in areas of higher Red fox density, i.e., a positive correlation. 2), to determine an association between hare habitat association in

http://www.aloki.hu ● ISSN 1589 1623 (Print) ● ISSN 1785 0037 (Online)
DOI: http://dx.doi.org/10.15666/aeer/1802_29212934

areas of high Red fox densities, with the underlying hypothesis that hares would be expected to have a heightened density were Red fox burrows would be low. In this study, we focused on the population density of Cape hare (*Lepus capensis*) and their predator, i.e., Red fox (*Vulpes vulpes montana*), since the surmised predator can change in habitat assortment of medium–sized prey by predation risks (Frid and Dill, 2002).

Materials and Methods

Study area

We conducted our study in 2015–2017 at Shigar Valley (8500 km^2; 35° 26′ N, 75° 44′ E) within the Karakorum range. The valley stretches approximately 80 km from the gateway of Shigar to Askole, Gilgit Baltistan Pakistan. The total survey area was approximately (5700 km^2) involved the current range of hare and observed predator. The valleys are dry with the annual precipitation around 200 mm with a maximum of almost 600 mm at elevations of 3962 m and snow depth maximum of 0.304 meter and a minimum of 0.127 meter. Shigar 1, is located in Karakorum range part, at the elevation of 2527 m above sea level (asl) the North–East. The major plant species are *Rosa webbiana*, *Hippophae rhamnoides*, and *Berberis lyceum*. The habitat and vegetation composition described by Zaman et al. (2019a).

Data collection

Cape hare and predator population density survey

The field surveys of Cape hare population abundance were made in three consecutive years. Our study was conducted in summer (3 June to 5 September 2015) and in winter (25 October to 27 December) in 2016, and in the summer of 2017 (27 May to 29 August) in Shigar Valley. Hare population density was estimated based on line transects (Langbein et al., 1999). The basic assumptions of distance sampling were for estimation of flushing-out distances (1) perfect detection of hare at line centers; (2) distance quantity are the initial positions, before reactive movement; (3) correct count of grouped Cape hare (4); measurement of detection distances without fault, and; (5) representative sampling of the study area (Marques et al., 2001; Buckland et al., 2008). Perpendicular distances (x) were measured from the line to each detected Single/ cluster of Cape hare. n hare was detected at perpendicular distances. Animals at the truncation distance from the transect line (w) and lengths of the transect (L) were recorded. The surveyed area was (a = 2wL) within which n animals were detected. Ṗa is the probability that a randomly chosen animal within the surveyed area was detected, and individual hare density (Ď$_s$) was estimated by

$$Ď_s = n/2WLṖa \quad \text{(Eq.1)}$$

To gain the estimated density of cluster, we multiplied by mean group size in the population, therefore:

$$E(s): Ď = (f(0)E(s))/2LṖa$$
$$Ṗa = 1/f(0) \quad \text{(Eq.2)}$$

http://www.aloki.hu ● ISSN 1589 1623 (Print) ● ISSN 1785 0037 (Online)
DOI: http://dx.doi.org/10.15666/aeer/1802_29212934

Probability is estimated of perpendicular distance at zero. E(s) estimated is expected cluster sized and Ď is the estimated density of cluster, respectively (objects/km). We designed 8 sample plots with 9 km lengths and each sample plots were divided into 4×4 km grid size and 5 to 10 parellel array 50 meter transects were laid out in each samples plots, the distance between one sample plot to another was 5 and 10 km. Each of the four study areas represented a huge variation in different habitat types, these were spaced between 3 km and 14 km apart in different selected sites (*Fig. 1*).

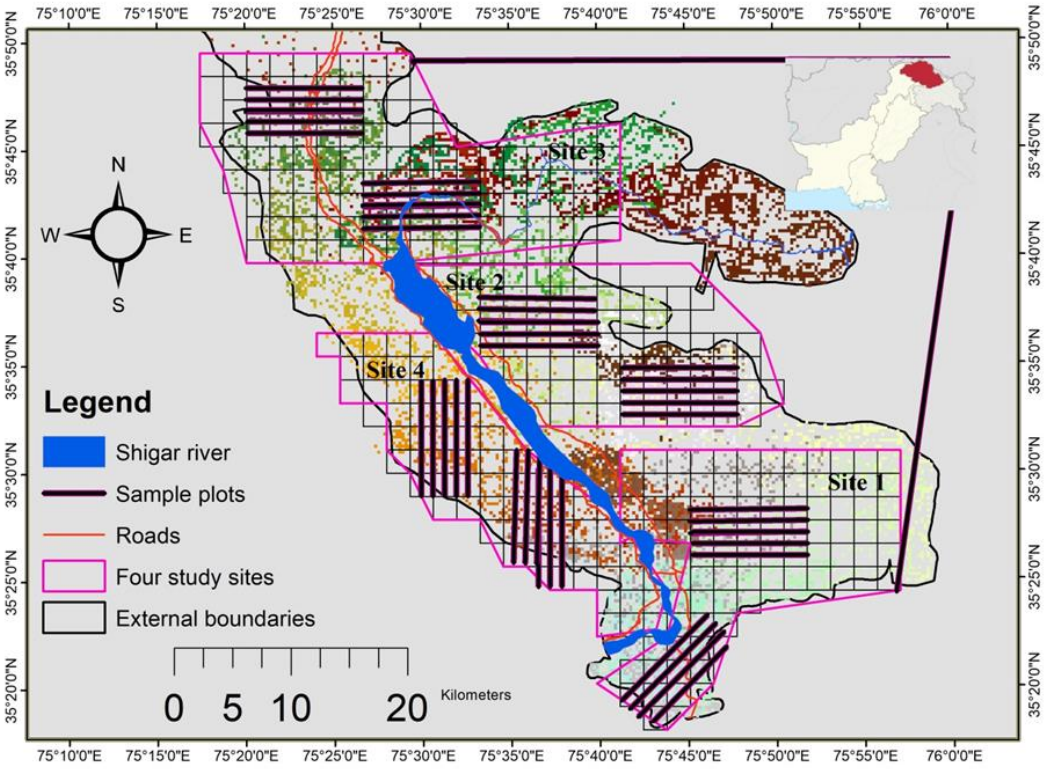

Figure 1. *Three consecutive years sampling sites and four selected area, in Shigar Valley Karakorum range in both winter (25 Oct to 27, Dec – 2015) and summer (3 June to 5 Sept – 2016 and 27 May to 29 August –2017. Hence, Shigar valley ~ 80 km from gateway of Shigar to Askole, Gilgit Baltistan Pakistan*

The study site 1, union council (UC) Marapi, extends from gateway of Sarfaranga (35°21'47.81"N, 75°44'24.82"E) to Ghazapa (35°25'5.05"N, 75°45'11.65"E), and Kanikernullah, Gangdrong nullah. Site 2, sampling areas were selected from UC Markunja nullah, Sarafa ranga thang, upper site of Chipping near historical Shigar fort (35°25'27.43"N, 75°44'34.83"E), to Taherping (35°26'17.90"N, 75°44'8.84"E), Chorkah ranga and extended from eastern part of valley to southern part. The 3rd study site containing sixteen different villages, UC Markuja extended from Bounpi ranga (35°26'3.02"N, 75°43'15.27"E) to UC Chorkah ranga (35°27'49.17"N, 75°41'15.65"E), Sildi, Hyderabad, Tiser. The study site 4, UC Gulapure and Barqzo contained Gulapur nullah (35°22'56.84"N,75°42'11.43"E) and, Nialinullah, Alochorinullah, Markunja nullah, Marapi nullah, Chorkah nullah, Azamkhan to second gateway of Shigar valley linked to Bonpa Gulapur (35°27'55.75"N, 35°27'55.75"N) near the catchment of the

http://www.aloki.hu ● ISSN 1589 1623 (Print) ● ISSN 1785 0037 (Online)
DOI: http://dx.doi.org/10.15666/aeer/1802_29212934

river. We only recorded distance for our targeted hare and each sample plots were sufficiently apart which was sufficient to avoid multiple recording of the same individuals across transects of different study areas (Smith et al., 2004). The abundance of hare pellet counts was used to estimate the hare abundance for broad–scale studies (Fa et al., 1999), counting fresh and old hare pellets within 10 plots of 10 m x 10 m at 30 m intervals, eluding counts on or proximate latrines. The abundances of pellets were counted in 30 plots along each transect to derive pellet abundance indices (the number of presences divided by the number of plots multiplied by transects length as pellet abundance indices/km). We used Pellet uncleared plots methodology (Perry and Robertson, 2012) to check habitat association of Cape hare. It is assumed that the hare defecation rates were incredibly high (300 to 700 pellets/day (Welch, 1982). The direct estimation of relative population density of Red fox is given by this formula, $D = n/A$, where n represents a number of sample efforts with a particular survey time and A stands for sampling area in each site. Whenever a Red fox was encountered, time, date and number of individuals were noted (Raza et al., 2015). We estimated Red fox number of individuals/4 km as described by Walton et al. (2017). We estimated Red fox abundance based on counts of active burrow entrances with a strip width of 30 m, considering the number of active burrow entrances/4 km as an index of Red fox abundance (Panek, 2009).

Habitat covariates sampling

We surveyed hare according to four different habitat features (Zaman et al., 2019a,b), and relative abundance, relative frequency, density and importance value index (IVI) of plant species were recorded as described by Mahmood et al. (2010). In a random stratified sample, 10 plots, each of the same size, were evaluated in all kinds of habitat types in each transect. The hare habitat types were extracted by polygons and we measured proximity factors: i.e., distance to rivers, roads, and agricultural lands and streams by ArcGIS (10.2) (Zaman et al., 2019a).

Data analyses

We calculated the seasonal density of hare population by the use of Distance 6.0 software (Thomas et al., 2010). The best model with the lowest delta akaike information criterion (Δ AICc = 0) values with the akaike information criterion (AICc) of the best–fitting model subtracted was selected for estimating population density (Thomas et al., 2010). We used Kolmogorov–Smirnov tests and quantile-quantile (Q–Q) plots to test the normality of data and data were normally distributed in selected sites (Thomas et al., 2010). We used Students samples t–test to compare the means of red Red fox population density. We used Pearson's correlation to analyze the relationships between pellets and burrow entrance abundance indices in two seasons. To measure the direct relationship between the hare and Red fox, we used the average means of population density in summer and winter. Multiple regression analysis was used to check seasonal habitat associations of hare pellet abundance index to the habitat variables in different sites (Broome, 2001). We used pellets abundance indices as dependent variables and independent categorical variables (habitat type) and ordinal variables (importance value index) for each habitat 10 plots of herbs, shrubs, trees, and grasses were used for analysis. The parameter estimates of variables were considered significant at $P < 0.05$. All data analyses were done in SPSS Statistics 21.0 (IBM SPSS, Chicago, IL, USA).

http://www.aloki.hu ● ISSN 1589 1623 (Print) ● ISSN 1785 0037 (Online)
DOI: http://dx.doi.org/10.15666/aeer/1802_29212934

Results

Spatial distribution of Cape hare and their predator population density

In summer, the population density of Cape hare in the selected site 3 was the highest and the lowest density of hare was found in selected site 1 (*Table 1a*). The average detection probability, Encounter rate and cluster size of Cape hare was the highest in selected site 1 (*Table 1b, Fig. 2b*). When using hazard rate key function with series expansion the observed and expected distances were significant (*Table 1b*). The lowest detection probability for hare was recorded in selected site 2, (*Table 1b, Fig. 2c*). The selected model key half–normal for Kolmogorov–Smirnov test was insignificant (*Table 1b*). In the selected site 4 (*Fig. 2d*) detection probability was low. Uniform normal key with extension key showed to be significant in Kolmogorov–Smirnov test. The detection probability, encounter rate and cluster size of hare in the study site 3, was low (*Table 1b, Fig. 2a*). Half–normal key function with series expansion revealed no significant differences between observed and expected distances (Kolmogorov–Smirnov test, *Table 1b*).

Table 1a. *Summary of candidate models (4 selected sites, key models; hazard–rate, half–normal, uniform and series expansion; cosine, simple–polynomial, harmite–polynomial), with an Akaike information criterion for small sample size (AICc) difference (Δ AICc = 0) of each Cape hare population density census (D) (animals per km), and 95% confidence interval (CI) in Shigar Valley, Karakorum range in both winter (25 Oct to 27, Dec – 2015) and summer (3 June to 5 Sept – 2016 and 27 May to 29 August – 2017) Gilgit Baltistan Pakistan*

Sites	Key models	AICc	D/km	Lower	Upper
Winter	–	–	–	–	–
1	Hazard rate/simple	38.14	1.05	0.49 –	2.28
2	Halfnormal/hermite	15.79	1.40	1.00 –	1.9
3	Hazardrate/simple	18.14	1.80	1.19 –	2 .7
4	Uniform/simple	15.38	1.38	1.0 –	1.94
Summer	–	–	–	–	–
1	Uniform/cosine,	97.45	2.41	1.95 –	2.98
2	Halfnormal/hermite	21.06	2.55	0.76 –	8.54
3	Halfnormal/simple	14.36	6.15	2.62 –	14.42
4	Uniform/cosine	13.46	4.67	1.76 –	12.37

Table 1b. *The summary of observed and expected distances significant Kolmogorov –Smirnov test (Dn), and The average detection probability (Ṗa), Encounter rate (Er) (n/survey effort (se) and cluster size (Ď) standard error (± SE), calculated from observation at different line transect of Cape hare in Shigar Valley, Karakorum range in both winter (25 Oct to 27, Dec – 2015) and summer (3 June to 5 Sept –2016 and 27 May to 29 August –2017)*

Sites	Er (n/se)	Ṗa	Ď	Dn	p
Winter	–	–	–	–	–
1	95.7	17.2	2.999 ± 0.160	0.1276	< 0.05
2	45.9	10.10	3.259 ± 0.179	0.1276	< 0.05
3	5.71	13.1	2.957 ± 0.196	0.2038	< 0.05
4	10.2	12.6	1.361 ± 0.345	0.1471	< 0.05
Summer	–	–	–	–	–
1	57.0	42.2	1.146 ± 0.274	0.2226	< 0.05
2	74.00	13.7	1.028 ± 1.162	0.1205	> 0.05
3	77.80	20.70	2.162 ±2.501	0.1628	> 0.05
4	85.7	19.4	1.048 ± 0.168	0.1103	< 0.05

http://www.aloki.hu ● ISSN 1589 1623 (Print) ● ISSN 1785 0037 (Online)
DOI: http://dx.doi.org/10.15666/aeer/1802_29212934

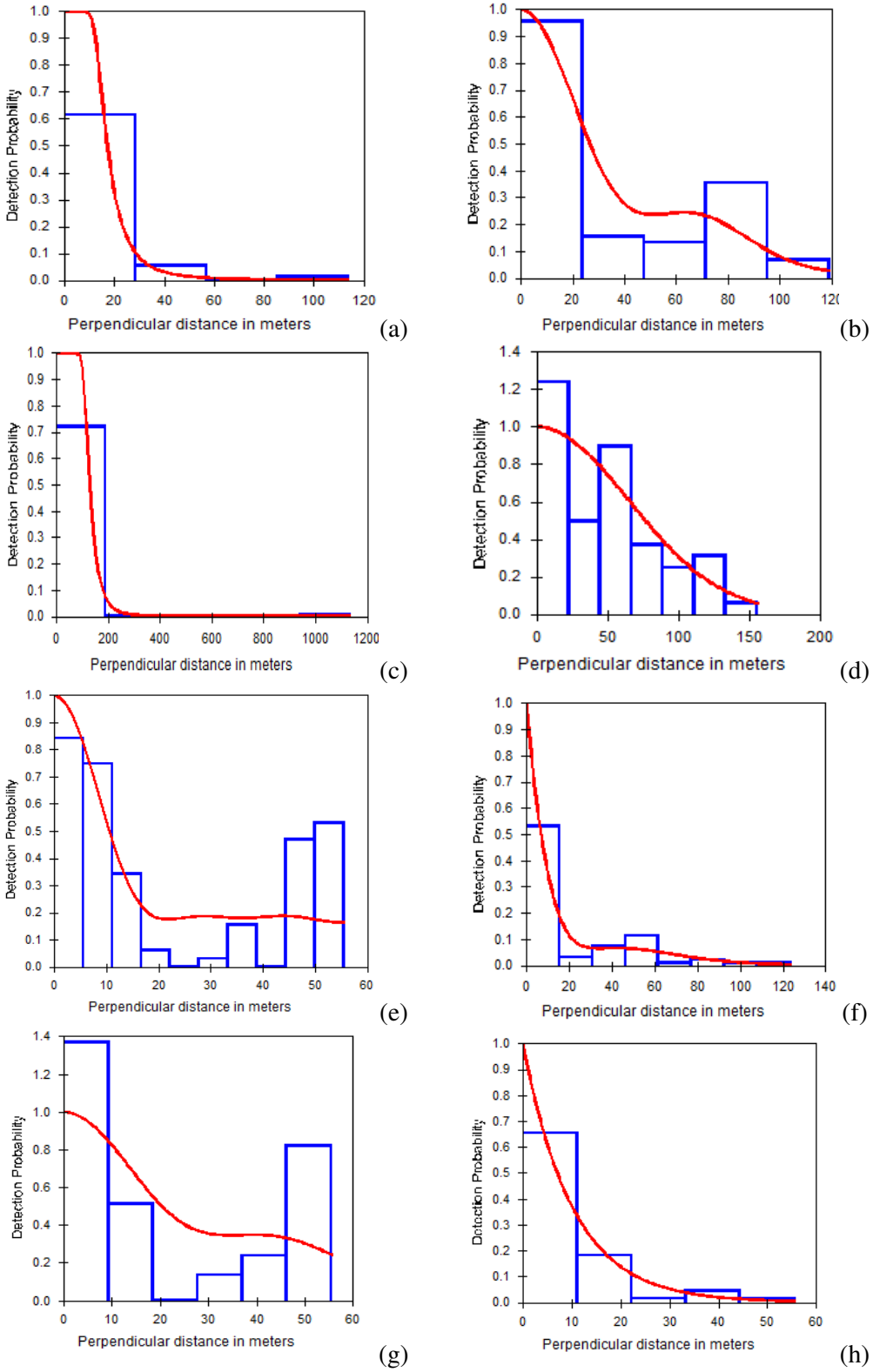

Figure 2. *The perpendicular detection probability of hare using different model key in the summer in the site 3 (a), site 1 (c). In the site 4, (d). In the winter in the site 1, (e), site 2 (f), in the site 3, (g). In the site 4, (h), hence the bar represented observed distance and the red curve showed the perpendicular distance at Shigar valley, Karakorum range in both winter (25 Oct to 27, Dec – 2015) and summer (3 June to 5 Sept – 2016 and 27 May to 29 August – 2017)*

http://www.aloki.hu ● ISSN 1589 1623 (Print) ● ISSN 1785 0037 (Online)
DOI: http://dx.doi.org/10.15666/aeer/1802_29212934

The relative density of Red fox was the lowest in the study site 3 and the highest in the selected site 1 (*Table 2a*).

In winter, the population density of Cape hare in the study site 3 was the highest and the lowest density of hare was found in selected site 2 (*Table 1a*). The average detection probability of Cape hare was the highest in the site 1 and average encounter rate was recorded and Hazard Rate key with extension key showed significant Kolmogorov–Smirnov test (*Table 1b, Fig. 2e*) and the lowest detection probability and encounter rate was observed in site 2. Half–normal key with extension key for Kolmogorov–Smirnov test was not significant (*Table 1b, Fig. 2f*). Detection rate and encounter rate was moderate in the site 4 (*Table 1b, Fig. 2h*) and observed and expected distance was significant (*Table 1b*) and, detection probability and encountered rate were accompanied by an expected cluster size; Uniform key with extension revealed significant differences for expected distance and observed distance (*Table 1b*). The relative density of Red fox was the lowest in site 4 and the highest in site 2 (*Table 2a*).

Table 2a. *The Summary of summer and winter populations' estimation means with degree of freedom (Df) for Students T –test, n number of surveyed in selected sites with particular time in both winter (25 Oct to 27, Dec – 2015) and summer (3 June to 5 Sept – 2015 and 27 May to 29 August – 2017) and (D) number of relatives density estimated from observation at different line transect of Red fox in Shigar Valley, Karakorum range Gilgit Baltistan Pakistan*

Sites	n	Means	PAI/km	n	means	ABE/4km
Cape hare	–	–	–	**Red fox**		
1	172	11.31±9.70	13.9	31	4.8 ±3.3	2.09
2	89	1.21± 0.52	0.05	15	0.1±1.20	0.21
3	43	0.12±1.31	0.91	24	2.1 ±7.9	2.09
4	37	0.02±0.12	0.01	–	–	–

Table 2b. *Seasonal counting dens and pellets Indices for predator–prey, (n) showing sample sizes and means difference in four selected sites in Shigar Valley, Karakorum range in both winter (25 Oct to 27, Dec – 2015) and summer (3 June to 5 Sept – 2016 and 27 May to 29 August – 2017) Gilgit Baltistan Pakistan. Hence, PAI denoted pellet abundance indices /km and ABE represented number of active burrow entrances / 4 km in Shigar Valley*

Sites	n	D/4km	Df	T	P
Summer					
1	112	0.028	37	3.34	< 0.05
2	73	0.018	40	2.77	< 0.05
3	44	0.001	40	2.27	< 0.05
4	37	0.009	26	2.76	< 0.05
Winter		–		–	
1	62	0.010	36	2.93	< 0.05
2	76	0.015	44	3.38	< 0.05
3	30	0.007	30	2.95	< 0.05
4	33	0.008	32	1.97	< 0.05

The relationships between Cape hare and their predator population density

The greatest abundance of pellets indices was recorded in site 1, and the lowest in site 2 (*Table 2b*), the greatest encounter rate of active burrows were in site 1 and the

http://www.aloki.hu ● ISSN 1589 1623 (Print) ● ISSN 1785 0037 (Online)
DOI: http://dx.doi.org/10.15666/aeer/1802_29212934

lowest in site 3 and in site 4 there were no encounter (*Table 2b*). In summer, Red fox density was significantly positively (r = 0.213; $p < 0.05$) related to hare density in site 3. Seasonal burrow entrance and pellets index negatively correlate (r = 0.922; $p < 0.05$) in site 1. In winter, Red fox density was significantly positively (r = 0.102; $p < 0.05$) related to Cape hare density in site 2. We found that seasonally hare pellet abundance indices were positively correlated with indices of herbs (site 1; site 2), grassland (site 1; site 2), shrubs (site 3; site 4), trees (site 3; site 4), distance to rivers (site 3), distance to agriculture land (site 2) and distance to roads (site 4) and streams (site 1; *Table 3*). Negative correlations were observed with distance to agricultural land (site 1; site 3; site 4), roads (site 1; site 2; Site 3), rivers (site 2) and streams (site 2; *Table 3*).

Table 3. *Linear relationship between the hares (Pellet uncleared plots) pellets abundance indices and habitat factors with 95% confidence interval (CL) in Shigar valley, Karakorum range in both winter (25 Oct to 27, Dec – 2015) and summer (3 June to 5 Sept – 2016 and 27 May to 29 August – 2017)*

Study sites	Independent Variables	Coefficients	P	95% CI Lower – upper
1	Herbs index	0.505	< 0.05	0.015 to 0.994
	Grasses index	0.925	< 0.05	0.422 to 1.428
	Distance to road	–0.327	> 0.05	–0.042 to 0.613
	Distance to agriculture	–0.032	< 0.05	–0.050 to 0.606
	Distance to stream	0.644	< 0.05	0.357 to 0.935
2	Herbs index	0.365	< 0.05	0.167 to 0.563
	Grasses index	0.387	< 0.05	0.033 to 0.741
	Distance to river	–0.278	< 0.05	–0.012 to 0.569
	Distance to agriculture	0.277	< 0.05	0.007 to 0.569
	Distance to road	–29.32	< 0.05	–17.783 to 40.867
	Distance to stream	–13.821	< 0.05	–0.46 to 27.687
3	Shrubs index	0.273	< 0.05	0.054 to 0.491
	Tree index	0.278	< 0.05	0.107 to 0.450
	Distance to river	0.175	< 0.05	0.019 to 0.330
	Distance to agriculture	–0.139	< 0.05	–0.083 to 0.887
	Distance to road	–0.490	< 0.05	–0.108 to 0.873
4	Shrubs index	0.300	< 0.05	0.120 to 0.481
	Tree index	0.338	< 0.05	0.165 to 0.510
	Distance to road	0.050	< 0.05	0.125 to 0.889
	Distance to agriculture	–0.387	< 0.05	–0.033 to 0.741

Discussion

Spatial relationships of predators and Cape hare population density relating to habitat factors

We found that the detection probability of Cape hare in the summer (site 1 and site 4) and in the winter, site 1and site 3 showed a higher broad shoulder in the histogram as compared to other selected sites. This situation led to a comparatively higher detection rate resulting in lower density estimates may influenced by biased or small sample size (Herrmann et al., 2010). It was an assumption that we were attentive to, that transects within dense vegetation show lower visibility despite the higher density, this is typical across the heterogeneous survey region (Buckland et al., 2001; Herrmann et al., 2010). While maximum detections of hares were single, we were attentive in counting hares in clusters, and regardless of vegetation structure (Rivera-Milán et al., 2015).

http://www.aloki.hu ● ISSN 1589 1623 (Print) ● ISSN 1785 0037 (Online)
DOI: http://dx.doi.org/10.15666/aeer/1802_29212934

Although there were a great number of Cape hares at 0 m distance from the 1 km length transect line. The 0 m distance assumption is critical (Buckland et al., 2001). Herrmann et al. (2010) studied spring Cape hare, and steenbok (*Raphicerus campestris)* densities in South Africa by distance sampling in different seasons in forestland with associated open land hare density, which was higher in summer. The European hare has been measured in numerous countries and its abundance has been found to be between 21 and 330/ ha, varying according to the landscape type (Smith et al., 2004). The abundance of lagomorph was counted in many countries using transects but was much higher than those found in our study area where e.g., Australia (25 rabbits/km, (Moreno et al., 2008)) and New Zealand (125 rabbits/km (Olsen et al., 2014)). European abundances of brown hares can extent densities in excess of 100 hares km^2 (Smith et al., 2005). Seasonally Pellets abundance also differed among the habitat, but high counted in site 1. The defecation rates of mountain hares *(Lepus timidus*) vary with season (Hewson, 1989). Pellet abundance index was greater in the site 1. We used the uncleared way to calculation pellets abundance due to some transect not accessible for winter and Cape hare defecation rates were also high, similar results were found in previous results described by (Welch, 1982). The abundance of pellets was higher in site 1, for examples, the accessibility of food resources and escape covers also influenced on latrines site selection of hare (Krebs et al., 1995).

In this study, we found that the seasonal and spatial distribution of Red fox density was altered among the habitat, although we have not previously reported of Red fox density in the study area so it was difficult to compare spatial Red fox abundance. In summer we encountered the highest density of Red fox 0.028/4 km in site 1 (*Table 2*), and less than 0.009/4 km in site 4, the highest den sites were encountered in site 1 3.01/4 km; site 1, in winter Red fox density (0.010/4 km) was the highest for site 1. Our density estimates were lesser because of revenge to damage, poisons, and inadequate baseline data reports available for Red fox in the current study area, than estimates found in areas of maximum density of Red fox in Europe (3.30 Red foxes/km^2, (Sarmento et al., 2009)). However, some English rural areas Red fox were recorded (0.64 Red foxes/km^2, (Heydon et al., 2000)) and in Portugal as well (0.63 Red foxes/km^2 (Sarmento et al., 2009)).

In the summer Red fox density was significantly positively related to hare density in the closed to open broadleaved or needle–leaved forest, for example Snow shoe hare (*Lepus americanus*) abundance is closely associated with habitat characteristics, and the primary reason for mortality for snow shoes hare is predation (Goszczyński and Wasilewski, 1992b). Seasonal Red fox burrow entrance were negatively correlated with hare pellets abundance in site 1, as others also report, according to those of the hares studies described by (Angelstam and Lindström, 1984). In this work, we investigated the distribution of Red fox per 4 km as considering that the variation in Red fox home range sizes (0.95 km^2 to 358 km^2; (Walton et al., 2017). It was not possible to census Red foxes using torch light counts in site 3, because of the large amount of dense vegetation (Heydon et al., 2000). We found that seasonally the Red fox utilizes dens for birthing and rearing offspring (‘breeding dens’) in the grassland and barren land, where higher accessibility afford less natural boulder, rock cervices dens as well as abundance of prey (Meia and Weber, 1992) in site 3 due to abundance of prey and shelters. We also expected that fuel wood collection and illegal hunting by local people reduced concealment throughout the landscape and increased the compensation of detection for example, den selection is influenced by prey availability in the cases of the Corsac Red

http://www.aloki.hu ● ISSN 1589 1623 (Print) ● ISSN 1785 0037 (Online)
DOI: http://dx.doi.org/10.15666/aeer/1802_29212934

fox (*Vulpes corsac*) (Murdoch et al., 2009), the Eurasian badger (*Meles meles*) and the Red fox (Márton et al., 2016). We assumed that high density of Red fox in site 1 and low density of Red fox in other habitats significantly depend on the abundance of prey species and avoid human conflicts.

Our study results explained that hare abundance is positively associated with vegetation such as shrubs, herbs, such a similar results also found in case of snowshoe hare (*Lepus americanus*) (Hodges et al., 2009). Roads are negatively linked with hare abundance (Roedenbeck and Voser, 2008). Hare abundance was also negatively associated with agricultural land at site 2 due to conflicts by farmers, such results were also described by (Santilli et al., 2015).

Agricultural land and roads were positively linked with hare abundance(Reichlin et al., 2006). The hare seasonal pellets abundance index was positively linked with herbs and trees , e.g. snow hare (Hodges et al., 2009). Similarly, Hodson et al. (2011) reported that shrubs and saplings provide lateral protective cover for hare. Furthermore, in Pakistan, the Cape hare prefers alpine meadows in the summer season while in winter it moved down to steppe meadows (Roberts, 2005).

Conclusions

Our finding also showed that Cape hare density plays a key role in the natal den site selection and spatial distribution of Red fox. Furthermore, we expected that prey density distribution, habitat association and behavioral response may result from the lethal (predation) or non–lethal (landscape fear) effect of a predator, or human. Human-wildlife interactions can result in conflict where perceived damage to livelihoods occurs in socio-economically poor areas. In the Shigar Valley, Karakorum Range, Pakistan, subsistence mixed farming is the predominant land use and Red foxes as well as preys are extensively persecuted. Understanding on the effects of human activity and habitat features of Red fox and Cape hare feeding behaviors in the region are lacking. The findings recommended that Red fox and Cape hare do not avoid human settlements area. In the future, further Red fox genetics studies are needed to be conducted with a focus on ecosystem functions via seed dispersal, carrion removal and regulation of prey populations. It is envisioned that this work can be offered to local authorities as the first piece of scientific literature for the area, serving as a valuable resource for local public education, and also for tourists and NGO community visitors of the Karakorum national park.

Acknowledgments. We would like to thank Dr. M. Anwar, M. Rais, T. Mahood, I. Hussain and Mr. J. Hussain for their moral support. We would also like to thank Mr. N. J. Roberts et al in Feline Research Center of National Forestry Administration, for their useful comments for revising the manuscript. This work was supported by the Fundamental Research Funds for the Central Universities (2572017PZ14) and NSFC (31872241; 31572285).

REFERENCES

[1] Angelstam, P. E., Lindström, P. W. (1984): Role of predation in short-term population fluctuations of some birds and mammals in fennoscandia. – Oecologia 62(2): 199-208.
[2] Arnold, G. W., Dudzinski, M. (1978): Ethology of free–ranging domestic animals. – Elsevier Scientific Publishing Co.

http://www.aloki.hu ● ISSN 1589 1623 (Print) ● ISSN 1785 0037 (Online)
DOI: http://dx.doi.org/10.15666/aeer/1802_29212934

[3] Berger, J., Swenson, J. E., Persson, I. L. (2001): Recolonizing carnivores and naive prey: Conservation lessons from pleistocene extinctions. – Science 291(5506): 1036-1039.
[4] Broome, L. S. (2001): Density, home range, seasonal movements and habitat use of the mountain pygmy-possum burramys parvus (marsupialia: Burramyidae) at mount blue cow, Kosciuszko national park. – Austral Ecology 26(3): 275-292.
[5] Brown, J. S., Laundré, J. W., Gurung, M. (1999): The ecology of fear: Optimal foraging, game theory, and trophic interactions. – Journal of mammalogy 80(2): 385-399.
[6] Buckland, S. T., Anderson, D. R., Burnham, K. P., Laake, J. L., Borchers, D. L., Thomas, L. (2001): Introduction to distance sampling: Estimating abundance of biological populations. – Oxford University press, 432p.
[7] Buckland, S. T., Marsden, S. J., Green, R. E. (2008): Estimating bird abundance: Making methods work. – Bird Conservation International 18(S1): S91-S108.
[8] Creel, S. (2011): Toward a predictive theory of risk effects: Hypotheses for prey attributes and compensatory mortality. – Ecology 92(12): 2190-2195.
[9] Fa, J. E., Sharples, C. M., Bell, D. J. (1999): Habitat correlates of european rabbit (oryctolagus cuniculus) distribution after the spread of rvhd in Cadiz province, Spain. – Journal of Zoology 249(1): 83-96.
[10] Frid, A., Dill, L. (2002): Human–caused disturbance stimuli as a form of predation risk. – Conservation Ecology 6(1): 11.
[11] Gilg, O., Hanski, I., Sittler, B. (2003): Cyclic dynamics in a simple vertebrate predator–prey community. – Science 302(5646): 866-868.
[12] Goszczyński, J., Wasilewski, M. (1992a): Predation of Red foxes on a hare population in central Poland. – Acta theriologica 37(4): 329-338.
[13] Hearn, B. J., Keith, L. B., Rongstad, O. J.(1987): Demography and ecology of the arctic hare (lepus arcticus) in southwestern Newfoundland. – Canadian journal of zoology 65(4): 852-861.
[14] Herrmann, E., Stenkewitz, U., Kamler, J. F. (2010): Distance sampling for estimating springhare, cape hare and steenbok densities in South Africa. – South African Journal of Wildlife Research 40(1): 87-92.
[15] Hewson, R. (1989): Grazing preferences of mountain hares on heather moorland and hill pastures. – Journal of Applied Ecology 26(1): 1-11.
[16] Heydon, M. J., Reynolds, J. C., Short, M. J. (2000): Variation in abundance of Red foxes (*vulpes vulpes*) between three regions of rural Britain, in relation to landscape and other variables. – Journal of Zoology 251(2): 253-264.
[17] Hodges, K. E., Mills, L. S., Murphy, K. M. (2009): Distribution and abundance of snowshoe hares in Yellowstone national park. – Journal of Mammalogy 90(4): 870-878.
[18] Hodson, J., Fortin, D., Bélanger, L. (2011): Changes in relative abundance of snowshoe hares (*lepus americanus*) across a 265–year gradient of boreal forest succession. – Canadian Journal of Zoology 89(10): 908-920.
[19] Kauhala, K., Helle, P., Helle, E., Korhonen, J. (1999): Impact of predator removal on predator and mountain hare populations in Finland. – Annales Zoologici Fennici 36(3): 139-148.
[20] Krebs, C. J., Boutin, S., Boonstra, R., Sinclair, A., Smith, J., Dale, M. R., Martin, K., Turkington, R. (1995): Impact of food and predation on the snowshoe hare cycle. – Science 269(5227): 1112-1115.
[21] Lima, S. L., Dill, L. M. (1990): Behavioral decisions made under the risk of predation: A review and prospectus. – Can J Zool 68(4): 619-640.
[22] Lima, S. L. (1998): Nonlethal effects in the ecology of predator–prey interactions. – Bioscience 48(1): 25-34.
[23] Macdonald, D. W. (1983): The ecology of carnivore social behaviour. – Nature 301(5899): 379.
[24] Macdonald, D. W. (2004): Dramatis personae. Wild Canids-an introduction and dramatis personae. – The Biology and Conservation of wild canids: 4-35.

http://www.aloki.hu ● ISSN 1589 1623 (Print) ● ISSN 1785 0037 (Online)
DOI: http://dx.doi.org/10.15666/aeer/1802_29212934

[25] Maheshwari, A. (2018): Foraging habits of the red Red fox vulpes vulpes (mammalia: Carnivora: Canidae) in the Himalaya, India. – Journal of Threatened Taxa 10(10): 12418-12421.
[26] Mahmood, S., Mahmood, T., Rais, M., Qureshi, I., Nadeem, M. (2010): A comparative study on the populations and habitats of the grey francolin francolinus pondicerianus and the black francolin francolinus francolinus in Lehri nature park, Punjab, Pakistan. – Podoces 5(1): 42-53.
[27] Marcström, V., Keith, L. B., Engren, E., Cary, J. R. (1989): Demographic responses of arctic hares (*lepus timidus*) to experimental reductions of red Red foxes (*vulpes vulpes*) and martens (*martes martes*). – Canadian Journal of Zoology 67(3): 658-668.
[28] Marques, F. F., Buckland, S. T., Goffin, D., Dixon, C. E., Borchers, D. L., Mayle, B. A., Peace, A. J. (2001): Estimating deer abundance from line transect surveys of dung: Sika deer in southern Scotland. – Journal of Applied Ecology 38(2): 349-363.
[29] Márton, M., Markolt, F., Szabó, L., Kozák, L., Lanszki, J., Patkó, L., Heltai, M. (2016): Den site selection of the European badger, meles meles and the red Red fox, vulpes vulpes in Hungary. – Folia Zoologica 65(1): 72-80.
[30] Meia, J., Weber, J. (1992): Characteristics and distribution of breeding dens of the red Red fox (*vulpes vulpes*) in a mountainous habitat. – Zeitschrift für Saugetierkunde 57: 137-143.
[31] Møller, A. P. (2008): Flight distance and population trends in European breeding birds. – Behavioral Ecology 19(6): 1095-1102.
[32] Moreno, S., Beltrán, J. F., Cotilla, I., Kuffner, B., Laffite, R., Jordán, G., Ayala, J., Quintero, C., Jiménez, A., Castro, F. (2008): Long–term decline of the European wild rabbit (*oryctolagus cuniculus*) in southwestern Spain. – Wildlife Research 34(8): 652-658.
[33] Murdoch, J. D., Munkhzul, T., Buyandelger, S., Reading, R. P. (2009): Body size and sexual dimorphism among a population of corsac and red Red foxes in central Mongolia. – Mammalia 73: 72-75.
[34] Newman, T. J., Baker, P. J., Harris, S. (2002): Nutritional condition and survival of red Red foxes with sarcoptic mange. – Canadian journal of zoology 80(1): 154-161.
[35] Olsen, J., Cooke, B., Trost, S., Judge, D. (2014): Is wedge–tailed eagle, aquila audax, survival and breeding success closely linked to the abundance of European rabbits, oryctolagus cuniculus? – Wildlife Research 41(2): 95-105.
[36] Panek, M. (2009): Factors affecting predation of red Red foxes vulpes vulpes on brown hares lepus europaeus during the breeding season in poland. – Wildlife Biology 15(3): 345-349.
[37] Perry, M. E., Robertson, A. W. (2012): Cleared and uncleared pellet plots as indices of brown hare density. – New Zealand Journal of Ecology 36(2): 1.
[38] Preisser, E. L., Bolnick, D. I., Benard, M. F. (2005): Scared to death? The effects of intimidation and consumption in predator–prey interactions. – Ecology 86(2): 501-509.
[39] Raza, G., Mirza, S. N., Anwar, M., Hussain, I., Khan, S. W., Khalil, A., Nawaz, M. A., Naseer, A. (2015): Population and distribution of himalayan ibex, capra ibex sibrica, in Hushe valley, central Karakoram national park, Pakistan. – Pakistan Journal of Zoology 47(4): 1025-1030.
[40] Reichlin, T., Klansek, E., Hackländer, K. (2006): Diet selection by hares (*lepus europaeus*) in arable land and its implications for habitat management. – European journal of wildlife research 52(2): 109-118.
[41] Rivera-Milán, F. F., Bertuol, P., Simal, F., Rusk, B. L. (2015): Distance sampling survey and abundance estimation of the critically endangered Grenada Dove (*Leptotila wellsi*). – The Condor 117(1): 87-93.
[42] Roberts, T. J. (2005): Field guide to the large and medium–sized mammals of Pakistan. – Oxford University Press.

http://www.aloki.hu ● ISSN 1589 1623 (Print) ● ISSN 1785 0037 (Online)
DOI: http://dx.doi.org/10.15666/aeer/1802_29212934

[43] Roedenbeck, I. A., Voser, P. (2008): Effects of roads on spatial distribution, abundance and mortality of brown hare (lepus europaeus) in Switzerland. – European Journal of Wildlife Research 54(3): 425-437.
[44] Santilli, F. (2007): Factors affecting brown hare (*lepus europaeus*) hunting bags in Tuscany region (central Italy). – Hystrix, Italian Journal of Mammalogy 17.2-4372.
[45] Santilli, F., Bagliacca, M., Paci, G. (2015): Density and habitat use of sympatric brown hares and European rabbits in a mediterranean farmland area of Tuscany (central Italy). – Ethology Ecology & Evolution 27(2): 233-243.
[46] Sarmento, P., Cruz, J., Eira, C., Fonseca, C. (2009): Evaluation of camera trapping for estimating red Red fox abundance. – The Journal of Wildlife Management 73(7): 1207-1212.
[47] Schneider, M. F. (2001): Habitat loss, fragmentation and predator impact: Spatial implications for prey conservation. – Journal of Applied Ecology 38(4): 720-735.
[48] Selås, V., Vik, J. (2006): Possible impact of snow depth and ungulate carcasses on red Red fox (vulpes vulpes) populations in Norway, 1897–1976. – Journal of Zoology 269(3): 299-308.
[49] Smith, R. K., Jennings, N. V., Robinson, A., Harris, S. (2004): Conservation of european hares lepus europaeus in Britain: Is increasing habitat heterogeneity in farmland the answer? – Journal of Applied Ecology 41(6): 1092-1102.
[50] Smith, R. K., Vaughan, N. J., Harris, S. (2005): A quantitative analysis of the abundance and demography of european hares lepus europaeus in relation to habitat type, intensity of agriculture and climate. – Mammal review 35(1): 1-24.
[51] Stankowich, T., Blumstein, D. T. (2005): Fear in animals: A meta –analysis and review of risk assessment. – Proceedings of the Royal Society of London B: Biological Sciences 272(1581): 2627-2634.
[52] Thomas, L., Laake, J., Strindberg, S., Marques, F., Buckland, S., Borchers, D., Anderson, D., Burnham, K., Hedley, S., Pollard, J. (2006): Distance 5.0. Release 2. – Research unit for wildlife population assessment, University of St. Andrews, United Kingdom.
[53] Thomas, L., Buckland, S. T., Rexstad, E. A., Laake, J. L., Strindberg, S., Hedley, S. L., Bishop, J. R., Marques, T. A., Burnham, K. P. (2010): Distance software: Design and analysis of distance sampling surveys for estimating population size. – Journal of Applied Ecology 47(1): 5-14.
[54] Waggett, R. J., Buskey, E. J. (2007): Calanoid copepod escape behavior in response to a visual predator. – Marine Biology 150(4): 599-607.
[55] Walton, Z., Samelius, G., Odden, M., Willebrand, T. (2017): Variation in home range size of red Red foxes vulpes vulpes along a gradient of productivity and human landscape alteration. – PloSone 12(4): e0175291.
[56] Welch, D. (1982): Dung properties and defecation characteristics in some scottish herbivores, with an evaluation of the dung –volume method of assessing occupance. – Acta theriologica 27(15): 191-212.
[57] Weston, M., McLeod, E. M., Blumstein, D., Guay, P. J. (2012): A review of flight–initiation distances and their application to managing disturbance to Australian birds. – Emu–Austral Ornithology 112(4): 269-286.
[58] Weterings, M. J., Zaccaroni, M., van der Koore, N., Zijlstra, L. M., Kuipers, H. J., van Langevelde, F., van Wieren, S. E. (2016): Strong reactive movement response of the medium–sized European hare to elevated predation risk in short vegetation. – Animal behaviour 115: 107-114.
[59] Zaman, M., Tolhurst, B. A., Zhu, M., Jiang, G. (2019a): Increased flight initiation distance (fid) in golden marmots (marmota caudata aurea) responding to domestic dogs in a landscape of human disturbance. – Animals 9(9): 605.
[60] Zaman, M., Tolhurst, B., Zhu, M., Heng, B., Jiang, G. (2019b): Do red Red foxes (vulpes vulpes) increase the detectability of scent marks by selecting highly conspicuous substrates? – Journal of Ethology and Animal Science 2(2): 000113.

http://www.aloki.hu ● ISSN 1589 1623 (Print) ● ISSN 1785 0037 (Online)
DOI: http://dx.doi.org/10.15666/aeer/1802_29212934

CHANGES OF SOIL PHOSPHORUS FRACTIONS IN PARENT MATERIAL OF A MOLLISOL AT THE EARLY PEDOGENIC STAGE IN NORTHEAST CHINA

LU, X. C.[1] – HAN, X. Z.[1] – CHEN, X.[1] – YAN, Y.[1] – YOU, M. Y.[1] – KWAW-MENSAH, D.[2] – HAO, X. X.[1] – ZOU, W. X.[1*]

[1]*Key Laboratory of Mollisols Agroecology, Northeast Institute of Geography and Agroecology, Chinese Academy of Sciences, Harbin 150081, China*

[2]*Department of Agronomy, Iowa State University, Ames, Iowa, 50011, USA*

**Corresponding author*
e-mail: zouwenxiu@iga.ac.cn

(Received 8th Nov 2019; accepted 30th Jan 2020)

Abstract. Fertility degradation of Mollisols affects world food security. Understanding the degradation mechanisms of Mollisols is essential in order to restore the soils' productivity. A long-term field experiment was conducted to assess soil phosphorus (P) concentrations and fractions in a Mollisol at its early development stage under different cropping systems in Northeast China. Parent material (PM) and mature Mollisol (OM) were used for comparison. Organic P (Po) concentrations under natural fallow (Pnat), alfalfa (*Medicago sativa L.*) (Palf) and soybean-maize (S-M) rotation without fertilizer application (PCS-F) increased by 68-74% after 10 years. S-M rotation with mineral fertilizer (PCS + F), organic matter amendment (PCS + F + OM), or crop straw return (PCS + F + BM) increased Po concentrations by 74.1-108 mg kg^{-1}, which is equivalent to 33% of total Po in the OM; and increased Ca_2-P, Ca_8-P, Al-P and Fe-P concentrations by 0.9-1.3, 7.1-8.8, 2.1-2.7 and 1.6-1.7 times, respectively. 67% of the applied fertilizer P was transformed to Pi for the treatments with chemical fertilizer. The results indicate that return of crop residue combined with chemical fertilizers enhances the accumulation of P in soils at their early development stage, which has important implications for the fertility restoration of a Mollisol in Northeast China and elsewhere in the world.
Keywords: *soil development, natural fallow, long-term restoration experiment, organic phosphorus, inorganic phosphorus*

Introduction

Phosphorus (P) is one of the essential elements for crop growth and development. Over 80% of P absorbed by crops comes from a soil reserve (Fageria et al., 2008) and applied fertilizer P reverts to less available forms in the soil (Han et al., 2005a, b). Therefore, the fractions and availability of soil P, and the transformation and availability of applied fertilizer P have received much attention in agronomic research (Milic et al., 2019; Sun et al., 2019). Soil P fractions include inorganic P (Ca_2-P, Ca_8-P, Al-P, Fe-P, O-P, Ca_{10}-P) and organic P (labile organic P, moderately labile organic P, moderately stable organic P and highly stable organic P). Generally, organic P (Po) accounts for 30-65% of the total P in soils (Pätzold et al., 2013; Jin et al., 2013), while organic P in Mollisol accounts for 42-69% of total P (Song et al., 2007), which can be attributed to the relatively high organic matter contents (Hou et al., 2014). Crops directly utilize inorganic P (Pi) in soil solution (generally orthophosphates), which is in dynamic equilibrium with phosphate minerals and surface adsorbed P in soil (Xiang et al., 2004). With the advancement of soil development, Po fractions become dominant and P availability is more closely related to the activity of soil microorganisms (van der

http://www.aloki.hu ● ISSN 1589 1623 (Print) ● ISSN 1785 0037 (Online)
DOI: http://dx.doi.org/10.15666/aeer/1802_29352948

Bom et al., 2019; Richardson et al., 2011). Generally, plant available P comes from the pools of Fe-P, Al-P, moderately labile organic P (MLOP) and labile organic P (LOP) in acid soil; while from the pools of Ca_2-P, Ca_8-P, LOP and MLOP in alkaline soil (Li et al., 2005). Therefore, Po fractions play an important role in P supply, especially in soils with relatively high organic matter content (Vanden Nest et al., 2016; Nobile et al., 2020).

The development and utilization of a Mollisol in Northeast China underwent both natural virgin stages through the stages of cultivation without fertilizer application, cultivation with organic matter application, and cultivation with the combination of organic matter and inorganic fertilizers. The impacts of different cropping systems and agricultural practices on the content and fractions of P in Mollisol have been reported (Song et al., 2007). Mollisol was fertile in nature and could sustain P supply under both natural and agricultural production systems. Excessive applications of chemical P fertilizers increased both available and unavailable P fractions (Song et al., 2007). However, the soils in Northeast China suffered from severe erosion as a result of intensive agricultural practices, which has caused 60% loss of soil organic matter content (Miao et al., 2019). In some extreme cases, soil erosion has removed the surface layer, with exposed parent material (C horizon). It is important to understand P transformations in soil during the period from parent material to current stage.

The restoration of degraded soil has been undertaken at a large-scale and proven to be successful in terms of above-ground ecosystem properties. However, it still lacks understanding regarding soil development in relation to vegetation changes (Griffiths et al., 2008; Harris, 2009), which could be attributed to the fact that it takes a long time to build a high level of soil fertility under natural conditions (Harrison et al., 2008). Anthropogenic activities can accelerate the pedogenic process as indicated by a significant increase in soil organic matter content with all the treatments including no fertilizer, chemical fertilizer and chemical fertilizer plus organic residue amendments during the first eight years of soil development from parent material (You et al., 2017). The inputs of crop residue and manure changed the distribution of carbon (C) density fraction and humic substances. High organic matter input first caused an increase in labile C pool, followed by stable C fractions (You et al., 2014). Soil microbial activity increased with tillage and organic amendment at the early pedogenic stage of parent material, as evidenced by an increase in soil microbial biomass-C and total PLFAs, as compared to the parent material (Li et al., 2014). The soil food web was quickly developed with fertility restoration practices (Li et al., 2016). However, information was limited about P transformations at the initial stage of soil development from the parent material.

Prior studies have focused on the impact of different vegetation types and agricultural practices on P fractionation in mature Mollisol, with much less attention being paid to young soils. Lu et al. (2015) reported that fertilizer P applied in Mollisol was transformed to Al-P and Fe-P, with less than 20% being accumulated as Po. Few reports are available about the effects of cropping systems (or vegetation types) and related agricultural practices on the changes of P fractions in the initial stages of soil development. Accordingly, a field experiment was established in 2004 to examine soil development from parent material (C horizon) of a Mollisol. To simulate the effects of cropping systems and agricultural practices on P fractions at the early development stage of soil, it was hypothesized that application of exogenous P including chemical fertilizer P and P in organic amendment can enhance the accumulation of P in parent

http://www.aloki.hu ● ISSN 1589 1623 (Print) ● ISSN 1785 0037 (Online)
DOI: http://dx.doi.org/10.15666/aeer/1802_29352948

material, which can reach relatively high levels within a short term. The objectives of this study were to: (1) identify P fractions in parent material and; (2) determine the effect of cropping systems and agricultural practices on P fraction in the initial stage of soil development.

Materials and methods

Site description and soil sampling

The long-term restoration experiment was located in the center of the Mollisol' area in Northeast China at the State Key Experimental Station of Agroecology, Chinese Academy of Sciences, Hailun, Heilongjiang province (47°26′N, 126°38′S). The Mollisol was derived from the sedimentary material of loamy loess parent material (Xiong et al., 1987). Typical soil profiles consist of A-AB-BC-C horizons (A, 0-60 cm; AB, 60-115 cm; BC, 115-150 cm; C, > 170 cm depth). The depth to bedrock is > 20 m. Soil classification is Pachic Haploborolls (fine-silty, mixed, superactive, mesic Pachic Ultic Haploxeroll) according to the USDA Soil Taxonomy (Soil Survey Staff, 2014). The climate in the region is typical temperate continental monsoon, characterized by cold winters and hot summer; with the mean annual temperature of 2.2 ℃. The average total annual precipitation is 550 mm, with approximately 358 mm occurring from June to August.

The long-term restoration experiment started in June 2004 with 24 enclosed plots (each plot measured 1.4 m long, 1.0 m wide and 0.8 m deep). The enclosures consisted of cement strips (0.2 m wide and 0.8 m deep) that protruded 0.1 m above the ground. These enclosures were refilled with parent material taken from the 2 m depth (C horizon) below surface near the experimental station. The parent material had a semi-blocky structure. Nylon mesh with 75 μm openings was placed on the parent material at 0.8 m depth to prevent root penetration, but it allowed water and nutrient exchange. The parent material contained 4.79 g C and 0.41 g N kg^{-1} soil, had a pH of 6.88 (soil: DI water 1:2.5), bulk density of 1.35 g cm^{-3}, 420 g kg^{-1} clay (< 0.002 mm) and 356 g kg^{-1} silt (0.02-0.002 mm). The dominant clay minerals were vermiculite, chlorite and illite (*Fig. 1*).

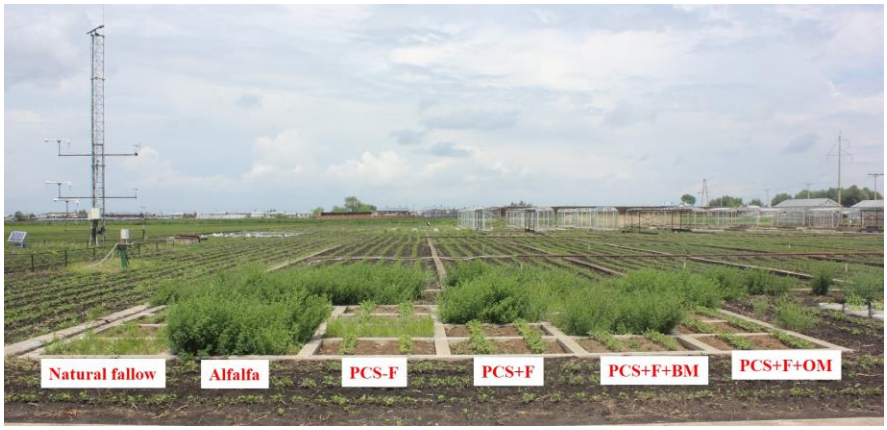

Figure 1. *The experimental plots in the field*

The following six treatments were assigned to the 24 plots with the parent materials as a randomized block design with four replications: natural fallow without weed

http://www.aloki.hu ● ISSN 1589 1623 (Print) ● ISSN 1785 0037 (Online)
DOI: http://dx.doi.org/10.15666/aeer/1802_29352948

control (*vegetation consisted mainly of Leymus chinensi, Poa annua L. and Equisetum tataricus*) (Pnat), N-fixing alfalfa (*Medicago sativa L.*) (Palf) and four Soybean (S)-Maize (M) rotation: (i) S-M without mineral fertilizer and biomass removed (PCS-F), (ii) S-M with mineral fertilizer and biomass removed (PCS + F), (ii) S-M with mineral fertilizer and partial return of residue as a soybean powder-maize straw mixture (PCS + F + OM) and (iv) S-M with mineral fertilizer and all biomass incorporated (PCS + F + BM) (*Table 1 and 2*). The biomass in each plot of Pnat and Palf treatments was left in the fields as mulch. In P + F-OM, 2250 kg ha^{-1} ground soybean seeds that had been baked at 200 ℃ and 4500 kg ha^{-1} chopped (20-50 mm long pieces) maize straw were incorporated into the soil at the same time as the other residue return treatments. The C content in the soybean powder and maize straw was equivalent to the C content of a typical organic manure application and return of maize straw C in this region (Qiao et al., 2014). In the PCS + F + BM treatment, the biomass of each year's crop was incorporated into the field, but the maize grain and soybeans were pulverized as above. The fertilizer sources were diammonium phosphate and potassium sulphate, applied at 54, 60, and 54 kg N, P and K ha^{-1} $year^{-1}$, respectively, for soybean and maize. An additional 140 kg N ha^{-1} $year^{-1}$ was applied as urea at the V8 stage of maize growth. The parent material was tilled to 20 cm depth with a spade to incorporate the chopped crop residue, and ridges (70 cm wide and 25 cm high) were made after applying the organic amendments. The first crop of rotation was soybean. The crop densities were 70000 and 270000 plants ha^{-1} for maize and soybean, respectively. The varieties of soybean and maize were Dongsheng 7 and Haiyu 6, respectively. The crops were sown in rows in May and harvested in October. At harvest, the above-ground biomass in each plot was cut and weighed, and subsamples were oven-dried at 60 ℃ to determine the dry weight of grain and non-grain biomass.

Table 1. *The list of abbreviations for field treatments*

Field treatments	Natural fallow	Alfalfa	Parent material	Mineral fertilizer	Biomass	The mixture of soybean powder-maize straw
Abbreviations	Pnat	Palf	PCS	F	BM	OM

Table 2. *Experimental treatments (i.e. crop rotations, inputs of plant material and mineral fertilizer, tillage) in the 10 years field experiments*

Field treatments	**Cropping systems[a]**	**Organic incorporation[b]**	**Mineral fertilizer input[c]**	**Tillage[d]**
Pnat	Natural fallow	Litter and roots	None	No
Palf	Alfalfa	Litter and roots	None	No
PCS-F	Crop rotation	Roots	None	Yes
PCS + F	Crop rotation	Roots	NPK	Yes
PCS + F + BM	Crop rotation	All crop straw, seeds and roots	NPK	Yes
PCS + F + OM	Crop rotation	Roots, and amended soybean seeds and maize straw	NPK	Yes

[a]Crop rotation is the rotation of soybean and maize in different years since 2004
[b]The amendment rates in PCS + F + OM were 2250 kg hm^{-1} of baked soybean powder and 4500 kg hm^{-1} of maize straw mixed homogeneously. The C:N ratios were 7.4:1 in soybean seeds, 33.5 in maize, 63.3:1 in maize straw and 59.1 in soybean straw
[c]Diammonium phosphate was source of N and P and applied at a rate of 300 kg hm^{-1} yr^{-1}; Potassium sulfate (K) was applied at a rate of 120 kg hm^{-1} yr^{-}
[d]Tillage was performed manually down to 20 cm with ridges made in October after harvest

http://www.aloki.hu ● ISSN 1589 1623 (Print) ● ISSN 1785 0037 (Online)
DOI: http://dx.doi.org/10.15666/aeer/1802_29352948

Soil samples at the surface layer (0-20 cm) were collected from the six treatments in all four replications after harvest in October 2013. Composite soil samples, consisting of four random subsamples, were removed with a spade from the ridge and furrow locations and mixed thoroughly. The soil surface layer (0-20 cm) of each treatment was air-dried after removing all visible roots and plant fragments and sieved through a 2 mm or 0.25 mm sieve. The samples of parent material (PM) were taken below 2 m depth in 2004. Mature Mollisol (OM) was sampled from the A horizon (0-20 cm) from an adjacent experimental field, which had been cropped to a maize and soybean rotation since 1993 and received only mineral N (120 g kg^{-1}, urea) and P (51.8 g kg^{-1}, diammonium phosphate) fertilizers for maize and N (20.3 g kg^{-1}, urea) and P (51.8 g kg^{-1} diammonium phosphate) fertilizers for soybean. All aboveground biomass had been removed from field of the mature Mollisol and soil tillage had been manually conducted to the 20 cm depth using a spade.

Soil sample analysis

The soil samples were air-dried and sieved through a 2-mm sieve for the laboratory experiment. Total P (T-P) in soil samples was determined by digesting soil in a tri-acid mixture (HNO_3, $HClO_4$, and H_2SO_4 at a 3:1:1 ratio) and P concentration in the digested samples determined calorimetrically using the vanado-molybdate-yellow color method (Jackson, 1973). Soil total organic P was determined after the soil was combusted at 550 °C and extracted with 4 M H_2SO_4 (Anderson, 1960). Available P was analyzed with the colorimetric molybdenum method following extraction with 0.5 M $NaHCO_3$ (Olsen et al., 1957).

Organic P fractions

Soil organic P (Po) was separated into four fractions using a modified sequential extraction procedure developed by Bowman et al. (1978) and modified by Fan et al. (1990). A flow diagram for the Po fraction procedure is given in *Figure 2*. Highly stable organic P (HSOP) was determined by subtracting the moderately stable organic P (MSOP) from the stable organic P.

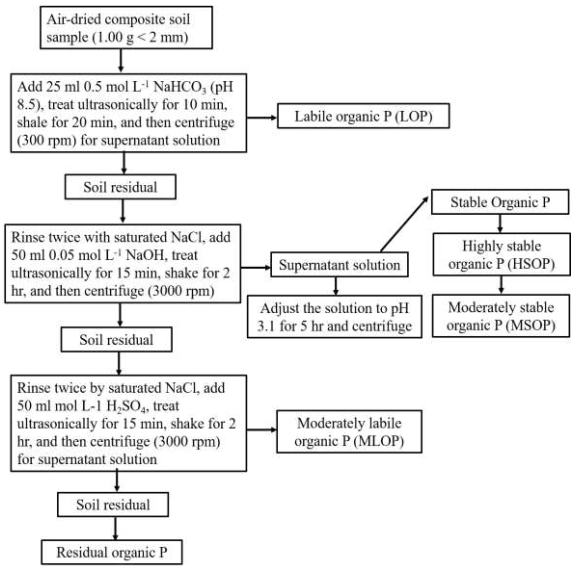

Figure 2. *Scheme of sequential extraction of organic P in a Mollisol (Yang et al., 2006)*

http://www.aloki.hu ● ISSN 1589 1623 (Print) ● ISSN 1785 0037 (Online)
DOI: http://dx.doi.org/10.15666/aeer/1802_29352948

Inorganic P fractions

Inorganic P fractions were measured according to the fractionation scheme of Jiang et al. (1989) modified from the method described by Chang et al. (1957) and Hedley et al. (1982). Briefly, the fractionation involved a sequential extraction with (1) 0.25 M $NaHCO_3$ (pH 7.5) to extract Ca_2-P, (2) 0.5 M CH_3COONH_4 (pH 4.2) to extract Ca_8-P, (3) 0.5 M NH_4F (pH 8.2) to remove Al-P, (4) 0.1 M NaOH-0.1 M Na_2CO_3 to obtain Fe-P, (5) 0.3 M sodium citrate-$Na_2S_2O_4$-0.5 M NaOH to obtain the occluded P and (6) 0.5 M H_2SO_4 to extract Ca_{10}-P. These fractions were designated as $NaHCO_3$-soluble P (Ca_2-P), NH_4Ac-soluble P (Ca_8-P), NH_4F-soluble P (Al-P), NaOH-$NaCO_3$-soluble P (Fe-P), occluded P (O-P), and H_2SO4-soluble P (Ca_{10}-P).

Statistical analysis

The analysis of variance (ANOVA) was performed using the SPSS (version 16, IBM SPSS Statistics, Somer, NY) to determine the significant difference between the treatments. Standard errors were calculated for mean values of determinations. The multiple comparison test was performed using Fisher's (protected) Least Significant Difference (LSD) at the 0.05 significant level. A principal component analysis (PCA) of the soil phosphorus fractions for all the field treatments, mature Mollisol and parent material was generated using CANOCO 5.0 software (written by Cajo J. F. ter Braak and Peter Smilauer, http://www.canoco5.com).

Results

Total P and Olsen P

Compared to parent material (PM), total P in unfertilized soils (Pnat, Palf and PCF-F) did not significantly increase ($P > 0.05$), but Olsen P did ($P < 0.05$) (*Fig. 3*). For the treatments with mineral fertilizers and organic matter amendment (PCS + F, PCS + F + OM and PCS + F + BM), total P concentrations increased by 282.1-330.6 mg kg^{-1} (*Fig. 3*), which was equivalent to the total P concentration in the OM. Olsen P concentrations increased by 93.3-114.9 mg kg^{-1}(*Fig. 3*), which was higher than that in the OM, indicating that application of chemical fertilizers and organic amendment enhanced P accumulation in soil after the initial10 years of treatments from parent material.

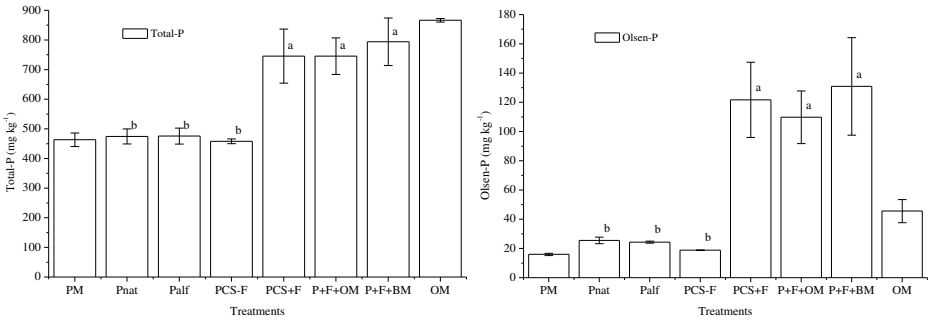

Figure 3. *The contents of total P and Olsen P in parent material of soil formation, parent material and mature Mollisol. (Pnat, natural fallow (grasses); Palf, alfalfa; PCS-F, unfertilized soybean-maize (S-M) control; PCS + F, chemical fertilizer S-M; PCS + F + OM, organic amendment plus chemical fertilizer S-M; PCS + F + BM, chemical fertilizer and all crop biomass returned S-M. Values followed by different letters differ significantly at* $P < 0.05$*)*

http://www.aloki.hu ● ISSN 1589 1623 (Print) ● ISSN 1785 0037 (Online)
DOI: http://dx.doi.org/10.15666/aeer/1802_29352948

Organic and inorganic P

Total organic and inorganic P

Compared to PM, the treatments without chemical fertilizers (Pnat, Palf and PCS-F) increased organic P (Po) but decreased inorganic P (Pi) (*Fig. 4*). However, the treatments with chemical fertilizers and organic amendment (PCS + F, PCS + F + OM and PCS + F + BM) significantly increased Pi concentrations with the highest value of 586.8 mg kg^{-1} occurred to the PCS + F treatment, which was higher than that in OM (348.7 mg kg^{-1}) (*Fig. 4*). The Po concentrations in all the field treatments increased by 68.2-138%, as compared to PM, and the highest value (186.2 mg kg^{-1}) was observed in the PCS + BM treatment, which was 39.4% of Po in the OM. OM had a similar Pi concentration as the PM, but had more Po (*Fig. 4*). The percentages of Po in the total P were lower in PM than OM, which were 57.4%, 18.2% and 20.6 - 31.9%, respectively for OM, PM and all the tested soil. The percentage of Po in total P within Pnat, Palf and PCS-F treatments was higher than those in the PCS + F, PCS + F + OM and PCS + F + BM treatments (*Fig. 4*).

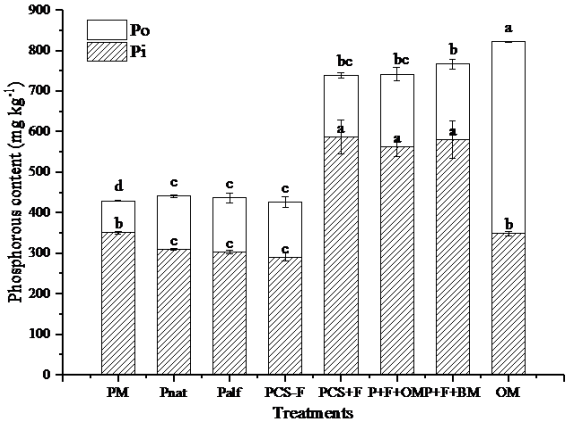

Figure 4. *The concentrations of organic p and inorganic P in parent material of soil formation, parent material and mature Mollisol. (Pnat, natural fallow (grasses); Palf, alfalfa; PCS-F, unfertilized soybean-maize (S-M) control; PCS + F, chemical fertilizer S-M; PCS + F + OM, organic amendment plus chemical fertilizer S-M; PCS + F + BM, chemical fertilizer and all crop biomass returned S-M; Po, organic P; Pi, inorganic P; PM, parent material; OM, mature Mollisol. Values followed by different letters differ significantly at* $P < 0.05$*)*

320 mg P kg^{-1} was applied to the soil as diammonium phosphate every year during the 10 years of the experiment in the treatments with chemical fertilizers (PCS + F, PCS + F + OM and PCS + F + BM) (*Table 2*). Compared to PM, total P concentrations in the treatments with chemical fertilizers increased by 282.1-330.6 mg kg^{-1}, which was comparable to the amount of P applied in fertilizers (*Fig. 4*). The different total P concentrations among treatments could be attributed to the removal of P in aboveground biomass, which possibly caused P loss in the PCS + F treatment. Total P concentrations in the PCS + BM treatment reached the highest value of 330.6 mg kg^{-1} (*Fig. 3*), which is higher than the total P input via fertilization. This can be attributed to biomass decomposition including aboveground and root biomass (*Fig. 3*). This indicates that most of the applied P accumulated in the top 0-20 cm of soil depth. This increased in

http://www.aloki.hu ● ISSN 1589 1623 (Print) ● ISSN 1785 0037 (Online)
DOI: http://dx.doi.org/10.15666/aeer/1802_29352948

total P was made up of the increase of 211.1-235.9 mg kg^{-1} of Pi and 74.1-108.0 mg kg^{-1} of Po over the 10-year period of the experiment (*Fig. 4*). Compared to PM, available P in the PCS + F, PCS + F + OM and PCS + F + BM treatments increased by 93.8-114.9 mg kg^{-1}, indicating that approximately 33% of the applied fertilizer P accumulated in the Olsen P pool (*Fig. 4*).

Phosphorus fractions

The total P concentrations in soil increased after the initial 10 years of experiment regardless of treatments, whilst vegetation types and agricultural practices showed different effects on Pi fractions (*Table 3*). There was an increase mainly in the concentrations of LOP and MLOP. Compared with the LOP of PM without P fertilizers, the highest concentration of LOP was found in the PCS + F + OM treatment, which accounted for approximately 25% of the amount in OM (*Table 3*). MLOP concentrations in all the tested soils increased by 2.9-5.3 times, with the highest value in the PCS + BM treatment, which was similar to that in OM (*Table 3*). Treatments with P fertilization increased MSOP by 15.3-62.2%, and this accounted for approximately 33% of the MSOP in the OM (*Table 3*). The PCS-F and PCS + F treatments decreased the contents of HSOP, but the rest of treatments did not affect HSOP concentrations. The HSOP concentrations in all the tested soil were much lower than that in OM (*Table 3*).

Table 3. *The contents of different P fractions in parent material under treatments, parent material and mature Mollisol*

Treatments	Organic P (mg kg^{-1})				Inorganic P (mg kg^{-1})					
	LOP	MLOP	MSOP	SOP	Ca_2-P	Ca_8-P	Al-P	Fe-P	O-P	Ca_{10}-P
PM	0.0 e	19.4 d	34.5 d	24.3 c	15.0 c	4.6 c	20.4 b	94.0 b	80.9 ab	135.9 a
Pnat	0.45 de	75.0 c	32.6 d	23.4 c	6.8 d	13.4 c	5.9 c	114.8 b	60.4 bc	108.2 b
Palf	0.97 cd	79.4 c	31.3 d	21.6 c	4.4 d	8.4 c	1.4 c	118.7 b	66.2 bc	109.5 b
PCS-F	1.68 c	90.9 bc	38.5 cd	5.1 d	3.0 d	7.0 c	5.7 c	104.8 b	65.2 bc	104.8 b
PCS + F	0.91 cd	98.1 abc	49.3 bc	4.0 d	32.1 b	37.1 a	76.5 a	253.8 a	80.1 ab	107.2 b
P + F + OM	4.00 b	96.3 abc	56.0 b	23.4 c	28.3 b	37.5 a	63.7 a	241.4 a	87.2 a	103.9 b
P + F + BM	1.45 c	116.4 ab	39.8 cd	28.6 b	34.3 b	45.1 a	67.9 a	252.4 a	77.0 ab	103.4 b
OM	16.7 a	122.1 a	149.6 a	184.2 a	42.2 a	26.1 b	55.7 a	122.9 b	44.2 c	57.6 c

Pnat, natural fallow (grasses); Palf, alfalfa; PCS-F, unfertilized soybean-maize (S-M) control; PCS + F, chemical fertilizer S-M; PCS + F + OM, organic amendment plus chemical fertilizer S-M; PCS + F + BM, chemical fertilizer and all crop biomass returned S-M; PM, parent material; OM, mature Mollisol; LOP, labile organic P; MLOP, moderate labile P; MSOP, moderate stable organic P; SOP, stable organic P; Ca_2-P, $NaHCO_3$-soluble P; Ca_8-P, NH_4Ac-soluble P, Al-P NH_4F-soluble P; Fe-P, NaOH-$NaCO_3$-soluble P; O-P, occluded P; Ca_{10}-P, H_2SO_4-soluble P. Values followed by different letters at same column differ significantly at $P < 0.05$

In contrast with PM, the treatments without fertilization (Pnat, Palf and PCS-F) decreased the concentrations of Ca_2-P, Al-P and Ca_{10}-P and increased the concentrations of Ca_8-P and Fe-P, whereas the treatments with fertilization (PCS + F, PCS + F + OM and PCS + F + BM) significantly increased the Pi fractions except for Ca_{10}-P and O-P (*Table 3*). The concentrations of Ca_2-P, Ca_8-P, Al-P, and Fe-P increased by 0.9-1.3, 7.1-8.8, 2.1-2.7 and 1.6-1.7 times (*Table 3*). The concentrations of Ca_2-P,

http://www.aloki.hu ● ISSN 1589 1623 (Print) ● ISSN 1785 0037 (Online)
DOI: http://dx.doi.org/10.15666/aeer/1802_29352948

Ca_8-P, Al-P, and Fe-P in OM were much higher than those in PM, but the concentrations of O-P and Ca_{10}-P in OM was lower than those in PM (*Table 3*).

Pedogenic process of parent material under Mollisol

Principal component analysis demonstrated that a large difference was found between OM and PM (*Fig. 4*), parent material with the field treatments had developed into mature Mollisol over the 10-year period of the experiment. Compared with the treatments without fertilizers (Pnat, Palf and PCS-F), the soils receiving fertilized treatments were closer to mature Moillisol (*Fig. 5*). Inorganic P concentrations in the soils treated with chemical fertilizers (PCS + F + BM, PCS + F + OM and PCS + F) were similar to the Pi in the OM, but a large difference in Po concentration exists between PM and OM (*Fig. 5*).

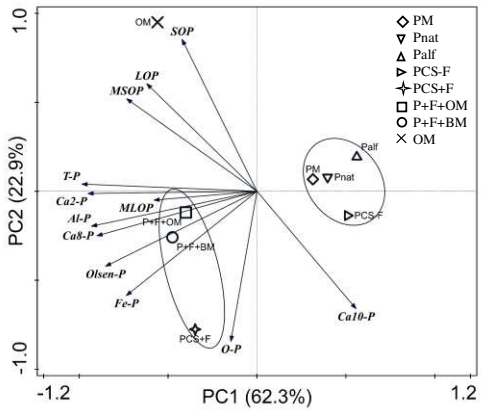

Figure 5. *The first two principal components (PC1 and PC2) of soil phosphorus fractions for all the field treatments, mature Mollisol and parent material. (Pnat, natural fallow (grasses); Palf, alfalfa; PCS-F, unfertilized soybean-maize (S-M) control; PCS + F, chemical fertilizer S-M; PCS + F + OM, organic amendment plus chemical fertilizer S-M; PCS + F + BM, chemical fertilizer and all crop biomass returned S-M)*

Discussion

Changes in different P fractions

Most P was present as calcium phosphates at the early pedogenic stage of rock, and vegetation occurrence converted Pi to Po in soil (Lu, 1980). In the parent material of Mollosil, the Pi concentration was 78.2 mg kg^{-1}, which accounted for 16.55% of that in mature Mollisol (*Fig. 4*). The unfertilized treatments (Pnat, Palf and PCS-F) did not increase total P, but increased Po to 131.5-136.1 mg kg^{-1}, accounting for 27.8-28.8% of Po in OM (*Fig. 4*), which is consistent with the organic carbon change measured by You et al. (2017), who reported that organic carbon increased by 7-60% in the same site. Soil organic carbon gradually increased in the parent material after vegetation occurrence, which resulted in an increase in Po, but a decrease in Pi concentration of a similar amount, indicating the transformation of Pi to Po during soil development from parent material. Specifically, Ca_2-P, Al-P, O-P and Ca_{10}-P were transformed to LOP and MLOP (*Table 3*), indicating that plants absorbed Pi and returned Po in residues to soil.

The Pnat and Palf treatments demonstrated a similar effect on the transformation of P fractions, which differed from the PCS-F treatment (*Table 3*) where SOC was only

http://www.aloki.hu ● ISSN 1589 1623 (Print) ● ISSN 1785 0037 (Online)
DOI: http://dx.doi.org/10.15666/aeer/1802_29352948

derived from root and litter. This resulted in a relatively low Po concentration with a decrease in HSOP in the PCS-F treatment. Perroni et al. (2014) has documented that Alfalfa growth resulted in an increase in Po in a desert scrub soil in Mexico. Parent material used in the present study had a low SOC (4.8 g kg^{-1}) in this study, and the field treatments rapidly increased SOC (You et al., 2017) and subsequently Po in the soil. However, Alfalfa did not show any advantage in the accumulation of Po fractions in the parent material.

A mature Mollisol had been cultivated for hundreds of years, underwent no fertilization stage, farmyard manure stage and chemical fertilization stage. The accumulation of Po increased during soil development and utilization. However, the accumulation of Po concentration became steady at a certain level without the application of inorganic P fertilizers (Song et al., 2011). The transformation of Pi to Po occurred at a lower rate in the treatments without fertilizers where Po accumulation per year accounted for 1% of that in the mature Mollisol (*Table 3*). Apparently, external P inputs could accelerate the accumulation of Po in soil under field conditions.

Effects of fertilizer application on P fractions

In this study we attempted to accelerate P formation in the parent material by adding P fertilizers to contrast with the natural soil development process. P fertilizer applied to soil was mainly presented as Pi in the plant-available fractions in parent material under the imposed cropping systems and agricultural practices (*Table. 3*). The rate of Po accumulation in the treated parent material was relatively slow, but approximately 33% of the fertilizer P was transformed to Po. Total P concentration in the treated parent material was close to that in the mature Mollisol, which may be attributed to the application of P fertilizers over the 10-year of the experiment (*Fig. 4*). Soil development in the Mollisol parent material was accelerated by P fertilization based on the result of PCA (*Fig. 5*), whilst soil development in the vegetation restoration contexts may take hundreds of years to accomplish this level of fertility (Harrison et al., 2008). Po accumulation was as high as 40% in the mature Mollisol, which is an evidence of the acceleration of soil development in the parent material used in this study.

Reddy et al. (2000) found that soil P fractionation was affected by soil type and fertilization practices, and the application of cattle manure increased the concentration of Po, activated fixed Pi in soil, and thus enhanced uptake of P by crops. Application of chemical fertilizers, straw and animal manure increased Pi concentration in the soils of Northwest China (Wei et al., 2011). Chemical fertilizers and organic manure also affected P sorption capacity in a Mollisol (Song et al., 2007). The long-term experiment with a Mollisol showed that chemical fertilizers (N and P), and the combination of chemical fertilizers with pig manure increased both total P and Olsen P, dominantly in the forms of Ca_2-P, Ca_8-P and Al-P, but no significant increase in Po was noted (Song et al., 2011). Similar results were obtained in present study. P fertilization enhanced Pi accumulation in the treated parent material, which resulted in a significant increase in Pi with the treatments of PCS + F, PCS + F + OM and PCS + F + BM.

The concentrations of Pi showed a decreasing order of PCS + F + AM, PCS + F + OM > PCS + F > Pnat, Palf, PCS-F. The highest value reached 186.2 mg kg^{-1}, accounting for 39.4% of that in the mature Mollisol (*Fig. 4*). Accumulated Po in the parent material was mainly derived from crop residues, and a higher rate of organic amendment resulted in more accumulation of Po in soil.

http://www.aloki.hu ● ISSN 1589 1623 (Print) ● ISSN 1785 0037 (Online)
DOI: http://dx.doi.org/10.15666/aeer/1802_29352948

Long-term field experiments have documented that organic amendment significantly increased the concentration of Olsen P and reduced soil adsorption capacity for P (Motavalli et al., 2002; Allen et al., 2006). Low molecular weight organic substances in organic amendment reduced the adsorption capacity of variable charge minerals for P by competition for adsorbing sites (Guppy et al., 2005). There was no significant difference in the total P and Olsen P concentrations between chemical fertilizers alone and the combination of chemical fertilizers and organic amendment. Applied fertilizer P was mainly presented in the Olsen P pools in the treated parent material. Compared with chemical fertilizer treatment alone (PCS + F), the treatments of chemical fertilizers with organic amendment (PCS + F + OM and PCS + F + BM) had no significant difference in Pi and Po concentrations or the Po : total P ratio.

Conclusions

The long-term field experiment was established in 2004 to determine the impact of cropping systems and agricultural practices on soil P concentration and fractionation during the first 10 years of soil development from parent material of a Mollisol. Po and Pi concentrations were 78.9 and 350.9 mg kg^{-1} in parent material, and 472.6 and 348.7 mg kg^{-1} in mature Mollisol. The treatments without chemical fertilizers (Pnat, Palf and PCS-F) enhanced P transformation from Ca_2-P, Al-P, O-P, Ca_{10}-P to Po in PM. The treatments with chemical fertilizers (PCS + F, PCS + F + OM and PCS + F + BM) increased total P concentration in PM to a level similar to that in OM, Po by 74.1-108 mg kg^{-1}, accounting for 20.6-31.9% of in the total P, lower than that in the Mollisol. The results from the present study indicate that agricultural practices with fertilizer application can enhance the accumulation of P during soil development from parent materials of a Mollisol in semi-arid and semi-humid climatic regions in a relatively short period. This information has important implications in the restoration of degraded Mollisols. The further studies are warranted to detect the mechanisms of P transformation during the process of fertility restoration.

Acknowledgement. The study was supported by the National Basic Research Program of China (No. 2016YFD0300806, 2016YFD0200309 and 2017YFD0300605), the Natural Science Foundation of China (NSFC) (41771327, 41671299 and 41807085), China Agriculture Research System (CARS04), Applied Technology Research and Development Program of Heilongjiang (GY2017ZB006). We are grateful to Zheli He for his modification for the manuscript.

REFERENCES

[1] Allen, B. L., Mallarino, A. P. (2006): Relationships between extractable soil phosphorus and phosphorus saturation after long-term fertilizer or manure application. – Soil Science Society of America Journal 70: 454-463.
[2] Anderson, G. (1960): Factors affecting the estimation of phosphate-esterin soils. – Journal of Food Agriculture & Environment 11: 497-503.
[3] Bowman, R. A., and Cole, C. V. (1978): An exploratory method for fractionation of organic phosphorus from grassland soils. – Soil Sciences 125: 95-101.
[4] Chang, S. C., Jackson, M. L. (1957): Fractionation of soil labile inorganic phosphorus. – Soil Sciences 84: 133-144.

http://www.aloki.hu ● ISSN 1589 1623 (Print) ● ISSN 1785 0037 (Online)
DOI: http://dx.doi.org/10.15666/aeer/1802_29352948

[5] Fageria, N. K., Baligar, V. C., Li, Y. C. (2008): The role of nutrient efficient plants in improving crop yield in the twenty first century. – Journal of Plant Nutrient 31(6): 1121-1157.
[6] Fan, Y. K., Xiong, H. D., Li, S. J. (1999): Some improvements of the fractionation method of organic phosphorus in calcareous soils. – Geoderma 193: 195-206.
[7] Griffiths, B. S., Liu, Q., Wang, H. L., Zhang, B., Kuan, H. L., McKenzie, B. M., Hallett, P. D., Daniell, T. J. (2008): Restoration of soil physical and biological stability are not coupled in response to plants and earthworms. – Restoration Ecology 26: 102-104.
[8] Guppy, C. N., Menzies, N. W., Moody, P. W., Blamey, F. P. C. (2005): Competitive sorption reactions between phosphorus and organic matter on soil: a review. – Australian Journal of Soil Research 43: 189-202.
[9] Han, X. Z., Song, C. Y., Wang, S. Y., Tang, C. (2005a): Impact of long-term fertilization on phosphorus status in black soil. – Pedosphere 319-326.
[10] Han, X. Z., Song, C. Y., Wang, S. Y., Qiao, Y. F. (2005b): Phosphorus characteristics correlate with soil fertility of albic luisols. – Plant and Soil 270: 47-56.
[11] Harris, J. (2009): Soil microbial communities and restoration ecology: facilitators or followers? – Science 325: 573-574.
[12] Harrison, R. B., Strahm, B. (2008): Soil Formation. – In: Jørgensen, S. E., Fath, B. D. (eds.) Encyclopedia of Ecology. Elsevier, Amsterdam, pp. 3291-3295.
[13] Hedley, M. J., Stewart, J. W. B., Chauhan, B. S. (1982): Changes in inorganic and organic soil phosphorus fractions induced by cultivation practices and by laboratory incubations. – Soil Science Society of America Journal 46: 970-976.
[14] Hou, E. Q., Chen, C. R., Wen, D. Z., Liu, X. (2014): Relationships of phosphorus fractions to organic carbon content in surface soils in mature subtropical forests, Dinghushan, China. – Soil Research 52: 55-63.
[15] Jackson, M. L. (1973): Soil Chemical Analysis. – Prentice Hall, New Delhi.
[16] Jiang, B. F., Gu, Y. C. (1989): A suggested fraction scheme of inorganic phosphorus in calcareous soils. – Scientia Agricultura Sinica 22: 58-66.
[17] Jin, X. D., He, Y. L., Kirumba, G., Haunas, Y., Li, J. B. (2013): Phosphorus fractions and phosphate sorption-release characteristics of the sediment in the Yangtze River estuary reservoir. – Ecology Engineer 55: 62-66.
[18] Li, L., Li, X. H., Li, X. Y., Li, Y. T., Zhao, B. Q. (2005): Effect of long term fertilization on accumulation, transformation and availability of phosphorous in Fluva-aquic soil. – Soil Fertility 3: 32-35.
[19] Li, N., Yao, S. H., You, M. Y., Zhang, Y. L., Qiao, Y. F., Zou, W. X., Han, X. Z., Zhang, B. (2014): Contrasting development of soil microbial community structure under no-tilled perennials and tilled cropping at the initial formation stage of a Mollisol from parent material. – Soil Biology Biochemistry 77: 221-232.
[20] Li, N., Pan, F. J., Han, X. Z., Zhang, B. (2016): Development of soil food web of microbes and nematodes under different agricultural practices during the early stage of pedogenesis of a Mollisol. – Soil Biology Biochemistry 98: 208-216.
[21] Lu, X. C., Zou, W. X., Han, X. Z., Hao, X. X., Jiang, H. (2015): Effect of long term fertilization on phosphorous and zinc fractions in a Mollisol. – Journal of Plant Nutrition and Fertilizers 21(6): 1536-1542.
[22] Miao, S. J., Qiao, Y. F., Yin, Y. F., Jin, J., Martin, B., Liu, X. B., Tang, C. X. (2019): Ten-year application of cattle manure contributes to the build-up of soil organic matter in eroded Mollisols. – Journal of Soils and Sediments 19(7): 3035-3043.
[23] Milic, S., Ninkov, J., Zeremski, T., Latković, D., Šeremešić, S., Radovanović, V., Žarković, B. (2019): Soil fertility and phosphorus fractions in a calcareous chernozem after a long-term field experiment. – Geoderma 339: 9-19.
[24] Motavalli, P. P., Miles, R. J. (2002): Soil fractions after 111 years of animal manure and fertilizer application. – Biology and Fertility of Soils 36: 35-42.

http://www.aloki.hu ● ISSN 1589 1623 (Print) ● ISSN 1785 0037 (Online)
DOI: http://dx.doi.org/10.15666/aeer/1802_29352948

[25] Nobile, C. M., Bravin, M. N., Becquer, T., Pailat, J. M. (2020): Phosphorus sorption and availability in an andosol after a decade of organic or mineral fertilizer applications: Importance of pH and organic carbon modifications in soil as compared to phosphorus accumulation. – Chemosphere 239: 1-10.
[26] Olsen, S. R., Cole, C., Watanabe, F. C., Dean, L. A. (1954): Estimation of Available Phosphorus in Soils by Extraction with Sodium Bicarbonate. – USDA Cir. 939. USDA, Washington, DC.
[27] Pätzold, S., Hejcman, M., Barej, J., Schellberg, J. (2013): Soil phosphorus fractions after seven decades of fertilizer application in the Rengen Grassland Experiment. – Journal of Plant Nutrition and Soil Science 176: 910-920.
[28] Perroni, Y., García-Oliva, F., Tapia-Torres, Y., Souza, V. (2014): Relationship between soil P fractions and microbial biomass in an oligotrophic grassland-desert scrub system. – Ecology Research 29: 463-472.
[29] Qiao, Y. F., Miao, S. J., Han, X. Z., You, M. Y., Zhu, X., Horwath, W. R. (2014): The effect of fertilizer practices on N balance and global warming potential of maize-soybean-wheat rotations in Northeastern China. – Field Crops Research 161: 98-106.
[30] Reddy, D. D., Rao, A. S., Rupa, T. R. (2000): Effects of continuous use of cattle manure and fertilizer phosphorus on crop yields and soil organic phosphorus in a Vertisol. – Bioresource Technology 75(2): 113-118.
[31] Richardson, A. E., Simpson, R. J. (2011): Soil microorganisms and phosphorus availability. – Plant Physiology 156(3): 989-996.
[32] Soil Survey Staff (2014): Keys to Soil Taxonomy. 12th Ed. – United States Department of Agriculture, Natural Resources Conservation Service, Government Printing Office, Washington, DC.
[33] Song, C., Han, X. Z. (2007): Phosphorous fertility characteristics of black soil under different types of land use. – Chinese Journal of Soil Science 38(5): 928-933.
[34] Song, C., Han, X. Z., Tang, C. (2007): Changes in phosphorus fractions, sorption and release in Udic Mollisols under different ecosystems. – Biology Fertility and Soils 44: 37-47.
[35] Song, C., Han, X. Z., Wang, E. L. (2011): Phosphorus budget and organic phosphorus fractions in response to long-term applications of chemical fertilizers and pig manure in a Mollisol. – Soil Research 49: 253-260.
[36] Sun, D. S., Bi, Q. F., Li, K. J., Dai, P. B., Yu, Y., Zhou. W. W., lv, T., Liu, X. P., Zhu, J., Zhang, Q. C., Jin, C. W., Lu, L. L., Lin, X. Y. (2018): Significance of temperature and water availability for soil phosphorus transformation and microbial community composition as affected by fertilizer sources. – Biology and Fertility of Soils 24: 229-241.
[37] van der Bom, F. J. T., McLaren, T. I., Doolette, A. L., Magid, J., Frossard, E., Oberson, A., Jensen, L. S. (2019): Influence of long-term phosphorus fertilisation history on the availability and chemical nature of soil phosphorus. – Geoderma 355: 1-12.
[38] Vanden Nest, T., Ruysschaert, G., Vandecasteele, B., Houot, S., Baken, S., Smolders, E., Cougnon, M., Reheul, D., Merckx, R. (2016): The long term use of farmyard manure and compost: Effects on P availability, orthophosphate sorption strength and P leaching. – Agriculture, Ecosystems & Environment 216: 23-33.
[39] Wei, X. R., Shao, M. A., Shao, H. B., Gao, J. L., Xu, G. (2011): Fractions and bioavailability of soil inorganic phosphorus in the Loess Plateau of China under different vegetations. – Acta Geological Sinica 85(1): 263-270.
[40] Xiang, W. S., Huang, M., Li, X. Y. (2004): Progress on fractioning of soil phosphorous and availability of various phosphorous fractions to crops in soil. – Journal of Plant Nutrition and Fertilizers 10(6): 663-670.
[41] Xiong, Y. Q., Li, K. (1987): Soils in China. – Science Press, Beijing.
[42] Yang, C. M., Yang, L. Z., Jianhua, L. (2006): Organic phosphorus fractions in organically amended paddy soils in continuously and intermittently flooded conditions. – Journal of Environmental Quality 35: 1142-1150.

http://www.aloki.hu ● ISSN 1589 1623 (Print) ● ISSN 1785 0037 (Online)
DOI: http://dx.doi.org/10.15666/aeer/1802_29352948

[43] You, M. Y., Burger, M., Li, L. J., Zou, W. X., Li, N., Qiao, Y. F. (2014): Changes in soil organic carbon and carbon fractions under different land use and management practices after development from parent material of Mollisols. – Soil Science 179: 205-210.
[44] You, M. Y., Li, N., Zou, W. X., Han, X. Z., Burger, M. (2017): Increase in soil organic carbon in a Mollisol following simulated initial development from parent material. – European Journal of Soil Science 68: 39-47.

http://www.aloki.hu ● ISSN 1589 1623 (Print) ● ISSN 1785 0037 (Online)
DOI: http://dx.doi.org/10.15666/aeer/1802_29352948

CULTIVAR AND FOLIAR FEEDING OF PLANTS AS FACTORS DETERMINING THE CHEMICAL COMPOSITION OF SPELT (*TRITICUM AESTIVUM* SSP. *SPELTA* L.) GRAIN

ANDRUSZCZAK, S.[1*] – KRASKA, P.[1] – KWIECIŃSKA-POPPE, E.[1] – SKOWROŃSKA, M.[2]

[1]*University of Life Sciences in Lublin, Department of Herbology and Plant Cultivation Techniques, Institute of Agricultural Ecology, Akademicka 13, 20-950 Lublin, Poland*

[2]*University of Life Sciences in Lublin, Department of Agricultural and Environmental Chemistry, Akademicka 15, Lublin, Poland*

[*]*Corresponding author*
e-mail: sylwia.andruszczak@up.lublin.pl; phone: +48-81-445-66 87

(Received 11th Nov 2019; accepted 12th Feb 2020)

Abstract. Due to the constantly increasing interest in growing spelt, research on the effects of different agronomic factors on grain quantity and quality is still valid and necessary. Nevertheless, the available literature lacks comprehensive studies on optimization of spelt mineral fertilization, especially concerning grain chemical composition. The aim of this study was to evaluate some grain quality characteristics and macro- and micronutrient content in grain of winter spelt cultivars ('Oberkulmer Rotkorn', 'Badengold', 'Frankenkorn') depending on foliar fertilizers applied (Santaura Pro+ or Prohorti Micro Amin Mg). Fertilizers were applied three times during the spelt growing season. The chemical composition of spelt grain was mostly dependent on cultivar and weather conditions during the crop growing season. The highest N, Ca, Mn, Fe, and Zn contents were determined in grain of the cultivar 'Oberkulmer Rotkorn'. Moreover, this cultivar contained most protein and gluten and was characterized by the highest sedimentation index. Grain of cv. 'Badengold', in turn, was poorest in terms of protein and gluten and, at the same time, exhibited the lowest N, P, Mg, Ca, Mn, Fe, and Zn content. Application of foliar fertilizers increased N, P, K, Cu and Mn content in spelt grain compared to plants grown without foliar fertilization.
Keywords: *macro- and micronutrients, protein, gluten, sedimentation index, biofortification*

Introduction

To reduce the dominant position of common wheat as a basic food material, a growing interest has been observed in the cultivation of ancient wheat forms in recent years. One of them is spelt wheat (*Triticum aestivum* ssp. *spelta* L.), belonging to the biological species *T. aestivum* L. Spelt played an important role in nutrition in old Europe, becoming the main bread cereal. With time, however, it lost its importance and its crop area gradually declined (Arzani and Ashraf, 2017). For some period of time, spelt was a forgotten cereal, but during the last 20 years its popularity has been growing. Spelt is valued due to its favorable chemical composition and high nutrient uptake (Ziegler et al., 2016). Its grain is particularly rich in some minerals and vitamins as well as in active biological substances with antioxidant properties (Suchowilska et al., 2012; Świeca et al., 2014; Andruszczak, 2017; Zrcková et al., 2019). According to some authors, it is characterized by a more favorable chemical composition compared to common wheat cultivars because it contains more protein, gluten, amino acids, dietary fiber, fat-soluble vitamins (A, D, and E), and unsaturated fatty acids (Ruibal-Mendieta et al., 2005; Gomez-Becerra et al., 2010; Escarnot et al., 2012; Jablonskyte-Rašče et al., 2013; Stępień et al., 2016). It has been proven that consumption of spelt wheat promotes a reduction in blood

http://www.aloki.hu ● ISSN 1589 1623 (Print) ● ISSN1785 0037 (Online)
DOI: http://dx.doi.org/10.15666/aeer/1802_29492958

cholesterol, supports digestive system activity, and reduces the risk of diseases related to the formation of gallstones in the body (Abdel-Aal and Rabalski, 2008).

The cultivar factor plays a major role in determining the chemical composition of cereal grains. Habitat conditions are also of essential importance, whereas agronomic practices, fertilization in particular, have a smaller impact (Cazzato et al., 2013). In modern agriculture, a proper cereal fertilization strategy should include not only soil fertilization, but also foliar feeding of plants. Such treatment enables quick supply of macro- and micronutrients both in the case of their deficiency in soil and inhibited nutrient uptake by root system (Mikos-Szymańska et al., 2018). Foliar fertilizer application is particularly advisable during the period of critical nutrient requirement of cereals, i.e. at stem elongation stage. In the case of micronutrients, foliar fertilization can essentially meet plants' requirement for these nutrients (Bharti et al., 2013). An insufficient amount of micronutrients in a plant leads to its reduced resistance to adverse habitat conditions and, as a consequence, to a decrease in yield and deteriorated grain quality (Potarzycki and Grzebisz, 2009).

The present study hypothesized that foliar application of the compound fertilizers Santaura Pro+ and Prohorti Micro Amin Mg would improve macro- and micronutrient supply to plants and beneficially affect the processing quality of spelt wheat grain. The aim of this study was to determine mineral content and also protein, gluten, and starch content as well as sedimentation index in spelt wheat grain depending on cultivar and foliar plant feeding.

Materials and methods

Field experiment and cultivation management

A field experiment was conducted over the period 2015–2017 at the Bezek Experimental Farm located near the city of Chełm (51°19′ N, 23°25′ E), Poland. The experiment was set up on *Rendzic Phaeozem* [WRB, 2006] derived from Cretaceous bedrock and with a texture of loam. It was characterized by alkaline pH, and the content of minerals was as follows: N_{total} – 3.05 g kg^{-1}, K – 194.7 mg kg^{-1}, P – 406.4 mg kg^{-1}, Mg – 17.9 mg kg^{-1}, S-SO_4 – 4.1 mg kg^{-1}, Zn – 22.33 mg kg^{-1}, Mn – 195.83 mg kg^{-1}, Cu – 2.55 mg kg^{-1}, Fe – 176.76 mg kg^{-1}. The content of C_{org} was 31.3 g kg^{-1}.

A two-factor field experiment was established in a split-plot design in triplicate with a plot area up to 12 m². The experimental design included three winter spelt wheat cultivars, i.e. 'Oberkulmer Rotkorn', 'Badengold', and 'Frankenkorn'. The second research factor was application of foliar fertilizers Santaura Pro+ (SDP – Société de Distribution et de Prestation, France) or Pro Horti Micro Amin Mg (Adob, Poland). The fertilizers were applied three times during the spelt growing season, i.e. at tillering (BBCH 23-25), stem elongation (BBCH 33-35), and heading (BBCH 53-55), at rates of 1 l ha^{-1} and 4 kg ha^{-1}, respectively. The fertilizers were dissolved in 300 l of water per hectare. The control treatment comprised plots without foliar fertilization. Santaura Pro+ is an organic fertilizer obtained from sea algae, which contains nitrogen in the organic form (8%), potassium (K_2O 3%), and micronutrients (iron, manganese, boron, zinc, copper), while its organic matter content is 20%. Pro Horti Micro Amin Mg fertilizer includes the following components: total nitrogen (2.0%), ammonium nitrogen (2%), magnesium oxide (20.0%), sulfur trioxide (39.3%), boron (0.05%), water soluble molybdenum (0.01%), amino acids (5.0%), IDHA (D,L-Aspartic acid, (N-1,2 dicarboxyethyl)-

http://www.aloki.hu ● ISSN 1589 1623 (Print) ● ISSN1785 0037 (Online)
DOI: http://dx.doi.org/10.15666/aeer/1802_29492958

tetrasodium salt) chelated zinc (0.1%), IDHA chelated copper (0.05%), IDHA chelated iron (0.15%) and IDHA chelated manganese (0.2%).

The previous crop of spelt was oats. Spelt spikelets were sown at the beginning of October at an amount of 350 kg per hectare. The thousand kernel weight of spelt was 41 g. Mineral fertilization was as follows (in kg of pure ingredient per hectare): N 60 (20+40); P 26.2; K 83. Phosphate and potassium fertilizers as well as 20 kg N ha^{-1} were applied before sowing spelt. In spring, 40 kg N ha^{-1} was applied at stem elongation stage (BBCH 32-34).

Chemical analysis of spelt grain

Grain for chemical analysis was harvested every year at fully ripe stage of spelt (BBCH 89) following the methodology used in experiments on cereals (Ostrowska et al., 1991). Spikelet samples were collected in triplicate in three randomly selected places on each plot, delineated by a 1 m x 0.5 m rectangular frame. After harvest, the collected spelt spikelets were threshed in a Wintersteiger LD 180 thresher. The following elements was determined: N (Kjeldahl method), P (spectrophotometrically), K and Ca (flame photometry), Mg, Cu, Zn, Mn, Fe (atomic absorption spectrometry (AAS)), and B (spectrophotometric curcumin method). The chemical analysis was carried out in an accredited laboratory (accreditation certificate No. AB 1375 issued by the Polish Centre for Accreditation), which meets the requirements of the PN-EN ISO/IEC 17025:2005 standard.

Grain total protein, gluten, and starch content as well as Zeleny sedimentation index were determined using an OmegAnalyzer G computer transmission analyzer of whole grain (Bruins Instruments, Germany).

Statistical analysis

The obtained results were statistically analyzed by analysis of variance. The means were compared using least significant differences based on Tukey's test ($P \leq 0.05$). Calculations were made using ARSTAT statistical software, developed at the Faculty of Applied Mathematics and Information Technology of the University of Life Sciences in Lublin.

Weather conditions

During the field experiment, the average air temperature was generally higher than the long-term average from 1.0°C in the 2016–2017 growing season to 2.2°C in the 2015-2016 season (*Fig. 1*). In the 2014–2015 season, the total rainfall was lower than the long-term average for the relevant period by 23%, while the highest rainfall deficit was found during the period from September to November and also from July to August. The second year of the experiment was much wetter and in that year the total rainfall was higher than the long-term average by 31%. The total rainfall during the 2016–2017 season was close to the long-term average, but the rainfall distribution during the crop growing season varied. The most moisture was recorded in October – in that month the total rainfall exceeded three times the long-term average. In June and August, in turn, a significant rainfall deficit was observed; compared to the long-term average, the amount of rainfall was lower by 65% and 44%, respectively.

http://www.aloki.hu ● ISSN 1589 1623 (Print) ● ISSN1785 0037 (Online)
DOI: http://dx.doi.org/10.15666/aeer/1802_29492958

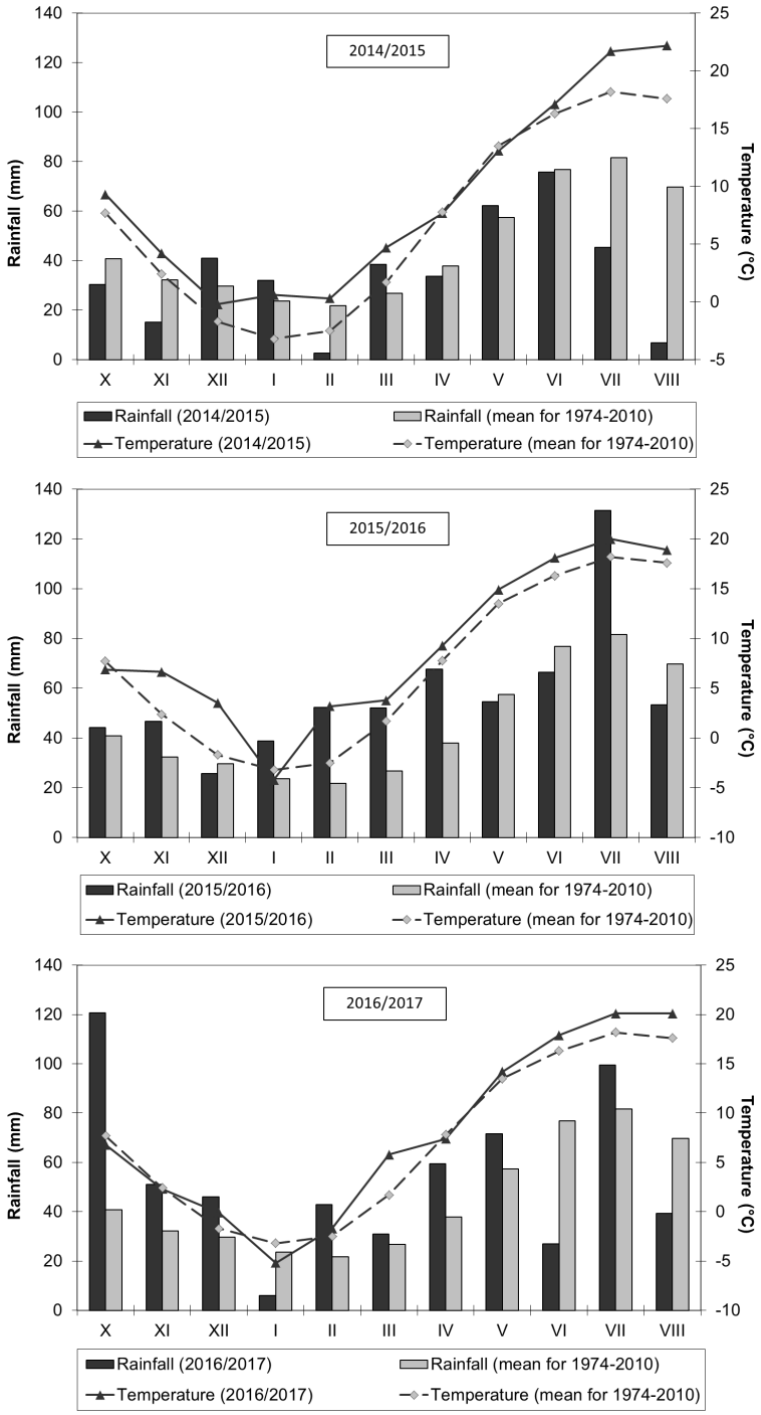

Figure 1. *Weather conditions during the research compared to the long-term period*

Results and discussion

This study shows that the genetic factor had a significantly differential effect on the contents of all macronutrients evaluated in spelt grain (*Table 1*). Among the cultivars studied, most N and Ca were found in grain of cv. 'Oberkulmer Rotkorn'. Cv. 'Frankenkorn' contained most P and Mg, while cv. 'Badengold', in turn, was characterized by the highest K content. At the same time, grain of cv. 'Badengold' was

http://www.aloki.hu ● ISSN 1589 1623 (Print) ● ISSN1785 0037 (Online)
DOI: http://dx.doi.org/10.15666/aeer/1802_29492958

found to have a significantly lower N, P, and Ca content in comparison to the other cultivars, whereas relative to cv. 'Frankenkorn' – a significantly lower Mg content. The obtained results corroborate the studies of other authors which indicate high variation in the mineral composition of spelt grain due to the genotype (Gomez-Becerra et al., 2010; Andruszczak, 2018; Kraska et al., 2019).

Table 1. *The content of macroelements in spelt wheat grain depending on experimental factors (g kg^{-1})*

Factor	N	P	K	Mg	Ca
Cultivars					
Oberkulmer R. (OR)	24.44 a*	3.937 a	3.295 a	1.184 ab	0.238 a
Badengold (B)	21.03 b	3.768 b	3.484 b	1.132 a	0.203 b
Frankenkorn (F)	23.25 c	4.019 c	2.766 c	1.250 b	0.225 a
Foliar fertilizers					
Control object (K)	22.71 a	3.826 a	3.103 a	1.169 a	0.219 a
Santaura Pro+ (S)	22.99 b	3.994 b	3.278 b	1.194 a	0.221 a
Prohorti Micro Amin Mg (P)	23.03 b	3.904 c	3.164 a	1.203 a	0.226 a
Years					
2015	22.07 a	3.874 a	3.162 a	1.619 a	0.308 a
2016	27.27 b	4.211 b	2.993 b	1.024 b	0.189 b
2017	19.39 c	3.639 c	3.390 c	0.923 b	0.168 b

* different letters indicate significant differences at $P \leq 0.05$)

Foliar feeding of plants did not have a significant effect on magnesium and calcium content in spelt grain. On the other hand, it resulted in a significant increase in nitrogen and phosphorus content compared to the control treatment. At the same time, this study demonstrated that spelt wheat fertilized with the fertilizer Prohorti Micro Amin Mg contained significantly less phosphorus and potassium in grain compared to plants fertilized with Santaura Pro+. Existing research shows different directions in changes in the chemical composition of cereal grains as influenced by foliar fertilization. Seadh et al. (2009) revealed a beneficial impact of foliar application of micronutrients on N, P, and K content in wheat grain. In turn, in a study by Majcherczak et al. (2006) foliar application of micronutrient fertilizer and copper caused a significant decrease in K content in spring barley grain, whereas zinc and manganese application reduced P concentration.

In the opinion of Kraska et al. (2013) and Gomez-Becerra et al. (2010), mineral content in spelt grain is significantly affected by habitat conditions, in particular weather conditions. This is confirmed by the present study which showed spelt wheat to exhibit high sensitivity to variable weather conditions during the study period. Spelt grain harvested in 2015 was characterized by a significantly higher Mg and Ca content compared to the other years. In the second year of the experiment, the highest grain N and P content and at the same time the lowest K content were obtained, whereas the pattern of weather conditions in 2017 was least favorable for macronutrient content. The then recorded rainfall deficit during spelt flowering and grain ripening, coupled with high air temperature, caused a significant decrease in N, P, Mg, and Ca content in grain, whereas the amount of K increased.

Micronutrient content is an important characteristic from the point of view of the consumer and the nutritional value of a food material. Even though micronutrients are taken up by plants in small amounts, they perform important physiological functions, participating in many metabolic reactions occurring in plants (Potarzycki and Grzebisz,

http://www.aloki.hu ● ISSN 1589 1623 (Print) ● ISSN1785 0037 (Online)
DOI: http://dx.doi.org/10.15666/aeer/1802_29492958

2009). The present study reveals that the cultivar factor caused significant differences in Mn, Zn, and Fe content in spelt grain, while Cu and B content showed small variations (*Table 2*). Most micronutrients were found in grain of cv. 'Oberkulmer Rotkorn', whereas cv. 'Badengold' grain was poorest in Mn, Fe, and Zn. The obtained Mn and Fe contents in spelt grain did not substantially differ from the values found for the same cultivars by Kraska et al. (2013). However, these authors demonstrated a much higher Cu and Zn content in grain.

Table 2. *The content of microelements in spelt wheat grain depending on experimental factors (mg kg^{-1})*

Factor	Cu	Mn	Fe	Zn	B
Cultivars					
Oberkulmer R. (OR)	3.747 a*	33.56 a	42.29 a	27.97 a	1.227 a
Badengold (B)	3.563 a	28.11 b	31.57 b	23.63 b	1.246 a
Frankenkorn (F)	3.472 a	31.10 c	40.91 a	26.27 c	1.271 a
Foliar fertilizers					
Control object (K)	3.391 a	30.11 a	37.49 a	25.51 a	1.223 a
Santaura Pro+ (S)	3.417 a	32.11 b	38.16 a	26.47 a	1.247 a
Prohorti Micro Amin Mg (P)	3.973 b	30.56 a	39.12 a	25.89 a	1.273 a
Years					
2015	3.408 a	48.23 a	39.92 a	23.74 a	1.251 a
2016	2.662 b	19.99 b	39.54 a	26.39 b	1.237 a
2017	4.712 c	24.56 c	35.31 b	27.74 c	1.256 a

* different letters indicate significant differences at P≤0.05)

Application of the compound foliar fertilizers Santaura Pro+ and Prohorti Micro Amin Mg, compared to the control treatment resulted in significant increase in Mn and Cu concentration in spelt grain, respectively. On the other hand, foliar fertilization did not affect Fe, Zn, and B content. In a study by Knapowski et al. (2017), foliar application of manganese and copper in the form of Adob Mn and Adob Cu fertilizers significantly increased the content of these elements in spelt grain, at the same time reducing Zn content. In turn, Wojtkowiak and Stępień (2015), who applied foliar fertilization of spelt wheat with copper, zinc, and manganese, found grain Fe, Zn, and Mn content to increase.

Micronutrient content (except for B) in spelt grain was significantly affected by weather conditions, which was also confirmed by Gomez-Becerra et al. (2010) as well as by Wojtkowiak and Stępień (2015) in their studies. In the first year of the experiment, spelt grain was characterized by the highest Mn and Fe content, whereas significantly more Cu and Zn were found in grain harvested in 2017 compared to the other years.

Baking quality, which characterizes the suitability of flour for making bread products with appropriate quality characteristics, can be indirectly determined using processing quality parameters such as total protein and gluten content. The present study demonstrates that the spelt cultivars compared differed in terms of grain protein content, which ranged from 13.2% to 15.9%. Cv. 'Oberkulmer Rotkorn' exhibited the significantly highest protein and gluten content, while cv. 'Badengold', in turn, was poorest in these components (*Figures 2* and *3*). Jablonskytė-Raščė et al. (2013) showed similar contents of this component in their research, while Wojtkowiak and Stępień (2015) determined protein content to range between 12.4% and 13.5%.

http://www.aloki.hu ● ISSN 1589 1623 (Print) ● ISSN1785 0037 (Online)
DOI: http://dx.doi.org/10.15666/aeer/1802_29492958

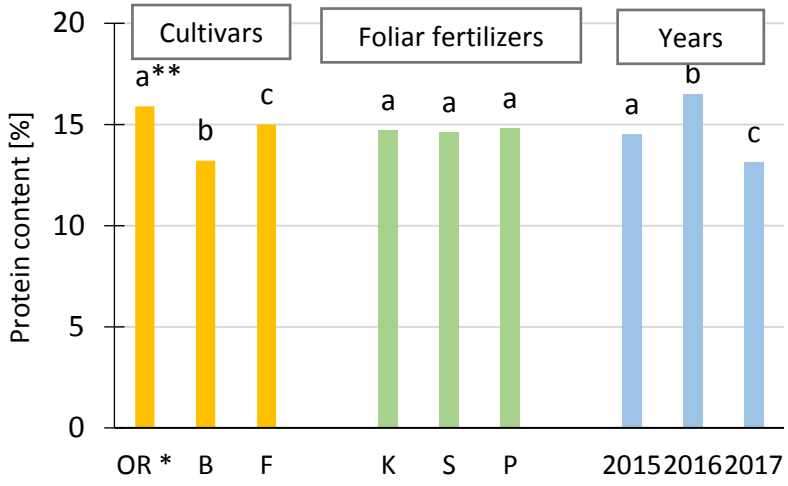

Figure 2. *The protein content in spelt wheat grain depending on experimental factors (* OR – Oberkulmer Rotkorn, B – Badengold, F – Frankenkorn, K – control object without foliar fertilization, S – Santaura Pro+, P – Prohorti Micro Amin Mg; ** different letters indicate significant differences at P≤0.05)*

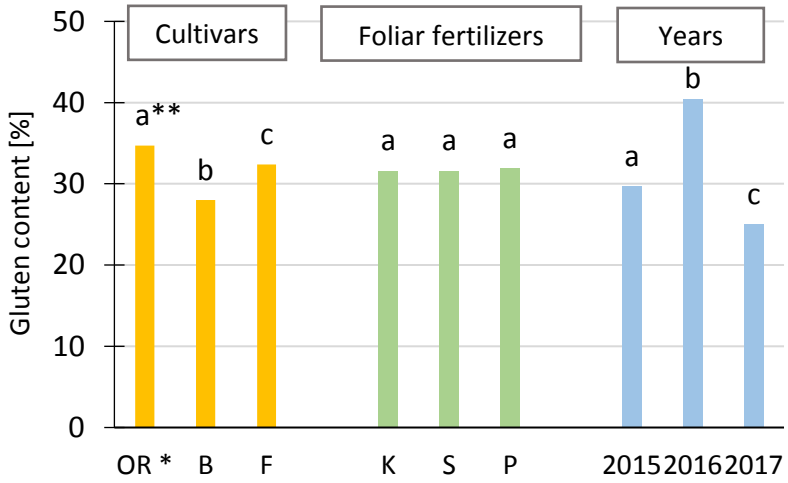

Figure 3. *The gluten content in spelt wheat grain depending on experimental factors (* OR – Oberkulmer Rotkorn, B – Badengold, F – Frankenkorn, K – control object without foliar fertilization, S – Santaura Pro+, P – Prohorti Micro Amin Mg; ** different letters indicate significant differences at P≤0.05)*

In a study on the winter spelt cultivar 'Rokosz', Knapowski et al. (2016) proved that foliar application of micronutrients has a beneficial effect on grain quality traits. This study did not confirm such a relationship. The protein and gluten content in spelt grain under application of the fertilizers Santaura Pro+ and Prohorti Micro Amin Mg and in the control treatment was similar. Significant differences were however found between years. Grain harvested in 2016 contained most protein and gluten, whereas the lowest contents of these components were shown in the last year of the study (*Figures 2* and *3*).

http://www.aloki.hu ● ISSN 1589 1623 (Print) ● ISSN1785 0037 (Online)
DOI: http://dx.doi.org/10.15666/aeer/1802_29492958

Starch content in spelt grain was significantly dependent on cultivar and weather conditions during the growing season, but foliar fertilizer application did not result in significant differences in this trait (*Figure 4*).

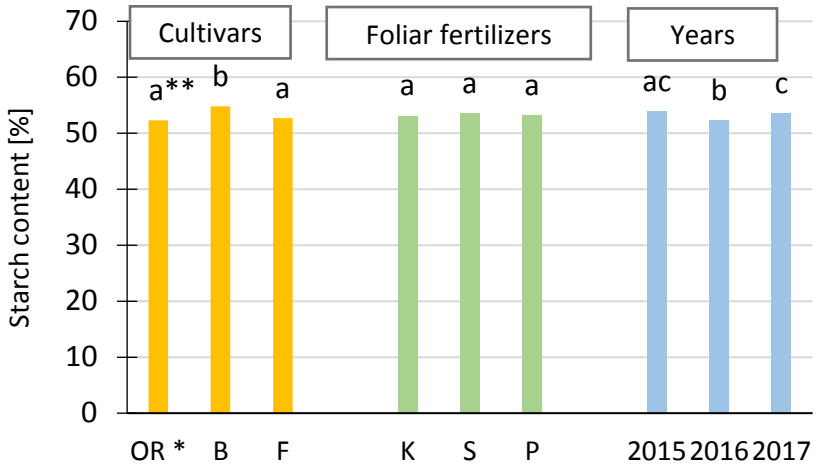

Figure 4. *The starch content in spelt wheat grain depending on experimental factors (* OR – Oberkulmer Rotkorn, B – Badengold, F – Frankenkorn, K – control object without foliar fertilization, S – Santaura Pro+, P – Prohorti Micro Amin Mg; ** different letters indicate significant differences at P≤0.05)*

Among the spelt cultivars in question, the highest sedimentation index was found in the case of cv. 'Oberkulmer Rotkorn', its value was significantly lower for cv. 'Frankenkorn', whereas the lowest value of this index was obtained for cv. 'Badengold' (*Figure 5*). The experiment did not prove that application of the fertilizers Santaura Pro+ and Prohorti Micro Amin Mg had a significant effect on Zeleny sedimentation index, but this study found significant differences in the values of this index between years – the highest sedimentation value was obtained for grain harvested in 2016.

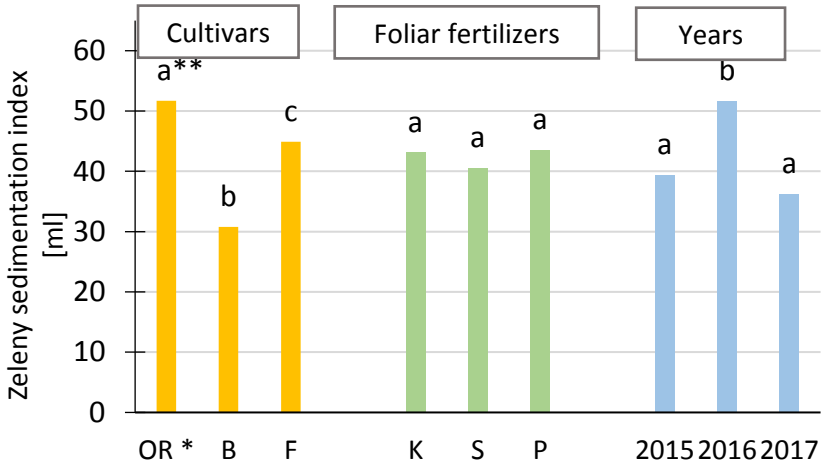

Figure 5. *The Zeleny sedimentation index of spelt wheat grain depending on experimental factors (* OR – Oberkulmer Rotkorn, B – Badengold, F – Frankenkorn, K – control object without foliar fertilization, S – Santaura Pro+, P – Prohorti Micro Amin Mg; ** different letters indicate significant differences at P≤0.05)*

http://www.aloki.hu ● ISSN 1589 1623 (Print) ● ISSN1785 0037 (Online)
DOI: http://dx.doi.org/10.15666/aeer/1802_29492958

Conclusions

To sum up, it should be stated that the chemical composition of spelt grain was determined by the individual characteristics of a specific cultivar, weather conditions during the crop growing season, as well as foliar application of the fertilizers Santaura Pro+ and Prohorti Micro Amin Mg.

Most N, Ca, Mn, Fe, and Zn were found in grain of the cultivar 'Oberkulmer Rotkorn'. This cultivar was also distinguished by the highest protein and gluten content as well as the highest sedimentation index. In turn, grain of cv. 'Badengold' was characterized by the least favorable chemical composition since it contained the least N, P, Mg, Ca, Mn, Fe, and Zn, and was also poorest in protein and gluten.

Application of foliar fertilizers significantly increased N and P content in spelt grain. In addition, Santaura Pro+ had a positive effect on the K and Mn content, while Prohorti Micro Amin Mg caused the increase in Cu content compared to spelt grown without foliar fertilization.

Due to the constantly growing interest in spelt cultivation, research on the effect of biofortification on grain quality is still valid and necessary. An interesting aspect, however, seems to be testing other foliar fertilizers to improve grain nutritional value. At the same time, it is worth considering more varieties of spelt in the study to draw more general conclusions.

Acknowledgements. This research was supported by the Ministry of Science and Higher Education in Poland.

REFERENCES

[1] Abdel-Aal, E. S. M., Rabalski, I. (2008): Bioactive compounds and their antioxidant capacity in selected primitive and modern wheat species. – The Open Agriculture Journal 2: 7-14.

[2] Andruszczak, S. (2017): Reaction of winter spelt cultivars to reduced tillage system and chemical plant protection. – Zemdirbyste-Agriculture 1: 15-22.

[3] Andruszczak, S. (2018): Spelt wheat grain yield and nutritional value response to sowing rate and nitrogen fertilization. – Journal of Animal and Plant Science 5: 1476-1484.

[4] Arzani, A., Ashraf, M. (2017): Cultivated ancient wheats (*Triticum* ssp.): a potential source of health-beneficial products. – Comprehensive Reviews in Food Science and Food Safety 16: 477-488.

[5] Bharti, K., Pandey, N., Shankhdhar, D., Srivastava, P. C., Shankhdhar, S. C. (2013): Improving nutritional quality of wheat through soil and foliar zinc application. – Plant, Soil and Environment 8: 348-352.

[6] Cazzato, E., Tufarelli, V., Laudadio, V., Stellacci, A. M., Selvaggi, M., Leoni, B., Troccoli, C. (2013): Forage yield and quality of emmer (*Triticum dicoccum* Schubler) and spelt (*Triticum spelta* L.) as affected by harvest period and nitrogen fertilization. – Acta Agriculturae Scandinavica, Section B: Soil and Plant Science 7: 571-578.

[7] Escarnot, E., Jacquemin, J. M., Agneessens, R., Paquot, M. (2012): Comparative study of the content and profiles of macronutrients in spelt and wheat (a review). – Biotechnology, Agronomy, Society and Environment (BASE) 16: 243-256.

[8] Gomez-Becerra, H. F., Erdemb, H., Yazici, A., Tutusa, Y., Torun, B., Ozturk, L., Cakmak, I. (2010): Grain concentrations of protein and mineral nutrients in a large collection of spelt wheat grown under different environments. – Journal of Cereal Science 3: 342-349.

http://www.aloki.hu ● ISSN 1589 1623 (Print) ● ISSN1785 0037 (Online)
DOI: http://dx.doi.org/10.15666/aeer/1802_29492958

[9] Jablonskytė-Raščė, D., Maikštėnienė, S., Mankevičienė, A. (2013): Evaluation of productivity and quality of common wheat (*Triticum aestivum* L.) and spelt (*Triticum spelta* L.) in relation to nutrition conditions. – Zemdirbyste-Agriculture 1: 45-55.
[10] Knapowski, T., Spychaj-Fabisiak, E., Kozera, W., Barczak, B., Murawska, B. (2016): Mineral fertilization and baking value of grain and flour of *Triticum aestivum* ssp. *spelta* L. – American Journal of Experimental Agriculture 4: 1-11.
[11] Knapowski, T., Kozera, W., Wszelaczyńska, E., Poberežny, J., Cieślewicz, J., Chmielewski, J. (2017): The effect of environmental conditions on the content of selected micronutrients in spelt grain. – Environmental Protection and Natural Resources 3: 26-31.
[12] Kraska, P., Andruszczak, S., Kwiecińska-Poppe, E., Pałys, E. (2013): Effect of chemical crop protection on the content of some elements in grain of spelt wheat (*Triticum aestivum* ssp. *spelta*). – Journal of Elementology 1: 79-90.
[13] Kraska, P., Andruszczak, A., Dziki, D., Stocki, M., Stocka, N., Kwiecińska-Poppe, E., Różyło, K., Gierasimiuk, P. (2019): Green grain of spelt (*Triticum aestivum* ssp. *spelta*) harvested at the stage of milk-dough as a rich source of valuable nutrients. – Emirates Journal of Food and Agriculture 4: 263-270.
[14] Majcherczak, E., Kozera, W., Nowak, K., Barczak, B. (2006): The content of macroelements and ionic ratios in spring barley grain under foliar fertilization with microelements. – Journal of Elementology 1: 43-48. (in Polish).
[15] Mikos-Szymańska, M., Borowik, M., Wyzińska, M., Rusek, P. (2018): Effects of different fertilizer treatments on grain yield and yield components of spring wheat. – Research for Rural Development 2: 100-106.
[16] Ostrowska, A., Gawliński, S., Szczubiałka, Z. (1991): Methods of analysis and assessment of soil and plant properties. – Institute of Plant Protection, Warsow.
[17] Potarzycki, J., Grzebisz, W. (2009): Effect of zinc foliar application on grain yield of maize and its yielding components. – Plant, Soil and Environment 12: 519-527.
[18] Ruibal-Mendieta, N. L., Delacroix, D. L., Mignolet, J. M. P., Marques, C., Rozenberg, R., Petitjean, G., Habib-Jiwan, J. L., Meurens, M., Qeentin-Leclerco, J., Delzenne, N. M., Larondelle, Y. (2005): Spelt (*Triticum aestivum* ssp. *spelt*a) as a source of breadmaking flours and bran naturally enriched in oleic acid and minerals but not phytic acid. – Journal of Agricultural and Food Chemistry 53: 2751-2759.
[19] Seadh, S. E., EL-Abady, M. I., El-Ghamry, A. M., Farouk, S. (2009): Influence of micronutrients foliar application and nitrogen fertilization on wheat yield and quality of grain and seed. – Journal of Biological Sciences 9: 851-858.
[20] Stępień, A., Wojtkowiak, K., Orzech, K., Wiktorski, A. (2016): Nutritional and technological characteristics of common and spelt wheats are affected by mineral fertilizer and organic stimulator Nano-Gro®. – Acta Scientiarum Polonorum, Agricultura 15(2): 49-63.
[21] Suchowilska, E., Wiwart, M., Kandler, W., Krska, R. (2012): A comparison of macro- and microelement concentrations in whole grain of four *Triticum* species. – Plant, Soil and Environment 3: 141-147.
[22] Świeca, M., Dziki, D., Gawlik-Dziki, U., Różyło, R., Andruszczak, S., Kraska, P., Kowalczyk, D., Pałys, E., Baraniak, B. (2014): Grinding and nutritional properties of six spelt (*Triticum aestivum* ssp. s*pelta* L.) cultivars. – Cereal Chemistry 3: 247-254.
[23] Wojtkowiak, K., Stępień, A. (2015): Nutritive value of spelt (*Triticum aestivum* spp. *spelta* L.) as influenced by the foliar application of copper, zinc and manganese. – Zemdirbyste-Agriculture 4: 389-396.
[24] Ziegler, J. U., Schweiggert, R. M., Würschum, T., Longin, C. F. H., Carle, R. (2016): Lipophilic antioxidants in wheat (*Triticum* spp.): A target for breeding new varieties for future functional cereal products. – Journal of Functional Foods 20: 594-605.
[25] Zrcková, M., Capouchová, I., Paznocht, L., Eliášová, M., Dvořák, P., Konvalina, P., Janovská, D., Orsák, M., Bečková, L. (2019): Variation of the total content of polyphenols and phenolic acids in einkorn, emmer, spelt and common wheat grain as a function of genotype, wheat species and crop year. – Plant, Soil and Environment 5: 260-266.

http://www.aloki.hu ● ISSN 1589 1623 (Print) ● ISSN1785 0037 (Online)
DOI: http://dx.doi.org/10.15666/aeer/1802_29492958

CORRELATION BETWEEN ECOTOURISM AND THE EVOLUTION LAW OF ZOOPLANKTON COMMUNITIES IN DONGTING LAKE TOURIST AREA OF CHINA'S HUNAN

HUANG, Z. Q.[1] – SHI, X. N.[2*]

[1]*Modern Logistics Department, Hunan Financial & Industrial Vocational-technical College, Hunan Hengyang 421002, China*

[2]*Economic and Trade Department, Hunan Financial & Industrial Vocational-technical College, Hunan Hengyang 421002, China*

[*]*Corresponding author*
e-mail: sxnxiaonong@sina.com

(Received 14th Nov 2019; accepted 12th Feb 2020)

Abstract. In order to understand the evolution of zooplankton communities in the Dongting Lake tourist area, Hunan, China, a one-year experiment was started in January 2018. Investigation of the water quality conditions and the evolution of zooplankton communities at 24 sampling points including the "three mouths" and "four waters" in the Dongting Lake area, including the incoming water section, the lake area and the exit section. The Wanshen AlgaeC type zooplankton and algae intelligent identification counter was used to obtain the relevant data of phytoplankton in the experimental water. By analyzing zooplankton diversity, water eutrophication results, zooplankton density, and the correlation between zooplankton abundance and environmental factors, conclusions are drawn. The results show that 4 phyla and 20 genera of zooplankton are detected. The density of zooplankton ranges from 5.0 to $3.4\times103\cdot L^{-1}$. The dominant genera of "three-port river structure" was Difflugia. The dominant genera of "four-port river structure" is the Difflugia and Tintinnopsis. The dominant genera of lake region are the Difflugia and Polyarthra. The eutrophication degree of Dongting Lake is evaluated by comprehensive trophic state index and plankton Shannon diversity index. The results of CCA show that salinity and water temperature are the main environmental factors influencing the distribution of zooplankton community in Dongting Lake tourist area. Different zooplankton have different tolerance to temperature and salinity changes, and their species composition and quantity distribution will vary with temperature and salinity changes. Temperature directly affects the body temperature of biological organisms. The temperature of the body determines the strength of zooplankton's metabolic process and affects the growth, development and reproduction of zooplankton.
Keywords: *eutrophication, plankton, diversity index, nutrition status index, ecotourism, environmental monitoring*

Introduction

Since the 1990s, tourism has rapidly developed globally. The growth of ecotourism market is the most significant (Xia et al., 2017). Relevant data shows that the growth rate of global ecotourism has increased from 10% to 30% (Hu and Li, 2017). Because the development of ecotourism is based on the natural environment and natural resource, it can't exist independently without the use of resource, the development of ecotourism must premised on the natural and cultural environment (Wang et al., 2017). The ecotourism uses the natural environment to create wealth continuously, but it will bring unexpected threats to the environment, culture and economic sustainable development. In order to promote the healthy development of ecotourism in China, it is necessary to research the sustainable mechanism to develop the regional ecotourism resource.

http://www.aloki.hu ● ISSN 1589 1623 (Print) ● ISSN1785 0037 (Online)
DOI: http://dx.doi.org/10.15666/aeer/1802_29592974

Dongting Lake (110°40'E—113°10'E, 28°30'N—30°20'N) is located in the north of Hunan Province and the South Bank of Yangtze River. Dongting Lake stretches across Hunan and Hubei, including eighteen counties and fifteen state-owned farms in the north of Hunan Province, with a land area of 3.2×104 km^2, in which the area of cultivated land is 8.93×104 hm^2, and the population is about 1/5 of Hunan, so Dongting Lake is a famous base of commodity grain and freshwater fishery (Wang et al., 2017). It is also an ecotourism area in China (Van Dorssen et al., 2017). Dongting Lake is the second largest fresh water lake in China (Duan and Liu, 2019). It receives the water from Songzikou, Taipingkou and Ouchikou of the Yangtze River (referred to as "san kou"), the inflow of Xiangjiang, Zijiang, Yuanjiang and Lishui (referred to as "si shui") in the local drainage area of Dongting Lake, and the inflow of Xinqiang River and Miluo River around the lake. After storing water in a reservoir or lake and regulating the volume of flow in the lower reaches, it flows into the Yangtze River from the Chenglingji in the north. The relationship between rivers and lakes is very complex. Due to the long-term joint action of special geographical environment, natural conditions and human activities, the unique wetland ecotourism resource landscape is formed. In recent years, with the rapid development of social economy in Dongting Lake basin, the water body is seriously over the standard of nutrients, and the water body pollution of Dongting Lake is prominent, leading to significant changes in biological community structure and function.

Zooplankton is small aquatic organisms suspended in the water (Xie et al., 2017). They feed on phytoplankton, bacteria and organic debris in the water. Meanwhile, they are an important part of the water ecosystem. On the one hand, the feeding relationship between zooplankton and phytoplankton can regulate the density and biomass change of phytoplankton community appropriately (Ye et al., 2017). On the other hand, zooplankton can provide important food for fish, shrimp, crab and other animals in the sea, so they play an important role in the food web of marine ecosystem. To some extent, the quantity, species and distribution of plankton can be used as indexes to reflect the ecological environment of the lake. Therefore, the research on the community structure and distribution characteristics of zooplankton is very important to the lake monitoring and management of the ecological environment.

In the early 21st century, Zhang and Ye (2017) found that the zooplankton community structure of Dongting Lake is relatively complete and the diversity level is high. Ou, L. found that the increase of nutrients and eutrophication level was the direct reason of the increase of zooplankton in the water of South Dongting Lake (Ou, 2018). In recent years, there are many researches on the community structure and diversity of zooplankton, but most of them are concentrated in Tai Lake and Chao Lake. There are few studies on zooplankton community in Dongting Lake (Shelley et al., 2017). As the only inland lake that is directly connected with the Yangtze River in the middle reaches, Dongting Lake has a variety of ecological service functions and it plays an important role in the regional ecotourism environment function. Therefore, it is urgent and important to investigate the zooplankton community of Dongting Lake under the influence of human activities in recent years, so as to understand its eutrophication status. On this basis, this article researches the correlation of evolution law of zooplankton community in Dongting Lake tourism area, and thus to provide scientific basis for the monitoring of ecotourism environment and technical support for controlling eutrophication.

http://www.aloki.hu ● ISSN 1589 1623 (Print) ● ISSN1785 0037 (Online)
DOI: http://dx.doi.org/10.15666/aeer/1802_29592974

Material and Methods

Layout of sampling points

In this survey, twenty-four sampling sections are arranged in Dongting Lake tourist area (Zheng et al., 2018). *Table 1* shows the section layout information. The actual geographical location is shown in *Figure 1* and the cross-sectional distribution is shown in *Figure 2*.

Table 1. *Layout of sampling points in Dongting Lake Tourist Area*

Monitoring point No.	Name of section	Longitude	Latitude	Control hydrological station	Remarks
1	Chen er kou	111°37′1.24″	30°18′16.35″	Zhicheng	Background section of the main stream of the Yangtze River
2	Da kou	111°48′24.03″	30°17′3.37″	New Jiangkou and SANDAOGUAN	Songzikou entrance
3	Taiping kou	112°7′42.99″	30°16′50.40″	Mito Temple	Taipingkou entrance
4	Lotus pond town	112°19′25.32″	29°44′31.33″	Kangjiagang, Guanjiapu	Lotus pond entrance
5	Tiao Guan town	112°37′19.80″	29°41′0.71″	Gate control	Tuning port entrance
6	Rock mountain	112°00′14.65″	29°24′1.96″	Rock mountain	Lishui entrance
7	Zhou Wen Temple	112°15′25″	28°54′45″	Zhouwenmiao (water level station)	Yuanshui entry
8	Sha Tau Village	112°29′32.69″	28°38′53.45″	Ganxi port and Shatou (2)	Water access
9	Zhangshu town	112°48′2.16″	28°34′3.28″	Baogong temple, Xiangyin	Xiangjiang entry
10	Leishishan	112°57′27.05″	28°59′58.32″	Leishishan (water level station)	Miluo River
11	Laohekou	113°6′20.40″	29°11′8.57″	-	New wall River
12	Chenglingji	113°09′3.64″	29°25′57.72″	Chenglingji	Exit
13	Lotus pond	113°12′40.18″	28°56′52″	Lotus pond	Converging the Yangtze River
14	Lo Shan	113°19′12.04″	29°37′43.28″	Lo Shan	Background of confluence of Yangtze River
15	Anxiang	112°10′16.07″	29°24′40.71″	Anxiang	Lake area
16	Nanxian	112°23′46.47″	29°21′40.825″	Nanxian	Lake area
17	Pinghu	112°13′47.69″	28°55′48.56″	-	West Dongting
18	Wan Zi Lake	112°17′6.27″	28°50′3.18″	Yangliutan	South Dongting
19	Junshan	113°0′23.17″	29°27′39.98″	Junshan	Dongdongting
20	Six door brake	112°46′16.53″	29°27′50.66″	-	East Dongting inward
21	Da tong hu	112°32′43.40″	29°10′35.07″	-	Typical Inner Lake in Lake area
22	Nan Ju	112°18′16.04″	29°03′5.78″	Nan Ju	Boundary of Dongting Lake in the West and North
23	Xiaohe Ju	112°18′37″	28°50′37″	Xiaohe Ju	Boundary between Dongting Lake in the West and Dongting Lake in the South
24	Lotus Leaf Lake	112°50′33.36″	28°36′33.35	Lotus Leaf Lake	Boundary between Dongting Lake and Dongting Lake

http://www.aloki.hu ● ISSN 1589 1623 (Print) ● ISSN1785 0037 (Online)
DOI: http://dx.doi.org/10.15666/aeer/1802_29592974

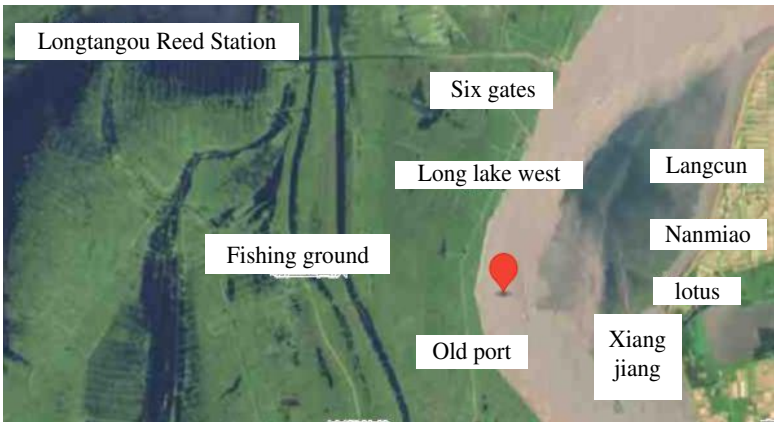

Figure 1. *Actual geographic location*

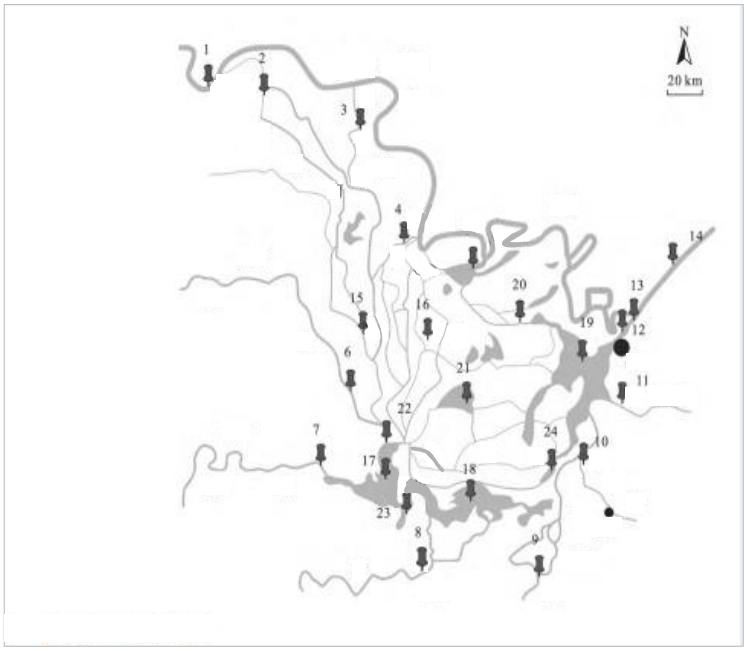

Figure 2. *Layout of sampling points in Dongting Lake Tourist Area*

In order to conduct a more comprehensive study on the evolution of zooplankton communities in the Dongting Lake Scenic Area, they were divided into zones. There is only one Yangtze River main stream background section (1#). There are four “three-port river structure” sections flowing into the lake (He et al., 2019) (2#~5#). There are four "four-port water system" sections flowing into the lake (Hu et al., 2018) (6#~9#). There are two inflow sections such as Miluo River, Xinxiang river (10#~11#). There are ten sections in Dongting Lake region (15#~24#). In addition, the number of exit and its background section are three (12#~14#). The experiment started on January 1, 2018, including the four seasons of spring, summer, autumn and winter, and the experiment cycle was one year. Among them, the sampling interval is 8 hours, and the samples are taken 3 times a day, respectively at 8am, 16pm, and 12 midnight. Record 11 environmental parameters including water temperature (WT), salinity (Sal),

http://www.aloki.hu ● ISSN 1589 1623 (Print) ● ISSN1785 0037 (Online)
DOI: http://dx.doi.org/10.15666/aeer/1802_29592974

transparency (T), dissolved oxygen (DO), chemical oxygen consumption (COD_{Mn}), and active phosphate (PO^{3-}_4) at these three time points Each sample is sampled 30 times and the average value is taken as the experimental sample data.

Sampling and sample processing

Zooplankton sampling: type I shallow plankton net (length is 145 cm, net internal diameter is 50 cm, net area 0.2 m^2) trawls from the sea bottom to the sea surface vertically. The samples were put into sample bottles, and then they are fixed and preserved with 5% formalin solution (Dai et al., 2017). After that, they are brought back to the laboratory for identification and analysis. Eleven environmental parameters such as water temperature (WT), salinity (SAL), transparency (T), dissolved oxygen (DO), chemical oxygen demand (COD_{Mn}), orthophosphate (PO^{3-}_4) were investigated simultaneously at each monitoring station. All operations were in accordance with the marine monitoring specification (GB17378-2007). Using the Wanshen AlgaeC type zooplankton and algae intelligent identification counter for plankton identification.

Sample analysis

The transparency of water samples collected from Dongting Lake in Hunan was measured by the method of Secchi disc (Hou et al., 2017). The chemical oxygen demand, chlorophyll a, total nitrogen and total phosphorus were determined in laboratory. The determination method refers to the monitoring and analysis method of water and wastewater (State Environmental Protection Administration, 2002). The plankton samples were identified and counted by microscope. Olympus BX53 microscope was adopted. Based on "China freshwater algae: system, classification and ecology" and "Research methods of freshwater plankton", the samples were identified.

The protozoa and rotifers were counted by 10×20 times microscope. The branch angle and copepoda were counted in full by 10×10 times microscope (Li and Jin, 2017). Genus was identified by qualitative analysis. The amount of zooplankton per litre of water should be calculated by following formulas:

$$N=\frac{nv}{VC} \quad \text{(Eq.1)}$$

In *formula (1)*, n is the number of calculating samples, v is the constant volume (mL) of concentrated sample, V is the sampling volume (L), C is the volume of counting sample (mL).

Data analysis

Eutrophication calculation

The eutrophication parameters of water quality are evaluated and calculated. The calculation method refers to “environmental quality evaluation method for surface water (Trial)” issued by Ministry of Environmental Protection. The eutrophication condition of Dongting Lake is evaluated by the comprehensive trophic state index TLI (∑) (Tang et al., 2019). Evaluation grade: TLI (∑) < 30, oligotrophy; 30 ≤ TLI (∑) < 50, mesotrophy; 50 < TLI (∑) < 60, light eutrophication; 60 < TLI (∑) < 70, moderate eutrophication; TLI (∑) > 70, severe eutrophication.

http://www.aloki.hu ● ISSN 1589 1623 (Print) ● ISSN1785 0037 (Online)
DOI: http://dx.doi.org/10.15666/aeer/1802_29592974

Calculation of zooplankton diversity

The diversity of zooplankton is denoted by Shannon-Weaver diversity index (*H'*) (Xiang et al., 2017). The evenness of community is denoted by Pielou evenness index (*J*) (Zhu and Yang, 2018). The richness of community is denoted by richness index of species (*D*) (Huang, 2017). The dominant species of community is denoted by dominance index (*Y*) (He et al., 2019). The formulas of indexes are as follows:

$$H' = -\sum P_i \ln P_i \quad \text{(Eq.2)}$$

$$J = \frac{H'}{\ln S} \quad \text{(Eq.3)}$$

$$D = \frac{(S-1)}{\ln N} \quad \text{(Eq.4)}$$

$$Y = \frac{n_i}{Nf_i} \quad \text{(Eq.5)}$$

In *formulas (2)-(5)*, P_i is the quantity proportion of species; *S* is the species quantity of zooplankton. *N* is the total number of zooplankton; *f* is the occurrence frequency of species. If the dominance index (*Y*) of species≥ 0.02, it will be selected as superior species (Yang et al., 2017). SPSS17.0 software is used to analyze the correlation between abundance, biomass and environmental factors. The Shannon-Weaver index and evenness index are calculated by Primer6 (Zhang et al., 2018). CANOCO for Windows5 is applied to CCA analysis, so that the relationship between zooplankton and environmental factors can be obtained. Google earth and MapInfo are used to draw the station distribution.

Results

Water quality and eutrophication assessment of Dongting Lake tourist Area

Analysis of water quality

The transparency, permanganate index, chlorophyll a, total nitrogen and total phosphorus of twenty-four in Dongting Lake tourist area were measured. The results are shown in *Table 2*.

Based on the results in *Table 2*, each single factor is evaluated by the environmental quality standard for surface water (GB3838-2002), so as to understand the water quality of Dongting Lake. From the physical and chemical monitoring results, we can see that the water quality of Dongting Lake tourist area is not optimistic, and the nutrient content is high. The fluctuation range of total nitrogen in Dongting Lake tourist area is 0.81-2.00 $mg \cdot L^{-1}$, with an average value of 1.49 $mg \cdot L^{-1}$. The results of monitoring points of "three-port water systems" and "four water systems" all exceed the class IV water standard, so the total nitrogen pollution of Dongting Lake is relatively serious. The fluctuation range of total phosphorus in Dongting Lake is 0.06-0.21 $mg \cdot L^{-1}$, and the average value is 0.09 $mg \cdot L^{-1}$. The average value of total phosphorus in lake area is

http://www.aloki.hu ● ISSN 1589 1623 (Print) ● ISSN1785 0037 (Online)
DOI: http://dx.doi.org/10.15666/aeer/1802_29592974

0.08 mg·L^{-1}, which meets the class IV water standard. The maximum value measured by No. 7 monitoring point (Zhouwenmiao) is 0.21 mg·L^{-1}. Zhouwenmiao is the entrance of Yuanjiang River to Dongting Lake. The reason for high total phosphorus is due to the aquaculture, agricultural production, soil erosion, feces and other pollution. As an index of organic pollution, when the concentration of COD_{Mn} exceeds 4 mg·L^{-1}, the water body has been polluted. The result of COD_{Mn} determination in Dongting Lake is 1.9-3.9 mg·L^{-1}, and the average value is 2.6 mg·L^{-1}. Therefore, some areas of Dongting Lake are close to the stage of pollution. We should pay enough attention to these areas.

Table 2. *Basic physical and chemical properties of Dongting Lake Tourist Area*

Monitoring point No.	COD_{Mn}/mg·L^{-1}	TN/mg·L^{-1}	SD/mg·L^{-1}	TP/mg·L^{-1}	Chlorophyll a/μg·L^{-1}
1	2.49	1.92	0.29	0.08	3.29
2	2.42	1.62	36	0.1	1.54
3	2.21	1.62	0.36	0.11	1.54
4	2.18	1.6	0.31	0.12	2.72
5	2.2	0.61	0.41	0.12	4.14
6	3.19	1.59	0.74	0.08	4.2
7	3.63	1.54	0.26	0.22	0.75
8	2.04	1.6	0.47	0.07	3.07
9	2.47	1.68	0.46	0.07	3.8
10	2.92	1.58	0.26	0.11	27.52
11	2.23	1.27	0.31	0.08	7.53
12	2.89	1.77	0.54	0.12	16.54
13	2.77	1.59	0.61	0.09	4.43
14	2.38	1.48	0.31	0.09	3.74
15	2.41	1.67	0.51	0.09	1.83
16	2.02	2.01	0.41	0.1	4.87
17	1.93	1.36	0.26	0.08	1.77
18	2.22	1.19	0.34	0.07	2.16
19	2.31	1.24	0.21	0.09	5.95
20	3.93	1.28	0.11	0.09	10.14
21	3.68	0.82	0.81	0.14	2.79
22	2.19	1.43	0.31	0.07	2.16
23	2.7	1.22	0.28	0.07	2.06
24	2.24	1.32	0.31	0.07	5.95

Eutrophication assessment

The eutrophication of Dongting Lake tourist area was evaluated according to the surface water environment quality evaluation method (Trial implementation), and the eutrophication is shown in *Figure 3*.

The transparency in the water body exceeds the average value by more than 500 px, the biochemical oxygen demand is greater than 10 mg/L, the concentration of chlorophyll a that marks the growth of algae is greater than 10 μg/L, the nitrogen content is greater than 0.2~0.3 mg/L, and the phosphorus content is greater than 0.01 mg/L, indicating that the water body is in a state of eutrophication. Through the calculation of trophic state index (TLI) of transparency, chemical oxygen demand, chlorophyll a, total nitrogen and total phosphorus, we can see that all monitoring points are in the state of eutrophication. Among all the monitoring points, TLI value in No. 20 monitoring point is the highest, 63.66, belonging to the moderate eutrophication state. This is consistent with the water bloom phenomenon found in the field sampling.

http://www.aloki.hu ● ISSN 1589 1623 (Print) ● ISSN1785 0037 (Online)
DOI: http://dx.doi.org/10.15666/aeer/1802_29592974

During field sampling, cyanobacteria bloom was found in No. 20 monitoring point (Liumen floodgate), and the water body of the monitoring point was green with odour. The causes of water bloom in Liumen sluice are analyzed. Firstly, the concentration of nutrients such as nitrogen and phosphorus is high. When the total nitrogen and total phosphorus are more than 0.5 and 0.02 $mg \cdot L^{-1}$ respectively, cyanobacterial blooms may occur. During the lake eutrophication, as the limiting factor of algal growth, the increase of phosphorus will lead to a large number of algal growths. Liumen sluice is in the state of moderate eutrophication. Respectively, the total nitrogen and total phosphorus of this monitoring point are 1.27 $mg \cdot L^{-1}$ and 0.08 $mg \cdot L^{-1}$. The high nitrogen and phosphorus content and eutrophic water create conditions for cyanobacteria bloom. The second is the impact of hydrological conditions. Generally, the cyanobacteria are difficult to gather effectively to form water bloom if the water retention time is too short. The longer the water retention time is, the greater the possibility of water bloom is. When the flow velocity is low, the flow velocity is the key regulating factor of nutrient concentration and transparency. When the flow velocity is low, the nutrient concentration increases and the transparency decreases. The average velocity at Liumen sluice is only 0.02 $m \cdot s^{-1}$. If the water retention time is too long, the high concentration of nutrients will provide sufficient nutrition for the mass propagation of algae, leading to water bloom. Therefore, the interaction of environmental factors and hydrological conditions led to the outbreak of cyanobacteria bloom.

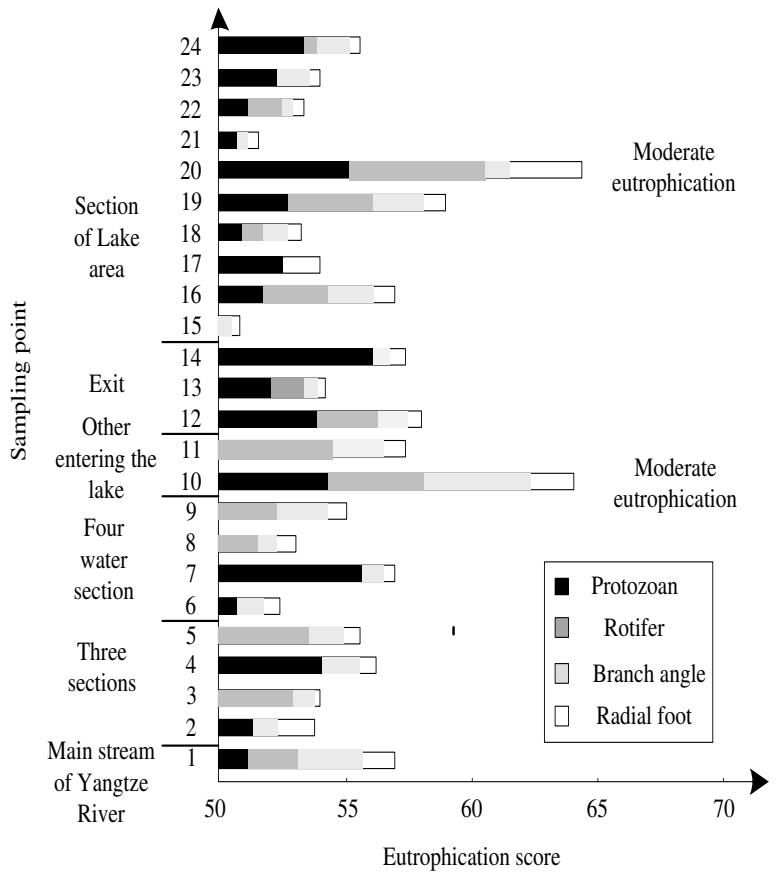

Figure 3. *Eutrophication in Dongting Lake Tourist Area*

http://www.aloki.hu ● ISSN 1589 1623 (Print) ● ISSN1785 0037 (Online)
DOI: http://dx.doi.org/10.15666/aeer/1802_29592974

Evolution law of zooplankton community in Dongting Lake tourist area

Composition of zooplankton

In this article, four phyla and twenty genera of zooplankton are found in Dongting Lake tourist area, in which six species are protozoa, and they account for 30.00% of the total number of zooplankton. Seven species are rotifers, accounting for 35.00%. Four species are Cladoceran, accounting for 20.00%. Three species are Copepoda, accounting for 15.00%. Nauplius is detected form all monitoring points, Cyclopoidea and Difflugia are more than 70% detection rate. Keratella and Bosmina are more than 50% detection rate. The composition of zooplankton is shown in *Figure 4*.

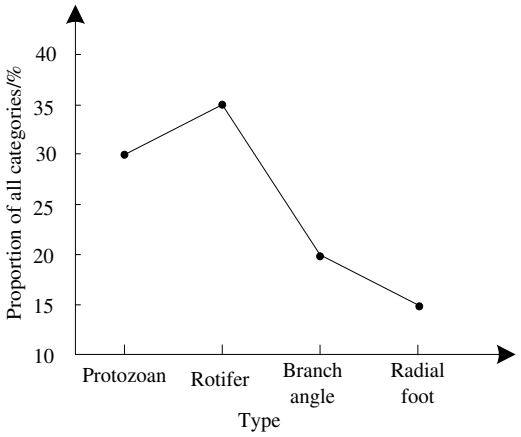

Figure 4. *Species composition of zooplankton*

The spatial distribution of zooplankton species is shown in *Figure 5*.

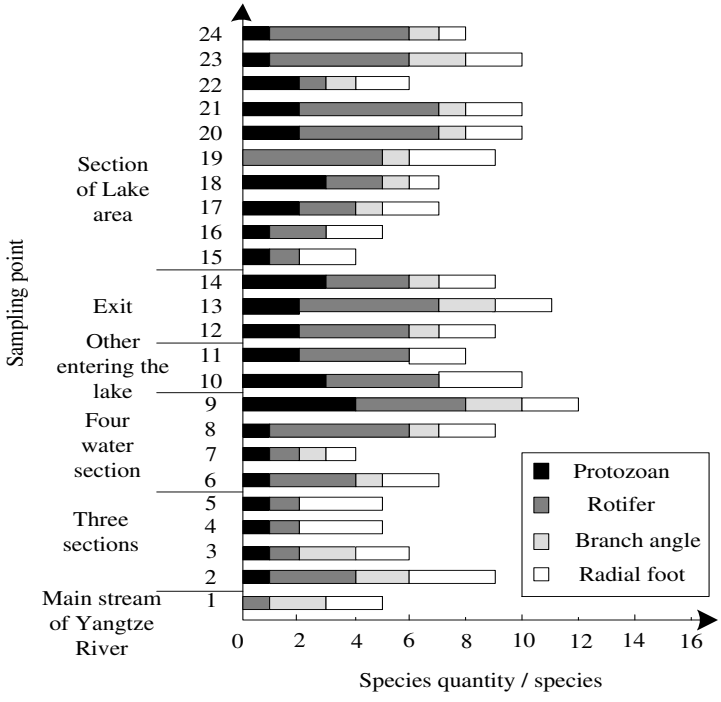

Figure 5. *Spatial distribution of zooplankton species composition*

http://www.aloki.hu ● ISSN 1589 1623 (Print) ● ISSN1785 0037 (Online)
DOI: http://dx.doi.org/10.15666/aeer/1802_29592974

Figure 5 shows that the number of zooplankton species in No.9 monitoring point is the most abundant, with a total of twelve species. No. 7 monitoring points and No.9 monitoring points have the least species. Only four species of zooplankton can be detected. There are ten species of zooplankton in the "three diversions river system" and there are fourteen species in the "four diversions river system". There are seventeen species in the lake area.

Zooplankton density

The spatial distribution of zooplankton is shown in *Figure 6*.

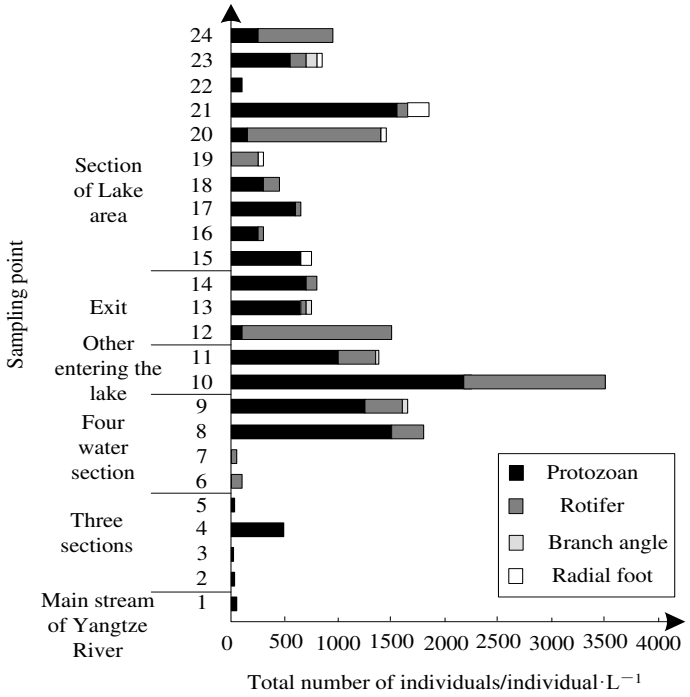

Figure 6. *Spatial distribution of zooplankton density*

The monitoring points in this paper are all equidistant, and the selection positions are random. *Figure 6* shows that the density of zooplankton changes from $5.0\sim3.4\times10^3\cdot L^{-1}$, and the average density is $802\cdot L^{-1}$. The density of No. 3 monitoring point is only $3.2*10^2\cdot L^{-1}$, almost no zooplankton can be detected. The distribution rule of density of zooplankton in Dongting Lake: three-port water system < lake area < four-water system. The average cell density of "three-port water system" is 140 L^{-1}. The average cell density of "four-water system" is 853 L^{-1}. The cell density of "four-water system" flowing the lake is 6.1 times of that of "three-port water system". The average cell density of Dongting Lake area is 791 L^{-1}. The distribution rule of density of zooplankton in lake area: East Dongting Lake < South Dongting Lake < West Dongting Lake. The dominant genera identified by zooplankton in Dongting Lake are as follows: the dominant genera of "three-port water system" are Difflugia; the dominant genera of "four-water systems" are Difflugia and Tininnidium; the dominant genera in lake area are Difflugia and Polyarthra. In addition, Difflugia are dominant in the whole Dongting Lake. *Figure 5* shows that Dongting Lake is dominated by protozoa and rotifers. Small

http://www.aloki.hu ● ISSN 1589 1623 (Print) ● ISSN1785 0037 (Online)
DOI: http://dx.doi.org/10.15666/aeer/1802_29592974

zooplanktons are dominant in species number and individual number, while Cladocera and copepod are less, and the trend of miniaturization is obvious. Some researches show that the community structure of zooplankton changes from large to small with the improvement of water nutrition level, and the eutrophication degree of water body in Dongting Lake is more serious, which is not conducive to the feeding of large zooplankton such as Cladocera. That is the main reason why the small zooplanktons in Dongting Lake become dominant. Meanwhile, some researches show that the filter-feeding way of silver carp and variegated carp will lead to the reduction of macro zooplankton. It will show a miniaturization trend. Due to the high culture rate of silver carp and variegated carp, the filter-feeding way of silver carp and variegated carp leads to the miniaturization of zooplankton. In addition, the cyanobacteria in Dongting Lake are the dominant species, which are not conducive to the feeding of Cladocera and other macro zooplankton. The rotifers can use Cyanobacteria for growth and reproduction, leading to the dominance of micro zooplankton in water.

Assessment of zooplankton diversity and eutrophication

The Shannon diversity indexes of zooplankton were calculated at 24 monitoring points in Dongting Lake. The spatial distribution of H-value measurement results is shown in *Figure 7*.

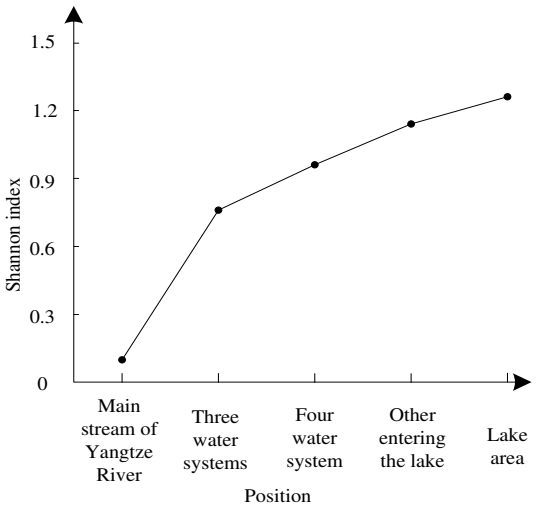

Figure 7. *Spatial distribution of Shannon diversity index and Margelef index*

When the Shannon diversity index in a water body exceeds 0.95, the water body is in a state of eutrophication. The range of H value in Dongting Lake is 0.02-1.59. The average value is 0.99. The average value of H in three diversions river systems is 0.75. The average value of H in four diversions river systems is 0.88. The average value of H in the lake region is 1.08. The distribution rule of zooplankton biodiversity is three diversions river system < four diversions river system < Lake region. The distribution law in lake region is West Dongting < South Dongting < East Dongting. The state of eutrophication in Dongting Lake was evaluated by Shannon index. All the results show that Dongting Lake is in the state of eutrophication.

http://www.aloki.hu ● ISSN 1589 1623 (Print) ● ISSN1785 0037 (Online)
DOI: http://dx.doi.org/10.15666/aeer/1802_29592974

Correlation between zooplankton abundance and environmental factors

The correlation of eleven physical and chemical factors such as zooplankton abundance, water temperature, salinity, nutrient salt and transparency is shown in *Table 3*.

Table 3. *Correlation coefficient between zooplankton abundance and environmental factors*

Correlation coefficient	2018		
	May	July	November
NO_2^-	0.134	-0.363	-0.099
NH_4^+	-0.318	-0.324	0.195
NO_3^-	-0.102	-0.248	0.347
PO_4^{3-}	0.017	-0.427	-3.433
T	-0.741**	0.080	-2.210
WT	0.611*	-0.082	-0.734**
Sal	0.611*	-0.452	0.589*
DO	-0.525	-0.079	0.481
pH	0.030	0.437	-0.472
COD	0.132	-0.118	-0.531
H	0.23	0.534	0.223

From *Table 3*, the zooplankton abundance has a significant negative correlation with water transparency in spring ($P < 0.01$) and a significant positive correlation with water temperature and salinity ($P < 0.05$). In summer, the zooplankton abundance does not have significant correlation with the monitored chemical parameters ($P > 0.05$). In autumn, the zooplankton abundance has a significant negative correlation with water temperature ($P < 0.01$) and a significant positive correlation with salinity ($P < 0.05$). There was no significant correlation between zooplankton abundance and other chemical parameters ($P > 0.05$). Therefore, the water temperature and salinity are important environmental factors influencing the community structure of zooplankton.

Discussion

Since the 1980s, a trend of thought has gradually emerged, which calls for strengthening the management of tourism resources in the process of tourism activities. Meanwhile, it calls for formulating a draft plan that can be generally agreed and abided by the relevant parties. This trend of thought developed in the late 1980s, and then the concepts of "Science to tourism", "Natural to tourism" and "E-tourism" appeared. The ecotourism has become the trend of tourism development in the world, but there is no clear definition of ecotourism. Mesfin et al. (2017) studied emerging zooplankton conservation methods in shallow tropical lakes supported by large aquatic plants. From January 2016 to August 2016, monthly monitoring of a large large-scale gushing plant, including monitoring of physical, chemical and biological parameters. Sampling points were selected to represent areas of large plant vegetation and open waters of the lake. Sites with large plants were found to be homes of more dense and diverse zooplankton communities. Based on this, the related methods are optimized, the experimental period is extended, and the research area is enlarged. The evolution of zooplankton community during this period is studied, and the following conclusions are drawn:

http://www.aloki.hu ● ISSN 1589 1623 (Print) ● ISSN1785 0037 (Online)
DOI: http://dx.doi.org/10.15666/aeer/1802_29592974

In this article, the evolution law of zooplankton community in Dongting Lake tourist area of Hunan Province is researched. Four phyla and twenty genera of zooplankton are found in Dongting Lake tourist area, in which six species are protozoa, and they account for 30.00% of the total number of zooplankton. Seven species are rotifers, accounting for 35.00%. Four species are Cladoceran, accounting for 20.00%. Three species are Copepoda, accounting for 15.00%. There are ten species of zooplankton in the "three diversions river system" and there are fourteen species in the "four diversions river system". There are seventeen species in the lake area. The average H value of zooplankton biodiversity is 0.99. The average D value of species richness is 1.02. The distribution rule of Shannon index of zooplankton is: three diversions river system < four diversions river system < lake region. The result of water quality evaluation by plankton Shannon diversity index shows that the water body is already in the state of eutrophication.

The composition and distribution characteristics of zooplankton are related to the ecological factors such as water temperature, salinity, dissolved oxygen, chlorophyll a, pH and nutrient content, in which temperature and salinity are the most important factors affecting zooplankton distribution. Different zooplanktons have different tolerance to the change of temperature and salinity, and their species composition and distribution will be different with the change of temperature and salinity. The temperature directly affects the body temperature of organisms, and the body temperature determines the intensity of the metabolism process of zooplankton and affects the growth, development and reproduction of zooplankton. When Jiang Huichao et al studied the community structure of zooplankton in Jincheng sea area of Laizhou Bay, they found that the species of zooplankton was positively correlated with the water temperature in the range of 2.2~27.4℃ ($P < 0.01$). The salinity is another important factor affecting the community structure of zooplankton, which is negatively related to the distribution of species. The cumulative contribution rate of selected environmental factors to explain species variables of zooplankton is as high as 90%, so the temperature and salinity are the main environmental factors affecting the distribution of zooplankton.

According to the resource characteristics of "particularity, diversity and fragility" of Dongting Lake tourist area and the current situation of utilization, the development of Dongting Lake tourist area should be positioned as a kind of protective resource development, which should develop towards the direction of ecotourism. The ecotourism can be used to improve and restore the quality of natural environment in lake area, so as to promote the virtuous cycle of ecosystem and sustainable development.

(1) return farmland to lake and ensure the area of natural ecosystem

The ecosystem of Dongting Lake belongs to the inland wetland ecosystem, including natural ecosystem and artificial ecosystem. According to its landscape, the natural ecosystem can be divided into river ecosystem, fresh water lake ecosystem, freshwater swamp ecosystem, wetland ecosystem dominated by trees, marsh wetland ecosystem dominated by reed. The artificial ecosystem mainly contains fish and shrimp pond, irrigation ditch, paddy field, irrigation land, seasonal flood farmland and other agricultural ecosystems. Zooplankton is one of the main biological groups in the natural ecosystem, and it is also the basic material element of forming the ecotourism landscape. Meanwhile, it is an important component of the ecological function of Dongting Lake.

http://www.aloki.hu ● ISSN 1589 1623 (Print) ● ISSN1785 0037 (Online)
DOI: http://dx.doi.org/10.15666/aeer/1802_29592974

To maintain natural ecosystem is the premise of developing Dongting Lake ecotourism and the fundamental guarantee of virtuous cycle of ecosystem. In the past, there were more people and less land in the lake area. In order to solve the problem of grain, the area of constructed wetland was expanded and the area of natural ecotourism resource was reduced. That is a problem of economic benefit between the whole and the part, the near term and the long term. The lake is reclaimed, leading to the sharp reduction of the flood storage capacity of the lake. Therefore, it is necessary to adjust the agricultural structure and promote “the avoiding calamity agriculture ", and develop "sightseeing agriculture". For example, reclaiming wetlands on low floodplain not only destroys the original eco-tourism resource, but also loses the proper benefits. It is necessary to return farmland to lakes and marshes, restore the original natural eco-tourism landscape, and make it play a variety of ecological functions. In conditional areas, it is necessary to build a pilot demonstration area of sightseeing agriculture and develop a sustainable sightseeing agriculture that adapts to the alternation of drought and flood. Aiming at shallow water, surrounding lakes, low lake waterlogged land and specific areas with more than one year of flooding, it is necessary to establish a variety of suitable composite and efficient tourism agricultural ecological engineering modes, so as to make overall arrangements for planting and breeding industries.

(2) restoration, reconstruction, standardization and expansion of nature reserves

According to the principle of ecology, the restoration and reconstruction of ecosystem is to change and eliminate the disadvantageous factors restricting the development of ecosystem, so as to restore the degraded ecosystem as soon as possible. Finally, it develops healthily. For a degraded ecosystem, it is necessary to establish a series of ecological sustainability indicators and conduct long-term monitoring before and after restoration to restore its ecological rationality and achieve its sustainability ultimately.

The primary task for the restoration and reconstruction of Dongting Lake ecosystem is to standardize and expand the nature reserve. The practice proves that the establishment of nature reserves is the most effective way to protect ecotourism resource. Dongting Lake Nature Reserve, established in Yueyang City since 1982, which has been listed in the list of international important wetlands, with an area of about 19×104 hm^2. The protected objects mainly include rare birds, wetlands and lakes. In 2000, World Wide Fund For Nature decided to take Qingshan Lake as the first implementation project of returning farmland to Lake, wetland restoration demonstration and "river of joint protection of life" in Qingshan Lake of Hanshou, West Dongting Lake. It is listed as a world wetland restoration demonstration area, with a total area of about 1100 hm^2. In the demonstration area, there are six functional areas. In South Dongting Lake, Dongting Lake environmental protection monitoring station of Hunan Province is established. In the past, some works had been done and great achievements have been made in the construction of wetland nature reserves, but it is far from the actual requirements. The number of protected areas (demonstration areas) is too small. The existing nature reserves still can’t effectively protect the ecotourism resources. It is necessary to strengthen the management and play a role in the established nature reserves. Meanwhile, we should increase the number of ecotourism resource reserves and increase the investment. Combined with scientific research institutes, the ecosystem research network is built. Based on "3S" technology, we should strengthen the monitoring of ecotourism resources, especially the monitoring of dynamic system and biodiversity change after the use of ecotourism resources, and then

http://www.aloki.hu ● ISSN 1589 1623 (Print) ● ISSN1785 0037 (Online)
DOI: http://dx.doi.org/10.15666/aeer/1802_29592974

prepare the ecotourism resource information management system, so as to promote the continuous improvement of reserve system. These provide scientific basis for scientific management and rational use of ecotourism resources. Moreover, it is necessary to establish a comprehensive planning and management organization of eco-tourism resources in lake area, study and formulate relevant laws and regulations, strengthen the management for the utilization of ecotourism resources, unify the planning, implement the environmental impact assessment system, and enforce the approval procedures for the development and utilization of ecotourism resources. In addition, the blind development and destruction of ecotourism resources are strictly prohibited, so that the tendency of paying attention to production function but neglecting its ecological function is completely changed. The comprehensive economic and ecological benefits are fully exerted and thus to achieve the sustainable utilization of ecotourism resource.

Conclusions

Dongting Lake in Hunan is one of the three major wetland resource areas in the middle and lower reaches of the Yangtze river. Under the long-term action of special geographical environment, natural conditions and human activities, the unique ecotourism resource landscape, obvious saucer-shaped basin landform, typical subtropical monsoon climate, rich animal and plant resources and other ecotourism resources. Zooplankton plays a bioindication role in the distribution of many important ocean currents and water masses and the climate change. Zooplankton is very sensitive to the changes of various hydrological factors due to their special life style. They often swim with the stream. The distribution and quantity change of species is corresponding to the hydrological conditions, water masses, ocean current and climate. To master the change dynamics of zooplankton community structure is an important content to understand the structure and function of the reservoir ecosystem. This article researches the evolution law of zooplankton community in Dongting Lake and analyzes the characteristics of zooplankton community structure, so as to provide basic data and theoretical basis for the rational construction and sustainable development of Dongting Lake.

In the future, this paper will use the results of this research to rationally plan the protection of the ecosystem and obtain a better ecological environment.

REFERENCES

[1] Dai, W., Kaminga, A. C., Tan, H. (2017): Long-term psychological outcomes of flood survivors of hard-hit areas of the 1998 Dongting Lake flood in China: Prevalence and risk factors. – Plos One 12(2): e0171557.

[2] Duan, P. P., Liu, L. (2019): Target Aspect Angle Estimation of SAR Images Based on Correlation Analysis. – Journal of China Academy of Electronics and Information Technology 14(1): 46-50.

[3] He, L., Zhang, X. R., Ni, Y. Q. (2019): Fabrication and Research on GaN-based Power Electronic Materials and Devices on 6-inch Si Substrate. – Journal of Power Supply 17(3): 26-37.

[4] Hou, Y., Chen, W., Liao, Y. (2017): Scenario analysis of the impacts of socioeconomic development on phosphorous export and loading from the Dongting Lake watershed, China. – Environmental Science & Pollution Research 24(34): 1-18.

http://www.aloki.hu ● ISSN 1589 1623 (Print) ● ISSN1785 0037 (Online)
DOI: http://dx.doi.org/10.15666/aeer/1802_29592974

[5] Hu, Y., Li, J. (2017): Analysis on evolution of drought-flood and its abrupt alternation in typical year from 1951 to 2015 in Dongting Lake area. – Transactions of the Chinese Society of Agricultural Engineering 33(7): 107-115.
[6] Hu, W., Wang, Z., Li, C. (2018): Assessment and prediction of land ecological environment quality change based on remote sensing-a case study of the Dongting lake area in China. – IOP Conference Series Earth and Environmental Science 121(3): 032053.
[7] Huang, X. Z. (2017): Simulation Study on the Scene of Three-Dimensional Image True Solid Modeling. – Computer Simulation 34(1): 249-252.
[8] Li, Q., Jin, X. J. (2017): Research on emergency communication network architecture and related technologies. – Automation & Instrumentation 12: 10-11.
[9] Mesfin, G., Demeke, K., Ludwig, T. (2017): Emergent Macrophytes Support Zooplankton in a Shallow Tropical Lake: A Basis for Wetland Conservation. – Environmental Management 60(6): 1-12.
[10] Ou, L. (2018): New Insights into the Pt-Catalyzed CH_3OH Oxidation Mechanism: First-Principle Considerations on Thermodynamics, Kinetics, and Reversible Potentials. – ACS Omega 3(1): 886-897.
[11] Shelley, E. A., Shakira, A., Alex, R. (2017): Calcium decline reduces population growth rates of zooplankton in field mesocosms. – Canadian Journal of Zoology 95(5): 25-29.
[12] Tang, L., Deng, S., Tan, D. (2019): Heavy metal distribution, translocation, and human health risk assessment in the soil-rice system around Dongting Lake area, China. – Environmental Science and Pollution Research 26(4): 1-11.
[13] Van Dorssen, C. F., Gordon, C. A., Li, Y. (2017): Rodents, goats and dogs - their potential roles in the transmission of schistosomiasis in China. – Parasitology 144(12): 1-10.
[14] Wang, S. R., Zhang, R., Guo, L. G. (2017): Study on the water ecological risk prevention and control technology system of dongting lake. – China Environmental Science 37(5): 1896-1905.
[15] Wang, W. X., Chen, F. Z., Gu, X. H. (2017): Community structures of zooplankton and its relation to environmental factors in five medium reservoirs in Nanjing City. – Journal of Lake Sciences 29(1): 216-223.
[16] Xia, H., Tang, Y., Lu, F. (2017): The effect of Aeromonas hydrophilainfection on the non-specific immunity of blunt snout bream (Megalobrama amblycephala). – Central-European Journal of Immunology 42(3): 239-243.
[17] Xie, Y. J., Xie, Y. H., Xiao, H. Y., Chen, X. S., Li, F. (2017): Controls on Litter Decomposition of Emergent Macrophyte in Dongting Lake Wetlands. – Ecosystems 20(7): 1383-1389.
[18] Yang, J. H., Zhang, X. W., Xie, Y. W., Song, C., Zhang, Y., Yu, H. X., Burton, G. A. (2017): Zooplankton Community Profiling in a Eutrophic Freshwater Ecosystem-Lake Tai Basin by DNA Metabarcoding. – Scientific Reports 7: 1773.
[19] Ye, G., Xie, Y. H., Zou, D. S. (2017): Using ANNs to analyse effects of the Three Gorges Dam on sedimentation in Dongting Lake, China. – Hydrological Sciences Journal/journal Des Sciences Hydrologiques 62(3): 1-8.
[20] Zhang, R. F., Ye, J. M. (2017): Adaptive Quasi-Newton Algorithm for Blind Source Separation Based on Canonical Correlation Analysis. – Journal of Jilin University (Science Edition) 55(3): 559-563.
[21] Zhang, H. B., Cao, W., Zhang, S. H. (2018): Quantitative Evaluation of Human-introduced Runoff Change of Three Streams in the Southern Jingjiang River of Dongting Lake Area, China. – Journal of Earth Sciences & Environment 40(1): 91-100.
[22] Zhu, G., Yang, Y. (2018): Variation laws and release characteristics of phosphorus on surface sediment of Dongting Lake. – Environmental Science & Pollution Research 25(13): 1-10.

http://www.aloki.hu ● ISSN 1589 1623 (Print) ● ISSN1785 0037 (Online)
DOI: http://dx.doi.org/10.15666/aeer/1802_29592974

RESPONSE OF SOIL ORGANIC CARBON AND TOTAL NITROGEN STOCKS TO DESERTIFICATION OF CHINA AGRO-PASTORAL TRANSITIONAL ZONE: A STUDY OF THE SOUTHEASTERN EDGE OF THE MU US SANDY LAND

YANG, M. H.[1*] – MA, Z. Z.[1] – ZHANG, M. C.[1]

College of Geomatics, Xi'an University of Science and Technology, 58 Yanta Road, Xi'an, Shaanxi, P. R. China

**Corresponding author*
e-mail: ymh8307024@163.com; phone: +86-29-8365-3727; fax: +86-29-8558-3176

(Received 14th Nov 2019; accepted 12th Feb 2020)

Abstract. Desertification, as one of the most severe socio-economic, environmental and ecological problems, has attracted widespread attention. In this study, the severity of desertification in the southeastern edge of the Mu Us sandy land of China was classified into five stages using the space-for-time method. A field experiment was conducted in July 2015 to investigate the dynamics of soil organic carbon (SOC) and total nitrogen (TN) concentrations and stocks. The results show that SOC and TN concentrations and stocks decreased significantly with the severity of desertification, reducing SOC and TN concentrations by 55.5% and 55.1% in 0-30 cm depth, SOC and TN stocks decreasing by 54.4% and 54.0%, respectively. The losses of SOC and TN stocks indicate that the impacts of desertification were more evident in upper soil, because the losses in them were higher than those in other layers, and early stages are vital to the restoration of desertification for more losses of SOC and TN stocks. SOC (4.25×10^8 kg) and TN (0.71×10^8 kg) accumulated from 2003 to 2015 indicate that desertification was reversed. Overall, key stages of combating desertification were identified, and the feasibility of integrating field experiment data and temporal-spatial data to evaluate the dynamics of desertification was verified.

Keywords: *soil property, desertification assessment, integrated method, desertification reverse, ecological restoration*

Introduction

During the past decades, carbon (C) and nitrogen (N) stocks in terrestrial ecosystems have attracted significant attention worldwide because of the enormous effect of C and N levels on the environment and human life (Agren et al., 1987; Deng et al., 2016; Jenkinson et al., 1977; Kelly et al., 1996). Soil, as the largest organic carbon pool in terrestrial ecosystems, plays a significant role in the soil carbon sequestration and global C cycle, and has intimate connections with atmospheric CO_2, for it could act as its source or sink (Dessie et al., 2017; Detwiler, 1986; Post et al., 1982). According to statistics proposed by Batjes and Emanuel, soil stores about 1500 Pg organic carbon in the top one meter, which is about 2.1 times the amount of organic carbon stored in the atmosphere and 2.7 times that in terrestrial plant biomass (Batjes, 1996; Emanuel et al., 1984). Soil also significantly affects N recycling, with values of 92–117 Pg to a depth of one meter, as a comparison the vegetation biomass held 10 Pg of N and microbial biomass holds about 2 Pg N (Batjes, 1996; Mehari et al., 2016; Wang et al., 2006). As key indicators for assessing soil quality and ecosystem productivity, the roles of soil organic carbon (SOC) and total nitrogen (TN) were recognized more than a century ago (Spycher et al., 1983; Twongyirwe et al., 2013). SOC and TN stocks in the soil vary as a result of climate change, land use changes, and even vegetation disturbances or

http://www.aloki.hu ● ISSN 1589 1623 (Print) ● ISSN 1785 0037 (Online)
DOI: http://dx.doi.org/10.15666/aeer/1802_29752988

succession (Alireza et al., 2017; Bouwman, 1990; Van Minnen et al., 2009). Therefore, understanding changes in SOC and TN stocks also plays a role of significance in determining regional, national, and even international carbon and nitrogen budgets.

Desertification is one of the most severe socio-economic, environmental, and ecological threats to the world, especially in arid, semi-arid, and dry subhumid areas (Carr et al., 1996; UNCCD, 1994). Desertification is estimated to affect 20% of the world's population and 25% of the world's land surface (Binns, 2000; UNCCD, 1994). As an extreme case of soil degradation, variation in the amounts of SOC and N stocks concerning desertification caused much concern in recent years (Hu et al., 2017; Tang et al., 2015; Zhao et al., 2009). Published studies have confirmed that desertification leads to a noticeable decline in SOC and N (Aweke et al., 2015; Huang et al., 2007; Zhou et al., 2008), which not only cause depletion of natural resource and losses of ecosystem services, but also enhance emissions of CO_2, NO_x, and other greenhouse gases to the atmosphere (Kirschbaum, 2000; Russell et al., 2005). Zhao et al. (2009) estimated SOC and N contents in the desertification process in Inner Mongolia (Zhao et al., 2009). Tang et al. (2015) analyzed changes in C and N concentrations and stocks in the desert steppe ecosystem in Ningxia (Qiu et al., 2012). However, there have been only few studies on changes in SOC and TN stocks in the Agro-pastoral transitional zone. The Mu Us sandy land is one of the four largest sandy lands in China. The southeast edge of the Mu Us sandy land in Shaanxi province of Chian is of particular concern as it is a typical Agro-pastoral ecotone and semi-arid grassland area of China (Li et al., 2017).

In the past two decades, numerous studies focus on the temporal and spatial monitoring and evaluating of the desertification process with the wide application of GIS and RS (Lamchin et al., 2016; Zhang et al., 2018). These researches could directly display desertification changes based on the dynamic area data of different desertification stages (Liu et al., 2018; Qi et al., 2012). However, these studies only show spatial changes (Duan et al., 2019; Gao et al., 2006), and could not precisely measure the desertification status (aggravation or reversion) along with a time series. Previous studies indicated that desertification processes directly resulted in the depletion of SOC and TN stocks, which declined sharply with the deterioration of desertification (Allington et al., 2010). Accordingly, we supposed that SOC and TN stocks can be used as indicators of desertification. In this study, an integrated method of experimental field data and temporal-spatial changing data was adopted to quantify the desertification process, and this is a new approach for desertification assessment.

This study aims to evaluate the effects of desertification on SOC and TN concentrations and stocks and assess changes of desertification status along with a time series. We selected the southeast edge of the Mu Us sandy land as the study area, used the space-for-time method to classify the desertification degradation gradient into five stages, analyzed variations in SOC and TN concentrations and stocks along the desertification gradient, and quantified total changes of SOC and TN stocks in study area since the Conversion of Cropland to Forest Project has implemented.

Materials and methods

Study area

In this investigation, the study area is located on the southeast edge of the Mu Us sandy land, in Yulin City, northern Shaanxi Province, China (*Fig. 1*).

http://www.aloki.hu ● ISSN 1589 1623 (Print) ● ISSN 1785 0037 (Online)
DOI: http://dx.doi.org/10.15666/aeer/1802_29752988

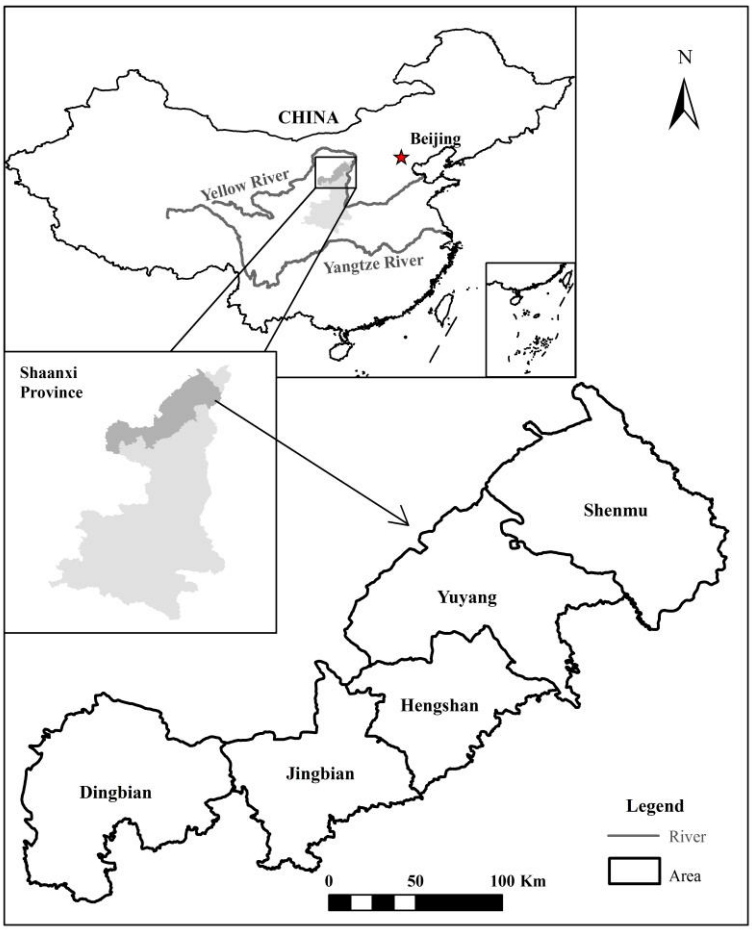

Figure 1. *The location of the study area*

Geographically, it is located from 36°49' to 39°27' E longitude and 107°15' to 110°54' N latitude, and the elevation is 2170 to 3054 m above sea level, with the relative altitude of 10 to 50 m. It is a temperate continental semi-arid monsoon climate. The mean annual precipitation ranges between 250 and 440 mm, with 60 to 75% of total yearly precipitation occurring from June to September. The mean annual temperature of this area is about 8 ℃. The main soil types are light chestnut soil and chestnut soil in the study area (according to the Chinese Soil Classification System), and according to FAO Soil Classification System, the main soil type is Kastanozem. About 80% of the study area is sandy land, among which each of fixed sand dunes, semi-fixed sand dunes, and moving sand dunes occupy one third. The dominant vegetation in the moving sand dunes is *Chenopodiun album*, which is an annual plant. The semi-fixed sand dunes are dominated by shrubs such as *Lespedeza davurica* and *Artemisia ordosica*. The fixed sand dunes are dominated by grasses such as *Stipa bungeana* and *Cleistogenes squarrosa*.

Sampling and laboratory analysis

Experimental design and sampling

In this study, we used the space-for-time method to classify desertification. According to the field survey and the classification of desertification degrees and types

http://www.aloki.hu ● ISSN 1589 1623 (Print) ● ISSN 1785 0037 (Online)
DOI: http://dx.doi.org/10.15666/aeer/1802_29752988

by Zhu and Wang (Wang et al., 2002), five different desertification stages were selected to represent desertification succession stages. The five stages were the non-desertification stage (ND), potential desertification stage (PD), light desertification stage (LD), moderate desertification stage (MD), and severe desertification stage (SD). *Table 1* shows the main characteristics (location, coverage, and dominant species) of each stage. *Figure 2* shows some photos of the sampling sites in the study area.

Table 1. *The classification of desertification and the main characteristics*

Desertification stages	Coverage	Main community	Constructive species	Coordinates
Non-desertification (ND)	> 70%	*Stipa bungeana* + *Cleistogenes squarrosa* + bunch grass	*Stipa bungeana*	E109°55′31″ N38°36′42″ E110°30′36″ N38°41′48″ E108°52′30″ N37°40′09″ E107°46′24″ N37°39′18″ E109°10′21″ N38°05′25″
Potential desertification (PD)	50-70%	*Cleistogenes squarrosa* + *Stipa bungeana* + *Lespedeza davurica*	*Cleistogenes squarrosa*	E109°54′25″ N38°38′21″ E110°23′32″ N38°47′35″ E108°45′31″ N37°38′37″ E107°41′35″ N37°33′17″ E109°15′43″ N38°08′15″
Light desertification (LD)	30-50%	*Lespedeza davurica* + *Artemisia ordosica*	*Lespedeza davurica*	E109°50′29″ N38°40′32″ E110°20′16″ N38°43′15″ E108°41′22″ N37°35′26″ E107°50′36″ N37°39′15″ E108°56′08″ N38°05′06″
Moderate desertification (MD)	10-30%	*Artemisia ordosica* + *Cynanchum komarovii*	*Artemisia ordosica*	E109°52′19″ N38°38′20″ E110°20′56″ N38°41′24″ E108°38′42″ N37°35′31″ E107°52′20″ N37°43′13″ E108°50′27″ N37°58′22″
Severe desertification (SD)	< 10%	Annual herb	*Chenopodiun album*	E109°48′22″ N38°32′43″ E110°29′31″ N38°40′48″ E108°37′15″ N37°42′43″ E108°04′17″ N37°48′28″ E108°42′11″ N37°52′49″

In this research, the fieldwork was conducted at the end of July 2015. We selected five study sites (10 m × 10 m) for each desertification stage. At each study site, five quadrats were selected to collect samples (*Fig. 2*). Four quadrants are located in the middle of the line connecting the center point to the center of each side, and one is at the center of all study sites. A total of 125 quadrats were dug for collecting soil samples. Soil samples were taken from six soil depth categories of 0–5 cm, 5–10 cm, 10–15 cm, 15–20 cm, 20–25 cm, and 25–30 cm. Then the soil samples were put into a sealed plastic bag. Soil bulk density at each site was calculated with a cylinder of 5 cm diameter and 5 cm height for each depth interval.

Laboratory analysis

When the soil samples were brought to the laboratory, they were passed through a 2 mm sieve to remove roots and litters and air-dried for chemical analysis. SOC was

http://www.aloki.hu ● ISSN 1589 1623 (Print) ● ISSN 1785 0037 (Online)
DOI: http://dx.doi.org/10.15666/aeer/1802_29752988

measured using the Walkley-Black method, and TN was determined using the Kjeldahl's method (Bao, 2008). Bulk density for each soil layer was calculated using the core method (Bao, 2008).

Figure 2. *Photos of the sampling sites*

Due to the lack of coarse fragments > 2 mm in the study area, SOC stocks in each soil sample were calculated by *Equation 1:*

$$SOC = \sum_{i=1}^{k} B_i \times C_i \times D_i \times 10 \quad \text{(Eq.1)}$$

where SOC is soil organic carbon stocks ($g \cdot m^{-2}$); k is the number of depth categories ($k = 6$); B_i denotes the soil bulk density ($g \cdot m^{-3}$); C_i is the soil organic carbon content ($g \cdot kg^{-1}$), and D_i presents soil thickness (cm).

TN stocks in each soil sample were calculated by *Equation 2:*

$$TN = \sum_{i=1}^{k} B_i \times N_i \times D_i \times 10 \quad \text{(Eq.2)}$$

where TN is total nitrogen stocks ($g \cdot m^{-2}$), and N_i is the soil nitrogen concentration ($g \cdot kg^{-1}$).

http://www.aloki.hu ● ISSN 1589 1623 (Print) ● ISSN 1785 0037 (Online)
DOI: http://dx.doi.org/10.15666/aeer/1802_29752988

Data analysis approach

Statistical analyses were performed using IBM SPSS Statistics software. One-way analysis-of-variance (ANOVA) and multiple comparisons were used to examine the differences of the concentrations and stocks of SOC and TN among different desertification stages and different depths (McHugh, 2011).

Results

Changes in soil bulk density

Table 2 shows that bulk density varied across soil depths and among different desertification stages. The bulk density in the top layer (0–5 cm) changed from 1.571 $g \cdot cm^{-3}$ in the ND stage to 1.694 $g \cdot cm^{-3}$ in the SD stage, but there was no significant difference among five desertification stages ($P > 0.05$). The minimum value of mean bulk density (0–30 cm) was 1.655 $g \cdot cm^{-3}$ in the ND stage, and the maximum value of mean bulk density (0–30 cm) was 1.671 $g \cdot cm^{-3}$ in the SD stage. There was no significant difference among the five desertification stages ($P > 0.05$). Bulk density fluctuated among different soil depths, and the largest values of bulk density were different in every profile. There were no significant differences among the profiles in every desertification stage ($P > 0.05$).

Table 2. *Changes of bulk density in the five stages of desertification*

Bulk density ($g \cdot cm^{-3}$)	0-5 cm	5-10 cm	10-15cm	15-20 cm	20-25 cm	25-30 cm
ND	1.571 ± 0.073	1.627 ± 0.069	1.667 ± 0.061	1.696 ± 0.146	1.674 ± 0.015	1.694 ± 0.038
PD	1.586 ± 0.139	1.612 ± 0.035	1.601 ± 0.128	1.656 ± 0.051	1.669 ± 0.077	1.652 ± 0.062
LD	1.613 ± 0.030	1.680 ± 0.058	1.588 ± 0.176	1.614 ± 0.079	1.633 ± 0.064	1.634 ± 0.066
MD	1.639 ± 0.157	1.673 ± 0.050	1.622 ± 0.086	1.609 ± 0.080	1.621 ± 0.078	1.635 ± 0.091
SD	1.658 ± 0.104	1.681 ± 0.077	1.663 ± 0.110	1.688 ± 0.046	1.668 ± 0.065	1.670 ± 0.023

Values are means ± SD. The values of bulk density were measured in five desertification stages: ND-non-desertification, PD-potential desertification, LD-light desertification, MD-moderate desertification, SD-severe desertification

Changes in SOC and TN concentration

Figure 3 shows that the SOC and TN concentrations decreased significantly across the desertification stages ($P < 0.05$). With the process of desertification, SOC concentrations (0–30 cm) ranged from 2.409 $g \cdot kg^{-1}$ in the ND stage to 1.072 $g \cdot kg^{-1}$ in the SD stage, whereas TN concentrations (0–30 cm) ranged from 0.251 $g \cdot kg^{-1}$ in the ND stage to 0.113 $g \cdot kg^{-1}$ in the SD stage, showing decreases of 55.5% and 55.1%, respectively. Both SOC and TN concentrations (0-30 cm) decreased significantly with the severity of desertification ($P < 0.05$). Compared with the ND stage, SOC concentration in the SD stage decreased by 63.45%, 56.74%, 51.22%, 48.56%, 53.84%, and 54.99% at soil depths of 0–5, 5–10, 10–15, 15–20, 20–25, and 25–30 cm, while the TN concentration decreased by 67.48%, 67.40%, 46.00%, 49.79%, 42.61%, and 37.48%, respectively. There also existed significant differences at different layers among different desertification stages ($P < 0.05$). The largest decreasing ranges of SOC

http://www.aloki.hu ● ISSN 1589 1623 (Print) ● ISSN 1785 0037 (Online)
DOI: http://dx.doi.org/10.15666/aeer/1802_29752988

and TN concentrations were all observed in the upper layer (0–5 cm), which showed that desertification had a greater impact on the upper layers than on the deeper layers.

Figure 3 also shows the comparing differences of SOC and TN concentrations between different desertification stages in different soil layers. For SOC concentration, there existed significant differences between PD and SD stage at most soil layers (except 10-15 cm) ($P < 0.05$). For TN concentration, significant differences existed between ND and PD stage (except 0–5 cm and 10–15 cm) ($P < 0.05$), and in the upper layer (0–5 cm), a significant difference existed between PD and SD stage ($P < 0.05$). The decreasing results also indicate that the decline ranges of SOC and TN concentrations differed among two desertification stages. The highest decreasing ranges of SOC concentration was existed in the PD to SD stage, with decreases of 24.9% throughout 0–30 cm layer and 37.42% in the top layer (0–5 cm). Influenced by the top layer, the greatest decreasing ranges of TN concentration also existed in the PD to SD stage, which were 18.8% in 0-30 cm layer and 43.13% in 0-5 cm layer. These results show that SOC and TN concentrations in different desertification stages were significantly affected by desertification, especially in the early stages.

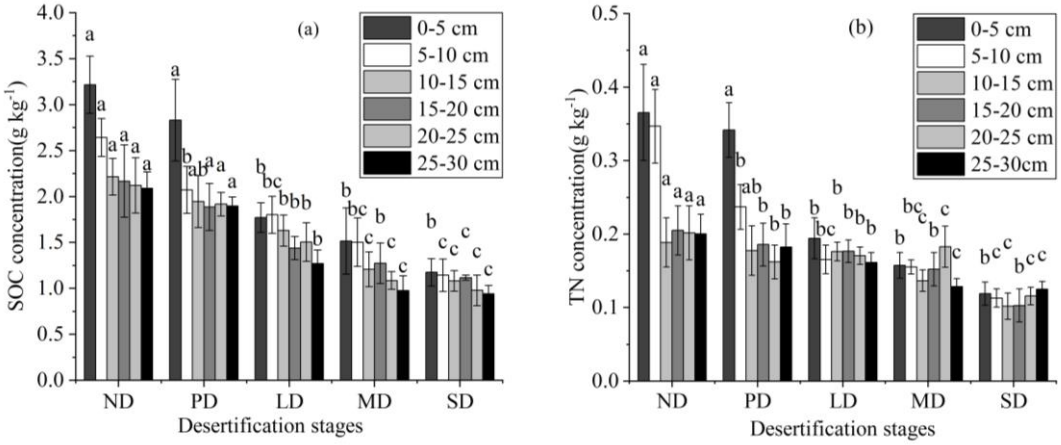

Figure 3. *Changes in the SOC and TN concentrations in five desertification stages. (a) SOC concentration; (b) TN concentration. SOC and TN concentrations were measured in five desertification stages: ND-non-desertification, PD-potential desertification, LD-light desertification, MD-moderate desertification, SD-severe desertification. Error bars indicate the standard deviation. Variations significant at the 0.05 level is indicated by different lowercase letters ($P < 0.05$)*

Changes in SOC and TN stocks

According to *Figure 4*, with the desertification development, SOC and TN stocks decreased significantly ($P < 0.05$). SOC stocks in the top soil layer (0–5 cm) ranged from 252.73 $g \cdot m^{-2}$ in the ND stage to 97.84 $g \cdot m^{-2}$ in the SD stage, and TN stocks in this layer declined from 28.86 $g \cdot m^{-2}$ in the ND stage to 9.90 $g \cdot m^{-2}$ in the SD stage, decreasing by 61.3% and 65.7%, respectively ($P < 0.05$). The SOC and TN stocks also decreased from the top soil layer to the deeper layer, but the decreasing magnitudes were different in different desertification stages. From 10–15 cm to deeper soil layers, there was no significant difference ($P > 0.05$) in both SOC and TN stocks.

http://www.aloki.hu ● ISSN 1589 1623 (Print) ● ISSN 1785 0037 (Online)
DOI: http://dx.doi.org/10.15666/aeer/1802_29752988

Figure 4 also shows the comparing differences of SOC and TN stocks between different desertification stages in different soil layers and at different soil depths. *Figure 4a* shows that, for SOC stocks, there existed significant differences between PD stage and the LD stage ($P < 0.05$) in most of the soil layers. *Figure 4b* shows that, for TN stocks, significant differences were observed mainly between PD stage and LD stage ($P < 0.05$) in 0–5 cm and 5–10 cm depths ($P < 0.05$). *Figure 4c* and *d* show that SOC and TN stocks decreased significantly at different soil depths ($P < 0.05$), and there existed significant differences between every two desertification stages ($P < 0.05$). These results show that desertification strongly influenced SOC and TN stocks in the study area.

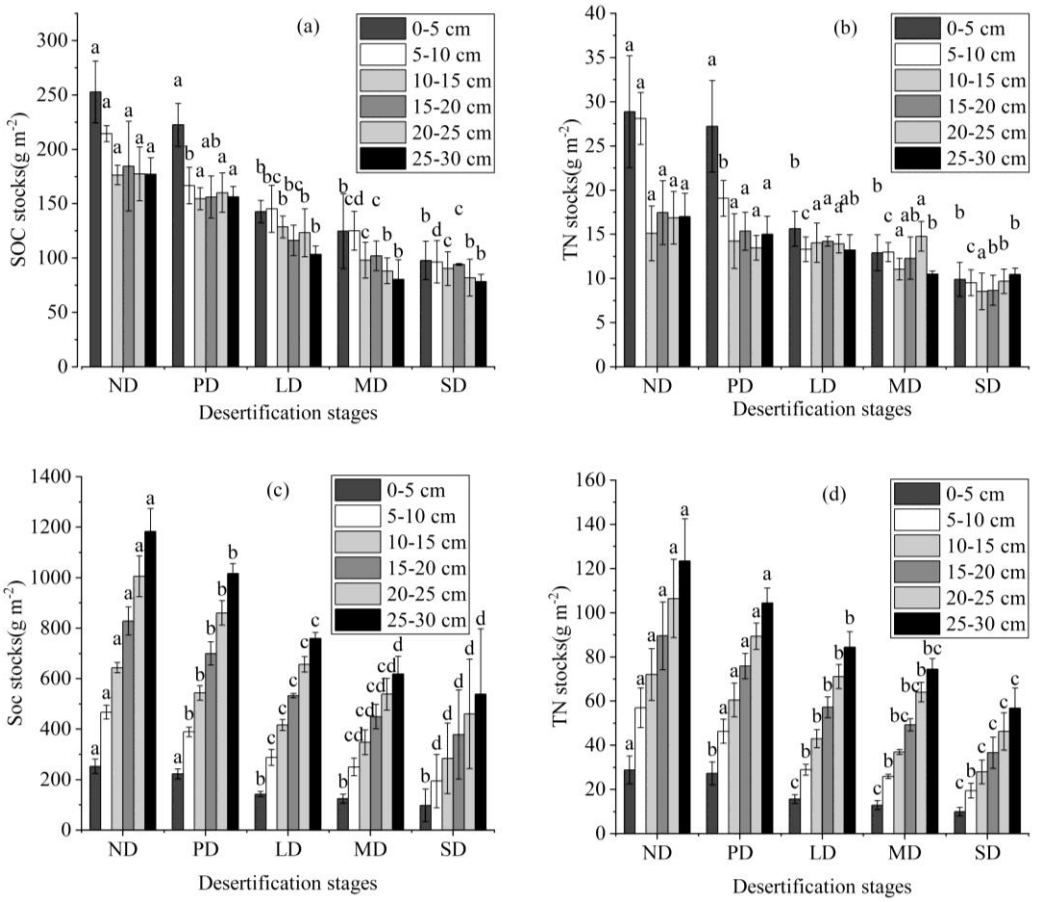

Figure 4. *Changes in the SOC and TN stocks in five desertification stages. (a) SOC stocks in different soil layers; (b) TN stocks in different soil layers; (c) SOC stocks at different soil depths; (d) TN stocks at different soil depths. SOC and TN stocks were measured in five desertification stages: ND-non-desertification, PD-potential desertification, LD-light desertification, MD-moderate desertification, SD-severe desertification. Error bars indicate the standard deviation. Variations significant at the 0.05 level are indicated by different lowercase letters ($P < 0.05$)*

Figure 5 shows that, with the process of desertification, SOC, and TN stocks in 0–30 cm depth reduced significantly ($P < 0.05$). SOC stocks (0–30 cm) decreased from 1182.73 $g \cdot m^{-2}$ in the ND stage to 539.21 $g \cdot m^{-2}$ in the SD stage, and TN stocks (0–30 cm) decreased from 123.42 $g \cdot m^{-2}$ in the ND stage to 56.75 $g \cdot m^{-2}$ in the SD stage, accounting for decreases of 54.4% and 54.0%, respectively ($P < 0.05$). The total losses of SOC and

http://www.aloki.hu ● ISSN 1589 1623 (Print) ● ISSN 1785 0037 (Online)
DOI: http://dx.doi.org/10.15666/aeer/1802_29752988

TN stocks in the SD stage compared to the ND stage were 653.52 $g \cdot m^{-2}$ and 66.67 $g \cdot m^{-2}$, respectively. The data also showed that the losses of SOD and TN stocks from the PD to LD stages were the most comparable to the losses between other contiguous stages.

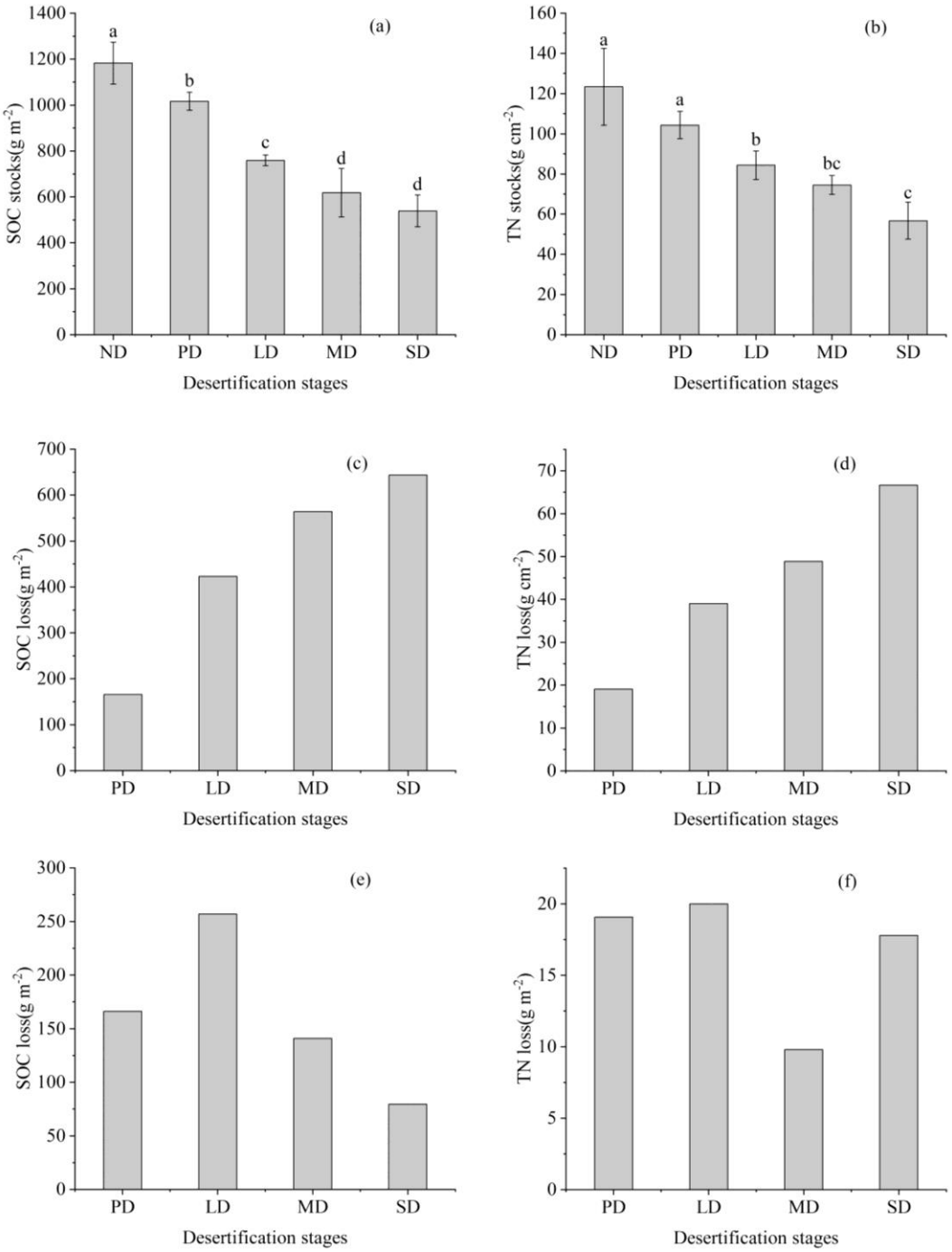

Figure 5. *Changes in the SOC and TN stocks in 0-30 depth in five desertification stages. (a) SOC stocks in 0-30 depth; (b) TN stocks in 0-30 depth; (c) SOC loss compared to ND; (d) TN loss compared to ND; (e) SOC loss compared to contiguous stages; (f) TN loss compared to contiguous stages. SOC and TN stocks and losses were measured in five desertification stages: ND-Non-desertification, PD-potential desertification, LD-light desertification, MD-moderate desertification, SD-severe desertification. Error bars indicate the standard deviation. Variations significant at the 0.05 level are indicated by different lowercase letters ($P < 0.05$)*

http://www.aloki.hu ● ISSN 1589 1623 (Print) ● ISSN 1785 0037 (Online)
DOI: http://dx.doi.org/10.15666/aeer/1802_29752988

Total changes in SOC and TN stocks from 2003 to 2015

According to *Table 3*, we monitored the area changes of different desertification stages from 2003 to 2015. The area changes between different desertification stages could be observed, but the reversal or aggravation of desertification could not be precisely assessed. Calculation of the total changes of SOC and TN stocks from 2003 to 2015 show that the SOC and TN stocks increased by 4.25×10^8 kg and 0.71×10^8 kg, respectively. Thus, the authors conclude that the same amounts of SOC and TN were accumulated during this period. Therefore, we could conclude that the desertification was a reversal from 2003 to 2015.

Table 3. *The total changes of SOC and TN stocks (0–30 cm) in the study area from 2003 to 2015*

Type		Area 2015 (km^2)						Stocks 2003 ($\times 10^8$ kg)	
		ND	**PD**	**LD**	**MD**	**SD**	**Total Area**	**SOC**	**TN**
Area 2003 (km^2)	ND	62.81	65.31	12.80	9.83	3.43	154.18	1.82	0.19
	PD	86.89	2554.57	735.65	1475.73	290.28	5143.11	52.29	5.37
	LD	12.07	1644.75	1217.18	2579.24	686.70	6139.95	46.64	5.18
	MD	12.93	1380.6	2029.89	5255.4	1707.69	10386.50	64.27	7.74
	SD	6.00	367.00	756.70	4834.03	3241.40	9205.14	49.64	5.22
	Total area	180.7	6012.23	4752.23	14154.23	5929.5	31028.87	214.66	23.7
Stocks 2015 ($\times 10^8$ kg)	SOC	2.14	61.12	36.1	87.58	31.97	218.91	**4.25**	
	TN	0.22	6.27	4.01	10.55	3.36	24.41		**0.71**

ND-non-desertification, PD-potential desertification, LD-light desertification, MD-moderate desertification, SD-severe desertification

Discussion

Desertification is a global disaster and has strongly affected many places and large populations around the world. Many studies have demonstrated that desertification would induce dramatic changes in the physical properties and nutrients of soil (Hu et al., 2017; Qiu et al., 2012). The results of our study demonstrate that the soil bulk density changed little in the upper layer (0–5 cm) with desertification, there was no significant difference among different desertification stages ($P > 0.05$).

Our results demonstrate that desertification had a remarkable effect on SOC and TN concentrations in the southeast edge of the Mu Us sandy land. The effects were observed not only in different desertification stages but also at different soil depths. SOC and TN concentrations decreased significantly with the process of desertification, which is similar to the outcome of Zhou et al. (2008). This could be mainly due to the decrease in vegetation cover and wind erosion (Albaladejo et al., 1998). Vegetation is the primary source of soil nutrients, and aeolian erosion is considered the trigger of desertification because it could remove fine soil particles rich in nutrients, and then leads to the reduction of SOC and TN concentrations. The results also indicate that the declining rates of SOC and TN concentrations were different between two contiguous stages. From the PD stage to the LD stage, the decreasing ranges of both SOC concentration and TN concentration were larger than those in other contiguous stages.

http://www.aloki.hu ● ISSN 1589 1623 (Print) ● ISSN 1785 0037 (Online)
DOI: http://dx.doi.org/10.15666/aeer/1802_29752988

This situation supports the results of Zhao et al. (2009) and Tang et al. (2015), which also demonstrated that SOC and TN decreased more sharply in early desertification stages.

In contrast, in a study on the impacts of desertification on alpine-cold grassland, Hu et al. (2017) reported that, with the progression of desertification, the rate of SOC loss accelerated, which is not consistent with our results (Hu et al., 2017). This may be because of the different climate between alpine-cold and semiarid areas. The results of our study also show that SOC and TN concentrations decreased with deeper soil layers, but they declined faster in the upper layer, which indicated that desertification has more significant effects on the top soil. Our results are consistent with the findings of Zhu et al. (1994), in which desertification was found to firstly affect the top soil.

This study shows that, with the aggravation of desertification, both SOC and TN stocks decreased significantly, with the highest SOC and TN stocks in the ND stage and lowest of them in the SD stage. Compared with the ND stage, the losses of SOC and TN stocks were the largest in the SD stage. The losses of SOC and TN stocks would result in the deterioration of land productivity, which will further lead to land degradation and increased desertification; it increases the release of CO_2, NO_x, and other greenhouse gases to the atmosphere, which could accelerate climate change. Besides, *Figure 5* shows that desertification effects on SOC and TN stocks were most severe in the LD stage, which confirmed the results of SOC and TN concentrations. This is also consistent with the viewpoint of Wang et al. (2002) and Zhou et al. (2008), their studies reported that the impact of desertification on C and N stocks were significantly different in five desertification stages. In the further control of desertification, the stages with the most severe changes should be given more attention because they are vital to the restoration of desertification.

Human factors, such as over-cultivation and overgrazing, are believed to be critical factors promoting desertification (Li et al., 2017). The Mu Us Sandy Land, which is located in the agropastoral ecotone of China, is extremely sensitive and fragile and has poor self-restoration ability to external disturbance (Liu et al., 2012). In the 20th century, this area suffered from extensive grazing and cultivating, and experienced the threat of sandy desertification (Li et al., 2017). Fortunately, since 1999; the Conversion of Cropland to Forest Project was implemented, and inappropriate land-use activities were forbidden (Li et al., 2017). Recently, many studies based on statistic data or RS and GIS reported that the Conversion of Cropland to Forest Project had practical impacts on combating land desertification and promoting vegetation restoration in this area (Liang et al., 2016; Wang, 2018; Zhang et al., 2008). These studies show that desertification reversion is associated with the restoration of soil nutrient levels. However, previous research only analyzed area changes of different land use or different desertification stages. Accordingly, this study calculated the total changes of SOC and TN stocks to evaluate the changes in soil nutrient levels for further assessing whether the desertification has reversed or not since the implementation of the Conversion of Cropland to Forest Project. Our results showed that 4.25×10^8 kg SOC and 0.71×10^8 kg TN were accumulated since 2003, which confirmed the findings of previous studies and indicates the active influence of the Conversion of Cropland to Forest Project on the restoration of the ecosystem. Indeed, this study not only presents a new method for the quantitative assessment of desertification but also has meaning for the calculation of the potential of soil carbon and nitrogen fixation in the reversal of desertification. At the same time, the results support the view that returning cultivated

http://www.aloki.hu ● ISSN 1589 1623 (Print) ● ISSN 1785 0037 (Online)
DOI: http://dx.doi.org/10.15666/aeer/1802_29752988

land to grassland and long-term livestock removal were effective in restoring desertification in this site and also provide encouragement for managers to re-establish the ecosystem of damaged grasslands.

Conclusions

In this investigation, results show that desertification affected SOC and TN concentrations significantly, especially in the top soil, and deeper soil depths. Desertification also resulted in remarkable losses of SOC and TN stocks (0–30 cm), with losses of 643.52 $g \cdot m^{-2}$ and 66.67 $g \cdot m^{-2}$, respectively. Besides, the losses of SOC and TN stocks from PD stages to LD stages were the largest between two contiguous stages, which means that the early stages of desertification are crucial periods for the restoration of desertification. More attention should be given to these stages of combating desertification. An integrated analysis of field experiment data and temporal-spatial changing data was used to calculate the total changes of SOC and TN stocks, the results show that, from 2003 to 2015, total SOC and TN stocks increased by 4.25×10^8 kg and 0.71×10^8 kg, respectively. The results not only indicate that the desertification reversed during this period, but also indicate that this method could provide a new quantitative method to assess the desertification process. The results of this study also support the effectiveness of the Conversion of Cropland to Forest Project in grassland ecosystems. For the future study, a more accurate method needs to be furtherly explored so that the fieldwork and experiment data can be in better accordance with the temporal-spatial analysis data.

Acknowledgements. This work was supported by the National Natural Science Foundation of China (41501571), Shaanxi Provincial Natural Science Foundation of China (2015JQ4110); China Scholarship Council Foundation (201808615052).

REFERENCES

[1] Agren, G. I., Bosatta, E. (1987): Theoretical-analysis of the long-term dynamics of carbon and nitrogen in soils. – Ecology 68: 1181-1189.
[2] Albaladejo, J., Martinez-Mena, M., Roldan, A., Castillo, V. (1998): Soil degradation and desertification induced by vegetation removal in a semiarid environment. – Soil Use Manage 14: 1-5.
[3] Alireza, R. A. H., Shahla, M. (2017): Organic and inorganic carbon storage in soils along an arid to dry sub-humid climosequence in northwest of Iran. – Catena 153: 66-74.
[4] Allington, G. R. H., Valone, T. J. (2010): Reversal of desertification: the role of physical and chemical soil properties. – Journal of Arid Environment 74: 973-977.
[5] Aweke, M., Gelaw, B. R. S., Lal, R. (2015): Organic carbon and nitrogen associated with soil aggregates and particle sizes under different land use in Trigay, Northern Ethiopia. – Land Degradation & Development 26: 690-700.
[6] Bao, S. D. (2008): Agricultural and chemical analysis methods of soils. – China Agriculture Press, Beijing.
[7] Batjes, N. H. (1996): Total carbon and nitrogen in the soils of the world. – European Journal of Soil Science 47: 151-163.
[8] Binns, T. (2000): World atlas of desertification., 2nd edition. – Applied Geography 20: 83-84.

http://www.aloki.hu ● ISSN 1589 1623 (Print) ● ISSN 1785 0037 (Online)
DOI: http://dx.doi.org/10.15666/aeer/1802_29752988

[9] Bouwman, A. F. (1990): Soils and the Greenhouse Effect - Introduction. – In: Bouwman, A. F. (ed.) Soils and the Greenhouse Effect. Wiley, Chichester, pp. 25-32.
[10] Carr, S., Mpande, R. (1996): Does the definition of the issue matter? NGO influence and the International Convention to Combat Desertification in Africa. – The Journal of Commonwealth & Comparative Politics 34: 143-166.
[11] Deng, L., Zhu, G. Y., Tang, Z. S., Shangguan, Z. P. (2016): Global patterns of the effects of land-use changes on soil carbon stocks. – Global Ecology and Conservation 5: 127-138.
[12] Dessie, A. B. R., Hans, S., Christoph, R., Abrham, A., Birru, Y., Douglas, L. G. (2017): Deforestation and land use strongly effect soil organic carbon and nitrogen stock in Northwest Ethiopia. – Catena 153: 89–99.
[13] Detwiler, R. P. (1986): Land-use change and the global carbon-cycle - the role of tropical soils. – Biogeochemistry 2: 67-93.
[14] Duan, H. C., Wang, T., Xue, X., Yan, C. Z. (2019): Dynamic monitoring of aeolian desertification based on multiple indicators in Horqin Sandy Land, China. – Science of Total Environment 650: 2374-2388.
[15] Emanuel, W. R., Killough, G. G., Post, W. M., Shugart, H. H. (1984): Modeling terrestrial ecosystems in the global carbon-cycle with shifts in carbon storage capacity by land-use change. – Ecology 65: 970-983.
[16] Gao, H. J., Jiang, Q. G. (2006): Research of desert and sandy desertification land partition in North China based on remote sensing technology. – Remote Sensing of the Environment: 15th National Symposium on Remote Sensing of China 6200, Guiyan City, China.
[17] Hu, Y. F., Jiang, S. L., Yuan, S., Deng, L. J., Xiao, H. H., Shu, X. Y., Chen, G. D., Xia, J. G. (2017): Changes in soil organic carbon and its active fractions in different desertification stages of alpine-cold grassland in the eastern Qinghai-Tibet Plateau. – Environmental Earth Science 76: 348.
[18] Huang, D., Wang, K., Wu, W. L. (2007): Dynamics of soil physical and chemical properties and vegetation succession characteristics during grassland desertification under sheep grazing in an agro-pastoral transition zone in northern China. – Journal of Arid Environment 70: 120-136.
[19] Jenkinson, D. S., Rayner, J. H. (1977): Turnover of soil organic-matter in some of Rothamsted classical experiments. – Soil Science 123: 298-305.
[20] Kelly, R. H., Burke, I. C., Lauenroth, W. K. (1996): Soil organic matter and nutrient availability responses to reduced plant inputs in shortgrass steppe. – Ecology 77: 2516-2527.
[21] Kirschbaum, M. U. F. (2000): Will changes in soil organic carbon act as a positive or negative feedback on global warming? – Biogeochemistry 48: 21-51.
[22] Lamchin, M., Lee, J. Y., Lee, W. K., Lee, E. J., Kim, M., Lim, C. H., Choi, H. A., Kim, S. R. (2016): Assessment of land cover change and desertification using remote sensing technology in a local region of Mongolia. – Advances in Space Research 57: 64-77.
[23] Li, S., Wang, T., Yan, C. Z. (2017): Assessing the role of policies on land-use/cover change from 1965 to 2015 in the Mu Us sandy land, northern China. – Sustainability 9: 1164.
[24] Liang, P., Yang, X. P. (2016): Landscape spatial patterns in the Maowusu (Mu Us) Sandy Land, northern China and their impact factors. – Catena 145: 321-333.
[25] Liu, Q. F., Zhao, Y. Y., Zhang, X. F., Buyantuev, A., Niu, J. M., Wang, X. J. (2018): Spatiotemporal patterns of desertification dynamics and desertification effects on ecosystem services in the Mu Us Desert in China. – Sustainability 10: 589.
[26] McHugh, M. L. (2011): Multiple comparison analysis testing in ANOVA. – Biochemia Medica 21: 203-209.

http://www.aloki.hu ● ISSN 1589 1623 (Print) ● ISSN 1785 0037 (Online)
DOI: http://dx.doi.org/10.15666/aeer/1802_29752988

[27] Mehari, A., Tesfaye, F. B., Ruiz, R. P., Valentín, P., Andrés, B. O. (2016): Impact of changes in land use, species and elevation on soil organic carbon and total nitrogen in Ethiopian Central Highlands. – Geoderma 261: 70-79.
[28] Post, W. M., Emanuel, W. R., Zinke, P. J., Stangenberger, A. G. (1982): Soil carbon pools and world life zones. – Nature 298: 156-159.
[29] Qi, Y. B., Chang, Q. R., Jia, K. L., Liu, M. Y., Liu, J., Chen, T. (2012): Temporal-spatial variability of desertification in an agro-pastoral transitional zone of northern Shaanxi Province, China. – Catena 88: 37-45.
[30] Qiu, L. P., Wei, X. R., Zhang, X. C., Cheng, J. M., Gale, W., Guo, C., Long, T. (2012): Soil organic carbon losses due to land use change in a semiarid grassland. – Plant Soil 355: 299-309.
[31] Russell, A. E., Laird, D. A., Parkin, T. B., Mallarino, A. P. (2005): Impact of nitrogen fertilization and cropping system on carbon sequestration in Midwestern Mollisols. – Soil Science Society of America Journal 69: 413-422.
[32] Spycher, G., Sollins, P., Rose, S. (1983): Carbon and nitrogen in the lightfraction of a forest soil - vertical-distribution and seasonal patterns. – Soil Science 135: 79-87.
[33] Tang, Z. S., An, H., Shangguan, Z. P. (2015): The impact of desertification on carbon and nitrogen storage in the desert steppe ecosystem. – Ecological Engineering 84: 92-99.
[34] Twongyirwe, R., Sheil, D., Majaliwa, J. G. M., Ebanyat, P., Tenywa, M. M., Van Heist, M., Kumar, L. (2013): Variability of soil organic carbon stocks under different land uses: a study in an afro-montane landscape in southwestern Uganda. – Geoderma 193: 282-289.
[35] UNCCD (1994): United Nations Convention to Combat Desertification in Those Countries Experiencing Serious Drought and/or Desertification, Particularly in Africa. – UNCCD, Paris.
[36] Van Minnen, J. G., Goldewijk, K. K., Stehfest, E., Eickhout, B., Van Drecht, G., Leemans, R. (2009): The importance of three centuries of land-use change for the global and regional terrestrial carbon cycle. – Climatic Change 97: 123-144.
[37] Wang, L., Jia, D., Shi, H. S., Lin, Q. Z., Ge, M. L., Xu, Y. M. (2006): Possibilities of multi-spectral data for the assessment of soil nitrogen content. – 2006 IEEE International Symposium on Geoscience and Remote Sensing, Denver, CO.
[38] Wang, T. (2018): Impacts of the Grain for Green Project on soil erosion: a case study in the Wuding River and Luohe River basins in the Shaanxi Province of China. – Applied Ecology and Environmental Research 16: 4165-4181.
[39] Wang, T., Zhu, Z., Wu, W. (2002): Sandy desertification in the north of China. – Science in China Series D 45: 23-34.
[40] Zhang, Y. Z., Chen, Z. Y., Zhu, B. Q., Luo, X. Y., Guan, Y. N., Guo, S., Nie, Y. P. (2008): Land desertification monitoring and assessment in Yulin of Northwest China using remote sensing and geographic information systems (GIS). – Environmental Monitoring Assessment 147: 327-337.
[41] Zhang, Z. H., Huisingh, D. (2018): Combating desertification in China: monitoring, control, management and revegetation. – Journal of Cleaner Production 182: 765-775.
[42] Zhao, H. L., He, Y. H., Zhou, R. L., Su, Y. Z., Li, Y. Q., Drake, S. (2009): Effects of desertification on soil organic C and N content in sandy farmland and grassland of Inner Mongolia. – Catena 77: 187-191.
[43] Zhou, R. L., Li, Y. Q., Zhao, H. L., Drake, S. (2008): Desertification effects on C and N content of sandy soils under grassland in Horqin, northern China. – Geoderma 145: 370-375.
[44] Zhu, Z. D., Chen, G. T. (1994): Sandy desertification in China. – Science Press, Beijing.

http://www.aloki.hu ● ISSN 1589 1623 (Print) ● ISSN 1785 0037 (Online)
DOI: http://dx.doi.org/10.15666/aeer/1802_29752988

IMPACT OF CLIMATIC FACTORS ON THE SUCCESS OF HUNTING VARIOUS GAME SPECIES IN CZECH REPUBLIC

RÖSSLOVÁ, M.[1] – VACEK, S.[2] – VACEK, Z.[2*] – PROKŮPKOVÁ, A.[2]

[1]*Czech University of Life Sciences Prague, Faculty of Environmental Sciences*
Kamýcká 129, 165 21 Prague 6 - Suchdol, Czech Republic

[2]*Czech University of Life Sciences Prague, Faculty of Forestry and Wood Sciences*
Kamýcká 129, 165 21 Prague 6 - Suchdol, Czech Republic

[*]*Corresponding author*
e-mail: vacekz@fld.czu.cz

(Received 14th Nov 2019; accepted 12th Feb 2020)

Abstract. The study evaluates the impact of climatic factors on the success of hunting in the Doupov Hills in the Czech Republic. The aim was to assess the impact of climatic factors on the success of individual and group hunting of various game species and their sex and age between 2005–2012. Overall, 27 thousand animals of the following game species were analyzed: red deer (*Cervus elaphus* L.), sika deer (*Cervus nippon* Temminck), fallow deer (*Dama dama* L.), mouflon (*Ovis musimon* L.), roe deer (*Capreolus capreolus* L.), wild boar (*Sus scrofa* L.), European badger (*Meles meles* L.) and red fox (*Vulpes vulpes* L.). The results show that mostly temperature co-determines the success of both hunting methods. Atmospheric pressure represents another important factor of influence, especially in group hunting. Snow cover supports variability of the probability of game hunting success. The success of hunting increased with decreasing temperature, increasing snow cover and increasing atmospheric pressure. Conversely, precipitation and wind speed had low effect on the success of hunting. Individual hunting was associated with significantly better climatic conditions in comparison to group hunting. Moreover, male game species were hunted in more favourable climatic conditions compared to female. Findings on the influence of climatic factors on the success of hunting can support planning the suitable time and method of hunting, thus increasing the success of hunting in montane and submontane regions of Central Europe.
Keywords: *hunting method, ungulate, temperature, precipitation, Czech Republic*

Introduction

Over the past decades and even centuries, European landscape has undergone significant changes due to the intensification of agriculture and land use (Ramankutty and Foley, 1999; Cukor et al., 2019a). As the landscape was being transformed and the demand for food was growing, agricultural production was increasing, field blocks widening, and structure of the crops changing (Levers et al., 2016; Wrzesień and Denisow, 2016). The new situation proved favourable for the ungulates that adapted well, and their populations increased in most European countries (Bleier et al., 2012; Hagen et al., 2014; Heurich et al., 2015; Thulin et al., 2015; Baltzinger et al., 2016).

The increase in numbers of large mammals does not derive only from the changes in landscape and intensification of agriculture – game populations are further influenced, for example, by climatic conditions (Hone and Clutton-Brock, 2007; Borowik et al., 2013; Koons et al., 2015). The 20th century witnessed gradual changes of climate; in most cases, studies have used summary factors such as mean temperature or total rainfall (Thomas et al., 2004, 2006). The changes influenced population dynamics (Balmford et al., 2003; Forsman and Mönkkönen, 2003; Sauerbrei et al., 2014), ecosystem functioning (Peñuelas et al., 2002; Hays et al., 2005) and also natural systems

http://www.aloki.hu ● ISSN 1589 1623 (Print) ● ISSN1785 0037 (Online)
DOI: http://dx.doi.org/10.15666/aeer/1802_29893014

(Böhning-Gaese and Lemoine, 2004; Hays et al., 2005; Parmesan, 2006). Recently, there has been a substantial increase in the amount of literature on climate change affecting populations of vertebrates. For large herbivorous mammals, most attention has been paid to distribution responses to climate variation. Much less information is available about how climate affects animal behaviour, i.e. the climate mechanisms (Rivrud et al., 2010, 2014). The dynamics of animal populations are influenced by climatic conditions, on both the local and regional scale (Newton, 1998; Hallett et al., 2004).

Climatic conditions during the year have a significant impact on the populations of ungulates and their dynamics, either directly through changes in mortality or indirectly through the quantity and quality of food (Post and Stenseth, 1999; Hone and Clutton-Brock, 2007; Borowik et al., 2013). Harsh winter conditions, for instance, have influenced the survival rate of domestic sheep (*Ovis aries* L.) (Milner et al., 1999; Coulson et al., 2001), red deer (*Cervus elaphus* L.) (Forchhammer et al., 1998) and roe deer (*Capreolus capreolus* L.) (Gaillard et al., 1993) and increased the numbers of mountain-dwelling woodland caribou (*Rangifer tarandus caribou* Gmelin) (Hegel et al., 2010). Autumn weather negatively influenced the reproduction rate of white-tailed deer (*Odocoileus virginianus* Zimmermann), while spring weather conditions supported successful reproduction (Simard et al., 2010). For red deer, the weight at birth was affected by rainfall in winter and spring temperatures (Sims et al., 2007).

Pettorelli et al. (2007), for example, report that forest mammals are very sensitive to the climate change of primary productivity and the phenological timing of green plants as their principal source of food. The annual fluctuation in weather affected the time and rate of the growth of plants that influenced juvenile growth of bighorn sheep (*Ovis canadensis* Shaw) and mountain goats (*Oreamnos americanus* Blainville), survival of bighorn sheep and Alpine ibex (*Capra ibex* L.) (Pettorelli et al., 2007) and the age of first reproduction of red deer (Langvatn et al., 1996).

Another major reason for the changes in populations of ungulates is the absence of natural predators, i.e. beasts of prey that play a key role in regulating the abundance of the ungulate populations (Buckland et al., 1996; Nilsen et al., 2009; Heurich et al., 2012). Gradually, hunting management became a tool to control game populations and regulate their distribution (Hothorn and Müller, 2010; Bischof et al., 2012; Heurich et al., 2015). In recent years, the importance of hunting management has been mentioned especially in the context of ever-increasing game-induced damage to field crops (Herrero et al., 2006; Bleier et al., 2012) and orchards (Mower et al., 1997; Marada et al., 2019). Moreover, increasing game populations significantly negatively affect forests by browsing of natural regeneration (Vacek et al., 2014, 2015; Ambrož et al., 2015; Slanař et al., 2017) and by bark stripping of young stands (Gerhardt et al., 2013; Månsson and Jarnemo, 2013; Cukor et al., 2019b, 2019c). The damage is caused not only by the native species of cloven-hoofed game but also by species introduced to the European continent in the past (Putman and Moore, 1998; Pitra and Lutz, 2005; Ward, 2005; Pérez-Espona et al., 2009). Due to the aforementioned, it is important to thoroughly monitor game populations using modern technology to determine appropriate wildlife management (Linchant et al., 2015; Cukor et al., 2019d).

Hunting management is a complex process driven by interactions between the dynamics of the natural system and stakeholders' decision-making and behaviour (Keuling et al., 2013; Quirós-Fernández et al., 2017). The effects of hunting pressure on spatial behaviour depend on several factors, including the hunting method (Root et

http://www.aloki.hu ● ISSN 1589 1623 (Print) ● ISSN1785 0037 (Online)
DOI: http://dx.doi.org/10.15666/aeer/1802_29893014

al., 1988; Millspaugh et al., 2000; Vieira et al., 2003), level of hunting pressure (Johnson et al., 2004), local laws and hunting philosophy (Williams et al., 2013). The social structure is also important for animals living in a group: the loss of an individual may have different consequences depending on the hierarchical role it played within the group (Tuytten and McDonald, 2000). Findings on game behaviour that could improve hunting success were investigated e.g. in sika deer (*Cervus nippon* Temminck), whose pasture practice was observed during autumn and winter, using a Global Positioning System (GPS) tracking collar. During the hunting season, the collared deer stayed in a hiding place and avoided the pasture the entire day, while after the hunting season, the collared deer preferred sunny and calm pastures during the day as there was no human disturbance (Kamei et al., 2010).

A successful hunt is also co-determined by the habitat characteristics of the hunting district (Vercauteren and Hyngstrom, 1998; Millspaugh et al., 2000; Conner et al., 2001) and current climatic conditions. An open site such as a field is exposed to harsh weather more intensively in comparison to forest stands (Solberg et al., 2010). Weather can also affect the behaviour of the hunter (Rivrud et al., 2010) but, as far as we know, no study on the extent to which the hunter's behaviour is influenced by specific weather conditions has been published. In accordance with a general notion, hunting at moonlit nights seems to be more successful than when the sky is overcast (Theuerkauf et al., 2003). Hunting is always more intensive over the weekend compared to working days regardless of weather (Ciuti et al., 2012). Ciuti et al. (2012) also state that hunting success depends on the behaviour of animals, which is different in an open site and in the forest. Animals of different age and sex behave differently depending on the type of environment. Younger individuals are less alert than the older and more experienced individuals (Ciuti et al., 2012), therefore they can be hunted more successfully than older individuals.

It is well known that some habitat features, including biotope characteristics and climate change, generally affect the predator-prey dynamics (Kunkel and Pletscher, 2000; Lebel et al., 2012; Kuijper et al., 2013). On hunting grounds, the hunters are sometimes considered to be predators and hunted animals the prey (Nugent and Choquenot, 2004). Ecological differences on the site affect the hunters as well. For example, extreme cold or heavy rainfall is less attractive for hunting than hot and rain-free weather (Rivrud et al., 2014).

The success of game observation and hunting depends on numerous factors, some of which can be taken advantage of by the hunters, improving their hunting success (Merkel, 2010). These include, for example, familiarity with the environment, biology of game and its resting haunts, and appropriate timing of the hunt (Bunnefeld et al., 2009). There are factors unsusceptible to our will, especially weather conditions at a given time and place (Rivrud et al., 2014).

Knowledge of the influence of detailed climatic characteristics on the success of hunting of various game species is still inadequate. The aim of this work is therefore to assess the influence of detailed climatic factors (maximum and minimum wind speed in m s^{-1}, mean, minimum and maximum daytime temperature in ^{o}C, 30-minute-interval temperature progress during the course of the day in ^{o}C, daily precipitation in mm, total daily snow cover in cm, atmospheric pressure reduced to sea level in Pa) on the method and success of hunting of various game species (red deer, sika deer, fallow deer */Dama dama* L./, mouflon */Ovis musimon* L./, roe deer, wild boar /*Sus scrofa* L./, European badger */Meles meles* L./, red fox /*Vulpes vulpes* L./) and their sex (male, female) and

http://www.aloki.hu ● ISSN 1589 1623 (Print) ● ISSN1785 0037 (Online)
DOI: http://dx.doi.org/10.15666/aeer/1802_29893014

age (adults, young animals) in 2005–2012 in the hunting grounds of the Karlovy Vary division of Military Forests and Estates, state enterprise (VLS) in Doupov Hills. In terms of game and hunting management it is important to know detailed information about the history of the study territory (Pohja-Mykrä et al., 2005; Rivrud et al., 2013). The settlement of the Doupov Hills, especially of their marginal parts and the Ohře River valley, dates back to the Neolithic (5500–4000 years BC). After the Thirty Years' War, the area was almost completely depopulated, and people were returning very slowly. After 1880, the area witnessed another depopulation as the inhabitants were leaving to seek work in nearby industrial cities. After the Second World War, prevailing German population was expelled. By Government resolution of March 4, 1953, Hradiště military training ground was set up on 290.4 km^2, gradually expanding to 331.6 km^2 (Culek et al., 2013), which helped to preserve natural landscape of the Doupov Hills and protect it from processes typical of the 20th century landscape (large-scale agricultural and forestry management, fertilization, application of chemical methods and amelioration) to the present day (Tscharntke et al., 2005; Lundmark et al., 2013; Cukor et al., 2017; Vacek et al., 2019).

The hypotheses of this research were that:

1) Favourable climatic characteristics (temperature, atmospheric pressure and precipitation) increase the success of particular game species hunting.
2) The hunting method is selected not only by climatic characteristics but also by particular hunting ground conditions, forest stand characteristics, and sex and age of particular game species.

Materials and Methods

Study area

The Doupov Hills are a geomorphological complex in the south of the Ore Mountains system in the north-west of the Czech Republic (*Fig. 1*). The area of the Doupov Hills is 607 km^2. Most of the range is situated on the right bank of the Ohře River, while a minor part is located also on its left bank. The Doupov Hills are composed of tertiary volcanic materials: lava (tephrites, leucitites) and tuff. The range is shaped as flat circular highlands, with the highest peaks reaching from 700 to 934 m a.s.l. (Vacek et al., 2003). According to Köppen world climate classification (Köppen, 1936), the study area predominantly belongs to humid continental climate characterized by a moderately warm to hot climate summers and cold winters (classification Dfb), while the highest parts belong to a boreal climate area characterized by long, usually very cold winters, and short, cool to mild summers (classification Dfc). Windward southwest and northwest slopes are wetter than the eastern, rain-shadowed slopes. The sunny exposures where the foothills verge into the basins are warmer than the inversion narrow steep-walled valleys and terrain depressions affected by water. The average annual air temperature ranges from 5.0 to 6.9°C and the precipitation ranges from 550 to 960 mm (*Fig. 1*). The average relative air humidity is in a range of 67-84%. The number of days with snow cover is around 80 (mean occurrence between October 27th and April 30th) and the average maximum snow depth is between 25-45 cm. The length of sunshine ranges from 30 hours in December to 225 hours in June (annually 1,554 hours). The length of the vegetation season varies from 110 to 150 days. Destructive winds come mainly from the west (Plíva and Žlábek, 1986; Tolasz, 2007).

http://www.aloki.hu ● ISSN 1589 1623 (Print) ● ISSN1785 0037 (Online)
DOI: http://dx.doi.org/10.15666/aeer/1802_29893014

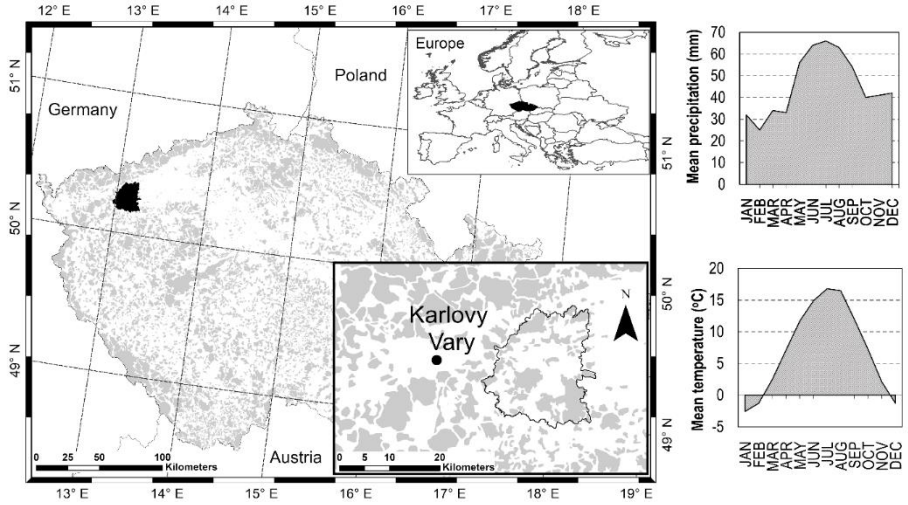

Figure 1. *The area of interest the Doupov Hills in the Czech Republic; the grey colour indicates the forest cover; mean monthly climate values (air temperature and precipitation) in 1939-2017 (right)*

Regarding soils, cambisols prevail in the lower and middle parts of the range, followed by cryptopodzols and podzols in the higher parts. Pseudogleys, gleys and organozems are common in terrain depressions (Demek et al., 2006). Plants of the area have typical features of Hercynian flora of montane and submontane zones. There are acidophilous oak forests on sunny exposures, verging into herb-rich beech forests and dominant woodrush beech forests on more nutrient soils. As the elevation rises, there are acidophilic montane beech forests, and in damp localities we observe water-drenched spruce forests and transitional peat bogs. Along the streams there are meadows and alder woods, and talus forests on the steep slopes. Sparse hornbeam oak, acidophilic and relic pine forest (Průša, 2001) should also be mentioned.

The landscape, essentially uninhabited and used only for training the troops, has acquired unusual features. The most striking – for a mountain range – are vast shrubby areas, pools in missile craters, rocket ranges battered by frequent fires, or exposed surface of tank roads, i.e. phenomena non-existent in civilian countryside. We also observe well-preserved genuine biotopes at sustaining stages of succession, such as herb-rich beech forests, ash-alder alluvial forests, oak-hornbeam, oak and talus forests. The most interesting vegetation is traditionally found on rocky steppes, dry grasslands and wetlands. We can also see managed species-rich meadows and extensively managed ponds rich in macrophyte vegetation (Matějů et al., 2016).

Hunting management

Hunting management reflects the specific regime of a military district. The Hradiště hunting grounds has a total area of 36,029 ha, of which 41.2% is forest land, 5.8% farm land, 0.2% water bodies and 52.8% other areas, largely covered by shrubs. The specific use of the landscape with its vast shrubby areas makes hunting considerably more complicated. Hunting from hides and stalking is used for individual hunting, while in the case of group hunting the hunters opt for battues and dog driving. Female animals, deer fawns and wild boar piglets are hunted in fee-charged battues and individually by gamekeeping staff; male animal hunting is usually subject to a charge. In the period

http://www.aloki.hu ● ISSN 1589 1623 (Print) ● ISSN1785 0037 (Online)
DOI: http://dx.doi.org/10.15666/aeer/1802_29893014

2005-2012, a total of 27,729 animals of the following species were hunted in this area: red deer (6,835 ind.), sika deer (8,294 ind.), fallow deer (103 ind.), mouflon (167 ind.), roe deer (4,292 ind.), wild boar (7,297 ind.), European badger (68 ind.) and red fox (673 ind.) (*Table 1*). Of these, animals shot for sanitary reasons were subtracted from the statistical evaluation, i.e. approximately 150 animals in the Hradiště hunting grounds every year. Northern raccoon (*Procyon lotor* L.) and pine marten (*Martes martes* L.) were also subtracted because of the low number of hunted animals (< 20 ind.). Moreover, in accordance with Act No. 449/2001 Coll., the Northern raccoon can be hunted only by professional gamekeepers or hunting guard.

Table 1. *The numbers of the hunted animals in Hradiště hunting grounds by the particular game species in 2005-2012*

Game species	Year								Total
	2005	2006	2007	2008	2009	2010	2011	2012	
Wild boar male	14	5	2	4	14	11	15	16	81
Wild boar female	76	25	36	26	33	37	58	110	401
Wild boar fawn	241	106	139	123	67	167	106	416	1,365
Wild boar piglet	795	303	651	676	633	696	675	1,021	5,450
Mouflon male	4	0	0	5	3	12	2	8	34
Mouflon female	22	9	8	12	12	9	6	2	80
Mouflon fawn	14	5	5	6	9	5	5	4	53
Roe deer male	110	84	118	180	225	200	202	226	1,345
Roe deer female	225	70	176	230	273	195	204	316	1,689
Roe deer fawn	192	49	129	155	211	178	126	218	1,258
Red deer male	119	76	126	169	194	193	290	287	1,454
Red deer female	223	206	248	310	361	471	491	481	2,792
Red deer fawn	268	212	203	281	338	403	421	463	2,589
Sika deer male	144	129	180	224	219	233	245	309	1,683
Sika deer female	217	161	330	404	439	636	655	772	3,614
Sika deer fawn	235	176	254	339	380	535	491	587	2,997
Fallow deer male	3	1	1	1	3	3	5	3	20
Fallow deer female	5	2	2	4	10	8	10	7	48
Fallow deer fawn	5	3	9	6	2	3	3	5	36
Red fox	85	34	69	57	93	140	73	122	673
European badger	0	0	4	11	9	8	12	24	68
Total	2,997	1,656	2,690	3,223	3,528	4,143	4,095	5,397	27,729

Data collection

The analysis of the impact of climatic data on the success of game hunting was based on climatic data provided by the Karlovy Vary meteorological station, Olšová vrata (603 m above sea level), which conveniently represents the climatic conditions in the Doupov Hills. Climatic data (maximum and minimum wind speed in m s^{-1}, mean, minimum and maximum daytime air temperature in °C, 30-minute-interval temperature progress in the course of the day in °C, daily precipitation in mm, total daily snow cover in cm, atmospheric pressure reduced to sea level in hPa and daily atmospheric pressure change) cover the period of 2005–2012. Data on hunting various game species (red deer, sika deer, fallow deer, mouflon, roe deer, wild boar, European badger, red fox), their sex (male, female) and age (adults, young animals), method and date of hunting in 2005-2012 were obtained from the VLS. In the VLS hunting grounds of the Doupov Hills, all hunted animals are recorded. Hunting seasons are strictly observed, as in the rest of the Czech Republic (*Table 2*). For generalized comparing, game species (including their age and sex) were divided in relation to hunting season to five groups.

http://www.aloki.hu ● ISSN 1589 1623 (Print) ● ISSN1785 0037 (Online)
DOI: http://dx.doi.org/10.15666/aeer/1802_29893014

Table 2. *The dates of hunting season for different species of game in the Czech Republic in 2005-2012*

The date of hunting	Game species	Group
01 Aug – 15 Jan	red deer, male and female	1
01 Aug – 31 Mar	red deer fawn	2
01 Aug – 15 Jan	sika deer, male and female	1
01 Aug – 31 Mar	sika deer fawn	2
16 Aug – 31 Dec	fallow deer, male and female	1
16 Aug – 31 Mar	fallow deer fawn	2
16 May – 30 Sep	roe deer	4
01 Sep – 31 Dec	roe deer fawn and female	1
01 Aug – 31 Dec	mouflon, male and female	1
01 Aug – 31 Mar	mouflon fawn	2
01 Jan – 31 Dec	wild boar	3
01 Jan – 31 Dec	red fox	3
01 Sep – 30 Nov	European badger	5

Statistical data processing

Testing for differences in values of selected climatic parameters was performed via Kruskal-Wallis tests with subsequent multiple comparisons. Game species were analysed in relation to their mean deviations from average climatic characteristic on the day of individual hunting and group hunting. Principal component analysis (PCA) was used to describe overall characteristics of analysed multivariate data. Climatic data (air temperature, precipitation, snow cover, wind speed, atmospheric pressure, atmospheric pressure change) were standardized according to hunting season of each species prior to statistical analyses. Furthermore, the success of hunting was focused on the period (November and December) with the highest occurrence of hunted animals (over 54% of the annual number), where the number of daily hunted animals was compared with climatic data by linear regression. All statistical tests were performed on significance level α=0.05. Statistically significant differences among game species in relation to climatic characteristic were marked by different indices (homogenous groups). Error bars indicate standard error of mean (SE). Computations were performed in R software (R Core Team, 2018).

Results

Climatic characteristics of the date of hunting for game species

The climatic characteristics for each game species at the time of hunting are shown in *Figs. 2-4*. *Fig. 2* shows average air temperatures in ºC on the hunting day by particular game species, varying considerably in relation to hunting time for each species. Average temperatures in the hunting time range from 0.5°C for wild boar piglets to 15.3°C for roe deer males. The greatest standard error of the mean (SE) of average temperature were found in fallow deer fawn (SE 1.22), mouflon male (SE 1.15) and fallow deer female (SE 1.00).

Comparing game species with the similar hunting season (same group in *Table 2*), red deer male showed the highest average air temperature in group 1, followed by fallow deer male, while the lowest temperature was observed in roe deer female and mouflon female. In hunting group 1, higher average air temperature (2.4ºC) was observed in all cases in male game species compared to female. In group 2, the highest temperature on hunting

http://www.aloki.hu ● ISSN 1589 1623 (Print) ● ISSN1785 0037 (Online)
DOI: http://dx.doi.org/10.15666/aeer/1802_29893014

day was in fallow deer fawn and the lowest in mouflon fawn. In wild boar, the highest temperature was found in the case of fawn and vice versa in piglet.

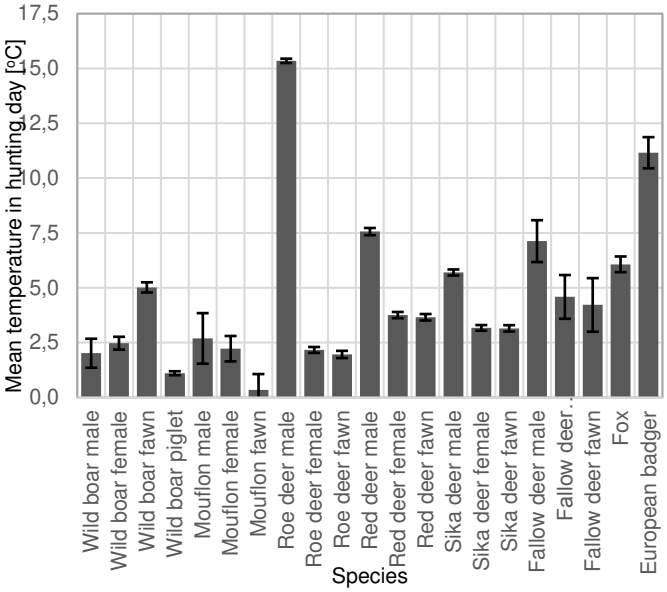

Figure 2. *Average air temperatures in ºC on the hunting day by particular game species in 2005-2012; error bars indicate standard error of the mean*

Fig. 3 shows average rainfall in mm on the day of hunting by particular game species, varying only insignificantly in each species (0.9–1.4 mm), being slightly higher only for European badger and roe deer male (1.8–2.1 mm). The greatest SE of average rainfall were found in European badger (SE 0.45), fallow deer fawn (SE 0.47) and fallow deer male (SE 0.54).

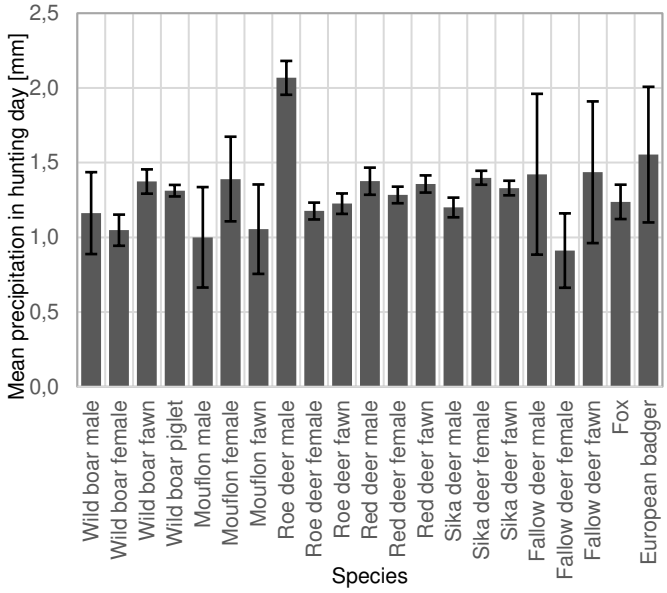

Figure 3. *Average precipitation in mm on the hunting day by particular game species in 2005-2012; error bars indicate standard error of the mean*

http://www.aloki.hu ● ISSN 1589 1623 (Print) ● ISSN1785 0037 (Online)
DOI: http://dx.doi.org/10.15666/aeer/1802_29893014

Regarding hunting group 1, fallow deer male showed the highest average precipitation, followed by mouflon female, while the lowest precipitation was observed in fallow deer female and mouflon male. Similarly, in group 2, the highest precipitation on hunting day was in fallow deer fawn, while the lowest was found in mouflon fawn. In wild boar, the highest temperature was found in the case of fawn and vice versa in female.

Fig. 4 shows the average snow cover in cm on the day of hunting by game species, varying from 0 to 8 cm for particular species. It was the highest in mouflon male (7.9 cm) and mouflon fawn (6.7 cm); it was also fairly high in wild boar piglet (6.0 cm), sika deer fawn (5.4 cm), sika deer female (5.3 cm), roe deer fawn (5.0 cm), while it was zero in roe deer male (0.0 cm) and only 0.1 cm in European badger. The greatest SE of average snow cover was found in fallow deer male (SE 1.88), mouflon male (SE 1.44), mouflon fawn (SE 1.21) and fallow deer female (SE 1.14).

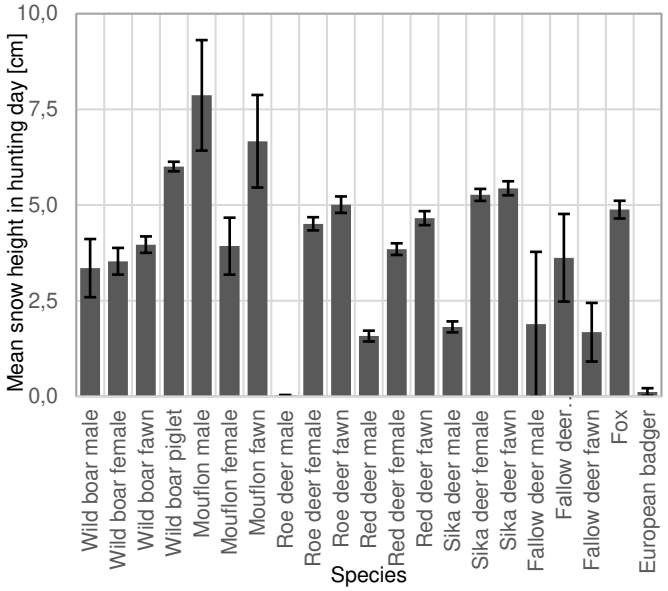

Figure 4. *Average snow cover in cm on the hunting day by particular game species in 2005-2012; error bars indicate standard error of the mean*

Comparing game species with the similar hunting season, fallow deer male showed the highest average snow cover in group 1, followed by fallow sika deer female, while the lowest snow height was observed in red deer male and sika deer male. In hunting group 1, higher average snow cover (0.9 cm) was observed in female game species compared to male (except mouflon). In group 2, the highest snow cover on hunting day was for mouflon deer fawn and the lowest for fallow fawn. In the wild boar group, the highest snow height was in the case of piglet and vice versa in male.

Fig. 5 shows the average atmospheric pressure in hPa on the hunting day by particular game species, varying inconsiderably and ranging from 1016.0 hPa (in fallow deer fawn) to 1020.7 hPa (in mouflon fawn). The greatest SE of average atmospheric pressure was found in fallow deer male, mouflon male, mouflon fawn and fallow deer fawn (SE 1.48-1.85).

Regarding hunting group 1, sika deer male showed the highest average atmospheric pressure, followed by fallow deer male, while the lowest atmospheric pressure was observed in roe deer female and sika deer female. In hunting group 1, higher average

http://www.aloki.hu ● ISSN 1589 1623 (Print) ● ISSN1785 0037 (Online)
DOI: http://dx.doi.org/10.15666/aeer/1802_29893014

atmospheric pressure (1.3 hPa) was observed in male game species compared to female. In group 2, the highest precipitation on hunting day was in mouflon fawn, while the lowest was found in fallow deer fawn. In group 3, the highest atmospheric pressure was in the case of wild board male, while it was lowest in female.

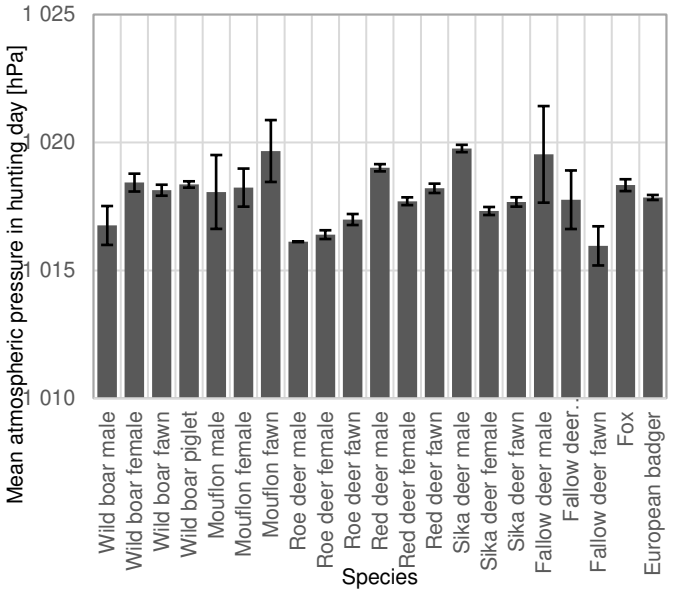

Figure 5. *Average atmospheric pressure in hPa on the hunting day by particular game species in 2005-2012; error bars indicate standard error of the mean*

Comparison of climatic characteristics of the hunting days by game species

Temperature impact

Standardized climatic characteristics for each game species at the time of hunting are shown in *Figs. 6-9*. *Fig. 6* shows average deviations from the average temperature in ºC on the hunting day for particular game species (for individual hunting and group hunting). Y-axis shows the mean temperature deviation on the hunting day from the average temperature over the whole investigated period. Game species reaching values above 0 are hunted when temperature is higher than mean value during the hunt and vice versa; the particular value then shows "how much temperature is higher or lower" it is than at usual hunting time.

Most game species were individually hunted at lower-than-average temperatures for the given time of hunting, except for yearling boar (0.1ºC), roe deer male (0.4ºC), fallow deer female (1.1ºC), red deer male (1.8ºC), fallow deer male (1.8ºC), fallow deer fawn (2.8ºC) and European badger (3.6ºC), which were hunted at higher-than-average temperatures. Markedly lower-than-average temperatures are suitable especially for individual hunting of wild boar piglets (-6.0ºC), mouflon females (-4.3ºC), wild boar males (-3.5ºC), mouflon fawns (-3.1ºC), mouflon males (-3.0ºC), sika deer females (-2.6ºC) and wild boar females (-2.0ºC). The standard errors of the mean are rather high in fallow deer fawns (SE 1.6), fallow deer females (SE 1.5), wild boar males (SE 1.3) and mouflon males (SE 1.3).

In terms of group-hunting, markedly lower-than-average temperatures are suitable especially for hunting of mouflon males (-10.5ºC), wild boar yearlings (-6.8ºC), wild boar

http://www.aloki.hu ● ISSN 1589 1623 (Print) ● ISSN1785 0037 (Online)
DOI: http://dx.doi.org/10.15666/aeer/1802_29893014

piglets (-6.8ºC), red deer males (-6.5ºC), red foxes (-6.4ºC), sika deer males (-6.3ºC), wild boar males (-6.2ºC), wild boar females (-6.0ºC), sika deer females (-5.9ºC), red deer females (-5.8ºC), roe deer fawns (-5.7ºC), mouflon females (-5.4ºC), roe deer females (-5.2ºC), fallow deer males (-4.8ºC), fallow deer females (-4.8ºC), mouflon fawns (-4.5ºC), sika deer fawns (-4.1ºC) and red deer fawns (-3.3ºC). The standard errors of the mean are rather large in fallow deer males (SE 3.5), mouflon males (SE 1.6), mouflon fawns (SE 1.2) and fallow deer fawns (SE 1.0).

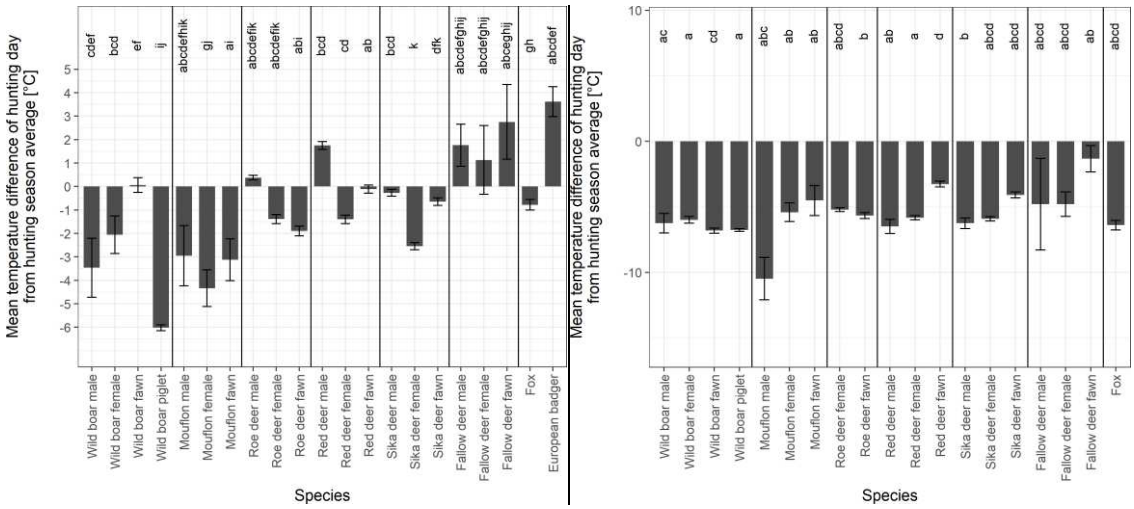

Figure 6. *Mean deviations from the average temperature in ºC on the day of individual hunting (left) and group hunting (right) by particular game species between 2005-2012; statistically significant differences among species are marked by different indices; error bars indicate standard error of the mean*

In the case of individual hunting, statistically significant differences were observed in the deviations from the average temperature between values for wild boar piglet, whose respective values were significantly different from the values of all species, except mouflon female, mouflon male, mouflon fawn and wild boar male. Mouflon and wild boar are generally hunted at temperatures lower than usual in their hunting season. In contrast, European badger, fallow deer fawn, red deer male and fallow deer male are generally hunted in weather with higher temperature than usual. The values for red deer male proved to be different from red deer female, sika deer female and sika deer male, while in the case of red deer and sika deer, we observed significant differences in values for females and fawns.

Significant differences between temperature deviations from the average for the particular hunting time can be identified in the case of group hunting of wild boar yearling and piglet in comparison with red deer female, sika deer male and roe deer fawn. Also, we find a difference in the value for red deer fawn and sika deer fawn, whose values differ significantly from those found for adults.

Precipitation impact

Fig. 7 shows average deviations from precipitation in mm on the day of hunting for particular species. Most game species were hunted individually at lower-than-average precipitation sums except for European badger (0.1 mm) that is hunted at higher

http://www.aloki.hu ● ISSN 1589 1623 (Print) ● ISSN1785 0037 (Online)
DOI: http://dx.doi.org/10.15666/aeer/1802_29893014

precipitation sums. Red deer fawns and sika deer fawns were hunted at boundary values of average precipitation. Significantly lower-than-average precipitation was suitable for hunting fallow deer females (-0.7 mm), mouflon males, fallow deer fawns, mouflon fawns (-0.4 mm), wild boar males, sika deer males, foxes (-0.3 mm), wild boar yearlings, mouflon females and wild boar females (-0.2 mm). The standard error of the mean was larger in fallow deer males, wild boar males (SE 0.6), mouflon males, mouflon females and European badgers (SE 0.4), mouflon fawns and fallow deer fawns (SE 0.3).

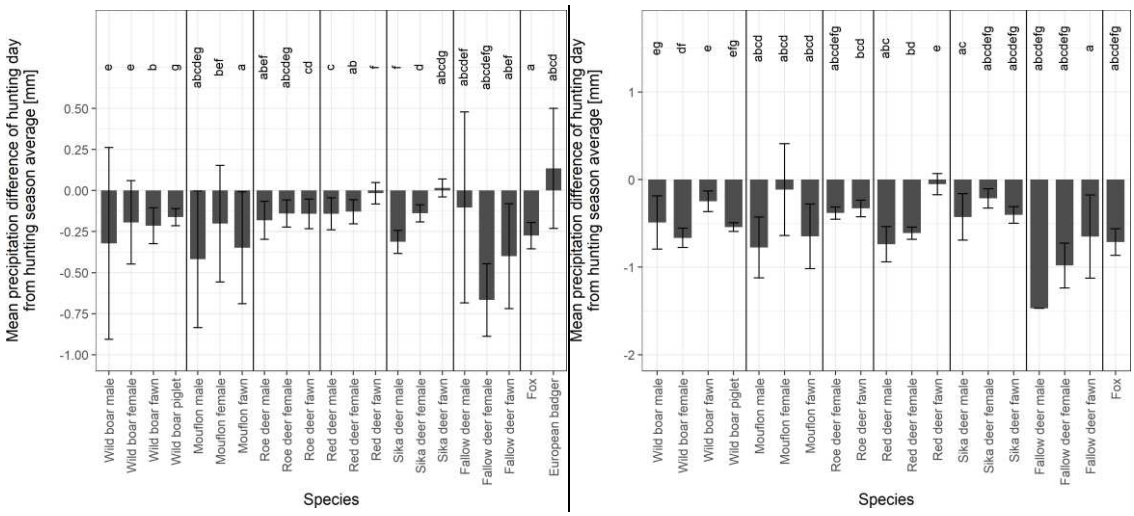

Figure 7. *Mean deviations from the precipitation in mm on the hunting day of individual hunting (left) and group hunting (right) by particular game species in 2005-2012; statistically significant differences among species are marked by different indices; error bars indicate standard error of the mean*

All game species were group-hunted at lower-than-average-precipitation. Markedly lower-than-average precipitation was suitable for hunting fallow deer males (-1.5 mm), fallow deer females (-1.0 mm), mouflon males (-0.8 mm), red deer males, foxes, wild boar females, fallow deer fawns, mouflon fawns (-0.7 mm), red deer females (-0.6 mm), wild boar piglets and wild boar males (-0.5 mm). The standard error of the mean was slightly higher in fallow deer fawns, mouflon females (SE 0.5), mouflon males, mouflon fawns (SE 0.4) and wild boar males (SE 0.3).

In the case of individual hunting, significant differences were not found between deviations from the average precipitation for red deer fawns and sika deer fawns, similarly to wild boar males and wild boar yearlings, and mouflon males, mouflon females and mouflon fawns, but in the case of wild boar yearlings and piglets there was a statistically significant difference, similar to that of roe deer males and roe deer fawns, whoes values did not differ from the value for the roe deer females. The values for red deer fawn and sika deer fawn differed from the values for the adult animals, but the values for red deer males and females showed no significant differences.

Group hunting also brought statistically significant results in wild boar yearlings and piglets, or red deer males and fawns in the case of red deer and sika deer. The average precipitation values were comparable, as in the previous case of fawns of both deer species.

http://www.aloki.hu ● ISSN 1589 1623 (Print) ● ISSN1785 0037 (Online)
DOI: http://dx.doi.org/10.15666/aeer/1802_29893014

Snow cover impact

Fig. 8 shows average deviations from the snow cover in cm on the hunting day by particular game species. Half of the game species are hunted individually at the lower-than-average snow cover, the other half at the higher-than-average snow cover, as compared with the average. The higher-than-average snow cover suits hunting wild boar piglets (3.3 cm), mouflon males (2.8 cm), sika deer females (2.5 cm), mouflon females (2.2 cm), foxes (1.7 cm), fallow deer females (1.5 cm) and roe deer fawns (1.2 cm). The lower-than-average snow cover suits hunting fallow deer fawns (-5.1 cm), fallow deer males (-2.2 cm), wild boar males (-1.5 cm) and red deer males (-1.3 cm). Snow cover of around the average is suitable for hunting red deer fawns and roe deer males. The standard error of the mean is rather large in fallow deer females (SE 1.8), mouflon males (SE 1.6), mouflon fawns (SE 1.5), wild boar males, mouflon females (SE 0.9).

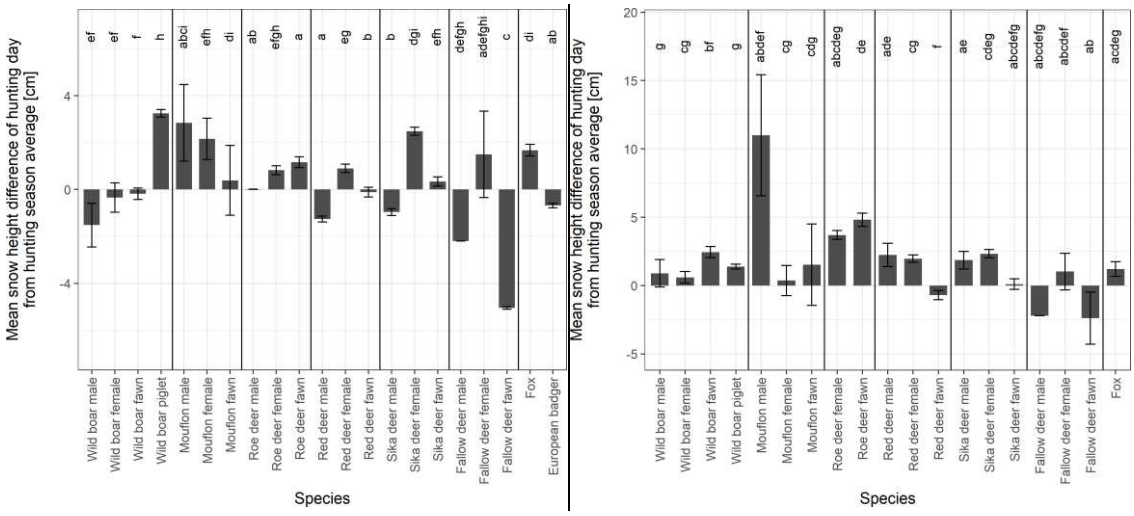

Figure 8. *Mean deviations from the snow cover in cm on the hunting day of individual hunting (left) and group hunting (right) by particular game species in 2005-2012; statistically significant differences among species are marked by different indices; error bars indicate standard error of the mean*

A vast majority of game species were group-hunted at higher-than-average snow cover. The highest levels of snow cover suited the group hunt of the mouflon male (11.0 cm), roe deer fawn (4.8 cm), roe deer female (3.7 cm), wild boar yearling (2.5 cm), sika deer female (2.3 cm), red deer male (2.2 cm) and sika deer male (1.9 cm). Lower-than-average snow cover suited group hunting of fallow deer fawn (-2.4 cm) and fallow deer males (-2.2 cm). Sika deer fawn was hunted at the average snow cover margin. The standard error of the mean was rather large in mouflon males (SE 4.4), mouflon fawns (SE 3.0), fallow deer females (SE 1.3), mouflon females (SE 1.1), wild boar males (SE 1.0) and red deer males (SE 0.9).

A statistically significant difference in height of the snow cover was recorded in the case of individual hunting of fallow deer fawn and fallow deer male, similarly to the case of wild boar yearling and piglet. Different values were observed in red deer male, red deer fawn and red deer female. Values for red deer males and sika deer males are similar to those found in previous cases, as well as for fawns of both species. In the case of

http://www.aloki.hu ● ISSN 1589 1623 (Print) ● ISSN1785 0037 (Online)
DOI: http://dx.doi.org/10.15666/aeer/1802_29893014

mouflon male and mouflon female, the values were also comparable, though significantly different from the mouflon fawn values.

In the case of group hunting, differences between red and sika deer adults and fawns were identified. There was no statistically significant difference between adult and young mouflons, similarly to the roe deer and fallow deer, or between the wild boar female, male and yearling, whose values, however, are statistically significantly different from piglet.

Atmospheric pressure impact

Fig. 9 shows average deviations from the atmospheric pressure in hPa on the hunting day by particular game species. Slightly over half of the game species (12) were hunted individually at higher-than-average atmospheric pressure, while the rest (10) at lower-than-average pressure. Average atmospheric pressure was suitable for hunting mouflon females (1018 hPa, SE 1.44). Lower-than-average pressure was suitable especially for hunting fallow deer fawns (-1.8 hPa), fallow deer females (-1.3 hPa), roe deer females, sika deer females and wild boar males (-0.8 hPa). The highest atmospheric pressure suited mouflon fawns (3.4 hPa), fallow deer males (2.5 hPa), sika deer males (1.6 hPa), wild boar piglets (1.0 hPa), red deer males (0.9 hPa) and foxes (0.7 hPa). A rather large SE was found in wild boar male (SE 2.3), mouflon fawn (SE 2.0), fallow deer fawn (SE 1.8), mouflon male (SE 1.7), fallow deer female, mouflon female (SE 1.4), wild boar female (SE 1.0) and European badger (SE 1.0).

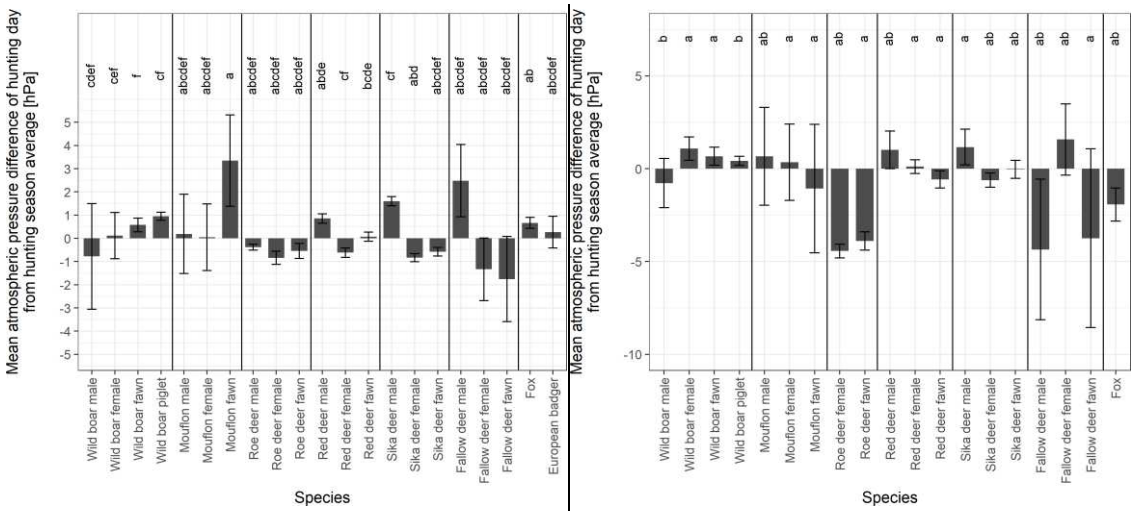

Figure 9. *Mean deviations from the atmospheric pressure in hPa on the hunting day of individual hunting (left) and group hunting (right) by particular game species in 2005-2012; statistically significant differences among species are marked by different indices; error bars indicate standard error of the mean*

Slightly over half of the game species (10) were group-hunted at lower-than-average atmospheric pressure, 2 species at average atmospheric pressure, and 8 species at higher-than-average atmospheric pressure. Average atmospheric pressure is suitable for hunting sika deer fawn and female (1018 hPa, SE 0.5 and 0.4). Lower-than-average pressure is suitable for hunting roe deer female, fallow deer male (-4.4 hPa), roe deer fawn (-3.9 hPa), fallow deer fawn (-3.7 hPa). Higher-than-average atmospheric pressure suits group-hunting of fallow deer female (1.6 hPa), sika deer male (1.2 hPa), wild boar female

http://www.aloki.hu ● ISSN 1589 1623 (Print) ● ISSN1785 0037 (Online)
DOI: http://dx.doi.org/10.15666/aeer/1802_29893014

(1.1 hPa) and red deer male (1.0 hPa). Very large SE was found in fallow deer fawn (SE 4.8), fallow deer male (SE 3.8), mouflon fawn (SE 3.5), mouflon female (SE 2.1), fallow deer female (SE 1.9); it was rather high in wild boar male (SE 1.3), red deer male and sika deer male (SE 1.0).

In the case of individual hunting, no statistically significant differences were identified in deviations from the average atmospheric pressure at the time of hunting between adult and juvenile fallow deer, roe deer or wild boar. Statistically significant differences were not detected even in the comparison of the females and fawns of both red and sika deer but significantly differed from the values of adult male deer. In the case of group hunting, there were no substantial differences between any of the game species mentioned.

Interaction of climate and success of hunting

The main part of data variability appeared to be caused by standardized values of temperature, which is an important parameter for both methods of hunting (*Figs. 10 and 11*). Standardized values of atmospheric pressure could be important as well, especially in the case of group hunting. Snow cover height is naturally negatively correlated with temperatures, similarly, negative correlation is observed between atmospheric pressure and precipitation. Increased variability in game hunting probability is observed when snow cover is present. In the case of individual method, roe deer male showed the lowest variability in relation to climatic factors in hunting days compared to high variability in mouflon fawn and wild board, where increasing atmospheric pressure, respectively snow cover had positive effect on success of hunting. Higher difference among game species was observed in the case of group hunting. For example, temperature had a positive effect on the success of hunting of European badger, respectively snow height on hunting of mouflon male.

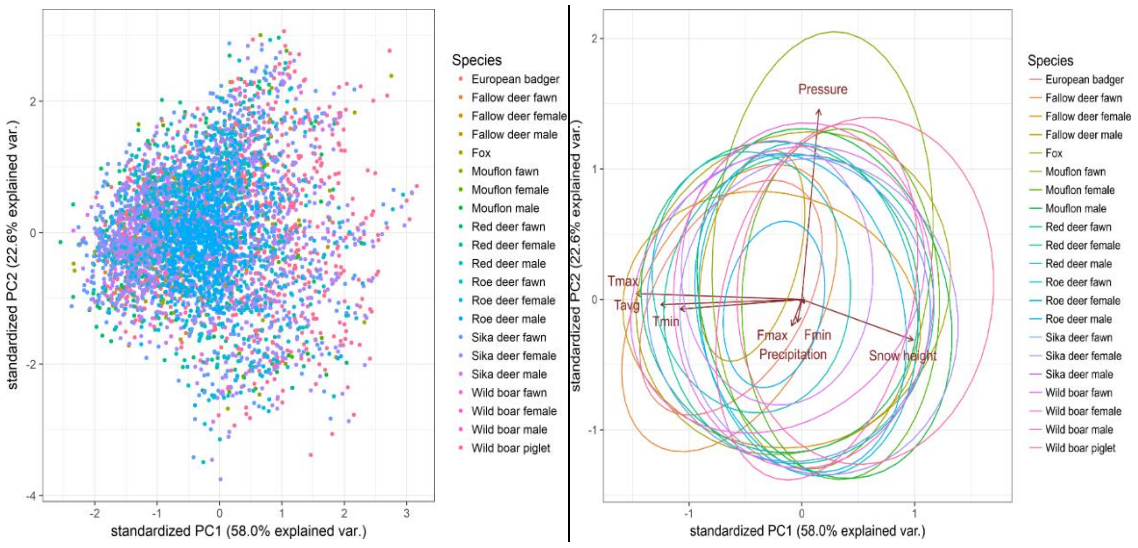

Figure 10. *Analysis of the main components for standardized climatic data (F – minimum and maximum wind speed, T – mean, minimum and maximum day time temperature, daily precipitation, daily snow cover, atmospheric pressure) for individual game species and respective individual hunting times – points (left) and ellipses of 50% probability of occurrence (right) are displayed*

http://www.aloki.hu ● ISSN 1589 1623 (Print) ● ISSN1785 0037 (Online)
DOI: http://dx.doi.org/10.15666/aeer/1802_29893014

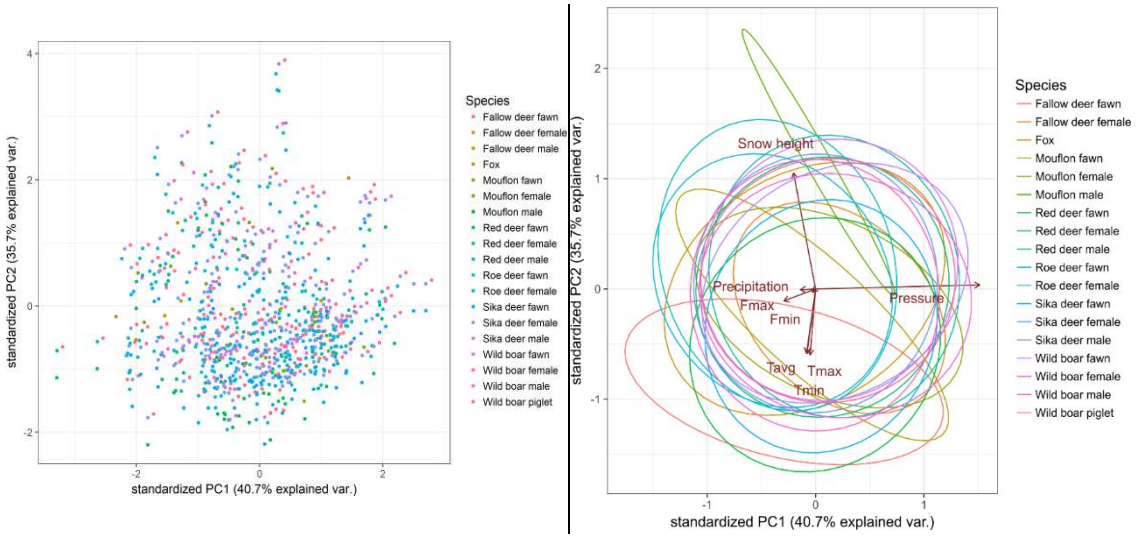

Figure 11. *Analysis of the main components for standardized climatic data (F – minimum and maximum wind speed, T – mean, minimum and maximum day time temperature, daily precipitation, daily snow cover, atmospheric pressure) for individual game species and respective group hunting times – points (left) and ellipses of 50% probability of occurrence (right) are displayed*

Focusing on November and December (period with the highest number of hunted game), the success of hunting (both methods together) of all game species was increasing with increasing snow cover, increasing atmospheric pressure change and decreasing temperature, while there was no effect of precipitation. In individual hunting, the factors which had the highest effect on the success of hunting were: decreasing temperature, increasing snow cover and increasing atmospheric pressure change. The lowest effect was observed also in term of precipitation. In more detail in relation to deer species, the highest effect on the success of hunting was connected with decreasing temperature, while in wild boar it was increasing atmospheric pressure. In group hunting method, the highest positive effect on success of hunting was connected with decreasing temperature and increasing snow cover. Generally, lower effect of climate was observed in group hunting compared to individual hunting method.

Discussion

Numerous studies generally admit that climatic factors have a significant impact on forest game species populations and their dynamics. Borowik et al. (2013), for example, report that the climatic conditions (temperature, precipitation and snow cover) greatly influence the dynamics of ungulate populations by affecting the productivity of plants and, consequently, the energy requirements of ungulates (Saether, 1997; Martinez-Jauregui et al., 2009). Loison and Langvatn (1998) analysed the stock density of the red deer population in Norway and found that deep snow and high wind velocities correlated with low density of red deer. In the case of Polish red deer populations, the average January temperature negatively affected its population dynamics due to mortality in winter months (Okarma et al., 1995). Borowik et al. (2013) further confirmed the positive influence of increasing average temperature in January on the number of red deer in Poland.

http://www.aloki.hu ● ISSN 1589 1623 (Print) ● ISSN1785 0037 (Online)
DOI: http://dx.doi.org/10.15666/aeer/1802_29893014

In our case, the assessment of temperature on the day of hunting of particular game species showed significant temperature fluctuations against an average value of the total hunting season for the given game species. In general, it is possible to observe – on the basis of the results found – that most game species are hunted at lower temperatures compared to the average at the time of hunting, especially in group hunting. However, this fact can be explained to some extent by the season of battues, which, most frequently, take place at the turn of the year, i.e. from November to January.

The influence of ambient temperature on ungulate populations has been verified and evaluated in relation to various habitat types used by the ungulates to relieve temperature stress (Merill, 1991; Mysterud and Østbye, 1995, 1999). The studies showed that high temperatures caused temperature stress, especially in the summer months, when the game seeks cover and is less active. Thus, the ungulates prefer habitats rich in cover and food, and significant reduction in their activity was observed (Godvik et al., 2009; Rivrud et al., 2014). Larger deer species are more susceptible to overheating (Mysterud and Østbye, 1999). An increase in the average temperature in January positively influenced the occurrence of roe deer in Poland (Borowik et al., 2013). Under unfavourable low temperature winter conditions, Holand et al. (1998) reported heavy leg strain, small body size and low chest height as factors hampering deer's survival. Okarma et al. (1995) in Poland and Kiili (1991) in Estonia found a relation between heavy frost, snow cover and the number of deer deaths from exhaustion, hunger and increased predatory pressure. In our research, analyses of numbers of hunted individuals confirmed that the assumption of a higher success rate was in lower-than-average temperature periods for particular game species. It was also confirmed inyear 2006, when winter temperature was extremely high (+ 3.2^{o}C above average) with almost no snow and the smallest number of animals was hunted in this period.

Body heat losses due to precipitation were measured in white-tailed deer – with the resulting observation that heavier body heat losses were observed than in the case of low-temperature-induced stress (Parker, 1988). Game seeks cover options to hide from fur-dampening, and thus reduces energy expenditure (Parker et al., 1984; Mysterud and Østbye, 1999). For these reasons, physical activity is minimized, and the game remains in the forest cover. It prefers mature forest habitats that provide more cover than young forest areas (König, 1987). A trend to hunt various game species in periods of less rainfall was also confirmed by our analyses. Fallow deer was hunted – both individually and in groups – on days of the lowest precipitation, both on group and on individual hunts. The original natural range of fallow deer is in Asia Minor and the Mediterranean (IUCN, 2018), i.e. in areas with lower precipitation totals compared to the Czech Republic. Another game species hunted in low-rainfall periods, is mouflon, which comes from the islands of Corsica and Sardinia and also from places of lower annual precipitation total (Schröder et al., 2016).

However, the native deer species are also hunted in periods of lower precipitation, which clearly confirms the theory of lower game activity on rainy days (Parker et al., 1984; König, 1987; Mysterud and Østbye, 1999). Low game activity reduces the chance for hunters to see it and successfully hunt it (Curtis, 1971). On the other hand, we can expect increased physical activity on days of lower-than-average rainfall from our results, which can be explained by the availability of good forage (Golodets et al., 2013; Lombardini et al., 2017). At the same time, the point of view of hunters also needs to be considered, as their effort to hunt and anticipation of worthwhile hunting experience on rainy days is reduced as well (Rivrud et al., 2014). However, to some extent, this fact can

http://www.aloki.hu ● ISSN 1589 1623 (Print) ● ISSN1785 0037 (Online)
DOI: http://dx.doi.org/10.15666/aeer/1802_29893014

be ruled out in the case of the studied Hradiště hunting grounds in hunting female and young game as hunting is performed by forest and hunting management staff who are required to fulfil the hunting quota. The influence of increased snow cover on the number of deer is very well documented from other studies, for example, for the sika deer. In the second half of the 19th century, Japanese islands witnessed a dramatic decline in sika deer numbers due to high snow cover, resulting in the banning of regulatory and commercial hunting (Kaji et al., 2000, 2010). On the other hand, the prediction for the development of sika deer numbers, which anticipates climate change and thus the reduction of snow cover, expects a significant increase in the population in the next decades (Ohashi et al., 2016).

Our direct assessment of the effect of the snow cover height on individual hunting success showed very varied values for particular game species. A dense canopy closure of forest stands reduces the height of snow cover; therefore, the game needs to emit less energy moving around the forest and finds fodder more easily (Mysterud and Østbye, 1999). However, in wild boar populations, Melis et al. (2006) indicate that deep snow and frozen soil significantly restrict their physical activity and ability to get food. Long and unfavourable winter conditions (low temperature at the beginning of spring) directly affected the survival rate of newborn wild boars in Switzerland (Geisser and Reyer, 2005). Okarma et al. (1995) in Poland and Kiili (1991) in Estonia found a correlation between high snow cover and the number of deer deaths caused by exhaustion.

Therefore, it appears that the success rate of hunting in the case of snow cover depends on the behaviour and nutritional requirements of the particular game species. In wild boar, for example, hunting from hides is considered the most effective as it takes only 18 man-hours to hunt an animal (Keuling et al., 2008). Efficiency of hunting from hides can be increased by sharpshooting at bait (Doerr et al., 2001). This method is popular in the Czech Republic especially for wild boar hunting in seasons of natural food deficiency. That explains, for example, a higher success rate of hunting piglets on days with higher-than-average snow cover in our study. Higher success rate of battues can probably be explained by the term they are organized, i.e. especially in winter months. Generally, most of the game is hunted in the winter months, while in our study we focused in particular on November and December (such as in other studies – Cupples and Jackson, 2014), when on average over 54% of the total number of animals was hunted during the year in the Doupov Hills. Our results showed that success of hunting of game species was increasing with increasing snow cover, increasing atmospheric pressure change and decreasing temperature.

The fluctuation of atmospheric pressure explains a large part of annual variability of temperatures and precipitation in Northern Europe (Hurrell, 1995). High pressure combined with high temperature and sufficient precipitation at nesting time had a beneficial effect on the reproduction of snow goose (*Chen caerulescens atlantica* Kennard) (Dickey et al., 2008). Atmospheric pressure, together with temperature and precipitation, are the most important variables in relation to weather conditions and also in relation to living organisms (Hawkins and Klimstra, 1970; Knape and de Valpine, 2010). Rapid changes in atmospheric pressure influence the animal-activity patterns (Ables, 1969; Bender and Hartman, 2015) and it can significantly affect the success of the hunting. Hynes (2014) documented that the best hunting time of white-tailed deer is when the pressure is changing, especially when the pressure immediately increases. Our study confirmed the effect of positive atmospheric pressure effect on the success of hunting, especially in individual hunting method and in wild boar. Slightly over a half of

http://www.aloki.hu ● ISSN 1589 1623 (Print) ● ISSN1785 0037 (Online)
DOI: http://dx.doi.org/10.15666/aeer/1802_29893014

game species are hunted at a lower-than-average atmospheric pressure in the the Doupov Hills. Also, in our case, a negative correlation between atmospheric pressure and precipitation was found. A comparison of the atmospheric pressure on the day of hunting showed no statistically significant differences between females and fawns of the two deer species, but they did differ significantly from the values for adult males.

Long-term influence of weather during the vegetation season is also indisputable, as it affects the quality and quantity of natural food (Albon and Langvatn, 1992; Solberg et al., 1999). It can be documented, for example, in the wild boar. The number of wild boar piglets was positively influenced by higher temperatures and higher precipitation in summer, as well as by the higher yield of acorns (Frauendofr et al., 2016) which is, together with beech nuts, the most important source of natural food (Jędrzejewska et al., 1994, 1997) and its yield is also very closely related to climatic influences. The success of the hunt is therefore indirectly influenced by the climate-supported higher numbers of game. The hunter is then more likely to see the game and successfully hunt it.

Borowik et al. (2013) report that, as part of the ongoing changes that are directly related to global warming, ever-milder winter conditions improve the lives of ungulates in Central Europe, leading to their increased numbers. In addition, rising temperatures cause changes in the utilization of the ungulates' habitats. In recent decades, a shift in phenology and tree composition has been observed, with coniferous stands being gradually replaced by mixed and deciduous forests (Sykes et al., 1996; Root et al., 2003; Hanewinkel et al., 2013), increasing the carrying capacity of hunting grounds (Gallo and Pejchar, 2016).

Conclusion

The success of game hunting depends on many factors that can be influenced to a certain extent, improving hunting success significantly. Hunters are supposed, for example, to be familiar with the hunting grounds, with biology of the game and its habitats, and should be able to choose suitable hunting and method (individual or group). There are more factors beyond the hunters' will. Among the most notable unavoidable factors influencing hunting activities are undoubtedly the weather patterns at a given time and place, e.g. air temperature, atmospheric pressure, precipitation, wind speed and snow cover height on the hunting day. In the Doupov Hills, it was the air temperature on the hunting day that had the greatest impact on hunting success. In the case of the snow cover, an increased variability in the values of the studied climatic parameters was observed on the day of hunting. Atmospheric pressure, together with temperature, was one of the most important variables in relation to weather conditions and to living organisms, substantially influencing their physiological processes and well-being and hence the success of hunting. Results showed that the success of hunting was increasing with decreasing air temperature, increasing snow cover and increasing atmospheric pressure change, especially in the case of individual hunting method. On the other hand, precipitation and wind speed had relatively low effect on the success of hunting. Individual hunting was associated with significantly better climatic conditions in comparison to group hunting, such as in the case of hunting of male game species compared to female. However, in relation to the success of the hunting, it is also necessary to focus on other factors not analysed in this study, for example habitat conditions, time of hunting, food source, air humidity, sunshine (clouds), wind direction, fog etc. The findings of this study can contribute to future research and planning of suitable times and methods of hunting and thus supporting successful hunting in montane and submontane regions of Central Europe.

http://www.aloki.hu ● ISSN 1589 1623 (Print) ● ISSN1785 0037 (Online)
DOI: http://dx.doi.org/10.15666/aeer/1802_29893014

Acknowledgements. This study was supported by the Czech University of Life Sciences Prague, Faculty of Environmental Sciences (No. IGA B13/14) and Faculty of Forestry and Wood Sciences. We are grateful to two anonymous reviewers and editor for their constructive comments and valuable suggestions that helped improve the manuscript.

REFERENCES

[1] Ables, E. D. (1969): Activity studies of Red Foxes in southern Wisconsin. – Journal of Wildlife Management 33: 145-153.

[2] Albon, S. D., Langvatn, R. (1992): Plant phenology and the benefits of migration in a temperate ungulate. – Oikos 65: 502-513.

[3] Ambrož, R., Vacek, S., Vacek, Z., Král, J., Štefančík, I. (2015): Current and simulated structure, growth parameters and regeneration of beech forests with different game management in the Lány Game Enclosure. – Central European Forestry Journal 61(2): 78-88.

[4] Balmford, A., Green, R. E., Jenkins, M. (2003): Measuring the changing state of nature. – Trends in Ecology & Evolution 18: 326-330.

[5] Baltzinger, M., Mårell, A., Archaux, F., Pérot, T., Leterme, F., Deconchat, M. (2016): Overabundant ungulates in French Sologne? Increasing red deer and wild boar pressure may not threaten woodland birds in mature forest stands. – Basic and Applied Ecology 17(6): 552-563.

[6] Bender, M. J., Hartman, G. D. (2015): Bat activity increases with barometric pressure and temperature during autumn in central Georgia. – Southeastern naturalist 14(2): 231-243.

[7] Bischof, R., Nilsen, E. B., Brøseth, H., Männil, P., Ozoliņš, J., Linnell, J. D. C. (2012): Implementation uncertainty when using recreational hunting to manage carnivores. – Journal of Applied Ecology 49(4): 824-832.

[8] Bleier, N., Lehoczki, R., Újváry, D., Szemethy, L., Csányi, S. (2012): Relationship between wild ungulates density and crop damage in Hungary. – Acta Theriologica 57(4): 351-359.

[9] Böhning-Gaesa, K., Lemoine, N. (2004): Importance of climate change for the ranges, communities and conservation of birds. – Advances in Ecological Research 35: 211-236.

[10] Borowik, T., Cornulier, T., Jędrzejewska, B. (2013): Environmental factors shaping ungulate abundances in Poland. – Acta Theriologica 58: 403-413.

[11] Buckland, S. T., Ahmadi, S., Staines, B. W., Gordons, I. J., Youngson, R. W. (1996): Estimating the minimum population size that allows a given annual number of mature red deer stags to be culled sustainably. – Journal of Applied Ecology 33: 118-130.

[12] Bunnefeld, N., Baines, D., Newborn, D., Milner-Gulland, E. J. (2009): Factors affecting unintentional harvesting selectivity in a monomorphic species. – Journal of Animal Ecology 78: 485-492.

[13] Ciuti, S., Muhly, T. B., Paton, D. G., McDevitt, D., Musiani, M., Boyce, M. S. (2012): Human selection of elk behavioural traits in a landscape of fear. – Proceedings of the Royal Society B: Biological Sciences 279: 4407-4416.

[14] Conner, S. R., Lee, J. T., Carey, J., Bailey, C. A. (2001): Nutrient characterization of guar meal fractions. – Poultry Science 80(1): 50.

[15] Coulson, T. E., Catchpole, A., Albon, S. D., Morgan, B. J. T., Pemberton, J. M., Clutton-Brock, T. H., Crawley, M. J., Grenfell, B. T. (2001): Age, sex, density, winter weather, and population crashes in Soay sheep. – Science 292: 1528-1531.

[16] Cukor, J., Vacek, Z., Linda, R., Remeš, J., Bílek, L., Sharma, R. P., Baláš, M., Kupka, I. (2017): Effect of mineral eco-fertilizer on growth and mortality of young afforestations. – Austrian Journal of Forest Science 134(4): 367-385.

[17] Cukor, J., Havránek, F., Vacek, Z., Bukovjan, K., Podrázský, V., Sharma, R. P. (2019a): Roe deer (*Capreolus capreolus*) mortality in relation to fodder harvest in agricultural landscape. – Mammalia 83(5): 461-469.

http://www.aloki.hu ● ISSN 1589 1623 (Print) ● ISSN1785 0037 (Online)
DOI: http://dx.doi.org/10.15666/aeer/1802_29893014

[18] Cukor, J., Vacek, Z., Linda, R., Sharma, R. P., Vacek, S. (2019b): Afforested farmland vs. forestland: Effects of bark stripping by Cervus elaphus and climate on production potential and structure of Picea abies forests. – PloS one 14(8): e0221082.
[19] Cukor, J., Vacek, Z., Linda, R., Vacek, S., Marada, P., Šimůnek, V., Havránek, F. (2019c): Effects of bark stripping on timber production and structure of Norway spruce forests in relation to climatic factors. – Forests 10(4): 320.
[20] Cukor, J., Bartoška, J., Rohla, J., Sova, J., Machálek, A. (2019d): Use of aerial thermography to reduce mortality of roe deer fawns before harvest. – PeerJ 7: e6923.
[21] Culek, M., Grulich, V., Laštůvka, Z., Divíšek, J. (2013): Biogeografické regiony České republiky. – Masarykova univerzita, Brno.
[22] Cupples, J. B., Jackson, D. H. (2014): Comparison of mule deer distributions during winter and hunting seasons in south-central Oregon. – Department of Fish and Wildlife, Oregon.
[23] Curtis, R. L. J. (1971): Climatic factors influencing hunter sightings of red deer on the broad run research area. – Virginia Polytech Institute, Blacksburg, VA.
[24] Demek, J., Mackovčin, P. (eds.) (2006): Zeměpisný lexikon ČR - Hory a nížiny. – Agentura ochrany přírody ČR, Brno.
[25] Dickey, M. H., Gauthier, G., Cadieux, M. C. (2008): Climatic effects on the breeding phenology and reproductive success of an arctic-nesting goose species. – Global Change Biology 14: 1973-1985.
[26] Doerr, M. L., McAninch, J. B., Wiggers, E. P. (2001): Comparison of four methods to reduce white-tailed deer abundance in an urban community. – Wildlife Society Bulletin 29: 1105-1113.
[27] Forchhammer, M. C., Stenseth, N. C., Post, E., Langvatn, R. (1998): Population dynamics of Norwegian red deer: densitydependence and climatic variation. – Proceedings of the Royal Society B: Biological Sciences 265: 341-350.
[28] Forsman, J. T., Mönkkönen, M. (2003): The role of climate in limiting European resident bird populations. – Journal of Biogeography 30: 55-70.
[29] Frauendorf, M., Gethöffer, F., Siebert, U., Keuling, O. (2016): The influence of environmental and physiological factors on the litter size of wild boar (*Sus scrofa*) in an agriculture dominated area in Germany. – Science of the Total Environment 541: 877-882.
[30] Gaillard, J. M., Delorme, D., Boutin, J. M., Vanlaere, G., Boisaubert, B., Pradel, R. (1993): Roe deer survival patterns—a comparative analysis of contrasting populations. – Journal of Animal Ecology 62: 778-791.
[31] Gallo, T., Pejchar, L. (2016): Improving habitat for game animals has mixed consequences for biodiversity conservation. – Biological Conservation 197: 4752.
[32] Geisser, H., Reyer, H. U. (2005): The influence of food and temperature on population density of wild boar Sus scrofa in the Thurgau (Switzerland). – Journal of Zoology 267: 89-96.
[33] Gerhardt, P., Arnold, J. M., Hacklander, K., Hochbichler, E. (2013): Determinants of deer impact in European forests – A systematic literature analysis. – Forest Ecology and Management 310: 173-186.
[34] Godvik, I. M. R., Loe, L. E., Vik, J. O., Veiberg, V., Langvatn, R., Mysterud, A. (2009): Temporal scales, trade-offs, and functional responses in red deer habitat selection. – Ecology 90: 699-710.
[35] Golodets, C., Sternberg, M., Kigel, J., Boeken, B., Henkin, Z., Seligman, N. G., Ungar, E. D. (2013): From desert to Mediiterranean rangelands: will increasing drough and inter-annual rainfall variability affect herbaceous annual primary productivity? – Climatic Change 119(3-4): 785-798.
[36] Hagen, R., Heurich, M., Kröschel, M., Herdtfelder, M. (2014): Synchrony in hunting bags: Reaction on climatic and human induced changes? – Science of the Total Environment 468-469: 140-146.

http://www.aloki.hu ● ISSN 1589 1623 (Print) ● ISSN1785 0037 (Online)
DOI: http://dx.doi.org/10.15666/aeer/1802_29893014

[37] Hallett, T. B., Coulson, T., Pilkington, J. G., Clutton-Brock, T. H., Pemberton, J. M., Grenfell, B. T. (2004): Why largescale climatic indices seem to predict ecological processes better than local weather. – Nature 430: 71-75.
[38] Hanewinkel, M., Cullmann, D. A., Schelhaas, M. J., Nabuurs, G. J., Zimmermann, N. E. (2013): Climate change may cause severe loss in the economic value of European forest land. – Nature Climatic Change 3: 203-207.
[39] Hawkins, R. E., Klimstra, W. D. (1970): Deer trapping correlated with weather factors. – Transactions of the Illinois State Academy of Science 63(2): 198-201.
[40] Hays, G. C., Richardson, A. J., Robinson, C. (2005): Climate chase and marine plankton. – Trends in Ecology & Evolution 20: 337-344.
[41] Hegel, T. M., Mysterud, A., Huettmann, F., Stenseth, N. C. (2010): Interacting effect of wolves and climate on recruitment in a northern mountain caribou population. – Oikos 119: 1453-1461.
[42] Herrero, J., Garcia-Serrano, A., Couto, S., Ortuno, V., Garcia-Gonzalez, R. (2006): Diet of wild boar Sus scrofa L. and crop damage in an intensive agroecosystem. – European Journal of Wildlife Research 52: 245-250.
[43] Heurich, M., Möst, L., Schauberger, G., Reulen, H., Sustr, P., Hothorn, T. (2012): Survival and causes of death of European Roe Deer before and after Eurasian Lynx reintroduction in the Bavarian Forest National Park. – European Journal of Wildlife Research 58: 567-578.
[44] Heurich, M., Brand, T. T. G., Kaandorp, M. Y., Sustr, P., Muller, J., Reineking, B. (2015): Country, Cover and Protection: What Shapes the Distribution of Red Deer and Roe Deer in the Bohemian Forest Ecosystem? – PloS One 10(3): 1-17.
[45] Holand, Ø., Mysterud, A., Wannag, A., Linnell, J. D. C. (1998): Roe deer in northern environments: physiology and behavior. – In: Andersen, R., Duncan, P., Linnell, J. D. C. (eds.) The European roe deer: the biology of success. Scandinavian University Press, Oslo..
[46] Hone, J., Clutton-Brock, T. H. (2007): Climate, food, density and wildlife population growth rate. – Journal of Animal Ecology 76: 361-367.
[47] Hothorn, T., Müller, J. (2010): Large-scale reduction of ungulate browsing by managed sport hunting. – Forest Ecology and Management 260: 1416-1423.
[48] Hurrell, J. W. (1995): Decadal trends in the North Atlantic oscillation: Regional temperatures and precipitation. – Science 269: 676-679.
[49] Hynes, R. (2014): Whitetail Movement and Barometric Pressure. – 365 Whitetail.
[50] IUCN (International Union for Conservation of Nature) (2018): The IUCN Red List of Threatened Species. – Available at: http://maps.iucnredlist.org/ (verified July 2018).
[51] Jędrzejewska, B., Okarma, H., Jędrzejewski, W., Miłkowski, L. (1994): Effects of exploitation and protection on forest structure, ungulate density and wolf predation in Białowieża Primeval Forest, Poland. – Journal of Applied Ecology 31: 664-676.
[52] Jędrzejewska, B., Jędrzejewski, W., Bunevich, A. N., Milkowski, L., Krasinski, Z. A. (1997): Factors shaping population densities and increase rates of ungulates in Białowieża Primeval Forest (Poland and Belarus) in the 19th and 20th centuries. – Acta Theriologica 42: 399-451.
[53] Johnson, J. B., Omland, K. S. (2004): Model selection in ecology and evolution. – Trends in Ecology & Evolution 19: 101-108.
[54] Kaji, K., Miyaki, M., Saitoh, T., Ono, S., Kaneko, M. (2000): Spatial Distribution of an Expanding Sika Deer Population on Hokkaido Island, Japan. – Wildlife Society Bulletin 28: 699-707.
[55] Kaji, K., Saitoh, T., Uno, H., Matsuda, H., Yamamura, K. (2010): Adaptive management of sika deer populations in Hokkaido, Japan: theory and practice. – Population Ecology 52: 373-387.
[56] Kamei, T., Takeda, K., Izumiyama, S., Ohshima, K. (2010): The Effect of Hunting on the Behavior and Habitat Utilization of Sika Deer (*Cervus nippon*). – Mammal Study 35: 235-241.

http://www.aloki.hu ● ISSN 1589 1623 (Print) ● ISSN1785 0037 (Online)
DOI: http://dx.doi.org/10.15666/aeer/1802_29893014

[57] Keuling, O., Stier, N., Roth, M. (2008): How does hunting influence activity and space use in wild boar Sus scrofa. – European Journal of Wildlife Research 54: 729-737.
[58] Keuling, O., Baubet, E., Duscher, A., Ebert, C., Fischer, C., Monaco, A., Podgórski, T., Prevot, C., Ronnenbert, K., Sodeikat, G., Stier, N., Thurfjell, H. (2013): Mortality rates of wild boar *Sus scrofa* L. in central Europe. – European Journal of Wildlife Research 59: 805-814.
[59] Kiili, J. (1991): Influences of climatic factors on roe deer population dynamics in Estonia. – In: Bobek, B., Regelin, W. (eds.) Global trends in wildlife management, transactions 18th IUGB Congress, Kraków 1987. Świat Press, Kraków-Warszawa.
[60] Knape, J., de Valpine, P. (2010): Effects of weather and climate on the dynamics of animal population time series. – Proceedings of the Royal Society B: Biological Sciences 278(1708): 985-992.
[61] König, K. P. (1987): Territory-holding over time by roe deer in closed woodland areas. – Zeitschrift für Jagdwissenschaft 33: 168-175.
[62] Koons, D. N., Colchero, F., Hersey, K., Gimenez, O. (2015): Disentangling the effects of climate, density dependence, and harvest on an iconic large herbivore's population dynamics. – Ecological Applications 25(4): 956-967.
[63] Köppen, W. P. (1936): Das Geographische System der Klimate. – In: Köppen, W., Geiger, R. (eds.) Handbuch der Klimatologie. Gebrüder Bornträger, Berlin.
[64] Kuijper, D. P. J., de Kleine, C., Churski, M., van Hooft, P., Bubnicki, J., Jędrzejewska, B. (2013): Landscape of fear in Europe: wolves affect spatial patterns of ungulate browsing in Białowieża Primeval Forest, Poland. – Ecography 36(12): 1263-1275.
[65] Kunkel, K. E., Pletscher, D. H. (2000): Habitat factors affecting vulnerability of moose to predation by wolves in southeastern British Columbia. – Canadian Journal of Zoology 78: 150-157.
[66] Langvatn, R., Albon, S. D., Burkey, T., Clutton-Brock, T. H. (1996): Climate, plant phenology and variation in age of first reproduction in a temperate herbivore. – Journal of Animal Ecology 65: 653-670.
[67] Lebel, F., Dussault, C., Massé, A., Côte, S. D. (2012): Influence of habitat features and hunter behavior on white-tailed deer harvest. – Journal of Wildlife Management 76: 1431-1440.
[68] Levers, C., Butsic, V., Verburg, P. H., Muller, D., Kuemmerle, T. (2016): Drivers of changes in agricultural intensity in Europe. – Land Use Policy 58: 380-393.
[69] Linchant, J., Lisein, J., Semeki, J., Lejeune, P., Vermeulen, C. (2015): Are unmanned aircraft systems (UAS s) the future of wildlife monitoring? A review of accomplishments and challenges. – Mammal Review 45(4): 239-252.
[70] Loison, A., Langvatn, R. (1998): Short- and long-term effects of winter and spring weather on growth and survival of red deer in Norway. – Oecologia 116: 489-500.
[71] Lombardini, M., Varuzza, P., Meriggi, A. (2017): Influence of weather and phenotypic characteristics on pregnancy rates of female roe deer in central Italy. – Population Ecology 59: 131-137.
[72] Lundmark, H., Josefsson, T., Östlund, L. (2013): The history of clear-cutting in northern Sweden–driving forces and myths in boreal silviculture. – Forest Ecology and Management 307: 112-122.
[73] Månsson, J., Jarnemo, A. (2013): Bark-stripping on Norway spruce by red deer in Sweden: level of damage and relation to tree characteristics. – Scandinavian Journal of Forest Research 28(2): 117-125.
[74] Marada, P., Cukor, J., Linda, R., Vacek, Z., Vacek, S., Havránek, F. (2019): Extensive Orchards in the Agricultural Landscape: Effective Protection against Fraying Damage Caused by Roe Deer. – Sustainability 11(13): 3738.
[75] Martinez-Jauregui, M., San Miguel-Ayanz, A., Mysterud, A., Rodriguez-Vigal, C., Clutton-Brock, T. H., Langvatn, R., Coulson, T. (2009): Are local weather, NDVI and

http://www.aloki.hu ● ISSN 1589 1623 (Print) ● ISSN1785 0037 (Online)
DOI: http://dx.doi.org/10.15666/aeer/1802_29893014

NAO consistent determinants of red deer weight across three contrasting European countries? – Global Change Biology 15: 1727-1738.
[76] Matějů, J., Hradecký, P., Melichar, V. (2016): Doupovské hory. – Česká geologická služba, Praha.
[77] Melis, C., Szafrańska, P. A., Jędrzejewska, B., Bartoń, K. (2006): Biogeographical variation in the population density of wild boar (Sus scrofa) in western Eurasia. – Journal of Biogeography 33: 803-811.
[78] Merill, E. H. (1991): Thermal constraints on use of cover types and activity time of elk. – Applied Animal Behaviour Science 29: 251-267.
[79] Merkel, F. R. (2010): Evidence of recent population recovery in common eiders breeding in Western Greenland. – Journal of Wildlife Management 74: 1869-1874.
[80] Millspaugh, J. J., Coleman, M. A., Bauman, B. J., Raedeke, K. J., Brundige, G. C. (2000): Serum profiles of American elk at the time of handling for three capture methods. – Canadian Field-Naturalist 114: 196-200.
[81] Milner, J. M., Elston, D. A., Albon, S. D. (1999): Estimating the contributions of population density and climatic fluctuations to interannual variation in survival of Soay sheep. – Journal of Animal Ecology 68: 1235-1247.
[82] Mower, K. J., Townsend, T. W., Tyznik, W. J. (1997): White-tailed deer damage to experimental apple orchards in Ohio. – Wildlife Society Bulletin 25(2): 337-343.
[83] Mysterud, A., Østbye, E. (1995): Bed-site selection by European roe deer (*Capreolus capreolus*) in southern Norway during winter. – Canadian Journal of Zoology 73: 924-932.
[84] Mysterud, A., Østbye, E. (1999): Cover as a habitat element for temperate ungulates: effects on habitat selection and demography. – Wildlife Society Bulletin 27: 385-394.
[85] Newton, I. (1998): Population limitation in birds. – Academic Press, London, U.K.
[86] Nilsen, E. B., Gaillard, J. M., Andersen, R., Odden, J., Delorme, D., van Laere, G., Linnell, J. D. C. (2009): A slow life in hell or a fast life in heaven: demographic analyses of contrasting roe deer populations. – Journal of Animal Ecology 78: 585-594.
[87] Nugent, G., Choquenot, D. (2004): Comparing cost-effectiveness of commercial harvesting, state-funded culling, and recreational deer hunting in New Zealand. – Wildlife Society Bulletin 32: 481-492.
[88] Ohashi, H., Kominami, Y., Higa, M., Koide, D., Nakao, K., Tsuyama, I., Matsui, T., Tanaka, N. (2016): Land abandonment and changes in snow cower period accelerate range expansion of sika deer. – Ecology and Evolution 6: 7763-7775.
[89] Okarma, H., Jędrzejewska, B., Jędrzejewski, W., Krasiński, Z. A., Miłkowski, L. (1995): The roles of predation, snow cover, acorn crop, and man-related factors on ungulate mortality in Białowieża Primeval Forest, Poland. – Acta Theriologica 40: 197-217.
[90] Parker, K. L., Robbins, C. T., Hanley, T. A. (1984): Energy expenditures for locomotion by mule deer and elk. – Journal of Wildlife Management 48: 474-488.
[91] Parker, K. L. (1988): Effects of heat, cold, and rain on coastal black-tailed deer. – Canadian Journal of Zoology 66: 2475-2483.
[92] Parmesan, C. (2006): Ecological and evolutionary responses to recent climate change. – Annual Review of Ecology, Evolution, and Systematics 37: 637-669.
[93] Peñuelas, J., Filella, I., Comas, P. (2002): Changed plant and animal life cycles from 1952 to 2000 in the Mediterranean region. – Global Change Biology 8: 531-544.
[94] Pérez-Espona, S., Pemberton, J. M., Putman, R. (2009): Red and sika deer in the British Isles, current management issues and management policy. – Mammalian Biology 79: 247-262.
[95] Pettorelli, N., Pelletier, F., von Hardenberg, A., Festa-Bianchet, M., Cote, S. D. (2007): Early onset of vegetation growth vs rapid green-up: impacts on juvenile mountain ungulates. – Ecology 88: 381-390.
[96] Pitra, C., Lutz, W. (2005): Population genetic structure and the effect of founder events on the genetic variability of introduced sika deer, *Cervus nippon*, in Germany and Austria. – European Journal of Wildlife Research 51: 95-100.

http://www.aloki.hu ● ISSN 1589 1623 (Print) ● ISSN1785 0037 (Online)
DOI: http://dx.doi.org/10.15666/aeer/1802_29893014

[97] Plíva, K., Žlábek, I. (1986): Přírodní lesní oblasti ČSR. – SZN, Prague.
[98] Pohja-Mykrä, M., Vuorisalo, T., Mykrä, S. (2005): Hunting bounties as a key measure of historical wildlife management and game conservation: Finnish bounty schemes 1647-1975. – Oryx 39(3): 284-291.
[99] Post, E., Stenseth, N. C. (1999): Climatic variability, plant phenology, and northern ungulates. – Ecology 80: 1322-1339.
[100] Průša, E. (2001): Pěstování lesů na typologických základech. – Lesnická práce, s. r. o., Kostelec nad Černými lesy.
[101] Putman, R. J., Moore, N. P. (1998): Impact of deer in lowland Britain on agriculture, forestry and conservation habitats. – Mammal Review 28: 141-164.
[102] Quirós-Fernández, F., Marcos, J., Acevedo, P., Gortázar, C. (2017): Hunters serving the ecosystem: the contribution of recreational hunting to wild boar population control. – European Journal of Wildlife Research 63(3): 57.
[103] R Core Team (2018): R: A language and environment for statistical computing. – R Foundation for Statistical Computing, Vienna, Austria. URL https://www.R-project.org/.
[104] Ramankutty, N., Foley, J. A. (1999): Estimating historical changes in global land cover: Croplands from 1700 to 1992. – Global Biogeochemical Cycles 13(4): 997-1027.
[105] Rivrud, I. M., Loe, L. E., Mysterud, A. (2010): How does local weather predict red deer home range size at different temporal scales? – Journal of Animal Ecology 79: 1280-1295.
[106] Rivrud, I. M., Sonkoly, K., Lehoczki, R., Csányi, S., Storvik, G. O., Mysterud, A. (2013): Hunter selection and long-term trend (1881–2008) of red deer trophy sizes in Hungary. – Journal of Applied Ecology 50(1): 168-180.
[107] Rivrud, I. M., Meisingset, E., Loe, L. E., Mysterud, A. (2014): Interaction effects between weather and space use on harvesting effort and patterns in red deer. – Ecology and Evolution 4(24): 2045-7758.
[108] Root, B. G., Fritzell, E. K., Giessman, N. F. (1988): Effects of intensive hunting on white-tailed deer movement. – Wildlife Society Bulletin 16(2): 145-151.
[109] Saether, B. E. (1997): Environmental stochasticity and population dynamics of large herbivores: a search for mechanisms. – Trends in Ecology & Evolution 12: 143-149.
[110] Sauerbrei, R., Ekschmitt, K., Wolters, V., Gottschalk, T. (2014): Increased Energy maize production reduces farmland bird diversity. – Global Change Biology Bioenergy 6(3): 265-274.
[111] Schröder, O., Lieckfeldt, D., Lutz, W., Rudloff, C., Frölich, K., Ludwig, A. (2016): Limited hybridization between domestic sheep and the European mouflon in Western Germany. – European Journal of Wildlife Research 62: 307-314.
[112] Simard, M. A., Coulson, T., Gingras, A., Cote, S. D. (2010): Influence of density and climate on population dynamics of a large herbivore under harsh environmental conditions. – Journal of Wildlife Management 74: 1671-1685.
[113] Sims, M., Elston, D. A., Larkham, A., Nussey, D. H., Albon, S. D. (2007): Identifying when weather influences life-history traits of grazing herbivores. – Journal of Animal Ecology 76: 761-770.
[114] Slanař, J., Vacek, Z., Vacek, S., Bulušek, D., Cukor, J., Štefančík, I., Bílek, L., Král, J. (2017): Long-term transformation of submontane spruce-beech forests in the Jizerské hory Mts.: dynamics of natural regeneration. – Central European Forestry Journal 63(4): 213-225.
[115] Solberg, E. J., Saether, B. E., Strand, O., Loison, A. (1999): Dynamics of a harvested moose population in a variable environment. – Journal of Animal Ecology 68: 186-204.
[116] Solberg, E. J., Rolandsen, C. M., Heim, M., Linnell, J. D. C., Herfindal, I., Sæther, B. E. (2010): Age and sex-specific variation in detectability of moose (Alces alces) during the hunting season: implications for population monitoring. – European Journal of Wildlife Research 56: 871-881.

http://www.aloki.hu ● ISSN 1589 1623 (Print) ● ISSN1785 0037 (Online)
DOI: http://dx.doi.org/10.15666/aeer/1802_29893014

[117] Sykes, M. T., Prentice, I. C., Cramer, W. (1996): A bioclimatic model for the potential distributions of north European tree species under present and future climates. – Journal of Biogeography 23: 203-233.
[118] Theuerkauf, J., Jedrzejewski, W., Schmidt, K., Okarma, H., Ruczynski, I., Sniezko, S., Gula, R. (2003): Daily patterns and duration of wolf activity in the Bialowieza Forest, Poland. – Journal of Mammalogy 84: 243-253.
[119] Thomas, C. D., Cameron, A., Green, R. E., Bakkenes, M., Beaumont, L., Collingham, Y., Erasmus, B. F., De Siqueira, M. F., Grainger, A., Hannah, L., Hughes, L., Huntley, B., Van Jaarsveld, A. S., Midgley, G. F., Miles, L., Ortega-Huerta, M. A., Peterson, A. T., Phillips, O. L., Williams, S. E. (2004): Extinction risk from climate change. – Nature 427: 145-148.
[120] Thomas, C. D., Franco, A. M. A., Hill, J. K. (2006): Range retractions and extinction in the face of climate warming. – Trends in Ecology & Evolution 21: 415-416.
[121] Thulin, C. G., Malmsten, J., Ericsson, G. (2015): Opportunities and challenges with growing wildlife populations and zoonotic diseases in Sweden. – European Journal of Wildlife Research 61(5): 649-656.
[122] Tolasz, R., Míková, T., Valeriánová, A., Voženílek, V. (eds.) (2007): Climatic Atlas of Czechia. – ČHMÚ, Prague.
[123] Tscharntke, T., Klein, A. M., Kruess, A., Steffan-Dewenter, I., Thies, C. (2005): Landscape perspectives on agricultural intensification and biodiversity–ecosystem service management. – Ecology letters 8(8): 857-874.
[124] Tuyttens, F. A. M., Macdonald, D. W. (2000): Social perturbation: consequences for wildlife management and conservation. – Behaviour and conservation, Cambridge University Press, Cambridge, United Kingdom.
[125] Vacek, S., Vančura, K., Zingari, P. C., Jeník, J., Simon, J., Smejkal, J. (2003): Mountain forests of the Czech Republic. – Ministry of Agriculture, Prague.
[126] Vacek, Z., Vacek, S., Bílek, L., Král, J., Remeš, J., Bulušek, D., Králíček, I. (2014): Ungulate Impact on Natural Regeneration in Spruce-Beech-Fir Stands in Černý důl Nature Reserve in the Orlické Hory Mountains, Case Study from Central Sudetes. – Forests 5: 2929-2946.
[127] Vacek, S., Vacek, Z., Bulušek, D., Bílek, L., Schwarz, O., Simon, J., Štícha, V. (2015): The role of shelterwood cutting and protection against game browsing for the regeneration of silver fir. – Austrian Journal of Forest Science 132(2): 81-102.
[128] Vacek, S., Vacek, Z., Ulbrichová, I., Remeš, J., Podrázský, V., Vach, M., Bulušek, D., Král, J., Putalová, T. (2019): The effects of fertilization on the health status, nutrition and growth of Norway spruce forests with yellowing symptoms. – Scandinavian Journal of Forest Research 34(4): 267-281.
[129] Vercauteren, K. C., Hyngstrom, S. E. (1998): Effects of agricultural activities and hunting on home ranges of female white-tailed deer. – Journal of Wildlife Management 62(1): 280-285.
[130] Vieira, M. E., Conner, M. M., White, G. C., Freddy, D. J. (2003): Effects of archery hunter numbers and opening dates on elk movement. – Journal of Wildlife Management 67: 717-728.
[131] Ward, A. I. (2005): Expanding ranges of wild feral deer in Great Britain. – Mammal Review 35: 165-173.
[132] Williams, S. C., DeNicola, A., Almendinger, T., Maddock, J. (2013): Evaluation of Organized Hunting as a Management Technique for Overabundant White-Tailed Deer in Suburban Landscapes. – Wildlife Society Bulletin 37(1): 137-145.
[133] Wrzesień, M., Denisow, B. (2016): The effect of agricultural landscape type on field margin flora in south eastern Poland. – Acta Botanica Croatica 72(2): 217-225.

http://www.aloki.hu ● ISSN 1589 1623 (Print) ● ISSN1785 0037 (Online)
DOI: http://dx.doi.org/10.15666/aeer/1802_29893014

OPTIMIZING THE SEEDING RATE IN SUBSOILING FOR DRYLAND WHEAT (*TRITICUM AESTIVUM* L.): A KEY TO IMPROVING WATER USE EFFICIENCY AND NITROGEN USE EFFICIENCY IN THE LOESS PLATEAU OF CHINA

LIN, W. – LI, H. – REN, A. – SUN, M.* – GAO, Z.*

College of Agronomy, Shanxi Agricultural University, Taigu, Shanxi 030801, China

**Corresponding author*
e-mail: sm_sunmin@126.com, gaosxau@163.com

(Received 16th Nov 2019; accepted 12th Feb 2020)

Abstract. The effects of seeding rate and tillage on water use and nitrogen use efficiencies were studied based on a field experiment carried out from 2012 to 2016. The results showed that subsoiling significantly increased the soil water storage before sowing in all years. The water consumption (ET) during the four years was, on average, 461 and 301 mm for subsoiling (SS) and CK, respectively. The average yield of SS was 4821 kg/ha, which was 944 kg/ha higher than that of CK. The average yield was highest at the mid-seeding rate for both SS and CK, with values of 5115 and 4394 kg/ha, respectively. Since the nitrogen fertilizer application rate was the same, a higher yield indicates a higher nitrogen use efficiency (NUE). Contribution analysis showed that the higher seeding rate led to a lower contribution of nitrogen uptake efficiency (UPE) and a higher contribution of NHIp to NUEp. In summary, subsoiling during summer fallow period increased the soil water retention and improved the wheat yield and WUE. It also increased nitrogen uptake and NUEp. The mid-seeding rate (approximately 90 kg/ha) under subsoiling is optimal for improving water use efficiency (WUE) and NUE in the Loess Plateau.
Keywords: *dryland farming, contribution analysis, water use efficiency, soil tillage, nitrogen fertilizer*

Introduction

In dryland farming areas, water is a limiting factor for crop production. In most regions of the Loess Plateau, the groundwater is deep, and no irrigation water can be obtained; hence, the crops are rain-fed (Kang et al., 2002). Winter wheat (*Triticum aestivum* L.) is one of the main crops in this area. With a continental monsoon climate, the rainfall in the Loess Plateau is low and mainly falls in July, August, and September (Wang et al., 2011). However, this period occurs during the fallow period of winter wheat, which grows from early October to the following June. The rainfall during the wheat growth season is insufficient for optimal crop growth; approximately 30-40% of the required water comes from the soil water stored before sowing (Zhang et al., 2013).

A higher temperature in the fallow period makes it easier for the soil water to be lost by evaporation (Han et al., 2015). To conserve more water in the soil for wheat growth, the precipitation storage efficiency (PSE) should be increased during that period. In agronomy, there are two main types of practices to increase the PSE: reduce soil evaporation and increase soil infiltration (Nielsen and Vigil, 2010). To reduce evaporation, soil surface mulching techniques can be applied, among which plastic mulching and straw mulching are widely used (Zhang et al., 2013). Research shows that plastic film increases soil moisture in topsoil by 12.9% (Ma et al., 2018). Soil infiltration is related to soil physical properties. Tillage modifies the soil physical properties, such as the soil bulk density, which will further influence soil infiltration (Gómez et al., 1999). Subsoiling is a tillage practice that decreases the soil bulk density

http://www.aloki.hu ● ISSN 1589 1623 (Print) ● ISSN 1785 0037 (Online)
DOI: http://dx.doi.org/10.15666/aeer/1802_30153026

and increases the amount of water infiltration. Previous studies have shown that subsoiling increases the water storage in drylands (Bhatt and Khera, 2006). In the Loess Plateau, soil water storage was increased by 76 mm in the 0-200 cm layer under subsoiling during the summer fallow period (Liao et al., 2002).

Nutrients represent another limiting factor in dryland farming. The nitrogen fertilizer use efficiency (NUE) is low in dryland farming areas (Zhu and Chen, 2002). Low soil moisture decreases nutrient availability sand impacts the uptake of nutrients by crops; thus, the NUE in the dryland farming area is low (Guntiñas et al., 2012). The improved soil water conditions under subsoiling may improve the nutrient conditions in the field by making nutrients such as nitrogen more available for crops (Zhu et al., 2018), which providing crops with a better growth environment and increases productivity (Basso et al., 2010).

The seeding rate influences the wheat population, which further influences the use of soil water and nutrients and finally influences wheat growth and yield formation (Kühling et al., 2017). Wheat yield increases with the increase in seeding rate under the low sowing rate and peaks at a certain threshold value, after which it might not increase and may even cause a decrease in grain yield (Bhatta et al., 2017). Whether the optimum seeding rate changes due to the application of subsoiling still need to be addressed.

The process of nitrogen use by winter wheat can be simplified into two stages (Sadras and Lawson, 2013). In the first stage, plants uptake N from the soil and store it in leaves and stems. In this process, the N availability impacts its uptake. In winter, wheat N uptake represents 75 to 90% of the total N in the plant at harvest (Delogu et al., 1998). In the second stage, N is translocated to grains during grain filling. Many previous studies have focused on the uptake and translocation of nitrogen. However, few studies have focused on how nitrogen absorption and transportation respond to subsoiling and seeding rates. To clarify this issue, a field experiment on subsoiling in the fallow period and different wheat seeding rates was carried out from 2012 to 2016 in the Loess Plateau of China.

Materials and methods

Site description

The study was conducted at the experimental station of Shanxi Agricultural University in Wenxi County, Shanxi Province, China (35°20'N, 111°17'E, and elevation 639 m), from 2012 to 2016. The experimental site is a dryland area, with an average precipitation of 484 mm, 60-70% of which is concentrated during the fallow period of winter wheat. To improve the water use, all the experiment was carried out based on plastic film mulch. The basic nutrient properties of the soil in the experimental field in 2012 are shown in *Table 1*.

Crop management

After harvesting the previous wheat, wheat stubble with a height of 20-30 cm was left in the field until mid-July. Subsoiling was performed during the fallow period by a subsoiler (IS-200, Xiuyuan Agricultural Machinery Co.) to a depth of 30-40 cm in mid-July, followed by rotary tillage to crumble large soil lumps and to level the field around 20 August. The winter wheat variety used in this study was 'Yunhan20410', which was

http://www.aloki.hu ● ISSN 1589 1623 (Print) ● ISSN 1785 0037 (Online)
DOI: http://dx.doi.org/10.15666/aeer/1802_30153026

the recommended variety by the local agricultural extension department due to its drought stress resistance ability. The suggested sowing rate of Yunhan20410 is 90 kg/ha, if the sowing date is delayed due to climate condition, the sowing rate may be increased to 105 kg/ha. During the four experimental years, wheat was sown in late September or early October and harvested around 20 June. Before sowing, chemical fertilizer was applied at a rate of 150 kg ha^{-1} nitrogen, 150 kg ha^{-1} P_2O_5 and 150 kg ha^{-1} K_2O. Since no irrigation was applied during the experiment, no fertilizer was applied during the entire growth period. Weeds and pests were controlled by herbicides as needed.

Table 1. *Main soil chemical properties before sowing in 2012*

Soil nutrients	Content
Organic matter (g kg^{-1})	11.88
Total nitrogen (g kg^{-1})	0.61
Alkali-hydrolysis nitrogen (mg kg^{-1})	38.62
Available phosphorous (mg kg^{-1})	14.61
Available potassium (mg kg^{-1})	238.16
pH	8.08

Experimental design

The experiment was conducted with a two-factor split plot design, taking the tillage practice as a main factor and the planting density as a sub-plot factor. The two tillage practices were the subsoiling (SS) and the no tillage (NT) condition, which was the control. Under each tillage method, three planting densities, low (L, 60-75 kg seed ha^{-1}, < 190 × 10^6 plants ha^{-1}), mid (M, 90-105 kg seed ha^{-1}, 190-260 × 10^6 plants ha^{-1}), and high (H, 112.5-120 kg seed ha^{-1}, > 320 × 10^6 plants ha^{-1}) were used in the experiment. Seeds were sown at rates of 67.5, 90 and 112.5 kg ha^{-1}, after which a 3-leaf stage planting density of 190, 260 and 320 plants m^{-2} was attained by thinning. Each treatment was repeated three times with a total of 18 plots. Each sub-plot (150 m^2) was 50 m long and 3 m wide with a line spacing of 30 cm.

Measurements

Soil water storage

The soil was sampled every 20 cm to a depth of 300 cm and soil water content was determined gravimetrically before planting and after harvest. The precipitation data were obtained from the meteorological station at the experimental site (*Table 2*).

Table 2. *Precipitation and mean temperature in fallow period and in growth stage during the experiment (mm)*

	Stage	2012-2013	2013-2014	2014-2015	2015-2016
Precipitation (mm)	Fallow period	188	288	284	95
	Growth stage	167	202	190	292
Temperature (℃)	Fallow period	24.9	26.7	24.8	24.7
	Growth stage	10.4	10.7	10.5	10.0

http://www.aloki.hu ● ISSN 1589 1623 (Print) ● ISSN 1785 0037 (Online)
DOI: http://dx.doi.org/10.15666/aeer/1802_30153026

As the plots were on a flat experimental field with ridges around them, the plots were not influenced by surface runoff. Moreover, the influence of groundwater can be ignored because the groundwater level is low in this region. The evapotranspiration (ET) and water use efficiency (WUE) were obtained through *Equations 1* and *2* (Li et al., 2013):

$$ET = P + \Delta W \quad \text{(Eq.1)}$$

$$WUE = \frac{Y}{ET} \quad \text{(Eq.2)}$$

where ΔW is the soil water depletion during the wheat growing stage, and Y is the grain yield.

Nitrogen content

Plant nitrogen content was determined using the semi-micro Kjeldahl method, and wheat protein content was obtained by multiplying the N content (%) by 5.7 (Halvorson et al., 2004).

Grain yield

At maturity, plants from three 1 m^2 size sample plots were harvested from each plot to determine the grain yield (kg ha^{-1}).

Contribution analysis

In this research, because soil available nitrogen was not measured, we focused on the use efficiency of nitrogen from fertilizer and then the NUE, which is defined as the ratio of the grain yield (Y) and nitrogen fertilizer application rate (Nf) (Moll et al., 1982). The nitrogen fertilizer use efficiency for protein (NUEp) is defined as the ratio of the grain nitrogen (Ng) and nitrogen fertilizer application rate. The NUE can be partitioned into the components of UTE (the ability of the plant to convert the absorbed N into harvested grain yield, Y/Nt) and UPE (nitrogen uptake efficiency, Nt/Nf). NUEp can be separated into the components of UPE and NHI (nitrogen harvest index, Ng/Nt) (Van Sanford and Mackown, 1986). *Equations 3* and *4* express the relationship between these indexes.

$$NUE = UPE \times UTE \quad \text{(Eq.3)}$$

$$NUEp = UTE \times NHI \quad \text{(Eq.4)}$$

To analyse the contribution of the components to NUE, we calculated the natural log of the three components using *Equation 5:*

$$ln\ NUE = ln\ UPE + ln\ UTE \quad \text{(Eq.5)}$$

Then, both individual components of NUE can be regressed with respect to NUE: ln UPE = a1 + b1 ln NUE; ln UTE = a2 + b2 ln NUE; (b1 + b2) must be = 1 and thus

http://www.aloki.hu ● ISSN 1589 1623 (Print) ● ISSN 1785 0037 (Online)
DOI: http://dx.doi.org/10.15666/aeer/1802_30153026

explains the complementary contribution of each component to NUE (Giuliani et al., 2011). Similarly, the contribution of each component to NUEp can be calculated by this means.

Statistical analysis

An analysis of variance was conducted on the experimental data using SAS 9.3 (SAS Institute Inc., Cary, NC, USA) to study the main effects of mulching methods and their interactions. The least significant difference (LSD) test was performed to calculate the significance of differences between means at $P < 0.05$.

Results

Yield and water use

Based on the boundary function concept proposed by French and Scultz (1984) and the improved boundary function establishment method developed by Lin and Liu (2016), we obtained the winter wheat boundary function of yield-ET in the Loess Plateau (*Fig. 1*). The upper boundary of the yield-ET relationship can be fitted using the function Yield = 14.8 (ET-42.3), which means that under plastic film mulch in this area, the maximum transpiration efficiency is 14.8 kg ha^{-1} mm^{-1}.

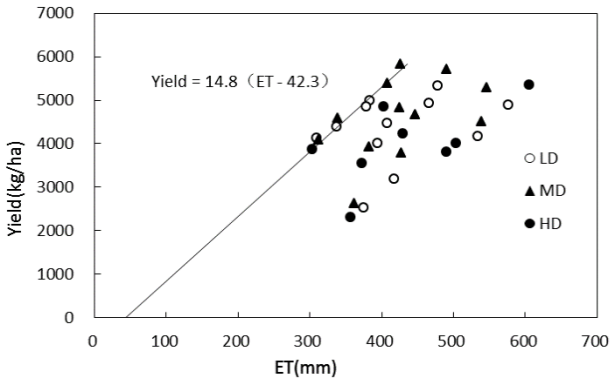

Figure 1. *Yield and ET relationship under different seeding rates. The boundary line was generated according to (Lin and Liu, 2016) and shows the maximum yield under different ET*

The results show that compared with CK, SS increased the soil water storage by an average of 58 mm during the 4 years ($p < 0.001$). The average yield under SS was 4821 kg/ha, which was 950 kg higher than the 3877 kg/ha of CK ($p < 0.001$). Higher soil water storage provided more water for crop use during the growth period; hence, the ET for SS was significantly higher than that of CK. The WUEs for SS and CK were 10.6 and 10.2 kg ha mm, respectively, without a significant difference. The WUEp for SS was significantly higher than that of CK (*Table 3*).

To evaluate the seeding rate impact on the yield and water use of winter wheat, we calculated the data based on the seeding rate (*Table 4*). The results showed that the wheat yields were 4324, 4787 and 3998 kg/ha for the low-, mid- and high-seeding rate treatments, respectively ($p < 0.05$). No significant difference was observed for ET among different seeding rates. The difference in WUE and WUEp under different

http://www.aloki.hu ● ISSN 1589 1623 (Print) ● ISSN 1785 0037 (Online)
DOI: http://dx.doi.org/10.15666/aeer/1802_30153026

seeding rates was much the same as that of yield, i.e., highest at the mid-seeding rate, second in the low-seeding rate and lowest in the high-seeding rate.

Table 3. *Yield, water consumption and WUE under different tillage measures*

Tillage	Yield (kg/ha)	Soil water storage before sowing (mm)	ET (mm)	WUE (kg ha^{-1} mm^{-1})	WUE$_P$ (kg ha^{-1} mm^{-1})
SS	4821	526	461	10.6	11.3
CK	3877	468	391	10.2	9.1
Prob	0.041**	0.045**	0.045**	0.064	0.041**

**Significant difference between SS and CK based on t test at the $p < 0.05$ significance level; ns: no significant difference was observed

Table 4. *Yield, water consumption and WUE under different seeding rates. L, M, and H represent low-, mid- and high-seeding rates, respectively. Values followed by different letters within the same row are significantly different ($P < 0.05$)*

Seeding rate	Yield (kg/ha)	ET (mm)	WUE (kg ha^{-1} mm^{-1})	WUE$_P$ (kg ha^{-1} mm^{-1})
L	4324 b	421 a	10.5 b	10.1 b
M	4787 a	431 a	11.3 a	11.1 a
H	3998 c	433 a	9.4 c	9.4 c
$LSD_{0.05}$	301	12.5	0.7	0.7

Nitrogen uptake and translocation

Under subsoiling, the NUE was 31.31, 34.10 and 30.43 kg/ha for the low-, mid- and high-seeding rates (*Table 5*). Under CK, the NUE decreased to 25.32, 26.51 and 21.91 kg/kg, respectively. The UTE for SS was significantly higher than that of CK under all seeding rates. However, the situation among different seeding rates was not the same for the NUE. The NUEs were highest under the mid-seeding rate. The UTE was highest at a low-seeding rate under SS and highest at a high-seeding rate under CK. The UPE is a component of both NUE and NUEp, and it was highest at the mid-seeding rate, with values of 1.06 and 1.01 in SS and CK, respectively (*Table 5*). However, for CK, there was no significant difference among seeding rates. The NUEp tended to be lower under CK than under SS. Under the same tillage method, the mid-seeding rate showed the highest NUEp. The average NHI was approximately 0.82, and no significant difference was observed between treatments.

Contributions of NUE and NUEp

Figure 2 shows the calculation process for NUEp under SS and CK. The slope of the regression function is the contribution of each component to NUEp. The contribution of NHI to NUEp was 20.84%, and under CK, it decreased to 12.92%. The contribution of UPE to NUEp was 79.16%, and under CK, it increased to 87.08%. Hence, SS led to a higher contribution of UPE and a lower contribution to NHI.

The contribution of UPE to NUEp was 84.96%, 81.12% and 76.59% for the high-, mid- and low-seeding rates, respectively (*Table 6*). The contribution of UPE to NUE was 67.05%, 48.95% and 36.06% for the high-, mid- and low-seeding rates,

http://www.aloki.hu ● ISSN 1589 1623 (Print) ● ISSN 1785 0037 (Online)
DOI: http://dx.doi.org/10.15666/aeer/1802_30153026

respectively (*Table 7*). The contribution of NHI to NUEp was 15.04%, 17.87% and 23.41% for the high-, mid- and low-seeding rates, respectively. The contribution of UTE to NUE increased as the seeding rate increased, ranking 32.95%, 51.05%, 63.94% for the high-, mid- and low-seeding rates, respectively.

Table 5. *N use efficiency and its components. NUE = Y/Nf, NUEp = Ng/Nf, UPE = Nt/Nf, UTE = Y/Nt, NHI = Ng/Nt. L, M, and H represent low-, mid- and high-seeding rates, respectively. Values followed by different letters within the same row are significantly different (P < 0.05). **Significance at p < 0.05*

Tillage	Seeding rate	NUE (kg/kg)	UTE (kg/kg)	UPE (kg/kg)	NUEp (kg/kg)	NHI (kg/kg)
SS	Low	31.31 b	33.50 a	0.96 b	0.80 b	0.83 a
	Mid	34.10 a	32.47 b	1.06 a	0.90 a	0.84 a
	High	30.43 c	31.09 c	0.98 b	0.82 b	0.84 a
CK	Low	25.32 e	26.82 e	0.95 b	0.79 b	0.82 ab
	Mid	26.51 d	26.36 e	1.00 b	0.83 b	0.82 ab
	High	21.91 f	27.88 d	0.78 c	0.63 c	0.80 b
ANOVA SS						
Tillage (F_T)		296.4**	275.6**	0.18**	0.12**	0.03
Seeding rate (F_S)		75.7**	87.5**	0.15**	0.10**	0.02
$F_T \times F_S$		26.8**	32.3**	0.03	0.05	0.02

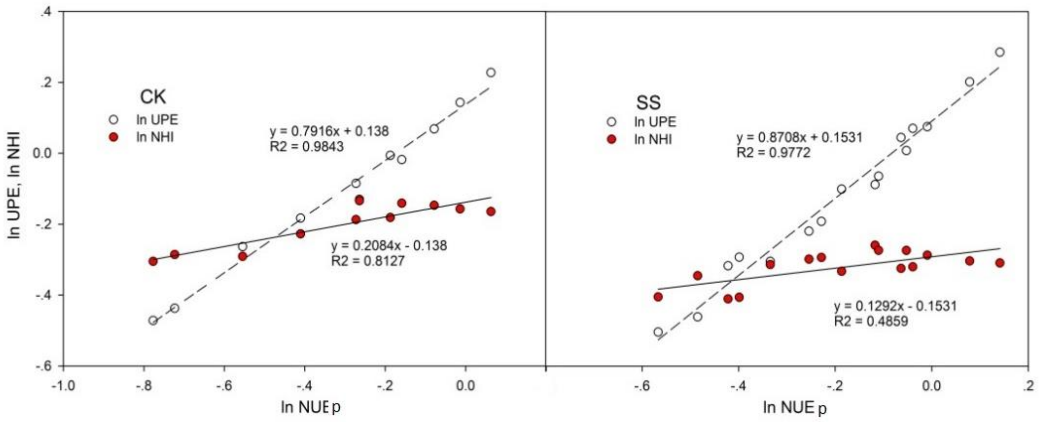

Figure 2. *Linear regression of nitrogen uptake efficiency (UPE) and nitrogen utilization for protein (NHIp) components on total nitrogen use efficiency for protein (NUEp) in CK and SS*

Table 6. *NUEp and its components under different seeding rates. L, M, and H represent low-, mid- and high-seeding rates, respectively. Values followed by different letters within the same row are significantly different (P < 0.05)*

D	NUEp (kg/kg)	UPE	Contribution	NHI	Contribution
L	0.80 b	0.95 b	84.96%	0.83 a	15.04%
M	0.87 a	1.04 a	81.12%	0.84 a	17.87%
H	0.74 c	0.89 c	76.59%	0.82 a	23.41%
$LSD_{0.05}$	0.59	0.05	-	0.03	-

http://www.aloki.hu ● ISSN 1589 1623 (Print) ● ISSN 1785 0037 (Online)
DOI: http://dx.doi.org/10.15666/aeer/1802_30153026

Table 7. *NUE and its components. L, M, and H represent the low-, mid- and high-seeding rates, respectively. Values followed by different letters within the same row are significantly different ($P < 0.05$)*

D	NUE (kg/kg)	UPE	Contribution	UTE	Contribution
L	28.92 b	0.95 b	67.05%	30.83 a	32.95%
M	31.06 a	1.04 a	48.95%	30.02 b	51.05%
H	26.78 c	0.89 c	36.06%	29.72 b	63.94%
$LSD_{0.05}$	1.58	0.05	-	0.55	-

Discussion

Seeding rate and wheat water yield potential

The boundary analysis results show that most of the dots close to the boundary line were the mid-seeding rate treatment and low-seeding rate treatment (*Fig. 1*). This result means that a high seeding rate is not appropriate for making full use of water resources in this region. The intercept of the boundary line represents the minimum soil evaporation in this area (Sadras and Angus, 2006). In this research, the intercept is 42.3 mm, which was lower than the value of 60 mm reported by Zhang (2013). The main reason is that plastic film was used in this research, and plastic is effective in reducing soil evaporation (Li et al., 2005).

Subsoiling influence on wheat yield and WUE

In SS, the ET and yield increased significantly, but no significant difference was observed in the WUE (*Table 3*). However, this does not mean that SS had no impact on water resource use in dryland wheat. SS increased precipitation infiltration into the soil in the summer period; hence, more water was stored in the soil before sowing (Williams et al., 2006), which means that more water was available for crop growth and soil evaporation. Hence, the ET was increased (Lin et al., 2016). Because ET and yield were increased in a similar ratio under SS in this research, the WUE remained the same. However, in dryland farming, a high WUE should be considered, but it makes no sense if the high WUE is based on a low yield and low ET. The effective use of water should be the goal to improve the crop yield in dryland areas (Blum, 2009). In the Loess Plateau, without irrigation and groundwater supplementation, soil water is supplied by precipitation; hence, precipitation is the only source of water for crop growth (Lin et al., 2019). However, more water was used under SS because more water was within reach for the crop. We further calculated the WUE of precipitation (WUEp) in a hydrological year (fallow period + growth period) and found that the WUEp under SS increased significantly (*Table 3*). SS significantly used the limited precipitation available in the dryland farming area.

Fang (2010) found that ET increased as the seeding rate increased. In this study, although ET showed an increasing trend as the seeding rate increased, no significant difference was found in the ET values among the different seeding rate treatments. This difference may be due to differences in the environment at the experimental sites. Compared with Fang's research, precipitation was lower in this research. Under a high-seeding rate, the large population calls for more water for transpiration use, but the shading effect of higher shoot coverage may reduce the soil evaporation; under a low-seeding rate, less water is used by transpiration, but more soil is exposed to the air

http://www.aloki.hu ● ISSN 1589 1623 (Print) ● ISSN 1785 0037 (Online)
DOI: http://dx.doi.org/10.15666/aeer/1802_30153026

directly, and hence more water is evaporated (Li et al., 2013). Iqbal et al. (2012) found that the mid-seeding rate helped obtain a high yield. In this research, we found a similar result. The wheat yield was highest in the mid-seeding rate treatment and lowest in the high-seeding rate treatment. Thus, a suitable seeding rate is important for achieving a high yield. This may be the reason why similar ET values were found among the different seeding rates in this study.

N uptake and utilization

SS increased the soil water content and improved the soil air condition, which increased the availability of nutrients and eased the uptake of nutrients by roots (Zhu et al., 2018); hence, UPE was higher in SS than in CK (*Table 1*). The higher UPE further led to a higher NUEp for SS, although there was no significant difference in the NHI among treatments. Contribution analysis showed that the contribution to NUEp was CK < SS for UPE and CK > SS for NHI. Giuliani et al. (2011) found that the contribution of UPE to NUEp was lower in dry years than in wet years. In this research, SS improved the soil water condition before sowing, which resembled a wetter condition compared with that in CK. A higher contribution of UPE means that the increased NUEp under SS was mainly due to the increased UPE.

NUE and NUEp were highest for the mid-seeding rate treatment. This result means that a moderate planting density helps make full use of nitrogen (Arduini et al., 2006). In agreement with several previous studies (Van Sanford and Mackown, 1986; Giuliani et al., 2011), the contribution of UPE to NUEp was higher than that of NHI under all seeding rates (*Table 6*). The contribution of UPE to NUEp decreased as the seeding rate increased, and the contribution of NHI increased as the seeding rate increased. For NUE, the contribution of UPE was higher than that of UTE at low-seeding rates, similar at mid-seeding rates and lower at high-seeding rates.

In this study, because the available soil N before seeding was not measured, nitrogen from fertilizer (Nf) was used instead of the nitrogen supply (Ns, expressed as Nf plus available soil nitrogen). This represents a limitation of this study. However, fertilizer N is an important N source for wheat growth; hence, the results still make sense for wheat production in dryland areas.

Conclusions

In order to make full use of the limited water resources and improve nitrogen fertilizer use efficiency (NUE) in the dryland farming area, the effects of seeding rate and tillage on water use and nitrogen use were analyzed. We found that under plastic film mulch, soil evaporation is effectively reduced for the winter wheat in the Loess Plateau. Subsoiling during the summer fallow period increased soil water retention and improved wheat yield and WUEp. It also increased nitrogen uptake and NUEp. The mid-seeding rate (approximately 90 kg/ha) increased the wheat yield and WUE and increased the contribution of NHI to NUEp but decreased the contribution of UPE to NUEp, which led to the highest NUEp. The results of this study focused on the overall use of N fertilizer absorption and utilization, to make a full understanding about how seeding rate and subsoiling influence N utilization process, N concentration in plant and enzymatic activity related to N enzymatic activity should be measured in future study.

http://www.aloki.hu ● ISSN 1589 1623 (Print) ● ISSN 1785 0037 (Online)
DOI: http://dx.doi.org/10.15666/aeer/1802_30153026

Acknowledgments. We gratefully acknowledge the anonymous reviewers for their constructive comments. This work was funded by Science & Technology Innovation Foundation of Shanxi Agricultural University (2017YJ24), Outstanding Doctor Funding Award of Shanxi Province (SXYBKY201749). This work was also supported by the earmarked fund for China Agriculture Research System (CARS-03-01-24), the National Natural Science Foundation of China (31771727).

REFERENCES

[1] Arduini, I., Masoni, A., Ercoli, L., Mariotti, M. (2006): Grain yield, and dry matter and nitrogen accumulation and remobilization in durum wheat as affected by variety and seeding rate. – European Journal of Agronomy 25(4): 309-318.

[2] Basso, B., Cammarano, D., Troccoli, A., Chen, D., Ritchie, J. T. (2010): Long-term wheat response to nitrogen in a rainfed Mediterranean environment: field data and simulation analysis. – European Journal of Agronomy 33(2): 132-138.

[3] Bhatt, R., Khera, K. (2006): Effect of tillage and mode of straw mulch application on soil erosion in the submontaneous tract of Punjab, India. – Soil and Tillage Research 88(1-2): 107-115.

[4] Bhatta, M., Eskridge, K. M., Rose, D. J., Santra, D. K., Baenziger, P. S., Regassa, T. (2017): Seeding rate, genotype, and topdressed nitrogen effects on yield and agronomic characteristics of winter wheat. – Crop Science 57(2): 951-963.

[5] Blum, A. (2009): Effective use of water (EUW) and not water-use efficiency (WUE) is the target of crop yield improvement under drought stress. – Field Crops Research 112(2-3): 119-123.

[6] Delogu, G., Cattivelli, L., Pecchioni, N., De Falcis, D., Maggiore, T., Stanca, A. (1998): Uptake and agronomic efficiency of nitrogen in winter barley and winter wheat. – European Journal of Agronomy 9(1): 11-20.

[7] Fang, Y., Xu, B.-C., Turner N. C., Li, F.-M. (2010): Grain yield, dry matter accumulation and remobilization, and root respiration in winter wheat as affected by seeding rate and root pruning. – European Journal of Agronomy 33(4): 257-266.

[8] French, R., Schultz, J. (1984) Water use efficiency of wheat in a Mediterranean-type environment. I. The relation between yield, water use and climate. – Aust. J. Agr. Res. 35: 743-764.

[9] Giuliani, M. M., Giuzio, L., Caro, A. D., Flagella, Z. (2011): Relationships between nitrogen utilization and grain technological quality in durum wheat: I. Nitrogen translocation and nitrogen use efficiency for protein. – Agronomy Journal 103(5): 1487-1494.

[10] Gómez, J., Giráldez, J., Pastor, M., Fereres, E. (1999): Effects of tillage method on soil physical properties, infiltration and yield in an olive orchard. – Soil and Tillage Research 52(3-4): 167-175.

[11] Guntiñas, M. E., Leirós, M., Trasar-Cepeda, C., Gil-Sotres, F. (2012): Effects of moisture and temperature on net soil nitrogen mineralization: a laboratory study. – European Journal of Soil Biology 48: 73-80.

[12] Halvorson, A. D., Nielsen, D. C., Reule, C. A. (2004) Nitrogen fertilization and rotation effects on no-till dryland wheat production. – Agron J 96: 1196-1201.

[13] Han, X., Liu, W., Lin, W. (2015): Spatiotemporal analysis of potential evapotranspiration in the Changwu tableland from 1957 to 2012. – Meteorological Applications 22(3): 586-591.

[14] Iqbal, J., Hayat, K., Hussain, S., Ali, A., Bakhsh, M. A. A. H. A. (2012): Effect of seeding rates and nitrogen levels on yield and yield components of wheat (Triticum aestivum, L.). – Pakistan Journal of Nutrition 11(7): 531.

http://www.aloki.hu ● ISSN 1589 1623 (Print) ● ISSN 1785 0037 (Online)
DOI: http://dx.doi.org/10.15666/aeer/1802_30153026

[15] Kang, S., Zhang, L., Liang, Y., Hu, X., Cai, H., Gu, B. (2002): Effects of limited irrigation on yield and water use efficiency of winter wheat in the Loess Plateau of China. – Agricultural Water Management 55(3): 203-216.
[16] Kühling, I., Redozubov, D., Broll, G., Trautz, D. (2017): Impact of tillage, seeding rate and seeding depth on soil moisture and dryland spring wheat yield in Western Siberia. – Soil and Tillage Research 170: 43-52.
[17] Li, F., Wang, J., Xu, J. (2005): Plastic film mulch effect on spring wheat in a semiarid region. – J. Sustain. Agr. 25(4): 5-17.
[18] Li, S., Wang, Z., Li, S., Gao, Y., Tian, X. (2013): Effect of plastic sheet mulch, wheat straw mulch, and maize growth on water loss by evaporation in dryland areas of China. – Agricultural Water Management 116: 39-49.
[19] Liao, Y., Han, S., Wen, X. (2002): Soil water content and crop yield effects of mechanized conservative tillage-cultivation system for dryland winter wheat in the Loess Tableland. – Transactions of the Chinese Society of Agricultural Engineering 2002(4).
[20] Lin, W., Liu, W. (2016): Establishment and application of spring maize yield to evapotranspiration boundary function in the Loess Plateau of China. – Agricultural Water Management. 178: 345-349.
[21] Lin, W., Liu, W., Xue, Q. (2016): Spring maize yield, soil water use and water use efficiency under plastic film and straw mulches in the Loess Plateau. – Scientific Reports 6: 38995.
[22] Lin, W., Liu, W., Zhou, S., Liu, C. (2019): Influence of plastic film mulch on maize water use efficiency in the Loess Plateau of China. – Agricultural Water Management 224: 105710.
[23] Ma, D., Chen, L., Qu, H., Wang, Y., Misselbrook, T., Jiang, R. (2018): Impacts of plastic film mulching on crop yields, soil water, nitrate, and organic carbon in Northwestern China: a meta-analysis. – Agricultural Water Management 202: 166-173.
[24] Moll, R. H., Kamprath, E. J., Jackson, W. A. (1982): Analysis and interpretation of factors which contribute to efficiency of nitrogen utilization. – Agronomy Journal 74(3): 562-564.
[25] Nielsen, D. C., Vigil, M. F. (2010): Precipitation storage efficiency during fallow in wheat-fallow systems. – Agronomy Journal 102(2): 537.
[26] Sadras, V. O., Angus, J. F. (2006): Benchmarking water-use efficiency of rainfed wheat in dry environments. – Australian Journal of Agricultural Research 57(8): 847-856.
[27] Sadras, V. O., Lawson, C. (2013): Nitrogen and water-use efficiency of Australian wheat varieties released between 1958 and 2007. – European Journal of Agronomy 46(2): 34-41.
[28] Van Sanford, D. A., Mackown, C. T. (1986): Variation in nitrogen use efficiency among soft red winter wheat genotypes. – Theoretical & Applied Genetics (Theoretische und angewandte Genetik) 72(2): 158.
[29] Wang, J., Liu, W., Dang, T. (2011): Responses of soil water balance and precipitation storage efficiency to increased fertilizer application in winter wheat. – Plant and soil 347(1-2): 41-51.
[30] Williams, J. D., Wuest, S. B., Schillinger, W. F., Gollany, H. T. (2006): Rotary subsoiling newly planted winter wheat fields to improve infiltration in frozen soil. – Soil and Tillage Research 86(2): 141-151.
[31] Zhang, S., Sadras, V., Chen, X., Zhang, F. (2013): Water use efficiency of dryland wheat in the Loess Plateau in response to soil and crop management. – Field Crops Research 151: 9-18.
[32] Zhu, Q., Castellano, M. J., Yang, G. (2018): Coupling soil water processes and nitrogen cycle across spatial scales: potentials, bottlenecks and solutions. – Earth-Science Reviews 4(2): 35-40.

http://www.aloki.hu ● ISSN 1589 1623 (Print) ● ISSN 1785 0037 (Online)
DOI: http://dx.doi.org/10.15666/aeer/1802_30153026

[33] Zhu, Z., Chen, D. (2002): Nitrogen fertilizer use in China. Contributions to food production, impacts on the environment and best management strategies. – Nutrient Cycling in Agroecosystems 63(2-3): 117-127.

http://www.aloki.hu ● ISSN 1589 1623 (Print) ● ISSN 1785 0037 (Online)
DOI: http://dx.doi.org/10.15666/aeer/1802_30153026

INFLUENCES OF SEWAGE SLUDGE-AMENDED SOIL ON HEAVY METAL ACCUMULATION, GROWTH AND YIELD OF ROCKET PLANT (*ERUCA SATIVA*)

EID, E. M.[1,2] – EL-BEBANY, A. F.[3*] – TAHER, M. A.[1,4] – ALRUMMAN, S. A.[1] – HUSSAIN, A. A.[1] – GALAL, T. M.[5] – SHALTOUT, K. H.[6] – SEWELAM, N. A.[6] – AHMED, M. T.[1] – EL-SHABOURY, G. A.[1]

[1]*Biology Department, College of Science, King Khalid University, Abha 61321, P.O. Box 9004, Saudi Arabia*

[2]*Permanent address: Botany Department, Faculty of Science, Kafr El-Sheikh University, Kafr El-Sheikh 33516, Egypt*

[3]*Plant Pathology Department, Faculty of Agriculture, Alexandria University, El-Shatby 21545, Alexandria, Egypt*

[4]*Permanent address: Botany Department, Faculty of Science, Aswan University, Aswan 81528, Egypt*

[5]*Botany and Microbiology Department, Faculty of Science, Helwan University, Cairo, Egypt*

[6]*Botany Department, Faculty of Science, Tanta University, Tanta 31527, Egypt*

[*]*Corresponding author*
e-mail: aelbebany@yahoo.com; phone: +20-112-315-8526; fax: +20-3592-2780

(Received 22nd Nov 2019; accepted 12th Feb 2020)

Abstract. The application of sewage sludge (SS) in agriculture is a wastewater recycling method for soil fertilization. The aim of this study was to assess the influences of SS amendment rates (0, 10, 20, 30, 40 and 50 g kg^{-1}) on the green-salad leafy plant *Eruca sativa*. The SS amendment increased soil salinity and organic matter and decreased soil pH. The heavy metal (HM) contents were below the permissible limits as recommended by the Council of the European Communities. An increase in *E. sativa* morphometric parameters was detected. The leaf, root and total biomasses of *E. sativa* increased at amendment rates 10, 20 and 30 g kg^{-1}. The applications of 40 and 50 g kg^{-1} negatively affected the biomass. The highest concentration of the measured HMs in the plant was detected at the 50 g kg^{-1} amendment rate. The bioaccumulation factors of Cd, Co, Cr, Fe, Mn, Ni, Pb and Zn were < 1.0, whereas those of Cu and Mo were > 1. The translocation factors for all HMs were < 1.0 except for Cd and Pb. Even though, SS increased the biomass of *E. sativa*, SS is not recommended as a fertilizer for *E. sativa*, since translocation factors of Cd and Pb were >1.
Keywords: *soil pollution, rocket plant, health hazards, environmental risks, metal bioaccumulation*

Introduction

Sewage sludge (SS) is a by-product of domestic wastewater treatment processes (Eid and Shaltout, 2016). SS has a variety of elements that are considered nutrients for plants in addition to organic components that increase agricultural soil fertility (Singh and Agrawal, 2008). However, the physical, chemical and microbial properties of SS have to be analyzed before use as agricultural soil fertilizers to avoid any harmful effects on plants, animals and humans (Carbonell et al., 2009). The effect of heavy metals (HMs) on crops differs according to the metal and/or plant (Hara and Sonoda,

http://www.aloki.hu ● ISSN 1589 1623 (Print) ● ISSN 1785 0037 (Online)
DOI: http://dx.doi.org/10.15666/aeer/1802_30273040

1979). Some HMs are required by plants for physiological processes, including Mn, Fe, Cu, Zn, and Mo, while other HMs are phytotoxic, such as Cd and Pb (Raskin et al., 1994).

The concerns in using SS as soil fertilizer relate to the possible transfer and accumulation of significant HMs in the food chain and, subsequently, their effect on human health (Shrivastava and Banerjee, 2004). Several factors influence the toxic HM accumulation in soil and plants, such as the origin and properties of the SS and agricultural soil, amendment level, metal availability, and plant species (Kabata-Pendias, 2011; Dede and Ozdemir, 2016). Even though use of SS in agriculture is an effective and economically beneficial method of disposal, the potential environmental and health issues should be considered.

Rocket (*Eruca sativa* Mill.) is a vegetable leafy crop belonging to the *Brassicaceae* family. Its fresh leaves are used as a green salad food because it is a fast-growing species, and is available nearly all year (Nail et al., 2017). The nutritional and medicinal benefits of *E. sativa* are documented as an anticarcinogenic, antimicrobial and antioxidant agent (Hassan et al., 2017). The biochemical constituents of *E. sativa* and their bio positive effects on health were explained in several studies (Garg and Sharma, 2014; Jilani et al., 2015). In the current study, SS was used as an amendment to agricultural soil for growing *E. sativa*. The objectives were to (1) evaluate the effect of SS on the growth and biomass of *E. sativa* and (2) assess the HM accumulation in *E. sativa* parts and in the agricultural soil.

Materials and Methods

Plant materials, sewage sludge treatments and experimental design

Eruca sativa seeds were obtained from a local market in Abha. The agricultural soil used in the experiment was collected at a depth of 0-20 cm from neighbouring cultivated fields. The SS was obtained from the Abha municipal sewage treatment plant, Aseer region, Saudi Arabia. The agricultural soil and SS were air-dried for 2 weeks and sieved through a sieve with 2-mm pore diameter. The experiment was performed in the greenhouse of the Biology Department, King Khalid University, Abha, Saudi Arabia.

The SS was mixed with agricultural soil at rates of 0 (the control soil), 10, 20, 30, 40 and 50 g kg^{-1}. Each treatment consisted of six replicates of a plastic pot (6-L volume), and each plastic pot was filled with 4 kg of the respective treatment. Twenty *E. sativa* seeds were planted in each pot. The experimental units were arranged in a complete randomized design. The plants were grown for 40 days, starting from the planting day of January 2nd, 2018 and were harvested on February 10th, 2018, in the greenhouse with a natural day/night regime and irrigated as needed. *Figure 1* shows the experiment setup and postharvest analyses.

Plant morphometric parameters and biomass

From the 120 plants in each treatment, 30 plants (5 plants/6 replicates) were used for morphological and biomass measurements. *E. sativa* plants were washed using running water. Shoot height and root length were measured, and the number of leaves were counted. Leaf area was measured using a leaf area metre (Dynamax AM 300, Dynamax Inc, USA). The absolute growth rate (AGR) was calculated according to the formula by Radford (1967) (*Eq. 1*):

http://www.aloki.hu ● ISSN 1589 1623 (Print) ● ISSN 1785 0037 (Online)
DOI: http://dx.doi.org/10.15666/aeer/1802_30273040

$$\text{AGR (g DM individual}^{-1}\text{ day}^{-1}) = (W_2 - W_1)/(t_2 - t_1) \quad \text{(Eq.1)}$$

where W_1 and W_2 are the total biomasses (g DM individual^{-1}) at times (days) t_1 and t_2, respectively. The value of t_1 is zero and t_2 is 40 which is the growing period of the plants.

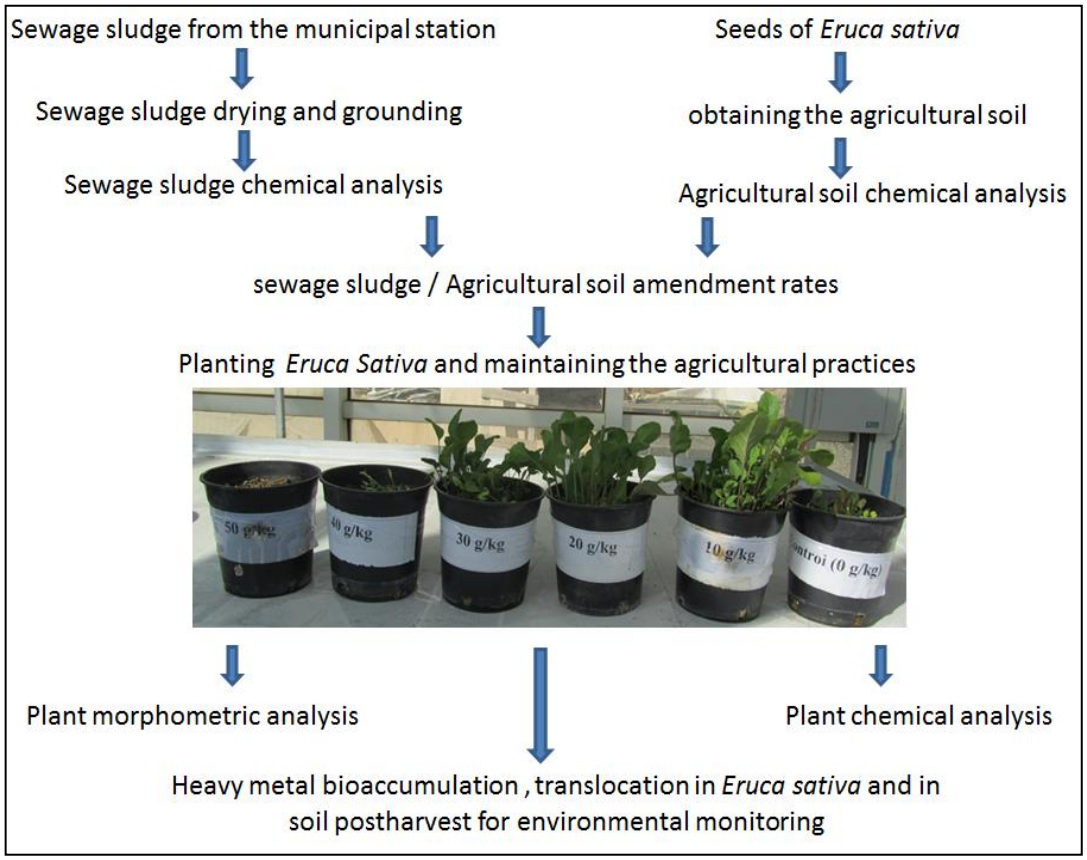

Figure 1. *A graphical demonstration of the experiment steps with pots represents the treatments of sewage sludge-soil amendment rates*

The plant leaves and roots were oven-dried at 60°C for one week and ground using a plastic mill. The biomass of the leaves and roots were determined. The total biomass refers to the summation of the leaf and root biomass.

Sample analyses

Pre-experiment analyses of the SS and agricultural soil were conducted. At the end of the experiment, the amended soil samples representing all treatments were air dried and sieved through a 2-mm sieve. The pre-used agricultural soil, SS and post-harvest amended soil samples (including the control) were analyzed for organic matter content using a loss-on-ignition method at 550ºC for two hours (Wilke, 2005). Soil-water extracts at a ratio of 1:5 were prepared for salinity and pH determination, using conductivity (Myron L Model DA-1, Myron L Company, USA) and pH metres (ICM Model 41150, ICM, USA), respectively. HMs in the pre-experiment agricultural soil, SS, post-harvest amended soil and plant parts samples were detected according to Allen

http://www.aloki.hu ● ISSN 1589 1623 (Print) ● ISSN 1785 0037 (Online)
DOI: http://dx.doi.org/10.15666/aeer/1802_30273040

(1989). HMs were extracted from approximately 0.5 g of each sample using a mixed-acid digestion method (HNO_3 and $HClO_4$; 3:1, v/v). Digestion was performed using a microwave sample preparation system (PerkinElmer Titan MPS, PerkinElmer Inc., USA). Blank samples were used to verify the accuracy. Analytical-grade chemicals were used for sample digestion. Cd, Co, Cr, Cu, Fe, Mn, Mo, Ni, Pb and Zn were determined using an inductively coupled plasma optical emission spectrometry (ICP-OES) (Thermo Scientific iCAP 7000 Plus Series; Thermo Fisher Scientific, USA). The instrument setting and operational conditions followed the manufacturer's specifications. Standard solutions with known concentrations of different HMs were prepared for the standardization of the system.

Estimation of bioaccumulation and translocation factors

Bioaccumulation and translocation factors were calculated as described by Ghosh and Singh (2005). The bioaccumulation factor (BF) was calculated to determine the effectiveness of the plants in accumulating a HM from the soil according the following formula (*Eq. 2*):

$$BF = \text{conc. of a metal in the roots/conc. of the same metal in the soil} \quad \text{(Eq.2)}$$

The translocation factor (TF) was calculated to determine the ability of the plants to translocate a metal from the roots to the shoot according the following formula (*Eq. 3*):

$$TF = \text{conc. of a metal in the shoot/conc. of the same metal in the roots} \quad \text{(Eq.3)}$$

Statistical analysis

The data were tested for normality of distribution and homogeneity of variance, and when necessary, the data were log-transformed. The data were assessed using one-way ANOVA. The significant differences between the means of the six amendment rates were identified using the Tukey HSD test at $P < 0.05$. A quadratic regression analysis (Eid et al., 2020) was performed to evaluate the response of the biomass and plant morphometric parameters of *E. sativa* grown in soils amended with different rates of SS. To evaluate the statistical relationships among the content of HM in plant parts and the amendment rate of SS, linear regression procedures were applied according to the following formula (*Eq. 4*):

$$y = a + bx \quad \text{(Eq.4)}$$

where y is the heavy metal concentration (mg kg^{-1}) in *E. sativa* tissue harvested after 40 days, x is the sewage sludge amendment rate (g kg^{-1}) and the regression coefficients used are a and b. Statistical analyses were conducted using Statistica 7.1 (Statsoft, 2007).

Results and discussion

The application of SS as an amendment to agricultural soils has been reported to play a role in soil fertilization (Jitariu et al., 2011; Eid et al., 2019). Analyses of SS and soil showed that SS had high organic matter content and acidity and was more saline compared

http://www.aloki.hu ● ISSN 1589 1623 (Print) ● ISSN 1785 0037 (Online)
DOI: http://dx.doi.org/10.15666/aeer/1802_30273040

to the cultivated soil. The analysis of the ten HMs' content in the SS showed the following order: Fe > Pb > Zn > Mn > Cr > Cu > Ni > Co > Cd > Mo. However, the order of these metals in the agricultural soil was as follows: Fe > Mn > Zn > Cr > Co > Ni > Cu > Cd > Pb > Mo (*Table 1*). The properties of soils amended with sludge depend on the initial constituents of both the soil and SS (Baghina et al., 2014). The HM contents in SS were under the allowed limits for soil application of SS recommended by the Council of the European Communities (1986). The HM contents in the SS were low because of the effective pre-treatment and monitoring of wastewater treatment processes in Saudi Arabia.

Table 1. *Selected chemical properties of sewage sludge and cultivated field soil used in the pot experiment (means ± standard error, n = 3)*

Properties	Sewage sludge	Cultivated fields soil
Salinity (mS cm^{-1})	1.39 ± 0.10	0.07 ± 0.00
pH	6.98 ± 0.02	8.68 ± 0.02
Organic matter (%)	65.0 ± 0.9	0.9 ± 0.2
Cd (mg kg^{-1})	1.17 ± 0.08	2.91 ± 0.05
Co (mg kg^{-1})	25.86 ± 1.31	35.49 ± 1.13
Cr (mg kg^{-1})	168.09 ± 4.45	44.11 ± 0.35
Cu (mg kg^{-1})	162.56 ± 2.32	15.01 ± 0.57
Fe (mg kg^{-1})	24410.0 ± 450.0	17120.0 ± 160.0
Mn (mg kg^{-1})	560.70 ± 9.81	340.43 ± 7.04
Mo (mg kg^{-1})	0.91 ± 0.04	0.40 ± 0.02
Ni (mg kg^{-1})	138.73 ± 3.71	23.20 ± 0.65
Pb (mg kg^{-1})	671.11 ± 6.22	1.51 ± 0.59
Zn (mg kg^{-1})	667.62 ± 13.44	70.59 ± 1.07

The chemical properties of the soil were monitored post-harvest at all the SS amendment rates (*Table 2*). Organic matter and salinity significantly increased, however, salinity gradually increased; the significant increasing was detected only at a SS amendment rate 50 g kg^{-1}. The soil pH significantly decreased at all SS application rates, reaching 7.33 at the highest amendment rate. These results agree with those of our previous study on the leafy plant spinach (Eid et al., 2017) and other studies (Indoria et al., 2013; Kumar et al., 2016). The decreasing soil pH post-addition of SS could be a result of organic acid production resulting from SS decomposition and/or nitrification and mineralization of sulphur-rich compounds (Singh and Agrawal, 2008). All HMs content a significant gradually increased in the soil at all SS amendment rates except Mo (*Table 2*). A significant increase in Cd, Co, Cu and Zn concentrations was detected at an amendment rate of 30 g kg^{-1}. However, Pb and Ni significantly increased at amendment rates of 40 and 50 g kg^{-1}, respectively. Although, the chemical composition of the applied SS and soil were analysed (*Table 1*) before planting *E. sativa*, the concentrations of HM in the soil 40 days after growing *E. sativa* were different according to the SS amendment rate.

The plant *E. sativa* was selected because it is grown in most cases on small farms around and within urban areas and is directly consumed as a fresh green plant. Effects of SS amendments on the morphological parameters of *E. sativa* are shown in *Figure 2*. A significant gradual increase in shoot length, leaf number, whole plant leaf area, single leaf area and AGR was observed in the SS application until an amendment rate of 30 g kg^{-1},

http://www.aloki.hu ● ISSN 1589 1623 (Print) ● ISSN 1785 0037 (Online)
DOI: http://dx.doi.org/10.15666/aeer/1802_30273040

with the highest growth improvement at 20 g kg^{-1}, followed by a decreasing trend at a SS application rate of 40 and 50 g kg^{-1}. However, the root length decreased at all SS amendment rates compared to that of the control plants. A similar trend was observed in terms of the *E. sativa* biomass, and a significant increase in leaf, root and total biomass was detected at amendment rates of 10, 20 and 30 g kg^{-1}. The *E. sativa* leaf/root ratio significantly increased at SS amendment rates of 10 and 20 g kg^{-1}. The application rates of 40 and 50 g kg^{-1} caused significant negative effects on the biomass measurements of *E. sativa* compared to those of the control (*Figure 3*). These findings agree with those of Indoria et al. (2013), who reported enhancement of *E. sativa* growth parameters when grown in sludge-amended soil, as well as our previous studies on the effect of SS applications on spinach growth (Eid et al., 2017). Plant growth improvement was a result of increased organic matter, macro- and micro-nutrients contents and availability, soil porosity and bulk density (Antolín et al., 2005). The reduction of the growth at high amendments rates may refer the high HM concentrations in soil which inhibit absorption of beneficial macronutrients such as K and Ca (Burzynski, 1987).

Table 2. *Selected chemical properties (means ± standard error, n = 6) of soil at different sewage sludge amendment rates after harvesting Eruca sativa that had been grown for 40 days*

Properties	Sewage sludge amendment rate (g kg^{-1})						*F*-value
	0	10	20	30	40	50	
Salinity (mS cm^{-1})	0.29 ± 0.01a	0.31 ± 0.02a	0.37 ± 0.04ab	0.38 ± 0.03ab	0.41 ± 0.03ab	0.49 ± 0.03b	5.5^{**}
pH	8.49 ± 0.01f	8.15 ± 0.05e	7.95 ± 0.03d	7.73 ± 0.03c	7.57 ± 0.06b	7.33 ± 0.05a	106.6^{***}
Organic matter (%)	0.98 ± 0.14a	2.52 ± 0.05b	3.57 ± 0.15c	4.20 ± 0.16d	5.19 ± 0.09e	6.56 ± 0.06f	286.3^{***}
Cd (mg kg^{-1})	2.02 ± 0.03a	2.07 ± 0.05a	2.18 ± 0.01ab	2.33 ± 0.01bc	2.48 ± 0.03cd	2.49 ± 0.08d	23.4^{***}
Co (mg kg^{-1})	24.37 ± 0.08a	25.65 ± 0.29ab	25.87 ± 0.86ab	26.60 ± 0.09b	26.76 ± 0.17b	26.99 ± 0.64b	4.4^{**}
Cr (mg kg^{-1})	56.79 ± 0.32a	63.54 ± 0.89b	65.04 ± 3.77bc	70.73 ± 0.16c	88.49 ± 1.31d	104.32 ± 1.31e	104.7^{***}
Cu (mg kg^{-1})	3.48 ± 0.08a	3.57 ± 0.15a	4.45 ± 0.15a	6.49 ± 0.48b	7.64 ± 0. 45bc	9.17 ± 0.88c	26.2^{***}
Fe (mg kg^{-1})	17303.1 ± 170.0a	19739.4 ± 1001.0b	21360.7 ± 120.1b	21558.4 ± 396.1b	26821.0 ± 493.4c	32585.9 ± 755.3d	91.7^{***}
Mn (mg kg^{-1})	244.29 ± 5.87a	269.07 ± 12.06ab	289.88 ± 0.42b	299.52 ± 4.81b	365.16 ± 9.94c	457.60 ± 12.04d	82.2^{***}
Mo (mg kg^{-1})	0.55 ± 0.08a	0.63 ± 0.04a	0.67 ± 0.06a	0.74 ± 0.06a	0.78 ± 0.19a	0.89 ± 0.08a	1.5^{ns}
Ni (mg kg^{-1})	30.63 ± 0.08a	31.43 ± 0.22ab	31.99 ± 1.39ab	32.24 ± 0.20ab	32.29 ± 0.03ab	33.84 ± 0.37b	3.2^{*}
Pb (mg kg^{-1})	5.85 ± 0.23a	5.94 ± 0.09a	6.28 ± 0.09a	6.71 ± 0.18a	8.55 ± 0.67b	8.68 ± 0.29b	15.7^{***}
Zn (mg kg^{-1})	67.44 ± 0.54a	70.34 ± 1.22a	80.21 ± 1.96ab	93.84 ± 5.67b	120.45 ± 0.71c	130.07 ± 7.98c	40.6^{***}

F-values represent one-way ANOVA; degrees of freedom (*df*) = 5. Means in the same row followed by different letters are significantly different at $P < 0.05$ according to Tukey's HSD test. *: $P < 0.05$, **: $P < 0.01$, ***: $P < 0.001$, *ns*: not significant (i.e., $P > 0.05$)

http://www.aloki.hu ● ISSN 1589 1623 (Print) ● ISSN 1785 0037 (Online)
DOI: http://dx.doi.org/10.15666/aeer/1802_30273040

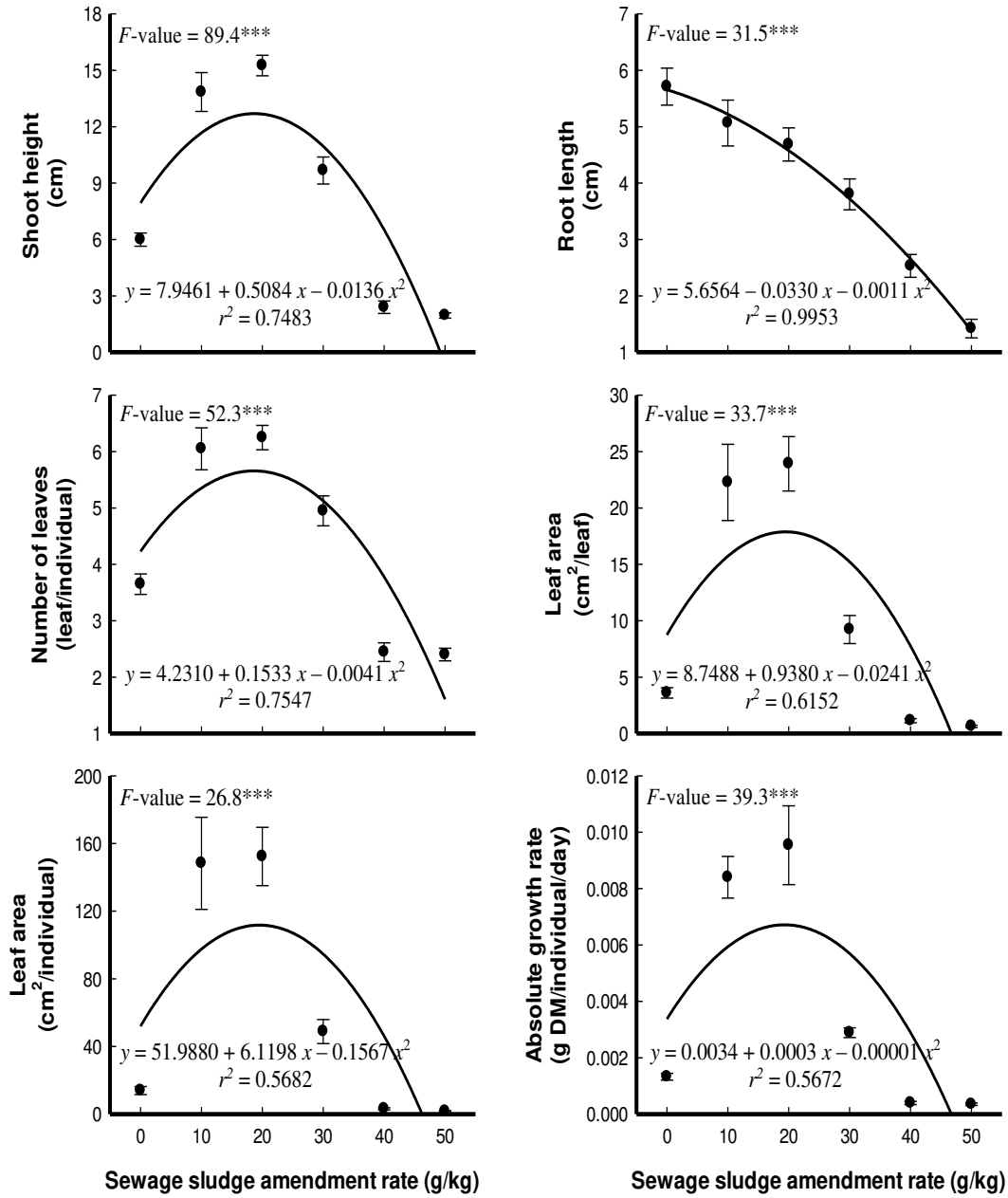

Figure 2. *Effects of different sewage sludge amendment rates on the morphometric parameters of Eruca sativa harvested after 40 days (means ± standard error, n = 30). The F-values represent one-way ANOVA and a degree of freedom (df) = 5. *** = P < 0.001*

The HMs uptake is a complicated method that is affected by numerous factors, comprising soil characteristics and type, environmental conditions, plant species, physiology and phenology, rhizosphere biochemistry and chelating effects of other HMs (Basta et al., 2005). In the current study, SS resulted in increasing shoot and root mass of the measured HMs at all the amendments rates (*Table 3*). The highest concentration of HMs was detected at a 50 g kg^{-1} as the shoot contents of Cd, Co, Cr, Cu, Fe, Mn, Mo, Ni, Pb and Zn increased to 304, 207, 210, 491, 380, 156, 246, 239, 363 and 323%, respectively, compared to the control plants. The high concentration of HMs in plants

http://www.aloki.hu ● ISSN 1589 1623 (Print) ● ISSN 1785 0037 (Online)
DOI: http://dx.doi.org/10.15666/aeer/1802_30273040

negatively affects several physiological processes (Kabata-Pendias, 2011). Substitution of Mg in chlorophyll by HMs results in the plants being incapable of photosynthesis (Kupper et al., 1996). HM toxicity in plants reduces the transpiration and photochemical light reactions (Singh and Agrawal, 2010).

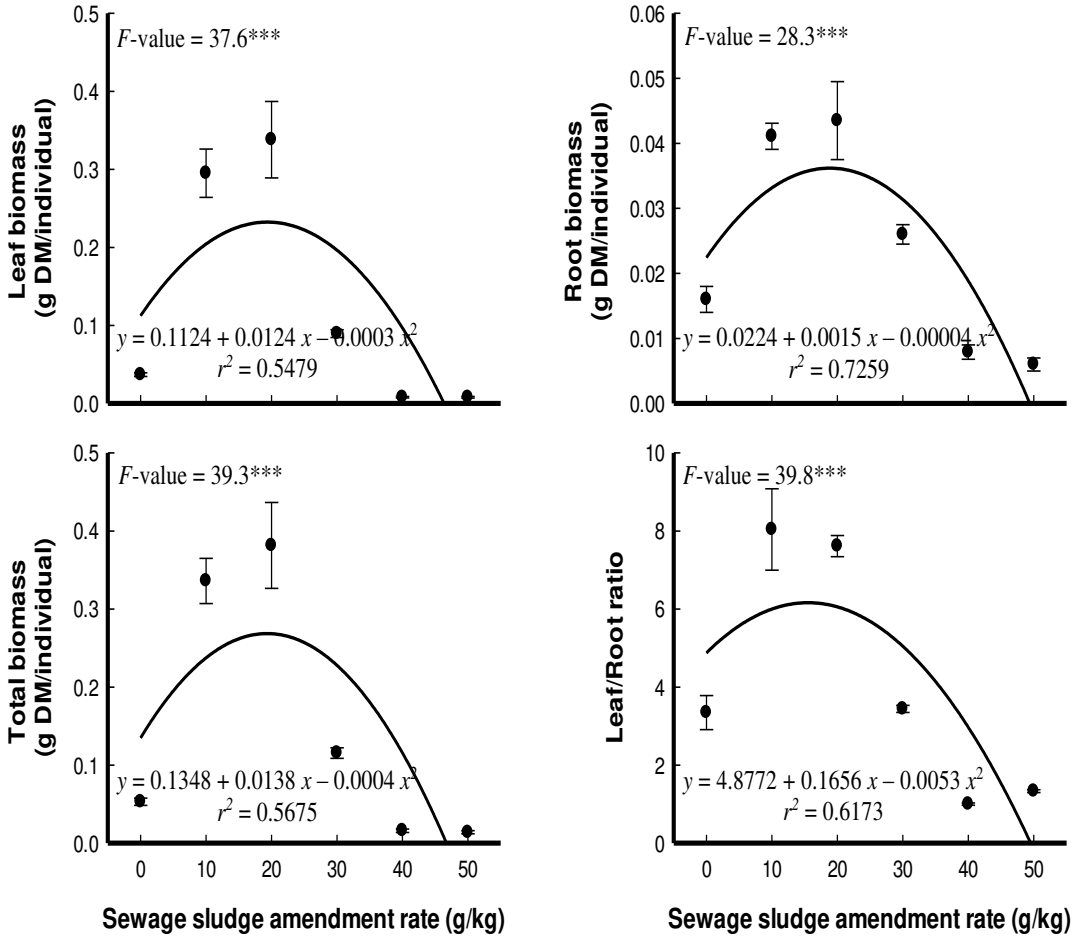

Figure 3. *Effects of different sewage sludge amendment rates on the biomass of Eruca sativa harvested after 40 days (means ± standard error, n = 30). F-values represent a one-way ANOVA and degrees of freedom (df) = 5. *** = P < 0.001*

The regression analysis showed that the increase in the HM contents was correlated with an increase in the SS amendment rates (*Table 4*). The highest R^2 values in the *E. sativa* roots and shoots were 0.942 and 0.936 for the HMs Cr and Zn, respectively. However, the lowest R^2 in the roots and shoots were 0.400 and 0.481 for Zn and Co, respectively (*Table 4*). This variation in R^2 could be related to the physiological role of each element in the plants. Decreasing soil pH increases HM bioavailability (Eid and Shaltout, 2016) as observed in the current study; thus, a follow-up study of the HM concentrations in edible parts of plants grown in sludge-amended soil is a necessity to avoid HM risks. Prediction models of HM concentrations in *Eruca sativa* grown in sewage sludge-amended soil have been developed by our research group and published recently (Eid et al., 2020).

http://www.aloki.hu ● ISSN 1589 1623 (Print) ● ISSN 1785 0037 (Online)
DOI: http://dx.doi.org/10.15666/aeer/1802_30273040

Table 3. *Effects of different sewage sludge amendment rates on heavy metal concentrations (mg kg^{-1}) in the shoots and roots of Eruca sativa harvested after 40 days (means ± standard error, n = 6)*

Metal	Tissue	Sewage sludge amendment rate (g kg^{-1})						*F*-value	Safe limit[+]	Phytotoxic range[‡]
		0	10	20	30	40	50			
Cd	Shoot	0.43 ± 0.03a	0.47 ± 0.05ab	0.54 ± 0.00b	0.67 ± 0.03c	1.14 ± 0.02d	1.31 ± 0.01e	184.3***	0.3	5-30
	Root	0.23 ± 0.00a	0.35 ± 0.05ab	0.40 ± 0.03ab	0.43 ± 0.09ab	0.48 ± 0.06b	0.56 ± 0.00b	5.0**		
Co	Shoot	1.26 ± 0.35a	1.28 ± 0.02a	1.36 ± 0.33ab	1.57 ± 0.04ab	2.12 ± 0.02bc	2.61 ± 0.01c	7.9***	-	30-40
	Root	3.03 ± 0.01a	6.06 ± 0.11b	6.38 ± 0.30b	7.72 ± 0.55c	10.20 ± 0.10d	11.27 ± 0.06e	130.3***		
Cr	Shoot	7.65 ± 0.41a	8.15 ± 0.03a	9.02 ± 0.51ab	9.81 ± 0.03b	14.86 ± 0.56c	16.10 ± 0.14c	103.4***	5	10-100
	Root	17.99 ± 0.28a	31.71 ± 3.38b	46.03 ± 3.74c	58.62 ± 3.78d	73.09 ± 0.05e	86.49 ± 0.50f	98.3***		
Cu	Shoot	5.45 ± 0.07a	5.47 ± 0.77a	6.34 ± 0.07a	6.85 ± 1.12a	10.41 ± 0.19b	26.76 ± 0.10c	219.8***	40	20-100
	Root	7.66 ± 0.02a	9.93 ± 1.50ab	11.56 ± 2.34ab	13.83 ± 2.09bc	18.34 ± 0.04c	19.26 ± 0.09c	10.6***		
Fe	Shoot	869.9 ± 81.7a	1215.5 ± 108.3b	1353.6 ± 35.7b	1854.1 ± 29.0c	2383.1 ± 74.9d	3312.2 ± 13.7e	191.1***	450	> 1000
	Root	3760.8 ± 278.2a	7141.0 ± 468.9b	9666.9 ± 446.8c	11403.1 ± 1065.9c	15364.9 ± 19.9d	17477.9 ± 98.2e	94.9***		
Mn	Shoot	78.08 ± 2.71a	79.38 ± 0.45a	98.31 ± 0.67b	102.74 ± 0.44b	102.80 ± 3.85b	122.06 ± 0.20c	71.4***	-	> 400
	Root	99.91 ± 2.55a	216.75 ± 9.71b	219.18 ± 18.73b	228.37 ± 8.67b	388.26 ± 1.98c	395.58 ± 0.29c	146.9***		
Mo	Shoot	1.16 ± 0.02a	1.82 ± 0.01b	1.98 ± 0.16b	1.98 ± 0.12b	2.61 ± 0.10c	2.86 ± 0.03c	53.4***	10	135
	Root	0.71 ± 0.08a	0.94 ± 0.04b	1.03 ± 0.01b	1.13 ± 0.07bc	1.26 ± 0.07cd	1.41 ± 0.01d	20.5***		
Ni	Shoot	3.00 ± 0.62a	3.43 ± 0.03a	3.82 ± 0.04a	3.98 ± 0.91a	6.36 ± 0.26b	7.18 ± 0.10b	13.7***	20	40-246
	Root	7.27 ± 0.30a	13.11 ± 1.28b	15.12 ± 1.76b	18.99 ± 0.76c	22.89 ± 0.05d	26.60 ± 0.14e	53.9***		
Pb	Shoot	0.86 ± 0.06a	0.87 ± 0.09a	1.11 ± 0.05a	1.31 ± 0.01ab	1.93 ± 0.21b	3.13 ± 0.38c	22.1***	5	30-300
	Root	0.23 ± 0.05a	0.38 ± 0.04a	0.42 ± 0.02a	0.57 ± 0.03ab	0.99 ± 0.28b	1.03 ± 0.01b	7.7***		
Zn	Shoot	25.02 ± 1.86a	40.42 ± 1.60b	47.05 ± 0.10c	49.40 ± 1.37c	70.98 ± 0.11d	80.94 ± 0.10e	315.9***	60	100-500
	Root	54.19 ± 6.09a	56.82 ± 7.63a	65.41 ± 9.79ab	70.92 ± 0.67ab	77.60 ± 0.04ab	83.02 ± 0.22b	4.1**		

F-values represent one-way ANOVA, degrees of freedom (*df*) = 5. Means in the same row followed by different letters are significantly different at $P < 0.05$, according to Tukey's HSD test. **: $P < 0.01$, ***: $P < 0.001$, [+]: FAO/WHO standard (Codex Alimentarius Commission, 2011), [‡]: Kabata-Pendias (2011)

http://www.aloki.hu ● ISSN 1589 1623 (Print) ● ISSN 1785 0037 (Online)
DOI: http://dx.doi.org/10.15666/aeer/1802_30273040

Table 4. *Linear regression equations of the form y = a + bx, where y is the heavy metal concentration (mg kg^{-1}) in Eruca sativa tissue harvested after 40 days and x is the sewage sludge amendment rate (g kg^{-1})*

y		*a*	*SE*	*b*	*SE*	R^2	*P*
Cd	Shoot	0.296	0.041	0.019	0.001	0.847	0.000
	Root	0.258	0.035	0.006	0.001	0.436	0.000
Co	Shoot	1.023	0.146	0.027	0.005	0.481	0.000
	Root	3.515	0.241	0.157	0.008	0.920	0.000
Cr	Shoot	6.419	0.436	0.180	0.014	0.822	0.000
	Root	18.081	1.760	1.370	0.058	0.942	0.000
Cu	Shoot	1.504	1.482	0.348	0.049	0.598	0.000
	Root	7.324	0.989	0.244	0.033	0.622	0.000
Fe	Shoot	673.197	78.526	46.329	2.594	0.904	0.000
	Root	4017.229	379.026	271.409	12.519	0.933	0.000
Mn	Shoot	76.180	1.912	0.843	0.063	0.840	0.000
	Root	115.001	12.638	5.720	0.417	0.847	0.000
Mo	Shoot	1.291	0.072	0.031	0.002	0.834	0.000
	Root	0.756	0.038	0.013	0.001	0.760	0.000
Ni	Shoot	2.496	0.359	0.085	0.012	0.603	0.000
	Root	8.054	0.676	0.371	0.022	0.890	0.000
Pb	Shoot	0.482	0.165	0.042	0.005	0.637	0.000
	Root	0.177	0.085	0.017	0.003	0.519	0.000
Zn	Shoot	25.618	1.447	1.067	0.048	0.936	0.000
	Root	52.854	3.855	0.606	0.127	0.400	0.000

SE: standard error, $n = 36$

HM accumulation in plants depends on the soil properties, SS origin and composition, amendment rate, plant species, plant physiology, climatic factors and metal chemical form (Mahdy et al., 2007). The bioaccumulation factors (BFs) and translocation factors (TFs) of all ten detected HMs in *E. sativa* were calculated (*Table 5*). The BFs of Cd, Co, Cr, Fe, Mn, Ni, Pb and Zn were < 1.0, whereas the BFs of Cu and Mo were > 1. The highest BF was detected for Cu at a SS amendment rate of 10 g kg^{-1}; however, there were no significant differences in the BFs of Cu and Mo between the control and all the SS amendment rates. The lowest BFs were found in the cases of Cd and Pb in roots of *E. sativa* grown in the control soil. The translocation factor (TF) varied among the HMs and soil treatments (*Table 5*). The TFs for all HMs were < 1.0 except for the HMs Cd and Pb. The accumulation of the majority of HMs was detected in roots rather than in the shoots (*Tables 3 and 5*). HMs, and particularly Cd, are inducible factors of phytochelatin which are low-molecular-weight proteins that form various complexes with Cd and as a result, prevent it from circulating as free Cd^{+2} inside the cytosol, subsequently aiding in the complexation and HM accumulation in roots (Clemens, 2006).

http://www.aloki.hu ● ISSN 1589 1623 (Print) ● ISSN 1785 0037 (Online)
DOI: http://dx.doi.org/10.15666/aeer/1802_30273040

Table 5. *Bioaccumulation factors (BFs), from soil to roots, and translocation factors (TFs), from roots to shoots, of heavy metals in Eruca sativa grown in soil at different sewage sludge amendment rates (means ± standard error, n = 6)*

Metal	Factor	Sewage sludge amendment rate (g kg^{-1})						*F*-value
		0	10	20	30	40	50	
Cd	BF	0.114 ± 0.002a	0.172 ± 0.026ab	0.181 ± 0.015ab	0.183 ± 0.041ab	0.196 ± 0.025ab	0.231 ± 0.005b	3.4*
	TF	1.887 ± 0.116ab	1.382 ± 0.060a	1.414 ± 0.106ab	2.196 ± 0.559ab	2.548 ± 0.314b	2.331 ± 0.009ab	3.2*
Co	BF	0.124 ± 0.001a	0.237 ± 0.007b	0.250 ± 0.020bc	0.290 ± 0.022c	0.381 ± 0.002d	0.426 ± 0.008e	83.8***
	TF	0.418 ± 0.116b	0.212 ± 0.001a	0.203 ± 0.042a	0.209 ± 0.018a	0.208 ± 0.002a	0.232 ± 0.001a	2.8*
Cr	BF	0.317 ± 0.007a	0.503 ± 0.060b	0.737 ± 0.100c	0.829 ± 0.053c	0.827 ± 0.012c	0.838 ± 0.009c	19.3***
	TF	0.424 ± 0.016c	0.272 ± 0.028b	0.207 ± 0.028ab	0.171 ± 0.011a	0.203 ± 0.008ab	0.186 ± 0.003a	26.3***
Cu	BF	2.206 ± 0.041a	2.714 ± 0.306a	2.708 ± 0.619a	2.310 ± 0.492a	2.443 ± 0.143a	2.359 ± 0.158a	0.4^{ns}
	TF	0.711 ± 0.011a	0.556 ± 0.008a	0.681 ± 0.132a	0.491 ± 0.007a	0.568 ± 0.010a	1.389 ± 0.006b	37.3***
Fe	BF	0.218 ± 0.018a	0.373 ± 0.043b	0.453 ± 0.023bc	0.527 ± 0.043cd	0.574 ± 0.011d	0.547 ± 0.009cd	25.6***
	TF	0.246 ± 0.039b	0.169 ± 0.004a	0.141 ± 0.003a	0.170 ± 0.015a	0.155 ± 0.005a	0.189 ± 0.001ab	4.4**
Mn	BF	0.411 ± 0.020a	0.822 ± 0.073b	0.756 ± 0.065b	0.761 ± 0.017b	1.067 ± 0.029c	0.885 ± 0.017b	26.3***
	TF	0.788 ± 0.047c	0.370 ± 0.019ab	0.464 ± 0.037b	0.454 ± 0.019b	0.265 ± 0.010a	0.309 ± 0.001a	47.7***
Mo	BF	1.601 ± 0.397a	1.528 ± 0.147a	1.628 ± 0.162a	1.610 ± 0.211a	2.116 ± 0.423a	1.544 ± 0.108a	0.7^{ns}
	TF	1.735 ± 0.181a	1.948 ± 0.078a	1.917 ± 0.156a	1.819 ± 0.206a	2.100 ± 0.118a	2.033 ± 0.028a	0.9^{ns}
Ni	BF	0.237 ± 0.009a	0.419 ± 0.044b	0.489 ± 0.076bc	0.589 ± 0.027cd	0.709 ± 0.001de	0.793 ± 0.007e	35.6***
	TF	0.399 ± 0.069b	0.275 ± 0.029ab	0.272 ± 0.033ab	0.202 ± 0.040a	0.278 ± 0.011ab	0.269 ± 0.001ab	2.9*
Pb	BF	0.037 ± 0.008a	0.064 ± 0.007ab	0.067 ± 0.004ab	0.086 ± 0.005bc	0.106 ± 0.025bc	0.122 ± 0.003c	9.2***
	TF	4.744 ± 0.835a	2.347 ± 0.304a	2.712 ± 0.250a	2.302 ± 0.112a	4.078 ± 1.551a	3.045 ± 0.365a	1.7^{ns}
Zn	BF	0.800 ± 0.084a	0.818 ± 0.123a	0.833 ± 0.142a	0.772 ± 0.054a	0.644 ± 0.004a	0.680 ± 0.029a	0.9^{ns}
	TF	0.513 ± 0.092a	0.761 ± 0.074ab	0.809 ± 0.119b	0.698 ± 0.026ab	0.915 ± 0.002b	0.975 ± 0.003b	5.6**
F-value$_{BF}$		31.9***	45.2***	14.2***	15.7***	30.2***	60.5***	
F-value$_{TF}$		24.3***	56.6***	55.7***	20.7***	7.1***	82.5***	

F-values represent one-way ANOVA, degrees of freedom (*df*) = 5. Means in the same row followed by different letters are significantly different at $P < 0.05$, according to Tukey's HSD test. *: $P < 0.05$, **: $P < 0.01$, ***: $P < 0.001$, *ns*: not significant (i.e., $P > 0.05$)

http://www.aloki.hu ● ISSN 1589 1623 (Print) ● ISSN 1785 0037 (Online)
DOI: http://dx.doi.org/10.15666/aeer/1802_30273040

Conclusions

The results of the current investigation indicate that a SS amendment to agricultural soils up to rate of 30 g kg^{-1} could be beneficial as a fertilizer for *E. sativa*. SS amendment rates of 40 and 50 g kg^{-1} caused negative effects on the growth, biomasses of *E. sativa.* The translocation factors for all the detected HMs were < 1.0 except for Cd and Pb. However, SS sludge used in the current study increased the biomass productivity of *E. sativa*, it is not recommended to be used as biofertilizer as the *E. sativa* is a green-salad freshly consumed plant. Also, the repeated application of SS at the same site may pose more environmental and health risks of consuming *E. sativa* plants. Thus, regular assessment and monitoring of HMs in agricultural products originating from plants grown in sludge-amended soils is recommended to avoid HM accumulation in the food chain. The future research should consider studying alteration of the crop rotation in cultivated areas that apply SS to introduce crops with low accumulation ability of HMs. Also, investigations of suitable methods for SS treatments are needed before the application in the agricultural system to avoid the health and environmental hazards.

Acknowledgements. This work was supported by the Deanship of Scientific Research at King Khalid University under Grant number R.G.P. 1/73/40.

REFERENCES

[1] Allen, S. (1989): Chemical analysis of ecological materials. – London: Blackwell Scientific Publications.
[2] Antolín, M. C., Pascual, I., García, C., Polo, A., Sánchez-Díaz, M. (2005): Growth, yield and solute content of barley in soils treated with sewage sludge under semiarid Mediterranean conditions. – Field Crop Res. 94: 224-237.
[3] Baghina, N., Radulov, I., Berbecea, A., Moisuc, A., Stroia, C. (2014): Sewage sludge fertilisation influence on main soil chemical features. – J Environ Prot Ecol. 15: 217-222.
[4] Basta, N. T., Ryan, J. A., Chaney, R. L. (2005): Trace element chemistry in residual-treated soil: Key concepts and metal bioavailability. – J Environ Qual. 34: 49-63.
[5] Burzynski, M. (1987): The influence of lead and cadmium on the absorption and distribution of potassium, calcium, magnesium and iron in cucumber seedlings. – Acta Physiol Plant. 9: 229-238.
[6] Carbonell, G., Pro, J., Gómez, N., Babín, M. M., Fernández, C., Alonso, E., Tarazona, J. V. (2009): Sewage sludge applied to agricultural soil: Ecotoxicological effects on representative soil organisms. – Ecotoxicol Environ Safe. 72: 1309-1319.
[7] Clemens, S. (2006): Toxic metal accumulation, responses to exposure and mechanisms of tolerance in plants. – Biochimie 88: 1707-1719.
[8] Council of the European Communities. (1986): Protection of environment and in particular of the soil, when sewage sludge is used in agriculture. – Off J Eur Comm. 181: 6-12.
[9] Dede, G., Ozdemir, S. (2016): Effects of elemental sulphur on heavy metal uptake by plants growing on municipal sewage sludge. – J Environ Manage. 166: 103-108.
[10] Eid, E. M., Shaltout, K. H. (2016): Bioaccumulation and translocation of heavy metals by nine native plant species grown at a sewage sludge dump site. – Int J Phytoremediat. 18: 1075-1085.

http://www.aloki.hu ● ISSN 1589 1623 (Print) ● ISSN 1785 0037 (Online)
DOI: http://dx.doi.org/10.15666/aeer/1802_30273040

[11] Eid, E. M., El-Bebany, A. F., Alrumman, S. A., Hesham, A., Taher, M. A., Fawy, K. F. (2017): Effects of different sewage sludge applications on heavy metal accumulation, growth and yield of spinach (*Spinacia oleracea* L.). – Int J Phytoremediat. 19: 340-347.
[12] Eid, E. M., Alrumman, S. A., El-Bebany, A. F., Fawy, K. F., Taher, M. A., Hesham, A., El-Shaboury, G. A., Ahmed, M. T. (2019): Evaluation of the potential of sewage sludge as a valuable fertilizer for wheat (*Triticum aestivum* L.) crops. – Environ Sci Pollut Res. 26: 392-401.
[13] Eid, E. M., Shaltout, K. H., Abdallah, S. M., Galal, T. M., El-Bebany, A. F., Sewelam, N. A. (2020): Uptake prediction of ten heavy metals by *Eruca sativa* Mill. cultivated in soils amended with sewage sludge. – Bull Environ Contam Toxicol. 104: 134-143.
[14] Garg, G., Sharma, V. (2014): *Eruca sativa* (L.): Botanical description, crop improvement, and medicinal properties. – J Herb Spi Med Plants 20: 171-182.
[15] Ghosh, M., Singh, S. P. (2005): A review on phytoremediation of heavy metals and utilization of its byproducts. – Appl Ecol Environ Res. 3: 1-18.
[16] Hara, T., Sonoda, Y. (1979): Comparison of the toxicity of heavy metals to cabbage growth. – Plant Soil 51: 127-133.
[17] Hassan, S. M., Ashour, M., Soliman, A. A. F. (2017): Anticancer sctivity, antioxidant activity, mineral contents, vegetative and yield of *Eruca sativa* using foliar application of autoclaved cellular extract of *Spirulina platensis* extract, comparing to N-P-K fertilizers. – J Plant Prod. (Mansoura Univ.) 8: 529-536.
[18] Indoria, A. K., Poonia, S. R., Sharma, K. L. (2013): Phytoextractability of Cd from soil by some oilseed species as affected by sewage sludge and farmyard manure. – Commun Soil Sci Plant 44: 3444-3455.
[19] Jilani, M. I., Ali, A., Rehman, R., Sadique, S., Nisar, S. (2015): Health benefits of arugula: a review. – Int J Chem Biochem Sci. 8: 65-70.
[20] Jitariu, D., Moise, I., Simionescu, V., Aurel, P. (2011): Some appreciations of chemical and biological features of the urban sludge in the Constanta County, Romania, in view of its usage as an organic fertiliser. – J Environ Prot Ecol. 12: 1406-1414.
[21] Kabata-Pendias, A. (2011): Trace elements in soils and plants. – Boca Raton, Florida: CRC Press.
[22] Kumar, V., Chopra, A. K., Srivastava, S. (2016): Assessment of heavy metals in spinach (*Spinacia oleracea* L.) grown in sewage sludge-amended soil. – Commun Soil Sci Plant Anal. 47: 221-236.
[23] Kupper, H., Kupper, F., Spiller, M. (1996): Environmental relevance of heavy metal-substituted chlorophylls using the example of water plants. – J Exp Bot. 47: 259-266.
[24] Mahdy, A. M., Elkhatib, E. A., Fathi, N. O. (2007): Cadmium, copper, nickel, and lead availability in biosolids-amended alkaline soils. – Aust J Basic Appl Sci. 1: 354-363.
[25] Nail, T. N. A., Ali, M. M., Salim, E. R. A. (2017): Phytochemical studies on Sudanese rocket (*Eruca sativa*) seeds and oil constituents. – Am J Phytomed Clin Ther. 5:1.
[26] Radford, P. J. (1967): Growth analysis formulae - their use and abuse. – Crop Sci. 7: 171-175.
[27] Raskin, I., Kumer, P. N., Dushenkov, S., Salt, D. E. (1994): Bioconcentration of heavy metals by plants. – Curr Opin Biotech. 5: 285-290.
[28] Shrivastava, S. K., Banerjee, D. K. (2004): Speciation of metals in sewage sludge and sludge-amended soils. – Water Air Soil Pollut. 152: 219-232.
[29] Singh, R. P., Agrawal, M. (2008): Potential benefits and risks of land application of sewage sludge. – Waste Manage. 28: 347-358.
[30] Singh, R. P., Agrawal, M. (2010): Biochemical and physiological responses of rice (*Oryza sativa* L.) grown on different sewage sludge amendments rates. – Bull Environ Contam Toxicol. 84: 606-612.
[31] Statsoft. (2007): Statistica version 7.1. – Tulsa, Oklahoma: Statsoft Inc.

http://www.aloki.hu ● ISSN 1589 1623 (Print) ● ISSN 1785 0037 (Online)
DOI: http://dx.doi.org/10.15666/aeer/1802_30273040

[32] Wilke, B. M. (2005): Determination of chemical and physical soil properties. – In: Margesin, R., Schinner, F. (eds.) Manual for soil analysis - monitoring and assessing soil bioremediation. Heidelberg: Springer-Verlag, pp. 47-95.

http://www.aloki.hu ● ISSN 1589 1623 (Print) ● ISSN 1785 0037 (Online)
DOI: http://dx.doi.org/10.15666/aeer/1802_30273040

MODELING A RIVER-LAKE INTERACTION SYSTEM IN THE TONLE SAP LAKE AREA

ZHU, X.[1,2] – WU, S.[3*] – ISHIDAIRA, H.[4]

[1]*Water Resources Department of Jiangsu Province, Nanjing, Jiangsu 210024, China*

[2]*College of Water Conservancy and Hydropower Engineering, Hohai University, Nanjing, Jiangsu 210098, China*

[3]*Jiangsu Hydraulic Research Institute, Nanjing, Jiangsu 210017, China*

[4]*Department of Civil and Environmental Engineering, University of Yamanashi, Kofu, Yamanashi 400-8511, Japan*

**Corresponding author*
e-mail: xk6sht@163.com

(Received 4th Dec 2019; accepted 9th Mar 2020)

Abstract. Mekong River-Tonle Sap Lake is a typical river-lake interaction system in a monsoon area. The Tonle Sap Lake (TSL) is the largest freshwater lake in Southeast Asia, and is an important component in lower Mekong River (MR) Basin. Water resource managers are highly concerned about the potential impact of climate change on the MR-TSL hydrological system in the future. Thus, it is necessary to develop a numerical model which can simulate MR-TSL interaction system for the assessment of potential impact of natural climatic variations on hydrological cycle in this area. The main objective of this study was to model a river-lake interaction system for water resource assessment in TSL area. The distinctive feature of this study is to develop an integrated River Lake Water Exchange (RLWE) model and couple it to a grid-based distributed hydrological model (YHyM) for MR-TSL system. Using the coupled model, discharge contribution to TSL from tributaries, lake water volume, water exchange between the MR and TSL, and consumptive water use in TSL area were simulated. The potential impact of climate change on TSL hydrological system was also assessed through the application of the coupled model. Several future scenarios were analyzed, and predictions of water budgets within the interaction system under different scenarios were made.
Keywords: *water resource, hydrological model, GCM, water exchange system, potential impact*

Introduction

River-lake interaction systems are significant in large river basins (Sutherland et al., 2018). The Mekong River (MR)-Tonle Sap Lake (TSL) is a typical example of such interaction in a monsoon area. The TSL plays a significant role, not only in the ecology of the lower Mekong River system, but also in the socio-economic life of Cambodia. Most of Cambodian population lives in the lower catchment of the MR basin, with more than 1 million people dependent on fishing for their livelihood (Keskinen, 2006; Kummu and Nikula, 2006; Campbell, 2016; Trisurat, 2018). Normal and reverse discharge occur in the Tonle Sap River. This unique hydrological phenomenon is a complicated river-lake interaction system. Due to rapid development in the upstream zone of TSL, hydrological changes in the TSL catchment have increased in the past decades. Climate changes and increased human activities in Mekong River Basin put the MR-TSL interaction system under a lot of stress, concerning water resources (Sverdrup, 2002; TERRA, 2007; Kummu et al., 2008; Ogston et al., 2017). However,

http://www.aloki.hu ● ISSN 1589 1623 (Print) ● ISSN 1785 0037 (Online)
DOI: http://dx.doi.org/10.15666/aeer/1802_30413055

not much is known about the interaction of hydrological processes, especially in the Tonle Sap Lake area, where insufficient historical gauge data is available (*Fig. 1*).

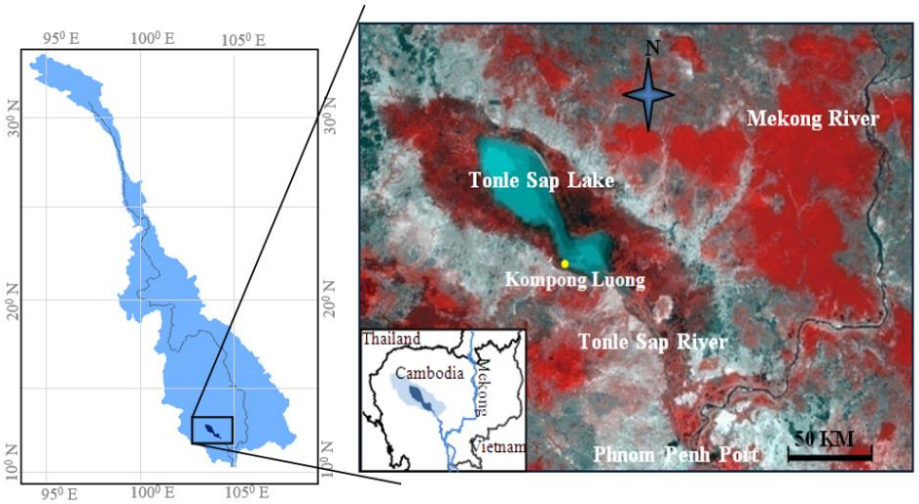

Figure 1. *Map of location of Tonle Sap Lake area*

It is important to investigate how future climate variations may affect the MR-TSL interaction system, and the consequences of these changes in the Mekong River Basin. This issue is highly important for the water resource managers. A comprehensive approach is needed to describe the complex interaction system and provide precise predictions under different future climate scenarios. The objective of this study is to understand the response of the hydrological system of TSL under future climate change, and to provide theoretical basis for water resource management.

Study area

The Mekong River Basin includes parts of China, Myanmar and Vietnam, and comprises nearly one third of Thailand and most of Cambodia and Lao PDR, with a total land area of 795000 km^2. Tonle Sap Lake is an integral part of the Mekong River, located in the northwest part of Cambodia. The lake area has abundant resource such as forests, fisheries, wetlands and agricultural land. It is an important region for socio-economic development of Cambodia. The TSL and its floodplains are located in the central part of Cambodia with the largest natural wetland habitats and the largest permanent freshwater body in Southeast Asia. This lake area is also a crucial source of food and livelihood in Cambodia. More than one million people who live in the area surrounding the Tonle Sap Lake and wetlands are highly dependent on agriculture and fishing (Sverdrup, 2002; Kummu et al., 2008; Chan et al., 2003).

The Tonle Sap Lake area has a tropical monsoon climate, with two distinct seasons i.e. rainy and dry seasons. The rainy season is from May to October. Normal and reverse discharge occur in the Tonle Sap River; this unique hydrological phenomenon constitutes a complicated river-lake interaction system. Mekong River-Tonle Sap Lake system includes Tonle Sap Lake, flood plain, Mekong River and Tonle Sap River. The Tonle Sap River connects the MR and TSL, with the confluence at Phnom Penh Port, as shown in *Figure 1*. Seasonal variations in Tonle Sap Lake floodplain are the determinants of the local ecosystem, fish production, livelihoods and inhabitants. In the

http://www.aloki.hu ● ISSN 1589 1623 (Print) ● ISSN 1785 0037 (Online)
DOI: http://dx.doi.org/10.15666/aeer/1802_30413055

rainy season, the increased rainfall rapidly accentuates the water level and discharge in Mekong River. In the Tonle Sap River, water flows from Mekong River into Tonle Sap Lake. At early May or late April, the water level in Tonle Sap Lake is about 1 m, and the in-site lake area is only about 2.5×10^9 m^2. As the incoming discharge from Tonle Sap River and tributaries is increased, the water level and inundation area of TSL rise gradually. In October, the water level of TSL peaks at over 10 m, and the inundation area reaches up to about 1.5×10^{10} m^2. After October, the rainfall in the MR basin decreases, thereby reducing the water level and discharge in the Mekong River. Meanwhile, the water level of TSL also drops, but at a slower rate than that in MR because of the storage nature of the lake. The delay in reduction of water level in lake makes the TSL water level higher than that of MR. This water level difference changes the direction of discharge in Tonle Sap River from Tonle Sap Lake to Mekong River (hereafter, the flow from the lake to river is referred to as "reverse flow"). This discharge continues throughout the dry season up to late April or early May. Due to the normal and reverse discharges existing in the Tonle Sap River, huge water exchange occurs between the Mekong River and Tonle Sap Lake every year, and influence the seasonal variation and duration of flood inundation of the plain.

Materials and methods

Yamanashi-distributed hydrological model

The Yamanashi Distributed Hydrological Model (YHyM) is a grid-based distributed hydrological model developed by the University of Yamanashi, Japan (Takeuchi et al., 1999; Ishidaira et al., 2000; Ao et al., 2003a, b; Zhou et al., 2006a). It is a comprehensive system integrated with different modules such as meso-scale precipitation module, potential evaporation module, sediment transport module, run-off generation module, snow accumulation/melt module, water quality module, and water use/control (dam operations) module.

In this study, the core module BTOPMODEL was applied to generate hydrological boundary conditions for the TSL balanced system. The core module of YHyM, run-off generation module is based on extended TOPMODEL concepts (Ao et al., 1999, 2000, 2001, 2006; Takeuchi et al., 1999; Kiem et al., 2004a, b, 2005; Zhou et al., 2005, 2006a, b). The BTOPMODEL was used to divide the whole basin into a number of blocks/sub-basins; each block/sub-basin may consist of several hillslopes, with water shared between hillslopes in each block, and no water exchange between blocks. The topographic index γ was re-defined in *Equations 1* and *2,* for effectiveness in the grid-based applications, especially for large basin analysis:

$$q_{bi} = [a_i f(a_i) r_k]/a_{0i} \quad \text{(Eq.1)}$$

$$\gamma_i = ln \frac{a_i f(a_i)/a_{0i}}{tan\beta_i} \quad \text{(Eq.2)}$$

where $f(a_i)$ ($0 \leq f(a_i) \leq 1$) is the effective contributing area ratio, i.e. the contribution rate of upstream net catchment area to discharge; q_{bi} (m day^{-1}) is the base flow of unit i, r_k (m day^{-1}) is the spatially homogeneous recharge rate over the block k, a_{0i} (m^2) is the area of the grid cell I, and D_i (m day^{-1}) is the ground water discharge ability:

http://www.aloki.hu ● ISSN 1589 1623 (Print) ● ISSN 1785 0037 (Online)
DOI: http://dx.doi.org/10.15666/aeer/1802_30413055

$$q_{bi} = D_i tan\beta_i exp\ (-\frac{SD_i}{m}) \quad \text{(Eq.3)}$$

where q_{bi} is the outlet discharge in *Equation 3,* the subscript *i* refers to the grid cell *i,* and a block-average value is used for *m*, the discharge decay factor.

The runoff routing used the Muskingum-Cunge method. The vertical column included vegetation zone, root zone, unsaturation zone and saturation zone. The runoff generation in each grid cell is shown in *Figure 2*.

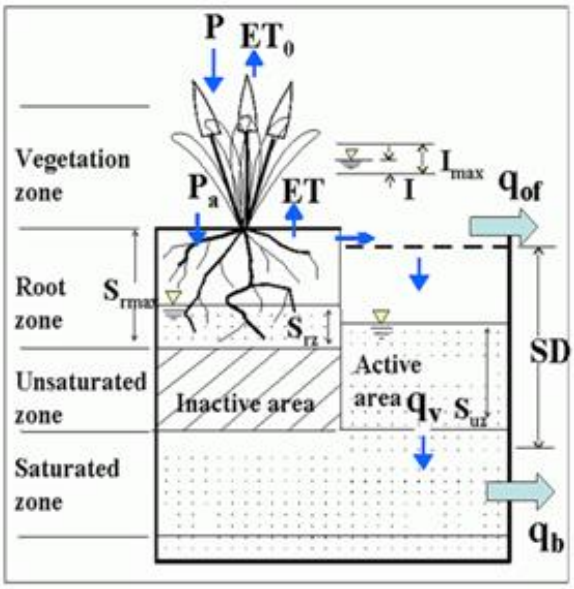

Figure 2. *BTOPMC runoff generation structure*

Three store layers are considered in this model: surface interception and depression store (S_1), near surface infiltration store (S_2) and saturated zone store (S_3). The variable contributing area be outlined and the rainfall on this area will immediately become overland flow. Once the interception store is filled, the infiltration to S_2 can happen. Evaporation is allowed from this store at the estimated potential rate until it is empty. A constant leakage rate i_0 be applied for the infiltration to the S_3. The rate into S_2 is at the rainfall rate *i* in *Equation 4*. However, if the rainfall rate is higher than the maximum infiltration rate i_{max}:

$$i > i_{max} = i_0 + {}^{b}/_{S_2} \quad \text{(Eq.4)}$$

The excess rainfall (i-i_{max}) becomes the infiltration excess overland flow. When the S_2 reach its maximum storage, the saturation excess overland flow will happen. Evaporation are allowed from the infiltration store at a decreasing rate depending on the level of the store S_2 in *Equation 5:*

$$e_a = e_r S_2 / S_c \quad \text{(Eq.5)}$$

where e_r is the potential evapotranspiration remaining once the interception store S_1 is depleted, and e_a is the actual loss from the infiltration store.

http://www.aloki.hu ● ISSN 1589 1623 (Print) ● ISSN 1785 0037 (Online)
DOI: http://dx.doi.org/10.15666/aeer/1802_30413055

RLWE model

The river-lake interactive system in this research consisted of Tonle Sap Lake, its floodplain, Tonle Sap River, and Kampong Cham section to Phnom Penh Port section in main Mekong River. River Lake Water Exchange (RLWE) model was developed to simulate the hydrological process of the interaction system and to have an accurate understanding of the water balance system components.

The model was established based on water balance equation (Szesztay, 1974):

$$V_{in} - V_{out} = \Delta V \quad \text{(Eq.6)}$$

where V_{in} is the water volume going into Tonle Sap Lake, V_{out} is the water volume going out from Tonle Sap Lake, and ΔV is the change in lake storage.

The water balance module was developed to simulate the hydrological cycle of TSL. Due to the huge seasonal area variation, the boundary of the TSL balance system was fixed in this research by the National Highway (NH) 5 and 6 as shown in *Figure 3*. Lake surface area fluctuates inside the NH boundary. The evapotranspiration in the balance system includes potential evaporation from water surface and actual evapotranspiration from flood plain not being inundated inside NH boundary.

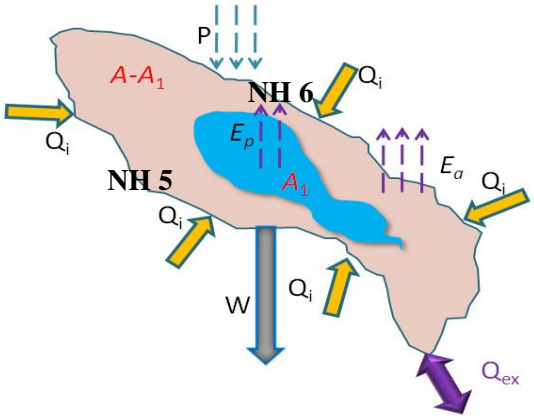

Figure 3. *Balanced system of RLWE model*

Thus, the water balance system for Tonle Sap Lake (*Fig. 4*) can be described in the following equation:

$$(P_j - E_{pj}) \times A_{1j} + (P_j - E_{aj}) \times (A - A_{1j}) + Q_{ij} \pm Q_{exj} - W_j = {}^{(V_{j+1} - V_j)}/_{\Delta t} \quad \text{(Eq.7)}$$

where j is the time step (day) of computation, P_j is the precipitation, E_{pj} is the potential evaporation, E_{aj} is the actual evaporation, A is the area of the National Highway (NH) 5 and 6 boundary which works as the boundary of TSL water balance system, A_{1j} is the area of lake water surface, $Q_{ij}$is the sum of the discharge from tributaries, Q_{exj} is the water exchange between the MR and TSL, W_j is the amount of water consumption, V_j is the lake water volume, and Δt is the time interval of computation.

River Lake Water Exchange model consists of five sub-modules (Wu, et al., 2010): water level-water volume relationship sub-module, water level and discharge convert sub-module, water consumption sub-module, lake-river water exchange sub-module,

http://www.aloki.hu ● ISSN 1589 1623 (Print) ● ISSN 1785 0037 (Online)
DOI: http://dx.doi.org/10.15666/aeer/1802_30413055

and water balanced system. In this research, lake water storage income components included precipitation, water flow from tributaries, water flow from Tonle Sap River and part of the flood directly flowing into lake through floodplain. Outcome items consisted of potential evaporation from lake water surface, actually evaporation from floodplain, water flow from lake to Mekong River through Tonle Sap River, recharge to ground water, and domestic and irrigation water consumption.

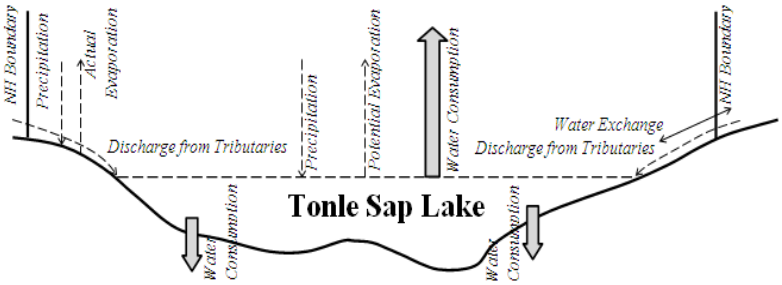

Figure 4. *Water budgets in Tonle Sap Lake water balance system*

Coupled model by YHyM and RLWE

Introduction

The hydrological system of TSL was simulated by coupling RLWE with YHyM. The structure of the coupling model system consisted of three layers (*Fig. 5*). The first layer (YHyM, a grid-based distributed hydrological model was applied to generate the boundary conditions including precipitation, evaporation, discharge from tributaries and discharge in certain cross sections in the main stream of the MR. These boundary conditions were regarded as the inputs for the second and third layers. The second layer was the RLWE model. Daily water consumption and water exchange between TSL and MR, and water level of TSL were calculated in this layer. The third layer was the water balance system of RLWE model. All the items in this system were derived from the first and the second layers. The daily water volume of TSL was calculated from the balance system, and used as the input in the next step.

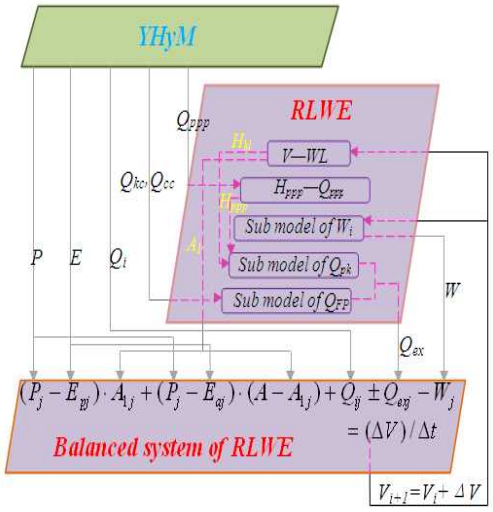

Figure 5. *Structure generated by coupling RLWE with YHyM*

http://www.aloki.hu ● ISSN 1589 1623 (Print) ● ISSN 1785 0037 (Online)
DOI: http://dx.doi.org/10.15666/aeer/1802_30413055

Data set

Observed daily water level data of Kompong Luong station from 1980 to 2002 were used to analyze the flood frequency of Mekong River. Daily observed water level data sets of Prek Kdam, Kompong Cham and Chroui Changvar stations from 1996 to 2004 (*Fig. 6*) are used for the calculation.

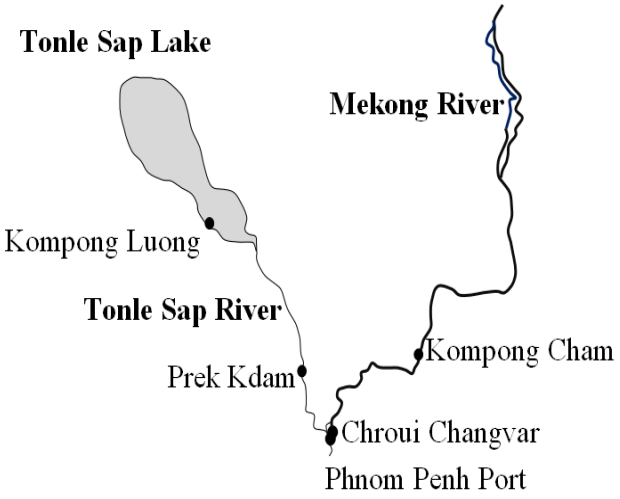

Figure 6. *Locations of the sections in river–lake interaction system*

In this study, BTOP Model was applied to generate the hydrological boundary conditions of TSL area. The implementation of the model in Mekong River basin needed topographic, land cover, soil type, NDVI and meteorological data sets.

The USGS-GTOPO30 was used in this paper to extract topographic information such as channel network, sub-basin division, basin boundary, flow accumulation and direction, and channel slope and length. Land cover data used the International Geosphere Biosphere Program (IGBP) Version 2 with 30 min resolution and 17 types of land cover. The data was converted into 8-km resolution by assigning the biggest potion of the type in each 8 × 8 cell. The soil map of the Food and Agriculture Organization (FAO) was used to describe the soil type. A total 23 soil textural classes in the MR basin and different percentage contents of three types of soil were considered: sand, silt and clay. With respect to NDVI data, average 10-day and monthly NDVI data from NOAA-AVHRR NDVI data set were used in this study. Spatial variation in precipitation was considered based on the Thiessen polygon method, and data from 65 gauging stations were used. Observed precipitation gauging data were obtained from the Mekong River Commission. Other meteorological input data sets including monthly mean temperature, diurnal temperature range, cloud cover and actual vapor pressure, mean monthly wind speed were provided by the Climate Research Unit (CRU), University of East Anglia in UK.

YHyM application in Tonle Sap

The river network system in Tonle Sap Lake catchment was generated from DEM data as shown in *Figure 7*. Ten points at which river network intersected the balance system boundary were acquired. Then, all the hydrological information in each block of

http://www.aloki.hu ● ISSN 1589 1623 (Print) ● ISSN 1785 0037 (Online)
DOI: http://dx.doi.org/10.15666/aeer/1802_30413055

the intersections were output using YHyM, which included runoff, precipitation (P), potential evaporation (E_p) and actual evaporation (E_a). These output data were used as input for the simulation of water balance.

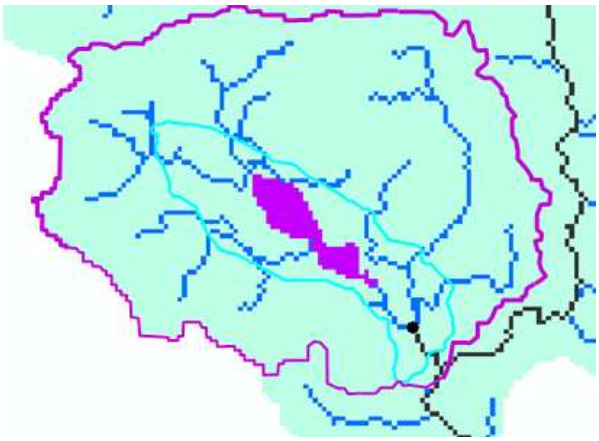

Figure 7. *River net in TSL catchment*

The sum of the runoff generated in these ten blocks was considered as the water flows into TSL contributed from tributaries, which varied from less than 100 m^3/s to more than 15,000 m^3/s in the period of 1987-2000, with an average discharge of 570 m^3/s. The average values of precipitation, potential evaporation and actual evaporation considered in the ten intersection grids provided by YHyM were used in the balance system of RLWE.

Daily observed water level data sets in Kompong Luong in 1980-2002 are used to analyze flood frequency in this region. Based on derived flood frequency curve of Kompong Luong, year 2000 and 1998 were selected as typical 1-20 wet year and typical 1-20 dry respectively.

Model calibration and validation

Based on the previous validation performance of YHyM and RLWE models, all the items in the balance system of RLWE were considered to be accurate, except the water consumption. Trial-and-error method was used to optimize parameter α by minimizing the difference between water volume of TSL calculated using the balanced equation and estimate, by converting observed water elevation Hkl (gauged stage at Kompong Luong) into water volume, based on the relationship between water level and lake water volume illustrated in the previous chapter.

The value of α obtained from optimization based on the data of 1987-1995 was 0.0051. For validation of the coupled model, the calibrated value of α was applied to estimate the daily water volume of TSL for the period of 1996-2000. The average daily absolute error in the period of 1996-2000 was 4×10^{10} m^3 (average V_{obs}: 21×10^{10} m^3), and comparison between observation and simulation is shown in *Figure 8*. The temporal variation of water volume was well reproduced by the simulation. According to the figure, the calculated V was underestimated, especially at the peak time. It probably results from the fact that the constant α cannot reflect the temporal variation of water consumption. Moreover, the assumption that water consumption was totally dominated by water volume at the specific day was another limitation.

http://www.aloki.hu ● ISSN 1589 1623 (Print) ● ISSN 1785 0037 (Online)
DOI: http://dx.doi.org/10.15666/aeer/1802_30413055

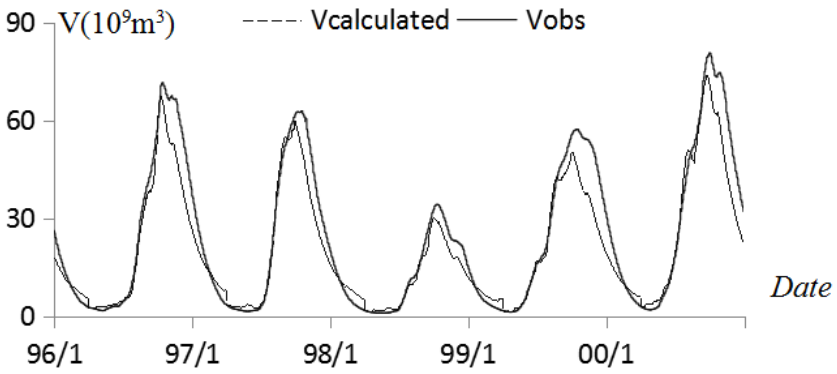

Figure 8. *Validation of daily water consumption*

GCMs

Methodology

Generally, future changes in climate are informed by the global climate models (GCM). In this study, 23 GCMs from IPCC were used for assessment of MR basin. Rainfall output of 23 GCMs and 65 gauge data from 1987 to 2000 were compared to check the performance of each GCM in upper, middle and lower MR basin. The details are shown in *Figure 9*.

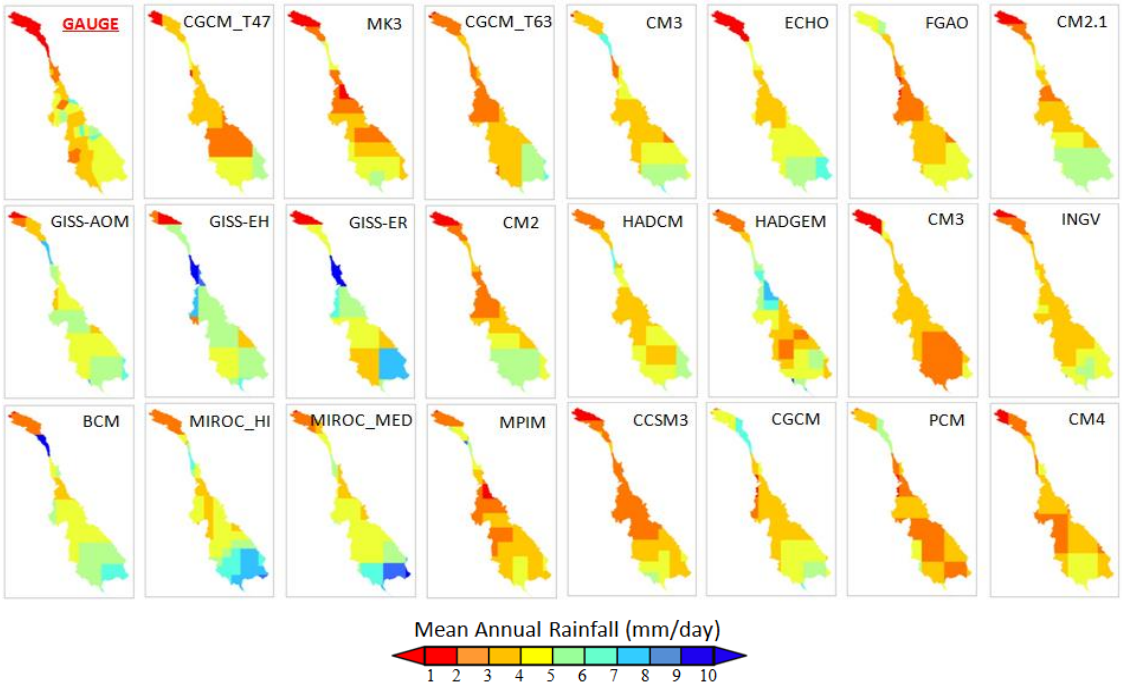

Figure 9. *Rainfall output of 23 GCMs and gauge data from 1987 to 2000*

Four indices were applied to describe the performance of each GCM:

1. Nash-Sutcliffe efficiency (NSE):

This is normalized statistic that determines the relative magnitude of the residual variance, compared to the observed data variance (Moriasi et al., 2006) in *Equation 8:*

http://www.aloki.hu ● ISSN 1589 1623 (Print) ● ISSN 1785 0037 (Online)
DOI: http://dx.doi.org/10.15666/aeer/1802_30413055

$$NSE = 1 - \left[\frac{\sum_{i=1}^{n}(Y_i^{obs} - Y_i^{sim})^2}{\sum_{i=1}^{n}(Y_i^{obs} - Y_i^{mean})^2}\right] \quad \text{(Eq.8)}$$

2. Correlation coefficient:
This describes the degree of collinearity between simulated and observed data.
3. Coefficient of variation (CV):
This is a normalized measure of dispersion of a probability distribution.
4. Skill scores/M-statistic:
These represent the goodness of fit at simulating rainfall (Perkins et al., 2007).

$$S_{score} = \sum_{1}^{n} minimum\ (Z_M, Z_O) \quad \text{(Eq.9)}$$

where *n* is the number of bins in *Equation 9, Zm* is the frequency of values in a given bin from GCM, and *Zo* is the frequency of values in a given bin from the observed data.

First, outputs of the 23 GCMS from IPCC (AR4, 1987-2000) were used to calculate the area average rainfall for upper, middle and lower parts of MR basin. Then, values of the 4 indices were calculated for each model in each part of the MR basin, relative to the gauge data in the same time period. Then, ranking was made, based on the values of each index in every part: R_i^n, where *i* is the index, *n* is the part of the MR basin. All ranks of each model were summed up in *Equations 10:*

$$S_m = \sum_{\substack{i=1-4 \\ n=1-3}} R_i^n \quad \text{(Eq.10)}$$

where *Sm* is the score of each GCM. Based on the scores in upper, middle and lower part in MR basin, the top five models were applied to derive an ensemble data. The information for these five GCMs are list in *Table 1*.

Table 1. *Information of the top five GCMs*

Model	Center	Horizontal resolution
NIES: MIROC3_2-HI	NIES, *Japan*	1.12 × 1.12
CNRM: CM3	INM, *Russia*	5.0 × 4.0
CONS: ECHO-G	MIUB, *Germany* METRI, *Korea* M&D, *Germany*	3.8 × 3.8
CSIRO: MK3	CSIRO, *Australia*	1.9 × 1.9
UKMO: HADGEM1	UKMO, *UK*	1.9 × 1.25

The potential impact of climate change on MR-TSL interaction system was analyzed using the coupled model. For the scenario analysis, future projected precipitation data were prepared using GCM output. In general, due to the difficulties in quantitative assessment of precipitation with GCM, "bias correction" was applied when GCM output was used for basin scale hydrological analysis.

As has been pointed out by Shibuo and Kanae (2010), proper bias correction method should be selected depending on the purpose of analysis. In this study, constant monthly scaling was used for bias correction. The modeled monthly changes (change ratio for each month) were applied to historical daily precipitation time series for producing future projected precipitation. This is one of the most widely used methods for assessing

http://www.aloki.hu ● ISSN 1589 1623 (Print) ● ISSN 1785 0037 (Online)
DOI: http://dx.doi.org/10.15666/aeer/1802_30413055

the impact of climate change on water resource, and is appropriate for long-term water balance analysis.

In this study, outputs from the 5 GCMs were obtained from IPCC AR4 for the 20th Century experiment (20c3m), and SRES SRA1B experiment was used for current and future precipitation. The A1 storyline and scenario family describe a future world of very rapid economic growth, global population that peaks in mid-century and the declines thereafter, and rapid introduction of new and more efficient technologies. For the A1B, balance was defined as not relying too heavily on one particular energy source, on the assumption that similar rates of improvement applied to all energy supplies and end-use technologies. In addition, modeled monthly changes were calculated using the data for 1981-2000 (for 20c3m) and 2046-2065, 2080-2099 (for SRA1B). The results of monthly ratios for upper, middle and lower parts in MR basin are shown in *Figure 10*.

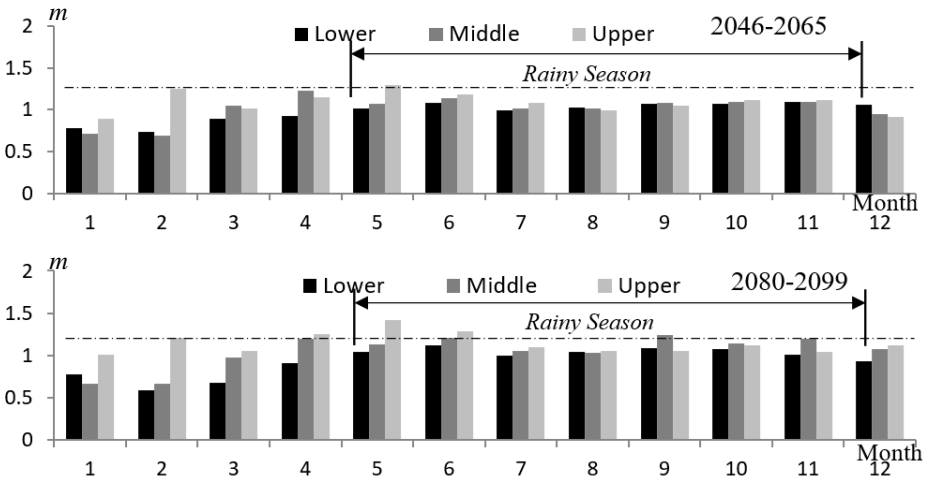

Figure 10. *Monthly ratios in MR basin*

Results and discussion

Typical wet year (20-year return period) and typical dry year (20-year return period) were chosen, based on the derived flood frequency curve of main MR. Through input, the future scenario precipitation in the YHyM and RLWE models, and daily water volume of TSL in a typical wet year and dry year were calculated. The results are shown in *Figure 11*.

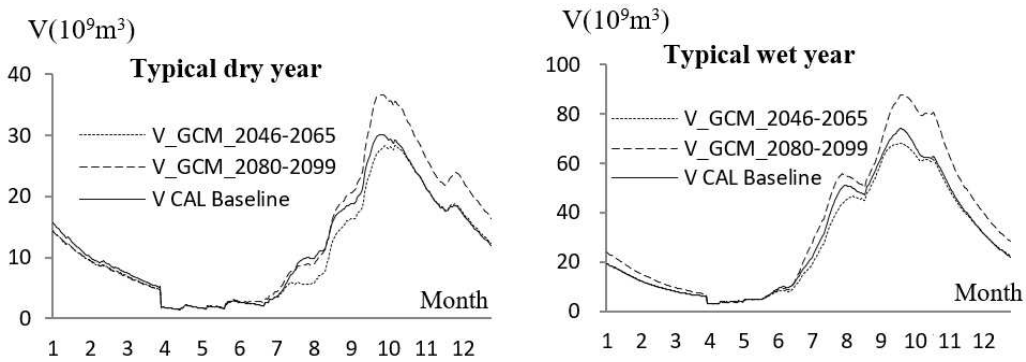

Figure 11. *Daily water volume of TSL in typical years under future scenario*

http://www.aloki.hu ● ISSN 1589 1623 (Print) ● ISSN 1785 0037 (Online)
DOI: http://dx.doi.org/10.15666/aeer/1802_30413055

In the later part of the rainy season (August–November), the total amount of precipitation changed more clearly than in other seasons, and runoff of main stream, tributary inflow, and water exchange between TSL and MR were also changed accordingly. These result in remarkable changes in water volume of TSL during this season. Values of the components in the water balance system in different typical years for the current period and future scenarios are listed in *Table 2* Vtri (10^{10} m^3) is the total water volume from tributaries within one year, Vex_{in} (10^{10} m^3) is the water volume from MR flow into TSL within one year, Vex_{out} (10^{10} m^3) is the water volume from TSL flow into MR within one year, W (10^{10} m^3) is the total water consumption within one year, P-E (10^{10} m^3) is the total volume of precipitation minus evaporation within balanced system boundary in one year, and max V (10^{10} m^3) is the maximum lake water volume calculated by coupling RLWE with YHyM.

Table 2. *Water budgets in balanced system of TSL*

Year	Vtri	Vex_{in}	Vex_{out}	W	P-E	max V
Wet (current)	2.8	6.6	4.5	5.3	0.9	7.4
Wet (46-65)	2.8	5.8	3.8	5.0	0.8	6.8
Wet (80-99)	3.2	8.2	5.2	6.3	0.5	8.7
Dry (current)	1.1	2.5	1.9	2.2	0.5	3.0
Dry (46-65)	1.1	2.2	1.7	2.0	0.4	2.8
Dry (80-99)	1.3	3.1	2.0	2.5	0.5	3.6

Based on comparisons, the maximum water volume of TSL will decrease in future in the period 2046-2065, and increase in the period 2080-2099. Water flow from the MR made the largest contribution to changes in maximum water volume of the TSL.

The predicted changes in the water income components (2046-2065) in TSL balanced system were as follows: max V will decrease by 0.6×10^{10} m^3 and 0.2×10^{10} m^3 in typical wet and dry years, respectively; P-E will decrease by 0.1×10^{10} m^3 in typical wet and dry year; Vtri will not change too much; Vexin decrease by 0.8×10^{10} m^3 and 0.3×10^{10} m^3 in wet and dry years, respectively. The predicted changes in water income components (2080-2099) in TSL balanced system were as follows: max V will increase by 1.3×10^{10} m^3 and 0.6×10^{10} m^3 in typical wet and dry years, respectively, P-E will decrease by 0.4×10^{10} m^3 in typical wet year, but there will be no obvious change in typical dry year; Vtriwill increase by 0.4×10^{10} m^3 and 0.2×10^{10} m^3 in typical wet and dry year, respectively, while Vex_{in} will increase by 1.6×10^{10} m^3 and 0.6×10^{10} m^3 in wet and dry years, respectively.

Conclusion

This study has successfully modeled the MR-TSL interaction system for water resource assessment and river basin management. The major contribution of this study is the development of an integrated River Lake Water Exchange (RLWE) model coupled with YHyM (a grid-based distributed hydrological model) in Tonle Sap Lake area. Using the coupled model, discharge contributions to TSL from tributaries, daily lake water volume, water exchange between the MR and TSL, and daily consumptive water use in TSL area were analyzed and discussed. In addition, the potential impact of

http://www.aloki.hu ● ISSN 1589 1623 (Print) ● ISSN 1785 0037 (Online)
DOI: http://dx.doi.org/10.15666/aeer/1802_30413055

climate change on TSL hydrological system were determined through the application of the coupled model.

The potential impact of climate change on MR-TSL interaction system was analyzed using the coupled model. The modeled monthly changes were applied to historical daily precipitation time series for producing future projected precipitation, and constant monthly scaling was used for bias correction. GCM output was obtained from IPCC AR4. The current and future scenarios in this study represent the periods 1981-2000 and 2046-2065, 2080-2099, respectively. Under future scenario, peak water volume will decrease in 2046-2065 and increase in 2080-2099 in typical dry and wet years. Water flow from the MR river the largest contribution to the reduction of maximum water volume of TSL.

The results from different future scenarios showed the potential impact on MR-TSL interaction system. The maximum water volume of TSL will decrease, while minimum water volume will increase under future climate change situations (2046-2065). Moreover, the maximum water volume of TSL will increase under future climate change situations (2080-2099). The range of variation in lake area will decrease as a result of these changes. These scenarios indicate that dams on lake tributaries will not have much effect on TSL, which implies that exchange water is the dominant item within the interaction system.

This study analyzed the hydrological response to future climate change, but does not consider water quality issue. Due to the economic development, water quality management will become a key point of water resource management in the near future. The water quality response study under global climate change can be a future research.

Acknowledgments. This work was financially supported by the Innovation capacity building project of Jiangsu provincial Department of science and technology (BM2018028), MEXT and G-COE Program of University of Yamanashi, Japan. Hydrological data for Tonle Sap Lake was provided by International Centre for Water Hazard and Risk Management (ICHARM) under the project of Research Revolution 2002 (RR2002). We also acknowledge the modeling groups, the Program for Climate Model Diagnosis and Inter-comparison (PCMDI) and the WCRP's Working Group on Coupled Modeling (WGCM) for their roles in making available the WCRP CMIP3 multi-model dataset.

REFERENCES

[1] Ao, T. (2001): Development of a distributed hydrological model for large river basins and its application to Southeast Asian rivers. – PhD Thesis, University of Yamanashi, Kofu, Japan, pp. 1-124.

[2] Ao, T., Ishidaira, H., Takeuchi, K., Kiem, A., Yoshitani, J., Fukami, K., Magome, J. (2006): Relating BTOPMC model parameters to physical features of MOPEX basins. – Journal of Hydrology 320(1-2): 84-102.

[3] Ao, T., Takeuchi, K., Ishidaira, H., Fukami, K., Kaneki, M. (1999): The Naka River floods analyses by BTOPMC method. – Proceedings of International Symposium on Floods and Droughts, Nanjing China, 18-21 October 1999, pp. 414-420.

[4] Ao, T., Takeuchi, K., Ishidaira, H. (2000): A distributed rainfall-runoff model for a large catchment—a preliminary application to the Mekong basin. – Proceedings of the AP FRIEND Workshop on Mekong Basin Study 19: 93-102.

[5] Ao, T., Yoshitani, J., Takeuchi, K., Fukami, K., Mutsuura, T., Ishidaira, H. (2003a): Effects of sub-basin scale on runoff simulation in distributed hydrological model:

http://www.aloki.hu ● ISSN 1589 1623 (Print) ● ISSN 1785 0037 (Online)
DOI: http://dx.doi.org/10.15666/aeer/1802_30413055

BTOPMC. – Weather Radar Information and Distributed Hydrological Modeling 282: 227-234.

[6] Ao, T., Takeuchi, T., Ishidaira, H., Yoshitani, J., Fukami, K., Matsuura, T. (2003b): Development and application of a new algorithm for automated pits removal for grid DEMs. – Hydrological Sciences Journal 48(6): 985-997.

[7] Campbell, I. C. (2016): Integrated management in the Mekong River Basin. – Ecohydrology & Hydrobiology 16(4): 255-262.

[8] Chan, S., Putrea, S., Sean, K., Hortle, K. G. (2003): Using local knowledge to inventory deep pools, important fish habitats in Cambodia. – Proceedings of the 6th Technical Symposium on Mekong Fisheries, Pakse, Lao PDR 26-28 November 2003, pp. 34: 65.

[9] Ishidaira, H., Takeuchi, K., Ao, T. (2000): Hydrological simulation of large river basins in Southeast Asia. Proceedings Fresh Perspectives on Hydrology and Water Resources in Southeast Asia and the Pacific, Christ Church. – Technical Document in Hydrology 7: 53-54.

[10] Keskinen, M. (2006): The lake with floating villages: socio-economic analysis of the Tonle Sap Lake. – International Journal of Water Resources Development 22: 463-480.

[11] Kiem, A. S., Hapuarachchi, H. P., Takeuchi, K. (2004a): Impacts of climate variability on streamflow in the Mekong River: an interesting challenge for hydrological modeling. – Proceedings of 7th International River Symposium 31: 4.

[12] Kiem, A. S., Hapuarachchi, H. P., Ishidaira, H., Magome, J., Takeuchi, K. (2004b): Uncertainty in hydrological predictions due to inadequate representation of climate variability impacts. – Proceedings of AOGS 1st Annual Meeting & APHW 2nd Conference 12: 5-9.

[13] Kiem, A. S., Geogievsky, M. V., Hapuarachchi, H. P., Ishidaira, H., Takeuchi, K. (2005): Relationship between ENSO and snow-covered area in the Mekong and Yellow River basins. – IAHS Publication 296: 255-264.

[14] Kummu, M., Nikula, J. (2006): Ecosystem management of Tonle Sap Lake: An integrated modelling approach. – International Journal of Water Resources Development 22: 497-519.

[15] Kummu, M., Sarkkula, K. (2008): Impact of the Mekong River Flow Alteration on the Tonle Sap Flood Pulse. – AMBIO A Journal of the Human Environment 37(3): 185-192.

[16] Kummu, M., Penny, D., Sarkkula, J., Koponen, J. (2008): Sediment - curse or blessing for Tonle Sap Lake? – AMBIO A Journal of the Human Environment 37(3): 158-163.

[17] Moriasi, D. N., Arnold, J. G., Van Liew, M. W., Binger, R. L., Harmel, R. D., Veith, T. (2006): Model evaluation guidelines for systematic quantification of accuracy in watershed simulations. – Transactions of the ASABE 50(3): 885.

[18] Ogston, A. S., Allison, M. A., Mullarney, J. C., Nittrouer, C. A. (2017): Sediment- and hydro-dynamics of the Mekong Delta: from tidal river to continental shelf. – Continental Shelf Research 147: 1-6.

[19] Perkins, S. E., Pitman, A. J., Holbrook, N. J. (2007): Evaluation of the AR4 climate models' simulated daily maximum temperature, minimum temperature, and precipitation over Australia using probability density functions. – Journal of Climate 20: 4356-4376.

[20] Shibuo, K., Kanae, S. (2010): Comparisons of bias correction methods for climate model's daily precipitation - from a heavy rainfall perspective. – Annual Journal of Hydraulic Engineering 54: 235-240.

[21] Sutherland, J. W., Norton, S. A., Short, J. W., Navitsky, C. (2018): Modeling salinization and recovery of road salt-impacted lakes in temperate regions based on long-term monitoring of Lake George, New York (USA) and its drainage basin. – Science of the Total Environment 637: 282-294.

[22] Sverdrup, J. S. (2002): Fisheries in the Lower Mekong Basin: Status and Perspectives. – MRC Technical Paper No. 6. Mekong River Commission, Phnom Penh, Cambodia.

[23] Szesztay, K. (1974): Water balance and water level fluctuations of lakes. – Hydrological Sciences-Bulletin-des Sciences Hydrologiques 1974: 73-84.

http://www.aloki.hu ● ISSN 1589 1623 (Print) ● ISSN 1785 0037 (Online)
DOI: http://dx.doi.org/10.15666/aeer/1802_30413055

[24] Takeuchi, K., Ao, T., Ishidaira, H. (1999): Introduction of block-wise use of TOPMODEL and Muskingum-Cunge method for the hydroenvironmental simulation of a large ungauged basin. – Hydrological Sciences Journal (Journal Des Sciences Hydrologiques) 44(4): 633-646.
[25] TERRA (2007): MRC silent as mainstream dams move forward. – TERRA Press Briefing, 8 November 2007, Bangkok.
[26] Trisurat, Y., Aekakkararungroj, A., Ma, H. (2018): Basin-wide impacts of climate change on ecosystem services in the Lower Mekong Basin. – Ecological Research 33: 73-86.
[27] Wu, S., Ishidaira, H., Sun, W. (2010): Potential impact of Sambor Dam project on interaction between Mekong River and Tonle Sap Lake. – Annual Journal of Hydraulic Engineering 54: 109-114.
[28] Zhou, M., Ishidaira, H., Hapuarachchi, H. P., Georgievsky, M., Takeuchi, K. (2005): Roles of snow, infiltration and saturation excess processes in runoff generation of Yellow River basin. – Symposium on Methodology in Hydrology 135: 196.
[29] Zhou, M., Ishidaira, H., Hapuarachchi, H. P., Magome, J., Kiem, A. S., Takeuchi, K. (2006a): Estimating potential evapotranspiration using Shuttleworth–Wallace model and NOAA-AVHRR NDVI data to feed a distributed hydrological model over the Mekong River basin. – Journal of Hydrology 327(1-2): 151-173.
[30] Zhou, M., Ishidaira, H., Hapuarachchi, H. P., Magome, J., Takeuchi, K. (2006b): Adaptive Muskingum-Cunge routing method for distributed hydrological modeling in large river basins. – 3rd APHW Conference 10: 16-18.

http://www.aloki.hu ● ISSN 1589 1623 (Print) ● ISSN 1785 0037 (Online)
DOI: http://dx.doi.org/10.15666/aeer/1802_30413055

GREEN EFFICIENCY OF INDUSTRIAL WATER RESOURCE IN CHINA AND ITS INFLUENCING FACTORS: EMPIRICAL EVIDENCE FROM CHINA'S 30 PROVINCES

LIU, X.-Y. – PENG, D.-Y.*

School of Statistics, Jiangxi University of Finance and Economics, Nanchang 330010, China

**Corresponding author*
e-mail: ukyo1823@163.com

(Received 28th May 2019; accepted 21st Jan 2020)

Abstract. Based on the theory of Cobb-Douglas production function, this paper introduces the Socio-Environmental Indicator, industrial blue water footprint and industrial grey water footprint to improve the traditional input-output indicator system, used the Epsilon-Based Measure (EBM) models, to measure green efficiency of industrial water resource (GEIWR) based on provincial panel data from 2004 to 2016 in China, and then applied Tobit model to explore the mechanism. First, the results show that distinct differences in the efficiency from different provinces in China. The efficiency from the eastern regions is higher than that in other regions. Then, some western provinces have a high efficiency with a shortage of water but effective waste water regulation, which indicates that the effective efficiency only symbolizes the region's optimal input-output allocation. In particular, the industrial water-saving potential showed a declining trend but there is still much room for improvement of provinces in central China, such as Hubei, Sichuan and Hunan. Lastly, the environmental regulation, technological progress, regional characteristics, industrial structure, foreign capital utilization and water resource consumption have certain impacts on the efficiency. This paper could be helpful in providing a reference for the evaluation of green efficiency of industrial water resource.
Keywords: *green efficiency of industrial water resource (GEIWR), undesirable output, industrial water footprint, industrial water-saving potential, epsilon-based measure (EBM), Tobit regression model*

Introduction

Water resource is one of the indispensable strategic resource for human survival and economic development. World Commission on Environment and Development (WECD) points out, "Water resource is an important factor that restricts socio-economic development". China is a country lacking in water resource. In addition, the uneven spatial distribution of water resource and water pollution from the extensive economic development have made the water resource to become the bottleneck of the sustainable development of our society and economy. In China's industrial structure, industry plays a leading role in the development of national economy, and industrial water consumption accounts for a large proportion in the total water consumption. Accompanied with the fast development of industrialization in China, the imbalance between water supply and demand and water environmental pollution have constantly challenged the growth quality of China's industrial economy. According to the 2016 Annual Statistic Report on Environment in China, industry is the main industry that consumes water resource and causes the continuous deterioration of water environment. China's industry urgently needs green transformation and takes the road of sustainable development. In particular, the spatial distribution of water resource is extremely uneven in China. Therefore, how to alleviate the contradiction between socio-economic development and resource to improve the efficiency of industrial water resource has become a hot topic among scholars. Water resource is an economic resource that can only generate economic benefits with the help

http://www.aloki.hu ● ISSN 1589 1623 (Print) ● ISSN 1785 0037 (Online)
DOI: http://dx.doi.org/10.15666/aeer/1802_30573072

of other production factors. Therefore, many scholars establish input-output indicator system to measure water resource efficiency. In 2006, Hu et al. (2006) established Data Envelopment Analysis (DEA) model to measure water resource efficiency. Based on this model, many scholars have improved the DEA model and the measurement indicator system. Chen et al. (2018) introduced water resource input into production function from the perspective of input. On this basis, taking the social benefits brought by water resource utilization into the measurement system, Sun et al. (2017) further proposed the concept of green efficiency of water resource, which can fully reflect the coordinated development of society, economy and environment. At the same time, scholars such as You Shaqiu and Ma Hailiang introduced undesirable output indicator into the measurement of green efficiency of water resource, considering the impact of environmental pollution output on water resource efficiency (You, 2017; Ma et al., 2012; Zhang and Liu, 2018). In the selection of DEA model, most scholars choose the traditional radial DEA model, such as Liu et al. (2007), Qian and He (2011) and Chemark et al. (2009). Some scholars choose non-radial SBM (Slack-Based Measure) model (Li and Ma, 2014; Sun et al., 2018; Ding et al., 2018), but both of them have their limitations. In order to comprehensively and objectively apply DEA model, we consider the EBM (Epsilon-Based Measure) model, with both radial and non-radial advantages, which was proposed by Tone and Tsutsui (2010). Once proposed, this model has been widely recognized and applied by scholars, but few studies have applied it to the measurement of green efficiency of industrial water resource (GEIWR).

In summary, scholars have conducted research into the efficiency of industrial water resource, laying the foundation for follow-up development in this field. On the whole, there are still some shortcomings in the current research. (1) The indicators of the efficiency measuring factors must be improved. Currently, there have been many researches on the evaluation and analysis of water resource efficiency from the perspective of economic output, but studies on the environmental and social benefits caused by water resource utilization in the process of economic development are insufficient. Scholars have mainly considered factors such as GDP, labor, capital and water input when studying the efficiency of industrial water resource without considering other factors that reflect socio-economic development (Chen et al., 2018; Li and Ma, 2014; Mai et al., 2014; Zhang et al., 2018; Wang, 2015). The lack of socio-economic development factors fails to reflect the fundamental requirements of the green development concept, will result in an efficiency overestimating or underestimating and deviations from the actual situation. This is not conducive to accurate measure of actual efficiency of industrial water resource and coordinated development of all the country's regions. (2) Most studies only calculated the efficiency and did not further evaluate the water potential regionally. At the same time, some researchers used statistical methods to evaluate the water potential but did not further explore the reasons for the efficiency results. (3) Taking all regions of China as the overall sample will neglect the influence of regional differences caused by various factors of water resource, geographic position and capital input, and lead to errors in the measurement of GEIWR.

Based on thee above understanding, this paper aims to further expand from the following two aspects: (1) Based on the provincial panel data from 2004 to 2016, this paper takes the GEIWR as the research core, chooses China's 30 provinces, cities and autonomous regions as the research object (excluding Tibet, Hong Kong, Macao and Taiwan), uses the EBM model as the main method, introduces SEI (Socio-Environmental Indicator), industrial blue water footprint and industrial gray water footprint to improve

http://www.aloki.hu ● ISSN 1589 1623 (Print) ● ISSN 1785 0037 (Online)
DOI: http://dx.doi.org/10.15666/aeer/1802_30573072

indicator system, analyzes the change and trend of the GEIWR in each provincial administrative region of China from the perspective of time and space. (2) In order to provide theoretical guidance for promoting the green transformation of China's industry and realizing the construction of water-saving society in the "13th Five-year plan", this paper estimates the water-saving potential of Chinese provinces, establishes Tobit panel model to explore possible ways to improve the GEIWR. Compared with existing research, the main innovative points of this paper are as follows: (1) It uses EBM to evaluate the GEIWR in China. DEA is a commonly used and effective method for multi-objective decision-making analysis. This paper innovatively applies the EBM method to the study of the GEIWR. At the same time, to eliminate the influence of subjectivity, this paper uses Principal Component Analysis (PCA) to determine the indicator weight of SEI. This method allows it to more objectively reflect the information, rendering the evaluation results more practical. (2) It enriches the indicator system of the efficiency of industrial water resource. In light of the shortcomings of most past studies that do not consider the social benefits of water utilization, this paper adds SEI as desirable output indicators, which can reflect socio-economic development and actual sewage-control situation. Besides, this paper also replaces industrial water utilization by industrial blue water footprint, adds industrial grey water footprint as undesirable output indicators to improve the indicator system. The concept and the indicator system of the GEIWR put forward in this paper better reflect current social development and the water control situation in all provinces, resulting in research results with more practical significance. (3) In the context of this research, we measure industrial water-saving potential by using the measured efficiency. At the same time, this paper also uses panel Tobit model to analyze influencing factors, exploring the underlying causes of the changes in the efficiency.

The structure of this paper as follows: the first section is 'Introduction', the second one, 'Methodology' describes the theoretical mechanism and the research methods, the next sections 'Empirical analysis' and 'Analysis on the influencing factors of GEIWR' demonstrate the results, and the last section provides the conclusion. The second part is the index system and model, the third part is the calculation of efficiency and water-saving potential, the fourth part is the analysis on the influencing mechanism, the fifth part is the conclusions, suggestions and discussions.

Methodology

The indicator system

The DEA approach does not require functional form assumptions between inputs and outputs and can avoid man-made subjectivity in parameter weighting Based on the Cobb-Douglas production function, from the perspective of input and output, this paper established an indicator system for the GEIWR. The indicator system is shown in *Table 1,* and the specific indicators are as follows:

(1) Labor input. The annual average number of employees was used to measure the actual labor input.

(2) Capital input. Referring to the method proposed by Shan Haojie to calculate the capital stock (Shan, 2018), the capital stock of each province is estimated as a measure of the capital input.[1] The perpetual inventory method is used to estimate the capital stock.

[1]Due to the lack of original data of Chongqing and Sichuan, we estimate the respective capital stock based on the population ratio of the two provinces.

http://www.aloki.hu ● ISSN 1589 1623 (Print) ● ISSN 1785 0037 (Online)
DOI: http://dx.doi.org/10.15666/aeer/1802_30573072

(3) Water resource input. Existing researches showed that the industrial blue water footprint can better reflect the water resource consumption in the process of industrial production, so we used the industrial blue water footprint to measure the input of water resource (Huang et al., 2013).

(4) Desirable output. We took the industrial added value and SEI as the desirable output.

To comprehensively, objectively and scientifically reflect the socio-economic development and the present situation of the pollution control in China, we selected 7 indicators from three aspects of industrial structure, social regulation and technology development.

1) Industrial structure

$$\text{Industrial Structure Proportion}(X1) = \frac{\text{Industrial Added Value}}{\text{Gross Regional Product}};$$

$$\text{Foreign Trade Dependence}(X2) = \frac{\text{Total Value of Imports and Exports}}{\text{Gross Regional Product}}.$$

2) Social regulation

$$\text{Water Resource Restriction}(X3) = \ln(\text{Per Capita Water Resource});$$

$$\text{Population Density}(X4) = \frac{\text{Population}}{\text{Area}};$$

$$\text{Government Waste Water Control}(X5) = \frac{\text{Investment in the Treatment of Industrial Waste Water}}{\text{Industrial Added Value}}.$$

3) Technology development

$$\text{Technical Progress}(X6) = \frac{\text{R\&D Expenditure}}{\text{Industrial Added Value}};$$

$$\text{Technical Market Development}(X7) = \frac{\text{Transaction Value in Technical Market}}{\text{Gross Regional Product}}.$$

Then, to solve the subjective question of the weight assignment, PCA was conducted to obtain the SEI. The weights determined by PCA depends on the characteristics of the data itself, which have strong objectivity and can simplify the statistical data on the premise of preserving the information contained in the original data as much as possible. The results showed that the standardized data passed the KMO-Bartlett test and was suitable for the process of dimension reduction. Through the obtained common factor score and the total variance of each common factor, we can get the factor composite score FAC, and finally the SEI is calculated by using *Equation 1*.

$$\text{SEI}_t = 0.1 + 0.9 * \frac{FAC_t - Min(FAC_t)}{(Max(FAC_t) - Min(FAC_t)} \quad \text{(Eq.1)}$$

http://www.aloki.hu ● ISSN 1589 1623 (Print) ● ISSN 1785 0037 (Online)
DOI: http://dx.doi.org/10.15666/aeer/1802_30573072

FAC_t is the factor composite score of the t th province; $Max(FAC_t)$ and $Min(FAC_t)$ are the maximum and minimum value of the corresponding factor composite score respectively.

(5) Undesirable output. The industrial grey water footprint can reflect the pollution degree of the water environment. It refers to the volume of fresh water needed to dilute certain industrial waste water pollutants based on the existing environmental water quality standards. As industrial waste water is directly discharged into water, the discharge amount of main pollutants, Industrial COD (Chemical Oxygen Demand) Emission and Industrial Ammonia Nitrogen, can usually be directly measured as the industrial grey water footprint (Zhang et al., 2017; Hoekstra et al., 2011). In order to consider the constraint effect of industrial water pollution, we take the industrial grey water footprint as the undesirable output part of the output indicator.

Table 1. *Indicator system*

Project	Inputs/outputs	Indicator selection		Measurement and explanations
Input	Labor input	Annual average number of employees		∑[Average number in (January, February, ..., December)] / 12. This input is used to measure the actual labor input
	Capital input	Capital stock		The actual capital stock at the end of year t = the nominal investment in year t / the fixed capital investment price index + (1-the replacement rate) × the actual capital stock at the end of the previous year
	Water resource input	Industrial blue water footprint		Industrial water consumption - industrial sewage discharge. This input can better reflect the water resource consumption in the process of industrial production
Output	Desirable output	Economic output: Industrial added value		This output is the most ideal variable to reflect industrial economic output, and its specific value can be obtained directly in the statistical yearbook of China
		Social output: SEI	Industrial structure proportion	The two rates describe the degree of government emphasis on industry and foreign trade
			Foreign trade dependence	
			Water resource restriction	The three rates describe the level of social regulation from the prospect of water resource, population and sewage treatment
			Population density	
			Government waste water control	
			Technical progress	The two rates indicate the technical level in China
			Technical market development	
	Undesirable output	Environmental output: Industrial grey water footprint		This output reflects the pollution degree of the water environment

http://www.aloki.hu ● ISSN 1589 1623 (Print) ● ISSN 1785 0037 (Online)
DOI: http://dx.doi.org/10.15666/aeer/1802_30573072

Data source

The data are mainly from the "China Environmental Yearbook", "China Statistical Yearbook", "China Water resource Bulletin", "China Industrial Economic Statistical Yearbook" and statistical yearbook of each province from 2004 to 2016. The study object is China's 30 provinces, because the data are from the yearbook statistics, are single-handed information, the reliability and validity of the data have been tested. Moreover, it needs to be noted that the sample includes panel data from 30 provinces in China, in which data in Tibet are missing and removed. In addition, the research range of this paper was selected from 2004 to 2016, mainly for the following reasons: 1) The availability of data. Some of the key variables used in the study do not have complete annual data until 2004, and the data for 2017 has not yet been released completely. 2) It is related to the research topic. Many scholars' similar researches are mainly published during this time. In conclusion, considering the availability of variables' data and the research theme, this paper selects data from 30 provinces in China from 2004 to 2016.

Methods

EBM models

The traditional DEA model can broadly fit into two types. The first classical DEA model is the CCR model, which is established on the basis of constant returns to scale. On the basis of CCR model, BCC model considering variable return on scale assumption can be proposed. But the two basic DEA models, CCR model and BCC model cannot cover slack variables. Other model extensions include slacks-based measure, SBM model. SBM allows all inputs, intermediate variables and outputs to vary in proportion. However, their work cannot guarantee the stage efficiency and efficiency decomposition of the process. In order to solve this problem, EBM, combining radial and non-radial measurement characteristics, was introduced in this paper to measure the GEIWR from 2004 to 2016 in China in order to get closer to the actual efficiency.

For n decision-making units with s input factors (x) and t output factors (y), EBM model can be expressed as follows.

$$
\begin{gathered}
\mathrm{X}=\sum_{j=1}^{n} x_{ij} \\
\mathrm{Y}=\sum_{j=1}^{n} \lambda_j y_{rj} \\
\sum_{i=1}^{m} w_i^- = 1 \\
\gamma^* = \min_{\theta,\lambda,t^-} \theta - \varepsilon_x \sum_{i=1}^{s} \frac{w_i^- t_i^-}{x_{i0}} \\
\text{s.t.}\, \theta x_{i0} - \sum_{j=1}^{n} \lambda_j x_{ij} = 0\,, i = 1, \cdots, s \\
\sum_{j=1}^{n} \lambda_j y_{rj} \geq y_{r0}\,, r = 1, \cdots, t \\
\lambda_i \geq 0 \\
t_i^- \geq 0
\end{gathered}
\qquad \text{(Eq.2)}
$$

http://www.aloki.hu ● ISSN 1589 1623 (Print) ● ISSN 1785 0037 (Online)
DOI: http://dx.doi.org/10.15666/aeer/1802_30573072

In the formula, γ^* represents the optimal efficiency value of EBM model considering undesirable output; X is the input value, Y is the output value, X, Y > 0; θ represents the radial efficiency value; t_i^- represents the slack vector of non-radial input elements; λ represents the relative weight value; w_i^- represents the weight value of the i th input variable; ε_x represents key parameters of radial θ and non-radial relaxation t_i^- contained in EBM model (Tone and Tsutsui, 2010).

Tobit model

After calculating the green efficiency of industrial water resources in all provinces and cities of China, this paper will further take the efficiency of industrial green water resources in all provinces and cities as the explanatory variable, and construct econometric model to investigate the influence mechanism of industrial green water resource efficiency in China. Since the range of industrial green water resource efficiency is 0-1, it is a limited dependent variable. If the ordinary least square method is still used, the parameter estimation will be biased and inconsistent. Therefore, Tobit regression model is used in this paper, which is an econometric model for dependent variables of partial continuous distribution and partial discrete distribution. Its specific form is as *Equation 3*.

$$Y_i = \begin{cases} X_i\beta + \mu_i & (\text{When } X_i\beta + \mu_i > 0) \\ 0 & (\text{Others}) \end{cases} \quad \text{(Eq.3)}$$

In *Equation 3,* Y_i is the limited dependent variable, X_i is the independent variable vector, β is the parameter vector to be estimated, and the random interference term $\mu_i \sim N(0, \sigma^2), i = 1,2, \ldots$ is the number of observation values. It can be proved that when the Tobit model is estimated by the maximum likelihood method, it can be concluded that $\hat{\beta}$ and $\hat{\sigma}^2$ are consistent estimators.

Empirical analysis

Measurement of GEIWR

Based on the panel data of 30 provinces in China from 2004 to 2016, the green efficiency of China's industrial water resource is calculated by using EBM model in MaxDEA6.0Pro.

The effective GEIWR indicates that its input-output allocation is optimal. As can be seen from *Table 2,* the GEIWR in different provinces showed different development trends from 2004 to 2016. Beijing, Guangdong, Tianjin, Shanghai, Shandong are characterized by having effective DEA value, which indicates that these regions have strong industrial economic strength, optimal allocation of various inputs and outputs in the development process, high level of scientific and technological development and strong ability of comprehensive social development. The GEIWR of these regions is at the optimal level nationwide. The result is consistent with the current situation of China's industrial water resource and social and economic development. In addition, Zhejiang, Chongqing and Fujian have obvious late-mover advantage advantages, and the efficiency value increases gradually from the low initial stage. For example, Zhejiang's efficiency value was only 0.5419 in 2004, but it increased to 0.9240 in 2016.

http://www.aloki.hu ● ISSN 1589 1623 (Print) ● ISSN 1785 0037 (Online)
DOI: http://dx.doi.org/10.15666/aeer/1802_30573072

On the contrary, Shanxi and Heilongjiang's efficiency values gradually get below 1.0000, which indicates that in the development process of these regions, the allocation of input and output may be unbalanced. In the western region of Inner Mongolia, Qinghai have high GEIWR. By consulting the input-output data of 2004-2016 and related literature, we found despite each of these areas is lack of water resource and has a low economic development level, but the per capita water resource possession ratio is high, the sewage control has been effective. The result proves that the GEIWR in a region is not necessarily related to the region's economic level.

Table 2. *EBM results of GEIWR*

Region	Province	2004	2005	2006	2007	2008	2009	2010	2011	2012	2013	2014	2015	2016	Average
Eastern Region	Beijing	1.0000	1.0000	1.0000	1.0000	1.0000	1.0000	1.0000	1.0000	1.0000	1.0000	1.0000	1.0000	1.0000	1.0000
	Tianjin	1.0000	1.0000	1.0000	1.0000	1.0000	1.0000	1.0000	1.0000	1.0000	1.0000	1.0000	1.0000	1.0000	1.0000
	Hebei	1.0000	1.0000	0.7413	1.0000	0.7171	0.7285	1.0000	1.0000	1.0000	1.0000	1.0000	0.8536	0.9092	0.9192
	Shanghai	1.0000	1.0000	1.0000	1.0000	1.0000	1.0000	1.0000	1.0000	1.0000	1.0000	1.0000	1.0000	1.0000	1.0000
	Jiangsu	0.6417	0.6169	0.5958	0.6353	0.6174	0.6619	0.5576	0.6831	0.4994	0.7236	0.6688	0.7454	0.7329	0.6446
	Zhejiang	0.5419	0.5620	0.5103	0.6054	0.6195	0.6777	0.7063	0.7854	0.6732	0.7720	0.7973	0.9165	0.9240	0.6993
	Fujian	0.7694	0.7329	0.6746	0.7287	0.7169	0.7787	0.8243	0.8294	0.7885	0.8750	0.9176	1.0000	0.9515	0.8144
	Shandong	1.0000	1.0000	1.0000	1.0000	1.0000	1.0000	1.0000	1.0000	1.0000	1.0000	1.0000	1.0000	1.0000	1.0000
	Guangdong	1.0000	1.0000	1.0000	1.0000	1.0000	1.0000	1.0000	1.0000	1.0000	1.0000	1.0000	1.0000	1.0000	1.0000
	Hainan	1.0000	1.0000	1.0000	0.9054	1.0000	1.0000	1.0000	1.0000	1.0000	1.0000	1.0000	1.0000	1.0000	0.9927
Western Region	Gansu	0.7027	1.0000	0.6997	0.6479	0.6406	0.6565	0.8334	0.8657	0.8512	0.7970	0.8571	0.6305	0.6185	0.7539
	Guangxi	0.5711	0.6085	0.4749	0.5471	0.4176	0.6492	0.6099	0.7066	0.5706	0.5891	0.7300	0.8006	0.7889	0.6203
	Guizhou	0.6771	0.7354	0.6836	0.5997	0.6838	0.7641	0.8206	0.7089	0.7231	0.7673	0.8432	0.8372	0.8354	0.7446
	Inner Mongolia	0.8786	0.8826	1.0000	1.0000	1.0000	1.0000	1.0000	1.0000	1.0000	1.0000	1.0000	1.0000	1.0000	0.9816
	Ningxia	1.0000	1.0000	1.0000	1.0000	0.6453	1.0000	0.6012	1.0000	0.7871	0.5783	0.5877	0.8660	0.6054	0.8208
	Qinghai	1.0000	0.8058	0.7081	1.0000	1.0000	0.8414	1.0000	1.0000	0.9230	1.0000	0.9225	1.0000	1.0000	0.9385
	Shaanxi	0.8612	0.8176	0.7843	0.8122	0.8022	0.7537	0.8527	0.8256	0.9177	1.0000	0.8828	0.8078	0.8370	0.8427
	Sichuan	0.4421	0.4967	0.4596	0.4861	0.5423	0.6167	0.6525	0.6914	0.6253	0.8346	0.8401	0.8107	0.7531	0.6347
	Xinjiang	1.0000	1.0000	1.0000	1.0000	1.0000	0.6626	0.8657	0.8457	0.7855	0.7544	0.7577	0.6813	0.6677	0.8477
	Yunnan	0.7846	0.7555	0.6548	0.7613	0.7622	0.7061	0.7583	0.6712	0.6884	0.5604	0.6849	0.6880	0.6952	0.7055
	Chongqing	0.8877	0.7905	0.7691	0.7704	0.8355	1.0000	1.0000	1.0000	1.0000	1.0000	1.0000	1.0000	1.0000	0.9272
Central Region	Anhui	0.6329	0.6278	0.6001	0.5907	0.6514	0.7464	0.8376	0.8372	0.7645	1.0000	1.0000	0.8611	0.8786	0.7714
	Henan	0.8592	1.0000	1.0000	1.0000	0.7391	0.5952	0.7546	0.6132	0.3173	0.7142	0.6462	0.6528	0.7313	0.7402
	Hubei	0.4978	0.5588	0.5484	0.5063	0.5657	0.7186	0.7446	0.7826	0.6874	0.8172	0.8173	0.7956	0.8225	0.6818
	Hunan	0.5191	0.5402	0.4990	0.5363	0.5754	0.5763	0.6352	0.6433	0.4686	0.7000	0.7023	0.7230	0.7146	0.6026
	Jiangxi	0.6493	0.6043	0.6465	0.6718	0.6662	0.6890	0.8466	0.7784	0.6692	0.9349	0.9188	0.8700	0.8135	0.7507
	Shanxi	1.0000	1.0000	0.8765	0.9073	0.8815	0.7093	0.8554	0.8730	0.7499	0.7908	0.7310	0.6300	0.6211	0.8174
Northeastern Region	Heilongjiang	1.0000	1.0000	1.0000	1.0000	1.0000	0.7812	0.9525	0.8943	0.7906	0.7633	0.7380	0.6444	0.6208	0.8604
	Jilin	0.8039	0.7670	0.6318	0.6515	0.6177	0.6399	0.6644	0.7261	0.5782	0.8275	0.8252	0.8247	0.8331	0.7224
	Liaoning	0.7920	0.6879	0.6409	0.6351	0.6460	0.7270	0.7915	0.8600	0.8579	0.8651	0.8803	0.8882	0.6419	0.7626
Average		0.8171	0.8197	0.7733	0.8000	0.7781	0.7893	0.8388	0.8540	0.7906	0.8555	0.8583	0.8509	0.8332	0.8199

*Efficiency value of 1.0000 means DEA value is effective

From the average efficiency of all provinces in China, we cannot get obvious data characteristics. Therefore, combined with the common regional classification in China, this paper divides 30 provinces into four regions: the east, the central, the west and the northeast, and analyzes the development trend of their average efficiency. The result clarifies that the change of the GEIWR in different regions of China shows certain regularity. The curves of average efficiency in East, middle, West and Northeast China are shown in *Figure 1*. It can be seen from *Figure 1* that the green efficiency of China's

http://www.aloki.hu ● ISSN 1589 1623 (Print) ● ISSN 1785 0037 (Online)
DOI: http://dx.doi.org/10.15666/aeer/1802_30573072

industrial water resource generally presents the law of fluctuation. From 2004 to 2016, except for the eastern region, the changes in the western, central and northeast regions are similar, with the overall efficiency value dropping first till 2006, and then rising, then falling to the lowest level in 2009, and finally rebounding slowly. Combined with China's national conditions in recent years, we find that all these changes show that the three regions especially the central region are greatly affected by different resource and governance policies in different periods. Moreover, the eastern region is always at the leading level of GEIWR in China. Whereas, the GEIWR in the central region is always at the backward level in China, which needs to be improved. This region should be the key area for optimal allocation of water resource.

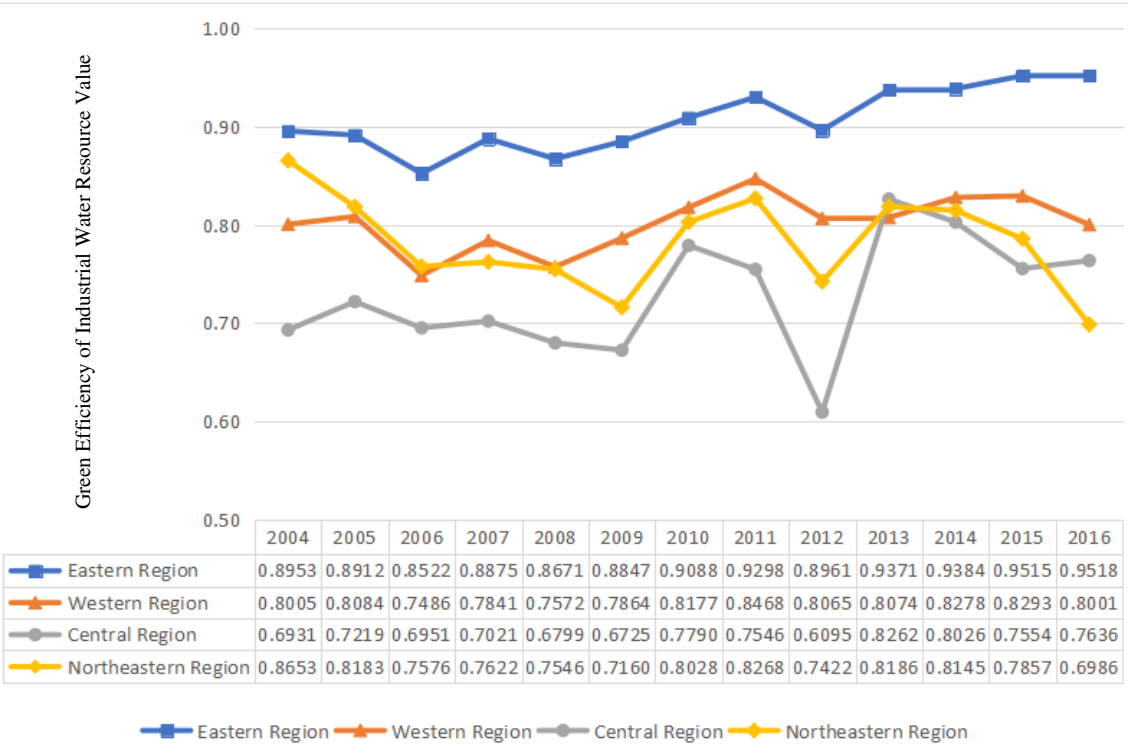

	2004	2005	2006	2007	2008	2009	2010	2011	2012	2013	2014	2015	2016
Eastern Region	0.8953	0.8912	0.8522	0.8875	0.8671	0.8847	0.9088	0.9298	0.8961	0.9371	0.9384	0.9515	0.9518
Western Region	0.8005	0.8084	0.7486	0.7841	0.7572	0.7864	0.8177	0.8468	0.8065	0.8074	0.8278	0.8293	0.8001
Central Region	0.6931	0.7219	0.6951	0.7021	0.6799	0.6725	0.7790	0.7546	0.6095	0.8262	0.8026	0.7554	0.7636
Northeastern Region	0.8653	0.8183	0.7576	0.7622	0.7546	0.7160	0.8028	0.8268	0.7422	0.8186	0.8145	0.7857	0.6986

Figure 1. *The GEIWR values of four regions in China over time*

Assessment of industrial water-saving potential

To sum up, we have analyzed and evaluated China's GEIWR through EBM model. In accordance with the above empirical results, till 2016, the GEIWR in most provinces in China is still less than 1, it proves that the utilization of industrial water resource has not reached the optimal level, and GEIWR can be further improved. We can tap the industrial water-saving potential.[2]

[2]The connotation of water-saving potential is defined in The Outline of National Water Resource Planning, which refers to the difference between the current water consumption and the water consumption at the optimal level. The industrial water-saving potential studied in this paper is the amount of water-saving stock, which refers to the amount of water-saving that can be achieved by water users under the current situation through water-saving measures to achieve effective utilization of Industrial water resource.

http://www.aloki.hu ● ISSN 1589 1623 (Print) ● ISSN 1785 0037 (Online)
DOI: http://dx.doi.org/10.15666/aeer/1802_30573072

Combined with the meaning of water resource efficiency, the industrial blue water footprint at the optimal industrial water level can be expressed as *Equation 4*.

$$\widehat{BW_{it}} = BW_{it} \times E_{it} \quad \text{(Eq.4)}$$

In the formula, $\widehat{BW_{it}}$ represents the industrial blue water footprint in the optimal input-output configuration; BW_{it} represents the current industrial blue water footprint; E_{it} represents the GEIWR; i represents the provincial region and t represents the year.

Then, the industrial water-saving potential ΔBW_{it} can be measured as *Equation 5* (Li, 2017).

$$\Delta BW_{it} = BW_{it} - \widehat{BW_{it}} = (1 - E_{it}) \times BW_{it} \quad \text{(Eq.5)}$$

We substituted the GEIWR (E_{it}) calculated by EBM into *Equations 4* and *5,* and the estimated results of China's industrial water-saving potential from 2004 to 2016 are shown in *Table 3*.

Table 3. *Industrial water-saving potential in China's provinces from 2004 to 2016 (100 million m^3)*

Region	Province	2004	2005	2006	2007	2008	2009	2010	2011	2012	2013	2014	2015	2016
Eastern Region	Beijing	0.00	0.00	0.00	0.00	0.00	0.00	0.00	0.00	0.00	0.00	0.00	0.00	0.00
	Tianjin	0.00	0.00	0.00	0.00	0.00	0.00	0.00	0.00	0.00	0.00	0.00	0.00	0.00
	Hebei	0.00	3.41	0.00	3.71	3.45	0.00	0.00	0.00	0.00	0.00	1.92	1.13	1.05
	Shanghai	0.00	0.00	0.00	0.00	0.00	0.00	0.00	0.00	0.00	0.00	0.00	0.00	0.00
	Jiangsu	68.30	77.45	72.35	70.17	57.12	73.20	53.32	84.84	54.74	72.04	55.59	60.84	65.84
	Zhejiang	17.02	20.94	17.38	15.59	11.28	11.15	9.35	14.10	9.68	8.26	3.08	2.54	12.18
	Fujian	13.46	17.62	16.04	17.40	13.92	12.09	11.22	13.76	8.07	5.36	0.00	2.90	10.99
	Shandong	0.00	0.00	0.00	0.00	0.00	0.00	0.00	0.00	0.00	0.00	0.00	0.00	0.00
	Guangdong	0.00	0.00	0.00	0.00	0.00	0.00	0.00	0.00	0.00	0.00	0.00	0.00	0.00
	Hainan	0.00	0.00	0.39	0.00	0.00	0.00	0.00	0.00	0.00	0.00	0.00	0.00	0.03
Western Region	Gansu	0.00	4.24	4.38	4.11	3.92	2.03	1.80	1.62	2.25	1.55	3.59	3.50	2.86
	Guangxi	11.93	17.67	13.32	18.13	13.26	15.10	13.84	17.36	19.91	13.37	9.81	9.25	14.27
	Guizhou	7.05	8.20	12.24	10.30	7.74	5.90	8.34	6.28	5.75	3.83	3.68	3.77	7.02
	Inner Mongolia	1.25	0.00	0.00	0.00	0.00	0.00	0.00	0.00	0.00	0.00	0.00	0.00	0.17
	Ningxia	0.00	0.00	0.00	0.46	0.00	0.77	0.00	0.69	1.45	1.44	0.37	1.12	0.48
	Qinghai	1.07	1.84	0.00	0.00	0.34	0.00	0.00	0.12	0.00	0.12	0.00	0.00	0.27
	Shaanxi	1.56	1.98	1.28	1.59	1.60	1.11	1.59	0.78	0.00	1.22	2.00	1.59	1.35
	Sichuan	22.41	24.84	24.42	21.45	19.55	18.62	17.45	17.87	8.57	6.07	9.13	11.98	17.48
	Xinjiang	0.00	0.00	0.00	0.00	2.58	1.16	1.50	2.02	2.29	2.43	2.86	2.95	1.37
	Yunnan	3.69	5.29	4.49	4.47	5.64	5.41	6.73	7.33	9.28	6.48	5.74	4.99	5.58
	Chongqing	5.13	6.88	7.81	6.46	0.00	0.00	0.00	0.00	0.00	0.00	0.00	0.00	2.22
Central Region	Anhui	22.84	29.04	31.30	27.43	21.89	14.12	13.59	21.38	0.00	0.00	11.99	10.56	17.31
	Henan	0.00	0.00	0.00	9.94	15.98	9.94	16.61	31.93	13.24	14.08	13.72	10.26	10.75
	Hubei	32.34	35.14	43.21	38.05	25.80	27.49	23.90	28.84	15.34	14.99	17.42	14.94	27.23
	Hunan	31.38	36.06	33.63	30.91	31.30	29.25	30.63	45.06	25.55	23.66	22.86	23.22	30.33
	Jiangxi	18.13	15.61	16.89	17.71	14.45	7.69	11.85	17.17	3.47	4.45	7.01	9.93	12.36
	Shanxi	0.00	1.36	0.96	1.11	1.91	1.10	1.31	2.67	2.12	2.49	3.54	3.24	1.68
Northeastern Region	Heilongjiang	0.00	0.00	0.00	0.00	11.44	2.48	5.16	7.51	6.92	6.50	7.17	6.43	4.12
	Jilin	3.42	5.59	5.42	5.90	7.15	7.47	6.14	9.54	3.84	3.95	3.39	2.96	5.18
	Liaoning	3.30	5.05	5.41	5.79	4.48	3.72	2.09	2.03	2.02	1.64	1.46	4.30	3.35

http://www.aloki.hu ● ISSN 1589 1623 (Print) ● ISSN 1785 0037 (Online)
DOI: http://dx.doi.org/10.15666/aeer/1802_30573072

As can be seen from *Table 3* and *Figure 2,* China's industrial water-saving potential showed an overall downward trend from 2004 to 2016, which indicates that with the accumulation of pollution treatment experience and the improvement of industrial water-saving technology over the years, China's industrial water resource green efficiency has been continuously improved. But industrial water-saving potential rebound in 2016, it showed that the gap of GEIWR among provinces has a declining trend. Provinces at the forefront of the GEIWR saw a smaller decline and maintained their leading level. However, provinces with low efficiency are restricted by many factors, such as water resource and management, and the decline rate is large, which caused the gap between them and frontier cities further widened. These provinces have a large space to improve industrial water saving in the future. Most of the provinces in central China, such as Hubei, Sichuan and Hunan, have a large space to tap the industrial water-saving potential. The governments of these regions should strengthen their drainage monitoring capacity, increase the intensity of industrial waste water treatment, and actively promote renewable water conservancy to improve the GEIWR.

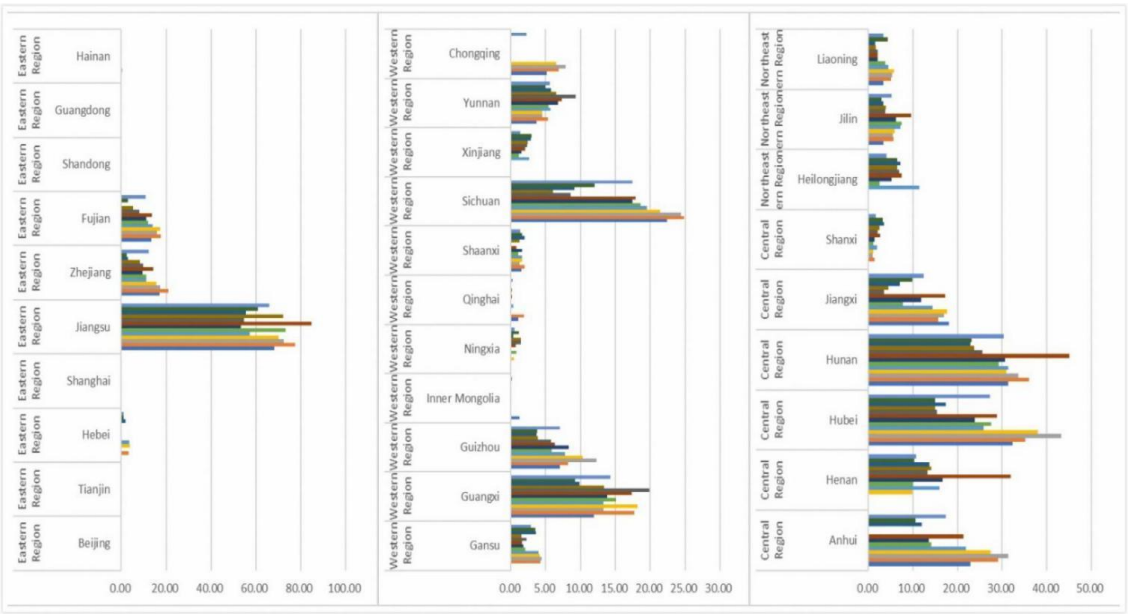

Figure 2. *Industrial water-saving potential of each region in China from 2004 to 2016*

Analysis on the influencing factors of GEIWR

We took the GEIWR in various provinces across the country from 2004 to 2016 as the explained variable; selected six indicators including Environmental Regulation (Government Waste Water Control), Technological Progress, Regional Characteristics[3], Industrial Structure (Industrial Structure Proportion), Foreign Capital Utilization (Foreign Trade Dependence) and Water Resource Consumption (Industrial Blue Water Footprint) as explanatory variables.

[3]Seen by the analysis results, there are obvious regional differences in China's green efficiency of industrial water resource. So we introduces dummy variable (0 represents the eastern region and 1 represents the central, western and the northeast regions) to reflect the influence of region on the green efficiency of industrial water resource.

http://www.aloki.hu ● ISSN 1589 1623 (Print) ● ISSN 1785 0037 (Online)
DOI: http://dx.doi.org/10.15666/aeer/1802_30573072

Because the explanatory variable value of regression equation is between 0 and 1, which is a limited dependent variable, this paper uses the panel Tobit model to test the efficiency effect mechanism. With the help of Stata software, the estimation results of Tobit regression model are obtained by using the maximum likelihood estimation (MLE) method, and are shown in *Tables 4* and 5.

Table 4. *Descriptive statistics*

Variable	Sample size	Mean	Standard deviation	Minimum	Maximum
Green efficiency of industrial water resources	390	0.840,4	0.159,1	0.3100	1.0000
Environmental regulation	390	0.115,5	0.118,9	0.0015	0.955,1
Technological progress	390	0.409,5	0.496,6	0.0000	2.601,8
Regional characteristics	390	0.666,7	0.4720	0.0000	1.0000
Industrial structure	390	40.171,2	8.193,9	11.904,2	56.491,6
Foreign capital utilization	390	31.644,6	36.781,5	1.343,9	187.500,4
Water resource consumption	390	379,480.6	405,716.7	128,52	227,748,3

Table 5. *The regression results of panel Tobit model*

Explanatory variable	Regression coefficient	Standard deviation	T-value	P > |t|
Environmental regulation	-0.243,4***	0.088,8	-2.74	0.006
Technological progress	0.091,4**	0.037	2.47	0.014
Regional characteristics	-0.213,4***	0.038,6	-5.52	0
Industrial structure	0.005,5***	0.001,5	3.58	0
Foreign capital utilization	0.001,9***	0.000,7	2.77	0.006
Water resource consumption	-1.95E-07***	3.07E-08	-6.35	0
Constant	0.844,8***	0.071,4	11.83	0
LR chi2(6)	206.22***			
Pseudo R2	0.730,6			
Log likelihood	-38.025,597			

***, **, * means that the variables are significant at the level of 1%, 5% and 10%, respectively

According to the regression results in *Table 5,* the influence mechanism of each factor is analyzed as follows:

(1) Although Environmental Regulation passed the significance test of 1% level, the regression coefficient was negative, which did not promote the improvement of the GEIWR. Generally speaking, increasing environmental regulation is conducive to the improvement of water resource efficiency. However, the regression results do not support this point. The main reason may be that the current government waste water control system is not perfect and the implementation effect is not satisfactory. The government should consider improving the waste water control system to better play the role of policy guidance.

(2) Technological Progress plays a role in promoting the GEIWR to some extent, but do not passed the significance test of 1% level. The positive impact is general.

(3) Regional Characteristic is significant at the 1% level, which shows that regional differences have a very significant impact on the GEIWR (Chen et al., 2016). However,

http://www.aloki.hu ● ISSN 1589 1623 (Print) ● ISSN 1785 0037 (Online)
DOI: http://dx.doi.org/10.15666/aeer/1802_30573072

the coefficient is negative, probably because the Inner Mongolia, Qinghai in the western region and other regions, despite the lack of water resource and the low level of economic development, have a higher proportion of water resource per capita, a more reasonable industrial structure and a better utilization and allocation of industrial water resource. Meanwhile, some provinces in the central region are constantly developing heavy industry, and problems such as high investment in water resource and high pollution arise. The GEIWR of these provinces is often low.

(4) The increase of the industrial structure proportion has a significant positive effect on promoting the GEIWR. The coefficient of the regression model is positive and significant at the level of 1%. The greater the industrial structure proportion, the greater the investment in the treatment of industrial water pollution, and the higher the GEIWR.

(5) The improvement of Foreign Capital Utilization has a positive impact on the GEIWR, and has passed the significance test at the 1% level.

(6) Although the Industrial Water resource Consumption passes the significance test of 1% level, its regression coefficient is negative, indicating that the increase of industrial water consumption does not promote the GEIWR. This is consistent with the fact that in the actual industrial development, the greater the industrial water consumption, the greater the cost of water resource paid by the industrial development. Therefore, effectively reducing industrial water resource consumption is an important way to improve the GEIWR.

Conclusions, suggestions and discussion

Conclusions and suggestions

In this paper, EBM model was used to objectively analyze and explore the development trend of the GEIWR in 30 provinces from 2004 to 2016, and it was found that the efficiency was differentiated in both time and space. From the perspective of time, the GEIWR in different regions showed different development trends during the period. Thereinto, the GEIWR in Beijing, Tianjin, Shanghai, Guangdong and other regions has maintained a stable and effective state, while efficiency in Yunnan, Sichuan and other regions has been low year by year, so there is a certain space to tap their water-saving potential. From the perspective of space, China's GEIWR has the problem of "central collapse", and the eastern region's efficiency is generally higher than the other regions'. This proves that the developed social services and industrialization level in the eastern region provide certain support for its higher efficiency. The overall low GEIWR in the central region is due to the continuous development of heavy industry in the central region since the implementation of the "rise of the central region" strategy in 2003. Along with the rapid economic growth, problems such as high investment in water resource and high pollution have also emerged. The green development of industrial water resource in the central region is worthy of attention. From the impact mechanism analysis results, increasing the proportion of industrial industry and expanding the utilization of foreign capital are acting the important role in promoting the GEIWR. However, the government's efforts in waste water control and the increase of industrial water consumption have significantly inhibited the improvement of efficiency. Technological progress, although there is a positive effect, the promoting impact is not obvious. Based on the above conclusions, on the premise of ensuring the gradual improvement of the GEIWR and realizing the coordination of economy, society and environment, we put forward the following two suggestions.

http://www.aloki.hu ● ISSN 1589 1623 (Print) ● ISSN 1785 0037 (Online)
DOI: http://dx.doi.org/10.15666/aeer/1802_30573072

(1) In view of the regional differences in China's GEIWR, each province should not cut at one stroke in dealing with problems, give full play to their regional characteristics, launch industrial water use strategy and water pollution prevention and control countermeasures in line with their own needs, so as to effectively improve the GEIWR. On the premise of ensuring the maximization of economic output and the minimization of environmental pollution, for provinces where the green efficiency of water resource has reached DEA efficiency, such as Beijing and Shanghai, the existing achievements should be consolidated, the steady economic and social development should be promoted, and the frontier level of GEIWR should be maintained. For provinces where the green efficiency of water resource is in the middle level, such as Jilin, Fujian and other regions should further improve the quality of economic growth, strengthen the guidance for the development of high-tech industries, limit the development of pollution-intensive industries, effectively reduce the intensity of industrial water, and improve the comprehensive service capacity of society on the basis of the achieved level. Provinces with low efficiency, such as Guangxi, Sichuan and other places should vigorously develop the economy, improve water management consciousness and ability, prefect the system of local government environmental regulation, develop water-saving potential on the basis of economic prosperity and development, emphasizes the synchronous development of the society to promote its positive role in GEIWR.

(2) In order to shorten the gap in the GEIWR among China's provinces, each province should break the regional blockade, avoid protectionism, increase the communication and cooperation in the field of industrial water-saving and water pollution prevention and control, optimize the industrial economic development pattern, and promote the coordinated development of all provinces.

Discussion

The study on the GEIWR is a complex and valuable subject with broad prospects. Indeed, regions with effective GEIWR are not completely devoid of water-saving space, and their water-saving potential still needs to be further explored. Moreover, there are many potential con-founders that could cause one region to be more efficient than another, including social factors, population health factors, environmental factors, and other economic factors. These factors may impact the GEIWR, and this issue warrants further investigation. Therefore, in terms of research methods, further research on EBM model and measurement ideas of water-saving potential can be carried out in the future to innovate research methods. In terms of research content, we can further enrich the content of the indicator system, such as exploring the impact on the GEIWR from the aspects of water resource price and tax.

Acknowledgments. This paper is supported by Jiangxi Humanities and Social Sciences Research Project (TJ161002), The Scientific Research Project of Jiangxi University of Finance and Economics (xskt18475), Student project of "The Marxist Youth Training Project" of Jiangxi University of Finance and Economics in 2019 (2019102509183036).

Conflict of interests. The authors declare no conflict of interests.

http://www.aloki.hu ● ISSN 1589 1623 (Print) ● ISSN 1785 0037 (Online)
DOI: http://dx.doi.org/10.15666/aeer/1802_30573072

REFERENCES

[1] Brundtland, G. H. (ed.) (1987): World Commission on Environment and Development (WCED). Our Common Future. – Oxford University Press, Oxford, UK.
[2] Chemark, F., Boussemart, J. P., Jacquet, F. (2009): Farming system performance and water use efficiency in the Tunisian semi-arid region: data envelopment analysis approach. – International Trans-actions in Operational Research 17(3): 381-396.
[3] Chen, C., Han, J., Fan, P. (2016): Measuring the level of industrial green development and exploring its influencing factors: empirical evidence from China's 30 provinces. – Sustainability 8(2): 153-154.
[4] Chen, W., Du, J., Chang, J. J. (2018): Utilization efficiency of water resource in Wuhan urban agglomeration. – Resource and Environment in the Yangtze Basin 27(06): 1251-1258.
[5] China Environmental Statistics Annual Report (2016). – http://www.jxepb.gov.cn/resource/uploadfile/file/20171227/20171227163909118.pdf.
[6] Ding, X. H., He, J. H., Wang, L. Y. (2018): Inter-provincial water resource utilization efficiency and its influencing factors considering undesirable outputs: based on SE-SBM and Tobit model. – China Population resource and Environment 28(1): 157-164.
[7] Hoekstra, A. Y., Chapagain, A. K., Mekonnen, M. M., Aldaya, M. M. (2011): The Water Footprint Assessment Manual: Setting the Global Standard. – Earthscan, London.
[8] Hu, J. L., Wang, S. C., Yeh, F. Y. (2006): Total-factor water efficiency of region in China. – Resource Policy 31: 217-230.
[9] Huang, S. L., Du, C., Li, W. Q., et al. (2013): Research on the theory and method of industrial water footprint. – Ecological Economy 1: 28-31.
[10] Li, J., Ma, X. C. (2014): The utilization efficiency of industrial water under the dual constraints of resource and environment—an empirical study based on SBM-Undesirable and Meta-frontier model. – Journal of Natural Resource 29(6): 920-933.
[11] Li, K. (2017): Research on Industrial Water Use Efficiency and its Influencing Factors in Anhui. – Hefei University of Technology, Hefei.
[12] Liu, Y., Du, J., Zhang, J. B. (2007): Estimation on utilization efficiency of agricultural water resource in Hubei Province. – China Population Resource and Environment 17(6): 60-65.
[13] Ma, H. L., Huang, D. C., Zhang, J. G. (2012): Water resource utility efficiency and its influencing factors considering undesirable goods. – China Population Resource and Environment 22(10): 35-42.
[14] Mai, Y. Z., Sun, F. L., Shi, L., et al. (2014): Evaluation of China's industrial water efficiency based on DEA model. – Journal of Arid Land Resource and Environment 28(11): 42-47.
[15] Qian, W. J., He, C. F. (2011): China's regional difference of water resource use efficiency and influencing factors. – China Population Resource and Environment 21(2): 54-60.
[16] Shan, H. J. (2008): Re-estimating the capital stock of China: 1952-2006. – The Journal of Quantitative & Technical Economics 10: 17-31.
[17] Sun, C. Z., Jiang, K., Zhao, L. S. (2017): Measurement of green efficiency of water utilization and its spatial pattern in China. – Journal of Natural Resource 32(12): 1999-2011.
[18] Sun, C. Z., Ma, Q. F., Zhao, L. S. (2018): Temporal and spatial evolution of green efficiency of water resource in China and its convergence analysis. – Progress in Geography 37(7): 901-911.
[19] Tone, K., Tsutsui, M. (2010): An epsilon-based measure of efficiency in DEA—a third pole of technical efficiency. – European Journal of Operational Research 207: 1554-1563.
[20] Wang, Y. S. (2015): Water use efficiency and related pollutants' abatement costs of regional industrial systems in China: a slack-based measure approach. – Journal of Cleaner Production 101: 301-310.

http://www.aloki.hu ● ISSN 1589 1623 (Print) ● ISSN 1785 0037 (Online)
DOI: http://dx.doi.org/10.15666/aeer/1802_30573072

[21] You, S. Q. (2017): Research on Green Total Factor Efficiency of Water Resource in China. – Harbin Institute of Technology, Harbin.
[22] Zhang, F., Song, X. N., Xue, H. F., et al. (2018): A spatial convergence effect analysis of China's industrial water use efficiency. – Journal of Capital University of Economics and Business 20(3): 50-60.
[23] Zhang, N., Li, C. H., Yang, Z. F., et al. (2017): Water resource assessment of Hebei Province by grey water footprint. – Journal of Beijing Normal University (Natural Science) 53(1): 75-79.
[24] Zhang, W., Liu, Y. (2018): Evaluation on utilization efficiency of green water resource in the Yangtze River Economic Zone: based on EBM model. – East China Economic Management 32(3): 67-73.

http://www.aloki.hu ● ISSN 1589 1623 (Print) ● ISSN 1785 0037 (Online)
DOI: http://dx.doi.org/10.15666/aeer/1802_30573072

IMPACT OF THE INVASIVE PLANT *ALTERNANTHERA PHILOXEROIDES* (MART.) GRISEB ON SOIL MESO- AND MICROFAUNAL COMMUNITY

ZHANG, Z.[1,2*] – LIU, J.[1] – WANG, L.-C.[1] – WANG, Y.[1] – DENG, L.-L.[1]

[1]*College of Resources and Environment, Anhui Agricultural University, Hefei 230036, Anhui, China*

[2]*Hefei Scientific Observing and Experimental Station of Agro-Environment, Ministry of Agriculture, P. R. China, Hefei 230036, China*

**Corresponding author*
e-mail: xjzhangzhen@163.com

(Received 2nd Aug 2019; accepted 21st Jan 2020)

Abstract. *Alternanthera philoxeroides* (Mart.) Griseb *i*s a plant species which has become one of the most damaging weeds in ecosystems. We examined potential effects of the invasive plant *A. philoxeroides* on soil animal community by considering four levels of plant invasion (including non-invaded, slightly invaded, moderately invaded and heavily invaded ecosystems) in Nanfeihe, Hefei, China. The following conclusions: A total of 2406 individuals of soil animals, belonging to 25 families, 13 orders and 7 classes, and Acarina and Collembola accounted for 64.52% of the total amount of soil animals captured, thus comprising the dominant species; Individual number of soil animals varied with different rate of invasion; the diversity and evenness indices of the soil fauna showed a pattern of non-invaded < heavily invaded < moderately invaded < slightly invaded, however, there were no significant differences between the moderately and slightly invaded plots. The vertical distribution of the species number and individual number of soil fauna had obvious surface segregation with the increased soil depth; The degree of invasion affects the soil physicochemical properties, and the total potassium content is significantly correlated with the number of soil fauna groups.
Keywords: *biological invasion, exotic plant invasion, Alternanthera philoxeroides, soil meso- and macrofaunal, community diversity, Nanfeihe*

Introduction

Biological invasion is a worldwide ecological phenomenon. Invasive species breed, reproduce, spread and form a stable population. Among them, exotic plant invasion, as an important group of invasive organisms, has seriously affected the biodiversity of the invaded land and the quality of the ecological environment, threatening the global ecological environment and economic development and have aroused worldwide concern, becoming one of the hot spots in global change research (Hui et al.2017).

In recent years, with the continuous increase in our understanding of soil ecosystem processes, research has focused on the impact of invasive plants on soil physicochemical properties, soil biodiversity and ecosystem processes, while soil fauna under the effect of invasive mechanisms has not been researched to such an extent (Yu et al., 2012; Pablo et al., 2014; Fernández et al., 2015; Nicola et al., 2015). Most studies have shown that the invasion of plants will increase the species and number of soil animals. Belnap et al. (2001) compared the numbers of invertebrates in early Brome intrusions and native Bromegrass in Utah, and found that species diversity and abundance were significantly reduced. Soil fauna, an important component of the soil ecosystem, can influence the soil environment through physical and chemical activities. Physical activities include plant

http://www.aloki.hu ● ISSN 1589 1623 (Print) ● ISSN 1785 0037 (Online)
DOI: http://dx.doi.org/10.15666/aeer/1802_30733085

debris crushing and decomposition, loosening and mixing of soil; The chemical activities include changing soil texture, crumb structure, aeration, water permeability and other physical properties, and influencing the soil pH, organic matter, carbon and nitrogen content and other chemical elements (Yin, 2000). Soil fauna play an important role in plant community succession and soil nutrient cycling (Shao et al., 2015) and some soil animals can also be used to monitor environmental pollution as indicator organisms (Xiang et al., 2007). The spatial distribution and community diversity of soil fauna are of great significance in assessing ecological health, and are important targets in the study of soil ecosystems (Ding et al., 2017)

The exotic plant invasion of *Alternanthera philoxeroides* (Mart.) Griseb, originated from South America, is now widely distributed in the United States, Australia, New Zealand, China and many other countries by virtue of its adaptability, rapid spread and vegetative reproduction (Van et al., 2002). *A. philoxeroides* in China was first introduced as horse feed in the 1930s and is now widely distributed in most parts of China (Zhou et al., 2017). Through investigating the effect of different rates of invasion by *A. philoxeroides* on soil faunal and soil physicochemical properties, this study aimed to improved our knowledge the impact of this invasive plant on the belowground compartment of terrestrial ecosystem. This would provide a theoretical basis to defend against this highly invasive plant.

Materials and methods

Study site

The sampling site was located on the north shore of the Nanfei River in Hefei city, Anhui Province (31.88°N, 117.26°E). The site belongs to a subtropical humid monsoon climate with annual average temperature of 15.8 °C and annual average rainfall of 995.3 mm with average annual sunshine of 1902.0 h (Yao et al., 2014). Along the plain of the river banks, the sampling sites are mainly located near the farmland (*Fig. 1*). According to vegetative ground cover rate (Niu et al., 2007; Chen et al., 2017). we established four rates of invasion by *A. philoxeroides*, that is, non-invaded (O, *A. philoxeroides* number is 0), slightly invaded (S, *A. philoxeroides* accounted for 30% of individuals in each plot), moderately invaded (M, *A. philoxeroides* accounted for 60% of individuals in each plot) and heavily invaded (L, *A. philoxeroides* accounted for > 90% of individuals in each plot).

Sample collection and processing

From July to October 2016, soil samples were collected four times. For each rate of invasion 5 quadrats of 50 cm × 50 cm were randomly selected; each sampling interval was more than 10 m, and the natural environment was basically similar. The aboveground vegetation and litter was removed and soil was collected from 4 depths for each quadrat (0–5, 5–10, 10–15 and 15–20 cm) by soil drilling (with a diameter of 7 cm). Soil samples were placed into labelled ziplock bags before being taken back to the laboratory for analysis. At the same time, soil from the top 0–20 cm in each quadrat was collected and mixed well for analysis of soil physical and chemical properties. Identification of soil animals according to relevant literature (Yin, 1998).

Using the Tullgren method (Yin, 2002), soil animals were extracted in the laboratory using a funnel suspended above a 60 W light with continuous irradiation for at least

http://www.aloki.hu ● ISSN 1589 1623 (Print) ● ISSN 1785 0037 (Online)
DOI: http://dx.doi.org/10.15666/aeer/1802_30733085

24 h; the photopathic instinct of the soil animals makes them move away from the light into beakers containing 75% alcohol that are placed underneath the funnel. The soil animals were collected and classified under the optical microscope, and the number of individuals was recorded.

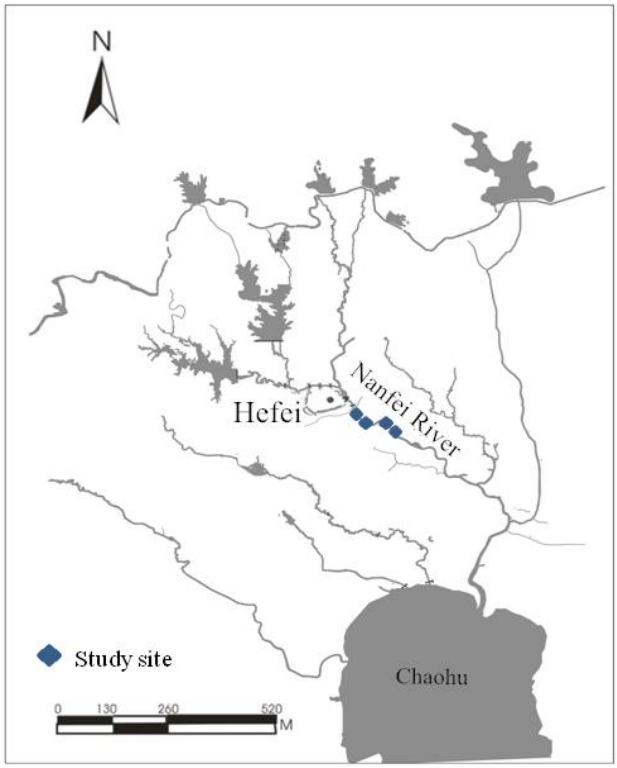

Figure 1. *The sampling site is at Nanfeihe, Hefei, Anhui, China*

Soil samples at depths of 0-5 cm, 5-10 cm, 10-15 cm and 15-20 cm were collected, and roots and stones were removed. Sufficient soil samples were taken by quartering method and air-dried in the room, and then ground through 40-mesh and 100-mesh soil sieves to make soil samples for the analysis of soil physical and chemical properties. Soil organic matter was assessed by potassium dichromate-sulfuric acid oxidation; soil total nitrogen was assessed by the Kjeldahl nitrogen method; soil total phosphorus and available phosphorus was determined by the Mo-Sb colorimetric method; total and available potassium content of soil were determined by flame photometry and soil moisture content measured by conventional drying and weighing method (Bao, 2000).

Data analyses

Diversity indices are usually used to determine the stability of a community or ecosystem; common indices include the Shannon-Wiener diversity index, Pielou's evenness index, Simpson's dominance diversity index and Margalef's richness index. The Shannon-Wiener index is an integrated indicator to measure richness and evenness. The community diversity of soil animals was analysed using the following indices:

$$H' = -\sum_{i=1}^{s} P_i \ln P_i \qquad \text{(Eq.1)}$$

http://www.aloki.hu ● ISSN 1589 1623 (Print) ● ISSN 1785 0037 (Online)
DOI: http://dx.doi.org/10.15666/aeer/1802_30733085

$$E = H' / \ln S \quad \text{(Eq.2)}$$

$$C = \sum (P_i)^2 \quad \text{(Eq.3)}$$

$$D = (S - 1) / \ln N \quad \text{(Eq.4)}$$

where *H'* is the Shannon-Wiener diversity index (*Eq. 1*); *E* is Pielou's evenness index (*Eq. 2*); *C* is the Simpson dominance index (*Eq. 3*); *D* is the Margalef richness index (*Eq. 4*); *S* is the number of species, *N* is the total individual number of soil animals; and *Pi* is the proportion of individuals belonging to species *i* in a sample.

All data were analysed using SPSS for Windows (SPSS, 20.0). Before the analysis, we conducted a diagnostic test of normal distribution and homoscedasticity, and the result is very satisfactory. Statistical analysis was performed by analysis of variance (one-way ANOVA and multiple comparison), and the means were subjected to the Duncan's multiple range test ($p < 0.05$) to obtain the main community differences between the treatments. In addition, to estimate the interaction of soil depth invasion degree among different degree of animal diversity was analyzed by two- way ANOVA analysis. SPSS's correlation analysis was used between soil animals species numbers and soil factors.

Results

Impact of plant invasion on soil physicochemical properties

The contents of soil organic carbon, total nitrogen, available potassium and available phosphorus in the heavily invaded areas were significantly higher than those in other plots (*Table 1*), The contents of available potassium and available phosphorus in the non-invaded area and the moderately invaded area were significantly lower than other treatments ($P < 0.05$), There was no significant difference in total phosphorus content between the four rates of invasion. The total potassium content was higher in the heavily and moderately invaded areas than in the other areas ($P < 0.05$), and there was no significant difference in total potassium content between the slightly invaded and non-invaded areas.

Soil animal composition

From four surveys, 2406 soil micro and meso-fauna were isolated, belonging to 7 classes, 13 orders and 25 families (*Table 2*). Among them, the dominant population (number of individuals accounting for more than 10% of the total number of individuals) consisted of acarina and collembola, accounting for 64.52% of the total amount of soil animals captured; common components of the population (individuals accounting for 1% to 10% of the total individuals) could be classified into nine categories: *Diptera*, *Isopoda, Hymenoptera, Diplura, Psocoptera, nematodes, Haplotaxida, Geophilella* and *Pauropus*, accounting for 32.51% of the total amount of soil animals captured. The rest of the individuals captured were rare populations (individuals accounting for 1% of the total number of individuals), accounting for 2.97% of the total amount of soil animals captured. From slight intrusion area to heavily intrusion area, total individual number of soil animals showed the trend of first increased and then decreased, number of species tends to be stable.

http://www.aloki.hu ● ISSN 1589 1623 (Print) ● ISSN 1785 0037 (Online)
DOI: http://dx.doi.org/10.15666/aeer/1802_30733085

Table 1. *Effects of A. philoxeroides invasion on soil chemical and physical properties*

	Organic matter (g/kg)	Total N (g/kg)	Total P (g/kg)	Total K (g/kg)	Available K (mg/kg)	Moisture content (%)	Available P (mg/kg)
O	6.8 ± 0.67d	0.5 ± 0.03b	0.2 ± 0.04ab	16.7 ± 0.36c	176.0 ± 1.73d	0.26 ± 0.03b	10.9 ± 1.47c
S	19.6 ± 0.64c	1.1 ± 0.11c	0.2 ± 0.02b	16.0 ± 0.10c	188.7 ± 0.58c	0.23 ± 0.01b	18.1 ± 2.23b
M	23.4 ± 0.73b	1.2 ± 0.05b	0.3 ± 0.03a	17.8 ± 0.85b	217.7 ± 7.09b	0.28 ± 0.01b	19.5 ± 1.86ab
L	29.0 ± 0.74a	1.7 ± 0.10a	0.2 ± 0.06ab	19.5 ± 0.44a	300.3 ± 0.58a	0.39 ± 0.06a	22.3 ± 2.76a

Values are mean ± SD. Different letters in the same column indicate that means are significantly different at $P < 0.05$.(a > b > c) O: non-invaded area, S: slight invaded area, M: moderate invaded area, L: heavily invaded area

Table 2. *The richness and abundance of soil fauna in different A. philoxeroides invasion area*

	Non-invaded		Slight invaded		Moderate invaded		Heavily invaded		Total	
	N	%	N	%	N	%	N	%	N	%
Parasiformes										
Ixodidae	159	6.61	132	5.49	204	8.48	183	7.61	678	28.18
Acariformes										
Chigger mites	6	0.25	12	0.5	6	0.25	0	0	24	1
Oribatulidae	78	3.24	72	2.99	111	4.61	102	4.24	363	15.09
Diptera										
Muscidae	24	1	36	1.5	30	1.25	36	1.5	126	5.24
Chironomidae	0	0	0	0	0	0	3	0.12	3	0.12
Collembola										
Isotomidae	39	1.62	78	3.24	105	4.36	87	3.62	309	12.84
Folsomides	0	0	0	0	6	0.25	3	0.12	9	0.37
Entomobrya	18	0.75	30	1.25	48	2	45	1.87	141	5.86
Sminthuridae	6	0.25	6	0.25	9	0.37	0	0	21	0.87
Onychiuridae dinghuensis	6	0.25	12	0.5	15	0.62	3	0.12	36	1.5
Isopoda										
Porcellio	3	0.12	45	1.87	21	0.87	24	1	93	3.87
Hymenoptera										
Aenictus	12	0.5	57	2.37	42	1.75	21	0.87	132	5.49
Coleoptera										
Family Nitidulidae	0	0	0	0	0	0	3	0.12	3	0.12
Staphylinidae	3	0.12	6	0.25	3	0.12	0	0	12	0.5
Corrodentia										
Psocidae	54	0.75	54	0.37	39	1.62	57	2.37	123	5.11
Entotrophi										
Japygidae	0	0	3	0.12	3	0.12	0	0	6	0.25
Thysanoptera										
Thripidae	6	0.25	18	0.75	0	0	0	0	24	1

http://www.aloki.hu ● ISSN 1589 1623 (Print) ● ISSN 1785 0037 (Online)
DOI: http://dx.doi.org/10.15666/aeer/1802_30733085

Plecoptera										
Perlidae larvae	3	0.12	3	0.12	3	0.12	0	0	9	0.37
Hemiptera										
Pentatomidae	0	0	6	0.25	0	0	0	0	6	0.25
Pseudoscorpionida										
Chthonioidea	3	0.12	0	0	0	0	0	0	3	0.12
Strongylida										
Meloidogynidae	0	0	21	0.87	45	1.87	18	0.75	84	3.49
Araneae										
Arachnid	3	0.12	3	0.12	12	0.5	6	0.25	24	1
Others										
Scolopendrellidae	15	0.62	15	0.62	36	1.5	21	0.87	87	3.62
Haplotaxis	0	0	6	0.25	9	0.37	54	2.12	66	2.74
Pauropus	0	0	6	0.25	3	0.12	15	0.62	24	1
Total individuals	402	16.71	576	23.94	750	31.17	678	28.18	2406	
Total species	17		21		21		17		27	

N: the number of individuals, %: representing the percentage of the total number of individuals

Community diversity of soil fauna under different rates of A. philoxeroides invasion

In the different degree of invasion of *Alternanthera philoxeroides*, there are some differences in community structure in soil animal (*Fig. 2*). The Margalef richness index was not significantly different ($p < 0.05$) among the four rates of invasion, but the Simpson dominance index ($p < 0.05$) in the non-invaded area was significantly different from those in the other three areas, and Shannon-Wiener diversity index space significant difference $p < 0.05$) In the non-invaded communities, soil animals are less and the number of species are relatively concentrated; In the *A. philoxeroides* invaded communities, There was no significant difference between the slight intrusion to heavily invasion areas, but the Simpson's dominance diversity index increased with the increase of the invasion degree, indicating *A. philoxeroides* invasion may affect to some extent of soil animal community, and in moderate intrusion conditions most suitable soil animal survival.

Community diversity of soil fauna at different soil depth

In the vertical direction, the number of species and individual density of soil animals showed a tendency of obvious aggregation, decreasing with the increase of soil depth. For all treatments, the number of individuals and species of soil animals was highest in the 0–5 cm soil layer and lowest in the 15–20 cm soil layer, although there was no obvious trend in the 5–15 cm soil layer (*Fig. 3*).

The Shannon-Wiener diversity index and Pielou's evenness index showed no significant difference with depth (*Fig. 4*), although they increased with increasing soil depth. The Simpson index was significantly different in the 15–20 cm soil layer when compared with the other soil layers ($P < 0.05$), but the Shannon-Wiener and Margalef indices were the lowest at this depth, indicating that as the soil depth increased, species

http://www.aloki.hu ● ISSN 1589 1623 (Print) ● ISSN 1785 0037 (Online)
DOI: http://dx.doi.org/10.15666/aeer/1802_30733085

diversity decreased, but there were some dominant species that adapted to the deep soil environment and were uniformly distributed.

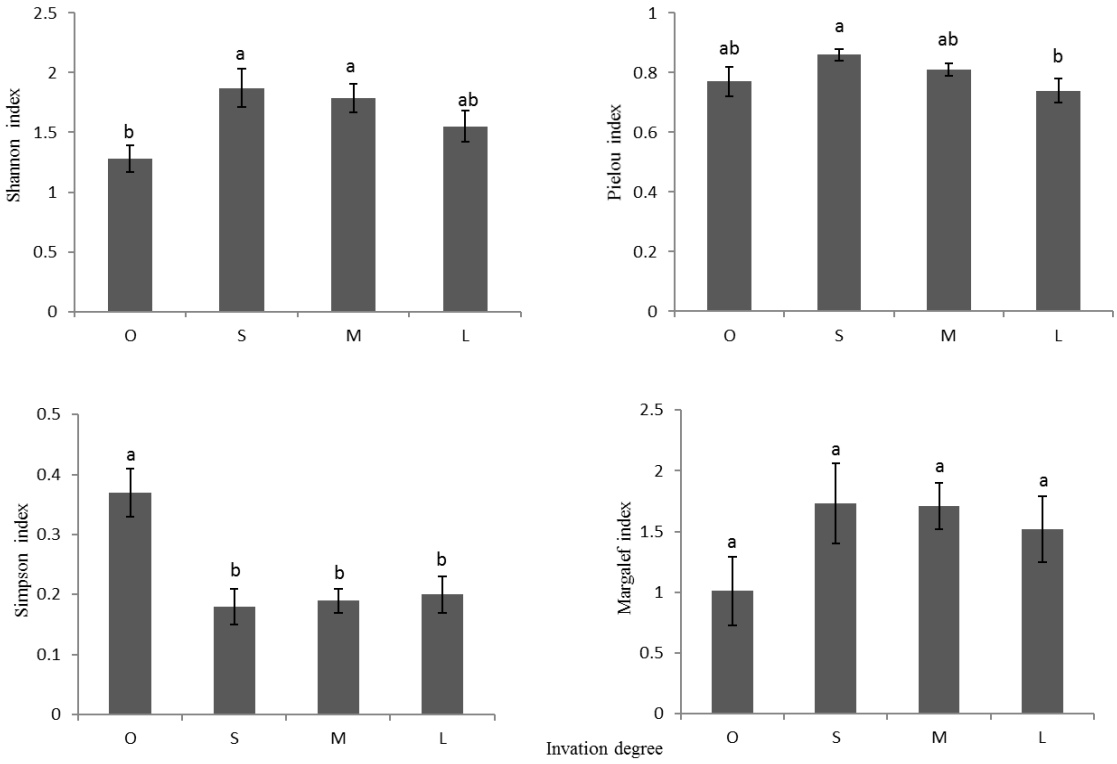

Figure 2. *Diversities of soil fauna community in in different A. philoxeroides invasion area (mean ± SE). (Different letters indicate that means are significantly different at $P < 0.05$ with $a > b > c$; O: non-invaded area, S: slight invaded area M: moderate invaded area, L: heavily invaded area)*

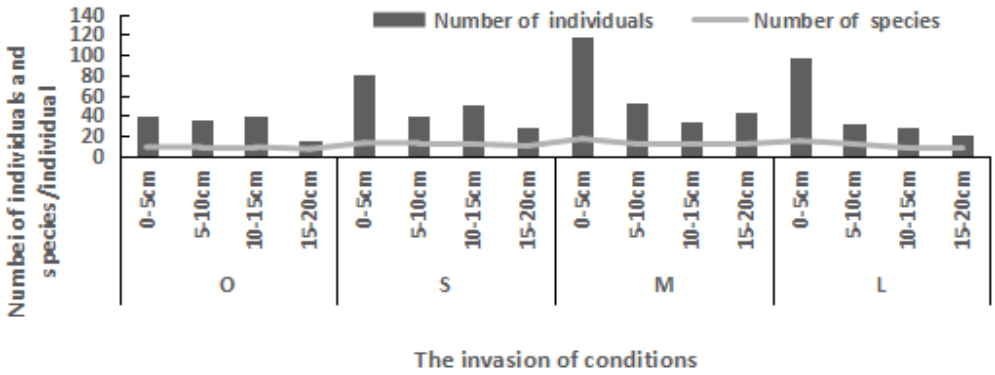

Figure 3. *Vertical distribution of the group number and individual number of soil fauna in different invasion area*

Different invasion degree and soil depth on soil animals community structure parameters

The two-way analysis of variance of invasion and depth and community showed that the degree of invasion has significant influence on community diversity ($P < 0.05$). Soil

http://www.aloki.hu ● ISSN 1589 1623 (Print) ● ISSN 1785 0037 (Online)
DOI: http://dx.doi.org/10.15666/aeer/1802_30733085

depth of different degree of invasion has significant effects on community diversity ($P < 0.01$), and significant impact on the community dominance index and evenness. he distribution of soil animals was affected by the rate of invasion and soil depth but no significant effect of the two factor interactions on the four community structure indices (*Table 3*). And the rate of invasion and soil depth were respectively affecting four indicators of diversity rather than a common effect.

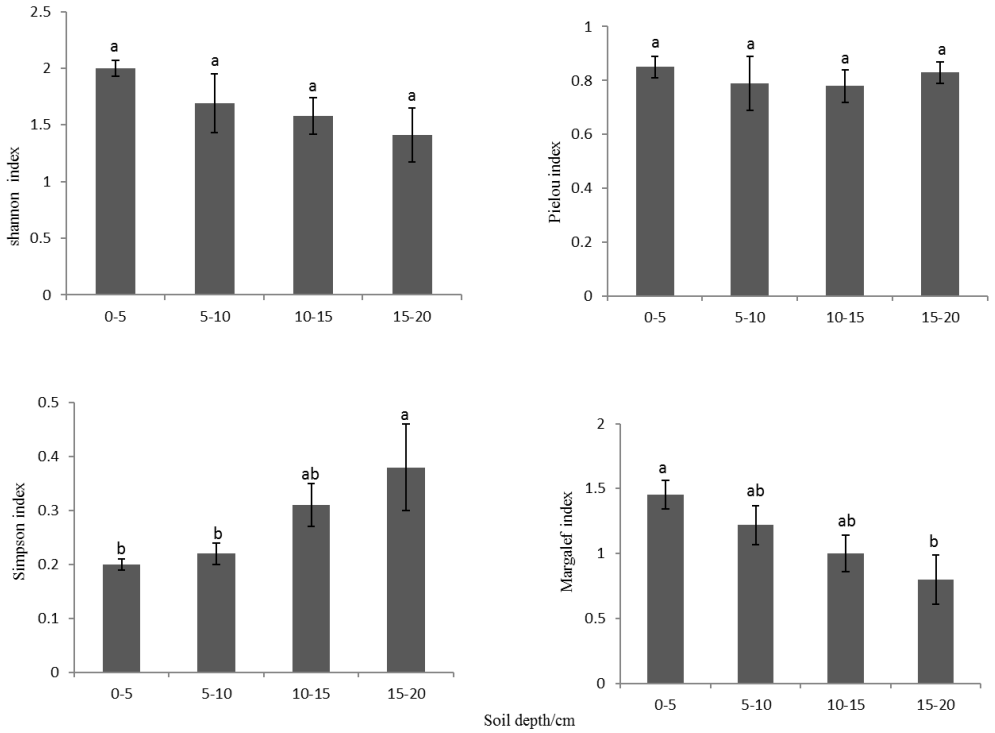

Figure 4. *Diversities of soil fauna community in different soil depth (mean ± SE). (Different letters indicate that means are significantly different at $P < 0.05$ with a > b > c)*

Table 3. *F-values of a two-way analysis of variance of soil animals community structure parameters in different invasion area and soil depth*

Variable	DF	Shannon-Wiener	Pielou	Simpson	Margalef
		F	F	F	F
Invasion degree	3	0.963*	2.657	0.321	0.617
Depth	3	5.214**	1.629	13.187*	24.294*
Invasion * depth	9	0.366	0.927	0.68	0.889

*Correlation is significant at the 0.05 level. **Correlation is significant at the 0.01 level

The relationship between soil physicochemical properties and soil animals in A. philoxeroides invaded areas

The correlation of soil animals species and soil physical and chemical properties under different rates of invasion is shown in *Table 4*. Except for the non-invasive area (O area), the number of soil animal species in the invaded area (S, M, L) was significantly negatively correlated with total potassium indicating that the distribution

http://www.aloki.hu ● ISSN 1589 1623 (Print) ● ISSN 1785 0037 (Online)
DOI: http://dx.doi.org/10.15666/aeer/1802_30733085

of soil animals was greatly influenced by total potassium content. The number of species in the slightly invaded area (S) was significantly correlated with total phosphorus ($P < 0.01$), but this relationship was not observed in other treatments (*Table 4*). The total potassium content increased significantly from the non-invaded area to the severely invaded area ($P < 0.05$). When comparing the numbers of individuals and species of soil animals in different invaded areas (*Fig. 3*), it was found that for both moderately and severely invaded areas, the numbers of soil fauna individuals and species were closely aligned with the total potassium distribution, further indicating that the distribution of soil animals might be affected by the total potassium content.

Table 4. *Correlations between soil animals species numbers and soil factors*

	Organic matter	Total N	Total P	Total K	Available P	Available K
O	0.11	0.30	0.17	-0.22	-0.31	0.22
S	0.05	0.32	0.71**	-0.43*	-0.24	0.02
M	0.34	0.30	0.48	-0.56*	-0.28	0.23
L	0.44	0.61	0.37	-0.11*	-0.41	0.42

**P < 0.01; *P < 0.05

Discussion

Effect of A. philoxeroides on the soil faunal community

The present study showed that with the increasing rate of invasion, the total number of individuals and groups of soil meso-and microfauna increased first and then decreased, and the number of individuals and species in some soil animals increased (*Table 2*). These results are consistent with those of several other studies: Gremmen (1998) found that communities dominated by exotic plants the grass *Agrostis stolonifera* have more soil invertebrates and mites at sub-Antarctic Marion Island; Kourtev (2002) found that the number of earthworms in invaded areas was significantly increased when compared with native plant communities; Quan et al. (2011) found that *Mikania micrantha* invasion significantly increased the number of soil nematodes and Acarina individuals, community density and the number of groups in the Huolushan Forest Park of Guangzhou, China; Xie et al. (2011) through found that ragweed invasion significantly increased the density of the community–group numbers of soil fauna, Simpson index and Margalef index by the field plot test method in the suburb of Lishi Town, Shaoguan City, Guangdong Province. These results showed the same results about that invasion by exotic plants can increase the biomass or diversity of soil animals.

A. philoxeroides is an amphibious herbaceous plant with strong adaptive and reproductive ability. Chang et al. (2013) research showed that it can quickly form a carpet cover distribution in the invaded area and change the local microclimate environment and soil physical and chemical properties. With the increasing rate of invasion, the soil water content increased and the environmental conditions were more conducive to hygrocoles such as *Nematodes, Mites* and *Collembola*. Soil animals feed on plant humus, radicle and caulicle, Alkemade et al. (2015) showed that after *Spartina anglica* invasion of the European coastal wetland, because of its high net primary productivity, the decomposition of a large number of aging stems provided additional resources into the detritus food web, leading to an increase in the number of soil invertebrates. The development of *A. philoxeroides* roots and stems can provide an

http://www.aloki.hu ● ISSN 1589 1623 (Print) ● ISSN 1785 0037 (Online)
DOI: http://dx.doi.org/10.15666/aeer/1802_30733085

abundant food source for soil animals (Pan et al., 2007). In our study, with the increasing rate of invasion by *A. philoxeroides*, the number of hygrophilous *Acarina* and *Collembola* drastically increased, and the biomass of the moderately invaded area was the highest, with slightly less biomass in the severely invaded area (*Table 2*). It could be due to the high vegetation coverage, environmental conditions are changed, such as increased humidity and poor ventilation, thus resulting in the disappearance of *Thysanoptera, Plecopterodae, Hymenoptera, Hemiptera* and other stomatal breathing soil animals, and a significant increase in the number of hygrophilous animals like *Earthworms*. Siersma et al. (2007) also suggested that invasive plant covers may lead to the changes of soil animals' number, but more research is also necessary to support the major claims of this study.

Effect of A. philoxeroides invasion on soil fauna diversity indices

It can be found in the study: with increasing rate of invasion, the Shannon-Wiener, Pielou and Margalef indices decreased, while the Simpson index increased, indicating that although invasion increased the biomass of small and medium-sized soil animals, the diversity, in terms of the number of groups, decreased, indicating that the increase in abundance of soil fauna was concentrated within a small number of groups, such as *Parasiforme, Acariformes* and *Collembola* (*Table 2*).

Many studies have shown that the density of soil animals decreases with depth, with the majority of soil fauna distributing in the top 0–5 cm and significant reductions in number and diversity in deeper soil (*Fig. 3*), for example, Chen and Aoki (1998) surveyed the distribution of soil mites in different soil layers in Changchun and found that the amount and type of mites in the soil layer vertical structure was sharply reduced with increasing soil depth, plummeted with the result what Aoki survey mites distribution in the soil layers (0–5) cm highest plummeted down) coincide. Yin et al. (2003a) studied the diversity of soil fauna in the Lesser Khingan forest and found that diversity in vertical direction of soil animals decreased with soil depth and that the surface aggregation of soil meso-and micro arthropods was more obvious than that of large soil animals. Similar results were found in our study, where the vertical distribution of soil fauna in both invaded and non-invaded areas was highest in the 0–5 cm soil layer and decreased with increasing soil depth (*Fig. 3*).

Effects of soil physicochemical properties on the distribution of soil fauna

There is a close relationship between soil animals and soil environmental factors. Some studies have shown that the soil environmental factors have little effect on the animal groups, just concerning with the number of individual soil animals (Kourtev et al., 1999; Yin et al., 2003b). But in our studies found that *A. philoxeroides* invasion influencing the soil physico-chemical properties, with increasing rate of invasion, soil organic carbon, total nitrogen, available phosphorus, available potassium and total potassium contents increased, there was a significant negative correlation between soil total potassium and the number of soil animal groups ($P < 0.05$), with the increase of total potassium in soil, the soil fauna decreased, it indicated that the regulation of soil potassium content may change the diversity of soil animal communities. Similar results have been found in invasive plants such as *Ambrosia artemisiifolia, Solidago canadensis* and *Ageratina adenophora* (Cruz-Ortega et al., 1998; Tan et al., 2002; Zhang, et al., 2009).

http://www.aloki.hu ● ISSN 1589 1623 (Print) ● ISSN 1785 0037 (Online)
DOI: http://dx.doi.org/10.15666/aeer/1802_30733085

Conclusion

In summary, changes in the soil faunal diversity indices with different rates of invasion and soil depth showed that *A. philoxeroides* invasion affects the species and quantity distribution of small and medium-sized soil animals. Among the communities invaded by *A. philoxeroides*, the *Acarina* and the *Collembola* were dominant members of the population. Soil animals communities were mainly distributed in the topsoil with high vegetation coverage rate and rich humus and litter, presenting a decreasing trend in abundance in the vertical direction under the common constraints of multiple environmental factors and climate conditions. In the future, comprehensive research on soil animals in *A. philoxeroides* should be strengthened to improve the invasion mechanism. Provide a theoretical basis for better prevention and control of invasive species.

Acknowledgments. This study was supported by the National Key Research and Development Program (2017YFD0200604); the National Natural Science Foundation of China under grant (31772235,31540051); State Key Laboratory for Biology of Plant Diseases and Insect Pests under grant (SKLOF201605). The experiments reported in this paper comply with the current laws of the People's Republic of China where they were conducted.

Conflict of interests. All of the authors in this paper declare that they have no conflict of interests.

REFERENCES

[1] Alkemade, R., Wielemaker, A., Hemminga, M. A. (2015): Correlation between nematode abundance and decomposition rate of Spartina anglica leaves. – Marine Ecology Progress 99(3): 293-300.

[2] Belnap, J., Phillips, S. L. (2001): Soil biota in an ungrazed grassland: response to annual grass (Bromus tectorum) invasion. – Ecological Applications 11(5): 1261-1275.

[3] Bao, S. D. (2000): Soil Agrochemical Analysis. – China Agriculture Press, Beijing.

[4] Chang, R. Y., Wang, R. Q., Zhang, Y. R., Liu, J. (2013): Invasion mechanism and integrated management of invasive plant *Alternanthera philoxeroides*. – Journal of Ecology and Rural Environment 29(1): 17-23.

[5] Chen, P. G., Aoki, J. (1998): Investigation on soil acarid in Jingyuetan area Changchun. – Acta Zoologica Sinica 34(3): 282-293.

[6] Chen, X. L., Zhang, L. N., Wang, J. H., et al. (2017): Effect of invasive degree of *Rhynchelytm repens* on microorganisms in rhizosphere soil. – Natural Science Edition 45(4): 165-172.

[7] Cruz-Ortega, R., Anaya, A. L., Hernández-Bautista, B. E., Laguna-Hernández, G. (1998): Effects of allelochemical stress produced by Sicyos deppei, on seedling root ultrastructure of Phaseolus vulgaris, and Cucurbita ficifolia. – Journal of Chemical Ecology 24(12): 2039-2057.

[8] Ding, X., Zhang, Y., Zhu, Y. H., et al. (2017): Advances in spatial distribution and influencing factors of soil animal population. – Hunan Agricultural Sciences 1: 119-122.

[9] Fernández, F. M., Gómez, R. M. X., González, P. S. J. (2015): Effects of fire and three fire-fighting chemicals on main soil properties, plant nutrient content and vegetation growth and cover after 10 years. – Science of the Total Environment 515–516: 92-100.

http://www.aloki.hu ● ISSN 1589 1623 (Print) ● ISSN 1785 0037 (Online)
DOI: http://dx.doi.org/10.15666/aeer/1802_30733085

[10] Gremmen, N., Chown, S. L., Marshall D. J. (1998): Impact of the introduced grass *Agrostis stolonifera* on vegetation and soil fauna communities at Marion Island, sub-Antarctic. – Biological Conservation 85(3): 223-231.
[11] Guo, H., Mazer, S. J., Xu, X., Luo, X., Huang, K., Xu, X. (2017): Biological Invasions in Nature Reserves in China. – In: Wan, F., Jiang, M., Zhan, A. (eds.) Invading Nature. Springer Series in Invasion Ecology. Springer, Dordrecht.
[12] Kourtev, P. S., Huang, W. Z., Ehrenfeld, J. G. (1999): Differences in earthworm densities and nitrogen dynamics in soils under exotic and native plant species. – Biological Invasions 1: 237-245.
[13] Kourtev, P. S., Ehrenfeld, J. G., Haggblom, M. (2002): Exotic plant species alter the microbial community structure and function in the soil. – Ecology 83(11): 3152-3166.
[14] Nicola, J. D., Pedro, M. A., Kari, E. D. (2015): Changes in *arbuscular mycorrhizal* fungal communities during invasion by an exotic invasive plant. – Acta Oecologica 67: 66-74.
[15] Niu, H. B., Liu, W. X., Wan, F. H. (2007): Invasive effect of *Ageratina adenophora Sprengel* (Asteraceae) on soil microbial community and physical and chemical properties. – Acta Ecology Sinica 27(7): 3051-3060.
[16] Pablo, S. A., Ana, N., Luís, G. (2014): Soil biochemical alterations and microbial community responses under Acacia dealbata Link invasion. – Soil Biology & Biochemistry 79: 100-108.
[17] Pan, X. Y., Geng, Y. P., Sosa, A. (2007): Invasive alternanthera philoxeroides: biology, ecology and management. – Acta Phytotaxonomica Sinica 45(6): 884-900.
[18] Quan, G. M., Liu, W. X., Xie, J. F., et al. (2011): Impact of Mikania micrantha invasion on soil meso- and micro-invertebrate community structure. – Chinese Journal of Applied Ecology 22(7): 1863-1870.
[19] Shao, Y. H., Zhang, W. X., Liu, S. J. (2015): Diversity and function of soil fauna – Acta Ecologica Sinica 35(20): 6614-6625.
[20] Siersma, H., Johnson, W., Mckeon, V. (2007): The effect of invasive plant species on invertebrate biodiversity in Great Lakes coastal wetlands. – ResearchGate 8: 15.
[21] Tan, W. Z., Li, Q. J., Qing, L. (2002): Biological control of alligator weed (*Alternanthera philoxeroides*) with a Fusarium sp. – Biocontrol (Dordrecht) 47(4): 463-479.
[22] Van Driesche, R., Blossey, B., Reardon, R. (2002): Biological Control of Invasive Plants in the Eastern United States. – Forest Health Technology Enterprise Team, USDA Forest Service, Morgantown.
[23] Xiang, C. G., Yang, S. J., Nie, Q. (2007): The biological indication of soil animals to soil. – Environment Chinese Agricultural Science Bulletin 23(04): 364-367.
[24] Xie, J. F., Quan, G. M., et al. (2011): Impacts of Ambrosia artemisia folia invasion on community structure of soil meso-and micro-fauna. – Acta Ecologica Sinica 31(19): 5682-5690.
[25] Yao, X. Y., Wei-Tao, L. I., Zheng, Y. L. (2014): Effect of community composition and species interactions on the invasion of alien plants. – Chinese Journal of Ecology 33(7): 1953-1959.
[26] Yin, W. Y. (1998): Chinese Soil Animal Search Illustrations. – Science Press, Beijing.
[27] Yin, W. Y. (2000): Soil animal of China. – Science Press, Beijing.
[28] Yin, X. Q., Ma, Z. Y. (2002): Efficiency of Tullgren method to middle-small-sized soil animal. – Journal of Northeast Normal University 34: 84-91.
[29] Yin, X. Q., Wu, D. H., Han, X. M. (2003a): Diversity of soil animals community in Xiao Hinggan Mountains. – Scientia Geographica Sinica 23(03): 316-322.
[30] Yin, X. Q., Wang, H. X., Zhou, D. W. (2003b): Characteristics of soil animals' communities in different agricultural ecosystem in the Songnen Grassland of China. – Acta Ecology Sinica 23(6): 1071-1078.

http://www.aloki.hu ● ISSN 1589 1623 (Print) ● ISSN 1785 0037 (Online)
DOI: http://dx.doi.org/10.15666/aeer/1802_30733085

[31] Yu, W. Q., Liu, W. X., Gui, F. R., et al. (2012): Invasion of exotic Ageratina adenophora Sprengel alters soil physical and chemical characteristics and arbuscular mycorrhizal fungus community. – Acta Ecologica Sinica 32(22): 114-122.
[32] Zhang, Z., Xu, L., Ma, Y. T., Li, J. (2009): Allelopathic effect of water extracts from the different organizations of *Alternanthera philoxeroides* on germination and seedling growth of Lolium perenne. – Acta Botanica Boreali - Occidentalia Sinica 29(1): 148-153.
[33] Zhou, F., Zhang, Z. J., Liu, M., et al. (2017): Effects of nutrient levels on defense against specialist insects in an invasive alligator weed. – Biodiversity Science 25(12): 1276-1284.

http://www.aloki.hu ● ISSN 1589 1623 (Print) ● ISSN 1785 0037 (Online)
DOI: http://dx.doi.org/10.15666/aeer/1802_30733085

EFFECTS OF MODIFYING SOIL MICROBES ON RESTORING VEGETATION DEGRADED BY AN INVASIVE PLANT CROFTON WEED (*AGERATINA ADENOPHORA*)

CHEN, L.[1,2,3] – SHI, Y. T.[1,3] – ZHANG, H. B.[1,2,3*]

[1]*State Key Laboratory for Conservation and Utilization of Bio-Resources in Yunnan, Yunnan University, Kunming 650091, China*

[2]*School of Ecology and Environmental Science, Yunnan University, Kunming 650091, China*

[3]*School of Life Sciences, Yunnan University, Kunming 650091, China*

**Corresponding author*
e-mail: zhhb@ynu.edu.cn; phone: +86-871-6503-4282

(Received 22nd Aug 2019; accepted 25th Nov 2019)

Abstract. Invasive plants commonly change soil microbial communities in their introduced range, promoting their own growth while inhibiting the growth of native species. This effect can persist even after invasive plants are removed, thereby hindering restoration of disturbed ecosystems. Our aim was to explore how modifying the altered soil microbe community affected the restoration of an area degraded by *Ageratina adenophora* (Crofton weed), one of the most notorious invasive plants in China. A three-year experiment was performed in the wild. After the removal of *A. adenophora*, the three antimicrobial drugs Chlorothalonil (BJQ), Carbendazim (DJL), and Streptomycin (LMS) were applied to inhibit the activity of soil microbes. The reestablishment of *A. adenophora* and recovery of other plant species were investigated, and soil characteristics were evaluated. All three drugs significantly decreased the total biomass of reestablished *A. adenophora*: relative to the control, BJQ decreased *A. adenophora* biomass by 46.73%, DJL by 70.69%, and LMS by 96.95%. Further, DJL and LMS significantly increased plant community diversity, as well as the biomass of other plant species. Drug treatment also significantly changed soil fertility and decreased soil enzyme activity. Our data indicated that inhibiting the activity of soil microbes is beneficial for both eradication and replacement of *A. adenophora*.
Keywords: *plant community, antimicrobial drugs, interruption, environmental degradation, recovering, exotic species*

Introduction

Invasive plants commonly change soil microbial communities in the introduced range to promote their own growth and inhibit the growth of native species (Klironomos, 2002; Callaway et al., 2004). To stimulate their own growth, invasive plants alter soil microbes such as mycorrhiza and nitrogen-fixing bacterial symbionts (positive feedbacks) (Richardson et al., 2000). However, invasive plants also inhibit the growth of native species (negative feedbacks) either indirectly by outgrowing and excluding native species in soils that lack soil pathogens in the novel range (i.e. enemy release) (Reinhart et al., 2005; Blumenthal et al., 2009), or directly by inhibiting beneficial microbe species that form mutualistic relationships with native plants (Vogelsang and Bever, 2009; Lankau, 2011). Moreover, some invasive plants can promote microbial species that are pathogenic to native plants in the rhizosphere of the soil (Mangla et al., 2008), referred to as the accumulating local pathogen (ALP) hypothesis (Eppinga et al., 2006).

http://www.aloki.hu ● ISSN 1589 1623 (Print) ● ISSN 1785 0037 (Online)
DOI: http://dx.doi.org/10.15666/aeer/1802_30873100

Restoring an ecosystem degraded by non-native plants is challenging and often unsuccessful, due in part to negative alterations to soil microbial communities that place native plants at a disadvantage (Hamman et al., 2013). This inability of ecosystems to recover from changes to the soil microbial community, referred to as the 'priority effect' (Grman and Suding, 2010) can persist even after non-native plants are removed (Marchante et al., 2009; Elgersma, 2011). Understanding priority effects is therefore essential for restoring degraded ecosystems because many native plants have been found to be especially vulnerable to such modifications (Kardol and Wardle, 2010). Further, eradication of a well-established invasive plant may result in the unexpected release of another, previously suppressed non-native species (Simberloff et al., 2013). For instance, Adler et al. (1998) demonstrated that the eradication of the invasive nitrogen-fixing species *Myrica faya* facilitated the invasion of other fast-growing non-native grasses. Thus, insight into the role of a well-established invasive plant species in an ecosystem is important before eradication is attempted, as risk of invasion by other non-native species can remain high after the removal or reduction in the prevalence of an invader (Simberloff et al., 2013).

Ageratina adenophora (Crofton weed) is one of the most notorious invasive plants in China (Feng and Zhu, 2010; Wang et al., 2011). In the 1940s, Crofton weed began to colonize the Yunnan Province in southwestern China and from there it dispersed north and east at an average rate of 20 km per year (Sang et al., 2010). Although the spread of *A. adenophora* stopped in Yunnan after 1990, it is still rapidly expanding its distribution in neighboring provinces (Wang and Wang, 2006). *Ageratina adenophora* is known to cause acute asthma, diarrhea, depilation, and even death in livestock, as well as cause a decline in crop yields (Wang et al., 2017). The economic losses to animal husbandry and grassland ecosystem services caused by the weed has been estimated at RMB 0.99 billion and 2.63 billion per year, respectively (Wang et al., 2017). Of the multiple mechanisms hypothesized to promote the invasion of *A. adenophora* (Feng et al., 2007, 2009; Wang et al., 2011), changes to soil microbial communities in introduced areas may play an important role in aiding the spread of *A. adenophora* (Yu, 2005). For example, Niu et al. (2007) demonstrated that *A. adenophora* invasion strongly increased both the abundance of soil vesicular-arbuscular mycorrhizal (VAM) fungi and the ratio of fungi to bacteria in soil, and that soil biota in a heavily invaded site had a greater inhibitory effect on native plant species than on *A. adenophora*. *A. adenophora* invasion has also been shown to significantly increase the amount and diversity of nitrogen-fixing bacterial (NFB) in soils (Xu et al., 2012; Zhao et al., 2019). Chen et al. (2019) indicated that this weed can selectively enrich the soil rare bacteria as endophytes in roots.

Currently, mechanical or manual eradication techniques are used to prevent invasion of *A. adenophora*. One study reported that *A. adenophora* was a susceptible plant to herbicide tenuazonic acid (TeA) (Chen et al., 2015), suggesting TeA is a potential chemical control for *A. adenophora* invasion. In some cases, native species are planted following eradication of *A. adenophora* to restore the degraded area (Wang et al., 2008). However, these methods have not been very effective, as *A. adenophora* frequently becomes reestablished after several years of eradication (unpublished data). Such poor restoration efforts may reflect a failure to integrate current ecological knowledge from belowground microbiotas and aboveground vegetation. Although Elliott et al. (2015) reported that microbial community structure is linked to restoration activity, it is unclear if the alteration of the soil microbe community by an invasive plant can affect the

http://www.aloki.hu ● ISSN 1589 1623 (Print) ● ISSN 1785 0037 (Online)
DOI: http://dx.doi.org/10.15666/aeer/1802_30873100

vegetation restoration in the management and control practices. Therefore, our objective was to determine if modifying the soil microbial community with antimicrobial drugs was sufficient to initiate successful reestablishment of native species after *A. adenophora* removal. In addition, we investigated if other soil characteristics, including soil chemistry and soil enzymes, play a role in the recovery of plant communities.

Materials and methods

Site description

The experimental field site, located on Xishan mountain in Kunming, Yunnan, China (24°58′24″N, 102°37′17″E; altitude 2,214 m), has been heavily invaded (>90% cover) by *A. adenophora* for at least 10 years. Climate data in this site were obtained from the WorldClim database using ArcGIS v10.3 (Yahdjian et al., 2011), with an annual mean temperature of 15.4 ℃ and an annual precipitation of 1024 mm. This site has experienced great changes in soil chemistry and in its soil microbial community since *A. adenophora* invasion (Xu et al., 2012), making it an ideal location for exploring soil priority effects on restoration.

Modifications to soil microbe community

Two plots, each 3 m × 3 m, were selected for manual removal of all *A. adenophora* individuals and other plant species. Each plot was subdivided into four 1 m × 1 m blocks, each separated by 20 cm. In June 2009, before the beginning of the rainy season, each block was randomly treated with one of three antimicrobial pesticides (Chlorothalonil (commercial name Baijunqing, BJQ), Carbendazim (commercial name Duojunling, DJL) or Streptomycin (commercial name Lianmeisu, LMS)) to inhibit soil microbes. BJQ is a broad-spectrum pesticide and inhibits both fungal and bacterial communities. DJL is also abroad-spectrum pesticide, but mainly inhibits the fungal community (Shao et al., 2011). LMS is used to treat soil-born bacterial pathogens. DJL, BJQ, and LMS were applied to the blocks at dosages of 31.96 g/m^2, 21.76 g/m^2, and 28 g/m^2, respectively, inhibiting soil microbes at a depth of 20 cm (Shao et al., 2011). Because pesticide activity continuously diminishes in the soil after initial application, an additional three supplemental treatments were applied to the blocks in July, August, and September 2009. Blocks treated with sterilized water were used as control.

Plant harvest and soil collection

At the end of October 2009, 2010, and 2011, all plants ≥ 10 cm in height were identified and counted in 0.2 m × 1 m subplots in each block (*Fig. 1*). Subsequently, each plant was cut down, placed into a paper bag, dried at 60 ℃ for 48 h, and weighed. About one kilogram of soil was collected from the top 10 cm of soil in each subplot and analyzed for chemical composition and enzyme activity.

Soil chemistry and enzyme analysis

At the end of October 2009 and 2010, soil chemistry and enzyme were analyzed. In 2011, we only harvested plant materials for measurement but did not collect soils, therefore missing of the soil properties for the third year. Soil pH, organic matter, and total and available N, P, and K in all soil samples were measured commercially (see

http://www.aloki.hu ● ISSN 1589 1623 (Print) ● ISSN 1785 0037 (Online)
DOI: http://dx.doi.org/10.15666/aeer/1802_30873100

Standard methods for observation and analysis in Chinese ecosystem research network, 1996). Briefly, soil pH was measured by the glass electrode method, after 2.5-fold water extraction. Organic matter was determined using the oil bath-K_2CrO_7 titration method. Total N was assessed by the Kjeldahl method, and available N was determined by the Conway microdiffusion method. Total and available P were measured by Mo–Sb colorimetric analysis. Total and available K were assessed with flame photometry.

Figure 1. *Experimental field (left) and plant harvest for measurement (right)*

Soil enzyme activity was assayed in triplicate. For invertase activity, 5 g of air-dried soil was incubated for 24 h at 37 °C with 15 mL 8% sucrose, 5 mL phosphate buffer at pH 5.5, and 0.1 mL toluene. The glucose released by invertase reacted with 3-5-dinitrosalicylic acid and 3-aminonitrosalicylic acid, which was then measured (as mg glucose released g^{-1} dry soil 24 h^{-1}) at 508 nm (UV 330, Unicam UV-vis). For Casein-hydrolyzing protease activity, 5 g of air-dried soil was incubated for 48 h at 30 °C with 25 mL 1% casein and 1 mL toluene, followed by addition of 25 mL of 10% Trichloroacetic acid to halt the enzyme reaction. The amount of amino acids released was determined by the Folin colorimetric method at 680 nm, measured as mg Tyrosine g^{-1} dry soil 48 h^{-1}. For catalase activity, 2 g air-dried soil was mixed with 40mL distilled water and 5 mL 0.3% H_2O_2, shaken for 20 min at 120 r/min, and the filtrate was titrated with 0.005 mol/L $KMnO_4$. Catalase activity was expressed as mL 0.005 mol L^{-1} $KMnO_4$ g^{-1} dry soil 20 min^{-1}. Soil polyphenol oxidase activity was measured by colorimetric method at 430 nm, determined by purpurogallin formation in soil samples using the substrate pyrogallic acid after 3 h incubation at 30 °C. Soil polyphenol oxidase activity was expressed as mg purpurogallin 100 g^{-1} dry soil 3 h^{-1} (Ma et al., 2003). Urease activity was determined by the modified colorimetric method (McGarity and Myers, 1967). Two milliliters of toluene was added to 20 g of soil and incubated for about 15 min to allow toluene to penetrate into the soil. Twenty milliliters of potassium citrate-citric acid buffer (pH 6.7) and 10 mL of 10% urea were then added and incubated for 3 h at 37 °C. The amount of NH_3-N released (expressed as mg NH_3-N 100 g^{-1} dry soil 3 h^{-1}) was measured using Indophenol Blue Method at 578 nm.

http://www.aloki.hu ● ISSN 1589 1623 (Print) ● ISSN 1785 0037 (Online)
DOI: http://dx.doi.org/10.15666/aeer/1802_30873100

Data analysis

The Shannon-Wiener index (H') was used to assess species diversity of the plant community (Spellerberg and Fedor, 2003). To account for the absence of *A. adenophora* in some subplots (recorded as zero), a value of one was added to all *A. adenophora* seedling records. Data were then transformed using a square root transformation for statistical analysis. The effects of each treatment on the plant community, soil chemistry, and soil enzymes were analyzed with a two-factor (year and drug) repeated-measures analysis of variance (ANOVA) to determine (1) whether these parameters changed over time and (2) whether drug treatments differed. Post hoc comparisons were made using least square differences (LSD). We reported F-tests adjusted for non-sphericity of the variance-covariance matrices using the Greenhouse-Geisser epsilon; hence some degrees of freedom were non-integer (Muller and Barton, 1989). All analyses were conducted in the SPSS software package (SPSS, Chicago, IL).

Results

Effects of soil microbes on the restoration of native plant community

The average biomass of individual *A. adenophora*, plant community diversity (H'), total biomass including *A. adenophora*, and the biomass of other plant species significantly changed cross years (*Table 1*). Moreover, these traits linearly increased over the period of three years of experiment (The biomass of *A. adenophora*, $F = 19.478$, $p = 0.022$; plant community diversity, $F = 34.896$, $p = 0.010$; total biomass including *A. adenophora*, $F = 80.511$, $p = 0.003$; the biomass of other plant species, $F = 32.254$, $p = 0.011$) (*Fig. 2*). But there was no significant change of population density and total biomass of *A. adenophora* over time (*Table 1*).

Table 1. *Repeated measures analysis of variance for plant community*

Source	Year			Drug			Year × drug		
	df	F	P	df	F	P	df	F	P
Population density	1.216	2.115	0.233	3	2.727	0.216	3.648	0.058	0.998
Total biomass of *A. adenophora*	1.096	3.251	0.162	3	15.909	0.024	3.287	0.696	0.620
Average biomass of individual *A. adenophora*	1.186	8.724	0.047	3	5.367	0.101	3.559	1.206	0.435
Diversity (H')	1.012	25.636	0.014	3	8.178	0.059	3.037	3.185	0.182
Total biomass	1.366	69.509	0.001	3	2.472	0.238	4.099	1.013	0.495
Biomass of other plant species	1.126	23.376	0.012	3	6.800	0.075	3.377	0.420	0.767

Drug treatment had a negative, though not significant, effect on the population density of *A. adenophora*, and significantly decreased the total biomass of *A. adenophora* (*Fig. 2A, D*). Relative to the control, BJQ, DJL, and LMS decreased *A. adenophora* biomass by 46.73%, 70.69%, and 96.95%, respectively. Although drug treatment also decreased individual biomass of *A. adenophora*, only streptomycin (LMS) was statistically significant ($p = 0.029$) (*Fig. 2B*). Interestingly, application of DJL ($p = 0.018$) and LMS ($p = 0.038$) significantly increased the biomass of other plant species by 68.5% and 43.87%, respectively (*Fig. 2E*), as well as plant community diversity (*Fig. 2C*).

http://www.aloki.hu ● ISSN 1589 1623 (Print) ● ISSN 1785 0037 (Online)
DOI: http://dx.doi.org/10.15666/aeer/1802_30873100

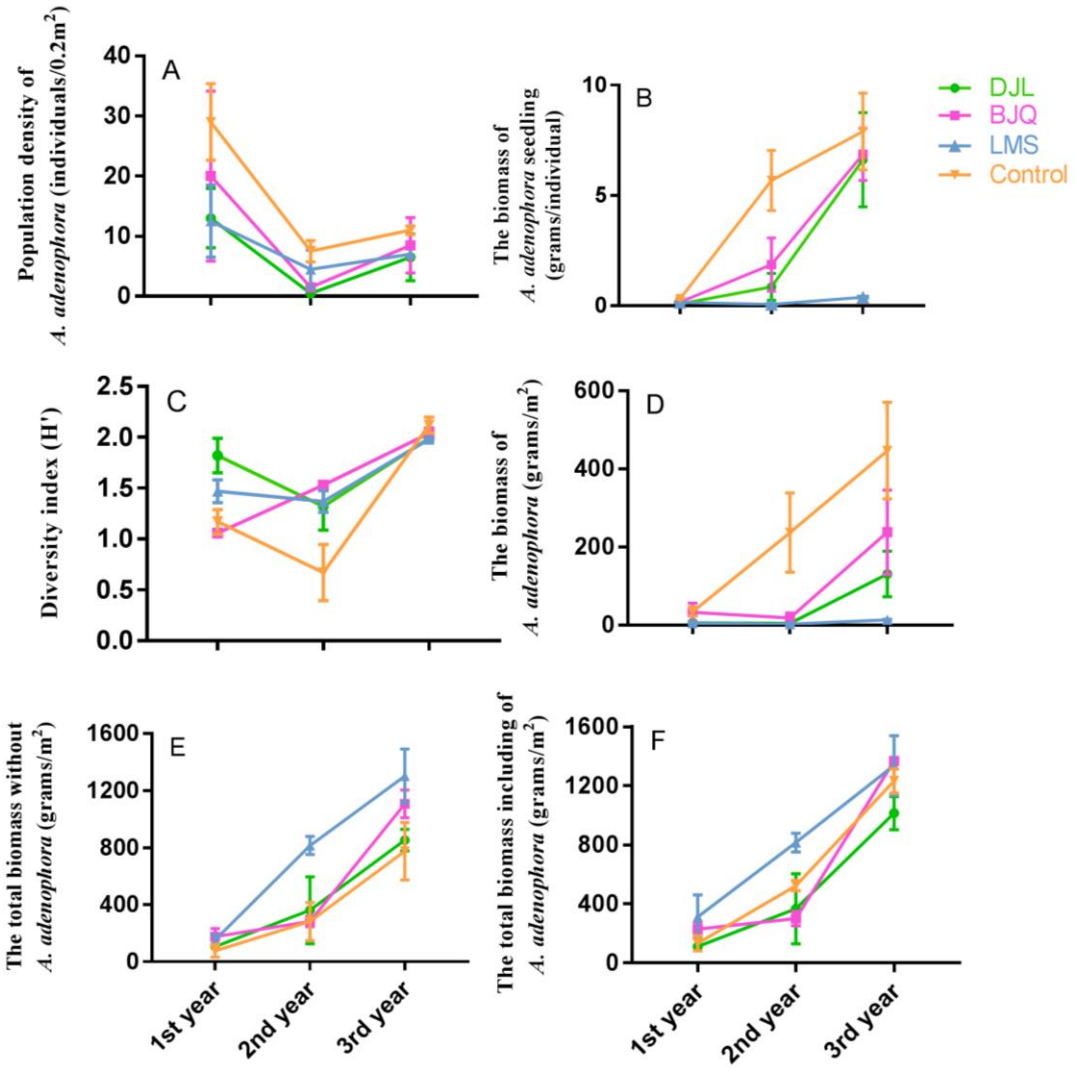

Figure 2. *Effects of modifying soil microbe activity with antimicrobial treatments on plant community. DJL (Carbendazim) is a broad-spectrum pesticide, mainly affecting the fungal community; BJQ (Chlorothalonil) is a broad-spectrum pesticide and is able to inhibit both fungal and bacterial communities; LMS (Streptomycin) is used to treat soil-born bacterial pathogens. Control is represented with water treatment. Error bar represents one standard error*

Soil chemistry enzyme

Only soil samples from 2009 and 2010 were analyzed. All chemistry characteristics significantly changed over years, except for total P ($F = 2.778$, $p = 0.194$) (*Table 2*; *Fig. 3*). Among of them, all pH values decreased from 2009 to 2010, while total K increased. Relative to the control, drug treatment changed most chemistry characteristics of soil, however, significant interactions were observed between treatment and year (*Table 2*). For example, three drugs significantly increased pH values at 2009 but decreased them at 2010; all drug treatments increased organic matter and total N at 2009 but decreased them at 2010 (*Fig. 3*). BJQ increased total P; LMS decreased available K at 2009 but increased it at 2010. DJL and BJQ increased available N and P at 2009 but decreased them at 2010.

http://www.aloki.hu ● ISSN 1589 1623 (Print) ● ISSN 1785 0037 (Online)
DOI: http://dx.doi.org/10.15666/aeer/1802_30873100

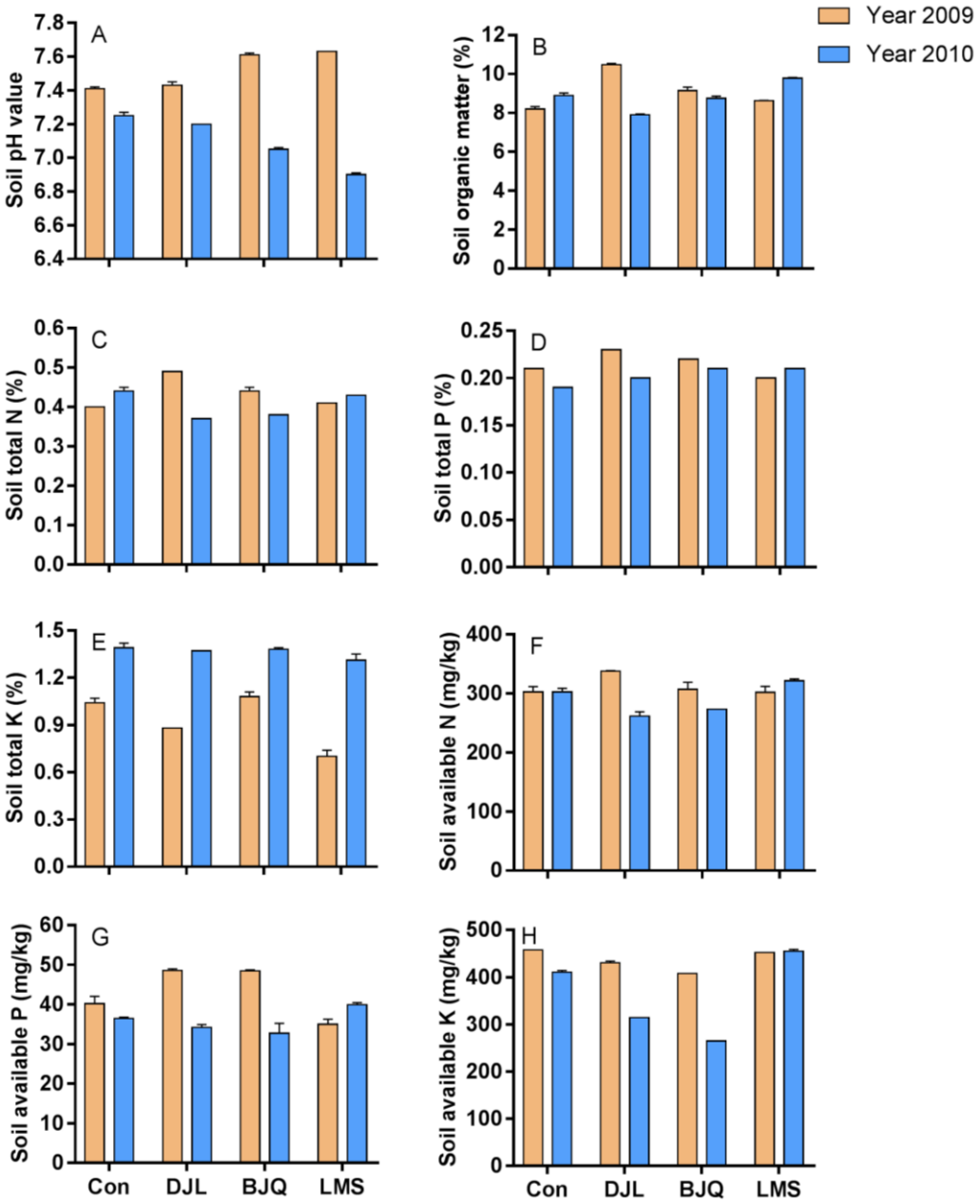

Figure 3. *Effects of pesticide treatment on soil chemical characteristics. Con: control; DJL (Carbendazim) is a broad-spectrum pesticide, mainly affecting the fungal community; BJQ (Chlorothalonil) is a broad-spectrum pesticide and is able to inhibit both fungal and bacterial communities; LMS (Streptomycin) is used to treat soil-born bacterial pathogens. Error bar represents one standard deviation*

From 2009 to 2010, soil protease activity significant increased, while the activity of catalase and polyphenol oxidase decreased over years, but urease and invertase had no changed (*Table 2*). Drug treatments significantly affected the activity of protease ($F = 30.182$, $p = 0.032$), catalase ($F = 55.364$, $p = 0.018$) and urease ($F = 28.358$, $p = 0.034$). However, relative to the control, BJQ significantly decreased protease activity; BJQ and LMS significantly decreased catalase activity; and DJL significantly increased urease activity.

http://www.aloki.hu ● ISSN 1589 1623 (Print) ● ISSN 1785 0037 (Online)
DOI: http://dx.doi.org/10.15666/aeer/1802_30873100

Table 2. *Repeated measures analysis of variance for soil chemistry and enzyme*

Source	Year			Drug			Year × drug		
	df	F	P	df	F	P	df	F	P
Soil enzyme									
Protease	1	1227.458	0.001	3	30.182	0.032	3	27.017	0.036
Polyphenol oxidase	1	90.632	0.011	3	2.751	0.278	3	6.485	0.137
Catalase	1	2174.738	0.000	3	55.364	0.018	3	43.868	0.022
Urease	1	7.621	0.110	3	28.358	0.034	3	1.397	0.443
Invertase	1	18.580	0.050	3	3.538	0.228	3	7.230	0.124
Soil chemistry									
pH	1	2048.000	0.000	3	421.000	0.000	3	151.000	0.001
Organic matter	1	4160.250	0.000	3	367.906	0.000	3	113.354	0.001
Total N	1	240.158	0.001	3	284.636	0.000	3	4.789	0.115
Total P	1	2.778	0.194	3	187.667	0.001	3	2.778	0.212
Total K	1	3264.000	0.000	3	106.022	0.002	3	142.235	0.001
Available N	1	101.999	0.002	3	123.741	0.001	3	9.293	0.050
Available P	1	1275.391	0.000	3	125.944	0.001	3	240.108	0.000
Available K	1	20557.989	0.000	3	1295.842	0.000	3	3877.301	0.000

Discussion

Ecosystems disturbed by non-native plants are often unable to be restored. Such a situation often results from the impact of non-native plants on soil biogeochemical characteristics and microbial communities, with negative effects persisting even after the removal of non-native plants (Hamman et al., 2013). There are three mechanisms commonly proposed for explaining how non-native plants influence the restoration of native communities by altering soil properties: changes in resource availability, buildup of allelochemicals, and alterations of soil microbial communities (Grman and Suding, 2010).

In general, resource availability increases in soil after invasion of non-native plants (Blumenthal, 2006; Littschwager et al., 2010; Sharma et al.,2010). Because most invasive plant species are adapted to high resource availability, native plants tend to be at a disadvantage when they co-occur with non-native plants (Blumenthal, 2006). In contrast, a low supply of nutrients likely reduces the potential of invasive species to grow (Kueffer, 2010). Previous research suggested *A. adenophora* invasion tends to increase soil fertility (Liu et al., 2007; Niu et al., 2007; Sun et al., 2013). Here, drug treatment decreased the growth of *A. adenophora* (*Fig. 2*) and increased soil fertility at 2009 (*Fig. 2*), indicating that increased resource availability is not the major reason for the soil priority effects of *A. adenophora*.

Although *A. adenophora* generally consumes soil nutrients at a high rate, its invasion tends to increase soil fertility (Liu et al., 2007; Sun et al., 2013). Such a conflict fact was considered resulting from the changed soil microbial community (Niu et al., 2007), for example, increased soil nitrogen-fixing bacterial number after *A. adenophora* invasion may facilitate *A. adenophora* to obtain more nutrients from surrounding soil (Xu et al., 2012). The fact that drug treatment decreased most soil nutrients in 2010 thus suggested that soil microbes play an important role in maintaining the high requirements of the growth of *A. adenophora*.

http://www.aloki.hu ● ISSN 1589 1623 (Print) ● ISSN 1785 0037 (Online)
DOI: http://dx.doi.org/10.15666/aeer/1802_30873100

Interestingly, urease, protease, polyphenol oxidase, and peroxidase activity in plant communities that included *A. adenophora* were greater than that in any native grass community (Liu et al., 2007; Sun et al., 2013). In this case, BJQ significantly decreased protease activity, while BJQ and LMS significantly decreased peroxidase activity (*Fig. 4*). Consequently, modifying the soil microbe community with antimicrobial drug treatments will likely helpful to restore soil enzyme activity to normal levels.

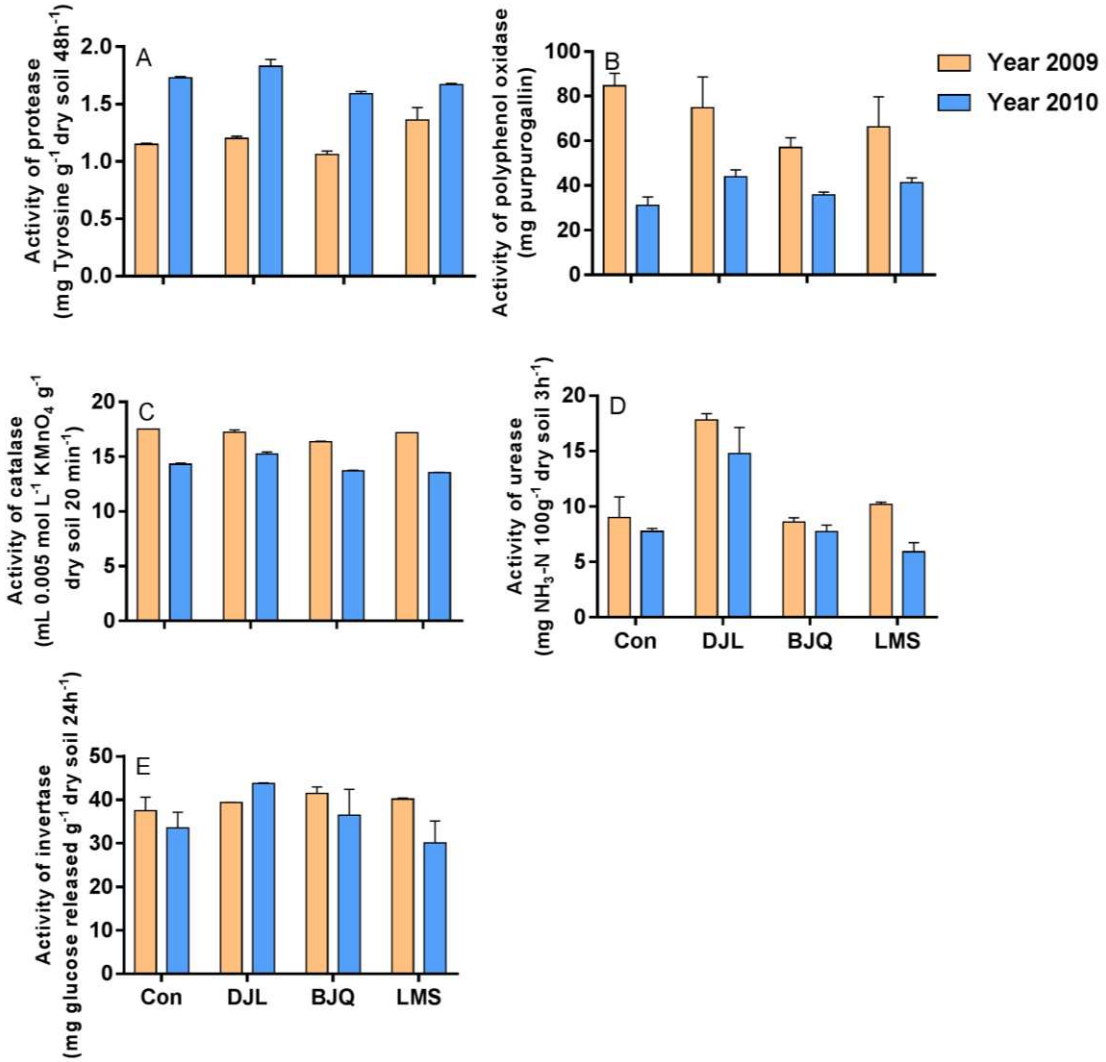

Figure 4. *Effects of pesticide treatment on the activity of soil enzymes. Con, control; DJL (Carbendazim) is a broad-spectrum pesticide, mainly affecting the fungal community; BJQ (Chlorothalonil) is a broad-spectrum pesticide and is able to inhibit both fungal and bacterial communities; LMS (Streptomycin) is used to treat soil-born bacterial pathogens. Error bar represents one standard deviation*

Allelochemical buildup in soil has been demonstrated to be important for the invasion of several plant species, including *Alliaria petiolata* (Bauer et al., 2010; Lankau, 2012) and *Centaurea maculosa* (Perry, 2005). However, the utilization of allelochemicals is also unlikely to be a key factor for the priority effects of *A. adenophora*. Although water extracts of *A. adenophora* leaves adversely affected the

http://www.aloki.hu ● ISSN 1589 1623 (Print) ● ISSN 1785 0037 (Online)
DOI: http://dx.doi.org/10.15666/aeer/1802_30873100

growth of some plant species (Zhong and Duan, 2006), allelochemicals were not found to persist in the soil after defoliation. Further, a greenhouse experiment also demonstrated that allelochemicals in soils of *A. adenophora* have little effect on native plants (Yu et al., 2005). More recently, *A. adenophora* has been verified to accumulate bacteria which can degrade the allelochemicals and thus decrease the allelopathic effects in soils (Li et al., 2017).

The invasion of *A. adenophora* strongly changes the soil microbial community, including both fungi and bacteria (Niu et al., 2007; Sun et al., 2013). For instance, Xu et al. (2012) found that *A. adenophora* accumulated a greater number and diversity of nitrogen-fixing bacteria than native plant species. In light of these studies, our results indicate that microbes may be the key factor inhibiting the growth of native plants after removal of *A. adenophora*. Moreover, LMS, which mainly inhibits soil bacterial growth, decreased *A. adenophora* biomass to the greatest degree, while DJL, which mainly inhibits soil fungal growth, increased the biomass of other plants the most (*Fig. 2*). This suggests that, if *A. adenophora* accumulates microbes beneficial for its own growth (*Fig. 2,* also see Yu et al., 2005; Niu et al., 2007), these microbes are likely to be bacteria, particularly nitrogen-fixing species (Xu et al., 2012; Zhao et al., 2019) or other selectively accumulated bacteria in roots (Chen et al., 2019). Therefore, the microbes inhibiting native plant growth are most likely pathogenic fungi. However, deciphering which group (or species) of fungi contributes to this inhibition depends on the comparison of the established microbial community by *A. adenophora* invasion with the changed one after the application of antimicrobial drugs, with the integration of the culture-dependent and culture-independent methods. It is too complex and beyond this study aim.

Although initial removal of non-native plants may be successful, reinvasion of non-native plants from remnant seed banks can be challenging to control and hinders restoration of the ecosystem (Adams and Galatowitsch, 2006; Simberloff, 2013). Like most invasive plants, *A. adenophora* produces a vast amount of seeds, and its seed bank persists in the soil for several years (Shen and Liu, 2004). Therefore, modifying the community of soil microbes becomes important for the restoration of the degraded area by *A. adenophora* after eradication. Aside from microbes, soil fauna may affect aboveground vegetation (Sackett et al., 2010); however, we were unaware if there were any side effects on soil fauna from the pesticides used in our experiment. In addition, the impact of an invasive plant on an ecosystem can change over time. For example, native species richness and productivity were initially reduced by the invasive plant *Heracleum mantegazzianum* but tended to recover about 30 years after invasion (Dostál et al., 2013). Therefore, future studies may want to focus on whether the negative effects of soil microbes on ecosystem restoration decrease over the invasion history of *A. adenophora*.

Conclusions

In this study we indicated the effects of soil microbes on the restoration of native plant. Drug treatment had significantly decreased the total biomass of *A. adenophora*. Relative to the control, BJQ, DJL, and LMS decreased *A. adenophora* biomass by 46.73%, 70.69%, and 96.95%, respectively. Meanwhile, application of DJL and LMS significantly increased the biomass of other native plant species, as well as plant community diversity.

http://www.aloki.hu ● ISSN 1589 1623 (Print) ● ISSN 1785 0037 (Online)
DOI: http://dx.doi.org/10.15666/aeer/1802_30873100

Chemistry characteristics, including pH, N and K, significantly changed over years, but total P had no changed. Relative to the control, drug treatment changed most chemistry characteristics of soil.

Soil protease activity significant increased, while the activity of catalase and polyphenol oxidase decreased over years, but urease and invertase had no changed. Drug treatments significantly affected the activity of protease, catalase and urease. Our data indicated that *A. adenophora* hinders the successful reestablishment of native species by changing the soil microbial community, and thus inhibiting the activity of soil microbes that promote non-native plant establishment and growth is beneficial for both eradication and replacement of *A. adenophora*.

Finally, although three chemical antimicrobial drugs we used in this study have been commonly applied in agricultural system for disease protection of crops (see materials and methods), the potential risk in natural ecosystems, e.g., carcinogenic and mutagenic effects, needs to be evaluated carefully in the case these drugs are utilized in the restoring vegetation degraded by invasive plants.

Acknowledgements. We thank Chen Yang, Zhen-Xin Zhou, Huan Jiang, Yun-Jiao Chen, and Li-Min Chen at Yunnan University for experimental assistance in the wild. This project was supported by the National Natural Science Foundation of China (Nos. 30960077, 31360153).

REFERENCES

[1] Adams, C. R., Galatowitsch, S. M. (2006): Increasing the effectiveness of reed canary grass (*Phalaris arundinacea* L.) control in wet meadow restorations. – Restoration Ecology 14: 441-451.

[2] Adler, P., D'Antonio, C. M., Tunison, J. T. (1998): Understory succession following a dieback of *Myrica faya* in Hawaii Volcanoes National Park. – Pacific Science 52: 69-78.

[3] Bauer, J. T., Anderson, R. C., Anderson, M. R. (2010): Competitive interactions among first-year and second-year plants of the invasive, biennial garlic mustard (*Alliaria petiolata*) and native ground layer vegetation. – Restoration Ecology 18: 720-728.

[4] Blumenthal, D. M. (2006): Interactions between resource availability and enemy release in plant invasion. – Ecology Letters 9: 887-895.

[5] Blumenthal, D. M., Mitchell, C. E., Pysek, P., Jarosik, V. (2009): Synergy between pathogen release and resource availability in plant invasion. – Proceedings of the National Academy of Sciences of the USA 106: 7899-7904.

[6] Callaway, R. M., Thelen, G., Rodriguez, A., Holben, W. E. (2004): Soil biota and exotic plant invasion. – Nature 427: 731-733.

[7] Chen, L., Fang, K., Zhou, J., Yang, Z. P., Dong, X. F., Dai, G. H., Zhang, H. B. (2019): Enrichment of soil rare bacteria in root by an invasive plant *Ageratina adenophora*. – Science of the Total Environment 683: 202-209.

[8] Chen, S. G., Kang, Y., Zhang, M., Wang, X. X., Strasser, R. J., Zhou, B., Qiang, S. (2015): Differential sensitivity to the potential bioherbicide tenuazonic acid probed by the JIP-test based on fast chlorophyll fluorescence kinetics. – Environmental and Experimental Botany 112: 1-15.

[9] Dostál, P., Müllerová, J., Pyšek, P., Pergl, J., Klinerová, T. (2013): The impact of an invasive plant changes over time. – Ecology Letters 16: 1277-1284.

[10] Elgersma, K. J., Ehrenfeld, J. G., Yu, S., Vor, T. (2011): Legacy effects overwhelm the short-term effects of exotic plant invasion and restoration on soil microbial community structure, enzyme activities, and nitrogen cycling. – Oecologia 167: 733-745.

http://www.aloki.hu ● ISSN 1589 1623 (Print) ● ISSN 1785 0037 (Online)
DOI: http://dx.doi.org/10.15666/aeer/1802_30873100

[11] Elliott, D. R., Caporn, S. J. M., Nwaishi, F., Nilsson, R. H., Sen, R. (2015): Bacterial and fungal communities in a degraded ombrotrophic peatland undergoing natural and managed re-vegetation. – PloS One 10(5): 20.
[12] Eppinga, M. B., Rietkerk, M., Dekker, S. C., De Ruiter, P. C., Van der Putten, W. H. (2006): Accumulation of local pathogens: a new hypothesis to explain exotic plant invasions. – Oikos 114: 168-176.
[13] Feng, J., Zhu, Y. (2010): Alien invasive plants in China: risk assessment and spatial patterns. – Biodiversity and Conservation 19: 3489-3497.
[14] Feng, Y., Wang, J., Sang, W. (2007): Biomass allocation, morphology and photosynthesis of invasive and noninvasive exotic species grown at four irradiance levels. – Acta Oecologica 31: 40-47.
[15] Feng, Y., Lei, Y., Wang, R., Callaway, R. M., Valiente-Banuet, A., Inderjitd Lia, Y., Zheng, Y. (2009): Evolutionary tradeoffs for nitrogen allocation to photosynthesis versus cell walls in an invasive plant. – Proceedings of the National Academy of Sciences of the USA 106: 1853-1856.
[16] Grman, E., Suding, K. (2010): Within-year soil legacies contribute to strong priority effects of exotics on native California grassland communities. – Restoration Ecology 18: 664-670.
[17] Hamman, S. T., Hawkes, C. V. (2013): Biogeochemical and microbial legacies of non-native grasses can affect restoration success. – Restoration Ecology 21: 58-66.
[18] Kardol, P., Wardle, D. A. (2010): How understanding aboveground–belowground linkages can assist restoration ecology. – Trends in Ecology and Evolution 25: 670-679.
[19] Klironomos, J. N. (2002): Feedback with soil biota contributes to plant rarity and invasiveness in communities. – Nature 417: 67-70.
[20] Kueffer, C. (2010): Reduced risk for positive soil-feedback on seedling regeneration by invasive trees on a very nutrient-poor soil in Seychelles. – Biological Invasions 12: 97-102.
[21] Lankau, R. A. (2011): Resistance and recovery of soil microbial communities in the face of *Alliaria petiolata* invasions. – New Phytologist 189: 536-548.
[22] Lankau, R. A. (2012): Interpopulation variation in allelopathic traits informs restoration of invaded landscapes. – Evolutionary Applications 5: 270-282.
[23] Li, Y. P., Feng, Y. L., Kang, Z. L., Zheng, Y. L., Zhang, J. L., Chen, Y. J. (2017): Changes in soil microbial communities due to biological invasions can reduce allelopathic effects. – Journal of Applied Ecology 54(5): 1281-1290.
[24] Littschwager, J., Lauerer, M., Blagodatskaya, E., Kuzyakov, Y. (2010): Nitrogen uptake and utilisation as a competition factor between invasive *Duchesnea indica* and native *Fragaria vesca*. – Plant and Soil 331: 105-114.
[25] Liu, C., Feng, Y., Tian, Y. (2007): Effects of *Eupatorium adenophorum* Sprengel invasion on soil enzyme activities and physical and chemical factors. – Bulletin of Botanical Research 27: 729-735.
[26] Ma, Y., Zhang, J. Y., Wong, M. H. (2003): Microbial activity during composting of anthracene-contaminated soil. – Chemosphere 52: 1505-1513.
[27] Mangla, S., Inderjit, Callaway, R. M. (2008): Exotic invasive plant accumulates native soil pathogens which inhibit native plants. – J Ecol 96: 58-67.
[28] Marchante, E., Kjøller, A., Struwe, S., Freitas, H. (2009): Soil recovery after removal of the N_2-fixing invasive Acacia longifolia: consequences for ecosystem restoration. – Biological Invasions 11: 813-823.
[29] McGarity, J. W., Myers, M. G. (1967): A survey of urease activity in soils of northern New South Wales. – Plant and Soil 27: 217-238.
[30] Muller, K. E., Barton, C. N. (1989): Approximate power for repeated-measures ANOVA lacking sphericity. – Journal of the American Statistical Association 84: 549-555.

http://www.aloki.hu ● ISSN 1589 1623 (Print) ● ISSN 1785 0037 (Online)
DOI: http://dx.doi.org/10.15666/aeer/1802_30873100

[31] Niu, H. B., Liu, W. X., Wan, F. H., Liu, B. (2007): An invasive aster (*Ageratina adenophora*) invades and dominates forest understories in China: altered soil microbial communities facilitate the invader and inhibit natives. – Plant and Soil 294: 73-85.
[32] Perry, L. G., Johnson, C., Alford, É. R., Vivanco, J. M., Paschke, M. W. (2005): Screening of grassland plants for restoration after spotted knapweed invasion. – Restoration Ecology 13: 725-735.
[33] Reinhart, K. O., Royo, A. A., Van der Putten, W. H., Clay, K. (2005): Soil feedback and pathogen activity in *Prunus serotina* throughout its native range. – Journal of Ecology 93: 890-898.
[34] Richardson, D. M., Allsopp, N., D'Antonio, C. M., Milton, S. J., Rejmanek, M. (2000): Plant invasions: the role of mutualisms. – Biological Reviews 75: 65-93.
[35] Sackett, T. E., Classen, A. T., Sanders, N. J. (2010): Linking soil food web structure to above- and belowground ecosystem processes: a meta-analysis. – Oikos 119: 1984-1992.
[36] Sang, W., Zhu, L., Axmacher, J. C. (2010): Invasion pattern of *Eupatorium adenophorum* Spreng in southern China. – Biological Invasions 12: 1721-1730.
[37] Shao, Y., Wang, Z., Zou, L., Wu, S. (2011): Effect of chlorothalonil on soil microbial communities of Larix artificial shelter-forest. – Acta Ecologica Sinica 31: 819-829.
[38] Sharma, G. P., Muhl, S. A., Esler, K. J., Milton, S. J. (2010): Competitive interactions between the alien invasive annual grass *Avena fatua* and indigenous herbaceous plants in South African Renosterveld: the role of nitrogen enrichment. – Biological Invasions 12: 3371-3378.
[39] Shen, Y., Liu, W. (2004): Persistent soil seed bank of *Eupatorium adenophora*. – Acta Phytoecologica Sinica 28: 768-772.
[40] Simberloff, D., Martin, J., Genovesi, P., et al. (2013): Impacts of biological invasions: what's what and the way forward. – Trends in Ecology and Evolution 28: 58-66.
[41] Spellerberg, I. F., Fedor, P. J. (2003): A tribute to clarde Shannon (1916–2001) and a plea for more rigorous use of species richness, species diversity and the 'Shannon–Wiener' index. – Global Ecology and Biogeography 12: 177-179.
[42] Sun, X., Gao, C., Guo, L. (2013): Changes in soil microbial community and enzyme activity along an exotic plant *Eupatorium adenophorum* invasion in a Chinese secondary forest. – Chinese Science Bulletin 58: 4101-4108.
[43] Vogelsang, K. M., Bever, J. D. (2009): Mycorrhizal densities decline in association with nonnative plants and contribute to plant invasion. – Ecology 90: 399-407.
[44] Wang, C., Lin, H. L., Feng, Q. S., Jin, C. Y., Cao, A. C., He, L. (2017): A new strategy for the prevention and control of *Eupatorium adenophorum* under climate change in China. – Sustainability 9(11): 11.
[45] Wang, H., Xie, M., Zhang, G. (2008): Investigation and study on using plants to control *Eupatorium adenophorum*. – Forest Inventory and Planning 33: 108-111.
[46] Wang, R., Wang, J., Qiu, Z., Meng, B., Wan, F., Wang, Y. (2011): Multiple mechanisms underlie rapid expansion of an invasive alien plant. – New Phytologist 191: 828-839.
[47] Wang, R., Wang, Y. (2006): Invasion dynamics and potential spread of the invasive alien plant species *Ageratina adenophora* (Asteraceae) in China. – Diversity and Distributions 12: 397-408.
[48] Xu, C., Yang, M., Chen, Y., Chen, L., Zhang, D., Mei, L., Shi, Y., Zhang, H. (2012): Changes in non-symbiotic nitrogen-fixing bacteria inhabiting rhizosphere soils of an invasive plant *Ageratina adenophora*. – Applied Soil Ecology 54: 32-38.
[49] Yahdjian, L., Gherardi, L. A., Sala, O. E. (2011): Nitrogen limitation in arid-subhumid ecosystems: a meta-analysis of fertilization studies. – Journal of Arid Environments 75(8): 675-680.
[50] Yu, X. J., Yu, D., Lu, Z. J., Ma, K. P. (2005): A new mechanism of invader success: exotic plant inhibits natural vegetation restoration by changing soil microbe community. – Chinese Science Bulletin 50: 1105-1112.

http://www.aloki.hu ● ISSN 1589 1623 (Print) ● ISSN 1785 0037 (Online)
DOI: http://dx.doi.org/10.15666/aeer/1802_30873100

[51] Zhao, M. X., Lu, X. F., Zhao, H. X., Yang, Y. F., Hale, L., Gao, Q., et al. (2019): *Ageratina adenophora* invasions are associated with microbially mediated differences in biogeochemical cycles. – Science of the Total Environment 677: 47-56.
[52] Zhong, S., Duan, X. (2006): Allelopathic effects of *Eupatorium adenophorum* Spreng on germination of two pastures. – Seed 25: 18-20.

http://www.aloki.hu ● ISSN 1589 1623 (Print) ● ISSN 1785 0037 (Online)
DOI: http://dx.doi.org/10.15666/aeer/1802_30873100

REVIEW PAPER ON TREATMENT OF INDUSTRIAL AND DOMESTIC WASTEWATERS USING UASB REACTORS INTEGRATED INTO CONSTRUCTED WETLANDS FOR SUSTAINABLE REUSE

ENGIDA, T. M.[1,2,] – WU, J. M. [2*] – XU, D.[2] – WU, Z. B. [1,2*]

[1]*School of Resources and Environmental Engineering, Wuhan University of Technology, Wuhan, P.R. China*
(e-mail: zewedenahomruhama@gmail.com)

[2]*State Key Laboratory of Freshwater Ecology and Biotechnology, Institute of Hydrobiology, Chinese Academy of Sciences, Wuhan, P.R. China*

**Corresponding authors*
e-mail (J.M. Wu): wujunmei@ihb.ac.cn;
e-mail/phone/fax (Z.B. Wu): wuzb@ihb.ac.cn/+86-27-6878-0020/+86-27-6878-0675

(Received 23rd Aug 2019; accepted 8th Feb 2020)

Abstract. The successful use of anaerobic technologies, especially up-flow sludge blanket (UASB) reactors for the treatment of raw domestic sewage and industrial wastewaters in tropical and subtropical countries opened the opportunity to substitute the aerobic processes with anaerobic reactors in removal of organic matter. Proper management of domestic and industrial wastewaters in developing nations is negligible. Even cost effective integrated green technologies like anaerobic reactor with constructed wetland technologies are not applied. Hence the objective of the present review was to assess the pollutant removal efficiency of the up flow anaerobic sludge blanket (UASB) reactor coupled with a constructed wetland (CW) in treating these wastewaters and their capability to produce quality water for sustainable reuse. To achieve the objectives, the review was organized using reputable journals, articles, and review papers. The interpretation of the result of each document was done using tables, bar graphs, Pie chart and lines. The results were reorganized again by calculating average flow rate, hydraulic loading rate, and percentage removal efficiencies. Most research results revealed that use of UASB-CW integrated treatment system is a promising technology in wastewater treatment and able to complying the effluent discharge standards. Globally, the following abatement efficiencies ranged from 79.2-93.9%, 89.2-92.9%, 87.2-96.3%, 22.6-96.9%, 33-85.9%, and 97.9-99.99% were achieved for Chemical oxygen demand (COD), Biological oxygen demand (BOD), Total suspended solid (TSS), Total Kjeldhal Nitrogen (TKN), Total phosphorus (TP) and fecal Coliforms (FC), respectively using UASB-CW treatment systems. UASB-CW technologies are effectively integrated treatment systems and can be used for resource scarce developing countries. Since, both treatment technologies are cost-effective, easy operation and maintenance and capable of meeting effluent standards. Hence, the indiscriminate disposal of wastewaters and their environmental impacts in Ethiopia can be resolved using these low-cost combined treatment technologies.

Keywords: *domestic sewage, industrial wastewaters, UASB reactor technology, constructed wetland, UASB-CW integrated treatment systems, effluent sustainable reuse*

Introduction

Ocean and river quality deterioration is primarily caused by the discharge of inefficiently treated industrial and municipal wastewater. To combat this increasing problem on aquatic environment, strict regulation on pollution discharge is being implemented by various governmental bodies, with the focus primarily of waste reduction (Chan et al., 2009). Nowadays, there are a wide range of wastewater treatment

http://www.aloki.hu ● ISSN 1589 1623 (Print) ● ISSN 1785 0037 (Online)
DOI: http://dx.doi.org/10.15666/aeer/1802_31013129

technologies in the world. However, the strategies of treating domestic, municipal and industrial wastewaters by common and aerobic processes were shifted to the anaerobic processes. Anaerobic treatment technologies were known to treat medium to high strength wastewaters. Many advanced anaerobic treatment reactors have been investigated in the past. Among the reactors, Up-flow Anaerobic Sludge Blanket (UASB) reactor is widely used as a sustainable technology to tackle the challenges faced in efficient treatment of various kinds of wastewater. The success of this reactor is due to its strong ability to remove in removal of chemical oxygen demand even at light loading rates and low temperature (Atashi et al., 2010). Besides this, anaerobic treatment of wastewater has recently gained worldwide attention due to its simplicity, low construction costs, small land requirements, plain operation and maintenance, low sludge production and low energy requirements and energy production capacity in the form of biogas compared to aerobic treatment (Bhatti et al., 2014; Kasaudhan et al., 2013; Khan et al., 2011; Airuk et al., 2010; Gomec, 2010; Tandukar et al., 2007). Earlier much attention was not given to the treatment of wastewaters and they were simply dumped into the natural sources of water. This led severe health problems by deteriorating natural water resources.

An organic waste from industries, domestics, municipalities and agricultural sector decomposes in the environment and resulting large scale contamination of land, water and air. In order to protect the environment and prevent health hazards it is necessary to provide adequate treatment for the wastewater to reduce its pollution potential (Lomte and Bobade, 2015). Similarly in Ethiopia, accelerated water quality change due to rapid growth of urbanization and industrialization becomes one of the major environmental concerns in the country. Release of large quantities of industrial wastes to the environment contributes large quantities of nutrients and toxic substances into the water bodies. The pollution of water bodies and human habitat in the major cities, rivers and lakes are one evident for enormous release of wastes (Kenatu, 2011). This rise of environmental protection issue, leads to put strict environmental regulations on the industrial pollutions in order to reduce the levels of discharge standards. To full fill the regulations, some industries begin to use anaerobic reactor technologies to handle ever-increasing complex generated wastes from their processing units (Kebena, 2014). Different investigations were carried out at pilot and full-scale levels to study the effectiveness of UASB reactor for the treatment of various industrial wastewaters like distillery, petroleum, canning industry, paper and pulp, pharmaceuticals, tannery, textile and food industries such as brewery, diary, slaughterhouse, and sugar factories (Atashi et al., 2010). However, the UASB reactor has become the most frequently used method in treating domestic and industrial wastewater and can produce two main valuable resources (i.e., methane and the effluent). The methane gas is produced during the COD removal which with a potential recovery rate of 28% to 75% and can be transformed into energy (Mutombo, 2004).

The successful use of anaerobic reactor technologies for the treatment of wastewaters was restricted in tropical and sub-tropical regions. In these regions, anaerobic reactors have been responsible for the removal of large fractions of organic matters (Foresti et al., 2006). However, despite this success, UASB reactors are usually unable to attain most of the existing effluent discharge standards due to presence of high residual COD and BOD, nutrients and pathogens (Foresti et al., 2006; Yasar and Tabinda, 2010). All these features make the UASB treatment of wastewater is a very important field of research, where improvements and new developments are needed to overcome the

http://www.aloki.hu ● ISSN 1589 1623 (Print) ● ISSN 1785 0037 (Online)
DOI: http://dx.doi.org/10.15666/aeer/1802_31013129

problem. Thus, additional post treatment strategy is mandatory for the anaerobic bioreactor treated effluents sustainable reuse for developing countries but also for advanced countries (Yasar and Tabinda, 2010). There are different types of post treatment configurations on combination with UASB reactor, such as UASB-Aerobic suspended growth, UASB-Aerobic attached growth, UASB-Final Polishing Units (FPU) or UASB-Polishing Ponds (PP) are some of them used at several sewage treatment plants in India, Colombia and Brazil (Von Sperling and Mascarenhas, 2005; Khan et al., 2011).

Recently, application of constructed wetlands (CW) for the treatment of wastewater has received much attention, due to their cost effectiveness and environmentally friendly approach. In this situation, application of integrated anaerobic pretreatment-constructed wetland for the removal of pollutants is promising (Jamshidi et al., 2014). Constructed wetland technologies can be effectively integrated with anaerobic processes because they require a low energy input, easy operation and maintenance, modest installation and maintenance costs, minor sludge production, and the creation of visually pleasing landscapes. However, they need a large land area. The UASB removes mainly organic matter in wastewater with low and high organic loads; while the Horizontal subsurface flow constructed wetland (HSSFCW) is capable of removing organic matter and nutrients and is commonly used to obtain secondary or tertiary effluent concentration levels. In other words, combining an anaerobic reactor with a constructed wetland brings important benefits to the constructed wetland system such as the reducing of the required planted area, reducing the hydraulic retention time and increasing their life cycle (Lopez-Lopez et al., 2015). In addition to this, for resource scarce developing countries to adopt wastewater treatment, the treatment technologies must be cost-effective and easy to adopt, requires less energy input, and maintenance costs and be capable of meeting effluent discharge standards (Kyambadde et al., 2005).

The objective of this review paper was to assess the potential use of UASB reactor followed by constructed wetland in treating domestic and industrial wastewaters to the discharge standard limit, to compare and contrast UASB-CW wastewater treatment system with other kinds of post-treatment technologies and to assess the limitation of UASB reactor technology for wastewater treatment.

Method of writing the review paper

This review paper was written using journals articles, review papers, master's and doctoral thesis downloaded from Springer Link, Science Direct, Library Genesis, Jester, and www.nap.orgsearching web pages. The interpretation of the result of each document was done using tables, bar graphs, Pie chart and lines in a Microsoft excel. Results were reorganized again by calculating average flow rate, hydraulic loading rate, and percentage removal efficiencies of the scholars for comparison. The pollutant removal rates (%) were calculated for the uncalculated wastewater parameters using the following equation:

$$R\ (\%) = \left[1 - \frac{Cf}{Ci}\right] x\ 100$$

where R is the removal rate, C_i and C_f are the influent and effluent.

http://www.aloki.hu ● ISSN 1589 1623 (Print) ● ISSN 1785 0037 (Online)
DOI: http://dx.doi.org/10.15666/aeer/1802_31013129

Overview of anaerobic reactors

The main anaerobic reactors types used for the treatment of wastewater can be classified as low rate or high rate treatment systems as shown in *Figure 1*. High-rate systems are characterized by retention of sludge (sludge retention time (SRT) > hydraulic retention time (HRT)) whereas most low-rate anaerobic systems have no sludge retention time (SRT = HRT) (Zhang, 2016).

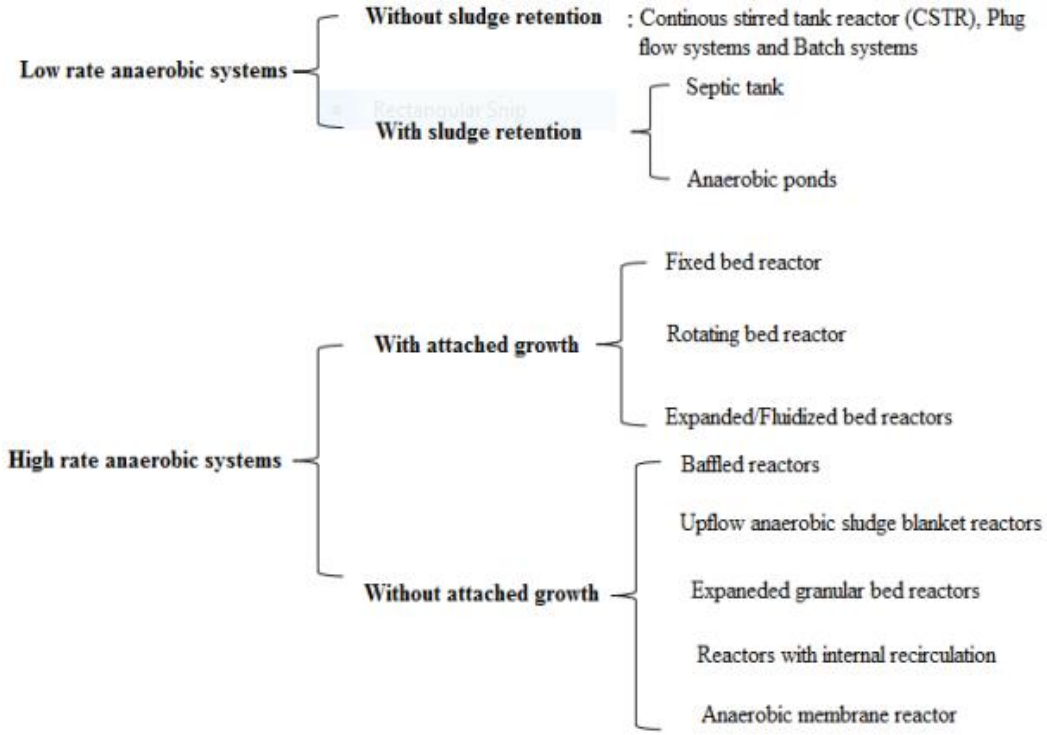

Figure 1. *Spectrums of anaerobic reactors used for wastewater treatment*

Among the spectrums, UASB reactor is one of the most distinguished anaerobic treatment technologies developed in Netherlands. Successful construction of a UASB process is capable of affording self-granulation of anaerobic microbes. The distinguished characteristic of this reactor is the presence of active biomass at the bottom of the reactor operating on suspended growth system. In this type of bioreactor, wastewater flows upwards direction through sludge bed and sludge blanket and is degraded by anaerobic microorganisms. Small sludge granules begin to form whose surface area is covered in aggregations of bacteria. Gas produced is then separated by a gas–liquid separator and the clarified liquid is discharged over a weir, while the granular sludge naturally settles at the bottom *Figure 2* (Saleh and Mahmood, 2003). Full-scale UASB reactors are now operational in Europe, US, Japan (Bani, 2011) and Ethiopia (Kebena, 2014).

Industries discharge wastes that contain high levels of organic materials which could adversely affect the environment. To meet the discharge limits, industries prefer economical and practical treatment methods. Anaerobic treatment has gained more attentions in developing countries due to their eco-friendly, low energy input, low biomass outputs, simple and inexpensive technologies to operate (Bukhari et al., 2015).

http://www.aloki.hu ● ISSN 1589 1623 (Print) ● ISSN 1785 0037 (Online)
DOI: http://dx.doi.org/10.15666/aeer/1802_31013129

Several anaerobic reactor technologies have been designed and constructed for the treatment of high strength wastewater. UASB reactors have received much attention due to their ability to treat high strength wastewater at higher organic loading rate (OLR) and a lower HRT. The treatment of high strength wastewater such as brewery wastewater using anaerobic digestion has been employed throughout the world. However, anaerobic digestion has some disadvantages like bad odor, and effluent that sometimes needing post-treatment to meet the discharging standards for nutrients levels, organic matter and pathogens content.

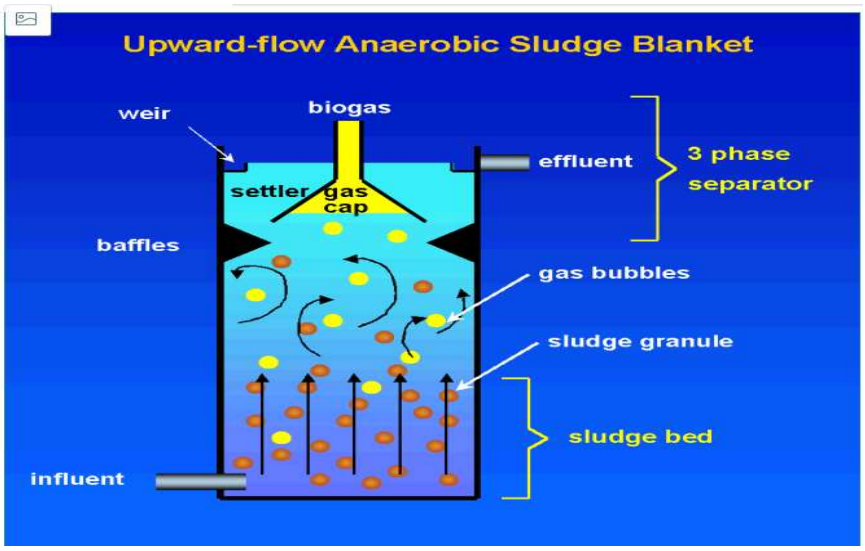

Figure 2. *Up-flow anaerobic sludge blanket reactor (UASB)*

Over the past times, different types of reactors have been developed and their installations have been commercialized. Among those, UASB reactor configuration is the most widely used high-rate anaerobic reactor for the treatment of high strength wastewater. An overview of the different anaerobic treatment systems used for different industrial wastewater pre-treatment and their proportions and types of anaerobic digestion systems that have been installed and commercialized for the treatment of industrial wastewater is presented in *Figure 3a* and *b* (Enitan, 2015).

Anaerobic reactor technologies have been widely applicable in the past decade for the treatment of various types of industrial wastewaters such as food processing, textile industry, paper and pulp industry (Pantea and Romocea, 2008). Anaerobic reactors have been used mainly for industrial wastewater treatment. This technology is also rarely applied for the treatment of municipal sewage, because municipal sewages are too weak (low BOD or COD) to maintain high biomass (i.e., in the form of granules-suspended solids or fixed film) content in the reactor. However, anaerobic wastewater treatment plants for municipal wastewater have been successfully operated in tropical countries such as Mexico, Colombia, India and China, the process until now has not been applied in countries with moderate and low temperatures.

According to Khan (2012) report indicates that there are 200 UASB reactors are used for municipal and industrial wastewater treatment application in India. The UASB reactor treating wastewater can produce main valuable resources (i.e., methane and the effluent) which can be recovered and utilized. Worldwide, more than 2000 anaerobic

http://www.aloki.hu ● ISSN 1589 1623 (Print) ● ISSN 1785 0037 (Online)
DOI: http://dx.doi.org/10.15666/aeer/1802_31013129

systems are also in operation for the treatment of industrial wastewater and landfill leachates (IEA, 2001). At lower temperature, the removal of COD by anaerobic reactor is limited and long HRT is needed for one step system to provide sufficient hydrolysis of particulate organics (Gašpariková et al., 2005) because low temperature causes deleterious effect on anaerobic digestion through relatively longer generation time of anaerobic bacterial populations and lower biochemical activity, resulting in the decrease of biogas yield and digester failure (Singh et al., 1999).

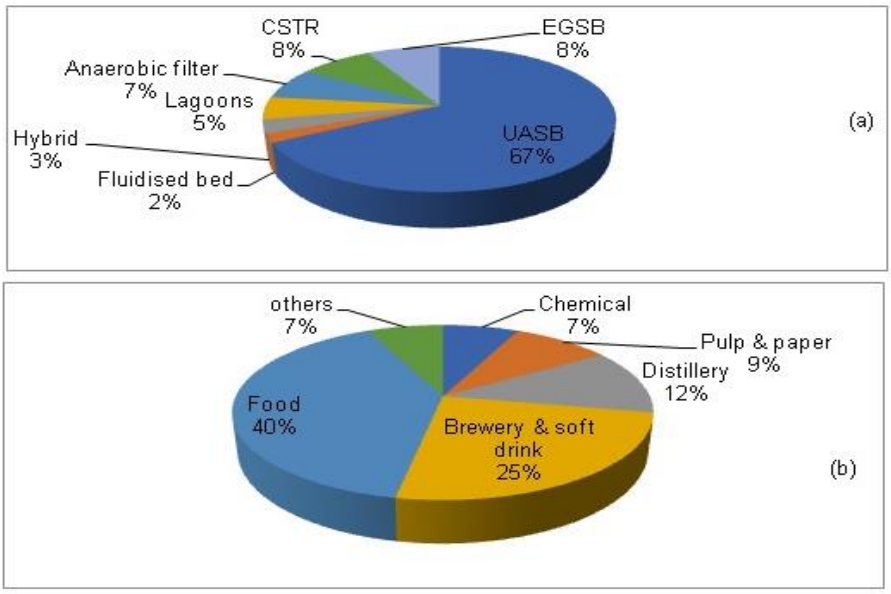

Figure 3. *(a) Proportions and types of anaerobic reactors that have been installed and commercialized for the treatment of industrial wastewater and (b) percentage of industries used anaerobic reactor technologies for wastewater treatment*

Anaerobic digestion process

Anaerobic reactors have a unique diverse group of bacteria that catalyzes the conversion of complex organic compounds to methane and carbon dioxide under a properly controlled and coordinated fashion. Degradation of organic matter in anaerobic process undergoes a complex microbial process consisting of several interdependent consecutive and parallel reactions. In this anaerobic digestion process, several groups of bacteria playing a vital role (Foresti et al., 2006) (*Fig. 4*).

Anaerobic effluents/UASB effluent characteristics

The output of anaerobic reactor indicates that the effluent contains residual organics in terms of BOD, COD, TSS and rich nutrients (N and P), microbial pathogens and reduced species such as sulfides, nitrate, ammonia, etc.

Organics and suspended solids

The concentration of BOD, COD, and TSS of anaerobic treatment system like UASB reactors in treating sewage without any post treatment system has been reported to vary from 60 to 150; 100 to 200; and 50 to 100 mg/l respectively (Foresti et al., 2006). The

http://www.aloki.hu ● ISSN 1589 1623 (Print) ● ISSN 1785 0037 (Online)
DOI: http://dx.doi.org/10.15666/aeer/1802_31013129

process efficiency depends on different factors like wastewater strength and composition, temperature, pH, and others. The dissolved mineralized compounds such as ammonia, phosphate and sulfides in the effluents also varied with these factors. The performance of these treatment systems highly depends on temperature and decrease with a decrease in temperature (Elmitwalli et al., 2001; Lew et al., 2003).

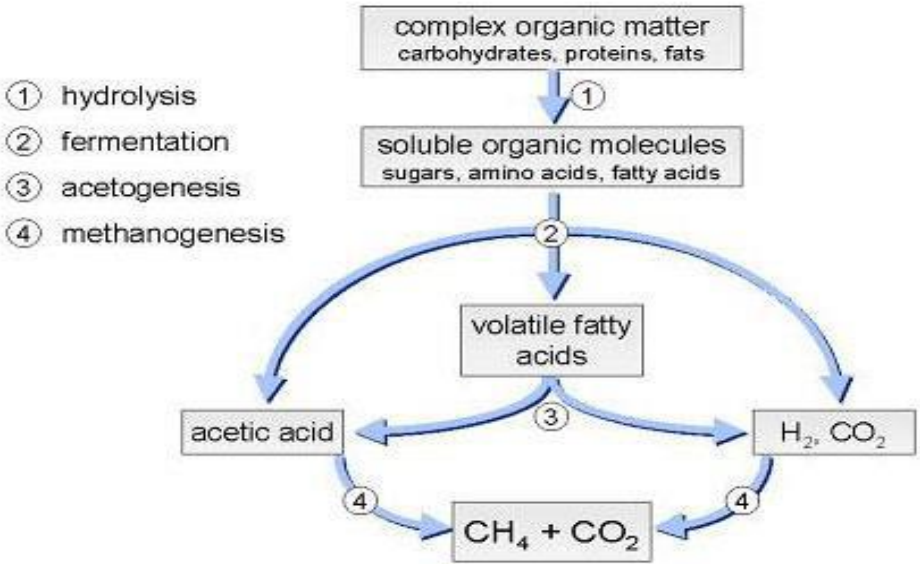

Figure 4. *The chemical reactions that occur during anaerobic digestion (Metcalf and Eddy, 2003)*

Nutrients

Insignificant or negligible removal of nutrients may be expected from anaerobic treatment systems (Foresti et al., 2006; Moawad et al., 2009). The poor removal of nutrients in anaerobic process is due to organic nitrogen and phosphorus hydrolysis into ammonia and phosphate respectively, which are not removed by this process and in consequence, their concentration increases in the liquid phase. Other highly mineralized sulfur compounds exist as sulfides in anaerobic systems effluent treating sewage. The effluent total sulfides concentration depends on the concentration of sulfates in the influents and sulfate reducing bacterial activity present in the reactor (Khan, 2012).

Indicators of microbial pathogens

The reduction of fecal coliforms is around one order of magnitude, i.e., from 108 to 107 in UASB treatment system which indicates that it is not designed for pathogenic removal, while helminth eggs removal efficiency has been reported to be 60-90% (Chernicharo et al., 2001; Von Sperling and Mascarenhas, 2005). In general, the UASB reactor effluent has a significant count of FC which is greater than the permissible limits specified by WHO (1989) for unrestricted irrigation. This indicates that the removal efficiency of UASB reactor is insufficient towards residual organics, nutrients and pathogens.

This may be due to the excessive hydraulic loading which consequently resulting higher up-flow velocities that may cause bypass of these pollutants with the final effluent without any microbial degradation. The temperature effect may be also one

http://www.aloki.hu ● ISSN 1589 1623 (Print) ● ISSN 1785 0037 (Online)
DOI: http://dx.doi.org/10.15666/aeer/1802_31013129

factor, because low temperature leads to insufficient mixing and more organic matter usually remains un-degraded as a result of slow hydrolysis of volatile solids at a given HRT. Considering the intrinsic limitations associated with the anaerobic systems and the stringent discharge standards, it is imperative to include a post-treatment stage for the effluents from anaerobic reactors. Therefore, the polishing stage has the purpose to improve the microbiological quality of the effluents, in view of the public health risks and limitations imposed on the use of treated effluents in agriculture. In an environmental approach, the post-treatment needs to guarantee the effluent quality in terms of organic matter and nutrients, in view of the environmental damages caused by the discharge of these remaining pollutants into the receiving surface water (Noykova et al., 2002).

Post-treatment of anaerobic reactor effluents

The insufficient removal of nutrients in anaerobic process is organic nitrogen and phosphorous hydrolyzed to ammonia and phosphate, respectively, which are not removed by anaerobic processes. Therefore, to minimize these problems, low rate natural settling systems (polishing ponds, constructed wetlands and duckweed pond), high rate aerobic methods (chemically enhanced primary treatment, Zeolite column, sequential batch reactor) and micro-aerobic methods (down-flow hanging sponge) are used for removal of the stabilized suspended matters, nutrients and fecal coliforms (FC) present in the UASB reactor (Khan et al., 2013).

Polishing ponds (PP)

Von Sperling and Mascarenhas (2005) found that the feasibility of PP (Polishing ponds) for the post treatment of effluent of UASB reactor in Brazil. The performance of the four series shallow depth PPs (i.e., 0.4 m) for the treatment of UASB effluent at a total of 7.4 day or 1.4 to 2.5 days results the final effluent concentration of BOD and COD, 44 and 170 mg/l, respectively. The mean overall FC removal efficiency was remarkably high (i.e., 99.99996%). The high FC removal efficiency together with total nitrogen concentration of 10 mg/l in the effluent were found compatible with the discharge standards for urban wastewater from European community, 15 mg/l or 70% removal. The ammonia nitrogen concentration in effluents from combined system was 7.3 mg/l or 67% removal. However, phosphorus removal was low (i.e., 28%). Other research study done on integrated anaerobic-aerobic systems carried out in Brazil also showed that shallow ponds in series even at short HRT, are able to produce effluents complying with the WHO guidelines for unrestricted irrigation in respect to FC concentration which is lower than 1000 MPN/100 ml. In general, all polishing pond systems were able to produce a quality effluent, which is a compliance with the WHO guidelines for unrestricted and restricted irrigation (Cavalcanti et al., 2001).

Constructed wetland (CW)

Constructed wetland system is technically and economically feasible alternative for wastewater treatment for small communities (Okurut, 1999). The systems consist of a solid medium (sand, soil or gravel) used to develop a natural process under suitable environmental conditions and wetland plant species provides a substrate (roots, stems and leaves) which microorganisms can grow as they break down organic matters. These plants species have a

http://www.aloki.hu ● ISSN 1589 1623 (Print) ● ISSN 1785 0037 (Online)
DOI: http://dx.doi.org/10.15666/aeer/1802_31013129

great role in utilization of the nutrients and other constituents, oxygen transfer to the solid medium and support medium for bio-films on the roots and rhizomes (De Sousa et al., 2001). According to Sousa et al. (2001) investigation, the pilot scale wetland system for the treatment of effluent of UASB reactor for the removal of residual organic matter, suspended solids, nutrients (N and P) and fecal coliforms. The 1500 L holding capacity of the UASB reactor was operated at HRT of 3 h and 6 h while the effluent of the UASB reactor was treated in four units of CW, each 10 m long and 1.0 m wide, filled with coarse sand substrate media and planted with Juncus sp. Macrophyte were planted in three CWs, whereas the other serves as a control unit without plants.

The final result revealed that the effluent COD from the four CW units had substantially constant concentration values, indicating that there was no influence of varied hydraulic load applied and presence of plant in CWs on its removal efficiency. The phosphorus removal was very efficient during the whole study periods; this removal was mainly due to the utilization by plants and microorganisms as well as adsorption and precipitation. In unplanted CW, the removal was due to precipitation and adsorption as well as assimilation by the bio-film developed on sand grains. The total nitrogen removal efficiency varied from 59 to 87% in wetlands containing macrophytes. This may be due to assimilation by plants and microorganisms present in wetlands, probably nitrification due to transport of oxygen from atmosphere by plants. The output indicated that the presence of macrophytes enhance the nitrogen removal efficiency significantly. The highest removal efficiency occurred in the unit with lowest hydraulic load corresponding to HRT of 10 day. The removal efficiency of the fecal coliforms was observed to be very high in wetlands with macrophytes. The increase in hydraulic load reduced the removal efficiency.

Duckweed pond (DP)

The aquatic macrophytes based treatment systems such as DP (Duckweed Pond) can be used to recover the nutrient and transformed them into easily harvested protein rich by products. The UASB effluents are highly rich in nutrients which should not be removed but, recovered. DP is covered by floating mat of macrophytes, which prevents light penetration into the pond resulting in shading. The high growth rates of the macrophytes permits regular harvesting of the biomass and hence nutrients are removed from the system. The produced biomass has economic value, since it can be applied as fodder for poultry and fish. El-Shafai et al. (2007) evaluated the performance of a combined UASB-DP system (3 pounds in series). The UASB reactor had a holding capacity of 40 L and run at 6 h HRT while each pond had 1 m^2 surface areas and 0.48 m depth and operated at HRT of 5 day in each pond. The duckweed ponds were inoculated with Lemna gibba, obtained from a local drain, at 600 grams fresh duckweed per m2. At the end, the system removed 93% COD, 96% BOD and 91% TSS during warm season. While residual values of ammonia, total nitrogen and total phosphorus were 98%, 85%, and 78%, respectively. The system also achieved 99.998% FC removals during the warm season. The removal efficiency of the system at the winter season was the same for BOD, COD, and TSS, but not for nutrients and fecal coliforms.

Chemically enhanced primary treatment (CEPT) and zeolite column

This treatment system was proposed by Aiyuk et al. (2004), which works in an integrated approach (i.e., coagulation and flocculation - UASB - Zeolite). In this integrate treatment system; domestic wastewater is initially treated with CEPT using

http://www.aloki.hu ● ISSN 1589 1623 (Print) ● ISSN 1785 0037 (Online)
DOI: http://dx.doi.org/10.15666/aeer/1802_31013129

$FeCl_3$ as a coagulant and polymer to remove suspended material and phosphorus followed by UASB to remove soluble organics. The UASB effluent was then subjected by re-generable zeolites to remove total ammonia nitrogen. The CEPT pre-treatment on average removed 73% COD, 85% TSS and 80% phosphate (PO_4^{3-}). The coagulation/flocculation step of this integrated system produced a concentrated sludge (8.4% solids), which can be stabilized in conventional anaerobic sludge digester used as fertilizer for agricultural purposes.

After, this step, UASB reactor consequently received pre-treated wastewater with COD loading of 140 mg/l and it was operated with hydraulic loading rate of 0.4 g COD/L/day. For these conditions, the system removed about 55% COD. The zeolite removed almost 100% NH_4^+. The integrated coagulation/flocculation - UASB - Zeolite system effectively decreased the TSS and COD up to 88% and more than 90% respectively. The nitrogen and phosphorus were decreased 99% and 94%, respectively. The column of zeolite proved most beneficial due to very high removal efficiency of ammonia and the oxidation of residual organic matter. Pathogenic indicators (FC) removal is 99%. The final effluent from the system can be used for crop irrigation or discharged into surface waters.

Down-flow hanging sponge (DHS)

This treatment system is a high rate micro-aeration treatment method. Micro-aeration implies that aeration of the treated effluent for about 30 min. The role of micro-aeration is to strip off and to oxidize the reduced species such as sulfides, ferrous ions etc., which exert immediate oxygen demand and remaining easily biodegradable organic pollutants and to remove the dissolved methane gas. In this DHS reactor designed, sponge cubes diagonally linked through nylon string have been used to provide a large surface area to accommodate microbial growth under non-submerged conditions. Then the wastewater trickled through the sponge cubes supplies nutrients to resident microorganisms. Oxygen is supplied through natural draught of air in the downstream without equipment. The system provides dissolved methane gas to be recovered. The performance efficiency of combined UASB-DHS cube process, with post-denitrification and an external carbon source, 84% in average nitrogen (NO3- + NO2-) was removed with HRT of less than 1 h. The DHS reactor was capable of stabilizing TN through nitrification, which ranged from 73 to 78% (Khan et al., 2013).

Sequential batch reactor (SBR)

SBR is a fill and draw type modified activated sludge process, where four steps of fill, aeration, settle and decant takes place sequentially in a single batch reactor. The operation of SBR can be adjusted to obtain aerobic, anoxic and anaerobic phases inside the standard cycles. The performance of the system was evaluated through a bench scale set-up comprising of a 4 L volume UASB reactor followed by two SBRs of 3.6 L each. The UASB reactor was fed with partially mixed synthetic substrate in sewage while SBR received effluent of UASB reactor. The HRT of 4 h in UASB was maintained constant throughout the study while the 4 h cycles in the following sequence of fill (0.1 h), reaction (1.9 h), sedimentation (1.6 h), discharge (0.25 h), idle (0.15 h) were maintained in SBR. The combined system removed 85% TN through nitrification. The COD removal in UASB reactor was around 86% while in SBR around 65% of the remaining, thus combined systems removed 95%. The combined system was also

http://www.aloki.hu ● ISSN 1589 1623 (Print) ● ISSN 1785 0037 (Online)
DOI: http://dx.doi.org/10.15666/aeer/1802_31013129

removed 96% of TSS and 98% of BOD (Khan et al., 2013). Mouawad et al. (2009) also studied the performance of the combined UASB-SBR system under different operating conditions for the treatment of domestic wastewater.

The reaction time was run for 3 h and the aeration time in the SBR cycle varied from 2 to 5 h, and then to 9 h. The observed average percentage removal for the three runs for COD, BOD and TSS was 94%, 97% and 98% respectively. Complete nitrification of ammonia was achieved after 5 h aeration in the SBR. The average percentage removal of phosphorus reached up to 65%. Increasing the HRT in the SBR from 2 to 9 h caused a significant improvement in FC removal. The overall removal efficiencies of the different post-treatment systems were mentioned in *Table 1*.

Table 1. *Treatment performance efficiency of UASB reactor integrated with different post-treatment systems in treating sewage (Khan et al., 2011)*

Treatment systems	Removal efficiencies of pollutants						
	BOD	**COD**	**TSS**	**NH_4 - N**	**TN**	**TP**	**FC (MPN/100 ml)**
CEPT + UASB + Zeolite	85%	91%	88%	99%	94%	94%	99%
UASB + PP	92%	79%	96%	50%	55%	-	99.999%
UASB + CWs	-	82%	79%	70%	70%	89%	99.998%
UASB + DWP	96%	93%	91%	98%	85%	78%	99.998%
UASB + DHS	96%	91%	93%	28%	40%	-	99.95%
UASB + SBR	97%	94%	98%	100%	77%	65%	-

Irrigation suitability of post-treated effluents

The UASB reactor process has been recognized as one of the environment friendly methods for treatment of urban wastewater in tropical countries due to its low capital investment, less land and energy requirements, less sludge generation, low maintenance cost and its potential to generate biogas. Effluent from this reactor, however, does not meet the disposal standards specifically in relation to organic content, suspended solids, nutrients and pathogen content. This makes the post-treatment of UASB reactor effluent necessary before its discharge into water bodies or its reuse in irrigation (Nair and Ahammed, 2013).

Domestic sewage treatment using UASB reactor is an interesting approach, provided the recovery of carbon in the form of energy-rich methane gas and nutrients. However, the effluent reusing for agriculture has some constraint because of the presence of pathogenic organisms and over nutrient dosage in the non-growing season. The UASB effluent still contain excess nutrients, salts and pathogens and is to be post-treated to remove pathogens after which the effluent can be used for irrigation and fertilization purposes. Unrestricted irrigation requires a high degree of pathogen removal and will increase the overall treatment costs. At presently, constructed wetland brings interesting results in removal of pathogens more effectively in a cost-effective way. The big advantage of this post-treatment system is its simplicity in operation, and the low investment costs when land prizes are low (van Lier et al., 2002) (*Fig. 5*).

http://www.aloki.hu ● ISSN 1589 1623 (Print) ● ISSN 1785 0037 (Online)
DOI: http://dx.doi.org/10.15666/aeer/1802_31013129

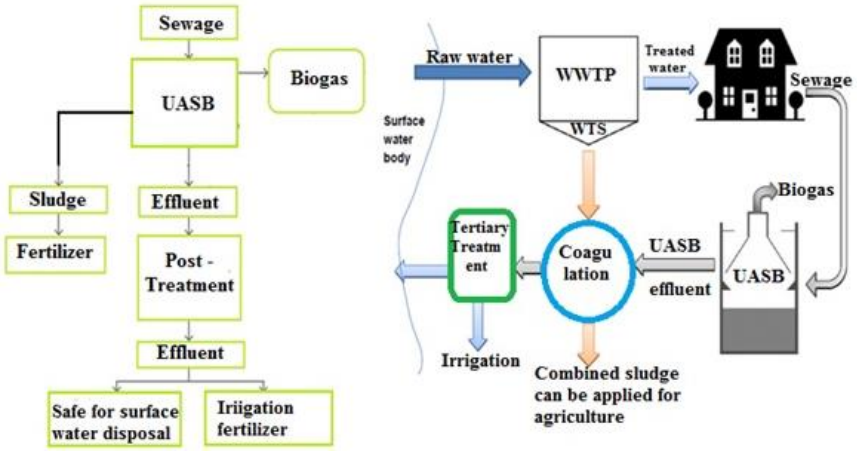

Figure 5. *(a) Post-treatment of UASB reactor domestic sewage effluents by onsite treatment options like CW for pathogen reduction and subsequent agricultural reuse (modified from van Lier et al., 1999) and (b) conceptual framework of reuse of treatment plant biosolids for UASB effluent post-treatment (Nair and Ahammed, 2013)*

Factors influencing the UASB reactors performance

The anaerobic process is a vital option for the treatment of industrial and domestic wastewater. The UASB reactor technology proved economically more attractive for treating sewage in both tropical and subtropical countries. However, a wide range of factors influence its performance efficiency. The most important factors are designing of UASB following parameters such as operational conditions (temperature, pH, organic loading rate, hydraulic retention time, and up-flow velocity), wastewater characteristics (influent concentration, influent particle size and influent particle charge), and sludge bed characteristics (particle size distribution, extra cellular polymeric substances and charge) and toxic substances should be considered as the most important factors affecting performance efficiency of UASB reactor (Sushma and Pal, 2013).

pH (potential hydrogen)

Due to the formation of different intermediates, anaerobic reactions are highly dependent on pH value particularly for methane producing bacterial ranging in 6.8-7.2. While, acid forming bacteria can survive in a more acidic condition. So, the pH of anaerobic system should be maintained between the methanogenic limits to avoid the predominance of the acid forming bacteria which may cause volatile acid accumulation. Therefore, microbial groups involved in each phase require different pH conditions for optimum growth. To achieve this, it is essential to provide buffering agents like sodium bicarbonate to neutralize any eventual VFAs accumulation. Addition of NaHCO3 is useful for supplementing the alkalinity, which shifts the equilibrium to the desired condition without disturbing the microbial population (Saleh and Mahmood, 2004).

Temperature

An aerobic occurs under a variety of temperatures depending on the species of microorganisms employed. In general, controlled anaerobic digestion is subdivided into

http://www.aloki.hu ● ISSN 1589 1623 (Print) ● ISSN 1785 0037 (Online)
DOI: http://dx.doi.org/10.15666/aeer/1802_31013129

three temperature ranges, psychrophilic (10-20 ℃), mesophilic (20-40 ℃), and thermophilic (50-60 ℃). The structures of the active microbial communities at each temperature optima are quite different. For example, bacterial growth and conversion of organic materials is slower under psychrophilic conditions.

The rate of methane production increases as temperature increases until maximum mesophilic temperature ranges, 35-37 ℃, because in this temperature ranges mesophilic microorganisms are actively involved. In general, biogas production yield depends on the choice of optimal temperature conditions for microorganism activity. most conventional anaerobic digestion processes occur under mesophilic temperatures. Because, this operation conditions are more stable and requires less energy input compared to operations under thermophilic conditions, and results in a higher degree of digestion (De Mes et al., 2003). The maximum (i.e., thermophilic) and minimum (psychrophilic) temperatures explains the limits of the temperature ranges for microbial optimal growth rate. The optimum temperature ranges are suitable conditions for maximum microbial growth rate. While the microbial growth become typically low below the optimal temperature levels and in some extent, it increases its growth exponentially at higher temperatures but some while microbial growth become restricted. The temperature effects on the removal efficiency of the anaerobic reactors depend on the type of the reactor as well. For example, a decline of the removal efficiency of the UASB reactor at lower temperature is due to the decreases in biological activity (Chernicharo, 2007).

C/N ratio

Unbalanced C/N ratio is one of a limiting factors of anaerobic digestion. Substrates with high C/N ratios, such as paper and most crop residues will be deficient in nitrogen, which is an essential nutrient for microbial cell growth. Thus, anaerobic digestion of very high C/N ratios may be limited by nitrogen availability. In the case of substrates with low C/N ratios, such as some animal manure, toxic ammonia build-up may become a problem. To overcome deficiencies in either carbon or nitrogen, co-digestion of low C/N materials with high C/N materials has been proven an effective solution (Martin-Ryals, 2012).

Organic loading rate (OLRs)

Organic loading rate is defined as the number of volatile solids or chemical oxygen demand fed to the system per unit volume per time. Higher OLRs can allow for smaller reactor volumes thereby reducing the associated capital cost. However, at high OLRs there is a danger in overloading of the reactor, especially during reactor start-up. At higher OLRs, retention times must be long enough such that the microorganisms have enough time to sufficiently degrade the material. Thus, there is a balance between OLR and HRT that must be determined in order to optimize digestion efficiency and reactor volume (Martin-Ryals, 2012). Hydraulic retention time (HRT) can be defined as the amount of time that waste remains in the digester and in contact with the biomass. For easily biodegradable compounds such as sugar, the HRT is low whereas more complex compounds need longer HRTs. HRT values influences the rate and extent of methane generation and is one of the most significant factors affecting the transformation of volatile substrates into gaseous products (De Kock, 2015).

http://www.aloki.hu ● ISSN 1589 1623 (Print) ● ISSN 1785 0037 (Online)
DOI: http://dx.doi.org/10.15666/aeer/1802_31013129

Nutrients

Nutrient at optimal levels are important for microorganisms for cellular building blocks and ensures that the cells are able to synthesize enzymes and co-factors responsible for driving metabolic activities. These include macronutrients such as nitrogen, phosphorous and Sulphur, vitamins and trace elements (iron, nickel, magnesium, selenium, copper, and cobalt). Even though, nutrients are required in very low amounts, lack of them causes significant effect on growth of microbes (De Kock, 2015).

UASB reactor removal efficiency

The efficiency and reliability the treatment system of a domestic sewage containing of an anaerobic reactor were assessed. Considering the slight balance of the micro-biota arose following the sludge extractions and these promoted reactor imbalances. This additional took about a reduction in reactor performance and hence of the over-all sustainability of the reactor development when treating domestic sewage directly. On the other hand, the system could not eliminate the nutrients such as nitrogen and phosphorus (Aiyuk et al., 2010). For example, performance assessment of complete scale UASB reactor in India by Sharda et al. (2013) indicates that, the high BOD and COD removal efficiencies. These high elimination efficiencies of the UASB reactor might be due to the proper functioning of the reactor.

While, the TSS removal efficiency was reduced, this may be attributed due to the high volatile suspended solids resulting in the creation of granular sludge bed in the UASB reactor. Similarly, performance assessment of full-scale UASB reactor in Ethiopia shows that higher removal efficiency in terms of COD while it was limited in removal of BOD, TSS and nutrients (Kebena, 2014). *Figure 6* demonstrates that the performance competence of full-scale anaerobic reactor treating domestic and industrial wastewaters.

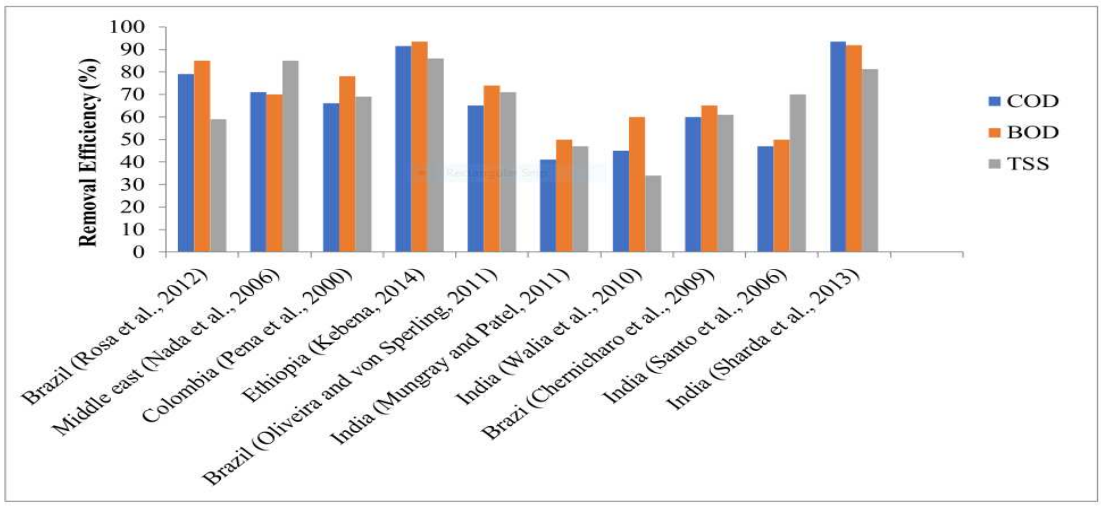

Figure 6. *Performance efficiency of full-scale anaerobic reactor treating sewage and brewery wastewater (Sharda et al., 2013; Kebena, 2014) treatment plants in different parts of the world*

The process efficiency of UASB reactor efficiency depends on diverse issues like strength and composition of wastewater, temperature and diurnal fluctuations. The

http://www.aloki.hu ● ISSN 1589 1623 (Print) ● ISSN 1785 0037 (Online)
DOI: http://dx.doi.org/10.15666/aeer/1802_31013129

dissolved mineralized compounds such as sulfides ortho-phosphate and ammonia, in the effluent also varied with factors. The performance of these treatment systems highly depends on temperature and decreases with a decrease in temperature (Khan et al., 2011) The performance efficiency of pilot and complete scale UASB reactor in treating sewage and industrial wastewater at different temperature and hydraulic retention time is summarized in *Table 2*.

Table 2. *Treatment performances of laboratory and full scale UASB reactors treating sewage and industrial wastewater (Khan et al., 2011; Bula, 2014)*

	Country	**Japan**	**Japan**	**India**	**Brazil**	**Cambodia**	**Brazil**	**Netherlands**	**Ethiopia**
	Capacity	_	1148 L	5 MLD	106 L	35 m^3	106 L	6 m^3	700 m^3
	Temp. (C)	-	-	25	21-25	23-24	20	20	-
	HRT	6	6	10	4.7	5.2	4	18	17
Influent mg/l	COD	600	532	590	265	475	424	550	2676
	BOD	291	240	167	150	-	195	-	1505
	TSS	-	-	-	123	225	188	-	686
Effluent mg/l	COD	222	197	201	133	170	170	165	228
	BOD	153	79	60	59	-	61	-	98
	TSS	-	-	-	33	65	59	-	96
Removal efficiency (%)	COD	63	63	66	50	66	60	70	91
	BOD	53	67	67	61	80	69	-	93.4
	TSS	-	-	-	73	69	69	-	82.6

India is a foremost country in terms of sewage wastewater treatment by UASB development where 37 UASB grounded sewage treatment plants (STPs) is already operating. It has been requested that 80% of total UASB reactors installed worldwide for sewage treatment are in India. The straightforward approach towards the selection of this technology for sewage treatment is due to its low capital cost, low energy requirements, small operation and maintenance costs and sustainability aspect. The performance of three STPs at Agra, Surat and Ludhiana (i.e., 78, 100, and 48 MLD) was greatest and the removal of COD, BOD and TSS was 45-48%, 29-43% and 40-51% respectively. The reason for poor performance was improper operation and maintenance and lack of screening control, grit removal and sludge wasting. The performance of 27 and 152 MLD at Noida and Ludhiana reactors was observed relatively good with the BOD, COD and TSS removal efficiencies of 53-59; 41-55 and 49-59%, respectively (Khan et al., 2014) (*Fig. 7*).

These results indicated that UASB reactor requires post treatment in order to obey with the removal standards. The monitoring of 10 STPs of diverse cities of India was agreed out in order to investigate their performance. The primary objective of research was to evaluate the treatment performance of full-scale UASB reactors and diverse post treatment systems. The general performance of these STPs was extended from 66 to 95% for BOD, COD and TSS removal (*Fig. 8*). However, three UASB reactors at 78, 100 and 48 MLD STPs at Agra, Surat and Ludhiana revealed minor treatment efficiency due to poor operation and maintenance (Khan et al., 2014).

http://www.aloki.hu ● ISSN 1589 1623 (Print) ● ISSN 1785 0037 (Online)
DOI: http://dx.doi.org/10.15666/aeer/1802_31013129

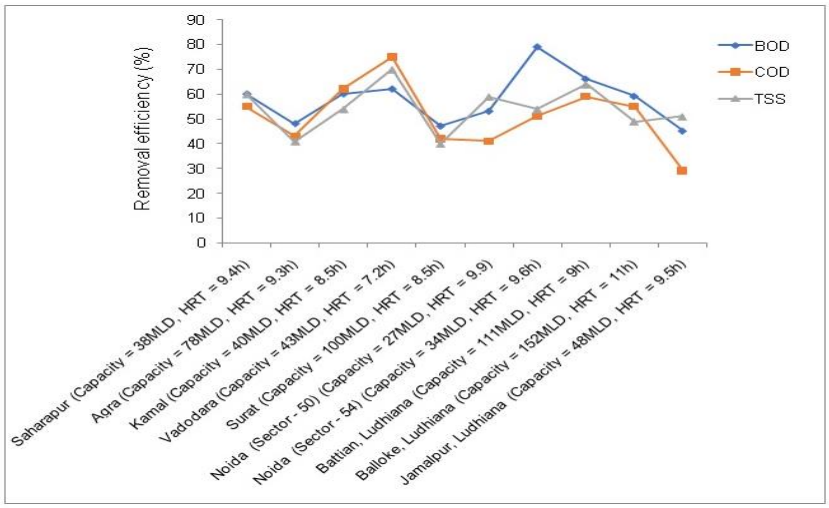

Figure 7. *Performance efficiency of full scale UASB reactor in treating sewage at different cities of Indian towns*

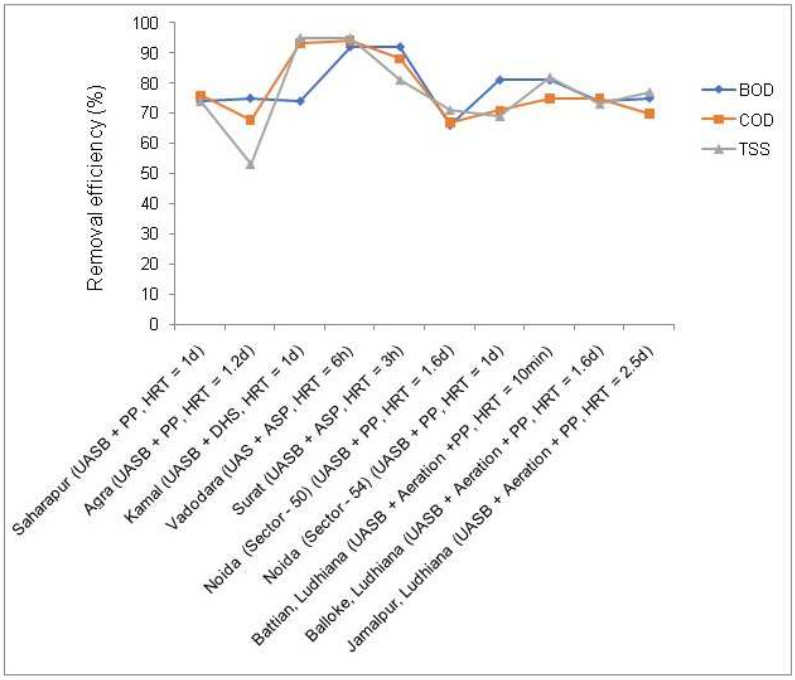

Figure 8. *Removal efficiency of the full-scale UASB reactor integrated with different post-treatment systems in different cities of India*

According to Mahmood et al. (2013) investigation, the laboratory scale UASB reactor performance for the treatment of original wastewater of COD concentration of 474 mg/l was reduced to 297 mg/l with 37.3% removal efficiency. Similarly, the TSS, BOD, NO_3 - N, and NH_4 - N were reduced from 1400 mg/l, 84.8 mg/l, 16 mg/l and 82 mg/l to 115 mg/l, 18.5 mg/l, 16 mg/l and 10 mg/l with removal efficiency of 91.7%, 78%, 88.9% and 87.8% respectively. Similarly, Khan et al. (2011) pilot scale of UASB reactor in treating sewage indicated that the performance efficiency of BOD, COD, and

http://www.aloki.hu ● ISSN 1589 1623 (Print) ● ISSN 1785 0037 (Online)
DOI: http://dx.doi.org/10.15666/aeer/1802_31013129

TSS was 66.3%, 60.1% and 62%, respectively. The indicators of pathogens that is FC in UASB reactor was reduced to 10%. The removal of reduced species like NH_4 - N, NO_3 - N and PO_4 - P were insignificant in both pilot and full scale UASB reactors. The performance efficiency of pilot scale and full scale UASB reactors operated at OLR of 60 L and HRT of 8 h in removal organics, nutrients and pathogens were shown in *Figure 9a* and *b*.

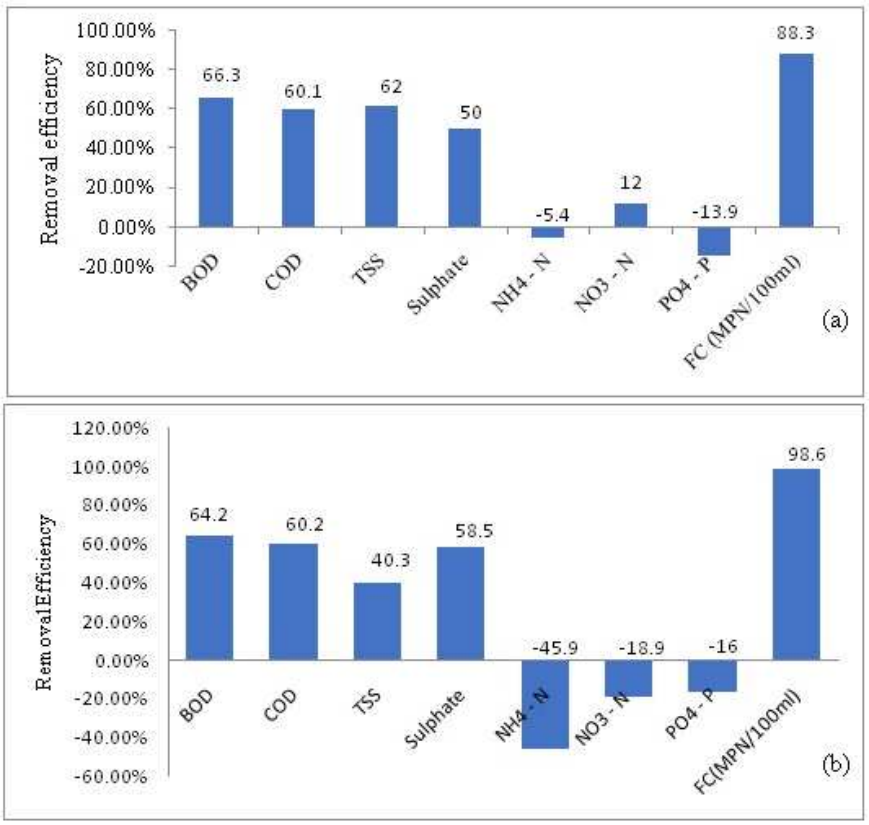

Figure 9. *Performance efficiency of UASB reactor at (a) pilot scale and (b) full scale levels in treating sewage wastewater*

The performance of the 111 ML/day full scale UASB reactor was also evaluated by Khan et al. (2011). The performance of full- and pilot-scale UASB reactors at ambient temperature (from 9 to 39 °C) was comparable. The percentage COD, TSS and BOD removal efficiency in the full-scale UASB reactor varied between 55 and 65%, whereas the removal in pilot scale ranged from 60 to 70%. The indicator of pathogens, which is FC in UASB reactors, was decreased to 10%. The removal of NH_4 - N, NO_3 - N and PO_4 - P were insignificant in both UASB reactors; the effluent pH remained within the optimal working range for anaerobic digestion (6.9-7.9). The research results were consistent with other UASB reactors investigated by El-Khateeb and El-Bahrawy (2003), i.e., the concentrations of COD, BOD, and TSS were decreased by 67.7%, 71.4% and 65.5%, respectively.

On the other hand, the TKN and TP were also reduced by removal efficiency of 11.3% and 23% respectively including fecal coliform removal efficiency of 96.7%. This high removal efficiency of COD, BOD and TSS is mainly attributed due to the

http://www.aloki.hu ● ISSN 1589 1623 (Print) ● ISSN 1785 0037 (Online)
DOI: http://dx.doi.org/10.15666/aeer/1802_31013129

relatively high sludge residence time (HRT = 38.1 days), which improves the hydrolysis and biodegradation of organic matter of wastewater content. Whereas the UASB reactor removed only the particulate nutrients by sedimentation and filtration and therefore, it had relatively low nutrient removal efficiency (El-Khateeb and El-Bahrawy, 2013).

Removal efficiency of UASB-CWs

Up-flow anaerobic sludge blanket (UASB) proved to be a cost-effective pretreatment system for wastewater. In addition, constructed wetlands provides a low-cost alternative for wastewater treatment in developing countries mainly in the arid and semi-arid regions. According to El-Khateeb et al. (2009) investigation, UASB reactor was used as a mainly treatment step followed by a horizontal subsurface constructed wetland for the treatment of grey municipal wastewater. The HRT and organic loading rate of the UASB reactor was 6 h and 1.88 Kg COD/m^3/day respectively. Within these operating conditions, the COD removal efficiency of the UASB reactor was 60%. Further enhancement of the quality of the treated wastewater was attained after the application of HSSFCW. The overall removal efficiency of the complete systems for COD, BOD and TSS were 87.7%, 89.5% and 94%, respectively (*Fig. 10*).

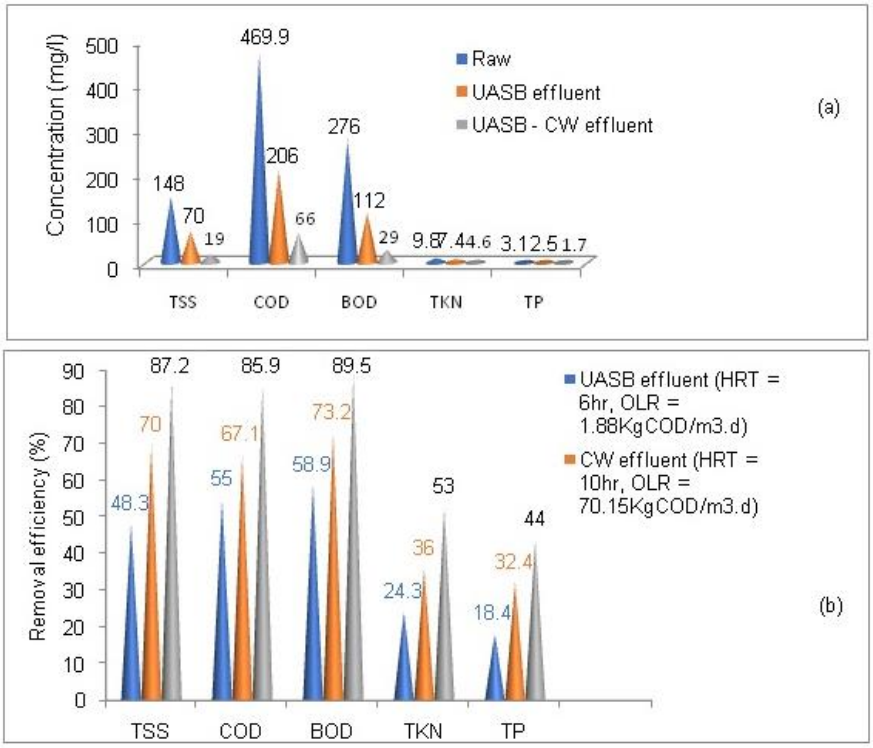

Figure 10. *(a) Concentration of raw grey wastewater and (b) removal efficiency of UASB-CWs in treating grey wastewater*

El-Khateeb and El-Bahrawy (2003) also found that the UASB reactor was operated at wastewater temperature varying from 15 °C during winter time to 30 °C during summer time. The UASB reactor efficiency at 8 h HRT was quite satisfactory. Average removal of COD and TSS were 63.2% and 66.5% respectively. The removal of FC in

http://www.aloki.hu ● ISSN 1589 1623 (Print) ● ISSN 1785 0037 (Online)
DOI: http://dx.doi.org/10.15666/aeer/1802_31013129

the reactor was 86%. After post-treatment with SSF CW COD reduction of 78%, BOD reduction of 78%, TSS and TP reduction of 78% and 79% were obtained respectively. The comparison of the removal competence of UASB reactor and its SSF CW integrated system in removal of COD, BOD, TSS, NH_4 - N, TKN, TP and FC are indicated in *Figure 11*.

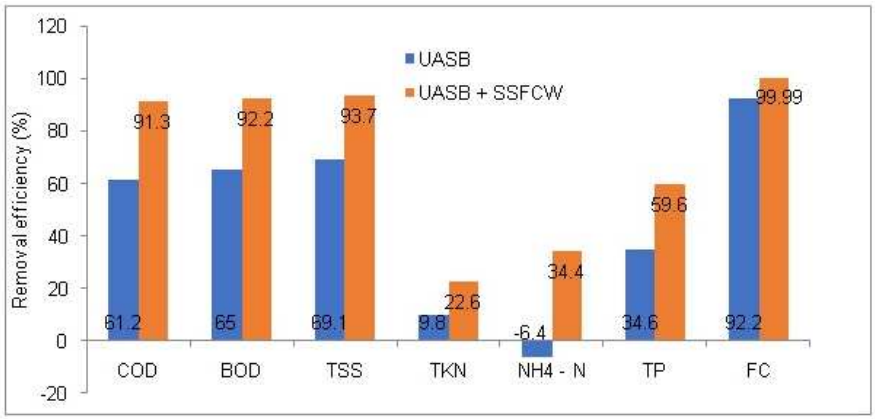

Figure 11. *Comparison between UASB reactor and UASB-SSFCW in removal of pollutants from sewage wastewater*

The likelihood of using treatment schemes consists of a UASB reactor tracked by subsurface flow constructed wetland for the treatment of sewage water is an effective system. The UASB reactor was designed at operating conditions of HRT (6 h), HLR (4 m^3//day), and OLR (2.45 Kg/m^3/day). The performance of this reactor for the treatment of raw sewage indicates that the concentration of COD, BOD, TSS, TN and TP were reduced by 67.7%, 71.4%, 65.5%, 11.3% and 23% respectively. The bacterial count was reduced to 96.7%. *Figure 12* shows that the performance of SSF wetland unit integrated with UASB reactor. The concentration of ammonia also greatly decreased in the final effluent of SSF unit. This may be due to aerobic conditions adjacent the root section of the plant in the CW unit (El-Khateeb and El-Bahrawy, 2013).

Research studies indicated that nitrogen and phosphorus elimination by plant uptake is not a significant mechanism for the removal of these elements in wetlands receipt moderately treated municipal wastewater because nitrogen and phosphorus are taken-up and free in the cycle of plant growth and death. In El-Khateeb and El-Bahrawy (2003) finding, the removal of TP was initiate to be high at the beginning of the experiment. As the plant reaches the maturation state the removal was decreased and there is some release of phosphorus from the dead parts of the plant. The removal efficiency the SSF CW was increased and noted that the final effluent was complying the WHO guidelines for treated effluent reuse.

According to Cheng et al. (2010) investigation, the removal percentage of pollutants in the influent and effluent following the UASB - CW1 - CW2 treatment systems achieved a greater reduction of pollutants (i.e., COD removal of 93.9%). The result indicates that the UASB reactor is capable of removing 60-80% of total COD, 75-85% of BOD, and 70-80% of total SS from the raw sewage, while the removal efficiency of nutrients such as TN and TP are only 10-25% and 10-20%, respectively. This removal limitation of UASB reactor can be improved by utilization of some aerobic processes such as activated sludge and constructed wetlands. *Figure 15* shows changes of NH_4 -

http://www.aloki.hu ● ISSN 1589 1623 (Print) ● ISSN 1785 0037 (Online)
DOI: http://dx.doi.org/10.15666/aeer/1802_31013129

N, NO_3 - N and PO_4 - P concentrations in the influent and effluent of the treatment units. From the data presented, the UASB reactor only removed 75% of NH_4 - N, 3.9% of NO_3 - N and 42.9% of PO_4 - P. However, the CWs removed almost over 85% of NH_4- N and PO_4 - P except NO_3 - N. The removal of NH_4 - N may be due to its oxidation into nitrite and nitrate–nitrogen compounds by microbial processes. Less removal of NO_3 - N may be due to the leaves of floating lettuces covered almost all the water surface in CW2 and protected direct sunlight from penetrating into the water body could suppress the growth of algae cells. As a result, the nitrogen removal capacity of the CW could be reduced. Whereas, the removal of TP levels in the UASB reactor was 42.9%, this may be achieved by metabolism of anaerobes and adsorption into the sludge. This less removal of TP can be improved by integrating with CW, in which the CW removes TP by microbial metabolism and plant uptake (*Fig. 13*).

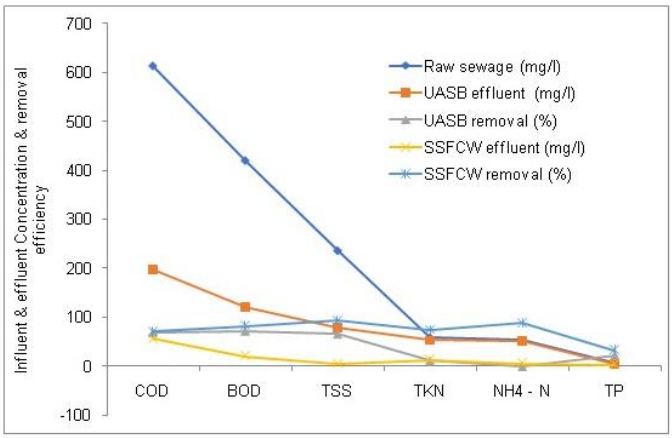

Figure 12. *Performance of the UASB reactor alone and post treated with SSFCW of raw sewage*

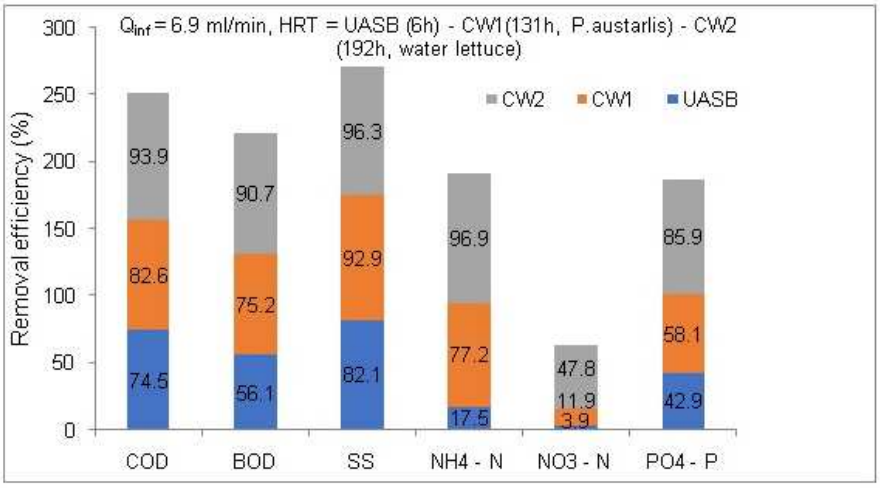

Figure 13. *Removal efficiency of UASB-CW1-CW2 in treating mixture of raw sewage and partially treated swine wastewater*

Similar study on the use of UASB reactor followed by a HSSFCW treatment system showed an important health advantage. In specific, there were no substantial odor

http://www.aloki.hu ● ISSN 1589 1623 (Print) ● ISSN 1785 0037 (Online)
DOI: http://dx.doi.org/10.15666/aeer/1802_31013129

emissions, and there was no indication of the proliferation of insects and other disease vectors. According to Raboni et al. (2015) investigations, the quality of raw sewage indicates that a high strength characteristic. Treatment of this sewage with UASB reactor results in the achievement of average removal efficiencies in the UASB reactor as high as 74% for BOD5, 71.15 for COD, and 65% for TSS. With regard to fecal indicators, the removal efficiency of UASB reactor appears low (i.e., 67.4% for fecal coliforms and 65.2% for fecal enterococci). Further treatment of UASB reactor effluents with SSFCW achieves removal efficiency of 92.9% for BOD5, 79.2% for COD, and 94% for TSS.

In addition to this, the SSFCW step concludes the removal of pathogens with an overall removal efficiency of 98.8% for fecal coliforms and 97.9% for fecal enterococci. The overall removal efficiency of the UASB reactor joint with subsurface flow constructed wetland on the removal of pollutants from raw sewage wastewater were indicated in *Figure 14*.

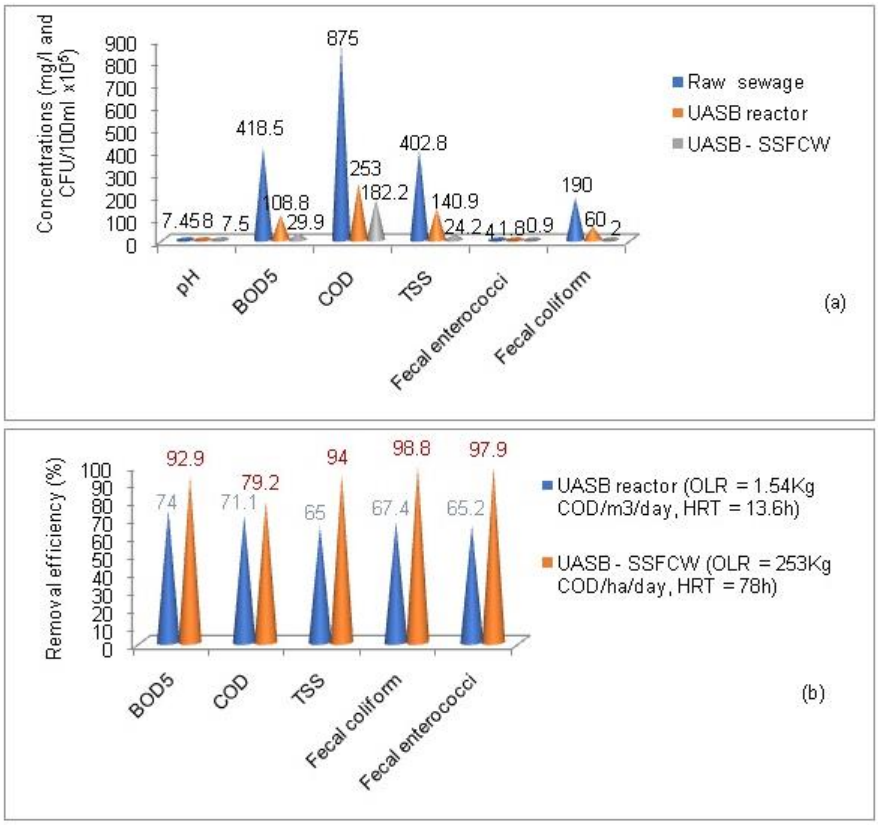

Figure 14. *(a) Concentration of pollutants in raw sewage, UASB and SSFCW and (b) removal efficiency of combined UASB-SSFCW treatment system*

It was observed that the effluent from the UASB reactor still contains significant count of fecal coliforms. These counts are larger than the permissible limit set by WHO (1989) for unrestricted irrigation. The feasibility of widespread post treatment using a horizontal subsurface flow constructed wetland for the treatment of sewage water has been studied by El-Khateeb and El-Bahrawy (2003). The result showed that the UASB-HSSFCW integrated treatment system was found to be efficient for removal of COD, BOD and TSS including nutrients and fecal coliforms. These may attribute due to the

http://www.aloki.hu ● ISSN 1589 1623 (Print) ● ISSN 1785 0037 (Online)
DOI: http://dx.doi.org/10.15666/aeer/1802_31013129

aerobic conditions near the root zone of the plants in the wetland units. Similarly, the water quality parameters at different sampling themes of hybrid system of UASB-CW were reduced due to through three systems. The overall removal competence of the UASB - SFCW - SSFCW was 91% for COD, 91.2% for BOD and 97.9% for TSS at applied organic loading rate in the range of 1200-6500 g BOD/m^2/day in UASB and 5-21 g BOD/m^2/day (10 g BOD/m^2/day on average for the two CW units) (de la Varga et al., 2013) (*Fig. 15*).

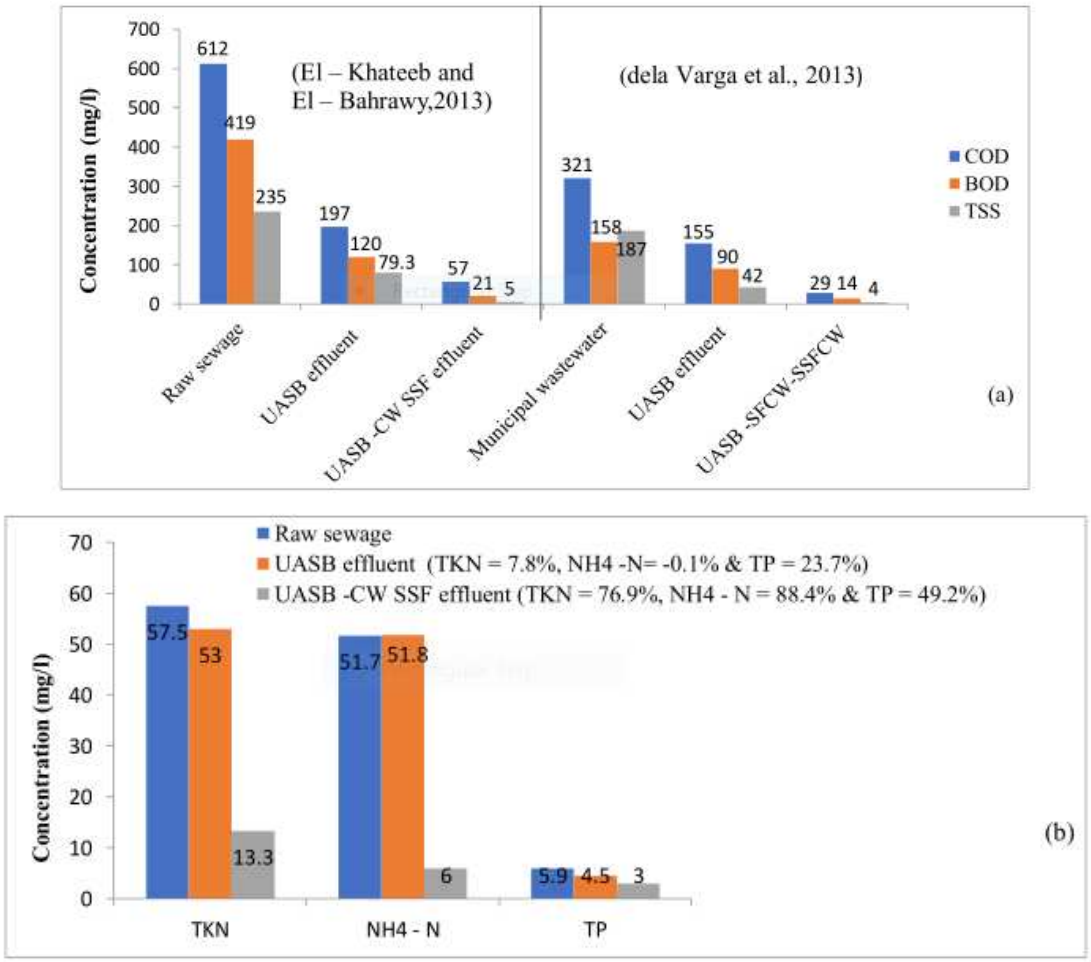

Figure 15. *Concentration of pollutants in raw sewage, UASB and SSFCW effluents and removal efficiency of combined UASB/SSFCW system (a and b)*

The anaerobic bioreactor indicates that removal of the residual concentration of organic (BOD and COD) less infective which usually exceeds the extreme permissible level prescribed by the effluent discharge standards of most developing countries. From this stand point; post treatment of anaerobic effluent is necessary to reduce the release of these contaminants to the required level. Due to this, the UASB effluent was further treated by CW at HRT of 3 days. The original wastewater fed into the UASB reactor and then post-treated by laboratory scale CW showed removal efficiencies of COD, BOD, TSS, nitrates and Ammonia were 82.4%, 78-82%, 91.7%, 88-92% and 100%, respectively (Mahmood et al., 2013). The overall results on the elimination efficiencies of the UASB-CW is summarized in *Table 3*.

http://www.aloki.hu ● ISSN 1589 1623 (Print) ● ISSN 1785 0037 (Online)
DOI: http://dx.doi.org/10.15666/aeer/1802_31013129

Table 3. *Lists and comparison of the performance efficiency of UASB-CWs in treating sewage*

Parameters	References					
	De souse et al. (2001)	**Chernic haro et al. (2001)**	**Ma (2005)**	**Cheng et al. (2010)**	**Raboni et al. (2014)**	**Ei-khataeb et al. (2009)**
Type of WW	Sewage	Sewage	Sewage	Sewage-swine	Sewage	Gray water
HRT of UASB (h)	3-6	5.5	1-6	2-6	13.6	6
HRT of CW (day)	5-10	4-20	2.3-13.5	4.5-13.5	78	10
COD removal (%)	79-85	70-80	90	91-94	79.2	85.9
BOD removal (%)	-	70-80	93	91	92.9	89.5
TSS removal (%)	48-71	90	90	93-96	94	87.2
NH_4-N removal (%)	45-70	33	75	89-97	-	-
TP removal (%)	90	-	100	78-86	-	44
FC removal (%)	-	-	-	-	98.8	-

The performance efficiency of constructed wetland integrated with UASB reactor is comparable with other post treatment techniques. According to Sharda et al. (2013) investigation, the assessment of the performance efficiency of a full scale brewery wastewater treatment plant, UASB reactor plus aeration (holding capacity of 380 m^3 at HRT of 23 h) followed by sand and activated carbon filter (holding capacity of 15 m^3 at HRT of 1 h) for a period of thirteen weeks showed an overall percentage reduction of COD, TSS and BOD values ranges from 96-98%, 88-98%, and 99% respectively. Similarly, Gasparikova et al. (2005) investigates, characterization of real wastewater treatment plant working on the principle of anaerobic-aerobic system, there was a problem with the high organic pollution on the effluent of anaerobic-aerobic treatment system. The high COD and BOD effluent concentration as well as TSS concentration are due to the incorrect operation of the wastewater treatment plant.

Among these operation problems, the primary settling tank was full of greases which lead to failure of the process. Another problem may rise from location of the air blower that used for oxygen delivery, which is inside the plastic tank of the wastewater treatment plant. The air circulates only there and no fresh air gets inside which means that there is not adequate oxygen for the aerobic post-treatment. This operation causes the presence of filamentous bacteria in the aerated part. Another study by Sharda et al. (2013), on the general performance of the brewery wastewater treatment plant indicates a reduction in TSS, COD and BOD. During the three-month study periods of the brewery's wastewater treatment plant, the overall removal efficiencies of TSS, COD and BOD were ranges from 96-98%,88-98% and 99% respectively which may be due to the proper functioning of the remaining treatment units such as aeration tank, sand filter and activated carbon filter. The comparison of overall performance of UASB reactor followed by different post treatment techniques are indicated in *Figure 16*.

According to Bhatti et al. (2014), UASB effluent was treated with 40% H_2 O_2 in a further step. A 2 ml/l dose of H_2O_2 was originate to be very effective and shows a removal of 73% for TSS, 99.9% for COD, 84% for TN and 19.8% for PO4 3 - Post-treatment of UASB effluents using H_2 O_2 was very attractive in removal of COD and TN. Similarly, the combined UASB-DHS system was operated continuously and the result showed that UASB-DHS system performs satisfactorily even at high organic loading rate. The total removal efficiency of the COD, BOD, and TSS were 93%, 93%,

http://www.aloki.hu ● ISSN 1589 1623 (Print) ● ISSN 1785 0037 (Online)
DOI: http://dx.doi.org/10.15666/aeer/1802_31013129

and 98%, respectively, during the first phase and decreased by 1% and 2% during the second and third phases, respectively (Doma et al., 2016) (*Fig. 17*).

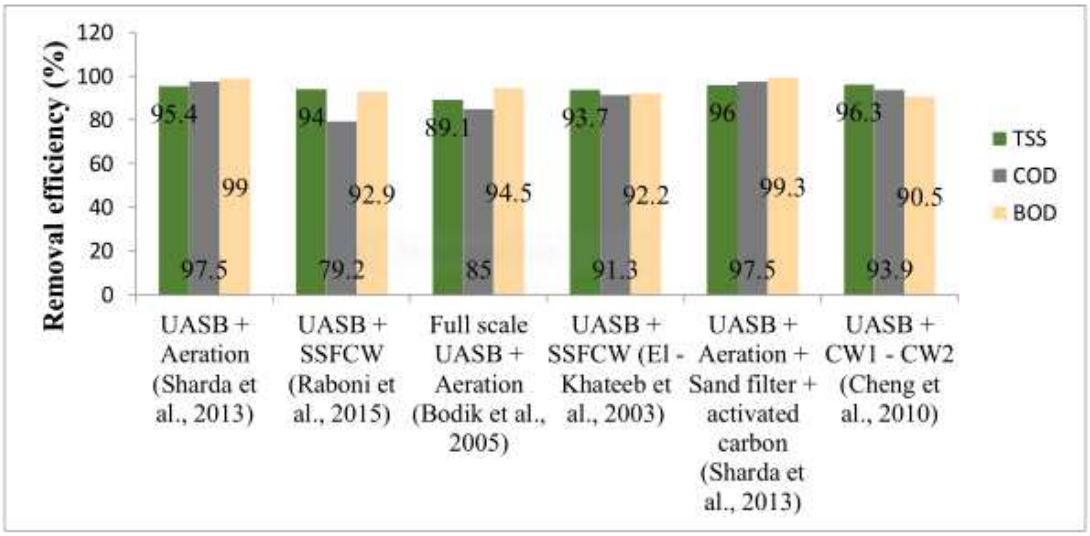

Figure 16. *TSS, COD and BOD removal efficiencies of UASB reactor integrated with different post-treatment system*

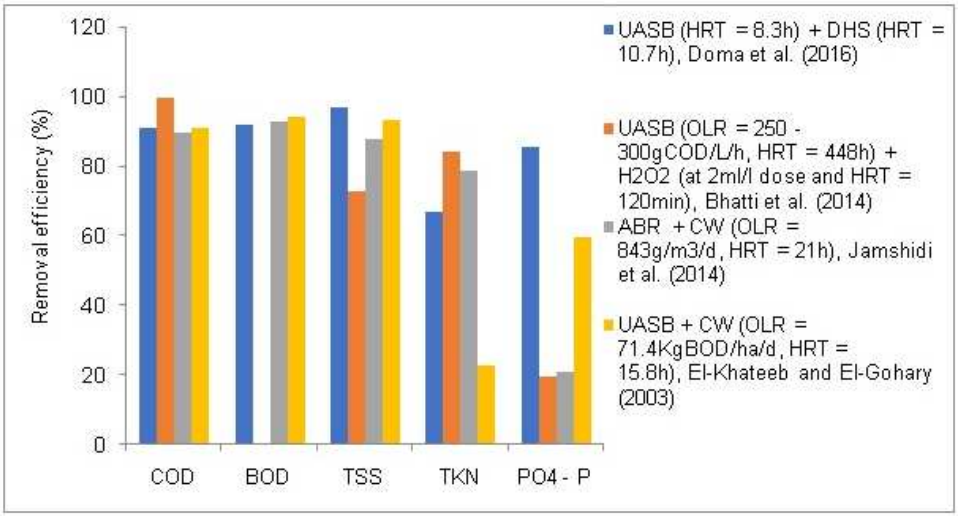

Figure 17. *Nutrient removal efficiencies of UASB reactor integrated with different post-treatment techniques*

Conclusion and recommendations

Conclusion

Now days, the strategies of treating domestic, municipal and industrial wastewaters by common and aerobic processes were shifted to the anaerobic processes. Globally, the following abatement efficiencies were achieved by UASB reactor: COD ranges from 29-92.9%, BOD ranges from 45-93.4%, TSS ranges from 40-82.6%, TKN and TP from negative values up to 74.8% and 23% and FC up to 98.6% respectively for both lab and

http://www.aloki.hu ● ISSN 1589 1623 (Print) ● ISSN 1785 0037 (Online)
DOI: http://dx.doi.org/10.15666/aeer/1802_31013129

full scales. Despite its success, UASB reactors are regularly unable to attain most of the present effluent discharge standards due to presence of high residual COD and BOD, nutrients and pathogens.

All these features make the UASB treatment of wastewater is a very significant field of research, where enhancements and new progresses are needed to overcome the problem. Thus, additional post treatment approach is compulsory for the anaerobic bioreactor treated effluents for sustainable reuse. At present, integrated constructed wetlands are recognized as a reliable wastewater technology because, they are low cost, simply functioned and sustained and have a strong potential for application in developing countries.

Most research investigation results revealed that use of a UASB reactor followed by a subsurface horizontal flow phytoremediation treatment system is a hopeful natural technology in the treatment of municipal or industrial wastewater. Because, the combined treatment system was found to complying with WHO (1989) standards for treated effluent reuse. Globally, the subsequent abatement efficiencies were achieved using UASB-CW treatment systems: COD ranges from 79.2-93.9%, BOD ranges from 89.2-92.9%, TSS ranges from 87.2-96.3%, TKN ranges from 22.6-96.9%, TP ranges from 33 to 85.9%, and FC ranges from 97.9 to 99.99%, respectively.

Recommendations

Enhanced water quality change due to industrial pollution is one of the great environmental concerns in the world. Most of the wastewaters in developing countries are still discharged directly to rivers, streams and open lands without adequate and comprehensive management. To reduce the indiscriminate disposal of these industrial and municipal wastewaters it is essential to provide a low-cost strategy which can bring comprehensive resource management. Literature review indicates that UASB-CW technologies are effectively integrated treatment particularly for resource scarce developing countries to adopt wastewater treatment, the treatment technologies must be cost-effective and easy to adopt, requires less energy input, easy operation and maintenance costs. Therefore, it is inevitable to adopt this technology in our country for in order to encounter effluent discharge standards with low costs.

Acknowledgments. The authors acknowledge to all authors of the original articles, books, and book chapters that we used freely for writing this reviewed article. The author also would like to thank the editor and the two reviewers for their constructive comments, which helped a lot to improve the original manuscript.

REFERENCES

[1] Aiyuk, S., Amoako, J., Raskin, L., van Haandel, A., Verstraete, W. (2004): Removal of carbon and nutrients from domestic wastewater using a low investment, integrated treatment concept. – Wat. Res. 38: 3031-3042.

[2] Aiyuk, S., Odonkor, P., Theko, N., et al. (2010): Technical evaluation of potential drawbacks in direct UASB treatment of raw domestic sewage. – 2010 International Conference on Environmental Engineering and Applications, IEEE, pp. 320-326.

[3] Atashi, H., Ajamein, H., Ghasemian, S. (2010): Effect of operational and design parameters on removal efficiency of a pilot-scale UASB reactor in a sugar factory. – World Applied Sciences Journal 11: 451-456.

http://www.aloki.hu ● ISSN 1589 1623 (Print) ● ISSN 1785 0037 (Online)
DOI: http://dx.doi.org/10.15666/aeer/1802_31013129

[4] Bani, R. (2011): Wastewater Management. – In: Einschlag, F. S. G. (ed.) Waste Water: Evaluation and Management. Intechopen, London.
[5] Bhatti, A. Z., Maqbool, F., Malik, H. A., Mehmood, Q. (2014): UASB reactor startup for the treatment of municipal wastewater followed by advanced oxidation process. – Brazilian Journal of Chemical Engineering 31: 715-726.
[6] Bodik, I., Gasparikova, E., Kapusta, S., Derco, J., Kratochvil, K. (2005): Evaluation of anaerobic-aerobic wastewater treatment plant operations. – Polish Journal of Environmental Studies 14: 29-33.
[7] Bukhari, F., Rizvi, H., Ahmad, N., Abbas, H. I., Yasar, A., Ali, S., Yasmeen, T., Riaz, M. (2015): Start-up of UASB reactors treating municipal wastewater and effect of temperature/sludge and hydraulic retention time (HRT) on its performance. – Arabian Journal of Chemistry 8: 781.
[8] Bula, K. (2014): Treatment and biogas production performances efficiency of St. George Brewery full scale waste water treatment system. – Thesis. Addis Ababa (ET), Addis Ababa University.
[9] Cavalcanti, P., Van Haandel, A., Lettinga, G. (2001): Polishing ponds for post-treatment of digested sewage. Part 1: Flow-through ponds. – Water Science and Technology 44: 237-245.
[10] Chan, Y. J., Chong, M. F., Law, C. L., et al. (2009): A review on anaerobic–aerobic treatment of industrial and municipal wastewater. – Chemical Engineering Journal 155: 1-18.
[11] Cheng, L. L., Lee, Y. H., Lin, H. J., Chou, S. M. (2010): Treatment of mixture of sewage and partially treated swine wastewater by a combination of UASB and constructed wetlands. – Pract. Period. Hazard. Toxic Radioact. Waste Manage. 14: 234-239.
[12] Chernic haro, C. (2007): Anaerobic Reactors. Vol. 4: Biological wastewater treatment Series. – IWA Publishing, London.
[13] Chernic haro, C., da Silva Cota, R., Zerbini, A. M., et al. (2001): Post-treatment of anaerobic effluents in an overland flow system. – Water Science and Technology 44: 229-236.
[14] De Kock, M. (2015): Anaerobic Bioconversion of Liquid and Solid Wastes from the Winemaking Process. – Stellenbosch University, Stellenbosch.
[15] De la Varga, D., Diaze, M. A., Ruiz, I., Soto, M. (2013): Heavy metal removal in UASB-CW system treating municipal wastewater. – Chemosphere 93(7): 1317-23.
[16] De Mes, T., Stams, A., Reith, J., et al. (2003): Methane Production by Anaerobic Digestion of Wastewater and Solid Wastes. – Reith, J. H. et al. (eds.) Bio-Methane and Bio-Hydrogen: Status and Perspectives of Biological Methane and Hydrogen Production. Dutch Biological Hydrogen Foundation, Petten, pp. 58-102.
[17] De Sousa, J., Van Haandel, A., Guimaraes, A. (2001): Post-treatment of anaerobic effluents in constructed wetland systems. – Water Science and Technology 44: 213-219.
[18] Doma, H. S., El-Kamah, H. M., El-Qelish, M. (2016): Slaughterhouse wastewater treatment using UASB reactor followed by down flow hanging sponge unit. – Research Journal of Pharmaceutical Biological and Chemical Sciences 7: 568-576.
[19] El-Khateeb, A. M., El-Bahrawy, Z. A. (2003): Extensive post-treatment using constructed wetland. – Life Science Journal 10: 560-565.
[20] El-Khateeb, M., El-Bahrawy, A. (2013): Extensive post treatment using constructed wetland. – Life Science Journal 10: 560-568.
[21] El-Khateeb, S. A., Regelsberger, M. A., El-Sheikh, R. M., Shehata, M. (2009): Integrated system for the treatment of black water and grey water via UASB and constructed wetland in Egypt. – Desalination and Water Treatment 8: 272-278.
[22] El-Shafai, S. A., El-Gohary, F. A., Nasr, F. A., van der Steen, P., Gijzen, H. J. (2007): Nutrient recovery from domestic wastewater using a UASB-duckweed ponds system. – Biores. Technol. 98: 798-807.

http://www.aloki.hu ● ISSN 1589 1623 (Print) ● ISSN 1785 0037 (Online)
DOI: http://dx.doi.org/10.15666/aeer/1802_31013129

[23] Elmitwalli, T., Zeeman, G., Lettinga, G. (2001): Anaerobic treatment of domestic sewage at low temperature. – Water Science and Technology 44: 33-40.
[24] Enitan, A. M. (2015): Microbial community analysis of a UASB reactor and application of an evolutionary algorithm to enhance wastewater treatment and biogas production. – http://hdl.handle.net/10321/1276.
[25] Foresti, E., Zaiat, M., Vallero, M. (2006): Anaerobic processes as the core technology for sustainable domestic wastewater treatment: consolidated applications, new trends, perspectives, and challenges. – Reviews in Environmental Science and Bio/Technology 5: 3-19.
[26] Gasparikova, E., Kapusta, S., Bodik, I., Derco, J., Kratochvil, K. (2005): Evaluation of anaerobic-aerobic wastewater treatment plant operations. – Polish Journal of Environmental Studies 14: 29-33.
[27] Gomec, C. Y. (2010): High-rate anaerobic treatment of domestic wastewater at ambient operating temperatures: a review on benefits and drawbacks. – Journal of Environmental Science and Health Part A 45: 1169-1184.
[28] Jamshidi, S., Akbarzadeh, A., Woo, K.-S., et al. (2014): Wastewater treatment using integrated anaerobic baffled reactor and bio-rack wetland planted with Phragmites sp. and Typha sp. – Journal of Environmental Health Science and Engineering 12: 131.
[29] IEA (2001): Biogas and More! Systems and Markets Overview of Anaerobic Digestion. – International Energy Agency (IEA), Paris.
[30] Kasaudhan, K. G., Mumtaz, N., Raj, V. (2013): Optimization of municipal wastewater treatment by UASB reactor and polishing pond. – An International Quarterly Journal of Biology and Life Sciences 1: 2000-207.
[31] Kebena, B. (2014): Treatment and biogas performance efficiency of St. George Brewery full scale-wastewater after treatment system. – Published MSc. Thesis, Addis Ababa University, Ethiopia.
[32] Kenatu, A. (2011): Evaluation of the performance of constructed wetland system for the treatment of brewery wastewater. – MSc Thesis, Addis Ababa University, pp. 1-3.
[33] Khan, A. A. (2012): Post treatment of UASB effluent: aeration and variant of ASP. – PhD Thesis. IIT, Roorkee, India.
[34] Khan, A. A., Gaur, R. Z., Tyagi, V., et al. (2011): Sustainable options of post treatment of UASB effluent treating sewage: a review. – Resources, Conservation and Recycling 55: 1232-1251.
[35] Khan, A. A., Gaur, R. Z., Kazmi, A. A., et al. (2013): Sustainable Posttreatment Options of Anaerobic Effluent. – In: Chamy, R. (ed.) Biodegradation - Engineering and Technology. – IntechOpen, London.
[36] Khan, A. A., Gaur, R. Z., Mehrotra, I., et al. (2014): Performance assessment of different STPs based on UASB followed by aerobic post treatment systems. – Journal of Environmental Health Science and Engineering 12: 43.
[37] Kyambadde, J., Kansiime, F., Dalhammar, G. (2005): Nitrogen and phosphorus removal in substrate-free pilot constructed wetlands with horizontal surface flow in Uganda. – Water, Air, and Soil Pollution 165: 37-59.
[38] Lew, B., Belavski, M., Admon, S., et al. (2003): Temperature effect on UASB reactor operation for domestic wastewater treatment in temperate climate regions. – Water Science and Technology 48: 25-30.
[39] Lomte, A. T., Bobade, V. (2015): Suitability of UASB reactor system in tropical developing countries like India. International – Journal of Science and Research 4: 801-807.
[40] Lopez-Lopez, A., Merino-Solis, L. M., Villegas, E., de Anda, J. (2015): The Effect of the hydraulic retention time on the performance of an ecological wastewater treatment system: an anaerobic filter with a constructed wetland. – Water 7: 1149-1162.

http://www.aloki.hu ● ISSN 1589 1623 (Print) ● ISSN 1785 0037 (Online)
DOI: http://dx.doi.org/10.15666/aeer/1802_31013129

[41] Ma, J. J. (2005): Study on the treatment of sewage by a combined upflow anaerobic sludge blanket (UASB)-constructed wetland process. – Published MSc Thesis, Institute of Environmental Engineering, National Sun Yat-sen Univ., Taiwan.
[42] Mahmood, B. S., Z., Q., Jadoon, S., Pervez, A., Irshad, M., Bilal, M., Bhatti, A. Z. (2013): Combined industrial wastewater treatment in anaerobic bioreactor post-treated in constructed wetland. – Biomed Research International 8: 1-7.
[43] Martin-Ryals, A. (2012): Evaluating the potential for improving anaerobic digestion of cellulosic waste via routine bioaugmentation and alkaline pretreatment. – MSc Thesis, University of Illinois at Urbana-Champaign.
[44] Metcalf & Eddy, Tchobanoglous, G., Burton, F., Stensel, H. D. (2003): Wastewater Engineering: Treatment and Reuse. 4th Ed. – McGraw-Hill, Boston.
[45] Moawad, A., Mahmoud, U., El-Khateeb, M., et al. (2009): Coupling of sequencing batch reactor and UASB reactor for domestic wastewater treatment. – Desalination 242: 325-335.
[46] Mungray, A. K., Patel, K. 2011. Coliforms removal in two UASB + ASP based systems. – International Biodeterioration and Biodegradation 65: 23-28.
[47] Mutombo, D. T. (2004): Internal circulation reactor: pushing the limits of anaerobic industrial effluents treatment technologies. – Proceedings of the 2004 Water Institute of Southern Africa (WISA) Biennial Conference, pp. 608-616.
[48] Nada, T., Moawad, A., El-Gohary, F. A., Farid, M. N. (2011): Full-scale municipal wastewater treatment by up-flow anaerobic sludge blanket (UASB) in Egypt. – Desalination and Water Treatment 30: 134-145.
[49] Nair, A. T., Ahammed, M. M. (2013): The reuse of water treatment sludge as a coagulant for post-treatment of UASB reactor treating urban wastewater. – Journal of Cleaner Production 96: 272-281.
[50] Noykova, N., Mueller, T. G., Gyllenberg, M., et al. (2002): Quantitative analyses of anaerobic wastewater treatment processes: identifiability and parameter estimation. – Biotechnology and Bioengineering 78: 89-103.
[51] Okurut, T. O., Rijs, G. B. J., van Bruggen, J. J. A. (1999): Design and performance of experimental constructed wetlands in Uganda, planted with Cyperus papyrus and Phragmites mauritianus. – Water Science and Technology 40: 265-271.
[52] Oliveira, S. C., von Sperling, M. (2011): Performance evaluation of different wastewater treatment technologies operating in a developing country. – Journal of Water Sanitation and Hygiene for Development 1: 37-56.
[53] Pantea, E. V., Romocea, T. (2008): Thermophilic anaerobic wastewater treatment. – Protectia Mediului, Analele Universitatii din Oradea 8: 454-458.
[54] Raboni, M., Gavasci, R., Urbini, G. (2014): UASB followed by sub-surface horizontal flow phytodepuration for the treatment of the sewage generated by a small rural community. – Sustainability 6(10): 6998-7012.
[55] Rosa, A. P., Lobato, L. C. S., Chernicharo, C. A. L., Martins, D. C. R. B., Maciel, F. M., Borges, J. M. (2012): Improving performance and operational control of UASB reactors via proper sludge and scum discharge routines. – Water Practice and Technology 7. https://doi.org/10.2166/wpt.2012.046.
[56] Saleh, M. M., Mahmood, U. F. (2003): UASB/EGSB applications for industrial wastewater treatment. – Seventh International Water Technology Conference, Cairo, Egypt, 1-3 April 2003.
[57] Saleh, M. M., Mahmood, U. F. (2004): Anaerobic digestion technology for industrial wastewater treatment. – Proceedings of the Eighth International Water Technology Conference, IWTC, Alexandria, Egypt, 26-28 March, 2004.
[58] Sharda, A. K., Sharma, M., Kumar, S. (2013): Performance evaluation of brewery waste water treatment plant. – International Journal of Engineering Practical Research 2: 105-111.

http://www.aloki.hu ● ISSN 1589 1623 (Print) ● ISSN 1785 0037 (Online)
DOI: http://dx.doi.org/10.15666/aeer/1802_31013129

[59] Singh, L., Alam, S., Ramana, K. (1999): Effect of fluctuating temperature regime on psychrophilic anaerobic digestion of nightsoil. – Defence Science Journal 49: 135-140.
[60] Sushma, P. J. (2013): Performance of UASB reactor at different flow rate treating sewage wastewater. – International Journal of ChemTech Research 5: 676.
[61] Tandukar, M., Ohashib, A., Harada, H. (2007): Performance comparison of a pilot-scale UASB and DHS system and activated sludge process for the treatment of municipal wastewater. – Water Res. 42: 297.
[62] Van Lier, J. B., Zeeman, G., Huibers, F. (2002): Anaerobic (pre-) treatment for the decentralised reclamation of domestic wastewater, stimulating agricultural reuse. – Proceedings of the VII Latin American Workshop and Symposium on Anaerobic Digestion, 22-25 October 2002, Merida, Mexico.
[63] Von Sperling, M., Mascarenhas, L. (2005): Performance of very shallow ponds treating effluents from UASB reactors. Water Science and Technology 51: 83-90.
[64] Walia, R., Kumar, P., Mehrotra, I. (2011): Performance of UASB based Sewage treatment plant in India: polishing by diffusers an alternative. – Water Science and Technology 63: 680-688.
[65] WHO (1989): Health Guidelines for the Use of Waste Water in Agriculture and Aqua Culture. – http.//apps.who int/iristhandle/10665139401.
[66] Yasar, A., Tabinda, A. B. (2010): Anaerobic treatment of industrial wastewater by UASB reactor integrated with chemical oxidation processes. An overview. – Pol. J. Environ. Stud 19: 1051-1061.
[67] Zhang, L. (2016): Anaerobic treatment of municipal wastewater in a UASB-Digester system: temperature effect on system performance, hydrolysis and methanogenesis. – Dissertation, Wageningen University, Wageningen.

http://www.aloki.hu ● ISSN 1589 1623 (Print) ● ISSN 1785 0037 (Online)
DOI: http://dx.doi.org/10.15666/aeer/1802_31013129

RESEARCH ON THE RUNOFF OF ARID DESERT GRASSLANDS UNDER CHANGING ENVIRONMENTS IN CHINA

HAO, W. G.[1,2] – LI, H. P.[1,2] – LIU, H.[1,2*] – WANG, L. X.[2] – JIAO, R.[2] – LIU, H. L.[2] – SONG, Y. F.[2] – CUI, L. P.[2]

[1]*State Key Laboratory of Simulation and Regulation of Water Cycle in River Basin, China Institute of Water Resources and Hydropower Research, Beijing 100044, China*

[2]*Ministry of Water Resources of Pastoral Water Institute of Science, Hohhot 010020, China (phone: +86-130-8712-1336)*

[*]*Corresponding author*
e-mail: 13087121336@163.com; phone: +86-130-8712-1336; fax: +86-047-1469-0603

(Received 30th Aug 2019; accepted 12th Feb 2020)

Abstract. Reasonable allocation of water resources in dryland pastures plays a decisive role in local ecological protection and economic development. Changes in the local climate and vegetation have a direct impact on the local runoff. With Darhan Muminggan Joint Banner (DM Banner) as the study area in China, we made use of the Soil and Water Assessment Tool (SWAT) hydrological model, calibrated and fitted the parameters into the model according to the local meteorological statistics and data on land utilization, soil texture and runoff. After fitting and calibration, we built a SWAT model for arid desert grasslands to simulate and forecast re-distribution of water resources in the study area under changes in the climate and vegetation. This study is expected to provide technical support for reasonable development and utilization of water resources in dryland pastures as well as ecological recovery in Inner Mongolia of China.
Keywords: *water resources, SWAT model, hydrological response unit, scenario simulation, efficient utilization*

Introduction

The hydrological process of surface runoff is a very complicated natural mechanism subject to impacts of multiple factors including the climate, geomorphological conditions and vegetation. This process follows varied working mechanisms under different dimensions of time and space, and the accompanying water dynamics and water circulation in the process is subject to changes by time, space and the conditions of the underlying surface. The hydrological process can be divided into three interconnected parts: the physical process, the chemical process and the ecological effect. The runoff yield and confluence are closely correlated with the hydrological process in dryland pastures (Wang et al., 2003, 2008; Zhang et al., 2003, 2005; Huang and Zhang, 2010).

To identify the mechanism of the hydrological cycle in the arid pastoral area under climate changes and intensive human activities in this region of China, this study used the SWAT model to simulate the runoff of the arid pastoral area in DM Banner in Inner Mongolia, China, and analyzed the changes in the runoff with changes in land utilization to provide a scientific basis for optimized management of land resources and water resources in this region.

http://www.aloki.hu ● ISSN 1589 1623 (Print) ● ISSN 1785 0037 (Online)
DOI: http://dx.doi.org/10.15666/aeer/1802_31313145

Review of Literature

The SWAT model is a distributed hydrological model developed by USDA Agricultural Research Center (USDA-ARS), which is a distributed hydrological model developed on the basis of CREAMS, EPIC, GLEAMS and other models. SWAT model can simulate the effects of land management activities on water volume and quality, sediment migration, pesticide and nutrient leaching in large and complex rivers (Hoang et al., 2017). Manoj and Friedrich (2016) applied SWAT model to conduct comparative evaluation on the simulation results of runoff and nutrient loads in Onkaparingacatchment basin of south Australia through single-station and multi-station calibration. Bannwarth et al. (2014) applied SWAT model to simulate the pesticide transport in Mae Sa basin in northern Chiang mai, Thailand. El-Khoury et al. (2015) used SWAT model to simulate the effects of future climate and land use changes on nitrogen and phosphorus content in Canadian river basins. On the basis of research achievements by international researchers, researchers in China have improved research methods and used new technologies in recent years, and they have made substantial progress in analysis, simulation and forecast of runoff generation and confluence. Many Chinese researchers have done research on changes of runoff in different regions via the SWAT model, such as studies on water basins in Loess Plateau, studies on the Black River basin by Lai et al. (2013), studies on the Wei River basin by Zhao et al. (2015), studies on the Jing River basin along the northern slope of Mount Tianshan in Xinjiang by Meng et al. (2014), and studies on the Kuye River basin by Cheng et al. (2009). Besides, Duan et al. (2014) and Guo et al. (2014) analyzed whether the SWAT model was applicable to research on the Huang-Huai-Hai region. Li et al. (2013) and Yuan et al. (2015) have studied the influence of land utilization and climate changes on the runoff of the Taihu basin and the Liuxi River basin, respectively, in 2013 and 2015. Li et al. (2014) analyzed the characteristics of changes in the land surface albedo on Loess Plateau. Chen et al. (2014) made forecasts on the runoff of the purple-soil slope land in basins and hills in southeast China. Wei et al. (2014) made sensitivity analysis of the SWAT model to landscape changes with the Old Guan River basin in Danjiangkou as the study case in 2014. Yu et al. (2013) improved the computing of the snowmelt module in SWAT with Yingluo Gorge in Shaanxi as the study case.

Studies mentioned above focused on regions including the Loess Plateau, mountainous areas in southwest China and hills in Sichuan and Shanxi; however, there are few studies made on arid grasslands in Inner Mongolia that are subject to semi-arid and arid continental climates in the temperate climate zone. Currently, few studies have been made on correlations between the hydrological process of surface runoff in in China's arid pastoral area and the local climate and ecology, so it is difficult to summarize the hydrological mechanism of this special region according to existing studies.

Materials and Methods

Study Area

Located in the north of Baotou City, Inner Mongolia Autonomous Region, China, Darhan Muminggan Joint Banner adjoins Mongolia on the north, the Wulate Middle Banner of Bayannur City on the west, Wuchuan County of Hohhot and Guyang County of Baotou on the south, and the Siziwang Banner of Ulanqab on the east. The

http://www.aloki.hu ● ISSN 1589 1623 (Print) ● ISSN 1785 0037 (Online)
DOI: http://dx.doi.org/10.15666/aeer/1802_31313145

geographic coordinates are between 41º16´N and 42º45´N, between 109º15´E and 111º25´E. Under the administration of this banner are Bayinhua Town, Mandula Town, Wuke Town, Shibao Town, Bailingmiao Town, Xilamuren Town, Mingan Town and Darhan Sumu, covering an area of 18177 km^2. Subject to the temperate continental climate, the DM Banner has cold winters, dry springs with strong sandstorms and hot summers. The average annual temperature in this region is 4.34℃, the highest annual temperature reaches 38℃ and the lowest reaches -39.4℃. The maximum precipitation is 425.2 mm, the minimum precipitation is 165.3 mm, and the average annual precipitation is 253.45 mm. The average amount of surface water evaporation is 2480.57 mm and the frost-free season lasts 90 to 120 days long. The Banner is located on the north of Mountain Daqing and the central area of the Inner Mongolian Plateau. With the southern region higher than the northern region, the study area has low mountains in the south, mild hills in the north and a flat and open plateau in the center, with an average altitude of 1376 m. With the highest altitude of 1846 m at Habtegegisu Ovoo, mountains in the study area is about 1300 m high, with a relative elevation of 30 m to 100 m. The Tengenor Lake marks the lowest point of the study area, with an altitude of 1058 m. Due to horizontal and vertical soil zones, the soil structure of the DM Banner has salient zonal features; meanwhile, because of differences in the landform and water resources, part of the soil in the study area shows intrazonal features.

The natural vegetation in DM Banner varies as the landform, soil, and hydrothermal conditions differ, forming three vegetation zones – typical arid grassland vegetation zone, desert grassland zone and steppe desert zone, from south to north, with vegetation of steppe deserts as the major type of vegetation. The typical arid grassland is mainly in the southern part of the Banner, accounting for 33% of the total area of grasslands there, the rate of grass coverage reaches 28%. The desert grassland is in the central area of the Banner, covering 27% of the area of the grassland in the Banner, the rate of grassland coverage is between 22% to 23%. The steppe desert is located in the north of the Banner, covering 35% of the area of the grasslands in the Banner, the vegetation is sparse and the rate of grassland coverage is between 15% and 22%.

Database Building and Data Analysis

Through the SWAT2009 model the paper builts a model for the basin of the arid pastoral area in DM Banner. The data required to build the SWAT model are shown in *Table 1*. Of all the parameters used by the model, rainfall uses the series daily precipitation provided by Bailingmiao Hydrological Station and Meteorological Station (not a site) from 1975 to 2015. And meteorological data includes mean daily maximum temperature for 12 months, mean daily minimum temperature for 12 months, daily deviation of monthly maximum temperature, daily deviation of monthly minimum temperature, monthly mean precipitation, monthly precipitation deviation, monthly day precipitation skewness coefficient, two precipitation probabilities of wet and dry transition, monthly mean precipitation days, most half hour precipitation, monthly mean net solar radiation, monthly average dew point temperature and monthly mean wind speed. All the parameters of the Bailingmiao Meteorological and Hydrological stations for 12 months are calculated by programming according to the daily data and written into the meteorological database according to the input format of the model.

http://www.aloki.hu ● ISSN 1589 1623 (Print) ● ISSN 1785 0037 (Online)
DOI: http://dx.doi.org/10.15666/aeer/1802_31313145

Table 1. *Basic Information and Source of Modelling Data*

Data	Resolution	Length of time	Format	Source
DEM	30m×30m		GRID	National Imagery and Mapping Agency (NIMA) & National Aeronautics and Space Administration (NASA)
Vegetation map	1:1,000,000		GRID	Institute of Grassland Research of CAAS
Soil type	1:1,000,000		GRID	Institute of Soil Science, CAS
Meteorological data	Daily scale	1975-2015	DBF	Bailingmiao Meteorological Station Daily precipitation, Daily maximum and minimum temperature, Mean daily temperature, Daily humidity, Daily wind speed, Daily solar radiation, etc
Hydrological data	Daily scale	1975-2015	XLSX	Bailingmiao Hydrological Station Monthly average runoff, Daily precipitation, Daily mean temperature, etc

DEM-based Hydrological Data Extraction

The basin map is produced based on the surface runoff model and according to the flow routes identified by the concept of hydrological overland flow. This method determines the direction of water flow according to the largest slope between a given grid cell in the DEM (*Figure 1*) and its eight adjacent cells, calculates the area of upstream catchment area of each cell, demarcates a drainage basin according to the threshold of a catchment area and extracts the hydrological features of the study area, as shown in *Figure 2*.

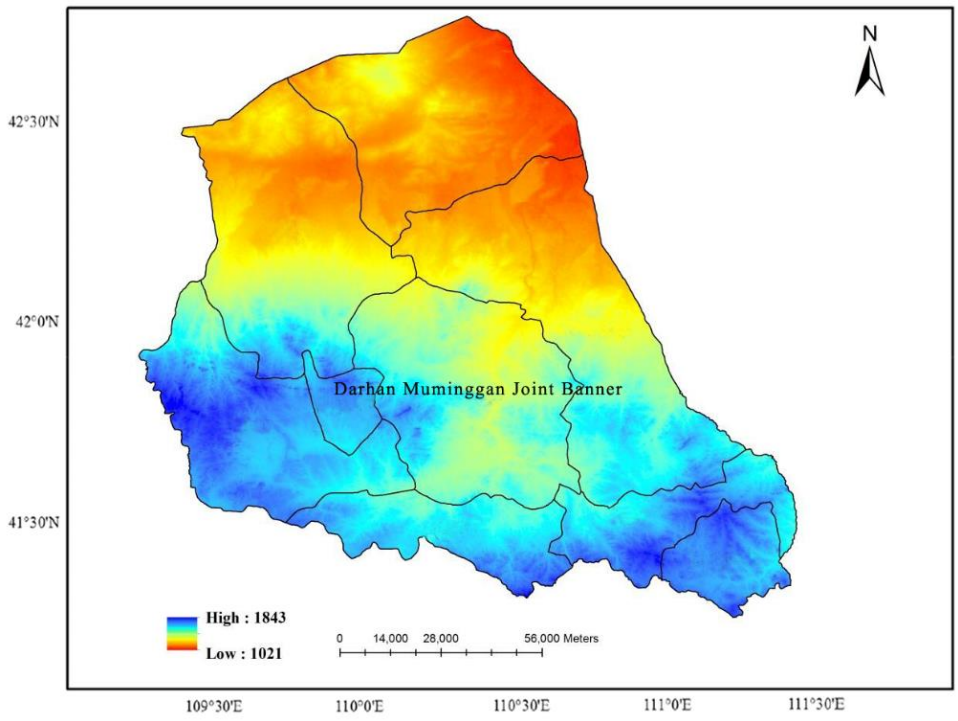

Figure 1. *Digital Elevation Model of DM Banner*

http://www.aloki.hu ● ISSN 1589 1623 (Print) ● ISSN 1785 0037 (Online)
DOI: http://dx.doi.org/10.15666/aeer/1802_31313145

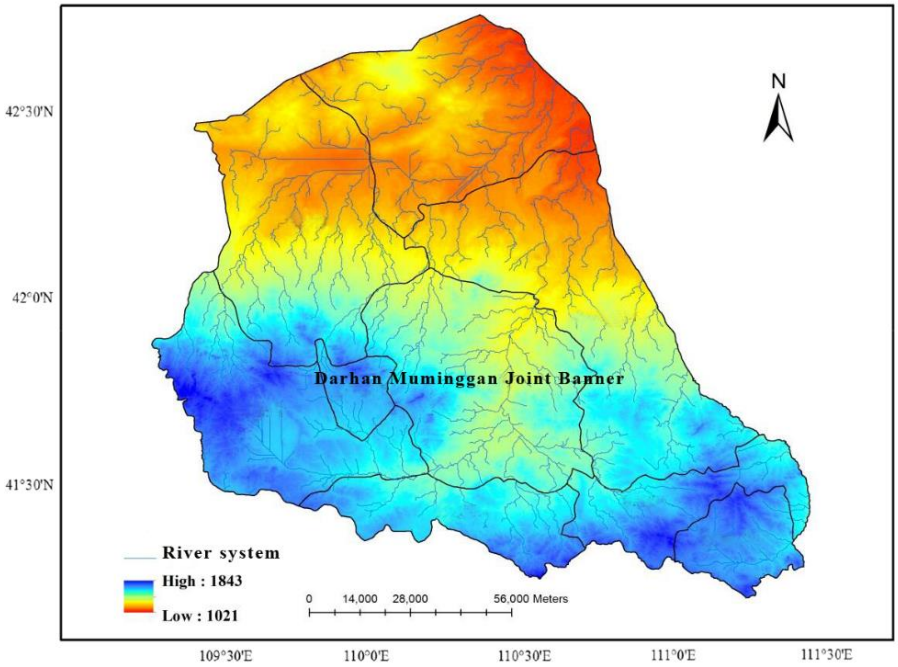

Figure 2. *Natural Drainage System of DM Banner*

Soil Database

The soil database uses the traditional "soil genetic classification" system and the basic charting unit is the subgroup level. There are 12 types of soil in the study area, including Calcic Gleysols (GLk), Cambic Arenosols (ARb), Calcaric Arenosols (ARc), Luvic Calcisols (CLl), Calcaric Fluvisols (FLc), Salic Fluvisols (FLs), Haplic Kastanozems (KSh), Calcic Kastanozems (KSk), Calcaric Phaeozems (PHc), Gleyic Phaeozems (PHg), Calcic Planosols (PLk) and Water Regime (WR), as shown in *Figure 3*.

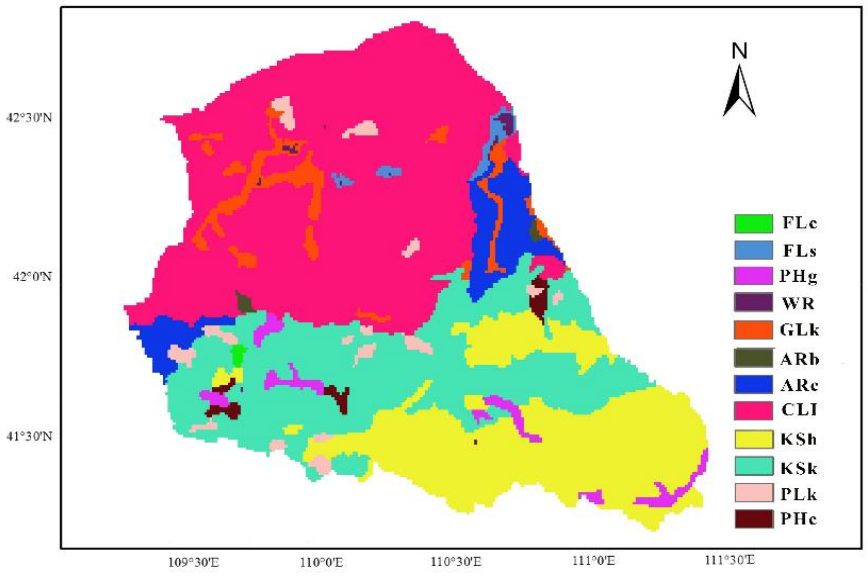

Figure 3. *Types of Soil in DM Banner*

http://www.aloki.hu ● ISSN 1589 1623 (Print) ● ISSN 1785 0037 (Online)
DOI: http://dx.doi.org/10.15666/aeer/1802_31313145

The soil database needs to input physical and chemical parameters of various types of soil, mainly including soil name, soil stratification number, soil hydrology grouping, total soil thickness, porosity and physical and chemical parameters of each layer of soil. These parameters are given by DM Banner Soil and the physical and chemical parameters' investigation results of typical soil profile.

Vegetation Database

The vegetation map reflects the types of vegetation, the formation and sub-formation of vegetation, the conditions of horizontal zonal features and vertical zonal features. This study classified the vegetation in the study area according to the national land utilization classification system and built a vegetation database, as shown in *Figure 4*. The vegetation map and the attribute data in the vegetation database were connected through the lookup table (luc.txt) of the land utilization data. The physiological parameters of the vegetation are mostly determined through actual surveying, and given the actual conditions, the measured types of vegetation were compared and matched with the configured types of vegetation in the database of the model so that the types of vegetation in the study area were converted to the configured types in the model. The respective physiological parameters were revised according to actual conditions.

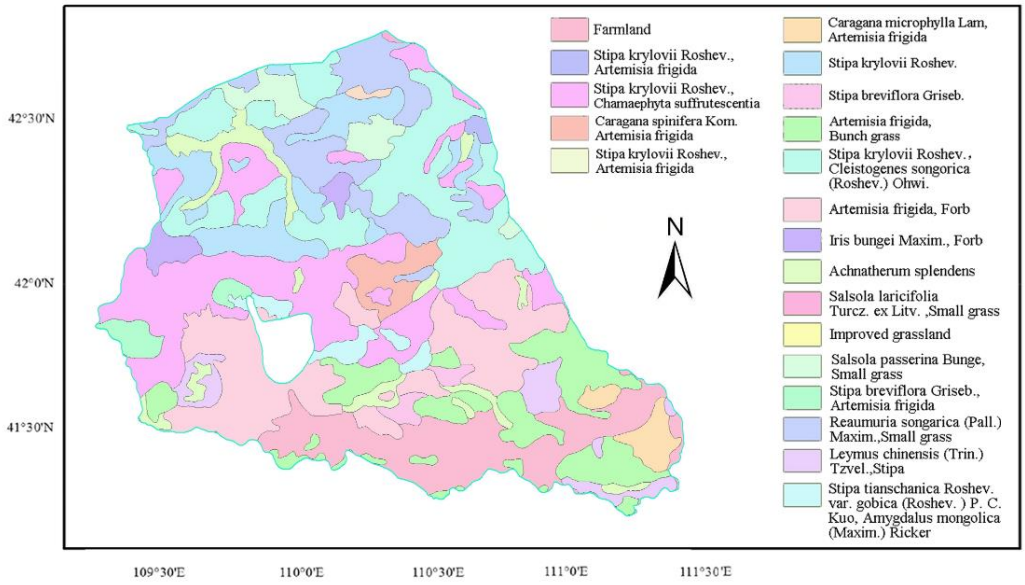

Figure 4. *Vegetation Map of DM Banner*

Hydrological Data

There was only one monitoring section in the study area, so a control node was set at the Bailinmiao Hydrologic Station to be used as runoff control and check section. The time scale was from 1975 to 1996. There are seven artificial reservoirs in the research area, as shown in *Figure 5*. Among them, the total reservoir capacity of Huanghua Beach reservoir, which is of medium and large size, accounts for 45.3% of the total reservoir capacity. And the total reservoir capacity of Yangyoufang reservoir accounts for 25.7% of the total reservoir capacity. The total storage capacity of the above two

http://www.aloki.hu ● ISSN 1589 1623 (Print) ● ISSN 1785 0037 (Online)
DOI: http://dx.doi.org/10.15666/aeer/1802_31313145

reservoirs accounts for 71% of the total storage capacity of the region. So the paper selects the above two reservoirs as a representative. In model, all of above two reservoirs' operation parameters, such as normal water level and its corresponding storage capacity, flood discharge level and corresponding storage capacity, hydraulic permeability coefficient of reservoir bottom, the year when the reservoir began to operate, the water storage way and drainage way, are input database. The water consumption data in the study area were obtained from statistical data and visits and surveys of relevant industry departments. According to the above data, the average annual total water consumption of each department in the region was 50,797,000 m³, which was mainly obtained from surface water and groundwater, and the total displacement is 6,688,800 m³, including 721,100 m³ for irrigation regression recharge of groundwater, 4,879,800 m³ for industry, 568,000 m³ for tertiary production, 520,000 m³ for urban residents living.

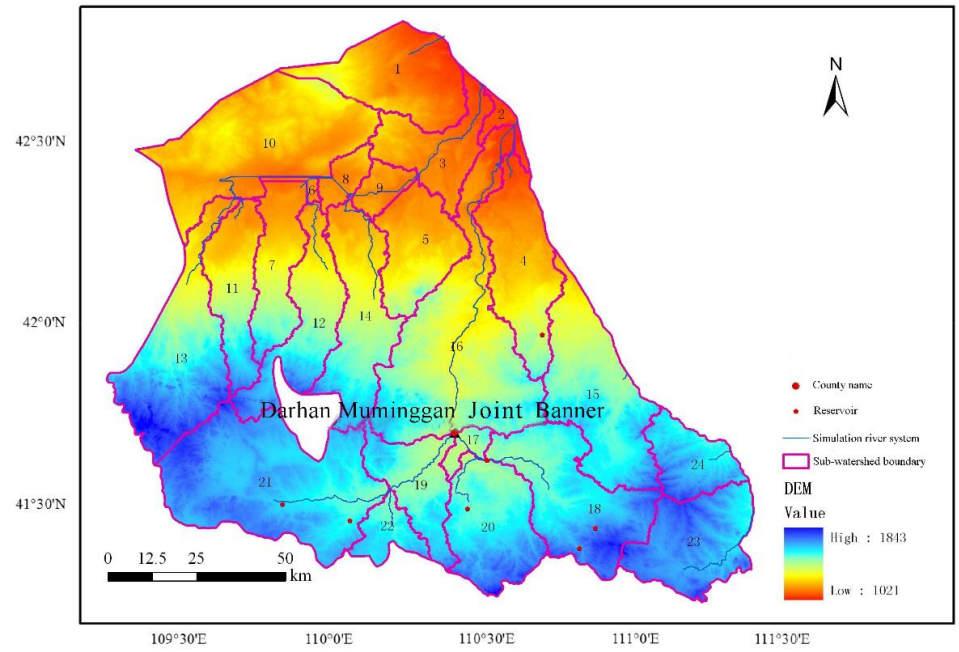

Figure 5. *Drainage System and Sub-Catchments*

The multi-year average water resources utilization and excretion data were modeled. Identifiable file by the model, which is composed of the position of intake and discharge ports, monthly water discharge and monthly water displacement, is input into the model.

Modelling and Result Analysis

Sub-Catchment and Division of Hydrological Response Unit (HRU)

On the distributed hydrological ArcSWAT model platform and according to the pre-set threshold of accumulated flow of 100 km^2, the study area was distributed into 24 sub-catchments, as shown in *Figure 5*. The hydrological response unit consisted of three layers of data including the types of vegetation, the types of soil and the types of slopes. The types of vegetation were defined according to the vegetation map and the vegetation classification link; the types of soil was defined according to the soil map

http://www.aloki.hu ● ISSN 1589 1623 (Print) ● ISSN 1785 0037 (Online)
DOI: http://dx.doi.org/10.15666/aeer/1802_31313145

and the soil link; as there are no large gradients of slopes in the study area, there types of slopes were defined: slopes with a gradient between 0 and 15°, slopes with a gradient between 15° and 30°, and slopes with a gradient of 30°. The hydrological response units were divided according to the percentage of data on each layer. We assume that when the rate of vegetation coverage in a region exceeds 15%, the area of a type of soil exceeds 15% and the area of a type of slope exceeds 15%, it forms a hydrological response unit. Each sub-catchment has multiple HRUs and there are 70 HRUs in the study area.

Model Calibration and Validation

Given that the underlying surface conditions including vegetation coverage and soil in the 1980s and the 1990s are distinct from those in the 1950s and 1960s due to rapid development, and one hydrological cycle was included during the calibration period, the years from 1975 to 1985 are selected as the period for calibration of model parameters, and the years from 1987 to 1996 are selected as the period for model validation. The SWAT model uses the Nash–Sutcliffe model efficiency coefficient (NSE), the relative coefficient (R^2) and the relative error (RE) to analyze the modelling accuracy to identify the modelling accuracy during the calibration period and the validation period at Bailingmiao Town Hydrological Station. On the yearly scale, the NSE during the model calibration period was 0.88, the relative coefficient was 0.91 and the average error over years was 5%; during the model validation period, the NSE was 0.41, the relative coefficient was 0.42 and the average error over years was -7%, as shown in *Table 2*. The results of modelling accuracy during the model calibration period and the model validation period on the yearly scale are shown in *Figure 6* and *Figure 7*.

Table 2. *Simulation Effect of Yearly Scale Runoff by SWAT Model*

Period of time	Year	Runoff (m^3/s)	Simulated runoff (m^3/s)	NSE	RE	R^2
Calibration period	1975	0.19	0.18	0.88	5%	0.91
	1976	0.50	0.49			
	1977	0.42	0.31			
	1978	0.10	0.09			
	1979	0.70	0.68			
	1980	0.25	0.21			
	1981	0.99	1.14			
	1982	0.12	0.12			
	1983	0.21	0.36			
	1984	0.37	0.22			
	1985	0.24	0.31			
Validation period	1987	0.089	0.22	0.41	-7%	0.42
	1988	0.55	0.27			
	1989	0.25	0.22			
	1990	0.34	0.35			
	1991	0.084	0.13			
	1992	0.25	0.41			
	1993	0.12	0.2			
	1994	0.4	0.42			
	1995	0.42	0.4			
	1996	0.13	0.21			

http://www.aloki.hu ● ISSN 1589 1623 (Print) ● ISSN 1785 0037 (Online)
DOI: http://dx.doi.org/10.15666/aeer/1802_31313145

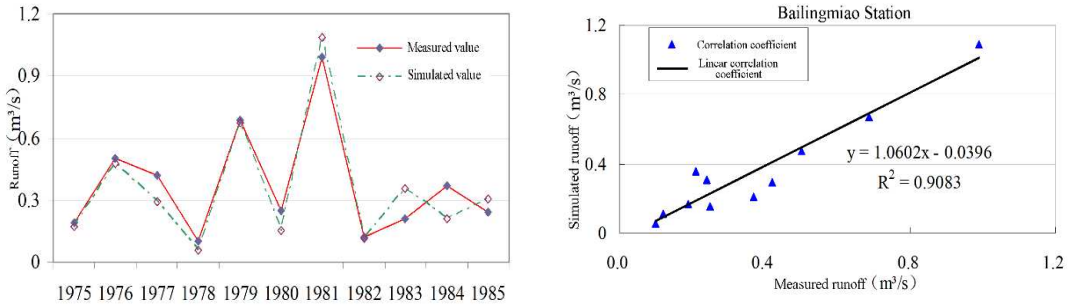

Figure 6. *Accuracy during Calibration Period on yearly scale*

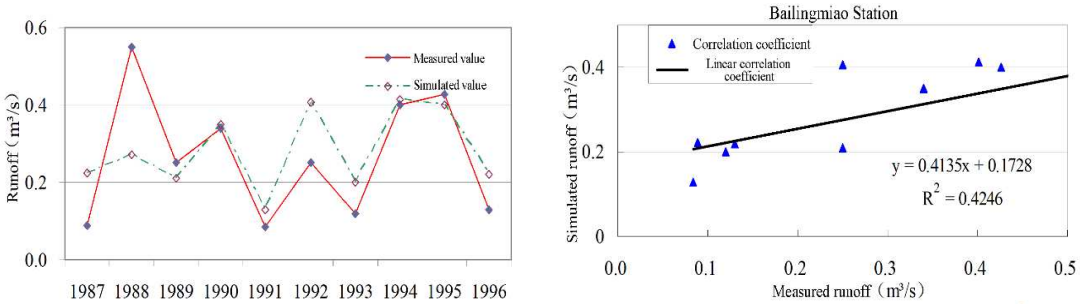

Figure 7. *Accuracy during Validation Period on yearly scale*

On the monthly scale, the NSE of Bailingmiao Town Hydrological Station during the calibration period was 0.70, the relative coefficient was 0.70 and the average relative error over years was 7%; during the validation period, the NSE was 0.47, the relative coefficient was 0.57 and the average relative error over years was 26%. Due to the large number of monthly scale data series, it is not detailed here, and the coefficients are shown in *Table 3*. On the monthly scale, the accuracy during the calibration period was shown in *Figure 8* and *Figure 9*, and that during the validation period was shown in *Figure 10* and *Figure 11*.

Table 3. *Simulation Effect of Monthly Scale Runoff by SWAT Model*

Period of time	Year	NSE	RE	R2
Calibration period	1975-1985	0.70	7%	0.70
Validation period	1987-1996	0.47	26%	0.57

The total water yield of the basin (WYLD) equals the sum of surface runoff (SURQ), lateral runoff (LATQ) and underground runoff (GWQ) subtracting the runoff losses (TLOSS) and the amount of water left in reservoirs and lakes(pond). The equation is as shown below:

$$WYLD = SURQ + LATQ + GWQ - TLOSS - pond \quad \text{(Eq.1)}$$

where, TLOSS can be neglected.

http://www.aloki.hu ● ISSN 1589 1623 (Print) ● ISSN 1785 0037 (Online)
DOI: http://dx.doi.org/10.15666/aeer/1802_31313145

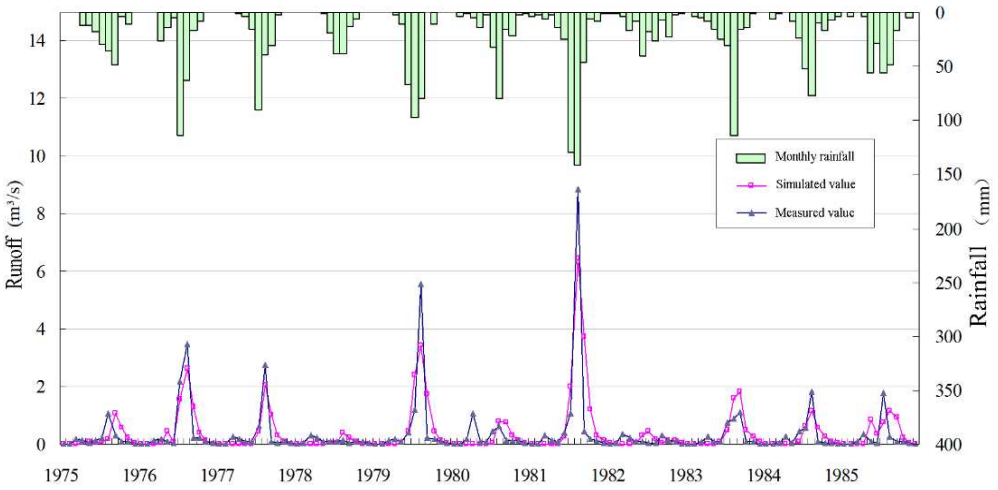

Figure 8. *Accuracy during Calibration Period on Monthly Scale*

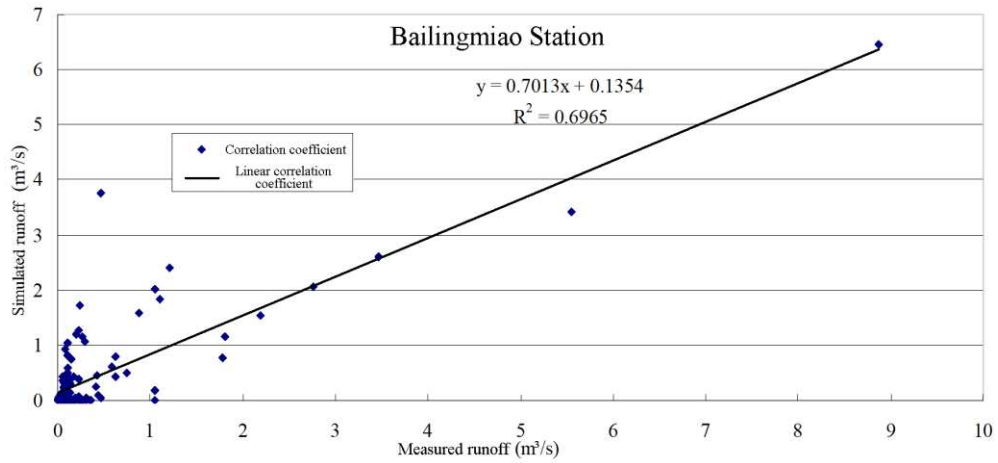

Figure 9. *Correlation between Measured Runoff and Simulated Runoff during Calibration Period on Monthly Scale*

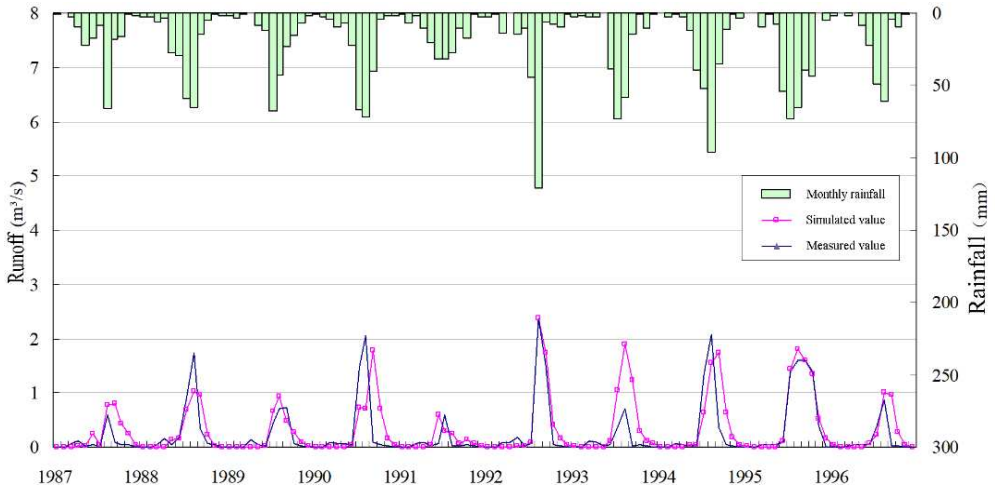

Figure 10. *Accuracy during Validation Period on Monthly Scale*

http://www.aloki.hu ● ISSN 1589 1623 (Print) ● ISSN 1785 0037 (Online)
DOI: http://dx.doi.org/10.15666/aeer/1802_31313145

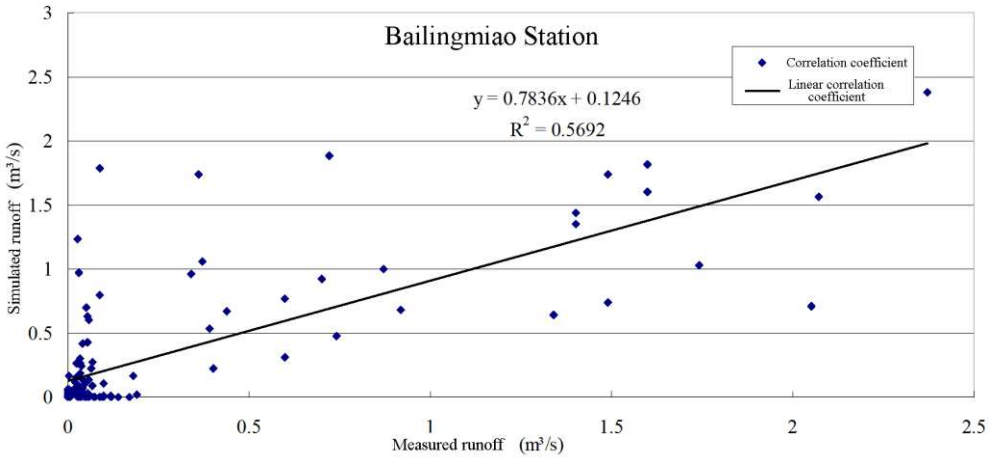

Figure 11. *Correlation between Measured Runoff and Simulated Runoff during Validation Period on Monthly Scale*

After verification with the data rate model parameters from 1975 to 1985 and the data from 1987 to 1996, the Nash coefficient and correlation coefficient were reasonable and the model parameters were reliable, the model could be used to predict the runoff changes under the changes of temperature and precipitation in the future.

Future Scenario Prediction

As the impact of the global and regional climate on forecast of climate changes in a small region is uncertain, this study defines the basic land use scenarios based on analysis of the trend of changes in meteorological factors and vegetation in the study area, and conducted quantitative modelling with calibrated model parameters to explore the impact of environmental changes on the water resources in the study area.

Climate Change

Since the end of 1980s, especially after 1995, the annual average temperature in the study area has been in the peak region, and the trend of temperature rising is very obvious, as shown in *Figure 12*.

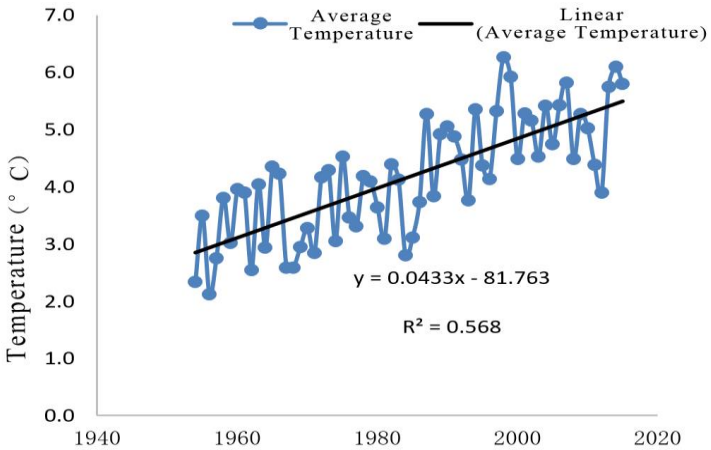

Figure 12. *Trend of Annual Average Temperature*

http://www.aloki.hu ● ISSN 1589 1623 (Print) ● ISSN 1785 0037 (Online)
DOI: http://dx.doi.org/10.15666/aeer/1802_31313145

The annual distribution of precipitation in the study area was extremely uneven, and the precipitation presented a wet - dry - wet - dry periodic change, as shown in *Figure 13*.

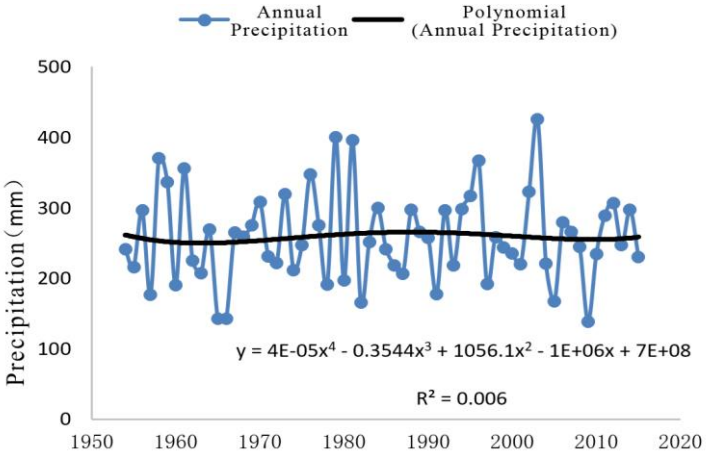

Figure 13. *Trend of Annual Precipitation*

Vegetation Changes

From 2000 to 2010, NDVI in DM Banner showed an overall trend of decrease. For many years, the maximum mean value of NDVI was 0.32, which appeared in 2004 and the minimum mean value of NDVI was 0.19, which appeared in 2009. From the above, difference degree of fluctuation was strong and there was no obvious linear relationship. It indicated that the anti-interference ability of desert steppe was poor, and the grassland showed a trend of degradation. The analysis of the relationship between the vegetation and the interannual variation of climate factors showed that temperature had positive and negative effects on the growth and development of herbage. The positive effects were mainly manifested in high temperature and good thermal conditions, which were conducive to the growth of herbage, but also the negative effects were caused by the increase of evapotranspiration consumption. And it could be showed that there was a significant positive correlation between precipitation and NDVI, with a correlation coefficient of 0.89 and increased precipitation is conducive to the growth of grass. The annual fluctuation of vegetation in DM Banner desert steppe was mainly controlled by the water condition, but the temperature was also an important factor, especially the minimum temperature (Hao et al., 2014).

Future Scenario Setting

As the result of analysis shows, the temperature in the study area increased, the precipitation showed cyclic changes, the area of surface vegetation was positively correlated to precipitation but showed no clear correlation to the temperature. Therefore, the following four future scenarios were set.

- Scenario 1: when the temperature rises 1℃ and the precipitation reduces by 10%, the rate of surface vegetation coverage drops by 10%.
- Scenario 2: when the temperature rises 1℃ and the precipitation increases by 10%, the rate of surface vegetation coverage increases by 10%.

http://www.aloki.hu ● ISSN 1589 1623 (Print) ● ISSN 1785 0037 (Online)
DOI: http://dx.doi.org/10.15666/aeer/1802_31313145

- Scenario 3: when the temperature rises 2℃ and the precipitation reduces by 10%, the rate of surface vegetation coverage drops by 10%.
- Scenario 4: when the temperature rises 2℃ and the precipitation increases by 10%, the rate of surface vegetation coverage increases by 10%.

Results

Table 4 shows the simulation result of changes in temporal and spatial distribution of water resources in four future scenarios, and the water yield in the study area in different scenarios was achieved. In Scenario 1, the water yield is 3.53 mm, equivalent to 64.16 million m^3 of water; In Scenario 2, the water yield is 5.68 mm, equivalent to 103.25 million m^3 of water; In Scenario 3, the water yield is 3.64 mm, equivalent to 66.16 million m^3; In Scenario 4, the water yield is 5.77 mm, equivalent to 104.88 million m^3. As the model requires input of lots of data, only the basic parameters available were input into the model in this study. In particular, the pastures in China are large and rivers abound in grasslands, but there are few hydrological stations which can produce only short-series data. Insufficient data may to some extent influence the accuracy of parameter model calibration and validation.

Table 4. *Forecast of Water Resources in Different Scenarios*

Scenario	Precipi-tation	Surface runoff	Underground runoff	Soil water content	Evapo-ration	Potential evaporation	Water yield	Measured Water yield
1	211.74	3.53	9.3	0.45	198.87	956.95	3.53	3.06
2	258.79	5.68	25.66	0.62	227.49	956.49	5.68	
3	211.74	3.64	8.68	0.45	199.2	996.43	3.64	
4	258.79	5.77	24.39	0.64	228.44	996.07	5.77	

Unit: mm

Discussion

Because of the lack of water resources and the fragile ecological environment in arid pastoral area of China, grassland ecological animal husbandry and regional economic and social development are mainly restricted by water resources. Reasonable and efficient use of limited water resources is the importance premise for the implementation of the corresponding industry development policy. And the ultimate goal is to achieve economic and social development of pastoral areas and grassland ecological protection win-win. So prediction of water resources in arid pastoral areas under future environmental changes is the basis of efficient utilization of local water resources.

In this paper, SWAT model was established in the study area to simulate and predict the change of local future runoff, so as to provide a scientific basis for the optimal allocation and management of region water resources in the future. Although the model input data required more, by the limit of the natural conditions of China's vast pastoral areas and numerous grasslands river, the study only collected the most basic input parameters for model. Now the number of corresponding hydrological stations is very small, and the data series is relatively short. Inadequate data input as mentioned above

http://www.aloki.hu ● ISSN 1589 1623 (Print) ● ISSN 1785 0037 (Online)
DOI: http://dx.doi.org/10.15666/aeer/1802_31313145

for parameter calibration and simulation accuracy may cause a certain influence. We have set up another long-term meteorological observatory in the Xilamuren Town of DM Banner. It's just that the monitoring time is short and it's not fully working. But we will continue to collect new meteorological and hydrological data in the future, in order to improve the model that we established and improve the accuracy of the model. This is a better support for sustainable use of water resources to support sustainable economic and social development in arid pastoral areas.

Acknowledgements. This study is supported by Natural Science Foundation of Inner Mongolia Autonomous Region of China (2017MS0516), National Natural Science Foundation of China (51009098), Special Fund of State Key Laboratory of Simulation and Regulation of Water Cycle in River Basin, China Institute of Water Resources and Hydropower Research (Grant NO. SKL2018ZY01), Xinjiang Science and Technology Support Project (201531115), and the Special Funds for Public Welfare Research of Ministry of Water Resources (201201008). Thanks are extended to the reviewers for their constructive comments.

REFERENCES

[1] Bannwarth, M. A., Sangchan, W., Hugenschmidt, C., Lamers, M., Ingwersen, J., Ziegler, A. D., Streck, T. (2014): Pesticide transport simulation in a tropical catchment by SWAT. – Enviromental Pollution 191: 70-79.

[2] Chen, Z. W., Liu, X. N., Zhu, B. (2014): Runoff estimation in hillslope cropland of purple soil based on SCS-CN model. – Transactions of the Chinese Society of Agricultural Engineering 30(7): 72-81.

[3] Cheng, L., Xu, Z. X., Luo, R., Mi, Y. J. (2009): SWAT application in arid and semi-arid region: A case study in the Kuye River Basin. – Geographical Research 28(01): 65-73.

[4] Duan, C. Y., Zhang, S., Li, J. R., Zhang, C. F., Qi, J. Y., Wu, Y. (2014): Analysis on Rainfall- Runoff Characteristics and Simulation of the Different Hydrologic Year Runoff of Xilin River Basin in Inner Mongolia Based on SWAT Model. – Research of Soil and Water Conservation 21(05): 292-297+341.

[5] El-Khoury, A., Seidou, O., Lapen, D. R., Que, Z., Mohammadian, M., Sunohara, M., Bahram, D. (2015): Combined impacts of future climate and land ues changes on discharge, nitrogen and phosphorus loads for a Canadian river basin. – Journal of Environmental Management 151: 76-86.

[6] Guo, J. T., Zhang, Z. Q., Wang, S. P., Strauss, P., Yao, A. (2014): Appling SWAT model to explore the impact of changes in land use and climate on the streamflow in a Watershed of Northern China. – Acta Ecologica Sinica 34(06): 1559-1567.

[7] Hao, W. G., Li, J. R., Guo, J. Y., Shen, J., Zhang, S. (2014): Dynamic changes of vegetation in desert grassland and precipitation and temperature responses. – Water Resources Protection 30(05): 56-59.

[8] Hoang, L., Griensven, A. V., Mynett, A. (2017): Enhancing the SWAT model for simulating denitrification in riparian zones at the river basin scale. – Environmental Modelling & Software 93: 163-179.

[9] Huang, Q. H., Zhang, W. C. (2010): Application and parameters sensitivity analysis of SWAT model. – Arid Land Geography 33(1): 8-15.

[10] Lai, Z. Q., Li, S., Li, C. G., Nan, Z. T., Yu, W. J. (2013): Improvement and Applications of SWAT Model in the Upper-middle Heihe River Basin. – Journal of Natural Resources 28(08): 1404-1413.

[11] Li, S., Lai, Z. Q., Wang, Q., Wang, Z. H., Li, C. G., Song, X. B. (2013): Distributed simulation for hydrological process in Plain River network region using SWAT model. – Transactions of the Chinese Society of Agricultural Engineering 29(6): 106-112.

http://www.aloki.hu ● ISSN 1589 1623 (Print) ● ISSN 1785 0037 (Online)
DOI: http://dx.doi.org/10.15666/aeer/1802_31313145

[12] Li, D. H., Wang, J. Y., Wang, S. G., Li, Z. C., Shang, K. Z., Shi, J. S. (2014): Change Features of Surface Albedo of Semi-Arid Grassland over the Loess Plateau of Middle Part Gansu. – Plateau Meteorology 33(01): 89-96.
[13] Manoj, K. S., Friedrich, R. (2016): Assessing SWAT models based on single and multi-site calibration for the simulation of flow and nutrient loads in the semi-arid Onkaparinga catchment in South Australia. – Agricultural Water Management 175: 61-71.
[14] Meng, X. Y., Ji, X. N., Liu, Z. H., Xiao, J. C., Chen, X., Wang, F. (2014): Research on Improvement and Application of Snowmelt Module in SWAT. – Journal of Natural Resources 29(03): 528-539.
[15] Wang, Z. G., Liu, C. M., Huang, Y. B. (2003): The Theory of SWAT Model and its Application in Heihe Basin. – Progress in Geography 22(1): 79-86.
[16] Wang, X. Y., Qin, F. L., Ou, Y., Xue, Y. F. (2008): SWAT- Based Simulation on Non-point Source Pollution in the Northern Watershed of Miyun Reservoir. – Journal of Agro-Environment Science 27(3): 1098-1105.
[17] Wei, C., Song, X., Chen, J. (2014): Sensitivity analysis of swat model on changes of landscape pattern:a case study from Lao Guanhe Watershed in Danjiangkou Reservoir Area. – Acta Ecologica Sinica 34(02): 517-525.
[18] Yu, W. J., Nan, Z. T., Zhao, Y. B., Li, S. (2013): Improvement of snowmelt implementation in the SWAT hydrologic model. – Acta Ecologica Sinica 33(21): 6992-7001.
[19] Yuan, Y. Z., Zhang, Z. D., Meng, J. H. (2015): Impact of changes in land use and climate on the runoff in Liuxihe Watershed based on SWAT model. – Chinese Journal of Applied Ecology 26(04): 989-998.
[20] Zhang, X. S., Hao, F. H., Yang, Z. F., Cheng, H. G., Li, D. F. (2003): Runoff and Sediment Yield Modeling in Meso-scale Watershed Based on SWAT Model. – Research of Soil and Water Conservation 10(4): 38-42.
[21] Zhang, D., Zhang, W. C., Zhu, L., Zhu, Q. (2005): Improvement and Application of SWAT-A Physically Based, Distributed Hydrological Model. – Scientia Geographica Sinica 25(4): 434-440.
[22] Zhao, A. Z., Liu, X. F., Zhu, X. F., Pan, Y. Z., Li, Y. Z. (2015): Spatiotemporal patterns of droughts based on SWAT model for the Weihe River Basin. – Progress in Geography 34(09): 1156-1166.

http://www.aloki.hu ● ISSN 1589 1623 (Print) ● ISSN 1785 0037 (Online)
DOI: http://dx.doi.org/10.15666/aeer/1802_31313145

COMPARATIVE STUDIES ON THE PHYSIOCHEMICAL PROPERTIES, PHENOLIC COMPOUNDS AND ANTIOXIDANT ACTIVITIES IN 13 JAPANESE PLUM CULTIVARS GROWN IN THE SUBTROPICAL REGION OF CHINA

YU, X. M.[1] – RIZWAN, H. M.[1] – LI, P.[1] – LUO, S. X.[2] – SHERAMETI, I.[3] – WU, W. F.[4] – LIN, J.[5] – ZHENG, S. X.[5] – OELMÜLLER, R.[3] – CHEN, F. X.[1*]

[1]*Institute of Subtropical Fruit, Fujian Agriculture and Forestry University, Fuzhou 350002, China*

[2]*Economic Crop Technology Extension Station, Agriculture Department, Liancheng, Fujian Province 366200, China*

[3]*Institute of General Botany and Plant Physiology, Friedrich-Schiller-University Jena, 07743 Jena, Germany*

[4]*Lushan Botanical Garden, Chinese Academy of Sciences, Jiujiang, Jiangxi 332900, China*

[5]*Detection and Analysis Section, Disease Prevention and Control Center, Fuzhou 350004, China*

**Corresponding author*
e-mail: cfaxing@126.com

(Received 26th Sep 2019; accepted 8th Jan 2020)

Abstract. The physiochemical parameters and antioxidant properties of plum cultivars, grown in subtropical regions of China are little known. However, in this comparative study, these properties of 6 landraces and 7 introduced cultivars showed evaluated. The major nonvolatile constituents were a significant difference among cultivars. Color parameter values were strongly influenced by cyanidin 3-*O*-glucoside and cyanidin 3-*O*-rutinoside. Remarkably high antioxidant activity, high total phenolic, and ascorbic acid contents were found in black or purple flesh genotypes. Catechinic acid, the most important phenolic acid in Japanese plum, together with vanillic acid, caffeic acid and syringic acid, accounted for > 96% of the total phenolic content. The total phenolics and ascorbic acid concentration revealed significant contributions to antioxidant capacity detected by α, α-diphenyl-β-picrylhydrazyl (DPPH), (r = 0.78**, 0.73**) and ferric reducing antioxidant power (FRAP) (r = 0.74**, 0.57*). Moreover, there was a clear correlation between the total phenolic compounds and the ascorbic acid content (r = 0.76**). Comparison of physicochemical characteristics and antioxidant profiles revealed that both introduced cultivars and landraces had good adaptability in the subtropical region.
Keywords: *Prunus salicina Lindl, chemical compounds, nutrient content, subtropical cultivation, correlation analysis*

Introduction

People consume fruits not only for their taste, but also their vital nutritional content (Liu, 2013), strong antioxidants and health promotion capabilities (Dai and Mumper, 2010; Goodarzi et al., 2018). Bioactive compounds including phenolics, anthocyanins and phytochemicals as well as vitamins E and C are considered to be beneficial properties of fruits (Mirmiran et al., 2009; Wang et al., 2018). Hence, a great deal of research has been carried out, in order to improve the quantity and quality of bioactive compounds in commonly consumed fruits.

http://www.aloki.hu ● ISSN 1589 1623 (Print) ● ISSN 1785 0037 (Online)
DOI: http://dx.doi.org/10.15666/aeer/1802_31473159

Plum (*Prunus salicina* Lindl) commonly known as Japanese plum, is an important stone fruit crop commercially grown in China, Spain and USA. China ranks first in plum production (Li et al., 2015; Vlaic et al., 2018). Likewise, other fruits, various kinds of polyphenolic compounds such as phenolic acids, flavonols, anthocyanins (Turturică et al., 2018) and antioxidant activities have been identified in plum (Gil et al., 2002). Plum are good source of antioxidant that protects from biomolecular damage including aging caused by free radicals (Cefali et al., 2018). However, European plums (*Prunus domestica* L.) and Japanese plums (*Prunus salicina* Lindl.) have several different concentrations of phytochemicals, nutritional properties and antioxidant activities (Arion et al., 2014; Fanning et al., 2014; Jaiswal et al., 2013). Different cultivars have a greater variation of phenolic composition and concentration under various environmental conditions (Bochi et al., 2015; Wang et al., 2018). Several reports have been found on Japanese plum cultivars focusing on large size and homogeneous color (red, purple or yellow) (Lozano et al., 2009). Recently, more attentions have been focused on the functional properties of plum, their reasonable source of dietary-fiber, ascorbic acid, phenolic compounds, anthocyanins and other compounds with antioxidant properties (Fanning et al., 2014; Jaiswal et al., 2013; Kim et al., 2003).

In the past 20 years, many plum cultivars such as Blackamber, Wickson, Fiar, and Methely have been introduced, in order to enhance the plum production scale. Most of the plums are adapted to subtropical regions of Southeastern China. However, little information is available about the phytochemical properties of Chinese genotypes growing in subtropical regions of China (Byrne et al., 2000; Liu et al., 2007). Assuming that physicochemical characteristic, phenolic compounds and antioxidant properties of different Japanese Plums cultivars are influenced in subtropical regions. The main objectives of this study were to analyze the physicochemical characteristics, phenolic compounds and antioxidant properties of 13 Japanese plum cultivars grown in southeastern China.

Materials and methods

Plant materials

Fruit samples of 13 plum cultivars were harvested at commercial maturity stage during early June to end of August from Fujian Agriculture and Forestry Experiment Station Orchard at the hillock reservoir of Gutian county, Fujian, located in Southeastern China (N26°38’56.67”, E118°49’1.02”, Elevation: 323 m). The daily effective accumulated temperature is > 10 ℃, and the annual average rainfall is about 5000 mm. Among 13 cultivars, 7 were introduced (Friar, Gariota, Blackamber, Santa Rosa, Elodrao, Methely, and Akihime) and 6 were landraces (Furongli, Hongnai, Yanzhili, and Xiguali as local cultivars of Fujian, Crown and Cuipingwannai were from the college of Horticulture, Fujian Agriculture and Forestry University. The dates of taking the samples are displayed in *Table A1* in the *Appendix*. After harvesting, fruits were immediately transported to the laboratory and sorted in a refrigerator up to 4 °C, according to the uniformity of their firmness. Plums without stones were cut into several pieces and then stored at -80 °C until extraction. To ensure the uniformity of frozen material before further experiments, the fruits were ground to a fine powder by using liquid nitrogen.

http://www.aloki.hu ● ISSN 1589 1623 (Print) ● ISSN 1785 0037 (Online)
DOI: http://dx.doi.org/10.15666/aeer/1802_31473159

Chemical standards

Standards for sucrose, glucose, fructose and sorbitol, as well as malic, citric, shikimic and fumaric acids were obtained from Fluka Chemical (New York, USA). Catechinic, vanillic, gallic, caffeic, syringic, ferulic and chlorogenic acids, quercetin, cyanidin 3-O-glucoside and cyanidin 3-O-glucoside were purchased from Sigma-Aldrich (Oslo, Norway).

Gas chromatography-mass spectrometer (GC-MS) determination of sugar compounds and organic acids

Organic acids and sugars were extracted according to the protocol described by Liu et al. (2007) and Glew et al. (2003) The extraction of derivatives was carried out by using the method of Jiao et al. (2010). 1 μl of the derivative sample was injected into GC-MS using the split mode 50:1 and injector temperature was 230 °C. Ultra-pure helium served as carrier gas at the constant flow of 1.0 $mL \cdot min^{-1}$. The oven was programmed at the following profile: initial temperature of the column was 70 °C (5 min hold), followed by an increasing the rate of 5 $°C \cdot min^{-1}$ to 310 °C and then hold for 1 min. The mass operating parameters were: interface temperature was 250 °C, ion trap temperature was 200 °C, ion source was EI mode, electron energy was 70 eV, the solvent delay was 8 min. All data were obtained from the full-scan mass spectra within the range of 50 - 600 amu. The organic acids and sugars were identified by comparing the retention times and mass spectral data with the corresponding standards. Concentrations were determined according to the calibration of external standard solution.

High performance liquid chromatography (HPLC) analysis of phenolic compounds and anthocyanins

Plum extraction was carried out by the method of Gil et al. (2002). Samples were filtered through a 0.45 μm filter and then used for the analysis of phenolic compounds by HPLC (Kelebek et al., 2015). Anthocyanins were analyzed at 530 nm by HPLC (Usenik et al., 2008).

Antioxidant activity evaluation

2 g sample was extracted with 15 ml solution of 80% methanol (v/v) at 30 °C, then by an ultrasonic extraction with the power of 300 W for 40 min. Furthermore, it was centrifuged at the acceleration of 10000×g for 10 min (4 °C). For the analysis of the antioxidant activities of the plum fruits, combined supernatants of two replications were filtered by using a 0.45 μm filter. Three methods, i.e., the DPPH(α, α-diphenyl-β-picrylhydrazyl, DDPH) (Arion et al., 2014), ABTS(2, 2'-azino-bis(3-ethylbenzothiazoline-6-sulfonic acid), ABTS) (Maria do Socorro et al., 2010) and FRAP (ferric reducing antioxidant power) (Benzie and Strain, 1996) were used in order to test the antioxidant activity of the plum fruits.

Statistical analysis

Three replications were used for each treatment (n = 3) and statistical analysis were conducted by using SPSS software (version 21.0). Results were expressed as mean values ± standard deviation (SD). To determine whether the bioactive compounds would contribute to the antioxidant capacity, Pearson's correlation coefficients were calculated at $p < 0.05$ and $p < 0.01$ confident levels for all variables. An analysis of

http://www.aloki.hu ● ISSN 1589 1623 (Print) ● ISSN 1785 0037 (Online)
DOI: http://dx.doi.org/10.15666/aeer/1802_31473159

variance was performed followed by Student's t-test (two-tailed distribution, unequal variance). Relationships between the physicochemical variables and either cultivar of P. salsida or antioxidants capacities of the known DPPH, FRAP and ABTS were analyzed using CCA (Canoco 4.5).

Results

Phenolic compounds and anthocyanins

Eight phenolic compound markers were identified in plums fruit at 280 nm. The acidic phenolics like caffeic acid, chlorogenic acid, ferulic acid and quercetin had more intense absorptance at 320 nm (*Fig. 1*). The concentration of the phenolic compounds of the 13 Prunus cultivars was shown in *Table 1*. The catechinic acid was the most abundant, especially in purple- or red-fresh cultivars Furongli, Xiguali and Yanzhili, which was two times higher than that 10 other cultivars. Additionally, abundant polyphenolic compounds were vanillic acid. Interestingly, the cultivars Xiguali, Gariota, Hongnai and Santa Rosa had outstanding high values of vanillic acid (*Fig. 2*). The hydroxycinnamic acid derivatives, caffeic acid, ferulic acid and chlorogenic in plums showed significant variation in 13 cultivars tested, in which caffeic acid predominated with the mean value of 7.68 $\mu g \cdot g^{-1}$ fresh weight (FW). The acidic phenolics such as chlorogenic acid, ferulic acid and quercetin had low levels, and the neutral phenolic gallic acid tended to have low values as well. It should be noted that catechinic and syringic acids made 84.8% and 11.9% of the phenolic materials, respectively in Furongli.

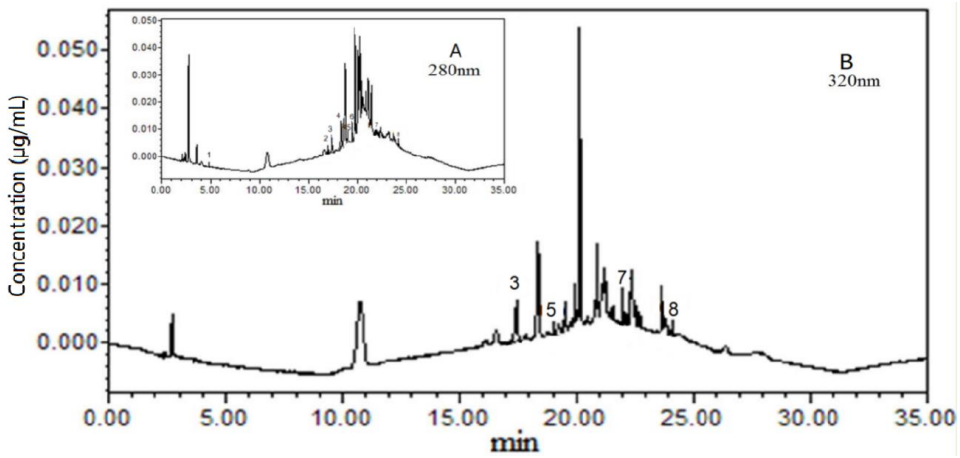

Figure 1. *Chromatogram of 8 polyphenol at 280 nm (A) and 320 nm (B) of plum samples. (1) Gallic acid, (2) catechin acid, (3) caffeic acid, (4) vanillic acid, (5) chlorogenic acid, (6) syringic acid, (7) ferulic acid, (8) quercetin*

Table 1. *Correlation matrix between anthocyanins with chromatic parameters of plum cultivars*

	L*	**a***	**b***	**Chroma (C)**	**Hue angle (H)**
Cyanidin 3-O-glucoside	-0.689**	0.707**	-0.738**	-0.632**	0.438**
Cyanidin 3-O-rutinoside	-0.682**	0.708**	-0.736**	-0.648**	0.428**
Total anthocyanins	-0.697**	0.717**	-0.748**	-0.646**	0.441**

**P < 0.01 by Pearson's test

http://www.aloki.hu ● ISSN 1589 1623 (Print) ● ISSN 1785 0037 (Online)
DOI: http://dx.doi.org/10.15666/aeer/1802_31473159

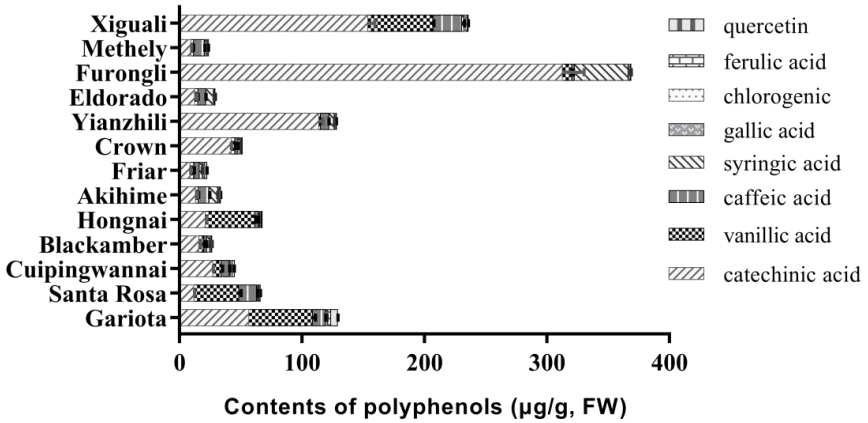

Figure 2. *Contents of polyphenols in 13 plum cultivars (μg/g FW). The bars represent the mean ± standard deviation*

Concerning the anthocyanins content, we observed that cyanidin 3-O-glucoside quantities were two times higher than that of cyanidin 3-O-rutinoside in plums (*Figs. 3* and *4*). Cyanidin 3-O-glucoside was the predominant compound among anthocyanins and detected in Xiguali, Methely and Blackamber, which corresponds to a mean content of 335.0 mg·100 g^{-1} FW among the 10 cultivars tested. The cyanidin 3-O-rutinoside was also detected in abundance and its mean value was 161.5 mg·100 g^{-1} FW in 10 cultivars. In all cases, the levels of cyanidin 3-O-glucoside, cyanidin 3-O-rutinoside and total anthocyanins correlated negatively or positively ($P < 0.01$) with each of the color parameters L*, a*, b*, C and H, respectively (*Table 1*). It seems that the highest values of a* and H corresponded positively to the samples with the highest anthocyanins content. The lowest values of b*, L* and C were negatively correlated with the anthocyanin levels. The darker the fruits, the more negative was the correlation of the color parameters of L*, b* and C to the amount of total anthocyanins, cyanidin 3-O-glucoside and cyanidin 3-O-rutinoside in plums. These results showed that chromatic parameters have a significantly correlate with the evolution of fruit color and anthocyanins levels and indicated that color parameters could be used to monitor pigment evolution and anthocyanins content of plum cultivars.

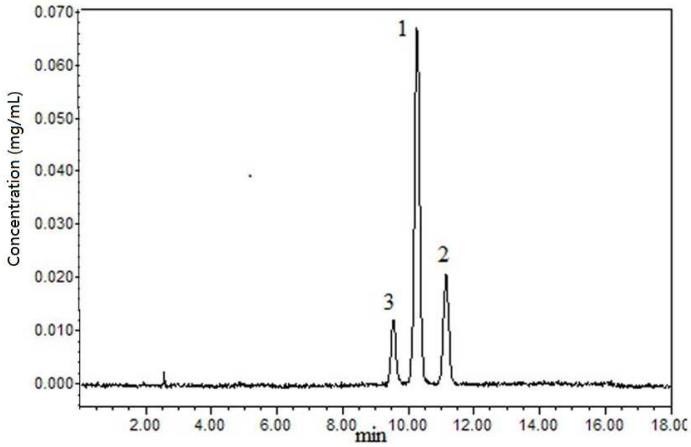

Figure 3. *Chromatogram of anthocyanins of plum cultivars. (1) Cyanidin 3-glucoside, (2) cyanidin 3-rutinosid, (3) unknown*

http://www.aloki.hu ● ISSN 1589 1623 (Print) ● ISSN 1785 0037 (Online)
DOI: http://dx.doi.org/10.15666/aeer/1802_31473159

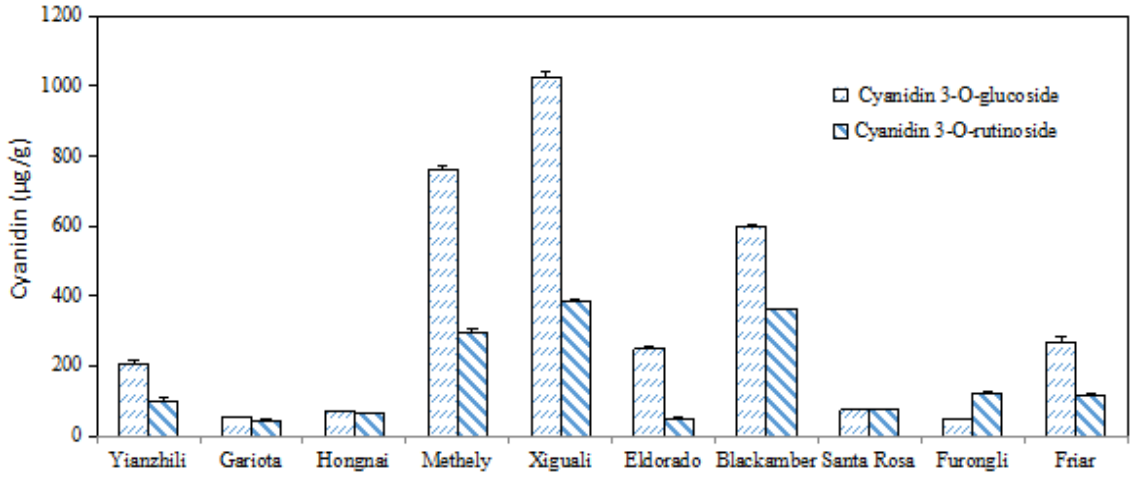

Figure 4. *Anthocyanin contents in 10 plum cultivars. The bars represent the mean ± standard deviation*

Total phenolics, ascorbic acid and antioxidant capacity

Thirteen cultivars were analyzed with respect to their content of total phenolics, ascorbic acid and antioxidant capacities (*Table 2*). Total phenolic contents were classified into three categories: low (150-200 mg of gallic acid equivalent (GAE) per 100 g FW), medium (200-250 mg of GAE per 100 gFW) and high (> 250 mg of GAE per 100 g FW). The highest contents of total phenolics were observed among the red- or purple-fresh fruits of Xiguali, Furongli and Yanzhili. The yellow-fresh fruits of Crown and Cuipingwannai had the lowest total phenolics except for Blackamber.

Table 2. *Antioxidant capacity, total phenolic content and ascorbic acid content of 13 plum cultivars*

Cultivars	Total phenolic contents (mg·100 g^{-1} Fw)	Ascorbic acid (mg·100g^{-1} FW)	DPPH (%)	FRAP (μmol·g^{-1} FW)	ABTS (%)
Gariota	192.68±15.62cd	20.04±1.78ef	93.95±0.31c	10.51±1.53b	99.84±0.00a
Santa Rosa	229.38±9.29bc	29.31±1.03c	93.30±0.10de	11.49±1.18ab	99.63±0.08a
Cuipingwannai	174.82±16.03d	7.92±0.46i	93.46±0.11cde	8.17±1.64c	95.78±3.02b
Blackamber	154.38±18.61e	18.83±0.49f	93.18±0.10e	7.46±1.51c	84.69±4.01c
Hongnai	216.74±29.49c	21.71±1.10e	93.75±0.06cd	10.78±1.79b	99.68±0.23a
Akihime	208.24±12.09c	5.74±0.63j	93.79±0.26cd	10.73±1.74b	99.20±0.57a
Friar	187.04±11.40cd	10.63±0.85h	92.49±0.41f	4.79±0.82d	55.10±4.35d
Crown	170.73±4.77d	12.16±0.24h	93.50±0.15cde	7.77±1.46d	85.22±3.83c
Yanzhili	257.53±16.57b	33.38±1.40b	94.52±0.00b	10.16±1.11b	99.44±0.33a
Eldorado	170.91±17.61d	16.85±0.63g	93.67±0.26cd	7.35±1.55c	96.06±4.23a
Furongli	281.05±9.59a	21.78±1.32e	94.48±0.11b	13.12±0.82a	99.84±0.00a
Methely	206.94±6.91c	26.29±1.33d	93.71±0.21cd	11.74±0.64b	99.68±0.13a
Xiguali	291.53±8.73a	44.00±1.82a	96.14±0.25a	12.12±1.12ab	99.79±0.08a

Values represent mean ± standard deviation (n = 3). Different letters denote significant differences in the level of $P < 0.05$ by Duncan's test

http://www.aloki.hu ● ISSN 1589 1623 (Print) ● ISSN 1785 0037 (Online)
DOI: http://dx.doi.org/10.15666/aeer/1802_31473159

In this study, 13 different cultivars were investigated for their total antioxidant capacity, using the DPPH, FRAP and ABTS methods as shown in *Table 2*. In general, the antioxidant activities of the black or red landraces Furongli and Xiguali were higher than those of the other cultivars. The results showed statistically significant correlation in antioxidant capacity on DPPH within 13 cultivars. The highest DPPH radical scavenging activities for the 13 cultivars fruit extracts was measured in Xiguali, followed by Furongli and Yanzhili, while the lowest values were observed in Friar. The reduction power towards ABTS radical cation was more than 95% in almost all plum cultivars except for Blackamber and Friar. The values obtained by FRAP were less than 10 $\mu mol \cdot g^{-1}$ FW for yellow-flesh cultivars like Crown, Cuipingwannai, Blackamber, Eldorada, and Friar. The FRAP values of red-flesh or red-skin cultivars were higher than those of yellow-flesh cultivars, except Akihime. In general, the measurement from the three methods (DPPH, ABTS and FRAP) demonstrated that Furongli and Xiguali had the highest levels of antioxidants but the lowest was in the Friar cultivar.

Relationships between organic acids and sugars

Correlation analysis of the typical biological characteristics on the components of sugar and organic acid in 13 plums cultivars (*Table 3*), found that, in terms of biological characteristics, succinic played a leading role, showed a extremely significantly positive correlation with Citric (r = 0.98**) and sorbitol (r = 0.54*). In addition, Shikimic showed a significantly positive correlated with Cis-aconitic (r = 0.59*) and a significantly negatively correlated with Ascorbic (r = -0.57*). In the relationship in soluble sugars, sucrose, fructose and glucose were the main three sugars in plums, and there was a significant correlation among them. In addition, sorbitol and glucose were also significantly correlated (r = 0.67**). It can be seen that the interdependent among soluble sugars is significantly stronger than that among organic acids, which may be due to a circulation of the metabolic pathways of these three sugars while not exist in organic acids. It is worth noting, the total phenolics and ascorbic indicated a significant positive correlation (r = 0.76**).

Table 3. *Correlation matrix between organic acids and sugars in 13 plum cultivars*

	Malic	**Citric**	**Shikimic**	**Succinic**	**Fumaric**	**Cis-aconitic**	**Sucrose**	**Glucose**	**Fructose**	**Sorbitol**	**Ascorbic**
Citric	-0.06										
Shikimic	0.24	0.27									
Succinic	-0.06	0.98**	0.20								
Fumaric	0.41	0.34	0.40	0.37							
Cis-aconitic	0.00	-0.12	0.59*	-0.15	0.36						
Sucrose	0.10	0.18	-0.18	0.27	-0.01	-0.11					
Glucose	0.25	0.09	0.35	0.14	0.05	0.00	0.75**				
Fructose	0.29	0.14	0.46	0.17	0.14	0.29	0.70**	0.97**			
Sorbitol	0.28	0.51	0.37	0.54*	0.17	-0.35	0.52	0.67**	0.65		
Ascorbic	-0.21	-0.53	-0.57*	-0.44	-0.47	-0.21	0.55*	0.34	0.22	-0.16	
Total phenolics	-0.13	-0.47	-0.45	-0.42	-0.45	0.22	0.37	0.04	0.03	-0.28	0.76**

* and ** indicate correlated significantly at the level of $P < 0.05$ and $P < 0.01$ respectively

Relationships between bioactive phytochemicals and antioxidant capacity

The amount of total phenolics, ascorbic acid, individual phenolic compounds and anthocyanins showed a good linear relationship with each other (*Table 4*). The total phenolics and ascorbic acid concentration of the 13 plum cultivars correlated

http://www.aloki.hu ● ISSN 1589 1623 (Print) ● ISSN 1785 0037 (Online)
DOI: http://dx.doi.org/10.15666/aeer/1802_31473159

significantly with the antioxidant capacity detected by DPPH (r = 0.78**, 0.73**) or FRAP (r = 0.74**, 0.57*), but not so significantly by ABTS (r = 0.41, 0.41). Moreover, there was a significant correlation between the total phenolic compounds and the ascorbic acid (r = 0.76**). We found that catechinic acid had a stronger contribution to the antioxidant constituents than DPPH (r = 0.63*), FRAP (r = 0.55*) and the total phenolics (r = 0.77**). The high significant correlations between caffeic acid and DPPH (r = 0.64*), ascorbic acid (r = 0.64*) and vanillic acid (r = 0.63*) indicated that catechinic- and caffeic acids contributed more than ascorbic acid to the total phenolics and antioxidant activity. Cyanidin 3-O-glucoside also shows a significantly correlated (r = 0.94**) with cyanidin 3-O-rutinoside in the flesh of plum cultivars (*Fig. 5; Table 5*). In addition, a positive significant correlation between the ascorbic acid, cyanidin 3-O-glucoside (r = 0.63*), and cyanidin 3-O-rutinoside (r = 0.60*) was identified. Anthocyanins were important bioactive compounds contributing to ascorbic acid. The clear trend between the antioxidant capacity and the Prunus genotypes was analyzed by Canonical correspondence analysis (CCA) (*Fig. 5*). The antioxidant capacity of the purple- or red-flesh cultivars Furongli, Xiguali and Yanzhili showed a bigger variation than that of the other cultivars and correlated with the contents of total phenolics (*Fig. 5*). In general, black and red Prunus cultivars had a higher antioxidant capacity compared with yellow-flesh genotypes such as Methely, Santa Rosa, Akihime, Crown, Hongnai, and Cuipingwannai (*Table 4*).

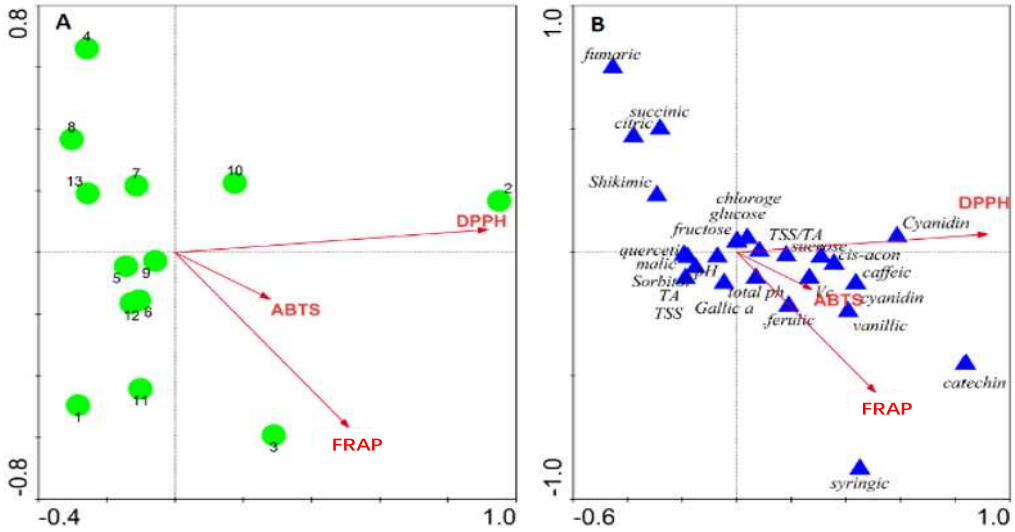

Figure 5. *CCA ordination of the 13 plum cultivars (green circles) for the 29 phytochemical profiles (blue triangles), with respect to antioxidant capacities (red arrows) using DPPH, FRAP and ABTS methods*

Discussion

The presence of polyphenolics correlated with previous investigations in which they showed that plums were rich in phenolic compounds and there are great differences among the phenolic contents in Prunus. Salicina and P. domestica (Arion et al., 2014; Mubarak et al., 2012; Slimestad et al., 2009). The occurrence of catechinic acid, vanillic acid and syringic acid has already been reported in plums (Jaiswal et al., 2013). However, some reports also showed smaller amounts of chlorogenic, caffeic acid and quercetin (Kim et al., 2003; Mubarak et al., 2012).

http://www.aloki.hu ● ISSN 1589 1623 (Print) ● ISSN 1785 0037 (Online)
DOI: http://dx.doi.org/10.15666/aeer/1802_31473159

Table 4. *Correlation matrix between phenolic compounds, anthocyanins, total phenolics content, ascorbic acid and antioxidant capacities using DPPH, FRAD and ABTS*

	Gallic acid	Catechinic acid	Caffeic acid	Vanillic acid	Chlorogenic	Syringic acid	Ferulic acid	Quercetin	Cyanidin 3-O-glucoside	Cyanidin 3-O-rutinoside	Total phenolics	Ascorbic acid	DPPH	FRAP
Catechinic acid	-0.26													
Caffeic acid	0.5	0.06												
Vanillic acid	0.29	0.1	0.63*											
Chlorogenic	-0.08	0.22	0.26	0.06										
Syringic acid	-0.26	0.85**	-0.29	-0.21	-0.04									
Ferulic acid	0.14	0.29	0.43	0.72*	-0.17	0.1								
Quercetin	-0.13	-0.1	0.25	0.49	-0.17	-0.19	0.78**							
Cyanidin 3-O-glucoside	0.02	0.05	0.52	0.17	0.22	-0.21	0.05	-0.21						
Cyanidin 3-O-rutinoside	-0.01	0.17	0.37	0.15	0.17	-0.04	0.05	-0.23	0.94**					
Total phenolics	0.2	0.77**	0.48	0.36	0.23	0.48	0.32	-0.25	0.33	0.39				
Ascorbic acid	0.06	0.39	0.65*	0.53	0.1	-0.01	0.27	-0.13	0.63*	0.6*	0.76**			
DPPH	-0.02	0.63*	0.64*	0.46	0.42	0.23	0.33	-0.09	0.46	0.39	0.78**	0.73**		
FRAP	0.09	0.55*	0.44	0.45	0.12	0.39	0.32	-0.05	0.13	0.19	0.74**	0.57**	0.66**	
ABTS	0.13	0.28	0.36	0.34	0.17	0.15	0.07	-0.02	-0.01	-0.02	0.41	0.41	0.59	0.81**

* and ** indicate correlated significantly at the level of $P < 0.05$ and $P < 0.01$ respectively

Table 5. *Correlation matrix between anthocyanins with chromatic parameters of plum cultivars*

	L^*	a^*	b^*	Chroma (C)	Hue angle (H)
Cyanidin 3-O-glucoside	-0.689**	0.707**	-0.738**	-0.632**	0.438**
Cyanidin 3-O-rutinoside	-0.682**	0.708**	-0.736**	-0.648**	0.428**
Total anthocyanins	-0.697**	0.717**	-0.748**	-0.646**	0.441**

* and ** indicate correlated significantly at the level of $P < 0.05$ and $P < 0.01$ respectively

http://www.aloki.hu ● ISSN 1589 1623 (Print) ● ISSN 1785 0037 (Online)
DOI: http://dx.doi.org/10.15666/aeer/1802_31473159

The plums contain mainly cyanidin 3-O-glucoside and cyaniding 3-O-rutinoside (Kim et al., 2003). Slimestad et al. (2009) reported that cyanidin 3-O-rutinoside represents more than 60% of the total anthocyanin content. It should be noted that cyanidin 3-Oglucoside and 3-O-rutinoside in fruit extracts of the yellow-flesh cultivars Crown, Akihime and Cuipingwannai were not detected due to their low contents, which is consistent to previous findings (Kim et al., 2003; Lozano et al., 2009).

The ascorbic acid content showed significant differences ($p < 0.05$) in the 13 selected cultivars. The ascorbic acid detected in our experiments was higher rather than previous reports. Most of the fruits contained considerable amounts of ascorbic acid (Asami et al., 2003; Fang et al., 2017) which were higher than 10 $mg \cdot 100\ g^{-1}$, and apparently higher than that in Spain (Gil et al., 2002). These results demonstrated that plum cultivars grown in subtropic areas have higher level of ascorbic acid than those grown in other regions.

Many assays were used for the determination of antioxidant activity in fruits and vegetables (Bustos et al., 2018; Moo-Huchin et al., 2015; Nayak et al., 2015).

These observations indicated that purple- or red-flesh Prunus cultivars had higher contents of the total phenolics (except cultivar Gariota) compared with other cultivars. However, Other researchers have also reported that plum is rich in total phenolic contents (Gil et al., 2002; Granato et al., 2018). Unfortunately, the range of total phenolics in plum differs among different reports due to their cultivar differences, agricultural practices, growth conditions and seasons (Arion et al., 2014; Kim et al., 2003).

These results indicated that the total phenolic compounds and ascorbic acid have a strong contribution to the antioxidant activity as also described in previous reports (Kim et al., 2003; Lozano et al., 2009; Mubarak et al., 2012). In some other reports, no correlation between antioxidant capacity and vitamin C was found (Hassimotto et al., 2005), even a negative influence of vitamin C was detected (Kalt et al., 1999). These similar results showed that cyanidin 3-O-rutinoside and cyanidin 3-O-glucoside were responsible for the pigmentation of the fruits (Kim et al., 2003; Raynal et al., 1989; Tomás-Barberán et al., 2001). These results were supported by previous reports which have shown that the main phytochemicals responsible for the antioxidant capacity in plums were total phenolics, ascorbic acid, and phenolic compounds (Gil et al., 2002; Vlaic et al., 2018), although other compounds may also be involved (Kim et al., 2003).

Conclusion

Overall, the results of this study demonstrated that many plum cultivars exhibited significant difference in levels of phenolic compounds, anthocyanins, total phenolics, ascorbic acid, and antioxidant capacities (DPPH, FRAP and ABTS). The highest levels of phenolic compounds, anthocyanins, and antioxidant capacities were observed in the black- or purple-flesh genotypes. Catechinic acid was the predominant polyphenolis in all tested plum cultivars and if combined with caffeic acid would make more important contributors to antioxidant capacities and total solute phenolic compounds, ascorbic acid in Japanese plums. The content of antioxidant capacities, polyphenols and anthocyanins has a certain correlation with the color of the peel and pulp, but it is not absolute, there were not found anthocyanins in yellow-skin or yellow-flesh cultivars. We conclude that phenolics, anthocyanin, and the antioxidant capacity could reflect the fruit quality and other important parameters for human health. It is not always a simple

http://www.aloki.hu ● ISSN 1589 1623 (Print) ● ISSN 1785 0037 (Online)
DOI: http://dx.doi.org/10.15666/aeer/1802_31473159

task to choose the most appropriate method to evaluate high-quality cultivars. Comparison of physicochemical characteristics and antioxidant profiles revealed that both introduced cultivars and landraces had good adaptability in the subtropical region. Thus, in order to achieve the maximum health-beneficial effects of plum consumption and their optimal organoleptic and nutritive properties, it would be advisable to get the cultivars with a high content of ascorbic acid, catechinic acid, caffeic acid, and syringic acid. The next work, we will conduct an depthly study on the main polyphenols and antioxidant activities in plums, and explore the best hybrid breeding model of plums to improve the functional components and nutrient content of fruits.

Acknowledgments. This work was funded by Fujian Agriculture Creative Projects from Fujian Development and Reform Commission, China (K6018203A), the Development of Local Science and Technology guided by central government, China (2017L3001) and the Project of Fujian Provincial Governor Fund.

REFERENCES

[1] Arion, M. C., Tabart, J., Kevers, C., Niculaua, M., Filimon, R., Beceanu, D., et al. (2014): Antioxidant potential of different plum cultivars during storage. – Food Chemistry 146: 485-491.
[2] Asami, D. K., Hong, Y.-J., Barrett, D. M., Mitchell, A. E. (2003): Comparison of the total phenolic and ascorbic acid content of freeze-dried and air-dried marionberry, strawberry, and corn grown using conventional, organic, and sustainable agricultural practices. – Journal of Agricultural & Food Chemistry 51(5): 1237-1241.
[3] Benzie, I. F., Strain, J. J. (1996): The ferric reducing ability of plasma (FRAP) as a measure of "antioxidant power": the FRAP assay. – Analytical Biochemistry 239(1): 70-76.
[4] Bochi, V. C., Godoy, H. T., Giusti, M. M. (2015): Anthocyanin and other phenolic compounds in Ceylon gooseberry (Dovyalis hebecarpa) fruits. – Food Chemistry 176: 234-243.
[5] Bustos, M. C., Rocha-Parra, D., Rueda Sampedro, I., De Pascual-Teresa, S., León, Alberto E. (2018): The influence of different air-drying conditions on bioactive compounds and antioxidant activity of berries. – Journal of Agricultural and Food Chemistry acs.jafc.7b05395.
[6] Byrne, D. H., Sherman, W. B., Bacon, T. A. (2000): Stone Fruit Genetic Pool and Its Exploitation for Growing under Warm Winter Conditions. – In: Erez, A. (ed.) Temperate Fruit Crops in Warm Climates. Springer, Dordrecht.
[7] Cefali, L. C., Maia, L., Stahlschimidt, R., Ataide, J. A., Tambourgi, E. B., Rosa, P. C. P., et al. (2018): Vitamin C in acerola and red plum extracts: quantification via hplc, in vitro antioxidant activity, and stability of their gel and emulsion formulations. – Journal of AOAC International 101(5): 1461-1465.
[8] Dai, J., Mumper, R. J. (2010): Plant phenolics: extraction, analysis and their antioxidant and anticancer properties. – Molecules 15(10): 7313-7352.
[9] Fang, T., Zhen, Q., Liao, L., Owiti, A., Zhao, L., Korban, S. S., et al. (2017): Variation of ascorbic acid concentration in fruits of cultivated and wild apples. – Food Chemistry 225: 132-137.
[10] Fanning, K. J., Topp, B., Russell, D., Stanley, R., Netzel, M. (2014): Japanese plums (Prunus salicina Lindl.) and phytochemicals - breeding, horticultural practice, postharvest storage, processing and bioactivity. – Journal of the Science of Food and Agriculture 94(11).

http://www.aloki.hu ● ISSN 1589 1623 (Print) ● ISSN 1785 0037 (Online)
DOI: http://dx.doi.org/10.15666/aeer/1802_31473159

[11] Gil, M. I., Tomás-Barberán, F. A., Hess-Pierce, B., Kader, A. A. (2002): Antioxidant capacities, phenolic compounds, carotenoids, andvitamin c contents of nectarine, peach, and plum cultivarsfrom california. – Journal of Agricultural and Food Chemistry 50(17): 4976-4982.
[12] Glew, R. H., Ayaz, F. A., Sanz, C., Vanderjagt, D. J., Huang, H. S., Chuang, L. T., et al. (2003): Changes in sugars, organic acids and amino acids in medlar (mespilus germanica l.) during fruit development and maturation. – Food Chemistry 83(3): 363-369.
[13] Goodarzi, S., Rafiei, S., Javadi, M., Haghighian, H. K., Noroozi, S. J. J. o. N. (2018): A review on antioxidants and their health effects. – Security 3: 106-112.
[14] Granato, D., Shahidi, F., Wrolstad, R., Kilmartin, P., Melton, L. D., Hidalgo, F. J., et al. (2018): Antioxidant activity, total phenolics and flavonoids contents: should we ban, in vitro, screening methods? – Food Chemistry 264: 471-475.
[15] Hassimotto, N. M. A., Genovese, M. I., Lajolo, F. M. J. J. o. A., F. (2005): Antioxidant activity of dietary fruits, vegetables, and commercial frozen fruit pulps. – Food Chemistry 53: 2928-2935.
[16] Jaiswal, R., Karaköse, H., Rühmann, S., Goldner, K., Kuhnert, N. (2013): Identification of phenolic compounds in plum fruits (Prunus salicina L. and Prunus domestica L.) by high-performance liquid chromatography/tandem mass spectrometry and characterization of varieties by quantitative phenolic fingerprints. – Journal of Agricultural & Food Chemistry 61(49).
[17] Jiao, Z., Deng, J., Li, G., Zhang, Z., Cai, Z. (2010): Study on the compositional differences between transgenic and non-transgenic papaya (Carica papaya L.). – Journal of Food Composition and Analysis 23(6): 640-647.
[18] Kalt, W., Forney, C. F., Martin, A., Prior, R. L. (1999): Antioxidant capacity, vitamin C, phenolics, and anthocyanins after fresh storage of small fruits. – Journal of Agricultural and Food Chemistry 47(11): 4638-4644.
[19] Kelebek, H., Selli, S., Gubbuk, H., Gunes, E. (2015): Comparative evaluation of volatiles, phenolics, sugars, organic acids and antioxidant properties of sel-42 and tainung papaya varieties. – Food Chemistry 173: 912-919.
[20] Kim, D. O., Chun, O. K., Kim, Y. J., Moon, H. Y., Lee, C. Y. (2003): Quantification of polyphenolics and their antioxidant capacity in fresh plums. – Journal of Agricultural and Food Chemistry 51(22): 6509-6515.
[21] Li, P., Wu, W., Chen, F., Liu, X., Lin, Y., Chen, J. J. H. (2015): Prunus salicina 'Crown', a yellow-fruited Chinese Plum. – HortScience 50(12): 1822-1824.
[22] Liu, R. H. (2013): Health-promoting components of fruits and vegetables in the diet. – Advances in Nutrition: An International Review Journal 4(3): 384S-392S.
[23] Liu, W., Liu, D., Zhang, A., Feng, C., Yang, J., Yoon, J., et al. (2007): Genetic diversity and phylogenetic relationships among plum germplasm resources in china assessed with inter-simple sequence repeat markers. – Journal of the American Society for Horticultural Science 132(5): 619-628.
[24] Lozano, M., Vidalaragon, M. C., Hernandez, M. T., Ayuso, M. C., Bernalte, M. J., Garcia, J., Velardo, B. (2009): Physicochemical and nutritional properties and volatile constituents of six Japanese plum (Prunus salicina Lindl.) cultivars. – European Food Research and Technology 228(3): 403-410.
[25] Rufino, M. S., Alves, R. E., De Brito, E. S., Perezjimenez, J., Sauracalixto, F., Mancinifilho, J. (2010): Bioactive compounds and antioxidant capacities of 18 non-traditional tropical fruits from Brazil. – Food Chemistry 121(4): 996-1002.
[26] Mirmiran, P., Noori, N., Zavareh, M. B., Azizi, F. (2009): Fruit and vegetable consumption and risk factors for cardiovascular disease. – Metabolism Clinical and Experimental 58(4): 460-468.
[27] Moohuchin, V. M., Moohuchin, M. I., Estradaleon, R. J., Cuevasglory, L., Estradamota, I., Ortizvazquez, E., ... Sauriduch, E. (2015): Antioxidant compounds, antioxidant activity

http://www.aloki.hu ● ISSN 1589 1623 (Print) ● ISSN 1785 0037 (Online)
DOI: http://dx.doi.org/10.15666/aeer/1802_31473159

and phenolic content in peel from three tropical fruits from Yucatan, Mexico. – Food Chemistry 166: 17-22.
[28] Mubarak, A., Swinny, E. E., Ching, S. Y. L., Jacob, S. R., Lacey, K., Hodgson, J. M., et al. (2012): Polyphenol composition of plum selections in relation to total antioxidant capacity. – Journal of Agricultural and Food Chemistry 60(41): 10256-10262.
[29] Nayak, B., Liu, R. H., Tang, J. (2015): Effect of processing on phenolic antioxidants of fruits, vegetables, and grains—a review. – C R C Critical Reviews in Food Technology 55(7): 887-918.
[30] Raynal, J., Moutounet, M., Souquet, J. M. (1989): Intervention of phenolic compounds in plum technology. 1. Changes during drying. – Journal of Agricultural and Food Chemistry 37(4): 1046-1050.
[31] Slimestad, R., Vangdal, E., Brede, C. (2009): Analysis of phenolic compounds in six norwegian plum cultivars (Prunus domestica L.). – Journal of Agricultural and Food Chemistry 57(23): 11370-11375.
[32] Tomasbarberan, F. A., Gil, M. I., Cremin, P., Waterhouse, A. L., Hesspierce, B., Kader, A. A. (2001): HPLC-DAD-ESIMS Analysis of phenolic compounds in nectarines, peaches, and plums. – Journal of Agricultural and Food Chemistry 49(10): 4748-4760.
[33] Turturică, M., Stănciuc, N., Mureşan, C., Râpeanu, G., Croitoru, C. (2018 Thermal degradation of plum anthocyanins: comparison of kinetics from simple to natural systems. – Journal of Food Quality. https://doi.org/10.1155/2018/1598756.
[34] Usenik, V., Kastelec, D., Veberi, R., Tampar, F. (2008): Quality changes during ripening of plums (Prunus domestica L.). – Food Chemistry 111(4): 830-836.
[35] Vlaic, R. A., Muresan, V., Muresan, A. E., Muresan, C., Paucean, A., Mitre, V., ... Muste, S. (2017): The changes of polyphenols, flavonoids, anthocyanins and chlorophyll content in plum peels during growth phases: from fructification to ripening. – Notulae Botanicae Horti Agrobotanici Cluj-Napoca 46(1): 148-155.
[36] Wang, R., Wang, L., Yuan, S., Li, Q., Pan, H., Cao, J., Jiang, W. (2018): Compositional modifications of bioactive compounds and changes in the edible quality and antioxidant activity of 'Friar' plum fruit during flesh reddening at intermediate temperatures. – Food Chemistry 254: 26-35.

APPENDIX

Table A1. *The dates of collecting samples in this work*

Cultivar	Time
Xiguali	6/20/2018
Methely	7/25/2018
Furongli	8/5/2018
Eldorado	7/25/2018
Yianzhili	6/8/2018
Crown	8/5/2018
Friar	7/25/2018
Akihime	8/10/2018
Hongnai	8/10/2018
Blackamber	8/10/2018
Cuipingwannai	8/20/2018
Santa Rosa	7/25/2018
Gariota	7/20/2018

http://www.aloki.hu ● ISSN 1589 1623 (Print) ● ISSN 1785 0037 (Online)
DOI: http://dx.doi.org/10.15666/aeer/1802_31473159

SPATIAL VARIATION OF SOIL MOISTURE CONTENT OF A STEPPED SLOPE UNDER SPRINKLER IRRIGATION AND ITS AFFECTING FACTORS

SUN, H. Y.[1#] – LIU, L.[1,2#*]

[1]*Northwest Institute of Eco-Environment and Resources, Chinese Academy of Sciences, Lanzhou, Gansu Province730000, China*

[2]*University of Chinese Academy of Sciences, Beijing 100049, China*

[#] *These authors contributed equally to this work.*

**Corresponding author*
e-mail: liule@lzb.ac.cn

(Received 27th Sep 2019; accepted 4th Feb 2020)

Abstract. In this study, the soil moisture migration pattern was studied under the sprinkler irrigation method with different modes of a stepped slope with 3 steps and its affecting factors. The results showed that at the early stage of the vegetation reconstruction, natural precipitation was enough to ensure the normal growth. This was found valid as long as the soil moisture content (SMC) was higher than 2.45% of the wilting coefficient at the non-irrigation stage. At the non-irrigation stage and at the stage of irrigation once every two days, the SMC increased with depth in the three slope surfaces. However, at the stage of irrigation once daily, the SMC decreased with depth. As the irrigation frequency decreased, the SMC dropped and the coefficient of variation (CV) of SMC rose. The order of CV of SMC within depths in 0-50 cm soil layer was the depths of 40-50 cm > 0-2 cm and 0-20 cm > 20-40 cm. The average soil moisture content (ASMC) increased from the top to the bottom of the stepped slope under different frequencies of sprinkler irrigation. The slope position and hardness and vegetation cover correlated negatively with the SMC ($P < 0.01$). Whereas, the slope gradient correlated positively with the SMC ($P < 0.05$).
Keywords: *Lanzhou New Area, Loess Plateau, ecological restoration, vegetation reconstruction, spatial differentiation, environmental factor*

Introduction

Excavation and filling of large mountains in Lanzhou New Area, located in the Loess Plateau of the Peoples Republic of China have produced a very high number of exposed stepped slopes during infrastructure construction. This has greatly changed the original ecological environment and led to water and soil loss (Cohen-Fernández and Naeth, 2013; Sharma et al., 2017). The total area suffering this loss was about 40 hm^2. Each exposed stepped slope usually consists of three steps and every two adjacent steps are isolated by a terrace. For these steep slope surfaces, vegetation slope protection is an effective pathway towards ecological restoration (Stokes et al., 2008). For this, the primary technical measures are available for sustainable development of the Loess Plateau (Wu and Yang, 1998). Soil moisture is a key factor affecting vegetation growth in the Loess Plateau (Engelbrecht et al., 2007; Wu and Yang, 1998). Small-scale topographical changes control secondary distribution of light, heat, precipitation and surface runoff (Crave and Gascuel-Odoux, 2015). All these, further affect the variability of soil moisture content (SMC) across the space. The spatial variation of SMC thus resulted, has a decisive impact on the surface vegetation type, density and structure (Vivoni et al., 2010). Steep slopes are usually associated with severe soil moisture shortage due to low permeability and high surface

http://www.aloki.hu ● ISSN 1589 1623 (Print) ● ISSN 1785 0037 (Online)
DOI: http://dx.doi.org/10.15666/aeer/1802_31613175

runoff (Miyazaki et al., 1993). The phenomenon is distinct especially for the slopes with greater hardness (Morgan, 1980). Hardness occurs because the slopes are formed via engineering construction. The process causes a compaction of particles which decreases the porosity and increases the bulk weight (Soane et al., 1980). The resultant condition hinders the circulation of moisture and nutrients, which is not conducive to the root growth of vegetation (Ishaq et al., 2001). Previous studies mostly dealt with the spatial variation of SMC in the gentle natural slopes of the Loess Plateau (Jia et al., 2013; Yang et al., 2015) and in typical roadbed side slopes (Yang et al., 2016). However, we know little about the spatial variation of SMC in stepped slopes. In this study, vegetation reconstruction was carried out for the steep slopes in Lanzhou New Area by sprinkler irrigation and mechanized grass growing. Then, a correlation analysis was conducted between the spatial variations of features of SMC in the 0-50 cm soil layer. In the correlation studies, different irrigation frequencies and four environmental factors namely, soil hardness, slope position and gradient and vegetation cover were considered. The soil moisture response to slope gradient and soil hardness in vegetation reconstruction of stepped slope was discussed. The present study provides a theoretical basis for developing irrigation regime and engineering measures for vegetation restoration in similar stepped slopes.

Study sites

Lanzhou New Area (103°29′22″-103°49′56″ E, 36°17′15″-36°43′29″ N), is located in Qinwangchuan Basin of the Peopole's Republic of China. The study area is about 60 km away from the city of Lanzhou (*Fig. 1*). The area is located in the intersect of Qinghai-Tibet-, Mongolian- and Loess Plateau. In that the eastward extending ranges of the Qilian Mountain run into the interlaced region of Longxi Basin. The primary landform of Lanzhou New Area is the Loess Plateau. The area enjoys typical temperate, continental and semiarid climate with an annual average temperature of 6.9 °C and annual precipitation of 300-350 mm. Because of the slope factor, the vegetation of the Loess Plateau near Lanzhou New Area shows two different categories i.e., shady and sunny slopes. The shady slope is predominantly grown with *Stipa breviflora* Desf. accompanied by undershrubs and perennial herbs such as *Caragana tibetica* (Maxim. *ex* C.K. Schneid.) Kom., *C. opulens* Kom., *Kraschenninnikovia ceratoides* (L.) Gueldenst., *Ajania achilleoides* (Turcz.) Poljakov *ex* Grubov, *Torularia humilis* (C.E. Mey) O.E. Schulz, *Peganum harmala* L., *Limonium aureum* (L.) Hill and *Reaumurta soongorica* (Pall.) Maxim. Whereas, the sunny slope is mainly grown with desert shrub *R. soongorica* accompanied by annual plants such as *Salsola collina* Pall., *Suaeda glauca* (Bunge) Bunge and *Setaria viridis* (L.) P. Beauv. The above undisturbed soil vegetation is an important indicator for vegetation reconstruction of steep slopes in Lanzhou New Area.

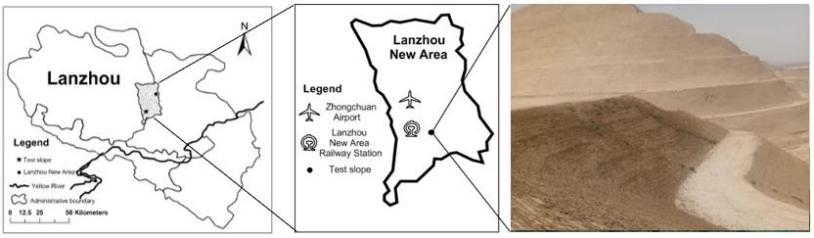

Figure 1. *Location map of study area*

http://www.aloki.hu ● ISSN 1589 1623 (Print) ● ISSN 1785 0037 (Online)
DOI: http://dx.doi.org/10.15666/aeer/1802_31613175

Methods

Time and location of the experiments

Experiments for the present study were performed from June 2nd to October 23rd, 2018. The experimental slopes (103°44′11″ E, 36°27′41″ N) was located on the west side of Nanraocheng Highway (from Shuiqin Road Overpass to Jingshiqi Road) (*Fig. 1*). The slopes were faced eastward and followed three successive steps having an elevation of 1930 m MSL. The slope surface was smooth, the soil characteristic had been analysed and the results showed that the soil was barren (*Table 1*) and without undisturbed soil vegetation. The wilting coefficient of the slope was 6.20 ± 0.60%.

Table 1. *Soil nutrient characteristics in the study area*

Organic matters (g/kg)	Total nitrogen (g/kg)	Total carbon (g/kg)	Total phosphorus (g/kg)	Alkali-hydrolyzable nitrogen (mg/kg)	Rapidly available phosphorus (mg/kg)	Rapidly available potassium (mg/kg)
1.742	0.268	15.405	1.28	10.50	11.46	120.00

Experimental layout

Slope engineering and grass growing

One study in 2017 indicated that a definite strip soil preparation (average length × width × depth = 45 × 8 × 5 cm) brought about the best water-retaining and vegetation restoration effects (Liu et al., 2019). Thus in 2018, after manually removing the rubbles and garbage from the slope, the experimental slope was prepared. To produce strip-like trenches with a depth of about 7 cm, a three-teethed harrow was used. The trenches were parallel with each other and spaced about 15 cm apart. From June 2nd to 6th, 2018 mechanized grass growing was carried out using sand-fixing mixture. Spray seeding was performed for the test slopes. The seeds of *Caragana korshinskii* Kom. (6 g/m^2), *Agropyron cristatum* (L.) Gaertn. (12 g/m^2) and *Medicago sativa* L. (2 g/m^2) were sown. After spray seeding, the test slope was covered with non-woven fabrics, which were fixed with disposable chopsticks. The date of first germination was June 11th, 2018 and the non-woven fabrics were removed after germination.

Sample plot layout

The bottom slope surface in the stepped slope (*Fig. 2a*) was considered the first (1st) one. It had a length of 12 m in the upper and lower direction and the slope gradient was 60°. The middle slope surface was considered the second (2nd) one which had a length of 14 m. In this case, the slope gradient was 40°. Between the first and second slope surfaces, there was a 3 m-wide terrace. The top slope surface was considered the third (3rd), with a length of 12 m. Here the slope gradient was 25°. There was a 12 m wide terrace between the second and third slope surfaces.

A 1×1 m sample plot was arranged at the upper (P), middle (M) and lower (D) positions of the first, second and third slope surfaces, respectively and each with three replicates. Thick iron wires and hemp ropes were used for immobilization (*Fig. 2b*). Nine plots were arranged for each slope surface. So, the entire test slope had 27 plots. The plot in the upper position of each slope surface was 1 m away from the top of this slope

http://www.aloki.hu ● ISSN 1589 1623 (Print) ● ISSN 1785 0037 (Online)
DOI: http://dx.doi.org/10.15666/aeer/1802_31613175

surface. The lower position was 1 m away from the bottom of the slope surface. The transverse spacing between adjacent plots was 10 m and the vertical spacing was 3-4 m.

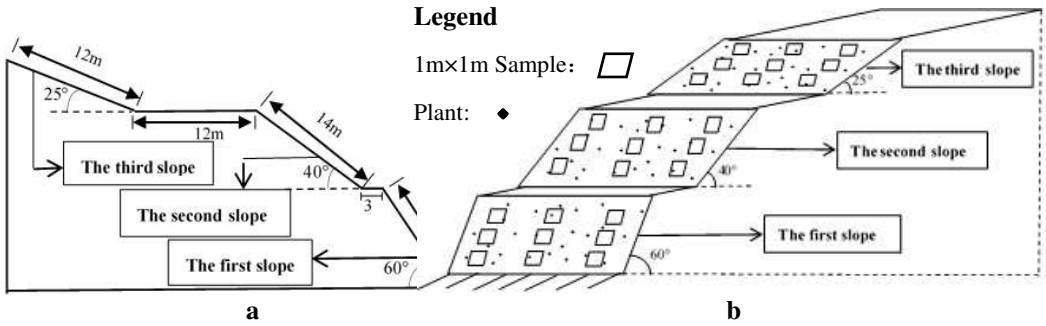

Figure 2. *The schematic diagram of profile and sample layout for the test slope.* ***a*** *Schematic for the s profile of the test slope.* ***b*** *Schematic for the sample plot layout of the test slope*

Sprinkler irrigation method and its application frequency

Sprinkler irrigation was performed for the experimental slopes. That is, all the three slope surfaces were irrigated by a sprinkling truck at 7-8 a.m. every day. The sprinkler irrigation amount was the same for different slope surfaces and the total sprinkler irrigation amount of the three slope surfaces was 12 MT/day. The frequency of irrigation followed three-time intervals. These are: (i) from June 2nd to July 10th sprinkler irrigation once daily; (ii) from July 11th to August 15th sprinkler irrigation once at every two days interval and (iii) from August 15th to November 23rd no irrigation, but natural precipitation was the only source of water. Sprinkler irrigation was avoided on the day of precipitation for all the experimental plots.

Sample collection, data collection and processing

Method of sample collection for SMC determination

At the irrigation stage, each plot was sampled once every 2 h since 9 a.m. on the morning of sprinkler irrigation. However, at the non-irrigation stage (natural precipitation), each plot was sampled at 9 a.m. once every 10 d.

A soil auger was used to collect samples for SMC determination. The sampling was carried out at randomly chosen positions for the soil depth of 0-50 cm under different irrigation frequencies. The soil was divided into 6 layers, namely, topsoil at 0-2 cm, 2-10 cm, 10-20 cm, 20-30 cm, 30-40 cm and 40-50 cm. The collected soil samples were put into specialized high-density ziplock bags prior to determination. The sampled soil pits were backfilled.

Determination of SMC

SF - 60 Moisture Tester (Shenzhen Houwang Electronic Technology Co., Ltd.) was used to determine the SMC. The measuring range was 0.01-100% and the measuring precision was 0.01%. During the first determination, the tester was calibrated by using the oven drying method (error 0.5-1%). For subsequent determinations, the SMCs were all detected using the electronic soil moisture tester. Each detection was repeated for three times and the average was taken.

http://www.aloki.hu ● ISSN 1589 1623 (Print) ● ISSN 1785 0037 (Online)
DOI: http://dx.doi.org/10.15666/aeer/1802_31613175

Determination of soil hardness

Soil hardness tester (Takemura Electric Works, Ltd) was placed perpendicular to the soil surface. The top length of the tester was 4.5 mm, and its bottom was inserted deep into the soil. The soil hardness tester was removed perpendicular out of the soil and the readings were taken. The measuring range of the soil hardness tester was 0-500 $kg \cdot cm^{-2}$ and the measuring precision was 0.1 $kg \cdot cm^{-2}$. A quincunx pattern was chosen for random selection of 5 points in each plot for each determination and average was taken after repeated determinations.

Determination of vegetation cover

Densities of different plants were calculated for each plot using the quadrat method. Three individuals were randomly selected for each plant species. After collection the crown breadth was measured and the average was taken. The vegetation cover was calculated for each plot based on the projected area of the stems and leaves on the ground.

Division of soil layers based on CV of SMC

According to the principle of soil layer division based on SMC variability (Yang and Shao, 2000), coefficient of variation (CV) was used to measure the degree of variation of SMC in the vertical direction. CV was calculated by

$$CV = \frac{SD}{S} \quad \text{(Eq.1)}$$

CV of *Equation 1* is the coefficient of variation, SD is the standard deviation and S is the average. The smaller the CV, the more stable the SMC was. On the other hand, the larger the CV, the stronger the changes of SMC. Soil layers with $CV > 30\%$, $20\% < CV \leq 30\%$, $10\% < CV \leq 20\%$ and $CV \leq 10\%$ were considered as rapid changing, active, less active and the relative stable layers, respectively.

Sources of precipitation data in Lanzhou New Area

Precipitation data of Lanzhou New Area during the test period (*Fig. 3*) came from the Meteorological Service Center of Gansu Province.

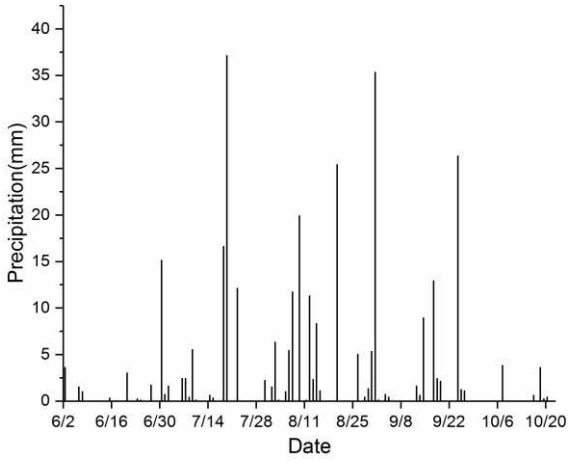

Figure 3. *Precipitation in Lanzhou New Area from June 2nd to October 23rd, 2019*

http://www.aloki.hu ● ISSN 1589 1623 (Print) ● ISSN 1785 0037 (Online)
DOI: http://dx.doi.org/10.15666/aeer/1802_31613175

Data analysis

Statistics was conducted using Microsoft Excel (2013), plots were drawn using Origin (2017) and data analysis was carried out using SPSS (20.0).

Results

Vertical spatial variation of SMC in the three slope surfaces of stepped slope

The SMC of each soil layer in different positions of the three slope surfaces have been presented in *Fig. 4*. At 34 d under the condition of irrigation once daily, the average soil moisture content (ASMC) ranged between 8.65 and 16.01% (*Fig. 4a*). In the 0-50 cm soil layer, the SMC decreased with increasing depth. At 50 d, under the condition of irrigation once every two days ASMC ranged between 9.81 and 16.28%. The variation trend of SMC in the 0-50 cm soil layer first increased and then decreased with increasing depth. The SMC, however, reached the highest in the 10-20 cm soil layer. At 60 d under the condition of irrigation once every two days, the ASMC ranged between 6.11 and 14.30%. In the 0-50 cm soil layer, the variation trend in the SMC increased with increasing depth. At 76-144th d and after grass growing, natural precipitation is the only source of recharge to soil moisture in the slope. The ASMC of each soil layer in different positions of the three slope surfaces ranged between 7.47 and 13.39%. Except for the lower position of the third slope surface, the ASMC of the 0-50 cm soil layer increased with depth. However, ASMC of the 0-50 cm soil layer in the lower position of the third slope surface remained basically constant with increasing depth. The magnitude of increase or decrease of SMC in each soil layer was below 1%.

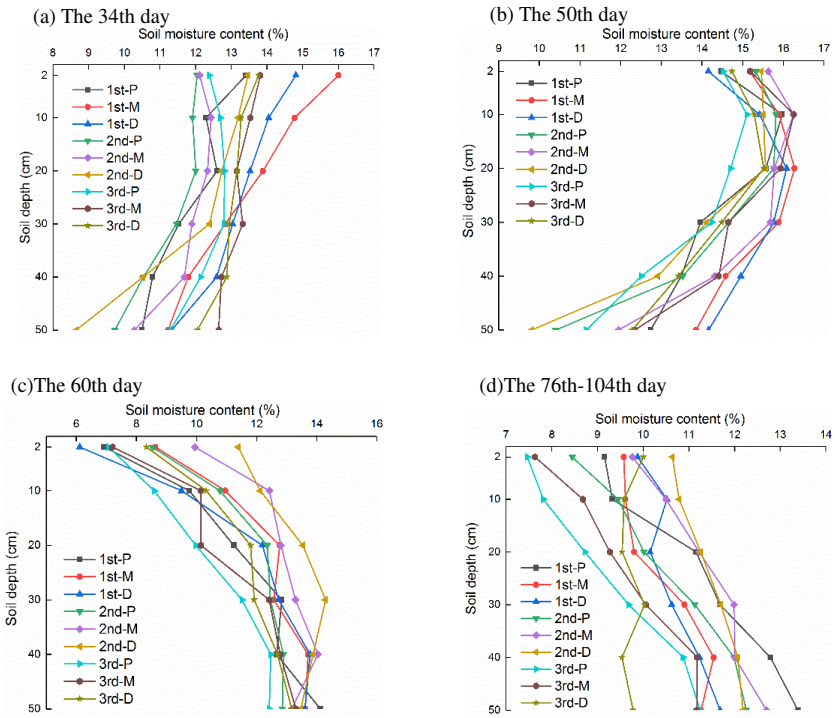

Figure 4. *The SMC of three slope positions on the first, second and third slopes in the stepped steep slope under different sprinkling irrigation frequency. (The first, second and third slope surfaces are represented by 1st, 2nd, 3rd and the upper, middle and lower slope positions are represented by P, M and D)*

http://www.aloki.hu ● ISSN 1589 1623 (Print) ● ISSN 1785 0037 (Online)
DOI: http://dx.doi.org/10.15666/aeer/1802_31613175

ASMC under different frequencies of sprinkler irrigation

Two factor analysis of variance was used to analyze the influence of different frequencies of sprinkler irrigation and slope positions on the variation of ASMC and based on the outcomes of this statistic data could be further processed with least significant difference method (LSD) test. The results showed that there was no significant difference in soil moisture between different slope positions ($P > 0.05$), different frequencies of sprinkler irrigation has a significant effect on ASMC ($P < 0.05$). ASMC after strong precipitation was significantly higher than that in other periods ($P < 0.05$) (*Table 2*), in addition, ASMC at the non-irrigation stage was significantly higher than that at the stage of sprinkler irrigation once every two days ($P < 0.05$).

Table 2. *LSD test of ASMC under different sprinkler irrigation*

Frequencies of sprinkler irrigation	The 34th day	The50th day	The 60th day	The 76th-104th day
The 34th day	1	-1.977*	-0.500	0.814
The 50th day		1	1.477*	2.792*
The 60th day			1	1.314*
The 76th-104th day				1

Figure 5 shows the variation of ASMC along 0-50 cm soil layer, error bars were expressed by standard deviation of ASMC. In addition, dotted lines with integer values close to range of the actual ASMC are added to the figure to make the change trend of ASMC clearer. In the second slope surface, the value was the highest in the lower position, followed by the middle and upper positions successively. However, no consistent variation pattern was found in different positions of the other two slope surfaces. Of the three slope surfaces, at 34 d (*Fig. 5a*) the value was the highest in the third slope surface. This was followed by the first and second slope surfaces successively. ASMC of the middle and lower positions of the first slope surface were significantly higher than that of the second slope surface ($P < 0.05$). However, the differences were not statistically significant as compared with the third slope surface. ASMC of the upper position in the second slope surface was significantly lower than that of the third slope surface ($P < 0.05$), but the difference was not significant as compared with the first slope surface. Of the three slope surfaces, ASMC at 50 d (*Fig. 5b*) was the highest in the first slope surface, followed by the third and second slope surfaces successively. But the value in the middle position of the first slope surface was significantly higher than that of the second slope surface ($P < 0.05$). However, the differences were not of statistically significant as compared with the third slope surface. ASMC in the upper and lower positions of the other slope surfaces were not significantly different. Of the three slope surfaces, at 60 d (*Fig. 5c*) ASMC was the highest in the second slope surface, followed by the first and third slope surfaces successively. In the lower position of the second slope surface, the value was significantly higher than that of the first and third slope surfaces ($P < 0.05$). However, the differences were not of statistically significant as compared with the upper and middle positions of each slope surface. At 76-104 d (*Fig. 5d*), the value was the highest in the first slope surface, followed by the second and third slope surfaces successively. In the upper position of the first slope surface it was higher than that of the second and

http://www.aloki.hu ● ISSN 1589 1623 (Print) ● ISSN 1785 0037 (Online)
DOI: http://dx.doi.org/10.15666/aeer/1802_31613175

third slope surfaces ($P < 0.05$). However, the differences were not statistically significant as compared with the middle and lower positions of each slope surface.

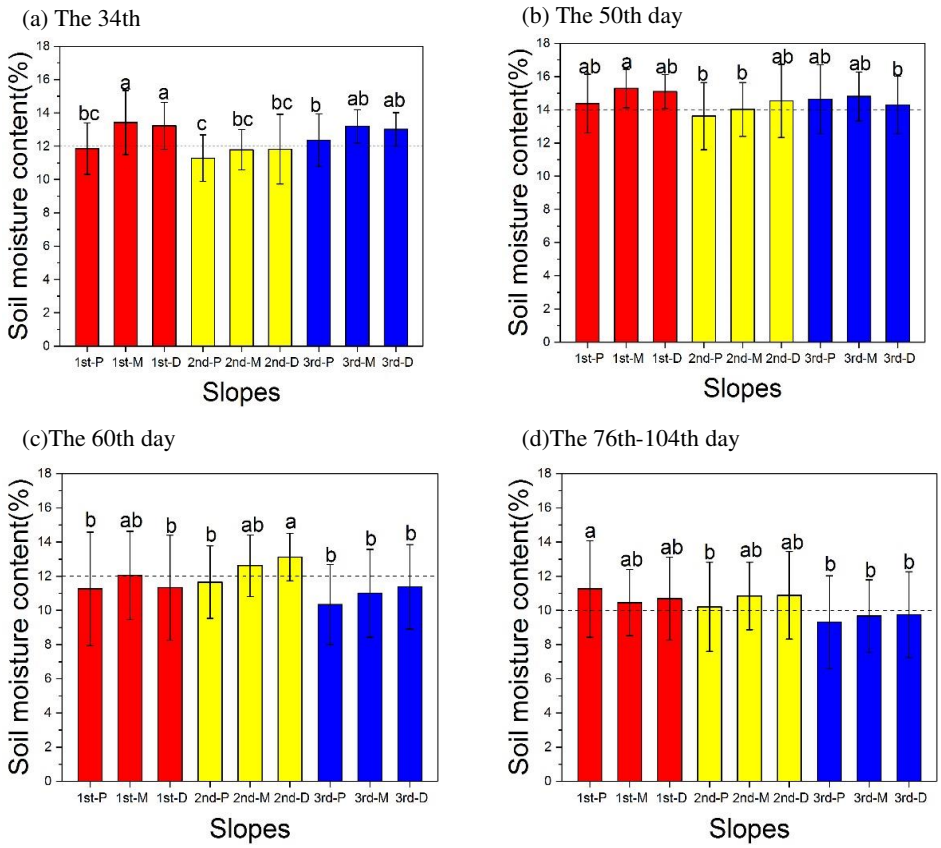

Figure 5. *Mean soil moisture content (ASMC) with error bars for different slope positions under different sprinkler irrigation. Different lower-case letters indicate levels of significance ($p < 0.05$) in mean soil water content at different slope positions in the same sprinkler irrigation. (Different lowercase letters are used to indicate significant difference in the ASMC at different slope positions under the same sprinkler irrigation condition ($P < 0.05$); first, second and third slope surfaces (1^{st}, 2^{nd} and 3^{rd}), upper, middle and lower slope surfaces (P, M and D))*

Stability of SMC of three slope surfaces in the stepped slope

Soil layers were divided vertically according to the SMC of each slope surface under different irrigation conditions (*Table 3*). At 34 d, the SMC was basically stable in the three slope surfaces, and CV based on *Equation 1* of ASMC was 8.9%. CV was larger in the 0-2 cm and 40-50 cm soil layers. These layers were thus considered as the less active layers. CV of other soil layers was all below 10%, indicating stable SMC. At 50 d, the SMC was generally stable in the three slope surfaces. The CV of ASMC was 6.7%. CV of each soil layer was below 10%, indicating stable SMC. At 60 d, the three slope surfaces were generally in a less active state and CV of the ASMC was 14.1%. CV of ASMC was larger in the 0-10 cm and 40-50 cm soil layers, corresponding to less active and active state, respectively. The CV was below 10% in the 10-40 cm soil layer, indicating stable SMC. At 76-104 d, the three slope surfaces were generally in an active state. In this finding the CV of ASMC was 21.9%. Recording of larger CV in the 0-

http://www.aloki.hu ● ISSN 1589 1623 (Print) ● ISSN 1785 0037 (Online)
DOI: http://dx.doi.org/10.15666/aeer/1802_31613175

20 cm and 40-50 cm soil layers, indicated an active state. The CV of the 20-40 cm soil layer showed a value below 20%, so the layer was in a less active state.

Table 3. *Vertical variation of SMC on slopes under different sprinkler irrigation conditions*

Item	The slope positions	Soil depth (cm)						
		0-2	2-10	10-20	20-30	30-40	40-50	Mean
The 34th day: *CV* (%)	1st	9.0	6.3	6.3	9.0	7.7	10.7	8.2
	2nd	11.7	6.7	5.3	5.7	11.3	15.7	9.4
	3rd	12.7	9.3	9.0	5.3	7.3	10.7	9.1
	Mean	11.1	7.4	6.9	6.7	8.8	12.3	8.9
The 50th day: *CV* (%)	1st	7.7	4.0	4.7	7.0	9.3	6.3	6.5
	2nd	3.7	3.0	5.3	4.7	4.7	9.3	5.1
	3rd	8.7	5.7	8.0	9.3	10.7	9.0	8.6
	Mean	6.7	4.2	6.0	7.0	8.2	8.2	6.7
The 60th day: *CV* (%)	1st	25.7	15.3	14.0	10.7	11.3	31.0	18.0
	2nd	13.7	10.3	6.3	8.0	6.7	16.3	10.2
	3rd	18.7	18.3	7.7	9.7	7.0	22.7	14.0
	Mean	19.3	14.7	9.3	9.4	8.3	23.3	14.1
The 76th - 104th day: *CV* (%)	1st	23.3	23.7	20.3	15.0	11.0	30.7	20.7
	2nd	25.3	26.3	20.0	17.7	13.3	26.7	21.6
	3rd	29.0	26.7	24.0	16.7	15.3	29.0	23.4
	Mean	25.9	25.6	21.4	16.4	13.2	28.8	21.9

Correlation between slope gradient, soil hardness and SMC of the three slope surfaces in the stepped slope

Of the three slope surfaces (*Table 4*), the slope gradient was the highest in the first slope surface (60°), followed by the second (40°) and third (25°) slope, successively. As to the average soil hardness, it was the highest in the third slope surface (5.3 ± 3.68 kg·cm^{-2}), followed by the second (4.1 ± 2.78 kg·cm^{-2}) and first (2.6 ± 1.24 kg cm^{-2}), successively. The ASMC in the 0-50 cm soil layer during the test period was the highest in the first slope surface (12.48 ± 1.80%), followed by the second (12.20 ± 1.44%) and the third slope (11.98 ± 2.19%), successively.

Table 4. *Slope gradient, soil hardness and the average soil moisture content in the 0-50 cm soil layer during the test period of the three slope surfaces in the stepped slope*

Slope position	Slope gradient	Soil hardness (kg·cm^{-2})	Soil moisture content (%)
The 1st slope	60°	2.6 ± 1.24	12.48 ± 1.80
The 2nd slope	40°	4.1 ± 2.78	12.20 ± 1.44
The 3rd slope	25°	5.3 ± 3.68	11.98 ± 2.19

Correlation analysis was conducted between SMC of each soil layer within the depth of 0-50 cm and four environmental factors, namely, slope position and gradient, soil hardness and vegetation cover (*Table 5*), Pearson correlation coefficient was used to express the magnitude of correlation between soil moisture content and environmental

http://www.aloki.hu ● ISSN 1589 1623 (Print) ● ISSN 1785 0037 (Online)
DOI: http://dx.doi.org/10.15666/aeer/1802_31613175

factors. The sample size was 90 for SMC determination in each soil layer. The SMC correlated negatively and significantly with the soil hardness ($P < 0.01$). In the 0-50 cm soil layer, the average correlation coefficient was -0.695. The correlation coefficient decreased between the SMC and soil hardness with increasing depth. The SMC correlated negatively with the soil hardness. The average correlation coefficient was -0.205 in the 0-50 cm soil layer. The correlation coefficient between SMC and slope position increased with increasing depth. The SMC in the 40-50 cm soil layer correlated negatively and significantly with the slope position ($P < 0.05$). The SMC correlated positively to slope gradient. The average correlation coefficient was 0.179 in the 0-50 cm soil layer and it increased with increasing depth. The SMC in the 40-50 cm soil layer correlated positively and significantly to slope gradient ($P < 0.05$). The SMC correlated negatively to vegetation cover. The average coefficient of correlation in the 0-50 cm soil layer was -0.155. It first increased and then decreased with increasing depth.

Table 5. *Correlation analysis between soil moisture content and environmental factors*

Soil depth (cm)	Environmental factors			
	Slope positions	**Slope gradient**	**Soil hardness**	**Vegetation coverage**
0-2	-0.176	0.110	-0.625**	-0.154
P value	0.097	0.300	0.000	0.147
2-10	-0.175	0.116	-0.625**	-0.197
P value	0.100	0.275	0.000	0.063
10-20	-0.173	0.146	-0.607**	-0.200
P value	0.103	0.169	0.000	0.059
20-30	-0.162	0.147	-0.651**	-0.106
P value	0.126	0.168	0.000	0.322
30-40	-0.176	0.206	-0.567**	-0.097
P value	0.097	0.051	0.000	0.361
40-50	-0.209*	0.266*	-0.463**	0.042
P value	0.048	0.011	0.000	0.695
0-50	-0.205	0.179	-0.695**	-0.155
P value	0.053	0.092	0.000	0.144

*Significant correlation at the 0.05 level; **significant correlation at the 0.01 level

Discussion

Vertical migration features of SMC in the stepped slope

At the stage of sprinkler irrigation once every two days and at the non-irrigation stage, the SMC in the 0-50 cm soil layer of the stepped slope increased with increasing depth (*Fig. 4*). The results are in agreement with the findings by Gwak and Kim (2017), Qiang et al. (2013) and Yang et al. (2015). At the stage of sprinkler irrigation once daily, the soil moisture content decreased with increasing depth in the 0-50 cm soil layer. This finding is just contrary to the variation pattern as described above. Strong precipitation under irrigation once every two days could alter the variation pattern as mentioned above. As a result, the SMC in the 10-20 cm soil layer was the highest. This is because irrigation once daily was a considerable source of recharge for the slope with

http://www.aloki.hu ● ISSN 1589 1623 (Print) ● ISSN 1785 0037 (Online)
DOI: http://dx.doi.org/10.15666/aeer/1802_31613175

shorter interval between the irrigations. Strong precipitation usually resulted significant rainwater infiltration and small evaporation and thus provided an efficient recharge to soil moisture in the 0-50 cm soil layer.

As the frequency of sprinkler irrigation decreased, the soil layer with strong changes in SMC extended from the depth of 0-2 to 0-10 cm and finally to 0-20 cm (*Table 5*). The SMC in the middle soil layer, i.e., at the depth of 20-40 cm, remained stable. The SMC was stronger at the greater depth of 40-50 cm, which was consistent with the findings by Choi and Jacobs (2007) and Yao et al. (2012). This is because in the semi-arid regions, the surface soil moisture is more vulnerable to the influence of precipitation, vegetation transpiration and soil evaporation (Seneviratne et al., 2011). Dense sprinkler irrigation (e.g., once daily) can timely recharge the surface soil moisture. As the frequency of irrigation decreased to once every two days, the surface soil moisture cannot be timely recharged after retention, evaporation and infiltration, leading to significant changes in SMC. In an absence of stable recharge from irrigation at the non-irrigation stage, precipitation served as the only recharge to soil moisture. At this stage, randomness of precipitation made the changes of SMC strongest. The local wilting coefficient was $6.20 \pm 0.60\%$. At the early stage of vegetation construction, natural precipitation was enough to ensure the normal growth of vegetation as long as the soil moisture content was higher than 2.45% of the wilting coefficient and that the vegetation entered the non-irrigation stage.

Spatial variation features of SMC in different slope positions

Of the three slope surfaces, the ASMC at the non-irrigation stage was the highest in the first slope surface, followed by the second and third slope surfaces, successively. On the whole, the SMC increased from the top to the bottom of the slope surface (Feng et al., 2013; Legates et al., 2011). The SMC of the three slope surfaces at the irrigation stage were different from the above. The reason was probably that the variability of environmental factors in the three slope surfaces of the stepped slope led to spatial differentiation features of soil moisture content. A correlation analysis was performed between the SMC and environmental factors (*Table 5*). The results showed that soil hardness and terrain factor had a larger impact on soil moisture in the stepped slope. As to the soil hardness, it was highest in the upper position of the second slope surface (3.14 $kg \cdot cm^{-2}$), followed by the middle (4.46 $kg \cdot cm^{-2}$) and lower (4.61 $kg \cdot cm^{-2}$) positions successively. However, the variation pattern was different for the other two slope surfaces. The average overall soil hardness was the highest in the third slope surface (5.3 $kg \cdot cm^{-2}$), followed by the second (4.1 $kg \cdot cm^{-2}$) and first (2.6 $kg \cdot cm^{-2}$) slope surfaces successively. The lower the soil hardness, the smaller the negative effect on the SMC was. As to the influence of terrain factor, the infiltration-excess surface runoff flowed from the third, then to the second and finally to the first slope surface. In relevant to the slope gradient, it was the highest in the first slope surface, followed by the second and third slope surfaces, successively. The larger the slope gradient, the more likely the runoff formation will be, thus leading to soil moisture loss. Therefore, under the joint influence of soil hardness and terrain factor, SMC of the stepped slope showed the above features of spatial variation.

Most studies would believe that soil hardness, slope position and slope gradient correlated negatively with SMC, while vegetation cover correlated positively with SMC (Ali et al., 2010; Cantón et al., 2004; Ishaq et al., 2001; Yang et al., 2015). In this study, we found that both the soil hardness and slope positive correlated negatively with soil

http://www.aloki.hu ● ISSN 1589 1623 (Print) ● ISSN 1785 0037 (Online)
DOI: http://dx.doi.org/10.15666/aeer/1802_31613175

moisture content, which agreed with the previous researches (Ali et al., 2010; Cantón et al., 2004; Ishaq et al., 2001; Yang et al., 2015). However, the findings that the SMC correlated positively with slope gradient and negatively with vegetation cover were consistent with the previous researches (Ali et al., 2010; Cantón et al., 2004; Ishaq et al., 2001; Yang et al., 2015). This was because soil hardness and slope position had a greater impact on SMC. Moreover, the test was conducted at the initial stage of vegetation reconstruction, where the root system of the vegetation was not fully developed. For this reason, the slope gradient and vegetation cover had little impact on SMC.

Influence of environmental factors on the stability of SMC in the stepped slope

Many studies have indicated that the main factors affecting spatial variation of SMC in slopes are soil properties (Fitzjohn et al., 1998; Zhang and Berndtsson, 1988), terrain (Crave and Gascuel-Odoux, 2015; Gómez-Plaza et al., 2001) and vegetation (Bromley et al., 1997; Rodriguez-Iturbe et al., 1999). But given the interaction between these factors and multiplicity of the effect of these factors on SMC, we can hardly determine their relative importance (Grayson et al., 1999). It is widely recognized that soil properties are important affecting factors of spatial distribution of soil moisture. For example, Martinez et al. (2010) opined that the effect of soil properties on spatial differentiation of SMC was greater than that of the terrain factor. However, the effect of terrain factor on spatial distribution of soil moisture was indescribable. Schneider et al. (2011) proposed that soil properties had greater impact on soil moisture, while the influence of vegetation on soil moisture was smaller. Famiglietti et al. (1998) suggested that under humid conditions, soil moisture content variability received the greatest impact from soil properties. While under dry condition, SMC variability was controlled jointly by terrain and soil properties. There are also contending opinions. For example, Tromp-van Meerveld and Mcdonnell (2006) showed that vegetation exerted a greater impact on the spatial distribution of soil moisture content than local terrain. Gwak and Kim (2017) and Kim (2012) opined that terrain was an important affecting factor of spatial distribution of SMC. The soil hardness had significant impact on the spatial variation of SMC. This explained why the SMC was still the smallest even when the gradient of the third slope surface was 25°. This agreed with the findings by Martinez et al. (2010) and Schneider et al. (2011), but disagreed with Gwak and Kim (2017), Kim (2012), Tromp-van Meerveld and Mcdonnell (2006). Ishaq et al. (2001) and Feng et al. (2013) showed that the correlation between soil hardness and SMC weakened with increasing depth, while the correlation of slope gradient and aspect to SMC was strengthened. Our results were in agreement with those. A correlation analysis was performed between the SMC and environmental factors (*Table 5*). The results showed that soil hardness and terrain factor had a larger impact on soil moisture in the stepped slope.

Conclusion

Our results indicated that the soil moisture migration of the three slope surfaces (bottom, middle and top) exhibited a similar pattern under different methods and significant of sprinkler irrigation. That is, at the non-irrigation stage and the stage of irrigation once every two days, the SMC increased with increasing depth. Whereas, at the stage of irrigation once daily, the SMC decreased with increasing depth. The SMC

http://www.aloki.hu ● ISSN 1589 1623 (Print) ● ISSN 1785 0037 (Online)
DOI: http://dx.doi.org/10.15666/aeer/1802_31613175

decreased and the CV of SMC increased with the decreasing frequency of sprinkler irrigation. However, the ASMC content increased from the top to the bottom of the stepped slope under different frequencies of sprinkler irrigation. The correlation analysis among the four environmental factors, namely, slope position and gradient, soil hardness and vegetation cover showed positive and negative relationships. The slope position, slope hardness and vegetation cover correlated negatively with the SMC ($P < 0.01$). On the other hand, the slope gradient correlated positively with the SMC ($P < 0.05$). In order to ensure better vegetation growth in the stepped slope under the water conservation context, the frequency and amount of sprinkler irrigation should be adjusted according to the growth status of vegetation. Moreover, reasonable tillage measures such as ploughing should be adopted to reduce soil hardness, increase SMC and promote fast vegetation restoration of the slopes.

The duration of the study is short, so it is difficult to assess and eliminate the impact of soil disturbance caused by infrastructure construction, and the spatial variation of SMC in different slope direction, number of steps and slope gradient needs further study.

Acknowledgement. This study was funded by Open Foundation of Northwest Institute of Eco-Environment and Resources, Chinese Academy of Sciences (KLDD-2017-004); 2017 Lanzhou Talent Innovation and Startup Project (2017-RC-26).

REFERENCES

[1] Ali, G. A., Roy, A. G., Legendre, P. (2010): Spatial relationships between soil moisture patterns and topographic variables at multiple scales in a humid temperate forested catchment. – Water Resources Research 46(10): 2290-2296.
[2] Bromley, J., Brouwer, J., Barker, A. P., et al. (1997): The role of surface water redistribution in an area of patterned vegetation in a semi-arid environment, south-west Niger. – Journal of Hydrology 198(1-4): 1-29.
[3] Cantón, Y., Solé-Benet, A., Domingo, F. (2004): Temporal and spatial patterns of soil moisture in semiarid badlands of SE Spain. – Journal of Hydrology 285(1): 199-214.
[4] Choi, M., Jacobs, J. M. (2007): Soil moisture variability of root zone profiles within SMEX02 remote sensin footprints. – Advances in Water Resources 30(4): 883-896.
[5] Cohen-Fernández, A. C., Naeth, M. A. (2013): Erosion control blankets, organic amendments and site variability influenced the initial plant community at a limestone quarry in the Canadian Rocky Mountains. – Biogeosciences 10(7): 5243-5253.
[6] Crave, A., Gascuel-Odoux, C. (2015): The influence of topography on time and space distribution of soil surface water content. – Hydrological Processes 11(2): 203-210.
[7] Engelbrecht, B. M. J., Comita, L. S., Condit, R., et al. (2007): Drought sensitivity shapes species distribution patterns in tropical forests. – Nature 447(7140): 80-82.
[8] Famiglietti, J. S., Rudnicki, J. W., Rodell, M. (1998): Variability in surface moisture content along a hillslope transect: Rattlesnake Hill, Texas. – Journal of Hydrology 210(1): 259-281.
[9] Feng, Q., Zhao, W., Qiu, Y., et al. (2013): Spatial heterogeneity of soil moisture and the scale variability of its influencing factors: a case study in the loess plateau of China. – Water 5(3): 1226-1242.
[10] Fitzjohn, C., Ternan, J. L., Williams, A. G. (1998): Soil moisture variability in a semi-arid gully catchment: implications for runoff and erosion control. – Catena 32(1): 55-70.

http://www.aloki.hu ● ISSN 1589 1623 (Print) ● ISSN 1785 0037 (Online)
DOI: http://dx.doi.org/10.15666/aeer/1802_31613175

[11] Gómez-Plaza, A., Martínez-Mena, M., Albaladejo, J., et al. (2001): Factors regulating spatial distribution of soil water content in small semiarid catchments. – Journal of Hydrology 253(1): 211-226.
[12] Grayson, R. B., Blöschl, G., Willgoose, G. R., et al. (1999): Observed spatial organization of soil moisture and its relation to terrain indices. – Water Resources Research 35(3): 797-810.
[13] Gwak, Y., Kim, S. (2017): Factors affecting soil moisture spatial variability for a humid forest hillslope. – Hydrol. Process 31(2): 431-445.
[14] Ishaq, M., Hassan, A., Saeed, M., et al. (2001): Subsoil compaction effects on crops in Punjab, Pakistan: I. Soil physical properties and crop yield. – Soil & Tillage Research 60(3): 153-161.
[15] Jia, Y. H., Shao, M. A., Jia, X. X. (2013): Spatial pattern of soil moisture and its temporal stability within profiles on a loessial slope in northwestern China. – Journal of Hydrology 495(15): 150-161.
[16] Kim, S. (2012): Characterization of annual soil moisture response pattern on a hillslope in Bongsunsa Watershed, South Korea. – Journal of Hydrology 448-449(15): 100-111.
[17] Legates, D. R., Mahmood, R., Levia, D. F., et al. (2011): Soil moisture: a central and unifying theme in physical geography. – Progress in Physical Geography: Earth and Environment 35(1): 65-86.
[18] Liu, L., Sun, H., Zhang, J., et al. (2019): Effect of several engineering measures on vegetation coverage on steep slope in the Loess region. – Arid Zone Research 36(4): 1041-1048.
[19] Martinez, C., Hancock, G. R., Kalma, J. D., et al. (2010): Spatio-temporal distribution of near-surface and root zone soil moisture at the catchment scale. – Hydrological Processes 22(14): 2699-2714.
[20] Miyazaki, T., Hasegawa, S., Kasubuchi, T. (1993): Water flow in soils. – Soil Science 157(4).
[21] Morgan, R. P. C. (1980): Implications. – In: Kirby, M. J., Morgan, R. P. C. (eds.) Soil Erosion. Wiley, New York, pp. 253-301.
[22] Rodriguez-Iturbe, I., D'Odorico, P., Porporato, A., et al. (1999): On the spatial and temporal links between vegetation, climate, and soil moisture. – Water Resources Research 35(12): 3709-3722.
[23] Schneider, K., Leopold, U., Gerschlauer, F., et al. (2011): Spatial and temporal variation of soil moisture in dependence of multiple environmental parameters in semi-arid grasslands. – Plant and Soil 340(1): 73-88.
[24] Seneviratne, S. I., Davin, E., Hirschi, M., et al. (2011): Soil moisture-ecosystem-climate interactions in a changing climate: – AGU Fall Meeting, 5-9 December, San Francisco, CA.
[25] Sharma, L. K., Umrao, R. K., Singh, R., et al. (2017): Stability investigation of hill cut soil slopes along National highway 222 at Malshej Ghat, Maharashtra. – Journal of the Geological Society of India 89(2): 165-174.
[26] Soane, B. D., Blackwell, P. S., Dickson, J. W., et al. (1980): Compaction by agricultural vehicles: a review I. Soil and wheel characteristics. – Soil & Tillage Research 1(3): 207-237.
[27] Stokes, A., Norris, J. E., Greenwood, J. R. (2008): Introduction to Ecotechnological Solutions. – Springer, Dordrecht.
[28] Tromp-van Meerveld, H. J., Mcdonnell, J. J. (2006): On the interrelations between topography, soil depth, soil moisture, transpiration rates and species distribution at the hillslope scale. – Advances in Water Resources 29(2): 293-310.
[29] Vivoni, E. R., Rinehart, A. J., Méndez-Barroso, L. A., et al. (2010): Vegetation controls on soil moisture distribution in the Valles Caldera, New Mexico, during the North American monsoon. – Ecohydrology 1(3): 225-238.

http://www.aloki.hu ● ISSN 1589 1623 (Print) ● ISSN 1785 0037 (Online)
DOI: http://dx.doi.org/10.15666/aeer/1802_31613175

[30] Wu, Q., Yang, W. (1998): Vegetation Construction and Sustainable Development in the Loess Plateau. – Science Press, Beijing.
[31] Yang, L., Chen, L., Wei, W. (2015): Effects of vegetation restoration on the spatial distribution of soil moisture at the hillslope scale in semi-arid regions. – Catena 124(1): 138-146.
[32] Yang, W., Shao, M. (2000): Study on Soil Moisture in Loess Plateau. – Science Press, Beijing.
[33] Yang, Y., Yang, J., Zhao, T., et al. (2016): Ecological restoration of highway slope by covering with straw-mat and seeding with grass–legume mixture. – Ecological Engineering 90: 68-76.
[34] Yao, X., Fu, B., Lu, Y. (2012): Spatial patterns of soil moisture at transect scale in the Loess Plateau of China. – Acta Ecologica Sinica 32(16): 4961-4968.
[35] Zhang, T., Berndtsson, R. (1988): Temporal patterns and spatial scale of soil water variability in a small humid catchment. – Journal of Hydrology 104(1): 111-128.

http://www.aloki.hu ● ISSN 1589 1623 (Print) ● ISSN 1785 0037 (Online)
DOI: http://dx.doi.org/10.15666/aeer/1802_31613175

CHANGE CHARACTERISTICS OF WATER EXCHANGE BETWEEN THE YANGTZE RIVER AND THE DONGTING LAKE DURING 1960–2018 IN CHINA

LI, Y. Y.[1,2] – YANG, G. S.[2,3*] – WAN, R. R.[2,3*] – LI, B.[2,3] – LAI, X. J.[2,3*]

[1]*School of Urban, Resources and Environment, Jiangsu Second Normal University, 210013 Nanjing, PR China*

[2]*Key Laboratory of Watershed Geographic Sciences, Nanjing Institute of Geography and Limnology, Chinese Academy of Sciences, 210008 Nanjing, PR China*

[3]*University of Chinese Academy of Sciences, 100049 Beijing, PR China*

**Corresponding author*
e-mail: gsyang@niglas.ac.cn, rrwan@126.com; phone: +86-025-8688-2003; fax: +86-025-5771-4759

(Received 27th Sep 2019; accepted 4th Feb 2020)

Abstract. Hydrological exchange between the trunk stream and the floodplains is the key factor maintaining ecological functioning. The water discharge diverting from the Yangtze River to the Dongting Lake has recently decreased considerably in China. However, their variation characteristics and major driving factors remained unclear. In this study, Mann Kendall trend and Pettitt abrupt tests were employed to determine the changes of time series. Double mass curve analysis and regression analysis were used for the qualitative analysis of the impacts of climate change and human activity. Results revealed that precipitation change trends significantly decreased in autumn. The water discharge at the trunk Yangtze River had a decreasing trend in autumn and an increasing trend in winter. The annual and seasonal water discharge diverting from the Yangtze River to the Dongting Lake, except at Xinjiangkou in summer, exhibited significant downward trends. No consistent trends in precipitation and water discharge were identified, thereby indicating that the seasonal relationships between them had been disturbed by human activities. Human activities had a dominant effect on the water discharge exchange between them during 1967–2018. Along with the intensification of human activities, the hydrological connectivity between the Yangtze River and the Dongting Lake would probably be further changed in the near future.
Keywords: *hydrological connectivity, river–floodplain systems, the Jingjiang Three Outlets, the Three Gorges Dam, Mann–Kendall test, Pettitt test*

Introduction

Floodplains have the highest levels of production and biodiversity worldwide (Tockner and Stanford, 2002) and not only provide habitat and refuge for species (Whited et al., 2007; Hung et al., 2012) but also supply important services for humankind (Kummu et al., 2014). The hydrological exchange between the trunk river and its floodplains is the most important factor for maintaining ecological function and biodiversity and for flood attenuation (Thomaz et al., 2007; Zurbrügg et al., 2012). In recent decades, river floodplain systems have been heavily disturbed by human activities (Heiler et al., 1995; Clilverd et al., 2013). Moreover, the hydrological cycle in major rivers worldwide has undergone dramatic spatiotemporal changes along with global climate changes (Palmer et al., 2008). Hydrological connectivity between the trunk river and its floodplains are changed by human activities and climate change significantly in many large rivers (Heiler et al., 1995; Knowlton and Jones, 1997;

http://www.aloki.hu ● ISSN 1589 1623 (Print) ● ISSN 1785 0037 (Online)
DOI: http://dx.doi.org/10.15666/aeer/1802_31773193

Amoros and Bornette, 2002; Tockner et al., 2010) and caused the biodiversity and bioproduction degradation in many river–floodplain systems, including the Danube in Europe (Besemer et al., 2005), the Missouri in the USA (Knowlton and Jones, 1997), and the Mackenzie in Canada (Lesack and Marsh, 2010). Numerous previous studies have concentrated on the benefits of river floodplain connections (Bullock and Acreman, 2003; Acreman et al., 2003; Zurbrügg et al., 2012). However, the effects of human activities and climate change on hydrological connectivity have not received significant attention. Therefore, quantitative assessments of the influences of human activities and climate change on the hydrological connectivity of these systems are extremely essential to make effective management and conservation plans for river–floodplain ecosystems.

The Yangtze River floodplain is characterized by a number of lakes of various sizes in China (Nie et al., 1999; Yang et al., 2008). The Yangtze River freely connected with many lakes in the history (Ru and Liu, 2013). Along with the intensive human activities such as the construction of dam, deforestation, water diversion, and sand extraction, the hydrological connectivity has been remarkably changed. At present, only three lakes (Dongting Lake, Poyang Lake, and Shijiu Lake) retain direct connections with the Yangtze River. The obstruction of hydrological connectivity changes the patterns of the lake wetland vegetation (Hu et al., 2015), damages the diversity of fish species (Xie et al., 2003), and increases flood risk (Nakayama and Shankman, 2013) in the Yangtze River floodplain. Thus, the obstruction of hydrological connectivity is one of the top threats to the Yangtze River floodplain (Liu and Wang, 2010; Pan et al., 2011).

The hydrological connectivity between the Yangtze River and the Dongting Lake is the most typical and complex in the floodplain of Yangtze River in China (Lai et al., 2014a). The Dongting Lake receives water from the Yangtze River through the tie channels of the Jingjiang Three Outlets (JTO). During 1956–1966, the JTO could recharge averaged 29.3% of the main river water discharge into the Dongting Lake; however, after 2003, it can divert only 11.8% (Zhu et al., 2015). The hydrological connectivity at the JTO has considerably decreased (Ou et al., 2014). Thus, significant attention is paid to investigate the reasons for the decreased hydrological connectivity at the JTO, especially after the Three Gorges Dam (TGD) in 2003. Chang et al. (2010) and Zhu et al. (2015) analyzed the variations in the water exchange at the JTO to determine the TGD influences on the water exchange capability, and they had different opinions on the effect factors of the water exchange changes at the JTO. Zhang et al. (2015a) found that the TGD impoundment was responsible for 31.1% of the decrease in the water exchange at the JTO. Li et al. (2016) found that river channel changes were responsible for 23.6% of the decrease in the water exchange at the JTO after the TGD. However, it still disagrees on how human activities influent the water exchange at the JTO (Chang et al., 2010; Zhu et al., 2015; Zhang et al., 2015a; Li et al., 2016). Furthermore, previous studies mainly focused on the influences of human activities, but the effects of climate change were neglected. The properties of changing water exchange and their influence factors at the JTO were not extensively analyzed. Therefore, this study objectives are as follows: (1) to detect the annual and seasonal variations in the water exchange at the JTO on the basis of the daily hydrologic data during 1960–2018; (2) to quantify the effects of precipitation changes on water exchange; and (3) to assess the contributions of human activities and climate change to water exchange reduction. This study hopes to provide an important scientific basis for

http://www.aloki.hu ● ISSN 1589 1623 (Print) ● ISSN 1785 0037 (Online)
DOI: http://dx.doi.org/10.15666/aeer/1802_31773193

the optimization control of the river–lake relationship and the protection of river–floodplain ecosystems.

Study area and data

Study sites

Human activities in the Yangtze River have remarkably intensified during the past half century, especially after the economic reform and opening-up policy was implemented in 1978 in China (Chen et al., 2014). The storage capacity of large reservoirs and dams has significantly increased, especially after 1981 and 2003 (*Fig. 1*). Water–soil conservation (i.e., terracing, planting trees, and protecting vegetation) was implemented in 1988. In 1992, the cumulative area of water–soil conservation displays an upward trend from 156.56×10^3 km^2 to 320.58×10^3 km^2.

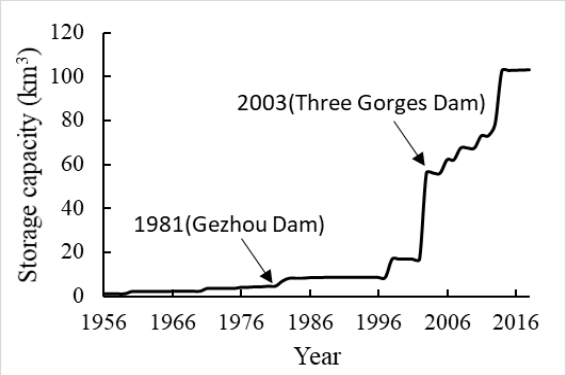

Figure 1. *Storage capacity of large reservoirs in the upper Yangtze River*

Local river channel cut-off events. As shown in *Table 1*, three instances of artificial and natural channel cut-offs occurred in the lower Jingjiang River from 1967 to 1972. Artificial channel cut-off projects at Zhongzhouzi in 1967 and Shangchewan in 1969 were carried out, which respectively shortened the channel lengths of the lower Jingjiang River (the lower Jingjiang River from the Ouchikou to the Chenglingji) to approximately 32.4 and 29.2 km. Natural channel cut-off at Shatanzi occurred in 1972, which resulted in a channel length decrease of 18.95 km.

Table 1. *River channel cut-off events in the lower Jingjiang River. (Data originated from Qin et al., 2013)*

Cut-off name	Cut-off year	Cut-off reason	Channel length before the cut-off (km)	Channel length after the cut-off	Channel length change
Zhongzhouzi	1967	Artificial	36.7	4.3	32.4
Shangchewan	1969	Artificial	32.7	3.5	29.2
Shatanzi	1972	Natural	20.3	1.35	18.95

The Songzi, Taiping, and Ouchi outlets comprise the JTO. The Zhicheng Hydrological Station situated 18 km upstream of the JTO was used to reflect the influence of the mainstream. Zhicheng is approximately 60.8 km distant from Yichang

http://www.aloki.hu ● ISSN 1589 1623 (Print) ● ISSN 1785 0037 (Online)
DOI: http://dx.doi.org/10.15666/aeer/1802_31773193

Hydrological Station that is the hydrological control station of the upper Yangtze River. They have very similar streamflows. Xinjiangkou and Shadaoguan are the hydrological stations at the Songzi outlet. Mituosi Hydrological Station controls the Taiping outlet. Ouchi (kang) and Ouchi (guan) are the hydrological stations at the Ouchi outlet (*Fig. 2*).

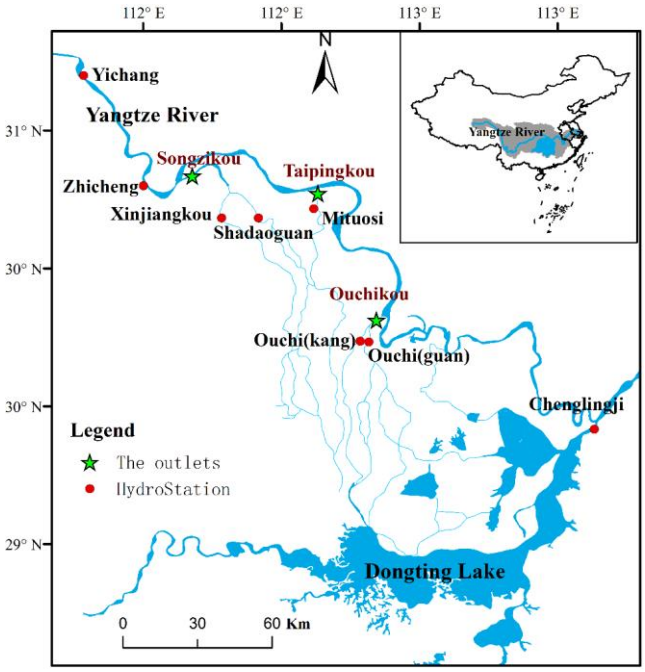

Figure 2. *Geophysical location of the JTO in the Yangtze River Basin*

Data

The daily water level and discharge data during 1960–2018 were obtained from the Bureau of Hydrology, Changjiang Water Resources Commission in China. The data of daily precipitation from 180 meteorological stations situated in the Yangtze River Basin were obtained from the China Meteorological Data Network (http://data.cma.cn/). A total of 70 meteorological stations with continuous precipitation record stations during 1960–2018 are located in the upstream of Zhicheng (*Fig. 3*). Based on the climate features in the Yangtze River Basin, there are four seasons divided: spring between March and May, summer between June and August, autumn between September and November, winter between December and February.

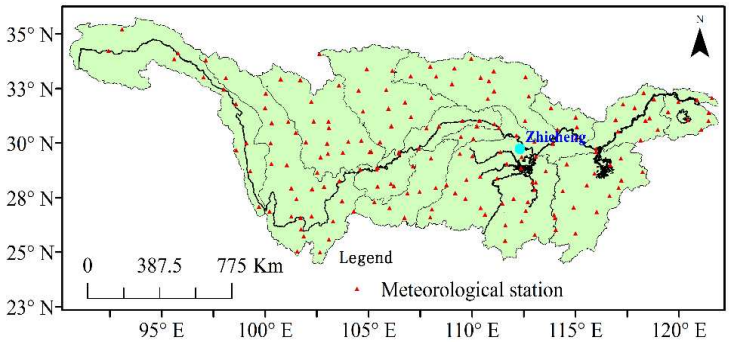

Figure 3. *Spatial distribution of meteorological stations in the Yangtze River Basin*

APPLIED ECOLOGY AND ENVIRONMENTAL RESEARCH 18(2):3177-3193.
http://www.aloki.hu ● ISSN 1589 1623 (Print) ● ISSN 1785 0037 (Online)
DOI: http://dx.doi.org/10.15666/aeer/1802_31773193

Methods

Mann–Kendall trend test

The trend analyses which are the hydrological-meteorological time series used the non-parametric Mann–Kendall (MK) test (Mann, 1945; Kendall, 1975). The test statistic for a time series $(x_1, x_2, x_3, \dots, x_n)$ is given as follows:

$$S = \sum_{i=1}^{n-1} \sum_{j=i+1}^{n} sgn(x_j - x_i) \quad \text{(Eq.1)}$$

$$\operatorname{sgn}(x_j - x_i) = \begin{cases} +1 & \text{if } (x_j - x_i) > 0 \\ 0 & \text{if } (x_j - x_i) = 0 \\ -1 & \text{if } (x_j - x_i) < 0 \end{cases} \quad \text{(Eq.2)}$$

where x_i and x_j respectively represent the data values at times i and j. n is the time series length.

$$\operatorname{Var}(S) = \frac{[n(n-1)(2n+5) - \sum_{i=1}^{m} t_i\,(t_i-1)(2t_i+5)]b}{18} \quad \text{(Eq.3)}$$

where m and t_i respectively represent the number of tied groups and data in the tied group. The standard normal variable Z is given by *Equation 4:*

$$Z = \begin{cases} \frac{S-1}{\sqrt{Var\,(S)}}, & \text{if } S > 0 \\ 0, & \text{if } S = 0 \\ \frac{S-1}{\sqrt{Var\,(S)}}, & \text{if } S < 0 \end{cases} \quad \text{(Eq.4)}$$

The positive Z value is an increasing trend, and the negative Z value is a decreasing trend. If $|Z|$ is greater than 1.96 at the 0.05 significance level, the null hypothesis of the absent trend is rejected.

Pettitt abrupt change test

The abrupt change of the hydrological-meteorological time series used the Pettitt test (Pettitt, 1979). The method uses a version of the Mann–Whitney statistic $U_{t,n}$, including two parts ($x_1, x_2, x_3, \dots, x_t$ and $x_{t+1}, x_{t+2}, x_{t+3}, \dots, x_T$) from the same time series. The test statistic $U_{t,n}$ is computed as follows:

$$U_{t,T} = \sum_{i=1}^{t} \sum_{j=1}^{T} sgn\,(x_t - x_j) \quad \text{for } t = 2, \dots, n \quad \text{(Eq.5)}$$

The largest $|U_{t,T}|$ value is the abrupt change point

$$K_T = max|U_{t,T}| \quad \text{(Eq.6)}$$

http://www.aloki.hu ● ISSN 1589 1623 (Print) ● ISSN 1785 0037 (Online)
DOI: http://dx.doi.org/10.15666/aeer/1802_31773193

The significance testing are as follows:

$$p \cong 2\exp\left\{-\frac{6(K_T)^2}{T^3+T^2}\right\} \quad \text{(Eq.7)}$$

Once the p value is less than the 5% significance level, a significant abrupt change point exists.

Double mass curve analysis

Double mass curve (DMC) is a common method to test the consistency and variation of the relationship between two parameters. A DMC is a line drawn between the continuous cumulative values of one variable and the continuous cumulative values of another variable for the same period. Generally, the Double mass curve analysis kept a straight line if water discharge was not affected by human activities. Therefore, evident abrupt change points in the DMCs suggest the variations influenced by human activities (Zhao et al., 2017).

Regression analysis for quantifying the influences of human activities and climate change

Reconstruction of the natural water discharge at the JTO is necessary to better understand and quantify the influences of human activities and climate change on hydrological connectivity between Dongting Lake and Yangtze River. The amount of water exchange at the JTO is impacted by various factors, such as the position between the JTO entrance and the trunk stream, the channel scouring and silting changes, and river regime variations in the mainstream (Lu et al., 2012). The changes of relative position and river channel gradually and slowly occur under natural conditions (Zhang et al., 2015b). Thus, the amount of water exchange at the JTO is directly related to the changes of water discharge at the mainstream of Zhicheng. To quantify the impact of precipitation changes and human activities on water exchange at the JTO, the regression analysis method was applied in the current study.

Previous studies indicated that the precipitation and streamflow in the Yangtze River Basin were minimally affected by human activities before the 1970s (Yang et al., 2015; Zhao et al., 2015). Thus, the period 1960–1966 was used as the reference period to achieve the requirement of this study. Although streamflow is related to many factors, such as precipitation, temperature, dam construction, and GDP in the Yangtze River Basin, numerous studies found that precipitation is the most correlated with streamflow at the mainstream which can explain 80% of the variance during the past 50 years (Chen et al., 2014; Zhao et al., 2015). Therefore, regression equations are established between annual precipitation and water discharge at Zhicheng based on data collected in the period 1960–1966 to estimate the natural water discharge at Zhicheng. Afterward, regression equations are established between the water discharge at Zhicheng and the water exchange at the JTO in the period 1960–1966. Thus, water exchange changes at the JTO in response to precipitation change in subsequent years can be quantified by estimating the natural water exchange at Zhicheng. The hydrological response to human activities can be provided by the difference between the estimated and the observed water discharge.

http://www.aloki.hu ● ISSN 1589 1623 (Print) ● ISSN 1785 0037 (Online)
DOI: http://dx.doi.org/10.15666/aeer/1802_31773193

Results and discussion

Annual and seasonal precipitation trends in the basin

The trends of the basin-averaged seasonal and annual precipitation in the upstream of Zhicheng from 1960 to 2018 on the basis of MK test are shown in *Figure 4*. The mean annual precipitation during 1960–2018 was 996.09 mm (from 756.50 mm to 1027.80 mm). Annual precipitation shows an inconspicuous tendency. On a seasonal basis, precipitation trends in spring, summer, and winter present no statistical significance. However, precipitation trends show a remarkable decreasing trend with a 99% confidence level in autumn.

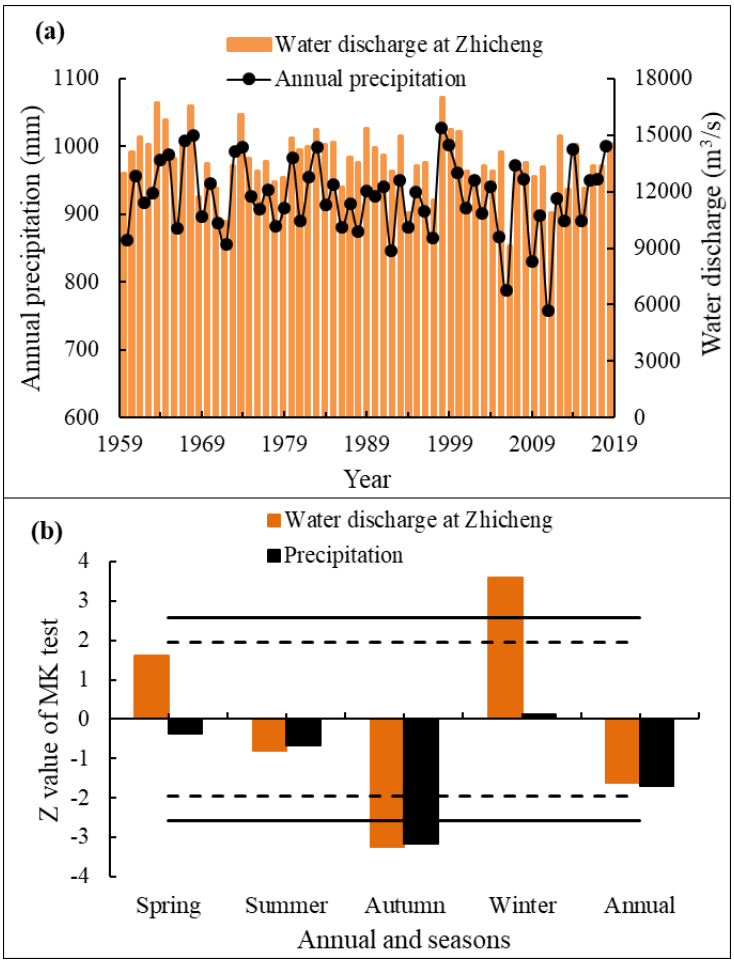

Figure 4. *Temporal trend changes in the annual-seasonal precipitation and water discharge at Zhicheng. (a) Annual precipitation and water discharge, (b) trends of the annual and seasonal precipitation and water discharge with the MK test. Horizontal dashed lines and solid lines in (b) denote confidence levels of 95% and 99% respectively*

Annual and seasonal water discharge trends at Zhicheng

Variations of the annual and seasonal water discharge at Zhicheng in the mainstream of Yangtze River are detected based on the observed data from 1960 to 2018 (*Fig. 4*). The annual average water discharge during 1960–2018 was 13,698.12 m^3/s, with a range from 12,995.85 m^3/s to 17,005.78 m^3/s (*Fig. 4a*). The annual average water discharge shows no significant decreasing trend and decreases by an average of 28.01

http://www.aloki.hu ● ISSN 1589 1623 (Print) ● ISSN 1785 0037 (Online)
DOI: http://dx.doi.org/10.15666/aeer/1802_31773193

m^3/s every year (*Fig. 4*). The seasonal water discharge time series exhibited different change trends (*Fig. 4b*). Water discharge shows an upward trend in spring and a downward trend in summer, with no statistically significant levels. However, a decreasing trend in autumn and an increasing trend in winter were detected with a 99% confidence level.

Annual and seasonal water discharge trends at the JTO

The changes of annual and seasonal water discharge at the JTO are shown in *Figure 5*. The annual and seasonal water discharge at different stations fluctuated and decreased from 1960 to 2018. The annual average water discharge at Xinjiangkou, Shadaoguan, Mituosi, Ouchi (kang), and Ouchi (guan) decreased by an average of 7.15, 6.42, 8.29, 1.91, and 27.91 m^3/s every year, respectively. Before the 1970s, the average water discharge at Ouchi (guan) was significantly larger than at the other outlets, whereas it was smaller than that at Xinjiangkou after the 1970s (*Fig. 5a*). The seasonal water discharge dramatically fluctuated throughout the year at all stations. More than 90% of water discharge at all stations occurred in summer and autumn. In winter, water discharge at the JTO, except at Xinjiangkou, almost presented a zero-water discharge state after the 1970s (*Figs. 5b–f*).

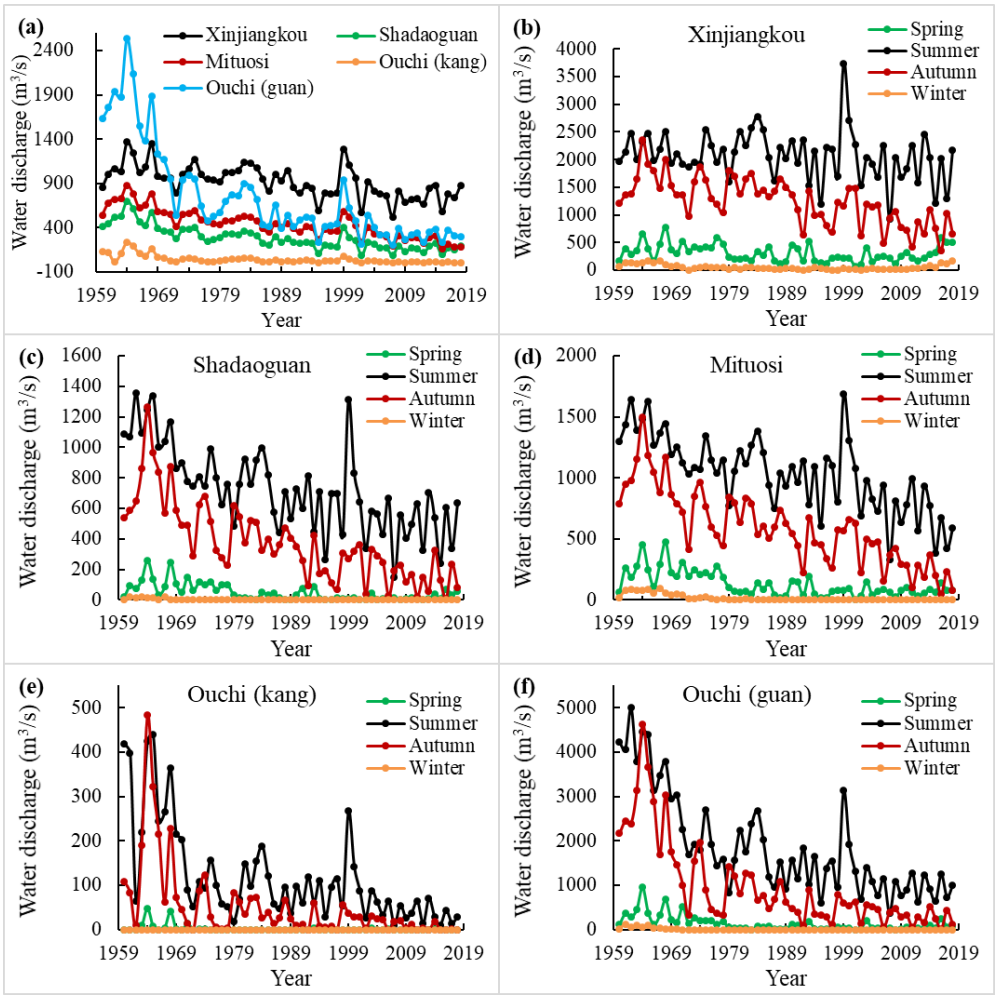

Figure 5. *Changes in the annual and seasonal water discharge at the JTO during 1960–2018. (a) Annual water discharge, (b–f) seasonal water discharge at different stations*

http://www.aloki.hu ● ISSN 1589 1623 (Print) ● ISSN 1785 0037 (Online)
DOI: http://dx.doi.org/10.15666/aeer/1802_31773193

The annual and seasonal water discharge except at Xinjiangkou, in summer exhibited significant downward trends with a 99% confidence level (*Fig. 6*). The consistent trend results of annual and seasonal water discharge indicated that they might experience similar driving factors.

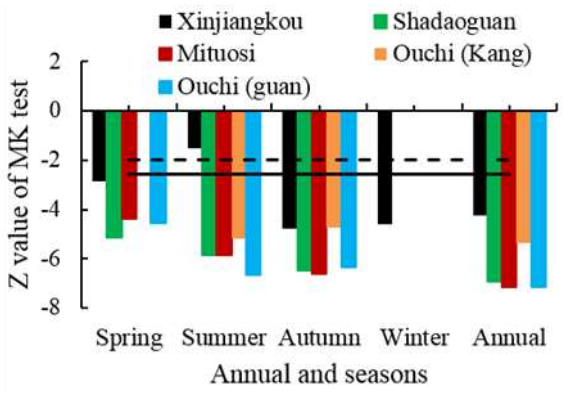

Figure 6. *Temporal trend changes in the annual and seasonal water discharge at the JTO with the MK test during 1960–2018. Horizontal dashed lines and solid lines denote confidence levels of 95% and 99% respectively*

Abrupt change point in annual-seasonal precipitation and water discharge

The Pettitt test was employed to detect abrupt change points in precipitation and water discharge for the control hydrological stations at the trunk stream of the Yangtze River and at the JTO during 1960–2018. The results are shown in *Table 2*. Only precipitation in autumn exhibited a downward abrupt change occurring in 1989. For the mainstream of Zhicheng, the water discharge in autumn and winter displayed significant abrupt changes in 1990 and 1999 with confidence levels of 99% and 95% respectively. On the other hand, every spring and summer, no significant abrupt changes occurred during 1960–2018. For the five control hydrological stations at the JTO, except water discharge in summer at Xinjiangkou and in spring at Ouchi (kang), significant abrupt changes were found in the annual and seasonal water discharge time series. All the stations at the JTO showed consistent outcomes with the test in spring (1977), summer (1982), and autumn (1989), whereas the abrupt stating times in annual and in winter were displayed differently. In general, abrupt stating times occurred mainly around 1980 and 1990. In particular, the abrupt stating times of the Ouchi (kang) and Ouchi (guan) at the Ouchi outlet were earlier than those of other outlets. Under the same conditions of the upstream, the change heterogeneity and inconsistency of annual and seasonal water discharge at the JTO indicated that local human activities affected the amount of water discharge in a complex way.

Impact of human activities and climate change on water exchange

The water exchange changes at the JTO have complex dynamic processes, which are not only closely associated with alterations in the hydrological regimes and channel morphology of the mainstream near the JTO, but also related to the scouring and silting changes in the diversion channels (Lu et al., 2012).

Precipitation and human activities in the upstream of Zhicheng caused the downstream water discharge changes, while water discharge changes at Zhicheng affected the amount

http://www.aloki.hu ● ISSN 1589 1623 (Print) ● ISSN 1785 0037 (Online)
DOI: http://dx.doi.org/10.15666/aeer/1802_31773193

of water exchange at the JTO. The decreasing trend of the average annual water discharge at the mainstream of Zhicheng was consistent with the annual precipitation change. This result is in agreement with previous findings. Chen et al. (2017) and Gao et al. (2012) used different methods to demonstrate that the annual streamflow at Yichang had a decreasing trend and confirmed that the decrease in annual precipitation was the primary driver. However, the seasonal change trends between the precipitation and the water discharge at Zhicheng displayed a complicated condition (*Fig. 4*).

Table 2. *Results of the Pettitt test for abrupt change points in the annual-seasonal precipitation and water discharge*

Type	Station name	Time scale	Change points	p value	Significance level
Precipitation	–	Annual	1984	0.3715353	–
		Spring	1978	0.3949851	–
		Summer	2003	0.9989329	–
		Autumn	1989	0.0007483	0.01
		Winter	2008	0.3949851	–
Water discharge	Zhicheng	Annual	2000	0.2811883	–
		Spring	2001	0.5568367	–
		Summer	2000	0.4449031	–
		Autumn	1989	0.0055008	0.01
		Winter	1999	0.0248369	0.05
	Xinjiangkou	Annual	1990	0.0001550	0.01
		Spring	1977	0.0007483	0.01
		Summer	2000	0.1400187	–
		Autumn	1989	0.0000104	0.01
		Winter	1979	0.0004053	0.01
	Shadaoguan	Annual	1985	0.0000015	0.01
		Spring	1977	0.0000038	0.01
		Summer	1982	0.0000351	0.01
		Autumn	1989	0.0000035	0.01
		Winter	1979	0.0000007	0.01
	Mituosi	Annual	1985	0.0000028	0.01
		Spring	1977	0.0000020	0.01
		Summer	1982	0.0000480	0.01
		Autumn	1989	0.0000058	0.01
		Winter	1983	0.0000002	0.01
	Ouchi (kang)	Annual	1993	0.0028987	0.01
		Spring	1973	0.0531960	0.01
		Summer	1982	0.0000480	0.01
		Autumn	1988	0.0036449	0.01
		Winter	Dried	Dried	–
	Ouchi (guan)	Annual	1985	0.0000053	0.01
		Spring	1977	0.0000041	0.01
		Summer	1982	0.0000088	0.01
		Autumn	1989	0.0000277	0.01
		Winter	1974	0.0000411	0.01

http://www.aloki.hu ● ISSN 1589 1623 (Print) ● ISSN 1785 0037 (Online)
DOI: http://dx.doi.org/10.15666/aeer/1802_31773193

To further address the reasons for the seasonal water discharge changes at Zhicheng, the DMCs were plotted to show the relationship between the precipitation and the water discharge (*Fig. 7*). Abrupt changes in the DMCs are inapparent, especially in summer (*Fig. 7*). In spring and winter, similar with precipitation, water discharge after the transition years was larger than the before in the DMCs. In autumn, water discharge after the transition years was smaller than the before. These results on the seasonal trends and the DMC analysis indicated that the seasonal relationship between water discharge and precipitation had been disturbed by human activities. The operations of reservoirs and dams changed the distribution of inner-annual water discharge downstream. For example, the Three Gorges Reservoir increased low flow in the winter and decreased flood flow in summer since 2003 (Gao et al., 2012). The implementation of water–soil conservation caused a decrease in streamflow from the upper Yangtze River Basin (Yang et al., 2015).

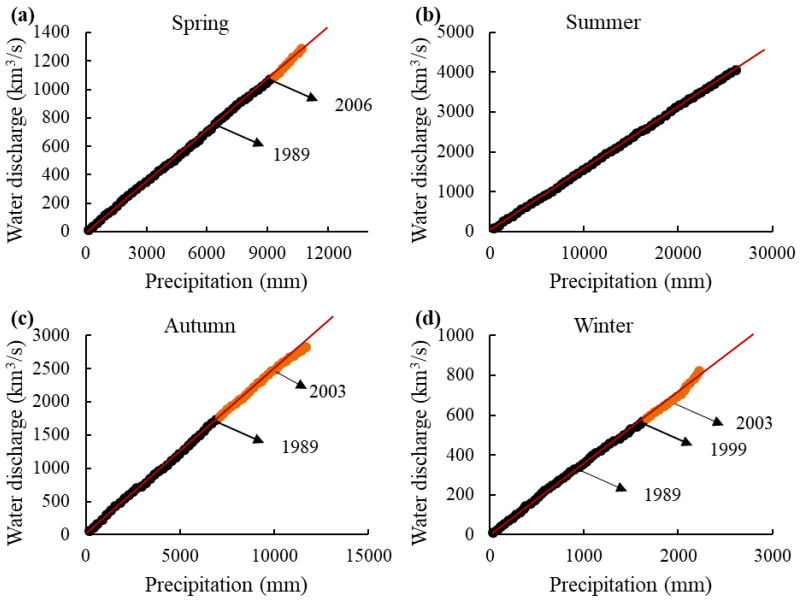

Figure 7. *DMC analysis between precipitation and water discharge at Zhicheng in different seasons*

The annual and seasonal trends of water discharge at the JTO were incompletely homologous to the hydrological variations at the mainstream of Zhicheng (*Figs. 4b* and *6*) because of alterations in the channel morphology (Lai et al., 2014b). The operations of reservoirs and dams trapped a large amount of sediment yield, especially after the operation of Gezhou Dam in 1981 (Zhang et al., 2006; Yang et al., 2014; Gao et al., 2015a, b). The implementation of water–soil conservation also caused a distinct in sediment yield from the upper Yangtze River Basin (Wang et al., 2011). Sediment yield decrease caused the channel erosion in the mainstream channel (Yua et al., 2018). The channel erosion resulted in the lowering water level with the same water discharge (*Figs. 8a*) which decreased the water level differences between the mainstream and the JTO, and resulted in the decline of water diversion ability. Meanwhile, the water level with the same water discharge at the JTO generally shifted up (*Figs. 8b–f*) because of the deposition at the diversion channel at the JTO. The alterations of the channel

http://www.aloki.hu ● ISSN 1589 1623 (Print) ● ISSN 1785 0037 (Online)
DOI: http://dx.doi.org/10.15666/aeer/1802_31773193

morphology counteracted the increase in water discharge of the mainstream and resulted in increased zero-discharge days at the JTO (Chang et al., 2010). Under the same precipitation and human activity conditions in the upper stream, the reduced magnitudes of water discharge at the different outlets during 1960–2018 were also different due to the different magnitudes of the scouring and silting changes in the diversion channels (*Figs. 8b–f*). River channel cut-offs caused strong channel erosions in the lower Jingjiang River and relative deposition in the diversion channels (Qin et al., 2013).

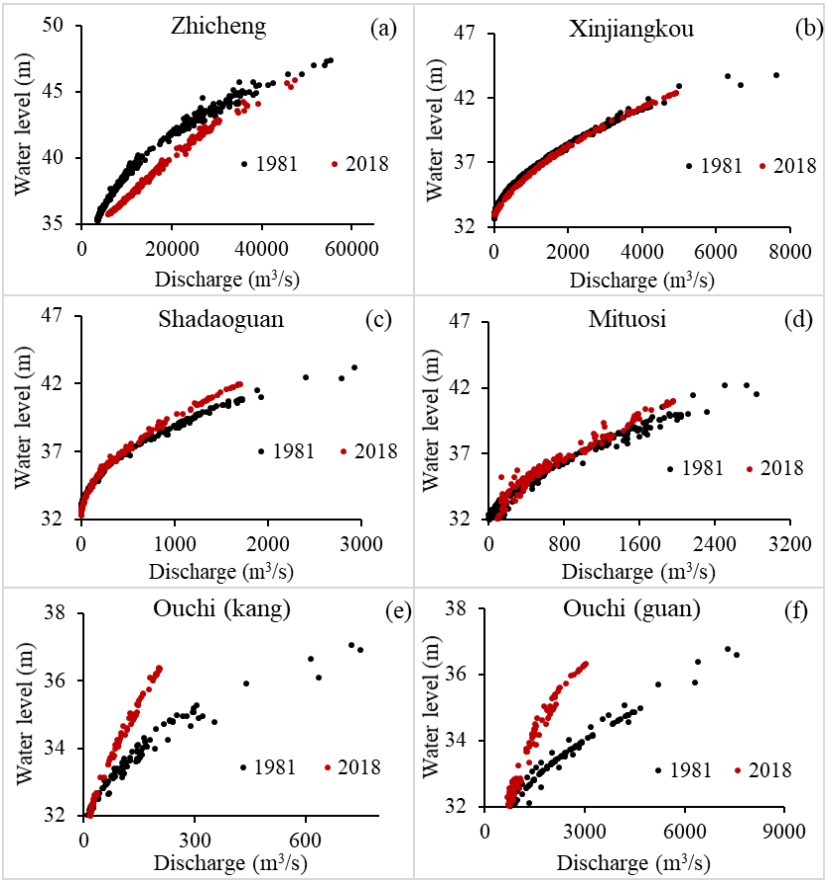

Figure 8. *Rating curves between water level and discharge at Zhicheng and the JTO after the 1981*

Regression analysis for quantifying the influences of precipitation and human activities on the water exchanges at the JTO

Regression analysis was used to quantify the relative contributions of precipitation and human activities to water exchanges at the JTO. The correlation equations are established as shown in *Equations 8–13* based on data observed in the reference period 1960–1966. Their significance levels are as follows:

$$Q_Z = 4.775P + 68.303, \quad R^2 = 0.7837, P = 0.002 \qquad \text{(Eq.8)}$$

$$Q_X = 0.124P - 232.06, \quad R^2 = 0.984, P < 0.001 \qquad \text{(Eq.9)}$$

$$Q_S = 0.0727Q_Z - 171.11, \quad R^2 = 0.964, P < 0.001 \qquad \text{(Eq.10)}$$

http://www.aloki.hu ● ISSN 1589 1623 (Print) ● ISSN 1785 0037 (Online)
DOI: http://dx.doi.org/10.15666/aeer/1802_31773193

$$Q_M = 0.08Q_Z - 146.98, \quad R^2 = 0.919, P < 0.001 \quad \text{(Eq.11)}$$

$$Q_{OK} = 0.0308Q_Z - 96.609, \quad R^2 = 0.763, P = 0.01 \quad \text{(Eq.12)}$$

$$Q_{OG} = 0.2395Q_Z - 507.04, \quad R^2 = 0.886, P = 0.002 \quad \text{(Eq.13)}$$

where Q_Z is the streamflow at Zhicheng; P is the basin-averaged annual precipitation above Zhicheng; and Q_X, Q_S, Q_M, Q_{Ok}, and Q_{OG} are the amounts of water discharge at Xingjiangkou, Shadaoguan, Mituosi, Ouchi (kang), and Ouchi (guan), respectively.

The modeling results are validated by comparing the observed and estimated water discharges in the reference period 1960–1966, as shown in *Table 3*. The calculated water discharges are consistent with the measured values. The comparison between the observed and the estimated is shown in *Figure 9*. The precipitation changes played a main role in the decreasing of streamflow in the the Yangtze River (*Table 4*), an effect that is consistent with previous studies (Chen et al., 2014; Yang et al., 2015; Zhao et al., 2015). However, the impact of human activities was gradually intensified and had a dominant status on the water discharge at the JTO. The impact degrees of human activities on water discharge were different at each outlet (*Fig. 9*). *Table 4* shows the contributions of human activities and climate change to impacts in water discharge from 1967 to 2018. At Xinjiangkou, human activities were responsible for 57.20% of the changes. In the other JTO stations, the impact of human activities on streamflow were 84.01% at Shadaoguan, 83.69% at Mituosi, 84.02% at Ouchi (kang), and 89.21% at Ouchi (guan). These results indicated that human activities played a more important influence than climate change in the decrease of water discharge at the JTO.

Table 3. *Results of regression analysis for the water discharge at the JTO in the reference period 1960–1966*

Station name	Duration	Water discharge (10^8 m^3/yr)		R^2
		Observed	Estimated	
Zhicheng	1960–1966	4,098.371	4,149.261	0.784
Xinjiangkou	1960–1966	342.510	337.368	0.853
Shadaoguan	1960–1966	165.892	163.524	0.778
Mituosi	1960–1966	223.622	220.741	0.912
Ouchi (kang)	1960–1966	46.104	46.022	0.715
Ouchi (guan)	1960–1966	602.649	593.825	0.850

Table 4. *Impact of climate change and human activities on water discharge at the JTO*

Station name	Period	Water discharge (10^8 m^3/yr)			Impact of climate change (%)	Impact of human activities (%)
		Observed	Estimated	Total change		
Zhicheng	1967–2018	4,689.641	4,636.272	390.427	62.63	37.37
Xinjiangkou	1967–2018	287.322	318.890	55.188	42.80	57.20
Shadaoguan	1967–2018	82.630	152.579	83.261	15.99	84.01
Mituosi	1967–2018	132.873	208.820	90.749	16.31	83.69
Ouchi (kang)	1967–2018	10.236	40.374	35.868	15.98	84.02
Ouchi (guan)	1967–2018	190.279	558.136	412.370	10.79	89.21

http://www.aloki.hu ● ISSN 1589 1623 (Print) ● ISSN 1785 0037 (Online)
DOI: http://dx.doi.org/10.15666/aeer/1802_31773193

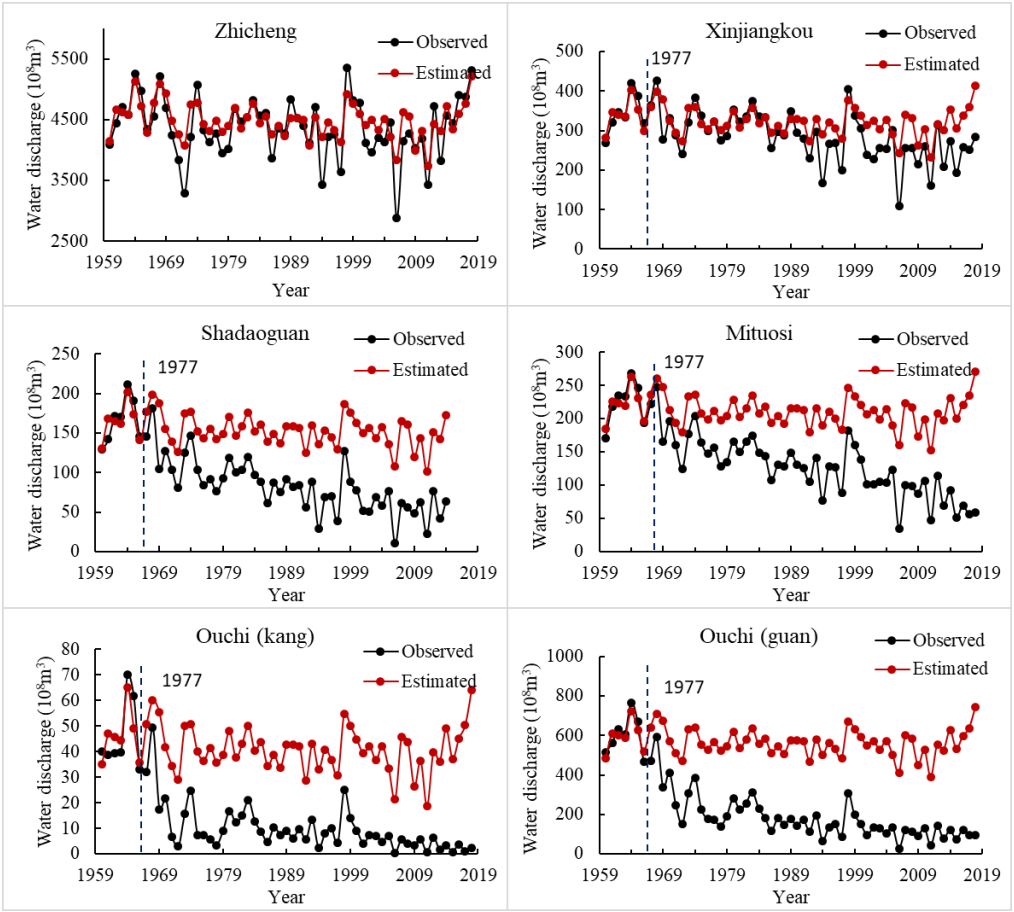

Figure 9. *Comparison between the observed mean annual streamflow and the estimated mean annual streamflow at the JTO with the regression analysis. The period 1960–1966 was the baseline period, and the period 1967–2018 was the prediction period*

Conclusions

This study utilized the MK Pettitt tests to analyze the spatial–temporal variations of precipitation and water discharge at the mainstream and at the JTO from 1960 to 2014. In addition, the impacts which human activities and climate change on water exchange between Yangtze River and Dongting Lake were assessed using the DMC method and regression analysis. Conclusions were summarized as follows:

(1) Precipitation change trends presented no statistical significance, except in autumn with a significant decrease at the 99% confidence level. Water discharge at Zhicheng showed a decreasing trend in autumn and an increasing trend in winter with a 99% confidence level. However, other periods displayed no significant trend changes. Annual and seasonal water discharge at the JTO, except at Xinjiangkou in summer, all exhibited significant downward trends with a 99% confidence level. The lack of consistent trends in the seasonal precipitation and water discharge at Zhicheng and at the JTO indicated that the seasonal relationships between them had been disturbed by human activities.

(2) Abrupt stating years of all the stations at the JTO were mainly around 1980 and 1990, and the Ouchi (kang) and Ouchi (guan) at the Ouchi outlet were earlier than the other stations. Under the same conditions of climate changes and human activities in the

http://www.aloki.hu ● ISSN 1589 1623 (Print) ● ISSN 1785 0037 (Online)
DOI: http://dx.doi.org/10.15666/aeer/1802_31773193

upstream of the Yangtze River, the change heterogeneity and inconsistency of annual and seasonal water discharge at the JTO indicate that local channel cut-off projects affect the amount of water discharge in a complex manner.

(3) Human activities had a dominant effect on the water discharge at the JTO, and the impact degrees of human activities on water discharge were different at each station. During 1967–2018, the impact of human activities on water discharge at Xinjiangkou were 57.20%. The impact of human activities on water discharge were 84.01% at Shadaoguan, 83.69% at Mituosi, 84.02% at Ouchi (kang), and 89.21% at Ouchi (guan).

(4) This research is an important step toward understanding the impact of climate changes and human activities on streamflow reduction at the JTO and provides an important scientific basis for the optimization control of the Yangtze River–Dongting Lake relationship.

Acknowledgements. This work is supported by the National Natural Science Foundation of China (41601041) and the Key Research Program of the Chinese Academy of Sciences (KFZD-SW-318). We thank Dr. Shi Kun for his detailed and helpful comments on the manuscript.

REFERENCES

[1] Acreman, M. C., Riddington, R., Booker, D. J. (2003): Hydrological impacts of floodplain restoration: a case study of the River Cherwell, UK. – Hydrology and Earth System Sciences 7(1): 75-86.

[2] Amoros, C., Bornette., G. (2002): Connectivity and biocomplexity in waterbodies of riverine floodplains. – Freshwater Biology 47(4): 761-776.

[3] Besemer, K., Moeseneder, M. M., Arrieta, J. M., Herndl, G. J., Peduzzi, P. (2005): Complexity of bacterial communities in a river-floodplain system (Danube, Austria). – Applied and Environmental Microbiology 71(2): 609-620.

[4] Bullock, A., Acreman, M. C. (2003): The role of wetlands in the hydrological cycle. – Hydrology and Earth System Sciences 7(3): 75-86.

[5] Chang, J., Li, J. B., Lu, D. Q., Zhu, X., Lu, C. Z., Zhou, Y. Y., Deng, C. X. (2010): The hydrological effect between Jingjiang River and Dongting Lake during the initial period of Three Gorges Project operation. – Journal of Geographical Sciences 20(5): 771-786.

[6] Chen, J., Wu, X. D., Finlayson, B. L., Webber, M., Wei, T. Y., Li, M. T., Chen, Z. Y. (2014): Variability and trend in the hydrology of the Yangtze River, China: annual precipitation and runoff. – Journal of Hydrology 513: 403-412.

[7] Chen, J., Finlayson, B. L., Wei, T. Y., Sun, Q. L., Webber, M., Li, M. T., Chen, Z. (2016): Changes in monthly flows in the Yangtze River, China - with special reference to the Three Gorges Dam. – Journal of Hydrology 536: 293-301.

[8] Clilverd, H. M., Thompson, J. R., Heppell, C. M., Sayer, C. D., Axmacher, J. C. (2013): River-floodplain hydrology of an embanked lowland Chalk river and initial response to embankment removal. – Hydrological Sciences Journal 58(3): 627-650.

[9] Gao, B., Yang, D. W., Zhao, T., Yang, H. B. (2012): Changes in the eco-flow metrics of the Upper Yangtze River from 1961 to 2008. – Journal of Hydrology 448-449: 30-38.

[10] Gao, J. H., Jia, J. J., Kettner, A. J., Xing, F., Wang, Y. P., Li, J., Bai, F. L., Zou, X. Q., Gao, S. (2015a): Reservoir-induced changes to fluvial fluxes and their downstream impacts on sedimentary processes: the Changjiang (Yangtze) River, China. – Quaternary International. DOI: 10.1016/j.quaint.2015.03.015.

[11] Gao, J. H., Jia, J. J., Wang, Y. P., Yang, Y., Li, J., Bai, F., Zou, X., Gao, S. (2015b): Variations in quantity, composition and grain size of Changjiang sediment discharging

http://www.aloki.hu ● ISSN 1589 1623 (Print) ● ISSN 1785 0037 (Online)
DOI: http://dx.doi.org/10.15666/aeer/1802_31773193

into the sea in response to human activities. – Hydrology and Earth System Sciences 19: 645-655.
[12] Heiler, G., Hein, T., Schiemer, F., Bornette, G. (1995): Hydrological connectivity and flood pulses as the central aspects for the integrity of a river–floodplain system. – Regulated Rivers: Research & Management 11(3-4): 351-361.
[13] Hu, Y. X., Huang, J. L., Du, Y., Han, P. P., Wang, J. L., Huang, W. (2015): Monitoring wetland vegetation pattern response to water–level change resulting from the Three Gorges Project in the two largest freshwater lakes of China. – Ecological Engineering 74: 274-285.
[14] Hung, N. N., Delgado, J. M., Tri, V. K., Hung, L. M., Merz, B., Bardossy, A., Apel, H. (2012): Floodplain hydrology of the Mekong Delta, Vietnam. – Hydrological Processes 26: 674-686.
[15] Kendall, M. G. (1975): Rank Correlation Methods. – Griffin, London.
[16] Knowlton, M. F., Jones, J. R. (1997): Trophic status of Missouri River floodplain lakes in relation to basin type and connectivity. – Wetlands 17(4): 468-475.
[17] Kummu, M., Tes, S., Yin, S., Adamson, P., Józsa, J., Koponen, J., Richey, J., Sarkkula, J. (2014): Water balance analysis for the Tonle Sap Lake–floodplain system. – Hydrological Processes 28: 1722-1733.
[18] Lai, X. J., Liang, Q. H., Jiang, J. H., Huang, J. (2014a): Impoundment effects of the Three-Gorges-Dam on flow regimes in two China's largest freshwater lakes. – Water resources management 28(14): 5111-5124.
[19] Lai, X. J., Jiang, J. H., Yang, G. S., Lu, X. X. (2014b): Should the Three Gorges Dam be blamed for the extremely low water levels in the middle–lower Yangtze River? – Hydrological Processes 28: 150-160.
[20] Lesack, L. F. W., Marsh, P. (2010): River–to–lake connectivities, water renewal, and aquatic habitat diversity in the Mackenzie River Delta. – Water Resources Research 46(12): 1-12.
[21] Li, Y. Y., Yang, G. S., Li, B., Wan, R. R., Duan, W. L., He, Z. (2016): Quantifying the effects of channel change on the discharge diversion of Jingjiang Three Outlets after the operation of the Three Gorges Dam. – Hydrology Research. DOI: 10.2166/nh.2016.016.
[22] Liu, X., Wang, H. (2010): Estimation of minimum area requirement of river-connected lakes for fish diversity conservation in the Yangtze River floodplain. – Diversity and Distributions 16(6): 932-940.
[23] Lu, J. Y., Yao, S. M., Shao, X. J., Zhang, X. B. (2012): Response Process of Downstream River–Lake Relation after the Early Operation of the Three Gorges Project. – Science Press, Shanghai (in Chinese).
[24] Mann, H. B. (1945): Nonparametric tests against trend. – Econometrica 13: 245-259.
[25] Nakayama, T., Shankman, D. (2013): Impact of the Three-Gorges Dam and water transfer project on Changjiang floods. – Global and Planetary Change 100: 38-50.
[26] Nie, P., Yao, W. J., Gao, Q., Wang, G. T., Zhang, Y. A. (1999): Diversity of intestinal helminth communities of carp from six lakes in the flood plain of the Yangtze River, China. – Journal of Fish Biology 54(1): 171-180.
[27] Ou, C. M., Li, J. B., Zhou, Y. Q., Chang, W. Y., Yang, Y. (2014): Evolution characters of water exchange abilities between Dongting Lake and Yangtze River. – Journal of Geographical Sciences 24(4): 731-745.
[28] Palmer, M. A., Reidy Liermann, C. A., Nilsson, C., Flörke, M., Alcamo, J., Lake, P. S., Bond, N. (2008): Climate change and the world's river basins: anticipating management options. – Frontiers in Ecology and the Environment 6(2): 81-89.
[29] Pan, B. Z., Wang, H. J., Liang, X. M., Wang, H. Z. (2011): Macrozoobenthos in Yangtze floodplain lakes: patterns of density, biomass, and production in relation to river connectivity. – Journal of the North American Benthological Society 30(2): 589-602.
[30] Pettitt, A. (1979): A non-parametric approach to the change-point problem. – Applied Statistics 28(2): 126-135.

http://www.aloki.hu ● ISSN 1589 1623 (Print) ● ISSN 1785 0037 (Online)
DOI: http://dx.doi.org/10.15666/aeer/1802_31773193

[31] Qin, H., Xie, Y., Zou, D. (2012): Changes of runoff and sediment discharge into Dongting Lake from the four rivers in Hunan Province. – Scientia Geographica Sinica 32(5): 609-615 (in Chinese).
[32] Ru, H. J., Liu, X. Q. (2013): River-lake migration of fishes in the Dongting Lake area of the Yangtze floodplain. – Journal of Applied Ichthyology 29(3): 594-601.
[33] Thomaz, S. M., Bini, L. M., Bozelli, R. L. (2007): Floods increase similarity among aquatic habitats in river-floodplain systems. – Hydrobiologia 579(1): 1-13.
[34] Tockner, K., Stanford, J. A. (2002): Riverine flood plains: present state and future trends. – Environmental Conservation 29: 308-330.
[35] Tockner, K., Pusch, M., Borchardt, D., Lorang, M. S. (2010): Multiple stressors in coupled river–floodplain ecosystems. – Freshwater Biology 55(s1): 135-151.
[36] Wang, H. J., Saito, Y., Zhang, Y., Bi, N. H., Sun, X. X., Yang, Z. S. (2011): Recent changes of sediment flux to the western Pacific Ocean from major rivers in East and Southeast Asia. – Earth Science Reviews 108(1-2): 80-100.
[37] Whited, D. C., Lorang, M. S., Harner, M. J., Hauer, F. R., Kimball, J. S., Stanford, J. A. (2007): Climate, hydrologic disturbance, and succession: drivers of floodplain pattern. – Ecology 88(4): 940-953.
[38] Xie, P. (2003): Three-Gorges Dam: risk to ancient fish. – Science 302(5648): 1149-1151.
[39] Yang, S. L., Milliman, J. D., Xu, K. H., Deng, B., Zhang, X. Y., Luo, X. X. (2014): Downstream sedimentary and geomorphic impacts of the Three Gorges Dam on the Yangtze River. – Earth Science Reviews 138: 469-486.
[40] Yang, S. L., Xu, K. H., Milliman, J. D., Yang, H. F., Wu, C. S. (2015): Decline of Yangtze River water and sediment discharge: impact from natural and anthropogenic changes. – Scientific Reports 5: 12581. DOI: 10.1038/srep12581.
[41] Yang, X., Anderson, N., Dong, X., Shen, J. (2008): Surface sediment diatom assemblages and epilimnetic total phosphorus in large, shallow lakes of the Yangtze floodplain: their relationships and implications for assessing long-term eutrophication. – Freshwater Biology 53(7): 1273-1290.
[42] Yua, Y., Meia, X., Daia, Z., Gaoa, J., Lic, J. (2018): Hydromorphological processes of Dongting lake in China between 1951 and 2014. – Journal of Hydrology 562: 254-266.
[43] Zhang, Q., Xu, C., Becker, S., Jiang, T. (2006): Sediment and runoff changes in the Yangtze River basin during past 50 years. – Journal of Hydrology 331(3): 511-523.
[44] Zhang, R., Zhang, S. H., Xu, W., Wang, B. B., Wang, H. (2015a): Flow regime of the three outlets on the south bank of Jingjiang River, China: an impact assessment of the Three Gorges Reservoir for 2003–2010. – Stochastic Environmental Research and Risk Assessment 29(8): 2047-2060.
[45] Zhang, W., Wang, W. G., Zheng, J. H., Wang, H. G., Wang, G., Zhang, J. S. (2015b): Reconstruction of stage–discharge relationships and analysis of hydraulic geometry variations: the case study of the Pearl River Delta, China. – Global and Planetary Change 125: 60-70.
[46] Zhao, G. J., Tian, P., Mu, X. M., Jiao, J. Y., Wang, F., Gao, P. (2014): Quantifying the impact of climate variability and human activities on streamflow in the middle reaches of the Yellow River basin, China. – Journal of Hydrology 519: 387-398.
[47] Zhao, Y., Zou, X., Liu, L., Yao, Y., Li, Y., Wu, X., Wang, C., Yu, W., Wang, T. (2017): Assessing natural and anthropogenic influences on water discharge and sediment load in the Yangtze River, China. – Science of The Total Environment 607-608: 920-932.
[48] Zhu, L. L., Chen, J. C., Yuan, J., Dong, B. J. (2015): Study on variation trends of flow diversion from Jingjiang River to Dongting Lake. – Journal of Hydroelectric Engineering 34(2): 103-111 (in Chinese).
[49] Zurbrügg, R., Wamulume, J., Kamanga, R., Wehrli, B., Senn, D. B. (2012): River-floodplain exchange and its effects on the fluvial oxygen regime in a large tropical river system (Kafue Flats, Zambia). – Journal of Geophysical Research 117(G3): 1-12.

http://www.aloki.hu ● ISSN 1589 1623 (Print) ● ISSN 1785 0037 (Online)
DOI: http://dx.doi.org/10.15666/aeer/1802_31773193

TEMPORAL AND SPATIAL CHANGES OF ≥ 10 °C ACCUMULATED TEMPERATURE IN HUANG-HUAI-HAI RIVER BASIN, CHINA

YIN, J.[1] – YUAN, Z.[2*] – YAN, D. H.[3*] – YANG, Z. Y. [3] – WANG, Y. Q.[2]

[1]*Faculty of Resources and Environmental Science, Hubei University, Wuhan 430062, China (phone: +86-159-2642-1064)*

[2]*Changjiang River Scientific Research Institute, Changjiang Water Resources Commission of the Ministry of Water Resources of China, Wuhan 430010, China (phone: +86-137-1656-5927)*

[3]*State Key Laboratory of Simulation and Regulation of Water Cycle in River Basin, China Institute of Water Resources and Hydropower Research, Beijing 100038, China (phone: +86-135-0103-8825)*

**Corresponding author*
e-mail: yuanzhe_0116@126.com; phone: +86-137-1656-5927

(Received 27th Sep 2019; accepted 4th Feb 2020)

Abstract. Huang-huai-hai River basin is an important grain production area and economic zone of China. Under the impact of global warming, energy resources are changing all around the world. Studying the ≥ 10 °C accumulated temperature (*AT*10) is of great importance for the food security and economy of Huang-huai-hai River basin. The slope of *AT*10 and Mann-Kendall statistical test were applied to quantify the trend magnitude and detect the significant trend respectively. And the distribution pattern and movement characteristics had been analysed with GIS technology. The results shown that *AT* 10 of Huang-huai-hai River basin has an increasing trend during since 1960s; *AT* 10 has a moving tendency towards the northwest and decreased from the southeast region towards the northwest region. The ratio between active area and stable area in different classes has fluctuated during the study period.
Keywords: *Huang-huai-hai River basin, accumulated temperature, spatiotemporal characteristic analysis, global warming*

Introduction

In the long-term interaction process between the climate system and land surface, climatic regionalization and agricultural distribution came into being, which are relatively stable. It has been proven that global mean surface temperature has increased by 0.85 °C during 1880-2012. Mean temperature of 2003-2012 has increased by 0.78 °C compared to that of 1850-1900 (IPCC, 2013) and the temperature in China also has shown a similar increasing trend (Wang et al., 2013). As a result, climatic zones and plant phenology have responded to these changes. Temperature determines crops' emergence, flowering and maturity dates (Skaugen and Tveito, 2004; Iannucci et al., 2008; Hou et al., 2014), while each plant species has a base temperature above which biological processes are able to function (Major et al., 1983; Stevens et al., 1986; McMaster and Smika, 1988; Hodges et al., 1994; Bonhomme et al., 1994; Olivier and Annandale, 1998; Kadioglu and Saylan, 2001; Berti and Johnson, 2008; Sacks and Kucharik, 2011). Most crops have a base temperature of 10 °C known as the active temperature. Previous researches have proven that the change of activity accumulated temperature will affect the growth rate of winter wheat and soybean (Li et al., 2015;

http://www.aloki.hu ● ISSN 1589 1623 (Print) ● ISSN 1785 0037 (Online)
DOI: http://dx.doi.org/10.15666/aeer/1802_31953209

Liang et al., 2015). Lv et al. (2019) has found that when the cumulative temperature was below 3300 °C·d, the maize yield increased with the cumulative temperature, while when the cumulative temperature was below 3800 °C·d, the soybean and rice yields increased with the cumulative temperature ≥ 10 °C accumulated temperature (hereinafter referred to as AT10) is the sum of mean daily temperature during the period in which mean daily temperature is above 10 °C for every day (Yan et al., 2011). Accumulated temperature plays a fundamental role in a plant's growth and spatial distribution (Xu et al., 2009). International research on AT10 is limited. Concerning researches on this subject has mainly been focused on the northeast of the China, while very little research has been carried out for Huang-huai-hai river basin (hereinafter referred to as HHHRB).

Using the meteorological data from Mikhelson station, Chirkov and Kononova (1984) analysed the spatial and temporal changes of ≥ 10 °C AAT in Moscow from 1890 to 1981. Dong et al. (2009) studied the spatiotemporal changes of accumulated temperatures ≥ 10 °C of China from the late 1980s to 2000 and found out that since the late 1980s it has increased on a national scale. Yan et al. (2011) studied the spatial-temporal changes of various decadal AT10 and the climatic means of ≥ 10 °C accumulated temperature in the north-eastern China. Significant increase of decadal AT10 since the 1980s was discovered and the change became larger and more obvious in the 1990s and 2000s. Wang et al. (2011) explored the tempo-spatial characteristics of AT10 and the results showed that the AT10 had a decreasing trend from southwest to northeast and also had 2.5-4a oscillations in Northeast China. Wu (2011) studied the changing trend of ≥ 10 °C accumulated temperature in Shenyang, Liaoning Province of China and found a significant increasing trend. Song et al. (2011) found a significant increase of accumulated temperature and length of growing season of North China Plain from 1961 to 2009. The start of growing season moved up and the end of growing season was delayed.

This paper analysed the spatial and temporal changes of *AT*10 in HHHRB, China. The tendency, distribution pattern and movement characteristics had been selected for the analysis, which can provide data for the basis of decision making for food security in HHHRB as well as give agriculture production technological support to respond to global warming.

Materials and methods

Study area

Huang-huai-hai River basin (HHHRB) encompasses the Yellow River basin, Huaihe River basin and Haihe River basin. HHHRB is located in the east of China and lies between 32°-42°N, 110°-120°E. The entire or partial part of the following provinces form HHHRB: Qinghai Province, Sichuan Province, Gansu Province, Ningxia Hui Autonomous Region, Inner Mongolia Autonomous Region, Shaanxi Province, Shanxi Province, Henan Province, Hebei Province, Shandong Province, Anhui Province, Jiangsu Province, Beijing and Tianjin (*Fig. 1*). The Yellow River basin has an area of 75.2×10^4 km^2. Temperature difference is large and stark regional differences can be seen. The catchment area of Huaihe River basin is 27.5×10^4 km^2 and its temperature increases from the north to the south with the temperature span from 11 to 16 °C. For Haihe River basin, it has an area of 31.8×10^4 km^2 and its mean annual temperature ranges from 1.5 to 14 °C.

http://www.aloki.hu ● ISSN 1589 1623 (Print) ● ISSN 1785 0037 (Online)
DOI: http://dx.doi.org/10.15666/aeer/1802_31953209

One third of China's population, grain yield and gross domestic product comes from HHHRB (Shen et al., 2002; Liu et al., 2010; Yu et al., 2012). As an important grain producing area and economic zone, HHHRB plays a fundamental role in guaranteeing China's economic and social development. Thus, studying AT10 in HHHRB is of great importance for safeguarding China's food security. In the meantime, data base will be provided for agriculture to response to global warming in the context of climate change.

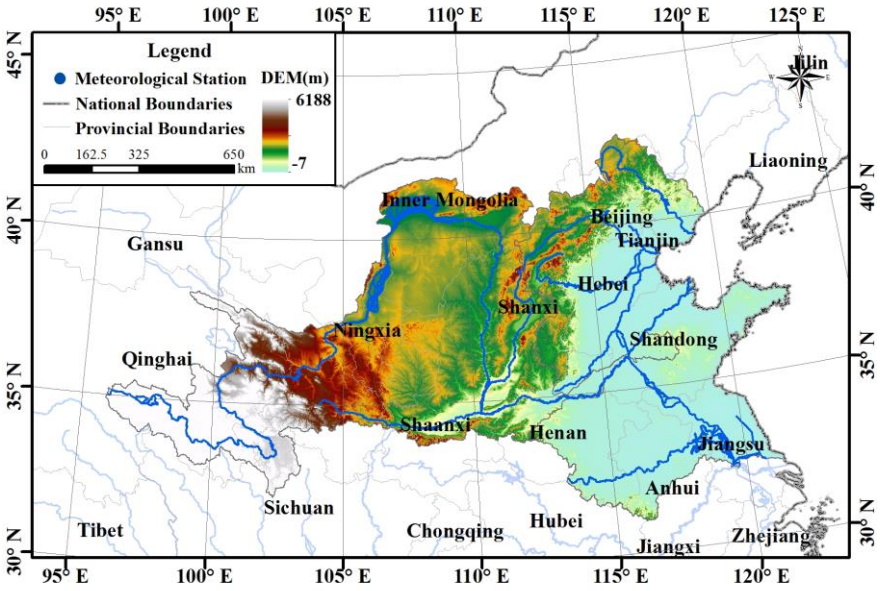

Figure 1. *The location of Huang-Huai-Hai River basin*

Dataset

The basic data for this study was the time series of daily air temperature, which were obtain from 982 meteorological stations within and surrounding HHHRB (*Fig. 2*). The daily air temperature was download from National Meteorological Information Centre (http://data.cma.cn/). Inverse Distance Weighted (IDW) spatial interpolation was used to create daily grid data (5 km × 5 km) of temperature. Data processing process was based on ArcInfo Workstation 10.0 platform using the ARC Macro Language (AML) to conduct the relevant calculations.

Methodology

Calculation of ≥ 10 °C accumulated temperature

The *AT*10 in each grid were calculated with 5-day simple moving average temperature in this study, which is defined as *Equation 1.*

$$AT10_n = \sum_{i=1}^{D} T_i \qquad \text{(Eq.1)}$$

$$T_i = \begin{cases} Ta_i & Ta_i \geq 10 \\ 0 & Ta_i < 0 \end{cases} \qquad \text{(Eq.2)}$$

http://www.aloki.hu ● ISSN 1589 1623 (Print) ● ISSN 1785 0037 (Online)
DOI: http://dx.doi.org/10.15666/aeer/1802_31953209

where $AT10_n$ is ≥ 10 °C accumulated temperature for the nth year. Ta_i is the 5-day simple moving average air temperature for ith day. D is days for the nth year.

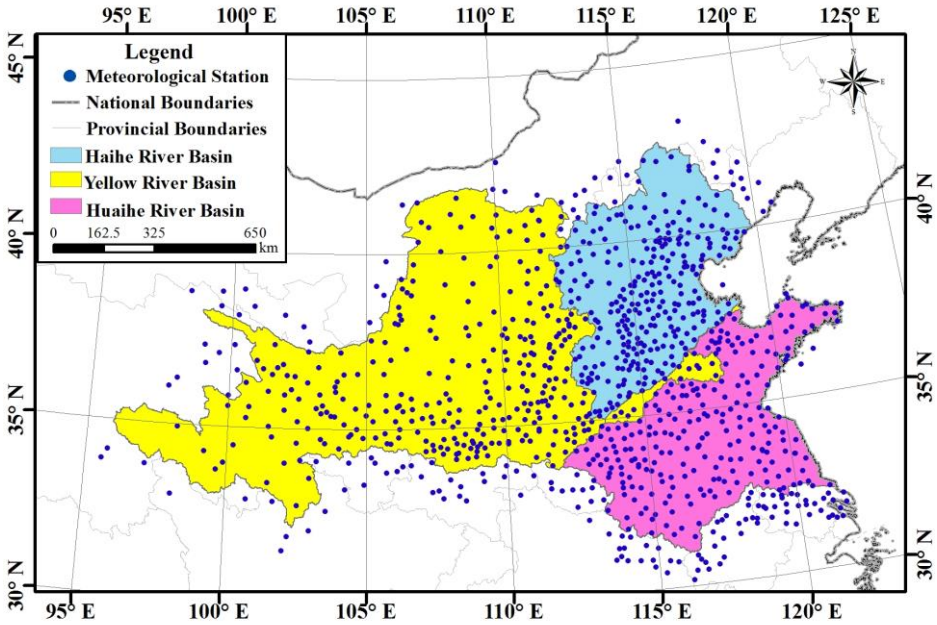

Figure 2. *The location of meteorological stations within and surrounding Huang-Huai-Hai River basin*

Mann-Kendall trend test

A non-parametric approach, Mann-Kendall statistical test (M-K) (Mann, 1945), is widely used in hydrology and climatology analysis because of less sensitive to outliers than parametric approaches (Hamed, 2009; Tian et al., 2012; Wang et al., 2008). In this study, the M-K method was used to was utilized to test the tendency of $AT10$ in the HHHRB. The test statistic U was established as *Equations 3–5*.

$$U = \frac{\tau}{\sqrt{V_{ar}(\tau)}} \quad \text{(Eq.3)}$$

$$\tau = \frac{4p}{n(n-1)} - 1 \quad \text{(Eq.4)}$$

$$V_{ar(\tau)} = \frac{2(2n+5)}{9n(n-1)} \quad \text{(Eq.5)}$$

where n is the length of the data sequence and p is the allelomorph of the random sequence. If U is positive the sequence has an increasing trend, if U is negative the sequence has a decreasing trend, and if $|U| > U\alpha = 1.96$ while the significance level is $\alpha = 0.05$, then the sequence has passed the significance test with a significant changing trend.

http://www.aloki.hu ● ISSN 1589 1623 (Print) ● ISSN 1785 0037 (Online)
DOI: http://dx.doi.org/10.15666/aeer/1802_31953209

Linear regression analysis and the slope

Linear regression method was utilized to calculate the slope of annual mean AT10 of HHHRB. Its tendency was analyzed and a test for significance was done (Zhang et al., 2011).

$$Slope = \frac{n \times \sum_{i=1}^{n}(i \times K_i) - \sum_{i=1}^{n} i \sum_{i=1}^{n} K_i}{n \times \sum_{i=1}^{n} i^2 - (\sum_{i=1}^{n} i)^2} \quad \text{(Eq.6)}$$

where slope is the tendency rate, n is the number of whole study years, and Ki is the AT10 in the ith year. If slope＞0 in a certain area, it means that the AT10 in this area has an increasing trend from 1956-2011.

Geographic center for ≥ 10 °C accumulated temperature

On the platform of ARCGIS10.0, the ARC Macro Language (AML) was used to conduct the analysis. For each different class of AT10 of HHHRB, CENTROIDLABLES was utilized to calculate the longitude and latitude of each continuous partition's centroid (*xi*,*yi*). After that, area was used as the weight to compute the centroid of each class of AT10 of HHHRB:

$$X_a = \frac{\sum_{i=1}^{n} x_i s_i}{\sum_{i=1}^{n} s_i} \quad \text{(Eq.6)}$$

$$Y_a = \frac{\sum_{i=1}^{n} y_i s_i}{\sum_{i=1}^{n} s_i} \quad \text{(Eq.7)}$$

where, x_a is the longitude of the centroid for a certain class of AT10 of HHHRB, x is the longitude of the centroid of each partition, s is the area of each partition, and n is the number of partitions in a certain class of AT10 of HHHRB. The calculation method for latitude is the same as that for longitude.

Results and analyses

Temporal changes of ≥ 10 °C accumulated temperature in HHHRB

The maximum value, minimum value, range (difference between maximum value and minimum value) and standard deviation of *AT*10 temperature of HHHRB were calculated (*Fig. 3*). The test statistic values for maximum value, minimum value, range and standard deviation of *AT*10 were 5.203, 3.223, 4.976 and 4.947, respectively. It could be concluded that all the characteristic values had a significant increasing trend at the 95% confidence level.

Annual accumulated temperature is an important factor which will affect the crop yield. The grain yield per hectare has a positive correlation with accumulated

http://www.aloki.hu ● ISSN 1589 1623 (Print) ● ISSN 1785 0037 (Online)
DOI: http://dx.doi.org/10.15666/aeer/1802_31953209

temperature (Wang et al., 2011). The range of AT10 of HHHRB increased while the maximum value and minimum value both increased as well which is consistent with the trend of global warming. What was also revealed was that since 1956, energy resources in the study area has increased, which will help to produce more food（Anwar et al., 2013). However, the risk of drought will be increased at the same time.

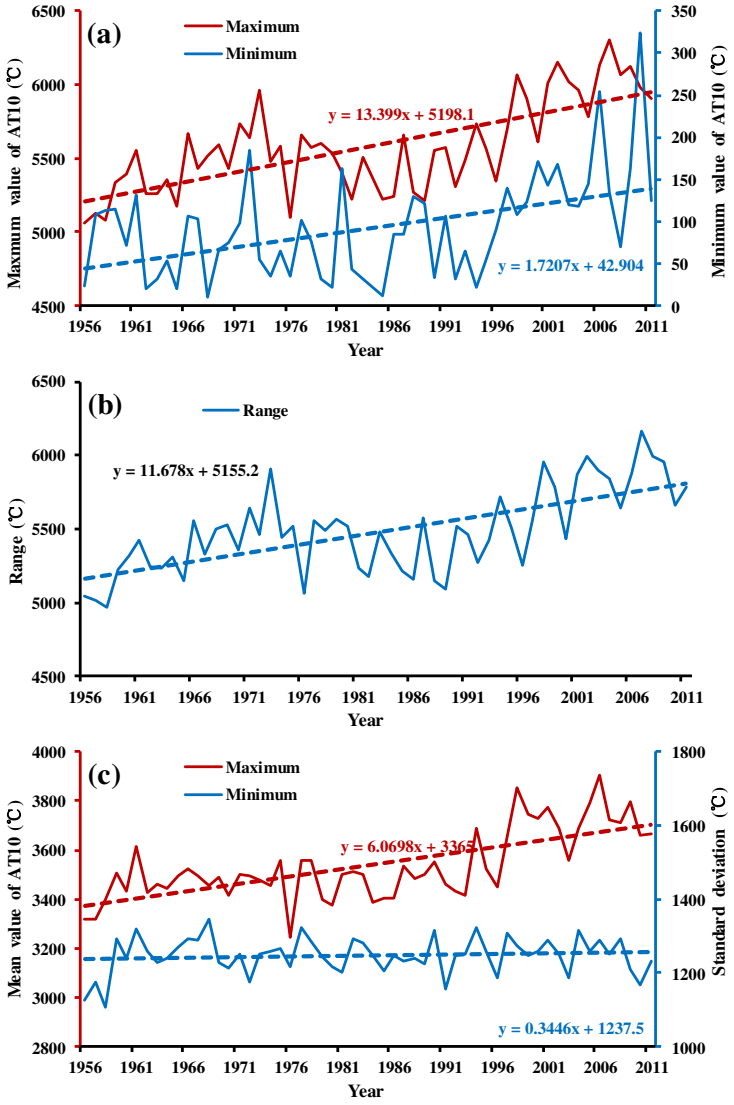

Figure 3. *Maximum/minimum value (a), range (b) and standard deviation (c) of AT10 of HHHRB*

Another factor which has great impact on crop growth is the length of thermal growing season. In this study the duration of development period, time started and ending time of *AT*10 were calculated for the HHHRB (*Fig. 4*). Since 1956, duration of thermal growing season of *AT*10 of HHHRB has an increasing trend. $U_{\text{duration}} = 4.142$ which has passed the significance test at the 95% level. The starting time of thermal growing season has moved forward with $U_{\text{time started-min}} = -1.145$, but it has not passed the significance test at the 95% level. The ending time has been postponed with $U_{\text{ended time-max}} = 0.297$, but it still has not passed the significance test at the 95% level.

http://www.aloki.hu ● ISSN 1589 1623 (Print) ● ISSN 1785 0037 (Online)
DOI: http://dx.doi.org/10.15666/aeer/1802_31953209

This result shows that the length of the thermal growing season of HHHRB from 1956-2011 has extended and may be a potential outcome of global warming in the river basin. The start of the growing season has moved forward while the end of growing season has lagged. To examine the effect of temporal changes in *AT*10 the whole study period (1956-2011) is be divided into 7 phases for each decade: A for 1956-1959, B for 1960-1969, C for 1970-1979, D for 1980-1989, E for 1990-1999, F for 2000-2009 and G for 2010-2011. Duration of thermal growing season of ≥ 10 °C accumulated temperature of HHHRB in each phase was calculated, which are 209.5 days, 214.3 days, 210.4 days, 212.0 days 218.1 days, 222.6 days and 225.2 days. Compared with that of phase A, the duration of F and G have increased significantly by 13.1 days and 15.7 days, respectively. The thermal conditions of HHHRB have improved for crop growth during 1956-2011, thus crop production may benefit from this increasing trend.

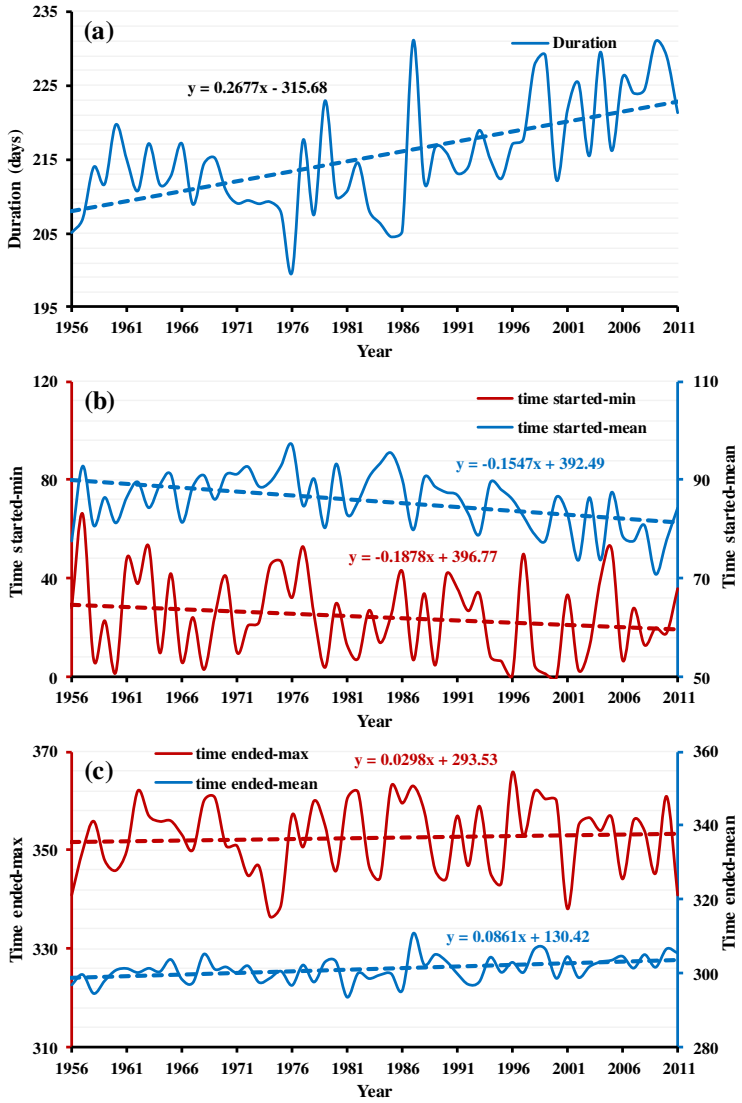

Figure 4. *Duration (a), time started (b) and ended time (c) of thermal growing season of AT10 of HHHRB. (Time started-min is the minimum value of the start time of all the grids in the study area, time started-mean is the mean value of the start time of all the grids in the study area, ending time-max is the maximum value of the ending time of all the grids in the study area, and ending time-mean is the mean value of the ending time of all the grids in the study area)*

http://www.aloki.hu ● ISSN 1589 1623 (Print) ● ISSN 1785 0037 (Online)
DOI: http://dx.doi.org/10.15666/aeer/1802_31953209

Spatial changes of ≥ 10 °C accumulated temperature of HHHRB

Distribution pattern of ≥ 10 °C accumulated temperature of HHHRB

Temperature belts are defined into 5 classes for *AT*10 to study its spatial distribution as follows: (1) Cold temperature zone where the *AT*10 is less than 1600 °C. The planting system is one crop a year and its main crops are early-matured spring wheat, barley, potato, etc. (2) Mid temperate zone where the *AT*10 is less than 3400 °C while more than 1600 °C. The planting system is one crop a year and its main crops are spring wheat, soybean, maize, millet, sorghum, etc. (3) Warm temperate zone where the *AT*10 is less than 4500 °C while more than 3400 °C. The planting system is three crops every two years or two crops a year consisting mainly of multiple cropping buckwheat after winter wheat or multiple cropping maize, millet and sweet potato after winter wheat, etc. (4) Subtropical zone where the *AT*10 is less than 8000 °C while more than 4500 °C. The planting system is two or three crops a year. The rotation system is wheat-rice rotation or double-rice rotation, etc. (5) Where the *AT*10 is more than 8000 °C, the planting system is three crops a year and its main crops are rice, sugarcane, etc.

According to the classification standard mentioned above, decadal spatial distribution patterns of *AT*10 of HHHRB from 1956-2011 were analysed. Since the AT10 of the whole study area is less than 8000 °C, only (1), (2), (3) and (4) were analysed. Generally speaking, AT10 of HHHRB decreased from southeast to northwest (*Fig. 5*). Distribution area of AT10 of different classes were calculated as well as the tendency of the distribution area: $U_{(1)} = -5.527$, $U_{(2)} = -4.919$, $U_{(3)} = 2.375$, $U_{(4)} = 4.227$. Distribution area of class (1) and (2) have a downward trend while that of class (3) and (4) have an upward trend. All of them have passed the significance test at 95% level (*Fig. 6*).

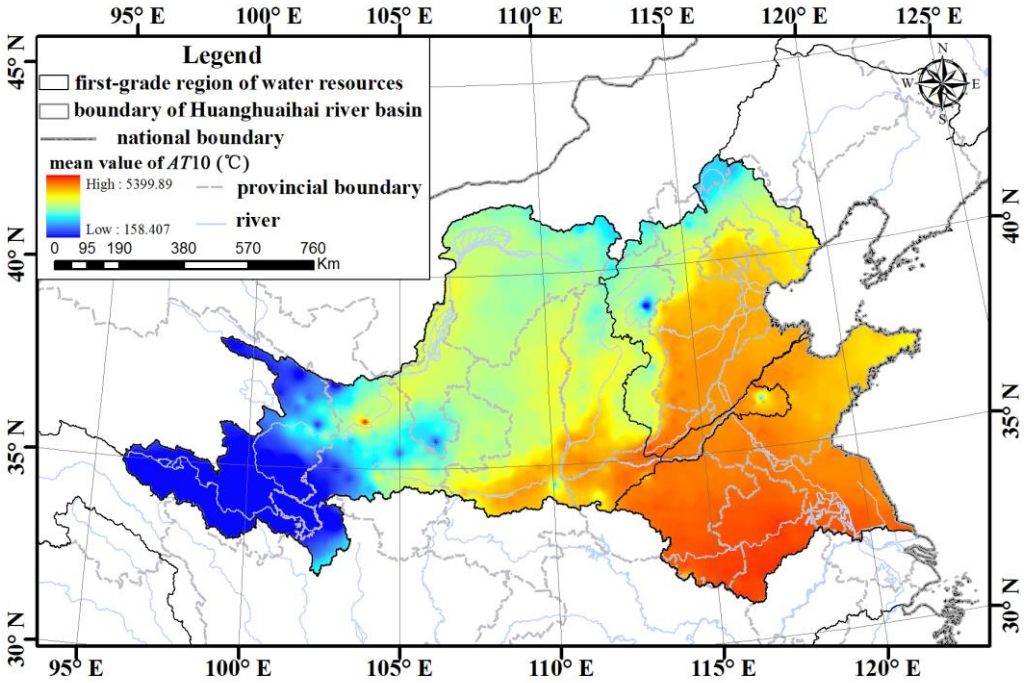

Figure 5. *Spatial distribution of AT10 of HHHRB*

http://www.aloki.hu ● ISSN 1589 1623 (Print) ● ISSN 1785 0037 (Online)
DOI: http://dx.doi.org/10.15666/aeer/1802_31953209

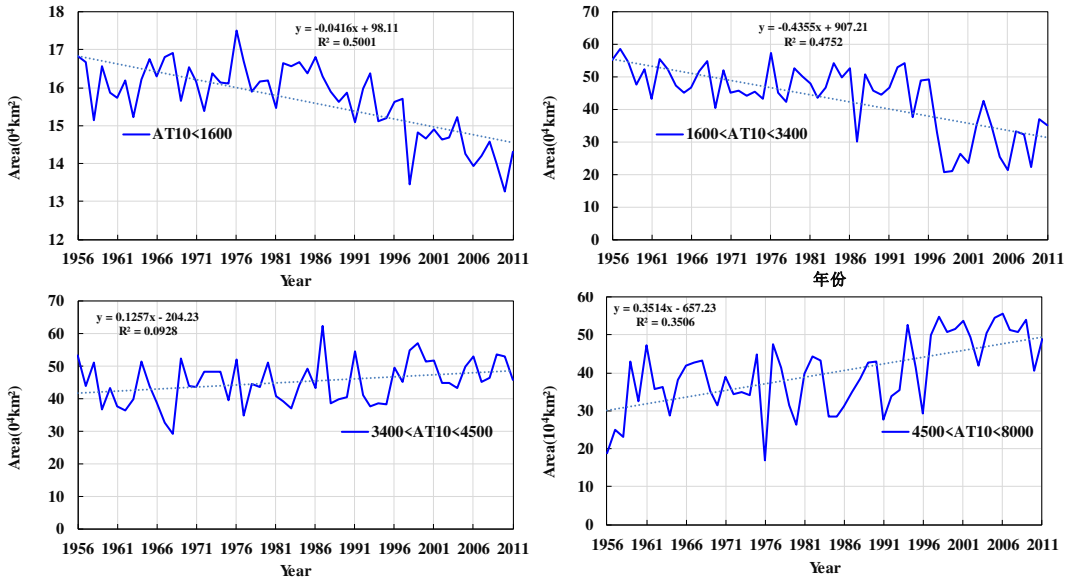

Figure 6. *Area of different classes of AT10 of HHHRB*

For each grid of a certain class of *AT*10 of HHHRB, the accumulated temperature either fits in the class or does not. By dividing the number of years when the accumulated temperature fits in a given class by the total number of years of the study period, the frequency of the occurrence of *AT*10 in a certain class in each grid can be obtained. The spatial distribution of the frequency of AT10 in HHHRB for each class are displayed in (*Fig. 7*).

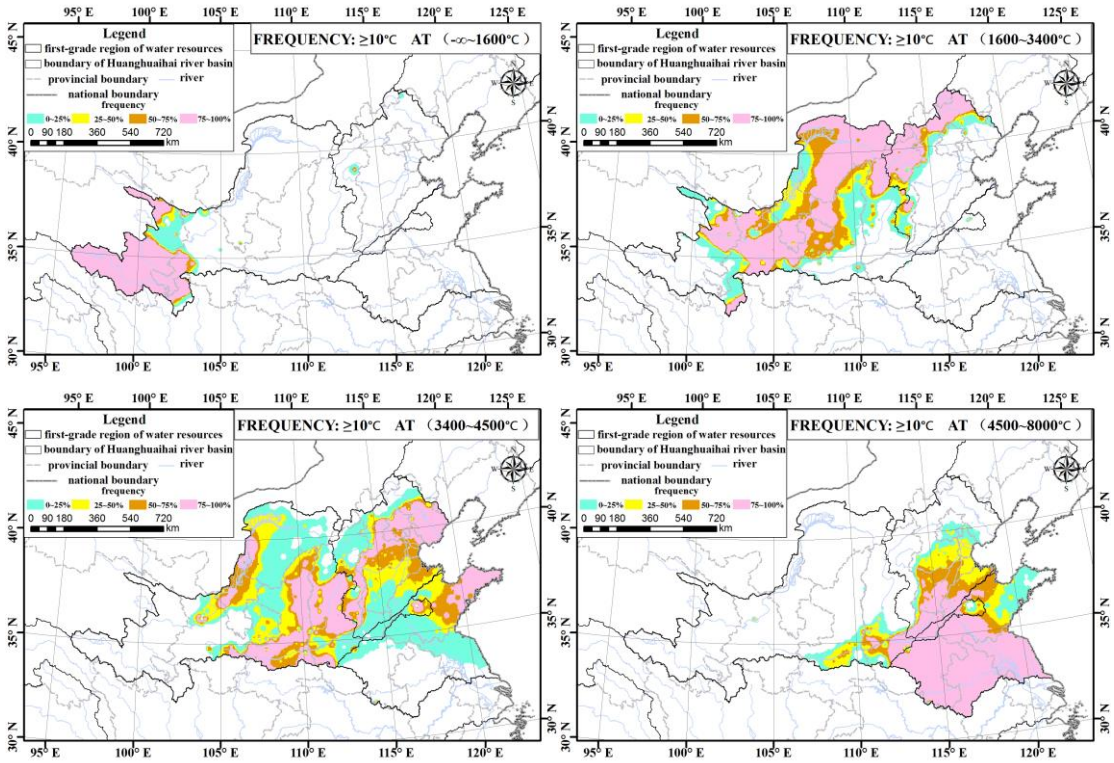

Figure 7. *Spatial distribution of the frequency of AT10 of HHHRB in different classes*

http://www.aloki.hu ● ISSN 1589 1623 (Print) ● ISSN 1785 0037 (Online)
DOI: http://dx.doi.org/10.15666/aeer/1802_31953209

Most of the regions in class (1) consist of high frequencies except in the northeast region. For class (2), the region of highest frequency lies mainly in the central region, while the periphery is the low frequency region. In addition, the area of high frequency region is significantly larger than the area of low frequency region. For class (3), the high frequency region lies in the middle and the low frequency region lies on its two sides. The area of high and low frequency regions is approximately the same. For class (4), most of its area is high frequency region, while the northwest rim is in the low frequency region.

From *Figures 8* and *9* we could see that except the most westerly part and some scattered areas, AT10 of HHHRB has an increasing trend. Additionally, the trend in most areas has passed the significance test at the level of 95%.

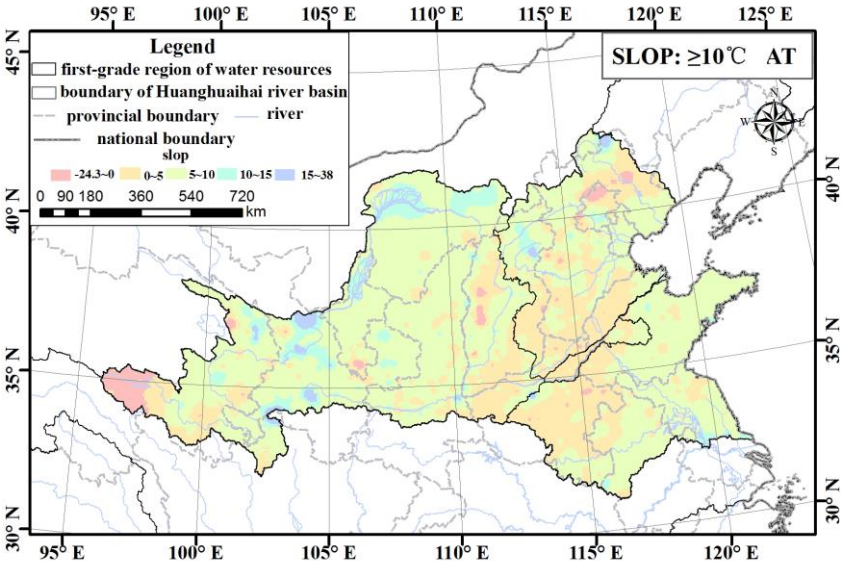

Figure 8. *Slope of AT10 of HHHRB*

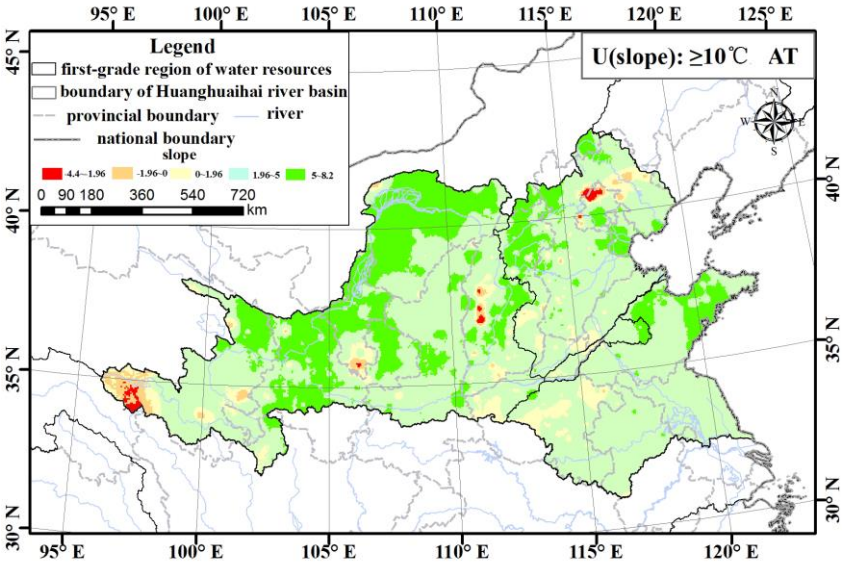

Figure 9. *U value of the slope of AT10 of HHHRB*

http://www.aloki.hu ● ISSN 1589 1623 (Print) ● ISSN 1785 0037 (Online)
DOI: http://dx.doi.org/10.15666/aeer/1802_31953209

Movement characteristics of ≥ 10 °C accumulated temperature of HHHRB

From *Figure 10* we can see that class (1) of AT10 of HHHRB has a moving tendency towards southwest. $U_{(1)\text{longitude}}$ = -5.710 and $U_{(1)\text{latitude}}$ = -6.742. They both have passed the significance test at 95% level. For class (2), $U_{(2)\text{longitude}}$ = -2.572 so the westward trend of class (2) is significant. $U_{(2)\text{latitude}}$ = -1.697, therefore class (2) has a southward trend but is not significant. For class (3), $U_{(3)\text{longitude}}$ = -5.612 and $U_{(3)\text{latitude}}$ = 3.703, thus class (3) has a significant trend moving towards northwest. For class (4), $U_{(4)\text{longitude}}$ = -1.682 and $U_{(4)\text{latitude}}$ = 4.311. So the northward trend is significant while the westward trend is not significant.

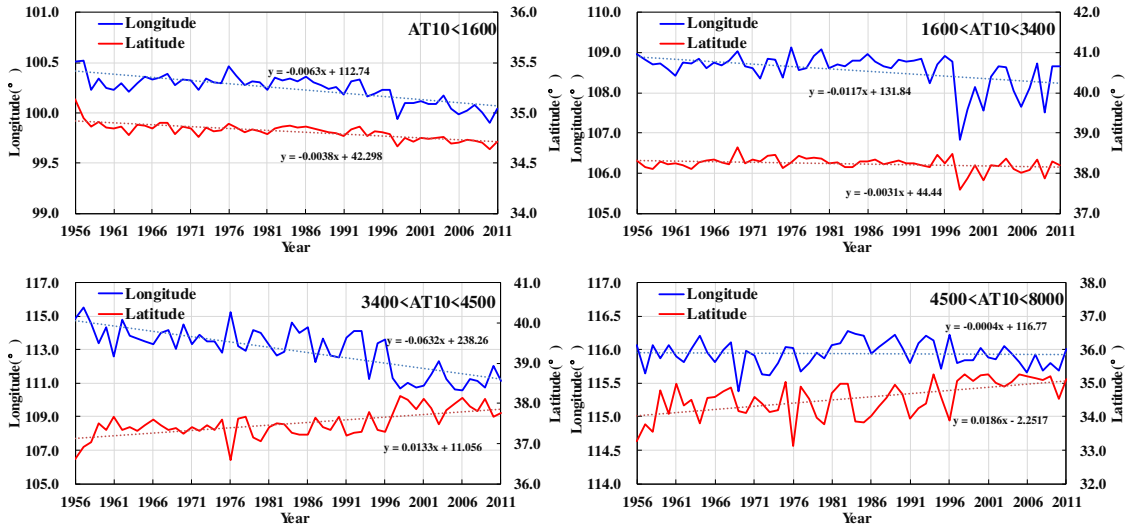

Figure 10. *Movement characteristics of AT10 of HHHRB*

The study period 1956-2011 was divided into 7 phases: A-G. Since phase A only includes four years, which are 1956, 1957, 1958 and 1959, and phase G only includes 2010 and 2011, phase A and G were deleted in the following analysis. For the remaining phases, spatial distribution of active area and stable area of the study area of AT10 were analysed (*Fig. 11; Table 1*). In a given phase, active area is the area where a certain class of AT10 appeared one or more times. Stable area is the area where the occurrence number of a certain class of AT10 is equal to the number of study years in a given phase.

For class (1), decadal change of active area and stable area are not obvious. For class (2), both stable area and active area are moving towards northwest and their areas are decreasing. For class (3), stable area and active area also have a moving trend towards northwest, which is particularly obvious in 2000-2010. For class (4), active area did not change much, while stable area moved northward notably during 2000-2010.

For class (1), the ratio between active and stable areas has been around 1:9. For class (2), the ratio between active and stable areas has changed from 4:6 to 6:4, thus the ratio of active area has increased. For class (3), the ratio between active and stable areas has changed from 7:3 to 6:4, thus the ratio of active has decreased. For class (4), the ratio between active and stable areas has changed from 4:6 to 5:5, and then back to 3:7, thus the ratio between these two areas have reversed.

http://www.aloki.hu ● ISSN 1589 1623 (Print) ● ISSN 1785 0037 (Online)
DOI: http://dx.doi.org/10.15666/aeer/1802_31953209

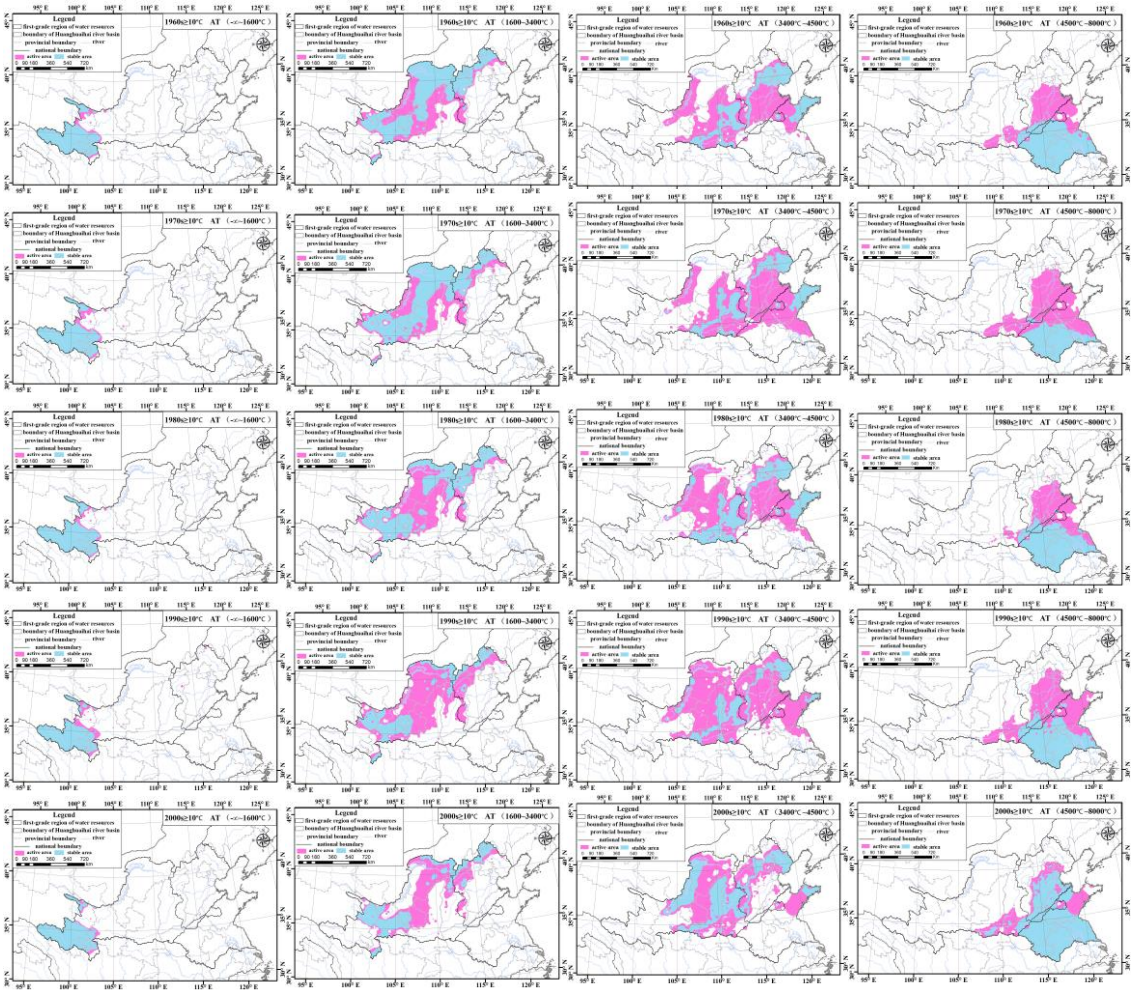

Figure 11. *Decadal spatial movement characteristics of active area and stable area of different classes of ≥ 10 °C ATT of HHHRB*

Conclusion and discussion

In general, *AT* 10 of HHHRB has an increasing trend during the study period, which is in accordance with the paradigm of global warming. Since 1956, energy resources in the HHHRB have increased. On one hand, this will contribute to the food production in the study area but on the other, the risk of drought could be increased. The maximum value, minimum value, range and standard deviation of *AT*10 of HHHRB all had a significant increasing trend, which verified significant warming and increasing energy resources in the study area. Duration of thermal growing season of *AT* 10 of HHHRB has an increasing trend. The starting time of thermal growing season has moved up and the ending time has been postponed. Compared with the duration of phase A, the duration of F and G have increased significantly by 13.1 days and 15.7 days respectively.

Generally speaking, *AT*10 of HHHRB has a moving tendency towards the northwest. *AT*10 of HHHRB decreased from the southeast region towards the northwest region. Except the west most part and some scattered area, *AT*10 of HHHRB has a significant increasing trend. Area of class (1) and (2) have a downward trend while that of class (3) and (4) have an upward trend. Class (1), (2), (3) and (4) of *AT*10 of HHHRB have a

http://www.aloki.hu ● ISSN 1589 1623 (Print) ● ISSN 1785 0037 (Online)
DOI: http://dx.doi.org/10.15666/aeer/1802_31953209

moving tendency towards southeast, west, northwest and north respectively. For class (2) and (3), stable area and active area are moving towards the northwest. The active area and stable area of class (1) have not experienced a notable change. For class (4), stable area moved northward but the active area remained changeless. What is more, the ratio between active area and stable area in different classes has fluctuated during the study period.

Table 1. *Decade ratio of active area and stable area of different classes of AT10 of HHHRB (100%)*

Class	**(1)**				
	1960s	1970s	1980s	1990	2000s
Active area	11.9	13.7	9.9	18.1	9.2
Stable area	88.1	86.3	90.1	81.9	90.8
Class	**(2)**				
	1960s	1970s	1980s	1990	2000s
Active area	40.2	39.5	50.5	69.9	58.3
Stable area	59.8	60.5	49.5	30.1	41.7
Class	**(3)**				
	1960s	1970s	1980s	1990	2000s
Active area	67.3	74.1	65.1	80.3	56.9
Stable area	32.7	25.9	34.9	19.7	43.1
Class	**(4)**				
	1960s	1970s	1980s	1990	2000s
Active area	43.4	66.0	45.2	54.5	27.2
Stable area	56.6	34.0	54.8	45.5	72.8

Ratio of active area in a certain phase and a certain class = (area of active area) / (area of active area + area of stable area); ratio of stable area in a certain phase and a certain class = (area of stable area) / (area of active area + area of stable area)

In the previous studies, Zhao et al. (2016) have found that the accumulated temperature had a strong positive effect on the components of maize yield in East Gansu. Wang et al. (2006) have detected that winter wheat yield increased with the increase of AT10, but decreased with the increase of AT20. The climate change would affect the crop productivity and food supply, which decrease the stability of the global food system. However, the potential impact on a regional scale is unclear (Wheeler et al., 2013). Global Climate change and regional climate change are not completely consistent due to the large regional differences in natural environment and human behavior. It is necessary to analyze the characteristics of regional accumulated temperature and its impact on local crop yield in the context of global climate change.

Acknowledgements. This research was funded by [National Key Research and Development Project] grant number [2017YFC1502404]; [National Natural Science Foundation of China] grant number [51909080;51709008]; [the Open Research Fund of State Key Laboratory of Simulation and Regulation of Water Cycle in River Basin (China Institute of Water Resources and Hydropower Research)] grant number [IWHR-SKL-KF201804]; [Young and middle-aged talent project of Hubei Province Education Department] grant number[Q20181001];. Natural Science Foundation of Hubei Province (2018CFB655).

http://www.aloki.hu ● ISSN 1589 1623 (Print) ● ISSN 1785 0037 (Online)
DOI: http://dx.doi.org/10.15666/aeer/1802_31953209

REFERENCES

[1] Anwar, M. R., Liu, D. L., Macadam, I., Kelly, G. (2013): Adapting agriculture to climate change: a review. – Theoretical and Applied Climatology 113: 225-245.
[2] Berti, M. T., Johnson, B. L. (2008): Physiological changes during seed development of cuphea. – Field Crops Res 106: 163-170.
[3] Bonhomme, R., Derieux, M., Edmeades, G. O. (1994): Flowering of diverse maize cultivars in relation to temperature and photoperiod in multi-location field trials. – Crop Sci 34: 156-164.
[4] Chirkov, Y. I., Kononova, N. K. (1984): Inter-annual variations of accumulated temperature from observation data of Mikhelson. – Meteorology and Hydrology 11: 102-106.
[5] Dong, J. W., Liu, J. Y., Tao, F. L., Xu, X. L., Wang, J. B. (2009): Spatio-temporal changes in annual accumulated temperature in China and the effects on cropping systems, 1980s to 2000. – Climate Research 40: 37-48.
[6] Hamed, K. (2009): Exact distribution of the Mann-Kendall trend test statistic for persistent data. – Journal of Hydrology 365: 86-94.
[7] Hodges, D. M., Hamilton, R. I., Charest, C. (1994): A chilling resistance test for inbred maize lines. – Can. J. Plant Sci 74: 687-691.
[8] Hou, P., Liu, Y., Xie, R. Z., Ming, B., Ma, D. L., Li, S. K., Mei, X. R. (2014): Temporal and spatial variation in accumulated temperature requirements of maize. – Field Crops Research 158: 55-64.
[9] Iannucci, A., Terribile, M. R., Martiniello, P. (2008): Effects of temperature and photoperiod on flowering time of forage legumes in a Mediterranean environment. – Field Crops Res 106: 156-162.
[10] IPCC (2013): Summary for Policymakers. – In: Stocker, T. F., Qin, D., Plattner, G.-K., Tignor, M., Allen, S. K., Boschung, J., Nauels, A., Xia, Y., Bex, V., Midgley, P. M. (eds.) Climate Change 2013: The Physical Science Basis. Contribution of Working Group I to the Fifth Assessment Report of the Intergovernmental Panel on Climate Change. Cambridge University Press, Cambridge.
[11] Kadioglu, M., Saylan, L. (2001): Trends of growing degree-days in Turkey. – Water Air Soil Pollut 126: 83-96.
[12] Li, X., Zhang, D., Wang, H., Shao, Y., Ma, F. (2015): Impact of temperature increment before the over-wintering period on growth and development and grain yield of winter wheat. – Chinese Journal of Applied Ecology 26(3): 839-846 (in Chinese).
[13] Liang, Q., Zhang, G., Yin, H. (2015): Effect of Temperature on the growth rate and yield of soybean based on stages seeding. – Anhui Agricultural Science Bulletin 21(5): 134-137 (in Chinese).
[14] Liu, M., Wu, J., Lv, A., Zhao, L., He, B. (2010): The water stress of winter wheat in Huang-Huai-Hai plain of China under rain-fed condition. – Prog. Geogr. 29(4): 427-432 (in Chinese).
[15] Lv, J., Yan, C., Jia, T., Wang, F., Sun, H., Dong, S., Gong, Z. (2019): The variation of accumulated temperature in Songnen Plain and its impact on crop yield. – Chinese Journal of Ecology 38(11): 3349-3356 (in Chinese).
[16] Major, D. J., Brown, D. M., Bootsma, A., Dupuis, G., Fairey, N. A., Grant, E. A., Green, D. G., Hamilton, R. I., Langille, J., Sonmor, G., Smeltzer, G. C., White, R. P. (1983): An evaluation of the corn heat unit system for the short-season growing regions across Canada. – Can. J. Plant Sci 63: 121-130.
[17] Mann, H. B. (1945): Non-parametric test against trend. – Econometrika 13: 245-259.
[18] McMaster, G. S., Smika, D. E. (1988): Estimation and evaluation of winter wheat phenology in the central Great Plains. Agric. – Forest Meteorol 43: 1-18.
[19] Olivier, F. C., Annandale, J. G. (1998): Thermal time requirements for the development of green pea (Pisum sativum L.). – Field Crops Res 56: 301-307.

http://www.aloki.hu ● ISSN 1589 1623 (Print) ● ISSN 1785 0037 (Online)
DOI: http://dx.doi.org/10.15666/aeer/1802_31953209

[20] Sacks, W. J., Kucharik, C. J. (2011): Crop management and phenology trends in the U. S. Corn Belt: impacts on yields, evapotranspiration and energy balance. – Agric. Forest Meteorol 151: 882-894.
[21] Shen, F., Geng, L., Qin, F., Xu, P. (2002): Analysis of water saving in received area in Huanghe-Huaihe-Haihe watersheds and Eastern and Middle Lines of water transferring project from South to North, China. – Adv. Water Sci. 13(6): 768-774 (in Chinese).
[22] Skaugen, T. E., Tveito, O. E. (2004): Growing-season and degree-day scenario in Norway for 2021-2050. – Clim. Res 26: 221-232.
[23] Song, Y. L., Zhao, Y. X., and Wang, C. Y. (2011): Changes of accumulated temperature, growing season and precipitation in the North China Plain from 1961 to 2009. – Acta Meteor. Sinica 25(4): 534-543.
[24] Stevens, E. J., Stevens, S. J., Flowerday, A. D., Gardner, C. O., Eskridge, K. M. (1986): Developmental morphology of dent corn and popcorn with respect to growth staging and growth models. – Agron. J. 78: 867-874.
[25] Tian, Y., Xu, Y., Booij, M., Lin, S., Zhang, Q., Lou, Z. (2012): Detection of trends in precipitation extremes in Zhejiang, East China. – Theoretical and Applied Climatology 107: 201-210.
[26] Wang, H., Chen, Y. N., Xun, S., Lai, D. M., Fan, Y. T., Li, Z. (2013): Changes in daily climate extremes in the arid area of northwestern China. – Theoretical and Applied Climatology 112(1-2): 15-28.
[27] Wang, W., Zhang, T., Huang, B., Li, Z., Wang, R., Yang, M., Pu, J. (2006): Responses of winter wheat in the Loess Plateau of east Gansu Province to climate warming. – Chinese Journal of Ecology 25(7): 774-778.
[28] Wang, W., Chen, X., Shi, P., van Gelder, P. H. A. J. M. (2008): Detecting changes in extreme precipitation and extreme streamflow in the Dongjiang River Basin in southern China. – Hydrology and Earth System Sciences 12(1): 207-221.
[29] Wang, Y. H., Ren, C. Y., Han, Y. D., Zhang, J., Zhang, W. Z., Huang, R. D. (2011): The tempo-spatial patterns of active accumulated and consecutive extreme low temperature and their impacts on grain crop yield in Northeast China. – Journal of Agro-Environment Science 30(9): 1742-1748.
[30] Wheeler, T., Von Braun, J. (2013): Climate change impacts on global food security. – Science 341: 508-513.
[31] Wu, K. (2011): Influence of climate warming on the agriculture in Shenbei New District of Shenyang. – Journal of Anhui Agri. Sci 39(16): 9918-9920.
[32] Xu, X. K., Wang, X. T., Jin, X. Q. (2009): Vegetation response to accumulated temperature patterns from 1960-2000 in China. – Acta Ecologica Sinica 29(11): 6042-6050.
[33] Yan, M. H., Liu, X. T., Zhang, W., Li, X. J., Liu, S. (2011): Spatio-temporal changes of ≥ 10°C accumulated temperature in Northeastern China since 1961. – Chin. Geogra. Sci 21(1): 17-26.
[34] Yu, S., Yang, J., Liu, G., Yao, R., Wang, X. (2012): Multiple time scale characteristics of rainfall and its impact on soil salinization in the typical easily salinized area in Huang-Huai-Hai Plain, China. – Stochastic Environmental Research and Risk Assessment 26(7): 983-992.
[35] Zhang, L., Li, M., Wu, Z., Liu, Y. (2011): Vegetation cover change and its mechanism in northeast China based on SPOT/NDVI data. – Journal of Arid Land Resources and Environment 25(1): 171-175 (in Chinese).
[36] Zhao, W., Zhang, Y., Zhang, F., Wang, Q., Zhai, X., Qiu, N., Zhang, M. (2016): Influence of meteorological factors variation on yield components during maize grain-filling stage in East Gansu. – Chinese Agricultural Science Bulletin 32(21): 62-66.

http://www.aloki.hu ● ISSN 1589 1623 (Print) ● ISSN 1785 0037 (Online)
DOI: http://dx.doi.org/10.15666/aeer/1802_31953209

ANALYSIS OF THE SPATIOTEMPORAL VARIATION CHARACTERISTICS OF MAIN EXTREME CLIMATE INDICES IN SICHUAN PROVINCE OF CHINA FROM 1968 TO 2017

LI, X. H. – CHEN, Z. F. – WANG, L.*

Plateau Atmosphere and Environment Key Laboratory of Sichuan Province, School of Atmospheric Sciences, Chengdu University of Information Technology, Chengdu 610225, China

**Corresponding author*
e-mail: 26107184@qq.com; phone: +86-134-0806-9773

(Received 27th Sep 2019; accepted 4th Feb 2020)

Abstract. With an increasing trend in global warming, extreme weather and a variety of related climate events frequently occur in the Southwestern China. In this research, we analyzed daily maximum and minimum temperatures, and daily precipitation data of 39 meteorological stations in the Sichuan Province between the years of 1968 and 2017. Nineteen different indices representing extreme climate change were selected, and linear regression analysis, Mann-Kendall mutation test, sliding T test, wavelet analysis and R/S analysis were applied. According to the results, we concluded that: (1) most extreme cold indices showed a decreasing trend, while the extreme warm indices displayed an increasing trend. There was no significant interannual variation for extreme precipitation indices. (2) Most extreme temperature indices presented no significant mutation years, and the significant periods were mainly 2-6 years long. The mutation years of heavy and very heavy precipitation events mainly appeared in the 1980 and the early 21st century, and the significant periods of most extreme precipitation indices were 2-7 years long. (3) As shown by the Hurst exponent analysis and interannual variation trends, it is very likely that the extreme temperature and extreme precipitation events in the Sichuan Province will increase in the future.
Keywords: *extreme temperature indices, extreme precipitation indices, M-K test, sliding T test, wavelet analysis, R/S analysis*

Introduction

According to the IPCC (Intergovernmental Panel on Climate Change, IPCC) Fifth Assessment Report, from 1880 to 2012 the global mainland and sea surface temperature increased by 0.85 °C. The change in temperature for the 2003-2012 period was 0.78 °C higher than for the period 1850 to 1990 (Stocker, et al., 2013). In the second half of the 20th century, the number of cold nights on land in over 70% of the areas worldwide began to show a significant decrease, while the number of warm nights increased (Alexander, et al., 2006). Extreme temperatures mainly manifest as more frequent incidences of extreme high and low temperature events and a prolongation of their duration. Extreme precipitation events mainly manifest with an increasing frequency and intensity of droughts, rainstorms, and extraordinary flood disasters (Ding, et al., 2018). As indicated by historical observations, in the past century global warming led to an increase in the intensity and frequency of extreme events (droughts, floods, and cold waves), as well as an expansion of the area of influence (Zhao, et al., 2016; Liu, et al., 2019).

At present, under the general context of global warming, extreme climate changes at different scales have attracted the attention of researchers all over the world. Alexander et al. (2006) have stated that, on a global scale, global warming has caused a significant reduction in the number of cold nights and a significant increase in the number of warm nights in many regions worldwide. The extreme precipitation indices including the number of continuous rainless days and number of continuous rainy days have also

http://www.aloki.hu ● ISSN 1589 1623 (Print) ● ISSN 1785 0037 (Online)
DOI: http://dx.doi.org/10.15666/aeer/1802_32113242

substantially increased (Easterling, et al., 2000). Song et al. (2013) analyzed the extreme temperature events all over the world from 1981 to 2010. They determined that the frequency of occurrence of heat and cold waves increased 2.7 and 6.4 times, respectively. On a regional scale, scholars have determined that the number of cold days and nights has been continuously decreasing, while the number of warm days and nights has been increasing. Similar variation trends have been observed for extreme temperature and precipitation events on a global scale. For example, in the United States, the increasing trends were identified for temperature, and the frost and ice days dwindled as growing season length, tropical nights and summer days increased (Sohrabi, et al., 2013). In Europe, significant increasing trends in annual precipitation extremes have been detected in different regions (Vogel, et al., 2018; Arnone, et al., 2018). The extreme temperature indices of Nile river basin decreased in cold, but increased in warm night/days, and most precipitation extreme indices increased (Tariku and Gan, 2018). For the Caribbean small islands, most extreme temperature indices at Piarco Point (Trinidad) showed significant warming trends on annual and seasonal scales as well as for most months. For Crown Point (Tobago), trends indicated an increase in annual precipitation totals and extremely wet days were observed (Dookie, et al., 2018). In some Asian country, with a large proportion of stations having statistically significant trends for all temperature indices, temperature extremes showed a warming trend over Iran (Soltani, et al., 2016). Sajjad and Ghaffar (2018) observed and projected extreme climate indices over Pakistan in changing climate, the results showed there were a significantly increasing trend in the mean maximum temperature and summer days, and frequency of heavy precipitation also significantly increased. In addition, studies on extreme temperatures and precipitation occurrences have shown that in most Chinese regions, the cold night index and warm night index displayed a similar intensity and yet an opposite trend of variation, which indicated a good symmetry (Yang, et al., 2010). Both, the frequency and intensity of extreme precipitation events have been increasing, though with apparent inter-regional differences (Jiang, et al., 2017; Yin and Sun, 2019). Some researchers have suggested that the extreme precipitation events have been increasing in the Yangtze River Basin and part of Southeastern China and Northwestern China. However, a decreasing trend was observed for some parts of Northern, Northeastern, and Southwestern China (Gao and Xie, 2014).

Two abnormal drought events occurring in 2005-2006 and 2009-2010 in Southwestern China have drawn widespread attention regarding extreme climate incidents in this region. Yuan and Zheng (2015) studied extreme temperature indices observed in Southwestern China during the period 1962 to 2012. In general, extreme high and low temperature events showed an increasing and decreasing tendency, respectively. An opposite variation trend was observed in some regions, which was a unique climate change feature of Southwestern China. In addition, when considering extreme precipitation events for the same period and region, results indicated that there was a large variability. The extreme precipitation events showed an overall increasing trend during the past 50 years; however, it was not significant. This may be related to abnormal changes in sea surface temperature and complex geographical environments (Yuan, et al., 2014). Luo et al. (2016) determined the trend for extreme temperatures in Southwestern China for the years of 1970 to 2010. Their results showed that there was a good local symmetry between the number of warm days and the number of cold days in this region, as well as a good symmetry between the number of warm nights and number of cold nights for the past 41 years. The warm indices increased in value, while

http://www.aloki.hu ● ISSN 1589 1623 (Print) ● ISSN 1785 0037 (Online)
DOI: http://dx.doi.org/10.15666/aeer/1802_32113242

the cold indices decreased. Ding (2014) studied the spatio-temporal changes of extreme precipitation in Southwestern China, and the results indicated that the frequency of extreme precipitations in this area have increased since the 1960s. There were significant inter-regional differences in inter-decadal variations. The frequency of extreme precipitations in the monsoon period significantly increased, while that in the non-monsoon period decreased.

The Sichuan Province is located in Southwestern China and marks the transition belt between the Tibetan Plateau of China and the eastern plain. With a complex landform and diverse climate types, it is a sensitive, vulnerable and strategic area affected by climate change. The inter-regional difference in temperature in this province can reach more than 20 °C, and the regional precipitation distribution varies significantly. In recent years, the occurrence of extreme climate events has led to frequent natural disasters in the Sichuan Province. For example, in 2006, this area suffered an extraordinary drought that was estimated to occur only once-in-a-hundred-year period. From the winter of 2009 to the spring of 2010, a persistent severe drought affected 71 cities, districts and counties of 13 Sichuanese municipalities. It was estimated that this drought affected a population of 8.282 million, a crop area of 511 000 hm^2, with a resulting direct economic loss of 1.38 billion RMB. In this same area, in 2011, the numbers were as follows: crop area affected by the drought reached the 346 000 hm^2, and the direct economic loss was of 1.2 billion RMB (Wang, et al., 2017). In 2012 and 2017, another historical extreme temperature hit the summer season in this same province. In July of 2007, the Sichuan Basin was struck by a once-in-a-hundred-year extraordinary heavy rain. On July 19th in the year of 2010, a heavy severe flood hit Guang'an City in Sichuan. In July of 2016, a persistent rainstorm occurred in Jiuzhaigou, which triggered a severe debris flow disaster and resulted in the shutdown of the Jiuzhaigou Scenic Area. In July of 2018, Mianyan area in Sichuan was hit by the most severe flood ever seen since the founding of New China. These extreme climate events have resulted in enormous economic losses to the Sichuan province, threatening people's life and property safety. A variety of studies related to the extreme temperatures and precipitation events in Sichuan have been conducted. For example, Liu (2013) defined extreme temperature events based on percentile thresholds at three representative stations in the Sichuan Basin (Chengdu, Nanchong, and Shapingba). His study showed that from the mid-1970s to the 1980s, the frequency and intensity of extreme high temperature events in the Sichuan Basin decreased. However, after the late-1990s, the frequency and intensity of extreme high temperature events increased, while the variation trend of extreme low temperature events was just the opposite. Sun et al. (2017) studied the extreme precipitation events of Sichuan that occurred between 1971 and 2014. They found out that in the past 44 years, the overall precipitation in this region slightly decreased. In addition, there was a general warming and drying trend in most parts of Sichuan, except for an increasing humidity pattern observed in the Western Sichuan Plateau. However, the investigations dealing with the distinctive topography and climate conditions in this area are far from being enough.

In view of the above, the objective of this study was to investigate the spatio-temporal and abrupt changes, as well as periodic trends in extreme temperature and precipitation in the Sichuan Province for the period 1968 to 2017 by using 10 extreme temperature indices and 9 extreme precipitation indices, which are recommended by the WMO (World Meteorological Organization, WMO). Furthermore, to explore the relationship between extreme climate indices and geographical factors and to project

http://www.aloki.hu ● ISSN 1589 1623 (Print) ● ISSN 1785 0037 (Online)
DOI: http://dx.doi.org/10.15666/aeer/1802_32113242

future change trends by using Hurst exponent. Through deep and comprehensive analysis, our research findings provide valuable information that may help in coping with climate change and for disaster prevention and relief in the Sichuan Province.

Materials and methods

Study area

The Sichuan Province is located in Southwestern China (97°21′~108°33′ longitude and 26°03′~34°19′ latitude). The entire region covers an area of 485 000 km^2, it is 1 075 km from east to west and 921 km from south to north (Zhan and Wen, 2006). The terrain is higher to the west and lower to the east. To the northwest, the area is mainly covered by plateaus and high mountains, while the southwest is a mountainous region, and the eastside is both, basin and mountains. Due to the varied landforms and the alternating influence of different monsoon winds, a unique climatic type has been formed. Taking into account temperature, precipitation, and sunshine conditions, the Sichuan Province can be divided into three major climatic zones: (1) A cold climatic zone in the high mountains and plateaus in the Northwestern area. Herein, there is an annual average temperature between 4~12 °C; the winter is cold and the summer is cool, and the total annual precipitation is only 500-900 mm. Also, the annual sunshine hours are as many as 1 600~2 600; (2) The subtropical semi-humid climatic zone in the mountainous areas in Southwestern Sichuan, where the annual average temperature oscillates between 12~20 °C, and the total annual precipitation is 900~1 200 mm; however, 90% of the precipitation occurs from May to October, and the annual sunshine hours are between 2 000~2 600; (3) The middle subtropical humid climatic zone in the Sichuan Basin with an intermediate annual average temperature of 16~18 °C; the winter is warm and the summer is hot; the annual precipitation is abundant (1 000~1 200 mm) and the annual sunshine hours are short (only 1 000-1 400) (Zhou, et al., 2011). The inter-regional climatic differences are significant in the Sichuan Province. Large climatic variations are related to altitude. Rapid climatic changes have led to a great number of meteorological disasters, such as droughts, rainstorms, floods and low temperature freezing events. These disasters have frequently occurred and they have affected extensive regions (Ma, 2016). *Figure 1* shows the geographical location of the Sichuan Province and a zoning map of this area based on terrain and climate.

Data sources

The main data source used in this study was collected from the MDSCC (Meteorological Data Service Center of China, MDSCC) (http://www.nmic.cn), and the principles of continuity and longest duration were considered. The data on daily maximum temperature, daily minimum temperature, 24h precipitation and annual precipitation at 39 meteorological stations from 1968 to 2017 were collected. Three quality control methods were used in handling these data, namely, internal consistency check, climate limit value check and station extreme check. Linear regression was applied in order to calculate missing data by interpolation using the available information on adjacent stations. In this endeavor, care was taken in order to ensure that the corrected meteorological data displayed high scientificity, accuracy, and continuity. *Figure 2* and *Table 1* show the spatial distribution, detailed information, and zone division for each station.

http://www.aloki.hu ● ISSN 1589 1623 (Print) ● ISSN 1785 0037 (Online)
DOI: http://dx.doi.org/10.15666/aeer/1802_32113242

Extreme climate indices

In this study, from all extreme climate indices recommended by the WMO, we selected 10 extreme temperature indices and 9 extreme precipitation indices (*Table 2*). These data were extracted by running the program.

Table 1. *Detailed information of meteorological stations in Sichuan Province used in the study*

Zoning	No.	Station names	Latitude (°N)	Longitude (°E)	Elevation (m)
Eastern Sichuan Basin (ESB)	1	WenJiang	103.94	30.82	548.9
	2	DuJiangYan	103.79	31.07	699.7
	3	MianYang	104.62	31.39	523.7
	4	Ya'an	103.10	29.98	629.4
	5	EMeiShan	103.33	29.51	3048.3
	6	LeShan	130.76	29.57	425.2
	7	YiBin	104.60	28.80	342.1
	8	GuangYuan	105.85	32.44	513.5
	9	WanYuan	108.05	32.07	675.0
	10	LangZhong	106.02	31.46	385.4
	11	BaZhong	106.86	31.87	416.3
	12	DaXian	107.50	31.19	344.4
	13	SuiNing	105.54	30.50	355.3
	14	GaoPing	106.09	30.76	311.0
	15	XuYong	105.46	28.19	378.6
	16	NanBu	106.07	31.35	406.9
	17	NaXi	105.40	28.79	369.4
Mountainous area in southwestern Sichuan (MSW)	18	MuLi	101.27	27.93	2424.6
	19	YueXi	102.52	28.65	1660.1
	20	ZhaoJue	102.86	28.02	2133.7
	21	LeiBo	103.58	28.27	1254.8
	22	YanYuan	101.51	27.44	2545.0
	23	XiChang	102.26	27.90	1592.7
	24	HuiLi	102.25	26.66	1788.6
Alpine and plateau area in northwestern Sichuan (PNW)	25	ShiQu	98.09	32.99	4201.0
	26	RuoErGao	103.02	33.64	3442.6
	27	DeGe	98.58	31.82	3185.0
	28	GanZi	100.00	31.63	3394.6
	29	SeDa	100.30	32.28	3895.8
	30	DaoFu	101.14	31.01	2959.2
	31	MaErKang	102.22	31.87	2666.3
	32	HongYuan	102.59	32.79	3492.8
	33	XiaoJin	102.34	31.00	2368.8
	34	SongPan	103.56	32.65	2852.1
	35	BaTang	99.07	30.01	2590.2
	36	XinLong	100.35	30.92	2999.2
	37	DaoCheng	100.30	29.14	3728.6
	38	KangDing	101.99	30.04	2615.5
	39	JiuLong	101.50	29.01	2931.4

http://www.aloki.hu ● ISSN 1589 1623 (Print) ● ISSN 1785 0037 (Online)
DOI: http://dx.doi.org/10.15666/aeer/1802_32113242

Table 2. *List of the 19 selected extreme climate indices*

Categories	No.	Indices	Descriptive names/units	Definitions
Extreme temperature indices	1	FD	Frost days/d	Annual count when Tn (daily minimum) < 0 °C
	2	Tnn	Min Tmin/°C	Annual minimum value of daily minimum temperature
	3	Tnx	Max Tmin/°C	Annual maximum value of daily minimum temperature
	4	Tn10	Cool nights/d	Number of days when Tn < 10th percentile
	5	Tx10	Cool days/d	Number of days when Tx (daily maximum) < 10th percentile
	6	SU	Summer days/d	Annual count when Tx > 25 °C
	7	Txn	Min Tmax/°C	Annual minimum value of daily maximum temperature
	8	Txx	Max Tmax/°C	Annual maximum value of daily maximum temperature
	9	Tn90	Warm nights/d	Number of days when Tn > 90th percentile
	10	Tx90	Warm days/d	Number of days when Tx > 90th percentile
Extreme precipitation indices	11	CDD	Consecutive dry days/d	Maximum number of consecutive days with RR > 1 mm
	12	CWD	Consecutive wet days/d	Maximum number of consecutive days with RR ≥ 1 mm
	13	R10	Number of heavy precipitation days/d	Annual count of days when PRCP ≥ 10 mm
	14	R20	Number of very heavy precipitation days/d	Annual count of days when PRCP ≥ 20 mm
	15	R50	Number of rainstorm days/d	Annual count of days when PRCP ≥ 50 mm
	16	R95p	Very wet days/mm	Annual total PRCP when RR > 95th percentile
	17	R99p	Extremely wet days/mm	Annual total PRCP when RR > 99th percentile
	18	SDII	Simple daily intensity index/(mm/d)	Annual total precipitation divided by the number of wet days
	19	PRCPTOT	Annual total wet-day precipitation/mm	Annual total PRCP in wet days (RR ≥ 1 mm)

RR: daily precipitation; PRCP: precipitation

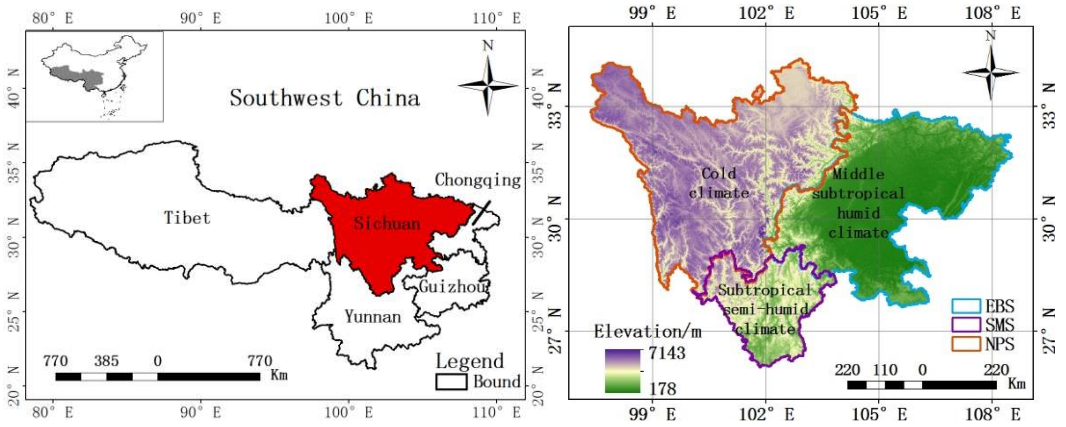

Figure 1. *Geographical location and zoning map based on terrain and climate in study area*

http://www.aloki.hu ● ISSN 1589 1623 (Print) ● ISSN 1785 0037 (Online)
DOI: http://dx.doi.org/10.15666/aeer/1802_32113242

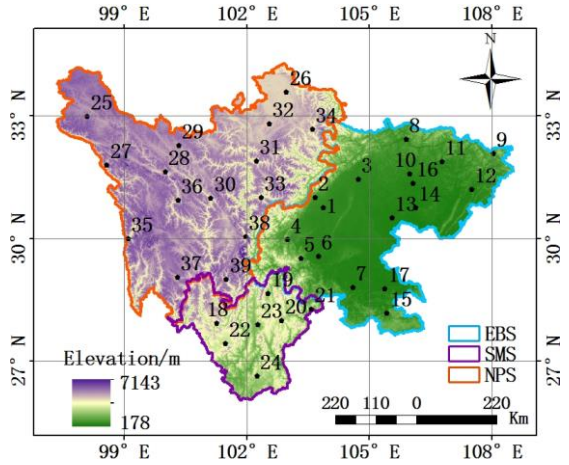

Figure 2. *The spatial distribution of 39 meteorological stations in Sichuan Province*

Main research methods

The following analyses or tests were performed: linear regression, Mann-Kendall trend test, sliding T test, wavelet, correlation, and R/S analyses. The main methods involved in the present study were as follows:

(1) Mann-Kendall trend test: it is also known as the M-K or nonparametric test. This method is recommended by the WMO, and is a valuable tool for effectively differentiating natural fluctuations from definite variation trends. It is a nonparametric statistical test to analyze the variation trends of climate and hydrological series over time. It is also used for the detection of precipitation trends as well as drought frequency under the influence of climate change (Liu, et al., 2011a). Samples used for M-K test may or may not conform to anormal distribution. In addition, analysis is not affected when samples display a few outliers. For these reasons, M-K test surpasses other tools when dealing with abrupt climate changes (Ma, et al., 2018). The main steps of M-K test are listed below (Wei, 2007):

For time series X comprising n samples, a rank sequence is constructed as:

$$S_k = \sum_{i=1}^{k} r_i = \begin{cases} 1, x_i > x_j \\ 0, x_i \le x_j \end{cases}, \quad j = 1, 2, \ldots, i \qquad \text{(Eq.1)}$$

where k is: the sample size; r_i is used to determine whether the value at time i is larger than that at time j; the rank sequence S_k represents the cumulative number when values are larger at time j than those at time i.

Statistics is defined as:

$$UF_k = \frac{S_k - E(S_k)}{\sqrt{Var(S_k)}}, k = 1, 2, \ldots, n \qquad \text{(Eq.2)}$$

where:

$$E(S_k) = \frac{n(n+1)}{4} \qquad \text{(Eq.3)}$$

http://www.aloki.hu ● ISSN 1589 1623 (Print) ● ISSN 1785 0037 (Online)
DOI: http://dx.doi.org/10.15666/aeer/1802_32113242

$$Var(S_k) = \frac{n(n-1)(2n+5)}{72} \quad \text{(Eq.4)}$$

where $UF_1 = 0$, $E(S_k)$, $Var(S_k)$ is the mean and variance of the rank sequence S_k. UF_i obeys a normal distribution. Through *Equation 2,* a positive UF trend was obtained. The same method was applied to the inverted series to obtain the corresponding UB curve, i.e., $UB_k = -UF_k$. When plotting the curves, if the UF test statistics result is above 0, the variable has an increasing trend. On the contrary, if the UF test statistics result is below 0, the variable has a decreasing trend. In addition, an intersection point between the UF and UB statistics result lying between the critical lines determines the starting time of climate alteration, i.e, the year of climate change.

(2) Sliding T test: This test is helpful in detecting climate mutations by determining if there is a significant difference in the means of two different groups. The basic principle is that the significant difference between the means of two subseries in one given climate series is tested by treating such difference as if it is the result of comparing two separate series. Should the difference in the means of the two subseries exceed a certain significance level, the means are considered to have undergone qualitative change, i.e., the mutation occurred.

For a time series $\{X_i, i=1, 2, \ldots, n\}$ composed of n samples, a given time is selected as the reference point. Before and after this point, n_1 and n_2 represent the number of elements in the samples for their corresponding two sub-sequences X_1 and X_2 (generally $n_1=n_2$). The means of the two sub-sequences are $\overline{X_1}$ and $\overline{X_2}$, and the variances s_1^2 and s_2^2, respectively. Statistics is defined as (Liu, et al., 2011b):

$$t = \frac{\overline{x}_1 - \overline{x}_2}{s\sqrt{\frac{1}{n_1} + \frac{1}{n_2}}} \quad \text{(Eq.5)}$$

where:

$$s = \sqrt{\frac{n_1 s_1^2 + n_2 s_2^2}{n_1 + n_2 - 2}} \quad \text{(Eq.6)}$$

Then, t obeys a t distribution with a degree of freedom n_1+n_2-2.

(3) Wavelet analysis: This is a method for the analysis of signal frequency and has a multi-resolution capacity. Wavelet analysis accurately provides information on local signal features in both, the time and frequency domains, and can be used for multi-scale detailed signal analysis. Since this method is more robust than Fourier transform, it has been widely used in multi-scale climate analysis in recent years (Xu, et al., 2004).

The wavelet function is defined as follows: Let the function φ(t) be a square-integrable function, i.e., $\varphi(t) \in L^2$ (R), where R is any real number. If the Fourier transform ψ(ω) satisfies the admissibility condition (Wei, 2007):

http://www.aloki.hu ● ISSN 1589 1623 (Print) ● ISSN 1785 0037 (Online)
DOI: http://dx.doi.org/10.15666/aeer/1802_32113242

$$\int_R \frac{|\psi(\omega)|^2}{\omega} d\omega < \infty \quad \text{(Eq.7)}$$

then φ(t) is called a basic wavelet or wavelet generating function. By expansion and translation of the wavelet function φ(t), the continuous wavelet is obtained as:

$$\varphi_{a,t}(t) = \frac{1}{\sqrt{a}} \varphi\left(\frac{t-\tau}{a}\right),\ a, \tau \in R, a > 0 \quad \text{(Eq.8)}$$

For any function $f(t) \in L^2(R)$, the continuous wavelet changes into

$$W_f(a, \tau) = \left\langle f(t), \varphi_{a,\tau}(t) \right\rangle = \frac{1}{\sqrt{a}} \int_R f(t) \varphi\left(\frac{t-\tau}{a}\right) dt \quad \text{(Eq.9)}$$

where a is the scale factor; τ is the translation factor; and $W_f(a,\tau)$ is the wavelet coefficient.

Herein, the Morlet wavelet was used for continuous wavelet transform of the extreme climate indices. The wavelet function is:

$$\psi(t) = e^{i\omega t} e^{-t^2/2} \quad \text{(Eq.10)}$$

(4) R/S analysis: This is also known as rescaled range analysis, which is an important analytical method under the chaos theory. It can be applied to analyze the fractal features and long-term memory process of a variety of time series. The calculation method is illustrated below:

A time series $\{X_t\}$ is divided into A subintervals with equal length N. For each subinterval, let

$$X_{t,n} = \sum_{u=1}^{t} \left(X_u - M_n\right) \quad \text{(Eq.11)}$$

Where M_n is the mean of the n^{-th} internal X_u; $X_{t,n}$ is the cumulative dispersion of the n^{-th} interval; u is the time series. Also,

$$R = \max\left(X_{t,n}\right) - \min\left(X_{t,n}\right) \quad \text{(Eq.12)}$$

where $\max(X_{t,n})$ and $\min(X_{t,n})$ are the maximum and minimum values, respectively. Let S be the standard deviation of the X_u series, then the rescaled range R/S can be defined. Through long-term practice, the following relationship can be established in terms of the Hurst exponent:

$$R / S = K(n)^H \quad \text{(Eq.13)}$$

http://www.aloki.hu ● ISSN 1589 1623 (Print) ● ISSN 1785 0037 (Online)
DOI: http://dx.doi.org/10.15666/aeer/1802_32113242

where H is the Hurst exponent and K(n) is a constant. Logarithm is taken on both sides to calculate the Hurst exponent, which can be used to measure the trend intensity and noise level variation over time. It is a measure of statistical correlation of time series (Zhao, et al., 2000).

Based on the above methods, first, a linear regression analysis was performed for the 19 extreme climate indices, and the spatio-temporal variation trend for each extreme climate index from 1968 to 2017 was obtained. In order to identify the major stages in the variation, a Mann-Kendall trend test and sliding T test were respectively implemented. By comparing and verifying the results of the two tests already mentioned, the year of abrupt change was determined. Next, a wavelet analysis with high resolution for the waveform characteristics was used to derive the periodic features of the climatic index changes. Given the relevant influence of terrain on climate, a correlation analysis between climate indices and geographical factors was performed. With this, it was possible to measure such degree of influence. Finally, R/S analysis was done with the purpose of predicting future climate trends in the Sichuan Province.

Results

Spatio-temporal variation characteristics of extreme temperature indices

Interannual temporal variations

Extreme weather events refer to a kind of rare events occurring at a specific area and time. The occurrence of extreme weather events can be estimated using extreme climate indices. *Figure 3* displays the interannual variation trend for extreme temperature indices observed in the Sichuan Province from 1968 to 2017. Specifically, *Figure 3a-e* shows the five extreme cold indices FD, Tnn, Tnx, Tn10, and Tx10, among the ten extreme temperature indices, where linear tendency rates indicated either a decreasing or a warming trend. The inter-decadal variation tendency rates for those indices were -133.73d/10a, 0.64 °C/10a, 0.23 °C/10a, -296.75d/10a, and -132.97d/10a, respectively. In *Figure 3f-j,* the five extreme warm indices include SU, Txn, Txx, Tn90, and Tx90, where their linear tendency rates indicated either an increasing or a warming trend. In this case, the inter-decadal variation tendency rates were 32.30d/10a, 0.28 °C/10a, 0.39 °C/10a, 272.1d/10a, and 273.7d/10a, respectively. For all these results, the tendency rates complied with the 0.05 significance level test. In addition, it was observed that the FD, Tnn, and Tx90 variation amplitudes were significantly higher than those corresponding to SU, Txn and Tx10 values. These results represented an asymmetry in temporal variation features of the extreme cold and warm indices. Generally speaking, warming was predominant in the Sichuan Province, which is a region with positive response to global warming.

Figure 4 shows the spatial distribution for the regression coefficients of extreme temperature indices observed in 39 meteorological stations of the Sichuan province for the past 50 years. Results indicated that among the five extreme cold indices, FD, Tn10, and Tx10 showed a decreasing trend in space, while Tnn and Tnx were the opposite. In general, the 5 extreme warm indices showed a warming or increasing trend, which was consistent with the interannual variation. For all these results, the regression coefficients complied with the 0.05 significance level test. The overall FD reduction was of -10~0d/10a, and the Muli Station displayed the largest reduction data

http://www.aloki.hu ● ISSN 1589 1623 (Print) ● ISSN 1785 0037 (Online)
DOI: http://dx.doi.org/10.15666/aeer/1802_32113242

with an inter-decadal variation of-19.5d/10a; Yuexi was the only station with a positive increase, showing an inter-decadal variation of 0.3d/10a. These two stations are both located in the MSW. More significant changes were observed in the mountainous regions, where the highest average variation rate was of -5.73d/10a. These types of changes were mostly insignificant in the basin regions, where the lowest average variation rate was obtained as -1.51d/10a. The overall Tnn increasing range was 0~0.5 °C/10a, and the fastest increase was found at the Muli Station (1.1 °C/10a). Tnn decreased only at the Yuexi Station (-0.21 °C/10a). These two stations are located in the mountainous region. The average variation trend of Tnn was 0.46 °C/10a in the MSW vs. 0.55 °C/10a in the PNW (a total of 9 stations had a variation rate larger than 0.5 °C/10a). The ESB displayed the smallest variation (0.27 °C/10a). Regarding Tnx, the Muli Station showed the highest increasing trend (0.64 °C/10a). In addition, only the Shaojue Station contained a negative change, which was -0.05 °C/10a. Among different terrain types, the largest average increasing trend was obtained in the PNW (0.29 °C/10a).

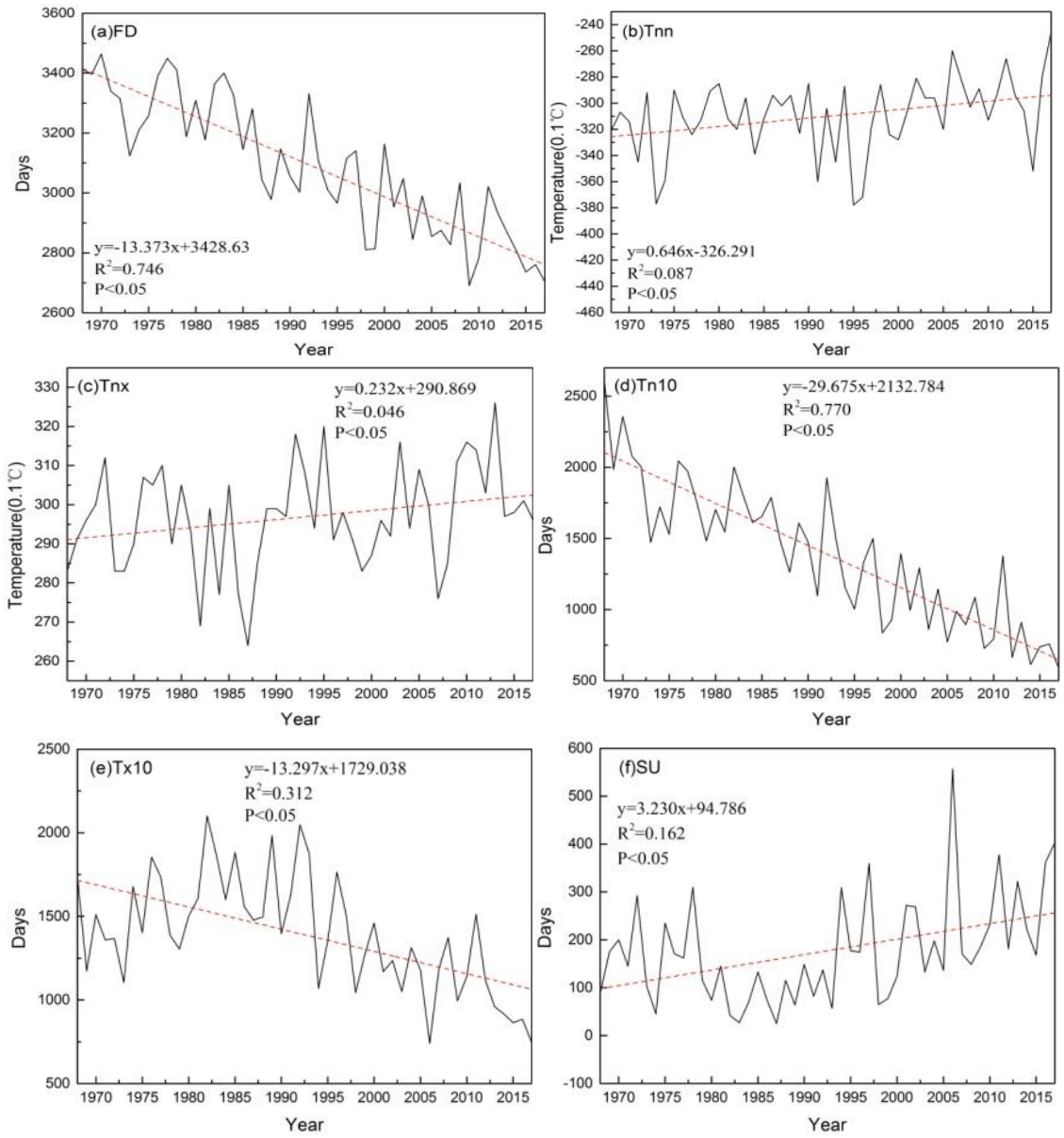

http://www.aloki.hu ● ISSN 1589 1623 (Print) ● ISSN 1785 0037 (Online)
DOI: http://dx.doi.org/10.15666/aeer/1802_32113242

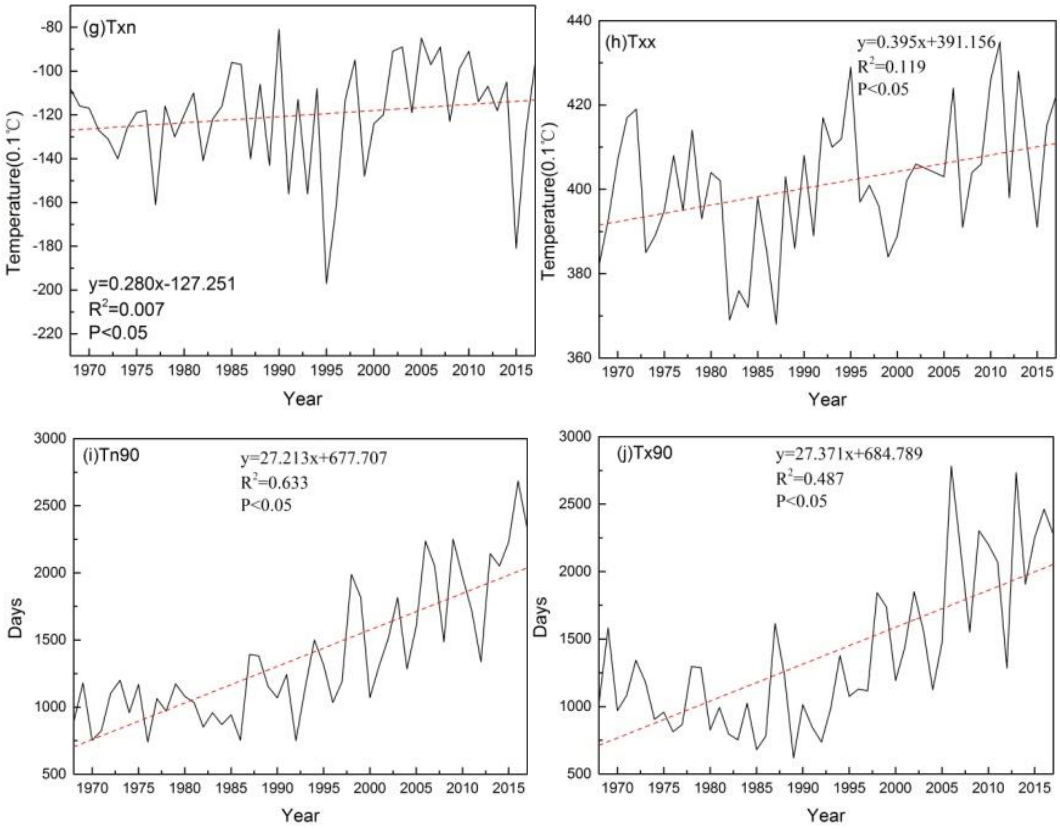

Figure 3. *Interannual temporal change trends of 10 extreme temperature indices from 1968 to 2017. (a) Frost days (FD), (b) Min Tmin (Tnn), (c) Max Tmin (Tnx), (d) Cool nights (Tn10), (e) Cool days (Tx10), (f) Summer days (SU), (g) Min Tmax (Txn), (h) Max Tmax (Txx), (i) Warm nights (Tn90),(j) Warm days (Tx90)*

Spatial change trends

It was also observed that Tn10 values gradually decreased from west to east. That is, the variation in the PNW (-9.0d/10a) was higher than that observed in the MSW (-8.5d/10a) as well as than that in the ESB (-6.0d/10a). In addition, the largest reduction was found at the Muli Station, which value was of -21.0d/10a. The Tx10 reduction range in the MSW (-4.7d/10a) was greater than those in both, the PNW (-3.7d/10a) and the ESB (-2.6d/10a). The largest reduction was determined at the Leibo Station, which was -11.9d/10a. Comparing the values for different terrain types, the average SU increase was larger in the ESB (1.7d/10a) than those in the PNW (0.05d/10a) and MSW (0.2d/10a). 13 stations in the plateau and 4 stations in the mountainous region showed a value of 0d/10a. In the case of Txn and Txx results, most of the stations showed an increasing trend, with an amplitude of 0~0.5 °C/10a. Also, the increasing rate value in the MSW (0.41 °C/10a, 0.4 °C/10a) was larger than those obtained for the PNW (0.31 °C/10a, 0.32 °C/10a) and the ESB (0.23 °C/10a, 0.39 °C/10a). The station with the highest increase (1.09 °C/10a, 0.78 °C/10a) was the Leibo Station, which is located in the mountainous area. Growth trends of Tn90 and Tx90 gradually decreased from west to east, and the increase was the fastest in the mountainous region (8.0d/10a, and 10.3d/10a, respectively). The largest increase was also found at the Muli Station in the mountainous area (19.2d/10a, 17.7d/10a).

http://www.aloki.hu ● ISSN 1589 1623 (Print) ● ISSN 1785 0037 (Online)
DOI: http://dx.doi.org/10.15666/aeer/1802_32113242

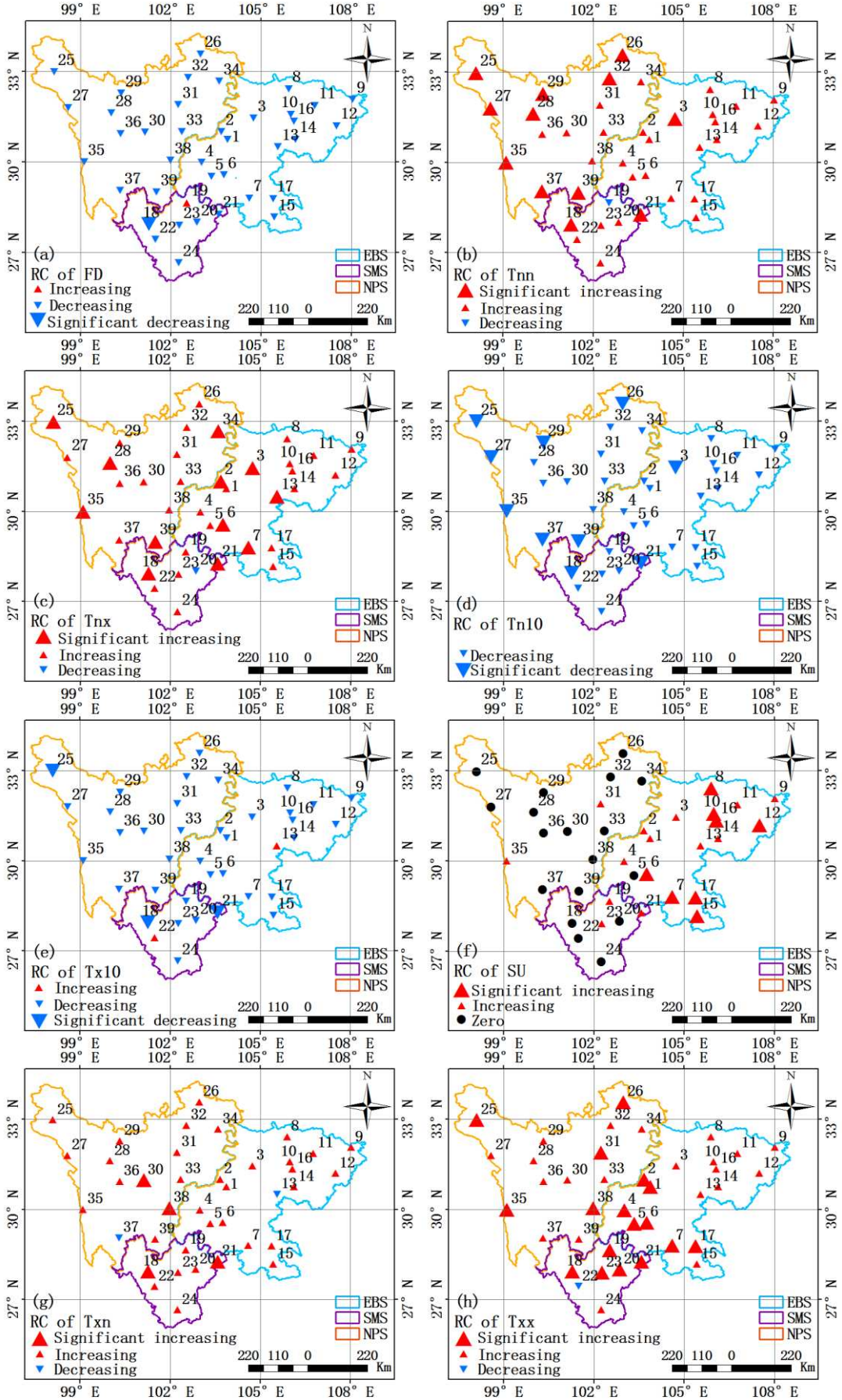

http://www.aloki.hu ● ISSN 1589 1623 (Print) ● ISSN 1785 0037 (Online)
DOI: http://dx.doi.org/10.15666/aeer/1802_32113242

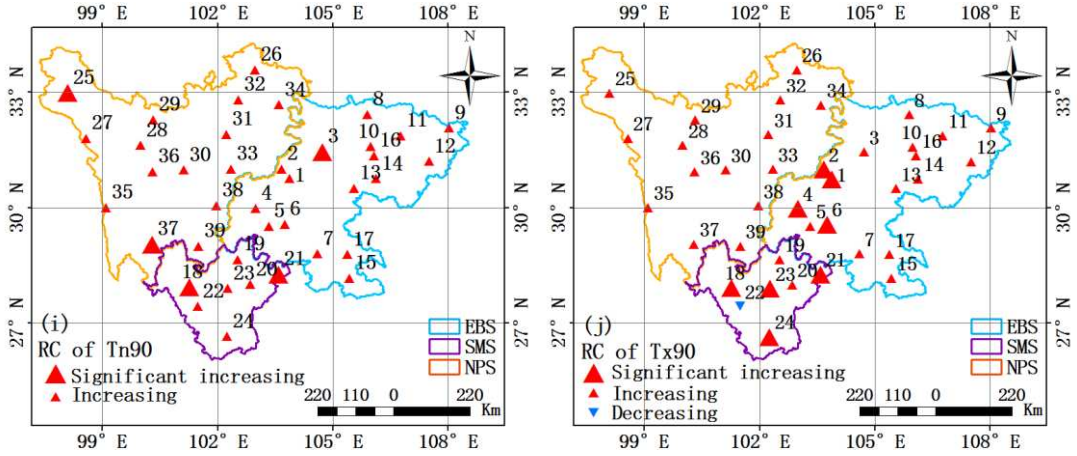

Figure 4. *Spatial change trends of 10 extreme temperature indices from 1968 to 2017, (a)Frost days (FD),(b) Min Tmin (Tnn),(c) Max Tmin (Tnx),(d) Cool nights (Tn10),(e) Cool days (Tx10), (f) Summer days (SU), (g) Min Tmax (Txn), (h) Max Tmax (Txx), (i) Warm nights (Tn90), (j) Warm days (Tx90)*

As these results showed, the extreme temperature in Sichuan exhibited an increasing trend during the past 50 years. The cold extreme events showed a warming or decreasing trend, while the warm extreme events showed a warming or increasing tendency. The variation trend in the west was more significant than that in the east, that is, the warming amplitude was higher in the PNW and MSW than in ESB. Particularly, the mountain to basin transition regions (Muli and Yuexi Station), as well as high-altitude areas were the most affected by global warming.

Mutation characteristics

Climate modifications are identified as abrupt changes in statistical spatio-temporal features, and can be represented by mutation points (Fu and Wang, 1992). To ensure the scientificity and accuracy of this research, the M-K and sliding T tests (subseries length 5) were simultaneously used for cross-validation. The purpose is to exclude false mutation points, which are identified by one of the two above-mentioned methods. This way, the reliability of the mutation analysis results is enhanced. *Table 3* shows the results for the M-K and the sliding T tests, as well as wavelet analysis for extreme temperature indices during the period of 1968 to 2017. Due to space constraints, only selected resulting diagrams are shown herein. Tnn diagrams for cold indices as well as SU diagrams for the warm indices are presented in *Figure 5*. It is important to state that other analysis yield similar results.

As shown in *Figure 5a,* the UF curve for Tnn showed overall increasing values over time. However, considering time stages, a decreasing trend was observed before the 1980s. Later, between the early 1980s and the mid-1990s, an increasing tendency occurred, followed by a slight decline. Finally, after the year of 2000, a growing trend was observed. The change was significant after 2010 ($P < 0.05$). The two UF and UB statistics intersected in the year of 2002, which indicated the starting mutation time and increasing. As data show in *Figure 5c,* the Tnn curve was both, concave and convex in shape; however, no mutation point appeared. Combining the results of the two tests, it was judged that there was no mutation year for Tnn, however this index steadily increased after the year of 2000. In *Figure 5b,* the UF curve for SU showed an

http://www.aloki.hu ● ISSN 1589 1623 (Print) ● ISSN 1785 0037 (Online)
DOI: http://dx.doi.org/10.15666/aeer/1802_32113242

increasing trend before the 1980s, while between the 1980s and the 21st century the tendency decreased. It was also observed that, before and after 1990, such decline was significant. In addition, after the 21st century SU increased, especially after 2012 when the change was significant ($P < 0.05$). The UF and UB statistics corresponding to SU intersected in 2009. This point indicated starting time of increasing change and mutation. As shown in *Figure 5d*, the t statistic exceeded the 0.05 significance level test in 1979. Since the t statistic is greater than zero, it indicated that SU experienced a significant mutation from lower to higher values in 1979. However, as two test cross-validation results indicated, no year for SU mutation occurred.

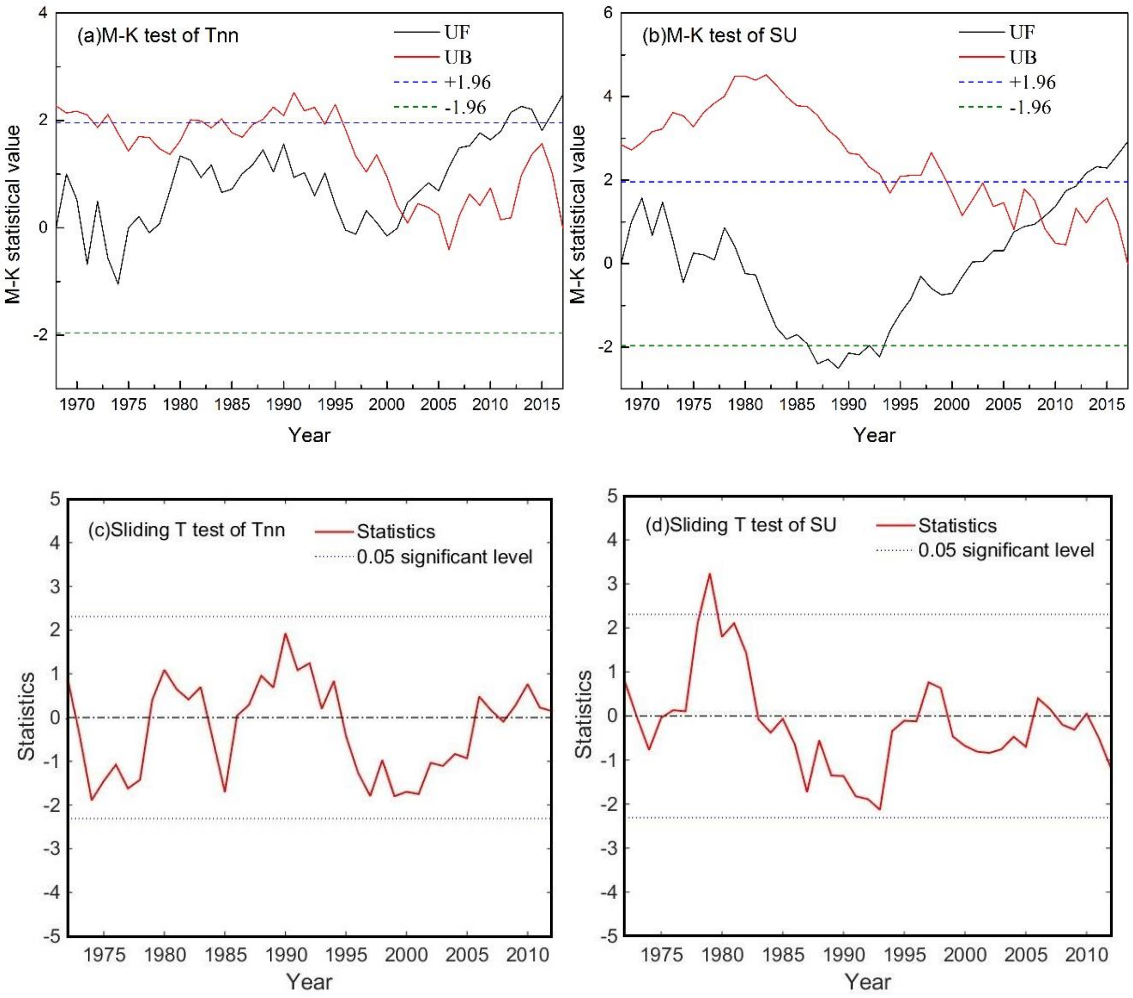

Figure 5. *M-K and sliding T test of Tnn and SU, (a) M-K test of Tnn, (b) M-K test of SU, (c) Sliding T test of Tnn, (d) Sliding T test of SU*

Table 3 displays the results of mutation points identified for all extreme temperature indices by the M-K and sliding T test. Taken together, except for the mutation year of Tnx in 1995, there were no significant mutation years in the other extreme temperature indices during the past 50 years. It was also determined that there was no significant mutation in extreme temperatures. However, increasing temperature trends were noticeable in the 1980s and the early 21stcentury.

http://www.aloki.hu ● ISSN 1589 1623 (Print) ● ISSN 1785 0037 (Online)
DOI: http://dx.doi.org/10.15666/aeer/1802_32113242

Periodic characteristics

Considering Tnn and SU as references, a detailed analysis in terms of wavelet periodic characteristics were performed (*Fig. 6*). *Figure 6a, d* shows the corresponding normalized time series. The threshold for the Tnn time series varied within ± 2.5 and changes were not significant. The threshold for the SU time series was about ± 2, with only a significant increase in the normalized value for the year of 2006. *Figure 6b, e* shows the wavelet power spectrum, which represents the fluctuation magnitude of the time series on the given wavelet scale and within a given time domain. The larger the wavelet power, the greener the color. The inverted cone-shaped lines in the figure correspond to the influence lines. The portion of the wavelet power spectrum below these influence lines indicates the marginal influence effect. Also, periodic features exhibit a greater uncertainty. Closed curves in the spectrum are related to regions with high power values. Tnn and SU closed regions corresponded to periods of significant interannual variation, which were all 2-6 years in length. Intense periodic change effects on this scale occurred in 1968~1980 and 1982~2017 for Tnn, while for SU happened from 1968 to1982 and from 1991 to 2017. Since time series variances of many physical quantities increase with time (red noise features), these red noises can be used as background when performing wavelet spectrum analysis. *Figure 6c, f* represents the full wavelet spectrum obtained when significance test is applied to the wavelet spectrum. When the solid lines (wavelet power spectrum curve) are smaller than the dotted line (this line represents the 0.05 significance level), it means that the periodic feature corresponding to this region passed the 0.05 significance level test. Thus, according to the data obtained, every Tnn and SU period that passed the significance test previously mentioned was all 2-6 years. In addition, when the period was 6 years long, the energy and oscillation were the strongest. As shown in the wavelet analysis results, between all the extreme temperature indices included in *Table 3,* the Txn period that passed the significance test was also the one which was 2-6 years. However, FD and Tn10 did not show significant wavelet periods. The periods for Tnx and Txx that passed the significance test were all 2-4 years, and for Tx10, Tn90 and Tx90 were all 3-4 years.

Table 3. *M-K test, sliding T test and wavelet analysis results of 10 extreme temperature indices*

Indices	M-K test	Sliding T test	Mutation years	Wavelet significant periods
FD	1993	1984,1985,1986	No	No
Tnn	2002	No	No	2~6
Tnx	1969,1973,1976,1979,1992,1995,2002	1988,1990,1995, 2008	1995	2~4
Tn10	1990	1976,2010	No	No
Tx10	1969,2005,2006,2007	No	No	3~4
SU	2009	1979	No	2~6
Txn	1985,1986,1988,1990,1997	No	No	2~6
Txx	2005	1980,1981,1987,1989,1991,1995,1996,2000,2001	No	2~4
Tn90	2015	1980,1981, 2009,2010,2011	No	3~4
Tx90	1970,2005,2006,2012,2014	No	No	3~4

http://www.aloki.hu ● ISSN 1589 1623 (Print) ● ISSN 1785 0037 (Online)
DOI: http://dx.doi.org/10.15666/aeer/1802_32113242

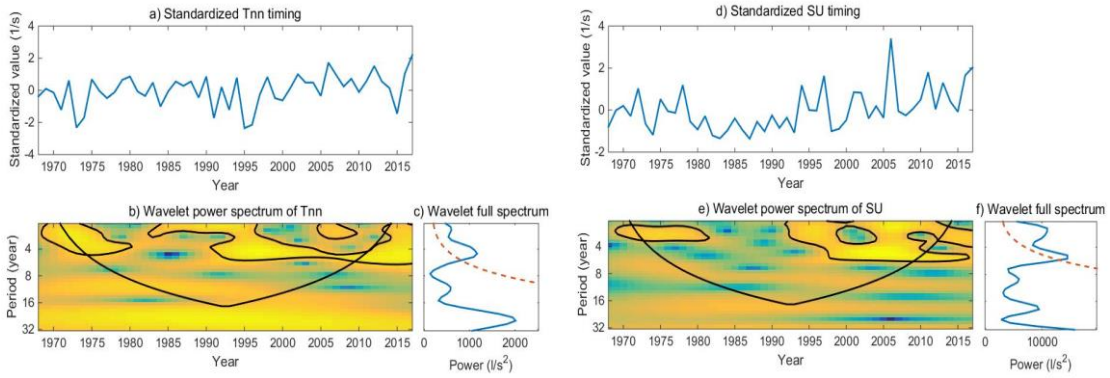

Figure 6. *Wavelet analysis of Tnn and SU. (a) Standardized Tnn timing, (b) Wavelet power spectrum of Tnn, (c) Wavelet full spectrum of Tnn, (d) Standardized SU timing, (e) Wavelet power spectrum of SU, (f) Wavelet full spectrum of SU*

Spatial and temporal variation characteristics of extreme precipitation indices

Interannual temporal variations

Considering the integrity and uniformity of data, 5 stations, namely, Batang (No.35), Huili (No.24), Guangyuan (No.8), Daxian (No.12), and Xuyong (No.15) where the precipitation data were incomplete, were excluded when analyzing extreme precipitation events in Sichuan. Therefore, only 34 stations were included in this type of analysis. As observed from the interannual variation trend of 9 extreme precipitation indices (*Fig. 7*), extreme precipitation occurred in the past 50 years; in addition, in the days of these events larger fluctuations were observed. Overall trend variation was not obvious, though. Also, R10, R95p, R99p and SDII displayed a mild increasing trend, with interannual variation tendency rate of 0.9d/10a, 79.5 mm/10a, 160.6 mm/10a and 0.05(mm/d)/10a, respectively. All remaining indices (CDD, CWD, R20, R50, and PRCPTOT) exhibited decreasing tendencies, with inter-decadal variation rates of -0.8d/10a, -0.4d/10a, -0.1d/10a, -0.5d/10a and -39.5 mm/10a, respectively. Inter-decadal variation tendency rates of every station analyzed in this research passed the 0.05 significance level test. On an overall perspective, the interannual variation of the extreme precipitation indices in Sichuan was not significant for the past 50 years. Nevertheless, some violent fluctuations occurred. Moreover, data also indicated that a regional peak appeared every 5 years.

Spatial change trends

Figure 8 shows the spatial distribution of extreme precipitation indices at 34 stations during the past 50 years. In the PNW area, CDD mostly showed a decreasing trend, with an average variation of -0.81d/10a. In contrast, in the MSW and ESB areas, this same index showed an increasing trend, with an average variation of1.57d/10a and 0.82d/10a, respectively. In every Sichuan region, except for 8 stations, CWD decreased. Among all geographical areas analyzed, the average PNW variation rate was of 0.04 d/10a, and those corresponding to MSW and ESB were -0.25 d/10a and -0.18 d/10a, respectively. R10 and R20 PNW showed an increasing trend (0.55d/10a, and 0.14d/10a, in that order), and the R50 variation rate at 12 stations was of 0d/10a. Thus, R50 for the PNW region basically remained unchanged (0.007d/10a). R10, R20,

http://www.aloki.hu ● ISSN 1589 1623 (Print) ● ISSN 1785 0037 (Online)
DOI: http://dx.doi.org/10.15666/aeer/1802_32113242

and R50 variation rates for the MSW area were of -0.03d/10a, 0.12d/10a, and 0.10d/10a, respectively. Values decreased in the ESB, where R10, R20 and R50 reduction rates were -0.40d/10a, -0.22d/10a, and -0.11d/10a, in that order. R95p and R99p showed an increasing trend, and PRCPTOT decreased. In general, the average variation rates of these three indices in PNW were 9.97 mm/10a, 6.70 mm/10a, and 12.64 mm/10a, respectively; those in the MSW region were 7.85 mm/10a, 4.68 mm/10a, and 1.37 mm/10a, in that order. However, the variation trend in ESB was slightly different (variation rates were -7.64 mm/10a, 2.06 mm/10a, and -15.56 mm/10a, correspondingly). SDII mostly increased in PNW and MSW (variation rates were 0.008 (mm/d)/10a and 0.003 (mm/d)/10a, respectively). However, a decreasing trend was observed in ESB, where the variation rate was -0.005 (mm/d)/10a. As shown, variation amplitude was rather small. According to the previous analysis, there were noticeable spatial and regional differences in the extreme precipitation events in Sichuan during the past 50 years. Precipitation increased in PNW and MSW, and significantly decreased in ESB. In particular, precipitations registered in the Ya'an, Emeishan, and Leshan Station where the precipitation used to be very abundant, showed a decrease. Among different regions, the precipitation as well as extreme precipitation events in PNW and MSW considerably increased. In detail, the number of heavy rain, rainstorm and very heavy precipitation events in the plateau increased. There was also arise in the number of extreme precipitation events in the mountainous regions. However, the amplitude was not as large as that observed in the plateau. The basin, however, displayed a drying trend with decreased precipitation, and the extreme precipitation was also reduced.

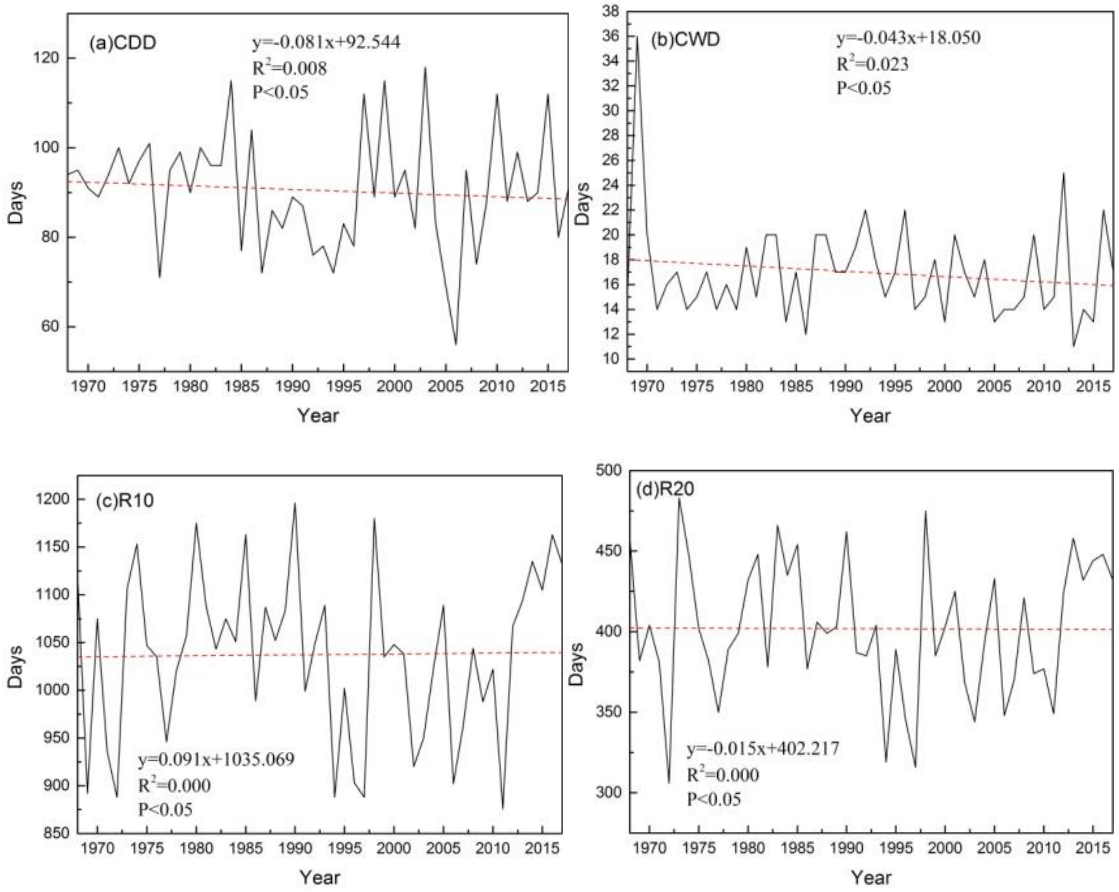

http://www.aloki.hu ● ISSN 1589 1623 (Print) ● ISSN 1785 0037 (Online)
DOI: http://dx.doi.org/10.15666/aeer/1802_32113242

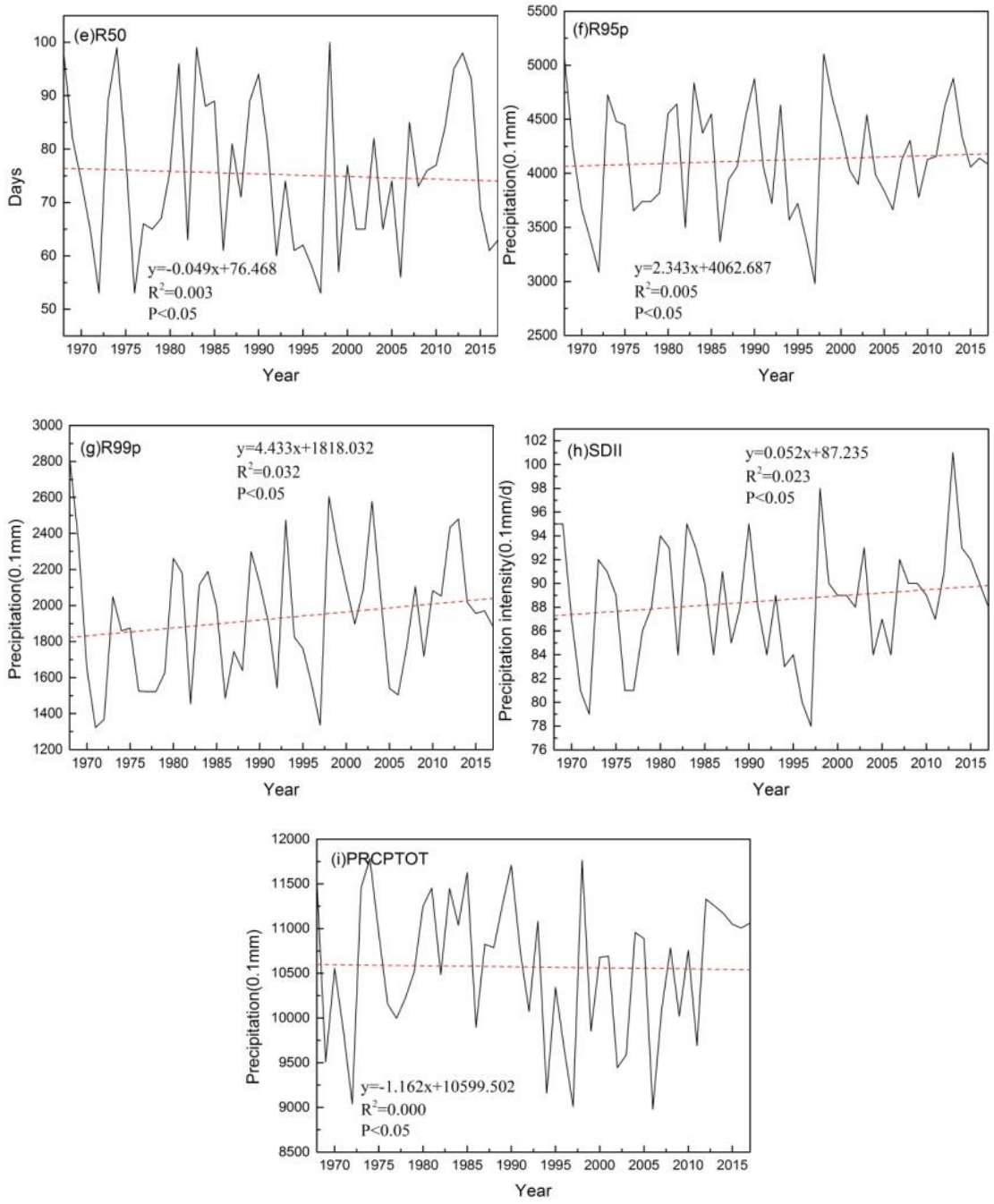

Figure 7. *Interannual temporal change trends of 10 extreme precipitation indices from 1968 to 2017. (a) Consecutive dry days (CDD), (b) Consecutive wet days (CWD), (c) Number of heavy precipitation days (R10), (d) Number of very heavy precipitation days (R20), (e) Number of rainstorm days (R50), (f) Very wet days (R95p), (g) Extremely wet days (R99p), (h) Simple daily intensity index (SDII), (i) Annual total wet-day precipitation (PRCPTOT)*

Mutation characteristics

Table 4 shows the results when extreme precipitation indices from 1968 to 2017 were assayed using the M-K test, sliding T test, and wavelet analysis. The process was similar to that applied to the extreme temperature indices. Only the CWD and

http://www.aloki.hu ● ISSN 1589 1623 (Print) ● ISSN 1785 0037 (Online)
DOI: http://dx.doi.org/10.15666/aeer/1802_32113242

PRCPTOT test results were analyzed as examples. *Figure 9* shows the M-K test and sliding T test statistical diagrams for these two indices. As our results showed, the CWD UF curve displayed an increasing trend during the period going from the 1980s to the early 21st century; also, in 1996 this curve over passed the 0.05 significance level line (*Fig. 9a*). CWD significantly increased in 1996, and after this point, it started decreasing. Moreover, UF and UB statistics intersected in 2013 and 2015. The CWD t-test statistic showed a wavy fluctuation, where no significant values or mutation points occurred (*Fig. 9c*). Combining the results of the two tests, it was concluded that there was no mutation year. For PRCPTOT (*Fig. 9b*), the intersections between the UF and UB statistics first occurred in 1973, and later in 1991, 2012, and 2014, successively. Combining this with the sliding T test results for the mutation points (*Fig. 9d*), it was verified that these were true in 1991. Due to limited space, other indices do not be analyzed in detail. A summary of the results is shown in *Table 4*. Taken together, CDD, CWD, R10, R20, and SDII extreme precipitation indices did not show significant mutation years in the past 50 years. In addition, mutation years for R50, R95p, R99p, and PRCPTOT occurred in 1980, 2010, 2004, and 1991, respectively. This means that mutation years corresponding to heavy and very heavy precipitation events mainly appeared in the 1980 and the early 21st century.

Table 4. *M-K test, sliding T test and wavelet analysis results of 9 extreme precipitation indices*

Indices	M-K test	Sliding T test	Mutation years	Wavelet significant periods
CDD	1970,1971,1984,1985,1986	1996,2003,2008	No	2~4
CWD	2013,2015	No	No	2~5
R10	1973,1975,1979,1989,1990,1991,2015	1992,2011,2012	No	2~6
R20	1974,1980,1981,1985,2015	1979,2011,2012	No	2~6
R50	1968,1973,1980,1981,1982,1985,2010,2015	1979,1980,1991, 1992,2008,2009	1980	2~7
R95p	1981,1983,2010	2009,2010,2011	2010	2~7
R99p	1997,2001,2003, 2004,2008	1979,2004,2009,2010,2011	2004	2~6
SDII	1969,1981,1983,1985,2007	1979,1991,1997	No	2~7
PRCPTOT	1973,1991,2012,2014	1979,1980,1991,2011	1991	2~6

Periodic characteristics

As previously mentioned, detailed analysis was performed for CWD and PRCPTOT test results in terms of wavelet cycle features (*Fig. 10*). *Figure 10a, d* shows the normalized time series. The threshold for CWD and PRCPTOT time series was about ± 2, and the normalized CWD value significantly increased in 1969. *Figure 10b, e* shows the wavelet power spectrum. The CWD closed region corresponded to a period of 2-7 years and that of PRCPTOT corresponded to a period of 2-8 years. In other words, intervals of significant interannual variation were of 2-7 and 2-8 years for CWD and PRCPTOT, correspondingly. Strong concentration periodic change effects on this scale appeared in the intervals 1968~1975, 1977~2002, and 2006~2017 for CWD. Also, in the case of PRCPTOT, time domains were 1968~1980 and 1982~2012. Red noises

http://www.aloki.hu ● ISSN 1589 1623 (Print) ● ISSN 1785 0037 (Online)
DOI: http://dx.doi.org/10.15666/aeer/1802_32113242

were used as background for the analysis of the wavelet spectrum. *Figure 10c, f* presents the full wavelet spectrum corresponding to the CWD and PRCPTOT period that passed the significance test. These periods were 2-4 and 2-6 years, respectively. The interval with the strongest wavelet energy was 4 years in length and that of PRCPTOT was 3 years. As indicated in *Table 4* that corresponds to the wavelet analysis of all extreme precipitation indices, periods where R10, R20, and R99p passed the significance test were also from 2-6 years. In the case of R50, R95p and SDII, interval was 2-7 years, and for CDD, it was 2-4 years.

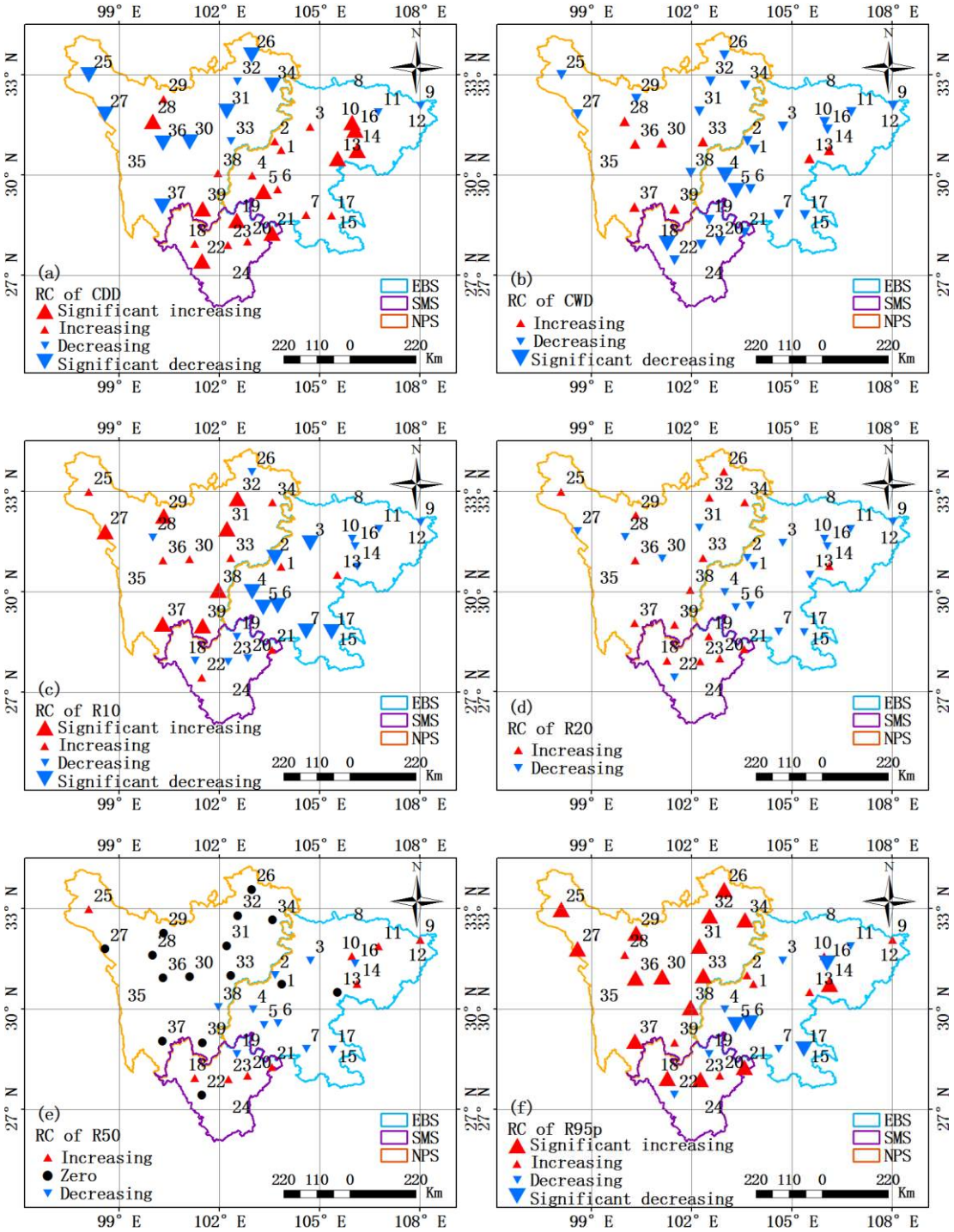

http://www.aloki.hu ● ISSN 1589 1623 (Print) ● ISSN 1785 0037 (Online)
DOI: http://dx.doi.org/10.15666/aeer/1802_32113242

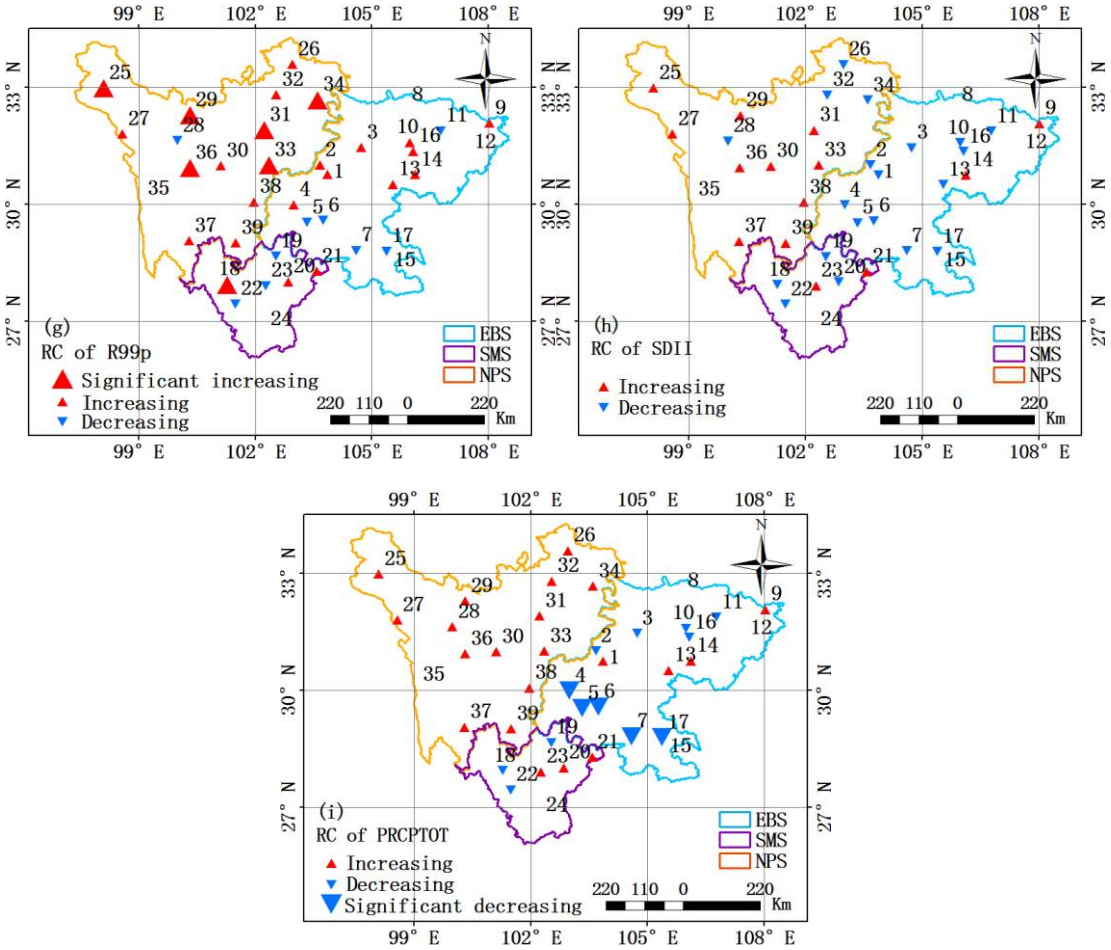

Figure 8. *Spatial change trends 0f 9 extreme precipitation indices from 1968 to 2017. (a) Consecutive dry days (CDD), (b) Consecutive wet days (CWD), (c) Number of heavy precipitation days (R10), (d) Number of very heavy precipitation days (R20), (e) Number of rainstorm days (R50), (f) Very wet days (R95p), (g) Extremely wet days (R99p), (h) Simple daily intensity index (SDII), (i) Annual total wet-day precipitation (PRCPTOT)*

Relationship between extreme climate index and geographical factors

According to the spatial distribution and regional difference analyses for extreme climate indices, it was demonstrated that topographical changes greatly affect extreme climate changes in the Sichuan Province. This region is roughly limited by the Guangyuan-Jiangyou-Dujiangyan-Yingjing-Muli line, and the topography is high to the northwest and low to the southeast. Extreme climate indices changes are highly related to longitude, latitude and altitude. In this research, the influence of these parameters on extreme climate indices was discussed (*Table 5*). Correlation analysis showed that Tnn, Tnx, SU, Txn and Txx were negatively correlated to elevation ($P < 0.01$), and positively to longitude ($P < 0.05$). Tnn, Tnx, Txn and Txx were negatively correlated to latitude; however, only Tnn and Txn passed the test at the 0.05 significance level. This indicated that the higher the altitude, the lower the longitude and the lower the latitude, the closer to the southwestern mountain area of Sichuan, the greater the change of the given extreme index value. Warmer extreme minimum and extreme maximum temperatures mainly occurred in the western alpine plateau area, and the warming range was larger as

http://www.aloki.hu ● ISSN 1589 1623 (Print) ● ISSN 1785 0037 (Online)
DOI: http://dx.doi.org/10.15666/aeer/1802_32113242

compared to that of the eastern basin. FD and Tn10 were positively correlated to elevation ($P < 0.01$) and latitude ($P < 0.05$), and negatively to longitude ($P < 0.05$). This indicated that the higher the altitude, the higher the latitude and the lower the longitude, the closer the alpine plateau area in northwest Sichuan, the greater the change of extreme index value, the greater the reduction of extreme cold events in the west, and the smaller the reduction in the eastern basin. There was no significant correlation between other extreme climate indices (Tx10, Tn90 and Tx90) and geographical factors. Of the extreme precipitation indices, CDD, CWD and SDII positively correlated to elevation ($P < 0.01$), and negatively to longitude (except SDII, others passed the test at the 0.05 significance level); other indices (R10, R20, R50, R95p, R99p, PRCPTOT) negatively correlated to elevation and latitude, and positively to longitude, and most of them passed the test at the 0.05 significance level. This indicated that the higher the altitude, the lower the longitude and the higher the latitude, the closer the plateau and mountainous area in west Sichuan, the greater the change of extreme index value. These results were consistent with those of the spatial distribution for the extreme climate indices previously mentioned. Terrain characteristics affect spatial variation of extreme climate indices in Sichuan Province.

Table 5. *Correlation analysis between extreme climate indices and geographical factors*

Extreme temperature indices	Longitude	Latitude	Elevation	Extreme precipitation indices	Longitude	Latitude	Elevation
FD	-0.465**	0.444**	0.940**	CDD	-0.380*	-0.231	0.479**
Tnn	0.452**	-0.447**	-0.899**	CWD	-0.510**	0.036	0.733**
Tnx	0.518**	-0.263	-0.982**	R10	0.147	-0.402*	-0.213
Tn10	-0.330*	0.344*	0.658**	R20	0.402*	-0.372*	-0.640**
Tx10	-0.193	-0.149	0.206	R50	0.506**	-0.078	-0.720**
SU	0.362*	0.009	-0.702**	R95p	0.545**	-0.180	-0.820**
Txn	0.338*	-0.397*	-0.753**	R99p	0.548**	-0.122	-0.838**
Txx	0.439**	-0.198	-0.891**	SDII	-0.266	0.540**	0.517**
Tn90	-0.028	0.203	0.199	PRCPTOT	0.417*	-0.336	-0.578**
Tx90	0.023	0.387*	-0.012				

**Passing the test at the 0.01 significance level ($P < 0.01$). *Passing the test at the 0.05 significance level ($P < 0.05$)

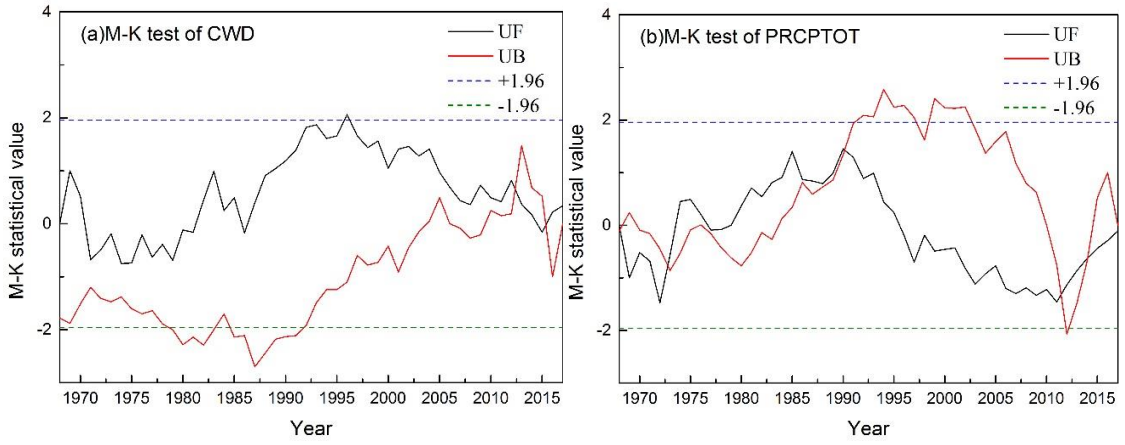

http://www.aloki.hu ● ISSN 1589 1623 (Print) ● ISSN 1785 0037 (Online)
DOI: http://dx.doi.org/10.15666/aeer/1802_32113242

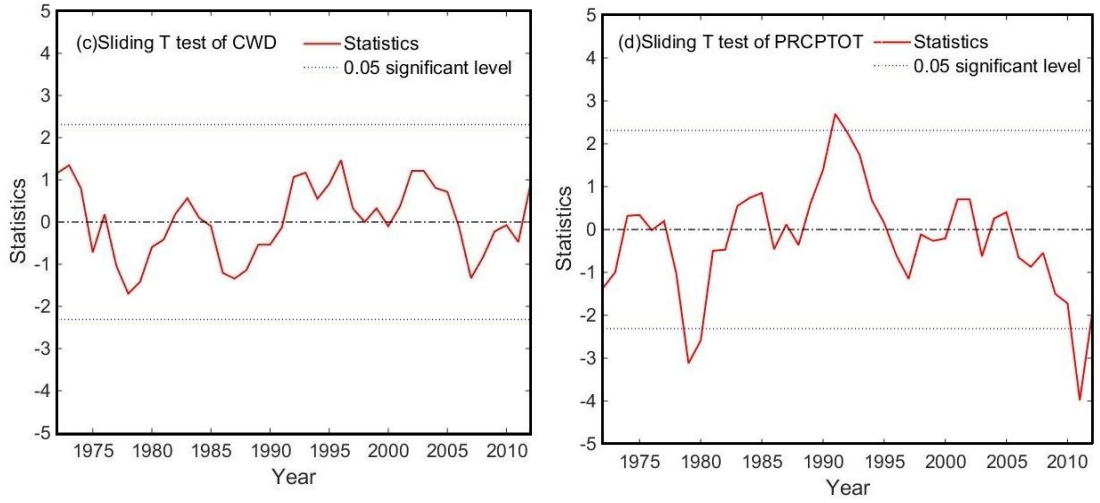

Figure 9. *M-K and sliding T test of CWD and PCRPTOT. (a) M-K test of CWD, (b) M-K test of PCRPTOT, (c) Sliding T test of CWD, (d) Sliding T test of PCRPTOT*

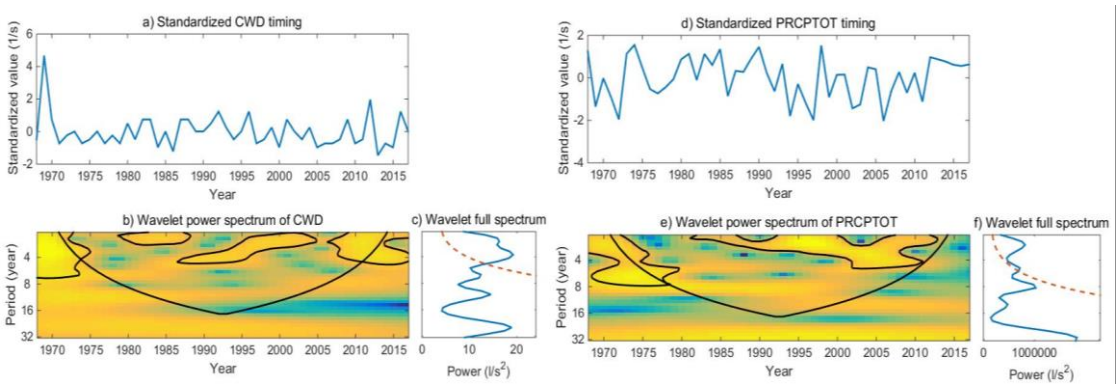

Figure 10. *Wavelet analysis of CWD and PCRPTOT. (a) Standardized CWD timing, (b) Wavelet power spectrum of CWD, (c) Wavelet full spectrum of CWD, (d) Standardized PCRPTOT timing, (e) Wavelet power spectrum of PCRPTOT, (f) Wavelet full spectrum of PCRPTOT*

Change trends of extreme temperature and precipitation in the future

In order to analyze future variation trends of extreme climate indices in Sichuan, Hurst exponents were calculated for every 19 extreme climate indices, and the results are shown in *Table 6*. As data indicated, Tn10, Tx10, SU, and Tn90 Hurst exponents were all obtained with values above 0.5, which indicated the hidden long-term trend in the time series, i.e., strong long-term memory and a positive effect as well as a high probability of continuing the current trend. The Hurst FD, Txx, R10, R20, R50, and PRCPTOT exponents were all smaller than 0.5, indicating that the time series was either not persistent or persistent in the inverse state. According to these results, they might well mark the beginning of weakened memory and inversion. The Hurst Tnn, Tnx, Txn, Tx90, CDD, CWD, R95p, R99p, and SDII exponents were close to 0.5, indicating that the variation approached a random series, and the accuracy of a future trend prediction decreased to a certain extent. Of all extreme climate indices, the Hurst exponent for

http://www.aloki.hu ● ISSN 1589 1623 (Print) ● ISSN 1785 0037 (Online)
DOI: http://dx.doi.org/10.15666/aeer/1802_32113242

Tn90 was the largest (0.802), and that of the PRCPTOT was the smallest (0.320). This was significantly greater (less) than the critical value of the random walk hypothesis. This means that an apparent positive (negative) continuity and fractal structure resulted in the time series. This is, an increment in the past might represent an increment (decrement) in the future. By combining the Hurst exponent analysis and the interannual variation trends for the 19 extreme climate indices (*Figs. 3* and *7*), it was determined that among all extreme temperature indices in Sichuan, FD, SU, and Tn90 may increase in the future. Conversely, Tn10, Tx10, and Txx may decrease, i.e., as a whole, extreme cold events will decrease and extreme warm events will increase. Of all extreme precipitation indices, R20, R50 and PRCPTOT may increase, while R10 may decrease. That is, it is very likely that the precipitation and the number of heavy precipitation and rainstorm events will increase in the future, and that both, the extreme temperature and extreme precipitation events of the Sichuan Province, will increase in the future.

Table 6. *Hurst exponents of 19 extreme climate indices*

Extreme temperature indices	Hurst exponents	Extreme precipitation indices	Hurst exponents
FD	0.353	CDD	0.440
Tnn	0.428	CWD	0.442
Tnx	0.433	R10	0.338
Tn10	0.556	R20	0.362
Tx10	0.691	R50	0.412
SU	0.570	R95p	0.446
Txn	0.440	R99p	0.494
Txx	0.405	SDII	0.493
Tn90	0.802	PRCPTOT	0.320
Tx90	0.473		

Conclusions and discussion

Under the general context of global warming, this study used daily meteorological data at 39 stations from MDSCC for the period 1968 to 2017. The 19 extreme climate indices recommended by the WMO were selected. Linear regression analysis, M-K test, sliding T test, wavelet analysis, correlation analysis and R/S analysis were performed for these indices. The interannual spatio-temporal variations, mutation and period features of extreme temperature and precipitation of Sichuan in the past 50 years were analyzed. On this basis, we further discussed the correlation between the extreme climate indices and geographical factors. Finally, some future trends were predicted based on the Hurst exponents. The main conclusions and discussion will cover the five aspects of this research.

(1) As to interannual temporal variations in the past 50 years (*Fig. 3*), in five extreme cold indices, the linear tendency rates of FD, Tn10 and Tx10 showed a decreasing trend, while those of Tnn and Tnx showed a warming trend. The five extreme warm indices include SU, Txn, Txx, Tn90 and Tx90, where their linear tendency rates indicated either an increasing or a warming trend. That is, most of extreme cold indices of Sichuan showed a decreasing trend, while the extreme warm indices showed a warming trend. Moreover, there was an asymmetry in temporal variation features of the extreme cold

http://www.aloki.hu ● ISSN 1589 1623 (Print) ● ISSN 1785 0037 (Online)
DOI: http://dx.doi.org/10.15666/aeer/1802_32113242

and warm indices. Generally speaking, warming was predominant in the Sichuan Province. The results observed are in agreement with other research previously carried out in the Southwestern China (Sun, et al., 2012; Qin, et al., 2015; Yuan and Zheng, 2015; Luo, et al., 2016) and Sichuan Province (Sun, et al., 2017). However, the inter-decadal variation tendency rates of extreme temperature indices are different. For instance, Sun et al. (2017) found that the inter-decadal variation tendency rates for Txx, Txn, Tnx and Tnn were 0.4 °C/10a, 0.3 °C/10a, 0.2 °C/10a, 0.3 °C/10a, respectively. The discrepancies may be caused by the data with different time periods and number of different meteorological stations used in the two studies.

The interannual variation of the extreme precipitation indices in Sichuan was not significant for the past 50 years (*Fig. 4*). Among them, R10, R95p, R99p and SDII displayed a mild increasing trend, and all remaining indices of CDD, CWD, R20, R50 and PRCPTOT exhibited decreasing tendencies. Nevertheless, some violent fluctuations occurred, and a regional peak appeared every 5 years. The temporal trends in our work are similar to previous studies in reporting trends of precipitation extremes over the past few decades in the Southwestern China (Sun, et al., 2012; Yuan, et al., 2014; Luo, 2015; Qin, et al., 2015) and Sichuan Province (Sun, et al., 2017; Li, et al., 2019a). For example, in Li's work (2019a), they found the trends in extreme precipitation indices constituted slight changes in the Sichuan Province and extreme precipitation was a fluctuation process from 1961 to 2017. Results showed that the ENSO (El Niño-Southern Oscillation, ENSO) events have long and strong relations with extreme precipitation. Sun et al. (2017) noted that the overall change trend of precipitation in Sichuan Province was not significant from 1971 to 2012.

(2) As to spatial change trends (*Fig. 7*), among 5 extreme cold indices, FD, Tn10 and Tx10 showed a decreasing trend in space, while Tnn and Tnx were the opposite. The 5 extreme warm indices showed a warming or increasing trend. The extreme temperature in Sichuan exhibited an increasing trend during the past 50 years. The cold extreme events showed a warming or decreasing trend, while the warm extreme events showed a warming or increasing tendency. The variation trend in the west was more significant than that in the east, that is, the warming amplitude was higher in the PNW and MSW than in ESB. Particularly, the mountain to basin transition regions (Muli and Yuexi Station), as well as high-altitude areas were the most affected by global warming. Li et al. (2012) studied the altitude dependency of trends of daily climate extremes in Southwestern China from 1960 to 2008. Characteristics of regional trends indicated the obvious warming with altitude. There is an enhanced sensitivity of climate extremes to elevation in southwestern China in the context of recent warming, and which are consistent with our results.

There were noticeable spatial and regional differences in the extreme precipitation events in Sichuan during the past 50 years (*Fig. 8*). Precipitation increased in PNW and MSW, and significantly decreased in ESB. In particular, precipitations registered in the Ya'an, Emeishan, and Leshan Station where the precipitation used to be very abundant, showed a decrease. Among different regions, the precipitation as well as extreme precipitation events in PNW and MSW considerably increased. In detail, the number of heavy rain, rainstorm and very heavy precipitation events in the plateau increased. There was also arise in the number of extreme precipitation events in the mountainous regions. However, the amplitude was not as large as that observed in the plateau. The basin, however, displayed a drying trend with decreased precipitation, and the extreme precipitation was also reduced. Previous studies have reported that the intensity,

http://www.aloki.hu ● ISSN 1589 1623 (Print) ● ISSN 1785 0037 (Online)
DOI: http://dx.doi.org/10.15666/aeer/1802_32113242

frequency, and duration of extreme precipitation increased in the Sichuan plateau, while the intensity and frequency of extreme precipitation decreased, but the duration of extreme precipitation did not change in the Sichuan basin (Li, et al., 2019a). Sun et al. (2017) determined that the precipitation distribution was low in the western Sichuan and high in the eastern Sichuan, and most of the extreme precipitation indices had no significant change trend. Although the average change trend and spatial distribution of CDD and CWD indicated that the Sichuan as a whole tended to dry, the humidity in some areas of the plateau increased from 1971 to 2014. Our results are roughly consistent with the previous work above.

(3) As shown by the M-K test, sliding T test and wavelet analysis (*Table 3*), of 10 extreme temperature indices, except for the mutation year of Tnx in 1995, there were no significant mutation years in the other extreme temperature indices. That is, there were no significant mutation in extreme temperature, but the increase and warming trend of temperature were obvious in the 1980s and the early 21st century. Except for FD and Tn10 that had no significant wavelet periods, Tnn, SU and Txn showed significant variation with a period of 2-6 years, and for Tnx and Txx were all 2-4 years, and for Tx10, Tn90 and Tx90 were all 3-4 years. Of 9 extreme precipitation indices (*Table 4*), except for R50, R95p, R99p and PRCPTOT that had mutation years occurred in 1980, 2010, 2004 and 1991, respectively, the other indices had no mutation years. Namely, mutation years corresponding to heavy and very heavy precipitation events mainly appeared in the 1980 and the early 21st century. Except for CDD and CWD that had significant variation with the periods of 2-4 years and 2-5 years, R50, R95p and SDII showed significant variation with a period of 2-7 years, and for R10, R20, P99p and PRCPTOT were all 2-6 years.

The method of M-K trend test is a valuable tool for effectively differentiating natural fluctuations from definite variation trends. It is a nonparametric statistical test to analyze the variation trends of climate and hydrological series over time (Song et al., 2019). But sometimes there are false mutation points in the results of the test. The method of sliding T test is also helpful in detecting climate mutations by determining if there is a significant difference in the means of two different groups. To ensure the scientificity and accuracy of this research, the M-K and sliding T tests (subseries length 5) were simultaneously used for cross-validation. By using M-K trend test, Luo et al. (2016) conducted mutation test of Tx90, Tx10, Tn90 and Tn10 in Southwestern China from 1970 to 2010. The results showed that there was an obvious mutation in the number of warm days in 2004, and there was a significant increase in the number of warm days from 2005 to 2010; the number of cold nights had an obvious mutation in 1994 and decreased significantly from 1995 to 2010; the number of cold days had a mutation in 1997, but it was not obvious; the number of warm nights had no mutation. Liu and Xu (2014) also discussed the mutation years of some extreme temperature indices in Southwestern China. Results indicated there were no mutation years of Tx90 and Tnn from 1951 to 2010; however, increasing temperature trends were noticeable in the early 21st century, which are in agreement with our results. Other discrepancies may be caused by the data with different time periods, extent of different study areas and singularity of mutation method used in the previous studies.

About the abrupt change point of extreme precipitation, Zhang and Ma (2011) indicated there was no mutation in the number of days of annual average extreme precipitation in Sichuan Province from 1961 to 2009. The intensity of extreme precipitation increased before 1990s, and there was a significant mutation point in 1980.

http://www.aloki.hu ● ISSN 1589 1623 (Print) ● ISSN 1785 0037 (Online)
DOI: http://dx.doi.org/10.15666/aeer/1802_32113242

After 1990s, the trend was decreased and there was a mutation before and after 2002, but it was not significant. Li et al. (2019a) analyzed mutation characteristics of extreme precipitation by using M-K test, and found R20, CWD and SDII were not detected the abrupt change point from 1961 to 2017 in Sichuan Province, moreover, most of the break points were in 1979 and 1991, which are consistent with our work.

Wavelet analysis can accurately provide information on local signal features in both, the time and frequency domains, and can be used for multi-scale detailed signal analysis. Luo et al. (2016) investigated the periodic characteristics of extreme temperature in Southwestern China, the results showed both the number of warm days and the number of warm nights had a short period of 3-4 years and a long period of 14 years, the number of cold days had a short period of 4 years, and two long periods of 7 years and 11 years, and the number of cold nights had a short period of 1-4 years, two long periods of 7 years and 10 years. The results of short period are in accord with our work, but the difference of long-period analysis may be caused by the data with different time periods, extent of different study areas and different specific method of wavelet analysis used in the two studies. In term of periodic characteristics of extreme precipitation, our results are roughly consistent with the previous work of Li et al. (2019a). As pointed by Li et al. (2019a), the ENSO events have the longest and strongest relations with extreme precipitation in the Sichuan Province.

(4) According to the correlation analysis between extreme temperature indices and geographical factors (*Table 5*), the results showed that Tnn, Tnx, SU, Txn and Txx were negatively correlated to elevation, and positively to longitude. Tnn, Tnx, Txn and Txx were negatively correlated to latitude. This indicated that the higher the altitude, the lower the longitude and the lower the latitude, the closer to the southwestern mountain area of Sichuan, the greater the change of the given extreme index value. Warmer extreme minimum and extreme maximum temperatures mainly occurred in the western alpine plateau area, and the warming range was larger as compared to that of the eastern basin. FD and Tn10 were positively correlated to elevation and latitude, and negatively to longitude. This indicated that the higher the altitude, the higher the latitude and the lower the longitude, the closer the alpine plateau area in northwest Sichuan, the greater the change of extreme index value, the greater the reduction of extreme cold events in the west, and the smaller the reduction in the eastern basin. The results of correlation analysis between extreme precipitation indices and geographical factors also indicated that the higher the altitude, the lower the longitude and the higher the latitude, the closer the plateau and mountainous area in west Sichuan, the greater the change of extreme index value.

The terrain of Sichuan is higher in the west and lower in the east, and the variation from west to east is mainly plateau-mountain-basin, and its position change is very related to longitude, latitude and altitude. Changes of extreme climate indices are highly related to longitude, latitude and altitude. Previous studies have reported that warming at high elevation regions appeared much more rapid than at low elevations on the basis of ice cores data from the Tibetan Plateau (Tian et al., 2006; Kang et al., 2007). Li et al. (2012) indicated for precipitation extremes, it was obvious that the larger decreasing in summit station than others, and following was flat stations, but the increase mainly in valley stations, which are also consistent with our studies.

(5) As shown by Hurst exponents and interannual variation trends of the 19 extreme climate indices (*Table 6*), in the future, FD, SU and Tn90 may increase, while Tn10, Tx10 and Txx may decrease, i.e., as a whole, extreme cold events will decrease and

http://www.aloki.hu ● ISSN 1589 1623 (Print) ● ISSN 1785 0037 (Online)
DOI: http://dx.doi.org/10.15666/aeer/1802_32113242

extreme warm events will increase. Of all extreme precipitation indices, R20, R50 and PRCPTOT may increase, while R10 may decrease. That is, the precipitation and the number of heavy precipitation and rainstorm events will increase, and that both the extreme temperature and extreme precipitation events of the Sichuan Province will increase, but there will be obvious regional differences under different topographic zones in the future. Among them, the results on the overall trend of future change are in agreement with many model projections of extreme climate change. (Liu et al., 2012; Li et al., 2019b; Peng et al., 2019; Zhao et al., 2019).

In this study, some future trends of extreme climate indices are predicted only based on the Hurst exponents. Because climate models are a powerful tool to study climate system and climate change, and its simulation results are an important data base for climate projection and climate change risk assessment. Furthermore, the use of climate models to assess and predict the future climate change features can provide a scientific basis for adjusting human development strategies to adapt to climate change. In the future research, we can use the simulation results of CMIP5 (Coupled Model Intercomparison Project Phase 5, CMIP5) model and high-resolution statistical downscaling data set, combined with RCPs (Representative Concentration Pathways, RCPs) proposed by IPCC, to project the possible future changes of extreme climate events in Southwestern China, even in Sichuan Province. Moreover, the mechanistic understanding of how some climate drivers impact extreme temperature and extreme precipitation in Sichuan Province through forcing large-scale atmospheric circulation changes need to be further investigated, especially, the relationships between ENSO events, SASM (South Asian Summer Monsoon, SASM), EASM (East Asian Summer Monsoon, EASM) and extreme climate indices need to be further discussed, and the analyses of the physical causes of these variability will also become the basis of our future work.

Acknowledgements. This research was funded by the Soft Science Research Project, Science & Technology Department of Sichuan Province, China (2017ZR0043, 2015GZ0238) and National Natural Science Foundation of China (NSFC) (41971308, 41505122, 41275033).

REFERENCES

[1] Alexander, L. V., Zhang, X., Peterson, T. C., Caesar, J., Gleason, B., Klein Tank, A. M. G., Haylock, M., Collins, D., Trewin, B., Rahimzadeh, F., Tagipour, A., Rupa Kumar, K., Revadekar, J., Griffiths, G., Vincent, L., Stephenson, D. B., Burn, J., Aguilar, E., Brunet, M., Taylor, M., New, M., Zhai, P., Rusticucci, M., Vazquez-Aguirre, J. L. (2006): Global observed changes in daily climate extremes of temperature and precipitation. – Journal of Geophysical Research Atmospheres 111(D05109). DOI: 10.1029/2005JD006290.

[2] Arnone, E., Cusshi, M., Gesso, S. D., Petitta, M. (2018): A multi-hazard extreme climate index across Europe. – EPiC Series in Engineering 3: 95-102.

[3] Ding, W. R. (2014): Spatial and temporal variability of the extreme daily precipitation in southwest China. – Resources and Environment in the Yangtze Basin 23(7): 1071-1079.

[4] Ding, Z. Y., Ge, Y. X., Abuduwaili, J., Pu, J. (2018): Trends of extreme temperature and precipitation in Ebinur Lake basin in Xinjiang during the period from 1957 to 2012. – Journal of University of Chinese Academy of Sciences 35(2): 160-171.

[5] Dookie, N., Chadee, X. T., Clarke, R. M. (2018): Trends in extreme temperature and precipitation indices for the Caribbean small islands: Trinidad and Tobago. – Theoretical and Applied Climatology. https://doi.org/10.1007/s00704-018-2463-z.

http://www.aloki.hu ● ISSN 1589 1623 (Print) ● ISSN 1785 0037 (Online)
DOI: http://dx.doi.org/10.15666/aeer/1802_32113242

[6] Easterling, D. R., Evans, J. L., Groisman, P. Y., Karl, T. R., Kunkel, K. E., Ambenje, P. (2000): Observed variability and trends in extreme climate events: a brief review. – Bulletin of the American Meteorological Society 81(3): 417-425.
[7] Fu, C. B., Wang, Q. (1992): The definition and detection of the abrupt climatic change. – Scientia Atmospherica Sinica 16(4): 482-493.
[8] Gao, T., Xie, L. A. (2014): Study on progress of the trends and physical causes of extreme precipitation in China during the last 50 years. – Advances in Earth Science 29(5): 577-589.
[9] Jiang, R. G., Xie, J. C., Zhao, Y., He, H. L., He, G. H. (2017): Spatiotemporal variability of extreme precipitation in Shaanxi province under climate change. – Theor Appl Climatol 130: 831-845.
[10] Kang, S. C., Qin, D. H., Zhang, D. Q. (2007): Recent temperature increase recorded in an ice core in the source region of Yangtze River. – Chinese Science Bulletin 52: 825-831.
[11] Li, J., Zhao, Y. D., Iqbal, J. (2019a): Variation patterns of extreme precipitation and relation to ocean-atmospheric climate in Sichuan province China from 1961 to 2017. – Theoretical and Applied Climatology 137: 3009-3026.
[12] Li, J. J., Wang, A. H., Guo, D. L., Wang, D. (2019b): Evaluation of extreme indices over China in the NEX-GDDP simulated by high-resolution statistical downscaling models. – Acta Meteorologica Sinica 77(3): 579-593.
[13] Li, Z. X., He, Y. Q., Wilfred, H. T., Wang, X. F., Zhang, W., Cao, W. H., Du, J. K., Xin, H. J., Chang, L. (2012): Altitude dependency of trends of daily climate extremes in southwestern China, 1961-2008. – J. Geogr. Sci. 22(3): 416-430.
[14] Liu, J. L. (2013): Study on Extreme Temperature and Precipitation Events in Sichuan Basin. – Southwest University, Sichuan.
[15] Liu, L., Xu, Z. Z. (2014): Spatiotemporal distribution of the extreme climate indices in the five southwestern provinces of China. – Resources and Environment in the Yangtze Basin 23(2): 294-301.
[16] Liu, M., Shen, Y. J., Qi, Y. Q., Wang, Y. F., Geng, X. X. (2019): Changes in precipitation and drought extremes over the past half century in China. – Atmosphere 10: 203. DOI: 10.3390/atmos10040203.
[17] Liu, X., Zhang, W. Y., Jia, D. Y., et al. (2011b): Research of abrupt changes of sandstorm frequency in Hexi Corridor in recent 50 years. – Journal of Desert Research 31(6): 1579-1584.
[18] Liu, X. R., Cheng, B. Y., Yang, Q., Zhang, T. Y., Wang, R. Y. (2012): Scenario projections of 21st century climate change in Southwest China. – Journal of Southwest University (Natural Science Edition) 34(9): 82-89.
[19] Liu, Z. F., Wang, Y. C., Yao, Z. J., Kang, H. M. (2011a): Trend and periodicity of precipitation, air temperature and runoff in the Taihu Lake Basin. – Journal of Natural Resources 26(9): 1575-1584.
[20] Luo, Y., Fan, G. Z., Zhou, D. W., Hua, W., Li, J. J. (2015): Extreme precipitation trend of Southwest China in recent 41 years. – Journal of the Meteorological Sciences 35(5): 581-586.
[21] Luo, Y., Fan, G. Z., Zhou, D. W., Hua, W., Zhang, Y. L. (2016): Trend of extreme temperature in southwest China in the recent 41 years. – Journal of Southwest University (Natural Science Edition) 38(5): 161-167.
[22] Ma, R., Zhang, M. J., Wang, S. J., Wang, J., Yang, S., Chen, Y. (2018): Variation characteristics of snow cover days in winter in arid region of northwest China in last 50 years. – Journal of Natural Resources 33(1): 127-138.
[23] Ma, X. B. (2016): Sichuan Yearbook. – Sichuan Yearbook Society, Chengdu.
[24] Peng, D. D., Zhou, T. J., Zhang, L. X., Zhang, W. X., Chen, X. L. (2019): Observationally constrained projection of the reduced intensification of extreme climate events in Central Asia from 0.5℃ less global warming. – Climate Dynamics https://doi.org/10.1007/s00382-019-05014-6.

http://www.aloki.hu ● ISSN 1589 1623 (Print) ● ISSN 1785 0037 (Online)
DOI: http://dx.doi.org/10.15666/aeer/1802_32113242

[25] Qin, N. X., Wang, J. N., Yang, G. S., Liang, H. Y., Zhang, J. B. (2015): Spatial and temporal variations of extreme precipitation and temperature events for southwest China in 1960-2009. – Geoenvironmental Disasters 2: 4. DOI: 10.1186/s40677-015-0014-9.
[26] Sajjad, H., Ghaffar, A. (2018): Observed, simulated and projected extreme climate indices over Pakistan in changing climate. – Theoretical and Applied Climatology 137: 255-281.
[27] Sohrabi, M. M., Ryu, J. H., Abatzoglou, J., Tracy, T. (2013): Climate extreme and its linkage to regional drought over Idaho, USA. – Nat Hazards 65: 653-681.
[28] Soltani, M., Laux, P., Kunstmann, H., Stan, K., Sohrabi, M. M., Molanejad, M., Sabziparvar, A. A., SaadatAbadi, A. R., Ranjbar, F., Rousta, J., Zawar-Reza, P., Khoshakhlagh, F., Soltanzadeh, I., Babu, C. A., Azizi, G. H. (2016): Assessment of climate variations in temperature and precipitation extreme events over Iran. – Theor Appl Climatol 126(3-4): 776-795.
[29] Song, X., Zhang, Z., Chen, Y., Wang, P., Ming, X., Shi, P. J., Tao, F. L. (2013): Spatiotemporal changes of global extreme temperature events (ETEs) since 1981 and the meteorological causes. – Nat Hazards 70(2): 975-994.
[30] Song, X. M., Zou, X. J., Zhang, C. H., Zhang J, Y., Kong, F. Z. (2019): Multiscale spatio-temporal changes of precipitation extremes in Beijing-Tianjin-Hebei region, China during 1958-2017. – Atmosphere 10(8): 462-490.
[31] Stocker, T. F., Qin, D., Platter, G. K., Tignor, M., Allen, S. K., Boschung, J., Nauels, A., Xia, Y., Bex, V., Midgley, P. M. (2013): IPCC: Summary for Policymakers. – In: Climate Change 2013: The Physical Science Basis. Contribution of Working Group I to the Fifth Assessment Report of the Intergovernmental Panel on Climate Change. Cambridge University Press, Cambridge.
[32] Sun, C., Cheng, Z. G., Mao, X. L., Mei, S. D., Yang, X., Y. (2017): Extreme climatic change trend and features in Sichuan for the latest 44 years. – Journal of Lanzhou University: Natural Sciences 53(1): 119-126.
[33] Sun, J. Q., Chen, H. P., Zhu, Y. L. (2012): Extreme climate in China: facts, simulation and projection. – Meteorologische Zeitschrift 21(3): 279-304.
[34] Tariku, T. B., Gan, T. Y. (2018): Regional climate change impact on extreme precipitation and temperature of the Nile River basin. – Climate Dynamics 51: 3487-3506.
[35] Tian, L. D., Yao, T. D., Li, Z., Kenneth, M. C., Wu, G. G., Xu, B. Q., Li, Y. F., Lu, A. X., Shen, Y., P. (2006): Recent rapid warming trend revealed from the isotopic record in Muztagata ice core, eastern Pamirs. – Journal of Geophysical Research 111: D13103. DOI: 10.1029/2005JD006249.
[36] Vogel, M. M., Zscheischler, J., Seneviratne, S. I. (2018): Varying soil moisture-atmosphere feedbacks explain divergent temperature extremes and precipitation projections in Central Europe. – Earth Syst. Dyn. 9(3): 1107-1125.
[37] Wang, C. X., Wei, Y. Y., Ye, X. B., Wu, X., Yan., Liu, Y. Y. (2017): Drought index estimation and drought characteristics in Sichuan province. – Journal of Agricultural Catastrophology 7(1): 36-48.
[38] Wei, F. Y. (2007): Modern Climate Statistical Diagnosis and Prediction Technology. Second Ed. – China Meteorological Press, Beijing.
[39] Xu, Y. Q., Li, S. C., Cai, Y. L. (2004): Study on precipitation variation in Hebei Plain based on Wavelet Analysis. – Science in China Ser. D Earth Sciences 34(12): 1176-1183.
[40] Yang, P., Liu, W. D., Wang, Q. G., Xiong, K. G., Hou, W. (2010): The climatic change trend and seasonal characteristics of daily temperature extremes in China for the latest 40 years. – Journal of Applied Meteorological Science 21(1): 29-36.
[41] Yin, H., Sun, Y. (2019): Characteristics of extreme temperature and precipitation in China in 2017 based on ETCCDI indices. – Climate Change Research 15(4): 363-373.

http://www.aloki.hu ● ISSN 1589 1623 (Print) ● ISSN 1785 0037 (Online)
DOI: http://dx.doi.org/10.15666/aeer/1802_32113242

[42] Yuan, W. D., Zheng, J. K. (2015): Spatial and temporal variations of extreme temperature events in southwest China during 1962-2012. – Resources and Environment in the Yangtze Basin 24(7): 1246-1254.
[43] Yuan, W. D., Zheng, J. K., Dong, K. (2014): Spatial and temporal variations in extreme precipitation events in southwest China during 1962-2012. – Resources Science 36(4): 0766-0772.
[44] Zhan, Z. Y., Wen, K. G. (2006): China Meteorological Disaster Ceremony (Volume Sichuan). – China Meteorological Press, Beijing.
[45] Zhang, S. Q., Ma, Z. F. (2011): Change tendency and cyclicity analysis of extreme precipitation over Sichuan province during 1961-2009. – Journal of Natural Resources 26(11): 1918-1929.
[46] Zhao, A. Z., Liu, X. F., Zhu, X. F., Pan, Y. Z., Zhao, Y., L., Wang, D. L. (2016): Trend variations and spatial difference of extreme air temperature events in the Loess Plateau from 1965 to 2013. – Geographical Research 35(4): 639-652.
[47] Zhao, J., Wang, N. A., Yang, S. H. (2000): R/S analysis of urbanization effect on climate in Lanzhou. – Journal of Lanzhou University (Natural Sciences) 36(6): 122-128.
[48] Zhao, Y. Q., Xiao, D. P., Bai, H. Z. (2019): Projection and application for future climate in China by CMIP5 climate model. – Meteorological Science and Technology. 47(4): 608-621.
[49] Zhou, C. Y., Cen, S. X., Li, Y. Q., Peng, G. Z., Yang, S. Q., Peng, J. (2011): Precipitation variation and its impacts in Sichuan in the last 50 years. – Acta Geographica Sinica 66(5): 619-630.

http://www.aloki.hu ● ISSN 1589 1623 (Print) ● ISSN 1785 0037 (Online)
DOI: http://dx.doi.org/10.15666/aeer/1802_32113242

STUDY ON THE CHANGE PROCESS AND CHARACTERISTICS OF LAND USE IN THE SHULE RIVER BASIN IN THE RECENT 20 YEARS

ZENG, J. J.[1] – LI, K. M.[1*] – CUI, Y. Q.[2] – CAO, S. Z.[1]

[1]*College of Geography and Environmental Engineering, Lanzhou City University, No.1, Jie Fang Road, An Ning District, Lanzhou 730000, China*

[2]*College of Geography and Environmental Science, Northwest Normal University, Lanzhou 730000, China*

**Corresponding author*
e-mail: lkm_wd@126.com; phone: +86-136-0932-3256

(Received 27th Sep 2019; accepted 4th Feb 2020)

Abstract. Based on the LandsatTM/ETM+/OLI remote sensing data (30 m resolution) of the Shule River basin in the past 20 years, the land use data was obtained by interpretation. By using Erdas9.2 and ArcGIS10.3 software, the land-use types were divided into 6 primary landscape types and 25 secondary landscape types, and the spatial database of watershed land use was established. By using GIS spatial analysis technology, transfer matrix, land use dynamics and many other spatial-temporal statistical analysis methods, the transformation process and temporal and spatial pattern analysis of land-use types in river basin in recent 20 years were carried out, with results showing that: In the past 20 years, different degrees of changes have taken place in land use in the Shule River basin. On the whole, the area of cultivated land, woodland, grassland and urban and rural industrial and mining residents increased, among which grassland increased the most, with an annual increase rate of 0.33%. The area of cultivated land increased, with an annual growth rate of 0.0959%. While water area and unused land decreased, with an annual decline rate of 0.4490%. The decrease of water area was the smallest, with an annual decline rate of 0.0122%. There are obvious differences in the speed and type of change in water area and unused land. The hot spot of land use type transformation in the basin is the middle reaches oasis, mainly Dunhuang, Guazhou and Yumen counties (cities).
Keywords: *land use, spatial change, transition matrix, characteristic study, Shule River basin*

Introduction

Land use is the most direct form of interaction between human activities and natural environment, and it is also a frontier and hot issue in the study of global change (Liu et al., 2003; Naef et al., 2002; Weng, 2002). The spatiotemporal change of land use can intuitively express the interaction between human activities and natural environment, reflect the relationship between the Earth's environmental system on which Human beings depend for their Survival and the growing production system of mankind (agriculture, industrialization/urbanization, etc.), it will also cause a variety of natural phenomena and ecological process changes (Wu et al., 2006; Guan et al., 2011). Under the background of global change, the change of land use pattern in river basin is gradually strengthening the imbalance and instability of hydrological cycle, thus affecting the controllability, reproducibility, total amount, composition and distribution of water resources. Furthermore, it brings great challenges to the safety of water supply, flood control, water ecology and so on (Ku, 2016; Ning et al., 2018). Therefore, in order to explore the interaction between human activities and natural environment in the inland river basin, we took the Shule River basin as the research area and carried out the analysis

http://www.aloki.hu ● ISSN 1589 1623 (Print) ● ISSN 1785 0037 (Online)
DOI: http://dx.doi.org/10.15666/aeer/1802_32433250

and study on the transformation process of land-use types and the temporal and spatial pattern in the past 20 years, which provide policy support and technical guarantee for the sustainable and healthy development of the river basin.

Overview of the study area

The Shule River basin is located in the hinterland of the arid area of northwest China, and is located between 93°22' - 98°59' E and 38°1' - 42°47' N. The watershed area is about 1.25×10^5 km^2, which is one of the three inland river basins in Hexi Corridor and one of the seven water rights pilot basins. The watershed location map is shown in *Figure 1*. The altitude of the river basin is between 914 and 5816 m, lower in the north and higher in the south. It belongs to continental desert climate. As a typical inland river basin, water supply is mainly composed of glacier melt water and mountain precipitation. There are 7 soil types, 31 subclasses and 63 soil genera in the watershed soil. By the end of 2018, the total population of the basin was 524200, and the agricultural population was 221400, with a natural population growth rate of 4.54% for many years. At present, the per capita share of water resources is 2933.7 m^3 (Yue et al., 2019).

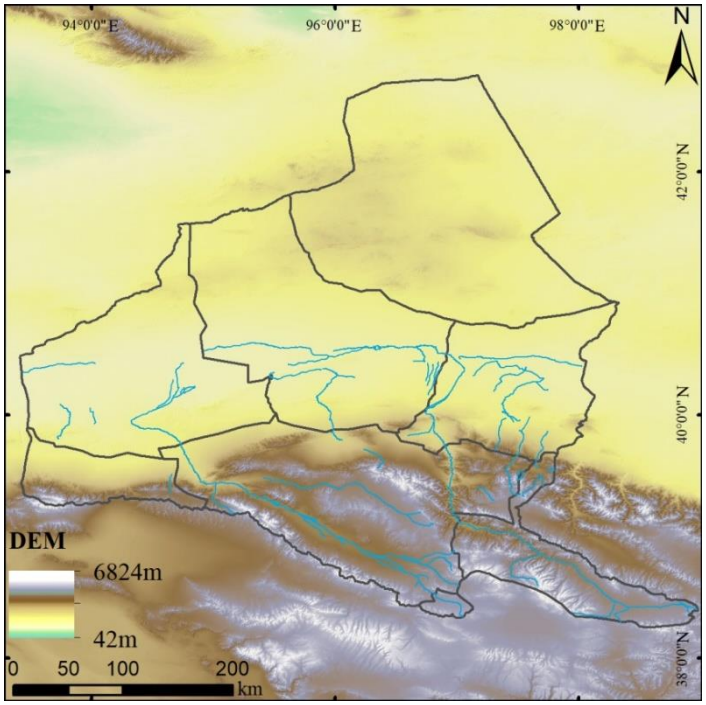

Figure 1. *The location of Shule River basin*

Research methods

According to the distribution of rivers and their tributaries, the boundary of the Shule River basin is delineated by using the digital elevation model of the study area in the SWAT hydrological model. The Landsat TM, ETM remote sensing image with spatial resolution of 30 m in watershed in summer and autumn is selected since in summer and autumn in 1995 and 2015, plants grow best with highest vegetation coverage and it is easy to distinguish from desert, which is conducive to visual interpretation. When extracting for land by information, the 4 (R), 3 (G), 2 (B) band of TM/ETM+ image is

http://www.aloki.hu ● ISSN 1589 1623 (Print) ● ISSN 1785 0037 (Online)
DOI: http://dx.doi.org/10.15666/aeer/1802_32433250

combined first to generate a standard false color image and unitedly conversed to Albers projection. Combined with the information of GPS measuring points in the field, geometric correction is carried out. The second is to establish the identification of remote sensing interpretation. First, the interpretation logo is initially established indoors. Then field observation and recording are carried out through GPS positioning and to correct and calibrate the interpretation in turn. The land-using information is extracted again. Adopting the visual interpretation method of human-computer interaction, taking the relevant drawings as a reference, with application of correlation analysis and comprehensive image feature, the boundary of various surface features is to be determined and then to generate the current land-using thematic map by using ArcGIS plug-in. On this basis, the thematic map of land-using change in two time periods is generated by applying ArcGIS spatial overlay analysis function. Finally, the type of surface features is determined while verifying the accuracy of the predicted map through comparing the high-resolution data view provided by GoogleEarth and combining with field observation and experience knowledge. By using Erdas9.2 and ArcGIS10.3 software, the land-use types were divided into 6 primary landscape types and 25 secondary landscape types, and a five-stage land use spatial database of river basin was established.

(1) Single land-use dynamic degree: Quantitative description of the speed of change and the type difference of change, its form of expression is as follows (Chen et al., 2012; Guo et al., 2015; Yang, 2018):

$$K = \frac{U_b - U_a}{U_a} \times \frac{1}{T} \quad \text{(Eq.1)}$$

In the formula, K is the dynamic attitude of land use in the study area; U_a and U_b are the number of land-use types before and after the change; T is the length of the study period.

(2) The integrate dynamic degree of land use: It is an index to describe the regional difference in the rate of change of land-use types, and reflects the comprehensive impact of human activities on the change of land-use types. Its mathematical model is (Le et al., 2018; Doelman et al., 2018; Bovet et al., 2018; Jin et al., 2013; Huang et al., 2014):

$$S = \left[\sum_{i=1}^{n} \Delta S_{i-j} / S_i \right] \times \frac{1}{T} \times 100\% \quad \text{(Eq.2)}$$

In the formula, S is the comprehensive dynamic attitude of land use, $\Delta S_{i\text{-}j}$ is the sum of the area of land-use types before and after conversion, S_i is the total area of type i land use, and t is the time of land use change.

Study on the change process and characteristics of land use in Shule River basin

Structural change of land-use types in watershed

As can be seen from *Table 1* and *Figure 2,* between 1995 and 2015: (1) The area of cultivated land, woodland, grassland and urban and rural industrial and mining residents increased, among which grassland increased the most, with an increase of 2069.54 km^2. The proportion of grassland increased from 19.88% in 1995 to 21.54% in 2015, with an

http://www.aloki.hu ● ISSN 1589 1623 (Print) ● ISSN 1785 0037 (Online)
DOI: http://dx.doi.org/10.15666/aeer/1802_32433250

annual increase rate of 0.33%. The area of cultivated land increased by 596.73 km^2, and the proportion of cultivated land increased from 0.85% to 1.33%, with an annual growth rate of 0.0959%. (2) The area of water area and unused land decreased, the area of unused land decreased the most, with a decrease of 2794.74 km^2. The proportion of unused land decreased from 78.03% in 1995 to 75.78% in 2015, with an annual decline rate of 0.4490%. The decrease of water area was the smallest, with an area of 76.06 km^2, and the proportion of grassland decreased from 0.66% in 1995 to 0.60% in 2015, with an annual decline rate of 0.0122%.

Table 1. *Land use change in Shule River basin from 1995 to 2015 (km^2)*

Land use type	1995		2015		Area of change	Annual rate of change
	Area	Proportion (%)	Area	Proportion (%)		
Cultivated land	1062.00	0.85	1658.73	1.33	596.73	0.0959
Woodland	583.35	0.47	627.02	0.50	43.67	0.0070
Grassland	24741.53	19.88	26811.07	21.54	2069.54	0.3325
Water	819.54	0.66	743.48	0.60	-76.06	-0.0122
Urban and rural	142.67	0.11	303.54	0.24	160.87	0.0258
Unused land	97127.90	78.03	94333.16	75.78	-2794.74	-0.4490

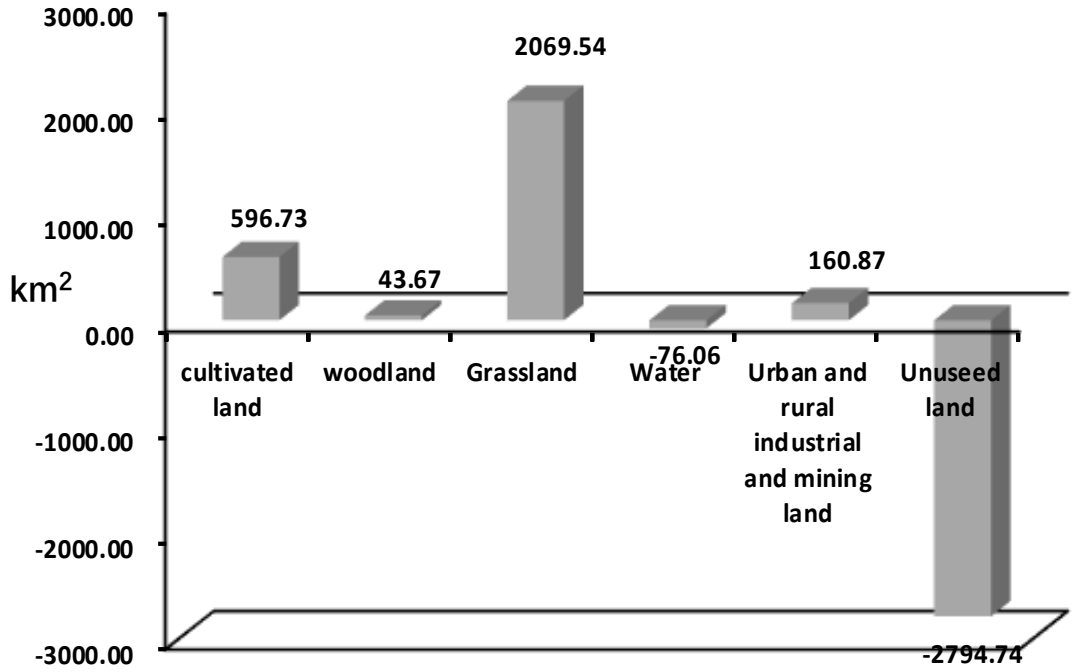

Figure 2. *Map of land use change in Shule River basin from 1995 to 2015*

Use *Equations 1* and *2*. Through the dynamic attitude analysis from 1995 to 2015, the dynamic degree of cultivated land, forest land, urban and rural industrial and mining land, water area, grassland and unused land were 0.03%, 0.0037%, 0.006%, -0.0046%, 0.0042% and -0.0014%, respectively. It can be seen that there are obvious differences in the speed and type of change in water area and unused land. The spatial distribution pattern of land-use types in Shule River from 1995 to 2015 is shown in *Figure 3*.

http://www.aloki.hu ● ISSN 1589 1623 (Print) ● ISSN 1785 0037 (Online)
DOI: http://dx.doi.org/10.15666/aeer/1802_32433250

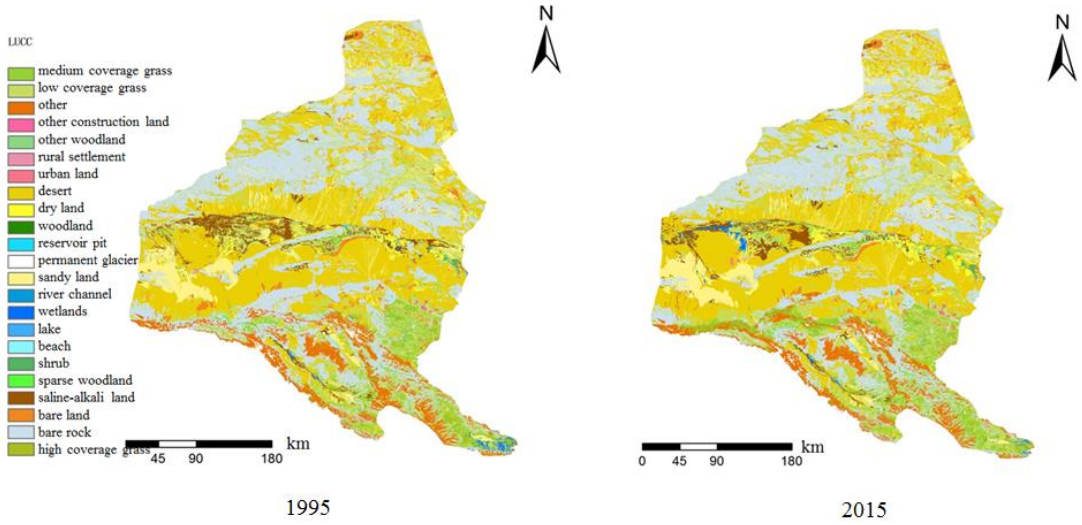

Figure 3. *Changes of land-use types in Shule River from 1995 to 2015*

From *Figure 3,* although the land use of the river basin has changed in the past 20 years, the main pattern has not changed. The north is mainly bare rock texture and Gobi; the middle and lower reaches are mainly dry land, grassland and Gobi; there are a lot of saline-alkali land and some grassland between Dunhuang city and Guazhou city, and there are a lot of sandy land in the south and southwest of Dunhuang city. There is bare land, a large area of grassland and permanent glacier snow fields in the upper reaches of the river basin.

Study on transformation of land-use types in river basin

In order to describe the conversion process of various land-use types from 1995 to 2015, the transfer matrix of land-use types in each period was calculated by using the function of ArcGIS spatial analysis (*Tables 2* and *3*), and the map of land use transfer matrix in each period was generated (Mishra et al., 2018; Andraschko et al., 2014; Dai et al., 2012).

Table 2. *Transfer matrix of land-use types in Shule River basin from 1995 to 2015 (km^2)*

1995 / 2015	Cultivated land	Woodland	Grassland	Water	Urban and rural	Unused land	Total
Cultivated land	859.70	40.44	332.52	2.47	20.69	402.70	1658.51
Woodland	9.68	445.80	76.57	0.92	0.81	93.16	626.94
Grassland	55.20	40.63	22188.93	17.55	1.87	4492.56	26796.75
Water	7.10	0.89	35.44	615.41	0.46	84.08	743.38
Urban and rural	72.96	1.83	22.16	0.04	115.43	91.07	303.51
Unused land	57.00	53.55	2075.50	180.54	3.34	91918.46	94288.39
Total	1061.63	583.14	24731.12	816.94	142.62	97082.03	124422.4

Table 3. *Transfer matrix of different land-use types from 1995 to 2015 (%)*

1995 / 2015	Cultivated land	Woodland	Grassland	Water	Urban and rural	Unused land

http://www.aloki.hu ● ISSN 1589 1623 (Print) ● ISSN 1785 0037 (Online)
DOI: http://dx.doi.org/10.15666/aeer/1802_32433250

Cultivated land	51.84	2.44	20.05	0.15	1.25	24.28
Woodland	1.54	71.11	12.21	0.15	0.13	14.86
Grassland	0.21	0.15	82.80	0.07	0.01	16.77
Water	0.95	0.12	4.77	82.79	0.06	11.31
Urban and rural	24.04	0.60	7.30	0.01	38.03	30.01
Unused land	0.06	0.06	2.20	0.19	0.00	97.49

The area of cultivated land showed an increasing trend as a whole. The cultivated land area was 1062 km^2 in 1995 and 1658 km^2 in 2015, which increased 597 km^2. Among them, the conversion amount is 798.81 km^2, accounting for 0.64% of the total land area, mainly converted to grassland and unused land. The amount of transfer is 201.94 km^2, and the main types of transfer are urban and rural areas, industrial and mining areas, residential land and unused land. The woodland area showed an increasing trend as a whole. The woodland area increased by 44 km^2 from 583 km^2 in 1995 to 627 km^2 in 2015, of which the transferred area reached 181.14 km^2, accounting for 0.15% of the total land area, and the main types of transfer were unused land and grassland. The amount of transfer was 137.34 km^2, and the main types of transfer were unused land and grassland. The grassland area is generally increasing. The grassland area increased by 20693 km^2 from 24741 km^2 in 1995 to 26811 km^2 in 2015, of which the transferred area reached 4607.82 km^2, accounting for 3.70% of the total land area, and the main types of transfer are unused land and cultivated land; the amount of transfer was 2542.19 km^2, and the main types of transfer were unused land and cultivated land. The water area showed a slight decreasing trend. The water area decreased 76 km^2 from 820 km^2 in 1995 to 743 km^2 in 2015, in which the transfer area reached 127.97 km^2, accounting for 0.10% of the total land area, the main types of transfer were unused land and grassland. The amount of transfer was 201.53 km^2, and the main types of transfer were unused land and grassland. The land use of urban and rural, industrial and mining, residents showed an increasing trend. The land area increased 161 km^2 from 304 km^2 in 1995 to 304 km^2 in 2015, of which the transfer area reached 188.08 km^2, accounting for 0.15% of the total land area, the main types of transfer were unused land and cultivated land; the amount of transfer was 27.19 km^2, and the main types of transfer were cultivated land and unused land. Unused land showed a decreasing trend, the unused land area decreased 2794 km^2 from 97128 km^2 in 1995 to 94333 km^2 in 2015, the transferred area reached 2369.93 km^2, accounting for 1.90% of the total land area. The amount of transfer was 5163.57 km^2, and the main types of transfer were grassland and cultivated land.

Conclusion and discussion

In order to solve the problem of ecological degradation of Shule River, the State Council approved The Comprehensive Plan for Rational Utilization of Water Resources and Ecological Protection in Dunhuang in June 2011. The plan studies and proposes the overall planning idea of “protecting water source in the south, establish oasis in the middle, resist sandstorm in the west, and dredge the Shule River in the north” and the overall planning layout of “coordination of internal and external adjustment, simultaneous protection in the west and dredge in the north, stability of water and oasis, and maintenance of economic and ecological balance”. The land use is the most direct manifestation pattern of the interaction between human activities and the natural

http://www.aloki.hu ● ISSN 1589 1623 (Print) ● ISSN 1785 0037 (Online)
DOI: http://dx.doi.org/10.15666/aeer/1802_32433250

environment. On the other hand, it can also reflect the regional ecological environment problems. In order to further protect the ecological environment of Shule river watershed, and to prevent ecological degradation, the research on the process and characteristics of land use change in Shule River watershed are developed.

The Landsat TM, ETM remote sensing image with spatial resolution of 30 m in watershed in summer and autumn is selected since in summer and autumn in 1995 and 2015. By using GIS spatial analysis technology, transfer matrix, land use dynamics and a variety of spatio-temporal statistical analysis methods, the transformation process and temporal and spatial pattern analysis of land-use types in river basins in recent 20 years were carried out: In the past 20 years, different degrees of changes have taken place in land use in Shule River basin:

(1) The area of cultivated land, woodland, grassland and urban and rural industrial and mining residents increased, among which grassland increased the most, with an annual increase rate of 0.33%. The area of cultivated land increased, with an annual growth rate of 0.0959%. The area of water area and unused land decreased, with an annual decline rate of 0.4490%. The decrease of water area was the smallest, with an annual decline rate of 0.0122%.

(2) Through the dynamic attitude analysis from 1995 to 2015, the dynamic degree of cultivated land, forest land, urban and rural industrial and mining land, water area, grassland and unused land were 0.03%, 0.0037%, 0.006%, -0.0046%, 0.0042% and -0.0014%, respectively. It can be seen that there are obvious differences in the speed and type of change in water area and unused land.

(3) Although the land use of the river basin has changed in the past 20 years, the main pattern has not changed. The north is mainly bare rock texture and Gobi; the middle and lower reaches are mainly dry land, grassland and Gobi; there are a lot of saline-alkali land and some grassland between Dunhuang city and Guazhou city, and there are a lot of sandy land in the south and southwest of Dunhuang city. There are is bare land, a large area of grassland and permanent glacier snow fields in the upper reaches of the river basin.

Acknowledgments. This research was supported by Doctor research launch aid of Lanzhou City University in 2019 (LZCU-BS2019-20), the National Natural Science Foundation of china (grant nos. 41661014), the National Natural Science Foundation of Gansu (grant nos. 18JR3RA221).

REFERENCES

[1] Andraschko, F., Sirker, J. (2014): Dynamical quantum phase transitions and the Loschmidt echo: a transfer matrix approach. – Physical Review B 89(12): 125120.

[2] Bovet, J., Reese, M., Köck, W. (2018): Taming expansive land use dynamics - sustainable land use regulation and urban sprawl in a comparative perspective. – Land Use Policy 77: 837-845.

[3] Chen, S., Liu, W., Qin, X., Liu, Y., Zhang, T., Chen, K., Hu, F., Ren, J., Qin, D. (2012): Response characteristics of vegetation and soil environment to permafrost degradation in the upstream regions of the Shule River Basin. – Environmental Research Letters 7(4): 045406.

[4] Dai, H., Wang, L., Qian, Q., Gan, J. (2012): Vibration analysis of three-dimensional pipes conveying fluid with consideration of steady combined force by transfer matrix method. – Applied Mathematics and Computation 219(5): 2453-2464.

[5] Doelman, J., Stehfest, E., Tabeau, A., Meijl, H., Lassaletta, L., Gernaat, D., Hermans, K., Daioglou, V., Biemans, H., Sluis, S., Vuuren, D. (2018): Exploring SSP land-use dynamics

http://www.aloki.hu ● ISSN 1589 1623 (Print) ● ISSN 1785 0037 (Online)
DOI: http://dx.doi.org/10.15666/aeer/1802_32433250

using the IMAGE model: regional and gridded scenarios of land-use change and land-based climate change mitigation. – Global Environmental Change 48: 119-135.

[6] Guan, D., Li, H., Inohae, T., Su, W., Nagaie, T., Hokao, K. (2011): Modeling urban land use change by the integration of cellular automaton and Markov model. – Ecological Modelling 222(20-22): 3761-3772.

[7] Guo, X., Feng, Q., Liu, W., Li, Z., Wen, X., Si, J., Xi, H., Guo, R. (2015): Stable isotopic and geochemical identification of groundwater evolution and recharge sources in the arid Shule River Basin of Northwestern China. – Hydrological Processes 29(22): 4703-4718.

[8] Huang, J., Yang, X., Cheng, G., Wang, S. (2014): A comprehensive eco-efficiency model and dynamics of regional eco-efficiency in China. – Journal of Cleaner Production 67: 228-238.

[9] Jin, S., Yang, L., Danielson, P., Homer, C., Fry, J., Xian, G. (2013): A comprehensive change detection method for updating the National Land Cover Database to circa 2011. – Remote Sensing of Environment 132: 159-175.

[10] Ku, C. A. (2016): Incorporating spatial regression model into cellular automata for simulating land use change. – Applied Geography 69: 1-9.

[11] Le, T., Bregt, A., van Halsema, G. E., Petra J. G., Hellegers, J., Nguyen, L. (2018): Interplay between land-use dynamics and changes in hydrological regime in the Vietnamese Mekong Delta. – Land Use Policy 73: 269-280.

[12] Liu, J., Liu, M., Zhuang, D., Zhang, Z., Deng, X. (2003): Study on spatial pattern of land-use change in China during 1995–2000. – Science in China Series D: Earth Sciences 46(4): 373-384.

[13] Mishra, P., Blaum, K., George, S., Grieser, A. W. (2018): Transfer matrix calculation for ion optical elements using real fields. – Nuclear Instruments and Methods in Physics Research Section A: Accelerators, Spectrometers, Detectors and Associated Equipment 885: 124-133.

[14] Naef, F., Scherrer, S., Weiler, M. (2002): A process-based assessment of the potential to reduce flood runoff by land use change. – Journal of Hydrology 267(1-2): 74-79.

[15] Ning, J., Liu, J., Kuang, W., Xu, X., Zhang, S., Yan, C., Li, R., Wu, S., Hu, Y., Du, G., Chi, W., Pan, T., Ning, J. (2018): Spatiotemporal patterns and characteristics of land-use change in China during 2010–2015. – Journal of Geographical Sciences 28(5): 547-562.

[16] Weng, Q. (2002): Land use change analysis in the Zhujiang Delta of China using satellite remote sensing, GIS and stochastic modelling. – Journal of Environmental Management 64(3): 273-284.

[17] Wu, Q., Li, H., Wang, R., Paulussen, J., He, Y., Wang, M., Wang, B., Wang, Z. (2006): Monitoring and predicting land use change in Beijing using remote sensing and GIS. – Landscape and Urban Planning 78(4): 322-333.

[18] Yang, J., Ji, Z., Chen, D., Chen, D., Kang, S., Fu, C., Duan, K., Shen, M. (2018): Improved land use and leaf area index enhances WRF-3DVAR satellite radiance assimilation: a case study focusing on rainfall simulation in the Shule River basin during July 2013. – Advances in Atmospheric Sciences 35(6): 628-644.

[19] Yue, D., Chen, G., Zou, M., Guo, X., Zhou, Y., Li, K., Wang, D., Guo, J., Zeng, J. (2019): Biocapacity and ecological water demand in Shule River basin over the past 20 years. Acta Ecologica Sinica 39(14): 5178-5187.

http://www.aloki.hu ● ISSN 1589 1623 (Print) ● ISSN 1785 0037 (Online)
DOI: http://dx.doi.org/10.15666/aeer/1802_32433250

ASSESSING THE IMPACTS OF CLIMATIC AND TELECONNECTION FACTORS ON MAIZE (*ZEA MAYS* L.) YIELD FROM BOTH MACROSCOPIC AND MICROSCOPIC PERSPECTIVES

LI, P. – HUANG, S. Z.* – HUANG, Q.

State Key Laboratory of Eco-hydraulics in Northwest Arid Regionof China, Xi'an University of Technology, Xi'an 710048, China
(phone: +86-29-8231-2801; fax: +86-29-8231-2797)

**Corresponding author*
e-mail: huangshengzhi7788@126.com; phone: +86-29-8231-2801; fax: +86-29-8231-2797

(Received 27th Sep 2019; accepted 4th Feb 2020)

Abstract. Maize (*Zea mays* L) as an important crop in the world is strongly affected by climatic and teleconnection factors, it is therefore necessary to fully assess their impacts on maize yield. Given the complexity and non-stationarity of the maize yield fluctuations in China, the empirical mode decomposition (EMD) and cross-wavelet methods were adopted to explore the correlations between maize yield including its whole series and various frequency series decomposed by the EMD and climatic and teleconnection factors from both macroscopic and microscopic perspectives. Results indicated that: (1) from the macroscopic perspective, sunspots were the main influencing factor of maize yield; (2) from the microscopic perspective, mainly precipitation, temperature, El Niño-Southern Oscillation (ENSO), Atlantic Oscillation (AO), and Pacific Decadal Oscillation (PDO) impact the high-medium frequency components (i.e., the frequency domain is 1~4 years and 6~10 years) of the detrended maize yield sequence, whilst solar activities (i.e., sunspots) primarily influence its low-medium frequency components (i.e., the frequency domain is 8~14 years); (3) three complete influencing hierarchical frameworks of sunspots-teleconnection factors-climatic factors on the various frequency components of the detrended maize yield were constructed, which help develop a physical significance of maize yield prediction model The study provides new insights into crop yield forecasting, thereby laying a solid scientific basis for crop yield decisions.
Keywords: *EMD, the cross wavelet method, climate change, different perspectives*

Introduction

Climate change has been one of the most studied topics during the last decades due to its socioeconomic, environmental and biological implications (IPCC, 2014; Fang et al., 2019; Guo et al., 2020). In the coming decades, global climate change will affect all sectors of the global economy (Huang et al., 2020; Ren et al., 2020; Li et al., 2020). But most of the impacts will concentrate on the agricultural sector, inducing food insecurity, particularly in developing countries (Ringler, 2008; Nelson et al., 2009). Despite significant advances in technology and in crop yield potential, food production and food security remain highly dependent on weather and climate change, as solar radiation, temperature and precipitation are the main drivers of crop growth (Angstrom, 1924; Hunt et al., 1998; Rosenzweig et al., 2001). Climate is one of the major uncontrollable factors affecting crop yield and causing global yield stagnation among the ones (You et al., 2009; Godfray et al., 2010). Maize is the crop with the largest planting area and production in China. According to FAO, the planted area of maize in 2016 was 36.8 million ha, and production was 219.6 million tons (Planting Industry Management Department, 2018; Tian et al., 2019; He et al., 2019). Therefore, it is necessary to explore the impact of climate change on corn yield to ensure the security of China's grain yield.

http://www.aloki.hu ● ISSN 1589 1623 (Print) ● ISSN 1785 0037 (Online)
DOI: http://dx.doi.org/10.15666/aeer/1802_32513275

Climate change is causing significant change in water supply and further threats to food production in various parts of the world (Hanjra et al., 2010; Knox et al., 2012; Smith et al., 2013; Zhao et al., 2013; Zhao et al., 2020a). As a result, food security problems caused by extreme climate events have sparked research and public interest in the analysis of climate change and agricultural production (Kummu et al., 2012). The increased rainfall recorded in the Pampas region led to yield increases of rainfed crops in the order of 38% for soybean, 18% maize, 13% wheat and 12% in sunflower (Zhang et al., 2008). The fluctuation of temperature has an adverse effect on food production (Magrin et al., 2005; Lobell et al., 2008; Battisti et al., 2009). ENSO condition has been related to agricultural yields in many parts of the world (Garnett et al., 1992; Cane et al., 1994; Hammer et al., 2001; Butler et al., 2013). Low maize yields in Zimbabwe were found to be a result of El Nino (Podestá et al., 2002; Butler et al., 2013). Similar negative effects caused by El Nino were also reported concerning lowland rice yields and total rice production during the wet season in the Philippines and Indonesia (Phillips et al., 1998; Lansigan et al., 2000). There was a significant negative correlation between the Atlantic oscillation (AO) index and maize and rice yield in northeast China (Naylor et al., 2001). Some complex impacts of the Pacific Decadal Oscillation (PDO) on dryland corn and wheat yields in the Missouri River Basin were found (Kim et al., 2005). Besides, solar radiation affects crop yield by affecting the process of crop growth (Angstrom et al., 1924; Hunt et al., 1998; Mehta et al., 2012), the change of crop yield is therefore affected to some extent by the intensity of solar activities (usually expressed by the number of sunspots). As mentioned above, long-term fluctuations in crop yield are closely related with climatic factors such as temperature and precipitation, teleconnection factors (i.e. ENSO, AO, PDO) (for the sake of brevity, climatic and teleconnection factors are collectively referred to as signals of climate variability) (Zhao et al., 2015a; Xu et al., 2018) and solar activities (i.e. sunspots). And, the above-mentioned research indicates that global climate change is slowly affecting the spatial pattern of global and regional food production and their yield levels, which plays an important role in investigating the food production changes and their possible causes under the context of global climate change. Nevertheless, these studies only considered the impact of a single factor on crop yield from a macroscopic perspective, neither comprehensively taking into account the combined effects of these factors on crop yield, nor exploring the differences of effects of the above-mentioned influencing factors on food production at different time scales including the macroscopic and microcosmic scales.

As previous studies mentioned that crop yield is affected by the signals of climate variability and solar activities. However, all of these factors possess different periodic signals. For instance, Plaut et al. (1995) reported the detection of 5.2, 7.7, 14.2 and 25.0 years periods in the 335 years the Central England Temperature by using the SSA technique. Chen et al. (2016) found that four significant cycles with alternation patterns of precipitation were detected mainly at the time scales of 3-5, 10-11, 20-23, and 31.2 years for each of the four subregions of Liaoning province. ENSO, first described in 1923 by Sir Gilbert Walker (Walker, 1923), is a coupled atmospheric-oceanic oscillation in the tropical Pacific with an average period of 2-7 years. Like ENSO, the PDO is dominated by oceanic temperature oscillations with a typical period of 20-30 years (Mantua et al., 1997; Zhang et al., 1997; Nigam et al., 1999; Stoner et al., 2009). The Arctic Oscillation is a mode of the climate variability with decadal-scale variability oscillation (Mokhov et al., 2013). Besides, average period of a sunspot number cycle is 11.2 years, actual periods have ranged from 7 to 14 years (Kane et al., 2008). In other words, the crop field under the influence of multiple signals of climate variability and solar activities must be provided with complex periodic

http://www.aloki.hu ● ISSN 1589 1623 (Print) ● ISSN 1785 0037 (Online)
DOI: http://dx.doi.org/10.15666/aeer/1802_32513275

signals. Therefore, studying the impact of the signals of climate variability and solar activities on crop yield from a macroscopic scale can only reveal the response characteristics of crop yield change to the changing environment in part.

In order to increase our awareness of the impacts of climate change and develop adaptation projects, it is necessary to separate the effects of climate change from the effects of each climate variable on observed changes in crop yields (Bai et al., 2015). Now that crop yield is the result of a combination of factors. Under the influence of multiple factors, its fluctuations do not move in a fixed cycle, but include changes in various time scales (periods) and local fluctuations, which lead it to change in multiple levels of time scales and localizations in the time domain. Hence, if the signal of which cycle of grain yield is affected specifically by the above factors can be explained clearly (that is, the effects of signals of climate variability and solar activities on different frequencies of maize yield are studied from the microcosmic scale), which will provide a very favorable forecasting approach for crop yield prediction, helping policy makers to accurately control the future trend of crop yield, and contributing to the reasonable development of national food security. The empirical mode decomposition (EMD) method is used to linearize and smooth the nonlinear and non-stationary signals step by step (Huang et al., 1998, 2013; Zhao et al., 2017; Yu et al., 2018; Zhao et al., 2020b). The method can separate the fluctuations of different scales step by step, and produce a series of intrinsic mode functions (IMFs) containing local characteristic information at different time scales of the original signal, and the residue (R), which retains the data itself in the process of decomposition characteristic. Therefore, this study will employ the EMD method for wave decomposition analysis, with a purpose of exploring the multi-scale characteristics of China's maize yield fluctuations and their correlations with major influencing factors (including the signals of climate variability and solar activities), which provide a new insight into the impact of various influencing factors on maize yield fluctuations at multiple scales including the macroscopic and microcosmic scales. This work helps to physically reveal the impact of climate change on grain production variations, thereby being helpful for reliable grain production forecasting. Additionally, since overall trend in increasing food production mainly caused by human activities (e.g. technological advances, fertilization, irrigation, etc.) (Lu et al., 2017), the yield data employed in this study is detrended in order to focus on analyzing climate effect on crop yield.

The main objectives of this study therefore are: (1) to examine the changing periods of detrended maize yield and the IMFs of maize yield in China; (2) to explore the possible causes of detrended maize yield variation from the perspective of climate change including the signals of climate variability (i.e. precipitation, temperature, AO, ENSO, PDO) and solar activities (i.e. sunspots) at the macroscopic scale; (3) to investigate the related implications of the signals of climate variability and sunspots on maize yield decompositions at the microcosmic scale; (4) to construct a complete influencing hierarchical framework of sunspots-teleconnection factors (ENSO, AO, PDO)-climatic factors (precipitation and temperature) on the various frequency components of the detrended maize yield. The remainder of the paper is structured in four sections. Section 2 describes the study database and methods. Results and discussion are provided in Section 3 and Section 4, Section 5 presents the conclusions.

http://www.aloki.hu ● ISSN 1589 1623 (Print) ● ISSN 1785 0037 (Online)
DOI: http://dx.doi.org/10.15666/aeer/1802_32513275

Data sources and methodology

Data sources

This study used annual, country-level yield data for corn during 1961-2016 from Food and Agriculture Organization of the United Nations (http://www.fao.org/fao-stat/en/#home). The meteorological data (included, precipitation, temperature) from the China meteorological data network (http://data.cma.cn/). The ENSO indices were derived from the National Oceanic and Atmospheric Administration (NOAA) Earth System Research Laboratory (www.esrl.noaa.go -v/psd/data/correlation/amon.us.data) and www.esrl.noaa.gov/psd/data/correlation/nina34.data), the AO index was derived from the NOAA National Climatic Data Center (www.ncdc.noaa.gov/tele -connections/ao/), and the PDO index was derived from the Tokyo Climate Center (ds.data.jma.go.jp/tcc/tcc/p-roducts/elnino/decadal/annpdo.txt).

Methods

The Empirical Mode Decomposition

Empirical Mode Decomposition (EMD) is an adaptive method for separating the spectrum of nonlinear and non-stationary signals (Wu et al., 2007). It decomposes a given time series, or signal, in components with different frequencies and amplitudes, known as Intrinsic Mode Functions (IMFs). IMFs have two attributes that differentiate them from other signals:

- The number of extreme and zero crossings must differ at most by one.
- The mean value between the upper and lower envelope is zero.

The original time series $X(t)$ can be written as *Eq.1*.

$$X(t) = \sum_{i=1}^{m} IMF_i(t) + r(t) \quad \text{(Eq.1)}$$

where m is the number of IMFs.

The Stopping Criterion for the extraction of each IMF consists of verifying whether or not the component h can be defined as an IMF, as well as optional criterion such as the component maintaining its characteristics after S additional number of siftings (S-number) and a maximum number of siftings. The sifting process runs iteratively, extracting IMFs from the signal until the residue becomes a monotonic function, a constant value or a function with only one extremum from which no more IMFs can be extracted (Zhao et al., 2017).

The cross wavelet analysis

The cross wavelet analysis developed by Hudgins et al. (1993) is a new technique in exploring the associations between two associated time series. It combines wavelet transform with cross-spectrum analysis to ideally reflect the variation characteristics and coupled oscillations of the two time series in the time and frequency fields. (Hudgins et al., 1993; Torrence et al., 1998).

The cross wavelet transform of two time series x_n and y_n is expressed as $W^{XY}=W^X W^{Y*}$ where * denotes their complex conjugation. The cross wavelet power can be expressed as $|W^{XY}|$. The complex argument arg(W^{XY}) can be regarded as the local relative phase

http://www.aloki.hu ● ISSN 1589 1623 (Print) ● ISSN 1785 0037 (Online)
DOI: http://dx.doi.org/10.15666/aeer/1802_32513275

between x_n and y_n in time-frequency field. The theoretical distribution of the cross wavelet power of these two series with their background power spectra P_K^X and P_K^Y is expressed as follows (Hudgins et al., 1993):

$$D\left(\frac{W_n^X(S)W_n^{Y*}}{\sigma_x\sigma_y} < p\right) = \frac{Z_\nu(P)}{\nu}\sqrt{P_K^X P_K^Y} \quad \text{(Eq.2)}$$

where $Z_\nu(P)$ is the confidence level associated with the probability P for a probability distribution function defined by the square root of two χ^2 distributions (Grinsted et al., 2004). The relevant codes can be freely downloaded from the website http://www.pol.ac.uk/home/rese-arch/waveletcoherence/.

Corn production shows fluctuating changes in time. The signals of climate variability can explain this variability to a certain extent (Talaee et al., 2014; Huang et al., 2016; Dai et al., 2020). Besides, photosynthesis must be conducted during the growth and development of maize. Therefore, solar activities are expected to have a certain impact on corn yield. Hence, the linkages between maize yield and the signals of climate variability/solar activities at both of the macroscopic and microcosmic scales were explored to fully reveal the impacts of these factors on corn yield in the China mainland, which has the largest population in the world. This work helps to physically reveal the impact of climate change and solar activities on the change in grain production China, thereby being helpful for its reliable maize yield prediction.

Results

Analysis of the changing periods of detrended maize yield and the IMFs of maize yield in China

Analysis of the changing periods of detrended maize yield in China

Lu et al. (2017) found that the all trends of yield of various crops are increasing, mainly caused by technological advances. The trends should be removed before other basic applications are implemented, such as computing the correlation function (Wu et al., 2007). The definition of the residual component in EMD method is almost identical to the definition of the trend when the data span in the trend covers the whole data length (Wu et al., 2007). Based on that, the study gets detrended maize yield data by eliminating the residual of original maize yield data. The continuous wavelet transform (CWT) is used to identify the period of the detrended maize yield data. The results are shown in *Fig. 1*. Detrended maize yield has a primary period of approximately 18 years, a secondary period of probably 12 years, a third period of roughly 6 years of corn yield and a fourth period of summarily 3 years. It is obviously seen that maize yield fluctuates at different frequencies in time domain (changing from low and medium frequencies to high frequency).

Analysis of the changing periods of the IMFs of maize yield in China

In this paper, the EMD method was used to decompose the detrended maize yield data. The results were shown in *Fig. 2*. It can be seen form *Fig. 2* that, 1961-2016, detrended maize yield time series in China was decomposed into 4 IMFs and 1 trend item R. Among them, 1) IMF1 reflects a fluctuation of 2~6 years, and the oscillations are more uniform

http://www.aloki.hu ● ISSN 1589 1623 (Print) ● ISSN 1785 0037 (Online)
DOI: http://dx.doi.org/10.15666/aeer/1802_32513275

throughout the scale period fluctuations. The peaks and valleys of the adjacent years appear one after another, indicating that the short-period maize yield fluctuations are more common, and the maize yield increase and decrease periodicity caused by the scale fluctuations is obvious; 2) IMF2 behaves a fluctuation of 6~11 years. The oscillation frequency is slower and the amplitude is relatively stable and small, as well as the fluctuation is relatively flat, which indicates that the maize yield fluctuation intensity of this scale is lighter; 3) there is a 12~19 years fluctuation displayed in IMF3. The period of the oscillation is relatively long and the amplitude is larger than IMF1 and IMF2, indicating that the fluctuation of maize yield at this scale does not occur often, but the intensity is relatively large; 4) it can be seen that IMF4 has a 27 years fluctuation with the long period, large amplitude and intensity indicating that fluctuations in maize yield at this scale rarely occur; 5) for the residual, Maize yield shows an upward trend at 1961-1990, and a downward trend at 1991-2016.

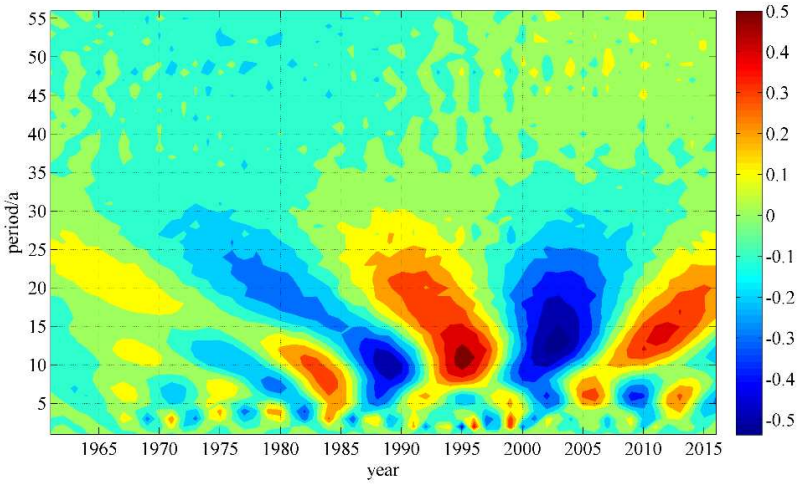

Figure 1. *Plot of the continuous wavelet transform of the detrended maize yield data*

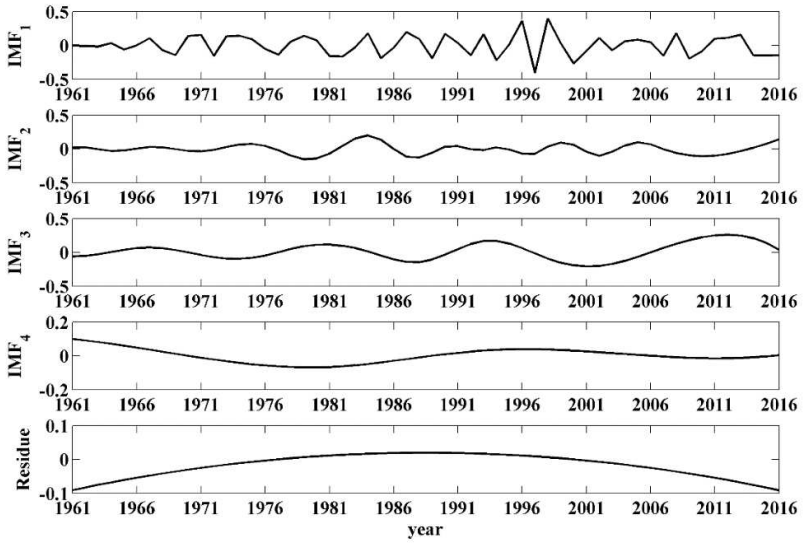

Figure 2. *The IMFs of detrended maize yield*

http://www.aloki.hu ● ISSN 1589 1623 (Print) ● ISSN 1785 0037 (Online)
DOI: http://dx.doi.org/10.15666/aeer/1802_32513275

Analysis of the effects of the signals of climate variability and solar activities on detrended maize yield at the macroscopic scale

As we all know, long-term fluctuations in corn yield are closely related with climatic factors. In this paper, the cross-wavelet analysis was used to analyze the correlations between influencing factors including precipitation, temperature, sunspots, AO, ENSO as well as PDO and detrended maize yield (*Fig. 3*).

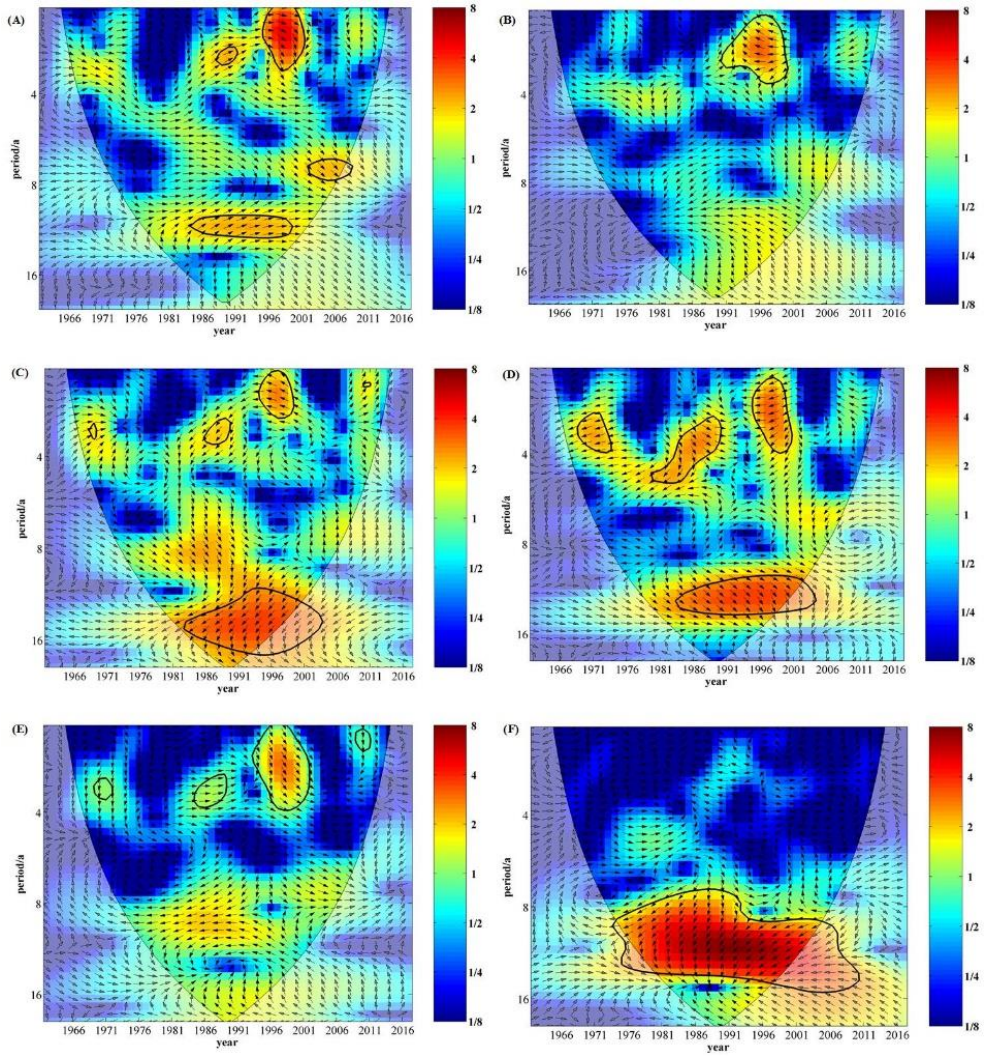

Figure 3. *The cross wavelet transforms of signals of climate variability (included precipitation (A), temperature (B), AO (C), ENSO (D), PDO (E)) and solar activities (sunspots (F)) and detrended maize yield, respectively*

To reveal the relationship between precipitation and detrended maize yield data in the Chinese mainland, the cross-wavelet analysis was performed and the results were shown in *Fig. 3A*. *Fig. 3A* displays that there are statistically positive correlations between precipitation and detrended maize yield with a 1-3 year signal in 1995-2001, a 2.5 year signal in 1987-1992, a 11~13 year signal in 1984~2000 and a 7.5 year signal in 2002~2008 at the 95% confidence level. There are some differences in the *Fig. 3B*. It exhibits the cross wavelet transforms between temperature and detrended maize yield. Temperature has relatively

http://www.aloki.hu ● ISSN 1589 1623 (Print) ● ISSN 1785 0037 (Online)
DOI: http://dx.doi.org/10.15666/aeer/1802_32513275

significant negative linkages with detrended maize yield at the 95% confidence level with a 1-3.5 year signal in 1990-2000. These directly demonstrate that precipitation and temperature play an important role in corn yield and have the opposite relationship with corn yield. The results were basically consistent with Zhao et al. (2015b). They found that precipitation and temperature had significant opposite effects on the climate-induced yield of maize from the macroscopic perspective.

AO has comparatively significant positive correlations with detrended maize yield with a 3 year signal in 1967-1970 and a 1.5 year signal in 2009-2011 (*Fig. 3C*). It also shows negative correlations with detrended maize yield with a 3-3.5 year signal in 1985-1990 and a 1-2.5 year signal in 1994-2000. Similarly, ENSO (Nino3.4) has relatively significant negative linkages with detrended maize yield at the 95% confidence level with a 3-4 year signal in 1967-1972 and a 1.5-4 year signal in 1995-2001, and it has significant positive correlations with detrended maize yield with a 3-5 year signal in 1980-1990 and a 11~14 year signal in 1982-2004 (*Fig. 3D*). In addition, *Fig. 3E* exhibits that PDO has a significant positive correlation with detrended maize yield at the 95% confidence level with a 1-4 year signal in 1992-2002. It also has a comparatively positive correlation with detrended data at the 95% confidence level with a 3.5 year signal in 1984-1990. It can be observed from *Fig. 3F* that sunspots show a statistically significant negative correlation with detrended maize yield at the 95% confidence level with a 7.5-15 year signal in 1973-2011. In addition, some relevant papers (Kim et al., 2005; Butler et al., 2013; Zhao et al., 2015b) reported that the linkages between maize yield and the signals of climate variability (AO, PDO and ENSO) and solar activities at macroscopic scale, which further verifies the reliability of our findings in this study.

Based on *Fig. 3A~Fig. 3F*, it was evident that the signals of climate variability (i.e., precipitation, temperature, ENSO (Nino3.4), AO, PDO) and solar activities (sunspots) had statistically correlations with detrended maize yield. These demonstrate that the short and long-medium periods of maize yield in China are subject to the interaction of above-mentioned factors. It is worth noting that sunspots had the most significant effects on corn yield, and their impacts were concentrated on low frequency regions of maize yield at the macroscopic scale. In contrast, the high-frequency fluctuations were mainly caused by the signals of climate variability at the macroscopic scale. According to influence intensity, this paper found that sunspots had the strongest influence on maize yield, followed by ENSO and AO, followed by precipitation, followed by PDO, and temperature had the weakest influence on maize yield found in *Fig. 3*.

Analysis of the effects of the signals of climate variability and solar activities on decomposition of detrended maize yield at the microcosmic scale

Section 3.2 shows that maize yield is the result of a combination of factors. Based on the above analysis, the application of the empirical mode decomposition (EMD) method in this manuscript to decompose maize yield data. Detrended maize yield data was decomposed into 4 intrinsic mode functions (IMF) and a residual component. The cross-wavelet analysis was employed to explore the correlations between the four IMFs and signals of climate variability, which is contributed to a deeper understanding of the impact of the signals of climate variability on maize yield at the microcosmic scale. Similarly, the cross-wavelet analysis was used to analyze the impact of solar activities on the decomposition of detrended maize yield. The results are displayed in *Fig. 4~Fig. 9.*

As seen from *Fig. 4A* that there was a statistically positive correlation between precipitation and the IMF1 of corn yield with a 3 year signal in 1987-1992, a 1-3.5 year signal

http://www.aloki.hu ● ISSN 1589 1623 (Print) ● ISSN 1785 0037 (Online)
DOI: http://dx.doi.org/10.15666/aeer/1802_32513275

in 1995-2001 and a 8 year signal in 2000-2010 at the 95% confidence level. There were some differences in *Fig. 4B* compared with *Fig. 4A*. In the figure, it shows that the cross wavelet transforms between precipitation and the IMF2. Precipitation had statistically significant positive linkages with the IMF2 at the 95% confidence level with a 4-13 year signal in 1970-2011. In addition, *Fig. 4C* displays that precipitation had a comparatively significant positive correlation with the IMF3 at the 95% confidence level with a 12 year signal in 1977-2002. *Fig. 4D* and *Fig. 4E* indicated that the correlations between precipitation and IMF4/residue were not significant. These results demonstrated that precipitation mainly impacted the medium-high frequency regions of maize yield and had a certain influence on the low frequency regions.

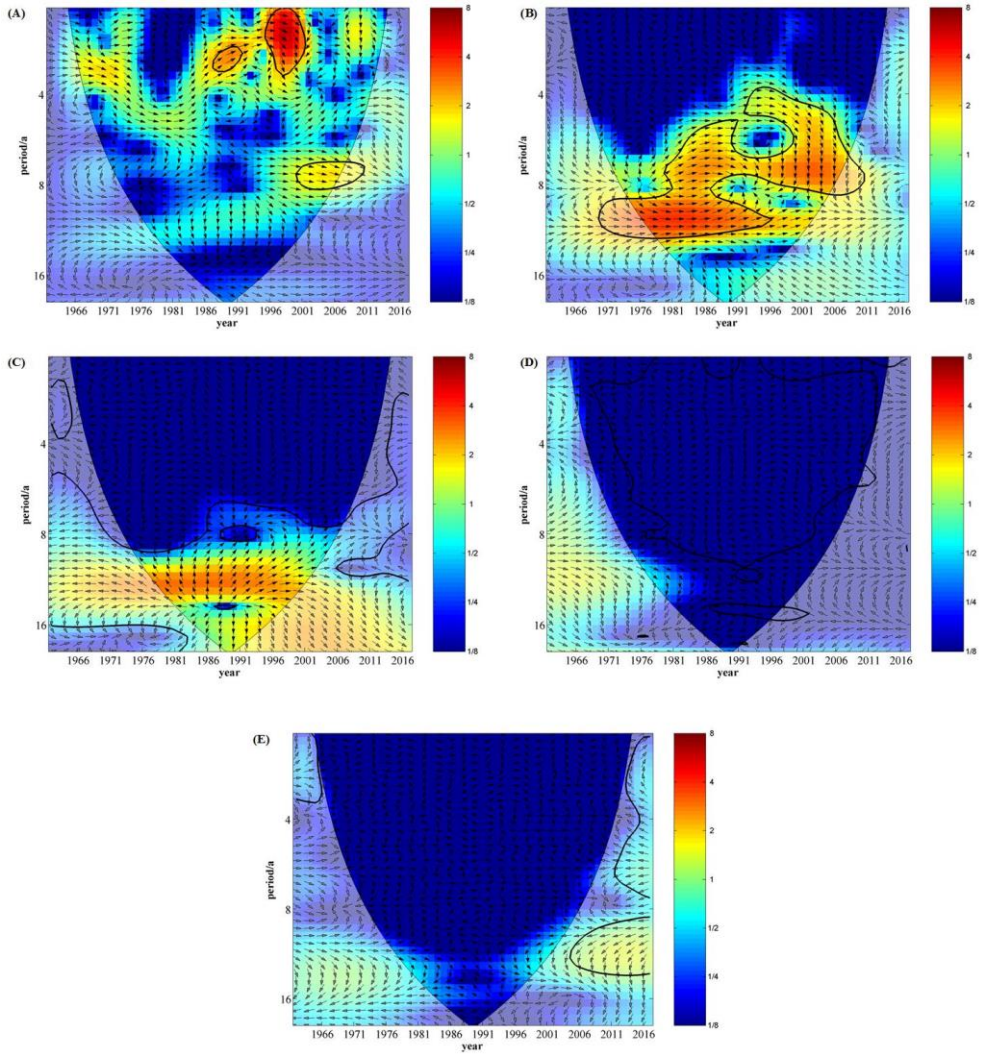

Figure 4. *The cross wavelet transforms of precipitation and IMF1~4 and residue of maize yield (A~E), respectively*

It can be observed from *Fig. 5A* that temperature showed a statistically significant negative correlation with IMF1 at the 95% confidence level with a 1.5-3.5 year signal in 1990–2001. There was a positive correlation between precipitation and the IMF1 of corn yield a 4 year signal in 1975-1982 at the 95% confidence level. There are some differences in *Fig. 5B*. It reveals that temperature has relatively significant positive

http://www.aloki.hu ● ISSN 1589 1623 (Print) ● ISSN 1785 0037 (Online)
DOI: http://dx.doi.org/10.15666/aeer/1802_32513275

linkages with the IMF2 at the 95% confidence level with a 4 year signal in 1992-1997 and a 6~7.5 year signal in 2000-2006. In addition, *Fig. 5C* displays that temperature has a comparatively significant positive correlation with the IMF3 at the 95% confidence level with a 13~15 year signal in 1976-2016. *Fig. 5D* and *Fig. 5E* have weaker correlations between temperature and IMF4/residue. In a word, temperature concentrated influence on medium and high frequency of corn yield.

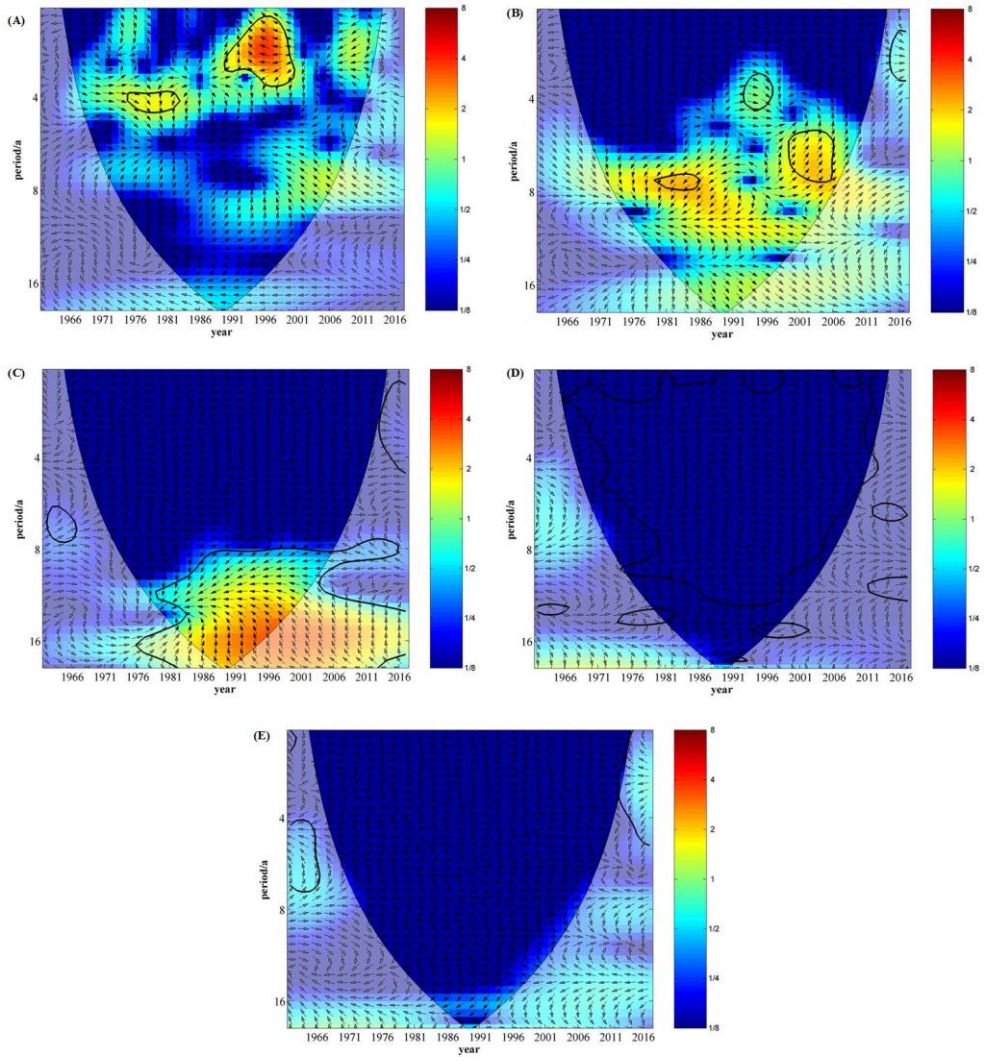

Figure 5. *The cross wavelet transforms of temperature and IMF1~4 and residual of maize yield (A~E), respectively*

Fig. 6A displays that there is a statistically positive correlation between AO and IMF1 of corn yield in the Chinese mainland with a 3-4 year signal in 1967-1972 and it has a significant negative linkages with IMF1with a 3-4 year signal in 1983-1991 and a 2 year signal in 1994-1999 at the 95% confidence level. There are some differences in the *Fig. 6B*. It exhibits the cross wavelet transforms between AO and IMF2 of corn yield. AO has significant positive linkages with IMF2 at the 95% confidence level with a 4-10 year signal in 1972-2000 and a significant negative correlation with IMF2 with a 5 year signal (*Fig. 6B*). It can be observed from *Fig. 6C* that there is a statistically negative correlation between AO and IMF3 of corn yield with a 9-17 year signal in 1961-2016. No significant relationship between AO and IMF4

http://www.aloki.hu ● ISSN 1589 1623 (Print) ● ISSN 1785 0037 (Online)
DOI: http://dx.doi.org/10.15666/aeer/1802_32513275

and residual term was found in the *Fig. 6D* and *6E*. We can see that AO primarily affects medium and low frequency of maize yield.

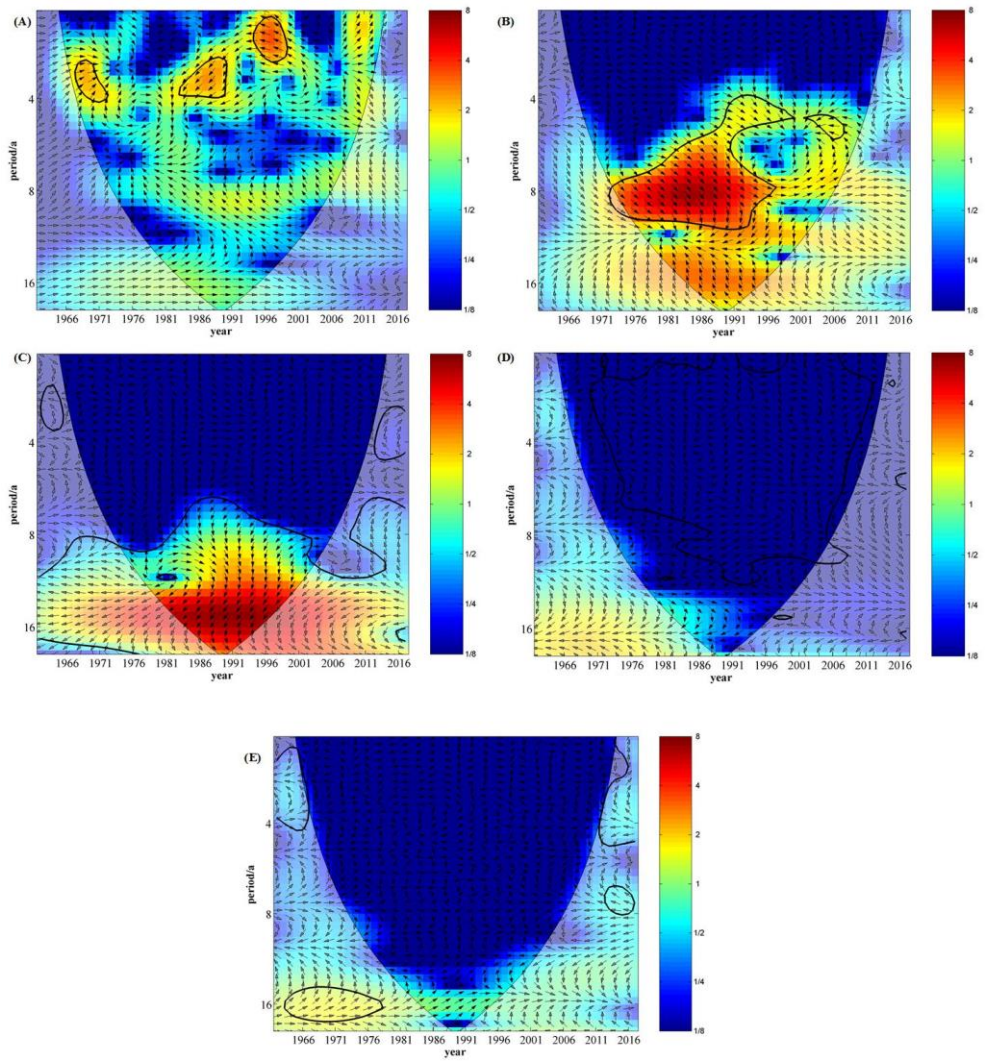

Figure 6. *The cross wavelet transforms of AO and IMF1~4 and residue of maize yield (A~E), respectively*

Similarly, the cross wavelet analysis was applied to reveal the correlations between ENSO (Nino3.4) and the IMFs of maize yield. There are the results shown in *Fig. 7* ENSO has a statistically positive correlation with IMF1 of corn yield with a 3-5 year signal in 1968-1991 and a 1.5-4 year signal in 1994-2001 (*Fig. 7A*). It also shows a significant correlation between ENSO and IMF2 with a 4-7 year in 1982-2007 and a significant positive linkage with IMF2 with a 14 year signal in 1977-2015 (*Fig. 7B*). Besides, *Fig. 7C* exhibits a comparatively significant positive correlation with IMF3 at the 95% confidence level with a 14 year signal in 1976-2016. There are weaker correlations between ENSO and IMF4 and residue seeing from *Fig. 7D* and *7E*. Above all, it is obviously seen that ENSO mainly impact on medium-high frequency of maize yield.

http://www.aloki.hu ● ISSN 1589 1623 (Print) ● ISSN 1785 0037 (Online)
DOI: http://dx.doi.org/10.15666/aeer/1802_32513275

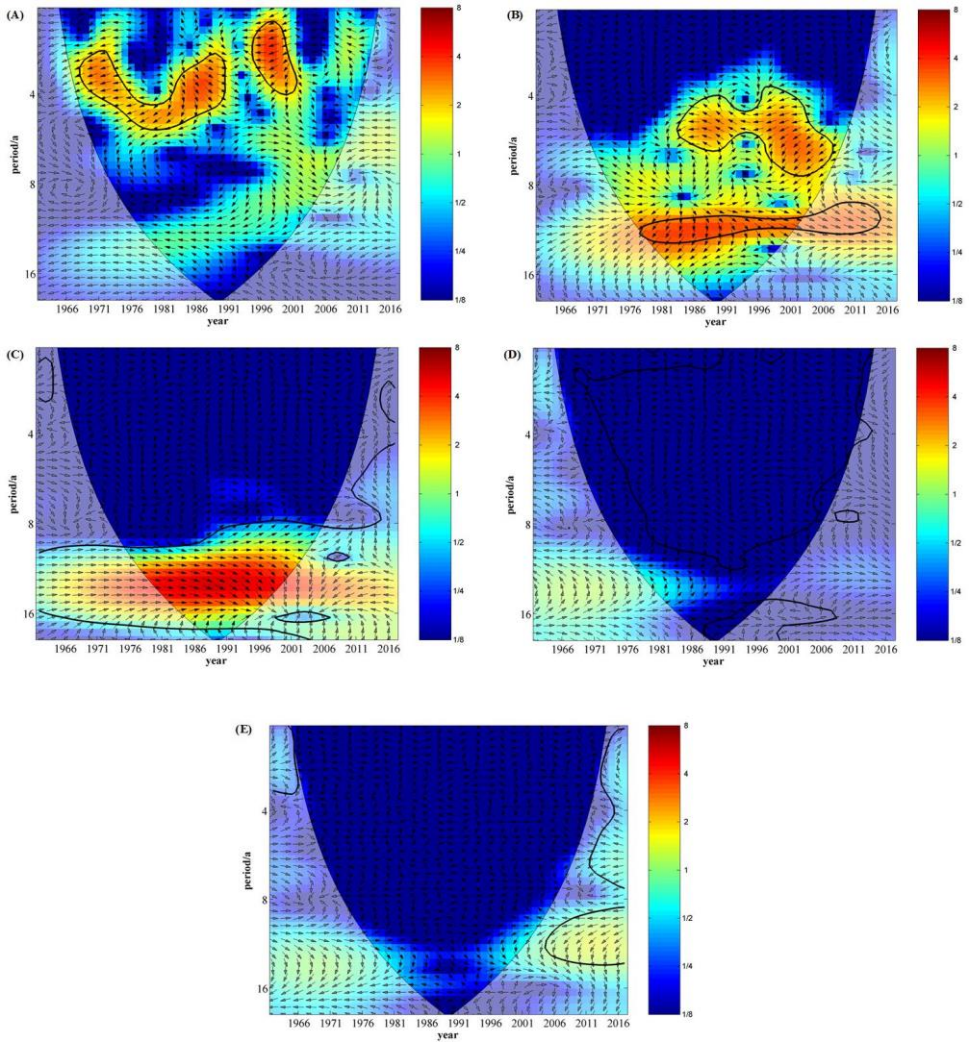

Figure 7. *The cross wavelet transforms of ENSO (Nino3.4) and IMF1~4 and residue of maize yield (A~E), respectively*

In addition, PDO has statistically significant positive linkages with IMF1 of corn yield at the 95% confidence level with a 1-4 year signal in 1992-2002 and a 3-4 year signal in 1982-1990 (*Fig. 8A*). It also shows that a comparatively significant correlation between PDO and IMF1 with a 3-4 year signal in 1967-1972. *Fig. 8B* exhibits PDO has a statistically significant linkage with IMF2 with a 6-9 year signal in 1972-2007. It can be seen from *Fig. 8C* that PDO has a relatively significant linkage with IMF3 with a 8~16 year signal in 1976-2016. Based on *Fig. 8*, we can see that PDO mainly influence medium frequency of maize yield.

In addition to analyzing the correlations between signals of climate variability and maize yield components, the cross-wavelet transform was used to explore the linkage the IMFs and solar activities (sunspots). The results are displayed in *Fig. 9*. It can be seen from *Fig. 9A* that sunspots have a relatively significant positive linkage with IMF1 of corn yield at the 95% confidence level with a 4-5 year signal in 1976-1982 and a statistically significant negative linkage with IMF1 with a 8-14 year signal in 1977-2005. *Fig. 9B* exhibits a statistically significant correlation between sunspots and IMF2 with a

http://www.aloki.hu ● ISSN 1589 1623 (Print) ● ISSN 1785 0037 (Online)
DOI: http://dx.doi.org/10.15666/aeer/1802_32513275

5-14 year signal in 1966-2016. Sunspots have a comparatively significant linkage with IMF3 with a 8-16 year signal in 1967-2016 (*Fig. 9C*). Interesting, sunspots mainly influence on medium and low frequency of maize yield components.

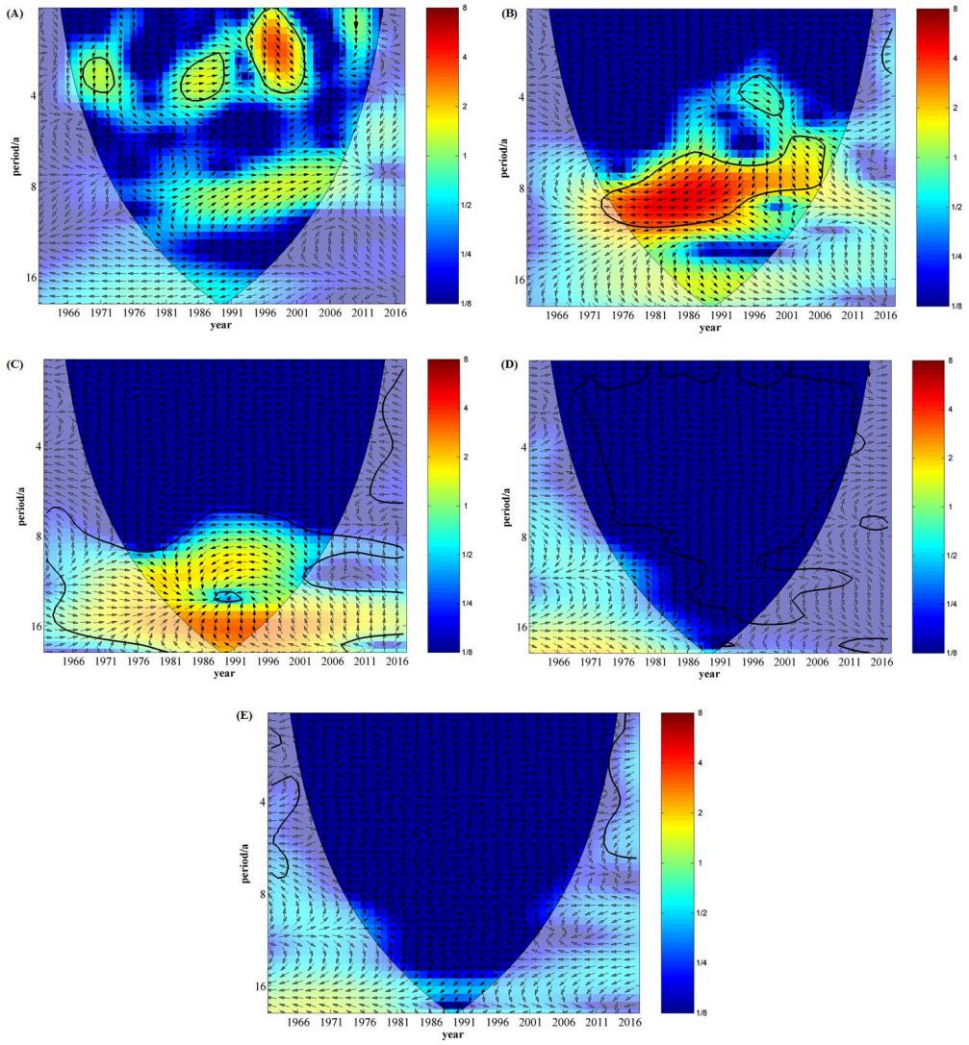

Figure 8. *The cross wavelet transforms of PDO and IMF1~4 and residue of maize yield (A~E), respectively*

Based on *Fig. 4* and *Fig. 9*, it was evident that PDO mainly affect the first and second components of detrended maize yield, and the second and third components of detrended maize yield were mainly impacted by sunspots and AO, whilst the first three components of detrended maize yield were influenced by ENSO and precipitation, moreover, the effect of temperature on detrended maize yield was relatively weak, and mainly affect the first and third component of detrended maize yield. These results indicated that the yield components of corn were not only affected by a single factor, but the result under the combined action of multiple factors, and the influence factors of different components were not the same. As far as was known, there were a number of papers (Plaut et al., 1995; Stonter et al., 2009; Mokhov et al., 2013; Zhao et al., 2015b; Chen et al., 2016) had proved that the signals of climate variability (i.e. precipitation, temperature, ENSO (Nino3.4), AO, PDO) and solar activities

http://www.aloki.hu ● ISSN 1589 1623 (Print) ● ISSN 1785 0037 (Online)
DOI: http://dx.doi.org/10.15666/aeer/1802_32513275

(sunspots) dominated by different periodic signals, which further verified the rationality and accuracy of the above findings.

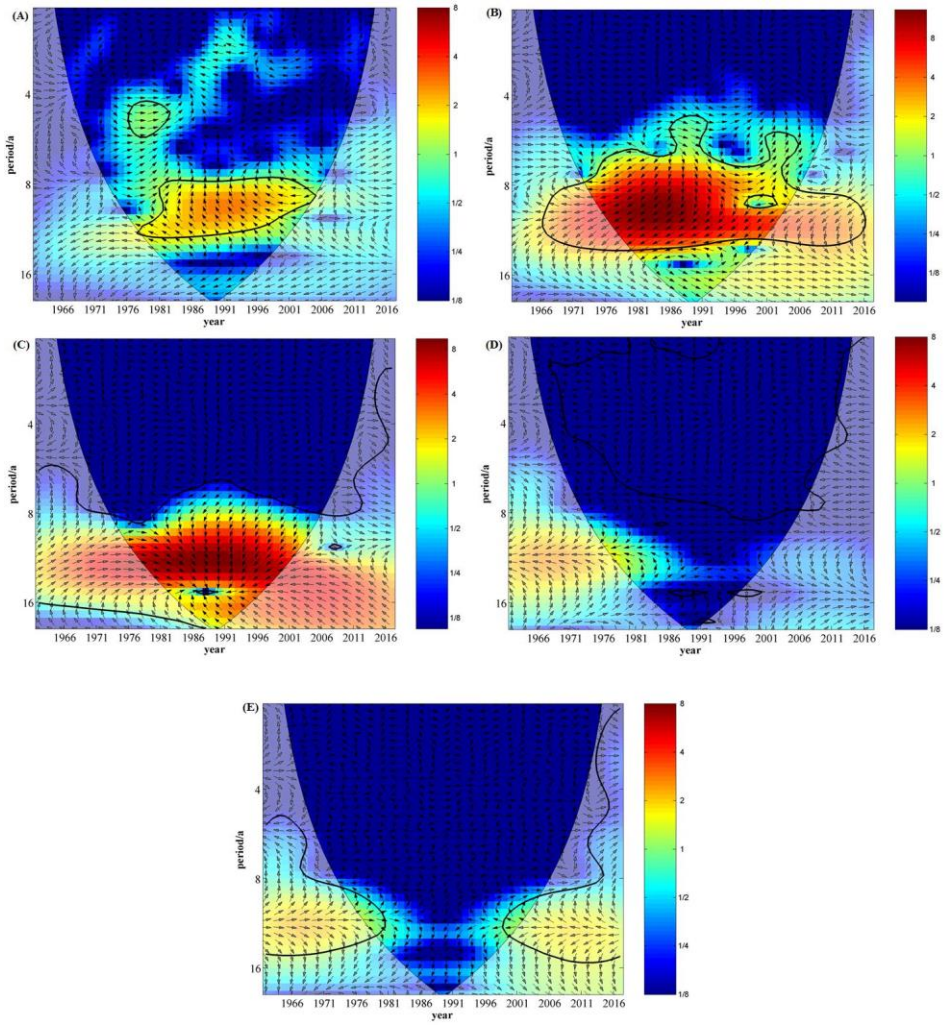

Figure 9. *The cross wavelet transforms of sunspots and IMF1~4 and residue of maize yield (A~E), respectively*

The complete influencing hierarchical framework

More and more studies indicate that teleconnection factors (e.g. ENSO, AO, PDO) and sunspots have major impact on global atmospheric circulation and regional climatic anomalies (Kenyon et al., 2008; Schubert et al., 2008; Alexander et al., 2009; Dikpati et al., 2010; Owens et al., 2011; Meehl et al., 2013). According to the analysis results in section 3.3, different impacting hierarchical frameworks were constructed for IMF1~3.

It can be seen from *Fig. 4A*, *Fig. 5A*, *Fig. 7A* and *Fig. 8A* that there were statistically positive correlations between precipitation, PDO and the IMF1 of detrended maize yield in 1980-2000, and ENSO had a significant positive linkage with IMF1 of detrended maize yield in 1983-1990. In contrast, temperature and ENSO showed statistically significant negative correlations with IMF1 in 1991-2001. These suggested that precipitation, PDO, ENSO and temperature had significant different effects on the growth of maize, and also suggested that the effect of ENSO on maize yield was different in different years. The effects of aforementioned factors on IMF1

http://www.aloki.hu ● ISSN 1589 1623 (Print) ● ISSN 1785 0037 (Online)
DOI: http://dx.doi.org/10.15666/aeer/1802_32513275

were extremely complicated and each factor had mutually reinforcing or weakening influence on maize yield. In view of the aforementioned results, the hierarchical framework of ENSO, PDO-climate variability (precipitation, temperature)-the IMF1 of detrended maize yield may be constructed. In other words, there was a chain effect, which was ENSO and PDO definitely showing impact to precipitation/temperature in some degree and in some land areas, and consequently the climate variability in such variables being certainly associated with detrended maize yield.

Compared the correlations in *Fig. 4B*, *Fig. 6B*, *Fig. 7B*, *Fig. 8B* and *Fig. 9B*, it can be found that precipitation and teleconnection factors had effect on IMF2 of detrended maize yield in the time domain of sunspots influencing IMF2. Therefore, the framework of sunspots-teleconnection factors (ENSO, AO and PDO)-precipitation-the IMF2 of detrended maize yield linkage may be constructed. In other words, there was a chain effect, which was sunspots definitely showing impact to teleconnection factors in some degree, and subsequently, the teleconnection factors exhibiting impact to precipitation in some degree and in some land areas, and consequently precipitation in such variables being certainly associated with detrended maize yield.

Combine the information of these figures (including *Fig. 4C*, *Fig. 5C*, *Fig. 6C*, *Fig. 7C* and *Fig. 8C*) to know that the framework of sunspots-teleconnection factors (ENSO, AO)-climatic variability (precipitation, temperature)-the IMF3 of detrended maize yield linkage may be constructed.

Based on that, the cross wavelet method was used to explore the correlation between sunspots and AO, ENSO as well as PDO (*Fig. 10*) in this study. *Fig. 10* showed that sunspots had significant linkages with AO, ENSO and PDO at the 95% confidence level with an 8~14 year signal in 1966-2001. The findings suggested that sunspots had significant effect on three teleconnection factors, and these also confirmed the first step of the chain effect (for IMF2 and IMF3).

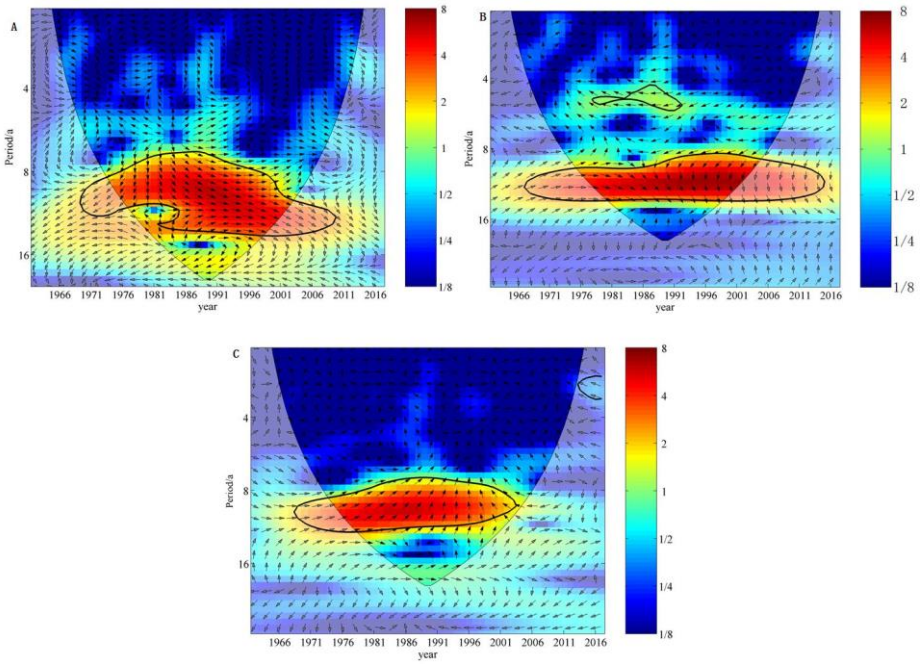

Figure 10. *The cross wavelet transforms of sunspots and AO (A), ENSO (B) and PDO (C), respectively*

http://www.aloki.hu ● ISSN 1589 1623 (Print) ● ISSN 1785 0037 (Online)
DOI: http://dx.doi.org/10.15666/aeer/1802_32513275

Both precipitation and temperature were decomposed by means of EMD decomposition in this paper, since they are also affected by various factors. Similar to the *Fig. 10*, the cross-wavelet method was utilized in the study, to explore the relationship between AO, ENSO, PDO and the components of precipitation and temperature (as shown in *Fig. 11* and *Fig. 12*). *Fig. 11* displayed that AO and ENSO were significantly correlated with the IMF2 and IMF3 of precipitation, and that there was a significant correlation between PDO and the IMF2 of precipitation. These results indicated that AO, ENSO and PDO had an important influence on precipitation. By contrast, the effects of AO and ENSO on precipitation were significantly stronger than that of PDO on precipitation. *Fig. 12* exhibited that there were significant linkages between AO, ENSO, PDO and the IMF1 and IMF2 of temperature. In comparison, AO and ENSO had a stronger effect on temperature than PDO. In a word, AO, ENSO and PDO had a certain influence on precipitation and temperature. And more, the findings confirmed the first step (for IMF1) and the second step (for IMF2 and IMF3) of the chain effect. As AO, ENSO and PDO had no significant influence on the IMF4 and residual term of precipitation and temperature, the correlations between them are explored in this paper. Three complete influencing hierarchical frameworks were shown in *Fig. 13*.

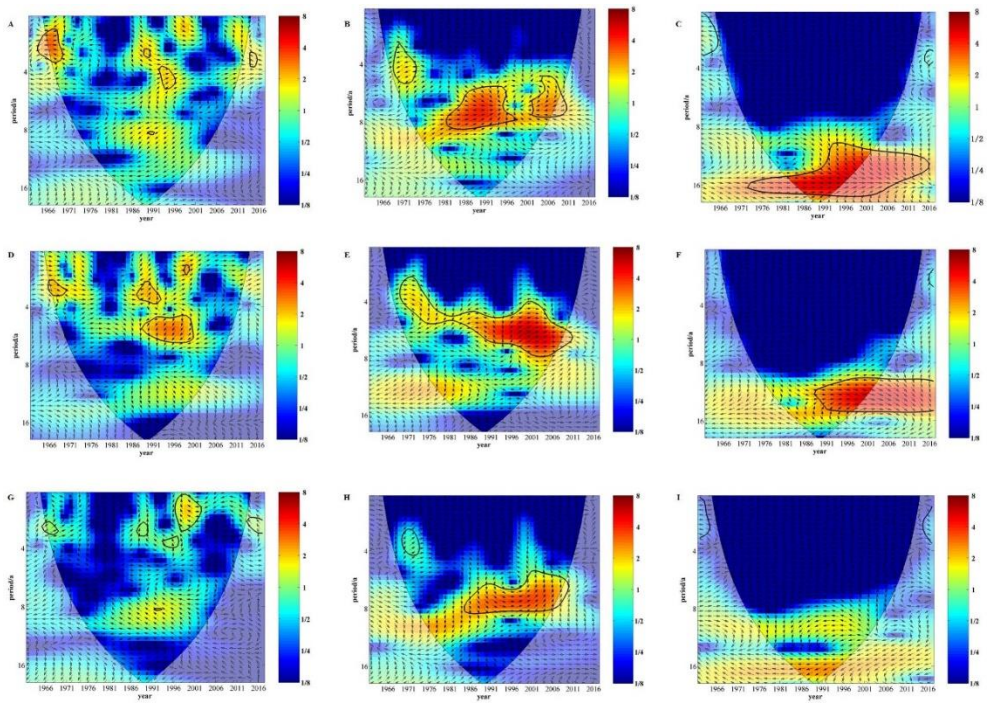

Figure 11. *The cross wavelet transforms of AO and the IMF1 (A), IMF2 (B) and IMF3 (C) of precipitation, ENSO and the IMF1 (D), IMF2 (E) and IMF3 (F) of precipitation as well as PDO and the IMF1 (G), IMF2 (H) and IMF3 (I) of precipitation, respectively*

Besides the above findings, we can also see from the figure that the signals of climate variability and solar activities have no significant influence on the IMF4 and residual terms of corn yield. This is mainly because the maize yield sequence was detrended in this paper, which made the low-frequency signals in the maize yield sequence be removed, so that the climatic factors had no obvious influence on the detrended maize yield sequence after decomposition.

http://www.aloki.hu ● ISSN 1589 1623 (Print) ● ISSN 1785 0037 (Online)
DOI: http://dx.doi.org/10.15666/aeer/1802_32513275

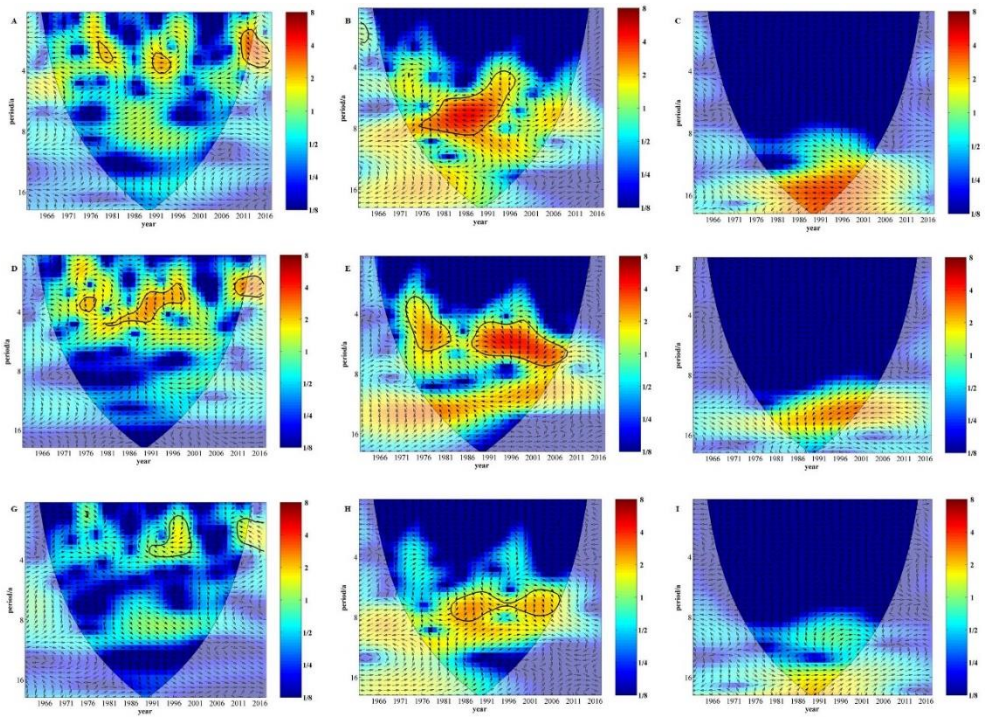

Figure 12. *The cross wavelet transforms of AO and the IMF1 (A), IMF2 (B) and IMF3 (C) of temperature, ENSO and the IMF1 (D), IMF2 (E) and IMF3 (F) of temperature as well as PDO and the IMF1 (G), IMF2 (H) and IMF3 (I) of precipitation, respectively*

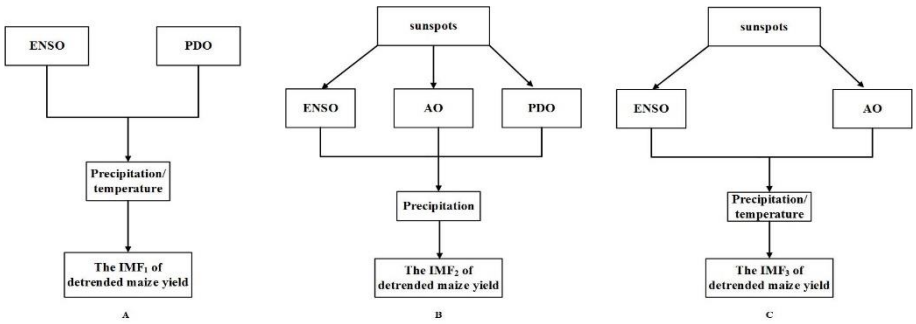

Figure 13. *Three complete influencing hierarchical frameworks for IMF1 (A), IMF2 (B) and IMF3 (C)*

Above all, three frameworks were constructed. These also showed that the effects of signals of climate variability and solar activities on the IMFs of corn yield can not only verify the accuracy of the effects of these factors on maize yield after detrending, but also demonstrate each single component of the IMFs was synthetically affected by the above factors. Based on these findings, this study can provide a new idea for the grain prediction model, that is, the above factors can be used to predict the different components of corn (i.e. ENSO, PDO, precipitation and temperature could be used to predict the IMF1 of maize yield; sunspots, ENSO, AO, PDO and precipitation could be used to predict the IMF2 of maize yield; and sunspots, ENSO, AO, precipitation and temperature could be used to predict the IMF3 of maize yield), and then the predicted results can be combined with relevant means to improve the prediction accuracy of grain yield to a certain extent.

http://www.aloki.hu ● ISSN 1589 1623 (Print) ● ISSN 1785 0037 (Online)
DOI: http://dx.doi.org/10.15666/aeer/1802_32513275

Discussion

The necessity of the signals of climate variability and solar activities affect the changes in detrended maize yield at microcosmic scale

Compared to the effects of precipitation on detrended maize yield and the IMFs of detrended maize yield (*Fig. 3A* and *Fig. 4*), it can be discovered that there were statistically positive correlations between precipitation and detrended maize yield with a 1-3 year signal in 1995-2001, a 2.5 year signal in 1987-1992 and a 7.5 year signal in 2002-2008 at the 95% confidence level (*Fig. 3A*), which was basically consistent with the effect of precipitation on detrended maize yield (*Fig. 4A*). Besides, the interesting findings in *Fig. 4B*, *Fig. 4C* and *Fig. 3A* were that a 11~13 year signal of significance in 1984-2000 (shown in *Fig. 3A*) was included in the time-frequency domains beyond significance of *Fig. 4B* and *Fig. 4C*. These findings suggested that precipitation had a significant positive effect on detrended maize yield and mainly affected the fluctuation of detrended maize field in the short and long-medium terms in macroscopic scale, which was fully verified on the microscopic scale (shown in *Fig. 4A~4C*). Notably, in *Fig. 3A*, the regions with high energy in the low and medium frequency regions but not exceeding the significance test all exceeded the significance test in *Fig. 4B* and *Fig. 4C*. On the one hand, the findings showed that the correlations of precipitation and the IMF1~3 of detrended maize yield were obviously superior to the relationship between precipitation and undecomposed detrended maize yield, suggesting that the microscopic scale to a certain extent, can isolate the influence of other factors; On the other hand, the feature that cannot be expressed on the macroscopic scale was observed on the microscopic scale, which indicated from the side that the yield of maize was subject to the influence of various factors. Similarly, temperature also influenced high frequency of detrended maize yield found from *Fig. 3B* and *Fig. 5A*, which was expressed in the time domain in 1990-2001. In contrast, there was a significant negative correlation between temperature and detrended maize yield (compared to *Fig. 3A* and *Fig. 3B*). In addition, the discoveries of temperature and detrended maize yield on macroscopic and microscopic scales were basically consistent with that of precipitation and detrended maize yield. In other words, the analyses of the correlations between temperature and the IMF1~3 of detrended maize yield in microscopic scale were the verification and supplement of the relationship between temperature and detrended maize yield.

It can be seen from *Fig. 3C~3E* and *Fig. 5~8* that the correlations between AO (ENSO, PDO) and detrended maize yield were roughly similar with the relationship between AO (ENSO, PDO) and the IMF1, which demonstrated that AO (ENSO, PDO) had strong effects on the high frequency of detrended maize yield. It was worth noting that sunspots influenced medium frequency of detrended maize yield (a period of 8~12 years in the frequency domain) exhibited in *Fig. 3F* and *Fig. 9A*, which was different with the effect of the signals of climate variability on detrended maize yield. As we all know, sunspots have an average period of 11 years, which was basically consistent with the frequency domain of sunspots impacting on detrended maize yield. Similar to the comparison of the correlations between precipitation or temperature and detrended maize yield in macroscopic and microscopic scales, the relationship between AO (ENSO, PDO and sunspots) and detrended maize yield had this feature, as well.

Based on the above analyses we all know that the signals of climate variability (including precipitation, temperature, AO, ENSO, PDO) made a difference to high frequency of detrended maize yield. It indicated that the short-term cycle changes of corn

http://www.aloki.hu ● ISSN 1589 1623 (Print) ● ISSN 1785 0037 (Online)
DOI: http://dx.doi.org/10.15666/aeer/1802_32513275

yield were mainly caused by meteorological factors (which is consistent with the results of Zhao et al. (2013) and Niu et al. (2018)), whilst mid-cycle changes in corn yield were mainly influenced by solar activities. The correlations between the above factors and the components of detrended maize yield proved the correctness of the above conclusion. For this reason, the above factors can be considered as input variables of corn production prediction model to improve the accuracy of the prediction when predicting the future corn production in China. In addition, this study found that not only the cross wavelet analysis between each influence factor and each component of detrended maize yield sequence can verify the relationship between the factors and detrended maize yield on the macroscopic factors and enhance the analysis accuracy, also found at the macroscopic scale some relevant information cannot be accurately captured on the microscopic scale to get the corresponding added. These findings indicate that correlation analysis from the microscopic scale can help reduce information distortion and ensure the accuracy of correlation analysis.

Potential application of the hierarchical frameworks

Past studies indicated that there were strong relations between solar activities and teleconnection factors (i.e. ENSO, PDO and NAO) (Kapala et al., 1998; Tudhope et al., 2001; Georgieva et al., 2012; Hassan et al., 2016; Maruyama et al., 2017; Liu et al., 2018; Han et al., 2019). Moreover, these teleconnection factors reflect on local weather conditions (precipitation and temperature) (Leathers et al., 1991; Thompson et al., 1998; Higgins et al., 2002; Huang et al., 2017 ; Zhao et al., 2019). In addition, climate variability, especially precipitation and temperature, have been shown to have important effects on crop yields in major crop growing regions in China (Tao, 2012; Wang et al., 2014; Zhang et al., 2015). The research content of the above literature fully shows that the three influencing hierarchical frameworks established in this paper are reasonable. Therefore, it is entirely possible to construct similar influencing hierarchical frameworks for other crops in other areas, such as rice in China, which can provide very reliable basis for food prediction model and reduce the error of food prediction.

Conclusions

In this study, we examined the effects of the signals of climate variability (i.e., precipitation, temperature, AO, ENSO, PDO) and solar activities (i.e., sunspots) on maize yield in China mainland during the period 1961-2016 at both of the macroscopic and microcosmic scales. First, we got rid of the trend of maize yield data sequence, and the periodical features of the detrended sequence was explored by means of CWT analysis. The detrended maize yield had a primary period of approximately 18 years, a secondary period of probably 12 years, a third period of roughly 6 years of corn yield and a fourth period of summarily 3 years. Then the effects of signals of climate variability and solar activities on detrended maize yield and the IMFs of original maize yield were investigated by cross-wavelet transforms. Findings showed that (1) sunspots had the strongest influence on maize yield, followed by ENSO and AO, followed by precipitation, followed by PDO, and temperature had the weakest influence on maize yield at macroscopic scale; (2) the signals of climate variability mainly impact the high-medium frequency (i.e., frequency domain is 1~4 years and 6~10 years) of maize yield and solar activities primarily influence medium frequency (i.e., frequency domain is 8~14 years) for detrended sequence; (3) PDO mainly affect the first and second components of detrended

http://www.aloki.hu ● ISSN 1589 1623 (Print) ● ISSN 1785 0037 (Online)
DOI: http://dx.doi.org/10.15666/aeer/1802_32513275

maize yield, and the second and third components of detrended maize yield were mainly impacted by sunspots and AO, whilst the first three components of detrended maize yield were influenced by ENSO and precipitation, moreover, the effect of temperature on detrended maize yield was relatively weak, and mainly affect the first and third component of detrended maize yield; (4) the hierarchical framework of ENSO, PDO-climate variability (precipitation, temperature)-detrended maize yield was constructed for IMF1; the hierarchical framework of sunspots-teleconnection factors (ENSO, AO and PDO)-precipitation-detrended maize yield was constructed for IMF2; the hierarchical framework of sunspots-remote correlation factors (ENSO, AO)-climate variability (precipitation, temperature)-detrended maize yield was constructed for IMF3. The results of the present study could contribute to improve the crop prediction (considering signals of climate variability and solar activities as the potential influence factors both on whole and decomposition of the maize yield sequence) and hence would provide possibilities for ensuring food security. This study explored the impact of climate change on maize yield on multi-temporal scales. Therefore, when predicting maize yield based on climatic conditions, it is possible to consider the prediction of grain component resynthesis from a multi-temporal perspective, which may improve the prediction accuracy of maize yield.

Acknowledgements. This research was jointly funded by the National Key Research and Development Program of China (grant number 2017YFC0405900), the Key laboratory research projects of the education department of Shaanxi province (grant number 17JS104), the National Natural Science Foundation of China (grant number 51709221), the Planning Project of Science and Technology of Water Resources of Shaanxi (grant numbers 2015slkj-27 and 2017slkj-19), the China Scholarship Council (grant number 201608610170), the Open Research Fund of State Key Laboratory of Simulation and Regulation of Water Cycle in River Basin (China Institute of Water Resources and Hydropower Research, grant number IWHR-SKL-KF201803 and the Doctorate Innovation Funding of Xi'an University of Technology (grant number 310-252071712).

REFERENCES

[1] Alexander, L. V., Uotila, P., Nicholls, N. (2009): Influence of sea surface temperature variability on global temperature and precipitation extremes. – J. Geophys. Res. Atmos. 114: D18116.

[2] Angstrom, A. (1924): Solar and terrestrial radiation. – Quarterly Journal of the Royal Meteorological Society 50(210): 121-125.

[3] Bai, H., Tao, F., Xiao, D., Liu, F., Zhang, H. (2015): Attribution of yield change for ricewheat rotation system in China to climate change, cultivars and agronomic management in the past three decades. – Climatic Change 135: 539-553.

[4] Battisti, D. S., Naylor, R. L. (2009): Historical warnings of future food insecurity with unprecedented seasonal heat. – Science 323: 240-244.

[5] Butler, E. E., Huybers, P. (2013): Adaptation of US maize to temperature variations. – Nat. Clim. Change 3: 68-72.

[6] Cane, M., Eshel, G., Buckland, R. (1994): Forecasting Zimbabwean maize yield using eastern equatorial Pacific sea surface temperature. – Nature 370: 204-205.

[7] Chen, T., Xia, G., Wilson, L. T., Chen, W., Chi, D. (2016): Trend and Cycle Analysis of Annual and Seasonal Precipitation in Liaoning, China. – Advances in Meteorology 2: 15.

[8] Dai, M., Huang, S., Z., Huang, Q., Leng, G. Y., Guo, Y., Wang, L., Fang, W., Li, P., Zheng, X.D. (2020): Assessing agricultural drought risk and its dynamic evolution characteristics. – Agricultural Water Management 231: 106003.

http://www.aloki.hu ● ISSN 1589 1623 (Print) ● ISSN 1785 0037 (Online)
DOI: http://dx.doi.org/10.15666/aeer/1802_32513275

[9] Dikpati, M., Gilman, P. A., Kane, R. P. (2010): Length of a minimum as predictor of nest solar cycle's strength. – Geophy. Res. Lett. 37.
[10] Fang, W., Huang, S. Z., Huang, Q., Huang, G., Wang, H., Leng, G., Wang, L., Guo, Y. (2019): Probabilistic assessment of remote sensing-based terrestrial vegetation vulnerability to drought stress of the Loess Plateau in China. – Remote Sensing of Environment 232: 111290.
[11] Garnett, E., Khandekar, M. (1992): The impact of large-scale atmospheric circulations and anomalies on Indian monsoon droughts and floods and on world grain yields: a statistical analysis. – Agricultural and Forest Meteorology 61: 113-128.
[12] Georgieva, K., Kirov, B., Koucká Knížová, P., Mosna, Z., Kouba, D., Asenovska, Y. (2012): Solar influences on atmospheric circulation. – Journal of Atmospheric and Solar-Terrestrial Physics 90-91(1): 15-25.
[13] Godfray, H. C. J., Beddington, J. R., Crute, I. R., Haddad, L., Lawrence, D., Muir, J. F., Pretty, J., Robinson, S., Thomas, S. M., Toulmin, C. (2010): Food security: the challenge of feeding 9 billion people. – Science 327: 812-818.
[14] Grinsted, A., Moore, J. C., Jevrejeva, S. (2004): Application of the cross wavelet transform and wavelet coherence to geophysical time series. – Nonlinear Proc. Geoph. 11: 561-566.
[15] Guo, Y., Huang, S. Z., Huang, Q., Leng, G. Y., Fang, W., Wang, L., Wang, H. (2020): Propagation thresholds of meteorological drought for triggering hydrological drought at various levels. – Sci. Total Environ. 712: 136502.
[16] Hammer, G. L., Hansen, J. W., Phillips, J. G., Mjelde, J. W., Hill, H., Love, A., Potgieter, A. (2001): Advances in application of climate prediction in agriculture. – Agricultural Systems 70: 515-553.
[17] Han, Z. M., Huang, S. Z., Huang, Q., Leng, G. Y., Wang, H., He, L., Fang, W., Li, P. (2019): Assessing GRACE-based terrestrial water storage anomalies dynamics at multi-timescales and their correlations with teleconnection factors in Yunnan Province, China. – Journal of Hydrology 574: 836-850. DOI: 10.1016/j.jhydrol.2019.04.093.
[18] Hanjra, M. A., Qureshi, M. E. (2010): Global water crisis and future food security in an era of climate change. – Food Policy 35(5): 365-377.
[19] Hassan, D., Iqbal, A., Hassan, S. A., Abbas, S., Ansari, M. R. K. (2016): Sunspots and ENSO relationship using Markov method. – Journal of Atmospheric and Solar-Terrestrial Physics 137: 53-57.
[20] He, Q., Zhou, G., Lü, X., Zhou, M. (2019): Climatic suitability and spatial distribution for summer maize cultivation in China at 1.5 and 2.0°C global warming. – Science Bulletin 64(10): 690-697.
[21] Higgins, R. W., Leetmaa, A., Kousky, V. E. (2002): Relationships between climate variability and winter temperature extremes in the United States. – Journal of Climate 15(13): 1555-1572.
[22] Huang, N. E., Shen, Z., Long, S. R., Wu, M. L. C., Shih, H. H., Zheng, Q., Yen, N. C., Tung, C.-C., Liu, H. H. (1998): The empirical mode decomposition and the Hilbert spectrum for nonlinear and non-stationary time series analysis. – Proceedings of the Royal Society of London A: Mathematical, physical and engineering sciences 454: 903-995.
[23] Huang, N. E., Wu, M.-L. C., Long, S. R., Shen, S. S. P., Qu, W. D., Gloersen, P., Fan, K. L. (2003): A confidence limit for the empirical mode decomposition and Hilbert spectral analysis. – Proceedings of the Royal Society of London A: Mathematical, physical and engineering sciences 459: 2317-2345.
[24] Huang, S. Z., Huang, Q., Chang, J. X., Leng, G. Y. (2016): Linkages between hydrological drought, climate indices and human activities: a case study in the Columbia River Basin. – Int. J. Climatol. 36(1): 280-290.
[25] Huang, S. Z., Li, P., Huang, Q., Leng, G. Y., Hou, B. B., Ma, L. (2017): The propagation from meteorological to hydrological drought and its potential influence factors. – Journal of Hydrology 547: 184-195.

http://www.aloki.hu ● ISSN 1589 1623 (Print) ● ISSN 1785 0037 (Online)
DOI: http://dx.doi.org/10.15666/aeer/1802_32513275

[26] Huang, S. Z., Zheng, X. D., Ma, L., Wang, H., Huang, Q., Leng, G. Y., Meng, E., Guo, Y. (2020): Quantitative contribution of climate change and human activities to vegetation cover variations based on GA-SVM model. – Journal of Hydrology 584: 124687.
[27] Hudgins, L., Friehe, C. A., Mayer, M. E. (1993): Wavelet transforms and atmospheric turbulence. – Phys. Rev. Lett. 71: 3279-3282.
[28] Hunt, L. A., Kuchar, L., Swanton, C. J. (1998): Estimation of solar radiation for use in crop modeling. – Agricultural and Forest Meteorology 91(3/4): 293-300.
[29] IPCC. (2014): Climate Change 2014: Synthesis Report. – In: Pachauri, R. K., Meyer, L. A. (eds.) Core Writing Team, Contribution of Working Groups I, II and III to the Fifth Assessment Report of the Intergovernmental Panel on Climate Change. IPCC, Geneva, Switzerland (151 pp).
[30] Kane, R. P. (2008): Prediction of solar cycle 24 based on the Gnevyshev-Ohl-Kopecky rule and the three-cycle periodicity scheme. – Annales Geophysicae 26(11): 3329-3339.
[31] Kapala, A., Mächel, H., Flohn, H. (1998): Behaviour of the centres of action above the Atlantic since 1881. Part II: Associations with regional climate anomalies. – Int. J. Climatol. 18(1): 23-36.
[32] Kenyon, J., Hegerl, G. C. (2008): Influence of modes of climate variability on global temperature extremes. – J. Clim. 21: 3872-3889.
[33] Kim, M., McCarl, B. A. (2005): The agricultural value of information on the North Atlantic oscillation: yield and economic effects. – Clim. Change 71: 117-139.
[34] Knox, J., Hess, T., Daccache, A., Wheeler, T. (2012): Climate change impacts on crop productivity in Africa and South Asia. – Environ. Res. Lett. 7(3): 034032.
[35] Kummu, M., de Moel, H., Porkka, M., Siebert, S., Varis, O., Ward, P. J. (2012): Lost food, wasted resources: global food supply chain losses and their impacts on freshwater, cropland, and fertiliser use. – Sci. Total Environ. 438: 477-489.
[36] Lansigan, F. P., de los Santos, W. L., Coladilla, J. O. (2000): Agronomic impacts of climate variability on rice production in the Philippines. – Agric. Ecosyst. Environ. 82(1-3): 129-137.
[37] Leathers, D. J., Yarnal, B., Palecki, M. A. (1991): The Pacific/North American teleconnection pattern and United States climate. Part I: Regional temperature and precipitation associations. – J. Clim. 4(5): 517-528.
[38] Liu, S. Y., Huang, S. Z., Xie, Y. Y., Leng, G. Y., Huang, Q., Wang, L., Xue, Q. (2018): Spatial-temporal changes of rainfall erosivity in the loess plateau, China: Changing patterns, causes and implications. – Catena 166: 279-289.
[39] Li, Z. Y., Huang, S. Z., Liu, D. F., Leng, G. Y., Zhou, S., Huang, Q. (2020): Assessing the effects of climate change and human activities on runoff variations from a seasonal perspective. Stochastic Environmental Research and Risk Assessment, in press. DOI: 10.1007/s00477-020-01785-1
[40] Lobell, D. B., Burke, M. B., Tebaldi, C., Mastrandrea, M. D., Falcon, W. P., Naylor, R. L. (2008): Prioritizing climate change adaptation needs for food security in 2030. – Science 319(5863): 607-610.
[41] Lu, J., Carbone, G. J., Gao, P. (2017): Detrending crop yield data for spatial visualization of drought impacts in the United States, 1895-2014. – Agricultural & Forest Meteorology 237-238: 196-208.
[42] Magrin, G. O., Travasso, M. I., Rodríguez, G. R. (2005): Changes in climate and crop production during the 20th century in Argentina. – Clim. Change 72: 229-249.
[43] Mantua, N. J., Hare, S. R., Zhang, Y., Wallace, J. M., Francis, R. C. (1997): A Pacific interdecadal climate oscillation with impacts on salmon production. – Bull. Amer. Meteor. Soc. 78: 1069-1079.
[44] Maruyama, F., Kai, K., Morimoto, H. (2017): Wavelet-based multifractal analysis on a time series of solar activity and PDO climate index. – Advances in Space Research 60(6): 1363-72.

http://www.aloki.hu ● ISSN 1589 1623 (Print) ● ISSN 1785 0037 (Online)
DOI: http://dx.doi.org/10.15666/aeer/1802_32513275

[45] Meehl, G. A., Arblaster, J. M., Marsh, D. R. (2013): Could a future \Grand Solar Minimum like the Maunder Minimum stop global warming? – Geophy. Res. Lett. 40.
[46] Mehta, V. M., Rosenberg, N. J., Mendoza, K. (2012): Simulated impacts of three decadal climate variability phenomena on dryland corn and wheat yields in the Missouri River Basin. – Agricultural & Forest Meteorology 152(1): 109-124.
[47] Mokhov, I. I., Eliseev, A. V. (2013): Temperature Patterns. – Reference Module in Earth Systems and Environmental Sciences.
[48] Naylor, R. L., Falcon, W. P., Rochberg, D., Wada, N. (2001): Using El Nino/Southern Oscillation climate data to predict rice production in Indonesia. – Climatic Change 50: 255-265.
[49] Nelson, G. C., Rosegrant, M. W., Koo, J., Robertson, R., Sulser, T., Zhu, T., Ringler, C., Msangi, S., Palazzo, A., Batka, M., Magalhaes, M., Valmonte-Santos, R., Ewing, M., Lee, D. (2009): Climate Change Impacts on Agriculture and Costs of Adaptation (Research report). – International Food Policy Research Institute, Washington, DC.
[50] Nigam, S., Barlow, M., Berbery, E. H. (1999): Analysis links Pacific decadal variability to drought and streamflow in United States. – EOS Trans. Amer. Geophys. Union 80(51): 621.
[51] Niu, J., Liu, Q., Kang, S., Zhang, X. (2018): The response of crop water productivity to climatic variation in the upper-middle reaches of the Heihe River basin, Northwest China. – Journal of Hydrology 563: 909-926.
[52] Owens, M. J., Lockwood, M., Barnard, L., Davis, C. J. (2011): Solar cycle 24: Implications for energetic particles and long-term space climate change. – Geophy. Res. Lett. 38.
[53] Phillips, J. G., Cane, M. A., Rosenzweig, C. (1998): ENSO, seasonal rainfall patterns and simulated maize yield variability in Zimbabwe. – Agric. For. Meteorol. 90: 39-50.
[54] Planting Industry Management Department, Ministry of Agriculture and Rural Affairs of the People's Republic of China (2018): http://202.127.42.157/mo-azzys/nongqing.aspx.
[55] Plaut, G., Ghil, M., Vautard, R. (1995): Interannual and interdecadal variability in 335 years of Central England temperatures. – Science 350: 324-327.
[56] Podestá, G., Letson, D., Messina, C., Royce, F., Ferreyra, R. A., Jones, J., Hansen, J., Llovet, I., Grondona, M., O'Brien, J. J. (2002): Use of ENSO-related climate information in agricultural decision making in Argentina: a pilot experience. – Agricultural Systems 74(3): 371-392.
[57] Ren, K., Huang, S. Z., Huang, Q., Wang, H., Leng, G.Y., Fang, W., Li, P. (2019): Assessing the reliability, resilience, and vulnerability of water supply system under multiple uncertain sources. – Journal of Cleaner Production 252: 119806.
[58] Ringler, C. (2008): Climate Variability and Change Impact on Water and Food Outcomes. – International Food Policy Research Institute (IFPRI), Washington, DC.
[59] Rosenzweig, C., Iglesias, A., Yang, X. B., Epstein, P. R., Chivian, E. (2001): Climate Change and Extreme Weather Events; Implications for Food Production, Plant Diseases, and Pests. – Global Change and Human Health 2(2): 90-104.
[60] Schubert, S. D., Chang, Y., Suarez, M. J., Pegion, P. J. (2008): ENSO and wintertime exreme precipitaton events over the contiguous United States. – J. Clim. 21: 22-39.
[61] Smith, P. (2013): Delivering food security without increasing pressure on land. – Glob. Food Sec. 2(1): 18-23.
[62] Stoner, A. M. K., Hayhoe, K., Wuebbles, D. J. (2009): Assessing general circulation model simulations of atmospheric teleconnection patterns. – Journal of Climate 22(22): 4348-4372.
[63] Talaee, P. H., Tabari, H., Ardakani, S. S. (2014): Hydrological drought in the west of Iran and possible association with large-scale atmospheric circulation patterns. – Hydrol. Process. 28: 764-773.
[64] Tao, F. L. (2012): Response of crop yields to climate trends since 1980 in China. – Clim. Res. 54: 233-247.

http://www.aloki.hu ● ISSN 1589 1623 (Print) ● ISSN 1785 0037 (Online)
DOI: http://dx.doi.org/10.15666/aeer/1802_32513275

[65] Thompson, D. W. J., Wallace, J. M. (1998): The Arctic oscillation signature in the wintertime geopotential height and temperature fields. – Geophys. Res. Lett. 25(9): 1297-1300.
[66] Tian, L., Li, J., Bi, W., Zuo, S., Li, L., Li, W., Sun, L. (2019): Effects of waterlogging stress at different growth stages on the photosynthetic characteristics and grain yield of spring maize (*Zea mays* L.) Under field conditions. – Agricultural Water Management 218: 250-258.
[67] Torrence, C., Compo, G. P. (1998): A practical guide to wavelet analysis. – Bull. Am. Meteorol. Soc. 79(1): 61-78.
[68] Tudhope, A. W., Chilcott, C. P., McCulloch, M. T., Cook, E. R., Chappell, J., Ellam, R. M., Lea, D. W., Lough, J. M., Shimmield, G. B. (2001): Variability in the El Niño-Southern Oscillation through a glacial interglacial cycle. – Science 291(5508): 1511-1517.
[69] Walker, G. T. (1923): Correlation in seasonal variations of weather. VIII. A preliminary study of world-weather. – Mem. Indian Meteor. Dep. 24(Part 4): 75-131.
[70] Wang, P., Zhang, Z., Song, X., Chen, Y., Wei, X., Shi, P., Tao, F. (2014): Temperature variations and rice yields in China: historical contributions and future trends. – Clim. Change 124: 777-789.
[71] Wu, Z., Huang, N. E., Long, S. R., Peng, C.-K. (2007): On the trend, detrending, and variability of nonlinear and nonstationary time series. – Proc. Natl. Acad. Sci. U.S.A. 104(38): 14889-14894.
[72] Xu, S., Yu, Z., Zhang, K., Ji, X., Yang, C., Sudicky, E. A. (2018): Simulating canopy conductance of the, Haloxylon ammodendron, shrubland in an arid inland river basin of northwest China. – Agricultural and Forest Meteorology 249: 22-34.
[73] You, L., Rosegrant, M. W., Wood, S., Sun, D. (2009): Impact of growing season temperature on wheat productivity in China. – Agric. For. Meteorol. 149: 1009-1014.
[74] Yu, Y. H., Zhang, H. B., Singh, V. P. (2018): Forward Prediction of Runoff Data in Data-Scarce Basins with an Improved Ensemble Empirical Mode Decomposition (EEMD) Model. – Water 10(4): 388.
[75] Zhang, Y., Wallace, J. M., Battisti, D. S. (1997): ENSO-like interdecadal variability: 1900-93. – J. Climate 10: 1004-1020.
[76] Zhang, T. Y., Zhu, J., Yang, X. G., Zhang, X. Y. (2008): Correlation changes between rice yields in North and Northwest China and ENSO from 1960 to 2004. – Agricultural and forest meteorology 148(6-7): 1021-1033.
[77] Zhang, Z., Song, X., Tao, F. L., Zhang, S., Shi, W. J. (2015): Climate trends and crop production in China at county scale, 1980 to 2008. – Theor. Appl. Climatol. 123: 291-302.
[78] Zhao, J., Wang, H. (2013): Development process, problem and countermeasure of maize production in China. – J. Agric. Sci. Technol. 15(3): 1-6.
[79] Zhao, J. F., Guo, J. P., Mu, J. (2015a): Exploring the relationships between climatic variables and climate-induced yield of spring maize in Northeast China. – Agric. Ecosyst. Environ. 207: 79-90.
[80] Zhao, J. F., Guo, J. P., Xu, Y. H., Mu, J. (2015b): Effects of climate change on cultivation patterns of spring maize and its climatic suitability in Northeast China. – Agric. Ecosyst. Environ. 202: 178-187.
[81] Zhao, X. H., Chen, X., Xu, Y. X., Xi, D. J., Zhang, Y. B., Zheng, X. Q. (2017): An EMD-Based Chaotic Least Squares Support Vector Machine Hybrid Model for Annual Runoff Forecasting. – Water 9(3): 153.
[82] Zhao, J., Huang, S. Z., Huang, Q., Wang, H. Leng, G. Y., Peng, J., Dong, H. X. (2019): Copula-Based Abrupt Variations Detection in the Relationship of Seasonal Vegetation-Climate in the Jing River Basin, China. – Remote Sensing 11: 1628.
[83] Zhao, J., Huang, S. Z., Huang, Q., Leng, G. Y., Wang H., Li, P. (2020a): Watershed water-energy balance dynamics and their association with diverse influencing factors at multiple time scales. – Sci. Total Environ. 711: 135189.

http://www.aloki.hu ● ISSN 1589 1623 (Print) ● ISSN 1785 0037 (Online)
DOI: http://dx.doi.org/10.15666/aeer/1802_32513275

[84] Zhao, J., Huang, S. Z., Huang, Q., Wang, H., Leng, G. Y., Fang, W. (2020b): Time-lagged response of vegetation dynamics to climatic and teleconnection factors. – Catena 189: 104474.

http://www.aloki.hu ● ISSN 1589 1623 (Print) ● ISSN 1785 0037 (Online)
DOI: http://dx.doi.org/10.15666/aeer/1802_32513275

SPATIOTEMPORAL CHANGES IN DAILY MAXIMUM AND MINIMUM TEMPERATURES AND THEIR RELATIONS WITH A LARGE-SCALE ATMOSPHERIC CIRCULATION PATTERN: A CASE STUDY IN THE WEI RIVER BASIN, CHINA

HUANG, S. Z.[1,2*] – LI, P.[2] – HUANG, Q.[2]

[1]*State Key Laboratory of Simulation and Regulation of Water Cycle in River Basin China Institute of Water Resources and Hydropower Research, Beijing 100038, China*

[2]*State Key Laboratory of Eco-hydraulics in Northwest Arid Region of China, Xi'an University of Technology, Xi'an 710048, China*
(phone: +86-29-8231-2801; fax: +86-29-8231-2797)

[*]*Corresponding author*
e-mail: huangshengzhi7788@126.com; phone: +86-29-8231-2801; fax: +86-29-8231-2797

(Received 27th Sep 2019; accepted 4th Feb 2020)

Abstract. The long-term mean air temperature has increased with continued greenhouse-gas emissions in the past decades in the Wei River Basin (WRB) (China), with little understanding of the changes in extreme temperatures. In this study, the change characteristics of both maximum (Tmax) and minimum (Tmin) temperatures at daily, monthly, and annual scales were fully examined, and their relations with the Arctic Oscillation (AO) were also explored. The modified Mann-Kendall trend test method (MMK) and heuristic segmentation method were employed to detect the trends and change points of the Tmax and Tmin at multiple scales, respectively. Subsequently, the cross wavelet transform was adopted to reveal the correlations between Tmax/Tmin and AO. Results indicated: (1) both monthly and annual Tmax and Tmin showed significantly increasing trends, whilst at daily scale they generally exhibited no obvious trends; (2) change points were found in monthly, seasonal, and annual Tmax and Tmin, implying that the stationarity of Tmax and Tmin series in the WRB has been ineffective; (3) AO had strong impacts on Tmax and Tmin changes in the WRB. Our results highlight the asymmetric response of Tmax and Tmin at the monthly, seasonal, and annual scales, which has great implications for ecosystem functions and agricultural production.
Keywords: *temperature extremes, Arctic Oscillation, the heuristic segmentation method, the cross wavelet transform, the Wei River Basin*

Introduction

The Fifth Assessment Report of the Intergovernmental Panel on Climate Change (IPCC, 2007) has stated that global average temperature has risen by nearly 0.85°C (IPCC, 2013) within the 1880-2012 period. Regionally, China has warmed by 0.45±0.05°C during 1860-2005 (CMA, 2006). Accompanying increased surface air temperature are the enhanced evaporation demand (Leng et al., 2015a), accelerated global hydrologic cycle (Menzel et al., 2002; Wang et al., 2013; Huang et al., 2016, 2017; Han et al., 2019; Fang et al., 2019a), and the increase of extreme events (WMO, 2003; Guo et al., 2013, 2019a,b; Leng et al., 2015b,c; Zhao et al., 2019a; Dai et al., 2020; Guo et al., 2020). Compared to the variations of mean conditions, variations of extremes can exert more adverse influences on both the natural environment and human society (Easterling et al., 2000a; Patz et al., 2005; Kapsomenakis et al., 2013; Zhao et al., 2019) and have attracted much attention during the last decades (Beniston et al., 2004; Lehner

http://www.aloki.hu ● ISSN 1589 1623 (Print) ● ISSN 1785 0037 (Online)
DOI: http://dx.doi.org/10.15666/aeer/1802_32773295

et al., 2006; Piao et al., 2010; Sheffield et al., 2012; Fang et al., 2019b; Zhao et al., 2019b; Ren et al., 2020).

Although many researchers have investigated the spatial and temporal changes in temperature extremes (Kunkel et al., 1999; Easterling et al., 2000b; Nasrallah et al., 2004; Fuhrer et al., 2006), the changing characteristics of temperature extremes vary regionally, showing obvious changes in some areas and no striking trends in other areas (Bonsal et al., 2001).

As for a time series, change point is a vital change characteristic. The statistical characteristics of a specific time series before a change point differ significantly from those after the change point. If a change point is found, it indicates the time series is not stationary and is characterized by a noticeable variation. Change point is a time when the temporal pattern of a time series changes significantly. Detection of change points in hydrological series is highly important not only for understanding the location and timing when there is a change in the factors driving the complex system, but also helps us make inference about the issue of non-stationarity (Li et al., 2020; Zhao et al., 2020a, b). Indeed, if the issue of non-stationarity in a hydrological time sequence exists, the conventional hydrological frequency analysis assuming the stationarity of time sequence would be useless in practice (Milly et al., 2008; Vogel et al., 2011; Gilroy et al., 2012). Many previous studies concerning temperature extremes focused on their trend variations, few of them paid attention to their change point detection. In view of the importance of identifying change points for a specific time series, the investigation on identifying change points in maximum (Tmax) and minimum (Tmin) temperatures series was conducted in this study.

Furthermore, majority of previous studies on temperature extremes paid attention to the spatial and temporal variations of Tmax and Tmin series, rare studies explained detected changes. Indeed, understanding of the cause of Tmax and Tmin series changes is extremely important, which helps better understand climate change. Therefore, this study attempts to reveal the possible relations between temperature extremes and the Arctic Oscillation (AO). AO is an important pattern of climate change in the Northern Hemisphere and has been shown to exert strong influences on the climate change in the middle and high latitude areas (Toreti et al., 2010; Wang et al., 2013). The meteorological and hydrological processes may show various characteristics at different spatial scales (Tudesquea et al., 2014). In order to fully reveal the scale effect on the correlations between temperature extremes and AO, the response of temperature extremes to AO at different spatial scales was also explored in this study.

Here, the Wei River Basin (WRB) is chosen as a case study. The WRB is located in a typical climatic zone (monsoon region) (Huang et al., 2014a). Tmax and Tmin series have been reported to exert strong adverse influences on both agricultural production and runoff variations. Investigation of the spatio-temporal changes in temperature extremes in the WRB can help to understand and effectively guide local water resources management in a changing climate. We focus on the temperature extremes at multiple time scales, i.e. daily, monthly, and annual Tmax and Tmin series. The major objectives of this study are: (1) to reveal the spatial and temporal variations of Tmax/Tmin; (2) to detect the change points in Tmax/Tmin series at different timescales in the WRB; (3) to analyze the possible relations between Tmax/Tmin and the AO series at different spatial scales.

http://www.aloki.hu ● ISSN 1589 1623 (Print) ● ISSN 1785 0037 (Online)
DOI: http://dx.doi.org/10.15666/aeer/1802_32773295

Materials and Methods

Introduction of the WRB

The WRB was selected as the study area in this study. It was partitioned into eight sub-basins based on the secondary basin boundary in China, and their zone ID are 26, 28, 29, 31, 33, 36, 40, and 41, respectively (*Figure 1*). Situated in a continental monsoon climate-impacted zone, the region is characterized by rich precipitation and high temperature in summer, and dominated by rare precipitation and low temperature in winter. Its annual precipitation is nearly 559 mm (Zhang et al., 2008; Liu et al., 2018a). The precipitation in the WRB varies obviously at seasonal scale, with flood season (from June to September) precipitation accounting for roughly 60% of the annual average (Huang et al., 2020).

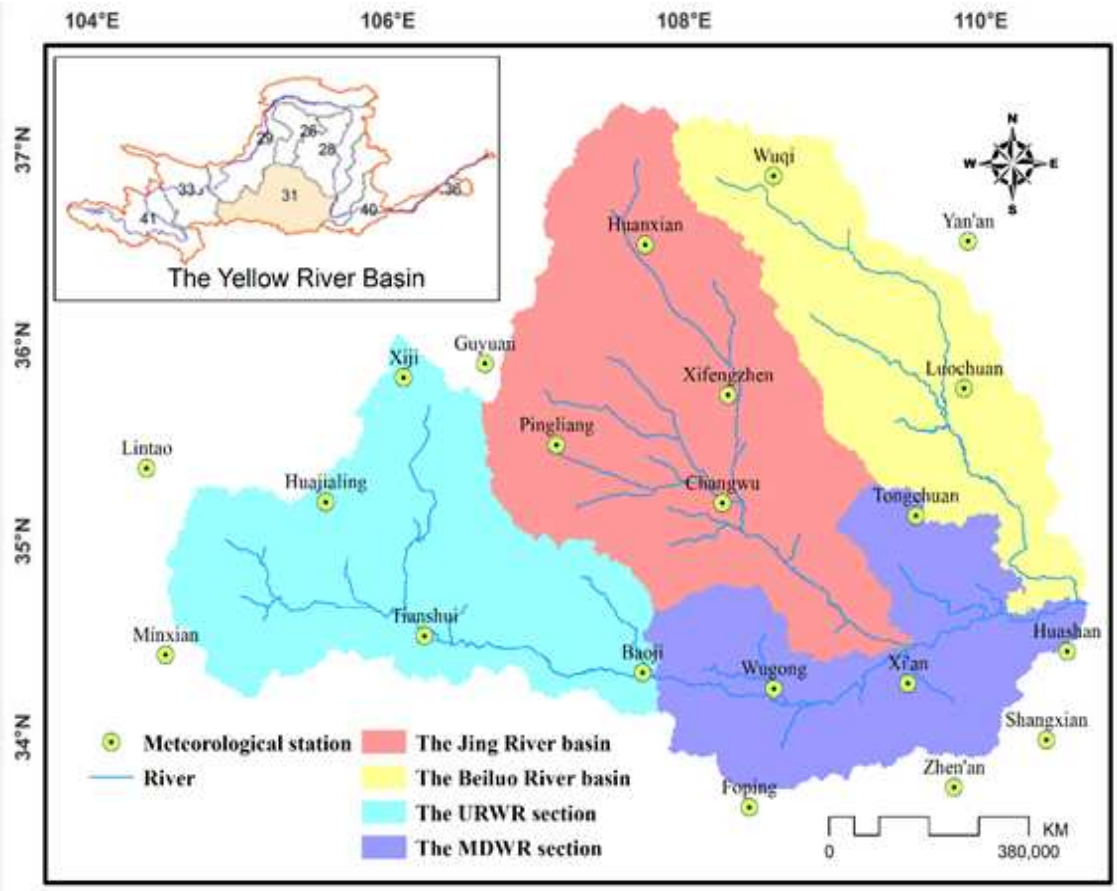

Figure 1. *Location of the WRB and related meteorological stations in the Yellow River Basin, China*

In order to explore the changing characteristics of temperature extremes and their correlation with AO at various spatial scales, the WRB was divided into four sub-basins primarily based on the distribution characteristic of its river system. The four sub-basins are the upper reaches of the Wei River (URWR) section, the middle and downstream of the Wei River (MDWR) section, the Jing River basin, and the Beiluo River basin (*Figure 1*).

http://www.aloki.hu ● ISSN 1589 1623 (Print) ● ISSN 1785 0037 (Online)
DOI: http://dx.doi.org/10.15666/aeer/1802_32773295

Data

Daily minimum and maximum air temperature are collected from 21 meteorological stations located in the WRB (*Figure 1*). The dataset is obtained from the National Climate Center (NCC) of the China Meteorological Administration (CMA), and are homogenized before their release. Note that monthly Tmax/Tmin was determined by the largest/lowest daily data in a month, and annual Tmax/Tmin was determined by the largest/lowest monthly data in a year. The sub-basin Tmax and Tmin are determined from point Tmax and Tmin based via calculating the arithmetic mean value of point Tmax and Tmin. The detailed information of these stations is summarized in *Table 1*. Each station has daily maximum and minimum temperature records spanning January 1st, 1958-December 31st, 2008. These data have been successfully applied in our previous studies (Huang et al., 2014b, c) in investigating drought evolution characteristics in the WRB. Additionally, the monthly AO series within 1958-2008 was obtained from the National Oceanic and Atmospheric Administration (NOAA).

Table 1. *Information on meteorological stations analyzed in this study*

Station name	Sub-basin	Station No.	Longitude (E)	Latitude (N)	Elevation (m)
Lintao	URWR	1	103.85	35.35	1893.8
Minxian	URWR	2	104.02	34.04	2315
Huajialing	URWR	3	105.00	35.38	2450.6
Xiji	URWR	4	105.72	35.97	1916.5
Tianshui	URWR	5	105.75	34.58	1141.7
Guyuan	JRB	6	106.27	36.00	1753
Pingliang	JRB	7	106.67	35.55	1346.6
Baoji	URWR	8	107.13	34.35	612.4
Huanxian	JRB	9	107.30	36.58	1255.6
Xifengzhen	JRB	10	107.63	35.73	1421
Changwu	JRB	11	107.80	35.20	1206.5
Foping	MDWR	12	107.98	33.52	827.2
Wuqi	BL	13	108.17	36.92	1331.4
Wugong	MDWR	14	108.22	34.25	447.8
Xi'an	MDWR	15	108.93	34.30	397.5
Tongchuan	MDWR	16	109.07	35.08	978.9
Zhen'an	MDWR	17	109.15	33.43	693.7
Yan'an	BL	18	109.50	36.60	958.5
Luochuan	BL	19	109.50	35.82	1159.8
Shangxian	MDWR	20	109.97	33.87	742.2
Huashan	MDWR	21	110.08	34.48	2064.9

URWR, MDWR, JRB and BL denote the upper reaches of the Wei River, middle and downstream of the Wei River, Jing River basin and Beiluo River basin, respectively

Methodology

The modified Mann-Kendall trend test method

Given initial Mann-Kendall (MK) trend test method is easily influenced by the persistence of hydro-meteorological series, Hamed and Rao (1998) proposed a modified MK (MMK) trend test method to remove the persistence through taking into account the lag-i autocorrelation. Daufresne et al. (2009) found that the MMK is more robust than MK in terms of examining the trends of hydro-meteorological series. Given the weakness of the MK mentioned above, the MMK trend test method was employed to in this study to calculate the change trends of Tmax/Tmin in the WRB. The detailed computation processes can be referred to Huang et al. (2014a, b).

http://www.aloki.hu ● ISSN 1589 1623 (Print) ● ISSN 1785 0037 (Online)
DOI: http://dx.doi.org/10.15666/aeer/1802_32773295

The heuristic segmentation method

Generally, traditional statistical test methods such as the sliding T test, rank sum test, sliding F test, and Mann-Kendell test are frequently adopted to detect change points, assuming the time series of interest is linear and stationary. Nevertheless, extreme temperature time series is extremely nonlinear owing to the high variability caused by many factors. Hence, it is difficult for them to obtain the real change points accurately. To this end, the heuristic segmentation method which was proposed by Pedro et al. (2001) was adopted to capture the change points in temperature extremes series in this study. The method is based on the sliding T test and further modified, which can be applied to identify the change points in highly nonlinear and nonstationary time series. The detailed calculation processes can be referred to Huang et al. (2017) and Liu et al. (2019).

The cross wavelet transform

The cross wavelet transform proposed by Hudgins et al. (1993) is a new technique in revealing the correlation between two-time series of interest. It is featured with combining the cross spectrum analysis with wavelet transform, and can reveal the changing features and the coupled oscillations of two-time series of interest in both time and frequency domains (Hudgins et al., 1996; Torrence et al., 1998). Hence, it was applied in this study to examine the correlation between Tmax/Tmin in the WRB and AO. The detailed calculation processes can be referred to Huang et al. (2018).

Results

Spatial and temporal changes in Tmax and Tmin

In order to vividly present the spatial change characteristics of Tmax and Tmin in the WRB, the stations adopted in this study were ranked according to the magnitude of their longitudes. Additionally, the MMK statistics of Tmax and Tmin in each month during 1958-2008 in the WRB were calculated, which were plotted in *Figure 2* and *Figure 3*, respectively, with x axis of station number ranked according to the magnitude of their longitudes and y axis of the MMK statistics of Tmax and Tmin in each month. A positive value of MMK statistics represents an increasing trend of Tmax/Tmin series, especially for the value is larger than 1.96, indicating a statistically significant increasing trend at the 95% confidence level. Otherwise, the detection trend is no obvious, and vice versa. Hence, the spatial and temporal changes in Tmax and Tmin at the monthly scale can be displayed in *Figure 2* and *Figure 3*, respectively.

Spatially, in the western and middle basin (*Figure 2*), increase of monthly Tmax is found for almost all months, especially for station 9 where significantly increasing trend is detected in February, April, June, and July. Changes in Tmax in the eastern basin is a little complex with decreasing trends in summer (June, July, and August) and increasing trends in Spring (February, march, April). The change pattern is especially evident for station 17, in which Tmax decreased significantly in June, but increased significantly in January, February, March, October, November, and December. Generally, changes in Tmax at the monthly scale exhibited a noticeable spatial difference. Temporally, the MMK of Tmax series is dominated by positive values in February, April and summer (June, July, and August), indicating a statistically increasing trend. Particularly, February and April show significant increasing trend. In contrast, the Tmax series for January, March, May, November, and December generally have decreasing trends.

http://www.aloki.hu ● ISSN 1589 1623 (Print) ● ISSN 1785 0037 (Online)
DOI: http://dx.doi.org/10.15666/aeer/1802_32773295

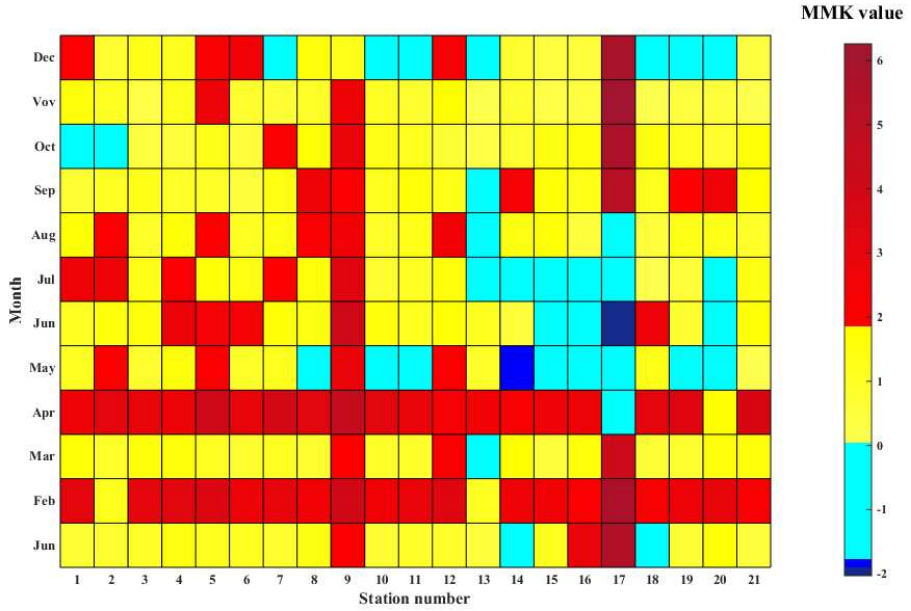

Figure 2. *The change trends of monthly maximum temperature in the WRB (Red, dark blue, yellow and sky blue represent significant increasing, significant decreasing, no obvious increasing and no obvious decreasing trends, respectively)*

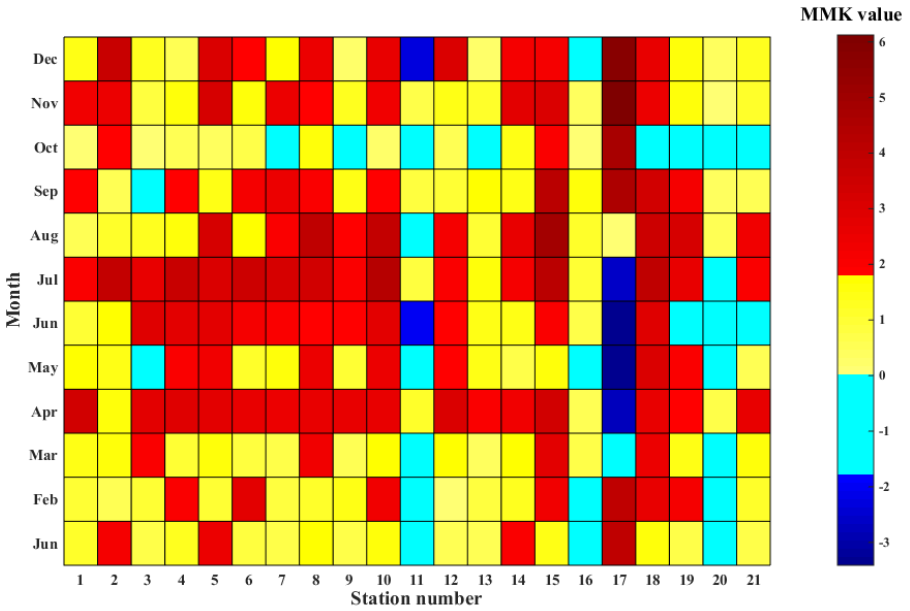

Figure 3. *The change trends of monthly minimum temperature in the WRB*

As for the changes in Tmin (*Figure 3*), spatially, being similar to the changes in Tmax, the western and middle basin is mainly characterized by increasing Tmin in almost all months except for station 11 experiencing decrease in January, February, March, May, June, October and December. In general, the eastern basin is characterized by increasing Tmin except for stations 17 and 20. Note that the Tmax and Tmin at station 17 have a significantly increasing trend at the 99% confidence level in autumn and winter and a significantly decreasing trend

http://www.aloki.hu ● ISSN 1589 1623 (Print) ● ISSN 1785 0037 (Online)
DOI: http://dx.doi.org/10.15666/aeer/1802_32773295

at the 99% confidence level in summer. The cause may be related to its location near to the edge of monsoon region compared with other meteorological stations, its temperature extremes therefore are easily impacted by the changing global climate (Huang et al., 2014c). The underlying causes of the strange behavior of station 17 need to be further investigated in the future study. Temporally, a statistical increase is detected in almost all months in most of the basin. In particular, April, June and July are dominated by significant increasing trends. In contrast, only October showed no obvious decreasing trends.

Overall, the spatial and temporal change patterns of Tmin are similar to that of Tmax. The MMK statistic of the diurnal temperature range in the whole basin is 0.16, which exhibits no obvious trend. The normalized annual Tmax and Tmin series during 1958-2008 in the four sub-basins are illustrated in *Figure 4*, which is based on the *Eq.1*. Note that the sub-basin Tmax and Tmin are determined from point Tmax and Tmin via calculating the arithmetic mean value of point Tmax and Tmin. It can be found that all of the sub-basins are characterized by increasing annual Tmax and Tmin. The MMK statistics of annual Tmax in the four sub-basins are 3.88, 4.51, 3.91 and 2.36, respectively, whilst those of annual Tmin are 5.11, 4.54, 3.64 and 3.89, respectively. The increase in annual Tmin is faster than that of annual Tmax in these sub-basins except for the Jing River basin.

$$\frac{x - x_{\min}}{x_{\max} - x_{\min}} \qquad \text{(Eq.1)}$$

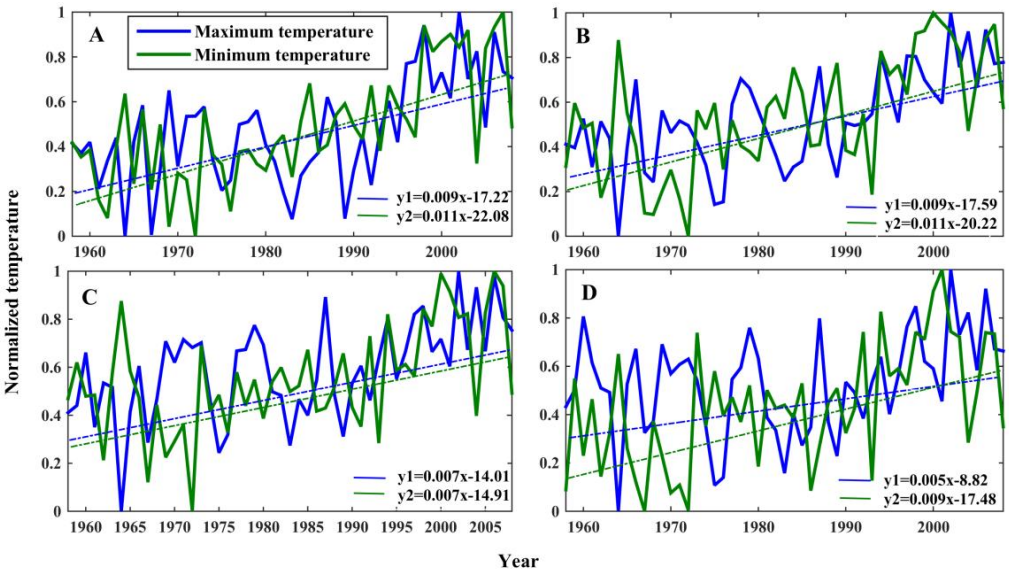

Figure 4. *The normalized annual maximum and minimum temperature series during 1958-2008 in the four sub-basins. A, B, C and D denote the URWB section, the MDWR section, the Jing River basin and the Beiluo River basin, respectively*

The MMK statistics of daily Tmax and Tmin were also calculated in this study, and the spatial and temporal distribution of daily Tmax and Tmin in the WRB is presented in *Figure 5*. It can be found that the MMK statistics of daily Tmax at all the stations are positive, and those at stations 2, 5, 12, and 17 are significant at the 95% confidence level (*Figure 5A*). Similarly, most of the MMK statistics of daily Tmin at all the stations are positive, and those at stations 5,

http://www.aloki.hu ● ISSN 1589 1623 (Print) ● ISSN 1785 0037 (Online)
DOI: http://dx.doi.org/10.15666/aeer/1802_32773295

10, 15, and 18 are significant at the 95% confidence level (*Figure 5B*). Differently, it also has a significant decreasing trend at stations 11 and 20 (*Figure 5B*).

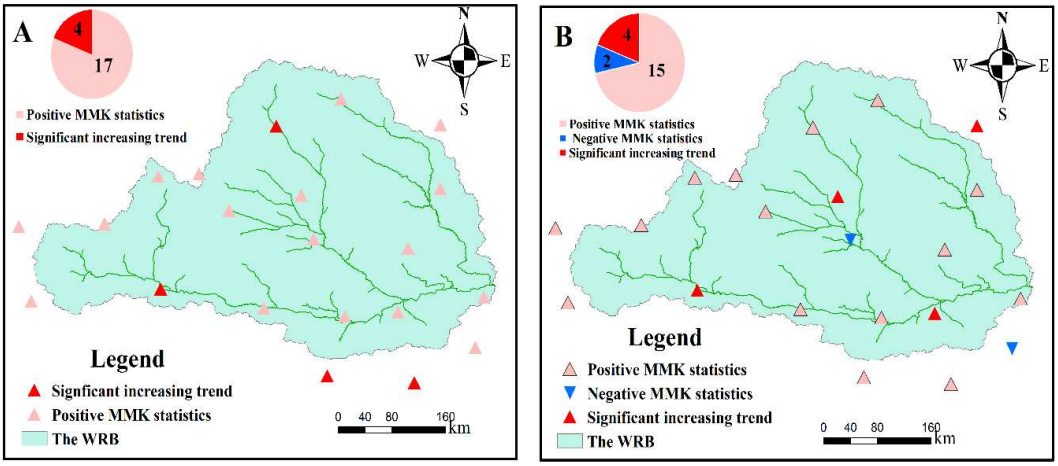

Figure 5. *The spatial and temporal distribution of daily Tmax (A) and Tmin (B) in the WRB*

Identification of change points of Tmax/Tmin and AO index series

The heuristic segmentation method introduced in previous was adopted to identify change points of Tmax and Tmin in the four sub-basins. The threshold P_0 was set to 0.95 and l_0 was set to 25. The segmentations and identified change points of the annual Tmax and Tmin in the four sub-basins are exhibited in *Figure 6* and *Figure 7*, respectively.

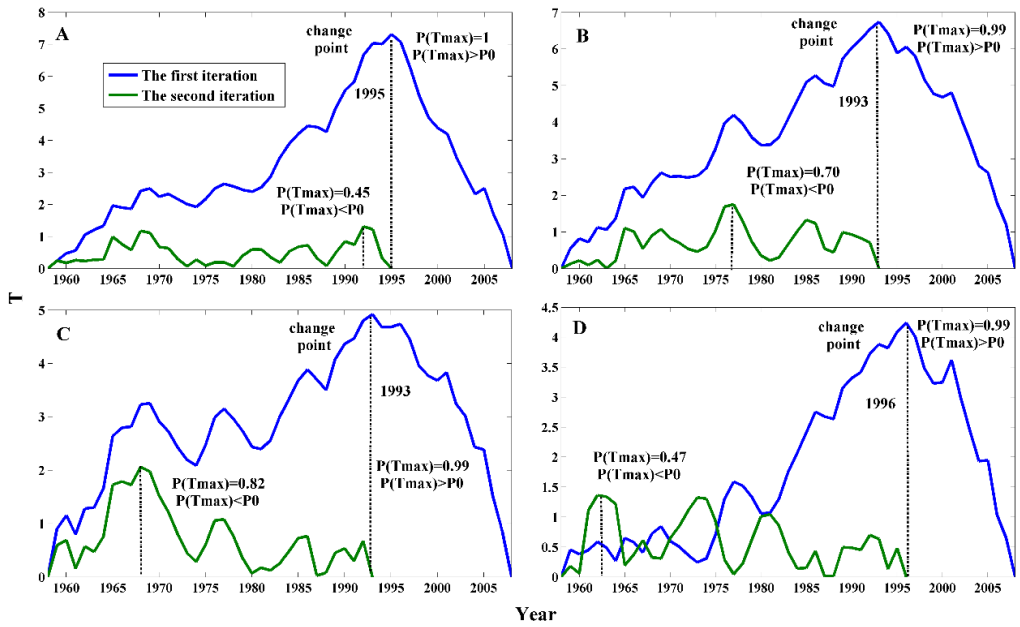

Figure 6. *Segmentations and identified change points of annual maximum temperature in the WRB. A, B, C and D denote the URWB section, the MDWR section, the Jing River basin and the Beiluo River basin, respectively*

http://www.aloki.hu ● ISSN 1589 1623 (Print) ● ISSN 1785 0037 (Online)
DOI: http://dx.doi.org/10.15666/aeer/1802_32773295

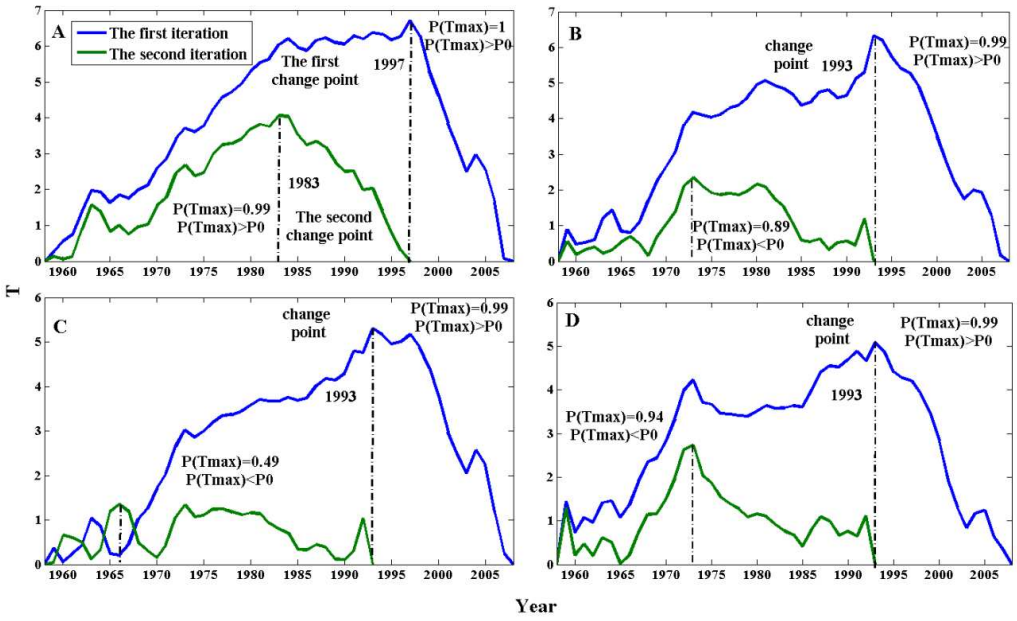

Figure 7. *Segmentations and identified change points of annual minimum temperature in the WRB. A, B, C and D denote the URWB section, the MDWR section, the Jing River basin and the Beiluo River basin, respectively*

In general, both of annual Tmax and Tmin series have change points, implying that the stationarity of temperature extremes in the WRB is invalid. As shown in *Figure 6A*, a change point of 1993 in Tmax was identified in the URWB section in the first iteration due to the condition that $P(t_{max})=1 > P_0$, while no change point was detected in the second iteration due to the condition that $P(t_{max})=0.45 < P_0$. For the MDWR section and the Jing River basin, a common change point (1993) was found in the first iteration due to the condition that $P(t_{max}) > P_0$, while no change point was detected in the second iteration due to the condition that $P(t_{max}) < P_0$. For the Beiluo River basin, a change point of 1996 was detected in the first iteration, whilst no change point was found in the second iteration. From *Figure 7A*, it can be found that a change point of 1997 was detected for the annual Tmin series in the URWB section. For the Tmin in the MDWR section, Jing River basin, and Beiluo River basin, a change point of 1993 was detected.

Moreover, the change points of monthly and seasonal Tmax in the four sub-basins in the WRB were also identified, and their results are displayed in *Table 2* and *Table 3*. It can be found that the change points of monthly Tmax in the four sub-basins vary from 1967 to 2003 with a striking variation (*Table 2*). Note that the monthly Tmax in May in the four sub-basins has no change point. As for the seasonal Tmax in the four sub-basins, their change points are concentrated in 1990s (*Table 2*). In general, the change points of the monthly and seasonal Tmax in the Beiluo River basin are less than those in the other sub-basins. The monthly Tmin in November and December in the four sub-basins has no change point (*Table 3*). Comparatively, the change points of the monthly and seasonal Tmin are less than those of the monthly and seasonal Tmax in the four sub-basins (*Table 3*). Similarly, the change points of the monthly and seasonal Tmin in the Beiluo River basin are less than those in the other sub-basins. Since the change points of monthly, seasonal, and annual Tmax and Tmin were found, the stationarity of temperature extremes in the WRB is ineffective.

http://www.aloki.hu ● ISSN 1589 1623 (Print) ● ISSN 1785 0037 (Online)
DOI: http://dx.doi.org/10.15666/aeer/1802_32773295

Table 2. *Identification of the change points of monthly and seasonal Tmax in the four sub-basins in the WRB*

Sub-basins	1	2	3	4	5	6	7	8	9	10	11	12	Sp	Sm	Am	Wt
URWR section	98	-	99/74	91	-	94	96	-	90	-	86	-	99	95	93	95
JRB	-	-	99	01	-	03	94	-	86	-	86	68	99	96	86	-
MDWR section	69	73	97	91	-	67/03	68/94	68	93	76	89/68	68	99	68/93	90	69/77
BL	-	-	99	03	-	-	94	-	86	-	-	-	99	96	86	-

1, 2,…, and 12 denote January, February,…, and December, respectively; Sp, Sm, Am, and Wt denote spring, summer, autumn, and winter, respectively

Table 3. *Identification of the change points of monthly and seasonal Tmin in the four sub-basins in the WRB*

Sub-basins	1	2	3	4	5	6	7	8	9	10	11	12	Sp	Sm	Am	Wt
URWR section	-	81/07	-	-	96	97	93	93	73	-	-	-	96	61/93	97	85
JRB	-	-	-	83	96	97	93	74	68	-	-	-	96	93	-	-
MDWR section	69	70	69	81	95	68/93	68/92	68	-	-	-	68	73/96	68/93	-	70
BL	72	-	-	80	96	84	92	-	-	-	-	-	-	90	97	-

In addition, identification of the change points of monthly and seasonal AO index was also conducted based on the heuristic segmentation method. Related results are displayed in *Table 4*. In general, from the monthly perspective, there are change points identified in January, February, May, July, August, September, November, and December. However, from the seasonal perspective, change points are detected in four seasons, indicating that the stationarity of AO status is also ineffective. Through comparison between the change points of Tmax/Tmin and AO, it can be observed that there is no solid linkage between Tmax/Tmin and AO at monthly and seasonal time scales.

Table 4. *Identification of the change points of monthly and seasonal AO index*

M/S	1	2	3	4	5	6	7	8	9	10	11	12	Sp	Sm	Am	Wt
Change points	82	88	-	-	07	-	73	70	03	-	69	70	67	70	71	87

M and S denote month and season, respectively

Tmax and Tmin variations are associated with the large-scale atmospheric circulations (Liang et al., 2014), underlying surface conditions (Yu and Li, 2015), as well as human activities such as carbon dioxide emissions (Pereira et al., 2013). To further explain the phenomenon in a quantitatively way is out of the scope of this study, since the major objective of this paper is to investigate the spatial and temporal variations of maximum and minimum temperature at various spatial and temporal scales, along with exploring the correlation between temperature extremes with the AO series. Therefore, the detailed reasons for the occurrence of the change points in annual maximum and minimum temperature series will be investigated in the future study.

http://www.aloki.hu ● ISSN 1589 1623 (Print) ● ISSN 1785 0037 (Online)
DOI: http://dx.doi.org/10.15666/aeer/1802_32773295

The linkages between temperature extremes and AO

As mentioned above, temperature extremes are associated with the large-scale atmospheric circulations (Liang et al., 2014), underlying land surface conditions (Yu and Li, 2015), as well as human activities such as carbon dioxide emissions (Pereira et al., 2013). To quantitatively separate the changes in Tmax and Tmin from various large-scale and local scale factors is important but not within the scope of this study. Arctic Oscillation (AO) is found to be closely associated with the climate variations in middle and high latitudes regions (Toreti, 2010; Wang, 2013). Hence, we attempt to examine the possible relations between AO and Tmax/Tmin variations. We focus the analysis on summer and winter seasons. The AO values corresponding annual Tmax were summer AO values (the average of those in June, July and August), and the AO values corresponding annual Tmin were the winter AO values (the average of those in December, January and February) (Xue et al., 2012). Based on the Morlet wavelet, the cross wavelet transform between Tmax/Tmin and AO are conducted, and relevant results are shown in *Figure 8* and *Figure 9*, respectively. The 95% significance confidence level against red noise is exhibited as a thick contour, and the relative phase relationship is denoted as arrows (with anti-phase pointing left, in-phase pointing right). It can be found that Tmax has a no obvious positive relationship with AO in the URWB section in the entire period except for the period of 1966-1973 when a statistically significant anti-phase relationship with a 2~3 signal is detected. Similarly, Tmax has a no obvious positive relationship with AO in the MDWR section in 1958-1989, with significant correlations with 4-year signal during 1962-1969. However, a significant negative correlation is detected in 1966-1970. As for the Jing River basin, Tmax has a no obvious positive correlation with AO in the entire period. With regards to the Beiluo River basin, the correlations between Tmax and AO are dominated by significant linkages with a 5-year signal during 1960-1966.

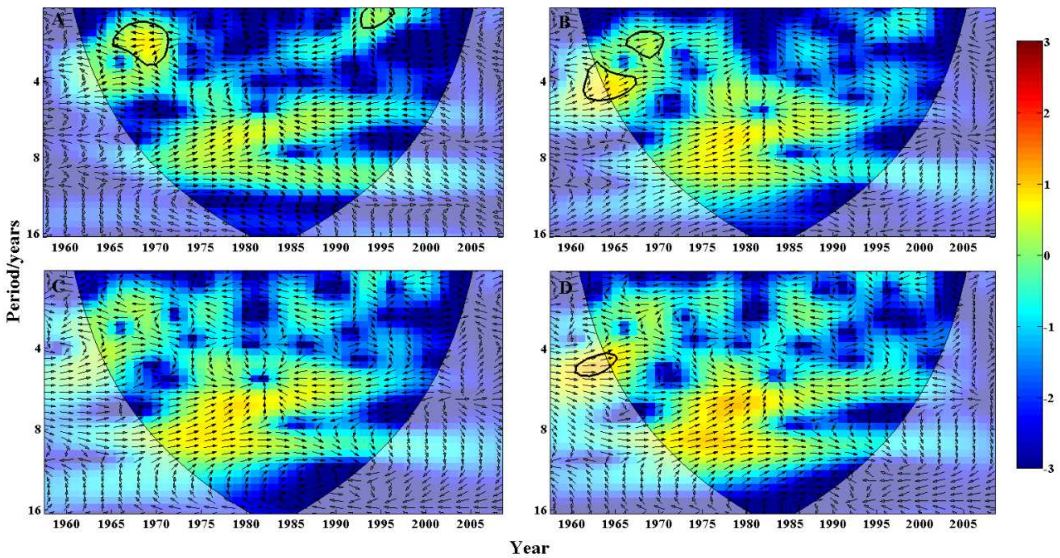

Figure 8. *The cross wavelet transform between maximum temperature and AO. The 95% significance confidence level against red noise is exhibited as a thick contour, and the relative phase relationship is denoted as arrows (with anti-phase pointing left, in-phase pointing right). A, B, C and D denote the URWB section, the MDWR section, the Jing River basin and the Beiluo River basin, respectively*

http://www.aloki.hu ● ISSN 1589 1623 (Print) ● ISSN 1785 0037 (Online)
DOI: http://dx.doi.org/10.15666/aeer/1802_32773295

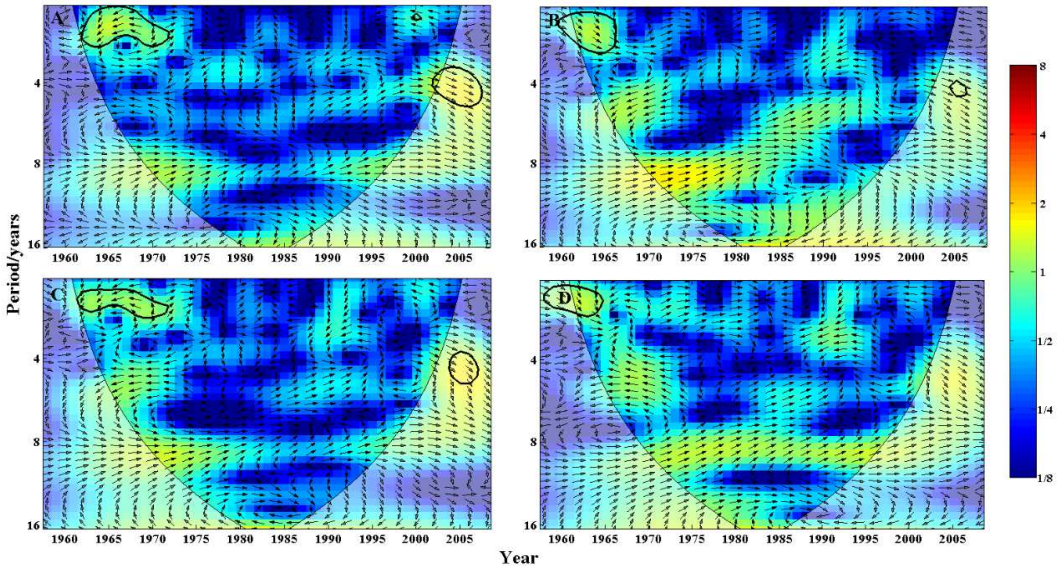

Figure 9. *The cross wavelet transform between minimum temperature and AO. The 95% significance confidence level against red noise is exhibited as a thick contour, and the relative phase relationship is denoted as arrows (with anti-phase pointing left, in-phase pointing right). A, B, C and D denote the URWB section, the MDWR section, the Jing River basin and the Beiluo River basin, respectively*

As for the relations between Tmin and AO in the URWB section, the significantly positive relationship is found with a period of 4 years during 2000-2007, and a significantly negative relationship with AO is detected in 1960-1970 with a 1~2-year signal. Regarding the MDWR section, Tmin has a generally no obvious positive correlation with AO, but the relation become significant in 1960-1969 with a 1~2-year signal. As regards to the Jing River basin, the relationship between Tmin and AO is also dominated by positive correlations, and that in 2003-2006 is significant with a period of 4 years, whilst they have a significantly negative association in 1961-1973 with a 2-year signal. With regards to the Beiluo River basin, the relationship between Tmin and AO is also primarily dominated by positive linkages, and that in 1958-1966 is significant with a 1~2-year signal. Generally, the relations between Tmax/ Tmin and AO in the four sub-basins have both similarity and difference. For example, both *Figures 8B* and *8D* show that the Tmax has a strongly positive correlation with AO with the same 4~5-year signal during 1960~1965 in the MDWR section and the Beiluo River basin. In addition, both *Figures 9A* and *9C* indicate that the Tmin has a strongly negatively relations with AO with the same 1~2-year signal during 1960~1970 and a significantly positive correlation with AO with the same 4~5-year signal in the URWR section and the Jing River basin. Through the comparison between *Figure 8* and *Figure 9*, it can be roughly observed that the area enclosed by the thick contour in *Figure 9* is larger than that in *Figure 8*, indicating that the correlation between Tmin and AO is stronger than that between Tmax and AO. Previous studies have reported that temperature extremes are modulated by the variability of precipitation (Liu et al., 2017), humidity (Krautgasser et al., 2015), wind speed (Jiménez-Hornero et al., 2011), and vegetation type (Migała et al., 2014) in addition to the anomaly of the large-scale atmospheric circulations. The combined effects of these factors may contribute to the different responses of temperature extremes to AO in the four sub-basins in the WRB. For example, Tabari et al. (2014) investigated the links

http://www.aloki.hu ● ISSN 1589 1623 (Print) ● ISSN 1785 0037 (Online)
DOI: http://dx.doi.org/10.15666/aeer/1802_32773295

between AO and inter-annual variability of Iranian evapotranspiration in 41 weather stations, and found that different stations had different characteristics in the response of evapotranspiration to AO. That is, the impacts of the large-scale circulation anomaly on local climatic variations may be different, especially for extreme events which is sensitive to climate change (Kapsomenakis et al., 2013; Zhao et al., 2019), depending on different climate types and underlying surface.

Furthermore, we selected the sub-basin 26 in the Yellow River Basin shown in *Figure 1* which is near to the WRB (the sub-basin 31) in the Yellow River Basin (YRB) to conduct a similar analysis. The cross wavelet transform between annual Tmax/Tmin and summer/winter AO in the sub-basin 26 in the YRB are exhibited in *Figure 10*. It can be observed from *Figure 10A* that Tmax temperature shows a strongly positive correlation with AO with a signal of 4~6 year during 1959~1966 in sub-basin 26 in the YRB. The response is similar to that in the Beiluo River Basin in the WRB which is close to the sub-basin 26 in the YRB. Importantly, it can be observed that a significantly positive relation is found between Tmax and AO with a signal of 2~3 year during 1975~1983 in the sub-basin 26, which is different from that in all the four sub-basins. The results further indicate that the relations between AO and Tmax would exhibit different features even in small areas in the WRB. Similar conclusions can be drawn for the relations between AO and Tmin as shown in *Figure 10B*.

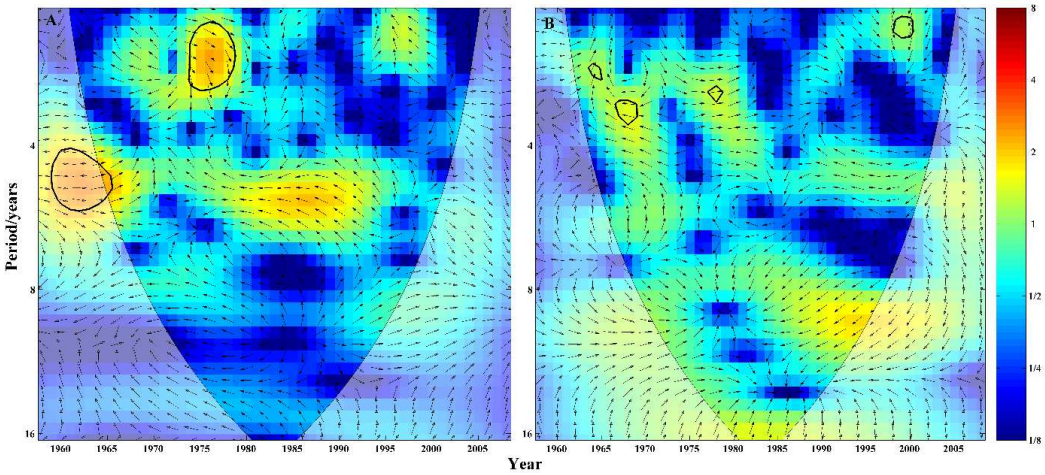

Figure 10. *The cross wavelet transform between maximum (A)/ minimum (B) temperature and summer/winter AO in sub-basin 26 in the Yellow River Basin*

In order to explore the response of temperature extremes to AO at different spatial scales, the correlations between Tmax/Tmin and AO in the whole WRB and YRB were obtained based on the cross wavelet analysis, and their cross wavelet transforms are shown in *Figure 11*. For the whole WRB, Tmax has a significantly negative correlation with AO with a signal of 2~3 year during 1965~1970 (*Figure 11A*), while Tmin exhibits a strongly positive correlation with AO with a signal of 4~5 year during 2002-2006 (*Figure 11B*). Regarding the whole YRB, Tmax has a strongly negative correlation with AO with a signal of 2~3 year during 1966~1980 and a significantly positive relation with AO with a signal of 4~6 year during 1959-1966 (*Figure 11C*), while Tmin exhibits a strongly positive association with AO with a signal of 2~3 year during 1965-1970 (*Figure 11D*). Therefore, the pattern of the correlations between temperature extremes and AO in the whole WRB has both

http://www.aloki.hu ● ISSN 1589 1623 (Print) ● ISSN 1785 0037 (Online)
DOI: http://dx.doi.org/10.15666/aeer/1802_32773295

similarity and difference compared with that in the whole YRB, but the difference is more obvious than its similarity. Generally, the URWB section in the WRB, the WRB, and the YRB has negative correlations between Tmax/Tmin and AO in 1965-1970. Differently, the WRB has significantly positive correlations between minimum temperature and AO in 2002-2007, whilst the YRB has significantly positive correlations between maximum temperature and AO in 1960-1965.

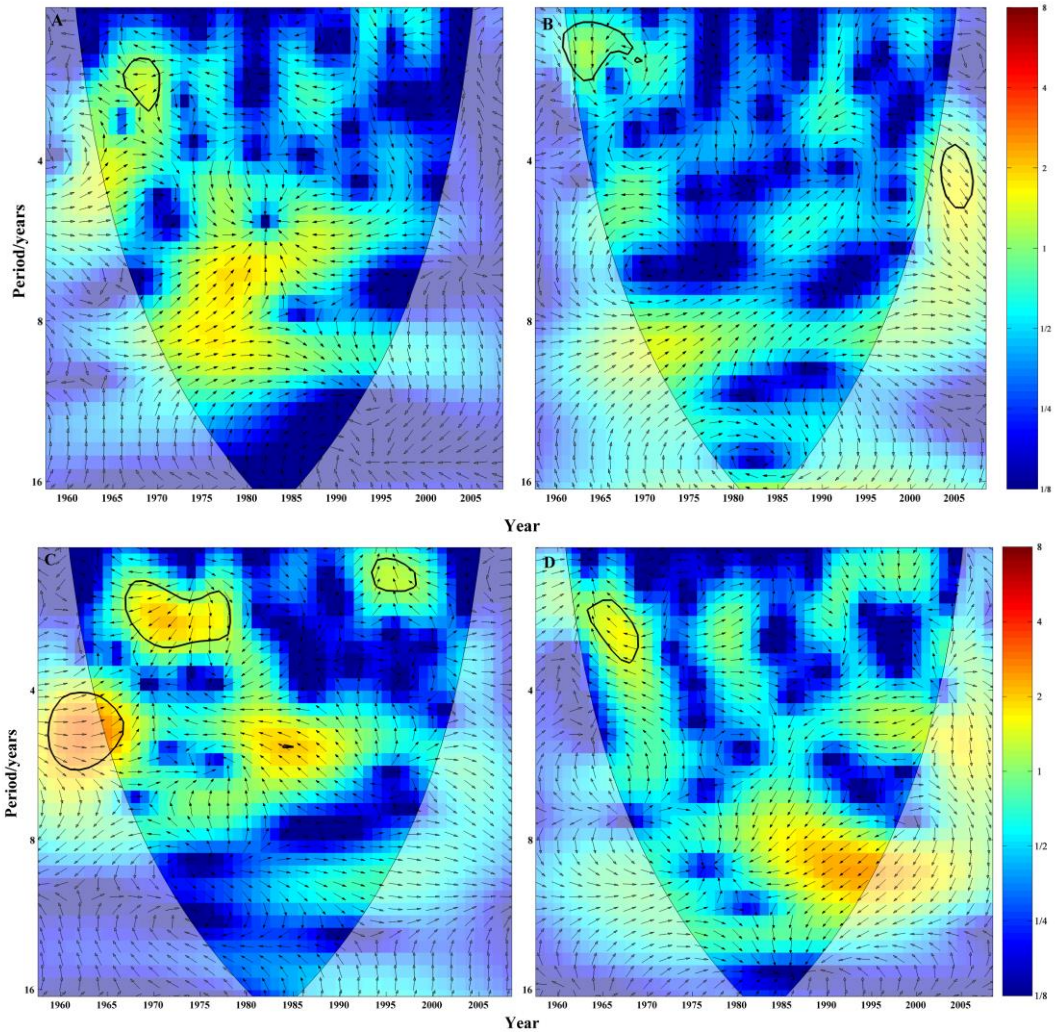

Figure 11. *The cross wavelet transform between maximum (AC)/minimum (BD) temperature and summer/winter AO in the whole Wei (AB) and Yellow (CD) River Basin*

Discussion

Extreme climatic events frequently occur in the context of global warming, including extreme temperature and extreme precipitation events. In this study, the spatiotemporal variation characteristics of extreme temperature (Tmax/Tmin) are discussed, and it is found that the maximum and minimum temperature in WRB showed an increasing trend at different degrees. Liu et al. (2018b) found that the frequency of extreme temperature is increasing. In particular, station 17 is dominated by significant increasing trends in autumn and winter, while the summer is reversed. It is near to the monsoon zone than

http://www.aloki.hu ● ISSN 1589 1623 (Print) ● ISSN 1785 0037 (Online)
DOI: http://dx.doi.org/10.15666/aeer/1802_32773295

other meteorological stations, thus is impacted by climate change. However, increasing extreme temperatures will lead to a change of the temperature difference, which will have a serious impact on crops. Therefore, extreme temperature events should be given more attention.

It is found that AO is a possible factor influencing the extreme temperature changes in WRB. Similarly, AO also affect temperature changes in other areas (Zhong et al., 2017; Gao et al., 2019; Liu et al., 2019). Therefore, this study can provide a reference for other areas of high concern.

In addition, the present research focuses on the spatiotemporal variation of extreme temperatures, and tries to explain possible causes of the changes at different scales from the perspective of atmospheric circulation. Note that the spatiotemporal variation of extreme temperatures are also related to underlying surface conditions, human activities and carbon dioxide emissions. Therefore, future work should extend current research to reveal the effects of different factors on extreme temperature dynamics.

Conclusion

Changing characteristics of Tmax and Tmin in time and space across the WRB were thoroughly investigated in this study. The modified Mann-Kendall trend test method was applied to identify the change trends, and the heuristic segmentation method was used to identify possible change points of Tmax and Tmin at the monthly, seasonal, and annual scales. Additionally, the cross wavelet transform was utilized to reveal the correlation between annual Tmax and Tmin and AO to explore the possible cause of temperature extremes variations from the perspective of atmospheric circulation anomaly. The primary conclusions are presented as follows:

(1) The WRB is primarily characterized by increasing monthly Tmax especially in the western and middle basin, whilst monthly Tmin is found to decrease in the eastern basin in summer, but increase in winter. Similar pattern of changes in Tmin is found with significant increase in most months. The annual Tmax and Tmin in the WRB have an obviously increasing trend. As for the daily scale, most of stations show no obvious trends. The increasing Tmax and Tmin are expected to accelerate the rate of water circulation, thus resulting in high frequent extreme events such as droughts and floods, which will affect local ecosystem functions and agricultural production.

(2) The change points in monthly, seasonal, and annual Tmax and Tmin series were identified, and all of them have change points found. This suggests that the stationarity of the temperature extremes in the WRB has been invalid in 1958-2008.

(3) The Tmax has a strongly positive correlation with AO with 4~5-year signal during 1960-1965, whilst the Tmin has a strongly negatively relations with AO with the 1~2-year signal during 1960-1970 in the WRB. Overall, Tmax and Tmin have strong correlations with AO, implying that the increasing temperature extremes in the WRB are closely related to the variation of AO.

Acknowledgements. This study was jointly funded by the Open Research Fund of State Key Laboratory of Simulation and Regulation of Water Cycle in River Basin (China Institute of Water Resources and Hydropower Research, grant number IWHR-SKL-KF201803), the Key laboratory research projects of the education department of Shaanxi province (grant number 17JS104), the National Natural Science Foundation of China (grant number 51709221 and 51779203), the Key laboratory research projects of the education department of Shaanxi province (grant number 17JS104), the Planning Project of Science and

http://www.aloki.hu ● ISSN 1589 1623 (Print) ● ISSN 1785 0037 (Online)
DOI: http://dx.doi.org/10.15666/aeer/1802_32773295

Technology of Water Resources of Shaanxi (grant numbers 2015slkj-27 and 2017slkj-19), and the Belt and Road Special Foundation of the State Key Laboratory of Hydrology-Water Resources and Hydraulic Engineering (2018490711).

REFERENCES

[1] Beniston, M., Stephenson, D. B. (2004): Extreme climatic events and their evolution under changing climatic conditions. – Global Planet. Change 44(1): 1-9.
[2] Bonsal, B. R., Zhang, X., Vincent, L. A. (2001): Characteristics of daily extreme temperatures over Canada. – J. Climate 14: 1959-1976.
[3] China Meteorological Administration. (2006): Climate and Environment in China. – Meteorology Press, Beijing. (in Chinese).
[4] Dai, M., Huang, S., Z., Huang, Q., Leng, G. Y., Guo, Y., Wang, L., Fang, W., Li, P., Zheng, X.D. (2020): Assessing agricultural drought risk and its dynamic evolution characteristics. – Agricultural Water Management 231: 106003.
[5] Daufresne, M., Lengfellner, K., Sommer, U. (2009): Global warming benefits the small in aquatic ecosystems. – Proceedings of the National Academy of Sciences USA 106(31): 12788-12793.
[6] Easterling, D. R., Meehl, G. A., Parmesan, C., Changnon, S. A., Karl, T. R., Mearns, L. O. (2000a): Climate extremes: observations, modeling, and impacts. – Science 289(5487): 2068-2074.
[7] Easterling, D. R., Evans, J. L., Groisman, P. Y., Karl, T. R., Kunkel, K. E., Ambenje, P. (2000b): Observed variability and trends in extreme climate events. – Bull Am. Meteorol. Soc. 81: 417-425.
[8] Fang, W., Huang, S. Z., Ren, K., Huang, Q., Huang, G. H., Cheng, G. H., Li, K. L. (2019a): Examining the applicability of different sampling techniques in the development of decomposition-based streamflow forecasting models. – Journal of Hydrology 568: 534-550.
[9] Fang, W., Huang, S. Z., Huang, Q., Huang, G. H., Wang, H., Leng, G. Y., Wang, L., Guo, Y. (2019b): Probabilistic assessment of remote sensing-based terrestrial vegetation vulnerability to drought stress of the Loess Plateau in China. – Remote Sensing of Environment, 232: 111290.
[10] Fuhrer, J., Beniston, M., Fischlin, A., Frei, C., Goyette, S., Jasper, K., Pfister, C. (2006): Climate Risks and Their Impact on Agriculture and Forests in Switzerland. – Climatic Change 79(1): 79-102.
[11] Gao, M., Yang, Y., Shi, H., Gao, Z. (2019): SOM-based synoptic analysis of atmospheric circulation patterns and temperature anomalies in China. – Atmospheric Research 220: 46-56.
[12] Gilroy, K. L., McCuen, R. H. (2012): A nonstationary flood frequency analysis method to adjust for future climate change and urbanization. – J. Hydrol. 414-415: 40-48.
[13] Guo, J. L., Guo, S. L., Li, Y., Chen, H., Li, T. Y. (2013): Spatial and temporal variation of extreme precipitation indices in the Yangtze River basin, China. – Stoch. Environ. Res. Risk Assess. 27: 459-475.
[14] Guo, Y., Huang, S. Z., Huang, Q., Wang, H., Fang, W., Yang, Y. Y., Wang, L. (2019a): Assessing socioeconomic drought based on an improved Multivariate Standardized Reliability and Resilience Index. – Journal of Hydrology 568: 904-918.
[15] Guo, Y., Huang, S. Z., Huang, Q., Wang, H., Wang, L., Fang, W. (2019b): Copulas-based bivariate socioeconomic drought dynamic risk assessment in a changing environment. – Journal of Hydrology 575: 1052-1064.
[16] Guo Y., Huang S., Huang Q., Leng G., Fang W., Wang L., Wang H. (2020): Propagation thresholds of meteorological drought for triggering hydrological drought at various levels. – Sci. Total Environ. 712: 136502.

http://www.aloki.hu ● ISSN 1589 1623 (Print) ● ISSN 1785 0037 (Online)
DOI: http://dx.doi.org/10.15666/aeer/1802_32773295

[17] Hamed, K. H., Rao, A. R. (1998): A modified Mann–Kendall trend test for autocorrelated data. – J Hydrol. 204: 182-196.
[18] Han, Z. M., Huang, S. Z., Huang, Q., Leng, G. Y., Wang, H., He, L., Fang, W., Li, P. (2019): Assessing GRACE-based terrestrial water storage anomalies dynamics at multi-timescales and their correlations with teleconnection factors in Yunnan Province, China. – Journal of Hydrology 574: 836-850.
[19] Huang, S. Z., Chang, J. X., Huang, Q., Chen, Y. T. (2014a): Monthly streamflow prediction using modified EMD-based support vector machine. – Journal of Hydrology 511: 764-775.
[20] Huang, S. Z., Chang, J. X., Huang, Q., Chen, Y. T. (2014b): Spatio-temporal changes and frequency analysis of drought in the Wei River Basin, China. – Water Resour. Manag. 28(10): 3095-3110.
[21] Huang, S. Z., Hou, B. B., Chang, J. X., Huang, Q., Chen, Y. T. (2014c): Copulas-based probabilistic characterization of the combination of dry and wet conditions in the Guanzhong Plain, China. – J. Hydrol. 519: 3204-3213.
[22] Huang, S. Z., Huang, Q., Chang, J. X., Leng, G. Y. (2016): Linkages between hydrological drought, climate indices and human activities: a case study in the Columbia River basin. – International Journal of climatology 36(1): 280-290.
[23] Huang, S. Z., Li, P., Huang, Q., Leng, G. Y., Hou, B. B., Ma, L. (2017): The propagation from meteorological to hydrological drought and its potential influence factors. – Journal of Hydrology 547: 184-195.
[24] Huang, S. Z., Zheng, X. D., Ma, L., Wang, H., Huang, Q., Leng, G. Y., Meng, E., Guo, Y. (2020): Quantitative contribution of climate change and human activities to vegetation cover variations based on GA-SVM model. – Journal of Hydrology 584: 124687.
[25] Hudgins, L., Friehe, C. A., Mayer, M. E. (1993): Wavelet transforms and atmospheric turbulence. – Phys. Rev. Lett. 71: 3279-3282.
[26] Hudgins, L., Huang, J. P. (1996): Bivariate Wavelet Analysis of Asia Monsoon and ENSO. – Adv. Atmos. Sci. 13(3): 299-312.
[27] IPCC. (2007): Summary for Policymakers of Climate Change 2007: the Physical Science Basis. – Contribution of Working Group I to the Fourth Assessment Report of the Intergovernmental Panel on Climate Change.
[28] IPCC. (2013): Summary for Policymakers of Climate Change 2013: the Physical Science Basis. – Contribution of Working Group I to the Fifth Assessment Report of the Intergovernmental Panel on Climate Change.
[29] Jiménez-Hornero, F. J., Pavón-Domínguez, P., Gutiérrez de Ravé, E., Ariza-Villaverde, A. B. (2011): Joint multifractal description of the relationship between wind patterns and land surface air temperature. – Atmos. Res. 99: 366-376.
[30] Kapsomenakis, J., Kolokotsa, D., Nikolaou, T., Santamouris, M., Zerefos, S. C. (2013): Forty years increase of the air ambient temperature in Greece: the impact on buildings. – Energ. Convers. Manage. 74: 353-365.
[31] Krautgasser, C., Danzer, R., Supancic, P., Bermejo, R. (2015): Influence of temperature and humidity on the strength of low temperature co-fired ceramics. – J. Eur. Ceram. Soc. 35: 1823-1830.
[32] Kunkel, K. E., Pritke, R. A., Changnon, S. A. (1999): Temporal fluctuation in weather and climate extremes that cause economic and human health impacts-a review. – Bull Am. Meteorol. Soc. 80: 1077-1098.
[33] Lehner, B., Döll, P., Alcamo, J., Henrichs, T., Kaspar, F. (2006): Estimating the impact of global change on flood and drought risks in Europe: a continental, integrated analysis. – Climatic Change 75(3): 273-299.
[34] Leng, G., Tang, Q., Huang, M., Hong, Y., Leung, L. R. (2015a): Projected changes in mean and interannual variability of surface water over continental China. – Sci. China Earth Sci. 58(5): 739-754.
[35] Leng, G., Tang, Q., Rayburg, S. (2015b): Climate change impacts on meteorological, agricultural and hydrological droughts in China. – Glob. Planet. Change 126: 23-34.

http://www.aloki.hu ● ISSN 1589 1623 (Print) ● ISSN 1785 0037 (Online)
DOI: http://dx.doi.org/10.15666/aeer/1802_32773295

[36] Leng, G., Tang, Q., Huang, S., Zhang, X. (2015c): Extreme hot summers in China in the CMIP5 climate models. – Clim. Change 135: 669-681.
[37] Liang, K., Bai, P., Li, J. J., Liu, C. M. (2014): Variability of temperature extremes in the Yellow River basin during 1961-2011. – Quatern. Int. 336: 52-64.
[38] Liu, S. Y., Huang, S. Z., Huang, Q., Xie, Y. Y., Leng, G. Y., Luan, J. K., Song, X. Y., Wei, X., Li, X. Y. (2017): Identification of the non-stationarity of extreme precipitation events and correlations with large-scale ocean-atmospheric circulation patterns: A case study in the Wei River Basin, China. – Journal of Hydrology 548: 184-195.
[39] Liu, S. Y., Huang, S. Z., Xie, Y. Y., Leng, G. Y., Huang, Q., Wang, L., Xue, Q. (2018a): Spatial-temporal changes of rainfall erosivity in the loess plateau, China: Changing patterns, causes and implications. – Catena 166: 279-289.
[40] Liu, S. Y., Huang, S. Z., Xie, Y. Y., Huang, Q., Leng, G. Y., Hou, B. B., Zhang, Y., Wei, X. (2018b): Spatial-temporal changes of maximum and minimum temperatures in the Wei River Basin, China: Changing patterns, causes and implications. – Atmospheric research 204: 1-11.
[41] Liu, S. Y., Huang, S. Z., Xie, Y. Y., Huang, Q., Wang, H., Leng, G. Y. (2019): Assessing the non-stationarity of low flows and their scale-dependent relationships with climate and human forcing. – Science of the Total Environment 687: 244-256.
[42] Liu, X., Xu, Z., Peng, D., Wu, G. (2019): Influences of the North Atlantic Oscillation on extreme temperature during the cold period in China. – International Journal of Climatology 39(1): 43-49.
[43] Li, Z. Y., Huang, S. Z., Liu, D. F., Leng, G. Y., Zhou, S., Huang, Q. (2020): Assessing the effects of climate change and human activities on runoff variations from a seasonal perspective. Stochastic Environmental Research and Risk Assessment, in press. DOI: 10.1007/s00477-020-01785-1
[44] Menzel, L., Bürger, G. (2002): Climate change scenarios and runoff response in the Mulde catchment (Southern Elbe, Germany). – J. Hydrol. 267: 53-64.
[45] Migała, K., Wojtuń, B., Szymański, W., Muskała, P. (2014): Soil moisture and temperature variation under different types of tundra vegetation during the growing season: A case study from the Fuglebekken catchment, SW Spitsbergen. – Catena 116: 10-18.
[46] Milly, P. C. D., Betancourt, J., Falkenmark, M., Hirsch, R. M., Kundzewicz, Z. W., Lettenmaier, D. P., Stouffer, R. J. (2008): Stationarity is dead: Whither water management? – Science 319: 573-574.
[47] Nasrallah, H. A., Nieplova, E., Ramadan, E. (2004): Warm season extreme temperature events in Kuwait. – J. Arid Environ. 56: 357-371.
[48] Patz, J. A., Campbell-Lendrum, D., Holloway, T., Foley, J. A. (2005): Impact of regional climate change on human health. – Nature 438(7066): 310-317.
[49] Pedro, B. G., Plamen, C. I., Luís, A. N. A. (2001): Scale invariance in the nonstationarty of human heart rate. – Phys. Rev. Lett. 87(16): 160815.
[50] Pereira, J., Figueiredo, N., Goufo, P., Carneiro, J., Morais, R., Carranca, C., Coutinho, J., Trindade, H. (2013): Effects of elevated temperature and atmospheric carbon dioxide concentration on the emissions of methane and nitrous oxide from Portuguese flooded rice fields. – Atmos. Environ. 80: 464-471.
[51] Piao, S., Ciais, P., Huang, Y., Huang, Y., Shen, Z., Peng, S., Li, J., Zhou, L., Liu, H., Ma, Y., Ding, Y., Friedingstei, P., Liu, C., Tan, K., Yu, Y., Zhang, T., Fang, J. (2010): The impacts of climate change on water resources and agriculture in China. – Nature 467(7311): 43-51.
[52] Ren, K., Huang, S. Z., Huang, Q., Wang, H., Leng, G.Y., Fang, W., Li, P. (2019): Assessing the reliability, resilience, and vulnerability of water supply system under multiple uncertain sources. – Journal of Cleaner Production 252: 119806.
[53] Sheffield, J., Wood, E. F., Roderick, M. L. (2012): Little change in global drought over the past 60 years. – Nature 491: 435-438.

http://www.aloki.hu ● ISSN 1589 1623 (Print) ● ISSN 1785 0037 (Online)
DOI: http://dx.doi.org/10.15666/aeer/1802_32773295

[54] Tabari, H., Talaee, P. H., Willems, P. (2014): Links between Arctic Oscillation (AO) and inter-annual variability of Iranian evapotranspiration. – Quaternary International 345: 148-157.
[55] Toreti, A., Xoplaki, E., Maraun, D., Kuglitsch, K. G., Wanner, H., Luterbacher, J. (2010): Characterisation of extreme winter precipitation in Mediterranean coastal sites and associated anomalous atmospheric circulation patterns. – Nat. Hazard. Earth Sys. 10: 1037-1050.
[56] Torrence, C., Compo, G. P. (1998): A Practical Guide to Wavelet Analysis. – Bull. Am. Meteorol. Soc. 79(1): 61-78.
[57] Tudesquea, L., Tisseuila, C., Leka, S. (2014): Scale-dependent effects of land cover on water physico-chemistry and diatom-based metrics in a major river system, the Adour-Garonne basin (South Western France). – Sci Total Environ. 466-467: 47-55.
[58] Vogel, R. M., Yaindl, C., Walter, M. (2011): Nonstationarity: flood magnification and recurrence reduction factors in the United States. – J. Am. Water Resour As. 47(3): 464-474.
[59] Wang, S. J., Zhang, M. J., Sun, M. P., Wang, B. L., Li, X. F. (2013): Changes in precipitation extremes in alpine areas of the Chinese Tianshan Mountains, central Asia, 1961-2011. – Quatern. Int. 311: 97-107.
[60] Wang, W. G., Shao, Q. X., Yang, T., Peng, S., Yu, Z., Taylor, J., Xing, W., Zhao, C., Sun, F. (2013): Changes in daily temperature and precipitation extremes in the Yellow River Basin, China. – Stoch. Env. Res. Risk A. 27(2): 401-421.
[61] World Meteorological Organization. (2003): Statement on the Status of Global Climate in 2003. – WMO, Geneva, Switzerland. Publication No. 966.
[62] Xue, H. X., Meng, D., Wu, D. L., Wang, L. X., Li, Q. (2012): Extreme temperature threshold changes and its association with AO index in Ningxia Hui Autonomous Region of China in 1959-2009. – Scientia Geographica Sinica 32(3): 380-385. (in Chinese).
[63] Yu, Z., Li, X. L. (2015): Recent trends in daily temperature extremes over northeastern China (1960-2011). – Quatern. Int. 380-381: 35-48.
[64] Zhang, H., Chen, Y., Ren, G. (2008): The characteristics of precipitation variation of Weihe River Basin in Shaanxi Province during recent 50 years. – Agricultural Research in the Arid Areas 26(4): 236-242. (In Chinese).
[65] Zhao, J., Huang, S. Z., Huang, Q., Wang, H., Leng, G. Y., Peng, J., Dong, H. X. (2019): Copula-Based Abrupt Variations Detection in the Relationship of Seasonal Vegetation-Climate in the Jing River Basin, China. – Remote Sensing 11: 1628.
[66] Zhao, J., Huang, S. Z., Huang, Q., Leng, G. Y., Wang H., Li, P. (2020a): Watershed water-energy balance dynamics and their association with diverse influencing factors at multiple time scales. – Sci. Total Environ. 711: 135189.
[67] Zhao, J., Huang, S. Z., Huang, Q., Wang, H., Leng, G. Y., Fang, W. (2020b): Time-lagged response of vegetation dynamics to climatic and teleconnection factors. – Catena 189: 104474.
[68] Zhao, M. L., Huang, S. Z., Huang, Q., Wang, H., Leng, G. Y., Xie, Y. Y. (2019a): Assessing socio-economic drought evolution characteristics and their possible meteorological driving force. – Geomatics, Natural Hazard and Risk 10(1): 1084-1101.
[69] Zhao, M. L., Huang, S. Z., Huang, Q., Wang, H., Leng, G. Y., Liu, S. Y., Wang, L. (2019b): Copula-Based Research on the Multi-Objective Competition Mechanism in Cascade Reservoirs Optimal Operation. – Water 11: 995.
[70] Zhong, K., Zheng, F., Wu, H., Qin, C., Xu, X. (2017): Dynamic changes in temperature extremes and their association with atmospheric circulation patterns in the Songhua River Basin, China. – Atmospheric research 190: 77-88.

http://www.aloki.hu ● ISSN 1589 1623 (Print) ● ISSN 1785 0037 (Online)
DOI: http://dx.doi.org/10.15666/aeer/1802_32773295

EFFECTS OF A CHEMICAL PLANT GROWTH REGULATOR AND PLANTING DENSITY ON THE LEAF SENESCENCE AND YIELD OF SPRING MAIZE IN NORTHEAST CHINA

MENG, Y. – LIU, X. M. – GU, W. R.* – WEI, S.*

Department of Crop Cultivation and Farming System, College of Agriculture, Northeast Agricultural University, 150030 Harbin, PR China

**Corresponding authors*
e-mail: wanronggu@163.com, weishi5608@126.com; phone: +86-451-5519-0472

(Received 27th Sep 2019; accepted 4th Feb 2020)

Abstract. The study aims to analyze the effects of chemical applications on the leaf senescence and yield of maize under different planting densities in Northeast China. Dongnong 253 (hybrid maize), was planted at four densities, i.e. 50,000, 60,000, 70,000, and 80,000 plants ha^{-1}. The leaves were sprayed with the plant growth regulator 'Yuhuangjin' (the main components of which include aminoacyl esters and ethephon) during the jointing stage. The results showed that the highest maize yield, i.e. 13290.95 kg ha^{-1}, was obtained when the plants were treated with 'Yuhuangjin' and 70,000 plants ha^{-1}. As the planting density increased in the water treatment, the height gradually increased, the dry weight of individuals decreased, and the barren stem proportion and lodging risk increased. In contrast, 'Yuhuangjin' reduced plant height, increased the dry weight of individual plants, and reduced both the barren stem proportion and the lodging risk. As planting density increased, the degree of reduction in leaf SPAD increased and the degree of leaf senescence increased in water. However, 'Yuhuangjin' increased leaf greenness and delayed senescence. During leaf senescence process, the activities of antioxidant enzymes (SOD, POD, CAT) decreased, the MDA content increased, and the soluble protein content decreased in the water treatment in response to increasing density. Compared to the water, 'Yuhuangjin' increased the activities of SOD, POD and CAT as well as the soluble protein content but reduced the MDA content. Under high planting densities, 'Yuhuangjin' have important values with respect to increasing maize yields and delaying leaf senescence during the late growth stage. This research provides a theoretical and experimental basis for maize production in Northeast China.
Keywords: *maize, plant growth regulator, density, leaf senescence, yield, antioxidant enzymes*

Introduction

Density is an important factor that determines maize yields (Ogunlela et al., 1988). The planting density of maize (*Zea mays* L.) in Northeast China is generally low, and increasing density is an important cultivation practice that can increase yields. Taking the United States as an example, maize planting density has been increasing since the 1960s, from 60000 plants ha^{-1} in the 1990s to more than 70000 plants ha^{-1} at the end of the 20th century. At present, high-yield fields are generally about 100000 plants ha^{-1} (Lu et al., 2011; Xu et al., 2019). However, a planting density that is too high will reduce individual plant production, and improper control may even reduce yields (Andrade and Calvino, 2002; Shin et al., 2014; Ren et al., 2017; Tokatlidis, 2017). The key to achieving high yields involves the ability to increase the density and sustain reasonable yields of individual maize plants. Plant growth regulators can effectively control maize growth and development. Many studies have recently shown that plant growth regulators play positive roles in improving crop quality, shaping ideal phenotypes and increasing yields (Zhao et al., 2006a; Chen et al., 2013; Cao et al., 2016; Xu et al., 2017). The process of maize leaf senescence reflects the length of its

http://www.aloki.hu ● ISSN 1589 1623 (Print) ● ISSN 1785 0037 (Online)
DOI: http://dx.doi.org/10.15666/aeer/1802_32973311

functional period, which is directly related to yield production (Pommel et al., 2006). Therefore, research conducted on maize yield and senescence physiology under different planting densities and in response to the applications of plant growth regulators has important practical significance.

Within a certain range, maize yield increases with increasing density. As maize planting density increases, light transmission within the canopy decreases, senescence increases, the grain number per spike and the 100-grain weight decrease, and the lodging rate increases (Li et al., 2011; Cao et al., 2013). Planting density significantly affects the leaf area index, plant height, ear length, and number of grains per ear, grain weight per ear, 100-grain weight, biological yield and grain yield (Shafi et al., 2012). Population yield increases with increasing density within a certain density range, and rational close planting is an important cultivation practice for achieving high yields (Zhang et al., 2006). The grain yield of an individual maize plant decreases as the plant density increases, and competition for photosynthate may lead to ear and grain abortion during the flowering phase (Andraski et al., 2000; Andrade and Calvino, 2002).

Exogenous substances can accelerate the rate of protein synthesis in plants, increase enzymatic activity and promote other physiological processes. Studies conducted on various plants have shown that exogenous substances can increase antioxidant enzyme (superoxide dismutase (SOD), guaiacol peroxidise (POD), catalase (CAT)) activity during leaf senescence, reduce malondialdehyde (MDA) contents, and increase soluble protein contents and as well as the stay-green ability of plant leaves (Bajguz and Hayat, 2009; Pan et al., 2013). 'Yuhuangjin' is a plant growth regulator that was developed for maize; the regulator consists of an aminoacyl ester combined with ethephon. 'Yuhuangjin' can improve lodging resistance, enhance the stay-green ability of leaves, and increase both the photosynthetic rate and number of aerial root layers. This plant growth regulator has shown clear effects on generating ideal phenotypes and increasing the lodging resistance of maize (Diallo et al., 2015). The planting density of spring maize in the northeastern region of China is relatively low, and the yield potential has not been attained. Research on the application of 'Yuhuangjin' has focused on morphological indexes, investigations of physiological indexes related to yield increases are scarce.

In this experiment, we studied the yield and senescence process of maize during the late growth stage in response to both 'Yuhuangjin' treatment and different planting densities. The results from this study provide a theoretical and experimental basis for further rational application of 'Yuhuangjin' to spring maize in Northeast China.

Materials and methods

Experimental materials and treatments

The field experiments were performed at the Xiangfang Experimental Station of Northeast Agricultural University (126°63′E, 45°44′N), Harbin, Heilongjiang Province, China, in 2014 and 2015. Dongnong 253 (compact growth habit, plant height of 280 cm, ear height of 110 cm) was used as the experimental material. The plant growth regulator 'Yuhuangjin' was provided by Fujian Haoluon Biology Engineering Technology Co. Ltd, China. The soil was previously planted with soybean and is classified as a chernozem (pH 6.85); the soil contained 25.25 g kg^{-1} organic matter, 1.7 g kg^{-1} total nitrogen (N), 179.35 mg kg^{-1} available potassium (K), 65.34 mg kg^{-1} available phosphorus (P), and 118.21 mg kg^{-1} alkaline N. The monthly weather data, i.e.

http://www.aloki.hu ● ISSN 1589 1623 (Print) ● ISSN 1785 0037 (Online)
DOI: http://dx.doi.org/10.15666/aeer/1802_32973311

air temperature, precipitation, the number of sunshine hours and wind speed, measured at the experimental site during the maize growing season in 2014-2015 are shown in *Table 1*.

Table 1. *Daily mean values of weather variables measured at the experimental site during the maize growing seasons in 2014 and 2015*

Month	Mean temperature (°C)		Precipitation (mm)		Sunshine hours (h)	
	2014	2015	2014	2015	2014	2015
April	10.30	8.56	6.10	6.60	267.00	191.00
May	14.30	14.25	91.40	77.60	127.50	156.90
June	22.90	22.06	56.80	77.30	216.80	226.70
July	23.10	23.60	115.50	52.90	159.90	262.90
August	21.90	22.76	83.80	110.50	208.10	152.80
September	15.50	16.17	32.20	24.80	184.40	209.20
Total[a]	18.00	17.89	385.80	349.70	1163.70	1199.50

[a] Precipitation and sunshine are monthly sums, while temperature is a monthly mean of daily means

The experiment was established as a two-factor, randomized block design consisting of three replications. Each plot was 10 m long and consisted of 12 rows with a 0.7-m row spacing. The experiment involved four planting densities, i.e. 50,000, 60,000, 70,000, and 80,000 plants ha^{-1}. Maize kernels were sown by hand on April 25th, 2014, at the same spacing across all replications via a planting density rope. The plant growth regulator 'Yuhuangjin' was applied evenly at the jointing stage (20 mL of liquid 'Yuhuangjin' in 30 kg water was applied per hectare), whereas only water was applied for the control treatment (CK represents the water treatment used for comparisons, and Y indicates the 'Yuhuangjin' treatment. 5CK represents the treatment in which plants at a planting density of 50,000 plants ha^{-1} were subjected to the water treatment, and 5Y represents the treatment in which plants at a planting density of 50,000 plants ha^{-1} were subjected to the 'Yuhuangjin' treatment. 6CK, 6Y, 7CK, 7Y, 8CK, 8Y and so on follow the same convention). The maize plants received 250 kg ha^{-1} diammonium phosphate, 75 kg ha^{-1} urea, and 150 kg ha^{-1} potassium sulphate at the seedling stage, and 300 kg ha^{-1} of urea was topdressed at the jointing stage.

Two 4-m-long sections of consecutive rows were selected in each treatment to calculate the numbers of plants, ears number, barren stalks and barren tip. All the maize plants were harvested, and twenty ears were randomly selected for calculating the number of ears per row, number of kernel per row, 100-grain weight and theoretical yield of each treatment. The average value of the three replications was calculated.

Measurement of SPAD values

The SPAD values were measured using a PAM-2100 chlorophyll meter (Heinz Walz GmbH, Eichenring 6·91090 Effeltrich, Germany). The degree of leaf senescence was considered the relative reduction in the SPAD value: degree of leaf senescence = $(SPAD_{t1}–SPAD_{t2})/ SPAD_{t1}\times100\%$. Beginning at the onset of pollen shedding (July 29th), sampling was conducted at 4 p.m. every 10 d. The ear leaf was placed in an ice box, transported to the laboratory, and maintained in a refrigerator at -80°C. On the following day, each physiological index was measured using the same part of the leaf that was washed and dried with absorbent paper.

http://www.aloki.hu ● ISSN 1589 1623 (Print) ● ISSN 1785 0037 (Online)
DOI: http://dx.doi.org/10.15666/aeer/1802_32973311

Measurement of antioxidant enzyme activity

To determine the antioxidant enzyme activity, fresh leaves (0.5 g) were homogenized by grinding with a mortar and pestle in 10 mL of ice-cold potassium phosphate buffer (KPB; pH 7.0) in an ice bath. The mixture was then centrifuged at 12000 rpm for 20 min at 4°C. CAT activity in the supernatant was determined in accordance with the methods of Aebi (1984). POD activity was assayed in accordance with previously described methods (Saba et al., 2012), with some modification. The change in absorbance at 410 nm was recorded during a 3-min period. One unit of POD activity was defined as an increase of 0.1/min. SOD activity was assayed as described by Huang method (Huang et al., 2008). The reaction mixture was incubated for 10 min under fluorescent light, after which the absorbance at 560 nm was measured. The ascorbic acid in maize leaves was assayed in accordance with the method reported by Mukherjee and Choudhuri (1983).

Measurement of Soluble protein

Soluble protein contents within fresh leaf extracts (0.1 g) were quantified in (KPB) (50 mM, pH 7.5). These extracts were filtered through four layers of cheese cloth and then centrifuged at 15500 rpm for 15 min at 4°C. The supernatant was collected and subsequently stored at 4°C for protein determination. The leaf soluble protein contents were measured via the protein dye-binding method of Bradford (1976); bovine serum albumin served as the standard.

Measurement of biomass and yield

To determine the biomass and yield, two consecutive four-meter lengths were selected for each process. The rows per ear, number of ear, kernels row, number of row and hundred grain weight were calculated. After harvest, 20 ears were selected to calculate the kernels row, number of row, hundred grain weight, and the theoretical yield. The biomass was determined by the drying method, and the stalks and grains were dried separately. Each process was repeated three times, and the results were averaged.

Statistical analyses

All the data are presented as the mean values of three replications. The data were collated using Microsoft Excel 2003 (Microsoft Corporation, Redmond, Washington, USA). Treatment effects on grain yield; yield components; plant height; dry weight; SOD, POD, and CAT activity; MDA content; and soluble protein contents were analysed in accordance with the principles of analysis of variance; the generalized linear model (GLM) package in SPSS 17.0 software (SPSS Inc. Chicago, Illinois, USA) was used.

Results

Effects of 'Yuhuangjin' and planting density on maize yields

The yield factors of maize include mainly the effective number of ears per unit area, grain number per spike and grain weight, among which ear per unit area is the most easily controlled. Therefore, increasing density is an effective way to obtain high yields.

http://www.aloki.hu ● ISSN 1589 1623 (Print) ● ISSN 1785 0037 (Online)
DOI: http://dx.doi.org/10.15666/aeer/1802_32973311

The results showed that, as the planting density increased, the grain number per ear and the 100-grain weight decreased, the effective number of ears increased, and the yield increased within a certain range (Abuzar et al., 2011; Li et al., 2015). Therefore, the tight coordination between the effective number of ears per unit area and the grain yield per plant is a key component of attaining high yields. *Table 2* shows that the yield in the water treatment increased initially but then decreased as the planting density increased; the highest yield, i.e. 12346.40 kg ha^{-1}, occurred at a planting density of 70,000 plants ha^{-1}. This value was 34.94% and 12.89% higher than the that in the 5CK and 6CK treatments, respectively, and reached an extremely high level, and this value was significantly higher (9.58% higher) than that in the 8CK treatment. The barren stem ratio in the 7CK and 8CK treatment was 1.857% and 4.037% higher, respectively, than that in the 5CK treatment. These results indicated that increasing density would lead to a decrease in airflow and light transmission within the canopy, affecting the pollination characteristics of plants and resulting in lower production capacity per plant (*Table 2*).

Table 2. *Effects of 'Yuhuangjin' application and plant density on maize yield components*

Treatment	Plant density (plants ha^{-1})	Effective number of ears (ears ha^{-1})	Rows per ear	Kernels per row	100-grain weight (g)	Theoretical yield (kg ha^{-1})
Water	50,000	49428.57	16.05^{a}	33.95^{bc}	33.97^{a}	9150.31^{d}
	60,000	59714.29	15.93^{a}	35.58^{abc}	32.31^{a}	10937.00^{c}
	70,000	67894.29	16.39^{a}	33.89^{bc}	32.74^{a}	12346.40^{b}
	80,000	75857.14	16.00^{a}	31.50^{de}	29.47^{b}	11266.74^{c}
'Yuhuangjin'	50,000	49571.43	15.80^{a}	33.95^{ab}	34.49^{a}	9711.98^{d}
	60,000	59857.14	15.95^{a}	33.50^{cd}	34.36^{a}	10989.10^{c}
	70,000	68085.71	15.45^{a}	36.50^{a}	34.61^{a}	13290.95^{a}
	80,000	76942.86	15.90^{a}	31.28^{e}	31.71^{ab}	11694.96^{bc}

The 100-grain weight and yield were both converted to those at a 14% moisture level. The different letters indicate a significant difference ($P<0.05$) between treatments

Compared with that in the water treatment, the maize yield in the 'Yuhuangjin' treatment increased but did not reach a significant level. The maximum maize yield (13290.95 kg ha^{-1}) occurred at a planting density of 70,000 plants ha^{-1}, which occurred for both the water and 'Yuhuangjin' treatments. Under different planting densities, compared with those in the respective water treatments, the yields in the 5Y, 6Y, 7Y and 8Y treatments increased by 6.14%, 0.48%, 7.65% and 3.81%, respectively. The 'Yuhuangjin' treatment had the best effect on increasing production of planted that were planted at a planting density of 70,000 plants ha^{-1}. Therefore, the proper combination of 'Yuhuangjin' and planting density can increase yields (*Table 2*).

Effects of chemical regulators and planting density on maize plant height and dry matter weight

Table 3 shows that, in the water treatment, plant height increased gradually and the dry matter weight of individual plants decreased gradually as the planting density increased. The height of plants that were planted at a planting density of 80,000 plants ha^{-1} was 23.3 cm higher than that of plants that were planted at a planting density of 50,000 plants ha^{-1}; however, the dry matter weight was 100.01 g lower. This result showed that an increase in the number of plants per unit area increased the plant

http://www.aloki.hu ● ISSN 1589 1623 (Print) ● ISSN 1785 0037 (Online)
DOI: http://dx.doi.org/10.15666/aeer/1802_32973311

height, reduced the dry matter weight and could greatly increase the risk of lodging. There are limits associated with trying to increase yields by altering the population structure.

Table 3. *Effects of 'Yuhuangjin' application and plant density on maize height and dry weight*

Treatment	Plant density (plants ha^{-1})	Plant height (cm)	Dry weight (g)
Water	50,000	305.00±5.00^{bcd}	354.79±36.27^{ab}
	60,000	318.33±1.53^{ab}	303.95±59.18^{bcd}
	70,000	310.33±4.51^{bc}	273.68±18.63^{de}
	80,000	328.33±8.50^{a}	243.00±10.16^{e}
'Yuhuangjin'	50,000	293.33±10.41^{d}	386.02±10.21^{a}
	60,000	310.00±5.00^{bc}	329.85±21.24^{bc}
	70,000	302.67±2.52^{cd}	295.19±22.13^{cde}
	80,000	314.33±14.36^{bc}	251.77±13.16^{de}

The values are the means ± standard deviations. The different letters indicate a significant difference ($P<0.05$) between treatments

The heights of plants in the 'Yuhuangjin' treatment were 3.83% (50,000 plants ha^{-1}), 2.47% (60,000 plants ha^{-1}), 2.62% (70,000 plants ha^{-1}) and 4.26% (80,000 plants ha^{-1}) lower than those in the water treatment, whereas the corresponding dry matter weights were 8.80% (50,000 plants ha^{-1}), 7.86% (60,000 plants ha^{-1}), 8.51% (70,000 plants ha^{-1}) and 3.61% (80,000 plants ha^{-1}) higher. The 'Yuhuangjin' treatment somewhat reduced plant height, increased the maize dry weight and promoted the transport of more nutrients to the grain, which increased both plant lodging resistance and grain yields. In conclusion, the application 'Yuhuangjin' improved the physiological function of individual leaves of plants at a high planting density, resulting in a reasonable plant phenotype and increased production depending on individual performance (*Table 3*).

Effects of 'Yuhuangjin' and planting density on ear leaf SPAD values after the pollen-shedding period

Chlorophyll is an important substance involved in the absorption and transformation of light energy during photosynthesis in leaves. The chlorophyll content reflects the degree of leaf senescence, and the SPAD value reflects the leaf chlorophyll content. Therefore, in this experiment, changes in SPAD values were used to represent changes in chlorophyll contents. *Table 4* shows that, during the process of leaf senescence, the SPAD values in the water treatment decreased as the planting density increased. Immediately after the pollen- shedding period began (0 d), the SPAD values in the 6CK, 7CK, and 8CK treatments were 11.16%, 17.59% and 20.28% lower, respectively, than those in 5CK treatment. In addition, compared with those at 0 d after pollen shedding, the SPAD values in the 5CK, 6CK, 7CK and 8CK treatments at 40 d after pollen shedding were 20.08%, 30.76%, 33.34% and 34.65% lower, respectively. The extent of the reduction in leaf SPAD values increased as the planting density increased, and the degree of leaf senescence increased.

Table 4 also shows that the SPAD values of the ear leaves treated with 'Yuhuangjin' also decreased after the pollen-shedding period, and compared with those in the water treatment, the SPAD values at different densities and during different periods in the

http://www.aloki.hu ● ISSN 1589 1623 (Print) ● ISSN 1785 0037 (Online)
DOI: http://dx.doi.org/10.15666/aeer/1802_32973311

'Yuhuangjin' treatment was higher. The SPAD values in the 5Y, 6Y, 7Y and 8Y treatments decreased by 18.52%, 16.54%, 12.30% and 16.71%, respectively, from 0 to 40 d after pollen shedding. The SPAD values in the 'Yuhuangjin' treatment were higher than those in the water treatment, i.e. the values increased by 4.83% (50,000 plants ha^{-1}), 19.16% (60,000 plants ha^{-1}), 26.12% (70,000 plants ha^{-1}) and 22.00% (80,000 plants ha^{-1}), at 40 d after pollen shedding (*Table 4*). In conclusion, the SPAD values of the ear leaves decreased as the planting density increased. The 'Yuhuangjin' treatment prolonged the functional period by delaying leaf senescence, allowing more nutrients to be transferred to the grain, resulting in higher yields. Under the experimental conditions, a planting density of 70,000 plants ha^{-1} resulted in optimal results.

Table 4. *Effects of 'Yuhuangjin' application and plant density on ear leaf SPAD values measured at different periods after pollen shedding*

Treatment	Plant density (plants ha^{-1})	Days after pollen shedding				
		0 d	10 d	20 d	30 d	40 d
Water	50,000	77.1±11.4^{b}	76.6±8.3^{a}	71.2±5.5^{a}	66.4±1.2^{ab}	64.2±9.8^{ab}
	60,000	68.5±2.4^{d}	63.4±3.0^{c}	59.1±3.9^{d}	58.3±1.8^{d}	52.4±4.0^{d}
	70,000	63.6±7.0^{e}	63.2±2.3^{c}	59.2±1.7^{d}	55.4±4.6^{de}	47.7±3.5^{e}
	80,000	61.3±6.2^{e}	59.3±3.6^{d}	53.0±1.3^{e}	53.7±4.2^{e}	45.5±9.0^{e}
'Yuhuangjin'	50,000	82.7±9.5^{a}	78.4±1.3^{a}	71.2±3.3^{a}	68.2±2.3^{a}	67.3±2.1^{a}
	60,000	74.8±4.7^{bc}	66.1±6.8^{b}	63.6±3.1^{bc}	62.6±3.4^{bc}	62.5±1.2^{bc}
	70,000	68.6±6.2^{d}	68.3±4.7^{b}	65.2±1.9^{b}	64.3±3.4^{b}	60.1±5.1^{c}
	80,000	66.6±4.1^{d}	64.7±1.8^{bc}	62.5±1.6^{c}	60.9±1.3^{c}	55.5±3.4^{d}

The values are the means ± standard deviations. The different letters indicate a significant difference ($P<0.05$) between treatments

Effects of 'Yuhuangjin' and planting density on ear leaf SOD activity after pollen shedding

SOD is a protective enzyme in organisms that can catabolise O_2^- into H_2O and O_2 and protect the biomembrane system. *Table 5* shows that the SOD activity of the ear leaf in the water treatment decreased as the planting density increased. After the pollen-shedding period, the SOD activity initially decreased, followed by an increase and then a decreasing trend; the peak value occurred at approximately 20 d after pollen shedding. The peak values in the 5CK, 6CK, 7CK and 8CK treatments were 208.58, 178.89, 169.49 and 147.84 U g^{-1} fresh weight (FW), respectively. The change trend of SOD activity in the 'Yuhuangjin' treatment was similar to that observed in the water treatment. The maximum values of SOD activity measured in the 'Yuhuangjin' treatments were 6.83% (5Y), 6.17% (6Y), 27.87% (7Y) and 23.42% (8Y) higher than those measured in the corresponding water treatments (*Table 5*).

In conclusion, increasing density led to a reduction in SOD activity in the ear leaf, which would reduce the scavenging ability of superoxide ion free radicals, aggravate the destruction of cell structure and accelerate the process of leaf senescence. The SOD activity in the ear leaf was greater in the 'Yuhuangjin' treatment than in the water treatment, which played a positive role in delaying the process of leaf senescence.

http://www.aloki.hu ● ISSN 1589 1623 (Print) ● ISSN 1785 0037 (Online)
DOI: http://dx.doi.org/10.15666/aeer/1802_32973311

Table 5. *Effects of 'Yuhuangjin' application and plant density on ear leaf SOD, POD, and CAT activities as well as MDA content after the pollen-shedding period*

Treatment		Plant density (plants/ha)	Days after pollen shedding				
			0 d	10 d	20 d	30 d	40 d
SOD	Water	50,000	188.22±22.65^{a}	175.48±20.58^{b}	208.59±21.59^{b}	174.62±20.38^{b}	108.52±21.78^{b}
		60,000	150.09±21.31^{c}	137.80±20.91^{d}	178.59±21.95^{cd}	116.02±23.14^{d}	87.52±21.08^{cd}
		70,000	120.00±20.35^{d}	135.81±21.00^{d}	169.49±20.31^{d}	84.83±20.58^{e}	78.00±21.78^{d}
		80,000	94.21±20.33^{e}	106.58±21.27^{e}	147.85±20.33^{e}	82.96±20.60^{e}	62.64±13.76^{e}
	'Yuhuangjin'	50,000	202.88±15.99^{a}	188.43±18.15^{a}	222.84±16.06^{a}	190.00±16.38^{a}	164.83±22.34^{a}
		60,000	199.45±20.17^{a}	140.00±20.01^{d}	189.61±20.39^{c}	160.92±20.01^{c}	109.40±22.18^{b}
		70,000	180.95±18.15^{b}	162.40±16.38^{c}	216.74±16.04^{ab}	150.11±16.06^{c}	112.24±16.04^{b}
		80,000	117.51±17.01^{d}	137.53±19.80^{d}	182.47±22.62^{cd}	123.86±21.47^{e}	96.10±18.65^{bc}
POD	Water	50,000	52.67±1.43^{c}	58.67±0.95^{c}	64.80±0.78^{bc}	63.07±0.85^{b}	45.97±0.83^{b}
		60,000	47.77±1.35^{c}	54.50±0.81^{c}	66.47±0.95^{b}	59.50±0.78^{c}	38.70±0.90^{c}
		70,000	40.37±1.42^{d}	46.50±0.88^{d}	56.13±0.80^{d}	52.13±0.77^{d}	35.40±0.92^{d}
		80,000	34.73±0.87^{e}	48.85±1.02^{d}	52.50±0.87^{e}	41.30±0.77^{e}	27.90±0.96^{e}
	'Yuhuangjin'	50,000	67.63±1.04^{a}	72.70±0.96^{a}	77.20±0.96^{a}	71.30±1.29^{a}	57.93±0.48^{a}
		60,000	58.57±0.79^{b}	68.30±0.77^{a}	70.43±0.77^{b}	65.03±0.96^{b}	46.83±0.61^{b}
		70,000	54.60±0.78^{b}	66.90±0.78^{b}	68.87±0.78^{b}	62.87±0.48^{b}	48.27±0.58^{b}
		80,000	48.53±1.22^{c}	55.57±0.77^{c}	60.67±0.78^{c}	51.43±0.57^{d}	32.27±0.40^{d}
CAT	Water	50,000	62.25±1.12^{a}	48.83±1.66^{b}	65.02±9.45^{a}	59.00±2.48^{a}	44.33±1.19^{b}
		60,000	54.25±0.91^{b}	47.50±0.96^{b}	58.21±0.61^{b}	47.33±1.48^{d}	31.17±1.21^{d}
		70,000	47.25±0.78^{c}	37.83±0.82^{d}	54.00±2.05^{c}	45.50±1.17^{d}	31.67±1.41^{d}
		80,000	38.33±1.50^{e}	30.67±1.55^{e}	42.12±1.17^{d}	37.00±0.79^{e}	27.17±1.39^{e}
	'Yuhuangjin'	50,000	64.13±3.32^{a}	58.67±3.63^{a}	68.00±0.68^{a}	55.33±0.67^{b}	49.33±2.15^{a}
		60,000	60.00±5.01^{a}	53.33±3.32^{b}	64.21±2.24^{a}	51.33±2.24^{c}	46.50±1.38^{b}
		70,000	52.50±2.40^{b}	42.75±1.57^{c}	60.32±3.32^{b}	47.25±1.14^{d}	40.67±9.21^{c}
		80,000	40.00±2.65^{d}	31.17±2.24^{e}	45.02±1.56^{d}	43.31±3.33^{d}	30.17±2.37^{d}
MDA	Water	50,000	5.46±0.71^{c}	7.18±0.47^{d}	7.55±0.49^{c}	8.37±0.51^{d}	9.91±0.66^{d}
		60,000	5.61±0.66^{c}	7.31±0.73^{cd}	7.98±0.48^{b}	8.64±0.48^{c}	11.09±0.43^{c}
		70,000	6.50±0.66^{a}	7.66±0.47^{b}	8.11±0.44^{a}	8.92±0.43^{c}	12.16±0.65^{b}
		80, 000	6.92±0.62^{a}	8.11±0.80^{a}	8.29±0.43^{a}	10.79±0.49^{a}	14.56±0.42^{a}
	'Yuhuangjin'	50,000	4.29±0.41^{e}	6.82±0.45^{e}	7.14±0.34^{d}	7.46±0.39^{e}	9.05±0.34^{e}
		60,000	5.09±0.39^{d}	7.46±0.34^{c}	7.81±0.40^{b}	8.11±0.51^{d}	10.22±0.49^{d}
		70,000	6.01±0.47^{b}	7.48±0.46^{c}	7.82±0.66^{b}	8.46±0.36^{d}	10.23±0.47^{d}
		80,000	6.59±0.40^{a}	7.66±0.35^{b}	8.14±0.47^{a}	9.26±0.37^{b}	12.48±0.47^{b}

SOD, superoxide dismutase; POD, peroxidase; CAT, catalase; MDA, malondialdehyde. The same conventions are used below. The values are the means ± standard deviations. The different letters indicate a significant difference ($P<0.05$) between treatments for each physiological and biological index

Effects of 'Yuhuangjin' and planting density on POD activity in ear leaves after pollen shedding

POD is another important enzyme involved in the plant protective enzyme system. POD can effectively eliminate the accumulation of peroxides in plants and reduce the

http://www.aloki.hu ● ISSN 1589 1623 (Print) ● ISSN 1785 0037 (Online)
DOI: http://dx.doi.org/10.15666/aeer/1802_32973311

degree of membrane lipid peroxidation, and this enzyme plays a positive role in maintaining leaf greenness. *Table 5* shows that the POD activity in the water treatment decreased as the planting density increased; the activity increased initially but then decreased over time after pollen shedding. The maximum POD activity occurred at approximately 20 d after pollen shedding. The maximum POD activity values in the 5CK, 6CK, 7CK and 8CK treatments were 64.8, 66.47, 56.13 and 53.5 (ΔA470 min^{-1}. g^{-1} FW), respectively. *Table 5* also shows that the POD activity in the 'Yuhuangjin' treatment increased at a later stage, and compared with those in the water treatment, the maximum values in the 'Yuhuangjin' treatment were 21.14% (50,000 plants ha^{-1}), 7.28% (60,000 plants ha^{-1}), 27.38% (70,000 plants ha^{-1}) and 16.72% (80,000 plants ha^{-1}) higher. These results indicate that maximum POD activity occurred at a planting density of 70,000 plants ha^{-1} (*Table 5*).

In summary, an increase in planting density led to a reduction in POD activity, which can cause hydrogen peroxide (H_2O_2) accumulations in the leaves, damage the cell membrane system, and reduce the ability of leaves to remain green. Spraying 'Yuhuangjin' can improve the canopy structure of a high-density population, increase both the POD activity in the ear leaves and the ability of leaves to remain green, and create favourable conditions for yield formation.

Effects of 'Yuhuangjin' and planting density on CAT activity in ear leaves after pollen shedding

CAT can promote the catabolism of H_2O_2 into molecular oxygen and water and can prevent the accumulation of H_2O_2 in cells. Table 5 shows that the CAT activity in the water treatment decreased as the planting density increased, and as the time after pollen shedding increased, an initial decrease followed by an increase and a subsequent decrease was observed; the peak value occurred at approximately 20 d after pollen shedding. The peak CAT activity values in the 6CK, 7CK and 8CK treatments were 10.47%, 16.95% and 35.22% lower, respectively, than the values in the 5CK treatment. The change trend of the 'Yuhuangjin' treatment was similar to that of the water treatment; the peak values were 4.62% (50,000 plants ha^{-1}), 10.34% (60,000 plants ha^{-1}), 11.11% (70,000 plants ha^{-1}) and 7.14% (80,000 plants ha^{-1}) higher than those of the corresponding controls (*Table 5*).

Therefore, increasing planting density reduced the physiological function of the ear leaves, and the CAT activity decreased. However, the 'Yuhuangjin' treatment improved the CAT activity, which positive affected the greening ability of the leaves.

Effects of 'Yuhuangjin' and planting density on the MDA content in the ear leaves after pollen shedding

MDA is one of the end products of membrane lipid peroxidation. The MDA content reflects leaf senescence to a certain extent, and the accumulation of MDA can severely damage the subcellular structure of plants. *Table 5* shows that, on the whole, the change trend of the MDA content in the water treatment was the same as that in the 'Yuhuangjin' treatment, i.e. an increase was observed in response to increasing planting density and time after pollen shedding. However, the 'Yuhuangjin' treatment caused a reduction in MDA contents, which, after 40 d, were 8.71% (50,000 plants ha^{-1}), 7.86% (60,000 plants ha^{-1}), 8.36% (70,000 plants ha^{-1}) and 7.41% (80,000 plants ha^{-1}) lower than those in the water treatment. The results showed that increasing planting density resulted in an increase both in membrane lipid peroxidation products and in leaf

http://www.aloki.hu ● ISSN 1589 1623 (Print) ● ISSN 1785 0037 (Online)
DOI: http://dx.doi.org/10.15666/aeer/1802_32973311

senescence. Less MDA accumulated in the 'Yuhuangjin' treatment than in the water treatment; in addition, the degree of membrane lipid peroxidation was lower in the former, and the leaf greenness retention ability was higher (*Table 5*).

Effects of 'Yuhuangjin' and planting density on the soluble protein contents in ear leaves after pollen shedding

Soluble protein enzymes in leaves include PEP carboxylase and RuBP carboxylase; changes in the contents of these enzymes reflect changes in enzyme activity. In addition, soluble protein contents are also associated with leaf metabolism, which is another important index of leaf senescence. *Table 6* shows that, as planting density increased in the water treatment, the soluble protein contents in the ear leaves decreased. As time after pollen shedding increased, the soluble protein content increased initially but then decreased; the peak value occurred at approximately 10 d after pollen shedding. The soluble protein contents in the 6CK, 7CK, and 8CK treatments were 20.72%, 23.37% and 27.11% lower, respectively, than those in the 5CK treatment. The results show that an increase in planting density can reduce light transmission within the canopy, resulting in poor environmental conditions for individual plants. In addition, increased planting density can reduce the soluble protein content, the activity of enzymes involved in N metabolism, and the yield of individual plants (*Table 6*).

Table 6. *Effects of 'Yuhuangjin' application and plant density on the soluble protein content of ear leaves after the pollen-shedding period*

Treatment	Plant density (plants ha^{-1})	Days after pollen shedding				
		0 d	10 d	20 d	30 d	40 d
Water	50,000	33.02±1.88^{b}	36.54±1.45^{a}	30.16±1.00^{bc}	27.16±1.06^{b}	25.28±0.73^{a}
	60,000	24.33±0.15^{de}	28.97±2.22^{c}	23.02±0.74^{d}	22.47±1.25^{d}	19.85±1.01^{d}
	70,000	25.84±0.93^{d}	28.00±1.73^{cd}	24.66±0.67^{d}	25.17±0.23^{c}	19.30±1.01^{d}
	80,000	22.64±0.91^{e}	26.63±0.73^{e}	21.13±1.00^{e}	20.17±1.18^{e}	16.54±0.69^{e}
'Yuhuangjin'	50,000	36.51±1.31^{a}	35.69±1.02^{a}	39.67±1.13^{a}	35.43±0.52^{a}	26.48±1.27^{a}
	60,000	32.94±1.49^{b}	30.82±1.08^{b}	33.99±1.49^{b}	27.04±0.93^{b}	25.32±0.82^{a}
	70,000	30.01±0.94^{c}	29.73±0.66^{bc}	32.31±1.12^{b}	26.90±1.29^{b}	22.76±1.55^{b}
	80,000	27.02±0.96^{d}	26.45±0.81^{e}	28.61±1.10^{c}	24.57±2.02^{c}	20.57±0.87^{c}

The values are the means ± standard deviations. The different letters indicate a significant difference ($P<0.05$) between treatments

Table 6 also shows that, compared with the water treatment, the 'Yuhuangjin' treatment led to increases in soluble protein contents at each period; the maximum values occurred at approximately 20 d after pollination and were 8.57% (50,000 plants ha^{-1}), 17.35% (60,000 plants ha^{-1}), 15.42% (70,000 plants ha^{-1}) and 7.43% (80,000 plants ha^{-1}) higher than those in the water treatment. The 'Yuhuangjin' treatment increased the metabolic activity of the maize ear leaf soluble proteins, which prolonged their functional period; increased the leaf greenness retention ability; and provided conditions for high yields.

http://www.aloki.hu ● ISSN 1589 1623 (Print) ● ISSN 1785 0037 (Online)
DOI: http://dx.doi.org/10.15666/aeer/1802_32973311

Discussion

Increased maize yield records have been reported in recent years, indicating that the average level of maize production in China may continue to improve (Zhao et al., 2006b). Increasing the planting density is the main cultivation practice to increase maize production. The results of this study showed that, when the planting density was between 50,000 and 70,000 plants ha^{-1}, the yield increased as the planting density increased, and when the planting density exceeded 70,000 plants ha^{-1}, the yield decreased as the planting density increased. Previous studies have shown that, under relatively high planting densities, an increase in the number of ears per unit area led to an increase in the number of grains per ear, which ultimately resulted in increased yields (Wei et al., 2017). The amount of dry matter is the material basis for the formation of grain yield, and the harvest index is an important factor affecting the yield (Gao et al., 2017). Increasing the planting density can significantly increase the amount of dry matter of groups and thus achieve the goal of increasing yield (Ogunlela et al., 1988). In the present study, the amount of dry matter per plant decreased as the planting density increased. The yield decreased after the planting density exceeded 70,000 plants ha^{-1}. The harvest index can decrease in response to increase of planting density, and the efficiency of dry matter allocation from the stem to the grain can decrease, which results in relatively lower yields when the planting density is too high (Wei et al., 2017). Previous studies have shown that a lack of source material is the main limiting factor for yields at low planting densities; therefore, increasing the planting density can increase production. However, the source and sink materials increased simultaneously, but the proportion of increase was different under the high planting density, causing the relative shortage of sink tissue to be the main limiting factor for production. Currently, measures such as increasing the grain number, grain weight and harvest index represent the main mechanisms for increasing yield (Wang et al., 2013). Previous studies have shown that applications of chemicals could increase the harvest index, increasing the distribution of photosynthetic products to the grain, promoting the development of the ear, increasing both the number of grains per ear and the 100-grain weight, and increasing yields (Zhang et al., 2014; Otie et al., 2016). In this study, the 'Yuhuangjin' treatment significantly increased the amount of dry matter per plant and increased the yield of the population. The yield was highest at a planting density of 70,000 plants ha^{-1} in the 'Yuhuangjin' treatment.

The flowering stage of maize is a critical period for yield formation, but it is also the time during which the physiological function of leaves gradually decreases. The length of the leaf functional phase directly influences the formation of maize yield. During the senescence process, the gradual loss of leaf chlorophyll is the most definitive characteristic of leaf senescence, and leaf chlorophyll content and senescence are significantly negatively correlated (Mohr and Schopfer, 1995; Taiz and Zeiger, 2006). Research has shown that delayed leaf senescence, the retention of green leaves, and high photosynthetic rates can prolong the late growth stage of maize, significantly increasing yields (Huffaker, 1990; Ma and Dwyer, 1998). The results of this study showed that increasing planting density reduced leaf chlorophyll contents after pollen shedding. In addition, leaf senescence increased as the number of days after pollen shedding increased. Previous studies have shown that chemical control was beneficial for delaying the senescence of leaves in the middle and lower parts of the plant and for maintaining a relatively greater effective photosynthetic area during the middle and late stages of grain filling. The results of this study showed that 'Yuhuangjin' could increase

http://www.aloki.hu ● ISSN 1589 1623 (Print) ● ISSN 1785 0037 (Online)
DOI: http://dx.doi.org/10.15666/aeer/1802_32973311

leaf chlorophyll contents, delay leaf senescence and increase the accumulation of photosynthetic products, ensuring high yields.

Increasing the planting density is one of the key ways to increase yields. However, as the planting density of maize increases, competition for light, temperature, water and other environmental resources increases, which affects plant growth and development (Wei et al., 2017); this competition reduces stem thickness, increases plant height, reduces stem mechanical strength and increases the risk of lodging (Zhang et al., 2017). Compared with normal-height plants, dwarf plants exhibit better lodging resistance, which lays a good foundation for close planting and high yields (Ren et al., 2016). The results of the present study showed that, as the planting density increased, the height of the maize plants significantly increased, and the plants were prone to lodging. 'Yuhuangjin' applications significantly reduced plant height, increased lodging resistance and ensured maize yields under high planting densities, which is consistent with previous results (Zhang et al., 2017).

Since Harman hypothesized the involvement of free radicals in senescence in 1956, research on the mechanism of the active oxygen defence response in plants has expanded (Shen, 2001). Many studies have shown that, under normal and abnormal metabolic conditions, plants produce reactive oxygen free radicals; however, reactive oxygen species can be controlled, mainly by protective enzymes (e.g. SOD, POD, CAT) and non-protective enzymes, vitamin C, and soluble proteins. When the metabolic balance is disturbed, free radicals accumulate in large amounts, leading to increased peroxidation of membrane lipids and increased MDA contents, which results in the destruction of the entire cell structure and function (Pan et al., 2006; Prochazkova and Wilhelmova, 2007). Previous studies have shown that leaf senescence is accompanied by the accumulation of reactive oxygen species and a decrease in antioxidant enzyme activities in cells (Prochazkova et al., 2001). Soluble protein contents are closely related to leaf function and senescence, which affect plant photosynthate accumulation and grain yields (Wang et al., 2016). The results of this study showed that increased planting density both led to a reduction in the activities of antioxidant enzymes (SOD, POD, CAT) in the ear leaves, an increase in MDA contents, and a decrease in soluble protein contents and accelerated leaf senescence. By regulating the balance of endogenous hormones, chemical controls can regulate plant growth and development, increase both the activity of plant protection enzymes and the soluble protein content, and improve plant adaptability to the environment, ultimately increasing crop yields (Wang et al., 2016). In the present study, 'Yuhuangjin' applications increased the activity of antioxidant enzymes, reduced the MDA content, increased the soluble protein content, increased the stay-green ability of the leaves and prolonged the functional period of the ear leaves, resulting in higher yields.

Conclusion

In a proper density extent, as the planting density increased, the 100-grain weight, rows per ear and number of grains per row decreased, whereas the barren stalk proportion and lodging risk increased. However, the increase in the effective number of ears per unit area compensated for the yield reduction caused by this density-induced stress. Under the premise of ensuring a specific density, 'Yuhuangjin' applications can reduce plant height, increase lodging resistance, shape a reasonable phenotype and delay leaf senescence to extend the functional period of the leaves, improve production

http://www.aloki.hu ● ISSN 1589 1623 (Print) ● ISSN 1785 0037 (Online)
DOI: http://dx.doi.org/10.15666/aeer/1802_32973311

conditions and increase production to a certain extent. Applications of chemical growth regulators and close planting at a reasonable density are therefore important ways for improving spring maize yields in Northeast China.

Acknowledgements. This work was supported by National Key Research and Development Program of China (grant no. 2016YFD0300103 and 2017YFD0300506), Heilongjiang Provincial Funding for National Key Research and Development Program of China (GX18B029), The "Academic Backbone" Project of Northeast Agricultural University (17XG23) and Postdoctoral Scientific Research Development Fund of Heilongjiang Province China (LBH-Q16031).

Conflict of Interests. Authors state no conflict of interests.

REFERENCES

[1] Abuzar, M. R., Sadozai, G. U., Baloch, M. S., Baloch, A. A., Shah, I. H., Javaid, T., Hussain, N. (2011): Effect of plant population densities on yield of maize. – Journal of Animal and Plant Sciences 21(4): 692-695.
[2] Aebi, H. (1984): Catalase in vitro. – Methods in Enzymology 105(105): 121-126.
[3] Andrade, F. H., Calvino, P. C. (2002): Yield response to narrow rows depends on increased radiation interception. – Agronomy Journal 94(5): 975-980.
[4] Andraski, T. W., Bundy, L. G., Brye, K. R. (2000): Crop management and corn nitrogen rate effects on nitrogen leaching. – Journal of Environmental Quality 29(4): 1095-1103.
[5] Bajguz, A., Hayat, S. (2009): Effects of brassinosteroids on the plant responses to environmental stresses. – Plant Physiology and Biochemistry 47(1): 1-8.
[6] Bradford, M. M. (1976): A rapid and sensitive method for the quantitation of microgram quantities of protein utilizing the principle of protein-dye binding. – Analytical Biochemistry 72(1-2): 248-254.
[7] Cao, C. Y., Li, W., Dang, H. K., Zheng, C. L., Ma, J. Y., Li, K. J., Wang, G. C., Zhang, S. G. (2013): Study on the influences of plant densities on yield, yield traits and canopy photosynthesis characteristics of summer maize. – Acta Agriculturae Boreali-sinica 28(S1): 161-166.
[8] Cao, Q. J., Gang, L., Diallo, L., Yang, F. T., Yao, L., Cui, J. H., Song, F. B. (2016): Effect of plant growth regulators on maize (*Zea Mays* L.) agronomic characteristics, stalk lodging and yield under high planting density in Northeast China. – Romanian Agricultural Research 33: 217-226.
[9] Chen, S. Q., Zhao, H. X., Yang, L. M., Du, X. D., Xue, Q. F., Jin, G. H., Zhou, T., Wang, C., Shan, L. L., Li, M., Wang, Q. Y. (2013): Preliminary study on regulate technique for resisting to lodging and high yielding cultivation of rice in cold region. – Acta Agriculturae Boreali-sinica 28(6): 159-165.
[10] Diallo, L., Cao, Q., Yang, F., Yang, Z., Cui, J., Gang, L., Dafaalla, T. I. M., Diarso, M., Ahmad, W. (2015): Seed priming effects of Yuhuangjin on spring maize. – The Journal of Animal and Plant Sciences 25(3): 747-754.
[11] Gao, J., Zhao, B., Dong, S. T., Liu, P., Ren, B. Z., Zhang, J. W. (2017): Response of summer maize photosynthate accumulation and distribution to shading stress assessed by using $^{13}CO_2$ stable isotope tracer in the field. – Frontiers in Plant Science 8: 1-12.
[12] Huang, R. H., Liu, J. H., Lu, Y. M., Xia, R. X. (2008): Effect of salicylic acid on the antioxidant system in the pulp of 'Cara cara' navel orange (*Citrus sinensis* L. Osbeck) at different storage temperatures. – Postharvest Biology and Technology 47(2): 168-175.
[13] Huffaker, R. C. (1990): Proteolytic activity during senescence of plants. – New Phytologist 116: 199-231.

http://www.aloki.hu ● ISSN 1589 1623 (Print) ● ISSN 1785 0037 (Online)
DOI: http://dx.doi.org/10.15666/aeer/1802_32973311

[14] Li, X. Y., Tang, Q. Y., Li, D. Q., Li, W. K., Li, H. L., Cai, Q. H. (2011): Effects of different plant densities on the photosynthetic-physiological characters and yield traits in spring maize grown on super-high yielding paddy field. – Acta Agriculturae Boreali-sinica 26(5): 174-180.
[15] Li, J., Xie, R. Z., Wang, K. R., Hou, P., Ming, B., Guo, Y. Q., Sun, L. Y., Zhang, G. Q., Zhao, R. L., Li, S. K. (2015): Changes in plant-to-plant variability among maize individuals and their relationships with plant density and grain yield. – Philippine Agricultural Scientist 98(1): 89-97.
[16] Lu, M., Liu, W. G., Yue, Y. H., Cai, Z., Wang, S. P., Zhang, H. W., Jin, M. H. (2011): Analysis on yield and relevant traits of maize varieties in Jilin province in the past twenty years. – Journal of Maize Sciences 19(5): 59-63.
[17] Ma, B. L., Dwyer, L. M. (1998): Nitrogen uptake and use of two contrasting maize hybrids in leaf senescence. – Plant and Soil 199(2): 283-291.
[18] Mohr, H., Schopfer, P. (1995): Plant physiology. – Springer-Verlag, Berlin, Heidelberg, Germany.
[19] Mukherjee, S. P., Choudhuri, M. A. (1983): Implications of water stress-induced changes in the levels of endogenous ascorbic acid and hydrogen peroxide in Vigna seedlings. – Physiologia Plantarum 58(2): 166-170.
[20] Ogunlela, V. B., Amoruwa, G. M., Ologunde, O. O. (1988): Growth, yield components and micronutrient nutrition of field-grown maize (*Zea mays* L.) as affected by nitrogen fertilization and plant density. – Nutrient Cycling Agroecosystems 17(2): 189-196.
[21] Otie, V., Ping, A., John, N. M., Eneji, A. E. (2016): Interactive effects of plant growth regulators and nitrogen on corn growth and nitrogen use efficiency. – Journal of Plant Nutrition 39: 1597-1609.
[22] Pan, Y., Wu, L. J., Yu, Z. L. (2006): Effect of salt and drought stress on antioxidant enzymes activities and SOD isoenzymes of liquorice (Glycyrrhiza uralensis Fisch). – Plant Growth Regulation 49(2-3): 157-165.
[23] Pan, S. G., Rasul, F., Li, W., Tian, H., Mo, Z. W., Duan, M. Y., Tang, X. R. (2013): Roles of plant growth regulators on yield, grain qualities and antioxidant enzyme activities in super hybrid rice (*Oryza sativa* L.). – Rice 6(1): 9.
[24] Pommel, B., Gallais, A., Coque, M., Quillere, I., Hirel, B., Prioul, J. L. (2006): Carbon and nitrogen allocation and grain filling in three maize hybrids differing in leaf senescence. – European Journal of Agronomy 24(3): 203-211.
[25] Prochazkova, D., Saiaram, R. K., Srovatava, G. C., Singh, D. V. (2001): Oxidative stress and antioxidant activity as the basis of senescence in maize leaves. – Plant Science 161(4): 765-771.
[26] Prochazkova, D., Wilhelmova, N. (2007): Leaf senescence and activities of the antioxidant enzyme. – Biologia Plantarum (Prague) 51(3): 401-406.
[27] Ren, B. Z., Li, L. L., Dong, S. T., Liu, P., Zhao, B., Yang. J. S., Wang, D. B., Zhang, J. W. (2016): Effects of Plant Density on Stem Traits and Lodging Resistance of Summer Maize Hybrids with Different Plant Heights. – Acta Agronomica Sinica 42(12): 1864-1872.
[28] Ren, B. Z., Liu, W., Zhang, J. W., Dong, S. T., Liu, P., Zhao, B. (2017): Effects of plant density on the photosynthetic and chloroplast characteristics of maize under high-yielding conditions. – Science of Nature 104(3-4): 12.
[29] Saba, M. K., Arzani, K., Barzegar, M. (2012): Postharvest polyamine application alleviates chilling injury and affects apricot storage ability. – Journal of Agricultural and Food Chemistry 60(36): 8947-8953.
[30] Shafi, M., Bakht, J., Ali, S., Khan, H., Khan, M. A., Sharif, M. (2012): Effect of planting density on phenology, growth and yield of maize (*Zea Mays* L.). – Pakistan Journal of Botany 44(2): 691-696.
[31] Shen, C. G. (2001): Plant senescence physiology and molecular biology. – China Agriculture Press, Beijing, China.

http://www.aloki.hu ● ISSN 1589 1623 (Print) ● ISSN 1785 0037 (Online)
DOI: http://dx.doi.org/10.15666/aeer/1802_32973311

[32] Shin, S., Lee, J. S., Son, B. Y., Kim, J. T., Kim, S. G., Kim, M. J., Kim, S. L., Kwon, Y. U., Baek, S. B., Woo, M. O., Bae, H. H. (2014): Effect of plant density on growth and yield of extremely late-planted korean sweet corn hybrids (*Zea mays L.*) for fresh market. – Journal of Crop Science Biotechnology 17(4): 289-295.
[33] Taiz, L., Zeiger, E. (2006): Plant physiology, 4th edition. – Sinauer Associates Inc. Publishers, Sunderland, Massachusetts, USA.
[34] Tokatlidis, I. S. (2017): Crop adaptation to density to optimise grain yield: breeding implications. – Euphytica 213(4): 92.
[35] Wang, Y. H., Wang, K. R., Zhao, R. L., Wang, K., Zhao, J., Wang, X. M., Li, J., Liang, M. X., Li, S. K. (2013): Relationship Between the Source and Sink of Spring Maize with High Yield. – Scientia Agricultura Sinica 46(2): 257-269.
[36] Wang, Y. C., Gu, W. R., Xie, T. L., Li, L. J., Sun, Y., Zhang, H., Li, J., Wei, S. (2016): Mixed compound of DCPTA and CCC increases maize yield by improving plant morphology and up-regulating photosynthetic capacity and antioxidants. – Plos One 11: e0149404.
[37] Wei, S. S., Wang, X. Y., Zhu, Q. C., Jiang, D., Dong, S. T. (2017): Optimising yield and resource utilisation of summer maize under the conditions of increasing density and reducing nitrogen fertilization. – Science of Nature 104(11-12): 86.
[38] Xu, C. L., Gao, Y. B., Tian, B. J., Ren, J. H., Meng, Q. F., Wang, P. (2017): Effects of EDAH, a novel plant growth regulator, on mechanical strength, stalk vascular bundles and grain yield of summer maize at high densities. – Field Crops Research 200: 71-79.
[39] Xu, T. J., Lv, T. F., Chen, C. Y., Liu, Y. E., Zhang, Y. T., Liu, X. Z., Zhao, J. R., Wang, R. H. (2019): Effects of Plant Density and Plant Growth Regulator on Stalk Traits of Maize and Their Regulation. – Scientia Agricultura Sinica 52(4): 629-638.
[40] Zhang, Y. K., Sun, M., Zhang, X. J., Wu, J. P., He, Z. Y., Ma, Y. P. (2006): Study on close planting and nutrient improvement of maize. – Journal of Maize Sciences 14(3): 129-132.
[41] Zhang, Q., Zhang, L. Z., Evers, J., Werf, W. V. D., Zhang, W. Q., Duan, L. S. (2014): Maize yield and quality in response to plant density and application of a novel plant growth regulator. – Field Crops Research 164: 82-89.
[42] Zhang, W. Q., Yu, C. X., Zhang, K., Zhou, Y. Y., Tan, W. M., Zhang, L. Z., Li, Z. H., Duan, L. S. (2017): Plant growth regulator and its interactions with environment and genotype affect maize optimal plant density and yield. – European Journal of Agronomy 91: 34-43.
[43] Zhao, M., Zhou, S. X., Cui, Y. H. (2006a): Research and application of plant growth regulators on maize in China. – Journal of Maize Sciences 14(1): 127-131.
[44] Zhao, M., Li, J. G., Zhang, B., Dong, Z. Q., Wang, M. Y. (2006b): The compensatory mechanism in exploring crop production potential. – Acta Agronomica Sinica 32(10): 1566-1573.

http://www.aloki.hu ● ISSN 1589 1623 (Print) ● ISSN 1785 0037 (Online)
DOI: http://dx.doi.org/10.15666/aeer/1802_32973311

REGIONAL FLOOD RISK ANALYSIS FOR HUAIHONG SOUTH FLOOD CONTROL PROTECTED AREA IN CHINA USING AN INTEGRATED METHOD

GAO, Y. Q.[1*] – ZHOU, X.[1] – ZHANG, Z. X.[2]

[1]*College of Water Conservancy and Hydropower Engineering, Hohai University, No. 1 Xikang Road, Gulou District, Nanjing 210098, China*

[2]*Illionis State Water Survey, Prairie Research Institute, University of Illinois Urbana-Champaign, 2204 Griffith Dr., Champaign IL, USA*

**Corresponding author*
e-mail: gyq_0909@163.com; phone: +86-139-5188-9955

(Received 27th Sep 2019; accepted 4th Feb 2020)

Abstract. Non-engineering flood control measures have gradually become an important part of flood disaster management in the past decades, and it cannot be separated from regional flood risk analyses. Flood risk analyses can be regarded as a complex of three aspects: flood hazard analyses, vulnerability analyses and comprehensive evaluation of both. In this paper, taking Huaihong South Flood Control Protected Area (simplified as HHS) of the Huaihe River Basin in China as an example, a one-dimensional (1-D) and two-dimensional (2-D) coupled hydrodynamic model of the study area was established to simulate the evolution process of the floods with different return periods and acquire inundation data in the flood hazard analysis. Concerning the vulnerability analysis, based on the composition mechanism of vulnerability and the available data of the study region, the vulnerability evaluation index system was established, then the magnitudes of vulnerability of the townships in the research were analyzed through the catastrophe progression method. Combined with the analysis results above, the flood risk of 15 townships in HHS can be classified into 6 magnitudes by factor analysis and hierarchical clustering analysis. The results show that the flood risk is medium or even higher in most zones of HHS. The integrated method used in this research can also be applied to other regions.
Keywords: *flood risk, vulnerability analysis, 1-D and 2-D coupled hydrodynamic model, catastrophe progression method, factor analysis, hierarchical clustering analysis*

Introduction

In recent decades, with the climatic changes, population growth and urban development in flood-prone areas, the ability of human beings to control floods has become stronger and stronger, but the devastating impacts on people's livelihood, economy and the environment due to floods had an increasing tendency in the past 25 years in China (Yu et al., 2018). A possible way to reduce the loss of flood disasters is the mapping of flood-prone areas to risk awareness and support sustainable land-use planning and urban development (Horritt et al., 2007). Flood risk analysis is a useful source of information in rescue and relief agencies for their operations. In 2007, the European Union has adopted Flood Directive, with the main objective of reducing and managing flood risk (Van Alphen et al., 2009).

Flood risk analyses can be basically divided into three parts: flood hazard analyses, vulnerability analyses and comprehensive evaluation of both. The researches on flood hazard analyses at domestic and abroad generally include two aspects: one is to explore the inner relationship between the different return periods and the actual scales of flood events; the other one is to predict future flow regime characteristics in flood-affected

http://www.aloki.hu ● ISSN 1589 1623 (Print) ● ISSN 1785 0037 (Online)
DOI: http://dx.doi.org/10.15666/aeer/1802_33133329

areas, and the flood hazard has usually been expressed by inundation information of flood (inundation range, depth, duration, etc.). The aim of vulnerability analyses is to assess the multi-dimensional vulnerability (Physical, Social, Economic and Environment) of the region. This exercise will be used to develop a vulnerability map as an input towards flood risk analysis.

In scientific literature, for both the hazard and vulnerability analyses, a number of approaches and models of different complexity levels are available (Kourgialas and Karatzas, 2011). Kourgialas and Karatzas (2011) presented a method to estimate the flood-hazard areas considering six factors: flow accumulation, slope, land use, rainfall intensity, geology and elevation. The study area was divided into five regions characterized by different magnitudes of flood risk ranging from very low to extremely high. Apel et al. (2009) tested numerous combinations of models of different complexity both on the hazard and on the vulnerability side in a case study. On the hazard side, the models selected include a mixed 1D/2D hydraulic model. On the vulnerability side, the models used for the estimation of direct damage to residential buildings are in order of increasing complexity, such as a rule-based micro-scale model applied to a detailed building inventory (Apel et al., 2011).

Materials and methods

Study area

The riverine area of the Huaihe River Basin in the Anhui Province (in China) has always been prone to flooding disasters (Wang, 2015). One of the most serious flooding areas in the Anhui Province is HHS which is located between 32°50′N–33°20′N latitude and 117°10′E–117°50′E longitude, covering an area of about 1480 km^2 (*Fig. 1*). It covers 15 townships in three counties, one district. The general trend of HHS is higher in the north and lower in the south.

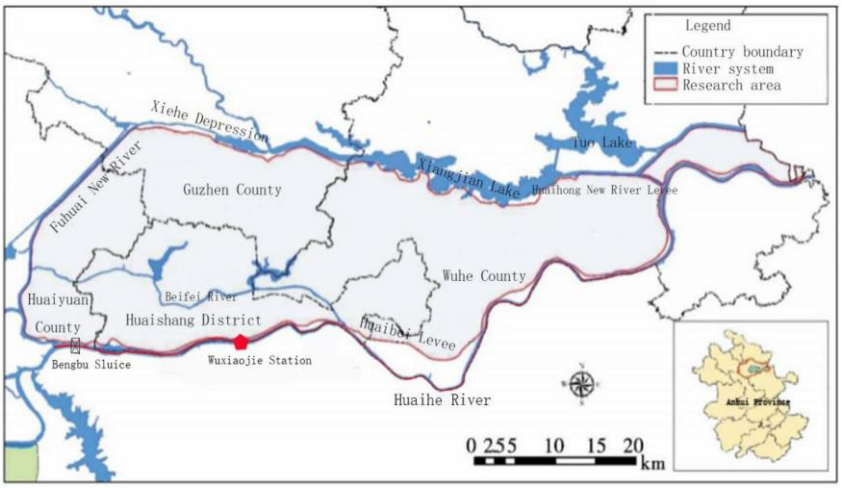

Figure 1. *Location of HHS*

Available data

The topographic data used in this research is based on 1:10000 topographic data and the DEM of the entire study area with a horizontal resolution of 5 m provided by Anhui

http://www.aloki.hu ● ISSN 1589 1623 (Print) ● ISSN 1785 0037 (Online)
DOI: http://dx.doi.org/10.15666/aeer/1802_33133329

Provincial Flood Control Office. Topographic map of the research region is shown in *Figure 2*. The cross-sectional data of the main stream of the Huaihe River are 104 cross-sections with 1-2 km spacing between the cross-sections measured in 1993.

Total length of the river reach in study is 110.0 km. Discharge curves of 50-, 100- and 200-year floods in Wujiadu Station are available (*Fig. 3*). Generalized river network of main stream of the Huaihe River considered in this research is shown in *Figure 4*.

According to the information sheet of key dangerous sections provided by the relevant water conservancy department, the Wuxiaojie Station on the Huaibei levee (indicated in *Fig. 1*) is selected as the possible dyke burst. *Table 1* shows the data of evaluation indicators (refer to Statistical Yearbook of Bengbu City in 2015) used in this research.

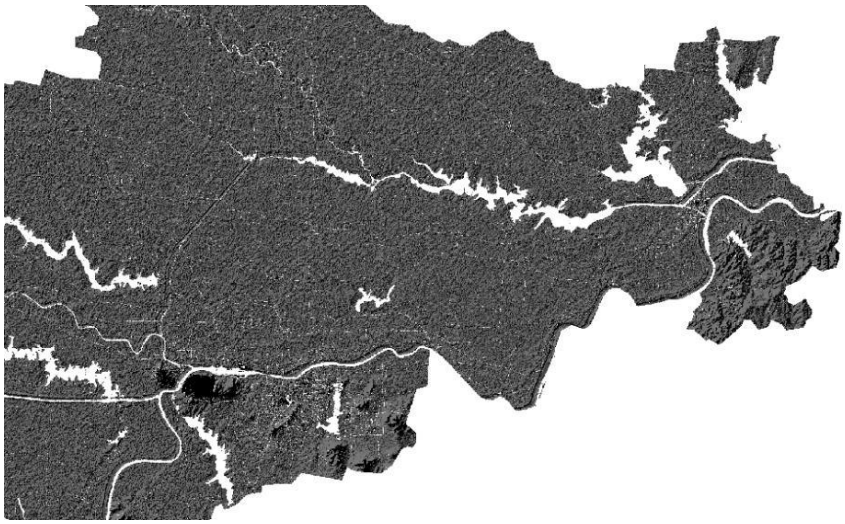

Figure 2. *Topographic map of the entire study area*

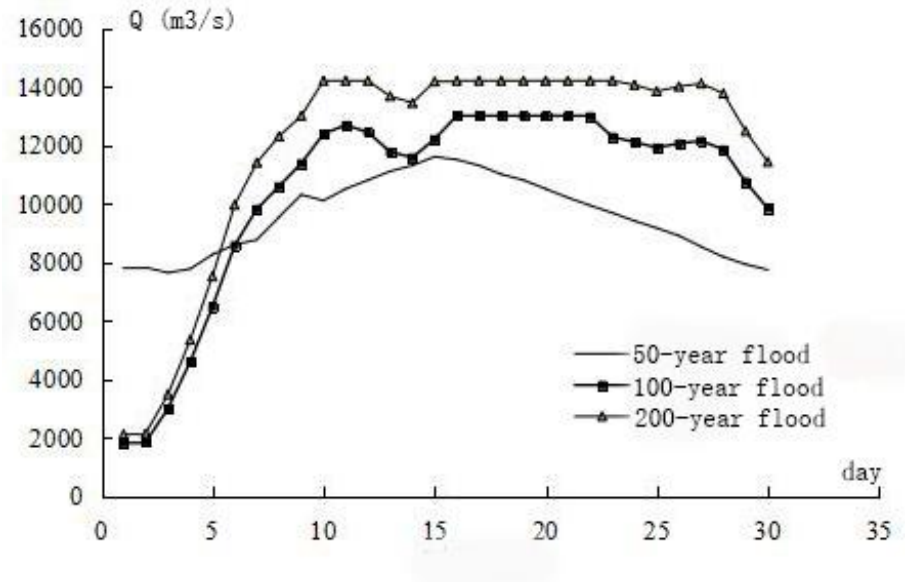

Figure 3. *Discharge curves of 50-, 100- and 200-year floods in Wujiadu Station*

http://www.aloki.hu ● ISSN 1589 1623 (Print) ● ISSN 1785 0037 (Online)
DOI: http://dx.doi.org/10.15666/aeer/1802_33133329

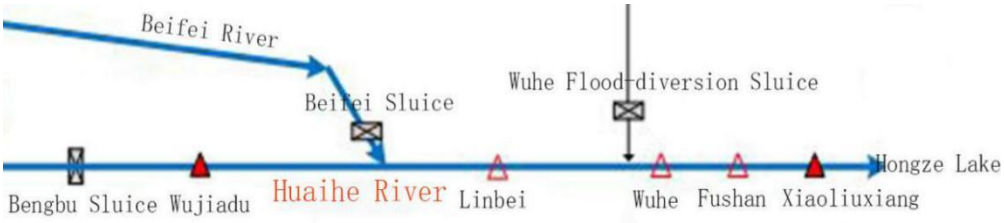

Figure 4. *Generalized river network of main stream of the Huaihe River considered in this research*

Table 1. *Original values of indicators used in this research*

Indicator	Evaluation township				
	Huinan (HN)	**Xinji (XJ)**	**Toupu (TP)**	**Daxin (DX)**	**Caoguzhang (CGZ)**
Drainage density ($m/10^3 m^2$)	0.007	0.008	0.008	0.006	0.008
GDP per unit area ($million/10^6 m^2$)	904.597	1351.741	1043.725	1160.379	1152.572
Density of population ($person/10^6 m^2$)	296.004	449.046	505.887	461.485	184.241
Density of residential structures (m^2/m^2)	0.014	0.021	0.023	0.022	0.007
Density of lifeline engineering structures ($m/10^3 m^2$)	0.407	0.482	0.593	0.512	0.271
Proportion of agricultural population (%)	0.964	0.941	0.962	0.964	0.828
Average elevation (m)	18.176	16.136	15.076	16.625	17.446
Land-use sensitive index	4.119	4.063	4.2	3.275	4.336
Proportion of female population (%)	0.468	0.47	0.478	0.473	0.485
GDP per capital (million/person)	2.663	2.64	1.882	2.219	6.256
Density of shelters ($number/10^6 m$)	0.288	0.03	0.101	0.146	0.083
Density of medical aid institutions ($one/10^6 m^2$)	0.09	0.296	0.172	0.255	0.193
Indicator	**Evaluation township**				
	North of the Muslim (NM)	**Xinmaqiao (XMQ)**	**Wangzhuang (WZ)**	**Meiqiao (MQ)**	**Caolaoji (CLJ)**
Drainage density ($m/10^3 m^2$)	0.017	0.007	0.007	0.008	0.009
GDP per unit area ($million/10^6 m^2$)	531.921	1285.729	1047.172	3926.926	2652.742
Density of population ($person/10^6 m^2$)	185.198	359.764	355.156	805.851	530.141
Density of residential structures (m^2/m^2)	0.007	0.014	0.013	0.031	0.021
Density of lifeline engineering structures ($m/10^3 m^2$)	1.62	0.631	0.343	0.685	0.473
Proportion of agricultural population (%)	0.862	0.946	0.968	0.93	0.951

http://www.aloki.hu ● ISSN 1589 1623 (Print) ● ISSN 1785 0037 (Online)
DOI: http://dx.doi.org/10.15666/aeer/1802_33133329

Average Elevation (m)	17.257	19.193	18.905	17.277	17.288
Land-use sensitive index	3.265	4.27	4.167	3.623	3.967
Proportion of female population (%)	0.465	0.475	0.466	0.459	0.477
GDP per capital (million/person)	2.872	3.274	2.774	4.873	5.004
Density of shelters (number/10^6 m)	0.081	0.061	0.037	0.298	0.104
Density of medical aid institutions (one/$10^6 m^2$)	0.228	0.155	0.203	0.265	0.166
Indicator	**Evaluation township**				
	Wuxiaojie (WXJ)	**Xiaobengbu (XBB)**	**Mohekou (MHK)**	**Weizhuang (WEZ)**	**Chengguan town in Huaiyuan county (CG)**
Drainage density ($m/10^3 m^2$)	0.008	0.006	0.006	0.008	0.013
GDP per unit area (million/$10^6 m^2$)	17638.226	62040.981	3567.112	254.26	14918.667
Density of population (person/$10^6 m^2$)	757.459	1217.154	707.183	125.8	691.251
Density of residential structures (m^2/m^2)	0.031	0.051	0.029	0.01	0.053
Density of lifeline engineering structures ($m/10^3 m^2$)	1.258	1.843	0.604	1.027	2.324
Proportion of agricultural population (%)	0.7	0.336	0.947	0.967	0.22
Average elevation (m)	16.991	17.656	17.492	18.281	18.67
Land-use sensitive index	3.662	3.146	4.367	2.847	2.831
Proportion of female population (%)	0.501	0.506	0.478	0.47	0.493
GDP per capital (million/person)	21.843	44.59	4.749	1.038	10.435
Density of shelters (number/10^6 m)	0.474	1.834	0.347	0.108	1.226
Density of medical aid institutions (one/$10^6 m^2$)	0.422	0.386	0.163	0.118	0.2

Flood hazard analysis

Flood hazard analysis is one of the methods of flood forecasting. In this paper, a 1-D hydrodynamic model was used to simulate the flood course of Huaihe River in the study area, a 2-D hydrodynamic model was used to simulate the flood routing in HHS, and a 1-D and 2-D coupled hydrodynamic model was used to simulate the flood course of a levee breach (Zhang et al., 2019). MIKE software with the advantage of stability, reliability and high accuracy was selected for modelling calculation.

1-D hydrodynamic modelling

For the 1-D hydrodynamic modelling, in terms of topographic data, it required a certain number of cross-sections to represent the river channel and its surrounding

http://www.aloki.hu ● ISSN 1589 1623 (Print) ● ISSN 1785 0037 (Online)
DOI: http://dx.doi.org/10.15666/aeer/1802_33133329

topography (Cook and Merwadee, 2009). The 104 cross-sections measured in 1993 were used in the model for describing the geometry of the river reach. Considering Wuxiaojie Station was the breach of Huaibei levee, the discharge curves of 50-, 100- and 200-year floods at the breach were taken as the upstream boundary condition, whereas the stage-discharge relation at Xiaoliuxiang Station was used as the downstream boundary condition (Brandimarte and Di Baldassarre, 2012). The 1-D model was established to simulate floods in the one-dimensional channel from Bengbu Sluice to Xiaoliuxiang Station with MIKE 11 (Ferdous, 2012). The initial discharge of the river is set to 0, and the initial water level is set to the measured water level at the beginning of the simulation.

2-D hydrodynamic modelling

The domain of the 2-D hydrodynamic model is described by a mesh consisting of nodes and triangular elements (Tewodros and Abdusselam, 2019; Jungkyu et al., 2019). The topographic data adopted in this model was the 1:10000 topographic data and DEM of the entire study area with a horizontal resolution of 5 m. In this model, a hybrid grid model was established to reflect the overall terrain variation characteristics of the region. The 2-D model was used to simulate the flood routing in HHS with MIKE 21.

1-D and 2-D coupled hydrodynamic modelling

The 1-D and 2-D coupled hydrodynamic model simulated the 1-D flow in river channels and the 2-D flow in floodplains with MIKE FLOOD to acquire inundation depth, inundation duration and velocity of the floods with different recurrence periods (Parto et al., 2009). During the coupling process, the left embankment of Huaihe River, the right embankment of Huaihong New River and the 20.5 m contour line of Fengshan in Sihong County of Jiangsu Province in China were taken as the external boundary; the dispatching process of dikes, roads, bridges, culverts and other structures were used as the internal boundary conditions. The 1-D model and 2-D model exchanged water level and flow information with each other. The 1-D model used the water level of the 2-D model's grid at the coupling point as the boundary water level, whereas the 2-D model used the outflow of the 1-D model at the coupling point as the inflow.

Vulnerability analysis

Vulnerability index system

In this study, vulnerability of the evaluation object at flood risk is regarded as a state variable. In the absence of a thorough study on the formation mechanism of vulnerability to flood, the index system method which is based on the hierarchy and the correlation between structural indicators of vulnerability is the most common method. It can reflect the overall macro-situation of the magnitudes of flood vulnerability in the region (Fan et al., 2000).

Defined as the inherent attribute of an element at risk, vulnerability was usually composed of three parts: exposure degree (Baldassarre et al., 2009), sensitivity, capacity of disaster prevention and mitigation. According to this, representative indicators (*Table 2*) are selected to construct the vulnerability index system of the evaluation object at flood risk.

http://www.aloki.hu ● ISSN 1589 1623 (Print) ● ISSN 1785 0037 (Online)
DOI: http://dx.doi.org/10.15666/aeer/1802_33133329

Table 2. *Vulnerability index system of the evaluation object at flood risk*

Target layer	Criterion layer	Index layer
Vulnerability (A)	Exposure degree (B1)	GDP per unit area (C1)
		Density of population (C2)
		Density of residential structures (C3)
		Density of lifeline engineering structures (C4)
	Sensibility (B2)	Average elevation (C5)
		Proportion of agricultural population (C6)
		Land-use sensitive index (C7)
		Proportion of female population (C8)
	Capacity of disaster prevention and mitigation (B3)	GDP per capital (C9)
		Density of shelters (C10)
		Density of medical aid institutions (C11)

Among these indicators, GDP per unit area refers to the gross domestic product of agriculture, industry and tertiary industry; density of lifeline engineering structures refers to the lifeline length per unit area; land use sensitive index is defined in the literature (Chen et al., 2012); density of shelters refers to the number of large and medium-sized sites, such as schools, shopping malls and hotels, that can accommodate the affected people on unit area of the evaluation township; density of medical aid institutions refers to the number of medical aid institutions on unit area of the evaluation township.

Catastrophe progression method

In order to avoid the subjectivity of determining the weight assignment of vulnerability indicators, this study used the catastrophe progression method to evaluate the magnitudes of vulnerability to flood of the townships in the region (Li et al., 2010; Liu et al., 2010).

When calculating the vulnerability indicators of evaluation townships, the original values of indicators in the *Table 1* should be uniformly normalized and transformed into positive indices in the range of [0,1].

For the larger-the-better indices:

$$r_{ij} = \frac{x_{ij} - \min(x_{ij})}{\max(x_{ij}) - \min(x_{ij})} \quad \text{(Eq.1)}$$

For the smaller-the-better indices:

$$r_{ij} = \frac{\max(x_{ij}) - x_{ij}}{\max(x_{ij}) - \min(x_{ij})} \quad \text{(Eq.2)}$$

where x_{ij} – original value of index 'j' of evaluation township 'i'; $\max(x_{ij})$ and $\min(x_{ij})$ – maximum and minimum value of index 'j'; r_{ij} – normalized value of x_{ij}.

http://www.aloki.hu ● ISSN 1589 1623 (Print) ● ISSN 1785 0037 (Online)
DOI: http://dx.doi.org/10.15666/aeer/1802_33133329

Catastrophe progression method is a multilevel objective decomposition for evaluation objects which combing the catastrophe theory and fuzzy mathematics, the ultimate catastrophe function is obtained through quantitative computing by the normalization formula of different catastrophe models, and thus the comprehensive assessment of alternatives is realized, then a catastrophe progression model is obtained to classify the vulnerability classification of evaluation townships.

In this paper, according to the number of variables, we chose the proper catastrophe progression model and used the corresponding normalization formula layer by layer to calculate until the ultimate catastrophe functional value (value of vulnerability to flood) was obtained. The mean value was taken as the upper index value when calculating the catastrophe progression of each layer for the reason that the evaluation indices considered in this study could make up for their deficiencies. Alternative catastrophic models are shown in *Table 3* (Li et al., 2010).

Table 3. *Alternative catastrophe progression models.*

Catastrophe progression model	Number of variables	Normalization formula
Cusp catastrophe	2	$X_a = a^{1/2}$; $X_b = b^{1/3}$
Swallowtail catastrophe	3	$X_a = a^{1/2}$; $X_b = b^{1/3}$; $X_c = c^{1/4}$
Butterfly catastrophe	4	$X_a = a^{1/2}$; $X_b = b^{1/3}$; $X_c = c^{1/4}$; $X_d = d^{1/5}$

X_a, X_b, X_c, X_d – catastrophe progression of a, b, c, d; a, b, c, d – normalized values of indices

Risk analysis

Flood risk index system

In a flood risk index system, according to the process of flood hazard analysis and vulnerability analysis (Fuchs et al., 2012; Merz et al., 2010; Masood and Takeuchi, 2012), inundation depth, inundation duration and velocity of 200-year flood were selected as indicators of flood hazard, drainage density, proportion of agricultural population, proportion of female population, land-use sensitive index, GDP per unit area, density of population, density of residential structures, density of lifeline engineering structures, GDP per capital and density of shelters were taken as vulnerability indicators.

Factor analysis

In the study of flood risk assessment, it generally involves multiple evaluation indicators and numerous evaluation objects (Li et al., 2003). Attempting to synthesize the characteristics reflected by various indicators and minimize the loss of raw information, we transformed several evaluation indicators into a few comprehensive factors through factor analysis (Helena et al., 2003). The basic idea of factor analysis approach is to divide the original indicator variables into several groups by making the correlation of variables in the same group become higher, while the correlation of variables from different groups become lower. Each group of indicator variables can be represented by an immeasurable comprehensive variable which is also called a common factor (Kuo et al., 2013). In this way, a few representative common factors can be used to summarize the information provided by the original variables (Muangthong and Shrestha, 2015). The part of the original variables which cannot be explained by the

http://www.aloki.hu ● ISSN 1589 1623 (Print) ● ISSN 1785 0037 (Online)
DOI: http://dx.doi.org/10.15666/aeer/1802_33133329

common factors will be regarded as special factors (Wan et al., 2013). It can be expressed by mathematical formula as follows (Ma et al., 2011; Zhang et al., 2009).

$$\begin{aligned} x_1 &= a_{11}F_1 + a_{12}F_2 + \cdots + a_{1m}F_m + \varepsilon_1 \\ x_2 &= a_{21}F_1 + a_{22}F_2 + \cdots + a_{2m}F_m + \varepsilon_2 \\ &\cdots \\ x_p &= a_{p1}F_1 + a_{p2}F_2 + \cdots + a_{pm}F_m + \varepsilon_p \end{aligned} \quad \text{(Eq.3)}$$

where x_i (i = 1,2,…,p) – original indicator variable; F_j (j = 1,2,…,m) – common factor; a_{ij} (i = 1,2,…,p; j = 1,2,…,m) – load of common factor F_j on variable x_i; $\varepsilon_i (i = 1,2,\ldots, p)$ – special factor.

F_j (j = 1,2,…,m) can be represented as follows:

$$F = BX \Leftrightarrow \begin{aligned} F_1 &= b_{11}x_1 + b_{12}x_2 + \ldots + b_{1p}x_p \\ F_2 &= b_{21}x_1 + b_{22}x_2 + \ldots + b_{2p}x_p \\ &\cdots \\ F_m &= b_{m1}x_1 + b_{m2}x_2 + \ldots + b_{mp}x_p \end{aligned} \quad \text{(Eq.4)}$$

where x_i(i = 1,2,…,p) – standardized variable; B – factor loading matrix.
Calculating the score 'S' of each evaluation unit:

$$S = \sum_{i=1}^{m} \left[(F_i \times (C_i / C) \right] \quad \text{(Eq.5)}$$

where C_i(i = 1,2,…,m) – contribution of variances of each common factor; C – accumulated contribution of variances.

Hierarchical clustering analysis

The evaluation objects are further classified by clustering to reveal the internal relationship among multiple evaluation objects with the method of hierarchical clustering algorithm in this research. Suppose there are 'n' samples to be clustered, for hierarchical clustering, the steps are as follows:
Step1: Initialization (take each sample as a class, and calculate the distance between each two classes, that is, the similarity between samples).
Step2: Find the two nearest classes among these classes, and classify them into one class (so that the total number of classes is one less).
Step3: Recalculate the similarity between the newly generated class and each old class.
Step4: Repeat Step2 and Step3 until all samples are in the same category.

Using MATLAB to perform the steps above can obtain the clustering dendrogram of hierarchical clustering analysis like *Figure 5*.

Based on clustering 15 samples (taking the comprehensive flood risk score 'S' and the vulnerability index value of one township as a sample) by the hierarchical clustering method, the townships falling in HHS were divided into various flood risk zones

http://www.aloki.hu ● ISSN 1589 1623 (Print) ● ISSN 1785 0037 (Online)
DOI: http://dx.doi.org/10.15666/aeer/1802_33133329

namely extremely-high-, high-, medium-high-, medium-, low-medium- and low-risk zones, taking township as a stratum.

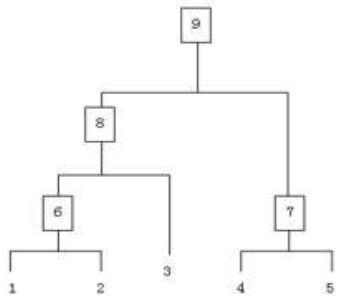

Figure 5. *Generalized dendrogram of Hierarchical clustering analysis*

Results

Flood hazard

A simulation was conducted according to the above-mentioned model (the 1-D and 2-D coupled hydrodynamic model) by MIKE software, the simulation inundation data based on the 50-year, 100-year and 200-year return period floods are presented in *Table 4*.

Table 4. *Simulation inundation data based on the 50-year, 100-year and 200-year return period flood*

Evaluation township	Inundation depth (m)			Inundation duration (h)			Flood velocity (m/s)		
	50-year	100-year	200-year	50-year	100-year	200-year	50-year	100-year	200-year
HN	0.684	1.808	2.181	104.302	248.028	273.860	0.036	0.056	0.062
XJ	2.514	3.879	4.253	209.447	317.023	327.933	0.080	0.098	0.105
TP	3.649	5.012	5.385	192.961	295.236	307.554	0.084	0.098	0.104
DX	2.053	3.399	3.772	226.367	335.816	346.401	0.062	0.083	0.091
CGZ	2.057	3.079	3.451	298.816	414.159	419.598	0.086	0.108	0.117
NM	1.735	2.961	3.330	252.017	354.912	362.313	0.090	0.108	0.115
XMQ	0.320	0.890	1.264	65.198	173.005	215.478	0.020	0.035	0.037
WZ	0.712	1.324	1.699	120.968	216.803	252.321	0.029	0.043	0.048
MQ	2.087	2.869	3.240	378.122	450.370	451.363	0.117	0.120	0.125
CLJ	2.183	2.993	3.365	299.140	396.235	404.646	0.146	0.191	0.197
WXJ	2.616	3.304	3.665	445.607	455.775	474.793	0.330	0.345	0.363
XBB	1.706	2.424	2.777	370.348	440.865	442.206	0.090	0.093	0.103
MHK	1.546	2.659	3.031	291.821	400.272	404.046	0.087	0.111	0.118
WEZ	1.139	1.857	2.222	212.028	315.534	331.058	0.043	0.051	0.055
CG	0.900	1.599	1.956	275.259	357.360	362.860	0.044	0.048	0.051

Vulnerability

Taking Chengguan town in Huaiyuan county (CG) as an example, the original values of indicators in the *Table 1* could be uniformly normalized and transformed into positive indicators in the range of [0,1], as shown in *Table 5*.

http://www.aloki.hu ● ISSN 1589 1623 (Print) ● ISSN 1785 0037 (Online)
DOI: http://dx.doi.org/10.15666/aeer/1802_33133329

Table 5. *Normalized values of indicators of CG.*

Target layer	Criterion layer	Index layer	Normalized values
Vulnerability of CG (A)	Exposure degree (B1)	GDP per unit area (C1)	0.2374
		Density of population (C2)	0.5181
		Density of residential structures (C3)	1
		Density of lifeline engineering structures (C4)	0
	Sensibility (B2)	Average elevation (C5)	0.1270
		Proportion of agricultural population (C6)	0
		Land-use sensitive index (C7)	0
		Proportion of female population (C8)	0.7234
	Capacity of disaster prevention and mitigation (B3)	GDP per capital (C9)	0.7842
		Density of shelters (C10)	0.3370
		Density of medical aid institutions (C11)	0.6687

C1, C2, C3, C4 in index layer could constitute a cusp catastrophe:

$$X_{c1} = C1^{1/2} = (0.2374)^{1/2} = 0.4872$$
$$X_{c2} = C2^{1/3} = (0.5181)^{1/3} = 0.8032 \quad \Rightarrow B1 = (X_{c1} + X_{c2} + X_{c3} + X_{c4})/4 = 0.5726$$
$$X_{c3} = C3^{1/4} = (1)^{1/4} = 1$$
$$X_{c4} = C4^{1/5} = (0)^{1/5} = 0$$

C5, C6, C7, C8 in index layer could constitute a cusp catastrophe:

$$X_{c5} = C5^{1/2} = (0.1270)^{1/2} = 0.3564$$
$$X_{c6} = C6^{1/3} = (0)^{1/3} = 0 \quad \Rightarrow B2 = (X_{c5} + X_{c6} + X_{c7} + X_{c8})/4 = 0.3234$$
$$X_{c7} = C7^{1/4} = (0)^{1/4} = 0$$
$$X_{c8} = C8^{1/5} = (0.7234)^{1/5} = 0.9373$$

C9, C10, C11 in index layer could constitute a swallowtail catastrophe:

$$X_{c9} = C5^{1/2} = (0.7842)^{1/2} = 0.8856$$
$$X_{c10} = C6^{1/3} = (0.3370)^{1/3} = 0.6959 \quad \Rightarrow B3 = (X_{c9} + X_{c10} + X_{c11})/3 = 0.8286$$
$$X_{c11} = C7^{1/4} = (0.6687)^{1/4} = 0.9043$$

B1, B2, B3 in criterion layer could constitute a swallowtail catastrophe:

$$X_{B1} = B1^{1/2} = 0.7567$$
$$X_{B2} = B2^{1/3} = 0.6864 \quad \Rightarrow A = (X_{B1} + X_{B2} + X_{B3})/3 = 0.7991$$
$$X_{B3} = B3^{1/4} = 0.9541$$

http://www.aloki.hu ● ISSN 1589 1623 (Print) ● ISSN 1785 0037 (Online)
DOI: http://dx.doi.org/10.15666/aeer/1802_33133329

Thus, the value of vulnerability to flood of CG is 0.7991 and the rest of townships could be calculated by analogy. The results are shown in *Table 6*.

Table 6. *The values of vulnerability of each evaluation township*

Evaluation township	Exposure degree (B1)	Sensibility (B2)	Capacity of disaster prevention and mitigation (B3)	Vulnerability
HN	0.5860	0.7926	0.9770	0.8951
XJ	0.6429	0.8860	0.9221	0.9141
TP	0.6487	0.9508	0.9695	0.9270
DX	0.6435	0.8265	0.9355	0.9081
CGZ	0.6011	0.7284	0.9599	0.8883
NM	0.4640	0.7569	0.9478	0.8598
XMQ	0.6017	0.6950	0.9717	0.8848
WZ	0.5251	0.8670	0.9465	0.8882
MQ	0.5135	0.6281	0.9107	0.8499
CLJ	0.6720	0.8563	0.9589	0.9196
WXJ	0.7789	0.8573	0.5443	0.8971
XBB	0.9346	0.7053	0.1913	0.8394
MHK	0.7169	0.8669	0.9446	0.9287
WEZ	0.3928	0.6344	0.9879	0.8277
CG	0.5726	0.3234	0.8286	0.7991

Vulnerability were classified into five magnitudes (micro vulnerability, light vulnerability, medium vulnerability, high vulnerability and severe vulnerability) by natural breakpoint method in ArcGIS (Wu and Li, 2013). The ranges of values for each level were [0.7991, 0.8277], [0.8394, 0.8598], [0.8848, 0.8971], [0.9081, 0.9141], [0.9196, 0.9287], respectively. The spatial distribution of the magnitudes of vulnerability in the study area is shown in *Figure 6*.

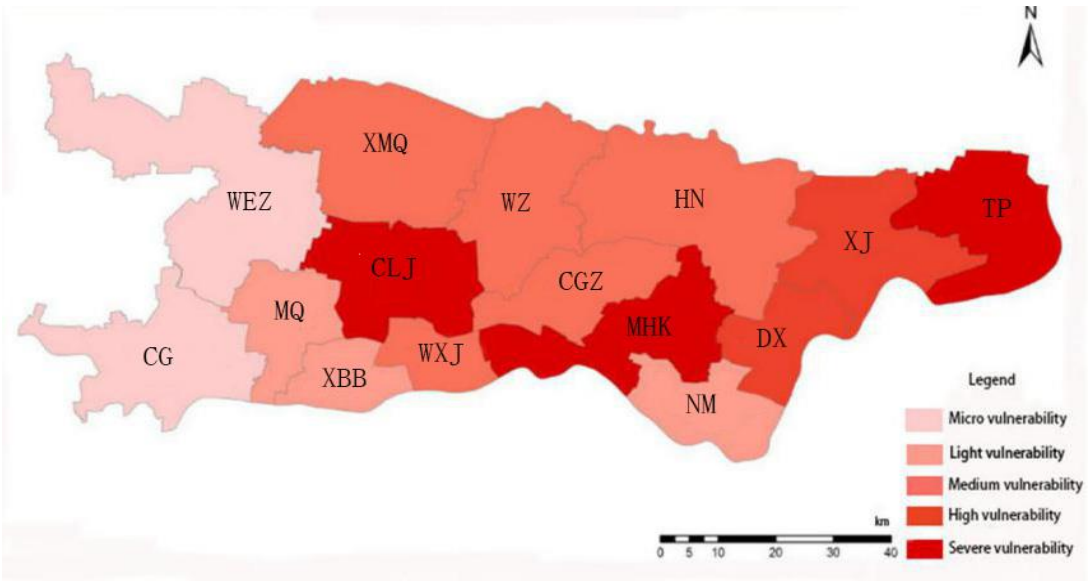

Figure 6. *Spatial distribution of the magnitudes of vulnerability in the study area*

http://www.aloki.hu ● ISSN 1589 1623 (Print) ● ISSN 1785 0037 (Online)
DOI: http://dx.doi.org/10.15666/aeer/1802_33133329

Risk

We standardized the original values of the indicators in flood risk index system (include 13 evaluation indicators and 15 evaluation objects) as the matrix firstly. Through factor analysis, it could be found that the accumulated contribution of variances of the first three factors could reach to 82.78% (close to 85%), so they were extracted as common factors to summarize the information provided by the original indicators. As computed, $C_1/C = 0.6357$; $C_2/C = 0.2057$; $C_3/C = 0.1586$, the comprehensive flood risk score 'S' of each evaluation township is presented in *Table 7*. With the application of hierarchical clustering analysis, the clustering dendrogram of evaluation townships was drawn by MATLAB, as shown in *Figure 7*. Based on *Figure 7*, we classified the flood risk in HHS into 6 magnitudes, as shown in *Table 7*.

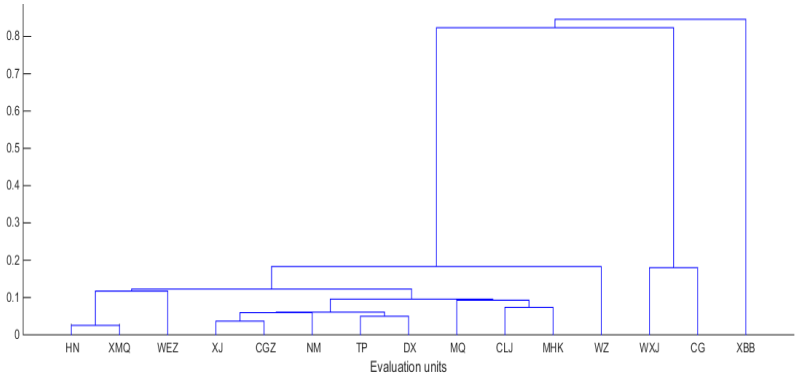

Figure 7. *The clustering dendrogram of evaluation townships*

Table 7. *The comprehensive flood risk score 'S' and the magnitudes of the flood risk of these evaluation townships*

Evaluation township	Comprehensive flood risk score (S)	Vulnerability index value	Magnitude of flood risk
HN	-0.509	0.8951	Low-risk
XJ	-0.326	0.9141	Low-medium-risk
TP	-0.253	0.9270	Low-medium-risk
DX	-0.207	0.9081	Low-medium-risk
CGZ	-0.300	0.8883	Low-medium-risk
NM	-0.248	0.8598	Low-medium-risk
XMQ	-0.532	0.8848	Low-risk
WZ	-0.715	0.8882	Medium-high-risk
MQ	0.010	0.8499	Medium-risk
CLJ	-0.112	0.9196	Medium-risk
WXJ	0.832	0.8971	High-risk
XBB	1.828	0.8394	Extremely-high-risk
MHK	-0.039	0.9287	Medium-risk
WEZ	-0.413	0.8277	Low-risk
CG	0.983	0.7991	High-risk

http://www.aloki.hu ● ISSN 1589 1623 (Print) ● ISSN 1785 0037 (Online)
DOI: http://dx.doi.org/10.15666/aeer/1802_33133329

Discussion

The results of the research show that the flood risk in most areas of HHS is medium or even higher, which are consistent with the facts (Guo and Zha, 2010; Zhang, 2018; Huang et al., 2011). Huang et al. (2011) demonstrated that the flood disaster prevention and mitigation capacity of areas in the south of the main stream of Huaihe River was relatively low. Most areas of HHS are in medium, high even severe vulnerability which calculated in this article corroborates the study by Huang et al. (2011). The hypothesis used in this study that the flood risk is a combination of the natural hazard and vulnerability which was schematized in an equation: Risk = Hazard × Vulnerability (Wisner et al., 2003; Kubal et al., 2009).

One of the planned extensions to the integrated method is a more comprehensive index system of flood risk assessment, which will inevitably involve more relevant regional indicators inputs associated with, for example, average age of population, type of housing and traffic situation in the region. In theory, the more considerate the indicators are, the more reliable the results become. A further possibility that could be considered for future development of the integrated method is to identify the evaluation units. The present-day results of flood risk are not completely actual because the administrative units (townships) are not the actual space units of flooding influence, thus it is difficult to distinguish the magnitudes of flood risk within a township. To a certain extent, this restricts the applicability of the integrated method in a small region. Besides, in the process of a flood, there is usually more than one breach in the floodplain. Therefore, the flood risk analysis considering multiple breaches is another future research direction to be supplemented and improved.

Conclusions

This paper fully understands the flood risk, considering that when assessing the flood risk for a specific region, we should investigate the flood hazard factors and different vulnerability indicators of the region at risk. In flood hazard analysis, a 1-D and 2-D coupled hydrodynamic model was established through MIKE software and used to simulate the floods with various return periods for obtaining the data of the flood hazard factors, such as inundation depth, inundation duration and flood flow velocity. In vulnerability analysis, according to the vulnerability evaluation index system of the object at flood risk, the catastrophe progression method was used to calculate the index value of vulnerability. Combining the flood hazard factors under the 200-year flood with the vulnerability indicators to flood disasters in HHS, a relatively complete index system of flood risk under the current conditions was established, and the flood risk were classified into 6 magnitudes by the method of factor analysis and hierarchical cluster analysis. The results are as follows:

The values of inundation depth, inundation duration and flood flow velocity of evaluation townships under 50-year, 100-year and 200-year floods in HHS show an increasing trend following the increasing return periods. When faced with the 50-year flood, the maximum inundation depth can reach 3.649 m and the maximum inundation duration can reach about 446 h. When faced with the 100-year flood, the maximum inundation depth can reach 3.879 m and the maximum inundation duration can reach about 456 h. When faced with the 200-year flood, the maximum inundation depth can reach 4.253 m and the maximum inundation duration can reach about 475 h.

http://www.aloki.hu ● ISSN 1589 1623 (Print) ● ISSN 1785 0037 (Online)
DOI: http://dx.doi.org/10.15666/aeer/1802_33133329

According to the spatial distribution map of the magnitudes of vulnerability, vulnerability in most areas of HHS towards flood disasters is high.

Among the 15 townships evaluated, XBB is an extremely high-risk zone, WXJ and CG are the high-risk zones, WZ is the medium-high-risk areas, MQ, CLJ, MHK are the medium-risk zones, while XJ, TP, DX, CGZ, NM are the low-medium-risk zones. HN, XMQ and WEZ are low-risk zones.

Acknowledgements. The authors would like to acknowledge the Associate Editor and two anonymous reviewers for providing useful and constructive comments. Special thanks to Zhang, Z. X. and Wu, J. J. for their contribution to this research. This paper is supported by Natural Science Foundation of Jiangsu Province of China (Program No. BK20181310) and the Fundamental Research Funds for the Central Universities of China (Program No. 2019B45314).

REFERENCES

[1] Apel, H., Aronica, G. T., Kreibich, H., Thieken, A. H. (2009): Flood risk analyses - how detailed do we need to be? – Nat Hazards 49: 79-98.

[2] Baldassarre, G. D., Castellarin, A., Montanari, A., Brath, A. (2009): Probability-weighted hazard maps for comparing different flood risk management strategies: a case study. – Natural Hazards 50(3): 479-496.

[3] Brandimarte, L., Di Baldassarre, G. (2012): Uncertainty in design flood profiles derived by hydrodynamic modelling. – Hydrology Research 43(6): 753-761.

[4] Chen, P., Wang, X. L., Chen, X. L. (2012): Spatio-temporal variation of flood vulnerability at the Poyang Lake Ecological Economic Zone, Jiangxi Province, China. – Water Science & Technology 65(7): 1332.

[5] Cook, A., Merwadee, V. (2009): Effect of topographic data, geometric configuration and modeling approach on flood inundation mapping. – Journal of Hydrology 377: 131-142.

[6] Fan, Y. X., Luo, Y., Chen, Q. S. (2000): Discussion on quantitative method of disaster-bearing body vulnerability evaluation index. – Journal of Catastrophology 15(2): 78-81.

[7] Ferdous, A. (2012): A hydrologic model of Kemptville Basin—calibration and extended validation. – Water Resources Management 26(9): 2583-2604.

[8] Fuchs, S., Birkmann, J., Glade, T. (2012): Vulnerability assessment in natural hazard and risk analysis: current approaches and future challenges. – Natural Hazards 64(3): 1969-1975.

[9] Guo, Y. F., Zha, L. S. (2010): Risk regionalization of flood and waterlogging disaster and analysis of variation tendency of damaged area in Anhui province. – Chinese Journal of Agrometeorology 31(1): 130-136.

[10] Helena, B., Pardo, R., Vega, M., Barrado, E., Fernandez, J. M., Fernandez, L. (2000): Temporal evolution of groundwater composition in an alluvial aquifer (Pisuerga River, Spain) by principal component analysis. – Water Research 34(3): 0-816.

[11] Horritt, M. S., Bates, P. D. (2002): Evaluation of 1-D and 2-D numerical models for predicting river flood inundation. – Journal of Hydrology 268(1-4): 87-99.

[12] Huang, D. P., Zheng, W., Zhang, R. H., Huo, Z. G., Li, J. L., Peng, S. F. (2011): Assessment of capacity of flood disaster prevention and reduction of Huaihe River Basin in Anhui Province. – Geographical Research 30(3): 523-530.

[13] Jungkyu, A., Yeji, N., Sung, W. P. (2019): Development of two-dimensional inundation modelling process using MIKE21 model. – KSCE Journal of Civil Engineering 23(9): 3368-3977.

[14] Kourgialas, N. N., Karatzas, G. P. (2011): Flood management and a GIS modelling method to assess flood-hazard areas—a case study. – Hydrological Sciences Journal 56(2): 212-225.

http://www.aloki.hu ● ISSN 1589 1623 (Print) ● ISSN 1785 0037 (Online)
DOI: http://dx.doi.org/10.15666/aeer/1802_33133329

[15] Kubal, C., Haase, D., Meyer, V., Scheuer, S. (2009): Integrated urban flood risk assessment - adapting a multicriteria approach to a city. – Natural Hazards and Earth System Science 9(6): 1881-1895.
[16] Kuo, Y. M., Jang, C. S., Yu, H. L., Chen, S. C., Chu, H. J. (2013): Identifying near shore groundwater and river hydrochemical variables influencing water quality of Kaoping River Estuary using dynamic factor analysis. – Journal of Hydrology 486(4): 39-47.
[17] Li, B., Pu, P. M., Han, A. M. (2003): Factor Analysis of Water Quality in Hongze Lake. – China Environmental Science Press, Beijing, pp. 70-74.
[18] Li, S. F., Feng, P., Sun, S. H. (2010): Application of catastrophe theory in flood risk assessment in flood storage and detention areas. – Journal of Natural Disasters 19(3): 132-138.
[19] Liu, J. T., Gao, J. F., Jiang, J. H., Xu, Y., Zhao, J. H. (2010): Zoning assessment of cyanobacterial blooms in Taihu Lake based on Catastrophe Theory. – Journal of Lake Sciences 4: 488-494.
[20] Ma, R., Shi, J. S. (2011): Assessing groundwater pollution using fuzzy factor analysis method: a case study of Luoyang City in Henan Province. – Acta Geoscientica Sinica 32(5): 611-622.
[21] Masood, M., Takeuchi, K. (2012): Assessment of flood hazard, vulnerability and risk of mid-eastern Dhaka using DEM and 1-D hydrodynamic model. – Natural Hazards 61(2): 757-770.
[22] Merz, B., Hall, J., Disse, M., Schumann, A. (2010): Fluvial flood risk management in a changing world. – Natural Hazards & Earth System Sciences 10(3): 509-527.
[23] Muangthong, S., Shrestha, S. (2015): Assessment of surface water quality using multivariate statistical techniques: case study of the Nampong River and Songkhram River, Thailand. – Environmental Monitoring & Assessment 187(9): 548.
[24] Parto, S., Chatterjee, C., Mohanty, S., Singh, R., Raghuwanshi, N. S. (2009): Flood inundation modeling using MIKE FLOOD and remote sensing data. – Journal of the Indian Society of Remote Sensing 37(1): 107-118.
[25] Tewodros, A. N., Abdusselam, A. (2019): Modeling the effect of urbanization on flood risk in Ayamama Watershed, Istanbul, Turkey, using the MIKE 21 FM model. – Natural Hazards 99(2): 1031-1047.
[26] Van Alphen, J., Martini, F., Looat, R., Slomp, R., Passchier, R. (2009): Flood risk mapping in Europe, experiences and best practices. – Journal of Flood Risk Management 2: 285-292.
[27] Wan, J., Bu, H., Zhang, Y., Meng, W. (2013): Classification of rivers based on water quality assessment using factor analysis in Taizi River basin, northeast China. – Environmental Earth Sciences 69(3): 909-919.
[28] Wang, Y. Z. (2015): Waterlogging Disaster and its Control in Huaihe River Basin. – Science Press, Beijing.
[29] Wisner, B., Blaikie, P., Cannon, T., Davis, I. (2003): At risk: natural hazards, people's vulnerability and disasters. – Econ. Geography 72(4): 460-463.
[30] Wu, H. Z., Li, T. (2013): The comprehensive performance evaluation of the high-tech development zone: analysis based on natural breakpoint method. – Statistics & Information Forum 28(3): 82-88.
[31] Yu, L., Xu, Y., Zhang, Y. X. (2018): Temporal and spatial variation of rainstorms and the impact of flood disasters due to rainstorms in China in the past 25 years. – Torrential Rain and Disasters 37(1): 67-72.
[32] Zhang, F. H., Cui, Q. L., Chen, L. J. (2019): Analysis of flood risk of the flood-protected area of lower Weihe River. – Yellow River 41(9): 65-69.
[33] Zhang, L., Wang, J. Q., Yang, F. R., Li, K. Q. (2009): Factor analysis and fuzzy clustering of driver behavior pattern. – Journal of Transportation Engineering 9(5): 121-126.

http://www.aloki.hu ● ISSN 1589 1623 (Print) ● ISSN 1785 0037 (Online)
DOI: http://dx.doi.org/10.15666/aeer/1802_33133329

[34] Zhang, Z. (2018): Research and development of flood analysis model subsystem that be part of the decision risk management system for flood discharge and retention zones in Huaihe river of Anhui province. – Pearl River 39(6): 101-106 + 112.

http://www.aloki.hu ● ISSN 1589 1623 (Print) ● ISSN 1785 0037 (Online)
DOI: http://dx.doi.org/10.15666/aeer/1802_33133329

PARTICLE SIZE, SPATIAL VARIATIONS, AND POLLUTION SOURCE APPORTIONMENT OF STREET DUST FROM A TYPICAL INDUSTRIAL DISTRICT, IN WUHAN, CHINA

LI, K. J.[1,2] – ZHU, X.[1,2*] – YU, W. X.[1,2] – YU, Y. N.[1,2]

[1]*Research Center for Environment and policy, Zhongnan University of Economics and Law, Wuhan 430073, China*

[2]*School of Information and Safety Engineering, Zhongnan University of Economics and Law, Wuhan 430073, China*

[*]*Corresponding author*
e-mail: zhuxi@zuel.edu.cn

(Received 27th Sep 2019; accepted 4th Feb 2020)

Abstract. To analyse the spatial distribution patterns and sources of heavy metals (Cr, Cu, Ni, Zn), 25 road dust samples were collected from a typical industrial area of Wuhan in July 2017. The multivariate statistics, geostatistics, and the field source survey were adopted to study the sources and pollution pattern of studied metals. The results indicated that the concentration distribution of heavy metals was related to dust particle size and pollution source. Cr had high spatial aggregation in QD, could be concentrated easily in 63-150 μm dust, and was discharged by industrial sources. Cu, Zn, and Ni were also enriched in 63-150 μm dust. Cu had high spatial aggregation in less than 45 μm and was derived from building construction sources. Zn and Ni were concentrated in 63-150 μm and originated from traffic sources and building construction sources. Pollution source influenced particle size and the content and distribution pattern of different heavy metals in atmospheric sediments, but the influence had obvious spatial limitations and compound effects.
Keywords: *Moran's I, heavy metal, ArcGIS, PMF, atmospheric sediments*

Introduction

The heavy metal contamination, such as Cr, Ni, Cu, Pb, Zn, and Cd, are high in urban soils and road dust (RD) in developed and industrial cities, and the pollution level of heavy metals in urban RD is usually much higher than that in urban soil (Wei and Yang, 2010; Chen et al., 2011) RD can easily enter the human body through uptake, absorption, and skin absorption, thereby threatening human health. RD also easily affects the urban environment quality through the hydrological cycle and atmospheric circulation. The damage is often hidden, potent, and long-term (Dockery and Pope, 1994; Sadiq et al., 1994; Crosby et al., 2006; Aelion et al., 2008; Wei et al., 2009, 2010; Wei and Yang, 2010; Sun et al., 2014). In China, most of the cities are dusty because a lot of infrastructures and buildings are under construction. Extensive research has been made on the human health risks and environmental ecological risks of heavy metals in urban RD, but the evaluation system of heavy metals in RD remains imperfect compared to soil standards (Soltani et al., 2015; Huang et al., 2016; Jayarathne et al., 2018). Heavy metal contamination in dust has obvious regional characteristics and mutable distribution and is interfered by many complicated pollution sources (Liang et al., 2011; Sun et al., 2014; Li et al., 2015, 2017; Dehghani et al., 2017; Škrbić et al., 2018; Alsubaie et al., 2019). The identification of heavy metal sources of RD is beneficial to risk management and control, and it can provide a theoretical basis for the uniform evaluation of dust pollution.

http://www.aloki.hu ● ISSN 1589 1623 (Print) ● ISSN 1785 0037 (Online)
DOI: http://dx.doi.org/10.15666/aeer/1802_33313347

Sources of heavy metals in RD are always classified into anthropogenic and natural sources. Anthropogenic sources include traffic pollution, industrial activities, and demolition or construction. Natural sources are mainly from secondary blowing dust of adjacent soils in the streets (Amato et al., 2009; Soltani et al., 2015). Heavy metals are greatly affected by different pollution sources (such as Pb, Cu, Zn, As, Mo, Ni, and Ti), industrial sources, and ground dust; Ni is mostly derived from alloy manufacturing; Cd, Hg, Zn, Fe, Ba, Cu, and Pb are mainly from vehicle traffic sources; Zn and Fe always come from multiple tires; Ba, Cu, Fe, Pb, and Zr are mostly derived from brake wear (Christoforidis and Stamatis, 2009; Soltani et al., 2015; Dehghani et al., 2017; Valotto et al., 2018; Urrutia-Goyes et al., 2018). Compared with point source pollution, such as industrial activities and dust removal at demolition or construction sites, traffic pollution has nonpoint source characteristics. Traffic density has a significant impact on RD and heavy metals and has regional characteristics. For instance, the concentration of heavy metals in the dust of Zhengzhou Branch Road is the highest, whereas the secondary trunk road has the lowest concentration. However, no obvious law exists on the concentration of heavy metals in RD of different sizes in Beijing. Among them, Ni, Cu, Zn, Cr, Pb, and Cd are affected by traffic (Shen et al., 2018). The heavy metal content in the dust on both sides of roads decreases exponentially with an increase in distance from highways, and it is affected by traffic flow, vehicle type, terrain and road conditions, green belt configuration, and wind and rainfall conditions (Guo et al., 2008). Pb and Zn often exist in the dust, and the Zn concentration is always high due to traffic pollution (Long et al., 2015). The measurement of traffic pollution always focuses on the division of main and secondary roads. Nevertheless, traffic volume can directly reflect the degree of traffic pollution because of the traffic congestion section and the main roads do not overlap completely in China.

The source identification of RD is complex because of the variation in regional features, the unstable influence of sources, and the unstable characteristics of components. For example, Zn, Cr, and Pb in Shanghai's surface dust are mainly concentrated in particles smaller than 75 μm, followed by 75-150 μm (Wang et al., 2009). Similarly, the heavy metals in the street dust of the old town of Zhenjiang City decrease with particle size, and the heavy metal content shows a highly progressive tendency (Xu et al., 2012). Cu, Pb, Zn, and Cr in the street dust of Xuchang City are remarkably correlated with 50-100 μm coarse silt, whereas Mn and Ni are highly correlated with 10-50 μm fine silt. Nonetheless, their content does not follow grain size. Co has a strong correlation with the component of clay smaller than 10 μm, and its particle size distribution is prominent (Yan et al., 2016).

An interaction occurs between the contamination of heavy metal and the grain size distribution of urban dust. For instance, Cu and Zn in the surface dust of a middle school in the Datong mining area are mainly concentrated in coarse particles, but no significant difference exists in Pd and Cd enrichment at different grain levels (Guo et al., 2013). The heavy metals in the construction site of Guiyang City indicate the largest fine particle enrichment (exceeding 40%) in all areas, whereas the coarse particle enrichment is the lowest (Liu et al., 2017). The particle size distributions of Cd and Cu in Luoyang City are obvious in densely populated areas, and Cd enrichment tends to be fine (75-96 and 75 μm). The mass fraction of Cu in 150-180 μm increases rapidly, and the particle size decreases and peaks at 75 μm. Zn is mainly concentrated in the 150-180 μm particle size in the traffic congestion zone, whereas Pb only has the grain size effect in the industrial zone (Li et al., 2018). However, in the process of rapid urban development in China, many

http://www.aloki.hu ● ISSN 1589 1623 (Print) ● ISSN 1785 0037 (Online)
DOI: http://dx.doi.org/10.15666/aeer/1802_33313347

cities have no strict boundary lines in commercial, industrial, residential, and transportation areas. The division of areas is difficult to equate with pollution sources. The effect of particle size of heavy metals in the dust on the study area cannot directly explain the law among pollution sources, particle size, and heavy metal.

From the preceding analysis, this study aims to investigate the sources of RD heavy metals in Qingshan District (QD) in Wuhan City, which is an old industrial area of developed cities. This study analyzes the correlation between heavy metal concentration and particle size of dust by ArcGIS and Moran's index (Moran's I). We discuss the relationship between grain size classification and pollution source and distinguish the main source of heavy metals in dust in the effective particle size range with the positive matrix factorization (PMF)-Environmental Protection Agency (EPA) method. This study reveals the interaction between heavy metal pollution in dust and pollution sources and particle size segments in a typical industrial city area under development and provides important data support and research reference to prevent and control RD heavy metal pollution in industrial cities.

Materials and methods

Study area and sample collection

QD covers an area of nearly 80.47 km^2 and is located in Wuhan City, Hubei Province, China. This old industrial area is built up around the Wuhan Iron and Steel Company, which is the fourth largest enterprise company in the world's steel industry, and has more than 5.4 million inhabitants. QD has a continental climate, with cool winters and hot summers. Winter lasts from mid-December to mid-March with southeast winds, whereas summer lasts from mid-June to mid-September with northwest winds. Twenty-five RD samples were collected by mesh points and expert point method. The sample plot was selected beside the main road, crossroads, and overpass from 25 different locations in QD during the summer (July 2017), as shown in *Fig. 1* and the original data is shown in *Table 1*. The sampling process was completed throughout the day of low wind speed (1.6 m/s-5.5 m/s), within 3 days after several days without any rain. One sample area contained multiple points and a plot area of 1 m width by the distance from the curb to the road centerline was demarcated at each study site to ensure the representative collection of solids distributed across the road surface (Christoforidis and Stamatis, 2009; Urrutia-Goyes et al., 2018; Shen et al., 2018). Plastic brushes were used to sweep RD up into a locked plastic bag. A cotton cloth was used to clean tools after sampling to avoid cross-contamination. Each sample of 500-1000 g of street dust (surface atmospheric sediments on cement road) was separated by a 2000 μm stainless steel sieve using a diagonal line method at a distance of a few centimeters away on the curb. The samples needed sufficient quality (500-1000 g) to classify particle size. Subsequently, the composite samples were thoroughly mixed and air-dried. Approximately 150 g of dust was dispersed in rotary vibration (BZS-200DC) and investigated by the weighing method to characterize the particle size distributions. Samples were sieved into six stages (more than 500, 500-250, 250-150, 150-63, 63-45, and less than 45 μm) as subsamples for the following experiment. These particle size ranges were selected in view of their significance in metal-solid adsorption and health risk characteristics, which can lead to variable contamination levels (Chang et al., 2009; Karmacharya and Shakya, 2012; Shi et al., 2018).

http://www.aloki.hu ● ISSN 1589 1623 (Print) ● ISSN 1785 0037 (Online)
DOI: http://dx.doi.org/10.15666/aeer/1802_33313347

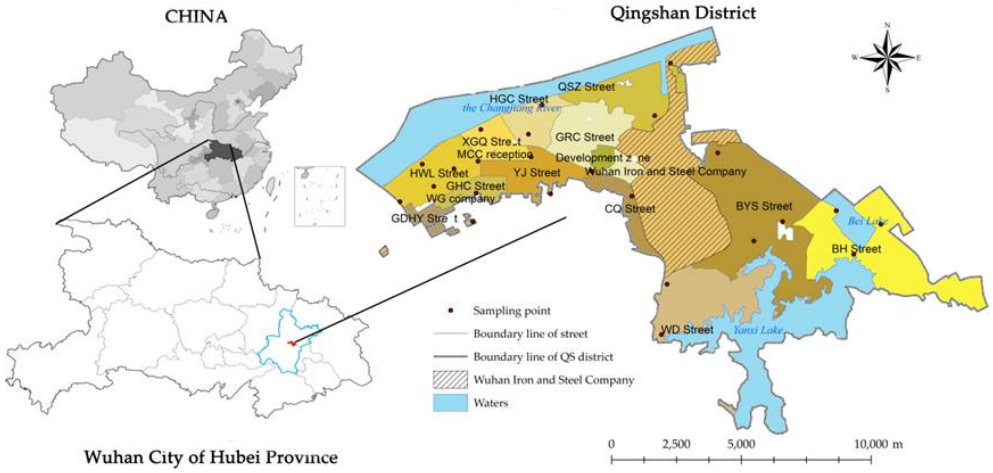

Figure 1. *Sampling sites of RD in Qingshan*

Table 1. *Original data and pollution sourcesof samplings sites*

Sample	Temperature (°C)	Relative humidity (%)	Longitude	Latitude	Pollution type
S1	30	76	E 114.359269	N 30.616601	Construction
S2	30	76	E 114.370969	N 30.621926	
S3	31	72	E 114.366978	N 30.6296021	Construction
S4	31	72	E 114.378029	N 30.628009	Construction
S5	32	66	E 114.385662	N 30.619633	
S6	32	66	E 114.387434	N 30.612799	
S7	32	66	E 114.387330	N 30.641614	
S8	32	66	E 114.386313	N 30.630564	Construction
S9	32	69	E 114.404692	N 30.632067	
S10	33	64	E 114.411466	N 30.619275	
S11	32	66	E 114.403818	N 30.639964	
S12	32	69	E 114.408505	N 30.650025	
S13	32	66	E 114.424812	N 30.645168	
S14	33	63	E 114.425704	N 30.627187	Construction
S15	33	64	E 114.439614	N 30.618538	Industry
S16	33	64	E 114.450361	N 30.641438	Industry
S17	33	64	E 114.452973	N 30.664559	
S18	30	74	E 114.44762997	N 30.589838244	
S19	29	75	E 114.44991619	N 30.570565216	Construction
S20	33	62	E 114.48188679	N 30.603038834	Construction
S21	33	66	E 114.46939278	N 30.633547111	
S22	34	62	E 114.52586251	N 30.608796659	Industry
S23	34	62	E 114.49180857	N 30.609703891	
S24	34	62	E 114.5165	N 30.598442	Industry
S25	33	62	E 114.5104	N 30.6135	Industry

The field source survey

In the data statistics process, we counted the local traffic flow three eight-hour shifts per day, in several sample collecting days. According to the Public Safety Industry Standards of the People's Republic of China, Road Traffic Congestion Degree, and Evaluation Method, we give value to various traffic conditions into 4 levels. In addition, population density (*Appendix Table 1*) is collected by China Statistical Yearbook, industry pollution and construction pollution statistics are from a field visit, both are shown in *Table 1*.

http://www.aloki.hu ● ISSN 1589 1623 (Print) ● ISSN 1785 0037 (Online)
DOI: http://dx.doi.org/10.15666/aeer/1802_33313347

Chemical analysis

Approximately 500 mg of each subsample was weighed with an analytical balance of nominal sensitivity of 0.01 mg and digested by an electric hot plate (5:5:3 nitric acid, hydrofluoric acid, and perchloric acid). All digested samples were then stored in Teflon bottles. The digested and properly diluted samples were analyzed with an atomic absorption spectrophotometer (AAS; ZEEnit-700P). Cu, Cr, Zn, and Ni were analyzed by flame method.

The content of heavy metals used in this study was calculated by *Equation (1)* to eliminate the diversity in dust's content in different particle sizes. In the formula, C_{1i} represents the heavy metal content of one grain-size segment in the dust sample (mg/kg), C_{0i} is the concentration analyzed by the AAS (mg/kg), m_{1i} (g) is the mass of the entire dust sample, m_{2i} (g) is the mass of dust of the grain-size segment, and i represents the sampling points.

$$C_{1i} = C_{0i} \times \frac{m_{2i}}{m_{1i}} \quad \text{(Eq.1)}$$

Receptor models

Moran's I

The global Moran's I method has been widely used to reflect the degree of spatial autocorrelation, spatial agglomeration, and distribution divergence. Moran's I was calculated by the following *Equation (2)*:

$$I = \frac{n\sum_{i=1}^{n}\sum_{j=1}^{n} w_{i,j}(D_i - \bar{D})\,(D_j - \bar{D})}{\sum_{i=1}^{n}\sum_{j=1}^{n} w_{i,j}(D_i - \bar{D})^2} \quad \text{(Eq.2)}$$

where i and j are the ith and jth sampling points, respectively; D represents the concentration of heavy metals; and $W_{i,\,j}$ is a matrix of spatial weights. The global Moran's I value range is [−1, 1]. A positive value indicates the spatial agglomeration distribution, whereas a negative value indicates the spatial divergence distribution. High Moran's I values indicate a strong spatial structure, whereas low Moran's I values indicate weak spatial structure. Zeroes represent random spatial distributions, i.e., no spatial correlation.

PMF

PMF has been applied in the source apportionment of various pollutants in the atmosphere, soil, and dust (Cao et al., 2015; Tian et al., 2018; Lv, 2019). PMF modeling was performed using the US-EPA PMF 5.0 program (Lv, 2019), which is a multivariate factor analysis tool. The initial data matrix X with the order of m × n can be expressed as *Equation (3)*:

$$\mathrm{X} = \mathrm{GF} + \mathrm{E} \quad \text{(Eq.3)}$$

E can be written as *Equation (4)*:

http://www.aloki.hu ● ISSN 1589 1623 (Print) ● ISSN 1785 0037 (Online)
DOI: http://dx.doi.org/10.15666/aeer/1802_33313347

$$e_{ij} = \sum_{k=1}^{p} g_{ik} f_{kj} - x_{ij} \quad \text{(Eq.4)}$$

where X_{ij} is the concentration of species j measured on sample i, p is the number of factors contributing to samples, g_{ik} is the relative contribution of factor k to sample i, f_{ik} is the concentration of species j in source profile km, and e_{ij} is the error of the PMF model for species j measured on sample i. The values of g_{ik} and f_{kj} are always positive and adjusted until a minimum Q value for a given p is found. The Q value can be expressed as *Equation (5)*:

$$Q = \sum_{i=1}^{n} \sum_{j=1}^{m} \left(\frac{e_{ij}}{u_{ij}} \right)^2 \quad \text{(Eq.5)}$$

where u_{ij} is the uncertainty of the jth species concentration in the ith sample, n is the number of samples, and m is the number of species.

PMF requires the concentration of heavy metals and uncertainty files to run the model. The uncertainty is calculated based on the element-specific method detection limit (MDL), and error percent is measured by standard reference materials. All measured contents are above the MDL; therefore, the equations of uncertainty are adopted as follows:

If the concentration is less than or equal to the MDL used, then the uncertainty (Unc) is calculated using the following *Equation (6)*:

$$U_{nc} = \frac{5}{6} \times MDL \quad \text{(Eq.6)}$$

If the concentration is greater than the MDL used, the uncertainty is calculated by *Equation (7)*:

$$U_{nc} = \sqrt{(ErrorFraction \times concentration)^2 + (0.5 \times MDL)^2} \quad \text{(Eq.7)}$$

Results

Granularity content

The dust of each sampling point is graded and screened. The particle size distribution characteristics of dust are calculated by the gravimetric method, as shown in *Table 2*, which indicates the particle size distribution proportion. MAX/MIN means the weight of the sample in the specific particle size over the total weight in that size, which can characteristics of special points and reduce the error and judgment of the sorting and analysis of individual cases. AVG is the mass of each particle size segment is a percentage of the total dust mass, shown in *Appendix Figure 1.* The particle size distribution is generally not uniform and concentrates in the range of 63-150 (33%), 150-250 (16%), and 250-500 μm (26%). The particle size with range below 45 μm accounts for 1%-14%, particulate matter (PM) = 45-63 μm for 3%-14%, PM = 63-150 μm for 19%-59%,

http://www.aloki.hu ● ISSN 1589 1623 (Print) ● ISSN 1785 0037 (Online)
DOI: http://dx.doi.org/10.15666/aeer/1802_33313347

PM = 150-250 μm for 10%-27%, PM = 250-500 for 10%-40%, and PM >500 μm for 3%-25% of the total dust at each sampling site. The coefficient of variation increases gradually with the decrease in particle size when it is less than 63 μm. The regularity occurrence suggests that fine particles are vulnerable to local sources; this result is consistent with the study of Xu, who showed that fine particles are enriched in heavy metals (Xu et al., 2012).

Table 2. *Distribution of dust particle size*

Particle size (μm)	AVG (%)	MAX (%)	MIN (%)	SD (%)	CV (%)
>500	11	25 (S11)	0 (S17)	6+-*/*-+	50
250-500	26	41(S17)	13(S14)	7	25
150-250	16	27(S20)	10(S9)	4	27
63-150	33	59(S24)	19(S23)	8	26
45-63	8	14(S24)	2(S23)	3	34
<45	6	14(S8)	0(S19-21)	4	67

Pollution sources

Particle size is a significant parameter which determines the environmental fate and the behavior of dust particles it has been found to be influential on the pollutant concentrations, while overestimation or underestimation would occur with improper strategies (Jayarathne et al., 2018). It is difficult to analysis of pollution sources precisely; the survey records can accurately reflect the current relationship between heavy metals in dust and pollution sources more than just Multivariate statistical analyses.

This study divides the pollution sources in QD into traffic, domestic, industrial, and building pollution sources (still under construction within one week of the sampling time), as shown in *Fig. 2*. The traffic source is considered from the vehicle speed, vehicle quantity, and residence time, and this study selects traffic flow as the index. According to GA115-1995 (Public Safety Industry Standards of the People's Republic of China, Road Traffic Congestion Degree, and Evaluation Method), the traffic pollution source is divided into four levels: speed not less than 30 km/h is defined as smooth level (1#), speed of 20-30 km/h is defined as mild traffic (2#), speed of 10-20 km/h is defined as traffic jam (3#), and speed less than 10 km/h is defined as serious traffic jam (4#). Traffic flow is obtained through collecting, arranging, and analyzing the data of the roads in QD for a long time. The main and secondary roads are highly congested in the northwest. The main roads, road traffic flow, and population density area do not overlap completely.

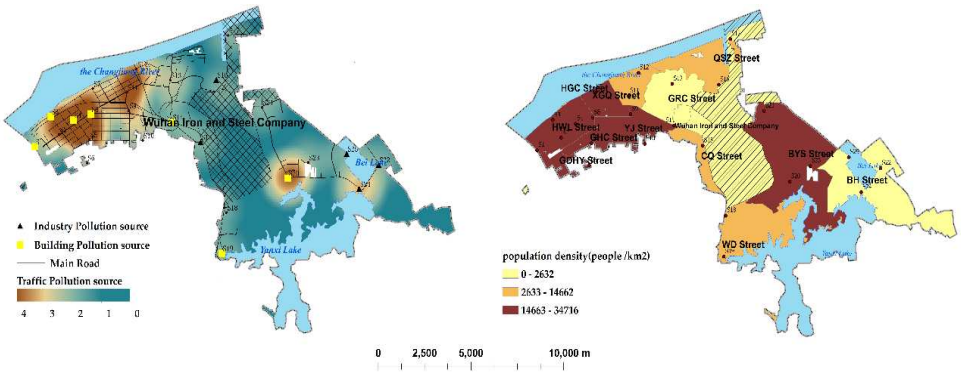

Figure 2. *Distribution of dust pollution sources*

http://www.aloki.hu ● ISSN 1589 1623 (Print) ● ISSN 1785 0037 (Online)
DOI: http://dx.doi.org/10.15666/aeer/1802_33313347

RD can contribute different PM10 rates in a different city area, the highest contributions were modeled in the commercial/residential district where most of the population live and work (Feng, 2016). The domestic pollution source measured by a population density responds to the frequency of human activities, such as waste disposal and cleaning. In this study, areas with population density between 14663 and 34716 people/km^2 are defined as a high-density zone, those between 2633 and 14662 people/km^2 are considered a medium-density zone (M zone), and those between 0 and 2632 people/km^2 are regarded as a low-density zone (L zone). *Figure 2* shows that most areas of the domestic pollution source overlap onto traffic pollution sources. For example, BH Street is an L zone but a traffic jam area with frequent starts and stops of large engineering vehicles, whereas WD Street is an M zone but a smooth-level area because of remoteness and residents' habit.

The identification of industrial sources mainly includes all existing industrial plants in QD, such as the coking plant and micropower factory. However, the main plant of the Wuhan Iron and Steel Company is excluded because of closed management. Five industrial pollution sources exist around the company. This research identifies the construction sites as building pollution sources at the sampling period. Seven building pollution sources are scattered around Hongwei Street and an important intersection.

Correlation between heavy metal distribution and grain size

The average contents of Cr, Ni, Cu, and Zn are 63.17, 26.49, 38.46, and 517.62 mg/kg, respectively, which are over the corresponding soil background values by 0.73, 0.71, 1.25, and 6.19 times, respectively. According to the background values of soil elements in China, Hubei (China National Environmental Monitoring Centre, 1990), Cr, Ni, Cu, and Zn are 86, 37.3, 30.7, and 83.6 mg/kg, respectively. Zn is the main contaminant. The Cr contaminant ranges are 6.14-191.54, 6.11-45.97, 0.69-37.91, and 0.14-13.89 mg/kg; the Cu contaminant ranges are 4.53-209.02, 6.07-73.49, 0.34-4.19, and 0.13-7.74 mg/kg; the Ni contaminant ranges are 7.4-39.0, 2.18-27.47, 1.15-6.21, and 0.15-9.80 mg/kg; and the Zn contaminant ranges are 131.2-1537, 625.29-744.18, 8.37-133.89, and 1.01-68.35 mg/kg. Cr, Cu, Zn, and Ni are all enriched in 63-150 μm.

The contamination distributions of Cr, Cu, Ni, and Zn in different grain sizes (all sizes, 63-150, 45-63 μm, and <45 μm) are shown in *Fig. 3*, which is drawn by ArcGIS kernel density method. Density calculation is conducted for the heavy metals' concentration data of the sampling points, which form a corresponding raster layer (the obtained data are reduced by 10^5) and present the trend of concentration in the search range. Spatial aggregation is measured by Moran's I model, as shown in *Table 3*. The contamination of Cr, Cu, Ni, and Zn in different grain sizes presents varying distribution trends.

Cr pollution is mainly present in the particle sizes of 63-150 and 45-63 μm (*Fig. 3a*). Various positive correlation distributions are observed in different grain sizes. The distribution in all sizes is close to the cluster tendency gathering in Ganghuacun Street, Hongwei Road Street, and Beihu Street, and the spatial distribution is positive and relevant. The distribution in 63-150 μm is similar to that in the all-size sample but more inclined to the random distribution, and the spatial distribution is positive but irrelevant. The distribution in 45-63 μm also presents cluster tendency but gathers in North Lake, and the spatial distribution is positively correlated and remarkable. The distribution in <45 μm shows cluster gathering in the streets of Hongwei Road, Xingouqiao, and the spatial distribution is positively correlated but unremarkable. Cr is generally concentrated in 45-63 μm, and the spatial aggregation is obvious and greatly affected by the influence of adjacent sources.

http://www.aloki.hu ● ISSN 1589 1623 (Print) ● ISSN 1785 0037 (Online)
DOI: http://dx.doi.org/10.15666/aeer/1802_33313347

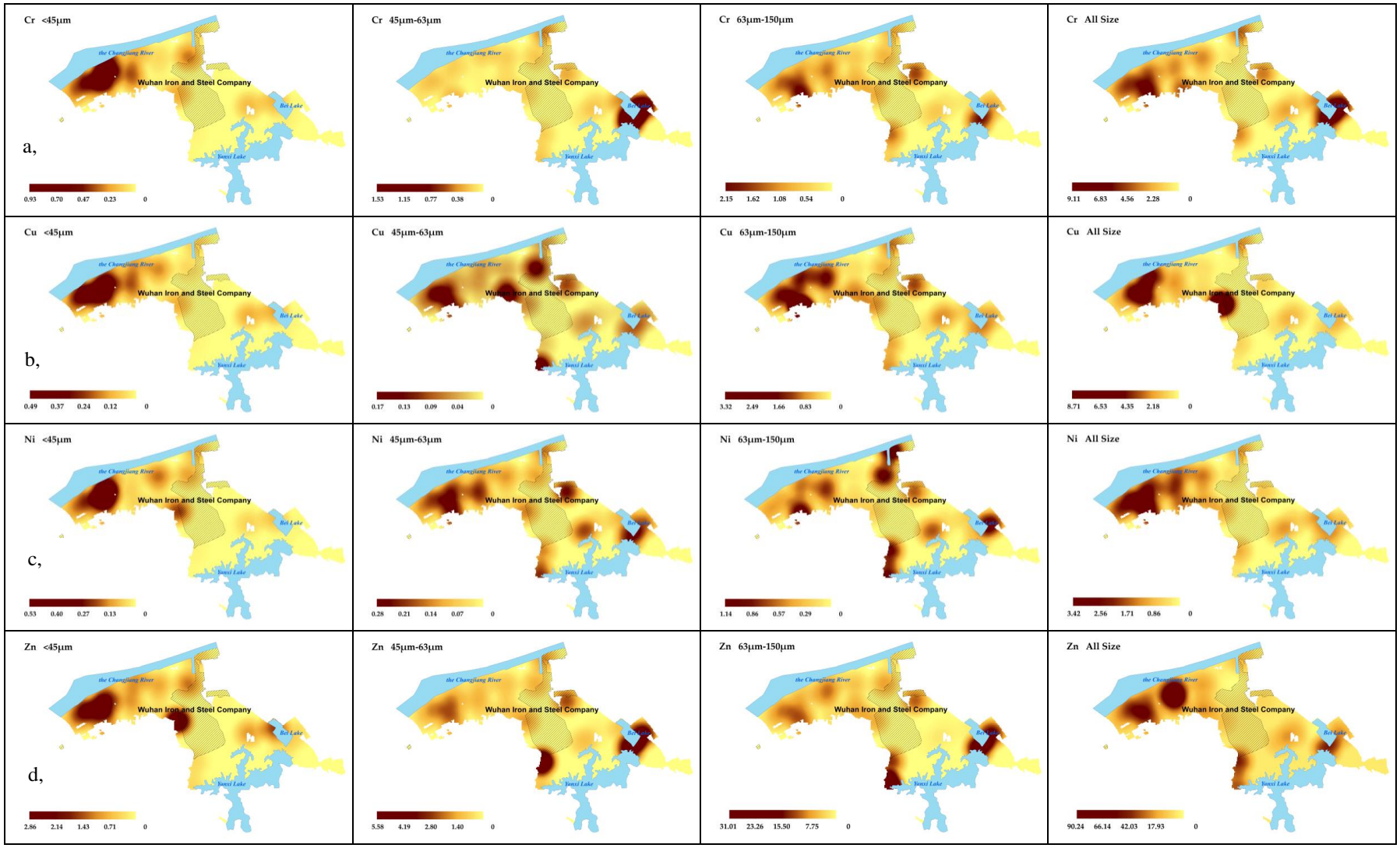

Figure 3. *Distribution of heavy metal content in different sizes (a: Cr ,b: Cu, c: Ni, d: Zn)*

http://www.aloki.hu ● ISSN 1589 1623 (Print) ● ISSN 1785 0037 (Online)
DOI: http://dx.doi.org/10.15666/aeer/1802_33313347

Table 3. *Moran's I of different heavy metal*

Heavy metal	Item	All Size	63 μm-150 μm	45 μm -63 μm	<45 μm
Cr	Moran's I	0.303725	0.218647	0.329085	0.179029
	z-score	2.196154	1.560779	2.362491	1.367709
	p-value	0.028081	0.118576	0.018153	0.171403
Cu	Moran's I	0.006938	-0.073557	0.007967	0.464664
	z-score	0.442169	-0.347610	0.372600	4.004758
	p-value	0.658367	0.728133	0.709446	0.000062
Ni	Mora's In	0.462726	0.309563	0.135859	0.060079
	z-score	3.930863	2.699898	1.348096	0.873931
	p-value	0.000085	0.006936	0.177628	0.382156
Zn	Moran's I	-0.113302	0.088300	0.226290	-0.071643
	z-score	-0.603821	1.098097	2.221055	-0.281705
	p-value	0.545962	0.272162	0.026347	0.778170

Cu in the full-grain segment is distributed in the cluster and is mainly concentrated in Ganghuacun Street, Hongwei Road Street, and Changqian Street, with a P-value of 0.66 (*Fig. 3b*). The distribution is positively correlated but irrelevant. Cluster distribution occurs in <45 μm; Cu is distributed in Ganghuacun Street and Hongwei Road Street, and the spatial distribution is positively correlated and remarkable. The distribution in 45-63 μm is random, and the spatial distribution is positively correlated but not prominent. Cluster distribution is observed in 63-150 μm; it is mainly located in Ganghuacun Street, Hongwei Road Street, and Xingouqiao Street (P = 0.73), and the spatial distribution is correlated positively but not significant. In summary, the spatial distribution of Cu is similar in different particle sizes. Cu accumulates in 63-150 μm, but the spatial distribution is relatively random.

Ni has different correlations in different particle size distributions (*Fig. 3c*). The Ni full-grain size segment is distributed in the cluster and is mainly concentrated in the streets of Hongwei Road and Ganghuacun, with a positively correlated and significant spatial distribution. Ni is clustered in <45 μm and concentrated in Hongwei Road Street with a normal phase but an insignificant spatial distribution. RD of 45-63 μm represents the random distribution, and the spatial distribution is positively correlated but unremarkable. Ni distribution in 63-150 μm is also random, and the spatial distribution is positively correlated and relevant. Ni mainly has accumulated of 63-150 μm, and the degree of aggregation in the particle size segment is high.

The autocorrelation of Zn at different particle sizes is not high, but the difference is obvious (*Fig. 3d*). Zn in all sizes is clustered in Honggangcheng, Xingouqiao, and Hongwei Road streets with an insignificant negative correlation (the area of high concentration is adjacent to the area of low heavy metal concentration). RD distribution in <45 μm is cluster concentrated in Hongwei Road Street, Ganghuacun Street, and Changqian Street, with an insignificant negative correlation as well. The RD distribution in 45-63 μm is random with a significantly positive correlation (the high concentration area is adjacent to the high heavy metal concentration area). The distribution is random in 63-150 μm, and the spatial distribution is positively correlated but insignificant. In general, the heavy metal Zn has a concentration characteristic in 63-150 μm, but the degree of aggregation is high in 45-63 μm.

Zn and Ni generally have a high degree of aggregation in 63-150 μm, but that of Cr is in 45-63 μm, whereas that of Cu is in less than 45 μm. This finding is consistent with several studies; e.g., heavy metals in surface dust are mainly concentrated in particle sizes

http://www.aloki.hu ● ISSN 1589 1623 (Print) ● ISSN 1785 0037 (Online)
DOI: http://dx.doi.org/10.15666/aeer/1802_33313347

of 75-150 μm (Shi and Lu, 2018); heavy metals are easily enriched in small particles, especially in the range of 63-75 μm; and Cu, Zn, and Cr are easy to concentrate in coarse silt (63-150 μm) (Chang et al., 2009). The accumulation space is mainly concentrated in the northwest direction of QD (Hongwei Road Street and Gangdu Garden Street), Beihu Street, and Changqian Street. The distribution analysis of pollution sources also shows that the northwest direction is the area where traffic pollution is mainly concentrated, and relatively small industrial factories exist around Beihu Street. Changqian Street is near the Wuhan Iron and Steel Company, which is the largest factory in QD. The particle size of dust and its medium-heavy metal concentration is affected by adjacent sources of pollution. The influence of different heavy metals on varying particle sizes must be clarified. The concentration distribution and concentration level of heavy metals are relatively different, and pollution does not have the pattern of diffusion distribution around the main plant area of the Wuhan Iron and Steel Company. The distribution of heavy metals in urban dust has strong block limitations.

Grain size distribution and pollution sources

The dust at the sampling points of different pollution sources is counted in this study. The distribution of the maximum, minimum, and mean values of different particle fractions are discussed, and the contribution of pollution sources to dust particle size is analyzed. *Figure 4* shows that the average amount of RD greater than 150 μm is above 50%, but heavy metal pollution is mostly concentrated in particles smaller than 150 μm. This condition is referred to as an effective heavy metal-enriched particle size segment. This segment is divided into particle sizes less than 45, 45-63, and 63-150 μm in accordance with the correlation of various metal contamination concentrations and particle sizes in the previous section. Different pollution sources have a spatial overlapping effect. For instance, the high-population-density area always has heavy traffic flow and building sources. By contrast, the industrial area is far away from the above source areas, and the influence of the industrial source on particle size has a high reference value.

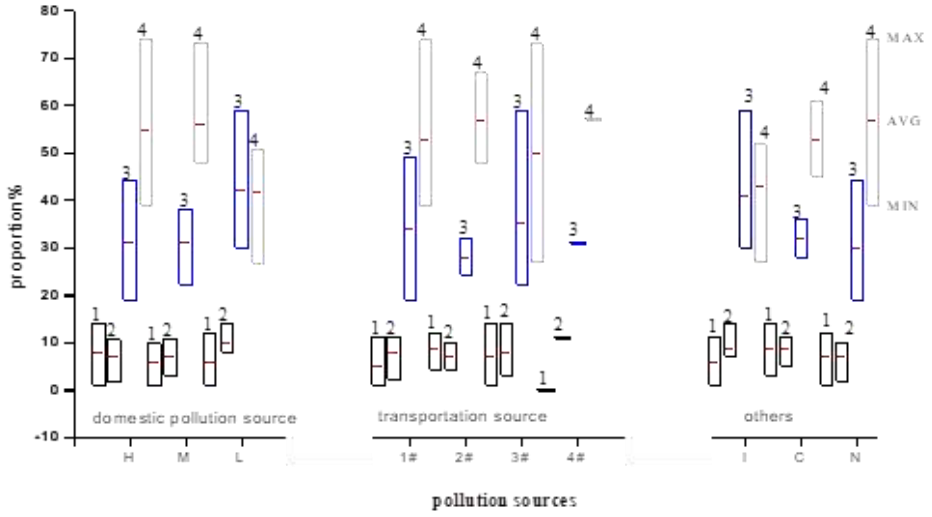

Figure 4. *Map of contribution rate of pollution source to RD particle level (I means the industrial source; C denotes the building source; N indicates no pollution source; and 1, 2, 3, and 4 correspond to particle sizes of <45, 45-63, 63-150, and >150 μm, respectively)*

http://www.aloki.hu ● ISSN 1589 1623 (Print) ● ISSN 1785 0037 (Online)
DOI: http://dx.doi.org/10.15666/aeer/1802_33313347

For particles smaller than 45 and 45-63 μm, the maximum and minimum spans are small and unaffected by various sources. In comparison, high-density populations, low traffic flow, and building sources have a slight advantage in the 45 μm average contribution rate, whereas low-density populations and high traffic flow have a slight advantage in 45-63 μm. The maximum and minimum spans are greatly affected by pollution sources for the 63-150 μm particle size segment. The industrial source mainly contributes to 63-150 μm, and the average value reaches 41%. Particles near other pollution sources are in this particle size segment, and the mean is only 28%-35%.

Heavy metal and pollution source

After PMF analyses of the sources of heavy metals in different particle sizes, the contribution rates of Cr, Cu, Ni, and Zn of domestic pollution, transportation, building, and industrial sources are summarized (*Fig. 5*). Differences in sources of different types of heavy metal pollution in RD in QD are observed. Several studies have found that different heavy metals are greatly affected by different pollution sources; Cu, Cr, As, Mo, Ni, and Ti are affected by industrial sources and ground dust from building operation; whereas Cd, Hg, Zn, Fe, Ba, Cu, and Pb are greatly affected by vehicle traffic sources (Soltani et al., 2015; Dehghani et al., 2017). We analyze the sources at different points.

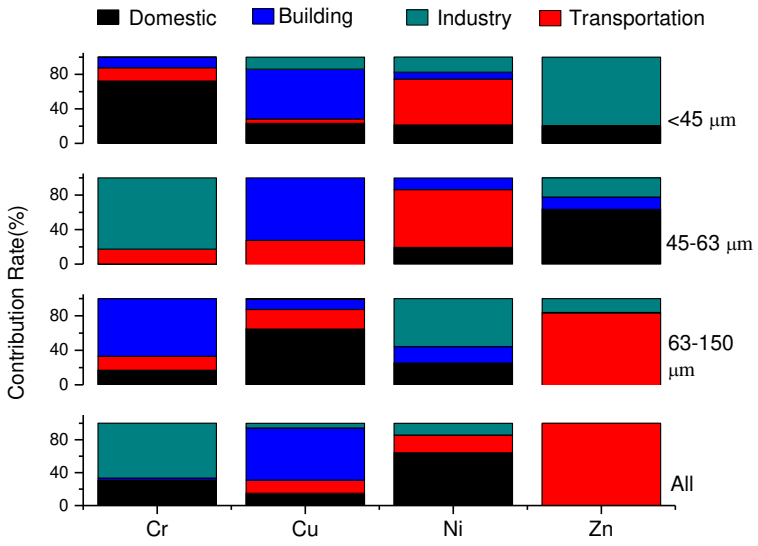

Figure 5. *Correlation diagram of heavy metal concentration and pollution source in characteristic particle size*

Industrial sources are the main sources of Cr and contribute to 45-63 μm dust. Cr is highly attached to 45-63 μm dust, so reducing the formation of 45-63 μm dust is beneficial to the reduction of Cr in urban dust. Traffic sources have the highest contribution to grain-level dust. On-site investigations indicate that large-scale transportation vehicles are frequent in such industrial active areas, with poor road conditions and large dust emission. Control of urban dust Cr pollution can be optimized by regulating pollution sources from car conditions, such as timely sprinklers and control of three waste emissions. Building pollution is the main source of Cu and contributes considerably to dust with a small particle size. The above analysis of construction sources contributes to dust with particle

http://www.aloki.hu ● ISSN 1589 1623 (Print) ● ISSN 1785 0037 (Online)
DOI: http://dx.doi.org/10.15666/aeer/1802_33313347

size less than 45 μm. The control of urban Cu pollution can reduce the formation of dust in urban construction. The source of Ni is relatively limited compared with that of Cu, and all four contamination sources have certain contributions. Dust that is less than 63 μm is susceptible to traffic sources, whereas dust larger than 63 μm is susceptible to industrial sources. In contrast to Ni, Zn is highly affected by traffic sources, especially in large particle size segments (greater than 63 μm), and by industrial sources at less than 45 μm. Joint control of industrial and traffic sources can be considered for the formation of Ni and Zn.

Different sources of pollution affect the amount and type of heavy metals, the differences can be observed in the distribution of particle size. The enrichment of heavy metals comes partly from the source discharge process, and other parts are from the process of contact with dust. Therefore, the concentration of heavy metals, pollution sources, and the particle sizes of dust are related. With the source control of different types and sizes of heavy metals in urban RD, dust pollution can be controlled in a targeted manner.

Discussion

Once we determined the sources related to various factors, the source contributions of heavy metals could be easily determined. PMF are widely used for the quantitative analysis of sources of various pollutants in the atmosphere, soil, and dust (Yang et al., 2017; Zhang et al., 2017; Duan et al., 2018; Garaga et al., 2018; Cai et al., 2019; Wang et al., 2019; Zhao et al., 2019). It can be used to calculate the source component spectrum and the contribution rate. Since the uncertainty is added in the calculation, the PMF can be used to solve the weighted factorization to achieve the individual processing of elements and reduce the requirements on the degree of connection between the data, making it suitable for analyzing complex pollution (Dong et al., 2019; Zhang et al., 2019). Khairy et al. found that PMF could afford better source apportionment of pollutants in the atmosphere, soils and sediments than APCS/MLR" (Jain et al., 2018). But The PMF method is unstable when directly used to describe dust sources (Cetin et al., 2018; Hu et al., 2018). The variation mainly stems from the differences in the volume of collected data and in the detection limits of the instruments used (Hu et al., 2018; Men et al., 2019) in this study, the result of the field source survey can match the regularity of PMF.

Conclusion

Our study analyzes the distribution and source of heavy metals in RD from the view of particle size distribution. The contributions of dust in 63-150, 45-63, and <45 μm sections are 33%, 8%, and 6%, respectively. Cr is enriched in 45-63 μm with obvious spatial aggregation; Cu accumulates in 63-150 μm, but the spatial distribution is relatively random; Ni accumulates in 63-150 μm with obvious spatial aggregation, and Zn has a concentration characteristic in 63-150 μm, but the degree of aggregation is higher than that in 45-63 μm. The distribution of these heavy metals has strong limitations and is not only around the main plant area of the Wuhan Iron and Steel Company. It is necessary to add spatiotemporal analysis in the follow-up studies to further discuss this conclusion. The distribution is affected by nearby sources, including traffic, domestic, industrial, and building pollution sources, in this old industrial area. The dominant sources of heavy metals differ in varying particle sizes and heavy metals. The effective size of dust particles

http://www.aloki.hu ● ISSN 1589 1623 (Print) ● ISSN 1785 0037 (Online)
DOI: http://dx.doi.org/10.15666/aeer/1802_33313347

must be confirmed for accurate source assessment and effective management of dust pollution. For the PMF model, the number of samples in this paper is relatively small, so it is very necessary to increase the number of analysis samples in subsequent studies.

Funding Information. This study was financially supported by the Fundamental Research Funds for Central University administered by Zhongnan University of Economics and Law (Project No.: 2722019PY050), Science and Technology Project of Hubei Education Department (B2018551).

Conflict of Interests. The authors declare no conflict of interests.

REFERENCES

[1] Aelion, C. M., Davis, H. T., McDermott, S., Lawson, A. B. (2008): Metal concentrations in rural topsoil in South Carolina: potential for human health impact. – Science of the total environment 402(2-3): 149-156.
[2] Alsubaie, A., Alsulaiti, L., Al-Dabbous, A. N., Chamakh, M., Jaafar, M., Daar, E., Bradley, D. A. (2019): A comparison of elemental presence in Riyadh and Doha road dust. – Radiation Physics and Chemistry 154: 58-63.
[3] Amato, F., Pandolfi, M., Viana, M., Querol, X., Alastuey, A., Moreno, T. (2009): Spatial and chemical patterns of PM10 in road dust deposited in urban environment. – Atmospheric Environment 43(9): 1650-1659.
[4] Cai, K., Li, C., Na, S. (2019): Spatial Distribution, Pollution Source, and Health Risk Assessment of Heavy Metals in Atmospheric Depositions: A Case Study from the Sustainable City of Shijiazhuang, China. – Atmosphere 10(4): 222.
[5] Cao, Z., Xu, F., Li, W., Sun, J., Shen, M., Su, X., Feng, J., Yu, G., Covaci, A. (2015): Seasonal and particle size-dependent variations of hexabromocyclododecanes in settled dust: implications for sampling. – Environmental science & technology 49(18): 11151-11157.
[6] Cetin, B., Yurdakul, S., Gungormus, E., Ozturk, F., Sofuoglu, S. C. (2018): Source apportionment and carcinogenic risk assessment of passive air sampler-derived PAHs and PCBs in a heavily industrialized region. – Science of The Total Environment 633: 30-41.
[7] Chang, J., Liu, M., Li, X., Lin, X., Wang, L., Gao, L. (2009): Primary research on health risk assessment of heavy metals in road dust of Shanghai. – China Environmental Science 29(5): 548-554.
[8] Chen, C. C., Lu, X. W., Wang, L. J., Lei, K. (2011): Health risk assessment of heavy metals in street dust in Baoji city. – Urban Environment & Urban Ecology 24(2): 35-38.
[9] China National Environmental Monitoring Centre (1990): Background values of soil elements in China. – China Environmental Science Press 1990: 87-90, 330-496.
[10] Christoforidis, A., Stamatis, N. (2009): Heavy metal contamination in street dust and roadside soil along the major national road in Kavala's region, Greece. – Geoderma 151(3-4): 257-263.
[11] Crosby, D. G. (2006): Environmental Toxicology and Chemistry. – Oxford Univ. Press, 336p.
[12] Dehghani, S., Moore, F., Keshavarzi, B., Beverley, A. H. (2017): Health risk implications of potentially toxic metals in street dust and surface soil of Tehran, Iran. – Ecotoxicology and environmental safety 136: 92-103.
[13] Dockery, D. W., Pope, C. A. (1994): Acute respiratory effects of particulate air pollution. – Annual review of public health 15(1): 107-132.
[14] Dong, B., Zhang, R., Gan, Y., Cai, L., Freidenreich, A., Wang, K., Guo, T., Wang, H. (2019): Multiple methods for the identification of heavy metal sources in cropland soils from a resource-based region. – Science of the Total Environment 651: 3127-3138.

http://www.aloki.hu ● ISSN 1589 1623 (Print) ● ISSN 1785 0037 (Online)
DOI: http://dx.doi.org/10.15666/aeer/1802_33313347

[15] Duan, S., Zhou, Z., Liu, Y., Xiao, Y., Chen, P., Fan, C., Chen, S. (2018): Distribution and source apportionment of soil heavy metals in central-south of Hunan province. – Journal of Agricultural Science and Technology (Beijing) 20(6): 80-87.
[16] Feng, J., Hu, P., Li, X., Liu, S., Sun, J. (2016): Ecological and health risk assessment of polycyclic aromatic hydrocarbons (pahs) in surface water from middle and lower reaches of the yellow river. – Polycyclic Aromatic Compounds 36(5): 656-670.
[17] Garaga, R., Sahu, S. K., Kota, S. H. (2018): A review of air quality modeling studies in India: local and regional scale. – Current Pollution Reports 4(2): 59-73.
[18] Guo, G. H., Lei, M., Chen, T. B., Song, B., Li, X. Y. (2008): Effect of road traffic on heavy metals in road dust and roadside soils. – Acta Scientiae Circumstantiae 28(10): 1937-45.
[19] Guo, F., Sheng, H., Fan, W. (2013): Particle Size Distribution and health risk assessment of heavy metal of surface dust in middle school of mining district in Daton city. – Journal of Soil and Water Conservation 1: 162-166.
[20] Hu, W., Wang, H., Dong, L., Huang, B., Borggaard, O. K., Hansen, H. C. B., He, Y., Holm, P. E. (2018): Source identification of heavy metals in peri-urban agricultural soils of southeast China: an integrated approach. – Environmental pollution 237: 650-661.
[21] Hu, W., Day, D. A., Campuzano-Jost, P., Nault, B. A., Park, T., Lee, T., Croteau, P., Canagaratna, M. R., Jayne, J. T., Worsnop, D. R., Jimenez, J. L. (2018): Evaluation of the new capture vaporizer for Aerosol Mass Spectrometers (AMS): Elemental composition and source apportionment of organic aerosols (OA). – ACS Earth and Space Chemistry 2(4): 410-421.
[22] Huang, J., Li, F., Zeng, G., Liu, W., Huang, X., Xiao, Z., Wu, H., Gu, Y., Li, X., He, X., He, Y. (2016): Integrating hierarchical bioavailability and population distribution into potential eco-risk assessment of heavy metals in road dust: A case study in Xiandao District, Changsha city, China. – Science of the Total Environment 541: 969-976.
[23] Jain, S., Sharma, S. K., Mandal, T. K., Saxena, M. (2018): Source apportionment of PM10 in Delhi, India using PCA/APCS, UNMIX and PMF. – Particuology 37: 107-118.
[24] Jayarathne, A., Egodawatta, P., Ayoko, G. A., Goonetilleke, A. (2018): Assessment of ecological and human health risks of metals in urban road dust based on geochemical fractionation and potential bioavailability. – Science of the Total Environment 635: 1609-1619.
[25] Karmacharya, N., Shakya, P. R. (2012): Heavy metals in bulk and particle size fractions from street dust of Kathmandu city as the possible basis for risk assessment. – Scientific World 10(10): 84-88.
[26] Li, Y. Y., Li, Z. P., Xiong, H. L., Chen, Y. C., Dai, Y. (2015): Health risk assessment of street dust and heavy metal pollution in Chongqing. – Journal of Southwest University (Natural Science Edition) 37(2): 18-23.
[27] Li, H. H., Chen, L. J., Yu, L., Guo, Z. B., Shan, C. Q., Lin, J. Q., Zhu, X. M. (2017): Pollution characteristics and risk assessment of human exposure to oral bioaccessibility of heavy metals via urban street dusts from different functional areas in Chengdu, China. – Science of the Total Environment 586: 1076-1084.
[28] Li, F., Zhang, J., Liu, W., Liu, J., Huang, J., Zeng, G. (2018): An exploration of an integrated stochastic-fuzzy pollution assessment for heavy metals in urban topsoil based on metal enrichment and bio accessibility. – Science of the total environment 644: 649-660.
[29] Liang, T., Shi, Z. T., Wu, F., Gu, X. M. (2011): Evaluation of heavy metal pollution and potential ecological risk in streets of Kunming. – Tropical Geography 31(2): 164-170.
[30] Liu, R., Tu, L. L., Gou, X., Yang, H. Y. (2017): Particle size distribution and health risk assessment of heavy metals of constructive dust in Guiyang. – Science Technology and Engineering 17(32): 187-195.
[31] Long, Y., Sun, C., Li, S., Liu, G. (2015): Comparative study on heavy metal pollution of surface dust in typical industries environment. – Environmental Engineering 02.
[32] Lv, J. (2019): Multivariate receptor models and robust geostatistics to estimate source apportionment of heavy metals in soils. – Environmental pollution 244: 72-83.

http://www.aloki.hu ● ISSN 1589 1623 (Print) ● ISSN 1785 0037 (Online)
DOI: http://dx.doi.org/10.15666/aeer/1802_33313347

[33] Men, C., Liu, R., Wang, Q., Guo, L., Miao, Y., Shen, Z. (2019): Uncertainty analysis in source apportionment of heavy metals in road dust based on positive matrix factorization model and geographic information system. – Science of The Total Environment 652: 27-39.
[34] Sadiq, M., Mian, A. A. (1994): Nickel and vanadium in air particulates at Dhahran (Saudi Arabia) during and after the Kuwait oil fires. – Atmospheric Environment 28(13): 2249-2253.
[35] Shen, M. H., Dong, W. J., Wang, M. L., Yang, S., Yang, T. F., Tang, L. F., Cao, Z. G. (2018): Pollution characteristics of heavy metals in road dust and its relationship with road levels: Taking Beijing and Zhengzhou as examples. – Environmental Chemistry 05.
[36] Shi, D., Lu, X. (2018): Accumulation degree and source apportionment of trace metals in smaller than 63 μm road dust from the areas with different land uses: A case study of Xi'an, China. – Science of the Total Environment 636: 1211-1218.
[37] Soltani, N., Keshavarzi, B., Moore, F., Tavakol, T., Lahijanzadeh, A. R., Jaafarzadeh, N., Kermani, M. (2015): Ecological and human health hazards of heavy metals and polycyclic aromatic hydrocarbons (PAHs) in road dust of Isfahan metropolis, Iran. – Science of the Total Environment 505: 712-723.
[38] Sun, Z. B., Zhou, J., Hu, B. B., Wang, Z. W., Meng, W. Q., Wang, Z. L. (2014): Characteristics of heavy metal pollution in urban street dust of Tianjin. – Ecol Environ Sci 23(1): 157-163.
[39] Škrbić, B. D., Buljovčić, M., Jovanović, G., Antić, I. (2018): Seasonal, spatial variations and risk assessment of heavy elements in street dust from Novi Sad, Serbia. – Chemosphere 205: 452-462.
[40] Tian, S., Liang, T., Li, K., Wang, L. (2018): Source and path identification of metals pollution in a mining area by PMF and rare earth element patterns in road dust. – Science of The Total Environment 633: 958-966.
[41] Urrutia-Goyes, R., Hernandez, N., Carrillo-Gamboa, O., Nigam, K. D. P., Ornelas-Soto, N. (2018): Street dust from a heavily-populated and industrialized city: Evaluation of spatial distribution, origins, pollution, ecological risks and human health repercussions. – Ecotoxicology and environmental safety 159: 198-204.
[42] Valotto, G., Zannoni, D., Rampazzo, G., Visin, F., Formenton, G., Gasparello, A. (2018): Characterization and preliminary risk assessment of road dust collected in Venice airport (Italy). – Journal of Geochemical Exploration 190: 142-153.
[43] Wang, L., Liu, M., Ou, N., Chang, J., Xu, S. (2009): Particle size distribution of heavy metals in urban surface dusts in Shanghai. – Journal of East China Normal University (Natural Science) 6.
[44] Wang, S., Cai, L. M., Wen, H. H., Luo, J., Wang, Q. S., Liu, X. (2019): Spatial distribution and source apportionment of heavy metals in soil from a typical county-level city of Guangdong Province, China. – Science of The Total Environment 655: 92-101.
[45] Wei, B., Jiang, F., Li, X., Mu, S. (2009): Spatial distribution and contamination assessment of heavy metals in urban road dusts from Urumqi, NW China. – Microchemical Journal 93(2): 147-152.
[46] Wei, B., Yang, L. (2010): A review of heavy metal contaminations in urban soils, urban road dusts and agricultural soils from China. – Microchemical journal 94(2): 99-107.
[47] Wei, B., Jiang, F., Li, X., Mu, S. (2010): Contamination levels assessment of potential toxic metals in road dust deposited in different types of urban environment. – Environmental Earth Sciences 61(6): 1187-1196.
[48] Xu, W., Lv, B., Chu, J. Y. (2012): The particle size distribution and source apportionment of heavy metal contaminated street dusts in different functional district of Zhenjiang. – Environmental Pollution & Control 34(10): 32-33.
[49] Yan, H., Xiao, J., Zhang, J. L. (2016): Concentration and particle size effect of heavy metals in the street dust of Xuchang City. – Journal of Earth Environment 7(2): 183-191.

http://www.aloki.hu ● ISSN 1589 1623 (Print) ● ISSN 1785 0037 (Online)
DOI: http://dx.doi.org/10.15666/aeer/1802_33313347

[50] Yang, Y., Christakos, G., Guo, M., Xiao, L., Huang, W. (2017): Space-time quantitative source apportionment of soil heavy metal concentration increments. – Environmental pollution 223: 560-566.
[51] Zhang, Y., Cai, J., Wang, S., He, K., Zheng, M. (2017): Review of receptor-based source apportionment research of fine particulate matter and its challenges in China. – Science of the Total Environment 586: 917-929.
[52] Zhang, J., Li, R., Zhang, X., Bai, Y., Cao, P., Hua, P. (2019): Vehicular contribution of PAHs in size dependent road dust: A source apportionment by PCA-MLR, PMF, and Unmix receptor models. – Science of The Total Environment 649: 1314-1322.
[53] Zhao, L., Hu, G., Yan, Y., Yu, R., Cui, J., Wang, X., Yan, Y. (2019): Source apportionment of heavy metals in urban road dust in a continental city of eastern China: Using Pb and Sr isotopes combined with multivariate statistical analysis. – Atmospheric environment 201: 201-211.

APPENDIX

Table A1. *Population density/km²*

Street	Population density/km²
Honggang	14662
Beihu	1024
Baiyushan	17688
Yejin	17444
Qingshanzhen	4352
Gangduhuayuan	32946
Wudong	3592
Xingouqiao	25647
Gongrencun	2632
Ganghuacun	34716
Hongweilu	20199
Changqian	3882

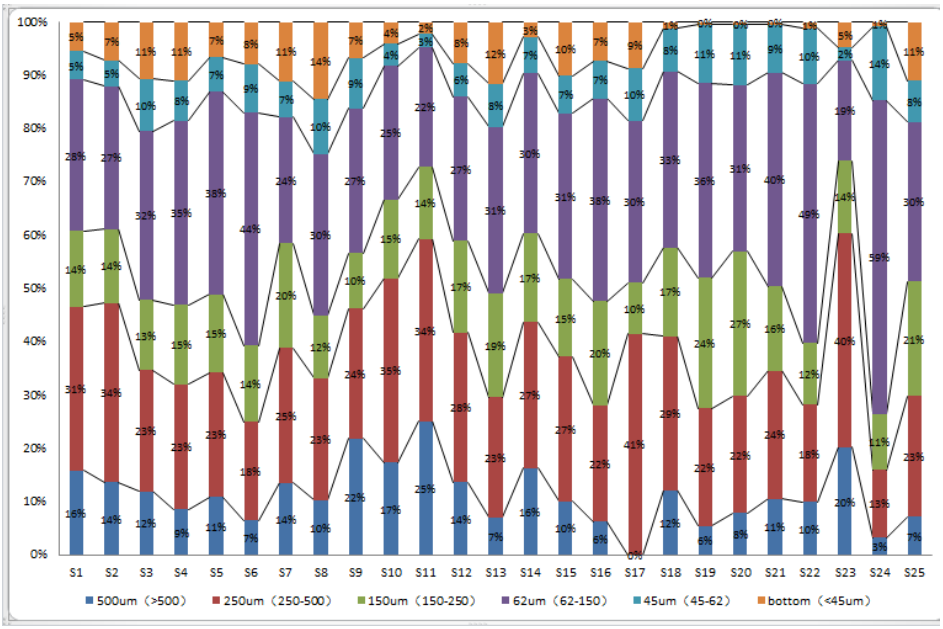

Figure A1. *Original grain size distribution*

http://www.aloki.hu ● ISSN 1589 1623 (Print) ● ISSN 1785 0037 (Online)
DOI: http://dx.doi.org/10.15666/aeer/1802_33313347

THE EFFECT OF SILICON FOLIAR AND ROOT APPLICATION ON GROWTH, PHYSIOLOGY, AND ANTIOXIDANT ENZYME ACTIVITY OF WHEAT PLANTS UNDER CADMIUM TOXICITY

UR RAHMAN, SH.[1,2] – QI, X.[1,2*] – ZHANG, Z.[3] – ASHRAF, M. N.[4] – DU, Z.[1,2] – ZHONG, Y. L.[1,2] – MEHMOOD, F.[5] – UR RAHMAN, S.[6] – SHEHZAD, M.[7]

[1]*Farmland Irrigation Research Institute, Chinese Academy of Agricultural Sciences, Xinxiang 453003, China*

[2]*Key Laboratory of High-efficient and Safe Utilization of Agriculture Water Resources of CAAS, Xinxiang 453003, China*

[3]*The James Hutton Institute, Craigiebuckler, Aberdeen AB15 8QH, UK*

[4]*National Engineering Laboratory for Improving Quality of Arable Land, Institute of Agricultural Resources and Regional Planning, Chinese Academy of Agricultural Sciences, 100081 Beijing, China*

[5]*Farmland Irrigation Research Institute of the Chinese Academy of Agriculture Sciences/Key Laboratory of Crop Water Use and Regulation, Ministry of Agriculture and Rural Affairs, Xinxiang, Henan 453003, China*

[6]*Department of Soil and Environmental Science, Arid Agriculture University, Rawalpindi, Pakistan*

[7]*Institute of Cotton Research, Chinese Academy of Agricultural Sciences, Anyang, China*

**Corresponding author*
e-mail: qxb6301@sina.cn; phone: +86-373-339-3277

(Received 7th Oct 2019; accepted 4th Dec 2019)

Abstract. Silicon (Si) application can boost plant growth and physiology under heavy metal toxicity. The article aimed to investigate how the foliar and root application of silicon (Si) affects the uptake, translocation, and concentration of cadmium (Cd) for winter wheat (*Triticum aestivum* L.), and in turn the plant's growth, physiology, and antioxidant enzyme activity, using a complete randomized block design (CRBD)? For this purpose, we used twelve treatments consisting of two levels of Si (0 and 3 mM Na_2SiO_3) against four levels of Cd (0, 50, 100, and 200 µM $CdCl_2$) with three replications. Results showed that all levels of Cd significantly enhanced membrane permeability measured as malonyldialdehyde (MDA) content, osmotic stress measured as hydrogen peroxide (H_2O_2) content, and triggered the enzymatic and non-enzymatic antioxidant system, resulting in a severe reduction in the growth of wheat seedlings. Besides, Si application either as root (SiR3) or foliar spray (SiF3) remarkably encountered Cd toxicity by further improving antioxidative enzymes activities, and by hindering Cd uptake, but more significant results were recorded for SiR3. Therefore, it might be established that Si root supplementation inhibited Cd translocation from root to shoot more effectively than foliar application, thereby lowering the potential health risk of Cd pollution.

Keywords: *enzymatic and non-enzymatic antioxidants, membrane permeability, osmoprotectants, photosynthetic pigments*

http://www.aloki.hu ● ISSN 1589 1623 (Print) ● ISSN 1785 0037 (Online)
DOI: http://dx.doi.org/10.15666/aeer/1802_33493371

Introduction

Wheat (*Triticum aestivum* L.) is the ultimate extensively grown cereal crop which fulfills 20% of the required daily protein for 4.5 billion people in the world (Flister and Galushko, 2016). It is the second most significant food crop in the developing world after rice. The wheat crop has the ability to adapt to various environmental circumstances but, considerable grain yield loss has been reported under heavy metals contamination, predominantly cadmium (Cd) contaminated soils (Rady et al., 2015). Most of the crop production area is under heavy metal stress caused by industrialization, anthropogenic activities, and other agricultural practices, which is currently becoming a worldwide serious threat (Zabin et al., 2015).

Among heavy metals, Cd is a highly lethal element because of its relative mobility, high water solubility, and phytotoxicity (Ali et al., 2011; Wuana and Okieimen, 2011). Due to its dynamic fates, Cd in an ionic form enters into plants through root and being shifted to shoot xylem and phloem through various active transporters and passive transporters (Dong et al., 2019; Takahashi et al., 2012). Higher uptake of Cd reduces photosynthesis by hindering root Fe (III) reductase, affects the activity of the enzyme involved in CO_2 fixation, affects mineral absorption causing a nutritional imbalance (such as N and K^+) and results in stomatal closure (Azevedo et al., 2012). It has been reported that in the intensified oxidative processes occur in cells of Cd-stressed plants which caused the formation of massive amount of reactive oxygen species (ROS) (Balakhnina et al., 2015; Gratão et al., 2005) which caused remarkable reduction of anti-oxidative enzymes activities in plants (Song et al., 2009). Additionally, Cd accumulates in the human body via the food chain, causing kidney, bone, and pulmonary damage (Ali et al., 2014; Fu and Wei, 2013; Li et al., 2014). Thus, developing positive approaches to minimize the potential health risk of heavy metal impurity in food chains is urgent for protecting edible parts of crops being polluted by heavy metals.

To alleviate heavy metals toxicity in plants, various means like soil phytoremediation and soil remediation engineering has been practiced (Rascio and Navari-Izzo, 2011). Although in most cases, these means did not work more effectively, as an alternative and/or accompanied by these means, silicon (Si) as soil or foliar application could be a more effective approach to diminish heavy metals accumulation in plants.

Silicon (Si), as a beneficial element, shows a crucial part in the growth and enlargement of various crops (Keeping, 2017; Zhao et al., 2017). Currently, Si has been conceived by Shi et al. (2014) as a compulsory element for numerous higher plants. However, Si is being proved as useful for plants, and it has the ability to alleviate biotic and abiotic stresses (Dong et al., 2019; Yu et al., 2016; Zhao et al., 2017). Si is the only element that can intake, translocate, and accumulate in considerable quantities in plants without any adverse effects (Ma et al., 2001a). Moreover, Si has been declared as a non-corrosive element (Wang et al., 2016). Consequently, Si, as being high-quality fertilizer may be used for eco-friendly agricultural enhancement.

It has been established in previous findings that Si can improve plant growth by mitigating the adverse influences of heavy metal toxicity (Dong et al., 2019). Numerous scientists have reported that Si treatments detoxify Cd-induced stress in various plants, particularly in graminaceous crops, which are deliberated as Si accumulators (Farooq et al., 2013; Howladar et al., 2018; Keeping, 2017; Zhao et al., 2017). Concerning abiotic stresses, Si counters various stresses, including drought, salinity, and heavy metals toxicity included Cd toxicity in growth medium (Alzahrani et al., 2018). Si, in the form

http://www.aloki.hu ● ISSN 1589 1623 (Print) ● ISSN 1785 0037 (Online)
DOI: http://dx.doi.org/10.15666/aeer/1802_33493371

of silicates, converts the exchangeable and the soluble fractions of metals into stable chemicals in soil. Such a decline in metal bioavailability is documented to redox reactions, humification, and precipitation (Vieira da Cunha et al., 2008). Besides, Silicates in soil encourages the polymerization of silicate composts and forms heavy-metals complexes (Sommer et al., 2006). However, evidence suggesting that Si addition improves photosynthetic activity modifies nutrient imbalance, minimizes mineral toxicity, and enhances abiotic tolerance (Ma et al., 2001a). Si maintains photosynthetic activity in Cd-stressed plants, reducing Cd uptake from nutrient solution to plant roots and restricts its translocation from root to shoots, which might be the possible mechanism of Cd detoxification (Kabir et al., 2016a).

Reactive oxygen species (ROS) produced in plants by Cd stress, causing a severe distraction of several metabolic processes in plants (Kim et al., 2017). Different responses have been reported against various environmental stresses within the crop, plant species, and/or cultivars according to their antioxidant defense system (Wael et al., 2015). Optimum ingredients of antioxidants in plants either stimulated and/or constitutive induce more tolerance in plants to oxidative burst (Kusvuran et al., 2016). It has been described by Kim et al. (2017) that Si increased plant tolerance to oxidative damage by regulating a substantial amount of different ROS in heavy metal stressed-plants. These findings can be justified based on Si amounts in plants, which involves improving activities of antioxidative enzymes; particularly those antioxidants which participated in the transformation of H_2O_2 in H_2O, and/or minimizing MDA activity to scavenge negative effects of ROS.

It has been widely studied the protective role of foliar as well as soil application of Si to alleviate the heavy metal toxicity in wheat crops. However, to our best knowledge, this is the first kind of study used Si foliar and root application method in wheat crop to evaluate the most effective Si application method to raise the capability of wheat to tolerate Cd toxicity.

Consequently, the primary aim of the present study was to find the constructive impact of Si in two Si application approaches and to identify the optimum way of Si supplementation for plant physiological traits, chlorophyll contents, anti-oxidative enzymes activities, proline, H_2O_2, and MDA content in Cd-stressed wheat plants grown hydroponically.

Materials and methods

Experimental layout

The experiment was conducted at the experimental site of the Farmland Irrigation Research Institute, Chinese Academy of Agricultural Sciences in Xinxiang City, China. Healthy seeds of winter wheat genotype Xin Mai 23 were immersed overnight in deionized water and sown in pasteurized quartz sand trays with the sand layer of 4 inches in width. The sand dishes were placed in a growing chamber of 16 h light/8 h dark with a light intensity of 375 μmole m^{-2} S^{-1}. The temperature of the growth chamber was set at 28 °C to 30 °C with a relative humidity of 85%. After two weeks of sowing, the five uniform seedlings were enfolded with foam at a root-shoot joint and relocated in each hole (15 in. ×17 in. in size) of plastic sheets fluctuating on 10 L capacity plastic basins. These basins occupied with 8 L modified Hoagland's solution (see *Appendix* heading 1). The pH was adjusted to 6.5 throughout the experiment by using acid (HCl) and base (NaOH). The air pumps were applied to the aerated nutrient solution. During

http://www.aloki.hu ● ISSN 1589 1623 (Print) ● ISSN 1785 0037 (Online)
DOI: http://dx.doi.org/10.15666/aeer/1802_33493371

the whole experiment, the nutrient solution was renewed after three days of intervals. After 65 days of transplantation Cd in the form of cadmium chloride ($CdCl_2$) and 3 mM per litter Si in the form of silicates nanoparticles (made by sodium silicate) (see *Appendix* heading 2) were added to nutrient solutions for 15 days to form twelve treatments with three replications as shown in *Table 1*. Si was applied by two different methods; 1) Si root-application (SiR3), 2) Si foliar-application (SiF3). In Si root application, 3 mM Si as silica gel was applied per liter of nutrient solution after every three days during 15 days of treatments. Alternatively, in Si foliar-application, Si with an amount of 3 mmol/L in the form of silica gel was sprayed five times during 15 days of treatment in 100 days experiment.

Table 1. *Experimental treatments*

Treatments	Cd (µM)	SiR (mM)	SiF (mM)
Ck	0	0	0
T2	0	3	0
T3	0	0	3
T4	50	0	0
T5	50	3	0
T6	50	0	3
T7	100	0	0
T8	100	3	0
T9	100	0	3
T10	200	0	0
T11	200	3	0
T12	200	0	3

Two levels of Si (0 & 3 mM) with two methods of Si applications (SiR3 & SiF3) along with four levels of Cd @ 0, 50, 100, and 200 µM

Determination of plant physiological traits

Growth parameters like roots and shoots fresh and dry weights were measured after 100 days of germination. Two plants from each replication were sampled and stored at -80 °C in the freezer (Thermo Fisher Scientific, USA 702) for enzymatic analysis. Remaining plants were detached into root and shoots and were measured for their fresh weights (kept at 70 °C temperatures in the oven till constant dry weight), which were subsequently measured for Si, Cd, K^+, total N, and total protein contents.

Measurements of photosynthetic pigments

Photosynthetic pigments (carotenoids. Chlorophyll a, b, and total chlorophyll) were measured by an ultraviolet-visible spectrophotometer (TU-1810) using the spectrophotometric method of Metzner et al. (1965).

Biochemical analysis

Anti-oxidative enzymes like superoxide dismutase (SOD), catalase (CAT), guaiacol peroxidase (POD), of leaves were analyzed with ultraviolet visible spectrophotometer (TU-1810) by using the kits of Beijing Solarbio Science & Technology Co., Ltd

http://www.aloki.hu ● ISSN 1589 1623 (Print) ● ISSN 1785 0037 (Online)
DOI: http://dx.doi.org/10.15666/aeer/1802_33493371

(http://www.solarbio.com). Briefly, 0.5 g weighted fresh samples of leaves were milled with the help of a motor and pestle and standardized in 0.05 M phosphate buffer with pH 7.8 under chilled condition. The standardized mixture was centrifuged at 12,000 rpm for 10 min at 4 °C after sieving through four layers of muslin cloth.

The activity of CAT was measured by the following formula:

$$CAT\left(\frac{\mu}{mgprot}\right)=\left(OD_{Control}-OD_{Test}\right)\times\frac{271}{60}\times\frac{1}{SQ}\times\frac{1}{Protein\,conc.} \quad \text{(Eq.1)}$$

where: SQ = sample quantity, $OD_{control}$ = absorption of light in control, OD_{test} = absorption of light in test samples.

After mixing all reagents in the standardized mixture, the supernatant was again centrifuged at 3500 rpm for 10 min. The light diameter of 1 cm was adjusted to zero by double streaming water. OD was measured at 420 nm wavelength. The activity of POD was measured by the following equation:

$$POD\left(\frac{\mu}{mgprot}\right)=\left(OD_{Test}-OD_{Control}\right)\times\frac{12}{1\text{ cm}}\times\frac{V_t}{SQ\times RT\times Protein\,conc.}\times 1000 \quad \text{(Eq.2)}$$

where: V_t = total volume of the reaction liquid, SQ = sample quantity, RT = reaction time, $OD_{control}$ = absorption of light in control, OD_{test} = absorption of light in test samples.

After mixing all reagents in a standardized mixture, the supernatant was placed at room temperature for 10 min. OD was measured at 550 nm wavelength. The activity of SOD was measured by the following equation:

$$SOD\left(\frac{\mu}{mgprot}\right)=\left(\frac{OD_{control}-OD_{test}}{OD_{Control}}\right)\times\frac{1}{50}\times\frac{V_t}{SQ\times Protein\,conc.} \quad \text{(Eq.3)}$$

where: V_t = total volume of the reaction liquid, SQ = sample quantity, $OD_{control}$ = absorption of light in control, OD_{test} = absorption of light in test samples.

The level of lipid peroxidation in the leaf tissue was assessed by measuring the contents of malondialdehyde (MDA, a by-product of lipid peroxidation. Briefly, 0.2-0.5 g weighted fresh samples of leaves were milled with the help of a motor and added 2 ml 10% TCA and a small amount of quartz sand, ground to homogenate, add 3 ml TCA, further ground. The homogenized sample was centrifuged at 12000 rpm for 10 min. Took 2 ml supernatant, added 0.67% TBA, mixed and boiled for 15 min in 100 °C water bath. Cooled the sample at room temperature and centrifuged again. Absorption values of samples were measured at 532 nm, 600 nm, and 450 nm, respectively. The activity of MDA was measured by the following formula:

$$CMDA=6.45\left(A532-A600\right)-0.56\times A450 \quad \text{(Eq.4)}$$

$$MDA\left(\frac{\mu mol}{g}\right)=CMDA\times\left(\frac{V_t}{SQ\times 1000}\right) \quad \text{(Eq.5)}$$

http://www.aloki.hu ● ISSN 1589 1623 (Print) ● ISSN 1785 0037 (Online)
DOI: http://dx.doi.org/10.15666/aeer/1802_33493371

where: V_t = total volume of the reaction liquid, SQ = sample quantity.

Proline was also assessed by using the kit of Beijing Solarbio Science & Technology Co., Ltd. Following formula was used to measure the proline contents:

$$Proline\left(\frac{\mu g}{g}\right)=\left(\frac{OD_{sample}-OD_{blank}}{OD_{st}-OD_{blank}}\right)\times C_{st}\frac{5\mu g}{ml}\times\frac{V_{reagent}}{M_{tissue}}\times COD \quad \text{(Eq.6)}$$

where: CoD = the coefficient of dilution in the pre-treatment process, C_{st} = concentration of standard, OD_{st} = absorption of standard sample.

Hydrogen peroxide levels in leaves of wheat plants were assessed by Sergiev et al. (1997) method (see *Appendix* heading 4).

Translocation and bioaccumulation factors

Cd translocation from shoot to root measured and calculated using the following equation:

$$TF=\left(\frac{C_{shoot}}{C_{root}}\right) \quad \text{(Eq.7)}$$

where C_{shoot} and C_{root} are the concentration of Cd in shoot and root, respectively. TF > 1 showed that metals effectively transported from root to shoot (Zhang et al., 2002).

The bioaccumulation factor (BAF) was calculated using the following equation:

$$BAF=\left(\frac{C_{shoot}}{C_{water}}\right) \quad \text{(Eq.8)}$$

where C_{shoot} and C_{water} presented Cd concentration in shoot and water, respectively. BAF was categorizing further as hyperaccumulators samples, which accumulated metals > 1 mg kg^{-1}, accumulator, and excluder samples, which accumulated metals < 1 mg kg^{-1}(Ma et al., 2001b).

Determination of nutrient elements in plant tissues

The N, K^+, Cd, and Si content in the plants were analyzed by inductively coupled plasma mass spectroscopy (ICP-MS, Agilent, and 7700 X, USA) after being oven-dried by following our previous study method (see *Appendix* heading 3) (Fırat et al., 2017).

Statistical analysis

The data were processed and analyzed using the SPSS 21.0 (SPSS, Chicago, IL), and all the graphs were made using the Sigma plot 12.5 software packages. The means of the three replicates were subjected to analysis of variance (two-way ANOVA), and multiple comparisons were performed using Duncan's multiple range test (DMR) at $P < 0.05$.

http://www.aloki.hu ● ISSN 1589 1623 (Print) ● ISSN 1785 0037 (Online)
DOI: http://dx.doi.org/10.15666/aeer/1802_33493371

Results

Cadmium attenuates growth parameters

Cadmium (Cd) caused a significant decrease in plant biomass without Si application (*Fig. 1*). Plant biomass in Cd50, Cd100, and Cd200 was decreased by 42%, 49%, and 68%, respectively, than that of the control plants. However, significantly higher biomass (root and shoot fresh weight) was recorded in Si treatments of combined SiR3 and SiF3 (*Fig. 1*). Plant biomass was increased, 71%, 62%, and 119% respectively, in SiR + Cd50, SiR + Cd100, and SiR + Cd200 than that of the Cd50, Cd100 and Cd200. While, in SiF + Cd50, SiF + Cd100, and SiF + Cd200 was increased, 45%, 40%, and 101%, respectively, than that of Cd50, Cd100, and Cd200. The maximum increase in plant biomass recorded in SiR3 while; minimum plant biomass was recorded in Cd200 than control (*Fig. 1*). Results showed that the overall SiR3 application performed well as compared to SiF3. Results showed that plant biomass in SiR3, SiR + Cd50, SiR + Cd100, and SiR + Cd200 was 10%, 18%, 15%, and 9%, respectively than that of SiF3, SiF + Cd50, SiF + Cd100, and SiF + Cd200. Si concentration was found positively correlated with plant growth parameters (*Fig. 2*).

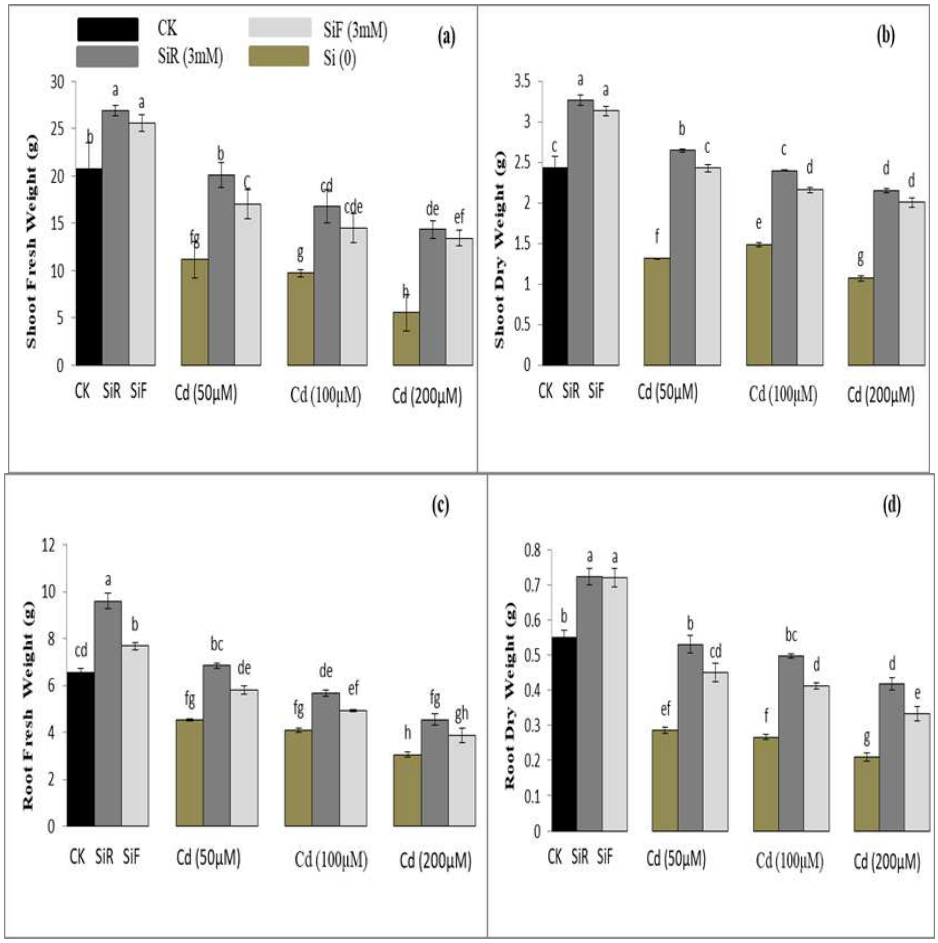

Figure 1. *The effects of silicon application (0, 3 mM) on shoot fresh weight (a), shoot dry weight (b), root fresh weight (c) and root dry weight (d) of the wheat plant grown under 0, 50, 100 and 200 µM Cd containing nutrient solution. Means ± SD (n = 3) with different letters in column indicates significant ($p \leq 0.05$) differences between treatments using Duncan's multiple range test (DMR)*

http://www.aloki.hu ● ISSN 1589 1623 (Print) ● ISSN 1785 0037 (Online)
DOI: http://dx.doi.org/10.15666/aeer/1802_33493371

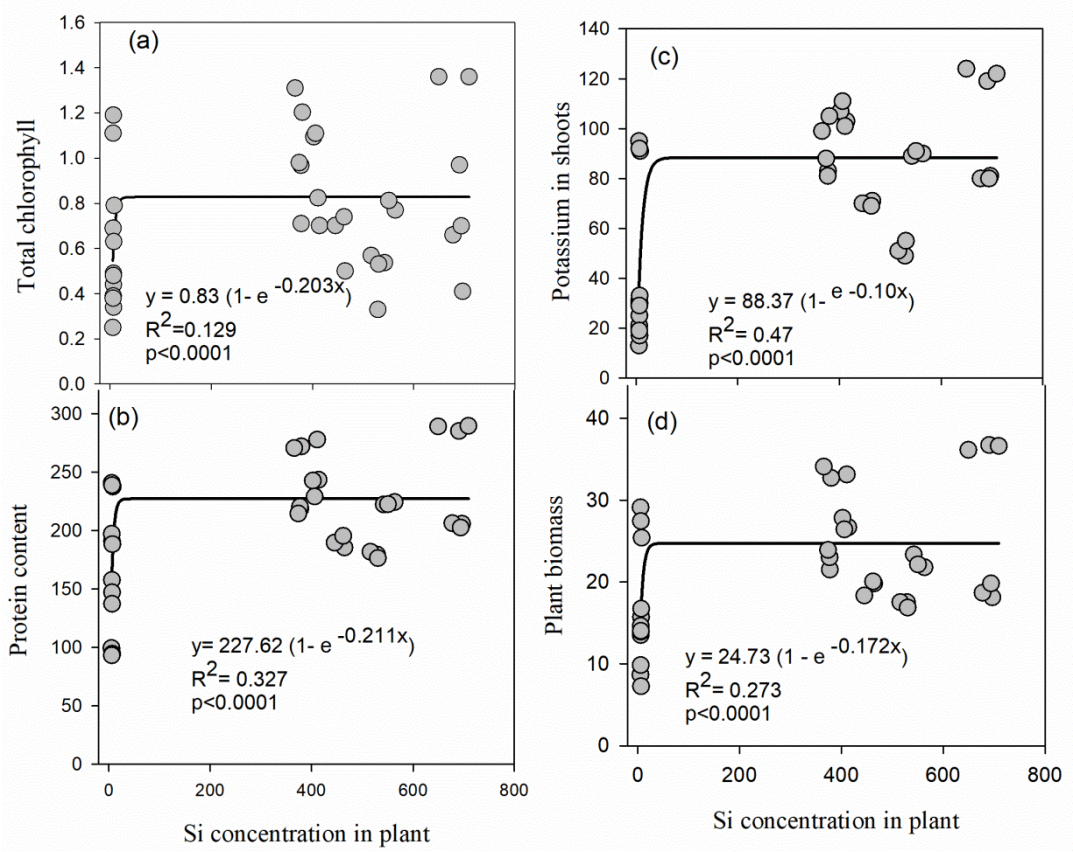

Figure 2. *Relationships among Si concentration in plants with (a) total chlorophyll content (b) protein content (c) potassium in plant and (d) plant biomass*

Cadmium attenuates the photosynthetic pigments

Cadmium (Cd) stress triggered a significant ($p < 0.05$) decline in carotenoids and total chlorophyll contents in wheat plants relative to control (*Table 2*). Total chlorophyll content in Cd50, Cd100, and Cd200 was decreased by 38%, 55%, and 71% respectively, as compared to control. Similarly, carotenoids contents in Cd50 were only 38%, while in Cd100 were 54% and in Cd200 were 71% compared to the control (*Table 2*). In the absence of Cd, Si treatment as SiF3 and SiR3 significantly ($p < 0.05$) elevated carotenoids and total chlorophyll contents. For instance, total chlorophyll contents in SiR + Cd50 were 34% that of Cd50, while, in SiR + Cd100 were 30% that of Cd100 and in SiR + Cd200 were 123% that of the Cd200. Correlation analysis was done between the means of the total concentration of Si in plant and total chlorophyll content, which showed a significantly ($p < 0.05$) positive correlation (*Fig. 2*). Similarly, carotenoids contents in SiR + Cd50 were 67% higher than Cd50, while, in SiR + Cd100 were 69% higher than Cd100 and in SiR + Cd200 were 83% higher than Cd200, respectively. Moreover, total chlorophyll contents in SiF + Cd50 were 43% higher than Cd50, while in SiF + Cd100 were 58% higher than Cd100 and in SiF + Cd200 were 90% higher than Cd200 respectively. Furthermore, the significant increase in total chlorophyll contents observed in SiF3 as compared to SiR3. For instance, total chlorophyll contents in SiF + Cd50 were 6% higher than SiR + Cd50, while in SiF + Cd100 were 18% higher than SiR + Cd100, and in SiF + Cd200 were 17% higher than

http://www.aloki.hu ● ISSN 1589 1623 (Print) ● ISSN 1785 0037 (Online)
DOI: http://dx.doi.org/10.15666/aeer/1802_33493371

SiR + Cd200 respectively. Contradictory results recorded in carotenoids content like maximum carotenoids contents observed in SiR3 than SiF3. Carotenoids contents in SiR + Cd50 were 29% higher than SiF + Cd50, while in SiR + Cd100 were 146% higher than SiF + Cd100, and in SiR + Cd200 were 66% higher than SiF + Cd200, respectively (*Table 2*).

Table 2. *Effect of different concentration of Cd (0, 50, 100, and 200 µM) and Silica sol. (0, 3 mM) along with different methods of Si application on chlorophyll contents of the wheat crop*

Treatments	Chl a (mg/g)	Chl b (mg/g)	Total Chl (mg/g)	Carotenoids (mg/g)
Ck	0.80 ± 0.005^{bc}	0.34 ± 0.03^{abc}	1.03 ± 0.12^{abc}	0.65 ± 0.02^{ab}
SiR 3mM	0.94 ± 0.017^{a}	0.42 ± 0.02^{a}	1.23 ± 0.13^{a}	0.83 ± 0.05^{a}
SiF 3mM	0.85 ± 0.030^{b}	0.39 ± 0.01^{ab}	1.11 ± 0.15^{ab}	0.71 ± 0.04^{ab}
Cd 50 µM	0.44 ± 0.014^{fg}	0.22 ± 0.01^{de}	0.59 ± 0.08^{ef}	0.34 ± 0.02^{de}
SiR3 + Cd50	0.75 ± 0.02^{cd}	0.32 ± 0.01^{bc}	0.97 ± 0.13^{bc}	0.57 ± 0.01^{bc}
SiF3 + Cd50	0.70 ± 0.00^{5d}	0.26 ± 0.02^{cd}	0.89 ± 0.09^{cd}	0.55 ± 0.21^{bc}
Cd 100 µM	0.36 ± 0.015^{g}	0.16 ± 0.02^{ef}	0.45 ± 0.03^{fg}	0.26 ± 0.01^{de}
SiR3 + Cd100	0.51 ± 0.013^{ef}	0.27 ± 0.02^{cd}	0.71 ± 0.09^{de}	0.44 ± 0.08^{cd}
SiF3 + Cd100	0.50 ± 0.005^{ef}	0.21 ± 0.02^{de}	0.65 ± 0.07^{ef}	0.41 ± 0.02^{cd}
Cd 200 µM	0.27 ± 0.011^{h}	0.08 ± 0.01^{f}	0.32 ± 0.04^{g}	$0.18 \pm 0.01e$
SiR3 + Cd200	0.41 ± 0.014^{e}	0.26 ± 0.01^{cd}	0.73 ± 0.09^{de}	0.33 ± 0.03^{de}
SiF3 + Cd200	0.37 ± 0.023^{g}	0.17 ± 0.02^{e}	0.48 ± 0.07^{fg}	0.28 ± 0.01^{de}

Values show the means of three replications ± SD. Means followed by same small letters are not significantly different at $P \leq 0.05$ by using the Duncan's multiple range test (DMR)

Cadmium accumulation in the wheat plant

Results showed that Cd content significantly enhanced when plants received Cd stress relative to control. Silicon (3 mM) addition as SiR3 and SiF3 significantly reduced Cd concentration in all parts of the plant, and the effect was more significant in SiR3 than SiF3. Moreover, results exhibited that Cd concentration in SiR + Cd50 was 25% less than SiF + Cd50, while in SiR + Cd100 was 25% less than SiF + Cd100, and SiR + Cd200 was 32% less than SiF + Cd200 in shoot (*Table 2*). Whereas, Cd concentration in SiR + Cd50 was 27% higher than SiF + Cd50, while SiR + Cd100 was 10% higher than SiF + Cd100, and SiR + Cd200 was 21% higher than SiF + Cd200 in root (*Table 3*). Both Si treatments minimized Cd accumulation significantly, but SiR3 bound more Cd in root cells and restricted its translocation from root to shoot and detoxify its deleterious effects more efficiently than Si foliar-application (*Table 3*).

Table 3. *Effect of different concentration of silica sol. (0, 3 mM) along with different methods of application and Cd (0, 50, 100 and 200 µM) on Cd and Si accumulation in wheat crop*

Treatments	Cd accumulation (µg/g) in root	Cd accumulation (µg/g) in shoot	Si accumulation (µg/g) in root	Si accumulation (µg/g) in shoot
Ck	5.07 ± 0.1^{j}	0.04 ± 0.02^{i}	2.57 ± 0.2^{g}	4.11 ± 0.5^{d}
SiR 3 mM	0.70 ± 0.1^{j}	0.03 ± 0.01^{i}	423.11 ± 5.9^{d}	139.88 ± 9.2^{c}
SiF 3 mM	0.53 ± 0.1^{j}	0.02 ± 0.005^{i}	85.98 ± 3.6^{ef}	299.55 ± 16.5^{a}

http://www.aloki.hu ● ISSN 1589 1623 (Print) ● ISSN 1785 0037 (Online)
DOI: http://dx.doi.org/10.15666/aeer/1802_33493371

Cd 50 µM)	1696.84 ± 40.6^{e}	1112.103 ± 7.1^{c}	3.17 ± 0.2^{g}	3.27 ± 0.3^{d}
SiR3 + Cd50	837.89 ± 9.4^{h}	229.1 ± 2.8^{h}	660.05 ± 6.0^{c}	130.98 ± 7.1^{c}
SiF3 + Cd50	659.50 ± 4.63^{i}	309.57 ± 12.3^{g}	93.15 ± 2.9^{ef}	213.48 ± 5.9^{a}
Cd 100 µM	2335.95 ± 18.7^{c}	1313.89 ± 9.9^{b}	3.25 ± 0.1^{g}	3.00 ± 0.2^{d}
SiR3 + Cd100	1347.83 ± 21.9^{f}	453.38 ± 23.3^{f}	797.88 ± 13.2^{b}	125.85 ± 3.7^{c}
SiF3 + Cd100	1216.36 ± 10.1^{g}	605.09 ± 7.9^{e}	101.78 ± 5.2e	210.68 ± 6.1^{d}
Cd 200 µM	3654.55 ± 7.3^{a}	1936.27 ± 26.4^{a}	3.07 ± 0.1^{g}	2.87 ± 0.3^{d}
SiR3 + Cd200	2037.04 ± 42.7^{b}	657.42 ± 23.6b^{d}	997.64 ± 6.9^{a}	117.03 ± 2.5^{c}
SiF3 + Cd200	2474.82 ± 8.3^{b}	978.08 ± 11.4^{c}	63.97 ± 15.8^{f}	281.45 ± 5.9^{b}

Values show the means of three replications ± S.D. Means by the same small letters are not significantly different at $P < 0.05$ by using the Duncan's multiple range test (DMR)

Silicon attenuates translocation factor and bioaccumulation factor of Cd

Results showed that a significant ($p < 0.05$) positive correlation was recorded between Cd concentration and translocation factor (TF) (*Table 4*), which means Cd translocation factor increased with the rise of Cd levels in the nutrient solution. While Si application as SiR3 and SiF3 both minimized Cd translocation from root to shoot, but more significant results observed in case of SiR3. TF of Cd in SiR + Cd50 was 41% less than SiF + Cd50, while in SiR + Cd100 was 32% less than SiF + Cd100, and in SiR + Cd200 was 33% less than SiF + Cd200, respectively. Moreover, in both SiR3 and SiF3, TF < 1 showed Cd incompetently transport from root to shoot in a wheat plant in the presence of Si. In the case of Cd, bioaccumulation factor recorded data showed significantly ($p < 0.05$) negative correlation between BAF of Cd and Cd existence in the nutrient solution (*Table 5*). Silicon both applications SiR3 or SiF3 showed a significantly negative correlation with both Cd bioaccumulation and translocation factors (*Fig. 4*). Moreover, Si treatments as SiR3 and SiF3 along with Cd (50, 100, and 200 µM) further minimized BAF of Cd, but results were more significant in SiR3 as compared to SiF3. For instance, BAF of Cd in SiR + Cd50 was 26% less than SiF + Cd50, while in SiR + Cd100 was 25% less than SiF + Cd100, and in SiR + Cd200 was 33% less than F3 + Cd200 respectively (*Table 4*).

Table 4. *Effect of different application methods as well as levels of Si on Cd translocation and bioaccumulation factors*

Treatments	Translocation factor (%)	Bioaccumulation factor (%)
Ck	0.007 ± 0.003^{f}	0 ± 0^{g}
SiR 3 mM	0.004 ± 0.012^{f}	0 ± 0^{g}
SiF 3 mM	0.05 ± 0.025^{f}	0 ± 0^{g}
Cd 50 µM	0.65 ± 0.011^{a}	0.121 ± 0.0007^{a}
SiR3 + Cd50	0.27 ± 0.003^{e}	0.025 ± 0.0003^{e}
SiF3 + Cd50	0.47 ± 0.001^{c}	0.034 ± 0.001^{d}
Cd 100 µM	0.56 ± 0.008^{b}	0.072 ± 0.0005^{b}
SiR3 + Cd100	0.34 ± 0.021^{de}	0.025 ± 0.001^{e}
SiF3 + Cd100	0.49 ± 0.01^{bc}	0.033 ± 0.0004^{d}
Cd 200 µM	0.55 ± 0.006^{bc}	0.053 ± 0.0007^{c}
SiR3 + Cd200	0.32 ± 0.017^{e}	0.018 ± 0.0006^{f}
SiF3 + Cd200	0.39 ± 0.005^{d}	0.027 ± 0.0003^{e}

Values show the means of three replications ± SD. Means followed by same small letters are not significantly different at $P \leq 0.05$ by using the Duncan's multiple range test (DMR)

http://www.aloki.hu ● ISSN 1589 1623 (Print) ● ISSN 1785 0037 (Online)
DOI: http://dx.doi.org/10.15666/aeer/1802_33493371

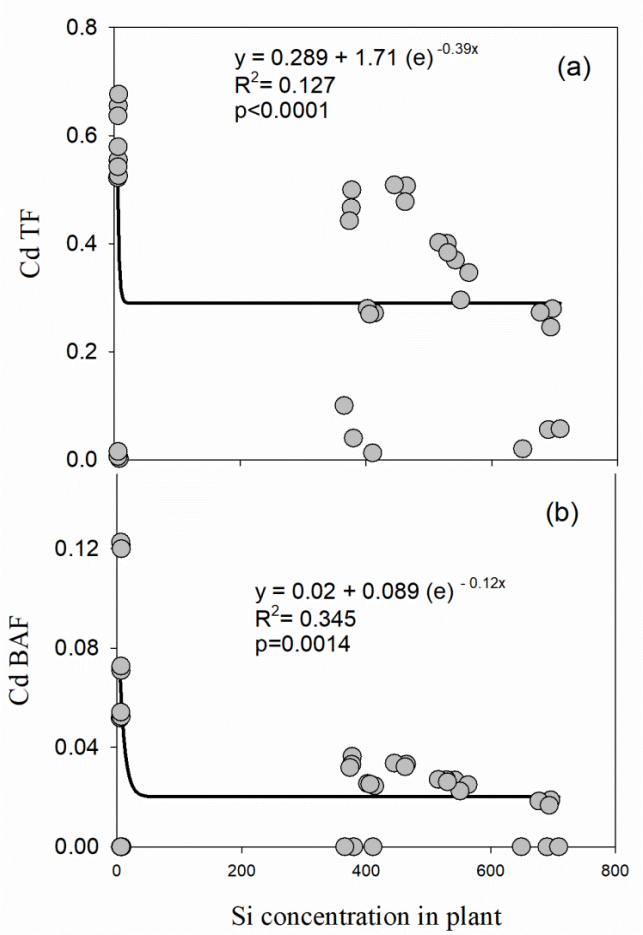

Figure 4. *The relationship among Si concentration in the plant, cadmium translocation factor (Cd TF), and cadmium bioaccumulation factor (Cd BAF)*

Silicon accumulation under cadmium toxicity

Silicon concentration was significantly ($p < 0.05$) increased when plants exposed to Si treatments as SiF3 and SiR3 relative to the control. Si concentration in SiF3 application was higher in shoots as compared to SiR3 application. For instance, Si concentration in SiF + Cd50 was 62% higher than in the SiR + Cd50, while, in SiF + Cd100 was 33% higher than in the SiR + Cd100, and in SiF + Cd200 was 31% higher than in the SiR + Cd200 respectively. While in SiR3 application, Si concentration in SiR3 was higher in root than shoot as compared to SiF3 application. For instance, our results showed that, Si concentration in SiR + Cd50 was 70% higher than in the SiF + Cd50, while, in SiR + Cd100 was 129% higher than in the SiF + Cd100, and in SiR + Cd200 was 189% higher than in the SiF + Cd200 respectively in root. The recorded data showed that Si concentration increased with the increase in Cd levels (*Table 3*). Si accumulation in root was more significant in SiR3 as relatively SiF3 while, Si accumulation in the shoot was more significant in SiF3 as relatively SiR3 (*Table 3*).

Cadmium enhances reactive oxygen species (ROS)

A significantly higher concentration of H_2O_2 and MDA in the shoot was recorded in Cd-treated plants than control (*Fig. 3b*).

http://www.aloki.hu ● ISSN 1589 1623 (Print) ● ISSN 1785 0037 (Online)
DOI: http://dx.doi.org/10.15666/aeer/1802_33493371

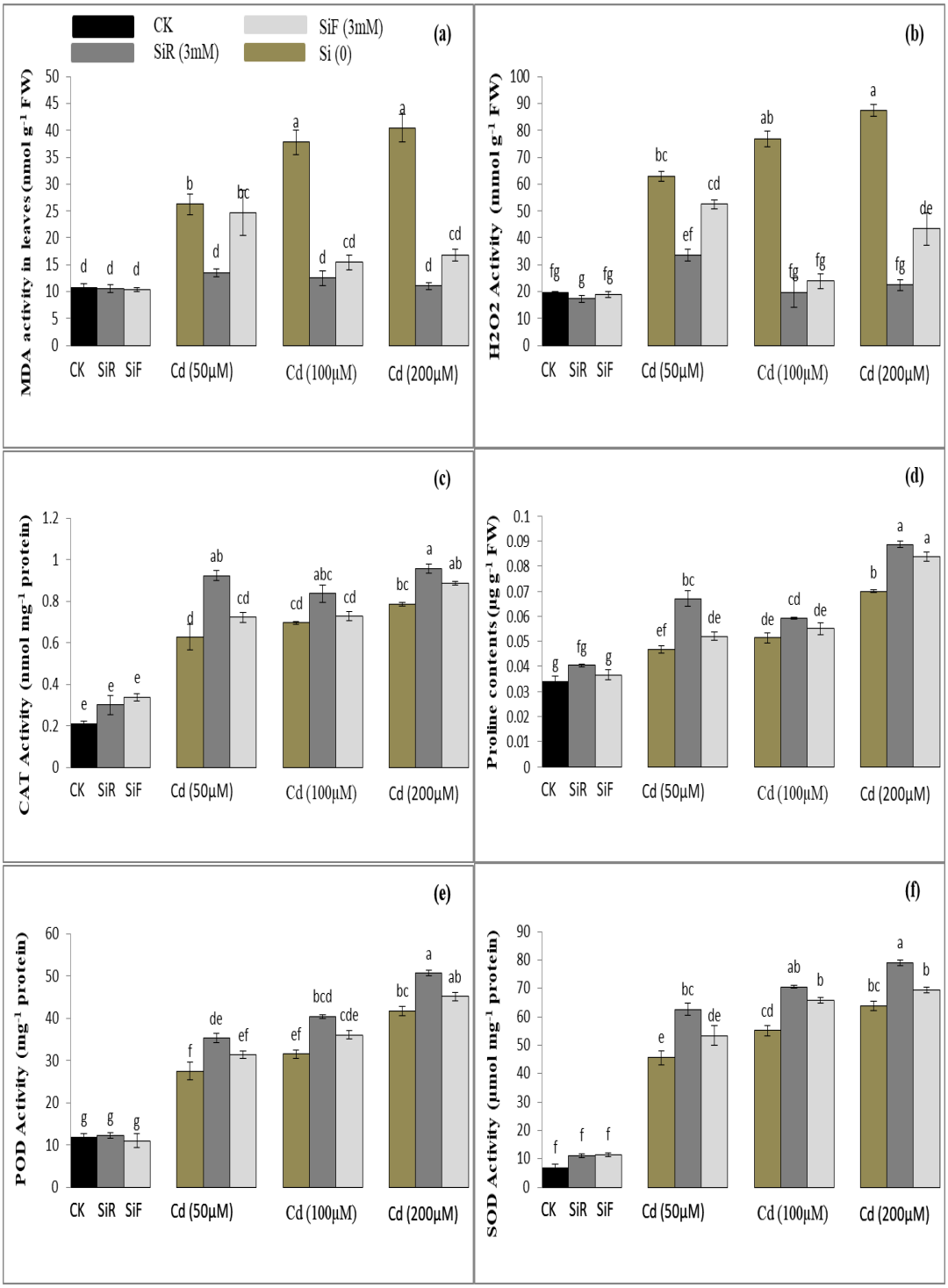

Figure 3. *The effects of silicon application (0, 3 mM) on reactive oxygen species (ROS) activity i.e. MDA (a), H_2O_2 (b), and antioxidative enzymes activity i.e. CAT (c), proline (d), POD (e) and SOD (f) of the wheat plant grown under 0, 50, 100 and 200 µM Cd containing nutrient solution. Bars show S.E. of three replications, the different letter above column within CAT, SOD, POD, MDA, H_2O_2, and proline represents a significant difference at $P < 0.05$ by using Duncan's multiple range test (DMR)*

http://www.aloki.hu ● ISSN 1589 1623 (Print) ● ISSN 1785 0037 (Online)
DOI: http://dx.doi.org/10.15666/aeer/1802_33493371

For instance, H_2O_2 concentration was 219% higher in Cd50, was 290% higher in Cd100, and was 343% higher in Cd200 than in control, respectively. Si application as SiR3 and SiF3 significantly ($P < 0.05$) decreased the concentration of H_2O_2 in shoots (*Fig. 3b*), but SiR3 proved more effective than SiF3. For instance, H_2O_2 concentration in SiR3 + Cd50 was 36% lower than in the SiF3 + Cd50, while in SiR + Cd100 was 17% lower than in SiF + Cd100, and in the SiR + Cd200 was 48% lower than in the SiF + Cd200 respectively (*Fig. 3*b). The same trend recorded in MDA contents. MDA concentration was significantly high in Cd-treated shoots as being compared to control. For instance, MDA concentration was, respectively, 144%, 251%, and 276% in Cd50, Cd100, and Cd200 that of the control (*Fig. 3a*). Added Si as SiR3 and SiF3 significantly lower MDA concentration in shoots of wheat plants at all Cd supply levels (*Fig. 3a*), but the maximum decreased in MDA concentration was noted in SiR3-treated plants along with or without Cd50, Cd100, and Cd200 as compared to all other treatments. For instance, MDA concentration was 45%, 18%, and 34% lower in SiR + Cd50, SiR + Cd100, and SiR + Cd200 that of the SiF + Cd50, SiF + Cd100, and SiF + Cd200 respectively (*Fig. 3a*).

Cadmium meliorates enzymatic and non-enzymatic antioxidants in wheat seedlings

A significant elevation was recorded in enzymatic (superoxide dismutase; SOD, peroxidase; POD and catalase; CAT) and non-enzymatic (proline) antioxidants concentration in Cd-treated plants as being compared to control. For instance, SOD activity was, 568%, 708%, 835% higher respectively, POD activity was 133%, 166%, 253% higher respectively, CAT activity was 198%, 231%, 275% higher respectively, and proline concentration was 37%, 51%, 106% higher in Cd50, Cd100, and Cd200 that of the control (*Fig. 3c, d, e, f*). Added Si as SiF3 and SiR3 further elevated SOD, POD, CAT, and proline activities significantly with or without Cd50, Cd100, and Cd200. Overall, SiR3 alone, as well as with Cd50, Cd100, and Cd200 performed well to boost up SOD, POD, CAT, and proline activities as compared to SiF3, but the difference was not significant. For instance, POD activity in SiR3 along with Cd (50, 100 and 200 µmol/L) was 31%, 36%, 45% respectively, SOD activity was 17%, 7%, and 14% higher, CAT activity was 27%, 15%, and 8% higher, and proline concentration was 28%, 8%, and 6% higher than that of higher than of SiF3 along with same levels of Cd (*Fig. 3*).

Cadmium attenuate essential nutrients in wheat

A significant decreasing trend was recorded in K^+ and N concentration in Cd-stressed plants than that of control (*Table 5*). For instance, K^+ and N concentration was, 66% and 73%, 82% and 19%, 38%, 59% respectively, in Cd50, Cd100, and Cd200 that of the control. Added Si as SiF3 and SiR3 alone, as well as with Cd50, Cd100, and Cd200, significantly increased K^+ and N concentration in the shoot of the wheat plant (*Table 5*). The maximum increase in results recorded in case of SiR3 compared to SiF3. For instance, K^+ and N concentration in shoot was, respectively, 27%, 28%, 55% and 24%, 51%, 113% higher in SiR + Cd50, SiR + Cd100, and SiR + Cd200 that of the SiF + Cd50, SiF + Cd100, and SiF + Cd200. Total Si concentration in plant showed a strong affirmative association with K^+ concentration in shoots of wheat plants (*Fig. 2*). With the increase of Si concentration from 0 to 3 mM significantly increased K^+ concentration from 16 mg g^-1 to 107 mg g^{-1} (*Table 5*).

http://www.aloki.hu ● ISSN 1589 1623 (Print) ● ISSN 1785 0037 (Online)
DOI: http://dx.doi.org/10.15666/aeer/1802_33493371

Table 5. *Effect of different concentrations of Cd (0, 50, 100, and 200 µM), and Silica sol. (0 and 3 mM) along with different ways of Si application on K^+, total N and total Protein concentration in shoots of the wheat plant*

Treatments	K^+ concentration in shoot (mg/g)	Total N in shoot (mg/g)	Total protein in shoot (mg/g)
Ck	92.67 ± 1.20^{c}	38.25 ± 0.15^{c}	239.06 ± 0.93^{c}
SiR 3 mM	121.67 ± 1.45^{a}	46.07 ± 0.22^{a}	287.96 ± 1.36^{a}
SiF 3 mM	101.67 ± 1.76^{b}	43.75 ± 0.35^{b}	273.44 ± 2.21^{b}
Cd 50 µM	31.33 ± 0.88^{h}	30.73 ± 0.43^{fg}	192.08 ± 2.68^{fg}
SiR3 + Cd50	107.00 ± 2.31^{b}	38.15 ± 0.74^{c}	238.41 ± 4.64^{c}
SiF3 + Cd50	84.00 ± 2.08^{de}	34.86 ± 0.27^{de}	217.84 ± 1.70^{de}
Cd 100 µM	25.00 ± 2.31^{h}	23.57 ± 0.94^{h}	147.32 ± 5.88^{h}
SiR3 + Cd100	90.00 ± 0.58^{cd}	35.68 ± 0.10^{d}	223.02 ± 0.64^{d}
SiF3 + Cd100	70.00 ± 0.58^{f}	30.42 ± 0.46^{g}	190.14 ± 2.87^{g}
Cd 200 µM	16.33 ± 1.76^{i}	15.32 ± 0.30^{i}	95.72 ± 1.90^{i}
SiR3 + Cd200	80.33 ± 0.33^{e}	32.77 ± 0.18^{ef}	204.81 ± 1.16^{ef}
SiF3 + Cd200	51.67 ± 1.76^{g}	28.67 ± 0.25^{g}	179.21 ± 1.59^{g}

Values show the means of three replications ± SD. Means followed by same small letters are not significantly different at $P \leq 0.05$ by using Duncan's multiple range test (DMR)

Discussion

Plants exposed to several biotic and abiotic stressors in different agriculture systems. Abiotic stressors like heavy metals stress, restrict plant biomass, and limit its yield. In present findings, Cd existence in nutrient solution at the concentration of 50 µM, 100 µM, and 200 µM severely decreased wheat plant growth (*Fig. 1*), silicon (Si) contents (*Table 2*), chlorophyll contents (*Table 2*), potassium (K^+) and nitrogen (N) contents (*Table 5*), while it significantly increased Cd content (*Table 3*), Cd translocation and bioaccumulation factors (*Table 4*), lipid peroxidation measured as malondialdehyde (MDA) content (*Fig. 3*), enzymatic and non-enzymatic antioxidative contents (*Fig. 3*). However, Si application either as root or foliar method at a level of 3 mM encountered the negativity of cadmium toxicity in wheat plants by further elevating of enzymatic and non-enzymatic antioxidative contents, reducing Cd, MDA, and H_2O_2 contents, resulting in high plant growth. These findings are consistent with Farooq et al. (2013), Howladar et al. (2018), Silva et al. (2017), Alzahrani et al. (2018), Wang et al. (2016), and Rady et al. (2015). The dominant and diverse thing in the current findings that two separate methods of Si supplementation (e.g., foliar spray, root treatment) were tested and the optimum results were attained with Si root application.

Results of the present study demonstrated that Cd stress interrupted several biological, chemical, and metabolic processes in various plant species (Kim et al., 2014; Shi et al., 2010; Zhang et al., 2014; Zhao et al., 2017). Foyer and Noctor (2005) has been identified Cd as a disruptor of antioxidant defense system by overproducing oxidative burst and reactive oxygen species (ROS), which enhances lipid peroxidation by MDA contents (Howladar et al., 2018). Cd accumulation gradually increased in plant various parts with preference of root, with the rise of Cd levels in growth medium. Our data showed that higher Cd accumulation in root than shoot of wheat plants. Plants take up lower amount of metal solution in upper ground part in any event with highest tolerance (Yang et al., 2004). In this study, Cd stress generated high levels of ROS,

http://www.aloki.hu ● ISSN 1589 1623 (Print) ● ISSN 1785 0037 (Online)
DOI: http://dx.doi.org/10.15666/aeer/1802_33493371

which indicated by severing reduction of photosynthetic gas exchange parameters in leaf, and significant elevations in MDA and H_2O_2 contents. Therefore, to meet these adverse conditions, plants are grown under Cd-induced oxidative damage to develop complex antioxidant systems (Dixit et al., 2001; Farooq et al., 2013; Howladar et al., 2018).

Silicon as a high-quality non-corrosive fertilizer enhanced plant existence against Cd toxicity by significantly interrupted uptake and/or accumulation of Cd in Cd-toxic plants (Farooq et al., 2013; Song et al., 2009; Wang et al., 2016; Zhao et al., 2017). The constructive effects of Si on plant physio-biochemical traits under various environmental stresses have been well documented (Hashemi et al., 2010). Previous researchers with different findings (Ali et al., 2013; Kabir et al., 2016b; Shi et al., 2005; Song et al., 2009; Zhao et al., 2017) have suggested optimum methods by which Si can enhance plant tolerance against abiotic stresses including Cd that considered the most critical toxic elements, causing limited crop yield in both arid and semiarid regions. The researchers have been conducting various studies to establish Si beneficial effects on the development and yield of wheat cultivars under Cd toxicity. In our present study, Si found effective fertilizer in demolishing Cd toxicity in the wheat plant. The growth traits were significantly elevated in stressed-plants to normal with Si supplementation. Si causes nutritional balance and increases dry matter production of plants while applied in suitable dose (Silva et al., 2017). According to the results of the present study, nutrient medium receiving Si or plants received Si as foliar spray increased growth of stress wheat plants. This upgrading in wheat growth may be recognized to that Si improved photosynthetic rate that is correlated to activity of ribulose biphosphate carboxylase, leaf ultrastructure, and leaf chlorophyll contents (Hamayun et al., 2010).

Oxidative damage generally caused in plants due to ROS, e.g., superoxide radical, H_2O_2, and hydroxyl radical (OH^{-1}) (Shahid et al., 2014; Tamás et al., 2017). Along with the overproduction of ROS, membrane permeability with lipid peroxidation is also the main mechanism in higher plants due to Cd exposure (Farooq et al., 2013). MDA, as a derivative of lipid peroxidation, destabilized cell membrane integrity, and higher the risk of its permeability in various crops (Moussa, 2006; Soylemezoglu et al., 2009). In our findings, Si supplementation significantly lowers the malondialdehyde (MDA) contents in Cd-stressed wheat plants, resulting in sustain cell membranes integrity and reduce their permeability in Cd stress. Plants have various enzymatic (CAT, SOD, and POD) and non-enzymatic (proline) antioxidant defense systems to control different productions of ROS. Among these protective defense systems, the fusion of osmolytes/osmoprotectants is one of the integral protective mechanisms of plants grown in stress conditions (Rios et al., 2017). Proline as osmoprotectants protects plant cells by neutralizing osmotic strength of external environment and the cytosol and vacuole osmotic strengths under salt stress (Gadallah, 1999).

Furthermore, proline, as an impotent osmolyte accumulated in response to osmotic stress, contributes to osmotic adjustments in plant cells (Gadallah, 1999). Proline contents scavenge free radicals of oxidative stress molecules, stabilizes protein and sub-cellular structures under Cd stress (Sharma and Dubey, 2005). As an optimum Si application method, Si root-application improved proline accumulation in wheat plants to increase plant chances to withstand under oxidative stress induced by Cd (*Fig. 3*).

http://www.aloki.hu ● ISSN 1589 1623 (Print) ● ISSN 1785 0037 (Online)
DOI: http://dx.doi.org/10.15666/aeer/1802_33493371

Enzymatic antioxidants included catalase (CAT), superoxide dismutase (SOD), peroxidase (POD), etc. is another defense system in various stresses including Cd (Şen, 2012). In the current study, enzymatic antioxidant activities were higher with Cd-induced oxidative stress and were further improved with Si supplementation with the preference of Si root-application. Cd-induced oxidative stress resulted superoxide radicals that were transformed into H_2O_2 by SOD. H_2O_2 is a powerful oxidant that is accumulated in plant tissues from SOD canalization reaction and is prohibited by the cycle of ascorbate-glutathione. Except H_2O_2, another lethal oxide is the OH^{-1}, which can combine with all macro-molecules. By assimilating their actions, both CAT and SOD can stop OH^{-1} formation in plant tissues (Kusvuran et al., 2016). It has established in previous findings that Si application elevated CAT and SOD (Howladar et al., 2018). Kabir et al. (2016b) found that addition of Si under stress considerably improved CAT and SOD activities in alfalfa plants. Peroxidases (PODs) due to their role in consuming and scavenging H_2O_2 can modify ROS levels in plants. Compared to SOD and CAT, PODs have high attraction to H_2O_2, though PODs can also produce H_2O_2 by the oxidation of NAD(P)H (Ranieri et al., 2005). Several scientists have reported in their findings that Si application elevated POD activity in plants grown under oxidative stress. In general, Si treatment reduced ROS generation and led to raising enzymatic and non-enzymatic anti-oxidants used to scavenge ROS (Rios et al., 2017). Therefore, Si uses ROS scavenging metabolic pathways more effectively, which makes it able to alleviate Cd-induced oxidative stress at cellular level, which may recover the integrity of cell membranes.

Cd accumulation in shoots and roots of wheat plants followed the same trend as shoots, and roots levels reduced with increasing Si dose as a foliar application. The same results found by previous reports (Treder and Cieslinski, 2005), but our results were conflicted with the finding of several studies that examined decreased shoots Cd concentration with increasing Si levels (Rizwan et al., 2012). Interestingly, contradictory results were obtained in case of Si root application as Cd concentration did not follow the same trend as Cd reduced in all three parts of plants than that of Cd alone treatments. But our consequences were conflicted with the finding of several studies which examined decreased Cd shoots concentration with increasing Si levels (Rizwan et al., 2012). Interestingly, contradictory results were obtained in case of Si root application as Cd concentration did not follow the same trend, i.e., Cd shoot concentrations declined while root concentrations elevated with increasing Si dose. Similar results were also found in durum wheat developed in a soil with aged impurity (Rizwan et al., 2012), rice is grown hydroponically (Shi et al., 2005; Zhang et al., 2008), in peanut and cucumber (Shi et al., 2010) and *Brassica Chinensis* (Song et al., 2009), but our results in case of SiR3 disagreed with authors who found Cd increased in both root and shoot with the increase in Si doses (Vaculík et al., 2009), or a decrease in Cd concentration in both roots and leaves with increase in Si levels (Nwugo and Huerta, 2008). In Si root application, increased Cd concentration in roots could be due to the deposition of Cd in roots and formed metal complexes with silicates as reported by numerous studies. i.e., Zhang et al. (2008) established that Cd usually deposited in the section of roots endodermis and epidermis in rice plants, while, Shi et al. (2010) found that Si often stored in the cell walls of the endodermis and formed metal complexes with silicates. However, in SiF3 application Cd concentration in both roots and shoots was decreased with increasing Si levels, it could be due to Si inhibitory behavior, Si deposited in leaves cells and translocated from leaves to shoot and then roots and

http://www.aloki.hu ● ISSN 1589 1623 (Print) ● ISSN 1785 0037 (Online)
DOI: http://dx.doi.org/10.15666/aeer/1802_33493371

inhibited Cd translocation through xylem and phloem (Treder and Cieslinski, 2005). In both methods of Si, application plant withstand against Cd toxicity may be attributed due to the improvement of plant tolerance and/or due to uptake and transport of Cd which was also reported by Wang et al. (2016). In our study Cd concentration was high in Cd alone treatments as compared to Cd + Si (*Table 2*) that were conflicted with the findings of various authors who found that the Cd concentration in both roots and shoots was higher in Cd + Si treated plants than alone Cd-treated plants (Prabagar et al., 2011; Ye et al., 2012). Our results showed TF < 1 suggesting that Cd could ineffectively be translocated from root to shoots in case of both SiF3 and SiR3, but more significant effects observed in the case of SiR3 (*Table 5*) which is in line of previous findings (Howladar et al., 2018). In our study Si concentration under Cd stress was significantly increased with Si supplementation (Silva et al., 2017), which clarified that in Si both application methods, Si absorbed by roots should have translocation into shoots, where it deposits in the leaf apoplast as a polymer, forming a crucial barrier to protect plants from various environmental stresses counting Cd stress. Furthermore, Si concentration in plant showed a negative correlation with TF, BAF, and BCF of Cd (*Fig. 4*), which suggests that with the increase of Si concentration in plants, Cd translocation and bioaccumulation will decrease simultaneously. Our results showed that BAF of Cd decreased with the rise of Cd concentration in nutrient solution (*Table 5*) which was in line of previous findings (Zhao et al., 2003) but was contrary with some scientists who found increase in BAF with increase of heavy metal accumulation in soil (Rezvani and Zaefarian, 2011).

Micro and macronutrients play an optimum role in the maintenance of biochemical processes, plant growth, and high plant yield if they are up taken in a controlled way, transported to a long distance, and then correctly utilize. Si application against chromium (Cr) and Cd stress improved the utilization of macro (Ca^{++}, Mg^{++}, and K^{+}) and microelements (Fe and Zn) (Tripathi et al., 2012). Our results showed a strong positive correlation between Si and K^{+} concentration, which means with the increase of Si concentration in solution K^{+} would also be increased simultaneously (*Fig. 4*). Previous studies (Jayakannan et al., 2013) showed that Si application increased K^{+} concentration plants under abiotic stresses. According to our hypothesis, Si might improve K^{+} concentration in stressed-plants by mitigating nutrient imbalance created by Cd-stress. Our study showed that Si and K^{+} have positive effects on the production of ROS in plants under stress conditions (*Table 4*).

Conclusion

In conclusion, the addition of Si has been proved high-quality non-corrosive fertilizer under the hostile conditions of Cd-stressed wheat seedlings as a study herein. Our data demonstrated that Si supplementation, with the preference of root application, significantly improved growth traits by successfully encountered toxic belongings of Cd stress. Si root-application enhanced all recorded parameters such as photosynthetic pigments, enzymatic (CAT, SOD, POD), and non-enzymatic (proline) antioxidants and demolished MDA, H_2O_2, and Cd contents. Si showed the antagonistic effect with Cd concentration in plants and showed synergetic effect with essential nutrients like K and N. After analyzing the recorded data, we can be strongly emphasized that Si supplementation with the preference of root-application must be used as an optimum approach to reduce Cd toxicity in wheat plants.

http://www.aloki.hu ● ISSN 1589 1623 (Print) ● ISSN 1785 0037 (Online)
DOI: http://dx.doi.org/10.15666/aeer/1802_33493371

Acknowledgments. The authors would like to extend their sincere gratitude to the Agriculture Water and Soil Environment Field Science Research Station, China, for the permission to carry out the research. The Central Public-Interest Scientific Institution supported this research Basal Research Fund (Farmland Irrigation Research Institute, CAAS, FIRI2013-17), by the Agricultural Science and Technology Innovation Program (Grant no. CAAS-ASTIP-FIRE-03), Chinese Academy of Agricultural Sciences and by the National Natural Science Foundation of China (Grant no. 51679241, 51709265).

REFERENCES

[1] Ali, B., Qian, P., Jin, R., Ali, S., Khan, M., Aziz, R., Tian, T., Zhou, W. (2014): Physiological and ultra-structural changes in Brassica napus seedlings induced by cadmium stress. – Biologia Plantarum 58: 131-138.

[2] Ali, S., Zeng, F., Cai, S., Qiu, B., Zhang, G. (2011): The interaction of salinity and chromium in the influence of barley growth and oxidative stress. – Plant Soil Environ 57: 153-159.

[3] Ali, S., Farooq, M., Jahangir, M., Abbas, F., Bharwana, S., Zhang, G. (2013): Effect of chromium and nitrogen form on photosynthesis and anti-oxidative system in barley. – Biologia Plantarum 57: 758-763.

[4] Alzahrani, Y., Kuşvuran, A., Alharby, H. F., Kuşvuran, S., Rady, M. M. (2018): The defensive role of silicon in wheat against stress conditions induced by drought, salinity or cadmium. – Ecotoxicol Environ Saf 154: 187-196.

[5] Azevedo, R. A., Gratão, P. L., Monteiro, C. C., Carvalho, R. F. (2012): What is new in the research on cadmium-induced stress in plants? – Food and Energy Security 1: 133-140.

[6] Balakhnina, T., Bulak, P., Nosalewicz, M., Pietruszewski, S., Włodarczyk, T. (2015): The influence of wheat Triticum aestivum L. seed pre-sowing treatment with magnetic fields on germination, seedling growth, and antioxidant potential under optimal soil watering and flooding. – Acta Physiologiae Plantarum 37: 59.

[7] Dixit, V., Pandey, V., Shyam, R. (2001): Differential antioxidative responses to cadmium in roots and leaves of pea (Pisum sativum L. cv. Azad). – Journal of Experimental Botany 52: 1101-1109.

[8] Dong, Q., Fang, J., Huang, F., Cai, K. (2019): Silicon amendment reduces soil Cd availability and Cd uptake of two Pennisetum species. – International Journal of Environmental Research and Public Health 16: 1624.

[9] Farooq, M. A., Ali, S., Hameed, A., Ishaque, W., Mahmood, K., Iqbal, Z. (2013): Alleviation of cadmium toxicity by silicon is related to elevated photosynthesis, antioxidant enzymes; suppressed cadmium uptake and oxidative stress in cotton. – Ecotoxicology and Environmental Safety 96: 242-249.

[10] Fırat, M., Bakırdere, S., Fındıkoğlu, M. S., Kafa, E. B., Yazıcı, E., Yolcu, M., Büyükpınar, Ç., Chormey, D. S., Sel, S., Turak, F. (2017): Determination of trace amount of cadmium using dispersive liquid-liquid microextraction-slotted quartz tube-flame atomic absorption spectrometry. – Spectrochimica Acta Part B: Atomic Spectroscopy 129: 37-41.

[11] Flister, L., Galushko, V. (2016): The impact of wheat market liberalization on the seed industry's innovative capacity: an assessment of Brazil's experience. – Agricultural and Food Economics 4: 11.

[12] Foyer, C. H., Noctor, G. (2005): Redox homeostasis and antioxidant signaling: a metabolic interface between stress perception and physiological responses. – The Plant Cell 17: 1866-1875.

[13] Fu, S., Wei, C. Y. (2013): Multivariate and spatial analysis of heavy metal sources and variations in a large old antimony mine, China. – Journal of Soils and Sediments 13: 106-116.

http://www.aloki.hu ● ISSN 1589 1623 (Print) ● ISSN 1785 0037 (Online)
DOI: http://dx.doi.org/10.15666/aeer/1802_33493371

[14] Gadallah, M. (1999): Effects of proline and glycinebetaine on Vicia faba responses to salt stress. – Biologia Plantarum 42: 249-257.
[15] Gratão, P. L., Polle, A., Lea, P. J., Azevedo, R. A. (2005): Making the life of heavy metal-stressed plants a little easier. – Functional Plant Biology 32: 481-494.
[16] Hamayun, M., Sohn, E.-Y., Khan, S. A., Shinwari, Z. K., Khan, A. L., Lee, I.-J. (2010): Silicon alleviates the adverse effects of salinity and drought stress on growth and endogenous plant growth hormones of soybean (Glycine max L.). – Pakistan Journal of Botany 42: 1713-1722.
[17] Hashemi, A., Abdolzadeh, A., Sadeghipour, H. R. (2010): Beneficial effects of silicon nutrition in alleviating salinity stress in hydroponically grown canola, Brassica napus L., plants. – Soil Science & Plant Nutrition 56: 244-253.
[18] Howladar, S. M., Al-Robai, S. A., Al-Zahrani, F. S., Howladar, M. M., Aldhebiani, A. Y. (2018): Silicon and its application method effects on modulation of cadmium stress responses in Triticum aestivum (L.) through improving the antioxidative defense system and polyamine gene expression. – Ecotoxicol Environ Saf 159: 143-152.
[19] Jayakannan, M., Bose, J., Babourina, O., Rengel, Z., Shabala, S. (2013): Salicylic acid improves salinity tolerance in Arabidopsis by restoring membrane potential and preventing salt-induced K+ loss via a GORK channel. – Journal of Experimental Botany 64: 2255-2268.
[20] Kabir, A. H., Hossain, M. M., Khatun, M. A., Mandal, A., Haider, S. A. (2016a): Role of silicon counteracting cadmium toxicity in alfalfa (Medicago sativa L.). – Frontiers in Plant Science 7: 1117.
[21] Kabir, A. H., Hossain, M. M., Khatun, M. A., Mandal, A., Haider, S. A. (2016b): Role of silicon counteracting cadmium toxicity in alfalfa (Medicago sativa L.). – Front Plant Sci 7: 1117.
[22] Keeping, M. G. (2017): Uptake of silicon by sugarcane from applied sources may not reflect plant-available soil silicon and total silicon content of sources. – Frontiers in Plant Science 8: 760.
[23] Kim, Y. H., Khan, A. L., Waqas, M., Shim, J. K., Kim, D. H., Lee, K. Y., Lee, I. J. (2014): Silicon application to rice root zone influenced the phytohormonal and antioxidant responses under salinity stress. – Journal of Plant Growth Regulation 33: 137-149.
[24] Kim, Y. H., Khan, A. L., Waqas, M., Lee, I.-J. (2017): Silicon regulates antioxidant activities of crop plants under abiotic-induced oxidative stress: a review. – Frontiers in Plant Science 8: 510.
[25] Kusvuran, S., Kiran, S., Ellialtioglu, S. S. (2016): Antioxidant Enzyme Activities and Abiotic Stress Tolerance Relationship in Vegetable Crops. – In: Shanker A., Shanker, C. (eds.) Abiotic and Biotic Stress in Plants. InTech Open, London, pp. 481-503.
[26] Li, W., Xu, B., Song, Q., Liu, X., Xu, J., Brookes, P. C. (2014): The identification of 'hotspots' of heavy metal pollution in soil–rice systems at a regional scale in eastern China. – Science of the Total Environment 472: 407-420.
[27] Ma, J., Miyake, Y., Takahashi, E. (2001a): Silicon as a Beneficial Element for Crop Plants. – In: Datnoff, L. E. et al. (eds.) Silicon in Agriculture. Series: Studies in Plant Science, Vol. 8. Elsevier, Amsterdam, pp. 17-39.
[28] Ma, L. Q., Komar, K. M., Tu, C., Zhang, W., Cai, Y., Kennelley, E. D. (2001b): A fern that hyperaccumulates arsenic. – Nature 409: 579.
[29] Metzner, H., Rau, H., Senger, H. (1965): Untersuchungen zur Synchronisierbarkeit einzelner Pigmentmangel-Mutanten von Chlorella. (Studies on synchronization of some pigment-deficient Chlorella mutants.) – Planta 65: 186-194.
[30] Moussa, H. R. (2006): Influence of exogenous application of silicon on physiological response of salt-stressed maize (Zea mays L.). – International Journal of Agriculture and Biology 8: 293-297.

http://www.aloki.hu ● ISSN 1589 1623 (Print) ● ISSN 1785 0037 (Online)
DOI: http://dx.doi.org/10.15666/aeer/1802_33493371

[31] Nwugo, C. C., Huerta, A. J. (2008): Effects of silicon nutrition on cadmium uptake, growth and photosynthesis of rice plants exposed to low-level cadmium. – Plant and Soil 311: 73-86.
[32] Prabagar, S., Hodson, M. J., Evans, D. E. (2011): Silicon amelioration of aluminium toxicity and cell death in suspension cultures of Norway spruce (Picea abies (L.) Karst.). – Environmental and Experimental Botany 70: 266-276.
[33] Rady, M. M., Hemida, K. A. (2015): Modulation of cadmium toxicity and enhancing cadmium-tolerance in wheat seedlings by exogenous application of polyamines. – Ecotoxicology and Environmental Safety 119: 178-185.
[34] Ranieri, A., Castagna, A., Scebba, F., Careri, M., Zagnoni, I., Predieri, G., Pagliari, M., di Toppi, L. S. (2005): Oxidative stress and phytochelatin characterisation in bread wheat exposed to cadmium excess. – Plant Physiol Biochem 43: 45-54.
[35] Rascio, N., Navari-Izzo, F. (2011): Heavy metal hyperaccumulating plants: how and why do they do it? And what makes them so interesting? – Plant Science 180: 169-181.
[36] Rezvani, M., Zaefarian, F. (2011): Bioaccumulation and translocation factors of cadmium and lead in 'Aeluropus littoralis'. – Australian Journal of Agricultural Engineering 2: 114.
[37] Rios, J. J., Martínez-Ballesta, M. C., Ruiz, J. M., Blasco, B., Carvajal, M. (2017): Silicon-mediated improvement in plant salinity tolerance: the role of aquaporins. – Frontiers in Plant Science 8: 948.
[38] Rizwan, M., Meunier, J.-D., Miche, H., Keller, C. (2012): Effect of silicon on reducing cadmium toxicity in durum wheat (Triticum turgidum L. cv. Claudio W.) grown in a soil with aged contamination. – Journal of Hazardous Materials 209: 326-334.
[39] Şen, A. (2012): Oxidative Stress Studies in Plant Tissue Culture. – In: El-Missiry, M. A. (ed.) Antioxidant Enzyme. InTech Open, London, pp. 59-88.
[40] Sergiev, P. V., Lavrik, I. N., Wlasoff, V. A., Dokudovskaya, S. S., Dontsova, O. A., Bogdanov, A. A., Brimacombe, R. (1997): The path of mRNA through the bacterial ribosome: a site-directed crosslinking study using new photoreactive derivatives of guanosine and uridine. – RNA 3: 464.
[41] Shahid, M., Pourrut, B., Dumat, C., Nadeem, M., Aslam, M., Pinelli, E. (2014): Heavy-metal-induced reactive oxygen species: phytotoxicity and physicochemical changes in plants. – Reviews of Environmental Contamination and Toxicology 232: 1-44.
[42] Sharma, P., Dubey, R. S. (2005): Modulation of nitrate reductase activity in rice seedlings under aluminium toxicity and water stress: role of osmolytes as enzyme protectant. – Journal of Plant Physiology 162: 854-864.
[43] Shi, G., Cai, Q., Liu, C., Wu, L. (2010): Silicon alleviates cadmium toxicity in peanut plants in relation to cadmium distribution and stimulation of antioxidative enzymes. – Plant Growth Regulation 61: 45-52.
[44] Shi, X., Zhang, C., Wang, H., Zhang, F. (2005): Effect of Si on the distribution of Cd in rice seedlings. – Plant and Soil 272: 53-60.
[45] Shi, Y., Zhang, Y., Yao, H., Wu, J., Sun, H., Gong, H. J. (2014): Silicon improves seed germination and alleviates oxidative stress of bud seedlings in tomato under water deficit stress. – Plant Physiol Biochem 78: 27-36.
[46] Silva, A., Nascimento, C., Gouveia-Neto, A. J. P. (2017): Assessment of cadmium phytotoxicity alleviation by silicon using chlorophyll a fluorescence. – Rev Environ Contam Toxicol 55: 648-654.
[47] Sommer, M., Kaczorek, D., Kuzyakov, Y., Breuer, J. J. (2006): Silicon pools and fluxes in soils and landscapes—a review. – Journal of Plant Nutrition and Soil Science 169: 310-329.
[48] Song, A., Li, Z., Zhang, J., Xue, G., Fan, F., Liang, Y. (2009): Silicon-enhanced resistance to cadmium toxicity in Brassica chinensis L. is attributed to Si-suppressed cadmium uptake and transport and Si-enhanced antioxidant defense capacity. – Journal of Hazardous Materials 172: 74-83.

http://www.aloki.hu ● ISSN 1589 1623 (Print) ● ISSN 1785 0037 (Online)
DOI: http://dx.doi.org/10.15666/aeer/1802_33493371

[49] Soylemezoglu, G., Demir, K., Inal, A., Gunes, A. (2009): Effect of silicon on antioxidant and stomatal response of two grapevine (Vitis vinifera L.) rootstocks grown in boron toxic, saline and boron toxic-saline soil. – Scientia Horticulturae 123: 240-246.
[50] Takahashi, R., Ishimaru, Y., Shimo, H., Ogo, Y., Senoura, T., Nishizawa, N. K., Nakanishi, H. (2012): The OsHMA2 transporter is involved in root-to-shoot translocation of Zn and Cd in rice. – Plant, Cell & Environment 35: 1948-1957.
[51] Tamás, L., Mistrík, I., Zelinová, V. (2017): Heavy metal-induced reactive oxygen species and cell death in barley root tip. – Environmental and Experimental Botany 140: 34-40.
[52] Treder, W., Cieslinski, G. (2005): Effect of silicon application on cadmium uptake and distribution in strawberry plants grown on contaminated soils. – Journal of Plant Nutrition 28: 917-929.
[53] Tripathi, D. K., Singh, V. P., Kumar, D., Chauhan, D. K. (2012): Rice seedlings under cadmium stress: effect of silicon on growth, cadmium uptake, oxidative stress, antioxidant capacity and root and leaf structures. – Chemistry and Ecology 28: 281-291.
[54] Vaculík, M., Lux, A., Luxová, M., Tanimoto, E., Lichtscheidl, I. (2009): Silicon mitigates cadmium inhibitory effects in young maize plants. – Environmental and Experimental Botany 67: 52-58.
[55] Vieira da Cunha, P. K., Araújo do Nascimento, W. C., da Silva, J. A. (2008): Silicon alleviates the toxicity of cadmium and zinc for maize (Zea mays L.) grown on a contaminated soil. – Journal of Plant Nutrition and Soil Science 171: 849-853.
[56] Wael, M. S., Mostafa, M. R., Taia, A. A. E.-M., Saad, M. H., Magdi, T. A. J. (2015): Alleviation of cadmium toxicity in common bean (Phaseolus vulgaris L.) plants by the exogenous application of salicylic acid. – The Journal of Horticultural Science and Biotechnology 90: 83-91.
[57] Wang, Y., Hu, Y., Duan, Y., Feng, R., Gong, H. (2016): Silicon reduces long-term cadmium toxicities in potted garlic plants. – Acta Physiologiae Plantarum 38: 211.
[58] Wuana, R. A., Okieimen, F. E. (2011): Heavy metals in contaminated soils: a review of sources, chemistry, risks and best available strategies for remediation. – International Scholarly Research Notices Ecology. https://doi.org/10.5402/2011/402647.
[59] Yang, X., Long, X., Ye, H., He, Z., Calvert, D., Stoffella, P. (2004): Cadmium tolerance and hyperaccumulation in a new Zn-hyperaccumulating plant species (Sedum alfredii Hance). – Plant and Soil 259: 181-189.
[60] Ye, J., Yan, C., Liu, J., Lu, H., Liu, T., Song, Z. (2012): Effects of silicon on the distribution of cadmium compartmentation in root tips of Kandelia obovata (S., L.) Yong. – Environmental Pollution 162: 369-373.
[61] Yu, H.-Y., Ding, X., Li, F., Wang, X., Zhang, S., Yi, J., Liu, C., Xu, X., Wang, Q. (2016): The availabilities of arsenic and cadmium in rice paddy fields from a mining area: the role of soil extractable and plant silicon. – Environmental Pollution 215: 258-265.
[62] Zabin, S. A., Howladar, S. M. (2015): Accumulation of Cu, Ni and Pb in selected native plants growing naturally in sediments of water reservoir dams, Albaha region, KSA. – Nature and Science of Sleep 13: 11-17.
[63] Zhang, C., Wang, L., Nie, Q., Zhang, W., Zhang, F. (2008): Long-term effects of exogenous silicon on cadmium translocation and toxicity in rice (Oryza sativa L.). – Environmental and Experimental Botany 62: 300-307.
[64] Zhang, Q., Yan, C., Liu, J., Lu, H., Duan, H., Du, J., Wang, W. (2014): Silicon alleviation of cadmium toxicity in mangrove (Avicennia marina) in relation to cadmium compartmentation. – Journal of Plant Growth Regulation 33: 233-242.
[65] Zhang, W., Cai, Y., Tu, C., Ma, L. Q. (2002): Arsenic speciation and distribution in an arsenic hyperaccumulating plant. – Science of the Total Environment 300: 167-177.

http://www.aloki.hu ● ISSN 1589 1623 (Print) ● ISSN 1785 0037 (Online)
DOI: http://dx.doi.org/10.15666/aeer/1802_33493371

[66] Zhao, F., Lombi, E., McGrath, S. (2003): Assessing the potential for zinc and cadmium phytoremediation with the hyperaccumulator Thlaspi caerulescens. – Plant and Soil 249: 37-43.
[67] Zhao, M., Liu, Y., Li, H., Cai, Y., Wang, M. K., Chen, Y., Xie, T., Wang, G. (2017): Effects and mechanisms of meta-sodium silicate amendments on lead uptake and accumulation by rice. – Environmental Science and Pollution Research 24: 21700-21709.

APPENDIX

1. Recipe of Hoagland's solution

The Hoagland's solution had composition (mg L^{-1}): (NH4)2SO4 48.2, MgSO4 65.9, K2SO4 15.9, KNO3 18.5, Ca (NO3)2 59.9, KH2PO4 24.8, Fe citrate 6.8, MnCl2.4H2O 0.9, ZnSO4.7H2O 0.11, CuSO4.5H2O 0.04, H3BO3 2.9, H2MoO4 0.01.

2. Recipe of Si treatment

Silicon (Si) as a silica nanoparticle prepared from sodium silicate. A measured amount of sodium silicate put into the double amount of boiling deionized distilled water in a petri dish for 10 min. For increasing its solubility, we added a small amount of KOH and further heated for 10 min. Continue stirring with a long-handled spoon and at the end added 2 to 3 drops of H_2O_2. The solution removed from heat stove and allowed it to cool at room temperature. Cooled solution transferred into a plastic bottle and sealed it up. From the prepared stock solution, we made subsolution of 3 mM/L and applied as SiF3 and SiR3. Both treatments Si and Cd were applied after 65 days of transplantation. The twelve treatments were arranged factorially in a randomized complete block design with three replications per treatments. A total number of pots were 36, and each pot contained 15 plants.

3. Recipe to determine nutrient elements in plant tissues

Cd and Si were measured in plant root and shoot dry masses by atomic absorption spectrometry method with some necessary modifications (Fırat et al., 2017). After 35 days of treatments, wheat plants were harvested and washed thoroughly with tap water, distilled water, and then with double distilled water. Plant samples were separated into roots and shoots and dried at 70 °C in the oven for 48 h, and ground into powder. Weighed 0.2 g of dried plant sample was placed into a microwave digestion tube. Added 10 ml of nitric acid and covered every sample with a lid. Later, it was put into the microwave digestion instrument and started to dissolve after selection of an appropriate program. After completion of digestion, tubes were removed and put the digestion solution into the PTFE digestion cup with a small number of repeated flushing. Digestion cups were placed on a hot plate at 220 °C temperature until the removal of 2-3 ml liquid. In the end, the digestion fluid was transferred into the 50 ml volumetric flask and made its volume up to 50 ml with double distilled water. Digestion solution used to measure Cd and Si concentrations in root and shoots by using an atomic absorption spectrophotometer (AAS) model AA-6300 SHIMADZU. The total contents of Cd and Si per plant were calculated from Cd and Si concentration (μg g^{-1}) and meant

http://www.aloki.hu ● ISSN 1589 1623 (Print) ● ISSN 1785 0037 (Online)
DOI: http://dx.doi.org/10.15666/aeer/1802_33493371

the dry weight of below- and above- ground parts. Total nitrogen was measured in plants by the method of (Brookes et al., 1985) with some modifications. Weighted 0.3 g of plant dry sample in digestion tubes with 4 ml of sulphuric acid was put on the curved stem small funnel into the digestion furnace and initiated to dissolve. The temperature was set to 220 °C for 2 h and boiled till brown, yellow endpoint. First, samples were heated at 380 °C and removed these digestion tubes from digestion furnace. Added 20 drops of hydrogen peroxide (H_2O_2) and samples were placed on hot plate and continue to heat again. This cycle was repeated 2-5 times to clear the digestion solution. At every cycle, the amount of H_2O_2 was decreased. The amount of H_2O_2 added to the blank was consistent with the maximum number of samples. After that, a few amounts of multiple flushing methods were transferred to the 100 ml volumetric flask. In the end, total nitrogen was determined in a solution using flow analyzer-3 of brand BRAN + LUEBBE, and potassium was determined in a solution using flame photometer FP6410.

4. Determination of biochemical parameters

For MDA measurement, 0.25 g leaf sample was homogenized in 5 ml 0.1% TCA. The homogenate was centrifuged at 10,000 ×g for 10 min. to 1 ml aliquot of the supernatant, 4 ml of 20% TCA containing 0.5% TBA was added. The mixture was heated at 95 °C for 30 min and then quickly cooled in the ice bath. After centrifugation at 10,000 ×g for 10 min, the absorbance of the supernatant at 532 nm was read and the value of the nonspecific absorption at 600 nm was subtract. The MDA content was calculated by using an extinction coefficient of 155 mM^{-1} cm^{-1}. For the measurement of H2O2, we weighted 0.5 g leaf tissues were homogenized in an ice bath with 5 ml 0.1% (W/V) trichloroacetic acid (TCA). The homogenate was centrifuged at 12000 × g for 15 min and 0.5 ml of the supernatant was added to 0.05 ml 10 mM potassium phosphate buffer (pH 7.0) and 1 ml 1 M KI. The absorbency of supernatant was assessed at 390 nm.

http://www.aloki.hu ● ISSN 1589 1623 (Print) ● ISSN 1785 0037 (Online)
DOI: http://dx.doi.org/10.15666/aeer/1802_33493371

EFFECT OF SALINITY STRESS ON SOME PHYSIOLOGICAL TRAITS OF BURNING BUSH

SHABANI, M.[1] – JAHANBAKHSH, S.[1*] – MEHRJERDI, M. Z.[2] – EBADI, A.[1]

[1]*Department of Agronomy and Plant Breeding, Faculty of Agriculture and Natural Resources, University of Mohaghegh Ardabili, End of University Street, Ardabil, Iran (phone: +98-45-3150-5106; fax: +98-45-3351-2204)*

[2]*Faculty of Agriculture, Shirvan Higher Education Complex, Shirvan, Iran*

**Corresponding author*
e-mail: jahanbakhsh@uma.ac.ir; phone: +98-91-4354-4213

(Received 18th Oct 2019; accepted 30th Jan 2020)

Abstract. Salinity is one of the most serious environmental stresses at the irrigated areas that causes problems for the plants and soil. *Kochia scoparia* is an annual plant of the Chenopodiaceae family, which can be a valuable source of forage growth using saline water. Salinity changes many traits and processes, including the amount of chlorophyll a and b, activity of antioxidant enzymes, protein content, and concentration of sodium and potassium in the plant. An experiment was performed with two salinity levels of 100 and 300 mM on *Kochia scoparia*. Among the measured traits, the levels of chlorophyll a, b, peroxidase and catalase specific enzyme activity, and protein content were not affected by salinity. In contrast, this plant limited sodium Influx and the amount entered accumulated in the stem. Also, the study results showed that potassium concentration in this plant significantly increased in the stem. The results of other studies indicate that potassium plays an important role in tolerance to salinity. Therefore, potassium has a function in tolerance to salinity in this plant.
Keywords: *catalase, K/Na ratio, peroxidase, potassium, sodium*

Introduction

In worldwide, the salinity is one of the main factors that cause losses of crop. The human activity including: extractions of oil, industrial waste production, salt usage for road way maintenance and intensive farming activity, are sources of soil salinization. The salinity of soil and freshwater exist in many places. The publication for this issue increased fivefold from 2004 to 2018 (Litalien and Zeeb, 2020).

Soil salinity is the most serious environmental constraint affecting the production of crops, which is estimated to affect 45 million hectares of irrigated lands and is expected to increase due to global climate changes and frequent irrigation operations (Rengasamy, 2010; Munns and Tester, 2008 quoted by Roy et al., 2014).

Kochia scoparia L. Schrad (Common name: burning bush) is an annual plant of the Chenopodiaceae family, tolerant to salinity and drought, which can be a valuable source of forage growth by saline water (Danesh Mesgaran and Stern, 2005; Riasi et al., 2008 quoted by Kafi et al., 2010).

Kochia scoparia exists in wide range of temperatures and climatic regions in the world, but this plant has adapted specifically to arid and semi-arid regions (Friesen et al., 2009 quoted by Casey, 2009). *Kochia* has shown that it is capable of rapid germination, which makes it possible to use the limited moisture content soil in the spring in arid and semi-arid regions (Eberlein and Fore, 1984 quoted by Casey, 2009). The seed germination occurs several times during the growing season, which enables the plant to use the advantage of moisture when available. The seeds of this plant are

http://www.aloki.hu ● ISSN 1589 1623 (Print) ● ISSN 1785 0037 (Online)
DOI: http://dx.doi.org/10.15666/aeer/1802_33733385

capable to germinate under severe stress conditions, such as lack of moisture, high salt, and high pH (Friesen et al., 2009 quoted by Casey, 2009).

An experiment was done on *Kochia scoparia* at five levels of 100:00, 75:25, 50:50, 25:75, and 00:100 tap water:seawater ratio, respectively. The total dry matter (g $plant^{-1}$) of *kochia* reduces in response to this condition. A trend of decline in linear phase was observed form the highest total dry matter in control plants (100:00) to 75:25, 50:50, 25:75, and 00:100 (the lowest) respectively. Additively, the relative growth rate (RGR, g g^{-1} d^{-1}) and Specific leaf area (SLA, cm^2 g^{-1}) were measured in this study. The RGR between 100:00, 75:25, 50:50 were not significant and between 25:75 and 00:100 it was significant. The SLA trait between 100:00, 25:75, and 00:100 were significant and between of 75:25, 50:50 it was not significant (Lopez-Aguilar et al., 2013).

The salinity effect was investigated on Indian and Sabzevar genotype of *kochia* at salinity of 5, 15, and 20 dS m^{-1}. Results show that salinity reduce yield of seed Sabzevar, although at high salinity levels the yield of seeds was 890 kg ha^{-1} that approximately 80% of yield at 5 dS m^{-1}. The seed production genotype of Indian great decreased with salinity raise (Kafi et al., 2010).

Salinity stress causes many physiological changes in plants, including the followings. According to the study of Agastian et al. (2000), chlorophyll and total carotenoid is significantly reduced by salinity. In tomato leaves, total chlorophyll (Chl-a + b) chlorophyll a and beta-carotene reduced with sodium chloride stress (Khavarinejad and Mostofi, 1998 quoted by Parida and Das, 2005).

With increasing salinity, the leaf protein content of *Bruguiera parviflora* reduced, which indicates that the protein synthesis process may be disturbed, or more probably, proteolytic activity increase (Parida et al., 2002). The soluble protein content in the berries increased under low salinity and reduced in high salinity (Agastian et al., 2000).

Salinity stress causes water deficiency as a result of osmotic effects on a wide range of metabolic activities of plants, and this water deficiency has resulted in oxidative stress due to the formation of reactive oxygen species (ROS) such as superoxides, proxy and hydroxy radicals. The (ROS) are by-products of hyper osmotic and ionic stress that interfere with cell membrane and cell death (Bohnert and Jensen, 1996 quoted by Parida and Das, 2005). With the increase of the formation of (ROS), enzyme activities of detoxification increase in these species (Apel and Hirt, 2004; Foyer and Noctor, 2005; Logan, 2005 quoted by Munns and Tester, 2008). In halophyte *Sesuvium portulacastrum*, antioxidant enzymes such as catalase, peroxidase and polyphenol oxidase increased to 600 mM and reduced slightly at higher levels (Rajaravindran and Natarajan, 2012). Agarwal and Pandey (2004) have been shown that salt treatment increased sodium and chloride ions in *Cassia angustifolia* seedlings and increased the activity of superoxide dismutase, catalase, peroxidase and polyphenol oxidase.

Sodium concentration in rice that was treated with NaCl was significantly higher. Also, potassium concentration was higher in older stems and leaves (Morales et al., 2012). For plants ability to distinguish between sodium and potassium, the K+/Na+ ratio index usage. There are many references for this index that can be determined for plants and their organs (Flowers, 2004). The K+/Na+ ratio in leaves of rice cultivars sensitive to salinity is significantly lower than that of salinity tolerant cultivars (Moradi and Ismail, 2007 quoted by Morales et al., 2012).

Regarding tolerance of *Kochia* to salinity, this study was done to investigate physiological cases mentioned above and to find some aspects of salinity response in this plant.

http://www.aloki.hu ● ISSN 1589 1623 (Print) ● ISSN 1785 0037 (Online)
DOI: http://dx.doi.org/10.15666/aeer/1802_33733385

Materials and methods

Sowing, sampling and experiment design

First, *Kochia* seed was sowed in sand and manure with a ratio of 3:1. Plant growth was carried out under greenhouse conditions (*Fig. 1*). About 3 to 4 weeks after planting, salt treatment at a concentration of 100 mM was performed. Two days after the treatment, samples from the roots, stems and leaves of treated and control plants were harvested in three replicates, and samples were transferred to a freezer at -70 °C. Then, the treatment was performed at a concentration of 300 mM and two days after treatment in three replications of leaves, stems and roots treatment and control plants, sampling was done with the same method as mentioned above. The experiment design which data can be analysis with two samples T-test.The controls for each treatment at 100 and 300 mM were selected separately and sampling was done. The controls for each treatment were selected separately, because environmental condition changed over time.

Figure 1. *Plants sowing in green house condition for salinity stress*

Extraction and measurement of chlorophyll

Wellburn (1994) method with partial modification was done to measure chlorophyll content. For this purpose, 50 mg of the leaf tissue well grinded with methanol in a mortar with pestle, and homogenized tissue was transferred to the microcentrifuge tubes. At the next stage, centrifugation was carried out at 5,000 rpm, the supernatant was transferred to a new tube and diluted with methanol. Using spectrophotometer (Smart Spec™ Plus, Bio-Rad), the absorbance of the resulting solution at wavelengths of 653 and 666 nm was read and chlorophyll a and b values were calculated using the following formulas:

$$Ca = 15.65\ A666 - 7.34\ A653$$

$$Cb = 27.05\ A653 - 11.21\ A666$$

http://www.aloki.hu ● ISSN 1589 1623 (Print) ● ISSN 1785 0037 (Online)
DOI: http://dx.doi.org/10.15666/aeer/1802_33733385

Sodium and potassium measurements

Munns et al. (2010) method with partial modification was used to measure sodium and potassium. The root, stem and leaf samples were dried in an oven at 70 °C for 48 h. The dried samples were then weighed, about 20 mg, and extracted using 1 Normal hydrochloric acid. The solution was thoroughly mixed with up and down movements and placed in a water bath for 45 min at 60 °C. During this period, the falcone is moved up and down to be mixed well with acid. Then, centrifuge was performed for 15 and 5 min at 5,000 rpm. The supernatant was transferred to the 50 ml falcon and the samples were diluted at a ratio of 1:10. Flame photometer model PFP7 (jenway) was used to measure sodium and potassium content.

Extraction of crude extract to measure enzyme activity and protein content

For this purpose, 50 mg of leaf was weighed and using sodium phosphate buffer (at a concentration of 0.1 M and pH = 6.8) based on Kar and Mishra (1976) method a homogenous solution was obtained. At the next stage, centrifugation at 10,000 (g) was carried out for 15 min at 2 °C. The supernatant was transferred to a new tube and kept at -20 °C until usage. At the extraction stage, the samples were kept on ice.

Measuring enzyme activity of peroxidase

The peroxidase enzyme activity was measured according to Mac Adam et al. (1992) method with partial modification. First 2810 µl of sodium phosphate buffer 0.1 M, 40 µl of 30 mM of hydrogen peroxide (H2O2) and 50 µl of Guaiacol solution of 200 mM were added to the 15 ml falcon. Then 100 µl of enzyme extract was added (total volume of the resulting solution was 3 ml). After moving the falcons up and down, the resulting solution was placed at room temperature for 10 min until the formation of tetraguaiacol from guaiacol (color of the solution was orange), and then absorption was read at 470 nm by spectrophotometer.

Measuring enzyme activity of catalase

Catalase activity was done according to Verma and Dubey (2003) procedure with partial modification. For this purpose, first 2840 µL of 0.1 M sodium phosphate buffer, 60 µl of hydrogen peroxide (H2O2) 1 M was added before starting the reaction and 100 µl of enzyme extract was also added. The falcon tube was moved up and down a few times to mix the reaction components and then placed at room temperature for 10 min to decompose hydrogen peroxide and the absorbance was read at 240 nm using spectrophotometer.

Measuring protein content

Protein content was measured according Bradford method (1976) with partial modification. First, a Stock 1 (mg/ml) of bovine serum albumin (BSA) was used to provide standards of protein. Then, using this we prepared series of dilutions of 10, 20, 30, 40, 50, 60, 70, 80, 90 and 100 (µg/ml) in a volume of 500 µl. At the next stage, 100 µl of each of these was mixed with 900 µl of Bradford solution (total volume of 1 ml), and absorption was read at 595 nm after 2 min. The final concentration of standards was 1, 2, 3, 4, 5, 6, 7, 8, 9 and 10 (µg/ml) in 1 ml of total volume.

In order to measure the protein content in extracted samples similar to the standard method. first 100 µl of the extracted solution was mixed with 900 µl of Bradford solution and absorption was read.

http://www.aloki.hu ● ISSN 1589 1623 (Print) ● ISSN 1785 0037 (Online)
DOI: http://dx.doi.org/10.15666/aeer/1802_33733385

Calculation of specific enzyme activity

In order to calculate the enzyme activity, volume activity was calculated according to *Equation 1* (Bisswanger, 2011, 2014):

$$\text{Volume activity}_{(\mu mol/min/ml)} = \frac{\text{absorption/min} \cdot \text{assay volume} \cdot \text{dilution factor}}{\text{absorption coefficient} \cdot \text{path length} \cdot \text{enzyme volume}} \quad \text{(Eq.1)}$$

Absorption coefficient of tetraguaiacol and H2O2 was 0.036 and 26.6 (mM^{-1}. cm^{-1}), respectively.

Then, the obtained value was used according to *Equation 2* in order to calculate the specific enzyme activity:

$$\text{Specific enzyme activity}_{(\mu mol/min/mg)} = \frac{\text{Volume activity}}{\text{protein concentration}} \quad \text{(Eq.2)}$$

Data analysis

The data obtained from the above were evaluated using software R version 3.2.3 for the normalization of the data. Comparison between control and treatment at 100 mM was done with two samples T-test. Also Comparison between control and treatment at 300 mM was done with two samples T-test. Two samples T-test were analyzed using software SAS 9.1. The correlation coefficients between traits were calculated by Pearson method with the R software. The figures were drawing by R software.

Results

Chlorophyll content

As shown in *Figure 2,* the levels of chlorophyll a and b at 100 mM level were higher in treatment than in control, and their level reduced to less than control with an increase at 300 mM. Of course, their difference was not significant.

Sodium and potassium content

The content of potassium and sodium in the stem, root and leaf is shown in *Figure 3,* which is described in the followings.

The concentration of potassium in the stem at level of 100 and 300 mM in treatment samples is higher than in control samples. These differences are significant at a concentration of 100 mM at $\alpha = 0.05$ and at a concentration of 300 mM at $\alpha = 0.01$.

The content of potassium in the root at treatment level of 100 and 300 mM in treatment samples was higher than in control samples. But these differences were not significant.

The content of potassium in the leaf samples at 100 mM in control was higher than in treatment samples. But at 300 mM, the content of potassium in the leaves in treatment was more than in control. The two concentrations of 100 and 300 mM were significant at $\alpha = 0.05$.

Sodium concentration in stem at both levels of 100 and 300 mM in treatment was higher than in control. As shown in *Figure 3,* this difference is only significant at $\alpha = 0.01$ at 100 mM.

http://www.aloki.hu ● ISSN 1589 1623 (Print) ● ISSN 1785 0037 (Online)
DOI: http://dx.doi.org/10.15666/aeer/1802_33733385

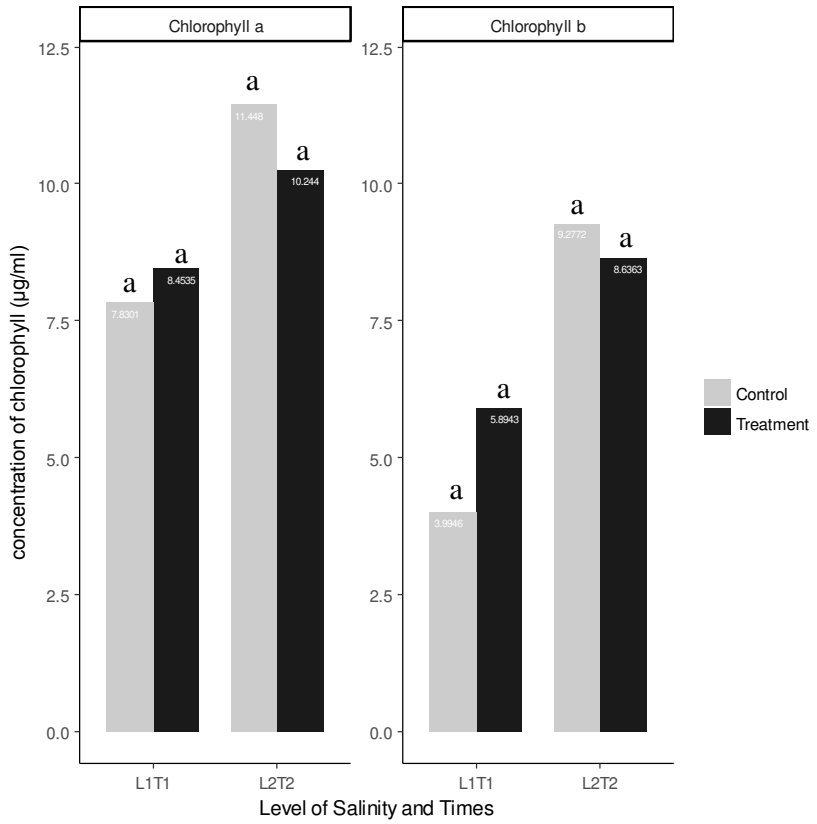

Figure 2. *Chlorophyll a and b content [L1T1: L1 = 100 mM level, T1 = two days after treatment] [L2T2: L2 = 300 mM level, T2 = two days after treatment]. Columns with a-a above are not significant*

Sodium content in the root at concentration of 100 mM is approximately not different in control and treatment samples, but in control samples it is more than in treatment samples at 300 mM. At both levels, the difference is not statistically significant.

Sodium concentration at leaf samples at 100 mM in control samples was more than in treatment samples. It is equal at 300 mM. Only at 100 mM level, a statistically significant difference was found at $\alpha = 0.05$.

K/Na ratio in stems, roots and leaves

As shown in *Figure 4,* the K/Na ratio in stem at 100 mM level in control sample was higher than in treatment samples, but at 300 mM at treatment it was higher than control. Neither of the two levels of this ratio was significant.

The K/Na ratio in root at both levels of 100 and 300 mM in treatment was higher than control and neither was statistically significant.

The K/Na ratio in leaf in treatment was higher than in control at both level and neither was statistically significant.

Protein content

As shown in *Figure 5,* protein content at the salinity level of 100 mM in control samples is higher than in treatment samples although it is reversed by increasing salinity to 300 mM. but neither was statistically significant.

http://www.aloki.hu ● ISSN 1589 1623 (Print) ● ISSN 1785 0037 (Online)
DOI: http://dx.doi.org/10.15666/aeer/1802_33733385

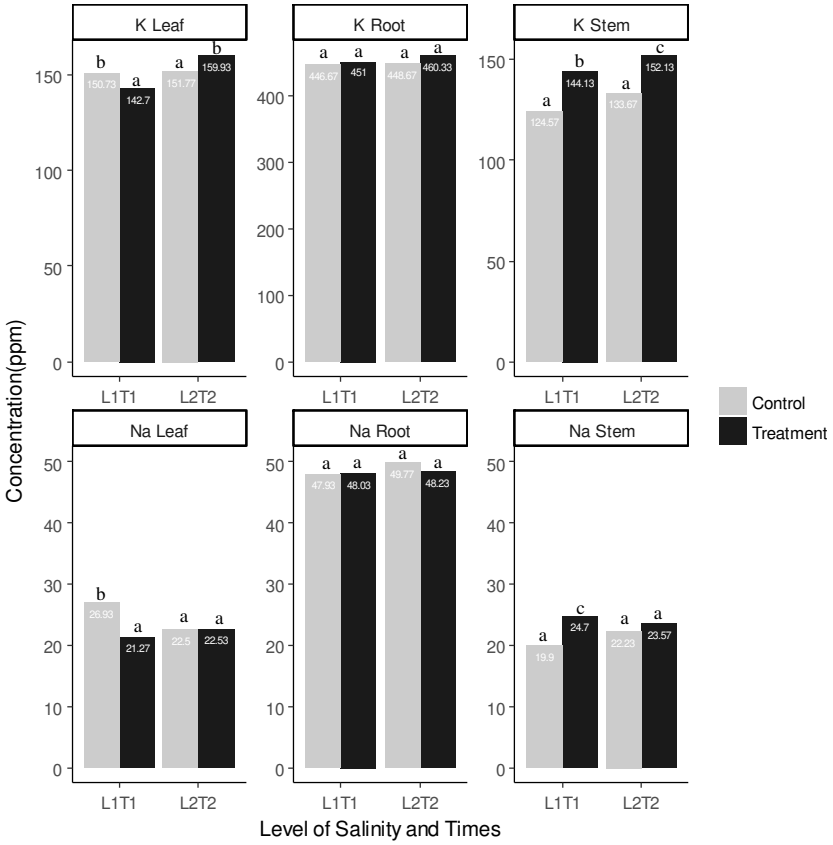

Figure 3. *Potassium and sodium content in stems, roots and leaves. columns with a-a above are not significant. Columns with a-b and a-c above are significant at α = 0.05 and α = 0.01 respectively. Legend same as Figure 2*

Peroxidase

According to *Figure 6,* the activity of this enzyme at 100 mM concentration and two days after the treatment was more than control, and it was equal at a concentration of 300 mM. Of course, there is no statistically significant difference between them.

Catalase

As showed in *Figure 6,* the specific enzyme activity of catalase at 100 mM concentration in control was higher than in treatment, but vice versa at 300 mM concentration. Although these differences were not significant.

Study of correlation coefficients

The values of correlation coefficients are given in *Figure 7*. Among all correlation coefficients, 14 cases were significant at $\alpha = 0.05$. Among correlation coefficients, chlorophyll a and protein, chlorophyll b and leaf K/Na ratio, stem Na and stem K, stem Na and leaf K/Na ratio, leaf K and protein, leaf K and stem K/Na ratio, stem K and root K, stem K and leaf K/Na ratio showed significant and positive correlation. However, between chlorophyll a and peroxidase, protein and peroxidase, leaf Na and stem Na, leaf Na and stem K, leaf Na and leaf K/Na ratio, root Na and root K/Na ratio a significant and negative correlation was found.

http://www.aloki.hu ● ISSN 1589 1623 (Print) ● ISSN 1785 0037 (Online)
DOI: http://dx.doi.org/10.15666/aeer/1802_33733385

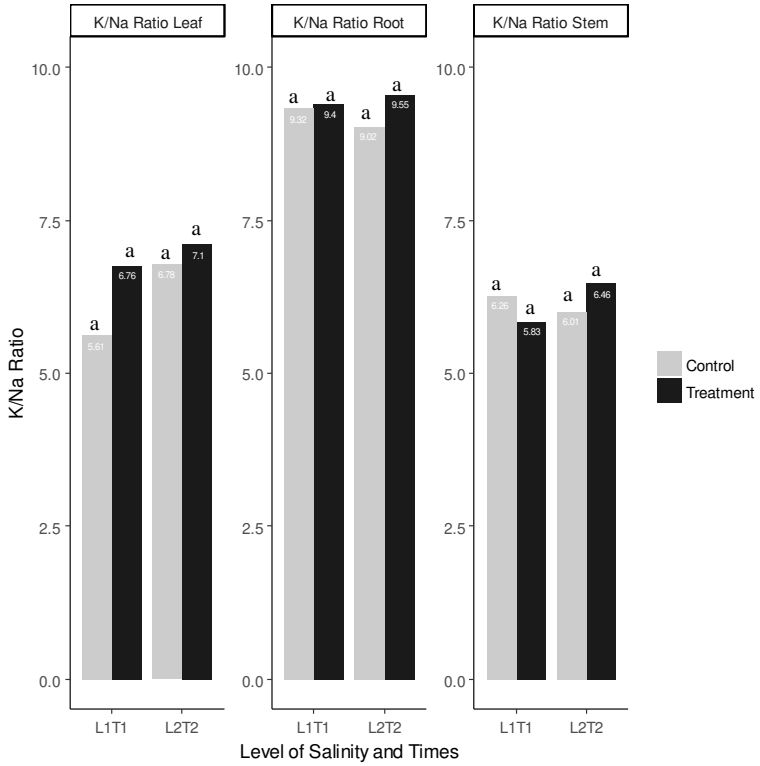

Figure 4. *The K/Na ratio in stems roots and leaves. Columns with a-a above are not significant. Legend same as Figure 2*

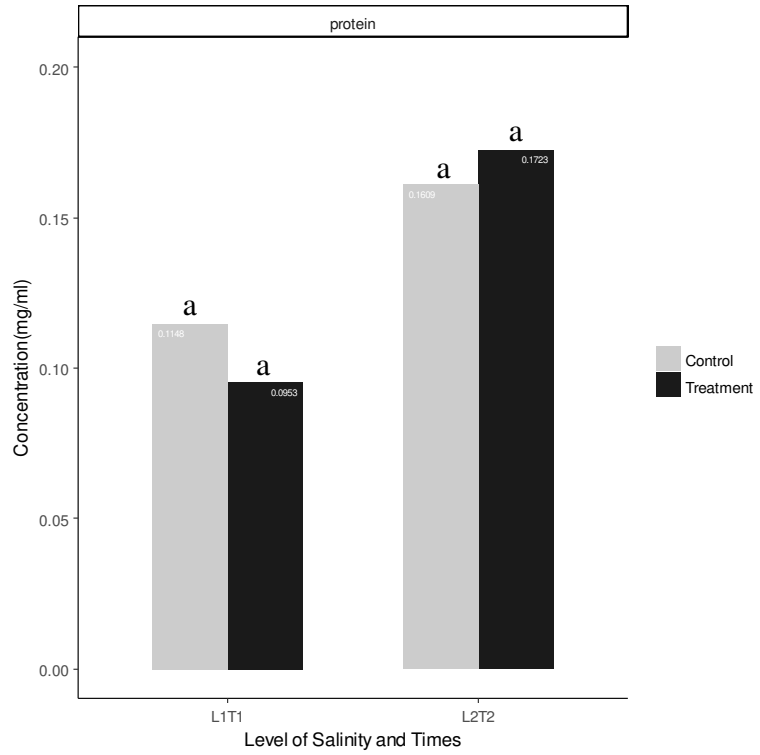

Figure 5. *Protein content in leaves. Columns with a-a above are not significant. Legend same as Figure 2*

http://www.aloki.hu ● ISSN 1589 1623 (Print) ● ISSN 1785 0037 (Online)
DOI: http://dx.doi.org/10.15666/aeer/1802_33733385

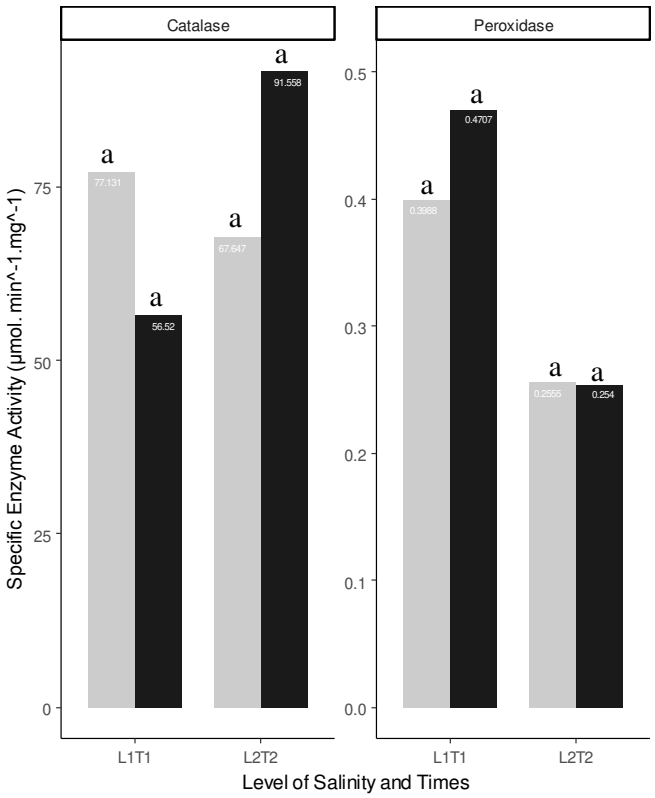

Figure 6. *Specific enzyme activity of peroxidase and catalase. Columns with a-a above are not significant. Legend same as Figure 2*

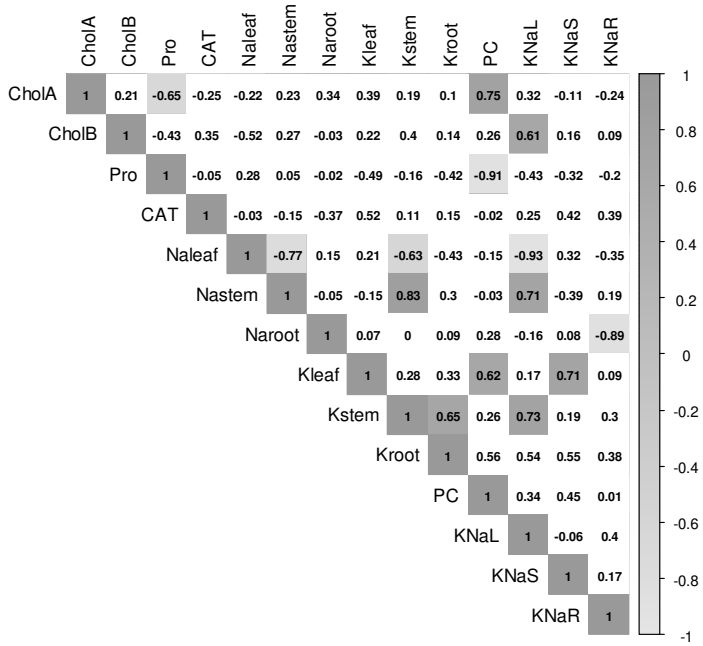

Figure 7. *Pearson correlation coefficients between the measured traits. Colour boxes are significant at α = 0.05, right bar shows the direction (positive and negative) and degree (colour intensity, from 1 to – 1) of correlation). CholA: chlorophyll a, CholB: Chlorophyll b, Pro: Peroxidase, CAT: Catalase, PC: Protein content, KNaL: leaf K/Na ratio, KNaS: Stem K/Na ratio, KNaR: Root K/Na ratio*

http://www.aloki.hu ● ISSN 1589 1623 (Print) ● ISSN 1785 0037 (Online)
DOI: http://dx.doi.org/10.15666/aeer/1802_33733385

Discussion

Chlorophyll a and b and total carotenoid in *Morus alba* L were affected differently by salinity, but their total amount reduced with salinity (Agastian et al., 2000).

The leaf chlorophyll content of *Bruguiera parviflora* increased by 6% in plants treated with 100 mM of NaCl compared to the control plants, and then reduced at 200 and 400 mM (Parida et al., 2004).

Leaf total chlorophyll and carotenoid reduced under salt stress (Parida and Das, 2005). But Wang and Nil (2000) quoted by Parida and Das (2005) reported that chlorophyll content increased under salinity conditions in Amaranthus.

But results of this study showed that Chlorophyll a and b at 100 mM level in treatment was higher than in control, while at 300 mM level this relationship was reversed, however, neither was significant. The study results showed that salinity had no significant effect on the amount of chlorophyll a and b.

The most important trait among salinity specific traits is the plant's ability to limit the high accumulation of sodium entering into xylems. This trait is described by the term "Na^+ exclusion". Within a species or even within a genus, sodium concentration in leaves can be considered as a sign of relative ability to "exclude Na^+", especially if well-defined tissues are sampled (Colmer et al., 2006). According to *Figure 3,* it seems that the plant allows low sodium entering the root, but the low amount entered accumulated in the stem. In leaves at L1T1, sodium is higher in control sample than in treatment sample with unknown reason, but in L2T2 it is reduced and equal in both samples.

The high salt uptake competes with other nutrient ions uptake, especially potassium, that cause deficiency of this element. An increase in sodium chloride treatment induces an increase in sodium and chloride and leads to a reduction in calcium, potassium and magnesium in a number of plants (Khan et al., 1999, 2000; Khan and Aziz, 2001 quoted by Parida and Das, 2005). As shown in *Figure 3,* in stems, roots and leaves at two levels and times, which for each element is six cases in total, in three cases potassium is higher in the treatment compared to the control, and in one case control is more than the treatment and is statistically significant. But sodium is significant in two cases, that one is more in control and one more in treatment. According to these results, it seems that in the competition between potassium and sodium, more potassium enters the plant, which is contrary to the above-mentioned works. With low sodium uptake, this substance accumulates less in the plant and prevents the toxicity it can cause.

The plant cells require high levels of potassium to maintain normal metabolic reactions. Potassium also plays an important role in maintaining turgor pressure (Sairam and Tyagi, 2004). It is possible that the plant at the early stages that is exposed to water deficiency stress also absorbs more potassium to maintain turgor pressure. It is also necessary to maintain the uptake of potassium and transfer to growing tissues for salinity tolerance (Greenway and Munns, 1980 quoted by Colmer et al., 2006). These reasons can be explanations to the increased K uptake of this plant.

Analysis of ions had shown that tolerant genotypes had lower sodium concentration in the shoot, and more potassium in the shoot that sensitive genotypes. Salt-tolerant crops are characterized by absorbing more potassium than sodium (Teakle and Tyerman, 2010; Kausar et al., 2014 quoted by Oyiga et al., 2016). The ratio of K/Na was significantly higher in the shoot compared to sensitive ones, which is due to high concentration of potassium in the shoot and low concentration of sodium in the shoot. The optimum ratio of K/Na plays an important role in maintaining the optimum osmotic

http://www.aloki.hu ● ISSN 1589 1623 (Print) ● ISSN 1785 0037 (Online)
DOI: http://dx.doi.org/10.15666/aeer/1802_33733385

potential and membrane potential for regulating cell volume in the plant under salinity stress and participate in increasing the tolerance of salinity in wheat (El-Hendawy et al., 2009 quoted by Oyiga et al., 2016). According to *Figure 4,* in most cases, K/Na ratio is higher in the treatment plants, which indicates the *kochia* tolerance to salinity and as mentioned above has a role in salinity tolerance of this plant.

As mentioned in Introduction, with the increase of hyperosmotic stresses, the activity of antioxidant enzymes increases. According to *Figure 6,* the activity of peroxidase in L1T1 in stressed plants is more than in the control, but catalase at this level and time in the control samples is more than in the treatment. In L2T2, the activity of catalase in treatment is more than in control, and peroxidase at this level and time is almost equal in the control and in the treatment. It can be said that the function of both enzymes is the opposite of each other except of L2T2 peroxidase that was different. Although these differences are not significant, they are remarkable. Probably a factor or process makes these two enzymes at any time and level one is higher for lower energy consumption.

As shown in *Figure 7,* a significant and negative correlation (r = -93) was found between the leaf Na and leaf K/Na ratio. Also, a significant and negative correlation was found between root Na and root K/Na ratio (r = -89). This result is consistent with the study results of Karimi et al. (2014) in safflower, which concluded that a negative and significant correlation was found between the leaf Na and leaf K/Na ratio, and the root Na and root K/Na ratio.

Furthermore, a significant and negative correlation was observed between chlorophyll a and peroxidase activity (r = -65). Moreover, a significant and positive correlation was found between chlorophyll a and protein content (r = 75). Anaya et al. (2017) reported a significant and positive correlation between chlorophyll a and peroxidase activity. They also observed a significant and negative correlation between chlorophyll a and protein. As mentioned, the study results were inconsistent with the study results of Anaya et al. (2017).

The results showed that salinity had no significant effect on chlorophyll a, b, peroxidase, catalase, and protein content. But this plant was limited sodium entering to the plant, and prevented its toxic effects. It also has been shown that potassium plays an important role in tolerance to salinity.

Acknowledgements. We thank to Masood Fakherfeshani, Ahmad Javai, Ghasem Parmoon, Jamshid Ardan, Ekhtiear Aghazade and others who helped in this work. This work was financed by a PhD fellowship from the University of Mohaghegh Ardabili.

REFERENCES

[1] Agarwal, S., Pandey, V. (2004): Antioxidant enzyme responses to NaCl stress in *Cassia angustifolia*. – Biologia Plantarum 48: 555-560.

[2] Agastian, P., Kingsley, S. J., Vivekanandan, M. (2000): Effect of salinity on photosynthesis and biochemical characteristics in mulberry genotypes. – Photosynthetica 38: 287-290.

[3] Anaya, F., Fghire, R., Wahbi, S., Loutfi, K. (2017): Antioxidant enzymes and physiological traits of *Vicia faba* L. as affected by salicylic acid under salt stress. – Journal of Materials and Environmental Sciences 8: 2549-2563.

[4] Bisswanger, H. (2011): Practical Enzymology. 2nd Ed. – Wiley-VCH Verlag & Co. KGaA, Weinheim.

http://www.aloki.hu ● ISSN 1589 1623 (Print) ● ISSN 1785 0037 (Online)
DOI: http://dx.doi.org/10.15666/aeer/1802_33733385

[5] Bisswanger, H. (2014): Enzyme assays. – Perspectives in Science 1: 41-55.
[6] Bradford, M. M. (1976): A rapid and sensitive method for the quantitation of microgram quantities of protein utilizing the principle of protein-dye binding. – Analytical Biochemistry 72: 248-254.
[7] Casey, P. A. (2009): Plant Guide for *Kochia* (*Kochia Scoparia*). – USDA-Natural Resources Conservation Service, Kansas Plant Materials Center, Manhattan, KS.
[8] Colmer, T. D., Flower, T. J., Munns, R. (2006): Use of wild relatives to improve salt tolerance in wheat. – Journal of Experimental Botany 57: 1059-1078.
[9] Flowers, T. J. (2004): Improving crop salt tolerance. – Journal of Experimental Botany 55: 307-319.
[10] Flowers, T. J., Flowers, S. A. (2005): Why does salinity pose such a different problem for plant breeders? – Agricultural Water Management 78: 15-24.
[11] Kafi, M., Asadi, H., Ganjeali, A. (2010): Possible utilization of high salinity waters and application of low amounts of water for production of the halophyte *Kochia scoparia* as alternative fodder in saline agroecosystems. – Agricultural Water Management 97: 139-147.
[12] Kar, M., Mishra, D. (1976): Catalase, peroxidase, and polyphenoloxidase activities during rice leaf senescence. – Plant Physiology 57: 315-319.
[13] Karimi, S., Arzani, A., Saeidi, G. (2014): Differential response of ion and osmolyte accumulation to salinity stress in salt-tolerant and salt-sensitive seedlings of safflower (*Carthamus tinctorius* L.). – Research on Crops 15: 802-809.
[14] Litalien, A., Zeeb, B. (2020): Curing the earth: A review of anthropogenic soil salinization and plantbased strategies for sustainable mitigation. – Science of the Total Environment 698: 1-15.
[15] Lopez-Aguilar, R., Rodriguez-Quezada, G., Lucero-Arce A., Naranjo-Murillo, A. (2013): Use of high-salinity waters to grow *Kochia scoparia* L. Schrad. as alternative fodder in saline environments in northwestern Mexico. – Interciencia 38(5): 325-331.
[16] Mac Adam, J. W., Sharp, R. E., Nelson, C. J. (1992): Peroxidase activity in the leaf elongation zone of tall fescue. – Plant Physiology 99: 872-878.
[17] Morales S. G., Tellez L. I. T., Merino, F. C. G., Caldana, C., Victoria, D. E., Cabrera, B. E. H. (2012): Growth, photosynthetic activity, and potassium and sodium concentration in rice plants under salt stress. – Acta Scientiarum Agronomy 34: 317-324.
[18] Munns, R., Tester, M. (2008): Mechanisms of salinity tolerance. – Annual Review of Plant Biology 59: 651-681.
[19] Munns, R., Wallace, P. A., Teakle, N. L., Colmer T. D. (2010): Measuring Soluble Ion Concentrations (Na+, K+, Cl−) in Salt Treated Plants. –In: Sunkar, R. (ed.) Plant Stress Tolerance. Methods in Molecular Biology Series, Vol. 639. Humana, Totowa, NJ, pp 371-382.
[20] Oyiga, B.C., Sharma, R. C., Shen, J., Baum, M., Ogbonnaya, F. C., Leonl, J., Ballvoral, A. (2016): Identification and characterization of salt tolerance of wheat germplasm using a multivariable screening approach. – Journal of Agronomy and Crop Science 202: 472-485.
[21] Parida, A. K., Das, A. B. (2005): Salt tolerance and salinity effects on plants: a review. – Ecotoxicology and Environmental Safety 60: 324-349.
[22] Parida, A., Das, A. B., Das, P. (2002): NaCl stress causes changes in photosynthetic pigments, proteins and other metabolic components in the leaves of a true mangrove, *Bruguiera parviflora*, in hydroponic cultures. – Journal of Plant Biology 45: 28-36.
[23] Parida, A. K., Das, A. B., Mittra, B. (2004): Effects of salt on growth, ion accumulation, photosynthesis and leaf anatomy of the mangrove *Bruguiera parviflora*. – Trees 18: 167-174.
[24] R core team. (2015). R: A language and environment for statistical computing. R Foundation for Statistical Computing, Vienna, Austria. URL https://www.R-project.org/.

http://www.aloki.hu ● ISSN 1589 1623 (Print) ● ISSN 1785 0037 (Online)
DOI: http://dx.doi.org/10.15666/aeer/1802_33733385

[25] Rajaravindran, M., Natarajan, S. (2012): Effects of salinity stress on growth and biochemical constituents of the halophyte *Sesuvium portulacastrum*. – International Journal of Research in Biological Sciences 2: 18-25.
[26] Roy, S. J., Negrao, S., Tester, M. (2014): Salt resistant crop plants. – Current Opinion in Biotechnology 26: 115-124.
[27] Sairam, R. K., Tyagi, A. (2004): Physiology and molecular biology of salinity stress tolerance in plants. – Current Science 86: 407-421.
[28] Verma, S., Dubey, R. S. (2003): Lead toxicity induces lipid peroxidation and alters the activities of antioxidant enzymes in growing rice plants. – Plant Science 164: 645-655.
[29] Wang, W., Vinocur, B., Altman, A. (2003): Plant responses to drought, salinity and extreme temperatures towards genetic engineering for stress tolerance. – Planta 218: 1-14.
[30] Wellburn, A. R. (1994): The spectral determination of chlorophylls a and b, as well as total carotenoids, using various solvents with spectrophotometers of different resolution. – Journal of Plant Physiology 144: 307-313.

http://www.aloki.hu ● ISSN 1589 1623 (Print) ● ISSN 1785 0037 (Online)
DOI: http://dx.doi.org/10.15666/aeer/1802_33733385

SEASONAL PHYTOPLANKTON COMMUNITY PATTERNS AND INFLUENCING FACTORS IN FISH-MUSSEL SYSTEMS

HU, B.J.[1,2] – HUANG, Y.Y.[1] – WU, L.Z.[1] – QIN, H.M.[3,4*] – HONG, Y.J.[1,2*]

[1]*School of Life Science, Nanchang University, Nanchang, Jiangxi Province, China*

[2]*Jiangxi Province Key Laboratory of Aquatic Animal Resources and Utilization, Nanchang University, Nanchang, Jiangxi Province, China*

[3]*Jiangxi Province Key Laboratory of Watershed Ecosystem Change and Biodiversity, Nanchang University, Nanchang, Jiangxi Province, China*

[4]*School of Life Sciences, Qufu Normal University, Qufu, Shandong Province, China*

**Corresponding author*
e-mail: qinhaiming@qfnu.edu.cn, yjhong@ncu.edu.cn

(Received 24th Oct 2019; accepted 12th Mar 2020)

Abstract. The rapid pearl farming industry causes environmental pollution to aquatic ecosystems. However, fish-mussel systems with highly productive, profitable and environment-friendly characteristics are appropriate aquaculture practices under the current polluted state of the environment in China. Phytoplankton are excellent indicators and play indispensable roles in maintaining the stability of a freshwater ecosystem. Therefore, samples were seasonally collected determine the seasonal phytoplankton community dynamics and potential driving factors in three subtropical reservoirs with integrated fish-mussel aquaculture. All water physicochemical parameters varied seasonally, and water quality had a trend of eutrophication. A total of 189 species were identified, among which Chlorophyta (83 species) dominated in species richness. Cyanophyta, in particular remained to be highly abundant (57.53% of the total seasonal biomass). The NMDS analysis indicated that summer was an independent branch. The CCA analysis and Spearman rank correlation analysis suggested that water temperature might be the main abiotic factor. Furthermore, pH, conductivity, DO, chlorophyll, TC and TN also significantly affected the community. The aquaculture enhanced the similarity in community structure which have happened due to predation pressure. The present study also identified the potential influences caused by the integrated fish-mussel aquaculture on phytoplankton seasonal succession, bringing some guidance to protect the reservoir ecosystem.
Keywords: *phytoplankton community structure, seasonal variation, reservoir ecosystem, predation pressure*

Introduction

Large scale freshwater pearl production began in the 1960s in China, and accounted for 95% of the freshwater pearl production of the world (Li, 2007), making China the most crucial contributor to the world's freshwater pearl production. However, rapid development of freshwater pearl farming causes environmental pollution. The traditional industry is facing urgent transformation and upgrading. Therefore, we have formed a fish-mussel system aiming at aquaculture water, "One Water, Two Treatments; One Mussel, Two Functions": the breeding of mussels and fish bring about the effective governance of aquaculture water, and mussels produce clean water and generate pearls (http://www.pyhfish.com/article-821-1.html). *Hyriopsis schlegelii* (*H. schlegelii*) was the very important producer of freshwater pearl in China due to its better quality of pearls, pretty breeding technology, and simple artificial pearl producing

http://www.aloki.hu ● ISSN 1589 1623 (Print) ● ISSN 1785 0037 (Online)
DOI: http://dx.doi.org/10.15666/aeer/1802_33873408

operation (Peng et al., 2012; He et al., 2013). Several aspects fundamentally accounted for the success of the freshwater pearl industry. Species with superduper performance of pearl production and continuously optimized culture models have contributed to the increasing annual freshwater pearl production, from approximately 3.5 tons during the period of 1958-1971 to approximately 4,448.34 tons during the period of 2002-2007 (Bai et al., 2014).

It is well known that freshwater pearl mussel, bighead carp and silver carp are aquaculture animals with high economic value, mainly grazing plankton. Among these culture models, integrated fish-mussel aquaculture, which cultures some filter fish, such as silver carp and bighead carp, into the water body with mussels, was practical, and improved water quality deterioration (Neori et al., 2004). Meanwhile, the concentrations of nitrogen, phosphorus and organics decreased in a planktivorous fish-mussel system, with an increase in the yield and growth of *H. cumingii* (Wang et al., 2009). Polyculture could improve the utilization efficiency of nutrients and water quality and increase yield, which has been widely applied for aquaculture (Milstein, 1992; Troell et al., 2003; Schneider et al., 2005). Water-quality deterioration and eutrophication might occur as a result of the significantly increased concentrations of nitrogen and phosphorus, which lead to cyanobacterial blooms, and bring negative impacts on photosynthesis in submerged plants on the account of blocking light (Hauxwell et al., 2001). This would further lessen the dissolved oxygen and might destroy aquatic ecosystems (Guo et al., 2009). However, various studies have focused on the optimization of the aquaculture production models, which were mainly on the integrated combination and management regimes. Researches with regard to production efficiency under the combination of various species were conducted by Tang et al. (2015) and Yan et al. (2009). Zheng et al. (2018) conducted a preliminary study on optimizing water quality and bacterial community in fish-mussel systems by regulating the C/N ratio. However, little attention was attached to the impact on the water ecosystem (including phytoplankton distribution, composition, etc.) caused by integrated fish-mussel aquaculture, even though phytoplankton was the most basic and nuclear primary producer, and contributed high effects on the dynamic equilibrium and relative stabilization. Furthermore, diatoms even affected the atmospheric CO_2 levels, considering that phytoplankton occupies a crucial position in the water ecosystem (Meyer et al., 2017; Leblanc et al., 2018; Milligan and Morel, 2012).

In particular, the diversity and richness of species generally exist in subtropical reservoirs, and Connell (1978) indicated determining factors that maintain the diversity in an ecosystem is crucial. Phytoplankton, as a kind of excellent bait for aquatic animals, and helps to better manage and maintain the sustainable utilization of water resources. Degefu et al. (2011) evaluated the potential impact of Nile Tilapia cage culture on water quality, and the zooplankton and phytoplankton community. It was indicated that cage culture enhanced the ammonium nitrogen levels and Cyanobacteria as a dominator, contributing 84% of the total phytoplankton abundance. In addition, And (1999) discovered that water quality deteriorated, and that the diversity and abundance of phytoplankton changed in shrimp ponds. Furthermore, Nile tilapia and *Macrobrachium rosenbergii* poluculture reduced the phytoplankton biovolume, and afternoon pH level was lower, when compared to prawn monoculture (Danaher et al., 2007). Rainbow trout cage cultures decreased the dissolved oxygen, and made *Daphnia sp.* dominant species (90% of the zooplankton), according to a study (Cornel and Whoriskey, 1993). Nevertheless, studies on the cumulative effect of natural- and

http://www.aloki.hu ● ISSN 1589 1623 (Print) ● ISSN 1785 0037 (Online)
DOI: http://dx.doi.org/10.15666/aeer/1802_33873408

human-induced processes on environment factors and phytoplankton in *H. schlegelii*-bighead carp and silver carp systems remains scarce. It is expected that the seasonal pattern of phytoplankton could be influenced by fish-mussel polyculture. In order to investigate the hypothesis, the seasonal investigation of phytoplankton was conducted from August 2017 to March 2018 in three sub-tropic reservoirs with integrated fish-mussel aquaculture. The specific aims were as follows: (1) to determine the seasonal variation and succession rules in the phytoplankton community, and the potential driving factors; (2) to clarify whether the fish-mussel polyculture might induce the similarity of phytoplankton community between seasons.

Materials and methods

Experimental design

Duchang county is the most important freshwater pearl production region in China. Experiments were carried out in Dagang (DG, with fish feed), Zhouxi (ZX, with bio-feeding) and Hetang (HT, with organic fertilizer) in reservoirs located in Duchang county. The three reservoirs are about 8 acers and 10 m deep. And these reservoirs were cleaned and sterilized by lime prior to experiments. The conditions and the placing of plots were similar for these three experimental plots, with alike water supply and husbandry management. Bighead carps and silver carps were left to swim freely, and H. schlegelii were hung in the water column at approximately 50 cm below the water surface (8 mussels in each water column, 600 columns in each acer). The whole aquatic organisms were purchased from local commercial farms.

Sampling design

Phytoplankton were seasonally sampled (spring = March, summer = August, autumn = October, and winter = December) at three points in three reservoirs from August 2017 to March 2018. The sampling points were set according to the occupation area of each reservoir, and sampling was performed for three times for each point (*Fig. 1*). At approximately 100 cm below the water surface, 10 L of mixed water were collected using a 10-L modified Schindler–Patalas sampler. A plankton net with a mesh size width of 64 μm was used to filter the water, and phytoplankton were collected from the end of the net and placed into a 10-ml plastic tubing with 1% Lugol's solution. Counting and identifying were conducted under a microscope (Olympus SZ61, Japan; Olympus CX23, Korea). The biomass of the phytoplankton (wet weight) was calculated, according to the study conducted by Zhang and Huang (1991). For the physico-chemical parameters, WT, pH, conductivity (Cond), dissolved oxygen (DO), turbidity (Turb) and Chl-a were measured for three times in situ using a Multifunction Water Quality Monitor (YSI 6600 V2, USA). Then, 25 ml of water was collected from each sampling point with two replications. The samples were storing at -20 ℃ in a laboratory, and the total nitrogen (TN) and total carbon (TC) were determined using a carbon-nitrogen analyzer.

The 1 L of collected water was filtered through a Whatman GF/F fiberglass filter membrane (burned at 450 ℃ for 2 h before removing the organic matter), which had a diameter of 25 mm. Then, the membrane was dried under 60 ℃ for 48 h, and allowed to cool after weighing in the dryer. The dried GF/F fiberglass filter membrane was burned at 450 ℃ for 2 h and weighted (ash weight after burning) again after cooling. The

http://www.aloki.hu ● ISSN 1589 1623 (Print) ● ISSN 1785 0037 (Online)
DOI: http://dx.doi.org/10.15666/aeer/1802_33873408

content of the particulate organic matter in the water sample was calculated according to the weight of the blank filter membrane, the dried sample filter membrane, and lost weight after burning, and the volume of the water sample.

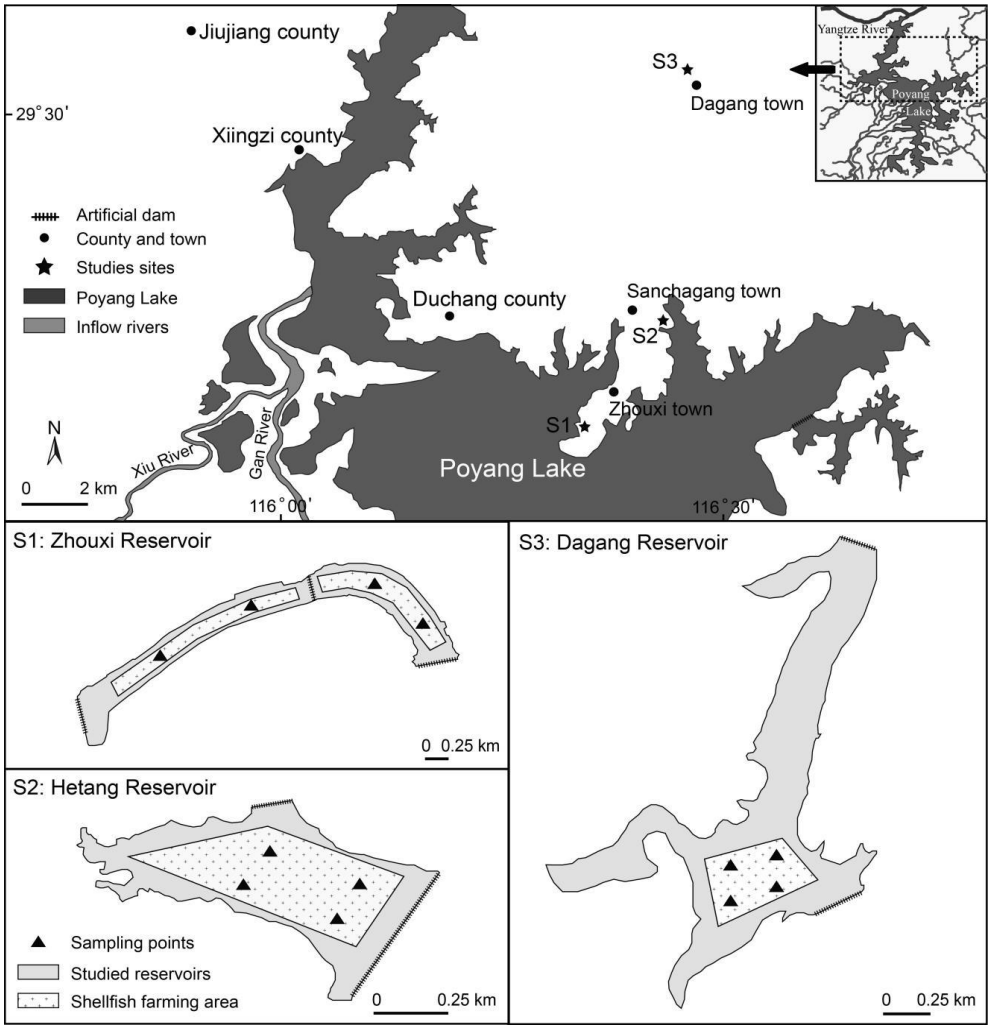

Figure 1. *Location of the studied sites and sampling points in the DG, HT and ZX reservoirs*

Statistical analysis

The Shannon–Weiner diversity index (H'), Margalef richness index (D) and Pielou evenness index (J') were calculated, as follows:

$$H' = -\sum Pi \ln (Pi)$$
$$D = (S-1) / \ln N \quad \text{(Eq.1)}$$
$$J' = H' / \ln S$$

where Pi is the proportion of i species densities in the total phytoplankton density, and S is species number.

The dominance index was as follows:

$$Y = n\,i \times f\,i / N \quad \text{(Eq.2)}$$

http://www.aloki.hu ● ISSN 1589 1623 (Print) ● ISSN 1785 0037 (Online)
DOI: http://dx.doi.org/10.15666/aeer/1802_33873408

where ni represents the number, fi represents the occurrence frequency of i species, and N represents the whole numbers. The species was deemed as dominant species when $Y \geq 0.02$.

The seasonal variations in water physico-chemical parameters (i.e. WT, pH, Cond, DO, Turb and Chl-a), TN, TC and phytoplankton parameters (i.e. biomass, H', D and J') were examined by one-way ANOVA, and the differences were further tested with LSD multiple comparison under various treatments. Spearman rank correlation analysis was performed to identify the correlation among physico-chemical parameters, TC, TN and the biomass of phytoplankton. $P < 0.05$ was the significant level. The seasonal variation in phytoplankton community structure was determined by NMDS analysis with the biomass data of dominant species using a ranked similarity matrix based on Bray–Curtis similarity measures.

A detrended correspondence analysis on species data was performed prior to the analysis of species-environmental correlation, and revealed the longest gradient length of 4.9, indicating that the Canonical correspondence analysis was applicable. Therefore, the correlation between water physico-chemical parameters and phytoplankton dominant species was examined with CCA, and the significance was determined by the Monte Carlo test using the Canoco for Windows 4.5 software (Microcomputer Power, Ithaca, USA). Then, one-way ANOVA, LSD multiple comparison and Spearman rank correlation analysis were performed with SPSS (version 22.0; IBM Corp., Armonk, USA). NMDS ordination analysis was performed with the PRIMER 5 computer package (Clarke and Warwick, 1994).

Results

Physico-chemical parameters

The one-way ANOVA indicated that all water physico-chemical parameters differed seasonally. The fluctuation rule for water temperature was that it increased from spring, reaching a maximum (±SE) of 30.93 ± 0.22 ℃ in summer, and continuously dropped from autumn to winter, reaching a minimum of 4.77 ± 0.31 ℃ (*Table 1*). A similar fluctuation rule was also observed in pH, conductivity and turbidity. In general, the water was characterized by alkalinity, ranging from 7.86 ± 0.04 to 8.80 ± 0.05. The DO concentrations ranged from 8.98 ± 0.11 mg/L in winter to 10.45 ± 0.17 mg/L in spring, indicating that a higher oxygen capacity occurred in spring. Conductivity and turbidity ranged from 101.61 ± 30.20 to 1,342.28 ± 85.87 μS/cm, and from 5.26 ± 0.69 to 14.48 ± 2.65 NTU, respectively. Furthermore, chlorophyll-a values and total carbon, which included total organic carbon and total inorganic carbon, peaked in autumn (24.64 ± 2.12 μg/L and 9.75 ± 0.62 mg/L, respectively), followed by a gradual decrease, reaching a minimum value in winter (2.39 ± 0.11 μg/L and 6.16 ± 0.35 mg/L, respectively). On the contrary, TN had a minimum of 0.63 ± 0.03 mg/L in autumn, but peaked to 1.10 ± 0.1 mg/L in summer.

Species composition

A total of 189 species were identified and belonged to seven groups: Cyanophyta, Chlorophyta, Bacillariophyta, Xanthophyta, Pyrrophyta, Euglenophyta and Chrysophyta. Chlorophyta was deemed as the most abundant group, which had 83 species (approximately 43.92% of the total species number), followed by Cyanophyta

http://www.aloki.hu ● ISSN 1589 1623 (Print) ● ISSN 1785 0037 (Online)
DOI: http://dx.doi.org/10.15666/aeer/1802_33873408

(59 species) and Bacillariophyta (25 species). The others, such as Xanthophyta, Pyrrophyta, Euglenophyta and Chrysophyta, were sporadically recorded (*Table A1* in the *Appendix*).

Table 1. *Mean values (±standard error) of the physicochemical factors*

	Spring	Summer	Autumn	Winter	F	P
WT (℃)	14.68±0.09^{b}	30.93±0.22^{d}	21.93±0.09^{c}	4.77±0.31^{a}	3002.41	<0.001
Cond (μS/cm)	911.06±61.25^{b}	1342.28±85.87^{d}	1107.28±74.13^{c}	101.61±30.20^{a}	66.269	<0.001
pH	7.87±0.05^{a}	8.80±0.05^{b}	8.05±0.13^{a}	7.86±0.04^{a}	32.149	<0.001
Turb (NTU)	7.80±1.64^{ab}	14.48±2.65^{c}	11.27±2.22^{bc}	5.26±0.69^{a}	4.294	0.008
DO (mg/L)	10.45±0.17^{b}	9.19±0.20^{a}	9.69±0.40^{a}	8.98±0.11^{a}	7.038	<0.001
Chl-a (μg/L)	17.17±2.14^{c}	9.03±1.25^{b}	24.64±2.12^{d}	2.39±0.11^{a}	35.122	<0.001
TC （mg/L）	7.07±0.29^{ab}	7.98±0.68^{b}	9.75±0.62^{c}	6.16±0.35^{a}	9.004	<0.001
TN （mg/L）	1.05±0.14^{b}	1.10±0.15^{b}	0.63±0.03^{a}	0.87±0.07^{ab}	3.684	0.016

The phytoplankton composition changed with the seasons and sites, which indicate a trend, in which taxa numbers gradually increased from spring to autumn, reached a peak period, and decreased (*Fig. 2*). A total of 112 species were recorded in spring, with a minimum (29) in DG, and these were similar in HT (42) and ZX (41). A total of 153 and 120 species were observed in summer and winter, respectively. In general, the taxa numbers exhibited a slight fluctuation of approximately 50 (in summer) and 40 (in winter) in three reservoirs. A total of 180 species were captured in autumn, with the minimum (50), and the number of taxa in HT (67) were slightly higher than those in ZX (63). In addition, 4, 6 and 5 species remained as co-existing species from spring to winter in DG, HT and ZX, respectively, and these mainly comprised of Bacillariophyta, in addition to Chlorophyta and Cyanophyta.

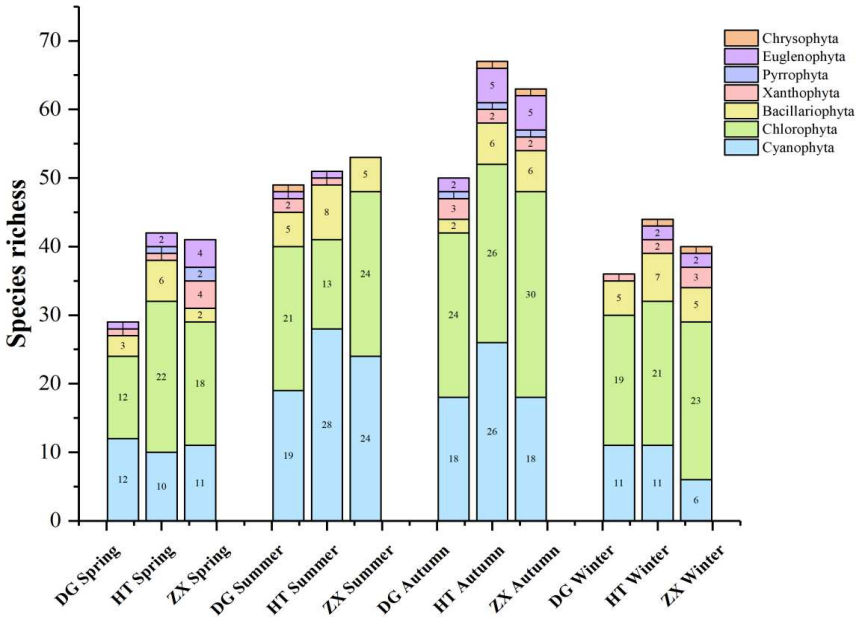

Figure 2. *Seasonal species richness of each phytoplankton group in the DG, HT and ZX reservoirs from August 2017 to March 2018*

http://www.aloki.hu ● ISSN 1589 1623 (Print) ● ISSN 1785 0037 (Online)
DOI: http://dx.doi.org/10.15666/aeer/1802_33873408

Dominant species

The number of dominant species were 9, 9 and 12 for DG, HT and ZX throughout the sampling period. Furthermore, 9, 3, 6 and 7 dominant species occurred from spring to winter. These dominant species changed with the seasons. *Microcystis pallida* dominated in spring and summer. S*ynechocystis aquatilis* and *Ulothrix tenerrima* were the dominant species in summer and winter, and in spring and winter, respectively. *Microspora stagnorum* dominated the four seasons, except for summer, and merely *Chlorella pyrenoidosa* was the dominant species from spring to winter.

The highest dominance was marked by Jaaginema angustissimum in spring, Synechocystis aquatilis in summer, Microcystis minutissima in autumn, and Oscillatoria tenuis in winter, with a dominance index of 0.57, 0.93, 0.25 and 0.20, respectively.

Biomass of phytoplankton

A similar trend was found in the seasonal dynamics of phytoplankton biomass. There was a relatively low biomass in spring, which peaked in summer on account of the outbreak of Cyanophyta, and progressively decreased to the minimum in winter. The fluctuation rule was consistent with the seasonal dynamics of Cyanophyta. Cyanophyta contributed to the seasonal total biomass, which ranged from 17.80% (winter in ZX) to 98.86% (summer in HT). The mean proportions were 52.74%, 90.68%, 53.72% and 32.72% for spring to winter, respectively. Therefore, a lot of Cyanophyta characterized the phytoplankton assemblages in these three reservoirs. This was followed by the main contributors to the total biomass of the phytoplankton community, which included Chlorophyta, Xanthophyta and Bacillariophyta (*Fig. 3*). From spring to winter, the mean value was 1,409.44 ± 228.51, 7,436.94 ± 1481.36, 1,187.5 ± 194.29 and 674.72 ± 138.55 ind/L. Summer significantly differed with the other seasons ($P < 0.01$). In addition, the phytoplankton biomass in ZX was higher than that in the rest of reservoirs, except for summer, and the maximum was 13,690 ± 2,682.11 ind/L in HT.

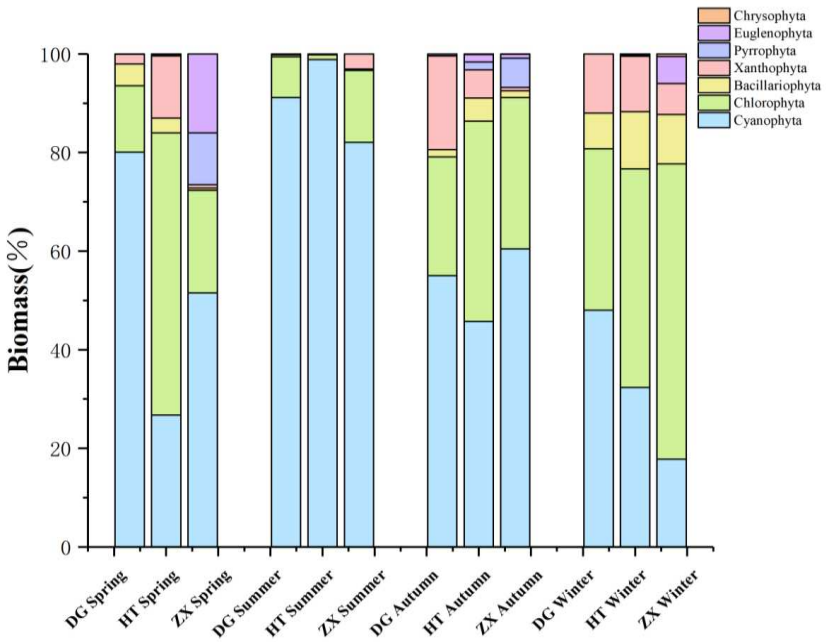

Figure 3. *Seasonal biomass that comprise of the proportion of each phytoplankton group in the DG, HT and ZX reservoirs from August 2017 to March 2018*

http://www.aloki.hu ● ISSN 1589 1623 (Print) ● ISSN 1785 0037 (Online)
DOI: http://dx.doi.org/10.15666/aeer/1802_33873408

Species of the diversity index

It was essential to study the Shannon–Weiner diversity index (*H'*), Margalef richness index (*D*) and Pielou evenness index (*J'*) to clarify the structure of the phytoplankton community. The overall pattern of the three diversity indexes represented a peak in autumn, and a minimum that was often shown in summer (*Fig. 4*). H', D and J' all indicated significant differences among the four seasons. The Shannon–Weiner index ranged from 0.58 (summer in DG) to 2.13 (autumn in HT), with an average of 1.50. The Margalef index ranged from 1.41 (spring in DG) to 3.46 (autumn in HT), with an average of 2.36. As for the Pielou's evenness index, this ranged from 0.16 (summer in HT) to 0.78 (winter in ZX), with an average of 0.58.

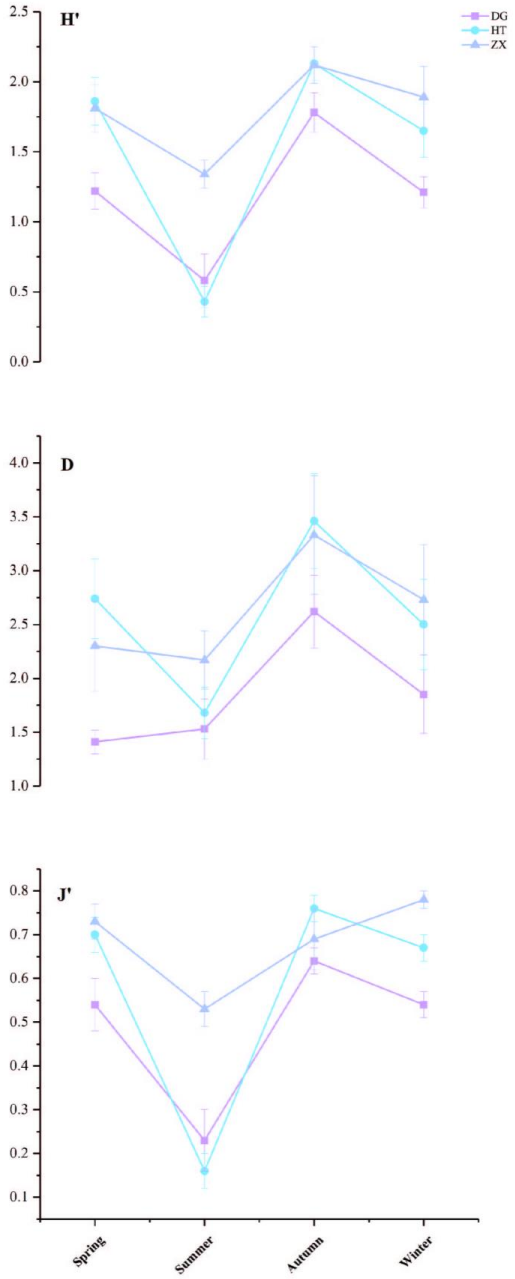

Figure 4. *Seasonal H' (Shannon–Weiner index), D (Margalef index) and J' (Pielou'sindex) in the DG, HT and ZX reservoirs from August 2017 to March 2018*

http://www.aloki.hu ● ISSN 1589 1623 (Print) ● ISSN 1785 0037 (Online)
DOI: http://dx.doi.org/10.15666/aeer/1802_33873408

Phytoplankton community structure

Temporal pattern

The result of the NMDS analysis based on the seasonal variance in dominant species biomass was presented in *Figure 5*. In the significant difference result for the component and biomass of dominant species between summer and others, summer was separated as an independent branch. Meanwhile, it was noteworthy that the other seasons did not gather together closely into a branch. In particular, a partial separation was observed in spring and winter, which meant that some variance in composition and abundance existed.

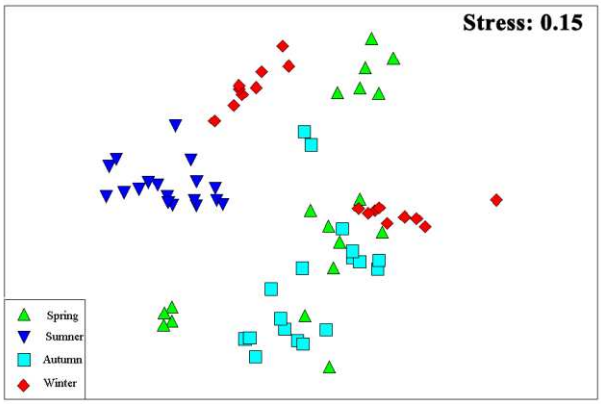

Figure 5. *Temporal pattern of the phytoplankton community structure of the DG, HT and ZX reservoirs by non-metric multidimensional scaling ordination (NMDS) analysis from August 2017 to March 2018*

Spatial pattern

NMDS was also conducted to determine whether the phytoplankton community structure expressed spatial differences. Different degrees of variance in phytoplankton structure among the three experimental plots was revealed from spring to winter (*Fig. 6*). Corresponding to the result of the temporal variance analysis, this strongly varied among the three plots in summer. In spring, DG exhibited a considerable difference with ZX and HT. However, no distinct rules were demonstrated in autumn and winter.

The relationship of the phytoplankton community with environmental parameters

The results of the CCA analysis indicated that 33.00% and 59.93% of the variance in the species-environmental relationship were carried out on the first and second axes, suggesting that there was some correlation between the environmental parameters and phytoplankton structure (*Fig. 7*). The Monte Carlo permutation test revealed that WT ($P = 0.002$), pH ($P = 0.002$), conductivity ($P = 0.002$), dissolved oxygen ($P = 0.002$), chlorophyll-a ($P = 0.002$), TC ($P = 0.022$) and TN ($P = 0.002$) were the crucial factors that had significant impacts on phytoplankton communities, and WT explains the largest variation, which was 10.4%. Along with the Spearman rank correlation analysis, pH, WT and conductivity had a strong positively correlation with total biomass, the biomass of *Cyanophyta*, and the main component, *Synechocystis aquatilis* (R value: pH > WT > conductivity; *Table 2*) However, pH, conductivity and TC were negatively correlated with *Bacillariophyta*. In addition, the

http://www.aloki.hu ● ISSN 1589 1623 (Print) ● ISSN 1785 0037 (Online)
DOI: http://dx.doi.org/10.15666/aeer/1802_33873408

occurrence of *Xanthophyta* and *Microcystis minutissima* was positively correlated with dissolved oxygen and chlorophyll-a.

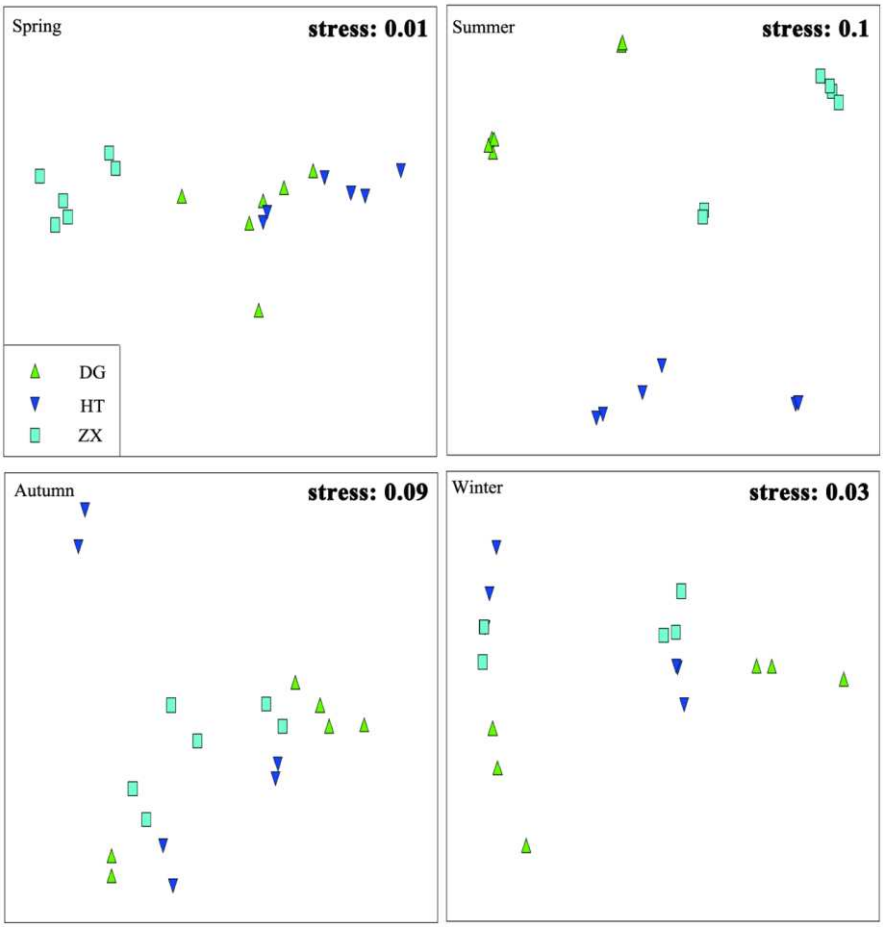

Figure 6. *Spatial pattern of the phytoplankton community structure of the DG, HT and ZX reservoirs based on the non-metric multidimensional scaling ordination (NMDS) analysis from August 2017 to March 2018*

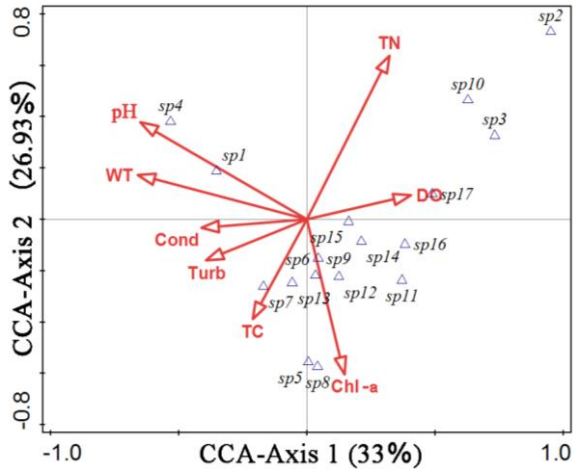

Figure 7. *Relationship of phytoplankton dominant species and environmental factors in the DG, HT and ZX reservoirs by Canonical Correspondence Analysis (CCA)*

http://www.aloki.hu ● ISSN 1589 1623 (Print) ● ISSN 1785 0037 (Online)
DOI: http://dx.doi.org/10.15666/aeer/1802_33873408

Table 2. *Spearman rank correlation analysis between the water factors and phytoplankton biomass*

	WT	**Cond**	**pH**	**Turb**	**DO**	**Chl-a**	**TC**	**TN**	**Cyanophyta**	**Chlorophyta**	**Bacillariophyta**	**Xanthophyta**	**Pyrrophyta**	**Euglenophyta**	**Chrysophyta**	**Total biomass**	**Jaaginema angustissimum**	**Synechocystis aquatilis**	**Microcystis minutissima**
WT																			
Cond	**.835****																		
pH	**.663****	**.348****																	
Turb	**.391****	**.539****	0.056																
DO	0.013	-0.135	**.307****	**-.508****															
Chl-a	**.299***	**.418****	0.143	0.11	**.464****														
TC	**.363****	**.679****	-0.057	**.620****	**-.407****	**.365****													
TN	0.068	0.163	0.119	**.239***	-0.134	-0.106	0.19												
Cyanophyta	**.556****	**.294***	**.614****	0.042	0.137	**-.237***	-0.084	-0.093											
Chlorophyta	0.029	-0.053	-0.026	-0.107	0.113	0.081	-0.189	-0.077	-0.076										
Bacillariophyta	**-.251***	**-.302****	-0.113	-0.224	0.154	-0.127	**-.293***	0.117	-0.052	0.192									
Xanthophyta	-0.039	-0.127	0.057	-0.139	**.266***	**.290***	-0.12	-0.13	-0.101	0.013	-0.056								
Pyrrophyta	0.003	0.216	-0.166	-0.083	0.04	0.11	**.266***	-0.035	-0.11	-0.08	-0.125	-0.099							
Euglenophyta	-0.116	0.148	-0.208	-0.086	0.117	0.087	0.072	-0.085	-0.148	-0.045	-0.154	-0.068	**.580****						
Chrysophyta	-0.113	-0.157	-0.102	-0.128	-0.081	-0.099	-0.037	-0.012	-0.069	0.166	-0.029	-0.126	0.143	-0.115					
Total biomass	**.557****	**.285***	**.613****	0.021	0.164	-0.22	-0.109	-0.105	**.994****	0.021	-0.023	-0.065	-0.107	-0.142	-0.058				
Jaaginema angustissimum	-0.109	-0.106	-0.023	**-.234***	**.431****	0.049	-0.178	**.517****	0	0.051	**.468****	-0.08	-0.071	-0.097	-0.082	0.007			
Synechocystis aquatilis	**.539****	**.281***	**.600****	0.079	0.063	**-.270***	-0.07	-0.143	**.988****	-0.077	-0.085	-0.158	-0.103	-0.13	-0.06	**.980****	-0.108		
Microcystis minutissima	0.12	0.041	0.21	-0.172	**.386****	**.490****	0.038	-0.187	-0.054	-0.058	-0.043	**.694****	0.119	-0.056	0.093	-0.033	-0.079	-0.115	

http://www.aloki.hu ● ISSN 1589 1623 (Print) ● ISSN 1785 0037 (Online)
DOI: http://dx.doi.org/10.15666/aeer/1802_33873408

Discussion

Effects of environmental factors on the phytoplankton community

The objectives of the present study were to investigate the seasonal variations in phytoplankton communities, and attempt to determine the potential factors that affected the community structure. In addition, the diversity, richness and components of the structure of the phytoplankton community were predicted, and all differed from natural reservoirs without aquaculture. The findings of the present study suggest that environmental factors and anthropogenic pressure affected the phytoplankton community structure in several aspects. However, to some extent, the results in some water physico-chemical parameters and species richness were within a reasonable range of fluctuations. However, these still exhibited different succession patterns between seasons, when compared to some natural subtropical reservoirs. That is, the hypothesis was partially supported.

On one hand, the physico-chemical parameters of water had a significant impact on the structure of phytoplankton and zooplankton, such as species richness, the value of the biomass, dominant species distribution, and the composition of the community (Li et al., 2019; Horváth et al., 2017; Zhao et al., 2013). The seasonal characteristics of these ecosystems could be explained by the variability of the environment, which was due to the temporal change. The present study also revealed all water physico-chemical factors, D, H' and J', were significantly different among the four seasons. In addition, the phytoplankton community structure could display a change when the temporal changed (Fabiana Schneck et al., 2011). Furthermore, the present study demonstrated that the composition of the phytoplankton community in these three reservoirs changed between seasons. In particular, Cyanophyta dominated the phytoplankton community mostly during the experimental periods. Water temperature, N levels, P levels and dissolved oxygen could contribute to the variation of the phytoplankton community (Xu et al., 2017). The present study indicated that water temperature, pH, conductivity, dissolved oxygen, chlorophyll-a, TC and TN were the primary factors that influenced the phytoplankton community, and that water temperature contributed the most variation. Simultaneously, the Spearman rank correlation analysis also indicated that water temperature occupied the crucial factors. These results agreed with the results reported by Wu et al. (2012). In addition, WT, pH, conductivity and turbidity revealed similar fluctuation patterns. Furthermore, abundant data have indicated the effect of water temperature on phytoplankton growth, photosynthesis, respiration and community succession in the water ecosystem (Williamson et al., 2010; Moore, 2010; Edwards and Richardson, 2004). The optimum temperature for microalgae belonging to various groups differed, in general, and high temperature always promoted the growth of phytoplankton (Wu et al., 2013). It is not surprising that the biomass of phytoplankton generally reached a peak in summer, and decreased in spring and winter. These findings indicate that the biomass in summer considerably increased, and was far greater than that in the other seasons. The NMDS results also suggested that the phytoplankton community in summer was separated as an independent branch. Diatoms were adapted to grow in cool water, with an optimum temperature of approximately 20 ℃, which tended to dominate in spring. As for others, such as A. tamarense, which are not eurythermal, these reached the greatest abundance at temperatures near 18 ℃ (Wang et

http://www.aloki.hu ● ISSN 1589 1623 (Print) ● ISSN 1785 0037 (Online)
DOI: http://dx.doi.org/10.15666/aeer/1802_33873408

al., 2009). However, Cyanobacterias thrived at relatively high temperatures (approximately 28-32 ℃), according to Ribeiro et al. (2018).

The phytoplankton community was characterized a lot of Cyanobacterias, which are indicators of an ecosystem with an excess of trophic state (Kangro et al., 2005). Cyanobacteria would show significant advantages, when compared to other groups, when facing an elevation in temperature. However, even in spring and winter, Cyanobacteria continued to play an important role in the phytoplankton community, and *Microcystis pallida* and *Microcystis pallida, Synechocystis aquatilis* and *Oscillatoria tenuis* were the dominant species in spring and winter, respectively. Therefore, temperature was not the only affecting factors that resulted in the abundance of Cyanobacteria in these three reservoirs. In addition, other factors also accounted for the phytoplankton temporal dynamics. The CCA analysis also indicated TN and pH had a significant impact on the structure of the phytoplankton community. Nevertheless, Cyanobacteria occupied over 90% of the biomass in summer. The Spearman rank correlation analysis revealed that pH, water temperature and conductivity had a strong positively correlation with Cyanobacteria. These results agree with other study conducted in a reservoir with cage farming (Degefu et al., 2011). Therefore, significant high biomass in summer could also be attributed to the blue-green algae outbreak. Based on previous studies on phytoplankton community structure, the rough features of Cyanobacteria could be demonstrated (Mwaura et al., 2002; Xiao et al., 2018; Smith, 1986; Sarma et al., 2005; Li et al., 2019). The Cyanobacteria exhibited better performance under high temperature, with relatively high pH and nutrition levels. These could shift to a position required for a suitable environment in the water column, and with a special allelopathy to dwindle other species that co-exist in the ecosystem with a possible competitive relationship. It was obvious, to some extent, that this might be attributable to the abundance of Cyanobacteria, which is advantageous of the better tolerance of grazing, homeostatic mechanism, and relatively suitable living environment for Cyanobacteria provided by these reservoirs. Meanwhile, the composition and succession rules were contrary to natural subtropical reservoirs (Yang et al., 2014). Among the four seasons, chlorophyta and cyanophyta were always the main dominant species, and the major contributors to the total biomass. However, no significant and clear phytoplankton community succession was observed. The diversity index could instruct the water trophic states, according to the study conducted by Kuang et al. (2005). These reservoirs were all in a moderately eutrophic state with the use of the method described as Kuang. That is, fish and mussels introduction might have brought some impact on the water quality, and further impacted the phytoplankton community.

Effects of aquaculture on the phytoplankton community

In addition to abiotic factors, biotic factors would affect the phytoplankton community structure, and may further bring a great impact on the water ecosystem (Reissig et al., 2006; Sarà, 2007). Integrated fish-mussel aquaculture might contribute to the variance in the composition and succession in several ways. On one hand, as far as aquatic organisms are concerned, a new predation pressure would be created, and the origin food web in the water ecosystem might be forced to change. Furthermore, the responses of the phytoplankton biomass in some groups of could be accurately predicted, based on food chain theory responses (Hansson et al., 2004). The predation pressure could be a direct or indirect major factor that affects the structure of phytoplankton, and the zooplankton community would also respond to the dynamics

http://www.aloki.hu ● ISSN 1589 1623 (Print) ● ISSN 1785 0037 (Online)
DOI: http://dx.doi.org/10.15666/aeer/1802_33873408

through the food web (Huston, 1979; He et al., 2017). He et al. discovered that the contribution and biomass of diatoms in the water column significantly increased due to the increasing competitiveness of microalgae with big cells caused by Crucian carp foraging activities. However, although a filter-feeder without capturing devices feeds majorly on phytoplankton and organics by forming a water flow to filter food, relying on the gill and cilium of the labial surface, cyanobacteria were a kind of inedible microalgae for these (Yan et al., 2009). Therefore, the specific selection of food by mussels has a significant impact on the food web composition, leading to a high quantity of cyanobacteria, when compared with other algae. This influenced the succession of phytoplankton communities, and possibly enhanced the similarity of species composition between seasons. Reissig et al. (2006) considered that the cyanobacteria dominated in lakes with introduced fishes. However, this phenomenon was absent in lakes without fishes. The proportion of cyanobacteria biomass in total biomass sharply plummeted, and was approximately equal to that of green algae, or even lower than that of green algae, in addition to environmental factors, and this may be correlated to the decrease in mussel population in autumn and winter. When the biomass of some microalgae occupied an absolute dominant position, this might lead to a relatively single species composition, thereby affecting the stability of the community structure and the balance of the ecosystem, while reducing the ecosystem to withstand this (Lawton, 1994). Mussels and fish polyculture had a limited effect on controlling blue-green algae blooms, but induced a decrease of some groups, which agrees to the study conducted by Soto and Mena (1999). Meanwhile, the increase in nitrogen, phosphorus concentrations and other water physico-chemical or trophic levels could be detected due to the feces, and maintenance respiration and activities. The bio-deposit degradation from aquatic organisms also may have toxic effects. On the other hand, husbandry management, such as feeding and fertilizing, were essential for some aquaculture types. Therefore, maintaining the balance and stabilization in water quality and tropical states meet greater challenges, and have an obvious impact on the microalgae community. Sarà et al. (2011) indicated that the N and P levels were continuously enhanced after the introduction of aquaculture, and approximately 34.2.5% of the relative N and P total input was caused by tuna fish-farming activities per year. In addition, relatively low dissolved oxygen, high total chlorophyll-a, and high phytoplankton abundances, but low species richness, were recorded by Er et al. (2018). However, different aquatic organisms affected the water column differentially, the dissolved inorganic nitrogen and total phosphorus concentrations in fish farms were significantly higher than that in bivalve cultures, and the bivalve cultures exerted lighter pressure than fish cultures (Sarà, 2007; Zhang et al., 2013). These reservoirs exhibited some obvious variations in oxygen capacity and community structure, including species composition and richness, which might be due to the various management schemes, based on the NMDS analysis. The physico-chemical parameters were mostly in the favorable range for aquaculture. For example, the dissolved oxygen was suitable for the fish-mussel system, and was not in a low level, which might be a relatively low abundant biomass. For silver carp, bighead carp and mussels, the filter feeder displayed crucial roles in the reservoir ecosystem, and this might have contributed to the low abundant biomass that further decreased the oxygen expended by the respiration of micro-algae. Calcium oxide was frequently applied to increase the calcium ion concentration and regulate water quality, and these might be reasonable to understand that the water was deemed alkaline in these three reservoirs. Seasonal phytoplankton

http://www.aloki.hu ● ISSN 1589 1623 (Print) ● ISSN 1785 0037 (Online)
DOI: http://dx.doi.org/10.15666/aeer/1802_33873408

community dynamics would be affected from a lot of aspects, but other factors were absent from the present study, such as phosphorus levels, bacteria, zooplankton and the interaction among fish, mussel and phytoplankton.

It remains challenging to clarify the mechanism of variation in water quality and the phytoplankton community caused by the hydrological regime and man-made disturbances based on the simple investigation environment factors and community component. Hence, monitoring is fundamental to clarify the internal correlation between affecting factors and the responses, and explain the complex ecological succession from a comprehensive point. Nevertheless, the present study demonstrated the seasonal dynamic characteristics of phytoplankton and its potential risks to water ecosystems attributed to integrated fish-mussel aquaculture.

Conclusion

The total water quality parameters revealed seasonal variations and an appropriate range for aquaculture, as well as a trend of eutrophication. The phytoplankton community was characterized by high species richness and abundance, and was dominated by cyanobacteria in the three reservoirs. The biomass in summer had a significant difference, when compared to other seasons. The community structure of phytoplankton had unclear patterns due to the fish-mussel polyculture, which possibly enhanced the similarity in species composition and dominance species. In a word, environment factors, aquaculture and human disturbances have an impact on its seasonal succession and structure, in direct and indirect means.

The planning of water areas and tidal flats for aquaculture has become a fundamental strategy in ecological civilization construction at present. Fish-mussel polyculture is the main culture model, and this has been continuously generalized for pearl production, which is an important industry in aquaculture. The present study was helpful in identifying the seasonal characteristics of phytoplankton and the potential risks of fish-mussel polyculture, which might bring some instructions to the better management and utilization of reservoir resources.

Acknowledgements. We are grateful to Liu Y, Luo HJ, Chen H, Li F for their assistance in the field. This work was supported by the Chinese Ministry of Science and Technology through the National Key Research and Development Program of China (2018YFD0901400); The National Natural Science Foundation of China (31660337); and Modern Agro-industry Technology Research System (CARS-49) and Modern agricultural cooperative research innovation special funds of Jiangxi(JXXTCX201602).

REFERENCES

[1] And, S. T., Songsangjinda, P. (1999): Water quality and phytoplankton communities in intensive shrimp culture ponds in Kung Krabaen Bay, Eastern Thailand. – Journal of the World Aquaculture Society 30: 36-45.

[2] Bai, Z. Y., Wang, G. L., Liu, X. J., Li, J. L. (2014): Current situation and development trend of freshwater pearl seed industry in China. – Journal of Shanghai Ocean University 23: 874-879 (in Chinese).

[3] Connell, J. H. (1978): Diversity in tropical rain forests and coral reefs. – Science 199: 1302-1310.

http://www.aloki.hu ● ISSN 1589 1623 (Print) ● ISSN 1785 0037 (Online)
DOI: http://dx.doi.org/10.15666/aeer/1802_33873408

[4] Danaher, J. J., Tidwell, J. H., Coyle, S. D., Dasgupta, S., Zimba, P. V. (2007): Effects of two densities of caged monosex Nile tilapia, Oreochromis niloticus, on water quality, phytoplankton populations, and production when polycultured with Macrobrachium rosenbergii in temperate ponds. – Journal of the World Aquaculture Society 38: 367-382.
[5] Degefu, F., Mengistu, S., Schagerl, M. (2011): Influence of fish cage farming on water quality and plankton in fish ponds: a case study in the Rift Valley and North Shoa reservoirs, Ethiopia. – Aquaculture 316: 129-135.
[6] Edwards, M., Richardson, A. J. (2004): Impact of climate change on marine pelagic phenology and trophic mismatch. – Nature 430: 881-884.
[7] Er, H. H., Lee, L. K., Lim, Z. F., Teng, S. T., Leaw, C. P., Lim, P. T. (2018): Responses of phytoplankton community to eutrophication in Semerak Lagoon (Malaysia). – Environmental Science and Pollution Research 25: 22944-22962.
[8] Cornel, G. E., Whoriskey, F. G. (1993): The effects of rainbow trout (Oncorhynchus mykiss) cage culture on the water quality, zooplankton, benthos and sediments of Lac du Passage, Quebec. – Aquaculture 109: 101-107.
[9] Guo, L., Li, Z., Xie, P., Ni, L. (2009): Assessment effects of cage culture on nitrogen and phosphorus dynamics in relation to fallowing in a shallow lake in China. – Aquacult Int 17: 229-241.
[10] Hansson, L., Gyllstrom, M., Stahl-Delbanco, A., Svensson, M. (2004): Responses to fish predation and nutrients by plankton at different levels of taxonomic resolution. – Freshwater Biol 49: 1538-1550.
[11] Hauxwell, J., Cebrián, J., Furlong, C., Valiela, I. (2001): Macroalgal canopies contribute to eelgrass (Zostera marina) decline in temperate estuarine ecosystems. – Ecology 82: 1007-1022.
[12] He, H., Hu, E., Yu, J., Luo, X., Li, K., Jeppesen, E., Liu, Z. (2017): Does turbidity induced by Carassius carassius limit phytoplankton growth? A mesocosm study. – Environmental Science and Pollution Research 24: 5012-5018.
[13] He, S., Peng, K., Hong, Y., Wang, J., Sheng, J., Gu, Q. (2013): Molecular properties and immune defense of two ferritin subunits from freshwater pearl mussel, Hyriopsis schlegelii. – Fish & Shellfish Immunology 34: 865-874.
[14] Horváth, Z., Vad, C. F., Preiler, C., Birtel, J., Matthews, B., Ptáčníková, R., Ptáčník, R. (2017): Zooplankton communities and Bythotrephes longimanus in lakes of the montane region of the northern Alps. – Inland Waters 7: 3-13.
[15] Huston, M. (1979): A general hypothesis of species diversity. – Am Nat 113: 81-101.
[16] Kangro, K., Laugaste, R., Peeter Nõges, Ott, I. (2005): Long-term changes and seasonal development of phytoplankton in a strongly stratified hypertrophic lake. – Hydrobiologia 547: 91-103.
[17] Kuang, Q., Ma, P., Hu, Z., Zhou, G. (2005): Study on the evaluation and treatment of lake eutrophication by means of algae biology. – Journal of Safety and Environment 5: 87-91 (in Chinese).
[18] Lawton, J. H. (1994): What Do Species Do in Ecosystems? – Oikos 71: 367-374.
[19] Leblanc, K., Quéguiner, B., Diaz, F., Cornet, V., Michel-Rodriguez, M., Durrieu De Madron, X., Bowler, C., Malviya, S., Thyssen, M., Grégori, G., Rembauville, M., Grosso, O., Poulain, J., de Vargas, C., Pujo-Pay, M., Conan, P. (2018): Nanoplanktonic diatoms are globally overlooked but play a role in spring blooms and carbon export. – Nature Communications 9: 953.
[20] Li, C., Feng, W., Chen, H., Li, X., Song, F., Guo, W., Giesy, J. P., Sun, F. (2019): Temporal variation in zooplankton and phytoplankton community species composition and the affecting factors in Lake Taihu-a large freshwater lake in China. – Environ Pollut 245: 1050-1057.
[21] Li, J. L. (2007): Utilization and protection of freshwater cultured pearl mussel germplasm resources. – Scientific Fish Farming 6: 1-2 (in Chinese).

http://www.aloki.hu ● ISSN 1589 1623 (Print) ● ISSN 1785 0037 (Online)
DOI: http://dx.doi.org/10.15666/aeer/1802_33873408

[22] Meyer, N., Bigalke, A., Kaulfuß, A., Pohnert, G. (2017): Strategies and ecological roles of algicidal bacteria. – Fems Microbiol Rev 41: 880-899.
[23] Milligan, A. J., Morel, F. M. M. (2002): A proton buffering role for silica in diatoms. – Science 297: 1848-1850.
[24] Milstein, A. (1992): Ecological aspects of fish species interactions in polyculture ponds. – Hydrobiologia 231: 177-186.
[25] Moore, J. W. (2010): Influence of temperature, photoperiod and trophic conditions on the seasonal cycles of phytoplankton and zooplankton in two deep subarctic lakes of northern Canada. – Int Rev Hydrobiol 66: 745-770.
[26] Mwaura, F., Mavuti, K. M., Wamicha, W. N. (2002): Biodiversity characteristics of small high-altitude tropical man-made reservoirs in the eastern Rift valley, Kenya. Lakes and reservoirs. – Res. Management 7: 1-12.
[27] Neori, A., Chopin, T., Troell, M., Buschmann, A. H., Kraemer, G. P., Halling, C., Shpigel, M., Yarish, C. (2004): Integrated aquaculture: rationale, evolution and state of the art emphasizing seaweed biofiltration in modern mariculture. – Aquaculture 231: 361-391.
[28] Peng, K., Wang, J., Sheng, J., Zeng, L., Hong, Y. (2012): Molecular characterization and immune analysis of a defensin from freshwater pearl mussel, Hyriopsis schlegelii. – Aquaculture 334-337: 45-50.
[29] Reissig, M., Trochine, C., Queimaliños, C., Balseiro, E., Modenutti, B. (2006): Impact of fish introduction on planktonic food webs in lakes of the Patagonian Plateau. – Biol Conserv 132: 437-447.
[30] Ribeiro, K. F., Duarte, L., Crossetti, L. O. (2018): Everything is not everywhere: a tale on the biogeography of cyanobacteria. – Hydrobiologia 820: 23-48.
[31] Sarà, G. (2007): Ecological effects of aquaculture on living and non-living suspended fractions of the water column: a meta-analysis. – Water Res 41: 3187-3200.
[32] Sarà, G., Lo Martire, M., Sanfilippo, M., Pulicanò, G., Cortese, G., Mazzola, A., Manganaro, A., Pusceddu, A. (2011): Impacts of marine aquaculture at large spatial scales: evidences from N and P catchment loading and phytoplankton biomass. – Mar Environ Res 71: 317-324.
[33] Sarma, S. S. S., Nandini, S., et al. (2005): Life history strategies of cladocerans: comparisons of tropical and temperature taxa. – Hydrobiologia 542: 315-334.
[34] Schneck, F., Schwarzbold, A., Rodrgues, S. C., Melo, A. S. (2011): Environmental variability drives phytoplankton assemblage persistence in a subtropical reservoir. – Austral Ecol 36: 839-848.
[35] Schneider, O., Sereti, V., Eding, E. H., Verreth, J. A. J. (2005): Analysis of nutrient flows in integrated intensive aquaculture systems. – Aquacult. Eng 32: 379-401.
[36] Smith, V. H. (1986): Light and nutrient effects on the relative biomass of blue-green in lake phytoplankton. – Can. J. Fish. Aquat. Sci 43: 148-153.
[37] Soto, D., Mena, G. (1999): Filter feeding by the freshwater mussel, Diplodon chilensis, as a biocontrol of salmon farming eutrophication. – Aquaculture 171: 65-81.
[38] Tang, J. Y., Dai, Y. X., Wang, Y., Qin, J. G., Su, S. S., Li, Y. M. (2015): Optimization of fish to mussel stocking ratio: development of a state-of-art pearl production mode through fish-mussel integration. – Aquacult Eng 66: 11-16.
[39] Troell, M., Halling, C., Neori, A., Chopin, T., Buschmann, A. H., Kautsky, N., Yarish, C. (2003): Integrated mariculture: asking the right questions. – Aquaculture 226: 69-90.
[40] Wang, Y., Wang, W. L., Qin, J. G., Wang, X. D., Zhu, S. B. (2009): Effects of integrated combination and quicklime supplementation on growth and pearl yield of freshwater pearl mussel, Hyriopsis cumingii (Lea, 1852). – Aquat Res 40: 1634-1641.
[41] Wang, Z., Zhao, J., Zhang, Y., Cao, Y. (2009): Phytoplankton community structure and environmental parameters in aquaculture areas of Daya Bay, South China Sea. – J Environ Sci (China) 21: 1268-1275.

http://www.aloki.hu ● ISSN 1589 1623 (Print) ● ISSN 1785 0037 (Online)
DOI: http://dx.doi.org/10.15666/aeer/1802_33873408

[42] Williamson, C. E., Salm, C., Cooke, S. L., Saros, J. E. (2010): Erratum to: how do UV radiation, temperature, and zooplankton influence the dynamics of alpine phytoplankton communities? – Hydrobiologia 652: 395-396.
[43] Wu, W. J., Yang, K., Wang, Z. C., Li, G. B., Liu, Y. D. (2012): Phytoplankton community structure and seasonal succession in Yudong reservoir, Yunnan-Guizhou plateau. – Journal of Hydroecology 33: 69-75 (in Chinese).
[44] Wu, Z. S., Cai, Y. J., Liu, X., Xu, C. P., Chen, Y. W., Zhang, L. (2013): Temporal and spatial variability of phytoplankton in Lake Poyang: the largest freshwater lake in China. – J Great Lakes Res 39: 476-483.
[45] Xiao, M., Li, M., Reynolds, C. S. (2018): Colony formation in the cyanobacterium Microcystis. – Biol Rev 93: 1399-1420.
[46] Xu, Y., Li, A. J., Qin, J., Li, Q., Ho, J. G., Li, H. (2017): Seasonal patterns of water quality and phytoplankton dynamics in surface waters in Guangzhou and Foshan, China. – Sci Total Environ 590-591: 361-369.
[47] Yan, L., Zhang, G., Liu, Q., Li, J. (2009): Optimization of culturing the freshwater pearl mussels, Hyriopsis cumingii with filter feeding Chinese carps (bighead carp and silver carp) by orthogonal array design. – Aquaculture 292: 60-66.
[48] Yang, L. J., Yu, P. F., Zhu, J. Q., Xu, Z., Lv, G. H., Jin, C. H. (2014): Phytoplankton community structure and its influencing factors in Hengshan reservoir, Zhejiang province. – Chinese Journal of Applied Ecology 25: 569-576 (in Chinese).
[49] Zhang, X., Huang, X., Huang, L. (2013): Phytoplankton community structure shaped by key environmental factors in fish and shellfish farms in Daya Bay, South China. – Aquat Ecosyst Health 16: 300-310.
[50] Zhang, Z. S., Huang, X. F. (1991): Research Methods on Freshwater Plankton. – Science Press, Beijing (in Chinese).
[51] Zhao, Z., Mi, T., Xia, L., Yan, W., Jiang, Y., Gao, Y. (2013): Understanding the patterns and mechanisms of urban water ecosystem degradation: phytoplankton community structure and water quality in the Qinhuai River, Nanjing City, China. – Environ Sci Pollut R 20: 5003-5012.
[52] Zheng, X., Zhang, D., Qin, J., Wang, Y. (2018): The effect of C/N ratio on bacterial community and water quality in a mussel-fish integrated system. – Aquac Res 49: 1699-1708.

APPENDIX

Table A1. *Collected species list of phytoplankton in the three reservoirs from August 2017 to March 2018*

Phytoplankton species	Spring			Summer			Autumn			Winter		
	DG	HT	ZX	DG	HT	ZX	DG	HT	ZX	DG	HT	ZX
Cyanophyta												
Jaaginema angustissimum	**											
Microcystis pallida	*	*	**	*	**	**	*	*				
Oscillatoria granulata	*		*					*	*			
Chroococcus limneticus	*				*	*	*	*	*	*	*	*
Anabaena cylindrica	*	*		*	*	*	*	*	*	*	*	*
Nostoc rivulare	*	*	*	*	*	*		*	*	*	*	
Raphidiopsis curvata	*			*	*						*	
Oscillatoria acuminata	*											
Geitlerinema acutissimum	*			*	*	*			*			
Dactylococcopsis acicularis	*			*	*	*		*		*	*	
Leptolyngyya valderiana	*											
Synechocystis millei		*	*									

http://www.aloki.hu ● ISSN 1589 1623 (Print) ● ISSN 1785 0037 (Online)
DOI: http://dx.doi.org/10.15666/aeer/1802_33873408

Rhabdogloea smithii		*	*	*	*	*	*	*	*	*	*	
Microcystis flos-aquae		*		*	*		*	*		*	*	
Oscillatoria princes		*	*		*		*	*		*	*	
Aphanothece nagelii		*					*					
Anabaena willei			*				*	*				
Cyanobium distomicala			*				*		*			
Synechocystis aquatilis				**	**	**	*	*	*	*	**	**
Cyanobium parvum				*			*	*	*		*	*
Chroococcus varius				*	*	*						
Aulosira laxa				*								
Chroococcus epiphyticus				*	*	*						
Oscillatoria limnetica				*	*	*						
Oscillatoria subcontorta				*	*	*						
Dactylococcopsis irregularis				*		*						
Chroococcus minor				*		*						
Dactylococcopsis mucicola				*	*	*						
Nostoc carneum					*			*				
Oscillatoria acutissima					*							
Spirulina maxima					*		*					
Microcystis marginata					*	*						
Phormidiumokenii					*			*	*			
Anabaena circinalis					*				*			
Dactylococcopsis rupestris					*	*						
Oscillatoria subtillissima					*							
Dactylococcopsis scenedesmoides						*						
Coelosphaerium dubium Grunow						*						
Chroococcus tenax						*						
Chroococcus minor			*	*	*	*		*	**			*
Merismopedia tenuissima						*	*	*				
Meriamopedia marssonii					*							
Microcystis minutissima							**	**	**			
Oscillatoria tenuis							*	*		**	*	*
Synechocystis minuscula							*					
Raphidiopsis sinensia								*				
Chroococcus cohaerens								*				
Raphidiopsis curvata								*	*			
Anabaena oscillarioides								*		*		
Anabaena hunanensis										*		
Microcystis elabena									*			
Anabaena variabilis								*				
Merismopedia elegans					*							
Aphanocapsa elachista		**					**	**	**			
Aphanocapsa pulchra					*	*		*				
Oscillatoria anguina	**	*	*				*		*			
Rhabdoderma lineare						*						
Aphanizomenon flosaquae								*				
Woronichinia campacta			*						*			
Chlorophyta												
Chlorella vulgaris	*	*	*	*	*	*		*	*	*		
Oocystis lacustris	*	*	**			*						
Ulothrix tenerrima	**									**	*	*
Closterium Ehrenbergü	*		*									
Actinastrum fluviatile	*								*	*		
Scenedesmus arcuatus	*			*	*	*	*	*	*	*	*	*
Chlorella pyrenoidosa	*	**	*	**			*	**	**	*	**	**
Scenedesmus armatus	*				*	*			*	*	*	*
Golenkinia paucispina	*											
Scenedesmus acuminatus	*					*	*	*	*	*	*	*
Staurastrum tetracerum	*			*			*	*		*		
Scenedesmus quadricauda		*	*	*	*	*	*	**	**	*	*	*

http://www.aloki.hu ● ISSN 1589 1623 (Print) ● ISSN 1785 0037 (Online)
DOI: http://dx.doi.org/10.15666/aeer/1802_33873408

Schroederia nitzschioides		*		*		*		*	*			*
Scenedesmus bicaudatus		*	*									
Microspora stagnorum		**	*			*		**	**	*	**	**
Pediastrum simplex var. duodenarium		*			*	*		*	*			
Scenedesmus bijuga		*		*		*	*	*	*	*	*	*
Ankistrodesmus acicularis		*	*				*	*		*	*	*
Ankistrodesmus angustus	**	*	*				*	*	*	*	**	*
Schroederia setigera		*	*			*	*	*	*	*	*	*
Gonatozygon monotaenium		*						*				
Scenedesmus ovalternus		*										
S.armatus var.boglariensis f.bicaudatus		*	*			*		*	*	*		*
Chloromonas mikroneusa		*	*								*	*
Ulothrix moniliformis		*	*							*	*	*
Pediastrum duplex var.gracillimum		*							*			
Closteriopsis longissima		*		*	*	*	*	*	*	*		
Ankistrodesmus falcatus var.mirabilis		*	*							*	*	*
Raphidonema longiseta			*									
Treubaria crassispina			*									
Eudorina elegans			*		*							*
Pediastrum biradiatum			*						*			
T. trigonum var.gracile				*					*			
Westellopsis linearis				*								
Staurastrum pingue				*			*					
Staurastrum gracile				*								
Gonatozygon kinahani				*	*	*						
Ulothrix variabilis				*								
Chodatella subsalsa				*			*					
Staurastrum aristiferum				*								
Cosmarium botrytis				*								
Staurastrum sexangulare				*								
Staurastrum pseudotetracerum				*								
Staurastrum retusum				*								
Staurastrum willsii Turn				*								
Scenedesmus dimorphus		*			*	*		*	*			
Staurastrum manfeldtii Delp.					*							
Crucigenia rectangularis					*							
Tetraëdron regulare var. incus					*	*			*			
Cosmarium nasutum					*							
Hormidium Kuetzing						*						
Chlorella ellipsoidea						*						
Spondylostium planum						*						
S.armatus var.boglariensis f.bicaudatus						*						
Schroederia spiralis						*						
Ankistrodesmus falcatus						*	*					*
Pediastrum biradiatum						*						
Planctonema lauterbornü						*						
Chlorococcum sp.							*					
Quadrigula chodatii							*					
Provasolialla cylintrica							*					
Tetraëdron tumidulum							*					
Tetrastrum elega							*					
Golenkinia radiata							*	*			*	*
Tetrallantos lagerkeim							*				*	*
Raphidonema longiseta							*	*	*			
Scenedesmus abundans var. asymmetrica							*					
Staurastrum planctonicum							*		*			
Staurastrum margaritaceum							*	*				
Scenedesmus acutiformis								*				
Tetraëdron trilobulatum								*	*			
Tetraëdron regulare var. torsum								*			*	*

http://www.aloki.hu ● ISSN 1589 1623 (Print) ● ISSN 1785 0037 (Online)
DOI: http://dx.doi.org/10.15666/aeer/1802_33873408

Pediastrum duplex var. clathratum								*	*			
Staurodesmus dejectus								*				
Chodatella quadriseta								*	*		*	
Pediastrum duplex									*			
Characium limneticum									*			
Crucigenia quadrata									*		*	*
Hirtusochloris ellipsoida									*			
Chlamydomonas globosa									*		*	
Chlamydomonas pseudolunata										*		
Crucigenia fenestrata		*									*	
Crucigenia tetrapedia												*
Bacillariophyta												
Navicula capitata	*				*					*	*	*
Melosira granulata	*	*	*		*		*	*	*	**	**	**
Synidra affinis Kütz	*				*							
Navicula pupula		*		*			*					
Tabellaria fenestrata		*		*				*	*		*	*
Pinnularia molaris		*										
Navicula viridula		*										
Mastogloia smithii		*								*		
Cymbella pusilla			*					*			*	*
Tabellaria flocculosa				*	*							
Synedra acusvar				*	*	*						
Frustulia vulgaris				*								
Synedra ulna					*				*			
Cyclotella stelligera					*	*						
Caloneis ventricasa var. truncatula					*	*						
Fragilaria virescens						*		*				
Tabellaria flocculosa								*				
Melosira granulata var. angustissima								*	*			
Synedra ulna var. biceps									*			
Fragilaria brevistriata										*		
Pinnularia nobilis										*		*
Nitzschia microcephala											*	
Fragilaria construens var. venter											*	
Navicula laevissima											*	
amphora ovalis						*			*			
Xanthophyta												
Tribonema minus	*	*	*				*	*	*	*	*	*
Ophiocytium parvulum			*				*	*	*		*	*
Ophiocytium capitatum				*								*
Tribonema affine			*	*	*		*					
Tribonema ulothrichoides			*									
Pyrrophyta												
Peridinium bipes Stein		*	**									
Ceratium hirundinella			*									
Peridinium gtunense							*					
Peridinium umbonatum								*	*			
Euglenophyta												
subgenus Catilliferae polymorpha		*	*					*	*		*	*
Strombomonas Schauinslandü			*						*			*
subgenus Rigidae gasterosteus			*								*	
Euglena gasterosteus				*	*							
Phacus inflexus							*	*	*			
Phacus longiauda								*				
Trachelomonas curta								*				
subgenus Rigidae wangü								*	*			
Lepocinclis teres									*			
Trachelomonas volvocina	*	*	**				*					
Chrysophyta												

http://www.aloki.hu ● ISSN 1589 1623 (Print) ● ISSN 1785 0037 (Online)
DOI: http://dx.doi.org/10.15666/aeer/1802_33873408

Chrysamoeba radians				*								
Epipyxis utriculus								*	*			
Dinobryon cylindricum											*	*

*: appeared;**: dominant species (dominance index > 0.02)

http://www.aloki.hu ● ISSN 1589 1623 (Print) ● ISSN 1785 0037 (Online)
DOI: http://dx.doi.org/10.15666/aeer/1802_33873408

INFLUENCE OF PHOSPHORUS FERTILIZER ON YIELD AND OIL OF SAFFLOWER *(CARTHAMUS TINCTORIUS)* VARIETIES UNDER RAINFED CONDITION

SOFY, S. O. – HAMA, S. J.* – HAMMA-UMIN, B. O.

Department of Biotechnology and Crop Science, College of Agricultural Engineering Sciences, University of Sulaimani, Sulaymaniyah, Iraq
(e-mails: shno.sofy@univsul.edu.iq, bestoon.omar@univsul.edu.iq)

**Corresponding author*
e-mail: shara.hama@univsul.edu.iq

(Received 30th Oct 2019; accepted 12th Feb 2020)

Abstract. This investigation was conducted during the winter seasons of 2017-2018 the Experimental Farm of the College of Agricultural Sciences, University of Sulaimani at Bakrajo, using split plot design to study the effect of three levels of phosphorus fertilizer on the growth, yield and yield components of safflower varieties. Three varieties namely Zaafarani, Aidn and; Al-shamia, were applied to the main plots, three phosphorus fertilizer levels (0, 50 and 100 kg P2O5/ha from Tsp. 48% source, were implemented in the subplots. Comparisons between means were carried out by the least significant difference (L.S.D) at 1% and 5% level of significance. The results showed that the Al-shaima varieties produced the best values at 15398.22 Kg/h and 1914.06 Kg/h followed by Aidn with values of 14508.77 Kg/h and 1655.72 for biological yield and seed yield respectively, finally the lowest values of 13662.88 Kg/h for biological yield and 1914.06 Kg/h for seed yield produced by Zaafarani. While the highest oil percentage was obtained from Zaafarani with values of 32.28% followed by Aiden with value of 29.62%, finally the lowest value of 28.10% was obtained from variety Al-shamia. The application of 100 Kg P/ha was found to be the best level for producing the highest seed yield with the highest percentage of oil. The trait of 100 seed weight showed a highly significant and positive correlation with seed yield, whereas the number of seeds/plant exerted the highest direct effect on seed yield Kg/ha, both traits were observed to be the most important trait for seed yield improvement in safflower.
Keywords: *safflower production, fertilization, growth parameters, protein percentage, oil components, correlation and path coefficient analysis*

Introduction

Safflower (*Carthamus tinctorius* L.) is an important annual industrial crop which is classified as a composite. It has more than 150 species that are scattered from Spain to North Africa, West Asia and India (Rastgou, 2013). These in turn are considered as the parental species of the cultivated species (*C. tinctorius* L.) in fact (*C. persicus,* and *flavenscens*) are the common subsidiary members of the Oak Forest association in Kurdistan (Guest, 1966). The stem, leaves, seeds and flowers are used as vegetable and industrial oil, bird feed, forage plant, medicinal purpose and for its colorful petals used as food coloring and flavoring agent (Dordas, and Sioulas, 2008). The oil content of seeds in Safflower is approximately 35 to 50 percent. Safflower oil preferred for its higher poly unsaturated fatty acid (78% linoleic acid) which reduces blood cholesterol level (Belgin and et al., 2007) also contains tocopherols, known to have antioxidant effect and high vitamin E content. For this reason, safflower oil is used in the diets of patients with cardiovascular disease, and bears great importance for its anti-cholesterol effect (Arsalan and Tuntruk, 2003). Safflower has different varieties from local to wild ones which are adapted to distinct climates in Iraq. This plant is considered as an almost tolerable plant to

http://www.aloki.hu ● ISSN 1589 1623 (Print) ● ISSN 1785 0037 (Online)
DOI: http://dx.doi.org/10.15666/aeer/1802_34093418

different conditions, because it is adapted to different weather conditions (Omidi-Tabrizi et al., 2000). In Safflower, some physiological treats like growth, seed quality and oil content are controlled by variety, different for instance plant density, and chemical fertilizer application (Weiss, 2000). But, the productivity of safflower is very low as the crop is cultivated under nutrient stress environment conditions. This necessitates rational application of these elements as they have become limiting factor for obtaining higher yields in safflower. Phosphorus (P) is vital to plant growth and is found in every living plant cell. It is involved in several key plant functions, including energy transfer, photosynthesis, transformation of sugars and starches, nutrient movement within the plant and transfer of genetic characteristics from one generation to the next (Sultenfuss and Doyle, 1999). Phosphorus (P) is the most limiting nutrient for crop growth and yield in many regions of the world (Rodriguez and Goudriaan, 1999), and application of P fertilizer represents an important measure to correct nutrient deficiencies and to replace nutrients having been removed in the products harvested (Dambroth and El-Bassam, 1990). However, recovery of fertilizer P in the first year is often below 15% and hardly reaches 50% after 30 years (Roy et al., 2000).

Therefore, the aim of this study was to evaluate the impact of phosphorous apply on growth, yield and oil percentage of safflower and to determine the best variety of safflower for yield and oil percentage.

Materials and methods

This study investigated in Sulaimani region, at Experimental Farm of the College of Agriculture Science Engineering, University of Sulaimani at Bakrajo located in the southwest of Sulaimani city (Latitude: 35° 33' N; Longitude 45° 27' Est altitude of approximately 830 m) during the winter season of 2017-2018. The meteorological data of Bakrajo location is shown in *Table 1*. The experimental area plots were ploughed twice, harrowed and well leveled. A brief account of some physical and chemical properties of the experimental soil is given in *Table 2*.

Three safflower varieties were selected for cultivation, which has been provided by The Sulaimani Agricultural Research Center, namely; Zaafarani, Aidn and; Al-shamia. The experiment was arranged as split- plot layout. The varieties were implemented in the main plots and conducted with Randomized Complete Block Design (RCBD), different levels of Phosphorus fertilizer (0, 50 and 100 Kg P_2O_5/ha) from TSP 46% were implemented in the subplots. Each main plot was consisted of three subplots with four rows (0.40 m between rows and 0.20 m between plants); thus, the plant population was 142,857plant/ha. Planting date was on 12th December of 2017. The cultural operations and weed control were accomplished according to normal field practices. Half of recommended dose of fertilization were added to the whole experiment which were 50 Kg Nitrogen/ha as urea and divided into two equal doses and were applied at the seeding time and after 20 days from germination.

The LSD test was done to find the significant differences between treatment means at 5% and 1% probability levels. Mature plants were harvested on 5th July, of 2018 for estimating seed yield, yield components and growth rate.

The studied characters were:

- 50% flowering.
- Dry matter/plant (g/plant): the mean weight of five plant sample were dried in oven for 48 h in 65 °C then weighted and recorded.

http://www.aloki.hu ● ISSN 1589 1623 (Print) ● ISSN 1785 0037 (Online)
DOI: http://dx.doi.org/10.15666/aeer/1802_34093418

- Plant height (cm): the mean height of the plant from ground level to the tip of five plants was recorded.
- No. of leaves/plant: the mean number of leaves per plant of the five plants was recorded.
- No. of seeds/plant: the mean number of seeds per plant of five plants was counted and recorded.
- 100 seed weight (g): 100 seeds were weighted and recorded and repeated three times.
- Oil %: 2 gm of the harvested seed of each treatment was powdered by electric blender. Digital soxhlet instrument used for oil distillation, with n-hexane solvent (Ferreira-Dias et al., 2000), the oil content calculated as follows:

$$\text{Oil percent} = \{(W2 - W1) \times 100\} / S \quad \text{(Eq.1)}$$

W1 = weight of empty flask (g), W2 = weight of flask and extracted oil (g), S = weight of sample.

- Protein (%): quantification of total protein by Bradford assay method (He, 2011).
- Ash content (%): seed ash content was estimated by muffle furnace on the 550 °C according to the following equation:

$$\text{Ash\%} = \text{Total ash / weight of the sample} \times 100 \quad \text{(Eq.2)}$$

- Biological yield (Kg/ha): the mean of weight of the five plant samples without the roots was recorded in each plot (g/plant) and converted to Kg/ha.
- Seed yield (Kg/ha): the mean of seeds weight of the five plant samples was recorded in each plot (g/plant) and converted to Kg/ha.

Correlation analysis

The correlation coefficient was conducted to determine the degree of association of characters with seed yield and also among all the criteria studied. Phenotypic correlations were computed between the characters in the growing season using the formula given by Singh and Chaudhary (1985).

Path coefficient analysis

The path coefficient analysis was carried out as suggested by Dewey and Lu (1959). Seedyield was kept as resultant variable and other characters as causal through (Analysis of Moment Structures) AMOS Ver. 18 Software.

Results and discussion

Data in *Table 3* confirm that the differences among varieties were highly significant for the studied criteria plant height, number of leaves per plant, dry matter weight oil % and seed yield, while it was significant for the characters100-seed weight, Protein % and biological yield. More leave number, and oil percentage was obtained by Zaafarani, as compared to Aidn and; Al-shamia with values of 616.22 and 32.58 respectively, followed by Aidn which was recorded value of 133.88 cm plant high, values of

http://www.aloki.hu ● ISSN 1589 1623 (Print) ● ISSN 1785 0037 (Online)
DOI: http://dx.doi.org/10.15666/aeer/1802_34093418

102.25 g total plant dry mater accumulate (leave, stem, and flower dry weight) and values of 3.76 g 100-seed weight. While, Al-shamia was significant in producing biological yield with value of 15398.22 Kg/ha and with value of 1914.06 Kg/ha for seed yield. This variation between the studied varieties was related to genetic variation and variation in their responses to the use of different levels of phosphorus fertilizer, as previously reported by Banna (2011) and Ryan et al. (2009).

Table 1. *Average air temperature and rainfall during the growing seasons of 2017-2018 at Bakrajo location*

Months	Average air temperature (°C)		Rainfall (mm)
	Max.	Min.	
October	33.1	10.4	10.0
November	23.9	7.6	114.6
December	17.8	-2.5	22.2
January	15.6	1.4	72.4
February	20.9	-2.3	323.0
March	24.4	1.0	44.6
April	31.6	2.2	98.6
May	38.1	13.0	70.4
Total			755.8

Table 2. *Physical and chemical properties of the studied soil*

Soil properties	Values
Texture class	Clay
Sand (g kg-1)	41.0
Silt (g kg-1)	430.50
Clay (g kg-1)	528.50
EC (dS m-1)	0.61
pH	7.32
OM (g kg-1)	21.60
CaCO3 (g kg-1)	107.0
Total N (mg kg-1)	1.07
K + (mmoles l-1)	0.32
Na + (mmoles l-1)	0.41
Ca + + (mmoles l-1)	1.49
Cl- (mmoles l-1)	0.57

Table 3. *Means of variety on the studied characters*

Varieties	Plant height (cm)	No. of leaves/plant	No. of seeds/plant	Dry matter (g/plant)	100 Seed weight (g)	Oil %	Protein %	Ashe %	Biological yield (Kg/ha)	Seed yield (Kg/ha)
V1	130.11 a	616.22 a	505.56	91.92 b	3.31	32.58 a	9.033	0.026	13662.88	1545.35b
V2	133.88 a	516.00 b	461.00	102.25 a	3.76	29.62 b	11.294	0.025	14508.77	1655.72b
V3	100.00 b	554.89 b	520.44	84.95 b	3.68	28.10c	9.243	0.026	15398.22	1914.06 a
LSD ($P \leq 0.05$)	9.72	59.99	N.S	7.91	0.34	0.90	1.595	N.S	1279.24	193.43
LSD ($P \leq 0.01$)	13.39	82.65	N.S	10.90	N.S	1.24	N.S	N.S	N.S	266.51

N.S: not significant

http://www.aloki.hu ● ISSN 1589 1623 (Print) ● ISSN 1785 0037 (Online)
DOI: http://dx.doi.org/10.15666/aeer/1802_34093418

The effect of phosphorus fertilizer application was found to be highly significant for all characters except of plant height and Ashe% (*Table 4*). The best values of 658.22, 561.78, 101.971 g, 3.897 g, 31.59%, 12.99, 16728.77 Kg/ha and 1972.433/ha for the number of leaves per plant, number of seeds per plant, dry matter weight, 100 seed weight, oil percentage, protein percentage, biological yield and seed yield respectively, were obtained by plants grown under 100 Kg P/ha except protein percentage was obtained by plants grown under 0 Kg P/ha. While the lowest values of 473.333, 422.67, 81.906 g, 3.177 g, 28.69%, 7.94%, 11118.88 Kg/ha and 1470.06 Kg/ha for the number of leaves per plant, number of seeds per plant, dry matter weight, 100 seed weight, oil percentage, protein percentage, biological yield and seed yield respectively, were obtained by plants grown under control, except protein percentage was obtained by the plants grown under 100 Kg P/ha. Because Phosphorus plays a major role in several physiological processes like photo-synthesis, respiration, energy storage and transfer, cell division, cell enlargement and development of meristematic tissues (Mengal and Kirkby, 2000). In addition, P is also an integral structural component of many biochemical, i.e. nucleic acids, which is the basic component of gene and chromosomes and asses to heredity (Blevins, 1999; Halvin et al., 1999). The P availability may affect yield formation by differential influence on individual yield components. However, little is known on this response in safflower as compared to sunflower (Kumar, 2000).

Data in *Table 5* confirm that the interaction between varieties and phosphorus application levels was significant only for the character Biological Yield Regarding the characters of Biological yield the interaction between Aidnand 100 Kg/ha of phosphorus fertilizer recorded maximum Biological yield reached 18113.00 Kg/h, while the minimum Biological yield was 9341.66 Kg/h recorded by the variety Aidnand the control treatment.

Data in *Table 6* explain the correlation coefficients among the characters. Highly significant and positive correlation represented between seed yield and 100 seed weight similar finding was showed by Singh (2004), while significantly and positively correlated with no. of seeds/plant and biological yield this agree with Pavithra (2016). The character no. of leaves/plant showed highly significant and negative correlation with protein percent, while correlated highly significantly and positively with no. of seed/plant and correlated positively with the character oil percent. Highly significant and positive correlation observed between the characters no. of seed/plant and biological yield, whereas the characters no. of seed/plant was highly significantly and negatively correlated with protein percent. Data in the same table confirm the presence of significant and positive correlation between the character dry matter weight and biological yield. The estimation of correlation coefficient between the character 100 seed weight and biological yield were significant and positive. The character biological yield showed significant and negative correlation with protein percent.

Data in *Table 7* represented the estimation of path coefficient analysis between characters. The character no. of Seeds/plant had maximum positive direct effect on seed yield/plant with 1.803 similar findings was also reported by Semahegn (2016), whereas the character oil% showed maximum negative direct effect on seed yield/plant with -0.690 this result is correspondence with Jadhav (2016). All characters except the plant height and protein% were exhibited maximum positive indirect effect via the character no. of seeds/plant on the seed yield/plant with 1.639, 1.494, 1.054, 0.852 and 0.781, while maximum negative indirect effect was showed by the character protein% via no. of seeds/plant on the seed yield/plant with -1.678.

http://www.aloki.hu ● ISSN 1589 1623 (Print) ● ISSN 1785 0037 (Online)
DOI: http://dx.doi.org/10.15666/aeer/1802_34093418

Table 4. *Effect of P fertilizer levels on the studied characters*

Phosphorus fertilizers levels (Kg/h)	Plant height (cm)	No. of leaves/plant	No. of seeds/plant	Dry matter (g/plant)	100 Seed weight (g)	Oil %	Protein %	Ashe %	Biological yield (Kg/ha)	Seed yield (Kg/ha)
0	120.78	473.33 c	422.67 b	81.90 b	3.17 b	28.69 c	12.99 a	0.026	11118.88 b	1470.067 c
50	121.33	555.56 b	502.56 ab	95.25 a	3.69 a	30.01 b	8.63 b	0.026	15722.22 a	1672.647 b
100	121.89	658.22 a	561.78 a	101.97 a	3.89 a	31.59 a	7.94 b	0.025	16728.77 a	1972.433 a
LSD ($P \leq 0.05$)	0.00	59.99	80.32	7.91	0.34	0.90	1.59	0.000	1279.24	193.433
LSD ($P \leq 0.01$)	N.S	82.65	110.65	10.90	0.46	1.24	2.19	N.S	1762.52	266.510

N.S.: not significant

Table 5. *The interaction effect of varieties and phosphorus fertilizer levels on studied characters*

Varieties × phosphorus fertilizer levels Kg/ha	Plant height (cm)	No. of leaves/plant	No. of seeds/plant	Dry matter weight (g/plant)	100 seed weight (g)	Oil %	Protein %	Ashe%	Biological yield (Kg/ha)	Seed yield (Kg/ha)
Zaafarani × 0	127.33 a	529.33 a	429.67 a	82.80 a	2.93 a	30.84 a	12.91 a	0.025 a	11689.33 e	1313.76 a
Zaafarani × 50	126.00 a	608.67 a	508.67 a	93.76 a	3.39 a	32.35 a	7.38 a	0.027 a	13914.00 cd	1440.93 a
Zaafarani ×100	137.00 a	710.67 a	578.33 a	99.22 a	3.63 a	34.55 a	6.80 a	0.025 a	15385.33 bc	1881.36 a
Aidn × 0	133.00 a	425.67 a	382.00 a	84.40 a	3.57 a	28.07 a	15.05 a	0.026 a	9341.66 f	1542.66 a
Aidn × 50	132.66 a	509.00 a	466.33 a	104.91 a	3.82 a	29.14 a	9.94 a	0.024 a	16071.66 abc	1600.40 a
Aidn × 100	136.00 a	613.33 a	534.67 a	117.43 a	3.90 a	31.10 a	8.89 a	0.025 a	18113.00 a	1824.10 a
Al-shamia × 0	102.00 a	465.00 a	456.33 a	78.51 a	3.02 a	27.09 a	11.03 a	0.027 a	12325.66 de	1553.76 a
Al-shamia× 50	105.33 a	549.00 a	532.67 a	87.09 a	3.87 a	28.14 a	8.56 a	0.026 a	17181.00 ab	1976.60 a
Al-shamia× 100	92.66 a	650.67 a	572.33 a	89.26 a	4.15 a	29.61 a	8.13 a	0.026 a	16688.00 ab	2211.83 a
L.S.D ($P \leq 0.05$)	N.S	N.S	N.S	N.S	N.S	N.S	N.S	N.S	2215.71	N.S
L.S.D ($P \leq 0.01$)	N.S	N.S	N.S	N.S	N.S	N.S	N.S	N.S	N.S	N.S

N.S: not significant

http://www.aloki.hu ● ISSN 1589 1623 (Print) ● ISSN 1785 0037 (Online)
DOI: http://dx.doi.org/10.15666/aeer/1802_34093418

Table 6. *Correlation coefficients among the characters*

	Seed yield (Kg/ha)	**Plant height (cm)**	**No. of leaves/plant**	**No. of seeds/plant**	**100 seed weight (g)**	**Dry matter (g/plant)**	**Biological yield (Kg/ha)**	**Oil %**	**Protein %**	**Ashe %**
Seed yield (Kg/ha)	1									
Plant height (cm)	-0.472$^{n.s}$	1								
No. of leaves/plant	0.555$^{n.s}$	0.037$^{n.s}$	1							
No. of seeds/plant	0.772*	-0.242$^{n.s}$	0.909**	1						
100 seed weight (g)	0.829**	-0.125$^{n.s}$	0.420$^{n.s}$	0.585$^{n.s}$	1					
Dry matter (g/plant)	0.235$^{n.s}$	0.555$^{n.s}$	0.471$^{n.s}$	0.433$^{n.s}$	0.540$^{n.s}$	1				
Biological yield (Kg/ha)	0.700*	-0.151$^{n.s}$	0.644$^{n.s}$	0.828**	0.713*	0.671*	1			
Oil %	-0.036$^{n.s}$	0.599$^{n.s}$	0.765*	0.472$^{n.s}$	0.011$^{n.s}$	0.500$^{n.s}$	0.227$^{n.s}$	1		
Protein %	-0.555$^{n.s}$	0.148$^{n.s}$	-0.849**	-0.931**	-0.453$^{n.s}$	-0.458$^{n.s}$	-0.789*	-0.534$^{n.s}$	1	
Ashe %	-0.048$^{n.s}$	-0.551$^{n.s}$	-0.151$^{n.s}$	-0.044$^{n.s}$	-0.284$^{n.s}$	-0.587$^{n.s}$	-0.323$^{n.s}$	-0.316$^{n.s}$	-0.024$^{n.s}$	1

N.S: Not significant; *: Significant; **: Highly significant

Table 7. *Path coefficient analysis confirming direct (diagonal values) and indirect effects among the characters*

	Plant height (cm)	**No. of seeds/plant**	**100 seed weight (g)**	**Dry matter (g/plant)**	**Biological yield (Kg/ha)**	**Oil %**	**Protein %**	**Ashe %**	**Correlation seed yield (Kg/ha)**
Plant height (cm)	0.266	-0.437	-0.049	-0.057	0.074	-0.413	0.067	0.077	-0.472
No. of leaves/plant	0.010	1.639	0.163	-0.048	-0.318	-0.528	-0.384	0.021	0.555
No. of seeds/plant	-0.064	1.803	0.227	-0.044	-0.409	-0.326	-0.421	0.006	0.772
100 Seed weight (g)	-0.033	1.054	0.389	-0.055	-0.352	-0.008	-0.205	0.040	0.829
Dry matter t (g/plant)	0.147	0.781	0.210	-0.102	-0.331	-0.345	-0.207	0.082	0.235
Biological yield (Kg/ha)	-0.040	1.494	0.277	-0.069	-0.494	-0.157	-0.357	0.045	0.700
Oil %	0.159	0.852	0.004	-0.051	-0.112	-0.690	-0.242	0.044	-0.036
Protein %	0.039	-1.678	-0.176	0.047	0.389	0.369	0.452	0.003	-0.555
Ashe %	-0.146	-0.079	-0.110	0.060	0.159	0.218	-0.011	-0.139	-0.048

http://www.aloki.hu ● ISSN 1589 1623 (Print) ● ISSN 1785 0037 (Online)
DOI: http://dx.doi.org/10.15666/aeer/1802_34093418

Conclusions and recommendation

From the results obtained in this study, it can be concluded that the variety of Zaafarani with non-phosphorus fertilizer application to cultivate for produce oil yield. However, the variety of Al-shamia with the level of 100 Kg P_2O_5/ha for produce economic seed yield under the rain fed condition of Sulaimani province and both traits observed to be the most important trait for seed yield improvement in safflower, so we recommended cultivation of these varieties in our region under the application of 100 Kg P_2O_5/ha to reach maximum yield.

REFERENCES

[1] Arslan, B., Altuner, F., Tuncturk, M. (2003): An investigation on yield and yield components of some safflower varieties which grown in Van. – 5th Field Crops Congress of Turkey 1: 468-472.
[2] Banna, M. N. (2011): Evaluation of 16 barley genotypes under calcareous soil conditions in Egypt. – J. Agric. Sci. 3(1): 105-121.
[3] Belgin, C., Bilal, G., Mustafa, K. (2007): Oil content and fatty acid composition of some safflower (*Cartham ustinctorius* L.) varieties sown in spring and winter. – Inter. J. Nat. and Eng. Sci. 1(3): 11-15.
[4] Blevins, D. G. (1999): Why plants need phosphorus. – Better Crops 83: 29-30.
[5] Dambroth, M., El-Bassam, N. (1990): Genotypic Variation in Plant Productivity and Consequences for Breeding of Low-Input Cultivars. – In: El-Bassam, N., Dambroth, M. C., Loughman, B. C. (eds.) International Symposium on Genetic Aspects of Plant Mineral Nutrition. Kluwer Academic Publishers, Dordrecht.
[6] Dewey, D. R., Lu, K. H. (1959): A correlation and path-coefficient analysis of components of crested wheatgrass grain production. – Agronomy Journal 51: 515-518.
[7] Dordas, C., Sioulas, C. (2008): Safflower yield, chlorophyll content, photosynthesis, and water use efficiency response to nitrogen fertilization under rainfed conditions. – Indian Crop Production 27: 75-85.
[8] Guest, E. (1966) Flora of Iraq. Vol. 1. – Ministry of Agricultural, Baghdad.
[9] Halvin, J. L., Beaton, J. D., Tisdale, S. L., Nelson, W. L. (1999): Soil Fertility and Fertilizers, an Introduction to Nutrient Management. 6th Ed. – Pearson Education, Singapore, pp.154-196.
[10] He, F. (2011) Bradford protein assay. – Bio 101: e45. DOI: 10.21769/BioProtoc.45.
[11] Jadhav, S. A., Dhuppe, M. V., Salunke, P. M. (2016): Correlation coefficient and path analysis in safflower (*Carthamus tincorius,* L.). – International Journal of Current Microbiology and Applied Sciences 2016(Special Issue). https: www.ijcmas.com.
[12] Kumar, H. (2000): Development potential of safflower in comparison to sunflower. – Sesame and Safflower Newsletter 15: 86-89.
[13] Mengal, K., Kirkby, E. A. (2000): Principles of Plant Nutrition. 5th Ed. – Int'l. Potash Instt., Switzerland.
[14] Omidi-Tabrizi, A. H., Ahmadi, M. R., Shahsavarii, M. R., Karimi, S. (2000): Evaluation of oil and seed yield stability on some of safflower winter variety and lines. – Seed and Plant Improvement Journal 16(2): 130-145 (in Persian with English abstract).
[15] Pavithra, K. P., Rajesh, Patil, S., Yallappa, H., Nishanth, G. K. (2016): Correlation and path analysis studies in safflower (*Carthamus tinctorius* L.) germplasm. – Research Journal of Agricultural Sciences 7(2): 428-432. https: www.rjas.org.

http://www.aloki.hu ● ISSN 1589 1623 (Print) ● ISSN 1785 0037 (Online)
DOI: http://dx.doi.org/10.15666/aeer/1802_34093418

[16] Rastgou, B., Ebadi, A., Vafaie, A., Moghadam, S. H. (2013): The effects of nitrogen fertilizer on nutrient uptake, physiological traits and yield components of safflower (Carthamus tinctorius L.). – Int. J. Agron. Plant Prod 4(3): 355-364.
[17] Rodriguez, D., Andrade, F. H., Goudriaan, J. (1999): Effects of phosphorus nutrition on tiller emergence in wheat. – Plant and Soil 209: 283-295.
[18] Roy, R. N., Finck, A., Blair, G. J., Tandon, H. L. S. (2006): Plant Nutrition for Food Security, a Guide for Integrated Nutrient Management. – FAO Fertilizer and Plant Nutrition Bulletin 16. FAO, Rome.
[19] Ryan, J., Abdel-Monem, M., Amir, A. (2009): Nitrogen fertilizer response of some barley varieties in semi-arid in Morocco. – J. Agric. Sci. Technol. 11: 227-236.
[20] Semahegn, Y., Tesfaye, M. (2016)*:* Characters Associations and Path Analysis in Safflower (*Carthamus tinctorious*) Accessions. – Holetta Research Center, Ethiopian Institute of Agricultural Research, Molecular Plant Breeding, Vol. 7, No. 31.
[21] Sing, R. K., Chaudhary, B. D. (1985): Biometrical Methods in Quantitative Genetic Analysis. Revised Edition. – Kalyani Publishers, Ludhiana.
[22] Sultenfuss, J. H., Doyle, W. J. (1999): Functions of Phosphorus in Plants. – Better Crops 83 (1): 6 -7.
[23] Vrijendra, S., Deshpande, M. B., Choudhari, S. V., Nimbkar, N. (2004): Correlation and Path Coefficient Analysis in Safflower (*Carthamus tinctorius* L.). – Nimbkar Agricultural Research Institute (NARI), Maharashtra.
[24] Weiss, E. A. (2000): Oilseed Crops. 2nd Ed. – Blackwell Science, Oxford.

http://www.aloki.hu ● ISSN 1589 1623 (Print) ● ISSN 1785 0037 (Online)
DOI: http://dx.doi.org/10.15666/aeer/1802_34093418

APPENDIX

Table A1. *Mean squares of variance analysis for seed yield and its components of studied characters*

S.O.V	d.f	Plant high (cm)	No. of leaves/plant	No. of seeds/plant	Dry weight/plant (g)	100 seed weight (gm)	Oil %	Protein%	Ashe%	Biological yield Kg/ha	Seed yield/ka/ha
Blocks	r-1 = 2	116.33	6188.25	6132.00	1.76	0.11	3.55	3.187	-0.006	19608914.37	44884.00
A (varieties)	a-1 = 2	3104.11**	22977.92**	8610.77 N.S	681.30**	0.51*	46.69**	14.046*	0.000 N.S	6777031.81 *	320265.44**
B (phosphorus fertilizer levels (Kg/ha)	b-1 = 2	2.77N.S	77227.25**	43862.11**	938.96**	1.24**	19.02**	67.688**	0.000 N.S	80512027.81 **	573808.00**
Varieties × phosphorus fertilizer levels (Kg/ha)	(a-1)(b-1) = 4	122.38N.S	9.48 N.S	354.22 N.S	100.86 N.S	0.13 N.S	0.55 N.S	3.173 N.S	0.000 N.S	7248454.25 N.S	44976.44 N.S
Error (b)	a(b-1)(r-1) = 16	94.62	3604.09	6460.08	62.70	0.11	0.81	2.548	0.001	1638641.78	37320.00
Total	abr-1 = 26	116.33	6188.25	6132.00	1.76	0.11	3.55	3.187	-0.006	19608914.37	44884.00

N.S: Not significant; *: Significant; **: Highly significant

Table A2. *Correlation coefficients among the characters*

	Seed yield (Kg/ha)	Plant height (cm)	No. of leaves/plant	No. of seeds/plant	100 seed weight (g)	Dry matter (g/plant)	Biological yield (Kg/ha)	Oil %	Protein %	Ashe %
Seed yield (Kg/ha)	1									
Plant height (cm)	-1.413	1								
No. of leaves/plant	1.767	0.098	1							
No. of seeds/plant	3.213	-0.661	5.767	1						
100 seed weight (g)	3.927	-0.334	1.226	1.907	1					
Dry matter weight (g/plant)	0.639	1.766	1.411	1.272	1.699	1				
Biological yield (Kg/ha)	2.592	-0.404	2.228	3.911	2.691	2.392	1			
Oil %	-0.094	1.979	3.140	1.418	0.029	1.530	0.617	1		
Protein %	-1.763	0.397	-4.247	-6.732	-1.345	-1.362	-3.394	-1.671	1	
Ashe %	-0.127	-1.746	-0.405	-0.116	-0.783	-1.919	-0.902	-0.882	-0.063	1
t(P ≤ 0.05)	2.365									
t(P ≤ 0.01)	3.499									

http://www.aloki.hu ● ISSN 1589 1623 (Print) ● ISSN 1785 0037 (Online)
DOI: http://dx.doi.org/10.15666/aeer/1802_34093418

PARASITES GOVERN THE TOPOLOGICAL PROPERTIES OF FOOD WEBS: A CONCLUSION FROM NETWORK ANALYSIS

CHEN, J. L. – ZHANG, W. J.*

School of Life Sciences, Sun Yat-sen University, Guangzhou 510275, China

**Corresponding author*
e-mail: zhwj@mail.sysu.edu.cn, wjzhang@iaees.org

(Received 12th Nov 2019; accepted 23rd Mar 2020)

Abstract. Parasitism has been ignored in most of the food web research. However, it has been found to play an important role in maintaining food web structure. In order to present further evidences and findings on the functionality of parasitism in food webs, this study used the methodology of network science and meta-analysis to analyze and compare topological properties of seven high-resolution marine and estuarine food webs that include free-living species only and all species with parasites respectively. The results showed that parasites significantly changed the species structure in the food webs. The number and proportion of top species declined and that of intermediate species increased once parasites were included in the food webs. The number of links and cycles, the connectance and link density of food webs significantly increased, among which most links are related to parasites and the complexity of food webs was thus enhanced. Parasitism increased food web spacing and overall clustering coefficient and food webs were made more closely connected. Parasitism was proved to have significant influence on the relative importance of species, and even to make some species crucial species in terms of food webs.
Keywords: *link density, connectance, clustering coefficient, network biology, meta-analysis*

Introduction

A food web is the network to describe between-species trophic relationships and energy / matter flows (Pimm et al., 1991; Kuang and Zhang, 2011; Jiang and Zhang, 2015), in which species are nodes and interacting species are connected by links. In a representative food web, plant species are at the trophic level of the first or primary producers, herbivores are at the second or primary consumer trophic level, and carnivorous animals are at the third or secondary consumer trophic level. In addition, if there are more advanced carnivores that feed on other carnivores, they will produce an even higher trophic level. Food webs are the focus of research on stability, diversity and complexity of ecosystems (Montoya and Pimm, 2006; Pascual and Dunne, 2006; Dunne et al., 2013). As self-organizing systems, they can be used to describe the nutritional relationship between species in the nature (Pimm et al., 1991; Williams and Martinez, 2000; de Araújo et al., 2017; de Araújo, 2018; Zhang, 2015, 2018). Studying food webs helps us understand the patterns of ecosystem organization and their relationship with ecological stability (Pimm, 1991; Pimm et al., 1991; Warren, 1994; McCann, 2000; Ferrarini, 2017; Wahab et al., 2017). A further objective of food web studies is to understand how they affect the functioning of ecosystems, thus further predict the environmental problems such as climate changes and species invasion (Ings et al., 2009).

The early studies of food webs began with MacArthur (1955). Major works during his period included: (1) food webs were in text and graphically expressed; (2) spatial uniformity and relationship linearity of between-species trophic relationships were assumed to analyze the stability and equilibrium of food webs. The studies during 1990s

http://www.aloki.hu ● ISSN 1589 1623 (Print) ● ISSN1785 0037 (Online)
DOI: http://dx.doi.org/10.15666/aeer/1802_34193437

to 2000s have focused on general principles of link distribution. How to find general and stable patterns in food webs was one of the focuses of those studies (May, 1973; Cohen et al., 1993; Navia et al., 2010). Studies have shown that food webs, including terrestrial, freshwater and marine food webs shared some common patterns and features as (Pimm et al., 1991; Jiang and Zhang, 2015): (1) cycles were rarely found in the food web; (2) the mean of the proportion top species (T) / intermediate species (I) / basal species (B), was an invariant value (Cohen and Newman, 1985); (3) the proportion, intermediate to top species links / basal to intermediate species links / basal to top species links, was averagely an invariant; (4) link density was nearly an invariant in the food webs with fewer species, and link density would increase with the increase of species; (6) omnivores were rarely found in certain food webs; (7) compartments were rarely found; (8) for top predators, their food chain length was generally 2 or 3, other chain lengths were rarely found.

As a biological network, the food web has various topological properties, including the number of species (S) and links (L), connectance (C; L/S^2), link density (L/S), cycles, chain length, etc (Kuang and Zhang, 2011; Dunne et al., 2013; Nuwagaba and Hui, 2015). Among these, the number of species and links represent species richness. Connectance and link density can be used to quantify the complexity of food webs and are thus important indicators of food web stability (Pimm and Lawton, 1980; Dunne et al., 2002; Montoya and Solé, 2003; Dunne, 2006; Montoya et al., 2006; Allesina et al., 2008; Allesina and Pascual, 2008; Zhang, 2012a,b). In addition, other topological properties such as Degree Centrality (DC) and Between Centrality (BC) help us measure the importance of a species in the food web (Zhang, 2018).

Unfortunately, most of the above findings have been achieved by analyzing the interactions between free-living species. Recent studies have found that parasites can profoundly affect food web properties. Parasites were found to have almost the same richness and productivity as their free-living hosts with the similar sizes and trophic levels. Studies have demonstrated that in terms of the trophic relationship, parasites had the body size ratio to their hosts that opposites the most free-living consumer-resource body size ratio, which helps them adjust the abundance of their host species. Parasites often have complex life cycles, and sometimes need to live in different host species with various body sizes. They may have the trophic specialization modes different from the free-living predators. They may be associated with their hosts in different topological positions. Their interactions with hosts can reorganize ecological communities and change the functioning of ecosystems. All these factors may lead to their difference with free-living organisms in adapting food webs and affecting food web structures. More and more evidence have been demonstrating that parasites may uniquely alter the food chain length, connectance and robustness of food webs, and thus change the topology of food webs or even the stability, interaction strength and energy flow of food webs (Anderson and May, 1978; McCallum and Dobson, 1995; Dobson et al., 2006; Wood, 2007; Allesina et al., 2008; Allesina and Pascual, 2008a,b; Kuris et al., 2008; Hechinger et al., 2011; Nedorezov, 2012; Sato et al., 2012; Dunne et al., 2013; Jiang et al., 2015; Shakil et al., 2015).

Although most of the food web studies have shown that the vulnerability at the highest trophic level is the smallest, if the parasites parasitize the species at the intermediate trophic level rather than at the lowest trophic level, those species may have the highest vulnerability to natural enemies' attack. These findings indicated that the food web without considering parasites is incomplete. Parasitic links are so important to

http://www.aloki.hu ● ISSN 1589 1623 (Print) ● ISSN1785 0037 (Online)
DOI: http://dx.doi.org/10.15666/aeer/1802_34193437

ecosystem stability because they can increase the link density and nestedness (Lafferty et al., 2006a,b). Parasites are always ignored mainly due to their small sizes, and lack of cross-disciplinary collaboration, identification and quantification of parasites in food webs, and parasitology skills (Lafferty et al., 2008).

Given the importance of parasites in food webs, how to include parasites in food web studies is becoming a very important topic in recent years and findings have been achieving (Huxham et al., 1995, 1996; Marcogliese and Cone, 1997; Memmott et al, 2000; Marcogliese, 2003; Lafferty et al., 2006a,b; Hernandez and Sukhdeo, 2008; Lafferty and Kuris, 2009; Amundsen et al., 2009, 2012; Warren et al., 2010; Kuang and Zhang, 2011; Dunne et al., 2013; Jiang et al., 2015; Jiang and Zhang, 2015). However, the further confirmation of above findings and deep exploration of the impact of parasites on topological structure of different food webs is still a problem to be addressed. For example, Kuang and Zhang (2011) studied the Carpinteria Salt Marsh (CSM) food web and have reached certain conclusions, such as the changes in species structure, and the increase in the number of cycles and links, and the increase of chain length and omnivorousness if parasites have been included, etc. Nevertheless, these results have been obtained from the topological analysis on a single food web with relatively low accuracy. In addition, although ecologists acknowledge the important role that parasites play in ecological communities, but few literatures have examined whether the addition of parasites changes the crucial species in the food web. In general, the specific mechanism of influence of parasites on the topology of food webs is still unclear and needed to be further exploited.

In recent years, with the advance of food web studies, we have been obtaining more and more full and fine quantitative data (Ings et al., 2009). These data make the findings of food webs more rigorous and credible. However, many of these results appeared to be non-natural laws because the data used was incomplete and the error has thus produced (Cohen et al., 1993; Winemiller and Polis, 1996). Aiming to present further evidences on the functionality of parasitism in food webs, the present study used the methodology of network biology and meta-analysis to analyze and compare the topological properties of seven high-resolution marine and estuarine food webs that include free-living species only and all species with parasites respectively.

Materials and Methods

Materials

Data sources

The food web data used in present study were achieved from seven sources: (1) Carpinteria Salt Marsh (CSM) (Hechinger et al., 2011); (2) Estero de Punta Banda (EPB) (Hechinger et al., 2011); (3) Bahía Falsa in Bahía San Quintín (BSQ) (Hechinger et al., 2011); (4) Flensburg Fjord on the Baltic Sea (FFB) (Zander et al., 2011); (5) Otago Harbour (OHR) (Mouritsen et al., 2011); (6) Sylt tidal basin in Germany and Denmark (STB) (Thieltges et al., 2011), and (7) the Athan estuary, Aberdeenshire (YEA) (Huxham et al., 1996). For the seven high-resolution coastal estuary food webs above, two versions of each network were analyzed: one containing predators and preys only (-FREE), and the other containing all species and links including parasitoid relationships (ALL).

http://www.aloki.hu ● ISSN 1589 1623 (Print) ● ISSN1785 0037 (Online)
DOI: http://dx.doi.org/10.15666/aeer/1802_34193437

These food webs are composed of basic species, free-living species and parasites. Among them, the BSQ ALL network contains 171 species, of which 52 species are parasitic. The CSM ALL network contains 165 species, of which 58 species are parasitic. There are 214 species in the EPB ALL network, of which 76 species are parasitic. FFB ALL includes 123 species, of which 46 are parasitic species. OHR ALL has 142 species, of which 19 species are parasitic. STB ALL network contains 161 species, of which 35 species are parasitic. YEA ALL contains 134 species, of which 42 species are parasitic. The raw data for each network consists of two columns, the first column is the consumer species, and the second column contains the species with the same category as the first column, but exists as predators or hosts.

Data transformation

Before making analysis, the format of the data obtained above should be transformed. First, we constructed the $n \times n$ food web matrix of n species based on the predation relationship between species, in which the elements were composed of 0 or 1. If there is the predation relationship between the two species and the column species is predator, the element is represented by 1. Otherwise, 0 means that there is no predation between the two species. Second, after constructing the food web matrix, UCINET and Netdraw software were used to transform the ".xlsx" file in Excel to the ".net" file in Pajek. And in UCINET, the command series was used: data→data editors→matrix editor, and then ".##h" format data was saved. In Netdraw, the command series was conducted: file→open→ucinet dataset→network, and the previously saved ".##h" file was opened by the command series: →file→save data as→pajek→net file, and finally, we saved the data as ".net" format file for forthcoming analyses (Jiang and Zhang, 2015; Zhang, 2012a, 2018).

Methods

Pajek

Pajek is the computational platform for analyzing and visualizing complex networks that contain up to millions of nodes. A variety of methods/algorithms for network analysis are embedded in Pajek. It is mainly used to conduct global analysis on complex networks (Batagelj and Mrvar, 2004; Kuang and Zhang, 2011; Jiang and Zhang, 2015; Zhang, 2018).

Network analysis

(1) Category of species

In the network analysis, the number of species (nodes) is generally denoted by S. The species in the food web can be divided into top species (T; i.e., the species that cannot be fed by other species), intermediate species (I; i.e., the species acting as both predators and preys), and basal species (B; i.e., the species unable to feed on other species) (Pimm et al., 1991; Dunne et al., 2013).

(2) Degree analysis

The degree of a node refers to the number of nodes connected to the node (Zhang, 2012c, 2018). Degree is the most basic topological property for complex networks. In general, the greater the degree of a node is, the higher the importance of the node in the network will be. In a directed network, the degree of a node is the sum of incoming degree and outgoing degree. Food webs are directed networks. In the Pajek software, we

http://www.aloki.hu ● ISSN 1589 1623 (Print) ● ISSN1785 0037 (Online)
DOI: http://dx.doi.org/10.15666/aeer/1802_34193437

can execute the command series, Net→Partions→Degree→In/Out/All under Net/Partitions/Degree menu, to achieve the incoming degree, outgoing degree and total degree.

(3) Food chain and food cycle analysis

A cycle (i.e., circuit) is a closed chain in the food web. In the food web, there are sometimes phenomena such as *A* feeds on *B*, *B* feeds on *C*, and *C* feeds on *A*. In such a situation, a closed loop is generated among the species *A*, *B* and *C*. Cannibalism is one of the food cycles. In the Pajek, the food cycles can be obtained by running the command series, Net→Count→4-rings→Directed→Cyclic.

(4) Link and connectance analysis

Two species (i.e., nodes) produce a link through predation relationship. The number of links in the network is represented by *L*. The link relationships are generally classified into basal species –intermediate species link (*B-I*), intermediate species - intermediate species link (*I-I*), basal species - top species link (*B-T*), and intermediate species - top species link (*I-T*).

Connectance (*C*) refers to the percentage of links *L* observed in the food web as a percentage of all possible connections that may be present in the web. That is, $C=L/S^2$ (Dunne et al., 2013). Link density refers to the ratio of the number of links in the food web to the number of total species (*L*/*S*) (Zhang, 2012a,b, 2018). If link density remains the same, the more species in the food web has, the greater the connectance will be (Pimm et al., 1991).

(5) Crucial species and node centrality analysis

Every species in the food web are different in maintaining ecosystem function. It is often necessary to identify crucial species that are extremely important or have a large impact on the food web, which is also due to the consideration of species protection (Jordán, 2009). Network topology analysis plays a powerful role in quantifying the importance of species (Livi et al., 2011). Node centrality measures can be used to quantify the importance of species in food webs. In present study, degree centrality (*DC*) and closeness centrality (*CC*) were used (Jiang and Zhang, 2015; Zhang, 2012a, 2018) to identify crucial species. In the Pajek, degree centrality can be obtained by implementing the command series: Net→Partions→DC→All. Closeness centrality is the average shortest path between a node and other nodes (Wasserman and Faust, 1994):

$$CC_i = \frac{N-1}{\sum_{j=1}^{N} d_{ij}} \quad \text{(Eq.1)}$$

where d_{ij} is the distance of the shortest path between node *i* and node *j*. Generally, the larger the *CC* value is, the smaller the average distance between the node *i* and all other nodes will be, and the greater the importance of the node *i* is.

(6) Triadic structure analysis

Three nodes (i.e., vertices, species) may maximally generate 16 possible structures (triadic structures) in a directed network. For example, all possible structures generated by three nodes A, B, and C are 003=A, B, C; 012=A→B, C; 102=A↔B, C; 021D=A←B→C; 021U=A→B←C; 021C= A→B→C; 111D=A↔B←C; 111U=A↔B→C; 030T=A→B←C, A→C; 030C=A←B←C, A→C; 201=A↔B↔C; 120D=A←B→C, A↔C; 120U=A→B←C, A↔C; 120C=A→B→C, A↔C; 210=A→B↔C, A↔C; 300=A↔B↔C, A↔C (Wasserman, 1977). However, four

http://www.aloki.hu ● ISSN 1589 1623 (Print) ● ISSN1785 0037 (Online)
DOI: http://dx.doi.org/10.15666/aeer/1802_34193437

possible structures exist in the undirected network, i.e., 003, 102, 201, and 300, in which the structure 300 is a complete network called triadic structure. The number of triadic structures can be used to reflect the spacing degree of a food web. The effect of parasites on the food web spacing can be understood by comparing the numbers of triadic structures that contain free-living species and all species respectively. Since the food web is a directed network, in Pajek we can analyze triadic structures by implementating the command series, Net→Transform→Arcs-Edges→All,Info→ Network→Triadic Census, or Nets→Fragment (First in Second)→Find.

(7) Clustering coefficient and similarity analysis

The clustering coefficient refers to the proportion of closed dual chains occupying the network (Dunne et al., 2013), which reflects the closeness of node connections in the network. The clustering coefficient of a node can be represented by the ratio of the observed number of links existing between adjacent nodes of the node and the total number of possible existing links. The clustering coefficient of the entire network can be achieved implementing the command series in Pajek: Net→Vector→Clustering coefficients→CC1. In addition, if two nodes share more adjacent nodes, the two nodes can be considered to have the higher similarity. In present study, we used the command series in Pajek to conduct hierarchical clustering analysis and, to compare the similarity between food webs with or without parasites, and to further understand whether parasites have any influence on the similarity of species in food webs: Cluster→Create Full Cluster→Operations→ Dissimilarity→Network based→Dl→All.

Results

Tropic structure of food webs

According to statistic survey, the number and proportion of top, basal and intermediate species for seven food webs, including the complete food webs with parasites (BSQ-ALL, EPB-ALL, etc.), and the food webs containing free-living species only (BSQ-FREE, EPB-FREE, etc.) are shown in *Table 1*.

From *Table 1*, we can find that the inclusion of parasites in each food web does not change the number of basal species. For instance, there are always four basal species in YEA-ALL and YEA-FREE, however, the number and proportion of intermediate and top species change greatly in all food webs. In general, the inclusion of parasites has greatly reduced the proportion of top species. For example, the number of top species in YEA reduced from 31 and 13, and the proportion reduced from 33.70% and 9.70%; the number of top species in STB decreased from 27 and 11, and the proportion decreased from 21.43% and 6.83%. These changes may have been due to the increase in the complexity of food web after the inclusion of parasites. In this process, some of the original top species were parasitized, and their role in the food web changed from the top species to the intermediate species. At the same time, the parasites that were temporarily the top species had the possibility of being preyed by other species, and transformed to intermediate species from the top species. As a consequence, the number of intermediate species increased and the number of top species declined drastically. Nevertheless, there were some exceptions. For instance, in the CSM food web, we can find that the number of species did not change although the species composition has changed, and the proportion increased correspondingly. This result is different from the previous research. It may be due to that other species joined the food web through migration or invasion during the later period (e.g., the number of species of free-living

http://www.aloki.hu ● ISSN 1589 1623 (Print) ● ISSN1785 0037 (Online)
DOI: http://dx.doi.org/10.15666/aeer/1802_34193437

species increased from 83 and 107), which changed the original trophic relationship in the food web, and further changed the proportion of top species. Taking the EPB food web as an example (*Figures 1 and 2*), it is obvious that the inclusion of parasites significantly led to the reduction of top species (from 9 and 3 species), which in turn changed the proportional relationship in the food web.

Table 1. *Number and proportion of top, basal and intermediate species in the seven food webs*[*]

Food web		Trophic Level	No. species	Total No. species	Proportion (%)	Species ID
BSQ	BSQ-ALL	T	3	171	1.75	34,37,77
		I	151		88.30	18-33,35,36,38-76,78-171
		B	17		9.94	1-17
	BSQ-FREE	T	9	119	7.56	34,37,71-73,75,77,118,119
		I	87		73.11	18-33,35,36,38-70,74,76,78-117
		B	17		19.33	1-17
CSM	CSM-ALL	T	6	165	7.56	17,35,45,63,65,154
		I	147		81.22	13-16,18-34,36-44,46-62,64,66-153,155-165
		B	12		11.22	1-12
	CSM-FREE	T	6	107	5.61	17,35,45,62,63,107
		I	89		83.18	13-16,18-34,36-44,46-61,64-106
		B	12		11.21	1-12
EPB	EPB-ALL	T	3	214	1.40	29,60,92
		I	197		92.06	13-28,30-59,61-91,93-214
		B	14		6.54	1-12
	EPB-FREE	T	9	138	6.52	29,60,83-85,88,91,92,138
		I	115		83.33	15-28,30-59,61-82,86,87,89-90,93-137
		B	14		10.15	1-14
FFB	FFB-ALL	T	2	123	1.63	40,57
		I	115		93.50	7-39,41-56,58-123
		B	6		4.87	1-6
	FFB-FREE	T	9	77	11.69	40,57,70-73,75-77
		I	62		80.52	7-39,41-56,58-69,74
		B	6		7.79	1-6
OHR	OHR-ALL	T	14	142	9.86	7-10,43,55-60,97,121,139
		I	124		87.32	4-5,11-42,44-54,61-96,98-120,121-138,140-142
		B	4		2.82	1-3,6
	OHR-FREE	T	32	123	26.02	7-10,55-60,97,103-123
		I	87		70.73	11-54,61-96,98-102
		B	4		3.25	1-3,6
STB	STB-ALL	T	11	161	6.83	10,15,17-19,45,46,74,75,124
		I	144		89.44	7-9,11-14,16,20-44,47-73,76-123,125-161
		B	6		3.73	1-6
	STB-FREE	T	27	126	21.43	10,15,17-19,45,46,51,65,74,75,91-96,111,113-116,122-126
		I	93		73.81	7-9,11-14,16,20-44,47-50,52-64,66-73,76-90,97-110,112,117-121
		B	6		4.76	1-6
YEA	YEA-ALL	T	13	134	9.70	19,21,23,43,53,57,65-69,82,86
		I	115		85.82	1-18,20,22,24-42,44-52,54-56,58-64,70-81,83-85,87-99,101-130
		B	4		3.73	131-134
	YEA-FREE	0	1	92	0.75	100
		T	31		33.70	43-49,51-69,73,75,82,83,86
		I	56		60.87	50,70-72,74,76-81,84-85,87-99,101-130
		O	1		1.10	100
		B	4		4.33	131-134

[*]Sources of food webs: (1) CSM (Hechinger et al., 2011); (2) EPB (Hechinger et al., 2011); (3) BSQ (Hechinger et al., 2011); (4) FFB (Zander et al., 2011); (5) OHR (Mouritsen et al., 2011); (6) STB (Thieltges et al., 2011); (7) YEA (Huxham et al., 1996)

http://www.aloki.hu ● ISSN 1589 1623 (Print) ● ISSN1785 0037 (Online)
DOI: http://dx.doi.org/10.15666/aeer/1802_34193437

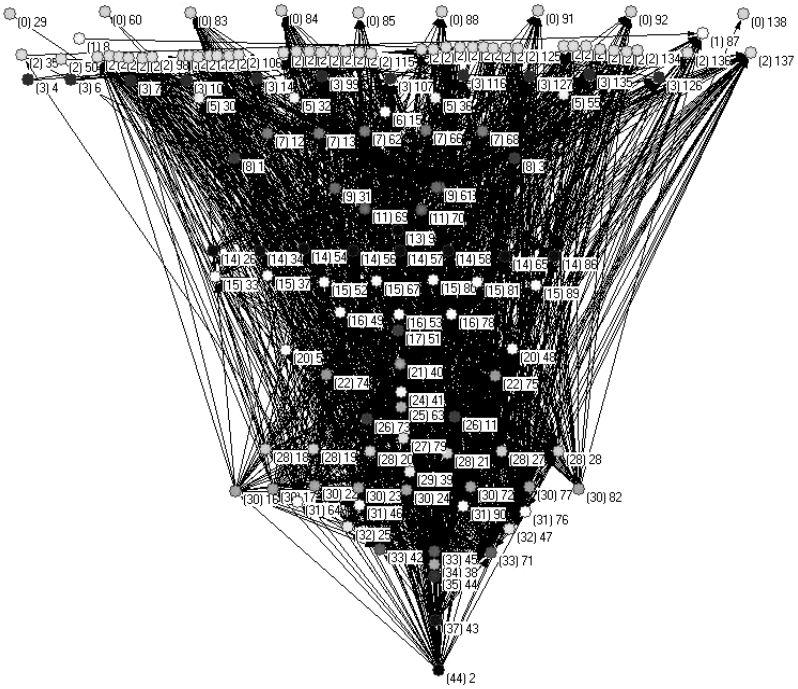

Figure 1. *The EPB-ALL food web. Each node in the figure represents a different species. The nodes are arranged in the order from the smallest to the largest outgoing degree, and the outgoing degree of nodes in the same layer are the same. Top species are all at the top layer of the food web*

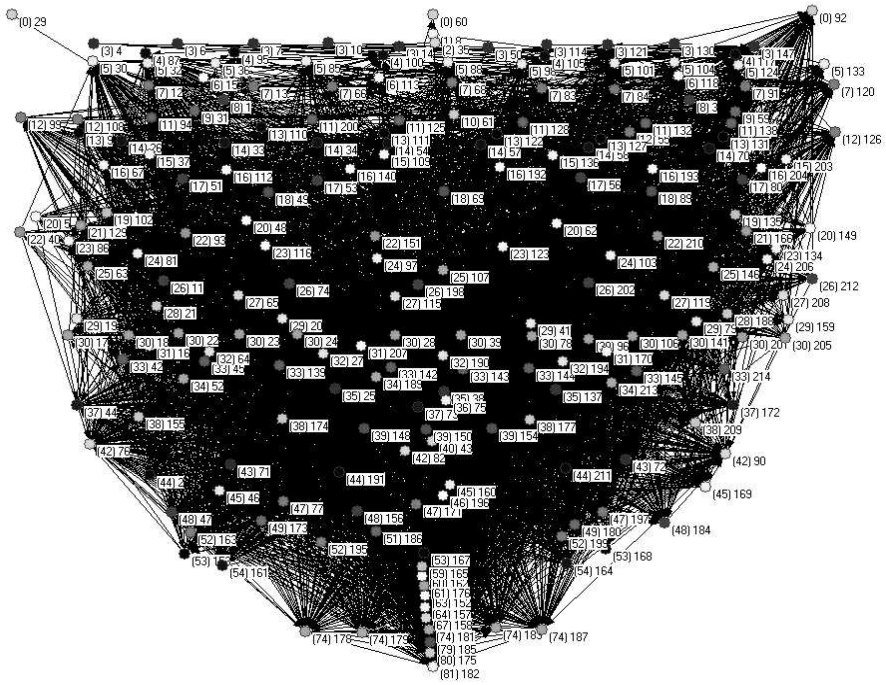

Figure 2. *The EPB-FREE food web. Each node in the figure represents a different species. The nodes are arranged in the order from the smallest to the largest outgoing degree, and the outgoing degree of nodes in the same layer are the same. Top species are all at the top layer of the food web*

http://www.aloki.hu ● ISSN 1589 1623 (Print) ● ISSN1785 0037 (Online)
DOI: http://dx.doi.org/10.15666/aeer/1802_34193437

Link analysis

There are in total of 1192 links (i.e., connections) in the predator-prey food web of BSQ-FREE. The connectance and link density of the predator-prey food web of BSQ-FREE are 0.08 and 10.02, respectively (*Figure 3*). For the BSQ-ALL, the total number of links, connectance and link density are 3889, 0.13, and 22.74, respectively. In addition, the total number of species in BSQ-FREE accounts for 0.696 (69.6%) of BSQ-ALL species, while the total number of links of the former is 0.307 only. Further details of link and connectance statistics are indicated in *Table 2*, and *Figures 3 and 4*.

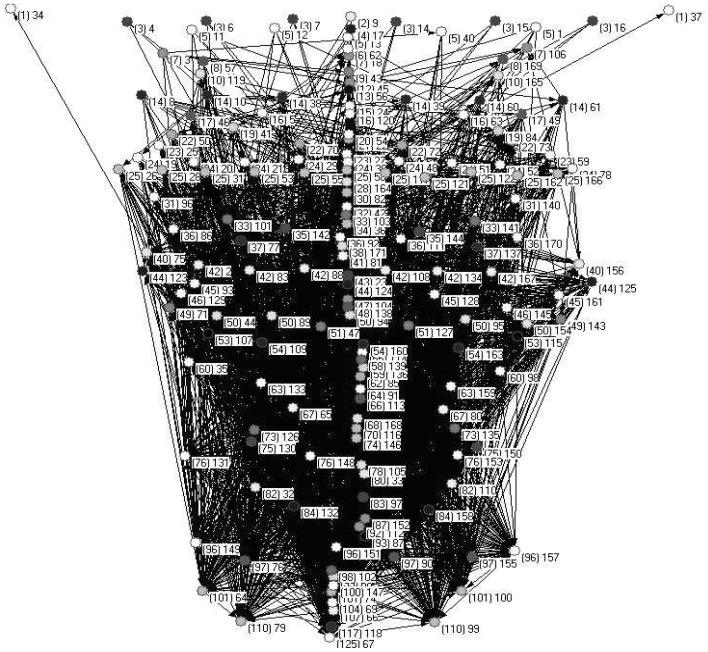

Figure 3. *The BSQ-ALL food web. The number outside the brackets is species ID and the number inside the brackets is total links of the species. From top layer to bottom layer, the species are arranged in the order from the smallest to the greatest number of links. There is the same number of links for the species at the same layer*

Table 2 indicates that in exception of FFB, the total number of links, connectance and link density of other free-living food webs increased significantly after parasites have been included, because the number of species in the predator-prey food webs accounts for nearly two-thirds of the complete web but the proportion of total links is rarely greater than one-third. Taking YEA as an example, the total number of YEA-FREE species accounts for 68.66% of YEA-ALL, while the proportion of total links is 33.34% only. Therefore, the inclusion of parasites has greatly enriched the trophic relationships in the food web and led the links in the food web, which increased the complexity of the food web.

Food cycles

Pimm et al. (1991) demonstrated that food cycles seldom occurred in most of the food webs. Conversely, our results indicated that food cycles frequently occurred in the food webs above, including the food webs without parasites. The inclusion of parasites may greatly increase cycles in the food web (*Table 3*).

http://www.aloki.hu ● ISSN 1589 1623 (Print) ● ISSN1785 0037 (Online)
DOI: http://dx.doi.org/10.15666/aeer/1802_34193437

Table 2. *Link and connectance statistics of the seven food webs*[*]

Food web		No. species	Proportion of species	Total links	Proportion of links	Connectance	Link density
BSQ	BSQ-ALL	171	0.696	3889	0.307	0.132998	22.743
	BSQ-FREE	119		1192		0.084175	10.017
CSM	CSM-ALL	165	0.648	3850	0.278	0.141414	23.333
	CSM-FREE	107		1068		0.093283	9.981
EPB	EPB-ALL	214	0.645	5859	0.305	0.127937	27.379
	EPB-FREE	138		1785		0.09373	12.935
FFB	FFB-ALL	123	0.623	1526	0.429	0.100866	12.407
	FFB-FREE	77		655		0.110474	8.506
OHR	OHR-ALL	142	0.867	1957	0.677	0.097054	13.781
	OHR-FREE	123		1325		0.08758	10.772
STB	STB-ALL	161	0.783	3157	0.372	0.121793	19.609
	STB-FREE	126		1174		0.073948	9.317
YEA	YEA-ALL	134	0.687	1512	0.334	0.084206	11.284
	YEA-FREE	92		505		0.059664	5.489

[*]Sources of food webs: (1) CSM (Hechinger et al., 2011); (2) EPB (Hechinger et al., 2011); (3) BSQ (Hechinger et al., 2011); (4) FFB (Zander et al., 2011); (5) OHR (Mouritsen et al., 2011); (6) STB (Thieltges et al., 2011); (7) YEA (Huxham et al., 1996)

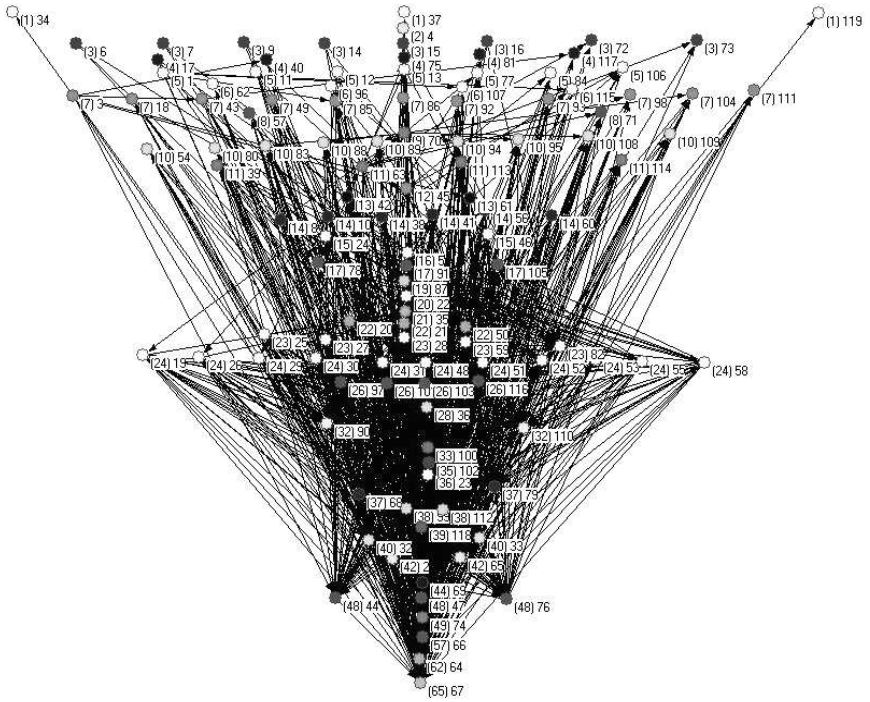

Figure 4. *The BSQ-FREE food web. The number outside the brackets is species ID and the number inside the brackets is total links of the species. From top layer to bottom layer, the species are arranged in the order from the smallest to the greatest number of links. There is the same number of links for the species at the same layer*

http://www.aloki.hu ● ISSN 1589 1623 (Print) ● ISSN1785 0037 (Online)
DOI: http://dx.doi.org/10.15666/aeer/1802_34193437

Table 3. *Number of cycles in the seven food webs*[*]

Food web		Number of cycles
BSQ	BSQ-ALL	164708
	BSQ-FREE	66
CSM	CSM-ALL	166947
	CSM-FREE	176
EPB	EPB-ALL	199420
	EPB-FREE	894
FFB	FFB-ALL	8464
	FFB-FREE	0
OHR	OHR-ALL	7805
	OHR-FREE	114
STB	STB-ALL	74494
	STB-FREE	0
YEA	YEA-ALL	2844
	YEA-FREE	0

[*]Sources of food webs: (1) CSM (Hechinger et al., 2011); (2) EPB (Hechinger et al., 2011); (3) BSQ (Hechinger et al., 2011); (4) FFB (Zander et al., 2011); (5) OHR (Mouritsen et al., 2011); (6) STB (Thieltges et al., 2011); (7) YEA (Huxham et al., 1996)

Crucial species and species centrality

From *Figures 5 and 6*, we can find that BSQ-ALL has more connections than BSQ-FREE, and the closeness centrality of species in BSQ slightly increases if parasites are included (BSQ-ALL). Parasitic species ID 147 shows some more importance in BSQ-ALL.

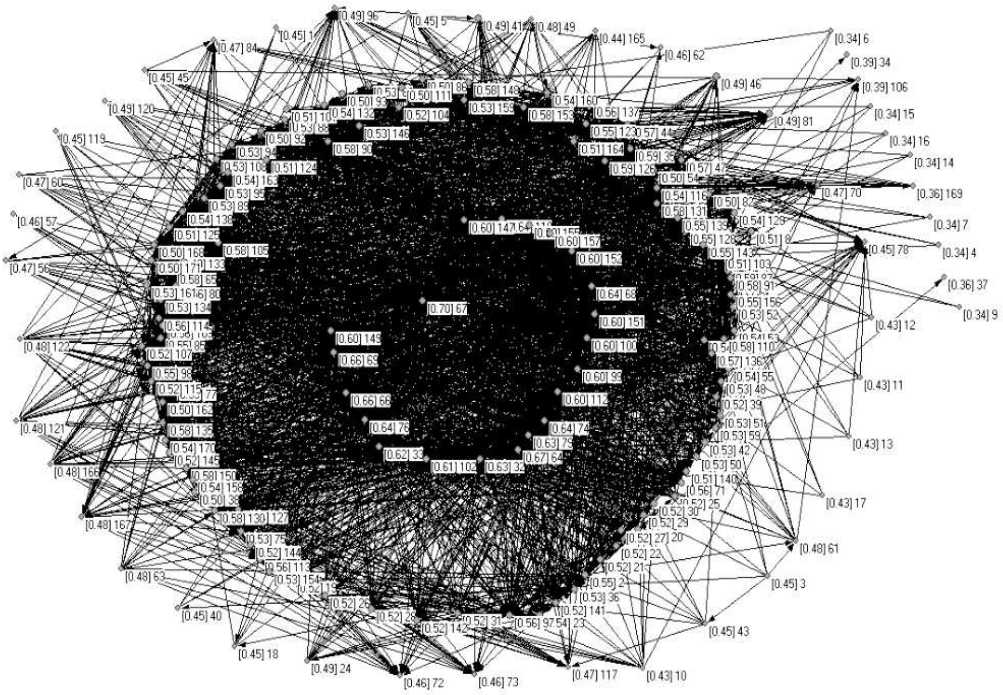

Figure 5. *Closeness centrality of species in BSQ-ALL food web. The number outside the brackets is species ID and the value inside the brackets is closeness centrality of species*

http://www.aloki.hu ● ISSN 1589 1623 (Print) ● ISSN1785 0037 (Online)
DOI: http://dx.doi.org/10.15666/aeer/1802_34193437

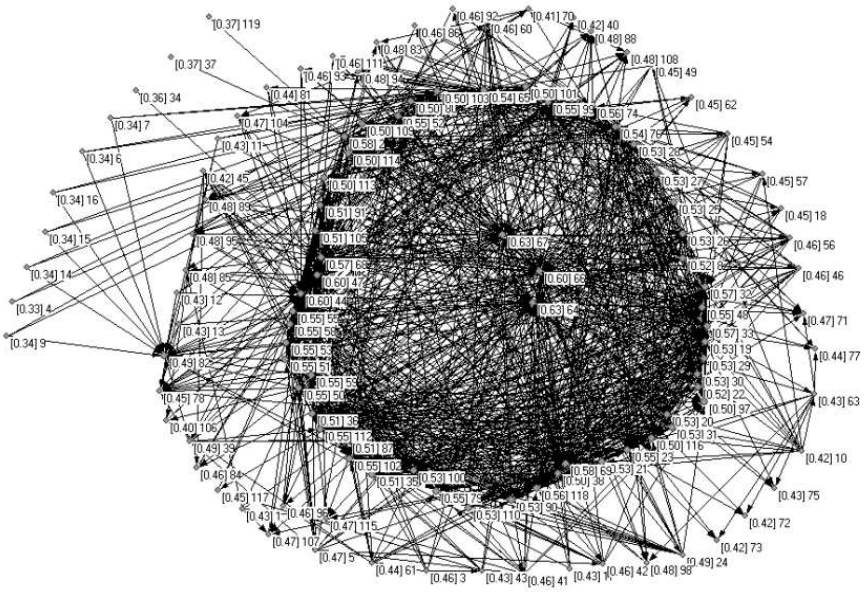

Figure 6. *Closeness centrality of species in BSQ-FREE food web. The number outside the brackets is species ID and the value inside the brackets is closeness centrality of species*

The species with the greater degree centrality (*DC*) and closeness centrality (*CC*) in the BSQ-ALL and BSQ-FREE food webs are shown in *Table 4*.

Table 4. *The species with greater degree centrality (DC) and closeness centrality (CC; Eq. (1)) in BSQ food web*[*]

BSQ-ALL		**BSQ-FREE**	
DC	***CC***	***DC***	***CC***
67	67	67	64
118	64	64	67
79	69	66	44
99	66	74	47
66	118	44	66
69	76	47	69
64	68	76	2
74	74	69	32
100	32	2	33
147	79	65	68

[*]Food web BSQ was sourced from Hechinger et al. (2011)

Since the *DC* value of a node can generally reflect the influence of other nodes on this node, and the *CC* value focuses on the local topology (Okamoto et al., 2008), *DC*s and *CC*s in *Table 4* can be combined to measure and rank nodes' importance, as indicated in *Table 5*. The results show that crucial species in the BSQ-ALL food web are the species IDs 67, 118, 64, 66 and 69, while the species with greater importance in the BSQ-FREE food web are the species IDs 64, 67, 44, 66 and 47.

http://www.aloki.hu ● ISSN 1589 1623 (Print) ● ISSN1785 0037 (Online)
DOI: http://dx.doi.org/10.15666/aeer/1802_34193437

Table 5. *Top 10 species (IDs) with greater importance in the seven food webs*[*]

CSM		EPB		FFB		OHR		STB		YEA	
CSM-ALL	CSM-FREE	EPB-ALL	EPB-FREE	FFB-ALL	FFB-FREE	OHR-ALL	OHR-FREE	STB-ALL	STB-FREE	YEA-ALL	YEA-FREE
51	34	72	72	75	75	5	2	60	60	85	43
57	37	77	77	59	39	42	5	58	58	5	48
137	57	81	71	61	41	91	6	127	33	89	47
139	51	137	76	63	1	2	42	137	1	9	46
143	50	76	59	39	4	125	22	133	4	77	59
145	22	71	27	66	9	100	100	138	9	6	38
134	24	175	28	41	12	102	43	139	34	80	35
59	55	181	38	58	59	114	91	131	65	90	74
55	21	185	42	71	15	6	75	131	33	32	92
135	26	38	61	64	61	124	114	33	89	61	61

[*]Sources of food webs: (1) CSM (Hechinger et al., 2011); (2) EPB (Hechinger et al., 2011); (3) BSQ (Hechinger et al., 2011); (4) FFB (Zander et al., 2011); (5) OHR (Mouritsen et al., 2011); (6) STB (Thieltges et al., 2011); (7) YEA (Huxham et al., 1996)

According to *Table 5*, the rank of species importance changes if the parasites are included the food web. In some food webs, parasites have the greater importance and become crucial species. For instance, there are seven parasite species in the top ten species list of STB-ALL. Parasites may have lowered the relative importance of some free-living species (e.g., the species ID 1 in FFB), or enhanced the importance of other species (e.g., the species ID 5 in YEA).

Triadic structures

Details of the triadic structures of the seven food webs are listed in *Table 6*.

According to *Table 6*, for example, FFB-ALL food web contains 3888 triadic structures while FFB-FREE food web contains 673 triadic structures only. It is obvious that the inclusion of parasites greatly increased the number of triadic structures in food webs.

Table 6. *Details of triadic structures of the seven food webs*[*]

Food web		No. triadic structures	Increase of proportion of triadic structures if parasites are included (%)
BSQ	BSQ-ALL	14093	577.22
	BSQ-FREE	2081	
CSM	CSM-ALL	18423	796.06
	CSM-FREE	2056	
EPB	EPB-ALL	32916	506.75
	EPB-FREE	5425	
FFB	FFB-ALL	3888	477.11
	FFB-FREE	673	
OHR	OHR-ALL	4717	98.11
	OHR-FREE	2381	
STB	STB-ALL	11379	477.91
	STB-FREE	1969	
YEA	YEA-ALL	2816	680.06
	YEA-FREE	361	

[*]Sources of food webs: (1) CSM (Hechinger et al., 2011); (2) EPB (Hechinger et al., 2011); (3) BSQ (Hechinger et al., 2011); (4) FFB (Zander et al., 2011); (5) OHR (Mouritsen et al., 2011); (6) STB (Thieltges et al., 2011); (7) YEA (Huxham et al., 1996)

http://www.aloki.hu ● ISSN 1589 1623 (Print) ● ISSN1785 0037 (Online)
DOI: http://dx.doi.org/10.15666/aeer/1802_34193437

Clustering coefficients

A greater clustering coefficient means the greater closeness of connections and species are thus more likely parasitized. As shown in *Table 7*, the clustering coefficients of each food web increase if the parasites are included.

Table 7. *Clustering coefficients of the seven food webs*[*]

Food web		Clustering coefficient
BSQ	BSQ-ALL	0.176856
	BSQ-FREE	0.106715
CSM	CSM-ALL	0.225561
	CSM-FREE	0.142477
EPB	EPB-ALL	0.187083
	EPB-FREE	0.169259
FFB	FFB-ALL	0.165141
	FFB-FREE	0.088927
OHR	OHR-ALL	0.140108
	OHR-FREE	0.112305
STB	STB-ALL	0.170479
	STB-FREE	0.109187
YEA	YEA-ALL	0.131878
	YEA-FREE	0.082545

[*]Sources of food webs: (1) CSM (Hechinger et al., 2011); (2) EPB (Hechinger et al., 2011); (3) BSQ (Hechinger et al., 2011); (4) FFB (Zander et al., 2011); (5) OHR (Mouritsen et al., 2011); (6) STB (Thieltges et al., 2011); (7) YEA (Huxham et al., 1996)

Conclusions

In present study, seven high-resolution riparian food webs were used to analyze topological properties of the complete food webs (-ALL) and the food webs containing only free-living species (-FREE). The conclusions on the importance of parasites were drawn or further confirmed in the following aspects:

(1) Parasitism changes trophic structure of species in the food web, i.e., the number and proportion of top species decline and the number and proportion of intermediate species increase. Although the number of top species in the CSM-ALL and CSM-FREE food webs was the same (Kuang and Zhang, 2011), the number and proportion of intermediate species increased significantly after parasites were included, which was basically consistent with the present conclusion.

(2) The presence of parasites increases the complexity of the food web. The number of links in food webs was proved to increase significantly as the inclusion of parasites, and most of the links were related to parasites, which means that parasites play an important role in the food web and the complexity of the food web is enhanced.

(3) Parasites significantly increase the number of cycles in the food web. Pimm (1991) found that there were few cycles in the predator-predator food webs. In present study, the results of FFB, STB, and YEA food webs coincided with his conclusion. In addition, the number of cycles in the food webs increased sharply after including parasites. On the one hand, the original connection relationship became more complex and thus the possibility of cycle occurrence increased due to the existence of parasites. On the other hand, considering the complicated life cycles of parasites, a series of cycles may also be produced among parasites.

http://www.aloki.hu ● ISSN 1589 1623 (Print) ● ISSN1785 0037 (Online)
DOI: http://dx.doi.org/10.15666/aeer/1802_34193437

(4) The presence of parasites alters the importance of species in the original food web. Network analysis demonstrated that parasites have produced a great impact on the relative importance of species in the food web, even as a crucial species in the complete food webs due to their great importance.

(5) Parasites increase the food web spacing. The number of triadic structures increased as the inclusion of parasites in the food web, thus making food web spacing significantly increased.

(6) Parasites increase the overall clustering coefficient of the food web, making the food web more closely connected. Parasitism is further enhanced with positive feedback mechanism as the increase of the clustering coefficient of the food web. The interaction between parasitism and the clustering coefficient is mutually reinforced.

Discussion

The food web is a major theme of fundamental ecology, which concerns with the stability, diversity and complexity of ecosystems (Pascual and Dunne, 2006). Traditional food web research mostly focuses on free-living species, while parasitism that are widespread in nature and are often difficult to detect has been ignoring (Price, 1980). As researchers become more aware of the importance of parasites and their possible effects on the structure, dynamics, and function of food webs, many have begun to focus on this potential area and a series of research have been conducting (Pascual and Dunne, 2006; Dunne et al., 2013; Michalska-Smith et al., 2018). More and more complete food webs containing parasites have been built and some research results were obtained. Studies have confirmed that parasites may change the structure and function of food webs (Sato et al., 2012). Nevertheless, the impact of parasites on the topological properties of the food web needs to be further exploited. The number of links, connectance and link density in the above food webs can reflect the potentiality of energy circulation paths, and thus may indicate the complexity of the food webs. MacArthur (1955) argued that the complexity of food webs can be considered as a key indicator of web stability. The research on the topological properties of networks also helps us measure the stability of food webs. In addition, studies have shown that parasites as pathogens of infectious diseases or as crucial species play an important role in maintaining the stability of ecological communities and ecosystems (McCallum and Dobson, 1995). Our conclusions further proved that parasites change the importance of the original species and may even become crucial species. They will increase the clustering coefficient of the food web and expand the epidemics of infectious diseases. It may be beneficial to the construction of relevant models in epidemiological studies (Shams and Khansari, 2019).

Some aspects should be further strengthened in the future studies: (1) network robustness of the food webs with parasites (Zhang, 2016), which is different from stability; (2) food web models specific to the food webs with parasites (Cohen and Newman, 1985; Cohen et al., 1990; Williams and Martinez, 2000), and (3) mechanisms of parasitism in maintaining food web structure.

Acknowledgments. This study was supported by The National Key Research and Development Program of China (2017YFD0201204) and Guangzhou Science and Technology Project (No. 201707020003).

http://www.aloki.hu ● ISSN 1589 1623 (Print) ● ISSN1785 0037 (Online)
DOI: http://dx.doi.org/10.15666/aeer/1802_34193437

REFERENCES

[1] Allesina, S., Pascual, M. (2008): Network structure, predator-prey modules and stability in large food webs. – Theoretical Ecology 1: 55-64.
[2] Allesina, S., Alonso, D., Pascual, M. (2008): A general model for food web structure. – Science 320(5876): 658-661.
[3] Amundsen, P. A., Lafferty, K. D., Knudsen, R., Primicerio, R., Klemetsen, A., Kuris, A. M. (2009): Food web topology and parasites in the pelagic zone of a subarctic lake. – Journal of Animal Ecology 78: 563-572.
[4] Amundsen, P. A., Lafferty, K. D., Knudsen, R., Primicerio, R., Kristoffersen, R., Klemetsen, A., Kuris, A. M. (2012): New parasites and predators follow the introduction of two fish species to a subarctic lake: implications for food-web structure and functioning. – Oecologia 171: 993-1002.
[5] Anderson, R. M., May, R. M. (1978): Regulation and stability of host-parasite population interactions: I. Regulatory processes. – Journal of Animal Ecology 47: 219-247.
[6] Batagelj, V., Mrvar, A. (2004): Pajek—analysis and visualization of large networks. – In: Mutzel, P., Jünger, M., Leipert, S. (eds.) Graph Drawing GD 2001. Lecture Notes in Computer Science 2265. Springer, Berlin, Heidelberg.
[7] Cohen, J. E., Newman, C. M. (1985): A stochastic theory of community food webs: I. Models and aggregated data. – Proceedings of the Royal Society of London B Biology 224(1237): 421-448.
[8] Cohen, J. E., Luczak, T., Newman, C. M., Zhou, Z. M. (1990): Stochastic structure and nonlinear dynamics of food webs – qualitative stability in a Lotka Volterra cascade model. – Proceedings of the Royal Society of London B Biology 240: 607-627.
[9] Cohen, J. E., Pimm, S. L., Yodzis, P., Saldana, J. (1993): Body sizes of animal predators and animal prey in food webs. – Journal of Animal Ecology 62: 67-78.
[10] de Araújo, W. S., Grandez-Rios, J. M., Bergamini, L. L., Kollár, J. (2017): Exotic species and the structure of a plant-galling network. – Network Biology 7(2): 21-32.
[11] de Araújo, W. S. (2018): Robustness of plant-plant networks with different levels of habitat modification and interaction intimacy. – Network Biology 8(2): 55-64.
[12] Dobson, A. P., Lafferty, K. D., Kuris, A. M. (2006): Parasites and food webs. – Oxford University Press, Oxford: 119-135.
[13] Dunne, J. A., Williams, R. J., Martinez, N. D. (2002): Food-web structure and network theory: The role of connectance and size. – Proceedings of the National Academy of Sciences of USA 99: 12917-12922.
[14] Dunne, J. A. (2006): The network structure of food webs. – Oxford University Press, Oxford: 27-86.
[15] Dunne, J. A., Lafferty, K. D., Dobson, A. P., Hechinger, R. F., Kuris, A. M., Martinez, N. D., McLaughlin, J. P., Mouritsen, K. N., Poulin, R., Reise, K., Stouffer, D. B., Thieltges, D. W., Williams, R. J., Zander, C. D. (2013): Parasites affect food web structure primarily through increased diversity and complexity. – Plos Biology 11(6): e1001579.
[16] Ferrarini, A. (2017): A deeper insight into the equilibrium of biological and ecological networks. – Network Biology 7(4): 98-104.
[17] Hechinger, R. F., Lafferty, K. D., McLaughlin, J. P., Fredensborg, B. L., Huspeni, T. C., Lorda, J., Sandhu, P. K., Shaw, J. C., Torchin, M. E., Whitney, K. L., Kuris, A. M. (2011): Food webs including parasites, biomass, body sizes, and life stages for three California/Baja California estuaries. – Ecology 92: 791.
[18] Hernandez, A. D., Sukhdeo, M. V. K. (2008): Parasites alter the topology of a stream food web across seasons. – Oecologia 156: 613-624.
[19] Huxham, M., Raffaelli, D., Pike, A. (1995): Parasites and food web patterns. – Journal of Animal Ecology 64(2): 168-176.
[20] Huxham, M., Beaney, S., Ra Aelli, D. (1996): Do parasites reduce the chances of triangulation in a real food web? – Oikos 76(2): 284-300.

http://www.aloki.hu ● ISSN 1589 1623 (Print) ● ISSN1785 0037 (Online)
DOI: http://dx.doi.org/10.15666/aeer/1802_34193437

[21] Ings, T. C., Montoya, J. M., Bascompte, J., Blüthgen, N., Brown, L., Dormann, C. F., Edwards, F., Figueroa, D., Jacob, U., Jones, J. I., Lauridsen, R. B., Ledger, M. E., Lewis, H. M., Olesen, J. M., van Veen, F. J. F., Warren, P. H., Woodward, G. (2009): Ecological networks - beyond food webs. – Journal of Animal Ecology 78(1): 253-269.
[22] Jiang, L., Zhang, W. J. (2015): Determination of keystone species in CSM food web: A topological analysis of network structure. – Network Biology 5(1): 13-33.
[23] Jiang, L., Zhang, W., Liu, G. (2015): Effects of parasitism on robustness of food webs. – Selforganizology 2(2): 21-34.
[24] Jordán, F. (2009): Keystone species and food webs. – Philosophical Transactions of the Royal Society B: Biological Sciences 364(1524): 1733-1741.
[25] Kuang, W. P., Zhang, W. J. (2011): Some effects of parasitism on food web structure: a topological analysis. – Network Biology 1(3-4): 171-185.
[26] Kuris, A. M., Hechinger, R. F., Shaw, J. C., Whitney, K. L., Aguirre-Macedo, L., Boch, C. A., Dobson, A. P., Dunham, E. J., Fredensborg, B. L., Huspeni, T. C., Lorda, J., Mababa, L., Mancini, F. T., Mora, A. B., Pickering, M., Talhouk, N. L., Torchin, M. E., Lafferty, K. D. (2008): Ecosystem energetic implications of parasite and free-living biomass in three estuaries. – Nature 454: 515-518.
[27] Lafferty, K. D., Dobson, A. P., Kuris, A. M. (2006a): Parasites dominate food web links. – Proceedingsof the National Academy of Sciences of the United States of America 103(30): 11211-11216.
[28] Lafferty, K. D., Hechinger, R. F., Shaw, J. C., Whitney, K., Kuris, A. M. (2006b): Food webs and parasites in a salt marsh ecosystem. – Oxford University Press, Oxford: 119-134.
[29] Lafferty, K. D., Allesina, S., Arim, M., Briggs, C. J., De Leo, G., Dobson, A. P., Dunne, J. A., Johnson, P. T. J., Kuris, A. M., Marcogliese, D. J., Martinez, N. D., Memmott, J., Marquet, P. A., McLaughlin, J. P., Mordecai, E. A., Pascual, M., Poulin, R., Thieltges, D. W. (2008): Parasites in food webs: the ultimate missing links. – Ecology Letters 11(6): 533-546.
[30] Lafferty, K. D., Kuris, A. M. (2009): Parasites reduce food web robustness because they are sensitive to secondary extinction as illustrated by an invasive estuarine snail. – Philosophical Transactions of the Royal Society of London B: Biological Science 364: 1659-1663.
[31] Livi, C. M., Jordán, F., Lecca, P., Okey, T. A. (2011): Identifying key species in ecosystems with stochastic sensitivity analysis. – Ecological Modelling 222(14): 2542-2551.
[32] MacArthur, R. (1955): Fluctuations of animal populations and a measure of community stability. – Ecology 36(3): 533-536.
[33] Marcogliese, D. J., Cone, D. K. (1997): Food webs: a plea for parasites. – Trends in Ecology and Evolution 12: 320-325.
[34] Marcogliese, D. J. (2003): Food webs and biodiversity: are parasites the missing link? – Journal of Parasitology 82(S): 389-399.
[35] May, R. M. (1973): Stability and Complexity in Model Ecosystems. – Princeton University Press, Chicago.
[36] McCallum, H., Dobson, A. (1995): Detecting disease and parasite threats to endangered species and ecosystems. – Trends in Ecology and Evolution 10(5): 190-194.
[37] McCann, K. S. (2000): The diversity-stability debate. – Nature 405(6783): 228-233.
[38] Memmott, J., Martinez, N. D., Cohen, J. E. (2000): Predators, parasitoids and pathogens: species richness, trophic generality and body sizes in a natural food web. – Journal of Animal Ecology 69: 1-15.
[39] Michalska-Smith, M. J., Sander, E. L., Pascual, M., Allesina, S. (2018): Understanding the role of parasites in food webs using the group model. – Journal of Animal Ecology 87(3): 790-800.

http://www.aloki.hu ● ISSN 1589 1623 (Print) ● ISSN1785 0037 (Online)
DOI: http://dx.doi.org/10.15666/aeer/1802_34193437

[40] Montoya, J. M., Sole, R. V. (2003): Topological properties of food webs: from real data to community assembly models. – Oikos 102: 614-622.
[41] Montoya, J. M., Pimm, S. L., Sole, R. V. (2006): Ecological networks and their fragility. – Nature 442: 259-264.
[42] Mouritsen, K. N., Poulin, R., McLaughlin, J. P., Thieltges, D. W. (2011): Food web including metazoan parasites for an intertidal ecosystem in New Zealand. – Ecology 92(10): 2006.
[43] Navia, A. F., Cortes, E., Mejia-Falla, P. A. (2010): Topological analysis of the ecological importance of elasmobranch fishes: A food web study on the Gulf of Tortugas, Colombia. – Ecological Modeling 221(24): 2918-2926.
[44] Nedorezov, L. V. (2012): Continuous-discrete model of population dynamics with time lag in a reaction of intra-population self-regulative mechanisms. – Network Biology 2(4): 139-147.
[45] Nuwagaba, S., Hui, C. (2015): The architecture of antagonistic networks: Node degree distribution, compartmentalization and nestedness. – Computational Ecology and Software 5(4): 317-327.
[46] Okamoto, K., Chen, W., Li, X. Y. (2008): Ranking of closeness centrality for large-scale social networks. – International Workshop on Frontiers in Algorithmics, Springer, Berlin, Heidelberg: 186-195.
[47] Pascual, M., Dunne, J. A. (2006): From small to large ecological networks in a dynamic world. – Ecological Networks: Linking Structure to Dynamics in Food Webs, Oxford University Press, Oxford: 3-24.
[48] Pimm, S. L., Lawton, J. H. (1980): Are food webs divided into compartments? – Journal of Animal Ecology 49: 879-898.
[49] Pimm, S. L. (1991): The balance of nature? Ecological issues in the conservation of species and communities. – University of Chicago Press, Chicago.
[50] Pimm, S. L., Lawton, J. H., Cohen, J. E. (1991): Food web patterns and their consequences. – Nature 350(6320): 669-674.
[51] Price, P. W. (1980): Evolutionary Biology of Parasites (Vol. 15). – Princeton University Press, Chicago.
[52] Sato, T., Egusa, T., Fukushima, K., Oda, T., Ohte, N., Tokuchi, N., Watanabe, K., Kanaiwa, M., Murakami, I., Lafferty, K. D. (2012): Nematomorph parasites indirectly alter the food web and ecosystem function of streams through behavioural manipulation of their cricket hosts. – Ecology Letters 15(8): 786-793.
[53] Shakil, M., Wahab, H. A., Naeem, M., Bhatti, S., Shahzad, M. (2015): The modeling of predator-prey interactions. – Network Biology 5(2): 71-81.
[54] Shams, B., Khansari, M. (2019): Average reachability: A new metric to estimate epidemic growth considering the network structure and epidemic severity. – Network Biology 9(3): 42-57.
[55] Thieltges, D. W., Reise, K., Mouritsen, K. N., McLaughlin, J. P., Poulin, R. (2011): Food web including metazoan parasites for a tidal basin in Germany and Denmark. – Ecology 92(10): 2005.
[56] Wahab, H. A., Ullah, R., Bhatti, S., Shahzad, M., Naeem, M., Hussain, F., Ahmad, S. (2017): An approximate solution for a generalized Hirota-Satsom coupled (Kdv): equation. – Computational Ecology and Software 7(1): 28-37.
[57] Warren, P. H. (1994): Making connections in food webs. – Trends in Ecology and Evolution 9: 136-141.
[58] Warren, C. P., Pascual, M., Lafferty, K. D., Kuris, A. M. (2010): The inverse niche model for food webs with parasites. – Theoretical Ecology 3(4): 285-294.
[59] Wasserman, S. S. (1977): Random directed graph distributions and the triad census in social networks. – Journal of Mathematical Sociology 5(1): 61-86.
[60] Wasserman, S., Faust, K. (1994): Social Network Analysis: Methods and Applications (Vol. 8). – Cambridge University Press, Cambridge.

http://www.aloki.hu ● ISSN 1589 1623 (Print) ● ISSN1785 0037 (Online)
DOI: http://dx.doi.org/10.15666/aeer/1802_34193437

[61] Williams, R. J., Martinez, N. D. (2000): Simple rules yield complex food webs. – Nature 404(6774): 180-183.
[62] Winemiller, K. O., Polis, G. A. (1996): Food Webs: Integration of Patterns and Dynamics. – Chapman and Hall, New York: 1-22.
[63] Wood, M. J. (2007): Parasites entangled in food webs. – Trends in Parasitology 23: 8-10.
[64] Zander, C. D., Josten, N., Detloff, K. C., Poulin, R., McLaughlin, J. P., Thieltges, D. W. (2011): Food web including metazoan parasites for a brackish shallow water ecosystem in Germany and Denmark. – Ecological Archives 92(10): 2007.
[65] Zhang, W. J. (2012a): Computational Ecology: Graphs, Networks and Agent-based Modeling. – World Scientific, Singapore.
[66] Zhang, W. J. (2012b): How to construct the statistic network? An association network of herbaceous plants constructed from field sampling. – Network Biology 2(2): 57-68.
[67] Zhang, W. J. (2012c): Several mathematical methods for identifying crucial nodes in networks. – Network Biology 2(4): 121-126.
[68] Zhang, W. J. (2015): A generalized network evolution model and self-organization theory on community assembly. – Selforganizology 2(3): 55-64.
[69] Zhang, W. J. (2016): Network robustness: Implication, formulization and exploitation. – Network Biology 6(4): 75-85.
[70] Zhang, W. J. (2018): Fundamentals of Network Biology. – World Scientific Europe, London.

http://www.aloki.hu ● ISSN 1589 1623 (Print) ● ISSN1785 0037 (Online)
DOI: http://dx.doi.org/10.15666/aeer/1802_34193437

ASSESSMENT OF THE ENVIRONMENTAL PURIFICATION OF TRIANGLE SAIL MUSSEL (*HYRIOPSIS CUMINGII*) IN RECIRCULATING AQUACULTURE SYSTEMS

YU, X. B.[1,2,3] – ZHAO, Z.[1,3] – TANG, R.[1,3] – XIONG, B.[1,2,3] – WU, Z. L.[1,2,3] – SU, S. Q.[1,2,3] – YAO, W. Z.[1,2,3*]

[1]*College of Animal Science and Technology, Southwest University, Chongqing, China*
(First author e-mail: yuxiaobo6@126.com)

[2]*Comprehensive Experimental Station of Chongqing, National Shellfish Industry Technology System, China*

[3]*Research Center of Fishery Resources and Environment, Southwest University, Chongqing, China*

[*]*Corresponding author*
e-mail: yaowz@swu.edu.cn

(Received 13th Nov 2019; accepted 12th Mar 2020)

Abstract. The current study was undertaken to assess the environmental adaptability and water capability of *Hyriopsis cumingii* in a recirculating aquaculture system in the Chongqing region, Southwestern China. A total of 175 species of planktonic algae belonging to 8 phylum and 75 genera were found at all sampling sites. 66.3% - 80.0% of them belong to the Chlorophyta and Bacillariophyta phyla, the main food sources of bivalve shellfish. The annual investigation results show that the range of water physical and chemical indexes fully meets the requirements of *H. cumingii* growth, with its average wet weight increasing from 359.4 g to 525.6 g. Concerning water purification, even though *H. cumingii* had no obvious effect on the composition of planktonic algae, it could reduce the phytoplankton biomass in all five sampling sites in the summer by 23.7% on average. Moreover, the transparency of the ecological purification area can be increased by 15.3% on average. Besides, the decrease of electro conductivity (4.9%), ammonia nitrogen (6.7%) and phosphate (7.2%) in *H. cumingii* purification area was determined in this study. Overall, *H. cumingii* showed excellent ecological purification function, and its mixed farming model based on the recirculating aquaculture system is worthy of further study.
Keywords: *Hyriopsis cumingii, recirculating aquaculture system, phytoplankton, ecological purification, freshwater*

Introduction

Human beings have complex social and ecological dependency on the freshwater ecosystem (Kingsford et al., 2011; Horton et al., 2015). In recent years, the environmental function of freshwater shellfish has gradually attracted the attention of the industry due to the policy guidance in China. Some mixed breeding modes, such as "fish and mussel mixed breeding" and "shellfish and shrimp mixed breeding", have been mentioned and developed again in freshwater aquaculture (Modesto et al., 2018; Wang et al., 2018). However, freshwater shellfish industry has been neglected for a long time in China due to its small scale and long economic cycle. The production of 0.20 million tons only accounts for 0.66% of the total freshwater aquaculture in 2018 (Zhang et al., 2019). Moreover, the freshwater shellfish industry is still in the infancy in southwest China, and its adaptability to the local environment and related water purification mechanisms need to be studied urgently. This project mainly focuses on the growth adaptation and water

http://www.aloki.hu ● ISSN 1589 1623 (Print) ● ISSN1785 0037 (Online)
DOI: http://dx.doi.org/10.15666/aeer/1802_34393454

purification function of *Hyriopsis cumingii* in the recirculating aquaculture system in the Chongqing region.

Recirculating aquaculture system (RAS) is a water circulation pond with an air stripping device to realize high-density intensive aquaculture in a rectangular mixed-cell rearing unit (Watten et al., 2000; Ebeling et al., 2005). It has transparent functional partitions including the aquaculture area, tail water discharge area and purification area. This mode has been applied and extended in the Chongqing region in recent years. Our group predicts that N, P and phytoplankton are abundant in the tail water discharge area, and potential water purification could be achieved by cultivating shellfish. On one hand, shellfishes may provide an ecosystem service through nutrient assimilation in soft tissues and adamant shells, and facilitate the permanent removal of carbon, nitrogen, phosphorus, bacteriological quality and so on (Cha et al., 2011; Kellogg et al., 2013; Bianchi et al., 2014). Meanwhile, the purification function and physiological responses of shellfish may be expected to vary with environmental conditions (Bianchi et al., 2014; Hoellein et al., 2015). On the other hand, phytoplanktons are primary producers in pond aquaculture, and their species, quantity, community structure and species diversity have significant influence on the growth of aquatic animals (Daines et al., 2014). Previous studies have suggested that freshwater shellfish can effectively control the content of chlorophyll and organic matter in ponds (Hawkins et al., 2013). Besides, bivalves show specific feeding selectivity in the process of filter feeding. For example, the digestibility of greenshell mussel *Perna canaliculus* to dinoflagellates is higher than that of diatoms, showing a carnivorous tendency (Ren et al., 2006). However, the studies remain unknown on phytoplankton growth and reproduction, diversity index and stability of the pond ecosystem.

China's commercial freshwater pearl industry has been developing for more than 50 years and has accounted for more than 90% of the world's total cultured pearl production in recent two decades (Dan and Ruobo, 2002). Among them, as a unique Unionidae family resource in China, bivalve mollusk triangle sail mussel *H. cumingii* is the best selection for producing high quality freshwater pearls and is widely distributed in the Yangtze River basin and Huaihe River basin (Jin et al., 2012; Qu et al., 2018). At present, despite the great development in the research of artificial propagation and seedling raising (Li and Li, 2009), genetic breeding (Bai et al., 2016), growth traits and pearl cultivation (Jin et al., 2019; Zhang et al., 2019), the applied research on the ecological function still lags in *H. cumingii*. Recently, the use of *H. cumingii* has been proposed as an alternative measure to control algal bloom in eutrophic water bodies (Liu et al., 2014). However, there is no comprehensive data on the dynamic response mechanism of phytoplankton and its correlation with water quality factors. Besides, the water environment in southwest China meets the requirements of *H. cumingii* farming in theory. The optimal conditions for *H. cumingii* growth mainly include water temperature (23-32℃), dissolved oxygen (DO, >4 mg/L), pH (>7.5) and salinity (<0.2‰), total alkalinity (24-219 mg/L), total hardness (40-218 mg/L), total nitrogen (TN, 0.52-1.91 mg/L) and total phosphorus (TP, 0.06-0.30 mg/L), etc. (Lin et al., 2004). Also, the growth of bivalve shellfish could be effected by the species of shellfish, the nutrition of the bait, the season changes and mixed culture mode (Naddafi et al., 2007). The aim of the present study was to comprehensively investigate the purification function of *H. cumingii* in a recirculating aquaculture system, including the influence on algal facies and water quality factors.

http://www.aloki.hu ● ISSN 1589 1623 (Print) ● ISSN1785 0037 (Online)
DOI: http://dx.doi.org/10.15666/aeer/1802_34393454

Methods

Sampling site and H. cumingii layout

In 2018, we first set up five recirculating aquaculture system testing bases in the Chongqing region, southwest China (*Figure 1A*), including Tongliang qinggang breeding bases (29°8449′N, 105°8609′E), Bishan xinyue aquaculture co., LTD (29°6844′N, 106°2537′E), Bishan zhubi breeding base (29°6853′N, 106°2559′E), Changshou dahonghu aquatic co., LTD (30°0406′N, 106°9742′E) and Liang ping hongyun fishery co., LTD (30°6791′N, 107°6472′E). Each flume is about 7 m in length and 2.5 m in width. Healthy *H. cumingii* (Wet weight: 368.9 ± 106.1 g, Shell length: 15.7 ± 1.4 cm; Shell width: 4.2 ± 0.3 cm; Shell height: 12.5 ± 1.2 cm) aged about 3 years were located about 30 cm underwater in the outlet area of the aquaculture pond (*Figure 1B*). Furthermore, the average amount of *H. cumingii* in the purification area is 400-600 per aquaculture pond. The water quality and algal facies of the shellfish purification area, tail water discharge area and ecological purification area were monitored for four quarters on March 21, June 20, September 3 and December 25. Sampling sites Bishan zubi were not fully sampled because the *H. cumingii* were not stocking in spring and the florfenicol induced shellfish death in winter.

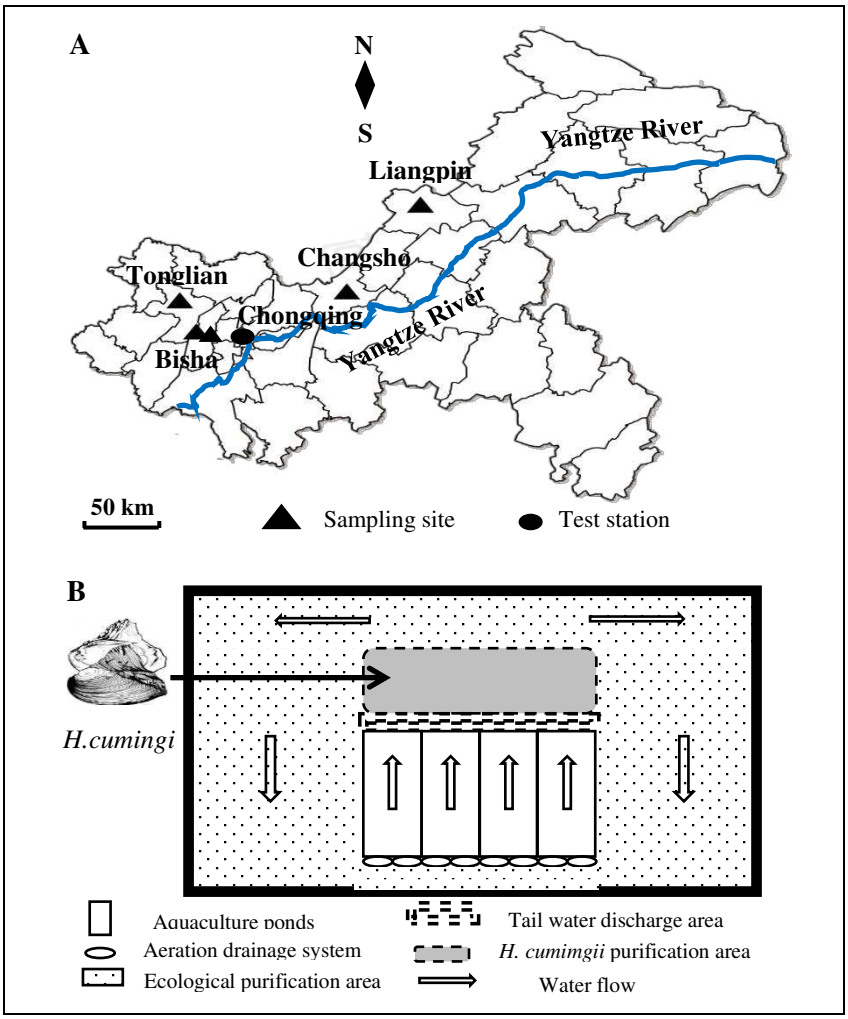

Figure 1. *Testing bases distribution for recirculating aquaculture system in the Chongqing region (A) and the schematic diagram of Hyriopsis cumingii aquaculture area selection (B)*

http://www.aloki.hu ● ISSN 1589 1623 (Print) ● ISSN1785 0037 (Online)
DOI: http://dx.doi.org/10.15666/aeer/1802_34393454

Phytoplankton quantitative collection

The collection of water samples from different sampling points and functional areas was accomplished according to the established methods in hydrobiology. Mixed water samples of about 0.5 m depth were collected with plexiglass water sampler, then fixed with 1.5% Lugol's iodine, placed in sedimentator for 24 h and concentrated into 50 mL centrifuge tube. Treated samples were qualitatively and quantitatively analysed by microscope counting. The phytoplankton composition of samples was determined by referring to "The common phytoplankton atlas of Chongqing region of the three gorges reservoir area" and "The common freshwater phytoplankton algae atlas of China" (Zhou and Zheng, 2005; Weng and Xu, 2010). The quantitative formula of phytoplankton is as follow:

$$C = N \times \frac{S_c}{S_f \times n} \times \frac{V_1}{V_2 \times V} \quad \text{(Eq.1)}$$

where, C is the phytoplankton density; N is the count result of phytoplankton in the observation field; S_c is the area of the counting box; S_f is the area per view; n is the number of views per slice; V_1 is the volume after concentration; V_2 is the volume of the counting box; V is the volume before concentration.

The calculation formula of preponderance degree is as follow:

$$Y = \frac{n_i}{N} \times f_i \quad \text{(Eq.2)}$$

where, Y is the preponderance degree; f_i is the frequency of algae i in the sample; n_i is the density of algae i; N is the total algal density. Among them, the dominant species is algae with Y value greater than 0.02, and the absolute dominant species is algae with Y value greater than 0.1.

Investigation in the physical and chemical index of water bodies

Electro conductivity, dissolved oxygen (DO) and pH values were detected by the portable dissolved oxygen meter (HQ30D, HACH Company, USA). Water temperature and transparency were detected by the water thermometer and transparency disc, respectively. Moreover, water samples were collected and brought back to the laboratory for water quality analysis according to relevant national standards (Wei et al., 2002). The collection, fixation and preservation of water samples were conducted following "the code for water environment monitoring (SL219-98, in Chinese)". Ammonia nitrogen was measured by the Nessler reagent colorimetry (NH_4^+-N, GB 7479-87). The phosphomolybdic acid methodologies measured phosphate (PO_4^{3-}-P, GB 9727-2007).

Statistical processing

Electro conductivity, water temperature, dissolved oxygen and pH values were measured twice with a calibrated portable dissolved oxygen meter. Each phytoplankton parameter and waterquality index was determined twice independently. All data expressed as mean.

http://www.aloki.hu ● ISSN 1589 1623 (Print) ● ISSN1785 0037 (Online)
DOI: http://dx.doi.org/10.15666/aeer/1802_34393454

Results

Phytoplankton composition and structure in sampling sites

A total of 175 species of planktonic algae belonging to 8 phyla and 75 genera were found in all five sampling sites (*Figure 2A*). Among them, Chlorophyta had the highest number of 33 genera and 67 species, accounting for 44.0% and 39.4% of the total. The second to the eighth are Bacillariophyta (16 genera, 45 species), Cyanophyta (13 genera, 24 species), Euglenophyta (5 genera, 21 species), Pyrrophyta (2 genera, 5 species), Cryptophyta (2 genera, 4 species), Xanthophyta (2 genera, 2 species) and Chrysophyta (2 genera, 2 species) phyla, respectively. Moreover, although the number of algae is different in each sampling site, the composition of algae facies is roughly consistent with the overall structure (*Figure 2B*). Moreover, the total number of species of Chlorophyta, Bacillariophyta, Cyanophyta and Euglenophyta phyla at all sampling sites were accounted for more than 90%. Among them, Chlorophyta and Bacillariophyta phyla are important bait categories of shellfish, accounting for 68.5%, 80.0%, 70.8%, 67.1% and 66.3% of the sampling sites respectively (*Figure 2B*). Also, there was a great difference in species classification among the sampling points. Fifty-five of the 175 species, or 32.4 percent, were observed at only one sampling site. And about half of the algae species were detected at only one or two sampling sites. Only 23.5% of the species were detected at all five sampling sites (*Figure 2C*).

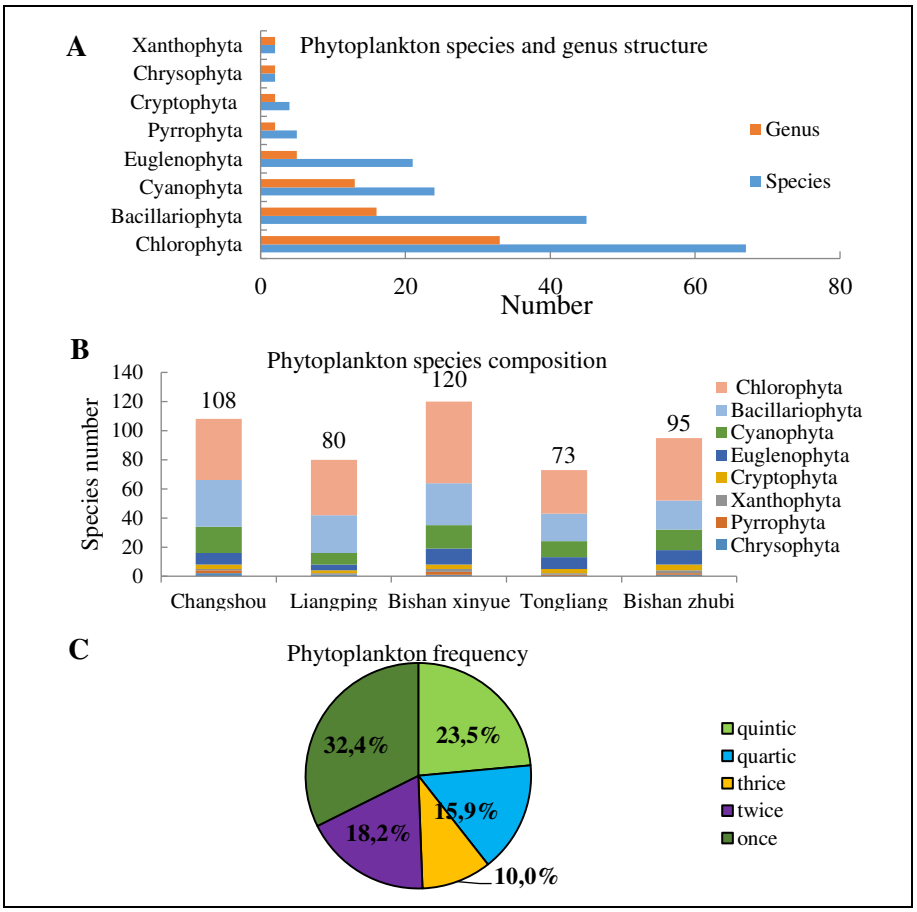

Figure 2. *Distribution of phytoplankton. (A) shows the species and genus structure in all sampling sites. (B) shows the phytoplankton species composition in each sampling sites. (C) shows the distribution characteristics of phytoplankton between sampling sites*

http://www.aloki.hu ● ISSN 1589 1623 (Print) ● ISSN1785 0037 (Online)
DOI: http://dx.doi.org/10.15666/aeer/1802_34393454

Filtering effect of H. cumingii on phytoplankton

H. cumingii filtering effects on phytoplankton were reflected in *Figure 3*. The results indicated that the phytoplankton biomass in summer and autumn were higher than those of spring and winter in Changshou, Liangping and Bishan xinyue. Sampling sites Bishan zubi were not fully sampled because the *H. cumingii* were not stocking in spring and the florfenicol induced shellfish death in winter. The results also revealed that *H. cumingii* could effectively reduce the biomass of phytoplankton. The phytoplankton biomass of the shellfish purification area and biological purification area were generally lower than that of the tail water discharge area. Results showed a 23.7% biomass reduction on average in all five samplings sites in the summer. Among them, the Liangping biomass of shellfish purification area and ecological purification has fallen by more than 85% in comparison with tail water discharge area in the summer. Besides, in some parts of the sampling sites phytoplankton biomass showed no noticeable change, such as Bishan zubi in winter, Changshou, Liangping and Tongliang in autumn (*Figure 3A-D*).

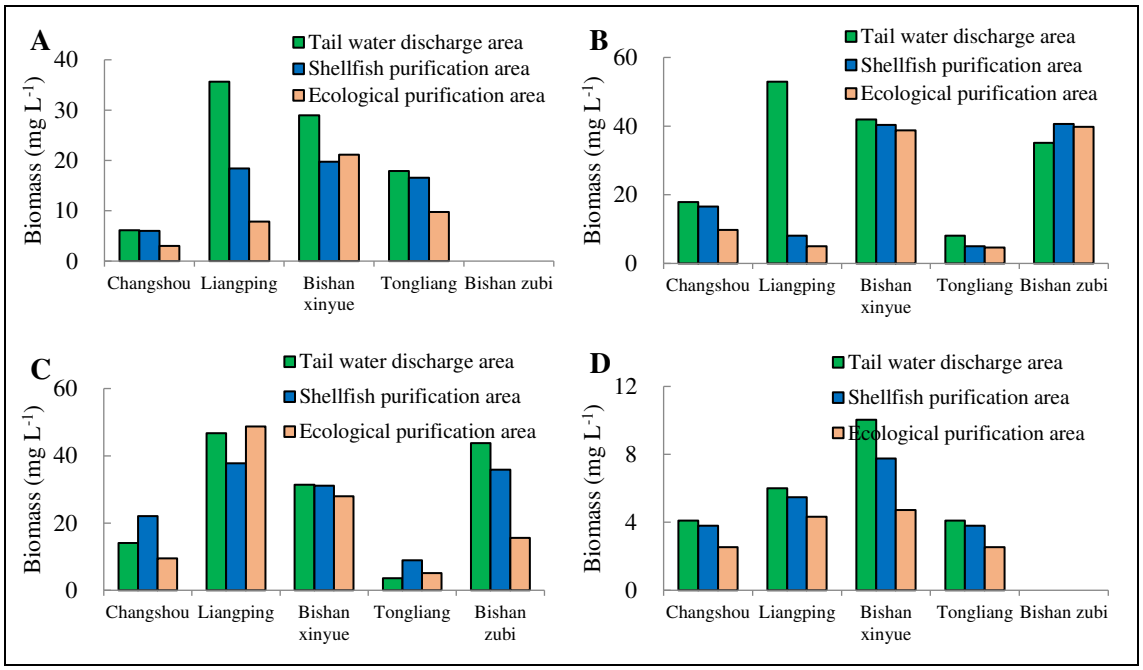

Figure 3. *Filtering effect of H. cumingii on phytoplankton biomass in four seasons (A, Spring; B, Summer; C, Autumn; D, winter)*

Although *H. cumingii* can significantly reduce the phytoplankton biomass, the total number of dominant algae has no obvious change. The preponderance degree and dominant species analysis results of higher biomass in summer and autumn are shown in *Tables 1 and 2*, respectively. Phytoplankton's dominant species mainly belong to the Cyanophyta, Chlorophyte and Bacillariophyta phyla in each sampling site. And a few numbers of dominant species mainly belong to the Xanthophyta, Euglenophyta and Cryptophyta phyla. However, the summer preponderance degree of all the Chlorophyte and Bacillariophyta in Bishan zubi, Tongliang and Bishan xinyue are less than 0.02, except *Chlorella vulgaris* Beij and *Coelastrum microporum* Nägeli (*Table 1*). The autumn preponderance degree of all the Chlorophyte and Bacillariophyta phyla in Changshou are less than 0.02, except *Pandorina morum* Bory and *Synedra acusvar* (*Table 2*).

http://www.aloki.hu ● ISSN 1589 1623 (Print) ● ISSN1785 0037 (Online)
DOI: http://dx.doi.org/10.15666/aeer/1802_34393454

Table 1. *Phytoplankton dominant species and preponderance degree in summer (Y > 0.02)*

Phytoplankton	Changshou			Liangping			Bishan zubi			Tongliang			Bishan xinyue		
	T	H	E	T	H	E	T	H	E	T	H	E	T	H	E
Cyanophyta															
Nostoc communes vauch.			0.054												
Merismopedia eleggans Br.		0.041			0.023		0.394	0.423	0.286	0.021				0.070	0.060
Merismopedia punctata Meyen	0.303	0.265	0.122										0.100		
Phormidium tenue (Menegh.) Gom.	0.118	0.102	0.078				0.023	0.030	0.026	0.022	0.025		0.180	0.160	0.090
Coelosphaerium dubium Grunow							0.387	0.352	0.411	0.865	0.876	0.845	0.390	0.440	0.560
Chroococcus minor (Kütz.) Näg.	0.091	0.073	0.074												
Chroococcus minutus (Kütz.) Näg.						0.034									
Anabaenopsis arnoldii Aptek.	0.113	0.136	0.132												
Microcystis flos-aquae (Wittr.) Kirchn.	0.317	0.051	0.083												
Anabaena sphaerica						0.065									
Microcystis incerta Lemm.	0.047	0.075	0.044												
Chlorophyta															
Sceaedesmus dimorphus (Turp.) Kütz.				0.034		0.029									
Sceaedesmus quadricauda (Turp.) Bréb.		0.049	0.034		0.077										
Coelastrum microporum Nägeli							0.022								
Planktosphaeria gelatinosa G.M.Smith				0.030	0.050										
Crucigenia tetrapedia (Kirch.) Morr.			0.026	0.042											
Crucigenia puadrata Morren				0.038	0.104										

http://www.aloki.hu ● ISSN 1589 1623 (Print) ● ISSN1785 0037 (Online)
DOI: http://dx.doi.org/10.15666/aeer/1802_34393454

Phytoplankton	Changshou			Liangping			Bishan zubi			Tongliang			Bishan xinyue		
	T	H	E	T	H	E	T	H	E	T	H	E	T	H	E
Selenastrum bibraianum Reinsch					0.073										
Chlorella vulgaris Beij.				0.380	0.276	0.079	0.120	0.091	0.085	0.038	0.028	0.028	0.160	0.120	0.100
Chlamydomonas globosa Snow					0.132										
Tetraspora			0.027			0.025									
Cosmarium formosulum Hoff.					0.033										
Bacillariophyta															
Asterionella formosa.						0.150									
Synedra amphicephala Kützing.					0.048										
Cymatopleura stelligera Grun.				0.186	0.029										
Melosira granulata (Ehr.) Ralfs						0.432									
Cocconeis placentula (Ehr.) Hust.				0.046											
Gyrosigma acuminatum (Kütz.) Rabenhorst															
Diatoma vulgure Borg.				0.051											
Fragilaria capucina Desm.						0.021									
Nitzschia longissima (Breb.) Ralfs															
Xanthophyta															
Monallantus brevicylindrus Pasch.				0.076	0.061										
Species number	6	8	10	10	11	8	5	4	4	4	3	2	4	4	4

T represents tail water discharge area, H represents H. cumingii purification area, E represents ecological purification area

http://www.aloki.hu ● ISSN 1589 1623 (Print) ● ISSN1785 0037 (Online)
DOI: http://dx.doi.org/10.15666/aeer/1802_34393454

Table 2. *Phytoplankton dominant species and preponderance degree in autumn (Y > 0.02)*

Phytoplankton	Changshou			Liangping			Bishan zubi			Tongliang			Bishan xinyue		
	T	H	E	T	H	E	T	H	E	T	H	E	T	H	E
Cyanophyta															
Merismopedia eleggans Br.									0.048						
Merismopedia punctata Meyen	0.352	0.288	0.267	0.619	0.599	0.598	0.135	0.392	0.248	0.650	0.553	0.229	0.280	0.270	0.220
Oscillatoria tenuis Ag.											0.027	0.062			
Oscillatoria princeps Vauch.															0.030
Phormidium tenue (Menegh.) Gom.				0.022		0.022					0.077	0.098			
Coelosphaerium dubium Grunow	0.429	0.075	0.376												
Aphanizomenon flos-aquae		0.040	0.072												
Aphanocapsa pulchra		0.326													
Chroococcus minor (Kütz.) Näg.							0.066	0.113	0.134		0.058	0.067	0.060	0.030	0.030
Anabaenopsis sp.	0.120	0.174	0.140								0.049	0.345			
Anabaena osicellarioides Bory.		0.031	0.034												
Chlorophyta															
Sceaedesmus cavinaus (Lemm.) Chod.								0.037							
Sceaedesmus dimorphus (Turp.) Kütz.					0.037					0.062	0.055	0.025	0.080	0.060	
Sceaedesmus quadricauda (Turp.) Bréb.								0.072	0.082	0.049		0.021	0.090	0.090	
Sceaedesmus perforatus Lemm.							0.045								
Coelastrum sp.									0.034				0.200	0.050	
Staurastrum gracile Ralfs							0.022								
Cosmarium									0.023						
Ankistrodesmus sp.									0.061						
Cosmarium laeve							0.097								
Tetrastrum staurogeniaeforme Schr.							0.038								
Sphaerocystis schroeteri Chodat										0.041					
Planktosphaeria gelatinosa G.M.Smith							0.022					0.044	0.050	0.040	0.030
Crucigenia tetrapedia (Kirch.) Morr.					0.023			0.036	0.030				0.090	0.110	

http://www.aloki.hu ● ISSN 1589 1623 (Print) ● ISSN1785 0037 (Online)
DOI: http://dx.doi.org/10.15666/aeer/1802_34393454

Phytoplankton	Changshou			Liangping			Bishan zubi			Tongliang			Bishan xinyue		
	T	H	E	T	H	E	T	H	E	T	H	E	T	H	E
Crucigenia puadrata Morren															0.090
Tetraspora lacustris Emm														0.040	
Chlorella vulgaris Beij.				0.187	0.154	0.189	0.199			0.086	0.042		0.250		
Chlamydomonas globosa Snow								0.020	0.030						
Chlamydomonas microsphaera Pasch						0.026									
Pandorina morum Bory.	0.049	0.048	0.067					0.088							
Tetraspora							0.027		0.041						
Bacillariophyta															
Synedra ulna Ehrenberg							0.026								
Synedra acusvar			0.029						0.039						
Navicula simplex Krassk.									0.032						
Cymatopleura stelligera Grun.										0.032					
Navicula viridula Kütz.							0.021			0.049	0.031				
Xanthophyta															
Monallantus brevicylindrus Pasch.							0.066								
Euglenophyta															
Trachelomonas oblonga Lemm.							0.026								
Cryptophyta															
Cryptomonas ovata Ehr.							0.065	0.026	0.025						
Cryptomonas rostrata								0.038	0.033						
Species number	4	7	7	3	4	4	14	9	14	7	8	8	8	8	5

T represents tail water discharge area, H represents H. cumingii purification area, E represents ecological purification area

http://www.aloki.hu ● ISSN 1589 1623 (Print) ● ISSN1785 0037 (Online)
DOI: http://dx.doi.org/10.15666/aeer/1802_34393454

Furtherly, phytoplankton dominant species in all sampling sites changed constitutively with the turn of seasons. For example, the dominant algae in Liangping mainly belong to Bacillariophyta and Chlorophyte phyla in the summer, and change into Cyanophyta phyla in autumn. Overall, *H. cumingii* showed an excellent filter-feeding feature to *Chlorella vulgaris* Beij, *Sceaedesmus dimorphus* Kütz, *Merismopedia punctata* Meyen, *Cymatopleura stelligera* Grun and *Navicula viridula* Kütz, as the preponderance degree of the shellfish purification area and ecological purification area are lower than that of the tail water discharge area (*Tables 1 and 2*).

Effects of H. cumingii on water environmental characteristics

The basic physical and chemical characteristics of the aquaculture water in the testing base are shown in *Figure 4*. The change of water temperature is basically consistent among five testing bases. Among them, Changshou base autumn water temperature can reach 35.6℃, and the temperature at the Liangping base is as low as 9.2℃ in winter. The results showed that *H. cumingii* adapted to the changes in water temperature in the Chongqing region (*Figure 4A*). The dissolved oxygen at different sampling sites and seasons varied greatly, but all the concentration was within the range of 4-12 mg L^{-1} (*Figure 4B*). Moreover, the water quality of the pond was weakly alkaline at all sampling sites, except Changshou in autumn and winter and Bishan in autumn (*Figure 4C*). Overall, the water environment in the Chongqing region fully meets the requirements of *H. cumingii* farming.

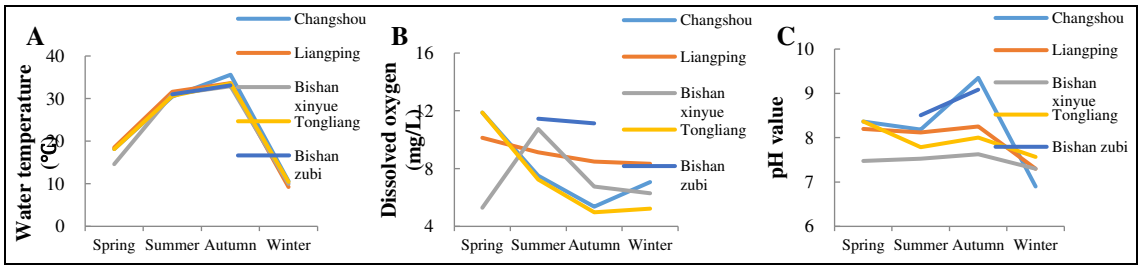

Figure 4. *Basic environmental factor of the aquaculture water in samplings sites. (A, water temperature; B, dissolve oxygen; C, pH value)*

The water purification effects of *H. cumingii* were reflected in *Figure 5*. The water transparency, electric conductivity, ammonia nitrogen and phosphate at different sampling sites and seasons are significantly different (*Figure 5A-D*). And the electro conductivity (4.9%), ammonia nitrogen (6.7%) and phosphate (7.2%) in purification area also decreased in this study. Besides, the results showed that the water transparency of spring and winter were higher than those of summer and autumn in each sampling sites. Generally, *H. cumingii* exhibited certain improvement effect on water transparency (*Figure 5A*). Conversely, the electro conductivity in spring and winter were lower than those in summer and autumn. However, the electro conductivity of the shellfish purification area and ecological purification area generally are equal to or lower than that of the tail water discharge area in sampling sites, except Tongliang and Bishan zubi in the summer (*Figure 5B*). The decrease of ammonia nitrogen and phosphate in the *H. cumingii* purification area has appeared only in part of sampling sites, such as Changshou, Liangping and Bishan xinyue (*Figure 5C-D*). To some extent, *H. cumingii* has improved water quality in inner circulation ponds.

http://www.aloki.hu ● ISSN 1589 1623 (Print) ● ISSN1785 0037 (Online)
DOI: http://dx.doi.org/10.15666/aeer/1802_34393454

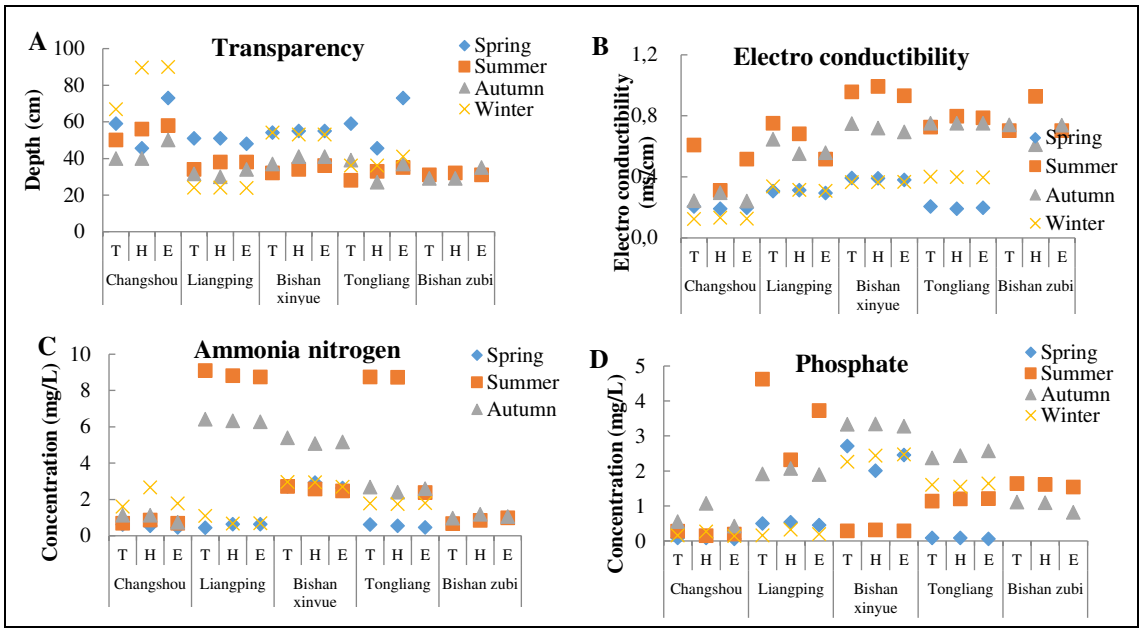

Figure 5. *Purifying effect of H. cumingii on transparency (A), electro conductivity (B), ammonia nitrogen (C) and phosphate (D). Where letter "T" represents tail water discharge area, "H" represents H. cumingii purification area and "E" represents ecological purification area*

Discussion

Southeast Asia has proved to be a global hotspot for freshwater mussel diversity due to the existence of 228 native and 3 non-native Bivalvia: Unionida (98% Unionidae, 2% Margaritiferidae). In this region, species richness was the highest in China (particularly Yangtze River basin) in absolute numbers and Cambodia when correcting for the country area, and decreased gradually towards the surrounding area (Zieritz et al., 2018). However, freshwater shellfish industry is still in its infancy in upper-middle reaches of the Yangtze River, especially in Chongqing, Sichuan, Guizhou and Yunnan provinces in southwest China, where the production of bivalve shellfish accounts for less than 0.04% of the total freshwater aquaculture in 2018 (Zhang et al., 2019). The newly established Chongqing Comprehensive Experimental Station, as the only freshwater comprehensive experimental station in the non-main producing areas, is mainly responsible for studying the ecological service function and fishery economic value of shellfish, and promoting the healthy development of freshwater shellfish industry in southwest China and even in wider regions. The present annual investigation results confirm that the water quality fully meets the requirements of *H. cumingii* growth in the Chongqing region (Lin et al., 2004; Liu et al., 2020). The average wet weight increased from 359.4 g to 525.6 g within 2018 in the five sampling sites. This investigation can be used as the basis for further development of shellfish industry in southwest China.

Automated closed recirculating aquaculture system, namely partitioned aquaculture system, was early designed in the United States (Brune et al., 2001). In recent years, this mode has been widely used in Zhejiang, Jiangsu and Chongqing regions in China. The renewed interest in recirculating aquaculture systems is also due to their perceived advantages, including significantly reduced water requirements, a high degree of environmental control, improved waste management, promoted nutrient recycling and so

http://www.aloki.hu ● ISSN 1589 1623 (Print) ● ISSN1785 0037 (Online)
DOI: http://dx.doi.org/10.15666/aeer/1802_34393454

on (Martins et al., 2010). Moreover, this water circulation system can realize high-density intensive aquaculture in rectangular mixed-cell rearing unit (Ebeling et al., 2005) and has clear functional partitions including aquaculture area, tail water discharge area and purification area. Our group predicted that N, P and phytoplankton are abundant in the tail water discharge area, and potential water purification could be achieved by cultivating *H. cumingii* in this area. Meanwhile, this "fish and mussel mixed breeding mode" can realize the regional division of *H. cumingii* and fish, and promote the more standardized production management in recirculating aquaculture system (Masser et al., 1999).

H. cumingii is mainly distributed in large lakes and rivers in east China and plays an important role in the fishery economy and aquatic ecosystem as a result of its value of ecological purification, edibility and pearl cultivation. However, despite the great development in the research of artificial propagation (Li and Li, 2009), genetic breeding (Bai et al., 2016), growth traits and pearl cultivation (Jin et al., 2012), the applied research on *H. cumingii* ecological function and environmental suitability still needs to be improved. Therefore, the main purpose of the investigation is to evaluate the adaptability to the local climate and the purification function of *H. cumingii* before popularized in the recirculating aquaculture system in the Chongqing region, southwestern China. Our results showed that *H. cumingii* adapted to the seasonal changes of water temperature, dissolved oxygen, pH and other water-chemistry factor in all the sampling sites. In addition to the influence of water environment factors (Lin et al., 2004), the growth and fertility of bivalve shellfish were also affected by the ratio of male to female (Zhao et al., 2013), different sized mussel (Davenport et al., 2011), phytoplankton composition (Vanderploeg et al., 1996), season variation (Naddafi et al., 2007) and fish-shellfish mixed breeding mode (Wang et al., 2018), such as the integrating culture of the mussel with herbivorous or omnivorous fish species in commercial farming (Wang et al., 2009).

At present, there are few studies on the ecological functions of *H. cumingii*, such as the influence on phytoplankton composition. Studies have shown that filter-feeding *H. cumingii* may potentially support submerged macrophyte growth by reducing cyanobacterial density, but bivalve communities in many lakes and rivers are in decline as a result of overharvesting (He et al., 2014). The present results also revealed that *H. cumingii* could effectively reduce the phytoplankton biomass. The measured value in the shellfish purification area and ecological purification area are generally lower than that of the tail water discharge area in recirculating aquaculture systems. However, the phytoplankton community structure and the total number of dominant algae have no visible change under lower *H. cumingii* stocking density. And more than 65% of them belong to the Chlorophyta, Cyanophyta and Bacillariophyta phyla, the primary food sources of bivalve shellfish (Marroni et al., 2014). Although there was no discernible effect on phytoplankton community structure and dominant algae in the present *H. cumingii* stocking density, the phytoplankton biomass could be significantly reduced. Therefore, the use of *H. cumingii* has been proposed as an alternative mean to control algal bloom in eutrophic water bodies in recent years (Liu et al., 2014).

This investigation revealed the potential role of *H. cumingii* in water purification, including increasing water transparency, decreasing electro conductivity, ammonia nitrogen and phosphate. Other results of different biological units show that *H. cumingii* can effectively enhance the contaminant removal rates from the ecological floating bed containing aquatic plant (*Ipomoea aquatica*), aquatic animal (*H. cumingii*), artificial medium (Wang et al., 2015). Furthermore, this purification of *H. cumingii* unit on nitrogen, phosphorus and COD was much lower than that of the aquatic plants unit and

http://www.aloki.hu ● ISSN 1589 1623 (Print) ● ISSN1785 0037 (Online)
DOI: http://dx.doi.org/10.15666/aeer/1802_34393454

microorganisms unit. These results suggest that the filter feeding of *H. cumingii* promotes the solubilization and mineralization of particulate organic matters, and improves the purification efficiency of the floating bed by microorganism purification (Wang et al., 2015). Therefore, the environmental response mechanism and interaction between *H. cumingii* and other aquatic organisms are worthy for further study.

Conclusion

Overall, the results of the annual investigation show that there is plenty of phytoplankton bait in the water environment in southwest China, and the seasonal variation range of physical and chemical indices completely meets the growth demand for *H. cumingii*. Meanwhile, the results also indicate that *H. cumingii* is an excellent way for algal bloom controlling and water quality regulating in the recirculating aquaculture system and the mixed farming model based on the recirculating aquaculture system is worthy for further study.

Acknowledgements. This research was supported by "Fundamental Research Funds for the Central Universities, Ministry of Education, China (SWU117047)", "Chongqing Municipal Social Livelihood Project (cstc2018jscx-msybX0235)" and "National Shellfish Industry Technology System Project, Ministry of Finance, China (CARS-49)". The authors thank the five testing sites for facilitating in the investigation. And we also thank the group members in Research Center of Fishery Resources and Environment for providing assistance.

REFERENCES

[1] Bai, Z. Y., Han, X. K., Liu, X. J., Li, Q. Q., Li, J. L. (2016): Construction of a high-density genetic map and QTL mapping for pearl quality-related traits in *Hyriopsis cumingii*. – Scientific Reports 32608.

[2] Bianchi, V. A., Castro, J. M., Rocchetta, I., Bieczynski, F., Luquet, C. M. (2014): Health status and bioremediation capacity of wild freshwater mussels (*Diplodon chilensis*) exposed to sewage water pollution in a glacial Patagonian lake. – Fish & shellfish Immunology 37(2): 268-277.

[3] Brune, D. E., John, A. C., Schwedler, T. E. (2001): Partitioned aquaculture system. – US Patent. No. 6,192,833.

[4] Cha, Y. K., Stow, C. A., Nalepa, T. F., Reckhow, K. H. (2011): Do invasive mussels restrict offshore phosphorus transport in Lake Huron? – Environmental Science & Technology 45: 7226-7231.

[5] Daines, S. J., Clark, J. R., Lenton, T. M. (2014): Multiple environmental controls on phytoplankton growth strategies determine adaptive responses of the N: P ratio. – Ecology Letters 17(4): 414-425.

[6] Dan, H., Ruobo, G. (2002): Freshwater pearl culture and production in China. – Aquaculture Asia 7(1): 6-8.

[7] Davenport, J., Ezgeta-Balić, D., Peharda, M., Skejić, S., Ninčević-Gladan, Ž., Matijević, S. (2011): Size-differential feeding in *Pinna nobilis* L. (Mollusca: Bivalvia): exploitation of detritus, phytoplankton and zooplankton. – Estuarine Coastal and Shelf Science 92(2): 246-254.

[8] Ebeling, J. M., Timmons, M. B., Joiner, J. A., Labatut, R. A. (2005): Mixedcell Raceway: Engineering design criteria, construction, and hydraulic characterization. – North American Journal of Aquaculture 67(3): 193-201.

http://www.aloki.hu ● ISSN 1589 1623 (Print) ● ISSN1785 0037 (Online)
DOI: http://dx.doi.org/10.15666/aeer/1802_34393454

[9] Hawkins, A. J. S., Pascoe, P. L., Parry, H., Brinsley, M., Cacciatore, F. (2013): Comparative feeding on chlorophyll-rich versus remaining organic matter in bivalve shellfish. – Journal of Shellfish Research 32(3): 883-898.
[10] He, H., Liu, X., Liu, X., Yu, J., Li, K., Guan, B., Jeppesen, E., Liu, Z. (2014): Effects of cyanobacterial blooms on submerged macrophytes alleviated by the native Chinese bivalve *Hyriopsis cumingii*: A mesocosm experiment study. – Ecological Engineering 71: 363-367.
[11] Hoellein, T. J., Zarnoch, C. B., Grizzle, R. E. (2015): Eastern oyster (*Crassostrea virginica*) filtration, biodeposition, and sediment nitrogen cycling at two oyster reefs with contrasting water quality in Great Bay Estuary (New Hampshire, USA). – Biogeochemistry 122(1): 113-129.
[12] Horton, M., Keys, A., Kirkwood, L., Mitchell, F., Kyle, R., Roberts, D. (2015): Sustainable catchment restoration for reintroduction of captive bred freshwater pearl mussels Margaritifera margaritifera. – Limnologica 50: 21-28.
[13] Jin, W., Bai, Z., Fu, L., Zhang, G., Li, J. (2012): Genetic analysis of early growth traits of the triangle shell mussel, Hyriopsis Cumingii, as an insight for potential genetic improvement to pearl quality and yield. – Aquaculture International 20(5): 927-933.
[14] Jin, C., Zhao, J. Y., Liu, X. J., Li, J. L. (2019): Expressions of shell matrix protein genes in the pearl sac and its correlation with pearl weight in the first 6 months of pearl formation in *Hyriopsis cumingii*. – Marine Biotechnology 21(2): 240-249.
[15] Kellogg, L. M., Cornwell, J. C., Owens, M. S., Paynter, K. T. (2013): Denitrification and nutrient assimilation on a restored oyster reef. – Marine Ecology Progress Series 480: 1-19.
[16] Kingsford, R. T., Biggs, H., Pollard, S. (2011): Strategic adaptive management in freshwater protected areas and their rivers. – Conservation Biology 16(1): 30-41.
[17] Li, J. L., Li, Y. S. (2009): Aquaculture in China-Freshwater pearl culture. – World Aquaculture 40: 60-62.
[18] Lin, Q. X., Wang, Y., Gao, J. H., Zhu, S. B., Wang, W. L. (2004): Water quality for culturing freshwater pearl mussel, *Hyriopsis cumingii* in waters scatted in different regions in China. – Journal of shanghai fisheries university 17(3): 327-332. (in Chinese).
[19] Liu, Q. G., Hu, M. H., Wu, Z. (2014): Can mussels change phytoplankton community structure and enhance prawn production in semi-enclosed prawn ponds? – Aquaculture Research 46: 2559-2564.
[20] Liu, Y., Li, L., Zheng, L., Fu, P., Wang, Y., Nguyen, H., Shen, X., Sui, Y. (2020): Antioxidant responses of triangle sail mussel *Hyriopsis cumingii* exposed to harmful algae *Microcystis aeruginosa* and high pH. – Chemosphere 243: 125241.
[21] Marroni, S., Iglesias, C., Mazzeo, N., Clemente, J., De Mello, F. T., Pacheco, J. P. (2014): Alternative food sources of native and non-native bivalves in a subtropical eutrophic lake. – Hydrobiologia 735(1): 263-276.
[22] Martins, C. I. M., Eding, E. H., Verdegem, M. C., Heinsbroek, L. T., Schneider, O., Blancheton, J. P., Roqued'Orbcastel, P., Verreth, J. A. J. (2010): New developments in recirculating aquaculture systems in Europe: A perspective on environmental sustainability. – Aquacultural engineering 43(3): 83-93.
[23] Masser, M. P., James, R., Losordo, T. M. (1999): Recirculating aquaculture tank production systems-Management of recirculating systems. – SRAC Publication 452.
[24] Modesto, V., Ilarri, M., Souza, A. T., Lopes-Lima, M., Douda, K., Clavero, M., Sousa, R. (2018): Fish and mussels: Importance of fish for freshwater mussel conservation. – Fish and Fisheries 19: 244-259.
[25] Naddafi, R., Pettersson, K., Eklöv, P. (2007): The effect of seasonal variation in selective feeding by zebra mussels (*Dreissena polymorpha*) on phytoplankton community composition. – Freshwater Biology 52(5): 823-842.
[26] Qu, X., Xia, W., Wang, R., Zhang, Y., Xie, Z., Trushenski, J., Chen, Y. (2018): Effects of Aquaculture on Lakes in the Central Yangtze River Basin, China, II: Benthic Macroinvertebrates. – North American Journal of Aquaculture 80(4): 369-378.

http://www.aloki.hu ● ISSN 1589 1623 (Print) ● ISSN1785 0037 (Online)
DOI: http://dx.doi.org/10.15666/aeer/1802_34393454

[27] Ren, J. S., Ross, A. H., Hayden, B. J. (2006): Comparison of assimilation efficiency on diets of nine phytoplankton species of the greenshell mussel *Perna canaliculus*. – Journal of shellfish research 25(3): 887-893.
[28] Vanderploeg, H. A., Liebig, J. R., Gluck, A. A. (1996): Evaluation of different phytoplankton for supporting development of zebra mussel larvae (*Dreissena polymorpha*): the importance of size and polyunsaturated fatty acid content. – Journal of Great Lakes Research 22: 36-45.
[29] Wang, Y., Wang, W. L., Qin, J. G., Wang, X. D., Zhu, S. B. (2009): Effects of integrated combination and quicklime supplementation on growth and pearl yield of freshwater pearl mussel, *Hyriopsis cumingii* (Lea, 1852). – Aquaculture Research 40(14): 1634-1641.
[30] Wang, G., Wang, X., Wu, L., Li, X. (2015): Contribution and Purification Mechanism of Bio components to Pollutants Removal in an Integrated Ecological Floating Bed. – Journal of Civil, Architectural & Environmental Engineering 4: 136-141.
[31] Wang, L., Ma, L., Sun, J., Zhang, Y., Zhou, Q., Wu, Z., He, F. (2018): Effects of different aquaculture methods for introduced bivalves (*Hyriopsis cumingii*) on seston removal and phosphorus balance at the water-sediment interface. – Journal of Freshwater Ecology 33(1): 251-265.
[32] Watten, B. J., Honeyfield, D. C., Schwartz, M. F. (2000): Hydraulic characteristics of a rectangular mixed-cell rearing unit. – Aquacultural engineering 24(1): 59-73.
[33] Wei, F. S., Qi, W. Q., Bi, T., Sun, Z., Huang, Y. (2002): Standard methods for water and wastewater monitoring and analysis. – China Environmental Science Press, Beijing.
[34] Weng, J. Z., Xu, H. S. (2010): The common freshwater phytoplankton algae atlas of China. – Shanghai Science and Technology Press, China 1-225.
[35] Zhang, G., Luo, Y., Zhang, W., Fang, A., Ye, R., Ren, G., Yang, S. (2019): The effect of two selected strains of mussels as donor or host on the color of cultivated pearls. – Journal of Shellfish Research 38(2): 363-369.
[36] Zhang, X. L., Cui, L. F., Li, S. M. (2019): China Fishery Statistical Yearbook 2018. – China Agriculture Press 1-172. (in Chinese).
[37] Zhao, Y., Bai, Z., Fu, L., Liu, Y., Wang, G., Li, J. (2013): Comparison of growth and pearl production in males and females of the freshwater mussel, *Hyriopsis cumingii*, in China. – Aquaculture International 21(6): 1301-1310.
[38] Zhou, X., Zheng, J. (2005): Hydrobiology atlas of Chongqing section of the three gorges reservoir area. – China Environmental Science Press 1-125.
[39] Zieritz, A., Bogan, A. E., Froufe, E., Klishko, O., Kondo, T., Kovitvadhi, U., Kovitvadhi, S., Jin, H. L., Lopes-Lima, M., Pfeiffer, J. M., Sousa, R., Van Do, T., Vikhrev, I., Zanatta, D. T., Sousa, R. (2018): Diversity, biogeography and conservation of freshwater mussels (Bivalvia: Unionida) in East and Southeast Asia. – Hydrobiologia 810(1): 29-44.

http://www.aloki.hu ● ISSN 1589 1623 (Print) ● ISSN1785 0037 (Online)
DOI: http://dx.doi.org/10.15666/aeer/1802_34393454

FLORAL ONTOGENESIS AND EMBRYOGENESIS FEATURES OF THE RELIC WILD LAPERRINE'S OLIVE (*OLEA EUROPAEA* SSP *LAPERRINEI*) IN ARID CENTRAL SAHARA

LAHMISSI, A.[1,2*] – VERDEIL, J. L.[3] – BOUGUEDOURA, N.[1]

[1]*Research Laboratory of Arid Zones (LRZA), Faculty of Biological Sciences, University of Sciences and Technology Houari Boumediene (USTHB), PO Box, 32 El Alia Bab-Ezzouar, 16111 Algiers, Algeria*

[2]*University Mouloud Mammeri, Faculty of Biological and Agronomical Sciences, Tizi-ouzou, Algeria*

[3]*International Center for Agronomic Research and Development, Montpellier, France*

[*]*Corresponding author*
e-mail: lahmissiaamina@gmail.com; phone: +213-551-496-538; fax: +213-2163-9141

(Received 13th Nov 2019; accepted 12th Feb 2020)

Abstract. *Olea europaea* subsp. *laperrinei* (Batt. & Trabut) Cif., is an endemic species of Ahaggar (Hoggar) and Tassili N'ajjer in southern Algeria, with powerful adaptation against harsh conditions. Several genetic and phylogenetic studies have been done on this taxon, offering awareness on its reproductive methods and its use as a genetic resource of the cultivated olive, but no attention was given to the ontogenesis and zygotic embryogenesis for this centenary desert plant. This work is focuses particularly on the morphology of the flower followed by the analysis of the cytological and histological changes during early zygotic embryogenesis, with the aim to identify and characterize gametophytes playing a role in this process. The results of this investigation showed different types of flowers as well as imperfections in the female gametophyte that is often absent or without nuclei in this species. These particular observations could be considered as adaptation behaviour of this plant relic against arid conditions.
Keywords: *Olea europaea subsp. laperrinei, cyto-histological study, genetic resource, male gametophyte, female gametophyte, embryos development*

Introduction

The Laperrine's olive tree, (*Olea europaea* subsp. *Laperrinei* (Batt. & Trabut) Cif.), is a relic taxon spread out across the central Saharan mountains (1400-2800 m altitude), considered as an endemic species from the Oleaceae family representing an important genetic resource due to its adaptation to arid conditions.

Note, that *Olea europaea* is a species composed of six subspecies with wild populations extended in large zones of south of Asia, Africa and southern Europe (Green, 2002).

Quézel (1965) has recognized a few individuals of (*Olea europaea* subsp. *laperrinei*) in Algerian Saharan areas. In contrast, the first inventories conducted by Baali-Cherif et al. (2007) indicated the presence of thousands of individuals in Hoggar and Tassili. In addition, it is found in granite massifs of Ahaggar Mountains (Tefedest) but rare at Tassili n'Ajjer and in Mouydir.

Besnard et al. (2007) and Anthelme et al. (2008) showed that this subspecies is distributed across fragmented habitats and locally exposed to extinction by the absence of the populations' regenerative capacities. These studies have reported that multi-centennial individuals which mainly reproduce vegetatively can restore sexuality under

http://www.aloki.hu ● ISSN 1589 1623 (Print) ● ISSN1785 0037 (Online)
DOI: http://dx.doi.org/10.15666/aeer/1802_34553469

favourable conditions. Recently, crosses between the Laperrine's olive and other olive diploid subspecies (subspp. *cuspidata* and *europaea*) have been reported.

Although, this plant species offers a plant matter for animals and prevent other plants disappearance, no natural regeneration was reported since several years (Maire, 1933; Quézel, 1978) causing its genetic diversity limit by the absence of fruits (self-incompatibility), due to the high separation of trees by high mountains reducing the pollen transportation and thus gene flow (Besnard et al., 2007).

Biological reproduction for this relic species is now becoming a priority, and hence its germplasm preservation is needed, among the ex situ methods available, the seed germination is considered the most efficient method (Benarar and Bouguedoura, 2003). Seeds are important starting materials for tree breeding and genetic improvement. Their use enables capturing the natural genetic variation (due to random mating or pollination). Indeed, several populations of this plant species identified by Baali-Cherif and Besnard (2005). These authors envisaged that through sexual hybridization, new and superior genotypes could be developed; they explained the possible sexual reproduction system role in genetic variation loss such as small populations could "turn-over" of the others causing strong genetic erosion and taxon's disappearance.

Therefore, this study reports for the first time a number of information about the reproductive biology by morphological and histological aspects of floral biology. The well knowledge of major steps could be helpful to understand how to prevent the production of abnormal flowers and seeds and enhance the genetic diversity of this important taxon considered as a green belt and rootstock of local varieties.

Material and methods

The present investigation was undertaken with the trees at 1400-2300 m of altitude of Ahaggar in Southern Algeria (*Fig. 1*), characterized by seasonal temperature and rain full regime variations (cold winter 15.40°C and 1.24 mm; hot summer 26.6°C and 8.60 mm).

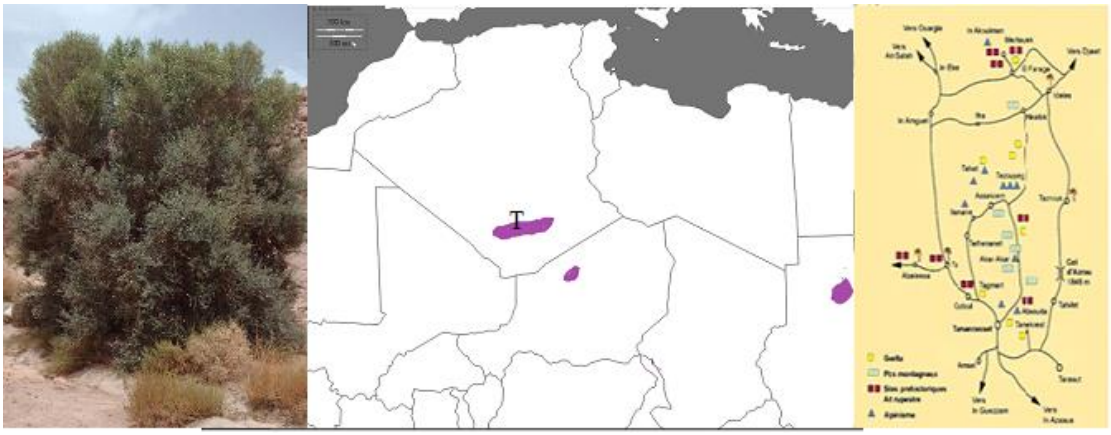

Figure 1. *Natural distribution of Olea europaea ssp laperrinei in southern Algeria (T: Tamanrasset) with some sampling areas (Akar-akar and Tezouyeg) according to website (Algerian agency. Tazrouk stays.com)*

Fresh plant parts (vegetative and floral buds, mature flowers) were collected from adult trees in flowering period for 3years (2013-2015) between March and June according to

http://www.aloki.hu ● ISSN 1589 1623 (Print) ● ISSN1785 0037 (Online)
DOI: http://dx.doi.org/10.15666/aeer/1802_34553469

areas location (*Table 1*). The vegetative and reproductive organs were examined and compared.

Table 1. *Location of sampling areas according to the altitude (m)*

Local name of Sampling areas	Altitude (m)	Latitude	Individuals number
Aguellala	from 1400 to 1500	22°38 127N 05°36 724E	11
Ainergiouene	1803	22°11 167N 06°02 874E	2
Akar-akar	from 1866 to 1885	23°03 306N 05°42 616E	7
Tagherra	1693	23°09 692N 06°01 529E	5
Tezouyeg	from 2150 to 2331	23°12 593N 05°42 413E	6

Morphological and anatomical studies

The morphological assessment was carried out by external aspects observation and measurement of fresh specimens. The organs were observed and photographs were taken by using Canon Power Shot A640 camera through the stereomicroscope StemiDV4 (Zeiss, Germany).

For the cyto-histological studies, the fresh samples were fixed in FAA fixator (Formaldehyde 37% (1 volume)-glacial acetic acid (1 volume)-Alcohol 70% (8 volume) or in Glutaraldehyde-Paraformaldhehyde-Caffeine fixator (Glutaraldehyde (25%) 4 ml-phosphate buffer pH 7.2-50 ml – paraformaldehyde (10%) 20 ml and caffeine 1% 1 g) (Schwendiman et al., 1990). The specimens were dehydrated and embedded in paraffin or in resin (Reichert-Jung Historesin). Thin sections of 2.5-5 µm were cut with microtome (Leica, Germany) and stained by Periodic Acid Schiff (PAS)-Naphthol Blue Black (NBB) (Feder and O'Brien, 1968; Fisher, 1968). Microphotographs were obtained using Canon camera, Power Shot A640 and Q-imaging Retiga 2000R camera combined with DM4500 microscope (Leica, Germany).

For transmission electron microscopy, floral parts were prefixed in 4% glutaraldehyde (1 volume)-cacodylate buffer pH 7.4 at 0.4 M (1 volume) and were fixed in 2% osmium tetroxide (1 volume)-cacodylate buffer pH 7.4 at 0.4 M (1 volume) - (Pottu-Boumendil, 1989) and then, embedded in Epoxy resin (Fluka). Ultra-thin sections of 0.01 µm were carried out with EM UC7 microtome (Leica, Germany) stained with positive contrast (2% uranyl acetate then lead citrate) (Pottu-Boumendil, 1989). Observations and microphotographs were made using the 1200EXII microscope (Jeol, Japan).

Results

Through sexual reproduction, Laperrine's olive tree individuals form four different types of flowers varying between trees, areas and sampling year (*Table 2*).

http://www.aloki.hu ● ISSN 1589 1623 (Print) ● ISSN1785 0037 (Online)
DOI: http://dx.doi.org/10.15666/aeer/1802_34553469

Table 2. *Variation rate of different flowers*

Sampling areas	Year	Percentage of flower types (%)			
		Type1	**Type2**	**Type3**	**Type4**
Aguellala	2013	75	15	10	0
	2014	80	10	10	0
	2015	80	15	5	0
Ainergiouene	2013	85	10	5	0
	2014	80	15	5	5
	2015	60	15	15	10

The flower (*Fig. 2A*) with fully developed parts: 4 sepals, 4 petals, 2 stamen (type 1) is the most frequent, following by flowers with less prominent and necrotic stigmas (type 2), male flowers with rudimentary and very insignificant pistils (type 3) and flowers with 3 stamen instead 2 (type 4) (*Fig. 3A and B*).

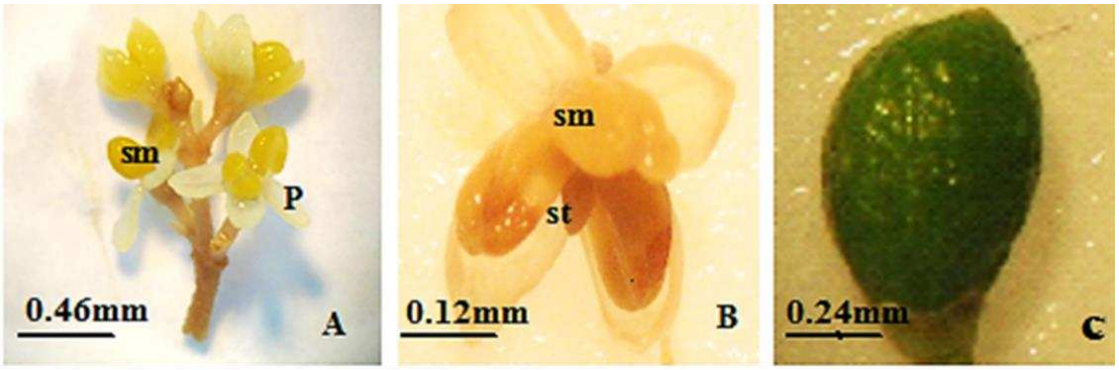

Figure 2. *Inflorescence (A), flower (B) and fruit (C) of Olea europaea ssp. laperrinei. p: petal, sm: staminate, st: stigma*

Mature flower structure

The flower of the Laperrine's olive tree is hermaphrodite or male flowers of 4.5 mm height, each with 4 greenish gamosepals, 4 whitish petals, 2 yellowish stamens with a longitudinal introrsely dehiscence and pistil formed of an ovary of two fused carpels bi-ovuled each, a style and of a two-lobbed dome shaped stigma. The pistil and the stamens have the same length (about 2.5 mm), stigma (1 mm), the style (0.5 mm) and ovary diameter (1-1.2 mm).

Flower ontogenesis: morphology and histology

The vegetative bud's foliar initiation is decussate corresponding to Laperrine's olive tree's phyllotaxis. The observation of axillary vegetative buds showed that previous year's twigs initiate floral buds in comparison to those of actual year which do not flowering.

http://www.aloki.hu ● ISSN 1589 1623 (Print) ● ISSN1785 0037 (Online)
DOI: http://dx.doi.org/10.15666/aeer/1802_34553469

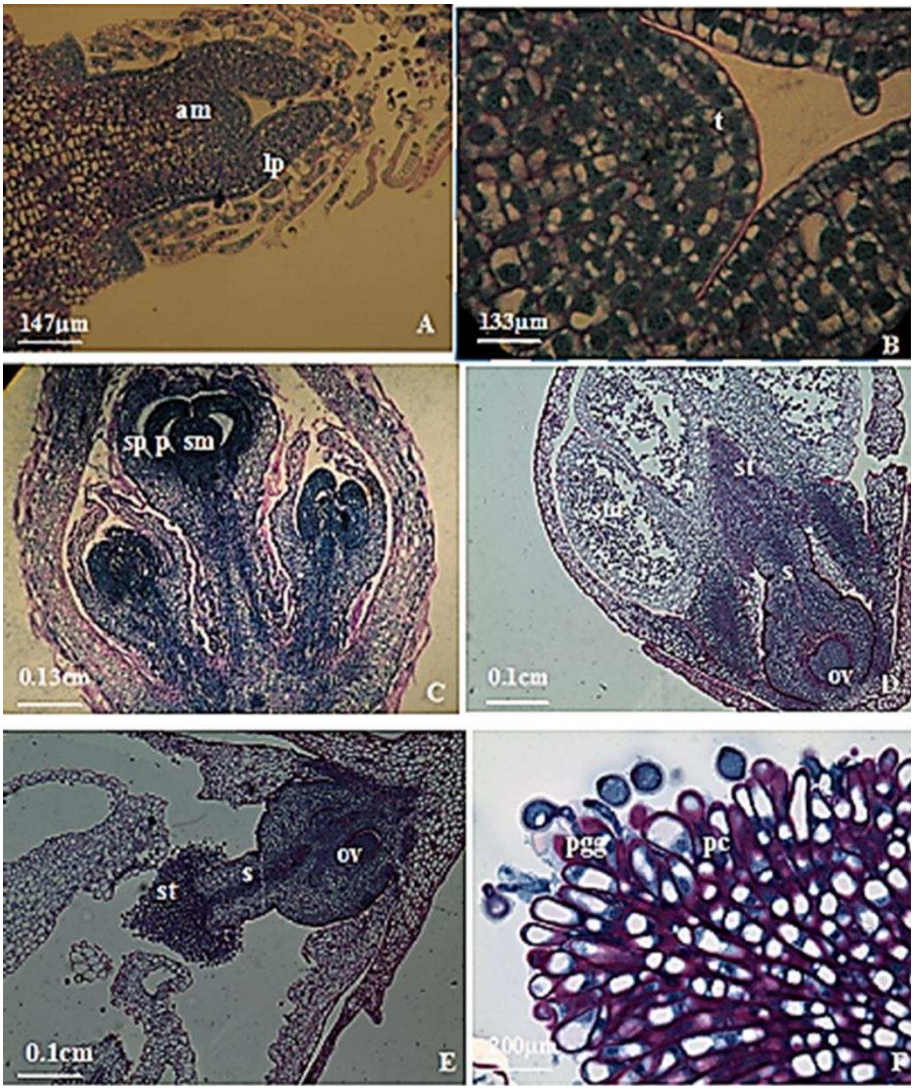

Figure 3. *Histological structures of vegetative and floral buds. A. Vegetative bud. B. Vegetative apical meristem. C. Youngflower bud. D. mature flower bud. E. Ovary. F. Stigma details. am: apical meristem, lp: leaf primordium, ov: ovary, p: petal,pc: papillar cells, pg: pollen grain germination, s:style, sm: stamen.,sp: sepal, st: stigma, t: tunica*

The morphological analysis of buds before flowering showed that the growth of vegetative twigs starts between March and April depending on the zone's altitude and temperature. The vegetative apical meristem (dome) is wide showing three heterogeneous zones; apical zone formed by tunica of one or two layers; lateral zone on the flanks enabling foliar initiation and the medullary zone located under the apical zone with lined up cells (*Fig. 3A and B*).

According to the histological study, it appears that the future flower bud's apical dome is more prominent (650 µm) than that of the vegetative bud (292,6 µm) covered by external bracts, formed by homogeneous structure of strongly meristematic cells called floral primordium (*Fig. 3C*), which develops into a flower bud (*Fig. 3D*).

Three types of flower buds were observed with variations in pistil; first type with two-lobed prominent stigma (*Fig. 3D*); the second type with less prominent and necrotic stigma (*Fig. 4A*) and the third type with a rudimentary pistil (*Fig. 4B*).

http://www.aloki.hu ● ISSN 1589 1623 (Print) ● ISSN1785 0037 (Online)
DOI: http://dx.doi.org/10.15666/aeer/1802_34553469

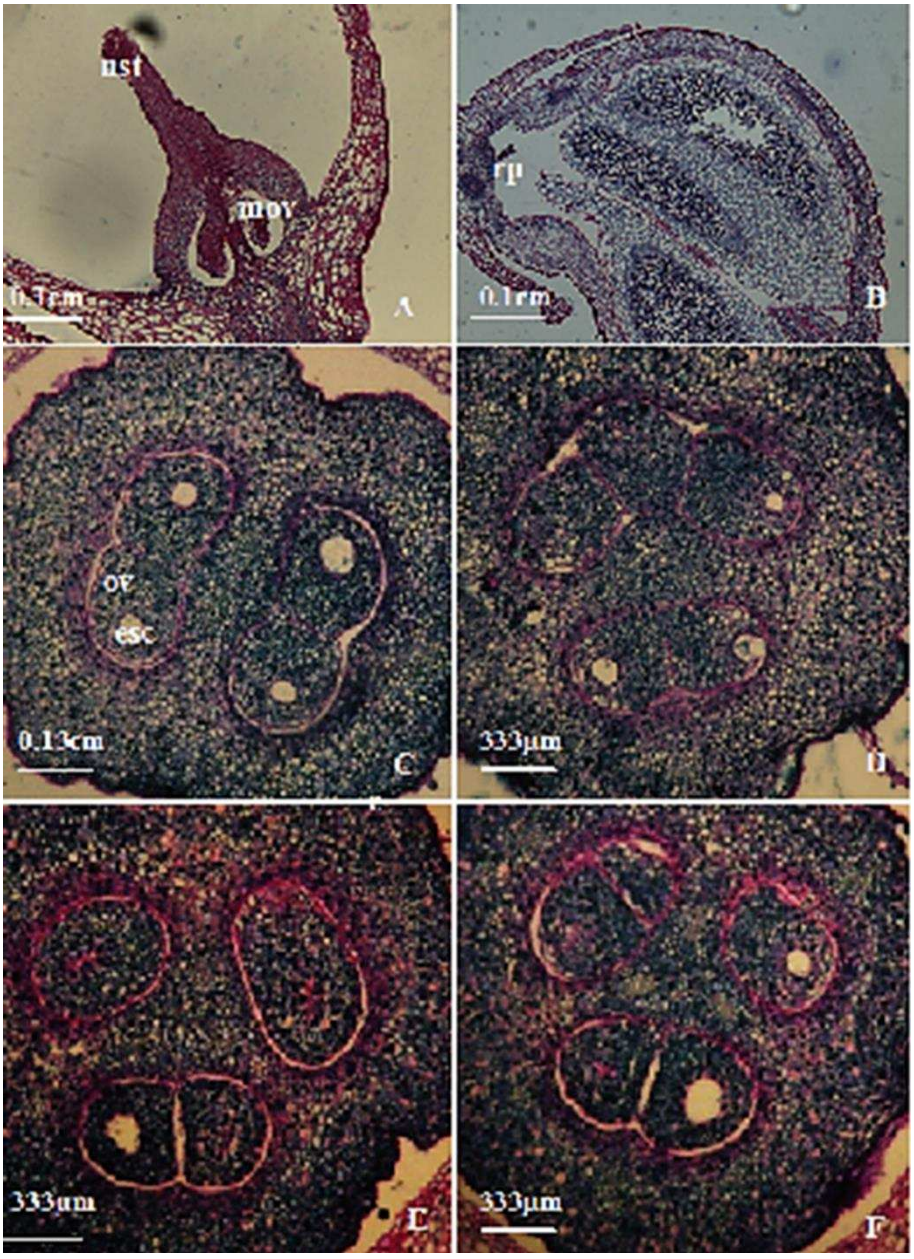

Figure 4. *Different abnormalities of ovarian development. A, B. Abnormal Pistil C. Ovary (2 carpels and 4 ovules). D. Abnormal ovary (2 carpels and 5 ovules). E. Abnormal ovary (3 carpels and 4 ovules). F. Abnormal ovary (3 carpels and 5 ovules). c: carpel, es: embryo sac, mov: malformed ovule, nst: necrotic stigma, ov: ovule, rp: rudimentary pistil, nst: necrotic stigma*

Androecium and male gametophyte

Anthers are composed of four pollen locules of different shape and size. Those with only two or three locules observed are due to their incomplete development.

From outside to inside, each anther contains an epidermis with wide cells, a mechanical layer, a layer of transitional cells, a medullar layer and a tapetum of two to three layers of protein-rich cells with a central big nucleus remembering meristematic cells (*Fig. 5A*).

http://www.aloki.hu ● ISSN 1589 1623 (Print) ● ISSN1785 0037 (Online)
DOI: http://dx.doi.org/10.15666/aeer/1802_34553469

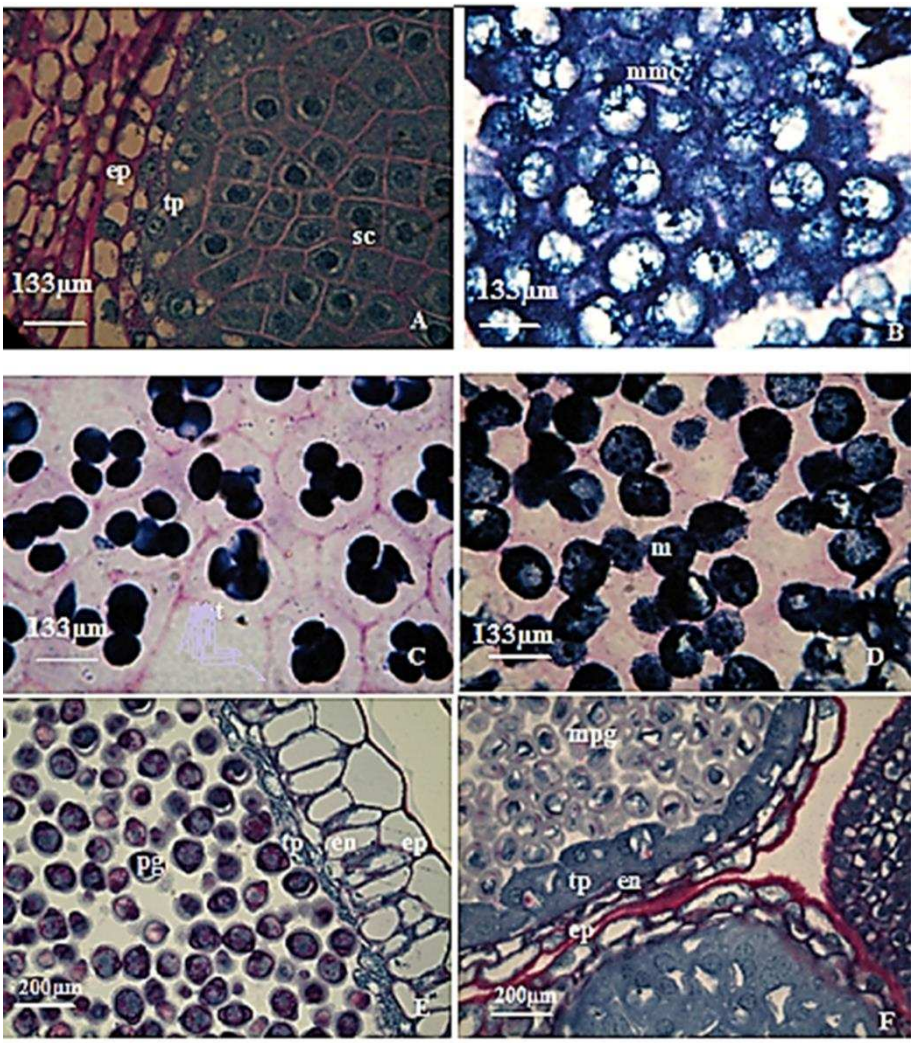

Figure 5. *Stages of male gametophyte development: A. Stamen and sporogen tissues.B. Mother cells. C. Tetrads. D. Microspores. E. Different stamen layers with fertile pollen. F. Different stamen layers with malformed pollen. en: endothecium,ep: epidermis,m: microspore, mmc: mother cell of microspore, mpg: malformed pollen grains, pg: pollen grain, sc: sporogenous tissue, t: tetrad, ta: tapetum*

The medullar layer begins to degenerate in the early stages of meiosis of microsporocytes. Indeed, the tapetum degeneration follows the first uninucleate microspores formation and continues until maturation. The sporogenous tissue is initially formed by polygonal-shaped cells (*Fig. 5B*), which differentiate into mother cells of spores forming tetrads surrounded by callose as tetrahedral type or rarely rhomboidal after meiosis (*Fig. 5C*).

The Electronic microscopy observation shows that mature pollen grains are bicellular and rich in starch at dehiscence time (*Fig. 5E*), the reproductive cell, previously found against the vegetative cell's wall, are in the middle of cells (*Fig. 6A and B*).

Triporate pollen grains presenting TEM images of apertures in equidistant positions composed of ecto aperture covered by a cross-linked tectum and of the endo aperture, these pollen grains can be observed onto the stigma surface and the ovary is fertilised

http://www.aloki.hu ● ISSN 1589 1623 (Print) ● ISSN1785 0037 (Online)
DOI: http://dx.doi.org/10.15666/aeer/1802_34553469

before the dehiscence of this flower's stamens. This situation induces the stigma's responsiveness before the stamens maturation and confirms the allogamy of the species.

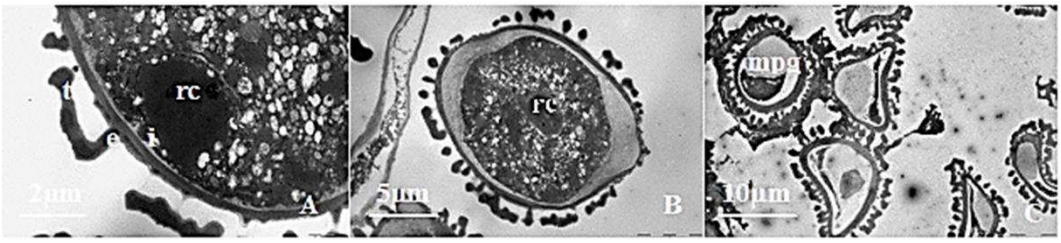

Figure 6. *Transmission electron micrographs of cross-sections through pollen grain during developmental stages. A. Non detached reproductive cell. B. Bicellular pollengrain, C. Malformed pollen grains, e: exina, i: intina, mgp: malformed pollenrc: reproductive cell, t: tectum*

The pollen locule can contain pollen grains showing a degeneration structure by deformation, cells are mostly empty formed of a tectum, exine, intine and a cytoplasm (*Figs. 5F and 6C*). This degeneration is only noted at pollen grain stage in 30% of flower buds observed.

Ovary and female gametophyte

The superior ovary is most commonly composed of two unilocular carpels, each one contains two anatropous ovules (*Fig. 4C*), and its epidermis contains elongate cells covered by a large polysaccharide layer.

Underneath the epidermis exists a layer of cells of different sizes with large active nuclei rich in proteins.

The two carpels reach maturity at the same time containing four ovules that will have a different development: three ovules decline and only one ovule will continue its structuration. Ovaries with three carpels or carpels with three ovules seldom seen are considered as anomalies (*Fig. 4 D, E and F*).

The narrower style covered by a polysaccharide layer (mucilage) is composed by an external epidermis and an intermediate tissue, organised into several cell layers with large vacuoles and of a vascular tissue as well as a transmission tissue that passes over its entire length.

The style widens into a bifid stigma sometimes mono or trifid whose surface is comprised of papilla cells with large vacuoles and covered by a layer of extracellular exudates of carbohydrate nature. The stigmas internal cells are non-papillary and surrounded by an accumulating substance in the intercellular area.

Unitegumented ovules with a very short funiculus, whose micropyle is narrow, develop at the same time but cases exist in which one or two of the four ovules are smaller (*Fig. 4C, D, E and F*).

For hermaphrodite flowers, cyto-histological study by photonic and electron microscopy has most often shown the absence of embryo sacs on a number of sliced ovules (*Table 3*). In some ovules, the embryo sac is involute; and in some rare cases, we could observe a typical embryo sac. This mature sac is of bisporic Allium type, which characterises the *Olea* type, therefore eight nuclei (Altamura et al., 1982). The nuclei located in the different levels of the sac are non-observable at the same time. The mature

http://www.aloki.hu ● ISSN 1589 1623 (Print) ● ISSN1785 0037 (Online)
DOI: http://dx.doi.org/10.15666/aeer/1802_34553469

embryo sac's cavity, narrow and fusiform, contains two synergids and one egg cell on the micropyle's side, two polar nuclei and three antipodal cells on the side of the chalaza (*Fig. 7 A, B, C and D*).

Table 3. *Frequencies of different embryo sacs types in hermaphrodite flowers*

Sampling areas	Year	Percentage of ovule with typical embryo sac per ovary	Percentage of ovule with absent or empty embryo sac per ovary
Aguellala	2013	8	92
	2014	11	89
	2015	10	90
Ainergiouene	2013	10	90
	2014	14	86
	2015	12	88

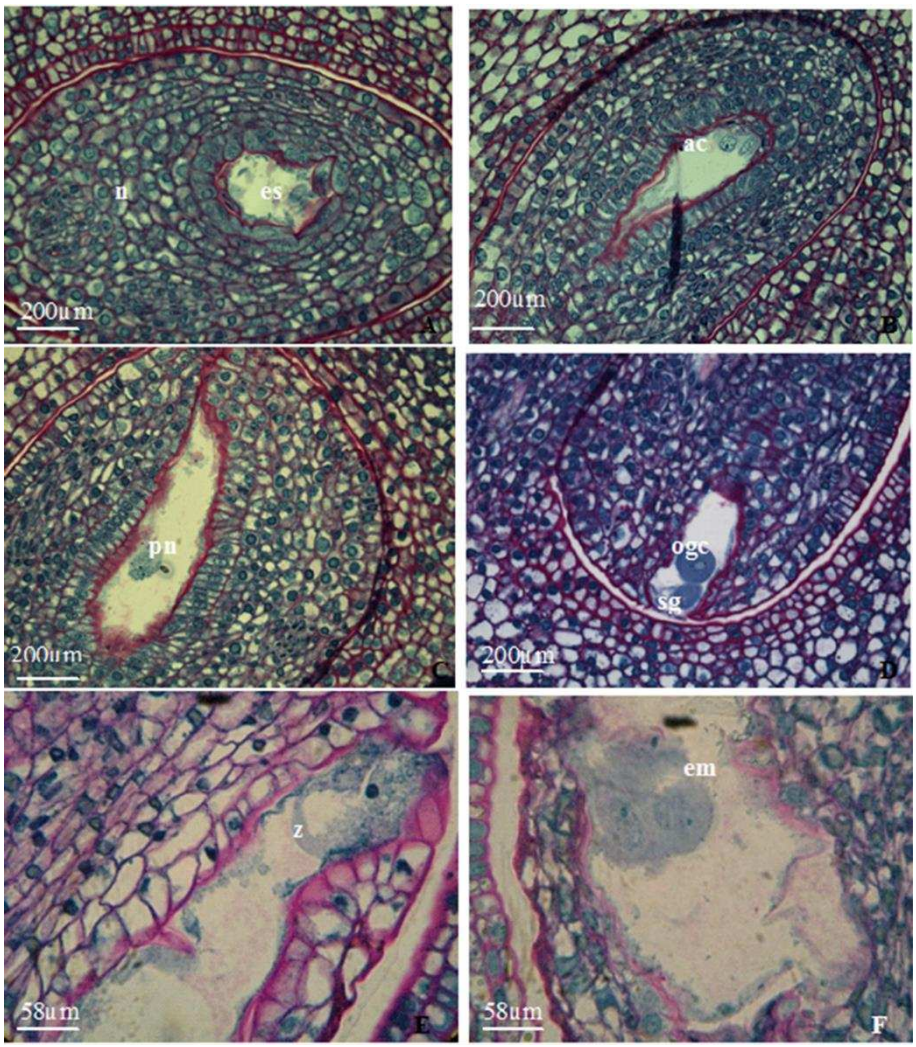

Figure 7. *Female gametophyte and embryogenesis. A. ovule with embryo sac cavity. B. Three antipodal cells. C. Two polar nuclei. D. Synergid and egg cell. E. Fertilised embryo sac: zygote. F. Young embryo (proembryo). ac: antipodal cells, egc: egg cell, em: embryo, es: embryo sac, n: nucellus, pn: polar nuclei, sg: synergids, z: zygote*

http://www.aloki.hu ● ISSN 1589 1623 (Print) ● ISSN1785 0037 (Online)
DOI: http://dx.doi.org/10.15666/aeer/1802_34553469

For flowers with a necrotic stigma, the embryo sac is deformed, empty or lacking, thus, the pistil's development is interrupted before the formation of the embryo sac. For male flowers, no embryo sac can be observed and the ovary kept rudimentary (*Fig. 4 A, B*).

Fertilisation and fruit formation

At fertilisation, only one ovule of four is fertilised. The ovules of the sterile carpel degenerate while those of the fertile carpel experience two different evolutions: one ovule is fertilised to become the seed and the other degenerate after long period comparing to sterile carpel's ovules. Note that, in the fruit development, it is possible to observe the remains of the locule surrounding the fertile carpel's non-fertilised ovule.

The ovule's fertilisation leads to the formation of the large spherical shaped zygote at the same time of beginnings of nuclear endosperm by central cells (*Fig. 7 E*).

An embryo is observed after this fertilisation while synergids and antipodal cells degenerate (*Fig. 7 F*).

Discussion

Floral anatomy

The study of Laperrine's olive tree showed that at flowering time, four types of flowers are formed on each tree; the normal hermaphrodite flower, the necrotic pistil flower, the male flower and three stamens flower. The first and the second types were observed by Reale et al. (2009), the third by Breton and Bervillé (2013) on the cultivated olive tree.

After the period of vegetative rest (autumn and winter), the buds have the same morphological structure and sprout from March to give new twigs and flowers for the next year. This seems to correspond to the bud burst and flowering period of the cultivated olive tree. Indeed, Aiachi-Mezghani et al. (2008) confirmed that for the cultivated olive tree, vegetative growth is more or less continuous from spring up to autumn. The typical structure of the vegetative apex is in line with angiosperms (Camort and Boué, 1997; Vallade, 1999) by zonation of the meristematic territory.

Floral differentiation begins at the end of March in some stations and can be delay until June in the others. Indeed, this differentiation depends on the altitude and temperature. In tropical zones, the flowering of Laperrine's olive trees takes place in spring like most olive cultivars in California (Fabbri and Benelli, 2000) due to the endogenous hormones variation (Badr Sayed et al., 1970). On the other hand, in Portugal, the Galega and Verdea cultivars flower as soon as February (Hartmann, 1951).

According to Malik and Pérez (2011), the low temperatures of winter are development of *Olea europaea* subsp. *lapperenei* follows the same steps of development as *Olea europaea* subsp. *europaea* (Yurukova-Grancharova et al., 2011), *Syringa vulgaris* (Jedrzejuk and Wladyslaw, 2005) and *Fraxinux angustifolia* (Rodriguez-Rajo et al., 2010).

After maturation, tetrads give bicellular pollen grains, rich in starch with dehiscence time similar on the cultivated olive tree (Serrano et al., 2010). Anthers' tissue layers develop the same as on cultivated olive trees (Yurukova-Grancharova et al., 2011). However, the difference observed concerns the tapetum cells that at tetrad stage are either mononuclear or binuclear like for *Colobanthus quitensis* (Kunth) Bartl (Gielwanowska et al., 2007).

http://www.aloki.hu ● ISSN 1589 1623 (Print) ● ISSN1785 0037 (Online)
DOI: http://dx.doi.org/10.15666/aeer/1802_34553469

Yurukova-Grancharova et al. (2011) observed that cell nuclei of the tapetum are divided and become binuclear, rarely tetra nuclear in 'Regalis', 'Chalkidis' and 'Pomiformis' cultivars of the cultivated olive tree compared to Pomiformis cultivar with 4 to 6 nuclei in tapetal cells.

Note that, Fernandez and Rodriguez-Garcia (1989, 1995) reported that Laperrine's olive pollen grains structure is similar to that of complex *Olea*.

Our results showed well-formed pollen grains and others with incomplete development or malformed (coloured in blue) indicating the absence of carbohydrates. Cuevas and Polito (2004) and Reale et al. (2006) have observed malformed pollen grains in *Olea europaea* subsp. *europaea.* According to Gielwanowscka et al. (2007), the pollen malformation can be a response to thermal or osmotic stress.

The allogamy and self-incompatibility in *Olea europaea* subsp. *laperrinei* confirmed by Besnard et al. (2007) could explain the low fruit production because the long distance separation between populations of *Olea europaea* subsp. *laperrinei*. Serrano et al. (2008) reported a high level of self-incompatibility in cultivated olive tree.

For the female gametophyte, the histological study often showed the absence of an embryo sac in ovules or existed but less developed (no nuclei), these cases are pointed out by Rapoport and Rallo (1991) for the cultivated olive tree, for the 'Manzanillo' cultivar and by Martin et al. (2006) for the 'Morisa' cultivar.

The mature embryo sac was observed only in hermaphrodite flowers belonging to Allium type of the *Olea* gender (Altamura et al., 1982; Yurukova-Grancharova et al., 2011) with eight-nucleate embryo sac.

For the flowers with necrotic stigmas, the embryo sac either was absent or is limited to its wall. These types of flowers and embryo sacs also exist in the cultivated olive tree (Cuevas and Polito, 2004; Martin et al., 2006; Reale et al., 2009). The proportion of each type depends of the tree genetics and climate conditions (Loussert and Brousse, 1978; Lavee et al., 1996). Indeed, according to these authors, the nutritional deficiency increases the pistil abscission leading to the formation of male flowers. For the Laperrine's olive tree, starch reserves are observed in different tissues of hermaphrodite flowers whereas no reserve is noted in the gynoecium of the necrotic pistil flowers.

Reale et al. (2006) made the same observations on the cultivated olive tree. It appears that, the carbohydrates are needed compounds from the flower initiation (Altamura et al., 1982) up to the complete differentiation of all floral organs (Rodrigo et al., 2000).

Abortion cases

Concerning the different abortion cases observed in different flowers studied, our results remind those obtained by Extremera (1985). This author specifies that the formation of ovules with malformed embryo sacs characterize Swan Hill cultivar not producing fruits; these structures can cause abscission of hermaphrodite flowers because the malformed embryo sac cannot be fertilised. This hypothesis can explain the substantial flowers drop for the Laperrine's olive tree by the higher rate of malformed embryo sacs within hermaphrodite flowers.

The production of male flowers following abortion of the olive tree's pistil is subject to genetic regulation and takes place one month before flowering (Reale et al., 2009). The lack of nutrients gives priority to pollen, thus to the production of male flowers (Cuevas and Polito, 2004).

http://www.aloki.hu ● ISSN 1589 1623 (Print) ● ISSN1785 0037 (Online)
DOI: http://dx.doi.org/10.15666/aeer/1802_34553469

In different non-grazing areas, the Laperrine's olive trees show abundant flowering with a high percentage of hermaphrodite flowers while the flower drop was significant and the olive production is low.

According to Breton and Bervillé (2013), the cultivated olive tree's fruit production is low when there is no synchronisation between responsiveness of pistils and pollination regardless of the number of hermaphrodite flowers. Indeed, the percentage of hermaphrodite flowers varies from 95% for the Lucques cultivar to 5% for the Salonenque cultivar (Ouksili, 1983) whereas for the oleaste, this percentage reaches 100% or 0% (Hannachi and Marzouk, 2012). For *Olea europaea* subsp *cuspidata,* the vegetative twigs from one year before could have different proportions of male and hermaphrodite flowers (Mukonyi et al., 2012).

In the previous studies of Cuevas and Polito (2004) and Yurukova-Grancharova (2011), the overproduction of flowers with a high level of imperfect flowers and the suppression of fruit constitute a reproduction strategy for olive trees. Indeed, induced abortion of the grains before sclerification of the nuclear (endocarp), about 7 or 8 weeks after complete flower formation, improves or increases the following flowering (Stephenson, 1981).

Abortion is an important phenomenon that allows the tree to control its fruit production according to the availability of nutrient inputs like those that it showed with vines (Lebon et al., 2004).

According to Argenson et al. (1999), there are critical periods for the olive tree during flowering that can have an impact on the potential of fruit-production. Thus, a water or nutrient stress, arising between outbreak and six weeks before the anthesis, reduces the number of flowers per inflorescence and increased ovule abortion.

The overproduction of flowers allows the control of quantity and quality of fruits that depend on environmental conditions and availability of nutrients like it is shown with citrus where only 2% of flowers make fruits (Troncoso et al., 1978). The most anomalies and abortion of *Olea lapperenei* reproductive organs (flowers and fruits) summarised in this investigation could be explained by the advanced age of the trees or by the arid climate conditions (Loussert and Brousse, 1978; Besnard et al., 2012).

Conclusion

This study clearly showed many morphological and reproductive characters of the Laperrine's olive tree summarizing different types of flowers on the same tree with several abortion cases in both male and female gametophytes. All of these features indicate that this woody tree developed reproductive traits to drought tolerance and high longevity.

The absence of regeneration of centenarian's olive tree would be due to the random flowering and fruit drop before ripening. This can be explained by the not fully developed pollen grain production but self-incompatible for sexual reproduction or by malformed sterile pollen grains.

Even if, the female gametophyte, mature and typical, is also capable to conduct the sexual reproduction, the arid conditions cause earlier abortion of flowers and fruits. The results suggest that the well knowledge of flower development and reproduction will be helpful to the conservation of this tree in its natural ecosystem. The involvement of both user cuttings and seed germination trials are suggested. Also, the use of biotechnology-based techniques is needed.

http://www.aloki.hu ● ISSN 1589 1623 (Print) ● ISSN1785 0037 (Online)
DOI: http://dx.doi.org/10.15666/aeer/1802_34553469

Acknowledgments. The authors acknowledge the General Direction of Scientific Research and Technological Development (DGRSDT) and the High Ministry of Research and Study (MESRS), Algeria for supporting this study. The authors also extend their thanks to the University Mouloud Mammeri, Faculty of Biological and Agronomical Sciences Tizi-Ouzou for providing the histological training in CIRAD-Montpellier and to Mr. Abdelaoui Mohamed Salah (head of INRF, Tamanrasset) for his help in collecting plant material.

REFERENCES

[1] Aichi-Mezghani, M., Ben El Hadj, S., Labidi, F., Jebari, A. (2008): Structure of the vegetative bud and relation with the result of growth in the olive tree (*Olea europaea L.*): characterization of winter and summer preformation. – Biotechnology, Agronomy, Society and Environment 12(3): 28-41.

[2] Altamura, B. M., Pasqua, G., Mazzolani, G. (1982): Development of the female gametophyte in *Olea europaea* L. – Annals of Botany 40: 111-117.

[3] Anthelme, F., Abdoulkader, A., Besnard, G. (2008): Distribution, shape and clonal growth of the rare endemic tree *Olea europaea* subsp.*laperrinei* (Oleaceae) in the Saharan mountains of Niger. – Plant Ecology 198: 73-87. DOI 10, 1007/s11258-007-9386-6.

[4] Argenson, C., Régis, S., Jourdain, J. M., Vaysse, P. (1999): The olive tree, monography. – Paris, international technical center for fruit and vegetables; Ctifl. 204p. (in French).

[5] Baali-Cherif, D., Besnard, G. (2005): High genetic diversity and clonal growth in relict populations of *Olea europaea* subsp.*laperrinei* (Oleaceae) from Hoggar, Algeria. – Annals of Botany 96: 823-830.

[6] Baali-Cherif, D., Bouguedoura, N., Besnaed, G., Bouhired, L. (2007): Study of populations of Laperrine olive (*Olea europaea subsp., Laperrinei* Batt.and Trab.) of Algerian central Sahara (Hoggar and Tassili): Biological aspects and molecular characterization. – Annals of the National Agronomic Institute (Algiers) 28(1-2): 35-71.

[7] Badr Sayed, A., Hartmann, H. T., Martin, G. C. (1970): Endogenous gibberellins and inhibitors in relation to flower induction and inflorescence development in the olive. – Plant Physiology 46: 674-679.

[8] Benarar, D., Bouguedoura, N. (2003): Germination test of the Laperrine olive tree (*Olea europaea* ssp *laperrinei* Batt. and Trab.). – The Algerian forest 5: 15-18. (in French).

[9] Besnard, G., Christin, P. A., Baali-Cherif, D., Bouguedoura, N., Anthelme, F. (2007): Spatial genetic structure in the Laperrine's olive (*Olea europaea* subsp. *laperrinei*), a long living tree from the central Saharan mountains. – Heredity 99: 649-657.

[10] Besnard, G., Anthelme, F., Baali-Cherif, D. (2012): The Laperrine's olive tree (Oleaceae):A wild genetic resource of the cultivated olive and a model species for studying the biogeography of the Saharan Mountains. – Acta Botanica Gallica 159(3): 319-629.

[11] Breton, C., Bervillé, A. (2013): From the olive flower to the drupe: Flower types, pollination, self and inter-compatibility. – In: Breton, C., Bervillé, A. (eds.) The Mediterranean Genetic Code-Grapevine and Olive. Quae, Versailles. Http// dx.doi.org/10.5772/55312.

[12] Camfort, H., Boué, H. (1997): Reproduction and biology of higher plants: bryophytes, pteridophytes, Spermaphytes. – Second edition Doin. 436p. (in French).

[13] Cuevas, J., Polito, V. S. (2004): The role of staminate flowers in the breeding system of *Olea europaea* (*Oleaceae*): an andromonoecious, wind-pollinated taxon. – Annals of Botany 93: 547-553.

[14] Extremera, G. (1985): Development of the embryo sac in two olive cultivars (*Oleaeuropaea* L.). – Bachelor's thesis, Faculty of Sciences. Univ. De Córdoba, Córdoba, Spain. (In Spanish).

[15] Fabbri, A., Benelli, C. (2000): Flower bud induction and differentiation in olive. – Journal of Horticultural Science and Biotechnology 75(2): 131-141.

http://www.aloki.hu ● ISSN 1589 1623 (Print) ● ISSN1785 0037 (Online)
DOI: http://dx.doi.org/10.15666/aeer/1802_34553469

[16] Feder, N., O'Brien, T. P. (1968): Plant microtechnique: sections for light microscopy. – American Journal of Botany 55: 123-142.
[17] Fernandez, M. C., Rodriguez-Garcia, M. I. (1989): Developmental changes in the aperture during pollen grain ontogeny in *Olea europaea* L. – New Phytology 111(4): 717-723.
[18] Fernandez, M. C., Rodriguez-Garcia, M. I. (1995): Pollen grain apertures in *Oleaeuropaea L.* (*Oleaceae*). – Revew of Palaeobotany and Palynology 85: 99-109.
[19] Fisher, D. B. (1968): Protein staining of ribonnedepon sections for light microscopy. – Histochimie 16: 90-92.
[20] Gielwanowska, I., Bochenek, A., Szczuka, E. (2007): Development of the pollen in the Antarctic flowering plant *Colobanthus quitensis* (Kunth). – Acta Agrobotanica 60(2): 3-8.
[21] Green, P. S. (2002): A revision of *Olea europaea* L. (*Oleaceae*). – Kew Bulletin 57(1): 91-140.
[22] Hannachi, H., Marzouk, S. (2012): Flowering in the wild olive (*Olea europaea* L.) tree (oleaster): phenology, flower abnormalities and fruit set. Traits for breeding the olive. – African Journal of Biotechnology 11: 8142-8148.
[23] Hartmann, H. T. (1951): Time of floral differentiation of the olive in California. – Botanical Gazette 112(3): 323-327.
[24] Jedrzejuk, A., Wladyslaw, S. (2005): Development of flower organs in common Lilac (*Syringa vulgaris L*) cv. Mme Florent Stepman. – Acta Biologica Cracoviensia, Series Botanica 47(2): 41-52.
[25] Lavee, S., Rallo, L., Rapoport, H. F., Troncoso, A. (1996): The floral biology of the olive: effect of flower number, type and distribution fruit set. – Scientia Horticulturae 66: 149-158.
[26] Lebon, G., Douchêne, E., Brun, O., Magne, C., Clément, C. (2004): Flower abscision and inflorescence carbohydrates in sensitive and non-sensitive cultivars of grapevine. – Sexual Plant Reproduction 17: 71-79.
[27] Loussert, R., Brousse, G. (1978): The olive tree. Agricultural techniques and Mediterranean productions. – G. P. Maisonneuve and Larose.
[28] Maire, R. (1933): Studies on the flora and vegetation of the central Sahara. – Memories of the Natural History Society of North Africa, No. 3, Hoggar II Mission. (Maps and planks), Algiers.
[29] Malik, N. S. A., Pérez, J. L. (2011): The effect of high temperature interruptions during inductive period on the extent of flowering and on metabolic responses in olives (*Olea europaea* L.). – Scientia Horticulturae 129(2): 207-212.
[30] Martins, P. C., Cordeiro, A. M., Rapoport, H. F. (2006): Flower quality in orchads of olive, *Olea europaea* L., cv Morisa. – Advances in Horticultural Science 20(4): 262-266.
[31] Mukonyi, K. W., Kyalo, N. S., Lusweti, A. M., Situma, C., Kibet, S. (2012): *Olea europaea* subsp. Cuspidate in Kenya. – African Journal of Biotechnology 11: 8142-8148.
[32] Ouksili, A. (1983): Contribution to the study of the floral biology of the olive tree *Olea europaea* L. from the formation of the flowers to the effective pollination. – USTL, Univ-Montpellier 2, 143p.
[33] Pottu-Boumendil, J. (1989): Electron microscopy: principles and methods of preparation. – INSERM, 221p.
[34] Quézel, P. (1965): The vegetation of the Sahara. From Chad to Mauritania. – Gustav Fisher Verlag, Stuttgart.
[35] Quézel, P. (1978): Analysis of the flora of the mediterranean and Sahara Africa. – Annals of the Missouri Botanical Garden 65: 479-534.
[36] Rapoport, H. F., Rallo, L. (1991): Flower and fruit abscission in Manzanillo olive *Olea europaea*. – Journal of the American Society for Horticultural Science 116(4): 720-723.
[37] Reale, L., Sgromo, C., Bonofiglio, T., Orlandi, F., Fornaciari, M., Ferranti, F., Romano, B. (2006): Reproductive biology of olive (*Olea europaea* L.) DOP Umbria cultivars. – Sexual Plant Reproduction 19: 151-161.

http://www.aloki.hu ● ISSN 1589 1623 (Print) ● ISSN1785 0037 (Online)
DOI: http://dx.doi.org/10.15666/aeer/1802_34553469

[38] Reale, L., Sgromo, C., Ederli, L., Pasqualini, S., Orlandi, F., Fornaciari, M., Ferranti, F., Romano, B. (2009): Morphological and cytological development and starch accumulation in hermaphrodite and staminate flowers of olive *Olea europaea* L. – Sexual Plant Reproduction 22(3): 109-119.
[39] Rodrigo, J., Hormaza, J. I., Herriro, M. (2000): Ovary starch reserves and flower development in apricot (*Prunus armeniaca* L). – Physiologia Plantarum 108: 35-41.
[40] Rodriguez-Garcia, M. I., Fernandez, M. C., Alché, J. D. (1995): Immunocytochemical localization of allergenic protein (Ole e I) in the endoplasmic reticulum of the developing pollen grain of olive (*Olea europaea* L.). – Planta 196: 558-563.
[41] Rodriguez-Rajo, F. J., Vega-Maray, A. M., Asturias, J. A., Jato, V., Seoane-Camba, J. A., Suarez-Cervera, M. (2010): The relationship between tapetum cells and microspores based on protein localization in *Fraxinus angustifolia* (*Oleaceae*) pollen grains. – Journal of Plant Sciences 171(1): 34-52.
[42] Schwendiman, J., Pannetier, C., Michaux-Ferriere, N. (1990): Histology of embryogenic formations during in vitroculture of oil palm (*Elaeis guineensis*Jacq). – Oleagineux 45(10): 409-418.
[43] Serrano, L., Suarez, C., Olmedilla, A. (2008): Structural organization and cytochemical features of the pistil in olive (*Olea europaea* L.) cv Picual at anthesis. – Sexual Plant Reproduction 21: 99-111.
[44] Serrano, I., Salvatore, P., Adela, O. (2010): Programmed-cell-death hallmarks in incompatible pollen and papillar stigma cells of *Olea europaea* L. under free pollination. – Plant cell reproduction 29: 561-572.
[45] Stephenson, A. G. (1981): Flower and fruit abortion: proximate causes and ultimate functions. – Annual Review of Ecology, Evolution and Systematics 12: 253-279.
[46] Troncoso, A., Prieto, J., Linan, J. (1978): Aclareoquimico of fruits in the Manzanillo de Seveilla olive grove. – Anales de Edafologia y Agrobiologia 37: 882-893. (In Spanish).
[47] Vallade, J. (1999): Structure and development of the plant: Morphogenesis and reproductive biology of angiosperms. – Collection Sciences Sup. Dunod Paris.
[48] Yurukova-Grancharova, P., Davidova, P., Jankova, E., Cantos, M., Linan, J., Troncoso, J., Troncoso, A. (2011): On the gametogenesis and early embryogenesis in some olive tree cultivars. – Flora 206: 47-51.

http://www.aloki.hu ● ISSN 1589 1623 (Print) ● ISSN1785 0037 (Online)
DOI: http://dx.doi.org/10.15666/aeer/1802_34553469

GROWTH-RELATED EXPRESSED SEQUENCE TAG - SAMPLE SEQUENCE REPEATS (EST-SSRS) SCREEN OF MUD IVORY WHELK (*BABYLONIA LUTOSA*) THROUGH TRANSCRIPTOME SEQUENCING

XIONG, G.[1*] – WANG, P.[2] – KANG, L.[1] – CHEN, Z. N.[2] – ZHOU, X. W.[3] – WU, Q. S.[4] – WANG, X. Q.[2*]

[1]*Hunan Biological and Electromechanical Polytechnic, Changsha 410127, China*

[2]*College of Animal Science and Technology, Hunan Agriculture University, Changsha 410128, China*

[3]*Aquatic science extension station, Xiangxi Autonomous State of Tujia and Miao Minorities, Jishou, 416000 Hunan, China*

[4]*Fisheries Research Institute of Fujian Province, Xiamen 361013, China*

[*]*Corresponding authors*
e-mail: xionggang709@126.com (Xiong, G.), wangxiao8258@126.com (Wang, X. Q.)

(Received 15th Nov 2019; accepted 30th Jan 2020)

Abstract. Mud ivory whelk (*Babylonia lutosa*) is one of the most economically important seawater mollusks in China. However, currently, there is no report on the molecular markers related to the growth of *Babylonia lutosa*, which hinders the its genetic breeding with dominant growth traits. The present study was the first to sequence the transcriptomes of *B. lutosa*, and then searched for EST-SSR in the growth-related genes. Wild *B. lutosa* samples were collected from the Lianjiang River, Fujian Province of China. The RNA of gastropods and hepatopancreas tissues from three *B. lutosa* were measured and mixed, and sequenced by Illumina HiSeq sequencer. A total of 24,829,460 reads containing 5,015,236,064 bp were obtained through sequencing. Eight growth-related genes (TBC-1-A, TBC-1-2B, FGFR-1, GFRBP2, GFR-15, FGFR-1-A, SMAD6, and TGFβR-1) containing EST-SSR sequences were detected in the *B. lutosa* transcriptomes. Our results would provide theoretical basis for *B. lutosa* breeding based on growth-related EST-SSRs.
Keywords: *aquaculture, Gastropoda, growth-related gene, insulin-like growth factors, microsatellites*

Introduction

Growth-related genes of aquatic animals have always been the focus of researchers. For instance, insulin-like growth factors (IGFs) of aquatic animals are a class of proteins with insulin-like metabolism and mitotic function. IGFs participate in the embryonic development and reproduction of vertebrates and are the main determinants of embryonic and postnatal growth (Reinecke et al., 1997; Upton et al., 1998; Zhang et al., 2011). In addition, IGFs mediate growth-promoting effects of growth hormones (Moriyama et al., 2000). Aquatic animal IGF system includes IGF-I, IGF-IR, IGF-II, IGF-IIR, and IGFBPs (Li et al., 2011), which play important roles in inducing myopoietin (MyoG) gene expression (Florini et al., 1991; Yano et al., 1999), promoting myocyte differentiation (Hembree et al., 1991; Le Roith et al., 2001; Buckingham et al., 2003), regulating skeletal muscle growth (Doumit et al., 1993; Lamberson et al., 1995; Davis et al., 2002), and other aspects. Growth-related genes have genetic polymorphism, and different genotypes correspond to different growth traits.

http://www.aloki.hu ● ISSN 1589 1623 (Print) ● ISSN 1785 0037 (Online)
DOI: http://dx.doi.org/10.15666/aeer/1802_34713482

Single nucleotide polymorphism (SNP) loci and microsatellites are important molecular markers commonly used in population genetic diversity research. Ruan et al. (2011) identified three SNPs by comparing the sequences of exon 1, exon 3, intron 2, and intron 4 of the IGF-1 gene in Giraffe tilapia (*Oreochromis niloticus*). Then they detected intron genotypes of 121 *G. tilapia* from five genetic families by PCR-RFLP, and screened two SNPs that correlated with weight gain. Therefore, the two SNPs could be used as molecular assisted markers for breeding. Microsatellites have been widely used in population genetic diversity analysis, because of their wide distribution in genome, good polymorphism, genetic stability, and easy detection (Nie, 2014). For instance, the population genetic diversities of blacklip abalone (*Haliotis rubra*) (Huang et al., 2000), scallop (*Pectinidae* sp.) (Feng et al., 2014), marine shrimp (*Fenneropenaeus chinensis*) (Zhang et al., 2005), whiteleg shrimp (*Litopenaeus vannamei*) (Tong et al., 2009), and Japanese pufferfish (*Fugu rubripes*) (Lu et al., 2013) have been studied using microsatellite markers. High-throughput sequencing technology provides a convenient way to transcriptome sequence and large-scale screen SNPs and microsatellite markers. Hou et al. (2011) sequenced transcriptomes of the larvae of scallop (*Patinopecten yessoensis*) at different development stages by high-throughput sequencing technology, and screened a large number of expressed sequence tag - sample sequence repeats (EST-SSRs) and SNPs that were correlated to growth, reproduction, and immune recognition.

Mud ivory whelk (*Babylonia lutosa*) is one of the most economically important seawater mollusks in China (Xiong et al., 2015). In 2018, the output of *B. lutosa* is approximately 4,000 tons in China. Although aquaculture output of marine snails has decreased by 6.17% compared with 2017 in China, the cultivation of *B. lutosa* increases (Fishery and Fishery Administration of the Ministry of Agriculture and Rural Areas of China et al., 2019). It is widely distributed in southeast coast of China, southeast Asia and Japan (Xiong et al., 2015). *B. lutosa* inhabits in the sediment bottom of several meters to tens of meters deep in the subtidal zone, mainly feeds on oyster eggs, organic debris, and protozoa in the juvenile stage, and small fish, shrimp, crab, and shellfish in the adult stage (Yin et al., 2007). Currently, studies on *B. lutosa* are mainly focused on morphological comparison (Wang et al., 2007; Pan et al., 2010; Huang et al., 2010; Qi et al., 2011), metamorphosis (Yang et al., 2008), environmental adaptation (Lin, 2012), genetic characteristics (Chen et al., 2011; Qin et al., 2014), and culture technologies (Yin et al., 2007). Molecular breeding is very important for the cultivation of snails with high growth characteristics. However, there is no report on the molecular markers related to the growth of *B. lutosa*, which hinders the genetic breeding of *B. lutosa* with dominant growth traits. The present study was the first time that sequenced the transcriptomes of *B. lutosa*, and then searched for EST-SSR in the growth-related genes. Our results would provide theoretical basis for *B. lutosa* breeding based on growth-related EST-SSRs.

Materials and Methods

Sample collection, RNA extraction, cDNA library construction and sequencing analysis

Wild *B. lutosa* samples were collected from the estuary of Lianjiang River, Fujian Province of China (26°20′ N, 119°42′ E) in 2015 (*Fig. 1*). Three living *B. lutosa* were dissected and their gastropods and hepatopancreas were quickly cut out and used to extract total RNA by a TRIzol reagent kit (TAKARA, China) (Xiong et al., 2015, 2019).

http://www.aloki.hu ● ISSN 1589 1623 (Print) ● ISSN 1785 0037 (Online)
DOI: http://dx.doi.org/10.15666/aeer/1802_34713482

The RNA concentration and purity were detected by an Ultrospec™ 2100UV/Visible spectrophotometer, and the RNA integrity was detected by 1% agarose gel electrophoresis. The RNA of gastropods and hepatopancreas tissues from the three *B. lutosa* were measured and mixed. After enrichment, purification, interruption and cDNA synthesis, the constructed cDNA library was sequenced by Illumina HiSeq sequencer at Beijing Biomarker Technologies Co., China.

Figure 1. *Map shows the sampling location*

Sequence assembly, annotation, and growth-related EST-SSR screening

The original reads were assembled to transcripts using Trinity software. Several sliceable transcripts were clustered into one gene, and finally obtained the unigene library. SSRs in the cDNA sequence of unigenes were searched using MISA software (http://pgrc.ipk-gatersleben.de/misa/) (Kanehisa et al., 2008). The searching parameters were set as a single base with a minimum repetition of more than 10 times, two bases with a minimum repetition of more than 6 times, and 3 - 6 bases with a minimum repetition of more than 5 times. The distance between two repetitions should not be greater than 100 bp. The ORFs were predicted using Getorf software based on the unigene sequences (Mortazavi et al., 2008). The software parameters were set to predict the forward and reverse directions of three bases at both ends of unigenes, and the longest sequence was as the ORF of unigenes. The reads obtained by the sequencing were aligned to unigenes library, and calculated the expression abundance (RPKM) of each unigene (Mortazavi et al., 2008). The unigenes were annotated using BlastX program referenced to the protein sequence databases of Swiss-Prot (Apweiler et al., 2004), TrEMBL (Apweiler et al., 2004), GenBank Nr (Deng et al., 2006), Gene Ontology (GO) (Ashburner et al., 2000), COG (Tatusov et al., 2000), and KEGG (Kanehisa et al., 2004). The parameter E value was set to $< 1e^{-6}$, and the maximum similar sequence was selected as the annotated gene. According to GO annotation information, functions of the unigenes were classified to molecular function, cellular component, and biological process (Ashburner et al., 2000). KEGG analysis was implemented by KEGG Automatic Annotation Service (KAAS) (Masoudi-Nejad et al., 2007). Growth-related genes were screened from the assembled annotated genes, and EST-SSR markers were excavated for the selected growth-related genes by SSR analysis.

The EST-SSRs were submitted to NCBI GenBank database with accession number from KM972681 to KM972698, and from KT763437 to KT784812.

http://www.aloki.hu ● ISSN 1589 1623 (Print) ● ISSN 1785 0037 (Online)
DOI: http://dx.doi.org/10.15666/aeer/1802_34713482

Results

Transcriptome characteristics and EST-SSR analysis of B. lutosa

A total of 24,829,460 reads containing 5,015,236,064 bp were obtained by sequencing. The GC content of the DNA sequences was 50.54%. CycleQ20 was 100%. A total of 119,113 unigenes that contained 16,877 unigenes with more than 1 kb were obtained through *de novo* assembling. N50 was 835 bp, and the average length of unigenes was 627.3 bp (*Table S1*).

A total of 13,962 EST-SSRs were found from 8,177 unigenes, which total length was 262,687 bp. We also found a large number of mixed repetitive nucleotide sequences. These mixed repetitive nucleotide sequences were distributed in 2,272 unigenes (*Table 1*). The frequency of EST-SSRs in the transcriptome of *B. lutosa* was 11.72% (ratio of the number of EST-SSRs detected to the total number of unigenes); and the frequency of EST-SSR occurrence was 6.86% (ratio of the number of unigenes with EST-SSR to the total number of unigenes). In the transcriptome of *B. lutosa*, an SSR occurred on average every 350.78 kb.

Table 1. *Occurrence of different types of EST-SSR in the B. lutosa transcriptome*

Repeat type	Number	Proportion	Frequency (%)	Average distance (kb)	Total length (bp)	Average length (bp)
Mononucleotide	5,536	39.65	4.65	884.70	75,641	13.7
Dinucleotide	3,906	27.98	3.28	1253.89	68,946	17.7
Trinucleotide	2,141	15.33	1.80	2,287.57	40,314	87.6
Tetranucleotide	100	0.72	0.08	48,976.91	2,536	25.4
Pentanucleotide	7	0.05	0.006	699,670.14	175	25
Compound SSR	2,272	16.27	1.907	2,155.67	75,075	75.5
Total	13,962	100	11.72	350.79	262,687	18.4

EST-SSR was abundant in the transcriptome of *B. lutosa*, and it could be found from mononucleotide repeat to pentanucleotide repeat types, but no hexanucleotide repeat type was found. The frequencies of occurrence of various EST-SSR types were quite different. It mainly focused on mononucleotide, dinucleotide, and trinucleotide repeats, which accounted for 39.65%, 27.98%, and 15.33% of the total EST-SSRs, respectively. The tetranucleotide and pentanucleodite repeats accounted for 0.72% and 0.05%, respectively. Among them, the largest number of SSR types was: A repeat primitives were 3,534 (25.31%), and T repeat primitives were 2,984 (21.37). The number of EST-SSR loci with different repeats was also quite different (*Fig. 2A*). The major EST-SSRs with more than 10 repeat elements were mononucleotides. The dinucleotide repeats with more than 10 repeat elements were very rare. TG repeats were 1,136 (8.14%), CA repeats were 866 (6.35%), AC repeats were 717 (5.14%), and AC/GT repeats were 3,409 (24.42%). In the trinucleotide repeats, GGA repeat was 151, GAG repeat was 114, GGT repeat was 108, GTG repeat was 104, TTG repeat was 100, AGG/CCT repeat was 560 (0.040%), and ACC/GGT repeat was 508 (0.036%; *Fig. 2B*). According to the overall distribution, polynucleotide repeats predominated in the frequency of six repeat.

Through analyzing the length of 13,962 EST-SSRs, the lengths of microsatellite sequences contained in the EST sequences of *B. lutosa* ranged from 9 to 265 bases with a total length of 262,687 bp. The average length of the microsatellite sequences was

http://www.aloki.hu ● ISSN 1589 1623 (Print) ● ISSN 1785 0037 (Online)
DOI: http://dx.doi.org/10.15666/aeer/1802_34713482

18.4 bp. The length of EST-SSRs was mainly in the range of 12 to 25 bp, of which 8928 (63.95%) were in the range of 12 to 20 bp. Number of SSRs with the length between 21 to 25 bp were 1,276 (9.14%), and the number of SSRs with the length of more than 25 bp were 225 (1.60%; *Fig. 2C*).

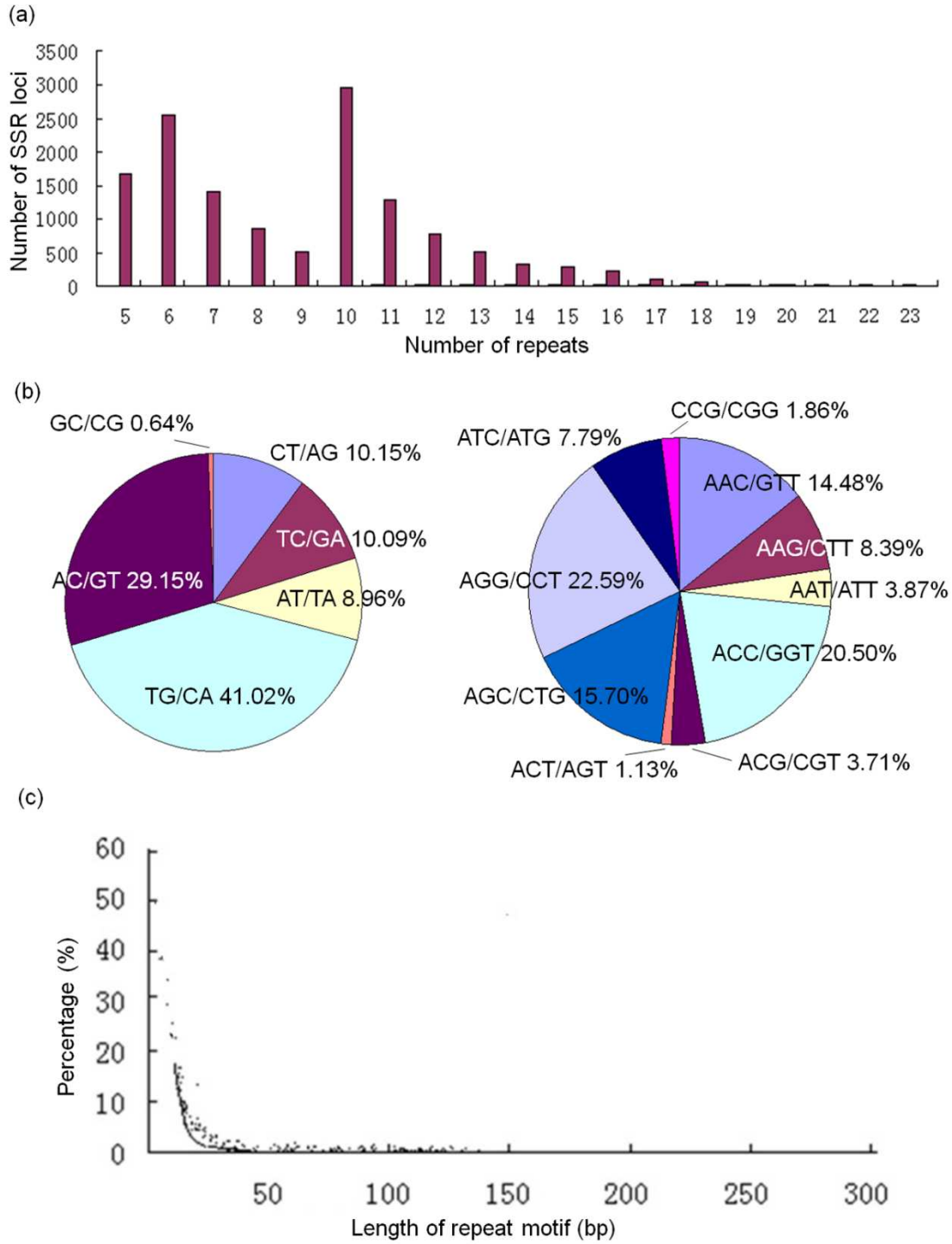

Figure 2. *Distribution of the number of repeats of EST-SSR (A), percentage of different motifs of dinucleotide and trinucleotide SSRs (B), and distribution of the repeat motif length of SSRs in B. lutosa transcriptome (C)*

http://www.aloki.hu ● ISSN 1589 1623 (Print) ● ISSN 1785 0037 (Online)
DOI: http://dx.doi.org/10.15666/aeer/1802_34713482

Functional annotation and Growth-related Genes Containing EST-SSR Sequences

Total of 118,608 unigenes were protein encoding unigenes, of which 78.84% were unigenes within 300 bp, and 6.18% were unigenes above 900 bp (*Appendix 1*). A total of 24,829,460 reads were belonged to the protein encoding unigenes, which showed the high reliability of the obtained transcriptome data (*Appendix 1*).

Total of 35,931 unigenes were annotated, which were in corresponding the sequences from sea-slug (*Aplysia californica*), oyster (*Crassostrea gigas*), polychaete worm (*Capitella teleta*), amphioxus (*Branchiostoma floridae*), sea urchin (*Strongylocentrotus purpuratus*), acorn worm (*Saccoglossus kowalevskii*), filarial nematode worm (*Brugia malayi*), eye worm (*Loa loa*), and sea anemone (*Nematostella vectensis*) (*Appendix 2*), and some sequences did not have similar homologous sequences in the databases, which was probably caused by the lack of mollusk EST sequences in these databases. A total of 35,931 annotated functions were obtained from the *B. lutosa* transcriptome annotation analysis (*Appendix 3*).

Total of 109,359 unigenes obtained GO information, of which 60,143 (55.0%) unigenes were belonged to biological process, 31,931 (29.2%) genes were belonged to cellular component, and 17,285 (15.8%) were belonged to molecular function. In the GO classification system, the biological process, cellular component, and molecular function were classified into more detailed 56 sub-categories (*Fig. 3*). In the biological process, there were 3,289 unigenes participated in the reproduction, 7,751 unigenes participated in the metabolic process, 353 unigenes participated in the immune system process, 387 unigenes participated in the cell proliferation, 8,826 unigenes participated in the cellular process, 2,876 unigenes participated in the reproductive process, and 5,562 unigenes participated in the biological regulation.

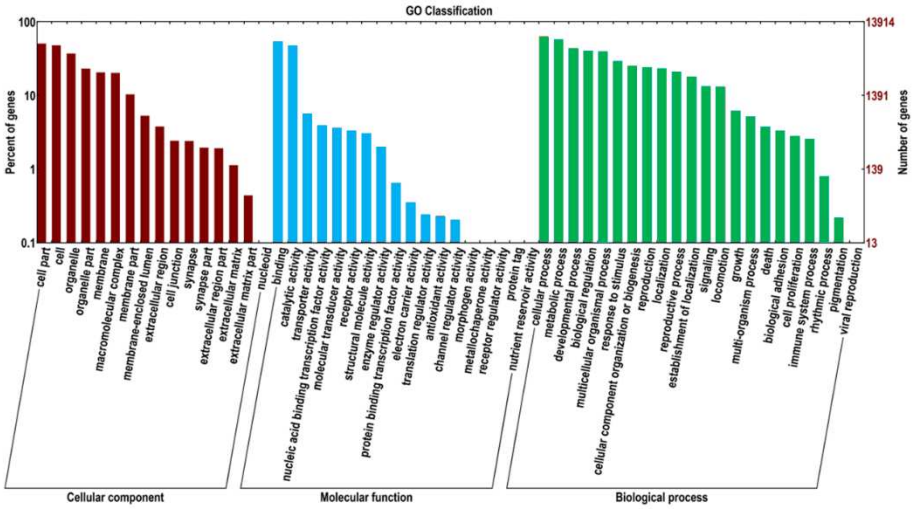

Figure 3. *GO function annotation results of B. lutosa transcriptome library*

Growth-related gene containing EST-SSR sequences were growth hormone-regulated TBC protein 1-A (TBC-1-A), growth hormone-regulated TBC 1 domain family member 2B (TBC-1-2B), fibroblast growth factor receptor 1 (FGFR-1), growth factor receptor-bound protein 2 (GFRBP2), growth factor receptor substrate 15 (GFR-15), fibroblast growth factor receptor 1-A (FGFR-1-A), SMAD family member 6 (SMAD6), and TGF-beta receptor type-1 (TGFβR-1, *Table 2*).

http://www.aloki.hu ● ISSN 1589 1623 (Print) ● ISSN 1785 0037 (Online)
DOI: http://dx.doi.org/10.15666/aeer/1802_34713482

Table 2. *Parameters of primer pairs for growth-relative EST-SSR*

Primer name		Primer sequence (5'-3')	Homologous gene	Core SSR sequence	Amplification location or target fragment length
3'RACE Olig(T)-Adaptor		CTGATCTAGAGGTACCGGATCCTTTTTTTTTTTTTT			3'-terminal amplification
3'RACE Adaptor		CTGATCTAGAGGTACCGGATCC			3'-terminal amplification
5'RACE Olig(T)-Adaptor		GACTCGAGTCGACATCGATTTTTTTTTTTTTTTT			5'-terminal amplification
5'RACE Adaptor		GACTCGAGTCGACATCG			5'-terminal amplification
TBC -1-A	(TG)7P1+	CAAGTGTGTGAATGATGTTGTCTAC	XM_005107837: *Aplysia californica* growth hormone-regulated TBC protein 1-A-like	(TG)7	297 bp
	(TG)7P1-	CACACATTCACATACATGCACA			
	GSPP1+	CCTTCCCAGAGAACATTTACTT			3'-terminal amplification
	NGSPP1+	CAAGTGTGTGAATGATGTTGTCTAC			3'-terminal amplification
	GSPP2-	ACTGATGTAGGACTGCACCGT			5'-terminal amplification
	NGSPP2-	TCCCTTCCTGCAGAACCGCTTGACT			5'-terminal amplification
TBC -1-2B	*P1+	GCATCACTCCGGTCACCAGCTT	XM_013087488: *Aplysia californica* TBC-1 domain family member 2B-like	(ACC)5*	225 bp
	*P1-	CCTGCTGCGGCACGGTCC		(GAG)5	BL-106
FGFR-1	(GGA)5P1+	TTGAGCAAGAGGGAAGAGC	XM_003974594.1: *Takifugu rubripes* fibroblast growth factor receptor 1-A-like	(GGA)5	206 bp
	(GGA)5P1-	ACCAGCGTGGCCTCGTCCCTT			
	(AGA)5P2+	TTCTCCGTGAACCTGACGCT		(AGA)5	250 bp
	(AGA)5P2-	AGGAAGAAGGTGTTGAGGGTGT			
FGFR-15	(CTG)6P1+	TTGACCGGACCTAGACTGC	XM_005110162.1: *Aplysia californica* epidermal growth factor receptor substrate 15-like	(CTG)6	217 bp
	(CTG)6P1-	TCTACGTGGCCCTCAAACT			
FGFR-1-p	(AC)8P1+	CGAGAACAGGCGGAGAAT	XM_005105989.1: *Aplysia californica* FGFR1 oncogene partner-like (LOC101862887)	(AC)8	261 bp
	(AC)8P1-	AAGGACGGAGGGAGACG			
	(GT)*P2+	TGCTGGGACTGACGGGCT		(GT)6*(G)16	245 bp
	(GT)*P2-	TCTTAGCAATTGCTTGGCGC			
GFR BP2	(CA)*P1+	TGCTACTACACACACATACCACACA	NM_001165306.1: *Salmo salar* growth factor receptor-bound protein 2	(CA)7*(TG)6	229 bp
	(CA)*P1-	GTGCTTTGTTTAGAATCTGGGC			
SMAD6	(CCT)5P1+	GCCAGTATTTGCCCAACAGT	XM_011385995.1: *Pteropus vampyrus* SMAD family member 6 (SMAD6)	(CCT)5	231 bp
	(CCT)5P1-	TGGAGGTGGTGGGGAGTGT			BL-120
TGFβR-1	(TG)*P1+	GTATCAACTACAAATGACACAACTT	XM_005103324.1: *Aplysia californica* TGF-beta receptor type-1-like	(TG)6*(TG)6	241 bp
	(TG)*P1-	ACTTGTGAAAGAAAAAGATTATTAT			
	(CA)7P2+	ATCATTACAGACAGGTTCTTAGC		(CA)7	202 bp
	(CA)7P2-	GGTAGGGAGGGCAAGGT			BL-151

* Intermediate non-repetitive sequence fragments of composite microsatellite sequences. Length of core sequence is amplification length of the EST-SSR

http://www.aloki.hu ● ISSN 1589 1623 (Print) ● ISSN 1785 0037 (Online)
DOI: http://dx.doi.org/10.15666/aeer/1802_34713482

Discussion

A total of 13,962 EST-SSRs was obtained from the *B. lutosa* transcriptome, which total length was 262,687 bp. The number and frequency of EST-SSRs in the *B. lutosa* transcriptome were more abundant than those in *P. yessoensis* (2,700 EST-SSRs; Hou et al., 2011). Besides the improvement of NGS technology provided more quantity and higher quality sequencing data of *B. lutosa* transcriptome, the reason caused the more SET-SSRs were detected from the *B. lutosa* transcriptome was we used a mixture of *B. lutosa* hepatopancreas and gastropodal muscle samples, which contain abundant transcriptional sequences. These EST-SSR molecular markers had laid an important foundation for large-scale development of *B. lutosa* molecular markers, evaluation of artificial multiplication effect, and population genetic diversity and molecular assisted breeding.

If EST-SSR markers can be directly identified on growth-related genes, it would effectively improve the breeding efficiency of *B. lutosa* with fast-growth traits. In the present study, we found eight growth-related genes that contain EST-SSR sequences in the *B. lutosa* transcriptome. These EST-SSR sequences were likely to participate in the expression and regulation of their representative genes, and affect the growth-related traits of *B. lutosa.*

TCB-1 gene was found in the growth-related genes containing EST-SST sequences. TBC-1 is a kind or nucleic acid protein. Richardson and Zon (1995) first discovered this nucleic acid protein in the mouse labrocyte cDNA library. A total of 29 proteins were found in the TBC-1 family, in which TBC-1-D4 and TBC-l-D1 have been extensive studied. Koumanov and Holman (2007) speculate that TBC-1-D4 and TBC-l-D1 play key roles in cell membrane transport and connection signal transduction. Bryant (2002) report that TBC-1D1 stimulates glucose transporter protein (GLUT4) from a cellular location to the cell surface in muscle and adipocytes, thereby completing signal transduction and substance transport. Hargett et al. (2015) confirm that TBC-1D1 regulates the expression of GLUT4 in skeletal muscle cells through knockout TBC-1D1 gene in mice.

Fibroblast growth factor (FGFR) belongs to tyrosinkinase (TK) receptor family (Kornbluth et al., 1988). Four kinds of FGFRs, i.e. FGFR-1, FGFR-2, FGFR-3, and FGFR-4, have been found. Deng et al. (1994) find that mouse embryos with defective FGFR-1 gene are severely blacked and died during development. Li (2008) shows that the FGFR1 regulates phosphorus metabolism and calcium metabolism in blood and bone through ALK3, and FGFR1 regulates osteoblasts proliferation and apotosis through inhibiting PI3K and promoting MAPK signaling pathway, and inhibits osteoblasts mineralization and proliferation physiologically. Gudernova et al. (2015) find that mutant FGFR3 causes human dwarfism-achondroplasia (ACH) symptoms.

Conclusion

In conclusion, we firstly sequenced the transcriptomes of *B. lutosa*, and detected eight growth-related genes (TBC-1-A, TBC-1-2B, FGFR-1, GFRBP2, GFR-15, FGFR-1-A, SMAD6, and TGFβR-1) that contain EST-SSR sequences in the *B. lutosa* transcriptome. However, which EST-SSR sequences should be used as biomarkers for breeding need to further study.

http://www.aloki.hu ● ISSN 1589 1623 (Print) ● ISSN 1785 0037 (Online)
DOI: http://dx.doi.org/10.15666/aeer/1802_34713482

Acknowledgments. This research was supported by the National Natural Science Foundation of China [31672640], the Natural Science Foundation of Hunan Province [2017JJ3134], Blue Granary [2018YFD0900200], and the Scientific Research Fund of Hunan Province Education Department [17C0935]. The authors thank anonymous technicians at Guangdong Meilikang Bio-Science Ltd., China for assistance with data analysis.

REFERENCES

[1] Apweiler, R., Bairoch, A., Wu, C. H., Barker, W. C., Boeckmann, B., Ferro, S., Gasteiger, E., Huang, H., Lopez, R., Magrane, M., Martin, M. J., Natale, D. A., O'Donovan, C., Redaschi, N., Yeh, L. S. L. (2004): UniProt: the universal protein knowledgebase. – Nucleic Acids Research 32: D115-D119.

[2] Ashburner, M., Ball, C. A., Blake, J. A., Botstein, D., Butler, H., Cherry, J. M., Davis, A. P., Dolinski, K., Dwight, S. S., Eppig, J. T., Harris, M. A., Hill, D. P., Issel-Tarver, L., Kasarskis, A., Lewis, S., Matese, J. C., Richardson, J. E., Ringwald, M., Rubin, G. M., Sherlock, G. (2000): Gene ontology: tool for the unification of biology. – Nature Genetics 25: 25-29.

[3] Bryant, N. J., Govers, R., James, D. E. (2002): Regulated transport of the glucose transporter GLUT4. – Nature Review Molecular Cell Biology 3: 267-277.

[4] Buckingham, M., Bajard, L., Chang, T., Daubas, P., Hadchouel, J., Meihac, S., Montarras, D., Rocancourt, D., Relaix, F. (2003): The formation of skeletal muscle: from somite to limb. – Journal of Anatomy 202: 59-68.

[5] Chen, F., Luo, X., Shen, M., Huang, M., Ke, C. (2011): Karyotypes of two species of the genus *Babylonia*. – Journal of Xiamen University (Natural Science) 50: 789.

[6] Davis, T. A., Fiorotto, M. L., Burrin, D. G., Vann, R. C., Reeds, P. J., Nguyen, H. V., Beckett, P. R., Bush, J. A. (2002): Acute IGF-I infusion stimulates protein synthesis in skeletal muscle and other tissues of neonatal pigs. – American Journal of Physiology-Endocrinology and Metabolism 283: E638-E647.

[7] Deng, C. X., Wynshaw-Boris, A., Shen, M. M., Daugherty, C., Ornitz, D. M., Leder, P. (1994): Murine FGFR-1 is required for early postimplantation growth and axial organization. – Genes & Development 8: 3045-3057.

[8] Deng, Y. Y., Li, J. Q., Wu, S. F., Zhu, Y. P., He, F. C. (2006): Integrated nr database in protein annotation system and its localization. – Computer Engineering 32: 71-74.

[9] Doumit, M. E., Cook, D. R., Merkel, R. A. (1993): Fibroblast growth factor, epidermal growth factor, insulin-like growth factors, and platelet-derived growth factor-BB stimulate proliferation of clonally derived porcine myogenic satellite cells. – Journal of Cellular Physiology 157: 326-332.

[10] Feng, L., Hu, L., Fu, X., Liao, H., Li, X., Zhan, A., Zhang, L., Wang, S., Huang, X., Bao, Z. (2014): An integrated genetic and cytogenetic map for Zhikong scallop, Chlamys farreri, based on microsatellite markers. – PLoS One 9: e92567.

[11] Fishery and Fishery Administration of the Ministry of Agriculture and Rural Areas of China, National Aquatic Technology Promotion Terminal of China, Chinese Society of Aquaculture. (2019): China Fisheries Statistics Yearbook. – China Agriculture Press, Beijing.

[12] Florini, J. R., Ewton, D. Z., Roof, S. L. (1991): Insulin-like growth factor-I stimulates terminal myogenic differentiation by induction of myogenin gene expression. – Molecular Endocrinology 5: 718-724.

[13] Gudernova, I., Vesela, I., Balek, L., Buchtova, M., Dosedelova, H., Kunova, M., Pivnicka, J., Jelinkova, I., Roubalova, L., Kozubik, A., Krejci, P. (2015): Multikinase activity of fibroblast growth factor receptor (FGFR) inhibitors SU5402, PD173074, AZD1480, AZD4547 and BGJ398 compromises the use of small chemicals targeting FGFR catalytic activity for therapy of short-stature syndromes. – Human Molecular Genetics 25: 9-23.

http://www.aloki.hu ● ISSN 1589 1623 (Print) ● ISSN 1785 0037 (Online)
DOI: http://dx.doi.org/10.15666/aeer/1802_34713482

[14] Hargett, S. R., Walker, N. N., Hussain, S. S., Hoehn, K. L., Keller, S. R. (2015): Deletion of the Rab GAP Tbc1d1 modifies glucose, lipid, and energy homeostasis in mice. – American Journal of Physiology Endocrinology and Metabolism 309(3): E233-E245.
[15] Hembree, J. R., Hathaway, M. R., Dayton, W. R. (1991): Isolation and culture of fetal porcine myogenic cells and the effect of insulin, IGF-I, and sera on protein turnover in porcine myotube cultures. – Journal of Animal Science 69: 3241-3250.
[16] Hou, R., Bao, Z., Wang, S., Su, H., Li, Y., Du, H., Hu, J., Wang, S., Hu, X. (2011): Transcriptome sequencing and de novo analysis for Yesso scallop (Patinopecten yessoensis) using 454 GS FLX. – PLoS One 6: e21560.
[17] Huang, B. X., Peakall, R., Hanna, R. J. (2000): Analysis of genetic structure of blacklip abalone (Haliotis rubra) populations using RAPD, minisatellite and microsatellite markers. – Marine Biology 136: 207-216.
[18] Huang, R., Huang, B., Tang, W., Chen, Z. (2010): Morphological observation of the early developmental stages of *Babylonia areolata*. – Journal of Oceanography in Taiwan Strait 29: 380-388.
[19] Kanehisa, M., Goto, S., Kawashima, S., Okuno, Y., Hattori, M. (2004): The KEGG resource for deciphering the genome. – Nucleic Acids Res 32: D277-D280.
[20] Kanehisa, M., Araki, M., Goto, S., Hattori, M., Hirakawa, M., Itoh, M., Katayama, T., Kawashima, S., Okuda, S., Tokimatsu, T., Yamanishi, Y. (2008): KEGG for linking genomes to life and the environment. – Nucleic Acids Res 36: D480-D484.
[21] Kornbluth, S., Paulson, K. E., Hanafusa, H. (1988): Novel tyrosine kinase identified by phosphotyrosine antibody screening of cDNA libraries. – Molecular and Cellular Biology 8: 5541-5544.
[22] Koumanov, F., Holman, G. D. (2007): Thrifty Tbc1d1 and Tbc1d4 proteins link signalling and membrane trafficking pathways. – Biochemical Journal 403: e9-e11.
[23] Lamberson, W. R., Sterle, J. A., Matteri, R. L. (1996): Relationships of serum insulin-like growth factor I concentrations to growth, composition, and reproductive traits of swine. – Journal of Animal Science 74: 1753-1756.
[24] Le Roith, D., Scavo, L., Butler, A. (2001): What is the role of circulating IGF-I? – Trends in Endocrinology and Metabolism 12: 48-52.
[25] Li, F. (2008): Role of FGFR1 signaling in bone development and remodeling in mice. – Chongqing: Third Military Medical University.
[26] Li, Y., Zhong, Y., Lu, L., Chen, C., Duan, C. (2011): Research progress of insulin-like growth factor binding protein IGFBP-3. – Periodical of Ocean University of China 41: 41-47.
[27] Lin, G. (2012): Acute toxicity tests of four heavy metal salts to juvenile snail of *Babylonia lutosa*. – Fujian Journal of Agricultural Sciences 27: 232-236.
[28] Lu, L., Ma, A., Wang, X., Yue, L., Meng, X., Zhai, J., Tan, L., Hou, S. (2013): Polymorphisms analysis of five populations of Takifugu rubripes with microsatellite. – Progress in Fishery Sciences 34: 27-33.
[29] Masoudi-Nejad, A., Goto, S., Jauregui, R., Ito, M., Kawashima, S., Endo, T. R., Moriya, Y. (2007): EGENES: transcriptome-based plant database of genes with metabolic pathway information and expressed sequence tag indices in KEGG. – Plant Physiol 144: 857-866.
[30] Moriyama, S., Ayson, F. G., Kawauchi, H. (2000): Growth regulation by insulin-like growth factor-I in fish. – Bioscience, Biotechnology and Biochemistry 64: 1553-1562.
[31] Mortazavi, A., Williams, B. A., McCue, K., Schaeffer, L., Wold, B. (2008): Mapping and quantifying mammalian transcriptomes by RNA-Seq. – Nature Methods 5: 621-628.
[32] Nie, Z. (2014): Transcriptome analysis and study on genetic diversity of different geographic populations in Megalobrama terminalis. – Wuhan: Huazhong Agricultural University.
[33] Pan, Y., Li, B., Li, G. (2010): Morphological comparison on radula from different populations of *Hemifusus*. – Journal of Tropical Oceanography 29: 125-129.

http://www.aloki.hu ● ISSN 1589 1623 (Print) ● ISSN 1785 0037 (Online)
DOI: http://dx.doi.org/10.15666/aeer/1802_34713482

[34] Qi, Z., Wang, Y., Chen, D., Li, Y. (2011): Effect of morphometric traits on body weight in clam *Nerita yoldi*. – Fisheries Science 30: 505-508.
[35] Qin, Q., Wang, X., Zeng, Z., Zhu, D., Xiong, G., Wu, Q., Ning, Y. (2014): Genetic distance in four populations of *Babylonia lutosa* (Lamer) assessed by AFLP makers. – Journal of Human Agricultural University (Natural Sciences) 40: 299-304.
[36] Reinecke, M., Schmid, A., Ermatinger, R., Loffing-Cueni, D. (1997): Insulin-like growth factor I in the teleost Oreochromis mossambicus, the tilapia: gene sequence, tissue expression, and cellular localization. – Endocrinology 138: 3613-3619.
[37] Richardson, P. M., Zon, L. I. (1995): Molecular cloning of a cDNA with a novel domain present in the tre-2 oncogene and the yeast cell cycle regulators BUB2 and cdc16. – Oncogene 11: 1139-1148.
[38] Ruan, R., Yu, J., Li, H., Li, J., Tang, Y. (2011): Effects of IGF-1 genotype on weight gain and body shape in GIFT strain *Oreochromis niloticus*. – Journal of Fishery Sciences of China 18: 682-688.
[39] Tatusov, R. L., Galperin, M. Y., Natale, D. A., Koonin, E. V. (2000): The COG database: a tool for genome-scale analysis of protein functions and evolution. – Nucleic Acids Research 28: 33-36.
[40] Tong, X., Gong, S., Yu, D., Huang, G., Du, B., Li, S. (2009): Genetic diversity of cultured pacific white shrimp (Litopenaeus vannamei) stocks of different generations in China. – Oceanologia et Limnologia Sinica 40: 214-220.
[41] Upton, Z., Yandell, C. A., Degger, B. G., Chan, S. J., Moriyama, S., Francis, G. L., Ballard, F. J. (1998): Evolution of insulin-like growth factor-I (IGF-I) action: in vitro characterization of vertebrate IGF-I proteins. – Comparative Biochemistry and Physiology Part B: Biochemistry and Molecular Biology 121: 35-41.
[42] Wang, W., Cai, L., Liu, W. (2007): Morphological classification of nassariids in Fujian coast. – Journal of Xiamen University (Natural Science) 46: 171-175.
[43] Xiong, G., Ma, X., Wang, X. Q., Zeng, Z. N., Zhu, D. L., Kang, L., Wu, Q. S. (2015): Development and characterization of 18 microsatellite markers for the *Babylonia lutosa*. – Conservation Genetics Resources 7: 471-472.
[44] Xiong, G., Wang, X. Q., Wang, P., Chen, Z. N., Zhou, X. W., Kang, L., Zeng, Z. N. (2019): Development and genetic diversity analysis of Babylonia lutosa with EST-SSR markers. – Progress in Fishery Sciences 40: 1-8.
[45] Yang, Z., Zheng, Y., Li, Z., Zheng, Y. (2008): The effect of KCl on induced metamorphosis of planktonic larvae of *Babylonia aerolato*. – Marine Sciences 32: 6-9.
[46] Yano, K., Bauchat, J. R., Liimatta, M. B., Clemmons, D. R., Duan, C. (1999): Down-regulation of protein kinase C inhibits insulin-like growth factor I-induced vascular smooth muscle cell proliferation, migration, and gene expression. – Endocrinology 140: 4622-4632.
[47] Yin, S., Liao, J., Huang, H., Gao, L. (2007): Research advancement on biology and cultural ecology in *Babylonia* sp. – Fisheries Science 26: 632-636.
[48] Zhang, T., Liu, P., Li, J., Kong, J., Wang, Q. (2005): Genetic diversity of cultured populations of Fenneropenaeus chinensis shrimp using microsatellites. – Journal of Fisheries of China 29: 6-12.
[49] Zhang, J., Shi, Z., Fu, Y., Cheng, Q. (2011): Gene expression and thyroid hormone regulated transcript of IGF-I during metamorphosis of the flounder, Paralichthys olivaceus. – Acta Hydrobiologica Sinica 35: 355-359.

http://www.aloki.hu ● ISSN 1589 1623 (Print) ● ISSN 1785 0037 (Online)
DOI: http://dx.doi.org/10.15666/aeer/1802_34713482

APPENDIX

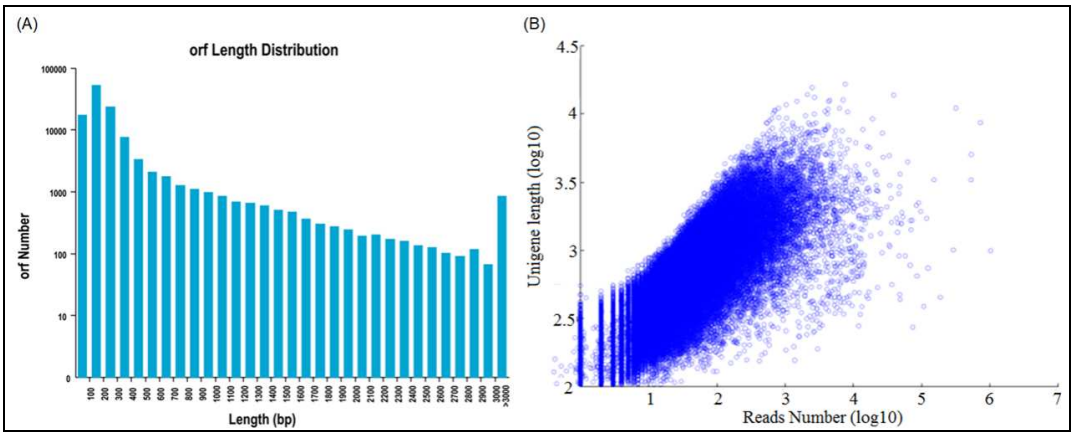

Appendix 1. *Length distribution of ORF in B. lutosa transcriptome (A) and the correlation between reads number and unigene length (B)*

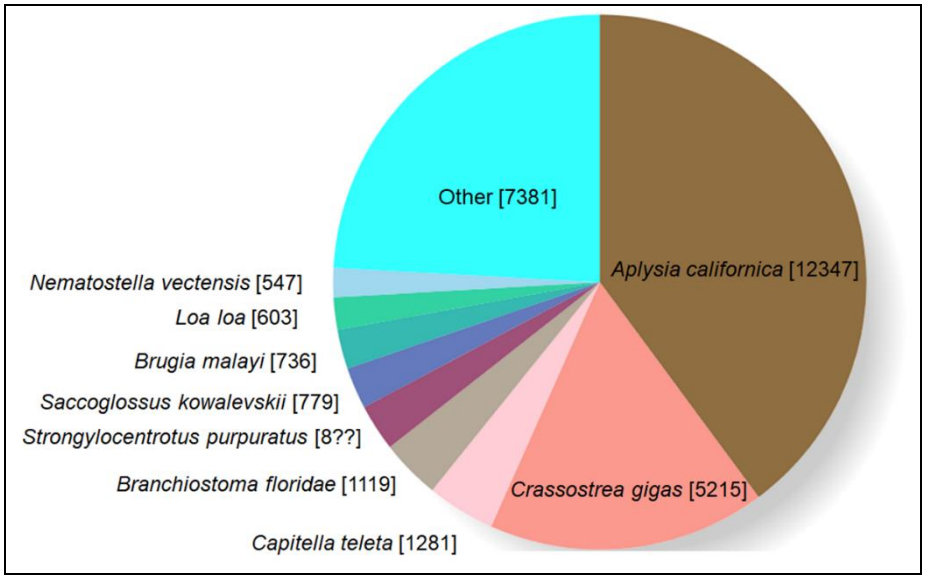

Appendix 2. *Distribution of species that were matched by unigenes in B. lutosa transcriptome*

Appendix 3. *Size distribution of Unigenes used for functional annotation of logarithmic transcriptome*

Annotated databases	All sequence	≥300 bp	≥1000 bp
NR	31,076	15,327	10,953
NT	17,033	7,483	7,093
SwissProt	18,413	7,892	8,409
TrEMBL	30,485	15,043	10,772
GO	14,106	6,025	6,300
KEGG	8,390	3,536	3,960
COG	7,191	2,852	3,685
Total	35,931	18,222	11,564

http://www.aloki.hu ● ISSN 1589 1623 (Print) ● ISSN 1785 0037 (Online)
DOI: http://dx.doi.org/10.15666/aeer/1802_34713482

EFFECT OF VARIOUS SYSTEMS OF TILLAGE ON WINTER BARLEY YIELD, WEED INFESTATION AND SOIL PROPERTIES

WOŹNIAK, A.

Department of Herbology and Plant Cultivation Techniques, University of Life Sciences in Lublin, Akademicka 13, Poland
(e-mail: andrzej.wozniak@up.lublin.pl)

(Received 21st Nov 2019; accepted 12th Mar 2020)

Abstract. A field experiment was performed to evaluate the yield of winter barley, weed infestation, and soil properties in various systems of tillage and crop rotation The following experimental factors were examined: tillage systems (TS): 1) CT – conventional tillage, 2) RT – reduced tillage, 3) NT – no-tillage; and crop rotation (CR): 1) winter wheat – winter barley, 2) pea – winter barley. Shallow ploughing and pre-sowing ploughing were performed in CT, cultivation in RT and glyphosate only was used in NT. The study found the highest barley grain yield in CT after pea, whereas the lowest one – in NT after wheat. A higher number and mass of weeds per m^2 was determined in RT than in CT and NT systems. Also the number and mass of weeds were found to be more affected by TS than by CR. The soil sampled from NT plots contained more organic C than that collected from RT and CT plots, and more total N than soil samples collected from CT plots. Higher contents of organic C and total N were also found in the soil from plots wherein barley was sown after pea compared to the soil from plot wherein barley was grown after wheat.
Keywords: *crop rotation, organic carbon, soil tillage, species composition of weeds, total nitrogen*

Introduction

The goal of soil tillage is to provide the best conditions for plant growth, development, and yield. Tillage systems determine soil properties (West and Marland, 2002; Tabaglio et al., 2008; Celik et al., 2011; Aziz et al., 2013), crop weed infestation (Hernández Plaza et al., 2015; Gawęda et al., 2018), water-air balance, and consequently crop yield and its quality (Ruisi et al., 2014; Montemurro and Maiorana, 2015; Rachoń et al., 2015; Woźniak and Stępniowska, 2017). Opinions on the effect of tillage systems on grain yield and weed infestation of crops are inexplicit and result mainly from various soil and weather conditions occurring during cultivation (Derpsch et al., 2010; Gruber et al., 2012; Zikeli et al., 2013). Soil tillage in the no-plough system (no-tillage, reduced tillage, strip-till) is practiced increasingly more often by farmers as it significantly reduces production costs compared to the conventional system (Haliniarz et al., 2018). Nevertheless, as reported by De Vita et al. (2007), there are strong correlations between wheat grain yield, tillage system, and total precipitation in the growing season. The no-tillage (NT) system has a positive effect on wheat grain yield when the total precipitation is low, whereas conventional tillage (CT) – when it is high. The better production effect in NT is due to the smaller evaporation of water the soil which results in its greater availability to plants (De Vita et al., 2007). Also in the study conducted by Ruisi et al. (2014), the no-tillage system ensured a higher grain yield of durum wheat after shortage of precipitation, whereas the conventional tillage system increased grain yield when water availability was sufficient. In turn, the experiment conducted by Woźniak and Kwiatkowski (2013) demonstrated a higher barley grain yield in the conventional tillage system than in reduced tillage and herbicide systems. In addition, it showed various responses of barley cultivars to the tillage system applied. In turn, López-Bellido et al. (2001) demonstrated a significant effect of tillage system on wheat grain quality. In their

http://www.aloki.hu ● ISSN 1589 1623 (Print) ● ISSN 1785 0037 (Online)
DOI: http://dx.doi.org/10.15666/aeer/1802_34833496

study, the conventional tillage had a more favorable effect on grain quality attributes than no-tillage, which was due to better availability of nitrogen for plants. Also in the experiment performed by Ruisi et al. (2014) the conventional tillage increased protein content of durum wheat grain, compared to the no-tillage system. In contrast, Woźniak and Stępniowska (2017) concluded that contents of protein and wet gluten in the grain as well as specific weight of the grain, and grain uniformity were affected by study years to a greater extent than by tillage systems. Tillage system was also found to differentiate the chemical composition of the grain. Conventional tillage facilitated accumulation of phytic-P and iron, reduced tillage – accumulation of calcium and manganese, whereas no-tillage – accumulation of phosphorus, potassium, magnesium, and copper. In addition, heavy rainfalls promoted the accumulation of phytic-P and copper in the grain, whereas precipitation shortages increased contents of potassium and magnesium in the grain.

Tillage system affects also the extent and structure of crop infestation with weeds. In a moderate climate, the no-plough and no-tillage systems increase the number and weight of weeds compared to the conventional system. Tillage systems influence also the species composition of weeds and their distribution in cereal stands. This, in turn, affects the competitiveness between weeds and crops, with the weeds of the upper level being more competitive to cereals than these off the ground and lower levels (Hernández Plaza et al., 2015; Woźniak, 2018). In the experiment performed by Gruber et al. (2012), a few to several times more weeds were found on plots cultivated in the no-tillage system than on these cultivated in the conventional tillage system. As reported by Hernández Plaza et al. (2015), tillage systems affect also the vertical distribution of weed seeds in the soil. The NT system promotes species with fine seeds and of high fertility, capable of germinating from soil surface. In turn CT plots are predominated by weed species having large seeds and capable of germinating from deeper soil layers. In the study conducted by Woźniak (2018), a high number of weed species belonging to the upper and middle layers of wheat crop was detected in the herbicide system (HT) than in conventional (CT) and reduced (RT) tillage systems. In the no-tillage system, weeds of the upper layer – *Apera spica-venti*, *Papaver rhoeas* and *Sonchus oleraceus* – spread mainly anemochorically by increasing the seedbank on soil surface. According to Koning et al. (2019), in this system weeds are eradicated with glyphosate which may form biotypes resistant to this herbicide. As claimed by Farooq et al. (2011), resistance of weeds to herbicides in the herbicide tillage system poses a problem across the world, while solution to this problem may be offered by conservation agriculture.

This study aimed to evaluate the effect of tillage systems and crop rotation on winter barley grain yield and its structure as well as on weed infestation and soil properties.

Material and Methods

Experiment location and description

A field experiment with tillage systems was established in 2007 at the Experimental Station Uhrusk belonging to the University of Life Sciences in Lublin, south-east Poland. The results presented in this manuscript were collected in the year 2018 from the 11-year CT, RT and NT systems. The experiment was established with the method of complete sub-blocks (6 m x 25 m in size), in three replications. The following experimental factors were tested: (I) tillage systems: 1) conventional tillage (CT), 2) reduced tillage (RT) and 3) no-tillage (NT); (II) crop rotation (CR): 1) winter wheat – winter barley and 2) pea –

http://www.aloki.hu ● ISSN 1589 1623 (Print) ● ISSN 1785 0037 (Online)
DOI: http://dx.doi.org/10.15666/aeer/1802_34833496

winter barley. The tillage plan is presented in *Table 1*. Winter barley cultivar 'Titus' was sown between 20 and 30 of September, at sowing density of 400 seeds per m^2.

Table 1. *Scheme of soil tillage*

Crops	Tillage system (TS)		
	conventional tillage (CT)	**reduced tillage (RT)**	**no-tillage (NT)**
After-harvest	shallow ploughing, depth of 10 cm	cultivator (twice)	Glyphosate (360 g L^{-1}, 4 L ha^{-1})
Pre-sowing cultivation	pre-sow ploughing (20 cm)	tillage unit for pre-sowing tillage (cultivator and roller)	

Soil and weather conditions

The experiment was established on *Rendzic Phaeozem* (WRB, 2014), which contains 24.5% of silty fraction and 13.7% of dust fraction. The soil has slightly alkaline pH (pH_{KCL} = 7.4), high contents of available phosphorus (120 mg kg^{-1} P dm) and potassium (194 mg kg^{-1} K), and a moderate content of magnesium (73 mg kg^{-1} Mg).

In the multi-year period of 2007-2017, the total atmospheric precipitation at the study area was 640 mm, including 230 cm since November till April (cold half-year) and 410 mm since May to October (warm half-year). In 2018, the total annual precipitation reached 440 mm, including 160 mm in the cold half-year and 280 mm in the warm half-year (*Fig. 1*). In the multi-year period, the average air temperature reached 1.8°C in the cold half-year and 15.6°C in the warm half-year. In 2018, the air temperature was slightly higher and reached 2.0°C and 17.1°C, respectively. The coldest months turned out to be January (average temperature: −2.7°C) and February (−2.1°C), whereas the warmest ones – July (20.2°C) and August (19.3°C). The growing season at the study area spans for 210–215 days; it begins from 20 to 31 of March and ends at the beginning of November.

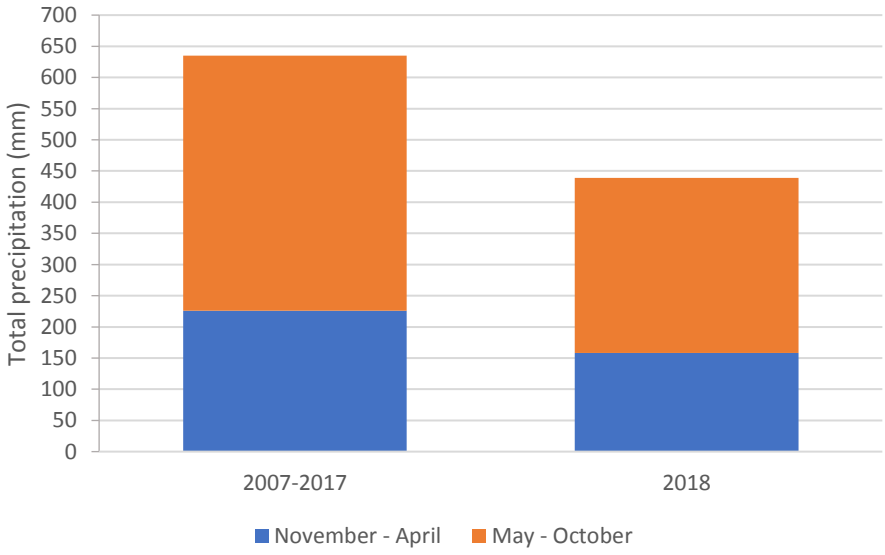

Figure 1. *Total annual precipitation at the Uhrusk Experimental Station, Poland*

http://www.aloki.hu ● ISSN 1589 1623 (Print) ● ISSN 1785 0037 (Online)
DOI: http://dx.doi.org/10.15666/aeer/1802_34833496

Fertilization and plant protection

Phosphorus-based (30 kg ha^{-1} P) and potassium-based (75 kg ha^{-1} K) fertilizers were used in the autumn before winter barley sowing. Nitrogen-based fertilizers were administered in three terms: in the autumn before barley sowing – 20 kg ha^{-1} N, in the spring at the tillering stage (23–24 BBCH) – 50 kg ha^{-1} N, and at the heading stage (52-53 BBCH) – 20 kg N ha^{-1} (BBCH Working Group, 2001). Fertilization doses were computed based on the chemical analysis of soil. Chemical protection of barley plants included administration of fungicides containing flusilazole + carbendazim at the shooting stage (31–32 BBCH) and propiconazole + fenpropidin at the heading stage (43-44 BBCH). Weeds were eradicated with a herbicide containing MCPA + mecoprop + dicamba at the tillering stage (23–24 BBCH), and herbicide treatment was performed after the first term of assessment of weed number and species composition.

Yield components and statistical analysis

The following yield components were analysed in the experiment: 1) plant number per m^2 at the tillering stage (23–24 BBCH); 2) spike number per m^2; 3) grain weight per spike; 4) 1000 grain weight; 5) number and species composition of weeds per m^2 at the tillering stage (23–24 BBCH); and 6) number, species composition, and air-dry weight of weeds in g m^{-2} at the milk maturity stage (73–74 BBCH). Additional determinations were conducted for contents of organic carbon (C) and total nitrogen (N) in the soil.

Grain was harvested using a plot harvester at 14% moisture content of the grain. Grain weight per spike was evaluated based on 40 plants randomly collected from each plot, whereas 1000 grain weight was determined by measuring out 2 × 500 grains. Weed infestation was evaluated with the botanical-gravimetric method which consists in determination of the number and species composition of weeds and of their air-dry weight from the surface area of one m^2 of each plot. This surface was determined at random (twice) using a frame (0.5 × 1.0 m). Determination of the air-dry weight of weeds consisted in their manual picking from frame surface, removing their root system, and placing them in a ventilated room until their constant weight has been achieved (Woźniak, 2018). Soil samples collected from all plots were determined for organic C content with the Tiurin method and total N content with the Kjeldahl method.

Results obtained were subjected to the analysis of variance (ANOVA), whereas significance of differences between mean values for tillage systems (TS), crop rotation (CR) and TS × CR interaction was evaluated using Tukey's HSD test, $p < 0.05$.

Results

Grain yield and its components

A higher barley grain yield was determined in CT system compared to RT system (by 24.8%) and NT (by 54.2%) systems (*Table 2*). A higher barley grain yield was also noted on plots where barley was sown after pea than after winter wheat. Tillage systems (TS) and crop rotation (CR) affected plant number per m^2 (*Table 3*). At the 23–24 BBCH stage, the number of barley plants per m^2 was higher in CT than in RT and NT. A higher plant number was also observed on plots where barley was sown after pea than after wheat. Likewise, the number of spikes per m^2 was higher in CT than in RT and NT, and on plots with barley sown after pea than after wheat. Tillage systems and crop rotation were also found to affect grain weight per spike and 1000 grain weight. Their values were more

http://www.aloki.hu ● ISSN 1589 1623 (Print) ● ISSN 1785 0037 (Online)
DOI: http://dx.doi.org/10.15666/aeer/1802_34833496

favourable in CT than in RT and NT, and also in plots where barley was sown after pea than after wheat.

Table 2. *Grain yield of winter barley in t ha^{-1}*

Crop rotation (CR)	Tillage system (TS)			Mean
	conventional tillage (CT)	reduced tillage (RT)	no-tillage (NT)	
Winter wheat – winter barley	4.43	3.38	1.89	3.23
Pea – winter barley	5.57	4.14	2.70	4.14
Mean	5.00	3.76	2.29	-
$HSD_{0.05}$ for TS = 0.24, CR = 0.16, TS × CR = ns				

ns – not significant

Table 3. *Biometric traits of winter barley*

Crop rotation (CR)	Tillage system (TS)			Mean
	conventional tillage (CT)	reduced tillage (RT)	no-tillage (NT)	
Plant number m^{-2} (23–24 BBCH)				
Winter wheat – winter barley	357	237	256	283
Pea – winter barley	383	281	269	311
Mean	370	259	262	-
$HSD_{0.05}$ for TS = 23, CR = 15, TS × CR = ns				
Spike number m^{-2}				
Winter wheat – winter barley	533	455	427	472
Pea – winter barley	572	541	448	520
Mean	553	498	437	-
$HSD_{0.05}$ for TS = 40; CR = 27; TS × CR = ns				
Grain weight per spike g				
Winter wheat – winter barley	0.86	0.76	0.44	0.69
Pea – winter barley	1.02	0.77	0.61	0.80
Mean	0.94	0.76	0.53	-
$HSD_{0.05}$ for TS = 0.07; CR = 0.05; TS × CR = 0.12				
1000 grain weight g				
Winter wheat – winter barley	48.2	44.6	43.4	45.4
Pea – winter barley	50.1	48.5	46.6	48.4
Mean	49.2	46.6	45.0	-
$HSD_{0.05}$ for TS = 1.6, CR = 1.1, TS × CR = ns				

ns – not significant

Variance component analysis indicates that barley grain yield, plant number per m^2, spike number per m^2, and grain weight per spike were affected to a greater extent by TS than by CR, whereas 1000 grain weight – to a greater extent by CR than by TS (*Table 4*).

http://www.aloki.hu ● ISSN 1589 1623 (Print) ● ISSN 1785 0037 (Online)
DOI: http://dx.doi.org/10.15666/aeer/1802_34833496

Table 4. *Analysis of variance for grain yield and its components*

Specification	Value	Tillage system (TS)	Crop rotation (CR)	TS × CR
Grain yield	*F*	473.1	158.1	2.8
	p	**	**	ns
Plant number m^{-2} (23–24 BBCH)	*F*	106.4	15,4	1.7
	p	**	**	ns
Spike number m^{-2}	*F*	29.7	15.5	2.5
	p	**	**	ns
Grain weight per spike	*F*	131.4	27.9	6.2
	p	**	**	*
1000 grain weight	*F*	23.1	36.1	1.2
	p	**	**	ns

$^{*}P < 0.05$, $^{**}P < 0.01$, ns – not significant

Indices of crop infestation by weeds

At the tillering stage of winter barley (23-24 BBCH), more weeds per m^2 occurred in RT than in CT and NT systems (*Table 5*).

Table 5. *Number of weeds per m^2 in winter barley crop*

Crop rotation (CR)	Tillage system (TS)			Mean
	conventional tillage (CT)	reduced tillage (RT)	no-tillage (NT)	
23–24 BBCH				
Winter wheat – winter barley	10.5	23.7	14.2	16.1
Pea – winter barley	8.9	15.2	11.0	11.7
Mean	9.7	19.4	12.6	–
$HSD_{0.05}$ for TS = 4.8, CR = 3.2, TS × CR = ns				
73-74 BBCH				
Winter wheat – winter barley	18.8	45.4	21.7	28.7
Pea – winter barley	13.5	27.5	15.6	18.9
Mean	16.2	36.4	18.6	–
$HSD_{0.05}$ for TS = 8.5, CR = 5.7, TS × CR = ns				

ns – not significant

The higher number of weeds was also observed on the plot where barley was sown after winter wheat than after pea. Also at the milk maturity stage of barley (73–74 BBCH) more weeds were found in RT than in CT and NT systems, and on plots where barley was sown after wheat than after pea. Similar observations were made for the air-dry weight of weeds (*Table 6*). The greatest biomass was developed by weeds in RT, smaller one in NT, and the smallest one in CT system. Variance component analysis indicates that, in both terms of evaluation, the number of weeds per m^2 and air-dry weight of weeds were more influenced by TS than by CR (*Table 7*).

http://www.aloki.hu ● ISSN 1589 1623 (Print) ● ISSN 1785 0037 (Online)
DOI: http://dx.doi.org/10.15666/aeer/1802_34833496

Table 6. *Air-dry weight of weeds in g m^{-2} at the 73–74 BBCH term of winter barley*

Crop rotation (CR)	Tillage system (TS)			Mean
	conventional tillage (CT)	reduced tillage (RT)	no-tillage (NT)	
Winter wheat – winter barley	10.9	29.1	18.7	19.6
Pea – winter barley	5.0	16.7	14.3	12.0
Mean	8.0	22.9	16.5	–
$HSD_{0.05}$ for TS = 5.9, CR = 4.0, TS × CR = ns				

ns – not significant

Table 7. *Analysis of variance conducted for the number and weight of weeds in winter barley*

Specification	Value	Tillage system (TS)	Crop rotation (CR)	TS × CR
Number of weeds 23–24 BBCH	*F*	15.5	9.1	2.0
	p	**	**	ns
Number of weeds 73–74 BBCH	*F*	24.1	14.3	2.5
	p	**	**	ns
Air-dry weight of weeds 73–74 BBCH	*F*	22.7	17.2	1.8
	p	**	**	ns

$^{*}P < 0.05$, $^{**}P<0.01$, ns – not significant

Tillage systems (TS) and crop rotation (CR) affected also the number and composition of weed species in barley stands (*Table 8*). At the tillering stage (23–24 BBCH), a higher number of weed species was observed on RT than on CT and NT plots, as well as on plots where barley was sown after pea than after wheat. Also at the milk maturity stage of barley (73–74 BBCH) was the number of weed species higher in RT than in CT and NT systems, and in plots where barley was sown after wheat than after pea.

Table 8. *Number of weed species in winter barley crop*

Crop rotation (CR)	Tillage system (TS)			Mean
	conventional tillage (CT)	reduced tillage (RT)	no-tillage (NT)	
23–24 BBCH				
Winter wheat – winter barley	8.0	11.0	4.0	7.7
Pea – winter barley	10.0	16.0	7.0	11.0
Mean	9.0	13.5	5.5	-
$HSD_{0.05}$ for TS = 3.6, CR = 2.7, TS × CR = 4.4				
73–74 BBCH				
Winter wheat – winter barley	13.0	22.0	15.0	16.6
Pea – winter barley	10.0	16.0	8.0	11.3
Mean	11.5	19.0	11.5	-
$HSD_{0.05}$ for TS = 4.1, CR = 3.7, TS × CR = ns				

ns – not significant

http://www.aloki.hu ● ISSN 1589 1623 (Print) ● ISSN 1785 0037 (Online)
DOI: http://dx.doi.org/10.15666/aeer/1802_34833496

In the CT, RT, and NT systems, most of the weed species belonged to the middle and upper level of barley stand, whereas a lower number of species were representatives of the ground level weed species (*Figs. 2 and 3*).

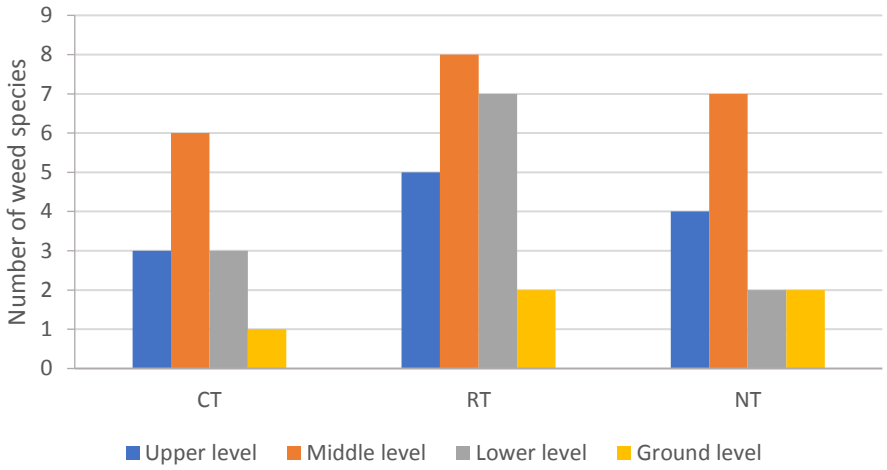

Figure 2. *Level distribution of weeds in winter barley crop at the milk maturity stage of barley (73–74 BBCH) in crop rotation: winter wheat – winter barley*

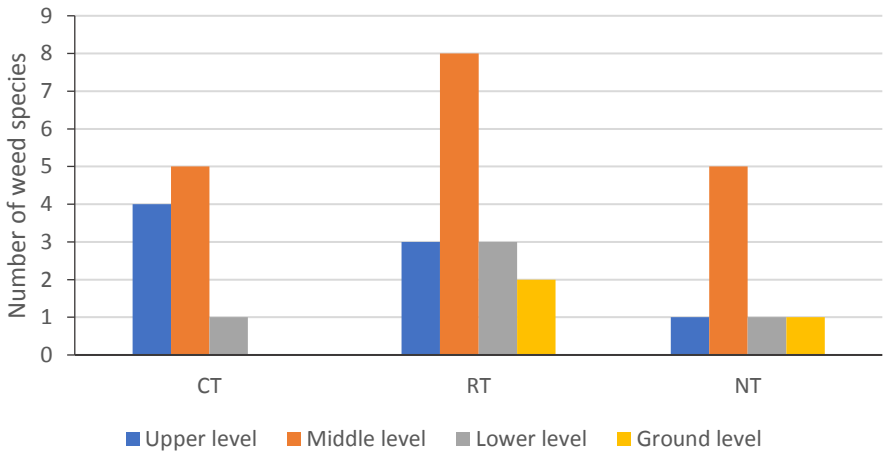

Figure 3. *Level distribution of weeds in winter barley crop at the milk maturity stage of barley (73–74 BBCH) in crop rotation: pea – winter barley*

At the tillering stage of barley (23–24 BBCH), the most abundant species on the plot where barley was sown after wheat included: *Thlaspi arvense*, *Apera spica-venti* and *Consolida regalis* in CT system, *Apera spica-venti*, *Consolida regalis* and *Veronica persica* in RT system as well as *Consolida regalis*, *Thlaspi arvense* and *Galium aparine* in NT system (*Fig. 4*).

The prevailing species observed on the plot with barley sown after pea included: *Apera spica-venti*, *Papaver rhoeas* and *Galium aparine* in CT system, *Apera spica-venti*, *Tripleurospermum inodorum* and *Consolida regalis* in RT system and *Galium aparine*, *Tripleurospermum inodorum* and *Apera spica-venti* in NT system (*Fig. 5*).

http://www.aloki.hu ● ISSN 1589 1623 (Print) ● ISSN 1785 0037 (Online)
DOI: http://dx.doi.org/10.15666/aeer/1802_34833496

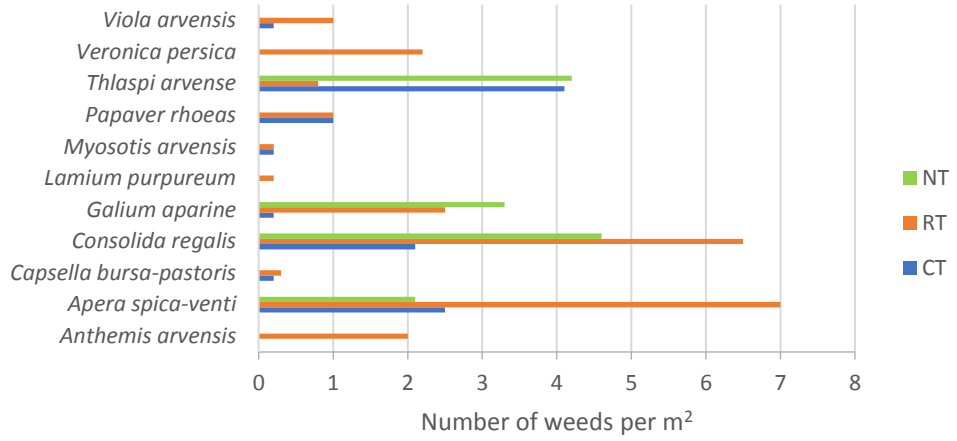

Figure 4. *Species composition of weeds in winter barley crop at the tillering stage of barley (23–24 BBCH) in crop rotation: winter wheat – winter barley; CT – conventional tillage, RT – reduced tillage, NT – no-tillage*

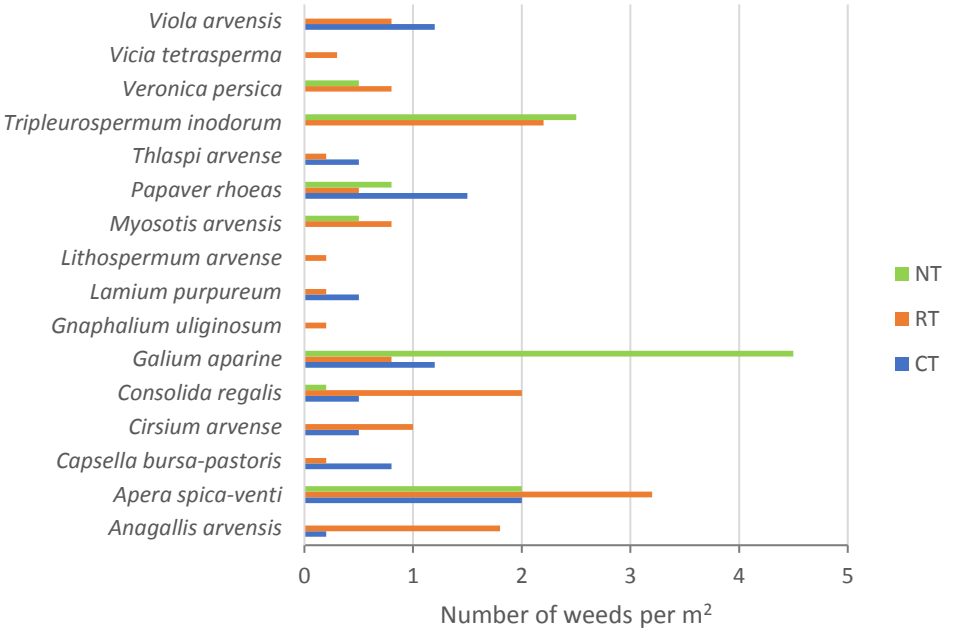

Figure 5. *Species composition of weeds in winter barley crop at the tillering stage of barley (23–24 BBCH) in crop rotation: pea – winter barley; CT – conventional tillage, RT – reduced tillage, NT – no-tillage*

At the milk maturity stage of winter barley (73-74 BBCH), the predominating weed species observed on the plot where barley was sown after wheat included: *Galeopsis tetrahit*, *Sinapis arvensis* and *Fallopia convolvulus* in CT system, *Apera spica-venti*, *Papaver rhoeas* and *Consolida regalis* in RT system and *Apera spica-venti*, *Consolida regalis* and *Galium aparine* in NT system (*Fig. 6*).

http://www.aloki.hu ● ISSN 1589 1623 (Print) ● ISSN 1785 0037 (Online)
DOI: http://dx.doi.org/10.15666/aeer/1802_34833496

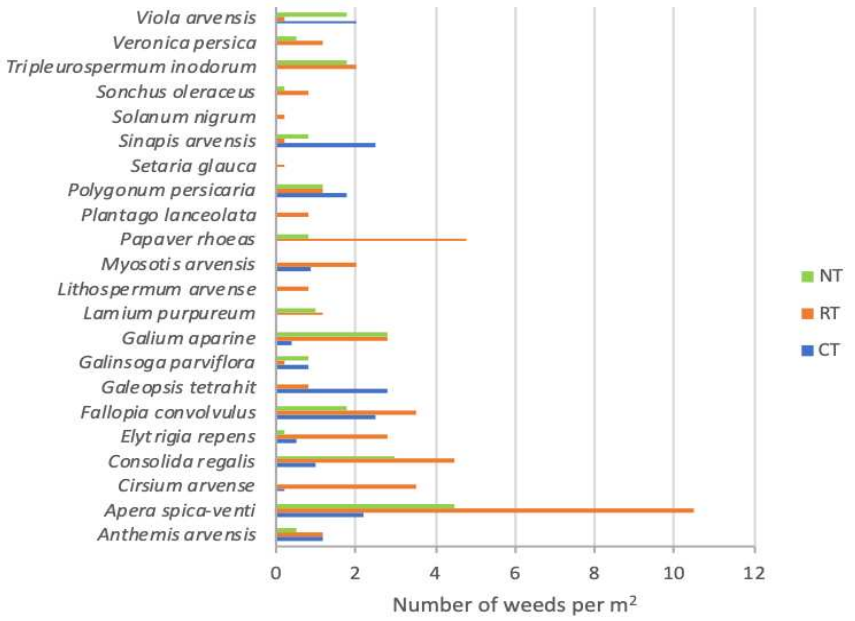

Figure 6. *Species composition of weeds in winter barley crop at the milk maturity stage of barley (73–74 BBCH) in crop rotation: winter wheat – winter barley; CT – conventional tillage, RT – reduced tillage, NT – no-tillage*

On the plot where barley was sown after pea, these were: *Fallopia convolvulus*, *Papaver rhoeas* and *Apera spica-venti* in CT system, *Apera spica-venti*, *Consolida regalis* and *Galium aparine* in RT system and *Apera spica-venti*, *Tripleurospermum inodorum* and *Consolida regalis* in NT system (*Fig. 7*).

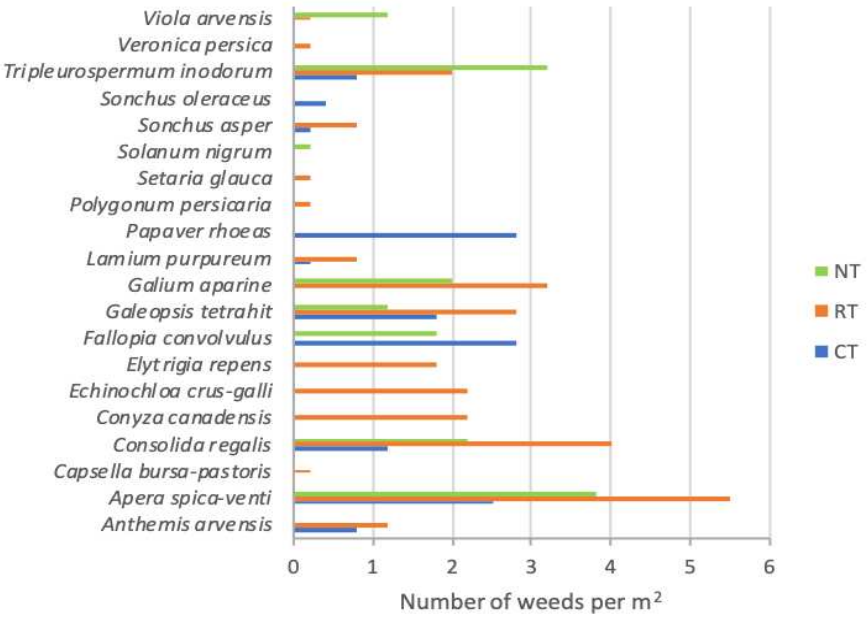

Figure 7. *Species composition of weeds in winter barley crop at the milk maturity stage of barley (73–74 BBCH) in crop rotation: pea – winter barley; CT – conventional tillage, RT – reduced tillage, NT – no-tillage*

http://www.aloki.hu ● ISSN 1589 1623 (Print) ● ISSN 1785 0037 (Online)
DOI: http://dx.doi.org/10.15666/aeer/1802_34833496

Soil properties

The soil sampled from NT plots contained more organic C than that from RT and CT plots (*Table 9*). Also more organic C was determined in the soil from plots where barley was sown after pea than after wheat. In turn, total N content was similar in soil samples from NT and RT plots, and significantly higher in the soil from CT plots. Also a higher N total content was determined in the soil sampled from plots where barley was sown after pea than after wheat.

Table 9. *Effect of crop rotation and tillage system on chemical properties of soil (0–30 cm)*

Crop rotation (CR)	Tillage system (TS)			Mean
	conventional tillage (CT)	reduced tillage (RT)	no-tillage (NT)	
Organic C (g kg^{-1} dm)				
Winter wheat – winter barley	8.33	11.03	12.43	10.60
Pea – winter barley	10.70	11.70	13.03	11.81
Mean	9.52	11.37	12.73	-
$HSD_{0.05}$ for TS = 1.08, CR = 0.72, TS × CR = ns				
Total N (g kg^{-1} dm)				
Winter wheat – winter barley	0.86	0.94	0.96	0.92
Pea – winter barley	0.91	1.06	1.08	1.01
Mean	0.88	1.00	1.02	-
$HSD_{0.05}$ for TS = 0.10, CR = 0.07, TS × CR = ns				

ns – not significant

Variance component analysis demonstrates that organic C content in the soil was influenced to a greater extent by TS than by CR, whereas total N content was similarly affected by CR and TS (*Table 10*).

Table 10. *Analysis of variance for chemical properties of soil*

Specification	Value	Tillage system (TS)	Crop rotation (CR)	TS × CR
Organic C	*F*	31.89	13.50	3.08
	p	**	**	ns
Total N	*F*	7.64	9.14	0.51
	p	**	*	ns

* $P < 0.05$, ** $P < 0.01$, ns – not significant

Discussion

Soil tillage aims to provide the best conditions for plant growth and yielding, and also to keep weed infestation at the level posing no threat to crop stands (Nichols et al., 2015; Santín-Montanyá et al., 2016). A study conducted by Gruber et al. (2012) indicates that, in moderate climate, the conventional tillage system is more effective in reducing weed infestation than the no-tillage system. Also Woźniak and Kwiatkowski (2013) demonstrated significantly lesser weed infestation in the conventional tillage than in the

http://www.aloki.hu ● ISSN 1589 1623 (Print) ● ISSN 1785 0037 (Online)
DOI: http://dx.doi.org/10.15666/aeer/1802_34833496

reduced and herbicide systems. In contrast, in the arid Mediterranean regions, better production results and smaller weed infestation are observed in the no-tillage system compared to the conventional tillage (López-Bellido et al., 2001; De Vita et al., 2007). According to Ruisi et al. (2014), caution should be exercised to the appropriate crop rotation in the no-tillage system (NT), with cereals cultivation after themselves found as the inappropriate sequence. Also in our study, the highest barley yield was determined in CT after pea (5.57 t ha^{-1}), whereas the lowest one – in NT after pea (1.89 t ha^{-1}). It is due to a lower number of plants per m^2 in NT than in CT, a lower spike number per m^2, a lower grain weight per spike, and also a lower 1000 grain weight. The outcomes of barley cultivation after wheat included also: a lower plant number and spike number per m^2, a lower grain weight per spike, and a lower 1000 grain weight than after its cultivation after pea. In the present study, values of these traits depended to a greater extent on tillage systems (TS) than on crop rotation (CR). Similar dependencies were observed by Jug et al. (2011).

The no-till systems and cereal monoculture are characterized by increased number and weight of weeds as well as by predominance and compensation of a few weed species, compared to the conventional tillage and crop rotation (Koning et al., 2019; Woźniak, 2019). As reported by Hernández Plaza et al. (2015), the NT system promotes species with fine grains and high fertility whose seeds accumulate mainly on soil surface from where they sprout under convenient conditions. According to Farooq et al. (2011), these weeds are effectively eradicated by herbicides, but the inappropriate use of these preparations may develop plant resistance to them. In turn, greater species diversity of weeds having seeds of various sizes and exhibiting various fertility is observed in the CT system (Hernández Plaza et al., 2011). During cultivation, these seeds are transferred into deeper soil layers from where only some of them are capable to sprout (Santín-Montanyá et al., 2016). Generally, it may be concluded that the conventional tillage system (ploughing) and the use of glyphosate in the no-tillage system reduce the number and weight of weeds and also affect their species composition. This has also been confirmed in the present study where a lower number of weed species and lower weed density were observed in CT and NT systems than in the RT system. Weed distribution in the crop is also of high importance. It may, generally, be concluded that weeds of the upper and the middle levels spread with wind (anemochorically) or during harvest of cereals, whereas weeds of the lower and the ground levels ripe and spread on the stubble field. In the study conducted by Woźniak (2018), 45% of weeds identified in the herbicide tillage system were represented by species with small grains belonging to the upper and middle levels. Also in the present study, most of the weed species formed the middle and the upper layer of the crop, from where they could easily spread before the harvest of cereals.

Tillage system and crop rotation affect also soil properties (Woźniak, 2019). Soil from the cereal monoculture contains less organic matter and organic carbon (Maillard et al., 2016) than the soil from crop rotation; in addition, its biological activity decreases (Kretzschmar and Monestiez, 1992). Also in the present study, the soil sampled after pea cultivation contained more organic C and total N than the soil after wheat cultivation. More organic C and total N was also determined in the soil samples from NT and RT systems than from CT system, which is in agreement with findings reported earlier by Tabaglio et al. (2008), Zikeli et al. (2013), Santín-Montanyá et al. (2016) and Woźniak (2019).

http://www.aloki.hu ● ISSN 1589 1623 (Print) ● ISSN 1785 0037 (Online)
DOI: http://dx.doi.org/10.15666/aeer/1802_34833496

Conclusion

Tillage systems and crop rotation caused significant differences in grain yield of winter barley, weed infestation, and soil properties. The highest grain yield was determined for barley grown in the conventional system after pea, whereas the lowest one for barley grown in no-till system after winter wheat. Grain yield, numbers of plants and spikes per m^2, and grain weight per spike depended to a larger extent on tillage systems than on crop rotation. A higher number and weight of weeds per m^2 was determined in the reduced tillage system compared to the conventional and no-till systems. Also, a higher number of weeds was found on the plot where barley was sown after winter wheat than after pea. The number and weight of weeds per m^2 were affected to a greater extent by tillage system than by crop rotation. Tillage systems differentiated also species number and composition of weeds. A higher number of weed species was found in the reduced tillage system than in the conventional and no-till systems. The soil sampled from plots cultivated in the no-till system contained more organic C than the soil collected from reduced and conventional systems as well as more total N than from the conventional system. Likewise, more organic C and total N was found in the soil sampled from the plot where barley was sown after pea than after wheat.

REFERENCES

[1] Aziz, I., Mahmood, T., Islam, K. R. (2013): Effect of long-term no-till and conventional tillage practices on soil quality. – Soil and Tillage Research 131: 28-35.

[2] BBCH Working Group (2001): Growth stages of mono-and dicotyledonous plants. – In: Meier, U. (ed.) Federal Biological Research Centre for Agriculture and Forestry (2nd ed.).

[3] Celik, I., Barut, Z. B., Ortas, I., Gok, M., Demirbas, A., Tulun, Y., Akpinar, C. (2011): Impacts of different tillage practices on some soil microbiological properties and crop yield under semi-arid Mediterranean conditions. – International Journal of Plant Production 5: 237-254.

[4] De Vita, P., Di Paolo, E., Fecondo, G., Di Fonzo, N., Pisante, M. (2007): No-tillage and conventional tillage effects on durum wheat yield, grain quality and soil moisture content in southern Italy. – Soil and Tillage Research 92: 69-78.

[5] Derpsch, R., Friedrich, T., Kassam, A., Hongwen, L. (2010): Current status of adoption of no-till farming in the world and some of its main benefits. – International Journal of Agricultural and Biological Engineering 3: 1-25.

[6] Farooq, M., Flower, K. C., Jabran, K., Wahid, A., Siddique, K. H. M. (2011): Crop yield and weed management in rainfed conservation agriculture. – Soil and Tillage Research 117: 172-183.

[7] Gawęda, D., Woźniak, A., Harasim, E. (2018): Weed infestations of winter wheat depend on the forecrop and the tillage system. – Acta Agrobotanica 71: 1744.

[8] Gruber, S., Pekrun, C., Möhring, J., Claupein, W. (2012): Long-term yield and weed response to conservation and stubble tillage in SW Germany. – Soil and Tillage Research 121: 49-56.

[9] Haliniarz, M., Nowak, A., Woźniak, A, Sekutowski, T. R., Kwiatkowski, C. A. (2018): Production and economic effects of environmentally friend.ly spring wheat production technology. – Polish Journal of Environmental Studies 27: 1523-1532.

[10] Hernández Plaza, E. H., Kozak, M., Navarrete, L., González-Andújar, J. L. (2011): Tillage system did not affect weed diversity in a 23-year experiment in Mediterranean dryland. – Agriculture, Ecosystems and Environment 140: 102-105.

http://www.aloki.hu ● ISSN 1589 1623 (Print) ● ISSN 1785 0037 (Online)
DOI: http://dx.doi.org/10.15666/aeer/1802_34833496

[11] Hernández Plaza, E., Navarrete, L., González-Andújar, J. L. (2015): Intensity of soil disturbance shapes response trait diversity of weed communities: The long-term effects of different tillage systems. – Agriculture, Ecosystems and Environment 207: 101-108.
[12] Jug, I., Jug, D., Sabo, M., Stipešević, B., Stošić, M. (2011): Winter wheat yield and yield components as affected by soil tillage systems. – Turkish Journal of Agriculture and Forestry 35: 1-7.
[13] Koning, L. A., de Mol, F., Gerowitt, B. (2019): Effects of management by glyphosate or tillage on the weed vegetation in a field experiment. – Soil and Tillage Research 186: 79-86.
[14] Kretzschmar, A., Monestiez, P. (1992): Physical control of soil biological activity due endogenic earthworm behaviour. – Soil Biology and Biochemistry 24: 1609-1614.
[15] López-Bellido, L., López-Bellido, R., Castillo, J. E., López-Bellido, F. J. (2001): Effects of long-term tillage, crop rotation and nitrogen fertilization on bread-making quality of hard red spring wheat. – Field Crops Research 72: 197-210.
[16] Maillard, É., Angers, D. A., Chantigny, M., Lafond, J., Pageau, D., Rochette, P., Lévesque, G., Leclerc, M. L., Parent, L. É. (2016): Greater accumulation of soil organic carbon after liquid dairy manure application under cereal-forage rotation than cereal monoculture. – Agriculture, Ecosystems and Environment 233: 171-178.
[17] Montemurro, F., Maiorana, M. (2015): Agronomic practices at low environmental impact for durum wheat in Mediterranean conditions. – Journal of Plant Nutrition 38: 624-638.
[18] Nichols, V., Verhulst, N., Cox, R., Govaerts, B. (2015): Weed dynamics and conservation agriculture principles: A review. – Field Crops Research 183: 56-68.
[19] Rachoń, L., Szumiło, G., Brodowska, M., Woźniak, A. (2015): Nutritional value and mineral composition of grain of selected wheat species depending on the intensity of a production technology. – Journal of Elementology 20: 705-715.
[20] Ruisi, P., Giambalvo, D., Saia, S., Di Miceli, G., Frenda, A. S., Plaia, A., Amato, G. (2014): Conservation tillage in a semiarid Mediterranean environment: results of 20 years of research. – Italian Journal of Agronomy 9: 560.
[21] Santín-Montanyá, M. I., Martín-Lammerding, D., Zambranab, E., Tenorio, J. L. (2016): Management of weed emergence and weed seed bank in response to different tillage, cropping systems and selected soil properties. – Soil and Tillage Research 161: 38-46.
[22] Tabaglio, V., Gavazzi, C., Menta, C. (2008): The influence of no-till, conventional tillage and nitrogen fertilization on physico-chemical and biological indicators after three years of monoculture barley. – Italian Journal of Agronomy 3: 233-240.
[23] West, T. O., Marland, G. (2002): A synthesis of carbon sequestration, carbon emissions, and net carbon flux in agriculture: Comparing tillage practices in the United States. – Agriculture, Ecosystems and Environment 91: 217-232.
[24] Woźniak, A. (2018): Effect of tillage system on the structure of weed infestation of winter wheat. – Spanish Journal of Agricultural Research 16: e1009.
[25] Woźniak, A. (2019): Effect of crop rotation and cereal monoculture on the yield and quality of winter wheat grain and on crop infestation with weeds and soil properties. – International Journal of Plant Production 13: 177-182.
[26] Woźniak, A., Kwiatkowski, C. (2013): Effect of long-term reduced tillage on yield and weeds of spring barley. – Journal of Agricultural Science and Technology 15: 1335-1342.
[27] Woźniak, A., Stępniowska, A. (2017): Yield and quality of durum wheat grain in different tillage systems. – Journal of Elementology 22: 817-829.
[28] WRB (2014): World reference base for soil resources. – World Soil Resources Reports No. 106. FAO.
[29] Zikeli, S., Gruber, S., Teufel, C. F., Hartung, K., Claupein, W. (2013): Effects of reduced tillage on crop yield, plant available nutrients and soil organic matter in a 12-year long-term trial under organic management. – Sustainability 5: 3876-3894.

http://www.aloki.hu ● ISSN 1589 1623 (Print) ● ISSN 1785 0037 (Online)
DOI: http://dx.doi.org/10.15666/aeer/1802_34833496

MUTAGEN EFFECT ON THE GROWTH, PHYSIOLOGY AND MICROSTRUCTURE OF ALFALFA (*MEDICAGO SATIVA* L)

SHEN, X. H.[1,2†] – JIANG, C.[2†] – ZHENG, W.[1†] – FENG, P.[1†] – WANG, Q.[3] – LAI, Y. C.[1*]

[1]*Postdoctoral Workstation of Heilongjiang Academy of Agricultural Sciences, Harbin 150086, China*

[2]*College of Life Sciences, Resources and Environment Sciences, Yichun University, Yichun, Jiangxi 336000, China*

[3]*Breeding Unit of the Academy of Agricultural Sciences in Heilongjiang Province, Harbin, Heilongjiang 150000, China*

[†]*These authors have contributed equally to this work*

**Corresponding author*
e-mail: nxysxh@163.com; phone/fax: +86-135-0360-5775

(Received 27th Nov 2019; accepted 24th Mar 2020)

Abstract. In order to study the effect of mutagenesis on growth, physiology and cell structure in alfalfa (*Medicago sativa* L), the seeds of *Longmu806* were treated with two kinds of mutagenesis methods including ^{60}Co-γ irradiation (50, 150, 300, 450, 600 Gy) and EMS (ethyl methane sulfonate 0.1%, 0.2%, 0.4% (v/v)). The results showed that the seed germination rate, seedling growth, fresh grass yield and plant height were significantly ($P < 0.05$) higher than their corresponding controls under 50-150 Gy, and then decreased with the increasing of radiation dose. However, these indicators decreased with the increasing of EMS concentration. Two mutagenic treatments increased alfalfa branch number. The chlorophyll content was promoted by a dose of 50-150 Gy and 0.4% EMS concentration. It was also found that mutagenic treatments could promote the activity of three anti-oxidant enzymes including superoxide dismutase (SOD), peroxidase (POD) and hydrogen peroxidase (CAT), and the highest antioxidant enzyme activity was 150 Gy ^{60}Co-γ irradiation and 0.4% EMS treatment. The leaf thicknesses increased, the vein protuberant degrees decreased and the compactness of cell structure was enhanced. Being more conducive for screening mutants, ^{60}Co-γ irradiation with 150 Gy and EMS with 0.4% were the ideal mutagenic treatments.
Keywords: *^{60}Co-γ irradiation, ethyl methane sulfonate, seedling growth, antioxidant enzyme activity, chlorophyll content*

Introduction

Alfalfa (*Medicago sativa* L.) is very important legume forage crop, which has been planted all over the world. However, in alpine areas such as northeast China, short frost-free period, narrow genetic basis, low harvest index and widespread biotic and abiotic stresses constrains alfalfa production, and feed supplies are often insufficient in some years, which seriously restricts the production productivity of livestock (Shen et al., 2016; Nan et al., 2011). Modern biotechnological approaches, including mutagenic technology, are gaining interest to augment the efforts of alfalfa genetic improvement (Jain, 2011).

The mutagen is very efficient for creating genetic variability in the natural gene pool of crops (Kumari et al., 2016; Kumar et al., 2010). It provides raw materials for the genetic improvement of any crop (Adamu et al., 2004). Artificial mutagenesis can be used to induce mutations in crop plants and subsequent improvement be done through

http://www.aloki.hu ● ISSN 1589 1623 (Print) ● ISSN 1785 0037 (Online)
DOI: http://dx.doi.org/10.15666/aeer/1802_34973510

selection. They made a significant contribution to agricultural development. Some scholars have screened a number of new varieties through mutagenic research on alfalfa. For example, Zhang et al. (2007) have selected a new alfalfa variety *Nongjing 1* from *Longmu 803* mutant through magnetic field free space; and selected alfalfa varieties *Nongjing 8 and Nongjing 10* from *Zhaodong* alfalfa *and Longmu 803* mutant by satellite.

Some reports provide evidence of a stimulating effect on growth and physiological characteristics when seeds or seedlings are treated at different mutation (Zhang et al., 2017). The growth and physiological responses of alfalfa to mutagens were elucidated (Dhawi and Al-Khayri, 2011). Mutagenesis inflicted modifications in seedling growth (Li et al., 2013); chlorophyll (Dhawi and Al-Khayri, 2008); SOD, POD, CAT and MDA (Dhawi and Al-Khayri, 2008); and water content as well as growth expressed in fresh weight (Dhawi and Khayri, 2009). Wu et al. (2015) discovered that the EMS mutagenesis treatment can inhibit the germination and growth of alfalfa seeds. In higher plants, the structure of the cell changes under different degrees of environmental and mutagenic stresses and is closely related to the degree of stresses implied and the inherent stress resistance capacity of the plant. Zhang et al. (2010) reported that after the space mutagenesis, the leaf thicknesses of alfalfa increased and the palisade tissues were significantly thickened. The mutants provide materials to be selected for breeding. The above studies have shown that mutagenesis can change the physiological and growth characteristics of alfalfa, and has practical production significance for alfalfa breeding research.

In this study, we selected ^{60}Co-γ radiation and EMS two types of mutagenesis treatments, because they had higher mutagenic efficiency, their mutant materials were more abundant, and can lead to be helpful to improve cold resistance of alfalfa. The two mutagenesis methods operations were simple and low in cost. The study aim to comprehensive understand the effects of physical mutagenesis and chemical mutagenesis on alfalfa growth, physiological characteristics and cell structure, and provide a theoretical basis for the selection of resistant mutant in the alpine region and the selection of new forage varieties.

Materials and methods

Climatic condition

An experimental field was established in the Jiamusi City, which was located in the east part of the Heilongjiang Province, P. R. of China, 2017. The longitude is 129°30′ – 135°5′E, and its latitude 45°56′ – 48°27′N. This region has a climate type of cold humid monsoon with annual average temperature of 3 ℃, annual average precipitation of 489.8 mm, annual sunshine of 2052.3 h, annual active accumulative temperature of 2500 ℃, and the annual average frost-free period is 128.9 d.

Growth condition

The row to row and plant to plant spacing were kept at 30 cm and 12 cm, respectively. The organic matter was 2.49% in the tested meadow black soil with available nitrogen 86.3 mg·kg^{-1}, available phosphorus 64.6 mg·kg^{-1}, available potassium 79.9 mg·kg^{-1}. Its total nitrogen, phosphorus, potassium was 0.14%, 0.15%, and 3.12%, respectively. Its soil pH was 6.5. The previous crop for this site was corn.

http://www.aloki.hu ● ISSN 1589 1623 (Print) ● ISSN 1785 0037 (Online)
DOI: http://dx.doi.org/10.15666/aeer/1802_34973510

Plant materials

The tested alfalfa (*Medicago sativa* L.) was local and widely cultivated variety *Longmu806* (Shen et al., 2015). It was supplied by the Jiamusi branch of the Heilongjiang Academy of Agricultural Sciences.

Experimental design

^{60}Co-ray irradiation

For ^{60}Co-γ irradiation treatment, the seeds taken from the aforementioned alfalfa were treated with 6 ^{60}Coγ-ray irradiation doses viz., 50 Gy, 150 Gy, 300 Gy, 450 Gy, 600 Gy (300 seeds per dose) from 60 cobalt source at the Institute of Atomic Energy Utilization of Chinese Academy of Agricultural Sciences. The dose of 0 was set as control. Each treatment lasted for 7 days.

Ethyl methyl sulfonate (EMS)

900 seeds taken from the aforementioned alfalfa were soaked with concentrated sulfuric acid for 5 min, and then rinsed with distilled water several times. The treated seeds were completely water-swelled by soaking in the phosphate buffer (100 mmol L^{-1}, pH 7.0) at 4 °C for 12 h. The seeds thus treated with phosphate buffer, were subjected to 0.1, 0.2 and 0.4% (v/v) EMS and incubated in the dark at room temperature for 15 h. During the procedure, the seeds were gently shaken. Finally, the seeds were rinsed with distilled water repeatedly for removing the residual EMS from the seed surface (Feng et al., 2018).

Germination percentage and seedling growth

After mutagenic treatments, the seeds along with its control seeds were germinated on moist filter paper at 28 ℃. After 2 weeks, the germinated seeds were counted and seedling growth was measured.

Germination percentage = Number of germinating seeds / Total number of seeds × 100

Sampling time

During alfalfa florescence (June 15th - June 25th), ten plantings were selected at random to record observations on planting height, the branches of each plant, the average yield of single plant and the stem-leaf ratio (Shen et al., 2018). The alfalfa functional leaves were taken and mixed from each treatment to measure physiological indexes.

Experimental method

Chlorophyll analysis

The plants leaves washed with distilled water, then weighed it about 0.2 g. Chlorophyll content in the leaves of treated and control plants were extracted in 80% acetone and 95% ethanol 20 ml, after 24 h dark extracted in 50 ℃ water bath, then determined the absorbance of the solution at 645 and 663 nm. Chlorophyll content was expressed by following equations (Ahmadreza et al., 2009):

$$Ca = (12.71A_{663} - 2.59A_{645}) \times (V / M) \times 1000 \quad \text{(Eq.1)}$$

http://www.aloki.hu ● ISSN 1589 1623 (Print) ● ISSN 1785 0037 (Online)
DOI: http://dx.doi.org/10.15666/aeer/1802_34973510

$$Cb = (22.88A_{645} - 4.67A_{663}) \times (V / M) \times 1000 \quad \text{(Eq.2)}$$

$$Ct = (8.04\ A_{663} + 20.29A_{645}) \times (V / M) \times 1000 \quad \text{(Eq.3)}$$

Ca, Cb, Ct were chlorophyll-a, chlorophyll-b, and total chlorophyll, V were solvent amount, M were leaf weight, A_{645}, A_{663} were the absorbance value at 645 nm and 663 nm.

Enzyme activities analysis

The SOD was determined with the nitroblue tetrazolium (NBT) method (Dai et al., 2011), while the POD determined with the guaiacol method (Shen et al., 2018); and the CAT determined with the ultraviolet absorption method. The content of malondialdehyde (MDA) was measured with the glucosinolate and pentobarbital acid colorimetric method (Nahla et al., 2015). The instrument used in the test was a 721 UV-visible spectrophotometer (model: U-T6, Made in China).

Microstructure

The functional leaves of the M0 generation plants were selected and cut along the middle veins in an inverted trapezoidal shape having a size of 5 × 5 mm. The samples were fixed with FAA (formalin-acetic acid-alcohol) solution and underwent conventional paraffin sections with a thickness of 5 μm and then stained with Safranin'O/Fast Green. The slides were observed under a Nikon-DIAPHOT (Model: Diaphot TMD, Made in Japan) microscope. The mean of the 4 values of leaf thickness, vein thickness, palisade thickness and spongy thickness of the tested alfalfa was determined by Motic Image 2000 1.3. Cell tense ratio, Spongy ratio, Vein protuberant degree were calculated as follows:

$$\text{Cell tense ratio (CTR \%)} = \text{Palisade tissue thickness / Leaf thickness} \times 100 \quad \text{(Eq.4)}$$

$$\text{Spongy ratio (SR \%)} = \text{Spongy tissue thickness / Leaf thickness} \times 100 \quad \text{(Eq.5)}$$

$$\text{Vein protuberant degree (VPD)} = \text{Vein thickness / Leaf thickness} \times 100 \quad \text{(Eq.6)}$$

Statistical analysis

The data were analyzed by using the Statistical Analysis System (SAS Inc. CARY, NC) and EXCEL software were used for the statistical analysis of data.

Results

Alfalfa seed germination after mutagenesis

The alfalfa seed germination rate is shown in *Figure 1a, b*. The results showed that the germination ability of the treated seeds was significantly increased by ^{60}Co-γ radiation from 50 Gy (85%) to 150 Gy (91.08%) as compared to the control (82.33%), and then the seed germination percentage decreased gradually from 73.67% (300 Gy) to 50.43% (600 Gy). However, for the chemical mutagen treatment, the significant reduction in seed germination percentage (72.67%) began at 0.1% of EMS and continued to decline to up to 44.57% at 0.4% (*Fig. 1b*). The results suggested that ^{60}Co-

http://www.aloki.hu ● ISSN 1589 1623 (Print) ● ISSN 1785 0037 (Online)
DOI: http://dx.doi.org/10.15666/aeer/1802_34973510

γ radiation could stimulate the alfalfa seed germination percentage at lower dose (50-50 Gy), but higher doses (300-600Gy), inhibit the germination rate. However, EMS mutagenesis could always inhibit seed germination. It can be seen that the inhibition rate of seed germination by EMS treatment was significantly ($P < 0.05$) higher than low-dose (50-150 Gy) ^{60}Co-γ radiation treatment (*Fig. 1*).

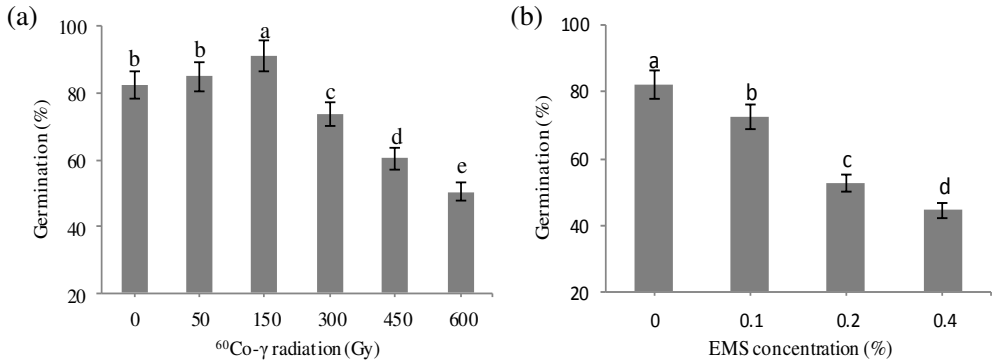

Figure 1. *Effects of different mutagenic treatments on germination rate of alfalfa seeds (a, b). Different small letters are significantly different ($p < 0.05$) in statistics. Each column represents the average of triplicate treatments, error bars represent the standard deviations of three replicates. (a) ^{60}Co-γ irradiation treatment and (b) ethyl methyl sulfonate treatment (EMS)*

Alfalfa seedling growth after mutagenesis

The measured root length of alfalfa is shown in *Table 1*. The root growth increased significantly from 50 Gy to 150 Gy of ^{60}Co-γ irradiation. The maximum root length was 4.50 cm at 150 Gy, after that the root length decreased gradually with increase in doses of the mutagen. The minimum root length was 1.88 cm at 600 Gy, which was significantly lower than their corresponding controls ($P < 0.05$). EMS mutagenesis inhibited root growth. The root length was significantly inhibited with increasing concentration ($P < 0.05$). Maximum root length was observed in 0.1% concentration (2.56 cm), and minimum root length was 1.38 cm in 0.4% concentration.

Table 1. *Effect of different mutagenic treatment on root length of alfalfa*

Treatments	Dose	Root length (cm)	Shoot length (cm)
CK	0 Gy	3.78 ± 0.3bc	3.19 ± 0.41b
^{60}Co-γ	50 Gy	3.86 ± 0.47bc	3.29 ± 0.29ab
	150 Gy	4.50 ± 0.38a	3.79 ± 0.11a
	300 Gy	3.21 ± 0.48c	3.00 ± 0.45b
	450 Gy	2.38 ± 0.46d	2.52 ± 0.42c
	600 Gy	1.88 ± 0.24e	2.06 ± 0.34d
EMS	0.10%	2.56 ± 0.26d	2.82 ± 0.36bc
	0.20%	2.01 ± 0.44d	2.51 ± 0.22c
	0.40%	1.38 ± 0.63e	2.06 ± 0.15d

Data in the table is the mean ± SE. Average is the value of different agronomic traits in the different treatments. Different small letters in same column are statistically different at $p < 0.05$ and same small letters in same column are not statistically different at $p < 0.05$. ^{60}CO-γ: ^{60}Co-γ irradiation treatment and EMS: ethyl methyl sulfonate treatment

http://www.aloki.hu ● ISSN 1589 1623 (Print) ● ISSN 1785 0037 (Online)
DOI: http://dx.doi.org/10.15666/aeer/1802_34973510

The variation trend of shoot length was consistent with that of root length. Maximum shoot length was observed in 150 Gy dose (3.79 cm) of ^{60}Co-γ radiation and 0.1% EMS concentration (2.82 cm) while the higher doses/concentrations retarded shoot length. In addition, it was found that the growth inhibition effect of EMS mutagenesis on seedlings was significantly ($P < 0.05$) greater than that of low-dose (50-300 Gy) ^{60}Co-γ radiation. The increase in mutagenic doses/concentration lead to decrease in seedling vigor because of increase in physiological damage induced in the seeds and seedlings and variations in stimulation due to cell division rates as well as an activation of growth hormones such as auxin.

Alfalfa agronomic traits after mutagenesis

Variable degree of agronomic traits response was observed in different dose/concentrations (*Table 2*). The variation range of agronomic characters increased with the increase of mutagenic dose/concentrations. The fresh grass yield increased from 5.24 to 13.85% when the ^{60}Co-γ treatment dose increased from 50 Gy to 150 Gy, and then it decreased with increasing dose. The fresh grass yield reduction ranged from 4.51% in 300 Gy to 21.23% in 600 Gy dose compare to control. While for EMS treatment, its reduction ranged from 3.24% in 0.1% EMS to 32.69% in 0.4% EMS. The change trend of plant height was consistent with that of fresh grass yield. The highest plant height was 139.70 cm in 150 Gy, and the lowest plant height was 59.30 cm in 0.4% EMS. In summary, compared with the control, the effects of ^{60}Co-γ radiation treatment on grass yield and plant height increased first and then decreased, while EMS treatment showed a significant inhibitory effect ($P < 0.05$).

Table 2. *Effect of mutagenic treatments on agronomic traits*

Treatments	Dose	Yield/plant (g)		Height (cm)		Branch/per plant		Stem-leaf ratio (%)	
		Amplitude	Mean	Amplitude	Mean	Amplitude	Mean	Amplitude	Mean
CK	0	168.65-198.52	185.63b	114.12-125.25	124.30b	17-20	14.19c	2.08-2.70	2.67a
^{60}Co-γ	50Gy	54.21-219.22	195.36b	126.55-141.62	133.70a	16-25	15.22bc	1.44-2.05	2.79a
	150Gy	77.87-264.44	211.34a	110.25-152.55	139.70a	18-28	17.17b	2.59-3.23	2.13b
	300Gy	69.14-197.25	177.25c	102.46-141.04	117.7c	15-28	17.80b	1.38-2.13	1.97b
	450Gy	46.14-297.34	164.23d	82.25-103.56	98.30d	14-25	19.56ab	1.45-2.26	1.55c
	600Gy	54.54-284.27	146.22e	86.51-105.65	94.70d	19-25	20.40a	1.28-2.49	1.47c
EMS	0.10%	79.14-198.57	179.62bc	92.45-132.22	104.13cd	15-22	17.73b	2.01-2.58	2.03ab
	0.20%	61.38-176.43	147.96e	56.34-90.21	86.70e	15-28	19.85ab	1.95-2.47	2.32a
	0.40%	44.51-160.37	124.95f	44.29-75.36	59.30f	17-27	21.94a	1.21-2.07	1.83b

Data in the table is the mean ± SE. Average is the value of different physiological indexes in the different treatments. Different small letters in same column are statistically different at $p < 0.05$ and same small letters in same rows are not statistically different at $p < 0.05$. CK: control treatment ^{60}Co-γ: ^{60}Co-γ irradiation treatment and EMS: ethyl methyl sulfonate treatment

Both mutagenesis treatments promoted alfalfa branching. The branch number of alfalfa enhanced with the increase in dose/concentration both in physical and chemical mutagens. It reaches the maximum value at 600 Gy, nearly 43.76% more than the control. Similarly, the branch number was improved from 24.95% in 0.1% EMS to 54.61% in 0.4% EMS. Overall, EMS treatments are more conducive to increasing the number of alfalfa branches, but it is not significantly different from ^{60}Co-γ radiation treatment. The stem-leaf ratio was also different with the different mutagenesis. The difference of stem-leaf ratio were not significantly affected between low dose (50 Gy-

http://www.aloki.hu ● ISSN 1589 1623 (Print) ● ISSN 1785 0037 (Online)
DOI: http://dx.doi.org/10.15666/aeer/1802_34973510

150 Gy) and low concentration (0.1%-0.2%), but there were significant reduction ($P < 0.05$) with the increase of dose and concentration. The decrease of the stem-leaf ratio indicates that alfalfa leaf increased and the nutrient content of alfalfa was improved.

Influence of mutagen on the chlorophyll content

The chlorophyll content and the ratio of chlorophyll a/b can reflect the adaptability of plant varieties, and also an important indicator for the utilization of environmental factors. The chlorophyll content obtained according to *Equations 1-3* is shown in *Table 3*. The chlorophyll a content of alfalfa leaves under the treatments with 150 Gy ^{60}Co-γ radiation and 0.4% EMS treatment were significantly higher than their corresponding controls ($p < 0.05$). The changes trend of chlorophyll b content was consistent with chlorophyll a content under different mutagenesis treatments. The change of total chlorophyll of alfalfa was increasing at first and then decreasing under the ^{60}Co-γ radiation, and it increased with the increase of EMS treatment concentration. Under low dose (50-150 Gy) ^{60}Co-γ radiation treatment and 0.4% EMS treatment, the total chlorophyll content was significantly ($p < 0.05$) higher than other treatments. The maximum was observed in 150Gy (4.36 mg•g^{-1}) and 0.4% EMS concentration (4.27 mg•g^{-1}). Except for 0.4% EMS treatment, the proportion of chlorophyll a/b in alfalfa leaves was basically lower than the control.

Table 3. *Effect of mutagenic treatments on chlorophyll content*

Treatments	Dose	Chl. content (mg•g^{-1})			
		Chl.a	Chl.b	Total Chl.	Chl. a/b
CK	0	2.94 ± 0.10b	0.94 ± 0.03a	3.88 ± 0.09b	3.13 ± 0.08a
^{60}Co-γ	50Gy	3.06 ± 0.19ab	1.07 ± 0.08a	4.13 ± 0.19a	2.86 ± 0.11b
	150Gy	3.21 ± 0.51a	1.15 ± 0.43a	4.36 ± 0.15a	2.79 ± 0.31b
	300Gy	2.90 ± 0.23b	0.95 ± 0.07a	3.85 ± 0.17b	3.05 ± 0.12a
	450Gy	2.93 ± 0.01b	0.95 ± 0.12a	3.89 ± 0.31b	3.07 ± 0.22a
	600Gy	2.81 ± 0.14b	0.91 ± 0.27a	3.72 ± 0.51b	3.09 ± 0.07a
EMS	0.10%	2.87 ± 0.28b	0.92 ± 0.03a	3.79 ± 0.06b	3.12 ± 0.07a
	0.20%	2.89 ± 0.11b	0.93 ± 0.14a	3.82 ± 0.38b	3. 11 ± 0.24a
	0.40%	3.26 ± 0.03a	1.01 ± 0.14a	4.27 ± 0.33a	3.23 ± 0.23a

Data in the table is the mean ± SE. Average is the value of different physiological indexes in the different treatments. Different small letters in same column are statistically different at $p < 0.05$ and same small letters in same rows are not statistically different at $p < 0.05$. CK: control treatment ^{60}Co-γ: ^{60}Co-γ irradiation treatment and EMS: ethyl methyl sulfonate treatment. Chl. content: chlorophyll content, Chl. a: chlorophyll a content, Chl. b: chlorophyll b content, Total Chl.: total chlorophyll content, Chl. a/b: the ratio of chlorophyll a to chlorophyll b

Influence of mutagen on the enzyme activity

The activity of SOD, POD, CAT and MDA content of alfalfa after treatments are shown in *Table 4*. The ^{60}Co-γ radiation treatment promoted the accumulation of SOD in alfalfa. The SOD activity was significantly increased ($P < 0.05$) in low dose, and after that it was decreased with the increase of dosage. However, the SOD activity increased with increasing of EMS treatment concentration, but was lower than that of control. The

http://www.aloki.hu ● ISSN 1589 1623 (Print) ● ISSN 1785 0037 (Online)
DOI: http://dx.doi.org/10.15666/aeer/1802_34973510

changes of POD activity and CAT activity were consistent in the two mutagenesis treatments and higher than their corresponding controls ($p < 0.05$). The POD and CAT activity increased when treated by 50-150 Gy, and decreased when treated by 300-600 Gy. The activity of the two enzymes decreased with the increase of EMS concentration. Furthermore, from the change of enzyme activity analysis it was shown that the promoted strength of activity was as follows: POD > CAT > SOD. The activity of three antioxidant enzymes in low-dose (50-150 Gy) ^{60}Co-γ radiation treatment were higher than in low-dose (0.1-0.2%) EMS treatment, and the enzyme activity at 150 Gy dose was significantly higher than all other treatments ($p < 0.05$). The activity of the three enzymes showed the tendency of increasing firstly and then decreasing, this is possibly because of that the higher dose of mutagen shifted from stimulation to inhibition or disturbances for the enzyme activity.

Compared with the control, the MDA content increased first and then decreased under the two mutagenesis treatments. In all the treatments, the MDA content under 0.1% EMS treatment was significantly higher than other treatments ($p < 0.05$).

Table 4. *Effect of different doses mutagenic treatments on physiological indexes*

Treatments	Dose	SOD (U•g^{-1})	POD (U•gFW•min^{-1})	CAT (U•gFW•min^{-1})	MDA (μmol•g^{-1})
CK	0 Gy	230.29±33.85b	2443.78±305.23d	250.00±75.85f	35.64±3.20c
^{60}CO-γ	50 Gy	242.63±22.47b	4218.44±746.86b	474.40±139.46b	37.89±1.52b
	150 Gy	271.37±9.12a	6753.78±421.58a	541.86±43.35a	37.77±8.33b
	300 Gy	233.42±7.81b	4087.56±708.19c	404.00±92.8c	36.51±13.83c
	450 Gy	219.70±16.53c	3930.22±2353.59c	417.49±89.24c	35.84±24.88c
	600 Gy	155.10±2.04d	3904.67±298.09c	300.93±38.95e	35.26±4.92cd
EMS	0.10%	209.52±19.46c	4004.67±28.09c	436.27±24.37bc	39.77±8.33a
	0.20%	214.70±16.53c	4130.22±23.59bc	331.20±39.83de	34.57±12.52d
	0.40%	221.46±14.50bc	6416.32±19.33a	441.73±43.03bc	36.95±0.46bc

Data in the table is the mean ± SE. Average is the value of different physiological indexes in the different treatments. Different small letters in same column are statistically different at $p < 0.05$ and same small letters in same rows are not statistically different at $p < 0.05$. CK: control treatment, ^{60}Co-γ: ^{60}Co-γ irradiation treatment, EMS: ethyl methyl sulfonate treatment. SOD: the abbreviation of superoxide dismutase, POD: the abbreviation of peroxidase, CAT: the abbreviation of hydrogen peroxidase, MDA: the abbreviation of malondialdehyde

Microstructure of leaves

In the experiment, different mutagenic treatments showed different effects on the microstructure of the alfalfa leaves from the M0 generation. The mutagenic direction and degrees varied with the mutagenic methods and doses (Loutou et al., 2016; Zhu et al., 2015). In this study (*Table 5*), the leaf thickness of Longmu806 alfalfa was significantly higher than its corresponding controls ($p < 0.05$). The leaf thickness under 0.1% EMS treatment was significantly ($p < 0.05$) higher than the control and ^{60}Co-γ radiation treatment. The vein protuberant degree (VPD) was calculated according to *Equation 6,* and the VPD of all the treatments were significantly less than their corresponding controls ($p < 0.05$) (*Table 5; Fig. 2*).

The leaf thickness of plants primarily depends upon the thickness of the palisade tissue and the spongy tissue. In this experiment, the thicknesses of the palisade tissues

http://www.aloki.hu ● ISSN 1589 1623 (Print) ● ISSN 1785 0037 (Online)
DOI: http://dx.doi.org/10.15666/aeer/1802_34973510

and the spongy tissues for all the treatments were higher than their corresponding controls. This proves that a thicker palisade tissue and spongy tissue could be the result of mutation treatment. In this study, the changes occurred in the compactness and looseness of cell structure of the alfalfa was different. The cell tense ratio (CTR) was calculated according to *Equation 4,* and the compactness of cell structure for the lower dose/concentration treatments was lower than control, but it was significantly ($p < 0.05$) higher than control under 600 Gy ^{60}Co-γ and 0.4% EMS treatment. However, the spongy ratio (SR) was calculated according to *Equation5,* the looseness of cell structure increased compared to control in all treatments.

Table 5. *Comparison of main structural features (mean ± SE) of alfalfa under different mutagenic treatments (μm)*

Treatments		Leaf thickness	Vein thickness	Palisade thickness	Spongy thickness	VPD (%)	CTR (%)	SR (%)
CK		298.93±7.61d	877.34±6.57a	129.00±3.25d	95.98±1.99e	294.34±5.54a	43.48±0.63c	31.37±0.27c
^{60}CO-γ	50	347.70±6.45c	776.94±8.61c	145.43±2.25c	119.52±3.72cd	223.41±2.84b	41.86±0.35c	34.84±0.26b
(Gy)	150	376.70±6.49b	786.94±8.01c	149.32±2.78bc	124.06±3.46c	209.67±2.44d	39.52±0.38c	32.51±0.64bc
	600	332.19±7.60c	690.55±2.76d	167.57±2.34b	181.34±3.53a	207.19±3.35d	50.71±0.45b	39.37±0.48a
EMS	0.1	432.42±8.65a	832.61±0.58b	170.95±3.98b	152.19±3.74b	192.25±9.63d	39.89±0.54c	35.52±0.35b
(%)	0.4	306.11±9.31d	659.65±4.53e	186.65±1.01 a	117.73±0.81d	215.03±2.74cd	60.14±0.25a	38.15±0.61ab

Data in the table is the mean ± SE. Average is the value of different physiological indexes in the different treatments. Different small letters in same column are statistically different at $p < 0.05$ and same small letters in same rows are not statistically different at $p < 0.05$. CK: control treatment, ^{60}Co-γ: ^{60}Co-γ irradiation treatment, EMS: ethyl methyl sulfonate treatment. VPD: vein protuberant degree, CTR: cell tense ratio, SR: spongy ratio

Discussion

Mutation induction through the use of different kinds of mutagens has proved vital in inducing variability that could be exploited in the improvements of alfalfa growth and types. It is therefore the origin of genetic variability as suggested by Tamarin (1999). The changed mean germination percent due to various EMS concentrations and ^{60}Co-γ radiation doses revealed the effects of the mutagen in the germination process. In this study, the germination of seeds decreased with increase in dose/concentration both in physical and chemical mutagens except 50 -150 Gy. This result is consistent with the findings of Dhakshanamoorthy et al. (2010) who reported the germination of Barbados nut decreased with the increase dose of irradiation mutagen. This reduction/stimulation in seed germination might have been due to the effect of mutagens on meristematic tissues of the seed, or may be either due to the inhibition or promotion in physiological and biological process necessary for seed germination (Wu et al., 2013).

The reduction in lengths of root and shoot due to mutagenic treatments has been observed in alfalfa (Shen et al., 2018). In the present study, the root and shoot length decreased with increased doses of radiation except 50 Gy, which is in agreement with the findings of Ge et al. (2011) who reported the seedling germination rate and seedling growth of *Chrysanthemu morifolium* Ramat. decreased obviously when treated with high dose of ^{60}Co-γ radiation. Li et al. (2013) demonstrated that the seedling emergence rate and seedling height of watermelon (*Citrullus lanatus* (Thunb.) Matsum. et Nakai) decreased significantly as the radiation dose increased. However, in this experiment, both root length and stem length of alfalfa seedlings were inhibited by EMS. Huo et al.

http://www.aloki.hu ● ISSN 1589 1623 (Print) ● ISSN 1785 0037 (Online)
DOI: http://dx.doi.org/10.15666/aeer/1802_34973510

(2014) using EMS treated the seeds of *Vicia sativa L.*, the result showed that the seedling growth were inhibited, and the inhibition enhanced with longer processing time. The increase in mutagenic doses lead to decrease in seedling vigor because of increase in physiological damage induced in the seeds and seedlings (Anbarasan et al., 2013) and variations in stimulation due to cell division rates as well as an activation of growth hormones such as auxin (Zaka et al., 2004). The reduced seedling growth in mutagenically treated seeds might be due to injury caused at cellular level because of gene controlled biochemical processes or acute chromosomal aberrations or both (Satpute et al., 2012).

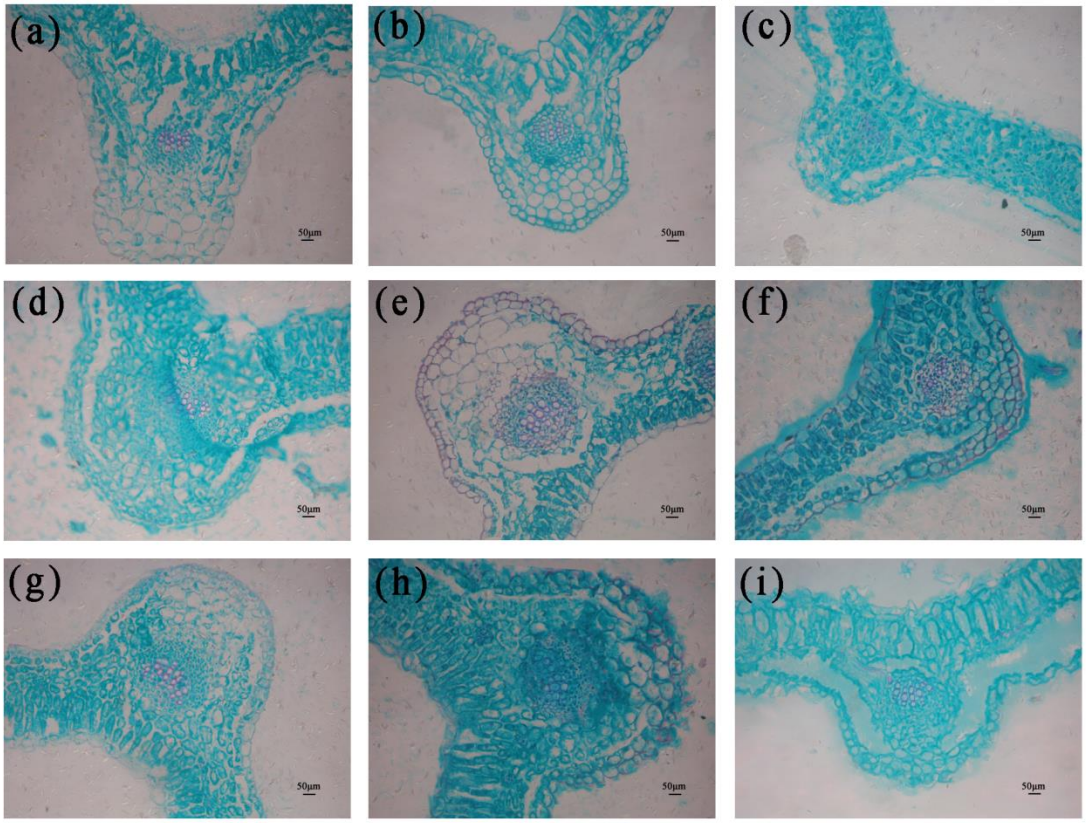

Figure 2. *Microstructure changes of leaf veins. a: control treatment, b: 0.1% ethyl methyl sulfonate treatment, c: 0.2% ethyl methyl sulfonate treatment, d: 0.4% ethyl methyl sulfonate treatment, e: 50 Gy ^{60}Co-γ irradiation treatment, f: 150 Gy ^{60}Co-γ irradiation treatment, g: 300 Gy ^{60}Co-γ irradiation treatment, h: 450 Gy ^{60}Co-γ irradiation treatment, i: 600 Gy ^{60}Co-γ irradiation treatment*

In this study, the change of fresh yield had the same trend with the plant height, which was firstly ascending and then descending following the dose increasing (*Table 2*). This might be due to the alteration of its genome integrated by environmental signals as reported by Wang et al. (2010). For the reason of the number of branch increased after mutagenesis, it might be caused by increasing the rates of cellular division and expansion at their meristematic regions. This is also in agreement with the findings of Yang et al. (2012) who reported that the increase of branch number of alfalfa was due to radiation mutagenesis. But it was in contrast with the findings of

http://www.aloki.hu ● ISSN 1589 1623 (Print) ● ISSN 1785 0037 (Online)
DOI: http://dx.doi.org/10.15666/aeer/1802_34973510

Maluszynski et al. (2001) who independently reported that the decrease of branch number was due to induced mutation in rice and other cereals. For the reason of that the stem-leaf ratio increased in lower dose (50 Gy) (*Table 2*), the explanation might be due to a greater increase in the yield of fresh forage. Following the dose increasing and the different concentrations of EMS, the stem-leaf ratio decreased, this means that the leaf area or leaf number was increasing, as leaf is a major nutrition tank and hence it would be helpful to improve the quality of alfalfa. This result was consistent with the reports of Yang et al. (2015) who reported that mutagen could decrease the stem-leaf ratio, and improve leaf number and increase leaf area.

In the present study, 150 Gy dose of ^{60}Co-γ radiation and 0.4% EMS all increased the content of chlorophyll in alfalfa. This is also in agreement with the findings of Yang et al. (2017) who reported increased in chlorophyll content of tomato and pepper due to radiation mutagenesis. Since the content of chlorophyll has a direct impact on the strength of photosynthesis, this also shows that mutagenesis could promote the photosynthesis of crops.

The active oxygen radical in plant cells is in a state of dynamic equilibrium under normal conditions. When plants are stimulated by mutagen, plants are equipped with antioxidant systems composed of low-molecular weight antioxidants and enzymes that protect the cell from the damaging effects (Ma et al., 2011). In the present study, the SOD activity increased in the range of 50-300 Gy, and then decreased as the dose gradually increased (*Table 4*). The later occurred decrease might be related to that the irradiated alfalfa suffered excessive mutagen stress. Both POD and CAT were found significantly increased in the leaf of alfalfa under ^{60}Co-γ radiation and EMS treatments, their activities also showed the trend of decreasing as the doses/concentrations increasing. The change of the antioxidant enzyme activity indicated that plants suffered oxidative stress induced by the over-production of the ROS, which was consistent with the results of Uruc and Demirezen (2012). The MDA is one of the membrane fat peroxidation products, its content can reflect the cell membrane fat peroxidation degree and the cell suffering injury degree (Pan et al., 2002). Under mutagen stress, the accumulation of reactive oxygen free radicals beyond a certain limit in alfalfa body will cause the membrane fat peroxidation, and its product MDA will accumulate (Gao et al., 2003) massively. In this study, the content of MDA was increased compared to their corresponding controls under the different mutagens stress, but the difference was not significant ($p < 0.05$). It indicates that the antioxidant enzyme system has certain protective effect on alfalfa under mutagenesis.

The structural characteristics of cells, including the thicknesses of the palisade tissue and the spongy tissue and the compactness and the looseness of the leaf tissue structures all contribute to the resistance mechanism of plants. According to Pavel et al. (2016) more compact the cell structure, the stronger the cold resistance of the species. Feng et al. (2008) demonstrated that after completing a space flight, leaves of alfalfa sowed increased thickness with high relative water content. In the same experiment, the thickness and compactness of spongy tissue was also increased. Zhang et al. (2015) showed that with respect to the microstructure of the alfalfa leaves, the spongy tissue and the palisade tissue reacted differently to the space mutagenesis, which had a bigger effect on the spongy tissue than on the palisade tissue. In this study, after mutagenesis, the thickness of the leaves increased, and the protrusion degree of the veins decreased. The thicknesses of the palisade tissues and the spongy tissues for all the treatments were significantly higher than their corresponding controls ($p < 0.05$), which was consistent

http://www.aloki.hu ● ISSN 1589 1623 (Print) ● ISSN 1785 0037 (Online)
DOI: http://dx.doi.org/10.15666/aeer/1802_34973510

with the conclusion of Dhakshanamoorthy et al. (2010). Compared to the control, the cell compactness structure of cells and looseness did not change obviously in the low dose/concentration of all mutagenesis treatments, but which were increased with the increase of dose/concentration. There are beneficial in increasing the adversity resistance and cold resistance capacity of alfalfa.

Conclusion

Artificial mutation by using of ^{60}Co-γ radiation and EMS proves vital in the improvement of genetic variability in alfalfa. Both mutagenesis treatments can enhance the physiological activity of alfalfa. Furthermore, ^{60}Co-γ-ray treatment can promote the growth of plant height and increase the yield. EMS treatment can inhibit the plant height and promote the branching of alfalfa. In this study the 150 Gy dose of ^{60}Co-γ radiation and 0.4% EMS are better mutagenic treatment for screening mutants. It shows that in the future research, the mutagenesis treatment method can be selected according to the actual production needs. This study analyzes the growth and physiological changes of alfalfa. In the future, it is necessary to further study the molecular mechanism of its mutation to provide a theoretical basis for the screening and breeding of new mutants.

Acknowledgments. This research was supported by the Heilongjiang province postdoctoral special funding (LBH-TZ06020). The authors are grateful to the Institute of Atomic Energy Utilization of Chinese Academy of Agricultural Sciences for providing technical support for this study.

REFERENCES

[1] Adamu, A. K., Chung, S. S., Abubakar, S. (2004): The effect of ionizing radiation (Gamma rays) on tomato (s.n.). – Nigerian Journal of Experimental Biology 5(2): 185-193.

[2] Ahmadreza, M., Alireza, N., Abdolrassoul, S. M., Hossein, M., Homan, L., Mohsen, K. (2009): Vegetation mapping of the Mond Protected Area of Bushehr Province (South-West Iran). – Journal of Integrative Plant Biology 3: 217-223.

[3] Anbarasan, K., Sivalingam, D., Rajendran, R., Anbazhagan, M., Chidambaram, A. A. (2013): Studies on the mutagenic effect of EMS on seed germination and seedling characters of sesame (Sesamum indicum L.) Var.TMV3. – International Journal of Research in Biological Sciences 3(1): 68-70.

[4] Dai, H. P., Zhang, P. P., Lu, C., Jia, G. L., Song, H., Ren, X. M., Chen, J. (2011): Leaf senescence and reactive oxygen cultivars metabolism of broomcorn millet (Panicum miliaceum L.) under drought condition. – Aust. J. Crop Sci. 5: 1655-1660.

[5] Dhakshanamoorthy, D., Selvaraj, R., Chidambaram, A. (2010): Physical and chemical mutagenesis in Jatropha curcas L. to induce variability in seed germination, growth and yield traits. – Rom. J. Biol. Plant Biol. 55: 113-125.

[6] Dhawi, F., Al-Khayri, J. M. (2008): Magnetic fields induce changes in photosynthetic pigments content in date palm (Phoenix dactylifera L.) seedlings. – Open Agr. J. 2: 121-125.

[7] Dhawi, F., Al-Khayri, J. M. (2009): Magnetic field increase weight and water content in date palm (Phoenix dactylifera L.). – J. Agr. Sci. Tech. 2: 23-29.

[8] Feng, P. (2008): Effects of Alfalfa Seed Moisture Content on Mutagenic of Satellite Carrying. – Gansu Agricultural University, LanZhou.

http://www.aloki.hu ● ISSN 1589 1623 (Print) ● ISSN 1785 0037 (Online)
DOI: http://dx.doi.org/10.15666/aeer/1802_34973510

[9] Feng, P., Shen, X. H., Li, R. L., Zheng, H. Y. (2018): Effect of different mutagenesis on microstructure and ultrastructure of alfalfa. – Pak. J. Bot. 50(4): 1387-1393.
[10] Gao, S. M., Chen, P. J., Guo, H. H. (2003): Study on cold acclimation and freezing-tolerance mechanism of Aucuba japonica cv. Variegata. – Acta BOT Boreal-Occidenta Sin 23(12): 2113-2119.
[11] Ge, W. Y., Chang, G. Z., Chen, L., Zhao, Y., Wang, T. T., Ge, H (2011): Effects of ^{60}Co γ-rays irradiation on seed growth of ground-cover chrysanthemum. – Journal of Nuclear Agricultural Sciences 25(1): 0067-0070.
[12] Huo, Y. X., Wang, N., Zhang, J. Y., Zhang, Y., Kong, L. F. (2014): Effects of three mutagens on seed germination of Vicia sativa. – Pratacultural Science 31(3): 438-445.
[13] Kumar, G., Yadav, R. S. (2010): EMS induced genomic disorders in sesame (Sesamum indicum L.). – Romanian Journal of Biology 55(2): 97-104.
[14] Kumari, V., Chaudhary, H. K., Prasad, R., Kumar, A., Singh, A., Jambhulkar, S. (2016): Effect of mutagenesis on germination, growth and fertility in sesame (Sesamum indicum L.). – Annual Research & Review in Biology 10(6): 1-9.
[15] Jain, S. M. (2011): Radiation-Induced Mutations for Date Palm Improvement. – In: Jain S., Al-Khayri J., Johnson D. (eds.) Date Palm Biotechnology. Springer, Dordrecht, pp. 271-286.
[16] Li, Y. M., Yang, S. M., Ji, H. B., Fang, C. Y., Pan, C. Y., Chen, N. L. (2013): Effects of ^{60}Co-γ irradiation intensity on watermelon seed germination and seedling growth. – Acta Agriculturae Boreali-occidentalis Sinica 22(3): 115-120.
[17] Loutou, M., Hajjaji, M., Mansori, M., Favotto, C., Hakkou, R. (2016): Heated blends of phosphate waste: microstructure characterization, effects of processing factors and use as a phosphorus source for alfalfa growth. – Environm. Manag. 4: 337-345.
[18] Ma, X. M., Zhang, Z. A., Deng, B., Zhang, Y. W., Gao, H. W., Pang, Y. Y., Yang, S. C., Liu, M. (2011): Study on protective enzyme activities of alfalfa leaves from satellite carrying seeds with different moisture contents. – Pratacultural Science 28(5): 783-787.
[19] Maluszynski, M., Szarejko, I., Barriga, P., Balcerzyk, A. (2001): Heterosis in crop mutant crosses and production of high yielding lines, using doubled haploid systems. – Euphytica 120: 387-398.
[20] Nahla, H., Noha, E. E. (2015): gamma irradiation effect on growth, physiological and molecular aspects of mustard plant. – American Journal of Agricultural Science 2(4): 164-170.
[21] Nan, L. L., Shi, S. L., Chen, J. G., Zhu, X. Q., Guo, Q. (2011): Field evaluation of the response and resistance to low temperature of alfalfa root with different root types during over-wintering. – Chinese Journal of Eco-Agriculture 19(3): 619-625 (in Chinese).
[22] Pan, X. Y., Cao, Q. D., Wang, G. X. (2002): Evaluation of lipid peroxidation for use in selection of cold hardiness cultivars of almond. – Acta Ecologica Sinica 22(11): 1902-1911.
[23] Pavel, L., Paul, K., Alexander, Z., Markku, P., Sergey, G. (2016): Recrystallization-based formation of uniform fine-grained austenite structure before polymorphic transition in high-strength steels for Arctic applications. – Int. Mech. and Mater. Eng. 11(1): 55-59.
[24] Satpute, R. A., Fultambkar, R. V. (2012): Effect of mutagenesis on germination, survival and pollen sterility in M 1 generation of soybean [Glycine max (L.) Merrill]. – International Journal of Recent Trends in Science and Technology 2(3): 30-32.
[25] Shen, X. H., Jiang, C., Li, R. L., Li, J. D., Zheng, H. Y., Feng, P. (2016): The study on the cold resistance and physiology change of root in meadow fescue – alfalfa mixture and monoculture in winter. – Pratacultural Science 33(2): 268-275 (in Chinese).
[26] Shen, X. H., Jiang, C., Li, R. L., Feng, P., Zheng, H. Y. (2018): Effect of Magnetic Field -free Space on Growth Characteristics of Alfalfa. – Journal of Nuclear Agricultural Sciences 32(4): 0633-0638 (in Chinese).
[27] Tamarin, R. H. (1999): Principles of Genetics. – WCB/McGraw Hill, New York.

http://www.aloki.hu ● ISSN 1589 1623 (Print) ● ISSN 1785 0037 (Online)
DOI: http://dx.doi.org/10.15666/aeer/1802_34973510

[28] Uruc, P. K., Demirezen, Y. D. (2012): Response of antioxidant defences to Zn stress in three duckweed species. – Ecotoxicol. Environ. Saf. 85: 52-58.
[29] Wang, M., Wei, J. M., Guo, H. Q. (2010): Selection of space flight mutation of alfalfa and its polymorphic analysis by RAPD. – Acta Agrestia Sinica 17(6): 841-844.
[30] Wu, Y., Mu, L. Q. (2013): Effect of soil Pb, Cd stress on the growth, physiological and accumulation characteristics of four ornamental trees. – Journal of Soil and Water Conservation 27(5): 234-240 (in Chinese).
[31] Wu, X. L., Sun, C., Yan, L. P., Liu, C. L., Li, L., Xiang, Y., Qu, X. (2015): Effect of EMS on alfalfa seed germination and growth of Zhongmu No.1. – Heilongjiang Agricultural Science 45(2): 1-3+106 (in Chinese).
[32] Yang, D. N., Luo, Y. F., Xie, J. Q., Zhang, Q., Yang, L. (2015): Effects of acidity and/or aluminum stress on seed germination and seedling growth of alfalfa. – Acta Prataculturae Sinica 24(8): 103-109.
[33] Yang, H. S., Chang, G. Z., Bao, W. S., Chai. X. Q., Zhou, X. H. (2012): Morphological variation of space mutation in alfalfas. – Acta Prataculturae Sinica 21(5): 222-2.
[34] Yang, J. C., Du, G. F., Peng, J. Z. (2017): Comparison of cold resistance and nutritional quality of six tropical and subtropical leguminous forages during overwintering period. – Pratacultural Science 34(04): 794-801.
[35] Zaka, R., Chenal, C., Misset, M. T. (2004): Effect of low doses of short-term gamma radiation on growth and development through two generations of Pisum sativum. – Science of the Total Environment 320: 121-129.
[36] Zhang, W. J., Deng, B., Zhang, Y. W., Chen, B. J., Wang, X. Y. (2010): Effect on the leaf microstructure of different alfalfa varieties from spaceflight. – Acta Agrestia Sinica 2: 233-236.
[37] Zhang, Y. W., Han, J. G., Ren, W. B., Sun, H. L. (2015): Breeding by spaceflight mutagenesis and its application in forage breeding. – Pratacultura Sinica 2(10): 59-63.
[38] Zhang, Y. X., Tang, F. L., Zhang, H. Q., Han, W. B., Li, D. M., Shen, Z. B., Liu, L. X. (2007): Breeding of new variety Nongjing No. 1 of *Medicago sativa* L. by magnetic field free space. – Journal of Nuclear Agricultural Sciences 1: 34-37 (in Chinese).
[39] Zhang, Z. W., Sun, X. C., Yang, Y. W., Tian, J., Yang, L. Y., Zhan, Y. H., Bai, X. F., Liu, F. (2017): Effects of EMS treatment on growth and development of Cowpea. – Chinese Journal of Tropical Crops 38(2): 218-225 (in Chinese).
[40] Zhu, H. S., Zhang, K., Dong, K. H., Yang, W. D., Zhao, X. (2015): Effect of drought stress on microstructural characteristic changes of medicago sativa 'Pingguan'. – Acta Prataculturae Sinica 4: 771-779.

http://www.aloki.hu ● ISSN 1589 1623 (Print) ● ISSN 1785 0037 (Online)
DOI: http://dx.doi.org/10.15666/aeer/1802_34973510

EVALUATION OF COMBINING ABILITY AND HETEROSIS IN VARIOUS TRAITS OF *ZEA MAYS* HYBRIDS

MASOOD, M.[1*] – AHSAN, M.[1] – SADAQAT, H. A.[1] – AWAN, F. S.[2]

[1]*Department of Plant Breeding and Genetics, University of Agriculture, Faisalabad, Pakistan*

[2]*Centre of Agriculture Biochemistry and Biotechnology, University of Agriculture, Faisalabad, Pakistan*

**Corresponding author*
e-mail: mmasoodmessage@gmail.com

(Received 28th Nov 2019; accepted 23rd Mar 2020)

Abstract. The selection of parents and superior genotypes is a primary task for plant breeders. In line × tester mating design, seven lines and three testers were crossed to create twenty-one hybrids. The hybrids and parents were evaluated together in the field for various yield and yield related traits at maturity under water stress conditions. The variance assessment implies prominent contrasts between the lines, and testers, crosses for various traits. The differences for GCA and SCA were observed significant for the traits. The line WM13RA and OH33-1 showed the highest general combining ability for most of the traits. The cross combination WM13RA C × Agati85 provided the highest positive better parents heterosis. Specific combining ability was also high, ML17 × Agati85 and ML3 × Agati85 produced higher grain yield in term of said production of early maturing hybrids. Concerning molecular component, ten SSR primers were used to check the hybrid purity. One primer showed the polymorphism with parents and hybrids, results showed that seventeen hybrids were confirmed based on the presence of the polymorphic bands. Genetic purity was 80.95%.
Keywords: *combining ability, line × tester, maize, heterosis, SSR markers, water stress*

Introduction

Agriculture is a main pillar of the economy in Pakistan adding 0.85% to GDP. Maize is the third largest cereal crop in Pakistan (Anonymous, 2019). It is grown on an area of 191 million ha and 1104 million metric tons are produced with a yield of 5.77 metric tons/ha (FAO, 2019). Maize is grown on an area of about 1318 thousand ha with grain production of 6.309 million tons in Pakistan. Punjab and Khyber Pakhtunkhwa (KPK) contribute significantly to maize production in Pakistan. The Province Punjab share 56.76% growing area with 80.12% grain production while KPK share 42.52% crop growing area with 19.59% grain production (Anonymous, 2019). In Punjab it is grown in spring and autumn but only in the spring season in KPK because of no space crop pattern (Rana, 2014). Maize is also a "5F" crop, i.e. food, feed, fuel, fiber and fodder crop. Its insoluble fiber used to cure the acidity of stomach. It is backbone of the feed for the poultry. Maize grain as food contains protein, starch, fiber, oil, sugar, ash 11, 71, 5.7, 4.8, 3.0 and 1.7%, respectively (Chaudhary, 1983). Pakistan generated about 52 thousand million liters of ethanol while the world produce 28.9 million liters (Anonymous, 2019). Maize fodder can be fed to animals at any time after sowing without toxicity of chemicals (Dahmardeh et al., 2009). The demand of maize increases as the population increase, due to multiple usage of the maize grains as food for human while maize fodder as feed for animals (Mishra and Cherkauer, 2010) Pakistan has deep rich soil in South Asia and it is one of the densely packed nations of the world. Agricultural production stayed low in 2018-19. The underperformance of the agricultural sector was due to a decrease in the cultivation region, a decrease in the supply

http://www.aloki.hu ● ISSN 1589 1623 (Print) ● ISSN 1785 0037 (Online)
DOI: http://dx.doi.org/10.15666/aeer/1802_35113523

of water and a decrease in fertilizer usage (Aaliya et al., 2016; Ali et al., 2015, 2017). Abiotic stresses make large area unfit for agriculture due to adverse effects such as drought. In the Punjab plain and Sindh provinces, there is low precipitation (< 200 mm) and warm spell throughout the year (Ali et al., 2013, 2016). Due to the enormous exploitation of fresh reservoirs, water shortages are severe threat to our agriculture. Drought has a serious impact on the development of maize plant (Wynne et al., 1970). Pakistan is unable to fulfill the requirements of the maize seed. The demand of maize seed is about 28892 metric tons from which the public sector provides 237 metric tons, the private sector companies provide 1222 metric tons, while 12776 metric tons of seeds is imported, in total 14235 metric tons are available. The supply of seed is about 50% of the demand so there is a shortage of seeds (Anonymous, 2019). There are various threats for maize grain and fodder yield throughout the globe, there is a need to develop such maize genotypes and hybrids which can produce higher grain yield. The present study is designed for the selection of the parents to develop local hybrids and synthetic varieties on the basis of combining ability and heterosis and to confirm hybrid nature with molecular analysis.

Materials and methods

The seven screened out tolerant lines (which showed higher root length, shoot length and ratio of root shoot length, were selected as tolerant maize genotypes) were grown during the spring season of 2016 and hybridized with three testers to produce 21 hybrids line × tester mating design. The location and average climate during the research period were the followings; Latitude = 31° 44' N, Longitude = 73° 06' E, Altitude = 184.4 m, the average temperature was 35.7 °C, rain fall was 2.6mm, pan evaporation was 8.4 mm, sun shine was 12.4 h, ETO was 7.9 mm and wind speed was 6.23 km/h. Both (parents and hybrids) were grown in triplicate randomized complete block design in the field during the autumn of 2016 and the performance of the hybrids were evaluated considering drought tolerance on the basis of PH (PH) in cm, Leaf area (LA) in cm^2, Leaf angle (La) in degree, chlorophyll contents (CC), leaf temperature (LT) in °C, Days to silking (DS), Days to tasseling (DT), Anthesis to silking interval (ASI) in days, Cob length (CL) cm, Cob diameter (CD) in cm, Kernels rows per cob (KR),100 grains weight (GRW) in grams, Grain yield per plant (GYPP: grams). The data were recorded for 10 plants from each of the three replications.

Biometrical and statistical analysis

The general combining ability and specific combining ability was calculated according to Kempthorne (1957). Heterosis was calculated as Meredith and Bridge (1972) suggested.

Molecular analysis

The samples of the leaves were taken from the parents and their hybrids after two weeks of germination in the evaluation field. The samples were stored at -80 °C for molecular analysis. The DNA extraction was done by modified CTAB method from each sample as described by Doyle and Doyle (1990). Quantification was done with the Nano Drop 2000 (spectrophotometer). The 1% agarose gel was used to check the quality of DNA containing (EDTA/Tris/borate) buffer. About 3 µL of bromophenol blue was added to parental DNA samples. Ten polymorphic SSR primers were selected from already available database as shown in *Table 1*. Working solutions both (parent and hybrid) contain 30 ng/µl sample. The

http://www.aloki.hu ● ISSN 1589 1623 (Print) ● ISSN 1785 0037 (Online)
DOI: http://dx.doi.org/10.15666/aeer/1802_35113523

reaction mixture for SSR analysis was 10X PCR buffer with $(NH_4)_2SO_4$, $MgCl_2$, concentrations of genomic DNA, SSR primers and polymerase enzyme (taq polymerase), dNTPS (dATP, dCTP, dGTP, dTTP) were optimized. The master mixture for 10 parental and 21 hybrids contained 2.5 µL of 10X PCR buffer, 2.5 µL $MgCl_2$, 1.0 µL dNTPs, 0. 2 µL of taq polymerase, 1.0 µL of forward primer, 1. 0 µL of reverse primer in 14.8 µL of d3 H_2O. 2 µL of diluted DNA was mixed with the master mixture in PCR tube. Initial denaturation was carried out at 94 °C for 5 min, subsequent cycle consisted of denaturation at 94 °C for 1 min, primer annealing at 45-60 °C for 1 min, primer extension at 71 °C for 2 min, final extension at 71 °C for 7 min. When all the samples were uploaded, gel was run at 100 V for 2 h. The gel was examined under gel documentation system GDC and photographed. Polymorphism was determined through visualization of the presence and absence of bands.

Table 1. *Hybrids used for evaluation under water deficit condition*

	Testers		**Lines**		
1	Golden	1	A50		
2	Agati85	2	A545		
3	EV189	3	AE204		
		4	OH33-1		
		5	WM13RA		
		6	ML13		
		7	Ml17		
	Hybrids		**Hybrids**		**Hybrids**
1	A50-2×Golden	8	AES204×Agati85	15	WM13RA×Ev189
2	A50-2×Agati85	9	AES204×Ev189	16	ML3×Golden
3	A50-2×Ev189	10	OH33-1×Golden	17	ML3×agati85
4	A545×Golden	11	OH33-1×Agati85	18	ML3×Ev189
5	A545×Agati85	12	OH33-1×Ev189	19	ML17×Golden
6	A545×Ev189	13	WM13RA×Golden	20	ML17×Agati85
7	AES204×Golden	14	WM13RA×Agati85	21	ML17×Ev 189

Results and discussion

Genetic variability

The analysis variance for the line × tester mating design for each trait was conducted under water deficit condition and their mean of square were given in *Table 2*. The genotypes showed highly significant contrast for PH, LA, La, CC, LT, KR, CL, CD, GRW, GYPP and significant in DS days to tasseling, and ASI. The parent showed prominent differences for most of the attribute except LA, DS, and DT. The crosses showed significant difference for all the traits except DT. The interaction parents vs crosses showed significant difference for PH, CD and KR. The lines revealed significant difference for most of the traits except La, LT, DS, ASI, GYPP. Tester showed significant difference for La, CC, ASI, CD, KR, GYPP. The interaction line × tester showed significant difference for most of the traits PH, LA, La, LT, DS, ASI, CL, CD GYPP. It revealed that variability was present among the genotypes for various traits (*Table 3*).

http://www.aloki.hu ● ISSN 1589 1623 (Print) ● ISSN 1785 0037 (Online)
DOI: http://dx.doi.org/10.15666/aeer/1802_35113523

Table 2. *List of simple sequence repeats (SSR) primers*

	Name	Forward primer (5'-3')	Reverse (5'-3')
1	bnlg439w1	AGTTGACATCGCCATCTTGGTGAC	GAACAAGCCCTTAGCGGGTTGTC
2	umc2007y4	TTACACAACGCAACACGAGGC	GCTATAGGCCGTAGCTTGGTAGACAC
3	bnlg1940k7 a	CGTTTAAGAACGGTTGATTGCATTCC	GCCTTTATTTCTCCCTTGCTTGCC
4	UMC1363	AAAGGCATTATGCTCACGTTGATT	TCTCCCTCCCCTGTACATGAATTA
5	UMC1004	CTGGGCATACAAAGCTCACA	TGCATAAACCGTTTCCACAA
6	UMC2002	TGACCTCAACTCAGAATGCTGTTG	CACAAAATCCTCGAGTTCTTGATTG
7	Phi053	CTGCCTCTCAGATTCAGAGATTGAC	AACCCAACGTACTCCGG
8	Umc1600	CGATCAGTGCGTGGAGAGTA	TAGGCATGCATTGTCCATTG
9	umc1166	CGATCAGATCATACACAACCTTGC	GAGGATCGATTCTTGGCGAGT
10	umc1859k1	AATCTCCAGGTTGGTGTTCAAAGG	AAAGATGACTTTGTGGGCAGTGG

Combining ability analysis

Identifying the highest performing lines and lines that can be used as parents in future crossings are two objectives in most crop breeding programs. Assessment of GCA and SCA effects is necessary to identify and select the better performing inbred lines and F1 crosses for each trait improvement (Areous et al., 2005; Danish et al. 2020, Ivy and Howlader, 2000; Oakey, 2006). General combining ability GCA can be defined as the performance of genotypes in the series of crosses while the SCA as the production in specific cross (Sprague and Tatum, 1942). The line WM13RA had high GC effect among the lines for La, CL, KR, GRW, GYPP and poor general combiner for LA, DT and DS. The line OH33-1 showed high GC effect for LA, CC, DT and low GC effect for ASI. The lineML17 had high GC effect for the LT while general combiner for La. The line ML3 had high GC effect for PH, DS, ASI and KR. The line A545 showed high GC effect among lines for CD. The line AES204 was noted low GC effect for PH. The line A50-2 proved to be poor combiner among the lines for CC, LT, CL, CD, GRW, GYPP (*Tables 3* and *4*). Specific combining ability WM13RA × EV189 top ranked among the negative SCA effects best for the reduction of PH. A545 × EV189 showed maximum negative SCA and proved to be good specific combiners for the leaf area. The cross ML 17 × Ev189 displayed the highest negative and significant SCA declared as good specific combiner for La. The cross ML3 × EV189 was found the highest positive and significant SCA was declared as good specific combiner for CC. The cross A50-2 × Ev189 *Table 5* was found to have maximum negative and significant SCA for the LT and revealed to be good specific combiners. The Cross combination ML3 × Agati85 displayed the highest negative and significant SCA, parent revealed to be good specific combiners for DS. The cross AES204 × Agati85 displayed the highest negative and significant SCA, and proved to be good specific combiner for DT. The Cross combination ML3 × Agati85 showed the maximum negative and significant SCA effects, and proved to be good specific combiner for ASI. The cross AES204 × Golden top ranked among positive and non -significant SCA, and revealed as good specific combiner for CL. The cross A545 × Ev189 showed the highest positive and significant SCA, and for CD it was a good specific combiner. The cross WM13RA × Golden showed the maximum positive and significant SCA for KR. The crossOH33-1 × Ev189 was found to have the highest positive and non-significant SCA and revealed as best specific combiners for GRW. The crossML17 × Agati85 showed the maximum positive and significant SCA for GYPP (*Table 5*) The results were in line with the results of Asif et al. (2020), Bibi et al. (2018), Kumar et al. (2004, 2016), Muraya et al. (2006), Uddin et al. (2008), Amiruzzaman et al. (2013), Gissa et al. (2013), Aminu et al. (2015), El-Shamarkaet al. (2015).

http://www.aloki.hu ● ISSN 1589 1623 (Print) ● ISSN 1785 0037 (Online)
DOI: http://dx.doi.org/10.15666/aeer/1802_35113523

Table 3. *Mean square values of line X tester of various traits under water deficit conditions*

Crosses	DF	Plant height (cm)	Leaf area (cm^2)	Leaf angle	Chlorophyll contents (mgg^{-1}fr.wt).	Leaf temperature (°C)	Days to silking	Days to anthesis	Anthesis to silking interval	Cob length (cm)	Cob diameter (cm)	Kernels per row	100 grain weight (g)	Grain yield per plant (g)
Replication	2	469.89NS	726.8NS	12.20NS	11.25NS	1.01NS	1.31NS	0.28NS	0.29NS	1.59NS	0.1NS	0.75 Ns	6.5NS	1409.3NS
Genotype	30	1452.9**	11525**	50.66**	38.70**	10.38**	1.32*	1.10*	0.5959*	31.61**	0.7**	2.62**	22**	12341.6**
Parents	9	1708**	4587NS	62.01**	51.82**	8.57**	0.99NS	1.03NS	0.732*	33.12**	1**	3.87**	34**	7792.7**
Parent vs crosses	1	8462**	3413NS	14.02NS	0.19NS	1.54NS	1.90NS	0.01NS	0.72NS	14.59NS	0.70*	4.03*	5.7NS	246.3NS
Crosses	20	987.38**	15052**	47.33**	34.73**	11.64**	1.44*	1.18*	0.53NS	31.77**	0.6**	1.98**	17**	14993.3**
Lines	6	2181.**	5963.6*	39.16NS	41.33*	2.16NS	0.59NS	1.03NS	0.82*	40.27**	1.3**	4.49**	46**	2877.2NS
Tester	2	30.60NS	1532NS	96.39**	77.91**	4.45NS	2.33*	1.33NS	0.77NS	26.86NS	0.7**	3.81**	9NS	18102.8**
LinesX tester	12	550.01*	21850**	43.33**	24.23NS	17.57**	1.72*	1.23*	0.34NS	28.35**	0.32*	0.42Ns	4.3NS	20533.1**
Error	60	308.31	2312.9	19.24	14.14	1.72	0.78	0.64	0.33	11.65	0.16	0.91	7.48	2171.1

Table 4. *General combining ability of various traits of maize under water deficit condition*

Nes	Plant height (cm)	Leaf area (cm^2)	Leaf angle	Chlorophyll contents (mgg^{-1} fr.wt)	Leaf temperature (°C)	Days to silking	Days to anthesis	Anthesis to silking interval	Cob length (cm)	Cob diameter (cm)	Kernels rows per cob	100 grain weight (g)	Grain yield per plant (g)
A50-2	-16.3*	-24.53	-0.79	-3.99*	3.76*	-0.12	-0.174	0.2	-2.3*	-0.358*	-0.244	-2.4*	-40.04*
A545	5.2	16.09	-1.16	0.12	0.2	-0.12	-0.174	0.23	0.03	0.52*	-0.941	-1.84*	29.112
AES204	15.4*	-2.46	0.68	0.49	-0.98*	-0.12	-0.396	0.222	2	0.39*	1.465*	1.576	15.08
OH33-1	13.7*	-47.15*	0.5	1.45	-1.26*	-0.12	-0.5	0.33	-1.58	0.16	0.021	0.601	-17.769
WM13RA	7.85	54.33*	-1.9	2	-0.28	0.76*	0.82*	-0.11	4.29*	-0.22	2.391*	2.86*	58.48*
ML3	-26*	9.54	0.24	0.263	-0.05	-0.34	0.38	-0.44*	-1.88	-0.14	-1.092	-1.442	-19.666
ML17	0.076	-5.82	2.42	-0.33	-1.381*	0.095	0.047	0.24	-0.51	0.34*	-0.598	0.637	-25.18
Tester													
Agati85	0.85	9.22	-0.27	1.28	0.435	-0.031	0.015	-0.09	0.042	-0.05	-0.488	-0.718	14.45
Ev189	3.91	-4.52	-0.94	-0.65	-0.09	-0.031	0.111	-0.04	0.82	-0.04	0.650	-0.52	-5.575
Golden	-4.76	-4.7	1.21	-0.63	-0.34	0.063	-0.12	0.14	-0.86	0.104	-0.162	0.19	-8.879

http://www.aloki.hu ● ISSN 1589 1623 (Print) ● ISSN 1785 0037 (Online)
DOI: http://dx.doi.org/10.15666/aeer/1802_35113523

Table 5. *Specific combining ability of various traits of maize under water deficit condition*

Hybrids	Plant height (cm)	Leaf area (cm^2)	Leaf angle	Chlorophyll contents (mgg^{-1} fr.wt)	Leaf temperature (°C)	Days to silking	Days to anthesis	Anthesis to silking interval	Cob length (cm)	Cob diameter (cm)	Kernels rows per cob	100 grain weight (g)	Grain yield per plant (g)
A50-2×Golden	2.04	58.57*	6.12*	-0.5	1.16	-0.301	-0.015	-0.23	-1.74	0.398	-0.28	-1.3	74.213*
A50-2×Agati85	-5.51	57.57*	6.09*	2.74	2.53*	0.031	-0.111	0.04	-0.97	-0.289	-0.089	1.358	0.436
A50-2×Ev189	3.53	-1.008	-0.03	-2.24	-1.36	0.26	0.126	0.19	2.69	-0.1	0.370	-0.056	-74.64*
A545×Golden	5.27	139.13*	-1.94	-1.26	-0.4	0.031	-0.01	0.095	3.63	-0.397	1.41	1.328	91.23*
A545×Agati85	-14.15	-49.73	-1.28	0.58	0.88	0.36	0.222	0.047	-2.88	-0.398	-0.169	-0.667	-31.433
A545×Ev189	8.88	-89.39	3.22*	0.68	-0.48	-0.39	-0.2	-0.14	-0.74	0.795*	-1.246	-0.661	-59.8*
AES204×Golden	-9.79	-16.9	-2.42	0.54	-0.38	-0.301	-0.12	-0.12	-3.46	-0.063	-3.88*	-0.564	-20.749
AES204×Agati85	6.62	-71.09	-1.02	-3.71	-0.26	0.365	-0.22	0.49	3.51	0.385	2.98	0.052	-48.631
AES204×Ev189	3.16	87.99*	-1.4	3.16	0.65	-0.06	0.34	-0.36	-0.052	-0.321	0.9	0.511	69.38*
OH33-1×Golden	-12.61	62.78*	-1.94	-2.22	-0.26	0.031	-0.015	0.095	2.94	-0.212	2.22*	-1.74	-53.086
OH33-1×Agati85	1.54	-14.28	3.71	0.15	0.64	0.031	-0.11	0.04	-3.6	0.253	-1.57	-0.876	12.619
OH33-1×Ev189	11.07	48.5	-1.77	2.07	-0.37	-0.063	0.126	-0.142	0.66	-0.04	-0.652	2.616	40.467
WM13RA×Golden	6.29	-30.4	-5.4*	2.25	-0.81	-0.52	-0.34	-0.12	-1.55	0.181	2.96*	1.185	-27.466
WM13RA×Agati85	11.13	83.67*	-0.53	2.09	-0.21	1.14*	1.22*	-0.174	2.97	-0.315	-0.612	1.05	61.279*
WM13RA×Ev189	-17.43	-53.27	5.96*	-4.35*	1.02	-0.61	-0.87	0.3	-1.41	0.134	-2.35	-2.241	-33.813
ML3×Golden	18.14	-7.372	-2.02	-1.42	-0.31	0.92	0.42	0.206	0.15	-0.031	-1.21	-1.305	33.143
ML3×agati85	-4.65	-5.16	1.2	-3.61	1.24	-1.74	-0.33	-0.84*	-0.62	0.024	-1.35	-0.821	-94.99*
ML3×Ev189	-13.48	12.54	0.81	5.04*	-0.93	0.82	-0.095	0.63	0.47	0.007	2.57	2.127	61.85*
ML17×Golden	-9.34	-80.25*	2.79	2.61	1.02	0.14	0.095	0.095	-0.001	0.125	-1.23	2.397	-97.29*
ML17×Agati85	5.08	85.6*	4.01	1.75	0.23	-0.19	-0.66	0.38	1.61	0.34	0.82	-0.101	100.72*
ML17×Ev 189	4.26	-5.35	-6.8*	-4.37*	-1.25	0.04	0.57	-0.47	-1.612	-0.465	0.410	-2.296	-3.429

http://www.aloki.hu ● ISSN 1589 1623 (Print) ● ISSN 1785 0037 (Online)
DOI: http://dx.doi.org/10.15666/aeer/1802_35113523

Heterosis and better parent heterosis

The cross combination ML3 × Ev189 maximum mid parent negative heterosis and the cross combination ML3 × Ev189 showed the maximum negative heterobeltiosis for PH. The cross combination ML17 × Golden maximal negative mid parent heterosis estimate and the cross ML17 × Golden showed the maximal positive better parent heterotic effects for leaf area. The cross combination WM13RA × Golden showed minimal mid parent negative heterosis and Cross WM13RA × Golden showed minimal better parent heterotic effects for La (Ali et al., 2014; Malook et al., 2016; Mahmood et al., 2019; Paul and Duara, 1991; Yaqoob et al. 2020). The cross combination 5 ML3 × Ev189 maximal positive mid parent heterosis estimate and, the cross WM13RA × Golden showed the maximal positive better parent heterosis for CC. ML17 × Ev189 showed maximum negative mid parent heterosis and the cross combination ML17 × Ev189 showed maximum negative better parent heterosis for LT (Aslam et al., 2012). ML3 × Agati85 showed maximum negative mid parent heterosis and Cross ML3 × Agati85 showed maximum better parent heterosis for DS. In developing early mature, high yield hybrids early silking is considered as basis of breeding. So early flowering can be useful to escape from water scarcity at critical stage of crop development. AES204 × Golden showed maximum negative mid parent heterosis and the cross combination Cross OH33-1 × Golden and AES204 × Golden both showed maximum better parent heterosis for DT. ML3 × Agati85 showed maximum negative mid parent heterosis and Cross ML3 × Agati85 showed the highest better parent heterosis for ASI. The cross combination WM13RA × Agati 85 maximal positive mid parent heterosis estimate and the cross WM13RA × Agati 85 showed maximal positive better parent heterotic effects for CL. The cross combination A545 × Ev189 maximal positive mid parent heterosis estimate and the cross A545 × Ev189 showed maximal positive better parent heterotic effects for CD. The cross combination OH33 -1 × Golden showed maximal positive mid parent heterosis estimate. The cross combination OH33 -1 × Golden showed maximal positive better parent heterotic effects for KR. The cross combination AES204 × Ev189 had maximal positive mid parent heterosis estimate for GRW and GYPP. The cross AES204 × Ev189 showed maximal positive heterobeltiosis for GRW. Cross WM13RA × Agati showed maximal heterobeltiosis for GYPP (*Tables 6* and 7).

Molecular analysis

The primer UMC 2002 was found polymorphic out of the ten SSRs primers used in the study. Hybrids confirmed on the presence and absence of the band in the gel for parents as well as for the hybrid. It was found that the hybrids of lines A50-2 × Golden showed the polymorphism and same fragment was found in the hybrid which confirm the inheritance of same fragment from the parent to offspring. The hybrid A50-2 × Golden was confirmed similarly for all the hybrid confirmed except for four hybrids AES 204 × Golden, OH33-1 × Golden, WM13RA × Ev189 and ML3 × Golden. These hybrids can be confirmed by applying more number of primers and extensive screening of primer 6 is needed to identify the polymorphic fragment in both parents that can be finally detected in the hybrid population *(Figure 1)*. The hybrid genetic purity was found 85.95% (*Table 8*) (Bibi et al., 2015; Hafeez et al., 2015; Farooq et al., 2017; Yaqoob et al. 2020).

http://www.aloki.hu ● ISSN 1589 1623 (Print) ● ISSN 1785 0037 (Online)
DOI: http://dx.doi.org/10.15666/aeer/1802_35113523

Table 6. *Better parent heterosis of various traits under water deficit condition*

Hybrids	Plant height (cm)	Leaf area (cm^2)	Leaf angle	Chlorophyll contents (mgg^{-1} fr.wt)	Leaf temperature (°C)	Days to silking	Days to anthesis	Anthesis to silking interval	Cob length (cm)	Cob diameter (cm)	Kernels per row	100 grain weight (g)	Grain yield per plant (g)
A50-2×Golden	-3.16	-1.85	9.01	-1.49	25.11*	-2.65*	-1.38	-21.67	-16.87*	-6.31	6.78	-23.1*	-0.67
A50-2×Agati85	-8.73	-39.76*	-27.58*	-4.81	-2.24	-0.45	0.15	-22.22	-8.07	-18.22*	-8.69*	-5.24	-39.06*
A50-2×Ev189	-4.99	-23.30	-2.05	-4.23	21.39*	0.3	-0.46	4.43	-1.29	8.8	-1.67	-13.23	-71.15*
A545×Golden	12.30	56.84*	-16.38	1.86	-5.92	-2.21*	-1.38	0.05	4.13	-4.5	0.77	-8.18	55.65*
A545×Agati85	-0.85	-8.09	-15.25	-2.71	-0.88	-0.14	-0.31	-22.22	-6.68	-0.82	-10.15*	-11.91	-7.3
A545×Ev189	11.91	-22.45*	5.09	1.88	-11.6*	-1.04	-1.23	4.94	-4.84	40.71*	3.9	0.65	-23.08
AES204×Golden	9.31	-3	-12.57	-6.19	-16.53*	-2.65*	-1.84*	1.04	-9.79	-0.072	-5.44	-1.15	-3.99
AES204×Agati85	17.91*	-18.70*	-23.15*	-12.4*	-14.82*	-0.44*	-1.38	0.05	17.24*	10.68*	-1.43	7.11*	-18.51*
AES204×Ev189	14.71*	41.38*	-18.58*	5.49*	-4.24*	-0.89*	-0.92	0.05	15.32*	-1.46	11.62*	25.04*	41.81*
OH33-1×Golden	6.50	34.059*	-11.36	0.98	-4.24	-2.21*	1.84*	2.33	-3.34	-10.55	18.88*	-11.65	-34.85*
OH33-×Agati85	13.82	-1.2	21.56	-1.74*	-10.85*	0.89*	-0.93	-11.11*	-18.79*	-0.49*	-10.1*	-2.01*	-1.64*
OH33-1×Ev189	18.67*	16.67	9.81	3.63	-10.85	-0.89	-0.93	2.43	11.88*	-3.47	-0.071	12.51	36.19
WM13RA×Golden	14.58*	11.84	-29.09*	5.95*	-16.14*	-1.76*	-0.46	-14.28	1.6	-8.2	7.5	12.89	13.36
WM13RA×Agati85	16.035*	55.07*	-10.7	0.93	-15.65*	2.25*	2.79*	-33.33*	22.22*	-15.88	-2.89	17.68*	55.82*
WM13RA×Ev19	-2.93	5.22	17.14	-3.47	-9.4	0.05	-0.46	14.28	18.29*	4.42	15.92*	10.76	6.07
ML3×Golden	-11.82	-0.67	-12.38	-0.45	-11.02*	-1.32	0.05	-14.28	-10.51	-10.96	-10.80*	-34.6*	0.62
ML3×agati85	-22.57*	-4.44	4.78	-7.07	-4.54	-3.15*	0.93	-66.66*	-5.71	-7.77	-13.52*	-28.3*	-66.54*
ML3×Ev189	-32.10*	1.27	10.66	4.54	-19.88*	0.9	0.01	26.38	-5.1	-4.74	-14.19*	-18.6*	3.06
ML17×Golden	-0.46	-33.88*	8.68	1.85	-4.38	-1.76*	-0.92	-36.36*	-8.41	-11.9*	5.08	-15.5*	-63.5*
ML17×Agati85	7.67	12.6	29.4*	-1.93	-13.34*	-0.89	0.04	-27.27*	-1.99	-3.61	-4.34	-20.0*	12.02
ML17×Ev 189	4.48	-15.25	-1.17	-7.8	-25.22*	-0.44	0.465	-45.45*	-15.17	-8.44	-1.67	-29.1*	-33.57*

http://www.aloki.hu ● ISSN 1589 1623 (Print) ● ISSN 1785 0037 (Online)
DOI: http://dx.doi.org/10.15666/aeer/1802_35113523

Table 7. *Heterosis of various various traits under water deficit conditions*

Hybrids	Plant height (cm)	Leaf area (cm^2)	Leaf angle	Chlorophyll contents ($mgg^{-1}fr.wt.$)	Leaf temperature (°C)	Days to silking	Days to anthesis	Anthesis to silking interval	Cob length (cm)	Cob diameter (cm)	Kernels per row	100 grain weight (g)	Grain yield per plant (g)
A50-2×Golden	7.62	6.035	10.69	-0.76	35.99*	-1.63*	-0.61	-18.14	-14.22*	17.59*	6.78	-23.04*	6.53
A50-2×Agati85	2.75	-31.37*	-20.15*	-1.77	7.13	-0.3	0.31	-15.96	-7.54	1.25	-1.55	-5.21	-30.87*
A50-2×Ev189	5.21	-11.05	16.4	-1.74	43.12*	0.37	-0.15	17.13	4.1	24.38*	1.19	-6.7	-54.58*
A545×Golden	22.529*	60.79*	-15.81*	2.077	1.16	-1.41*	-1.07	2.41	7.16	1.15	3.285	1.332	59.6*
A545×Agati85	9.62	-4.94	5.84	-0.53	7.47	-0.07	0.31	-10.65	-6.4	3.25	-5.35	-2.66	-3.85
A545×Ev189	21.678*	-18.17	25.77*	5.5*	3.21	-0.75	-1.08	10.49	0.61	48.81*	4.35	3.7	15.77
AES204×Golden	34.776*	1.74	-5.7	-1.02	-8.87	-2.004*	-1.61*	0.05	2.15	0.2915	-1.22	6.05	1.061
AES204×Agati85	47.022*	-17.85	-8.2	-9.78*	-11.01*	-0.224	-0.69	12.5	29.75*	12.28*	1.88	15.07*	-17.71
AES204×Ev189	41.03*	45.83*	4.0018	2.86	0.822	-0.45	-0.69	7.69	20.7*	9.64	13.34*	25.12*	110.53*
OH33-1×Golden	7.92	-23.14*	-4.32	1.84	2.58	-1.55*	-1.38*	6.66	-2.75	-9.42	20.86*	-11.36	-24.35
OH33-×Agati85	17.02*	9.2799	-26.26*	-0.165	1.18	0.67	-0.46	5.88	-16.17*	2.55	-4.59	-1.82	8.14
OH33-1×Ev189	19.79*	26.72	23.62*	7.965*	-0.99	-0.45	-0.93	14.28	-3.74	8.952	1.18	21.16*	90.145*
WM13RA×Golden	23.60*	15.12	26.76*	7.165*	-7.78	-0.89	0.05	-14.28	13.77*	-3.51	8.40*	17.92	17.098
WM13RA×Agati85	26.86*	59.73*	-3.09	2.25	-6.49	2.25*	3.27*	-25*	33.7*	-13.1*	3.88	23.09*	60.454*
WM13RA×Ev189	4.32	10.6	37.23*	0.84	7.92	0.22	-0.465	23.07	22.28*	11.27	18.35*	13.98	59.07*
ML3×Golden	-5.90	1.78	-8.23	0.892	-2.37	0.15	0.93	-9.97	-7.07	-10.08*	-0.744	-27.49*	2.79
ML3×agati85	-18.50*	3.58	12.2	-6.05*	5.58	-2.56*	0.938	-60.86*	-4.55	-7.02	-10.50*	-20.51*	-63.71*
ML3×Ev189	-27.27*	11.9	28.08*	9.44*	-4.75	1.28	0.467	29.76	-0.54	5.4	-6.99*	-3.76	58.64*
ML17×Golden	-0.23	-30.10*	17.32*	3.965	1.49	-1.11	0.467	-22.22*	-7.83	-5.27	6.43	-5.13	-61.51*
ML17×Agati85	9.01	25.68*	34.4*	-1.561	-7.22	-0.67	0.47	-20*	1.19	1.91	4.35	-10.34	25.106*
ML17×Ev 189	5.14	-3.65	11.25	-2.82	-13.7*	0.05	1.40*	-29.41*	-7.31	-4.66	2.46	-15.33*	3.78

http://www.aloki.hu ● ISSN 1589 1623 (Print) ● ISSN 1785 0037 (Online)
DOI: http://dx.doi.org/10.15666/aeer/1802_35113523

Table 8. *Hybrid confirmation by UMC2002 SSR marker*

Sr no	Hybrid/parent	Parent 1	Parent 2	Confirmation
1	A50-2×Golden	+	+	Confirmed
2	A50-2×Agati85	+	+	Confirmed
3	A50-2×Ev189	+	+	Confirmed
4	A545×Golden	+	+	Confirmed
5	A545×Agati85	+	+	Confirmed
6	A545×Ev189	+	+	Confirmed
7	AES204×Golden	+	-	Not confirmed
8	AES204×Agati85	+	+	Confirmed
9	AES204×Ev189	+	+	Confirmed
10	OH33-1×Golden	+	+	Not confirmed
11	OH33-1×Agati85	+	+	Confirmed
12	OH33-1×Ev189	+	+	Confirmed
13	WM13RA×Golden	+	+	Confirmed
14	WM13RA×Agati85	+	+	Confirmed
15	WM13RA×Ev189	+	-	Not confirmed
16	ML3×Golden	+	-	Not confirmed
17	ML3×agati85	+	+	Confirmed
18	ML3×Ev189	+	+	Confirmed
19	ML17×Golden	+	+	Confirmed
20	ML17×Agati85	+	+	Confirmed
21	ML17×Ev 189	+	+	Confirmed
Purity of hybrid				**80.9524**

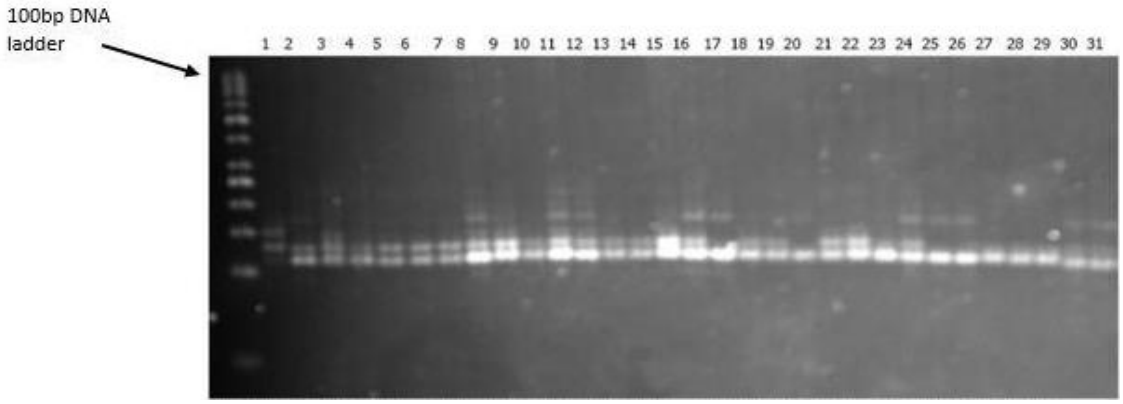

Figure 1. *The lanes indicated lines, testers and hybrids; 1) Golden, 2) A50, 3) Agati85, 4) A545, 5) EV189, 6) AE204, 7) OH33-1, 8) WM13RA, 9) ML13, 10) Ml17, 11) A50-2 × Golden, 12) AES204 × Agati85, 13) WM13RA × Ev189, 14) A50-2 × Agati85, 15) AES204 × Ev189, 16) ML3 × Golden, 17) A50-2 × Ev189, 18) OH33-1 × Golden, 19) ML3 × Agati85, 20) A545 × Golden, 21) OH33-1 × Agati85, 22) ML3 × Ev189, 23) A545 × Agati85, 24) OH33-1 × Ev189, 25) ML17 × Golden, 26) A545 × Ev189, 27) WM13RA × Golden, 28) ML17 × Agati85, 29) AES204 × Golden, 30) WM13RA × Agati85, 31) ML17 × Ev 189*

http://www.aloki.hu ● ISSN 1589 1623 (Print) ● ISSN 1785 0037 (Online)
DOI: http://dx.doi.org/10.15666/aeer/1802_35113523

Conclusion

It is a need among plant breeders to be able to select and develop tolerant genotypes for water deficit conditions. The research displayed that the line WM13RA and OH33-1 showed the highest and 6 general combining ability for most of the traits. The cross combination WM13RA× Agati85was found to have the highest positive better parents heterosis. Specific combing ability was also high in ML17 × Agati85 for grain yield and ML3 × Agati85 for the production of early maturing hybrids. The genetic purity of the hybrids was found about 80.95% in molecular analysis with SSR markers.

REFERENCES

[1] Aaliya, K., Qamar, Z., Nasir, I. A., Ali, Q., Munim, A. F. (2016): Transformation, evaluation of gtgene and multivariate genetic analysis for morpho-physiological and yield attributing traits in Zea mays. – Genetika 48(1): 423-443.

[2] Ali, F., Kanwal, N., Ahsan, M., Ali, Q., Bibi, I., Niazi, N. K. (2015): Multivariate analysis of grain yield and its attributing traits in different maize hybrids grown under heat and drought stress. – Scientifica. https://doi.org/10.1155/2015/563869.

[3] Ali, F., Ahsan, M., Ali, Q., Kanwal, N. (2017): Phenotypic stability of Zea mays grain yield and its attributing traits under drought stress. – Frontiers in Plant Science 8: 1397.

[4] Ali, Q., Ahsan, M., Ali, F., Aslam, M., Khan, N. H., Munzoor, M., Mustafa, H. S. B., Muhammad, S. (2013): Heritability, heterosis and heterobeltiosis studies for morphological traits of maize (*Zea mays* L.) seedlings. – Advancements in Life Sciences 1(1): 52-63.

[5] Ali, Q., Ali, A., Ahsan, M., Ali, S., Khan, N. H., Muhammad, S., Abbas, H. G., Nasir, I. A., Husnain, T. (2014): Line × tester analysis for morpho-physiological traits of Zea mays L. seedlings. – Advancements in Life Sciences 1(4): 242-253.

[6] Ali, Q., Ahsan, M., Malook, S., Kanwal, N., Ali, F., Ali, A., Ahmed, W., Ishfaq, M., Saleem, M. (2016): Screening for drought tolerance: comparison of maize hybrids under water deficit condition. – Advancements in Life Sciences 3(2): 51-58.

[7] Aminu, D., Garba, M., Muhammad, A. (2015): Combining ability and heterosis for phonologic and agronomic traits in maize (Zea mays L.) under drought conditions in the Northern Guinea Savanna of Borno State, Nigeria. – Afr. J. Biotechnol. 13(24): 2400-2406.

[8] Amiruzzaman, M., Islam, M. A., Hasan, L., Kadir, M., Rohman, M. (2013): Heterosis and combining ability in a diallel among elite inbred lines of maize. *Zea mays* L. – J. Food Agric. 25(2): 132-137.

[9] Anonymous (2019): Ministry of Food and Agriculture, Bureau of Statistics. – Government of Pakistan, Islamabad.

[10] Areous, L., Slafer, G., Royo, C., Serret, M. D. (2005): Breeding for yield potential and stress adaptation in cereals. – Crit. Rev. Plant Sci. 27: 377-412.

[11] Asif S, Ali Q, Malik A. (2020): Evaluation of salt and heavy metal stress for seedling traits in wheat. –Biol. Clin. Sci. Res. J. 2020: e005.

[12] Aslam, M., Khan, J. A., Basra, S. M. A. (2012): Combing ability estimates ability estimates and mode of inheritance for drought related traits in genetically distant maize accessions (Zea mays L.). – Anim. Plant Sci. 22(3): 679-682.

[13] Bibi, T., Mustafa, H. S. B., Hasan, E. U., Rauf, S., Mahmood, T., Ali, Q. (2015): Analysis of genetic diversity in linseed using molecular markers. – Life Sci J 12(4): 28-37.

[14] Bibi, T., Mustafa, H. S. B., Mahmood, T., Hameed, A., Ali, Q. (2018): Multivariate analysis for adaptability and yield stability of rapeseed (*Brassica napus* L.) strains in different agro-climatic zones. – Genetika (0534-0012) 50(2): 369-378.

[15] Chaudhary, A. R. (1983): Maize in Pakistan. – Punjab Agri. Res. Coordination Board, Uni. Agri. Faisalabad, Pakistan.

http://www.aloki.hu ● ISSN 1589 1623 (Print) ● ISSN 1785 0037 (Online)
DOI: http://dx.doi.org/10.15666/aeer/1802_35113523

[16] Danish P, Ali Q, Hafeez MM, Malik A, (2020): Antifungal and antibacterial activity of aloe vera plant extract. –Biol. Clin. Sci. Res. J. 2020: e003.
[17] Dahmardeh, M., Ghanbari, A., Syasar, B., Ramroudi, M. (2009): Effect of intercropping maize with cowpea on green forage yield and quality evaluation. – Asian J. Plant Sci 8(3): 235-239.
[18] Doyle, J. J., Doyle, J. L. (1990): Isolation of plant DNA from fresh tissue. – Focus 12: 13-15.
[19] El-Shamarka, S. A., Ahmed, M. A., El-Nahas, M. M. (2015): Heterosis and combining ability for yield and its components through diallel cross analysis in maize, *Zea mays* L. – Alex. J. Agric. Res. 60(2): 87-94.
[20] FAO (2019): Statistical Database. – http://faostat.fao.org.
[21] Farooq, A. M., Nasir, I. A., Ali, Q., Tabassum, B., Husnain T. (2017): Identification and interrelationship of yield related traits through DNA fingerprinting in *Zea mays*. – International Journal of Biology, Pharmacy and Allied Sciences 6(6): 1276-1303.
[22] Gissa, D. W., Zelleke, H., Labuschagne, M. T., Hussien, T. Singh, H. (2013): Heterosis and combining ability for grain yield and its components in selected maize inbred lines. – Afr. J. Plant Soil. 24(3): 133-137.
[23] Hafeez, M. N., Sadique, S., Hassan, S., Sarwar, M. B., Rashid, B., Ali, Q., Husnain, T. (2015): Physiological, morphological, biochemical and molecular basis of drought tolerance in cotton. – Int. J. Biol. Pharm. Allied Sci 4: 1091-1112.
[24] Ivy, N. A., Howlader, M. S. (2000): Combining ability in maize. – Bangladesh J. Agril. Res. 25(3): 385-92.
[25] Kepmthorne, O. (1957): An Introduction to Genetic Statistics. – John Wiley and Sons Inc., New York.
[26] Kumar, P., Gupta, S. (2004): Genetic analysis in maize (Zea mays L.). – J. Res. Birsa Agri. Univ. 16(l): 113-117.
[27] Kumar, S. V. V. P., Babu, D. R. (2016): Combining ability and heterosis in maize, *Zea mays* L. for grain yield and yield components. – IJAEB 9(5): 763-772.
[28] Mahmood, T., Mustafa, H. S. B., Aftab, M., Ali, Q., Malik, A. (2019): Super canola: newly developed high yielding, lodging and drought tolerant double zero cultivar of rapeseed (Brassica napus L.). – Genetics and Molecular Research 18(2): gmr16039951.
[29] Malook, S., Ali, Q., Ahsan, M., Shabaz, M., Waseem, M., Mumtaz, A. (2016): Combining ability analysis for evaluation of maize hybrids under drought stress. – Journal of the National Science Foundation of Sri Lanka 44(2): 223-230.
[30] Meredith, W. E., Bridge, R. R. (1972): Heterosis and gene action in cotton Gossypium hirsutum L.). – Crop Sci. 12: 304-310.
[31] Mishra, V., Cherkauer, K. A. (2010): Retrospective droughts in the crop growing season: implications to corn and soybean yield in the mid-western united states. – Agr. Meteorol. 150: 1030-1045.
[32] Muraya, M. M., Ndirangu, C. M., Omolo, E. O. (2006): Heterosis and combining ability in diallel crosses involving maize (Zea mays L.) S1 lines. – Australian J. Exp. Agri. 46(4): 387-394.
[33] Oakey, H., Verbyla, A., Pitchford, W., Cullis, B., Kuchel, H. (2006): Joint modeling of additive and non-additive genetic line effects in single field trials. – Theor Appl Genet 113(5): 809-819.
[34] Paul, S. K., Duara, R. K. (1991): Combining ability studies in maize (Zea mays L.). Intl. adaptation in cereals. – Crit. Rev. Plant Sci. 27: 377-412.
[35] Rana, M. A. (2014): The seed industry in Pakistan: regulations, politics, and entrepreneurship. PSSP Working Paper 19, Washington, DC. – International Food Policy Research Institute (IFPRI) Res. 25: 385-392.
[36] Sprague, G. F., Tatum, L. A. (1942): General versus specific combining ability in single crosses of corn. – J. Americ. Soc. Agron. 34: 923-932.

http://www.aloki.hu ● ISSN 1589 1623 (Print) ● ISSN 1785 0037 (Online)
DOI: http://dx.doi.org/10.15666/aeer/1802_35113523

[37] Uddin, M. S., Amiruzzaman, M., Bagum, S. A., Hakim, M. A., Ali, M. R. (2008): Spring maize (Zea mays L.) S1 lines. – Aust J. Exp. Agri. 46(4): 387-394.
[38] Wynne, J. C., Emery, D. A., Rice, P. W. (1970): Combining ability estimates in Arachis hypogaea L. II. Field performance of F1 hybrids. – Crop Sci. 10: 713-715.
[39] Yaqoob S, Fatima N, Khan S, Ali Q, Hafeez MM, Malik A. (2020): Begomoviruses and betasatellites associated with CLCuD. –Biol. Clin. Sci. Res. J. 2020: e002.

http://www.aloki.hu ● ISSN 1589 1623 (Print) ● ISSN 1785 0037 (Online)
DOI: http://dx.doi.org/10.15666/aeer/1802_35113523

ECOTOXICOLOGICAL EFFECT OF MESOTRIONE ON ENZYME ACTIVITY AND MICROBIAL COMMUNITY IN AGRICULTURAL SOILS

SUN, Y. B.[1,2] – WANG, L.[1,2] – XU, Y. M.[1,2*] – LIANG, X. F.[1,2] – ZHENG, S. N.[3*]

[1]*Key Laboratory of Agro-Environmental Pollution Prevention and Control, Ministry of Agriculture and Rural Affairs, Tianjin 300191, China*

[2]*Tianjin Key Laboratory of Agro–environment and Agro–product Safety, Agro–Environmental Protection Institute, Ministry of Agriculture and Rural Affairs, Tianjin 300191, China*

[3]*Rural Energy & Environment Agency, Ministry of Agriculture and Rural Affairs, Beijing 100125, China*

**Corresponding authors*
e-mail: ymxu1999@126.com, zhengshunan1234@163.com; *phone: +86-22-2361-8061; fax: +86-22-2361-8060*

(Received 3rd Dec 2019; accepted 26th Mar 2020)

Abstract. Multiple experiments were performed to evaluate the ecotoxicological effect of mesotrione on soil enzymatic activity, functional diversity, and genetic microbial biodiversity. The results showed that catalase and invertase activity initially increased with higher mesotrione concentration and then declined slightly. However, urease activity experienced a 11.9–23.2% reduction in comparison to control soil. The average well-color development (AWCD) was positively affected by the mesotrione treatment, the amount of carbohydrate, amino acid, and phenolic acid increased by 1.7–2.1, 1.1–1.6, and 1.7–2.5 times, respectively, when compared with the blank treatment. However, the utilization of carboxylic and acid amine was prohibited after applying 50–100 mg kg^{-1} and 20–100 mg kg^{-1} mesotrione. Denaturing gradient gel electrophoresis (DGGE) analysis showed that the shift in the bacterial community structure for different mesotrione treatments can be mainly attributed to an increment in band intensity, while the dissimilarity in the bacterial genetic structure decreased with increasing mesotrione content in the soil. Sequencing and phylogenetic analyses showed that the four bands in the denaturing gradient gel electrophoresis results were closely related to *Bacillus subterraneus*, *Clostridium sp*., and *Bacillus sp*. Obtained results show that abuse of mesotrione may pose a potential risk for soil microbial functioning.
Keywords: *mesotrione, Biolog EcoPlates, denaturing gradient gel electrophoresis, eco-environmental impact*

Introduction

Soil microbes are fundamental components of a soil's ecosystem playing an important role in many metabolic processes, e.g. the biogeochemical cycling of nutrients, decomposition of organic matter, formation of structural and hydrological properties, and various other biological–physical–chemical processes in the soil (Hu et al., 2011; Liu et al., 2015). Microorganisms can also serve as environmental bioindicators of quality due to their rapid and sensitive response to small environmental disturbances (Zhang et al., 2010; Cycoń et al., 2013b; Gryta et al., 2014). Thus, the microbial properties of the soil, and particularly those related to the diversity and activity of the soil's microbial communities, can be a most useful predictor of the fluctuation in soil health (Zhang et al., 2010; Chen et al., 2014; Allegrini et al., 2015). Soil enzyme also plays an important role in the microbial soil ecology by catalyzing various reactions, including those involved in the decomposition of organic residues and

http://www.aloki.hu ● ISSN 1589 1623 (Print) ● ISSN1785 0037 (Online)
DOI: http://dx.doi.org/10.15666/aeer/1802_35253541

nutrient cycling in soil–plant systems (Bhattacharyya et al., 2008; Sun et al., 2013a; Giacometti et al., 2014). In general, microbial activity and soil enzyme activity are usually influenced by various soil management practices, e.g. crop rotation, mulching, tillage, and the application of fertilizers and herbicides (Johnsen et al., 2001; Hua et al., 2009; Lupwayi et al., 2010). Therefore, these can all be used as potential indicators of microbial activity, soil fertility, and land quality (Ciarkowska et al., 2014).

Mesotrione [2-(4-methylsulfonyl-2-nitrobenzoyl)-1,3-cyclohexanedione] is a triketone herbicide that has recently been registered for the pre- and post-emergence control of annual broadleaved weeds in maize fields, and constitutes a replacement for atrazine (Sun et al., 2013b; Pose-Juan et al., 2015). Armel et al. (2009) reported that a dose equal to 235 g ai ha^{-1} was required to provide effective (≥80%) control of some common weeds (lamb's quarters, smooth pigweed, and common ragweed). Vyn et al. (2006) documented successful control (≥90%) of another *Amaranthus* species (*Amaranthus tuberculatus* var. rubis) at mesotrione doses of 175 (pre-emergence) and 100 g ai ha^{-1} (post-emergence). However, our previous studies found that the adsorption isotherms of mesotrione fit well into first-order and Freundlich equations. The hysteresis indices in phaeozem and red soil indicated that it had weak–moderate soil retention properties (Sun et al., 2015) and its degradation time (DT_{50}) varies from 6 to 34 d (Crouzet et al., 2010). Therefore, the continuous and extensive use of the herbicides would pose side-effects on the function and fertility of agricultural soils. A few studies have attempted to determine the effects of mesotrione on the nitrogen cycle, enzyme activity, and microbes in soil (Crouzet et al., 2010, 2013; Cycoń et al., 2013a; Pose-Juan et al., 2015). Crouzet et al. (2010) found that mesotrione applied at a dose of 0.45 mg kg^{-1} did not have any effect on the substrate-induced respiration, regardless of the post-treatment exposure time. However, higher doses (45 and 450 mg kg^{-1}) of mesotrione induced significant increases. Similarly, mesotrione had a strong negative impact on soil chlorophyll concentration and cyanobacterial genetic structure and diversity when its content was up to 450 mg kg^{-1} (Crouzet et al., 2013).

Non-targeted effects of herbicides on soil microorganisms can reduce microbial diversity but increase functional diversity. There may even be a tendency towards reversible stimulatory/inhibitory effects on microbial community structure and activity (Zabaloy et al., 2010; Pose-Juan et al., 2015). It has been reported that herbicides are adsorbed by organic matter in the soil to form bound or recalcitrant states, which, in turn, reduces the possibility of microbial attack (Crouzet et al., 2010). This might also account for the insignificant effect (or masking) of the impact of herbicides on the activity of enzymes (Cai et al., 2015). These effects depend on the herbicide's properties and environmental chemical behavior, soil type, environmental conditions, and functioning of the soil's microorganisms (Lupwayi et al., 2010; Pose-Juan et al., 2015). It is therefore essential to assess the ecological and environmental impact of newly marketed xenobiotics such as mesotrione in China. Unfortunately, information on the environmental impact of mesotrione in the soil (on enzyme activity and diversity of the microbial communities) is lacking. Therefore, the experiments reported here are the first aimed at extending our knowledge of these aspects. The objectives of the present study are to determine mesotrione's effects on: (1) soil enzymatic activity (via a microcosm approach), (2) functional diversity (using the Biolog method), and (3) genetic microbial biodiversity (using a method based on denaturing gradient gel electrophoresis, DGGE).

http://www.aloki.hu ● ISSN 1589 1623 (Print) ● ISSN1785 0037 (Online)
DOI: http://dx.doi.org/10.15666/aeer/1802_35253541

Materials and methods

Test chemicals

The mesotrione ($C_{14}H_{13}NO_7S$) was purchased from Sigma-Aldrich (St. Louis, MO, USA) in the form of dispersible granules (high performance liquid chromatography (HPLC) grade with a purity of 99.9%). The solubility of mesotrione in water increases with pH value (being 2.2, 15, and 22 g L^{-1} at pH 4.8, 6.9, and 9.0, respectively), and the stability stable to hydrolysis is at pH 4–9 (pKa 3.12).

Experimental design and treatment regime

The present research was conducted in Agro-environmental Protection Institute, Ministry of Agriculture and Rural Affairs, China. 10 kg soil samples were collected from 0-20 cm layer of agricultural fields in Changsha City, China (28º03' N and 113º 11' E) and then passed through a 20 mesh sieve for the analysis of physical and chemical fraction. The basic characteristics of this ferralsol soil are that it consists of 44.9% clay, 8.6% silt, and 46.5% sand. The amount of organic matter, total N, pH, available P, and available K equate to 1.03%, 0.84 g kg^{-1}, 4.92, 3.95 mg kg^{-1}, and 40 mg kg^{-1}, respectively.

Weighed amounts (500 g) of dried and sieved soil were placed in plastic pots and preincubated under controlled experimental conditions for two weeks. The effect of mesotrione on soil enzymatic activity and the microbial communities was investigated using 4 different doses of 0, 20, 50 and 100 mg kg^{-1}, respectively. After mixing thoroughly, the treated soils were incubated in a dark experimental chamber at 21 ± 1°C for 30 d, and changed randomly every week. To make moisture conditions comparable to those in the field, the soil's moisture content was adjusted to 40% of the maximum (saturated) value. This was subsequently maintained throughout the experiment by weighing the microcosms on a weekly basis and adding sterile distilled water as needed.

Enzyme assay

Catalase activity was assayed according to the method used by Sun et al. (2015). The measured enzymatic activities were then calculated and expressed using units of mg g^{-1} h^{-1}. Urease activity was measured using the method adopted by Chen et al. (2014) with slight modification. The enzymatic activity was calculated and expressed as NH_4–N mg g^{-1} h^{-1}. Invertase activity was determined using an 8% sucrose solution as substrate and incubation at 37°C for 24 h, after which the glucose produced was measured at 508 nm using a colorimetric method. The enzymatic activity was finally expressed as mg g^{-1} h^{-1} (Kandeler et al., 1999).

Microbiological analyses

Functional diversity determination

The community-level physiological profiles (CLPPs) of the bacteria in the soil samples were evaluated using a Biolog EcoPlate™ system (Biolog Inc., CA, USA). This procedure tests the ability of a microbial community to utilize different carbon substrates contained in microplates. The soil samples (10 g) were mixed with 0.85% NaCl and then shaken for 1 h. After this time, aliquots (150 µL) of the soil suspension were added to the Biolog EcoPlate® microplates containing 31 sole carbon sources and

http://www.aloki.hu ● ISSN 1589 1623 (Print) ● ISSN1785 0037 (Online)
DOI: http://dx.doi.org/10.15666/aeer/1802_35253541

a water control. The plates were incubated at 24°C in the dark. Color development in each well was recorded in terms of the optical density (OD) at 590 nm (color development + turbidity) and 750 nm (turbidity). This was carried out after inoculation and at 24 h intervals for 168 h using a microplate reader (Victor TM X5 multilabel plate reader, PerkinElmer) (Osem et al., 2007; Cycoń et al., 2013b). Negative readings, after correction, were adjusted to zero.

Analysis of the microbial structure diversity

The total bacterial DNA in the test soils was extracted and purified according to previously published methods (Qing et al., 2007; Huang et al., 2008). It was then amplified via PCR using forward primer F_{357} (5'-CCT ACG GGA GGC AGC AG-3') and reverse primer R_{518} (5'-ATT ACC GCG GCT GCT GG-3'). As for the forward primer, a 40-base GC clamp (5'-CGC CCG CCG CGC GCG GCG GGC GGG GCG GGG GCA CGG GGG G-3') was added to the 5' end to stabilize the melting behavior of the DNA fragments. The gradient concentrations used in the denaturing gradient gel electrophoresis (DGGE) analysis ranged from 35% to 65% for bacterial DNA. Initial denaturation was carried out at 94°C for 4 min. Amplification was carried out using 35 cycles including denaturation at 94°C for 1 min, annealing at 55°C for 1 min, and DNA extension at 72°C for 1 min, followed by a final extension cycle at 72°C for 10 min.

PCR products from the soils were characterized using a DGGE run on a vertical acrylamide gel in a D-Code System (Bio-Rad Laboratories Ltd., Hertfordshire, UK). The DGGE gels were made from 8% (w/v) acrylamide stock solutions (37.5:1 of acrylamide:bis acrylamide solution) containing 100% denaturant (7 mol L^{-1} urea and 40% (v/v) formamide). The DGGE bands of interest were cut from the gel and soaked overnight at 4°C in 50 μL TAE buffer (10 mmol L^{-1} tris-acetate, pH 7.5, 1 mmol L^{-1} EDTA). The gel was stained for 15 min with ethidium bromide after electrophoresis and visualized using a UV transilluminator table using a gel documentation system (Bio-Rad, Hercules, CA, USA).

The 16S rDNA gene sequences of the excised DGGE bands were compared with existing sequences in the GenBank database using the BLAST 2.0 program (http:/www.ncbi.nlm.nih.gov/BLAST) to determine the nearest matches. The GenBank sequences were added to the data set for CLUSTAL W multiple sequence alignment and the phylogenetic distance tree was constructed using MEGA 4.0.

Statistical analysis

All of the experiments were replicated three times. The means and standard deviations (SDs) of the replicated data were calculated using Microsoft Office Excel 2010. One-way analysis of variance was performed using the SPSS (v10.0) software package. When a significant difference ($P < 0.05$ or $P < 0.01$) was observed between the treatments, multiple comparisons were made by performing an LSD test. Principal component analysis (PCA) was used to identify distinct differences in the soil microbial community functions under different mesotrione treatments.

Average well-color development

The average well-color development (AWCD) can be calculated to reflect the sole-carbon utilization of the soil microorganisms via *Equation 1*:

http://www.aloki.hu ● ISSN 1589 1623 (Print) ● ISSN1785 0037 (Online)
DOI: http://dx.doi.org/10.15666/aeer/1802_35253541

$$AWCD = \sum (C_i - R)/31 \quad \text{(Eq.1)}$$

where C_i is OD in each carbon source well and R is OD of the control. When C_i–R < 0, the value is considered to be zero.

Microbial functional diversity indices

Several diversity indices can be calculated using the equations that follow. These are referred to as the Shannon index (H), Simpson index (D), Shannon evenness index (E), McIntosh index (U), and Dice index (C_s), and are given by *Equations 2-6*:

$$H = -\sum P_i \ln\left(P_i\right) \quad \text{(Eq.2)}$$

$$D = 1 - \sum P_i^2 \quad \text{(Eq.3)}$$

$$E = \frac{H}{H_{\max}} = \frac{H}{\ln S_i} \quad \text{(Eq.4)}$$

$$U = \left(\sum N_i^2\right)^{1/2} \quad \text{(Eq.5)}$$

$$C_s = \frac{2j}{a+b} \quad \text{(Eq.6)}$$

In these expressions, N_i is the metabolic activity on each substrate, P_i is the ratio of n_i to the sum of the activities on all substrates, S_i is the natural logarithm of the number of species, j is the number of bands common to samples A and B, and a and b are the number of bands in samples A and B, respectively.

Results and discussion

Soil enzymatic activity

In the present study, the catalase activity initially increased and then declined as the amount of mesotrione increased. Under the application of 20 and 50 mg kg^{-1} mesotrione, the increase was amounted to 11.2% and 12.6%, respectively (*Fig. 1*). However, catalase activity fell by 2.7% when the concentration of mesotrione was increased up to 100 mg kg^{-1}. There was no significant difference in catalase activity across the 20–100 mg kg^{-1} mesotrione treatment range (P > 0.05). Similar results have been obtained by Baćmaga et al. (2014), who found that metazachlor applied at doses of 6.7–106.7 mg kg^{-1} stimulated the activity of catalase in the range of 7.5–92.5%. Moreover, Liu (2000) reported that imidacloprid can also stimulate catalase activity, and that the higher the concentration used, the stronger the observed effect on soil catalase for imidacloprid doses in the range 1–40 mg kg^{-1}. However, there was no obvious effect on catalase activity after application of 0.5 to 50 mg kg^{-1} of acetamiprid for 14 days (Yao et al., 2006).

http://www.aloki.hu ● ISSN 1589 1623 (Print) ● ISSN1785 0037 (Online)
DOI: http://dx.doi.org/10.15666/aeer/1802_35253541

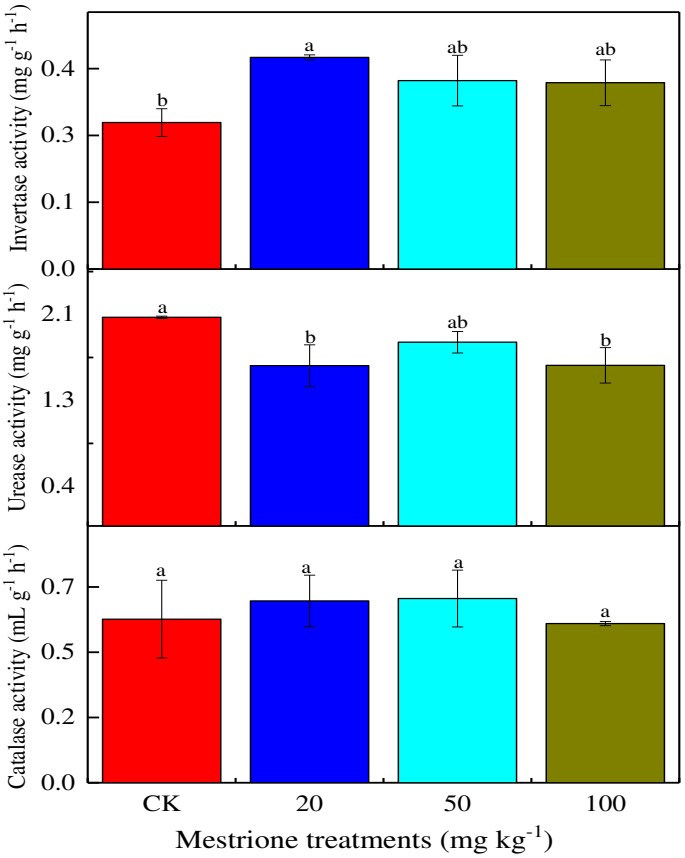

Figure 1. *Effects of mesotrione on soil enzyme activities. Letters above the bar diagram refer to the difference at significance level $P < 0.05$ among different treatments of mesotrione. The same as below*

Urease, which involves in the hydrolysis of urea-type substrates, is an enzyme that quickly responds to changes in the soil environment (Yao et al., 2006). Furthermore, contamination of soil with mesotrione has a destructive influence on the activity of urease. The application of mesotrione caused a 11.9–23.2% reduction in urease activity compared with control soil (*Fig. 1*), and amending the soil with 20 and 100 mg kg^{-1} mesotrione resulted in a significant decrease in urease activity ($P < 0.05$). Results similar to ours concerning the inhibitory effects of herbicides on urease activity have been reported by Baćmaga et al. (2014) who investigated metazachlor and by Sukul (2006) who tested metalaxyl. In turn, Yao et al. (2006), who investigated the eco-toxicology of the herbicide acetamiprid, did not detect any obvious influence on urease activity.

Another enzyme used in assays evaluating the quality of soil is invertase, which is involved in the hydrolysis of sucrose to glucose and fructose. Invertase is more efficient than other enzymes in reflecting soil fertility and biological activity levels (Cang et al., 2009). *Fig. 1* exhibits the promotion effect of mesotrione on invertase activity in the soil, which increased at first and then decreases with increasing concentration. It was, however, always 27.1–44.4% greater than that of the control soil over the 20-100 mg kg^{-1} mesotrione range. In particular, there was a significant increase using 20 mg kg^{-1} of mesotrione ($P < 0.05$). Positive effects of buprofezin and acephate on invertase had already been noted by Raju and Venkateswarlu (2014).

http://www.aloki.hu ● ISSN 1589 1623 (Print) ● ISSN1785 0037 (Online)
DOI: http://dx.doi.org/10.15666/aeer/1802_35253541

The results above clearly indicate that soil enzyme activity differs in sensitivity upon application of herbicide. Ye et al. (2003) likewise found that mefenacet strongly prohibited soil dehydrogenase activity in a concentration-dependent manner, but stimulated phosphatase activity. Indeed, both significantly positive and negative, as well as neutral, responses have been recorded compared to untreated soils (Floch et al., 2011; Baćmaga et al., 2014). Herbicides may change enzyme protein or interact directly by binding with protein-active groups which subsequently affects their catalytic activity. Another possible reason is that a herbicide may indirectly affect soil enzyme activity by acting on soil microorganisms (Johnsen et al., 2001; Floch et al., 2011; Baćmaga et al., 2014; Jacobsen and Hjelmsø, 2014). Baćmaga et al. (2014) demonstrated that in soil contaminated with excessive quantities of metazachlor there are significant effects on the biochemical activity of the soil (with correlation coefficients that are negative). In another report, no significant differences ($P > 0.05$) were found in enzyme activity in treated soil compared to a control in the initial 2 weeks, while enzyme activity was stimulated from the third week on (Yao et al., 2006). Moreover, the influence of pesticide on soil was generally a long-term process and closely related to the soil's characteristics (Yao et al., 2006).

Microbial community substrate utilization profile

Color development in the Biolog EcoPlates was analyzed to qualitatively and quantitatively assess the community-level physiological profile of the microbe communities in treated soils (Osem et al., 2007; Gryta et al., 2014). The average well-color development in the Biolog generally followed similar patterns (*Fig. 2a*), i.e. an apparent lag phase was experienced during the first 48 h. After this time, the AWCD values increased rapidly with incubation time for all treatments which is attributable to more rapid bacterial growth taking place. The period selected for metabolic activity analysis was 120 h as this period corresponded to the occurrence of the largest AWCD change. The slope of the AWCD curve at this time can be used to represent the average metabolic activity of a microbial sample (Kong et al., 2013). Thus, the slopes of the AWCD curves after 120 h were selected for use in the metabolic activity analysis. The analysis of the variation in AWCD in the stressed soils over the incubation time (during the period 0–120 h), showed that the AWCD values using 20–100 mg kg^{-1} of mesotrione were all higher than those of the control. Strong oxidation of the supplied carbon sources (high AWCD) usually reflects an increase in bacterial density (Loranger-Merciris et al., 2006). A possible reason for this might be that soil microbes tolerate and adapt to the herbicide after repeated applications, and/or degrade the herbicide as a source of carbon and energy (Yao et al., 2006; Xu et al., 2014). However, after an incubation time of 168 h, the AWCD values decreased with an increase in mesotrione, and a dose–effect relationship could be discerned.

The substrate utilization patterns currently established via the Biolog Ecoplates can be used to determine the changes in the functioning of the soil microbial communities (Floch et al., 2011). As shown in *Fig. 2b*, there were remarkable differences in the substrate utilization profiles of the mesotrione treated soil samples. Carbon source metabolism by the microbial population decreased in the following order: polymer > amino acid > carbohydrate > phenolic acid > acid amine > carboxylic acid. This suggested that the carboxylic acid could be more easily utilized by the microbes subjected to the different mesotrione treatments. Although the variation in the carbon sources appeared to be irregular under the series of mesotrione treatments, the increase

http://www.aloki.hu ● ISSN 1589 1623 (Print) ● ISSN1785 0037 (Online)
DOI: http://dx.doi.org/10.15666/aeer/1802_35253541

in the amount and rate of carbohydrate, amino acid, and phenolic acid utilization observed in the soils subjected to different mesotrione treatments corresponded to increases of 1.7–2.1, 1.1–1.6, and 1.7–2.5 times, respectively (compared to the control). Significant increases ($P < 0.05$) in substrate utilization were observed with a mesotrione concentration of 20 mg kg^{-1} for carbohydrate and amino acid, and 100 mg kg^{-1} for polymer and phenolic acid. However, there appeared a decrease in polymer, carboxylic, and acid amine by 3.0%, 12.5–17.1%, and 13.3–48.1%, respectively, in mesotrione treated soil of 50, 50–100, and 20–500 mg kg^{-1}, respectively, and the amount of acid amine decreased sharply at a mesotrione content of 20 mg kg^{-1} ($P < 0.05$).

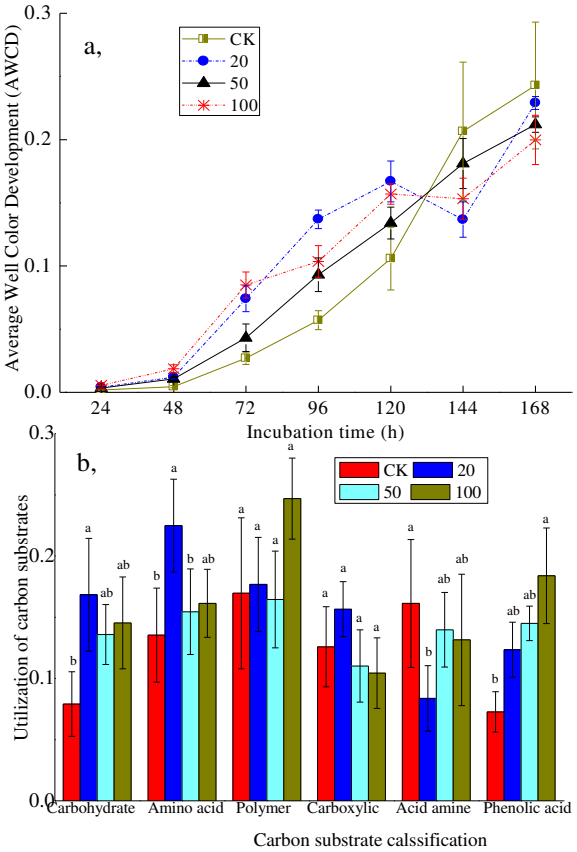

Figure 2. *Microbial community level physiological profiles (CLPP) under different treatments of mesotrione. Note: (a) and (b) refers the variations in AWCD over time and utilization of 6 groups carbon sources, respectively*

Principal component analysis (PCA) was used to assess the microbial communities in the stressed-soil environment (Kong et al., 2013; Shrestha et al., 2015). The PCA results from the Biolog Ecoplates data explained 67.3% of the total variance and components, and the first principal components (PC1) and the second principal components (PC2) accounted for 37.1% and 30.2%, respectively (*Fig. 3a*). Therefore, the first two principal components (PC1 and PC2) were used to describe the effects of the different treatments of mesotrione (0–200 mg kg^{-1}) on the utilization of 31 carbon sources. PC1 and PC2 are plotted against each other in *Fig. 3* for illustration purposes. The PCA plots indicated that bacterial functional diversity changes with the level of mesotrione used.

http://www.aloki.hu ● ISSN 1589 1623 (Print) ● ISSN1785 0037 (Online)
DOI: http://dx.doi.org/10.15666/aeer/1802_35253541

Most of the points were clustered in the first and second quadrants of the loading plot, and the plots amended with 20–100 mg kg^{-1} mesotrione were clustered together and are differentiated from the control. *Fig. 3b* also compares the Biolog Ecoplates utilization patterns for each substrate guild (i.e. carbohydrate, amino acid, polymer, carboxylic, acid amine, and phenolic acid) for different mesotrione treatments, using PCA. The first variable (PC1) accounted for 54.8% and the second variable (PC2) accounted for 28.7% of the total variance in the data. Rotation of the matrix revealed that the substrate utilization can be separated into three groups: (a) amino acid and carboxylic (relatively negatively related with PC2), (b) carbohydrate and phenolic acid (positively associated with values of PC1 and PC2), and (c) polymer and acid amine (associated with negative values of PC1 and PC2). The PCA plots indicate that the bacterial communities originally present in the tested soil were shifted after application of mesotrione.

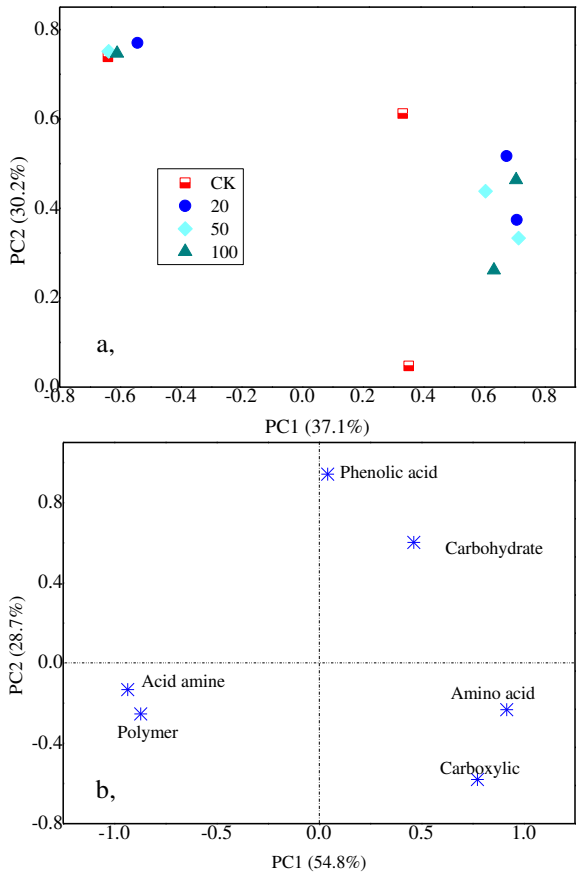

Figure 3. *Scatterplots of principal components scores for soil samples based on (a) different treatments of mesotrione and (b) 6 carbon sources. Numbers in parentheses on axis labels is the percentage of the variation according to principal components analysis (PCA)*

To further investigate the effect of mesotrione on the bacterial properties of the soil, the diversity indices of *H*, *D*, *E*, and *U* are calculated to assess the soil's microbial functional diversity (Gomez et al., 2006), *H* and *E* values indicate the richness and evenness of the soil microorganisms (Zhou et al., 2008), index *D* is often used to emphasize the dominant microbe population, and while *U* (which is based on Euclidean distance) indicated the evenness or homogeneity of the microbial community (Zhou et

http://www.aloki.hu ● ISSN 1589 1623 (Print) ● ISSN1785 0037 (Online)
DOI: http://dx.doi.org/10.15666/aeer/1802_35253541

al., 2008). The calculated values of the diversity indices of *H*, *D*, *E*, and *U* are presented in *Table 1*. In general, the *H*, *D*, and *U* values gradually increased with incubation time and then fell. However, the amount of *H*, *D*, and *U* was still 6.6–36.1%, 2.0–12.2%, and 70.1–894.0% greater than those of the control, respectively. Index *E* decreased by 1.6-14.1%, 18.1–32.1%, 7.6–14.6%, and 12.9–27.8%, under mesotrione treatments of 0, 20, 50, and 100 mg kg^{-1}, respectively, when compared with the control. The microbial community analysis was consistent with substantial increases in microbe diversity in the treated soil. The *H*, *E*, *D*, and *U* values were stimulated by the various mesotrione treatments, corresponding to increases of 2.7–3.4%, 1.3–10.2%, 1.4–2.2%, and 6.6-20.0%, respectively (compared to the control). The increase in the microbial activity in the soil may have been higher and the microorganisms more active if the mesotrione was used as an energy source (Crouzet et al., 2010; Zabaloy et al., 2010). The regression coefficients between the richness and Shannon–Weaver indices and organic carbon in the soil suggested that the increase in microbial community functional potential may be explained by the increase in carbon availability resulting from incorporation of the amendment (Gomez et al., 2006). The microorganism communities may have been indirectly stimulated by the dead biomass arising from more sensitive organisms together with a concomitant stimulation of the resistant microbial populations resulting from the loss of protozoan grazers or competitors (Crouzet et al., 2010). The number of live bacteria present was generally higher ($P < 0.01$) in linuron amended soil than in unamended soil (Grenni et al., 2009). However, there were no significant differences observed in the functional diversity parameters *H*, *E*, and *U* among the different mesotrione treatments ($P > 0.05$).

Table 1. *Diversity indices of Biolog in soils treated with mesotrione*

Diversity indices	Mesotrione (mg kg^{-1})	Time (h)							Mean + S.D.
		24	48	72	96	120	144	168	
Shannon index (*H*)	0	1.94±0.08c	2.61±0.17a	2.56±0.15a	2.65±0.11a	2.63±0.10a	2.64±0.07a	2.64±0.11a	2.52±0.26a
	20	2.37±0.01a	2.94±0.12a	2.53±0.12a	2.57±0.10a	2.59±0.09a	2.55±0.07a	2.71±0.05a	2.61±0.18a
	50	2.15±0.11b	2.91±0.18a	2.59±0.19a	2.68±0.26a	2.63±0.14a	2.61±0.15a	2.57±0.13a	2.59±0.26a
	100	2.24±0.04a	2.56±0.34a	2.74±0.17a	2.66±0.15a	2.73±0.12a	2.61±0.13a	2.68±0.15a	2.60±0.22a
		$P < 0.01$	$P > 0.05$	$P > 0.05$	$P > 0.05$	$P > 0.05$	$P > 0.05$	$P > 0.05$	$P > 0.05$
Shannon evenness index (*E*)	0	2.80±0.12c	2.81±0.64a	2.76±0.64	2.41±0.10a	2.39±0.09a	2.40±0.06a	2.41±0.10a	2.57±0.36b
	20	3.42±0.01a	2.67±0.11a	2.73±0.63	2.78±0.68a	2.80±0.69a	2.32±0.06a	2.47±0.05a	2.74±0.49ab
	50	3.10±0.16b	2.65±0.17a	2.79±0.59	2.86±0.54a	2.84±0.63a	2.81±0.62a	2.77±0.63a	2.83±0.45a
	100	3.23±0.06ab	2.33±0.31a	2.49±0.15	2.42±0.14a	2.49±0.11a	2.81±0.64a	2.44±0.14a	2.60±0.38ab
		$P < 0.01$	$P > 0.05$	$P > 0.05$	$P > 0.05$	$P > 0.05$	$P > 0.05$	$P > 0.05$	$P > 0.05$
Simpson index (*D*)	0	0.81±0.02b	0.91±0.02ab	0.86±0.04b	0.89±0.03a	0.90±0.02a	0.91±0.00a	0.91±0.00a	0.89±0.04b
	20	0.89±0.00a	0.94±0.00a	0.90±0.00a	0.91±0.01a	0.91±0.00a	0.88±0.02b	0.91±0.01ab	0.90±0.02a
	50	0.87±0.01a	0.94±0.00a	0.90±0.00a	0.91±0.02a	0.91±0.00a	0.90±0.01a	0.89±0.01b	0.90±0.02a
	100	0.87±0.11a	0.87±0.05b	0.91±0.01a	0.91±0.01a	0.92±0.01a	0.90±0.01ab	0.90±0.01ab	0.90±0.03ab
		$P < 0.01$	$P < 0.05$	$P < 0.05$	$P > 0.05$	$P > 0.05$	$P < 0.05$	$P > 0.05$	$P < 0.05$
McIntosh index (*U*)	0	0.02±0.00b	0.04±0.00b	0.32±0.09b	0.59±0.14c	1.03±0.31b	1.92±0.05a	2.22±0.47a	0.88±0.88a
	20	0.04±0.00ab	0.09±0.01b	0.72±0.11a	1.27±0.11a	1.59±0.17a	1.47±0.25a	2.17±0.11sa	1.05±0.76a
	50	0.04±0.00b	0.08±0.01b	0.42±0.12b	0.85±0.19bc	1.25±0.10ab	1.74±0.13a	2.16±0.10a	0.93±0.79a
	100	0.06±0.03a	0.21±0.07a	0.78±0.14a	0.97±.17b	1.42±0.15a	1.51±0.23a	1.91±0.28a	0.98±0.67a
		$P < 0.05$	$P < 0.01$	$P < 0.01$	$P < 0.01$	$P < 0.05$	$P > 0.05$	$P > 0.05$	$P > 0.05$

The same letters are not significantly at P=0.05 (n=3) between different treatments of mesotrione according to the LSD test

http://www.aloki.hu ● ISSN 1589 1623 (Print) ● ISSN1785 0037 (Online)
DOI: http://dx.doi.org/10.15666/aeer/1802_35253541

Effect of mesotrione on microbial community structure diversity

The changes in the bacterial structures of the tested soils were elucidated according to PCR–DGGE phylotype. The *H* and *D* indices were calculated to estimate the bacterial diversities in the mesotrione-amended and control soils (*Table 2*). The value of *H* increased after different amounts of mesotrione were applied to the soil, being 0.7-3.6% higher than the *H* value of the control group. However, differences in the *D* index were negligible for the different mesotrione treatments. This indicated the stimulation effect or toxicity of the mesotrione on the soil microbial community was small (Hu et al., 2007).

Table 2. *Diversity indices of DGGE in soils treated with mesotrione*

Treatment of mesotrione (mg kg^{-1})	Shannon index (*H*)	Shannon evenness index (*E*)
0	3.02±0.78	0.93±0.13
20	3.13±1.02	0.96±0.24
50	3.04±0.81	0.95±0.34
100	3.12±0.93	0.95±0.29

The bacterial DGGE profiles generated using universal bacterial primers (F357 and R518) revealed the structural compositions of the communities in the soil samples (*Fig. 4a*). The results showed that there are certain differences in the bacterial community diversities in the soils – some bands disappeared and several new bands appeared – following mesotrione application. The disappearance of bands A and B revealed that the bacterial community structures and genetic diversity were affected by the increase in mesotrione concentration. It appeared that the number of bands is related to the mesotrione content. Nine bands (labeled a–i in *Fig. 4a*) were shared in all profiles. This suggested that the bacterial groups represented by these bands may play an important role in mesotrione ecology (Gu et al., 2010). However, the number of bands in the soil samples initially increased with increasing mesotrione content, and then decreased slightly. Significant increases in microbial biomass were found afterwards (compared to the biomass values in unamended soil) in all cases. The microbial biomass was thus significantly increased. Moreover, the similarity indices decreased with increasing mesotrione content (varying from 68.0% to 47.6%). Similarly, the maximum dissimilarity in the bacterial and fungal genetic structures between the control and 100-fold field rate (FR) treated soil did not exceed 12% and 28%, respectively (Crouzet et al., 2010). This may be due to excessive stimulation of cellular redox processes which reflects an unspecified stress response of the microorganisms in the soil.

Clustering of the DGGE profiles was performed (to elucidate the similarities among the different banding patterns) and the results presented using a dendrogram (Zhang and Fang, 2000). The advantage of this method of presentation was that the coherence in the fingerprinting patterns can be rapidly assessed (Fromin et al., 2002). It can be seen that the 20–100 mg kg^{-1} mesotrione treatments belong to a common cluster which had a similarity among them of over 60%, and 53% difference with the control group profiles (*Fig. 4a*). This showed that the bacterial communities in the soil changed upon addition of herbicide. El Fantroussi et al. (1999) compared the microbial communities in soil treated with three phenylurea herbicides (diuron, linuron, and chlorotoluron) using cluster analysis. They found that the microbial communities were significantly different compared to untreated soil.

http://www.aloki.hu ● ISSN 1589 1623 (Print) ● ISSN1785 0037 (Online)
DOI: http://dx.doi.org/10.15666/aeer/1802_35253541

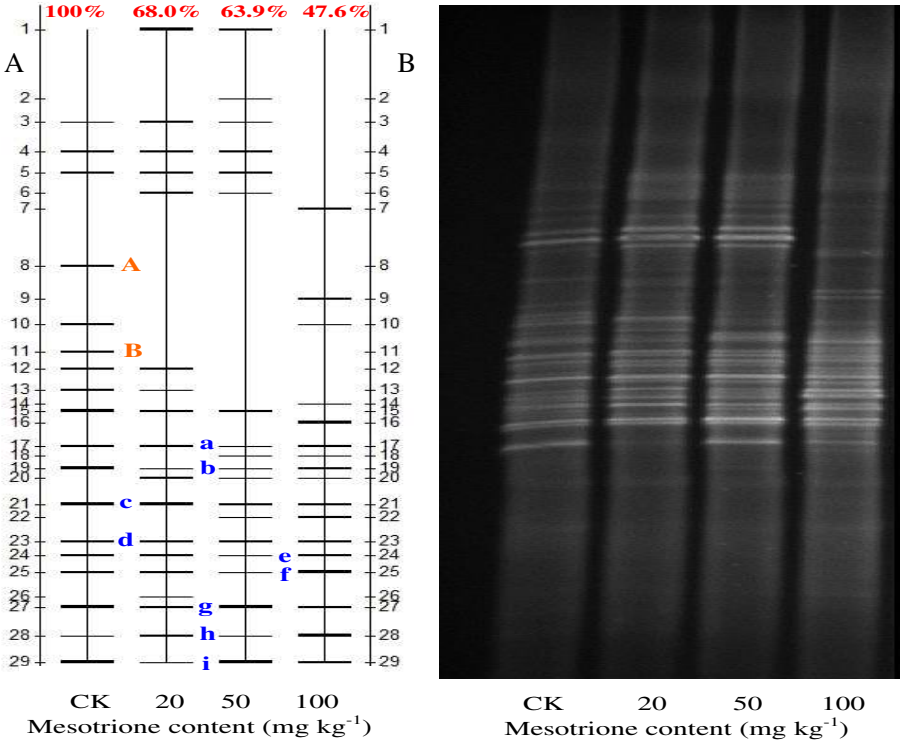

Figure 4. *Comparison of bacterial communities between the control and the three treatments. Note: (A) the analysis results of lane comparison from the DGGE gels using Quantity One V4 4.0.0 software, and (B) DGGE profiles for PCR-amplified fragments of 16 sDNA. A, B, and a-i refer the bands of bacterial DGGE profiles*

To obtain insight into the identities of the major bacterial populations, the discernible DGGE bands in the different mesotrione-treated samples (*Fig. 4b*) were all excised and used for nucleotide sequence analysis. Then, a BLAST search was conducted using the GenBank database to determine their phylogenetic types (*Table 3*). The sequences from bands a, c, and d were found to be closely related to members of the genus *Desulfitobacterium sp*. These are sulfate-reducing bacteria that can grow using meta-chlorinated benzoic acids as electron acceptors and are known to dechlorinate chlorinated phenols and other chlorinated compounds (Yoshida et al., 2007; Jing et al., 2013). The 16S rDNA of the isolated band b closely matched that of *Herbaspirillum sp.* (98%). Bacteria of this genus fall into the β-*Proteobacteria* class and include known nitrogen-fixing endophytes (Doty et al., 2009) and can enhance the phytoremediation of volatile organics and herbicides (Ryan et al., 2008). Band e can be identified (99%) with *Burkholderia caledonica* which had been found to degrade compounds such as herbicides (Hunter and Shaner, 2012), pentachlorophenols (Caliz et al., 2011), and a variety of aromatic hydrocarbons (Stopnisek et al., 2015). Band f showed 100% sequence similarity to a taxonomically unidentified bacterium. Bands g and h were identical to those from strains *Bacillus subterraneus* and *Clostridium sp.*, with 100% similarity. This also showed the capacity of these strains to acclimatize to organic compound pollution. The 16S rDNA sequences of band i were 100% similar to the 16S rDNA sequences of *Bacillus sp*. These bacteria commonly occurred in mesotrione-treated soil and was able to completely and rapidly biotransform mesotrione (Batisson et al., 2009). Biodegradation assays showed that *only* the *Bacillus sp*. strain

http://www.aloki.hu ● ISSN 1589 1623 (Print) ● ISSN1785 0037 (Online)
DOI: http://dx.doi.org/10.15666/aeer/1802_35253541

was able to completely and rapidly bio-transform mesotrione (Durand et al., 2006a, 2006b; Batisson et al., 2009). This is because of the bacterial reductase that is involved in the enzymatic step in which the nitro group of mesotrione is reduced to an hydroxylamine moiety during the degradation process (Durand et al., 2010).

Table 3. *Sequence analysis of bands excised from DGGE gels derived from bacterial 16S rDNA fragments*

Band	Closest organisms in the GenBank database	Accession no.	Similarity (%)
a	*Desulfitobacterium sp.*	AB596883.1	99
b	*Herbaspirillum sp.*	AB769218.1	98
c	*Desulfitobacterium sp.*	AB596883.1	98
d	*Desulfitobacterium sp.*	AB596883.1	97
e	*Burkholderia caledonica*	KM019850.1	99
f	*Uncultured bacterium*	KM153196.1	100
g	*Bacillus subterraneus*	LN774202.1	100
h	*Clostridium sp.*	JQ420069.1	100
i	*Bacillus sp.*	KJ769178.1	100

Conclusions

The results described in this study show that the treatment of soil with mesotrione was able to stimulate 7.5–92.5% and 27.1–44.4% increase for catalase and invertase activity, while urease activity was inhibited by 11.9–23.2%. CLPPs were obtained that reflect the increase in the amount and rate of carbon utilization of carbohydrate, amino acid polymer and phenolic acid observed in soil subjected to different mesotrione treatments. In contrast, the AWCD of carboxylic and acid amine was inhibited after the application of 50–100 mg kg^{-1} and 20–100 mg kg^{-1} mesotrione, and principal component analysis plots showed that microbial function diversity changed with mesotrione level and each substrate guild. The resulting diversity indices (*H*, *D*, *E*, and *U*) indicate that mesotrione-treated soil had a greater number of more active microorganisms. Our DGGE analysis showed that mesotrione caused slight changes to be made to the biodiversity of the soil bacteria. However, the appearance of some new bands in the DGGE profiles suggests that mesotrione treatment does not have significantly toxic effects on the soil function. In future, it would be useful if further research on the impact of mesotrione could be more integrated with the farming procedures employed, especially herbicide continuous and extensive use. This should provide a more comprehensive understanding of the response of the microbial community in the soil.

Acknowledgements. This work was supported by the National Natural Science Foundation of China (21107056; 31971525) and the Central Public Research Institutes Basic Funds for Research and Development.

REFERENCES

[1] Allegrini, M., Zabaloy, M. C., Gómez, E. D. V. (2015): Ecotoxicological assessment of soil microbial community tolerance to glyphosate. – Science of The Total Environment 533: 60-68.

[2] Armel, G. R., Wilson, H. P., Richardson, R. J., Hines, T. E. (2009): Mesotrione Combinations in No–Till Corn (*Zea mays*). – Weed Technology 17(1): 111-116.

http://www.aloki.hu ● ISSN 1589 1623 (Print) ● ISSN1785 0037 (Online)
DOI: http://dx.doi.org/10.15666/aeer/1802_35253541

[3] Baćmaga, M., Kucharski, J., Wyszkowska, J., Borowik, A., Tomkiel, M. (2014): Responses of microorganisms and enzymes to soil contamination with metazachlor. – Environmental Earth Sciences 72: 2251-2262.
[4] Batisson, I., Crouzet, O., Besse–Hoggan, P., Sancelme, M., Mangot, J. F., Mallet, C., Bohatier, J. (2009): Isolation and characterization of mesotrione–degrading *Bacillus sp*. from soil. – Environmental Pollution 157: 1195-1201.
[5] Bhattacharyya, P., Tripathy, S., Kim, K., Kim, S. H. (2008): Arsenic fractions and enzyme activities in arsenic–contaminated soils by groundwater irrigation in West Bengal. – Ecotoxicology and Environmental Safety 71: 149-156.
[6] Cai, Z. Q., Li, S. S., Zhang, W. J., Ma, J. T., Wang, J., Cai, J. Y., Yang, G. H. (2015): Effects of the novel pyrimidynyloxybenzoic herbicide ZJ0273 on enzyme activities, microorganisms and its degradation in Chinese soils. – Environmental Science and Pollution Research 22: 4425-4433.
[7] Caliz, J., Vila, X., Martí, E., Sierra, J., Cruañas, R., Garau, M. A., Montserrat, M. (2011): Impact of chlorophenols on microbiota of an unpolluted acidic soil: microbial resistance and biodegradation. – FEMS Microbiology Ecology 78: 150-164.
[8] Cang, L., Zhou, D. M., Wang, Q. Y., Wu, D. Y. (2009): Effects of electrokinetic treatment of a heavy metal contaminated soil on soil enzyme activities. – Journal of Hazardous Materials 172: 1602-1607.
[9] Chen, Q. L., Wang, H., Yang, B. S., He, F. (2014): The combined effects of atrazine and lead (Pb): Relative microbial activities and herbicide dissipation. – Ecotoxicology and Environmental Safety 102: 93-99.
[10] Ciarkowska, K., Sołek-Podwika, K., Wieczorek, J. (2014): Enzyme activity as an indicator of soil-rehabilitation processes at a zinc and lead ore mining and processing area. – Journal of environmental management 132: 250-256.
[11] Crouzet, O., Batisson, I., Besse-Hoggan, P., Bonnemoy, F., Bardot, C., Poly, F., Bohatier, J., Mallet, C. (2010): Response of soil microbial communities to the herbicide mesotrione: a dose-effect microcosm approach. – Soil Biology and Biochemistry 42: 193-202.
[12] Crouzet, O., Wiszniowski, J., Donnadieu, F., Bonnemoy, F., Bohatier, J., Mallet, C. (2013): Dose–dependent effects of the herbicide mesotrione on soil cyanobacterial communities. – Archives of Environmental Contamination and Toxicology 64: 23-31.
[13] Cycoń, M., Markowicz, A., Piotrowska–Seget, Z. (2013a): Structural and functional diversity of bacterial community in soil treated with the herbicide napropamide estimated by the DGGE, CLPP and r/K–strategy approaches. – Applied Soil Ecology 72: 242-250.
[14] Cycoń, M., Wójcik, M., Borymski, S., Piotrowska–Seget, Z. (2013b): Short–term effects of the herbicide napropamide on the activity and structure of the soil microbial community assessed by the multi–approach analysis. – Applied Soil Ecology 66: 8-18.
[15] Doty, S. L., Oakley, B., Xin, G., Kang, J. W., Singleton, G., Khan, Z., Vajzovic, A., Staley, J. T. (2009): Diazotrophic endophytes of native black cottonwood and willow. – Symbiosis 47: 23-33.
[16] Durand, S., Amato, P., Sancelme, M., Delort, A. M., Combourieu, B., Besse–Hoggan, P. (2006a): First isolation and characterization of a bacterial strain that biotransforms the herbicide mesotrione. – Letters in Applied Microbiology 43: 222-228.
[17] Durand, S., Legeret, B., Martin, A. S., Sancelme, M., Delort, A. M., Besse–Hoggan, P., Combourieu, B. (2006b): Biotransformation of the triketone herbicide mesotrione by a Bacillus strain. Metabolite profiling using liquid chromatography/electrospray ionization quadrupole time–of–flight mass spectrometry. – Rapid Communications in Mass Spectrometry 20: 2603-2613.
[18] Durand, S., Sancelme, M., Besse–Hoggan, P., Combourieu, B. (2010): Biodegradation pathway of mesotrione: complementarities of NMR, LC–NMR and LC–MS for qualitative and quantitative metabolic profiling. – Chemosphere 81: 372-380.

http://www.aloki.hu ● ISSN 1589 1623 (Print) ● ISSN1785 0037 (Online)
DOI: http://dx.doi.org/10.15666/aeer/1802_35253541

[19] El Fantroussi, S., Verschuere, L., Verstraete, W., Top, E. M. (1999): Effect of phenylurea herbicides on soil microbial communities estimated by analysis of 16S rRNA gene fingerprints and community–level physiological profiles. – Applied and Environmental Microbiology 65: 982-988.
[20] Floch, C., Chevremont, A. C., Joanico, K., Capowiez, Y., Criquet, S. (2011): Indicators of pesticide contamination: soil enzyme compared to functional diversity of bacterial communities via Biolog® Ecoplates. – European Journal of Soil Biology 47: 256-263.
[21] Fromin, N., Hamelin, J., Tarnawski, S., Roesti, D., Jourdain–Miserez, K., Forestier, N., Teyssier–Cuvelle, S., Gillet, F., Aragno, M., Rossi, P. (2002): Statistical analysis of denaturing gel electrophoresis (DGE) fingerprinting patterns. – Environmental Microbiology 4: 634-643.
[22] Giacometti, C., Cavani, L., Baldoni, G., Ciavatta, C., Marzadori, C., Kandeler, E. (2014): Microplate–scale fluorometric soil enzyme assays as tools to assess soil quality in a long–term agricultural field experiment. – Applied Soil Ecology 75: 80-85.
[23] Gomez, E., Ferreras, L., Toresani, S. (2006): Soil bacterial functional diversity as influenced by organic amendment application. – Bioresource Technology 97: 1484-1489.
[24] Grenni, P., Caracciolo, A. B., Rodríguez–Cruz, M., Sánchez–Martín, M. (2009): Changes in the microbial activity in a soil amended with oak and pine residues and treated with linuron herbicide. – Applied Soil Ecology 41: 2-7.
[25] Gryta, A., Frąc, M., Oszust, K. (2014): The application of the Biolog Ecoplate approach in ecotoxicological evaluation of dairy sewage sludge. – Applied biochemistry and biotechnology 174: 1434-1443.
[26] Gu, L. K., Bai, Z. H., Jin, B., Hu, Q. L., Wang, H. L., Zhuang, G. Q., Zhang, H. X. (2010): Assessing the impact of fungicide enostroburin application on bacterial community in wheat phyllosphere. – Journal of Environmental Sciences 22: 134-141.
[27] Hu, Q., Qi, H. Y., Zeng, J. H., Zhang, H. X. (2007): Bacterial diversity in soils around a lead and zinc mine. – Journal of Environmental Sciences 19: 74-79.
[28] Hu, J. L., Lin, X. G., Wang, J. H., Dai, J., Chen, R. R., Zhang, J. B., Wong, M. H. (2011): Microbial functional diversity, metabolic quotient, and invertase activity of a sandy loam soil as affected by long–term application of organic amendment and mineral fertilizer. – Journal of Soils and Sediments 11: 271-280.
[29] Hua, F., Yu, Y. L., Chu, X. Q., Wang, X. G., Yang, X. E., Yu, J. Q. (2009): Degradation of chlorpyrifos in laboratory soil and its impact on soil microbial functional diversity. – Journal of Environmental Sciences 21: 380-386.
[30] Hua, G., Chen, G. F., Lv, Z. P., Hua, Z., Hong, Y. (2009): Alteration of microbial properties and community structure in soils exposed to napropamide. – Journal of Environmental Sciences 21: 494-502.
[31] Huang, A. Q., Chen, H., Ling, C., Dai, Y. L., Zhao, J. F. (2008): Effects of Cd (II) and Cu (II) on microbial characteristics in 2–chlorophenol–degradation anaerobic bioreactors. – Journal of Environmental Sciences 20: 745-752.
[32] Hunter, W. J., Shaner, D. L. (2012): Removing hexazinone from groundwater with microbial bioreactors. – Current microbiology 64: 405-411.
[33] Jacobsen, C. S., Hjelmsø, M. H. (2014): Agricultural soils, pesticides and microbial diversity. – Current Opinion in Biotechnology 27: 15-20.
[34] Jing, Z. Q., Hu, Y., Niu, Q. G., Liu, Y. Y., Li, Y. Y., Wang, X. C. (2013): UASB performance and electron competition between methane–producing archaea and sulfate–reducing bacteria in treating sulfate–rich wastewater containing ethanol and acetate. – Bioresource Technology 137: 349-357.
[35] Johnsen, K., Jacobsen, C. S., Torsvik, V., Sørensen, J. (2001): Pesticide effects on bacterial diversity in agricultural soils–a review. – Biology and Fertility of Soils 33: 443-453.

http://www.aloki.hu ● ISSN 1589 1623 (Print) ● ISSN1785 0037 (Online)
DOI: http://dx.doi.org/10.15666/aeer/1802_35253541

[36] Kandeler, E., Luxhøi, J., Tscherko, D., Magid, J. (1999): Xylanase, invertase and protease at the soil–litter interface of a loamy sand. – Soil Biology and Biochemistry 31: 1171-1179.
[37] Kong, X., Wang, C., Ji, M. (2013): Analysis of microbial metabolic characteristics in mesophilic and thermophilic biofilters using Biolog plate technique. – Chemical Engineering Journal 230: 415-421.
[38] Liu, W., Liu, H. J., Liu, W. P. (2000): Influence of pesticide imidacloprid and its metabolites on catalase activity in soil. – China Environmental Science 20: 524-527.
[39] Liu, B., Li, Y. X., Zhang, X. L., Wang, J., Gao, M. (2015): Effects of chlortetracycline on soil microbial communities: Comparisons of enzyme activities to the functional diversity via Biolog EcoPlates™. – European Journal of Soil Biology 68: 69-76.
[40] Loranger–Merciris, G., Barthes, L., Gastine, A., Leadley, P. (2006): Rapid effects of plant species diversity and identity on soil microbial communities in experimental grassland ecosystems. – Soil Biology and Biochemistry 38: 2336-2343.
[41] Lupwayi, N. Z., Brandt, S. A., Harker, K. N., O'Donovan, J. T., Clayton, G. W., Turkington, T. K. (2010): Contrasting soil microbial responses to fertilizers and herbicides in a canola–barley rotation. – Soil Biology and Biochemistry 42: 1997-2004.
[42] Osem, Y., Chen, Y., Levinson, D., Hadar, Y. (2007): The effects of plant roots on microbial community structure in aerated wastewater–treatment reactors. – Ecological Engineering 29: 133-142.
[43] Pose–Juan, E., Sánchez–Martín, M. J., Herrero–Hernández, E., Rodríguez–Cruz, M. S. (2015): Application of mesotrione at different doses in an amended soil: Dissipation and effect on the soil microbial biomass and activity. – Science of The Total Environment 536: 31-38.
[44] Qing, H., Qi, H. Y., Zeng, J. H., Zhang, H. X. (2007): Bacterial diversity in soils around a lead and zinc mine. – Journal of Environmental Sciences 19: 74-79.
[45] Raju, M. N., Venkateswarlu, K. (2014): Effect of repeated applications of buprofezin and acephate on soil cellulases, amylase, and invertase. – Environmental Monitoring and Assessment 186: 6319-6325.
[46] Ryan, R. P., Germaine, K., Franks, A., Ryan, D. J., Dowling, D. N. (2008): Bacterial endophytes: recent developments and applications. – FEMS Microbiology Letters 278: 1-9.
[47] Shrestha, K., Stevens, S., Shrestha, P., Adetutu, E. M., Walsh, K. B., Ball, A. S., Midmore, D. J. (2015): Characterisation of the soil microbial community of cultivated and uncultivated vertisol in Australia under several management regimes. – Agriculture, Ecosystems & Environment 199: 418-427.
[48] Stopnisek, N., Zühlke, D., Carlier, A., Barberán, A., Fierer, N., Becher, D., Riedel, K., Eberl, L., Weisskopf, L. (2015): Molecular mechanisms underlying the close association between soil Burkholderia and fungi. – The ISME Journal 10(1): 253-264.
[49] Sukul, P. (2006): Enzymatic activities and microbial biomass in soil as influenced by metalaxyl residues. – Soil Biology and Biochemistry 38: 320-326.
[50] Sun, Y. B., Sun, G. H., Xu, Y. M., Wang, L., Liang, X. F., Lin, D. S. (2013a): Assessment of sepiolite for immobilization of cadmium–contaminated soils. – Geoderma 193: 149-155.
[51] Sun, Y. B., Xu, Y. M., Sun, Y., Qin, X., Wang, Q. (2013b): Dissipation and dynamics of mesotrione in maize and soil under field ecosystem. – Bulletin of Environmental Contamination and Toxicology 90: 242-247.
[52] Sun, Y. B., Li, Y., Xu, Y. M., Liang, X. F., Wang, L. (2015): In situ stabilization remediation of cadmium (Cd) and lead (Pb) co–contaminated paddy soil using bentonite. – Applied Clay Science 105: 200-206.
[53] Sun, Y. B., Xu, Y. M., Sun, Y., Qin, X. (2015): Adsorption–desorption characteristics of mesotrione in phaiozem and red soils. – Environmental Chemistry 34: 1832-1838.

http://www.aloki.hu ● ISSN 1589 1623 (Print) ● ISSN1785 0037 (Online)
DOI: http://dx.doi.org/10.15666/aeer/1802_35253541

[54] Vyn, J. D., Swanton, C. J., Weaver, S. E., Sikkema, P. H. (2006): Control of *Amaranthus tuberculatus* var. rudis (common waterhemp) with pre and post–emergence herbicides in *Zea mays* L. (maize). – Crop Protection 25: 1051-1056.

[55] Xu, J., Zhang, Y., Dong, F. S., Liu, X. G., Wu, X. H., Zheng, Y. Q. (2014): Effects of repeated applications of chlorimuron–ethyl on the soil microbial biomass, activity and microbial community in the greenhouse. – Bulletin of Environmental Contamination and Toxicology 92: 175-182.

[56] Yao, X. H., Min, H., Lü, Z. H., Yuan, H. P. (2006): Influence of acetamiprid on soil enzymatic activities and respiration. – European Journal of Soil Biology 42: 120-126.

[57] Ye, Y. F., Min, H., Zhou, X. C. (2003): Effects of mefenacet on microbial respiration and enzyme activities in paddy soil. – Acta Pedologica Sinica 41: 93-96.

[58] Yoshida, N., Yoshida, Y., Handa, Y., Kim, H. K., Ichihara, S., Katayama, A. (2007): Polyphasic characterization of a PCP–to–phenol dechlorinating microbial community enriched from paddy soil. – Science of The Total Environment 381: 233-242.

[59] Zabaloy, M. C., Garland, J. L., Gomez, M. A. (2010): Assessment of the impact of 2, 4–dichlorophenoxyacetic acid (2, 4–D) on indigenous herbicide–degrading bacteria and microbial community function in an agricultural soil. – Applied Soil Ecology 46: 240-246.

[60] Zhang, T., Fang, H. P. (2000): Digitization of DGGE (denaturing gradient gel electrophoresis) profile and cluster analysis of microbial communities. – Biotechnology Letters 22: 399-405.

[61] Zhang, C. P., Liu, X. G., Dong, F. S., Xu, J., Zheng, Y. Q., Li, J. (2010): Soil microbial communities response to herbicide 2, 4–dichlorophenoxyacetic acid butyl ester. – European Journal of Soil Biology 46: 175-180.

[62] Zhang, W., Zhang, M., An, S., Xiong, B., Li, H., Cui, C. Z., Lin, K. F. (2012): Ecotoxicological effects of decabromodiphenyl ether and cadmium contamination on soil microbes and enzymes. – Ecotoxicology and Environmental Safety 82: 71-79.

[63] Zhou, J., Guo, W. H., Wang, R. Q., Han, X. M., Qiang, W. (2008): Microbial community diversity in the profile of an agricultural soil in northern China. – Journal of Environmental Sciences 20: 981-988.

http://www.aloki.hu ● ISSN 1589 1623 (Print) ● ISSN1785 0037 (Online)
DOI: http://dx.doi.org/10.15666/aeer/1802_35253541

VEGETATION DYNAMICS AND THEIR RELATIONS WITH CLIMATE CHANGE AT SEASONAL SCALES IN THE YANGTZE RIVER BASIN, CHINA

CUI, L. F.[1*] – WANG, Z. D.[1] – DENG. L. H.[1] – QU, S.[2]

[1]*School of Geography and Tourism, Huanggang Normal University, Huanggang 43800, China*

[2]*School of Resources and Environmental Sciences, Wuhan University, Wuhan 430079, China*
(phone: +86-186-7403-2566)

[*]*Corresponding author*
e-mail: cuilifang1104@126.com

(Received 3rd Dec 2019; accepted 26th Mar 2020)

Abstract. Knowledge on vegetation dynamics and its response to climate change is important for the sustainability of natural resources and understanding the changes in the ecosystems and its impact on the Earth's environment. We have carried out an analysis of GIMMS (Global inventory modelling and mapping studies) NDVI3g (third generation normalized difference vegetation data), daily temperature (T) and precipitation (P) for the 1982-2015 period based on Linear Regression (LR) analysis, the Mann-Kendall (MK) test with Sen's slope estimator and Kriging interpolation method. We have investigated the spatiotemporal variations of NDVI and climatic factors in the Yangtze River Basin (YRB), China. The relationship between NDVI and climatic factors was also analyzed quantitatively. The results show that the mean NDVI has an increasing trend in all four seasons during 1982-2015, the increasing trend during spring and autumn seasons was higher compared to winter and summer seasons. The response of vegetation dynamics to temperature was more prominent than precipitation. The correlation analysis shows that the mean NDVI had a significant and positive correlation with seasonal temperature, and the correlation coefficients were the highest during spring, followed by winter, summer and autumn seasons.
Keywords: *vegetation variation, NDVI, temperature, precipitation, YRB*

Introduction

Vegetation, as the link between the soil, atmosphere and water, plays an important role in characterizing the energy exchange, carbon cycle and regional human activities (Eugster et al., 2010). Vegetation dynamics has become an indicator of global environmental changes (Qu et al., 2018). In addition, vegetation dynamics (degradation and restoration) can reflect natural evolution and the impact of human activities on the ecological environment (Jiang et al., 2017). Therefore, investigating vegetation dynamics is crucial to protect the ecological environment (Yu and Hu, 2013).

Remote sensing data is one of the most important data sources to monitor vegetation dynamics, which has become a widely used tool in the field of ecological protection due to their advantages, including large coverage area and time savings (Qu et al., 2018). The satellite-based normalized difference vegetation index (NDVI) has been considered to be an effective indicator to monitor vegetation dynamics at regional, continental and global scales (Pinzon and Tucker, 2014). The commonly used NDVI data mainly include NOAA/AVHRR data, EOS/MODIS data and SPOT Vegetation NDVI data. Recently, many scholars have used these datasets to investigate vegetation dynamics at different spatial scales (Peng et al., 2011; Pan et al., 2018). Recent studies show that vegetation activities have increased in the northern mid–high latitudes and vegetation

http://www.aloki.hu ● ISSN 1589 1623 (Print) ● ISSN 1785 0037 (Online)
DOI: http://dx.doi.org/10.15666/aeer/1802_35433556

stability is changing with the external environment (Nemani et al., 2003; Xu et al., 2013). Climate, especially the factors of temperature and precipitation, has an important impact on vegetation dynamics (Piao et al., 2003; Goetz et al., 2005). In the context of global warming, studies on the relationship between vegetation dynamics and climate change have become hot topics worldwide (Chu et al., 2019; Yao et al., 2019).

Many studies reveal that NDVI showed dramatic spatial variations in response to climate changes (Gong and Shi, 2003; Piao et al., 2015). Ichii et al. (2002) and Xu et al. (2013) found that vegetation dynamics has been strongly influenced by increasing temperature at a global scale. Pan et al. (2018) pointed out that drought possibly has an important impact on the increasing global vegetation browning trend and global vegetation growth is at risk of reversal from greening to browning in the future due to climate warming. Temperature has a positive impact on vegetation dynamics in China (Song and Ma, 2011; Piao et al., 2015). However, the correlation between precipitation and NDVI is characterized by the geographical heterogeneity. Precipitation has a positive effect on NDVI in most dry regions whereas in humid regions, there was a negative correlation between NDVI and precipitation (Wang et al., 2010; Xu et al., 2016). To data, most of the previous studies mainly focused on the correlation between vegetation dynamics and climate factors at annual scale (Zhou et al., 2001). However, climate factors in different seasons might have different impacts on vegetation changes. Therefore, it is meaningful to study the relationship at seasonal scale.

The Yangtze River basin (YRB) is the third-largest river basin in the world. The vegetation cover in YRB plays an important role in regulating ecological balance in China, adjacent areas and even in the world. In the past few decades, the YRB has experienced significant climate change (Cui et al., 2019). The vegetation in the basin has changed obviously (Qu et al., 2018). The present study focused on the spatiotemporal trends of vegetation, as well as its relations with climate factors at annual scale. This paper focuses on long-term vegetation variation and the correlation with climate change at seasonal scale in YRB, which will serve as a reference for further scientific understanding of vegetation dynamics at a large basin scale and provide a reliable scientific basis for vegetation planting and protection. This paper aims to (1) study the spatial and temporal variation of seasonal mean NDVI in YRB during 1982-2015; (2) investigate the correlation between the seasonal mean NDVI and climate factors in YRB; and (3) detect the response of NDVI to climate variables to investigate the major climate factors affecting the vegetation dynamics in YRB.

Materials and methods

Study area

The Yangtze River, with the length of about 6300 km, is the longest river in Asia. The river originates from the Tibetan Plateau (TP) in western China and finally flows into the East China Sea (Zhang et al., 2014). The YRB lies between 91-122° E and 25-35° N (*Fig. 1*) with an area of about 1.8×10^6 km^2 (Niu et al., 2019). The annual average temperature ranges from 12.6 to 28.0°C and annual average precipitation is about 476 mm (Qu et al., 2018). The northern YRB is adjacent to the temperate zone, and the southern YRB is near to the tropical zone (Sang et al., 2013).

http://www.aloki.hu ● ISSN 1589 1623 (Print) ● ISSN 1785 0037 (Online)
DOI: http://dx.doi.org/10.15666/aeer/1802_35433556

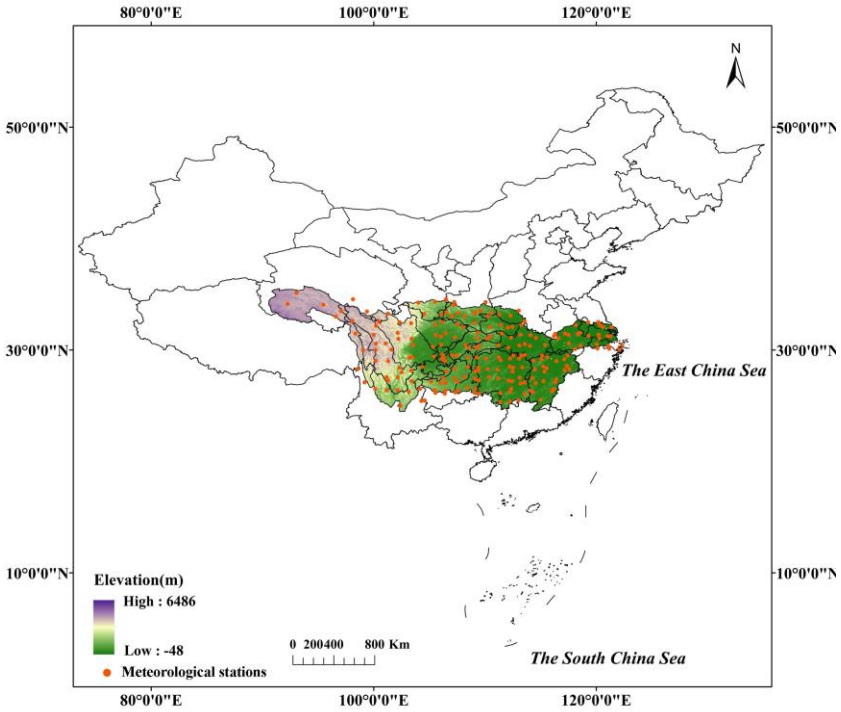

Figure 1. *Location of the YRB in China*

Data

Meteorological data

The daily climate datasets that included temperature (*T*) and precipitation (*P*) were acquired from the Chinese Meteorological Science Data Sharing Service Network. In this study, the daily climate data from 214 meteorological stations in YRB (*Fig. 1*) were used to analyse the variations of temperature and precipitation during the period of 1982-2015.

NDVI data

This study used the GIMMS 3g dataset developed by the NASA Global Inventory Modeling and Mapping Studies group, with a spatial resolution of 8 km and a temporal interval of 15 days (Li et al., 2018). The dataset covering the period from 1982 to 2015 is helpfull for detecting long-term vegetation dynamics at regional and global scales (Qu et al., 2018). To avoid the partial effects from clouds and atmosphere, we calculated a monthly NDVI by Maximum-Value Composites (MVCs) method.

Methods

This study investigates the trends in the annual and seasonal NDVI, temperature and precipitation using the Linear Regression (LR) analysis and the Mann-Kendall (MK) test with Sen's slope estimator.

The linear equation is as follows:

$$y=ax + b, (x=n, n+1 ,..., N) \quad \text{(Eq.1)}$$

http://www.aloki.hu ● ISSN 1589 1623 (Print) ● ISSN 1785 0037 (Online)
DOI: http://dx.doi.org/10.15666/aeer/1802_35433556

where *y* is the trend of NDVI, temperature and precipitation; *x* is the year; *a* and *b* are the slope and intercept respectively; n represents the starting year of the time series.

A positive value of *a* indicates increasing trends, while a negative value of *a* denotes decreasing trends. The significance level (*p*-values) of 10%, 5% and 1% was used for the LR analysis.

In this study, we use the MK test to investigate long-term trends in meteorological data and NDVI time series. This method mainly contains two parameters: Z and β. The standard normal test statistic Z, used for detecting a significant trend of the time series (Cui et al., 2019). The parameter β estimates the slope within the time series.

The correlation coefficients between the NDVI and climatic variables were calculated using Pearson correlation coefficients (Jiang et al., 2017). A prewhitening procedure was applied to the series prior to correlation analysis to improve the accuracy.

Results

Vegetation dynamics in YRB

The mean NDVI during spring (March-May), summer (June-August), autumn (September-November) and winter (December-February) was approximately 0.50, 0.67, 0.56 and 0.41, respectively during 1982-2015 (*Figs. 2a-d*), and increased at the rate of 0.02/10yr (Z_{MK} = 4.12, p < 0.01), 0.002/10yr (Z_{MK} = 0.47, p = 0.58), 0.02/10yr (Z_{MK} = 2.70, p < 0.01) and 0.006/10yr (Z_{MK} = 1.25, p = 0.18), respectively (*Table 1*). A significant turning point (TP) of NDVI during spring, summer, autumn and winter was found in 1996, 1997, 1994 and 1994, respectively (*Fig. 3*), and the abrupt change was statistically significant detected by MK test (*Fig. 4*). The mean NDVI during spring, summer and autumn was 0.47 and 0.52, 0.68 and 0.67, 0.54 and 0.58, 0.40 and 0.41, respectively before and after TP (*Figs. 2a-d*). The seasonal changes in NDVI before and after TP did not reach the statistically confidence level except the trend before TP during summer season (*Table 1*).

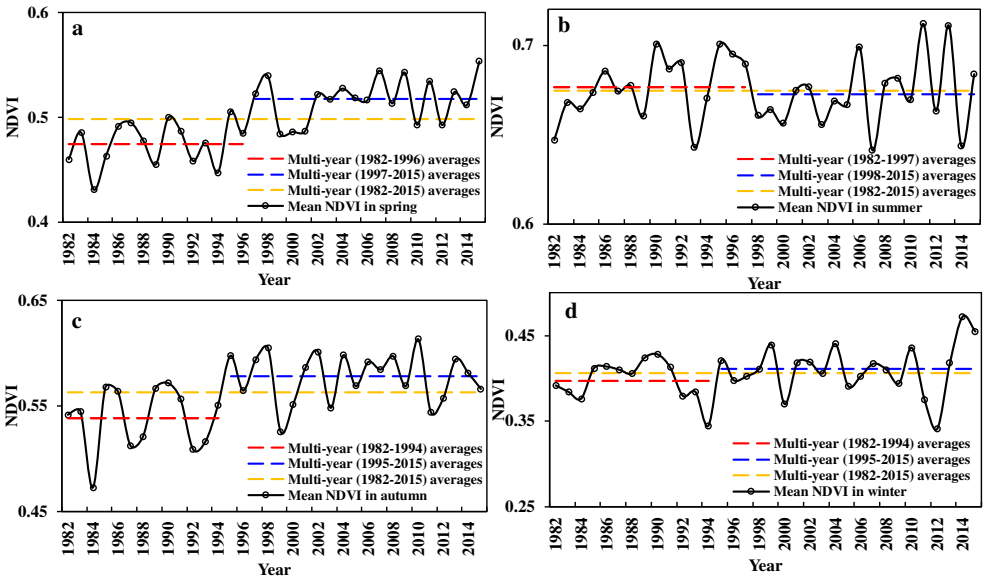

Figure 2. *Seasonal (a-d) mean NDVI of YRB during 1982-2015 and their Accumulated Anomaly Curve (f)*

http://www.aloki.hu ● ISSN 1589 1623 (Print) ● ISSN 1785 0037 (Online)
DOI: http://dx.doi.org/10.15666/aeer/1802_35433556

Table 1. *Trend test results (/10yr) of seasonal NDVI in YRB during 1982-2015, before and after the TP based on MK and LR analysis*

	Trend during1982-2015	Trend before TP	Trend after TP
Spring	0.02^{***}/0.02^{***}	0.01/0.01	0.01/0.01
Z_{MK}/*p*	<0.01	ns	ns
Summer	0.002/0.002	0.02^{**}/0.02^{*}	0.01/0.01
Z_{MK}/*p*	ns	<0. 1	ns
Autumn	0.02^{***}/0.02^{***}	0.00/0.00	0.00/0.00
Z_{MK}/*p*	<0.01	ns	ns
Winter	0.006/0.006	-0.004/-0.01	0.006/0.006
Z_{MK}/*p*	ns	ns	ns

ns denotes Not significant. *Trends at the 10% confidence level, **Trends at the 5% confidence level, ***Trends at the 1% confidence level

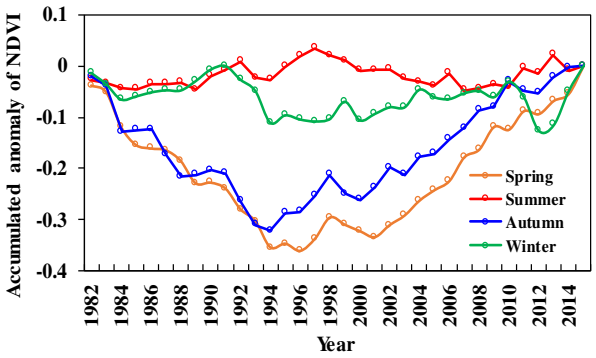

Figure 3. *Accumulated Anomaly Curve of seasonal mean NDVI of YRB during 1982-2015*

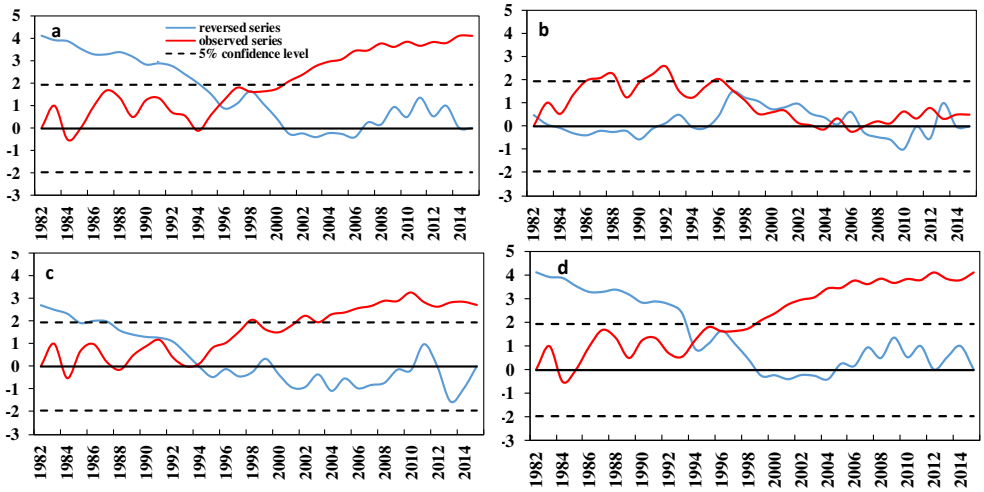

Figure 4. *The significant test of abrupt change in spring, summer autumn and winter NDVI (a, b, c, d) in YRB during 1982-2015*

The seasonal mean NDVI during spring, summer and autumn was generally high over the whole YRB except the north-western dry region and a small part of eastern YRB during 1982-2015 (*Figs. 5a-c*). The mean NDVI during winter was lower over the study area except the south-western and south-eastern YRB (*Fig. 5d*). The seasonal

http://www.aloki.hu ● ISSN 1589 1623 (Print) ● ISSN 1785 0037 (Online)
DOI: http://dx.doi.org/10.15666/aeer/1802_35433556

changes in NDVI also show strong spatial heterogeneity during 1982-2015 (*Fig. 6*). Parts of the eastern YRB show a significant and continuous increase in vegetation greenness (NDVI ≤0.03/10yr), especially during spring season. However, in most parts of YRD vegetation greenness decrease (NDVI ≤0.03/10yr), especially during summer season. Most parts of the central-south YRB show an increasing trend during spring (NDVI ≤0.05/10yr), and show decreasing trend during winter season (*Figs. 6a, g*). In addition, the mean NDVI in the north-western parts of YRB increase during summer and decrease during autumn (*Figs. 6c, e*).

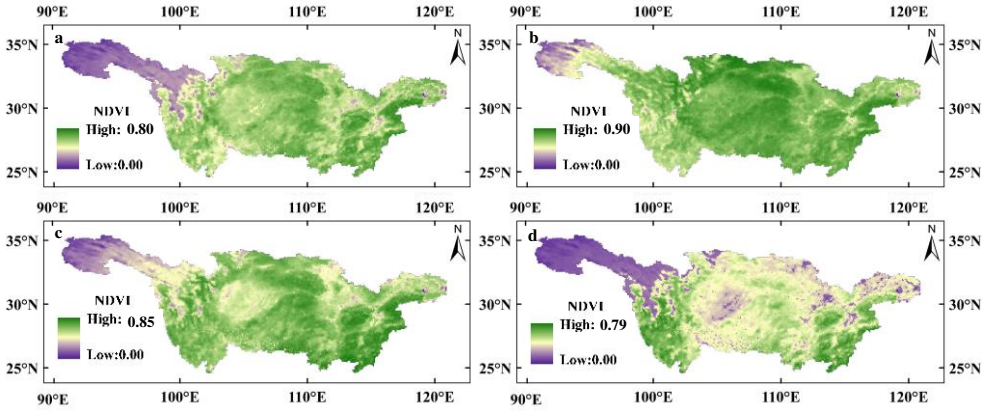

Figure 5. *Spatial distribution of seasonal mean NDVI in YRB during 1982-2015 (spring (a), summer (b), autumn (c) and winter (d))*

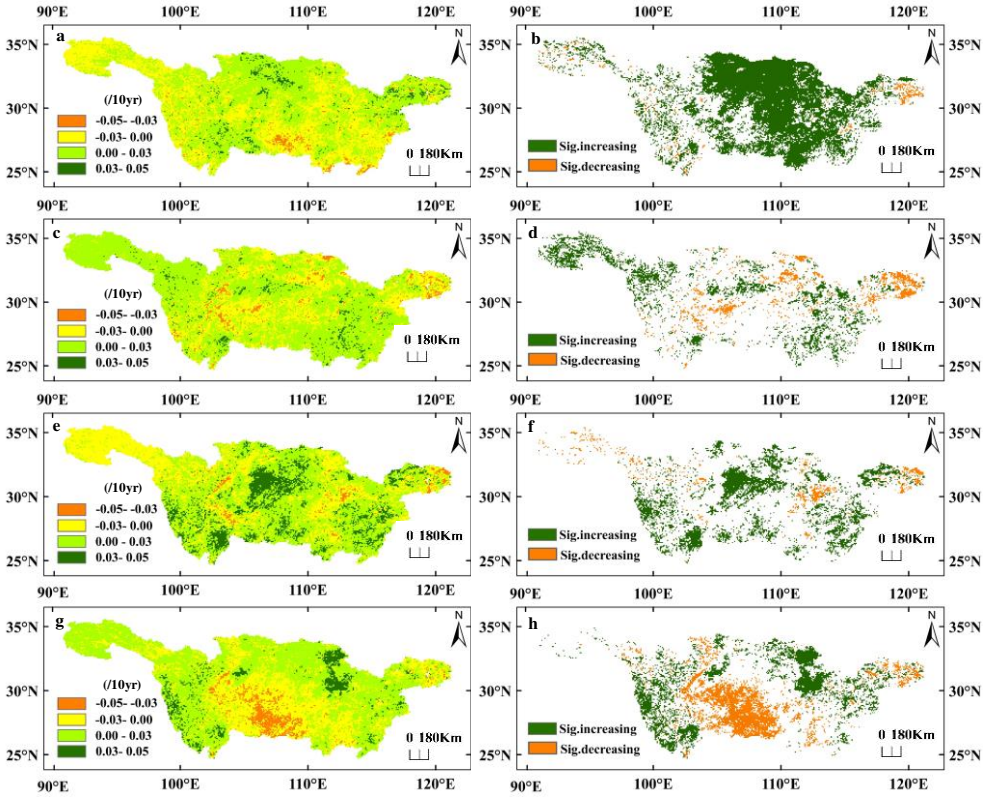

Figure 6. *Spatial distribution of NDVI variation trend in spring, summer autumn and winter (a, c, e, g) and its significant test (b, d, f, h) in YRB during 1982-2015*

http://www.aloki.hu ● ISSN 1589 1623 (Print) ● ISSN 1785 0037 (Online)
DOI: http://dx.doi.org/10.15666/aeer/1802_35433556

Long-term climate variability in YRB

The seasonal mean temperature during spring, summer, autumn and winter were 14.44, 23.70, 15.33 and 4.40°C, respectively over the whole YRB during 1982-2015 (*Table 2*).

Table 2. *Multi-year means of seasonal NDVI, temperature (T) and precipitation (P) in YRB during 1982-2015*

	NDVI	T(°C)	P(mm)
Spring	0.50	14.44	322.23
Summer	0.67	23.70	518.90
Autumn	0.56	15.33	225.90
Winter	0.41	4.40	108.70

The seasonal mean temperature shows statistically significant increasing trends, and the highest warming magnitude during spring ($p < 0.01$), followed by winter ($p < 0.05$), autumn ($p < 0.01$) and summer ($p < 0.01$) during 1982-2015 (*Table 3*). *Table 3* shows that seasonal mean temperature before TP and after TP also presents an increasing trend in four seasons. The spatial distribution of seasonal mean temperature shows strong seasonal variability (*Figs. 7a-d*): the mean temperature during spring and autumn seasons has a significant increasing trend in the whole YRB, while a decreasing trend during summer and winter seasons was detected in a small part of the YRB (*Figs. 7b-d*). *Figs. 7a-d* also shows the most warming areas in the four seasons were located in the western source region of the Yangtze River and Yangtze River Delta (YRD) due to the rapid population growth and the rapid expansion of built-up areas.

Table 3. *Trend test results of temperature (°C/10yr) and precipitation (mm/10yr) in YRB during 1982-2015, before and after the TP of NDVI trend based on MK and LR analysis*

	Trend during1982-2015		Trend before TP		Trend after TP	
	T	P	T	P	T	P
Spring	0.55^{***}/0.51^{***}	-3.56/-8.12	0.00/0.05	63.95^{***}/67.07^{***}	0.22/0.18	-21.19/-30.47
p	<0.01	ns	ns	<0.01	ns	ns
Summer	0.25^{***}/0.30^{***}	-8.05/-13.43	0.32/0.35	93.56^{**}/98.04^{**}	0.17/0.33	-85.16/-70.80
p	<0.01	ns	ns	<0.05	ns	ns
Autumn	0.32^{***}/0.31^{***}	-8.65/-8.58	-0.31/-0.22	-48.53/-31.40	0.32/0.27	14.63/10.12
p	<0.01	ns	ns	ns	ns	ns
Winter	0.41^{**}/0.29^{**}	-2.95/-2.86	0.82^{**}/0.94^{**}	50.33^{*}/52.73^{**}	0.30/0.12	-14.75/-13.95
p	<0.05	ns	<0.05	<0.05	ns	ns

ns denotes Not significant. *Trends at the 10% confidence level, **Trends at the 5% confidence level, ***Trends at the 1% confidence level

Seasonal precipitation shows a decreasing trend in the four seasons during 1982-2015 (*Table 3*). However, precipitation presents a significant increasing trend during spring ($p < 0.01$), summer ($p < 0.05$) and winter season ($p < 0.05$) before TP. The spatial variation of seasonal precipitation trend (*Figs. 7e-h*) shows regional differences. The region where precipitation increased was located in parts of the western YRB during spring season (*Fig. 7e*) and in eastern parts of YRB during summer and winter seasons (*Figs. 7f, h*). A decreasing seasonal precipitation was found in located in middle YRB during summer, most parts of YRB during winter season (*Figs. 7f, h*) and in the eastern parts of YRB during spring and autumn seasons (*Figs. 7e, g*).

http://www.aloki.hu ● ISSN 1589 1623 (Print) ● ISSN 1785 0037 (Online)
DOI: http://dx.doi.org/10.15666/aeer/1802_35433556

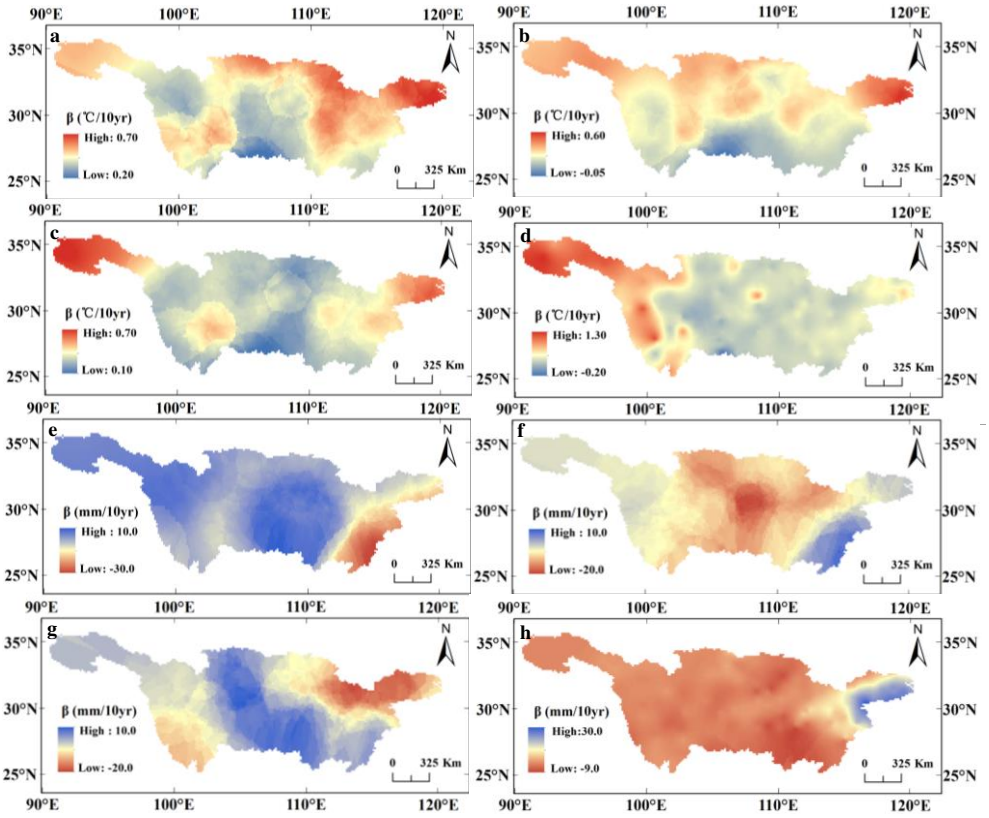

Figure 7. *Spatial distribution of seasonal mean temperature (a-d) and precipitation (e-h) trends in YRB during 1982-2015*

Correlation between vegetation dynamics and climatic variations

Table 4 shows that the mean NDVI had a statistically significant and positive correlation with seasonal temperature, and the correlation coefficients were the highest during spring (R = 0.65, p<0.01), followed by winter (R = 0.50, p<0.01), summer (R = 0.43, p<0.01) and autumn (R = 0.38, p<0.05) seasons. Moreover, the increasing rate of seasonal mean NDVI and temperature during spring season was also the highest during 1982-2015 (*Tables 1, 3*). These results show that climate warming in the beginning of the growing season has a positive effect on NDVI in YRB during 1982-2015. In addition, the mean NDVI shows a significant and positive correlation with temperature during winter season after TP (R = 0.60, p < 0.05) and during summer season before and after TP (R = 0.60, p < 0.01; R = 0.46, p < 0.05). *Fig. 8a* shows a significant and positive correlation between the mean NDVI and seasonal temperature during spring over most of the study area, with the correlation coefficients upto 0.50-0.80. The correlation coefficients in other seasons show spatial heterogeneity. During summer season, the significant and positive correlations were detected in the source region of Yangtze River and eastern YRB, whereas negative correlations were found in parts of the northern and southern YRB (*Fig. 8b*). During autumn season, the correlation coefficients were statistically significantly positive correlation in western and middle YRB, and statistically negative in parts of eastern YRB (*Fig. 8c*). During winter season, the mean NDVI was positively correlated with temperature in the whole YRB, especially statistically significant in the western and southern YRB (*Fig. 8d*).

http://www.aloki.hu ● ISSN 1589 1623 (Print) ● ISSN 1785 0037 (Online)
DOI: http://dx.doi.org/10.15666/aeer/1802_35433556

Table 4. *Correlation coefficients between seasonal NDVI and temperature (precipitation) during 1982-2015, before and after TP of NDVI trend*

Indicator		NDVI		
		1982-2015	Before TP	After TP
Temperature	Spring	0.65***	0.03	0.38*
	Summer	0.43***	0.60**	0.46**
	Autumn	0.38**	0.11	0.09
	Winter	0.50***	-0.04	0.60***
	Annual	-0.23	-0.07	-0.23
Precipitation	Spring	-0.26	-0.11	-0.26
	Summer	-0.13	-0.05	-0.37*
	Autumn	-0.15	0.13	-0.15
	Winter	-0.11	-0.23	-0.06

* At the 10% confidence level, ** At the 5% confidence level, *** At the 1% confidence level

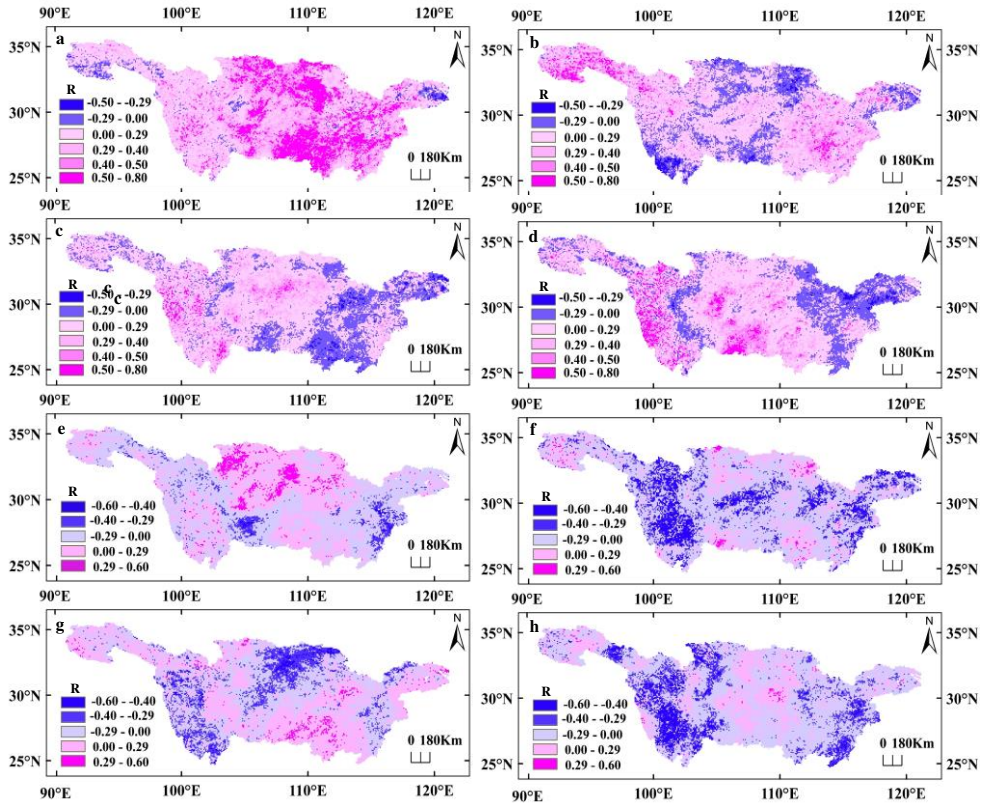

Figure 8. *Spatial distribution of correlation coefficients between seasonal mean NDVI and temperature (a-d), precipitation (e-h) during 1982-2015. (The values of 0.29 is corresponding to 5% significant level of those correlation coefficients during 1982-2015)*

Table 4 shows that the mean NDVI was negatively correlated with seasonal precipitation over the whole study period, before and after TP, but a statistically significant trend was observed during summer season after TP (R = -0.37, p < 0.1). The correlation coefficients between NDVI and seasonal precipitation were characterized by seasonal and spatial differences (*Figs. 8e-h*). *Fig. 6e* shows that during spring, the

http://www.aloki.hu ● ISSN 1589 1623 (Print) ● ISSN 1785 0037 (Online)
DOI: http://dx.doi.org/10.15666/aeer/1802_35433556

regions with significant and negative correlation were located in a small parts of the eastern and southern YRB, while those with significant and positive correlation in parts of the northern YRB. During summer and winter seasons, a negative correlation was observed in most parts of YRB, and the correlation coefficients were significant in the eastern and western YRB (*Figs. 8f, h*). During autumn, the significant and negative correlations were observed in the northern, parts of the western and eastern YRB (*Fig. 8g*).

Discussion

Climate change in YRB

Global warming has influenced the climatic pattern of YRB (Cui et al., 2019). The increasing rate of global mean land-surface air temperature was 0.18 ± 0.04°C/10yr in 1951-2012, while the most significant warming was found during 1979-2012, with the highest warming rate of 0.25 ± 0.05°C/10yr (IPCC, 2013). With economic development in China, especially in the past 30 years, the urbanization has been made a large contribution to climate warming (Jin et al., 2015). The amount of urban area rapidly increased from 3376 km^2 to 13073 km^2 in the eastern YRB during 2001-2013. Moreover, a significant and positive correlation existed between land surface temperature and urban area (Yao et al., 2017). Under global warming, the continual increases in temperature in QTP will seriously accelerate the melting of glaciers (Jiapaer et al., 2015). Glacier melt will lead to a drop in river and groundwater recharge, which would be fatal for ecological environment in the source region of Yangtze River due to most vegetation growth relying on rivers and groundwater. Thus local governments should focus on such environments and propose feasible countermeasures to alleviate these risks.

Seasonal precipitation shows a decreasing trend in YRB during 1982-2015. However, a statistically wetting trend was observed in the source region of Yangtze River (Zhang et al., 2017). A similar wetting trend was also found in the western inland river basin and south-eastern China (Zhang et al., 2013). The increase in precipitation is helpful to improve local ecological environments. Recent research reported that the area of the closed inland lake on the QTP has expanded from 2.56×10^4 km^2 to 3.23×10^4 km^2 in approximately the past 20 years, and the number of new lakes reached 99 in approximately the past 40 years, which was mainly caused by a change to a warm and humid climate on the QTP (Zhang et al., 2017).

Variations of NDVI in YRB

This study analysed the spatiotemporal dynamics of seasonal mean NDVI in YRB for the period 1982-2015. The results provide a new understanding of vegetation dynamics in YRB in recent decades. In our past study, we found a significant statistically increasing trend in annual mean NDVI. However, the changes of annual mean NDVI before and after TP (1994) was slight without showing the statistically confidence level (Cui et al., 2019). The spatial distribution of NDVI observed was similar to those of Wang et al. (2015). At seasonal scale, the mean NDVI during spring and autumn increased faster. Earlier study suggested that the vegetation growth in China increased faster during spring (Piao et al., 2003).

http://www.aloki.hu ● ISSN 1589 1623 (Print) ● ISSN 1785 0037 (Online)
DOI: http://dx.doi.org/10.15666/aeer/1802_35433556

Relationship between NDVI and climatic variables

In this study, the correlation analysis between seasonal mean NDVI and temperature/ precipitation was performed. The statistically significant and positive correlations between seasonal NDVI and temperature were generally observed in YRB. These results were consistent with those from Richardson et al. (2010) and Peng et al. (2011). However, it was found in this study that the correlation was negative between NDVI and precipitation over the whole YRB and did not reach a statistically confidence level, which indicated that vegetation growth was least affected by precipitation condition in this region during the study period. A widely accepted viewpoint is that vegetation growth is mainly affected by temperature in humid regions, while precipitation is not a limited factor for vegetation growth due to abundant rainfall (Wang et al., 2015). For example, the climate in the source region of Yangtze River is characterized by lower temperature and relatively abundant precipitation, which indicates that the effect of temperature on vegetation in this region is more than that of moisture (Zhang et al., 2016). Karnieli et al. (2010) found that when energy was the limiting factor for vegetation growth in the North American continent at higher latitudes and elevations, the NDVI was positively correlated with temperature. On the contrary, precipitation for vegetation growth is more important compared to the temperature due to lower rainfall in the arid region (McGwire et al., 2000). The increasing temperature will have a positive impact on vegetation growth by extending growing season and increasing photosynthesis if the temperature ranges from baseline to optimum value (Thornthwaite, 1948; Slayback et al., 2003; Hua et al., 2017). However, vegetation growth will be limited if the increasing temperature exceeds the optimum value (Thornthwaite, 1948). Hence, the regions with higher increasing rate of temperature should pay more attention to protecting ecological environments to mitigate and adapt to climate warming.

Conclusion

In this study, the daily meteorological data (T and P) were used to analyze the spatiotemporal variation of seasonal temperature and precipitation in YRB during 1982-2015. Additionally, the vegetation dynamic and the response to climate change were also investigated. The main findings of the present study are summarized as:

(1) Seasonal mean temperature show significant increasing trend over the whole YRB during 1982-2015 which is mainly attributed to an obvious warming during spring season. The warming rates in the north of the study area were observed to be higher compared to those in the south and the highest warming rate was observed in the eastern YRB with intense human activities and the western source region of Yangtze River in QTP.

(2) The mean NDVI during spring and autumn show significant increasing trends over the whole study area. The seasonal NDVI also shows strong spatial heterogeneity.

(3) The correlation coefficients between the mean NDVI and seasonal temperature (precipitation) were strongly dependent on the season with pronounced spatial difference.

Acknowledgements. This work was financially supported by National Natural Science Foundation of China (No.41601044), the High-level Nurturing Project, Huanggang Normal University (No.204201911503). We would like to thank the China Meteorological Administration (CMA) for providing the meteorological data.

http://www.aloki.hu ● ISSN 1589 1623 (Print) ● ISSN 1785 0037 (Online)
DOI: http://dx.doi.org/10.15666/aeer/1802_35433556

REFERENCES

[1] Chu, H., Venevsky, S., Wu, C., Wang, M. (2019): NDVI-based vegetation dynamics and its response to climate changes at Amur-Heilongjiang River Basin from 1982 to 2015. – Science of the Total Environment 650: 2051-2062.

[2] Cui, L. F., Wang, L. C., Qu, S., Singh, R. P., Lai, Z. P., Yao, R. (2019): Spatiotemporal Extremes of Temperature and Precipitation during 1960-2015 in the Yangtze River Basin (China) and Impacts on vegetation dynamics. – Theoretical and Applied Climatology 136: 675-692.

[3] Eugster, W., Rouse, W. R., Pielke Sr, R. A., McFadden, J. P., Baldocchi, D. D., Kittel, T. G. F., Chapin, F. S., Liston, G. E., Vidale, P. L., Vaganov, E. (2010): Land-atmosphere energy exchange in Arctic tundra and boreal forest: available data and feedbacks to climate. – Global Change Biology 6: 84-115.

[4] Goetz, S. J., Bunn, A. G., Fiske, G. J., Houghton, R. A. (2005): Satellite-observed photosynthetic trends across boreal North America associated with climate and fire disturbance. – Proceedings of the National Academy of Sciences of the USA 102: 13521-13525.

[5] Gong, D., Shi, P. (2003): Northern hemispheric NDVI variations associated with large-scale climate indices in spring. – Internatinal Jounal of Remote Sensing 24: 2559-2566.

[6] Hua, W., Chen, H., Zhou, L., Xie, Z., Qin, M., Li, X., Ma, H., Huang, Q., Sun, S. (2017): Observational quantification of climatic and human influences on vegetation greening in China. – Remote Sensing 9: 425.

[7] Ichii, K., Kawabata, A., Yamaguchi, Y. (2002): Global correlation analysis for NDVI and climatic variables and NDVI trends: 1982-1990. – Internatinal Jounal of Remote Sensing 23(18): 3873-3878.

[8] IPCC AR5 (2013): Climate Change 2013: The Physical Science Basis. – In: Stocker, T. F., Qin, D., Plattner, G. K., Tignor, M., Allen, S. K., Boschung, J., Nauels, A., Xia, Y., Bex, V., Midgley, P. M. (eds.) Contribution of Working Group I to the Fifth Assessment Report of the Intergovernmental Panel on Climate Change. Cambridge University Press, Cambridge, United Kingdom and New York, NY, USA.

[9] Jiang, L. L., Jiapaer, G., Bao, A. M., Guo, H., Ndayisaba, F. (2017): Vegetation dynamics and responses to climate change and human activities in Central Asia. – Science of the Total Environment 599-600: 967-980.

[10] Jiapaer, G. L., Liang, S. L., Yi, Q. X., Liu, J. P. (2015): Vegetation dynamics and responses to recent climate change in Xinjiang using leaf area index as an indicator. – Ecological Indicator 58: 64-76.

[11] Jin, K. J., Wang, F., Chen, D. L., Jiao, Q., Xia, L., Fleskens, L., Mu, X. M. (2015): Assessment of urban effect on observed warming trends during 1955–2012 over China: a case of 45 cities. – Climatic Change 132(4): 631-643.

[12] Karnieli, A., Agam, N., Pinker, R. T., Anderson, M., Imhoff, M. L., Gutman, G. G. (2010): Use of NDVI and Land Surface Temperature for Drought Assessment: Merits and Limitations. – Journal of Climate 23: 618-633.

[13] Li, C., Filho, W. L., Wang, J., Yin, J., Fedoruk, M., Bao, G., Bao, Y., Yin, S., Yu, S., Hu, R. (2018): An assessment of the impacts of climate extremes on the vegetation in Mongolian Plateau: Using a scenarios-based analysis to support regional adaptation and mitigation options. – Ecological Indicator 95: 805-814.

[14] McGwire, K., Minor, T., Fenstermaker, L. (2000): Hyperspectral mixture modeling for quantifying sparse vegetation cover in arid environments. – Remote Sensing of Environment 72(3): 360-374.

[15] Nemani, R. R., Keeling, C. D., Hashimoto, H., Jolly, W. M., Piper, S. C., Tucker, C. J., Myneni, R. B., Running, S. W. (2003): Climate-driven increases in global terrestrial net primary production from 1982 to 1999. – Science 300: 1560-1563.

http://www.aloki.hu ● ISSN 1589 1623 (Print) ● ISSN 1785 0037 (Online)
DOI: http://dx.doi.org/10.15666/aeer/1802_35433556

[16] Niu, Z., Wang, L., Fang, L., Li, J., Yao, R. (2019): Analysis of spatiotemporal variability in temperature extremes in the Yellow and Yangtze River basins during 1961–2014 based on high-density gauge observations. – International Journal of Climatology 40(1): 1-21.
[17] Pan, N. Q., Feng, X. M., Fu, B. J., Wang, S., Ji, F., Pan, S. F. (2018): Increasing global vegetation browning hidden in overall vegetation greening: Insights from time-varying trends. – Remote Sensing of Environment 214: 59-72.
[18] Peng, S. S., Chen, A. P., Xu, L., Cao, C. X., Fang, J. Y., Myneni, R. B., Pinzon, J. E., Tucker, C. J., Piao, S. L. (2011): Recent change of vegetation growth trend in China. – Environmental Research Letters 6(4): 044027.
[19] Piao, S. L., Fang, J. Y., Zhou, L. M., Guo, Q. H., Henderson, M., Ji, W., Li, Y., Tao, S. (2003): Interannual variations of monthly and seasonal normalized difference vegetation index (NDVI) in China from 1982 to 1999. – Journal of Geophysical Research Atmospheres 108(4401D14).
[20] Piao, S. L., Yin, G. D., Tan, J. G., Cheng, L., Huang, M. T., Li, Y., Liu, R., Mao, J., Myneni, R. B., Peng, S. S. (2015): Detection and attribution of vegetation greening trend in China over the last 30 years. – Global Change Biology 21(4): 1601-1609.
[21] Pinzon, J., Tucker, C. (2014): A non-stationary 1981–2012 AVHRR NDVI3g time series. – Remote Sensing 6: 6929-6960.
[22] Qu, S., Wang, L. C., Lin, A. W., Zhu, H. J., Yuan, M. X. (2018): What drives the vegetation restoration in Yangtze River basin, China: Climate change or anthropogenic factors? – Ecological Indicator 90: 438-450.
[23] Richardson, A. D., Black, T. A., Ciais, P., Delbart, N., Friedl, M. A., Gobron, N., Hollinger, D. Y., Kutsch, W. L., Longdoz, B., Luyssaert, S., Migliavacca, M., Montagnani, L., Munger, J. W., Moors, E., Piao, S., Rebmann, C., Reichstein, M., Saigusa, N., Tomelleri, E., Vargas, R., Varlagin, A. (2010): Influence of spring and autumn phenological transitions on forest ecosystem productivity. – Philosophical Transactions of the Royal Society B 365: 3227-3246.
[24] Sang, Y. F., Wang, Z. G., Liu, C. M. (2013): Spatial and temporal variability of daily temperature during 1961-2010 in the Yangtze River Basin, China. – Quaternary International 304: 33-42.
[25] Slayback, D. A., Pinzon, J. E., Los, S. O., Tucker, C. J. (2003): Northern hemisphere photosynthetic trends 1982-99. – Global Change Biology 9: 1-15.
[26] Song, Y., Ma, M. (2011): A statistical analysis of the relationship between climatic factors and the normalized difference vegetation index in China. – International Journal of Remote Sensing 32: 3947-3965.
[27] Thornthwaite, C. W. (1948): An approach toward a rational classification of climate. – Geographical Review 38(1): 55-94.
[28] Wang, W., Wang, W. J., Li, J. S., Wu, H., Xu, C., Liu, T. (2010): The impact of sustained drought on vegetaion ecosystem in Southwest China based on remote sensing. – Procedia Environmental Sciences 2: 1679-1691.
[29] Wang, H. L., Chen, A. F., Wang, Q. F., He, B. (2015): Drought dynamics and impacts on vegetation in China from 1982 to 2011. – Ecological Engineering 75: 303-307.
[30] Xu, L., Myneni, R. B., Chapin III, F. S., Callaghan, T. V., Pinzon, J. E., Tucker, C. J., Zhu, Z., Bi, J., Ciais, P., Tommervik, H., Euskirchen, E. S., Forbes, B. C., Piao, S. L., Anderson, B. T., Ganguly, S., Nemani, R. R., Goetz, S. J., Beck, P. S. A., Bunn, A. G., Cao, C., Stroeve, J. C. (2013): Temperature and vegetation seasonality diminishment over northern lands. – Nature Climate Change 3: 581-586.
[31] Xu, Y. F., Yang, J., Chen, Y. N. (2016): NDVI-based vegetation responses to climate change in an arid area of China. – Theoretical and Applied Climatology 126: 213-222.
[32] Yao, R., Wang, L. C., Gui, X., Zheng, Y. K., Zhang, H. M., Huang, X. (2017): Urbanization effects on vegetation and surface urban heat islands in China's Yangtze River Basin. – Remote Sensing 9(6): 540.

http://www.aloki.hu ● ISSN 1589 1623 (Print) ● ISSN 1785 0037 (Online)
DOI: http://dx.doi.org/10.15666/aeer/1802_35433556

[33] Yao, J., Hu, W., Chen, Y., Huo, W., Zhao, Y., Mao, W., Yang, Q. (2019): Hydro-climatic changes and their impacts on vegetation in Xinjiang, Central Asia. – Science of the Total Environment 660: 724-732.
[34] Yu, K., Hu, C. (2013): Changes in vegetative coverage of the Hongze Lake national wetland nature reserve: a decade-long assessment using MODIS medium-resolution data. – Journal of Applied Remote Sensing 7: 3589.
[35] Zhang, Q., Li, J., Singh, V. P., Xiao, M. (2013): Spatio-temporal relations between temperature and precipitation regimes: implications for temperature-induced changes in the hydrological cycle. – Global and Planetary Change 111(4): 57-76.
[36] Zhang, Y., Song, C., Zhang, K., Cheng, X., Band, L. E., Zhang, Q. (2014): Effects of land use/land cover and climate changes on terrestrial net primary productivity in the Yangtze River Basin, China, from 2001 to 2010. – Journal of Geophysical Research Biogeosciences 119: 1092-1109.
[37] Zhang, Y., Zhang, C., Wang, Z., Chen, Y., Gang, C., An, R., Li, J. (2016): Vegetation dynamics and its driving forces from climate change and human activities in the Three-River Source Region, China from 1982 to 2012. – Science of the Total Environment 563-564: 210-220.
[38] Zhang, G. Q., Yao, T. D., Piao, S. L., Bolch, T., Xie, H. J., Chen, D. L., Gao, Y. H., O'Reilly, C. M., Shun, C. K., Yang, K., Yi, S., Lei, Y. B., Wang, W. C., He, Y., Shang, K., Yang, X. K., Zhang, H. B. (2017): Extensive and drastically different alpine lake changes on Asia's high plateaus during the past four decades. – Geophysical Research Letters 44: 252-260.
[39] Zhou, L. M., Tucker, C. J., Kaufmann, R. K., Slayback, D., Shabanov, N. V., Myneni, R. B. (2001): Variations in northern vegetation activity inferred from satellite data of vegetation index during 1981 to 1999. – Journal of Geophysical Research Atmospheres 106: 20069-20083.

http://www.aloki.hu ● ISSN 1589 1623 (Print) ● ISSN 1785 0037 (Online)
DOI: http://dx.doi.org/10.15666/aeer/1802_35433556

SMALL-SCALE SPATIAL PATTERNS OF TWO TERRICOLOUS LICHENS IN A CONIFER PLANTATION

SEVGI, E.[1] – YILMAZ, O. Y.[2*] – SEVGI, O.[3]

[1]*Department of Pharmaceutical Botany, Faculty of Pharmacy, Bezmialem Vakif University, Istanbul, Turkey*

[2]*Department of Surveying and Cadastre, Faculty of Forestry, Istanbul University-Cerrahpaşa, Istanbul, Turkey*

[3]*Department of Soil Science and Ecology, Faculty of Forestry, Istanbul University-Cerrahpaşa, Istanbul, Turkey*

[*]*Corresponding author*
e-mail: yilmazy@istanbul.edu.tr

(Received 9th Dec 2019; accepted 23rd Mar 2020)

Abstract. Various studies have been conducted on the factors affecting the spatial distribution of terricolous lichen species at regional and landscape scales, yet not on small-scales. In our study, the distribution of lichens was obtained by objective classification and spatial analysis of RGB camera images taken from two different heights by an unmanned aerial vehicle at a reforested area of 1575 m^2. Black pine and cypress are species that have been introduced, while the, native species are oak and mock privet. The total area covered by *Cladonia rangiformis* Hoffm., (26.17 m^2) in the study area was 5 times higher than that covered by the *Cladonia foliacea* (Huds.) Willd. (5.01 m^2). These species were found to be located mostly to the north and sometimes at the east of the tree species. *C. rangiformis* was found under the crown projection area of cypress; however, no such result has been found for black pine, mock privet, and oak. Therefore, tree species affect the distribution of terricolous lichen species. The patch sizes of both of these lichen species fit the power law distribution and demonstrate inhomogeneous spatial distribution in the area. *C. rangiformis* and *C. foliacea* patch size classes generally clustered at short distance (2-2.5 meters) and demonstrated regular distribution beyond this distance.
Keywords: *directional interaction, inhomogeneous distribution, patch-size distribution, unmanned aerial vehicles, Cladonia*

Introduction

Lichens can grow on human-made materials such as fences, tombstones, walls, surfaces of wooden or concrete buildings, just as they can on many natural substrates (Aptroot and James, 2002). The classification of lichens is sometimes based on these substrates; hence the lichens examined in this study are named terricolous lichens since they are located on the ground (Purvis et al., 1992).

The saxicolous lichens on rocks can affect the soil formation process both physically and chemically by weathering the rocks with the acids they produce (Chen et al., 2000; Adamo et al., 2002; Sevgi and Makineci, 2005). Similarly, terricolous lichens contribute to soil formation by changing the physical and chemical properties of the soil by covering it and releasing lichen acids (Asta et al., 2001; Maestre et al., 2011; Gypser et al., 2015; Jackson, 2015). For instance, the terricolous lichens *Cladonia rangiformis* Hoffm., and *Peltigera neckeri* Hepp ex Müll. affect soil mineralization and bacteria growth with the secondary metabolites they produce (Akpinar et al., 2009).

Some studies have been carried out on biological soil crusts (biocrust), including terricolous lichens (Eldridge, 1996, 1999; Martínez et al., 2006; Ochoa-Hueso and

http://www.aloki.hu ● ISSN 1589 1623 (Print) ● ISSN 1785 0037 (Online)
DOI: http://dx.doi.org/10.15666/aeer/1802_35573576

Manrique, 2011; Ochoa-Hueso et al., 2011, 2017; Pietrasiak et al., 2011; Concostrina-Zubiri et al., 2014, 2018; Gypser et al., 2015). Terricolous lichen cover is positively related to organic carbon, nitrogen, and aggregate stability in soil (Rai and Upreti, 2014). Terricolous lichens take place in different habitats as an important component of the ecosystem and are an indicator of habitat heterogeneity (Will-Wolf et al., 2002a). Besides general distribution in arid, semi-arid ecosystems or cold climate conditions (Eldridge, 1996; Zouaoui et al., 2014), terricolous lichens also prefer the gaps in shrublands and forests in Mediterranean ecosystems (Loppi et al., 2004; Ochoa-Hueso et al., 2011).

Terricolous lichen species require comparatively longer time for dispersal and establishment in the ecosystem (Zouaoui et al., 2014). Elevation and soil type are the leading factors affecting the occurrence of terricolous lichens in large areas (Will-Wolf et al., 2002b; Bowker et al., 2006; Zouaoui et al., 2014). It is also stated that gypsiferous soil is also rich in terms of the diversity of terricolous lichen (Concostrina-Zubiri et al., 2014). In a study conducted in arid and semi-arid ecosystem in Australia, the presence and diversity of terricolous lichen species contributing to the soil crusts is explained through landscape types with non-calcareous soils (Eldridge, 1996). A positive relationship exists between soil pH, Fe, Ca and spatial distribution of lichens and mosses forming soil crusts in the gaps of kermes oak scrubs in semi-arid Spain has been determined (Ochoa-Hueso et al., 2011). The species diversity of terricolous lichen communities of Northern Italy grasslands depends on soil pH, light, and humidity requirements of lichen species (Gheza et al., 2016). Especially some terricolous lichens (*Cladonia* spp.) are limited by light compared to mosses (Tilk et al., 2018).

Unlike studies on factors affecting regional and landscape-level distribution of terricolous lichens, (Pietrasiak et al., 2011; Nelson et al., 2013; Concostrina-Zubiri et al., 2018) there are limited papers on understanding their spatial distribution in small-scale. In the steppe of south-eastern Spain, the microsite created by *Stipa tenacissima* L. may alter the small-scale spatial pattern of *Cladonia convoluta* (Lam.) Anders and *Squamarina cartilaginea* (With.) P. James (Maestre, 2003).

Remote sensing data has been used for determining lichens and biocrusts on a regional scale at deserts and arid areas (Chen, 2005), badlands (Rodríguez-Caballero, 2014), and drylands (Panigada, 2019). RGB, NIR, and hyperspectral images acquired using terrestrial and aerial photography, which are lately often used in other ecology studies, have also been used in lichen studies (Hinchliffe, 2017). However, to the best of our knowledge, this study represents the first application of aerial images in lichen studies at small-scale.

In this study, determining the spatial distribution of terricolous lichens on a small-scale with the RGB images captured by an unmanned aerial vehicle at a reforested degraded forest area was aimed. According to the hypothesis of this study lichen species are expected to a) be distributed inhomogeneously, b) cluster in the area, c) attract each other interspecifically. Lichen size classes are anticipated to fit power law distribution. Determining the effects of tree species, distance from trees, and azimuth of lichen patches cluster centroids on the spatial distribution of terricolous lichens are other objectives of the study.

Materials and methods

Study area

The study area is located in Değirmenköy (Istanbul), northwest Turkey (latitude; 41^0 08’ 11” and longitude; 28^0 03’ 30”) at an altitude of 200 m a.s.l., and the distance

http://www.aloki.hu ● ISSN 1589 1623 (Print) ● ISSN 1785 0037 (Online)
DOI: http://dx.doi.org/10.15666/aeer/1802_35573576

from the sea is 9 km. Mean annual precipitation is 509 mm, and mean annual temperature is 16°C. Presence of summer drought and drops in precipitation in winter show that mediterranean climate is dominant in the area. In 1983, the degraded forest area was reforested with mainly black pine, and cypress trees were planted as road buffer zone. While black pine (*Pinus nigra* J. F. Arnold) and cypress (*Cupressus sempervirens* L.) are species planted into the field, native species are oaks (*Quercus* spp.) and mock privet (*Phillyrea latifolia* L.). Some of the cypress species in the area were cut in 2018 (20 trees) and 2013-2014 (32 trees).

The study area is 1575 m^2 and has a near flat topographic structure (*Figure 1*). In the study area there are 12 black pines, 102 cypresses, 44 oaks, and 29 mock privets (*Table 1*). Black pine is present only along the east side of the area. Among the reforestation species, blackpine has mean height 7.58 m and cypress has 7.56 m, while among the natural species oak has mean height 2.42 m and mock privet 1.70 m. Mean crown projection areas of the trees were 12.01 m^2 for black pine, 5.68 m^2 for cypress, 4.46 m^2 for oak, and 3.55 m^2 for mock privet (*Table 1*).

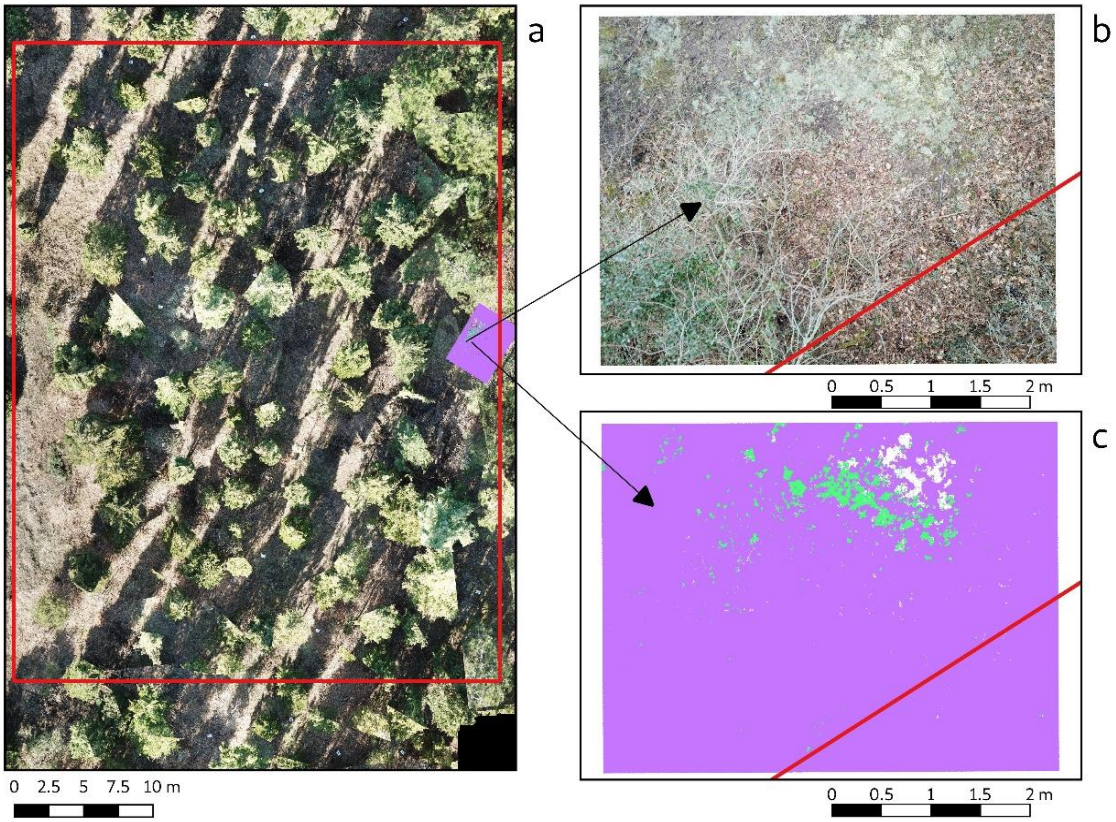

Figure 1. *a) Orthophoto produced from aerial photographs taken from 12 meters height, b) aerial photographs taken from 3-5 meters height, c) classified raster map of lichen species (white pixels: C. foliacea, green pixels: C. rangiformis)*

When the branching structure of the trees is analyzed, it is seen that (except few individuals) black pine and cypress do not ramify down to the breech of the trees; whereas oak and mock privet branch down to the bottom of the trees. Crown base height for black pine is 2.83 m and 0.97 m for cypress on average.

http://www.aloki.hu ● ISSN 1589 1623 (Print) ● ISSN 1785 0037 (Online)
DOI: http://dx.doi.org/10.15666/aeer/1802_35573576

Table 1. *Summary statistics of crown projection area, height, and distance to nearest neighbor of plants in the study area*

variable	species	n	Mean	Std. Deviation	Minimum	Maximum	sum
crown projection (m^2)	mock privet	29	3.55	2.22	0.97	9.68	105.66
	black pine	12	12.01	5.4	5.95	21.87	145.32
	oaks	44	4.46	4.24	0.53	25	188.5
	cypress	102	5.68	3.98	0.31	22.81	568.56
height (m)	mock privet	29	1.7	0.69	0.5	3	
	black pine	12	7.58	0.63	6.5	8.5	
	oaks	44	2.42	1.07	0.5	5	
	cypress	102	7.56	1.73	1	12	
nearest neighbor distance (m)	mock privet	29	3.41	2.17	0.93	7.84	
	black pine	12	4.75	7.02	2.17	27.01	
	oaks	44	2.87	1.21	1.33	6.74	
	cypress	102	2.44	0.8	0.97	5.51	

Species data

Three species of terricolous lichens; *Cladonia foliacea* (Huds.) Willd. (Syn.: *Cladonia convoluta* (Lam.) Anders), *Cladonia furcata* (Huds.) Schrad. subsp. *furcata* and *Cladonia rangiformis* Hoffm. were collected from the study area in March 2019. The lichen specimens were treated with a chemical spot test and identified with a stereomicroscope (Nikon SMZ445) according to the keys of references (Hodgetts, 1992; Purvis et al., 1992; Nimis and Martellos, 2004; Eversham, 2015; AFL, 2019; British lichens, 2019; Irish lichens, 2019). Nomenclature of the species mainly follows the Index Fungorum (2019) and MycoBank Database (2019).

Thallus of *C. foliacea* is fruticose when with podetia, but mostly squamulose greenish grey, forming compact mats (Nimis and Martellos, 2004), squamules 4-10 mm x 1-3 mm (Hodgetts, 1992). Thallus of *C. rangiformis is* fruticose, greenish grey to whitish grey, shrubby, (1-3 mm long and broad), forming tuft, (Nimis and Martellos, 2004), podetia 20-60 mm tall (Hodgetts, 1992; Nimis and Martellos, 2004). Thallus of *C. furcata* subsp. *furcata* is fruticose, podetia 20-70 mm tall, forming irregular tufts (Hodgetts, 1992).

C. foliacea was easily noticed in the aerial photos since it has a quite bright color. It was not possible to distinguish *C. furcata* subsp. *furcata* which is mixed with the predominant species in the study area, *C. rangiformis,* in the aerial photos, therefore these two species were considered together, and their mention in the text as *C. rangiformis* should be considered as *C. rangiformis* (+*C. furcata*).

The crown projection of the trees and the shrubs present at the survey area were digitized using the orthophoto generated by aerial photographs taken from 12 m height and the centroids of crown projections were regarded as trees (or shrubs) position coordinates. Minimum enclosing circles surrounding the crown projection were produced and accepted as crown projection (*Figure 2*) and the radius and areas of these circles were calculated (*Table 1*). The plant species were identified, their height and crown base height were measured in the field.

http://www.aloki.hu ● ISSN 1589 1623 (Print) ● ISSN 1785 0037 (Online)
DOI: http://dx.doi.org/10.15666/aeer/1802_35573576

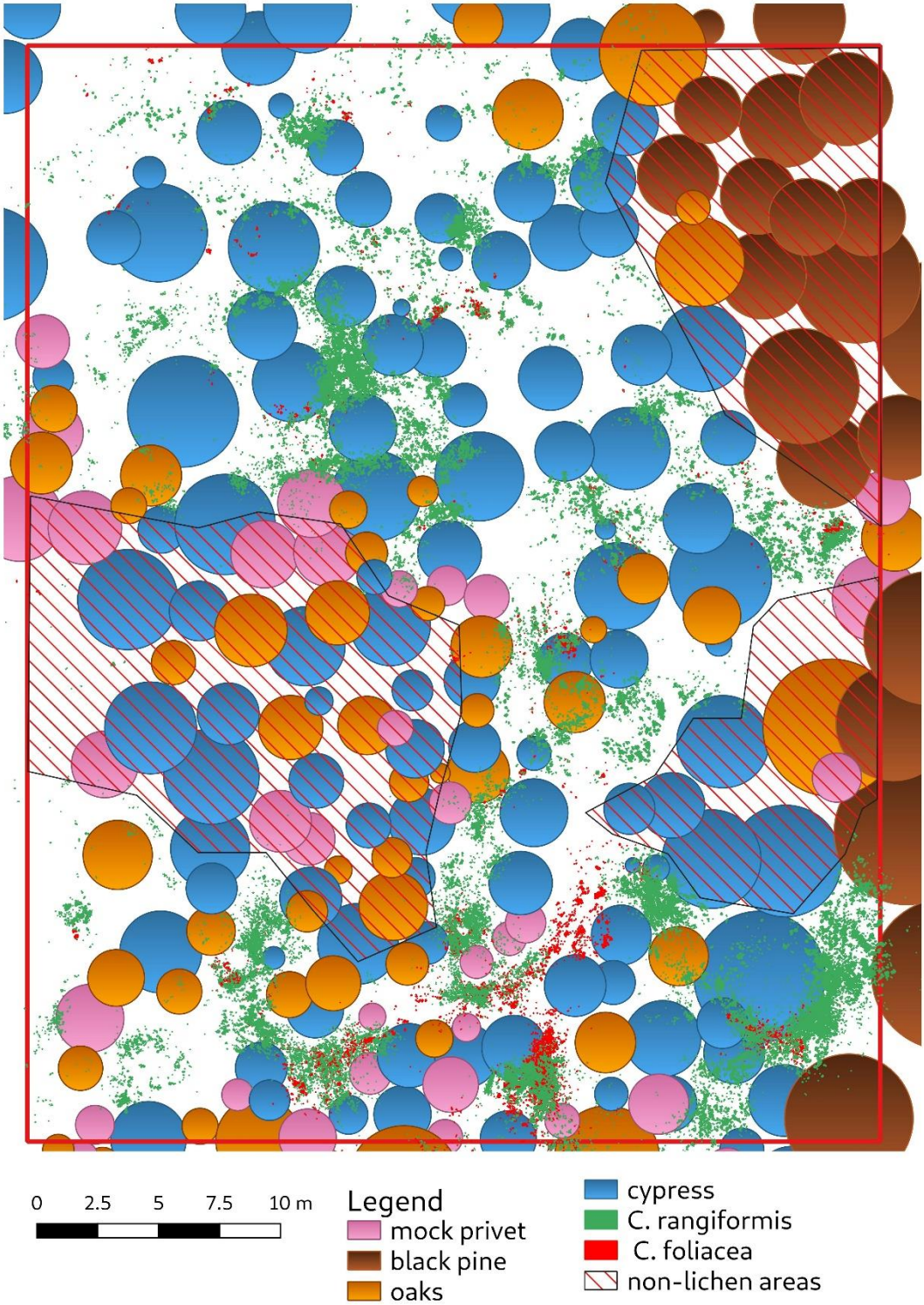

Figure 2. *Distribution of trees, shrubs, and lichens in the survey area. No or very few lichens were detected in the red hatched areas*

http://www.aloki.hu ● ISSN 1589 1623 (Print) ● ISSN 1785 0037 (Online)
DOI: http://dx.doi.org/10.15666/aeer/1802_35573576

Data collection and preparation for analysis

In regional, landscape, ecosystem and small-scale terricolous lichen studies, data were collected through sampling based surveying in the field such as transect based sampling (Pietrasiak et al., 2011; Bowker et al., 2013), random sampling (Maestre, 2003; Concostrina-Zubiri, 2018; Gutiérrez et al., 2018) or systematic sampling in the field (Ochoa-Hueso et al., 2011; Tilk et al., 2018). In our study, data regarding the lichen population in the study area was collected total count by aerial survey using one of the advanced technology's opportunities, "unmanned aerial vehicle-UAV" with the 12 megapixel resolution RGB camera in March 2019. With this goal in mind, the two-step aerial survey was conducted. First, an orthophoto of the survey area was produced using the photogrammetric method (Open Drone Map, 2019) with images captured from 12 m above the ground through an autonomous aerial photography covering the entire survey area (*Figure 1a*). It has been detected that the spatial resolution of these images (ca. 5 mm) was insufficient in distinguishing lichens. Thereupon new aerial images of lichens with a higher spatial resolution (<=2 mm) were obtained by manual flight of an unmanned aerial vehicle between trees at a height of approximately 3-5 meters above ground.

Since sizes of lichen individuals are rather small, it is very arduous to distinguish them individually in aerial photographs. As a result, lichen patches formed by individual lichens getting together were used as the material in this study. To objectively determine the boundaries of lichen patches from images obtained from a 3-5 meters height, "Trainable Weka Segmentation" (Arganda-Carreras et al., 2017) method was used. 188 aerial photographs were classified in this method, and so objectively determined lichen patches' boundaries were saved as raster data. RGB images captured from 3-5 meters height and the classified raster data (*Figure 1b,c*) were transformed into geo-registered raster data through georectification with the help of the orthomosaic map of the survey area. These geo-registered raster maps were first converted to vector data and then merged to obtain the boundaries of lichen patches as vector maps. The area corresponding to each lichen patch was calculated (*C. rangiformis* n= 25025, *C. foliacea* n= 5598 polygon) and these areas were used to create patch size classes (*Table 2*). In order to use the lichen patches in analysis, their polygon centroids were obtained. In order to investigate the relationships between the lichen patches and trees, lichen patch centroids were clustered.

Table 2. *Total area and number of lichen patches*

size class / species	*Cladonia rangiformis* (cm^2)	*Cladonia foliacea* (cm^2)
VSLP	6.48 (n=18003)	2.09 (n=4226)
SLP	46834.83 (n=4900)	9671.67 (n=1011)
MLP	38617.97 (n=1258)	6823.80 (n=230)
LLP	53010.72 (n=636)	8759.78 (n=101)
DLP	123216.02 (n=228)	24916.91(n=30)
Totals of size classes	261679.54 (n=25025)	50172.16 (n=5598)
Totals	311851.70 (n=30623)	

Lichen patch centroids were clustered using density-based spatial clustering of applications with noise (DBSCAN) algorithm (Ester et al., 1996). In this process, lichen

http://www.aloki.hu ● ISSN 1589 1623 (Print) ● ISSN 1785 0037 (Online)
DOI: http://dx.doi.org/10.15666/aeer/1802_35573576

patch clusters (hereafter LPC) were generated with a minimum of 5 neighbors in each cluster and a maximum distance of 0.25 meters between LPCs.

Trees and shrubs at a distance below 4 meters to the centers of LPCs were selected. The distances and azimuth values between the center of LPCs and the position of trees and shrubs were calculated (*Figure 3*).

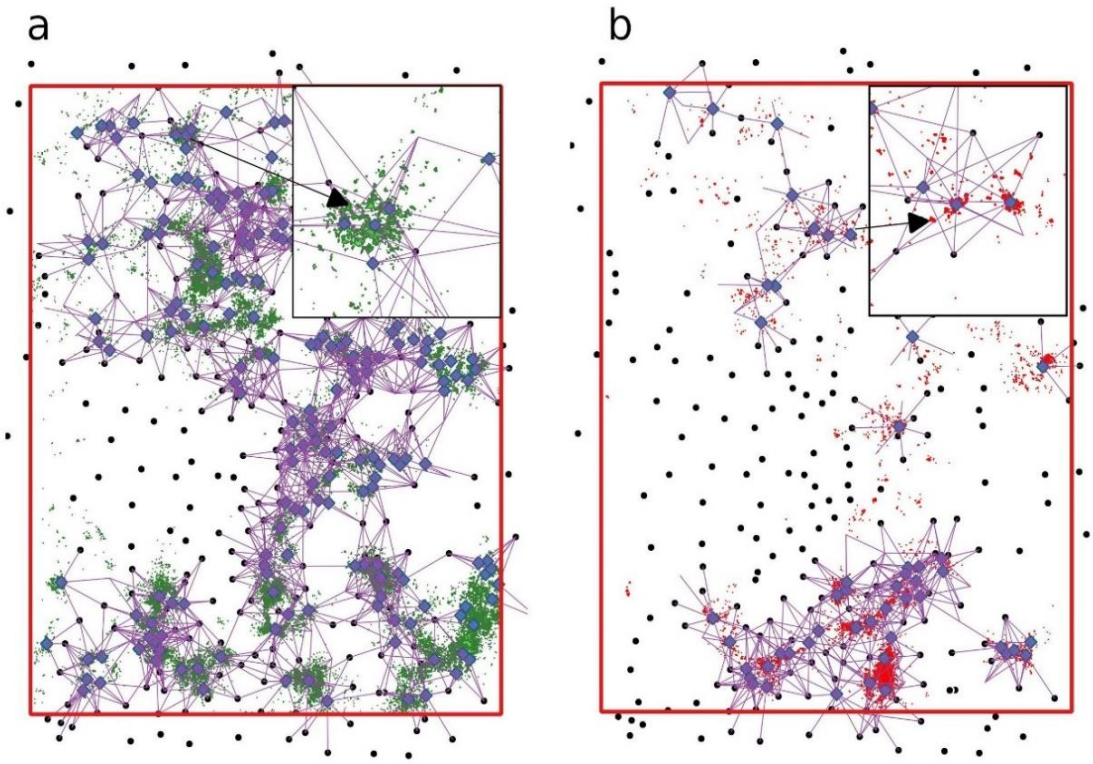

Figure 3. *Hublines for the calculation of azimuth and distance between centers of LPC and position of trees and shrubs; a) C. rangiformis b) C. foliacea*

Statistical Analysis

Since the studied objects were represented areally as lichen patches and the aerial survey was conducted over the entire area, analyses were conducted using a two-tiered approach: a cluster of lichen patches and whole lichen patches. In order to fulfill this objective, the relationships between LPC centers and surrounding trees and shrubs were investigated with circular statistics methods. Whether whole lichen patches fit the power-law distribution was tested and their distribution was inspected using spatial point pattern analyses.

In order to be able to evaluate differences between lichen patches based on their sizes, both lichen patches were sorted into 4 size classes as: Small lichen Patch (SLP) (5-20 cm^2), Middle Lichen Patch (MLP) (20-50 cm^2), Large Lichen Patch (LLP) (50-150 cm^2), Dead Lichen Patch (DLP) (> 150 cm^2). Patches covering areas less than 5 cm^2 (Very Small Lichen Patch) were not used in analyses in order to minimize classification and geometrical accuracy errors.

For analyses regarding the distribution of LPC centers around trees (or shrubs), the circular package (Agostinelli and Lund, 2017) of the R software was employed (R Core

http://www.aloki.hu ● ISSN 1589 1623 (Print) ● ISSN 1785 0037 (Online)
DOI: http://dx.doi.org/10.15666/aeer/1802_35573576

Team, 2018). To test whether whole community lichen patches fit power-law distribution (Kefi, 2007; Bowker et al., 2013, 2014) the "poweRlaw" package of the R software (Gillespie, 2015) was used. For the spatial point pattern analysis, firstly whether the lichen distribution is homogeneous was tested with quadrattest (Wang et al., 2010) and it was determined that the distribution is not homogeneous. Therefore the mentioned analyses were conducted inhomogeneously over the entire area (the word inhomogenous is synonymous with the word heterogeneous, but since the word inhomogeneous is used in spatstat package, this word was preferred in our study). The univariate pair correlation function g(r) was employed in order to determine the spatial pattern of the *C. rangiformis* and *C. foliacea*, (Stoyan and Stoyan, 1994; Wiegand and Moloney, 2014) under a inhomogeneous Poisson null model. To detect spatial relationships between lichen pathes in different size classes, and between lichen pathes and trees/shrubs, the bivariate pair correlation functioning $g_{12}(r)$ was used. For spatial point pattern analyses, the "spatstat" package (Baddeley et al., 2015) of the R software was used.

In the followed methodological approach (*Figure 4*) all spatial analyses were performed with Quantum GIS (Quantum GIS Development Team, 2019) and "weka trainable segmentation" FIJI (Schindelin et al., 2012), and all statistical analyses were performed using R (R Core Team, 2018) software.

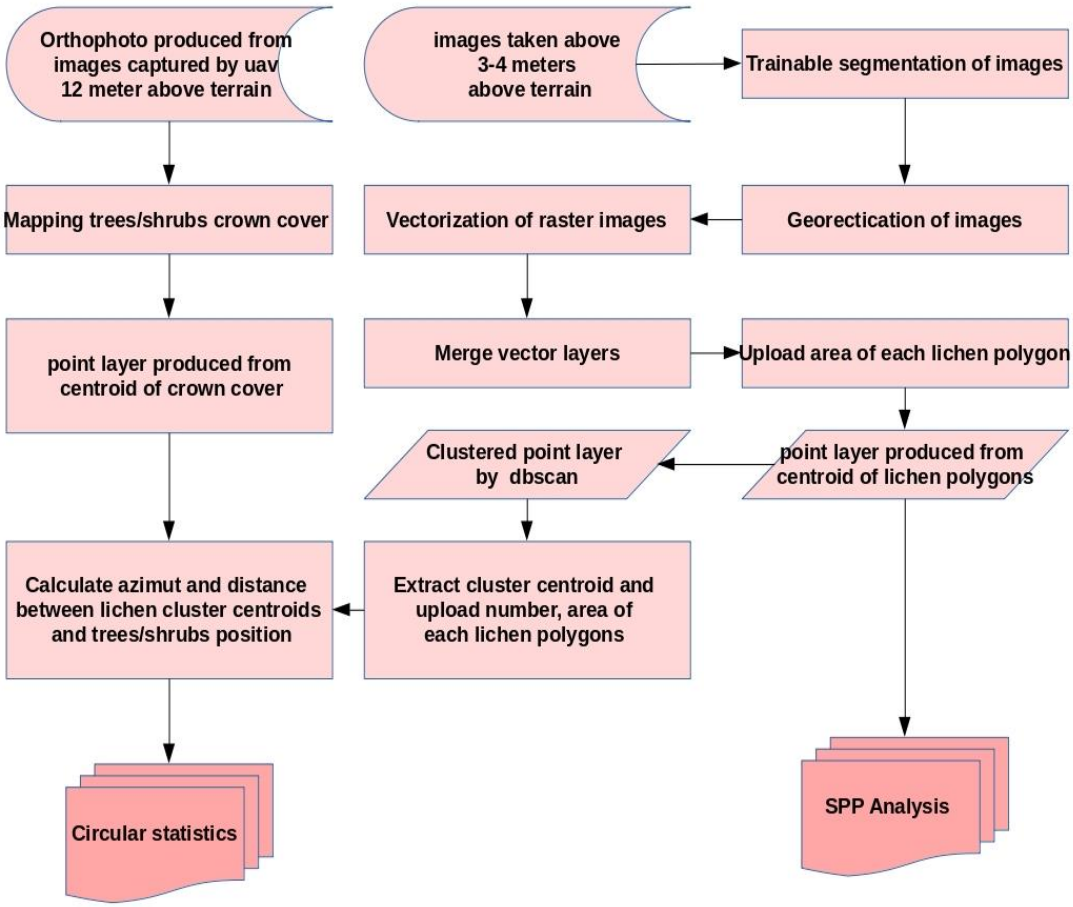

Figure 4. *Workflow of the methodological approach followed in the study*

http://www.aloki.hu ● ISSN 1589 1623 (Print) ● ISSN 1785 0037 (Online)
DOI: http://dx.doi.org/10.15666/aeer/1802_35573576

Results

Cover area of trees (or shrubs) and lichens

In the study area, the crown projection area of black pine, cypress, oak, and mock privets were calculated to be 145.32 m^2, 568.56 m^2, 188.50 m^2, and 105.66 m^2, respectively and the gap area was calculated to be 684.55 m^2. Since the crown projections were intertwined, the total coverage area resulted to be 184 m^2 more than the exact area of the study area.

The total area covered by the *C. rangiformis* (+*C. furcata*) in the study area was 5 times higher than that of the *C. foliacea* (*Table 2*). The total area covered by the lichen species is 31.19 m^2 which lies over 2% of the area. When the total area covered by lichen species were analyzed according to their size classes, 25025 lichen patches in *C. rangiformis*, 5598 lichen patches in *C. foliacea*, and 30623 lichen patches in total were determined (*Table 2*). For both lichen species, the highest lichen patch number was seen in VSLP; however, this size class' total cover is very low (*Table 2*). Among the size classes, DLP was the one with the highest total area, and it was measured 5 times higher for *C. rangiformis* than that for *C. foliacea* on average (*Table 2*).

Cluster of lichen patches analysis

Directional distribution of LPC centers around trees (or shrubs)

For the directional analyses of the lichen patch clusters, SLP, MLP, LLP, and DLP were utilized. In consequence of the conducted clustering process 199 clusters for *C. rangiformis* (*Figure 3a*), and 49 clusters for *C. foliacea* (*Figure 3b*) were determined. The average size of *C. rangiformis* patches was 37.27 cm^2, and the average size of *C. foliacea* patches was 36.57 cm^2. The average distance of lichen patches to cluster centers was 0.74 m for *C. rangiformis*, whereas it was 0.41 m for *C. foliacea*.

When the mean directions of trees and stumps closer than 4 m to LPC centers are considered, *C. rangiformis* LPC centers are located at the north of mock privet, east of oaks, and northeast of stumps (*Figure 5*). *C. rangiformis* LPC centers are located at the north of cypresses until 2.5 m distance, whereas at around 3-3.5 m they are at the northwest (*Figure 5*). Even though *C. foliacea* interaction with trees and shrubs is more erratic, its LPC's are located approximately towards the north of cypress and oak (*Figure 5*).

The amount of trees around *C. rangiformis* LPC centers are higher than those around *C. foliacea* LPC centers (*Figure 5*). The number of trees sorted from high to low at all distances from *C. raniformis* LPC centers are; cypress, stumps, oak, and mock privet (*Figure 5*). Also, while until 2 m stump and cypress individuals amounts are close, after 2 m, cypress amount is ahead (*Figure 5*). For *C. foliacea* cluster centers, the same ranking is: cypress, mock privet, stumps, and oak (*Figure 5*).

Whole lichen patches analysis

Power-law distribution analysis of lichen patches

The fact that lichen patch sizes differ between 0.5 mm^2 and 2.20 m^2 encouraged testing the aptitude of power-law distribution. According to the results of the hypothesis test, the logarithmic values of the number of *C. rangiformis* (p-value=0.38) and *C. foliacea* (p-value=0.44), and their patch-sizes fit power-law distribution (*Figure 6*). It was observed that while the more abundant ones with small lichen patch-sizes fit the

http://www.aloki.hu ● ISSN 1589 1623 (Print) ● ISSN 1785 0037 (Online)
DOI: http://dx.doi.org/10.15666/aeer/1802_35573576

power-law distribution better, the ones with big patch-size are relatively further from power-law distribution (*Figure 6*).

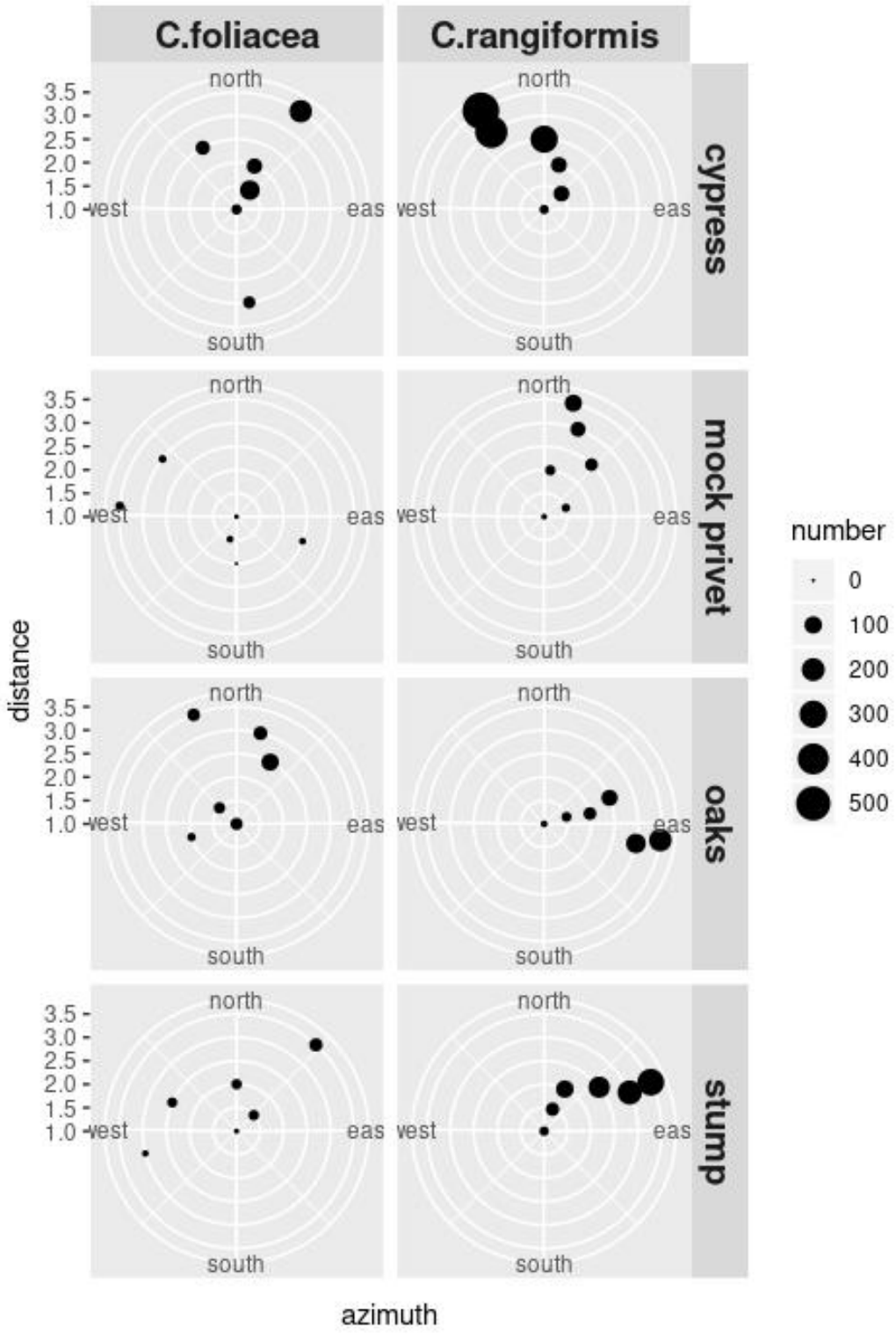

Figure 5. *Directional interaction based on distance and mean azimuth between the cluster of lichen patches and trees and shrubs. White circles show the distance from LPC centers, black-filled circles show plant cumulative count*

http://www.aloki.hu ● ISSN 1589 1623 (Print) ● ISSN 1785 0037 (Online)
DOI: http://dx.doi.org/10.15666/aeer/1802_35573576

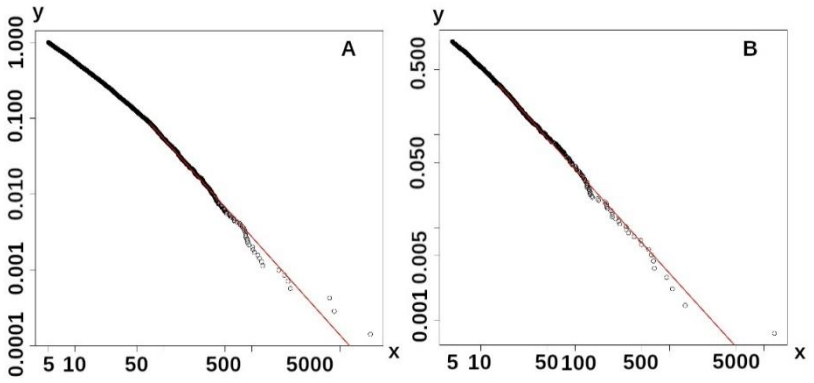

Figure 6. *Cumulative distributions of lichen patches for a) C. rangiformis, b) C. foliacea, shown with logarithmic scales*

Univariate point patterns analysis of lichens patches

According to the results of univariate point pattern analyses, *C. rangiformis* and *C. foliacea* show significant clustering in short distance (*Figure 7a,b*). g(r) values of *C. foliacea* resulted to be higher than the values of *C. rangiformis*. Clustering distance was observed to be same for *C. rangiformis* (r<2.5 m) as *C. foliacea* (r< 2.5 m) (*Figure 7*). When the two species are together, similar clustering was observed in short distance (r<2.5 m) (*Figure 7c*). Besides this, both species demonstrate significant regular distribution after short distance clustering (r>2.5 m).

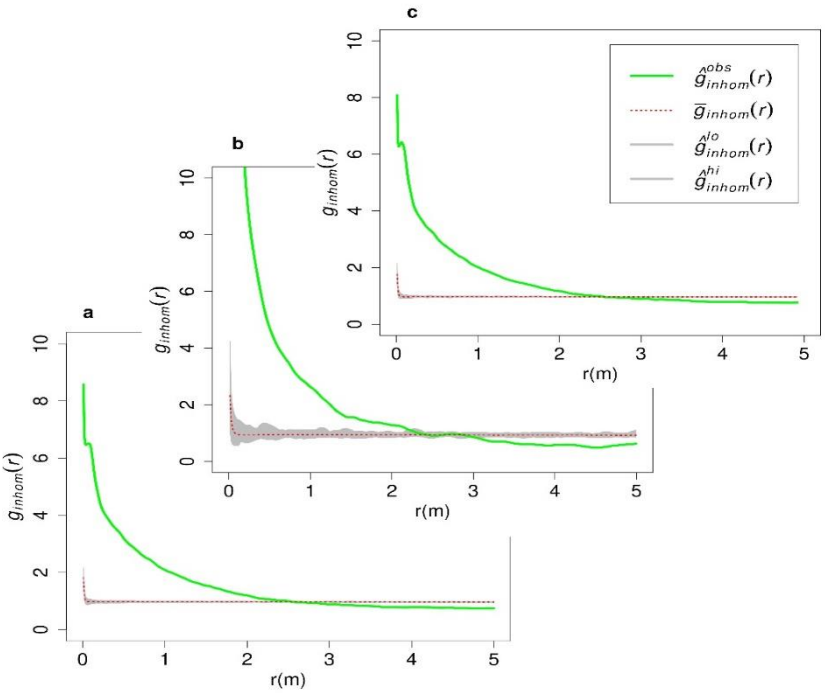

Figure 7. *Univariate point patterns analyses of a) C. rangiformis b) C. foliacea c) whole lichen patches using inhomogeneous pair-correlation function. $g_{inhom}(r)$ = green line; gray areas indicate boundaries of the simulation envelope constructed from 99 simulations of an inhomogeneous Poisson process with inhomogeneity given by kernel smoothed intensity function from a point pattern*

http://www.aloki.hu ● ISSN 1589 1623 (Print) ● ISSN 1785 0037 (Online)
DOI: http://dx.doi.org/10.15666/aeer/1802_35573576

The patterns created by all size classes of the species, both separately and together, univariate point pattern analyses done according to size classes gave similar results (*Figure 8*). According to the results of univariate analyses conducted considering size classes, random distribution was observed after 1-1.5 meters for *C. foliacea* at LLP and DLP, and after 5 and 6 meters at DLP for *C. rangiformis* (*Figure 8*).

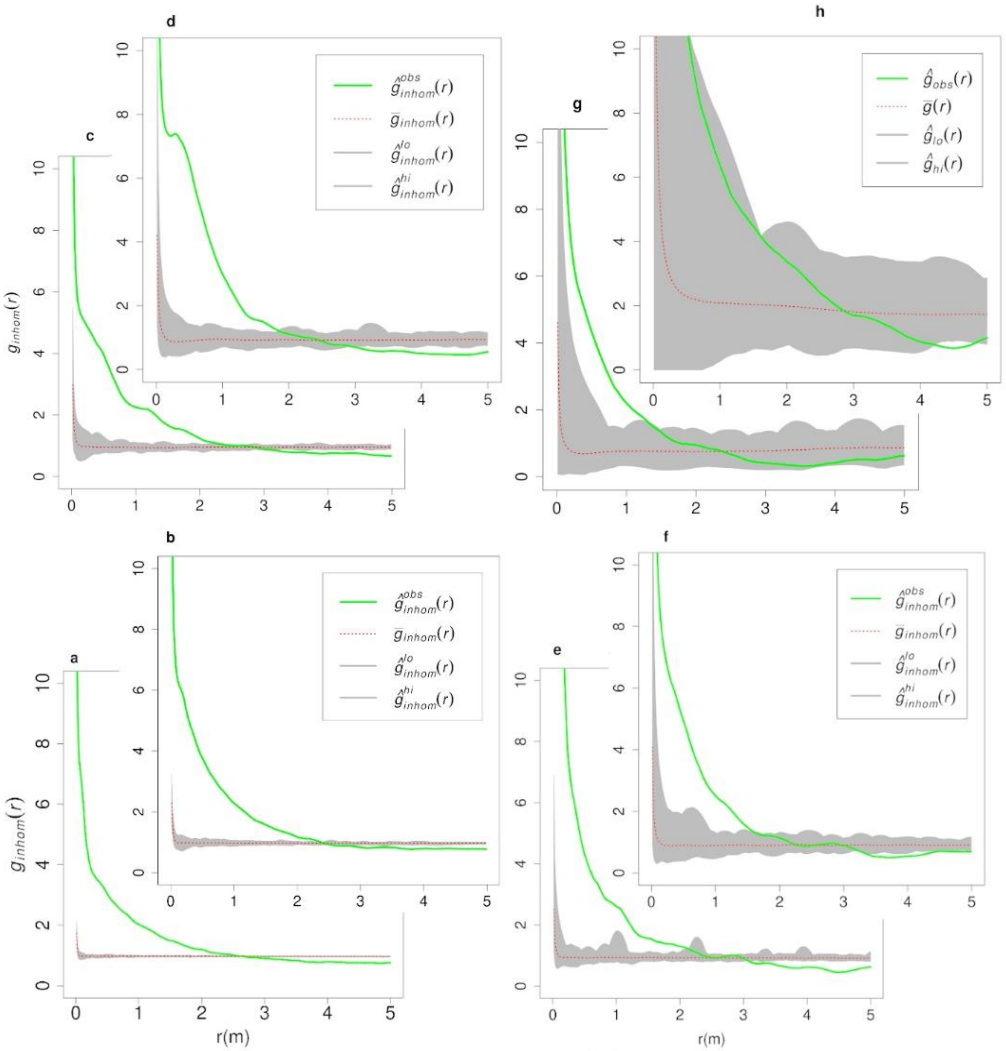

Figure 8. *Univariate point patterns analyses of C. rangiformis based on size class; a) SLP, b) MLP, c) LLP, d)DLP and Univariate point patterns analyses of C. foliacea based on size class e) SLP, f) MLP, g) LLP, h)DLP using inhomogeneous pair-correlation function. $g_{inhom}(r)$ = green line; gray areas indicate boundaries of the simulation envelope constructed from 99 simulations of an inhomogeneous Poisson process with inhomogeneity given by kernel smoothed intensity function from a point pattern*

Bivariate point pattern analysis of lichen patches size classes

SLP of *C. rangiformis* is attracted by other size classes of lichen patches in short distance (r<2 m); however, after this distance (r>2 m), repulsion is observed (*Figure 9*). A similar situation exists between MLP and LLP, between MLP and DLP, and between LLP and DLP (*Figure 9*).

http://www.aloki.hu ● ISSN 1589 1623 (Print) ● ISSN 1785 0037 (Online)
DOI: http://dx.doi.org/10.15666/aeer/1802_35573576

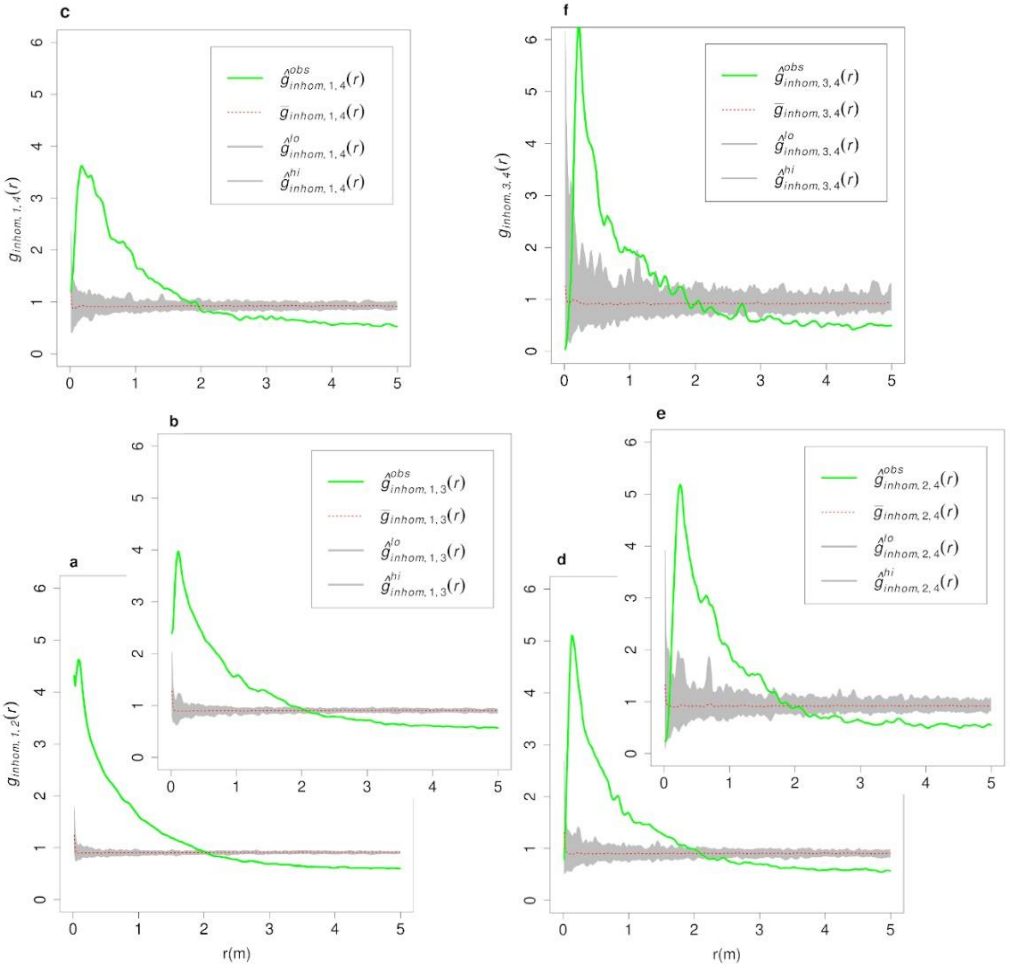

Figure 9. *Bivariate point pattern analysis of C. rangiformis based on a) SLP to MLP, b) SLP to LLP, c) SLP to DLP, d) MLP to LLP, e) MLP to DLP, f)LLP to DLP using inhomogeneous cross-type pair-correlation function $g_{inhom}(r)$ = green line; gray areas indicate boundaries of the simulation envelope constructed from 99 simulations of an inhomogeneous Poisson process with inhomogeneity given by kernel smoothed intensity function from a point pattern*

SLP of *C. foliacea* species is attracted by MLP and LLP in short distance (r<2 m), but after this distance (r>2 m), repulsion is observed. MLP is again attracted by LLP at short distance (r<2 m) (*Figure 10*). Other bivariate analyses were conducted, but since the DLP had n=30 and as a consequence the resulting envelopes were highly irregular, it was not evaluated.

Between *C. rangiformis* and *C. foliacea*, attraction is observed in short distance (r<1.5 m), however after this distance, repulsion is observed (*Figure 11*).

Bivariate point pattern analysis of lichen patches and trees/shrubs

It was determined that both lichen species are repulsed by the cypress (*Figure 12*). Other bivariate analyses were performed, but since n values were very low and therefore the resulting envelopes were irregular they were not evaluated.

http://www.aloki.hu ● ISSN 1589 1623 (Print) ● ISSN 1785 0037 (Online)
DOI: http://dx.doi.org/10.15666/aeer/1802_35573576

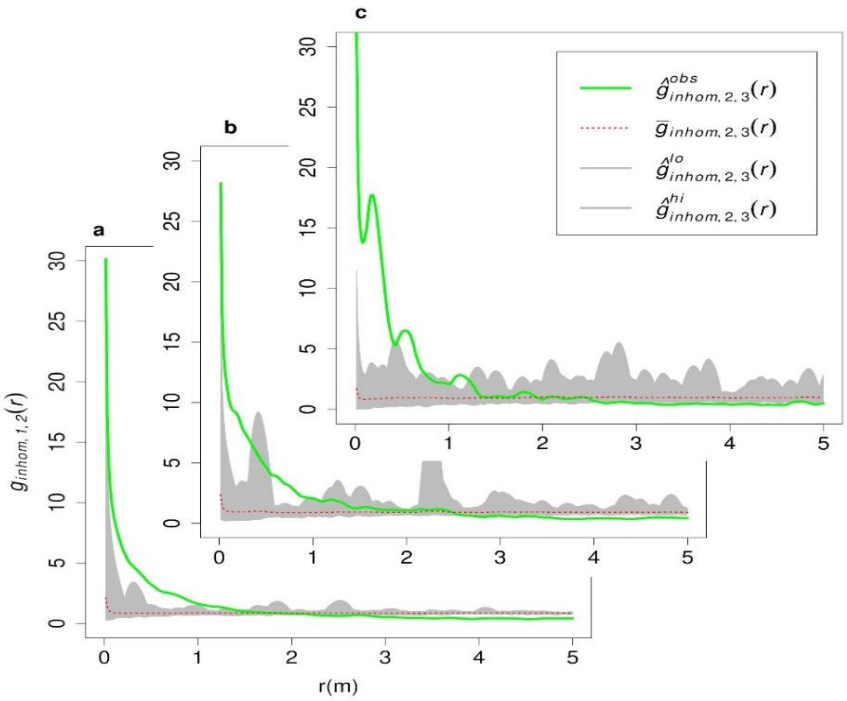

Figure 10. *Bivariate point pattern analysis of C. folicaea based on a) SLP to MLP, b) SLP to LLP, c) SLP to DLP using inhomogeneous cross-type pair-correlation function.* $g_{inhom}(r)$ *= green line; gray areas indicate boundaries of the simulation envelope constructed from 99 simulations of an inhomogeneous Poisson process with inhomogeneity given by kernel smoothed intensity function from a point pattern*

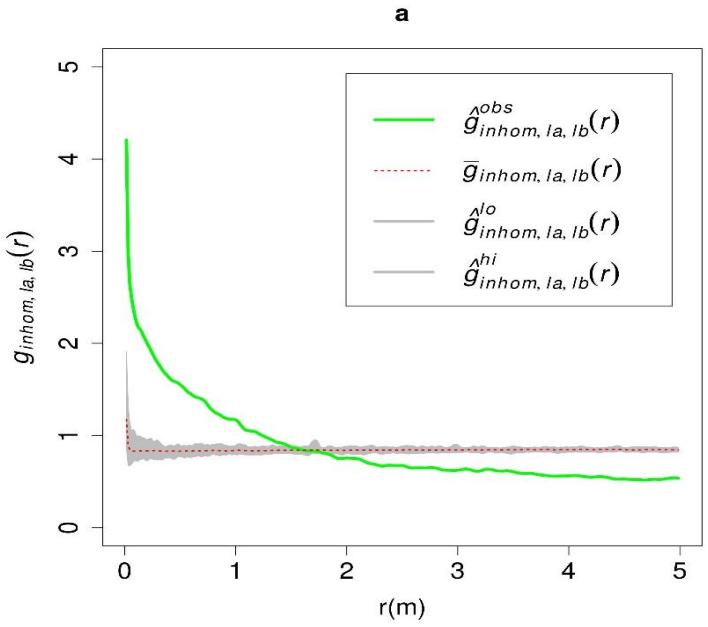

Figure 11. *Bivariate point pattern analysis of C. folicaea and C. rangiformis based on whole patches using inhomogeneous cross-type pair-correlation function.* $g_{inhom}(r)$ *= green line; gray areas indicate boundaries of the simulation envelope constructed from 99 simulations of an inhomogeneous Poisson process with inhomogeneity given by kernel smoothed intensity function from a point pattern*

http://www.aloki.hu ● ISSN 1589 1623 (Print) ● ISSN 1785 0037 (Online)
DOI: http://dx.doi.org/10.15666/aeer/1802_35573576

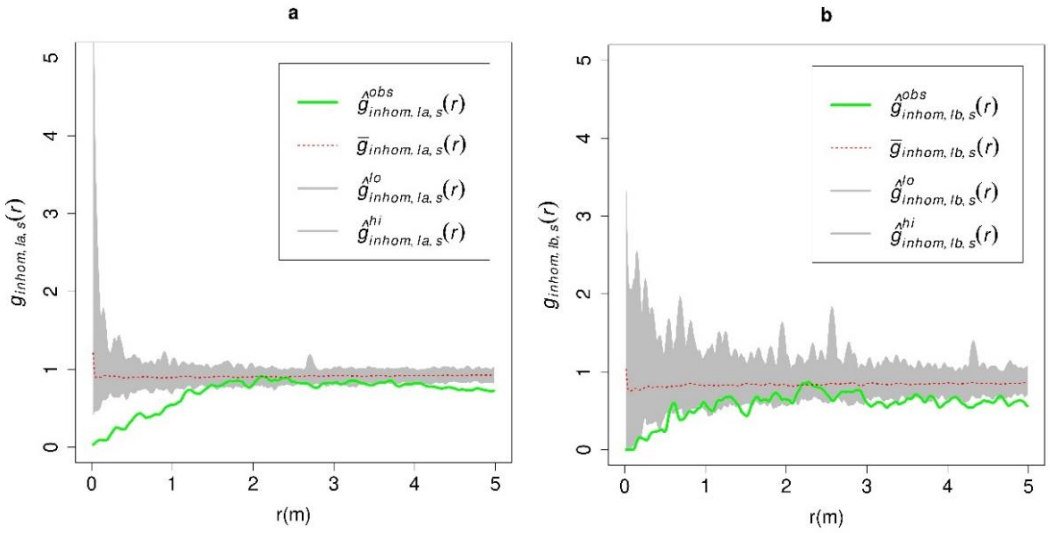

Figure 12. *Bivariate point pattern analysis between cypress and a) C. rangiformis, b) C. folicaea using inhomogeneous cross-type pair-correlation function $g_{inhom}(r)$ = green line; gray areas indicate boundaries of the simulation envelope constructed from 99 simulations of an inhomogeneous Poisson process with inhomogeneity given by kernel smoothed intensity function from a point pattern*

Discussion

Factors affecting the distribution of the important genus of terricolous lichens *Cladonia* have been studied for a long time (Yarranton, 1975). *Cladonia* generally can grow on soil, but can also be found in other substrates such as bark, rotting wood, dune system and among moss (Bowker et al., 2006; Osyczka, 2006; Gheza et al., 2016; Tilk et al., 2018; Sevgi et al., 2019). We contributed by investigating the spatial distribution of the species *C. foliacea* and *C. rangiformis* (+*C. furcata*) and their interactions with tree/shrub species. The complicated relationships based on direction and distance between the studied objects were investigated with an aerial survey. These relationships can also be investigated with different re/sampling methods and/or new studies could be done, because the area of such size (1575 m^2) captured aerially is 17500 times the size of the 30 cm x 30 cm (0.09 m^2) sample areas which are widely used in lichen studies. Hence just as different research can be done by resampling this permanent research area, temporal monitoring studies can also be conducted.

In afforestation areas in the Mediterranean region, new species brought into the area through planting and the presence of dominated natural species in the environment affects the distribution of terricolous lichens (Loppi et al., 2004; Concostrina-Zubiri et al., 2018). Similarly, in our study species brought into the area and natural species affected the distribution of terricolous lichens in small-scale. In the spatial clustering of two terricolous lichen species, 199 clusters for *C. rangiformis* (*Figure 3*), and 49 clusters for *C. foliacea* were found. Based on these results, *C. rangiformis* has a higher number of the lichen patches that has joined in size classes and their spatial distribution in small-scale is high. Another evidence that shows this effect more clearly is the mean direction of LPC centers with respect to trees (*Figure 5*). LPC centers are inclined to be on specific sides of tree species even at various distances (*Figure 5*). This inclination is more apparent for the *C. rangiformis*. Both species' cluster centers interacted 'by distance' most with

http://www.aloki.hu ● ISSN 1589 1623 (Print) ● ISSN 1785 0037 (Online)
DOI: http://dx.doi.org/10.15666/aeer/1802_35573576

cypress, then with other species (*Figure 5*). Oaks and mock privet being fewer in number and them gathering together at specific parts of the area may have made cypress' effects on lichens more obvious compared to other species. Results obtained for the *C. rangiformis* supports previous studies (Loppi et al., 2004).

When the distance from LPC centers at which trees were located was investigated, it has been found that lichen species were found under the crown projection area of cypress; however, no such result has been found for mock privet and oak. While the branching until bottom of oak and mock privet individuals block lights from passing through, the fact that branching begins at 97 cm on average and the branching angle is greater may have allowed more light to pass through the crown. As a result, while lichens with low shade tolerance were not able to disperse beneath the canopy of mock privet and oak, they were able to disperse beneath the canopy of some cypress individuals (Eldridge, 1999). These results are in line with studies which have revealed the negative effects of oak on *Cladonia* species' distribution (Ochoa-Hueso et al., 2011; Goldberg and Heine, 2014). Distribution of *Cladonia* species in open microsites is affected by trees (Crittenden, 1999). Another factor which augments this effect is forest litter (Eldridge, 1999). Although in our study forest litter-related evaluations were not conducted, the dense amounts of forest litter often produced by oak may have contributed in hindering lichens to enter beneath the crown projection area. In our study, besides this effect of oak, it has been determined that there are nearly no lichens in the region where oak is present with mock privet (non-lichen area in the left of *Figure 2*).

Power-law distribution is being utilized successfully in vegetation studies (Kefi et al., 2007) and explains the relationship between epiphytic lichen species diversity and tree diameter (Buckley, 2011). Bowker et al. (2013, 2014) stated that analysis of the patch-size distributions of biological biosoil crusts including terricolous lichens fit power-law distribution. Our study validated that terricolous lichen species' patch sizes directly demonstrate power-law distribution, which is in line with our expectations.

It is thought that the inhomogeneity of lichen distribution arises from the distribution of the trees and shrubs in the area, which proves our hypothesis to be true. It is considered that the intensity and distribution of pine, oak, and mock privet species in the area causes this. It is possible to perform the point pattern analysis of an irregular area by excluding these regions; however, in that case, the reasons behind in-homogeneous distribution and the actual distribution patterns of the lichens would not have been revealed, therefore this method was not preferred.

Considering all lichen size classes together, the occurrence of clustering at short distance (2-2.5 meters) and regular distribution beyond this distance is thought to be related to both the distance among trees in the afforestation area (the average distance of all trees; 1.91 m, the average distance among cypress; 2.44 m) and the fact that lichens form large colonies in the gaps of forest/shrublands by colonization. The highness of the g(r) value of *C. foliacea* results from its clustering in only specific regions of the area. Both *Cladonia* species demonstrating clustering and not distributing randomly goes along with Maestre's (2003) results. However, the random distribution of *C. foliacea* and *C. rangiformis*' large size classes, discovered through the univariate analyses conducted based on size classes, may indicate that they initially disperse randomly in the region. The existence of a positive or negative correlation between lichen patch size classes were investigated using bivariate analyses. According to the results, small size classes in both lichen species show a positive correlation with large size classes at short distance ($r<2$ m);

http://www.aloki.hu ● ISSN 1589 1623 (Print) ● ISSN 1785 0037 (Online)
DOI: http://dx.doi.org/10.15666/aeer/1802_35573576

however, after this distance (r>2 m) a negative correlation was observed. This may be due to the effects of colonization, competition for space and nutrition.

The relationship between *C. rangiformis* and *C. foliacea* which is positive at short distance (r<0.5 m), is negative after this distance. The investigation of the bivariate relationship between lichens and trees revealed significant repulsion from cypress trees.

Conclusions

This study has shown that aerial photography can be used for determining the spatial distribution of terricolous lichen species. Captured photographs will allow for comparison with photos taken at a later time period, which will in turn contribute to understanding the spatial distribution of terricolous lichen species over long periods of time. Futher studies should take into consideraiton of spatial modelling of environmental factors (i.e., tree height, crown width, shade, microtopography, soil properties) affecting the spatial distribution of lichens. Also, the effect of herbaceous plants between trees on the spatial distribution of terricolous lichens should be made clear.

Acknowledgements. The authors report that they have no conflicts of interests. We would like to thank to İstanbul Regional Directorate of Forestry and İstanbul Forest Service. Our special thanks are due to Dr. Hatice Yılmaz for her contribution to field studies. The authors are grateful to Lale Yılmaz for the language editing of this paper.

REFERENCES

[1] Adamo, P., Vingiani, S., Violante, P. (2002): Lichen-rock interactions and bioformation of minerals. – Developments in Soil Science 28(2): 377-391.

[2] AFL (2019): Association Française de Lichénologie. – Retrieved from https://www.afl-ichenologie.fr/Photos_AFL/Photos_AFL_C.htm (10.07.2019).

[3] Agostinelli, C., Lund, U. (2017): R package 'circular': Circular Statistics (version 0.4-93). – URL Retrieved from https://r-forge.r-project.org/projects/circular/.

[4] Akpinar, A. U., Ozturk, S., Sinirtas, M. (2009): Effects of some terricolous lichens [*Cladonia rangiformis* Hoffm., *Peltigera neckerii* Hepp ex Müll. Arg., *Peltigera rufescens* (Weiss) Humb.] on soil bacteria in natural conditions. – Plant Soil and Environment 55(4): 154-158.

[5] Aptroot, A., James, P. W. (2002): Monitoring Lichens On Monuments. – In: Nimis, P. L., Schedegger, C., Wolseley, P. A. (eds.) Monitoring with Lichens- Monitoring Lichens., Kluwer Academic Publishers, Netherlands.

[6] Arganda-Carreras, I., Kaynig, V., Rueden, C., Eliceiri, K. W., Schindelin, J., Cardona, A., Sebastian Seung, H. (2017): Trainable Weka Segmentation: a machine learning tool for microscopy pixel classification. – Bioinformatics 33(15): 2424-2426. PMID28369169, doi:10.1093/bioinformatics/btx180 (on Google Scholar).

[7] Asta, J., Orry, F., Toutain, F., Souchier, B., Villemin, G. (2001): Micromorphological and ultrastructural investigations of the lichen-Soil interface. – Soil Biology and Biochemistry 33(3): 323-337.

[8] Baddeley, A., Rubak, E., Turner, R. (2015): Spatial point patterns: Methodology and applications with R. – London, UK: Chapman and Hall/CRC Press. Retrieved from http://www.crcpress.com/Spatial-Point-Patterns-Methodology-and-Applications-with-R/Baddeley-Rubak-Turner/9781482210200/.

http://www.aloki.hu ● ISSN 1589 1623 (Print) ● ISSN 1785 0037 (Online)
DOI: http://dx.doi.org/10.15666/aeer/1802_35573576

[9] Bowker, M. A., Belnap, J., Miller, M. E. (2006): Spatial modeling of biological soil crusts to support rangeland assessment and monitoring. – Rangeland Ecology and Management 59(5): 519-529.
[10] Bowker, M. A., Maestre, F. T., Mau, L. R. (2013): Diversity and patch-size distributions of biological soil crusts regulate dryland ecosystem multifunctionality. – Ecosystems 16: 923-933.
[11] Bowker, M. A., Maestre, F. T., Eldridge, D., Belnap, J., Castillo-Monroy, A., Escolar, C., Soliveres, S. (2014): Biological soil crusts (biocrusts) as a model system in community, landscape and ecosystem ecology. – Biodiversity and Conservation 23: 1619-1637.
[12] British lichens (2019): Retrieved from http://www.lichens.lastdragon.org (10.07.2019).
[13] Buckley, H. L. (2011): Isolation affects tree-scale epiphytic lichen community structure on New Zealand mountain beech trees. – Journal of Vegetation Science 22: 1062-1071.
[14] Chen, J., Blume, H. P., Beyer, L. (2000): Weathering of rocks induced by lichen colonization- a review. – Catena 39: 121-146.
[15] Chen, J., Zhang, M. Y., Wang, L., Shimazaki, H., Tamura, M. (2005): A new index for mapping lichen-dominated biological soil crusts in desert areas. – Remote Sensing of Environment 96: 165-175.
[16] Concostrina-Zubiri, L., Martínez, I., Rabasa, S. G., Escudero, A. (2014): The influence of environmental factors on biological soil crust: from a community perspective to a species level approach. – Journal of Vegetation Science 25: 503-513.
[17] Concostrina-Zubiri, L., Martínez, I., Escudero, A. (2018): Lichen-biocrust diversity in a fragmented dryland: Fine scale factors are better predictors than landscape structure. – Science of the Total Environment 628-629: 882-892.
[18] Crittenden, P. D. (1999): Aspects of the ecology of mat-forming lichens. – Rangifer 20(2-3): 127-139.
[19] Eldridge, D. J. (1996): Distribution and floristics of terricolous lichens in soil crusts in arid and semi-arid New South Wales, Australia. – Australian Journal of Botany 44: 581-599.
[20] Eldridge, D. J. (1999): Distribution and floristics of moss- and lichen-dominated soil crusts in a patterned *Callitris glaucophylla* woodland in eastern Australia. – Acta Oecologica 20(3): 159-170.
[21] Ester, M., Kriegel, H.-P., Sander, J., Xu, X. (1996): A density-based algorithm for discovering clusters in large spatial databases with noise. – In: Proceedings of the International Conference on Knowledge Discovery and Data Mining (KDD '96): 226-231.
[22] Eversham, B. (2015): Heathland Lichens. – Retrieved from https://www.wildlifebcn.org › sites › default › files (10.07.2019).
[23] Gheza, G., Assini, S., Passadore, M. V. (2016): Terricolous lichen communities of *Corynephorus canescens* grasslands of Northern Italy. – Tuexenia 36: 121-142.
[24] Gillespie, C. S. (2015): Fitting Heavy Tailed Distributions: The poweRlaw Package. – Journal of Statistical Software 64(2): 1-16. URL http://www.jstatsoft.org/v64/i02/.
[25] Goldberg, N. A., Heine, J. N. (2014): Effects of canopy and leaf litter on the distribution of mat-forming terricolous lichens (*Cladonia* spp.) in northeastern Florida xeric scrub. – Florida Scientist 77(2): 87-97.
[26] Gutıérrez, M., Pando-Moreno, M., Jurado, E., González-Rodríguez, H., Marmolejo, J. G., Mendoza, D. (2018): Non-random distribution of biocrust in a natural arid environment in the Northern Mexican. – Applied Ecology and Environmental Research 16(3): 2441-2451.
[27] Gypser, S., Veste, M., Fischer, T., Lange, P. (2015): Formation of soil lichens crusts at reclaimed post-mining sites, Lower Lusatia, North-east Germany. – Graph. Scr. 27: 3-14.
[28] Hinchliffe, G., Bollard-Breen, B., Cowan, D. A., Doshi, A., Gillman, L. N., Maggs-Kolling, G., de los Ríos-Murillo, A., Pointing, S. B. (2017): Advanced photogrammetry to assess lichen colonisation in the hyper-arid Namib Desert. – Frontiers in Microbiology 8: 2083.
[29] Hodgetts, N. G. (1992): *Cladonia*: a field guide. – Joint Nature Conservation Committee, ISBN 1 873701 08 X.

http://www.aloki.hu ● ISSN 1589 1623 (Print) ● ISSN 1785 0037 (Online)
DOI: http://dx.doi.org/10.15666/aeer/1802_35573576

[30] Index Fungorum (2019): Retrieved from http://www.indexfungorum.org/ (10.07.2019).
[31] Irish lichens (2019): Retrieved from http://www.irishlichens.ie/pages-lichen/l-209.html (10.07.2019).
[32] Jackson, T. A. (2015): Weathering, secondary mineral genesis, and soil formation caused by lichens and mosses growing on granitic gneiss in a boreal forest environment. – Geoderma 251-252: 78-91.
[33] Kéfi, S., Rietkerk, M., Alados, C., Pueyo, Y., Papanastasis, V. P., Elaich, A., de Ruiter, P. C. (2007): Spatial vegetation patterns and imminent desertification in Mediterranean arid ecosystems. – Nature 449: 213-217.
[34] Loppi, S., Boscagli, A., Dominicis, V. (2004): Ecology of soil lichens from Pliocene clay badlands of central Italy in relation to geomorphology and vascular vegetation. – Catena 55: 1-15.
[35] Maestre, F. T. (2003): Small-scale spatial patterns of two soil lichens in semi-arid Mediterranean steppe. – Lichenologist 35(1): 71-81.
[36] Maestre, F. T., Bowker, M. A., Cantón, Y., Castillo-Monroy, A. P., Cortina, J., Escolar, C., Escudero, A., Lázaro, R., Martínez, I. (2011): Ecology and functional roles of biological soil crusts in semi-arid ecosystems of Spain. – Journal of Arid Environments 75(12): 1282-1291.
[37] Martínez, I., Escudero, A., Maestre, F. T., de la Cruz, A., Guerrero, C., Rubio, A. (2006): Small-scale patterns of abundance of mosses and lichens forming biological soil crusts in two semi-arid gypsum environments. – Australian Journal of Botany 54: 339-348.
[38] MycoBank Database (2019): Retrieved from http://www.mycobank.org/ (10.07.2019).
[39] Nelson, P. R., Roland, C., Macander, M. J., McCune, B. (2013): Detecting continuous lichen abundance for mapping winter caribou forage at landscape spatial scales. – Remote Sensing of Environment 137: 43-54.
[40] Nimis, P. L., Martellos, S. (2004): Keys to the lichens of Italy I. Terricolous species. – Le Guide di Dryades 1 - Serie Licheni I (LI). Trieste: Edizioni Goliardiche. ISBN 88-88171-73-8.
[41] Ochoa-Hueso, R., Manrique, E. (2011): Effects of nitrogen deposition and soil fertility on cover and physiology of *Cladonia foliacea* (Huds.) Willd., a lichen of biological soil crusts from Mediterranean Spain. – Environmental Pollution 159: 449-457.
[42] Ochoa-Hueso, R., Hernandez, R. R., Pueyo, J. J., Manrique, E. (2011): Spatial distribution and physiology of biological soil crusts from semi-arid central Spain are related to soil chemistry and shrub cover. – Soil Biology and Biochemistry 43(9): 1894-1901.
[43] Ochoa-Hueso, R., Mondragon-Cortés, T., Concostrina-Zubiri, L., Serrano-Grijalva, L., Estébanez, B. (2017): Nitrogen deposition reduces the cover of biocrust-forming lichens and soil pigment content in a semiarid Mediterranean shrubland. – Environmental Science and Pollution Research 24(34): 26172-26184.
[44] Open Drone Map [Computer software]. (2019): Retrieved from https://github.com/OpenDroneMap/OpenDroneMap.
[45] Osyczka, P. (2006): The lichen genus *Cladonia* (Cladoniaceae, lichenized Ascomycota) for Spitsbergen. – Polish Polar Research 27: 207-242.
[46] Panigada, C., Tagliabue, G., Zaady, E., Rozenstein, O., Garzonio, R., Di Mauro, B., De Amicis, M., Colombo, R., Cogliati, S., Miglietta, F., Rossini, M. (2019): A new approach for biocrust and vegetation monitoring in drylands using multi-temporal Sentinel-2 images. – Progress in Physical Geography: Earth and Environment 43(4): 496-520. https://doi.org/10.1177/0309133319841903.
[47] Pietrasiak, N., Johansen, J. R., Drenovsky, R. E. (2011): Geologic composition influences distribution of microbiotic crusts in the Mojave and Colorado Deserts at the regional scale. – Soil Biology & Biochemistry 43: 967-974.
[48] Purvis, O. W., Coppins, B. J., Hawksworth, D. L., James, P. W., Moore, D. M. (1992): The Lichen Flora of Great Britain and Ireland. – Natural History Museum Publications, London.

http://www.aloki.hu ● ISSN 1589 1623 (Print) ● ISSN 1785 0037 (Online)
DOI: http://dx.doi.org/10.15666/aeer/1802_35573576

[49] Quantum GIS Development Team (2019): Quantum geographic information system. – Open source geospatial foundation project. Retrieved from http://qgis.osgeo.org.
[50] R Core Team (2018): R: A language and environment for statistical computing. – Vienna, Austria: R Foundation for Statistical Computing. Retrieved from https://www.R-project.org/.
[51] Rai, H., Upreti, D. K. (2014): Terricolous Lichens in India: Volume 1: Diversity Patterns and Distribution Ecology. – Springer-Verlag, New York.
[52] Rodríguez-Caballero, E., Escribano, P., Cantón, Y. (2014): Advanced image processing methods as a tool to map and quantify different types of biological soil crust. – ISPRS Journal of Photogrammetry and Remote Sensing 90: 59-67.
[53] Schindelin, J., Arganda-Carreras, I., Frise, E., Kaynig, V., Longair, M., Pietzsch, T., Preibisch, S., Rueden, C., Saalfeld, S., Schmid, B., Tinevez, J. Y., White, D. J., Hartenstein, V., Eliceiri, K., Tomancak, P., Cardona, A. (2012): Fiji: an open-source platform for biological-image analysis. – Nature methods 9(7): 676-682. PMID 22743772, doi:10.1038/nmeth.2019 (on Google Scholar).
[54] Sevgi, O., Makineci, E. (2005): Functions of lichens on disintegration and weathering of rocks (Likenlerin kaya parçalanması ve ayrışmasında işlevleri). – İstanbul Üniversitesi, Orman Fakültesi Dergisi, Seri B 55(2): 75-83.
[55] Sevgi, E., Yılmaz, O. Y., Özyiğitoğlu, G. Ç., Tecimen, H. B., Sevgi, O. (2019): Factors influencing epiphytic lichen species distribution in a managed mediterranean Pinus nigra Arnold forest. – Diversity 11(59): 1-21.
[56] Stoyan, D., Stoyan, H. (1994): Fractals, random shapes and point fields: Methods in geometrical statistics. – Chichester, UK: John Wiley & Sons.
[57] Tilk, M., Ots, K., Tullus, T. (2018): Effect of environmental factors on the composition of terrestrial bryophyte and lichen species in Scots pine forests on fixed sand dunes. – Forest Systems 27(3): 1-12.
[58] Wang, X., Wiegand, T., Hao, Z., Li, B., Lin, F. (2010): Species associations in an old-growth temperate forest in north-eastern China. – Journal of Ecology 98: 674-686.
[59] Wiegand, T., Moloney, K. A. (2014): Handbook of spatial point pattern analysis in ecology. – Boca Raton, FL: CRC Press.
[60] Will-Wolf, S., Scheidegger, C., McCune, B. (2002a): Methods for monitoring biodiversity and ecosystem function-Monitoring scenarios, sampling strategies and data quality. – In: Nimis, P. L., Schedegger, C., Wolseley, P. A. (eds.) Monitoring with Lichens- Monitoring Lichens., Kluwer Academic Publishers, Netherlands.
[61] Will-Wolf, S., Esseew, P. A., Neitlich, P. (2002b): Monitoring Biodiversity and Ecosystem Function: Forests. – In: Nimis, P. L., Schedegger, C., Wolseley, P. A. (eds.) Monitoring with Lichens- Monitoring Lichens., Kluwer Academic Publishers, Netherlands.
[62] Yarranton, G. A. (1975): Population growth in Cladonia stellaris (Opiz.) Pouz. and Vezda. – The New Phytologist 75(1): 99-110.
[63] Zouaoui, S., Boudreault, C., Drapeau, P., Bergeron, Y. (2014): Influence of time since fire and micro-habitat availability on terricolous lichen communities in Black Spruce (Picea mariana) Boreal Forests. – Forests 5(11): 2793-2809.

http://www.aloki.hu ● ISSN 1589 1623 (Print) ● ISSN 1785 0037 (Online)
DOI: http://dx.doi.org/10.15666/aeer/1802_35573576

DETERMINING THE WATER QUALITY INDEX OF TREATED WASTE WATER FOR REPELLENT AND WETTABLE SANDY LOAM BASED ON INFILTRATION CHARACTERISTICS

ZHAO, X.[1A] – CHAI, H. Y.[1,2A] – CAI, Y. H.[1] – CHEN, J. Y.[1*] – WU, P. T.[1] – LI, Y.[1] – CHEN, H. Y.[3]

[1]*College of Water Resources and Architectural Engineering, Key Laboratory of Agricultural Soil and Water Engineering in the Ministry of Education, Northwest A&F University, Yangling, Shaanxi 712100, China*

[2]*Northwest Research Institute of Engineering Investigations and Design, Xi'an, Shaanxi 710000, China*

[3]*Department of Foreign Languages, Northwest A&F University, Yangling, Shaanxi 712100, China*

[A]*These authors contributed equally to this work.*

[*]*Corresponding author*
e-mail: cjyrose@126.com

(Received 10th Dec 2019; accepted 24th Mar 2020)

Abstract. Treated waste water (TWW) has been replacing fresh water (FW) partly in irrigation. However, irrigation with TWW can cause soil water repellency that affects infiltration characteristics. In order to determine the water quality index with full consideration taken into infiltration characteristics, one dimensional infiltration experiments were conducted in wettable and repellent sandy loams with TWW irrigation. Five kinds of TWW and one tap water (TW) were chosen. The effect of water quality on the wetting front and cumulative infiltration volume was analyzed. The comprehensive water quality index (ZF) was obtained by principal component analysis. The results show that the water quality has a great effect on the cumulative infiltration and wetting front of wettable soil. The more significant the comprehensive water quality index is, the greater the cumulative infiltration volume and wetting front are. The water quality has a great effect on the cumulative infiltration and no effect on wetting front of repellency soil. Power correlation exists between sorptivety (S) and chemical oxygen demand (COD). Meanwhile, a quadratic polynomial relationship exists between the ratio of S for the wetting front coefficient and ZF, and there is a minimum value in the curve.
Keywords: *soil water repellency, soil moisture, wetting front, cumulative infiltration, COD*

Introduction

Treated waste water (TWW) irrigation has become a common practice in arid and semiarid areas to deal with water scarcity and reduce the consumption of fresh water (FW) (Wallach et al., 2005). However, such irrigation may have an impact on the chemical and hydraulic properties of soils. Long-term TWW irrigation will increase soil organic matter (OM) and form a layer of hydrophobic organic compounds on the surface of soil particles (Chen et al., 2009; Nadav et al., 2012a, 2012b), which will cause soil water repellency. The water drop penetration time (WDPT) of repellent soils could reach 802 s for sandy soils (Mataix-Solera et al., 2011) and 3600 s in clay loam with long-term TWW irrigation (Wallach et al., 2005). The occurrence of water repellency leads to a decrease of soil infiltration rate and water conductivity, which affects irrigation efficiency (Wallach et al., 2005; Leuther et al., 2018).

http://www.aloki.hu ● ISSN 1589 1623 (Print) ● ISSN 1785 0037 (Online)
DOI: http://dx.doi.org/10.15666/aeer/1802_35773592

The reduction of irrigation efficiency is shown in the decrease of the infiltration rate and the migration rate of wetting front which becomes irregular and unstable during irrigation process. Rye and Smettem (2017) found water repellency reduced the rate of water migration and the evaporation of soil surface water. It is easy to form a preferential flow in repellency soil due to the big difference in the movement of water in horizontal and gravitational directions (DeBano, 2000; Wallach et al., 2008, 2010). The water tends to accumulate on the surface of repellent soil (DeBano, 2000) and cannot infiltrate when the depth of water accumulation is less than the matrix suction of the soil during irrigation (Jordán et al., 2009). However, the above researches mainly aim to obtain the discipline of water movement by FW irrigation in repellent soil. Irrigation water source seldom changes after the soil repellency appears for a long time of TWW irrigation. Therefore, it is very important to study the infiltration law of TWW in repellent soil.

TWW has many components such as grease, OM, suspended solids, salt and so forth (Halliwell et al., 2001). Each component will affect the characteristics of the soil, and then change its infiltration characteristics during the infiltration. Suspended particulate matter and dissolved organic matter (DOM) can clog the soil pores (Vries, 1972; Vinten et al., 1983; Levy et al., 1999). High concentration of sodium ions causes swelling and dispersion of soil clay (Durgin et al., 1984; Frenkel et al., 1992; Levy et al., 1999; Halliwell et al., 2001). Inorganic salt increases the alkalinity and salinity of the soil (Balks et al., 1998; Halliwell et al., 2001; Lado et al., 2009; Bedbabis et al., 2014). These components reduce the pores of the soil, the hydraulic conductivity of the soil and the cumulative infiltration volume. However, some components of TWW can increase soil infiltration in repellent soils. Surfactants alleviates the repellency degree of the soil which increases the cumulative infiltration after a long period of TWW irrigation (Chaney et al., 1986; Fortun et al., 1989; Piccolo et al., 1997; Dekker et al., 2018; Liu et al., 2019). Both characters of irrigated soil and irrigation water quality have great effect on soil water infiltration, and they are always interacting, continuous development and evolution (Sheng et al., 2016). Therefore, selection of right water quality index for different soils is of great significance in irrigation with TWW.

The water quality indexes standards, including biochemical oxygen demand (BOD), chemical oxygen demand (COD), suspended solids, anionic surfactants, pH, total salt, chloride, sulfide, heavy metal content, fecal coliforms, aphid eggs, and so on, have been established for agricultural irrigation all over the world. However, these water quality indexes standards have taken the ecological environmental protection into account, but the impact of irrigation water quality on infiltration characteristics is not considered. There is no uniform comprehensive index, so it is applicative to find a comprehensive water quality index to guild TWW irrigation. The objective of this study was to determining the water quality index of TWW for repellent sandy loam (R) and wettable sandy loam (W) based on irrigation infiltration characteristics.

Materials and Methods

Soil sampling and pretreatment

The soil depth of 0~5 cm shows a certain degree water repellency after long-term TWW irrigation (Wallach et al., 2005; Mataix-Solera et al., 2011). Soil water repellency is not obvious below the depth of 5 cm. The soil samples were collected in 0~5 cm surface sandy loam in the first terrace of Wei River, Yangling (34º18′N, 108º24′E), Shaanxi Province, China. The bulk density, grain-size distribution of the soil was measured by the drying

http://www.aloki.hu ● ISSN 1589 1623 (Print) ● ISSN 1785 0037 (Online)
DOI: http://dx.doi.org/10.15666/aeer/1802_35773592

method and Mastersizer 2000 laser particle size analyzer in the laboratory, respectively. The soil, whose bulk density is 1.65 g/cm^3, is composed of 14.4% of clay, 24.7% of silt and 60.9% of sand. Therefore, the soil texture is identified as wettable sandy loam. The soil, after air-drying and impurity removal, was subjected to standard sieving of 10-mesh (2 mm). The soil moisture after air drying and saturated soil moisture were 0.029 cm^3/cm^3 and 0.363 cm^3/cm^3, respectively.

The field water-repellent soil is prone to disturbance in the sampling, which may destroy its original water-repellent characteristics. Therefore, surface active material, octadecylamine ($C_{18}H_{39}N$), is added to wettable soil to obtain a relatively stable water-repellent soil (J&K Scientific Ltd.). Octadecylamine, a white waxy solid crystal with alkalinity, is practically insoluble in water. Its melting point is 52.3°C. The repellency soil was obtained by mixing $C_{18}H_{39}N$ with the air-dried soil sample at a ratio of 0.1 g/kg. Then the mixed soil was placed in an oven at 80°C for 24 hours, and the soil sample was stirred for 5 minutes every 2 hours to make the liquid $C_{18}H_{39}N$ fully mixed with the soil particles (Li et al., 2017). This approach eliminated the confounding time effects associated with unstable water repellency systems and allowed for the identification of basic mechanisms (Carrillo et al., 2000). The relatively stable water-repellent sandy loam was obtained after the whole process. The repellency was determined by water drop penetration time test (WDPT) (Letey, 1969; Dekker et al., 1990). According to the water repellency classification standard proposed the mixed soil is slightly water repellent (Bisdom et al., 1993).

Water sampling and water quality index

The TWW sample was taken from pools under different treatments, namely the catchment, the anaerobic pool, the oxidation pool, the sedimentation pool and the outlet pool, in a domestic sewage treatment plant in China. The reference water is tap water in Yangling, China. The water quality index is given in *Table 1*.

Table 1. *Water quality index of TW and pools under different treatment*

The location of the water	Tap water	Catchment	Anaerobic pool	Oxidation pool	Sedimentation pool	Outlet pool
pH	7.92	7.29	7.31	7.31	7.36	7.07
Electric conductivity(μS·cm^{-1})	143	811	825	811	849	799
Dissolved oxygen(mg·L^{-1})	7.52	0.24	0.43	3.00	4.61	4.03
Total hardness(mmol·L^{-1})	0.89	0.49	0.64	0.61	0.68	0.79
Total alkalinity(CaO mg·L^{-1})	27.96	169.81	176.32	164.37	167.67	153.21
Sodium adsorption ratio a	1.23	6.12	6.16	6.98	6.77	7.01
Turbidity	0	125	187	510	4.77	3.95
Total dissolved substances(mg·L^{-1})	95	226	360	260	412	420
Total suspended solids(mg·L^{-1})	0	170	198	780	325	242
Total nitrogen(mg·L^{-1})	18.23	69.27	100.3	63.83	36.22	30.12
Chemical oxygen demand(mg·L^{-1})	0	331.5	423	588	37.15	22.15
Biochemical oxygen demand (mg·L^{-1})	0	171	100	143	11	11

a. The sodium adsorption ratio (SAR) refers to the ratio of the sodium ion concentration to the square root of the mean value of the calcium ion concentration and the magnesium ion concentration in the cation exchange reaction of calcium, magnesium, sodium, etc. The formula of the sodium adsorption ratio is $SAR = \frac{C_{(Na^+)}}{\sqrt{C_{(Ca^{2+})}+C_{(Mg^{2+})}}}$ (Bughici and Wallach, 2016), where, the values are expressed in mmol·l^{-1}.

http://www.aloki.hu ● ISSN 1589 1623 (Print) ● ISSN 1785 0037 (Online)
DOI: http://dx.doi.org/10.15666/aeer/1802_35773592

There are 12 water quality parameters, including pH, Electric conductivity, dissolved oxygen, total hardness, total alkalinity, sodium adsorption ratio (SAR), turbidity, total dissolved substances (TDS), total suspended solids (TTS), total nitrogen (TN), Chemical oxygen demand (COD) and Biochemical oxygen demand (BOD). Principal component analysis was conducted on each water quality index using SPSS software (v. 21.0, SPSS Inc, 2013) in order to quantitatively evaluate the water quality. First, three principal components are extracted, and then the water quality comprehensive evaluation index is established according to the contribution rate of the characteristic value of each principal component in initial eigenvalues *Eq.1*.

The formula for the comprehensive index of water quality is as follows.

$$Z_F = \frac{\lambda_1}{\lambda_1+\lambda_2+\lambda_3}\cdot F_1 + \frac{\lambda_2}{\lambda_1+\lambda_2+\lambda_3}\cdot F_2 + \frac{\lambda_3}{\lambda_1+\lambda_2+\lambda_3}\cdot F_3 \qquad \text{(Eq.1)}$$

where λ_1, λ_2 and λ_3 are eigenvalues of the first, second and third principal components, respectively. F_1, F_2 and F_3 are the calculated values of the three components, respectively.

Infiltration experiments

The infiltration experiments were carried out in Key Laboratory of Agricultural Soil and Water Engineering in Arid and Semiarid Areas, Ministry of Education, Northwest A&F University, China.

Two kinds of soils (wettable soil and repellency soil) were irrigated by six kinds of water with different quality in one-dimensional water infiltration experiments. The experiments consisted of 12 treatments, and each treatment was repeated 3 times. For convience, in the rest part of the paper, R and W are repellent sandy loam and wettable sandy loam, respectively; R-TW and R-TWW1~5 refer to the six water quality experiment waters that are ranked according to the comprehensive water quality index from small to large. Among them, TW is tap water, R-TWW1 is the water from outlet pool, R-TWW 2～5 are waters from sedimentation pool, catchment, anaerobic pool and oxidation pool, the same below.

The experiment device is shown in *Fig. 1*. The water supply device is a Marriotte bottle to provide a stable water head. The column is 80 cm in height 12 cm in diameter. The bottom of the column is equipped with a 10 cm of quartz sand filter layer to prevent air resistance. The soil sample is loaded into the soil column according to the actual bulk density of 1.65 g/cm^3. The soil is layered into the soil column and each layer is 5 cm. The layers were slightly roughened to prevent delamination. The soil column is 65 cm in height. The soil columns were placed for 24 hours after loading to make the soil moisture distribute evenly. A filter paper is placed on the surface of the soil column to resist the impact of water on the soil. Three paper scales are placed on the column to record wetting front. The water head is 3 cm in the experiments. The infiltration time was recorded using the stopwatch. During the first half hour of the experiments, the Mariotte scale and the wetting front were recorded at 5-min intervals. Subsequently they were recorded at intervals of 10-min from 0.5 h to 1.5 h, and 30-min after 1.5 h.

The Philip model (Philip, 1957) was used to fit the soil cumulative infiltration with time to further analyze the effect of water quality on soil infiltration. The mathematical expression of the model is as follows.

http://www.aloki.hu ● ISSN 1589 1623 (Print) ● ISSN 1785 0037 (Online)
DOI: http://dx.doi.org/10.15666/aeer/1802_35773592

$$I = St^{0.5} + At \quad \text{(Eq.2)}$$

where, I is the cumulative infiltration, cm; S is the soil sorptivety, cm·min$^{-0.5}$; A is the stable infiltration rate, cm/min; t is the infiltration time, min.

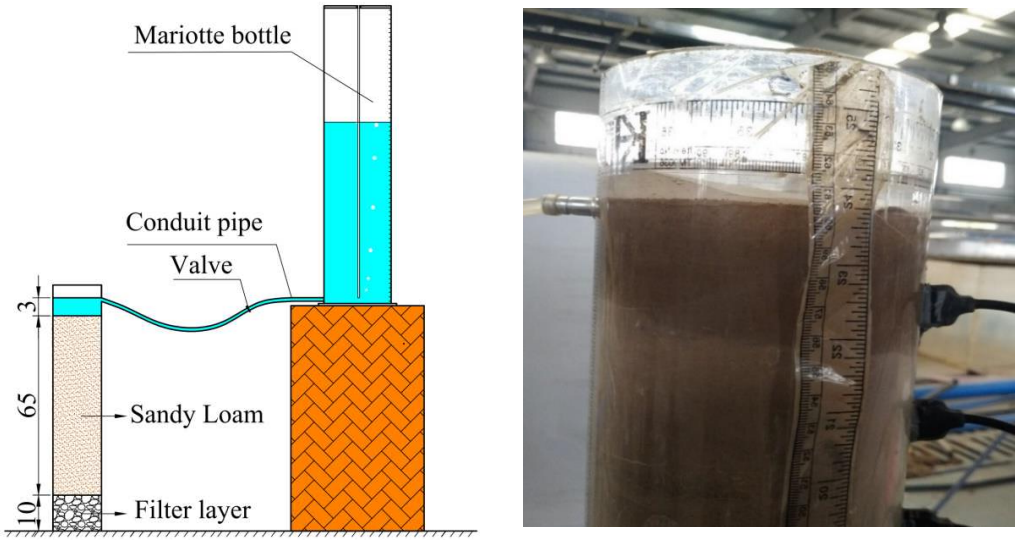

Figure 1. *Laboratory setup of one-dimensional TWW infiltration*

When the infiltration time of the experiment is as short as a couple of hours, the soil sorptivety (S) becomes the main influencing factor of water infiltration. That is, the effect of the stable infiltration rate A can be neglected. Then the *Eq.2* can be expressed as follows.

$$I = St^{0.5} \quad \text{(Eq.3)}$$

Then this paper uses the *Eq.3* to fit the cumulative infiltration and time.

In this study, SPSS 22.0 was used to conduct analysis of variance between means, and significant differences between the treatments were compared by the least significant differences test at a 5% probability, orthogonal design, Standard analysis of variance (ANOVAR) were used to evaluate the effect of the water quality on the infiltration.

Results and Discussion

Comprehensive evaluation result of water quality

Three principal components were extracted using principal component analysis of SPSS. The first principal component eigenvalue has the highest contribution rate of 38.35%. Total dissolved substances, sodium adsorption ratio and conductivity are the main factors of water quality index of the first principal component. The contribution rate of the second principal component eigenvalue is 35.89%. BOD, COD, the total dissolved oxygen, total nitrogen and total hardness are the main factors of the second main component. The total suspended matter and turbidity take up a larger proportion of the third principal component. The cumulative contribution rate of the three principal

http://www.aloki.hu ● ISSN 1589 1623 (Print) ● ISSN 1785 0037 (Online)
DOI: http://dx.doi.org/10.15666/aeer/1802_35773592

components eigenvalue reaches 95.21%, which can basically represent the information of all 12 water quality indexes. A comprehensive evaluation index is established according to the contribution rate of the eigenvalues as is shown in *Eq.4*.

$$Z_F = 40.29\% \cdot F_1 + 37.70\% \cdot F_2 + 22.02\% \cdot F_3 \quad \text{(Eq.4)}$$

The comprehensive evaluation result of water quality is given in *Table 2*.

Table 2. *Principal component analysis results, the water quality comprehensive index and the naming of water samples*

Water sampling location	First principal component F_1	Second principal component F_2	Third principal component F_3	The water quality comprehensive index Z_F	Levels of TWW
Tap water	-1.812	-0.834	-0.415	-1.136	TW
Catchment	-0.133	1.372	-0.557	0.341	TWW 3
Anaerobic pool	0.197	1.007	-0.388	0.374	TWW 4
Oxidation pool	-0.063	0.117	2.032	0.466	TWW 5
Sedimentation pool	0.809	-0.748	-0.265	-0.014	TWW 2
Outlet pool	1.002	-0.914	-0.407	-0.030	TWW1

According to the water quality comprehensive index, the irrigation waters taken from different locations in the domestic sewage treatment plant are ranked from small to large of Z_F. The comprehensive water quality index of the outlet pool is the smallest, and the oxidation pond outlet is the largest. That might be because TWW needs to add biological bacteria such as nitrates for denitrification and absorption of easily degraded BOD before treated in the oxidation pond. After entering the sedimentation pond, mud and water are separated under the effect of coagulant drugs, and the water quality is greatly improved. For the convenience of the following description, TW represents tap water, TWW1, TWW2, TWW3, TWW4 and TWW5 represent the water of the outlet pool, sedimentation pool, catchment, anaerobic pool and oxidation pool respectively.

Effect of water quality on cumulative infiltration

The variation of cumulative infiltration of wettable and repellent sandy loams under different water infiltration conditions are shown in *Fig. 2*. The cumulative infiltration of different water quality in wettable sandy loam is significant (P value<0.05) (*Fig. 2a*). The cumulative infiltration amount increases with the increase of water quality comprehensive index. That is, the greater the comprehensive water quality index is, the faster the infiltration in wettable soil is. Taking 90 min as an example, the cumulative infiltration amounts of W-TW and W-TWW1~5 are 7.19, 13.13, 13.70, 15.48, 17.18 and 16.02 cm, respectively. When the wetting front reaches the end of 40 cm infiltration, the cumulative infiltration amount is 12.65, 17.3, 17.18, 18.19, 19.96 and 18.21 cm, respectively.

There is a significant difference between TWW and TW during the infiltration of water-repellent sandy loam (*Fig. 2b*). However, the difference among the five groups of TWW is significantly reduced relative to the wettable sandy loam. Taking 90 min as an example, the cumulative infiltration of R-TW and R-TWW1~5 is 6.17, 11.58, 11.74, 12.06, 15.53 and 13.15 cm, respectively. The cumulative infiltration of R-TW and R-TWW1~5 was 10.50, 16.85, 17.36, 17.68, 19.84 and 17.88 cm, respectively at the end of infiltration. Comparing

http://www.aloki.hu ● ISSN 1589 1623 (Print) ● ISSN 1785 0037 (Online)
DOI: http://dx.doi.org/10.15666/aeer/1802_35773592

Fig. 2a and *Fig. 2b*, it is found that the cumulative infiltration in the water-repellent soil is smaller than that in the wettable soil with the same water quality. Taking W-TWW3 and R-TWW3 as examples, the cumulative infiltration of W-TWW3 is 13.70 cm and the R-TWW3 is 11.73 cm at 90 min. Therefore, it can be inferred that regardless of tap water or sewage water, the water-repellent soil will hinder its water migration and affect its infiltration rate.

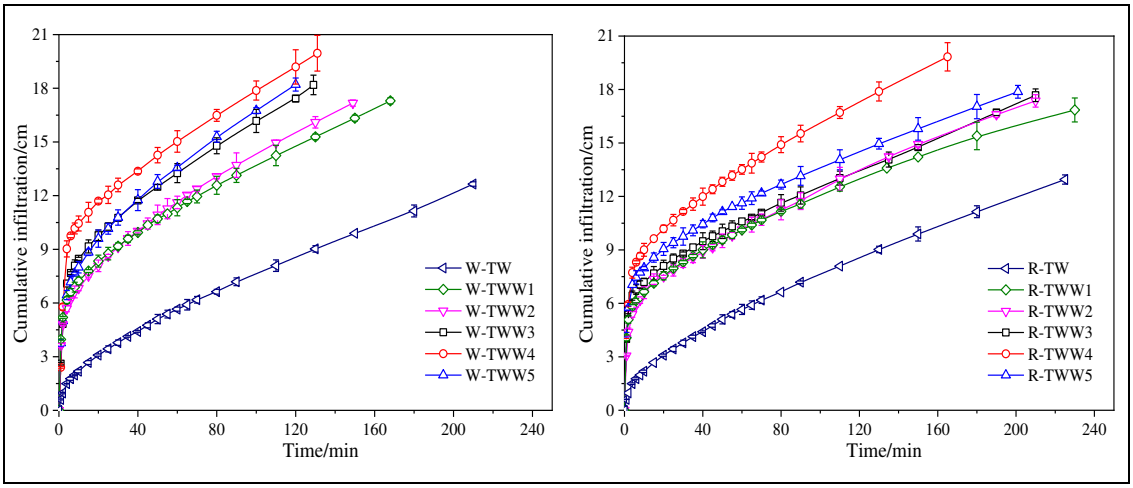

Figure 2. *The cumulative infiltration versus time for different water quality in repellent and wettable sandy loams, (a) Wettable sandy loam, (b) Repellent sandy loam*

Table 3 shows the relationship between the cumulative infiltration and time. The fitting accuracy of the Philip model of TWW infiltration is worse than that of tap water, but the coefficient of determination is greater than 0.7 and the root mean square error is small. Therefore, the curves fit well with the data with high Determination coefficient (R^2>0.988). There is a positive correlation between the infiltration rate and water quality (water from TW, TWW1 to TWW5) of wettable and repellent sandy loams. The infiltration rate of the wettable soil is higher than that of the water-repellent soil with the same kind of water. The regularity of the infiltration rate is the same as the law of cumulative infiltration.

Table 3. *The fitting parameters of the infiltration model*

Soil type	Treatment	Philip formula			Wetting front model		
		Sorptivety S (cm·min$^{-0.5}$)	Determination coefficient R^2	Root mean square error RMSE	Fitting parameter a (cm·min$^{-0.5}$)	Determination coefficient R^2	Root mean square error RMSE
Wettable sandy loam	W-TW	0.776	0.982	0.450	2.652	0.990	0.342
	W-TWW1	1.463	0.809	1.700	2.982	0.994	0.912
	W-TWW2	1.522	0.880	1.385	3.192	0.993	0.895
	W-TWW3	1.769	0.825	1.985	3.394	0.997	0.980
	W-TWW4	2.002	0.701	2.825	3.347	0.995	0.907
	W-TWW5	1.837	0.862	1.707	3.618	0.995	1.218
Repellent sandy loam	R-TW	0.648	0.971	0.426	2.593	0.988	1.234
	R-TWW1	1.268	0.759	1.775	2.692	0.995	1.161
	R-TWW 2	1.299	0.860	1.476	2.590	0.993	0.691
	R-TWW 3	1.338	0.737	1.933	2.530	0.990	1.032
	R-TWW 4	1.695	0.721	2.202	2.950	0.990	0.888
	R-TWW 5	1.449	0.710	2.231	2.710	0.998	1.406

http://www.aloki.hu ● ISSN 1589 1623 (Print) ● ISSN 1785 0037 (Online)
DOI: http://dx.doi.org/10.15666/aeer/1802_35773592

Effect of water quality on wetting front movement

The wetting front depth versus time for different water quality in wettable and repellent sandy loams is shown in *Fig. 3*. The variation of the wetting front depth is similar to that of cumulative infiltration in wettable sandy loam (*Fig. 3a*). When different water infiltrates the wettable sandy loam, the greater the comprehensive water quality index is, the greater the depth of the wetting front is at the same infiltration time. The infiltration times of W-TW and W-TWW1~5 are 210, 168, 149, 129, 131 and 120 min, respectively, when the wetting front depth reaches 40 cm in wettable sandy loam. The water quality has little effect on the wetting front depth of repellent sandy loam (*Fig. 3b*). The infiltration times of R-TW and R-TWW1~5 are 210, 168, 149, 129, 131 and 120 min, respectively, when the wetting front depth reaches 40 cm in repellent sandy loam. There is no significance difference between infiltration time and wetting front depth among the different irrigation water quality from TW, TWW1 to TWW5 in repellent sandy loam (P>0.05). The wetting front depth of the water-repellent sandy loam is smaller than that of the wettable sandy loam with the same water quality (*Fig. 3a* and *Fig. 3b*). The infiltration time of the water-repellent sandy loam is greater than that of the wettable sandy loam when the wetting front depth reaches 40 cm.

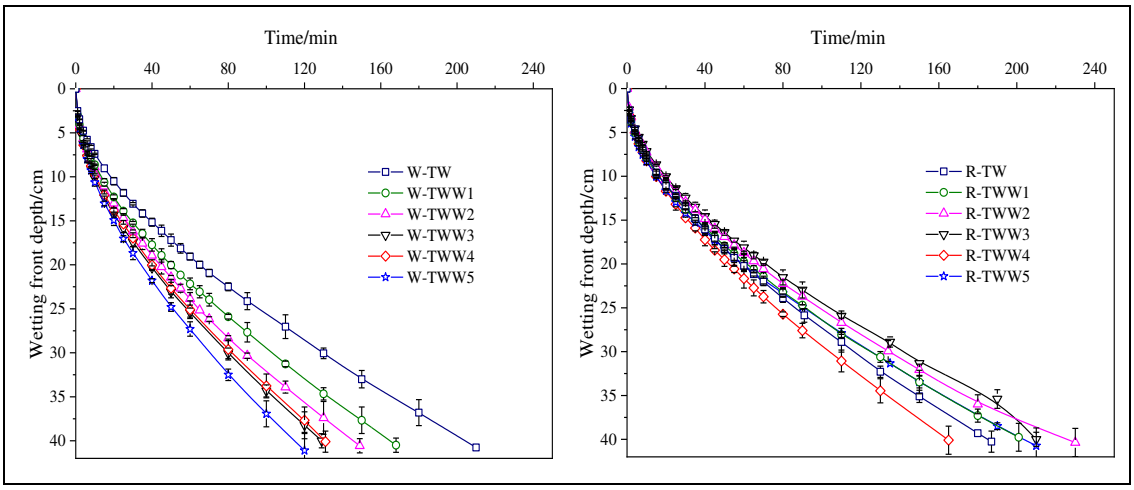

Figure 3. *Wetting front depth versus time for different water quality in wettable and repellent sandy loams, (a). Wettable sandy loam, (b) Repellent sandy loa*

The power function is used to fit the relationship between wetting front depth and infiltration time to analyze the effect of water quality on the soil wetting front. The mathematical expression of the model is as follows:

$$H = at^{0.5} \quad \text{(Eq.5)}$$

where H is wetting front depth, cm; a is the wetting front coefficient, cm·min$^{-0.5}$.

The wetting front model fitting result is given in *Table 3*. The fitting accuracy of the wetting front model (R^2> 0.98, RMSE <1.3) is high. Water quality has little effect on a in repellent sandy loam. The parameter a increases with the increase of the comprehensive water quality index in wettable sandy loam.

http://www.aloki.hu ● ISSN 1589 1623 (Print) ● ISSN 1785 0037 (Online)
DOI: http://dx.doi.org/10.15666/aeer/1802_35773592

The effect of irrigation water quality on the infiltration is significant (*Fig. 2* and *Fig. 3*). The cumulative infiltration and infiltration rates generally increase with the increase of water quality comprehensive index.

The sorptivety of repellent sandy loam is smaller than that of wettable sandy loam with the same water (*Table 3*). According to the comprehensive water quality index from small to large (TW and TWW1~5), sorptivety decreases by 16.5%, 13.3%, 14.7%, 24.4%, 15.3% and 21.1%, respectively.

The effect of irrigation water quality on infiltration is mainly reflected in the influence of soil solute potential which is closely related to the conductivity in the water quality index. The higher the conductivity is, the greater the soil solute potential is, and the more obvious effect the water has on soil water movement. The electric conductivity value of TW is smaller than TWW (*Table 1*). Therefore, the cumulative infiltration of TWW is larger than that of TW irrigation. The cumulative infiltration shows little difference among the TWW due to the small difference in conductivity among them. It also shows the larger the conductivity is, the greater the cumulative infiltration is. The wetting front depth decreases with the increase of water quality comprehensive index in wettable sandy loam due to the large difference of solute potential. The solute potential is different because TWW contains many solute ions. The wetting front changes greatly with the same cumulative infiltration due to the different solute potential under the same condition of the matrix potential and the gravitational potential.

The water quality comprehensive index has no significant effect on the wetting front in repellent sandy loam because water repellency seriously hinders the water infiltration. So the solute potential caused by the substances contained is smaller than that of the water repellency of both TW and TWW in repellent soil. Therefore, the wetting front has no significance among TW and TWW1~5.

TWW contains many components. It's insufficient to use a single water quality index to analyze the effect of infiltration. For example, the total suspended matter in the water quality index describes the amount of insoluble matter in the water. The suspended matter will deposit on the surface layer or block the soil pores which make the soil surface crust and soil porosity reduction during the infiltration process. Then the soil infiltration rate and the hydraulic conductivity are significantly reduced. It is one of the causes of soil water repellency. However, the effect of suspended matter in TWW on soil pores during the short-term infiltration is not obvious due to the short experiments period in this study. The clogging is weak because of the large particles and soil pores in sandy loam. Soil infiltration rate and hydraulic conductivity decline significantly because the clogging, caused by sewage or TWW irrigation in soils with higher clay content, is obvious (Lado and Ben-Hur, 2009). Therefore, the suspended matter is an important index for long-term irrigation with TWW.

The water movement rate is high in the irrigation of wettable soil with the TWW. The irrigation time must be shortened when the irrigation volume is fixed, or it will cause deep leakage. The TWW contains more polluting ions which may cause groundwater pollution and soil nutrients loss (Lado and Ben-Hur, 2009). However, wetting front is of no difference under the same irrigation time interval in the irrigation of the repellent soil with the TWW. Then the greater the water quality index is, the greater the irrigation volume is. This will cause the water to stay in the upper layer of the soil for a long time, and it is difficult to reach the planned wetting layer of the irrigation design. At the same time, the evaporation of the surface layer increases, resulting in a decrease in water use efficiency. Therefore, the irrigation time should be

http://www.aloki.hu ● ISSN 1589 1623 (Print) ● ISSN 1785 0037 (Online)
DOI: http://dx.doi.org/10.15666/aeer/1802_35773592

reduced and high frequency and small flow discharge should be used in order to increase the effective irrigation depth for the soil for high water quality index in repellent soil.

Effect of COD on infiltration parameters

There are many causes of the water repellency in the soil (Bond, 1964; McGhie et al., 1980; King et al., 1981; DeBano, 1981; Jex et al., 1985; Stenstrom et al., 1989; Shakesby et al., 1993, 2006; Dekker et al., 2000; Chau et al., 2012; Jiménez-Pinilla et al., 2016). For sewage water irrigation, water repellency is caused by the increase of the organic matter in the soil (Morales et al., 2010; Chen et al., 2013). In the irrigation with TWW, the oil and grease content in the water has a great influence on the soil water repellency, and the soil water repellency increases with the increase of oil and grease (Travis et al., 2008). As the organic matter in the soil increases, the water repellency of sandy and clay increases. The organic matter in water is measured by COD value. During the infiltration, the organic matter and grease affect the surface tension of the liquid, which in turn affects the interaction between the soil particles and the water molecules. It will affect the capillary force during the movement of soil water. And these can be described by the COD value. The relationship between COD and sorptivety is shown in *Fig. 4*. The relationship between sorptivity *S* and COD is a power function.

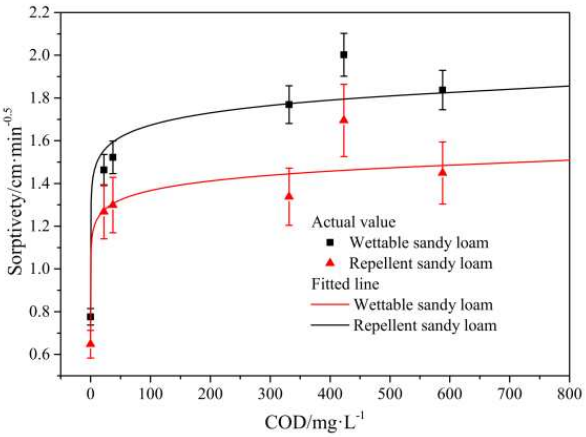

Figure 4. *The relationship between the soil sorptivety (S) and chemical oxygen demand (COD)*

The function is as follows.
Wettable sandy loam:

$$S_w = 1.322 \cdot (\mathrm{COD})^{0.053}, \ R^2 = 0.931 \quad \text{(Eq.6)}$$

Repellent sandy loam:

$$S_r = 1.104 \cdot (COD)^{0.046}, R^2 = 0.955 \quad \text{(Eq.7)}$$

The effect of COD on infiltration is obvious when COD is less than a certain value for wettable and repellent soils. When the COD exceeds the set value, the change of the infiltration rate is small although the COD has a large change.

http://www.aloki.hu ● ISSN 1589 1623 (Print) ● ISSN 1785 0037 (Online)
DOI: http://dx.doi.org/10.15666/aeer/1802_35773592

With the infiltration change rate of 0.05 cm/min0.5 as the critical point, when the COD value of the irrigation water is greater than 170 mg/L for wettable sandy soil and 140 mg/L for repellent sandy soil, the COD has little effect on irrigation.

Therefore, the influence of COD on soil water infiltration must be considered. The Farmland Irrigation Water Quality Standard GB5084-2005 in China stipulates that the COD of irrigation water should be less than 200 mg/L for dry crop irrigation. According to this study, considering the effect of COD values on infiltration, we recommend that the COD value should be less than 170 mg/L for wettable sandy soil and 140 mg/L for repellent sandy soil in sewage irrigation.

Effect of comprehensive water quality indicators on infiltration parameters

The effect of water quality on infiltration can be seen from the above research. EC, TSS and COD all have an effect on infiltration. Previous studies focused on the impact of a water quality index on infiltration, but research shows that many water quality indexes affect soil infiltration (Singh et al., 2017; Misaghi et al., 2017; Leuther et al., 2018). Therefore, it is necessary to use comprehensive water quality indicators to analyze the impact of water quality on infiltration. The relationship between Z_F and sorptivety S was shown in *Fig. 5a*. The S of sandy loam increases with the increase of Z_F, and there is a positive linear correlation between them (R^2 is 0.980 and 0.950 for wettable and repellent sandy loams).

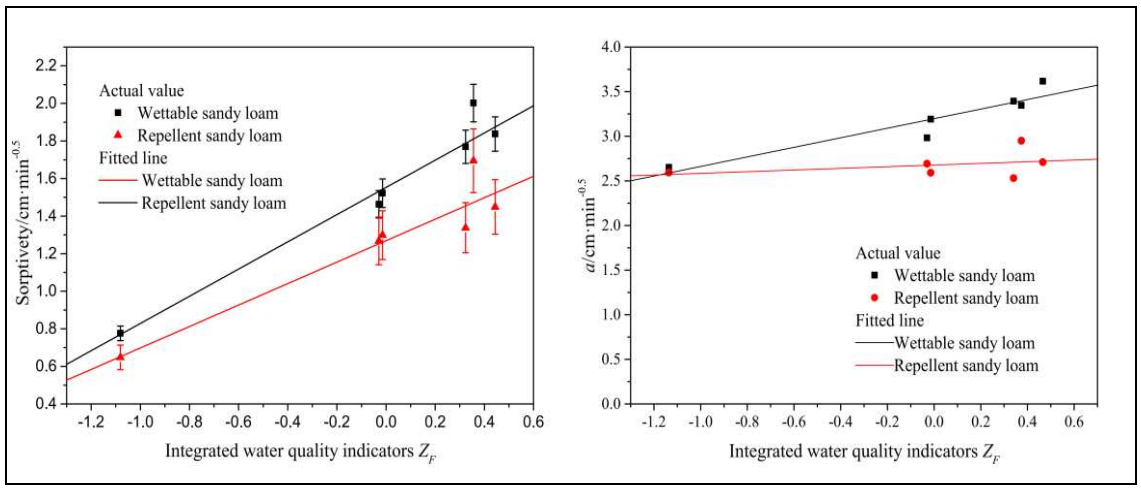

Figure 5. *Relationships between soil sorptivety (S), the wetting front coefficient a and comprehensive water quality index Z_F (a). soil sorptivety, (b) the wetting front coefficient a*

The function is as follows.
Wettable sandy loam:

$$S_{\mathrm{w}} = 1.553 \cdot Z_F + 0.724, \qquad R^2 = 0.980 \tag{Eq.8}$$

Repellent sandy loam:

$$S_r = 1.269 \cdot Z_F + 0.571, \mathrm{R}^2 = 0.950 \tag{Eq.9}$$

http://www.aloki.hu ● ISSN 1589 1623 (Print) ● ISSN 1785 0037 (Online)
DOI: http://dx.doi.org/10.15666/aeer/1802_35773592

It can be seen that the larger the comprehensive water quality index is, the faster sorptivety of the soil is (*Eq.8*, *Eq.9*, *Fig. 5a*). The quality of TWW significantly facilitates soil infiltration. However, soil water repellency will lead to a decrease in soil infiltration rate when water infiltrates, and also slow down the tendency of infiltration rate to increase with the increase of the comprehensive water quality index. Soil water repellency will decrease soil infiltration and also slow down the tendency of sorptivety to increase with the increase of ZF. For wettable soils, the water quality of TWW is more significant in increasing soil infiltration. The sorptivety of the wettable sandy loam is larger than that of the repellent sandy loam with the same water quality (*Fig. 2* and *Table 3*). The effect of ZF on sorptivety of the wettable sandy loam is larger than that of the repellent sandy loam. Therefore, it is not advisable to increase the infiltration rate of the soil in order to reduce the irrigation time and simply increase the comprehensive water quality index. The selection of the comprehensive water quality index should be within a reasonable range.

It can be seen that the larger the comprehensive water quality index is, the faster sorptivety of the soil is (*Eq.8*, *Eq.9*, *Fig. 5a*). The quality of TWW significantly facilitates soil infiltration. However, soil water repellency will lead to a decrease in soil infiltration rate when water infiltrates, and also slow down the tendency of infiltration rate to increase with the increase of the comprehensive water quality index. Soil water repellency will decrease soil infiltration and also slow down the tendency of sorptivety to increase with the increase of Z_F. For wettable soils, the water quality of TWW is more significant in increasing soil infiltration. The sorptivety of the wettable sandy loam is larger than that of the repellent sandy loam with the same water quality (*Fig. 2* and *Table 3*). The effect of Z_F on sorptivety of the wettable sandy loam is larger than that of the repellent sandy loam. Therefore, it is not advisable to increase the infiltration rate of the soil in order to reduce the irrigation time and simply increase the comprehensive water quality index. The selection of the comprehensive water quality index should be within a reasonable range.

The relationship between the wetting front coefficient a and Z_F of the sandy loam is shown in *Fig. 5b*. The wetting front coefficient a increases with the increase of Z_F, and there is a positive linear correlation between them for wettable sandy loam. However, Z_F has little effect on the wetting front coefficient a due to the effect of water repellency in repellent sandy loam.

The relationship between the ratio of sorptivety S to the wetting front coefficient a and Z_F is shown in *Fig. 6*. There is a nonlinear relationship between S/a and Z_F. As Z_F increases, S/a shows a minimum point. The minimum point appears near 0.59 and 0.10 for wettable and repellent sandy loams respectively. S/a reflects the volume of water in the wetting body, i.e., the average increase in moisture content in the wetting front range. When Z_F exceeds 0.10 for the water-repellent sandy loam, the increase of S/a indicates that the wetting front coefficient is reduced with the same irrigation volume. That is to say, the increase of irrigation volume does not make the effective wetting depth increase significantly. Therefore, the value of Z_F should be less than 0.10 of TWW when irrigating repellent sandy soil. However, when the minimum Z_F value is around 0.59 for the wettable sandy loam, the water quality indicators have seriously exceeded the agricultural irrigation water quality standards in China, and it is not suitable for irrigation. Therefore, in the irrigation of wettable sandy loam with sewage, it is necessary to consider the impact of crop growth, environment, and long-term

http://www.aloki.hu ● ISSN 1589 1623 (Print) ● ISSN 1785 0037 (Online)
DOI: http://dx.doi.org/10.15666/aeer/1802_35773592

irrigation on soil water repellency rather than simply consider its influence on infiltration characteristics.

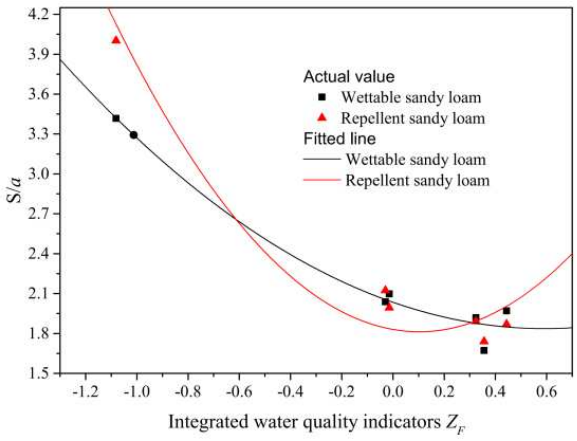

Figure 6. *Relationship between S/a (the ratio of sorptivety to the wetting front coefficient) and comprehensive water quality index* Z_F

Conclusions

Infiltration experiments were conducted on a wettable and a water repellent sandy loam with TWW to determine the water quality index and analyze the effect of water quality on wetting front and cumulative infiltration volume.

(1) The water quality has a great effect on the cumulative infiltration and wetting front of wettable sandy loam. The greater the comprehensive water quality index is, the greater the cumulative infiltration volume and wetting front are. But the water quality has a great effect on the cumulative infiltration but no effect on wetting front of repellency soil. Soil water repellency will decrease soil sorptivety (S). There is a power function relation and positive linear correlation between S and COD, S and Z_F, respectively. Meanwhile a quadratic polynomial relationship exists between the ratio of soil sorptivety S to the wetting front coefficient a and the comprehensive water quality index, and there is a minimum value in the curve.

(2) When both cumulative infiltration and wetting front requirements in TWW irrigation are taken into consideration, COD and Z_F should be less than 170 mg/L and 0.59, respectively, in wettable sandy loam while the two values should be less than 140 mg/L and 0.10, respectively, in repellency sandy loam. However, the study of this paper is relatively macroscopic, the changes in the microstructure between the reclaimed water and the soil pores need to be studied. When the soil water content is same, as the contact angle increases, the matrix suction will continue to decrease, making the soil infiltration rate slow down. Analyzing the relationship between the contact angle and the microstructure of soil pores during soil infiltration is a future research direction.

Acknowledgements. This work was supported by the National Natural Science Foundation of China (51409221, 51979234) and Basic Research Business Fee of Northwest A&F University (2452017116) and Humanities and Social Science Program of Northwest A&F University (Z109021405) and National Key R&D Program of China (2017YFC0403503).

http://www.aloki.hu ● ISSN 1589 1623 (Print) ● ISSN 1785 0037 (Online)
DOI: http://dx.doi.org/10.15666/aeer/1802_35773592

REFERENCES

[1] Balks, M. R., Bond, W. J., Smith, C. J. (1998): Effects of sodium accumulation on soil physical properties under an effluent-irrigated plantation. – Australian Journal of Soil Research 36: 821-830.
[2] Bedbabis, S., Rouina, B. B., Boukhris, M., Ferrara, G. (2014): Effect of irrigation with treated wastewater on soil chemical properties and infiltration rate. – Journal of Environmental Management 133: 45-50.
[3] Bisdom, E. B. A., Dekker, L. W., Schoute, J. F. T. (1993): Water repellency of sieve fractions from sandy soils and relationships with organic material and soil structure. – Geoderma 24-28: 105-118.
[4] Bond, R. D. (1964): The influence of the microflora on the physical properties of soils. Ⅱ. field studies on water repellent sands. – Australian Journal of Soil Research 2(1): 123-131.
[5] Bughici, T., Wallach, R. (2016): Formation of soil-water repellency in olive orchards and its influence on infiltration pattern. – Geoderma 262: 1-11.
[6] Carrillo, M. L. K., Letey, J., Yates, S. R. (2000): Unstable Water Flow in a Layered Soil: II. Effects of an Unstable Water-Repellent Layer. – Soil Science Society of America Journal 64: 456-459.
[7] Chaney, K., Swift, R. S. (1986): Studies on aggregate stability. Ⅱ .The effect of humic substances on the stability of re-formed soil aggregates. – Journal of Soil Science 37(2): 337-343.
[8] Chau, H. W., Goh, Y. K., Vujanovic, V., Si, B. C. (2012): Wetting properties of fungi mycelium alter soil infiltration and soil water repellency in a γ-sterilized wettable and repellent soil. – Fungal Biology 116(12): 1212-1218.
[9] Chen, X. H., Song, J. X., Cheng, C., Wang, D. M., Lackey, S. O. (2009): A new method for mapping variability in vertical seepage flux in streambeds. – Hydrogeology Journal 17(3): 519-525.
[10] Chen, J., Zhang, Z., Gillerman, L., Wang, Z. (2013): Analysis of principal components of wastewater affecting soil water repellency. – Journal of Drainage and Irrigation Machinery Engineering 31(5): 434-439.
[11] DeBano, L. F. (1981): Water repellent soils: a state-of-the-art. – United States Department of Agriculture Forest Service General Technical Report PSW-46.
[12] DeBano, L. F. (2000): Water repellency in soils: A historical overview. – Journal of Hydrology 231-232: 4-32.
[13] Dekker, L. W., Jungerius, P. D. (1990): Water repellency in the dunes with special reference to the Netherlands. – Dunes of the European coasts 18: 173-183.
[14] Dekker, L., Ritsema, C. J. (2000): Wetting patterns and moisture variability in water repellent Dutch soils. – Journal of Hydrology 231-232: 148-164.
[15] Dekker, L. W., Ritsema, C. J., Oostindie, K., Wesseling, J. G., Geissen, V. (2018): Effects of a soil surfactant on grass performance and soil wetting of a fairway prone to water repellency. – Geoderma: 10.1016/j.geoderma.2018.09.016.
[16] Durgin, P. B., Chaney, J. G. (1984): Dispersion of Kaolinite By Dissolved Organic Matter From Douglas-Fir Roots. – Canadian Journal of Soil Science 64: 445-455.
[17] Fortun, A., Fortun, C., Ortega, C. (1989): Effect of farmyard manure and its humic fractions on the aggregate stability of a sandy–loam soil. – Journal of Soil Science 40(2): 293-298.
[18] Frenkel, H., Levy, G. J., Fey, M. V. (1992): Organic and Inorganic Anion Effects on Reference and Soil Clay Critical Flocculation Concentration. – Soil Science Society of America Journal 56(6): 1762-1766.
[19] Halliwell, D. J., Barlow, K., Nash, D. (2001): A review of the effects of wastewater sodium on soil physical properties and their implications for irrigation systems. – Australian Journal of Soil Research 39(6): 1259-1267.

http://www.aloki.hu ● ISSN 1589 1623 (Print) ● ISSN 1785 0037 (Online)
DOI: http://dx.doi.org/10.15666/aeer/1802_35773592

[20] Jex, G. W., Bleakley, B. H., Hubbell, D. H., Munro, L. L. (1985): High Humidity-induced Increase in Water Repellency in Some Sandy Soils. – Soil Science Society of America Journal 49(5): 1177-1182.
[21] Jiménez-Pinilla, P., Lozano, E., Mataix-Solera, J., Arcenegui, V., Jordán, A., Zavala, L. M. (2016): Temporal changes in soil water repellency after a forest fire in a Mediterranean calcareous soil: Influence of ash and different vegetation type. – Science of the Total Environment 572: 1252-1260.
[22] Jordán, A., Zavala, L. M., Nava, A. L., Alanís, N. (2009): Occurrence and hydrological effects of water repellency in different soil and land use types in Mexican volcanic highlands. – Catena 79(1): 60-71.
[23] King, P. M. (1981): Comparison of methods for measuring severity of water repellence of sandy soils and assessment of some factors that affect its measurement. – Australian Journal of Soil Research 19: 275-285.
[24] Lado, M., Ben-Hur, M. (2009): Treated domestic sewage irrigation effects on soil hydraulic properties in arid and semiarid zones: A review. – Soil and Tillage Research 106(1): 152-163.
[25] Letey, J. (1969): Measurement of contact angle, water drop penetration time and critical surface tension. – Symposium on Water Repellent soils, May 6-10, Univ. of California.
[26] Leuther, F., Weller, U., Wallach, R., Vogel, H-J. (2018): Quantitative analysis of wetting front instabilities in soil caused by treated waste water irrigation. – Geoderma 319: 132-141.
[27] Levy, G. J., Rosenthal, A., Tarchitzky, J., Shainberg, I., Chen, Y. (1999): Soil hydraulic conductivity changes caused by irrigation with reclaimed waste water. – Journal of Environmental Quality 28(5): 1658-1664.
[28] Li, Y., Wang, X. F., Cao, Z. K., Si, B. C. (2017): Water repellency characteristic curve influenced by drying and wetting processesSoil. – Canadian Journal of Soil Science 97(2): 226-240.
[29] Liu, Z., Rahav, M., Wallach, R. (2019): Spatial variation of soil water repellency in a commercial orchard irrigated with treated wastewater. – Geoderma 333(7): 214-224.
[30] Mataix-Solera, J., García-Irles, L., Morugán, A., Doerr, S. H., Garcia-Orenes, F., Arcenegui, V., Atanassova, I. (2011): Longevity of soil water repellency in a former wastewater disposal tree stand and potential amelioration. – Geoderma 165(1): 78-83.
[31] McGhie, D. A., Posnerk, A. M. (1980): Water repellence of a heavy-textured Western Australian surface soil. – Australian Journal of Soil Research 18(3): 309-323.
[32] Misaghi, F., Delgosha, F., Razzaghmanesh, M., Myers, B. (2017): Introducing a Water Quality Index for Assessing Water for Irrigation Purposes: A Case Study of the Ghezel Ozan River. – Science of the Total Environment 589(C): 107-116.
[33] Morales, V. L., Parlange, J. Y., Steenhuis, T. S. (2010): Are preferential flow paths perpetuated by microbial activity in the soil matrix? A review. – Journal of Hydrology 393(1-2): 29-36.
[34] Nadav, I., Arye, G., Tarchitzky, J., Chen, Y. (2012): Enhanced infiltration regime for treated-wastewater purification in soil aquifer treatment (SAT). – Journal of Hydrology 420-421: 275-283.
[35] Nadav, I., Tarchitzky, J., Chen, Y. (2012): Soil cultivation for enhanced wastewater infiltration in soil aquifer treatment (SAT). – Journal of Hydrology 470-471: 75-81.
[36] Philip, J. R. (1957): The theory of infiltration: 4. Sorptivity and algebraic infiltration equations. – Soil Science 84: 257-264.
[37] Piccolo, A., Pietramellara, G., Mbagwu, J. S. C. (1997): Use of humic substances as soil conditioners to increase aggregate stability. – Geoderma 75(32): 267-277.
[38] Rye, C. F., Smettem, K. R. J. (2017): The effect of water repellent soil surface layers on preferential flow and bare soil evaporation. – Geoderma 289: 142-149.

http://www.aloki.hu ● ISSN 1589 1623 (Print) ● ISSN 1785 0037 (Online)
DOI: http://dx.doi.org/10.15666/aeer/1802_35773592

[39] Shakesby, R. A., Coelho, C. D. A., Ferreira, A. D., Terry, J. P., Walsh, R. P. D. (1993): Wildfire impacts on soil erosion and hydrology in wet mediterranean forest, Portugal. – International Journal of Wildland Fire 3(2): 95-110.
[40] Shakesby, R. A., Doerr, S. H. (2006): Wildfire as a hydrological and geomorphological agent. – Soil Science Society of America Journal 74: 269-307.
[41] Sheng, F., Wu, D., Zhang, L. (2016): Review on effect of reclaimed water irrigation on soil water movement in cropland. – Transactions of the Chinese Society of Agricultural Engineering 32: 46-51.
[42] Singh, B., Sihag, P., Singh, K. (2017): Modelling of impact of water quality on infiltration rate of soil by random forest regression. – Modeling Earth Systems and Environment 3: 999-1004.
[43] Stenstrom, T. A. (1989): Bacterial Hydrophobicity, an Overall Parameter for the Measurement of Adhesion Potential to Soil Particles. – Microbiology 55(1): 142-147.
[44] Travis, M. J., Weisbrod, N., Gross, A. (2008): Accumulation of oil and grease in soils irrigated with greywater and their potential role in soil water repellency. – Science of the Total Environment 394(1): 68-74.
[45] Vinten, A. J. A., Mingelgrin, U., Yaron, B. (1983): The effect of suspended solids in wastewater on soil hydraulic conductivity: II. vertical distribution of suspended solids. – Soil Science Society of America Journal 47(686): 408-412.
[46] Vries, D. J. (1972): Soil filtration of wastewater effluent and the mechanism of pore clogging. – Journal of the Water Pollution Control Federation 44: 565-573.
[47] Wallach, R., Ben-Arie, O., Graber, E. R. (2005): Soil Water Repellency Induced By Long-Term Irrigation with Treated Sewage Effluent. – Journal of Environment Quality 34(5): 1910-20.
[48] Wallach, R., Jortzick, C. (2008): Unstable finger-like flow in water-repellent soils during wetting and redistribution - The case of a point water source. – Journal of Hydrology 351(1-2): 26-41.
[49] Wallach, R. (2010): Effect of soil water repellency on moisture distribution from a subsurface point source. – Water Resources Research 46(8): 1-9.

http://www.aloki.hu ● ISSN 1589 1623 (Print) ● ISSN 1785 0037 (Online)
DOI: http://dx.doi.org/10.15666/aeer/1802_35773592

SELECTING THE SUPERIOR GENOTYPE OF SUMMER MAIZE HYBRIDS IN MEGA-ENVIRONMENTS USING AMMI MODEL AND GGE BIPLOT IN CHINA

WANG, S. Q.[1] – GUO, Q.[2*] – WANG, S. D.[1] – CHEN, Z. Y.[3]

[1]*College of Computer and Communication Engineering, China University of Petroleum, Qingdao 266580, China*

[2]*College of Environmental Science & Engineering, Chang'an University, Xi'an 710054, China*

[3]*Dryland Farming Institute, Hebei Academy of Agriculture and Forestry Sciences/Hebei Provincial Key Laboratory of Crops Drought Resistance Research, Hengshui 053000, China*

**Corresponding author*
e-mail: guoqian818@outlook.com

(Received 12th Dec 2019; accepted 23rd Mar 2020)

Abstract. Effective analysis of genotype by environment interactions (GEI) is helpful to screen stable genotypes in a variety of environments. Therefore, the purpose of this study is to test the stability and adaptability of the agronomic traits of maize hybrids from different ecological environments. Thirteen maize hybrids in twenty-six locations over two years (2017-2018) in Huanghuaihai region was conducted to compare the performance and stability of six agronomic traits using AMMI (additive main effect and multiplicative interaction) model and GGE (genotype, genotype × environment) biplot. The analysis of variance through AMMI model showed that genotype (G), environment (E), and GEI had significant effects on agronomic traits. E explains a larger portion of the total variation in grain yield (GY), ear weight (EW) and 100-grain weight (100-GW), to a much higher degree than GEI and G. However, compared to E and G, GEI contributed more to total variation in ear length (EL), kernel row number (KRN) and bald tip length (BTL). Comprehensive analysis of the AMMI model and the GGE biplot results showed that genotypes G2, G3, and G4 had better agronomic performance and stability than other genotypes and are ideal for planting.
Keywords: *genotype by environment interaction, stability, adaptability, agronomic traits, yield, agronomic traits*

Introduction

Maize (*Zea mays* L.) originated in Central and South America and is an important food crop in the world, widely distributed in the United States, China, Brazil and other countries. In China, maize is used as an important food, feed and industrial raw material. The domestic maize cultivation area was 42 million ha with the annual maize production was 260 million tons in 2017 (Wang et al., 2019). Since 2012, maize has surpassed rice and became China's largest food crop variety (Yang et al., 2019). The Huanghuaihai summer maize region is China's largest concentrated maize production area. The annual planting area accounts for more than 40% of the country's total area, and the planting area accounts for about 32% of the country's total planting area, the total output accounts for about 34% of the country's total output. In recent years, the planting area and yield of summer maize in this region have shown a gradual increasing trend, which plays an important role in ensuring national food security (Yue et al., 2018a). The farming system, soil, fertilizer, variety, cultivation management and climatic factors all have different effects on maize yield (Li et al.,

http://www.aloki.hu ● ISSN 1589 1623 (Print) ● ISSN 1785 0037 (Online)
DOI: http://dx.doi.org/10.15666/aeer/1802_35933614

2019). There is a wide difference in maize yield between the Huanghuaihai region, with an average yield of 5.3 tons/ha, a large area with a high yield of 7.5-9 tons, and a small area with a high yield of 15 tons. For most regions, there is a huge potential for increased production (Huang et al., 2019). High yielding and stable yielding of summer maize has always been one of the research goals of scientists all over the world, and it is also one of the difficulties. Analysis of the high yielding and stability of the representative hybrids, as well as the contribution of various yield components to yield, can effectively guide the production and breeding of maize in the Huanghuaihai region.

Screening and identifying good genotypes are very difficult due to the genotype (G) by environment (E) interaction (GEI). But assessing this interaction is important because it is the primary factor in genotypic performance changes under different environments. The GEI can weaken the association between maize phenotypes and genotype values, and leading to bias in the terms of genotypic effect assessment (Farshadfar et al., 2011; Mohamed, 2013). The GEI can make summer maize genotypes behave differently in different environments, especially in the Huanghuaihai region where the climate is complex and variable (Yue et al., 2019). The selection and breeding of important traits of maize genotypes is complicated by the cross-interaction between hybrids in different environments, and the result is that high-yielding and stable genotypes are easily overlooked (Mulema et al., 2008; Nzuve et al., 2013). In order to breed hybrids that meet people's living needs, it is necessary to systematically evaluate the yield, resistance and quality of the tested genotypes, and obtain basic data on adaptability, high yielding and stability in different ecological regions, comprehensive evaluation and screen out hybrids with excellent yield traits. At the same time, the discriminative power and representativeness of each testing site are evaluated, and the basis for selecting the ideal site for resource and hybrid screening is provided. Multi-environment trials (Mets) is a well-established method for identifying the high yielding and adaptability of different crop varieties. In the Mets, the newly bred varieties were tested according to uniform specifications, and their important characteristics such as high yield, stability, adaptability, stress resistance and quality were comprehensively identified (Navas-Lopeza et al., 2019).

There were many statistical methods for evaluating the GEI, such as, scientists have earlier proposed the coefficient of variation (CV) (Döring and Reckling, 2018), analysis of variance (ANOVA) (Fry, 1992), principal component analysis (PCA) (Perkins, 1972) and linear regression analysis (LRA) (Kang, 1993), but each method has its shortcomings. The coefficient of variation method describes the stability of genotypes, this method can only explain the difference in genotype effects, and does not explain the environmental effects and the interaction between genotypes and the environment. The study of the stability of the variety by linear regression does not reflect the adaptability of the genotype to the environment. The application of analysis of variance to evaluate the adaptability of genotypes cannot analyze the relationship between environmental effects and interaction effects (Blouin et al., 2015). In recent years, with the deepening of research methods, scientists have proposed two analysis methods of the additive main effects and multiplicative interaction (AMMI) model (Gauch, 1988) and the genotype plus genotype by environment (GGE) biplot (Yan et al., 2000) for GEI research. The AMMI model is a graphically unique linear-bilinear model based on a biplot, combining both the ANOVA and the multiplicative model (Yan et al., 2007). The AMMI model is an effective tool for studying genotypic

http://www.aloki.hu ● ISSN 1589 1623 (Print) ● ISSN 1785 0037 (Online)
DOI: http://dx.doi.org/10.15666/aeer/1802_35933614

stability analysis and distinguishing the environment, and has been successfully applied to the research of various crops (Suwaero et al., 2011; Mortazavian et al., 2014; Ndhlela et al., 2014; Raggi et al., 2017; Mehdipour et al., 2019). The GGE biplot takes into account the G and GE effects and can simultaneously evaluate genotypes and the environments. At the same time, the GGE biplot gives information on the genotype and environment and their relationship, including determining the best variety in a particular environment, the most appropriate environment for a particular variety, and the performance of any two varieties in different environments. Which variety is a high yielding and stable yield. Which environment is conducive to the screening the varieties with high yielding and stable yield (Yan, 2001; Kaya et al., 2006; Dehghani et al., 2017; Oral et al., 2018).

In this study, the multi-environment test was conducted to analyze the yield and yield component traits of 13 tested maize hybrids using the AMMI model and GGE biplot data through the data of 26 test sites for 2 consecutive years, and the genotype-environment interaction effect was evaluated. The actual effect of maize grain yield and yield components, and the comprehensive yield components screen out excellent hybrids. At the same time, the GGE biplot is used to analyze the representativeness and discriminative power of the test sites.

Material and methods

Data of 13 tested genotypes used were maize hybrids recently approved by the National Crop Variety Approval Committee (NCVAC), including one check hybrid Zhengdan958 (G13), were evaluated in 26 locations during two consecutive years (2017-2018 growing seasons) in Huanghuaihai region, and the basic information of tested genotypes is given in *Table 1*. In this study, there were 26 testing sites in the multi-environment trials (Mets), which were derived from seven provinces of Hebei province, Shanxi province, Henan province, Shandong province, Anhui province, Jiangsu province and Shanxi Province. Agro-climatic description and the code of testing sites is given in *Table 2*.

Table 1. *The description of the tested maize hybrids and its code in this study*

Cultivars	Code	Plant type	Female	Male	Ear axis color	Year
Weike702	G1	Compact	WK858	WK798-2	White	2017-18
Liyu86	G2	Semi-compact	L5895	L5012	Red	2017-18
Nonghua101	G3	Compact	NH60	S121	Red	2017-18
Liangyu99	G4	Compact	M03	M5972	Red	2017-18
Meiyu5	G5	Compact	M2325	M1826	Red	2017-18
Nonghua032	G6	Semi-compact	7P402	LS121	Red	2017-18
Wugu704	G7	Compact	6320	WG5603	Red	2017-18
Mingyu19	G8	Semi-compact	M84	M71	White	2017-18
Tunyu808	G9	Semi-compact	T88	T172	White	2017-18
Luyu36	G10	Semi-compact	LZM2-18	LZF4	White	2017-18
Xianyu335	G11	Compact	PH6WC	PH4CV	Red	2017-18
Denghai605	G12	Compact	DH351	DH382	Red	2017-18
Zhengdan958	G13	Compact	Z58	C7-2	White	2017-18

http://www.aloki.hu ● ISSN 1589 1623 (Print) ● ISSN 1785 0037 (Online)
DOI: http://dx.doi.org/10.15666/aeer/1802_35933614

Table 2. *The agro-climatic description of the sites in the trials in 2017-2018*

Sites	Province	Code	Longitude	Latitude	Altitude (m)	Sowing date	Harvest date
Luquan	Hebei	E1	114°18′	38°05′	155	12 June	10 Oct.
Xingtai	Hebei	E2	114°30′	37°08′	102	13 June	11 Oct.
Anping	Hebei	E3	115°21′	38°18′	25	11 June	10 Oct.
Wuqiang	Hebei	E4	115°15′	38°16′	18	13 June	11 Oct.
Wuqiao	Hebei	E5	116°20′	37°43′	55	13 June	11 Oct.
Yuanshi	Hebei	E6	114°49′	37°77′	165	14 June	12 Oct.
Gaoyang	Hebei	E7	115°38′	38°30′	408	15 June	13 Oct.
Yuncheng	Shanxi	E8	110°35′	35°29′	226	9 June	4 Oct.
Yongqiao	Anhui	E9	116°95′	33°65′	48	6 June	1 Oct.
Taihe	Anhui	E10	115°30′	33°10′	12	5 June	30 Sep.
Qianxian	Shanxi	E11	108°12′	34°26′	520	4 June	1 Oct.
Xinxiang	Henan	E12	113°92′	35°30′	70	5 June	2 Oct.
Zhoukou	Henan	E13	114°69′	33°62′	49	3 June	1 Oct.
Runan	Henan	E14	114°23′	33°10′	80	3 June	30 Sep.
Fangcheng	Henan	E15	113°12′	33°29′	155	2 June	3 Oct.
Fugou	Henan	E16	114°75′	33°60′	52	2 June	1 Oct.
Wenxian	Henan	E17	112°51′	34°52′	105	3 June	2 Oct.
Anyang	Henan	E18	113°45′	36°02′	68	7 June	5 Oct.
Ningjin	Shandong	E19	116°38′	37°41′	35	11 June	9 Oct.
Linqing	Shandong	E20	115°59′	36°36′	35	8 June	7 Oct.
Laizhou	Shandong	E21	119°95′	37°17′	56	8 June	5 Oct.
Weishan	Shandong	E22	116°35′	34°28′	38	4 June	2 Oct.
Lanling	Shandong	E23	117°48′	34°57′	75	7 June	5 Oct.
Dongping	Shandong	E24	116°12′	35°76′	56	8 June	5 Oct.
Peixian	Jiangsu	E25	116°57′	34°38′	35	1 June	30 Sep.
Siyang	Jiangsu	E26	118°29′	33°26′	15	1 June	1 Oct.

We used the randomized block design with three repetitions in each testing site, and the experimental plot contained five lines (6.7 m long). The width between each line is 0.7 m, and the sowing density was used 7,5000 plants in per hectare which is widely used in local agricultural production. The grain yield (GY) was calculated in the middle three rows of each plot when harvested by manual harvesting. The two side rows were used to sample the ear length (EL), ear row number (ERN), bald tip (BT), kernel weight (KW) and 100-grain weight (100-GW). The fertilization situation of each plot depends on the soil nutrient analysis results of the plot.

Statistical analysis

AMMI model

The formula for the AMMI model was used (Gauch, 1992):

$$y_{ge} = \mu + \alpha_g + \beta_e + \sum_{n=1}^{N} \lambda_n \gamma_{gn} \delta_{en} + \theta_{ge} \quad \text{(Eq.1)}$$

http://www.aloki.hu ● ISSN 1589 1623 (Print) ● ISSN 1785 0037 (Online)
DOI: http://dx.doi.org/10.15666/aeer/1802_35933614

where y_{ge} represents the value of the genotype (g) in the environment (e); μ is the grand mean; is the average deviation of the *g*th genotype from the grand mean; is the average deviation of the *e*th environment from the grand mean; is the *n*th eigenvalue of interaction principal component axis (IPCA); and are the genotypic and environmental principal component score representing the *n*th principal component, respectively; is the error term. The AMMI model can also be used to rank genotypes in accordance with yield stability of the tested varieties. The AMMI stability values (ASVs) calculation can be performed according to the formula of Purchase (Purchase et al., 2000).

$$\mathrm{ASV} = \sqrt{\left[\frac{\mathrm{SS}_{IPCA1}}{SS_{IPCA2}}(IPCA_1)\right]^2 + (\mathrm{IPCA}_2)^2} \quad \text{(Eq.2)}$$

In the formula, SS_{IPCA1} and SS_{IPCA2} are the sum of squares of interaction principal component analysis 1 (IPCA1) and IPCA2, respectively.

GGE biplot

The GGE biplot is called the principal component analysis of environmental centralization. After subtracting the average value of the environment from the original data, the genotype is singularly decomposed in the interaction effect, and the formula as follows:

$$Y_{ge} - y_e = \lambda_1 \xi_{g1} \eta_{e1} + \lambda_2 \xi_{g2} \eta_{e2} + \varepsilon_{ge} \quad \text{(Eq.3)}$$

where Y_{ge} is the value of the *g*th genotype in the *e*th environment; y_e is the yield performance of all genotypes in the *e*th environment; ξ_{g1} and ξ_{g2} are the first and second principal component scores of the *g*th genotype in the *e*th environment, respectively; λ_1 andλ_2 are the eigenvectors of the first and second principal components, respectively; η_{e1} andη_{e2} represent the first and second eigenvector scores of the *e*th environment, respectively; ε_{ge} is the residuals in the model (Balestre et al., 2009).

Data analysis

In this study, the effects of the genotypes, environments and their interactions were calculated by analysis of variance (ANOVA) using Data Processing System (DPS) software (Tang and Zhang, 2013) in the AMMI model. The GGE biplot analysis using the Genstat 64-bit Release (Payne et al., 2013) to select the optimal environments and superior genotypes.

Results

Variations in six agronomic traits

It can be seen from *Figure 1* that the agronomic traits are significantly different. The coefficient of variation of the six agronomic traits is between 5.08 and 77.97%, with an average of 20.18%, and the coefficient of variation of the bald tip length is the largest. Statistics on six agronomic traits of thirteen hybrids in the twenty-six tested environments

http://www.aloki.hu ● ISSN 1589 1623 (Print) ● ISSN 1785 0037 (Online)
DOI: http://dx.doi.org/10.15666/aeer/1802_35933614

are shown in *Table 3*. The grain weight varied between 7227.91 and 12321.56 kg/t across environments, the ear length and bald tip length are between 12.85-21.35 cm and 0.00-9.90 cm, respectively. The change range of ear weight and 100-grain weight are between 103.00-214.25 g and 24.25-42.30 g, respectively. The minimum and maximum values of the kernel row number are 12.00 and 17.60, respectively. Further statistical values for six agronomic traits can also be seen from *Table 3*.

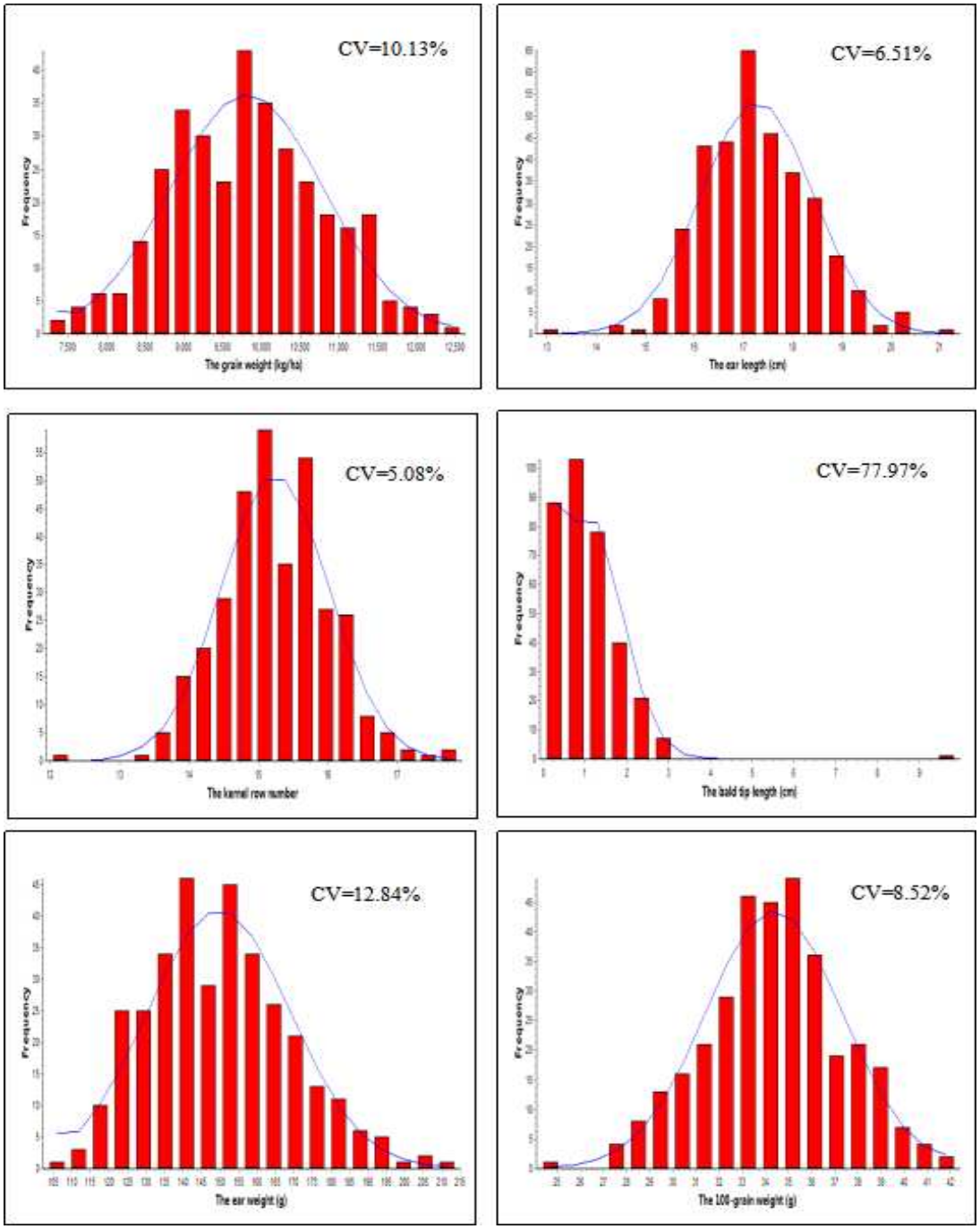

Figure 1. *Normal distribution map of agronomic traits of tested hybrids. CV: coefficient of variation*

http://www.aloki.hu ● ISSN 1589 1623 (Print) ● ISSN 1785 0037 (Online)
DOI: http://dx.doi.org/10.15666/aeer/1802_35933614

Table 3. *Statistical value of each agronomic trait*

Agronomic traits	NS	Min	Max	Mean	AD	R	V	STD	SEM
Grain weight (kg/ha)	338	7227.91	12321.56	9807.43	804.05	5093.64	987716.60	993.84	54.06
Ear length (cm)	338	12.85	21.35	17.27	0.88	8.50	1.27	1.13	0.07
Kernel row number	338	12.00	17.60	15.24	0.61	5.60	0.60	0.77	0.04
Bald tip length (cm)	338	0.00	9.90	1.04	0.56	9.90	0.65	0.81	0.04
Ear weight (g)	338	103.00	214.25	149.70	15.36	111.25	369.71	19.22	1.05
100-grain weight (g)	338	24.25	42.30	34.38	2.31	18.05	8.58	2.93	0.16

NS: Number of samples; Min: minimum; Max: Maximum; AD: Average deviation; R: range; V: variance; STD: Standard deviation; SEM: Standard error of mean

The AMMI model analysis

The results of AMMI model analysis exhibited the variations across mega-environments and genotype by environment interaction (GEI) had a significantly differences ($P < 0.001$, $P < 0.01$ and $P < 0.05$) for tested maize hybrid agronomic traits in 2017-2018 (*Table 4*). The genotype (G) and environment (E) of each agronomic trait had very highly significant effects ($P < 0.001$). The GEI effects on grain yield, bald tip length and 100-grain weight also reached very highly significant effects ($P < 0.001$). The GEI effects on ear length exhibited highly significant effects ($P < 0.01$), and there are significant differences ($P < 0.05$) were observed for kernel row number and ear weight. Furthermore, the AMMI model analysis decomposed the SS of GEI into eight interaction principal component axes (IPCAs), of which the first four IPCAs exhibited very highly significant differences ($P < 0.001$) for all agronomic traits. In terms of the ratio of the variance to the total SS, among the three agronomic traits of grain yield, ear weight and 100-grain weight, environmental effects accounted for 57.48%, 66.62% and 50.52% of the total sum of squares, respectively. The GEI as a second main effect contributed to 47.89%, 54.74% and 44.48% of the total sum of squares of ear length, kernel row number and bald tip length, respectively. Among all the six agronomic traits, genotype effects accounted for the lowest proportion. The first four IPCAs explained 64.62%, 70.71%, 65.22%, 84.41%, 69.72% and 62.97% of the interaction sum of squares of grain yield, ear length, kernel row number, bald tip length, ear weight and 100- grain weight, respectively, with IPCA1 contributing 22.23%, 30.82%, 21.30%, 60.42%, 25.74% and 19.71%, in which greater than other IPCAs.

The IPCA values, average performance of the agronomic traits and the ASV values of the tested maize hybrids are presented in *Table 4*. The IPCA value for a specific genotype in the AMMI model indicates the stability of this genotype throughout the environment. The difference in IPCA values (positive or negative) shows the genotype adapted to the specific environment, and the closer the IPCA value is to zero, the more stable the adaptation to the environment (Gerrano et al., 2019). Genotypes vary widely in yield performance between traits. The average grain yield of the genotypes G7 and

http://www.aloki.hu ● ISSN 1589 1623 (Print) ● ISSN 1785 0037 (Online)
DOI: http://dx.doi.org/10.15666/aeer/1802_35933614

G9 was the lowest and highest in different environments, 9304 kg/ha and 10222 kg/ha, respectively. Other genotypes such as G1, G2, G3, G4, G5 and G8 have higher grain yields. Genotypes G8 and G10 are 16.11 cm and 18.20 cm, which are the worst and best hyrids of ear length, respectively. The performance range of the kernel row number of the tested hybrids was 14.36 to 15.66, which belonged to G4 and G3, respectively. The lightest of the bald tip length is G12, which is 0.38 cm. In contrast, bald tip length of genotype G6 has the highest value of 1.65 cm. Genotypes such as G10 and G5 is the champion of ear weight and 100-grain weight, respectively, and the yield performance is 159.00 g and 36.56 g, respectively.

Table 4. *The performances of IPCA1 to IPCA8 for interaction effect components of 6 agronomic traits of 13 maize hybrids*

Trait	Genotype code	Trait yield	IPCA1	IPCA2	IPCA3	IPCA4	IPCA5	IPCA6	IPCA7	IPCA8	ASV
Grain yield (kg/ha)	G1	9803	8.78	24.00	-27.02	18.61	-2.09	5.57	-29.72	-7.43	27.08
	G2	10237	-2.72	16.29	-8.32	3.01	-25.97	5.99	16.79	14.07	16.74
	G3	10088	9.25	1.47	-15.11	-5.32	21.55	10.44	16.20	-13.33	13.29
	G4	10208	4.02	-12.05	16.54	-13.49	-10.46	-3.34	-20.94	16.01	13.35
	G5	10112	-23.60	17.49	-12.64	-24.14	17.63	-28.38	4.22	6.68	37.97
	G6	9736	1.98	1.33	23.78	-18.90	-11.98	-6.96	-8.68	-29.05	3.12
	G7	9304	10.66	-18.14	-17.84	-16.81	5.14	6.88	-8.35	7.09	23.68
	G8	10157	-10.17	-11.36	9.07	-9.73	15.86	31.43	1.26	3.63	18.44
	G9	10222	-46.17	-21.51	2.09	29.58	3.03	-4.80	-3.48	-3.70	69.34
	G10	9204	26.09	12.69	28.50	22.56	25.78	-9.11	1.24	11.11	39.35
	G11	9417	2.45	8.89	6.04	7.35	-9.74	2.02	14.70	-14.88	9.55
	G12	9257	26.45	-33.56	-14.12	9.15	-11.18	-17.41	10.40	-0.49	50.53
	G13	9753	-7.03	14.46	9.03	-1.89	-17.57	7.68	6.36	10.29	17.6
Ear length (cm)	G1	16.87	0.38	0.50	0.69	-0.57	-0.67	0.21	0.56	-0.46	0.84
	G2	17.28	0.00	0.51	-0.15	0.03	-0.34	0.81	0.43	0.07	0.51
	G3	17.33	0.22	-0.18	0.72	0.09	0.77	-0.59	0.50	0.58	0.43
	G4	17.47	1.30	-0.97	-0.03	0.43	-1.12	-0.52	-0.44	0.30	2.50
	G5	17.69	0.86	-0.01	0.54	0.26	0.59	-0.01	-0.37	-0.77	1.53
	G6	17.19	-0.42	1.15	0.09	0.17	-0.57	0.30	-0.47	0.23	1.37
	G7	17.00	0.21	0.99	-0.11	1.16	0.41	-0.38	0.30	0.10	1.06
	G8	16.11	1.20	-0.25	-0.99	-0.86	0.50	0.23	0.29	-0.24	2.16
	G9	17.63	-0.44	0.09	0.39	-0.48	0.47	0.10	-1.24	-0.07	0.79
	G10	18.20	-0.72	0.14	0.11	-1.10	-0.12	-0.69	0.15	0.53	1.28
	G11	17.56	-0.79	-1.35	0.67	0.37	0.14	0.94	0.25	0.22	1.94
	G12	17.16	-1.50	-0.49	-0.52	0.25	-0.27	-0.69	0.23	-0.88	2.72
	G13	17.08	-0.29	-0.14	-1.41	0.25	0.22	0.29	-0.20	0.39	0.53
Kernel row number	G1	15.30	0.16	-0.43	-0.13	-1.11	0.24	0.22	-0.14	0.60	0.83
	G2	15.52	-0.44	0.45	0.76	0.58	0.74	-0.29	0.18	-0.34	0.98
	G3	15.66	0.73	-0.55	0.13	0.10	-0.34	-0.83	-0.20	0.22	1.25
	G4	14.36	0.64	-0.78	-0.49	0.89	0.23	0.84	0.49	0.06	0.59
	G5	15.01	0.26	0.01	0.14	-0.14	0.63	-0.04	0.06	-0.22	1.60
	G6	15.43	0.17	-0.66	0.55	-0.69	-0.27	0.29	-0.08	-1.00	1.73
	G7	15.51	0.23	-0.35	0.42	0.56	-0.49	-0.10	-0.30	0.36	9.48

http://www.aloki.hu ● ISSN 1589 1623 (Print) ● ISSN 1785 0037 (Online)
DOI: http://dx.doi.org/10.15666/aeer/1802_35933614

	G8	15.11	-0.13	0.07	0.07	0.09	0.24	-0.83	-0.11	0.17	0.89
	G9	15.63	0.28	0.57	-1.15	-0.35	0.13	-0.46	0.66	-0.19	2.28
	G10	15.07	-0.32	0.61	0.75	-0.31	0.25	0.60	0.28	0.59	2.21
	G11	15.38	-1.79	-0.61	-0.42	0.09	-0.51	-0.05	0.19	0.02	3.83
	G12	15.21	-0.16	0.53	-0.76	0.21	0.30	0.41	-1.17	-0.16	3.35
	G13	14.94	0.35	1.14	0.12	0.06	-1.15	0.25	0.15	-0.09	1.43
Bald tip length	G1	1.48	-2.61	0.22	0.06	0.03	0.12	0.05	0.07	0.03	15.90
	G2	0.85	0.08	-0.34	0.11	-0.49	0.20	0.02	-0.09	-0.64	0.62
	G3	0.74	0.22	0.15	0.31	-0.51	-0.10	-0.97	0.56	0.08	1.37
	G4	1.13	0.49	0.85	-0.29	0.03	0.23	-0.13	-0.36	0.13	3.08
	G5	1.56	0.11	0.24	-0.68	0.40	-0.14	-0.19	-0.21	-0.69	0.69
	G6	1.65	0.01	-0.61	-0.64	-0.10	-0.95	0.25	0.30	0.13	0.61
	G7	0.82	0.15	-0.44	0.20	0.17	0.32	0.50	0.09	0.13	0.99
	G8	1.08	0.33	0.72	0.64	0.82	-0.48	0.13	0.20	0.05	2.15
	G9	0.69	0.35	0.28	-0.08	-0.52	-0.03	0.47	-0.13	0.16	2.13
	G10	1.20	0.01	-0.92	0.50	0.42	-0.08	-0.47	-0.67	0.18	0.92
	G11	1.23	0.20	-0.12	-0.89	0.22	0.54	-0.20	0.10	0.49	1.22
	G12	0.38	0.15	0.26	0.39	-0.68	-0.18	0.23	-0.40	0.16	0.98
	G13	0.66	0.52	-0.27	0.37	0.21	0.54	0.30	0.55	-0.20	3.17
Ear weight (g)	G1	149.00	3.03	3.54	2.49	0.33	-1.24	-1.63	1.46	-0.41	5.48
	G2	151.90	4.09	-4.60	-1.76	-2.15	1.00	-2.17	-1.77	-0.15	7.27
	G3	149.10	1.55	0.32	1.72	-0.37	2.77	0.49	0.54	-1.92	2.17
	G4	155.90	-0.88	-3.51	3.57	2.27	1.33	-0.06	-0.04	3.32	3.71
	G5	152.30	-4.74	0.26	0.58	-0.44	-2.04	0.34	-1.86	1.53	6.54
	G6	150.50	1.46	0.12	-2.15	-4.41	-2.33	0.65	1.15	1.87	2.02
	G7	144.20	0.48	1.67	-4.62	2.78	0.52	0.77	2.35	1.74	1.80
	G8	142.70	0.02	2.44	1.56	-2.07	3.57	2.32	0.31	0.65	2.44
	G9	153.1	-2.11	2.47	-3.18	1.53	2.08	-2.42	-2.65	-0.57	3.82
	G10	159.00	-5.07	-3.01	-0.87	-1.33	0.17	1.01	2.08	-2.79	7.61
	G11	143.30	-1.05	2.62	2.10	-1.38	-1.92	-1.25	-1.33	-0.70	2.99
	G12	148.90	2.94	-0.72	-0.33	2.63	-2.15	4.28	-2.30	-1.50	4.12
	G13	146.30	0.28	-1.61	0.88	2.62	-1.76	-2.31	2.06	-1.08	1.65
100-grain weight (g)	G1	32.86	1.23	-0.67	0.62	-1.13	0.03	-1.64	-0.12	1.09	1.66
	G2	33.49	1.05	-0.85	0.48	1.28	1.13	-0.33	-0.24	-0.87	1.56
	G3	34.57	-1.67	0.20	0.42	0.02	-0.14	0.07	-1.97	0.01	2.09
	G4	36.47	-0.37	-0.94	-2.21	0.66	0.72	-0.14	-0.18	0.95	1.05
	G5	36.56	0.78	-0.40	-0.02	-1.15	-0.13	1.93	-0.13	0.69	1.05
	G6	34.35	0.63	0.86	1.51	0.72	0.46	0.19	0.18	0.29	1.17
	G7	32.54	0.63	0.09	-0.26	0.36	0.35	0.48	-0.43	-0.89	0.79
	G8	35.68	0.18	-0.76	-0.83	-0.90	-0.52	-0.07	0.69	-1.38	0.79
	G9	35.27	0.35	-0.57	0.62	0.13	-1.34	0.50	0.06	0.06	0.71
	G10	34.11	-2.07	-1.14	0.86	0.02	-0.46	-0.45	0.79	-0.16	2.81
	G11	32.57	0.24	1.90	-0.76	-1.02	-0.35	-0.80	-0.39	-0.58	1.93
	G12	35.24	-1.11	1.11	0.17	-0.64	1.55	0.36	1.09	0.22	1.77
	G13	33.16	0.14	1.16	-0.58	1.65	-1.30	-0.10	0.66	0.56	1.17

IPCA: Interaction principal component axes; ASV: AMMI stability value

http://www.aloki.hu ● ISSN 1589 1623 (Print) ● ISSN 1785 0037 (Online)
DOI: http://dx.doi.org/10.15666/aeer/1802_35933614

In the AMMI model, genotypes with lower ASV values are considered to be more stable. Therefore, genotypes G6 and G11 have better stability of grain yield than other maize hybrids. By the same method and so on, the genotypes G3, G2, and G13 have better stability in ear length performance, G4, G1, G8, and G2 belong to the genotypes with better stability of ear row number, genotypes G6, G2, and G5 belong to the hybrids with better stability in bald tip length. We can also see from *Table 4* that genotype G13 followed by G7 and G9 followed by G8, G7, which belong to the hybrids with better stability of ear weight and 100-grain weight, respectively.

The adaptive analysis using GGE biplot

The "who-wins-where" views of the GGE biplot of grain yield, ear length, kernel row number, bald tip length, ear weight and 100-grain weight are shown in *Figure 2a, b, c, d, e* and *f*. The biplot consists of genotypes that are furthest from the origin in the same direction, and all genotypes are included. The biplot is divided into several sectors by vertical lines from the origin to the sides of the polygon, and the test sites fall in different areas in the sector. Test sites in the same sector are considered to have similar yield performance to genotypes, and these sites also belong to the same ecological group. In the same way, genotypes located in the same sector are considered to have similar performance to the environments of this sector. In the biplot, the genotype at the "vertex" position is considered to be the best-performing genotype in this sector (Duma et al., 2019).

GGE biplot analysis showed that the first two principal components (PC1 + PC2) accounted for 54.27%, 54.88%, 46.62%, 77.56%, 49.65% and 59.14% of the total variation in GEI of grain yield, ear length, kernel row number, bald tip length, ear weight and 100-grain weight, respectively. For grain yield, G9, G12, G10, G1, and G2 are connected into a polygon, and the five rays divide the polygon into 5 sectors. The first sector contains the test sites E1, E2, E5, E9, E10, E14, E15, E16, E17, E18, E20, E21, E23, E24 and E25, genotype G9 has the highest yield performance. There are no sites in the second, third, and fourth sectors, indicating that the "vertex" genotypes G12, G10, and G1 of these sectors did not perform well in all the sites. The fifth sector contains the remaining sites, with G2 performing best (*Fig. 1a*). For ear length, PC1 and PC2 in the GGE biplot explained 36.60% and 18.28% of the total variation of GEI, respectively. In this biplot, it can be divided into four ecological groups. The first ecological group contains twelve test sites, environments E2, E4, E5, E6, E7, E8, E10, E12, E14, E16, E19, and E23 fell into the first ecological group, environments E1, E11, E15, E20, E21 and E24 belong to the second ecological group, E13 fell into the third ecological group, and E3 and E9 belong to the fourth ecological group. The genotypes G10, G4, G8 and G12 belong to the champion hybrids of the first to fourth ecological regions, respectively (*Fig. 1b*). For kernel row number, PC1 contributed 31.48% while PC2 accounted for 15.14% of the total variation. This biplot consisted of three ecological group; where E1, E2, E5, E6, E8, E9, E10, E13, E15, E16, E19, E20, E22, E24 and E26 belong to the first ecological group; E23 fell in one group; the remaining sites are combined belong to the third ecological group. Genotype G11 had the highest yielding performance in the first ecological group, G12 was the winner in the second ecological group, whereas genotype G7 was the vertex hybrid in the third group (*Fig. 1c*). For bald tip length, the percentages of 53.10% and 24.46% are attributed to PC1 and PC2, respectively. In this biplot, only two ecological groups were found;

http://www.aloki.hu ● ISSN 1589 1623 (Print) ● ISSN 1785 0037 (Online)
DOI: http://dx.doi.org/10.15666/aeer/1802_35933614

where E10 and E18 belong to one group; the remaining sites were divided into another group. Genotype G1 and G6 in the first and second ecological group are the vertex genotypes, respectively, which had the most bald performance (*Fig. 1d*). For ear weight, PC1 and PC2 accounted 30.63% and 19.02% of GEI, respectively. GGE biplot for ear weight grouped E2, E4, E12, E13, E14, E15, E16, E18, E19, E21, E24 and E25 as the first group and E1, E5, E6, E7, E8, E10, E20 and E22 belong to the second group. E26 and E1, E9, E9 were found in the third and fourth group, respectively. Genotypes G10, G2, G1 and G5 were found suited for the first to fourth group, respectively (*Fig. 1e*). For 100-grain weight, PC1 accounted for 48.16% of the variation caused by GEI, while PC2 accounted for 10.98% (*Fig. 1f*). Genotype G4 had the highest 100-grain weight performance in E1, E2, E5, E7, E9, E11, E12, E14, E16, E17, E18 and E22. No genotypes fell on E16, indicating that all genotypes did not perform well on E16. Genotype G5 was the top-ranking hybrid at the remaining sites.

Mean performance and stability analysis of the tested genotypes using GGE biplot

The use of the first two principal components axises formed a biplot related to genotypic performance. GGE biplot is an effective tool for assessing two aspects (mean performance and genotypic stability). The longer the vertical line of the genotype relative to axis 1, the lower the stability, and the longer the distance between the genotype and axis 2 (vertical to axis 1), indicated the higher yield (Badu-Apraku et al., 2012). *Figure 3* showed the average environment coordinate (AEC) of the GGE biplot of the agronomic traits of the tested hybrids. Thus, the genotypes G3, G4, G5, G8 and G13 had high grain yield combined with high stability. Genotypes G6 and G11 had good stability, however, these genotypes had no promising performance with grain yield. Based on these interpretations, although G9 has a high grain yield, it has poor stability and is not an ideal genotype (*Fig. 3a*). Genotypes G3, G9, G10 and G11 had longer ear length and good stability, whereas G4, G5 and G12 were highly unstable with longer ear length performance. Genotypes G4 and G5 had higher ear length performance, but had poor stability (*Fig. 3b*). The mean kernel row number of tested genotypes were arranged in the following order: G11 > G5 > G3 > G10 > G2 > G7 > G1 > G4 > G8 > G6 > G13 > G9 > G12. The performance of genotypes G7 and G11 had the worst stability, whereas genotypes G5, G3 and G10 were highly stable with high kernel row number (*Fig. 3c*). Genotype G6 had the highest mean bald tip length, followed by G5, G1, G11, etc.; and G12 had the lowest mean bald tip length. In terms of stability, genotype G2 was the most stable hybrid whereas, G1 was the least stable genotype (*Fig. 3d*). G13 was the most stable genotype with an average ear weight performance. Genotypes G2, G5 and G10 were the most unstable with a high average performance of ear weight (*Fig. 3e*). The biplot showed the ranking of 13 tested maize genotypes based on their average 100-grain weight and stability performance (*Fig. 3f*). The 100-grain weight performance of genotype G5 was the highest and that of G11 was the lowest among all 13 tested genotypes. From the perspective of crop breeding, breeders prefer genotypes with high average yield and high stability as potential ideal genotypes. In the biplot, the more stable genotype should be close to the average environment (the center of the small circle), and it should also have the shortest vector (Bai et al., 2014). Based on this information, although G5 had the highest 100-grain yield performance among all the genotypes, it is still less stable compared with genotypes G7, G8 and G9.

http://www.aloki.hu ● ISSN 1589 1623 (Print) ● ISSN 1785 0037 (Online)
DOI: http://dx.doi.org/10.15666/aeer/1802_35933614

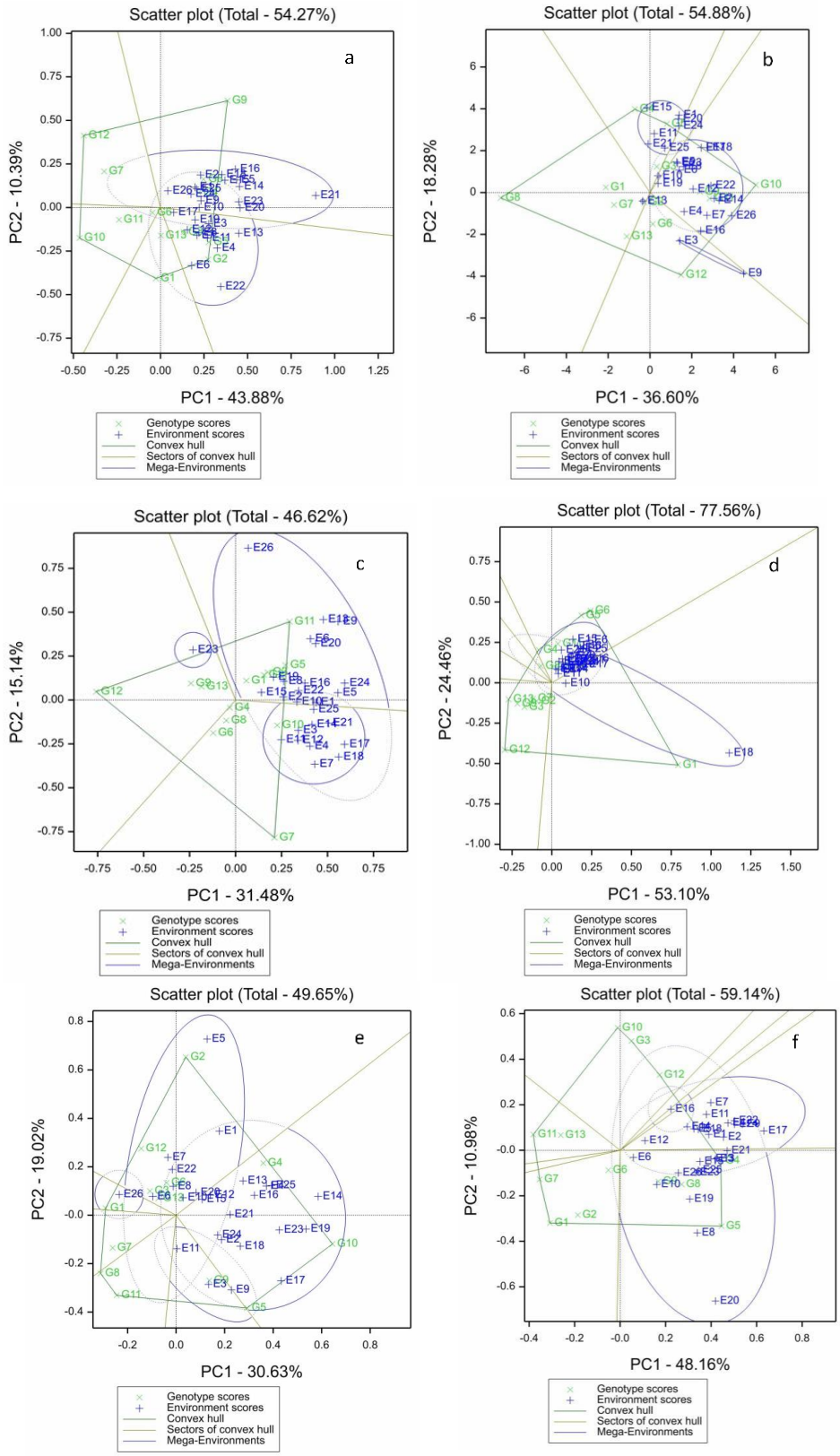

Figure 2. *The "who-wins-where" view for agronomic traits of the GGE biplot of 13 maize hybrids in 26 environments to display which genotype performs best in which environment. See Table 1 for genotypes and Table 2 for environments codes. a: grain yield; b: ear length; c: kernel row number; d: bald tip length; e: ear weight; f: 100-grain weight (the same as below)*

http://www.aloki.hu ● ISSN 1589 1623 (Print) ● ISSN 1785 0037 (Online)
DOI: http://dx.doi.org/10.15666/aeer/1802_35933614

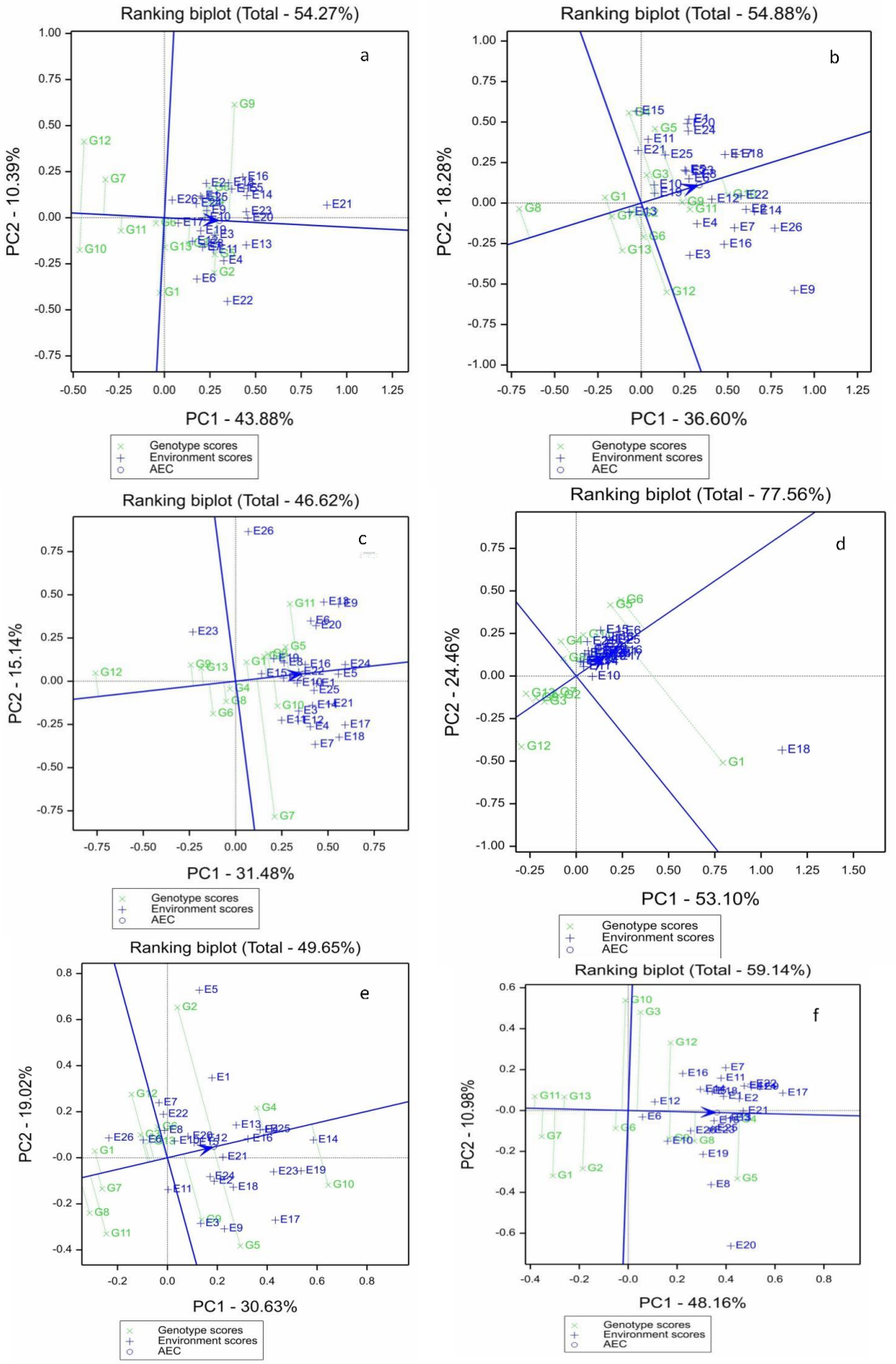

Figure 3. *The mean performance and stability of the tested 13 maize hybrids evaluated in 26 environments using GGE biplot*

http://www.aloki.hu ● ISSN 1589 1623 (Print) ● ISSN 1785 0037 (Online)
DOI: http://dx.doi.org/10.15666/aeer/1802_35933614

Judging the best genotypes based on the GGE biplot

The concept of 'ideal genotypes' should show high yielding and stability within a mega- environments (Yan and Tinker, 2006). However, we know that ideal genotypes do not exist in reality. Studies have also shown that, compared to average performance and stability, different concentric circles were drawn to help clearly distinguish the distance between each genotype and the ideal genotype, the distance between a genotype and an ideal genotype is also an important parameter for evaluating genotype performance. The closer the genotype is to the center of the circle (the position of ideal genotype), the better the average yield and stability of this genotype. On the contrary, being far away from the center of the circle represents the worst performance of this genotype is defined as the undesired genotype (Erdemci et al., 2018). Based on these, the genotypes G5 and G2 were located on the innermost concentric circle of the biplot, and are closer to the center of the circle than other genotypes. Therefore, these two genotypes (G5 and G2) can be considered as the genotypes closest to the ideal genotypes. In addition, genotypes G6 and G8 were located on the next concentric circle, and these two genotypes were considered desirable genotypes in terms of grain yield. In contrast, genotypes G10 and G12 were located on the outermost concentric circles, which are farther from the center of the concentric circles than other genotypes, may be regarded as undesirable genotypes (*Fig. 4a*). Given that the genotype G10 was located near the first concentric circle and closer to the ideal genotype position, it can be used as the genotype closest to the ideal genotype for evaluation in terms of ear length. Next to genotype G10, compared to other maize hybrids, G9 and G11 were the more desirable genotypes. On the other side, genotype G8 belong to the undesirable hybrid and implying poor performance in all environments (*Fig. 4b*). Genotype G5 belong to the most favorable genotype owing to was closest to the center of the concentric circle, whereas, G12 had the worst performance of kernel row number (*Fig. 4c*).

In the first circle, genotype G15 was found. Therefore, this was an ideal genotype in terms of obtaining a higher average bald tip length and good stability in the tested environments. Genotype G12 was located in the last circle, with the worst average baldness length and general stability compared to other tested maize genotypes (*Fig. 4d*). According to *Fig. 4e,* genotype G10 was highly "ideal", followed by genotypes G4, G5, G9, etc., and these genotypes can be considered as desirable genotypes. On the other hand, G1, G7, G11 and G8 were very poorest for average ear weight, classify them as undesirable genotypes in all environments. Compared with other maize genotypes, G4 fell into the center of concentric circles was ideal genotype, with higher 100-grain weight and good stability. In addition, next to G4 were the genotypes G5, G8 and G9, which were considered as the promising genotypes. In contrast, G11 was the furthest from the center of the circle, followed by genotypes G7, G1, G13, and G2, which were considered the least promising genotypes (*Fig. 4f*).

Discussion

In view of the vast area of the Huang-Huai-Hai region and as the largest area of centralized maize cultivation in China, it is particularly important to test and evaluate the stability and adaptability of different maize genotypes before large-scale planting (Yue et al., 2018). The performance of maize agronomic traits was affected by multiple factors, such as the genotype itself, environmental conditions, and the interaction between genotype and environment. Compared with genotype (G) and environment (E),

http://www.aloki.hu ● ISSN 1589 1623 (Print) ● ISSN 1785 0037 (Online)
DOI: http://dx.doi.org/10.15666/aeer/1802_35933614

the genotype by environment interaction (GEI) was the most difficult to grasp and control due to its uncertainty. The expression of many traits, such as crop yield, ear length, 100-grain, etc., were significantly affected by the GEI, and it effects on yield will affected yield stability directly. If the GEI effect was greater, the genotypes' stability was worse. Genotypes with high yielding and stable under multi-environmental trials (Mets) generally had broad adaptability and great value for promotion and utilization, genotypes with poor yielding and unstable but had special adaptability to local environments also had high recommendation. Screening and evaluating high-yielding and stable genotypes in various of environments has been an ongoing challenge for agronomy breeders worldwide (Lin et al., 1992; Alwala et al., 2010). The analysis of the Mets data of most genotypes were based on the data of a single trait (such as yield, quality or resistance), but multiple traits need to be considered simultaneously during the breeding practice. The conclusion based on the comprehensive analysis of single trait components is more important than the conclusion of single trait analysis (Kendal et al., 2016a). According to the analysis of single-yield traits of hybrid maize, only genotype total yield data can be obtained. ear length, ear row number, bald tip length, ear weight and 100-grain weight data and the main factors affecting these data cannot be obtained from the total yield. The purpose of Mets was to identify superior genotypes under different environments. Because of the existence of unpredictable environmental factors, researchers have developed different analytical models (GE, GEI, GGE, AMMI) to explain the effects of genotype, environment, and their interactions. So far, the AMMI model and the GGE biplot were the recommended methods for analyzing the GEI effect across the mega-environments (Kendal et al., 2019). According to reports, the AMMI model was a comprehensive and effective method because it can classify genotypes based on the genotype level combined with the target environment and classify them according to their advantages and disadvantages in different environments. Compared with other methods (such as joint regression methods), this model was a valuable statistical tool for identifying genotypes with specific or broad adaptability, which may be an important advantage of this method. On the other hand, the GGE biplot has been successfully used in Mets of various crops, which can concisely and effectively distinguish the best performing genotypes in the entire environment, so that specific genotypes can be recommended to specific large environments and the yield and stability were fully evaluated (Kendal et al., 2016b).

In this study, the AMMI model analysis indicated that the main effect of G, E and GEI were important among agronomic traits (*Table 5*). By analyzing the proportions of G, E, and GEI of the total variation, the six traits can be divided into two categories. The first category was grain yield (GY), ear weight (EW) and 100-grain weight (100-GW). These three agronomic indicators reflect a phenomenon that the proportion of environment effect was the greatest, followed by GEI and G, which ranged from 3.89-, 11.37- and 2.37-fold the genotype effect for GY, EW and 100-GW, respectively. This suggesting that maize breeders can either choose to set a specific genotype for each environment, or can choose excellent genotypes in a wide range of environments. Correspondingly, ear length (EL), kernel row number (KRN) and bald tip length (BTL) belong to the second category. This type of agronomic traits reflected the largest proportion of the total variation was GEI effect, followed by E and G, which ranged from 2.68-, 6.00- and 2.10- fold the genotype effect for EL, KRN and BTL. It has often been shown in the Mets that agronomic traits variations due to GEI effect exceed that due to genotypes effects (Dehghani et al., 2016).

http://www.aloki.hu ● ISSN 1589 1623 (Print) ● ISSN 1785 0037 (Online)
DOI: http://dx.doi.org/10.15666/aeer/1802_35933614

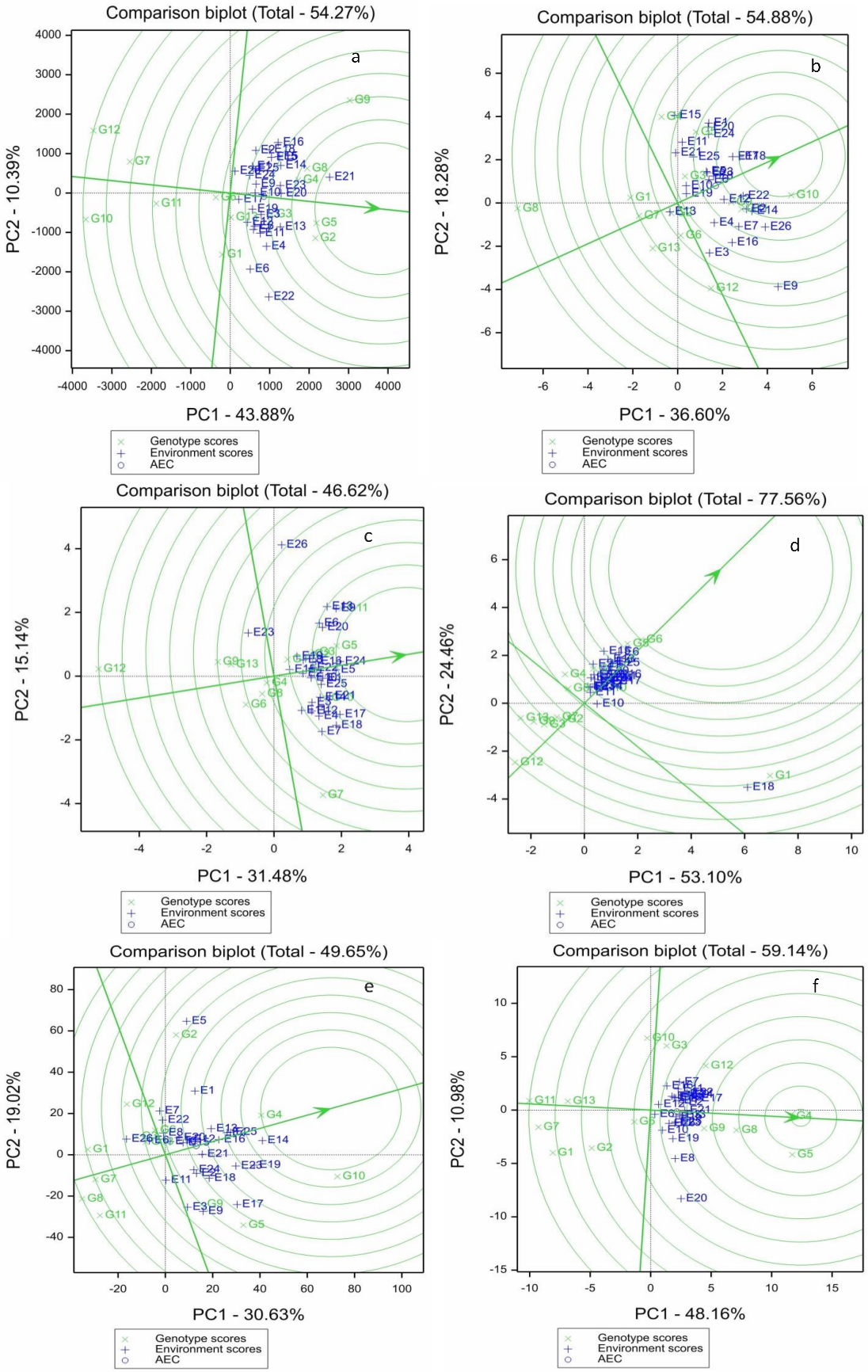

Figure 4. *Comparison of distance between tested genotypes and ideal genotype in GGE biplot*

http://www.aloki.hu ● ISSN 1589 1623 (Print) ● ISSN 1785 0037 (Online)
DOI: http://dx.doi.org/10.15666/aeer/1802_35933614

Table 5. *Analysis of variance of 13 maize hybrids in 26 environments for agronomic traits using the additive main effects and multiplicative interaction (AMMI) model analysis in China*

Traits	Source	DF	SS	MS	*F*	%SS	*P* value
Grain yield (kg/ha)	Total	337	332860498	987716.6			
	Genotype (G)	12	49171359	4097613	13.31^{***}	14.77^{a}	< .001
	Environment (E)	25	191327413	7653097	24.86^{***}	57.48^{a}	< .001
	Genotype and environment interaction (GEI)	300	92361726	307872	1.15^{***}	27.75^{a}	< .001
	IPCA 1	36	20532503	570347	6.19^{***}	22.23^{b}	< .001
	IPCA 2	34	14379975	422940	4.59^{***}	15.57^{b}	< .001
	IPCA 3	32	12681392	396293	4.30^{***}	13.73^{b}	< .001
	IPCA 4	30	11615878	387196	4.20^{***}	12.58^{b}	< .001
	IPCA 5	28	10161779	362921	3.94^{***}	11.00^{b}	< .001
	IPCA 6	26	6494016	249770	2.71^{***}	7.03^{b}	< .001
	IPCA 7	24	5800433	241685	2.62^{**}	6.28^{b}	0.0012
	IPCA 8	22	4426879	201222	2.18^{**}	4.79^{b}	0.0076
	Residuals	68	6268872	92189		6.79^{b}	
	Error	262	70130640	267674.2			
Ear length (cm)	Total	337	426.73	1.2662			
	Genotype (G)	12	76.17	6.347	9.32^{***}	17.85^{a}	< .001
	Environment (E)	25	146.19	5.848	8.58^{***}	34.26^{a}	< .001
	Genotype and environment interaction (GEI)	300	204.36	0.681	1.34^{**}	47.89^{a}	0.0072
	IPCA 1	36	62.98	1.749	7.85^{***}	30.82^{b}	< .001
	IPCA 2	34	35.38	1.041	4.67^{***}	17.31^{b}	< .001
	IPCA 3	32	26.89	0.84	3.77^{***}	13.16^{b}	< .001
	IPCA 4	30	19.26	0.642	2.88^{***}	9.42^{b}	< .001
	IPCA 5	28	15.14	0.541	2.43^{**}	7.41^{b}	0.0016
	IPCA 6	26	12.56	0.483	2.17^{**}	6.15^{b}	0.0058
	IPCA 7	24	10.14	0.422	1.89^{*}	4.96^{b}	0.0211
	IPCA 8	22	6.84	0.311	1.39^{ns}	3.35^{b}	0.1495
	Residuals	68	15.16	0.223		7.42^{b}	
	Error	262	132.89	0.5072			
Kernel row number	Total	337	202.15	0.5998			
	Genotype (G)	12	38.92	3.2437	8.79^{***}	9.12^{a}	< .001
	Environment (E)	25	51.22	2.0489	5.55^{***}	12.00^{a}	< .001
	Genotype and environment interaction (GEI)	300	110.66	0.3689	1.16^{*}	54.74^{a}	0.0270
	IPCA 1	36	23.57	0.6547	5.76^{***}	21.30^{b}	< .001
	IPCA 2	34	20.53	0.6038	5.31^{***}	18.55^{b}	< .001
	IPCA 3	32	16.07	0.5021	4.42^{***}	14.52^{b}	< .001
	IPCA 4	30	12.01	0.4005	3.52^{***}	10.85^{b}	< .001
	IPCA 5	28	10.83	0.3867	3.40^{***}	9.79^{b}	< .001
	IPCA 6	26	9.7	0.3732	3.28^{***}	8.77^{b}	< .001
	IPCA 7	24	5.63	0.2344	2.06^{*}	5.09^{b}	0.0105
	IPCA 8	22	4.60	0.2091	1.84^{*}	4.16^{b}	0.0294
	Residuals	68	7.73	0.1136		6.99^{b}	
	Error	262	83.9685	0.3205			

http://www.aloki.hu ● ISSN 1589 1623 (Print) ● ISSN 1785 0037 (Online)
DOI: http://dx.doi.org/10.15666/aeer/1802_35933614

Bald tip length (cm)	Total	337	219.9935	0.6528			
	Genotype (G)	12	46.65	3.8874	11.92***	21.21[a]	< .001
	Environment (E)	25	75.49	3.0195	9.26***	34.31[a]	< .001
	Genotype and environment interaction (GEI)	300	97.86	0.3262	2.30***	44.48[a]	< .001
	IPCA 1	36	59.13	1.6424	34.09***	60.42[b]	< .001
	IPCA 2	34	9.70	0.2852	5.92***	9.91[b]	< .001
	IPCA 3	32	8.14	0.2544	5.28***	8.32[b]	< .001
	IPCA 4	30	5.64	0.1882	3.9***	5.76[b]	< .001
	IPCA 5	28	3.95	0.1412	2.93***	4.04[b]	< .001
	IPCA 6	26	3.82	0.1471	3.05***	3.90[b]	< .001
	IPCA 7	24	2.48	0.1033	2.14**	2.53[b]	0.0075
	IPCA 8	22	1.71	0.0778	1.61ns	1.75[b]	0.0688
	Residuals	68	3.28	0.0482		3.35[b]	
	Error	262	37.17	0.1419			
Ear weight (g)	Total	337	124591.40	369.71			
	Genotype (G)	12	7297	608.10	5.32***	5.86[a]	< .001
	Environment (E)	25	83004	3320.20	29.05***	66.62[a]	< .001
	Genotype and environment interaction (GEI)	300	34290	114.30	1.2501*	27.52[a]	0.0318
	IPCA 1	36	8826	245.20	5.73***	25.74[b]	< .001
	IPCA 2	34	6403	188.30	4.40***	18.67[b]	< .001
	IPCA 3	32	4895	153.00	3.58***	14.28[b]	< .001
	IPCA 4	30	3783	126.10	2.95***	11.03[b]	< .001
	IPCA 5	28	2540	90.70	2.12**	7.41[b]	0.0062
	IPCA 6	26	2132	82.00	1.92*	6.22[b]	0.0171
	IPCA 7	24	1492	62.20	1.45ns	4.35[b]	0.1165
	IPCA 8	22	1310	59.60	1.39ns	3.82[b]	0.1506
	Residuals	68	2908	42.80		8.48[b]	
	Error	262	23956.31	91.44			
100-grain weight (g)	Total	337	2892.55	8.58			
	Genotype (G)	12	616.2	51.35	18.90***	21.30[a]	< .001
	Environment (E)	25	1461.4	58.45	21.52***	50.52[a]	< .001
	Genotype and environment interaction (GEI)	300	815	2.72	1.01***	28.18[a]	< .001
	IPCA 1	36	161.1	4.48	4.66***	19.77[b]	< .001
	IPCA 2	34	129.5	3.81	3.97***	15.89[b]	< .001
	IPCA 3	32	116.1	3.63	3.78***	14.25[b]	< .001
	IPCA 4	30	106.4	3.55	3.70***	13.06[b]	< .001
	IPCA 5	28	75.2	2.68	2.80***	9.23[b]	< .001
	IPCA 6	26	64.7	2.49	2.60***	7.94[b]	< .001
	IPCA 7	24	50.7	2.11	2.20**	6.22[b]	0.0059
	IPCA 8	22	46.1	2.09	2.18**	5.66[b]	0.0076
	Residuals	68	65.2	0.96		8.00[b]	
	Error	262	640.43	2.44			

df: degree of freedom; SS: sum of squares, a: Percentage of total SS; b: Percentage of sum of squares of GEI; MS: mean square; IPCA, Interaction principal component axes; *, **, *** significant at $P < 0.05$, $P < 0.01$ and $P < 0.001$, respectively; ns: non-significant ($P > .05$)

http://www.aloki.hu ● ISSN 1589 1623 (Print) ● ISSN 1785 0037 (Online)
DOI: http://dx.doi.org/10.15666/aeer/1802_35933614

The effect of GEI on agronomic traits can be confirmed by the ear length of each genotype varied from 12.85 cm (corresponding to G8 at environment E26) to 21.35 cm (corresponding to G11 at environment E18) (*Table 3*), it was shown that the ear length performance of 13 genotypes in 26 environments had considerable variation. Further analysis of the AMMI model, in the face of different parameters, because of the stability analysis using multiple IPCA numbers, it was better than the stability analysis using the first IPCA score. Hence, combined with the ASV results in this study, G9 had a higher performance of GY, but the worst stability. However, G6 had the best stability, the GY was moderate. According to comprehensive analysis, genotypes G2, G3, G4 and G8 were high yielding with outstanding stable in GY. Similarly, genotypes G2, G3 and G4 also showed better agronomic performance and stability in agronomic traits, like EL, KN, GTL, EW and 100-WG compared with other genotypes. In production practice, genotypes with showing good adaptability in agronomic traits across all the environments were favored by plant breeders. Conceptually, successful genotypes not only had high agronomic trait values, but also showed good stable performance in different ecological environments (Mohammadi et al., 2017). However, we should not ignore those genotypes that had special adaptability to individual environments. For instance, genotypes showed higher EL (i.e. G8 at environment E13 and G12 at environments E3, E9), genotype G5 showed higher EW at environments E3, E9 and E11. Because of the existence of GEI, both the AMMI model and GGE biplot could well explore the variations in Mets data, and the two methods had proven to be similar in practice, which leads to basically the same conclusion (Mitrovic et al., 2012; Vaezi et al., 2017; Yue et al., 2020).

Conclusions

This result of research revealed that agronomic traits like GY, EW and 100-GW of tested maize hybrids were highly influenced by E effect, followed by GEI effect and G contributed the least, other agronomic traits EL, KRN and BTL were highly influenced by GEI effect, followed by E effect and G. For the maize agronomic traits GY, EL, KRN, EW and 100-GW, the larger the field performance value, the more the breeder likes, but the BTL was just the opposite. The results of the GEI study indicated that the environments in this research had an opposite effect on genotypes performance. For instance, genotypes G2 and G5 had opposite results for 100-KW in the tested environments. Genotypes G2, G3 and G4 showed the best performance and stability in agronomic traits. These genotypes could be considered as the desirable hybrids with similar ecological region. It turns out that the AMMI model and GGE biplot were approximately equal for the analysis results of this study, and thus the conclusions of the genotypes with the highest agronomic performance and stability were basically the same. Considering the enormous impact of environment and genotype by environment interactions on agronomic traits of summer maize hybrids, maize breeders across China are encouraged to conduct further experiments in more seasons and elsewhere in agro-climatic regions.

Acknowledgements. This research was supported by the National Natural Science Foundation of China (31601386).

Conflict of interests. The authors declare no conflict of interests.

http://www.aloki.hu ● ISSN 1589 1623 (Print) ● ISSN 1785 0037 (Online)
DOI: http://dx.doi.org/10.15666/aeer/1802_35933614

REFERENCES

[1] Alwala, S., Kwolek, T., Mcpherson, M., Pellow, J., Meyer, D. (2010): A comprehensive comparison between Eberhart and Russell joint regression and GGE biplot analyses to identify stable and high yielding maize hybrids. – Field Crops Research 119: 225-230.
[2] Badu-Apraku, B., Oyekunle, M., Obeng-Antwi, K., Osuman, A. S., Ado, S. G., Coulibay, N., Yallou, C. G., Abdulai, M., Boakyewaa, G. A., Didjeira, A. (2012): Performance of extra-early maize cultivars based on GGE biplot and AMMI analysis. – Journal of Agricultural Science 150: 473-483.
[3] Balestre, M., Von Pinho, R. G., Souza, J. C., Oliverira, R. L. (2009): Genotypic stability and adaptability in tropical maize based on AMMI and GGE biplot analysis. – Genetics and Molecular Research 8(4): 1311-1322.
[4] Bai, J., Zhao, F., He, J., Wang, C., Chang, H., Zhang, J., Wang, D. (2014): GGE biplot analysis of genetic variations of 26 potato genotypes in semi-arid regions of Northwest China. – New Zealand Journal of Crop and Horticultural Science 42(3): 161-169.
[5] Blouin, D. C., Webster, E. P., Bond, J. A. (2015): On the analysis of combined experiments. – Weed Technology 25(1): 165-169.
[6] Dehghani, M. R., Majidi, M. M., Mirlohi, A., Saeidi, G. (2016): Study of genotype by environment interaction in tall fescue genotypes and their polycross progenies in Iran based on AMMI model analysis. – Crop and Pasture Science 67(7): 792-799.
[7] Dehghani, M. R., Majidi, M. M., Saeidi, G., Mirlohi, A., Amiri, R., Sorkhilalehloo, B. (2017): Application of GGE biplot to analyse stability of Iranian tall fescue (*Lolium arundinaceum*) genotypes. – Crop and Pasture Science 66(9): 963-972.
[8] Döring, T. F., Reckling, M. (2018): Detecting global trends of cereal yield stability by adjusting the coefficient of variation. – European Journal of Agronomy 99: 30-36.
[9] Duma, S. W., Shimelis, H., Ramburan, S., Shayanowako, A. I. T. (2019): Genotype-by-region interactions of released sugarcane varieties for cane yield in the South African sugar industry. – Journal of Crop Improvement 33(4): 478-504.
[10] Erdemci, I. (2016): Investigation of genotype × environment interaction in chickpea genotypes using AMMI and GGE biplot analysis. – Turkish Journal of Field Crops 23(1): 20-26.
[11] Farshadfar, E., Mahmodi, N., Uagjptopoor, A. (2011): AMMI stability value and simultaneous estimation of yield and yield stability in bread wheat (*Triticum aestivum* L.). – Australian Journal of Crop Science 5(13): 1837-1844.
[12] Fry, J. D. (1992): The mixed-model analysis of variance applied to quantitative genetics: biological meaning of the parameters. – Evolution 46(2): 540-550.
[13] Gauch, H. G. (1988): Model selection and validation for yield trials with interaction. – Biometrics 44(3): 705-715.
[14] Gauch, H. G. (1992): Statistical Analysis of Regional Yield Trials: AMMI Analysis of Factorial Designs. – Elsevier, Amsterdam.
[15] Gerrano, A. S., Rensburg, W. S. J. V., Adebola, P. O., Manjeru, P., Bairu, M. W., Venter, S. L. (2019): Evaluation and selection of taro [*colocasia esculentra* (L.) Schott] accessions under dryland conditions in South Africa. – Acta Agriculturae Scandinavica, Section B – Soil and Plant Science 69(3): 219-227.
[16] Huang, C. D., Liu, Q. Q., Li, X. L., Zhang, C. C. (2019): Effect of intercropping on maize grain yield and yield components. – Journal of Integrative Agriculture 18(8): 2-12.
[17] Kang, M. S. (1993): Simultaneous selection for yield and stability in crop performance trials: consequences for growers. – Agronomy Journal 85(3): 754-757.
[18] Kendal, E., Sayar, M. S. (2016a): The stability of some spring triticale genotypes using biplot analysis. – The Journal of Animal and Plant Science 26(3): 754-765.
[19] Kendal, E., Sayar, M. S., Tekdal, S., Aktas, H., Karaman, M. (2016b): Assessment of the impact of ecological factors on yield and quality parameters in triticale using GGE biplot and AMMI analysis. – Pakistan Journal of Botany 48(5): 1903-1913.

http://www.aloki.hu ● ISSN 1589 1623 (Print) ● ISSN 1785 0037 (Online)
DOI: http://dx.doi.org/10.15666/aeer/1802_35933614

[20] Kendal, E., Tekdal, S., Karaman, M. (2019): Proficiency of biplot methods (AMMI and GGE) in the appraisal of triticale genotypes in multiple environments. – Applied Ecology and Environmental Research 17(3): 5995-6007.
[21] Kaya, Y., Akcur, A. M., Taner, S. (2006): GGE-biplot analysis of multi-environment yield trials in bread wheat. – Turkish Journal of Agriculture and Forestry 30(5): 325-337.
[22] Li, S., Lei, Y. D., Zhang, Y. Y., Liu, J. G., Shi, X. Y., Jia, H., Wang, C., Chen, F., Chu, Q. Q. (2019): Rational trade-offs between yield increase and fertilizer inputs are essential for sustainable intensification: a case study in wheat–maize cropping systems in China. – Science of the Total Environment 679: 328-336.
[23] Lin, C. S., Butler, G., Hall, I., Nault, C. (1992): Program for investigating genotype-environment interaction. – Agronomy Journal 84(1): 121-124.
[24] Mehdipour, S., Rezaeiad, A., Azizinezhad, R., Etminan, A. (2019): Yield stability of rapeseed genotypes under drought stress conditions. – Indian Journal of Genetics and Plant Breeding 79(1): 40-47.
[25] Mitrovic, B., Stanisavljevi, D., Treski, S., Stojakovic, M., Ivanovic, M., Bekavac, G., Rajkovic, M. (2012): Evaluation of experimental maize hybrids tested in multi-location trials using AMMI and GGE biplot analysis. – Turkish Journal of Field Crops 17(1): 35-40.
[26] Mohamed, N. E. (2013): Genotype by environment interactions for grain yield in bread wheat (*Triticum aestivum* L.). – Journal of Plant Breeding and Crop Science 7(5): 150-157.
[27] Mohammadi, R., Armion, M., Zadhasan, E., Ahmadi, M. M., Amri, A. (2017): The use of AMMI model for interpreting genotype × environment interaction in durum wheat. – Experimental Agriculture 54(5): 670-683.
[28] Mortazavian, S. M., Nikkhah, H. R., Hassani, F. A., Harif-Al-Hosseini, M., Taheri, M., Mahlooji, M. (2014): GGE biplot and AMMI analysis of yield performance of barley genotypes across different environments in Iran. – Journal of Agricultural Science and Technology 16(3): 609-622.
[29] Mulema, J. M. K., Adipal, A. E., Olanya, O. M. (2008): Yield stability analysis of late blight resistant potato selections. – Experimental Agriculture 44(2): 145-155.
[30] Navas-Lopeza, J. F., Leóna, L., Trentacosteb, E. R., de la Rosaa, R. (2019): Multi-environment evaluation of oil accumulation pattern parameters in olive. – Plant Physiology and Biochemistry 139: 485-494.
[31] Nzuve, F., Githiri, S., Mukunya, D. M., Gethi, J. (2013): Analysis of genotype × environment interaction for grain yield in maize hybrids. – Journal of Agricultural Science 5(11): 75-85.
[32] Ndhlela, T., Herselman, L., Magorokosho, C., Labuschagne, M. (2014): Genotype × environment interaction of maize grain yield using AMMI biplots. – Crop Science 54(5): 1992-1999.
[33] Oral, E., Kendal, E., Dogan, Y. (2018): Selection the best barley genotypes to multi and special environments by AMMI and GGE biplot models. – Fresenius Environmental Bulletin 27(7): 5179-5187.
[34] Payne, R. W., Murray, D. A., Harding, S. A., Baird, D. B., Soutar, D. M. (2013): Introduction to GenStat for Windows. 15th Ed. – VSN International, Hemel Hempstead.
[35] Perkins, J. M. (1972): The principal component analysis of genotype-environmental interactions and physical measures of the environment. – Heredity 29(1): 51-70.
[36] Purchase, J., Hatting, H., Van Deventer, C. (2000): Genotype× environment interaction of winter wheat (*Triticum Aestivum* L.) in South Africa: II. stability analysis of yield performance. – South African Journal of Plant and Soil 17(3): 101-107.
[37] Raggi, L., Ciancaleoni, S., Torricelli, R., Terzi, V., Ceccarelli, S., Negri, V. (2017): Evolutionary breeding for sustainable agriculture: selection and multi-environmental evaluation of barley populations and lines. – Field Crops Research 204: 76-88.

http://www.aloki.hu ● ISSN 1589 1623 (Print) ● ISSN 1785 0037 (Online)
DOI: http://dx.doi.org/10.15666/aeer/1802_35933614

[38] Suwaero, N. (2011): Genotype × environment interaction for iron concentration of rice in central Java of Indonesia. – Rice Science 18(1): 75-78.
[39] Tang, Q. Y., Zhang, C. X. (2013): Data Processing System (DPS) software with experimental design, statistical analysis and data mining developed for use in entomological research. – Insect Science 20(2): 254-260.
[40] Vaezi, B., Pour-Aboughadareh, A., Mohammadi, R., Armion, M., Mehraban, A., Hossein-Pour, T., Dorii, M. (2017): GGE biplot and AMMI analysis of barley yield performance in Iran. – Cereal Research Communications 45(3): 500-511.
[41] Wang, S. Q., Jiang, X. W., Wang, S. D., Bu, J. Z., Wei, J. W., Chen, S. P., Peng, H. C., Xie, J. L., Yue, H. W., Li, H. S. (2019): Genotype by environment interaction analysis in summer maize hybrids for grain yield under multi-environment trials in Huang-Huai-Hai Area, China. – International Journal of Agriculture and Biology 22(6): 1573-1580.
[42] Yang, J. Z., Li, Y. C., Cao, H. B., Yao, H. L., Han, W., Sun, S. X. (2019): Yield-maturity relationships of summer maize from 2003 to 2017 in the Huanghuaihai plain of China. – Scientific Reports 9: 11417.
[43] Yan, W., Tinker, A. N. (2006): Biplot analysis of multienvironment trial data: principles and applications. – Canada Journal of Plant Science 86(3): 623-645.
[44] Yan, W., Kang, M. S., Ma, B., Woods, S., Cornelius, P. L. (2007): GGE biplot vs. AMMI analysis of genotype-by-environment data. – Crop Science 47(2): 643-655.
[45] Yan, W. K. (2001): GGE biplot-A windows application for graphical analysis of multienvironment-trial data and other types of two-way data. – Agronomy Journal 93(5): 1111-1118.
[46] Yan, W. K., Hunt, L. A., Sheng, Q., Szlavnics, Z. (2000): Cultivar evaluation and mega-environment investigation based on the GGE biplot. – Crop Science 40(3): 597-605.
[47] Yue, H. W., Bu, J. Z., Wei, J. W., Peng, H. C., Xie, J. X., Zheng, S. H., Jiang, X. W., Xie, J. L. (2018a): Effect of planting density on grain-filling and mechanized harvest grain characteristics of summer maize varieties in Huang-huai-hai plain. – International Journal of Agriculture and Biology 20(6): 1365-1374.
[48] Yue, H. W., Li, Y., Li, C. J., Bu, J. Z., Wei, J. W., Guo, A. Q., Chen, S. P., Peng, H. C., Xie, J. L., Jiang, X. W. (2018b): Grain filling characteristics of maize hybrids with different maturity periods. – International Journal of Agriculture and Biology 20(7): 1650-1656.
[49] Yue, H. W., Bu, J. Z., Wei, J. W., Zhang, Y. L., Chen, S. P., Peng, H. C., Xie, J. L., Jiang, X. W. (2019): Evaluation of the adaptability and stability of maize cultivars through GGE biplot analysis. – Fresenius Environmental Bulletin 28(9): 6719-6732.
[50] Yue, H. W., Wang, Y. B., Wei, J. W., Meng, Q. M., Yang, B. L., Chen, S. P., Xie, J. L., Peng, H. C., Jiang, X. W. (2020): Effects of genotype-by-environment interaction on the main agronomic traits of maize hybrids. – Applied Ecology and Environmental Research 18(1): 1437-1458.

http://www.aloki.hu ● ISSN 1589 1623 (Print) ● ISSN 1785 0037 (Online)
DOI: http://dx.doi.org/10.15666/aeer/1802_35933614

APPLICATION OF LIQUID PHOSPHORUS FERTILIZER IMPROVES THE AVAILABILITY OF PHOSPHORUS IN CALCAREOUS SOILS

ERENOĞLU, E. B.* – DÜNDAR, Ş.

Department of Soil Science and Plant Nutrition, Faculty of Agriculture, Çukurova University, Adana, Turkey

**Corresponding author*
e-mail: berenoglu@cukurova.edu.tr

(Received 17th Dec 2019; accepted 23rd Mar 2020)

Abstract. Increasing the efficiency of phosphorus (P) fertilizers is very important for using natural sources as well as minimizing possible environmental risks. Therefore, the effects of P, applied as mono-ammonium phosphate (MAP) in different forms (liquid and granule) and soil amendment containing humic-fulvic acids (HA + FA), on the growth and P uptake of model plant bread wheat (*Triticum aestivum* L. cv. Adana-99) and vertical movement of P in a calcareous soil were investigated. The application of P in a liquid form enhanced both P uptake and shoot growth in comparison to its granule form. However, HA + FA application had no effect on either P uptake or plant growth. Although the HA + FA did not affect biomass yield, it had a strengthening effect on vertical movement, even for P applied as a granule. The application of P in liquid form not only increased P movement in the soil but also enhanced the P nutritional status of wheat. In conclusion, the results, in a supportive manner to formerly obtained limited results, showed that the application of P containing liquid fertilizers, in comparison to granular ones as well as HA + FA addition might increase the efficiency of P fertilizers; and thus enhance yield and minimize the environmental concerns, as well.
Keywords: *nutrient efficiency, fluid, granule, phosphorus uptake, soil amendment*

Introduction

Increasing human population together with incorrect and unconscious consumption of natural resources necessitates a specific need to increase crop productivity per area. That is why the main objectives of today's agriculture are as follows: i) raising of crop yields to higher levels and ii) sustainability. Increasing the agricultural production to maximum levels will be possible by either expanding production areas or obtaining better yields per area. Since a further increase in existing agricultural areas does not seem feasible/possible, obtaining a higher yield per area appears to be the real target. One of the most critical factors that may ensure higher yields per area in a sustainable manner is sustainable plant production practices. As a well-known phenomenon, nutrient deficiencies are in the forefront among factors limiting the development of sustainable plant production (Fageria and Baligar, 2005) and 30-50% of the total increase in world food production since the 1950s has come about due to fertilizer additions (Stewart et al., 2005).

Agricultural production depends on phosphorus (P), which is a non-renewable natural resource derived from phosphate rocks (Cordell et al., 2009). However, a conflict exists with regard to how many years the available phosphate resources will last. While van Kauwenbergh (2010) opined that existing phosphate rocks reserves would be exhausted in 300-400 years or more, others emphasize that they would only last for 50-100 years (Cordell et al., 2009).

http://www.aloki.hu ● ISSN 1589 1623 (Print) ● ISSN 1785 0037 (Online)
DOI: http://dx.doi.org/10.15666/aeer/1802_36153626

As it is well recognized, P has the highest far-reaching effect after nitrogen (N) in both natural and agricultural ecosystems among fertilizer nutrients (Brady and Weil, 2008). However, approximately 5.7 billion ha of agricultural land on Earth contains P lower than the optimum level (Mouazen and Kuang, 2016).

Soil organic matter, pH, and exchangeable and soluble aluminum (Al), iron (Fe), and calcium (Ca) affect the availability of P for plant growth (Ulrich and Schnug, 2013). Since the mobility of P in soils is limited and, what is considered worse, exposed to fixation at high rates, plants cannot use it effectively. Plants can use only 10-25% of the P in fertilizers applied to the soil during the application season (Syers et al., 2008). In such a way, plants in the year of application use only a few portions of P in fertilizers, and the effectiveness of any residual P fertilizer decreases with time (Lombi et al., 2004a, b).

Alkaline soils represent a very significant part of the agricultural production area of the world (Holloway et al., 2001). According to the Food and Agriculture Organization (FAO), almost 800 million ha of soils worldwide are calcareous and mainly located in arid or semi-arid climates of both hemispheres (FAO, 2001). In general, high pH, clay, lime, and low organic matter are known as factors limiting the availability of P in soils (Gallet et al., 2003; Franson et al., 2003).

In calcareous soils, the application of fluid forms of P fertilizers results in higher P mobility (Lombi et al., 2004 a, b) and availability (Holloway et al., 2001). In the andisols and oxisols, as well, greater P diffusion is observed with the fluid form in comparison to the granular one (Montalvo et al., 2014), However, in contrast to calcareous soils, the liquid form of P does not have an enhancing effect on P availability in andisols and oxisols - lability and solubility (Montalvo et al., 2014).

It is well-known that the addition of soil amendments such as HA + FA may have positive effects on plant growth (Arjumend et al., 2015; Canellas and Olivares, 2014; Quilty and Cattle, 2011) and support the root development (Canellas and Olivares, 2014; Quilty and Cattle, 2011). Also, this application may increase the mobility/availability of fertilizer P (Zhen-Yu et al., 2013) and its recovery (Delgado et al., 2002).

For the above-mentioned reasons, it was evident that studies aimed at increasing the efficiency of P containing fertilizers may have outstanding contributions to plant production, thereby quelling the environmental concerns. Therefore, using a subsoil known for its low P availability and low P fertilizer use efficiency due to high pH, clay content, lime, and few organic matter, two experiments were designed. In the first experiment, to view the effects of different forms of MAP (fluid or granular) and soil amendment (HA + FA) applications on growth and P uptake, a pot experiment was set up using bread wheat (*Triticum aestivum*) as a model plant. Also, a column experiment was set up to analyze the effects of the above-mentioned variants on vertical P transport.

Materials and methods

Experimental soil and basal fertilization

The soil material used in the present work was clayey (63.5% clay, 19.6% sand, 16.9% silt), calcareous (17.8% $CaCO_3$), alkaline (pH 7.5), and low organic matter containing (0.12% OM) subsurface soil. The available P and potassium (K) contents of soil were found to be 1.5 kg $P_2O_5 \cdot ha^{-1}$ and 462 kg $K_2O \cdot ha^{-1}$, respectively.

http://www.aloki.hu ● ISSN 1589 1623 (Print) ● ISSN 1785 0037 (Online)
DOI: http://dx.doi.org/10.15666/aeer/1802_36153626

The experimental soil was fertilized with the following rates of basal nutrients (in $mg \cdot kg^{-1}$ soil): 200 N (as NH_4NO_3 + [MAP]), 100 K (as K_2SO_4), 5.0 Fe (as Fe(III)EDDHA, 2.5 Zn (as $ZnSO_4 \cdot 7H_2O$), 2.5 Mn (as $MnSO_4$), and 1.0 Cu (as $CuSO_4 \cdot 7H_2O$). As mentioned earlier, the soil had very low P availability, so a basal P fertilization was also included in the amount of 5.0 $mg \cdot kg^{-1}$ soil as TSP. Since varied amounts of NH_4-N came from different rates of MAP, after subscription of those NH_4-N amounts from the total N (200 $mg \cdot kg^{-1}$ soil), the rest of it was added using NH_4NO_3.

Fertilizer forms, HA + FA, and P uptake - Experiment I

In this part, a pot experiment was conducted in a growth chamber under controlled climatic conditions [light:dark periods, 16:8 h; temperature (light:dark), 22:18 °C; relative humidity (light:dark), 60:70%; photosynthetic flux density, 250 μmol $m^{-2}s^{-1}$] to view the effects of fertilizer forms and their application rates, presence of HA + FA mixture as soil amendments on plant growth, and P uptake using pots contained 1 kg of soil in each. For this, a bread wheat cultivar (*Triticum aestivum* L cv. Adana-99) was used as a model plant. While MAP-P was added at three rates (0, 25, 50, and 100 mg $P \cdot kg^{-1}$ soil) as either granule or fluid, HA + FA mixture was applied at two rates (0 and 125 mg $[HA + FA] \cdot kg^{-1}$ soil) using a commercial product (TKI-Hümas, Coal Enterprises Association of Turkey). The HA + FA mixture, together with other basal nutrients (given above) was mixed with soil. Thereafter, all of the granular and fluid MAP applications were performed 2.5 cm below the soil surface shortly before sowing. While granule numbers were kept equal for each rate of P (6 granules per pot) to eliminate the effect of spatial variations, liquid applications were performed in 50 mL of distilled water. After sowing five seeds per pot, seedlings were thinned to 3 $plants \cdot pot^{-1}$. Every two days, pots were regularly weighed and watered at 50% of the field capacity for the first week and 75% for the following weeks. At the end of the 30-day experimental period, the shoots were harvested, dried at 65 °C, weighed, and dry ashed; then, P concentrations were determined. After the above-ground parts were cut off, the roots in pots were washed carefully with deionized water, and dried at 65 °C to measure their dry weights. Thereafter, their P contents were determined as well.

Fertilizer forms, HA + FA, and vertical P transport - Experiment II

A disrupted soil column experiment was designed to investigate the effects of fertilizer forms and HA + FA on the vertical transport of P in soil. Here, columns prepared with an inner diameter of 6.9 cm and a height of 23 cm were used (*Fig. 1A*). In the middle of the 0-5 cm, 5-10 cm, 10-15 cm, and 15-20 cm sections below the first 3 cm from the top, there were 4 mm holes in which soil solution sampling sticks of 2.5 mm diameter existed. The columns were filled with soil subjected to incubation with 5 or 100 mg $P \cdot kg^{-1}$ soil, with or without application of HA + FA at 125 mg HA + $FA \cdot kg^{-1}$ soil level for two weeks, at a bulk density of 1.1 $g\ cm^3$. In the experiment, the application forms were a granular and fluid MAP, and the application dose was 100 mg $P \cdot kg^{-1}$ soil. Both types of MAP were employed 2.5 cm below the soil surface, and deionized water was added to the columns until they reached field capacity. Twenty-four hours after application, the samples of soil solution were taken using soil solution samplers (Rhizone Sampling), which were made of a porous plastic material (*Fig. 1B*) and sucking them with the help of vacuum tubes. Since the pore diameters of the samplers are 0.15 μm, the P measured in the solutions obtained is deemed to be colloid-

http://www.aloki.hu ● ISSN 1589 1623 (Print) ● ISSN 1785 0037 (Online)
DOI: http://dx.doi.org/10.15666/aeer/1802_36153626

free soil solution P (McDowell and Sharply, 2001; Shand et al., 2000). Since the sophistication of experimental design (especially solution sampling step) would not let us have multiple replicas in *Experiment II*, statistical analysis was *not applicable*.

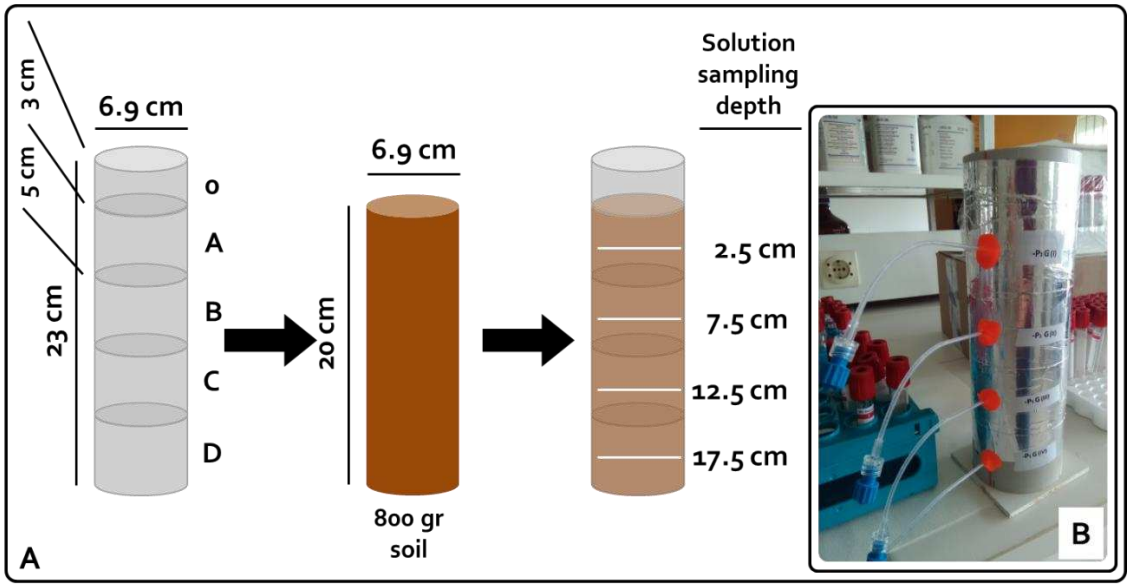

Figure 1. *Experimental design of fertilizer forms, HA + FA, and vertical P transport experiment. (A) Design of a column and solution sampling points in it and (B) a column ready for sampling*

Statistics

All the values obtained in *Experiment I* were subjected to analysis of variance using the statistical package software 'SPSS STATISTICS 20'. Since there was no statistical effect of HA + FA recorded for each parameter measured, traits with or without HA + FA application were evaluated separately. The averages of measured parameters with different traits were compared using the Duncan test at the probability level of $P \leq 0.05$, and the differentiating averages were shown with different characters.

Results

Fertilizer forms, HA + FA, and P uptake - experiment I

Plant growth

Even though soils fertilized with a basal P level of 5 mg $P \cdot kg^{-1}$ soil, due to shallow Olsen P level of soil, were used in the experiment, the control plants showed very severe P deficiency symptoms. On day 24, grayish-brown necrosis, which was different from typical P deficiency symptoms such as growth regression in shoot growth and purpling on old leaves, was visible. As the symptoms on control plants became severe, the experiment was terminated on day 30.

The plant observations at harvest showed that P application, together with increments in P rates, had a positive effect on plant growth. In *Table 1*, there are some growth parameters such as shoot and roots dry weights and root-to-shoot ratios. As given in this

http://www.aloki.hu ● ISSN 1589 1623 (Print) ● ISSN 1785 0037 (Online)
DOI: http://dx.doi.org/10.15666/aeer/1802_36153626

table and *Figure 2*, the P applied in the fluid form of the MAP showed a statistically important higher effect on the shoot growth of plants compared to the ones supplied with the granular MAP. Compared to plants provided with the fluid MAP, root/shoot ratios, an indicator of P nutrition of plants, of plants fertilized with granule MAP in both the presence and absence of HA + FA were higher, and this was statistically important (*Table 1*). Although increasing P application rates had a positive effect on both shoot and root dry weights of bread wheat, HA + FA mixture used as soil amendments did not affect plant growth (*Table 1*). Also, *Figure 2* taken on the day of harvest shows that independent of HA + FA application, tillering density and stalk thickness was higher in plants supplied with a fluid MAP than granule MAP.

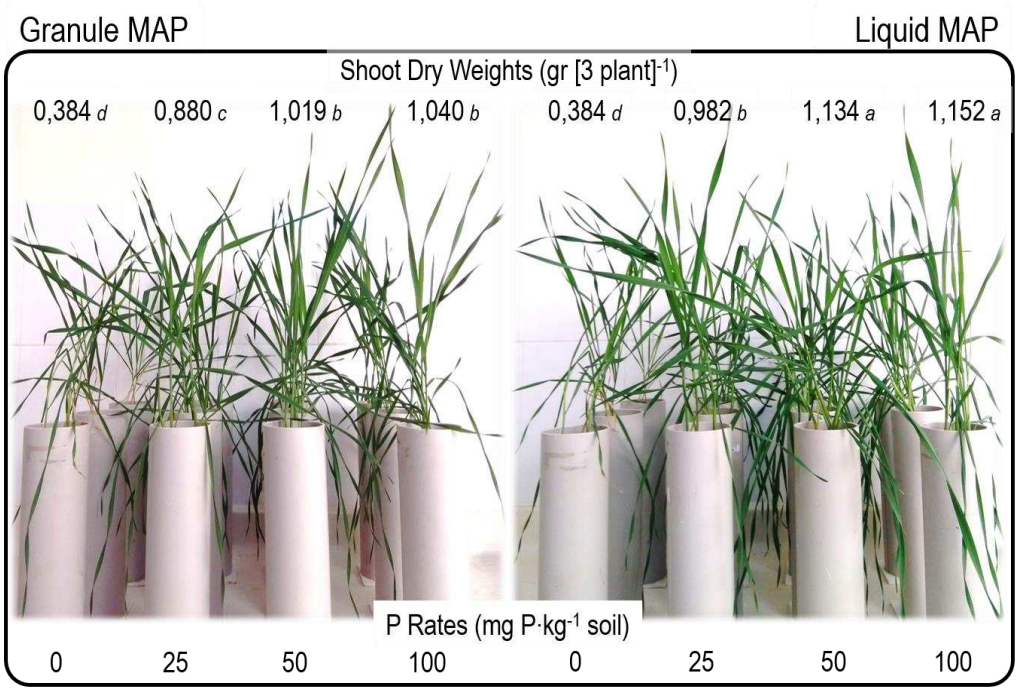

Figure 2. *Shoot dry weights and growth of model plant bread wheat grown with fluid or granule forms of the MAP and different P rates (- [HA + FA]). Dry weight values are means of three independent replicates. For each trait, numbers with different letters are significantly different from each other at $p < 0.05$, according to ANOVA and Duncan's test*

Phosphorus uptake

As clearly seen in *Table 2,* independent of the application form of MAP-P and HA + FA addition, increasing rates of P moved the P contents per shoot or root dry matter up in comparison to the control plant. However, this increment was more evident for the plants grown with fluid MAP, and the effect was statistically significant as well. Even the P concentration in the shoot of plant supplied with the fluid MAP at the lowest P rate was higher than granule applications at all P levels without HA + FA (*Table 2*). Parallel to this, when plants were supplied with HA + FA, the P concentration in the shoot of plants supplied with the fluid MAP at the lowest P rate was similar to plants provided with granule MAP at the highest P rate and higher than the other two lower P rates (*Table 2*).

http://www.aloki.hu ● ISSN 1589 1623 (Print) ● ISSN 1785 0037 (Online)
DOI: http://dx.doi.org/10.15666/aeer/1802_36153626

Table 1. *Shoot and root dry weights and roots to shoot ratio of model plant bread wheat grown with granule or fluid forms of the MAP and different P rates and with or without HA + FA application. The values are the means of three independent replicates. For each trait, numbers with different letters are significantly different from each other at $p < 0.05$, according to ANOVA and Duncan's test*

Fertilizer form	P rates (mg P kg^{-1} soil)	Dry weights (g [3 plants]$^{-1}$)		Roots/shoot
		Shoot	Roots	
		-[HA + FA]		
-	0	0.38 d	0.16 c	0.41 ab
Granule	25	0.88 c	0.39 ab	0.45 a
	50	1.02 b	0.43 a	0.42 a
	100	1.04 b	0.43 a	0.41 ab
Fluid	25	0.98 b	0.38 ab	0.39 ab
	50	1.13 a	0.35 b	0.31 c
	100	1.15 a	0.42 a	0.36 bc
		+[HA + FA]		
-	0	0.37 e	0.19 d	0.49 a
Granule	25	0.83 d	0.36 abc	0.43 abc
	50	0.92 cd	0.42 ab	0.45 a
	100	1.00 bc	0.44 a	0.44 ab
Fluid	25	0.92 cd	0.33 c	0.36 bcd
	50	1.07 ab	0.34 bc	0.32 d
	100	1.12 a	0.39 abc	0.35 cd

Table 2. *Phosphorus contents per shoot and roots dry weights (%) in shoot and roots of model plant bread wheat grown with granule or fluid forms of the MAP and different P rates and with or without HA + FA application. The values are the means of three independent replicates. For each trait, numbers with different letters are significantly different from each other at $p < 0.05$, according to ANOVA and Duncan's test*

Fertilizer form	P rates (mg P·kg^{-1} soil)	P concentration (%)			
		- [HA + FA]		+ [HA + FA]	
		Shoot	Roots	Shoot	Roots
-	0	0.17 *d*	0.11 *e*	0.16 *d*	0.13 *d*
Granule	25	0.22 *c*	0.14 *de*	0.21 *c*	0.16 *cd*
	50	0.26 *b*	0.16 *cd*	0.24 *c*	0.15 *cd*
	100	0.28 *b*	0.21 *ab*	0.28 *b*	0.20 *b*
Fluid	25	0.30 *b*	0.18 *bc*	0.27 *b*	0.18 *bc*
	50	0.37 *a*	0.22 *a*	0.36 *a*	0.25 *a*
	100	0.39 *a*	0.21 *ab*	0.37 *a*	0.26 *a*

As a result of better growth and higher P uptake, independent of the application forms of MAP and HA + FA application, increasing rates of P enhanced the P content

http://www.aloki.hu ● ISSN 1589 1623 (Print) ● ISSN 1785 0037 (Online)
DOI: http://dx.doi.org/10.15666/aeer/1802_36153626

per shoot, roots, and whole plant in comparison to control plants (*Table 3*). Moreover, with or without soil amendment application, the P content per shoot, roots, and whole plant in plants grown with fluid or granule form of MAP considered together, it was seen that plants supplied with fluid ones had higher P contents and this difference was statistically significant (*Table 3*). The P content per plant with or without HA + FA application showed that there was no difference among the plants.

Table 3. *Phosphorus contents per shoot, roots, shoot, and the whole plant in shoot and roots of model plant bread wheat grown with granule or fluid forms of the MAP and different P rates and with or without HA + FA application. The values are the means of three independent replicates. For each trait, numbers with different letters are significantly different from each other at $p < 0.05$, according to ANOVA and Duncan's t-test*

Fertilizer form	**P rates (mg P kg^{-1} soil**	**P uptake (mg P·[3 plants]$^{-1}$)**		
		Shoot	**Roots**	**Shoot + roots**
		-[HA + FA]		
-	0	0.66 *d*	0.17 *e*	0.84 *d*
Granule	25	1.97 *c*	0.53 *d*	2.50 *c*
	50	2.67 *b*	0.70 *bc*	3.37 *b*
	100	2.88 *b*	0.90 *a*	3.78 *b*
Fluid	25	2.90 *b*	0.68 *cd*	3.58 *b*
	50	4.17 *a*	0.77 *abc*	4.94 *a*
	100	4.50 *a*	0.85 *ab*	5.35 *a*
		+ [HA + FA]		
-	0	0.60 *f*	0.23 *d*	0.83 *f*
Granule	25	1.75 *e*	0.57 *c*	2.33 *e*
	50	2.18 *d*	0.61 *b*	2.81 *d*
	100	2.84 *c*	0.90 *a*	3.74 *c*
Fluid	25	2.53 *c*	0.59 *b*	3.12 *d*
	50	3.81 *b*	0.84 *a*	4.65 *b*
	100	4.18 *a*	1.03 *a*	5.21 *a*

Fertilizer forms, HA + FA, and vertical P transport - Experiment II

The results of the disrupted soil column experiment, which was conducted to investigate the effects of fertilizer forms and rates and HA + FA on the vertical transport of P in the soil, are displayed in *Table 4*. As mentioned above, the columns prepared with an inner diameter of 6.9 cm and a height of 23 cm were used (*Fig. 1A*), and P was applied either as fluid or granule to the horizontal mid-point of the top cylinder. After a 24-h incubation period, the soil solution samples were taken from the middle of each cylinder using a soil solution sampler to analyze them for P (*Fig. 1B*).

Table 4 shows the P concentrations in soil solution samples. As it is clearly reflected, the vertical movement of MAP-P, which was applied as granule with or without HA + FA application, was much lower than when it was applied as fluid. In the columns supplied with the granule MAP-P and no soil amendment, and in the soil solution samples taken from 7.5 cm and deeper, no P was measurable, showing bordered movement of P (*Table 4*). However, even in the soil solution samples taken from the

http://www.aloki.hu ● ISSN 1589 1623 (Print) ● ISSN 1785 0037 (Online)
DOI: http://dx.doi.org/10.15666/aeer/1802_36153626

mid-point (15 cm away from application point) of the bottom-standing cylinder of columns, the P could be measured 24 h after application. Phosphorus could be detected even in the soil solution samples taken 5 cm below application points of columns pre-cultured with HA + FA and to which the granule MAP-P was applied, as opposed to columns precultured without HA + FA.

Table 4. *The P concentrations in the soil solution samples taken from the application points and vertically 5, 10, and 15 cm away from them in the columns pre-cultured 5 or 100 mg P·kg^{-1} soil and with or without HA + FA for two weeks*

Pre-culture (mg kg^{-1} soil)		**Fertilizer form**	**P concentration in soil solution (µg mL^{-1}) The position of sampling stick (cm from the top of soil surface**			
HA + FA	P		2.5	7.5	12.5	17.5
–	5	Granule	6.34	0.00	0.00	0.00
	100		19.24	0.00	0.00	0.00
	5	Fluid	2.91	1.31	1.00	0.26
	100		3.87	4.18	0.50	0.00
+	5	Granule	5.87	1.37	0.00	0.00
	100		5.09	1.15	0.00	0.00
	5	Fluid	1.29	1.10	0.30	0.10
	100		1.97	7.26	1.60	1.20

Moreover, the mobility of P in the columns supplied with the fluid MAP and pre-cultured with HA + FA and 100 mg P·kg^{-1} soil was even better than columns without HA + FA; even the solution samples taken from 15 cm away from application point contained higher P concentrations. However, there were no apparent differences in the P movement of soils pre-cultured with different amounts of P within a given form of MAP fertilizer.

Discussion

According to Fageria and Baligar (2005), one of the essential details that cause problems in sustainable crop production is the inadequacy of nutrient element(s). The nutrient capital of soils is not unlimited and should be renewed depending on the amounts of nutrients removed from the land. In addition to this renewal, the primary aim involves minimizing the risk of environmental contamination and maximizing the contribution of plant nutrients to vegetative production by ensuring the most effective use of the nutrients by plants.

Although the most critical roles of P in vegetative life are energy transfer and storage, it is also found in the structure of many components, which are essential for growth and development, such as nucleic acids, nucleotides, coenzymes, phospholipids, phosphoproteins, and sugar phosphates (Vance et al., 2003). Incongruity involves an increase in the shoot growth of model plant wheat with the P application as well as an increase in P rates (*Table 2*) fitted well in those roles of P in plant nutrition. However, gray-brown necrosis and very severe growth regression differed from the typical P deficiency symptoms of regressive growth and purpling in old leaves (Snowball and Robson, 1983) of control plants cultivated on the experimental soil with very low

http://www.aloki.hu ● ISSN 1589 1623 (Print) ● ISSN 1785 0037 (Online)
DOI: http://dx.doi.org/10.15666/aeer/1802_36153626

available P being observed. The reason for this might be the problems encountered with the use of photosynthesis products and that occur in severe P deficiency (Carstensen et al., 2018). Moreover, independent of HA + FA application, the higher roots-to-shoot ratios of plants supplied with granule MAP in comparison to the plants provided with the fluid form of MAP (*Table 3*) may be an indicator of severe P deficiency (Andrews et al., 1999; Zhang et al., 2012).

Although increasing rates of P increased both shoot and roots growths, the soil amendment application had no positive effect on plant growth (*Table 3*). This result was in contrast to the results of those studies in which the HA + FA mixture had positive effects on plant growth (Arjumend et al., 2015; Canellas and Olivares, 2014; Quilty and Cattle, 2011). The possible reason for this might be the termination of the experiment after 30 days, as the control plant showed fast and severe P deficiency stress due to very low organic matter content (0.12%) or very low Olsen P in the soil. It is a well-known phenomenon that the root growth is very active on P uptake (Wang et al., 2016), and HA + FA supports the development of root growth (Canellas and Olivares, 2014; Chunhua et al., 1998; Quilty and Cattle, 2011). Due to the limited volume of soil in a narrow design pot, the superior effect of HA + FA application on root growth in comparison to plants grown without HA + FA might have been prevented, since the roots of plants grown without HA + FA application could easily reach to the nutrients in the pots.

Consistent with a study carried out in the calcareous soils of Australia by Holloway and colleagues (2001), the plant observations as well as the shoot dry weights (*Table 1*) obtained from the harvested plants on the 30th day after planting indicated that fluid P improved the plant development relative to granule. As mentioned before, roots/shoot ratio is an indication of P nutrition in plants, as it increases when they suffer from P deficiency (Andrews et al., 1999; Zhang et al., 2012). Accordingly, the model plant wheat supplied with no P or granular MAP-P, irrespective of soil amendments application, had higher root-to-shoot ratio values than plants supplied with fluid MAP-P with the same rates of granule ones (*Table 1*). It is well known that P moves in soil with diffusion (Marschner, 2012), and its application in fluid form in calcareous soils showed higher mobility and distribution than its granular forms (Lombi et al., 2004a, b). Therefore, the higher root/shoot ratios of plants, grown with granule MAP-P as in control plants and in comparison to plants fertilized with fluid MAP-P (*Table 1*), might be the higher P deficiency stress as a result of limited P mobility in case of granular MAP-P application. Lower P concentrations in the shoots of plants supplied with granular MAP-P compared to the plants grown with the same rates of the fluid MAP (*Table 2*) also supports the argument. This result is consistent with the knowledge that P applied to the band as a fluid responds better than in the granular form (Holloway et al., 2001). However, although they had found a supporting effect of fluid P application on grain yield of wheat in the field conditions, they did not observe any increase in P concentrations in the leaf tissue (Holloway et al., 2001).

According to the growth parameters (*Table 1*) and P nutritional status (*Tables 2* and *3*) of model plant wheat, the application of P as fluid instead of granular improved its mobility in the soil (*Table 4*). In the common opinion, while the P precipitation occurs at high concentrations of soil solution P, the P adsorption takes place at low levels (Castro and Torrent, 1998; Saavedra and Delgado, 2005). Therefore, it might be assumed that the precipitation of Ca-phosphates arises in the soil surrounding fertilizer granule where the P concentration is higher than the bulk soil (Holloway et al., 2001;

http://www.aloki.hu ● ISSN 1589 1623 (Print) ● ISSN 1785 0037 (Online)
DOI: http://dx.doi.org/10.15666/aeer/1802_36153626

Lombi et al., 2004a, b). So, the reason for higher mobility (or longer vertical movement) of P applied as the fluid MAP (*Table 4*) might be less Ca-phosphate precipitation in comparison to the granular MAP application. However, in contrast to calcareous soils, although the liquid form of P may increase the mobility of P in andisols and oxisols, it does not have an enhancing effect on P availability - lability and solubility (Montalvo et al., 2014). It is known that organic compounds may decrease the P fixation capacity of soils (Brady and Weil, 2008), and humates can bind P (von Wandruszka, 2006). Parallel to this, the application of HA + FA caused an increment even in the mobility of P applied in the granular form. This result fits well with the results of a study showing that HA application supports the movement of MCP-P to long distances, thereby increasing its mobility (Zhen-Yu et al., 2013).

Moreover, in a survey conducted by Delgado et al. (2002), the soil amendment with HA + FA increased the recovery of fertilizer P. However, in that study, they had tested extremely high amounts of HA + FA (from 1000 to 5000 mg [HA + FA]·kg^{-1} soil) which were much higher than applied in practice. Also, all the experiments related to the mobility of P in soils had been conducted during an extended incubation period (Delgado et al., 2002; Lombi et al., 2004a, b; Zhen-Yu et al., 2013), but in the present work, we analyzed the mobility of P in a period as limited as 24 h.

Conclusions

Our study, propelled by limited previous research activities, showed that liquid forms of P containing fertilizers might increase the efficiency of P fertilizers, expanding both P mobility and availability in soils with high $CaCO_3$ and clay. As a natural result of it, the P application in the form of the fluid MAP led to higher uptake of P than plants supplied with the granular MAP. Therefore, under suitable conditions/regions, the growers may prefer liquid forms of P containing fertilizers to ensure higher yields and protect the environment from the hazardous effect of excess P. However, to test the actual contribution of this phenomenon, additional experiments are needed under field conditions. Moreover, the addition of HA + FA enhanced the mobility of P in the soil in both forms of MAP, in particular, fluid form of it. Although such an amendatory effect of HA + FA on P mobility existed, its application did not play a decisive role in either the growth or P uptake of the model plant. The reason for this might be the extreme behaviors of experimental materials such as soil with extremely low OM and plant available P or very narrow designed pots. Further detailed experiments are required to clarify this point.

Acknowledgments. The present manuscript was prepared using the results of Şeyhmus Dündar's MSc thesis, which was granted by the Scientific Research Projects Coordination Unit at Çukurova University.

REFERENCES

[1] Andrews, M., Sprent, J. I., Raven, J. A., Eady, P. E. (1999): Relationships between shoot to root ratio, growth and leaf soluble protein concentration of *Pisum sativum*, *Phaseolus vulgaris* and *Triticum aestivum* under different nutrient deficiencies. – Plant Cell & Environment 22: 949-958.

http://www.aloki.hu ● ISSN 1589 1623 (Print) ● ISSN 1785 0037 (Online)
DOI: http://dx.doi.org/10.15666/aeer/1802_36153626

[2] Arjumend, T., Abbasi, M. K., Rafique, E. (2015): Effects of lignite derived humic acid on some selected soil properties, growth and nutrient uptake of wheat (*Triticum aestivum* L.) grown under greenhouse conditions. – Pakistan Journal of Botany 47: 2231-2238.
[3] Brady, N. C., Weil, R. R. (2008): The Nature and Properties of Soils. – Pearson-Prentice Hall, Upper Saddle River, NJ.
[4] Canellas, L. P., Olivares, F. L. (2014): Physiological responses to humic substances as plant growth promoter. – Chemical and Biological Technologies in Agriculture 1: 3. https://doi.org/10.1186/2196-5641-1-3.
[5] Carstensen, A., Herdean, A., Schmidt, S. B., Sharma, A., Spetea, C., Pribil, M., Husted, S. (2018): The impacts of phosphorus deficiency on the photosynthetic electron transport chain. – Plant Physiology 177: 271-284.
[6] Castro, B., Torrent, J. (1998): Phosphate sorption by calcareous Vertisols and Inceptisols as evaluated from extended P-sorption curves. – European Journal of Soil Science 49: 661-667.
[7] Chunhua, L., Cooper, R. J., Bowman, D. C. (1998): Humic acid application affects photosynthesis, root development, and nutrient content of creeping bentgrass. – HortScience 33: 1023-1025.
[8] Cordell, D., Drangert, J. O., White, S. (2009): The story of phosphorus: global food security and food for thought. – Global Environmental Change 19: 292-305.
[9] Delgado, A., Madrid, A., Kassem, S., Andreu, L., del Campillo, M. D. C. (2002): Phosphorus fertilizer recovery from calcareous soils amended with humic and fulvic acids. – Plant and Soil 245: 277-286.
[10] Fageria, N. K., Baligar, V. C. (2005): Enhancing nitrogen use efficiency in crop plants. – Advances in Agronomy 88: 97-185**.**
[11] FAO (2001): World Soil Resources Reports 94. – Lecture Notes on the Major Soils of the World. FAO, Rome.
[12] Franson, A., Aarle, I. M., Olsson, P. A., Tyler, G. (2003): *Plantago lanceolata* L. and *Rumex acetosella* L. differ in their utilization of soil phosphorus fractions. – Plant and Soil 248: 285-295.
[13] Gallet, A., Flish, R., Ryser, J., Nosberger, J., Frossard, E., Sinaj, S. (2003): Uptake of residual phosphate and freshly diammonium phosphate by Lolium perenne and Trifolium repens. – Journal of Plant Nutrition and Soil Science166: 557-567.
[14] Holloway, R. E., Bertrand, I., Frischke, A. J., Brace, D. M., McLaughlin, M. J., Shepperd, W. (2001): Improving fertilizer efficiency on calcareous and alkaline soils with fluid sources of P, N, and Zn. – Plant and Soil 236: 209-219.
[15] Lombi, E., McLaughlin, M. J., Johnston, C., Armstrong, R. D., Holloway, R. E. (2004a). Mobility and lability of phosphorus from granular and fluid mono-ammonium phosphate differs in calcareous soil. – Soil Science Society of America Journal 68: 682-689.
[16] Lombi, E., McLaughlin, M. J., Johnston, C., Armstrong, R. D., Holloway, R. E. (2004b). Mobility, solubility, and lability of fluid and granular forms of P fertilizer in calcareous and non-calcareous soils under laboratory conditions. – Plant and Soil 269: 25-34.
[17] Marschner, P. (2012): Mineral Nutrition of Higher Plants. – Academic Press Elsevier, New York.
[18] McDowell, R. W., Sharply, A. N. (2001): Soil phosphorus fractions in solution: influence of fertilizer and manure, filtration and method of determination. – Chemosphere 45: 737-748.
[19] Montalvo, D., Degryse, F., McLaughlin, M. J. (2014): Fluid fertilizers improve phosphorus diffusion but not lability in andisols and oxisols. – Soil Science Society of America Journal 78(1): 214-224.
[20] Mouazen, A. M., Kuang, B. (2016): On-line visible and near-infrared spectroscopy for in-field phosphorous management. – Soil & Tillage Research 155: 471-477.
[21] Quilty, J., Cattle, S. (2011): Use and understanding of organic amendments in Australian agriculture: a review. – Soil Research 49: 1-26.

http://www.aloki.hu ● ISSN 1589 1623 (Print) ● ISSN 1785 0037 (Online)
DOI: http://dx.doi.org/10.15666/aeer/1802_36153626

[22] Saavedra, C., Delgado, A. (2005): Phosphorus fractions and release patterns in typical Mediterranean soils. – Soil Science Society of America Journal 69: 607-615.
[23] Shand, C. A., Smith, S., Edwards, A. C., Fraser, A. R. (2000): Distribution of phosphorus in particulate, colloidal and molecular-sized fractions of soil solution. – Water Research 34: 1278-1284.
[24] Snowball, K., Robson, A. D. (1983): Symptoms of Nutrient Deficiencies: Subterranean Clover and Wheat. – University of Western Australia, Perth.
[25] Stewart, W. M., Dibb, D. W., Johnston, A. E., Smyth, T. J. (2005): The contribution of commercial fertilizer nutrients to food production. – Agronomy Journal 97: 1-6.
[26] Syers, J. K., Johnston, A. E., Curtin, D. (2008): Efficiency of soil and fertilizer phosphorus use: reconciling changing concepts of soil phosphorus behavior with agronomic information. – FAO Fertilizer and Plant Nutrition Bulletin; 2008/18. Food and Agriculture Organization of the United Nations (FAO), Rome.
[27] Ulrich, A., Schnug, E. (2013): The modern P sustainability movement: a profiling experiment. – Sustainability 5: 4523-4545.
[28] Van Kauwenbergh, S. (2010): World Phosphate Rock Reserves and Resources. – IFDC Technical Bulletin 75. International Fertilizer Development Centre, Muscle Shoals, Alabama.
[29] Vance, P. C., Uhde-Stone, C., Allan, D. (2003): Phosphorus acquisition and use: Critical adaptations by plants for securing a nonrenewable resource. – New Phytologist 157: 423-447.
[30] Von Wandruszka, R. (2006): Phosphorus retention in calcareous soils and the effect of organic matter on its mobility. – Geochemical Transactions 7: 6.
[31] Wang, Y., Thorup-Kristensen, K., Jensen, L. S., Magid, J. (2016): Vigorous root growth is a better indicator of early nutrient uptake than root hair traits in spring wheat grown under low fertility. – Frontiers in Plant Sciences 7: 865. DOI: 10.3389/fpls.2016.00865.
[32] Zhang, B. G., Chen, Q. X., Yang, Q., Liu, K. D. (2012): Effects of NPK deficiencies on root architecture and growth of cucumber. – International Journal of Agriculture and Biology 14: 145-148.
[33] Zhen-Yu, D., Qing-Hua, W., Fang-Chun, L., Hai-Lin, M., Bing-Yao, M., Malhi, S. S. (2013): Movement of phosphorus in a calcareous soil as affected by humic acid. – Pedosphere 23: 229-235.

http://www.aloki.hu ● ISSN 1589 1623 (Print) ● ISSN 1785 0037 (Online)
DOI: http://dx.doi.org/10.15666/aeer/1802_36153626

COMPARISON OF BREAD WHEAT (*Triticum aestivum* L.) LINES WITH REGISTERED CULTIVARS IN TERMS OF YIELD AND QUALITY CHARACTERISTICS

KARAMAN, M.[1*] – AKTAS, H.[2]

[1]*Department of Plant Production Technologies, Faculty of Applied Sciences, Mus Alparslan University, Mus, Turkey*

[2]*Kiziltepe Vocational School, Mardin Artuklu University, Mardin, Turkey*

**Corresponding author*
e-mail: karaman2178@hotmail.com; phone: +90-530-600-9136; fax: +90-436-231-2201

(Received 19th Dec 2019; accepted 24th Mar 2020)

Abstract. The study was carried out under rainfall conditions during the 2011-2012 and 2012-2013 growing seasons in Diyarbakir province of Turkey. The experiment had designed as a randomized block design with 3 replications. The aim of the study was to determine the lines that were superior in terms of yield and quality to the varieties. The experimental material consisted of 20 bread wheat lines and 5 standard varieties. According to the results of variance analysis; significant differences were observed between genotypes in all features at 1%. Grain yield (GY) had a significant positive relationship with test weight (TW), and a significant negative relationship with wet gluten (WG). Also, grain hardness (GH) (PSI: Particle size index) had significant negative relationship with TW, and a significant positive relationship with plant height (PH) and heading time (HT). 4 lines in grain yield, 3 lines in test weight, 1 line in protein content, 4 lines in zeleny sedimentation and 1 line in wet gluten showed superior performance than all standards. It is concluded that the G19 and G24 lines may be candidates for registration.
Keywords: *correlation, grain hardness, protein content, wet gluten*

Introduction

Wheat has been a main source of nutrient throughout the ages, and it continues to strengthen its role in human life. 23.4 million hectare of agricultural land is cultivated in Turkey, It is reported that the area allocated for agricultural activities except fallow areas is 66.4%. Also, it is reported that cereal sowing amount has 71% share in this area and wheat cultivation takes first place among cereals in proportion (TSI, 2018).

The center of origin of wheat in the world and also the first place where wheat and barley cultivation is made is called fertile crescent. Southeast Anatolia Region is located in fertile crescent region. So, of Turkey it is considered to have a significant track record in wheat breeding and commissioning culture of wheat (Cıvgın, 2016; Aktas, 2017).

Central Anatolia Region in wheat production in Turkey takes first place with rate of 33.5%. Southeastern Anatolia Region ranks second in wheat production with a rate of 16.5% (TSI, 2018). Diyarbakir is one of the important provinces of Southeastern Anatolia Region in wheat production. 1.1 million tons of wheat is produced in Diyarbakir. This amount constitutes 3.5% of the total wheat production in Turkey (TSI, 2018). The annual per capita wheat consumption in Turkey is over 200 kg. Due to the high daily consumption per capita and being one of the most important caloric sources of Turkish people, wheat maintains its strategic importance (Morgounov et al., 2016).

It has been reported that the amount of protein in the grain is affected significantly by environmental conditions (climate, fertilizer amount, irrigation, etc.) and also the

http://www.aloki.hu ● ISSN 1589 1623 (Print) ● ISSN 1785 0037 (Online)
DOI: http://dx.doi.org/10.15666/aeer/1802_36273638

inheritance factor is an important determinant on quality parameters in wheat grown in both irrigated and rainfall conditions (Grausgruber et al., 2000; Souza et al., 2004).

It is emphasized that the amount of protein in bread wheat is important in determining quality. However, since the amount of protein alone is not sufficient, it has been reported that the amount of sedimentation and gluten should be taken into account (Gooding et al., 2003). Plant breeders aim to develop genotypes with high grain yield, quality and ability to adapt to different environments (Kendal and Sener, 2015).

With this purpose, study was conducted in Diyarbakir conditions in Turkey. After comparing the wheat lines of abroad origin with registered varieties in terms of yield and quality characteristics, the lines that can be high performance candidates were determined.

Materials and methods

The study was carried out under rainfall conditions in Diyarbakir province of Turkey in 2011-2012 and 2012-2013 growing seasons with 5 standard varieties and 20 advanced bread wheat lines (*Fig. 1; Table 1*).

Table 1. *Origins of bread wheat genotypes used in the research*

Genotypes (G)	Character	Pedigree	Origin
G1	Spring	Attila-7 (Check) Ndvg9144//Kal/Bb/37yaco/4/Vee#5 Cm85836...	CIMMYT
G2	Spring	Nadia-15 Van's'/3/Cndr's/Ana//Cndr's/Mus's/4/Tevee-5 Icw99…	CIMMYT
G3	Spring	Sisaban-4shuha-5/Asfoor-1 Icw00-0207-0ap-0ap-0ap-56ap-0ap...	CIMMYT
G4	Spring	Morsud-22bt1735//Achtar//Hubara-8 Icw01-00162-0ap-3ap-0ap..	CIMMYT
Nurkent	Spring	Check	GAP UTAEM
G6	Spring	Qafzah-14/Asfoor-1 Icw01-00223-0ap-11ap-0ap-0ap-1ap-0ap…	CIMMYT
G7	Spring	Usher-16 Crow's'/Bow's'-1994/95//Asfoor-5 Icw01-00257-0ap…	CIMMYT
G8	Spring	Pastor//Hxl7573/2*Bau/3/Sokoll/Wbll1 Ptss02b00098t-0topy…	CIMMYT
G9	Spring	Croc_1/Ae.Squarrosa(213)//Pgo/3/Cmh81.38/2*Kauz/4/Berkut…	CIMMYT
Pehlivan	Winter	Check	TTAEM
G11	Spring	Croc_1/Ae.Squarrosa(213)//Pgo/3/Cmh81.38/2*Kauz/4/Berkut…	CIMMYT
G12	Spring	Chen/Aegılops Squarrosa (Taus)//Bcn/3/Bav92/4/Berkut Cmsa…	CIMMYT
G13	Spring	Serı//Au/Up301/3/Je93 7.20/4/Mılan/Amsel See02528-0s-0s-0sd.	CIMMYT
G14	Spring	Opata*2/Wulp/3/Sara1/Yaco//Attıla/4/Har 1685 See02556-0tops.	CIMMYT
Cemre	Spring	Check	GAP UTAEM
G16	Spring	V763.2312/V879.C8.11.11/Sn.64/Hn.4//Rex/3/Edch/Mex/4/…	CIMMYT
G17	Spring	Basribey/3/Agri/Nacozari-Sd…	CIMMYT
G18	Spring	Tam200/Pastor//Toba97Cmss99y02667t-060m-040y-040m…	CIMMYT
G19	Spring	Oasis/Skauz//4*Bcn/3/Pastor/4/Kauz*2/Yaco//Kauzcmss…	CIMMYT
Sagittario	Alternative	Check	TASACO TARM.
G21	Spring	Qafzah-31(Check) Sha5//Carc/Auk/3/Vee//5//Dobuc's Cmss93…	CIMMYT
G22	Spring	Misket-12-Bti735/Achtar//Asfoor-1 Icw01-00164-0ap-1ap-0ap...	CIMMYT
G23	Spring	Rebwah-12/Zemamra-8-Rebwah-12/Zemamra-8 Icw01-00193…	CIMMYT
G24	Spring	Qafzah-14/Asfoor-1-Qafzah-14/Asfoor-1 Icw-0100223-0ap…	CIMMYT
Adana-99	Spring	Check	DATAE

G: Genotypes, CIMMYT: International Maize and Wheat Improvement Center, GAP UTAEM: GAP International Agricultural Research and Training Center, DATAE: Eastern Mediterranean Agricultural Research Institute, TASACO TARM.: Tasaco Agriculture, TTAEM: Directorate of Trakya Agricultural Research Institute

http://www.aloki.hu ● ISSN 1589 1623 (Print) ● ISSN 1785 0037 (Online)
DOI: http://dx.doi.org/10.15666/aeer/1802_36273638

Figure 1. *Experiment location's place in the Turkey map*

In the first year of the study, rainfall was below the average of long years, while in the second year there was rainfall above the average of long years (*Fig. 2*).

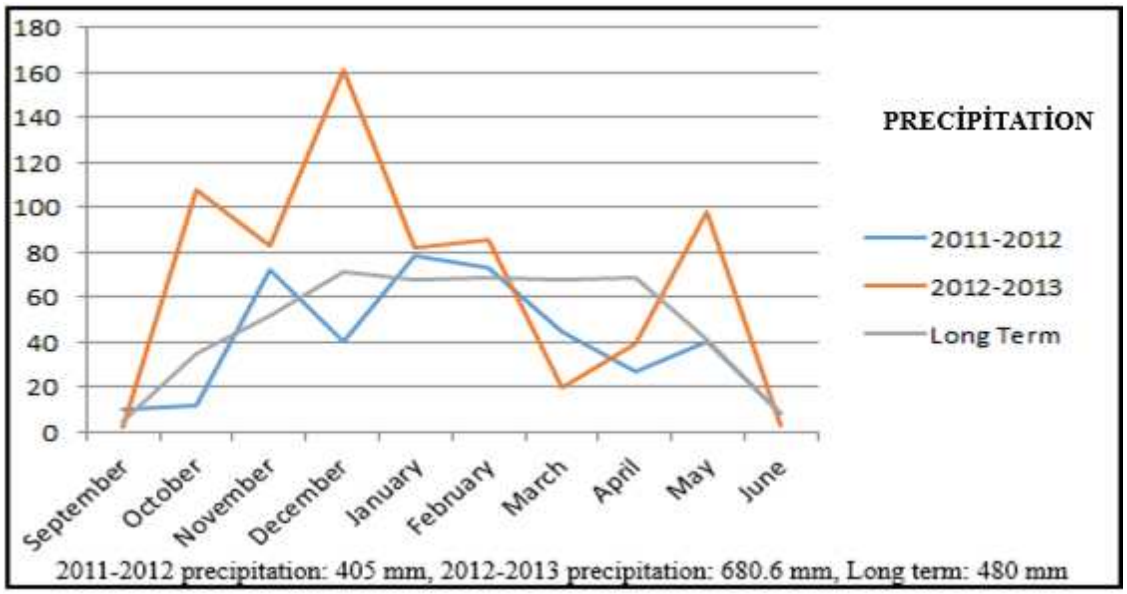

Figure 2. *The amount of precipitation of Diyarbakir's in 2011-2012 and 2012-2013 growing seasons and long terms (mm)*

However, it was determined that the amount of precipitation was not reflected to the grain yield at the expected level since the distribution of rainfall was irregular on months basis.

In the first year of the study, the average temperatures based on months were below long years. However, the second year has been more than long years (*Fig. 3*).

The experiment was conducted in randomized block design with 3 replications. All of the lines used in the study are of spring nature. Additionally, Pehlivan winter, Sagittario alternative, Nurkent, Cemre and Adana-99 varieties are of spring character. 450 seeds were sowed in the square meter and the size of the parcel was 6 m^2.

http://www.aloki.hu ● ISSN 1589 1623 (Print) ● ISSN 1785 0037 (Online)
DOI: http://dx.doi.org/10.15666/aeer/1802_36273638

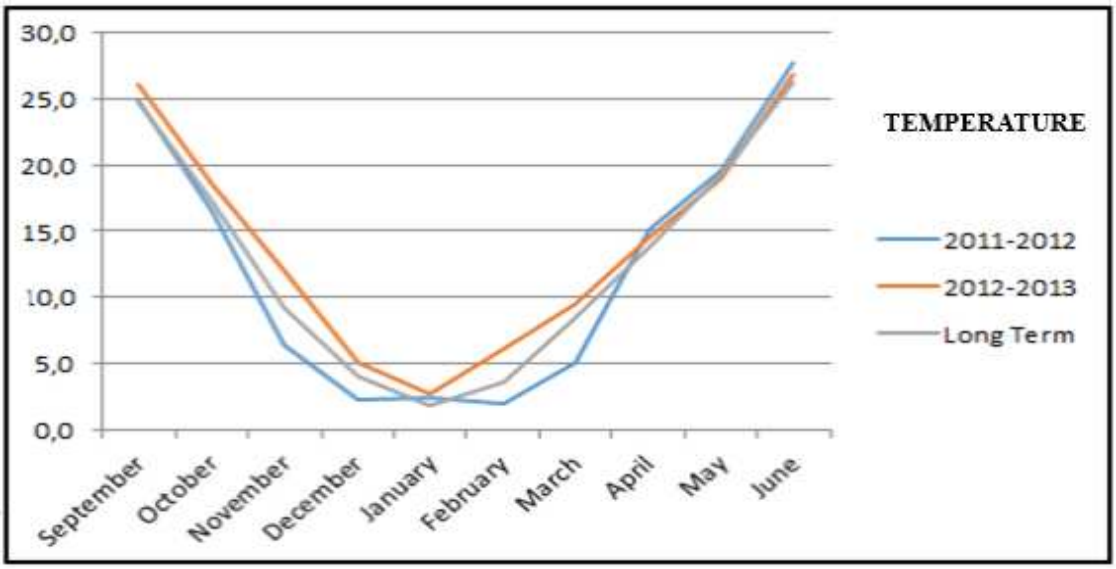

Figure 3. *Average temperature of Diyarbakir's in 2011-2012 and 2012-2013 growing seasons and long terms (°C)*

The amount of fertilizer to be used in the experiment was calculated over 120 kg ha^{-1} pure nitrogen (N) and 60 kg ha^{-1} pure phosphorus (P_2O_5). Half of the total nitrogen and all of the phosphorus were used with sowing and the remaining half of the nitrogen was given at the end of the tillering period. Experiment was sowed in the first week of November and harvesting was done with the combine harvester in the second week of June. The study area is 37° 56 north latitude and 43° 15 east longitude and has a height of 599 m. It is determined that the soil formation class is clayey, the salt content is 0.25%, PH: 7.8, the amount of organic matter is 0.68% and the saturation rate with water is 77%. (Anonymous, 2013).

In the study, heading time (HT) was determined as the number of days as of January 1, taking into account the date when 50% of the plants in each parcel were spiked. When determining plant height (PH), 10 plants were randomly selected per plot. Then, the length from soil level to the highest spikelet except for awns was measured in cm. Grain yield (GY) was determined by turning the yield in kg ha^{-1} after the whole parcel was harvested. When determining the thousand grain weight (TGW), 100 seeds were counted 4 times and weighed on a 0.01 precision scale, then averaged and multiplied by 10 and determined in grams.

To determine the test weight (TW), the seed obtained from each parcel after harvest was weighed after being put into a 1-L container and its weight was multiplied by 100. Protein content (PR) was determined with the Near Infrared Model 6500 device according to the AACC 39-10 method (Anonymous, 1990). Amount of zeleny sedimentation (ZS) ICC-No. according to the 115 was determined (Anonymous, 1982). Wet gluten (WG) ratio was determined by the Glutomatic 2200 device according to ICC standard 155/1 method (Anonymous, 1994). Grain hardness (GH) (Particle size index) was made according to the AACC 39-70 A method (Anonymous, 2000). In the research, variance analysis of the data was performed with JMP 13.0 statistical package program. Differences in mean values were examined by LSD test ($p \leq 0.01$ or $p \leq 0.05$) (Gomez and Gomez, 1984).

http://www.aloki.hu ● ISSN 1589 1623 (Print) ● ISSN 1785 0037 (Online)
DOI: http://dx.doi.org/10.15666/aeer/1802_36273638

Results and discussion

According to the results of ANOVA analysis, of squares mean and significance levels of the investigated features are given in *Tables 2* and *3*. In terms of other features, except for grain yield (n.s.) and zeleny sedimantasyon (5%), between years were observed significant differences at the level of 1%. In addition, except for grain hardness, it is seen that the responses (YxG) of genotypes by years are different from each other (*Tables 2* and 3).

Table 2. *Mean of squares according to variance analysis results*

Variance resources	Degree of freedom	Heading time	Plant height	Grain yield	Test weight	Thousand grain weight
Y	1	3591.7**	8816.6**	994762.5 n.s.	77.3**	518.1**
R	4	12.0**	110.9**	1695965.4**	2.5**	4.1 n.s
G	24	28.2**	228.5**	1007080.0**	8.5**	19.9**
Y*G	24	19.7**	101.6**	1330460.1**	9.5**	36.4**
CV (%)		0.7	1.8	9.5	0.7	8.2

**: 0.01 level, *: 0.05 level statistically significant, Y: Year, R: Replication, G: Genotype, Y * G:: Year * Genotype interaction, n.s.: not significant

Table 3. *Mean of squares according to variance analysis results*

Variance resources	Degree of freedom	Protein content	Zeleny sedimantasyon	Wet gluten	Grain hardness (PSI)
Y	1	77.6**	468.8*	141.7**	949.0**
R	4	0.2n.s.	48.9**	1.1n.s.	3.9n.s.
G	24	0.5**	51.6**	4.7**	134.0**
Y*G	24	0.6**	30.6**	6.4**	0.07n.s.
CV (%)		2.9	10.3	4.1	4.1

In the study, the average values of heading time are given in *Table 4*. The average experiment of heading time was 119.4 days. While the early heading genotypes were G14 (115.3 days) and G22 (115.3 days), in terms of heading time means, Pehlivan (124.0 days) was the late heading genotype. In terms of heading time, it was determined that all lines were earlier heading than the earliest heading standard cultivar (Adana-99; 121.2 days).

Because temperature stress is an important problem in the Southeastern Anatolia Region, early heading genotypes not exposed to heat stress are preferred. In this case, early heading varieties rather than late heading varieties are in demand (Tekdal and Yildirim, 2017). In the selection study, early heading and medium early heading varieties were selected. Kiseleva and Salina (2018) reported that many genes interact for determination of heading time in bread wheat. Also, they emphasized that the genes that affect the heading time of wheat are not studied sufficiently, but the number of studies is increasing day by day.

Average plant height was determined as 99.4 cm. Cemre cultivar had the longest plant length with 110.8 cm and Sagittario cultivar had the shortest plant height with 80.8 cm (*Table 4*). In studies conducted on wheat under different conditions, it was

http://www.aloki.hu ● ISSN 1589 1623 (Print) ● ISSN 1785 0037 (Online)
DOI: http://dx.doi.org/10.15666/aeer/1802_36273638

determined that heredity had a significant effect on plant height. In addition, climate, soil structure and agronomical application (fertilization, soil processing, etc.) has been reported to be effective on plant height (Caierao, 2006).

Table 4. *Statistical significance groups for heading time, plant height and grain yield*

Genotypes	HT (day)			PH (cm)			GY (kg ha^{-1})		
	1. year	2. year l	Av.	1. year	2. year	Av.	1 year	2. year	Av.
G1	124.0 ^{f}	113.7 ^{gh}	118.8 ^{fh}	97.7 ^{f}	96.0 $^{b-d}$	96.8 $^{j-k}$	7258^{ab}	7338 $^{a-d}$	7298^{ab}
G2	125.0 ^{e}	114.0 $^{f-h}$	119.5 $^{e-g}$	102.7 ^{e}	100.0 ^{a}	101.3$^{f-ı}$	6148 $^{b-e}$	6272 ^{fg}	6210 $^{g-h}$
G3	123.8 ^{f}	117.9 ^{abc}	120.9 ^{cd}	95.7 ^{f}	99.7 ^{abc}	97.7 ^{j}	6096 ^{cde}	6474 $^{d-g}$	6285 ^{fgh}
G4	124.0 ^{f}	115.0 $^{d-g}$	119.5 $^{e-g}$	107.7 ^{d}	92.7 ^{def}	100.2^{hı}	6558 ^{abc}	6280 ^{fg}	6419 ^{efg}
Nurkent	127.0 ^{d}	118.3^{ab}	122.7 ^{b}	117.5 ^{b}	97.9 ^{abc}	107.7 ^{b}	6104 ^{cde}	7188 $^{b-f}$	6646 ^{bg}
G6	121.0 ^{ı}	116.7^{bcd}	118.8 $^{f-h}$	112.7 ^{c}	87.7 ^{h}	100.2 ^{hı}	6992 ^{abc}	7291 $^{a-e}$	7142 $^{a-e}$
G7	120.0 ^{j}	115.7^{def}	117.8 ^{ıj}	97.5 ^{f}	88.5 ^{gh}	93.0 ^{lm}	7028 ^{abc}	5875 ^{g}	6452 $^{d-g}$
G8	122.5 ^{g}	114.8 $^{e-g}$	118.7 $^{g-ı}$	111.7 ^{c}	92.7 $^{e-g}$	102.2 $^{e-h}$	7562 ^{a}	6349 $^{d-g}$	6956 $^{a-f}$
G9	122.0 ^{h}	114.3 $^{e-g}$	118.2 $^{h-j}$	112.2 ^{c}	88.8 ^{gh}	100.5 ^{gı}	6689 ^{abc}	6327^{efg}	6508 $^{c-f}$
Pehlivan	129.0 ^{b}	119.0 ^{a}	124.0 ^{a}	112.6 ^{c}	95.1 ^{cde}	103.9 ^{de}	6737 ^{abc}	7069 $^{b-f}$	6903 $^{a-g}$
G11	122.0 ^{h}	114.3 $^{e-g}$	118.2 $^{h-j}$	112.4 ^{c}	93.6 ^{de}	103.0 ^{ef}	7019 ^{abc}	6547 $^{d-g}$	6783 $^{a-g}$
G12	122.0 ^{h}	114.7 $^{e-g}$	118.3 $^{h-j}$	112.8 ^{c}	94.2 ^{cde}	103.5 ^{de}	7178 ^{abc}	5858 ^{g}	6518 $^{c-g}$
G13	121.0 ^{ı}	114.3 $^{e-g}$	117.7 ^{j}	117.6 ^{b}	92.8 ^{def}	105.2 ^{cd}	6866 ^{abc}	6452 $^{d-g}$	6659 $^{b-g}$
G14	117.3 ^{k}	113.3 $^{g-h}$	115.3 ^{k}	112.3 ^{c}	92.3 ^{def}	102.3 $^{e-g}$	7444 ^{a}	7127 $^{b-f}$	7286 ^{ab}
Cemre	130.0 ^{a}	116.7 ^{bcd}	123.3 ^{ab}	122.7 ^{a}	99.0 ^{ab}	110.8 ^{a}	6558 ^{abc}	7816 ^{ab}	7187 $^{a-d}$
G16	125.0 ^{e}	112.3 ^{h}	118.7 $^{g-ı}$	102.4 ^{e}	89.3 $^{f-h}$	95.9 ^{jk}	5138 ^{de}	8227 ^{a}	6683 ^{bg}
G17	125.0 ^{e}	114.3 $^{e-g}$	119.7 $^{e-f}$	97.9 ^{f}	87.5 ^{h}	92.7 ^{m}	6508 ^{abc}	6636 $^{d-g}$	6572 ^{bg}
G18	124.0 ^{f}	113.3 ^{gh}	118.7 $^{g-ı}$	97.4 ^{f}	92.6 ^{def}	95.0 ^{kl}	7242 ^{ab}	6669 $^{c-g}$	6955 $^{a-f}$
G19	124.0 ^{f}	113.7 ^{gh}	118.8 $^{f-h}$	102.3 ^{e}	87.3 ^{h}	94.8 ^{kl}	6672 ^{abc}	7811 ^{ab}	7242 ^{abc}
Sagittario	130.0 ^{a}	116.0 $^{c-e}$	123.0 ^{b}	82.7 g	79.0 ^{ı}	80.8 ^{n}	5083 ^{e}	6230 ^{fg}	5657 ^{h}
G21	128.0 ^{c}	108.3 ^{ı}	118.2 $^{h-j}$	97.3 f	89.0 $^{f-h}$	93.2 ^{lm}	6514 ^{abc}	6805 $^{c-g}$	6660 $^{b-g}$
G22	123.3 ^{fg}	107.3 ^{ı}	115.3 ^{k}	108.3 d	81.7 ^{ı}	95.0 ^{kl}	7014 ^{abc}	6730 $^{c-g}$	6872 $^{a-g}$
G23	125.2 ^{e}	114.8 $^{e-g}$	120.0 ^{de}	112.3 c	87.7 ^{h}	100.0 ^{ı}	6211 $^{b-d}$	7058 $^{b-f}$	6635 $^{b-g}$
G24	123.3 ^{fg}	114.3 $^{e-g}$	118.8 $^{f-h}$	112.2 c	100.5 ^{a}	106.4 ^{bc}	7239 ^{ab}	7658 ^{abc}	7449 ^{a}
Adana-99	126.7 ^{d}	115.7 $^{d-f}$	121.2 ^{c}	112.7 c	92.3 ^{def}	102.5 $^{e-g}$	7225 ^{ab}	7069 $^{b-f}$	7147 $^{a-e}$
Average	124.0	114.5	119.4	107.0	91.7	99.4	6683	6846	6765
Passed of check	19	17	20	0	0	0	5	1	4
LSD (0.05)	0.7**	1.9**	1.0**	1.3**	3.9**	2.1**	1120**	990.0**	738.1**

In terms of grain yield, the experiment average was 6765 kg ha^{-1} and G24 (7449 kg ha^{-1}) line had the highest grain yield. In terms of grain yield, 4 lines passed the standard variety with the highest grain yield (Cemre; 7187 kg ha^{-1}) (*Table 4*). It has been reported that grain yield and quality parameters in wheat are generally affected by genotypes, environmental conditions and genotype environment interaction. (Barutcular et al., 2016; Kizilkeci, 2019).

The average experiment for test weight was 81.7 kg hl^{-1}. In addition, G14 (83.1 kg hl^{-1}), G18 (83.1 kg hl^{-1}) and G21 (83.1 kg hl^{-1}) lines by share the same group and were the highest test weight (*Table 5*). In terms of test weight, 3 lines showed higher performance than the highest standard variety (Adana-99; 83.0 kg hl^{-1}) (*Table 5*). In a

http://www.aloki.hu ● ISSN 1589 1623 (Print) ● ISSN 1785 0037 (Online)
DOI: http://dx.doi.org/10.15666/aeer/1802_36273638

study conducted on bread wheat in India conditions, it was reported that the weight of test ranged from 70.0 to 84.6 kg hl^{-1}. In this study, the results were similar since the average test weight was 81.7 kg hl^{-1} (Panghal et al., 2019).

Table 5. *Test weight, thousand grain weight and protein content values obtained*

Genotypes	TW (kg hl^{-1})			TGW (g)			PR (%)		
	1. year	2. year	Av.	1. year	2. year	Av.	1. year	2. year	Av.
G1	82.1 de	82.6 b-g	82.4 bcd	28.4 ı	45.6 a	37.0 a-d	13.8 h-j	12.9 a-e	13.3 d-h
G2	79.2 ıj	82.0 f-k	80.6 gh	29.6 hı	39.5 bcd	34.6 c-g	13.8 g-j	13.1 a-d	13.5 cg
G3	77.6 lm	81.9 f-k	79.8 ıj	34.3 b-g	38.3 b-f	36.3 b-f	14.7 bc	13.1 a-d	13.9 abc
G4	83.5 ab	81.8 g-k	82.6 abc	32.5 f-ı	34.0 e-f	33.3 fg	14.1 e-h	13.0 a-e	13.5 c-g
Nurkent	76.2 n	83.5 abc	79.9 ıj	33.4 d-h	35.4 def	34.4 c-g	14.2 c-h	12.6 c-f	13.4 d-h
G6	82.5 cd	83.3 a-d	82.9 ab	31.6 f-ı	33.9 e-f	32.8 g	14.2 c-h	12.5 c-f	13.4 d-h
G7	77.8 lm	82.5 c-h	80.2 hı	34.3 b-g	36.8 c-f	35.5 c-g	14.3 c-g	12.4 def	13.4 d-h
G8	81.1 fg	83.0 a-f	82.0 cde	31.1 ghı	37.9 b-f	34.5 c-g	13.8 h-j	12.3 e-f	13.0 h
G9	81.8 d-f	81.2 k	81.5 e-f	37.4 a-d	35.9 c-f	36.6 b-e	14.7 bcd	13.6 a	14.1 a
Pehlivan	82.0 d-f	83.3 a-d	82.7 abc	36.9 a-e	37.8 b-f	37.3 abc	14.1 e-h	12.7 c-f	13.4 d-h
G11	83.7 a	81.3 j-k	82.5 a-d	34.0 b-g	35.3 def	34.7 c-g	13.4 j	13.1 a-d	13.3 f-h
G12	81.5 e-g	81.6 h-k	81.5 e-f	39.4 a	39.1 b-e	39.3 ab	13.8 h-j	13.5 ab	13.6 b-f
G13	84.2 a	81.3 k	82.7 abc	32.3 f-ı	38.8 b-e	35.5 c-g	15.0 ab	13.0 a-e	14.0 ab
G14	84.0 a	82.2 e-k	83.1 a	37.7 abc	33.1 f	35.4 c-g	14.4 c-f	12.1 f	13.3 f-h
Cemre	79.8 ıij	83.2 a-e	81.5 e-f	39.4 a	40.9 abc	40.1 a	14.4 c-f	12.4 def	13.4 d-h
G16	77.1 mn	81.5 h-k	79.3 j	29.8 hı	40.8 abc	35.3 c-g	14.5 b-e	12.4 def	13.5 c-g
G17	78.2 kl	83.2 a-e	80.7 gh	30.8 ghı	35.9 cdf	33.4 e-g	14.3 c-f	13.1 a-d	13.7 a-e
G18	82.5 cd	83.8 a	83.1 a	33.6 c-h	40.2 bcd	36.9 a-d	14.3 c-g	12.8 b-f	13.6 b-g
G19	82.0 df	81.8 g-k	81.9 def	37.9 ab	33.1 f	35.5 c-g	14.7 bcd	12.6 c-f	13.7 b-f
Sagittario	79.0 jk	81.5 ı-k	80.2 hı	33.5 c-h	39.6 bcd	36.6 b-f	15.4 a	12.6 c-f	14.0 ab
G21	83.3 abc	82.9 a-f	83.1 a	33.5 c-h	33.1 f	33.3 e-g	13.5 iij	13.1 a-d	13.3 e-h
G22	80.8 gh	82.4 d-ı	81.6 e-f	34.3 b-g	38.0 b-f	36.1 b-f	14.2 d-h	12.5 c-f	13.3 d-h
G23	80.1 hı	82.3 d-j	81.2 fg	35.8 a-f	36.5 c-f	36.2 b-f	14.5 b-e	13.0 a-e	13.7 a-d
G24	82.6 b-d	82.8 a-g	82.7 abc	32.8 e-h	42.5 ab	37.7 abc	14.3 c-g	13.2 abc	13.8 a-d
Adana-99	82.4 de	83.6 ab	83.0 ab	31.3 gı	36.0 c-f	33.7 d-g	13.9 f-ı	12.5 c-f	13.2 g-h
Average	81.0	82.4	81.7	33.8	37.5	35.7	14.2	12.8	13.5
Passed of check	8	1	3	0	2	0	0	13	1
LSD (0.05)	0.9**	1.0**	0.7**	4.2**	5.4**	3.4**	0.5**	0.7*	0.5**

Av: Average

Cemre (40.1 g) cultivar took the first place in terms of thousand grain weight (*Table 5*). In a study carried out in bread wheat related to thousand grain weight, it was reported that thousand grain weight ranged between 29.6 and 53.8 g, and the average was 40.7 g. In this study, a thousand grain weight ranged between 32.8 and 40.1 g. The average of the experiment was 35.7 g. The results of the studies are similar (Panghal et al., 2019).

The average of protein content was 13.5%. The highest protein content was obtained from G9 (14.1%) line. In addition, the highest value in terms of protein content of the varieties used as standard in the study was obtained from Sagittario cultivar with 14.0%

http://www.aloki.hu ● ISSN 1589 1623 (Print) ● ISSN 1785 0037 (Online)
DOI: http://dx.doi.org/10.15666/aeer/1802_36273638

(*Table 5*). Karaman (2019), in his study based on precipitation conditions in bread wheat has reported that the average protein rate is 14.5%. Also, there is a significant relationship between protein content and grain hardness. This has been reported to result from the strong interaction between carbohydrates and proteins. This result was confirmed by our study. (*Table 5*) (Preston, 1998; Dobraszczyk et al., 2002; Pasha et al., 2010; Baslar et al., 2012).

The average amount of zeleny sedimentation was 28.5 ml and the G12 (35.1 ml) line have the highest sedimentation amount. In addition, it was determined that 4 lines had higher sedimentation amount than the highest standard variety (Sagittario; 31.6 ml) (*Table 6*). In the study of Koçak et al. (1992), the sedimentation value ranged from 18.8 to 43.8 ml, reported that the hereditary effect in sedimentation is higher than the effect of environmental factors. The obtained values are similar to our findings. It is emphasized that the amount of sedimentation is of great importance in determination of protein quality in bread wheat (Peterson et al., 1992).

Table 6. *Zeleny sedimentation, wet gluten and grain hardness values*

Genotypes	ZS (ml)			WG (%)			GH (PSI)		
	1. year	2. year	Av.	1. year	2. year	Av.	1. year	2. year	Av.
G1	24.0 ^{def}	34.5 ^{bcd}	29.3 $^{d-g}$	29.9 $^{e-h}$	29.4 $^{a-f}$	29.6 $^{d-g}$	52.1 ^{h}	47.0 ^{gh}	49.6^{h}
G2	36.5 ^{a}	29.0 $^{h-k}$	32.8 ^{abc}	29.4 $^{g-h}$	30.1 $^{a-e}$	29.8 $^{d-g}$	56.2 $^{d-g}$	51.2 ^{def}	53.7 ^{def}
G3	28.5 $^{b-e}$	31.0 $^{e-h}$	29.8 $^{c-f}$	32.7 ^{bc}	29.9 $^{a-e}$	31.3 ^{abc}	57.2 $^{c-e}$	52.2 $^{c-e}$	54.7 ^{cd}
G4	23.5 ^{ef}	31.7 $^{e-g}$	27.6 $^{e-k}$	29.9 $^{e-h}$	29.6 $^{a-f}$	29.7 $^{d-g}$	49.0 ^{iij}	43.9 ^{hı}	46.5 ^{ı}
Nurkent	25.5 $^{c-f}$	28.3 $^{e-k}$	26.9 $^{f-k}$	30.7 ^{def}	28.3 $^{c-g}$	29.5 $^{d-g}$	48.8 ^{iij}	43.7 ^{hı}	46.3 ^{ı}
G6	24.0 ^{def}	26.7 ^{k}	25.3 $^{j-k}$	30.7 $^{d-g}$	28.1 $^{c-g}$	29.4 ^{efg}	56.2 $^{d-g}$	51.2 ^{def}	53.7 ^{def}
G7	35.0 ^{a}	33.3 $^{b-e}$	34.2 ^{ab}	31.5 ^{cd}	27.7 $^{d-g}$	29.6 $^{d-g}$	54.1 $^{e-h}$	49.1 ^{efg}	51.6 ^{fgh}
G8	23.5 ^{ef}	30.7 $^{f-ı}$	27.1 $^{f-k}$	29.6 $^{f-h}$	27.6 ^{efg}	28.6 ^{g}	59.0 ^{bcd}	54.0 ^{bcd}	56.5 ^{bc}
G9	30.3 $^{a-d}$	29.7 $^{g-j}$	30.0 $^{c-f}$	31.6 $^{b-d}$	31.7 ^{a}	31.6 ^{a}	52.7 ^{h}	47.7 ^{g}	50.2 ^{gh}
Pehlivan	23.5 ^{ef}	28.8 $^{h-k}$	26.2 $^{g-k}$	30.2 $^{e-h}$	28.5 $^{c-g}$	29.3 ^{efg}	54.8 $^{e-h}$	49.7 ^{efg}	52.3 $^{e-g}$
G11	32.5 ^{ab}	33.0 $^{c-f}$	32.8 ^{abc}	28.0 ^{ı}	30.2 $^{a-d}$	29.1 ^{efg}	49.1 ^{iij}	44.0 ^{hı}	46.6 ^{ı}
G12	35.0 ^{a}	35.2 ^{abc}	35.1 ^{a}	29.2 ^{hı}	31.4 ^{ab}	30.3 $^{a-f}$	60.7 ^{ab}	55.7 ^{ab}	58.2 ^{b}
G13	25.5 $^{c-f}$	28.7 $^{h-k}$	27.1 $^{f-k}$	32.8 ^{ab}	29.6 $^{a-f}$	31.2 ^{abc}	47.6 ^{j}	42.6 ^{ı}	45.1 ^{ı}
G14	22.0 ^{f}	27.0 ^{k}	24.5 ^{k}	31.5 ^{cd}	26.5 ^{g}	29.0 ^{fg}	47.7 ^{j}	42.6 ^{ı}	45.2 ^{ı}
Cemre	24.0 ^{def}	27.8 ^{jk}	25.9 $^{g-k}$	32.4 ^{bc}	27.8 $^{d-g}$	30.1 $^{b-f}$	63.8 ^{a}	58.8 ^{a}	61.3 ^{a}
G16	24.5 ^{def}	27.0 ^{k}	25.8 $^{h-k}$	31.1 ^{de}	27.6 $^{e-g}$	29.3 $^{e-g}$	53.5 ^{gh}	48.9 ^{efg}	51.2 ^{gh}
G17	31.0 ^{abc}	27.0 ^{k}	29.0 $^{d-ı}$	30.8 ^{def}	28.3 $^{c-g}$	29.5 $^{d-g}$	56.4 $^{d-g}$	51.4 ^{def}	53.9 ^{def}
G18	24.0 ^{def}	37.6 ^{a}	30.8 $^{b-e}$	32.6 ^{bc}	29.1 $^{b-g}$	30.8 $^{a-d}$	53.7 ^{fh}	48.7 ^{fg}	51.2 ^{gh}
G19	23.0 ^{ef}	29.0 $^{h-k}$	26.0 $^{g-k}$	31.6 ^{bcd}	28.3 $^{c-g}$	29.9 $^{c-g}$	48.9 ^{iij}	43.9 ^{hı}	46.4 ^{ı}
Sagittario	27.5 $^{b-f}$	35.7 ^{ab}	31.6 $^{b-d}$	34.1 ^{a}	29.0 $^{b-g}$	31.5 ^{a}	60.3 ^{bc}	55.3 ^{bc}	57.8 ^{b}
G21	24.5 ^{def}	28.0 ^{jk}	26.3 $^{g-k}$	29.5 $^{f-h}$	30.4 ^{abc}	30.0 $^{b-g}$	48.2 ^{j}	43.2 ^{ı}	45.7 ^{ı}
G22	24.0 ^{def}	27.3 ^{jk}	25.7 $^{ı-k}$	30.5 $^{d-g}$	27.5 $^{e-g}$	29.0 ^{fg}	48.4 ^{j}	42.4 ^{ı}	45.4 ^{ı}
G23	26.5 $^{b-f}$	27.0 ^{k}	26.8 $^{f-k}$	31.6 ^{bcd}	31.1 ^{ab}	31.4 ^{ab}	56.3 $^{d-g}$	51.3 ^{def}	53.8 ^{def}
G24	25.0 $^{c-f}$	31.7 $^{e-g}$	28.3 $^{d-j}$	31.0 ^{de}	30.0 $^{a-e}$	30.5 $^{a-e}$	57.1 $^{c-f}$	52.1 $^{c-f}$	54.6 ^{cde}
Adana-99	26.0 $^{c-f}$	32.2 ^{def}	29.1 $^{d-h}$	30.6 $^{d-g}$	27.3 ^{fg}	28.9 $^{f-g}$	59.4 ^{bcd}	54.4 $^{b-d}$	56.9 ^{bc}
Average	26.8	30.3	28.5	30.9	29.0	30.0	54.0	49.0	51.5
Passed of check	7	1	4	0	12	1	0	0	0
LSD (0.05)	6.4**	2.4**	3.4**	1.3**	2.6**	1.4**	3.4**	3.4**	2.4**

http://www.aloki.hu ● ISSN 1589 1623 (Print) ● ISSN 1785 0037 (Online)
DOI: http://dx.doi.org/10.15666/aeer/1802_36273638

The mean of wet gluten ratio was found to be 30.0%, while G9 (31.6%) and Sagittario (31.5%) had the highest value by sharing the same group (*Table 6*). It has been reported that wet gluten ratio in bread wheat is important and the amount of gluten formed as a result of swelling of gliadin and gluten, which are subcomponents of protein, by absorbing water, is affected significantly by environmental conditions. The researchers reported that wet gluten content varied between 11.3 and 45.2% (Keçeli et al., 2017).

In the study, the mean experiment value of grain hardness was found to be 51.5 (PSI). Nurkent (46.3 PSI) had the hardest grain type and Cemre (61.3 PSI) had the softest grain type. In the interpretation of the grain hardness parameter, it is interpreted that the grain hardness increases with decreasing PSI value and decreases with increasing PSI value (Sahin et al., 2017). According to this, G13 (45.1) was found to be the genotype with the highest grain hardness. G4 (46.5), Nurkent (46.3), G11 (46.6), G14 (45.2), G19 (46.4), G21 (45.7) and G22 (45.4) lines were also good genotypes for grain hardness (*Table 6*). Because grain hardness is positively associated with protein *(Table 7).*

Grain hardness (PSI) parameter is important in bread wheat. Especially when flour is obtained from hard wheat, starch damage is more than soft wheat. It was emphasized that this was not preferred by bakers. Also, dough made from a high damaged starch content flour was reported to have more water-holding capacity (Khan and Shewry, 2009; Sahin et al., 2017).

Correlation analysis

Respect to correlation analysis, there was a positive correlation between grain yield and test weight and a negative correlation with wet gluten ratio. While test weight increased, wet gluten ratio and grain hardness (PSI) values were found to decrease. Thousand grain weight was found to be inversely related to protein content and wet gluten ratio. In addition, the content of protein and wet gluten was found to be inversely related to the amount of zeleny sedimentation (*Table 7*). This situation is contrary to the literature. Because many researchers have reported that the amount of zeleny sedimentation positively correlated with protein content and wet gluten ratio (Surma et al., 2012; Keceli et al., 2017).

Table 7. *Correlation coefficients and significance levels between parameters*

Features	GY	TW	TGW	PR	ZS	WG	GH	HT
TW	0.325**							
TGW	0.096	0.227**						
PR	-0.149	-0.432**	-0.329**					
ZS	-0.146	-0.070	0.256	-0.284**				
WG	-0.201*	-0.364**	-0.185*	0.860**	-0.165*			
GH	0.037	-0.274**	-0.047	0.397**	-0.076	0.323**		
HT	-0.091	-0.394**	-0.368**	0.703**	-0.356**	0.459**	0.565**	
PH	0.093	-0.105	-0.147	0.540**	-0.342**	0.295**	0.350**	0.629**

** 1%, * 5% important

http://www.aloki.hu ● ISSN 1589 1623 (Print) ● ISSN 1785 0037 (Online)
DOI: http://dx.doi.org/10.15666/aeer/1802_36273638

This may be due to the low protein quality despite the high protein content of the genotypes or vice versa. Additionally, grain hardness (PSI) was positively correlated with heading time and plant height. Kılıç et al. (2014) obtained similar results in their study.

Conclusion

In the study, early heading cultivars were found to be prominent in terms of grain yield and test weight. However, it was determined that the same situation was not observed in terms of quality parameters. It was found that there was a positive correlation between grain yield and test weight and a negative correlation with wet gluten. There was a negative correlation between grain hardness (PSI) and test weight and a positive correlation between plant height and heading time. G1, G14, G19, G24 for grain yield, G14, G18, G21 for test weight; G9 for protein ratio and wet gluten amount, G2, G7, G11, G12, for zeleny sedimentation outperformed all standards. In the study, it is determined that the lines which are superior to standard varieties in terms of one or a few features should be taken into consideration in grain yield or quality-oriented breeding studies. It was concluded that G19 and G24, which have superior features, can be registered candidates. In the future, if collaboration with modern breeding (molecular) is done, genotypes of superior will be studied and the results will shed light on future research.

REFERENCES

[1] Aktas, H. (2017): Evaluation of some barley (*Hordeum vulgare L.*) cultivars commonly cultivated in Turkey under supplemented irrigation and rainfall conditions. – J. Tekirdag Agr. Fac. 14(03): 86-97.
[2] Anonymous (1982): ICC-Standard No: 115/1. – International Association for Cereal Chemistry, Vienna.
[3] Anonymous (1990): Approved Methods of the American Association of Cereal Chemistry, USA. – AACC, Washington, DC.
[4] Anonymous (1994): ICC - Standard No: 155/1. – International Association for Cereal Chemistry, Vienna.
[5] Anonymous (2000): AACC. Approved Methods. Vol. 2. 8th Ed. – Repr. American Association of Cereal Chemists, St. Paul, MA.
[6] Anonymous (2013): GAP International Agricultural Research and Training Center. – Soil Analysis Laboratory, Diyarbakir.
[7] Barutcular, C., Yildirim, M., Koç, M., Akinci, C., Toptas, I., Albayrak, O., Tanrikulu, A., EL Sabagh, A. (2016): Evaluation of SPAD chlorophyll in spring wheat genotypes under different environments. – Fresenius Env. Bul. 25(4): 1258-1266.
[8] Baslar, M., Kalkan, F., Kara, M., Ertugay, M. F. (2012): Correlation between the protein content and mechanical features of wheat. – J. Agr. and Forest. 36: 601-607.
[9] Caierao, E. (2006): Brazilian society of plant breeding. Printed in brazil effect of induced lodging on grain yield and quality of brewing barley. – Crop Breed. Appl. Biotech. 6: 215-221.
[10] Cıvgın, İ. (2016): The factors that affect plant domestication process in the fertile crescent: climate, natural habitat and cross-cultural encounters (11000-7000 BCE.) Mehmet Akif Ersoy Univ. – J. of the Ins. of Soc. Sci. 8(17): 463-488.
[11] Dobraszczyk, B. J., Whitworth, M. B., Vincent, J. F. V., Khan, A. A. (2002): Single kernel wheat grain hardness and fracture features in relation to density and the modelling of fracture in wheat endosperm. – J. Cereal Sci. 35: 245-263.

http://www.aloki.hu ● ISSN 1589 1623 (Print) ● ISSN 1785 0037 (Online)
DOI: http://dx.doi.org/10.15666/aeer/1802_36273638

[12] Gomez, K. A., Gomez, A. A. (1984): Statistical Procedures for Agricultural Research. 2nd. Ed. – John Willey and Sons, Inc. New York.
[13] Gooding, M. J., Ellis, R. H., Shewry, P. R., Schofield, J. D. (2003): Effects of restricted water availability and increased temperature on the grain filling, drying and quality of winter wheat. – J. Cereal Sci. 37: 295-309.
[14] Grausgruber, H., Oberforster, M., Werteker, M., Ruckenbauer, P., Vollmann, J. (2000): Stability of quality traits in Austrian-grown winter wheats. – Field Crop. Res. 66: 257-267.
[15] Karaman, M. (2019): Evaluation of bread wheat genotypes in irrigated and rainfed conditions using biplot analysis. – Applied Ecol. Env. Res. 17(1): 1431-1450.
[16] Keçeli, A., Kaplan Evlice, A., Pehlivan, A., Şanal, T., Karaca, K., Külen, S., Seis Subaşı, A., Salantur, A. (2017): Investigation of the relationship between zeleny sedimentation analysis and other quality parameters in bread wheat (*Triticum aestivum L.*). Kahramanmaraş Sütçü İmam Univ. – J. Natur. Sci. 20(Special Issue): 292-296.
[17] Kendal, E., Sener, O. (2015): Examination of genotype × environment interactions by GGE biplot analysis in spring durum wheat. – Indian J. Gen. Plant Breed. 75(3): 341-348.
[18] Khan, K., Shewry, P. R. (2009): Criteria of Wheat and Flour Quality. – In: Gordon, R., Carson, N., Edwards, M. (eds.) Wheat and Chemistry. Fourth Ed. Chap. 4. AACC International Inc., St. Paul.
[19] Kilic, H., Kendal, E., Aktas, H., Tekdal, S. (2014): Assessment of advanced bread wheat lines for yield and some quality traits at different environment. – Iğdir Univ. J. Inst. Sci. Tech. 4(4): 87-95.
[20] Kiseleva, A. A., Salina, E. A. (2018): Genetic regulation of common wheat heading time. – Russian J. Genetic. 54: 375-388
[21] Kizilgeci, F. (2019): Physiological, agronomical and quality response of bread wheat to phosphorus application under dryland condition. – Applied Ecol. Env. Res. 17(2): 1979-1987.
[22] Kocak, N., Atli, A., Karababa, E., Tuncer, T. (1992): Macar-Yugoslav (MAYEB) A research on the quality properties of Hungarian Yugoslavia bread wheat varieties. – J. Field Crop. Cent. Res. Inst. 1(1): 27-45.
[23] Morgounov, A., Keser, M., Kan, M., Küçükçongar, M., Özdemir, F., Gummanow Muminjanov, H., Zuev, E., Qualset, C. O. (2016): Wheat landraces currently grown in Turkey: distribution, diversity and use. – Crop Sci. 56: 1-13.
[24] Panghal, A., Chhikara, N., Khatkar, B. S. (2019): Characterisation of Indian wheat varieties for chapatti (flat bread) quality. – J. Saudi Soc. Agr. Sci. 18(1): 107-111.
[25] Pasha, I., Anjum, F. M., Morris, C. F. (2010): Grain hardness: a major determinant of wheat quality. – Food Sci. Tech. Inter. 16: 511-522.
[26] Peterson, C. J., Graybosch, R. A., Baenziger, P. S., Grombacher, A. W. (1992): Genotype and environment effects on quality characteristics of hard red winter wheat. – Crop Sci. 32: 98-103.
[27] Preston, K. R. (1998): Protein-Carbohydrate Interactions. – In: Hamer, R. J., Hoseney, R. C. (eds.) Interactions: The Keys to Cereal Quality. AACCI, St. Paul, MN, pp. 83-91.
[28] Souza, E., Martin, J. M., Guttieri, M. J., O'Brien, K. M., Habernicht, D. K., Lanning, S. P., McLean, R., Carlson, G. R., Talbert, L. E. (2004): Influence of genotype, environment, and nitrogen management on spring wheat quality. – Crop Sci. 44: 425-432.
[29] Sahin, M., Gocmen Akcacik, A., Aydogan, S., Hamzaoglu, S., Demir, B., Yakişir, E. (2017): Investigation of the relationship between zeleny sedimentation and yield and some quality traits in winter bread wheat varieties. – J. Bahri Dag. Crop Res. 6(1): 10-21.
[30] Surma, M., Adamski, T., Banaszak, Z., Kaczmarek, Z., Kuczynska, H., Majcher, M., Ługowska, B., Obuchowski, W., Salmanowicz, B., Krystkowiak, K. (2012): Effect of genotype, environment and their interaction on quality parameters of wheat breeding lines of diverse grain hardness. – Plant Product. Sci. 15(3): 192-203.

http://www.aloki.hu ● ISSN 1589 1623 (Print) ● ISSN 1785 0037 (Online)
DOI: http://dx.doi.org/10.15666/aeer/1802_36273638

[31] Tekdal, S., Yildirim, M. (2017): Relation of physiological and morphological parameters with heat stress in some durum wheat genotypes. – Turkish J. Nat. Sci. 6(2): 73.
[32] TSI (2018): Turkish Statistical Institute. – Crop Production Statistics, www.tuik.gov.tr.

http://www.aloki.hu ● ISSN 1589 1623 (Print) ● ISSN 1785 0037 (Online)
DOI: http://dx.doi.org/10.15666/aeer/1802_36273638

GROWTH RESPONSES OF THE SUBMERGED MACROPHYTE SAGO PONDWEED (*POTAMOGETON PECTINATUS*) TO DISTURBANCE BY THREE OMNIVOROUS FISHES

WANG, H. L.[1,2] – LI, Z. F.[1,3*] – LIU, Y.[1] – ZHANG, J. W.[1] – ZHANG, X. K.[2] – XIE, J.[1,3*]

[1]*Key Laboratory of Tropical and Subtropical Fishery Resource Application and Cultivation, Pearl River Fisheries Research Institute, Chinese Academy of Fishery Sciences, Guangzhou, Guangdong 510380, China*

[2]*College of Life Science, Anqing Normal University, Anqing, Anhui 246133, China*

[3]*Guangdong Ecological Remediation of Aquaculture Pollution Research Center, Guangzhou, Guangdong 510380, China*

[*]*Corresponding authors*
e-mail: xiejunhy01@126.com, lzf@prfri.ac.cn

(Received 19th Dec 2019; accepted 23rd Mar 2020)

Abstract. In China, the distribution area and ecological function of *Potamogeton pectinatus* have been adversely affected by aquaculture. To evaluate the effects of omnivorous fishes on submerged plant recovery in cultured lakes, growth responses of *Potamogeton pectinatus* to disturbance by three such fishes (gold fish (*Carassius auratus*), common carp (*Cyprinus carpio*), and yellow catfish (*Pelteobagrus fulvidraco*)) were analyzed. Three stocking densities (low, medium, and high) were selected for each fish species. Fish stocking obviously increased total nitrogen, total phosphorus, conductivity, and total dissolved solids and decreased dissolved oxygen and pH of the water. Fish species had significant effects on plant height, root length, root dry weight, and aboveground dry weight, which were the lowest after *Cyprinus carpio* treatment. Stocking density had significant effects only on root length, root dry weight, and aboveground dry weight. The fish species, stocking density, and their interaction had significant effects on total dry weight and biomass allocation. The total dry weight and root:aboveground part values were significantly lower after *Cyprinus carpio* treatment than after the other treatments. Therefore, the dominant fish species should be scientifically assessed before restoring submerged vegetation, and fish stocking density needs to be controlled to promote submerged macrophyte establishment in cultured lakes.
Keywords: *cultivated lakes, aquaculture, ecological restoration, stocking density, aquatic plants*

Introduction

Submerged macrophytes are the dominant primary producers in lake ecosystems, and they play important roles in stabilizing embankments, purifying water, and providing shelter for other aquatic organisms (Zhang et al., 2017, 2019; Ge et al., 2018). In China, the distribution area of submerged macrophytes in many freshwater lakes has been greatly reduced due to human activities (Fang et al., 2006; Zhang et al., 2017). The lakes have gradually shifted from a macrophyte-dominated state to a phytoplankton-dominated state (Wu et al., 2019), and the ecological service function is seriously degraded. In addition to factors such as land use change, dam construction, and eutrophication, aquaculture is often considered to be a major reason for the degradation of submerged macrophytes in lakes (Wang et al., 2005; Fang et al., 2006; Wu et al., 2019).

In China, aquaculture is an important part of fisheries. Aquaculture production in the country accounts for 60.5% of the total production worldwide (Mo et al., 2018).

http://www.aloki.hu ● ISSN 1589 1623 (Print) ● ISSN 1785 0037 (Online)
DOI: http://dx.doi.org/10.15666/aeer/1802_36393649

However, high fish production in China is mainly achieved through high-density farming. For more economic benefits, many cultured lakes generally stock a high density of fish. Previous studies have shown that high-density stocking of herbivorous or omnivorous fishes can affect submerged plants directly or indirectly (Pipalova, 2006). The direct effects mainly include direct feeding and physical damage by the fishes, for example, grass carp (*Ctenopharyngodon idellus*) can directly graze on the rhizomes, shoots, and stems of submerged plants, resulting in the decline of aquatic plant resources (Hanlon et al., 2000; Domingues et al., 2017), and the foraging activities of some bottom fishes such as common carp (*Cyprinus carpio*) and tilapia (*Oreochromis mossambicus*) which often uproot submerged macrophytes (Chen and Guo, 2005). The indirect effects are mainly attributable to the activities of the fishes. After fish stocking, the suspended matter in the water increases, and more nutrients (such as N and P) are released into the sediment, leading to decreased water transparency and overpopulation of algae and, thus, inhibition of the growth of aquatic plants (Pipalova, 2006; Wang et al., 2016; Hansen et al., 2019).

Recently, the negative impacts of aquaculture have received widespread attention. To restore lake environments, ecological restoration projects have been conducted in many cultured lakes in China (Gu et al., 2018). However, the growth response of aquatic plants affected by different fish disturbances has rarely been reported, and it is difficult to provide a theoretical basis for the restoration of aquatic plants in cultured lakes. Therefore, in this study, we selected three omnivorous fishes, (*Carassius auratus*, *Cyprinus carpio*, and *Pelteobagrus fulvidraco*) that are commonly cultured in lakes in China to determine the growth responses of *Potamogeton pectinatus* to disturbances by the different fishes at different stocking densities. Although all the three fishes are omnivorous, *Pelteobagrus fulvidraco* mainly feeds on benthic invertebrates and is less active and causes minimal disturbance in the water body; *Carassius auratus* mainly feeds on plants and shows relatively strong activity; and *Cyprinus carpio* mainly feeds on both animals and plants and may cause the strongest disturbance to the water body. Therefore, we hypothesized that the growth responses of *Potamogeton pectinatus* to disturbances by the different fish species may be different, and its growth was the worst when disturbed by *Cyprinus carpio* at high stocking density.

Materials and methods

Experimental design

Potamogeton pectinatus L. is a perennial submerged macrophyte that can reproduce via vegetative fragments, underground stems, and seeds. On July 22, 2018, similar fragments of *Potamogeton pectinatus* (35-cm-long apical shoots without developed roots) were collected from Baiyangdian Lake, Hebei Province; transferred to the Baiyangdian field station (N: 115°59′30.31″; E: 38°50′37.12″); and randomly cultivated in rectangular plastic pots (40 cm × 15 cm × 20 cm). Each plastic pot contained 10 cm of the substrate (obtained from Baiyangdian Lake). The nutrient content of the substrate (dry weight) was determined to be 1.64 mg g^{-1} N, 0.52 mg g^{-1} P, and 24.53 mg g^{-1} organic matter. Each rectangular plastic pot had 12 seedlings, and three pots were placed in a cement pond (2.0 m × 2.0 m × 1.8 m) as three replicates. A total of 10 cement ponds were used in this study. Lake water was added to each cement pond. The total nitrogen (TN) and total phosphorus (TP) in the water were 0.980 and

http://www.aloki.hu ● ISSN 1589 1623 (Print) ● ISSN 1785 0037 (Online)
DOI: http://dx.doi.org/10.15666/aeer/1802_36393649

0.048 mg/L, respectively; the temperature, dissolved oxygen (DO), conductivity (Cond), total dissolved solids (TDS), and pH in the water were 28.9℃, 7.70 mg/L, 904 uS/cm, 587.9 mg/L, and 8.90, respectively. The water depth was initially maintained at 100 cm to promote the survival and growth of the seedlings. After half a month, the water depth in the cement pond was increased to 150 cm, and two plants from each pot with large differences in plant size were removed, so that the average plant height of the remaining 10 seedlings was maintained at about 135 cm.

Three omnivorous fishes (*Carassius auratus*, *Cyprinus carpio*, and *Pelteobagrus fulvidraco*) were used, and all of them were captured from Baiyangdian Lake. For each fish species, individuals with a weight of about 100 g were selected. Three stocking densities were selected for each fish species: high density (HD), medium density (MD), and low density (LD); correspondingly, the number of fishes for the three treatments was 15, 10, and 5, respectively, and the total weight was 1500, 1000, and 500 g, respectively. On August 9, 2019, the three fish species at different stocking densities were placed randomly in each pond. The cement pond with no fish was used as control group. During the experiment, if a fish was found dead, it was replaced with a fish of similar size. No fish were fed throughout the experiment. At the end of the experiment, the temperature, DO, Cond, TDS, and pH were measured using a portable multi-parameter water quality analyzer (YSI Professional Plus, USA). The transparency of the water body was measured using a Secchi disc. The TN and TP of the pond water were determined using standard methods (Lu, 2000).

Data analyses

The experiment ended on September 22, 2018. All plants were harvested from the plastic pots, and plant height and root length were measured with a meter stick. Then, the plants were divided into root and aboveground (including stems and leaves) parts and dried in an oven at 80℃ for three days. The dry weight (DW) of the roots, aboveground parts, and whole plants was determined. Two-way analysis of variance (ANOVA) was used to analyze the effects of the fish species and stocking density on plant height, root length, aboveground DW, root DW, and total DW of *Potamogeton pectinatus*. The normality and homogeneity of all the variables were tested before ANOVA. For variables that satisfied the homogeneity, Tukey's HSD multiple comparisons were used to test for differences between groups, whereas Tamhane's T2 method was used for unequal variances (Li et al., 2018). All analyses were performed using Excel and SPSS 13.0 software.

Results

Physiochemical parameters

At the end of the experiment, the physiochemical parameters in the different treatment groups showed some differences (*Table 1*). The TN, TP, Cond, and TDS in all the treatments were obviously higher after fish stocking and transparency was obviously lower than the control. Small differences in the water temperature were observed in all the treatments. The DO and pH in all treatments with stocked fish (except for *Pelteobagrus fulvidraco* at LD) were lower than the control values.

http://www.aloki.hu ● ISSN 1589 1623 (Print) ● ISSN 1785 0037 (Online)
DOI: http://dx.doi.org/10.15666/aeer/1802_36393649

Table 1. *Comparison of the physiochemical parameters in the different treatment groups*

Variable	Control group	*Pelteobagrus fulvidraco*			*Cyprinus carpio*			*Carassius auratus*		
		HD	MD	LD	HD	MD	LD	HD	MD	LD
Temperature (℃)	22.9	22.9	22.6	22.5	23.3	23.2	23.0	23.2	23.0	22.9
DO (mg/L)	10.16	9.08	8.98	10.45	9.40	9.61	9.28	9.69	9.15	9.84
Cond (uS/cm)	586	945	852	869	860	811	665	846	716	664
TDS (mg/L)	443.5	617.5	552.5	565.5	559.0	529.0	526.5	552.5	499.0	468.0
pH	9.48	9.15	9.16	9.69	9.08	8.82	8.90	8.81	9.02	8.95
Transparency (cm)	150	42	103	105	16	25	32	25	32	62
TN (mg/L)	0.215	0.393	0.341	0.232	1.243	0.646	0.477	0.656	0.341	0.246
TP (mg/L)	0.039	0.045	0.048	0.058	0.198	0.100	0.079	0.082	0.069	0.069

Morphological parameters

The fish species had significant effects on plant height, root length, root DW, and aboveground DW of *Potamogeton pectinatus*, and the values of all four parameters were the lowest after *Cyprinus carpio* treatment (*Table 2*; *Fig. 1*). The root DW and aboveground part DW were lower than the control values after fish stocking; however, the plant height and root length did not show similar trends (*Fig. 1*).

Table 2. *Two-way ANOVA of the effects of fish species, stocking density, and their interactions on plant height, root length, root dry weight (DW), and aboveground DW of Potamogeton pectinatus*

Source of variation	Plant height	Root length	Root DW	Aboveground DW	Total DW	Ratio
Fish species	77.19**	45.62**	64.25**	35.66**	42.29**	3.87*
Stocking density	0.78	5.65**	11.76**	22.86**	23.32**	4.57*
Fish species × Stocking density	3.70**	6.78**	14.70**	4.37**	5.16**	9.13**

Note: * $P < 0.05$; ** $P < 0.01$

The stocking density had significant effects on root length, root DW, and aboveground DW of *Potamogeton pectinatus*; however, it had no significant effects on plant height (*Table 2*). With the increase in stocking density, the root length, root DW, and aboveground DW of the plants showed a significant decrease (*Fig. 2*). The highest values of all three parameters were observed in the control group, whereas the lowest values were detected in the HD treatment groups (*Fig. 2*). In addition, the fish species and stocking density had significant interactions with respect to all four morphological parameters (*Table 2*).

Biomass allocation

Fish species, stocking density, and their interactions had significant effects on the total DW and root:aboveground part values (*Table 1*), which were significantly lower in the *Cyprinus carpio* treatment groups than in the other two fish groups and control group. Although the total DW values after *Carassius auratus* and *Pelteobagrus fulvidraco* treatments were lower than the control values, the ratio was not significantly different among the three groups (*Fig. 3*). With the increase in stocking density, the total DW and ratio showed a tendency to significantly decrease, and both were the lowest after HD treatment (*Fig. 4*).

http://www.aloki.hu ● ISSN 1589 1623 (Print) ● ISSN 1785 0037 (Online)
DOI: http://dx.doi.org/10.15666/aeer/1802_36393649

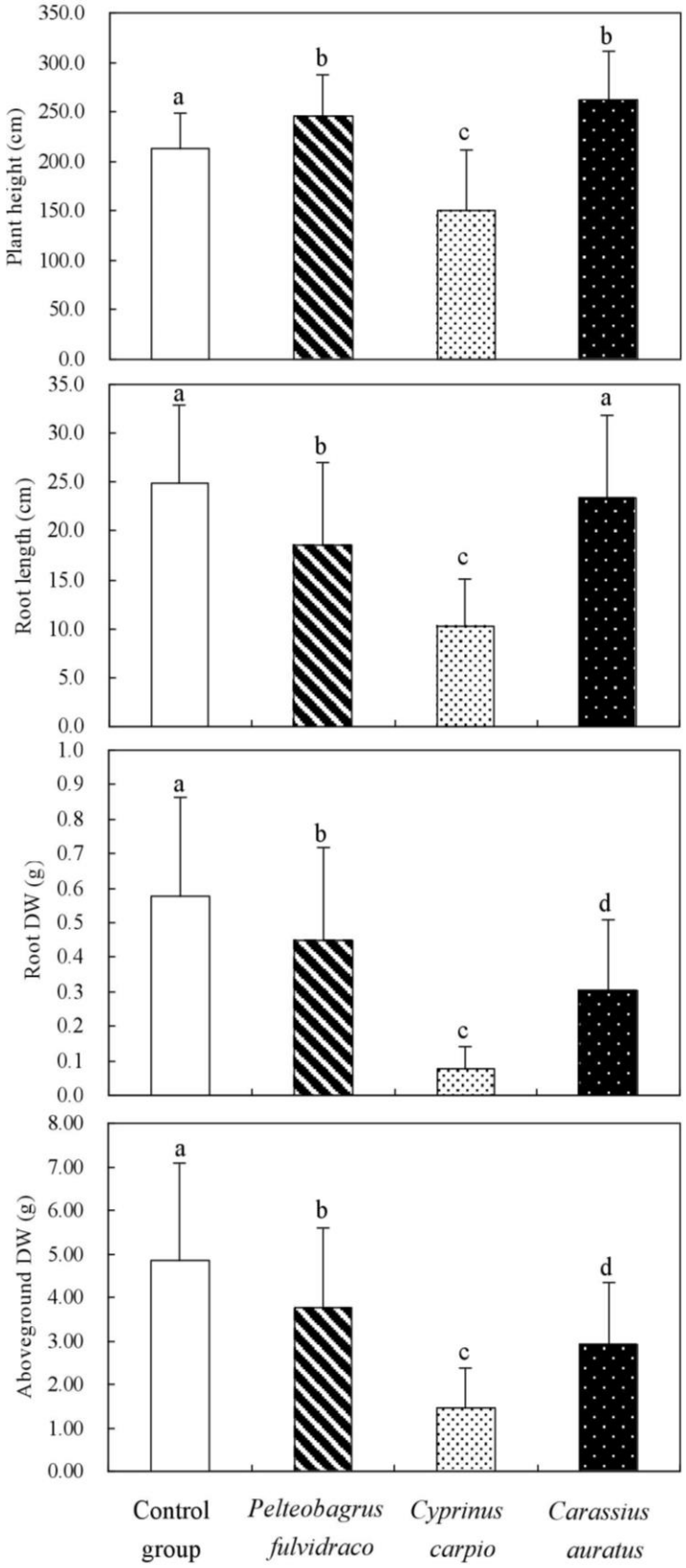

Figure 1. *Comparisons of plant height, root length, root dry weight (DW), and aboveground DW after treatment with different fishes. Different lowercase letters indicate significant differences ($P < 0.05$). Error bars indicate the standard deviation of the mean*

http://www.aloki.hu ● ISSN 1589 1623 (Print) ● ISSN 1785 0037 (Online)
DOI: http://dx.doi.org/10.15666/aeer/1802_36393649

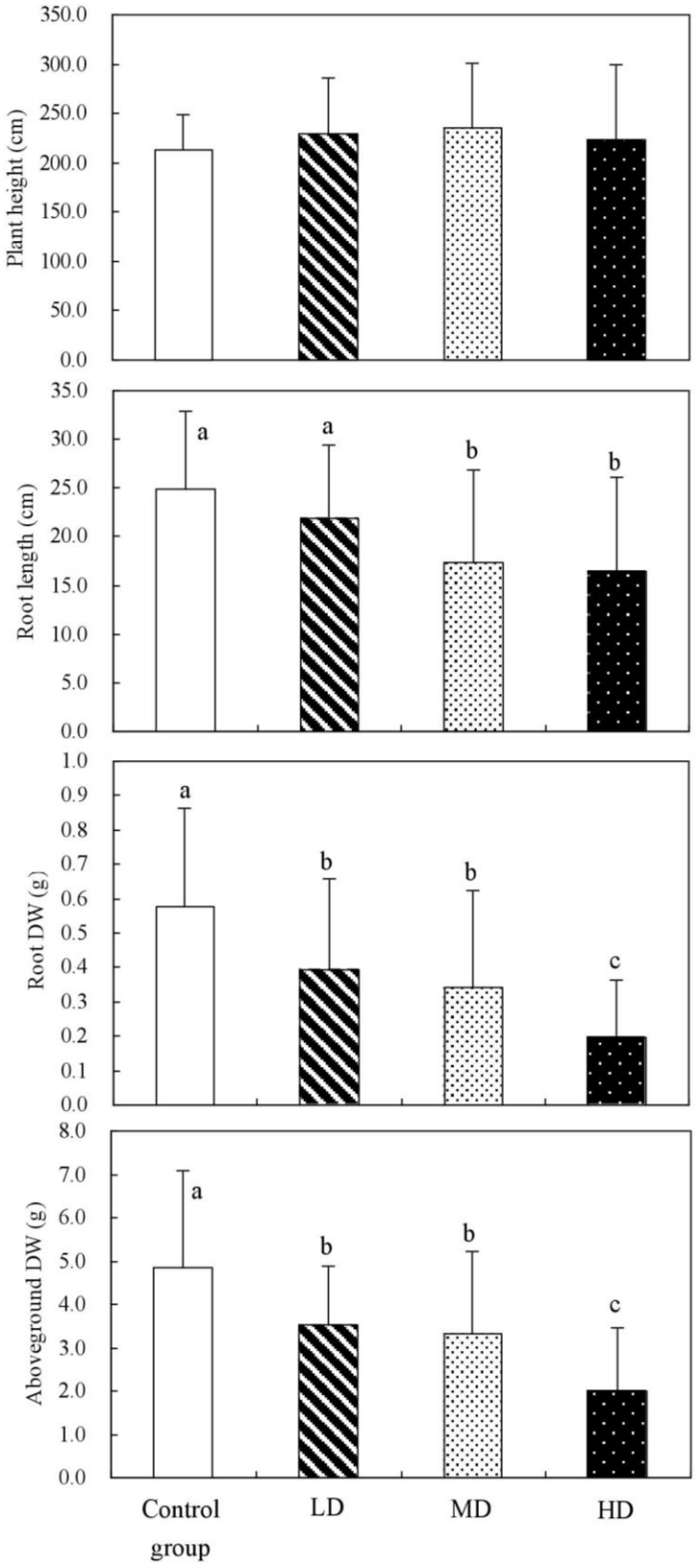

Figure 2. *Comparisons of plant height, root length, root dry weight (DW), and aboveground DW under different stocking densities. Different lowercase letters indicate significant differences ($P < 0.05$). Error bars indicate the standard deviation of the mean*

http://www.aloki.hu ● ISSN 1589 1623 (Print) ● ISSN 1785 0037 (Online)
DOI: http://dx.doi.org/10.15666/aeer/1802_36393649

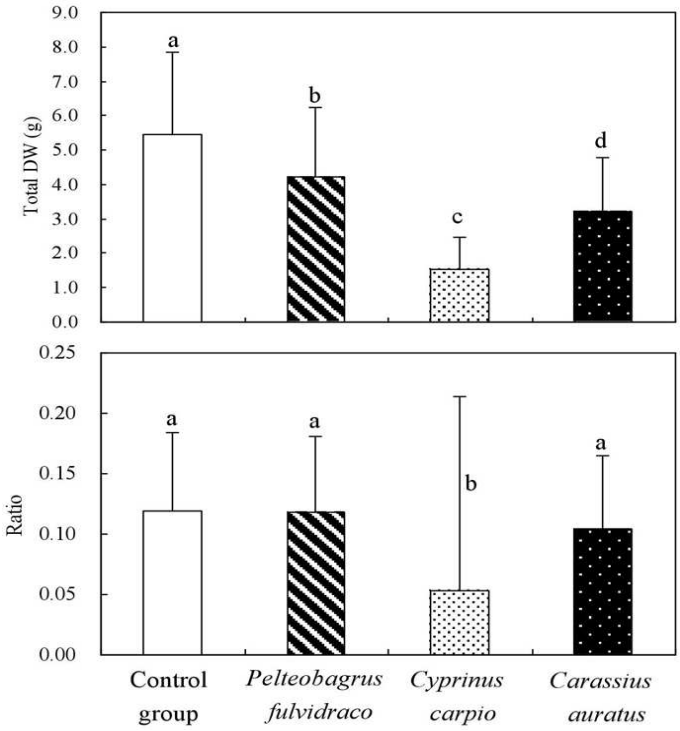

Figure 3. *Comparisons of total dry weight (DW) and root:aboveground part values after treatment with the different fishes. Different lowercase letters indicate significant differences ($P < 0.05$). Error bars indicate the standard deviation of the mean*

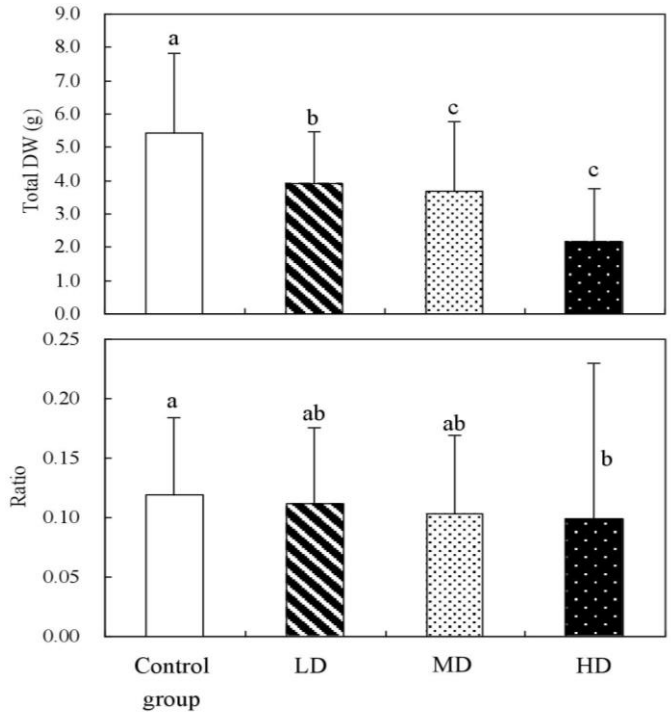

Figure 4. *Comparisons of the total dry weight (DW) and root:aboveground part values under different stocking densities. Different lowercase letters indicate significant differences ($P < 0.05$). Error bars indicate the standard deviation of the mean*

http://www.aloki.hu ● ISSN 1589 1623 (Print) ● ISSN 1785 0037 (Online)
DOI: http://dx.doi.org/10.15666/aeer/1802_36393649

Discussion

In China, fishery plays a very important role in socio-economic development. With the rapid development of freshwater aquaculture fisheries, many freshwater lakes and reservoirs in China are being used intensively (Gu et al., 2018). In 2015, freshwater aquaculture production from the lakes and reservoirs account for 18% of the total freshwater aquaculture in China (Fisheries Bureau of the Ministry of Agriculture, 2016). Although aquaculture has made great advances in China, its negative impacts on the environment have also received increased attention. The most significant negative impacts are the deterioration of water quality and degradation of aquatic plants because of high-density aquaculture. In this study, the TN, TP, Cond, and TDS were obviously higher in all the treatment groups than in the control group after fish stocking; however, water transparency was obviously lower in all the treatment groups than in the control group. This is consistent with the results of other studies, which indicates that fish stocking increases disturbance to aquatic plants and accelerates the release of nutrients in the sediment (Pipalova, 2006; Wang et al., 2016; Hansen et al., 2019). The *Cyprinus carpio* treatment groups showed the lowest transparency and highest nutrient content at the same stocking density, whereas the *Pelteobagrus fulvidraco* treatment groups showed the opposite trend (*Table 1*). This may because, of the three fish species, *Cyprinus carpio* disturbs water bodies and aquatic plants to the greatest extent.

Changes in morphology and biomass allocation because of external disturbances are adaptive strategies developed by aquatic plants during long-term evolution (Lytle and Poff, 2004; Merritt et al., 2010; Zhang, 2013). The results of this study show that the fish species and stocking density had significant effects on the morphological parameters and biomass allocation of *Potamogeton pectinatus*, and the morphological parameters differed in response to fish disturbance. The plant height was significantly higher in the *Pelteobagrus fulvidraco* and *Carassius auratus* treatment groups than in the control group, whereas the plant height was significantly lower in the *Cyprinus carpio* treatment groups than in the control group. This may be mainly because the transparency of the water body gradually decreases with an increase in fish disturbance. To a certain extent, *Potamogeton pectinatus* can increase its height to avoid the lack of underwater light; however, excessive disturbance significantly inhibits the growth and survival of the plant. Many studies have shown that light availability is the main factor that determines the growth of submerged plants. Aquatic plants tend to produce taller shoots, which is associated with decreased investment in the belowground part in response to decreased light availability (Strand and Weisner, 2001; Zhang et al., 2013; Li et al., 2018). In this study, the root length of the plants after the three different fish treatments was lesser than that of the plants in the control group, which indicates that *Potamogeton pectinatus* reduced root investment after the stocking of omnivorous fishes. The root:aboveground part value was significantly lower in the *Cyprinus carpio* groups than in the control group and other two fish groups (*Fig. 3*); this suggested that the *Cyprinus carpio* groups caused the largest disturbance, and the plants in the *Cyprinus carpio* groups invested more resources into aboveground parts than those in the other groups.

The plant height in the different treatment groups did not demonstrate any significant differences as the stocking density increased, but the root length and root:aboveground part values significantly decreased (*Fig. 2*). The reason for the similar plant heights may be mainly attributable to the shallow water depth in the cement ponds during the experiment (always maintained at 150 cm), which limited the space for plant growth.

http://www.aloki.hu ● ISSN 1589 1623 (Print) ● ISSN 1785 0037 (Online)
DOI: http://dx.doi.org/10.15666/aeer/1802_36393649

The significantly decreased root length and root:aboveground part values indicated the active adaptation of *Potamogeton pectinatus* to gradually increasing external disturbances. In addition, regardless of the stocking density, the total DW, root DW, and aboveground DW values significantly decreased and were the lowest in the *Cyprinus carpio* treatment groups. This may be mainly due to the reduced branch number and stem diameter of *Potamogeton pectinatus* after the fish stocking, which is an active adaptation to weak light conditions caused by the fish stocking. Other studies on the morphological responses of emergent or submerged plants in low light environments have also reported similar findings (Stand and Weisner, 2001; Zhang, 2013; Wang et al., 2018).

Changes in the fish community structure will inevitably affect other aquatic communities and the structure and function of the entire lake ecosystem (Gu et al., 2018; Zhen et al., 2018). A previous study on some temperate lakes has shown that the ultimate cause for the transition from a macrophyte-dominated state to a phytoplankton-dominated state is changes in the fish community structure (Brönmark and Weisner, 1992). Therefore, appropriate regulation of fish resources is very important for lake management and submerged plant restoration. To date, studies on the relationships between fish and aquatic plants mainly focused on herbivorous fishes, especially grass carp (Garner et al., 2013; Domingues et al., 2016). Some studies have indicated that irrational stocking of grass carp often leads to the disappearance of many submerged macrophytes in freshwater lakes (Chen and Guo, 2005; Wang et al., 2016; Zhen et al., 2018). However, our study showed that, although the consumption of submerged macrophytes by omnivorous fishes was lower than that by the grass carp, the effects of different omnivorous fishes on the growth of submerged macrophytes have significant differences. For the restoration of submerged plants in cultivated lakes, in addition to reducing the adverse effects of some herbivorous fishes (such as grass carp) on submerged macrophytes, the adverse disturbances caused by omnivorous fishes (such as *Cyprinus carpio*) need to be considered. On the basis of the results of this study, we suggest strict control of the number of *Cyprinus carpio*, appropriate control of the number of *Carassius auratus*, and relaxed control of omnivorous fishes (such as *Pelteobagrus fulvidraco*) that do not cause much disturbance to submerged macrophytes.

Conclusion

Both the fish species and stocking density had significant effects on the growth of *Potamogeton pectinatus*. Generally, the disturbance caused by *Cyprinus carpio* was the greatest, and the disturbance caused by *Pelteobagrus fulvidraco* was the lowest. With the increase in stocking density, the disturbance gradually increased. To a certain extent, *Potamogeton pectinatus* can adapt through changes in the morphological parameters or biomass allocation, but excessive disturbance by fishes significantly inhibits the growth and survival of the plant. Therefore, the dominant fish species should be scientifically assessed before the restoration of submerged vegetation, and appropriate control of fish stocking density is necessary to promote the establishment of submerged macrophytes in cultured lakes. Finally, more field studies are required to determine the joint or single effects of dominant fishes with different feeding habits on the growth of submerged macrophytes and provide a quantitative basis for the restoration of submerged macrophytes.

http://www.aloki.hu ● ISSN 1589 1623 (Print) ● ISSN 1785 0037 (Online)
DOI: http://dx.doi.org/10.15666/aeer/1802_36393649

Acknowledgements. This study was supported by Test and Demonstration of Agricultural Technology and Service Support (2130106-ZJBYD); Open Foundation of Key Laboratory of Tropical and Subtropical Fishery Resource Application and Cultivation, Ministry of Agriculture; Key Project of Natural Science Foundation for Universities of Anhui Province (KJ2019A0550); and Aquatic Plant Regulation and Landscape Design Program in Baiyangdian Lake (604-180025).

REFERENCES

[1] Brönmark, C., Weisner, S. E. B. (1992): Indirect effects of fish community structure on submerged vegetation in shallow, eutrophic lakes: an alternative mechanism. – Hydrobiologia 243: 293-301.
[2] Chen, X., Guo, Y. (2005): Succession of aquatic vegetation in Lake Xiannv of Lake Xinghu, Zhaoqing City, Guangdong Province. – Journal of Lake Science 17(4): 334-339.
[3] Domingues, F. D., Starling, F. L. R. M., Nova, C. C., Loureiro, B. R., Souza, L. C., Branco, C. W. C. (2016): The control of floating macrophytes by grass carp in net cages: experiments in two tropical hydroelectric reservoirs. – Aquaculture research 48(7): 3356-3368.
[4] Fang, J., Wang, Z., Zhao, S., Li, Y., Tang, Z., Yu, D., Ni, L., Liu, H., Xie, P., Da, L., Li, Z., Zheng, C. (2006): Biodiversity changes in the lakes of the central Yangtze. – Frontiers in Ecology and the Environment 4(7): 369-377.
[5] Fisheries Bureau of the Ministry of Agriculture of China. (2016): China fishery statistical yearbook. – China Agriculture Press, Beijing.
[6] Garner, A. B., Kwak, T. J., Manuel, K. L., Barwick, D. H. (2013): High-density grass carp stocking effects on a reservoir invasive plant and water quality. – Journal of Aquatic Plant Management 51: 27-33.
[7] Ge, Y., Zhang, K., Yang, X. (2018): Long-term succession of aquatic plants reconstructed from palynological records in a shallow freshwater lake. – Science of the Total Environment 643: 312-323.
[8] Gu, X., Mao, Z., Ding, H., Wang, Y., Zeng, Q., Wang, L. (2018): Progress and prospect of lake fishery in China. – Journal of Lake Science 30: 1-14.
[9] Hanlon, S. G., Hoyer, M. V., Cichra, C. E., Canfield, D. E. (2000): Evaluation of macrophyte control in 38 Florida lakes using triploid grass carp. – Journal of Aquatic Plant Management 38: 48-54.
[10] Hansen, J. H., Brodersen, J., Baktoft, H., Skov, C. (2019): Relationship between bream (*Abramis brama*) activity and water turbidity in a shallow lake under different season conditions. – Journal of Limnology 78(2): 259-269.
[11] Li, Z., Zhang, X., Wan, A., Wang, H., Xie, J. (2018): Effects of water depth and substrate type on rhizome bud sprouting and growth in *Zizania latifolia*. – Wetlands Ecology and Management 26: 277-284.
[12] Lu, R. S. (2000): Soil and Agriculture Chemical Analysis Methods. – Chinese Agricultural Science and Technology Press, Beijing.
[13] Lytle, D. A., Poff, N. L. (2004): Adaptation to natural flow regimes. – Trends in Ecology and Evolution 19(2): 94-100.
[14] Merritt, D. M., Scott, M. L., Poff, N. L., Auble, G. T., Lytle, D. A. (2010): Theory, methods and tools for determining environmental flows for riparian vegetation: riparian vegetation-flow response guilds. – Freshwater Biology 55: 206-225.
[15] Mo, W. Y., Man, Y. B., Wong, M. H. (2018): Use of food waste, fish waste and food processing waste for China's aquaculture industry: Needs and challenge. – Science of the Total Environment 613: 635-643.
[16] Pipalova, I. (2006): A review of grass carp use for aquatic weed control and its impact on water bodies. – Journal of Aquatic Plant Management 44: 1-12.

http://www.aloki.hu ● ISSN 1589 1623 (Print) ● ISSN 1785 0037 (Online)
DOI: http://dx.doi.org/10.15666/aeer/1802_36393649

[17] Strand, J. A., Weisner, S. E. B. (2001): Morphological plastic responses to water level depth and wave exposure in an aquatic plant (*Myriophyllum spicatum*). – Journal of Ecology 89: 166-175.
[18] Wang, H. Z., Wang, H. J., Liang, X. M., Ni, L. Y., Liu, X. Q., Cui, Y. D. (2005): Empirical modelling of submersed macrophytes in Yangtze lakes. – Ecological Modelling 188(2): 483-491.
[19] Wang, X., Wang, Y., Yang, G., Qin, B., Yang, H. (2016): The effects of different fish species on growth of submerged macrophytes. – Journal of Lake Science 28(6): 1354-1360.
[20] Wang, H. L., Zhang, X. K., Wan, A. (2018): Morphological responses of Zizania latifolia seedlings at different ages to short-term submergence. – Journal of Lake Science 30(1): 192-198.
[21] Wu, Z. G., Xiong, W., Hou, H. W. (2019): Biodiversity pattern and conservation of aquatic vascular plants in the Yangtze River basin, China. – Acta Hydrobiologica Sinica 43(S1): 27-41.
[22] Zhang, X. (2013): Water level fluctuation requirements of plants in the Yangtze floodplain lakes. – Ph.D. Thesis of University of Chinese Academy of Sciences, Beijing, China.
[23] Zhang, X., Liu, X., Ding, Q. (2013): Morphological responses to water level fluctuations of two submerged macrophytes Myriophyllum spicatum and Hydrilla verticillata. – Journal of Plant Ecology 6: 64-70.
[24] Zhang, Y., Jeppesen, E., Liu, X., Qin, B., Shi, K., Zhou, Y., Thomaz, S. M., Deng, J. (2017): Global loss of aquatic vegetation in lakes. – Earth-Science Reviews 173: 259-265.
[25] Zhang, X., Liu, X., Yang, Z., Wang, H. (2019): Restoration of aquatic plants after extreme flooding and drought: a case study from Poyang Lake National Nature Researve. – Applied Ecology and Environmental Research 17(6): 15657-15668.
[26] Zhen, W., Zhang, X., Guan, B., Yin, C., Yu, J., Jeppesen, E., Zhao, X., Liu, Z. (2018): Stocking of herbivorous fish in eutrophic shallow clear-water lakes to reduce standing height of submerged macrophtes while maintaining their biomass. – Ecological Engineering 113: 61-64.

http://www.aloki.hu ● ISSN 1589 1623 (Print) ● ISSN 1785 0037 (Online)
DOI: http://dx.doi.org/10.15666/aeer/1802_36393649

A COMPARATIVE STUDY ON THE NUTRITIONAL CHARACTERISTICS OF MALE AND FEMALE CHINESE HOOK SNOUT CARP (*OPSARIICHTHYS BIDENS*)

CHEN, K. J.[1#] – TANG, Y.[1#] – LIU, D. Z.[2*] – GENG, B.[1] – LIU, X. Y.[1*]

[1]*College of Animal Science and Technology, Hunan Agricultural University, Changsha 420128, China*

[2]*Rural Agriculture Bureau of Taojiang County, Yiyang 413400, China*

[*]*Corresponding authors*
e-mail: 502732837@qq.com (Liu, D. Z); 1176450971@qq.com (Liu, X. Y.)

[#] *These authors contributed equally to this work.*

(Received 24th Dec 2019; accepted 24th Mar 2020)

Abstract. The nutritional composition of fish muscle is an important reference data for the design of fish feed formulae. However, the nutritional composition of the muscle of Chinese hook snout carp has not been analyzed at present. In addition, considering the obvious individual difference between male and female Chinese hook snout carp, there may also be significant difference in nutritional composition. To provide a reference for the feed formula design of artificially cultured Chinese hook snout carp, the muscle nutrient composition of five wild male and female individuals was analyzed in this study. Our results showed that water, crude protein, crude fat, and crude ash contents had no significant differences between male and female fish. Although there was no significant difference in the contents of most amino acids between male and female fish, the contents of flavored amino acids, essential amino acids and total amino acids in male fish muscle were significantly higher than those in female fish muscle. The proportion of saturated fatty acids, monounsaturated fatty acids, and polyunsaturated fatty acids was 1.37:1:1.80, and most of fatty acids showed significant difference between male and female fish.
Keywords: *regional environment, culture method, feed, muscle nutrition, nutrient determination*

Introduction

Chinese hook snout carp (*Opsariichthys bidens* Günther) is one of the most widely distributed small Asiatic cyprinids. It generally occupies fast-flowing mountainous steams (Perdices et al., 2005; Fu et al., 2012). However, due to habitat destruction caused by human activities and overfishing, the natural resources of the fish decreased dramatically in recent years (Chen, 2015).

To avoid extinction of wildlife resources due to over hunting, it is an important and feasible way to establish artificial breeding technology instead of the market demand for the wildlife resources (Chen, 2015; Xiang et al., 2018). For example, only in a Chinese county, Anhua County, 26505 kg of commercial adult Chinese hook snout carp and 994000 fries produced in 2012. However, although the nutritional composition of fish muscle is an important reference data for the design of fish feed formulae (Schaeffer et al., 2012), and a large number of studies have been reported on the nutritional composition of fishes (e.g. Hang et al., 2001; Xu et al., 2005; Lou et al., 2010; Liu et al., 2010; Yang et al., 2010), the nutritional composition of the muscle of Chinese hook snout carp has not been analyzed yet. In addition, considering the obvious individual difference between male and female of Chinese hook snout carp, there may also be significant difference in nutritional composition.

http://www.aloki.hu ● ISSN 1589 1623 (Print) ● ISSN1785 0037 (Online)
DOI: http://dx.doi.org/10.15666/aeer/1802_36513658

The lack of nutritional composition of muscle seriously limits the development of feed formula and the efficiency of artificial propagation and cultivation of Chinese hook snout carp. For example, to provide more suitable feed for the parent fish of Chinese hook snout carp in the breeding stage, it is necessary to clarify the nutritional requirements of the male and female fish, and the muscle nutritional components of the male and female fish provide an important reference data for the development of such feed. To provide a reference for the feed formula design of artificial cultured Chinese hook snout carp, the muscle nutrient composition of wild male and female Chinese hook snout carp was analyzed in this study.

Materials and Methods

Sample collection

The Chinese hook snout carp samples were collected from Chetianjiang Reservoir, Anhua, China (27.85° N, 111.60° E) on March 15. The fish samples were transported to the laboratory by oxygenation and then fasted for 1 days. Each 5 male and female samples with the same size (approximately 50 g of each fish; *Fig. 1*) were selected and anesthetized 5 min using 100 mg/L of neutralized MS222 (tricaine methanesulfonate, Sigma-Aldrich, Germany) (Tuo et al., 2020). Then, the muscles on both sides of the back above the lateral scale below the dorsal fin were dissected for the determination of nutritional components.

Figure 1. *Photos of male (A) and female (B) Chinese hook snout carp*

Analysis of nutrients

Dry matter content was determined by 105°C constant temperature and atmospheric pressure drying method. Crude protein content, crude fat content, and crude ash content was determined by Kjeldahl nitrogen method, Soxhlet extraction method, and muffle

http://www.aloki.hu ● ISSN 1589 1623 (Print) ● ISSN1785 0037 (Online)
DOI: http://dx.doi.org/10.15666/aeer/1802_36513658

furnace burning method respectively according to previous studies (Saalah et al., 2010; Sun et al., 2011).

Amino acids were measured by a L8800 amino acid analyzer (Hitachi, Japan) (Sun et al., 2016). Fish oil was extracted by Soxhlet extraction (Ozogul et al., 2012). Composition of fatty acids was measured using a 6890-5973N gas chromatography - mass spectrometer (Agilent, USA) (Mazurek et al., 2017).

Data analysis

The data were showed as mean ± standard deviation (S.D.) (Jiang et al., 2019). Independent *t*-test was conducted to test statistical difference between different groups using R software with basic packages (Everitt and Hothorn, 2010; Horton and Kleinman, 2011). Results with $p \leq 0.05$ were considered statistically significant (Ni et al., 2019).

Results

Contents of the crude protein, crude fat, and crude ash in male Chinese hook snout carp muscles were 17.23 ± 1.54%, 2.71 ± 0.61%, and 1.32 ± 0.10%, respectively. Contents of the crude protein, crude fat, and crude ash in female fish muscles were 16.71 ± 0.99%, 2.23 ± 0.92, and 1.36 ± 0.02%, respectively (*Fig. 2*). Water content in muscle was no significant difference between the male and female fish (independent *t*-test, $t = 0.90$, $p = 0.38$). No significant difference of crude protein (independent *t*-test, $t = 0.49$, $p = 0.64$), crude fat (independent *t*-test, $t = 1.38$, $p = 0.18$), and crude ash (independent *t*-test, $t = 1.20$, $p = 0.25$) contents in muscle between male and female Chinese hook snout carp was found.

Figure 2. *Nutritional compositions in muscle of male and female Opsariichthys uncirostris bidens Günther (% wet weight)*

Among the amino acids in the muscle of male and female Chinese hook snout carp samples, the highest amino acids were glutamic acid, proline, aspartic acid and lysine, all of which were more than 1.5 g in 100 g of muscle (*Table 1*). Only content of cystine in the muscle of male fish was significantly higher than that of female (independent *t*-test, $t = 3.16$, $p = 0.01$; *Table 1*). Although there was no significant difference in the contents of most amino acids between male and female fish, the contents of flavored amino acids, essential amino acids and total amino acids in male fish muscle were significantly higher than those in female fish muscle (*Table 1*).

http://www.aloki.hu ● ISSN 1589 1623 (Print) ● ISSN1785 0037 (Online)
DOI: http://dx.doi.org/10.15666/aeer/1802_36513658

Table 1. *The compositions and contents of amino acids in muscle of male and female Opsariichthys uncirostris bidens Günther*

Amino acid	Sampling size	Male (g/100 g)	Female (g/100 g)	*t*	*p*
Asp	5	1.86±0.06	1.86±0.07	0.03	0.96
Ser	5	0.78±0.02	0.77±0.03	0.62	0.55
Glu	5	2.73±0.10	2.65±0.06	1.53	0.16
Ala	5	1.04±0.03	1.04±0.04	0.02	0.98
Gly	5	0.80±0.04	0.79±0.05	0.35	0.74
Arg	5	0.98±0.04	0.97±0.04	0.40	0.70
Pro	5	2.23±0.03	2.23±0.03	0.01	1.00
Cys	5	1.28±0.01	1.26±0.01	3.16	0.01*
Tyr	5	0.63±0.03	0.62±0.02	0.62	0.55
NH_3	5	0.21±0.01	0.21±0.01	0.01	0.99
Val	5	1.03±0.02	1.02±0.02	0.79	0.45
Met	5	1.18±0.01	1.16±0.02	2.00	0.08
Ile	5	0.86±0.01	0.86±0.02	0.01	0.99
Leu	5	1.45±0.04	1.44±0.04	0.40	0.70
Phe	5	1.09±0.01	1.08±0.01	1.58	0.15
Lys	5	1.72±0.05	1.72±0.05	0.01	0.96
His	5	0.60±0.01	0.60±0.05	0.16	0.88
Thr	5	0.84±0.03	0.84±0.04	0.01	0.98
∑DAA	5	7.19±0.03	7.10±0.01	6.36	<0.001***
∑EAA	5	8.76±0.01	8.73±0.02	3.00	0.02*
∑TAA	5	21.28±0.02	21.11±0.02	13.44	<0.001***

∑DAA, flavored amino acid; ∑EAA, essential amino acid; ∑TAA, total amino acids. * $p < 0.05$; ** $p < 0.01$; *** $p < 0.001$

The saturated fatty acids detected in the muscle of the Chinese hook snout carp samples were c13:0, c14:0, c15:0, c16:0, c18:0 and c20:0. Methyl palmitate (c16:0) was the major saturated fatty acids, which accounted for 68.18% of the saturated fatty acids (*Table 2*). This result was similar to those reported in other fishes (Lv et al., 1995). The main monounsaturated fatty acids were c16:1n-9 and c18:1, which accounted for 80.08% of the monounsaturated fatty acids (*Table 2*). The main polyunsaturated fatty acids were c22:6n-4, which accounted for 58.57% of the polyunsaturated fatty acids (*Table 2*). The proportion of saturated fatty acids, monounsaturated fatty acids, and polyunsaturated fatty acids was 1.37:1:1.80 (*Table 2*). Although the concentration distribution of various fatty acids in muscle of male and female fish was similar, the contents of most of fatty acids in muscle were significant differences between the male and female Chinese hook snout carp samples, in which c15:0 and c18:1 in male muscle were more than one time than those in female, while c27:2n-3 in female muscle was more than one time than that in male (*Table 2*).

http://www.aloki.hu ● ISSN 1589 1623 (Print) ● ISSN1785 0037 (Online)
DOI: http://dx.doi.org/10.15666/aeer/1802_36513658

Table 2. *The compositions and contents of ratty acids in muscle of male and female Opsariichthys uncirostris bidens Günther*

Fatty acid	Sampling size	Female (g/100 g)	Male (g/100 g)	*t*	*p*
c13:0	5	0.50±0.03	0.43±0.01	4.95	0.07
c14:0	5	1.86±0.05	1.10±0.02	31.56	<0.001***
c15:0	5	2.35±0.03	5.10±0.09	64.82	<0.001***
c16:0	5	19.35±0.45	16.54±0.33	11.26	<0.001***
c16:1n-9	5	5.96±0.36	6.55±0.28	2.89	0.02*
c18:0	5	4.11±0.03	4.40±0.07	8.51	<0.001***
c18:1	5	10.68±0.57	25.49±0.65	38.31	<0.001***
c18:2n-9	5	4.05±0.19	7.77±0.32	22.35	<0.001***
c20:0	5	0.11±0.01	0.18±0.01	11.07	<0.001***
c20:1n-9	5	0.35±0.02	0.90±0.01	55.00	<0.001***
c20:1n-11	5	0.74±0.08	1.18±0.07	9.26	<0.001***
c20:2n-11	5	1.11±0.08	0.80±0.02	8.41	<0.001***
c20:4n-5	5	3.64±0.15	3.35±0.12	3.38	0.01**
c20:5n-5	5	1.93±0.12	1.91±0.11	0.27	0.79
c22:6n-4	5	21.94±1.25	17.17±1.75	4.96	0.001**
c27:2n-3	5	6.72±0.45	0.47±0.09	30.45	<0.001***
SFA	5	28.38±1.69	27.75±1.23	0.67	0.52
MUFA	5	20.78±1.32	33.70±1.75	13.18	<0.001***
PUFA	5	37.46±2.11	32.21±1.44	4.60	0.001**

SFA, saturated fatty acids; MUFA, monounsaturated fatty acids; PUFA, polyunsaturated fatty acids. * $p < 0.05$; ** $p < 0.01$; *** $p < 0.001$

Discussion

There is a close relationship between the nutritional composition of fish muscle and its feeding habits (Wang et al., 2010a). Generally, contents of crude protein and crude fat in muscle of carnivorous fishes are higher than those of herbivorous fishes, while the content of crude ash is lower than that of herbivorous fishes (Wang et al., 2010a). Our results showed that the content of crude protein in the Chinese hook snout carp was higher than that of yellow catfish (*Pelteobagrus fulvidraco*) (Jiang et al., 2013) and Qinling lenok (*Brachymystax lenok*) (Xu et al., 2010), lower than that of *Phoxinus lagowskii* (Zhang et al., 2013), and closed to that of *Neosalanx brevirostris* (Jiang et al., 2011) and other carnivorous fishes (Sun et al., 2008; Jiang et al., 2013). These results implied that the muscle of Chinese hook snout carp contained high protein level and conformed to its carnivorous attribute.

Sex is one of the most important factors that affect the composition of muscle nutrients in fish (Jiang et al., 2011; Zhang et al., 2013). Although contents of most of amino acids in muscle are significant difference between male and female *Neosalanx brevirostris* (Jiang et al., 2011) and *Silurus asotus* (Jiang et al., 2012), our results showed that only cystine content was significant difference between male and female Chinese hook snout

http://www.aloki.hu ● ISSN 1589 1623 (Print) ● ISSN1785 0037 (Online)
DOI: http://dx.doi.org/10.15666/aeer/1802_36513658

carp, which was consistent with previous report in *Pelteobagrus fulvidraco* (Jiang et al., 2013). However, contents of most of fatty acids were significant differences in muscle between male and female Chinese hook snout carp, which was consistent with previous reports in *Neosalanx brevirostris* (Jiang et al., 2011).

Fish species is an important factor affecting the nutritional composition in muscle. Choi et al. (2008) reported that the protein in the muscle of *Sophorae fructus* is composed of a total of 18 different kinds of amino acids, and the contents of saturated fatty acids, monounsaturated fatty acids, and polyunsaturated fatty acids in the muscle of *Sophorae fructus* are 24.94%, 32.40%, and 32.86%, respectively. Our results showed that the contents of saturated fatty acids, monounsaturated fatty acids, and polyunsaturated fatty acids in the muscle of were 28.38%, 20.78%, and 37.46%, respectively. In addition, culture patterns, food sources and fish strains affect the compositions of fish nutrients (Wang et al., 2010b; Zhou et al., 2014).

Conclusion

In conclusion, contents of the crude protein, crude fat, and crude ash in male Chinese hook snout carp muscles were 17.23 ± 1.54%, 2.71 ± 0.61%, and 1.32 ± 0.10%, respectively. Contents of the crude protein, crude fat, and crude ash in female fish muscles were 16.71 ± 0.99%, 2.23 ± 0.92%, and 1.36 ± 0.02%, respectively. No significant difference of the crude protein, crude fat, and crude ash was detected between male and female fish. Although there was no significant difference in the contents of most amino acids between male and female fish, the contents of flavored amino acids, essential amino acids and total amino acids in male fish muscle were significantly higher than those in female fish muscle. The proportion of saturated fatty acids, monounsaturated fatty acids, and polyunsaturated fatty acids was 1.37:1:1.80, and most of fatty acids were significant difference between male and female fish. However, the influence of feed formulae designed according to our results on the reproduction and growth of Chinese hook snout carp should be further studied.

Acknowledgements. This research was supported by the Basic R & D Project of Key R & D Plan of Science and Technology Department of Hunan Province (No. 2015JC3104). The authors thank anonymous technicians at Guangdong Meilikang Bio-Science Ltd., China for assistance with data re-analysis.

REFERENCES

[1] Chen, C. (2015): Study on reproductive biological characteristics and breeding technology of Chinese hook snout carp (*Opsariichthys bidens*). – Changsha: Hunan Agricultural University.

[2] Choi, Y. S., Shin, E. H., Park, S. J., Kim, J. D. (2008): Nutritional characteristics and some bioactive components contents of *Sophorae fructus*. – Journal of the Korean Society of Food Science and Nutrition 37(9): 1154-1161.

[3] Everitt, B. S., Hothorn, T. (2010): A handbook of statistical analyses using R (Second edition). – CRC press, Boca Raton.

[4] Fu, S. J., Peng, Z., Cao, Z. D., Peng, J. L., He, X. K., Xu, D., Zhang, A. J. (2012): Habitat-specific locomotor variation among Chinese hook snout carp (*Opsariichthys bidens*) along a river. – PLoS ONE 7(7): e40791.

http://www.aloki.hu ● ISSN 1589 1623 (Print) ● ISSN1785 0037 (Online)
DOI: http://dx.doi.org/10.15666/aeer/1802_36513658

[5] Hang, X., Tang, Y., Liu, X. (2001): Progress in the research on polyunsaturated fatty acids. – Progress in Biotechnology 21.
[6] Horton, N. J., Kleinman, K. (2011): Using R for data management, statistical analysis, and graphics. – CRC press, Boca Raton.
[7] Jiang, J., Han, X., Fu, Z., Sun, Z. (2011): Analysis and assessment of muscle nutritive composition between female and male *Neosalanx brevirostris* Pellegrin. – Journal of Guangdong Ocean University 31(4): 23-29.
[8] Jiang, J., Han, X., Fu, Z., Xie, G., Li, W., Meng, Y., Sun, Z. (2012): Comparative analysis of the main nutritional components in muscle and skin of male and female *Silurus asotus*. – Journal of Jimei University (Natural Science) 17(1): 6-12.
[9] Jiang, J., Fu, Z., Zhang, W., Li, W., Meng, Y., Sun, Z. (2013): Comparative analyses of the main nutritional components in edible tissues of male and female *Pelteobagrus fulvidraco* Richardson. – Journal of Bijie University 31(04): 96-103.
[10] Jiang, H., Liu, S., Xiao, T. Y., Cao, Y. K., Xie, M., Yin, Z. F. (2019): Cellular biological and eumelanin-related gene expressional bases of pigment deviation of *Leptobotia taeniops*. – Applied Ecology and Environmental Research 17(5): 12181-12189.
[11] Liu, Y., Xu, G., Mou, Z., Li, Y. (2010): Evaluation of nutritive quality and nutritional components of the muscle of *Brachymystax lenok*. – Acta Nutrimenta Sinica 32(1): 99-100.
[12] Lou, B., Gao, L., Mao, G., Shi, H., Luo, J. (2010): Analysis and Evaluation of the nutritional components in the muscle of *Paralichthys olivaceus*. – Acta Nutrimenta Sinica 32(02): 195-197.
[13] Lv, X., Li, M., Yao, Y., Gao, W., Yun, X., Kou, D. (1995): Preliminary analysis of fatty acid of some economical fishes. – Acta Scientiarum Naturalium Universitatis Nankaiensis 28(4): 20-25.
[14] Mazurek, B., Chmiel, M., Górecka, B. (2017): Fatty acids analysis using gas chromatography-mass spectrometer detector (GC.MSD) - method validation based on berry seed extract samples. – Food Analytical Methods 10(8): 2868-2880.
[15] Ni, J., Huang, R., Zhou, H., Xu, X., Li, Y., Cao, P., Zhong, K., Ge, M., Chen, X., Hou, B., Yu, M., Peng, B., Li, Q., Zhang, P., Gao, Y. (2019): Analysis of the relationship between the degree of dysbiosis in gut microbiota and prognosis at different stages of primary hepatocellular carcinoma. – Frontiers in Microbiology 10: 1458.
[16] Ozogul, Y., Şimşek, A., Balikçi, E., Kenar, M. (2012): The effects of extraction methods on the contents of fatty acids, especially EPA and DHA in marine lipids. – International Journal of Food Sciences and Nutrition 63(3): 326-331.
[17] Perdices, A., Sayanda, D., Coelho, M. M. (2005): Mitochondrial diversity of *Opsariichthys bidens* (Teleostei, Cyprinidae) in three Chinese drainages. – Molecular Phylogenetics and Evolution 37: 920-927.
[18] Saalah, S., Shapawi, R., Othman, N. A., Bono, A. (2010): Effect of formula variation in the properties of fish feed pellet. – Journal of Applied Sciences 10(21): 2537-2543.
[19] Schaeffer, T. W., Hennen, M. J., Brown, M. L., Rosentrater, K. A. (2012): Nutritional composition and use of common carp muscle in yellow perch diets. – North American Journal of Aquaculture 74: 297-305.
[20] Sun, Z., Li, C., Yin, H., Wang, B. (2008): Analysis of the nutritional composition in muscle of five varieties of *Oncorhynchus mykiss*. – Acta Nutrimenta Sinica 30(3): 298-302.
[21] Sun, H., Liu, X., Miao, Y. (2011): Speciation analysis of trace inorganic arsenic in dietary supplements by slurry sampling hydride generation atomic absorption spectrometry. – Food Anal Methods 4: 251-257.
[22] Sun, J., Zhang, S., Hu, Q., Mao, X. H., Ji, S. (2016): Determination of 16 kinds of amino acids in health foods by high performance liquid chromatography with pre-column derivatization. – Journal of Food Safety & Quality 7(7): 2715-2719.
[23] Tuo, Y., Xiao, T., Wang, H. (2020): Discrimination of sexual dimorphism through external morphology of Hemibarbus maculatus in the Yuanhe River, China. – Applied Ecology and Environmental Research 18(1): 1539-1550.

http://www.aloki.hu ● ISSN 1589 1623 (Print) ● ISSN1785 0037 (Online)
DOI: http://dx.doi.org/10.15666/aeer/1802_36513658

[24] Wang, G., Sun, L., Li, Z., Guo, G., Niu, X., Lu, H. (2010a): Nutritional composition and evaluation in muscles and flesh content of various fishes with different feeding habits. – Feed Industry Magazine 31: 94-98.
[25] Wang, J., Li, P., Song, Z., Wang, S., Li, B., Huang, B., Zhang, L. (2010b): Comparsion of amino acid composition in different tissues of the wild and the cultured *Paralichthys olivaceus* broodstock. – Journal of Fisheries of China 34(11): 1736-1743.
[26] Xiang, J., He, T., Wang, P., Xie, M., Xiang, J., Ni, J. (2018): Opportunistic pathogens are abundant in the gut of cultured giant spiny frog (*Paa spinosa*). – Aquaculture Research 49: 2033-2041.
[27] Xu, J., Zhu, Y., Yan, X., Ye, F., Xu, S. (2005): Comparison of fatty acids composition between farmed and wild yellow croaker *Pseudosciaena crocea* (Richardson). – Acta Nutrimenta Sinica 27(3): 256-257, 260.
[28] Xu, G., Ye, Y., Liu, Y., Mou, Z., Li, Y. (2010): Comparative analyses of nutritional composition in muscle of male and female lenok (*Brachymystax lenok*). – Chinese Journal of Fisheries 23(2): 29-33.
[29] Yang, P., Wang, Z., Xia, D., Li, M., Xie, C., Liu, L., Wang, W. (2010): Analysis of nutritional compositions and evaluation of nutritional quality of muscle of *Aristichthys nobilis* blackspot and *Aristichthys nobilis* whitespot. – Oceanologia et Limnologia Sinica 41(4): 549-554.
[30] Zhang, Y., Yin, J., Du, J., Geng, L., Bai, Q., Xu, W. (2013): Comparative analysis of nutritional compositions in muscle of female and male *Phoxinus lagowskii* Dybowski. – Food Science 34(17): 259-262.
[31] Zhou, P., Jin, M., Wu, W., Shentu, J., Li, M., Zhou, Q. (2014): Comparison of nutrient components of large yellow croaker (*Pseudosciaena crocea* Richardson) cultured in different modes, fed different feeds and from different strains. – Chinese Journal of Animal Nutrition 26(4): 969-980.

http://www.aloki.hu ● ISSN 1589 1623 (Print) ● ISSN1785 0037 (Online)
DOI: http://dx.doi.org/10.15666/aeer/1802_36513658

PRECISE CLASSIFICATION OF FOREST SPECIES BASED ON MULTI-SOURCE REMOTE-SENSING IMAGES

ZHANG, R.[1,2] – LI, Q.[3] – DUAN, K. F.[4*] – YOU, S. C.[1*] – ZHANG, T.[1] – LIU, K.[1] – GAN, Y. H.[1]

[1]*Land Satellite Remote Sensing Application Center, Ministry of Natural Resources, Beijing 100048, China*

[2]*College of Resources Environment and Tourism, Capital Normal University, Beijing 100048, China*

[3]*College of Forestry and Horticulture, Xinjiang Agricultural University, Urumqi 830052, China*

[4]*School of Economics and Management, Tongji University, Shanghai 200092, China*

*****Corresponding authors*
e-mail: kefee920729@tongji.edu.cn, youusc@126.com

(Received 28th Dec 2019; accepted 26th Mar 2020)

Abstract. *Picea schrenkiana var. tianshanica* (*PSVT*) is an endemic tree species in Xinjiang, and serves as windbreak and soil consolidation, to ensure the stability of ecological environment. To efficiently and quickly grasp the ecological status of *PSVT* and the stability of forest ecosystem, we used images of different resolutions (GF-2 (1 m), GF-1 (8 m), GF-1 (16 m), Landsat 8 (30 m)) combined with field survey data, and performed multi-resolution segmentation to select the best segmentation scales. Based on the spectrum, texture and terrain factors, the canopy closure inversion of *PSVT* was performed to select the characteristic factors suitable. Then, we applied three object-oriented methods (i.e. support vector machine (SVM), classification and regression tree (CART), and nearest neighbor classification (NNC)) to classify the forest land. The result shows that the near-infrared (NIR) band is highly independent and makes an important contribution to the optimum index factor (OIF), in which the real-time adjustments of segmentation results are made to achieve better effect. There is a significant relationship between textural features of each band. The canopy closure estimation model performs better with a combination of spectral, terrain, and texture factors. Compared to CART and NNC models, SVM classification achieved better accuracy.
Keywords: *multi-resolution segmentation, remote sensing, environmental factors, canopy closure, supervised classification*

Introduction

Picea Schrenkiana var. tianshanica (*PSVT*) is a unique tree species in Xinjiang that is important to the wind resistance, soil stabilization, and overall stability of the ecological environment. The fast and efficient monitoring of forest resource information (Fernandez et al., 2019) and changes has become an important basis for scientific management and the efficient use of forest resources. Canopy closure (Perea et al., 2019; Adepoju et al., 2020), an important aspect of forest information surveys, reflects the growth status and density of forests, and plays a very important role in forest monitoring, so it is widely used in forest resource information surveys and forest ecology evaluations.

With the increasing number of satellite image sources, high-spatial-resolution remote-sensing images now contain more abundant spectral, spatial, shape, and textural information (Abdulhakim, 2019). Using only the spectral information of a single image will very likely cause the problems of "same substance and different spectrum" and

http://www.aloki.hu ● ISSN 1589 1623 (Print) ● ISSN 1785 0037 (Online)
DOI: http://dx.doi.org/10.15666/aeer/1802_36593681

"different substance and same spectrum" (Gilcher et al., 2019). The reasonable and effective selection of image data sources along with spectral factors, textural information, and terrain factors is very important for ensuring the accuracy and classification of canopy closure. Object-oriented methods can make better use of detailed information regarding an image's spectrum, space, shape, and texture (Baatz, 2000; Hofmann, 2001; Sun, 2009; Guo, 2012). For instance, Baatz (2000) and Hofmann (2001) conducted extensive experiments and research on high-resolution remote-sensing images and proposed a method for processing target features and an object-oriented classification. Hofmann (2001) used an object-oriented method to process IKONOS remote-sensing images to effectively classify buildings and highways. Piazza (2016) used aerial imagery to produce a graphic drawing of the tropical rain forest area in southern Brazil, and compared object-oriented and pixel-based classification methods. Guo (2012) took HJ-1 image and used an object-oriented method to effectively classify forest land information in Mentougou district, Beijing. Based on IKONOS images, Sun (2009) used the object-oriented and pixel-based fuzzy classification methods to extract urban-forest-park land in Fuzhou. Data with different resolutions often require different classification methods (Maas, et al., 2019). The canopy closure of a forest stand is used to achieve effective and precise forest classification (Donato et al., 2019), and the relationship between the internal information and depression in images has been widely studied. Linear regression modeling is performed, using the measured value of the degree of sample depression as the dependent variable (Rajasekhar et al., 2019) to obtain the correlation between the image feature factor and the degree of depression. Finally, the precise classification of a forest is realized based on its canopy closure.

In this study, we investigated the effects of spatial resolution on forest classification accuracy and selected the appropriate classification model based on images with different resolutions. Combining field survey data from GF-2 (1 m), GF-1 (8 m), GF-1 (16 m), and Landsat 8 (30 m) images, we established a canopy closure estimation model, selected sensitive feature factors, and used the classification and regression tree (CART), nearest neighbor classification (NNC), and support vector machine (SVM) methods to classify the *PSVT*. Then, we compared the accuracies of the different classifiers. Our aim in this work was to explore the effect of using data with different spatial resolutions and different classification methods on the precision of forest classification.

Materials and methods

Study area

The study area is located in the middle of the Tianshan Mountains (Dilixiati et al., 2019), 110 km southwest of Urumqi (86°46′ E–86°57′ E, 43°16′ N–43°26′ N). The total forest farm area is approximately 10444 hm^2 with a woodland core area 5116 hm^2. The terrain in the study area is complex, with high terrain in the south and low terrain in the north. The altitude ranges between 1700 and 3200 m. Topographic changes are obvious, and the slope mainly ranges between 10° and 40°. A wide range of rivers flows within the forest farm, with the Toutunhe River flowing from south to north, and small tributaries flowing throughout the area. The drinking water of local herders is mainly from these rivers. The annual precipitation in the study area is unevenly distributed. The annual average precipitation is about 600 mm, with great seasonal differences. The

http://www.aloki.hu ● ISSN 1589 1623 (Print) ● ISSN 1785 0037 (Online)
DOI: http://dx.doi.org/10.15666/aeer/1802_36593681

concentrated precipitation in summer and autumn accounts for a large proportion of the precipitation over the whole year. The annual average temperature is 3 °C, and the average temperature in July is 14 °C (Aizezitiyuemaier et al., 2019). The total annual sunshine is 1300 h, and the frost-free period lasts 140 d. *Figure 1* shows the specific location of this area, with the forest mainly distributed on the northeast and northwest slopes, comprising mainly grasses and *Picea Schrenkiana var. tianshanica* (*PSVT*), and the soil of the forest being ordinary taupe forest soil. As the main dominant conifer species in Xinjiang mountain forests (Li et al., 2019), *PSVT* comprises an important part of the northern forest. It also plays an irreplaceable role in the conservation of water resources (Liu et al., 2019), maintaining both the water and soil and the ecological balance of the Xinjiang oasis.

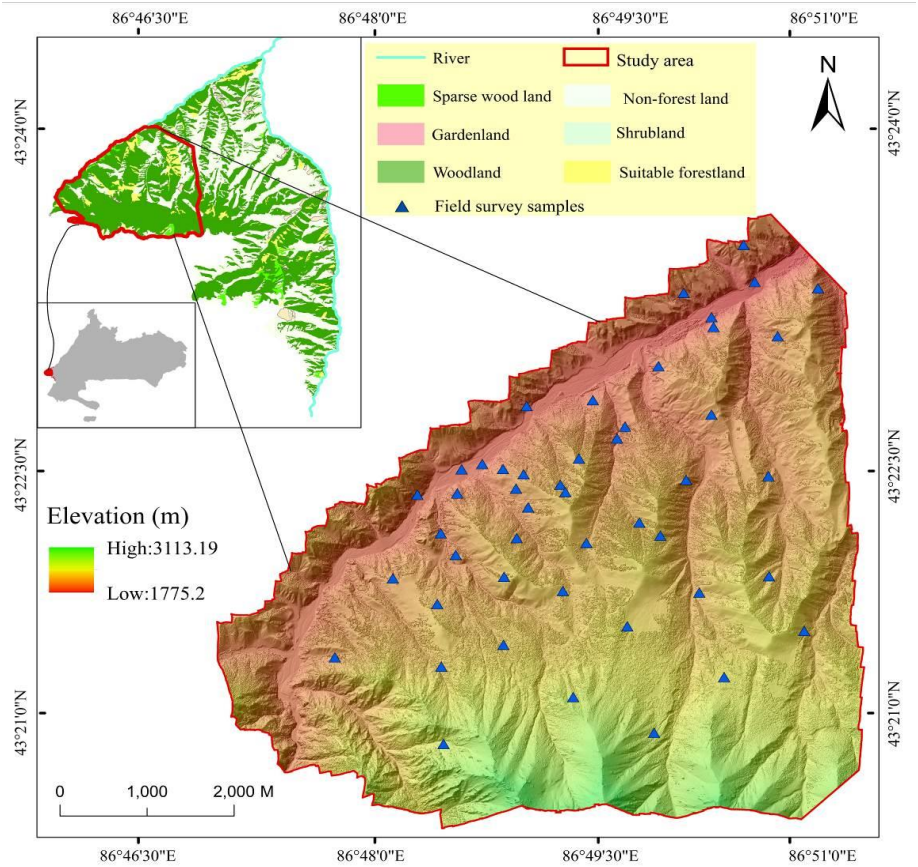

Figure 1. *Study area showing study plots and forest types*

Data and processing

Remote sensing data

Data with different scales reflect the spatial heterogeneity of forest stands. In this study, we used remote-sensing images with four scales, including GF-2 (1 m), GF-1 (8 m), GF-1 (16 m), and Landsat 8 (30 m). According to multispectral satellite imagery data in the study area (*Table 1*), we performed extensive pre-processing, including radiometric calibration, atmospheric correction, orthorectification, projection definition, cropping, and image fusion. We then used these satellite remote-sensing images to invert the canopy closure for classification experiments.

http://www.aloki.hu ● ISSN 1589 1623 (Print) ● ISSN 1785 0037 (Online)
DOI: http://dx.doi.org/10.15666/aeer/1802_36593681

Table 1. *Main parameters of satellite images*

Type	Payload	Band	Spectral range (μm)	Spatial resolution (m)	Width (km)	Revisit period (d)	Acquisition time
GF-1	PMS	1	0.45~0.52	8	60	4	3/8/2017
		2	0.52~0.59	8			
		3	0.63~0.69	8			
		4	0.77~0.89	8			
		Panchromatic	0.45~0.90	2			
	WFV	1	0.45~0.52	16	800		16/8/2017
		2	0.52~0.59	16			
		3	0.63~0.69	16			
		4	0.77~0.89	16			
GF-2		1	0.45~0.52	2.4	45	5	3/8/2017
		2	0.52~0.59	2.4			
		3	0.63~0.69	2.4			
		4	0.77~0.89	2.4			
		Panchromatic	0.45-0.90	0.61			
Landsat 8	OLI	1	0.43~0.45	30	185	16	4/8/2017
		2	0.45~0.52	30			
		3	0.53~0.60	30			
		4	0.63~0.68	30			
		5	0.85~0.89	30			
		6	1.56~1.66	30			
		7	2.10~2.30	30			
		8	0.50~0.68	15			
		9	1.36~1.39	30			
	TIRS	10	10.6~11.2	100			
		11	11.5~12.5	100			

Field survey data

The field data mainly included data from 47 plots with the dimensions 30 m × 30 m surveyed from July to September 2017 (*Fig. 2*), including their latitudes and longitudes, along with their wooden height, crown width, slope, aspect, elevation, and canopy closure. We used GPS to record the center point of the sample square and the positions of the four corner points and matched the measured sample plots with the corresponding remote-sensing images. The measurement process of the canopy closure was as follows: First, we set the sample points and captured images of five crowns with the Win SCANOPY canopy analyzer, include center point, 2 diagonal lines formed by southeast-northwest and northeast-southwest. Then, we used Win SCANOPY 2016 software to calculate the light transmission porosity of the five canopy images, using the mean value as the true value of the measured light transmittance in the ground field. To eliminate the influence of shrubs and weeds on the canopy measurements, we set the height of the fisheye lens to 1.5 m. Using the Win SCANOPY 2016 software to analyze the fisheye photos, we obtained two measures of light transmittance porosity, the gap fraction and the openness. The openness measure eliminates the effect of nonlinear projection on the transparency of the canopy to generate a result equal to the true canopy transparency. Therefore, we used the openness measure as the canopy transparency.

http://www.aloki.hu ● ISSN 1589 1623 (Print) ● ISSN 1785 0037 (Online)
DOI: http://dx.doi.org/10.15666/aeer/1802_36593681

Figure 2. *Field survey of PSVT in Tianshan Mountain*

Methods

Multi-scale segmentation

Multi-scale segmentation, an algorithm based on region segmentation, performs bottom-up segmentation of target image data. The objective is to gather one or more groups of pixels with similar features to identify a set of regions and thereby obtain different image objects as carriers for the next image classification. In the process of segmentation, a different level of network structure is established and each segmentation is based on the image object layer of the following layer for segmentation, which is then merged in the segmentation process. The segmentation parameters mainly include the segmentation scale and weight factor. Spectral and shape factors and smoothness and tightness factors are two important pairs of parameters in multi-scale segmentation. The sum of the spectral and shape factors is equal to 1, and that of the

http://www.aloki.hu ● ISSN 1589 1623 (Print) ● ISSN 1785 0037 (Online)
DOI: http://dx.doi.org/10.15666/aeer/1802_36593681

smoothness and tightness factor is also 1, so the reasonable adjustment of parameters has an important impact on multi-scale segmentation.

Best factor index (OIF) method

We used the best factor index (OIF) method (Goodchild, 1995; Singh, 2013) to select the bands of the GF-2 (1 m), GF-1 (8 m), GF-1 (16 m), and Landsat 8 (30 m) images. By calculating the standard deviation of each of the four types of data and the correlation coefficients between the bands, we could select the band combination most suitable for the region. This is because the standard deviation indicates the amount of information contained, and the correlation coefficient between each band reflects the independence of the image data and their degree of redundant information. To calculate the OIF, we use *Equation 1:*

$$OIF = \frac{\sum_{i=1}^{n} Y_i}{\sum_{i=1}^{n} \sum_{j=i+1}^{n} |Y_{ij}|} \quad \text{(Eq.1)}$$

where n is the band of the remote-sensing images, Y_i is the standard deviation of each band, and Y_{ij} is the correlation coefficient between band i and band j.

Principal component analysis (PCA)

We used the PCA algorithm to reduce the number and dimensions of the feature factors and improve processing efficiency (Lin et al., 2004). First, we analyzed the correlation between individual feature factors, after which we used the variance matrix to orthogonally rotate the load matrix of the feature factors and select the factors with a load factor of 0.85 or higher in each principal component. The selected feature factors were then used as independent variables to construct the canopy-closure estimation model. PCA not only ensures that unrelated comprehensive factors can be extracted to minimize the loss of information, but also reduces the spatial dimensions.

Multiple stepwise regression

Multivariate stepwise linear regression is the basic modeling method used in regression modeling, whereby the model selects the variable x_1 that has the most significant effect on the dependent variable among all the n independent variables. Then it selects the variable $x_2 \ldots x_1$ with the most significant effect on the dependent variable among the remaining n-1 independent variables. In this way, $x_2 \ldots x_n$ establishes a multivariate equation, and another multivariate equation is established for significant x_1, x_2, … x_m variables. Next, the model selects and verifies all the independent variables that have a significant effect on the dependent variable. The multivariate stepwise linear regression equation (*Eq. 2*) is:

$$y = k + ax_1 + bx_2 + cx_3 + \ldots + nx_m \quad \text{(Eq.2)}$$

where k is a regression constant term, a, b, c…n are the regression coefficients, and x_1, x_2, … x_m are the significant independent variables.

http://www.aloki.hu ● ISSN 1589 1623 (Print) ● ISSN 1785 0037 (Online)
DOI: http://dx.doi.org/10.15666/aeer/1802_36593681

Classification method and accuracy evaluation

We used three methods to classify forest land and compare the classification results (Wang et al., 2019; Wei et al., 2019), including CART, NNC, and SVM. CART, a common classification method (Cai et al., 2019), uses the Gini Index to select the best test variable. It achieves fast classification and has strong practicability. NNC classifies by determining the distance between sample objects, with the degree of membership of a sample determining the classification accuracy. SVM improves the generalization ability of a model by reducing the amount of sample error by transforming the sample space into a high-dimensional space and then constructing an optimal classification hyperplane as the decision surface. In this study, we correlated the main evaluation indicators, i.e., overall accuracy, mapping accuracy, and user accuracy, based on the confusion matrix method. Using the coefficient of determination (R^2), root mean square difference (RMSE) (*Eq. 3*), and estimation accuracy (EA%) (*Eq. 4*), we could determine the accuracy of the different types of canopy-closure models, and using the confusion matrix to calculate classification accuracy, include overall accuracy (OA) (*Eq. 5*), user accuracy (UA) (*Eq. 6*), and producer accuracy (PA) (*Eq. 7*).

$$RMSE = \sqrt{\frac{\sum_{i=1}^{n} (s_i - y_i)^2}{n}} \quad \text{(Eq.3)}$$

$$EA = (1 - \frac{RMSE}{Ave(y_i)}) \times 100\% \quad \text{(Eq.4)}$$

$$OA = \frac{TP + TN}{T} \quad \text{(Eq.5)}$$

$$UA = \frac{TP}{TP + FP} \quad \text{(Eq.6)}$$

$$PA = \frac{TP}{TP + FN} \quad \text{(Eq.7)}$$

y_i, s_i represent the measured and estimated values, respectively; Ave(y_i) are the average values of the samples, and n is the number of samples; TP is the correctly extracted objects; FP is the incorrectly extracted objects; TN is the non-samples that are correctly rejected; FN is the samples that are not detected.

Results

Canopy features extraction

Vegetation index factor

When considering the spectral features (Twisa and Buchroithner, 2019; Brabant et al., 2019), we selected three vegetation indices, the ratio vegetation index (RVI),

http://www.aloki.hu ● ISSN 1589 1623 (Print) ● ISSN 1785 0037 (Online)
DOI: http://dx.doi.org/10.15666/aeer/1802_36593681

normalized vegetation index (NDVI), and the transformed normalized difference vegetation index (TNDVI) (*Table 2*). The RVI changes significantly with changes in the vegetation coverage. When the coverage exceeds or is lower than 50%, the sensitivity of the RVI to vegetation increases or decreases, which reflects the vegetation coverage. NDVI, which is derived from RVI by simple nonlinear normalization, reflects the growth of the vegetation and the effective coverage, and effectively eliminates the influence of atmospheric radiation to show the same trend as shown by the vegetation coverage (*Fig. 3*). TNDVI is mainly used to adjust the NDVI when the sensitivity of the vegetation coverage is higher or lower, and it more intuitively reflects the comprehensive condition and growth of vegetation.

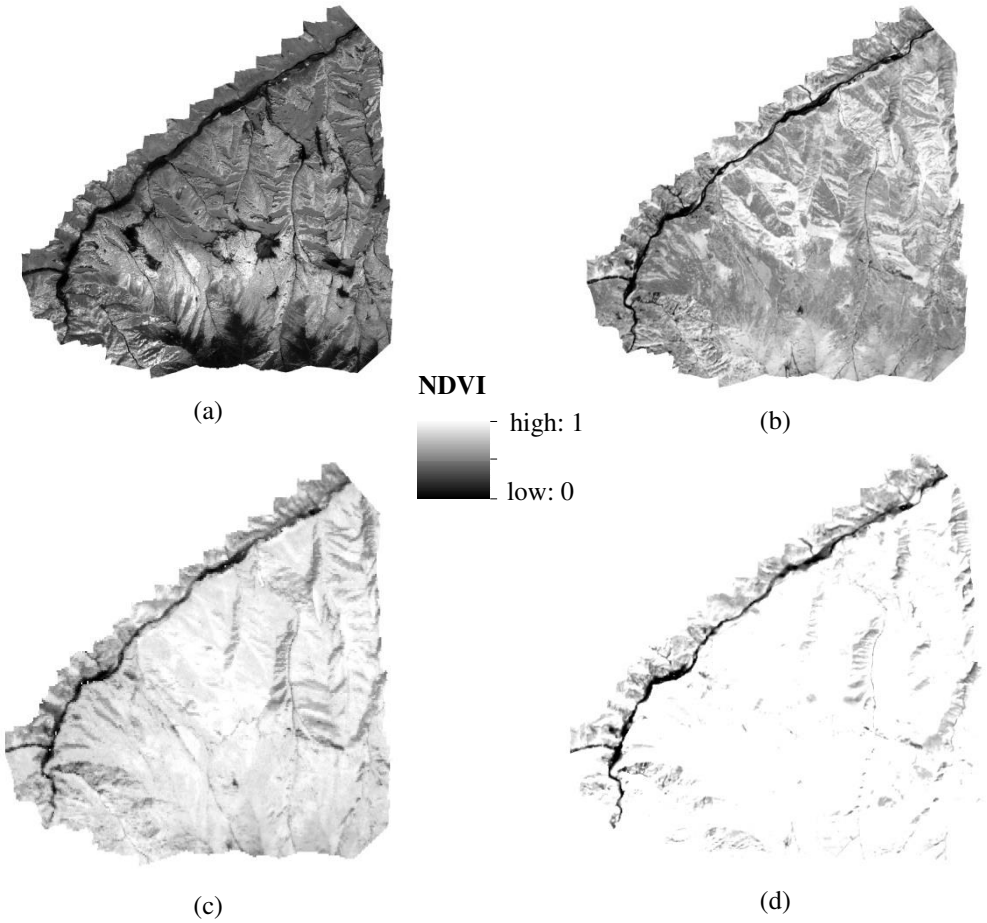

Figure 3. *Vegetation index features of remote-sensing images. (a) GF-2 (1 m); (b) GF-2 (8 m); (c) GF-2 (16 m); (d) Landsat 8 OLI (30 m)*

Terrain and shadow index factor

Due to the height angle of the sun, the height of the object itself, and the varied topography in the study area, a remote-sensing image will contain more shadows, which can affect the estimation of the canopy closure in the study area. Using ENVI 5.3 software, we found the slope, slope direction, and height of the study area to have a direct impact on the canopy closure of the stand and the extraction of the shadow index,

http://www.aloki.hu ● ISSN 1589 1623 (Print) ● ISSN 1785 0037 (Online)
DOI: http://dx.doi.org/10.15666/aeer/1802_36593681

slope, aspect, and height of the image. In particular, the shadow index is the ratio of the fourth to the third band based on the image data.

Table 2. *Alternative factors for vegetation index*

Modeling factor	Calculation formula
Ratio vegetation index (RVI)	$RVI = \frac{DN_{NIR}}{DN_R}$
Normalized vegetation index (NDVI)	$NDVI = \frac{NIR - R}{NIR + R}$
Conversion vegetation index (TNDVI)	$TNDVI = \sqrt{\frac{DN_{NIR} - DN_R}{DN_{NIR} + DN_R + 0.5}}$

R: Red band; NIR: Near infrared band

Texture factors

The simple use of spectral features will result in a large loss of spatial information of the image, whereas the addition of textural features can make full use of the spatial information. In the same kind of remote-sensing images, the textural features of different canopy regions can differ, with the texture of a canopy with a larger canopy closure being more uniform and that with a smaller canopy closure being less uniform. Choosing the right type of textural feature will greatly improve the accuracy of canopy estimation. The gray level co-occurrence matrix (GLCM) (Haralick, 1973) describes the correlation and spatial structures of pixel pairs based on the spatial relationship of the gray values of an image. GLCM is the most commonly used method used for textural analysis. In this study, we used the GLCM to extract eight textural features from Tianshan spruce forest images in the study area. *Figure 4* shows the specific textural feature factors and extraction results.

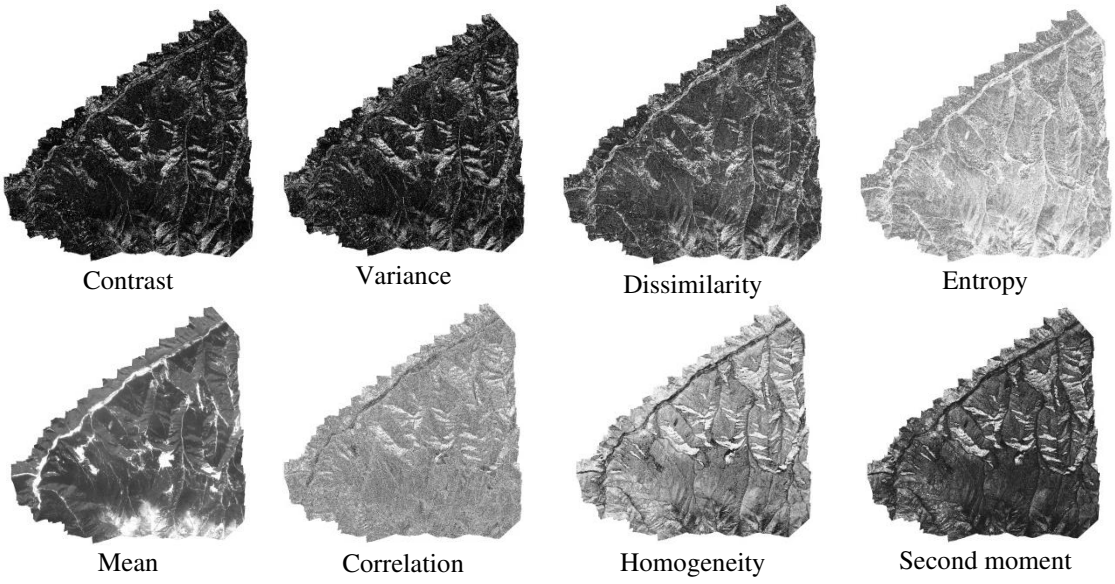

Figure 4. *Textural features of band 1 of GF-2 remote-sensing image*

http://www.aloki.hu ● ISSN 1589 1623 (Print) ● ISSN 1785 0037 (Online)
DOI: http://dx.doi.org/10.15666/aeer/1802_36593681

Multi-resolution segmentation

Each band of multispectral remote-sensing data with different spatial resolutions contains different amounts of information. Using the weight ratio method, the spectral information of these different bands can be biased or discarded to improve the segmentation efficiency and effect of different remote-sensing images. In this study, we used the OIF method to compare and screen the bands by calculating the standard deviation of each band and the correlation coefficient between bands in the remote-sensing images with different spatial resolutions. When the standard deviation between the bands is larger, the correlation coefficient between the bands will be smaller, and the more information is contained in the band, the stronger is the independence of the data.

In *Table 3* we can see that for band combination GF-2 (1 m), the highest OIF value is the combination with band 234. Compared to the band combinations 123, 124, and 1234, it can be seen that when the 1st and 2nd bands are fixed, the 4th band is introduced, and the OIF value is increased from 64.357 to 74.392, and when the 234 band combination is fixed, band 1 is introduced to the band combination, and the OIF value is reduced from 78.665 to 67.15. For GF-1 images (8 m), when the first and second bands are fixed, the fourth band is introduced, and the OIF value does not change significantly. When the band combination 234 is fixed, band 1 is introduced to the band combination, and the obtained OIF value is significantly reduced from 69.014 to 55.134. For GF-1 images (16 m), when the 1st and 2nd bands are fixed, the 4th band is introduced, and the OIF value does not increase significantly. When the band combination 234 is fixed, band 1 is introduced to the band combination, and the obtained OIF value is significantly reduced from 68.836 to 47.402. For Landsat 8 images (30 m), in the band combination (*Table 4*), the combination of the 146th and 456th bands has a higher OIF value.

Table 3. *GF data OIF values of each combination band*

Combined band	123	124	134	234	1234
GF-2 (1 m)	64.357	74.392	76.811	78.665	67.165
GF-1 (8 m)	51.233	52.736	59.236	69.014	55.134
GF-1 (16 m)	44.987	47.496	57.246	68.836	47.402

Table 4. *Landsat 8 data (30 m) OIF values of each combination band*

Combined band	OIF value	Combined band	OIF value
124	45.714	234	51.012
125	47.175	235	49.674
126	63.411	236	69.563
127	28.622	237	31.552
134	48.259	245	77.243
135	49.489	247	47.701
136	66.268	256	103.057
137	30.522	257	46.752
145	73.640	345	73.134
146	105.206	346	95.913
147	44.188	347	45.584
157	45.919	456	100.173
167	63.410	457	67.020

http://www.aloki.hu ● ISSN 1589 1623 (Print) ● ISSN 1785 0037 (Online)
DOI: http://dx.doi.org/10.15666/aeer/1802_36593681

In short, for remote-sensing image data with different resolutions, the image information contained in the near-infrared band is rich, the image information contained in this band is relatively independent, and the contribution to the OIF is also obvious. In addition, to extract forest land information, the near-infrared band shows high reflectivity of the vegetation, which has obvious benefit for the extraction of forest land information. When setting the weight of the split band and the weights of the GF-2 (1 m), GF-1 (8 m), and GF-1 (16 m) bands, we set the data to 0 (band 1), 1 (band 2), 1 (band 3), and 2 (band 4). For Landsat 8 (30 m), we set each band weight to 0 (band 1), 1 (band 2), 0 (band 3), 1 (band 4), 2 (band 5), 2 (band 6), and 1 (band 7).

In the multi-resolution segmentation process, the segmentation scale can either too small or too large, which will affect the accuracy of the target object classification. As such, it is important to set the optimal segmentation scale for different image data in the target region to ensure that the multi-resolution segmentation can effectively segment different remote-sensing data, which lays the foundation for information extraction and classification of different images. Depending on the target of the extracted features, the types of bands involved in the segmentation will differ, so no single classification method can be used. Using eCognition Developer 9.0, we scaled and processed the remote-sensing data with four different resolutions, and intercepted some regions with richer terrestrial types to compare the segmentation effects of different data sources, categories, and scales.

In terms of GF-2 (1 m), GF-1 (8 m), GF-1 (16 m), and Landsat 8 (30 m), we set the segmentation scale from 90, 65, 30, and 20 respectively (Zhang et al., 2015), with a step size of 5, and simultaneously set the compactness and smoothness of the remote sensing data with different resolutions to be 0.5, to study and analyze the spectrum and shape factors. Specifically, the compactness value is set to be 0.5 (remain unchanged), the initial value of the shape factor is set to 0.1, and we increase the shape factor from 0.1 to 0.8 with a step size of 0.1, to conduct the multi-scale segmentation experiments in turn (Zhang et al., 2014). After several experimental comparisons, we obtained the optimal segmentation scales for GF-2 (1 m), GF-1 (8 m), GF-1 (16 m), and Landsat 8 (30 m), which are 115, 85, 55, and 35, respectively. We set the shape and compactness of the weighting factors to 0.3, 0.5, 0.3, 0.5, 0.5, 0.6, 0.2, and 0.5, respectively, and achieved superior results for each image (*Fig. 5*). The results indicate that the topography of the study area comprises mostly natural landforms, and that most of the features are Tianshan spruce forest land and grassland, which means the shape factor accounts for only a small proportion and the spectral factor accounts for a large proportion.

With respect to the band weights of the remote-sensing image bands, during the segmentation process, we set different band weights for different remote-sensing data from the same research area. In this study, we calculated the standard deviation and correlation coefficient of each band based on remote-sensing data with different spatial resolutions, and used the OIF value to determine the best combination of bands for performing image segmentation. From the analysis, we found that the combination of different bands of the remote-sensing images with the same resolution and the same bands of images with different resolutions yielded different OIF values. The correlation coefficient is relatively small between the near-infrared band (NIR) and other bands in the remote-sensing image data. The independence of the band information is also strong, and the contribution rate to the OIF value is also large. When segmenting the Tianshan spruce forest based on GF-2 (1 m) remote-sensing

http://www.aloki.hu ● ISSN 1589 1623 (Print) ● ISSN 1785 0037 (Online)
DOI: http://dx.doi.org/10.15666/aeer/1802_36593681

data, when the weights of the first, second, third, and fourth bands are set to 0, 1, 1, and 2, respectively, and the division scale, shape, and compactness factor are respectively set to 115, 0.3, and 0.5, the obtained segmentation result is optimal. For GF-1 (8 m), when the weights of the 1st, 2nd, 3rd, and 4th bands are set to 0, 1, 1, and 2, respectively, and the division scale, shape, and compactness factors are set to 85, 0.3, and 0.5, the best image segmentation is obtained. For GF-1 (16 m) data, we set the weights of the first, second, third, and fourth bands to 0, 1, 1, and 2, respectively, the scale selection to 55, and the shape and compactness factors are to 0.5. At 0.6, the segmentation results are the best. For Landsat 8 (30 m) remote-sensing images, we set the weights of the 1st, 2nd, 3rd, 4th, 5th, 6th, and 7th bands to 0, 1, 0, 1, 2, 2, and 1, respectively. When the shape and the compactness factor are 0.2 and 0.5, the image segmentation effect is the best.

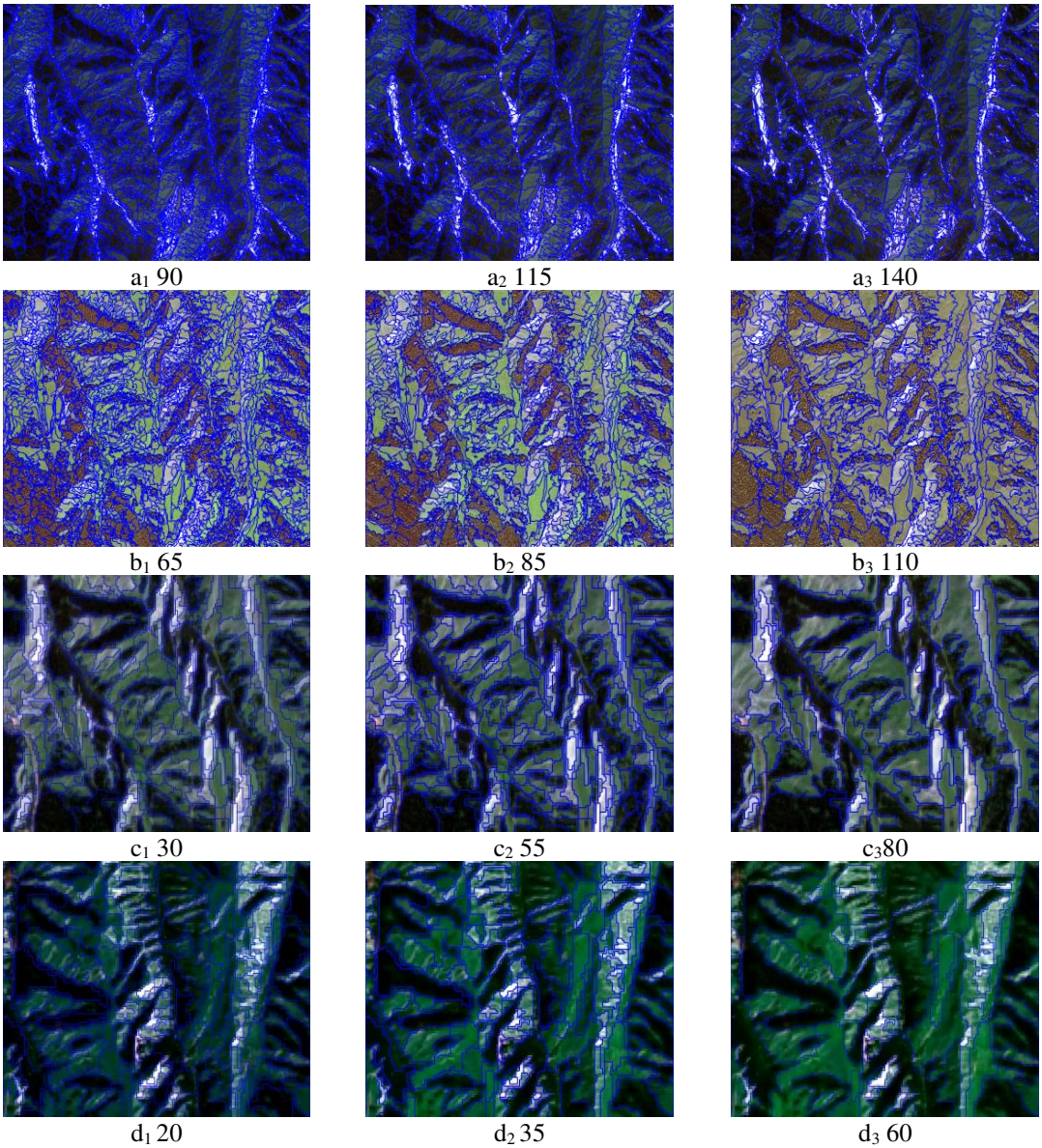

Figure 5. *Maps of multi-scale segmentation effects of remote-sensing data with different resolutions. a_1, a_2, a_3 are GF-2 (1 m) images, b_1, b_2, b_3 are GF-1 (8 m) images, c_1, c_2, c_3 are GF-1 (16 m) images, d_1, d_2, d_3 are Landsat 8 (30 m) images*

http://www.aloki.hu ● ISSN 1589 1623 (Print) ● ISSN 1785 0037 (Online)
DOI: http://dx.doi.org/10.15666/aeer/1802_36593681

Canopy closure simulation

Next, we conducted an experiment using the GF-2 (1 m), GF-1 (8 m), GF-1 (16 m), and Landsat 8 (30 m) images. Using the image and feature factor variables, we constructed a canopy-closure estimation model based on the measured values of the canopy closure in the field, and then evaluated its accuracy. We calculated 39 features related to the spectra, texture, shape, topography, and shadow index. Spectral factors included the NDVI, RVI, TNDVI, SI; topographic factors including the slope, aspect, and altitude; and textural factors including the mean, variance, homogeneity, contrast, dissimilarity, entropy, second moment, and correlation. Using SPSS 19.0 software, we performed correlation analysis of the 39 extracted feature factors and the measured canopy-closure values, and selected the factors with a small correlation. As independent variables, we used spectral and topographical features, textural features, spectral and topographic features + textural features, and used canopy closure as the dependent variable. We used the multi-step regression method to construct the canopy closure model. In *Table 5*, the fit of the canopy-closure regression model based on the spectral, topographic features and texture features is significantly better than that achieved when using a single spectrum, topographical features, or textural features. R^2 and corrected R^2 reflect degree of advantages for simulation results.

Table 5. *Estimation models of canopy density of spruce in Picea Schrenkiana var tianshanica based on different characteristic factors*

Type	Variable	Estimation model	R^2	Correction R^2
Spectral	SI, Slope (GF-1 2 m)	y=1.123-2.256×SI-0.004×Slope	0.671**	0.643
	SI, NDVI, RVI (GF-1 8 m)	y=0.772+2.398×NDVI-0.636×RVI-0.638×SI	0.602**	0.594
	TNDVI, RVI, NDVI (GF-1 16 m)	y=1.205-1.438×NDVI-0.152×RVI-0.996×TNDVI	0.573**	0.558
	SI, RVI, NDVI (OLI 30 m)	y=0.867+0.606×NDVI-0.245×RVI-0.526×SI	0.573**	0.558
Texture	Con_1, Con_2, Con_3, Con_4, Ent_3, SeM_3 (GF-1 2 m)	y=5.280-0.394×Con_2+0.129×Con_4+0.125×Con_3+0.236×Con_1-2.143×Ent_3-4.929×SeM_3	0.774**	0.759
	M_4, Va_4, Dis_1, Dis_2, Dis_3 (GF-1 8 m)	y=0.646+0.091×Dis_3-0.045×Dis_2+0.012×Dis_1-0.006×Va_4+0.010×M_4	0.623**	0.604
	M_4, Va_4, Dis_1, Dis_2, Dis_3 (GF-1 16 m)	y=0.646+0.091×Dis_3-0.045×Dis_2+0.012×Dis_1-0.006×Va_4+0.010×M_4	0.623**	0.604
	M_7, Ent_2 (OLI 30 m)	y=0.859-0.147×Ent_2+0.233×M_7	0.623**	0.604
Spectral + texture	SI, Con_2, Con_3, Con_4 (GF-1 2 m)	y=1.355-4.936×SI+0.232×Con_3-0.271×Con_2+0.091×Con_4	0.823**	0.797
	SI, NDVI, Slope, M_4 (GF-1 8 m)	y=0.480+6.265×SI-0.054×M_4-0.005×Slope+0.208×Cor_4+0.808×NDVI	0.724**	0.701
	SI, TNDVI, Dis_1, Dis_2, Dis_3, Va_4 (GF-1 16 m)	y=0.270+3926×SI-0.006×Va_4-0.052×Dis_2-0.008×Dis_1+0.118×Dis_3+0.426×TNDVI	0.654**	0.691
	TNDVI, M_7, Cor_1, Ent_2 (OLI 30 m)	y=0.859+0.076×Cor_1-0.141×Ent_2-0.070×TNDVI+0.224×M_7	0.654**	0.691

SI: Shadow index; **represents significantly correlated at the 0.01 level ($P < 0.01$); *represents significantly correlated at the 0.05 level ($P < 0.05$); M, Va, H, Con, Dis, Ent, SeM, Cor represent mean, variance, homogeneity, contrast, dissimilarity, entropy, second moment, correlation, respectively. The subscripts 1, 2, 3, 4, 5, 6, and 7 represent the B1, B2, B3, B4, B5, B6, and B7 bands, respectively

http://www.aloki.hu ● ISSN 1589 1623 (Print) ● ISSN 1785 0037 (Online)
DOI: http://dx.doi.org/10.15666/aeer/1802_36593681

To test the universality of the estimated model, we tested its accuracy. The remaining 15 test samples were used in three regression models to obtain predicted canopy-closure values, and we calculated the RSME and EA (%) of each group. As can be seen from *Table 6,* the determined coefficient of the estimation model based on textural features is better than that based on spectral and topographic features, the determined coefficient of the estimation model based on spectral, topographic, and textural features is significantly improved, and the estimation accuracy is greatly improved.

Table 6. *Comparison of measured and estimated results of the three models*

Data	Fitting equation	R^2	RMSE	EA (%)
GF-2 (1 m)	y = 0.6418x + 0.2543	0.723	0.123	84.11
	y = 1.181x - 0.1929	0.761	0.096	87.41
	y = 1.1919x – 0.2017	0.868	0.079	89.82
GF-1 (8 m)	y = 0.7858x + 0.1757	0.699	0.132	81.11
	y = 0.5068x + 0.3883	0.676	0.110	84.28
	y = 0.5564x + 0.3211	0.784	0.132	87.28
GF- 1(16 m)	y = 0.7374x + 0.0452	0.587	0.167	76.86
	y = 0.8297x + 0.0359	0.652	0.117	83.75
	y = 0.6282x + 0.2453	0.708	0.104	85.67
Landsat OLI (30 m)	y = 0.6317x + 0.2502	0.516	0.101	85.61
	y = 0.7266x + 0.2033	0.527	0.097	86.15
	y = 0.8489x + 0.1052	0.621	0.092	86.87

Object-oriented classification

According to the image features in the study area and the actual survey results for GF-2 (1 m), GF-1 (8 m), GF-1 (16 m), and Landsat 8 (30 m), these four kinds of images were segmented at multiple scales. We selected the image objects at the optimal segmentation scale and established classification levels. We used the NNC, SVM, and CART methods to classify the forest land. According to the classification standards and the actual conditions of the study area, with reference to land-use classification standards, we divided the ground objects within the study area into six categories, including buildings, water, shrub land, grassland, bare land, and forest. We then divided the forest land into dense forest land, middle wood land, and sparse wood land according to the degree of canopy closure. *Figure 6* shows the results of classification based on four kinds of images using NNC, SVM, and CART methods, respectively, a1, a2, a3, a4 are the results of using CART classifier; b1, b2, b3, b4 are the results of using NNC classifier; c1, c2, c3, c4 are the results of using SVM classifier.

The evaluation of accuracy is a key step in remote-sensing image classification. In this study, we selected a total of 200 sample verification points in the study area to evaluate the accuracy of the three image-classification methods. To calculate their accuracies, we constructed a confusion matrix. The selected sample verification points were mainly derived from field sampling points, drone aerial sampling points, a distribution map of a second-class survey of forest resources, and forest phase maps of the study area. *Tables 5-8* list the classification accuracies of these methods for GF-2 (1 m), GF-1 (8 m), GF-1 (16 m), and Landsat 8 (30 m) images, respectively.

http://www.aloki.hu ● ISSN 1589 1623 (Print) ● ISSN 1785 0037 (Online)
DOI: http://dx.doi.org/10.15666/aeer/1802_36593681

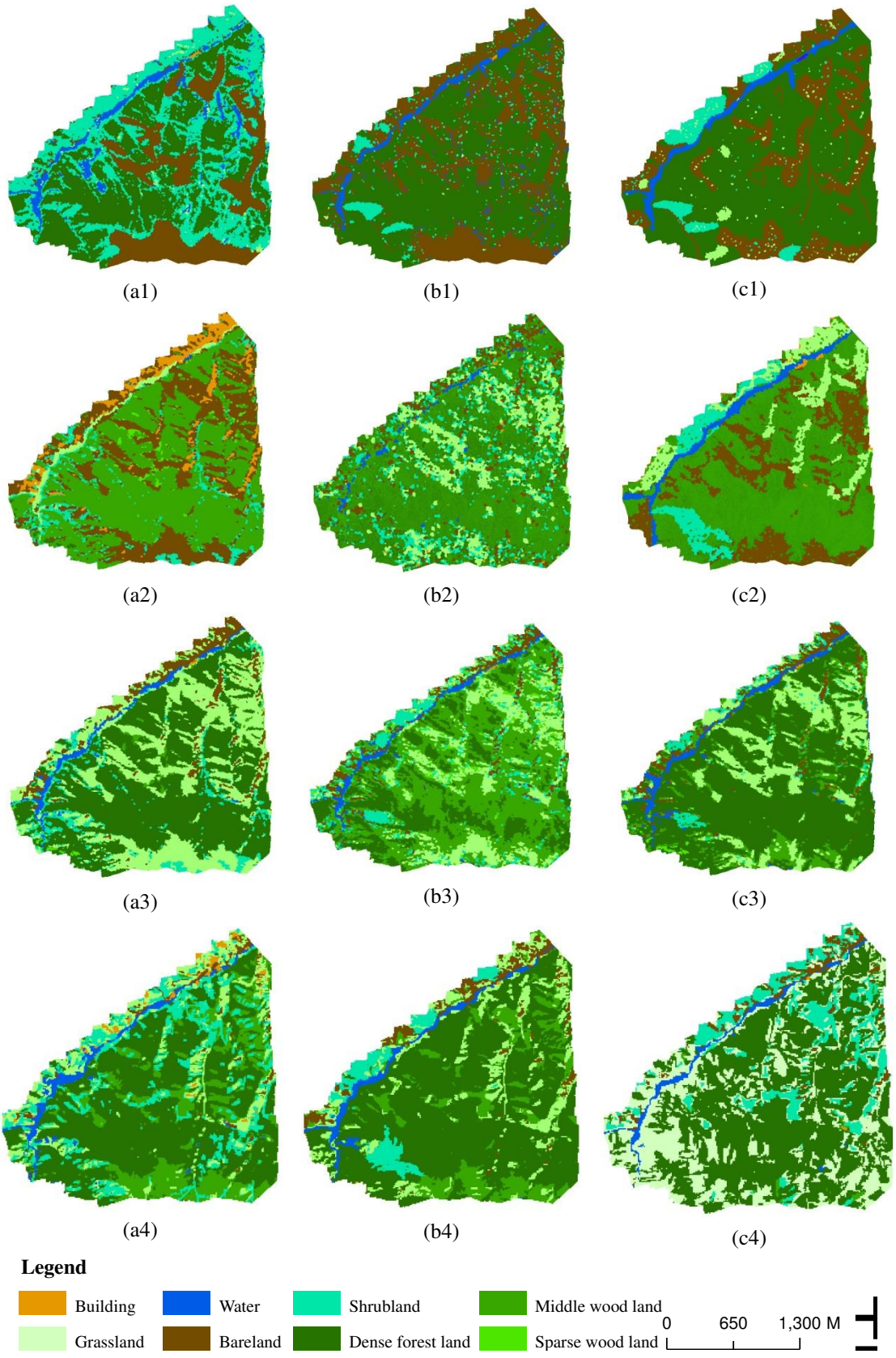

Figure 6. *Classification results of different classifiers. a1, a2, a3, a4: CART; b1, b2, b3, b4: NNC; c1, c2, c3, c4: SVM; a1, b1, c1 from GF-2 (1 m), a2, b2, c2 from GF-1 (8 m), a3, b3, c3 from GF-1 (16 m), a4, b4, c4 from Landsat 8 OLI (30 m)*

http://www.aloki.hu ● ISSN 1589 1623 (Print) ● ISSN 1785 0037 (Online)
DOI: http://dx.doi.org/10.15666/aeer/1802_36593681

As shown in *Table 7,* in terms of overall accuracy, the classification accuracy of the SVM method was 84.50%, which is better than those of the other two classification methods. This result demonstrates that classification based on the SVM method is more suitable for forest land classification of GF-2 (1 m) remote-sensing images. Regarding SVM's classification accuracy for different land types, the classification accuracies of buildings and sparse forests were the best, and those of middle and dense forests were good. The best classification result for middle and dense forests were also obtained by the SVM method, with user accuracies of 96.67% and 85.71% and mapping accuracies of 90.63% and 73.0%, respectively.

Table 7. *Accuracies of three classification methods of GF-2 (1 m)*

Type	NNC		CART		SVM	
	UA	PA	UA	PA	UA	PA
Building	100.00	100.00	100.00	100.00	100.00	100.00
Grassland	84.00	70.00	100.00	33.33	91.67	73.33
Water	100.00	100.00	63.64	100.00	87.50	100.00
Bare land	43.33	100.00	27.78	38.46	42.31	84.62
Shrub land	42.86	37.50	17.95	87.50	38.46	62.50
Dense forest land	93.44	89.06	94.64	82.81	96.67	90.63
Middle wood land	71.43	41.67	100.00	66.67	85.71	73.00
Sparse wood land	100.00	100.00	100.00	100.00	100.00	100.00
OA	82.50		72.50		84.50	

For the GF-1 (8 m) image classification, the SVM method also achieved a higher accuracy of 84.01%, which is 10% higher than that of the other two methods. When classifying middle and dense forests, the classification result for dense forest was relatively good, but that for middle forest was poor. Better classification results for dense forests was achieved by the CART and SMV methods, with user accuracies of 93.70% and 93.02% and mapping accuracies of 92.97% and 93.75%, respectively. In the classification of bare land, the NNC method obtained relatively good results, with a user and mapping accuracies of 64.29% and 69.23%, respectively (*Table 8*). The SVM method achieved better recognition of shrub land, with user and mapping accuracies of 71.43% and 62.50%, respectively.

Table 8. *Accuracies of three classification methods for GF-1 (8 m)*

Type	NNC		CART		SVM	
	UA	PA	UA	PA	UA	PA
Buildings	100.00	100.00	100.00	100.00	100.00	100.00
Grassland	73.68	46.67	66.67	53.33	76.92	66.67
Water	100.00	100.00	66.67	85.71	77.78	100.00
Bare land	64.29	69.23	35.71	38.46	50.00	61.54
Shrub land	16.67	75.00	35.71	62.50	71.43	62.50
Dense forest land	87.93	79.69	93.70	92.97	93.02	93.75
Middle wood land	100.00	50.00	60.00	50.00	54.55	50.00
Sparse wood land	100.00	100.00	100.00	100.00	100.00	100.00
OA	73.00		79.50		84.01	

http://www.aloki.hu ● ISSN 1589 1623 (Print) ● ISSN 1785 0037 (Online)
DOI: http://dx.doi.org/10.15666/aeer/1802_36593681

For GF-1 (16 m) images, the classification of sparse forest land by the SVM method was also the best. The classification accuracy of the SVM method for dense forest was higher than that for middle-closed forest land for both user and mapping accuracy, i.e., higher than 80% (*Table 9*). The NNC method made obvious misclassifications and misjudgments in this category, which also occurred for bare land and shrub land, yielding only a fair classification accuracy.

Table 9. *Accuracy of three classification methods for GF-1 (16 m)*

Type	NNC		DTC		SVM	
	UA	PA	UA	PA	UA	PA
Buildings	100.00	100.00	100.00	100.00	100.00	100.00
Grassland	60.00	50.00	42.86	70.00	50.00	46.67
Water	100.00	100.00	100.00	85.71	77.78	80.00
Bare land	57.14	61.54	42.86	46.15	50.00	53.85
Shrub land	31.25	62.50	39.41	62.50	66.67	50.00
Dense forest land	96.10	57.81	89.62	74.22	88.89	81.25
Middle wood land	48.62	41.67	33.33	16.67	49.17	58.33
Sparse wood land	50.00	100.00	50.00	100.00	100.00	100.00
OA	58.00		68.00		72.50	

For Landsat 8 (30 m) images, in terms of overall accuracy (*Table 10*), the NNC classification accuracy was 73.50%. Compared with the CART and SVM methods, the NNC accuracy was 4.5% and 12% higher, respectively, which indicates that the NNC method is more suitable for forest land classification in the area. Regarding the classification accuracy for different land types, those for buildings and sparse forests were the best, and that for moderately closed forest land was fair. The classification accuracy of dense forest by NNC was the best, with user and mapping accuracies of 92.44% and 85.94%, but the classification accuracies of bare land and shrub land were low.

Table 10. *Accuracy of three classification methods of Landsat 8 (30 m)*

Type	NNC		CART		SVM	
	UA	PA	UA	PA	UA	PA
Buildings	100.00	100.00	100.00	100.00	100.00	100.00
Grassland	46.43	43.33	42.86	40.00	23.73	46.67
Water	63.64	100.00	77.78	100.00	100.00	100.00
Bare land	55.56	38.46	83.33	38.46	55.56	38.46
Shrub land	33.33	50.00	22.00	37.50	27.14	22.50
Dense forest land	92.44	85.94	92.86	81.25	88.79	74.22
Middle wood land	31.58	50.00	25.00	41.67	50.00	48.33
Sparse wood land	100.00	100.00	100.00	100.00	100.00	100.00
OA	73.50		69.00		62.50	

In summary, in terms of overall classification accuracy, the best classification effect was achieved for GF-2 (1 m) remote-sensing images, and the worst for Landsat 8

http://www.aloki.hu ● ISSN 1589 1623 (Print) ● ISSN 1785 0037 (Online)
DOI: http://dx.doi.org/10.15666/aeer/1802_36593681

(30 m) remote-sensing images. The overall classification accuracies for the GF-1 (8 m) and GF-1 (16 m) images were 78.83% and 66.17%, respectively, which indicates that the classification accuracy of forest land in the study area depends to some degree on the spatial resolution of the image. Regarding classification methods, when using the CART method for classification, the overall classification accuracies for GF-2 (1 m), GF-1 (8 m), GF-1 (16 m), and Landsat 8 (30 m) remote-sensing images were 72.50%, 79.50%, 68.00%, and 69.00%, respectively. However, the classification method that is most suitable for the study area varies with the data source. In terms of GF-2 (1 m) images, our results indicate that the best classification for this study area is the SVM method, followed by the NNC and CART methods. For GF-1 (8 m) and GF-1 (16 m) images, the best classification method was SVM, followed by NNC. For Landsat 8 (30 m) images, the best to worst classification methods are the NNC, CART, and SVM methods.

Discussion

Superiority and summary

High-precision land use/cover remote sensing classification mapping is widely used in precision agriculture, vegetation ecology, wetland water quality, urban heat island, mineral resources, atmospheric environment, and other research fields. In this study, multi-source data was based on agreement analysis and refined classification (Jung et al., 2006). Compared with traditional remote sensing forest land classification methods, the object-oriented method can not only make full use of the spectral information of remote sensing images, but also can add texture information, shape information, and custom information according to the classification of ground features to more accurately compare effective extraction and classification of target features (Judah and Hu, 2019). In the case of determining the optimal segmentation scale, the selection of remotely sensed images that do not use spatial resolution and the use of different object-oriented classifiers will have a certain impact on the classification effect. Therefore, a reasonable selection of remotely sensed images to determine the spatial resolution of data and classification method has become the key to the fine classification of forest land types.

From the perspective of the spatial resolution of remote sensing images, when the resolutions of remote sensing images are 1 m, 8 m, 16 m, and 30 m, their average overall classification accuracy is 80.00%, 78.83%, 66.17% and 68.33% It shows that the higher the resolution, the higher the classification accuracy of the image. This is because the high-resolution images contain more feature information and categories, and the information utilization rate is higher, which leads to the improvement of the classification accuracy of the image. However, in practical applications, although the classification of images with a resolution of 1 m and 8 m is good, but because of the large amount of data it contains, the processing time is long, and the process is more complicated, you can choose to ensure certain accuracy Fast processing speed of 16 m and 30 m images.

From the perspective of the classification method, the classification method that is most suitable for the study area varies with different data sources. For example, in the GF-2 (1 m) remote sensing image, the classification effect of the study area is better by the support vector machine method, followed by the nearest neighbor method and the decision tree method; for the medium resolution GF-1 (8 m), GF-1 (16 m) remote sensing image, the effect is better is support vector machine, the worst is the nearest

http://www.aloki.hu ● ISSN 1589 1623 (Print) ● ISSN 1785 0037 (Online)
DOI: http://dx.doi.org/10.15666/aeer/1802_36593681

neighbor method; in Landsat8 (30 m) remote sensing image, the classification effect is the nearest neighbor classification, decision tree classification Support vector machine method.

This is due to a series of reasons such as different study areas, different image data sources, and the scale selected during segmentation. As a result, for each data source, the forest land classification method that is most suitable for the region is different. Due to the particularity of geographical location and terrain in this study area, the distribution of forest stands is complex. Different classification methods have been adopted for different data sources. It can be seen from the accuracy analysis that the adopted classification method has certain effectiveness and reliability, which meets the requirements for extraction of *Picea Schrenkiana var. tianshanic*a (*PSVT*).

Limitation and outlook

This study comprehensively uses the spectrum, terrain, texture, shape and other information contained in the image to estimate the canopy closure model and forest land classification of the study area (Amani et al., 2017; Dendoncker et al., 2007), which has certain limitations. (1) The study area is small, and large-scale verification and improvement are needed in other areas to ensure the universality of the estimation model. (2) The accuracy of results is affected by landscape heterogeneity in the study area. Therefore, although this research has made important progress in remote sensing classification mapping of land use/cover based on multi-source data, many follow-up studies need to be completed to obtain the best results. (3) In the future more attention should be paid to the fusion between different classifiers, because it is difficult for a single type of classifier to classify all the forest types better.

For example, the target classification system can be further refined. This study divided *PSVT* into eight main types: building, water, shrubland, middle woodland, grassland, bareland, dense woodland, sparse woodland. Specifically, these types are high generalizations of actual land types, avoiding as much confusion as possible due to the complexity of classification. However, in view of the particularity of forest areas, reasonable attention should be paid to *PSVT* resources in follow-up studies.

Conclusions

Taking GF-2 (1 m), GF-1 (8 m), GF-1 (16 m), Landsat 8 (30 m) images combined with field survey data, and performed multi-resolution segmentation to select the best segmentation scales. Based on the spectrum, texture and terrain factors, the canopy closure inversion of PSVT was performed to select the characteristic factors suitable for different images. Then, we applied three object-oriented methods (i.e. the support vector machine (SVM), classification and regression tree (CART), and the nearest neighbor classification (NNC) methods) to classify the forest land. The conclusions show that (1) the near-infrared (NIR) band is highly independent and makes an important contribution to the optimum index factor (OIF), in which the real-time adjustments of segmentation results are made to achieve better effect. (2) In the canopy-closure estimation model, a combination of the spectrum, terrain remote-sensing factors, and textural feature factors yields the best result. For GF-2 (1 m) images, the combination of the four characteristic factors SI, Con_2, Con_3, and Con_4 yields the best estimation model. The model estimation accuracy is an EA of 89.82%, an RMSE of 0.079, and a determination coefficient R^2 of 0.868. (3) In terms of GF-2 images, the classification performs better when using the

http://www.aloki.hu ● ISSN 1589 1623 (Print) ● ISSN 1785 0037 (Online)
DOI: http://dx.doi.org/10.15666/aeer/1802_36593681

SVM method, which achieved an overall classification accuracy of 84.5%, thereby being an effective classification method for the forest land types in the study area. In terms of their economics and practicality, each data source has its own advantages.

Additionally, forest canopy estimation algorithm can be further developed. As there are many variables introduced, and there is a strong correlation between the texture feature factors, it is important to find a reasonable and effective modeling method. With the improvement of image resolution, the influence of the shadow index on the estimation of occlusion is getting larger and larger. Due to the differences in the selected remote sensing images or the differences in the ecological and geographical environments in different regions, the factors for estimating canopy closure in different regions should take into account the actual local conditions.

Acknowledgments. This research was funded by the National Key Research and Development Program of China (grant number 2016YFB0501403).

Conflict of interests. The authors declare that they have no conflicts of interests.

REFERENCES

[1] Abdulhakim, M. A. (2019): Land cover and land use classification performance of machine learning algorithms in a boreal landscape using Sentinel-2 data. – GIScience & Remote Sensing 57(1): 1-20.
[2] Adepoju, K. A., Adelabu, S. A. (2020): Improving accuracy evaluation of Landsat-8 OLI using image composite and multisource data with Google Earth Engine. – Remote Sensing Letters 11(2): 107-116.
[3] Aizezitiyuemaier, M., Yusufujiang, R., He, H., Baihetinisha, A. (2019): Spatio-temporal characteristics of vegetation water use efficiency and its relationship with climate factors in Tianshan Mountains in Xinjiang from 2000 to 2017. – Chinese Journal of Plant Ecology 43(6): 490-500.
[4] Amani, M., Salehi, B., Mahdavi, S., Granger, J., Brisco, B. (2017): Wetland classification in Newfoundland and Labrador using multi-source SAR and optical data integration. – GIscience & Remote Sensing 54(6): 779-796.
[5] Baatz, M., Schape, A. (2000): Multiresoulution segmentation: an optimization approach for high quality mufti scale image segmentation. – Angewandte Geographische Informationsverarbeitung 12(12): 12-23.
[6] Brabant, C., Alvarez-Vanhard, E., Laribi, A., Morin, G., Nguyen, K. T., Thomas, A., Houet, T. (2019): Comparison of hyperspectral techniques for urban tree diversity classification. – Remote Sensing 11(11): 1-19.
[7] Cai, G. Y., Ren, H. Q., Yang, L. Z., Zhang, N., Du, M. Y., Wu, C. S. (2019): Detailed urban land use land cover classification at the metropolitan scale using a three-layer classification scheme. – Sensors 19(14): 1-24.
[8] Dendoncker, N., Rounsevell, M., Bogaert, P. (2007): Spatial analysis and modelling of land use distributions in Belgium. – Computers, Environment and Urban Systems 31(2): 188-205.
[9] Donato, D. C., Halofsky, J. S., Reilly, M. J. (2019): Corralling a black swan: natural range of variation in a forest landscape driven by rare, extreme events. – Ecological Applications 30(1): 1-16.
[10] Dilixiati, M., Rusuli, Y., Namaiti, H. (2019): The phenological characteristics and climatic response of vegetation in the Xinjiang Tianshan Mountains, China. – Climate Change Research 15(6): 624-632.

http://www.aloki.hu ● ISSN 1589 1623 (Print) ● ISSN 1785 0037 (Online)
DOI: http://dx.doi.org/10.15666/aeer/1802_36593681

[11] Fernandez-Guisuraga, J. M., Suarez-Seoane, S., Calvo, L. (2019): Modeling Pinus pinaster forest structure after a large wildfire using remote sensing data at high spatial resolution. – Forest Ecology and Management 446: 257-271.
[12] Gilcher, M., Ruf, T., Emmerling, C., Udelhoven, T. (2019): Remote sensing based binary classification of maize. dealing with residual autocorrelation in sparse sample situations. – Remote Sensing 11(18): 2172.
[13] Goodchild, M. F. (1995): Attribute accuracy elements of spatial data quality by Guptill and Morrison. – International Cartographic Association 37(9): 59-79.
[14] Guo, Y. G., Yu, X. F., Jiang, D., Wang, S. K., Jiang, X. S. (2012): Study on forest classification based on object oriented techniques. – Journal of geo-information science 14(4): 514-522.
[15] Haralick, R. M., Shanmugam, K., Dinstein, I. (1973): Textural features for image classification. – IEEE transactions on systems man and cybernetics SCM-3: 610-621.
[16] Hofmann, P. (2001): Detecting informal settlements from IKONOS image data using methods of object oriented image analysis-an from cape town. – Urban Remote Sensing 20(12): 85-88.
[17] Judah, A., Hu, B. X. (2019): The integration of multi-source remotely-sensed data in support of the classification of wetlands. – Remote Sensing 11(13): 1537.
[18] Jung, M., Henkel, K., Herold, M., Churkina, G. (2006): Exploiting synergies of global land cover products for carbon cycle modeling. – Remote Sensing of Environment 101(4): 534-553.
[19] Li, Q., Wang, Z. X., Wang, Y. P., Liu, M. T., Yang, Y. Q. (2019): Study on canopy density inversion of Picea schrenkiana forest based on GF-2 remote sensing image. – Journal of Central South University of Forestry & Technology 39(8): 48-54.
[20] Lin, W. H., Yang, Y. Q., Hou, C. M. (2004): A study of spectral features of stands and their related factors with principal component analysis. – Journal of South China Agricultural University (Natural Science Edition) 25(2): 22-25.
[21] Liu, M. T., Wang, Z. X., Wang, Y. P., Li, Q., Shi, Y. X. (2019): Plant communities pattern of Picea tianschanica forest and their interrelations with environmental factors in Tianshan area. – Forest Research 32(6): 90-98.
[22] Maas, A. E., Rottensteiner, F., Heipke, C. (2019): A label noise tolerant random forest for the classification of remote sensing data based on outdated maps for training – Computer Vision and Image Understanding 188: 1-18.
[23] Perea-Ardila, M. A., Oviedo-Barrero, F., Leal-Villamil, J. (2019): Mangrove forest mapping through remote sensing imagery: study case for Buenaventura, Colombia. – Revista De Teledeteccion 53: 73-85.
[24] Piazza, G. A., Vibrans, A. C., Liesenberg, V., Refosco, J. C. (2016): Object-oriented and pixel-based classification approaches to classify tropical successional stages using airborne high spatial resolution image. – Remote Sensing 53(2): 11-21.
[25] Rajasekhar, M., Raju, G. S., Raju, R. S., Ramachandra, M., Kumar, B. P. (2019): Accuracy assessment of land use/land cover classification in parts of Kadapa district (Andhra Pradesh, India), using remote sensing and GIS. – Journal of Indian Geophysical Union 23(4): 356-366.
[26] Singh, P. P., Garg, R. D. (2013): Information extraction from high resolution satellite imagery using integration technique. – Communications in Computer and Information Science 276: 231-245.
[27] Sun, X. D. (2009): Object-oriented forestry land extraction based on semantic correlation. – Journal of Fujian Forestry Science and Technology 36(3): 36-40.
[28] Twisa, S., Buchroithner, M. E. (2019): Land-use and land-cover (LULC) change detection in Wami River basin, Tanzania. – Land 8(9): 136.
[29] Wang, X. X., Gao, X. W., Zhang, Y. Z., Fei, X. W., Chen, Z., Wang, J., Zhang, Y. Y., Lu, X., Zhao, H. M. (2019): Land-cover classification of coastal wetlands using the RF algorithm for Worldview-2 and Landsat 8 images. – Remote Sensing 11(16): 1927.

http://www.aloki.hu ● ISSN 1589 1623 (Print) ● ISSN 1785 0037 (Online)
DOI: http://dx.doi.org/10.15666/aeer/1802_36593681

[30] Wei, Y. F., Tong, X. H., Chen, G., Liu, D. Q., Han, Z. F. (2019): Remote detection of large-area crop types: the role of plant phenology and topography. – Agriculture 9: 150.
[31] Zhang, L., Jia, K., Li, X. S., Yuan, Q. Z., Zhao, X. F. (2014): Multi-scale segmentation approach for object-based land-cover classification using high-resolution imagery. – Remote Sensing Letters 5(1): 73-82.
[32] Zhang, X. L., Feng, X. Z., Xiao, P. F. (2015): Multi-scale segmentation of high spatial resolution remote sensing images using adaptively increased scale parameter. – Photogrammetric Engineering and Remote Sensing 81(6): 461-470.

APPENDIX

Table A1. *The attribute table of field survey samples*

Site	Longitude (°)	Latitude (°)	Elevation (m)	Slope (°)
1	86.838	43.403	1959.28	33.34
2	86.839	43.399	1786.17	1.19
3	86.848	43.398	1951.00	43.69
4	86.829	43.398	1890.05	68.49
5	86.833	43.395	1793.27	3.52
6	86.834	43.394	1861.85	52.39
7	86.843	43.393	1987.05	60.01
8	86.826	43.390	1877.12	26.90
9	86.816	43.386	1870.91	39.76
10	86.807	43.385	1844.58	25.71
11	86.833	43.384	2028.59	21.07
12	86.821	43.383	1902.19	51.62
13	86.820	43.382	1889.79	16.32
14	86.814	43.380	2134.94	66.23
15	86.801	43.379	1836.07	7.34
16	86.798	43.378	1837.18	1.63
17	86.804	43.378	1944.42	26.03
18	86.807	43.378	2056.10	19.65
19	86.841	43.378	2061.99	37.98
20	86.830	43.377	2078.59	35.17
21	86.812	43.377	2151.87	38.58
22	86.806	43.376	2027.58	33.40
23	86.797	43.376	1914.21	28.05
24	86.813	43.376	2187.08	55.85
25	86.792	43.376	1886.56	44.32
26	86.807	43.374	2049.24	27.76
27	86.823	43.373	2168.12	77.74
28	86.795	43.371	1921.97	57.97
29	86.826	43.371	2238.82	34.35
30	86.806	43.371	2106.82	34.82
31	86.816	43.370	2158.13	46.48
32	86.797	43.369	1989.59	36.31
33	86.804	43.367	2210.87	51.00

http://www.aloki.hu ● ISSN 1589 1623 (Print) ● ISSN 1785 0037 (Online)
DOI: http://dx.doi.org/10.15666/aeer/1802_36593681

34	86.841	43.367	2203.04	46.69
35	86.788	43.366	2060.14	24.80
36	86.832	43.365	2162.08	26.23
37	86.812	43.365	2213.90	67.97
38	86.794	43.364	2164.53	46.44
39	86.821	43.361	2315.67	2.88
40	86.846	43.361	2261.91	28.68
41	86.804	43.359	2255.38	24.79
42	86.780	43.358	2063.56	42.75
43	86.795	43.357	2251.45	55.42
44	86.835	43.356	2379.38	33.86
45	86.814	43.353	2513.09	52.06
46	86.825	43.350	2523.30	41.09
47	86.795	43.348	2511.50	55.02

http://www.aloki.hu ● ISSN 1589 1623 (Print) ● ISSN 1785 0037 (Online)
DOI: http://dx.doi.org/10.15666/aeer/1802_36593681

DIFFERENCES IN RHIZOSPHERE MICROBIOTA COMPOSITIONS BETWEEN HEALTHY AND DISEASED POTATO (*SOLANUM TUBEROSUM*) IN CHINA

MAO, L. T.* – LAI, L. E. – LIN, G. G. – XU, L. X. – CHEN, Z. G. – ZHU, W. J.

School of Life Science, Huizhou University, Huizhou 516007, China

**Corresponding author*
e-mail: mlt@hzu.edu.cn; phone: +86-075-2252-9555

(Received 2nd Jan 2020; accepted 26th Mar 2020)

Abstract. Potato (*Solanum tuberosum*) is the fourth most important food crop worldwide, but soil-borne diseases lead to serious decline of potato yield and quality. Rhizosphere microbiota (RM) play an important role in the health of potato. However, the number of reports on the RM of potatoes with soil-borne diseases is still insufficient. To explore the correlation between RM and the potato soil-borne diseases, 3 rhizosphere samples of potatoes with blackleg disease (PBD), bacterial wilt (BW), and healthy controls were collected from a Chinese potato base and analyzed by Actinomycetes culturing and culture-free high-throughput sequencing technology. Our results showed that the amount of Actinomycetes in the healthy control was higher than that in the PBD and the BW. The RM composition of the healthy control was significantly different from that of the PBD and the BW. The increased bacterial species in the PBD group mainly concentrated in Firmicutes, while those in the BW mostly belonged to Betaproteobacteria. Soil pH and content of organic matter (OM), available phosphorus (P) and available potassium (K) were most significantly positively correlated with the bacteria that were enhanced in the healthy potato RM. The results implied that the RM of diseased potatoes were significantly different from the healthy controls, and moderately improved the soil pH, OM, P and K probably aid in the prevention of the PBD and the BW through regulating the RM.
Keywords: *high-throughput sequencing, potato blackleg disease, bacterial wilt, soil physicochemical indicators, soil-borne bacterial diseases*

Introduction

Potato (*Solanum tuberosum*) is the crop with the fourth largest planting area worldwide, following rice, corn and wheat (Bera et al., 2015). However, potato diseases, especially soil-borne bacterial diseases, have caused serious reduction in yield and quality (Mao et al., 2019). The soil-borne bacterial diseases have caused 22% of global potato loss, and the loss reaches to 65 million tons per year (FAO, 2008; Mao et al., 2019).

Potato blackleg disease (PBD) and bacterial wilt (BW) are two common soil-borne bacterial diseases. PBD is caused by *Pectobacterium atroseptica* and mainly damages the base of stem and tuber of potato. It can occur from seedling stage to late growth stage and storage period. In seeding stage, symptoms usually begin to appear when the plant height is 15-20 cm. The symptoms are that the leaves are chlorotic and yellow flowers roll up, the internodes of the plants are shortened, the tissues above the stem base are black and rotten, and eventually wilt and die (Mao et al., 2019). Potato BW is a destructive bacterial disease caused by *Ralstonia solanacearum*. The BW plants withered in the early daytime and returned to normal at dusk. Leaves remained green and did not turn yellow. Later stem rotted with mucus, and finally withered and died. Generally, the disease begins at the middle stage of plant growth, resulting in serious yield reduction (Jiang et al., 2017). In addition, the pathogens of the above diseases can

http://www.aloki.hu ● ISSN 1589 1623 (Print) ● ISSN 1785 0037 (Online)
DOI: http://dx.doi.org/10.15666/aeer/1802_36833691

invade the potato disability tissues to survive in winter. High temperature and humidity promote the diseases (Mao et al., 2019).

There are many rhizosphere microorganisms, such as bacteria and fungi, which play an important role in the nutrition and health of plants. For instance, the amount of actinomycetes in rhizosphere soil is collected to soil microecological balance (Chen et al., 2013; Zheng et al., 2016; Mao et al., 2019). Soil actinomycetes could inhibit soil-borne diseases of crops in potato-maize intercropping system (Zhao, 2013). Additionally, Ma et al. (2015) reported that change of soil microbial species in pepper root was related to its pathogenesis. These studies provide a direction for prevention and control of plant bacterial diseases through regulating the composition of rhizosphere microbiota (RM). However, there still are few comparative studies on the RM compositions of PBD, BW, and healthy potatoes, which implements the prevention of bacterial diseases of potato through regulating the composition of RM.

To elucidate the composition characteristics of the RM of potatoes with BW, PBD, and healthy controls for providing reference information to control the BW and PBD, the community structure of rhizosphere soil microorganisms of diseased and healthy potatoes were collected and analyzed using Actinomycetes culturing and culture-free high-throughput sequencing technology. The results could provide important reference for biological control of the potato soil-borne diseases.

Materials and methods

Sample collection

Potato rhizosphere soil samples were collected from the Jiuhua Potato Base in Huidong County, Huizhou City of China (22.86° N, 114.93° E) on September 20, 2017. The elevation of sampling sites was 11.03 m. A total of 9 rhizosphere soil samples including 3 samples of PBD, 3 samples of BW, and 3 healthy controls (*Fig. 1*), were collected according to our previous description (Mao et al., 2019). Diagnoses of PBD and BW were conducted according to previous descriptions (Jiang et al., 2017; Mao et al., 2019).

Determination of soil physicochemical indicators

Rhizosphere soil pH, content of organic matter (OM), alkali-hydrolyzable nitrogen (N), available phosphorus (P) and available potassium (K) in the rhizosphere soils was measured according to previous reports (Xiong et al., 2008; Shen et al., 2013).

Amount counting of actinomycetes

Amount counting of actinomycetes in the rhizosphere samples was conducted according to a previous report (Guan et al., 2018). Briefly, ten grams rhizosphere soil of each sample was weighted and added into a triangular bottle containing 90 ml sterile water and glass beads, then the triangular bottle was shaken for 20 min with 150 r/min at 28 °C to obtain the 10^{-1} suspension of rhizosphere soil. The 10^{-2}, 10^{-3}, and 10^{-4} gradient suspensions were prepared by the 10-fold dilution method. Each 100 μL suspension was added to the Gauze's synthetic medium No. 1 and the humic acid medium, then was inversely cultured 7 days at 28 °C to count the colony forming units (CFUs). Two replicates were set up in each sample. The CFUs in per ml were calculated (*Eq. 1*) as follows:

http://www.aloki.hu ● ISSN 1589 1623 (Print) ● ISSN 1785 0037 (Online)
DOI: http://dx.doi.org/10.15666/aeer/1802_36833691

$$CFUs = N_{two} \times DM \times 10 \quad \text{(Eq.1)}$$

where N_{two} was the average colony number of two repeats, and *DM* was the dilution multiplier.

Figure 1. *Photos of healthy potatoes (A), potatoes with potato blackleg disease (B) and bacterial wilt (C), and symptoms of the diseases (D). PBD, potato blackleg disease; BW, bacterial wilt*

RM DNA extraction and high-throughput sequencing

DNA of RM was extracted using CTAB method according to previous reports (Fang et al., 2015; Ni et al., 2017). Then the DNA was purified using a DNA fast purifying kit (Dingguo Changsheng, China). One μL of each DNA sample was used to measure purity and concentration by a NanoDrop 2000 micro-spectrophotometer (Thermo, USA).

The V4 hypervariable region of the 16S rRNA gene was amplified using the 515F and 806R primers with sample-specific barcodes (Douglas et al., 2014; Li et al., 2017). PCR reaction mixture and the thermal cycling conditions were as reported in Li et al. (2017). The PCR producted were mixed at equimolar ratios and purified using an AxyPrep DNA gel extraction kit (Axygen, China), then sequenced using the Illumina MiSeq platform at BIG (China) and 250 bp paired-end reads were generated (Douglas et al., 2014).

The raw sequences were filtered for quantity control, merged, and assigned to each sample according to previous descriptions (Magoc and Salzberg, 2011; Huang et al., 2018; Xiang et al., 2018; Ni et al., 2019). The remaining sequences with > 97% similarity were assigned to the same operational taxonomic unit (OTU) using USEARCH v7.0.1090 (Edgar, 2013). Then the chimeric OTUs were detected and removed using UCHIME v4.2.40 (Edgar et al., 2011), the remaining OTUs were used as valid OTUs for subsequent analysis. The representative sequence of each OTU was annotated by RDP classifier v2.2 with reference to Greengene gg_13_8 dataset. The alpha-diversity indices were calculated using mothur v1.31.2.

http://www.aloki.hu ● ISSN 1589 1623 (Print) ● ISSN 1785 0037 (Online)
DOI: http://dx.doi.org/10.15666/aeer/1802_36833691

The sequences were submitted to the Genome Sequence Archive (https://bigd.big.ac.cn/gsa/) database under accession number subCRA001900.

Data analysis

The results are presented as the mean ± standard error for each group. Principal component analysis (PCA) of OTUs was conducted using R ade4 package. Kruskal-Wallis rank sum test was conducted using R. Boxplots were drawn using R ggpubr package. Circular layout was drawn using R Statnet and circlize packages. LDA effect size (LEfSE) analysis (Segata et al., 2011) was conducted at Galaxy platform (http://huttenhower.sph.harvard.edu/galaxy/). Parametric multivariate analysis of variance (Per-MANOVA) was conducted using R vegan package.

Results

Amount differences of actinomycetes in RM between healthy and diseased potatoes

Amounts of actinomycetes in the RM of the healthy control, the PBD, and the BW were 16.52×10^5, 6.18×10^5, and 7.58×10^5 CFU/g in the humic acid medium, respectively; and those were 23.38×10^5, 7.72×10^5, and 6.23×10^5 CFU/g in the Gauze's synthetic medium No.1, respectively (*Fig. 2*). Although no significant difference was found (Kruskal-Wallis rank sum test, $\chi^2 = 5.60$, $p = 0.061$ for humic acid medium; $\chi^2 = 5.42$, $p = 0.066$ for Gauze's synthetic medium No.1), the amount of actinomycetes in the healthy control was much higher than those in the PBD and the BW, suggesting that the amount of actinomycetes had a positive effect on maintaining the ecological balance of the potato RM.

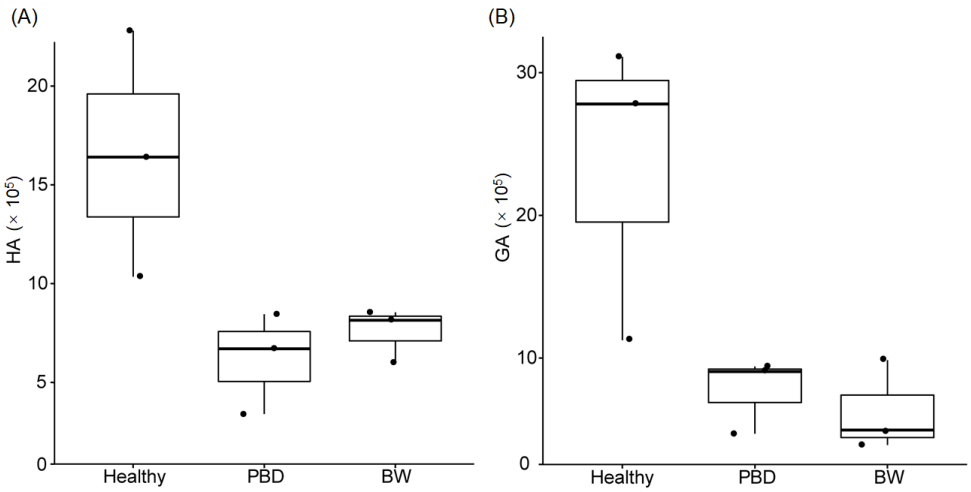

Figure 2. *Boxplots shows the amount differences of actinomycetes in different rhizosphere microbiota of potato. HA, humic acid medium; GA, Gauze's synthetic medium No.1. PBD, potato blackleg disease; BW, bacterial wilt*

Significant difference of RM between healthy and diseased potatoes

After removing low-quality and chimerism sequences, total of 263173 (29241.44 ± 365.93) merged sequences were obtained from the 9 samples. Total of

http://www.aloki.hu ● ISSN 1589 1623 (Print) ● ISSN 1785 0037 (Online)
DOI: http://dx.doi.org/10.15666/aeer/1802_36833691

4096 (2200.56 ± 65.63) OTUs were detected under 97% sequence similarity. PCA result showed that the microbiota from the healthy control were significantly distinguished to PBD and BW groups, but those from PBD and BW groups did not distinguish to each other (Per-MANOVA, $F = 2.121$, $p = 0.045$; *Fig. 3A*). Although it has been reported that the alpha-diversity of RM of diseased potatoes was significantly decreased, no significantly decrease in the alpha-diversity of RM of diseased potatoes was found in the present study (Kruskal-Wallis rank sum test, $\chi^2 = 2.40$, $p = 0.301$; *Fig. 3B*).

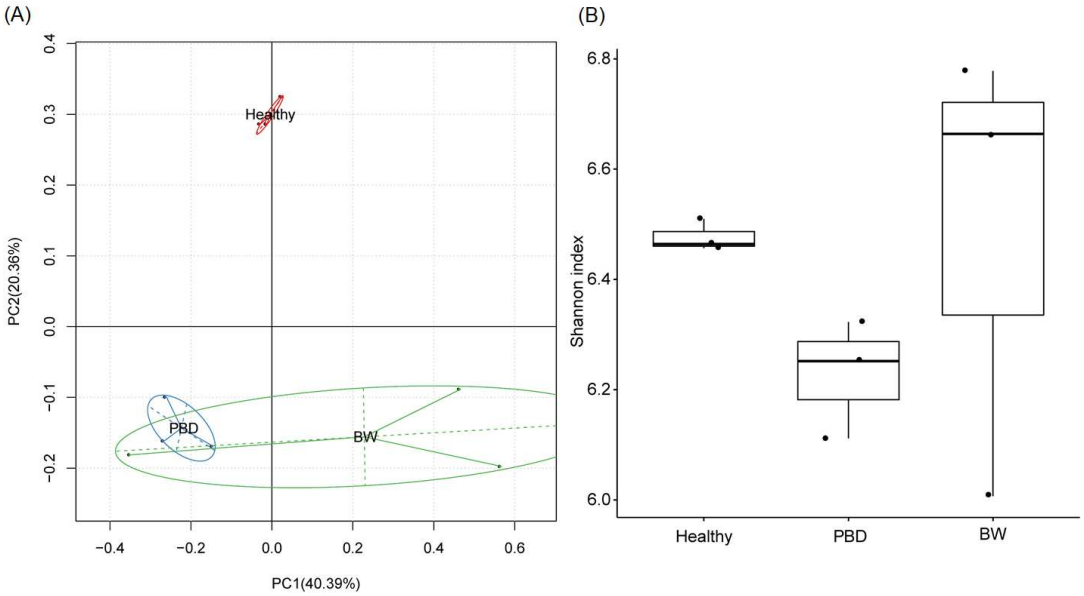

Figure 3. *PCA profile (A) shows the differences between the healthy, PBD, and BW groups; and boxplot (B) shows the Shannon index between the groups. PBD, potato blackleg disease; BW bacterial wilt*

Except rare tags (0.98 ± 0.08%) that could not ascertain their classification, other tags were classified into 50 phyla. However, only 15 phyla - Acidobacteria, Actinobacteria, Bacteroidetes, Chlorobi, Chloroflexi, Crenarchaeota, Euryarchaeota, Firmicutes, Gemmatimonadetes, Nitrospirae, Ploteobacteria, TM6, TM7, and Verrucomicrobia - dominated the microbiota, which contained 96.19 ± 0.32% of the high-quality analyzed sequences (*Fig. 4A*). Except TM6 (Kruskal-Wallis rank sum test, $\chi^2 = 6.489$, $p = 0.039$), other phyla were not detected significant difference between the groups. In addition, no significant difference was detected in TM6 between the groups through pairwise comparison using Wilcoxon test (*Fig. 4B*).

Considering there was a significant difference at OTU level between the healthy and diseased groups (*Fig. 3A*), we screened significantly different OTUs using LEfSe method. Our results showed that the increased bacteria in the PBD group mainly concentrated in Firmicutes, such as *Paenibacillus*, *Sporosarcina*, and *Caloramator*, while those in the BW group mainly concentrated in Betaproteobacteria, such as *Novosphingobium*, and *Rubrivivax*. Comparing with the two diseased groups, the bacteria species in the healthy controls mainly concentrated in Chloroflexi and Proteobacteria, such as *Anaerolinea*, *Desulfovibrio*, and *Geobacter* (*Fig. 5*).

http://www.aloki.hu ● ISSN 1589 1623 (Print) ● ISSN 1785 0037 (Online)
DOI: http://dx.doi.org/10.15666/aeer/1802_36833691

To analyze potential impacts of soil chemical indices on the RM OTUs, we analyzed their correlation and screened the significantly correlated soil chemical indices and the OTUs. Our results showed that soil pH, and soil content of OM, P and K mainly significantly positive correlated with the OTUs that significantly higher in the RM of heathy potatoes (*Fig. 5*). These results implied that moderately improved the soil pH, and content of OM, P and K probably aid in the prevention of PBD and BW through regulated the RM.

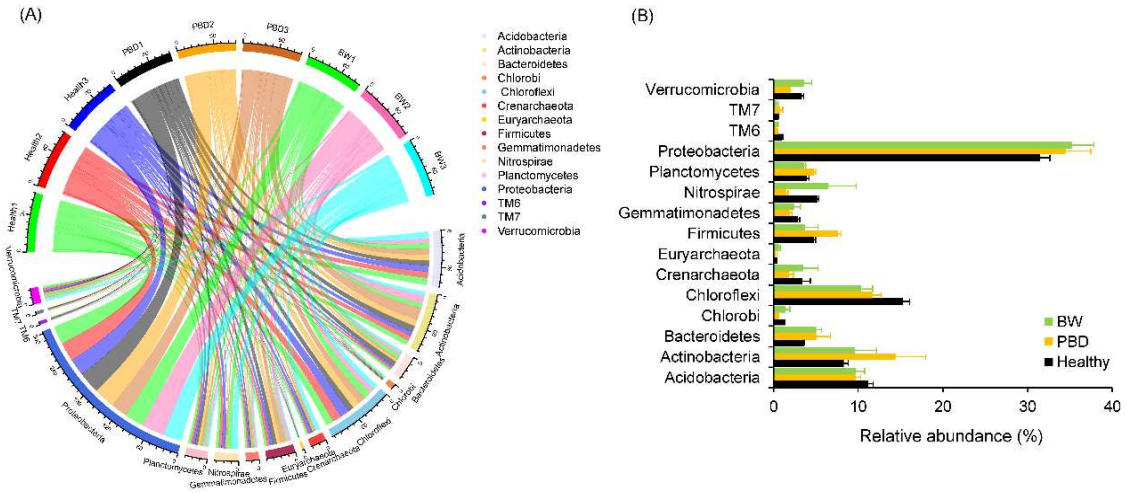

Figure 4. *Circular layout (A) and bar plot (B) show the distribution of dominant phyla in potato rhizosphere microbiota. PBD, potato blackleg disease; BW bacterial wilt. The error bars showed the standard errors of the relative abundances of the dominant phyla*

Discussion

Previous reports showed that amount of actinomycetes in the healthy potato RM was higher than that in the diseased potatoes (Chen et al., 2013), which implied that the actinomycete abundance has a positive effect on maintaining soil microecological balance and improving crop disease resistance. In present study, we also found that the amount of actinomycetes in the healthy potato RM was slightly higher than the diseased potatoes (the PBD and the BW groups). However, it is still need to further verify whether actinomycetes can effectively prevent the occurrence of potato bacterial diseases.

Our previous study showed that the PBD was closely related to the composition of the RM, and found *Flavobacterium*, *Acinetobacter*, *Dickeya*, *Sphingobacterium*, and *Myroides* were more abundance in the RM of the PBD than the healthy potatoes, while *Bacillus*, *Rhodophlanes*, *Kaistobacter*, and *Pedobacter* were less abundant in the PBD (Mao et al., 2019). In the present study, we found the increased bacteria in the PBD group mainly concentrated in Firmicutes, such as *Paenibacillus*, *Sporosarcina*, and *Caloramator*, while those in the BW group mainly concentrated in Betaproteobacteria, such as *Novosphingobium*, and *Rubrivivax* (*Fig. 5*). The inconformity was probably caused by sampling time and position, as season and geography are the two major factors that impact the compositions of soil microbiota and RM (Schloter et al., 2000; Wang et al., 2015).

Soil physicochemical indices play an important role in balancing the plant RM and preventing disease outbreaks (Zaccardelli et al., 2012; Vilvert et al., 2014; Wang et al.,

http://www.aloki.hu ● ISSN 1589 1623 (Print) ● ISSN 1785 0037 (Online)
DOI: http://dx.doi.org/10.15666/aeer/1802_36833691

2015; Gudeta et al., 2016; Bonanomi et al., 2018; Liu et al., 2019). Soil pH, content of P and K are highly correlated with the occurrence of plant diseases (Anderson et al., 1990; Sun et al., 2004; Burdon et al., 2014). Our results showed that properly increasing soil pH, and P and K content could help to increase relative abundances of the OTUs that were significantly enhanced in the healthy potato RM, and presumably helped to prevent PBD and BW, which was consistent with production practice that improvs potato disease resistance through using the plant ash and P and K fertilizers. Plant ash riches in minerals, which can provide K for potato seeding, and plant ash is alkaline, which can improve the rhizosphere soil pH.

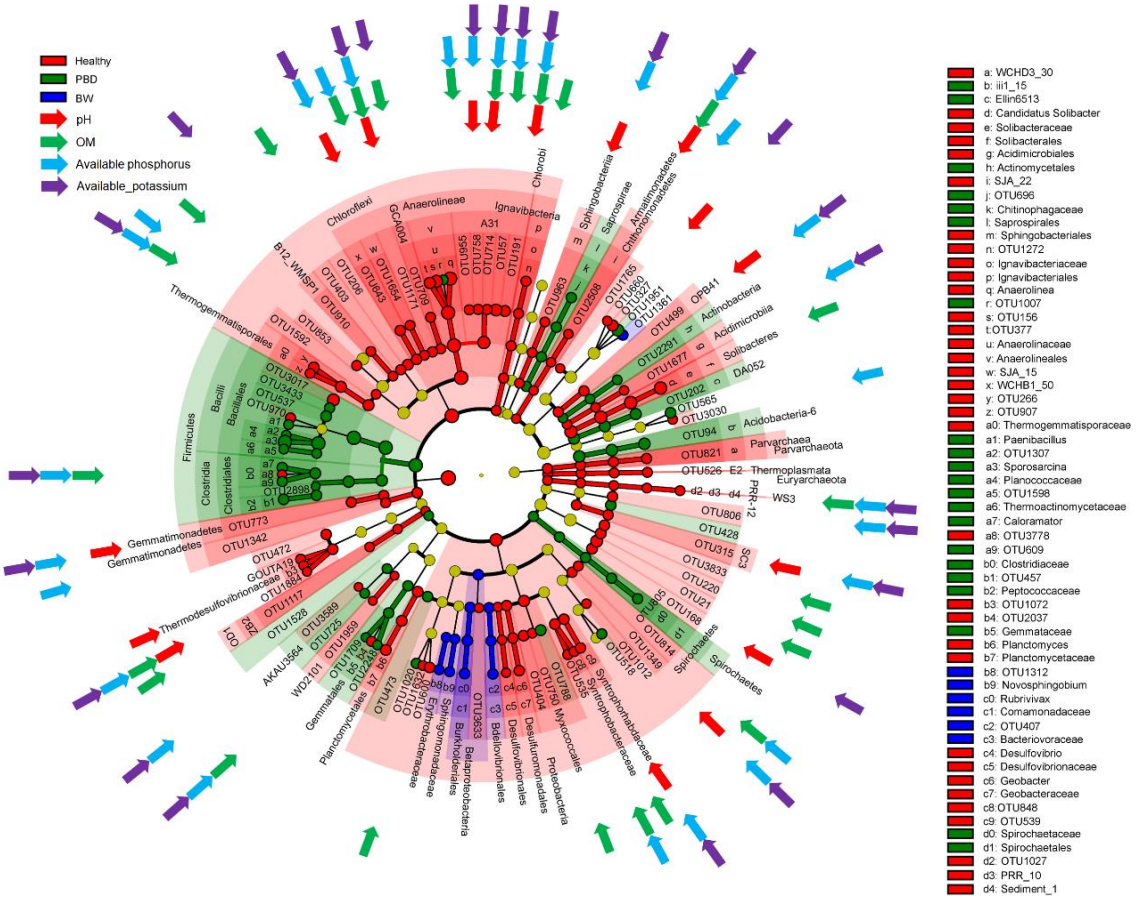

Figure 5. *LDA effect size (LEfSE) profile showed the significantly taxa between the PBD, BW, and healthy potatoes. PBD, potato blackleg disease; BW bacterial wilt. The arrows showed the OTUs that significantly positively correlated with soil chemical indices*

Conclusion

In conclusion, there were significant differences in the structure of RM between the healthy and diseased potatoes with PBD and BW. The occurrence of the PBD and the BW is closely corrected to the potato RM. Moderately improved the soil pH, and content of OM, P and K probably aid in the prevention of PBD and BW through regulated the RM. However, how to improve the soil pH, and the content of OM, P and K, and the mechanism to prevent the PBD and BW still need to be further studied and assessed, respectively.

http://www.aloki.hu ● ISSN 1589 1623 (Print) ● ISSN 1785 0037 (Online)
DOI: http://dx.doi.org/10.15666/aeer/1802_36833691

Acknowledgements. This work was supported by the Huizhou Science and Technology Planning Project (grant number 2017C0423039); and the National Science Foundation of China (grant number 31772032). The funding sources had not participated in the study design, collection, analysis and interpretation of data, writing of the report, and decision to submit the article for publication. The authors thank anonymous technicians at Guangdong Meilikang Bio-Science Ltd., China for assistance with data re-analysis and figure preparation.

REFERENCES

[1] Anderson, D. L., Raid, R. N., Irey, M. S., Henderson, L. J. (1990): Association of sugarcane rust severity with soil factors in Florida. – Plant Dis 74: 683-686.
[2] Bera, S., Poddar, R., Ghosh, R. (2015): Effect of weed management on the performance of potato and microflora population in rhizosphere. – Potato J 42: 29-35.
[3] Bonanomi, G., Lorito, M., Vinale, F., Woo, S. L. (2018): Organic amendments, beneficial microbes, and soil microbiota: toward a unified framework for disease suppression. – Annu Rev Phytopathol 56: 1-20.
[4] Burdon, J. J., Ericson, L., Thrall, P. H. (2014): Emerging plant disease. – Encyclopedia of Agriculture and Food Systems 2014: 59-67.
[5] Chen, J., Guo, T. W., Tan, X. L., Zhu, W. B., Wei, X. L., Wang, D. S., Xue, Q. H. (2013): Comparison of microecological characterization in rhizosphere soil between healthy and diseased plants in continuous cropping potato fields. – Acta Agronomica Sinica 39(11): 2055-2064.
[6] Douglas, W. F., Bing, M., Pawel, G., Naomi, S., Sandra, O., Rebecca, M. B. (2014): An improved dual-indexing approach for multiplexed 16S rRNA gene sequencing on the Illumina MiSeq platform. – Microbiome 2: 6.
[7] Edgar, R. C. (2013): UPARSE: highly accurate OTU sequences from microbial amplicon reads. – Nature Methods 10(10): 996-998.
[8] Edgar, R. C., Haas, B. J., Clemente, J. C., Quince, C., Knight, R. (2011): UCHIME improves sensitivity and speed of chimera detection. – Bioinformatics 27: 2194-2200.
[9] Fang, Y., Xu, M., Chen, X., Sun, G., Guo, J., Wu, W., Liu, X. (2015): Modified pretreatment method for total microbial DNA extraction from contaminated river sediment. – Front Environ Sci Eng 9: 444-452.
[10] FAO (2008): International Year of the Potato 2008. New Light on a Hidden Treasure. – Food and Agriculture Organization of the United Nations, Rome.
[11] Guan, T., Xiang, H., Feng, X., Yang, Y., Jiao, S., Zhao, H. (2018): Diversity and antibacterial activity of culturable actinobacteria from Xiaoerkule Lake. – Acta Microbiologica Sinica 58(10): 1864-1874.
[12] Gudeta, D. D., Bortolaia, V., Amos, G., Wellington, E. M. H., Brandt, K. K., Poirel, L., Nielsen, J. B., Westh, H., Guardabassi, L. (2016): The soil microbiota harbors a diversity of carbapenem-hydrolyzing β-lactamases of potential clinical relevance. – Antimicrobial Agents and Chemotherapy 60(1): 151-160.
[13] Huang, R., Li, T., Ni, J., Bai, X., Gao, Y., Li, Y., Zhang, P., Gong, Y. (2018): Different sex-based responses of gut microbiota during the development of hepatocellular carcinoma in liver-specific Tsc1-knockout mice. – Frontiers in Microbiology 9: 1008.
[14] Jiang, G., Wei, Z., Xu, J., Chen, H., Zhang, Y., She, X., Macho, A. P., Ding, W., Liao, B. (2017): Bacterial wilt in China: history, current status, and future perspectives. – Frontiers in Plant Science 8: 1549.
[15] Li, X., Zhou, L., Yu, Y., Ni, J., Xu, W., Yan, Q. (2017): Composition of gut microbiota in the gibel carp (Carassius auratus gibelio) varies with host development. – Microb Ecol 74: 239-249.

http://www.aloki.hu ● ISSN 1589 1623 (Print) ● ISSN 1785 0037 (Online)
DOI: http://dx.doi.org/10.15666/aeer/1802_36833691

[16] Liu, L., Huang, X., Zhao, J., Zheng, J., Cai, Z. (2019): Characterizing the key agents in a disease-suppressed soil managed by reductive soil disinfestation. – Appl Enivron Microbiol 85(7): e02992-18.
[17] Ma, Y., Wang, D., Li, Y., Xue, Q., Lin, Y. (2015): Micro-ecology in the rhizosphere soil of the phytophthora blight infected plants and healthy plants. – Acta Agriculturae Boreali-occidentalis Sinica 24(4): 129-137.
[18] Magoc, T., Salzberg, S. (2011): FLASH: fast length adjustment of short reads to improve genome assemblies. – Bioinformatics 27(21): 2194-2200.
[19] Mao, L., Chen, Z., Xu, L., Zhang, H., Lin, Y. (2019): Rhizosphere microbiota compositional changes reflect potato blackleg disease. – Applied Soil Ecology 140: 11-17.
[20] Ni, J., Li, X., He, Z., Xu, M. (2017): A novel method to determine the minimum number of sequences required for reliable microbial community analysis. – Journal of Microbiological Methods 139: 196-201.
[21] Ni, J., Huang, R., Zhou, H., Xu, X., Li, Y., Cao, P., Zhong, K., Ge, M., Chen, X., Hou, B., Yu, M., Peng, B., Li, Q., Zhang, P., Gao, Y. (2019): Analysis of the relationship between the degree of dysbiosis in gut microbiota and prognosis at different stages of primary hepatocellular carcinoma. – Frontiers in Microbiology 10: 1458.
[22] Schloter, M., Lebuhn, M., Heulin, T., Hartmann, A. (2000): Ecology and evolution of bacterial microdiversity. – FEMS Microbiology Reviews 24: 647-660.
[23] Segata, N., Izard, J., Waldron, L., Gevers, D., Miropolsky, L., Garrett, W. S., Huttenhower, C. (2011): Metagenomic biomarker discovery and explanation. – Genome Biology 12: R60.
[24] Shen, C., Xiong, J., Zhang, H., Feng, Y., Lin, X., Li, X., Liang, W., Chu, H. (2013): Soil pH drives the spatial distribution of bacterial communities along elevation on Changbai Mountain. – Soil Biology & Biochemistry 57: 204-211.
[25] Sun, X., Stall, R. E., Jones, J. B., Cubero, J., Gottwald, T. R., Graham, J. H., Dixon, W. N., Schubert, T. S., Chaloux, P. H., Stromberg, V. K., Lacy, G. H., Sutton, B. D. (2004): Detection and characterization of a new strain of citrus canker bacteria from Key/Mexican lime and alemow in South Florida. – Plant Dis 88: 1179-1188.
[26] Vilvert, R. M., Aguiar, D., Gimenes, R. M. T., Alberton, O. (2014): Residual effect of transgenic soybean in soil microbiota. – African Journal of Agricultural Research 9(30): 2369-2376.
[27] Wang, Z., Silva, L. C. R., Sun, G., Luo, P., Mou, C., Horwath, W. R. (2015): Quantifying the impact of drought on soil-plant interactions: a seasonal analysis of biotic and abiotic controls of carbon and nutrient dynamics in high-altitudinal grasslands. – Plant Soil 389: 59-71.
[28] Xiang, J., He, T., Wang, P., Xie, M., Xiang, J., Ni, J. (2018): Opportunistic pathogens are abundant in the gut of cultured giant spiny frog (Paa spinosa). – Aquaculture Research 49: 2033-2041.
[29] Xiong, Y., Xia, H., Li, Z., Cai, X., Fu, S. (2008): Impacts of litter and understory removal on soil properties in a subtropical Acacia mangium plantation in China. – Plant Soil 304: 179-188.
[30] Zaccardelli, M., Villecco, D., Campanile, F., Pane, C. (2012): Metagenomic profiles of soil microbiota under two different cropping systems detected by STRs-based PCR. – Agricultural Sciences 3: 98-103.
[31] Zhao, L. (2013): Screening and Functional Study of Antagonistic Actinomycetes against Soil-Borne Diseases. – Lanzhou Jiaotong University, Lanzhou.
[32] Zheng, Y., Chen, B., Song, P., Li, Z., Xiao, G. (2016): Diversity of actinomycetes in rhizosphere soil of potato intercropping maize system and antagonistic activity against plant pathogenic fungi. – Acta Agriculturae Boreali-Occidentalis Sinica 25(6): 912-920.

http://www.aloki.hu ● ISSN 1589 1623 (Print) ● ISSN 1785 0037 (Online)
DOI: http://dx.doi.org/10.15666/aeer/1802_36833691

IS FOREST LANDSCAPE PATTERN MORE AFFECTED IN ROAD OVERLAP ZONE: EVIDENCE FROM AN UPSTREAM AREA OF THE MINJIANG RIVER OF FUJIAN PROVINCE IN THE SUB-TROPICAL REGION OF CHINA

LIN, Y. Y.[1,2,3] – HU, X. S.[4*] – LIN, M. S.[2] – QIU, R. Z.[4] – LIN, J. G.[5]– LI, B. Y.[3*]

[1]*Postdoctoral Research Station of Ecology， Fujian Normal University，Science and Technology Road, 350117 Fuzhou, P.R. China*

[2]*College of Tourism, Fujian Normal University, Science and Technology Road, 350117 Fuzhou, P.R. China*

[3] *School of Geographical Sciences, Fujian Normal University, Science and Technology Road, 350117 Fuzhou, P.R .China*

[4]*College of Transportation and Civil Engineering, Fujian Agriculture and Forestry University, Xiyuangong Road, 350108 Fuzhou, Fujian, P.R . China*

[5]*College of Material Engineering, Fujian Agriculture and Forestry University, Xiyuangong Road, 350108 Fuzhou, Fujian, P.R . China*

*****Corresponding authors*
e-mail: xshu@fafu.edu.cn; byli985@126.com

(Received 3rd Jan 2020; accepted 24th Mar 2020)

Abstract. Despite there is a rich literature base that strives to characterize and understand the influencing factors of landscape ecology, the fact that we still know very little about the ecological impact in the road overlap areas. Taking the upstream area of the Minjiang River of Fujian Province in China, as a case, quantitative landscape metrics were employed to analyze the forest landscape fragmentation and degradation associated with road networks in five zones, including the whole landscape (WL), non-road effect zone (NREZ), road effect zone (REZ), mono-road effect zone (MONREZ) and multi-road effect zone (MULREZ). Our findings showed that 5.4% of the forest landscape within the REZ experienced changes from 2007 to 2015, while only 4.1% in the NREZ. Landscape metrics also identified more scattered habitats in the REZ than in the NREZ. As a result, these leaded to more severe forest landscape degradation in the REZ. Notably, the outcomes showed that the landscape pattern in the MULREZ has been more affected by road networks than the REZ and the MONREZ. Furthermore, the growing rate of landscape degradation from 2007 to 2015 in the REZ was about 1.2 times higher of the NREZ.
Keywords: *sub-tropical forest, road effect zone, fragmentation, landscape degradation index, landscape pattern*

Introduction

As the element of social development and economic prosperity, road networks tend to occupy a growing percentage of land surface worldwide (Gutiérrez and Urbano, 1996; Wang et al., 2007; Patarasuk, 2013). Development of road network increases accessibility and mobility, meanwhile opening land for resource extraction and other human activities, thus aggravating human interference on ecosystems (Jaeger et al., 2007; Selva et al., 2011). This negative impact on the environment may occur at multiple spatial scales from local to global (Forman, 1998; Coffin, 2007). At the local scale, individual road segment change the ecological process of the landscape, resulting

http://www.aloki.hu ● ISSN 1589 1623 (Print) ● ISSN 1785 0037 (Online)
DOI: http://dx.doi.org/10.15666/aeer/1802_36933711

in the increased abundance of invasive species, alternating hydrologic flows, and blocking the movement for animals (Forman, 1998). At the landscape scale, road network causes habitat fragmentation and degradation by creating high contrast linear edges, removing, alternating or subdividing the continuous forests into pieces (Hawbaker et al., 2005; Mehdipour et al., 2019). Moreover, landscape speeding changes associated with road network extensions often aggravate habitat fragmentation and degradation (Liu et al., 2014). However, most researches on the effects of roads on ecosystems have examined them at separate scales, few studies have integrated multiple scales in their observation. At the local scale, previous studies have focused on biodiversity conservation, such as traffic mortality, animal movement patterns, species distributed patterns, and species invasion (Spooner et al., 2004; Gibbs and Steen, 2010; Bordadeágua et al., 2011). At the landscape level, landscape structure, pattern and cover change dynamics have been quantified using geographical information system (GIS) tools. Considering the complexity and irreversibility due to the cumulative and time-lagged effects of road network on biodiversity (Selva et al., 2011), conservation evaluations on a local scale are far from comprehensive due to the lack of related knowledge (e.g. the habitats' alternations or forest displacement), while landscape-level analyses, such as landscape transitions, often have limited ecological meanings for biodiversity, owing to number of land cover classes restricted by satellite imagery (Wimberly and Ohmann, 2004; Fu et al., 2010; Li et al., 2010). For example, typical analysis of road effect on landscape pattern based on previous studies usually does not distinguish among forest categories, instead they view on "forests" as an implicitly homogenous category, thereby ignoring variations between forests and their effects on the ecological processes (Wang et al., 2007; Patarasuk, 2013; Angelstam et al., 2017). Only a few of studies on road disturbances subdivided forests into coniferous forest, mixed forest and broad-leaved forest (Freudenberger et al., 2013; Liang et al., 2014). Fortunately, the implement of Forest Resources Inventory Program in China involves an intensive survey of permanent sampling plots, thus establishing an extensive database covering many aspects of the forest resources at the biome level, such as forest type, and tree species type (Ren et al., 2011; Xie et al., 2011). This large database provides an excellent and unique opportunity to assess forest composition at the finer level. In this study, we classified landscape into relatively homogeneous forest types to address the environmental heterogeneity across the region basing on the dominant tree species (group) at the patch level, then relating patterns of forest change with road network. This combining the biome level (sampling plots) with the patch level (spatial information) datasets in an analysis of forest landscape structure overcomes the deficiencies of local-scale empirical studies and landscape-scale studies separately (Redo et al., 2012).

Although biodiversity exists at the multiple levels (e.g. genetic, species, population, community, ecosystem, and landscape level) (Lindenmayer et al., 2000), all levels of biodiversity could be enhanced from improved connectivity and stability of forest from a landscape-level perspective (Forman, 1998). In this context, landscape structure, fragmentation and connectivity should be included into the biodiversity indicator system (Liu et al., 2014; Karadağ and Şenik, 2019), e.g., the efficiency of biodiversity conservation is often assessed by landscape metrics representing the spatial structure in a quantitative manner (Sowińska-Świerkosz and Soszyński, 2014). Such landscape metrics consist of a set of indexes at the patch, class and landscape levels, which are always calculated for both administrative borders (Hargis et al., 1998) and for different

http://www.aloki.hu ● ISSN 1589 1623 (Print) ● ISSN 1785 0037 (Online)
DOI: http://dx.doi.org/10.15666/aeer/1802_36933711

kinds of natural units, such as a park (Peng, 2019) or a watershed (Syrbe and Walz, 2012). They are also used to suggest the level of anthropogenic interference in landscape (Moser et al., 2007).

Habitat fragmentation and the subsequent effects of roads have been widely studied in America (Airey, 1992; Mcgarigal et al., 2001; Forman et al., 2002) and Europe (Jaeger et al., 2007; Freudenberger et al., 2013; Psaralexi et al., 2017), while similar research has just begun in China (Forman et al., 2002; Li et al., 2010). Since the implementing of the government's reform policy, China's road network construction has made brilliant achievements during the past four decades. As one of the most developed regions in China, Fujian Province also experienced rapid development in the construction of road infrastructure during 2007 and 2015, and in the coming years, more roads will be built to improve the accessibility for the region according to the provincial strategic plan. Moreover, Fujian Province is also one of the four major forest regions in China, with the highest forest coverage rate (66.8%, 2018) in the country (http://lyt.fujian.gov.cn/). It is noteworthy that a recent study indicated that active transformations occur among forest cover types with high conversion rates (e.g. from primary and secondary forest to planted forests) in this region (Zhang et al., 2010; Hansen et al., 2014), which can lead to the reduction of forest biodiversity and carbon storage of forest biomass (Carnus et al., 2006; Stephens and Wagner, 2007). Therefore, the direct and underlying driving forces of such landscape dynamics need to be further investigated in the upcoming studies to habitat conservation (Zhang et al., 2010). Especially, with the expansion of the road network, more and more roads are built parallelly, e.g., parallel roads of different levels are very common here; moreover, the numbers of road intersections increase greatly. These both lead to the overlapping and overlapping road effect zones. However, quantitative research on the impact of these zones on the landscape is still lacking. Thus, researches on the ecological effects of road network, especially of road overlap areas, on the forest landscape structure and degradation will have significant practical applications for this region.

Taking a typical forest landscape in the sub-tropical region, the upstream area of the Minjiang River, Fujian Province, as a case, we hypothesized five zones in this paper firstly, including the whole landscape (WL), non-road effect zone (NREZ), road effect zone (REZ), mono-road effect zone (MONREZ) and multi-road effect zone (MULREZ). Then, different rates and trajectories of forest cover changes among these zones were compared in this study. Specified, the objectives are: (1) investigate the effects of the road network on forest landscape structures (habitat fragmentation, connectivity and heterogeneity) in the five zones; (2) comprehensively evaluate the forest landscape degradation dynamics in the five zones by a comprehensive index (landscape degradation index, LDI); (3) examine whether the 'scaling up' level of human disturbance on ecosystems exists in the MULREZ zones.

Materials and methods

Study area

The study area, the upstream area of the Minjiang River (26°5′N, 117°5′E) is in a catchment basin between the Wuyi Mountains and the Daiyun Mountains, the skeletons of the terrain in Fujian Province, China. The area belongs to a typical sub-tropical forest. In the study area, 82.7% of the land area was covered by forest in 2007 and was selected as the study site, with total area of 672 km^2. Three reasons make it suitable for

http://www.aloki.hu ● ISSN 1589 1623 (Print) ● ISSN 1785 0037 (Online)
DOI: http://dx.doi.org/10.15666/aeer/1802_36933711

this study: (1) intensive extensions of road network in recent years, e.g. Quan-Shan and Yong-Ning express ways, have enforced biodiversity in this region to be subjected to severe disturbances by these roads; (2) this area is located in the upper reaches of the Minjiang River, therefore, the water quality of these rivers highly depends on the protection the forests in the study area; (3) the mixed forest with Chinese fir, pine and hardwood is a major type in the southeastern China, and of national and international importance in terms of its provision of both plant diversity and community stability of the ecosystem.

Data sources

The road data was digitized as a vector map based on the transportation maps of Sanyuan District in 2015. According to the study by Liu et al. (2008) the roads were divided into six categories (*Fig. 1a*): (1) first level (expressway), (2) second level (national roads), (3) third level (provincial road), (4) fourth level (county road), (5) fifth level (country road) and (6) sixth level (the other main road).

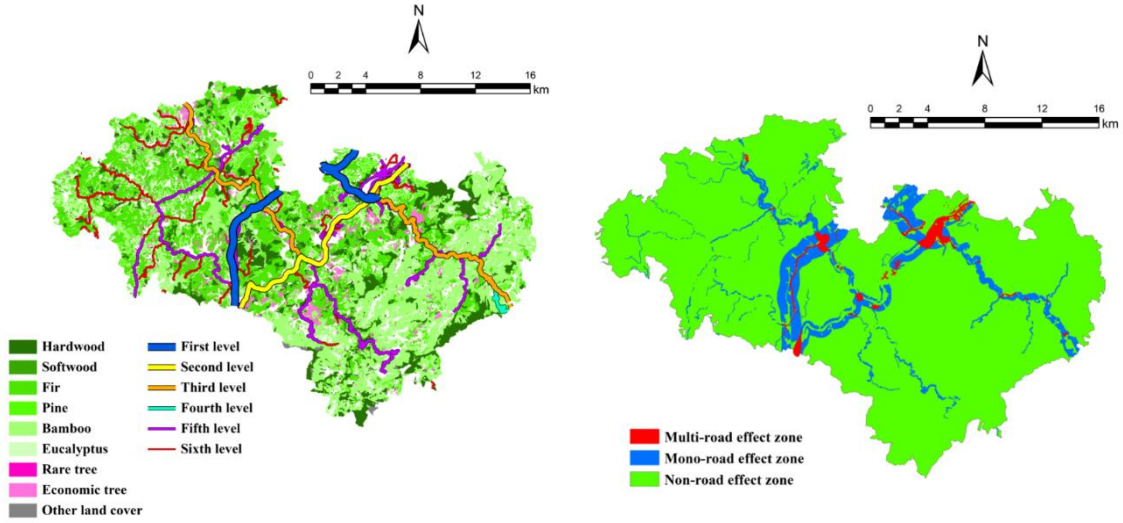

Figure 1. *(a) Road network of study area, (b) study zones, including multi-road effect zone (MULREZ), non-road effect zone (NREZ), mono-road effect zone (MONREZ), road effect zone (REZ) is composed of MONREZ and MULREZ, and whole landscape (WL) is composed of NREZ and REZ*

The forest landscape maps were derived from Forest Resources Inventory Databases (vector maps) for 2007 and 2015, collected from the local forestry department. In China, the database is the second type of forest resource survey based on forest management units such as state-owned forest farms, nature reserves, forest parks, or county-level administrative areas, to meet the needs of forest management plans, overall design, forestry zoning, and planning and design. The outcome of the survey is the establishment and update of forest resource inventory database, which is the basis for forestry engineering planning and design and forest resource management, is also an important basis for formulating regional national economic development plans and forestry development plans, implementing forest ecological benefit compensation and

http://www.aloki.hu ● ISSN 1589 1623 (Print) ● ISSN 1785 0037 (Online)
DOI: http://dx.doi.org/10.15666/aeer/1802_36933711

forest resource asset management, and guiding and standardizing forest scientific management. The database is prepared and updated yearly by the combining of field investigation (*Fig. 2*) and remote sensing. Sample plots systematically located on 1-by-1 km grid cells across the study area and are used for remote sensing verification as well (see (Xie et al., 2011) for detail). The database provides miscellaneous information at the landscape pixel level, such as land type, terrain factors, vegetation type, and dominant tree species so on.

Figure 2. *Field investigation*

Landscape classification

In this study, we classified the forests into nine categories according the dominant tree species (i.e., with the highest percentage in quantity of all individuals) of each biome when mapping forest landscapes. The nine categories of forests were fir, pine, rare tree, softwood, hardwood, Eucalyptus, bamboo, economic tree and other land cover (*Table 1*). Then, transitions between forest cover categories between 2007 and 2015 were calculated using area tabulation tool of ArcGIS software for each studied zone.

Definition of road effect zones and zones

The first-, second-, third-, fourth-, fifth- and six-level roads were buffered at 1000 m, 500 m, 250 m, 100 m, 50 m and 25 m, respectively, depending on the impact degree on the ecosystems (Wang et al., 2007; Liu et al., 2014). A minor portion of buffer zones of different level roads overlapped each other. Theoretically, these overlapped areas are more accessible than others, with more chances to be interrupted. In this context, it is interesting to better understand several fundamental questions. Are these areas more vulnerable? Is the 'scaling up' level of human disturbance on ecosystems in these areas higher than that of the other? To answer these questions, the road effect zone was separated into mono-road effect zone and multi-road effect zone here, thus as a whole five zones were hypothesized in this study, including WL (672 km^2), NREZ (607 km^2), REZ (65 km^2), MONREZ (62 km^2) and MULREZ (3 km^2) (*Fig. 1b*). Then, landscape metrics for these five zones were calculated respectively for the comparisons of their Landscape change, habitat fragmentations, isolation, heterogeneity and landscape degenerations between 2007 and 2015.

http://www.aloki.hu ● ISSN 1589 1623 (Print) ● ISSN 1785 0037 (Online)
DOI: http://dx.doi.org/10.15666/aeer/1802_36933711

Table 1. *Description of the nine classes of forest cover*

Forest cover classes	Classification criteria	Biomes
Fir	Taxodiaceae family species	*Cunninghamia lanceolata*
Pine	Pinaceae family species	*Pinus massoniana*, *P. elliottii*, *P. taeda*, *Tsuga chinensis* var. *tchekiangenesis*
Rare tree	The first reference list of the main rare species in Fujian Province (2007), compiled by the Fujian Province Department of Forestry	*Cinnamomum camphora*, *Phoebe bournei*, *Fokienia hodginsii*, *Taiwania cryptomerioide*, *Liquidamba formosana*, *Cryptomeria fortunei*
Softwood	Hard timber trees, are generally more durable and denser than softwoods or soft timbers although not all are harder than softwoods the main differences between them are botanical, these types of trees have broader leaves than soft timber trees	*Paulownia chinense*
Hardwood		*Castanopsis* species, *Schima superba*
Eucalyptus	Plants of *Eucalyptus* (Myrtaceae family)	*Eucalyptus grandis*, *E. citriodora*
Bamboo	The woody bamboos	*Phyllostachys edulis*, *Dendrocalamus olhami*, *D. latiflorus*
Economic tree	Those where the main management emphasis is on forest products rather than timber, such as fruit, bark, leaves, tree sap, branches, flower buds and tender sprouts	*Citrus maxima*, *C. reticulate*, *C. mollissima*, *Camellia oleifera*, *C. Sinensis*, *Magnolia officinalis*, *Vernicia fordii*
Other land cover	Other forest covers apart from the above, besides which non-forest covers are included in this category in the 2015's landscape	2007: shrub land and minor forest; 2015: shrub land, minor forest, no standing forest and non-forest

Calculation of landscape change rate

Landscape change rate (LCR) indicates the transfer rate between all landscape types in a study period in a region, and can be used to characterize the intensity of landscape type transformation in a particular region (e.g., a road buffer zone) in order to find a hot spot for change. It can be calculated as follows (*Eq. 1*):

$$LCR = \frac{\sum_{i=1}^{n} \Delta LA_{i-j}}{\sum_{i=1}^{n} LA_i} \times 100 \quad \text{(Eq.1)}$$

where, *LCR* is the landscape change rate (%) of the integrated landscape during the study period, LA_i is the total area of the initial landscape type *i*, $\Delta\ LA_{i\text{-}j}$ s the area of landscape type *i* converted to the landscape type *j* during the study period.

Calculation of landscape degradation

The Fragstats software presents the most comprehensive overview of the landscape metrics, which are algorithms that quantify the specific spatial characteristics of three hierarchical levels: patch level, class level and landscape level (Šímová and Gdulová, 2012). To investigate the effects of road network extensions on landscape structure, we measured commonly used landscape metrics to analyze the habitat changes for each landscape using the Fragstats 3.4 program (Mcgarigal and Marks, 1995; Mcgarigal et

http://www.aloki.hu ● ISSN 1589 1623 (Print) ● ISSN 1785 0037 (Online)
DOI: http://dx.doi.org/10.15666/aeer/1802_36933711

al., 2001). Among which, area related indices were calculated to describe the features of patches, such as mean patch area (AREA_MN), standard deviation of patch area (PSSD) and coefficient variation of patch area (AREA_CV). Number of patch (NP), patch density (PD), edge density (ED), and mean fractal dimension index (FRAC_MN) were used to examine habitat fragmentation at the class level. The isolation, connection and heterogeneity of the entire landscape were indicated by landscape level metrics: aggregation index (AI), contagion index (CONTAG) and Shannon's evenness index (SHEI). For the formulas and detailed descriptions of all landscape indices, please refer to reference (Mcgarigal and Marks, 1995; Mcgarigal et al., 2001).

Quantitatively measuring the fragmentation, isolation, connection and heterogeneity of the entire landscape have been extensively applied to the analysis of landscape pattern using landscape metrics (Turner et al., 2003). However, these metrics were calculated as separate indicators in the most of the landscape structure studies (Tinker et al., 1998; Mcgarigal et al., 2001), with little contribution to the comprehensive comparisons of different ecological processes between different landscapes. In this context, an integral index, LDI, was selected to evaluate the landscape pattern as a whole. LDI measures the fragmentation and the stability of the entire landscape, which is proportionally composed of a series of metrics, such as AREA_CV, PD, ED, FRAC_MN, CONTAG, AI and SHEI. The formulas were given by the following expressions (Wang et al., 2007; *Eqs. 2-4*).

$$LFDI = aAREA\_CV + bPD + cED + dFRAC\_MN \quad \text{(Eq.2)}$$

$$LSI = \sqrt[3]{CONTAG \times SHEI \times AI} \quad \text{(Eq.3)}$$

$$LDI = LFDI/LSI \quad \text{(Eq.4)}$$

where the LDI includes landscape fragmentized degree intensity (LFDI) and landscape stability index (LSI); *a, b, c* and *d* are the weights of the indexes of AREA_CV, PD, ED, and FRAC_MN, which is 0.27, 0.26, 0.24 and 0.23 respectively (Wang et al., 2007).

We assumed that in a region with relatively homogeneous biophysical interference, higher value of LDI indicates higher level of anthropogenic interference (e.g., road network, cutting) in the habitats, which, in turn, influences the abundance and distribution of plant and animal species (Geneletti, 2003; Eigenbrod et al., 2008).

Results

Forest landscape composition and dynamics in different senarios

For the whole landscape, NREZ and REZ occupied 90.3% and 9.7% of the study area respectively. In the REZ, MONREZ and MULREZ occupied 95.0% and 5.0%, respectively (*Fig. 3*).

Figure 2 also indicated that forest landscape changes were active during the study period in all the zones. 5.4% of the landscape in the REZ experienced forest cover change between 2007 and 2015. By contrast, only 4.1% of the landscape in the NREZ was transformed between 2007 and 2015. In the REZ, 5.6% of the landscape experienced forest cover change in the MONREZ, while it was unexpectedly that only 2.3% of the landscape was transformed in the MULREZ between 2007 and 2015.

http://www.aloki.hu ● ISSN 1589 1623 (Print) ● ISSN 1785 0037 (Online)
DOI: http://dx.doi.org/10.15666/aeer/1802_36933711

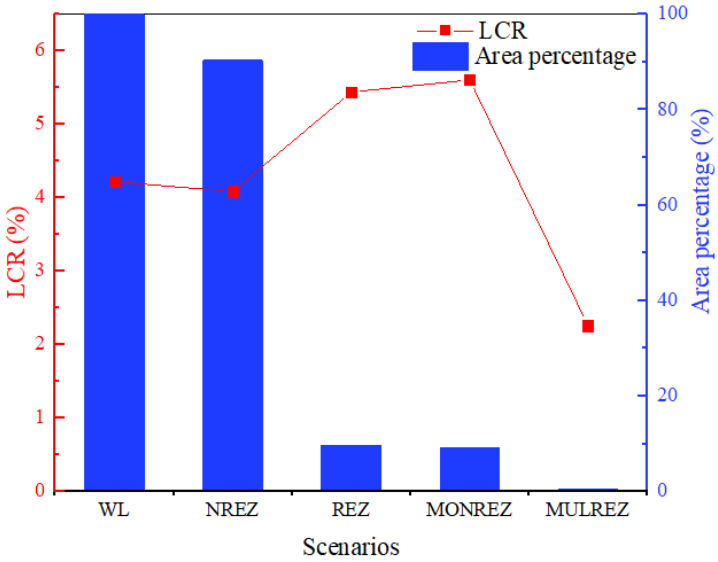

Figure3. *Proportion of each zone and its landscape change dynamics. The curve represents the landscape change rate of d different zones (left Y-axis); the columns represent the area proportion of each zone to the total area of the study area (right Y-axis). LCR is landscape change rate*

Figure 4 showed the forest landscape compositions and dynamics from 2007 to 2015 for the five zones. The dominant forest cover classes were fir and bamboo, predominating in 34.1% and 31.7% in 2007, and 32.7% and 31.7% in 2015, respectively, in the WL zone. Compared to the NREZ, the REZ had a relatively smaller proportion of bamboo, accounted for 21.5% and 21.7% of the area, respectively in 2007 and 2015. On the contrary, the proportion of fir and economic tree in the REZ were about 5% higher than that in the NREZ in the both years. Furthermore, it was worth to mention that the proportions of other land cover in the REZ (especially in the MULREZ) were uncommonly several-fold beyond those in the NREZ.

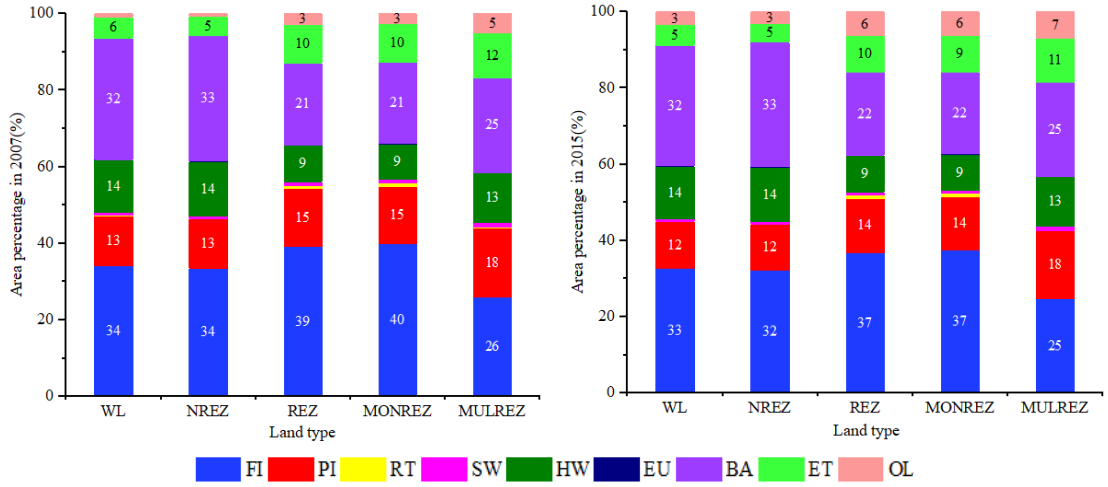

Figure 4. *Forest landscape composition in each zone. The nine categories of forests were Fir (FI), Pine (PI), Rare tree (RT), Softwood (SW), Hardwood (HW), Eucalyptus (EU), Bamboo (BA), Economic tree (ET) and other land cover (OL). The numbers on the columns indicates the percentage of each landscape in each zone*

http://www.aloki.hu ● ISSN 1589 1623 (Print) ● ISSN 1785 0037 (Online)
DOI: http://dx.doi.org/10.15666/aeer/1802_36933711

Figure 5 indicated that, in all the zones, bamboo and hardwood showed high stability during the studied period, fir, pine, softwood and economic tree decreased steadily, while eucalyptus and other land cover increased dramatically over time. Between 2007 and 2015, fir in the NREZ was reduced by 4.0% of its area, while the reduction increased to 6.1% in the REZ; the proportion of pine was also slightly reduced by 6.7% and 5.5% in the NREZ and REZ, respectively. The opposite trend was observed in other land cover, which increased more than four times in the NREZ, whereas, only increased 127.0% in the REZ. Eucalyptus also increased 22.8% and 74.2% in the NREZ and REZ, respectively. Simultaneously, the change of rare tree showed a different trends and directions in different zones. Specifically, in the NREZ zone, the area of rare tree increased, while in the case of road zones (i.e., REZ, MONREZ, MULREZ), the area of rare tree species decreased, especially all the area of rare tree was encroached in the MULREZ zone.

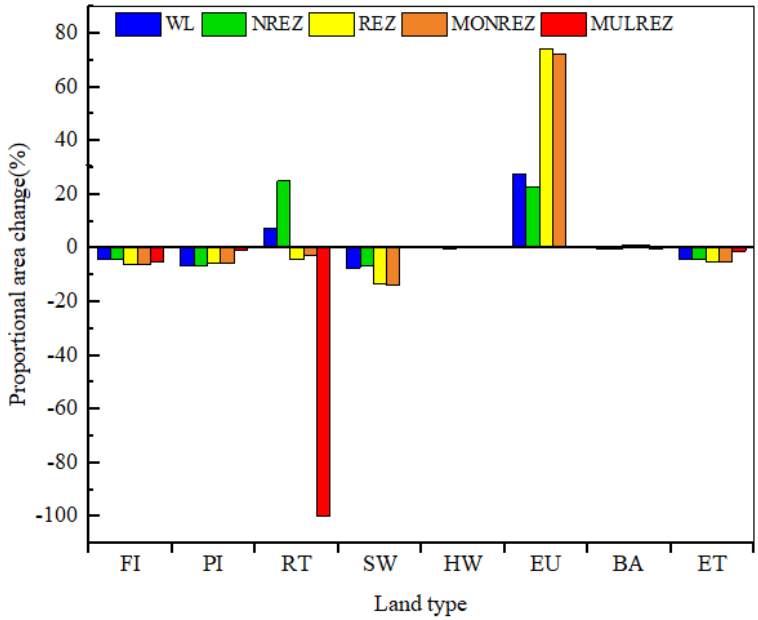

Figure 5. *Forest landscape change dynamics in each zone during 2007-2015*

Forest landscape patterns and dynamics in different scenarios

Table 2 showed the calculated results of the landscape metrics for the years of 2007 and 2015. In this studied case, the AREA_MN index in the NREZ (10.853-12.150 ha) was much higher than that of the REZ (2.989-3.215 ha) (P-value = 0.000), which indicated that the forest landscape structure of the NREZ was much more stable, and distinguished by a number of larger area patches. The PD index was substantially higher in the REZ (31.102-33.461) than that in the NREZ (8.231-9.214) (P-value = 0.000), especially in the MULREZ (80.021-81.571) even ten times or so as much as that in the NREZ (P-value = 0.000). Analogically, the ED index in the REZ (71.410-77.496) was significantly higher than that of the NREZ (57.372-61.697) (P-value = 0.000), moreover, MULREZ had a greater ED than the former two as well. These findings clearly indicated that the landscape spatial structure in the REZ (especially in the MULREZ) was much more fragmented than that in the NREZ.

http://www.aloki.hu ● ISSN 1589 1623 (Print) ● ISSN 1785 0037 (Online)
DOI: http://dx.doi.org/10.15666/aeer/1802_36933711

The AI and CONTAG values were close in all the zones, with the highest in the NREZ, and then in the REZ, followed by the MULREZ. The study results showed that patch types with a similar area (lower AREA_CV and PSSD values) in the REZ were generally much more dispersed than those of the NREZ. The SHEI value was bit higher in the REZ (0.742-0.770) (P-value = 0.005), much higher in the MULREZ (0.835-0.843) (P-value = 0.000) than that in the NREZ (0.683-0.712). This finding confirmed a lower landscape diversity of the REZ than that of the NREZ.

Table 2. *Statistics of forest landscape metrics under different zones*

Metrics	Year	NP	AREA_MN	PSSD	AREA_CV	PD	ED	FRAC_MN	SHEI	AI	CONTAG	LDI
WL	2007	4607	14.562	162.124	1113.309	6.867	58.865	1.106	0.692	97.892	63.18	1.181
	2015	5266	12.74	112.673	884.404	7.849	63.368	1.107	0.72	97.78	61.615	1.22
NREZ	2007	4988	12.15	90.725	746.722	8.231	57.372	1.107	0.683	97.862	63.693	1.122
	2015	5584	10.853	79.467	732.205	9.214	61.697	1.108	0.712	97.756	62.105	1.193
REZ	2007	2017	3.215	10.513	326.974	31.102	71.41	1.12	0.742	96.308	60.254	1.621
	2015	2170	2.989	9.461	316.565	33.461	77.496	1.119	0.77	96.159	58.634	1.742
MONREZ	2007	2141	2.879	9.452	328.359	34.741	70.836	1.12	0.738	96.163	60.459	1.672
	2015	2293	2.688	8.48	315.51	37.207	77.106	1.119	0.767	96.009	58.773	1.797
MULREZ	2007	258	1.25	2.352	188.175	80.021	77.493	1.119	0.835	94.459	55.224	2.459
	2015	263	1.226	2.316	188.897	81.571	80.052	1.119	0.843	94.393	54.737	2.522

Number of patch (NP), mean patch area (AREA_MN), standard deviation of patch area (PSSD), coefficient variation of patch area (AREA_CV), patch density (PD), edge density (ED), mean fractal dimension index (FRAC_MN), aggregation index (AI), contagion index (CONTAG) and Shannon's evenness index (SHEI), landscape degradation index (LDI)

Figure 6 showed that the trends of the landscape metrics between 2007 and 2015 were relatively unanimous in all the zones, indicating a decreasing trend as the increasing intensity of road disturbance, in order of WL, NREZ, MONREZ and REZ and MULREZ.

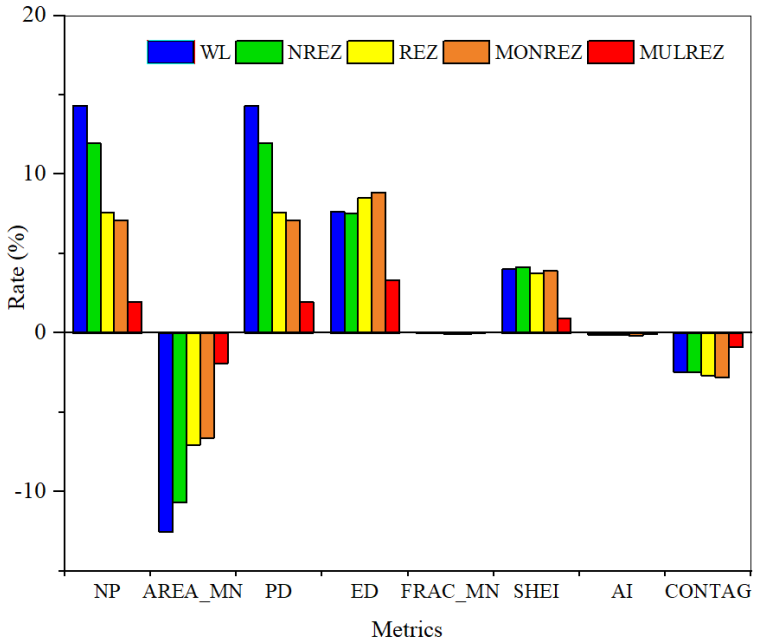

Figure 6. *Change rates in landscape metrics in each zone (2007-2015)*

http://www.aloki.hu ● ISSN 1589 1623 (Print) ● ISSN 1785 0037 (Online)
DOI: http://dx.doi.org/10.15666/aeer/1802_36933711

Forest landscape degradation and dynamics in different scenarios

The dynamics of the landscapes showed that the fragmentations of the landscape structures were obviously strengthened under the disturbance of road network (*Table 2*). In *Figure 7,* the composite index of landscape fragmentation (LFDI) also showed that the degree of fragmentation of forest landscape increases with the increase of road disturbance intensity, moreover, the trend was relatively stable for the index of LSI. Referring these results directly to identify the level of degradation of the entire landscape requires the analysis of the LDI. In this case, the LDI was significantly higher in the REZ (1.621-1.742) than that in the NREZ (1.193-1.122), and the MULREZ (2.459-2.522) had much higher LDI than MONREZ (1.672-1.797). Furthermore, the growing rate of landscape degradation from 2007 to 2015 in the REZ was about 1.2 times as that in the NREZ, however, the change rate in the MULREZ was relatively low (*Fig. 8*). This finding confirms that road networks have broken the landscape into pieces and resulted in fragmented ecosystems and complicated ecosystem structures, eventually accelerating the degradation of the ecosystem.

Discussion

Landscape transitions

As a permanent modification of the landscape, road network threatens the existing habitats and the wildlife populations depending on it, e.g., interrupting ecological flows, inhibiting interior species, and promoting landscape fragmentation (Forman, 1998). Landscape fragmentation is a breakup to transform a continuous habitat into smaller, more dispersal patches, which can impose destructive and irreversible consequences on regional biodiversity (Trakhtenbrot et al., 2005). Such negative impacts of road network have been hot topics in the study of landscape ecology and biodiversity conservation (Zhu et al., 2006; Benítez-López et al., 2010). In this study, we detected considerable transitions among different forest landscapes types in each zone. Though landscape dynamics patterns varied through zones, most of the changed forest cover was transformed into other land cover in all the zones. However, the key differences were that the percentages (the area changed to other land cover divided by the total area experienced change in each zone) were significantly higher in the REZ (67.4%) than that in the NREZ (60.9%) (*Table A1* in the *Appendix*). Moreover, the MULREZ was among the most surprising zone, in which more than 80% of the forest cover change happened to shift into other land cover. In the NREZ, gain of other land cover area was largely from fir, which accounted for more than 60% of the total area gained by other land cover in the study periods; while, in the REZ, the gain of other land cover was from relatively diversified forest covers, among which fir, pine and economic tree accounted for 38.5%, 10.0% and 8.6% of the total area gained by other land cover, respectively. All these findings indicated that the forest covers have suffered greater human disturbance in the REZ (MULREZ in particular) than in the NREZ. Previous studies on the ecological impacts of road network at the landscape level, with no effort identifying habitat changes among forest types, which have limited ecological meanings to devise more effective strategies for biodiversity conservation (Li et al., 2010; Patarasuk, 2013). In this study, we overcame these difficulties by conducting a Forest Resources Inventory Database-based analysis of changes in forest landscape, stratified

http://www.aloki.hu ● ISSN 1589 1623 (Print) ● ISSN 1785 0037 (Online)
DOI: http://dx.doi.org/10.15666/aeer/1802_36933711

by dominant species in respective biomes, which it very helpful in identifying the dynamics of forest landscape changes from a finer scale.

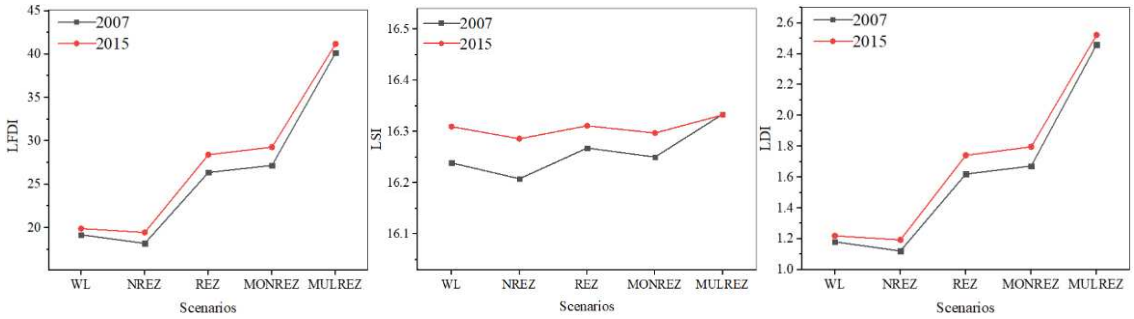

Figure 7. *Landscape degradation dynamic in each zone (2007-2015)*

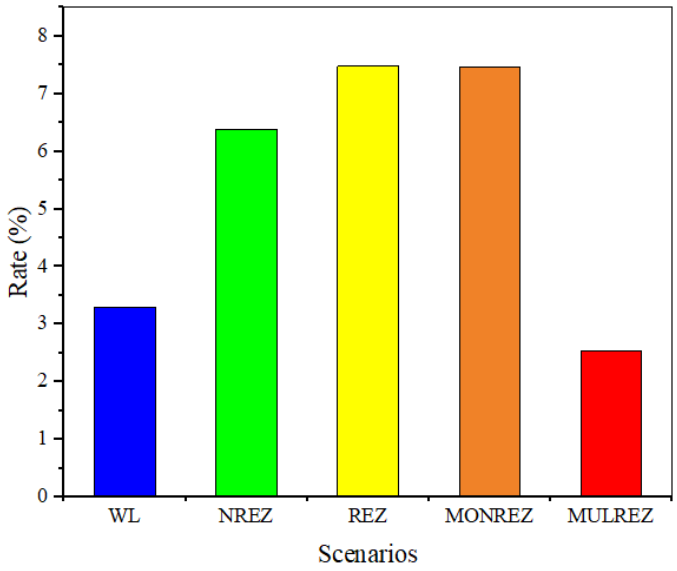

Figure 8. *Change rate of landscape degradation index from 2007 to 2015*

Landscape degradation

In our study, it was obvious that the landscape metrics varied greatly across different zones, revealing that the landscape spatial structure in the REZ (especially in the MULREZ) was much more fragmented than that in the NREZ, and a lower landscape diversity in the REZ than that of the NREZ. This finding indicates a higher level of interference imposing on the forests in the REZ, leading to the increasing of habitat fragmentation and isolation, the decreasing of heterogeneity in forest landscape near roads. Our results agree with previous researches, documenting habit fragmentation causing by the changes of landscape patterns near road corridors (Hawbaker et al., 2005; Liu et al., 2008), which have been reported as a contribution to the declining in forest species (Arnold et al., 1995; Mcintyre, 1995). However, different from many of these studies (Heilman et al., 2002; Liu et al., 2014), we further separated the REZ into two segments, i.e., MONREZ and MULREZ. Our result indicated that the level of

http://www.aloki.hu ● ISSN 1589 1623 (Print) ● ISSN 1785 0037 (Online)
DOI: http://dx.doi.org/10.15666/aeer/1802_36933711

habitat fragmentation and isolation in the MULREZ was much higher than that of the MONREZ, implying that there exists superimposed effect of the roads on the forest landscape.

For the change ratios between 2007 and 2015, landscape fragmentation indices (NP, AREA_MN, PSSD, PD and ED) had larger values than landscape stability index (AI, CONTAG and SHEI). In all the zones except the MULREZ, the rates of change of NP, AREA_MN, PSSD, PD and ED indices were 7.1~14.3%, 6.6~12.5%, 10.3~30.5%, 7.1~14.3% and 7.5~8.9%, respectively, while those for the AI, CONTAG and SHEI indices were -0.2~-0.1%, -2.8~-2.5% and 3.8~4.2%, respectively (*Table 2*). The relatively major changes in landscape fragmentation and relatively minor changes in overall landscape structure of the forest may be attributed to the high rate of persistence in area size of each forest category between 2007 and 2015, while a relatively rapid transition intra/inter- these cover categories occurred. This provided a good reason for us to classify landscape into forest types basing on the dominant tree species.

As landscape fragmentation indices concerned, the change ratios of NP, AREA_MN, PSSD, and PD in the NREZ were higher than those in the REZ, while it was versa for the change ratios of ED. Similarly, the comparisons of the change ratios for landscape stability indices also showed a bidirectional diagram between the NREZ and the REZ. Though, much greater in habitat fragmentation and landscape degradation was evident on the REZ, more significant changes of habitat fragmentation were detected in the NREZ between 2007 and 2015. Also, an unexpected outcome of the study was the lowest change ratios of such indices in the MULREZ. The reasons are followed: the study area has always been a key base of forestry industry in Fujian Province, a large proportion of forest is designated as suitable for commercial timber use. Therefore, logging often happens in the currently designated as suitable timberlands, which as a result is sufficient to cause rather dramatic changes in landscape structure. These can be proved by the fact that more than 60% of the total area changed has been converted into other land cover (shrub land, minor forest, no standing forest and non-forest) in all the zones (*Table A1*). Therefore, the increase in other land cover was partly caused by frequent regeneration failures or time-lagged regenerations following clear-cut logging in the study area. This implies that both road network extensions and forest management practices lead to the increasing of landscape degradation in all the zones, with a higher change rate in the REZ in the study area.

Several indices have been developed to quantify the influence of road disturbance on landscape structure (Mcgarigal et al., 2001; Liu et al., 2014). Most of the current indices focus on habitat fragmentation, isolation, connection or heterogeneity separately, without joint consideration of comprehensive evaluation of these landscape metrics. In this study, LDI, an approach that combines these measures of landscape metrics, was employed to examine the disturbance of road network on landscape. An expected outcome was that the LDI in the REZ was higher than that of the NREZ, and showed an aggravated influence on the forest landscape in the REZ during the study period. Thus, in the REZ, habitat fragmentation may switch from being predominantly internally driven (i.e., logging) to being predominantly externally driven (i.e., road construction). Simultaneously, remnant patches become more and more isolated, thereby resulting in further ecological degradation across the landscapes.

These findings are consistent with other studies from the Rocky Mountains (Reed et al., 1996; Mcgarigal et al., 2001) and the north-central Wyoming (Tinker et al., 1998), which documented that forests were more highly fragmented from roads than from

http://www.aloki.hu ● ISSN 1589 1623 (Print) ● ISSN 1785 0037 (Online)
DOI: http://dx.doi.org/10.15666/aeer/1802_36933711

clear-cuts. However, we also found that the change ratios of some landscape metrics were higher in the NREZ than in the REZ, these can be explained by the following reasons other than logging mentioned above: (1) Roads provide access and allow landscape pattern to change during the construction and in the early stage, however these changes may be constrained by environmental factors such as topography in the later period after road been built (Hawbaker et al., 2005). In this case, land use changes near roads may be mediated by the constrain of the topographic feature prevailed with the mountain terrain in the study area; (2) a large portion of forest buffer belts were designed for various ecological purpose (e.g. conservation of water and soil, prevention of traffic noise, protection of slope and greening of road), where logging and constructing cannot occur frequently.

Extensions and limitations

As described by different authors, the simple landscape metrics, e.g., NP, ED, PD and AREA_MN, are the most suitable indices to analyze landscape structure (Frohn and Hao, 2006; Šímová and Gdulová, 2012), so the cutting and fragmentizing effect of road networks on landscape can be revealed from the changes of such landscape metrics (Sowińska-Świerkosz and Soszyński, 2014). The ED is among a positive index identifying the level of provision of habitats for alien plants, posing a great threat to the existence of native species. Still more important is the dissecting effect of road network, the ED value has also been proven to be crucial for local hydrologic and erosion effects and downstream peak-flow and sediment impacts (Forman, 1998; Uuemaa et al., 2009). In our case, the ED values of REZ were greater than those of NREZ, and the differences incline to be enlarged during the study period. This finding shows that biodiversity in the REZ and water quality in the watersheds has been subjected to severe disturbances by these roads during the study period.

Yet, it is insufficient to assess landscape changes due to road network disturbances within a specific zone/a fixed temporal extent using landscape metrics (Liu et al., 2008), because the extent of REZ may be different for different regions (Forman et al., 2002), moreover, effects of roads on landscape may vary over time (Forman, 1998), while the analysis performed here to the five zones was in the same period and the REZ was at a fixed spatial scale. Such approach does not give answer if a particular stage is up surging for the landscape changes near roads, and if the effects of road network on landscape vary with different extents of REZ. Moreover, the road network has continued to expand over time, and although the overall change has been small, we have failed to consider the impact of new roads on the landscape during the study period.

Conclusions

Our results showed that there were obvious different forest landscape structures and their dynamics between the NREZ and REZ during the study periods, so the LDI did. In addition, we found that the change ratio of LDI value in the REZ was much higher than that in the NREZ, while it was versa for some landscape fragmentation indices. This is because the high rate of persistence in area size of each forest category between 2007 and 2015, while a relatively faster transition intra/inter- these cover categories occurred in the NREZ. These results indicate that the potential effects of road network on biodiversity maybe severer than the direct effects of logging, while logging may be also an important factor contributing to the habitat fragmentations in the study area. And it

http://www.aloki.hu ● ISSN 1589 1623 (Print) ● ISSN 1785 0037 (Online)
DOI: http://dx.doi.org/10.15666/aeer/1802_36933711

also shows the necessity of the landscape classification according to the dominant tree species, which will provide more finer information on forest cover change.

Our result indicated that the level of habitat fragmentation and isolation in the MULREZ was much higher than that of the MONREZ, implying that there exists superimposed effect of the roads on the forest landscape. While, an unexpected outcome of the study was the lowest change ratios of landscape metrics in the MULREZ during the study period. The reasons were still unclear so far as from our study. Therefore, we suggest that further investigations should be carried out for this region and beyond by conducting a gradient analysis with changing road buffer zones and a comparison analysis across time periods (e.g., pre- and post- construction of a road). Furthermore, it is also necessary to further quantify forest landscape structure, such as forest edge dynamic and landscape connectivity, analyze the underlying causes of these habitat changes, and to evaluate the effect of such active forest change in this area on carbon emission, which will help to prevent adverse impacts of human dimensions on biodiversity and climate warming. Finally, understanding how the spatial distribution of road networks affects forest landscape pattern should take at least the following factor into account: control for bias that arises when observable biophysical (e.g., topography) and artificial (e.g., logging and mining) factors affect both which landscapes are in REZ and which are in NREZ.

Acknowledgments. This research was funded by the National Natural Science Foundation of China (No. 41901221 and 31971639), to which we are very grateful. We are also very grateful for the support provided by the Natural Science Foundation of Fujian Province, China (No.2019J01406 and 2019J01430). Finally, many thanks to the Forestry Bureau of Sanyuan District, Fujian Province, China for providing us with a validation dataset.

REFERENCES

[1] Airey, T. (1992): The impact of road construction on the spatial characteristics of hospital utilization in the Meru district of Kenya. – Social Science & Medicine 34(10): 1135-1146.

[2] Angelstam, P., Khaulyak, O., Yamelynets, T., Mozgeris, G., Naumov, V., Chmielewski, T. J., Elbakidze, M., Manton, M., Prots, B., Valasiuk, S. (2017): Green infrastructure development at European Union's eastern border: effects of road infrastructure and forest habitat loss. – Journal of Environmental Management 193: 300-311.

[3] Arnold, G. W., Weeldenburg, J. R., Ng, V. M. (1995): Factors affecting the distribution and abundance of Western grey kangaroos (Macropus fuliginosus) and euros (M. Robustus) in a fragmented landscape. – Landscape Ecology 10(2): 65-74.

[4] Benítez-López, A., Alkemade, R., Verweij, P. A. (2010): The impacts of roads and other infrastructure on mammal and bird populations: a meta-analysis. – Biological Conservation 143(6): 1307-1316.

[5] Bordadeágua, L., Navarro, L., Gavinhos, C., Pereira, H. M. (2011): Spatio-temporal impacts of roads on the persistence of populations: analytic and numerical approaches. – Landscape Ecology 26(2): 253-265.

[6] Carnus, J. M., Parrotta, J., Brockerhoff, E., Arbez, M., Jactel, H., Kremer, A., Lamb, D., O'Hara, K., Walters, B. (2006): Planted forests and biodiversity. – Journal of Forestry 104(2): 65-77.

[7] Coffin, A. W. (2007): From roadkill to road ecology: a review of the ecological effects of roads. – Journal of Transport Geography 15(5): 396-406.

http://www.aloki.hu ● ISSN 1589 1623 (Print) ● ISSN 1785 0037 (Online)
DOI: http://dx.doi.org/10.15666/aeer/1802_36933711

[8] Eigenbrod, F., Hecnar, S. J., Fahrig, L. (2008): Accessible habitat: an improved measure of the effects of habitat loss and roads on wildlife populations. – Landscape Ecology 23(2): 159-168.
[9] Forman, R. T. T. (1998): Road ecology: a solution for the giant embracing us. – Landscape Ecology 13(4): III-V.
[10] Forman, R. T. T., Reineking, B., Hersperger, A. M. (2002): Road traffic and nearby grassland bird patterns in a suburbanizing landscape. – Environmental Management 29(6): 782-800.
[11] Freudenberger, L., Hobson, P. R., Rupic, S., Pe Er, G., Schluck, M., Sauermann, J., Kreft, S., Selva, N., Ibisch, P. L. (2013): Spatial road disturbance index (SPROADI) for conservation planning: a novel landscape index, demonstrated for the State of Brandenburg, Germany. – Landscape Ecology 28(7): 1353-1369.
[12] Frohn, R. C., Hao, Y. (2006): Landscape metric performance in analyzing two decades of deforestation in the Amazon Basin of Rondonia, Brazil. – Remote Sensing of Environment 100(2): 237-251.
[13] Fu, W., Liu, S., Degloria, S. D., Dong, S., Beazley, R. (2010): Characterizing the "fragmentation–barrier" effect of road networks on landscape connectivity: a case study in Xishuangbanna, Southwest China. – Landscape & Urban Planning 95(3): 122-129.
[14] Geneletti, D. (2003): Biodiversity impact assessment of roads: an approach based on ecosystem rarity. – Environmental Impact Assessment Review 23(3): 343-365.
[15] Gibbs, J. P., Steen, D. A. (2010): Trends in sex ratios of turtles in the united states: implications of road mortality. – Conservation Biology 19(2): 552-556.
[16] Gutiérrez, J., Urbano, P. (1996): Accessibility in the European Union: the impact of the trans-European road network. – Journal of Transport Geography 4(1): 15-25.
[17] Hansen, M., Potapov, P., Margono, B., Stehman, S., Turubanova, S., Tyukavina, A. (2014): Response to comment on "High-resolution global maps of 21st-century forest cover change". – Science 342(6187): 850-853.
[18] Hargis, C. D., Bissonette, J. A., David, J. L. (1998): The behavior of landscape metrics commonly used in the study of habitat fragmentation. – Landscape Ecology 13(3): 167-186.
[19] Hawbaker, T. J., Radeloff, V. C., Hammer, R. B., Clayton, M. K. (2005): Road density and landscape pattern in relation to housing density, and ownership, land cover, and soils. – Landscape Ecology 20(5): 609-625.
[20] Heilman, G. E., Strittholt, J. R., Slosser, N. C., Dellasala, D. A. (2002): Forest fragmentation of the Conterminous United States: assessing forest intactness through road density and spatial characteristics. – Bioscience 52(5): 411-422.
[21] Jaeger, J. A. G., Schwarzvon Raumer, H. G., Esswein, H., Müller, M., Schmidtlüttmann, M. (2007): Time series of landscape fragmentation caused by transportation infrastructure and urban development: a case study from Baden-Württemberg, Germany. – Ecology & Society 12(1): 181-194.
[22] Karadağ, A. A., Şenik, B. (2019): Landscape sensitivity analysis as an ecological key: the case of Duzce, Turkey. – Applied Ecology and Environmental Research 17: 14277-14296.
[23] Li, T., Shilling, F., Thorne, J., Li, F., Schott, H., Boynton, R., Berry, A. M. (2010): Fragmentation of China's landscape by roads and urban areas. – Landscape Ecology 25(6): 839-853.
[24] Liang, J., Liu, Y., Ying, L., Li, P., Xu, Y., Shen, Z. (2014): Road impacts on spatial patterns of land use and landscape fragmentation in three parallel rivers region, Yunnan Province, China. – Chinese Geographical Science 24(1): 15-27.
[25] Lindenmayer, D. B., Margules, C. R., Botkin, D. B. (2000): Indicators of biodiversity for ecologically sustainable forest management. – Conservation Biology 14(4): 941-950.
[26] Liu, S., Dong, Y., Deng, L. I., Liu, Q. I., Zhao, H., Dong, S. (2014): Forest fragmentation and landscape connectivity change associated with road network extension and city

http://www.aloki.hu ● ISSN 1589 1623 (Print) ● ISSN 1785 0037 (Online)
DOI: http://dx.doi.org/10.15666/aeer/1802_36933711

expansion: a case study in the Lancang River Valley. – Ecological Indicators 36(36): 160-168.
[27] Liu, S. L., Cui, B. S., Dong, S. K., Yang, Z. F., Yang, M., Holt, K. (2008): Evaluating the influence of road networks on landscape and regional ecological risk—a case study in Lancang River Valley of Southwest China. – Ecological Engineering 34(2): 91-99.
[28] Mcgarigal, K., Marks, B. J. (1995): FRAGSTATS: spatial pattern analysis program for quantifying landscape structure. – General Technical Report Pnw 351.
[29] Mcgarigal, K., Romme, W. H., Crist, M., Roworth, E. (2001): Cumulative effects of roads and logging on landscape structure in the San Juan Mountains, Colorado (USA). – Landscape Ecology 16(4): 327-349.
[30] Mcintyre, N. E. (1995): Effects of forest patch size on avian diversity. – Landscape Ecology 10(2): 85-99.
[31] Mehdipour, N., Fakheran, S., Soffianian, A., Pourmanafi, S. (2019): Road-induced fragmentation and the environmental value of roadless areas in a partly protected landscape in central Iran. – Environmental Monitoring and Assessment 191: 461.
[32] Moser, B., Jaeger, J., A. G., Tappeiner, U. E., Eiselt, B. (2007): Modification of the effective mesh size for measuring landscape fragmentation to solve the boundary problem. – Landscape Ecology 22(3): 447-459.
[33] Patarasuk, R. (2013): Road network connectivity and land-cover dynamics in Lop Buri province, Thailand. – Journal of Transport Geography 28: 111-123.
[34] Peng, Y. (2019): Influence of environmental landscape structure on the distribution features of plant communities in green parks. – Applied Ecology and Environmental Research 17: 14599-14609.
[35] Psaralexi, M. K., Votsi, N. E. P., Selva, N., Mazaris, A. D., Pantis, J. D. (2017): Importance of roadless areas for the European Conservation Network. – Frontiers in Ecology and Evolution 5: 2.
[36] Redo, D. J., Grau, H. R., Aide, T. M., Clark, M. L. (2012): Asymmetric forest transition driven by the interaction of socioeconomic development and environmental heterogeneity in Central America. – Proceedings of the National Academy of Sciences 109(23): 8839-8844.
[37] Reed, R. A., Johnson-Barnard, J., Baker, W. L. (1996): Fragmentation of a forested Rocky Mountain landscape, 1950-1993. – Biological Conservation 75(3): 267-269, 271-277.
[38] Ren, Y., Wei, X., Zhang, L., Cui, S., Chen, F. (2011): Potential for forest vegetation carbon storage in Fujian Province, China, determined from forest inventories. – Plant & Soil 345(1/2): 125-140.
[39] Selva, N., Kreft, S., Kati, V., Schluck, M., Jonsson, B. G., Mihok, B., Okarma, H., Ibisch, P. L. (2011): Roadless and low-traffic areas as conservation targets in Europe. – Environmental Management 48(5): 865-877.
[40] Šímová, P., Gdulová, K. (2012): Landscape indices behavior: a review of scale effects. – Applied Geography 34: 385-394.
[41] Sowińska-Świerkosz, B. N., Soszyński, D. (2014): Landscape structure versus the effectiveness of nature conservation: Roztocze region case study (Poland). – Ecological Indicators 43(43): 143-153.
[42] Spooner, P. G., Lunt, I. D., Okabe, A., Shiode, S. (2004): Spatial analysis of roadside Acacia populations on a road network using the network K-function. – Landscape Ecology 19(5): 491-499.
[43] Stephens, S. S., Wagner, M. R. (2007): Forest plantations and biodiversity: a fresh perspective. – Journal of Forestry 105(6): 307-313.
[44] Syrbe, R. U., Walz, U. (2012): Spatial indicators for the assessment of ecosystem services: providing, benefiting and connecting areas and landscape metrics. – Ecological Indicators 21(3): 80-88.

http://www.aloki.hu ● ISSN 1589 1623 (Print) ● ISSN 1785 0037 (Online)
DOI: http://dx.doi.org/10.15666/aeer/1802_36933711

[45] Tinker, D. B., Resor, C. A. C., Beauvais, G. P., Kipfmueller, K. F., Fernandes, C. I., Baker, W. L. (1998): Watershed analysis of forest fragmentation by clearcuts and roads in a Wyoming forest. – Landscape Ecology 13(3): 149-165.
[46] Trakhtenbrot, A., Ran, N., Perry, G., Richardson, D. M. (2005): The importance of Long-Distance dispersal in biodiversity conservation. – Diversity & Distributions 11(2): 173-181.
[47] Turner, M. G., Gardner, R. H., O'Neill, R. V. (2003): Landscape ecology in theory and practice. – Geography 83(5): 479-494.
[48] Uuemaa, E., Antrop, M., Roosaare, J., Marja, R., Mander, Ü. (2009): Landscape metrics and indices: an overview of their use in landscape research. – Living Reviews in Landscape Research 3(1): 1-28.
[49] Wang, J., Cui, B. S., Liu, S. L., Dong, S. K., Wei, G. L., Liu, J. (2007): Effects of road networks on ecosystem service value in the Longitudinal Range-Gorge Region. – Chinese Science Bulletin 52(2 Suppl.): 180-191.
[50] Wimberly, M. C., Ohmann, J. L. (2004): A multi-scale assessment of human and environmental constraints on forest land cover change on the Oregon (USA) coast range. – Landscape Ecology 19(6): 631-646.
[51] Xie, X., Wang, Q., Dai, L., Su, D., Wang, X., Qi, G., Ye, Y. (2011): Application of china's national forest continuous inventory database. – Environmental Management 48(6): 1095-1106.
[52] Zhang, X. H., Huang, Q. L., Zhang, C. (2010): Analysis of forest landscape dynamics based on Forest Landscape Restoration: a case study of Yong'an city, Fujian province, China. – European Journal of Forest Research 129(5): 975-980.
[53] Zhu, M., Jiangang, X. U., Jiang, N., Jianlong, L. I., Fan, Y. (2006): Impacts of road corridors on urban landscape pattern: a gradient analysis with changing grain size in Shanghai, China. – Landscape Ecology 21(5): 723-734.

APPENDIX

Table A1. *Landscape transfer matrix between 2007 and 2015*

2007	2015									
	Landscape	**FI**	**PI**	**RT**	**SW**	**HW**	**EU**	**BA**	**ET**	**OL**	**% (2007)**
FI	WL	93.1	0.1	0.1	0.0	0.3	0.0	0.7	0.0	5.8	34.1
	NREZ	93.3	0.1	0.1	0.0	0.2	0.0	0.6	0.0	5.7	33.6
	REZ	92.1	0.0	0.0	0.0	0.4	0.0	1.3	0.0	6.2	39.2
	MONREZ	92.0	0.0	0.0	0.0	0.4	0.0	1.4	0.0	6.2	39.9
	MULREZ	93.8	0.0	0.0	0.0	0.0	0.0	0.1	0.0	6.2	26.1
PI	WL	4.9	92.6	0.0	0.0	0.5	0.0	0.4	0.0	1.6	13.1
	NREZ	5.3	92.4	0.0	0.0	0.6	0.0	0.4	0.0	1.3	12.9
	REZ	1.5	94.3	0.0	0.0	0.0	0.0	0.0	0.0	4.2	15.1
	MONREZ	1.6	94.0	0.0	0.0	0.0	0.0	0.0	0.0	4.4	14.9
	MULREZ	0.0	99.0	0.0	0.0	0.0	0.0	0.0	0.0	1.0	18.0
RT	WL	6.3	0.0	91.4	0.0	0.0	0.0	0.0	0.0	2.2	0.1
	NREZ	3.9	0.0	90.4	0.0	0.0	0.0	0.0	0.0	5.7	0.1
	REZ	7.9	0.0	92.1	0.0	0.0	0.0	0.0	0.0	0.0	0.9
	MONREZ	6.8	0.0	93.2	0.0	0.0	0.0	0.0	0.0	0.0	0.9
	MULREZ	100.0	0.0	0.0	0.0	0.0	0.0	0.0	0.0	0.0	0.2

http://www.aloki.hu ● ISSN 1589 1623 (Print) ● ISSN 1785 0037 (Online)
DOI: http://dx.doi.org/10.15666/aeer/1802_36933711

ST	WL	0.7	1.9	0.5	92.2	1.6	2.2	0.2	0.0	0.7	0.7
	NREZ	0.8	1.8	0.0	93.1	0.9	2.6	0.3	0.0	0.5	0.6
	REZ	0.1	2.2	3.2	86.9	6.3	0.0	0.0	0.0	1.4	1.0
	MONREZ	0.1	2.3	3.4	86.1	6.6	0.0	0.0	0.0	1.5	1.0
	MULREZ	0.0	0.0	0.0	100.0	0.0	0.0	0.0	0.0	0.0	1.2
HW	WL	0.8	0.3	0.0	0.0	98.6	0.0	0.1	0.0	0.2	13.8
	NREZ	0.8	0.3	0.0	0.0	98.6	0.0	0.0	0.0	0.2	14.3
	REZ	1.0	0.0	0.0	0.0	98.0	0.0	0.2	0.2	0.6	9.4
	MONREZ	1.1	0.0	0.0	0.0	97.9	0.0	0.2	0.2	0.7	9.2
	MULREZ	0.1	0.0	0.0	0.0	99.9	0.0	0.0	0.0	0.0	13.0
EU	WL	0.0	0.0	0.0	0.0	0.0	82.7	0.0	0.0	17.3	0.1
	NREZ	0.0	0.0	0.0	0.0	0.0	81.0	0.0	0.0	19.0	0.1
	REZ	0.0	0.0	0.0	0.0	0.0	100.0	0.0	0.0	0.0	0.1
	MONREZ	0.0	0.0	0.0	0.0	0.0	100.0	0.0	0.0	0.0	0.1
	MULREZ	0.0	0.0	0.0	0.0	0.0	0.0	0.0	0.0	0.0	0.0
BA	WL	0.3	0.0	0.0	0.0	0.1	0.0	99.0	0.1	0.5	31.7
	NREZ	0.3	0.1	0.0	0.0	0.1	0.0	99.0	0.0	0.5	32.8
	REZ	0.8	0.0	0.0	0.0	0.0	0.0	98.6	0.5	0.1	21.5
	MONREZ	0.8	0.0	0.0	0.0	0.0	0.0	98.5	0.5	0.1	21.3
	MULREZ	0.4	0.0	0.0	0.0	0.0	0.0	99.6	0.0	0.0	24.9
ET	WL	0.5	0.0	0.0	0.0	0.0	0.6	0.2	95.0	3.7	5.6
	NREZ	0.6	0.0	0.0	0.0	0.1	0.6	0.2	95.3	3.3	5.1
	REZ	0.0	0.0	0.0	0.0	0.0	0.8	0.2	93.6	5.3	10.1
	MONREZ	0.0	0.0	0.0	0.0	0.0	0.8	0.2	93.3	5.6	10.0
	MULREZ	0.0	0.0	0.0	0.0	0.0	0.4	0.0	98.9	0.8	11.6
OL	WL	1.8	0.0	0.0	0.0	0.1	0.0	0.0	0.0	98.1	0.8
	NREZ	0.0	0.0	0.0	0.0	0.0	0.0	0.0	0.0	100.0	0.6
	REZ	5.4	0.0	0.0	0.0	0.2	0.0	0.0	0.0	94.5	2.8
	MONREZ	5.9	0.0	0.0	0.0	0.2	0.0	0.0	0.0	93.9	2.6
	MULREZ	0.0	0.0	0.0	0.0	0.0	0.0	0.0	0.0	100.0	5.0
% (2015)	WL	32.7	12.2	0.1	0.6	13.8	0.1	31.7	5.4	3.4	100.0
	NREZ	32.2	12.0	0.1	0.6	14.2	0.1	32.7	4.9	3.1	100.0
	REZ	36.8	14.2	0.8	0.9	9.4	0.2	21.7	9.6	6.3	100.0
	MONREZ	37.5	14.1	0.9	0.9	9.3	0.2	21.6	9.4	6.2	100.0
	MULREZ	24.8	17.8	0.0	1.2	13.0	0.0	24.8	11.5	6.9	100.0

Fir (FI), Pine (PI), Rare tree (RT), Softwood (SW), Hardwood (HW), Eucalyptus (EU), Bamboo (BA), Economic tree (ET) and other land cover (OL)

http://www.aloki.hu ● ISSN 1589 1623 (Print) ● ISSN 1785 0037 (Online)
DOI: http://dx.doi.org/10.15666/aeer/1802_36933711

THE POSSIBILITY OF USING SCOTS PINE (*PINUS SYLVESTRIS* L.) NEEDLES AS BIOMONITOR IN THE DETERMINATION OF HEAVY METAL ACCUMULATION

ALAQOURI, H. A. A.[1] – OZER GENC, C.[1] – ARICAK, B.[1] – KUZMINA, N.[2] – MENSHIKOV, S.[2] – CETIN, M.[3*]

[1]*Department of Forestry, Faculty of Forestry, Kastamonu University, Kastamonu, Turkey*

[2]*Institute of Botanical Garden, Russian Academy of Sciences, Ural Branch, Yekaterinburg, Russia*

[3]*Department of Landscape Architecture, Faculty of Engineering and Architecture, Kastamonu University, Kastamonu, Turkey*

**Corresponding author*
e-mail: mcetin@kastamonu.edu.tr; phone: +90-366-280-2920; fax: +90-366-280-2900

(Received 11th Jan 2020; accepted 26th Mar 2020)

Abstract. Heavy metals can remain in nature for a long time without deterioration and their concentration in the environment is constantly increasing. In addition, some may have toxic or carcinogenic effects even at low concentrations, while some others which act as micronutrients can have toxic effects for humans at high concentrations. Therefore, determining heavy metal concentrations is of great importance towards identifying risk zones and risk levels. The main sources of heavy metals are industrial plants where heavy metal ores are processed. In this study, the Combine Magnesite operating in Russia which entails -"processing and mining of magnesite ore"- was examined for Mg, Al, Fe, Mn and Ca concentrations by analysing the samples taken from the 1- and 2-year-old needles of scots pines grown at 1, 3, 10 and 25 km distances. As a result of the study, it was determined that the concentrations of heavy metals subject to the study vary depending on the distance, especially the Mg concentration which exhibited a significant decrease the farther the trees were. We determined that the concentrations recorded in the 2-year-old needles at almost all points were higher than the 1-year-old needles, and could even exceed this difference several times.
Keywords: *pollution, Satkinsky Combine Magnesite, forest, Mg, Al, Fe*

Introduction

With the rapid increase in the world population, industrial activities have witnessed an identical rise, and the air pollution which increased in parallel with these activities has reached dangerous levels (Cetin and Sevik, 2016a, b; Cetin et al., 2017,2020; Turkyilmaz et al., 2020; Bozdogan Sert et al., 2019; Ozel et al., 2019; Kaya et al., 2019; Cetin, 2019; Zeren Cetin and Sevik, 2020). So much so that today air pollution has become a global problem that causes millions of deaths annually (Cetin, 2016a, b, c, 2017, 2019; Bozdogan Sert et al., 2019; Cetin et al., 2018a,b, 2019a, b; 2020).

Industrial activities are the biggest culprit for air pollution (Shahid et al., 2017). Although mineral resources are extremely important for socio-economic development, mineral extraction and its use in different industrial processes play a leading role in increasing environmental pollution, and air pollution in particular (Li et al., 2014; Goix et al., 2015; Niazi and Burton, 2016).

The change in heavy metal pollution can be determined by direct and indirect methods. The direct approach is expensive, and the direct impact of atmosphere

http://www.aloki.hu ● ISSN 1589 1623 (Print) ● ISSN 1785 0037 (Online)
DOI: http://dx.doi.org/10.15666/aeer/1802_37133727

pollution on the ecosystem cannot be determined, and data about the measurement period cannot be examined (Yucedag et al., 2019a, b, c; Cesur, 2019; Gemici et al., 2019). These methods often require expensive measuring instruments and carry a higher risk of contamination than biomonitors. The use of biomonitors in the determination of air pollution is an inexpensive and easy method and provides more reliable data on the periodic changes of heavy metal concentrations (Aricak et al., 2019a, b). Plants that grow in areas with heavy pollution show heavy metals concentrations in the body, branches and hands, and show the increase in heavy metal concentrations in the air over time (Turkyilmaz et al., 2019; Bozdogan Sert et al., 2019). Therefore, instead of the direct detection of heavy metal pollution, biomonitors are frequently used (Sevik et al., 2019a; Cetin et al., 2018a, 2019 a, b, 2020; Turkyilmaz et al., 2019; Bozdogan Sert et al., 2019; Cetin, 2019; Ozel et al., 2019).

In this study, we aimed to determine the change of pollution level depending on distance and pointer age by using 1 and 2 wet hands of scotch pines grown in different distances around a process and mining of Magnesite ore operating in Russia.

Materials and methods

In the conditions of modern cities, aerotechnogenic pollution is a permanent environmental factor that has a negative impact on the environment and human health. One of the objects of large foci of destruction of forest vegetation is located in the Southern Urals in the Chelyabinsk region city Satka the Combine Magnesite in Russia, (the GPS coordinates of 55°6'10.663" N and 58°58'27.53" E) (*Fig. 1a, b*). Experimental sites (ES) were planting trees created in rows in 1980-1983. Employees of the Botanical Garden in order to study the suitability of soils for reforestation in various zones of magnesite pollution. ES are located at different distances from the Combine.

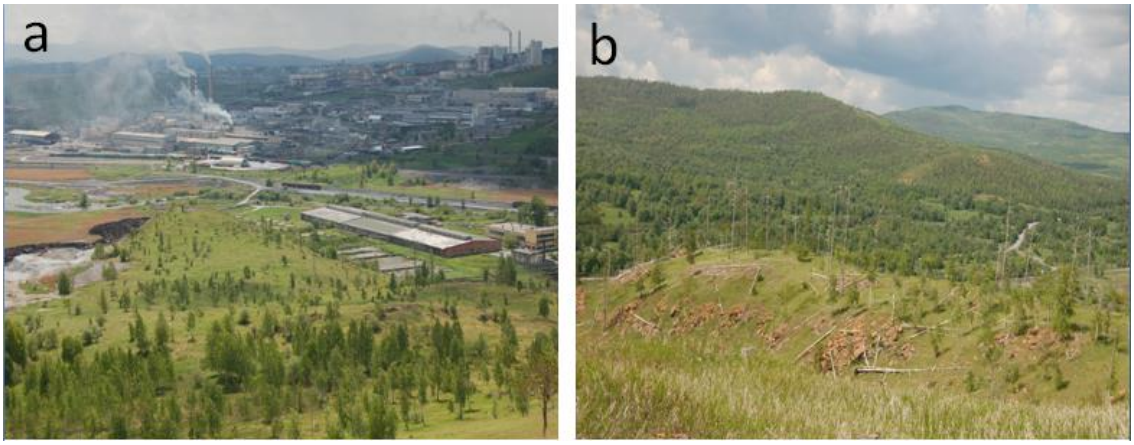

Figure 1. *Satkinsky Combine Magnesite (a) and the surrounding forests (b)*

In the pollution gradient to the northeast, in the direction of the prevailing winds from the emission source, the following areas are located: ES-2 at 1 km from the plant in the zone of strong influence, ES-5 at 3 km - zone of average influence and ES-4 at 10 km - zone of weak influence at the Combine Magnesite. Near the village of Sibirka settlement area (conditional control) - 25 km south of the Combine in background

http://www.aloki.hu ● ISSN 1589 1623 (Print) ● ISSN 1785 0037 (Online)
DOI: http://dx.doi.org/10.15666/aeer/1802_37133727

conditions is located Control. During planting of *Pinus sylvéstris* L., peat was deposited at ES-2 and ES-5 at a layer of 2 cm. Peat was not added to the site at ES-4. The type of forest in all ES is the Scots pine (*Fig. 2*).

The raw material for the production of sintered Pericles powders is raw magnesite. High-carbonate feedstock is burned in such a way that raw magnesite of Satkinsky groups of deposits (fractions 0–40 mm) is loaded into a rotary kiln. After burning natural magnesite, a large amount of caustic dust is formed which undergoes repeated burning. When burning dust, a large amount of flue gases, carbon monoxide, alkali, fluorine and sulfuric anhydride, nitrogen oxides are released into the atmosphere. Near the Combine Magnesit and within a radius of 1.5–2 km, the forest completely died (*Fig. 1b*). The maximum volumes of magnesite dust into the atmosphere in 1963 reached 182.5–328.5 thousand tons per day. In 1978, new electrostatic precipitators were installed at the plant, and dust emissions dropped to 70–90 tons per day.

Figure 2. *Location of experimental sites depending on the Combine Magnezit*

Samples were taken from the ends of the longest lateral branches of the trees at the designated points on the source of pollution by cutting branches with a needle. Under the conditions of the region, the pine needles can remain on the tree for two years and with the help of the formed nodes. The cut branches were then cut according to their age, and the shoots formed in the last year were classified as 1 year, shoots formed in the previous year were classified as 2 years, and labelled by packaging. This classification process in trees such as pine, spruce and fir has also been used in different studies (Turkyilmaz et al., 2018c; Cobanoglu, 2019; Kececi, 2019). The needle samples used in the study were collected at the end of the 2018 vegetation season and the study was carried out in 5 replications.

http://www.aloki.hu ● ISSN 1589 1623 (Print) ● ISSN 1785 0037 (Online)
DOI: http://dx.doi.org/10.15666/aeer/1802_37133727

Heavy metal analyses

The samples, which were classified and labeled in the laboratory, were stored and air dried for 15 days. The air-dried samples were then dried in a drying oven at 45 °C for a week. Experiments were started for heavy metal analysis in dried samples on the same day. Plant samples were pulverized and were weighed as 0.5 g and put into tubes designed for microwave. 10 mL of 65% HNO_3 were added to the samples. During this process, the fume cupboard was used. The prepared specimens were then burnt at 280 PSI pressure in a microwave and at 180 °C for 20 min. The tubes were removed from the microwave after being processed and left to cool. Deionized water was added to the cooled samples and tubes were filled until 50 ml was completed. The filtered solutions were analyzed for heavy metal concentrations of Mg, Al, Fe, Mn and Ca using GBC Integra XL–SDS-270 ICP-OES.

Statistical analyses

The obtained data were evaluated with the help of SPSS package program, variance analysis was applied to the data and homogeneous groups were obtained by applying the Duncan test to the values having at least 95% confidence level differences statistically. The obtained data is simplified and tabulated and interpreted.

Results

The change in Mg levels according to distance and pointer age was determined and mean values and P value obtained by analysis of variance, error rate and groupings formed as a result of the Duncan test are given in *Table 1*.

Table 1. *The element of Mg (ppm) of the change depending on distance and needle age variance*

Distance	1 Age needle	2 Age needle	P value	Error
1 km	3659.24 Ad	4566.64 Bd	42.598	0.000
3 km	2907.08 Ac	4179.28 Bc	50.364	0.000
10 km	2687.33 Ab	2902.48 Bb	9.415	0.007
25 km	2282.17 Aa	2597.37 Ba	12.012	0.003
P Value	65.505	83.040		
Error	0.000	0.000		

It is statistically different from the values contained in different groups, starting with the letter A-a, the numerical value grows

When the results of the table are examined, it is observed that the concentration changes of Mg element are statistically significant ($p < 0.001$). When the average values and Duncan test results are examined, it is seen that Mg concentration decreases significantly in both 1-year-old and 2-year-old needles depending on the distance, Mg concentration values determined at 25 km distance are more than 1.6 times of Mg concentration values determined at 1 km. It is seen that the changes in all distances in terms of pointer age are statistically significant ($p < 0.01$ in 1 and 3 km at other distances $p < 0.001$), and the values determined in 2-year-old needles at all distances are higher than those determined in 1-year-old needles.

http://www.aloki.hu ● ISSN 1589 1623 (Print) ● ISSN 1785 0037 (Online)
DOI: http://dx.doi.org/10.15666/aeer/1802_37133727

The change of Al element according to distance and pointer age was determined and the mean values and P value obtained by the analysis of variance, error rate and the groupings formed as a result of Duncan test are given in *Table 2*.

Table 2. *The element of Al (ppm) of the changing depending on distance and needle age*

Distance	1 Age needle	2 Age needle	P value	Error
1 km	23.64 Aa	62.57 Bb	116.168	0.000
3 km	20.97 Aa	65.52 Bb	197.77	0.000
10 km	16.42 Aa	39.28 Ba	262.687	0.000
25 km	71.48 Ab	125.29 Bc	22.618	0.000
P Value	65.32	47.825		
Error	0.000	0.000		

The letters A, B, a, b, c, etc. means according to Duncan's test results; show that the group is located. It is statistically different from the values contained in different groups, starting with the letter a, the numerical value grows

Al-element concentration in both 1- and 2-year-old needles is statistically significant ($p < 0.001$), but it is difficult to say that there is a linear relationship between distance and Al concentration when the mean values and groupings formed by Duncan test are examined, because, the lowest value is determined at 10 km and the highest value is 25 km at both 1-year and 2-year-old needles. As a result of the variance analysis, it was observed that the changes in all distances were statistically significant ($p < 0.001$) in terms of pointer age, and the values determined in the 2-year-old needles were higher than those determined in the 1-year-old needles. In fact, it was calculated that this difference was quite high and the difference, which was 1.75 times at a distance of 25 km, could reach up to 3.12 times.

The change of Fe element according to distance and pointer age was determined and P values, error rate and groupings resulting from Duncan test obtained from mean values and variance analysis are given in *Table 3*.

Table 3. *The element of Fe (ppm) of the changing depending on distance and needle age*

Distance	1 Age needle	2 Age needle	P value	Error
1 km	66.56 Ac	110.41 Ba	21.641	0.000
3 km	55.20 Ab	156.48 Bb	224.086	0.000
10 km	31.15 Aa	91.34 Ba	901.938	0.000
25 km	38.69 Aa	108.86 Ba	29.160	0.000
P Value	28.092	4.367		
Error	0.000	0.011		

The letters A, B, a, b, c, etc. means according to Duncan's test results; show that the group is located. It is statistically different from the values contained in different groups, starting with the letter a numerical value grows

According to the analysis of variance, the change of Fe element concentration depending on distance was statistically significant ($p < 0.001$ in 1-year-old needles and $p < 0.01$ in 2-year-old needles). According to the average values and Duncan test

http://www.aloki.hu ● ISSN 1589 1623 (Print) ● ISSN 1785 0037 (Online)
DOI: http://dx.doi.org/10.15666/aeer/1802_37133727

results, it can be said that Fe concentration decreases in 1-year-old needles while it is difficult to say that there is a significant change in 2-year-old needles. As a result of variance analysis, it was seen that the changes in all distances were statistically significant ($p < 0.001$) in terms of pointer age, and the values determined in 2-year-old needles were higher than those determined in 1-year-old needles. In fact, this difference is quite high, ranging from 1.6 times to 2.9 times.

The variation of Mn element according to distance and pointer age was determined and the mean values and P value obtained by analysis of variance, error rate and the groupings formed as a result of Duncan test are given in *Table 4*.

Table 4. *The element of Mn (ppm) of the changing depending on distance and needle age*

Distance	1 Age needle	2 Age needle	P value	Error
1 km	40.95 Ab	77.78 Bb	28.326	0.000
3 km	65.52 Ac	100.52 Bc	62.199	0.000
10 km	28.18 Aa	48.10 Ba	13.131	0.002
25 km	95.42 Ad	169.47 Bd	81.932	0.000
P Value	172.674	72.060		
Error	0.000	0.000		

The letters A, B, a, b, c, etc. means according to Duncan's test results; show that the group is located. It is statistically different from the values contained in different groups, starting with the letter a numerical value grows

It was determined that the concentration of Mn element was statistically significant ($p < 0.001$). However, it is difficult to say that there is a linear relationship between distance and Mn concentration when the mean values and the groupings formed by Duncan test are examined because the lowest value is determined at 10 km and the highest value is 25 km at both 1 year and 2-year-old needles. As a result of the analysis of variance, it was found that the changes in all distances were statistically significant ($p < 0.01$ at 10 km distance, $p < 0.001$ at other distances) in terms of pointer age, between 5 and 1.9 times.

It was determined that the concentration of Mn element was statistically significant ($p < 0.001$). However, it is difficult to say that there is a linear relationship between the distance and the Mn concentration because the lowest value is determined at 10 km and the highest value is 25 km at both 1 year and 2-year-old needles. ($P < 0.01$ at 10 km distance, $p < 0.001$ at other distances) in terms of pointer age. Between 5 and 1.9 times.

According to the variance analysis results, are given in *Table 5,* it was found that the change of Ca element depending on distance was statistically significant ($p < 0.01$) in both 1 and 2 year old needles, and when the mean values and Duncan test results were examined, it was found that there was an inverse relationship between Ca concentration and distance. As a result of the analysis of variance, it was found that the changes in all distances were statistically significant ($p < 0.001$) in terms of pointer age, and the values determined in 2-year-old needles were 1.9 times to 2.3 times higher than those in 1-year-old needles.

http://www.aloki.hu ● ISSN 1589 1623 (Print) ● ISSN 1785 0037 (Online)
DOI: http://dx.doi.org/10.15666/aeer/1802_37133727

Table 5. *The element of Ca (ppm) of the changing depending on distance and needle age*

Distance	1 Age needle	2 Age needle	P value	Error
1 km	1298.71 Aa	2985.44 Ba	28.489	0.000
3 km	2002.73 Ab	4312.44 Bb	26.576	0.000
10 km	1992.97 Ab	4538.26 Bb	51.147	0.000
25 km	2451.64 Ab	4750.71 Bb	44.374	0.000
P Value	7.126	6.025		
Error	0.001	0.002		

The letters A, B, a, b, c, etc. means according to Duncan's test results; show that the group is located. It is statistically different from the values contained in different groups, starting with the letter a numerical value grows

Discussion

The concentrations of Mg, Al, Fe, Mn and Ca elements in the 1 and 2-year-old needles of the scots pine grown around 1, 3, 10 and 25 km distances around the "process and mining of magnesite ore" were determined. Although many studies on heavy metals have studied some of these elements, it is noticeable that in general, studies focus on elements such as Pb, Ni, Cd, Cr, Zn, Co (Turkyilmaz et al., 2019, 2018a, b, c, d; Sevik et al., 2019b). The reasons that these elements may cause toxic effects and are carcinogens even at low concentrations can be shown as the main factors in the prominence of these elements (Turkyilmaz et al., 2019, 2018a, b, c, d; Saleh, 2018). Some recent studies are shown that conform the temporal changes in magnesite pollution released by the factory to the air (Blanár et al., 2019; Pišút and Pišút, 2006).

However, the studies show that although micronutrients such as Mn and Fe, which are considered in this study, are necessary, they can create harmful effects at high levels (Shahid et al., 2017). Fe and Al are defined as carcinogenic to humans (Goney, 2018). In addition, it is stated that the elements that are required as a nutrient can cause serious health hazards if taken by mouth or respiration (Batır, 2019). For example, Mn, which reaches people through the food chain, causes hallucinations, fatigue, insomnia, weakness, forgetfulness and nerve damage by causing damage to the respiratory system and brain, and may cause Parkinson's, lung embolism and bronchitis, and impotence in men (Pak, 2011; Mossi, 2018). It is therefore very important to monitor the concentrations of these elements in the air.

The results of the study show that Mg concentration decreases significantly depending on the distance. In studies conducted to date, it has been shown that the concentration of heavy metals in plants decreases as they move away from the source (Turkyilmaz et al., 2018c; Aricak et al., 2019a, b). However, as a result of the study, no linear relationship was found between distance and concentration decrease in other elements. This has been demonstrated in other similar studies and it has been stated in many studies that there is no significant difference between the distance to the source of pollution and the concentration of heavy metals (Mossi, 2018; Saleh, 2018; Sevik et al., 2019a).

There are two possible explanations for this situation. The first is that the source of pollution is not a source of pollution in terms of these elements. The second explanation is that the change in heavy metal concentration in plants is a complex mechanism that has not been fully solved under the influence of many factors (Sevik et al., 2019b; Turkyilmaz et al., 2019). Indeed, studies show that heavy metals can be transported

http://www.aloki.hu ● ISSN 1589 1623 (Print) ● ISSN 1785 0037 (Online)
DOI: http://dx.doi.org/10.15666/aeer/1802_37133727

hundreds of kilometers away from their original source (Shahid et al., 2017). However, the accumulation of heavy metal concentrations in plants is shaped by the interaction of many factors and their sub-factors (Mossi, 2018; Turkyilmaz et al., 2018b, c).

Studies carried out to this day have shown that the diffusion of heavy metals in the atmosphere and entry into the plant is a very complex process. The heavy metal accumulation potential of the plants grown in the same environment as well as plant species and plant organ, organelle structure, physico-chemical properties of metals, organelle morphology and surface area, organelle surface texture and size, plant habitus, duration of exposure to heavy metal and amount of particulate matter (Pearce et al., 2006; Xu and Zhou, 2008; Schreck et al., 2012).

The accumulation of heavy metals in the plant is closely related to environmental conditions. It is stated that there is a significant relationship between the entry of heavy metals into the plant and especially air humidity and precipitation (Shahid et al., 2017; Ozel, 2019). In addition, environmental factors directly affect plant growth and there is a significant relationship between plant growth and heavy metal uptake. Therefore, the introduction of heavy metals into the plant and its accumulation in organs are shaped under the interaction of many factors and their sub factors (Shahid et al., 2017; Aricak et al., 2019a).

The study shows that the concentration of all elements subject to the study at 2-years-old needles is higher than their concentration at 1-years-old needles at all distances. This can be explained by the longer exposure of the 2-year-old needles to the same environmental conditions and therefore to heavy metals. Similarly, similar results were obtained from studies on different aged needles on the same plant (Turkyilmaz et al., 2018c; Cobanoglu, 2019; Kececi, 2019).

Although a number of studies have been conducted on the use of plants as biomonitor for monitoring heavy metal pollution in the air, it is not yet possible to determine which plants are most suitable for monitoring heavy metal concentrations. There are many reasons for this, but the most obvious is the limited number of plants, since it is very difficult and costly to work with many plants at the same time. The studies can be done by comparing 8-10 plants at most and in this case only the plants subject to the study can be compared with each other. However, studies show that there is a very high-level difference between the species growing in the same environment (Mossi, 2018; Sevik et al., 2019a, b; Saleh, 2018).

The first question to be answered is which kind of heavy metal pollution should be used. Lichen and algae are the most important plant groups in biomarkers for heavy metal pollution.

Bryophytes covering these plants, especially algae, have been used as biomonitor since the 1970s (Ayres et al., 2006; Harmens et al., 2010). However, one of the biggest problems in using lichen and algae as biomonitors is that it is not easy to determine how long these plants have been exposed to pollution. Therefore, it is not known clearly how long any concentration of metal accumulates, and this results in questioning the reliability of the data obtained (Cobanoglu, 2019).

In deciduous high-structured plants the problem of time is relatively eliminated. Because the foliage in these plants occurs at the beginning of the vegetation season, which is in the spring and is exposed to air pollution, i.e. heavy metals, until the leaves are shed. Therefore, the amount heavy metals accumulation in the leaves can be known. Therefore, deciduous plants are often used to monitor heavy metal pollution (Anicic et al., 2011; Petrova et al., 2014; Mossi, 2018).

http://www.aloki.hu ● ISSN 1589 1623 (Print) ● ISSN 1785 0037 (Online)
DOI: http://dx.doi.org/10.15666/aeer/1802_37133727

By using deciduous plants as biomonitors, the amount of heavy metals deposited on the leaves during the vegetation period of the year in which the samples collected can be determined. However, as much as the determination of the concentration of heavy metal is possible, it is extremely important to determine the change of this concentration depending on the year. Few studies have been conducted to determine the amount of heavy metal accumulation in plants in the past years. Rather, the studies are done on the trunks of trees by taking samples from annual rings. This type of sampling usually involves the analysis of heavy metals deposited on annual rings in the trunks of trees (Panyushkina et al., 2016; Xu et al., 2017; Turkyilmaz et al., 2018b, c). This method is not suitable for sustainable monitoring because trees need to be cut down.

In some variegated species, the leaves can remain on the plant for many years. However, there is a problem in interpreting what heavy metal concentration means because the leaf age is not known in these studies. However, in many types of hands, the hands remain on the tree for a few years, and it is possible to know the age of hands by the means of the nodes formed. In addition, since the hands of these plants are exposed to the same environmental conditions outside the vegetation season, the accumulation in the old hands can be much higher (Cobanoglu, 2019; Kececi, 2019). As a matter of fact, in this study, it was found that the concentrations obtained in the 2-year-old hands were much higher than the 1-year-old hands.

Heavy metals can enter the plant through root or leaf uptake, but it is very difficult to distinguish whether heavy metals in the plant's internal tissues are taken from the soil or atmosphere, because both intake pathways can work simultaneously (Pourrut et al., 2013; Shadid et al., 2017). Therefore, it is thought that leaves are the most suitable organs especially for monitoring heavy metal pollution in the air. Because the leaves are the most exposed to heavy metal pollution in the air and are affected most by them due to the entry of air through their stomata during photosynthesis (Cetin et al., 2019a,b, 2020; Turkyilmaz et al., 2018c; Shahid et al., 2017; Saleh, 2018).

There is also a significant relationship between heavy metal accumulation in the plant and particulate matter in the air. Studies show that the interaction of fine particles with plant leaves is especially important in contamination with heavy metals (Temmerman et al., 2012; Schreck et al., 2012). Particulate matter acts as a pharynx for heavy metals in the air, and the concentration of heavy metals in these organs can vary significantly with the adherence of particulate matter contaminated with these heavy metals to plant surfaces and especially leaves (Mossi, 2018; Turkyilmaz et al., 2018d). Heavy metals in the air may accumulate in plant leaves by leaf transfer following precipitation of atmospheric particles on leaf surfaces. The potential for absorbing nutrients, water and metals from leaf parts of plants has long been recognized. However, information about the uptake of metal by plant leaves from the atmosphere is very limited (Shahid et al., 2017). To date, there have been few studies on leaf or pointer ages in determining the concentration of heavy metals in the past (Turkyilmaz et al., 2018c; Cobanoglu et al., 2019; Kececi, 2019).

Heavy metal accumulation in plants varies significantly on organ basis. However, there are many factors that affect this accumulation. Particularly with the adhesion of particulate materials contaminated with heavy metals to plant organs, heavy metal concentrations in these organs increase significantly. Adhesion of particulate materials contaminated with heavy metals causes heavy metal concentrations to be quite high, especially in the bark of trees with cracks. However, heavy metal concentrations in branches, leaves and fruits other than this vary significantly by species. In the wood,

http://www.aloki.hu ● ISSN 1589 1623 (Print) ● ISSN 1785 0037 (Online)
DOI: http://dx.doi.org/10.15666/aeer/1802_37133727

which is located in the interior of the tree and does not have a direct connection with the external environment, many heavy metal concentrations remain at lower levels (Sevik et al., 2020a, b, c).

As a result, there are many factors that affect the penetration and accumulation of heavy metals in the air. These factors include plant species, rainfall and moisture content, plant habitus, organelle structure, type of heavy metal and interaction with the plant (Sevik et al., 2019a; Aricak et al., 2019a) There are also many factors that may directly or indirectly affect the concentration of heavy metals. For example, the change in heavy metal concentration depending on plant species has been demonstrated in many studies (Sevik et al., 2019a, b, c, 202a, b, c; Saleh, 2018; Erdem, 2018; Bozdogan Sert et al., 2019; Cetin et al., 2019a). However, it can be expected that the heavy metal concentrations in the subspecies, forms, varieties and origins of the plant will be at different levels. Because, studies show that many phenological, morphological and anatomical structures change depending on these characteristics (Yucedag et al., 2019a; Cetin et al., 2018a; Sevik et al., 2019c). In this case, it is inevitable that plant metabolism changes and this affects heavy metal absorption (Shahid et al., 2017; Sevik et al., 2019a, b).

Heavy metal absorption in plants is also closely related to plant metabolism (Shahid et al., 2017; Sevik et al., 2019a, b). Therefore, the stress level of the plant significantly affects plant metabolism (Sevik and Cetin, 2015; Yigit et al., 2016), plant origin (Sevik and Topacoglu, 2015), and the genetic structure of the plant (Hrivnak et al., 2017), and many other factors such as heavy metal absorption and thus heavy metal concentration. However, the factors affecting the accumulation of heavy metal concentrations in plants and their effect levels have not been clearly determined yet. Therefore, studies on this subject should be continued, diversified and increased.

Conclusions

We have attempted to determine the change of some heavy metal concentrations depending on the distance to the point which is thought to be the source of pollution and the age of the pointer in *Pinus sylvestris* L. whose needles can remain on the tree for a few years. The results of the study showed that Mg concentration decreased significantly in relation the distance. Considering that the source of pollution is "processing and mining of magnesite ore", this result is very logical and also shows that *Pinus sylvestris* L. needles are very suitable for monitoring the change of Mg concentration in the air.

One of the most important results of the study is that the concentrations obtained in the 2-year-old needles in all elements are significantly higher than in the 1-year-old needles. This can be explained by the fact that older needles are exposed to heavy metals in the air longer than younger needles. According to this result, the needles of trees such as *Abies* and *Picea,* whose needles can remain on the trees for up to 8-10 years and the age of the pointer can be calculated clearly, can be good biomonitor in monitoring the recent heavy metal pollution.

No connection between the distance and the Al, Fe, Mn and Ca could be observed, but sometimes those concentrations were lower close to the factory. This shows that there is no direct connection between the source of pollution and the elements, and the source of these elements is probably soil. It is suggested that the source of these elements should be determined clearly by doing soil analysis in further studies.

http://www.aloki.hu ● ISSN 1589 1623 (Print) ● ISSN 1785 0037 (Online)
DOI: http://dx.doi.org/10.15666/aeer/1802_37133727

It has been determined that Mg concentration varies significantly depending on the distance to the source. While the concentration of Mg in 1-year-old hands taken at a distance of 1 km from the source is 3659 ppm, it decreases to 2907 ppm at 3 km distance, 2687 ppm at 10 km distance and 2282 ppm at 25 km distance. In the 2-year-old hands, the concentration of 4566 ppm in 1 km distance to the source decreased to 4179 ppm at 3 km, 2902 ppm at 10 km and 2597 ppm at 25 km. However, in order to determine how much of this decrease originates from air and how much from soil, it is recommended to make measurements in soil samples and evaluate the results comparatively.

Acknowledgements. The work was carried out as part of the state assignment of the Botanical Garden of the Ural Branch of the Russian Academy of Sciences and Kastamonu University, Faculty of Forestry and Faculty of Architecture and Engineering.

REFERENCES

[1] Anicic, M., Spasic, T., Tomasevic, M., Rajsic, S., Tasic, M. (2011): Trace elements accumulation and temporal trends in leaves of urban deciduous trees (Aesculus hippocastanum and Tilia ssp.). – Ecol Indic 11: 824-830. https://www.sciencedirect.com/science/article/abs/pii/S1470160X10001937.

[2] Aricak, B., Cetin, M., Erdem, R., Sevik, H., Cometen, H. (2019a): The change of some heavy metal concentrations in Scotch pine (Pinus sylvestris) depending on traffic density, organelle and washing. – Appl Ecol Env Res 17(3): 6723-6734.

[3] Aricak, B., Cetin, M., Erdem, R., Sevik, H., Cometen, H. (2019b): The usability of Scotch pine (Pinus sylvestris) as a biomonitor for traffic originated heavy metal concentrations in Turkey. – Pol J Environ Stud 29(2): 1051-1057. http://www.pjoes.com/The-Usability-of-Scotch-Pine-Pinus-sylvestris-nas-a-Biomonitor-for-Traffic-Originated,109244,0,2.html.

[4] Ayres, E., Van der Wal, R., Sommerkorn, M., Bardgett, R. D. (2006): Direct uptake of soil nitrogen by mosses. – Biol Lett 2(2): 286-288. https://royalsocietypublishing.org/doi/abs/10.1098/rsbl.2006.0455.

[5] Batır, D. (2019): Heavy metal accumulation in some edible landscape plants breeding in Eskişehir. – MSc Thesis, Kastamonu University Graduate School of Natural and Applied Sciences Department of Landscape Architecture, Kastamonu.

[6] Blanár, D., Guttová, A., Mihál, I., Plášek, V., Hauer, T., Palice, Z., Ujházy, K. (2019): Effect of magnesite dust pollution on biodiversity and species composition of oak-hornbeam woodlands in the Western Carpathians. – Biologia 74(12): 1591-1611. https://link.springer.com/article/10.2478/s11756-019-00344-6.

[7] Bozdogan Sert, E., Turkmen, M., Cetin, M. (2019): Heavy metal accumulation in rosemary leaves and stems exposed to traffic-related pollution near Adana-İskenderun Highway (Hatay, Turkey). – Environ Monit Assess 191(9): 553. https://rd.springer.com/article/10.1007/s10661-019-7714-7.

[8] Cesur, A. (2019): Determination of heavy metal accumulation in air through annual rings: The case of Cupressus arizonica species. – MSc Thesis, Kastamonu University Graduate School of Natural and Applied Sciences Department of Landscape Architecture, Kastamonu.

[9] Cetin, M. (2016a): A change in the amount of CO2 at the center of the examination halls: case study of Turkey. – Studies on Ethno-Medicine 10(2): 146-155. https://www.tandfonline.com/doi/abs/10.1080/09735070.2016.11905483.

http://www.aloki.hu ● ISSN 1589 1623 (Print) ● ISSN 1785 0037 (Online)
DOI: http://dx.doi.org/10.15666/aeer/1802_37133727

[10] Cetin, M. (2016b): Changes in the amount of chlorophyll in some plants of landscape studies. – Kastamonu University Journal of Forestry Faculty 16(1): 239-245. https://www.researchgate.net/publication/319242469_Changes_in_the_Amount_of_Chlo: ophyll_in_Some_Plants_of_Landscape_Studies.
[11] Cetin, M. (2016c): Determination of bioclimatic comfort areas in landscape planning: a case study of Cide Coastline. – Turkish Journal of Agriculture - Food Science and Technology 4(9): 800-804. http://www.agrifoodscience.com/index.php/TURJAF/article/view/872/374.
[12] Cetin, M. (2017): Change in amount of chlorophyll in some interior ornamental plants. – Kastamonu University Journal of Engineering and Sciences 3(1): 11-19. https://dergipark.org.tr/download/issue-file/5600.
[13] Cetin, M. (2019): The effect of urban planning on urban formations determining bioclimatic comfort area's effect using satellitia imagines on air quality: a case study of Bursa city. – Air Qual Atmos Health 12(10):1237-1249. https://rd.springer.com/article/10.1007/s11869-019-00742-4.
[14] Cetin, M., Sevik, H. (2016a): Measuring the impact of selected plants on indoor CO2 concentrations. – Pol J Environ Stud 25(3): 973-979. http://www.pjoes.com/Measuring-the-Impact-of-Selected-Plants-on-Indoor-CO2-Concentrations,61744,0,2.html.
[15] Cetin, M., Sevik, H. (2016b): Change of air quality in Kastamonu city in terms of particulate matter and CO2 amount. – Oxid Commun 39(4-II): 3394-3401.
[16] Cetin, M., Sevik, H., Saat, A. (2017): Indoor air quality: the samples of Safranbolu Bulak Mencilis Cave. – Fresen Environ Bull 26(10): 5965-5970.
[17] Cetin, M., Sevik, H., Yigit, N., Ozel, H. B., Aricak, B., Varol, T. (2018a): The variable of leaf micromorphogical characters on grown in distinct climate conditions in some landscape plants. – Fresen Environ Bull 27(5): 3206-3211.
[18] Cetin, M., Zeren, I., Sevik, H., Cakir, C., Akpinar, H. (2018b): A study on the determination of the natural park's sustainable tourism potential. – Environ Monit Assess 190(3): 167. https://link.springer.com/article/10.1007/s10661-018-6534-5
[19] Cetin, M., Onac, A. K., Sevik, H., Sen, B. (2019a): Temporal and regional change of some air pollution parameters in Bursa. – Air Qual Atmos Health 12(3): 311-316. https://link.springer.com/article/10.1007/s11869-018-00657-6.
[20] Cetin, M., Adiguzel, F., Gungor, S., Kaya, E., Sancar, M. C. (2019b): Evaluation of thermal climatic region areas in terms of building density in urban management and planning for Burdur, Turkey. – Air Qual Atmos Health 12(9): 1103-1112. https://rd.springer.com/article/10.1007/s11869-019-00727-3.
[21] Cetin, M., Sevik, H., Cobanoglu, O. (2020): Ca, Cu, and Li in washed and unwashed specimens of needles, bark, and branches of the blue spruce (Picea pungens) in the city of Ankara. – Environ Sci Pollut Res (2020). DOI: 10.1007/s11356-020-08687-3; https://doi.org/10.1007/s11356-020-08687-3
[22] Cobanoglu, O. (2019): The possibilities of using blue spruce (Picea pungens Engelm) as a bio-monitor by measuring the recent accumulation of heavy metals in its leaves. – Msc. Thesis, Kastamonu University Institute of Science, Kastamonu.
[23] Erdem, T. (2018): Variation of heavy metal concentrations depending on species, organelles and traffic density in some plants. – Msc. Thesis, Kastamonu University Institute of Science, Kastamonu.
[24] Gemici, E., Yücedağ, C., Özel, H. B., İmren, E. (2019): Predicting cone production in clonal seed orchard of Anatolian black pine with artificial neural network. – Appl Ecol Env Res 17(2): 2267-2273.
[25] Goix, S., Mombo, S., Schreck, E., Pierart, A., Lévêque, T., Deola, F., Dumat, C. (2015): Field isotopic study of lead fate and compartmentalization in earthworm-soil-metal particle systems for highly polluted soil near Pb recycling factory. – Chemosphere 138: 10-17. https://www.sciencedirect.com/science/article/pii/S0045653515004671.

http://www.aloki.hu ● ISSN 1589 1623 (Print) ● ISSN 1785 0037 (Online)
DOI: http://dx.doi.org/10.15666/aeer/1802_37133727

[26] Goney, G. (2018): Poisoning due to the use of electronic cigarette (e-cigarette). – Journal of Dependence 19(2): 40-44.
[27] Harmens, H., Norris, D., Steinnes, E., Kubin, E., Piispane, J., Alber, R., Aleksiayenak, Y., Blum, O., Cos, K. M., Dam, M. (2010): Mosses as biomonitors of atmospheric heavy metal deposition: spatial patterns and temporal trends in Europe. – Environ Pollut 158: 3144-3156.
[28] Hrivnák, M., Paule, L., Krajmerová, D., Kulac, S., Sevik, H., Turna, I., Tvauri, I., Gömöry, D. (2017): Genetic variation in Tertiary relics: the case of Eastern-Mediterranean Abies (Pinaceae). – Ecol Evol 7(23): 10018-10030. https://onlinelibrary.wiley.com/doi/full/10.1002/ece3.3519.
[29] Kaya, E., Agca, M., Adiguzel, F., Cetin, M. (2019): Spatial data analysis with R programming for environment. – Human and Ecological Risk Assessment: An International Journal 25(6): 1521-1530. https://www.tandfonline.com/doi/abs/10.1080/10807039.2018.1470896.
[30] Kececi, B. (2019): The using elements of Zn, Ni, Cr, Co, Cd and Pb as biomonitor in the monitoring of heavy metal contamination of Picea pungens in needles, bark and branches. – Msc. Thesis, Kastamonu University Institute of Science, Kastamonu.
[31] Li, Z., Ma, Z., van der Kuijp, T. J., Yuan, Z., Huang, L. (2014): A review of soil heavy metal pollution from mines in China: pollution and health risk assessment. – Sci Total 843-853. https://www.sciencedirect.com/science/article/pii/S0048969713010176.
[32] Mossi, M. M. M. (2018): Determination of heavy metal accumulation in some shrub formed landscape plants. – PhD Thesis, Kastamonu University Institute of Science Department of Forest Engineering, Kastamonu.
[33] Niazi, N. K., Burton, E. D. (2016): Arsenic sorption to nanoparticulate mackinawite (FeS): an examination of phosphate competition. – Environ Pollut 218: 111-117. https://www.sciencedirect.com/science/article/pii/S0269749116307709.
[34] Ozel, H. U., Ozel, H. B., Cetin, M., Sevik, H., Gemici, B. T., Varol, T. (2019): Base alteration of some heavy metal concentrations on local and seasonal in Bartin River. – Environ Monit Assess 191(9): 594. https://rd.springer.com/article/10.1007%2Fs10661-019-7753-0.
[35] Ozel, S. (2019): The variation of heavy metal accumulation in some fruit tree organelles due to traffic density. – MSc Thesis. Kastamonu University Graduate School of Natural and Applied Sciences Department of Sustainable Agriculture and Natural Plant Resources, Kastamonu.
[36] Pak, O. (2011): An investigation of some heavy metal pollution along the TEM motorway soils in Kırklareli. – MSc. Thesis. Namık Kemal University Graduate School of Natural and Applied Sciences Main Science Division of Soil Science and Plant Nutrition, Tekirdağ.
[37] Panyushkina, I. P., Shishov, V. V., Grachev, A. M., Knorre, A. A., Kirdyanov, A. V., Leavitt, S. W., Vaganov, E. A., Chebykin, E. P., Zhuchenko, N. A., Hughes, M. K. (2016): Trends in elemental concentrations of tree rings from the Siberian Arctic. – Tree-Ring Research 72(2): 67-77. https://treeringresearch.org/doi/abs/10.3959/1536-1098-72.02.67.
[38] Pearce, D. W., Millard, S., Bray, D. F., Rood, S. B. (2006): Stomatal characteristics of riparian poplar species in a semi-arid environment. – Tree Physiology 262: 211-218. https://academic.oup.com/treephys/article/26/2/211/1676809.
[39] Petrova, S., Yurukova, L., Velcheva, I. (2014): Possibilities of using deciduous tree species in trace element biomonitoring in an urban area (Plovdiv, Bulgaria). – Atmospheric Pollution Research 5(2): 196-202. https://www.sciencedirect.com/science/article/pii/S1309104215303184.
[40] Pišút, I., Pišút, P. (2006): Changes of epiphytic lichens in the surroundings of magnesite factories near Jelšava (SE Slovakia) in the period 1973-2004. – Ekológia 25(2): 176-187. http://147.213.211.222/sites/default/files/ek206tlac06_pisut.pdf.

http://www.aloki.hu ● ISSN 1589 1623 (Print) ● ISSN 1785 0037 (Online)
DOI: http://dx.doi.org/10.15666/aeer/1802_37133727

[41] Pourrut, B., Shahid, M., Douay, F., Dumat, C., Pinelli, E. (2013): Molecular Mechanisms Involved in Lead Uptake, Toxicity and Detoxification in Higher Plants. – In: Gupta, D. K. et al. (eds.) Heavy Metal Stress in Plants. Springer, Berlin, pp. 121-147.

[42] Saleh, E. A. A. (2018): Determination of heavy metal accumulation in some landscape plants. – PhD. Thesis. Kastamonu University Institute of Science Department of Forest Engineering, Kastamonu.

[43] Schreck, E., Foucault, Y., Sarret, G., Sobanska, S., Cécillon, L., Castrec, R. M., Uzu Dumat, C. (2012): Metal and metalloid foliar uptake by various plant species exposed to atmospheric industrial fallout: mechanisms involved for lead. – Sci Toplam Environ 427-428: 253-262. https://www.sciencedirect.com/science/article/pii/S0048969712004123.

[44] Sevik, H., Cetin, M. (2015): Effects of water stress on seed germination for select landscape plants. – Pol J Environ Stud 24(2): 689-69. http://www.pjoes.com/Effects-of-Water-Stress-on-Seed-Germination-for-Select-Landscape-Plants,50860,0,2.html.

[45] Sevik, H., Topacoglu, O. (2015): Variation and inheritance pattern in cone and seed characteristics of scots pine (Pinus sylvestris L.) for evaluation of genetic diversity. – Journal of Environmental Biology 36(5): 1125-1130.

[46] Sevik, H., Ozel, H. B., Cetin, M., Özel, H. U., Erdem, T. (2019a): Determination of changes in heavy metal accumulation depending on plant species, plant organism, and traffic density in some landscape plants. – Air Qual Atmos Health 12(2): 189-195. https://link.springer.com/article/10.1007/s11869-018-0641-x.

[47] Sevik, H., Cetin, M., Ozel, H. B., Pinar, B. (2019b): Determining toxic metal concentration changes in landscaping plants based on some factors. – Air Qual Atmos Health 8: 983-991. https://rd.springer.com/article/10.1007/s11869-019-00717-5.

[48] Sevik, H., Cetin, M., Ozturk, A., Yigit, N., Karakus, O. (2019c): Changes in micromorphological characters of Platanus orientalis L. leaves in Turkey. – Appl Ecol Env Res 17(3): 5909-5921.

[49] Sevik, H., Cetin, M., Ozel, H. B., Akarsu, H., Zeren Cetin, I. (2020a): Analyzing of usability of tree-rings as biomonitors for monitoring heavy metal accumulation in the atmosphere in urban area: a case study of cedar tree (Cedrus sp.). – Environ Monit Assess 192(1): 23. https://link.springer.com/article/10.1007/s10661-019-8010-2.

[50] Sevik, H., Cetin, M., Ozel, H. B., Ozel, S., Zeren Cetin, I. (2020b): Changes in heavy metal accumulation in some edible landscape plants depending on traffic density. – Environ Monit Assess 192(2): 78. https://link.springer.com/article/10.1007/s10661-019-8041-8.

[51] Sevik, H., Cetin, M., Ucun Ozel, H., Ozel, H. B., Mossi, M. M. M., Zeren Cetin, I. (2020c): Determination of Pb and Mg accumulation in some of the landscape plants in shrub forms. – Environ Sci Pollut Res 27(2): 2423-2431. https://doi.org/10.1007/s11356-019-06895-0, https://rd.springer.com/article/10.1007/s11356-019-06895-0

[52] Shahid, M., Dumat, C., Khalida, S., Schreck, E., Xiong, T., Nabeel, N. K. (2017): Foliar heavy metal uptake, toxicity and detoxification in plants: a comparison of foliar and root metal uptake. – Journal of Hazardous Materials 325: 36-58. https://www.sciencedirect.com/science/article/pii/S0304389416310937.

[53] Temmerman, D. L., Ruttens, A., Waegeneers, N. (2012): Impact of atmospheric deposition of As, Cd and Pb on their concentration in carrot and celeriac. – Environ Pollut 166: 187-195. https://www.sciencedirect.com/science/article/pii/S0269749112001443.

[54] Turkyilmaz, A., Sevik, H., Cetin, M., Saleh, E. A. A. (2018a): Changes in heavy metal accumulation depending on traffic density in some landscape plants. – Pol J Environ Stud 27(5): 2277-2284. http://www.pjoes.com/Changes-in-Heavy-Metal-Accumulation-Depending-non-Traffic-Density-in-Some-Landscape,78620,0,2.html.

[55] Turkyilmaz, A., Sevik, H., Isinkaralar, K., Cetin, M. (2018b): Using Acer platanoides annual rings to monitor the amount of heavy metals accumulated in air. – Environ Monit

http://www.aloki.hu ● ISSN 1589 1623 (Print) ● ISSN 1785 0037 (Online)
DOI: http://dx.doi.org/10.15666/aeer/1802_37133727

Assess 190(10): 578. https://doi.org/10.1007/s10661-018-6956-0. https://rd.springer.com/article/10.1007%2Fs10661-018-6956-0.

[56] Turkyilmaz, A., Sevik, H., Cetin, M. (2018c): The use of perennial needles as bio-monitors for recently accumulated heavy metals. – Landsc Ecol Eng 14(1): 115-120. https://doi.org/10.1007/s11355-017-0335-9. https://rd.springer.com/article/10.1007/s11355-017-0335-9.

[57] Turkyilmaz, A., Cetin, M., Sevik, H., Isinkaralar, K., Saleh, E. A. A. (2018d): Variation of heavy metal accumulation in certain landscaping plants due to traffic density. – Environ Dev Sustain. DOI: https://doi.org/10.1007/s10668-018-0296-7. https://link.springer.com/article/10.1007%2Fs10668-018-0296-7.

[58] Turkyilmaz, A., Sevik, H., Isinkaralar, K., Cetin, M. (2020): Use of tree rings as a bioindicator to observe atmospheric heavy metal deposition. – Environ Sci Pollut R 26(5): 5122-5130. DOI: 10.1007/s11356-018-3962-2. https://rd.springer.com/article/10.1007/s11356-018-3962-2.

[59] Xu, J., Jing, B., Zhang, K., Cui, Y., Malkinson, D., Kopel, D., Song, K., Da, L. (2017): Heavy metal contamination of soil and tree-ring in urban forest around highway in Shanghai, China. – Human and Ecological Risk Assessment: An International Journal 23(7): 1745-1762. https://www.tandfonline.com/doi/abs/10.1080/10807039.2017.1340826.

[60] Xu, Z., Zhou, G. (2008): Responses of leaf stomatal density to water status and its relationship with photosynthesis in a grass. – Journal of Experimental Botany 59(12): 3317-3325. https://academic.oup.com/jxb/article/59/12/3317/627451.

[61] Yigit, N., Sevik, H., Cetin, M., Gul, L. (2016): Clonal variation in chemical wood characteristics in Hanönü (Kastamonu) Günlüburun black pine (Pinus nigra Arnold. subsp. pallasiana (Lamb.) Holmboe) seed orchard. – J Sustain Forest 35(7): 515-526. https://www.tandfonline.com/doi/abs/10.1080/10549811.2016.1225512.

[62] Yucedag, C., Ozel, H. B., Cetin, M., Sevik, H. (2019a): Variability in morphological traits of seedlings from five Euonymus japonicus cultivars. – Environ Monit Assess t 191: 285. https://doi.org/10.1007/s10661-019-7464-6.

[63] Yucedag, C., Bilir, N., Ozel, H. B. (2019b): Phytohormone effect on seedling quality in Hungarian oak. – Forest Systems 28(2): 5. https://doi.org/10.5424/fs/2019282-14604.

[64] Yucedag, C., Sanders, J., Musah, M., Gailing, O. (2019c): Stomatal density in Quercus petraea and Q. robur natural populations in Northern Turkey. – Dendrobiology 81: 58-64.

[65] Zeren Cetin, I., Sevik, H. (2020): Investigation of the relationship between bioclimatic comfort and land use by using GIS and RS techniques in Trabzon. – Environ Monit Assess 192(2): 71. DOI: 10.1007/s10661-019-8029-4. https://doi.org/10.1007/s10661-019-8029-4

http://www.aloki.hu ● ISSN 1589 1623 (Print) ● ISSN 1785 0037 (Online)
DOI: http://dx.doi.org/10.15666/aeer/1802_37133727

ANALYSIS ON WATER QUALITY OF THE TIBETAN PLATEAU BASED ON THE MAJOR IONS AND TRACE ELEMENTS IN THE NIYANG RIVER BASIN

WU, J.[1,2,3] – ZHAO, Z. Q.[4*] – MENG, J. L.[1,3] – ZHOU, T.[1,3]

[1]*State Key Laboratory of Environmental Geochemistry, Institute of Geochemistry, Chinese Academy of Sciences, Guiyang 550081, China*

[2]*School of Chemistry and Materials Science, Guizhou Education University, Guiyang 550018, China*

[3]*University of Chinese Academy of Sciences, Beijing 100049, China*

[4]*School of Earth Science and Resources, Chang'an Unveristy, Xi'an 710054, China*

[*]*Corresponding author*
e-mail: zhaozhiqi@chd.edu.cn

(Received 14th Jan 2020; accepted 13th Apr 2020)

Abstract. Niyang River is the second largest tributary of the Yarlung Tsangpo River on the Tibetan Plateau. To establish the controlling factors of water quality in the river basin, this paper explores the hydro-chemical features of the major ions in the river water, and evaluates the water quality and health risk of trace elements. Multiple advanced technical instruments were adopted for our exploration including, the principal component analysis (PCA) and Water Quality Index (WQI). The hydro-chemical results show that the major ions in the river mainly originate from the weathering of rocks, with Ca-Mg-HCO_3 being the dominant type of hydro-chemical facies. Through PCA-based water quality assessment, we learned that the trace elements of Tl, Hg, Cd, Mo, Ti, U, As, Cr, Pb, Rb, Li, Sr, Ba, Fe and Al mostly come from rock weathering and groundwater leaching, while Cu, Zn and Mn are mainly attributable to natural and human sources. According to international and domestic standards, virtually no trace element surpassed the permissible limit, and the WQI values were basically low across the river basin, indicating that the river water is suitable for drinking directly.
Keywords: *Water Quality Index, trace elements, Niyang River, dissolved ion chemistry, principal component analysis*

Introduction

Water is one of the most important resources on the Earth. However, freshwater only makes up 2.5% of the total volume of the world's water. The Tibetan Plateau has an abundance of water resources, which greatly affect the local economy and ecology (Huang et al., 2008; Qu et al., 2019). Hailed as the water tower of Asia, the plateau is the source of the ten largest rivers on the continent, such as the Yangtze River, the Yellow River and the Nujiang River (Huang et al., 2010, 2008; Wu et al., 2005; Xu et al., 2019). Among the various rivers on the Tibetan Plateau, more than 20 rivers have a catchment greater than 10, 000 km^2 (Guan and Chen, 1980). The largest catchment (>240, 000 km^2) belongs to the Yarlung Tsangpo River (Jiang et al., 2015; Zeng et al., 2018). On the Tibetan Plateau, the most important tributary of the Yarlung Tsangpo River is the Niyang River, the catchment of which catchment is larger than 10,000 km^2 (Liu et al., 2018). The existing studies on this river mainly focus on the potential effects of global warming on the chemical weathering of rocks in the catchment and on the eco-environmental changes

http://www.aloki.hu ● ISSN 1589 1623 (Print) ● ISSN 1785 0037 (Online)
DOI: http://dx.doi.org/10.15666/aeer/1802_37293740

in the downstream (Liu et al., 2018; Yu et al., 2019). There is little report on the water quality in the Niyang River, from the perspectives of major ions and trace elements.

Water quality reflects the potential of river water to serve drinking and production purposes. It is generally agreed that the water quality of rivers is influenced by human factors (e.g. mining, wastewater discharge, and land use changes) and natural processes (e.g. rock weathering, grassland degradation, and glacier melting) (Huang et al., 2015; Wijesiri et al., 2018; Chen et al., 2019; Haldar et al., 2019; Jahin et al., 2020). For instance, rapid economic growth, which is accompanied by intense human activity, can push up the pollutant content in water systems, while rivers in pristine areas maintain good water quality (Wijesiri et al., 2018; Haldar et al., 2019). Under global warming, the pollutants accumulated in glaciers are released into the rivers, reducing the water quality (Huang et al., 2008). However, it is very difficult to assess the water quality of rivers in a comprehensive manner, because of the complex interplay between human factors and natural processes.

In recent years, both anthropogenic factors and natural processes are posing a serious threat to the water quality of the Niyang River. About 94, 000 people now live along this water course, and economic activities (e.g. mining, agriculture and tourism) have been in full swing in the downstream. In addition, the water chemistry in the catchment is being changed by the growing volume of meltwater and rainwater. Through the above analysis, this paper aims to identify the chemical features of river water, assess the controlling factors of water quality, track the source of trace elements, and evaluate the water quality in the Niyang River basin. First, water samples were collected from the Niyang River and its major tributaries. Then, the major ions and trace elements were analyzed in the water samples. In addition, the suitability of the water samples as drinking water was evaluated based on multiple water quality indices. The research results shed new light on water management and health protection on the Tibetan Plateau.

Materials and Methods

General situation of research area

The Niyang River (92°10'-94°35'E; 29°28'-30°31'N) originates at 5,000 m above the sea level (m a.s.l.) from the Cuomuliangla, west of the Mila Mountain, China's Tibet Autonomous Region (TAR). With a catchment of 17, 679 km^2, the river flows 307.5 km from west to east, before entering the Yarlung Tsangpo River at 2,920 m a.s.l. The elevation difference between the source and confluence is up to 2,080 m (Zhang et al., 2009). Being the second largest tributary of the Yarlung Tsangpo River, Niyang River is of great importance to the regional water balance on the Tibetan Plateau. The annual runoff of river is estimated to be 17.23 billion m^3. Meltwater and rainwater contribute to 47 and 40% of the annual runoff, respectively (Wang, 2011). The precipitation in the river basin is unevenly distributed, and largely controlled by the warm current in the Indian Ocean and the cold current from the north. The mean annual rainfall stands at 650 mm, 90% of which occurs in the summer months from June through September. The climate in the river basin changes significantly with the elevations. The annual mean temperature rises from 7.6℃ in the upstream to 8.6°C in the downstream.

The river basin has a complex lithology. The bedrocks are mainly composed of granite, diorite and granodiorite. The dominant minerals include mica, feldspar and quartz. Quaternary deposits are widely developed on both banks of the river. Located in the downstream of the Niyang River, the Bayi District is home to more than 39,000 people,

http://www.aloki.hu ● ISSN 1589 1623 (Print) ● ISSN 1785 0037 (Online)
DOI: http://dx.doi.org/10.15666/aeer/1802_37293740

serving as an important agricultural base on the Tibetan Plateau (Li, 2009). Every year, a large volume of agricultural and domestic wastewater is discharged into the river. What is more, fertilizers and pesticides are widely applied in this district to guarantee the agricultural output (Shi, 2015).

Experimental methods

In August, 2018, water samples were collected at 10 cm below the water surface from the Niyang River and its major tributaries (*Fig. 1*). The physical and chemical compositions of the samples are reported by Liu et al. (2018). The temperature (T), electrical conductivity (EC) and pH of the samples were measured in-situ by a Multi 3630 IDS multi-parameter portable meter (WTW, Germany). The alkalinity of the samples was obtained through Gran titration analysis in the field, using 0.02 mol/L HCl. The water samples were processed by 0.45 μm cellulose acetate (CA) membrane filters, and then stored in pre-cleaned polyethylene bottles. The filtrate was divided into two parts: one part was used directly for anion analysis (e.g. SO_4^{2-}, F^-, Cl^-, NO_3^-), and the other was acidified to pH < 2 with ultrapure 1:1 HNO_3 for cation analysis (e.g. Na^+, K^+, Ca^{2+}, Mg^{2+}, SiO_2). The cations were analyzed by inductively coupled plasma atomic emission spectroscopy (ICP-OES) system (Vista MPX, US), while the anions were measured by ionic chromatography (IC), using an ICS-90 IC system (Dionex, US). The contents of trace elements were obtained through inductively coupled plasma mass spectrometry (ICP-MS) system (Agilent 7700X, US). The contents of anions, cations and trace elements were all measured in The State Key Laboratory of Environmental Geochemistry, Institute of Geochemistry, Chinese Academy of Sciences. The measurement reproducibility was determined through repeated analysis, showing ± 5% precision for the anions, cations and trace elements. For all the samples, the calculated total anion charge TZ^- was balanced by the total cation charge TZ^+ within the analytical uncertainties, and the normalized inorganic charge balance (NICB) fell within ± 5% are reported in Liu et al. (2018).

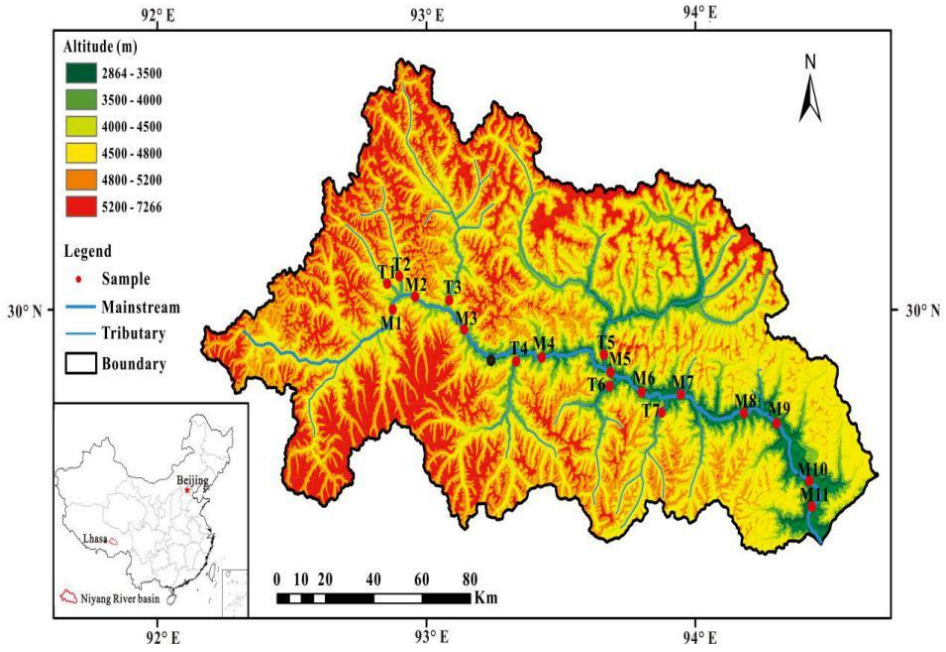

Figure 1. *Sampling location map of Nyang River. Modified from Liu et al. (2018)*

http://www.aloki.hu ● ISSN 1589 1623 (Print) ● ISSN 1785 0037 (Online)
DOI: http://dx.doi.org/10.15666/aeer/1802_37293740

Statistical methods

Pearson correlation analysis was performed to disclose how different trace elements influence the water quality. If the Pearson correlation coefficient (r), is greater than or equal to 0.7, then the two variables have a strong correlation; if $0.4 < r < 0.7$, then the two variables have a moderately strong correlation; if $r \leq 0.4$, then the two variables have a weak correlation (Gidey and Amanuel, 2018).

The Water Quality Index (WQI) was introduced to evaluate the combined effects of several toxic elements considered detrimental to the aquatic ecosystem (Qu et al., 2019):

$$WQI = \frac{1}{n}\sum_{i=1}^{n} A_i = \frac{1}{n}\sum_{i=1}^{n} C_i/Q_i \quad \text{(Eq.1)}$$

where C_i (μg/L) is the content of the i-th toxic element in the water sample; Q_i (μg/L) is the content limit of the i-th toxic element specified by the World Health Organization (WHO, 2011) and the Chinese national standard (GB) (MOH and SAC, 2006). According to the WQI value, the pollution level was divided into four classes: $WQI \leq 1$ (Class 1, unpolluted); $1 < WQI \leq 2$ (Class 2, slightly polluted); $2 < WQI \leq 3$ (Class 3, moderately polluted); and $WQI > 3$ (Class 4, heavily polluted) (Qu et al., 2019).

Results and Discussion

Characterization of the major ions of Niyang River systems

As mentioned before, the chemical compositions of the water in the Niyang River basin are reported in Liu et al. (2018). The pH of the water samples varied from 8.08 to 7.71, indicating the mild alkalinity of the water in the river basin. Due to the specific hydrology and geology, the major ion contents of the Niyang River were lower than those of other rivers in the world (*Fig. 2*). The total dissolved solids (TDS) of the samples ranged from 51.7 to 112 mg/L, averaging at 81.7 mg/L. This is far lower than the global mean level of 120 mg/L (Wetzel, 1975). In the mainstream of the Niyang River, the TDS decreased from 112 mg/L in the upstream to 72.3 mg/L in the downstream, owing to the dilution effect. The Ca^{2+} accounts for 60.5-80% of all cations (TZ^+) in the water samples, followed by Mg^{2+} (10.8-34.9%), Na^+ (3.58-8.74%) and K^+ (0.67-1.9%), while HCO_3^- accounts for 60.2% of all anions (TZ^-) in the samples, followed by SO_4^{2-} (36.4%).

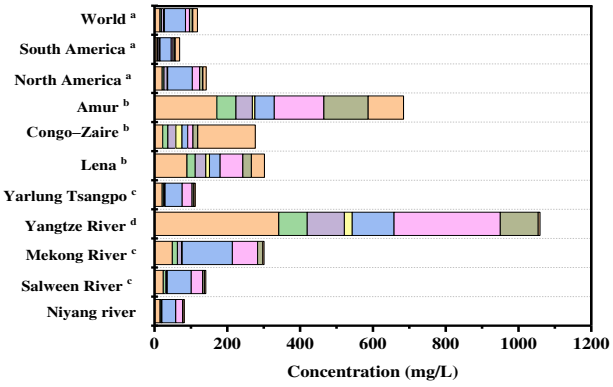

Figure 2. *Average concentrations of major ions in Niyang River and other rivers of the world. Data source: a. Wetzel (1975); b. Gaillardet et al. (1999); c. Huang et al. (2011); d. Chetelat et al. (2008)*

http://www.aloki.hu ● ISSN 1589 1623 (Print) ● ISSN 1785 0037 (Online)
DOI: http://dx.doi.org/10.15666/aeer/1802_37293740

To evaluate the hydrogeochemical facies and types of the samples, the relative equivalent proportions of major ions were plotted as ternary diagrams. As shown in *Fig. 3*, the data clustered near the [Ca^{2+} + Mg^{2+}] peak (*Fig. 3a*) and the HCO_3^- peak (*Fig. 3b*), suggesting the water in the Niyang River basin belongs to the type of Ca-Mg-HCO_3 river water. This is similar to that in the Yangtze River (Chetelat et al., 2008), but differs from that of the Wujiang River (Han and Liu, 2004) and the Yellow River (Fan et al., 2014).

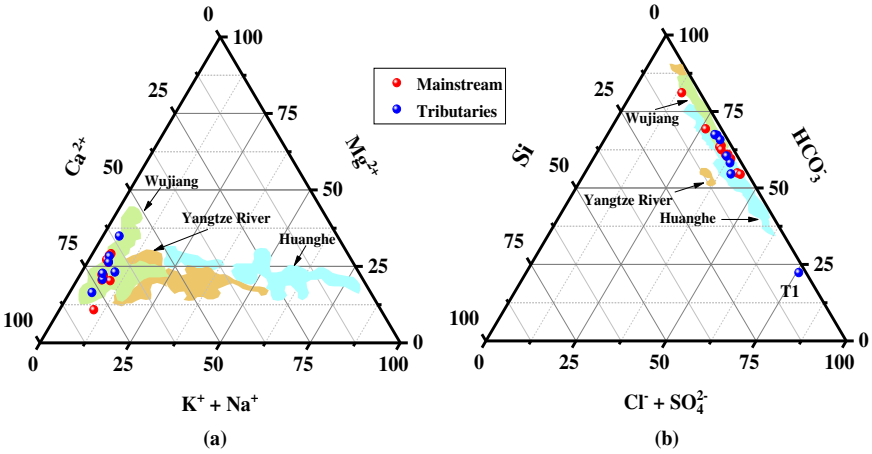

Figure 3. *Ternary diagram of the relative equivalent proportions of major cations (a) and major anions (b) for the river waters, indicating that the Niyang River was dominated by Ca^{2+} and HCO_3^-*

Major sources and controlling factors of the ions

The major elements dissolved in river water generally come from precipitation, groundwater leaching, human inputs (e.g. agriculture, industry and urbanization), and chemical weathering of rocks (e.g. silicate, evaporite, carbonate, and sulfide) in the catchment (Meybeck and Ragu, 1997; Gaillardet et al., 1999). On the Tibetan Plateau, the meltwater and rainwater are the two leading sources of the major elements in rivers (Hasnain and Thayyen, 1999). Zhang et al. (2003) calculated how much atmospheric inputs contribute to the total cations based on the measured ion/Cl^- ratio in rainwater in Lhasa region, assuming that rainwater has the lowest Cl^- content measured in the catchment (Ding et al., 2017). In the Niyang River basin, the lowest Cl^- content was observed at the site T-2 (3.30 μM). According to Liu et al. (2018), the atmospheric inputs contribute to 5.5-12.9% of the total cations, with an average of only 8.0%. Thus, the contribution of atmospheric inputs to the major ions of our samples is very limited. Considering the major impact of human activities on water chemistry via wastewater input (Sun et al., 2017), it is necessary to evaluate the contribution of human inputs to the major ions in the water samples. In many large rivers, NO_3^-, among the dissolved ions, is generally associated with anthropogenic sources (Chetelat et al., 2008). In our water the NO_3^- content was below the global mean value of 21.7 μM (Meybeck, 1987). According to Liu et al. (2018), the human activities are responsible for 0-0.5% of all cations. Hence, the human inputs also have a limited contribution to the major ions in our samples. TDS contents and low weight ratios of [Na^+]/[Na^+ + Ca^{2+}] and [Cl^-]/[Cl^- + HCO_3^-]. This means the dominant source of major ions in the Niyang River catchment is the chemical weathering of rocks. In general, the Mg^{2+}, Ca^{2+} and HCO_3^- in our samples are most likely

http://www.aloki.hu ● ISSN 1589 1623 (Print) ● ISSN 1785 0037 (Online)
DOI: http://dx.doi.org/10.15666/aeer/1802_37293740

to originate from the weathering of carbonates and silicates, while the K^+, Na^+, SO_4^{2-} and Cl^- from the weathering of silicates and the dissolution of evaporites. To identify which type of rock weathering controls the ions in the water samples, the plotted the mixing diagrams of the Na-normalized of Ca^{2+} versus HCO_3^- and Ca^{2+} versus Mg^{2+} for identifying three endmembers of carbonates, silicates and evaporates. As shown in *Fig. 4*, our water samples were close to the carbonate endmember in the mixing diagrams, indicating that the weathering of carbonate is crucial to the major ion chemistry of the river water.

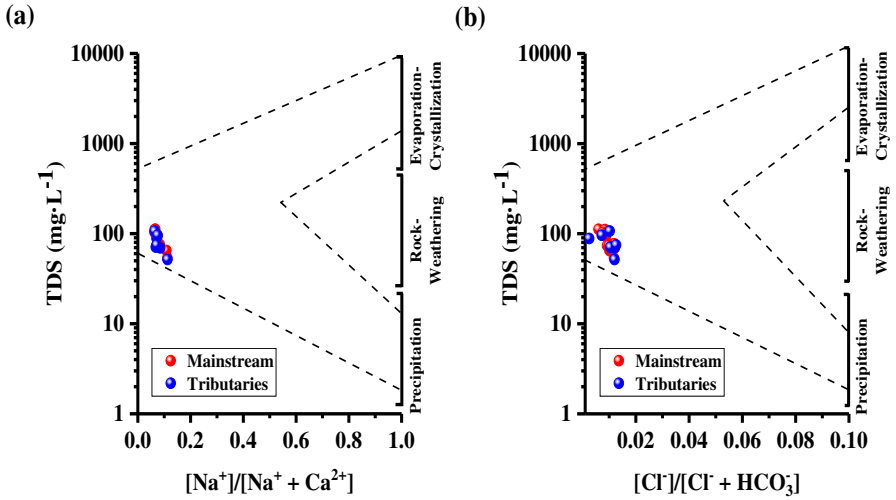

Figure 4. *Gibbs diagram (weight ratios) of major ion compositions in Niyang River basin*

This conclusion echoes with the previous results on the rivers in other parts of the High Himalaya region (Wu et al., 2008; Jiang et al., 2018; Zeng et al., 2018), and is supported by the relatively high mean $[Ca^{2+} + Mg^{2+}]/[Na^+ + K^+]$ molar ratios of 7.62 and mean $[HCO_3^-]/[Na^+ + K^+]$ molar ratios of 9.28. The molar ratios confirm that the river basin is dominated by the weathering of dolomite and calcite minerals in *Fig. 5*.

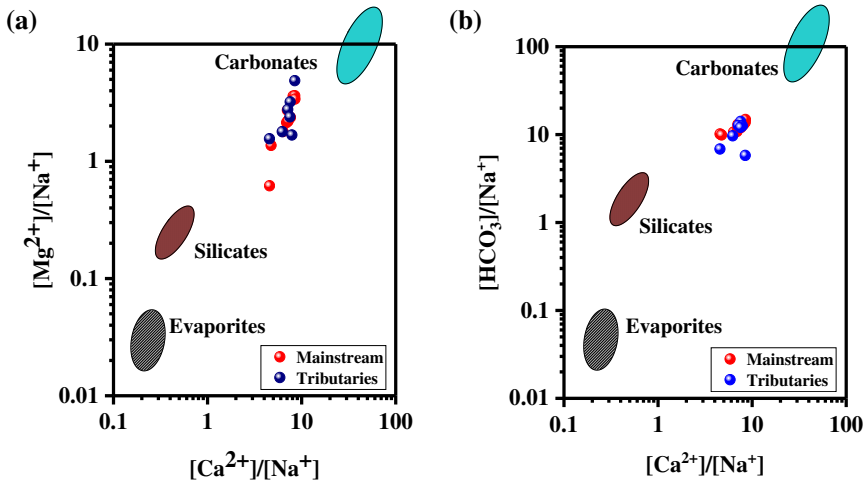

Figure 5. *Mixing diagram of the Na-normalized molar ratios of (a) Ca^{2+} versus Mg^{2+} and (b) Ca^{2+} versus HCO_3^- in the Niyang River basin. The data for the three endmembers, i.e., carbonates, silicates and evaporites, are obtained from Gaillardet et al. (1999)*

http://www.aloki.hu ● ISSN 1589 1623 (Print) ● ISSN 1785 0037 (Online)
DOI: http://dx.doi.org/10.15666/aeer/1802_37293740

Dissolved trace elements and water quality assessment

Dissolved trace elements

Despite their excessively low content (<1 mg/L), the trace elements play an important role in human health (Xiao et al., 2019). This subsection discusses the features and possible sources of trace elements in our water samples, and assesses their risks to the residents in the river basin in *Table 1*.

Table 1. *The trace elements and WQI in Niyang River basin*

Sample	***Mn***	***Cu***	***Zn***	***Pb***	***Cr***	***As***	***Rb***	***Sr***	***Ba***
	μg/L	μg/L	μg/L	μg/L	μg/L	μg/L	μg/L	μg/L	μg/L
M-1	98.3	6.24	24.6	5.02	0.54	2.55	1.88	76.2	45.6
M-2	78.7	1.39	6.62	0.41	0.13	1.73	1.61	77.4	49.2
M-3	48.2	1.78	6.45	0.57	0.14	1.17	1.62	59.7	46.5
M-4	30.6	0.83	4.47	0.12	0.1	1.04	1.54	54.7	45.0
M-5	9.6	0.48	4.71	0.13	0.08	0.52	1.93	41.8	38.3
M-7	4.08	0.22	2.54	0.07	0.04	0.25	1.25	19.6	41.6
M-10	11.5	0.59	2.55	0.36	0.12	0.75	1.81	43.9	9.89
M-11	11.2	0.57	3.63	0.27	0.13	0.66	1.87	41.9	46.0
T-1	451	1.59	76.9	0.40	0.08	0.24	2.26	52.6	46.6
T-2	3.83	0.49	5.26	0.10	0.09	0.43	1.24	47.7	49.8
T-3	2.22	0.19	3.00	0.03	0.05	0.31	1.69	58.1	50.7
T-4	3.29	0.55	3.39	0.11	0.16	1.41	1.65	47.8	41.5
T-5	4.55	0.31	3.13	0.11	0.07	0.32	2.05	37.3	43.3
T-7	11.0	0.51	3.95	0.10	0.07	0.69	1.85	44.1	42.0
Sample	***U***	***Li***	***Al***	***TI***	***Fe***	***Mo***	***Cd***	***Hg***	***Tl***	***WQI***
	μg/L	*μg/L*	*μg/L*	*μg/L*	*μg/L*	*μg/L*	*μg/L*	*μg/L*	*μg/L*	
M-1	0.76	2.84	113	0.51	69.6	0.89	0.09	0.03	0.01	0.41
M-2	0.51	2.48	9.99	0.08	5.96	1.49	0.01	0.06	0.01	0.14
M-3	0.66	3.4	136	1.64	53.1	0.73	0.07	na	0.01	0.27
M-4	0.49	3.09	85.4	0.64	41.7	0.84	0.07	na	0.01	0.23
M-5	0.68	3.18	17.3	0.06	4.52	1.03	0.02	0.02	0.01	0.08
M-7	0.21	1.34	18.7	0.11	9.6	0.4	0.01	0.01	na	0.05
M-10	0.59	1.86	41.3	0.6	32.4	0.47	0.02	0.01	0.01	0.10
M-11	0.56	2.74	40.8	0.57	21.34	0.79	0.02	0.01	0.01	0.10
T-1	0.17	3.43	19.9	0.1	5.92	0.41	0.76	0.03	0.05	1.74
T-2	0.4	0.85	20.6	0.1	8.34	0.38	0.03	0.03	na	0.10
T-3	0.5	4.73	11.7	0.13	8.1	0.75	0.02	0.01	na	0.07
T-4	0.42	1.71	19.2	0.4	16.5	1.36	0.01	0.03	na	0.07
T-5	0.75	3.15	7.47	0.14	6.55	0.89	na	0.02	na	0.03
T-7	0.54	2.88	11.6	0.07	4.66	1.06	0.01	0.01	0.01	0.06

na, not determine

The Niyang River has fewer dissolved elements than most rivers around the world. The contents of trace elements were extracted to identify the correlations and covariances between varying sample parameters through the principal component analysis (PCA). Three main parameter clusters were observed in the PCA loading-plot (PC1, PC2 vs PC3) in *Fig. 6*, which represent 74.0% of the total variances in the data of river waters. The Sr, Cu, Cr, Al, Fe, Ti, and Pb in PC1 had the highest loadings among the PCs, which explains

http://www.aloki.hu ● ISSN 1589 1623 (Print) ● ISSN 1785 0037 (Online)
DOI: http://dx.doi.org/10.15666/aeer/1802_37293740

33.1% of the variance. This is supported by the positive correlation among these elements (*Table 2*): the correlation coefficients of Cu and Pb, Al and Fe, and Cr and Pb were 0.975, 0.952, 0.944 and 0.971, respectively. Meanwhile, the Cd, Mn, Zn, Rb and Tl in PC2 could explain 26.6% of the variance; the Mo and Hg in PC3 was responsible for 14.2% of the variance.

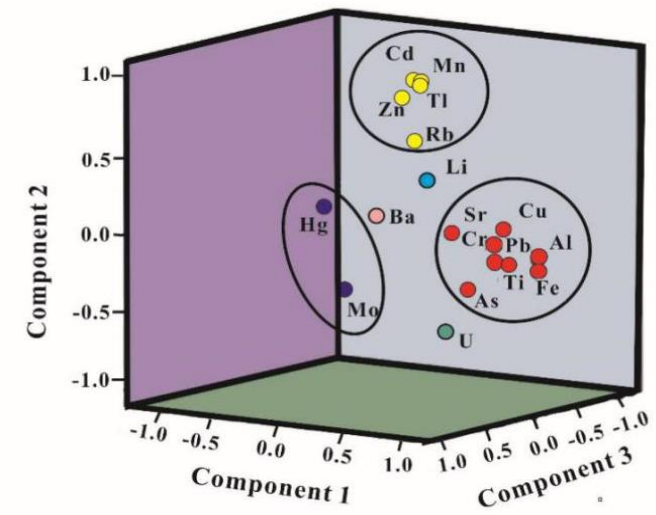

Figure 6. *Principal component analysis (PCA) for dissolved trace elements in the Niyang River basin*

Table 2. *Correlation coefficientc matrix of trace elements in Niyang River basin*

	Mn	***Li***	***U***	***Cu***	***Zn***	***Pb***	***Cr***	***As***	***Rb***	***Sr***	***Ba***	***Al***	***Ti***	***Fe***	***Mo***	***Cd***	***Hg***	***Tl***
Mn	1																	
Li	0.241	1																
U	-0.461	0.305	1															
Cu	0.301	0.103	0.345	1														
Zn	**.986****	0.225	-0.434	0.361	1													
Pb	0.161	0.056	0.402	**.975****	0.244	1												
Cr	0.086	-0.021	0.443	**.952****	0.161	**.971****	1											
As	-0.04	-0.059	0.425	**.793****	-0.037	**.759****	**.855****	1										
Rb	.544	.563	0.275	0.213	.562	0.182	0.146	-0.026	1									
Sr	0.255	0.344	0.318	.650	0.222	.549	.592	**.747****	0.138	1								
Ba	0.166	0.285	-0.155	0.14	0.166	0.068	0.041	0.075	-0.143	0.308	1							
Al	0.019	0.156	0.387	.635	0.03	.564	.594	.564	-0.072	0.426	0.028	1						
Ti	-0.098	0.131	0.335	0.256	-0.129	0.172	0.254	0.332	-0.089	0.231	-0.109	**.861****	1					
Fe	-0.035	0.074	0.444	**.741****	-0.002	**.719****	**.759****	**.688****	-0.036	0.457	-0.118	**.944****	**.749****	1				
Mo	-0.249	0.155	0.38	0.081	-0.301	0.055	0.18	.541	0.125	0.43	0.204	-0.111	-0.084	-0.07	1			
Cd	**.980****	0.239	-0.52	0.188	**.978****	0.059	-0.019	-0.186	0.528	0.121	0.137	-0.008	-0.092	-0.078	-0.363	1		
Hg	0.298	-0.248	-0.107	0.257	0.268	0.21	0.246	0.387	0.071	0.476	0.239	-0.367	-0.478	-0.281	0.453	0.16	1	
Tl	**.946****	0.283	-0.371	0.223	**.920****	0.081	0.019	-0.082	.624	0.202	0.013	0.06	-0.016	-0.014	-0.233	**.938****	0.15	1

** Correlation is significant at $p < 0.05$ level (2-tailed). The bold number indicates the strong correlation ($r \geq 0.7$)

http://www.aloki.hu ● ISSN 1589 1623 (Print) ● ISSN 1785 0037 (Online)
DOI: http://dx.doi.org/10.15666/aeer/1802_37293740

Overall, the contents of trace elements in samples varied with the differences in the weathering of rocks, groundwater supply, rainwater and human inputs (Tatsi et al., 2015; Qu et al., 2017). In the Niyang River systems, Fe and Al mainly come from the weathering of chlorite and calcite (Yokoo et al., 2004), Cu, Zn and Mn mostly originate from mineral exploration, due to the abundance of mineral deposits (e.g., manganese ore, copper ore and lead zinc ore) in the river basin (Lü et al., 2019). As shown in *Table 2*, Tl and Cd had a positive correlation coefficient of 0.93, suggesting that the two trace elements are both attributable to mining and meltwater (Tatsi et al., 2015). Note that the heavy metals Mn and Zn at site T-I were 13 times and 128 times more concentrated than those in other rivers (Gaillardet et al., 1999), respectively, reflecting the major contribution of the human activity of metal mining.

Water quality assessment

The water quality indices of our samples were compared against the drinking water standards of the World Health Organization (WHO) (WHO, 2011) and the GB (MOH and SAC, 2006). The comparison shows that most of the Al, As, Ba, Hg, Pb, Tl, Cr, Cu, Fe, Mo, Sr and Zn in our samples were below the lower limits of toxic elements for drinking water. As shown in *Table 1*, the trace element contents and the Water Quality Index (WQI) were relatively high in the upstream of the Niyang River, owing to high evaporation and limited precipitation. Across the river basin, the WQI values ranged from 0.03 to 0.4, except for the relative high WQI at site T-1. The latter is attributable to the mineral exploration at the site. Therefore, almost all samples from the river basin belong to the unpolluted class.

The Niyang River supplies agricultural water to the entire Bayi District. More than half of the population in that district live along the water course. The tourism and agriculture are booming along the river. This research reveals that water in the Niyang River is still undisturbed, because the impacts from agriculture and industrial activities (mining) are mitigated by the strong dilution and buffering capacity of the river. However, the boom in tourism, coupled with the mining activities, will put heavy burdens on the water quality in the region. The degradation of water quality is foreseeable, due to the intensified weathering of rocks and growing human activities in the river basin. Therefore, the local government should implement strict environmental regulations on solid waste and waste water treatment.

Conclusions

In the context of sustainable development, water quality is an important environmental issue across the globe, especially in the Tibetan Plateau, the water tower of Asia. This paper mainly explores the geochemistry features of major ions in the Niyang River, and assesses the water quality in the river basin. It is learned that the water chemistry in the river is greatly affected by the natural process of rock weathering, with Ca-Mg-HCO_3 being the dominant type of hydro-chemical facies. Under the alkaline aquatic environment, the river basin has low contents of trace elements, which originate from bedrock weathering. Through water quality assessment, the rivers water in the basin was found safe for direct drinking, for no trace element surpasses the lower limit in international and domestic water quality standards, except for Mn and Zn at site T-I. However, the elemental abundances in the air, soil, and water of the river basin may be perturbed by the growth in economy, human activities (e.g. mining and wastewater

http://www.aloki.hu ● ISSN 1589 1623 (Print) ● ISSN 1785 0037 (Online)
DOI: http://dx.doi.org/10.15666/aeer/1802_37293740

discharge) and natural processes (e.g. rock weathering). Considering the potential damages of this possibility to human health and the essential role that rivers on the Tibetan Plateau play in terms of water resources of Asia, the region should consistently monitor the pollutant loads and implement pollutant control in the rivers, e.g. increasing of the sampling and adding the analysis of water quality parameters.

Acknowledgments. This work was jointly supported by the National Natural Science Foundation of China (Grant No. 41661144042, 41673124, 41603018, 91647205) and National Basic Research Program (973 project) of China (2013CB956401).

REFERENCES

[1] Chen, M., Li, C., Zeng, C., Zhang, F., Raymond, P. A., Hur, J. (2019): Immobilization of relic anthropogenic dissolved organic matter from alpine rivers in the Himalayan-Tibetan Plateau in winter. – Water research 160: 97-106.

[2] Chetelat, B., Liu, C. Q., Zhao, Z. Q., Wang, Q. L., Li, S. L., Li, J., Wang, B. L. (2008): Geochemistry of the dissolved load of the Changjiang Basin rivers: Anthropogenic impacts and chemical weathering. – Geochimica et Cosmochimica Acta 72: 4254-4277.

[3] Ding, H., Liu, C.-Q., Zhao, Z.-Q., Li, S.-L., Lang, Y.-C., Li, X.-D., Hu, J., Liu, B.-J. (2017): Geochemistry of the dissolved loads of the Liao River basin in northeast China under anthropogenic pressure: Chemical weathering and controlling factors. – Journal of Asian Earth Sciences 138: 657-671.

[4] Fan, B.-L., Zhao, Z.-Q., Tao, F.-X., Liu, B.-J., Tao, Z.-H., Gao, S., Zhang, L.-H. (2014): Characteristics of carbonate, evaporite and silicate weathering in Huanghe River basin: A comparison among the upstream, midstream and downstream. – Journal of Asian Earth Sciences 96: 17-26.

[5] Gaillardet, J., Dupré, B., Louvat, P., Allègre, C. J. (1999): Global silicate weathering and CO_2 consumption rates deduced from the chemistry of large rivers. – Chemical Geology 159: 3-30.

[6] Gidey, A. (2018): Geospatial distribution modeling and determining suitability of groundwater quality for irrigation purpose using geospatial methods and water quality index (WQI) in Northern Ethiopia. – Applied Water Science 8: 82.

[7] Guan, Z.-H., Chen, C.-Y. (1980): River water resources in Tibet (Xizang). – Resour Sci 2: 25-35.

[8] Haldar, K., Kujawa-Roeleveld, K., Dey, P., Bosu, S., Datta, D. K., Rijnaarts, H. H. M. (2019): Spatio-temporal variations in chemical-physical water quality parameters influencing water reuse for irrigated agriculture in tropical urbanized deltas. – Sci Total Environ 708: 134559.

[9] Han, G., Liu, C.-Q. (2004): Water geochemistry controlled by carbonate dissolution: a study of the river waters draining karst-dominated terrain, Guizhou Province, China. – Chemical Geology 204(1-2): 1-21.

[10] Hasnain, S. I., Thayyen, R. J. (1999): Discharge and suspended-sediment concentration of meltwaters, draining from the Dokriani glacier, Garhwal Himalaya, India. – Journal of Hydrology 218: 191-198.

[11] Huang, X., Sillanpää, M., Duo, B., Gjessing, E. T. (2008): Water quality in the Tibetan Plateau: metal contents of four selected rivers. – Environmental pollution 156: 270-277.

[12] Huang, X., Sillanpää, M., Gjessing, E. T., Peräniemi, S., Vogt, R. D. (2010): Environmental impact of mining activities on the surface water quality in Tibet: Gyama valley. – Science of The Total Environment 408: 4177-4184.

http://www.aloki.hu ● ISSN 1589 1623 (Print) ● ISSN 1785 0037 (Online)
DOI: http://dx.doi.org/10.15666/aeer/1802_37293740

[13] Huang, X., Sillanpää, M., Gjessing, E. T., Peräniemi, S., Vogt, R. D. (2011): Water quality in the southern Tibetan Plateau: chemical evaluation of the Yarlung Tsangpo (Brahmaputra). – River Research and Applications 27: 113-121.
[14] Huang, J., Kang, S., Zhang, Q., Guo, J., Sillanpaa, M., Wang, Y., Sun, S., Sun, X., Tripathee, L. (2015): Characterizations of wet mercury deposition on a remote high-elevation site in the southeastern Tibetan Plateau. – Environmental pollution 206: 518-526.
[15] Jahin, H. S., Abuzaid, A. S., Abdellatif, A. D. (2020): Using multivariate analysis to develop irrigation water quality index for surface water in Kafr El-Sheikh Governorate, Egypt. – Environmental Technology & Innovation 17: 100532.
[16] Jiang, M., Peng, M., Yang, J., Tan, H., Qian, R., Zhang, Y., Xu, L., Zhang, L., Li, Q. (2015): Seismic reflection and magnetotelluric profiles across the Luobusa ophiolite: Evidence for the deep structure of the Yarlung Zangbo suture zone, southern Tibet. – Journal of Asian Earth Sciences 110: 4-9.
[17] Jiang, H., Liu, W., Xu, Z., Zhou, X., Zheng, Z., Zhao, T., Zhou, L., Zhang, X., Xu, Y., Liu, T. (2018): Chemical weathering of small catchments on the Southeastern Tibetan Plateau I: Water sources, solute sources and weathering rates. – Chemical Geology 500: 159-174.
[18] Li, F. (2009): Research on the Aquatic Organisms and Advance Estimate of Effects of Hydropower Engineering in Nanyang River Basin, Tibet. – Xi'an, Northwest University, pp: 26.
[19] Liu, X., Zhang, D., Gao, S., Wu, J., Guo, J. Y., Zhao, Z. Q. (2018): Chemical weathering and CO_2 consumption flux in Tibetan Plateau: A case of Niyang River catchment Chinese. – Journal of Ecology 37: 688-696.
[20] Lü, L., Li, Z., Huang, Y., Cui, C. (2019): Distribution characteristics and risk assessment of heavy metals in Niyang River, Tibet. – Transactions of the Chinese Society of Agricultural Engineering 35: 193-199.
[21] Meybeck, M. (1987): Global Chemical Weathering of Surficial Rocks Estimated From River Dissolved Loads. – American Journal of Science 287: 401-428.
[22] Meybeck, M., Ragu, A. (1997): River Discharges to the Oceans: An Assessment of Suspended Solids, Major Ions and Nutrients. – Environment information and assessment technical report, UNEP, WHO.
[23] MOH & SAC (Ministry of Health of the People's Republic of China & Standardization Administration of P. R. China). (2006): Chinese National Standards GB 5749-2006: Standards for Drinking Water Quality. – Available online at: http://www.nhc.gov.cn/.
[24] Qu, B., Zhang, Y., Kang, S., Sillanpää, M. (2017): Water chemistry of the southern Tibetan Plateau: an assessment of the Yarlung Tsangpo river basin. – Environmental Earth Sciences 76: 74-86.
[25] Qu, B., Zhang, Y., Kang, S., Sillanpää, M. (2019): Water quality in the Tibetan Plateau: Major ions and trace elements in rivers of the "Water Tower of Asia". – Sci Total Environ 649: 571-581.
[26] Shi, X.-P. (2015): Investigation and Analysis on Cognitive of Agricultural Materials Used by Farmers in Nyingchi--Case on Niyanghe Valley in Tibet. – Science and Technology of Qinghai Agriculture and Forestry 3: 45-49.
[27] Sun, X., Mörth, C.-M., Humborg, C., Gustafsson, B. (2017): Temporal and spatial variations of rock weathering and CO_2 consumption in the Baltic Sea catchment. – Chemical Geology 466: 57-69.
[28] Tatsi, K., Turner, A., Handy, R. D., Shaw, B. J. (2015): The acute toxicity of thallium to freshwater organisms: Implications for risk assessment. – Sci Total Environ 536: 382-390.
[29] Wang, H.-L. (2011): Study on situation of water environment and protection countermeasure in Niyang River valley. – Linzhi, Agricultural and Animal Husbandry college of in Tibet University, pp: 17-18.
[30] Wetzel, R. G. (1975): Limnology. – W. B. Saunders Co., Philadelphia, USA, 743 p.

http://www.aloki.hu ● ISSN 1589 1623 (Print) ● ISSN 1785 0037 (Online)
DOI: http://dx.doi.org/10.15666/aeer/1802_37293740

[31] WHO (World Health Organization). (2011): Guidelines for Drinking-Water Quality. Recommendations, Vision 4. – Available at: http://www.who.int/watersanitation health/dwq/gdwq3rev/en/.
[32] Wijesiri, B., Deilami, K., Goonetilleke, A. (2018): Evaluating the relationship between temporal changes in land use and resulting water quality. – Environmental pollution 234: 480-486.
[33] Wu, L., Huh, Y., Qin, J., Du, G., van Der Lee, S. (2005): Chemical weathering in the Upper Huang He (Yellow River) draining the eastern Qinghai-Tibet Plateau. – Geochimica et Cosmochimica Acta 69: 5279-5294.
[34] Wu, W., Yang, J., Xu, S., Yin, H. (2008): Geochemistry of the headwaters of the Yangtze River, Tongtian He and Jinsha Jiang: Silicate weathering and CO_2 consumption. – Applied Geochemistry 23: 3712-3727.
[35] Xiao, J., Wang, L., Deng, L., Jin, Z. (2019): Characteristics, sources, water quality and health risk assessment of trace elements in river water and well water in the Chinese Loess Plateau. – Sci Total Environ 650: 2004-2012.
[36] Xu, R., Hu, H., Tian, F., Li, C., Khan, M. Y. A. (2019): Projected climate change impacts on future streamflow of the Yarlung Tsangpo-Brahmaputra River. – Global and Planetary Change 175: 144-159.
[37] Yokoo, Y., Nakano, T., Nishikawa, M., Quan, H. (2004): Mineralogical variation of Sr–Nd isotopic and elemental compositions in loess and desert sand from the central Loess Plateau in China as a provenance tracer of wet and dry deposition in the northwestern Pacific. – Chemical Geology 204: 45-62.
[38] Yu, Z., Wu, G., Keys, L., Li, F., Yan, N., Qu, D., Liu, X. (2019): Seasonal variation of chemical weathering and its controlling factors in two alpine catchments, Nam Co basin, central Tibetan Plateau. – Journal of Hydrology 576: 381-395.
[39] Zeng, C., Zhang, F., Lu, X., Wang, G., Gong, T. (2018): Improving sediment load estimations: The case of the Yarlung Zangbo River (the upper Brahmaputra, Tibet Plateau). – Catena 160: 201-211.
[40] Zhang, D. D., Jim, C. Y., Peart, M. R., Shi, C. (2003): Rapid changes of precipitation pH in Qinghai Province, the northeastern Tibetan Plateau. – Science of The Total Environment 305: 241-248.
[41] Zhang, N., Li, H.-j., Wen, Z.-z., Yu, C.-l., Liu, P.-s. (2009): Spatio-Temporal Characteristics of Niyang River in Tibet. – Journal of Henan Normal University (Natural Science) 37: 79-82.

http://www.aloki.hu ● ISSN 1589 1623 (Print) ● ISSN 1785 0037 (Online)
DOI: http://dx.doi.org/10.15666/aeer/1802_37293740

EFFECTS OF SLIPPERY JACK (*SUILLUS LUTEUS*) ON THE HEAVY METAL ACCUMULATION AND SOIL PROPERTIES OF MASSON'S PINE (*PINUS MASSONIANA* LAMB) IN A MINING AREA OF CHINA

SUN, Y. J.[1#] – YU, P. Y.[1#] – CHEN, J. Z.[2] – LI, S. M.[1] – JIANG, L. J.[1*]

[1]*College of Life Science and Technology, Central South University of Forestry and Technology, 498 South Shaoshan Road, Changsha, Hunan 410004, China*

[2]*Hunan Academy of Forestry, 658 South Shaoshan Road, Changsha, Hunan 410004, China*

[#]*These authors contributed equally to this work*

**Corresponding author*
e-mail: znljiang2542@163.com

(Received 17th Jan 2020; accepted 24th Mar 2020)

Abstract. Plant-microbial bioremediation is an efficient way to treat heavy metal contaminated soils. In order to reveal the potential mechanisms of ectomycorrhizal fungi mutualistic symbiosis for remediating heavy metal contaminated soils, the masson's pine associated with ectomycorrhizal fungi (*Suillus luteus*) and control treatments (plant roots without ectomycorrhizal fungi) were planted in a Pb and Zn contaminated mining area in the south of China. The results showed that the growth of masson's pine seedlings were significantly higher in the treated group than in the control group. The bioconcentration factor (BCF) of heavy metals inoculated with *Suillus luteus* was 1 to 5 times higher than that of those in control group. However, the translocation factor (TF) of heavy metals in treated group decreased by 50% compare to the control group. Both selenium and potassium content significantly improved the functions of oxidation and stress resistance in symbiotic systems. The activity of the urease and alkaline phosphatase in the soil was significantly improved in treated group. The soil available N, P and K contents, and the ratio of C/N was increased compared to the control. In conclusion, the ectomycorrhizal fungi could improve soil physicochemical properties, and enhance nutrient absorption by the plants, which would be favorable to the growth of plants in the soil contaminated with heavy metals.
Keywords: *bioremediation, heavy metal toxicity, enzyme activities, mycorrhiza, symbiosis systems*

Introduction

Soils may be contaminated by the accumulation of heavy metals through emissions from the rapidly expanding mine tailings. The water and soil erosion caused by deforestation in abandoned mining area had polluted the surrounding soil with heavy metals severely, which resulted in impacts on the growth and development of wild life, plants and human activities in central south of Hunan, China (Ayangbenro and Babalola, 2017; Huang et al., 2012). To remediate hazardous pollutants of heavy metal ions have attracted more attention (Li et al., 2019).

There were many methods reported to restore or remediate heavy metal contaminated soil, for example, physcio-chemically, to fix available heavy metals in soils by means of welding, stabilizing, excavating and electrodynamics, so that the effective concentration (EC) of heavy metals were reduced to harmless level (Sheoran et al., 2011; Wuana and Okieimen, 2011). However, these methods would inevitably damage the natural structure of soil by adding curing agent. Also the improper storage

http://www.aloki.hu ● ISSN 1589 1623 (Print) ● ISSN 1785 0037 (Online)
DOI: http://dx.doi.org/10.15666/aeer/1802_37413755

of the contaminated soil after curing might result in secondary pollution. In contrast, the bioremediation method constructed by plant roots and ECM fungi was environmentally friendly. The symbiotic system could immobilize, accumulate and transfer excessive heavy metals through the absorption of water and nutrients in soil (Ma et al., 2019; Guo et al., 2020).

Many reports, in recent years, showed that the heavy metal contaminated soils, such as abandoned mining areas and tailings reservoir areas, did harm to the growth and development of plants considering the physiologically and the survival of herbaceous plants (Zhang and Ji, 2019; Zhang et al., 2018). However, some woody plants such as Fagaceae (Tam, 1995; Sozoniuk et al., 2019) or Pinaceae (Wang et al., 2019) coexisted with ectomycorrhizal (ECM) fungi, which could supply the host plants with water and nutrient (Colpaert, 2008), and promote these plants to survive in the toxicity of heavy metals in mining areas (Lalancette et al., 2019). According to Jentschke and Godbold (2000), the roots of almost all forest tree seedlings rely on mycorrhizal fungi, which could shift the absorption and translocation of heavy metal stress in roots system and ameliorate the toxicity of heavy metals to the aboveground of host plants (Jentschke and Godbold, 2000). Compared with the plants inoculated without ECM fungi, *Pinus sylvestris* inoculated with six strains of ECM fungi immobilized larger numbers of zinc in the roots, and limiting the transportation of zinc to the host plants of *Pinus sylvestris* (Colpaert, 2008). As well as Sousa et al. (2012) mentioned that ECM fungi (*Suillus bovinus*) would improve shoot development of *Pinus pinaster* seedlings up to 30% exposure to the soil contaminated by Cd, and the accumulation of Cd in the aboveground parts of the seedlings inoculated with *S. bovinus* seedlings also increased (Sousa et al., 2012). Other studies also showed that masson's pine inoculated with ECM fungi was more tolerant to higher concentrations of heavy metals than the non-ECM fungi inoculation, and ECM fungi had a great effect on the absorption and fixation of heavy metals (Huang et al., 2012).

Masson's pine, a pioneer tree species with large biomass, is regarding as an important timber and industrial material tree species that has ectomycorrhizal in southern China (Sun et al., 2010). Masson's pine exhibits many advantages, such as fast growth, high yield, strong adaptability to drought-stressed soils, and high potential for the phytoremediation of soils that contaminated by heavy metals (Wang et al., 2019; Zhang et al., 2017). Therefore, masson's pine was considered to be an appropriate reforestation tree species in heavy metal contaminated soils in abandoned mining tails area. *Suillus luteus* could form symbiotic systems with masson's pine (Zhang et al., 2017), *Larix principis-rupprechtii* (Huai et al., 2003), P*icea abies* (Krznaric et al., 2009a), *Pinus sylvestris* (Yin et al., 2014) and so on, and could increase the absorption of nutrients and water, and then promote the growth of symbiotic plants (Luo et al., 2014). However, so far, the effect of ECM fungi on the improvement of host plant remediation potential and adaption under excessive stress of heavy metals in soil are not very clear.

In this study, the effects of masson's pine inoculated with or without ECM fungi on soil properties were investigated. The objectives of the study were 1) the characteristics of absorption, accumulation and transportation of heavy metals and nutrients of masson's pine inoculated with *Suillus luteus* compared to the control (without ECM fungi) in the mining areas contaminated soil by lead-zinc; 2) to address the mechanisms of mycorrhiza and plant mutualistic symbiosis system on the soil physicochemical properties and the activities of enzymes in masson's pine rhizosphere.

http://www.aloki.hu ● ISSN 1589 1623 (Print) ● ISSN 1785 0037 (Online)
DOI: http://dx.doi.org/10.15666/aeer/1802_37413755

Materials and methods

Experimental site

The experimental site is located in an abandoned lead-zinc mining tails of mountain Manao in the southeast of Chenzhou city, Hunan Province, China (*Fig. 1*). *Miscanthus* sp, *Equisetum ramosissimum, Elsholtzia cypriani* are the dominate plants species growing in the abandoned mining tails area that are seriously polluted by lead (Pb) and zinc (Zn) heavy metals. The area is at the northern foot of middle section of the mountain Nanling (13°08′00″~113°08′30″E, 25°35′00″~25°44′00″N). It is a continental subtropical monsoon humid climate, with distinct four seasons, abundant sunshine and the rainfall, but unevenly distributed. As "hometown of non-ferrous metals", the mountainous and hilly are rich in mineral resources, have less arable land and water. Due to extensive mining, there is a series of problems such as soil erosion, eco-environment deterioration, and heavy metals pollution. Therefore, the native plant species, such as *Koelreuteria paniculata*, *Sapium sebiferum*, *Pinus massoniana* Lamb, and *Quercus*, growing in the polluted site are endangered. It is urgently needed to protect and reforest plants and tree species in the whole area, particularly the mining tailings.

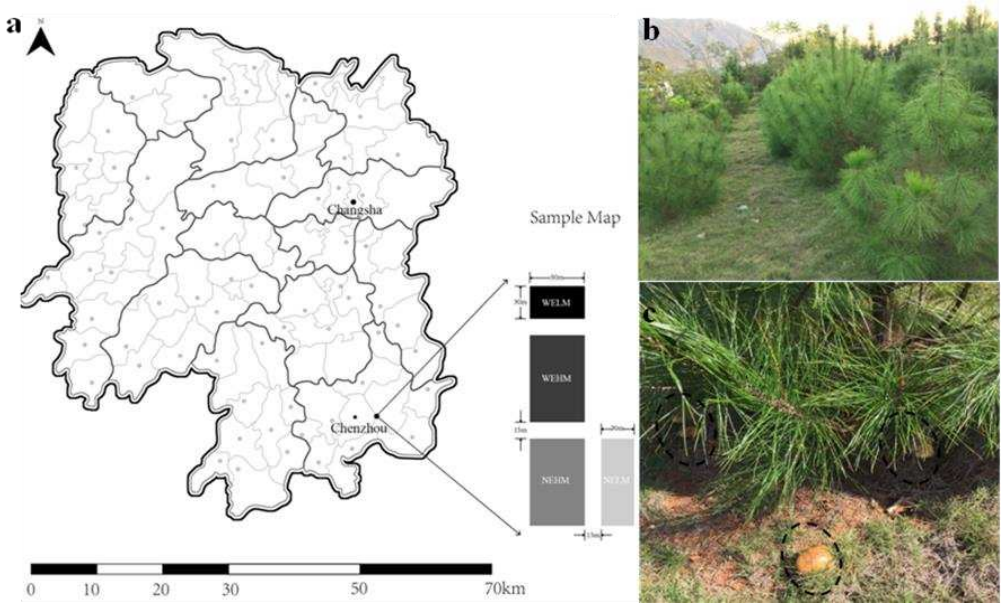

Figure 1. *Location of the study area and plot setting. (Note: a refers to the experimental site, b refers to the growth condition of masson's pine, and c refers to the sampling site inoculated with Suillus luteus; the capital letter WELM refers to low heavy metals contaminated soil inoculated with ECM fungi, WEHM refers to high heavy metals contaminated soil inoculated with ECM fungi, NELM refers to low heavy metals contaminated soil inoculated without ECM fungi, NEHM refers to high heavy metals contaminated soil inoculated without ECM fungi)*

Experiments design

The plants used in this experiment were two-year-old masson's pine seedlings inoculated with and without ECM fungi, which were provided by Hunan academy of forestry. The seedlings inoculated with EMC were cultivated by the way of Yu et al. (2020). At the end of 2016, the masson's pine seedlings inoculated with ECM fungi (WE) and without inoculation (NE) were planted in two polluted areas with two different levels of Pb and Zn

http://www.aloki.hu ● ISSN 1589 1623 (Print) ● ISSN 1785 0037 (Online)
DOI: http://dx.doi.org/10.15666/aeer/1802_37413755

contamination degree in soil, the low heavy metal contaminated soil (LM) and the high heavy metal contaminated soil (HM). The polluted soils combine with the treatment inoculated with ECM fungi (WE) named as WELM, WEHM, and the polluted soils inoculated without ECM fungi (NE) named as NELM, NEHM. There was no polluted soil (NM) based on the Pb and Zn contaminated degree below the Hunan background and national standard II (see *Table 1*) with NE treatment only (names as CK) in the experiment. There were three replications in both LM and HM soils. Before the experiment to set up, we have measured the no polluted soil samples with WE and NE treatments, and we found that no significant difference between the treatment and control. So that there were three WELM, three WEHM, three NELM, three NEHM, and three NENM of the treatments, the total of 15 sampling plots in the experimental study, and each plot included 3 trees. The heavy metal contents in different plots were showed in *Table 1*.

Table 1. *Heavy metals content of soil in different planting areas of masson's pine (mg/kg)*

Soil type	Pb	Zn	Cu	Cd	Mn
CK	20.93	87.47	23.69	0.13	686.10
LM	602.35	400.93	44.93	0.32	1222.93
HM	2555.20	496.75	57.52	0.473	2010.83
Hunan background	29.7	94.4	27.3	0.17	–
National standard II	≤ 250	≤ 200	≤ 150	≤ 0.30	–

CK refers to no heavy metal polluted soil without ECM fungi; LM refers to the low heavy metal contaminated soil; HM refers to the high heavy metal contaminated soil

Plant growth determination and sampling

From June 2017 to May 2019, the plant heights, ground diameters, crown width and annual branch length of masson's pine were measured. Meanwhile, three root, stem and leaf samplings of each masson's pine inoculated with ECM fungi (including WELM and WEHM), without ECM fungi (including NELM and NEHM) and CK treatment were collected, and the root, stem and leaf samplings from each plot was mixed into one sample, respectively, we totally got 15 root samplings, 15 stem samplings, and 15 leaf samplings. Then, heavy metals and nutrient element contents were determined. Notably, root samplings of each plant were carefully excavated by soil core sampler (φ108 mm × φ100mm × 130mm), the soil attached to the root surface was took as rhizospheric soils, and the depth of sampling was 10 to 20cm.

Soil sampling

The soil samples were taken in each plot before the seedlings of masson's pine planting and the soil physicochemical properties were measured (*Table 1*). Two years after planting the seedlings of masson's pine, root samplings of each plant were carefully excavated and the soil attached to the root surface of masson's pine was collected and packed in a sealed plastic bag. The gravel, plant litter and other visible impurities were removed. The sampled soil was divided into two categories: one was stored in refrigerator at -20 ℃ for the determination of soil enzyme activities of the soil, and the other one was air-dried at room temperature for the determination of soil physicochemical properties.

http://www.aloki.hu ● ISSN 1589 1623 (Print) ● ISSN 1785 0037 (Online)
DOI: http://dx.doi.org/10.15666/aeer/1802_37413755

Determination of soil physicochemical properties

The soil was dried in oven at 70 ℃ for 48 h for measuring water content. Took 1 g soil dissolved in 5 ml distilled water and shaken for 30 min, and was measured by glass electrode (Sartorius PB-10). Soil total carbon (TC) and total nitrogen (TN) were determined by element analyzer (VarioEL III, Germany). The available phosphorus (AP) in soil was extracted by sodium bicarbonate and determined with molybdenum-blue method, the available potassium (AK) was determined by flame spectrophotometry, and available nitrogen (AN) was measured by means of alkaline hydrolysis diffusion method (Bao, 2000).

Determination of total heavy metal concentrations in plants and soils

The dried plants were divided into two parts, belowground part and aboveground (stem and leaf) parts. After smashed, both of 0.3 g plant and soil samples were weighed accurately, then digested by microwave acid digestion (EPA 3051; USEPA, 2004). The heavy metal concentrations were determined by Inductively Coupled Plasma Emission Spectrometer (ICP-MS, X-7, Thermo Electron, Waltham, MA, USA) (Zhao et al., 2013). All samples were repeated for three times and then took the average value was taken.

Determination of soil enzyme activities

The activity of catalase was defined as decomposing one milligram of soil hydrogen peroxide every 30 min, and determined by ultraviolet spectrophotometry. A unit (μ) of urease active was defined as producing the mass of NH_3-N by hydrolyzing 1 g soil for 1 min, and determined by sodium phenol-sodium hypochlorite colorimetry. The activity of alkaline phosphatase was defined as producing the mass of phenol with 1 g of soil after 24 h, and determined by disodium phosphate colorimetric method. The activity of sucrose enzyme was defined as producing the mass of glucose with 1 g of soil after 24 h, and determined by 3, 5 dinitrosalicylate colorimetric method (Guan et al., 1986).

Statistical analysis

The means of the growth vigor of masson's pine, the absorption of heavy metals and nutrient elements, and soil physicochemical properties had been compared within Microsoft s Excel (Office' 2000), One-way analysis of variance (ANOVA) and The correlation between the soil physicochemical properties and plant nutrients was performed to determine the effects of above factors by using SPSS (version 19.0; SPSS, Chicago, IL, USA)

Results

Effects of ECM fungi on the growth of masson's pine

The mean height, ground diameter, annual branch length and crown width of masson's pine seedlings inoculated with/without EMC and the control in different contaminated soils are shown in *Figure 2*. The mean height and annual branch growth of seedlings with NE treatment were decreased compared to the no polluted soil treatment (CK), especially, there was a significantly difference in plant height ($P < 0.05$) (*Fig. 2a*). Seedlings of WELM treatment have improved the mean plant height, annual branch length, ground base diameter and crown width than in others

http://www.aloki.hu ● ISSN 1589 1623 (Print) ● ISSN 1785 0037 (Online)
DOI: http://dx.doi.org/10.15666/aeer/1802_37413755

($p < 0.05$). The mean ground diameter of seedlings in WELM and WEHM plots were increased by 53.12% and 43.38%, respectively, compared to the NELM and NEHM plots (*Fig. 2b*).

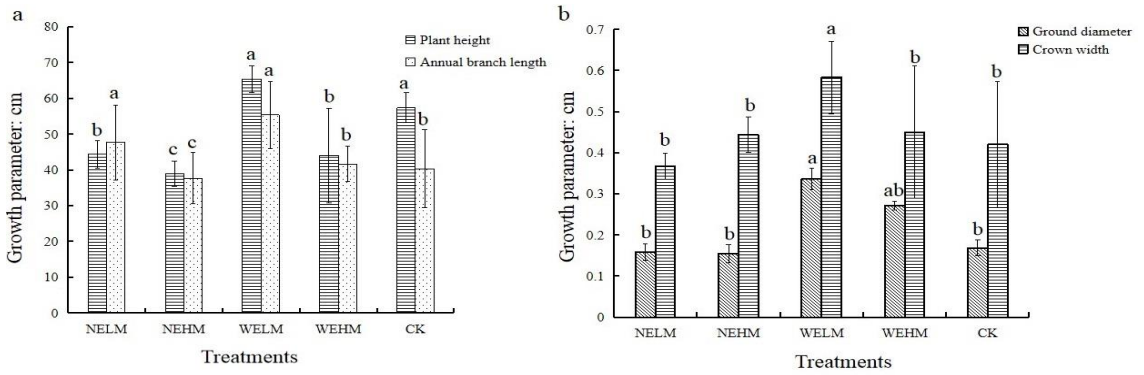

Figure 2. *Effects of ectomycorrhizal fungi on the growth of masson's pine. (Note: a refers to the plant height and annual branch length, and b refers to the plant ground base diameter and crown width; the capital letter CK refers to no heavy metal polluted soil without ECM fungi, WELM refers to low heavy metals contaminated soil inoculated with ECM fungi, WEHM refers to high heavy metals contaminated soil inoculated with ECM fungi, NELM refers to low heavy metals contaminated soil inoculated without ECM fungi, NEHM refers to high heavy metals contaminated soil inoculated without ECM fungi; means followed with same letters are not significantly different by Tukey's test multiple comparison at $p < 0.05$, mean ± standard error of three measurements)*

Effect of ECM fungi on accumulation and transportation of heavy metals in masson's pine

The distribution of heavy metal concentrations of masson's pine in different treatments were analyzed (*Table 2*). The results showed that accumulation of heavy metals of Pb, Zn, Cd, Cu and Mn in WE treatment was higher than that of NE in the plant roots ($p < 0.05$). The translocation factor (TF) of Pb was 0.93, and the bioconcentration factor (BCF) of the root was 0.09 in NEHM plot, which was nearly reach to that of CK (TF = 1.26, BCF = 0.55). However, the TF and BCF of Pb in WEHM plots were 0.51 and 0.44, respectively; the TF was about 45% while the BCF was almost five times of that in NE treatment. The accumulation of Zn, Cd, Cu and Mn in the roots of WE treatment was increased by 1 to 2 times, while TF was significantly decreased compared to the NE soil.

Effects of ECM fungi on the absorption and distribution of nutrient elements in masson's pine

The results showed that the TF of selenium in WELM and WEHM treatments were 2.33 and 1.57 times higher than that of NELM and NEHM treatments, respectively (*Table 3*). The Iron (Fe) in the root system was significantly increased in WEHM treatment, while decreased in aboveground part, especially, in the plant leaves ($p < 0.05$). In soil with the same degree of pollution, the average content of N and P of the plants in the WE treatment plant were higher than that of NE treatment, but the content ratio of the belowground part to the underground part was lower in WE treatment than that in NE treatment ($p < 0.05$), except for the N content of NELM and

http://www.aloki.hu ● ISSN 1589 1623 (Print) ● ISSN 1785 0037 (Online)
DOI: http://dx.doi.org/10.15666/aeer/1802_37413755

WELM. The content of K in the plant is lower in WE treatment than that in NE treatment, while the TF of K is higher in WE treatment than that in NE treatment.

Table 2. *The effects of accumulation and transport of heavy metals in masson's pine on different treatments*

Element	Treatment	Soil (mg/kg)	Roots (mg/kg)	Stem (mg/kg)	Leaf (mg/kg)	Upper part/ground part (TF)	Roots/soil (BCF)
Pb	CK	20.93±0.17c	11.60±0.58d	16.53±2.43d	12.81±1.84d	1.26±0.12a	0.55±0.02a
	NELM	602.35±15.26b	87.21±3.11bc	92.93±4.24b	60.40±3.82b	0.88±0.13b	0.12±0.02bc
	NEHM	2555.2±50.22a	229.56±20.14a	73.00±3.61bc	21.33±1.53c	0.93±0.15b	0.09±0.01c
	WELM	602.35±15.26b	121.60±10.40b	57.07±7.69c	64.67±2.01b	0.55±0.08c	0.19±0.08b
	WEHM	2555.2±50.22a	279.23±18.12a	149.43±8.74a	132.88±3.03a	0.51±0.12c	0.44±0.10a
Zn	CK	87.47±2.15c	41.77±7.48d	45.07±3.02d	57.83±0.51ab	1.23±0.12a	0.48±0.08b
	NELM	400.93±9.51b	40.67±5.83d	53.47±3.78c	44.13±1.51b	1.2±0.59ab	0.10±0.08c
	NEHM	496.75±4.37a	67.73±2.05c	90.60±2.76b	43.10±2.00b	0.99±0.26b	0.14±0.01bc
	WELM	400.93±9.51b	145.87±3.26ab	66.53±2.05cd	73.60±5.25a	0.48±0.01c	0.36±0.12a
	WEHM	496.75±4.37a	181.77±16.06a	119.20±3.54a	69.20±4.61a	0.52±0.15c	0.37±0.11a
Cd	CK	0.13±0.01c	0.28±0.07d	0.19±0.06c	0.21±0.11b	0.71±0.08bc	2.15±0.13ab
	NELM	0.32±0.13b	0.38±0.05c	0.44±0.03b	0.28±0.01a	0.95±0.12a	1.18±0.22c
	NEHM	0.47±0.11a	0.45±0.01bc	0.50±0.05a	0.28±0.03a	0.87±0.13b	0.96±0.16c
	WELM	0.32±0.13b	0.82±0.02a	0.49±0.16a	0.31±0.09a	0.49±0.15c	2.56±0.82a
	WEHM	0.47±0.11a	0.62±0.26b	0.53±0.14a	0.29±0.13a	0.67±0.22bc	1.31±0.16c
Cu	CK	23.69±1.22c	6.77±0.35c	6.42±0.87bc	6.91±0.43a	0.98±0.02a	0.29±0.02c
	NELM	44.93±10.11b	5.47±0.61d	5.33±1.93c	5.73±0.46bc	1.01±0.13a	0.12±0.06c
	NEHM	57.52±9.86a	7.00±0.46c	5.47±0.59c	5.00±0.61d	0.75±0.11b	0.12±0.05c
	WELM	44.93±10.11b	16.13±1.61a	7.20±1.39b	6.13±1.01b	0.41±0.08c	0.36±0.11a
	WEHM	57.52±9.86a	11.08±2.01b	14.52±4.13a	5.47±3.03c	0.90±0.11a	0.19±0.05b
Mn	CK	686.10±14.98c	346.47±5.88c	549.55±13.51a	1324.72±36.11a	2.70±0.78a	0.50±0.05c
	NELM	1222.93±111.42b	521.33±10.20b	421.20±11.15a	1015.33±21.63b	1.38±0.15b	0.43±0.15c
	NEHM	2010.83±65.45a	426.97±28.96b	524.57±13.12a	1072.73±16.40b	1.87±1.10b	0.21±0.09b
	WELM	1222.93±111.42b	1336.67±8.25a	507.87±27.13a	1366.40±44.20a	0.70±0.55c	1.09±0.08b
	WEHM	2010.83±65.45a	1529.00±26.51a	538.58±24.51a	1083.33±38.40b	0.53±0.09c	0.76±0.17a

The capital letters CK refer to no heavy metal polluted soil without ECM fungi, WELM refers to low heavy metals contaminated soil inoculated with ECM fungi, WEHM refers to high heavy metals contaminated soil inoculated with ECM fungi, NELM refers to low heavy metals contaminated soil inoculated without ECM fungi, NEHM refers to high heavy metals contaminated soil inoculated without ECM fungi; means followed with same letters within column are not significantly different by Tukey's test multiple comparison at $p < 0.05$, mean ± standard error of three measurements

Effect of ECM fungi on physicochemical properties of soil

The physicochemical properties of soil were changed significantly between WE and NE treatments (*Fig. 3*). The water content of soil was increased by 84% in WELM and 45% in WEHM treatment than that in NE treatment, respectively. The available N content was increased by 64% in WELM and 13.3% in WEHM than that in NE treatment, respectively. The C/N ratio of the soil in WE treatment changed greatly, especially in WELM soil, and the soil C/N is about 22% higher than that in NE treatment. The contents of P and K in WELM plot was significant increased compared to CK. The highest N content was found in WE treatment of the soil ($p < 0.05$). The overall results showed that the inoculation of ECM fungi could significantly improve the soil structure and physicochemical properties.

http://www.aloki.hu ● ISSN 1589 1623 (Print) ● ISSN 1785 0037 (Online)
DOI: http://dx.doi.org/10.15666/aeer/1802_37413755

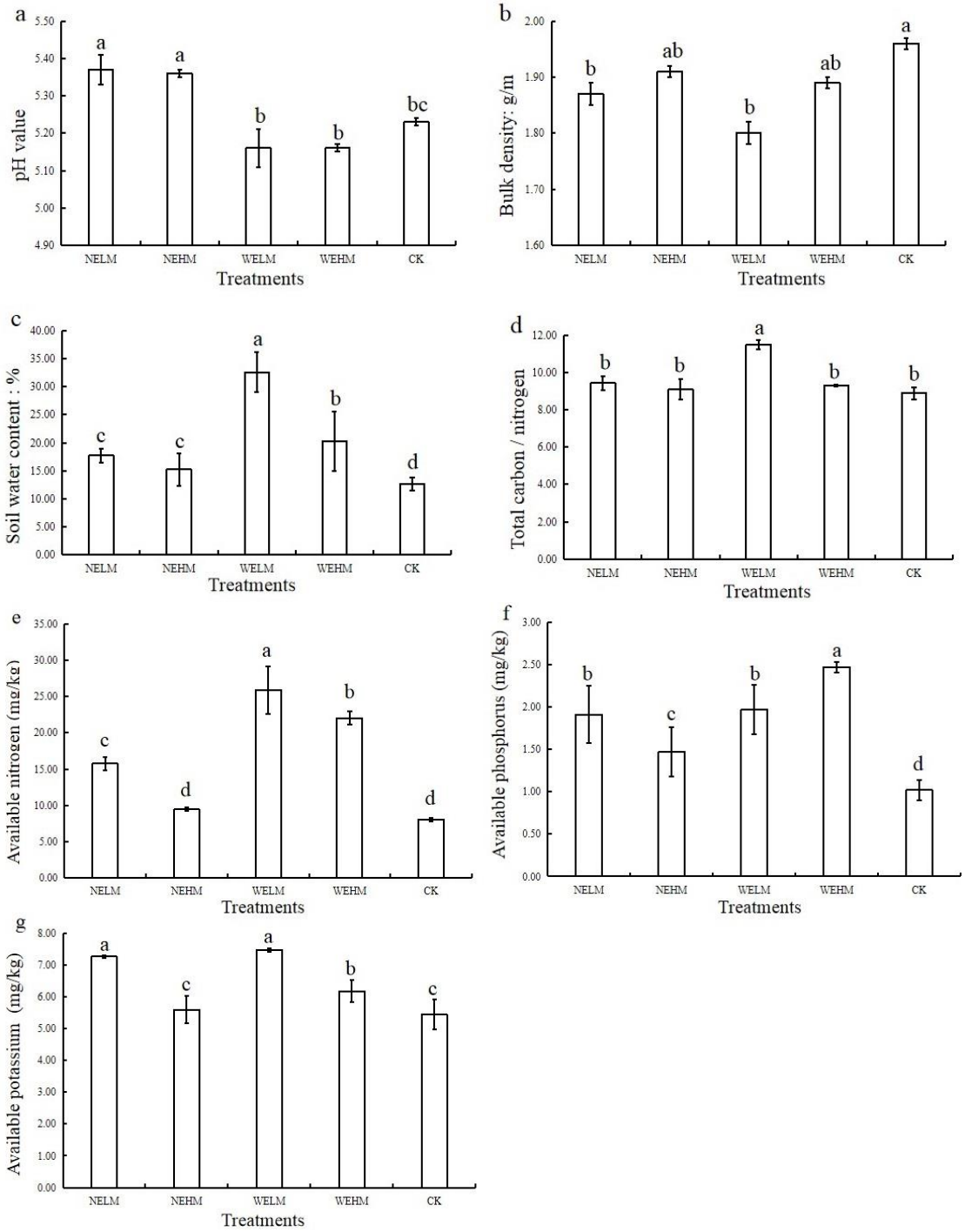

Figure 3. *The soil physicochemical properties of soil under different treatments. (Note: a refers the soil pH value, b refers the soil bulk density, c refers the soil water content, d refers the ratio of total carbon to total nitrogen, e refers the soil available nitrogen, f refers the soil available phosphorus, g refers the soil available potassium; the capital letter CK refers to no heavy metal polluted soil without ECM fungi, WELM refers to low heavy metals contaminated soil inoculated with ECM fungi, WEHM refers to high heavy metals contaminated soil inoculated with ECM fungi, NELM refers to low heavy metals contaminated soil inoculated without ECM fungi, NEHM refers to high heavy metals contaminated soil inoculated without ECM fungi; means followed with same letters are not significantly different by Tukey's test multiple comparison at* $p < 0.05$*, mean ± standard error of three measurements)*

http://www.aloki.hu ● ISSN 1589 1623 (Print) ● ISSN 1785 0037 (Online)
DOI: http://dx.doi.org/10.15666/aeer/1802_37413755

Table 3. *Accumulation and transport of nutrient elements in masson's pine under different treatments*

Element	Treatment	Average plant content	Root (mg/kg)	Stem (mg/kg)	Leave (mg/kg)	Above-/underground
Se	CK	2.82±0.14ab	3.12±0.41a	2.74±0.62b	2.61±0.32bc	0.86±0.29c
	NELM	2.27±0.42b	1.33±0.83c	2.00±0.40c	3.47±0.61a	2.01±1.53a
	NEHM	2.61±0.33b	3.00±0.52a	3.77±0.35a	1.07±0.42d	0.81±0.31bc
	WELM	3.02±0.58a	3.33±0.83a	2.93±0.83b	2.80±1.06b	0.86±0.42c
	WEHM	2.73±0.67ab	1.75±0.76b	2.18±0.95c	2.27±1.22c	1.27±0.22b
Fe	CK	1121.57±54.53b	2887±112.67cd	166.43±15.91cd	311.27±53.61b	0.08±0.01a
	NELM	1263.34±21.64b	3241.07±78.54cd	187.47±5.90c	361.47±124.45a	0.08±0.05a
	NEHM	3172.16±64.36a	8916.83±179.21b	216.77±20.23b	382.87±56.08a	0.07±0.01b
	WELM	1334.04±15.67b	3528.80±81.86c	229.20±21.70b	244.13±14.52c	0.07±0.03b
	WEHM	3415.45±43.40a	9694.10±629.86a	405.73±59.97a	146.53±21.87d	0.03±0.01c
P	CK	955.89±21.33b	786.82±22.06b	924.71±83.19c	1156.13±24.63b	1.32±0.22b
	NELM	834.31±4.33b	1493.60±50.61a	881.47±37.13cd	1127.87±48.50b	2.04±1.63a
	NEHM	922.58±8.67b	759.33±4.55b	892.27±20.87cd	1116.13±30.44b	1.32±0.51b
	WELM	1149.41±21.57a	788.97±38.89b	1282.00±97.96b	1377.27±50.04a	1.69±1.81ab
	WEHM	1358.98±27.33a	1362.48±44.27a	1321.52±49.71a	1392.93±41.46a	1.00±0.41c
K	CK	5902.64±126.30b	7382.41±134.3b	5006.57±102.31b	5318.95±85.33c	0.70±0.51bc
	NELM	4834.62±59.77b	6082.67±50.6c	4125.20±130.83bc	4296.00±154.35cd	0.69±0.12bc
	NEHM	7584.53±121.57a	8269.53±296.19a	7572.10±462.22a	6911.97±326.31a	0.88±0.25b
	WELM	2980.53±67.53c	2387.73±86.43d	2932.27±90.55d	3621.60±138.28d	1.37±0.38a
	WEHM	6022.83±156.71a	7530.65±860.35ab	4361.85±329.59bc	6176.00±207.88b	0.70±0.11bc
N	CK	3034.64±63.43a	1793.5±35.1b	2505.67±112.30b	4804.76±76.19c	2.04±0.81ab
	NELM	2542.74±27.36b	1537.23±114.52c	2536.52±103.32b	3554.46±200.87d	1.98±0.98b
	NEHM	2690.92±151.31b	1855.63±89.51b	2125.36±115.69bc	3256.47±187.58d	1.45±0.11c
	WELM	3910.35±51.31a	2050.53±91.88a	3144.29±196.38a	6536.23±285.48a	2.36±0.53a
	WEHM	3451.41±136.67a	1998.86±105.32ab	2856.35±123.56ab	5499.01±324.25b	2.09±1.01ab

The capital letters CK refer to no heavy metal polluted soil without ECM fungi, WELM refers to low heavy metals contaminated soil inoculated with ECM fungi, WEHM refers to high heavy metals contaminated soil inoculated with ECM fungi, NELM refers to low heavy metals contaminated soil inoculated without ECM fungi, NEHM refers to high heavy metals contaminated soil inoculated without ECM fungi; means followed with same letters within column are not significantly different by Tukey's test multiple comparison at $p < 0.05$, mean ± standard error of three measurements

Effect of ECM fungi on soil enzymes

Soil enzyme plays an important role in recycling of nutrients, which is closely related to soil microorganisms and plant community structure. It is a sensitive index to evaluate soil fertility and soil quality. The results showed that the enzyme activity in WE treatment was significantly different from that of control treatment (CK) and NE treatment ($p < 0.05$) (*Table 4*). The urease and alkaline phosphatase contents in WE treatment was significantly higher than that of NE treatment ($P < 0.05$), while there was no significant different in catalase and sucrase content among different treatments.

The correlation between the soil physicochemical properties and plant nutrients

The correlations between the soil physicochemical properties of soil and the contents of macro nutrients in masson's pine seedlings were analyzed (*Table 5*). The results showed that there were correlations between soil physicochemical properties and the

http://www.aloki.hu ● ISSN 1589 1623 (Print) ● ISSN 1785 0037 (Online)
DOI: http://dx.doi.org/10.15666/aeer/1802_37413755

accumulation of macro nutrient. The soil pH correlated negatively with all the nutrient elements of plant, excepting the K. Especially, the significantly negative correlation was found between the concentration of N and soil pH (*Table 5*). The soil water content was positively correlated with plant Se, N, P elements, while the negatively correlation was found between soil water content and the plant Fe and K (*Table 5*). There was positive correlation of N and P between the plants and the LM and HM soils, while the content of K in plant was negatively correlated with the available K content in the soil. The results of correlation analysis of soil enzymes and soil physicochemical properties showed that urease had a significantly negative relationship with soil pH, while there was no significant relationship between the soil urease and bulk density (*Table 5*). Both Urease and alkaline phosphatase positively correlated with soil nutrient elements. Sucrase negatively correlated with the soil properties (excepting the soil pH and the soil bulk density), especially with the available nitrogen (N) and phosphorus (P) contents of the soil. Altogether, plants inoculated with ECM fungi could increase the activities of catalase, urease and alkaline phosphates and therefore improved the soil physicochemical properties.

Table 4. *Enzyme activity indexes of soil main enzymes under different treatments*

Treatment	Catalase (mg/g)	Urease (mg/g)	Alkaline phosphatase (mg/g)	Sucrase (mg/g)
CK	3.13±0.04 a	0.39±0.05b	52.96±3.52ab	0.40±0.10a
NELM	2.96±0.09ab	0.27±0.03b	41.86±1.71b	0.26±0.04a
WELM	3.13±0.09a	0.58±0.06a	69.66±9.44a	0.35±0.08a
NEHM	2.77±0.13b	0.17±0.05c	40.13±4.09b	0.22±0.04a
WEHM	3.02±0.08ab	0.46±0.05ab	51.72±5.1ab	0.23±0.04a

The capital letters CK refer to no heavy metal polluted soil without ECM fungi; WELM refers to low heavy metals contaminated soil inoculated with ECM fungi, WEHM refers to high heavy metals contaminated soil inoculated with ECM fungi, NELM refers to low heavy metals contaminated soil inoculated without ECM fungi, NEHM refers to high heavy metals contaminated soil inoculated without ECM fungi; means followed with same letters within column are not significantly different by Tukey's test multiple comparison at $p < 0.05$, mean ± standard error of three measurements

Table 5. *The correlations between the soil physicochemical properties and the soil nutrient elements contents in masson's pine seedings*

	Soil pH	Bulk density	Moisture content	Available nitrogen	Available phosphorus	Available potassium
Se	-0.370	-0.201	0.412	0.041	-0.495	0.013
Fe	-0.024	0.143	-0.152	0.040	0.428	-0.414
N	-0.929*	-0.563	0.807	0.773	0.408	0.331
P	-0.856	-0.282	0.479	0.690	0.683	0.054
K	0.457	0.776	-0.817	-0.728	-0.311	-0.854
Catalase	-0.750	-0.182	0.406	0.409	-0.013	0.285
Urease	-0.927*	-0.518	0.747	0.764	0.335	0.431
Alkaline phosphatase	-0.838	-0.570	0.804	0.676	0.119	0.424
Sucrase	0.379	0.854	-0.785	-0.944*	-0.912*	-0.813

*Significantly different by Tukey's test multiple comparison at $p < 0.05$, mean ± standard error of three measurements

http://www.aloki.hu ● ISSN 1589 1623 (Print) ● ISSN 1785 0037 (Online)
DOI: http://dx.doi.org/10.15666/aeer/1802_37413755

Discussion

Tolerance and adaptability of ECM fungi on masson's pine seedlings in mining area

Soil bioremediation based on plant-microorganism symbiotic system has become a hot topic of researches (Kurzawova et al., 2012; Becerra-Castro et al., 2012). Many studies have shown that herbaceous plants have a strong ability to absorb and accumulate heavy metals (Leguizamo et al., 2017; Xue et al., 2014). In recent years, researchers have also tried to use woody plants with larger amount of biomass for forest restoration (Shi et al., 2011). For example, Shukla et al. (2011) chose five species of woody plant for the phytoremediation of heavy metals of sludge dumps in India, and the results showed that all the five plants had high bioconcentration factor for different metals and the remove rate of heavy metals were from 14.05 to 70.22% (Shukla et al., 2011). It is worth noting that many plant species largely rely on mycorrhizal fungi, which enhance nutrient uptake and protect against environmental stresses (Krznaric et al., 2009a), especially in the heavy metal contaminated stress (Adriaensen et al., 2006; Krznaric et al., 2009b).

In our research, the growth parameters, height, lateral branches and the ground diameter of the masson's pine inoculated with ECM fungi were significantly higher than those of the control and the masson's pine inoculated without ECM fungi during the experimental study in the mining area (*Fig. 1*). Moreover, masson's pine inoculated with ECM fungi could enhance the accumulation of heavy metals (*Table 2*), and the absorbed metals such as Pb, Zn, Cd, Cu, Mn elements were immobilized in roots system, which reduced the transportation of heavy metals to the aboveground part and alleviated the toxicity of heavy metals to the plant (*Table 3*). Our result was consistent with Reddy et al. (2016) that growth performance of plants was improved significantly inoculated with ectomycorrhizal fungi (*Pisolithus albus*) in the stress of Cu and Cd, which proved that ectomycorrhizal fungi could help plants to adapt to the heavy metal stress environment (Reddy et al., 2016). Similar results were also reported by other ectomycorrhizal fungi studies where heavy metals transfer to the host plants was significantly reduced (Krznaric et al., 2009b; Colpaert et al., 2005). Mycorrhizal fungi contribute not only to the uptake and detoxification of various environmental pollutants including heavy metals, but also to plant nutrition (Perotto and Martino, 2001). The result was consistent with our results that ECM fungi inoculation could promote the plant absorption and accumulation of essential elements Fe, N, P, K, and Se in the aboveground and underground parts of masson's pine under heavy metals stress in soil. The Se element could enhance the activity of plant antioxidant enzymes and the resistance of heavy metals stress.

Effects of ECM fungi on nutrient elements and soil enzyme in heavy metals contaminated soils

Soil enzyme is the most important catalyst of all biochemical reactions in soil biological activity (Nannipieri et al., 2018), and it is the most active bioactive substance in the degradation, transformation, and mineralization of soil organic matter (SOM) thereby maintaining energy flow and change the composition and structure of nutrient elements in soil, which was of great significance to plant growth (Sinsabaugh, 2010), and further alleviate the stress of the environment to the plants (Angelovičová et al., 2015).

In our study, the ECM fungi could activate the soil urease and the phosphatase, and increased the available nitrogen and the phosphorus contents in the soil for the plants to

http://www.aloki.hu ● ISSN 1589 1623 (Print) ● ISSN 1785 0037 (Online)
DOI: http://dx.doi.org/10.15666/aeer/1802_37413755

uptake it. Furthermore, the enzyme activities had significant negative correlation with soil pH, and positively correlated with available N, P, and K contents in soil, while the soil pH had significantly negative correlation with the N, P contents in plants, so that there was a significantly positive correlation between N, P contents in masson's pine plants and urease and alkaline phosphates in soil. ECM fungi could form mutual symbiotic system with majorities of plants' roots (Burke et al., 2011), and play a vital role in enzyme activities which correlated with nutrient absorption such as nitrogen and/or phosphorus (Eichlerová et al., 2015). Previously studies shown that ECM fungi could expand the absorption area of plant roots through hyphae, and then increase the nutrient uptake in plant rhizosphere, especially in soil available P (Cairney, 2011; Köhler et al., 2018). According to Taniguchi et al. (2008), the inoculation of ECM fungi significantly increased the growth of plants, which significantly related to the content of phosphorus, the ratio of nitrogen to phosphorus and plant rhizosphere soil phosphatase (Taniguchi et al., 2008).

Conclusions

In this study, we investigated the effects of masson's pine inoculated with ECM fungi (*Suillus luteus*) on soil physicochemical properties by evaluating the soil bulk density, water content, soil available nutrients and soil pH. The heavy metals accumulation and translocation in multi-metals of mining areas was also analyzed. The results showed that the masson's pine inoculated with ECM fungi growing in the heavy metals contaminated soils increased the growth of masson's pine in ground base diameter, annual branch length and crown width. Soil enzymatic activities were significantly improved in the mutualistic symbiosis systems of *Suillus-Pine*, especially the activities of urease and alkaline phosphatase, indicating the potential to obtain more nutrient elements. An immobilization of Pb, Zn, Cd, Cu, Mn was observed in the roots of plant inoculated with S*uillus luteus*, and correspondingly decreased the translocation of heavy metals in the plants' roots may due to the detoxification. Two enzymes decreased the soil pH and increased the soil available of N, P, K contents, enhancing the growth of masson's pine. Our results provided the information to understand the adaptation and bioremediation of plants mycorrhizal to detoxify the heavy metals from the environment, and provided a theoretical basis in allocation and transformation of heavy metals in the case of multi-metals contaminated soil in mining area.

Considered that, future research should pay more attention to the difference of rhizosphere microbial community diversity in different contaminated sites and its influence on the restoration effect of heavy metals.

Acknowledgements. This work supported by The Key R&D Project of Science and Technology Granted by Hunan Government (2019Sk2191), Scientific Innovation Fund for Post-graduates of Central South University of Forestry and Technology (20183038) and Changsha Municipal Government (kq1801080). And we helpful comments by the following graduate students for their assistance in laboratory chemical analysis: Xiao Zhou, Xuechun Feng and Qinyi Wang.

REFERENCES

[1] Adriaensen, K., Vangronsveld, J., Colpaert, J. V. (2006): Zinc tolerant *Suillus bovinus* improves growth of Zn-exposed *Pinus sylvestris* seedlings. – Mycorrhiza 16: 553-558.

http://www.aloki.hu ● ISSN 1589 1623 (Print) ● ISSN 1785 0037 (Online)
DOI: http://dx.doi.org/10.15666/aeer/1802_37413755

[2] Angelovičová, L., Bobuľská, L., Fazekašová, D. (2015): Toxicity of heavy metals to soil biological and chemical properties in conditions of environmentally polluted area middle Spiš (Slovakia). – Carpathian Journal of Earth and Environmental Sciences 10(1): 193-201.
[3] Ayangbenro, A., Babalola, O. (2017): A new strategy for heavy metal polluted environments: a review of microbial biosorbents. – International Journal of Environmental Research and Public Health 14(1): 94.
[4] Bao, S. (2000): The Soil Agricultural Chemistry Analysis. – Chinese Agriculture Press, Beijing (in Chinese).
[5] Becerra-Castro, C., Monterroso, C., Prieto-Fernández, A., Rodríguez-Lamas, L., Loureiro-Viñas, M., Acea, M. J., Kidd, P. S. (2012): Pseudometallophytes colonising Pb/Zn mine tailings: a description of the plant–microorganism–rhizosphere soil system and isolation of metal-tolerant bacteria. – Journal of Hazardous materials 217: 350-359.
[6] Burke, D. J., Weintraub, M. N., Hewins, C. R., Kalisz, S. (2011): Relationship between soil enzyme activities, nutrient cycling and soil fungal communities in a northern hardwood forest. – Soil Biology and Biochemistry 43(4): 795-803.
[7] Cairney, J. W. (2011): Ectomycorrhizal fungi: the symbiotic route to the root for phosphorus in forest soils. – Plant and Soil 344(1-2): 51-71.
[8] Colpaert, J. V. (2008): Heavy Metal Pollution and Genetic Adaptations in Ectomycorrhizal Fungi. – In: Avery, S. V., Stratford, M., Van West, P. (eds.) Stress in Yeasts and Filamentous Fungi. British Mycological Society Symposia Series, Vol. 27. Academic, Amsterdam, pp. 157-174.
[9] Colpaert, J. V., Adriaensen, K., Muller, L. A. H., Lambaerts, M., Faes, C., Carleer, R., Vangronsveld, J. (2005): Element profiles and growth in Zn-sensitive and Zn-resistant Suilloid fungi. – Mycorrhiza 15: 628-634.
[10] Eichlerová, I., Homolka, L., Žifčáková, L., Lisá, L., Dobiášová, P., Baldrian, P. (2015): Enzymatic systems involved in decomposition reflects the ecology and taxonomy of saprotrophic fungi. – Fungal Ecol. 13: 10-22.
[11] Guan, S., Zhang, D., Zhang, Z. (1986): Soil Enzyme and Its Research Methods. – Agricultural, Beijing (in Chinese).
[12] Guo, J., Lv, X., Jia, H., Hua, L., Ren, X., Muhammad, H., Ding, Y. (2020): Effects of EDTA and plant growth-promoting rhizobacteria on plant growth and heavy metal uptake of hyperaccumulator Sedum alfredii Hance. – Journal of Environmental Sciences 88: 361-369.
[13] Huai, W., Guo, L., He, W. (2003): Genetic diversity of an ectomycorrhizal fungus *Tricholoma terreum* in a *Larix principis-rupprechtii* stand assessed using random amplified polymorphic DNA. – Mycorrhiza 13(5): 265-270.
[14] Huang, J., Nara, K., Lian, C., Zong, K., Peng, K., Xue, S., Shen, Z. (2012): Ectomycorrhizal fungal communities associated with Masson pine (*Pinus massoniana* Lamb.) in Pb-Zn mine sites of central south China. – Mycorrhiza 22: 589-602.
[15] Jentschke, G., Godbold, D. L. (2000): Metal toxicity and ectomycorrhizas. – Physiol Plant 109: 107-116.
[16] Köhler, J., Yang, N., Pena, R., Raghavan, V., Polle, A., Meier, I. C. (2018): Ectomycorrhizal fungal diversity increases phosphorus uptake efficiency of European beech. – New Phytologist 220(4): 1200-1210.
[17] Krznaric, E., Verbruggen, N., Wevers, J. H. L., Carleer, R., Vangronsveld, J., Colpaert, J. V. (2009a): Cd-tolerant *Suillus luteus*: a fungal insurance for pines exposed to Cd. – Environ Pollut 157: 1581-1588.
[18] Krznaric, E., Wevers, J. H. L., Cloquet, C., Vangronsveld, J., Vanhaecke, F., Colpaert, J. V. (2009b): Zn pollution counteracts Cd toxicity in metal-tolerant ectomycorrhizal fungi and their host plant, *Pinus sylvestris.* – Environ Microbiol 12: 2133-2141.

http://www.aloki.hu ● ISSN 1589 1623 (Print) ● ISSN 1785 0037 (Online)
DOI: http://dx.doi.org/10.15666/aeer/1802_37413755

[19] Kurzawova, V., Stursa, P., Uhlik, O., Norkova, K., Strohalm, M., Lipov, J., Mackova, M. (2012): Plant–microorganism interactions in bioremediation of polychlorinated biphenyl-contaminated soil. – New Biotechnology 30(1): 15-22.
[20] Lalancette, S., Lerat, S., Roy, S., Beaulieu, C. (2019): Fungal endophytes of *Alnus incana* ssp. rugosa and *Alnus alnobetula* ssp. crispa and their potential to tolerate heavy metals and to promote plant growth. – Mycobiology 1-15.
[21] Leguizamo, M. A. O., Gómez, W. D. F., Sarmiento, M. C. G. (2017): Native herbaceous plant species with potential use in phytoremediation of heavy metals, spotlight on wetlands-a review. – Chemosphere 168: 1230-1247.
[22] Li, K., Yang, B., Wang, H., Xu, X., Gao, Y., Zhu, Y. (2019): Dual effects of biochar and hyperaccumulator Solanum nigrum L. on the remediation of Cd-contaminated soil. – Peer J. 7: e6631.
[23] Luo, Z., Wu, C., Zhang, C., Li, H., Lipka, U., Polle, A. (2014): The role of ectomycorrhizas in heavy metal stress tolerance of host plants. – Environ. Exp. Bot. 108: 47-62.
[24] Ma, Y., Rajkumar, M., Oliveira, R. S., Zhang, C., Freitas, H. (2019): Potential of plant beneficial bacteria and arbuscular mycorrhizal fungi in phytoremediation of metal-contaminated saline soils. – Journal of Hazardous Materials 379: 120813.
[25] Nannipieri, P., Trasar-Cepeda, C., Dick, R. P. (2018): Soil enzyme activity: a brief history and biochemistry as a basis for appropriate interpretations and meta-analysis. – Biology and Fertility of Soils 54(1): 11-19.
[26] Perotto, S., Martino, E. (2001): Molecular and cellular mechanisms of heavy metal tolerance in mycorrhizal fungi: what perspectives for bioremediation? – Minerva Biotecnol. 13: 55-63.
[27] Reddy, M. S., Kour, M., Aggarwal, S., Ahuja, S., Marmeisse, R., Fraissinet-Tachet, L. (2016): Metal induction of a P isolithus albus metallothionein and its potential involvement in heavy metal tolerance during mycorrhizal symbiosis. – Environmental Microbiology 18(8): 2446-2454.
[28] Sheoran, V., Sheoran, A., Poonia, P. (2011): Role of hyperaccumulators in phytoextraction of metals from contaminated mining sites: a review. – Crit. Rev. Environ. Sci. Technol. 41: 168-214.
[29] Shi, X., Zhang, X., Chen, G., Chen, Y., Wang, L., Shan, X. (2011): Seedling growth and metal accumulation of selected woody species in copper and lead/zinc mine tailings. – Journal of Environmental Sciences 23(2): 266-274.
[30] Shukla, O. P., Juwarkar, A. A., Singh, S. K., Khan, S., Rai, U. N. (2011): Growth responses and metal accumulation capabilities of woody plants during the phytoremediation of tannery sludge. – Waste Management 31(1): 115-123.
[31] Sinsabaugh, R. L. (2010): Phenol oxidase, peroxidase and organic matter dynamics of soil. – Soil Biol Biochem 42: 391-404.
[32] Sousa, N. R., Ramos, M. A., Marques, A. P., Castro, P. M. (2012): The effect of ectomycorrhizal fungi forming symbiosis with Pinus pinaster seedlings exposed to cadmium. – Science of the Total Environment 414: 63-67.
[33] Sozoniuk, M., Nowak, M., Dudziak, K., Bulak, P., Leśniowska-Nowak, J., Kowalczyk, K. (2019): Antioxidative system response of pedunculate oak (*Quercus robur* L.) seedlings to Cd exposure. – Physiology and Molecular Biology of Plants 25(6): 1377-1384.
[34] Sun, F., Wen, D., Kuang, Y., Li, J., Zuo, W. (2010): Concentrations of heavy metals and polycyclic aromatic hydrocarbons in needles of Masson pine (*Pinus massoniana* L.) growing nearby different industrial sources. – J. Environ. Sci. 22: 1006-1013.
[35] Tam, P. C. (1995): Heavy metal tolerance by ectomycorrhizal fungi and metal amelioration by *Pisolithus tinctorius*. – Mycorrhiza 5(3): 181-187.
[36] Taniguchi, T., Kataoka, R., Futai, K. (2008): Plant growth and nutrition in pine (*Pinus thunbergii*) seedlings and dehydrogenase and phosphatase activity of ectomycorrhizal

http://www.aloki.hu ● ISSN 1589 1623 (Print) ● ISSN 1785 0037 (Online)
DOI: http://dx.doi.org/10.15666/aeer/1802_37413755

root tips inoculated with seven individual ectomycorrhizal fungal species at high and low nitrogen conditions. – Soil Biology and Biochemistry 40(5): 1235-1243.

[37] Wang, Z., Qin, H., Wang, J. (2019): Needle pigment responses of *Pinus massoniana* L. to soils polluted with the heavy metals Zn, Pb and Cu. – Geochemistry: Exploration, Environment, Analysis 19(1): 1-5.

[38] Wuana, R. A., Okieimen, F. E. (2011): Heavy metals in contaminated soils: a review of sources, chemistry, risks and best available strategies for remediation. – ISRN Ecol. 2011: 1-20.

[39] Xue, L., Liu, J., Shi, S., Wei, Y., Chang, E., Gao, M., Jiang, Z. (2014): Uptake of heavy metals by native herbaceous plants in an antimony mine (Hunan, China). – CLEAN–Soil, Air, Water 42(1): 81-87.

[40] Yin, D., Deng, X., Chet, I., Song, R. (2014): Physiological responses of *Pinus sylvestris* var. mongolica seedlings to the interaction between *Suillus luteus* and *Trichoderma virens*. – Current Microbiology 69(3): 334-342.

[41] Yu, P., Sun, Y., Huang, Z., Zhu, F., Sun, Y., Jiang, L. (2020): The effects of ectomycorrhizal fungi on heavy metals' transport in *Pinus massoniana* and bacteria community in rhizosphere soil in mine tailing area. – Journal of Hazardous Materials 381: 121203.

[42] Zhang, T., Wen, X., Ding, G. (2017): Ectomycorrhizal symbiosis enhances tolerance to low phosphorous through expression of phosphate transporter genes in masson pine (*Pinus massoniana*). – Acta Physiol. Plant 39: 101.

[43] Zhang, X., Li, M., Yang, H., Li, X., Cui, Z. (2018): Physiological responses of Suaeda glauca and Arabidopsis thaliana in phytoremediation of heavy metals. – Journal of Environmental Management 223: 132-139.

[44] Zhang, Y., Ji, H. (2019): Physiological responses and accumulation characteristics of turfgrasses exposed to potentially toxic elements. – Journal of Environmental Management 246: 796-807.

[45] Zhao, X., Liu, J., Xia, X., Chu, J., Wei, Y., Shi, S., Chang, E., Yin, W., Jiang, Z. (2013): The evaluation of heavy metal accumulation and application of a comprehensive bio-concentration index for woody species on contaminated sites in Hunan, China. – Environ. Sci. Pollut. Res. 21: 5076-5085.

http://www.aloki.hu ● ISSN 1589 1623 (Print) ● ISSN 1785 0037 (Online)
DOI: http://dx.doi.org/10.15666/aeer/1802_37413755

EFFECT OF CADMIUM STRESS ON THE POLYPHENOL CONTENT, MORPHOLOGICAL, PHYSIOLOGICAL, AND ANATOMICAL PARAMETERS OF COMMON BEAN (*PHASEOLUS VULGARIS* L.)

BENHABILES AIT EL HOCINE, K.[1,2*] – BELLOUT, Y.[1] – AMGHAR, F.[1,2]

[1]*Department of Biology, Faculty of Sciences, University Mhamad Bougara, Boumerdes, Algeria*

[2]*Laboratory of Biodiversity, Biotechnology, Environment and Sustainable Development, University Mhamad Bougara, Boumerdes, Algeria*

**Corresponding author*
e-mail: k.benhabiles@univ-boumerdes.dz; phone: +213-671-172-603; fax: +213-24-799-012

(Received 9th Dec 2019; accepted 24th Mar 2020)

Abstract. Cadmium (Cd) is one of the most notable heavy metals because of its high mobility and toxicity towards plants. In the present study, we aimed to evaluate the effect of cadmium on growth, physiological parameters, anatomical changes and phenolic compounds content in *Phaseolus vulgaris* L plant. Seedlings were exposed to cadmium at 0.25; 0.5 and 1 $g.l^{-1}$ for 21 days. Results indicated that cadmium significantly decreased percent seed germination, embryonic radical elongation, plant dry weight, stem/root length and numbers of leaves and lateral roots. Cadmium also induced a decrease in chlorophyll and protein content with all treatments; however, sugar and proline increased significantly with 1 $g.l^{-1}$. Total phenolic content increased by around 43% and 32% in the above ground part and roots respectively. Flavonoids, flavonols, hydrolysable tannins and condensed tannins showed a significant increase with higher cadmium concentration. Cadmium also changed plant root and stem anatomy; a decrease in both number and size of xylem vessels and a delay in xylem differentiation were observed.
Keywords: *cadmium, Phaseolus vulgaris L., growth, histological changes, phenolic compounds*

Introduction

Modern agro-ecosystems have continually received ever-increasing cadmium (Cd) pollution from several domestic and industrial activities, as well the agricultural application of phosphate fertilizers, sewage sludge and irrigation water contaminated with this element; leading to soil Cd contamination and increased Cd uptake by plants grown in those mediums (McLaughlin et al., 2006; Escudey et al., 2007). Cadmium can be found in soils, reaching levels of approximately 1 $mg.kg^{-1}$ for most of surface soils (Kabata-Pendias, 2000). It is relatively easily available for plant uptake because it is predominantly found in soil solution or bound to solid phase systems (Verbruggen et al., 2009).

In plants, exposure to cadmium induces phytotoxicity symptoms, such as biomass reduction, inhibition of root elongation (Gratao et al., 2009) and causes a reduction of several physiological processes including photosynthesis, respiration and transpiration (Seregin and Ivanov, 2001; He et al., 2017; Yazdi et al., 2019), seed germination (Chugh et al., 1995; Fattahi et al., 2019) and interferes with uptake, transport, and distribution of essential and non-essential mineral elements, especially in the form of Cd^{2+}(He et al., 2017). Cd toxicity triggers the over-accumulation of reactive oxygen

http://www.aloki.hu ● ISSN 1589 1623 (Print) ● ISSN 1785 0037 (Online)
DOI: http://dx.doi.org/10.15666/aeer/1802_37573774

species, ultimately resulting in oxidative stress in plants (Cuypers et al., 2011; Anjum et al., 2015; Gupta et al., 2017)

Antioxidant molecules produced by plants as a response to Cd uptake, are considered a defense mechanism to metal stress. In this context, many studies have shown the radical scavenging properties of phenols, mainly by yielding electrons (Michalak, 2010; Cruces et al., 2015; Manquián-Cerda et al., 2016). Plants exposed to heavy metal stress have been observed to exude high levels of phenolic compounds (Posmyk et al., 2009; Mongkhonsin et al., 2016; Manquián-Cerda et al., 2018).

The harmful effects of Cd in soils include also anatomical changes such as variation in root tissues organization, development of apoplastic barriers (Vaculík et al., 2012), structural changes in plant's vascular system (Barcelo et al., 1988).

Common bean (*Phaseolus vulgaris* L.) is one of the most important grain legumes worldwide; it is a valuable food source for humans around the world and accounts for higher consumption and economic importance. This crop is potentially exposed to Cd due to a component of fungicide and fertilizer formulations and amendment that is commonly used in agriculture throughout the word.

The purpose of this study was to evaluate Cd effect on: (i) morphological and physiological parameters, (ii) polyphenol accumulation in seedlings, (iii) root and stem structure in order to obtain detailed picture of Cd-induced structural disorders in vessels. It should help to explain responses of common bean to Cd stress.

Materials and methods

Plant material, treatments and growth conditions

Study was done in Algeria northern Africa under laboratory conditions. Common bean (*Phaseolus vugaris* L.) Djadida genotype commonly cultivated there was used. Seeds were selected, surface-disinfected using 0.1% sodium hypochlorite (NaClO) for 10 min, rinsed and soaked in distilled water at room temperature for 12 h. Seeds were then germinated in sealed plastic dishes with moistened filter paper at 25 °C in dark for 3 days. Uniform seedlings were selected and transplanted to pots containing mould with 16 h light and 8 h dark cycle at average day/night temperature of 25 °C/20 °C and average relative humidity of 75%, watered as needed according to field capacity calculated in gram of water per gram of soil and afterwards, till the end of the experiment for 21 days. The following treatments were considered: (1) 0.25 $g.l^{-1}$ of Cd, (2) 0.5 $g.l^{-1}$ of Cd, (3) 1 $g.l^{-1}$ of Cd. The Cd concentration was supplied us $CdCl_2$ water solution. For control experiment, Cd was omitted.

Seed germination and root elongation test

This test serves to verify the effect of cadmium on seeds germination. After selection and disinfection, seeds were placed in boxes containing filter paper moistened with cadmium solution at different concentrations 0.25 $g.l^{-1}$, 0.5 $g.l^{-1}$, 1 $g.l^{-1}$ and control moistened with distilled water. In each box 50 seeds were putted at 25 °C temperature in dark, with three repetitions for each concentration. Seeds were watered as needed by distilled water during 7 days.

To calculate the germination rate, we counted seeds sprouted per box every day until the seventh day, knowing that germination is positive when its radical reaches 5 mm in

http://www.aloki.hu ● ISSN 1589 1623 (Print) ● ISSN 1785 0037 (Online)
DOI: http://dx.doi.org/10.15666/aeer/1802_37573774

length. After the seventh day of seed germination, radical's length of germinated seeds was measured on cm.

To obtain percentage of germination, we used the formula:

$$G(\%) = (\text{number of germinated seeds / total number of seeds}) \times 100$$

Morphological parameters

The different studied parameters are: Stem height and root length measured in cm; number of leaves and lateral roots. After sampling, roots were separated from above-ground part of plants and dried at 80 °C temperature for 48 h and weighed until we obtained a fixed weight in order to have the dry matter yield per pot.

Determination of tolerance index

Tolerance index (TI) was calculated as a ratio of the mean dry weight of plants grown in presence of Cd and mean dry weight of control plants. TI values lower than 1 suggests that plants are stressed due to metal pollution. Whereas, TI values equal to 1 indicate no difference relative to control treatments. Also, TI values higher than 1 indicate that plant is a hyper accumulator (Audet and Charest, 2007).

Biochemical and physiological parameters

Photosynthetic pigments determination

For photosynthetic pigments (chlorophyll *a* and *b*, carotenoids) analysis, fully developed trifoliate leaves were extracted with 80% acetone. Pigments contents were determined spectrophotometrically (spectrophotometer Shimadzu UV 1800) at following wavelengths: 663, 646 and 470 nm and calculated according to Lichtenthaler and Wellburn (1983).

Total soluble sugars

Leaves were used for soluble sugar determination; extraction was done with 80% (v/v) ethanol. Sugar content of resulting solution was determined following to Dische (1962) using anthrone reagent. Absorbance was measured at 620 nm. Standards of glucose were prepared and analyzed in the same way to obtain a calibration curve. Soluble sugars content was calculated as mg glucose equivalent g^{-1} FW.

Total protein content

The protein content in leaf tissue was determined according to Bradford (1976), Fresh leaves were homogenized and extracted with 5 mM buffer Tris-HCl, pH 7.2, 0.25 M sucrose and 1 mM $MgCl_2$. The extract was incubated with Bradford reagent in darkness. Absorbance was measured at 595 nm and the amount of proteins was expressed in equivalents of BSA bovin serum albumin (mg eq. BSA g^{-1} FW), used as standard.

Proline content

Proline content was determined following to Bates et al. (1973), using ninhydrin reagent. The absorbance was measured at 520 nm. Reference standards of proline were

http://www.aloki.hu ● ISSN 1589 1623 (Print) ● ISSN 1785 0037 (Online)
DOI: http://dx.doi.org/10.15666/aeer/1802_37573774

prepared and analyzed in the same way to obtain a calibration curve. Results were expressed on $\mu g.g^{-1}$ DW.

Estimation of phenolic compounds

Phenolic compounds were extracted from shoot and roots dried samples of *Phaseolus vulgaris* L. The amount of total phenolics in the extract was determined using Folin Ciocalteu reagent as described by Meyers et al. (2003). Absorbance was measured at 750 nm and the results expressed in equivalents of gallic acid (mg eq. GA g^{-1} DW), used as standard.

Colorimetric aluminum chloride method was used for flavonoids and flavonols determination, using optimized protocols established by Bahorun et al. (1996); Kumaranand Karunakaran (2007a, b), respectively. Absorbance was measured at 430 and 440 nm respectively, and the amount of flavonoids and flavonol were expressed in equivalents of Quercetin (mg eq. Q g^{-1} DW), used as standard.

Hydrolysable tannins content was determined as described by Mole and Waterman (1987) and was quantified according to standard curve prepared for tannic acid. Results were expressed in equivalent of tannic acid (mg eq. TA g^{-1} DW).

Condensed tannins contents were determined following the method described by Swain and Hillis (1959). The absorbance was measured at 500 nm. The amount of condensed tannins was expressed in equivalents of catéchin (mg eq. CAg^{-1} DW), used as standard.

Anatomical study

At day 21 from sowing, samples were taken for light microscopy study. Sections were performed on fresh plants. Cross sections were made on the main root (1 cm of the collar; area of lateral roots), and those of stem are represented between first and second internodes. Samples were cut with a vibratome in order to obtain 100-µm transverse sections; fresh sections were collected and stained with iodine green carmine as described in Locquin and Langeron (1978).

Specimens were analyzed using a light microscope (optika B-350, Italy) using ×100 and × 400 magnifications, light micrographs were acquired by a digital camera and the images were processed and archived with TS view software version 6.2.4.5, tucsen imagin technology.

Statistical analyses

All data presented are the mean values of tree replicates ± standard deviation (SD). Statistical analysis was carried out by student analysis at 5%, 1% and 0.1% significance level, using statistical software package STATISTICA version 8.0

Results

Effect of Cd on germination and root elongation

Smaller number of seeds germinated in comparison with control variant was identified when Cd was added. Percent seeds germination was affected by different cadmium concentrations, it was lowered by about 68% with 0.25 $g.l^{-1}$ of metal, 84% with 0.5 $g.l^{-1}$ and 98% with 1 $g.l^{-1}$ Cd concentration ($p < 0.05$*) in contrast to control (*Fig. 1A*).

http://www.aloki.hu ● ISSN 1589 1623 (Print) ● ISSN 1785 0037 (Online)
DOI: http://dx.doi.org/10.15666/aeer/1802_37573774

However, elongation of embryonic radical was impaired by about 70%, 87%, 91% (*Fig. 1B*) by 0.25; 0.5 g.l^{-1} and 1 g.l^{-1} Cd respectively ($p<0.01$**) compared to control.

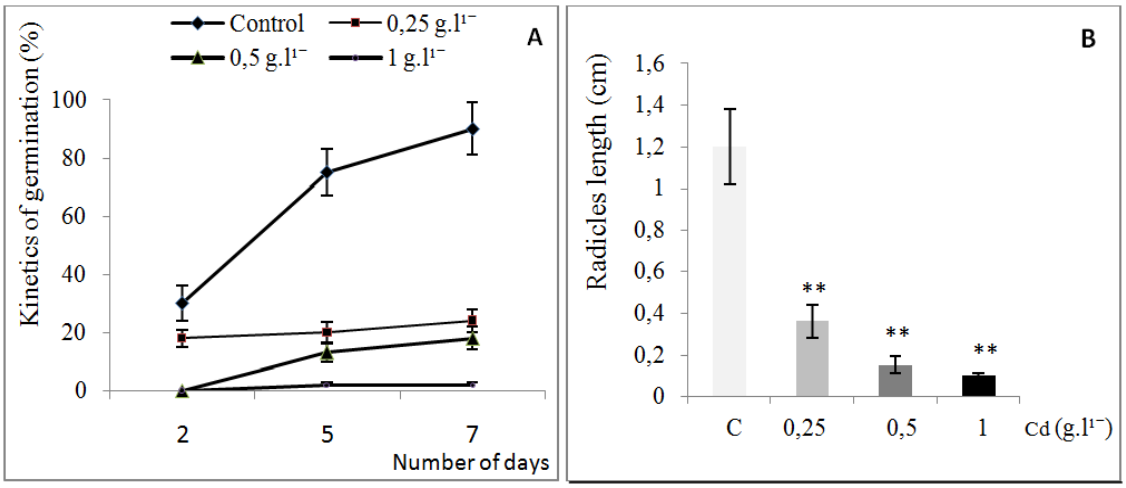

Figure 1. *Effects of cadmium (Cd) on (A) germination kinetics, (B) radicles length of common bean seeds (Phaseolus vulgaris L.). Results represent the mean ± SE (n = 3) (*p < 0.05, **p < 0.01, ***p < 0.001 according to Student test)*

Effect of Cd on plant growth

Morphological changes in *Phaseolus vulgaris* L. plants treated with concentrations of Cd showed leaf chlorosis, growth inhibition; stem weakening and dark brown root tips. We noted that 21-day-old, bean seedlings on polluted soil developed all aerial organs but shorter compared to control plants. Dark brown root tips and reduced growth are the most common physiological effects of heavy metal exposure in plants (Ovečka and Takáč, 2014). Stem and main root length is 68.58% and 71.43% shorter respectively in bean plants grown in 1 g.l^{-1} Cd concentration compared with those of controls (*Fig. 2A*); in this same concentration, bean plants had 50% fewer leaves and 20% fewer lateral roots per plant (*Fig. 2B*). The above ground part-roots dry weight and TI which represent relative plant growth were adversely affected by Cd concentrations; they decreased gradually with increase of Cd concentrations. This decrease was around 77.27% in above ground part length, and 47.97% in roots length comparing to their respective control under 1 g.l^{-1} Cd (*Fig. 2C*). According to results shown in *Table 1,* Tolerance Index of bean plants is less than 1 for all Cd concentrations in both part of plant, this confirmed a net decrease in biomass and suggests that *Phaseolus vulgaris* L. plants are stressed.

Treatment with 0.5 and 1 g.l^{-1} of Cd elicited significant decrease in all growth parameters as compared with control value ($P<0.05$ *), except for lateral roots number and roots dry weight; no changes were observed.

Table 1. *Value of tolerance index of bean plants according to Cd concentrations*

	Cadmium treatments		
TI	0.25 g.l^{-1} Cd	0.5 g.l^{-1} Cd	1 g.l^{-1} Cd
Above ground part	0.65	0.34	0.22
Roots	0.82	0.58	0.52

http://www.aloki.hu ● ISSN 1589 1623 (Print) ● ISSN 1785 0037 (Online)
DOI: http://dx.doi.org/10.15666/aeer/1802_37573774

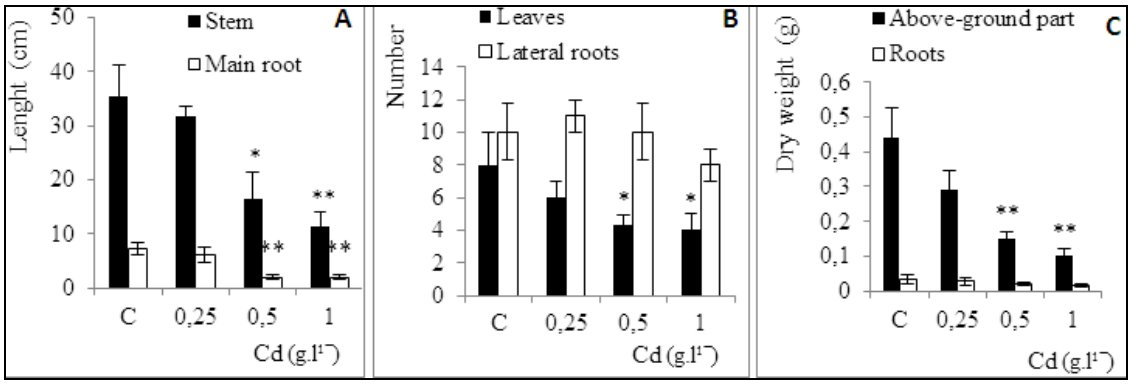

Figure 2. *Effects of cadmium (Cd) on (A) stem and main root length, (B) leaves and lateral roots number, and (C) dry weight of common bean seedling (Phaseolus vulgaris L.). Results represent mean ± SE (n = 3) (*p < 0.05, **p < 0.01, ***p < 0.001 according to Student test)*

Biochemical and physiological parameters

Cd treatment results in decline in chlorophyll content with increasing Cd concentrations. Chl *a* decreased significantly (P<0.01**) under all treatments till 56.87% compared to control. However, Chl *b* decrease was significant only under 1 g.l^{-1} Cd (p<0.05*) till 31.19% compared to control (*Fig. 3A*). When total carotenoids content showed a decrease reaching their lowest value under 1 g.l^{-1} Cd treatment (p<0.05*) in contrast to control (*Fig. 3B*).

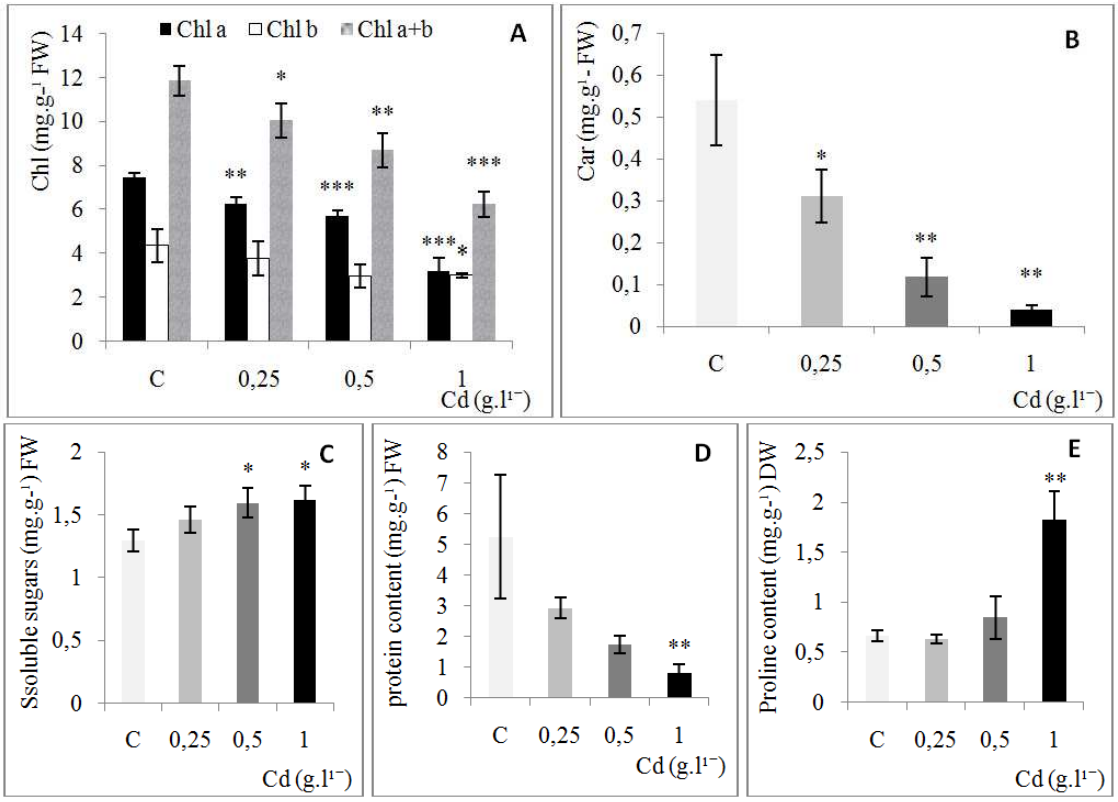

Figure 3. *Effects of cadmium (Cd) on biochemical parameters of common bean seedling (Phaseolus vulgaris L.). Results represent the mean ± SE (n = 3) (*p < 0.05, **p < 0.01, ***p < 0.001 according to Student test)*

http://www.aloki.hu ● ISSN 1589 1623 (Print) ● ISSN 1785 0037 (Online)
DOI: http://dx.doi.org/10.15666/aeer/1802_37573774

It is obvious from *Figure 3C* that total soluble sugars content, appeared to increase under Cd treatment; increase was significant under 0.5 and 1 $g.l^{-1}$ Cd ($p<0.05$*) as compared with control value, it reached 24.80%.

Bean plants exhibited a significant decrease in proteins content with 1 $g.l^{-1}$ Cd concentration ($p<0.01$**) reaching 84.67% compared to control (*Fig. 3D*) when proline appeared to increase progressively with increase of Cd concentrations till 63.80% with 1 $g.l^{-1}$ Cd concentration ($P<0.01$*) (*Fig. 3E*).

Changes in phenolic compounds

Phenolic content in *Phaseolus vulgaris* L. extract is shown in *Figure 4*. Increasing levels of Cd markedly increased synthesis of these metabolites in all treatments in both above ground part and roots ($p<0.05$*) in contrast to control, aside from roots hydrolysable tannins. The rates of increase were till 43, 63, 58, 106, 239% in above ground part, and till 32, 34, 65, 31 and 20% in roots for total phenolics, flavonoids, flavonols, hydrolysable tannins and condensed tannins respectively.

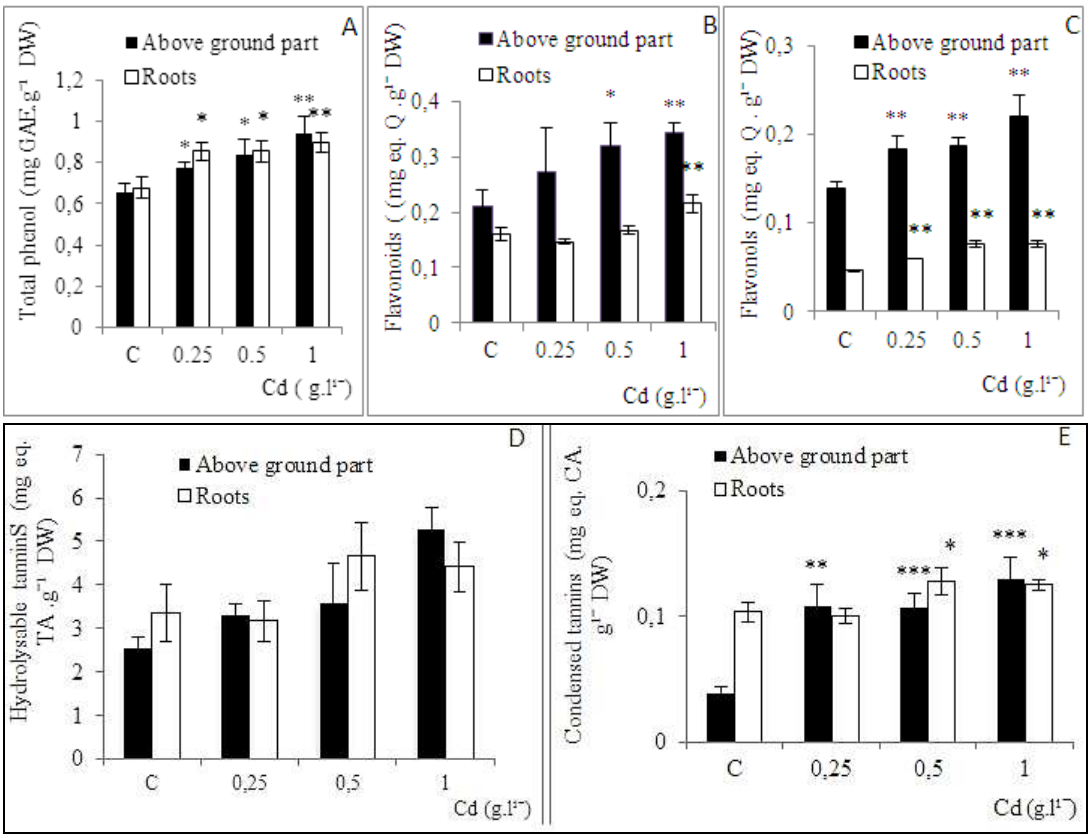

Figure 4. *Effects of cadmium (Cd) on phenolic compounds content of comman bean seedling (Phaseolus vulgaris L.). Results represent the mean ± SE (n = 3) (*p < 0.05, **p < 0.01, ***p < 0.001 according to Student test)*

Anatomical study

Our results showed that stem (*Fig. 5A, B, C, D*) and root (*Fig. 6A, B, C, D*) diameter sections were similar in control and all Cd treatment plant samples, with slight flattening of stem section. Cortex cells are similar in size in all samples; however, there

http://www.aloki.hu ● ISSN 1589 1623 (Print) ● ISSN 1785 0037 (Online)
DOI: http://dx.doi.org/10.15666/aeer/1802_37573774

was a slight enlargement of cortex zone in primary roots and stem that had been exposed to Cd. At high magnification (*Figs. 5E, F, G, H, 6E, F, G, H*), a decrease of both number and size of xylem vessels in root and stem sections was observed and xylem differentiation appears retarded in plants grown in presence of Cd. which probably led to a decrease in raw sap flow.

Development of plant led to progressive disappearance of cortical parenchyma resulting to medular lacunae formation in plants stem; our results showed that medular lacunae diameter decreased with increase of Cd concentration till its disappearance with 1 $g.l^{-1}$ Cd concentration (*Fig. 5*), which suggests a delay in development of bean plant. In addition, sections showed appearance of secondary tissues in control, in contrast these tissues were retarded in plants grown with Cd treatment with a high number of cambial cells (*Figs. 5E, F, G, H, 6E, F, G, H*).

In root, higher Cd concentrations can result in rhizodermis disintegration in some location of root, but lateral root initiation was observed in all samples (*Fig. 6A, B, C, D*).

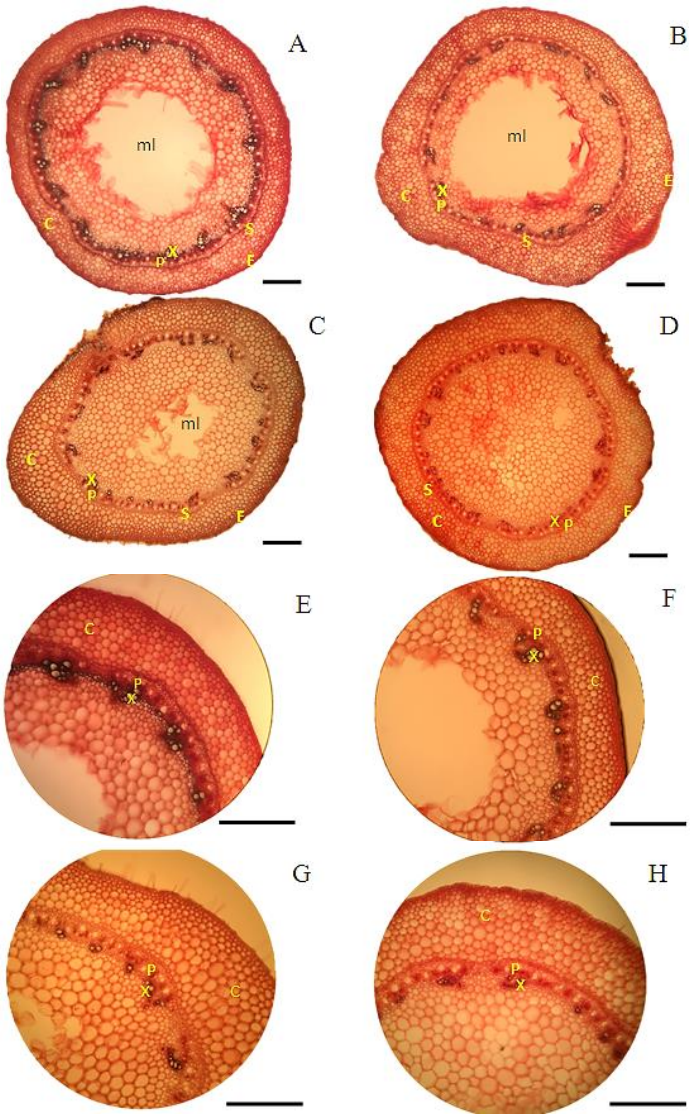

Figure 5. *Light micrographs of control (A, E) and Cd-treated plants: 0.25 $g.l^{-1}$ (B, F); 0.5 $g.l^{-1}$ (C, G); 1 $g.l^{-1}$ (D, H) showing transversal stem sections. C: cortex, X: xylem, P: phloem, S: sclerenchyma, E: epidermis, ml: medular lacunae; Scale bar, 500 µm*

http://www.aloki.hu ● ISSN 1589 1623 (Print) ● ISSN 1785 0037 (Online)
DOI: http://dx.doi.org/10.15666/aeer/1802_37573774

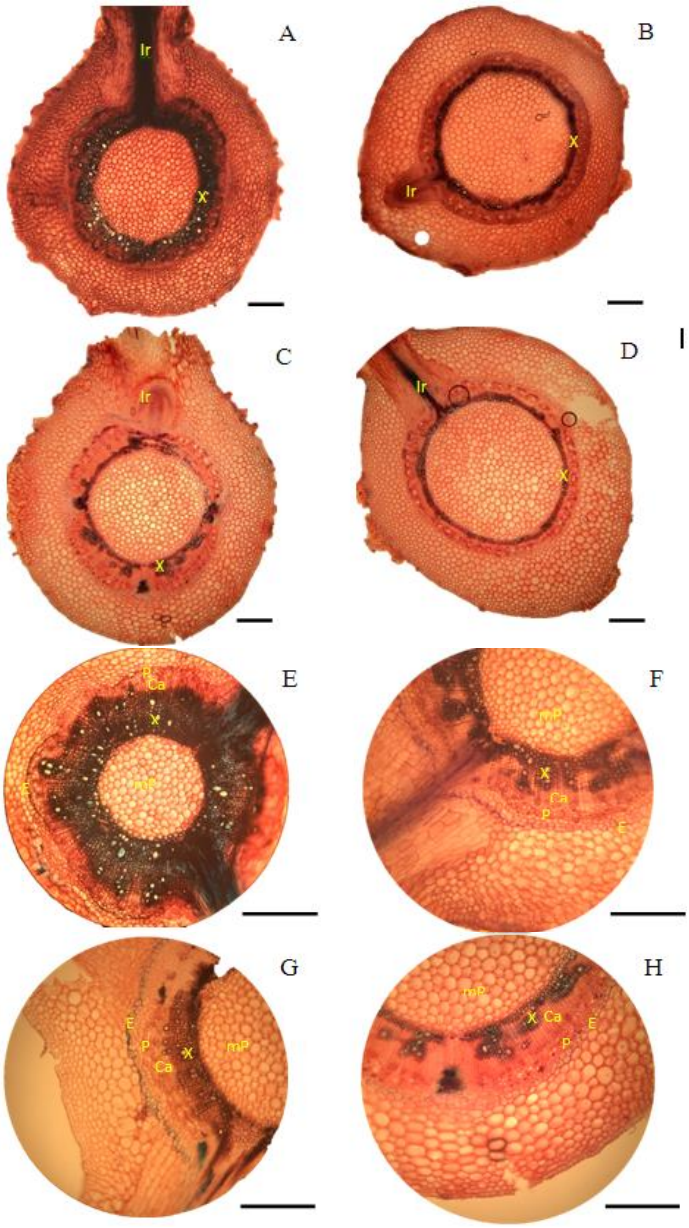

Figure 6. *Light micrographs of control (A, E) and Cd-treated plants: 0.25 g.l^{-1} (B, F); 0.5 g.l^{-1} (C, G); 1 g.l^{-1} (D, H) showing transversal root sections. C: cortex, X: xylem, P: phloem, E: endodermis, Ca: cambium; lr: lateral root; mP: medular parenchyma; Scale bar, 500 µm*

Discussion

Effect of Cd on germination and root elongation

Seed germination and root elongation tests are frequently used for assessing heavy metal phytotoxicity (Wang and Keturi, 1990; Munzuroglu and Geckil, 2002). Our results indicated significant inhibition of seed germination and root elongation under Cd stress which is in agreement with previous results of Li et al. (2005) on *Arabidopsis thaliana*. Hsu and Chang-Hung Chou (1992) reported that among heavy metals tested, Cd showed more toxicity to seed germination of *Miscanthus*, Fattahi et al. (2019) also

http://www.aloki.hu ● ISSN 1589 1623 (Print) ● ISSN 1785 0037 (Online)
DOI: http://dx.doi.org/10.15666/aeer/1802_37573774

indicated that the increase in Cd concentrations led to an increase in germination time and a reduction in germination percentage.

According to Kranner and Colville (2011), Cd hamper water uptake inhibiting seed germination, and prolonged their dormancy under room temperature, Munzuroğlu et al. (2008) demonstrate that the inhibition of germination was related with abscisic acid accumulation in seeds. In addition, starch is the most abundant stored material in seeds used in germination after being degraded by enzymes such as amylase; so, inhibition of specific enzymatic reactions by heavy metals causes a negative effect on germination (Ko et al., 2012).

Effect of Cd on plant growth

Plant growth is one of the best indicators to evaluate plant response to environmental stress. Cadmium stress is a major environmental factor which induces various phytotoxicity symptoms such as stunted growth, root browning, chlorosis, necrosis and cell apoptosis (Chang et al., 2013; Zemanová et al., 2015; Younis et al., 2018a).

Our experimental data revealed that cadmium stress inhibited the growth of bean plants; similar behavior was reported by Yazdi et al. (2019), who found that seedlings of lettuce treated with low doses of Cd (100, 200, and 300 $\mu g.g^{-1}$ perlite) had phytotoxic effects. In addition, Younis et al. (2018a) reported that (*Phaseolus vulgaris*) treated with (10^{-6}, 10^{-3}M Cd) showed a significant decrease in growth parameters. The same result was observed in research conducted on three Miscanthus species (Guo et al., 2016). Growth inhibition could be attributed to inhibiting photosynthesis, respiration, water and nutrient uptake by Cd (Dias et al., 2013; Xue et al., 2013). The production of various forms of reactive oxygen species under inductive oxidative stress due to heavy metals presence, results in retardation of plant growth that could eventually led to plant death (Loi et al., 2018). It has been proposed that inhibition of root and shoot growth in presence of heavy metals may be mainly due to abnormal cell division as well as interference of heavy metals with cofactors that play a vital role in photosynthesis, respiration and protein synthesis in root and shoot of plants (Volland et al., 2014).

Biochemical and physiological parameters

Cadmium treatments cause a decrease in pigmentation of common bean shoots wich is in accordance with results of Molnarova et al. (2012) on *Sinapis alba* shoots., Younis et al. (2018a) on *P. vulgaris* L., Yazdi et al. (2019) on *Lactuca sativa* Linn. and Chen et al. (2019) on *Kandelia obovata*.

Decrease in chlorophyll content is attributed to inhibition of chlorophyll synthesis either by affecting key enzymes synthesis such as d-aminolevulinic acid dehydratase (ALA-dehydratase) and proto-chlorophyllide reductase (Stobart et al., 1985; Van Assche and Clijsters,1990), or indirectly by induction of Fe deficiency by inhibiting Fe(III) reductase and seriously affecting photosynthesis (Alkantara et al., 1994; Lang et al.,1995; He et al., 2017). Cd is also known to enhance chlorophyll enzymatic degradation (Somashekaraiah et al., 1992).

Sugars are involved in many mechanisms of biotic or abiotic stress response, their action in abiotic stress is very wide, they can act as an osmoprotectants by stabilising cellular membranes and maintaining turgor (Peshev and Ende, 2013) or as antioxidant molecules (Keunen et al., 2013).

http://www.aloki.hu ● ISSN 1589 1623 (Print) ● ISSN 1785 0037 (Online)
DOI: http://dx.doi.org/10.15666/aeer/1802_37573774

Our results indicate that Cd treatment led to an increase in total soluble sugars content in common bean. Similar results have been reported by Li et al. (2013) on wheat plants and Vezza et al. (2018) on soybean plants under Zn and As stress, respectively. Contrary to these results, reducing sugar content was observed in *Phaseolus vulgaris L.* under Pb and Cd stress (Bhardwaj et al., 2009; Younis et al., 2018a). In fact, cadmium induced perturbation in metabolism of carbohydrates by modulating their enzymes activities and causes sugar accumulation (Devi et al., 2007; Mishra and Dubey, 2013)

Protein content is inversely proportional to Cd concentrations, it decreases with Cd increasing. This is may be due to enhanced protein hydrolysis either by increased protease activity (Palma et al., 2002; Melnichuk et al., 1982) or by fragmentation of proteins due to toxic effects of reactive oxygen species. In fact, denaturant ion of functional and structural proteins is known as a result of reactive oxygen species (ROS) production in cells under stress conditions (Davies et al., 1987; Bowler et al., 1992). Moreover, decrease in protein content can also be attributed to their slowdown biosynthesis due to a decrease in nitrate reductase activity (Fresneau et al., 2007). Similar effects have been showed in several other plant species under Cd stress (Tamas et al., 1997; John et al., 2008; Aslam et al., 2014) or in *Phaseolus vulgaris* L. Plant (Bhardwaj et al., 2009; Younis et al., 2018a).

Proline has always been considered as a biomarker of drought or salt stress. Actually, several studies associated its accumulation with heavy metal stress (Alia and Pardha, 1991; Choudhary et al., 2007; Vezza et al., 2018; Younis et al., 2018a). Proline promotes photosynthetic activity, water status, antioxidative enzymes activities (Zouari et al., 2016) and assures osmotic adjustment at cellular level (Kasai et al., 1998). According to Alia and Pardha (1991), increase in proline level could be either due to its fresh synthesis and/or due to decrease in its utilization in stressed plants. Li et al. (2013) reported that accumulation of proline is due to ornithine pathway involving in OAT (ornithine d-aminotransferase) stimulation a biosynthesis enzyme of proline; on the other hand, a decrease in GK (glutamate kinase) and PDH (proline dehydrogenase) activities involved in catabolism of proline.

Changes in phenolic compounds

Oxidative stress is an important mechanism of cadmium toxicity (Smeets et al., 2005). Plants use a complex antioxidant defense system to prevent oxidative damage and keep reactive oxygen species concentrations within a narrow functional range (Ozgur et al., 2013). The primary components of this system include non-enzymatic radical scavengers among them carotenoids, flavonoides, and phenolic compounds. These components keep plant cells away from oxidative damage by scavenging ROS (Schafer et al., 2002). A better understanding of underlying antioxidant mechanisms mediated by phenolic compounds is necessary to develop strategies for contaminated crop soil.

Phaseolus vulgaris L. grown under Cd treatments showed a significant increase of phenolic compounds and total flavonoids contents in both parts of plant. Under heavy metal stress, phenolic compounds can act as transition metal ions chelators, ROS scavengers (Vollmannova et al., 2014; Manquian-Cerda et al., 2016) and can suppress lipid peroxidation by breaking radical chain reactions during lipid peroxidation (Arora et al., 2000; Sakihama and Yamasaki, 2002).

Chen et al. (2019) reported that the activity of Shikimate dehydrogenase (SKDH), cinnamyl alcohol dehydrogenase (CAD), and polyphenol oxidase (PPO) increased at the

http://www.aloki.hu ● ISSN 1589 1623 (Print) ● ISSN 1785 0037 (Online)
DOI: http://dx.doi.org/10.15666/aeer/1802_37573774

meantime when total phenolic compounds increase in *Kandelia obovata* exposed to higher concentrations of cadmium (Cd) and zinc (Zn), which indicate that Cd and Zn play a previously unrecognized but major role in phenolic compounds synthesis, transport, and metabolism. Kovácik et al. (2006) affirmed that activation of the phenylalanine ammonia-Liaza (PAL) enzyme is the main cause of increase in the phenolic metabolits concentration, since it is the main biosynthetic pathway of phenolic compounds. Increase of total phenolic compounds under Cd pollution has been reported in several plants, including *P. vulgaris* (Manquian-Cerda et al., 2016; Mongkhonsin et al., 2016; Younis et al., 2018b; Chen et al., 2019).

Flavonoids are frequently induced by abiotic stress especially by heavy metals and promote roles in plant protection (Grace and Logan, 2000; Dai et al., 2006). Biological and antioxidant activities of flavonols, among others quercetin, have been proven (Tsai et al., 2002). Posmyk et al. (2009) reported that at 0.5 mM Cu^{2+} stress, anthocyanins concentration increased and that anthocyanins synthesis was the effective strategy against ROS generated by Cu^{2+} stress. Flavonoids are known that are inhibitors of lipoxygenase enzyme, which converts polyunsaturated fatty acids to oxygen-containing derivatives (Nijveldt et al., 2001).

Posmyk et al. (2009), Mongkhonsin et al. (2016) and Younis et al. (2018b) examined common bean plant treated with metals such as Cu and Cd, and reported an increase in flavonoids concentration in both shoots and roots.

In the present study, Cd led to a marked increase of tannins. Tannins have great anti-oxidant capacities due to their phenol nuclei. According to Bruneton (1999), hydrolysable tannins are ROS and superoxide anion scavengers and are very good proton donors to ROS produced during peroxidation, resulting in more stable tannic radical formation. Tannins are known to remove heavy metals from solutions using green technology (Sun et al., 2019). Oo (2009) reported that the metal ions could interact with hydroxyl groups of mangrove tannins through an ion exchange and/or complexation process.

Anatomical changes

Plant anatomy is known to be sensitive to physical and chemical conditions, like Cd pollution area. Anatomical changes in response to Cd have been long reported (Barcelo et al., 1988; Lux et al., 2011; Pereira et al., 2018) on *Phaseolus vulgaris*, *Zea mays L.* and, *Solidago chilensis* respectively.

Presence of Cd in soil causes a decrease of both number and size of xylem vessels and a slight enlargement of cortex zone. As mentioned by Maksimovic et al. (2007), the enlargement of cortical tissues had a functional role by decreasing radial flows of water and solutes showed in maize with Cd and Ni pollution. Little information is available on development of central cylinder cells and tissues under Cd stress; this topic requires more attention, especially considering the importance of xylem translocation in regulating cadmium movement from roots to aerial tissues (Lux et al., 2011).

Our result were in accord with Aloni (1987), Barcelo et al. (1988) and Vazquez et al. (1992) who reported that Cd reduces cell division and differentiation in vascular cylinder of Cd-treated bean plants, which seems essential for both production of cambium and cambium cells differentiation into vessels and fibers leading to poor development of vascular bundles. Moreover, the differentiation of cambium to these conducting elements depends on phytohormones like auxins and cytokinins (Aloni, 1987; Bhalerao et Bennett, 2003). Lower auxin concentrations, result in slower differentiation and therefore fewer

http://www.aloki.hu ● ISSN 1589 1623 (Print) ● ISSN 1785 0037 (Online)
DOI: http://dx.doi.org/10.15666/aeer/1802_37573774

vessels (Aloni, 1988). It seems that Cd stimulates Auxin degradation (Chaoui et al., 2005). Cytokinins seem crucial for formation and maintenance of cambial cells (Fukuda, 2004), furthermore Cd may decrease cambium size and fiber differentiation in stems by inhibiting cytokinin export from roots (Aloni, 1982).

Cd exposure had not any effect on diameters of bean roots, which is in concordance with Vázquez et al. (1992). However, higher Cd concentrations can result in rhizodermis disintegration in some location of root, similar abnormal effects have been also described in tomato (Gratão et al., 2009).

Conclusion

The present study showed clearly that Cd had negative impact on seed germination, plant growth and caused several physiological and biochemical modifications in *Phaseolus vulgaris* L. Furthermore, it resulted in noticeable effects on phenolic compounds contents as antioxidant response to Cd. It is supposed that the revealed anatomical changes in xylem under Cd impact hamper fluid movement from root to shoot and are one of the reasons of nutrients decrease and pollutants translocation from roots to shoots. It might be a tolerance to abiotic stress limiting Cd impact on plant.

For future studies, evaluation of Cd effect on phenolic compounds profile and non-enzymatic antioxidants seems to be important.

REFERENCES

[1] Alia, P., Pardha, S. (1991): Proline accumulation under heavy metal stress. – Journal of Plant Physiology 138: 554-558.

[2] Alkantara, E., Romerza, F. J., Canett, M., De LaGuardia, M. D. (1994): Effect of heavy metals on both induction and function of root Fe (III) reductase in Fe-deficient cucumber (*Cucumis sativus* L.). plants. – J. Exp. Bot. 45: 1893-1898.

[3] Aloni, R. (1982): Role of cytokinin in differentiation of secondary xylem fibers. – Plant Physio. 70: 1631-1633.

[4] Aloni, R. (1987): Differentiation of vascular tissues. – Ann. Rev. Plant Physio. 38: 179-204.

[5] Aloni, R. (1988): Vascular Differentiation of within Plants. – In: Roberts, L. W., Mahan, P. B., Aloni, R. (eds.) Vascular Differentiation and Plant Growth Regulators. Springer-Verlag, Berlin, pp. 39-59.

[6] Anjum, S. A., Tanveer, M., Hussain, S., Bao, M., Wang, L., Khan, I., Shahzad, B. (2015) Cadmium toxicity in Maize (*Zea mays L.*): consequences on antioxidative systems, reactive oxygen species and cadmium accumulation. – Environ SciPollut Res 22: 17022-17030.

[7] Arora, A., Byrem, T. M., Nair, M. G., Strasburg, G. M. (2000): Modulation of liposomal membrane fluidity by flavonoids and isoflavonoids. – Archives of Biochemistry and Biophysics 373: 102-109.

[8] Aslam, R., Ansari, M. Y. K., Choudhary, S., Bhat, T. M., Jahan, N. (2014): Genotoxic effects of heavy metal cadmium on growth, biochemical, cyto-physiological parameters and detection of DNA polymorphism by RAPD in *Capsicum annuum* L. - an important spice crop of India. – Saudi Journal of Biological Sciences 21: 465-472.

[9] Audet, P., Charest, C. (2007): Heavy metal phytoremediation from a meta-analytical perspective. – Environ. Pollut. 147: 2337.

[10] Bahorun, T., Gressier, B., Trotin, F., Brunet, C., Dine, T., Luyckx, M., Vasseur, J., Cazin, M., Cazin, J. C., Pinkas, M. (1996): Oxygen species scavenging activity of phenolic extracts from hawthorn fresh plant organs and pharmaceutical preparations. – Arzneim Forsch 46: 1086-1108.

http://www.aloki.hu ● ISSN 1589 1623 (Print) ● ISSN 1785 0037 (Online)
DOI: http://dx.doi.org/10.15666/aeer/1802_37573774

[11] Barcelo, J., Vazquez, M. D., Poschenrieder, C. (1988): Structural and ultrastructural disorders in cadmium-treated bush bean plants (*Phaseolus vulgaris* L.). – New Phytol 108: 37-49.
[12] Bates, L. S., Waldren, R. P., Teare, I. D. (1973): Rapid determination of free proline for water stress studies. – Plant Soil 39: 205-207.
[13] Bhalerao, R., Bennett, M. (2003): The case for morphogens in plants. – Nature Cell Biology 5: 939-943.
[14] Bhardwaj, P., Chaturvedi, A. K., Prasad, P. (2009): Effect of enhanced lead and cadmium in soil on physiological and biochemical attributes of *Phaseolus vulgaris* L. – Nat. Sci 7: 63-75.
[15] Bowler, C., Van Montagu, M., Inze, D. (1992): Superoxide dismutase and stress tolerance. – Annu. Rev. Plant Physiol. Plant Mol. Biol. 43: 83-116.
[16] Bradford, M. M. (1976): A rapid and sensitive method for the quantitation of microgram quantities of protein utilizing the principle of protein-dye binding. – Anal. Biochem 72: 248-254.
[17] Bruneton, J. (1999): Pharmacognosie, phytochimie, plantes médcinales. – Thechnique et Documentation. Ed. Lavoisier., Paris, pp. 227-401.
[18] Chang, Y. S., Chang, Y. J., Lin, C. T., Lee, M. C., Wu, C. W., Lai, Y. H. (2013): Nitrogen fertilization promotes the phytoremediation of cadmium in *Pentas lanceolata*. – Int Biodeter Blodegr. 85: 709-714.
[19] Chaoui, A., El Ferjani, E. (2005): Effects of cadmium and copper on antioxidant capacities, lignification and auxin degradation in leaves of pea (*Pisum sativum* L.) seedlings. – C R Biol. 328: 23-31.
[20] Chen, S., Wang, Q., Lu, H., Li, J., Yang, D., Liu, J., Yan, C. (2019): Phenolic metabolism and related heavy metal tolerance mechanism in *Kandelia obovata* under Cd and Zn stress. – Ecotoxicology and Environmental Safety 169: 134-143.
[21] Choudhary, M., Jetley, U. K., Abash, M., Zutshi, K. S., Fatma, T. (2007): Effect of heavy metal stress on proline, malondialdehyde, and superoxide dismutase activity in the *cyanobacterium spirulina* platensis-S5. – Ecotoxicology and Environmental Safety 66: 204-209.
[22] Chugh, L. K., Sawhney, S. K. (1995): Effect of cadmium on germination, amylases and rate of respiration of germinating pea seeds. – Environmental Pollution 92: 1-5.
[23] Cruces, E., Rojas-Lillo, Y., Ramirez-Kushel, E., Atala, E., López-Alarcón, C., Lissi, E., Gómez, I. (2015): Comparison of different techniques for the preservation and extraction of phlorotannins in the kelp *Lessonia spicata* (Phaeophyceae): assays of DPPH, ORAC-PGR, and ORAC-FLas testing methods. – J. Appl. Phycol. 28: 573-580.
[24] Cuypers, A., Smeets, K., Ruytinx, J., Opdenakker, K., Keunen, E., Remans, T., Horemans, N., Vanhoudt, N., Van Sanden, S., Van Belleghem, F. (2011): The cellular redox state as a modulator in cadmium and copper responses in *Arabidopsis thaliana* seedlings. – J. Plant Physiol 168: 309-316.
[25] Dai, L. P., Xiong, Z. T., Huang, Y., Li, M. J. (2006): Cadmium-induced changes in pigments, total phenolics, and phenylalanine ammonialyase activity in fronds of *Azolla imbricate*. – Environ. Toxicol. 21: 505-512.
[26] Davies, C. S., Nielsen, S. S., Nielsen, N. C. (1987): Flavor improvement of soybean preparations by genetic removal of lipoxygenase-2. – J. Am. Oil Chem. Soc 64: 1428-1433.
[27] Devi, R., Munjral, N., Gupta, A. K., Kaur, N. (2007): Cadmium induced changes in carbohydrate status and enzymes of carbohydrate metabolism, glycolysis and pentose phosphate pathway in pea. – Environ. Exp. Bot. 61: 167-174.
[28] Dias, M. C., Monteiro, C., Moutinho-Pereira, J., Correia, C., Gonçalves, B., Santos, C. (2013): Cadmium toxicity affects photosynthesis and plant growth at different levels. – ActaPhysiol Plant 35: 1281-1289.
[29] Dische, Z. (1962): Color Reactions of Hexoses. – In: Whistler, R. L., Wolfrom, M. L. (eds.) Methods in Carbohydrate Chemistry. Vol. 1. Academic Press, New York, pp. 488-490.

http://www.aloki.hu ● ISSN 1589 1623 (Print) ● ISSN 1785 0037 (Online)
DOI: http://dx.doi.org/10.15666/aeer/1802_37573774

[30] Escudey, M., Forster, J. E., Becerra, J. P., Quinteros, M., Torres, J., Arancibia, N., Galindo, G., Chang., A. C. (2007): Disposal of domestic sludge and sludge ash on volcanic soils. – J. Hazard. Mater. 139: 550-555.
[31] Fattahi, B., Arzani, K., Souri, M. K., Barzegar, M. (2019): Effects of cadmium and lead on seed germination, morphological traits, and essential oil composition of sweet basil (*Ocimum basilicum* L.). – Industrial Crops & Products 138: 111584.
[32] Fresneau, C., Ghashghaie, J., Cornic, G. (2007): Drought effect on nitrate reductase and sucrose phosphate synthase activities in wheat (*Triticum durum* L.): role of leaf internal CO2. – Journal of Experimental Botany 58: 2983-2992.
[33] Fukuda, H. (2004): Signals that control plant vascular cell differentiation. – Nature Reviews Molecular Cell Biology 5: 379-391.
[34] Grace, S. C., Logan, B. A. (2000): Energy dissipation and radical scavenging by the plant phenyl propanoid pathway. – Philosophical Transactions of the Royal Society B 355: 149510.
[35] Gratao. P. L., Monteiro, C. C., Rossi. M. L., Martinelli, A. P., Peres, L. E. P., Medici, L. O., Lea, P. J., Azevedo, R. A. (2009): Differential ultrastructural changes in tomato hormonal mutants exposed to cadmium. – Environ Exp Bot 67: 387-394.
[36] Guo, H., Hong, C., Chen, X., Xu, Y., Liu, Y., Jiang, D. (2016): Different growth and physiological responses to cadmium of the three Miscanthus species. – PLoS One 11: 0153475.
[37] Gupta, D. K., Pena, L. B., Romero-Puertas, M. C., Hernández, A., Inouhe, M., Sandalio, L. M. (2017): NADPH oxidases differentially regulate ROS metabolism and nutrient uptake under cadmium toxicity. – Plant Cell Environ 40: 509-526.
[38] He, S. Y., Yang, X. E., He, Z., Baligar, V. C. (2017): Morphological and physiological responses of plants to cadmium toxicity: a review. – Pedosphere 27: 421-438.
[39] Hsu, F. H., Chang-Hung Chou (1992): Inhibitory effects of heavy metals on seed germination and seedling growth of Miscanthus species. – Bot. Bull. Acad. Sin. 33: 3342.
[40] John, R., Ahmad, P., Gadgil, K., Sharma, S. (2008): Effect of cadmium and lead on growth, biochemical parameters and uptake in *Lemna polyrrhiza* L. – Plant Soil Environ. 54: 262-270.
[41] Kabata-Pendias, A. (2000): Trace Elements in Soils and Plants. 3rd Ed. – CRC Press, Boca Raton.
[42] Kasai, Y., Kato, M., Aoyama, J., Hyodo, H. (1998): Ethylene production and increase in 1 aminocyclopropane-1 carboxylate oxidase activity during senescence of broccoli florets. – Acta Horticulturae 464: 153-157.
[43] Keunen, E., Peshev, D., Van gronsveld, J., Van den ende, W. (2013): Plant sugars are crucial players in the oxidative challenge during abiotic stress: extending the traditional concept. – Plant, Cell & Environment 36: 1242-1255.
[44] Ko, K. S., Lee, P. K., Kong, I. C. (2012): Evaluation of the toxic effects of arsenite, chromate, cadmium, and copper using a battery of four bioassays. – Appl Microbiol Biotechnol 95: 1343-1350.
[45] Kovcik, J., Tomko, J., Backor, M., Repcak, M. (2006): *Matricaria chamomilla* is not a hyperaccumulator, but tolerant to cadmium stress. – Plant Growth Regul 50: 239-247.
[46] Kranner, I., Colville, L. (2011): Metals and seeds: biochemical and molecular implications and their significance for seed germination. – Environ. Exp. Bot. 72: 93-105.
[47] Kumaran, A., Karunakaran, R. J. (2007a): Activity-guided isolation and identification of free radical-scavenging components from an aqueous extract of *Coleus aromaticus*. – Food Chemistry 100: 356-361.
[48] Kumaran, A., Karunakaran, R. J. (2007b): In vitro antioxidant activities of methanol extracts of Phyllanhtus species from India. – Lebens-Wiss Technol 40: 344-352.
[49] Lang, F., Sarvari, E., Szigeti, Z., Fodor, F., Cseh, E. (1995): Effects of Heavy Metals on the Photosynthetic Apparatus in Cucumber. – In: Mathis, P. (ed.), Photosynthesis: From Light to Biosphere. Kluwer Academic Publishers, Dordrecht, pp. 533-536.

http://www.aloki.hu ● ISSN 1589 1623 (Print) ● ISSN 1785 0037 (Online)
DOI: http://dx.doi.org/10.15666/aeer/1802_37573774

[50] Li, W., Khan, M. A., Yamaguchi, S., Kamiya, Y. (2005): Effects of heavy metals on seed germination and early seedling growth of *Arabidopsis thaliana*. – Plant Growth Regulation 46: 45-50.
[51] Li, X., Yang, Y., Jia, L., Chen, H., Wei, X. (2013): Zinc-induced oxidative damage, antioxidant enzyme response and proline metabolism in roots and leaves of wheat plants. – Ecotoxicol. Environ. Saf. 89: 150-157.
[52] Lichtenthaler, H. K., Wellburn, A. R. (1983): Determinations of total carotenoids and chlorophylls *a* and *b* of leaf extracts in different solvents. – Biochem Society Transactions 11: 591-592.
[53] Locquin, M., Langeron, M. (1978): Manuel de microscopie. – Ed. Masson, France.
[54] Loi, N. N., Sanzharova, N. I., Shchagina, N. I., Mironova, M. P. (2018): The effect of cadmium toxicity on the development of lettuce plants on contaminated sod-podzolic soil. – Russ. Agric. Sci. 44: 49-52.
[55] Lux, A., Martinka, M., Vaculık, M., White, P. J. (2011): Root responses to cadmium in the rhizosphere: a review. – J. Exp. Bot. 62: 21-37.
[56] Maksimovic, I., Kastori, R., Krstic, L., Lukovic, J. (2007): Steady presence of cadmium and nickel affects root anatomy, accumulation and distribution of essential ions in maize seedlings. – Biologia Plantarum 51: 589-592.
[57] Manquián-Cerda, K., Escudey, M., Zúñiga, G., Arancibia-Miranda, N., Molina, M., Cruces, E. (2016): Effect of cadmium on phenolic compounds, antioxidant enzyme activity and oxidative stress in blueberry (*Vaccinium corymbosum* L.) plantlets grown in vitro. – Ecotoxicol. Environ. Saf. 133: 316-326.
[58] Manquián-Cerda, K., Cruces, E., Escudey, C., Zúñiga, G., Calderon, R. (2018): Interactive effects of aluminum and cadmium on phenolic compounds, antioxidant enzyme activity and oxidative stress in blueberry (*Vaccinium corymbosum* L.) plantlets cultivated in vitro. – Ecotoxicology and Environmental Safety 150: 320-326.
[59] McLaughlin, M. J., Whatmuff, M., Warne, M., Heemsbergen, D., Barry, G., Bell, M., Nash, D., Pritchardet, D. (2006): A field investigation of solubility and food chain accumulation of biosolid-cadmium across diverse soil types. – Environ Chem: 3428-432.
[60] Melnichuk Yu, P., Lishko, A. K., Kalinin, F. L. (1982): Cd effect on free amino acid content in germs of pea seeds at early germination stages. – Fiziologiya biokhimiya kulturnyh Rasstenii 14: 383-385.
[61] Meyers, K. J., Watkins, C. B., Pritts, M. P., Liu, R. H. (2003): Antioxydant and antiproliferative activities of strawberries. – Journal of Agricultural and Food Chemistry 51: 6887-6892.
[62] Michalak, A., 2010. Phenolic compounds and their antioxidant activity in plants growing under heavy metal stress. – Pol. J. Environ. Stud.15: 523-530.
[63] Mishra, P., Dubey, R. S. (2013): Excess nickel modulates activities of carbohydrate metabolizing enzymes and induces accumulation of sugars by up regulating acid invertase and sucrose synthase in rice seedlings. – Biometals 26: 97-111.
[64] Mole, S., Waterman, P. G. (1987): A critical analysis of techniques for measuring tannins in ecological studies. II. Techniques for biochemically defining tannins. – Oecologia 72: 148-156.
[65] Molnarova, M., Fargasova, A. (2012): Relationship between various physiological and biochemical parameters activated by cadmium in *Sinapisalba* L. and *Hordeum vulgare* L. – Ecological Engineering 49: 62.
[66] Mongkhonsin, B., Nakbanpote, W., Hokura, A., Nuengchamnon, N., Maneechai, S. (2016): Phenolic compounds responding to zinc and/or cadmium treatments in *Gynura pseudochina* (L.) DC. Extracts and biomass. – Plant Physiol. Biochem. 109: 549-560.
[67] Munzuroglu, O., Geckil, H. (2002): Effects of metals on seed germination, root elongation, and coleoptile and hypocotyl growth in *Triticuma estivum* and *Cucumis sativus*. – Bull. Environ. Contam. Toxicol. 43: 203-213.

http://www.aloki.hu ● ISSN 1589 1623 (Print) ● ISSN 1785 0037 (Online)
DOI: http://dx.doi.org/10.15666/aeer/1802_37573774

[68] Munzuroğlu, O., Zengin, F. K., Yahyagil, Z. (2008): The abscisic acid levels of wheat (*Triticuma estivum* L. Cv. Cakmak 79) seeds that were germinated under heavy metal (Hg^{++}, Cd^{++}, Cu^{++}) stress. – J. Fac. Pharm. Gazi. 21: 1-7.
[69] Nijveldt, R. J., Van Nood, E., Van Hoorn, D. E. C., Boelens, P. G., Van Norren, K., Van Leeuwen, P. A. M. (2001): Flavonoids: a review of probable mechanisms of action and potential applications. – American Society for Nutrition 74: 418-425.
[70] Oo, C. W., Kassima, M. J., Pizzib, A. (2009): Characterization and performance of *Rhizophora apiculata* mangrove polyflavonoid tannins in the adsorption of copper (II) and lead (II). – Industrial Crops and Products 30: 152-161.
[71] Ovecka, M., Takac, T. (2014): Managing heavy metal toxicity stress in plants: biological and biotechnological tools. – Biotechnol. Adv. 32: 73-86.
[72] Ozgur, R., Uzilday, B., Sekmen, A. H., Turkan, I. (2013): Reactive oxygen species regulation and antioxidant defence in halophytes. – Functional Plant Biology 40: 832-847.
[73] Palma, J. M., Sandalio, L. M., Javier Corpas, F., Romero-Puertas, M. C., McCarthy, I., del Rio, L. A. (2002): Plant proteases protein degradation and oxidative stress: role of peroxisomes. – Plant Physiol. Biochem 40: 521-530.
[74] Pereira, L. S., Pereira de Araújob, R., Souza de Oliveirac, P., Dias da Silvac, L., CasaesAlvesa, P. A., Fernandesd, V. F., Gross, E. (2018): Cadmium induced changes in *Solidago chilensis Meyen* (Asteraceae) grown on organically fertilized soil with reference to mycorrhizae, metabolism, anatomy and ultrastructure. – Ecotoxicology and Environmental Safety 150: 75.
[75] Peshev, D., Van den Ende, W. (2013): Sugars as Antioxidants in Plants. – In: Tuteja, N., Gill, S. S. (eds.) Crop Improvement under Adverse Conditions. Springer-Verlag, Berlin.
[76] Posmyk, M. M., Kontek, R., Janas, K. M. (2009) Antioxidant enzymes activity and phenolic compounds content in red cabbage seedlings exposed to copper stress. – Ecotoxicology and Environmental Safety 72: 596-602.
[77] Sakihama, Y., Yamasaki, H. (2002): Lipid peroxidation induces by phenolics in cinjunction with aluminium ions. – Biol. Plantarum 45: 249-254.
[78] Schafer, F. Q., Wang, H. P., Kelly, E. E. (2002): Comparing beta-carotene, vitamin E and nitric oxide as membrane antioxidants. – The Journal of Biological Chemistry 383: 671-681.
[79] Seregin, I. V., Ivanov, V. B. (2001): Physiological aspects of cadmium and lead toxic effects on higher plants. – Russ. J. Plant Physiol 48: 523-544.
[80] Smeets, K., Cuypers, A., Lambrechts, A., Semane, B., Hoet, P., Van Laere, A., Vangronsveld, J. (2005): Induction of oxidative stress and antioxidative mechanisms in *Phaseolus vulgaris* after Cd application. – Plant Physiology and Biochemistry 43: 437-444.
[81] Somashekaraiah, B. V., Padmaja, K., Prasad, A. R. K. (1992): Phytotoxicity of cadmium ions on germinating seedlings of mung bean (*Phaseolus vulgaris*): Involvement of lipid peroxides in chlorphyll degradation. – Physiol Plant. 85: 85-89.
[82] Stobart, A. K., Griffiths, W. T., Ameen-Bukhari, I., Sherwood, R. P. (1985): The effect of Cd^{2+} on the biosynthesis of chlorophyll in leaves of barley. – Physiol. Plant. 63: 293-298.
[83] Sun, H., Xia, N., Liu, Z., Kong, F., Wang, S. (2019): Removal of copper and cadmium ion from alkaline solution using chitosan-tannin functional paper materials as adsorbents. – Chemosphere 236: 124370.
[84] Swain, T., Hillis, W. E. (1959): The phenolics constituants of *Prunus domestica*-I. The quantitative analysis of phenolics constituents. – Journal of the Science of Food and Agriculture 10: 13.
[85] Tamas, L., Huttova, J., Zigova, Z. (1997): Accumulation of stress protein in intracellular spaces of barley leaves induced by biotic and abiotic factors. – Biol. Plant. 39: 387-394.
[86] Tsai, P. J., McInstosh, J., Pearce, P., Camden, B., Jordan, B. R. (2002): Anthocyanin and antioxidant capacity in Roselle (*Hibiscus sabdariffa* L.) extract. – Food Res. Int. 35: 351-356.

http://www.aloki.hu ● ISSN 1589 1623 (Print) ● ISSN 1785 0037 (Online)
DOI: http://dx.doi.org/10.15666/aeer/1802_37573774

[87] Vaculík, M., Konlechner, C., Langer, I., Adlassnig, W., Puschenreiter Alexander., Hauser, L. M. T. (2012): Root anatomy and element distribution vary between two *Salix caprea* isolates with different Cd accumulation capacities. – Environmental Pollution 163: 117-126.
[88] Van Assche, F., Clijsters, H. (1990): Effects of metals on enzyme activity in plants. – Plant Cell Environ. 13: 195-206.
[89] Vazquez, M. D., Poschenrieder, C., Barcelo, J. (1992): Ultrastructural effects and localization of low cadmium concentrations in bean roots. – New Phytologist 120: 215-226.
[90] Verbruggen, N., Hermans, C., Schat, H. (2009): Molecular mechanisms of metal hyperaccumulation in plants. – New Phytol 181: 759-77.
[91] Vezza, M. E., Llanes, A., Travaglia, C., Agostinia, E., Talanoa, M. A. (2018): Arsenic stress effects on root water absorption in soybean plants: physiological and morphological aspects. – Plant Physiology and Biochemistry 123: 8-17.
[92] Volland, S., Bayer, E., Baumgartner, V., Andosch, A., Lutz, C., et al. (2014): Rescue of heavy metal effects on cell physiology of the algal model system Micrasterias by divalent ions. – J. Plant Physiol. 171: 154-163.
[93] Vollmannova, A., Musilova, J., Toth, T., Arvay, J., Bystrick, J., Medvecky, M., Daniel, J. (2014): Phenolic compounds, antioxidant activity and Cu, Zn, Cd and Pb content in wild and cultivated cranberries and blue berries Intern. – J. Environ. Anal. Chem 94: 1445-1451.
[94] Wang, W., Keturi, P. H. (1990): Comparative seed germination tests using ten plant species for toxicity assessment of metals engraving effluent sample. – Water, Air, Soil Pollut. 52: 369-376.
[95] Xue, Z. C., Gao, H. Y., Zhang, L. T. (2013): Effects of cadmium on growth, photosynthetic rate and chlorophyll content in leaves of soybean seedlings. – Biol Plant 57: 587-590.
[96] Yazdi, M., Kolahi, M., MohajelKazemi, E., GoldsonBarnaby, A. (2019): Study of the contamination rate and change in growth features of lettuce (*Lactuca sativa* Linn.) in response to cadmium and a survey of its phytochelatin synthase gene. – Ecotoxicology and Environmental Safety 180: 295-308.
[97] Younis, M. E., Tourky, S. M. N., Elsharkawy. E. A. (2018a): Element content, growth and metabolic changes in Cu- and Cd stressed *Phaseolus vulgaris* plants. – Journal of Plant and Environmental Research 3: 9.
[98] Younis, M. E., Tourky, S. M. N., Elsharkawy, S. E. A. (2018b): Symptomatic parameters of oxidative stress and antioxidant defensesystem in *Phaseolus vulgaris* L. in response to copper or cadmium stress. – South African Journal of Botany 117: 207-214.
[99] Zemanova, V., Pavlík, M., Pavlíkova, D., Kyjakova, P. (2015): Changes in the contents of amino acids and the profile of fatty acids in response to cadmium contamination in spinach. – Plant Soil Environ 61: 285-290.
[100] Zouari, M., Ben Ahmed, Ch., Zorrig, W., Elloumi, N., Rabhi, M., Delmail, D., Ben Rouina, B., Labrousse, P., Ben Abdallaha, F. (2016): Exogenous proline mediates alleviation of cadmium stress by promoting photosynthetic activity, water status and antioxidative enzymes activities of young date palm (*Phoenix dactylifera L.*). – Ecotoxicology and Environmental Safety 128: 100-108.

http://www.aloki.hu ● ISSN 1589 1623 (Print) ● ISSN 1785 0037 (Online)
DOI: http://dx.doi.org/10.15666/aeer/1802_37573774